nature

INTERNATIONAL WEEKLY JOURNAL OF SCIENCE

Volume 321 No 6065 1-7 May 1986 £1.90

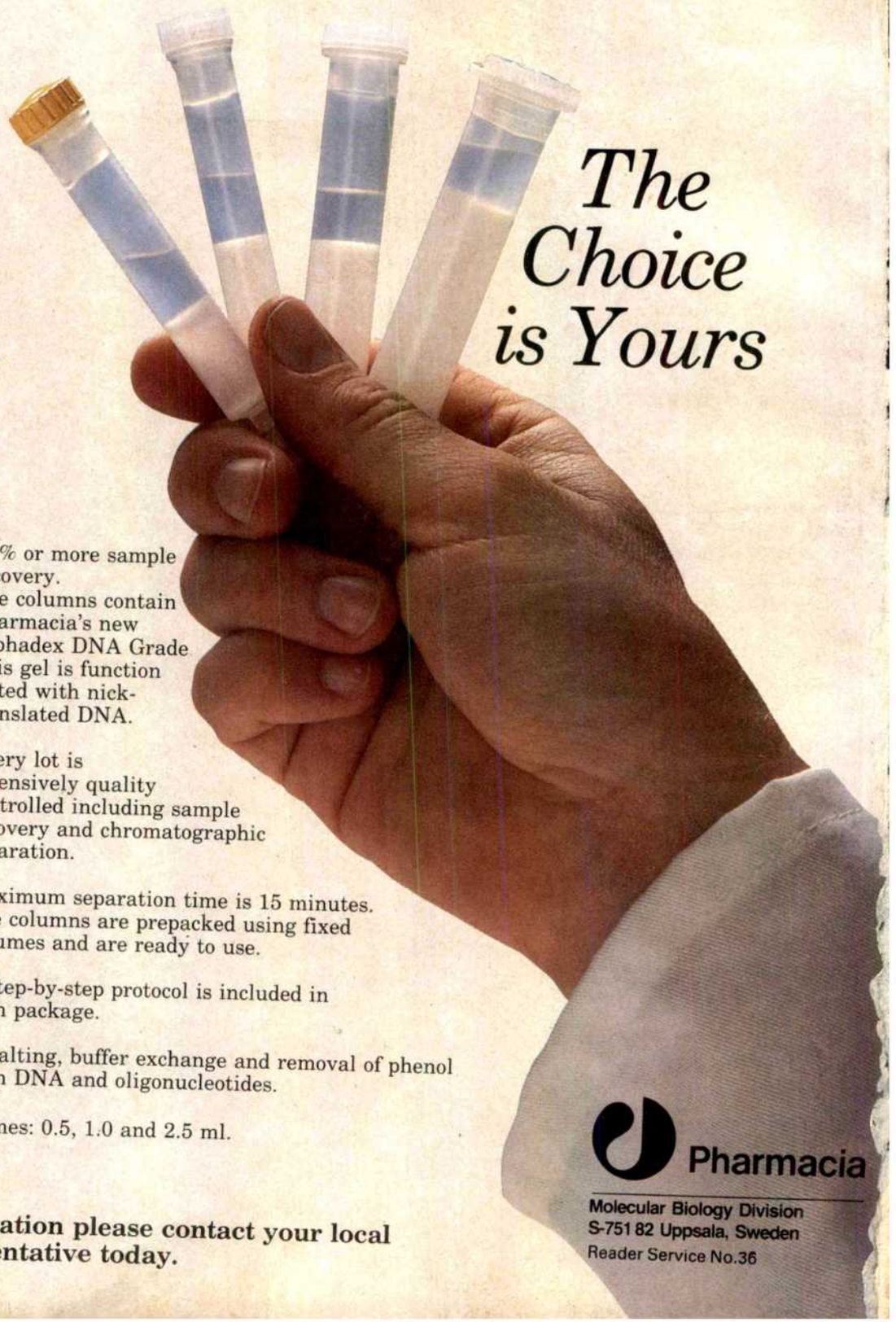


SELF-INCOMPATIBILITY IN FLOWERING PLANTS

COMPUTER CHEMISTRY

product review

NAP™-columns for DNA and Oligonucleotide Purification



The Choice is Yours

HIGH YIELDS: 90 % or more sample recovery. The columns contain Pharmacia's new Sephadex DNA Grade This gel is function tested with nick-translated DNA.

REPRODUCIBLE: Every lot is extensively quality controlled including sample recovery and chromatographic separation.

TIME SAVING: Maximum separation time is 15 minutes. The columns are prepacked using fixed volumes and are ready to use.

EASY TO USE: A step-by-step protocol is included in each package.

APPLICATIONS: Desalting, buffer exchange and removal of phenol from DNA and oligonucleotides.

Maximum sample volumes: 0.5, 1.0 and 2.5 ml.

For further information please contact your local Pharmacia representative today.

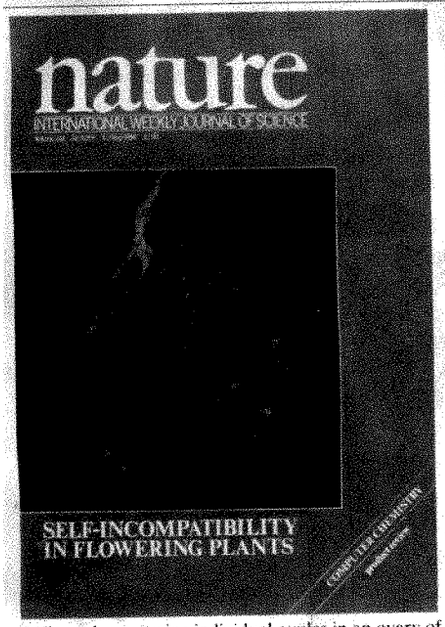
Pharmacia

Molecular Biology Division
S-751 82 Uppsala, Sweden
Reader Service No.36

CUL-H0685 S-312 — RP439

nature

ATURE VOL. 321 1 MAY 1986



Pollen tubes entering individual ovules in an ovary of the wild-tomato *Lycopersicon peruvianum*. Successful pollination in this species, as in many other plants, is determined by a highly polymorphic genetic locus (the *S*-gene) in such a way that self-fertilization is prevented. The cloning of the *S*-gene of tobacco (*Nicotiana alata*) is reported on pages 38 – 44 of *Nature*, and discussed in News and Views on page 20.

OPINION

What will emerge from Tokyo? 1
What's in a name? 2
Cloud over Chernobyl

NEWS

Virus nomenclature 3
British astronomy 4
SDI in Japan 5
Animal protection
Japanese education 6
Soviet science
Biology at Berkeley 7
Engineered vaccines
Britain squeezed
French budget cut 8
Military research
Lawrence Berkeley laboratory 9
UK flood channel

CORRESPONDENCE

New name for AIDS virus, UK civil plutonium 10

NEWS AND VIEWS

Is there inanimate memory? 11
Molecular genetics of colour vision
J D Mollon 12
Taxonomic tangles from Australia
Tony Thulborn 13
Ocean Drilling Program: Mid-Atlantic bare-rock drilling and hydrothermal vents
Leg 106 shipboard scientific party 14
Adrenergic receptors: Some similarities and surprises
Peter Newmark 15
The most reliable black hole yet
M G Watson 16
Mathematics: Hermann Grassman was right
Ian Stewart 17
Origins of the cytoskeleton
Carl M Cohen 18
Information technology: New flow of ideas in networks
Alistair Mees 19
Molecular biology: Self-incompatibility in plants
John Fincham 20

SCIENTIFIC CORRESPONDENCE

Keeping supercomputers under control
J H Cushman & F J Wobber 21
The real hazards of nuclear fallout
J B Knox & C S Shapiro 21

BOOK REVIEWS

Evolution Through Group Selection
by V C Wynne-Edwards
Eric Charnov 23
Low Temperature Methods in Biological Electron Microscopy
by A W Robards and U B Sleytr
Daniel Branton 25
Numerical Methods in Quaternary Pollen Analysis
by H J B Birks and A D Gordon
and
Pollen Records of Late-Quaternary North American Sediments
V M Bryant Jr and R G Holloway, eds
Peter Moore
The Brain Machine: The Development of Neurophysiological Thought
by M Jeannerod
Richard Passingham 26

REVIEW ARTICLE

The mean mass density of the Universe
P J E Peebles 27

ARTICLES

Black smokers, massive sulphides and vent biota at the Mid-Atlantic Ridge
P A Rona, G Klinkhammer, T A Nelsen, J H Trefry & H Elderfield 33
[C]loning of cDNA for a stylar glycoprotein associated with expression of self-compatibility in *Nicotiana alata*
M A Anderson, E C Cornish, S-L[illegible] E G Williams, R Hoggart, A [illegible]on, I Bonig, B Grego, R S [illegible]pson, P J Roche, J D Haley, J D [illegible]nschow, H D Niall, G W [illegible]egear, J P Coghlan, R J Crawford & A E Clarke 38

LETTERS TO NATURE

'Missing image' in gravitational lens systems?
D Narasimha, K Subramanian & S M Chitre 45
Resolution of Crab nebula filaments into chains of quasistellar knots
S van den Bergh & C J Pritchet 46
A flare-induced cascade model of γ-ray bursts
P A Sturrock 47
Tidal reorientation and the fracturing of Jupiter's moon Europa
A S McEwen 49
Ionic structure in aqueous electrolyte solution by the difference method of X-ray diffraction
N T Skipper, S Cummings, G W Neilson & J E Enderby 52
Constant-geometry edge-flaking of brittle materials
E A Almond & N J McCormick 53
Inferred oxygen isotope profile of Archaean oceanic crust, Onverwacht Group, South Africa
S E Hoffman, M Wilson & D S Stakes 55
Input of excess CO_2 to the surface ocean based on $^{13}C/^{12}C$ ratios in a banded Jamaican sclerosponge
E R M Druffel & L M Benavides 58
Molecular evidence for a terrestrial component of organic matter dissolved in ocean water
K J Meyers-Schulte & J I Hedges 61
Fluorescently labelled Na^+ channels are localized and immobilized to synapses of innervated muscle fibres
K J Angelides 63
Single cyclic GMP-activated channel activity in excised patches of rod outer segment membrane
L W Haynes, A R Kay & K-W Yau 66

Contents continued overleaf

Nature® (ISSN 0028-0836) is published weekly on Thursday, except the last week in December, by Macmillan Journals Ltd and includes the Annual Index (mailed in February). Annual subscription for USA and Canada US $240. USA and Canadian orders to: *Nature*, Subscription Dept, PO Box 1501, Neptune, NJ 07753, USA. Other orders to *Nature*, Brunel Road, Basingstoke, Hants RG21 2XS, UK. Second class postage paid at New York, NY 10012 and additional mailing offices. Authorization to photocopy material for internal or personal use, or internal or personal use of specific clients, is granted by *Nature* to libraries and others registered with the Copyright Clearance Center (CCC) Transactional Reporting Service, provided the base fee of $1.00 a copy plus $0.10 a page is paid directly to CCC, 21 Congress Street, Salem, Massachusetts 01970, USA. Identification code for *Nature*: 0028-0836/86 $1.00 + $0.10. US Postmaster send address changes to: *Nature*, 65 Bleecker Street, New York, NY 10012. Published in Japan by Macmillan Shuppan K.K., Eikow Building, 1-10-9 Hongo, Bunkyo-ku, Tokyo, Japan. © 1986 Macmillan Journals Ltd

The Quest for Process Perfection – Q and S Sepharose® Fast Flow Gels

Q and S Sepharose Fast Flow gels are strong ion exchangers that have been developed for the biotechnology industry where biologically active compounds are purified from large volumes of raw material. Processing time is now minimized without compromise in end-product quality.

Industrially dedicated

Physical stability

The rigidity of the matrix allows for outstanding flow rates, compatible with production requirements, even at elevated pressures.

Chemical stability

The outstanding gel performance enables effective operation in industrial environments. The gel may be stored at 40°C in 2 M NaOH for at least 7 days with no change in gel properties. This stability allows for;

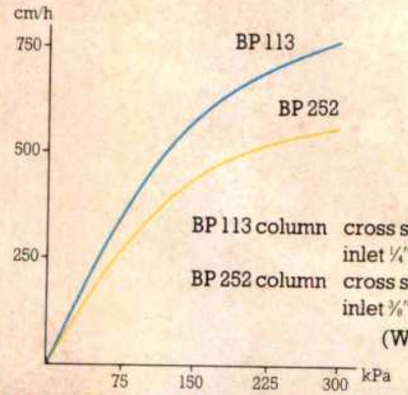
- Process directed sanitation.
- Cleaning in place procedures.

Pharmacia is dedicated to developing media to meet the exacting demands of your industry.

Try Q and S Sepharose Fast Flow today, contact Pharmacia and join the quest.

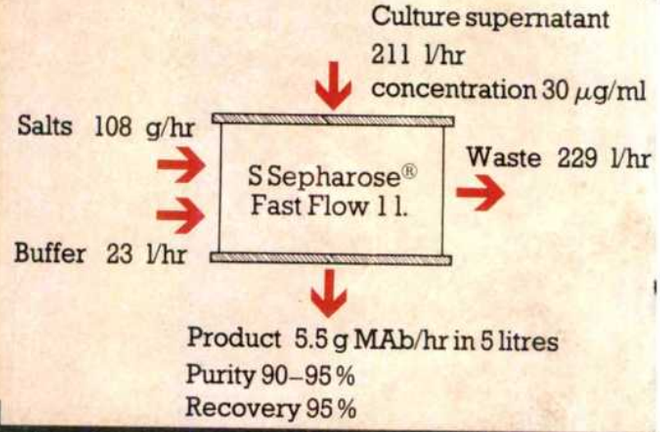
Process Scale Flow Rates

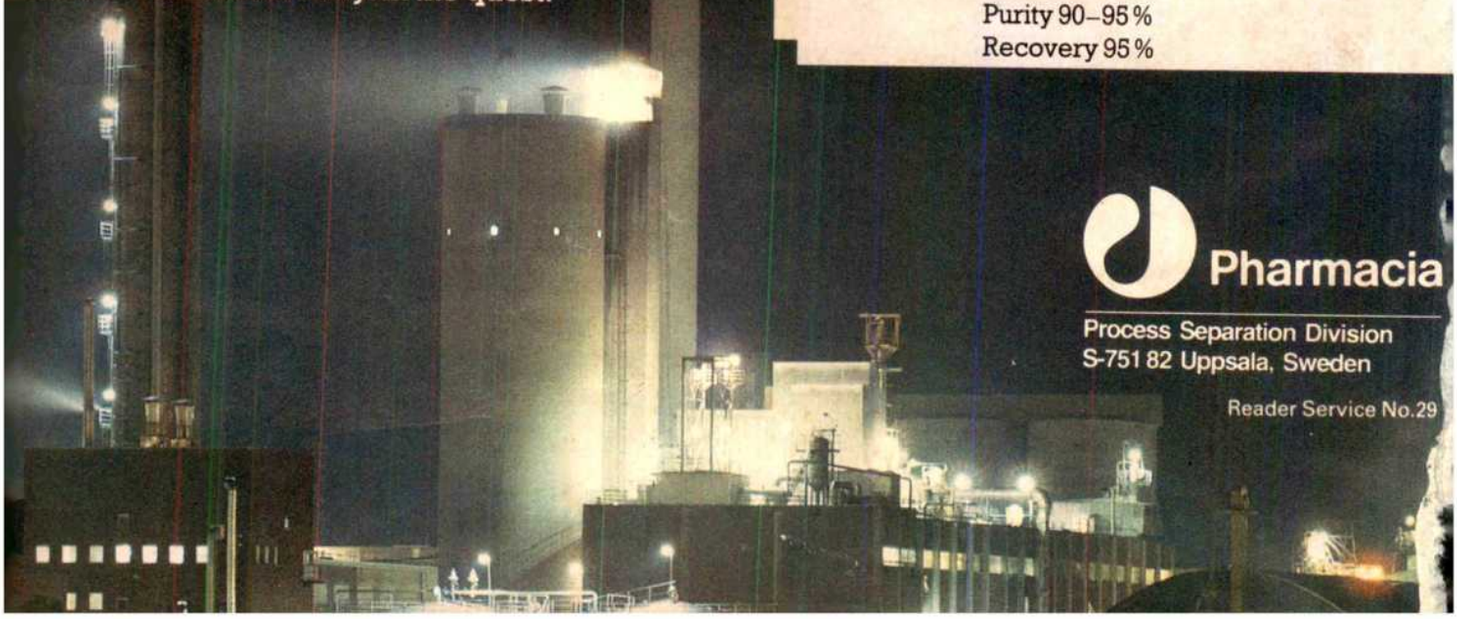
Pressure/flow rate curves for Q Sepharose Fast Flow



BP 113 column cross sectional area 100 cm^2 inlet ¼". Bed height 15 cm.
BP 252 column cross sectional area 500 cm^2 inlet ⅜". Bed height 15 cm.
(Work from Pharmacia)

Cost Effective Production





Pharmacia

Process Separation Division
S-751 82 Uppsala, Sweden

Reader Service No.29

HALLEY'S COMET

SPECIAL SUPPLEMENT

Nature's May 15 issue will carry a 100 page supplement on Halley's Comet.

The supplement brings together for the first time the results of missions being carried out from Russia, Europe and Japan.

Among other items, reports will include extensive data on the composition of cometary gases, the density of the dust storm near the comet's core and the interactions between the comet and the solar winds buffeting it, as well as the first ever photos of the comet's nucleus.

RESERVE YOUR EXTRA COPIES OF THE SUPPLEMENT TODAY BY WRITING TO OUR BASINGSTOKE OFFICE (prices as for back issues below).

Supply can be guaranteed only if we receive your order before May 9.

Annual Subscription Prices

UK & Irish Republic		£104
USA & Canada		US$240
Australia, NZ & S. Africa	Airspeed	£150
	Airmail	£190
Continental Europe	Airspeed	£125
India	Airspeed	£120
	Airmail	£190
Japan	Airspeed	Y90000
Rest of World	Surface	£120
	Airmail	£180

Orders (with remittance) to:

USA & Canada
Nature
Subscription Dept
PO Box 1501
Neptune
NJ 07753
USA

UK & Rest of World
Nature
Circulation Dept
Brunel Road
Basingstoke
Hants RG21 2XS, UK
Tel: 0256 29242

(The addresses of Nature's editorial offices are shown facing the first editorial page)

Japanese subscription enquiries to:
Japan Publications Trading Company Ltd
2-1 Sarugaku-cho 1-chome
Chiyoda-ku, Tokyo, Japan
Tel: (03) 292 3755

Personal subscription rates: These are available in some countries to subscribers paying by personal cheque or credit card. Details from:

USA & Canada
Nature
65 Bleecker Street
New York
NY 10012, USA
Tel: (212) 477-9600

UK & Europe
Felicity Parker
Nature
4 Little Essex Street
London WC2R 3LF, UK
Tel: 01-836 6633

Back issues: UK, £2.50; USA & Canada, US$6.00 (surface), US$9.00 (air); Rest of World, £3.00 (surface), £4.00 (air)

Binders
Single binders: UK, £5.25; USA & Canada $11.50; Rest of World, £7.75. Set of four: UK, £15.00; USA & Canada $32.00; Rest of World, £22.00

Annual indexes (1971-1985)
UK, £5.00 each; Rest of World, $10.00

Nature First Issue Facsimile
UK, £2.00; Rest of World (surface), $3.00; (air) $4.00

Nature in microform
Write to University Microfilms International, 300 North Zeeb Road, Ann Arbor, MI 48106, USA

Cyclic GMP-sensitive conductance of retinal rods consists of aqueous pores
A L Zimmerman & D A Baylor 70

Neural control of the forms of acetylcholinesterase in slow mammalian muscles
J Lai, J Jedrzejczyk, J A Pizzey, D Green & E A Barnard 72

Cloning of the gene and cDNA for mammalian β-adrenergic receptor and homology with rhodopsin
R A F Dixon, B K Kobilka, D J Strader, J L Benovic, H G Dohlman, T Frielle, M A Bolanowski, C D Bennett, E Rands, R E Diehl, R A Mumford, E E Slater, I S Sigal, M G Caron, R J Lefkowitz & C D Strader 75

***In vitro* osteoclast generation from different bone marrow fractions, including a highly enriched haematopoietic stem cell population**
B A A Scheven, J W M Visser & P J Nijweide 79

Epidermal growth factor-dependent phosphorylation of lipocortin
R B Pepinsky & L K Sinclair 81

Ha-*ras* hypervariable alleles in myelodysplasia
S L Thein, D G Oscier, J Flint & J S Wainscoat 84

Spectrin assembly in avian erythroid development is determined by competing reactions of subunit homo-and hetero-oligomerization
C M Woods & E Lazarides 85

Template-free RNA synthesis by Qβ replicase
C K Biebricher, M Eigen & R Luce 89

PRODUCT REVIEW

Computer-assisted model building
W C Ripka 93

Chemical design takes to the terminals 94

EMPLOYMENT

Bringing home the technology
R Pearson 98

MISCELLANY

100 years ago 16

NATURE CLASSIFIED

Professional appointments — Research posts — Studentships — Fellowships — Conferences — Courses — Seminars — Symposia: Back Pages

Next week in *Nature*:

- Self-splicing *Tetrahymena* RNA
- Muon-catalysed fusion
- 2.6 arc min gravitational lens separation
- Lymphocyte repertoire development
- Carbonate recrystallization
- Oncogenes and steroid receptors
- Comet Halley coma structures
- Benzodiazepines and the biological clock
- Mechanism of flying in bats
- South China Sea spreading
- Protein translocation across membranes

GUIDE TO AUTHORS

Authors should be aware of the diversity of *Nature*'s readership and should strive to be as widely understood as possible.

Review articles should be accessible to the whole readership. Most are commissioned, but unsolicited reviews are welcome (in which case prior consultation with the office is desirable).

Scientific articles are research reports whose conclusions are of general interest or which represent substantial advances of understanding. The text should not exceed 3,000 words and six displayed items (figures plus tables). The article should include an italic heading of about 50 words.

Letters to *Nature* are ordinarily 1,000 words long with no more than four displayed items. The first paragraph (not exceeding 150 words) should say what the letter is about, why the study it reports was undertaken and what the conclusions are.

Matters arising are brief comments (up to 500 words) on articles and letters recently published in *Nature*. The originator of a Matters Arising contribution should initially send his manuscript to the author of the original paper and both parties should, wherever possible, agree on what is to be submitted.

Manuscripts may be submitted either to London or Washington. Manuscripts should be typed (double spacing) on one side of the paper only. Four copies are required, each accompanied by copies of lettered artwork. No title should exceed 80 characters in length. Reference lists, figure legends, etc. should be on separate sheets, all of which should be numbered. Abbreviations, symbols, units, etc. should be identified on one copy of the manuscript at their first appearance.

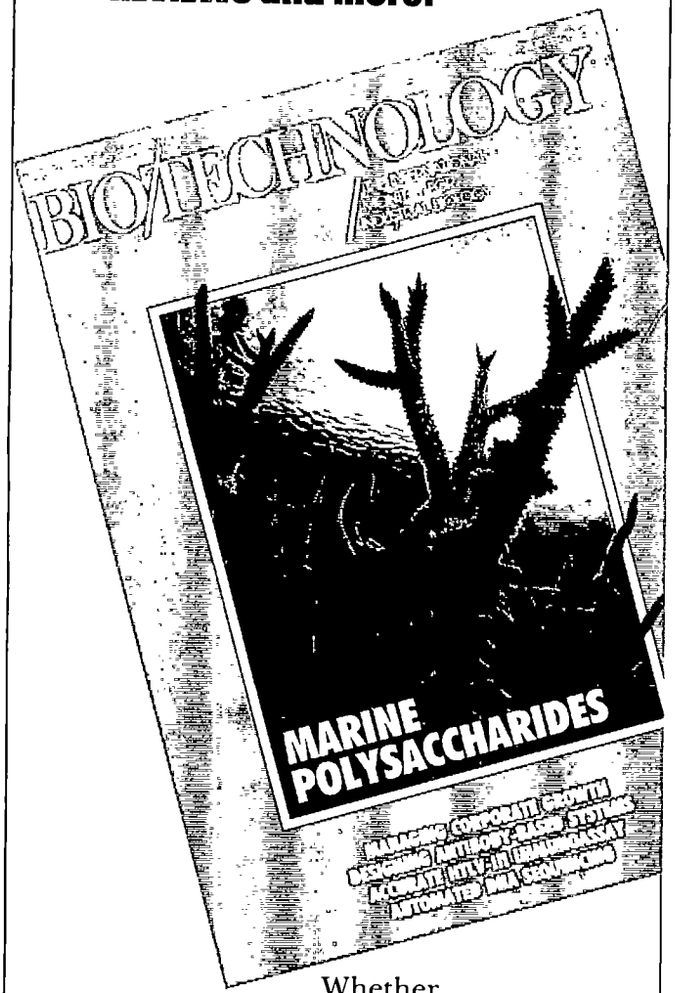
References should appear sequentially indicated by superscripts, in the text and should be abbreviated according to the *World List of Scientific Periodicals*, fourth edition (Butterworth 1963-65). The first and last page numbers of each reference should be cited. Reference to books should clearly indicate the publisher and the date and place of publication. Unpublished articles should not be formally referred to unless accepted or submitted for publication, but may be mentioned in the text.

Each piece of artwork should be clearly marked with the author's name and the figure number. Original artwork should be unlettered. Suggestions for cover illustrations are welcome. Original artwork (and one copy of the manuscript) will be returned when manuscripts cannot be published.

Requests for permission to reproduce material from Nature *should be accompanied by a self-addressed (and, in the case of the United Kingdom and United States, stamped) envelope.*

- **NEWS**
- **FEATURES**
- **ORIGINAL RESEARCH**
- **PRODUCT EVALUATIONS**
- **INDUSTRIAL APPLICATIONS**
- **JOB OPENINGS**

BOOK and PRODUCT REVIEWS and more!



Whether you are involved in the engineering, scientific or commercial aspects of biotechnology, this is the one magazine you can't afford to be without.
For details of our special 2-year subscription offer and a FREE SAMPLE COPY phone Za Dale on (01) 836 6633 (UK) or Paige Beaver (212) 477 9600 (US) OR write to

Bio/Technology
Macmillan Journals Ltd
4 Little Essex Street
London WC2R 3LF
UK

Bio/Technology
65 Bleeker Street
New York
NY 10012
USA

BURN YOUR REFERENCE CARDS!

REF-11™

Computerizes your REFERENCES and prepares your BIBLIOGRAPHIES

- ☐ Maintains a data base of references
- ☐ Searches for any combination of authors, years of publication, reference title (or any words in the title), and topics covered by the reference
- ☐ Formats bibliographies exactly as you want them
- ☐ Alphabetizes references
- ☐ Abbreviates journal titles
- ☐ Runs on any video terminal and printer
- ☐ Menu driven dialogue
- ☐ Compact storage format
- ☐ 20 lines of comments for each reference

IBM PC/XT/AT, MS-DOS, CP/M 80 ... **$195.00**

RT-11, TSX-Plus, RSX-11, P/OS **$250.00**

VAX/VMS (native mode) **$350.00**

DG™ SYSTEMS

ANY MANUAL **$15.00**

ANY MANUAL & DEMO **$20.00**

322 Prospect Ave., Hartford, CT 06106
(203) 247-8500
Connecticut residents add 7½% sales tax.

Reader Service No.123

SCIENCE AND TECHNOLOGY

Whatever the subject... refer to MACMILLAN DICTIONARIES

DESIGNED FOR STUDENTS

The paperback *Macmillan Dictionary Series* combines new and established works of teaching and reference with an attractive series format.

* authoritative definitions and explanations of all current terminology written by experts
* lucidly written entries with thorough cross referencing
* regular new editions keep the student up to date with the latest research, practice and technology
* a clear layout for easy reference
* prices range from just £7.95 to £9.95

RP439

NEW IN 1986...

MACMILLAN DICTIONARY OF BIOTECHNOLOGY
JIM COOMBS March 1986 320pp 0 333 40875 6 £9.95

MACMILLAN DICTIONARY OF THE HISTORY OF SCIENCE
Edited by W. F. BYNUM, E. J. BROWNE and ROY PORTER
March 1986 528pp 0 333 34901 6 £8.95

MACMILLAN DICTIONARY OF PERSONAL COMPUTING AND COMMUNICATIONS DENNIS LONGLEY and MICHAEL SHAIN
August 1986 320pp 0 333 42170 1 £8.95

MACMILLAN DICTIONARY OF PHYSICS
MARY P. LORD August 1986 320pp 0 333 42377 1 £8.95

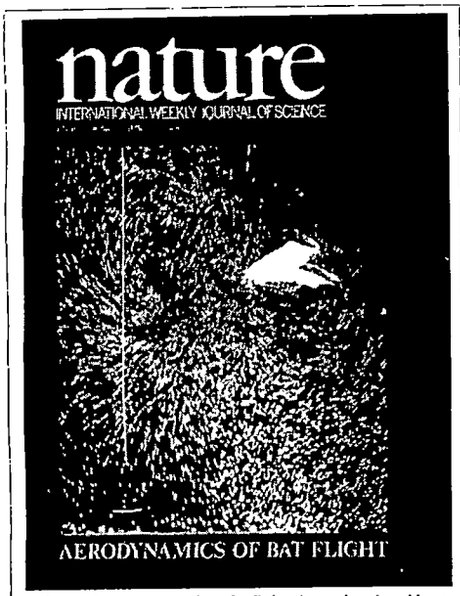
MACMILLAN DICTIONARY OF IMMUNOLOGY
FRED ROSEN, LISA STEINER and EMIL UNANUE
August 1986 256pp 0 333 39248 5 £8.95

Macmillan Press, Houndmills, Basingstoke, Hants RG21 2XS, UK
Not available in USA.

MACMILLAN PRESS

nature

NATURE VOL. 321 8 MAY 1986



Air vortices in the wake of a flying bat, visualized by a cloud of helium-filled soap bubbles. As described on pages 162–164 of this issue, these vortex patterns allow the gait of flying bats to be visualized, and have shown how the gait changes with flight speed. These observations are discussed in News and Views on page 113.

OPINION

The long shadow from Chernobyl 99

NEWS

Chernobyl 100
Soviet nuclear reactors
Nuclear prognostications 101
France in Tokyo 102
ESF joins Ocean Drilling Program
Good week for Pasteur institute
US technology 103
AIDS in India
Archaeology congress 104
Biotechnology
Research planning 105
AIDS in California
Degrees by consent

CORRESPONDENCE

Future of UK observatory/ Sexism/MRC unit closure 106

NEWS AND VIEWS

Mechanizing cellular automata 107
Protein translocation: A common mechanism for different membrane systems?
Gottfried Schatz 108
Archaeology: Late Saxon ceramic utensils
Richard Hodges 109
Predation by drilling gastropods
Michael J Benton 110
Unravelling fates of black holes
Don N Page 111
Oncogenes as hormone receptors
J Michael Bishop 112
Three kinds of flying in animals
R McNeill Alexander 113
Benzodiazepines set the clock
A T Winfree 114
Is there coherence between Earth tides and earthquakes?
Paul W Burton 115
Development and modification of the lymphocyte repertoire
Malcolm Gefter
and Philippa Marrack 116

SCIENTIFIC CORRESPONDENCE

First isolation of HTLV-III
R C Gallo, P S Sarin, B Kramarsky, Z Salahuddin, P Markham & M Popovic; J Schüpbach 119
Keeping supercomputers under control
J H Cushman & F J Wobber 120
Are light head loads carried free?
D Mitchell; D A H Taylor 120
State of preservation of the Dead Sea Scrolls
T B Kahle & N Caldararo
Reply: S Weiner, Z Kustanovich, E Gil-Av & W Traub 121
Nuclear winter and the greenhouse effect
S B Idso 122
Competition amongst desert perennials
T J King & S R J Woodell 122

BOOK REVIEWS

Inward Bound: Of Matter and Forces in the Physical World
by A Pais
Nicholas Kemmer 123
Reconstitutions of Transporters, Receptors, and Pathological States
by E Racker
Miles Houslay 124
Taking Darwin Seriously: A Naturalistic Approach to Philosophy
by M Ruse
Peter J Bowler 125
The Connection Machine
by W D Hillis
Igor Aleksander 126

REVIEW ARTICLE

Muon-catalysed fusion revisited
S E Jones 127

ARTICLES

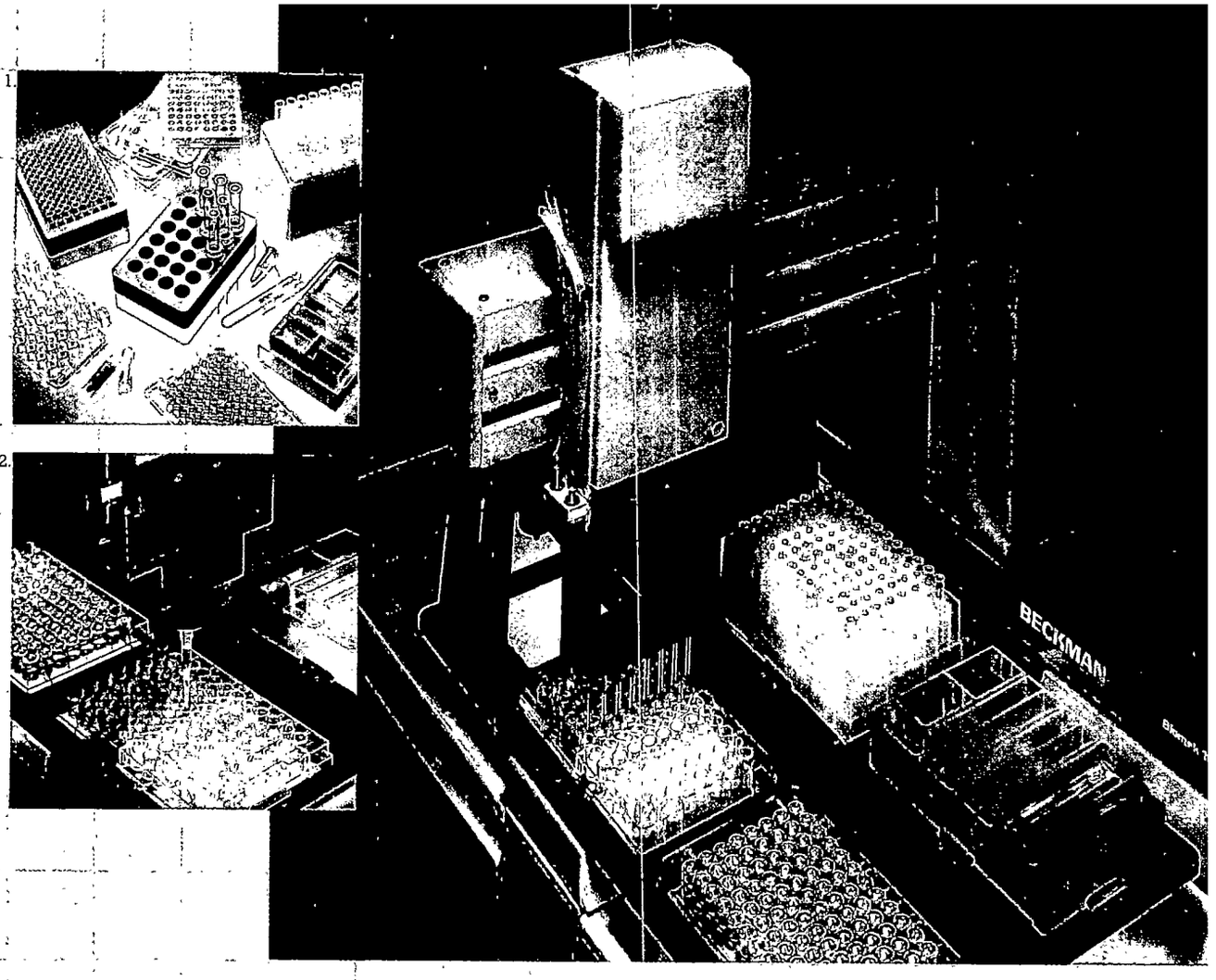
Splice-site selection by a self-splicing RNA of *Tetrahymena*
R B Waring, P Towner, S J Minter & R W Davies 133

LETTERS TO NATURE

High-resolution imaging from Mauna Kea: the triple quasar in 0.3-arc s seeing
J P Henry & J N Heasley 139
An apparent gravitational lens with an image separation of 2.6 arc min
E L Turner, D P Schneider, B F Burke, J N Hewitt, G I Langston, J E Gunn, C R Lawrence & H Schmidt 142
Structures in the coma of comet Halley
E Grün, U Graser, L Kohoutek, U Thiele, L Massonne & G Schwehm 144
Nitrogen dioxide emitted from space shuttle surfaces and shuttle glow
U von Zahn & E Murad 147
Atmospheric CH_4, CO and OH from 1860 to 1985
A M Thompson & R J Cicerone 148
Spreading direction in the central South China Sea
G Pautot, C Rangin, A Briais, P Tapponnier, P Beuzart, G Lericolais, X Mathieu, J Wu, S Han, H Li, Y Lu & J Zhao 150
Propagation of internal tides from the upper slopes of the Bay of Biscay
R D Pingree, G T Mardell & A L New 154
Carbonate recrystallization in basal sediments: evidence for convective fluid flow on a ridge flank
M Kastner, J M Gieskes & J-Y Hu 158
Mutual diffusion in a miscible polymer blend
R A L Jones, J Klein & A M Donald 161

Contents continued overleaf

Nature® (ISSN 0028-0836) is published weekly on Thursday, except the last week in December, by Macmillan Journals Ltd and includes the Annual Index (mailed in February). Annual subscription for USA and Canada US $240. USA and Canadian orders to: *Nature*, Subscription Dept, PO Box 1501, Neptune, NJ 07753, USA. Other orders to *Nature*, Brunel Road, Basingstoke, Hants RG21 2XS, UK. Second class postage paid at New York, NY 10012 and additional mailing offices. Authorization to photocopy material for internal or personal use, or internal or personal use of specific clients, is granted by *Nature* to libraries and others registered with the Copyright Clearance Center (CCC) Transactional Reporting Service, provided the base fee of $1.00 a copy plus $0.10 a page is paid directly to CCC, 21 Congress Street, Salem, Massachusetts 01970, USA. Identification code for *Nature*: 0028-0836/86 $1.00 + $0.10. US Postmaster send address changes to *Nature*, 65 Bleecker Street, New York, NY 10012. Published in Japan by Macmillan Shuppan K.K., Eikow Building, 1-10-9 Hongo, Bunkyo-ku, Tokyo, Japan. © 1986 Macmillan Journals Ltd



New from Beckman

The Most Advanced Robot To Enter The Laboratory

The Biomek™ 1000 Automated Laboratory Workstation. It's a new concept in laboratory automation, and it's changing the way researchers spend their time.

Ideal for immunoassays such as ELISA, hybridoma screening and selection, or other bioassays, Biomek takes over all liquid handling steps. Pipetting, diluting, dispensing, plate washing, even photometry can be completed at this single workstation.

Fast

With Biomek™ 1000, plate-based enzyme immunoassays, from sample transfer to OD measurement, can take just 12 minutes, excluding incubations. And a tenfold, 96-tube serial dilution and transfer, with tip changes, can be completed in just over 3 minutes.

Flexible

With Biomek™ 1000, you're not restricted to a manufacturer-supplied program. Biomek does your work the way *you* want it done. A proprietary assay language lets you easily program methods from simple to complex. And you can use labware you're accustomed to: multiwell plates, cryovials, tubes, or our new modular reservoirs.

As cost and labor savings become more critical to the research lab, the demand grows for instruments that speed research and stretch research dollars. Biomek 1000 does both.

To find out more, call toll-free (800) 742-2345, or write to Beckman Instruments, Inc., Spinco Division, 1050 Page Mill Rd., Palo Alto, CA 94304. Offices in major cities worldwide.

1. With the Biomek™ 1000 Automated Laboratory Workstation, you can use the labware you're accustomed to.
2. Complex procedures, from pipetting through photometry, can be performed at this single workstation.

BECKMAN

Reader Service No.281

HALLEY'S COMET

SPECIAL SUPPLEMENT

Nature's May 15 issue will carry a 100 page supplement on Halley's Comet.

The supplement brings together for the first time the results of missions being carried out from Russia, Europe and Japan.

Among other items, reports will include extensive data on the composition of cometary gases, the density of the dust storm near the comet's core and the interactions between the comet and the solar winds buffeting it, as well as the first ever photos of the comet's nucleus.

RESERVE YOUR EXTRA COPIES OF THE SUPPLEMENT TODAY BY WRITING TO OUR BASINGSTOKE OFFICE (prices as for back issues below).

Supply can be guaranteed only if we receive your order before May 9.

Annual Subscription Prices

UK & Irish Republic		£104
USA & Canada		US$240
Australia, NZ & S. Africa	Airspeed	£150
	Airmail	£190
Continental Europe	Airspeed	£125
India	Airspeed	£120
	Airmail	£190
Japan	Airspeed	Y90000
Rest of World	Surface	£120
	Airmail	£180

Orders (with remittance) to:

USA & Canada
Nature
Subscription Dept
PO Box 1501
Neptune
NJ 07753
USA

UK & Rest of World
Nature
Circulation Dept
Brunel Road
Basingstoke
Hants RG21 2XS, UK
Tel: 0256 29242

(The addresses of Nature's editorial offices are shown facing the first editorial page)

Japanese subscription enquiries to:
Japan Publications Trading Company Ltd
2-1 Sarugaku-cho 1-chome
Chiyoda-ku, Tokyo, Japan
Tel: (03) 292 3755

Personal subscription rates: These are available in some countries to subscribers paying by personal cheque or credit card. Details from:

USA & Canada
Nature
65 Bleecker Street
New York
NY 10012, USA
Tel: (212) 477-9600

UK & Europe
Felicity Parker
Nature
4 Little Essex Street
London WC2R 3LF, UK
Tel: 01-836 6633

Back issues: UK, £2.50; USA & Canada, US$6.00 (surface), US$9.00 (air); Rest of World, £3.00 (surface), £4.00 (air)

Binders
Single binders: UK, £5.25; USA & Canada $11.50; Rest of World, £7.75. Set of four: UK, £15.00; USA & Canada $32.00; Rest of World, £22.00

Annual indexes (1971-1985)
UK, £5.00 each; Rest of World, $10.00

Nature First Issue Facsimile
UK, £2.00; Rest of World (surface), $3.00; (air) $4.00

Nature in microform
Write to University Microfilms International, 300 North Zeeb Road, Ann Arbor, MI 48106, USA

Vortex flow visualizations reveal change in upstroke function with flight speed in bats
J M V Rayner, G Jones & A Thomas **162**

Genetics and evolution of female choice
M E N Majerus, P O'Donald, P W E Kearns & H Ireland **164**

A benzodiazepine used in the treatment of insomnia phase-shifts the mammalian circadian clock
F W Turek & S Losee-Olson **167**

Replication of the neurochemical characteristics of Huntington's disease by quinolinic acid
M F Beal, N W Kowall, D W Ellison, M F Mazurek, K J Swartz & J B Martin **168**

Channel properties of an insect neuronal acetylcholine receptor protein reconstituted in planar lipid bilayers
W Hanke & H Breer **171**

Potentiation of synaptic transmission in hippocampus by phorbol esters
R C Malenka, D V Madison & R A Nicoll **175**

Platelet activation — a role for a 40K anti-phospholipase A_2 protein indistinguishable from lipocortin
L Touqui, B Rothhut, A M Shaw, A Fradin, B B Vargaftig & F Russo-Marie **177**

Equivalence of intracellular *p*H of differentiating *Dictyostelium* cell types
D I Ratner **180**

MISCELLANY

100 years ago **117**

NATURE CLASSIFIED

Professional appointments — Research posts — Studentships — Fellowships — Conferences — Courses — Seminars — Symposia: Back Pages

Next week in *Nature*:

- Comet Halley: results from the Halley flotilla
- Why DNA is methylated
- Transfer RNA transformed
- T-cell specificity
- Archaebacterial virus
- Visual inhibition
- New papillomavirus
- Cytoimmunotherapy in virus infection
- WIMPs and solar oscillations
- Global ethane
- Antarctic helium

GUIDE TO AUTHORS

Authors should be aware of the diversity of *Nature*'s readership and should strive to be as widely understood as possible.

Review articles should be accessible to the whole readership. Most are commissioned, but unsolicited reviews are welcome (in which case prior consultation with the office is desirable).

Scientific articles are research reports whose conclusions are of general interest or which represent substantial advances of understanding. The text should not exceed 3,000 words and six displayed items (figures plus tables). The article should include an italic heading of about 50 words.

Letters to *Nature* are ordinarily 1,000 words long with no more than four displayed items. The first paragraph (not exceeding 150 words) should say what the letter is about, why the study it reports was undertaken and what the conclusions are.

Matters arising are brief comments (up to 500 words) on articles and letters recently published in *Nature*. The originator of a Matters Arising contribution should initially send his manuscript to the author of the original paper and both parties should, wherever possible, agree on what is to be submitted.

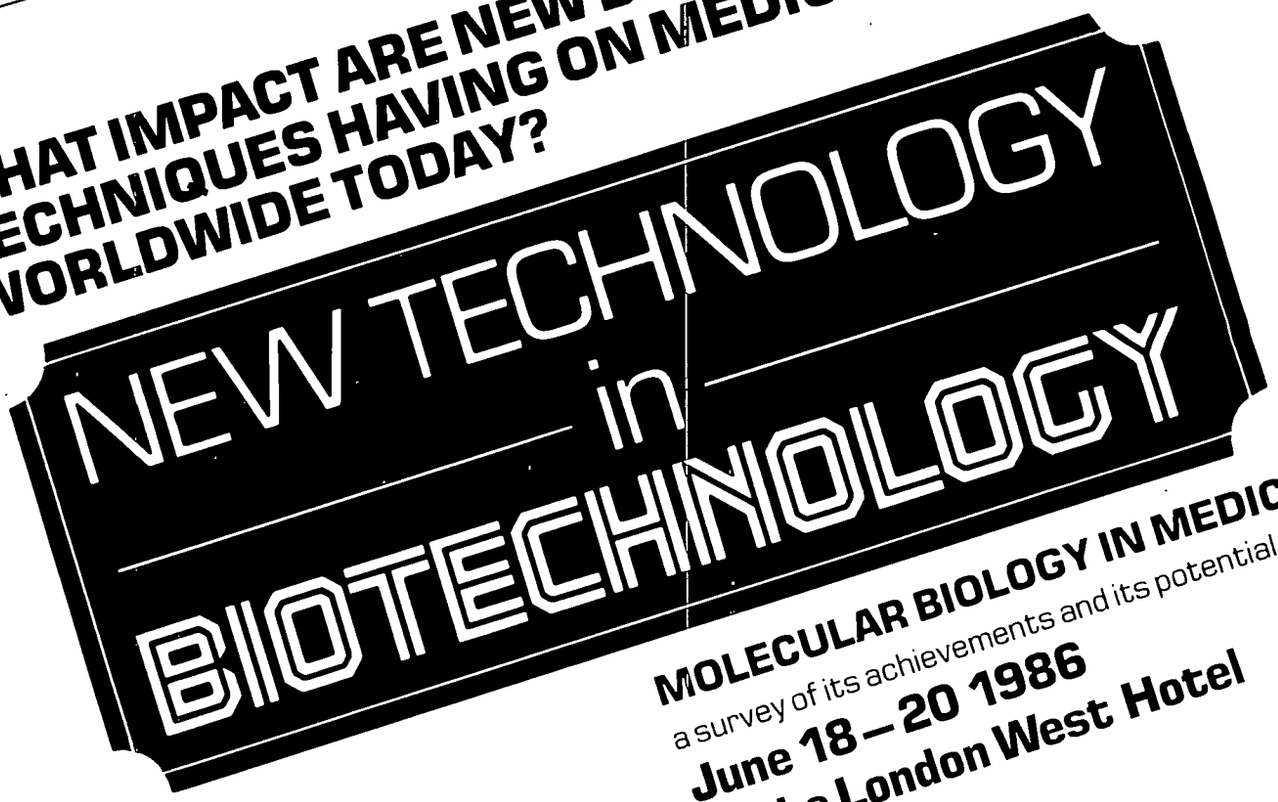
Manuscripts may be submitted either to London or Washington. Manuscripts should be typed (double spacing) on one side of the paper only. Four copies are required, each accompanied by copies of lettered artwork. No title should exceed 80 characters in length. Reference lists, figure legends, etc, should be on separate sheets, all of which should be numbered. Abbreviations, symbols, units, etc, should be identified on one copy of the manuscript at their first appearance.

References should appear sequentially indicated by superscripts, in the text and should be abbreviated according to the *World List of Scientific Periodicals*, fourth edition (Butterworth 1963-65). The first and last page numbers of each reference should be cited. Reference to books should clearly indicate the publisher and the date and place of publication. Unpublished articles should not be formally referred to unless accepted or submitted for publication, but may be mentioned in the text.

Each piece of artwork should be clearly marked with the author's name and the figure number. Original artwork should be unlettered. Suggestions for cover illustrations are welcome. Original artwork (and one copy of the manuscript) will be returned when manuscripts cannot be published.

Requests for permission to reproduce material from Nature *should be accompanied by a self-addressed (and, in the case of the United Kingdom and United States, stamped) envelope.*

WHAT IMPACT ARE NEW BIOTECHNOLOGY TECHNIQUES HAVING ON MEDICINE WORLDWIDE TODAY?



MOLECULAR BIOLOGY IN MEDICI

a survey of its achievements and its potential

June 18–20 1986

at the London West Hotel

It is clear that the modern techniques of biotechnology are set to have a major impact on medicine. Over the next few years many new opportunities will emerge. This important conference will provide a wide-ranging survey of the most recent research in the fast changing field of molecular biology in medicine, and a look into the future. If you want an opportunity to see and hear for yourself what leading exponents have achieved in recent years – and to learn what new opportunities are on the horizon, come and join us.

The **CONFERENCE FEE** is just £189 plus VAT for the three days of the conference. This includes entrance to all sessions, mid-morning coffee, afternoon tea and reading material. Group discounts are available on application to Janine Slipman, see booking form for address and phone no.

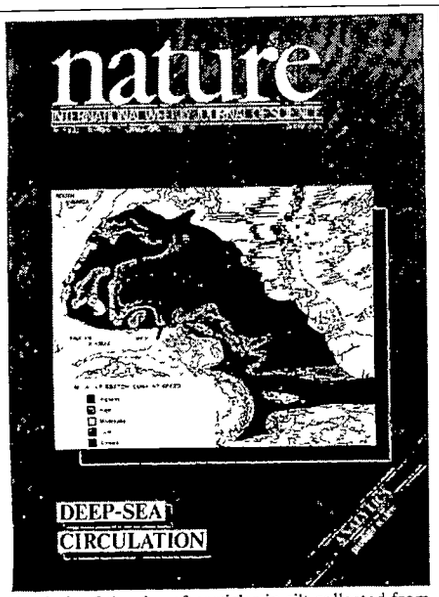
ACCOMMODATION has been reserved in the London West Hotel for conference participants. A booking form will be sent to you as soon as we receive your registration.

TECHNICAL SEMINARS and **POSTER SESSIONS** will be held each day. Anybody wishing to present a poster should send a title and a brief synopsis.

To: Dr Peter Newmark Deputy Editor Nature
4 Little Essex Street London WC2R 3LR

nature

NATURE VOL. 321 22 MAY 1986



Analysis of the size of particles in silt collected from the sea bed can be used to work out the patterns of ocean currents at great depths. Here the contours represent mean silt particle size in the region of the Argentine Basin. See p.423. This week's Product Review (p.451) includes details of new instruments on display at the Analytica exhibition in Munich.

OPINION

What future for nuclear power? 367

NEWS

Chernobyl 369
SDI
Particle accelerators 370
British research
Human genome 371
The numbers game
US research costs 372
Strident report
US space
French science 373
SDI
Supercomputers 374
Japan Prize
Japan's forests 375

CORRESPONDENCE

French nuclear safety/Human embryos 376

NEWS AND VIEWS

Disappointment over double quasar 377
AIDS virus: More and better *trans*-activation
A Burny 378
Gravitational waves: Observatories of the future
M G Edmunds 378
Embryology goes fishing
David Marcey & Christiane Nüsslein-Volhard 380
Theoretical physics: Supertwistors and superstrings
L P Hughston 381
Structure and function of acetylcholine-receptor ion channels
David Colquhoun 382
A microcosm of ocean basin evolution in the Mediterranean
Leg 107 shipboard scientific party 383
Spurious *Babesia* antigens
F E G Cox 384

SCIENTIFIC CORRESPONDENCE

Predicting that comet Halley is dark
J M Greenberg 385
Multiple sclerosis viruses and glycolipids
J K Fazakerley & H E Webb 386
Ventral activation process in insect oocytes
L F Jaffe 386

BOOK REVIEWS

How to Obtain Biomedical Research Funding
J T Dingle, ed.
Walter Gratzer 387
Diffraction Methods for Biological Macromolecules
H W Wyckoff, C H W Hirs and S N Timasheff, eds
Kenneth C Holmes 388
Growth Factors and Transformation
J Feramisco, B Ozanne and C Stiles, eds
A R Rees
The Human Skeleton
by P Shipman, A Walker and D Bichell
Bernard Wood 389
The Machinery of Nature
by P R Ehrlich
John H Lawton 390

COMMENTARY

Space observations of comet Halley
J C Brandt 391

REVIEW ARTICLE

Chaos in light
R G Harrison & D J Biswas 394

ARTICLES

Observation of an unexplained event from a magnetic monopole detector
A D Caplin, M Hardiman, M Koratzinos & J C Schouten 402
Molecular distinction between fetal and adult forms of muscle acetylcholine receptor
M Mishina, T Takai, K Imoto, M Noda, T Takahashi, S Numa, C Methfessel & B Sakmann 406
A second post-transcriptional *trans*-activator gene required for HTLV-III replication
J Sodroski, W C Goh, C Rosen, A Dayton, E Terwilliger & W Haseltine 412

LETTERS TO NATURE

Towards the geometrization of physics
G A J Sparling 417
Is there a black hole in the sky?
B Paczyński 419
Is QSO1146 + 111B,C due to lensing by a cosmic string?
J R Gott III 420
Relation between solar narrow-band decimetre-wave bursts and associated X-ray bursts
S Enome & L E Orwig 421
Bottom-current pathways in the Argentine Basin revealed by mean silt particle size
M T Ledbetter 423
Ubiquitous occurrence of 2-nitrofluoranthene and 2-nitropyrene in air
T Ramdahl, B Zielinska, J Arey, R Atkinson, A M Winer & J N Pitts Jr 425
Influence of Saharan dust on the rain acidity and atmospheric input to the Mediterranean
M D Loÿe-Pilot, J M Martin & J Morelli 427
Amino-acid sequence of the β-subunit of the $(Na^+ + K^+)$ATPase deduced from a cDNA
G E Shull, L K Lane & J B Lingrel 429

Contents continued overleaf

Nature® (ISSN 0028-0836) is published weekly on Thursday, except the last week in December, by Macmillan Journals Ltd and includes the Annual Index (mailed in February). Annual subscription for USA and Canada US $240. USA and Canadian orders to: *Nature*, Subscription Dept, PO Box 1501, Neptune, NJ 07753, USA. Other orders to *Nature*, Brunel Road, Basingstoke, Hants RG21 2XS, UK. Second class postage paid at New York, NY 10012 and additional mailing offices. Authorization to photocopy material for internal or personal use, or internal or personal use of specific clients, is granted by *Nature* to libraries and others registered with the Copyright Clearance Center (CCC) Transactional Reporting Service, provided the base fee of $1.00 a copy plus $0.10 a page is paid directly to CCC, 21 Congress Street, Salem, Massachusetts 01970, USA. Identification code for *Nature*: 0028-0836/86 $1.00 + $0.10. US Postmaster send address changes to: *Nature*, 65 Bleecker Street, New York, NY 10012. Published in Japan by Macmillan Shuppan K.K., Eikow Building, 1-10-9 Hongo, Bunkyo-ku, Tokyo, Japan. © 1986 Macmillan Journals Ltd.

CUSTOM SYNTHETIZED DNA AT EXTREMELY LOW PRICES

Prices (USD) per purified oligomer up to the length of 35:

		Basic fee	Per base
0.05	A260 units (~ 1.5 μg)	85	5.50
0.2	A260 units (~ 6 μg)	125	7.50
1	A260 unit (~30 μg)	170	10.00

SPECIAL OFFER: FREE OLIGONUCLEOTIDES

FOR EVERY FIVE OLIGOMERS YOU BUY
YOU GET ONE ADDITIONAL OLIGOMER FOR FREE

WHY BUY MORE THAN YOU ACTUALLY NEED?

1 μg OF OLIGONUCLEOTIDE IS SUFFICIENT FOR:

- 10 oligonucleotide-directed mutagenisis experiments.
- 100 hybridization and gene synthesis experiments.
- 1000 dideoxy sequencing experiments.
- More than 1000 cloning experiments.

EVALUATE YOUR ACTUAL NEEDS BEFORE ORDERING!

FOR PRICE LIST AND PRODUCT INFORMATION, CONTACT:

SYN-TEK AB
Box 1010
S-901 20 Umeå, SWEDEN
Phone +46-90-13 24 10
Telefax +46-90-12 32 05
Telex 54920 syntek s

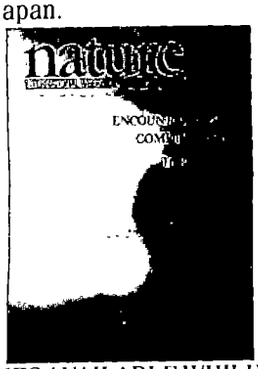
SYN-TEK CORP.
P.O. Box 50068
Palo Alto, CALIFORNIA 94303
Phone 415-494-8690
Telefax 415-494-0762

SYN-TEK AB
INNOVATORS IN BIOLOGICAL SCIENCES
Reader Service No.20

HALLEY'S COMET

SPECIAL SUPPLEMENT

AVAILABLE NOW – Nature's supplement on Halley's Comet containing results of missions carried out from Russia, Europe and Japan.



COPIES AVAILABLE WHILE STOCKS LAST FROM OUR OFFICES IN BASINGSTOKE
Prices as for back issues below

Annual Subscription Prices

UK & Irish Republic		£104
USA & Canada		US$240
Australia, NZ & S. Africa	Airspeed	£150
	Airmail	£190
Continental Europe	Airspeed	£125
India	Airspeed	£120
	Airmail	£190
Japan	Airspeed	Y90000
Rest of World	Surface	£120
	Airmail	£180

Orders (with remittance) to:

USA & Canada
Nature
Subscription Dept
PO Box 1501
Neptune
NJ 07753
USA

UK & Rest of World
Nature
Circulation Dept
Brunel Road
Basingstoke
Hants RG21 2XS, UK
Tel: 0256 29242

(The addresses of Nature's editorial offices are shown facing the first editorial page)

Japanese subscription enquiries to:
Japan Publications Trading Company Ltd
2-1 Sarugaku-cho 1-chome
Chiyoda-ku, Tokyo, Japan
Tel: (03) 292 3755

Personal subscription rates: These are available in some countries to subscribers paying by personal cheque or credit card. Details from:

USA & Canada
Nature
65 Bleecker Street
New York
NY 10012, USA
Tel: (212) 477-9600

UK & Europe
Felicity Parker
Nature
4 Little Essex Street,
London WC2R 3LF, UK
Tel: 01-836 6633

Back issues: UK, £2.50; USA & Canada, US$6.00 (surface), US$9.00 (air); Rest of World, £3.00 (surface), £4.00 (air)

Binders
Single binders: UK, £5.25; USA & Canada $11.50; Rest of World, £7.75. Set of four: UK, £15.00; USA & Canada $32.00; Rest of World, £22.00

Annual indexes (1971-1985)
UK, £5.00 each; Rest of World, $10.00

Nature First Issue Facsimile
UK, £2.00; Rest of World (surface), $3.00; (air) $4.00

Nature in microform
Write to University Microfilms International, 300 North Zeeb Road, Ann Arbor, MI 48106, USA

Isolation of cDNA clones encoding the 20K non-glycosylated polypeptide chain of the human T-cell receptor/T3 complex
D P Gold, J M Puck, C L Pettey, M Cho, J Coligan, J N Woody & C Terhorst 431

Isolation of an HTLV-III-related retrovirus from macaques with simian AIDS and its possible origin in asymptomatic mangabeys
M Murphey-Corb, L N Martin, S R S Rangan, G B Baskin, B J Gormus, R H Wolf, W A Andes, M West & R C Montelaro 435

Mechanism of activation of *HuBlym*-1 gene unresolved
J M Devine 437

Specific inhibition of herpesvirus ribonucleotide reductase by synthetic peptides
B M Dutia, M C Frame, J H Subak-Sharpe, W N Clark & H S Marsden 439

Specific inhibition of herpesvirus ribonucleotide reductase by a nonapeptide derived from the carboxy terminus of subunit 2
E A Cohen, P Gaudreau, P Brazeau & Y Langelier 441

Re-routing of a secretory protein by fusion with human growth hormone sequences
H-p H Moore & R B Kelly 443

Expression of biologically active viral satellite RNA from the nuclear genome of transformed plants
D C Baulcombe, G R Saunders, M W Bevan, M A Mayo & B D Harrison 446

Sequence-directed curvature of DNA
P J Hagerman 449

Errata... page 450

Danish Basin subsidence by Triassic rifting on a lithosphere cooling background
K Sørensen

An *Agrobacterium* transformation in the evolution of the genus *Nicotiana*
I J Furner *et al*

PRODUCT REVIEW

Carbohydrate detection gains potential
D C Johnson 451

Analytica instrumentation 452

NATURE CLASSIFIED

Professional appointments — Research posts — Studentships — Fellowships — Conferences — Courses — Seminars — Symposia: Back Pages

Next week in *Nature*:

- Solar structure
- Aerial acetone/ammonia
- Ecology of nuclear war
- Dead Sea salinity
- Black Sea phosphate
- Earthquake pyrotechnics
- Insulin gene expressed
- Monoclonal construction
- Segmentation gene cloned
- Plant virus vector
- Sweet-tasting protein

GUIDE TO AUTHORS

Authors should be aware of the diversity of *Nature*'s readership and should strive to be as widely understood as possible.

Review articles should be accessible to the whole readership. Most are commissioned, but unsolicited reviews are welcome (in which case prior consultation with the office is desirable).

Scientific articles are research reports whose conclusions are of general interest or which represent substantial advances of understanding. The text should not exceed 3,000 words and six displayed items (figures plus tables). The article should include an italic heading of about 50 words.

Letters to *Nature* are ordinarily 1,000 words long with no more than four displayed items. The first paragraph (not exceeding 150 words) should say what the letter is about, why the study it reports was undertaken and what the conclusions are.

Matters arising are brief comments (up to 500 words) on articles and letters recently published in *Nature*. The originator of a Matters Arising contribution should initially send his manuscript to the author of the original paper and both parties should, wherever possible, agree on what is to be submitted.

Manuscripts may be submitted either to London or Washington. Manuscripts should be typed (double spacing) on one side of the paper only. Four copies are required, each accompanied by copies of lettered artwork. No title should exceed 80 characters in length. Reference lists, figure legends, etc, should be on separate sheets, all of which should be numbered. Abbreviations, symbols, units, etc, should be identified on one copy of the manuscript at their first appearance.

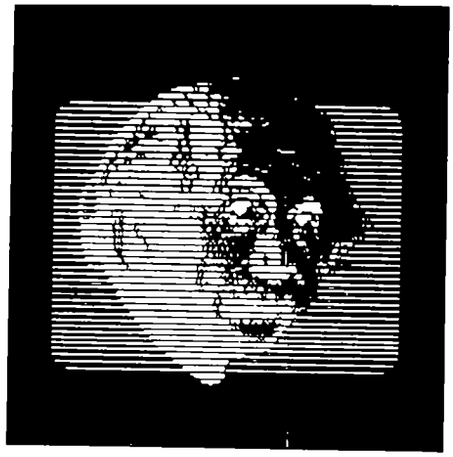
References should appear sequentially indicated by superscripts, in the text and should be abbreviated according to the *World List of Scientific Periodicals*, fourth edition (Butterworth 1963-65). The first and last page numbers of each reference should be cited. Reference to books should clearly indicate the publisher and the date and place of publication. Unpublished articles should not be formally referred to unless accepted or submitted for publication, but may be mentioned in the text.

Each piece of artwork should be clearly marked with the author's name and the figure number. Original artwork should be unlettered. Suggestions for cover illustrations are welcome. Original artwork (and one copy of the manuscript) will be returned when manuscripts cannot be published.

Important: Manuscripts of proofs sent by air courier should be declared as "manuscripts" and "value $5" to prevent the imposition of Customs duty and Value Added Tax in the United Kingdom.

Requests for permission to reproduce material from Nature *should be accompanied by a self-addressed (and, in the case of the United Kingdom and United States, stamped) envelope.*

BIO '86



MLSE

LABORATORY
LABORATORY
LABORATORY
LABORATORY
LABORATORY
LABORATORY

ANALYTICON
ANALYTICON
ANALYTICON
ANALYTICON
ANALYTICON

SEE YOU AT "THE WEEK"!

The British Laboratory Week is Britain's leading scientific event – by a mile.

This year TWO new disciplines will be introduced.

Firstly, Bio '86, the exhibition and conference for bio-technology and genetic engineering.

Secondly, the Computer-Aided-Sciences exhibition and conference. C-A-S for short.

With "The Week's" cornerstone – Laboratory '86 exhibition and Analyticon conference – now in its ninth year – plus Medical Laboratory Sciences Exhibition (MLSE), there will be no less than FOUR exhibitions and THREE conferences to attend.

In fact, with the products on display, and the subjects for discussion, that we've got lined up, you'd be crazy to stay away.

CUT OUT AND MAIL FOR YOUR FREE TICKET!

To: Brian Curtis, Organiser, British Laboratory Week, The Hub, Emson Close, Saffron Walden, Essex CB10 1HL, United Kingdom.

Please send me_____FREE ticket(s) to "The Week" and information on my principal area of interest:
Laboratory '86 ☐ Medical Laboratory Sciences ☐ Bio '86 ☐
Computer-Aided-Sciences ☐

Name Title

Company/Organisation

Address

Also, please send me details of the following conferences:
Bio '86 ☐ Analyticon ☐ Computer-Aided-Sciences ☐

THE BRITISH LABORATORY WEEK.

THE COUNTRY'S LARGEST SCIENTIFIC EVENT

23-25 SEPTEMBER, 1986
OLYMPIA, LONDON, ENGLAND

The British Laboratory Week is organised by Curtis Steadman & Partners Limited, The Hub, Emson Close, Saffron Walden, Essex CB10 1HL, United Kingdom.
Telephone: (0799) 26699.
Telex: 81653 INFORM G.
Fax: (0799) 26088.

"Hip hip, hooray!"

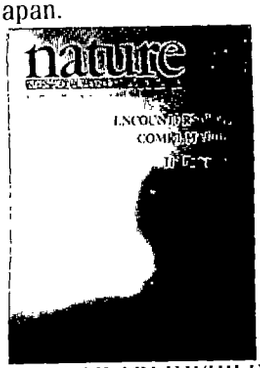


Reader Service No.22

HALLEY'S COMET

SPECIAL SUPPLEMENT

AVAILABLE NOW – Nature's supplement on Halley's Comet containing results of missions carried out from Russia, Europe and Japan.



COPIES AVAILABLE WHILE STOCKS LAST FROM OUR OFFICES IN BASINGSTOKE
Prices as for back issues below

Annual Subscription Prices

UK & Irish Republic		£104
USA & Canada		US$240
Australia, NZ & S. Africa	Airspeed	£150
	Airmail	£190
Continental Europe	Airspeed	£125
India	Airspeed	£120
	Airmail	£190
Japan	Airspeed	Y90000
Rest of World	Surface	£120
	Airmail	£180

Orders (with remittance) to:

USA & Canada
Nature
Subscription Dept
PO Box 1501
Neptune
NJ 07753
USA

UK & Rest of World
Nature
Circulation Dept
Brunel Road
Basingstoke
Hants RG21 2XS, UK
Tel: 0256 29242

(The addresses of Nature's editorial offices are shown facing the first editorial page)

Japanese subscription enquiries to:
Japan Publications Trading Company Ltd
2-1 Sarugaku-cho 1-chome
Chiyoda-ku, Tokyo, Japan
Tel: (03) 292 3755

Personal subscription rates: These are available in some countries to subscribers paying by personal cheque or credit card. Details from:

USA & Canada
Nature
65 Bleecker Street
New York
NY 10012, USA
Tel: (212) 477-9600

UK & Europe
Felicity Parker
Nature
4 Little Essex Street
London WC2R 3LF, UK
Tel: 01-836 6633

Back issues: UK, £2.50; USA & Canada, US$6.00 (surface), US$9.00 (air); Rest of World, £3.00 (surface), £4.00 (air)

Binders
Single binders: UK, £5.25; USA & Canada $11.50; Rest of World, £7.75. Set of four: UK, £15.00; USA & Canada $32.00; Rest of World, £22.00

Annual indexes (1971-1985)
UK, £5.00 each; Rest of World, $10.00

Nature First Issue Facsimile
UK, £2.00; Rest of World (surface), $3.00; (air) $4.00

Nature in microform
Write to University Microfilms International, 300 North Zeeb Road, Ann Arbor, MI 48106, USA

Mechanosensitivity of mammalian auditory hair cells *in vitro*
I J Russell, G P Richardson & A R Cody — 517

NMDA-receptor activation increases cytoplasmic calcium concentration in cultured spinal cord neurones
A B MacDermott, M L Mayer, G L Westbrook, S J Smith & J L Barker — 519

Replacing the complementarity-determining regions in a human antibody with those from a mouse
P T Jones, P H Dear, J Foote, M S Neuberger & G Winter — 522

Regulation of human insulin gene expression in transgenic mice
R F Selden, M J Skośkiewicz, K B Howie, P S Russell & H M Goodman — 525

Genetic recombination between RNA components of a multipartite plant virus
J J Bujarski & P Kaesberg — 528

A tobacco mosaic virus-induced tobacco protein is homologous to the sweet-tasting protein thaumatin
B J C Cornelissen, R A M Hooft van Huijsduijnen & J F Bol — 531

MATTERS ARISING

Was there 26-Myr periodicity of extinctions?
J J Sepkoski Jr & D M Raup; N L Gilinsky; J A Kitchell & G Estabrook
Reply: A Hoffman — 533

Endocast morphology of Hadar hominid AL 162–28
R L Holloway & W H Kimbel
Reply: D Falk — 536

Maternal investment in mammals
S I Zeveloff & M S Boyce
Reply: R D Martin & A M MacLarnon — 537

PRODUCT REVIEW

Molecular dynamics resolved — 539
Biochemists converge at the capital — 540

MISCELLANY

Books received — 546

NATURE CLASSIFIED

Professional appointments — Research posts — Studentships — Fellowships — Conferences — Courses — Seminars — Symposia: Back Pages

Next week in *Nature*:

- Galactic mock gravity
- Multiple quasar
- Altamira cave paintings
- Chernobyl fallout
- Oceanic East African Rift
- Seafloor sediment subduction
- Microtubules visualized
- Muscle cell replication
- Interleukin-2 stimulates glial cells
- DNase I structure
- Modular striate cortex

GUIDE TO AUTHORS

Authors should be aware of the diversity of *Nature*'s readership and should strive to be as widely understood as possible.

Review articles should be accessible to the whole readership. Most are commissioned, but unsolicited reviews are welcome (in which case prior consultation with the office is desirable).

Scientific articles are research reports whose conclusions are of general interest or which represent substantial advances of understanding. The text should not exceed 3,000 words and six displayed items (figures plus tables). The article should include an italic heading of about 50 words.

Letters to *Nature* are ordinarily 1,000 words long with no more than four displayed items. The first paragraph (not exceeding 150 words) should say what the letter is about, why the study it reports was undertaken and what the conclusions are.

Matters arising are brief comments (up to 500 words) on articles and letters recently published in *Nature*. The originator of a Matters Arising contribution should initially send his manuscript to the author of the original paper and both parties should, wherever possible, agree on what is to be submitted.

Manuscripts may be submitted either to London or Washington. Manuscripts should be typed (double spacing) on one side of the paper only. Four copies are required, each accompanied by copies of lettered artwork. No title should exceed 80 characters in length. Reference lists, figure legends, etc. should be on separate sheets, all of which should be numbered. Abbreviations, symbols, units, etc. should be identified on one copy of the manuscript at their first appearance.

References should appear sequentially indicated by superscripts, in the text and should be abbreviated according to the *World List of Scientific Periodicals*, fourth edition (Butterworth 1963-65). The first and last page numbers of each reference should be cited. Reference to books should clearly indicate the publisher and the date and place of publication. Unpublished articles should not be formally referred to unless accepted or submitted for publication, but may be mentioned in the text.

Each piece of artwork should be clearly marked with the author's name and the figure number. Original artwork should be unlettered. Suggestions for cover illustrations are welcome. Original artwork (and one copy of the manuscript) will be returned when manuscripts cannot be published.

Important: Manuscripts or proofs sent by air courier should be declared as "manuscripts" and "value $5" to prevent the imposition of Customs duty and Value Added Tax in the United Kingdom.

Requests for permission to reproduce material from Nature *should be accompanied by a self-addressed (and, in the case of the United Kingdom and United States, stamped) envelope.*

BIOSYSTEMS UPDATE

For People who make Peptides

Here are five reasons why.

1 It's the Truly Efficient Way to Make Peptides

The Model 430A Peptide Synthesizer doesn't waste time, amino acids, or reagents. It consistently produces high yields of quality peptide which reduces post-synthesis purification and characterization significantly. You get more peptide for your effort *and* for your dollar.

2 It's More Flexible, Easier to Operate

The 430A meets the needs of every user whether new to peptide synthesis or very experienced. Software is written in plain English using familiar terminology. All control is implemented by simply touching the screen. Standard synthesis cycles and functions can be selected or new ones designed quickly and easily.

3 Its Chemistry is Proven and Unique

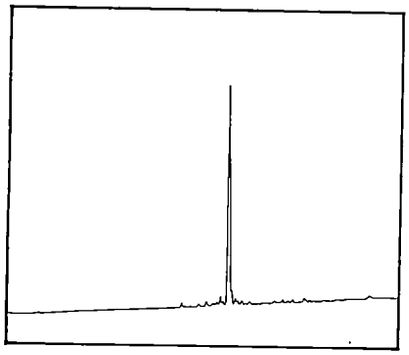
High stepwise yields, high purity and reproducibility are routine. Each step of the chemistry is specific to the requirements of the various amino acids. Coupling failures are eliminated or greatly reduced resulting in fewer double couplings. Both *t*-BOC and FMOC chemistries can be accommodated.

4 It Produces Superb Short Peptides

Step Yield (% Coupled) Standard ABI *t*-boc cycles, version 1.0

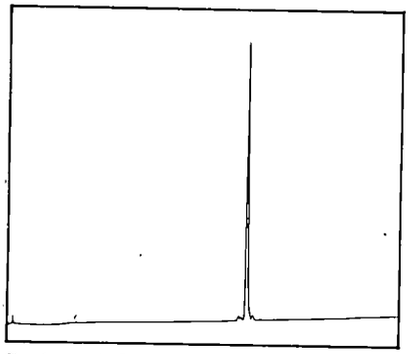
PEPTIDE SEQUENCE	LEU	HIS	PHE	PRO	HIS	ILE	TYR	VAL	ARG	ASP	AVG. STP. YIELD %
Ninhydrin Analysis	•	96.7	99.7	99.7	†99.6	98.9	99.5	98.3	99.5	99.4	99.0
Preview Sequence Analysis	•	•	•	99.5	99.2	94.9	96.6	96.5	97.1	97.9	97.4
RESIDUE NUMBER	10	9	8	7	6	5	4	3	2	1	

†Ninhydrin values for amino acids coupled to proline are not quantitative.



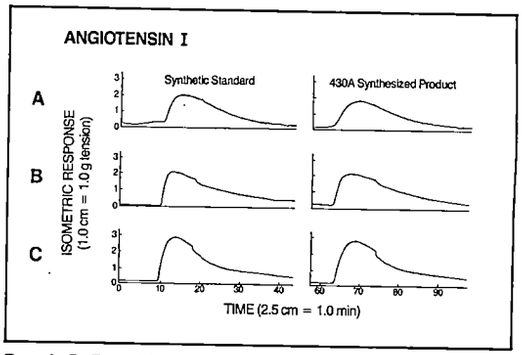
Angiotensin I, Crude

mobile phase	0.1% TFA/CH_3CN
gradient	0 to 60% in 60 minutes
flow rate	1.0 mL/min
detector	216 nm
column	Brownlee, C-8, 300Å, 10μm 4.6 mm x 250 mm



Angiotensin I, HPLC Purified

mobile phase	0.1% TFA/CH_3CN
gradient	0 to 60% in 60 minutes
flow rate	1.0 mL/min
detector	216 nm
column	Brownlee, C-8, 300Å, 10μm 4.6 mm x 250 mm



Panels A, B and C are isometric responses of two different Ile^5-Angiotensin I—a synthetic standard and the 430A-produced, purified peptide—on three separate rabbit aortic strips. The responses produced by the Applied Biosystems Ile^5-Angiotensin I were not significantly different than those of the standard. Sample concentrations were: in panel A, 564 ng/mL; in panels B and C, 500 ng/mL.

These response data were furnished by Drs. M. C. Khosla and A. Husein of the Cleveland Clinic Foundation.

Copyright 1986, Applied Biosystems, Inc.

he 430A is the No. 1 Choice.

5 It Produces Superb Long Peptides

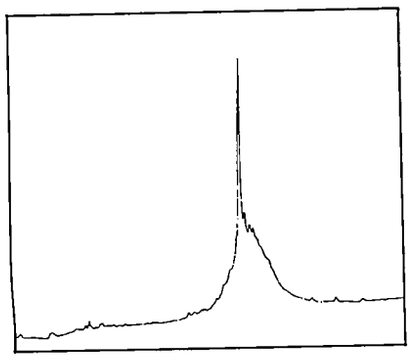
Step Yield (% Coupled) Standard ABI *t*-boc cycles, version 1.0

PEPTIDE SEQUENCE	GLY	GLY	LYS	GLU	SER	ARG	GLY	GLN	GLN	VAL	PRO	PRO	GLY	ASP	ARG	GLN	ALA	GLU	VAL	LEU →
Ninhydrin Analysis	99.7	99.8	99.5	99.4	99.2	*99.6	99.4	*99.6	*99.2	98.0	97.0	†99.8	†99.1	98.9	99.0	99.1	98.7	98.6	98 5	98 5
Preview Sequence Analysis	•	•	99.6	99.6	99.5	99.6	99.5	•	•	99.1	•	1	98.9	99.0	99.0	98.6	98.7	98.6	98 5	98 4
RESIDUE NUMBER	67	66	65	64	63	62	61	60	59	58	57	56	55	54	53	52	51	50	49	48 →

→ LYS	SER	TYR	ASP	PHE	SER	ASP	GLY	SER	GLU	GLU	TYR	GLU	ALA	ASN	LEU	GLU	ALA	ASP	LEU	THR	THR	GLN	ALA	LEU →
95.8	97.4	97.2	97.8	98.3	98.3	97.9	96.9	98.5	98.3	98.0	97.1	97.2	98.2	*96.9	98.1	97.7	98.0	98.0	98.2	97.6	95.0	*82.7	96 0	96 *
98.5	98.5	98.5	98.5	98.8	97.9	98.0	97.8	97.0	•	•	98.8	•	99.3	99.3	99.3	98.9	99.1	98.9	93.9	•	•	98.4	99 0	98.*
→ 47	46	45	44	43	42	41	40	39	38	37	36	35	34	33	32	31	30	29	28	27	26	25	24	23 →

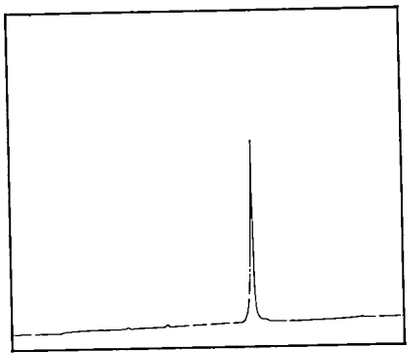
→ VAL	ARG	ALA	GLN	SER	SER	GLN	ARG	ASN	ARG	SER	SER	SER	SER	SER	ALA	PRO	ARG	SER	SER	SER	NET	AVG. STP. YIELD %
96.1	*94.9	95.2	*94.6	95.5	95.5	*96.4	*92.5	*92.2	*91.7	93.9	95.0	96.7	96.2	94.5	94.8	94.4	†*95.0	97.2	•	95.9	96.5	*96.9
98.3	98.5	98.0	96.8	•	•	•	•	97.9	•	•	•	•	•	•	95.2	95.1	97.2	•	•	•	•	98.9
→ 22	21	20	19	18	17	16	15	14	13	12	11	10	9	8	7	6	5	4	3	2	1	

*These are amino acid resin samples from the first coupling of the HOBT ester double couple cycles used for the Arg, Asn and Gln couplings. The calculation of the average step yield excludes these (*) residues. †Ninhydrin values for amino acids coupled to proline are not quantitative.



M-67-G ($CONH_2$), Crude

mobile phase	0.1% TFA/CH_3CN
gradient	0 to 60% in 60 minutes
flow rate	1.0 mL/min
detector	214 nm
column	Brownlee, C-8, 300Å, 10 µm 4.6 mm x 100 mm



M-67-G, ($CONH_2$), Purified

mobile phase	0.1% TFA/CH_3CN
gradient	0 to 60% in 60 minutes
flow rate	1.0 mL/min
detector	214 nm
column	Brownlee, C-8, 300Å, 10 µm 4.6 mm x 250 mm

Met-67-Gly ($CONH_2$) is a 69-residue peptide that is part of a 124k-dalton plant protein, Avena Phytochrome. This peptide is from an area of the Phytochrome protein that has been shown to be essential for complete biological activity. Although sequence analysis suggests the purified product contains minor peptide impurities, initial experiments have shown good peptide binding activity to antibodies made against the native protein. Work is continuing with efforts to map the exact reading frame of these antibodies by using deprotected, resin-bound peptides directly in the antibody binding assays.

This peptide was synthesized for collaborative research with Dr. Peter Quail, University of Wisconsin—Madison

You Can Prove It for Yourself

Compare a 430A-synthesized peptide made to *your* specifications (and at a very reasonable price) with what you've been getting so far. The quality will convince you that the 430A is the first choice of more people who make peptides.

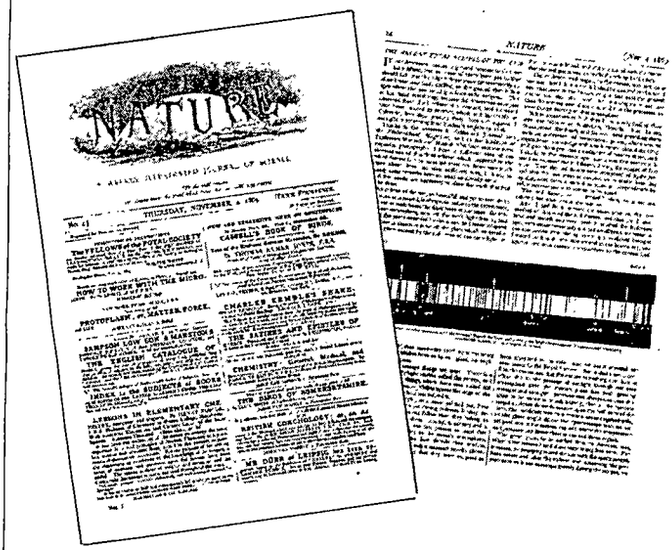
For more information, contact Jan Bowen at our U.S.A. office, your local Applied Biosystems Representative, or indicate Reader Service Number 218

Applied Biosystems

Sales and Service Worldwide: U.S.A. 850 Lincoln Centre Drive, Foster City, California 94404, U.S.A., Tel. (415) 570-6667 (800) 874-9868, in Calif (800) 831-[illegible] • U.K. Birchwood Science Park, Warrington, Cheshire, U.K., Tel. 925-825650, Telex 629[illegible] • W.Germany Bergstrasse 104, D6102 Pfungstadt, B R D , Tel 6157 6[illegible] • Australia Suite 2, 1401 Burke Road KEW, Victoria, Australia 3101, Tel. (03) 859-9571

THURSDAY, NOVEMBER 4, 1869 WAS THE PUBLICATION DAY OF

Nature's first issue



Now in 1986 you can add this unique and fascinating issue to your own collection or offer it as an unusual gift to a friend or colleague.

Browse through J. Norman Lockyer's famous article "The Recent Total Eclipse of the Sun", discover how science was taught in schools in *1869* with W. Tuckwell or delve into T. H. Huxley's absorbing report on "Triassic Dinosauria".

These and other original articles are reproduced in **NATURE**'s high quality first issue facsimile available **NOW** from the address given below.

To: **Nature**, Macmillan Journals Ltd, Brunel Road, Basingstoke, Hampshire RG21 2XS, UK.

Please send me .....facsimile(s) of the first issue of NATURE.

I enclose ☐ **UK £2.00** ☐ **$3.00** Surface Rest of World ☐ **$4.00** Airmail Rest of World

Name

Address

Payment may be made in any currency at the prevailing exchange rate. Cheques should be made payable to **Nature**. Prices include postage and packing.

Forma Scientific International Technical Sales and Service

Australia
Selby Anax, Oakleigh, Victoria Phone 03-544-4844
Austria
Kurt Bartelt GmbH, A-8010, Graz Phone 316-45328
Belgium
Technical Trading Office, B-1641 Alsemberg Phone 02-3802223
China
Novelact, Ltd., Kowloon, Hong Kong Phone 3-668363
Denmark
Teknunc A/S, Roskilde Phone 02-756311
Finland
Kaukomarkkinat Oy, Espoo 63 Phone 0-5215211
France
Bioblock Scientific, S.A., Illkirch Cedex Phone 88-671414
Germany
Labotect GmbH, Goettingen, Phone 551-82835
Greece
Anti-Sel O.E., Selidis Bros., Thessaloniki Phone 31-276303
India
Oriental Electromeds, Pvt. Ltd., Bombay 400 034 Phone 22-494259
Research Instrumentation Assoc., Madras 600 102 Phone 44-611210
Omega Instruments, Calcutta 700-016 Phone 29-7940
Ireland
Medlabs, Dublin, Phone 1-952101
Italy
Analytical Control Italia S.P.A. Cinisello Balsamo Phone 02-612-28-41
Japan
Sanyo Electric Tokki Co., Ltd., Osaka Phone 06-447-1171
Korea
Tech Express Korea & Co., Seoul Phone 02-7844385-7
Mexico
INTEKSA, 06760, Mexico Phone 5-5433630
Netherlands
Brouwer Scientific bv, P J DeMeern Phone 03406-64299
Norway
Dipl. Ing. Houm Oslo 3, Phone 2-159250
Portugal
ELNOR Equipamentos Tecnicos e de Laboratorio, P-4000 Porto Phone 29-490791
Puerto Rico
LIRCO, Caguas 00626 Phone 809-758-1770
Singapore
Mecomb Singapore, 2158 Phone 4698833
Spain
Hucoa Erloss, S.A. Madrid, 16 Phone 1-7337212
Sweden
AB Nino Lab, 19422 Uplands Vasby 1 Phone 760-86070
Switzerland
Brouwer Engineering, Lucerne Phone 041-44-44-48
Taiwan
Bestway Corporation, Taipei Phone 02-771-8337-9
United Kingdom
JENCONS (Scientific) Ltd., Leighton Buzzard Bedfordshire Phone (0525) 372010
Venezuela
Sersuinca Div., Medica SDM, Caracas 1062 Phone 2-329906
With Additional Dealers Serving 53 Other Countries.

Forma Scientific
DIVISION OF MALLINCKRODT, INC.
BOX 649 MARIETTA OHIO 45750 614-373-4763
USA AND CANADA 800-848-3080 TELEX 29-8205

nature

NATURE VOL. 321 5 JUNE 1986



Voltage-sensitive dyes reveal a modular organization of ocular dominance and orientation selectivity in the monkey striate cortex. In the cover picture (part of Fig. 5*b* on page 583), colours represent a gradient of orientation selectivity, with orange, yellow, green, blue, red and black indicating increasingly rapid rates of change in the orientation response. See also *News and Views* page 564.

OPINION

Scrapping treaties is wrong 547
Who pays for AIDS? 548
Who will pity Africa?

NEWS

US research funds 549
Space launchers
Chernobyl 550
British universitites
Bone marrow transplants
Chilean physicians 551
SDI 552
Neolithic Jericho
Japanese psychiatry 553
Ageing research
Yellow rain 554
French research
Optical computer
Beckman anniversary 555

CORRESPONDENCE

Japanese psychiatry/Dutch law/Truth 556

NEWS AND VIEWS

Danger of delay for genetic tests
Peter Newmark 557
Finding the defective gene
Peter Little 558
Wirechambers in Vienna
David J Miller 559
Immunology: A common form of killing
Peter J Lachmann 560
Low-dimensional electrons in a magnetic field
Paul Chaikin 561
Desertification or xerification?
N E West 562
Obituary: Albert L Lehninger
E C Slater 562
Crossbridges, force and motion
Richard T Tregear 563
Optical mapping of activity in primate visual cortex
D Van Essen & H S Orbach 564
Why do disused proteins become genetically lost or repressed?
Jared M Diamond 565
Magnetotelluric evidence for subduction of seafloor sediments
D Ian Gough 566

SCIENTIFIC CORRESPONDENCE

Weather forecasts still tricky
C Nicolis & G Nicolis 567
Activation of cellular calcium entry
O H Petersen 567
Beam balance test of weak equivalence principle
C C Speake & T J Quinn 567
***Blym* clone could be contaminant**
J Devine 568
Writing enzyme units in the correct way
M Paolini 568
Gamma-ray spectrum of Chernobyl fallout
D M Pringle, W J Vermeer & K W Allen 569
Q1146+111B,C double quasar pair: illusion or delusion?
E S Phinney & R D Blandford 569
Beware the cups that cheer
A-M Coriat & R D Gillard 570
Frequency of dizygotic twinning
M Sipser 570

BOOK REVIEWS

Comprehensive Biotechnology: The Principles, Applications and Regulations of Biotechnology in Industry, Agriculture and Medicine
M Moo-Young, editor-in-chief
A N Emery and A Lyddiatt 571
Schistosomiasis: The St Lucia Project
by P Jordan
G Webbe 572
Ecology and Natural History of Desert Lizards
by E R Pianka
Paul H Harvey 573
Thermoluminescence Dating
by M J Aitken
D J Huntley
Geology and Radwaste
by A G Milnes
J L Knill 574

ARTICLES

Galaxy formation by mock gravity
C J Hogan & S D M White 575
Voltage-sensitive dyes reveal a modular organization in monkey striate cortex
G G Blasdel & G Salama 579

LETTERS TO NATURE

Test of the gravitational lens hypothesis for the quasar pair 1146+111B,C
P A Shaver & S Cristiani 585
Natural ventilation of the Paintings Room in the Altamira cave
P L Fernández, I Gutierrez, L S Quindós, J Soto & E Villar 586
Global distribution of peroxyacetyl nitrate
H B Singh, L J Salas & W Viezee 588
Geometry of accretion and oceanic thrusting of the Spongtang Ophiolite, Ladakh-Himalaya
I Reuber 592
A magnetotelluric sounding across Vancouver Island detects the subducting Juan de Fuca plate
R D Kurtz, J M DeLaurier & J C Gupta 596
Seaward extension of the East African Rift
D Mougenot, M Recq, P Virlogeux & C Lepvrier 599
Eutectoid phase transformation of olivine and spinel into perovskite and rock salt structures
J P Poirier, J Peyronneau, M Madon, F Guyot & A Revcolevschi 603

Contents continued overleaf

Nature® (ISSN 0028-0836) is published weekly on Thursday, except the last week in December, by Macmillan Journals Ltd and includes the Annual Index (mailed in February). Annual subscription for USA and Canada US $240. USA and Canadian orders to: *Nature*, Subscription Dept, PO Box 1501, Neptune, NJ 07753, USA. Other orders to *Nature*, Brunel Road, Basingstoke, Hants RG21 2XS, UK. Second class postage paid at New York, NY 10012 and additional mailing offices. Authorization to photocopy material for internal or personal use, or internal or personal use of specific clients, is granted by *Nature* to libraries and others registered with the Copyright Clearance Center (CCC) Transactional Reporting Service, provided the base fee of $1.00 a copy plus $0.10 a page is paid directly to CCC, 21 Congress Street, Salem, Massachusetts 01970, USA. Identification code for *Nature*: 0028-0836/86 $1.00 + $0.10. US Postmaster send address changes to *Nature*, 65 Bleecker Street, New York, NY 10012. Published in Japan by Macmillan Shuppan K.K., Eikow Building, 1-10-9 Hongo, Bunkyo-ku, Tokyo, Japan.

© 1986 Macmillan Journals Ltd.

< Next to in vivo >

Heraeus

CO_2 Incubators

Experience and service: Nothing can replace them

- Competent supplier of equipment for cell labs worldwide
- More than 20 years of experience with high-quality CO_2 incubators
- Close co-operation with leading research institutes at home and abroad
- Detailed sales guidance and instruction
- Installation and putting into operation by own team of specialists
- Everything from one supplier: numerous peripheral units and special fittings available

Indispensable technical advantages

- Exact adherence to in vivo parameters by means of patented CO_2-Auto-Zero system: no drifting of the CO_2 content
- O_2 Clark electrode: automatic zero correction at the press of a button
- High constant humidity or psychrometric humidity control
- Perfect protection against contamination provided by copper inner casing or heat sterilization
- Exceptionally short recovery times due to heavy-duty heating and control system

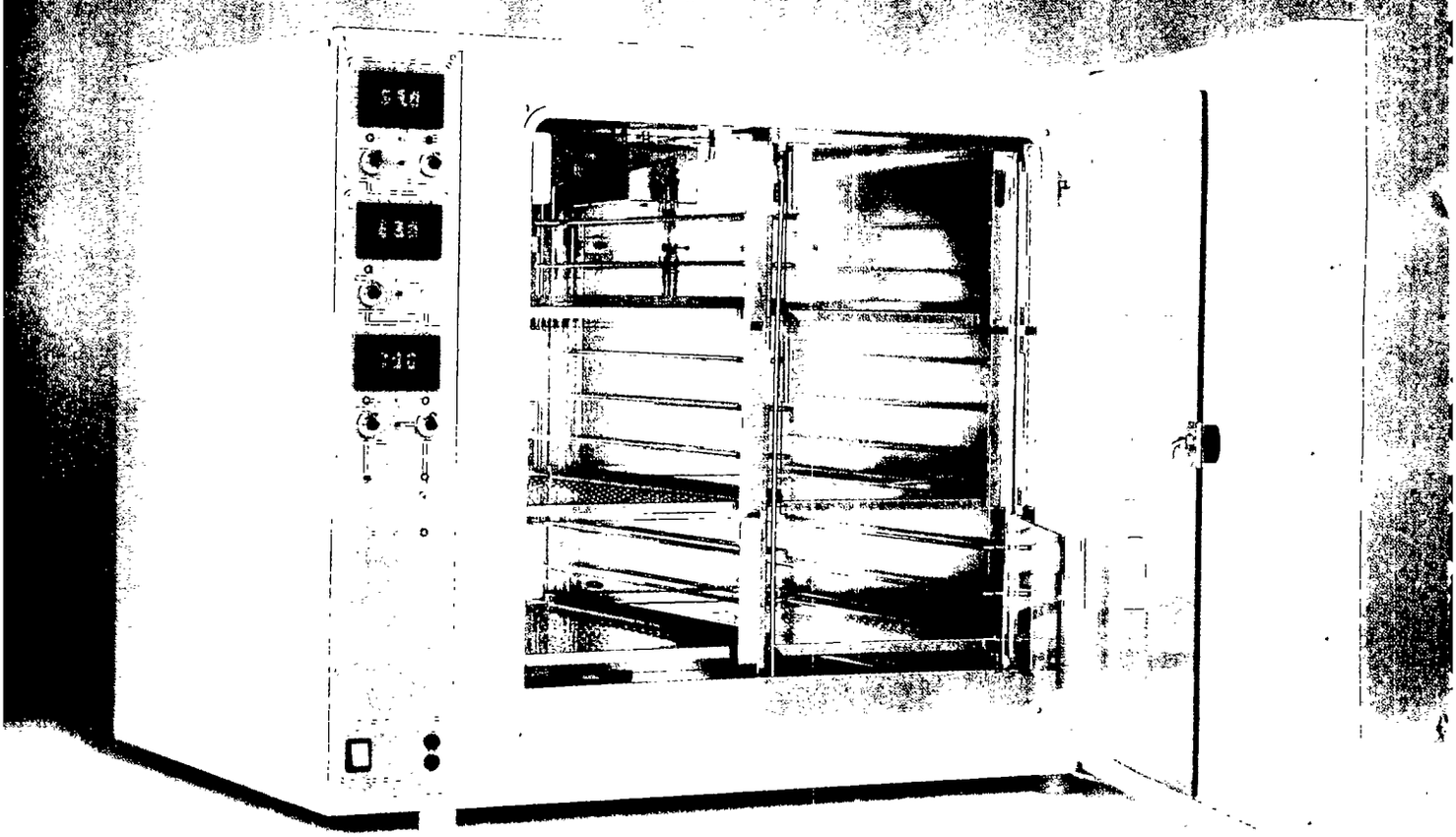
Heraeus: Recognized symbol of quality in cell research

Heraeus incubators are trend-setters in their quality, perfection and built-in know-how. So before you buy a CO_2 or O_2 incubator, make sure to find out in detail about the many advantages and extras of the Heraeus models

- B 5061 CO_2-Auto-Zero
- Cytoperm® and
- B 5060.

The scope of our range means that we provide "the perfect fit" for every in vivo situation.

Heraeus: For decades a leader in the sector of accurate cell research



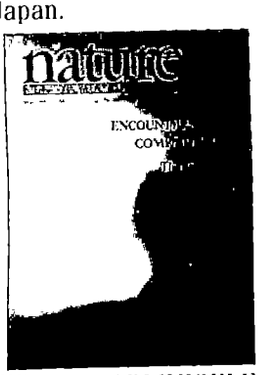
Heraeus W. C. Heraeus GmbH · Produktbereich Elektrowärme
P.O.B. 1553 · D-6450 Hanau 1 · Telephone (06181) 35-1

Reader Service No. 168

HALLEY'S COMET

SPECIAL SUPPLEMENT

AVAILABLE NOW – Nature's supplement on Halley's Comet containing results of missions carried out from Russia, Europe and Japan.



COPIES AVAILABLE WHILE STOCKS LAST FROM OUR OFFICES IN BASINGSTOKE
Prices as for back issues below

Annual Subscription Prices

UK & Irish Republic		£104
USA & Canada		US$240
Australia, NZ & S. Africa	Airspeed	£150
	Airmail	£190
Continental Europe	Airspeed	£125
India	Airspeed	£120
	Airmail	£190
Japan	Airspeed	Y90000
Rest of World	Surface	£120
	Airmail	£180

Orders (with remittance) to:

USA & Canada
Nature
Subscription Dept
PO Box 1501
Neptune
NJ 07753
USA

UK & Rest of World
Nature
Circulation Dept
Brunel Road
Basingstoke
Hants RG21 2XS, UK
Tel: 0256 29242

(The addresses of Nature's editorial offices are shown facing the first editorial page)

Japanese subscription enquiries to:
Japan Publications Trading Company Ltd
2-1 Sarugaku-cho 1-chome
Chiyoda-ku, Tokyo, Japan
Tel: (03) 292 3755

Personal subscription rates: These are available in some countries to subscribers paying by personal cheque or credit card. Details from:

USA & Canada
Nature
65 Bleecker Street
New York
NY 10012, USA
Tel: (212) 477-9600

UK & Europe
Felicity Parker
Nature
4 Little Essex Street
London WC2R 3LF, UK
Tel: 01-836 6633

Back issues: UK, £2.50; USA & Canada, US$6.00 (surface), US$9.00 (air); Rest of World, £3.00 (surface), £4.00 (air)

Binders
Single binders: UK, £5.25; USA & Canada $11.50; Rest of World, £7.75. Set of four: UK, £15.00; USA & Canada $32.00; Rest of World, £22.00

Annual indexes (1971-1985)
UK, £5.00 each; Rest of World, $10.00

Nature First Issue Facsimile
UK, £2.00; Rest of World (surface), $3.00; (air) $4.00

Nature in microform
Write to University Microfilms International, 300 North Zeeb Road, Ann Arbor, MI 48106, USA

Visualization of the dynamic instability of individual microtubules by dark-field microscopy
T Horio & H Hotani 605

Evidence that reserve cells are a source of regenerated adult newt muscle *in vitro*
J A Cameron, A R Hilgers & T J Hinterberger 607

Stimulation of oligodendroglial proliferation and maturation by interleukin-2
E N Benveniste & J E Merrill 610

Mechanism of membrane damage mediated by human eosinophil cationic protein
J D-E Young, C G B Peterson, P Venge & Z A Cohn 613

A novel cell surface molecule on early B-lineage cells
M D Cooper, D Mulvaney, A Coutinho & P-A Cazenave 616

Chloroquine and ammonium chloride prevent terminal glycosylation of immunoglobulins in plasma cells without affecting secretion
B Thorens & P Vassalli 618

Structure of DNase I at 2.0 Å resolution suggests a mechanism for binding to and cutting DNA
D Suck & C Oefner 620

L1 family of repetitive DNA sequences in primates may be derived from a sequence encoding a reverse transcriptase-related protein
M Hattori, S Kuhara, O Takenaka & Y Sakaki 625

MATTERS ARISING

Physiological relevance of erythroid-potentiating activity or TIMP
G P Stricklin & H G Welgus
Reply: J C Gasson & D W Golde 628

PRODUCT REVIEW

Growth factors spawn new cell cultures
W L McKeehan 629

Hi-tech for tissue culture: a growing endeavour 630

EMPLOYMENT

No quick cure for skill shortages
R Pearson 634

NATURE CLASSIFIED

Professional appointments — Research posts — Studentships — Fellowships — Conferences — Courses — Seminars — Symposia: Back Pages

Next week in *Nature*:

- Solar X rays
- Metallic cometary tails
- Nature of Na^- anion
- $CuInS_2$ for solar conversion
- Pacific lead isotopes
- Therian mammal metabolism
- Phorbol ester mechanisms
- Tumour necrosis factor
- Chromosomal replication
- Leguminous gene regulation
- Automated DNA sequencing

GUIDE TO AUTHORS

Authors should be aware of the diversity of *Nature*'s readership and should strive to be as widely understood as possible.

Review articles should be accessible to the whole readership. Most are commissioned, but unsolicited reviews are welcome (in which case prior consultation with the office is desirable).

Scientific articles are research reports whose conclusions are of general interest or which represent substantial advances of understanding. The text should not exceed 3,000 words and six displayed items (figures plus tables). The article should include an italic heading of about 50 words.

Letters to *Nature* are ordinarily 1,000 words long with no more than four displayed items. The first paragraph (not exceeding 150 words) should say what the letter is about, why the study it reports was undertaken and what the conclusions are.

Matters arising are brief comments (up to 500 words) on articles and letters recently published in *Nature*. The originator of a Matters Arising contribution should initially send his manuscript to the author of the original paper and both parties should, wherever possible, agree on what is to be submitted.

Manuscripts may be submitted either to London or Washington. Manuscripts should be typed (double spacing) on one side of the paper only. Four copies are required, each accompanied by copies of lettered artwork. No title should exceed 80 characters in length. Reference lists, figure legends, etc, should be on separate sheets, all of which should be numbered. Abbreviations, symbols, units, etc, should be identified on one copy of the manuscript at their first appearance.

References should appear sequentially indicated by superscripts, in the text and should be abbreviated according to the *World List of Scientific Periodicals*, fourth edition (Butterworth 1963-65). The first and last page numbers of each reference should be cited. Reference to books should clearly indicate the publisher and the date and place of publication. Unpublished articles should not be formally referred to unless accepted or submitted for publication, but may be mentioned in the text.

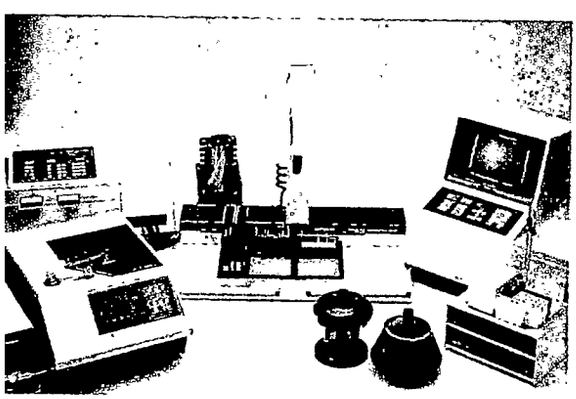
Each piece of artwork should be clearly marked with the author's name and the figure number. Original artwork should be unlettered. Suggestions for cover illustrations are welcome. Original artwork (and one copy of the manuscript) will be returned when manuscripts cannot be published.

Important: Manuscripts or proofs sent by air courier should be declared as "manuscripts" and "value $5" to prevent the imposition of Customs duty and Value Added Tax in the United Kingdom.

Requests for permission to reproduce material from Nature *should be accompanied by a self-addressed (and, in the case of the United Kingdom and United States, stamped) envelope.*

LIFE SCIENCE LEADERSHIP:

We're with you every step of the way... and before.



Before?

The accuracy of the analytical process is only as good as the preparation that takes place before the measurements are made.

But in addition to the care which must be exercised, sample preparation and handling can be tedious and extremely labor intensive.

Beckman's commitment to provide solutions to this crucial area of laboratory operations continues with new advances that increase lab productivity and optimize efficiency.

It begins with our new Biomek™ 1000 Automated Laboratory Workstation, a unique robotic system designed specifically to improve throughput and productivity in sample preparation and handling.

The new Biomek 1000 joins an illustrious line-up of sample preparation and handling solutions that includes batch and automatic samplers for virtually unattended analyses of large sample batches using HPLC systems and UV/Visible spectrophotometers. And a self-operating dissolution testing system that integrates sample handling with data gathering.

The Biomek 1000 and other Beckman systems for sample handling and preparation exemplify our commitment to being with you in every step of your laboratory process. Not surprisingly because, here at Beckman, we consider our efforts to be part of a permanent partnership with the entire life science process.

The commitment continues. For more product information, contact your local Beckman representative. Or write to: Beckman Instruments, Inc., 2500 Harbor Boulevard, Mail Station E-33-D, Fullerton, CA 92634-3100.

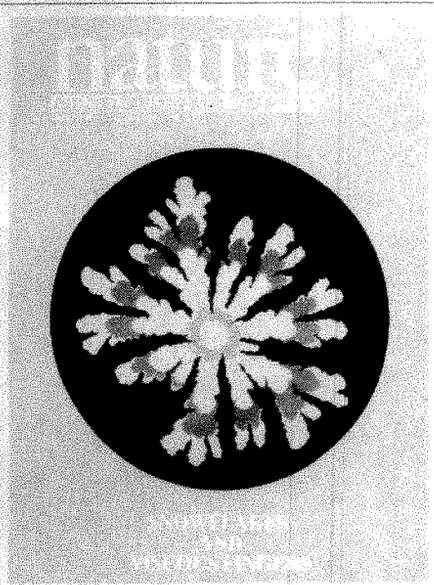
©1986, Beckman Instruments, Inc.

BECKMAN

Reader Service No.19

nature

NATURE VOL. 321 12 JUNE 1986



A new theoretical model for the tip splitting phenomenon: an object initially grows by adding successive circular rings, then suddenly forms a random proliferation of bifurcations. This ubiquitous phenomenon is especially striking in developmental biology and fluid mechanics. Six successive snapshots of this growing fractal structure are indicated by six different colours. The tips screen the inner regions, as a newly formed region rarely touches the older regions. See p. 663.

OPINION

What happens to NASA now? 635
Observers in arms 636

NEWS

Shuttle catastrophe
Other avenues? 637
Seismic monitoring
Soviet industry 638
AIDS research
Rice breeding 639
Germany and Chernobyl 640
US biotechnology
Chernobyl 641
French science
US policy 642
Laboratory accidents
Foreign students in science and engineering
Corrigendum: Chernobyl fallout 643

CORRESPONDENCE

For AIDS read human immunodeficiency virus/French basic research/Chance and Chernobyl 644

NEWS AND VIEWS

Towards understanding snowflakes 645
Energy and signal transduction by transmembrane protein complexes
Alexander N Glazer 646
Obituary: Robert Day Allen
D Lansing Taylor 647
Energetic costs of reproduction
Paul H Harvey 648
Laser technology: Microfabrication of thin films
Ian W Boyd & F Micheli 649
Immunology: Approaches to tolerance in man
Leslie Brent 650
Do computers need attention?
Anya Hurlbert & Tomaso Poggio 651
Epstein–Barr virus: Infection and tumour induction
M A Epstein 653
Pesticides and pollination
Peter D Moore 654

SCIENTIFIC CORRESPONDENCE

Iodine-131 in human thyroids in Britain following Chernobyl
C R Hill, I Adam, W Anderson, R J Ott & F D Sowby 655
Do mammals need P elements?
I J Jackson 656
Initiating boiling with ice
R E Apfel & R L Day 657
In defence of bacterial phylogeny
J A Lake 657
Testis size and zygotic twins
L R Willat & D J Bartlett 658

BOOK REVIEWS

Profiles of Social Research: The Scientific Study of Human Interactions
by M Hunt
Marie Jahoda 659
The Inflammatory Reaction
by H Z Movat
Gerry Higgs & Brendan Whittle 660
Genetically Altered Viruses and the Environment
B Fields, M A Martin and D Kamely, eds
D H L Bishop
The Citadel of the Senses and Other Essays
by M Critchley
John C Marshall 661
General Features of the Paleobiological Evolution of Cetacea
by G A Mchedlidze
Samuel A McLeod 662

ARTICLES

Tip splitting without interfacial tension and dendritic growth patterns arising from molecular anisotropy
J Nittmann & H E Stanley 663

Nodule-specific expression of a chimaeric soybean leghaemoglobin gene in transgenic *Lotus corniculatus*
J S Jensen, K A Marcker, L Otten & J Schell 669

Fluorescence detection in automated DNA sequence analysis
L M Smith, J Z Sanders, R J Kaiser, P Hughes, C Dodd, C R Connell, C Heiner, S B H Kent & L E Hood 674

LETTERS TO NATURE

Coordinated Exosat and spectroscopic observations of flare stars and coronal heating
C J Butler, M Rodono, B H Foing & B M Haisch 679

Metallic ions in cometary comae and plasma tails
W-H Ip & W I Axford 682

Gas-like nature of the sodium anion in solution
A S Ellaboudy, D M Holton, N C Pyper, P P Edwards, B Wood & W McFarlane 684

Distribution of atoms at the surface of liquid mercury
S W Barton, B N Thomas, F Novak, P M Weber, J Harris, P Dolmer, J M Bloch & S A Rice 685

Efficient solar energy conversion with $CuInS_2$
H J Lewerenz, H Goslowsky, K-D Husemann & S Fiechter 687

Vertical profile of lead isotopic compositions in the north-east Pacific
A R Flegal, K Itoh, C C Patterson & C S Wong 689

Basal metabolic rate and energetics of reproduction in therian mammals
S D Thompson & M E Nicoll 690

Contents continued overleaf

Nature® (ISSN 0028-0836) is published weekly on Thursday, except the last week in December, by Macmillan Journals Ltd and includes the Annual Index (mailed in February). Annual subscription for USA and Canada US $240. USA and Canadian orders to: *Nature*, Subscription Dept, PO Box 1501, Neptune, NJ 07753, USA. Other orders to *Nature*, Brunel Road, Basingstoke, Hants RG21 2XS, UK. Second class postage paid at New York, NY 10012 and additional mailing offices. Authorization to photocopy material for internal or personal use, or internal or personal use of specific clients, is granted by *Nature* to libraries and others registered with the Copyright Clearance Center (CCC) Transactional Reporting Service, provided the base fee of $1.00 a copy plus $0.10 a page is paid directly to CCC, 21 Congress Street, Salem, Massachusetts 01970, USA. Identification code for *Nature*: 0028-0836/86 $1.00 + $0.10. US Postmaster send address changes to: *Nature*, 65 Bleecker Street, New York, NY 10012. Published in Japan by Macmillan Shuppan K.K., Eikow Building, 1-10-9 Hongo, Bunkyo-ku, Tokyo, Japan. © 1986 Macmillan Journals Ltd.

FPLC*pure*™ MODIFYING ENZYMES



Pharmacia's 30 years of pioneering in biomolecule purification techniques has resulted in the remarkable state-of-the-art FPLC® System.

Pharmacia P-L purification expertise utilizes optimized FPLC technology and offers you modifying enzymes of unsurpassed purity and reproducibility unique in the biotechnology market.

The label FPLC*pure* on the package of a Pharmacia Modifying Enzyme is your guarantee that this batch of enzyme is functionally identical to the last batch you bought and will give the same outstanding performance.

A working partnership with Pharmacia gives you dependability and unique solutions that greatly improve your molecular biology applications.

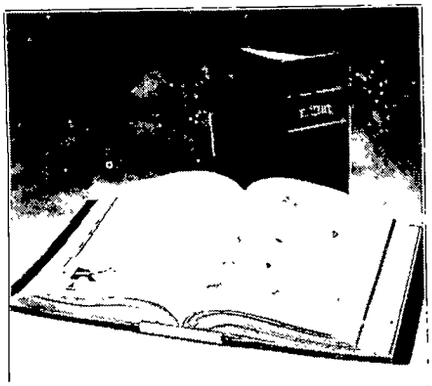
- ☐ FPLC*pure* Klenow Fragment – CLONED
- ☐ FPLC*pure* T4 Ligase – CLONED
- ☐ FPLC*pure* T7 RNA Polymerase – CLONED
- ☐ FPLC*pure* T4 DNA Polymerase
- ☐ FPLC*pure* Mung Bean Nuclease
- ☐ FPLC*pure* AMV Reverse Transcriptase
- ☐ FPLC*pure* Polynucleotide Kinase
- ☐ FPLC*pure* Terminal Transferase

Pharmacia. Unique Solutions in Molecular Biology.

Life's Thread: Sculpture in glass by Alberius, Orrefors. Commissioned by Molecular Biology Division, Pharmacia AB.

Pharmacia

Molecular Biology Division
S-751 82 Uppsala, Sweden
Reader Service No.76



NATURE BINDERS

Your copies of Nature are invaluable for future reference so why not give them the treatment they deserve and file them neatly in our special Nature binders?

Ordering address and prices for one or a set of four are listed below.

Annual Subscription Prices

UK & Irish Republic		£104
USA & Canada		US$240
Australia, NZ & S. Africa	Airspeed	£150
	Airmail	£190
Continental Europe	Airspeed	£125
India	Airspeed	£120
	Airmail	£190
Japan	Airspeed	Y90000
Rest of World	Surface	£120
	Airmail	£180

Orders (with remittance) to:

USA & Canada
Nature
Subscription Dept
PO Box 1501
Neptune
NJ 07753
USA

UK & Rest of World
Nature
Circulation Dept
Brunel Road
Basingstoke
Hants RG21 2XS, UK
Tel: 0256 29242

(The addresses of Nature's editorial offices are shown facing the first editorial page)

Japanese subscription enquiries to:
Japan Publications Trading Company Ltd
2-1 Sarugaku-cho 1-chome
Chiyoda-ku, Tokyo, Japan
Tel: (03) 292 3755

Personal subscription rates: These are available in some countries to subscribers paying by personal cheque or credit card. Details from:

USA & Canada
Nature
65 Bleecker Street
New York
NY 10012, USA
Tel: (212) 477-9600

UK & Europe
Felicity Parker
Nature
4 Little Essex Street
London WC2R 3LF, UK
Tel: 01-836 6633

Back issues: UK, £2.50; USA & Canada, US$6.00 (surface), US$9.00 (air); Rest of World, £3.00 (surface), £4.00 (air)

Binders
Single binders: UK, £5.25; USA & Canada $11.50; Rest of World, £7.75. Set of four: UK, £15.00; USA & Canada $32.00; Rest of World, £22.00

Annual indexes (1971-1985)
UK, £5.00 each; Rest of World, $10.00

Nature First Issue Facsimile
UK, £2.00; Rest of World (surface), $3.00; (air) $4.00

Nature in microform
Write to University Microfilms International, 300 North Zeeb Road, Ann Arbor, MI 48106, USA

Enhanced detection in the aperture of focal attention during simple discrimination tasks
D Sagi & B Julesz — 693

Phorbol esters block a voltage-sensitive chloride current in hippocampal pyramidal cells
D V Madison, R C Malenka & R A Nicoll — 695

Phorbol ester facilitates ^{45}Ca accumulation and catecholamine secretion by nicotine and excess K^+ but not by muscarine in rat adrenal medulla
A R Wakade, R K Malhotra & T D Wakade — 698

Mediation of mouse natural cytotoxic activity by tumour necrosis factor
J R Ortaldo, L H Mason, B J Mathieson, S-M Liang, D A Flick & R B Herberman — 700

A block to elongation is largely responsible for decreased transcription of c-*myc* in differentiated HL60 cells
D L Bentley & M Groudine — 702

Idealization of the hydrophobic segment of the alkaline phosphatase signal peptide
D A Kendall, S C Bock & E T Kaiser — 706

Stringent control of initiation of chromosomal replication in *Bacillus subtilis*
S J Séror, F Vannier, A Levine & G Henckes — 709

MISCELLANY

100 years ago — 653
Books received — 711

NATURE CLASSIFIED

Professional appointments — Research posts — Studentships — Fellowships — Conferences — Courses — Seminars — Symposia:
Back Pages

Next week in *Nature*:

- Merging galaxies
- Earth's orbit and climate
- Antarctic ozone depletion
- Sweden's acid rain
- Ancient zircons
- Man's arrival in South America
- α-Thalassaemia and malaria
- Inhibins and FSH
- Primate α-globins
- Axon growth
- Prehistoric oligonucleotide synthesis

GUIDE TO AUTHORS

Authors should be aware of the diversity of *Nature*'s readership and should strive to be as widely understood as possible.

Review articles should be accessible to the whole readership. Most are commissioned, but unsolicited reviews are welcome (in which case prior consultation with the office is desirable).

Scientific articles are research reports whose conclusions are of general interest or which represent substantial advances of understanding. The text should not exceed 3,000 words and six displayed items (figures plus tables). The article should include an italic heading of about 50 words.

Letters to *Nature* are ordinarily 1,000 words long with no more than four displayed items. The first paragraph (not exceeding 150 words) should say what the letter is about, why the study it reports was undertaken and what the conclusions are

Matters arising are brief comments (up to 500 words) on articles and letters recently published in *Nature*. The originator of a Matters Arising contribution should initially send his manuscript to the author of the original paper and both parties should, wherever possible, agree on what is to be submitted

Manuscripts may be submitted either to London or Washington. Manuscripts should be typed (double spacing) on one side of the paper only. Four copies are required, each accompanied by copies of lettered artwork. No title should exceed 80 characters in length. Reference lists, figure legends, etc., should be on separate sheets, all of which should be numbered. Abbreviations, symbols, units, etc. should be identified on one copy of the manuscript at their first appearance.

References should appear sequentially indicated by superscripts, in the text and should be abbreviated according to the *World List of Scientific Periodicals*, fourth edition (Butterworth 1963-65). The first and last page numbers of each reference should be cited. Reference to books should clearly indicate the publisher and the date and place of publication. Unpublished articles should not be formally referred to unless accepted or submitted for publication but may be mentioned in the text.

Each piece of artwork should be clearly marked with the author's name and the figure number. Original artwork should be unlettered. Suggestions for cover illustrations are welcome. Original artwork (and one copy of the manuscript) will be returned when manuscripts cannot be published.

Important: Manuscripts or proofs sent by air courier should be declared as "manuscripts" and "value $5" to prevent the imposition of Customs duty and Value Added Tax in the United Kingdom.

Requests for permission to reproduce material from Nature *should be accompanied by a self-addressed (and, in the case of the United Kingdom and United States, stamped) envelope.*

DAY RATES
NOW AVAILABLE
— phone 01-836 6633
YOUR LAST CHANCE TO BOOK

WHAT IMPACT ARE NEW BIOTECHNOLOGY TECHNIQUES HAVING ON MEDICINE WORLDWIDE TODAY?

NEW TECHNOLOGY in BIOTECHNOLOGY

MOLECULAR BIOLOGY IN MEDICIN
a survey of its achievements and its potential

June 18–20 1986
at the London West Hotel

It is clear that the modern techniques of biotechnology are set to have a major impact on medicine. Over the next few years many new opportunities will emerge. This important conference will provide a wide-ranging survey of the most recent research in the fast changing field of molecular biology in medicine, and a look into the future. If you want an opportunity to see and hear for yourself what leading exponents have achieved in recent years — and to learn what new opportunities are on the horizon, come and join us.

The **CONFERENCE FEE** is just £189 plus VAT for the three days of the conference. The daily rate is £69 plus VAT. This includes entrance to all sessions, mid-morning coffee, afternoon tea and reading material. Group discounts are available on application to Janine Slipman, see booking form for address and phone no.

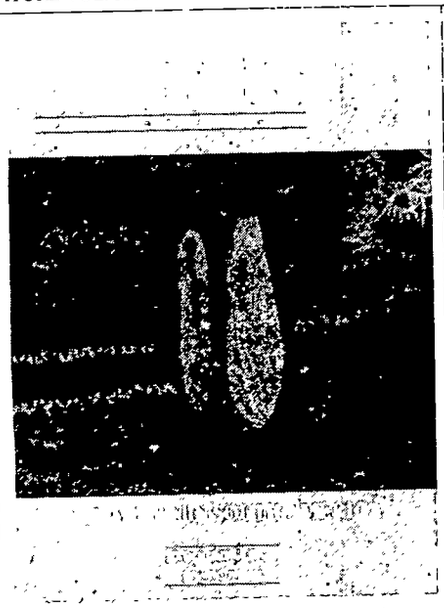
ACCOMMODATION has been reserved in the London West Hotel for conference participants. A booking form will be sent to you as soon as we receive your registration.

TECHNICAL SEMINARS and **POSTER SESSIONS** will be held each day. Anybody wishing to present a poster should send a title and a brief synopsis.

To: Dr Peter Newmark Deputy Editor Nature
4 Little Essex Street London WC2R 3LR

nature

NATURE VOL. 321 19 JUNE 1986



Sao Raimundo Nonato in north-east Brazil is famous for the richness of prehistoric art decorating the numerous rockshelters in the region. Carbon-14 dates from an excavation of one of these shelters, "Toca do Boqueirao do Sitio da Pedra Furada", establish human occupation beginning 32,000 years ago. This is the oldest site of Early Man presently known in America. The excavation is described on page 769 and discussed in *News and Views* on page 726.

OPINION

Where next with the greenhouse? 713

NEWS

Atmospheric greenhouse 714
French universities
US copyright 715
British software
Cancer research 716
Soviet education
Chemical weapons 717
Estonian protest
Biotechnology 718
European research
Materials science 719
US research overheads
Test-tube babies
Japanese gynaecology 720
Brown eggs catch on in Japan
Colombian immunology 721

CORRESPONDENCE

The Paluxy River mystery/ Cometary first/Nuclear energy 722

NEWS AND VIEWS

When reference means deference 722
Dual gonadal control of follicle-stimulating hormone
Con G Tsonis & Richard M Sharpe 724
The most ancient rocks revisited
Stephen Moorbath 725
Finding the earliest Americans
Warwick Bray 726
Thin filament regulatory proteins of smooth- and non-muscle cells
Anthony Bretscher 726
The fibronectin receptor family
Maria Leptin 728
Depletion of Antarctic ozone
A F Tuck 729
Globin gene monkey business
Nick Proudfoot 730
Clues about glues in development
Colin J Barnstable 731
Sedimentological use of dinosaurs
Michael J Benton 732

SCIENTIFIC CORRESPONDENCE

Portuguese role in spread of HTLV-I virus
S S Kantha 733
Commercial samples of subtilisin BPN'
A J Russell & A R Fersht 733
***Alu* sequences in the LDL receptor messenger RNA**
J Auwerx, H de Loof, &G Verhoeven 733
How to test special relativity
H Aspden
Reply: M Psimopoulos & T Theocharis 734

BOOK REVIEWS

The Politics of Uncertainty: Regulating Recombinant DNA Research in Britain
by D Bennett, P Glasner and D Travis
and
Cloning and the Constitution: An Inquiry into Governmental Policymaking and Genetic Experimentation
by I H Carmen
Sheldon Krimsky 735
Hormones and Human Behaviour
by B T Donovan
Robert T Rubin 736
Natural Zeolites
by G Gottardi and E Galli
William S Wise
Mind from Matter? An Essay on Evolutionary Epistemology
by M Delbrück, G S Stent et al. *eds*
H C Longuet-Higgins 737

ARTICLES

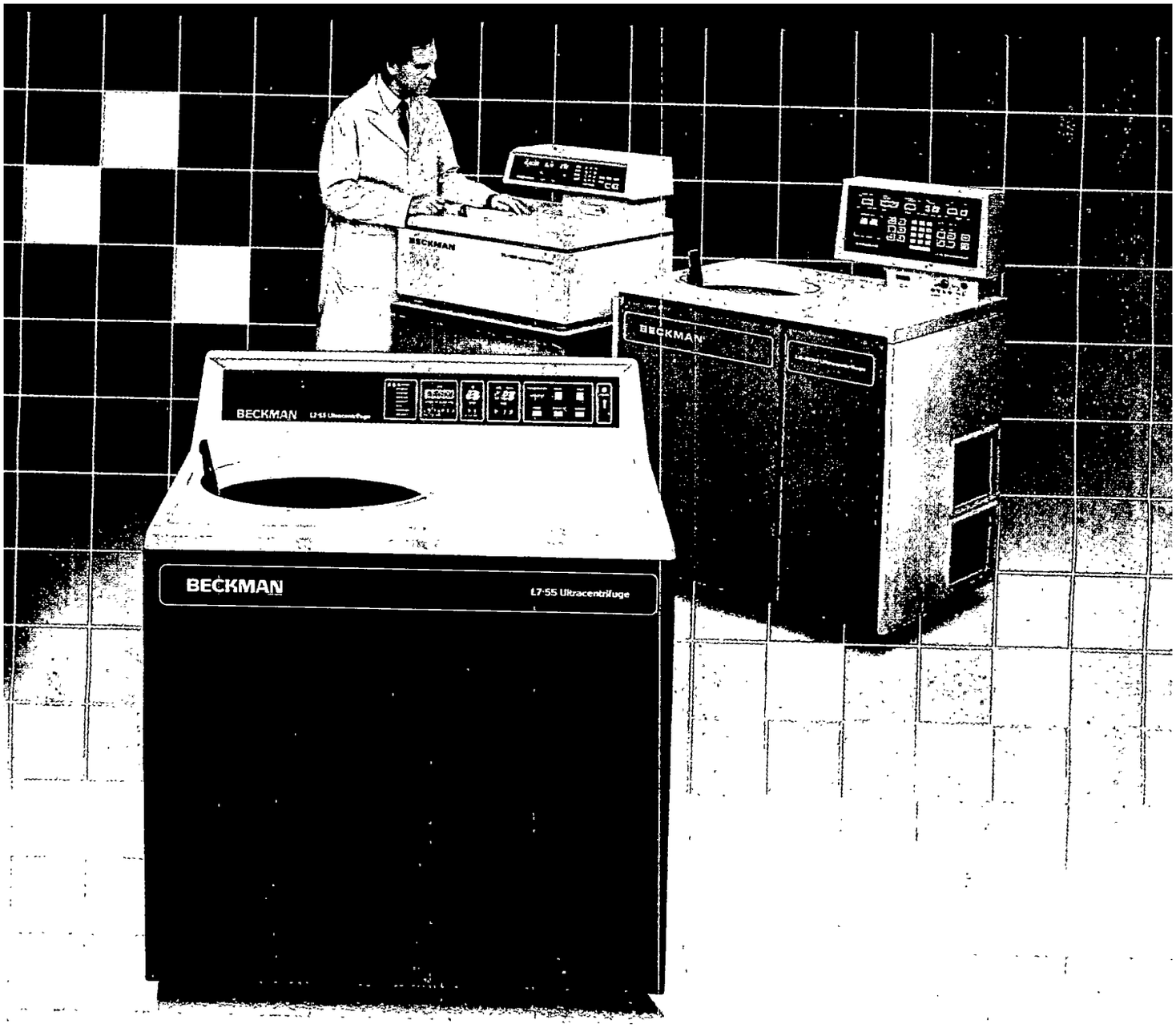
Milankovitch climatic origin of mid-Cretaceous black shale rhythms in central Italy
T D Herbert & A G Fischer 739
High frequencies of α-thalassaemia are the result of natural selection by malaria
J Flint, A V S Hill, D K Bowden, S J Oppenheimer, P R Sill, S W Serjeantson, J Bana-Koiri, K Bhatia, M P Alpers, A J Boyce, D J Weatherall & J B Clegg 744

LETTERS TO NATURE

PKS1345+125: a Seyfert nucleus merging with a powerful radio galaxy
G Gilmore & M A Shaw 750
A compact radio source in the nucleus of M87
R E Spencer & W Junor 753
On the depletion of Antarctic ozone
S Solomon, R R Garcia, F S Rowland & D J Wuebbles 755
Reductions of Antarctic ozone due to synergistic interactions of chlorine and bromine
M B McElroy, R J Salawitch, S C Wofsy & J A Logan 759
Temporal evolution of nitrogen compounds in Swedish precipitation since 1955
H Rodhe & M J Rood 762
High-temperature fluid–rock interactions in a layered syenite pluton
I Parsons & S M Becker 764
Jack Hills, evidence of more very old detrital zircons in Western Australia
W Compston & R T Pidgeon 766
Carbon-14 dates point to man in the Americas 32,000 years ago
N Guidon & G Delibrias 769
Synaptosomes possess an exocytotic pool of glutamate
D G Nicholls & T S Sihra 772

Contents continued overleaf

Nature® (ISSN 0028-0836) is published weekly on Thursday, except the last week in December, by Macmillan Journals Ltd and includes the Annual Index (mailed in February). Annual subscription for USA and Canada US $240. USA and Canadian orders to: *Nature*, Subscription Dept, PO Box 1501, Neptune, NJ 07753, USA. Other orders to *Nature*, Brunel Road, Basingstoke, Hants RG21 2XS, UK. Second class postage paid at New York, NY 10012 and additional mailing offices. Authorization to photocopy material for internal or personal use, or internal or personal use of specific clients, is granted by *Nature* to libraries and others registered with the Copyright Clearance Center (CCC) Transactional Reporting Service, provided the base fee of $1.00 a copy plus $0.10 a page is paid directly to CCC, 21 Congress Street, Salem, Massachusetts 01970, USA. Identification code for *Nature*: 0028-0836/86 $1.00 + $0.10. US Postmaster send address changes to *Nature*, 65 Bleecker Street, New York, NY 10012. Published in Japan by Macmillan Shuppan K.K., Eikow Building, 1-10-9 Hongo, Bunkyo-ku, Tokyo, Japan. © 1986 Macmillan Journals Ltd



Something Special

Imagine the world's simplest operating ultracentrifuge. Add the most reliable drive ever designed—the Ultra-Smooth vacuum-encased induction system. Include automatic "Soft-Start," built-in diagnostics and the ability to run every Beckman high performance rotor. Top it off with a most attractive purchase price. And you have the new Model L7-55—the one you have been asking for.

With speeds to 55,000 rpm, forces to 408,000 *g*, integrated circuit logic and remarkably simple controls, the L7 is ideal for everyday applications. It's the perfect addition to the Beckman family of induction drive ultracentrifuges, joining the premier L8M models—the ultimate in centrifugal research tools—and the Benchtop TL-100 for rapid microvolume separations.

Use the L7 for the routine jobs. Save your L8M for investigations where microprocessor control and memory are an advantage, where delicate gradients call for acceleration/deceleration versatility, where computer interfacing is needed for remote control or record keeping. When you want to cut run times for these jobs by more than half, use the TL-100.

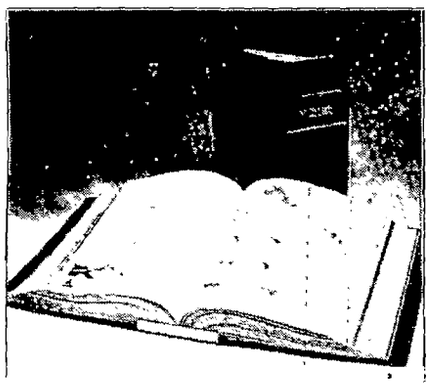
The workaday Model L7-55: it's something special—especially for you!

To get better acquainted, ask for Brochure SB-667. Beckman Instruments, Inc., Spinco Division, 1050 Page Mill Road, Palo Alto, CA 94304.

BECKMAN 50 1935-1985

BECKMAN

Reader Service No.149



NATURE BINDERS

Your copies of Nature are invaluable for future reference so why not give them the treatment they deserve and file them neatly in our special Nature binders?

Ordering address and prices for one or a set of four are listed below.

Annual Subscription Prices

UK & Irish Republic		£104
USA & Canada		US$240
Australia, NZ & S. Africa	Airspeed	£150
	Airmail	£190
Continental Europe	Airspeed	£125
India	Airspeed	£120
	Airmail	£190
Japan	Airspeed	Y90000
Rest of World	Surface	£120
	Airmail	£180

Orders (with remittance) to:

USA & Canada
Nature
Subscription Dept
PO Box 1501
Neptune
NJ 07753
USA

UK & Rest of World
Nature
Circulation Dept
Brunel Road
Basingstoke
Hants RG21 2XS, UK
Tel: 0256 29242

(The addresses of Nature's editorial offices are shown facing the first editorial page)

Japanese subscription enquiries to:
Japan Publications Trading Company Ltd
2-1 Sarugaku-cho 1-chome
Chiyoda-ku, Tokyo, Japan
Tel: (03) 292 3755

Personal subscription rates: These are available in some countries to subscribers paying by personal cheque or credit card. Details from:

USA & Canada
Nature
65 Bleecker Street
New York
NY 10012, USA
Tel: (212) 477-9600

UK & Europe
Felicity Parker
Nature
4 Little Essex Street
London WC2R 3LF, UK
Tel: 01-836 6633

Back issues: UK, £2.50; USA & Canada, US$6.00 (surface), US$9.00 (air); Rest of World, £3.00 (surface), £4.00 (air)

Binders
Single binders: UK, £5.25; USA & Canada $11.50; Rest of World, £7.75. Set of four: UK, £15.00; USA & Canada $32.00; Rest of World, £22.00

Annual indexes (1971-1985)
UK, £5.00 each; Rest of World, $10.00

Nature First Issue Facsimile
UK, £2.00; Rest of World (surface), $3.00; (air) $4.00

Nature in microform
Write to University Microfilms International, 300 North Zeeb Road, Ann Arbor, MI 48106, USA

Phosphorylation of the nicotinic acetylcholine receptor regulates its rate of desensitization
R L Huganir, A H Delcour, P Greengard & G P Hess **774**

Purification and characterization of an FSH releasing protein from porcine ovarian follicular fluid
W Vale, J Rivier, S-Y Ying, J Vaughan, R McClintock, A Corrigan, W Woo, D Karr & J Spiess **776**

Pituitary gland FSH is released by a heterodimer of the β-subunits from the two forms of inhibin
N Ling, S-Y Ying, N Ueno, S Shimasaki, F Esch, M Hotta & R Guillemin **779**

Inducible cellular transformation by a metallothionein-*ras* hybrid oncogene leads to natural killer cell susceptibility
W S Trimble, P W Johnson, N Hozumi & J C Roder **782**

Sequence organization and genomic complexity of primate θ1 globin gene, a novel α-globin-like gene
J Marks, J-P Shaw & C-K Shen **785**

Assembly of microtubules at the tip of growing axons
J R Bamburg, D Bray & K Chapman **788**

Template-directed oligonucleotide ligation on hydroxylapatite
O L Acevedo & L E Orgel **790**

PRODUCT REVIEW

Focusing on hormone release **793**
L S Frawley, F R Boockfor & J P Hoeffler
Endocrinology outlook **794**

MISCELLANY

100 years ago **731**

NATURE CLASSIFIED

Professional appointments — Research posts — Studentships — Fellowships — Conferences — Courses — Seminars — Symposia:
Back Pages

Next week in *Nature*:

- Cosmic rays from supernovae
- Acid raindrops
- Is El Niño coming?
- The making of gold
- China's Devonian/Carboniferous boundary
- New echinoderm from New Zealand
- Memory-enhancing drugs
- Haematopoiesis stimulant
- Wilms' tumour genetics
- Ethanol from plant biomass

GUIDE TO AUTHORS

Authors should be aware of the diversity of *Nature*'s readership and should strive to be as widely understood as possible.

Review articles should be accessible to the whole readership. Most are commissioned, but unsolicited reviews are welcome (in which case prior consultation with the office is desirable).

Scientific articles are research reports whose conclusions are of general interest or which represent substantial advances of understanding. The text should not exceed 3,000 words and six displayed items (figures plus tables). The article should include an italic heading of about 50 words.

Letters to *Nature* are ordinarily 1,000 words long with no more than four displayed items. The first paragraph (not exceeding 150 words) should say what the letter is about, why the study it reports was undertaken and what the conclusions are.

Matters arising are brief comments (up to 500 words) on articles and letters recently published in *Nature*. The originator of a Matters Arising contribution should initially send his manuscript to the author of the original paper and both parties should, wherever possible, agree on what is to be submitted.

Manuscripts may be submitted either to London or Washington. Manuscripts should be typed (double spacing) on one side of the paper only. Four copies are required, each accompanied by copies of lettered artwork. No title should exceed 80 characters in length. Reference lists, figure legends, etc. should be on separate sheets, all of which should be numbered. Abbreviations, symbols, units, etc. should be identified on one copy of the manuscript at their first appearance.

References should appear sequentially indicated by superscripts, in the text and should be abbreviated according to the *World List of Scientific Periodicals*, fourth edition (Butterworth 1963-65). The first and last page numbers of each reference should be cited. Reference to books should clearly indicate the publisher and the date and place of publication. Unpublished articles should not be formally referred to unless accepted or submitted for publication, but may be mentioned in the text.

Each piece of artwork should be clearly marked with the author's name and the figure number. Original artwork should be unlettered. Suggestions for cover illustrations are welcome. Original artwork (and one copy of the manuscript) will be returned when manuscripts cannot be published.

Important: Manuscripts or proofs sent by air courier should be declared as "manuscripts" and "value $5" to prevent the imposition of Customs duty and Value Added Tax in the United Kingdom.

Requests for permission to reproduce material from Nature *should be accompanied by a self-addressed (and, in the case of the United Kingdom and United States, stamped) envelope.*

Several hundred new products and services will be announced this year. But it's unlikely the press will give you all the facts – answer all your questions.

You need to talk to the people responsible.

The makers. The suppliers.

Because only then can you expect to get the information you want to make valued judgements.

NOT TO BE MISSED

Which is why Bio '86 at London's Olympia, September 23rd to 25th, is not to be missed.

Bio '86 is the new exhibition and conference for the biotechnology and genetic engineering industry.

And it has all the right credentials.

It was created with the active support of the AABB (Association for the Advancement of British Biotechnology) in collaboration with SIRA (Scientific Industries Research Association).

And it sensibly justifies the title "biggest and best."

With the largest, most comprehensive display of biotechnology products and services ever mounted in the UK.

And it's international.

Visitors and delegates to Bio '86 will be coming from all over the world. With strong representations from Europe and America.

Not just biotechnologists (although there will be a significant number), but research directors, department heads, biochemists, process engineers, chief technicians, lab technicians. Bio'86 is an allgrades event.

And it's part of the British Laboratory Week, this country's most successful scientific get-together – over 450 stands, nearly twice that number of exhibitors.

FREE TRANSPORT

Admission to Bio '86 is gratis. Free! Just return the coupon on this page.

Better than that, the Organisers will lay on free transport for you.

Make up a party of eight or more. We'll arrange for you to be collected from your lab or company Head Quarters and bussed to Olympia.

This is a terrific offer and should be taken up before our troglodyte accountant returns from holiday and reads us the Riot Act!

For this reason we suggest you use our:

CONFERENCE INFORMATION HOT LINE (0799) 25495

Leave your name and address on our answering service. Full details of Bio '86 plus tickets (you must say how many you want) will be sent by return post.

Another money-saving Bio '86 advantage is college accommodation. From as little as £17.00 + VAT per night.

Or, if you prefer to stay in a higher-priced hotel, we can arrange that too.

Use our Hot Line or tick the appropriate box on our coupon.

On registration at Olympia, you'll get a free exhibition catalogue. A handy item. It doubles as a guide and new product directory for the year ahead.

Bio '86.

You really should visit.

It's a thoroughbred event.



CUT AND MAIL FOR YOUR FREE TICKET!

"I like my product info straight from the horse's mouth."

Name _____

Title _____

Company/Organisation _____

Address _____

_____

_____

Please tick

I would like... ticket(s)

Please send Bio '86 Conference Registration information ☐

Please send details of FREE group travel ☐

Please send details of discount accommodation ☐

Post to: Kathryn Venn, British Laboratory Week, The Hub, Emson Close, Saffron Walden, Essex CB10 1HL, England.

OLYMPIA, LONDON, SEPTEMBER 23-25, '86.

BIO '86 IS ORGANISED BY CURTIS/STEADMAN & PARTNERS LIMITED, THE HUB, EMSON CLOSE, SAFFRON WALDEN, ESSEX CB10 1HL, ENGLAND. TEL: (0799) 26699. TELEX: 81653 INFORM G.

BIO '86



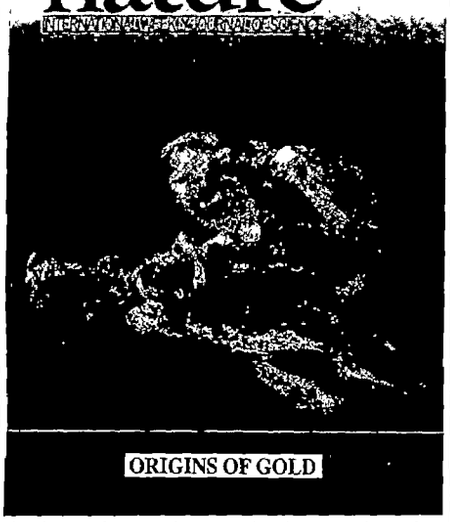
PART OF THE BRITISH LABORATORY WEEK.

"Hip hip hooray!"

42128

nature

NATURE VOL. 321 26 JUNE 1986



ORIGINS OF GOLD

Native gold encrusting crystals of quartz, from the Hollinger mine in north Ontario. The mine forms part of the second largest Archaean gold-quartz deposit in the world. On page 851 of this issue, Burrows *et al.* demonstrate that the gold was deposited from a magmatic, rather than a metamorphic fluid. The specimen measures 6.5×3.5 cm. Photograph courtesy of the Royal Ontario Museum, Toronto. See also News and Views page 812.

OPINION

Social security for students 797
Selling lamb short 798

NEWS

British astronomy 799
Monoclonal antibodies
US space science 800
Chinese rockets
Environment 801
Turkey turns away Israeli scientists
US defence research 802
A prize for Tooze from EMBO
Soviet science 803
Telecommunications
Scientific fraud 804
JET Britons seek to double pay
US biological weapons 805
Chernobyl

CORRESPONDENCE

Future of lion tamarins/Last word in metric/Sex discrimination/etc. 806

NEWS AND VIEWS

New technology of medicine 807
A new class of echinoderms
David Nichols 808
The double tilt of Uranus
Fran Bagenal 809
Predictability of El Niño
S G H Philander 810
Acid rain: Predictions and applications
Nurtan A Esmen 811
Archaean gold: Exploring for magmatic origins
Neil Williams 812
Mathematics: The costs of calculation
Ian Stewart 812
Looking for missing xenon
Minoru Ozima 813
One molecular machine transduces diverse signals
Henry R Bourne 814

SCIENTIFIC CORRESPONDENCE

Agricultural impact of Chernobyl: a warning
C Hohenemser, M Deicher, H Hofsass, G Lindner, E Recknagel & J I Budnick 817
First assessment of Chernobyl radioactive plume over Paris
A J Thomas & J M Martin 817
High level radioactive nuclides in Japan in May
M Aoyama, K Hirose, Y Suzuki, H Inoue & Y Sugimura 818
Monitoring Minsk and Kiev students after Chernobyl
B Holliday, K C Binns & S P Stewart 820
Radiation levels in Eastern Europe
G A M Webb, J R Simmonds & B T Wilkins 821

BOOK REVIEWS

The History of the Countryside
by O Rackham
and
Countryside Conflicts
by P Lowe et al.
George Peterken 823
Biochemistry of Lipids and Membranes
D E Vance and J E Vance, eds
Howard Goldfine 824
Atmospheric Chemistry and Physics of Air Pollution
by J H Seinfeld
Richard P Wayne
One World: The Interaction of Science and Theology
by J Polkinghorne
Robert John Russell 825
Science and Civilisation in China, Vol. 6: Part 1. Biology and Biological Technology: Botany
by J Needham
James Cullen 826

ARTICLES

Experimental forecasts of El Niño
M A Cane, S E Zebiak & S C Dolan 827
Secular variation in carbon isotope ratios from Upper Proterozoic successions of Svalbard and East Greenland
A H Knoll, J M Hayes, A J Kaufman, K Swett & I B Lambert 832

LETTERS TO NATURE

Enhancement of high-energy cosmic-ray spectrum by type-II supernovae
Y Takahashi, S Miyaji, T A Parnell, M C Weisskopf, T Hayashi & K Nomoto 839
Are bipolar jets precessing?
J Fukue & T Yokoo 841
Measurements of *p*H versus drop size in natural rain
S J Adams, S G Bradley, C D Stow & S J de Mora 842
Palaeolatitude drift history of displaced terranes in southern and Baja California
L K Morris, S P Lund & D J Bottjer 844
Domain observations of titanomagnetites from room temperature to Curie point and the nature of thermo-remanent magnetism in fine particles
M Metcalf & M Fuller 847
Magnetotactic bacteria and single-domain magnetite in hemipelagic sediments
J F Stolz, S-B R Chang & J L Kirschvink 849
Carbon isotope evidence for a magmatic origin for Archaean gold-quartz vein ore deposits
D R Burrows, P C Wood & E T C Spooner 851

Contents continued overleaf

Nature® (ISSN 0028-0836) is published weekly on Thursday, except the last week in December, by Macmillan Journals Ltd and includes the Annual Index (mailed in February). Annual subscription for USA and Canada US $240. USA and Canadian orders to: *Nature*, Subscription Dept, PO Box 1501, Neptune, NJ 07753, USA. Other orders to *Nature*, Brunel Road, Basingstoke, Hants RG21 2XS, UK. Second class postage paid at New York, NY 10012 and additional mailing offices. Authorization to photocopy material for internal or personal use, or internal or personal use of specific clients, is granted by *Nature* to libraries and others registered with the Copyright Clearance Center (CCC) Transactional Reporting Service, provided the base fee of $1.00 a copy plus $0.10 a page is paid directly to CCC, 21 Congress Street, Salem, Massachusetts 01970, USA. Identification code for *Nature*: 0028-0836/86 $1.00 + $0.10. US Postmaster send address changes to *Nature*, 65 Bleecker Street, New York, NY 10012. Published in Japan by Macmillan Shuppan K.K., Eikow Building, 1-10-9 Hongo, Bunkyo-ku, Tokyo, Japan. © 1986 Macmillan Journals Ltd

The ELISA productivity machine.

Bio-Rad's new Model 2550 EIA reader packs fully automated capability into a compact, affordable system that doesn't sacrifice performance.

In fact, the 2550 combines the latest in fiber optics with a proven vertical pathlength design for exceptional sensitivity and accuracy in two measurement modes: absorbance and matrix (for rapid screening).

All this, plus simple, dependable operation.

All 2550 functions are entered on a touch-sensitive keypad with a minimum number of steps. Audible beeper and "ERROR" function indicators help to insure correct function entry. And on-board self-diagnostics let you know in advance if problems exist.

Multiple wavelength capability, too.

The 2550 is available with filters from 380 to 700 nm. Four of the more popular wavelength filters are provided as standard equipment.

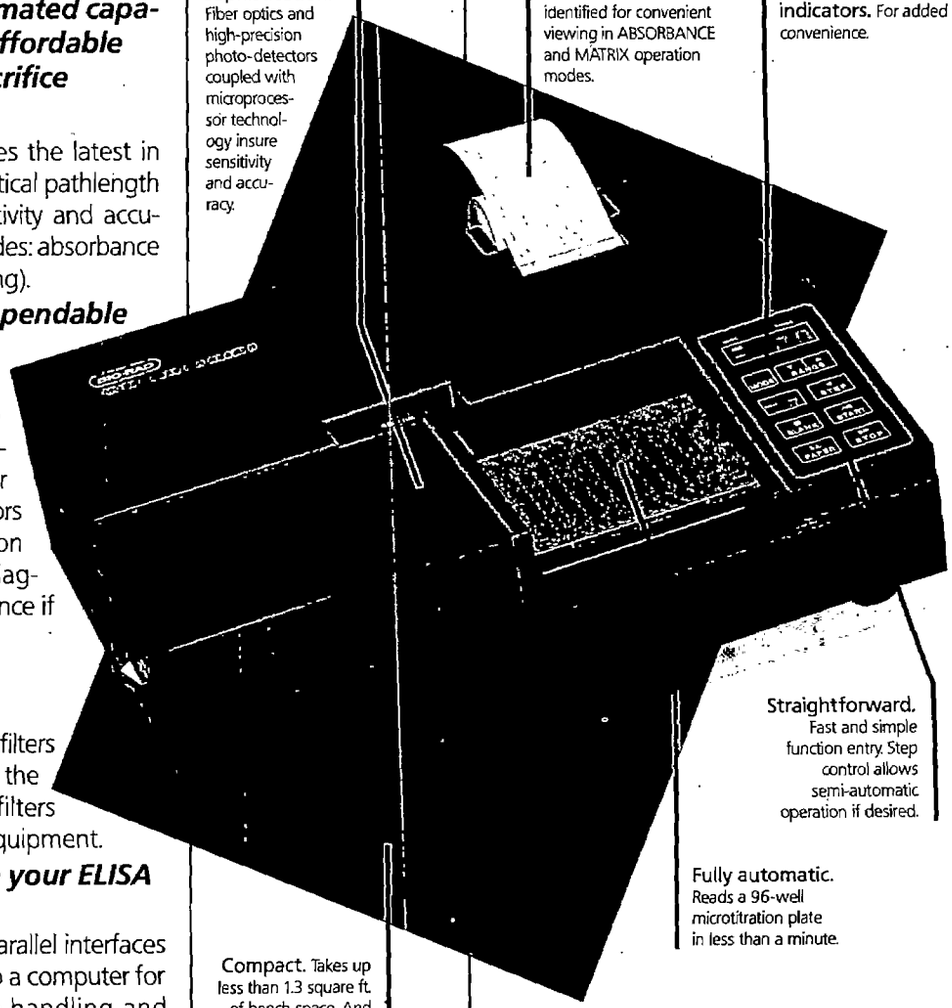
More ways to increase your ELISA productivity.

With optional serial and parallel interfaces you can hook the 2550 up to a computer for high sample volume data handling and sophisticated data analysis.

For routine protein determinations, the 2550 and Bio-Rad's Protein Assay Kit combine for simple, accurate automated protein determinations—at rates up to 80 samples per minute!

And Bio-Rad also offers an extensive line of affinity purified antibodies, enzyme-antibody conjugates, pipets, tips, and plates for all ELISA applications.

In other words, the Model 2550 EIA reader is part of a comprehensive line of products developed for ELISA screening, protein determination, and related applications. It's a system that will save your time, money—and bench space.



Microprocessor sophistication. Fiber optics and high-precision photo-detectors coupled with microprocessor technology insure sensitivity and accuracy.

Easy-to-read data. Columns and rows are identified for convenient viewing in ABSORBANCE and MATRIX operation modes.

RANGE, ERROR, and OVERFLOW indicators. For added convenience.

Straightforward. Fast and simple function entry. Step control allows semi-automatic operation if desired.

Fully automatic. Reads a 96-well microtitration plate in less than a minute.

Compact. Takes up less than 1.3 square ft. of bench space. And that's not much!

Now linear to 2.0 absorbance units.

Put our ELISA expertise to work.

For complete information on the Bio-Rad Model 2550 EIA reader and any of our other ELISA products, call our toll-free number (800) 4-BIORAD or write:

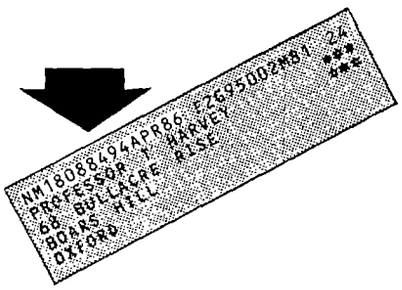
BIO-RAD

Bio-Rad Laboratories
Chemical Division
2200 Wright Avenue
Richmond, CA 94804
(415) 234-4130

Also in Rockville Centre, N.Y., Australia, Austria, Canada, Germany, Italy, Japan, the Netherlands, Switzerland and the United Kingdom.

SUBSCRIPTION SERVICE

Your mailing label contains your unique subscriber identification number



To ensure prompt service, please quote this number whenever you speak or write to us about your subscription

HELP US TO HELP YOU

Annual Subscription Prices

UK & Irish Republic		£104
USA & Canada		US$240
Australia, NZ & S. Africa	Airspeed	£150
	Airmail	£190
Continental Europe	Airspeed	£125
India	Airspeed	£120
	Airmail	£190
Japan	Airspeed	Y90000
Rest of World	Surface	£120
	Airmail	£180

Orders (with remittance) to:

USA & Canada
Nature
Subscription Dept
PO Box 1501
Neptune
NJ 07753
USA

UK & Rest of World
Nature
Circulation Dept
Brunel Road
Basingstoke
Hants RG21 2XS, UK
Tel: 0256 29242

(The addresses of Nature's editorial offices are shown facing the first editorial page)

Japanese subscription enquiries to:
Japan Publications Trading Company Ltd
2-1 Sarugaku-cho 1-chome
Chiyoda-ku, Tokyo, Japan
Tel: (03) 292 3755

Personal subscription rates: These are available in some countries to subscribers paying by personal cheque or credit card. Details from:

USA & Canada
Nature
65 Bleecker Street
New York
NY 10012, USA
Tel: (212) 477-9600

UK & Europe
Felicity Parker
Nature
4 Little Essex Street
London WC2R 3LF, UK
Tel: 01-836 6633

Back issues: UK, £2.50; USA & Canada, US$6.00 (surface), US$9.00 (air); Rest of World, £3.00 (surface), £4.00 (air)

Binders
Single binders: UK, £5.25; USA & Canada $11.50; Rest of World, £7.75. Set of four: UK, £15.00; USA & Canada $32.00; Rest of World, £22.00

Annual indexes (1971-1985)
UK, £5.00 each; Rest of World, $10.00

Nature First Issue Facsimile
UK, £2.00; Rest of World (surface), $3.00; (air) $4.00

Nature in microform
Write to University Microfilms International, 300 North Zeeb Road, Ann Arbor, MI 48106, USA

Significance of a $\delta^{13}C$ anomaly near the Devonian/Carboniferous boundary at the Muhua section, South China
D-Y Xu, Z Yan, Q-W Zhang, Z-D Shen, Y-Y Sun & L-F Ye 854

Organically preserved microbial endoliths from the late Proterozoic of East Greenland
A H Knoll, S Golubic, J Green & K Swett 856

More than one event in the late Triassic mass extinction
M J Benton 857

A new class of Echinodermata from New Zealand
A N Baker, F W E Rowe & H E S Clark 862

Benzodiazepine impairs and β-carboline enhances performance in learning and memory tasks
P Venault, G Chapouthier, L Prado de Carvalho, J Simiand, M Morre, R H Dodd & J Rossier 864

The structural gene coding for myelin-associated proteolipid protein is mutated in *jimpy* mice
A Dautigny, M -G Mattei, D Morello, P M Alliel, D Pham-Dinh, L Amar, D Arnaud, D Simon, J -F Mattei, J -L Guenet, P Jollès & P Avner 867

Light-dependent phosphorylation of rhodopsin by β-adrenergic receptor kinase
J L Benovic, F Mayor Jr, R L Somers, M G Caron & R J Lefkowitz 869

Stimulation of haematopoiesis in primates by continuous infusion of recombinant human GM-CSF
R E Donahue, E A Wang, D K Stone, R Kamen, G G Wong, P K Sehgal, D G Nathan & S C Clark 872

No functional γ-chain transcripts detected in an alloreactive cytotoxic T-cell clone
F Rupp, G Frech, H Hengartner, R M Zinkernagel & R Joho 876

A functional γ gene formed from known γ-gene segments is not necessary for antigen-specific responses of murine cytotoxic T lymphocytes
E B Reilly, D M Kranz, S Tonegawa & H N Eisen 878

Corticotropin releasing factor induction of leukocyte-derived immunoreactive ACTH and endorphins
E M Smith, A C Morrill, W J Meyer III & J E Blalock 881

The β-subunit of follicle-stimulating hormone is deleted in patients with aniridia and Wilms' tumour, allowing a further definition of the *WAGR* locus
T Glaser, W H Lewis, G A P Bruns, P C Watkins, C E Rogler, T B Shows, V E Powers, H F Willard, J M Goguen, K O J Simola & D E Housman 882

Ethanol production from sugars derived from plant biomass by a novel fungus
J F Wu, S M Lastick & D M Updegraff 887

MISCELLANY

100 years ago 810

NATURE CLASSIFIED

Professional appointments — Research posts — Studentships — Fellowships — Conferences — Courses — Seminars — Symposia: Back Pages

GUIDE TO AUTHORS

Authors should be aware of the diversity of *Nature*'s readership and should strive to be as widely understood as possible.

Review articles should be accessible to the whole readership. Most are commissioned, but unsolicited reviews are welcome (in which case prior consultation with the office is desirable).

Scientific articles are research reports whose conclusions are of general interest or which represent substantial advances of understanding. The text should not exceed 3,000 words and six displayed items (figures plus tables). The article should include an italic heading of about 50 words.

Letters to *Nature* are ordinarily 1,000 words long with no more than four displayed items. The first paragraph (not exceeding 150 words) should say what the letter is about, why the study it reports was undertaken and what the conclusions are.

Matters arising are brief comments (up to 500 words) on articles and letters recently published in *Nature*. The originator of a Matters Arising contribution should initially send his manuscript to the author of the original paper and both parties should, wherever possible, agree on what is to be submitted.

Manuscripts may be submitted either to London or Washington. Manuscripts should be typed (double spacing) on one side of the paper only. Four copies are required, each accompanied by copies of lettered artwork. No title should exceed 80 characters in length. Reference lists, figure legends, etc, should be on separate sheets, all of which should be numbered. Abbreviations, symbols, units, etc, should be identified on one copy of the manuscript at their first appearance.

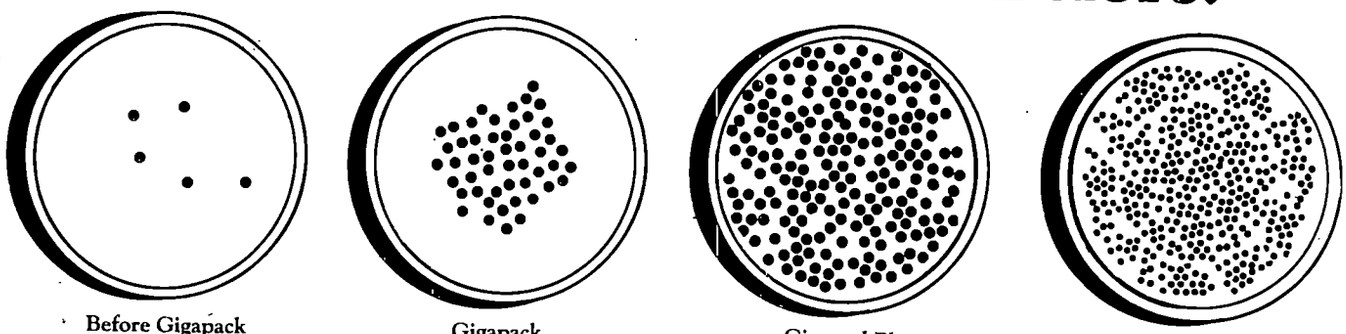
References should appear sequentially indicated by superscripts, in the text and should be abbreviated according to the *World List of Scientific Periodicals*, fourth edition (Butterworth 1963-65). The first and last page numbers of each reference should be cited. Reference to books should clearly indicate the publisher and the date and place of publication. Unpublished articles should not be formally referred to unless accepted or submitted for publication, but may be mentioned in the text.

Each piece of artwork should be clearly marked with the author's name and the figure number. Original artwork should be unlettered. Suggestions for cover illustrations are welcome. Original artwork (and one copy of the manuscript) will be returned when manuscripts cannot be published.

Important: Manuscripts of proofs sent by air courier should be declared as "manuscripts" and "value $5" to prevent the imposition of Customs duty and Value Added Tax in the United Kingdom.

Requests for permission to reproduce material from Nature *should be accompanied by a self-addressed (and, in the case of the United Kingdom and United States, stamped) envelope.*

Even More Efficient Than Before!



Before Gigapack | Gigapack | GigapackPlus | Gigapack Gold

Gigapack Plus & Gigapack Gold

3 to 5 times better than the original!

Most in vitro lambda packaging extracts are made from Eco K12 derivatives, which express the Eco K restriction endonuclease system. Packaging extracts contain residual Eco K activity[1]. Thus genomic and cDNA inserts containing the sequences AACNNNNNNGTGC or GCACNNNNNNGTT are under-represented significantly in lambda and cosmid libraries. Eco K sites occur at a frequency of one in 8000 random nucleotides. Most 20 kb fragments will contain 2 or 3 Eco K sites; and approximately one in five cDNA inserts will have an Eco K site. Eco K sites can account for a 3 to 5 fold bias in DNA packaging efficiencies.

Gigapack Plus

Gigapack Plus is Gigapack without Eco K activity. It packages unmethylated DNA (such as eukaryotic DNA) 3 to 5 times more efficiently than the old Gigapack. The effect is most pronounced with large DNA inserts, and is striking with cosmids. But why take the 1 in 5 chance that your cDNA will have an Eco K site? In vitro methylation with Eco RI methylase does not protect against Eco K digestion.

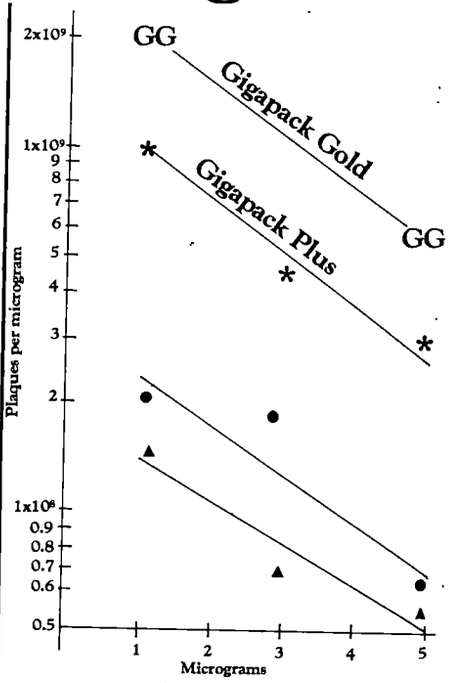
The graph illustrates the superior efficiency of Gigapack Plus compared with two leading extracts. Note that Gigapack Plus outperformed the others 5 to 1, even when 5 micrograms were added to a single reaction. Gigapack Plus has the highest efficiency and highest total DNA *capacity* of any extract available. Even with these new improvements, price has remained stable. We even offer significant discounts for large purchases.

Gigapack Gold

For the connoisseur, we also offer Gigapack Gold. This is our highest quality extract, doubling the efficiency of Gigapack Plus. It too has no Eco K bias and offers the highest efficiencies available anywhere. For those really valuable libraries Gigapack Gold is worth the investment.

Figure Legend

Packaging efficiencies were compared using varying amounts of Eco K unmethylated (unprotected from Eco K cleavage — just like eukaryotic DNA) cI857 Sam7 DNA. The specified amount of DNA was added to a single packaging reaction according to manufacturer's instruction. All phage were plated on strain DP50 supF. Experiments were all performed in duplicate on the same day. *Gigapack Plus, GG Gigapack Gold, ● Popular single tube system, ▲Popular double tube system.



1. Rosenberg, S.M. Gene 39 313-315, 1985

STRATAGENE
Cloning Systems

Where Satisfaction Multiplies

(Formerly Vector Cloning Systems)

3770 Tansy Street/San Diego, CA 92121/Call TOLL FREE 1-800-424-5444
In California call (619) 458-9151/TELEX 910380 9841

Distributors: ***Exclusive Japanese Distributor:*** **Funakoshi Pharmaceutical Co., Ltd.,** Telephone: Tokyo 03-293-2352, Telex: J28489 FUNA/**Genofit, S.A., 5 Rue des Falaises,** 1205 Geneva, Switzerland, Telephone: 022-29-84-30, Telex: 423082 STER CH/**Nbl Enzymes Limited,** South Nelson Industrial Estate Cramlington, Northumberland NE 23 9hl, England, Telephone: Cramlington (0670) 732992, Telex: 538239/**Integrated Sciences,** 13 Mobbs Lane, Carlingford NSW 2118 Australia, Telephone: (2) 8585644, Telex: 176482

Reader Service No.91

nature

NATURE VOL. 321 1 MAY 1986

What will emerge from Tokyo?

The economic summit meeting that opens in Tokyo on 4 May could be a chance to put the West's affairs in better order. But the precedents are discouraging.

THERE could be no better place than Tokyo for this year's meeting of the leaders of the seven large industrialized nations of the West. Although the city may not yet be the financial capital of the world, Japan as a whole has become the world's industrial pacemaker. Even as the participants are shuttled quickly from one event to another, they will not be able to avoid the question of how the most orderly of all the world's metropolitan conurbations can also be the source of repeated innovation which, elsewhere, is more usually marked by chaos. Those who can afford the time should stay on for a day or so after the two-day meeting; they will not be able in that time to come to grips with all the secrets of Japan's success, but they might be able to pick up a few tips that could help with the domestic problems awaiting their return and which will be waiting unchanged, as they have been for the past decade, unless this year's summit is markedly more successful than its predecessors.

Tokyo is planned as a largely economic meeting, and for good reason. These meetings became regular and annual only after the price of oil shot up in 1973; they were well established in the top politicians' calendar by the time of the 1979 meeting in Venice, when those present could do little but wring their hands about the second round of the price increase decreed by the Organisation of Petroleum Exporting Countries (OPEC). By that token, this year's meeting could have been an occasion for celebrating the demise of OPEC, at least temporarily, and for planning what should happen next. If the United States can avoid reading too many lessons to too many people about the horrors of terrorism, that could be a useful exercise.

Balance

What the Tokyo meeting might usefully do is to strike a better balance between the optimists and the pessimists about the likely course of events. The collapse of OPEC's policies has wonderfully increased the population of the optimists, who are especially thick on the ground where there are equity shares in industrial companies to buy and sell, and whose eagerness to buy has driven most of the world's stock exchanges to record price peaks (which means that shareholders forgo income now in the belief that there are capital gains to come). Nobody can conclusively quarrel with the view that the world stands on the threshold of a new period of economic growth from which everybody will benefit. The snag is that there is no evidence conclusively to support this cheerful view, nor sufficient evidence for the opposite conclusion that this may be the threshold of a time of honours. For the pessimists' case is not so much a case as a collection of gloomy speculations: what if countries such as Mexico should declare themselves bankrupt because selling oil at reduced prices will not allow them to service their debt? What if the US dollar, which now buys only two-thirds as many Japanese yen as at the beginning of 1985, should keep on falling? Or if the industrialized countries fearful of losing their place in the competition should seek to save themselves by trade protection, beggaring everybody in the process? A few years ago, when catastrophe theory in mathematics was fashionable, this would be recognized as a time of incipient bifurcation: events could go one way or the other.

World leaders may be no better able than the rest of us to tell which view is right, but what they decide in Tokyo could help to show which way the dice will fall. There are three groups of issues to be settled: money, trade and debt. The largest countries have been congratulating themselves in the past few months for having using their inner club (called the group of five) successfully to make the value of the US dollar decline. Central banks seem to have been able to trigger a substantial movement at very little cost, but may in the process have destroyed the source of the dollar's previous strength, the belief from which only a few sceptics dissented that it would always be a rock-solid currency. The problem now is whether bankers could as cheaply stop the continuing slide if they thought that necessary.

Usefulness

The devaluation will serve three useful purposes. By making imported goods and services more expensive in the United States, it will reduce the external deficit of the United States. Indirectly, it may help to simplify the funding of the US budget deficit, which means that interest rates will be given a further downward push. And it will mark a step towards realism, the recognition that industrial power has partly migrated from the United States, almost certainly for good. Even for the United States, this is a step towards enlightenment. The grounds for pessimism are different, and concern the capacity of the world's institutions, mostly financial institutions, to accommodate the rapid readjustments now under way. What can the summit-goers do to make the promise of prosperity less fragile?

Two things to begin with. The most urgent need is for a reaffirmation and an extension of the Western doctrine that trade protection is an abomination. The West free-traders echo closely St Augustine's plea to be made chaste, but "not just yet". The US government is rightly complaining about European agricultural protection through the Common Agricultural Policy of the European Communities, while protecting both its own farmers and a variety of other declining industries by quota arrangements that conflict with the spirit if not the letter of the General Agreement on Tariffs and Trade. In Europe as well as the United States, advanced industries and their sponsoring governments complain that Japan is selling unfairly in their mutual competition, whence another battery of quotas and "voluntary agreements" to limit imports. Japan is probably right to protest its injured innocence of these charges, but is equally guilty of what may be the most pernicious form of protection in modern circumstances, restraint on the free flow of capital. To ask that these and other restraints on trade should be promptly thrown out of the window would be to ask too much, but to ask that governments should plan eventually to practise what they preach is mere prudence.

The second urgent need is to face up to the reality of international debt. The lenders and the borrowers are at present playing chicken with each other, but everybody knows that the West will not, for example, let Mexico or the Philippines go bankrupt. Politically, these countries are too important, while the collapse of the commercial banks that would be carried with them would cause untold damage in the industrialized world. So

why wait until disaster stares these governments directly in the face? Why not find a way out of the mess before it actually exists? The US administration has shown signs of willing in this direction, although the Secretary of the US Treasury's plan for dealing with international debts (which would have the commercial banks lend more, but with an implicit government guarantee) will not be generally acceptable. A better and more durable plan is needed. That is what Tokyo should be for. □

What's in a name?

The latest name for the AIDS virus is in trouble before the christening is over.

EVERYTHING about Acquired Immune Deficiency Syndrome (AIDS) seems to be controversial. That will be many people's reaction to the report (see p.3) of the arguments that attend the launching this week (see p.10) of the proposed name for the causative virus. The Varmus committee which has laboured for more than a year on the design of a single name to replace the two now in common use will get none of the thanks it deserves for the trouble it has taken. The most serious danger now is that an important field of investigation already too much soured by contending passions will be further embittered by personal considerations. Everybody's interest is that a corrosive rivalry between research groups should be mollified.

The identification of the virus responsible for AIDS is in every sense a remarkable piece of modern history, the significance of which for the treatment of disease is not yet fully appreciated. AIDS as a recognizable disease is barely five years old. Its recognition as an infection, first on epidemiological grounds, is naturally more recent. The first published evidence that a virus is responsible is due to Dr Luc Montagnier, at the Institut Pasteur in Paris, and consists essentially of a number of clinical cases and an electron micrograph including virus-like particles. Soon afterwards, Dr Robert Gallo and his associates at the National Cancer Institute (NCI) of the US National Institutes of Health in Bethesda, Maryland, were able to publish evidence that virus-like particles isolated from patients with AIDS are indeed able to infect other lymphocytes in culture; with his then recent interest in human retroviruses infecting lymphocytes fresh in his mind, Gallo was naturally tempted to think of his virus as one of a series (of which there were then already two). This is how the Pasteur virus and the NCI virus are differently named; Montagnier's is called LAV (for lymphadenopathy-associated virus), Gallo's HTLV-III (for human T-cell lymphotropic virus). Further investigation, which has been breathtaking in its speed, shows the two viruses to be essentially identical, give or take the replacement of a sizeable percentage of the bases in the nucleotide sequence of the virus.

This would not be the first time the same organism has been discovered independently by two different routes. In the past, there has even been confusion of this kind about the naming of chemical elements. Ultimately, of course, there is usually a felt need to make sense of such confusion. What the Varmus committee has been doing, on behalf of the International Committee on the Taxonomy of Viruses, is to force the pace a little, to bring order to a field in which disorder appears rife. The snag is that this laudable attempt should have coincided with a serious dispute between the French and US groups. The two groups have been edgy about each other's proprietary interests in the discovery for some two years. Last year, after techniques for the diagnosis of AIDS antibodies were developed separately in Paris and Bethesda, the Pasteur Institute filed a claim against its US colleagues (or, strictly, against the US Department of Health and Human Services) on the grounds that US reagents were developed with the use of French material. The matter has been made to seem worse (but it may be only an appearance) by the discovery that one of the electron micrographs in Gallo's first paper about the virus was mistakenly an image of the French virus.

Trying to win agreement on a common name at a time like this is therefore a little like trying to win agreement on a national anthem in the middle of a civil war. It was courageous of the Varmus committee to attempt the task. (A letter from Gallo and his associates explaining how the mix-up happened, and remarking on some of the attendant issues, will appear in *Nature* next week.) Meanwhile, the committee's chances of winning acceptance for its proposals have been diminished by Montagnier's premature announcement of what the Varmus committee had decided. The issue has nothing to do with the recommended name but with the circumstances: bearers of important news are supposed to run on an inside track. It is understandable that Gallo should now be unwilling to use the recommended name for any but generic purposes; he was probably a reluctant member of the naming committee from an earlier stage.

There is nothing much that can be done about all this. It will not make sense to hope that there can be agreement on a common name for the virus that causes AIDS if one or other of the principal investigators in the field should decline to use it. Even if one should be compliant and the other should demur, enforcing commonality would be a disservice. That is why *Nature* will not attempt to lay down the law, but instead seek only to ensure that its readers are not confused. We shall (like our readers) wait and see. Meanwhile, the biomedical research community should do more than it has done so far to resolve the issue that has arisen. The Montagnier and Gallo groups stand out among several working in basic research laboratories that have thrown light on the way that AIDS infections work. Neither has yet cured a patient, but each has given hope to many. In passing, they have given everybody good cause to believe that the investigation of novel infections is now well within the competence of well-organized laboratories. It would be shabby, even disgraceful, if the contribution of these two men and their associates were not widely recognized, even by the principals. That is what the community owes its heroes, or near-heroes: for in this case, that of an infection for which there is still no therapy, the real heroes are the physicians who must deal with patients in ignorance of what may yet be possible. And, of course, the patients themselves. □

Cloud over Chernobyl

The first Soviet nuclear accident to be made public may bring unlikely comrades together.

LAST weekend's nuclear accident north of Kiev is a sobering reminder of the problems of running high-technology enterprises safely. The fact that the first sign of trouble was reported not from the Soviet Union, but more than 1,000 miles away, in Sweden, suggests that the Soviet managers of the plant that released the cloud of activity should have had a better telephone system at their disposal or that there should have been somebody able by other means to tell Sweden about the cloud of radioactivity on the way. Neighbourliness requires no less.

The important question, when the dust settles, is not so much how accidents like these can be prevented, but how we can learn to live with them safely. For, from time to time, even with nuclear plants (which go wrong less often than other kinds of machinery), accidents will happen. There is nothing particularly secret about the Chernobyl plant, whose general characteristics have been declared by the Soviet Union to the International Atomic Energy Agency at Vienna; it consists of six reactors, two still under construction, in which the neutron moderator is graphite and the coolant consists of steam (also a moderator). On paper, such a plant should have a degree of built-in safety. (Let coolant escape, and the chain reaction should be less efficient.) But something went wrong. The Soviet Union's neighbours have a right to know what it was, and also a right to some assurance that the same will not happen a second time. □

Virus nomenclature

Controversy over AIDS virus extends to name

Washington

MORE than a year of patient negotiations to choose a new name for the virus associated with acquired immune deficiency syndrome (AIDS) ended last week in a hectic torrent of letters, leaks and rearranged release dates. Two key members of the naming committee have refused to go along with human immunodeficiency virus (HIV) as a replacement for HTLV-III/LAV, but support for a new name is strong; HIV could well be the eventual choice.

The name change is proposed in a letter published elsewhere in this issue (see p. 10) and simultaneously in *Science*. The letter is the result of a year's deliberations by a specially empanelled subcommittee of the International Committee on the Taxonomy of Viruses (ICTV). Chaired by Harold Varmus of the University of California at San Francisco, the subcommittee consisted of the six members of the ICTV retrovirus study group (John Coffin, Natalie Teich, Kumao Toyoshima, Varmus, Robert Gallo and Max Essex), as well as seven members directly involved in AIDS research or familiar with the field (Ashley Haase, Jay Levy, Luc Montagnier, Steven Oroszlan, Howard Temin, Peter Vogt and Robin Weiss).

By February this year, the committee had tentatively agreed on HIV, and the name was proposed to ICTV's executive committee. David W. Kingsbury, who heads ICTV's human virus subcommittee, says that all 12 of the responses received so far from the 17 executive committee members are favourable to the new name.

But HIV never had unanimous support from Varmus's subcommittee. Nearly half of the members preferred the current compound name, HTLV-III/LAV. Others, including Gallo of the National Institutes of Health (NIH) in Bethesda, Essex of the Harvard School of Public Health and Temin of the University of Wisconsin, preferred human retrovirus (HRV), with numbers assigned sequentially for every new virus. But committee members were anxious to find a name that would eliminate disputes over priority of discovery; for that purpose, HRV was too nonspecific for most committee members.

Armed with a positive response from the ICTV executive committee, Varmus then sent to *Nature* and *Science* a letter proposing the new name, saying a full list of signatories would follow. But the announcement of new human retroviruses late in March dashed hopes for unanimity for HIV.

The new viruses, called LAV-2 by Montagnier of the Institut Pasteur and HTLV-IV by Essex, may turn out to be variations of the same virus. Montagnier announced his discovery at a meeting in Lisbon before it had been accepted for publication in any journal (see *Nature* **320**, 3; 1986). Montagnier's announcement



came slightly more than a week before publication (in *Science*) of Essex's discovery. Essex was incensed by Montagnier's action, and he informed Varmus that he would have nothing to do with the new name, already supported by Montagnier.

Essex says he had never been satisfied with HIV as a name for the AIDS virus. He feels that the name HTLV-III/LAV is so ingrained in the literature that it will not be possible to change it, and calls the committee's efforts "shortsighted". He is also concerned that the new nomenclature would not be appropriate for HTLV-IV, as it does not cause immune deficiency.

Shortly after Essex's decision, Gallo indicated that he would not go along with HIV either. Gallo's attitude hardened further when, two weeks ago, Montagnier delivered a lecture at NIH where he mentioned HIV. A reporter, alerted by Institut Pasteur's New York public relations company, attended the meeting, and a report that HIV would replace HTLV-III/LAV appeared in the *Washington Post* on 19 April.

Gallo was furious. Varmus had decreed that no subcommittee member should discuss the new name with the press before it appeared in a scientific journal. Outraged that Montagnier should have made his announcement "right under my nose", Gallo wrote to Varmus exhorting him to withdraw his letter to *Science* and *Nature*, and saying that he should reconsider the new name.

Varmus was also furious with Montagnier for leaking the new name prematurely, but felt that Essex and Gallo were being churlish not to go along. After consultation with editors John Maddox of *Nature* and Dan Koshland of *Science*, it was agreed that the letter proposing the new name would appear as soon as possible. A contentious sentence asking editors printing the letter to "urge" authors to use the new name was dropped in the final version.

As for the name itself, even Varmus concedes that HIV has problems, but he believes it represents a reasonable compromise. Several committee members conceded that HIV was not their first chose, but were willing to compromise and to accept it.

David Baltimore, who is heading a study of AIDS for the National Academy of Sciences Institute of Medicine, says the AIDS virus was "crying out" for a name change. Baltimore shares the opinion voiced by many that, because HTLV-III is too dissimilar from its numerical ancestors HTLV-I and II to share the name, a change is needed to eliminate confusion on that point. But supporters of the name HTLV, chosen originally by Gallo in the mistaken belief that it would be closely related to HTLV-I and II, argue that hepatitis A and B are even more dissimilar from each other than are the HTLV viruses, but that those two names coexist without controversy.

Gallo says that he used HTLV-III only after a protocol for naming new human retroviruses had been agreed by an international *ad hoc* committee formed at a Cold Spring Harbor symposium in September 1983. But it is precisely because controversy has arisen over the virus responsible for AIDS, says Kingsbury, that the committee has sought a new name

Steve Gillis of Immunex Corporation at Seattle, Washington, who is familiar with controversies over new names from his own experience with lymphokines, questions whether a name that is not supported by Gallo can win general support. In addition to Gallo and Essex, a prominent AIDS researcher who asked not to be identified indicated that he will not use the new name.

But support for HIV is already growing among people in the field. Baltimore has already begun to use the name, and Jerome Groopman of Harvard Medical School has included it in a draft of a paper he is preparing.

By the end of the week before publication of the Varmus letter, Gallo was insisting that he would never use HIV when referring to his original isolates, but he might consider using HIV to refer to a "generic" AIDS virus.

Formal endorsement from ICTV for HIV is expected to come in May. But, as ICTV chairman Fred Brown puts it, any name is acceptable "so long as people know what you are talking about".

Joseph Palca

British astronomy

Observatory move stirs passions

THE plan to move the Royal Greenwich Observatory (RGO) from its present location in Sussex to somewhere else in Britain has evoked mixed passions among British astronomers. If possible, feelings run even more strongly than in the high-energy physics community when British membership of the European Organisation for Nuclear Physics (CERN) was being examined more than a year ago. But British astronomers are divided between those who think RGO should stay where it is and those who wish it to be moved to one



or other of the three candidate locations.

The decision that RGO should be moved was taken by the Science and Engineering Research Council (SERC) in March (see *Nature*, **320**, 297; 1986). SERC is to decide at its meeting in June whether RGO should, while retaining its identity, go the Universities of Cambridge or Manchester or, alternatively, unite with the Royal Observatory, Edinburgh (ROE), on its Blackford Hill site.

SERC's announcement of these developments followed an invitation to seven British universities to offer hospitality to a transplanted RGO. Dr E.J.W. Mitchell, SERC's chairman, explained in March that the decision to move RGO had arisen in part from disappointment with the strength of its present relationship with university astronomers. Of the three future locations for RGO, the council said that Edinburgh was the most favoured.

Some of the fiercest reactions to this development have come from universities not now on the short-list of candidate locations. The University of Oxford, one of those invited to provide a site for RGO earlier in the year, is up in arms at what local astronomers consider to have been a change in the rules of SERC's competition when the finishing post was in sight. In a strongly worded protest to SERC, Oxford astronomers have complained that, when they had identified a building capable of providing the 2,000 m^2 of floor space required by SERC, they were told that the requirement of floor space had doubled.

According to a SERC spokesman this week, there is some confusion on this point. He acknowledged that there had been a change of specification, but said that the present requirement for 4,000 m^2 of space was intended to be a gross figure; usable floor space would be three-quarters of the total. This does not fully meet the Oxford contention that the hospitality the university offers includes a large workshop equipped for work in nuclear physics which will be under-used when SERC ceases to support the tandem electrostatic generator on the site.

The lobbying of the two universities on the short-list is, for Britain, unusually direct. The University of Manchester makes a great deal of its offer of rent-free accommodation, on the site of the Christie Hospital, for RGO. At Cambridge, on the other hand, it seems to be accepted that SERC would have to meet the cost of a building to house RGO, presumably out of the proceeds of the sale of the Herstmonceux buildings: SERC has said that the move will have to be self-financing. In the nature of things, the sale of the castle is at the speculative end of the real-estate spectrum.

Intellectually, Cambridge offers propinquity to the Institute of Astronomy and the Cavendish Laboratory, with RGO to be sited in the grounds of the university observatory adjoining the institute. Manchester, by contrast, emphasizes its own close academic links with other universities and polytechnics in the Midlands and northern England. In a letter addressed to all fellows of the Royal Astronomical Society, the Astronomer-Royal, Sir Francis Graham Smith, who is also director of the Jodrell Bank Observatory of the University of Manchester, argues first against the preferred move to Edinburgh on the grounds of geography, the tenuous academic link between the Edinburgh observatory and the university and by saying that the continued separate existence of RGO and the Edinburgh observatory offers the best scientific value. He then goes on, after declaring his interest, to put the case for Manchester on the grounds of geography and facilities.

Astronomers elsewhere appear mostly to wish that a decision could be avoided. All speak highly of the work done by the two public observatories in commissioning new telescopes on Hawaii (ROE) and La Palma (RGO); there is particularly high praise for the support offered by RGO to academic astronomers using the 2.5-m Isaac Newton telescope at La Palma.

This argument is lent support by the lack so far of an estimate of the savings that may result from the proposed move, which SERC says is being made on scientific grounds within the constraint that the cost of the move should be supported by the sale of assets. The staff at RGO has already shrunk from its peak of about 240 to a present complement of 190. By the time planned for the move in 1990, it is intended that the observatory's staff should consist of about 100 people in Britain with a further 30 at La Palma.

The opinions of the RGO staff are also divided, but favour Cambridge. A survey carried out last month (to which 55 per cent of the staff responded) showed that 80 per cent would be prepared to move somewhere, of whom 90 per cent gave Cambridge as their preference. Asked to identify the sites to which they would not move, only two per cent of the staff came out against Cambridge. In response to the same question, 60 per cent said they would not move to Edinburgh and 50 per cent dug in their heels against Manchester.

Meanwhile, a regional political lobby is forming to preserve RGO at its present site. The East Sussex County Council and the North Weald District Council, both of which have an interest in the tourists attracted by Herstmonceux, are seeking to influence official opinion, as are local members of parliament.

There is no precedent for political forces such as these influencing the autonomous decisions of research councils, yet SERC will need strong nerves if it is to stick to its timetable of a decision next month. Matters have not been much simplified by reports that Dr Harry Atkinson, the senior official of SERC in charge of astronomy spending (and also chairman of the European Space Research Organisation) had given the members of one committee the impression that there were political considerations in the decision not to vacate the Edinburgh site. Dr Atkinson explained on the telephone this week that he meant only that, in his opinion, SERC should pay attention to the regional distribution of its establishments, but even that may be enough for the Sussex lobby to keep the door ajar.

John Maddox

SDI in Japan

Growing interest in joint venture

Tokyo

AT the eleventh hour, two Japanese scientific groups have joined forces to organize a signature-gathering campaign across the country in protest against the US Strategic Defense Initiative (SDI). "Physicists and Mathematicians against SDI" claim to have gathered nearly 3,000 signatures from their colleagues at 145 universities and research institutes across the nation. But it looks as though their protest may be too late.

Last week, a report was submitted to the government from a fact-finding mission of government and business groups (see *Nature* **320**, 294; 1986). The 55-member mission had spent ten days in the United States visiting SDI-related research facilities and being briefed on the projects' technical aspects. The mission was the third to visit the United States but the first to include representatives from private companies, itself a pointer to the growing likelihood of participation.

Even before the mission left, business leaders had privately admitted that they had been approached by government and that a generally favourable attitude towards participation had developed. Their main worry, one said, is whether the United States would guarantee that SDI would be a long-term project and not susceptible to sudden cancellation. Without that guarantee, some of the smaller companies would find a commitment to SDI research too risky. Given these behind-the-scenes developments, it is no surprise that the fact-finding mission's eight-page report recommends that Japan take part in the "research phase of SDI".

The report describes SDI as being "non-nuclear" and aimed at abolishing nuclear arms, thus making it compatible with Japan's commitment to peace, enshrined in its constitution and in a Diet resolution never to permit nuclear weapons research. It also stresses that SDI is only a research programme and not a plan for deployment of a defence system. But the chief advantages it sees in participation are more practical.

The report says that progress has already been made in the SDI programme and raises the spectre of a "widening technology gap between the United States and Japan". It also asserts that there will be significant spin-offs for the civilian sector including new air-control radars and remote sensors from the surveillance, acquisition, track, kill and assessment (SATKA) section of SDI. The sensors used to detect heat from rocket exhausts will also find applications in medical sensors. Kinetic-energy weapons research will aid aircraft technology with development of new lightweight materials. And high-power lasers and particle beams can be used in the control of industrial chemical reactions. Altogether, participation will "greatly improve the level of related technologies in this country".

Further consultations will now take place and the final decision made by a group of five cabinet ministers — Defense, International Trade and Industry, Science and Technology, Foreign Affairs and the Cabinet Secretary — along with the Prime Minister. If the answer is positive, as is now expected, they will determine the form of Japanese participation. The decision is not expected to be in time for the Tokyo summit of the leaders of industrial nations next week.

With the SDI bandwagon already rolling, it is hard to see that a protest from scientists will have much impact. But many of those who have signed the petition opposing SDI are the very people – physicists, mathematicians and computer scientists — who might be expected to be involved in SDI research. They are concerned not only that science is being "increasingly militarized" but also that their research will be diverted into SDI and their publications become restricted "military secrets".

Alun Anderson

Animal protection

Critics assail West German law

Hamburg

THE Bundestag (the West German parliament) has now passed the amended form of the 1972 Animal Protection Act, introduced by the minister of agriculture, nutrition and forestry in the federal government, Ignaz Kiechle. But it seems unlikely that this development will silence the arguments about the use of animals in experiments that have become common in the past few years.

The new law is the first in a series of measures intended to cover several issues in the field of biological ethics. The dispute about animal experiments, involving industrial companies and scientists on one side and anti-vivisectionists on the other, has been especially fierce in recent months. Individual protesters continue to release experimental animals from institute laboratories, but the bombing of a Cologne laboratory last year has not yet been repeated.

On the face of things, the requirements of the new law are tough, and cover all experiments leading to "pain or injury of the animal", a definition that leaves the use of the organs of dead animals exempt from regulation. In future, investigators will have to justify the need for their use of experimental animals by reference to the investigation of the environmental impact of materials on human beings or the risk of new chemical substances used in medicine. The study of human and vertebrate physiology, like basic research in general, will be a valid justification of experiments.

The new law will require that laboratories where experiments with vertebrates are carried out must appoint animal protection officers (*Tierschutzbeauftragten*) who must be qualified physicians, veterinarians or zoologists, and who will be required to supervise the application of the new regulations, such as an interdiction of needless duplication of experiments.

The new law forbids the use of animals in the development and testing of weapons; animal tests are also forbidden in the testing of tobacco products, washing powders and cosmetics. While the immediate effect of the new law is to restrict animal experiments, there are provisions to encourage the use of alternative methods to the use of animals in research.

Authorization procedures are to be tightened, chiefly by the appointment of a network of commissions to supervise the authorization procedure. The animal protection organizations will have a powerful influence on the proceedings of these advisory commissions, having established the right to nominate up to a third of the members of the commissions.

The argument is certain to continue, if only because its philosophical and legal implications have not yet been talked out. Some jurists argue that the West German constitution (*grundgesetz*) is relevant in that a guarantee of human dignity on the principles laid down by Kant and Schopenhauer cannot also be used to justify the killing of countless animals so as to protect people from over-indulgence.

It is significant that there have been several recent decisions of the constitutional court to the effect that the "absolute" right of freedom of research can be in conflict with novel ethical principles, which may imply that guarantees such as this in the 1949 constitution may be mutable in changed circumstances.

Of the political implications of the new developments, there seems no question. The critics of the new law complain that "those to be controlled are the controllers", and their argument is consistent enough to continue at least until the next federal election in January 1987. The Social Democrats have said that they will amend the law if they win power; both they and the Greens also want the law to be extended to cover the extensive keeping of animals as pets. But scientists consistently oppose the new law as an impediment to research.

Jürgen Neffe

Japanese education

Further iteration towards reform

Tokyo

ATTEMPTS to reform Japan's educational system have taken another halting step forward with the publication last Thursday of Prime Minister Yasuhiro Nakasone's Special Educational Advisory Council's second full-length report.

The report met the barrage of criticism that has greeted every pronouncement of the special council (see *Nature* **319**, 347; 1986) and was preceded by the publication of counter-reports from women's groups, teachers groups and unions, proving, as other nations have found, that although it may be hard to effect educational reform, it is certainly not hard to whip up opposition to it. In the new report, for the first time, details begin to emerge of how universities might be reformed.

The central criticisms of the universities are that they are too inflexible, too homogeneous and do not make a contribution to the international research community commensurate with Japan's status as a world power. Furthermore, the universities are resistant to change and do not sufficiently influence educational policy.

The solution to this last problem is seen in the establishment of a "university council" which would have the right of direct access to the Minister of Education, Science and Culture. Its brief would be wide: as well as conducting surveys and collecting information, it would expect to proffer advice on the structure of the universites, their planning and construction, on what areas needed developing to provide trained manpower, the content of university education and the methods of teaching. There are at present a number of bodies representing the universities but none that can speak for all universities — including state and private universities and the junior (two-year) colleges.

To the problems of inflexibility and homogeneity come one familiar solution: the use of a credit system that would allow students to transfer between faculties, or even universities. If necessary, a special institution should be set up to grant degrees to those who have gained sufficient credits from several sources. Inputs to the universities could be made more diverse with quotas set for the enrolment of ordinary citizens and junior college graduates into the four-year universities.

Suggestions for the reform of university research begin with the surprising statistic that the ratio of graduate students to undergraduate students in Japan is the lowest of all the developed countries. In part, of course, this reflects the high number of engineering students who quickly enter industry. Less surprising is the recognition of the lack of technical back-up in the universities: the general rule is that if you want a piece of equipment you must build it yourself. To bring about reform, young people need better treatment.

The report gives the average age for completion of a PhD course as 27. To make things move faster, it is suggested that it should be made possible to complete a master's course in one year and a doctoral course in three years, with direct entry to a doctoral course after graduation possible for especially talented students.

Postdoctoral fellowships (of which there are still only a few hundred in Japan) should be made much more easily available. And thought should go to the establishment of an independent graduate university for research students. This is something those in the new research institutes for joint use by universities (like those at Okazaki) would particularly welcome, for without attachment to any particular university they have no ready source of graduate students. A graduate university could well find a home at Okazaki.

The role of "joshu", the lowly position of research assistant which is often the first rung on the ladder to professor but which is sometimes mistaken by professors as a post providing personal attendants, also needs to be looked at afresh, the report says. Low staff turnover is another problem: possible solutions are the usual early retirement, untenured short-term posts and contract research.

Reforms are,of course, expensive, particularly the provision of increased technical assistance, more fellowships, graduate universities and increased foreign exchange. The report points out that 330 thousand million yen will be spent on academic research this year. But estimates of how much reform of postgraduate education would cost suggest that the same amount again would need to be spent over the next ten years. This is unlikely to find favour with the Ministry of Finance, which is already complaining that spending on education is high enough. How high is high enough is hard to measure: the Japan Teachers Union claims that Japan's 1985 education budget accounted for 4.6 per cent of its gross national product compared with 9.1 per cent in Sweden, 8.1 per cent in The Netherlands, 7.2 per cent in the Soviet Union and 6.4 per cent in the United States. **Alun Anderson**

Soviet science

Lenin prizes return to basics

THIS year's Lenin Prizes for Science and Technology in the Soviet Union concentrate on fundamental research. Only two of the eight prizes awarded last week have any immediate relevance to the application of research results in production, hailed for the past two decades as the principal target for Soviet science.

Pravda's editorial preamble to the review of the prizes by Academician Anatolii Aleksandrov, president of the Soviet Academy of Sciences, still emphasizes the need to "accelerate scientific and technical progress", but the stress is now on the mobilization of "creative forces" in science rather than on the rapid implementation of results.

All but one of the awards are cumulative, for "cycles" of research and publications going back, in some cases, more than 20 years. The exception is the prize for Yurii Aleksandrov and his team from the Institute of Radio and Electronics of the Soviet Academy of Sciences and the Special Design Bureau of Moscow University, who won the prize for developing a special radar system for mapping the surface of Venus from the Venera-15 and Venera-16 probes. (This is the only prize-winning work for which Academician Aleksandrov mentions spin-off; the system, he says, has also been applied in the study of flooding, irrigation, salination, and soil and water studies in many parts of the Soviet Union.)

The longest "cycle" to be honoured is that of Academician Grigorii Devatykh, for his development of methods of obtaining high-purity volatile substances, which he began in 1959. Almost as early, and far more significant, is the starting date assigned to Dr Roman Khesin-Lur'e's work on "molecular principles of the functioning of the genome", which he apparently began to publish in 1960. Lysenkoism was then in full swing, and, according to the Soviet biological establishment, the gene was considered an "empty abstraction", accepted only by reactionaries. It would be interesting to know where Khesin-Lur'e published his work at that time, and what part, if any, he played in the overthrow of Lysenkoism.

Another interesting award is that for "inclusive processes in strong interactions of high-energy elementary particles and the discovery of scale invariance in these processes". Aleksandrov goes out of his way to stress that the new directions opened up by the work done at Serpukhov were afterwards confirmed at CERN and the Fermi National Accelerator Laboratory in the United States, and the team includes not only Soviet citizens but also Dr Nguyen Van Hue, president of the Vietnamese National Centre for Scientific Research. Lenin prizes are normally a purely Soviet affair, but this year there seems to have been a greater emphasis on their place in world science. **Vera Rich**

Biology at Berkeley

New order prompts fund-raising

Berkeley, California

THE University of California (UC) at Berkeley has started mailing thousands of glossy brochures to alumni and academic philanthropists in order to raise $50 million towards a planned $150 million refurbishment of its biology department. Spurred by the perception that Berkeley has lost pre-eminence in molecular biology and genetic engineering to other UC campuses, the scheme has snowballed into what must be one of the most ambitious reorganizations ever of an academic department.

Hundreds of reports and untold numbers of faculty meetings have resulted in a grand plan aimed at making the most of the new biology by merging and reshuffling most of the seventeen existing departments into three new super-departments based on affinities between research interests. The biggest problem at present is the condition of the life sciences building, completed in 1932 and by all accounts a continual frustration for its inhabitants. Researchers speak of overloaded power lines, frequent floods caused by faulty plumbing and insufficient storage space.

The grand plan calls for two new buildings (one for cell biology and molecular genetics, one for plant and molecular biology, microbiology and biochemistry) and the complete reconstruction of the existing life sciences building (for "integrative biology": organismic botany and zoology, ecology and some genetics, more or less). A special chancellor's advisory committee is making recommendations on all appointments.

Berkeley lacks the tradition of alumni support that private universities such as Stanford have relied upon. Undeterred, the Berkeley campus development office has compiled a table indicating how the required $50 million might be raised: one donation of $15 million, two of $5 million, and so on down to 40 gifts of $25,000. The state of California has agreed to pay two-thirds of the total cost of the project; overtures will also be made to foundations which have been traditional sources of support for private universities but which have been less generous elsewhere.

Not surprisingly, some professional feathers have been ruffled by the proposed reorganization, often of smaller departments fearful that they might be swallowed up, so disappearing without trace. Biophysics has yet to find a satisfactory home, and is pressing for joint departmental status with cell physiology, for example.

Another problem seems to be that biology at Berkeley is found in two largely autonomous units, the College of Natural Resources (which receives most of its funds from the state as an agricultural experiment station) and the College of Letters and Sciences. The College of Natural Resources, with its applied emphasis, has reservations about throwing in its lot with basic scientists, and some departments in the college (such as entomology) have indicated their desire to retain their independent status, although some of their staff might be affiliated with the new groupings.

Vice-chancellor Roderic Park sees the reorganization as an interim step towards a single new College of Biology (although no such decision has yet been approved) that would encompass both the existing colleges. Park believes that the device of the Experiment Station (which dates back to the last century) is an inefficient way of supporting research. In his view, California could buy better applied agricultural research if it were to put its grant money up for competitive bids from all comers instead of tying it to a permanent institution which is solely an administrative entity. But such a change would be resisted.

Although there is now general support for the planned changes, many details remain to be sorted out. Curriculum content, for example, has hardly been considered yet. Park says that one result of the reorganization that he would like to see is a better unification of theory and applied development. Wood replies that good researchers will continue to do good research, including collaborations, wherever they are. The debates on reorganization are far from over. **Tim Beardsley**

Engineered vaccines

Instant approval

Washington

THE US Department of Agriculture (USDA) has found a genetically engineered live-virus vaccine to be "pure, safe, potent and efficacious", and has enabled Biologics Corporation of Omaha, Nebraska, the manufacturer, to resume sales after a two-week voluntary suspension.

The suspension came about after charges appeared in the press that USDA had failed to follow proper procedures in approving the vaccine licence. USDA had not notified its own Agricultural Recombinant DNA Research Committee about the application (see *Nature*, **320**, 473; 1986). The vaccine, called Omnivac, protects swine from pseudorabies, a potentially fatal disease caused by a herpesvirus. Omnivac lacks a normally present gene for thymidine kinase that allows the virus to enter a latent state in an animal's nervous system, leading to future outbreaks of disease.

USDA's Animal and Plant Health Inspection Service conducted an "environmental assessment" of the vaccine based on available data, but critics of recombinant DNA research are not satisfied, calling instead for a full environmental impact statement. The Foundation on Economic Trends, headed by Jeremy Rifkin, has filed suit in federal court to suspend Omnivac's licence, and a congressional committee is also investigating USDA's procedures in this case.

Meanwhile, the Scientific Advisory Panel to the Environmental Protection Agency (EPA) has issued a favourable report on Monsanto's permit application to test a genetically engineered microbial pesticide in the field. Final EPA approval is expected later this month. **Joseph Palca**

Britain squeezed

THE proposed cuts in French research spending may have a knock-on effect elsewhere and, in particular, on British participation in the European Synchrotron Radiation Facility (ESRF) to be built at Grenoble. The British Science and Engineering Research Council (SERC), which has been keen to participate, has insisted that the principal members of the Grenoble consortium, France, Italy and West Germany, should in return join (and help pay for) Britain's Spallation Neutron Source (SNS) at the Rutherford Appleton Laboratory near Oxford. But now France, the least reluctant of the trio, seems less likely than ever to participate.

According to Pierre Papon, director-general of the Centre National de la Recherche Scientifique (CNRS), which with the Commissariat à l'Energie Atomique (CEA) would have been the leading French partner in SNS, the British have asked potential partners that the costs to Britain of participation at Grenoble should be matched, pound for pound, by European contributions to the planned second phase of SNS development.

"What advantage would there be in that for us?", Papon demanded last week. He is already conscious of the cuts that lie ahead, while CNRS and CEA apparently agree that French investigators already have "quite enough neutrons", and buying a share in SNS would entail an obligation for continuing operating costs.

Although the present ESRF partners would still like to see Britain contribute some 20 per cent of the Grenoble facility, Papon said last week that negotiations are also under way with a consortium of smaller European states, including Austria, Switzerland and Spain. If the negotiations succeed, Papon says, the remaining gap of 10 per cent may be closed without British participation. Robert Walgate

French budget cut

Chirac takes knife to fatted calf

AFTER five years of socialist expansion, French science is about to go into reverse under the new right-wing Chirac government. In the revised budget for 1986 announced last week, roughly half of all the budget cuts affect science and research. Under the new government, spending on civil research and development will fall by 9 per cent. Since the previous government had planned a 4 to 5 per cent increase in real terms, the result will be a real cut in resources for research and development, the first cut in spending since 1981.

In numbers, FF1,974 million (£84 million) is to be taken from research, most of it from the budgets set aside for the programmes in the gift of the old ministry of research and technology. Funds for the ministry's strategic research in support of new technology (*programmes mobilisateurs*), as well as for other research programmes independent of the research councils, are to be slashed by half, saving FF1,000 million.

Applied research will suffer most, although the chief French programmes in space and nuclear technology are to be protected. ANVAR (Agence National pour la Valorisation de la Recherche), intended to assist technology transfer to small businesses, will be cut by 40 per cent, and the French organization for alternative energy and conservation, AFME (Agence Française pour la Maîtrise de l'Energie), by a third.

The research councils are to lose 10 per cent of their operating budgets, but (with the exception of AFME) the large technology agencies such as the Commissariat à l'Energie Atomique (CEA) will be cut very little if at all. This means that the agencies transferred to the ministry of industry will be left intact but that the organizations left with the rump belonging to the ministry of research and higher education will have been cut.

One small mercy is that funds for the direct support of university research through the ministry of education will also be unchanged, although these are small compared with the sums awarded to universities by the research councils. As yet, the councils have not finally decided how to administer the budget cuts, but the medical council (INSERM) is likely to pass on a 10 per cent cut in laboratory operating costs according to a spokesman last week. The principal research council, the Centre National de la Recherche Scientifique (CNRS), which has to save FF230 million (£21 million), has yet to decide between the deletion of a "whole programme" of research and a general cut of 10 per cent in operating budgets.

The Chirac government is defending the cuts by saying that they are no greater than the amounts removed from the research budget by the Socialists in 1983, when the previous government was converted from Keynesian to conservative economics. But the government's critics point out that the cuts in mid-1983 were reductions of a budget which had been increased by 16 per cent over that for 1982. Then, there was a real increase of 4–5 per cent in science spending, not the reduction by that amount now in prospect.

M. Alain Devaquet, minister of research in the new government, says that he is "unhappy" with the cuts but that he "understands" the reasons for them. Speaking to journalists in Paris on Thursday last week, he insisted that research remains on the government's list of priorities.

At the same time, Devaquet disarmed fears that the French research councils CNRS and INSERM would be dismembered, as some members of Chirac's right-wing party were demanding during the election campaign. The minister now says that the research councils have some "small problems" which can be solved without radical change.

The new division of responsibility between the ministries of research and of industry has been partly clarified. Devaquet said last week that his ministry would be left with programmes (now halved in value) intended to encourage industrial research, while the industrial ministry would be responsible for the whole field of industrial development.

This seems to be a victory for those in the industry ministry who have always been suspicious of the upstart initiatives of the research ministry. By the same test, the development is a defeat for the influence of science on French industrial policy.

Robert Walgate

Military research

Campus protests at nuclear tests

Berkeley, California

THE University of California is yet again wracked by protests about military research on its campus at Berkeley. The university administration has now replied to campus petitions alleging failure to oversee the nuclear weapons laboratories it manages for the US government, saying it affirms that work at the laboratories must allow for progress towards nuclear disarmaments as well as design of nuclear weapons.

The issue arises in acute form at the University of California, which has had since the end of the Second World War contracts for the managements of the two principal weapons laboratories in the United States, as well as the Lawrence Berkeley physics laboratory.

The university's present position is spelled out in letters of reply sent to several groups of faculty petitioners who had written to university president David Gardner expressing concern over reports suggesting that nuclear bomb designers at the Los Alamos and Lawrence Livermore laboratories were designing unnecessarily sophisticated nuclear bombs that need constant testing. The charge was made most recently by Hugh DeWitt and Gerald Marsh, physicist at Livermore and at the IIT Research Institute, in the November 1985 issue of the journal *Bulletin of the Atomic Scientists*.

De Witt and Marsh argued that weapons laboratories are now operating under the assumption that continued testing of nuclear weapons will be possible, thus in practice making them necessary and making a comprehensive nuclear test ban impossible. This conflicts with declared US policy, at least until 1971, when weapons were designed on the assumption that there would eventually be a comprehensive test ban.

The current US administration is the first not to support the idea of a test ban in principle, arguing that continued testing is necessary to ensure the effectiveness and reliability of the weapons stockpile. One petition expressing concern was distributed on the Berkeley campus; its organizers say they believe several hundred faculty members wrote to Gardner on the topic.

The petition argued that any unnecessary testing represented a serious failure of oversight by the university, which manages the laboratories under contract. The university's management contract is voted on by the university every five years, and there have been enough close calls for the administration to be sensitive about allegations such as those of De Witt and Marsh.

Although nobody expects there to be any immediate changes at the weapons laboratories as a result of the university statement, faculty members opposed to the university's role regard it as a step in the right direction. William Frazer, the vice-president for academic affairs at the University of California, says the university is confident that weapons are not being designed deliberately to require nuclear testing and says there are no grounds for thinking the conduct of Livermore improper.

Nevertheless, Gardner is to ask a standing academic review committee to "delve deeper" into the matter, according to Frazer.

Tim Beardsley

Lawrence Berkeley laboratory

SDI brings back old problem

Berkeley, California

THE steep decline in federal support for magnetic fusion research and the concurrent growth in the Strategic Defense Initiative (SDI) budget are posing hard questions at Lawrence Berkeley Laboratory (LBL). Administrators and staff are having to confront again a question many thought had been settled in the early 1970s, when the laboratory's remaining classified research projects were either wound down or transferred to Lawrence Livermore Laboratory, 40 miles away.

Should LBL pursue weapons-related research for the Department of Defense that might, if successful, end up being classified? Recent hard-fought negotiations over publication restrictions on strategic defence research at LBL have now thrown the issue into new relief.

The ability of the national laboratories to set their own policies on classified research was challenged last summer, when the Department of Energy proposed (*Federal Register*, 26 August, p.34662) that they should agree to accept defence work, whether classified or not. That proposal was withdrawn after strong opposition from virtually all quarters, and led LBL director David Shirley to issue a clarifying statement last November to the effect that research at LBL could be "freely communicated to the scientific and technical community". Occasional use of laboratory facilities for classified work by investigators from other institutions would need case-by-case approval in advance by the director.

Similar questions have now been raised by research, supported by the SDI organization, into neutral-particle beam accelerators and high-current beam instability. The "very objectionable" restrictions on publication originally proposed by the SDI organization have been "fought very hard", according to LBL's general counsel Aleetha Owens. But the fighting is apparently not yet over.

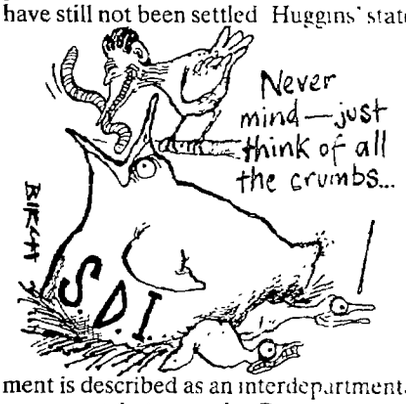
The neutral beam research includes theoretical and experimental work on the development of hydrogen-ion accelerators, and was until recently supported by the Department of Energy's magnetic fusion programme; neutral beams formed by neutralizing hydrogen ions might be a means of heating plasmas to achieve conditions required for fusion. But the magnetic fusion budget at LBL has fallen from around $6 million to $2 million in the past two years, and substantial layoffs were likely without an alternative source of funds.

After what sounds like much heart-searching, investigators in LBL's accelerator and fusion research division decided last year to make two applications for SDI funds. A third proposal, for a radio frequency quadrupole accelerator to operate at extremely low temperatures in outer space, was vetoed by the division on the grounds that it had no feasible non-military justification. The result of the applications submitted was a contract for the work on neutral particle beams worth $2.2 million in the current year, with another $600,000 for theoretical studies of instabilities in high current beams. SDI also supports work at LBL on infrared sensors.

Laboratory staff say they have been left in no doubt that SDI research results must now be submitted for pre-publication review to ensure that classified information is not disclosed, although the research itself will not be secret. This apparently represents a change of policy by the SDI organization, which insisted last year that there should be no such restrictions on earlier particle beam work. A statement dated 14 February 1986 and signed by James Huggins of the the US Army's Strategic Defense Command now circulating among LBL staff says that, following pre-publication review, "any information deemed classified shall not be published".

Staff see Huggins' declaration as drawing a "mighty fine line" between classified and unclassified research. Huggins also states that new interviews and press releases on neutral particle beam work will require advance review for classification and that information that is "non-releasable based on the Militarily Critical Technologies List" shall be revised in consultations with the author.

Owens says she doubts that pre-publication review would be used to classify LBL research retroactively, but sceptics point to the free electron laser as an example of LBL research that was classified and moved to Livermore when it became militarily important. Although the SDI money at LBL is already flowing for the neutral beam and beam instability research, the official LBL line is that the publication conditions of the contract have still not been settled. Huggins' statement is described as an interdepartmental agreement between the Departments of Defense and Energy which has still not been agreed by the director of LBL.



A further complication is that the University of California, which manages LBL, has endorsed the "no classified research" policy and would take a keen interest in any erosion of that position.

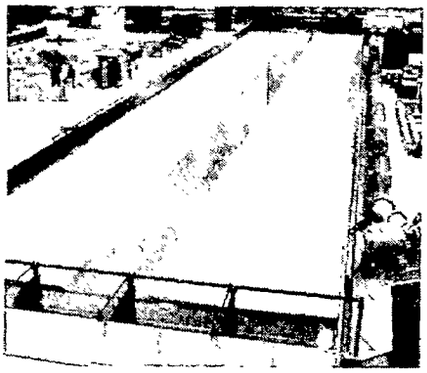
Another concern, according to Jay Marx, assistant director of the accelerator and fusion research division, is the feeling in the division that SDI funds should not exceed 10 per cent of the division's budget because "frankly we're worried about the volatility of the funding". Director Shirley adds that if the laboratory is to undertake a multi-million dollar project, it should have confidence that support will continue for a substantial period, say ten years. But SDI is hoping to achieve breakthroughs by the early 1990s and "that is not research".

There is a conspicuous absence of security controls at LBL; all buildings are open, and visitors can enter the site without so much as a name check by hopping on a shuttle bus at the University of California's Berkeley campus, just a mile down Cyclotron Road. Researchers say they value the unrestricted exchange of ideas with university faculty and others, and are wary of the change in atmosphere that security restrictions would bring about.

Thus James Symons, head of LBL's nuclear chemistry division, says "most people much prefer the present system and hope we can keep it that way". Symons is clearly speaking for the majority in saying that he would react "very strongly and very negatively" to the imposition of restrictions on what he could publish. But the alternative, at least for some researchers, seems to be no research at all. Some might say the objectors had better decide whether they want to have their cake or eat it.

Tim Beardsley

UK flood channel



THE UK Science and Engineering Research Council has this week opened a new flood channel facility built at a cost of £0.75 million at Hydraulics Research Limited, Wallingford. The facility is designed to investigate the interaction between flow in a river channel and over a flood plain; it is 56 m long and 10 m wide, with a discharge capacity of up to 1.1m^{3}s^{-1}. □

What to call the AIDS virus?

SIR—The undersigned are members of a subcommittee empowered by the International Committee on the Taxonomy of Viruses to propose an appropriate name for the retrovirus isolates recently implicated as the causative agents of the acquired immune deficiency syndrome (AIDS). Adoption of an internationally acceptable name for this group of viruses has become an important issue because of the widespread interest in AIDS and its origins and because of the multiplicity of names currently in use. Thus the several isolates of what are now evidently closely related members of the same virus group have been called lymphadenopathy-associated virus (LAV), human T-lymphotropic lymphotropic virus type III (HTLV-III), immunodeficiency-associated virus (IDAV), and AIDS-associated retrovirus (ARV). At present, two compound names (HTLV-III/LAV and LAV/HTLV-III) are also used in publications, while the colloquial name, the AIDS virus, is often used by the general press.

We propose that the AIDS retroviruses be officially designated as the human immunodeficiency viruses, to be known in abbreviated form as HIV.

We have considered several issues bearing on this proposal.

(1) The name should conform to common nomenclature for retroviruses, beginning with the host species ("human"), ending with "virus", and containing a word that denotes a major (though not the only) pathogenetic property of the prototypic members of the group ("immunodeficiency"). ("Feline leukaemia virus" and "mouse mammary tumour virus" are two well-known examples of such names for retrovirus species.)

(2) Though the name should clearly link the viruses to the disease with which they are associated, it should not incorporate the term "AIDS", which many clinicians urged us to avoid.

(3) The name should be readily distinguished from all existing names for this group of viruses and has been chosen without regard to priority of discovery.

(4) The name should be sufficiently distinct from the names of other retroviruses to imply an independent virus species, a group of isolates that can presumably exchange genetic information readily with each other but not with members of other known retrovirus species. These other species include the human T-cell leukaemia viruses (for example, HTLV-1 and HTLV-2), which will continue to be named according to a convention adopted by several leading investigators in September 1983. (Though roman numerals are often used to indicate the type of HTLV, arabic numbers were originally prescribed in the agreement and are thus used here.)

(5) Retroviruses isolated from subhuman primates and found to be genetically related and biologically similar to HIVs should be designated as immunodeficiency viruses of the appropriate host species (for example, simian immunodeficiency virus [SIV] or African green monkey immunodeficiency virus [AGMIV]).

(6) Because HIV isolates are numerous and display considerable genetic heterogeneity, particularly in the *env* gene, it will be necessary for each laboratory to assign subspecies designations to their isolates. We recommend that each laboratory adopt a code with geographically informative letters and sequential numbers to identify their isolates (for example, the 42nd isolate at the University of Chicago could be described as HIV [CHI-42]). Initially, the existing, well-characterized isolates, such as LAV-1, HTLV-IIIB or ARV-2, should be identified as such in publications to ease the transition to a unified nomenclature.

(7) Any future isolates of human retroviruses with clear but limited relationship to isolates of HIV (for example, more than 20 per cent but less than 50 per cent nucleic acid sequence identity) should not be called HIV unless there are compelling biological and structural similarities to existing members of the group.

We hope that this proposal will be adopted rapidly by the research community working with viruses.

JOHN COFFIN (Tufts University, Medford, Massachusetts, USA), ASHLEY HAASE (University of Minnesota, Minneapolis, Minnesota, USA), JAY A. LEVY (University of California, San Francisco, California, USA), LUC MONTAGNIER (Institut Pasteur, Paris, France), STEVEN OROSZLAN (Frederick Cancer Research Center, Frederick, Maryland, USA), NATALIE TEICH (Imperial Cancer Research Fund, London WC2, UK), HOWARD TEMIN (University of Wisconsin, Madison, Wisconsin, USA), KUMAO TOYOSHIMA (University of Tokyo, Tokyo, Japan), HAROLD VARMUS, chairman (University of California, San Francisco, California, USA), PETER VOGT (University of Southern California, Los Angeles, California, USA), ROBIN WEISS (Institute of Cancer Research, Chester Beatty Laboratories, London SW3, UK)

• An earlier version of this letter asked that journals publishing it should make use of the name HIV a condition for the publication of research articles. There is much to be said for the general use of a common name, while the present proposal seems to have much to commend it (except for the possibility of misreading the last two initials as a roman "four"). Nevertheless, *Nature* will continue its present practice of allowing its contributors to use whatever nomenclature seems to them appropriate, while reserving the right to add a clarifying note if this should seem necessary to avoid confusion. Editor, *Nature*.

Disposal of British civil plutonium

SIR—The stated position of the Central Electricity Generating Board (CEGB) on British civil plutonium (*Nature* **318**, 406; 1985) has for its keystone an apparent material inaccuracy of very considerable magnitude, namely, the claim that "no plutonium produced in CEGB reactors has been... exported for use in weapons". Three apparent facts indicate that the claim is false.

First, CEGB is party to a statement that "... approximately four tonnes..." of such plutonium has been exported to the United States under the provisions of the 1958 Mutual Defence Agreement and its 1959 Amendment, Cmnd 859 (*The Electrical Power Engineer*, p.163, August/September 1984).

Second, Paragraph C of Article V of Cmnd 859 specifies an *exclusive* use of this plutonium: "the preparation or implementation of defence plans". (Colloquially, this appears to mean bomb tests and bombs.)

Third, and setting the issue beyond reasonable doubt, a spokesman for the US government has recently stated that "...the Mutual Defence Agreement actually requires the United States to use *all* plutonium obtained from the United Kingdom under the Agreement for military purposes..." (*The Electrical Power Engineer*, February 1985, p38; my italics).

The apparent material inaccuracy is very considerable. Approximately 4,000 kg of plutonium is enough for a thousand bombs, perhaps two thousand if the design is sophisticated, more than enough to devastate the whole of Europe, or the whole of the Soviet Union, or both. Thus, the apparent involvement of the UK "civil" nuclear power programme in weapons production is on a very large scale indeed.

A similar, apparently false statement occurs in a written Parliamentary Answer published in the first weeks of the Sizewell Inquiry: "...no plutonium from the CEGB nuclear programme has ever been exported for use in weapons..." (*Hansard*, Commons, 4 February 1983, col. 206).

R.V. HESKETH

Faculty of Science,
Bayero University,
Kano,
Nigeria

Is there inanimate memory?

It is too easy to forget that pre-Victorian physics ascribed memory to lumps of iron. Now this still surprising phenomenon has a mathematical basis to call its own.

EVERYBODY knows what is meant by hysteresis, chiefly from what school physics teachers have had to say. Take a piece of magnetic material such as iron, put it in a magnetic field whose strength can be varied and, starting with unmagnetized iron, let the strength of the magnetic field increase steadily. To begin with, the magnetization of the iron increases less quickly than the field; anthropomorphically, the iron hankers after its unmagnetized condition. But then the rate of increase becomes greater; magnetization grows on what the economists call an S-shaped curve, the kind of thing that might be represented by a factor such as $[1 - \exp(-x)]$.

The surprise is that the same happens on the way down. Decreasing the external magnetic field gives the impression that the lump of iron hankers after its magnetized condition. Plotting the values for magnetization and external magnetic field on a piece of graph paper, there is a gap between the two S-shaped curves. Many young people are asked to record the difference, but are rarely asked to think what it means. But these days, when school administrators are so concerned with technology, young people may be expected to know that the area of the hysteresis curve is a measure of the energy loss of a transformer using iron as a magnetic inductor.

The more interesting question is that of the physics of the process. How is it that a lump of iron can remember its past history in such a reproducible fashion that its hysteresis curve can be counted as a function of its constitution? To be sure, the area within the hysteresis curve is a function of the frequency with which the cycle is traversed (the faster, the greater the area), which implies that lumps of iron have not merely a memory, but a time-dependent capacity to forget. I.D. Mayergoyz from the University of Maryland has now provided a framework in which to ask how such odd behaviour may arise (*Phys. Rev. Lett.* **56**,1518; 1986).

Mayergoyz's starting point is in 1935, and the work of the German physicist Preisach who is said (a little disdainfully) to have constructed a model of hysteresis on "some hypotheses concerning the physical mechanisms of magnetization. Abstractly, of course, magnetization followed by demagnetization must entail some kind of energy expenditure. A magnetized state is ordered, and so has lesser entropy than that from which it was formed. Simple thermodynamics proclaims that achieving such a state in a finite time requires that some work should be done (which will eventually appear as heat). But that is no more illuminating about the underlying mechanism than the calculations economists make to show that a trade surplus (deficit) must always be balanced by an export (import) of capital, whence (in physics) concepts such as magnetostrictive friction, fashionable enough in the 1930s.

That is why the mathematical framework of the discussion may be helpful in its own right. Mayergoyz borrows heavily from the Soviet mathematician Kasnoselski, whom he describes as having distilled from earlier work a way of describing hysteresis. The problem is this. A hysteresis curve is a function in some appropriate space. An input, in the simplest case the changing strength of the external field as a function of time, yields an output characteristic of itself. If the speed of the transition from the unmagnetized to the magnetized condition is immaterial, or is ignored, there remains a problem in that the shape is a function of the initial and final values of the external field. More generally, at any point of the planar graph in which magnetization is represented as a function of external field, there is an infinity of curves that may represent the future behaviour of a lump of iron, each one dependent on a particular past history.

What emerges from this argument is a description very similar to what the statisticians would call a Markov system. The future behaviour (magnetization) of a lump of iron may be determined from a knowledge of its state at some instant and from a knowledge of the magnetic field then and at subsequent times. How could it be otherwise, when causality applies? So there must be something about the initial state that embodies the memory of recent past history. In dynamical systems, it may be the rate at which the system is changing on a microscopic scale (the velocity field); in the relatively static context of magnetization, the pattern of magnetization is the clue to the past.

The important part of Mayergoyz's result is his demonstration that it should be possible to calculate the properties of the operator that transforms the input function of the system (the external magnetic field) by means of a simple series of experiments in which the output (magnetization) is recorded. The demonstration is mathematical, and in a novel way, but the result is to suggest what the history of mathematical physics has consistently shown to be significant, the forging of relationships between functions of one kind and functions of another. The fact that, in the simplest case of hysteresis, that of magnetism, the results must accord with the thermodynamics of entropy and the explanation may lie in microscopic physics is, for the time being, irrelevant.

One practical implication of the argument stands out. Although a system showing hysteresis will behave in a particular way determined by its starting condition and the external influences upon it, there are general rules that determine the behaviour of systems exposed to extreme conditions that appear to be unaffected by the details of the case This is mirrored, in Mayergoyz's treatment, by the way in which the local microscopic conditions (say, local magnetic domains), which are the local repositories of memories of the past, will be smeared out or extinguished by extreme conditions.

What may this mean for the concept of memory? The simple and oversimple answer is that there can be no connection between inanimate physical systems such as lumps of iron and biological systems, some even blessed with what is called consciousness, in which memory must be an infinitely more subtle business. But can that in reality be the case? Nobody seriously suggests that human beings, who can remember the past, are on that account exceptions to causality.

On the contrary, it is simplest to suppose that the state of the nervous system at any instant somehow mirrors past experience in such a way as to be able to regenerate images of the past that people call memories. What Mayergoyz has done is merely to show that such a model can represent what happens with inorganic materials that appear to have a memory of the past. That is not surprising in itself. The fun will come if it turns out that the equations explain some of the properties of memory as people know it. And if the physical analogy of magnetization shows that exceptional local patterns tend to be smeared out, what can explain in the human case the enhancement of especially vivid memories? It will be interesting if the tricks that people play on themselves can be derived from theorems of some kind. **John Maddox**

Molecular genetics

Understanding colour vision

from J.D. Mollon

THOSE with deficient or anomalous colour vision live in different subjective worlds from the rest of us. Psychologists have been slow to take an interest in molecular genetics, but two recent papers by Jeremy Nathans and collaborators[1,2] allow us to trace one detailed mechanism by which specific variations in DNA lead to individual differences in perceptual ability and in subjective experience.

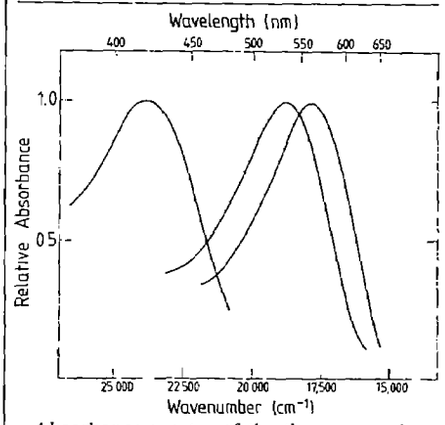
We already know that normal colour vision depends on the presence in the retina of three classes of cone cell, each containing a different photopigment[3] (see figure). A fourth pigment, contained in the rod cells, underlies our colourless vision at twilight. Each of these pigments consists of a protein molecule to which is bound a derivative of vitamin A_1, 11-*cis*-retinal. The 11-*cis*-retinal is common to all the pigments, but the pigment absorbs maximally at different wavelengths according to the protein component. We know in some detail how the photopigment, embedded in the infolded membranes of receptor cells, initiates electrical signals when light is absorbed. To work out the wavelengths falling on a local region of the retina, the nervous system must then find the ratio of the quantum catches in different classes of cone. We have a good idea of how this is done[4,5]. And we know something of how the local ratio is compared with those measured elsewhere in the visual field, so as to give us accurate colour perception despite changes in the spectral composition of the illumination[6].

A major addition to our knowledge is provided by the new reports of Nathans *et al.*, who isolated and sequenced the genes that specify the three proteins underlying normal vision[1] and show how the genes are altered in cases of colour deficiency[2]. Nathans *et al.* began with a radioactively labelled fragment of DNA derived from the gene that specifies the rod pigment of cattle. With this probe they were able to identify in human DNA not only the rather similar gene specifying the human rod pigment, but also — by manipulating the experimental temperature and thus the readiness of DNA to 'hybridize' with a partially mismatching probe — they were able to identify other, rather less similar, genes that were likely to be those that specify the cone pigments.

To localize genes on particular chromosomes, probes were prepared from each of the genes and were hybridized with DNA from a panel of mouse–human hybrid cells that retain various subsets of the human chromosomes. From the pattern of results, the gene for the rod pigment is localized on chromosome 3 and one of the putative cone genes is localized on chromosome 7; the latter gene was taken to be that for the short-wave pigment because disorders of this pigment are known not to be sex-linked. The other genes lie on the q-arm of the X-chromosome. To distinguish genes for the middle- and long-wave pigments, Nathans *et al.* examined 25 colour-deficient men, collating subjective measurements of colour vision with the pattern of hybridization to probes derived from the X-chromosome genes. One curious finding was that more than one middle-wave gene might be present on the X-chromosome of a colour-normal man. But there was never evidence for more than one long-wave gene.

Evolution of colour vision

Why are inherited anomalies of the short-wave cones very rare whereas anomalies of the middle- and long-wave receptors are so very common? Why are the absorbance curves of our photopigments (see figure) so unequally spaced in the spectrum? Why is our visual resolution in space and time so poor when it depends only on signals originating in the short-wave cones of the retina? These and other features of human vision can be explained by an evolutionary scheme that has recently been suggested by various lines of evidence and is now supported by the work of Nathans *et al.*



Absorbance spectra of the three cone pigments of human vision. These curves are plotted from Table 2 of ref. 3 and are based on microspectrophotometric measurements of cone cells from human retinas. Peak sensitivities lie in the violet (short-wave), green (middle-wave) and yellow–green (long-wave) regions of the spectrum.

Widespread among mammals is an ancient, dichromatic form of colour vision that depends on a comparison of the quantum catches in a short-wave class of cones with peak sensitivity near 430 nm; and in a second class of cones with peak sensitivity varying between species but usually in the range 510 to 570 nm (ref. 7). The short-wave cones are sparse[3,8,9] and are probably used only for colour vision, whereas all the other business of daytime vision (such as spatial discrimination and the detection of movement or flicker) depends on the second, more numerous, class of cones. The explicitly chromatic information — provided by the ratio of quantum catches in the two kinds of cone — is carried within the visual system by a sub-channel that seems to be electrophysiologically and morphologically distinct[10,11].

No doubt a trichromatic, or three-variable, system of colour vision has more than once appeared in the mammals. But our own form of trichromacy seems to be shared only with the Old World monkeys and the apes[12]. We, and these primate relatives, enjoy a second dimension of colour vision, provided by a comparison of the quantum catches of the 530- and 560-nm cones. This comparison allows us to make fine discriminations in the red–green part of the spectrum. A distinct retinal channel may not yet have evolved to handle this second type of chromatic information. It is carried by a class of retinal ganglion cells that also extract spatial contrast[4].

The very recent differentiation of the middle- and long-wave photopigments has probably been achieved by duplication of a single gene on the X chromosome. Nathans *et al.*[1,2] confirm that the genes for the middle- and long-wave pigments lie in the same region of the X chromosome and they show that 96 per cent of the inferred amino-acid sequence is identical for the two. By contrast, the short-wave pigment shows only a 43 per cent identity with the middle- and long-wave pigments. This is comparable with the degree of identity between the latter pigments and the human rod pigment.

Colour blindness

About 8 per cent of males in Caucasian populations inherit some form of colour deficiency or anomaly. About 2 per cent are dichromats, requiring only two primary wavelengths to match all colours. From reflection densitometry of the living fovea[12], and from microspectrophotometry of individual receptors[13], there is direct evidence that dichromats lack one of the three cone pigments. Six per cent of Caucasian males are anomalous trichromats, who, like normal observers, require three variables in a colour-matching experiment but who make matches that are different from the normal[14]. The most favoured explanation of anomalous trichromacy is that one of the three photopigments is shifted in its spectral position.

What are the genetic abnormalities that

underline dichromacy and anomalous trichromacy? Visual scientists have probably entertained rather simple notions of these disorders, assuming that local mutations of the gene lead to local substitutions in the sequence of amino acids. Nathans *et al.* show that such point mutations are unlikely to be a common source of colour deficiency. Rather, they suggest, the trouble lies in the juxtaposition and the similarity of the genes for the middle- and long-wave pigments. During the formation of ova and sperm cells, when crossing-over occurs between members of a pair of chromosomes, misalignments of the DNA may occur in the region that encodes the middle- and long-wave pigments. Because the sequences are so similar, the long-wave gene on one chromosome might get itself apposed to a middle-wave gene on the other chromosome. If now crossing-over occurs and if the breakpoint lies in the duplicated spacers between genes, then one chromosome might lose its middle-wave gene and the other chromosome end up with two. If, on the other hand, the breakpoint occurs within a gene, a hybrid gene might be formed that consists of part of the long-wave gene and part of the middle-wave gene.

A man who inherits an X chromosome that lacks the middle-wave gene will be a dichromat, but if the X chromosome carries a hybrid gene, then the outcome will depend on where the breakpoint occurred at the time of crossing-over. There is one sub-region of the gene that seems to determine the actual spectral sensitivity of the resulting photopigment. If this sub-region is drawn from the long-wave gene, then the hybrid gene may produce a photopigment very similar to the normal long-wave pigment; the owner of this chromosome will again be a dichromat. But there may be a whole range of possible breakpoints and some of these may produce hybrid genes that encode photopigments with spectral sensitivities intermediate between those of the normal long- and middle-wave pigments; a man who inherits such a hybrid gene will be an anomalous trichromat. □

1. Nathans, J., Thomas, D. & Hogness, D.S. *Science* **232**, 193 (1986).
2. Nathans, J., Piantanida, T.P., Eddy, R.L., Shows, T.B. & Hogness, D.S. *Science* **232**, 203 (1986).
3. Dartnall, H.J.A., Bowmaker, J.K. & Mollon, J.D. *Proc. R. Soc.* B**220**, 115 (1983).
4. Gouras, P. *Progr. Retinal Res.* **3**, 227 (1984).
5. Boynton, R.M. *Human Color Vision* (Holt-Rinehart-Winston, New York, 1979).
6. Zeki, S.M. *Nature* **284**, 412 (1980).
7. Jacobs, G.H. *Comparative Color Vision*, (Academic, New York, 1981).
8. Mollon, J.D., Bowmaker, J.K. & Jacobs, G.H. *Proc. R. Soc.* B**222**, 373 (1984).
9. Sperling, H.G. in Cool, S.J. & Smith, E.L. *Frontiers in Visual Science* (eds Cool, S.J. & Smith, E.L.) 138 (Springer, New York, 1978).
10. Gouras, P. & Zrenner, E. in *XXIII Concilium Opthalmologicum, Kyoto* (ed. Shimizu, K.) 379 (North-Holland, Amsterdam, 1978).
11. Mariani, A.P. *Nature* **308**, 184 (1984).
12. Rushton, W.A.H. *Nature* **206**, 1087 (1965).
13. Mollon, J.D., Bowmaker, J.K., Dartnall, H.J.A. & Bird, A. C. in *Colour Vision Deficiencies VII* (ed. Verriest, G.) 303 (Junk, The Hague, 1984).
14. Rayleigh, Lord *Nature* **25**, 64 (1881).

J.D. Mollon is a Lecturer in the Department of Experimental Psychology, University of Cambridge, Cambridge CB2 3EB, UK.

Taxonomy

Taxonomic tangles from Australia

from Tony Thulborn

IN THE next few years, many of the world's biologists may find themselves beset by taxonomic problems originating from Australia, where a pair of taxonomists is engaged in upsetting the stability of zoological nomenclature. So far, the pair have confined their attention to the Australian herpetofauna, which has been augmented by no fewer than 577 questionable taxa in the past 18 months. As a result, the comparatively stable nomenclature of Australia's reptiles has threatened to collapse into near chaos. Readers will be alarmed to know that the perpetrators now plan to turn their attention to the rest of the world's reptiles.

The saga began in 1981, when R.W. Wells undertook to edit a new periodical, *Australian Journal of Herpetology*, on behalf of the Australian Herpetologists League. Manuscripts were solicited on the understanding that they would undergo rigorous review by an editorial board comprising three renowned herpetologists. The first two issues of *Aust. J. Herp.* appeared on schedule, and the journal began to draw subscriptions from individuals and libraries throughout Australia and overseas. Things started to go wrong after Wells left his undergraduate studies at the University of New England (Armidale, New South Wales) and moved to Sydney. *Aust. J. Herp.* failed to appear for the next two years, although Wells maintained an address at New England and continued to receive manuscripts.

In 1984 Wells unveiled the third issue of *Aust. J. Herp.* It contained only one paper — a 56-page 'Synopsis of the Class Reptilia in Australia', by Wells and his co-author C.R. Wellington. Manuscripts that had been refereed and accepted for publication in order of receipt had been pushed aside for the Wells and Wellington paper; in fact none of the manuscripts processed by the editorial board has yet been published, although information from at least one of them was transplanted into the Wells and Wellington 'Synopsis'. Authors requesting the return of their manuscripts have so far met with no success. The third issue of *Aust. J. Herp.* revealed another surprise: its copyright had been transferred to an organization called 'Australian Biological Services', with Wells as 'Managing Editor' and Wellington as 'Advertising Sales Manager'.

The 'Synopsis' itself can only be described as shoddy work — there are no illustrations, and the diagnoses of taxa are so perfunctory as to be useless. Nevertheless, Wells and Wellington designated 33 new genera and 14 new species and elevated 208 synonyms or sub-specific names to the rank of species. The reactions of professional herpetologists ranged from disbelief to outrage. Most dismayed of all were those who found that their casual remarks about their research findings had been published as definitions for new taxa. At its annual general meeting in 1984 the Australian Society of Herpetologists discussed the possibility of suppressing the Wells and Wellington nomenclature, and several individual workers expressed their opinions in letters to *Herpetological Review* (**16**, 4; 1985).

Wells and Wellington were not deterred. In a 98-page publication dated 1 March 1985, identified as *Aust. J. Herp. Supplementary Series* No. 1, and titled 'A Classification of the Amphibia and Reptilia of Australia' they update their previous synopsis of the reptiles and proceed to treat the frogs in similar fashion. The document enumerates 66 new genera (9 of them resurrected from synonymy) and 256 new species (119 of them as resurrected synonyms). It also claims to designate lectotypes for 108 species.

In the bibliography to this second paper there is a list of more than 500 papers said to have been published by Wells in *Australian Herpetologist* since 1983. The existence of those papers is questionable: *Australian Herpetologist* is a 'phantom' publication that cannot be located by librarians, and Wells has not responded to requests for copies of his papers. Also mentioned in the bibliography is a 10-volume work on 'The Herpetology of Australia' by Wells and M. Peterson; this is stated to be 'in press' under the imprint of Australian Biological Services.

Wells and Wellington have created much confusion. Thanks to the convenience of modern word-processing equipment they have been able to exploit existing databases (for example, *The Zoological Catalogue of Australia* Vol. 1, Reptilia and Amphibia) and to re-shuffle them into chaos. The resulting taxonomic work is hopelessly inadequate. Names have been coined for animals on the grounds that they were mentioned by previous authors as local variants. Other taxa are based on nothing more than a reference to a photograph published elsewhere. Type specimens are not identified (unless their registration numbers appear in existing

publications). In several instances there is an attempt to designate a lectotype from an unseen series of syntypes by the ploy of nominating the 'large specimen'. More than 300 names have been elevated to species rank without any explanation or definition beyond "We herein resurrect from synonymy . . .".

The choice of formal names is odd, to say the least. For example, Wells and Wellington introduce the genus names *Licentia* (meaning 'freedom to do as one pleases'), *Phthanodon* ('to anticipate' or 'to do first'), *Contundo* ('to crush') and *Solvonemesis* ('to set free the goddess of retributive justice'). Then there are names that can only be regarded as frivolous: the bestowal of a patronymic species on the Australian Prime Minister, the naming of a species for Telecom Australia, and *Vaderscincus* ('named for Mr Darth Vader'). The name *Eroticoscincus* needs no comment.

While the taxonomic practices of Wells and Wellington would not be tolerated in conventional publications, it is not absolutely clear that they contravene the rules and recommendations of the International Code of Zoological Nomenclature. Unfortunately, it seems certain that some of their name-games will amount to technically valid combinations.

What is to be done? First of all, biologists outside Australia should be alerted to the situation. Wells and Wellington have placed themselves beyond the pale of legitimate science, and their publications and taxonomic revisions should be treated with extreme scepticism. The Australian Society of Herpetologists plans to approach the International Commission on Zoological Nomenclature with a view to seeking formal suppression of the Wells and Wellington nomenclature. However, such a procedure could be expensive, protracted and somewhat uncertain in its outcome — especially if the Commission refuses 'blanket' suppression and examines each of the 577 cases on their individual merits. Meanwhile, it may suffice that taxonomists are aware of what has been happening to the nomenclature of Australian herpetology. □

Tony Thulborn is in the Department of Zoology, University of Queensland, St Lucia, Brisbane, Australia 4067.

Ocean Drilling Program

Mid-Atlantic bare-rock drilling and hydrothermal vents

*from the Leg 106 shipboard scientific party**

LEG 106 of the Ocean Drilling Program (ODP) has taken two significant steps in the study of geological processes at mid-ocean ridges. The first essentially 'zero-age' crustal hole was drilled on the plateau at the summit of a small axial volcano in the Mid-Atlantic Ridge Rift Valley 2,200 km south-east of Bermuda; and engineers demonstrated the feasibility of 'bare-rock', spud-in drilling and coring. The survey of a hydrothermal area in the rift valley also led to the discovery of an active vent field with large sulphide chimneys, hot 'black smoker' vents and a unique biological community. Several drill holes in this area, the first ever drilled in an active, submarine hydrothermal system, recovered massive sulphides (Fe and Cu) and unconsolidated hydrothermal deposits of Zn, Cu and Fe sulphides. Despite the need for technical developments to improve drilling rates and core recovery in these difficult conditions, Leg 106 opens up exciting possibilities for crustal drilling at oceanic spreading centres.

In submarine volcanic areas, cold seawater circulates close to hot, intrusive rocks deep within the crust where it is heated to very high temperatures and upwells as hot springs on the sea floor. Although at least six active hydrothermal vent areas have been identified along medium- and fast-spreading ridges in the eastern Pacific, until recently no direct evidence for such activity was known along the slow-spreading Mid-Atlantic Ridge. During a pre-drilling site survey in May 1985, W.B.F. Ryan (Lamont-Doherty Geological Observatory) and L. Mayer (Dalhousie University) took photographs of pockets of greenish-white, mottled hydrothermal sediment, crabs and small, spindly worms indicative of recent hydrothermal activity in an area about 25 km south of the Kane Fracture Zone. The new hydrothermal vent field was discovered during a 36-hour video survey of this area on ODP Leg 106. The sulphide chimneys range up to several metres in diameter and more than 11 m in height, and display the spectacular dendritic, tubular structures and elaborate ornamentation previously seen on the East Pacific Rise and Juan de Fuca Ridge.

Ten shallow holes were drilled at this site to sample the hydrothermal deposits and the underlying basement rocks, two of which are located at the foot of a large black smoker. The hydrothermal deposits are surprisingly thick — more than 13 m at the foot of the black smoker and at least 3–6 m more than 17 m away from the vent. Recovery of the sand-sized sulphide deposits was generally poor, but our analyses indicate that they are composed mainly of chalcopyrite ($CuFeS_2$), sphalerite (ZnS), pyrite (FeS), marcasite (FeS_2) and pyrrhotite (Fe_{1-x}) in varying proportions. Lenses of massive (Fe + Cu) sulphide were also drilled and recovered from a hole at the base of the black smoker. Where recovered, the underlying basalts were fresh.

The vent field is also associated with a diverse biological community that is surprisingly different from that observed in the Pacific. We did not observe any clams, mussels or large, sessile tube worms near the vents. The most common forms of life are large swimming crustacea, small shrimp-like organisms and long (30–60 cm), flat, snake-like swimmers (possibly eels) that give the area the name of the Snake Pit. The shrimp-like organisms seem to congregate on rock surfaces near the vent orifices while sessile little white balls (possibly some type of anemone) litter the sea floor around the vents. In general, the community appears to consist of smaller, more mobile organisms than those previously found at submarine hydrothermal vents.

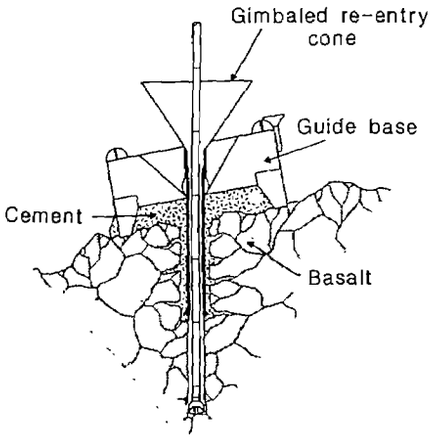
Previous attempts to drill to significant depths in young oceanic crust have been unsuccessful because of difficult drilling conditions in the fresh, abrasive and highly fractured basaltic rocks found at

Co-chief scientists: Robert S. Detrick (Univ. Rhode Island, Kingston) and Jose Honnorez (Univ. Louis Pasteur, Strasbourg, France and Univ. Miami). ODP Staff scientist, Andrew C. Adamson (Texas A & M Univ.). Also Garret W. Brass (NSF), Kathryn M. Gillis (Dalhousie Univ.) Susan E. Humphris (Woods Hole Oceanographic Inst.), Catherine Mevel (Univ. Pierre et Marie Curie), Peter S. Meyer (Woods Hole Oceanographic Inst.), Nikolai Petersen (Univ. Muenchen) Martina Rautenschlein (Max-Plank-Inst. fur Chemie), Tsugio Shibata (Okayama Univ.), Hubert Staudigel (Scripps Inst. Oceanography), Anita Wooldridge (Univ. Miami) and Kiyohiko Yamamoto (Tohoku Univ.).

THE three-man deep-sea submersible *Alvin* is going to take a close look at some hydrothermal vents, but this time in the waters of the Atlantic rather than the Pacific Ocean, where all the vents have so far been found. These sites where hot brines emerge from the sea floor, together with their characteristic 'black smokers', sulphide chimneys and peculiar ecology, have now been found on the Mid-Atlantic Ridge by two groups. On page 33 of this issue, Rona *et al.* describe vents found by dredging and video cameras during a cruise in July–August 1985, and on this page, the ODP Leg 106 scientists reveal similar finds made quite close by in December of last year. The level of excitement generated by these discoveries can be judged by the fact that Rona has managed to get time to use *Alvin* in the early summer of 1986. Normally he would have had to wait until at least 1988 to stand a chance of getting a slot on a cruise. But the *Alvin* team just happened to be planning a visit to the mid-Atlantic, and a few extra days have been found to look more closely at the hydrothermal vents. Peter Gambles

mid-ocean ridges. The requirement for significant thicknesses of sediment (>100 m) on the basement to spud-in to the crust also precluded any drilling within the narrow, zero-age crust of the accretionary zone itself.

The main objective of ODP Leg 106 was to test and evaluate new bare-rock drilling techniques at the site in the Mid-Atlantic Ridge Rift Valley and to establish a zero-age crustal hole that could be re-occupied and deepened on subsequent legs. Among the new engineering systems tested were a hard-rock guide base to confine the drill bit during initial spud-in on sediment-free rock (see figure); a low-light television camera system for imaging the sea floor and monitoring drilling operations; and



The hard rock guide base used on Leg 106, designed to provide the lateral support necessary for the drill bit to spud-in to hard, volcanic rock on slopes up to 20 degrees and water depths of up to 6,000 m. The 20-ton guide base stands on four legs and is 5.7 m square and 2.3 m high. It is lowered to the sea floor and cemented in place with 56 m^3 of cement. A cone 5.3 m in diameter and 2 m deep is built into the base and serves as a temporary re-entry cone. Once the hole is started and cased, a permanent, gimbaled re-entry cone is positioned in the base.

new downhole drilling and coring motors to facilitate bare-rock spud-in.

The site chosen for the first bare-rock drill hole is about 70 km south of the Kane Fracture Zone on the flat summit plateau of a small axial volcano. This site is characterized by bulbous and tubular pillow lavas up to 1–2 m in diameter with a light dusting of pelagic sediment. The hard-rock guide base was successfully lowered 3,344 m to the sea floor, released and cemented without incident. A positive-displacement, downhole drilling motor was used to spud-in to the basaltic crust. The drilling motor and conventional rotary drilling advanced the hole to a total depth of 33.3 m below the sea floor before drilling was terminated after 25 days.

The average recovery for the 26.7 m of cored hole was 23 per cent, comparable with that experienced during previous drilling in young volcanic rocks. All the recovered rocks are very fresh, plagioclase–olivine, sparsely phyric basalt. The texture of the groundmass ranges from glassy to subvariolitic to intersertal to intergranular, indicating that most samples are probably derived from parts of pillow lavas. The presence of plagioclase and olivine glomerocrysts and the absence of chromian spinel suggest that the basalts are typical, moderately evolved mid-ocean ridge basalts. The drill hole was left cased and open so that it can be deepened when the ship returns later this year. □

Adrenergic receptors

Some similarities and surprises

from Peter Newmark

Two particularly striking results have emerged from the sequence, reported by Richard Dixon *et al.* on page 75 of this issue, of the gene for one of the most studied of all receptors, the β-adrenergic receptor through which adrenaline and other catecholamines exert their physiological effects. The first is that there are some structural resemblances between the receptor and rhodopsin, the protein at the front end of the machinery in rod cells of the retina that converts light into the visual response. The second surprise is that the protein-coding sequence of the gene that encodes the hamster β-adrenergic receptor is not interrupted by non-coding sequences (introns).

Adrenergic receptors have been subject to the relentless prying of endless ranks of scientists. Physiologists have established the responses to catecholamines mediated by them. Pharmacologists have categorized them into types (α_1, α_2, β_1 and β_2) and established their behaviour (for example, desensitization and down-regulation, to use the operational terms beloved of pharmacologists) in response to various types of exposure to catecholamines. And biochemists have elucidated the initial events that follow the binding of catecholamine to the receptor.

What biochemists (biochemical pharmacologists?) have established is that catecholamine binding to β-adrenergic receptors induces their coupling to so-called G (or N) proteins (which come in several types, each of which has three subunits, α,β and γ). The coupling is followed by the binding of GTP to the α-subunit of the G protein, which then dissociates from its partners to activate adenylate cyclase, and thus the synthesis of cyclic AMP. This is a transient event, lasting only until the α-subunit has hydrolysed the GTP that is bound to it. The cyclic AMP produced during that time mediates the eventual physiological responses to the catecholamine.

Dixon *et al.* report two ways in which the structure of the β-adrenergic receptor protein, whose amino-acid sequence they deduce from the DNA sequence, resembles rhodopsin. First, there are three peptides within the receptor sequence that have a considerable number of amino acids in common with peptides in roughly equivalent positions within rhodopsin; and second, rhodopsin and the receptor have "remarkably similar" hydropathicity profiles (providing some measure of which parts of a protein lie within the cell membrane and thus how the protein is threaded through the membrane).

These structural resemblances make sense in the context of biochemical parallels between the two systems. When rhodopsin is stimulated by light, it couples to transducin, a G protein whose α-subunit binds GTP and, until the bound GTP is hydrolysed, activates a phosphodiesterase that in turn hydrolyses cyclic GMP. The resulting closure of ion channels on the rod cell membrane produces the visual response (see Altman, J. *Nature News and Views* **313**, 264; 1985).

It is because of the structural resemblances between the two proteins that it comes as a particular surprise to find that the gene for the β-adrenergic receptor contains no introns. In any case, it joins a very select band: histone and interferon genes are the only other mammalian genes to lack introns; and introns have so far turned up in each of the genes for cell-surface receptors. In the particular case of the rhodopsin gene and its relatives, there are four introns in the mammalian gene, four or five in the genes that encode the three human colour pigments (Nathans, J., Thompson, D. & Hogness, D.S. *Science* **232**, 193; 1986) and three or four in two different opsin genes of the fruitfly (see Cowman, A.F., Zucker, C.S. & Rubin, G.M. *Cell* **44**, 705; 1986). Dixon *et al.* are confident that they have sequenced the real gene for the receptor rather than a pseudogene, so their discovery will be interesting grist for the mill of those who try and explain the evolutionary goings (and comings?) of introns.

And for those with an interest in β-adrenergic receptors either as a prime example of a receptor or as a target for drugs that modify the physiological responses to catecholamines, the structure of the receptor itself, quite apart from its resemblance to rhodopsin, should prove immensely valuable. □

Peter Newmark is Deputy Editor of Nature.

Astrophysics

The most reliable black hole yet

from M.G. Watson

BLACK holes are frequently invoked by astronomers to explain the vast amount of energy radiated from the nuclei of many galaxies. The energy is produced, in this picture, as material surrounding the black hole falls down its extremely steep gravitational potential well. The same phenomenon is believed to occur on a much smaller scale in a few X-ray-emitting binary stars in or near our Galaxy, providing the best available evidence that these theoretically predicted objects exist at all. In these X-ray binaries the infalling matter eventually accreted by the black hole is supplied by the companion star. A recent investigation of a system of this type — an X-ray transient — has produced results which arguably place the existence of black holes on considerably firmer ground (McClintock, J.E. & Remillard, R.A. *Astrophys. J.* in the press).

X-ray transients are a small but important subclass of X-ray binaries. Most are believed to be systems containing a faint red star and an accreting compact object (a neutron star or black hole). As such they are closely similar to the persistent low-mass X-ray binaries (White, N.E. & Mason, K.O. *Space Sci. Rev.* **40**, 167; 1985), the principal difference being that X-ray transients are only luminous X-ray emitters during their relatively short (of the order of months) outbursts which recur on timescales of years, a pattern of behaviour which presumably reflects a highly variable mass transfer rate onto the compact object. The X-ray transient A0620−00 is perhaps the most famous member of its class as it was, for a few months in 1975, the brightest celestial X-ray source ever recorded (Elvis, M *et al. Nature* **257**, 656; 1975). Despite the enormous observational attention that it attracted then, little was learnt about the properties of the underlying binary system. A decade later, the new detailed optical study of the A0620−00 system (now in its quiescent state) by McClintock and Remillard provides compelling evidence that the binary system contains a black hole.

McClintock and Remillard's result is based on several years of photometric observation of A0620−00 in quiescence that provide a unique orbital period of 7.75, together with just one night's spectroscopy which allowed them to determine the radial velocity curve of the faint red companion to the compact object by measuring the periodic Doppler shifts of its absorption lines. The amplitude of the radial velocity curve, 457 ± 8 km s^{-1}, is very large for a binary with such a short period, and this measurement alone sets a firm lower limit to the mass of the compact object of 3.2 solar masses. This is significantly above the maximum mass for a neutron star for the stiffest equation of state of neutron matter considered realistic, leading inexorably to the conclusion that the compact object must be a black hole. A more realistic estimate of the compact object mass can be made by assuming a reasonable mass for the red companion star, and using the constraints on the orbital inclination placed by the lack of X-ray eclipses and the modelling of the photometric light curve. On this basis McClintock and Remillard conclude that the mass of the compact object is likely to be greater than 7 solar masses.

The X-ray transient A0620−00 thus joins CygX−1 and two systems in the Large Magellanic Cloud, LMC X−1 and LMC X−3, as the fourth system which is a good candidate for a black-hole binary on the basis of dynamical measurements of the compact object mass. In contrast to the other three black-hole binaries which have hot, luminous, massive companions, the companion in A0620−00 is clearly a faint, low-mass red star. The presence of a massive black hole in this system may pose a fresh set of evolutionary questions. In particular it is difficult to understand how the black hole could have formed in this system without the binary being totally disrupted. The mass of the progenitor star would have had to be at least 20 solar masses (probably more), hence it seems very likely that the formation of the black hole would have involved the loss of more than half the system mass, leading to the binary becoming unbound. The present short binary period is also difficult to reconcile with the size of the original binary system required to accommodate the large, massive progenitor of the present black hole. The difficulties associated with understanding the evolutionary history of A0620−00 suggest that it is a rather rare system. It is too early to say whether this is indeed the case, because the binary system parameters of a large fraction of all X-ray binaries, transient or otherwise, have yet to be measured, but it is interesting to note that the empirical X-ray spectral classification scheme proposed by White and F.E. Marshall (*Astrophys. J.* **281**, 354; 1984) suggested several new black-hole candidates, one of which was A0620−00.

In the case of A0620−00 there can be little doubt about either the correctness of the radial velocity measurements or their interpretation. One of the standard sceptical responses to any unlikely dynamical measurement has been to suggest that the system is a triple, rather than a binary. This argument cannot be applied to A0620−00, given the small size of the system implied by the 8-hour period. Thus, A0620−00 is arguably the most reliable (or the least unreliable) black-hole candidate yet discovered. Because of this, and because it is a nearby galactic system, it may be that the impact of this result will be mainly psychological in making the possibility, if not the reality, of black holes of stellar mass seem more appealing to many astronomers. □

M.G. Watson is in the X-ray Astronomy Group, Department of Physics, University of Leicester, Leicester LE1 7RH, UK.



100 years ago

New System of Earthquake Observations in Japan

OWING to the invention of new seismographs by the members of the Seismological Society of Japan, there has been of late a complete change in the system of earthquake observations in this country. The Meteorological Bureau now employs the horizontal pendulum and vertical-motion seismographs of Profs. J. Milne and T. Gray, and of Prof. J.A. Ewing for systematic observation, while the Imperial University of Tokio publishes from time to time detailed accounts of particular and more interesting shocks by the use of similar instruments. These seismographs register on a revolving glass plate or drum automatically started by the earthquake motion, components of horizontal and vertical motions of the earth on a magnified scale, thus producing continuous diagrams, and indicating successive displacement of the ground in conjuction with the time. The account of the earthquake of December 28, 1885, the largest shock during the last three months, is here given as a sample of seismic record now issued in this country. The motion is slowly commenced, not accompanied by quick tremors, as is usually the case. At the 14th second from the commencement a considerable E.–W. motion occurred; in another second the maximum movement appeared in the same direction, which was followed by smaller shocks during about one minute; and from thence the oscillations, gradually subsided. As usual, the particles of the ground did not move to and fro, but traced a curvilinear path, although the E.–W. components always remained greater than the S.–N. components. In all, over 130 shocks or complete waves were registered. I may add in respect to the above earthquake, and in general, that the vertical motions are always — in our experience — smaller than horizontal ones, and the maxima and minima of these two kinds of motions are not synchronous. I shall have occasion before long to communicate to you the general results of all observations made during past years.

SEIKEI SEKIYA

The Imperial University of Tokio, Japan.

From *Nature* **33**, 603; 29 April 1886.

Mathematics

Hermann Grassmann was right

from Ian Stewart

THE late nineteenth century witnessed many attempts to develop an algebra of n-dimensional space, by analogy with the representation of the plane by complex numbers. Prominent among them was Hermann Grassmann's *Die lineale Ausdehnungslehre* (*The Calculus of Extension*), published in 1844. Grassmann had the misfortune to write in a discursive, philosophical and obscure style at the time when axiomatic presentation was becoming *de rigeur* in the mathematical world. Further, he was a high-school teacher with no formal training in mathematics. Not surprisingly, his ideas were at first not taken very seriously — but later, Élie Cartan used Grassmann's 'exterior algebra' as the basis of his theory of differential forms. This work proved highly influential and established the importance of Grassmann's work. But, as Marielena Barnabei, Andrea Brini and Gian-Carlo Rota write in a recent paper (*J. Algebra* **96**, 120; 1985) "In the process Cartan paid a price of omission from which we are yet to recover." They argue that mathematicians have still not fully understood what Grassmann was trying to say, and propose a formulation of his ideas in modern terms which provides a natural language for the study of invariants.

In Grassmann's original work the same notation was used to denote two different operations performed on vectors, called the progressive and regressive products. This was not an oversight, but a deliberate choice. Every mathematician knows that what Bourbaki calls "abuse of notation" can, when wielded with care, greatly illuminate what would otherwise be a confusing situation. Unfortunately Grassmann managed to confuse greatly what might otherwise have been an illuminating situation. The tale has two main threads: differential forms and invariants.

Cartan's theory of differential forms attempts to make sense of the idea that expressions such as dx and dy in calculus can have a perfectly sensible meaning. The intuitive idea of 'a very tiny bit of x' runs into severe difficulties, and is not very helpful; but the basic idea that the derivative dy/dx satisfies an equation $dy=(dy/dx)dx$ is crucial. So is the idea that an integral $\int dx$ can be thought of as an operation $\int$ applied to a differential form dx. The fundamental observation is that products of differential forms, such as $dx.dy$, do not obey the usual laws of algebra. This is because the double integral $\iint dx.dy$ represents a signed area, positive or negative; and interchanging x and y turns a left-handed coordinate system into a right-handed one, multiplying all areas by -1. In other words, one must set up the formation to make $dx.dy=-dy.dx$. Grassmann's progressive product obeys the same kind of law. Cartan found that the regressive product added nothing to his theory, and he quietly abandoned it. Until now, its demise has gone unmourned.

The new work of Barnabei *et al.* is part of an extensive programme of research that Rota has carried out for more than a decade, applying combinatorial methods to invariant theory. Classical invariant theory is the study of expressions that remain unchanged when their variables are transformed in particular ways. A simple example arises in connection with quadratic equations $ax^2+bx+c=0$, for which there is a well-known formula involving square roots of b^2-4ac. This quantity is called the discriminant, because it vanishes precisely when the two roots of the equation are equal. Suppose the variable is changed from x to $x+h$. Then the quadratic becomes $(x+h)^2+b(x+h)+c$, or $ax^2+(2ah+b)x+(ah^2+bh+c)$. Write this as Ax^2+Bx+C. Now compute the new discriminant: $B^2-4AC=(2ah+b)^2-4a(ah^2+bh+c)=b^2-4ac$. Thus the formula for the discriminant does not change, although the variable x does. It is called an invariant of the transformation.

Invariant theory was invented around 1850 by Arthur Cayley and James Joseph Sylvester. It considers more complicated expressions than only quadratics, and more complicated transformations than $x \to x+h$. The fundamental problem in the theory is to prove that, in any particular case, the full system of invariants can be expressed in the terms of a finite subsystem, called a basis. The main classical method is to describe explicitly all invariants and to exhibit such a basis. By such methods Paul Gordan, the 'king of the invariants', proved in 1868 that for any expression in two variables, a finite basis exists. Limited extensions were proved by Gordan and others, but progress became painfully slow as ideas were overwhelmed by a swelling mountain of calculation.

In 1888 David Hilbert created a tremendous stir by proving that a finite basis always exists — and he did it without calculating any invariants at all. He used only very general abstract properties of systems of polynomials. "This is not mathematics", Gordan complained, "it is theology". But theology won the day, and explicit computation of invariants went out of fashion, being replaced by a much more abstract, higher level approach that gave conceptual ideas pride of place. But history tends to run in spirals, and in recent decades there has been something of a classical revival, inspired in part by the needs of other branches of mathematics, and by applications. Explicit formulas, rather than existence results, are often desirable. Rota, an expert in combinatorics, has developed a powerful approach to such problems: his methods manage to be both conceptual and computational at once. How does one achieve such a balancing act? By making the notation reflect the concepts. As a result Rota has become the Edgar Allen Poe of mathematics, exhuming Grassmann's regressive product from its premature burial.

Barnabei *et al.* motivate their ideas in terms of three important types of transformation: orthogonal transformations are essentially rotations in a multidimensional space; symplectic transformations arise from mechanics; and a general linear transformation is, as its name implies, the most general transformation that keeps straight lines straight. Barnabei *et al* summarize the standard results in the first two cases as follows: (1) a Hilbert space is a vector space having a symmetric form (x,y). That is, $(x,y)=(y,x)$. A transformation T is orthogonal if it preserves this form, that is, $(Tx,Ty)=(x,y)$. Invariants under orthogonal transformations are polynomials in the symmetric form. Computations in Hilbert space are carried out in a naturally associated algebra, the Clifford algebra; (2) a symplectic space is a vector space having an antisymmetric (or symplectic) form $[x,y]$, that is, one such that $[y,x]=-[x,y]$. A transformation is symplectic if it preserves this form. Invariants under symplectic transformations are polynomials in the symplectic form. Computations occur in a naturally associated algebra, the Weyl algebra.

The parallel between these two theories is striking, and it suggests a fruitful question: is there an analogous setting for the general linear group? Barnabei *et al.* show that the answer is yes. They define a Peano space to be a vector space having a bracket $[x,y,z,\ldots]$. Invariants under the general linear group are polynomials in the bracket. Computations are carried out in a naturally associated algebra, the double algebra. It is so called because it has two operations (rather than the usual one). They are, of course, modern versions of Grassmann's regressive and progressive product. *Plus ça change...*

Ideas that are ahead of their time do not always find immediate favour, and those that are not appreciated tend to be forgotten. But it is hard to keep a really good idea down. It was Grassmann's tragedy to be ahead of his time, but it is a mark of his genius that his ideas are now coming to full flower. □

Ian Stewart is in the Mathematics Institute, University of Warwick, Coventry CV4 7AL, UK.

Cell biology

Origins of the cytoskeleton

from Carl M. Cohen

A REPORT by Catherine Woods and Elias Lazarides on page 85 of this issue[1] shows that our understanding of membrane skeletal biogenesis shares at least one characteristic with the cells in which it has most recently been studied — both are embryonic. Lazarides and co-workers have recently provided us with fascinating insights into membrane skeletal biogenesis in chick embryo erythroid cells. Although these cells are nucleated, they nonetheless contain a membrane skeleton composed of the protein complex spectrin–actin–band 4.1 as well as the spectrin-binding protein ankyrin (goblin) which links spectrin to the integral membrane protein band 3. Lazarides' group has interpreted their observations in terms of a 'receptor-driven' membrane skeletal assembly, that is, that the amount of band 3 (the 'ultimate' membrane skeletal receptor) limits the amount of newly synthesized ankyrin that gets incorporated into the skeleton. Ankyrin is then thought to limit the amount of spectrin β chain (containing the ankyrin-binding site) which in turn limits spectrin α-chain incorporation[2]. According to this scheme, spectrin chains that are not incorporated into the skeleton as α/β heterodimers, α_2/β_2 heterotetramers or higher hetero-oligomers are degraded[3,4].

A major question raised by this model is how the unassembled chains are targeted for destruction. Woods and Lazarides' new work[1] suggests that α and β chains not incorporated into the skeleton pass their brief existence as homo-oligomers, either α_2 or β_4. These oligomers are largely incapable of forming stable functional associations within the membrane skeleton and the cytosol, and are somehow marked for destruction.

The possible existence of spectrin homo-oligomers runs counter to a small body of literature suggesting that such complexes do not form, or are rare, in solutions of purified α or β chains[5–8]. But these studies were done on mammalian erythrocyte or brain spectrins, and there may be important differences between chicken and mammalian spectrins. Although chicken non-erythroid and human erythroid spectrin chains have much in common, these two forms are probably the most widely divergent among the spectrin-chain family[9–11]. (Because chickens apparently possess only a single spectrin gene, the same must hold for chicken erythroid spectrin.) More to the point, recent unpublished studies by M. Mooseker, J. Coleman and J. Morrow at Yale University show that purified chicken erythroid β-spectrin chains have a remarkable propensity to self-aggregate. This is apparently true of fodrin chains as well[12]. Taken together, these studies suggest that for most spectrins, self-oligomerization of spectrin chains, particularly the β chain, may be the rule rather than the exception.

Intriguingly, the chains making up homo-oligomers in the chick cytosol seem to be perfectly capable of forming heterodimers if the homo-oligomers are first denatured and then mixed with their partners under appropriate renaturing conditions. Thus, there is nothing inherently different about those chains that end up as homo-oligomers. What, then determines the proportion of spectrin chains that end up as heterodimers? Is the proportion regulated by membrane-bound ankyrin? If not, what happens to the heterodimers that are synthesized in excess of ankyrin? Woods and Lazarides find no evidence for unassembled heterodimers in the cytosol of chick erythroid cells after translation *in vivo*. Are unassembled heterodimers also somehow targeted for destruction?

It seems likely that heterodimerization would take place in the cytosol during or soon after synthesis in order for the chains to be protected from self-oligomerization. In fact, the proposition that the α/β heterodimer (or α_2/β_2 heterotetramer) may form before its incorporation in the skeleton makes sense in the context of the known functional capabilities of spectrin chains. Several groups have shown that the high affinity association of spectrin in the spectrin–actin–band 4.1 complex requires an α/β heterodimer (or α_2/β_4 heterotetramer) even though isolated α and β chains bind to band 4.1 quite well[5,8]. Even fodrin, which can apparently bind to actin filaments without the need for band 4.1, must be heterodimeric for the association to occur[7]. Thus, it is more appealing to envision a fully competent heterodimer or heterotetramer forming a stable link in the nascent membrane skeleton than a single β chain arriving and waiting for its α mate.

If the homo-oligomer degradation route is operative in mammalian cells it may be less stringent, but the same principles may still apply. For example, in mice with any one of several genetic defects at the *sph* locus there is no α spectrin synthesized, whereas β spectrin is synthesized at a nearly normal rate. Almost normal amounts of β spectrin are bound to the reticulocyte membrane skeleton, and about 20 per cent of normal



More stamps for comet Halley (courtesy of Crown Agents Stamp company). First results from the Soviet, Japanese and European spacecraft encounters with comet Halley will be published in a special supplement in *Nature* on 15 May.

1. Lazarides, E. & Woods, C.M. *Nature* **321**, 85 (1986).
2. Lazarides, E. & Moon, R.T *Cell* **37**, 354 (1984).
3. Blikstad, I., Nelson, W.J., Moon, R.T. & Lazarides, E. *Cell* **32**, 1081 (1983).
4. Woods, C.M. & Lazarides, E. *Cell* **40**, 959 (1985).
5. Calvert, R., Bennett, P. & Gratzer, W. *Eur. J. Biochem.* **107**, 355 (1980).
6. Yoshino, H. & Marchesi, V.T. *J. biol. Chem.* **259**, 4496 (1984).
7. Davis, J. & Bennett, V. *J. biol. Chem.* **258**, 7757 (1983).
8. Cohen, C.M. & Langley, R.C. *Biochemistry* **23**, 4488 (1984).
9. Birkenmeyer, C.S. *et al. Proc. natn. Acad. Sci. U.S.A.* **82**, 5671 (1985).
10. Glenney, J.R. & Glenney, P. *Eur. J. Biochem.* **144**, 529 (1984).
11. Wasenius, V.-M., Saraste, M., Knowles, J., Virtanen, I. & Lehto, V.-P. *EMBO J.* **4**, 1425 (1985).
12. Glenney, J.R. & Weber, K. *Analyt. Biochem.* **150**, 364 (1985).
13. Barker, J.E., Bodine, D.M. & Birkenheimer, C.S. in *Membrane Skeletons and Cytoskeletal Membrane Associations* (eds Cohen, C.M., Bennett, V. Lux, S. & Palek, J. (Liss, New York, in the press).

is retained in red cell membranes at steady state[13]. This suggests that whatever form the β chain is in, most of it makes it to the reticulocyte membrane skeleton without being degraded. Subsequently, 80 per cent of the β chains are degraded, presumably because they fall off the membrane (as oligomers?). These and other instances documented in mice[13] show that the mere presence of single chains (be they monomers or homo-oligomers) does not dictate immediate destruction. Possibly, if the chains make it to the membrane soon enough they are spared. In cases where there are no heterodimers to compete for membrane binding, the β chains may have a higher probability of associating with the membrane and escaping degradation, if only transiently.

Interesting as these studies are for those in the membrane skeleton field, there are also paradigms emerging which may be more general. The notion that post-translational folding, and hence the fate of a protein, may depend as much on the presence or availability of other protein subunits as on primary structure clearly has wide implications (see ref. 2 for review). Also, the rather unorthodox characteristics of the degradation of excess α and β chains (the former ATP dependent and lysosome-like, and the latter ATP independent) suggests that more surprises are in store the deeper we probe membrane skeletal beginnings. □

Carl M. Cohen is in the Department of Biomedical Research at St Elizabeth's Hospital, Tufts University School of Medicine, Boston, Massachusetts 02135, USA.

Information technology

New flow of ideas in networks

from Alistair Mees

FLOWS in networks are a common feature of today's world — they may involve physical quantities such as traffic in a city, or information in a telephone or computer network. Many problems that do not at first sight directly concern network flows can easily be converted to that form: railway scheduling and project management are well-known examples. Until recently only simple versions of such problems have been easy to solve. But now a new mathematical approach opens the way for greatly improving the efficiency of the solution of common, hard problems.

With the advent of ever more complicated networks, particularly in telecommunications, rapidly increasing amounts of computer time are needed to answer questions such as: what is the capacity of a particular network and how should the flows be arranged to attain it; and what is the cheapest way to expand a network to have a particular capacity?

For the simplest sort of network flow, in which there is only one commodity flowing (for example a network of pipes carrying water, or an electricity grid), many problems can be solved by existing methods (Ford, L.K. & Fulkerson, D.K. *Flows in Networks* Princeton University Press, 1962). The methods are good both because they are intuitively 'right' — a feature which is more important in mathematics than is often admitted — and because they are efficient for use on computers. For instance, think of a network with capacity limits on the arcs (the lines), where there is a single source and a single destination, and we want to find the maximum traffic capacity. The famous Ford–Fulkerson method finds a route from source to destination; looks for the bottleneck on it which determines the maximum capacity of that route; and pushes through that amount of traffic. That particular route is now blocked because the bottleneck is operating at maximum capacity. The method now finds another route and does the same, continuing until all routes are blocked by previous traffic. We now have the maximum flow that the network is capable of carrying.

More sophisticated problems, for example those in which there are costs associated with different routes, can be solved by related methods. The 'out-of-kilter' algorithm is one, in which certain conditions are checked for each arc, which it is said to be out of kilter if they do not hold: the algorithm uses a route-search-and-block method successively to put arcs into kilter. (This is the only time I have ever heard the expression 'in kilter'.)

The most important mathematical feature of these methods is that they are based on results from duality theory. Duality refers to the fact that for every optimization problem there is a related problem which (under some convexity conditions that hold in the cases under discussion) has the same solution. For example, the basic Ford–Fulkerson result is actually a duality theorem which states that maximum flow equals minimum cut, meaning that if the network is cut so that the source is in one part and the destination in the other, the sum of the capacities of the broken arcs is always at least as big as any allowed flow, and for certain cuts it will equal the biggest possible flow. Duality theory pervades the mathematical theory of optimization and often has a price or a game-theoretic interpretation: if we let the capacity of an arc be the cost of breaking it, the Ford–Fulkerson result could be expressed in terms of an attacker who tries to isolate the source from the destination, and a defender who tries to make the attack as expensive as possible. The conditions for an arc to be in kilter in the more general problem come directly from duality theory.

Things get harder when we talk about multicommodity flows, in which there may be distinct kinds of traffic, with different sources and destinations, all sharing the same capacitated network. This is a lot closer to many real-world problems, but the ideas that were good for single-commodity flows do not work well: if one kind of traffic is maximized, another kind may be blocked, although some different arrangement would allow both flows to coexist. Trying out different arrangements from scratch quickly leads to a combinatorial explosion in which the number of options to try grows exponentially fast with the size of the network or with the number of commodities. Exponential growth of the time taken to solve a problem means that beyond a certain size of problem (in this case probably rather a small size) it becomes impossible to find solutions with present technology, and any future improvements in computing power will only marginally increase the size that can be managed. There is nothing for it but to look for better algorithms.

Multicommodity problems have been solved by linear programming methods (Assad, A.A. *Networks* **8**, 37; 1978), but because they transform to very special and degenerate linear programs this is an inefficient way to proceed: only problems of a rather modest size can be solved.

Recent work by Soviet mathematicians shows promise in solving multicommodity problems in the same sort of nice way that single-commodity problems are solved. An entire issue of the journal *Discrete Applied Mathematics* (**11**; 1985) is devoted to a paper by M.V. Lomonosov describing combinatorial approaches to multicommodity flow problems. There are many theoretical and algorithmic ideas in this long paper, some of them new and some of them summarizing recent work by the author and his colleagues, particularly A.V. Karzanov, most of which has not previously been published outside the Soviet Union. Duality theory is as central as ever, with Ford and Fulkerson's max-flow min-cut theorem being extended, but perhaps the most practically useful ideas are switching techniques that give systematic ways to unlock a multicommodity network and allow different flow patterns. Switching and draining transformations are introduced to allow flows to be rearranged without reducing the traffic amounts. Providing systematic transformations between different flow patterns is an important step towards overcoming the combinatorial explosion: the

fact that these transformations do not reduce flow may mean that, as with the simplex algorithm for linear programming, rather a small number of different arrangements can be stepped through to reach the optimum.

It is too early to say whether these new ideas will lead to significantly greater efficiency in solving multicommodity problems. The paper deals only with certain specialized flow problems, so it is roughly analogous to the situation with the Ford–Fulkerson approach before the out-of-kilter algorithm was developed. Lomonosov does not discuss algorithmic efficiency directly, nor does he give explicit examples, but it is likely that his methods will prove good for some kinds of problems. If this turns out to be the case, we may hope for extensions to more practically realistic problems and perhaps a large increase in the size of multicommodity problems that can be solved. □

Alistair Mees is in the Department of Mathematics at the University of Western Australia, Nedlands, Western Australia 6009, Australia.

Molecular biology

Self-incompatibility in plants

from John Fincham

In many families of flowering plants, exemplified by the Solanaceae (which includes the genera *Nicotiana* and *Lycopersicon*), self-pollination is prevented by a genetic system based on multiple alleles at what appears to be a single locus which is given the symbol *S*. Impressive progress towards the goal of discovering what the products of the *S* allele are and how they relate to each other in molecular terms has recently been made by two groups, first by J. B. Nasrallah *et al.* from Cornell University (*Nature* **318**, 263; 1985) and now by Anderson *et al.* of Melbourne University and reported elsewhere in this issue (*Nature* **321**, 38; 1986).

It is known that pollination is blocked only when the same allele is present in the germinating pollen grain and the style down which it is trying to grow. Because wild populations of outbreeding species usually have tens or even hundreds of *S* alleles, this system ensures that the great majority of random cross-pollinations are fertile. In some plant families, including the Cruciferae and its best-known genus *Brassica*, there is a variant system in which pollen expresses one or both of the *S* alleles present in the diploid plant which bore it, even though each pollen grain, as a haploid product of meiosis, retains only one allele. The difference between the two systems is presumably one of timing of *S*-locus expression — post-meiotic in the Solanaceae and pre-meiotic in the Cruciferae — and does not necessarily imply any fundamental difference in the functions of the products of the respective *S* loci. In each case, incompatibility evidently results from some kind of interaction between products of identical *S* alleles.

What is the mechanism of this self-recognition by *S* alleles? There are two possibilities. If one supposes that the *S* locus is really a single gene, encoding the same protein in pollen and style, one can think in terms of dimerization of similar protein monomers, located respectively on the cell surface of the pollen tube and in the cell sap of the style. The alternative is to postulate that the *S* locus is a complex of at least two genes expressed respectively in pollen and style, with each *S* allele encoding a stylar product and a different but complementary pollen product. The second model does not require the products of any particular *S* allele (more accurately termed a haplotype) to bear any specific structural relationship to those of any other — each haplotype could evolve independently, subject to selection only for self-recognition. A bipartite structure of the *S* locus has, in fact, long been postulated as an explanation of *S* mutations, which tend to affect pollen and style reactivities independently.

The breakthrough by the Cornell group was the molecular cloning of a complementary (c)DNA sequence representing an abundant style-specific messenger (m)RNA in *Brassica oleracea* of genotype S_6S_6 (obtained by forced self-pollination). When used to probe restriction-endonuclease digests of DNA from plants carrying other *S* alleles, this cDNA clone revealed a restriction fragment size polymorphism that was closely and perhaps inseparably linked to the *S* locus; each *S* allele was associated with its own specific array of restriction sites within the region covered by the probe. Moreover the cDNA, when cloned into an expression vector, was translated in *Escherichia coli* into a protein product that reacted with an antiserum made against a glycoprotein of relative molecular mass (M_r) ~ 85,000 that had been found specifically in styles of plants bearing allele S_6. Only a partial sequence of the cDNA clone has been published so far.

The starting point for the Australian group was the finding of an abundant glycoprotein of M_r ~ 32,000 in styles of *Nicotiana alata* (tobacco) plants carrying allele S_2. Somewhat surprisingly, no glycoprotein of comparable abundance was isolated by the same method from plants carrying other *S* alleles, which raises the possibility that different *S* alleles have very different stylar products. Determination of part of the N-terminal amino-acid sequence of the M_r 32,000 protein permitted the synthesis of a mixed DNA probe for the encoding gene, and the gene was indeed recovered by this means from a cDNA library made from mRNA of styles carrying S_2. Sequencing of the cDNA clone revealed an open reading frame encoding a 204-residue polypeptide chain with a 22-residue N-terminal hydrophobic portion (presumed signal sequence) leading into the sequence already found at the N-terminus of the mature glycoprotein. The cDNA hybridized strongly to DNA of plants carrying S_2 and much more weakly to DNA of plants with other *S* alleles, suggesting again that the different *S* alleles have very subtantially different coding sequences and only remotely related stylar products. There is as yet no direct evidence about the extent and nature of the inter-allele differences within *N. alata*, but Anderson *et al.* do present some preliminary information from another Solanaceous species, the wild tomato *Lycopersicon peruvianum*. A part of the N-terminal sequence has been obtained from two different stylar glycoproteins associated with different *Lycopersicon S* alleles; these are clearly homologous with each other (although there are also several differences) and also with the N-terminal sequence of the *N. alata* S_6 protein. Disappointingly, but not surprisingly, no similarity is visible as yet between the *Nicotiana* or *Lycopersicon* sequences and the limited amount of sequence available from the *Brassica* S_2 protein.

Clearly we are at the beginning of what is bound to be a period of intense activity as these highly promising observations are carried further. Several questions are now readily answerable. We should soon see some full-length comparisons between the DNA sequences of different *S* alleles (or at least those parts of them governing the stylar products); it should soon become apparent if there is any homology between the *Nicotiana*/*Lycopersicon* and *Brassica S* loci. More difficult, but probably not long delayed, will be the identification of *S*-allele products in the pollen tube and the cloning of the corresponding DNA sequences. If the *S* locus really does have separate pollen- and style-specific products with seperate coding sequences, much may depend on how close together these sequences are in the genomic DNA. If they are separated by only tens of kilobases, walking from one to the other should not be difficult; but if they are hundreds of kilobases apart, as they could be and still be almost inseparably linked, there will be more of a problem. □

John Fincham is Professor of Genetics at the University of Cambridge, Downing Street, Cambridge CB2 3EH, UK.

Keeping supercomputers under control

SIR—The Purdue Water Resources Reseach Center in conjunction with the Office of Health and Environmental Research of the US Department of Energy recently co-sponsored a meeting on the current uses of, and future needs for, supercomputers in hydrology. 'Supercomputers in Hydrology: Future Directions', the first meeting of its kind, aimed to evaluate the need for large-scale vector and parallel processing machines and their peripherals in the hydrologic sciences, especially in subsurface hydraulics. While the charge of the seminar was to specifically deal with hydrologic applications of supercomputers, the conclusions drawn at the meeting apply equally well to many other fields of science and technology.

Almost all technical issues involving the use of supercomputers were presented either by a computer scientist, a programmer or an applied mathematician. Because the architecture of most supercomputers is radically different from scalar processing machines, this is no surprise. The real importance of this observation is the implied increase in need for multidisciplinary research teams to solve major ecological problems. Unfortunately, in the United States, many of the larger supercomputer funding initiatives do not address this issue at all.

This defect in the supercomputer initiatives leads to two major problems: scientists not doing 'science' and the inefficient use of supercomputers. If funds were available to support programmers with expertise on a machine of a certain architecture, the scientist would only need to communicate effectively with the programmer. The projected changes in architecture affect the programmer and not the scientist; hence the scientist is free to do science.

An alternative to long-run funding of programmer-consultants is for the initiatives to increase their effort in the development of very high level languages. Rice of Purdue's Computer Science Department gave a talk on projected advances in hardware and software over the next 10 years. From 1975 to 1985 computing speed increased by a factor of 25. Between 1985 and 1995 the speed is projected to increase by a factor of 2,000. On the other hand, from 1975 to 1985, computer languages have been improved by a factor of only 1.4. Unless more funding is made available for the development of high-level languages, improvement in ease of coding is not expected to increase nearly as fast as machine computational power. In fact, because of radical changes in architecture, programming may well become more difficult.

Another important point brought out at the seminar is that advances in science should not be overpowered by advances in computational capability. Do we really improve our fundamental understanding of science by looking at larger and larger computational problems? Many would argue that the understanding of complex chemical and physical interactions in the subsurface and the ability to estimate parameters is so poor that the large supercomputer models may in fact be totally incorrect. In this instance, supercomputer modelling efforts may turn out to be a greater obstacle to real progress than no model at all.

So there is clearly a role for supercomputers, but the extent of this role will depend on the availability of high level languages, expert programmer consultants working closely with multidisciplinary teams, exposure to different computational systems, and a judicious choice of problems with the aim of advancing our understanding of science.

JOHN H. CUSHMAN
Water Resources Research Center,
Lilly Hall of Life Sciences,
Purdue University,
West Lafayette,
Indiana 47907, USA

FRANK J. WOBBER
US Department of Energy,
Office of Energy Research,
Washington, DC 20545, USA

The real hazards of nuclear fallout

SIR—In his article "On minimizing the consequences of nuclear war"[1], Carl Sagan is misleading in his discussion of the dangers of radioactive fallout. Our remarks on this question are made in the spirit that the goal of scientists is to be as accurate and unbiased as possible in assessing the potential or alleged impacts of an event such as nuclear war, and that either minimizing or maximizing these consequences is a disservice to the general public and to decision makers who seek guidance. If scientists are not accurate, credibility is lost and messages from the scientific community will eventually be ignored.

To our knowledge, the serious consequences of local (or early) fallout, that which is deposited during the first 24 hours, have been accepted by the scientific community for over three decades. Projections of the intensity and extent of local fallout are highly sensitive to a number of variables, which helps explain why different assessments have produced widely different results. Uncertainties in these projections can be divided into three categories, those due to (1) the targeting scenario, (2) the fallout calculation model and (3) the selected meteorological conditions.

The targeting scenario contains variables such as numbers of weapons, the yield mix, fission fraction, height of burst and precise target locations. The height of burst (HOB) is of particular significance because air bursts do not produce significant local fallout, except for the possible rainout of debris from tactical yield weapons. Only when the fireball interacts with the ground (a ground level or near ground burst) does significant local fallout ensue. A reasonable assumption often made is that hardened military targets are targeted with ground bursts. For the 'softer' industrial and other military targets, maximum damage is accomplished by air bursts where the HOB can be optimized. The primary fires hypothesized in urban areas in 'nuclear winter' studies are assumed to be initiated by airbursts, because ground bursts have shorter range for initiating fires. Hence, maximizing smoke production implies minimizing local fallout. (2) Uncertainties in dose calculations in the best fallout models originate from several sources. These uncertainties are due to limited experimental calibration data, whether the modelled radioactivity is rigorously conserved, and whether time of arrival is properly accounted for. (3) Assumptions about selected meteorology — such as wind velocities, shears, precipitation patterns — affect the results. Hence local fallout assessments can vary greatly depending on these many assumptions.

In assessing the human impact of local fallout, additional factors must be considered. By far the most sensitive of these is the protection factor afforded by structures, such as homes, buildings, basements, and shelters. These structures can dramatically mitigate the unprotected dose assessments normally cited. An additional important consideration is the assummed lethal acute external whole body dose levels. Finally, for radiation exposure that is protracted in time, biological repair of the resulting damage is important in mitigating the effects'. This is especially important with regard to global fallout, where the dose is received slowly over many years. Dose effectiveness factors from 0.1 to 0.5 for chronic exposures have been suggested[2]. This means that a large chronic dose will have an effect equivalent to a much smaller acute dose. Any presentation that implies that our planet would be a radioactive desert of certain demise is not including these important factors in a balanced sense; hence, inaccurate and biased estimates can be created. Calculations of total fatalities produced by large-scale attacks on the continental United States undertaken by our group have produced estimates of fallout fatalities (after subtracting those already killed by blast and thermal effects) that range over almost two orders of mag-

R439

nitude. This large variation in fallout fatalities is well understood in terms of variations in the parameters discussed above.

As part of our contribution to the recent International Council of Scientific Unions (ICSU) SCOPE-ENUWAR study of the environmental effects of nuclear war[3], we undertook calculations of local fallout using the computer model KDFOC2[4], using single burst fallout patterns and a semi-empirical approach for multiple explosions. Calculations were done for a 6,000-megaton multi-phase counterforce-countervalue nuclear exchange. Results indicated that about 7 per cent of the land areas of the United States, Soviet Union and Europe would receive a minimum of 450 rads within 48 hours. This assumed no shielding and would apply to a population unprotected by structures. The SCOPE-ENUWAR study[3] was primarily concerned with direct effects on unprotected plants and animals and excluded direct effects on humans. In considering the direct effects on humans, protection factors and population distribution should be added into the picture, with the result that land area envelopes are reduced below 7 per cent by factors of several (land area envelopes scale very roughly as the inverse of the protection factor). As an example, a recent study[5] used protection factors of 3 for rural areas and 10 for urban areas. The figure of 30 per cent of all northern-midlatitude land areas receiving an acute mean lethal dose to humans obtained by TTAPS and quoted by Sagan[1] is clearly much higher than our SCOPE result, and we believe inaccurate and misleading.

There is a hint of *On the Beach* in Sagan's discussions of global fallout; the spectre of a cloud of lethal levels of radioactivity spreading around the globe. Our group first reported in 1983 that long-term total doses of 100 rem or larger in global fallout hot spots are possible[6]. Sagan refers to this, and then interjects the possible effects of a 100 rem acute dose on the immune system (a speculative new result). This may mislead the reader as there is an immense difference in the effects of an acute compared with a long-term (lifetime or 50-year) dose.

The calculations at Livermore on global fallout reported in 1983[6] were supplemented by additional work in 1984[7]. The original results using the GLODEP2 code[8] assumed an atmosphere unperturbed by smoke. These were supplemented by new work utilizing GRANTOUR[9], a fully interactive microphysical, three-dimensional global circulation model code developed at LLNL. Doses were calculated with and without smoke in the atmosphere to assess the impact of a perturbed climate on global fallout.

Our GLODEP2 calculations for strategic nuclear exchanges of 5,000 to 6,000 megatons predict that the 50-year unsheltered unweathered average external total body gamma dose levels in the Northern Hemisphere would be about 15 rads, and about 0.5 rad in the Southern Hemisphere. The maximum of 30 to 40 rads appears in the 30° to 50° north latitude band. Values predicted for the global population (chronic) dose are typically about 6×10^{10} person-rads. The dose in hot spots, obtained using an area grid of 10° latitude by 10° longitude, are a factor of 6 to 8 higher than the Northern Hemisphere averages. These results have an estimated confidence level of about a factor of 2. Some 50–75 per cent of the global fallout dose is due to the tropospheric injections of radionuclides that are deposited in the first month.

The additional calculations, utilizing GRANTOUR involving a perturbed nuclear winter atmosphere indicate that the above dose assessments would be about 15 per cent lower in the Northern Hemisphere and marginally higher (approximately 1 rad) in the Southern Hemisphere compared to the unperturbed atmosphere predictions. These results are consistent with the projection that smoke injections can increase vertical stability, inhibit precipitation, and increase interhemispheric transport. We note that the GRANTOUR calculations utilizing a fully interactive microphysical approach with a three dimensional global circulation model produced results that were in good general agreement with the GLODEP2 results that depended on empirical observations from past atmospheric tests.

These calculations have been presented at a number of scientific meetings, including the ICSU-SCOPE workshop on radiation held in Paris in October 1984. There, an international array of radiation experts reviewed this work in detail, and it then became a basis of the chapter of radioactivity in the SCOPE-ENUWAR report[3] and underwent additional external review by dozens of international experts. The effects of these levels of global fallout were summarized in the Report of the Paris Commission on Radiological Dose Assessments and Biological Effects[10]. It concluded "The long-term increase in genetic and carcinogenic effects on humans from global fallout is of the order of 1 per cent of the natural incidence and should be considered a second order effect." No mention is made of pro-dromal effects on humans because at these lifetime dose levels and considering biological repair, pro-dromal effects from global fallout would not be observed. This does not sound anything like the *On the Beach* scenario or the impression transmitted to the audience at the Washington Sheraton Hotel briefing held by Sagan and others on Halloween, October 1983.

It is true that our original calculations have not been published in a refereed journal, nevertheless they have undergone extensive external review. Sagan should perhaps heed the Biblical injunction "let he who has not sinned cast the first stone". Reference 2 in his paper[1] (EOS, **63**, 1018; 1982) is a 250-word unreviewed abstract of a paper that was to be given at the San Francisco meeting of the American Geophysical Union but was cancelled before presentation. Authored by the "TTAPS team", this unpublished paper was cited in Sagan's recent *Nature* article 10 times!

This work was performed under the auspices of the US Department of Energy by the Lawrence Livermore National Laboratory under contract No. W-7405-Eng-48.

JOSEPH B. KNOX

Atmospheric and Geophysical Science Division,
Lawrence Livermore National Laboratory,
Livermore,
California 94550, USA

CHARLES S. SHAPIRO

Department of Physics,
San Francisco State University,
1600 Holloway Avenue,
San Francisco,
California 94132, USA

1. Sagan, C. *Nature* **317**, 485–488 (1985).
2. *NCRP84 National Council on Radiation Protection and Measurement, Report 64* (Government Printing Office, Washington, DC, 1980).
3. Pittock, A.B., Ackerman, T.A., Crutzen, P., MacCracken, M., Shapiro, C.S. & Turco, R.P. *The Environmental Consequences of Nuclear War* Vol. 1 (Wiley, Chichester, 1985).
4. Harvey, T.F. & Serduke, F.J.D. *Fallout Model For System Studies* (Lawrence Livermore National Laboratory Report UCRL-52858, 1982).
5. Daugherty, W., Levi, B. & von Hippel, F. *Symposium on Medical Aspect of Nuclear War, Washington DC,* (National Academy Press, Washington, 1986).
6. Knox, J.B. *Proceedings of the Third Inernational Conference on Nuclear War,* Erice, Sicily, Italy (Laboratori Nazionali di Frascati dell' INFN); Lawrence Livermore National Laboratory Report (UCRL-89907).
7. Shapiro, C.S. & Edwards, L.L. *Scenario and Parameter Studies on Global Deposition of Radioactivity Using the Computer Model GLODEP2* (Lawrence Livermore National Laboratory Report UCID-20548, 1984).
8. Edwards, L.L., Harvey, T.F. & Peterson, K.R. *GLODEP2: A Computer Model for Estimating Gamma Dose Due to Worldwide Fallout of Radioactive Debris* (University of California, Lawrence Livermore National Laboratory Report UCID-20033, 1984).
9. Walton, J.J. & MacCracken, M.C. *Preliminary Report on The Global Transport Model GRANTOUR* (Lawrence Livermore National Laboratory Report UCID-19985, 1984).
10. Report of Commission of Radiological Dose Assessments and Biological Effects – Paris Workshop (*SCOPE-ENUWAR Newsletter,* October 1984).

Scientific Correspondence

Scientific Correspondence is intended to provide a forum in which readers may raise points of a rather technical character which are not provoked by articles or by letters previously published (where the Matters Arising section remains appropriate).

WAIT

until 14 August 1986

S.H.Yang

JAPAN

ANNOUNCING Volumes 10 & 11 in the internationally acclaimed series

PRACTICAL METHODS IN ELECTRON MICROSCOPY

edited by Audrey M. Glauert

"This is the standard manual that could hardly be improved, a must in any electron microscopical laboratory, and equally important to the beginner and the experienced investigator."
Bjoïn Afzelius Science Tools

Volume 11

Thin foil Preparation for Electron Microscopy

by **P. J. Goodhew**

This comprehensive volume covers all the commonly-used techniques for preparing thin specimens for transmission electron microscopy in material science. Full descriptions are given of both simple laboratory techniques and sophisticated commercial thinning equipment for electropolishing, ion beam milling and replica making.
All the stages involved in the production of a thin foil from a large piece of metal, ceramic, polymer or semi-conductor are described.

CONTENTS: Chapters. 1. Introduction. 2. Initial preparation of bulk specimens. 3. Final thinning: chemical and electropolishing. 4. Final thinning: ion beam thinning and mechanical techniques. 5. Preparation of specimens with difficult geometry. 6. Replica techniques. 7. Mounting and storing specimens. Appendix. List of suppliers. Subject index.

1985: xiv + 216 pages
Price: US $ 64.75/Dfl. 175.00
ISBN 0-444-80701-2
Hardback
Price: US $ 24.00/Dfl. 65.00
ISBN 0-444-80699-7
Paperback

Volume 10

Low Temperature Methods in Biological Electron Microscopy

by **A. W. Robards** *and* **U. B. Sleytr**

This volume gives a comprehensive description of the state of the art of low temperature methods for ultrastructural studies on biological specimens. The theory behind each technique is described to form a scientific basis upon which to build.
Methods given in each chapter are complete and self-explanatory. Clear flow diagrams and schematic drawings allow a fast access to each technique and possible combination of procedures.
The chapter on freezing is essential introductory reading for the other chapters. It gives an unique survey and analysis of the theoretical and practical aspects of the freezing of water and of biological tissues.
Although written for biologists, this book is highly recommended to materials scientists studying hydrated specimens by electron microscopy.

CONTENTS: Chapters. 1. Introduction. 2. Freezing. 3. Direct viewing and analysis of cold specimens. 4. Freeze-sectioning. 5. Freeze-drying. 6. Freeze-fracture replication. 7. Freeze-substitution and low temperature embedding. 8. Future Outlook. Appendix 1. Safety. Appendix 2. List of suppliers. Subject index.

1985: xx + 528 pages
Price: US $ 111.00/Dfl. 300.00
ISBN 0-444-80685-7
Hardback
Price: US $ 48.25/Dfl. 130.00
ISBN 0-444-80684-9
Paperback

Recent volumes in the series

Volume 9
Dynamic Experiments in the Electron Microscope
by E. P. Butler *and* K. F. Hale

Volume 8
Replica Shadowing and Freeze-Etching Techniques
by J. H. Martin Willison *and* Arthur J. Rowe

Volume 7
Image Analysis, Enhancement and Interpretation
by D. L. Missell

Volume 6
Part I
Autoradiography and Immunocytochemistry
by M. A. Williams
Part II
Quantitative Methods in Biology
by M. A. Williams

Volume 5
Part I
Staining Methods for Sectioned Material
by P. R. Lewis *and* D. P. Knight
Part II
X-Ray Microanalysis in the Electron Microscope
by John A. Chandler

Volume 4
Design of the Electron Microscope Laboratory
by Ronald H. Alderson

Series folder available on request, please apply to the publisher for details.

ELSEVIER

ELSEVIER SCIENCE PUBLISHERS
P.O. Box 211, 1000 AE Amsterdam, The Netherlands

Distributor in the U.S.A. and Canada:
ELSEVIER SCIENCE PUBLISHING CO. INC., P.O. Box 1663, Grand Central Station, New York, NY 10164-0028, U.S.A.

The Dutch guilder price is definitive. US $ prices are subject to exchange rate fluctuations. Prices are excl. B.T.W. for Dutch customers.

FL37A377

Reader Service No.8

Group selection revisited

Eric Charnov

Evolution Through Group Selection. By V.C. Wynne-Edwards. *Blackwell Scientific:1986. Pp.386. Hbk £29.50, $58; pbk £14.95, $29.*

NEARLY 25 years ago, V.C. Wynne-Edwards published a provocative and important book about the evolution of social behaviour. It was entitled *Animal Dispersion in Relation to Social Behaviour,* and in it Wynne-Edwards proposed that most features of vertebrate reproductive and social behaviour are adaptations whereby populations regulate their numbers and so avoid over-exploitation of their food resources. Most of the book was a discussion of biological examples of this process at work. Thus, clutch size, territoriality, dispersal, male display and competition for females, as well as other aspects of social interaction, were assigned functions in terms of population regulation — individuals practised reproductive restraint when necessary for the good of the group's resource management. Of course, such group-level adaptations would seem to require that natural selection acts mainly on the group, and not through individual reproductive success.

Animal Dispersion had an immediate impact. It drew an enormous following, and during the 1960s various ideas based on "group selection" became popular among many biologists and social scientists. The book's appeal may have stemmed from the intellectual climate of the time, combined with the facts that the main thesis was both morally satisfying and a *tour de force* of radical thinking: to explain so much with one simple principle!

Wynne-Edwards himself realized that *some* form of group selection was required by his theory; he clearly said so. And his main critics (D. Lack, W.D. Hamilton, J. Maynard Smith and G.C. Williams) immediately fired back. To them it seemed unlikely that natural selection at a group (or population) level could overcome selection at the level of individuals. Furthermore, most of the biological examples he discussed, and which he saw as beneficial in regulating a population, could, they considered, be more easily explained in terms of individual reproductive success. This latter criticism was even more important than those of the notion of group selection; alternative hypotheses, not considered by Wynne-Edwards, did a better job with the data, and his vision of individual reproductive restraint was illusory. So said the critics. However, by taking such a strong stand on the "why's" of social evolution, his book focused attention on the subject: ideas that were developed over the past two decades in opposition to his theory are prominent in much of the current thinking in sociobiology and behavioural ecology.

This new book is an up-date of *Animal Dispersion.* The first half includes a restatement of the hypothesis that populations manage their resources; again, most social interaction (at least in vertebrates) is seen as operating to regulate the population concerned. Following this is an account of the population and social dynamics of red grouse, the fruit of a superb long-term field study. In the second half of the book Wynne-Edwards discusses group selection as a process, both in theory and as seen against the data. He introduces one major new "population level benefit" hypothesis, describes a few case histories and ends with a good summarizing chapter. His new hypothesis, to which I shall come in more detail at the end of this review, is that populations benefit from managing their genetic structure; somehow, natural selection has favoured populations which control their mating system (for example monogamy versus polygamy), dispersal and other genetic characteristics which may be involved in the working of group selection. Simply, these controls exist and they function to facilitate the evolution of group benefits. They both facilitate group selection, and are themselves examples of it.



Subject of study — the red grouse, well-camouflaged in its natural habitat.

This new book is bound to be widely read and discussed. In my opinion, however, it suffers from many of the same problems as its predecessor. At issue here is not the *possibility* of group selection, but whether it has produced all (or many of) the behaviours and reproductive phenomena that Wynne-Edwards considers.

To develop this point, let us first consider the "resource management" hypothesis. Here I will pose three questions. Is it needed (in theory)? Is it supported by the evidence? Is it a likely outcome of a group selection process? This critique applies equally to the conceptual development of the author's theory and his case history of red grouse.

Wynne-Edwards claims that predator populations *must* regulate their numbers socially or they would typically decimate their prey populations; this applies also to herbivores and their food plants. But I know of nothing in population dynamics theory which generally supports this proposition. Numerous equations describing predator–prey interaction have stable or cyclical solutions. Predators may often be limited by their own predators, by parasites or by the availability of food of adequate quality. Density-dependent birth and death effects may operate in many ways, and may often stabilize the population at numbers far short of those required for resource destruction. The fact that individuals use social interaction to compete for food, space or mates does not necessarily support any hypothesis of population regulation; indeed, even if social interaction *does* sometimes regulate population size, such a density-dependent effect may simply be viewed as a by-product of individual reproductive competition. Wynne-Edwards's blanket claim — that we need social regulation or else . . . — is much too strong. (While I accept his key observation that predators do not usually decimate their prey, I doubt that anyone has studied how often this does or does not occur.) Of course, that "resource management" may not be needed *generally* does not mean it does not or cannot ever happen.

In the past 20 years we have greatly increased our knowledge of social evolution and natural selection, including group selection. Wynne-Edwards discusses a fair bit of this newer work on group selection, but he mentions none of the rest of sociobiological thought. Modern ideas on mating systems, sexual selection, sex allocation, territoriality and group structure, game theory and evolutionarily stable strategies — almost the entire contents of books such as *Behavioural Ecology*, edited by J. Krebs and N. Davies (Blackwell Scientific, 1984) or M. Daly and M. Wilson's *Sex, Evolution and Behavior* (Duxbury, 1983) — are virtually ignored. This is perhaps the book's greatest failing. At the very least, the author ought to have attempted to convince us by a fair contest of various ideas set against the evidence, especially when many workable alternatives were put forth in response to his

previous book. Although plenty of data are discussed, critical tests of hypotheses are not. We are, then, left with a work of advocacy.

Professor Wynne-Edwards appears to have adopted the position that the criticisms of *Animal Dispersion* simply mandated his finding, demanding only that he should demonstrate a mechanism of group selection which he has now found in the works of M.J. Wade and D.S. Wilson.

"Group selection is *not* different from natural selection. ..."

The concept of group selection has had a chequered history, and here I can give only a necessarily simplistic account of the arguments. Readers who wish to follow things up should refer to the review articles by M.J. Wade (*Q. Rev. Biol.* **53**, 101–114; 1978) and D.S. Wilson (*A. Rev. Ecol. Syst.* **14**, 159–187; 1983).

Group selection is *not* different from natural selection. Suppose a population is split into groups where the members within a group interact mostly with each other. As a result of social interaction, feeding, predator escape and so on, individuals produce offspring. Clearly, natural selection will favour attributes (genes building phenotypes) which confer higher reproductive success. But a phenotype's reproductive success or fitness may be thought to consist of two parts: the first is an individual's contribution of genes, relative to other members of its group; the second is the group's contribution of genes to the overall population. These are the within-group and between-group components of fitness. While not all theorists agree with this distinction, it is useful in showing that attributes may sometimes be selected for if they increase group productivity, even if their bearers do worse at reproducing relative to other members of their own group.

Of course, some attributes may increase *both* group productivity *and* an individual's fitness relative to other group members; these two components of fitness need not conflict. The strength of each component depends upon factors such as group size and stability, how groups are formed, dispersal patterns and so forth. Using a fairly extreme form of differential group productivity (extinction), Wade has demonstrated in laboratory experiments with *Tribolium* that the between-group component of fitness is sufficient to produce a fair amount of phenotypic change. A group-selection effect has also been shown in the field for the evolution of sex ratio in group-structured populations of parasitoid wasps and mites. Briefly, a sex ratio of 1:1 is favoured within each group, but the migrants or dispersers are all females and so the group productivity component of fitness favours a female-biased sex ratio. It is the within-group component of fitness that favours an equal sex ratio. The resulting sex ratio *is* often female biased, reflecting a balance of the between- and within-group components of fitness. This group-selection interpretation for the female-biased sex ratio is not accepted by everyone, and other explanations are possible. Yet I think it is a reasonable interpretation. So, the between-group component of fitness can influence evolution; it can sometimes affect the value of characters. In his 1983 review, Wilson suggested that the evolution of traits containing a strong component of self-sacrifice would probably require small groups with one or a few founders (or kin selection, see below), and he made the sensible suggestion that the traits most likely to be favoured with more diffuse groups would be those with high social (group) benefit and little personal costs. Altogether, biologists would do well to pay closer attention to the thoughts of Wilson and Wade.

Wynne-Edwards is doing much more, however, than arguing that selection can sometimes favour traits which benefit the group. He is claiming that such traits will *usually* evolve and will include traits for population regulation for resource management. He further asserts that such traits will often not be opposed by the within-group component of fitness; what benefits the group will usually benefit the individual within the group. Although this latter assumption supports his hypothesis, I can think of no compelling reason why we would find it to be true for the multitude of examples that Wynne-Edwards discusses. Furthermore, nothing in the literature particularly suggests population regulation as the typical or expected outcome; the example of sex ratio in wasps and mites was not at all related to potential over-exploitation of food resources.

"Wynne-Edwards is doing much more, however, than arguing that selection can sometimes favour traits which benefit the group. ..."

Another response to *Animal Dispersion* was the development of the theory of kin selection, mainly by W.D. Hamilton. There are several approaches to this question, one of which shows kin selection to be a special case of group selection, as discussed above. In the new book, Wynne-Edwards shows a curious love–hate relationship with kin selection. Early on he claims that it is a form of group selection; then, in the final two chapters, he totally rejects it in favour of group selection. Scattered throughout the book are various discussions of the inadequacy of kin selection to explain this or that; these are invariably followed by a glib claim that group selection will do the trick. I really do not know what to make of such statements.

I will end this review with a brief discussion of Wynne-Edwards's new proposal: that is, populations genetically structure themselves to foster beneficial processes such as group selection. I find this notion difficult to understand in terms of population-level adaptation. Let us consider an example. In Chapter 16, Wynne-Edwards uses the idea to explain a long-standing puzzle in the reproductive biology of Atlantic salmon. Immature fish (called parr) first spend a few years in fresh water, and then go to the sea to feed, grow and mature, before returning as adults to spawn in fresh water. The puzzle is that some parr (young males, who have not yet gone to sea) become reproductive, spawn and then turn off sperm production to join the usual out-migration to the sea. Some of these parr will undoubtedly return to spawn as adults. Wynne-Edwards's answer to this puzzle (why do parr become reproductive?) is that these fish are assigned the role of keeping genes in the group. Field data suggest that many adult fish do not return to their home stream to spawn; thus, the parr are the main bearers of in-group genes to the local group and this role is a form of genetic structuring favoured by group selection.

Three observations are in order. First, the population structure (with lots of mixing of fish from different groups during reproduction) is just that where group selection would not really work. Second, the population-level benefits of this "in-breeding" are not really specified (and totally escape me). Third, small breeding males are common in fish species and have now been studied in salmonids. The idea of the frequency-dependent fitness advantage of small males, in reproductive competition with larger males, has proved a very powerful tool in the analysis of these systems; this involves no postulated group benefit whatsoever. Readers of Wynne-Edwards's present book should compare carefully his explanation for the existence of these small breeding males with the evidence and interpretation of the same phenomenon by M. Gross (*Nature* **313**, 47–48; 1985). A fair contest of ideas would seem to be in order.

Animal Dispersion, or rather the responses to the extreme position adopted by Wynne-Edwards in that book, did much to discredit notions of group selection. For many people, the pendulum has swung from uncritical acceptance to equally uncritical rejection of the idea. I hope that the similarly extreme tone of *Evolution Through Group Selection* does not add further to that process. Natural selection, operating in a group-structured population, can sometimes produce the unexpected. And we still have so much to learn. □

Eric Charnov is a Professor in the Department of Biology, University of Utah, Salt Lake City, Utah 84112, USA.

Coming in to the cold

Daniel Branton

Low Temperature Methods in Biological Electron Microscopy. By A.W. Robards and U.B. Sleytr. *Elsevier:1985. Pp.551. Hbk $111, Dfl. 300; pbk $48.25, Dfl. 130.*

GREATER USE of low-temperature methods and frozen specimens in biological electron microscopy has resulted from recent advances in a variety of morphological and analytical applications, especially freeze-etching, immunocytochemistry and the direct examination of hydrated frozen specimens. While all of these applications depend upon the use of frozen specimens, workers experienced in one particular area will, upon reading Robards and Sleytr's book, discover well-developed traditions and critical manipulations that have simply not crossed the boundary between, for example, those laboratories engaged in freeze-etching and those doing cytochemistry of frozen sections. For the expert, this book is the equivalent of an informative tour of distant laboratories. Here they will learn of the latest "tricks" in freezing biological materials, direct viewing of frozen specimens, freeze-sectioning, freeze-drying, freeze-substitution, low-temperature embedding and freeze-fracturing.

The book will also be very helpful for the non-expert. It is a clear and accurate survey of a large number of methods, almost all of which are illustrated and wisely accompanied by detailed description and discussion. Although the amount of detail may appear excessive, success with low-temperature methods often hinges on apparently minute points. Freezing and freeze-etching methods are particularly well covered, and attention is given to tissue differences and important principles of sampling and interpretation that are often overlooked in "methods" books. Throughout, the authors provide critical comparisons and sufficient background and theory so that readers can decide for themselves what they can hope to gain by using low-temperature methods, and which method should be selected from the many available.

The book is abundantly illustrated but the graphics are often disappointing. The authors' attempt to be comprehensive is admirable, but the introductory diagrams are sometimes so cluttered with details of alternative pathways that many readers will have the impression of being given an unabridged chart of intermediary metabolic pathways before even having been introduced to the tricarboxylic acid cycle. An appendix listing suppliers of commercially available equipment is included, but it is not as useful as it could have been: there are too few listings under specific categories and little attention has been given to suppliers outside Europe.

A breakthrough in low-temperature electron microscopy has been the demonstration that biological specimens can be vitrified. Although some of the techniques for the preparation and direct viewing of vitrified specimens at high resolution are included, the coverage here is neither as well organized nor as complete as this promising area deserves. To be fair, these methods are very recent; but it is regrettable that Robards and Sletyr did not have more of an opportunity to comment on these advances, for they have otherwise produced a discerning and up-to-date reference work. □

Daniel Branton is Higgins Professor in the Department of Cellular and Developmental Biology, Biological Laboratories, Harvard University, 16 Divinity Avenue, Cambridge, Massachusetts 02138, USA.

Graded grains

Peter D. Moore

Numerical Methods in Quaternary Pollen Analysis. By H.J.B. Birks and A.D. Gordon. *Academic:1985. Pp.317. $59, £45.*

Pollen Records of Late-Quaternary North American Sediments. Edited by Vaughn M. Bryant Jr and Richard G. Holloway. *American Association of Stratigraphic Palynologists Foundation, PO Box 819047, Dallas, Texas 75381, USA:1985. Pp.426. $35.*

ONE of the most valuable features of pollen grains as palaeoecological material is their sheer abundance. Combine this with their capacity to survive well in peats and lake sediments, and we have in fossil pollen assemblages a splendid opportunity to use numerical methods for their analysis. This was immediately apparent to von Post when he first came upon pollen in peat and it has been exploited by all subsequent research workers in the area. Until the 1960s numerical analysis was restricted to the expression of pollen counts in terms of percentage values, but since then there has been rapid growth in ways of treating data in order to improve their value to the palaeoecologist. Among those who have led this field of enquiry, few have contributed more to its development than the authors of *Numerical Methods in Quaternary Pollen Analysis*.

In their book, Birks and Gordon present a critical review of the current state of each aspect of Quaternary palynology to which numerical techniques have been applied, commencing with the most obvious, the presentation of pollen data. The use of binomial and multinomial models, as originally described by Mosimann, is explained in some detail, though, as a basis for establishing homogeneity within a section of the stratigraphic profile, ordination methods are preferred. This involves the classification of samples, using spatial models, on the basis of dissimilarity indices.

This approach provides a number of opportunities to the palynologist, one of which is the establishment of objectively determined zones. These are subdivisions of the pollen profile into relatively homogeneous subunits for the sake of simplicity. In the early days a subjective approach to this process was considered perfectly adequate, since zones are simply aids to description of pollen proportions in time (that is, vertical space in the sediments) Recently many research workers have questioned the need for such zones at all, because they have led to a great deal of confusion in the past, while others feel that each of the main pollen taxa should be zoned independently. One wonders, therefore, whether sophisticated methods of zonation based on tests of homogeneity are necessary, but the practice is unlikely to do any harm and it may give confidence in the location of lines of maximum change.

Much more useful, in my opinion, is the application of the same group of techniques to follow the course of development of pollen assemblages through time, to compare one sequence with another and to set a fossil sequence in the context of modern pollen studies. Here the numerical approach comes into its own and many of those who doubted the value of these methods in the past, myself among them, have now become regular users.

Several variants of ordination methods are currently available for this type of work and they are well known to phytosociologists. These techniques are well explained by Birks and Gordon, and their application to palaeoecology is set out with clarity and enthusiasm. Many waverers have already been converted to their use and this book will be a means of initiating yet more palynologists into an increasingly fruitful type of analysis. Altogether, no palynological laboratory can afford to be without this compendium.

The second book under review, a manual of results rather than methods, is a long overdue synthesis of the vegetation history of North America through the late Pleistocene and Holocene. It is divided into geographical regions, ranging from Mexico to Alaska and Texas to Quebec, each dealt with by a different author. In each chapter representative pollen diagrams are reproduced and the variation in vegetation history is described, together, where appropriate, with assessments of climatic variations and human impact.

The emphasis is naturally upon vegeta-

tion change rather than methodology, but there are some helpful discussions of techniques such as the interpretation of alluvial pollen data in the drier regions, as in New Mexico, and the development of the isopoll vegetation maps in the north-east. The bibliographies supplied with each chapter are extensive and are a splendid point of entry to the relevant literature.

The timing of this volume is somewhat surprising, coming as it does on the heels of the two-volume *Late Quaternary Environments of the United States* (University of Minnesota Press/Longman, 1984). There is obviously a fair degree of overlap with that work, but the book reviewed here is confined to pollen data and is thus more detailed in vegetation descriptions and in its attention to regional variation.

Bringing so much information into one volume must have been a formidable undertaking and it has been brought off successfully only by careful planning and editing. Apart from finding a wide audience in North America, the book will be welcomed by palynologists on this side of the Atlantic who, perhaps, may be inspired to perform a similar service for Europe. □

Peter D. Moore is Reader in Ecology in the Department of Biology, King's College London (KQC), 68 Half Moon Lane, London SE24 9JF, UK.

"OUTSTANDING"

THE ATOMIC COMPLEX
by BERTRAND GOLDSCHMIDT

An accurate, complete and fascinating worldwide political history and personal memoir of nuclear energy — from the development of the bomb in World War II to today's nuclear energy complex and proliferation problems.

"READS EASILY"

Goldschmidt, a leading French scientist turned international statesman, reviews half a century of political moves, countermoves, international intrigue and manipulation. *The Atomic Complex* is a pragmatic look at the nuclear world today, carefully examining the terror nuclear weapons represent, but at the same time stressing the benefits of nuclear energy.

Order this 500 page best seller today.
$31 Hardbound $24 Softbound

American Nuclear Society
555 North Kensington Avenue
La Grange Park, IL 60525 USA

Reader Service No.12

Done with a will

Richard Passingham

The Brain Machine: The Development of Neurophysiological Thought. By Marc Jeannerod. Translated by David Urion. *Harvard University Press:1985. Pp.171. $16.95, £14.50.*

THE subtitle of *The Brain Machine* says that it deals with *The Development of Neurophysiological Thought.* It doesn't. In the original French the subtitle is *Physiologie de la Volonte,* and indeed the book turns out to be about the history of neurophysiological speculation about willed movement.

In Descartes' time people were credited with a will but animals were not. Descartes correctly conceived of the brain as a machine, although his conception of its workings was quaint. However, he also believed that by some mysterious process the machine was controlled by an indwelling soul.

Later physiologists, such as Hughlings Jackson, suggested a class division within the brain: based on the observation that damage to the motor cortex interfered with willed movements while leaving many automatic movements intact, the idea was that the lower centres catered for our animal needs, while the higher neocortical centres supervised our voluntary activities. Certainly, it is true that patients with such damage report that it is their subjective impression that moving the affected limb requires them to summon up an effort of will.

Jeannerod argues that "the elucidation of the term 'will', and the multiple concepts it covered, without doubt constitutes the central problem in comprehending the physiologic bases of the different aspects of movement" (p. 20), and in the various chapters of his book he covers some of these concepts. One issue is how a movement is triggered. We carry out some movements in response to external prompts, but there are others that we perform at our own direction and at our own pace. In accounting for spontaneous movement, the author mentions the spontaneous rhythms of the electroencephalogram and the oscillators proposed by von Holst. He also describes studies in which slow potentials are recorded from the cortical motor areas while subjects make simple movements. These potentials differ in their pattern and timing when it is the subject rather than the experimenter who decides when the movements are to be made.

A second idea is that of intention. Jeannerod argues that if a movement is intended the brain knows "what will happen as a result of its own action" (p. 97); that is, the brain is aware of its own commands and can therefore compare what happens with what was intended. A copy of the command to the motor system is sent to other centres, but if a movement occurs which is not intended there will be no such copy.

There is, too, a third notion: "Human action, when it is voluntary, intentional, or propositional, has the distinction of being dominated by language, in the sense that language precedes the action and is an integral part of the representation" (p. 121). More generally there must be a plan; people can try out possible actions in their heads before performing them. Recent technology has allowed us to detect evidence of such planning. When brain regions increase their activity they increase their metabolic requirements, and we can use the flow of blood to an area as a measure of its metabolic activity. It is now possible to take these measurements from the outside of the skull and thus to investigate the activity of brain regions in human subjects while they carry out mental work. If subjects are asked to rehearse mentally a set of finger movements without actually performing them, activity can be detected in the supplementary motor area.

Jeannerod's book gives the history of these and other ideas. He includes chapters on such topics as the natural history of the soul; hierarchy and integration of movements; the motor cortex; the physiology of spontaneity; representation, plan, programme; and action, the force of self-organization. He ranges widely, his theme taking him from animal spirits to electrical conduction, and from spinal reflexes in frogs to apraxia in the hospital clinic, and also into the realms of European philosophers such as Schopenhauer, Cassirer and Merleau-Ponty. Because the thrust of the book is primarily historical, Jeannerod says little of modern experiments in modern physiology. But the history of ideas on this subject is intriguing, and makes an altogether fascinating story.

The book is illustrated with line drawings, some of which are delightful: for example, the author reprints Descartes' splendid drawing of the mechanism for muscular contraction, a naive diagram by an alchemist of mental function and a beautiful drawing of a brain dissection done in 1827. The text has been well translated by David Urion, and it is to his particular credit that if the book were handed to someone who did not know they might fail to guess the language of the original. □

Richard Passingham is a Lecturer in the Department of Experimental Psychology, University of Oxford, South Parks Road, Oxford OX1 3UD, UK.

• Recently published by Raven is *The Citadel of the Senses,* by Macdonald Critchley, a collection of 30 short essays on episodes and personalities in the "prescientific age of neurology". The book costs $32.50, and will be reviewed in a future issue of *Nature.*

MICRO 86/ EUROSEM 86 7-11 JULY 1986

AT THE
BLOOMSBURY CREST HOTEL
CORAM STREET, LONDON WC1
(Close to Russell Square Underground (Piccadilly Line))

FIRST EUROPEAN SCANNING ELECTRON MICROSCOPY CONFERENCE

TO BE HELD IN CONJUNCTION WITH MICRO 86 (in Association with NATURE)

Topics will include

Monday 7 July 1986
AM Low Voltage SEM
PM High Resolution SEM

Tuesday 8 July 1986
ALL DAY Image Processing and Analysis

Wednesday 9 July
ALL DAY SEM in Semiconductor Technology

Thursday 10 July 1986
ALL DAY Surface Imaging and Analysis

Friday 11 July 1986
ALL DAY Biological SEM

For details of this and of the parallel MICRO Conference, please contact:
The Royal Microscopical Society,
37/38 St Clements, Oxford OX4 1AJ
Telephone: Oxford (0865) 248768/721081

MICRO 86 EXHIBITION

An important part of this unique International Exhibition will be a wide range of instruments and other equipment essential for Scanning Electron Microscopy and its Associated Techniques.

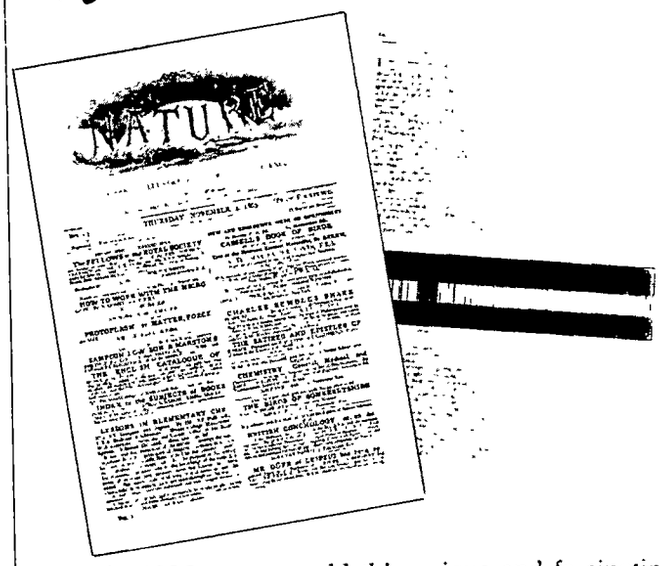
Admission to the Exhibition is FREE.

Further information is available from:
The Royal Microscopical Society,
37/38 St Clements, Oxford OX4 1AJ
Telephone: Oxford (0865) 248768/721081

Reader Service No.150

THURSDAY, NOVEMBER 4, 1869 WAS THE PUBLICATION DAY OF

Nature's first issue



Now in 1986 you can add this unique and fascinating issue to your own collection or offer it as an unusual gift to a friend or colleague.

Browse through J. Norman Lockyer's famous article "The Recent Total Eclipse of the Sun", discover how science was taught in schools in *1869* with W. Tuckwell or delve into T. H. Huxley's absorbing report on "Triassic Dinosauria".

These and other original articles are reproduced in **NATURE**'s high quality first issue facsimile available **NOW** from the address given below.

To: **Nature**, Macmillan Journals Ltd, Brunel Road, Basingstoke, Hampshire RG21 2XS, UK.

Please send me .....facsimile(s) of the first issue of NATURE.

I enclose ☐ **UK £2.00** ☐ **$3.00** Surface Rest of World ☐ **$4.00** Airmail Rest of World

Name _____

Address _____

Payment may be made in any currency at the prevailing exchange rate. Cheques should be made payable to **Nature**. Prices include postage and packing

Pharmaceutical Medicine

Editor Dr R. N. Smith
Assistant Editor P. J. Keen

. . . "a quarterly journal, which includes papers on the validation of new and established methods of testing drugs in man written by investigators both inside and outside the pharmaceutical industry. It also provides a forum for the exchange of ideas about issues affecting drug development. These new developments merit support from all involved in the management, sale and use of drugs." *Lancet*

Contents of Issue Three

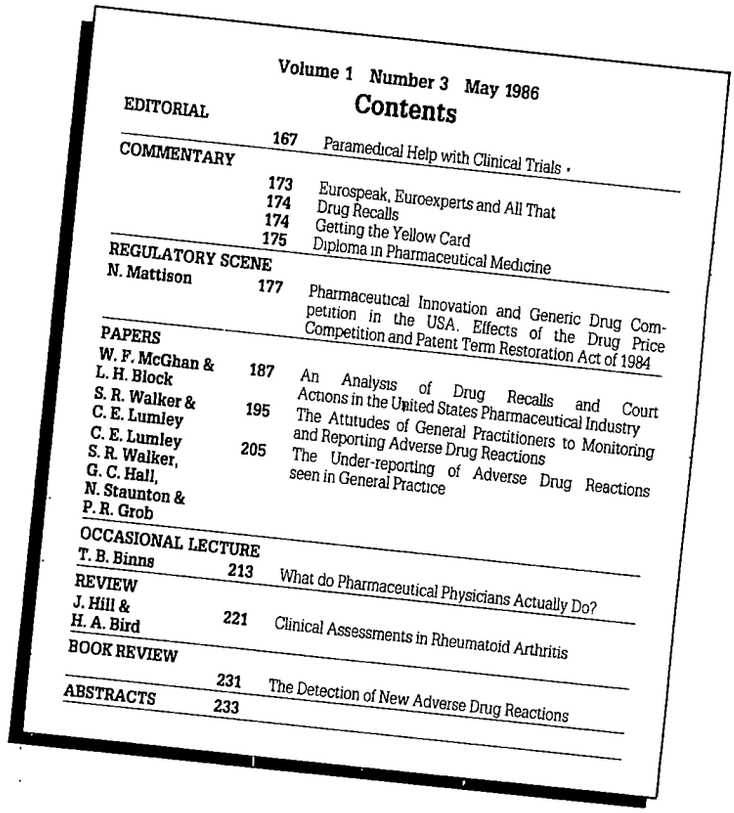
SUBSCRIPTION DETAILS:
Quarterly; one volume per year.

Rates: UK £45.00.

USA & Canada $168.00 accelerated surface post; $210.00 airmail.

Rest of World £120.00 accelerated surface post; £150.00 airmail.

Subscribe for two years and save money – simply double the payment sent!



Volume 1 Number 3 May 1986

Contents

EDITORIAL	167	Paramedical Help with Clinical Trials
COMMENTARY	173	Eurospeak, Euroexperts and All That
	174	Drug Recalls
	174	Getting the Yellow Card
	175	Diploma in Pharmaceutical Medicine
REGULATORY SCENE N. Mattison	177	Pharmaceutical Innovation and Generic Drug Competition in the USA. Effects of the Drug Price Competition and Patent Term Restoration Act of 1984
PAPERS W. F. McGhan & L. H. Block	187	An Analysis of Drug Recalls and Court Actions in the United States Pharmaceutical Industry
S. R. Walker & C. E. Lumley	195	The Attitudes of General Practitioners to Monitoring and Reporting Adverse Drug Reactions
C. E. Lumley, S. R. Walker, G. C. Hall, N. Staunton & P. R. Grob	205	The Under-reporting of Adverse Drug Reactions seen in General Practice
OCCASIONAL LECTURE T. B. Binns	213	What do Pharmaceutical Physicians Actually Do?
REVIEW J. Hill & H. A. Bird	221	Clinical Assessments in Rheumatoid Arthritis
BOOK REVIEW	231	The Detection of New Adverse Drug Reactions
ABSTRACTS	233	

☐ I would like to subscribe to **Pharmaceutical Medicine.** Please invoice me for:

two years/one year. Please invoice me for: _____

NAME _____

POSITION _____

ADDRESS _____

_____

Sample copies are available on request.
Return to Alison Baverstock, Macmillan Press, Houndmills, Basingstoke, Hants RG21 2XS, UK.

Macmillan Press Scientific & Medical

The mean mass density of the Universe

P. J. E. Peebles

Joseph Henry Laboratories, Princeton University, Princeton, New Jersey 08544, USA

Observations of galaxy clustering indicate that the mean mass density is only about one-third of that predicted by the popular Einstein–de Sitter cosmological model. Theory and observation can be reconciled if there has been large-scale segregation of galaxies from mass, but the gravitational instability of the expanding universe would tend to destroy such a segregation. Thus either conventional ideas about galaxy formation are wrong, or the Einstein–de Sitter model is not a useful approximation.

THE mass distribution of the universe is approximately uniform on a large scale, and can be described by two parameters: the mean mass density ρ and the expansion rate H. Conventional general relativity gravity theory indicates that if ρ is large enough the expansion eventually stops and the universe collapses to a singularity, while for small ρ the universe continues to expand forever. This conventional theory has two defects: it fails to explain why the large-scale mass distribution should be so close to uniform and its requires that the expansion can be extrapolated back to a singularity at a definite time in the past. As will be indicated below, Guth's[1] inflation model offers a partial solution to both problems. In the usual interpretation, inflation requires that the mean mass density ρ be equal to the critical value that separates universes that eventually collapse from those that expand forever, so that ρ has a definite value fixed by the expansion rate, H. However, as will be described, estimates of ρ based on derived masses of clusters of galaxies and counts of these objects are lower than the critical value by a factor of ~3. It is impressive that the observed density is so close to the expected critical value, but it is also apparent that the discrepancy is real. We can avoid the problem by recalling that the gravitational acceleration of a hollow spherical mass is zero inside the sphere. Thus estimates of the mass of a cluster of galaxies based on the accelerations of the galaxies in the cluster would miss any mass on the outskirts beyond the observed galaxies. The 'biased galaxy formation' model, in which galaxies form in islands surrounded by a sea of dark mass, can thus reconcile the observed mass density with the larger theoretically expected value. However, there is yet another consideration. The universe is gravitationally unstable, which means that gravity is drawing galaxies together to form an ever larger hierarchy of clusters. Because different forms of mass fall at the same gravitational acceleration, the gravitational instability draws mass together with galaxies. Thus if galaxies formed in tight islands, then the collections of islands formed later by gravity would be expected to yield a higher apparent mean mass density. The fact that this is not observed suggests that either galaxies formed in a different way from the standard picture, in islands large enough that all available observations miss the sea, or else that ρ really is smaller than the critical value.

The idea that the mean mass density might be expected to equal the critical value predates the inflation model. The historical development of this idea is reviewed in the next section, in order to show why the value of ρ has received so much attention and has so strongly influenced the direction of research in cosmology. There follows a review of observational estimates of ρ, which shows that the measurements are now sufficiently detailed to merit serious attention. Possible ways to reconcile the observations with the higher critical mass density are discussed next. Finally, I indicate how we might most simply adapt our ideas on cosmology if a low value of ρ is accepted.

Historical remarks

Cosmological models. In the general relativity cosmological model the rate of expansion, measured by the Hubble constant, H, and the mean mass density, ρ, are related by the equation

$$H^2=\frac{8}{3}\pi G\rho\pm\frac{c^2}{(aR)^2}+\frac{\Lambda}{3} \qquad (1)$$

The radius of curvature of space (measured at a fixed cosmic time, t) is $a(t)R$ (where R is the cosmic scale factor). Λ is Einstein's cosmological constant, and the dimensionless expansion parameter $a(t)$ is proportional to the mean proper distance between conserved particles (such as galaxies). G is the universal gravitational constant, and c is the speed of light. The mass density term is often written as $\frac{8}{3}\pi G\rho = H^2\rho/\rho_c = \Omega H^2$, where $\rho_c = 1.88\times10^{-29}h^2\,\mathrm{g\,cm^{-3}}$ and $H = 100\,h\,\mathrm{km\,sec^{-1}\,Mpc^{-1}}$. The length unit is 1 Mpc (megaparsec) = $3.1\times10^{24}\,\mathrm{cm}\simeq3\times10^6$ light yr. The dimensionless parameter h reflects the uncertainty in the Hubble constant; it is thought to be in the range $0.5\leq h\leq1$. The critical density is ρ_c. If $\Lambda=0$, as is usually assumed, then if $\rho<\rho_c$ the universe continues expanding indefinitely, and if $\rho>\rho_c$ the universe eventually collapses. The density parameter is the ratio $\Omega=\rho/\rho_c$ of the mean mass density to the critical value.

Arguments for $\rho=\rho_c$. The value of Ω is of course an observational question, but one gets a useful guide to its significance by reviewing the theoretical arguments which have been advanced in support of $\Omega=1$.

The cosmological model with $\Lambda=0$ and $\Omega=1$ is named after Einstein and de Sitter[2,3], who argued as follows: in the original static Einstein cosmological model the presence of a non-zero mean mass density ρ (with a reasonable pressure) requires that Λ and space curvature both assume specific non-zero values. By 1932 it was recognized that the static model is a special case; a positive mean mass density generally requires evolution in time (expansion or contraction of the universe). Einstein and de Sitter noted that in evolving models with non-zero mass density there is no requirement that Λ or space curvature be non-zero, and suggested that these terms might be dropped. De Sitter recognized that if $\Lambda=0$ and $R^{-2}=0$ it would require a rather large mean mass density, but he argued that this is not inconsistent with the observations. However, his estimates of the number density of galaxies and the mean mass per galaxy exceed the values found by Hubble[4], and in the more recent work summarized below.

In a second argument, one observes that the mass density term in equation (1) $\frac{8}{3}\pi G\rho$, varies at least as rapidly as $(a(t))^{-3}$,

the curvature term varies as $(aR)^{-2} \propto (a(t))^{-2}$ and the last term is $\Lambda/3 =$ constant. The three terms thus vary with time in three different ways. The values of these terms were presumably set as initial conditions in the very early universe when classical general relativity theory became a useful approximation and when the expansion parameter $a(t)$ was very much smaller than it is now. If $\Omega \neq 1$, at least two of the terms on the right-hand side of equation (1), density and one other, make an appreciable contribution to the present expansion rate, H. But because these terms vary with $a(t)$ in different ways, in the very early universe the two terms that are comparable now would have been vastly different, but by the highly special factor needed to make the terms comparable just now. This is an unlikely arrangement. The advantage of the Einstein–de Sitter model is that the one term we know is present, the mass density, always dominates. This attractive argument based on the undesirability of coincidences is not easy to find in the literature before the introduction of the inflation model, although Dicke[5,6] has advanced it for 25 years.

Wheeler[7] has long argued that Mach's principle, which states that inertial motion is defined by the mean motion of mass in the universe, sets boundary conditions for general relativity, requiring that space be closed, like the surface of a sphere. This eliminates Minkowski space (which is the limit to which an open expanding universe with $\Lambda = 0$ tends as $t \to \infty$), in which test particles have inertia but there is no background matter to define inertial motion. If $\Lambda = 0$ a spatially closed universe requires $\Omega > 1$, which means the density is high.

In Guth's[1] inflation model, the expansion of the universe can be traced back to a phase transition before which the energy density of space would have had a large, nearly constant term (which behaves like a large Λ-term) that would have caused space to expand as an exponential function of time (instead of the power-law expansion of the usual models). If this exponential 'inflationary' phase lasted long enough it could have stretched all characteristic lengths, in whatever chaos the inflation started from, to values larger than the maximum distance we can see, $cH^{-1} \simeq 3{,}000\ h^{-1}$ Mpc. That would account for the fact that we see such very small density gradients around the sky at depths $\simeq cH^{-1}$. But then it would have to follow that the radius of curvature $|aR|$, is also much larger than cH^{-1}, so the curvature term would have to be negligibly small in equation (1). The coincidence argument mentioned above says that Λ ought to be negligible. Particle physicists observe that Λ has the units of mass to the fourth power (with suitable factors of G, c and Planck's constant). A reasonable mass from particle physics yields a value of Λ suitable for the inflationary phase but more than 100 orders of magnitude larger than is now observationally acceptable[1]. The only other 'reasonable' value is $\Lambda = 0$, which brings us to $\Omega = 1$.

Finally, galaxy formation seems to be easier to understand if $\Omega \simeq 1$ because if $\Omega \ll 1$ the kinetic energy of expansion dominates the gravitational potential energy, thus suppressing the growth of mass concentrations by gravity[8], so that to get the observed degree of small-scale clustering of mass in galaxies and clusters of galaxies we would have to postulate larger initial mass-density fluctuations in the early universe, which would cause fluctuations in the microwave background that are uncomfortably large compared with the observational limits[9].

Exotic matter. Evidence for a low mean mass density in baryons comes from the computed production of elements in the hot Big Bang. It is difficult to see how the abundance of deuterium in our stellar neighbourhood could have been produced in stars. If an appreciable part of the deuterium were to have been produced in the early universe in the conventional hot Big Bang cosmology it would require a mass density of baryonic matter that (with a value of H in the standard range) would imply $\Omega \lesssim 0.1$ (ref. 10). However, as noted by Chapline[11] and Gott *et al.*[10], that constraint would be lifted if the mass of the universe were dominated by non-baryonic matter such as small black holes or massive neutrinos; the list of such possible exotic forms of dark matter is now quite long[12]. Thus it appears that if $\Omega = 1$ the mass of the universe must be dominated by exotic matter other than the material out of which we and stars and the bright parts of galaxies are made. There are some prospects for the experimental detection of exotic matter if it is present in our neighbourhood of the Galaxy[13].

Segregation of galaxies from mass. It was well established by the early 1970s that the 'seen' mass in the dense central parts of galaxies is well below what is required in the Einstein–de Sitter model, but there were already indications that there is considerably more mass in 'massive faint extended haloes' of galaxies[14]. Gott *et al.*[10], arguing partly from the nucleosynthesis constraint on the baryon density, concluded that $\Omega \simeq 0.06 \pm 0.02$. Ostriker *et al.*[15] and Einasto *et al.*[16] argued that there is in fact a lot of mass outside the bright parts of galaxies, the observations suggesting that the mass of a galaxy increases almost linearly with radius to at least ~1 Mpc, which would bring the density parameter to $\Omega \simeq 0.2$. If the trend of mass with radius extrapolated to the mean separation between galaxies, $\sim 4\ h^{-1}$ Mpc, it would bring Ω quite close to unity[17]; however, there has recently been considerable improvement in the dynamical estimates of masses on scales larger than that of a single galaxy and, as described below, it appears that the trend does not continue. If the mean mass per galaxy derived from the dynamics of groups and clusters were assigned to all galaxies it would yield $\Omega \simeq 0.3$, quite close to the estimates of a decade ago.

Although dynamical estimates of Ω use whole-galaxy masses (because they consider systems of galaxies) they could nonetheless underestimate Ω if there were a smoothly distributed mass component that has little effect on clustering dynamics. In the now standard version of this idea it is argued that galaxy formation would be expected to be biased toward regions of higher than average mass density, where galaxies could more readily form and survive. The current interest in this idea largely developed out of a series of papers that appeared in published or preprint form in 1984. Kaiser's[18] argument that clusters of galaxies may cluster more strongly than do galaxies themselves, because clusters are unusually dense spots that tend to have dense surroundings, was soon generalized to the suggestion that galaxies cluster more strongly than mass because galaxies form at unusually dense spots[19,20]. Rees[21] emphasized that it is easy to think of ways in which the formation of a galaxy could influence the formation of neighbours; and Davis *et al.*[22] found that N-body model simulations of the motion of pressureless matter in an Einstein–de Sitter model would give reasonable results if galaxies were located at the high (2.5 standard deviations) mass density peaks. Biased galaxy formation is the framework for most recent papers on galaxy formation[22–28].

Estimates of Ω

Three methods have yielded useful measures of Ω from galaxy clustering dynamics. We are in a small collection of galaxies, the Local Group, on the edge of a large cloud, the Local Supercluster (LSC), which is roughly centred on the Virgo cluster of galaxies. The mass concentration in the LSC produces an inward peculiar velocity field, v_v. We can hope to measure v_v and so derive the local peculiar gravitational field and hence the mass excess, δM, in the LSC. If this is a fair sample then the mean mass per galaxy in the LSC multiplied by the global mean number density of galaxies yields the global mean mass density[29,30]. Recent estimates[31,32] of v_v are in the range $150 \lesssim v_v \lesssim 450\ \mathrm{km\ s^{-1}}$. The concentration of bright galaxies within our radius in the LSC is $\delta N/N = 2.2 \pm 0.3$, where N is the expected mean number of galaxies for a homogeneous distribution and δN the observed number minus N. The recession velocity of the Local Group from the Virgo cluster is $cz = HR_v - v_v = 980 \pm 50\ \mathrm{km\ s^{-1}}$, where R_v is our distance from the centre of the mass concentration. (z is the redshift corresponding to this recession velocity.) If the material in the LSC is a fair sample,

so that the mass concentration is $\delta M/M = \delta N/N$, then these numbers yield[31-33]

$$0.05 < \Omega_{LSC} < 0.45 \quad (2)$$

The large spread results mainly from the uncertainty in v_v. To obtain $\Omega = 1$, v_v would have to be $\simeq 900$ km sec^{-1}, but it is unlikely that the observations could have missed such a large value. With the numbers given above, $\Omega = 1$ requires that the mass constrast in the LSC be $\delta M/M = 0.5$-1, which is a factor of 2-4 less than $\delta N/N$, and it is difficult to believe that the counts could be that far off. The connection between v_v and $\delta M/M$ assumes either linear perturbation theory or spherical symmetry. In an interesting cautionary example, Bushouse *et al.*[34] find that in N-body models the value of Ω derived from the mean v_v may be wrong by 30-50% (after correction for nonlinearity; A. Melott, personal communication). However, what such N-body models mainly show is a model velocity field considerably rougher than observed, indicating that the real mass distribution somehow stays a good deal smoother than in the models. One can estimate the possible effect of departure from spherical symmetry another way, by asking what transverse velocity, v_t, of our Galaxy (and its neighbours) relative to the LSC would be needed if the present gravitational acceleration of the LSC were balanced by the present centrifugal acceleration due to v_t. If $\Omega = 1$ the result is

$$v_t^2 = \frac{1}{2}\frac{\delta M}{M}(HR)^2 \quad (3)$$

With $\delta M/M = \delta N/N$ and the above numbers this yields $v_t \simeq$ 1,200 km sec^{-1}, which is about three times bigger than could be allowed, so it is difficult to see how the estimate could be spoilt by departures from radial motion. Thus the evidence is that if $\Omega = 1$, the mass concentration $\delta M/M$ in the LSC is less than about half the galaxy concentration $\delta N/N$.

For the discussion of biased galaxy formation it will be useful to have an estimate of what the LSC would have been like when galaxies formed. The numbers here assume the Einstein-de Sitter model, with $\Omega = 1$, and assume pressure may be neglected in estimating the growth of clustering. As quasars are seen at redshifts z (where $1+z$ is the ratio of observed to emitted wavelength) $\simeq 4$, it is reasonable to assume that the sites of galaxy formation were fixed at a redshift z_i no less than about 5. The mass concentration in the LSC can be extrapolated back from its present value, $\delta M/M \simeq 0.5$-1, to $(\delta M/M)_i \leqslant 0.10$ at $z_i = 5$, and $(\delta M/M)_i$ scales as $(1+z_i)^{-1}$. The galaxy concentration extrapolates back to $(\delta N/N)_i \simeq 1$, very nearly independent of z_i. The mean number density of bright galaxies is $\langle n\rangle \simeq 0.02\, h^3$ Mpc^{-3} (ref. 35). (The bright galaxies are those that contribute 75% of the net mean luminosity per unit volume.) The number of bright galaxies N_{is} within our radius in the LSC is the product of $\langle n\rangle$ with the volume and $(1+\delta N/N)$: $N_{is} \simeq 600$. Thus in the biased galaxy formation model the Local Supercluster would have originated as a moderately prominent island of ~600 bright galaxies, with $(\delta N/N)_i \simeq 1$, but with a modest mean-mass-density enhancement, $(\delta M/M)_i \leqslant 0.1$.

The second method of estimating Ω is based on the mean mass distribution around pairs of galaxies. If galaxy redshifts are used to derive distances assuming pure Hubble flow (that is, distance $= cz/H$), then random relative motions make the galaxy clustering pattern appear elongated along the line of sight. The size of the effect is a measure of the relative velocity of pairs of galaxies[36,37]. This measure has been applied to three moderately deep samples of galaxies selected by apparent magnitude and to two samples of more or less isolated pairs of galaxies[37-40]. The root-mean-square (r.m.s.) relative line-of-sight velocity dispersion, σ, of pairs of galaxies as a function of the projected separation, r_p, is found to increase slowly with increasing separation at 5 kpc $\leqslant r_p \leqslant$ 1 Mpc; typical values are $\sigma = 200 \pm 20$ km sec^{-1}, $hr_p = 10$ kpc; $\sigma = 300 \pm 75$ km sec^{-1}, $hr_p =$ 1 Mpc. The first number agrees with what is expected from observed velocities within galaxies at $hr \simeq 10$ kpc (where r is the radial distance from the galaxy centre). The flatness of $\sigma(r_p)$ is an extension of the nearly flat rotation or velocity dispersion curves observed in spiral and some elliptical galaxies[41,42].

The relative motions of close galaxy pairs must be balanced on average by gravity, because otherwise the clustering pattern observed at $hr \leqslant 1$ Mpc would dissolve within a Hubble time (H^{-1}). If we model the mass distribution as the linear sum of spherical haloes with mass (within r) $\delta M(<r)$ centred on each galaxy, then the condition for statistical support of the clustering pattern at small r, where typically two galaxies are involved, is $\delta M(<r) \simeq \sigma^2 r/G$. (This assumes isotropic velocites. If orbits tended to be radial then, as discussed below, this would reduce δM and Ω.) We can compare δM with the known mean number of galaxies in excess of random within a distance r of a galaxy:

$$\delta N(<r) = \langle n\rangle \int \xi_{gg}(r)\, d^3r \simeq r^{3-\gamma} \quad (4)$$

where $\xi_{gg} = (r_0/r)^\gamma$, $\gamma = 1.77$ and $hr_0 = 5.4 \pm 0.3$ Mpc. $\xi_{gg}(r)$ is a two-point correlation function measured from galaxy counts, and $\langle n\rangle$ is the global mean galaxy number density. The power-law model is a good approximation at $hr \leqslant 10$ Mpc[38,43,44]. We see that because σ varies roughly as $r^{0.1}$, δM and δN scale with r in about the same way, as $r^{1.2}$. This invites us to consider the assumption that whatever gathered galaxies together to make the present clustering pattern gathered mass in the same proportion, so that $\xi_{g\rho} = \xi_{gg}$ and therefore $\delta M(<r)/\delta N(<r) = \langle\rho\rangle/\langle n\rangle$, where $\langle\rho\rangle$ is the global mean mass density. The result of solving the above equations for $\Omega = \langle\rho\rangle/\rho_c$ is

$$0.3 \leqslant \Omega_{gg} \leqslant 0.6 \quad (5a)$$

This applies at $hr \leqslant 100$ kpc, where the galaxy pair typically has no bright close neighbours.

At $hr \simeq 1$ Mpc, where a galaxy pair typically has many ($N_{is} \simeq$ 10) bright neighbours that can contribute to the mean relative gravitational acceleration, we assume that each galaxy has mass m and then use the known statistics of the galaxy distribution to compute the mean relative acceleration. This yields[38,39]

$$0.1 \leqslant \Omega_{gg} \leqslant 0.3 \quad (5b)$$

The third dynamical estimate is based on the mean distribution of galaxies and mass around the rich compact clusters of galaxies catalogued by Abell[45]. Let $n(r)$ and $\rho(r)$ be the mean values of the galaxy number density and the mass density at distance r from an Abell cluster and averaged across a fair sample of clusters, and write $n(r) = \langle n\rangle[1+\xi_{cg}(r)]$ and $\rho(r) = \langle\rho\rangle[1+\xi_{c\rho}(r)]$, where $\langle n\rangle$ and $\langle\rho\rangle$ are the large-scale mean values, and ξ_{cg} and $\xi_{c\rho}$ are analogous to ξ_{gg} and $\xi_{g\rho}$, but for clusters. The Lick[46] galaxy counts around the positions of Abell richness class 1 clusters yield[47]

$$\xi_{cg} = \left(\frac{7.0\ \text{Mpc}}{hr}\right)^{2.5} + \left(\frac{12\ \text{Mpc}}{hr}\right)^{1.7} \quad (6)$$

at $0.5 \leqslant hr \leqslant 40$ Mpc. Gravity will have caused $n(r)$ and $\rho(r)$ to have grown considerably since galaxies formed. If gravity pulled in mass and galaxies alike, then at large enough r, $\xi_{c\rho}$ must approach ξ_{cg}, in which case the known ξ_{cg} fixes $\rho(r)/\langle\rho\rangle$. If we can estimate $\rho(r$ from dynamics we have an estimate of $\langle\rho\rangle$[47].

The following assumes $\xi_{cg} = \xi_{c\rho}$ at $r \simeq 2\, h^{-1}$ Mpc. This avoids the dense central parts of the cluster (where the galaxies are gas-poor so the mean mass per galaxy might be anomalous) but is still close enough to the centre to permit a reasonable estimate of $\rho(r)$. The Struble-Rood catalogue (M. F. Struble & H. J. Rood, unpublished) lists 17 Abell clusters of richness class 1 in which enough redshifts are known to permit estimates of the line-of-sight galaxy velocity dispersion σ_0; the r.m.s. value is $\langle\sigma_0^2\rangle^{1/2} = 830 \pm 80$ km sec^{-1}. The measurements of σ_0 are concentrated well within the Abell radius ($hr_A = 1.5$ Mpc). For the

four clusters in which the variation of velocity dispersion with radius has been fairly well measured (the Coma, Perseus, Hydra I and Virgo clusters), the $\sigma(r)$ estimates decrease with increasing r outside a possible slight central minimum[48–51]. These results suggest that $\sigma(r)$ at $hr \simeq 2$ Mpc is down from the central value by a factor of 1.3 to 1.5.

If the galaxy orbits in the cluster are isotropic, with velocity dispersion $\sigma(r)$ varying only slowly with radius, the mass density needed for statistical equilibrium is $\rho(r) = \sigma(r)^2/(2\pi G r^2)$. This implies $\rho \simeq r^{-2}$, consistent with the above estimate of $\xi_{cg}(r)$. The above numbers at $hr = 2$ Mpc give

$$0.2 < \Omega_{cg} < 0.35 \tag{7}$$

This assumes an isotropic velocity distribution. A spherical system is described by two components of dispersion, σ_r in the radial direction and σ_t in one transverse direction. Following White[52], we assume that at $hr \simeq 2$ Mpc, σ_r and σ_t have reached constant values and the galaxy number density scales as a power law, $n \propto r^{-\varepsilon}$. Then the equilibrium gravitational acceleration, g is

$$g = \frac{GM(<r)}{r^2} = \frac{2\sigma_t^2 + (\varepsilon - 2)\sigma_r^2}{r} \tag{8}$$

and the line-of-sight velocity dispersion is $\sigma^2 = \sigma_r^2/\varepsilon + \sigma_t^2(1 - 1/\varepsilon)$. It is a reasonable approximation to take $\varepsilon = 2$; this simplifies the equations to

$$\frac{GM}{r\sigma^2} = \frac{4\sigma_t^2}{\sigma_t^2 + \sigma_r^2} \tag{9}$$

Equation (7) assumes σ_t. If orbits were purely circular, with $\sigma_t \gg \sigma_r$, this would double M and Ω_{cg}, but it is hard to see how this could come about. If clusters formed by collapse it would tend to produce radial orbits, with $\sigma_r > \sigma_t$, which would depress Ω_{cg} from the value in equation (7).

If Ω were unity, clusters would have to be stronger concentrations of galaxies than of mass, and we would expect that gravity would attract to the cluster material rich in mass per galaxy, making the mass per bright galaxy $m(r)$ increase with increasing radius r in the cluster. Attempts to measure $m(r)$ using galaxy velocity dispersion data alone are complicated by the uncertainty in how the velocity anisotropy parameter σ_t^2/σ_r^2 varies with r; for the Coma cluster Kent and Gunn[48] could only conclude that they saw no need to assume that m varies with r. Cowie *et al.* (L. L. Cowie, J. Henriksen and R. Mushoksky, in preparation) have shown that the constraints on $m(r)$ are improved if one also imposes the condition that the gravitational field must balance the pressure-gradient force in the plasma in the cluster. Using the integrated cluster X-ray spectrum as a constraint on the distribution of plasma temperatures in the cluster, the rather accurately measured plasma density as a function of r, and the galaxy velocity dispersion data, they conclude that $m(r)$ has to be a decreasing function of r in the Coma cluster. The constraints are weaker for the Perseus cluster, but there is no evidence that $m(r)$ increases with increasing r, contrary to what we would have expected to see if Ω were unity.

We avoid this problem if we assume that cluster galaxies were created in large islands with roughly uniform mass per galaxy within the island. (The gradient in $m(r)$ in the Coma cluster is then given the usual interpretation, that galaxies near the centre suffered earlier loss of gas, which would have suppressed formation of younger stars and so lowered the galaxy luminosities.) The minimum number of bright galaxies per island is the mean number within our matching radius of $2\,h^{-1}$ Mpc: $N_{is} \geqslant 70$.

It may be possible to extend this constraint by using the fact that the concentration of galaxies around rich clusters extends well beyond $2\,h^{-1}$ Mpc. For example, the mean number of galaxies within distance $r = 20\,h^{-1}$ Mpc of an Abell cluster is about twice the number expected for a homogeneous distribution[47]. If there were a like concentration of mass within $r = 20\,h^{-1}$ Mpc the gravitational attraction of the mass would cause the galaxies at $r \simeq 20\,h^{-1}$ Mpc to have an appreciable streaming motion toward the cluster (relative to the Hubble flow), as in the LSC. When galaxy distances are estimated from redshifts using Hubble's law, $r = cz/H$, this streaming motion would make the galaxy distribution around a cluster tend to appear flattened along the line of sight[53]. Application of this test would require a large redshift sampling program, which now seems feasible and would be of considerable interest.

A more indirect constraint on the mass distribution might be mentioned. The new Center for Astrophysics (CfA) survey catalogues 1,100 galaxy redshifts in a field 6° wide by ~100° long[54]. The redshift map shows holes with diameters $\simeq 30\,h^{-1}$ Mpc, which is about what would be expected, given the clustering seen on smaller scales. The surprising result is that the holes are so empty and that the galaxies tend to distribute themselves so smoothly along the walls of the holes. If the mass were distributed like the galaxies and if Ω were close to unity this would be a strongly unstable arrangement, gravity causing mass to drain along the walls toward intersections, as is seen in the numerical N-body model simulations of the pancake model for galaxy formation[55]. Thus if $\Omega = 1$ it is doubtful that the mass is in the walls; it is more reasonable to assume that there is a general segregation of galaxies from mass on a scale of $\sim 30\,h^{-1}$ Mpc. If so then we have no problem in reconciling the low apparent densities in equations (2), (5) and (7) with a high mean mass density, but we substantially increase the demands on a theory for biased galaxy formation. If $\Omega \ll 1$, then gravity is suppressed relative to the general expansion, and a mass distribution like the galaxy distribution in the CfA redshift map might reasonably be expected to persist.

The direct way to measure Ω is through the classical cosmological model tests, as discussed many years ago by Tolman[56] and others. This approach has not received much attention in recent years because it has become apparent that galaxy evolution can mask the effects one is looking for, but the classical tests may be due for a renaissance. Loh and Spillar[57,58] have shown that a measurement of the joint distribution, $f(m, z)$, of galaxy apparent magnitude and redshift is feasible and substantially reduces the evolution problem. The standard tests depend on the curvature of a function of one variable, such as apparent magnitude as a function of redshift, and a given curvature can be produced by many reasonable combinations of galaxy evolution and cosmological effects. The function $f(m, z)$ depends on two variables, which offers a much better chance of separating the effects of galaxy evolution and cosmology. The current result[28] is $0.6 < \Omega < 2.0$ if $\Lambda = 0$. This is encouraging for the Einstein–de Sitter model but it should be considered a preliminary result because it assumes all galaxy luminosities evolve at the same fractional rate: the possible effect of evolution of the shape of the galaxy luminosity function has yet to be tested.

Models for biased galaxy formation

Three points are worth noting from the dynamical estimates of Ω described above. First, the independent estimates in equations (2), (5) and (7) yield consistent results, $\Omega \simeq 0.3$. If Ω were unity and the estimates were biased because mass clusters less strongly than galaxies, then we would have expected the Ω estimates to increase with increasing clustering scale (as measured by N_{is}). Second, if Ω were unity then galaxies would have to be placed on islands of tens to hundreds of bright galaxies each; a bias extending to nearest neighbours alone would not do. Third, whatever put the galaxies in islands cannot have perturbed the mass very much. If the Local Supercluster formed at redshift $z_i \simeq 5$, the initial mass concentration would have been $\delta M/M \simeq 0.1$, which is 10% of the original galaxy concentration. Even if

galaxies were put in place by non-gravitational forces it would require a special arrangement to keep the resulting mass perturbation so small.

One model for biased galaxy formation starts from the idea[19-21] that the first generation of stars that formed in the densest spots in the primeval mass distribution might have suppressed star formation elsewhere (perhaps blast waves from supernovae push the gas out of protogalaxies that have not yet managed to collapse to stars), so that bright galaxies would have survived only at rare extreme positive mass density fluctuations. Because the peaks of the mass distribution can be more strongly clustered than is the general mass distribution[18] (assuming the distribution is a random gaussian process with positive autocorrelation function), galaxies would be segregated from mass in the desired way. In a common implementation of this idea one assumes that a galaxy forms wherever the primeval mass density, smoothed through a window with size typical of a galaxy, exceeds the mean by more than a fixed multiple, $\nu \simeq 3$, of the standard deviation. This prescription has been studied in some detail under the assumptions that the mass of the universe is dominated by exotic dark matter with negligible primeval pressure and that the primeval mass distribution is a random gaussian process (random phases) with power spectrum P (square of the Fourier transform) that scales as $P \propto \langle|\rho_k|\rangle^2 \propto k$, where k is the wavenumber. (The assumption $P \propto k$ comes from the expected spectrum of quantum fluctuations resulting from inflation[1].)

Analytical[19] and N-body model[22] calculations show that these assumptions with the above prescription for the sites of galaxy formation make galaxies cluster more strongly than mass, as desired. However, one can use the same analytical computation to show that the bias does not extend much beyond the nearest neighbour galaxy. Thus this model would help account for the low value of Ω derived from relative motions of close pairs of galaxies (equation (5)), but would not help with the estimates based on larger clustering scales (if $\Omega = 1$).

To extend the scale of biasing one can assume that the spectrum, P, of density fluctuations increases with increasing length scale, rather than decreasing as in the above model. In this case we have to discuss in more detail whether the prescription for galaxy formation sites is reasonable. Three points should be considered.

First, the prescription uses the mass distribution averaged over a typical scale of a galaxy. Unless one assumes that the spectrum P is cut off on scales below that of a galaxy, one would expect that the first generation of stars formed in clusters much smaller than a galaxy and well before objects the size of a galaxy could have formed (because mass fluctuations tend to increase with decreasing length scales). It is hard to see how such pre-galaxy star clusters could be eliminated once formed. (The star clusters once formed could coalesce later to form galaxies.) This suggests that our criterion for star-forming regions should be the peaks in the primeval mass distribution averaged over scales well below that of a galaxy. But the analytical argument mentioned above indicates that this would suppress biasing on the scales of galaxies and larger.

Second, as mentioned above, the biased galaxy formation model requires that the Local Supercluster form at a mass excess $(\delta M/M)_i < 0.1$ and with a galaxy excess $(\delta N/N)_i \simeq 1$. I doubt that it is reasonable to expect that a 10% change in the ambient mass density could have caused a factor of two change in the survival of galaxies, because if protogalaxies were easily destroyed, survival surely would depend on many factors other than ambient mass density. Examples are the degree of subclustering in a protogalaxy, which determines how many star clusters form early and so resist dispersal, and the degree of sheltering of a protogalaxy by its neighbours. These additional random variables would tend to suppress the sensitivity of the survival probability to one variable, the ambient mass density.

Third, one might have thought that the dispersal effect which is supposed to inhibit galaxy formation would decrease with increasing distance from a new galaxy. This would tend to suppress galaxy clustering, leading to a reverse bias in which galaxies are less strongly clustered than mass, which would make the true value of Ω less than the dynamical estimates. To get the desired sign of bias, we would have to assume that tens to hundreds of bright galaxies form in islands and become robust enough to withstand disruption by their immediate neighbours, while protogalaxies well outside the islands must so lag in star formation that they can be destroyed by blast waves from the islands. My impression is that no very convincing way to do this has been proposed.

Another approach to biasing starts not from the statistics of the primeval mass distribution, but from the expected rearrangement of the mass distribution as stars form and die in supernova explosions. In this model, discussed by Ostriker and Cowie[59] and by Ikeuchi[60], a blast wave from supernovae in an early star cluster compresses the surrounding gas into a ridge, which can fragment into new star clusters whose blast waves can make still larger ridges. Islands of galaxies would be produced wherever the last and largest ridges form. As noted above, if we adopt $\Omega = 1$ and we accept the constraint on the baryon density from nucleosynthesis, we must assume that the mass of the universe is dominated by exotic, weakly interacting dark matter. The dark matter would be left behind when the blast waves gather the hydrogen to make galaxies, but then would participate in clustering once gravity takes over, giving the desired partial segregation of galaxies from mass.

This model requires two special arrangements. First, the explosions must be adjusted so as to fill space without making most of the matter so hot it cannot cool and contract to stars. Second, we must find some other way to account for the tendency of galaxies to appear in clusters and of clusters to appear in superclusters, because there is no way known to make the blast waves travel distances comparable to the sizes of superclusters. If these objects formed by the gravitational growth of primeval mass density fluctuations, as in the first model discussed above, it would require a special coincidence to account for the observations that galaxies and clusters of galaxies fit quite well into a scale-invariant clustering hierarchy[8,43]. It remains to be seen how serious these two problems are.

There are still other ways in which galaxies might have been segregated from mass. If the baryons were initially distributed in a wispy fashion in a sea of exotic dark matter, galaxies could form only in the wisps. A roughly similar effect might be obtained if galaxy formation were triggered by a network of massive cosmic strings. Both models are *ad hoc* for our purpose, but not without supporting arguments[61,62]. Another possibility is that the mass of the universe is dominated by gravitational radiation, or by weakly interacting particles with velocities that have always been high enough to resist the graviatational attraction of the mass concentrations in galaxies. However, either would significantly increase the mean mass density at high redshift, which would speed expansion and so spoil the nucleosynthesis calculations[63]. An ingenious variant of this scheme proposes that galaxies and clusters of galaxies formed by gravitational clustering of massive, weakly interacting, unstable particles[64]. These particles are then supposed to have decayed into low-mass, high velocity, weakly interacting particles, leaving behind islands of galaxies in a nearly smooth sea of dark matter. This is not without cosmological problems[65,66]. For example, if clusters of galaxies lost two-thirds of their mass, which would make the apparent density parameter derived from clustering dynamics $\simeq 0.3$, the clusters would expand by a factor of ~ 3 in radius. That means the clustering pattern would have been stronger in the past, which is contrary to the usual assumption that the clustering pattern has been growing to the present epoch. This would substantially increase the density fluctuations needed to make clusters of galaxies form by gravitational instability, and thus would increase the problem of reconciling the gravitational

instability picture with the isotropy of the microwave background[9,66].

Cosmology with low mass density

As the above models as presently understood are not very persuasive, we might consider the alternative: cosmological models with low mass density. The Einstein–de Sitter model could fail because we are assuming the wrong physics. An example is Milgrom's conjecture, that we are using the wrong gravity theory to compute masses[67]. A less spectacular mode of failure is the possibility that general relativity theory is valid, and that space sections have zero curvature, in accordance with inflation, but that the cosmological constant is non-zero[68]. This is distasteful, because of the coincidence argument mentioned at the beginning of this review, but such arguments must be examined closely. For example, suppose $\Omega = 0.2$, $h = 0.75$, $R^{-2} = 0$, and assume that initial conditions for classical cosmology were set at the end of inflation at redshift $z_{c1} = 10^{27}$. Expansion starts from $a = 1$ at $z = z_{c1}$. Four important epochs are: equal relativistic and non-relativistic mass densities, $a_1 = 10^{23.6}$; decoupling of baryons from radiation, $a_2 = 10^{24.0}$; equal values of the Λ and ρ terms in equation (1), $a_3 = 10^{26.8}$; and development of astronomy on Earth, $a_4 = 10^{27.0}$. It is curious that a_1 is relatively close to a_4, and striking that a_1 is so close to a_2; but surely it is no more startling that a_3 might be so close to a_4. It might be counted as a distinct advantage that if $\Omega \simeq 0.1$, the mass indicated by clustering dynamics is at least roughly consistent with the baryon density allowed by current estimates of element production in the hot Big Bang[63] without invoking exotic matter.

Conclusions

The Einstein–de Sitter cosmological model has been considered to be the most reasonable choice by the majority of those who cared to adopt an opinion in advance of a convincing observational test. We are now entering a very interesting period as the tests improve and, among the dynamical methods, fail to support the Einstein–de Sitter model. The observations can be reconciled with our expectations by assuming that galaxies formed in islands in a more nearly uniform sea of dark mass, but my impression is that we have seen no model that does this without a considerable degree of special arrangement. This impasse is a part of the normal process of development of an active but still immature subject, and will probably be resolved soon. It seems likely that in the next few years, as redshift surveys proceed, we will be able to improve considerably the measures of the large-scale mass distribution and so sharpen the constraints on Ω and the related problem of how galaxies form. It is somewhat more optimistic to hope for a tight constraint on Ω from the classical cosmological tests[58]. More optimistic still, but not unreasonably so, is the hope that observations of objects at high redshift will help show us how galaxies formed[69]. Meanwhile, the tension between what is observed and what we think ought to be is a most useful stimulus to research, as long as we remember that it is only a stimulus.

I thank P. Campbell, Len Cowie, Bob Dicke, George Efstathiou, John Huchra, Steve Kent, Ed Loh, Ardrian Melott, Jerry Ostriker, Jeff Peterson, Martin Rees, Dave Schramm, Joe Silk, Chris Thomson and Dave Wilkinson for stimulating discussions. This research was supported in part by NSF.

1. Guth, A. *Ann. N. Y. Acad. Sci.* **422**, 1–14 (1984).
2. Einstein, A. & de Sitter, W. *Proc. natn. Acad. Sci. U.S.A.* **18**, 213–214 (1932).
3. Einstein, A. *Sur la Structure Cosmologique de l'Espace*, 108 (Hermann, Paris, 1933).
4. Hubble, E. *Realm of the Nebulae*, 188–189 (Yale University Press, 1936).
5. Dicke, R. H. *Gravitation and the Universe*, 62 (American Philosophical Society, Philadelphia, 1970).
6. Dicke, R. H. & Peebles, P. J. E, in *General Relativity: an Einstein Centenary Survey* (eds Hawking, S. W. & Israel, W.) 504–517 (Cambridge University Press, New York, 1979).
7. Misner, C. W., Thorne, K. S. & Wheeler, J. A. *Gravitation*, 549 (Freeman, San Francisco, 1973).
8. Peebles, P. J. E. *Astrophys. J.* **189**, L51–L53 (1974).
9. Bond, J. R. & Efstathiou, G. *Astrophys. J.* **285**, L45–L48 (1984).
10. Gott, J. R., Gunn, J. E., Schramm, D. N. & Tinsley, B. M. *Astrophys. J.* **194**, 543–554 (1974).
11. Chapline, G. F. *Nature* **253**, 251–252 (1975).
12. Pagels, H. R. *Ann. N. Y. Acad. Sci.* **442**, 15–32 (1984).
13. Goodman, M. W. and Witten, E. *Phys. Rev.* D**31**, 3059–3063 (1985).
14. Peebles, P. J. E. *Physical Cosmology*. 116 (Princeton University Press, 1971).
15. Ostriker, J. P., Peebles, P. J. E. & Yahil, A. *Astrophys. J.* **193**, L1–L4 (1974).
16. Einasto, J., Kaasik, A. & Saar, E. *Nature* **250**, 309–310 (1974).
17. Peebles, P. J. E. *Ann. N.Y. Acad. Sci.* **375**, 159 (1981).
18. Kaiser, N. *Astrophy. J.* **284**, L9–L12 (1984).
19. Bardeen, J. in *Inner Space/Outer Space* (eds Kolb, E. W. *et al.*) (University of Chicago Press, in the press).
20. Kaiser, N. in *Inner Space/Outer Space* (eds Kolb, E. W. *et al.*) (University of Chicago Press, in the press).
21. Rees, M. J. in *Clusters and Groups of Galaxies* (eds Mardirossian. F. *et al.*) 485–497 (Reidel, Dordrecht, 1984).
22. Davis, M., Efstathiou, G., Frenk, C. S. & White, S. D. M. *Astrophys. J.* **292**, 371–394 (1985).
23. Faber, S. M. in *Dark Matter in the Universe* (eds Kormedny, J. & Knapp, G.) (Reidel, Dordrecht, in the press).
24. Rees, M. J. *Mon. Not. R. astr. Soc.* **213**, 75P–81P (1985).
25. Schaeffer, R. & Silk, J. *Astrophys. J.* **292**, 319–329 (1985).
26. Dekel, A. & Silk, J. *Astrophys. J.* **303**, 39–55 (1986).
27. Melott, A. L. & Fry, J. N. *Astrophys. J.* **305** (in the press).
28. Kaiser, N. & Davis, M. *Axtrophys. J.* **297**, 365–370 (1985).
29. Silk, J. *Astrophys. J.* **193**, 525–527 (1974).
30. Peebles, P. J. E. *Astrophys. J.* **205**, 318–328 (1976).
31. Davis, M. & Peebles, P. J. E. *A. Rev. Astr. Astrophys.* **21**, 109–130 (1983).
32. Tammann, G. A. & Sandage, A. *Astrophys. J.* **294**, 81–95 (1985).
33. Hoffman, G. L. & Salpeter, E. E. *Astrophys. J.* **263**, 485–500 (1982).
34. Bushouse, H., Melott, A. L., Centralla, J. & Galagher, J. S. *Mon. Not. R. astr. Soc.* **217**, 7P–11P (1985).
35. Kirschner, R. P., Oemler, A., Schechter, P. & Shectman, S. A. *Astr. J.* **88**, 1285–1300 (1983).
36. Geller, M. J. & Peebles, P. J. E. *Astrophys. J.* **184**, 329–341 (1973).
37. Peebles, P. J. E. *Astr. J.* **84**, 730–734 (1979).
38. Davis, M. & Peebles, P. J. E. *Astrophys. J.* **267**, 465–482 (1983).
39. Bean, A. J. *et al. Mon. Not. R. astr. Soc.* **205**, 605–624 (1983).
40. Peebles, P. J. E. *Science* **224**, 1385–1391 (1984).
41. Rubin, V. C. *Science* **220**, 1339–1344 (1983).
42. Fabricant, D. & Gorenstein, P. *Astrophys. J.* **267**, 535–546 (1983).
43. Groth, E. J. & Peebles, P. J. E. *Astrophys. J.* **217**, 385–405 (1977).
44. Stevenson, P. R. F. *et al. Mon. Not. R. astr. Soc.* **213**, 953–969 (1982).
45. Abell, G. O. *Astrophys. J. Suppl. Ser.* **3**, 211–288 (1958).
46. Shane, C. D. & Wirtanen, C. A. *Univ. Calif. Publs Lick Obs.* **22**, 1–60 (1967).
47. Seldner, M. & Peebles, P. J E. *Astrophys. J.* **214**, L1–L4 (1977).
48. Kent, S. M. & Gunn, J. E. *Astr. J.* **87**, 945–971 (1982).
49. Kent, S. M. & Sargent, W. L. W. *Astr. J.* **88**, 697–708 (1983).
50. Ftaclas, C., Fanelli, M. N. & Struble, M. F. *Astrophys. J.* **282**, 19–28 (1984).
51. Fuchs, B. & Marterne, J. *Astr. Astrophys.* **113**, 85–93 (1982).
52. White, S. D. M. *Mon. Not. R. astr. Soc.* **195**, 1037–1056 (1981).
53. Peebles, P. J. E. *Large-Scale Structure of the Universe*, 297–299 (Princeton University Press, 1980).
54. De Lapparent, V., Geller, M. J. & Huchra, J. P. *Astrophys. J.* **302**, L1–L5 (1986).
55. Melott, A. *Mon. Not. R. astr. Soc.* **202**, 595–604 (1983).
56. Tolman, R. C. *Relativity, Thermodynamics and Cosmology*, (Clarendon Press, Oxford, 1934).
57. Loh, E. D. & Spillar, E. J. *Bull. Am. astr. Soc.* **61**, 488–489 (1984).
58. Loh, E. D. & Spillar, E. J. *Astrophys. J.* (in the press).
59. Ostriker, J. P. & Cowie, L. L. *Astrophys. J.* **243**, L127–L131 (1981).
60. Ikeuchi, S. *Publs astr. Soc. Japan* **33**, 211–222 (1981).
61. Stecker, F. W. *Nucl. Phys.* B**252**, 25–36 (1985).
62. Turock, N. & Schramm, D. N. *Nature* **312**, 598–599 (1984).
63. Yang, J., Turner, M. S., Steigman, G., Schramm, D. N. & Olive, K. A. *Astrophys. J.* **281**, 493–511 (1984).
64. Turner, M. S., Steigman, G. & Krauss, L. M. *Phys. Rev. Lett.* **52**, 2090–2093 (1984).
65. Efstathiou, G. *Mon. Not. R. astr. Soc.* **213**, 29P–34P (1985).
66. Silk, J. & Vittorio, N. *Phys. Rev. Lett.* **54**, 2269–2272 (1985).
67. Milgrom, M. *Astrophys. J.* **270**, 365–389 (1983).
68. Peebles, P. J. E. *Astrophys. J.* **284**, 439–444 (1984).
69. Djorgovski, S., Spinrad, H., McCarthy, P. & Strauss, M. A. *Astrophys. J.* **299**, L1–L5 (1985).

Black smokers, massive sulphides and vent biota at the Mid-Atlantic Ridge

P. A. Rona*, G. Klinkhammer†, T. A. Nelsen*, J. H. Trefry‡ & H. Elderfield§

* NOAA/AOML, 4301 Rickenbacker Causeway, Miami Florida 33149, USA
† Department of Earth, Atmospheric and Planetary Sciences, MIT, Cambridge, Massachusetts 02139, USA
‡ Department of Oceanography and Ocean Engineering, Florida Institute of Technology, Melbourne, Florida 32901, USA
§ Department of Earth Sciences, University of Cambridge, Cambridge CB3 0EZ, UK

The discovery of black smokers, massive sulphides and vent biota in the rift valley of the Mid-Atlantic Ridge demonstrates that this assemblage of hydrothermal phenomena is not limited to intermediate-to-fast-spreading oceanic ridges. Hydrothermal exchange processes may thus be important at the ridges which extend through the Atlantic Ocean and western Indian Ocean, comprising more than half of the 55,000-km global length of seafloor spreading centres.

AN assemblage of hydrothermal phenomena including active black smokers, inactive chimneys, massive sulphides and vent biota has been discovered at a site[1] in the rift valley of the Mid-Atlantic Ridge near latitude 26°08′ N (Fig. 1). This is the first report of such an assemblage at a slow-spreading oceanic ridge (half-rate ≤ 2 cm yr^{-1}). The association of black-smoker-type hydrothermal venting, chimney-like edifices precipitated by the venting solutions, and vent biota was previously known only at sites on intermediate-to-fast-spreading ridges in the eastern Pacific Ocean, including the East Pacific Rise[2–4], the Guaymas Basin of the Gulf of California[5] and the Juan de Fuca Ridge[6,7]. Vent biota have been reported from sites at cold seeps in the Gulf of Mexico[8,9] and at the axis of the Mid-Atlantic Ridge ~310 km south of the present study site[10], and vent clams were tentatively identified near the present site[1].

The black smokers and associated phenomena were found using a combination of methods to sense far- and near-field properties of the water column and sea floor on a July–August 1985 cruise of the NOAA ship *Researcher* as part of the NOAA Vents program. Shipboard measurements of elevated values of dissolved manganese[11] and light scattering due to suspended particulate matter[12] in the water column delineated an area of hydrothermal activity. A systematic survey of that area with a deep-towed instrumented sled located active vents by measuring near-bottom water temperature anomalies and recording images of the sea floor[13]. We report here preliminary results of the seafloor imaging, near-bottom water temperature measurements and analyses of dredged hydrothermal precipitates[14]. These data complement other data sets pertaining to water chemistry[11], suspended particulate matter[12,15], and bottom sediment[16].

Instrumentation

Twelve transects were made across the study site with an instrumented sled. The sled was towed at an average speed of 1.8 km h^{-1} within 10 m of the sea floor, using an acoustic pinger to monitor and a winch to adjust altitude above the sea floor. The position of the sled was determined every 15 s to an accuracy of ±20 m relative to a net of four long-baseline (5–10 km) bottom-mounted acoustic transponders. The geographical positions of the acoustic transponders were determined using shipboard satellite navigation (Global Positioning System for three of the four transponders); the acoustic navigation net was converted to geographical coordinates with an estimated accuracy of ±150 m. In addition to the acoustic pinger and a relay transponder, the sled carried a 35-mm still camera system programmed to fire at 7.5-s intervals (inoperative 50% of the time due to malfunction); a continuously operating video camera system with recorder; a 1.5-m-long vertical array of four temperature sensors (thermistors accurate to ±0.01 °C) which recorded sequentially for 2 s every 10 s; and a pressure sensor with recorder from which pressures were converted to sled depth[17] (accuracy ± 2 m) and summed with pinger altitude for seafloor depth.

Geological setting

The discovery was made within the previously known TAG (Trans-Atlantic Geotraverse) hydrothermal field[18–21], which is located on a 10-km segment of the east wall of the rift valley between small-offset (<10 km) right-lateral transform faults[22]. The two walls of the rift valley of a slow-spreading ridge are normally nearly straight and subparallel to the bathymetric axis of the rift valley. At the TAG hydrothermal field the east wall projects westward as a broad salient which narrows the rift valley floor from a full width of ~6 km to only 3 km, coincident with a bathymetric high along the rift valley axis (Fig. 1). Thus, the east wall may be close to the subjacent intrusive heat sources that provide the increased thermal gradients which drive the upwelling limb of a sub-seafloor hydrothermal convection system. The sea floor is spreading asymmetrically at half-rates (averaged over 10 Myr) of 1.1 cm yr^{-1} to the west and 1.3 cm yr^{-1} to the east[23,24], indicative of asymmetric crustal accretion to the east[1,21].

The east wall rises from the rift valley floor near 4,000 m depth to the top of the rift mountains at ~2,000 m in a series of steps formed by underlying fault blocks. The steps are up to hundreds of metres in horizontal and vertical dimension, and tilt eastward away from the rift valley at angles up to 30° (refs 25, 26). Previous work identified a zone of hydrothermal phenomena between 2,400 and 3,100 m on the east wall[1]. These phenomena comprise layered deposits and surface stains of manganese oxide, iron oxide, iron hydroxide and iron silicate[27], as well as anomalous values of temperature[1] and helium concentration[28] in the near-bottom water, and metal enrichment in the sediment[29]. Analysis of metals in cores recovered from thin (<1.5 m) sediment between 3,100 m and the rift valley floor revealed layers with anomalously high contents (calculated on a carbonate-free basis) of copper (>1,000 p.p.m. (parts per 10^6 by weight)), iron (>8%) and zinc (>1,000 p.p.m.) at the surface and 30 cm beneath the surface, attributed to past and recent episodes of high-temperature black-smoker-type venting[1,29]. The layered hydrothermal precipitates, surface stains and near-bottom water temperature anomalies exhibit a linear distribution along fault zones, primarily between fault blocks that trend subparallel to the rift valley. The fault zones are inferred to tap hydrothermal sources, channel upwelling hydrothermal solutions and focus their discharge[20,21].

Black smokers, sulphides and vent biota

The black smokers, massive sulphides and vent biota occur at the juncture between the floor and east wall of the rift valley at

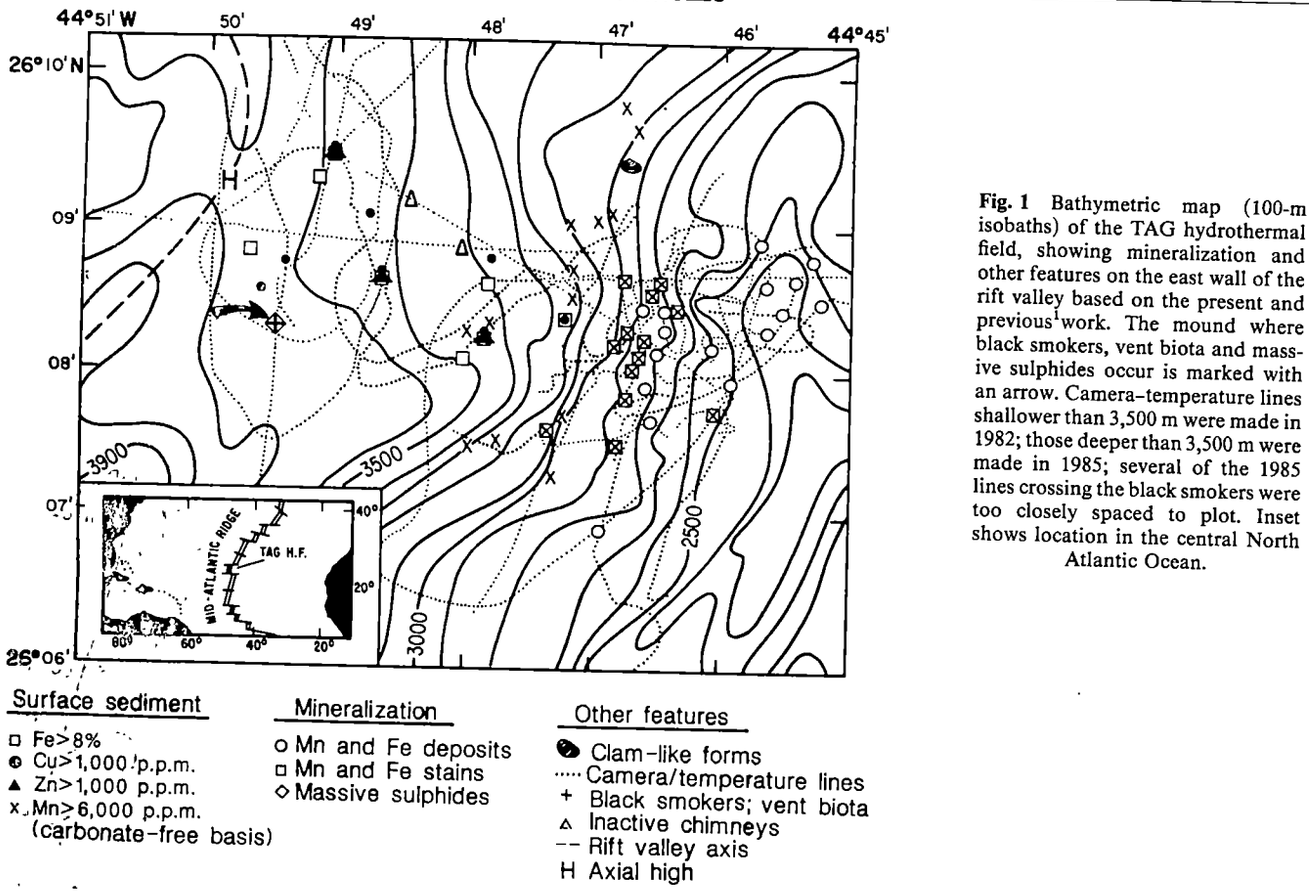


Fig. 1 Bathymetric map (100-m isobaths) of the TAG hydrothermal field, showing mineralization and other features on the east wall of the rift valley based on the present and previous[1] work. The mound where black smokers, vent biota and massive sulphides occur is marked with an arrow. Camera–temperature lines shallower than 3,500 m were made in 1982; those deeper than 3,500 m were made in 1985; several of the 1985 lines crossing the black smokers were too closely spaced to plot. Inset shows location in the central North Atlantic Ocean.

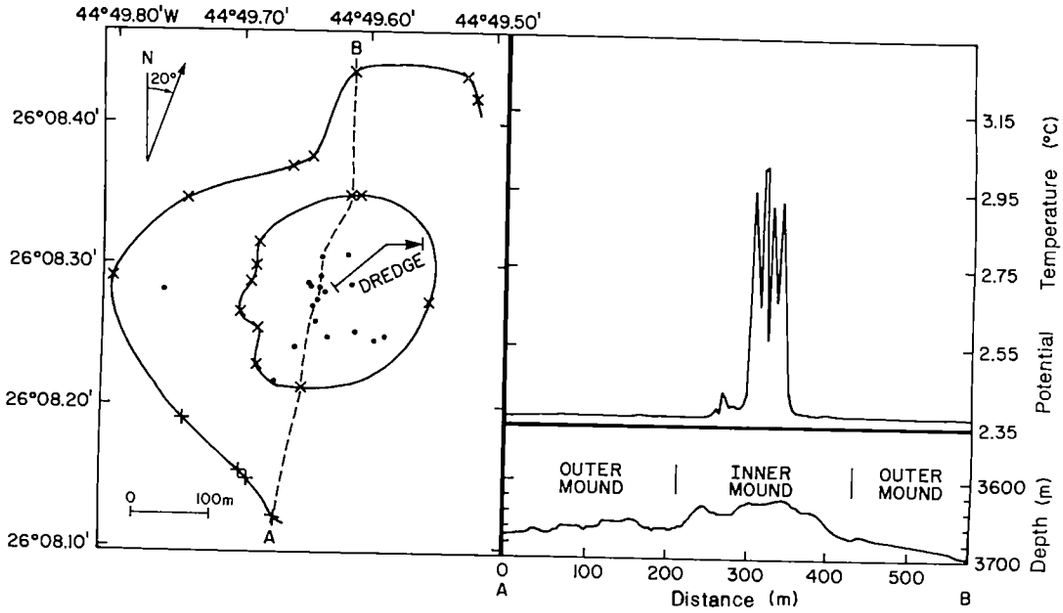


Fig. 2 Characteristics of the mound where black smokers, vent biota and massive sulphides occur at the juncture between the east wall and floor of the rift valley (Fig. 1), as delineated by camera–temperature–depth transects. Left, plan view showing boundaries of concentric inner and outer mounds (crossings marked '×'), distribution of vents (dots), azimuth of axis of rift valley (020°), and positions of transect A–B and a dredge. Lower right, bathymetric profile across the mound along transect A–B. Upper right, potential temperature profile in the water column within 10 m of the sea floor along transect A–B; the four central spikes correspond to black smokers.

water depths of 3,620–3,700 m (Fig. 1). They lie between the previously delineated hydrothermal zone 3.7 km up-slope to the east and the bathymetric axis of the rift valley 1.5 km down-slope to the west. The axial high of the rift valley lies 2 km up-slope to the north-west. The camera–temperature–depth tows delineated a compound mound with concentric inner and outer portions, each with an elliptical shape in plan view (Fig. 2). The inner mound lies between water depths of ~3,620 and 3,675 m and is up to 55 m higher than the outer mound, which lies between 3,675 and 3,700 m. The inner mound is ~250 m wide along azimuth 020° by 220 m wide along azimuth 110°; the outer mound is ~580 m wide along azimuth 020°.

A representative transect shows principal features of the compound mound (Fig. 2, transect A–B). The sea floor surrounding the mound is covered by basalt talus interspersed with sediment. The talus ranges from cobble- to boulder-sized, including angular fragments and whole pillows; some of the pillows may be in place. The sediment is thin (<1.5 m), light tan to pale red, mottled with light-coloured spots several centimetres in diameter made by burrowing organisms (~5 spots m^{-2}), fine-grained and resuspends in the wake of the sled. At the perimeter of the outer mound the talus is predominantly boulder-sized and sharply angular. Some of these talus blocks display regular, repetitive layers ~5 cm thick, which resemble successive basalt flows

Table 1 Petrography and mineralogy of representative samples

Sample no.	Petrography*	Pyrite (FeS_2) Content†	Pyrite (FeS_2) Wt %‡	Marcasite (FeS_2) Content	Marcasite (FeS_2) Wt %	Chalcopyrite ($CuFeS_2$) Content	Chalcopyrite ($CuFeS_2$) Wt %	Mineralogy sphalerite (ZnS) Content	Mineralogy sphalerite (ZnS) Wt %	Anhydrite ($CaSO_4$) Content	Anhydrite ($CaSO_4$) Wt %	Gypsum ($CaSO_4 \cdot 2H_2O$) Content	Gypsum ($CaSO_4 \cdot 2H_2O$) Wt %	Silica (SiO_2) Content	Silica (SiO_2) Wt %
1	Spongy-textured intergrown yellow pyrite and black sphalerite	Major	82.0§	Minor	—	Very low	0.8	Minor	13.6	ND	—	ND	—	Very low	0.4
2	Fragment of chimney wall 2 cm thick with inner zone of chalcopyrite and pyrite and outer zone of sphalerite	Minor	24.2§	Low	—	Major	63.1	Very low	4.7	ND	—	ND	—	Very low	0.4
3	Coarsely crystalline anhydrite (density 3.07) with fine pyrite crystals and an orange mineral (molysite?) on surfaces and in cavities	Very low	0.7	ND	—	Very low	2.9	Very low	0.04	Major	68.0‖	Low	—	Very low	0.9
4	Fragment of chimney wall similar to sample 2	Very low	—	ND	—	Major	86.1	Very low	1.4	ND	—	ND	—	Very low	0.4
5	Fine-grained, unconsolidated, cohesive pyrite particles with some euhedral crystals of pyrite	Major	92.8§	Low	—	ND	—	ND	—	ND	—	ND	—	Very low	0.4

Major, >25 wt %; minor, 10–25 wt %; low, 5–10 wt %; very low, <5 wt %; ND, not detected.
* Polarizing and scanning electron microscopy.
† X-ray diffraction.
‡ Wt % estimated from mineralogy and major element analysis by B. W. Haynes, US Bureau of Mines.
§ Wt % FeS_2 includes both pyrite and marcasite.
‖ Wt % $CaSO_4$ includes both anhydrite and gypsum.

ponded in lava lakes, such as are observed at the axis of the East Pacific Rise[30]. Alternatively, the layering may have been produced by bedded volcaniclastics. The sea floor within the outer mound is covered by angular talus fragments, basalt flows and interspersed sediment. The talus consists of a mixture of angular basalt fragments and reddish-yellow layered rocks inferred to be hydrothermal precipitates. Basalt pillows are present, both detached in the talus and attached as part of lava flows partially buried by talus and sediment. The sediment is red, mottled with abundant light-coloured spots at burrows (~10 spots m^{-2}), fine-grained and resuspends in the wake of the sled. Typically one large fish (≤25 cm long) was observed within each 100 m of horizontal advance of the sled.

The inner mound contrasts with the outer mound as regards substrate, hydrothermal activity and biota. The substrate is predominantly composed of reddish-yellow layered rocks which form irregular protuberances: ledges, dome-shaped masses and columns with horizontal and vertical dimensions of the order of metres. During tows across the inner mound the sled occasionally hit bathymetric highs while travelling at an altitude of ~5 m above the sea floor; thus the towing procedure systematically missed imaging the tops of the higher protuberances which may have been chimneys.

Shimmering water emanates from broad areas of fractured rocks inside the boundary of the inner mound. By analogy with temperature measurements made by submersibles in shimmering water at the Galapagos spreading centre[31] and the Guaymas Basin[32], this water could be up to 200 °C hotter than the ambient water potential temperature of 2.37 °C (Fig. 2). Towards the centre of the inner mound, suspended particulate matter in the water column increases in quantity, and changes from discrete, neutrally buoyant white flocks inferred to be pieces of bacterial mats, to wisps of white smoke, to wisps followed by plumes of black smoke.

The black smokers emanate from fractures in the layered rocks (Fig. 3), rather than from distinct chimneys. The buoyant plumes of black smoke appear to rise more slowly than those investigated on the East Pacific Rise[33,34], which ascend at rates between 1 and 5 m s^{-1}. At the TAG site, the rate of plume ascent was estimated to be <1 m s^{-1} from videotapes and from the down-current inclination of plumes (Fig. 3) in currents flowing south at several centimetres per second (estimated from particle movement at the time of observation). Particle loading in the plumes is high, as evidenced by the fact that the sea floor behind the plumes is obscured by the density of the black smoke (Fig. 3). Also, the camera sled was coated with fine, cohesive black particulate matter after tows through the smokers. Effects of the hydrothermal plumes were detected up to 400 m above the sea floor, as anomalies in dissolved manganese[11] and suspended particulate matter[12,15].

At least 11 black smokers clustered near the centre of the inner mound were seen during various transects (Fig. 2). The highest potential temperature anomaly measured from the sled at an altitude of 5 m above the sea floor was 3.86 °C. This temperature is 1.43 °C above ambient, and is associated with a

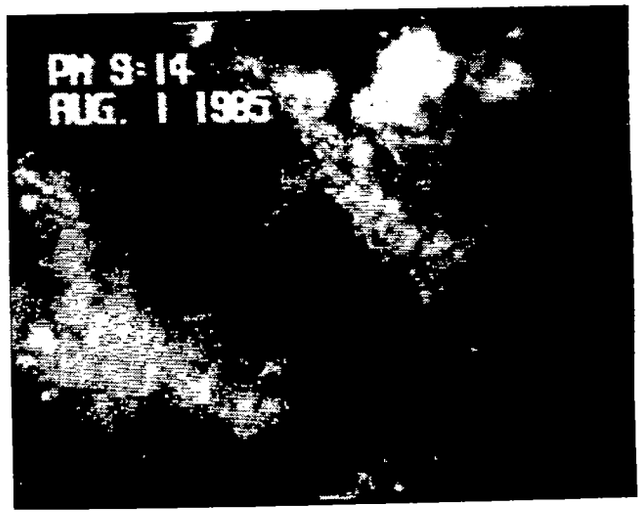


Fig. 3 A black smoker photographed from a video image recorded at an altitude of 5 m over the central portion of the inner mound (Fig. 2). The hydrothermal solutions are being discharged from seafloor fractures and the plume is inclined down-current.

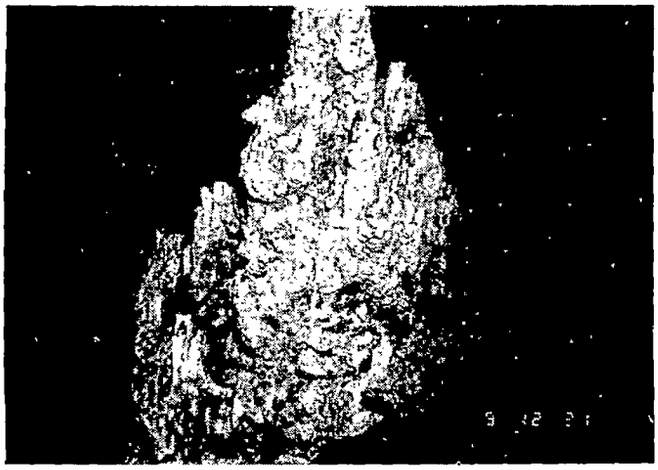


Fig. 4 A toppled chimney ~4 m from base to top, lying on the sea floor in an area of inactive chimneys at 3,500 m water depth on the lower portion of the east wall of the rift valley (Fig. 1). The sea floor around the chimney is littered with fragments of layered rocks with the appearance of hydrothermal precipitates and thin sediments with patchy black mineralized stains.

gradient of 0.21 °C m^{-1} (warming downward) over the 1.5-m vertical length of the temperature sensor array. The highest water temperature previously reported from a sled towed over hydrothermal vents in the Pacific Ocean was 0.18 °C (ref. 35), because the anomalies are attenuated by rapid heat dissipation in moving water. Direct measurements made from a submersible in similar Pacific vents have recorded water temperatures up to 400 °C (ref. 36).

The colour of the sediment interspersed between seafloor protuberances changes from red near the margins of the inner mound to black next to the black smokers. The black sediment and adjacent rocks exhibit a spectacular glitter on the videotape, interpreted as reflections from faces of euhedral pyrite crystals that settle from the black smoke. Euhedral pyrite crystals were identified in the black sediment that coated the instrument sled after tows through the black smokers (Tables 1, 2; sample 5).

The biota exhibits systematic changes from the margins to the centre of the inner mound. Translucent anemones several centimetres in diameter appear at the boundary between the outer and inner mound. Such anemones are the predominant sessile benthic invertebrate on the inner mound, with the densest population in shimmering water. Sparse translucent worms tentatively identified as vestimentiferans (M. L. Jones, personal communication) lie recumbent on rocks in limited areas closer to the centre: the thickets of vestimentiferan worms conspicuous at Pacific hydrothermal sites at shallower depths (2,600 m) were not observed. Occasional white patches (~1 m in diameter) on the rocks appear to be bacterial mats. Thousands of shrimp bask in beds around the black smokers and are highly mobile. About 200 of these shrimp, ranging in length from 3.8 to 5.1 cm, were recovered in a dredge with rocks from the inner mound (Fig. 2); the shrimp were preserved and are being studied[41]. A few crabs identified as brachyurans (A. B. Williams, personal communication) were present on rocks near the shrimp beds. Large fish (up to 25 cm long), including an eel-like form, were more abundant on the inner than on the outer mound, especially near the shrimp beds. Clams and other shelled organisms were not observed, although vesycomyid clams had been tentatively identified previously, in photographs from 3,000 m in the hydrothermal zone[1] (Fig. 1).

Area of inactive chimneys

A group of chimneys was observed on bottom images from two transects of an area at 3,500–3,600 m depth, located 2 km northeast of the mound (Fig. 1). One of the transects imaged toppled chimneys (Fig. 4) and related fragmental material at 3,500 m, with interspersed sediment marked by dark stains similar to mineralized stains observed higher on the east wall, there attributed to active hydrothermal seepage (Fig. 1). The other transect imaged 35 standing chimneys up to 5 m high along a horizontal distance of 100 m at 3,600 m depth. The absence of near-bottom water temperature anomalies over either the toppled or standing chimneys indicates that they are inactive; however, the fresh appearance of the chimneys (Fig. 4) suggests that hydrothermal venting stopped quite recently. By analogy with chimneys of similar appearance at sites in the Pacific, it is likely that these chimneys contain massive sulphides.

Hydrothermal precipitates

A single dredge of the inner mound (Fig. 2) recovered 59 kg of hydrothermal precipitates without any basalt. The hydrothermal precipitates recovered are predominantly sulphides (66 wt % of dredged material); sulphates, oxides, hydroxides, silicates and carbonates were also recovered. Preliminary petrographic descriptions and mineralogical and compositional analyses of five representative samples were performed at the Avondale Research Center of the US Bureau of Mines (B. W. Haynes, personal communication). The consolidated sulphides are broadly classified as two types. The first type (93 wt % of sulphides recovered) is a spongy-textured intergrowth of yellow pyrite and black sphalerite with irregular layering and cavities

Table 2 Composition of representative samples (wt%, dry basis)

	Method*	Sample no. 1	2	3	4	5
Major elements						
Fe	1	38.4	30.5	1.20	22.3	43.2
Cu	1	0.28	21.9	1.00	29.8	0.008
Zn	1	9.15	3.13	0.03	0.95	0.02
Ca	1	0.04	0.04	31.2	0.04	0.04
Mo	1	0.03	0.02	<0.01	0.05	<0.01
Ni	1	<0.004	0.06	<0.004	0.04	<0.004
Pb	1	0.06	0.19	<0.01	0.25	0.02
Si	1	0.2	0.2	0.4	0.2	0.2
S	4	46.9	36.1	17.4	30.7	50.9
Minor elements						
Al	1	0.05	0.19	0.02	0.47	0.04
Ag	2	<0.03	<0.03	<0.03	<0.03	<0.03
Ba	1	0.03	0.01	<0.01	<0.01	0.03
Co	1	<0.001	0.003	<0.001	0.003	<0.001
K	3	0.08	0.11	0.20	0.09	0.19
Mg	1	<0.01	0.01	<0.01	<0.01	<0.01
Mn	1	<0.005	<0.005	<0.005	<0.005	<0.005
Na	2	0.25	0.33	0.05	0.15	1.21
Sr	1	<0.01	<0.01	0.21	<0.01	<0.01
Ti	1	0.06	0.09	0.05	0.12	0.01
V	1	<0.01	<0.01	<0.01	0.02	<0.01
H_2O	(105 °C)	0.33	0.32	0.23	0.42	1.16

* Method of analysis: 1, inductively coupled plasma spectrometer; J. Zink and C. Hammet, US Bureau of Mines; 2, semi-quantitative optical emission spectrographic analysis; 3, atomic absorption spectrometer; 4, sulphur analyser. Oxygen content undetermined.

(Tables 1, 2; sample 1). It is high in iron (38 wt %) and zinc (9 wt %) and low in copper (≤1 wt %). Oxidized crusts typically several millimetres thick are present on exposed surfaces. The characteristics of this predominant sulphide type suggest precipitation from moderate-temperature solutions discharging into open spaces and forming irregularly layered deposits of diverse shapes on the sea floor. The second type of sulphide (7 wt % of sulphides recovered) occurs in dense, curved plates up to several centimetres thick exhibiting distinct mineral zonation (Tables 1, 2; samples 2, 4). A relatively thick zone on the concave side of the plates is composed of chalcopyrite and pyrite; a thinner contiguous zone on the convex side is composed of sphalerite (Tables 1, 2; samples 2, 4). The convex surface has a yellowish- to reddish-brown oxidation crust several millimetres thick; the concave surface of some of the samples is coated with soft, black, botryoidal and reddish-brown, fine-grained iron and manganese oxides and hydroxides up to 1 cm thick. The copper content of these sulphides is high (22–30 wt %), and the zinc content is low (1–3 wt %). The characteristics of this second type of sulphide suggest precipitation in a chimney that vented high-temperature solutions. Unconsolidated sulphide particles that accumulated on the instrument sled during tows through the black smokers consist of cohesive particulate material primarily composed of pyrite (Tables 1, 2; sample 5), as described above.

Sulphates (~1 kg) were recovered in the form of coarsely crystalline aggregates of anhydrite with fine crystals of pyrite on surfaces and in cavities (Tables 1, 2; sample 3). The presence of anhydrite indicates seafloor temperatures of ~140 °C: at lower temperatures it would re-dissolve in sea water, at the ambient pressure of ~370 bar[37,38]. Studies are in progress of the mineralogy, composition and isotopic characteristics of the various hydrothermal mineral phases in the recovered samples (G. Thompson and P.A.R., unpublished data).

Conclusions

The discovery of black smokers, chimneys, massive sulphides and vent biota fills a major gap in the understanding of slow-spreading oceanic ridges. The low-temperature hydrothermal zone previously delineated at mid-depth on the east wall of the rift valley at the TAG hydrothermal field is not an isolated phenomenon, but is part of a larger hydrothermal system, probably related by physical and chemical gradients to the high-temperature area at the juncture between the wall and the floor of the rift valley (Fig. 1). The high-temperature area, with vigorous venting of black smokers and precipitation of massive sulphides, is laterally contiguous with the low-temperature zone, with weak venting of warm springs and precipitation of oxides, hydroxides and silicates.

The elliptical configuration of the compound mound, with black smokers venting from the inner mound and evidence of lava flows and extensive fracturing at the perimeter of the outer mound, suggests that the mound may overlie a crater partially collapsed over an off-axis magma chamber (Fig. 2). The parallelism between the long axis of the ellipse and the axis of the rift valley (020°) suggests the additional influence of faulting subparallel to that axis. The observation that the black smokers vent from fractures rather than from chimneys suggests that the fractures opened in response to an episode of seismicity so recent that chimneys have not had time to grow. The massive sulphides recovered and the inactive chimneys imaged formed during previous episodes of black smoker activity. The relatively slow observed rate of ascent of the plumes indicates either hydrothermal fluid temperatures lower than that of Pacific black smokers or, alternatively, high temperatures with thermal expansion partially compensated by the observed dense particle loading and/or phase separation[39]. Fluid temperature measurements and sampling by submersible are needed to resolve this question. Assuming that the inner mound is constructed primarily of hydrothermal precipitates (average density 3.0 g cm^{-3}) in the form of a semi-ellipsoid, the deposit would weigh 4.5×10^6 tonnes. The similarities in size, shape and structure of this mineral deposit to certain ancient massive sulphide deposits in the form of convex-upward mounds, such as Noranda-type deposits[40], is striking, although differences exist in petrological associations.

The record of hydrothermal activity at the TAG hydrothermal field is partially preserved in localized ponded sediment. Fluctuations in activity through time may be distinguished from spatial variations within the field by examination of this sedimentary record[1,16,29]. The relation between inactive chimneys (Figs 1, 4) and black smokers (Fig. 3) may also be deciphered from the sedimentary record. The occurrence of the full range of seafloor hydrothermal phenomena at this site on the Mid-Atlantic Ridge suggests a role for slow-spreading oceanic ridges in the hydrothermal exchange processes that affect ocean chemistry, seafloor mineralization, heat transfer and biological adaptation.

We thank E. Bernard, director, and S. Hammond, manager of the NOAA Vents program, for encouragement and support, H. Bezdek and D. K. Atwood of NOAA, AOML for support; A. Meyer, S. Jones and G. Eberhart for work with the camera/temperature system and assistance in data processing; acting commanding officer C. Molyneaux, operations officer K. A. Doggett, other officers and crew of the NOAA ship *Researcher* for capable support at sea; the NOAA Vents program and NERC (UK) for funding; L. Burk (Oceano Instruments) for acoustic navigation; J. R. Delaney (University of Washington) for discussion of pressure–temperature–density effects on hydrothermal solutions; B. W. Haynes for sample analysis as part of the Characterization of Seafloor Minerals project of the US Bureau of Mines; and J. F. Grassle (Woods Hole Oceanographic Institution) for guidance of biological studies.

Received 15 January; accepted 11 March 1986.

1. Rona, P. A. *et al. J. geophys. Res.* **89**, 11365–11377 (1984).
2. Francheteau, J. *et al. Nature* **277**, 523–528 (1979).
3. Spiess, E. N. *et al. Science* **207**, 1421–1444 (1980).
4. Hekinian, R., Fevrier, M., Bischoff, J. L., Picot, P. & Shanks, W. C. *Science* **207**, 1433–1444 (1980).
5. Lonsdale, P. F., Bischoff, J. L., Burns, V. M., Kastner, M. & Sweeney, R. E. *Earth planet. Sci. Lett.* **49**, 8–20 (1980).
6. Normark, W. R. *et al. Mar. Technol. Soc. J.* **16**, 46–53 (1982).
7. Chase, R. L. *et al. Nature* **313**, 212–214 (1985).
8. Paull, C. K. *et al. Science* **226**, 965–967 (1984).
9. Kennicutt, M. C. II *et al. Nature* **317**, 351–353 (1985).
10. Kong, L. *et al. Eos* **66**, 936 (1985).
11. Klinkhammer, G., Rona, P., Elderfield, H. & Greaves, M. *Eos* **66**, 936 (1985).
12. Nelsen, T. A., Klinkhammer, G. & Trefry, J. *Eos* **66**, 936 (1985).
13. Rona, P. A. *Eos* **66**, 682–683 (1985).
14. Rona, P. A. *Eos* **66**, 936 (1985).
15. Trefry, J. E. & Trocine, R. P. *Eos* **66**, 936 (1985).
16. Metz, S. & Trefry, J. H. *Eos* **66**, 936 (1985).
17. Saunders, P. M. & Fofonoff, N. P. *Deep Sea Res.* **23**, 109–111 (1976).
18. Rona, P. A. *Ocean Mgmt* **1**, 145–159 (1973).
19. Rona, P. A. & Scott, R. B. (convenors) *Eos* **55**, 292–295 (1974).
20. Scott, R. B., Rona, P. A. McGregor, B. A. & Scott, M. R. *Nature* **251**, 301–302 (1974).
21. Rona, P. A. *J. geol. Soc. Lond.* **137**, 385–402 (1980).
22. Rona, P. A., Harbison, R. N., Bassinger, B. G., Scott, R. B. & Nalwalk, A J *Geol Soc Am. Bull.* **87**, 661–674 (1976).
23. Lattimore, R. K., Rona, P. A. & DeWald, G. *J. geophys. Res.* **79**, 1207–1209 (1974).
24. McGregor, B. A. & Rona, P. A. *J. geophys. Res.* **80**, 3307–3314 (1975).
25. Temple, D. G., Scott, R. B. & Rona, P. A. *J. geophys. Res.* **84**, 7453–7466 (1979).
26. Karson, J. A. & Rona, P. A. *Eos* **63**, 1103 (1982).
27. Thompson, G., Mottl, M. J. & Rona, P. A. *Chem. Geol.* **49**, 243–257 (1985).
28. Jenkins, W. J., Rona, P. A. & Edmonds, J. M. *Earth planet. Sci. Lett.* **49**, 39–44 (1980).
29. Shearme, S., Cronan, D. S. & Rona, P. A. *Mar. Geol.* **51**, 269–291 (1983).
30. Francheteau, J., Juteau, T. & Rangan, C. *Nature* **281**, 209–211 (1979).
31. Corliss, J. B. *et al. Science* **203**, 1073–1083 (1979).
32. Edmond, J. M. *Eos* **66**, 918 (1985).
33. Macdonald, K. C., Becker, K., Spiess, F. N. & Ballard, R. D *Earth planet Sci. Lett* **48**, 1–7 (1980).
34. Converse, D. R., Holland, H. D. & Edmond, J. M. *Earth planet. Sci. Lett.* **69**, 159–175 (1984).
35. Weiss, R. F., Lonsdale, P., Lupton, J. E., Bainbridge, A. E. & Craig, H. *Nature* **267**, 600–603 (1977).
36. Delaney, J. R., McDuff, R. E. & Lupton, J. E. *Eos* **65**, 973 (1984).
37. Blount, C. W. & Dickson, F. W. *Geochim. cosmochim. Acta* **33**, 227–245 (1969).
38. Janecky, D. R. & Seyfried, W. E. Jr *Am. J. Sci.* **283**, 831–860 (1983).
39. Delaney, J. R. & Cosens, B. *Mar. Technol. Soc. J.* **16**, 62–66 (1982).
40. Franklin, J. M., Lydon, J. W. & Sangster, D. F. *Econ. Geol.* 75th Anniv Vol 485–627 (1981).
41. Williams, A. B. & Rona, P. A. *J. crustacean Biol.* (in the press).

Cloning of cDNA for a stylar glycoprotein associated with expression of self-incompatibility in *Nicotiana alata*

M. A. Anderson*, E. C. Cornish*, S.-L. Mau*, E. G. Williams*, R. Hoggart*, A. Atkinson*, I. Bonig*, B. Grego†, R. Simpson†, P. J. Roche‡§, J. D. Haley‡§, J. D. Penschow‡§, H. D. Niall‡§, G. W. Tregear‡§, J. P. Coghlan‡§, R. J. Crawford‡§ & A. E. Clarke*

* Plant Cell Biology Research Centre, School of Botany, University of Melbourne, Parkville, Victoria 3052, Australia
† Joint Protein Structure Laboratory, Ludwig Institute for Cancer Research (Melbourne Branch) and The Walter and Eliza Hall Institute for Medical Research, Parkville, Victoria 3052, Australia
‡ Xerogen Pty Ltd, c/o 121 William Street, Melbourne, Victoria 3052, Australia

Self-incompatibility in flowering plants is controlled by the S *gene. A complementary DNA clone encoding a style protein of* Nicotiana alata *which segregates with the* S_2 *allele has now been sequenced. The* S*-allele-associated style components in different genotypes of* N. alata *and in* Lycopersicon peruvianum, *another self-incompatible species in the family Solanaceae, are homologous.*

OVER half the flowering plant families have specific self-incompatibility genes (*S* genes) which prevent inbreeding (for reviews see refs 1–6). Among homomorphic multi-allelic incompatibility systems there are two major types, showing either gametophytic or sporophytic control of the self-incompatibility response. Gametophytic incompatibility is the more common and, in many cases, is controlled by a single nuclear gene locus (*S* locus) with multiple alleles. Pollen expresses its haploid *S* genotype and matings are incompatible if the *S* allele of the pollen is matched by one of two *S* alleles expressed in the diploid tissue of the pistil. During both incompatible and compatible matings, pollen germinates and the pollen tubes grow through the stigma into the transmitting tissue of the style. Tube growth from incompatible pollen grains is arrested in the style; the tip of the tube becomes thickened, there is often a characteristic deposit of callose close to the tip, and the tip may burst. In sporophytic incompatibility, on the other hand, pollen behaviour is determined by the genotype of the pollen-producing plant; inhibition usually occurs on the stigma surface and is often associated with deposition of callose in the stigma cells. The gametophytic system is generally considered to be the ancestral form of self-incompatibility in flowering plants, with the sporophytic system being derived from it[1].

The genetics of gametophytic self-incompatibility systems has been studied extensively (see, for example, refs 1, 7–11). Several attempts have been made to identify the active product(s) of the *S* gene in both gametophytic and sporophytic systems[12–14], and recently a clone encoding part of an *S*-locus-specific glycoprotein from *Brassica oleracea* stigmas has been described[15]. In general, the early studies point to the presence of *S*-genotype-associated antigens or proteins in the pistil, but have so far failed to positively identify corresponding molecules in pollen or pollen tubes. Although several genetic and molecular models have been constructed to account for the breeding behaviour of *S* alleles[16–18], the detailed nature of the *S*-gene product and its mode of action in preventing fertilization are still unknown.

The major criteria for positive identification of an *S*-allelic product are, first, that its presence in reproductive tissues of the plant must consistently be associated with the corresponding breeding behaviour and, second, that it should show specific biological activity under appropriate bioassay conditions (for example, it should inhibit growth of pollen tubes bearing the same allele but not tubes bearing a different allele).

To elucidate the molecular basis of incompatibility, we have isolated an *S*-genotype-associated glycoprotein from styles of an ornamental tobacco, *Nicotiana alata* Link and Otto, a species which displays gametophytic self-incompatibility. Here we report the association of this glycoprotein with expression of the S_2 allele and describe a complementary DNA clone encoding the protein. We have used this cDNA to examine both expression of self-incompatibility in female tissues of the flower and the homology between different *S* alleles of *N. alata*.

The present study represents an initial step in understanding how plants discriminate between self and non-self[19]. We examine how 'self' pollen tubes are recognized and how their growth is arrested within the female tissues of the style. This system is defined in terms of classical genetics by breeding techniques, and we have now started to define it in terms of molecular genetics.

Expression of S_2 allele

From the original acquisition, S_2S_3, S_2S_2 and S_3S_3 homozygotes were produced by bud self-pollination. Bud self-pollination of a second acquisition, S_1S_3, provided the homozygote S_1S_1, and a third heterozygote, S_1S_2, was obtained by intercrossing the two acquisitions. Extracts from styles of mature plants revealed an association of a component of relative molecular mass (M_r) 32,000 (32K) with the presence of the S_2 allele; this was apparent on single-dimension SDS-polyacrylamide gels (not shown) and in two-dimensional gels (Fig. 1*A*), which showed that the 32K component had a high *p*I. The high-*p*I proteins in extracts of styles bearing different *S* alleles could be compared on the same isoelectric focusing gel by selecting from the gel those components in the high-*p*I range (>9.5) and subjecting them to SDS-polyacrylamide gel electrophoresis (SDS-PAGE) in the second dimension[20]. Association of the 32 K band with S_2 allele was clearly demonstrated in this selective two-dimensional gel electrophoresis (Fig. 1*B*).

Style proteins were analysed for 53 plants resulting from reciprocal crosses involving the genotypes S_2S_2, S_3S_3, S_2S_3 and S_1S_3, using conventional two-dimensional gel electrophoresis and selective two-dimensional gel electrophoresis. The results demonstrated genetic segregation of the 32K component with breeding behaviour identifying the S_2 allele. Forty progeny plants in which the 32K component was present in style extracts, all rejected S_2 pollen. The remaining 13 plants, apparently lacking the 32K component, all accepted S_2 pollen. Thus, no recombination was observed between S_2 breeding behaviour and presence of the 32K component in the style.

§ Present addresses: Howard Florey Institute of Experimental Physiology and Medicine, University of Melbourne, Parkville, Victoria 3052, Australia (P.J.R., J.D.P., G.W.T., J.P.C., R.J.C.); Imperial Cancer Research Fund, London WC2A 3PX, UK (J.D.H.); Genentech Inc., South San Francisco, California 94080, USA (H.D.N.).

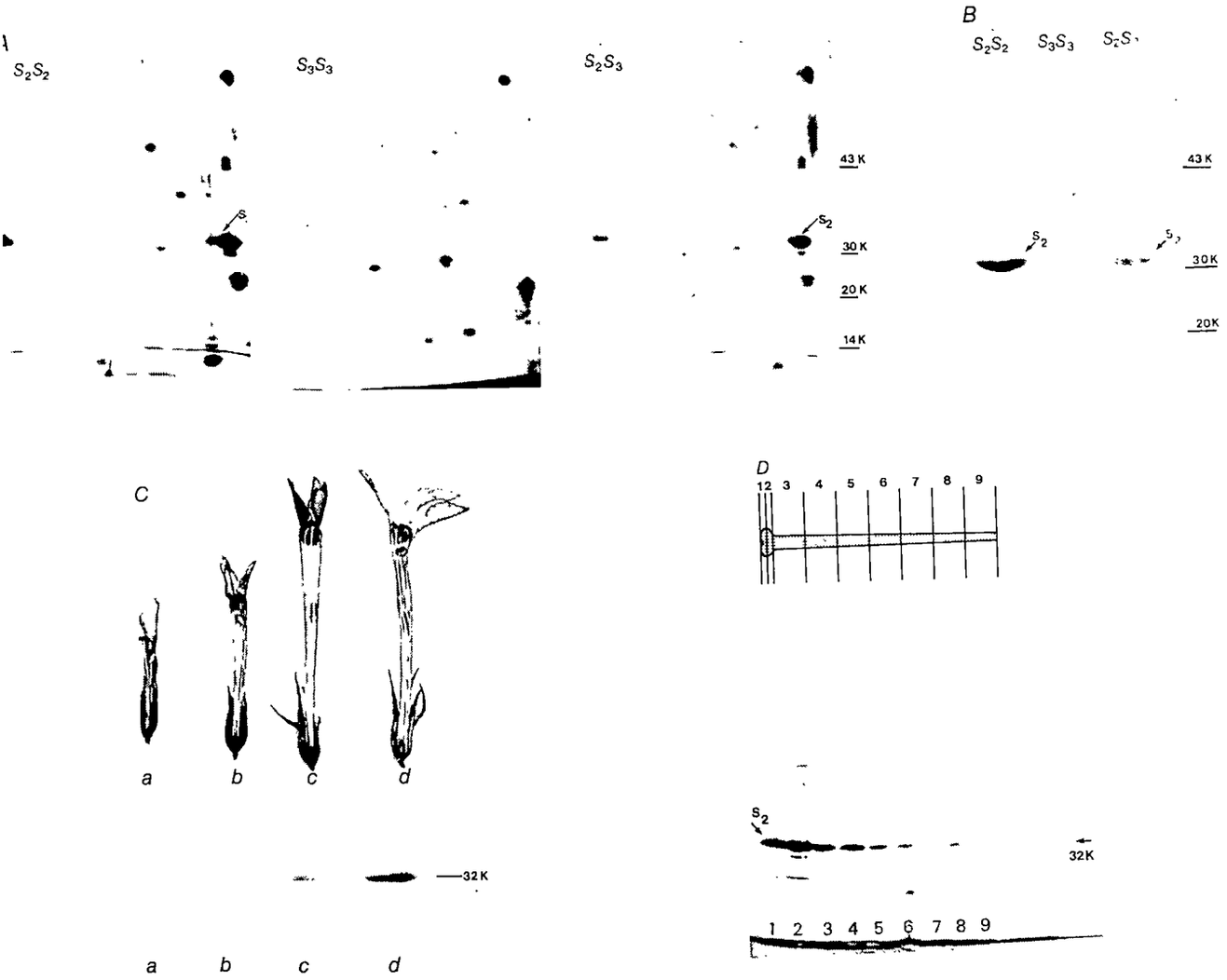
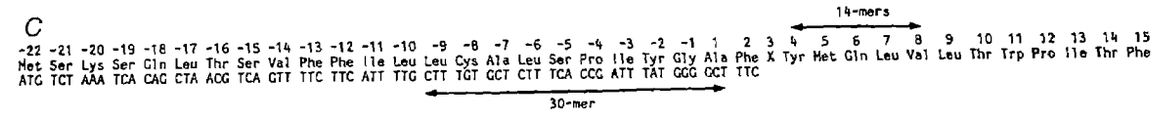


Fig. 1 Correlation of expression of the S_2 allele of *Nicotiana alata* with the presence of a 32K glycoprotein in style extracts, *A*, Two-dimensional gel electrophoresis of style extracts from mature plants of *N. alata*, genotypes S_2S_2, S_3S_3 and S_2S_3. A high-*p*I component of M_r 32,000 is present in the parent acquisition S_2S_3 and in bud-selfed progeny with the genotype S_2S_2, assigned by test crossing. The 32K component is absent from progeny of the same bud-selfing with an assigned genotype of S_3S_3. *B*, Selective two-dimensional gel electrophoresis of style extracts from mature plants as shown in *A*. The 32K band is present in style extracts of all plants which carry a functional S_2 allele. *C*, Selective two-dimensional gel electrophoresis of style extracts from flowers of genotype S_2S_3 at different developmental stages. The 32K band is absent from style extracts prepared at the green-bud stage when the self-incompatibility response is absent (*a*), but appears, together with expression of self-incompatibility, at the time of petal colouration (*b*) and is present in higher concentrations in extracts prepared from styles of mature flowers (*c*, *d*). *D*, Selective two-dimensional gel electrophoresis of extracts from segments of mature styles. A diagram representing the stigma and upper part of the style is shown; the stigma sections were 1 mm long and the style sections 6 mm long. The 32K glycoprotein is present at highest concentrations in the sections which include the stigma (1 and 2), and in the upper segments of the style (3, 4 and 5).

Methods. *A*, Seed of *N. alata* of incompatibility genotypes S_2S_3 and S_1S_3 was provided by Dr K. K. Pandey. Crosses were made by hand on emasculated flowers in a pollinator-proof glasshouse and scored as incompatible if flowers abscised without capsule development, or compatible if filled seed capsules were formed. Plants homozygous for the S_2 and S_3 alleles were obtained by self-pollination of immature flowers at the green-bud stage using mature pollen from the same plant and stigmatic secretion from a mature, emasculcated flower to aid pollen germination on the surface of the immature stigma. As incompatibility is first expressed at the petal colouration stage, self-pollen tubes are not always arrested when flowers are pollinated at the green-bud stage. Abscission of fruits containing low numbers of 'selfed' seeds was prevented by smearing the floral pedicels with 1% indoleacetic acid (IAA) in crude lanolin. Genotypes were assigned by test crossing to original acquisitions. Style extracts were prepared by crushing six styles lightly in 0.3 ml of extraction buffer [50 mM Tris-HCl *p*H 8.5, 10 mM EDTA, 1 mM $CaCl_2$, 1 mM phenylmethylsulphonyl fluoride (PMSF), 1 mM dithiothreitol (DTT)]. The extracts were centrifuged and the protein concentations measured[30]. Extracts containing 15 μg of protein were analysed on two-dimensional gels run according to Mau *et al.*[20].Protein spots were visualized by silver staining. *B*, Extracts were prepared from six mature styles as described for *A*, and samples containing 15 μg of protein were loaded onto the isoelectric focusing gel. After running according to Mau *et al.*[20], the region corresponding to the *p*I range >9.5, which contains the S_2-glycoprotein, was excised and run on a 15% SDS-polyacrylamide gel and stained with Coomassie blue. As many of the proteins present in the extract are of low *p*I, the pattern shown in conventional two-dimensional gels is considerably simplified by this procedure. *C*, Style extracts of flowers at the developmental stages shown were prepared and examined by selected two-dimensional gel electrophoresis as described for *B*. *D*, Six mature styles were harvested, aligned and sectioned with a razor blade according to the diagram. Each group of sections was extracted separately with 0.3 ml of buffer and the extracts examined by selective two-dimensional gel electrophoresis as described for *B*. Protein bands were visualized by silver staining.

Selective two-dimensional gel electrophoresis was also used to demonstrate the association of the 32K component with development of S_2 function in maturing styles (Fig. 1*C*). The 32K component was present at highest concentrations in upper segments of the style (Fig. 1*D*), the zone in which the arrest of incompatible pollen tubes occurs. Thus, the 32K glycoprotein segregates with S_2 breeding behaviour, appears concomitantly with S_2 function in maturing styles and occurs in highest concentration in the part of the style in which inhibition of incompatible pollen tube growth occurs. This 32K glycoprotein is termed the S_2-glycoprotein. The appearance of *S*-allele-associated style proteins in mature but not immature styles has been noted for other self-incompatible species, and the concentration of *S*-allele-associated proteins in the stigma and upper style



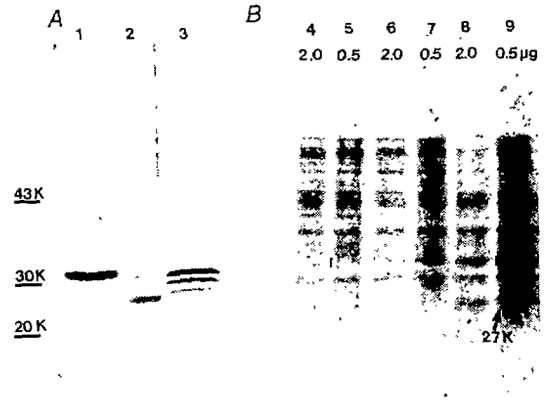


Fig. 2 Protein products specific to the S_2 allele. *A*, Purification and deglycosylation of the S_2-glycoprotein. Lane 1, S_2-glycoprotein isolated by chromatographic procedures (M_r 32,000); lane 2, S_2-glycoprotein after chemical deglycosylation (M_r 26,000); lane 3, S_2-glycoprotein after enzymatic deglycosylation. Four species are detected by silver staining: a strongly staining band of 32K which corresponds to the undegraded glycoprotein, two 30K species running closely together (the separation of these is not clear in the photograph) and a fourth species of M_r 28,000. *B*, Identification of an *in vitro* translation product specific to mature styles. The figure shows *in vitro* translation products of mRNA isolated from *N. alata* ovary (lanes 4 and 5), green-bud style (lanes 6 and 7) and mature style (lanes 8 and 9). The amount of mRNA used in each experiment is indicated. The 27K translation product unique to mature style mRNA is indicated. *C*, Amino-acid sequence of the N-terminus of the mature S_2-glycoprotein and the C-terminus of a putative signal sequence for this protein, as determined by N-terminal analysis and deduced from DNA sequence analysis. Amino acids 1–15 were determined by N-terminal analysis of the isolated glycoprotein where X denotes no clear assignment. From the sequence Tyr-Met-Gln-Leu-Val (amino acids 4–8), the following three pools of oligodeoxyribonucleotide 14-mers, each of 8-fold degeneracy, were prepared: 5′ d(ACA^{G}AGT^{C}TGCATA^{G}TA (pool I), 5′ d(ACC^{T}AGT^{C}TGCATA^{G}TA (pool II) and 5′ d(ACC^{T}AAT^{C}TGCATA^{G}TA (pool III). The nucleotide sequence complementary to a portion of cDNA synthesized when pool I was used to prime cDNA synthesis is shown. This sequence is in the same sense as the mRNA and encodes 22 amino acids of a putative signal peptide and two amino acids at the N-terminus of the mature S_2-glycoprotein. A synthetic 30-mer probe complementary to the sequence indicated was synthesized as described below.

Methods. *A*, Flowers were emasculated at the onset of petal colouration; 2 days later, the fully mature styles were removed and stored at −70 °C. (Styles refer to stigma and style which were removed together; the ovary was not included.) Frozen styles (3 g; 220 styles) were ground to a fine powder in liquid nitrogen using a mortar and pestle, then ground further in 50 ml of extraction buffer [0.1 M Tris-HCl *p*H 8.5, 1 mM $CaCl_2$, 0.1 M NaCl, 1 mM PMSF, 1 mM DTT, 10 mM EDTA and 1% (w/w) insoluble polyvinyl pyrrolidone (Polyclar AT)]. The homogenate was centrifuged (10,000g; 15 min) and the supernatant equilibrated with 5 mM ammonium bicarbonate *p*H 8.6, 1 mM NaCl, 1 mM $CaCl_2$, 1 mM EDTA, by passage through a Sephadex G-25 column (1.6×22 cm; void volume 11 ml). The first 16 ml that eluted after the void volume was collected (28.6 mg total protein as bovine serum albumin) and applied to DEAE-Sepharose (2×13 cm), equilibrated with the same ammonium bicarbonate buffer. As the S_2-associated glycoprotein is known from isoelectric focusing experiments to have a high *p*I (>9.5), it does not bind to DEAE-Sepharose at *p*H 8.6, but was present in the unbound fraction together with one other major component and several minor components. The unbound fractions were combined (2.78 mg protein as BSA), concentrated to 16 ml and fractionated further by chromatography on concanavalin A (Con A)–Sepharose. Then the Con A–Sepharose was washed with 5 vol. 0.1 M methyl-α-D-mannoside in 10 mM sodium acetate *p*H 7.0, 0.1 M NaCl, 1 mM $MgCl_2$, 1 mM $CaCl_2$, 1 mM $MnCl_2$ and subsequently with sodium bicarbonate (0.25 M, *p*H 8.8) (four changes during a 1-h period). Four volumes of sodium bicarbonate (0.25 M *p*H 8.8) containing 0.03% glutaraldehyde were added to the beads, the two were mixed and then the beads were washed with 0.1 M sodium bicarbonate *p*H 8.0, containing 0.5 M NaCl, resuspended in the sodium acetate buffer (without methyl-α-D-mannoside) and packed into a column (0.8×14 cm). The unbound fraction from DEAE-Sepharose was equilibrated in acetate buffer by passage through a Sephadex G-25 column equilibrated with acetate buffer, then applied to the Con A-Sepharose column. Unbound material was collected, the column was washed with 10 vol. acetate buffer, and the bound material eluted with 0.2 M methyl-α-D-mannoside in acetate buffer. The eluted material was separated from the methyl-α-D-mannoside by passage through a Biogel P150 column. Yield was 490 μg of protein (1.7% of total style protein). Chemical deglycosylation of the S_2-associated glycoprotein: the isolated S_2-glycoprotein (lane 1) was deglycosylated (lane 2) using the trifluoromethanesulphonic acid (TFMS) procedure[31], and the deglycosylated proteins were analysed on 15% SDS-polyacrylamide gels which were stained with Coomassie blue. Enzymatic deglycosylation of the S_2-associated glycoprotein: Isolated glycoprotein (5 μg) in SDS sample buffer (10 μl) was heated at 100 °C for 2 min, then cooled and 46.5 U endoglycosidase F (Miles Laboratories) added. The mixture was incubated at 35 °C for 2 h, then applied to a 15% SDS-polyacrylamide gel, which was stained with silver stain. *B*, Poly(A)$^+$ mRNA (0.5 or 2.0 μg) was isolated from mature styles, green-bud styles or ovary[32], and translated using an amino-acid-depleted rabbit reticulocyte lysate kit (Amersham) in the presence of tritiated leucine, lysine, phenylalanine, proline and tyrosine. Translation products were separated by SDS-PAGE using 12.5–20% SDS-polyacrylamide gradient gels. The products were visualized by autoradiography after treatment of the gel with Amplify (Amersham). *C*, N-terminal sequencing of the S_2-glycoprotein purified as described in *A* was performed using an Applied Biosystems Model 470 A gas-phase sequencer. Isolated glycoprotein (~200 μg) was applied in aqueous solution to a glass fibre disk and evaporated to dryness. The resultant phenylthiohydantoin amino-acid derivatives were identified on an IBM-CN column (IBM, Danbury, Connecticut) using a sodium acetate–acetonitrile trifluoroacetic acid gradient, in a Beckman-Altex high-pressure liquid chromatograph. From the N-terminal sequence, three pools of 14-mers (oligodeoxyribonucleotides) of 24-fold degeneracy to Tyr-Met-Gln-Leu-Val were synthesized by the solid-phase phosphoramidite method[33] using an Applied Biosystems (ABI) Model 380A DNA Synthesizer. The 14-mers were labelled at the 5′ end using [α-^{32}P]ATP (5,000 Ci mmol^{-1}) and T_4 polynucleotide kinase. The labelled 14-mers (500 μg ml^{-1}) were used to prime cDNA synthesis. Specifically primed cDNA products were separated on an 8% acrylamide/7 M urea gel. Oligonucleotide pool I primed the synthesis of a cDNA fragment of ~100 nucleotides, whereas no cDNA products were detected when either pool II or pool III was used to prime cDNA synthesis. The cDNA fragment was purified and sequenced[34] to give unequivocal assignment for 72 nucleotides as shown. From this sequence, a single 30-mer (oligodeoxyribonucleotide) complementary to the cDNA sequence encoding amino acids −9 to +1 was synthesized[33]. This 30-mer was used to screen a cDNA library as described in Fig. 3 legend.

segments has been noted for *Lycopersicon peruvianum*[20], another member of the Solanaceae that has a gametophytic self-incompatibility system. Previous studies with *N. alata*[21] also demonstrated the developmental regulation and distribution of *S*-allele-associated style components.

The absolute correlation between the presence of the 32K glycoprotein component in the style and the ability of the style to reject S_2 pollen, represented strong evidence that the 32K protein was a product of either the S_2 allele or of a gene closely linked to it that does not appear to recombine with S_2 in the present breeding programme. We attempted to isolate the S_2 product and to clone the cDNA encoding the protein.

Isolation of S_2-glycoprotein cDNA

A method for isolating the 32K component from styles was established, based on the fact that it is a glycoprotein with a high *p*I. Chemical deglycosylation of the 32K component, isolated by a combination of ion-exchange and affinity chromatography, yielded a single product (M_r 26K) (Fig. 2*A*). The carbohydrate component contains fucose, arabinose, xylose, mannose, galactose and possibly glucose, but the organization of these monosaccharide residues into carbohydrate chains is unknown. At least part of the carbohydrate occurs as *N*-linked chains, as the isolated component was susceptible to degradation with endoglycosidase F (Endo F), yielding three products as well as the undegraded glycoprotein of M_r 32K (Fig. 2*A*). The Endo F products comprised two species running closely together, each with an estimated M_r of 30,000, and a single species of M_r 28,000. A product of M_r 27,000, which is slightly larger than the chemically deglycosylated protein, was found on *in vitro* translation of messenger RNA isolated from a mature style but was absent from translation products of

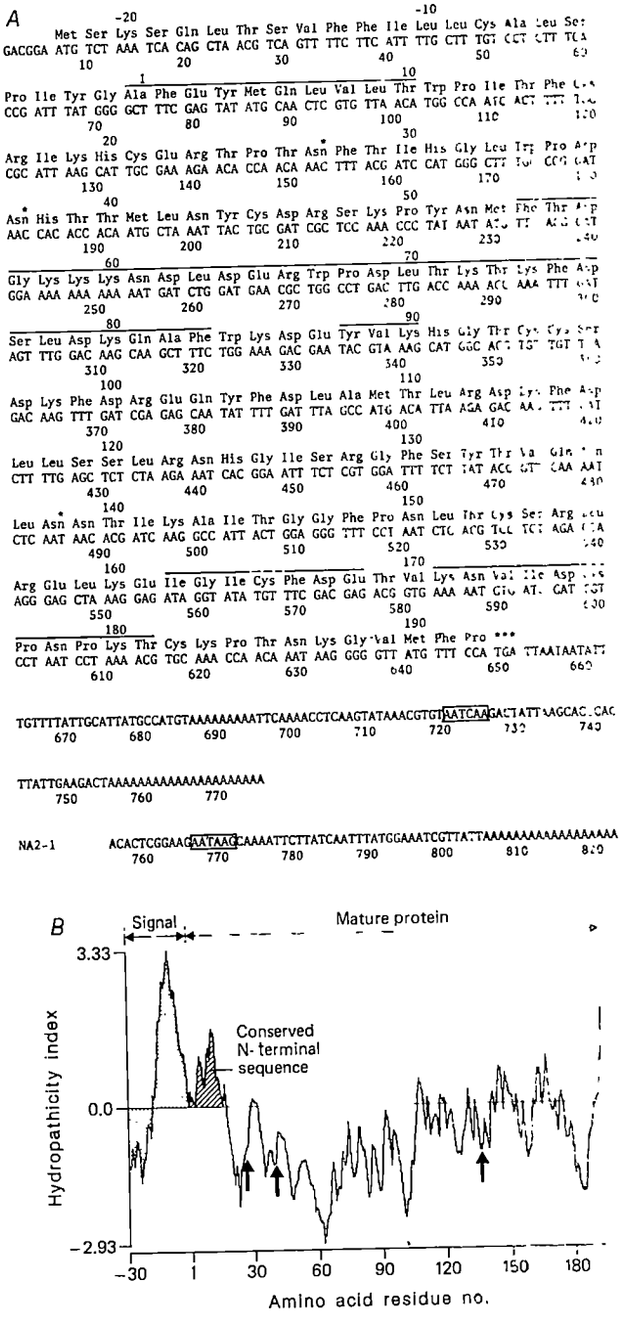


Fig. 3 *A*, The nucleotide sequence and predicted amino-acid sequence of the cDNA encoding the S_2-glycoprotein of *N. alata*, as defined by the sequence of clone NA-2-2. Nucleotides 19–754 are identical to those of clone NA-2-1. The cDNA insert from clone NA-2-1 had an additional 50 nucleotides at the 3′-untranslated end preceding a polyadenylation site, as shown beneath the last line of the NA-2-2 sequence. Only one strand with the polarity of the mRNA is shown. Nucleotides are numbered beneath the DNA sequence. The predicted amino-acid sequence is given above the nucleotide sequence and is numbered beginning with 1 for the first amino acid of the mature protein. The putative signal peptide is indicated by negative numbers. The overlined amino acids are those residues identified by protein sequencing. Broken overlining indicates those residues that could not be identified unambiguously by amino-acid sequencing. Potential glycosylation sites are indicated by asterisks, and potential polyadenylation signals at residues 720–725 and 766–771 (for NA-2-1) are boxed. *B*, A hydrophobicity plot of the deduced amino-acid sequence of the unprocessed S_2-glycoprotein. The region of the profile corresponding to the putative signal peptide (amino acids −22 to −1) is stippled. The hydrophobic N-terminal sequence, which exhibits striking homology to the *S*-allele-associated style components from *L. peruvianum*, is shaded. The positions of the three putative *N*-glycosylation sites are indicated by arrows.

Methods. *A*, Poly(A)$^+$ mRNA isolated from mature S_2S_3 styles[32] was used to construct a cDNA library in λgt10 (ref. 35). The library was screened for sequences specific to mature style by differential hybridization to single-stranded ^{32}P-cDNAs prepared from ovary, green-bud style and mature style poly(A)$^+$ mRNAs. Prehybridization (2 h at 42 °C) was in 5×Denhardt's, 5×SSC, 50 μg ml^{-1} sonicated salmon sperm DNA, 50 mM Na-phosphate *p*H 6.8, 1 mM Na-pyrophosphate, 100 μM ATP and 50% deionized formamide. The cDNA probes were used at 4×10^7 c.p.m. ml^{-1}. Filters were washed in 0.1×SSC, 0.1% SDS at 42 °C. One clone (NA-2-1) which hybridized to mature style cDNA, but not to cDNA from ovary or green-bud style, also hybridized to the synthetic 30-mer described in the legend to Fig. 2*C*. The same hybridization solution as described above was used for hybridizations with the 30-mer (10^8 c.p.m. μg^{-1}, $0.4–1\times10^6$ c.p.m. ml^{-1}), except that the formamide concentration was 20% and the temperature was decreased to 37 °C. A second cDNA library in λgt10 was constructed by a method designed to optimize isolation of full-length clones[22]. A library containing 200,000 plaques was obtained from 5 μg of mature style poly(A)$^+$ RNA. From this library, a clone, designated NA-2-2, which hybridized to the *Eco*RI insert from NA-2-1 and the synthetic 30-mer, was identified. The insert was labelled with [α-^{32}P]dATP using DNA polymerase I (Klenow fragment)[36]. The 30-mer was labelled with [γ-^{32}P]ATP using T_4 polynucleotide kinase. The cDNA inserts from clones NA-2-1 and NA-2-2 were ligated into the bacteriophage vector M13mp8 RF DNA[37] and sequenced by the chain termination method[38,39]. Sequence data obtained in this way were analysed and manipulated using the computer programs of Staden[40], as modified by Dr A. P. Kyne. Peptide sequencing: The 32K glycoprotein was electroeluted from selective two-dimensional SDS-polyacrylamide gels (60 μg) and purified by 'reverse-gradient' HPLC[20] before reduction and alkylation[41] and desalting by 'reverse-gradient' HPLC[20]. The sample was divided into two equal portions and fragmented by either CNBr cleavage[42] or *S. aureus* protease digestion using an enzyme/substrate ratio of 1:50 in 1% ammonium bicarbonate[43]. The peptides were purified for sequence analysis by multi-dimensional microbore HPLC[41]. HPLC was performed on a Perkin-Elmer liquid chromatograph (model LC4) equipped with a model LC95 ultraviolet detector, a model LS4 fluorimeter and a model LS1 100 integrator. Fractions were collected either with a Pharmacia Frac 100 or manually. *B*, The hydrophobicity profile was determined using the predictive rules of Kyte and Doolittle[44] and a span of nine consecutive residues.

mRNA from both ovary and styles harvested at the green-bud stage (Fig. 2*B*). As the 32K S_2-glycoprotein was not detected in extracts of ovary or styles from flowers at the green-bud stage, it was concluded that the 27K component corresponds to the *in vitro*-translated product of S_2 mRNA. This component is slightly larger than the 26K chemically deglycosylated glycoprotein, consistent with the presence of a signal peptide that is cleaved during secretion of the S_2-glycoprotein from the transmitting tract cells to the extracellular space.

The N-terminal sequence of the isolated glycoprotein was determined and three pools of 14-mers of 24-fold degeneracy to amino acids 4–8 were prepared and used to prime cDNA synthesis (see Fig. 2 legend). A specifically primed fragment of ~100 nucleotides, produced using one of the three pools of 14-mers, was purified and sequenced. From this sequence a single 30-mer complementary to the cDNA sequence encoding amino acids −9 to +1 was synthesized (Fig. 2*C*). A cDNA library was prepared in λgt10 using mRNA isolated from mature styles of *N. alata* of genotype S_2S_3. The library was subjected to differential screening using ^{32}P-labelled cDNA prepared from mRNA isolated from mature and green-bud styles. Plaques that hybridized strongly only to the mature style cDNA were selected and rescreened using cDNA prepared from mature style and ovary mRNA. Ovary cDNA was chosen for the second screen because electrophoretic analysis of extracts of mature style and ovary indicated that these tissues have in common some proteins that are not present in green-bud styles (data not shown). The protein profiles of other plant organs were too diverse compared with mature style to be useful for differential screening. Clones that hybridized to mature style cDNA, but not to ovary or green-bud style cDNA, were screened with the synthetic oligodeoxyribonucleotide 30-mer described above. One of the clones that hybridized with the 30-mer as well as the cDNA prepared from mature style mRNA, but not ovary or green-bud style mRNA, was chosen for further study. This clone was designated NA-2-1.

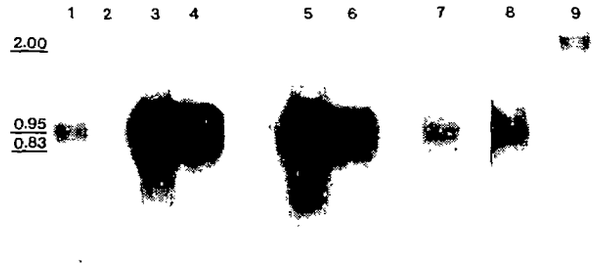


Fig. 4 Northern blot analysis of mRNAs from styles of different *S* genotypes isolated from *N. alata* and *L. peruvianum*. Lanes 1–4, *N. alata* genotypes S_2S_3 (lane 1, ovary 5 μg; lane 2, green bud 5 μg; lane 3, mature style 2 μg; lane 4, mature style 0.5 μg); lanes 5, 6, *N. alata* genotype S_2S_2 (lane 5, mature style 5 μg; lane 6, mature style 0.5 μg); lane 7, *N. alata* genotype S_3S_3 (mature style 5 μg); lane 8, *N. alata* genotype S_1S_3 (mature style 5 μg); lane 9, *L. peruvianum* mature style (5 μg). Numbers on the left are size markers.

Methods. mRNAs were isolated as described previously[32] and electrophoresed in formaldehyde/1.2% agarose gels[45] using a running buffer containing 20 mM morpholinopropanesulphonic acid *p*H 7.0, 5 mM sodium acetate and 0.1 mM EDTA *p*H 8.0. The RNAs were transferred to nitrocellulose filters and probed with ^{32}P-labelled[36] S_2 cDNA (10^8 c.p.m. μg^{-1}, 2×10^6 c.p.m. ml^{-1}). The size markers used were *Eco*RI/*Hin*dIII restriction fragments of λDNA. Prehybridization (2 h at 42 °C) and hybridization (16 h at 42 °C) was carried out in 5×Denhardt's, 5×SSC, 50 μg ml^{-1} sonicated salmon sperm DNA, 100 μM ATP and 50% deionized formamide. Filters were washed in 0.1×SSC, 0.1% SDS at 42 °C. All exposures were for 3 h, except for S_1S_3 *N. alata* mRNA (lane 8) and S_1S_3 *L. peruvianum* mRNA, where films were exposed for 18 h.

Nucleotide sequence analysis of the cDNA insert in clone NA-2-1 showed that it contained an open reading frame, but had no ATG that could act as an initiation codon. To obtain a clone containing a full-length cDNA insert, another cDNA library was prepared using a method[22] which optimizes the recovery of full-length clones. This library (200,000 plaques) was screened with both the cDNA insert from NA-2-1 and the 30-mer shown in Fig. 2*C*. A second clone, designated NA-2-2, hybridized to both these probes. Figure 3*A* shows the nucleotide sequence of the cDNA insert from NA-2-2. The cDNA sequence at the 5′ end of the NA-2-2 insert is identical to the sequence of the cDNA fragment synthesized by primer extension (Fig. 2*C*), and includes an ATG that could act as an initiation codon. In addition, the sequence of the NA-2-2 insert matches exactly the sequence of the NA-2-1 insert from nucleotide 19 of the NA-2-2 cDNA (Fig. 3*A*). The NA-2-2 sequence contains an open reading frame of 642 base pairs (bp) which encodes a protein with a predicted M_r of 24,847, including a putative signal sequence of 22 amino acids. Figure 3*A* shows the sequence regions that have been confirmed by sequencing of peptides generated from the S_2-glycoprotein by either CNBr cleavage or digestion with *Staphylococcus aureus* protease. Of the predicted 192 amino-acid residues of the mature S_2-glycoprotein, 61 have been confirmed by amino-acid sequencing of peptides. We therefore conclude that the sequence shown in Fig. 3*A* encodes the mature S_2 protein and a signal sequence that directs the transfer of the S_2-glycoprotein from the transmitting tract cells to the extracellular space. This putative signal sequence has features that are typical of eukaryotic signal sequences[23]—a relatively hydrophilic sequence of five amino acids at the C-terminal end, a relatively hydrophobic sequence (−6 to −14) and a more hydrophilic sequence at the N-terminal end (see Fig. 3*B*). The amino acids at the C-terminal end include glycine at the cleavage site, an aromatic residue at −2 and a helix breaker, proline, at −4, all of which are common features of the C-terminal region of signal sequences. In the mature protein sequence there is relatively hydrophobic sequence at the N-terminus (Fig. 3*B*) which is homologous with that of *S*-allele-associated style components from *L. peruvianum*[20] (see Fig. 6). There are also three predicted glycosylation sites (residues 27, 37 and 138), based on the consensus glycosylation sequence (Asn-X-Ser/Thr)[24], in the hydrophilic region of the protein. As six moles of *n*-acetylglucosamine were detected per mole of isolated S_2-glycoprotein (unpublished observations), it is possible that each of these glycosylation sites carries an *N*-linked carbohydrate chain. The fact that enzymatic deglycosylation with Endo F (Fig. 2*A*) yielded three products separable by SDS-polyacrylamide gel electrophoresis, suggests that these sites are in fact *N*-glycosylated. As well as these potential *N*-linked carbohydrate chains, there may also be *O*-linked chains. As no hydroxyproline was detected in the amino-acid analysis (unpublished observations), there is no opportunity for Hyp-glycosylation. As there are nine cysteine residues in the mature protein, there is considerable potential for internal sulphydryl linkages as well as at least one free sulphydryl group which might be functionally significant.

Apart from differences at the 5′ end, clones NA-2-1 and NA-2-2 also differed in the lengths of their 3′-untranslated sequences. The two clones were identical as far as nucleotide 754, the polyadenylation site in clone NA-2-2; from this point the cDNA insert from clone NA-2-1 had an additional 50 nucleotides of untranslated mRNA and a poly(A) tail of 18 residues (see Fig. 3*A*). This difference at the 3′ end suggests that there are alternative polyadenylation sites in S_2 RNA transcripts. The putative signals for the two sites are indicated in Fig. 3*A*; neither has the sequence AATAAA which is typically found in animal messages[25,26], but the polyadenylation signals in plant genes apparently show much greater sequence variation than is found in animal genes[27,28].

Hybridization analyses

The S_2 cDNA was used as a probe in Northern blot hybridization experiments with mRNAs prepared from mature styles of *N. alata* genotypes S_1S_3, S_2S_3, S_2S_2 and S_3S_3, as well as from mature styles of *L. peruvianum* genotype S_1S_3 and green-bud styles and ovaries of *N. alata* genotype S_2S_3 (Fig. 4). In all mature styles bearing the S_2 allele, a predominant mRNA species of ~940 nucleotides hybridized to the cDNA probe. A mRNA of identical size was detected in preparations of poly(A)$^+$ mRNA isolated from S_3S_3 and S_1S_3 styles of *N. alata*, the extent of hybridization being ≤1% the level obtained in styles bearing the S_2 allele. This result indicates that the transcripts of the different *S* alleles are homologous. The same probe did not hybridize to green-bud mRNA; however, a weak signal corresponding to 940 nucleotides was detected in S_2S_3 ovary mRNA.

Self-incompatibility is not expressed in green buds, nor is the S_2-glycoprotein detected in extracts of green buds; it is therefore not surprising that the S_2 cDNA probe did not hybridize with green-bud mRNA. The hybridization with ovary mRNA was unexpected as the S_2-glycoprotein is not detected in extracts of ovary; it is possible that low levels of the glycoprotein are produced in the ovary to ensure arrest of any self-pollen tubes that manage to evade the self-incompatibility mechanisms expressed in the style. The RNA blot analysis also revealed that styles from *L. peruvianum* (genotype S_1S_3) synthesized readily detectable levels of a 2.5-kilobase (kb) mRNA that hybridized with the NA-2-1 cDNA insert. This finding is consistent with the extensive homology observed at the N-terminal sequences of the S_2-glycoprotein from *N. alata* and both the S_1 and S_3 proteins from *L. peruvianum* (Fig. 6). The S_1 and S_3 proteins from *L. peruvianum* each have an estimated M_r of 28,000 and the RNA blot analysis indicated that the mRNA transcripts encoding these proteins are also identical in size. The predicted proportion of noncoding mRNA in the *L. peruvianum* S_1 and S_3 transcripts is significantly greater than for the S_2 transcript from *N. alata*.

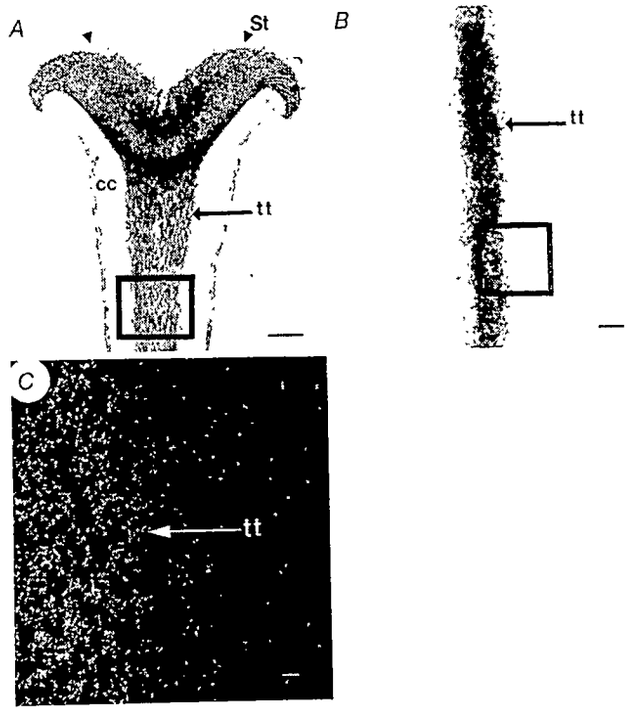


Fig. 5 Hybridization histochemistry of probe for cDNA encoding the 32K style glycoprotein from *N. alata*, genotype S_2S_3. *A*, Light micrograph of longitudinal section through a mature style (genotype S_2S_3) embedded in JB-4 resin (Polysciences) and stained with Richardson's blue. The central core of transmitting tissue (tt) is surrounded by the cortex (cc). The stigma surface (St) is indicated. Scale bar, 250 μm. *B*, Autoradiograph of a frozen longitudinal section through the style after hybridization with ^{32}P-labelled S_2 cDNA (obtained by direct exposure to X-ray film). Scale bar, 100 μm. The area shown corresponds to the boxed area in *A*. *C*, Darkfield photograph of a longitudinal section through the style shown in *B* after hybridization (obtained by liquid emulsion autoradiography). Scale bar, 10 μm. The area shown corresponds to the boxed section *B*.

Methods. Mature styles of *N. alata* (genotypes S_2S_3 and S_1S_3) were placed in a mould with OCT Tissue Tec and frozen in Freon 22 cooled in liquid nitrogen. Longitudinal sections (6–8 μm thick) were cut at −20 °C using a Frigocut microtome (Reichert Jung) and attached to glass slides precoated with 1% gelatin using 0.25% formaldehyde as a crosslinking agent. The sections were fixed at 4 °C for 5–10 min in 2% glutaraldehyde in 33% ethylene glycol and 0.1 M sodium phosphate buffer. Prehybridization and hybridization conditions were as described by Rall *et al.*[46]. The ^{32}P-labelled S_2 cDNA (5×10^8 c.p.m. μg^{-1}) was hybridized to the sections at 40 °C for 60 h; direct exposure time was 2 days using Cronex MRF 31 Medical Recording Film (Du Pont); exposure with liquid emulsion (Emulsion K5, Ilford Nuclear Research) was 7 days.

Hybridization to style sections

The cDNA encoding the S_2-glycoprotein was also used in hybridization histochemical experiments using longitudinal sections of mature S_2S_3 and S_1S_3 styles. Figure 5 shows that there was specific binding of the cDNA probe to the cells of the S_2S_3 transmitting tissue, with no binding to the cortical or epidermal cells. The transmitting tract is the tissue through which the pollen tubes grow on their way to the ovary and it is in this tissue that we would expect the *S* gene to be expressed. The cDNA probe also bound to the transmitting tissue of S_1S_3 styles; although identical conditions were used, binding was very faint compared with that obtained using mature S_2S_3 styles. This result is consistent with the weak hybridization detected in the Northern blot experiments. In control experiments there was essentially no hybridization.

Homology between *N. alata* and *L. peruvianum*

N-terminal sequence analysis of the proteins associated with *L. peruvianum* self-incompatibility alleles S_1 and S_3 revealed striking homologies to the N-terminus of the *N. alata* S_2-glycoprotein[20]. The proteins associated with the S_1 and S_3 alleles of *L. peruvianum* were identified by electrophoretic analysis of style extracts and were purified by electroelution and sequenced as described by Mau *et al.*[20]. Figure 6 shows the extent of homology between the *N. alata* S_2-glycoprotein and the two *S*-associated proteins isolated from *L. peruvianum*. The homology at the N-terminal ends of the *S*-allele-associated style components of *N. alata* and *L. peruvianum* is consistent with the hypothesis that the *S* gene has been conserved in evolution to prevent inbreeding of plant species[1].

Discussion

We have cloned the cDNA encoding a glycoprotein from the female sexual tissue of *N. alata* which segregates with the S_2 allele of the gene controlling self-incompatibility. This cDNA hybridizes with mRNAs from styles of other *S* genotypes of *N. alata* and also with mRNAs from styles of *L. peruvianum*, another species in the family Solanaceae which has a gametophytic self-incompatibility system. Specific homology in the N-terminal sequences of *S*-genotype-related style proteins for these two species has also been demonstrated.

Taken together, the segregation of the S_2-glycoprotein with function of the S_2 allele, the *in vitro* activity of the isolated S_2-glycoprotein as a pollen tube inhibitor[29], and the homology at the N-terminus of *S*-genotype-associated style components from *N. alata* and *L. peruvianum*, provide strong evidence that the cDNA described here encodes the product of the S_2 allele. However, conclusive evidence can only come from transformation of the *S* genotype by gene transfer.

The *S* gene is considered to have a tripartite structure—two conserved portions encoding pollen activity and style activity and a variable part encoding the allelic specificity[1]. The conservation of the hydrophobic N-terminal sequences of the *S*-allele-associated components from *N. alata* and *L. peruvianum*[20] is compatible with this model; these sequences may represent a fragment of the conserved portion encoding style activity. The S_2 cDNA can now be used as a probe to obtain cDNA clones for other *S*-alleles from *N. alata* as well as other related species, an approach which should elucidate the expression of different allelic specificities. Although it is likely that the allelic differences are expressed as differences in the protein component of the style glycoprotein, the possibility that the allelic differences reside in the glycosyl moiety cannot be excluded. In this case, the allelic differences would be expressed primarily as glycosyl transferases of different specificities, and differences would then be detected in the structures of the glycosyl moieties of the products of different *S* alleles. Analysis of the carbohydrate moiety of the *S*-glycoprotein is presently limited by difficulties in obtaining sufficient material.

Comparison of the *N. alata* S_2 cDNA sequence with nucleotide sequences encoding *S*-genotype-associated proteins from female tissues of other plant species may provide some insight into the evolution of self-incompatibility. Recently, a cDNA clone encoding part (~30%) of an *S*-locus-specific glycoprotein from *Brassica oleracea*, a species having a sporophytic self-incompatibility system[15], has been described; there is no apparent homology between this partial sequence and that of the *N. alata* S_2 cDNA. However, the possibility of homology with the other undescribed 70% of the molecule remains. Once a full-length clone for the *B. oleracea* protein is available, comparison of the two sequences should give a greater under-

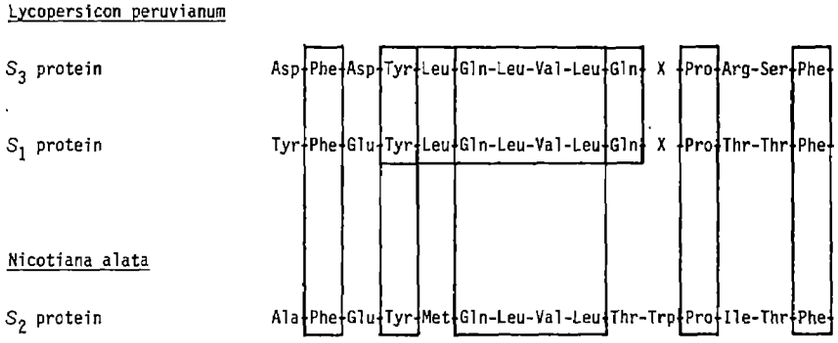


Fig. 6 A comparison of the amino-terminal sequences of *L. peruvianum* S_1- and S_3-associated proteins with *N. alata* S_2 protein. Identical amino acids are boxed.

standing of the evolutionary relationship between the sporophytic and gametophytic systems.

A fundamental question in understanding how self-incompatibility is expressed is whether the pollen tube and style *S*-gene products are identical. To date, we have not been able to identify a protein from pollen which corresponds to the *S* genotype. There are two reasons for expecting the products of a particular *S* allele to differ in pollen and style: first, it is difficult to envisage how two identical molecules could interact to cause inhibition of pollen tube growth. It is possible that the *S*-gene products from the style and pollen tube, although generated from the same allele, are not identical. Non-identical products could be generated by different splicing of the same transcriptional unit to produce different mRNAs, or there may be different post-translational modifications such as glycosylation[29]. In this way, differences leading to complementary sites on the two *S*-gene products might be generated. The second reason for expecting differences in the structures of the two *S*-gene products relates to their secretion. It is assumed that the cells of the style transmitting tract secrete the *S*-gene product into the extracellular matrix; the presence of the signal sequence predicted by the S_2 cDNA sequence is compatible with secretion of the product. The pollen tubes grow through the style in the extracellular matrix and must in some way recognize the *S*-gene product. It is difficult to envisage how the recognition which results in pollen tube arrest could occur if the pollen *S*-gene product, as well as the style *S*-gene product, is secreted. It is more likely that the pollen *S*-gene product is either membrane-associated or wall-associated, so that the interaction with the style *S*-gene product could signal cytoplasmic events leading to arrest of pollen-tube growth.

The cloning of the cDNA encoding the S_2-glycoprotein represents the initial step in resolving these questions, which have broader implications in the field of cell–cell recognition in plants. It is likely that an understanding of how allelic differences are expressed by plant genes and how products of these alleles interact to initiate a response involving changes in cell-wall metabolism, will lead to principles which may apply to more complex systems involving plant cell–cell interactions, for example, in host–pathogen and host–parasite interactions.

We thank Dr K. K. Pandey (Grasslands, Palmerston North, New Zealand), for providing *N. alata* seed of genotypes S_2S_3 and S_1S_3, Mr Darron Broom for management of the glasshouse and Ms Susan Mau for collection of plant material. We also thank Lucy Duncan for assistance in preparation of the synthetic oligonucleotide probes; Marie John for assistance with amino-acid sequencing; Dr Tony Bacic for the monosaccharide analyses; Marg Strode for preparation of the manuscript; and Tony Kyne for making the MELBDBSYS suite of computer programs available to us. The work was supported in part by funds from Agrigenetics Research Associates.

Received 21 October 1985; accepted 12 March 1986.

1. de Nettancourt, D. *Incompatibility in Angiosperms* (Springer, Berlin, 1977).
2. Heslop-Harrison, J. *Proc. R. Soc.* **B202**, 73–92 (1978).
3. Lewis, D. *N.Z. Jl Bot.* **17**, 637–644 (1979).
4. Pandey, K. K. *N.Z. Jl Bot.* **17**, 645–663 (1979).
5. Harris, P. J., Anderson, M. A., Bacic, A. & Clarke, A. E. *Oxford Surveys of Plant Molecular and Cell Biology* Vol. 1 (ed. Miflin, B. J.) 161–203 (Oxford University Press, 1984).
6. Knox, R. B. in *Encyclopaedia of Plant Physiology, New Series* Vol. 17 (eds Linskens, H. F. & Heslop-Harrison, J.) 508–608 (Springer, Berlin, 1984).
7. Larsen, K. *Hereditas* **85**, 227–248 (1977).
8. Pandey, K. K. *Heredity* **22**, 255–283 (1967).
9. Lawrence, M. J. *Proc. R. Soc.* **B188**, 275–285 (1975).
10. Lawrence, M. J., Afzal, M. & Kenrick, J. *Heredity* **40**, 239–253 (1978).
11. Linskens, H. F. *Proc. R. Soc.* **B188**, 299–311 (1975).
12. Nishio, T. & Hinata, K. *Jap. J. Genet.* **54**, 307–311 (1979); *Genetics* **100**, 641–647 (1982).
13. Ferrari, T. E., Bruns, D. & Wallace, D. H. *Pl. Physiol.* **67**, 270–277 (1981).
14. Mau, S-L., Raff, J. & Clarke, A. E. *Planta* **156**, 505–516 (1982).
15. Nasrallah, J. B., Kao, T.-H., Goldberg, M. L. & Nasrallah M. E. *Nature* **318**, 263–267 (1985).
16. Lewis, D. *Heredity* **3**, 339–345 (1949); *Proc. R. Soc.* **B151**, 468–477 (1960); in *Genetics Today* Vol. 3 (ed. Geerts, S. J.) 656–663 (Pergamon, Oxford, 1965).
17. Nasrallah, M. E., Barber, J. T. & Wallace, D. H. *Heredity* **24**, 23–27 (1969).
18. Heslop-Harrison, J. *A. Rev. Pl. Physiol.* **26**, 403–425 (1975); *Proc. R. Soc.* **B218**, 371–395 (1983).
19. Burnet, F. M. *Nature* **232**, 230 (1971).
20. Mau, S.-L. *et al. Planta* (submitted).
21. Bredemeijer, G. M. M. & Blass, J. *Theor. appl. Genet.* **59**, 185–190 (1981).
22. Okayama, H. & Berg, P. *Molec. cell. Biol.* **2**, 161–170 (1982).
23. von Heijne, G. *Eur. J. Biochem.* **133**, 17–21 (1983); *J. molec. Biol.* **184**, 99–105 (1985).
24. Wagh, P. V. & Bahl, O. P. *CRC Crit. Rev. Biochem.* **10**, 307–377 (1981).
25. Proudfoot, N. J. & Brownlee, G. G. *Nature* **263**, 211–214 (1976).
26. Beinoist, C., O'Hare, K., Beathnach, R. & Chambon, P. *Nucleic Acids Res.* **8**, 127–140 (1980).
27. Lycett, G. W., Delauney, A. J. & Croy, R. R. D. *FEBS Lett.* **153**, 43–46 (1983).
28. Messing, J. *et al.* in *Genetic Engineering of Plants* (*Basic Life Sci. Ser.*) (eds Kosuge, T., Meredith, C. P. & Hollaender, A.) 211–227 (Plenum, New York, 1983).
29. Clarke, A. E., Anderson, M. A., Bacic, T., Harris, P. J. & Mau, S.-L. *J. Cell Sci. Suppl.* **2**, 261–285 (1985).
30. Bradford, M. M. *Analyt. Biochem.* **72**, 248–253 (1976).
31. Edge, A. S. B., Faltynek, C. R., Hof, L., Reichert, L. E. & Weber, P. *Analyt. Biochem.* **118**, 131–137 (1981).
32. Malmberg, R., Messing, J. & Sussex, I. in *Molecular Biology of Plants: A Laboratory Course Manual* (Cold Spring Harbor Laboratory, New York, 1985).
33. Beaucage, S. L. & Caruthers, M. H. *Tetrahedron Lett.* **22**, 1859–1862 (1981).
34. Maxam, A. M. & Gilbert, W. *Meth. Enzym.* **65**, 499–560 (1980).
35. Huynh, T. V., Young, R. A. & Davis, R. W. in *DNA Cloning: A Practical Approach* (ed. Glover, D.) (IRL, Oxford, 1984).
36. Feinberg, A. P. & Vogelstein, B. *Analyt. Biochem.* **132**, 6–13 (1983).
37. Messing, J. & Vieira, J. *Gene* **19**, 269–276 (1982).
38. Sanger, F., Nicklen, S. & Coulson, A. R. *Proc. natn. Acad. Sci. U.S.A.* **74**, 5463–5467 (1977).
39. Sanger, F., Coulson, A. R., Barrell, B. G., Smith, A. J. H. & Roe, B. A. *J. molec. Biol.* **143**, 161–718 (1980).
40. Staden, R. *Nucleic Acids Res.* **4**, 4037–4051 (1977); *Nucleic Acids Res.* **5**, 1013–1015 (1978).
41. Grego, B. *et al. Eur. J. Biochem.* **148**, 485–491 (1985).
42. Simpson, R. J. & Nice, E. C. *Biochem. Int.* **8**, 787–791 (1984).
43. Nice, E., Grego, B. & Simpson, R. J. *Biochem. Int.* **11**, 187–195 (1985).
44. Kyte, J. & Doolittle, R. F. *J. molec. Biol.* **157**, 105–132 (1982).
45. Maniatis, T., Fritsch, E. F. & Sambrook, J. *Molecular Cloning: A Laboratory Manual* (Cold Spring Harbor Laboratory, New York, 1982).
46. Rall, L. B. *et al. Nature* **313**, 228–231 (1985).

'Missing image' in gravitational lens systems?

D. Narasimha*, K. Subramanian† & S. M. Chitre‡

* Department of Physics, University of Calgary, Calgary, Alberta, Canada T2N 1N4
† Astronomy Centre, University of Sussex, Brighton BN1 9QH, UK
‡ Tata Institute of Fundamental Research, Homi Bhabha Road, Bombay 400 005, India

Gravitational lens models involving extended mass distributions generally predict an odd number of images[1], with one of the images close to the centre of the principal lens galaxy. In all the lens systems observed up to now, only an even number of images have been unambiguously detected. A number of suggestions[2-4] have been advanced to explain the absence of the 'odd' image, but none of these is sufficiently compelling. We suggest here that the presence of a compact nucleus with mass in the range 5×10^9 to 5×10^{10} solar masses ($M_\odot$), contained within a region of size $\leq$50 pc at the centre of a lens galaxy, would dim the odd image significantly without affecting the rest of the image configuration.

We argue that a massive compact nucleus with even a small fraction ($\leq$2%) of the total galaxy mass contained within ~50 pc would have negligible influence on the properties of the images located outside the core of the galaxy. But the proximity of the odd image to the nucleus allows it to be pulled closer to the galactic centre, at the same time becoming significantly dimmer. We demonstrate below that the effect becomes pronounced for a nuclear mass exceeding $\sim5\times10^9\ M_\odot$ contained within ~50 pc. It turns out that the exact size of the nucleus is not particularly important, although the intensity of the odd image increases as the nucleus becomes more extended.

Consider a spherically symmetric density distribution of matter for the core of the underlying lens galaxy. The scattering function[5] representing the bending of light rays for an impact parameter small compared with the radius of the galactic core is given by

$$I_G(Z_0)=\pi\sigma_G Z_0^* \tag{1}$$

Here, in the usual notation, σ_G is the central surface density of the galaxy and Z_0 is the complex number giving the image position in the deflector plane. Suppose, in addition we consider the effect of a nucleus of mass M_N and radius R_N, with a constant surface density. Then the scattering function of the nucleus can be written as

$$\begin{aligned} I_N(Z_0)&=\frac{M_N}{R_N^2}Z_0^*, \quad |Z_0|<R_N \\ &=M_N/Z_0, \quad |Z_0|>R_N \end{aligned} \tag{2}$$

With the help of the above scattering functions we can relate the image position Z_0 to the source position Z, through the equation[5]

$$\begin{aligned} Z&=Z_0-\frac{4GD}{c^2}I_G^*-\frac{4GD}{c^2}I_N^* \\ &=Z_0(1-\kappa_G-\kappa_N), |Z|<R_N \end{aligned} \tag{3}$$

where

$$\kappa_G=\frac{4GD}{c^2}\pi\sigma_G, \qquad \kappa_N=\frac{4GD}{c^2}\pi\left(\frac{M_N}{\pi R_N^2}\right)\equiv\frac{R_0^2}{R_N^2} \tag{4}$$

$R_0=[(4GD/c^2)M_N]^{1/2}$ is the radius of influence of the nucleus and $D=\mathrm{DD}\times\mathrm{DDS}/\mathrm{DS}$, where DD, DDS and DS are the distances between observer and deflector, deflector and source, and observer and source, respectively. G is the gravitational constant and c is the speed of light in vacuum.

Table 1 Image properties in the presence of the galactic nucleus

Lens system	$M_N\ (M_\odot)$	$M_G\ (M_\odot)$	Intensity ratio: Without nucleus	Intensity ratio: With nucleus	Ref.
0957+561	1.4×10^{10}	4.8×10^{11}	2.5×10^{-2}	1.0×10^{-6}	6
2345+007	1.3×10^{10}	1.4×10^{12}	1.8×10^{-2}	8.0×10^{-5}	7
2016+112	2.5×10^{10}	3.4×10^{12}	1.5×10^{-2}	4.0×10^{-6}	8

M_N, mass of galactic nucleus; M_G, mass of parent lens galaxy (both in units of solar mass, $M_\odot$). The intensity ratio is that between the odd (third) image and the external bright image.

In the absence of the nucleus the image would have been located at a position Z_0^I given by

$$Z=Z_0^I(1-\kappa_G) \tag{5}$$

Let $Z=\gamma e^{i\theta}$, $Z_0=\gamma_0 e^{i\phi}$ and $Z_0^I=\gamma_0^I e^{i\psi}$. In the context of the present problem, as will become clear later, both κ_G and κ_N exceed unity. Then, without the presence of the nucleus, the 'odd image' is located at

$$\gamma_0^I=\frac{\gamma}{(\kappa_G-1)} \tag{6}$$

The introduction of the nucleus shifts the image to the position

$$\gamma_0=\frac{\gamma}{(\kappa_G+\kappa_N-1)}=\frac{(\kappa_G-1)\gamma_0^I}{(\kappa_G+\kappa_N-1)} \tag{7}$$

Note that for values of κ_G exceeding unity and for the location, in the absence of the compact nucleus, of the odd image γ_0^I within a critical radius, $\simeq\kappa_G^{1/2}R_0$, the nucleus does not create additional sub-images of the odd image (ref. 3, section 2(e), (f)). The amplification A^I of the image in the absence of the nucleus is obtained using equation (6):

$$A^I=\frac{\gamma_0^I}{\gamma}\frac{d\gamma_0^I}{d\gamma}=\frac{1}{(\kappa_G-1)^2} \tag{8}$$

whereas after the introduction of the nucleus the amplification A follows from equation (7):

$$A=\frac{\gamma_0}{\gamma}\frac{d\gamma_0}{d\gamma}=\frac{1}{(\kappa_G+\kappa_N-1)^2} \tag{9}$$

Suppose the parent galaxy has a mass $M\simeq5\times10^{11}\ M_\odot$, within a core-radius $\simeq$3 kpc. Assuming $D\simeq600$ Mpc, we get $\kappa_G\simeq6.5$. If we now consider a nucleus with mass $M_N\simeq10^{10}\ M_\odot$ and radius $R_N\simeq50$ pc, then we have $\kappa_N\simeq470$. Clearly κ_N is very large compared with κ_G, so that from equations (4) and (7) we have

$$\gamma_0\simeq\frac{\kappa_G}{\kappa_N}\gamma_0^I=\kappa_G\left(\frac{R_N}{R_0}\right)\left(\frac{\gamma_0^I}{R_0}\right)R_N \tag{10}$$

Thus for $\gamma_0^I\leq\kappa_G^{1/2}R_0$ and for the foregoing choice of parameters, the image in the presence of the nucleus is located at

$$\gamma_0\leq\kappa_G^{3/2}\left(\frac{R_N}{R_0}\right)R_N\leq\tfrac{3}{4}R_N.$$

The amplifications before and after the introduction of the nucleus are given by equations (8) and (9):

$$A^I\simeq3\times10^{-2}; \qquad A\simeq4\times10^{-6} \tag{11}$$

It is evident from this idealized example that after the introduction of the nucleus the odd image is depressed in intensity by a factor of $\sim10^4$, or equivalently dimmed by ~10 mag, in addition to being brought closer to the centre of the galaxy (and the nucleus) by a factor of ~80.

We now incorporate the effects of the compact nucleus on the image properties by adopting the prescription outlined for

realistic lens models[6]. In fact, we merely add the gravitational effect of the compact nucleus to the lens models which we have previously constructed[6-8], without altering any of the parameters of those models.

Table 1 summarizes the numerical results for three multiple quasar systems: 0957+561, 2345+007 and 2016+112. In these models, without the inclusion of the effects of the nucleus the intensity of the odd (third) image is a few percent of that of the external bright image. But in the presence of the nucleus the intensity of the third image is enormously diminished, and the intensity ratio is lowered by a factor anywhere from 10^2 to 10^4; that is, the odd third image is dimmed by ~6–9 mag. A remarkable feature is that the properties of the main images, such as their positions and intensities, are left practically unaltered by the presence of the nucleus, while the third image is pulled significantly closer to the centre of the nucleus. The masses of the parent lens galaxy required to obtain the observed configuration are in the range 5×10^{11}–$3.4\times10^{12}\ M_\odot$, with the mass of the nucleus $\simeq1.3\times10^{10}$–$2.5\times10^{10}\ M_\odot$ contained within ~50 pc. Further, the intensity of the third image would increase if the nucleus is assumed to be more extended or the mass of the nucleus lower than the values given in Table 1.

We note that the present model does not necessarily involve any singularities (for example, black holes or strings) in the density distribution of matter, although such singularities can also play a similar role in explaining the absence of the odd image. We consider that it is better to try to account for most of the observed features of the gravitational lens system, including the missing odd image, in the framework of a conventional, smooth density distribution, before invoking the presence of singularities. Indeed, Young *et al.*[9] have inferred from photometric and spectroscopic observations that the nucleus of the giant elliptical galaxy M87 contains a compact mass $\simeq5\times10^9\ M_\odot$ within 100 pc (see also Sargent *et al.*[14]).

The presence of a black hole in the central region of a lens galaxy could cause the complete disappearance of the third image, due to the action of the black hole as a 'mini-lens'. In contrast, a massive compact nucleus will merely dim the image by a substantial amount[3]. The dimmed image could be detected if the source size (for example, the extended narrow-emission-line region in the quasar) is comparable to the radius of influence of the nucleus, for, in such a situation, some fraction of the large emission-line region is unlikely to be significantly affected by the lens action of the massive nucleus.

Will the existence of clumpiness in the lens affect the intensity of the odd image? For parameters appropriate to the present problem and for clumps in the form of solar-mass stars, neither the overall bending nor the intensity amplification of the large radio and emission-line regions are sensibly influenced. But for the compact optical continuum region we cannot neglect the effects of minilensing. However, in such a situation arguments[10,11] based on flux conservation and the large optical depth to mini-lens action[12] enable us to assign a probability distribution[13], $P(A)$, to the intensity amplification of the odd image which peaks at $A\simeq4\times10^{-6}$. As a result the clumpiness in the lens galaxy or the nucleus is not expected to affect our conclusions about the dimness of the odd image.

A testable prediction of the present suggestion is the observation of an image of the quasar optical continuum region within ~0.2 arc s from the centre of the lens galaxy, with visual magnitude fainter by nearly 6 mag than the external bright image. Equally, if the source size is large compared with R_0 in some frequency, such as the narrow-emission-line region, then in the present model the image could still be observed near the centre of the lens galaxy. On the other hand, the detection of a bright odd image in the optical continuum will invalidate the hypothesized presence of a compact massive nucleus in the core of the lens galaxy and would imply that the nucleus is either less massive than $5\times10^9\ M_\odot$ or has a linear size larger than 50 pc.

The numerical computations were carried out on the CYBER 175 and CDC 205 computers at the University of Calgary. D.N. was supported by a Canadian NSERC grant to S. R. Sreenivasan. K.S. was supported by SERC.

Received 2 January; accepted 25 February 1986.

1. Burke, W. L. *Astrophys. J.* **244**, L1–LX (1981).
2. Chang, K. & Refsdal, S. *Astr. Astrophys.* **132**, 168–178 (1984).
3. Subramanian, K., Chitre, S. M. & Narasimha, D. *Astrophys. J.* **289**, 37–51 (1985).
4. Narayan, R., Blandford, R. & Nityananda, R. *Nature* **310**, 112 (1984).
5. Bourassa, R. R. & Kantowski, R. *Astrophys. J.* **195**, 13–21 (1975).
6. Narasimha, D., Subramanian, K. & Chitre, S. M. *Mon. Not. R. astr. Soc.* **210**, 79–83 (1984).
7. Subramanian, K. & Chitre, S. M. *Astrophys. J.* **276**, 440–448 (1984).
8. Narasimha, D., Subramanian, K. & Chitre, S. M. preprint, Tata Institute, Bombay (1985).
9. Young, P. J., Westphal, J. A., Kristian, J., Wilson, C. P. & Landauer, F. P. *Astrophys. J.* **221**, 721–730 (1978).
10. Weinberg, S. *Gravitation and Cosmology* (Freeman, San Francisco, 1972).
11. Cowling, S. A. preprint, Imstitute of Astronomy, Cambridge 1985).
12. Vietri, M. & Ostriker, J. P. *Astrophys. J.* **267**, 488–510 (1983).
13. Paczynski, B. preprint, Princeton University Observatory (1985).
14. Sargent, W. L. W., Young, P. J., Boksenberg, A., Shortridge, K., Lynds, C. R. & Hartwick, F. D. A., *Astrophys. J.* **221**, 731–744 (1978).

Resolution of Crab nebula filaments into chains of quasistellar knots

Sidney van den Bergh* and Christopher J. Pritchet†

* Dominion Astrophysical Observatory, Herzberg Institute of Astrophysics, 5071 W. Saanich Road, Victoria, British Columbia, Canada V8X 4M6
† Department of Physics, University of Victoria, PO Box 1700, Victoria, British Columbia, Canada V8W 2Y2

We have clearly resolved a number of the Hα emitting filaments in the Crab nebula into chains of knots with diameters ≤1.0 arc s. This resolution was possible because sub-arcsecond seeing is common on Mauna Kea, Hawaii (altitude 4,204 m) but quite rare at the sites of other large telescopes situated at lower altitudes. Individual filaments resemble beads on a string which shows that these objects are rope-like structures. In the brightest filament close to the Crab pulsar the quasistellar knots are slightly displaced from the spine of the low-density filament on which they are superposed. This segregation might be understood if the dense knots have been accelerated outwards by a lesser amount than the low-density filament in which they were originally embedded. The present results show that a substantial fraction of the line emission of the Crab nebula originates in the small and very dense quasistellar knots that lie along the spines of filaments. This will affect estimates of the mass and composition of the Crab nebula, and observations of the motions of quasistellar knots should enable one to study the expansion (and eventually perhaps even the acceleration) of the Crab nebula with much greater precision than was possible previously.

On 12 October 1985 (UT) we obtained frames of two fields in the Crab nebula with the 320×512 pixel RCA charge-coupled device (CCD) detector at the prime focus of the Canada–France–Hawaii Telescope. These 600-s exposures were made in 0.8-arc-s seeing through a ~100-Å-wide filter centred on Hα. The scale of the resulting images was 0.41 arc s per pixel. On these frames many of the Hα emission filaments resemble necklaces (see Figs 1 and 2) composed of 'beads' of differing sizes. Some of these beads appear stellar whereas others are barely resolved with diameters ~1.0 arc s. Typically such knots are strung out along the spines of individual filaments at separations of a few seconds of arc. Bright and faint filaments appear to have the same basic structure. However, in bright filaments individual knots tend to be more luminous (and more closely spaced) than they are in fainter filaments. The appearance of the Hα emission filaments, and the fact that most knots are located in filaments, suggests that they are (in three dimensions) rope-like structures rather than sheets seen edge-on. One might

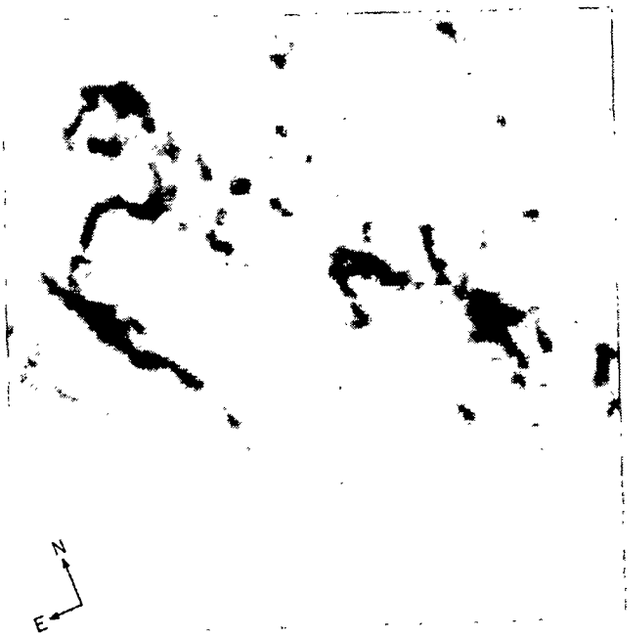


Fig. 1 Hα filament located north of centre of the Crab nebula. The filament is seen to be resolved into a string of quasistellar knots with diameters ≤1.0 arc s. The figure is 60 arc s on a side. Pixel size is 0.41 arc s.



Fig. 2 Filament located west of the Crab pulsar, which is marked by an arrow. This frame was taken in 0.8-arc-s seeing. The figure is 60 arc s on a side.

speculate that individual knots are due to instabilities within these filaments. The distribution of these knots and the pressures needed to form and confine them should provide information about the otherwise unprobed small-scale distribution and properties of the hot thermal plasma and magnetic field between and around the filaments.

Our CCD frames cover two 2×3-arc-min fields. One of these was centred on the Crab pulsar and the other is located slightly to the west of the base of the Crab jet[1]. We estimate that the total number of Hα emission knots in the Crab nebula is a few hundred. At an assumed distance[2,3] of 2 kpc the ≤1.0-arc-s diameters of individual knots correspond to linear dimensions ≤0.01 pc. The total emitting volume of all knots in the Crab nebula is therefore only a few $\times 10^{-4}$ pc^3. A substantial fraction of the total Hα emission of the Crab nebula must originate within this very small volume.

Important questions that remain to be answered by future observations are: (1) Do the quasistellar Hα knots also radiate in the light of elements other than hydrogen? (2) What is the range of physical conditions within these knots? (3) What are the lifetimes of quasistellar knots? (4) How do the spectra of knots differ from those of the filaments in which they are embedded?

The observations reported above were obtained with the Canada-France-Hawaii Telescope, which is operated by the NRC of Canada, CNRS of France and the University of Hawaii. We thank Peter Stetson and David Duncan for their assistance with the processing and reproduction of the digital images shown in the figures.

Received 6 January; accepted 5 March 1986.

1. van den Bergh, S. *Astrophys. J. Lett.* **160**, L27 (1970).
2. Woltjer, L. *Bull. astr. Inst. Neth.* **14**, 39–80 (1958).
3. Trimble, V. *Astr. J.* **73**, 535–547 (1968).

A flare-induced cascade model of γ-ray bursts

P. A. Sturrock

Center for Space Science and Astrophysics, Stanford University, Stanford, California 94305, USA

Although there is no agreement concerning the model and mechanisms responsible for γ-ray bursts, it is generally agreed that they are produced by neutron stars[1]. With few exceptions[2], it is thought that an intense magnetic field plays a key role. The favoured radiation mechanism is optically thin synchrotron radiation[3], but it is difficult to find any way of maintaining the electron energy since the radiation cooling time is extremely short. As a resolution of this difficulty, I propose that the basic energy-release mechanism is a flare in the magnetosphere of a neutron star. This involves reconnection that leads to an electric field parallel to the magnetic field. This accelerates an electron along the magnetic field, producing high-energy γ rays (by curvature radiation) that promptly annihilate in the magnetic field, resulting in an electron-positron cascade as in radio pulsars[4]. This model offers an explanation of the continuum spectrum, of the 511-keV annihilation line, and possibly of the optical radiation that seems to accompany some γ-ray bursts.

An electron of energy E_e (eV) moving in a magnetic field B (gauss) at a large pitch angle produces predominantly photons of energy E_ϕ (eV) where

$$E_\phi = 10^{-19.7} E_e^2 B \quad (1)$$

Hence if observed photons of energy 10^5 eV are in fact produced in a magnetic field of order 10^{12} gauss, the emitting electrons must have energy of the order of $10^{6.4}$ eV. Since the power S emitted by a single electron by this process is given by

$$S_1 = 10^{-26.1} E_e^2 B^2 \quad (2)$$

we see that the timescale characteristic of radiation cooling of the emitting electron is given by

$$\tau_R = 10^{14.4} E_e^{-1} B^{-2} \quad (3)$$

For the parameters of interest, τ_R is of the order of 10^{-16} s. The problem is to find a process that can energize electrons as rapidly as, or more rapidly than, they are being de-excited by synchrotron radiation.

Basically, the excitation must be achieved by an electric field. One possibility is that this electric field is intrinsic to the photon

flux itself, so that absorption of photons is going on at the same high rate as the emission of photons. This occurs only if the optical depth of the emitting region is of order unity or more, and this possibility is ruled out since observed spectra do not display a Wien peak. (On the other hand, as Hameury *et al.*[5] have shown, excitation of electrons by a distinct 'primary' beam of photons that have *not* been produced by synchrotron radiation, *can* lead to optically thin synchrotron radiation. Their model is in some respects similar to the one to be presented herein.)

Another possibility is that the electric field required to excite an electron is provided by a close encounter with another charged particle—electron, positron, or ion. However, we find that the particles responsible for exciting the radiating electrons must have an enormous density, of order 10^{31} cm^{-3} or more. Clearly, the focus of the inquiry then changes to a study of radiation from that very dense plasma. Hence we have not solved a difficult problem, but merely replaced it by another problem more difficult still.

For the above reasons, it has been proposed[3,6,7] that excitation of the electrons is maintained by a collective plasma process. This process must generate an intense electric field since, to maintain the electron energy against loss by synchrotron radiation for the parameters proposed, the electric field must have a value of $10^{9.5}$ e.s.u. or more. A further requirement is that the electric field must be transverse to the magnetic field and have a frequency comparable with the orbital frequency of the electrons in the magnetic field. For the parameters quoted, this frequency is of the order of $10^{17.8}$ Hz, corresponding to a photon energy of $10^{3.4}$ eV. If this were the case, we would expect the source to emit more energy in X rays than in γ rays, which is normally not the case.

It is clearly very difficult to propose an acceptable mechanism by which electrons may be energized as rapidly as they are being cooled by synchrotron radiation. As a resolution of this dilemma, I propose that energy lost by synchrotron radiation is not restored to the emitting electron.

The impulsive nature of γ-ray bursts and the 'light curves' of the γ-ray flux are reminiscent of solar flares[8]. It is not inconceivable that the energy released during a γ-ray burst has been stored as magnetic free energy in a neutron-star magnetosphere, so it is attractive to consider the consequences of a neutron-star flare. Although there are several models of solar flares, all current models involve magnetic-field reconnection by the tearing mode or a similar processes.[9] Magnetic reconnection violates the 'frozen-flux' condition and therefore develops electric fields that have a non-zero component parallel to the magnetic field. We now examine the consequence of the development of such an electric field in a neutron-star magnetosphere. Since this same situation arises in most models of radio pulsars, we may draw upon pulsar theory in investigating the present problem.

In the presence of a strong electric field parallel to the magnetic field, electrons rapidly accelerate, but their acceleration is soon limited by curvature radiation[4]. The radiation-reaction limited energy, measured in eV, is given by

$$E_{eRL} = 10^{8.1}\, \mathscr{E}^{1/4}\, R_c^{1/2} \tag{5}$$

where $\mathscr{E}$ (e.s.u.) is the electric field strength and R_c (cm) is the radius of curvature. During magnetic reconnection, the strength of the electric field may approach $10^{-2}(v_A/c)B$, where v_A is the Alfvèn speed[10]. In the present situation, the Alfvèn speed is likely to be close to the speed of light so that $\mathscr{E}$ might well be of the order of 10^{10} e.s.u. Adopting $R_c \approx 10^6$, we then see that E_{eRL} will be of the order of $10^{13.6}$ eV. On using the formula

$$E_\phi = 10^{-22.2}\, E_e^3\, R_c^{-1} \tag{6}$$

we see that these electrons will emit photons with energy of the order of $10^{12.6}$ eV by curvature radiation.

As in the case of radio pulsars, a photon of this energy would not escape from the magnetosphere but would rapidly annihilate to produce an electron and a positron, each of which has approximately half the energy of the annihilated photon. As shown some time ago[4], annihilation occurs approximately at a location where the photon 'sees' a transverse magnetic field $B_\perp$ that satisfies

$$E_\phi B_\perp = 10^{18.6} \tag{7}$$

The newly created electrons and positrons have non-zero pitch angles and so radiate by the synchrotron process. These photons also will have such high energy that they will be immediately annihilated by the magnetic field. This cascade ends when photons are produced that are of sufficiently low energy that they may escape. If the above process were to occur only in a small region where the magnetic field strength is constant, the emitted spectrum will be of limited extent. The lower limit of the spectrum, $E_{\phi,L}$, is given approximately by the gyrofrequency:

$$E_{\phi,L} \approx 10^{-7.9}\, B \tag{8}$$

The upper limit to the spectrum, $E_{\phi,U}$, is given approximately by

$$E_{\phi,U} = 10^{18.6}\, B^{-1} \tag{9}$$

Between these limits, the shape of the spectrum is essentially that of a single electron as it radiates away its energy by the synchrotron process. We find, from Equation (B.18) of ref. 4, that the spectrum of a single electron is given by

$$N_{\phi,1} = 10^{9.9}\, B^{-1/2}\, E_\phi^{-3/2} \tag{10}$$

where $N_{\phi,1}\, dE_\phi$ us the number of photons with energy in the range E_ϕ to $E_\phi + dE_\phi$. The γ-ray burst spectra compiled in refs 11 and 12 exhibit great variation. However, a few cases are found to approximate a power-law form over a substantial range of energy. In these cases, we find that the index is indeed close to -1.5.

In most cases, it is likely that radiation will be produced by an extended volume of the magnetosphere in which the field strength varies over a wide range. The resultant spectrum will then differ from the above form, the actual spectrum depending on the magnetic-field geometry, and on the way that energy release is distributed.

One simple model is to assume that the flare occupies most of the volume of a dipole magnetic field and that the free energy density is proportional to B_0^2, where B_0 is the potential field of the dipole. In this case, we find that the emergent gamma-ray spectrum is composed of three sections: below $E_{\phi,LM}$, the spectrum is flat; between $E_{\phi,LM}$ and $E_{\phi,UM}$, the slope is $-3/2$ as in equation (10); above $E_{\phi,UM}$, the slope is -3. $E_{\phi,LM}$ and $E_{\phi,UM}$ are given by equations (8) and (9), with B replaced by B_M, the maximum value of the magnetic field strength in the magnetosphere. Some observed spectra fit this form reasonably well; the required values of B_M are found sometimes to be as high as 10^{13} gauss or more. It is possible that curvature radiation will make some contribution to the observed spectrum, and this may be the origin of the high-energy tail to the spectrum as measured in some cases by the the γ-ray spectrometer on board the Solar Maximum Mission[13].

If N_L is the total number of leptons (electrons and positrons) produced in the terminal stage of the cascade, the total spectrum of the fluence from the gamma-ray burst is given by

$$N_\phi = N_L N_{\phi,1} \tag{11}$$

However, N_L will also be the total number of photons emitted in the 511 keV line when the electrons and positrons annihilate. In some circumstances, the plasma will be so dense that annihilation occurs in the magnetosphere, and the line will be broad due both to particle velocities and the variation of gravitational potential energy. In other circumstances, the plasma will be sufficiently thin that most annihilation occurs at the surface of the star. In this case, the line should be fairly sharp. It is clear from the above formulas that comparison of the fluence in the annihilation line to the fluence in the continuum gives an esti-

mate of the mean strength of the magnetic field in the emitting region.

By using equation (11) to estimate the total number of electrons and positrons involved in a gamma-ray burst, and estimating the lifetime of the electrons either from *in situ* annihilation or flow to the surface of the star, we may estimate the electron-positron number density. This may vary over a wide range, but a typical value would be 10^{20} cm^{-3}. The fact that synchrotron radiation is optically thin implies that $\sigma_T nc < 1$, where σ_T is the Thomson cross-section and b is the instantaneous thickness of the radiating region of the magnetosphere. One is thus led to infer that b is less than about 10^4 cm—perhaps much less—but this is not unreasonable if energy release occurs in the neighbourhood of a thin (possibly moving and evolving) current sheet.

An electric field acting on an electron-positron plasma will tend to develop a two-stream flow. In solar physics, an electron stream moving at high speed through the corona develops plasma oscillations that then radiate at radio frequencies to produce a 'type III radio burst'[14]. In the present situation, the plasma frequency will be in the infrared, optical, or possibly (as Liang[15] has already suggested) in the ultraviolet part of the spectrum. Since the radiation is produced by a collective process, the brightness temperature can be much higher than the plasma temperature. Hence the development of plasma oscillations and radiation from these oscillations could be responsible for the optical radiation that is believed to accompany some γ-ray bursts[16,17].

Many questions remain, the most pressing of which is the origin of the free magnetic energy released during the flare. We know that all large solar flares, and possibly all small ones also, are due to the interplay of two flux systems. It is believed that in some flares 'new' flux slowly intrudes into an 'old' flux system, followed at some later stage by reconnection[18]. On the other hand, it appears that in most large flares a magneto-hydrodynamic (MHD) process leads to the rapid injection of new flux into the old flux, and that 'driven' reconnection occurs during this process[19]. In the case of a neutron-star magnetosphere, it is hard to understand why spontaneous reconnection in the magnetosphere should be so slow as to produce a burst lasting many seconds, so it seems more likely that the reconnection accompanies a slower MHD process which must therefore involve a dense plasma.

It is natural to suppose that the process responsible for stressing the magnetosphere is external to the star. For instance, the stressing could be caused by the sudden infall of material due possibly to a tidally disrupted comet or to an instability of an accretion disk. However, one should bear in mind also the possibility that the stressing might arise from a process internal to the star. It is known from studies of radio pulsars that the magnetic field of a neutron star slowly decays[20]. This requires a loss of flux from the interior and from the crust. This loss of flux might conceivably occur episodically. For instance, if the internal magnetic field is sufficiently strong and the crust sufficiently weak, the accumulation of dense magnetic flux just below the crust may on occasion lead to the fracture of the crust and the sudden injection of new flux into the magnetosphere. If this indeed occurs, a γ-ray burst may be the detectable signal of a 'magnetic volcano' on a neutron star.

I acknowledge with thanks valuable conversations with Spiro Antiochos, Fred Lamb, Edison Liang, and Vahè Petrosian. This work was supported by NASA Grants NGL 05-020-272 and NGR 05-020-668.

Received 18 November 1985; accepted 24 February 1986.

1. Woosley, S. E. (ed.) *High Energy Transients in Astrophysics* (American Institute of Physics, New York, 1984).
1. Colgate, S. A., Petschek, A. G. & Sarracino, R. in *High-Energy Transients in Astropphysics* (ed. Woolsey, S. E.) 548–554 (American Institute of Physics, New York, 1984).
3. Lamb, D. Q. in *High Energy Transients in Astrophysics* (ed. Woosley, S. E.) 512–547 (American Institute of Physics, New York, 1984).
4. Sturrock, P. A. *Astrophys. J.* **164**, 529–556 (1971).
5. Hameury, J. M., Lasota, J. P., Bonazzola, S. & Heyvaerts, J. *Astrophys. J.* **293**, 56–68.
6. Liang, E. P. in *High Energy Transients in Astrophysics* (ed. Woosley, S. E.) 597–604 (American Institute of Physics, New York, 1984).
7. Liang, E. P. & Antiochos, S. K. *Nature* **310**, 121–122 (1984).
8. Svestka, Z. *Solar Flares* (Reidel, Dordrecht, 1976).
9. Sturrock, P. A. in *Solar Flares* (ed. Sturrock, P. A.) 411–449 (Colorado University Press, Boulder, Colorado, 1980).
10. Soward, A. M. & Priest, E. R. *Phil. Trans. R. Soc.* **A284**, 369–417 (1974).
11. Barat, C. in *Positron-Electron Pairs in Astrophysics* (eds Burns, M. L., Harding, A. K. & Ramaty, R.) 54–58 (American Institute of Physics, New York, 1983).
12. Nolan, P. L., Share, G. H., Forrest, D. J., Chupp, E. L., Matz, S. & Rieger, E. in *Positron Electron Pairs in Astrophysics* (eds Burns, M. L., Harding, A. K. & Ramaty, R.) 59–63 (American Institute of Physics, New York, 1983).
13. Nolan, P. L., Share, G. H., Matz, S., Chupp, E. L., Forrest, D. J. & Rieger, E. in *High Energy Transients in Astrophysics* (ed. Woosley, S. E.) 399–402 (American Institute of Physics, New York, 1984).
14. Kundu, M. R. *Solar Radio Astronomy* (Interscience, New York, 1965).
15. Liang, E. P. *Nature* **313**, 202–204 (1985).
16. Schaefer, B. E. *Nature* **294**, 722–724 (1981).
17. Schaefer, B. E., Seitzer, P. & Bradt, H. V. *Astrophys. J. Lett.* **270**, L49–L52 (1983).
18. Heyvaerts, J., Priest, E. R. & Rust, D. M. *Astrophys. J.* **216**, 123–137 (1977).
19. Sturrock, P. A., Kaufman, P., Moore, R. L. & Smith, D. F. *Solar Phys* **94**, 341–357 (1984).
20. Manchester, R. N. & Taylor, J. H. *Pulsars*, 164 (Freeman, San Francisco, 1977).

Tidal reorientation and the fracturing of Jupiter's moon Europa

Alfred S. McEwen

Department of Geology, Arizona State University, Tempe, Arizona 85287 and US Geological Survey, 2255 N. Gemini Drive, Flagstaff, Arizona 86001, USA

The most striking characteristic of Europa is the network of long linear albedo markings over the surface, suggestive of global-scale tectonic processes. Various explanations for the fractures have been proposed: freezing and expansion of an early liquid water ocean[1], planetary expansion due to dehydration of hydrated silicates[2], localization by weak points in the crust generated by impacts[3], and a combination of stresses due to planetary volume change and tidal distortions from orbital recession and orbital eccentricity[4,5]. Calculations by Yoder[6] and Greenberg and Weidenschilling[7] have shown that Europa may rotate slightly more rapidly than the synchronous rate, with a rotation period (reorientation through 360°) ranging from 20 to >10^3 yr if a liquid mantle is present, or up to 10^{10} yr if the satellite is essentially solid[7]. Helfenstein and Parmentier[8] modelled the stresses due to nonsynchronous rotation, and concluded that this could explain the long fractures in part of the anti-jovian hemisphere. In this note, I present a global map of lineaments with long arc lengths (>20° or 550 km), and compare the lineament orientations to the tensile stress trajectories due to tidal distortions (changes in the lengths of three principal semiaxes) and to nonsynchronous rotation (longitudinal reorientation of two of the principal semiaxes). An excellent orthogonal fit to the lineaments is achieved by the stresses due to nonsynchronous rotation with the axis radial to Jupiter located 25° east of its present position. This fit suggests that nonsynchronous rotation occurred at some time in Europa's history.

The global lineaments on Europa appear to be major extensional openings, ~10–50 km in width, filled with new crustal material. They are darker and redder than the terrain they transect, so are probably composed of a different material[3]. Water ice makes up at least 95 wt% of Europa's surface[9], so both the bright areas and the dark bands probably consist of mostly water ice, but with a greater percentage of dark contaminants in the bands. The band widths are very uniform, and are probably intrusions confined by the fracture walls rather than extrusions onto the surface. Some of the widest bands have central bright stripes, perhaps due to late-stage injections of clean ice[2].

Extension fractures may form either when the principal stresses are tensile or when the principal (macroscopic) stresses are compressive[10]. Extension fracturing during compression may be due to local tensile stresses at flaws or heterogeneities when confining pressures are low[10] or the fracturing may be caused

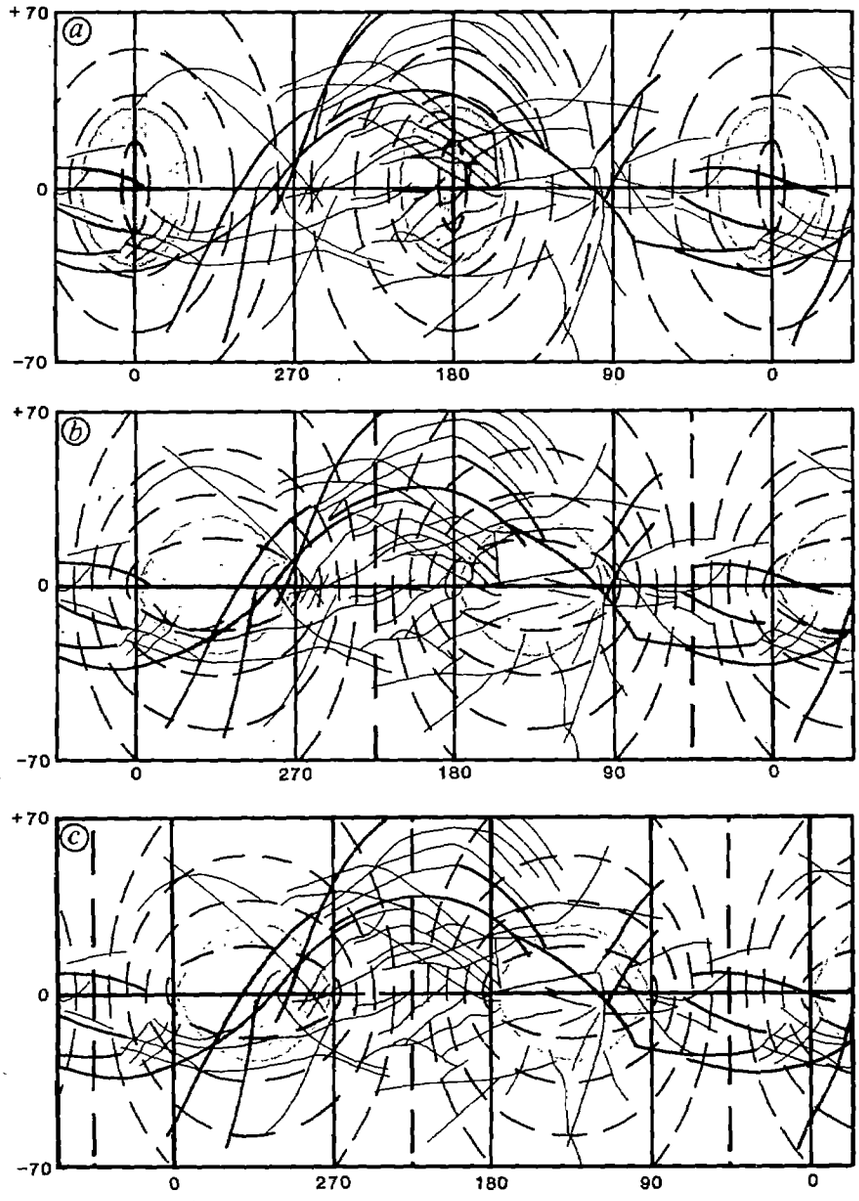


Fig. 1 Map of lineaments on Europa in Mercator projection. Heavy lines indicate great-circle lineaments. Superimposed over map (dashed lines) are trajectories for *a*, tensile and/or compressive stresses due to tidal distortions (data from ref. 5); *b*, tensile stresses due to nonsynchronous rotation with the axis radial to Jupiter at its present position (continuing nonsynchronous rotation; stress trajectories from ref. 8); and *c*, tensile stresses due to nonsynchronous rotation with the axis radial to Jupiter shifted 25° east. Shaded areas are where both principal surface stresses are compressional; applies to *a* only if trajectories are tensile.

by intrusions into the cracks resulting in forces on the crack faces[11]. In either case, extension fractures form nearly perpendicular to the most tensile or least compressive stresses.

The best evidence for strike-slip faulting on Europa consists of minor apparent rotations near the anti-jovian region[12]. A strike-slip mechanism has been proposed for some of the long global lineaments on the basis of preferred 60° orientations of lineament intersections to each other[4] and to the tensile stresses due to tidal distortions[5]. However, there were errors in the longitudinal positions of the lineaments used in these analyses, as great as 15° (ref. 4) and 40° (refs 5, 8), so the preferred orientations are suspect. Furthermore, the tidal stresses are probably much too weak to fracture the crust in shear[5,13]. If fractures initiate at depths where the vertical stress is the most compressive, then normal faults or graben may form[14], but may become extension faults due to intrusions[11]. Therefore, I interpret the majority of the global lineaments as extension fractures.

The lineament map, produced from Mercator projections of global mosaics of Europa[15], is shown in Fig. 1. Only those lineaments visible in the global mosaics (resolution 11–23 km per pixel) and with arc lengths of at least 20° are mapped. Images utilized in the mosaics are acquired at low phase angles (3–32°), so all of the lineaments are identified by albedo markings rather than topography. Positions are accurate to within 5°, determined by comparison with geodetic control[16]. Lineaments are uniformly distributed over Europa's surface, although they appear concentrated at low latitudes in Mercator projections.

Superimposed on the lineament map are the stress trajectories for tidal distortion of a thin elastic shell (Fig. 1*a*), nonsynchronous rotation with the axis radial to Jupiter at its present position (Fig. 1*b*) and nonsynchronous rotation with the axis radial to Jupiter located 25° east of the present position (Fig. 1*c*). The tidal stress trajectories (Fig. 1*a*) can represent either (1) tensile stresses due to orbital recession, or (2) compressive stresses due to orbital contraction, or (3) cyclical tensile and compressive stresses due to orbital eccentricity. Stress trajectories for nonsynchronous rotation (Fig. 1*b*,*c*) are tensile. The principal surface stresses are tangential (most tensile or least compressive) and normal (least tensile or most compressive) to the tensile trajectories; the stresses are reversed for compressive trajectories. Three regions of the surface may be defined by the signs of the surface stresses (++, +−, and −−, with tensile stresses positive). Extension fractures (in all three regions) should be concentrated at a 90° angle to the tensile stress trajectories, but are least likely to form in the areas of compress-

ive (−−) surface stresses, so these regions (shaded in Fig. 1) are excluded from the analysis of lineament orientations.

Very long lineaments oriented along great circles seem most likely to be due to global stresses, whereas the shorter, small-circle, and irregular lineaments may have been influenced by impacts or crustal heterogeneities. Therefore, the approximately great-circle lineaments (those whose plane passes within 15° of the centre of the sphere) of long arc length (>30°) are shown as heavy lines on Fig. 1.

Lineament orientations to the stress trajectories were measured at intervals of 12° arc length (330 km) along each lineament. No preferred orientation with respect to tidal stresses is seen (Fig. 2*a*), contrary to previous reports [4,5], and the tidal-stress magnitudes are probably not sufficient to fracture the ice crust[5,13].

The lineaments are generally oriented at high angles to the tensile stress trajectories predicted for ongoing nonsynchronous rotation (Fig. 2*b*), consistent with extension fractures. However, if the satellite (or its crust) is continually rotating at a rate faster than synchronous, as expected[7] if a liquid water mantle is present[17], then the stresses would continuously change and fractures of different ages would not follow the same stress pattern. This can be simulated by moving the stress trajectories in Fig. 1*b* along the equator (with the lineaments fixed); only fractures that lie along the equator are consistent with all positions. The position giving the best fit (most orthogonal) occurs with the axis radial to Jupiter located ~25° east (relative to the surface) of its current position (Figs 1*c* and 2*c*). The 25° east position may represent the mean of stresses from reorientation through ~50° to its present position. This suggests that the fracturing resulted from an epoch of nonsynchronous rotation resulting in ~25–50° eastward reorientation of the satellite or its crust relative to the radial to Jupiter. Several additional observations support this hypothesis: (1) the great-circle lineaments give an especially good fit to the stresses (Fig. 2*c*); (2) a region of isotropic stress near the anti-jovian point[18] may be explained by stretching this region over the tidal bulge[7]; (3) many lineaments terminate or break up into discontinuous spots[3] in the regions of compressive surface stresses; and (4) the predicted stress magnitude due to a 25° reorientation is 2–3 times greater than the probable tensile strength of the ice crust[8].

An eastward reorientation of the satellite, preserving the equator, is the direction of movement that would result from faster-than-synchronous rotation. Therefore, the proposed reorientation seems best explained by the mechanism described by Yoder[6] and Greenberg and Weidenschilling[7], that is, orbital eccentricity forced by resonant interaction with Io and Ganymede, resulting in non-zero tidal torque on a Europa in synchronous rotation. An alternative hypothesis is reorientation due to a large impact[19], but this seems unlikely for Europa because (1) no large impact scar is apparent on the surface; (2) a 25–50° reorientation, preserving the equator, is improbable by this mechanism; and (3) the global fracture pattern is not like that expected from a large impact[20]. Stable synchronous rotation is expected if the satellite has a perfectly circular orbit (not true of Europa) or if the satellite has a permanent mass asymmetry (like the Earth's Moon). The remarkable absence of topographic relief on Europa[1] is consistent with the absence of a mass asymmetry.

One possible explanation for the fracture pattern is continuous nonsynchronous rotation but with episodic fracturing when stresses have built up to exceed the tensile strength of the crust. However, this model requires some mechanism to synchronize the failure of many separate fractures. Another possibility is that venting of water vapour is very rapid[17], resulting in complete resurfacing by condensed frost in a fraction of the rotation period, so that only very recent fractures ($\sim 10^3$ yr or less)[7,8] are seen. However, the observed impact craters imply an age of at least 10^7 yr (refs 1, 3), Europa's photometric function does not support the contention that a very low-density (condensed) frost

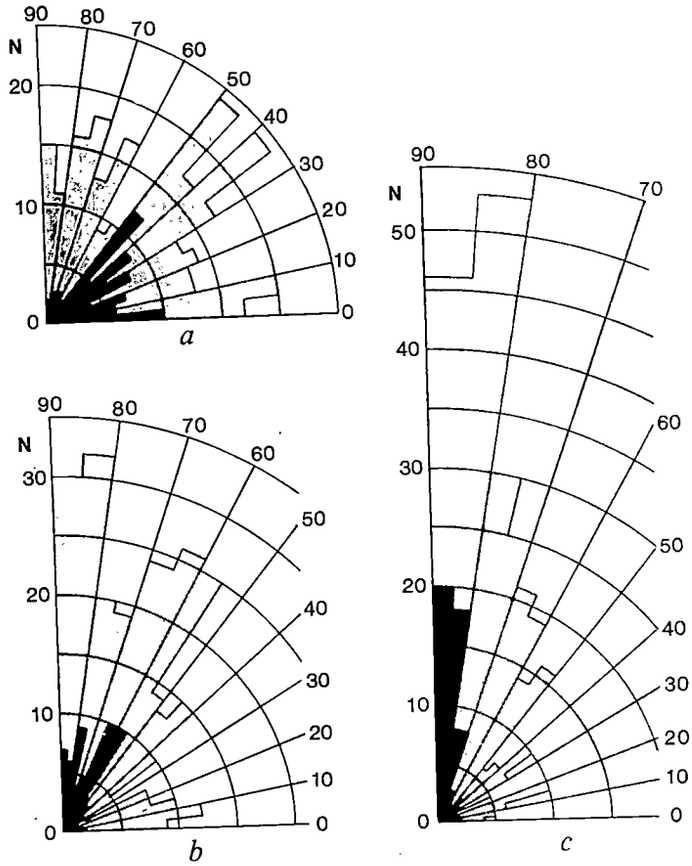


Fig. 2 Rose diagrams for angles of intersection between stress trajectories and lineaments. Black areas are for great-circle lineaments. *a*, *b* and *c* correspond to stress trajectories in Fig. 1.

layer is present[21], and a thin ice shell of variable thickness[17] seems unlikely to form such long, linear fractures.

Assuming that the satellite is essentially solid, there are several alternative scenarios: (1) its figure may gradually creep to a new configuration over time, resulting in very slow nonsynchronous rotation[7], (2) an asymmetry may be dynamically supported by solid-state convection[2], with slowly changing convection patterns leading to epochs of nonsynchronous rotation separated by periods of synchronous rotation, or (3) the fracturing may be due to the final stages of nonsynchronous rotation before a mass asymmetry was frozen into place.

I thank R. Greenberg, E. M. Shoemaker, M. C. Malin, P. Helfenstein, B. K. Lucchitta, and J. M. Moore for critical reviews. This research was supported by NASA Planetary Geology grant NAGW-1 to Arizona State University.

Received 7 October 1985; accepted 7 March 1986.

1. Smith, B. A. *et al. Science* **204**, 951–972 (1979).
2. Finnerty, A. A., Ronsford, G. A., Pieri, D. C. & Collerson, K. D. *Nature* **289**, 24–27 (1981).
3. Lucchitta, B. K. & Soderblom, L. A. in *Satellites of Jupiter* (ed. Morrison, D.) 521–555 (University of Arizona Press, Tucson, 1982).
4. Helfenstein, P. & Parmentier, E. M. *Proc. 11th lunar planet. Sci. Conf.*, 1987–1998 (1980).
5. Helfenstein, P. & Parmentier, E. M. *Icarus* **53**, 415–430 (1983).
6. Yoder, C. F. *Nature* **279**, 767–770 (1979).
7. Greenberg, R. & Weidenschilling, S. J. *Icarus* **58**, 186–196 (1984).
8. Helfenstein, P. & Parmentier, E. M. *Icarus* **61**, 175–184 (1985).
9. Clark, R. N. *Icarus* **44**, 388–409 (1981).
10. Griggs, D. T. & Handin, J. *Mem. geol. Soc. Am.* **79**, 347–364 (1960).
11. Brace, W. F. in *State of Stress in the Earth's Crust* (ed. Judd, W. R.), 111–174 (Elsevier, New York, 1964).
12. Schenk, P. M. *NASA TM-86247*, 3–111 (1984).
13. Cassen, P. M., Peale, S. J. & Reynolds, R. T. in *Satellites of Jupiter* (ed. Morrison, D.) 93–128 (University of Arizona Press, Tucson, 1982).
14. Golombek, M. P. *J. geophys. Res.* **90**, 3065–3074 (1985).
15. McEwen, A. S. *J. geophys. Res.* (in the press).
16. Davies, M. E. & Katayama, F. Y. *J. geophys. Res.* **86**, 8635–8657 (1981).
17. Squyres, S. W., Reynolds, R. T., Cassen, P. M. & Peale, S. J. *Nature* **301**, 225–226 (1983).
18. Pieri, D. C. *Nature* **289**, 17–21 (1981).
19. Melosh, H. J. *Earth Planet Sci. Lett.* **26**, 353–360 (1975).
20. Fleitout, L. & Thomas, P. G. *Earth planet Sci. Lett.* **58**, 104–115 (1982).
21. Buratti, B. J. *Icarus* **61**, 208–217 (1985).

Ionic structure in aqueous electrolyte solution by the difference method of X-ray diffraction

N. T. Skipper, S. Cummings*, G. W. Neilson† & J. E. Enderby*

H. H. Wills Physics Laboratory, University of Bristol, Bristol BS8 1TL, UK

Neutron diffraction difference methods based on isotopic substitutions offer a means of directly probing the detailed structure around a solute dissolved in a host solvent[1], but there are two main drawbacks to their implementation. First, they rely on the use of separated isotopes which are expensive and sometimes of limited availability. Second, the experiments have to be performed at a sophisticated central facility to obtain sufficiently intense beams of thermal neutrons. We have therefore initiated a series of experiments aimed at introducing difference methods to X-ray diffraction studies of liquid and amorphous systems. Difference methods have been attempted before[2], but the absence of definitive neutron data did not allow the method to be made fully quantiative. We now present the first results obtained from such a study in which the difference technique is applied to a concentrated aqueous electrolyte solution and the cation–cation distribution function $g_{MM}(r)$ is determined directly. The success of the method rests on the ability to identify nearly isomorphic pairs of elements, whose isomorphism can be quantified by reference to similar results obtained from the first-order difference method of neutron diffraction[3].

For the case of a salt MX dissolved in water, there are ten partial structure factors, $S_{\alpha\beta}(k)$ which contribute in varying degrees to the total structure factor $F(k)$ (ref. 1). However, the (first-order) difference, $\Delta_M(k)$, between the total structure factors for any two chemically identical but isotopically distinct solutions can be written in terms of a linear combination of only the four correlations associated with the isotopically substituted ion species[1]. Furthermore, the second-order difference[4] between three such solutions gives information directly about the partial structure factor of the substituted species $S_{\alpha\alpha}(k)$. Fourier transformaiton of $\Delta_M(k)$ and $S_{\alpha\alpha}(k)$ gives information regarding the structural properties of the ion-water subsystem and the ions themselves through the radial pair distribution functions:

$$g_{\alpha\beta}(r)-1=\frac{1}{2\pi^2 nr}\int \mathrm{d}k(S_{\alpha\beta}(k)-1)k\sin kr$$

where n is the total number density of the system and is typically 0.1 Å^{-3}.

The electrolytes chosen for this study were nickel chloride and magneisum chloride, and X-ray diffraction experiments were carried out on the following three aqueous solutions (all 4.2 M): $NiCl_2$ in H_2O (I), $MgCl_2$ in H_2O (II) and a 50:50 mixture of $MgCl_2$ and $NiCl_2$ in H_2O (III).

The X-ray structure factors, $F(k)$, of the three solutions were obtained from the raw intensity data by standard correction and normalization procedures[1].

By adopting the same formalism as in the neutron diffraction case[4], but with the important difference that X-ray atomic form factors, f, are k-dependent, the first-order difference $\Delta_{Ni}(k)$ of the X-ray diffraction patterns for two isomorphic solutions can be written as:

$$\Delta_{Ni}(k)=A(S_{NiO}(k)-1)+B(S_{NiH}(k)-1)+C(S_{NiCl}(k)-1)+D(S_{NiNi}(k)-1) \quad (1)$$

* Present addresses: Shuster Laboratory, University of Manchester, M13 7PL, UK (S.C.); Institute Laue Langevin, BP 156X, 38042 Grenoble Cedex, France (J.E.E.).
† To whom correspondence should be addressed.

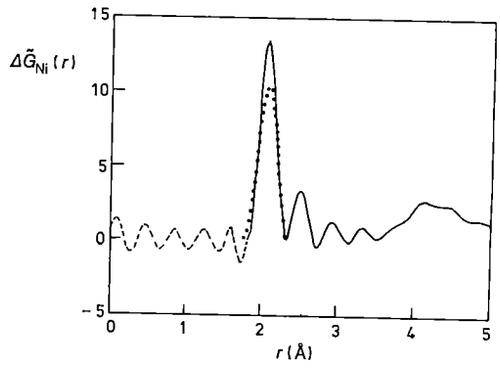


Fig. 1 The nickel ion total radial distribution function in 4.2 M aqueous chloride solution, derived from X-ray diffraction. The oscillations (dashed line) at low r are caused by termination errors in the Fourier transformation. The dotted curve is the nearest neighbour Ni–O correlation derived from neutron diffraction.

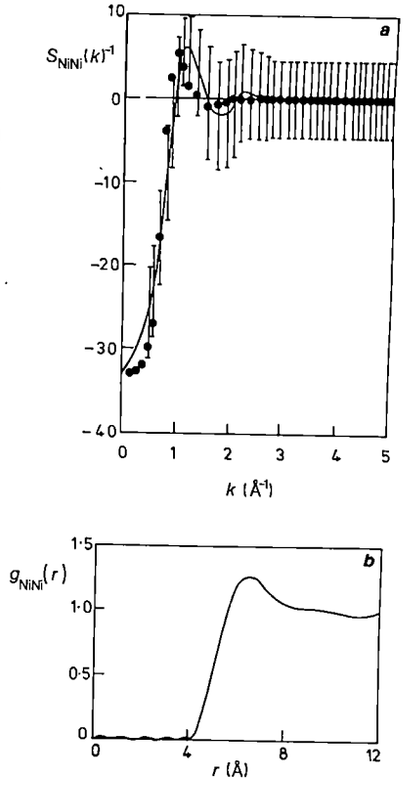


Fig. 2 *a*, The nickel–nickel partial structure factor, $S_{NiNi}(k)$ in 4.2 M aqueous nickel chloride solution. Curve (with error bars), X-ray diffraction; solid circles, neutron diffraction. The errors were determined by the same means as used in the neutron diffraction study[4]: a 1% systematic error was introduced into the coefficients of the $F(k)$s. *b*, The corresponding Ni–Ni radial distribution function $g_{NiNi}(r)$ obtained by Fourier transformation of the curve in *A* after a damping function was used.

where $A=2f_O(k)\Delta f_M(k)c_Oc_{Ni}$, $B=2f_H(k)\Delta f_M(k)c_Hc_{Ni}$, $C=2f_{Cl}(k)\Delta f_M(k)c_{Cl}c_{Ni}$, $D=\Delta f^2{}_M c^2_{Ni}$, and $\Delta f_M(k)=(f_{Ni}(k)-f_{Mg}(k))$, $\Delta f^2_M=f^2_{Ni}(k)-f^2_{Mg}(k)$, c_β is the concentration of species β.

The coefficients are such that A and $C \gg B$, D so that $\Delta_{Ni}(k)$ is dominated by the nickel-oxygen and nickel chloride terms. The Fourier transformation of $\Delta_{Ni}(k)/A$, written as $\Delta\tilde{G}_{Ni}(r)$, gives $g_{NiO}(r)$ directly, together with a convolution of the other three radial distribtion functions, and has the form

$$\Delta\tilde{G}_{Ni}(r)=g_{NiO}(r)+\sum_{\beta\neq o} a_\beta \int H_\beta(|\mathbf{r}-\mathbf{r}'|)g_{Ni\beta}(|\mathbf{r}'|)^{-1}\,\mathrm{d}\mathbf{r}' \quad (2)$$

where β = H, Cl or Ni, $H_\beta(|\mathbf{r}-\mathbf{r}'|)$ is a convolution function associated with the k-dependence of the form factor and a_β are constants which relate to the concentration of species β.

Three $\Delta G_{Ni}(r)$ were calculated for the three possible differences between the $\tilde{F}$(k) values for the three solutions studied. The largest and therefore the most accurately defined difference is

that calculated from solutions I and II, and is shown in Fig. 1. Because the first peak in $g_{NiO}(r)$ is well separated from any peaks in $g_{NiCl}(r)$, $\Delta G_{Ni}(r)$ can be used to check the isomorphism of Ni and Mg. This is achieved by comparing the result for the Ni–Ô nearest-neighbour correlation with that derived from the formally exact difference method of neturon diffraction. As can be seen from Table 1 and Fig. 1, the two methods yield structural parameters which are in excellent agreement. The fact that the width of $g_{NiO}(r)$ is smaller in the X-ray case reflects the superior instrument resolution obtained with our X-ray diffractometer (a θ–θ D/MAX system manufactured by Rigaku, Tokyo), relative to that of the D4 neutron diffractometer (now improved) at the Institut Laue–Langevin, even though the k-range of the scattering was about the same in both cases.

Having established that Ni and Mg are isomorphic, the cation–cation structure factor $S_{NiNi}(k)$ can be determined from a double difference[4] between the $F(k)$ values for the three solutions:

$$S_{NiNi}(k)-1=\frac{1}{c_{Ni}^2(f_{Mg}-f_{Ni/Mg})}\times\left[\frac{(F_I(k)-F_{II}(k))}{(f_{Ni}-f_{Mg})}-\frac{(F_I(k)-F_{III}(k))}{(f_{Ni}-f_{Ni/Mg})}\right] \quad (3)$$

where $f_{Ni/Mg}(k)=(f_{Ni}(k)+f_{Mg}(k))/2$.

The Fourier transformation of $S_{NiNi}(k)$ yields $g_{NiNi}(r)$. The results shown in Fig. 2 are in good agreement with those obtained from an earlier neutron diffraction experiment in which isotopic substitution was used and represent the first ion–ion radial distribution function obtained by X-ray methods alone.

Table 1 Comparison of peak position $\bar{r}_{NiO}$, coordination number $\bar{n}$ and half-width Δr for $g_{NiO}(r)$ derived from X-ray and neutron diffraction

Method	$\bar{r}_{NiO}$ (Å)	$\bar{n}$	Δr (Å)
X-ray	2.07 (2)	6.0 (2)	0.23 (2)
Neutron	2.07 (2)	5.8 (2)	0.26 (2)

The above results clearly demonstrate the power of the X-ray difference method. The proof that Ni and Mg are isomorphic in aqueous electrolyte solution means that a comprehensive study in which counter-ion, concentration and temperature are varied, can now be undertaken. For example, it will be possible to obtain accurate information regarding the ion–oxygen distribution at a much lower concentration than is currently practicable with the neutron difference method. Experiments on $NiBr_2$ and $MgBr_2$ aqueous solutions will help resolve the controversy regarding the existence of inner-sphere complexing in bromide solution.

The X-ray difference method may play an increasingly important role in the determination of the structural properties of a variety of liquid and amorphous systems, and a systematic procedure is being developed in order to identify other isomorphic pairs.

We thank SERC for their continuing support of the aqueous solution programme, and Mr Philip Gullidge for assistance in the calibration and preparation of samples. J.E.E. thanks NATO for the award of a travel grant (RG125/80) which allowed some of the ideas contained in this paper to be discussed with Professor Harold Friedman at SUNY, Stony Brook.

2 September 1985; accepted 13 February 1986.

1. Enderby, J. E. & Neilson, G. W. *Rep. Prog. Phys.* **44**, 593–653 (1981).
2. Bol, W., Gerrits, G. J. A. & Eck, C. L. vP. *J. appl. Crystallogr.* **3**, 486–492 (1970).
3. Soper, A. K., Neilson. G. W., Enderby, J. E. & Howe, R. A. *J. Phys.* **C10**, 1793–1801 (1977).
4. Neilson, G. W. & Enderby, J. E. *Proc. R. Soc.* **A390**, 353–371 (1985).
5. Habenschuss, A. & Spedding, F. H. *J. chem. Phys.* **70**, 2797–2806 (1979).

Constant-geometry edge-flaking of brittle materials

E. A. Almond & N. J. McCormick

National Physical Laboratory, Teddington, Middlesex TW11 0LW, UK

Lithic tool manufacture was the earliest technological exploitation of the brittle fracture of hard materials, and archaeologists have traced and reproduced the evolution of flake tools through various stages of development from the early simple flake knives (Fig. 1) to the sophisticated multi-faceted edges of stone axes. The technology advanced during the period of gunflint manufacture. Of special interest are the simple geometrical relationships between the dimensions of flakes formed in certain controlled conditions[1,2]. The phenomenon of edge-flaking is also encountered in the attrition of tool cutting edges and in the chipping of precision edges of metrological components, where it is avoided rather than understood, by empirical radiusing (rounding-off). In our effort to improve the efficiency of cutting edges, we have observed that a law of constant geometry seems to apply to the flakes formed at rectangular edges, and the effect is relatively insensitive to the test material.

Our experimental approach has been to indent rectangular blocks of the test material with increasing loads at different distances from an edge until a flake breaks off. The distance at which flaking occurs is approximately equal to the flake thickness (Fig. 2). We used a conical diamond indentor with a tip radius of 0.2 mm and an apex angle of 120°. We initially observed that the size of the flakes formed in a tungsten carbide/cobalt tool material decreased with decrease in distance from the edge, and the width-to-height and thickness-to-height ratios of the flakes were approximately constant (Fig. 3). When the same test procedure was extended to other materials it was found that similar height-to-width and thickness-to-width ratios applied for flakes formed in various glasses, a high-carbon steel, an alumina ceramic, a Thames Valley flint (Fig. 4*a*), a polymethyl methacrylate polymer and a range of tungsten carbide/cobalt tool materials. Furthermore, when the boxed volume (defined as the product of the height, width and thickness of the flake) was plotted against the true volume (calculated from the weight and



Fig. 1 Heavily struck flake from lower gravels, Barnfield, Swanscombe, Kent (UK); Clactonian culture, 300,000 yr old.

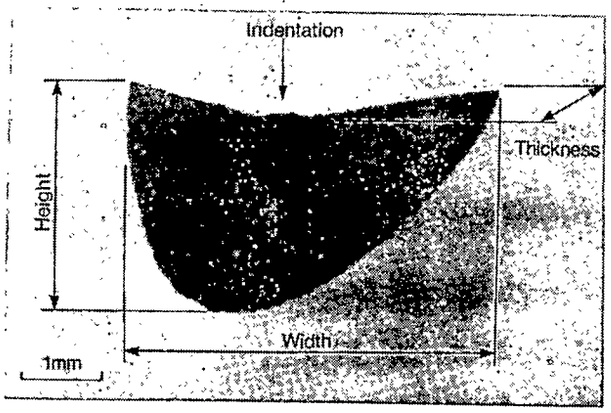


Fig. 2 Flake produced by static loading of the edge of a tungsten carbide/cobalt tool materials.

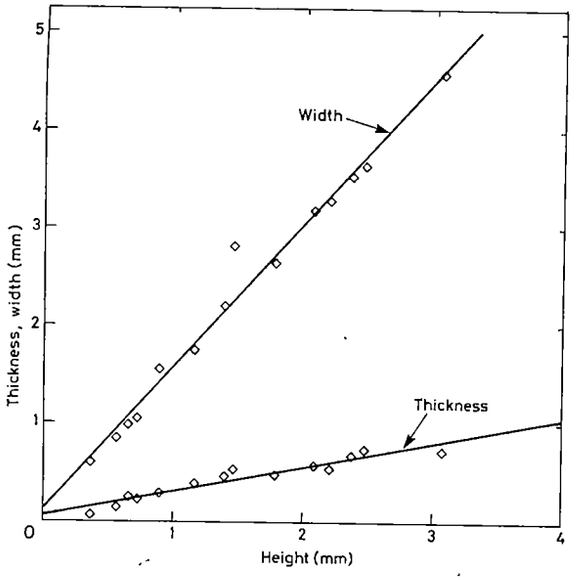
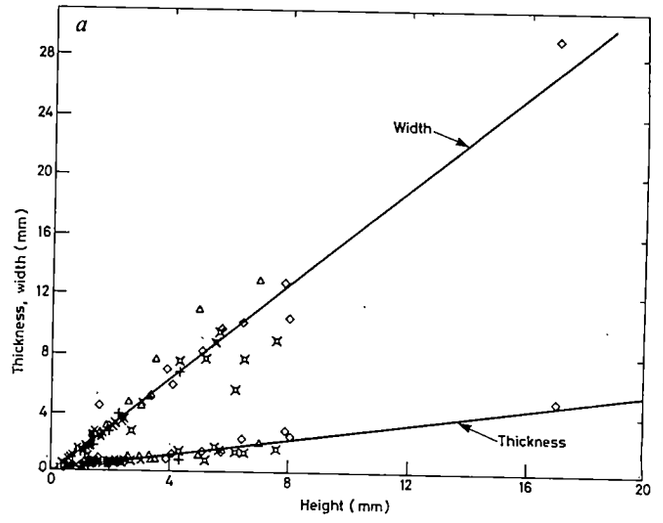


Fig. 3 Variation of flake width and thickness with flake height for a 9 wt% cobalt tungsten carbide tool material; correlation coefficients, $r = 0.9901$ and 0.9564, respectively. (The correlation coefficient r is defined as[7] $r = \sum(x-\bar{x})(y-\bar{y})/(\sum(x-\bar{x})^2 \sum(y-\bar{y})^2)^{1/2}$, where x, y and $\bar{x}, \bar{y}$ are respectively the coordinates of a data point and the corresponding point on the best straight line obtained by minimizing the sum of the squares of the residuals.)



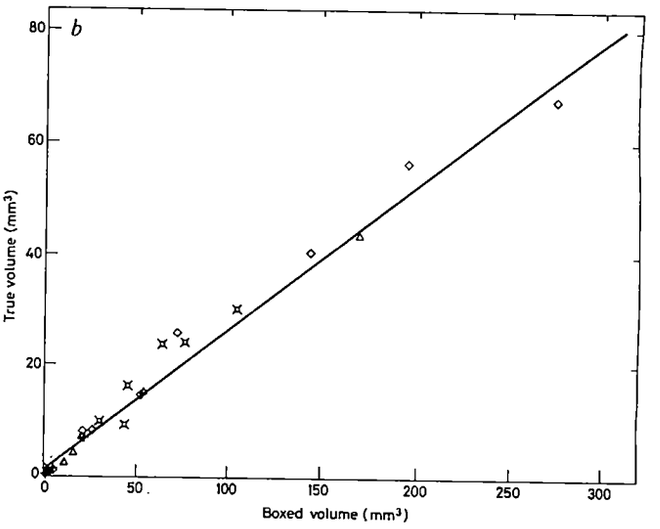


Fig. 4 *a*, Variation of flake width and thickness with flake height ($r = 0.9685$ and 0.9579, respectively); *b*, relation between flake volume and boxed volume ($r = 0.9997$). Data for various glasses ( ), Thames Valley flint (◇), an alumina ceramic (△), a 9 wt% cobalt tungsten carbide tool material (×) and a high-carbon steel (+); *b* also contains results from ref. 3.

density of the flake) a linear relationship was observed (Fig. 4*b*), with a slope of ~0.25 for all the materials tested.

Although detailed inspection of the data in Fig. 4 indicates that they may belong to separate curves according to the size of the test piece, manufacturing technique and hardness, the observed linear relationship has unexpected implications. Thus, for edge flakes produced by statically loaded indenters: (1) the volume lost from the edge depends only on the distance of the loading point from the edge and is relatively independent of the material; and (2) the shape of the flake varies little; it is scaled in proportion to the distance from the edge.

Examination of previous data[3] showed that the observations of constant geometry also held for flakes produced by ball indenters of 2–5 mm diameter using tungsten carbide/cobalt tool materials for the indenter and the test materials. However, in the earlier work the measurement techniques were not sufficiently sensitive to detect the flake size dependence on distance from the edge.

The existence of a constant-geometry law for the dimensional ratios implies that a similar law might apply for the angle of inclination between the flat and curved vertical faces of the flake, and for the angle subtended by the flake faces at the indentation. However, although the latter tended towards 146°, (as expected from the ratio of 20:3 for the width and thickness dimensions), it was not possible to develop a consistent measurement criterion because the faces were convex and the curvatures varied considerably. This applied even more to the angle of inclination, because the flake surface was also convex in the thickness direction and the flakes were not normally symmetric about a vertical plane through the indentation, as can be seen in Fig. 2.

There must be a materials dependence of the flaking phenomenon, and this is found in the magnitude of the load required to initiate flaking at a given distance from the edge, which varies, for example, from 164 N for a silica glass to 6.15 kN for a 9 wt% cobalt tungsten carbide tool material at a distance of 0.71 mm from an edge. The mechanism of flake formation is not yet understood, but it is not restricted to fracture nucleation by hertzian cracking and conical fracturing as has been suggested for flakes produced in lithic tools with blunt hammers in percussive conditions[1,2]. In our tests, although circumferential crack paths of hertzian origin have been observed at some of the

fracture initiation sites, the fracture path more commonly passes through the centre of the indentation, which is characteristic of the tensile stress field resulting from plastic deformation or densification under the loading point[4]. It would probably be more appropriate to consider flaking as two energy-dissipative processes: a load-dependent crack initiation mechanism which occurs in the deformed region below the indenter, and a crack propagation stage determined by the strain energy release rate in linear elastic fracture mechanics conditions[5].

The fact that good reproducibility of flake geometry was obtained with different indenter shapes and different materials may be related to the quasi-static loading mode used in our tests. Thus, stone-age humans adopted pressure loading 25,000 yr ago to dress the edges of cutting tools[6], and it is tempting to conclude that this technique was favoured because it was more precise and reproducible than the percussive loading methods developed by their ancestors.

We acknowledge valuable discussions with Dr Mark Newcomer of the Institute of Archaeology, London, and the loan from his collection of the tool shown in Fig. 1.

Received 31 December 1985; accepted 26 February 1986.

1. Speth, J. D. *Am. Antiq.* **37**, 34–60 (1972).
2. Speth, J. D. *Am. Antiq.* **40**, 203–207 (1975).
3. Almond, E. A. & Roebuck, B. *Proc. int. Conf. Science of Hard Materials* (eds Viswanadham, R. K. *et al.*) 597–614 (Plenum, New York, 1983).
4. Evans, A. G. & Wilshaw, T. R. *Acta metall.* **24**, 939–956 (1976).
5. Fonseca, J. G., Eshelby, J. D. & Atkinson, C. *Int. J. Fracture Mech.* **7**, 421–433 (1971).
6. Clark, G. & Piggot, S. *Prehistoric Societies* (Penguin, Harmondsworth, 1970).
7. Sachs, L. *Applied Statistics* (Springer, New York, 1982).

Inferred oxygen isotope profile of Archaean oceanic crust, Onverwacht Group, South Africa

S. E. Hoffman*, M. Wilson† & D. S. Stakes‡

* College of Oceanography, Oregon State University, Corvallis, Oregon 97331, USA
† Department of Geological Sciences, University of Saskatchewan, Saskatoon, Saskatchewan, Canada S7N 0W0
‡ Department of Geology, University of South Carolina, Columbia, South Carolina 29208, USA

Whole-rock oxygen isotope data from a suite of mafic and ultramafic samples from the Onverwacht Group, the basal unit of the Archaean greenstone succession of the Barberton Mountain Land, South Africa, show a range of values from $\delta^{18}O \simeq +3$ to $\delta^{18}O \simeq +14$, a range which coincides with those of Phanerozoic ophiolites and oceanic crust. When the samples are arranged in an inferred ophiolitic pseudostratigraphy, from basal serpentinized ultramafic cumulates through altered mafic extrusives, they have an oxygen isotope distribution profile which is indistinguishable from that of Phanerozoic ophiolites. The distinctive isotopic profiles and secondary mineral assemblages in Phanerozoic ophiolites are caused by hydrothermal interaction between seawater ($\delta^{18}O \simeq 0$) and oceanic crust ($\delta^{18}O \simeq +5.8$). The existence of a similar isotopic and metamorphic profile in the Onverwacht Group argues strongly that these rocks were hydrothermally altered by an Archaean ocean whose isotopic composition was indistinguishable from modern sea water.

The Barberton Mountain Land is one of the oldest surviving Archaean greenstone belts. Whole-rock Sm-Nd measurements have given the oldest ages: 3.54 ± 0.03 Gyr (ref. 1) and 3.56 ± 0.24 Gyr (ref. 2). Other isotopic systems have given ages clustered about 3.3 Gyr (refs 3–8).

The rocks of the greenstone belt are divided stratigraphically into the Moodies, Fig Tree, and Onverwacht Groups. The Onverwacht Group, in the stratigraphy of Viljoen and Viljoen[9], encompasses six formations of mafic and ultramafic extrusive and intrusive rocks which have been altered to chloritic greenschists, actinolitic amphibolites, and serpentinites, and which include minor intercalations of felsic volcanics and volcaniclastic and carbonate sediments[9,10]. The lithologies of each formation are described in detail by Viljoen and Viljoen[9] and by Tankard *et al.*[10]. The upper subgroup, the Geluk, also known as the Mafic to Felsic Unit, is composed of the Swartkoppie, Kromberg, and Hoogenoeg Formations[9]. The lower subgroup, the Tjakastad, also known as the Lower Ultramafic Unit, is composed of the Komati, Theespruit, and Sandspruit Formations[9]. In order to account for what they described as repetitious cycles of volcanics and sediments up to 20 km in total thickness, Viljoen and Viljoen[11] proposed a model of cyclical volcanism and sedimentation.

Table 1 Multiple runs of rose quartz standard (RQ) and duplicate runs of selected Onverwacht samples

Sample ID	$\delta^{18}O$ (SMOW)	Average	Plotted
RQ-CIT	+8.48		—
RQ-CIT	+8.49		—
RQ-CIT	+8.50	+8.45	—
RQ-CIT	+8.18		—
RQ-CIT	+8.83		—
RQ-CIT	+8.24		—
RQ-US	+8.26		—
RQ-US	+8.29		—
RQ-US	+8.36	+8.30	—
RQ-US	+8.27	(2σ<0.1)	—
RQ-US	+8.31		—
RA5052(US)	+4.58	+4.52	+4.5
RA5052(US)	+4.45		
RA5054(US)	+5.47	+5.27	+5.3
RA5054(US)	+5.06		
RA5055(US)	+6.47	+6.56	+6 6
RA5055(US)	+6.65		
RA5063(US)	+5.20	+5.24	+5.2
RA5063(US)	+5.28		
RA13175(US)	+2.45	+2.58	+2.6
RA13175(US)	+2.70		

CIT, California Institute of Technology; US, University of Saskatchewan. Gregory and Taylor[20] reported a $\delta^{18}O$ value for RQ of +8.45‰ obtained at CIT. Analytical reproducibility for the data plotted in Fig. 1 is calculated as 2σ<0.3‰.

More recent mapping in the Barberton Mountain Land[12–15] has produced evidence that the stratigraphic succession may not be one of simple supercession. Williams and Furnell[12] recognized structural unconformities within the Onverwacht Group which suggested isoclinal folding and faulting, and De Wit[13] proposed that thrust faulting had occurred, resulting in tectonic repetition of strata. These studies[12–15] suggest that the 20-km thickness is a tectonic artefact rather than the result of volcanological or sedimentological processes.

De Wit[14] has compiled a revised stratigraphy which consists of the layered ultramafic complexes at the base, progressively overlain by the Komati Formation, the Hoogenoeg and Kromberg Formations, the rhyodacites and silicic porphyries of the Mafic to Felsic Unit, the Fig Tree Group, and the Moodies Group. De Wit and Stern[16] previously proposed that the Onverwacht Group constitutes an Archaean ophiolite sequence. In this paper, we report an additional parallel between the Onverwacht Group and Phanerozoic ophiolites and oceanic crust: a whole-rock oxygen isotope distribution which reflects cooling and alteration by convective seawater hydrothermal activity.

A total of thirty-three powdered 'whole-rock' samples from rocks collected in the Komati Formation, the Hoogenoeg Formation, and the Stolzburg Ultramafic Complex by Roger Hart and

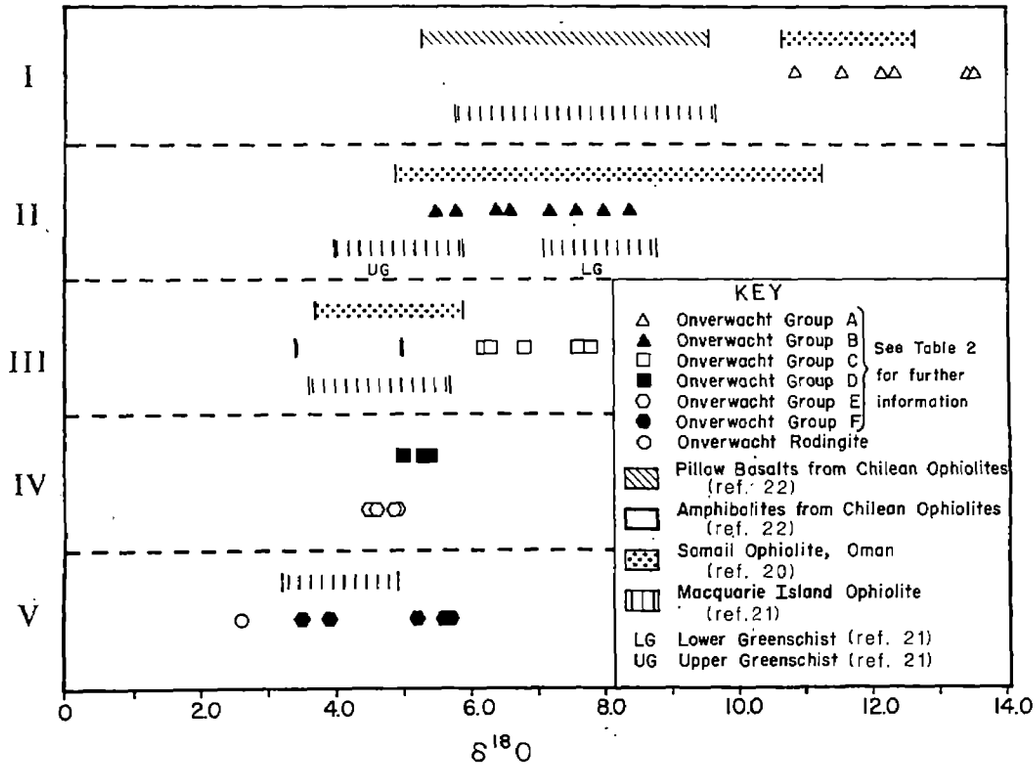


Fig. 1 Whole-rock ^{18}O distribution in the Onverwacht Group plotted in an ophiolitic pseudostratigraphy (size of symbols is larger than range of calculated experimental error), along with data from the Oman ophiolite[20], the Macquarie Island ophiolite[21], and Chilean ophiolites[22]. The Onverwacht data are compared with the following lithologies from the Phanerozoic ophiolites: I, pillow basalts; II, sheeted dykes; III, gabbros; IV, (only Onverwacht data shown); V, serpentinized harzburgites.

Maarten De Wit were analysed for their bulk oxygen isotope composition at the California Institute of Technology and at the University of Saskatchewan. Oxygen was liberated using the fluorine technique[17] at CIT, and the bromine pentafluoride technique[18] at the University of Saskatchewan. Data are reported relative to standard mean ocean water (SMOW, $\delta^{18}O = 0‰$). On this scale, NBS-28 (quartz) has a $\delta^{18}O$ value of +9.6[19]. Statistical data on analytical precision and accuracy as well as interlaboratory comparisons are shown in Table 1.

The data from sixteen whole-rock analyses at CIT and 32 whole-rock analyses at the University of Saskatchewan are listed in Table 2. The samples are grouped according to their alteration mineralogies and relict textures. The results of the 32 analyses from the University of Saskatchewan and the analysis of RA13177 from CIT are shown in Fig. 1. The Onverwacht rocks are plotted according to an ophiolitic pseudostratigraphy which is derived in part from the revised stratigraphic model of De Wit[14]. The pseudostratigraphy proceeds 'upsection' from ultramafic rocks (Groups D, E, and F in Table 2, and IV and V in Fig. 1) through progressively less mafic rocks to altered pillow basalts (Groups A, B, and C in Table 2 and I, II, and III in Fig. 1). Figure 1 also shows ranges of $\delta^{18}O$ for corresponding samples from the Samail ophiolite in the Sultanate of Oman[20], the Macquarie Island ophiolite[21], and ophiolites of Southern Chile[22]. There is a rough correlation between $\delta^{18}O$ and lithology for the samples from Oman, Macquarie Island, Chile, and the Onverwacht Group, although there are also significant overlaps between fields. The range of whole-rock $\delta^{18}O$ values relative to SMOW for the Onverwacht Group ($\delta^{18}O = +2.6$–$13.6‰$) coincides almost entirely with the combined range of the Macquarie Island, Samail, and Chilean ophiolites ($\delta^{18}O = +3.2$–$12.7‰$). If the rodingite from the Stolzburg Ultramafic Complex is excluded (RA13175, Table 2), the ranges completely coincide except for two Onverwacht samples, RA5061 and RA5062, which are dominantly composed of smectite[23], a mineral which is enriched in ^{18}O (ref. 24).

Chemical data from the samples listed in Table 2[23] show that the concentrations of all major oxides and most minor elements are distinctly correlated with oxygen isotope value, water content, and CO_2 content[23]. This indicates that chemical alteration of the rocks was coincident with the redistribution of their oxygen isotope content.

Basaltic rocks altered in subaerial hydrothermal systems by meteoric water have substantially different oxygen isotope signatures from those altered in submarine systems by seawater because meteoric water is depleted in ^{18}O relative to seawater. This depletion results from isotopic fractionation during evaporation and increases with increasing latitute[25]. The average whole-rock $\delta^{18}O$ value for rocks altered in meteoric hydrothermal systems is significantly lower than that of rocks altered by seawater at the same temperatures of alteration[25]. That is, metamorphic assemblages of the same grade will be much more depleted in ^{18}O, and thus have lower $\delta^{18}O$ values, in a meteoric hydrothermal system. For example, greenschist-facies rocks altered in meteoric hydrothermal systems at temperatures sufficient for the formation of actinolite and chlorite have $\delta^{18}O$ values relative to SMOW between roughly −2 and +4 (ref. 25). In contrast, oxygen isotope studies of Phanerozoic submarine greenstones have revealed that their $\delta^{18}O$ values range from +2.8 to >+10 (refs 24–26). Taking into account the analytical accuracy of the study, Fig. 1 shows that the Onverwacht rocks fall totally within the combined fields for Phanerozoic oceanic crust and ophiolites ($\delta^{18}O \simeq +2.8$ to $>+10$)[20–22,24–26].

This coincidence of isotopic and lithologic characteristics between samples from the Onverwacht Group and those from Phanerozoic ophiolites and oceanic crust could indicate that the Onverwacht rocks were altered by Archaean sea water in an oceanic environment. If one assumes that the $\delta^{18}O$ value of the Archaean ocean was essentially equivalent to that of the present ($\simeq 0‰$), then it is possible that the same conditions and processes which produced the oxygen isotope distribution in the Samail[20], Macquarie Island[21], and Chilean[22] ophiolites were also responsible for the oxygen isotope distribution observed in samples from the Onverwacht.

There have been relatively few stable isotope studies on samples from Archaean greenstone belts, but there is some evidence that the $\delta^{18}O$ value of the ocean has changed very little over the past 3 Gyr. Beaty[27] analysed more than 150 samples from six areas within the Abitibi greenstone belt (2.8 Gyr). In each of the six areas, he found an increase in $\delta^{18}O$ with strati-

Table 2 Whole-rock oxygen isotope values for samples from the Onverwacht Group

Sample	$\delta^{18}O$ Caltech	$\delta^{18}O$ U. Sask.
A Clay-calcite		
RA5060	—	+12.4
RA5061	—	+13.6
RA5062	—	+13.5
RA13256	—	+10.9
RA13257	—	+12.2
RA13258	—	+11.6
B Chlorite-calcite-(epidote)-(qtz)		
RA5055	+6.1	+6.6
RA5056	+6.0	+5.8
RA5057	+6.1	+5.5
RA13173	+7.0	+7.6
RA13180	+7.2	+7.2
RA13182	—	+6.4
RA13227	+8.1	+8.4
RA13228	—	+8.0
C Actinolite-albite-epidote		
RA5048	+7.2	+7.6
RA5049	—	+6.2
RA5050	+6.8	+6.8
RA13172	+6.8	+6.3
RA13260	—	+7.7
D Spinifex-textured komatiites*		
RA5054	+5.3	+5.3
RA13174	—	+5.0
RA13259	—	+5.4
E Serp. dunites, Komati Formation		
RA5052	—	+4.5
RA5053	+4.5	+4.9
RA13178	+5.5	+4.9
RA13181	—	+4.6
F Samples from ultramafic complexes†		
RA5063	+5.1	+5.2
RA5068	—	+3.9
RA5069	—	+3.5
RA13175	+2.7	+2.6
RA13176	+6.0	+5.6
RA13177	+5.8	—

Samples are divided into groups according to their alteration mineralogies and their relict igneous textures. Results from California Institute of Technology were obtained in 1982 using the fluorine extraction method[17]. Results from the University of Saskatchewan were obtained in 1984 using the bromine pentafluoride method[18]. The average difference between analyses from the two different laboratories is 0.3‰, with $2\sigma < 0.5$‰.

* Mineralogy of spinifex-textured komatiites: spinifex blades now altered to serpentine (and magnetite); interstices between blades now altered to tremolite and magnetite.

† RA5063 and RA13176 are partially altered orthopyroxenites; RA5068 and RA5069 are serpentinized dunites; RA13175 is a rodingite with a probable orthopyroxenite precursor; RA13177 is a massive serpentine whose precursor is not determinable.

graphic height which correlated with the hydrothermal alteration of the sequence, and in five of the six areas, he found that the altering fluid was probably sea water with a $\delta^{18}O$ value between −2 and +2 (ref. 27). Thus, the data of Beaty[27] and Beaty and Taylor[28,36] support the assumption that the $\delta^{18}O$ of sea water has varied little for at least the past 3 Gyr.

The Onverwacht oxygen isotope data also strongly imply that the range of temperatures over which submarine hydrothermal alteration occurs has not markedly changed over the past 3.4 Gyr. The range of temperatures at which rocks are altered in a submarine hydrothermal system is mainly dependent upon the temperature of the magma and the tectonically controlled configuration of the seawater convection system relative to the magma chamber, not on the temperature of the intake water (that is, ambient bottom water). Thus, the Onverwacht rocks provide little data to clarify the debate on Archaean bottom water temperatures. However, it should be noted that most estimates of Archaean seawater temperatures and $\delta^{18}O$ values are based upon analyses of cherts. In a study of Phanerozoic cherts recovered from Deep Sea Drilling Project cores, Hein and Yeh[29] determined that the samples did not reflect palaeoenvironmental (bottom water) temperatures but rather diagenetic temperatures of formation which were generally greater than 30 °C. While bottom water temperatures have fluctuated in the Cretaceous, Phanerozoic ambient bottom temperatures have been generally less than 10 °C.

Based predominantly on studies of Onverwacht cherts, Perry and Tan[30] suggested that the $\delta^{18}O$ value of the Archaean ocean was significantly lower than at present and that there has been a secular increase in the ^{18}O content of the oceans over the history of the Earth. However, their evaluation of their samples as having no significant post-depositional diagenetic history is suspect in view of more recent studies. The evidence for intense hydrothermal alteration, silicification, and recrystallization in Onverwacht strata is overwhelming[6,23,31]. In addition, many Onverwacht "cherts" are in fact silicified pyroclastic deposits[31,32], and the silicifying fluids appear to have been evolved hydrothermal solutions resulting from the interaction between seawater and underlying mafic and ultramafic strata[31]. Thus, the $\delta^{18}O$ values of Onverwacht cherts reflect their interaction with diagenetic fluids significantly different from Archaean ambient bottom water.

On the basis of oxygen isotope measurements of oceanic crustal samples and mass balance calculations, Muehlenbachs and Clayton[33] proposed that the $\delta^{18}O$ value of the oceans has been buffered via "processes associated with the creation, aging, and destruction of the oceanic crust"[33]. They calculated that at present-day seafloor creation rates, the oceans would achieve a $\delta^{18}O$ value of ~0 roughly 250 Myr after the onset of seafloor spreading[33]. If seafloor creation rates were five times the present day values[34], this 'time constant' would equal only 60 Myr (ref. 33).

Abbott and Hoffman[34] proposed a model for the evolution of plate tectonic processes as a function of the aging of oceanic crust over time. This model postulates that seafloor creation rates 3.8 Gyr ago were as much as five times present-day values. If the time constant calculated for this seafloor creation rate is indeed 60 Myr (ref. 33), then the oxygen isotope composition of the oceans would have been buffered by hydrothermal alteration before the formation of the Onverwacht Group. Therefore, the oxygen isotope distribution in the Onverwacht could be the result of the same types of processes which Gregory and Taylor[20] and Cocker *et al.*[21] proposed to explain the distributions observed in the Samail and Macquarie Island ophiolites.

In such a system[35], sea water with $\delta^{18}O = 0$‰ interacts with ultramafic and gabbroic rocks (~ +5.7–6.0‰) at depth, altering their mineralogies and isotopically exchanging oxygen (and hydrogen) at temperatures above 500 °C over a range of mostly low (<1) water/rock ratios. The interaction leaches ^{18}O from the rocks, enriching the fluids in ^{18}O. These ^{18}O-enriched fluids percolate upward into overlying strata where they alter those rocks to greenschist mineralogical assemblages at somewhat lower temperatures. The interaction of these rocks with ^{18}O-enriched fluids at lower temperatures causes them to be relatively enriched in ^{18}O. The high positive $\delta^{18}O$ values of the overlying basalts result from low-temperature seafloor alteration (weathering). Stratigraphic preservation in the Onverwacht may not permit the kind of detailed modelling of the structure of the hydrothermal system as was performed by Gregory and Taylor[20] and Cocker *et al.*[21], particularly with regard to the effects of magma chamber configuration on the fluid flow regime. However, the general principle of oxygen isotope redistribution under conditions of subseafloor hydrothermal metamorphism is undoubtedly applicable.

Detailed descriptive information on the samples analysed in this study may be obtained by writing to S.E.H. We thank R. Hart for permission to analyse rock samples from his Onverwacht collection and Drs H. P. Taylor Jr and K. Kyser for access to their laboratories. Thanks also to K. Kyser, E. Nesbit, E. Suess, R. Duncan, M. Lyle, D. Abbott and M. De Wit, all of whom reviewed earlier drafts of the manuscript and substantially improved it through their comments. S.E.H. was funded by grant no. DPP-8120473 from the NSF Division of Polar Programs. M.W. and laboratory expenses at the University of Saskatachewan were funded by a grant from the Natural Sciences and Engineering Research Council (NSERC) of Canada to T. K. Kyser. D.S.S. was at the California Institute of Technology during part of this study. Isotopic analyses at CIT were funded

by a grant from NSF Division of Ocean Sciences, OCE80-19021, to Dr H. P. Taylor Jr.

Received 18 March 1985; accepted 28 January 1986.

1. Hamilton, P. J. *et al. Nature* **279**, 298–300 (1979).
2. Jahn, B. M., Gruau, G. & Glikson, A. Y. *Contr. Miner. Petrol.* **80**, 25–40 (1982).
3. Jahn, B. M. & Shih, C. *Geochim. cosmochim. Acta* **38**, 611–627 (1974).
4. Van Niekirk, C. B. & Burger, A. J. *Trans. geol. Soc. S. Afr.* **72**, 9–25 (1969).
5. Hurley, P. M., Nagy, B. & Pinson, W. H. Jr *Earth planet. Sci. Lett.* **14**, 360 (1972).
6. De Wit, M. J. *et al. Econ. Geol.* **77**, 1783–1802 (1982).
7. York, D. *et al. Eos* **62**, 429 (1981).
8. Martinez, M. L. *et al. Nature* **307**, 352–354 (1984).
9. Viljoen, M. J. & Viljoen, R. P. *Spec. Pub. geol. Soc. S. Afr.* **2**, 9–151 (1969).
10. Tankard, A. J. *et al. Crustal Evolution of Southern Africa* (Springer, New York, 1982).
11. Viljoen, M. J. & Viljoen, R. P. in *African Magmatism and Tectonics* (eds Clifford, T. N. & Gass, I. G.) 27–49 (Oliver and Boyd, Edinburgh, 1970).
12. Williams, D. & Furnell, R. G. *Precamb. Res.* **9**, 325–347 (1979).
13. De Wit, M. J. *J. struct. Geol.* **4**, 117–136 (1982).
14. De Wit, M. J. *Spec. Pub. geol. Soc. S. Afr.* **9**, 185–187 (1983).
15. De Wit, M. J., Fripp, R. E. P. & Stanistreet, I. G. *Spec. Pub. geol. Soc. S. Afr.* **9**, 21–29 (1983).
16. De Wit, M. J. & Stern, C. R. *2nd int. Archaean Symp., Perth* 85–87 (Geological Society of Australia, 1980).
17. Taylor, H. P. Jr & Epstein, S. *Geol. Soc. Am. Bull.* **73**, 461–480 (1962).
18. Clayton, R. N. & Mayeda, T. K. *Geochim. cosmochim. Acta* **27**, 43–52 (1963).
19. Coplen, T. B., Kendall, C. & Hopple, J. *Nature* **302**, 236–238 (1983).
20. Gregory, R. T. & Taylor, H. P. Jr *J. geophys. Res.* **86**(B4), 2737–2755 (1981).
21. Cocker, J. D., Griffin, B. J. & Muehlenbachs, K. *Earth planet. Sci. Lett.* **61**, 112–122 (1976).
22. Stern, C. R., De Wit, M. J. & Lawrence, J. R. *J. geophys. Res.* **81**, 4370–4380 (1976).
23. Hoffman, S. E. thesis, Oregon State Univ. College of Oceanography (1985).
24. Stakes, D. S. & O'Neil, J. R. *Earth planet. Sci. Lett.* **57**, 285–304 (1982).
25. Taylor, H. P. Jr in *Hydrothermal Processes at Seafloor Spreading Centers* (eds Rona, P. A. *et al.*) 83–139 (Plenum, New York, 1983).
26. Muehlenbachs, K. & Clayton, R. N. *Can. J. Earth Sci.* **9**, 471–478 (1972).
27. Beaty, D. W. thesis, California Institute of Technology (1980).
28. Beaty, D. W. & Taylor, H. P. Jr *Econ. Geol.* **77**, 95–108 (1982).
29. Hein, J. R. & Yeh, H.-W. *Init. Rep. DSDP* **62**, 749–758 (1981).
30. Perry, E. C., Jr & Tan, F. C. *Geol. Soc. Amer. Bull.* **83**, 647–664 (1972).
31. Heinrichs, T. *Precamb. Res.* **24**, 237–283 (1984).
32. Lowe, D. R. & Knauth, L. P. *J. Geol.* **85**, 699–723 (1977).
33. Muehlenbachs, K. & Clayton, R. N. *J. geophys. Res.* **81**, 4365–4369 (1976).
34. Abbott, D. H. & Hoffman, S. E. *Tectonics* **3**, 439–448 (1984).
35. Taylor, H. P. Jr *J. geol. Soc. Lond.* **133**, 509–558 (1977).
36. Beaty, D. W. & Taylor, H. P. Jr in *Komatiites* (ed Arndt, N. T. & Nisbet, E. G.), 267–280 (Allen & Unwin, London, 1982).

Input of excess CO_2 to the surface ocean based on $^{13}C/^{12}C$ ratios in a banded Jamaican sclerosponge

Ellen R. M. Druffel & Livia M. Benavides*†

Department of Chemistry, Woods Hole Oceanographic Institution, Woods Hole, Massachusetts 02543, USA
* Department of Civil Engineering, Massachusetts Institute of Technology, Cambridge, Massachusetts 02139, USA

The CO_2 content of the atmosphere has increased during the past two centuries as a result of the combustion of fossil fuels for energy[1] and the reduction of forest and soil carbon reservoirs on land[2]. The amount of CO_2 added to the atmosphere from fossil-fuel burning is known from historical records[1] (±10%), but the contribution from reduction of the terrestrial biosphere is far less certain. Several authors have estimated the relative contributions from the two sources by measuring the change in the $^{13}C/^{12}C$ ratio in atmospheric CO_2 as revealed in tree rings[3–8] (CO_2 derived from these two sources is depleted in ^{13}C with respect to that in the atmosphere). Using trees in the Northern Hemisphere, recent estimates of the integrated CO_2 release from the terrestrial biosphere since AD 1800 ranged from 70% (ref. 5) to 90% (ref. 9) of that released from fossil fuels. Here we present surface ocean $\delta^{13}C$ and $\delta^{18}O$ records measured in the skeleton of a living sclerosponge (*Ceratoporella nicholsoni*), which accretes aragonite in isotopic equilibrium with the surrounding sea water/dissolved inorganic carbon (DIC) system. The $\delta^{13}C$ record reveals a decrease

† Present address: Avenue Pardo 239, Apto 1310, Lima 18, Peru.

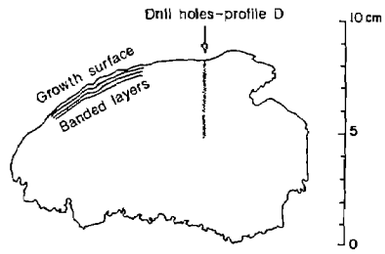


Fig. 1 Schematic diagram showing the sampling intervals for stable isotopes along profile D (0.5-mm drill holes) and for ^{210}Pb and ^{14}C analyses (0.5–1.0 mm bands)[19]. The $\delta^{18}O$ and $\delta^{13}C$ measurements obtained from the profile with the highest resolution are discussed in the text. Data obtained from three other profiles are not reported because an unexpected ageing effect after drilling was observed for these samples. Although it is standard practice to store aragonitic $CaCO_3$ samples indefinitely, we found that the $\delta^{18}O$ values of these drilled samples were lower by 0.3–0.4‰ after storage periods of a few months; most of the $\delta^{13}C$ results were decreased by 0.1–0.15‰. When samples were stored for a period of months after baking this effect was even greater. The effect of baking was observed previously by Land *et al.*[17], but these workers did not mention storage effects. We suspect that high-speed drilling of dense aragonite heats up the material sufficiently to cause partial conversion to calcite, a mineral that can exchange its CO_3^{2-} with other sources of CO_2. The results reported here are for samples that were analysed within 48 h of drilling, thus ensuring the smallest possible ageing effect.

of 0.50‰ from 1820 to 1972. Using a model of the world carbon cycle and a deconvolution of our $\delta^{13}C$ data, we estimate that the amount of excess CO_2 derived from the terrestrial biosphere is ~38% of that from fossil-fuel sources. Our model calculations support a preindustrial CO_2 concentration in the atmosphere of 280 p.p.m.v. (parts per million by volume), in agreement with direct measurements of air occluded in Antarctic ice cores[10].

Tree-ring records may not accurately reflect changes in atmospheric $\delta^{13}C$ with time because of kinetic isotope fractionation during the diffusion of CO_2 through the leaf stomata and during carboxylation of ribulose diphosphate during photosynthesis[11,12]. Small variations of the fractionation associated with these and other[11,12] processes may alter the tree-ring $\delta^{13}C$ record, rendering it unrepresentative of the actual change in the atmosphere due to excess CO_2 input.

Another approach for determining the relative contributions of fossil-fuel and forest/soil CO_2 is to examine $\delta^{13}C$ records obtained from the surface waters of the oceans. Nozaki *et al.*[13] found a reduction in $\delta^{13}C$ of 0.50‰ from 1900 to 1974 in a banded coral (*Diploria*) from Bermuda. However, other authors have found changes in coral $\delta^{13}C$ for this period that are too large to be attributed solely to the input of excess CO_2 from the atmosphere (ref. 14 and E.R.M.D., unpublished data). Corals contain symbiotic algae (zooxanthellae) whose photosynthetic activities fractionate the DIC pool from which the coral accretes its aragonite. This and other processes constitute the 'vital effect' which, as in trees, might vary with time masking the actual $\delta^{13}C$ change in sea water. Isotopic studies of corals devoid of symbiotic algae reveal a $\delta^{13}C$ record more representative of the ambient DIC in sea water, as that part of the vital effect associated with photosynthesis is absent[15,16]. However, Land *et al.*[17] found a direct correlation between the $\delta^{13}C$ and $\delta^{18}O$ in several shallow-water ahermatypic corals, indicating a common effect on both stable isotope ratios. Land *et al.* proposed that this was caused by variable retention rates of metabolic CO_2 in the internal DIC pool, another process contributing to the vital effect.

In the present study, we used the sclerosponge *Ceratoporella nicholsoni* as a recorder of $^{13}C/^{12}C$ and $^{18}O/^{16}O$ ratios in sea water. This animal has no symbiotic algae and appears to precipitate aragonite without a vital effect. The sclerosponge was

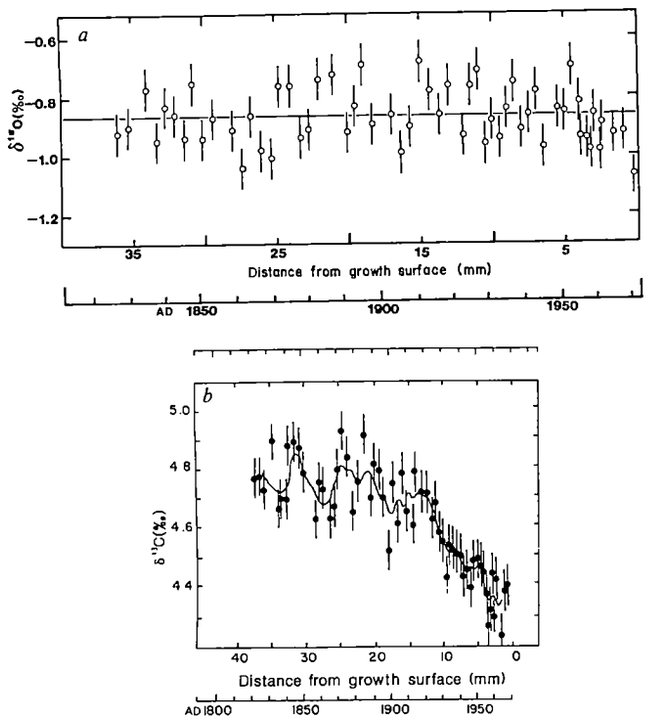


Fig. 2 *a*, $\delta^{18}O$ measurements for drilled samples along profile D. There is no apparent trend in these data, suggesting that there was no significant change in the long-term averaged SST, salinity and water composition from 1820 to 1972 on the reef. The solid line represents a least-squares fit of the data. Error bars represent 1σ error of ±0.07‰, determined from numerous triplicate analyses. *b*, $\delta^{13}C$ measurements for drilled samples along profile D. A decrease of 0.50‰ from the mid-1800s to 1972 is apparent. The solid line represents a cubic spline function fitted to the data (with 4-point smoothing). The error bars represent a 1σ error of ±0.07‰.

collected in 1972 in the fore-reef zone of Chalet Caribe Reef from the north-west coast of Jamaica at a depth of 26 m. This area is laved by open ocean waters. The major current system influencing this western Caribbean location is the precursor to the Gulf Stream.

The sclerosponge (~7 cm in diameter) was cut into slabs 3–4 mm wide which were studied using a dissecting microscope to ensure that they had been cut parallel to the growth axis. The slabs were cleaned ultrasonically to eliminate remnants of worm tubes and dust from cutting. A thin slab (1 mm) was X-rayed in an attempt to discern growth bands of varying density; however, despite the use of high-contrast film, no bands were detected. Dark-light band pairs, approximately 1 mm wide, were visible to the naked eye. These bands were identified by Hartman and Goreau[18] as a part of the organic matrix of the sclerosponge. The slabs were mapped using these organic bands (a total of 26) and sectioned for radioacarbon and ^{210}Pb analyses[19]. To obtain higher resolution of the stable isotope records, samples were drilled along a profile on a single slab (see Fig. 1). The profiles were drilled at intervals of 0.5 to 1.0-mm. For stable isotope analyses, the samples were baked at 375 °C for 1 h and converted to CO_2 by acidification with 100% orthophosphoric acid under vacuum at 50 °C. A VG Micromass 602E mass spectrometer was used to make the measurements.

The growth rate of this Jamaican sclerosponge was determined[19] using ^{210}Pb and bomb ^{14}C distributions in growth layers near the active growing surface. From these measurements and from the pre-bomb ^{14}C distributions in the sclerosponge bands, the specimen was estimated to have lived from ~AD 1700 to 1972; the average growth rate was 0.25 ± 0.05 mm yr^{-1} using the two methods. This gives an uncertainty of ±30 yr for our oldest year assignment (AD 1825).

Figure 2*a* and *b* shows the $\delta^{18}O$ and $\delta^{13}C$ results, plotted against distance from the growing surface and also against date of formation based on the bomb ^{14}C chronology[19].

The $\delta^{18}O$ measurements in Fig. 2*a* show no obvious trends. The entire data set gives an average $\delta^{18}O$ value of −0.87‰ (s.d. = 0.07‰). These data suggest that there was no significant long term variation in any of the factors controlling the $^{18}O/^{16}O$ ratio of the accreted aragonite[20–25] (that is, sea surface temperature (SST), salinity or seawater composition). Variations in $\delta^{18}O$ caused by seasonal SST changes are insignificant, as each sample represents a 2.5-yr growth interval. Surface salinity measurements were made along a transect extending from the shore to the collection site, which was ~600 m offshore. These results reveal that salinity values at the collection site (36.055–36.059‰) were within the range of values present in the western Caribbean Sea. The slight salinity gradient away from shore (on the order of +0.03‰) may represent a small input of fresh water from the island. A variation of this magnitude, however, would not significantly affect the $\delta^{18}O$ values (±0.015‰).

A cubic spline function was fitted to the $\delta^{13}C$ data set, with 4-point smoothing (solid line in Fig. 2*b*). $\delta^{13}C$ values from sclerosponge layers accreted during the nineteenth century average $+4.78 \pm 0.09$‰ (1 s.d.). Superimposed on this average value is an inter-annual oscillation of 0.2‰ with a timescale of approximately two decades. A trend toward values that are 0.40–0.50‰ lower is evident in the upper 15 mm of the sclerosponge skeleton. This result is similar to that of Nozaki *et al.*[13], who revealed a decline in $\delta^{13}C$ of 0.50‰ in a Bermuda coral. Although there is little correlation between the short-term variations of $\delta^{13}C$ as recorded in the surface ocean by the sclerosponge and the Bermuda coral (Fig. 3), partially because of the uncertainty in the chronology of the sclerosponge bands, the overall trend toward lower values by 1972 is the same.

There is no apparent correlation between the $\delta^{13}C$ and $\delta^{18}O$ values in samples from the sclerosponge, in contrast to the direct relationship found in ahermatypic corals[17]. Thus, the two quantities are independent, which is essential if we are to conclude that the isotopic ratios in the skeletal material represent accretion in equilibrium with the seawater/carbonate system.

The $\delta^{18}O$ and $\delta^{13}C$ values expected for equilibrium inorganic precipitation of calcite in surface waters of the northwestern Atlantic Ocean are −1.4 to −2.3‰ (at SST of 28 ± 1 °C) and 2.4 to 2.6‰, respectively[17,26–28]. To compare these ranges with our data, we had to take into account the additional fractionation that occurs during the accretion of aragonite as opposed to calcite, which is +0.6‰ for $\delta^{18}O$ (ref. 29) and 1.8‰ for $\delta^{13}C$ (ref. 28). Thus, values for aragonite precipitated recently in equilibrium with surrounding sea water in the northern Jamaican region are −0.8 to −1.7‰ for $\delta^{18}O$ and 4.2 to 4.4‰ for $\delta^{13}C$. Our results fall within these ranges (average $\delta^{18}O$ of −0.87‰, $\delta^{13}C$ range of 4.2–4.5‰). This evidence, in addition to the fact that there is no apparent correlation between $\delta^{13}C$ and $\delta^{18}O$, suggests that the vital effect is insignificant and that the sclerosponge precipitates aragonite in equilibrium with the DIC/water

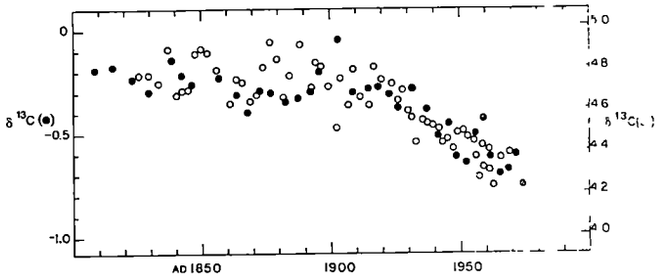


Fig. 3 $\delta^{13}C$ trend in surface ocean water in the north-west Atlantic as revealed by a Bermuda coral[13] (●, 5-yr averages) and by a Jamaican sclerosponge (present study) (○, 2.5-yr averages). A decrease of 0.50 ± 0.10‰ is apparent from the mid-1800s to 1972.

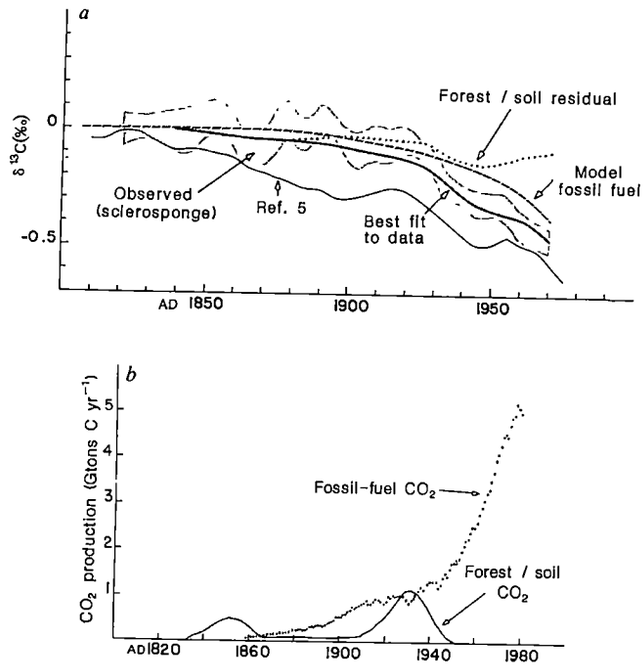


Fig. 4 *a*, Model calculations of the $\delta^{13}C$ trend in surface ocean waters. The stippled area represents the observed values from the sclerosponge. The decrease due to fossil-fuel CO_2 alone (– – –) was calculated from historical records[1,33]. The forest/soil component (.....) was calculated by eliminating the fossil-fuel curve from the model-derived best fit of the observed sclerosponge measurements (heavy solid line). The surface-ocean curve calculated from the tree-ring data of Stuiver *et al.*[5] is shown for comparison (light solid line). *b*, Annual CO_2 production from fossil-fuel burning[1] and from forest/soil sources (present work) during the past two centuries. Integration of the two curves reveals that ~28% of the total excess CO_2 released into the atmosphere during 1820–1972 was derived from the terrestrial biota.

system in which it lives. In contrast to corals, sclerosponges pump large amounts of water through their channels[18]; this may provide a mechanism for the removal of metabolic CO_2 from the animal tissue, thus eliminating significant retention of respired CO_2 in the calcioblastic layer, and hence in the accreted aragonite.

Assuming that sclerosponges accrete aragonite in equilibrium with the surrounding sea water, their skeletons contain valuable information regarding the input of excess CO_2 to the oceans. Knowledge of both the timing and magnitude of the $\delta^{13}C$ change obtained from the stable isotope records in banded sclerosponge layers enables us to estimate the relative contributions to the atmosphere and oceans of the two major sources of CO_2: fossil fuels and forest/soil carbon.

A one-dimensional mixing model of the world carbon cycle, similar to that of Emanuel *et al.*[30], was used to estimate the timing and magnitude of excess CO_2 input to the atmosphere from the two major sources mentioned above. In this model, the ocean is constructed of 19 layers that are mixed diffusively, in a manner similar to the box-diffusion model of Oeschger *et al.*[31]. The biota is represented by the five major terrestrial carbon reservoirs. Values of the atmospheric P_{CO_2} (partial pressure of CO_2) calculated using the model agreed (to within ±2 p.p.m.v.) with measurements obtained by Keeling *et al.*[32] from 1958 to 1982 at Mauna Loa.

The stippled region in Fig. 4*a* shows the range of $\delta^{13}C$ values in the surface ocean as recorded in the sclerosponge bands. Using the model, we calculate that the reduction in $\delta^{13}C$ expected in average surface ocean waters due to the input of fossil CO_2 alone[1,33] is 0.37‰ by 1972 (broken line); this is two-thirds of the value observed in the sclerosponge record. If we assume that the north-west Atlantic is representative of average global surface ocean water, then it seems that there is an additional source of excess CO_2, presumably from deforestation and soil manipulation on land. In the model, we have added CO_2 derived from the reduction of the forest/soil reservoir ($\delta^{13}C = -26$‰) in order to obtain the best fit of the observed ocean $\delta^{13}C$ curve (heavy solid line in Fig. 4*a*). The change in $\delta^{13}C$ in the surface ocean calculated from the composite tree-ring curve of Stuiver *et al.*[5] is slightly greater than our observed trend (Fig. 4*a*). Figure 4*b* shows the annual CO_2 production (in gigatons C yr^{-1}) from the two sources of excess CO_2. The forest/soil contribution is approximately 38% the size of the fossil fuel contribution, representing a net input to the atmosphere of 53 G tons C from the terrestrial biosphere between 1820 and 1972. Using the combined observed ocean trend (Fig. 3) from the Bermuda coral and Jamaican sclerosponge, the estimate of the forest/soil CO_2 contribution remains the same.

Although the shape of the forest/soil curve is difficult to determine with any certainty because of the large signal-to-noise ratio in the ocean $\delta^{13}C$ records, these data do suggest that the change in $\delta^{13}C$ due to forest/soil CO_2 input was minimal between 1950 and 1972; this is in agreement with the results of studies of tree rings[5,9] and atmospheric CO_2 (ref. 34). Also, there was a significant decrease in $\delta^{13}C$ from 1845 to 1865, suggesting that the forest/soil component was an important net source of CO_2 to the atmosphere during the nineteenth century. However, it appears from the sclerosponge data that most of the excess terrestrial CO_2 was expelled into the atmosphere during the period 1920–1950 (Fig. 4*b*).

The bimodal nature of the forest/soil CO_2 input, as revealed here, has also been demonstrated by deconvolution of ice-core CO_2 data[35] and of tree-ring $\delta^{13}C$ records[5,36]. The similarity of recent results derived from independent geochemical data sets indicates that our understanding of the excess CO_2 problem is approaching a consensus—(1) the net input of CO_2 to the atmosphere from the biosphere between 1800 and 1975 was approximately half of that from fossil fuels, and (2) the net production of biospheric CO_2 has undergone two periods of peak production in the past two centuries, at 1820–1850 and 1880–1930.

An estimate of the partial pressure of CO_2 in the atmosphere during the early 1800s can be made using these data. Using historical records of the industrial production of CO_2 from fossil fuels[1,33] and the P_{CO_2} record in the atmosphere[32], the preindustrial P_{CO_2} is estimated at 292 p.p.m.v., if the biosphere was neither a sink nor a source of CO_2. Considering the biotic source of excess CO_2, which is estimated here to have been ~38% the size of the fossil-fuel source, the preindustrial P_{CO_2} is decreased to 280 p.p.m.v.; this value is in agreement with measurements made by Neftel *et al.*[10] of air trapped in ice cores from Siple Station, Antarctica.

We thank Peter Williams, Peter Brewer, Phil Dustan, Dave Keeling, Lloyd Keigwin, Ann McNichol, Barrien Moore, Bill Emanuel and Werner Deuser for helpful discussions; Phil Dustan for providing the sclerosponge; Sheila Griffin for technical support; Debbie Shafer for helping with the modelling efforts; Stephen Rodriguez for collecting the salinity samples; and Molly Lumping for typing the manuscript. This research was supported by NSF grants OCE81-11954 and OCE83-15260.

Received 11 November 1985; accepted 27 February 1986.

1. Keeling, C. D. *Tellus* **25**, 174–198 (1973).
2. Houghton, R. A. *et al. Ecol. Monogr.* **53**, 235–262 (1983).
3. Rebello, A. & Wagener, K. *Environmental Biogeochemistry* (ed. Nriagu, J. O.) 13–23 (Ann Arbor Science, Ann Arbor, 1976).
4. Pearman, G. J., Francey, R. J. & Fraser, P. J. B. *Nature* **260**, 771–773 (1976).
5. Stuiver, M., Burk, R. L. & Quay, P. D. *J. Geophys. Res.* **89**, (D7), 11731–11748 (1984).
6. Harkness, D. D. & Miller, B. F. *Radiocarbon* **22**, 291–298 (1980).
7. Francey, R. J. *Nature* **290**, 232–235 (1981).
8. Freyer, H. D. *Proc. 6th ORNL Life-Sci. Symp.*, Oak Ridge (eds Trabalka, J. R. & Reichle, D. E.) (Springer, New York, in the press).
9. Peng, T. -H. *Geophys. Monogr.* **32**, 123–131 (1985).
10. Neftel, A., Moore, E., Oeschger, H. & Stauffer, B. *Nature* **315**, 45–47 (1985).

11. Farquhar, G. D., O'Leary, M. H. & Berry, J. A. *Aust. J. Pl. Physiol.* **9**, 121–137 (1982).
12. Francey, R. J. & Farquhar, G. D. *Nature* **297**, 28–31 (1982).
13. Nozaki, Y., Rye, D. M., Turekian, K. K. & Dodge, R. E. *Geophys. Res. Lett.* **5**, 825–828 (1978).
14. Chivas, A. R., Aharon, P., Chappell, J., Vlastuin, C. & Kiss, E. *Proc. Inaugural Great Barrier Reef Conf.*, Townsville, 77–81 (J.C.U. Press, Townsville, 1983).
15. Weber, J. N. *Deep Sea Res.* **20**, 901–910 (1973).
16. Emiliani, C., Hudson, J. H., Shinn, E. A. & George, R. Y. *Science* **202**, 627–629 (1978).
17. Land, L. S., Lang, J. C. & Barnes, D. J. *Geochim. cosmochim. Acta* **41**, 169–172 (1977).
18. Hartman, W. D. & Goreau, T. F. *Symp. zool. Soc. Lond.* **25**, 205–243 (1970).
19. Benavides, L. & Druffel, E. R. M. *Coral Reefs* (in the press).
20. Swart, P. K. *Earth Sci. Rev.* **19**, 51–80 (1983).
21. Weber, J. N. & Woodhead, P. M. J. *J. geophys. Res.* **77**, 463–473 (1972).
22. Fairbanks, R. G. & Dodge, R. E. *Geochim. cosmochim. Acta* **43**, 1009–1020 (1979).
23. Weil, S. M., Buddemeier, R. W., Smith, S. V. & Kroopnick, P. M. *Geochim. cosmochim. Acta* **45**, 1147–1153 (1981).
24. Dunbar, R. B. & Wellington, G. M. *Nature* **293**, 453–455 (1981).
25. Druffel, E. R. M. *Geophys. Monogr.* **32**, 111–122 (1985).
26. Kroopnick, P. *Deep Sea Res.* **32**, 57–84 (1985).
27. Epstein, S., Buchsbaum, R., Lowenstam, H. A. & Urey, H. C. *Bull. geol. Soc. Am.* **64**, 1315–1326 (1953).
28. Rubinson, M. & Clayton, R. N. *Geochim. cosmochim. Acta* **33**, 997–1002 (1969).
29. Tarutani, T., Clayton, R. N. & Mayeda, T. K. *Geochim. cosmochim. Acta* **33**, 987–996 (1969).
30. Emanuel, W. R., Killough, G. G., Post, W. M., Shugart, H. H. & Stevenson, M. P. *Dep. Envir. Docum.* No. DOE/NBB-0062, UC-11, 79 (1984).
31. Oeschger, H., Siegenthaler, U., Schotterer, U. & Gugelmann, A. *Tellus* **27**, 168–192 (1975).
32. Keeling, C. D., Bacastow, R. B. & Whorf, T. P. *Carbon Dioxide Review: 1982* (ed. Clark, W. C.) 377–385 (Oxford University Press, 1982).
33. Rotty, R. M. *Carbon Cycle Modelling, SCOPE 16* (ed. Bolin, B.) 121–123 (Wiley, New York, 1981).
34. Keeling, C. D., Mook, W. G. & Tans, P. P. *Nature* **277**, 121–123 (1979).
35. Siegenthaler, U. & Oeschger, H. *Tellus* (in the press).
36. Peng, T.-H. & Freyer, H. D. *Proc. 6th ORNL Life Sci. Symp.* Oak Ridge (eds Trabalka, J. R. & Reichle, D. E.) (Springer, New York, in the press).

Molecular evidence for a terrestrial component of organic matter dissolved in ocean water

Kathleen J. Meyers-Schulte & John I. Hedges

School of Oceanography, WB-10, University of Washington, Seattle, Washington 98195, USA

Dissolved organic matter (DOM) in seawater represents one of the largest active carbon reservoirs on Earth[1]. Although mass-balance calculations suggest a substantial riverine input to the marine DOM pool[2], a terrestrial organic component has not been positively identified in open-ocean water. By using lignin-derived phenols as molecular-level probes of DOM (analogous to previous studies in sediments[3–5]), we report here the first unambiguous evidence for the presence of terrestrially derived DOM in open ocean water. Dissolved humic substances, isolated by resin adsorption from near-surface water of the eastern equatorial Pacific, yield lignin-derived phenols in compositional patterns which resemble those obtained from Amazon River water[6,7]. Total phenol yields from these open-ocean humic isolates are, on average, ~10% of those from Amazon humic substances, indicating that ~10% of dissolved marine humic material (and at least 0.5% of the bulk marine DOM) is terrestrially derived.

The concentration of terrestrially derived organic matter in the marine DOM pool is one of the most ill-defined factors in the global carbon cycle[1]. The potential for a significant terrestrial contribution is evident from the calculation that the global DOM input by rivers[2] is sufficient to support ~70% of the oceanic DOM pool at its measured (^{14}C) average age of 3,400 yr[8]. Evidence that riverine DOM mixes conservatively in selected estuaries[9] suggests that most riverine DOM passes through estuaries to coastal waters[10], where its subsequent fate is unknown.

Direct biochemical analyses of marine DOM have yielded limited source-related information because the overall abundance of recognizable biochemicals is low (10–20%)[11–13] and their geographic origins are usually ambiguous. A portion of the DOM is comprised of a complex mixture of acidic polymers called humic substances which are produced by microbial degradation and condensation of biochemicals and can be isolated by adsorption onto resin[14]. Bulk isotopic and chemical analyses of humic isolates from seawater indicate a predominant marine origin[15–18], but these measurements are not well suited for detection of minor constituents, and cannot preclude a terrestrial component. Degradative analyses of humic substances allow the greater sensitivity inherent in molecular level analyses, but to date have either yielded products of unclear geographic origin[18], have been applied to landlocked marine water[10] which may not be representative of the open ocean, or have not detected a terrestrial component of marine humus[19].

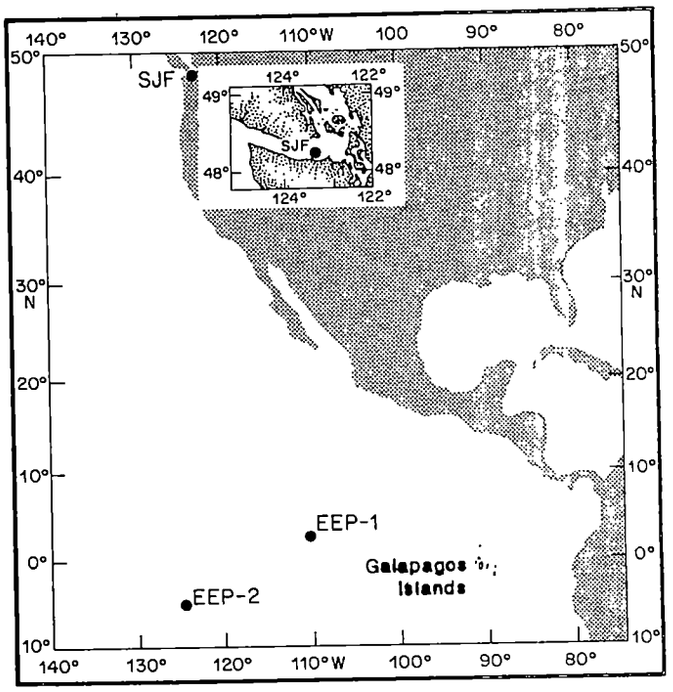


Fig. 1 Seawater sampling sites.

Using the lignin-biomarker technique[5], we report here the first direct evidence for the presence of terrestrially derived organic matter in open-ocean DOM. Lignin is a phenolic polymer which is produced solely by vascular land plants as structural units of their cell walls[20]. Its exclusive terrestrial source, high natural abundance on land, inherent chemical stability[21] and unmistakable suite of cupric oxide oxidation products render lignin an attractive molecular tracer for terrestrial organic matter in aquatic environments[6,7,22]. On oxidation by cupric oxide, lignin of all vascular plant tissues produces vanillyl phenols, which can be used as unambiguous general tracers of terrestrially derived material. In addition, syringyl phenols (produced only from angiosperm lignin) and cinnamyl phenols (produced only from non-woody tissues) denote specific vascular tissue sources[4,22]. Finally, the weight ratio of vanillic acid to vanillin, symbolized as $(Ad/Al)_V$ of fresh (undergraded) vascular plant tissues ranges from 0.1 to 0.2 (ref. 23), whereas higher values are characteristic of biodegraded lignin[6].

Previous applications of the lignin-biomarker technique to dissolved humic substances from lakes and rivers have demonstrated the ubiquitous presence of lignin structural units[6,7,22]. In particular, humic substances from the Amazon River system produce high yields of lignin oxidation products characterized by low syringyl/vanillyl (S/V) and cinnamyl/vanillyl (C/V) weight ratios and relatively high $(Ad/Al)_V$ values[6,7]. Because the Amazon is by far the world's largest river system and contributes approximately 20% of the total freshwater input to the ocean[2], it serves as a good model for the expected terrestrial component within the marine DOM pool.

We chose to study water from the Pacific Ocean which is at the most extreme end of the global ocean circulation pattern and least affected by direct river input. Both surface (depth 5 m) and sub-thermoclinic (150 m) water samples (400 l) were collected from two stations in the eastern equatorial Pacific Ocean

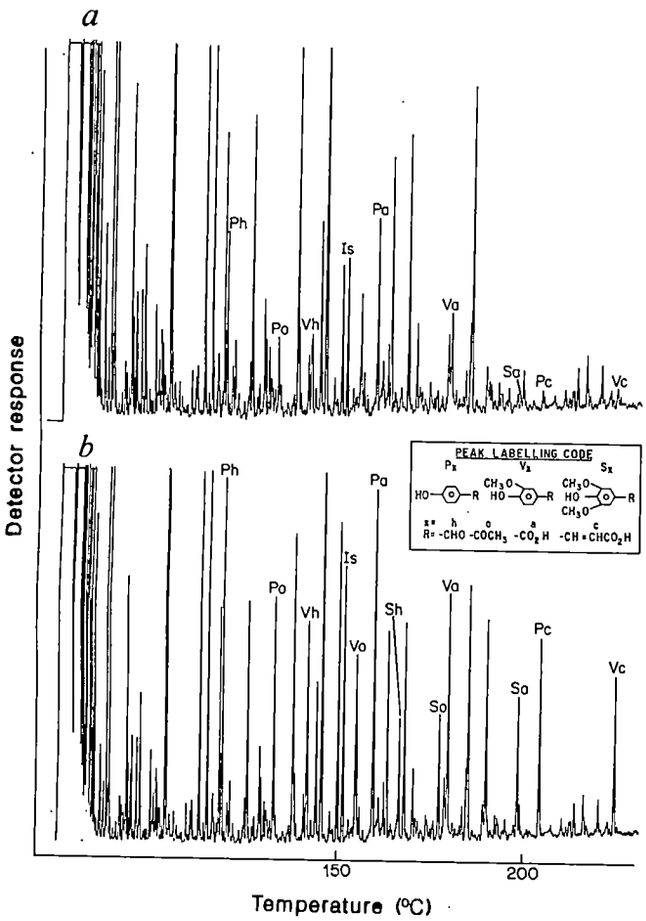


Fig. 2 Gas chromatographic traces of the cupric oxide oxidation products of the humic substance isolates from station EEP-1 (Fig. 1), sub-thermoclinic water: *a*, analysed directly as TMS derivatives; *b*, coinjected with a standard mixture of TMS-phenols. Peak identities (named as unsilylated forms): Ph, *p*-hydroxybenzaldehyde; Po, *p*-hydroxyacetophenone; Vh, vanillin; Is, ethylvanillin (GC internal standard); Vo, acetovanillon; Pa, *p*-hydroxybenzoic acid; Sh, syringaldehyde; So, acetosyringone; Va, vanillic acid; Sa, syringic acid; Pc, *p*-coumaric acid; Vc, ferulic acid. For chromatographic method, see ref. 22.

(EEP-1 and EEP-2, Fig. 1). In addition, a sample from coastal inland waters (SJF, Fig. 1; Salinity $S = 33.3‰$) was analysed. We chose to use XAD-2 (rather than XAD-8) resin to isolate and concentrate humic substances from seawater because XAD-2 gave comparable DOM recoveries in the coastal sample and produced no phenolic contamination peaks in the gas chromatographic trace of its procedural blank. The isolation procedure was carried out with 3-l resin columns as described by Thurman and Malcolm[24], with the exceptions that we used in-line glass-fibre filters (0.45 μm) in addition to the primary silver filters, and we required two recycling steps to concentrate the bulk humic isolate, which was not subsequently fractionated. By this method, 33.6–95.8 mg of humic material was isolated, corresponding to ~5–15% of the total dissolved organic carbon (DOC), assuming a DOC concentration of 0.8 mg l^{-1}. A procedural blank of 0.04 mg organic carbon was obtained for the entire isolation scheme, which corresponds to ~0.2% of the total organic carbon in the smallest humic isolate sample. Elemental compositions were determined in duplicate using a Carlo Erba Model 1106 CHN analyser. Stable carbon isotope compositions were determined in duplicate by Coastal Science Laboratories and are reported here in $\delta^{13}C$ notation, relative to PDB[25]. Cupric oxide lignin oxidation products were quantified as trimethylsilyl (TMS) derivatives by gas capillary chromatography[26] only after identities were verified against commercial standards by coinjection of TMS and methoxime derivatives[27], and by gas chromatography–mass spectrometry (GC–MS).

The average percentage of organic carbon in the humic isolates from the equatorial Pacific samples (50 ± 0.8%) agrees well with values previously reported for the open ocean[15] and the Amazon River[6,7], and reflects a low ash content. Atomic C/N ratios of the Pacific coastal and open-ocean humic isolates (32.4–37.2) are intermediate between reported ratios for open ocean (8.63; ref. 16) and Amazon (44.6 ± 5.2; refs 6, 7) isolates, but are significantly higher than the previously reported oceanic value. The mean H/C ratio for the ocean samples (1.58 ± 0.07) is similar to previously determined values for seawater humics (1.57 and 1.61; refs 18, 28), confirming the aliphatic nature of this material[17]. The somewhat lower H/C ratio of the coastal sample (1.27) is still higher than values reported for lake (1.2; ref. 14) and Amazon River (0.88–1.1; refs 6, 7) waters. All open-ocean H/C values are much higher than that of the polystyrene XAD-2 resin (1.09), indicating minimal sample contamination by the resin. The $\delta^{13}C$ values for the marine humic substances (−21.8 to −22.2‰) are within the range of values reported for humic isolates from coastal and open-ocean waters (−23.7‰ and −22.8‰, respectively)[16], and are also consistent with reported values for bulk DOC from the south (−19.9 to −22.2‰)[29] and north-east (−21.2 to −24.2‰)[30] Pacific Ocean. These $\delta^{13}C$ values for marine DOM are all more positive than reported values for humic substances from streams and rivers (−25.9 to −26.6‰)[14] and for bulk XAD-2 resin (−28.0‰), confirming the predominance of uncontaminated marine-derived material in the seawater humic isolates.

Gas chromatographic traces of the cupric oxide oxidation products for all Pacific samples (coastal and open-ocean) are remarkably similar and are dominated by non-lignin-derived compounds (Fig. 2). These traces have many peaks in common with the cupric oxide oxidation product mixtures of Amazon humic isolates[6,7], although some additional and as yet unidentified major peaks appear in the marine samples. For the coastal marine humic sample, all characteristic lignin oxidation products (aldehydic, ketonic and acidic forms of vanillyl and syringyl phenols, plus two acidic cinnamyl phenols) can be clearly identified by their mass spectra. In the open-ocean samples, neither syringaldehyde nor acetosyringone can be convincingly discriminated, and although the presence of acetovanillon is verified by GC–MS, it cannot be sufficiently separated from other compounds to be quantified in the gas chromatographic traces (Fig. 2).

In all five marine humic isolate samples, vanillyl phenols are the dominant lignin products, contributing an average 58 ± 5% to the total definable lignin yield. The S/V and C/V weight ratios of the coastal marine sample (0.21 and 0.10, respectively)

Table 1 Elemental and lignin compositions of humic substances isolated from coastal and open-ocean waters

Station	Depth (m)	%OC	C/N	H/C	Λ	$(Ad/Al)_V$	$\delta^{13}C$ (‰)
SJF	100	45.0	34.5	1.27	0.19	1.3	−22.2
EEP-1	5	49.9	32.4	1.65	0.16	1.3	−22.2
EEP-1	150	50.0	37.2	1.55	0.11	2.1	−21.8
EEP-2	5	51.1	35.7	1.57	0.12	1.1	−22.0
EEP-2	150	51.5	35.8	1.56	0.11	1.5	−22.2

SJF, Strait of Juan de Fuca sample, 48°13.2′ N, 123°21.1′ W; EEP-1, eastern equatorial Pacific station 1, 2°06.1′ N, 110°09.9′ W; EEP-2, eastern equatorial Pacific station 2, 5°00.9′ S, 124°58.4′ W; %OC, weight per cent organic carbon of freeze-dried humic isolates (uncorrected for ash); C/N and H/C, atomic ratios of freeze-dried isolates; Λ, sum of the eight lignin oxidation products in mg per 100 mg organic carbon; $(Ad/Al)_V$, weight ratio of vanillic acid to vanillin; $\delta^{13}C$ of freeze-dried humic isolates is given relative to PDB standard.

are very close to the values for the Amazon River system (S/V = 0.22–0.47; C/V = 0.01–0.10)[6,7]. The $(Ad/Al)_V$ ratios of all the marine humic isolates (1.1–2.1) also lie within the range for dissolved humic substances from the Amazon River system (1.1–2.2; refs 6, 7) but are, on average, higher than values reported for dissolved humic isolates from temperate freshwaters (0.79–0.98; ref. 22). The similar high $(Ad/Al)_V$ ratios for the marine and Amazon humic isolates reveal extensive oxidative biodegradation of the component lignin structural units. In all five marine samples, *p*-hydroxyl phenols are abundant relative to vanillyl compounds and *p*-hydroxyacetophenone is depleted, indicating a predominantly non-lignin source[6,7].

Because the relative yields of lignin oxidation products from the oceanic humic isolates are low, their quantification by means of gas chromatographic integration is crude. However, we obtain yields of total lignin phenols normalized to 100 mg of organic carbon (Λ) for open ocean humic materials that are uniformly near 0.14 (Table 1). These Λ-values are low compared with those reported for lake (2.5–3.4; ref. 22) and Amazon (0.90–2.1; refs 6, 7) humic isolates, and correspond to only 0.2% of the bulk humic carbon present as lignin structural units. Thus, the concentration of chemically recognizable lignin present in these marine humic substances is too low to account for a significant fraction of the aromatic carbon indicated by previous spectroscopic studies[17,18]. Assuming that the lignin content of riverine humic substances is unaltered at sea, the ratio $\Lambda_{ocean}/\Lambda_{Amazon}$ (0.14/1.2; refs 6, 7) provides a crude estimate that approximately 10% of open-ocean humic material is terrestrially derived. At the minimum (assuming all terrestrially derived material is confined to this 10% humic-fraction of DOC) this corresponds to roughly 1% of the bulk DOC, with a probably upper limit of 10%, if the resin-isolated material is typical of DOC in general.

With regard to the global carbon cycle, further data is necessary to better quantify the terrestrial contribution to oceanic DOM. Additional investigations of lignin-derived phenols from various ocean-water masses and geographical locations may provide compositional trends related to locations, patterns and rates of lignin removal as well as information applicable to oceanic mixing processes.

We thank J. Ertel for advice and consultation; T. Bates and P. Murphy (PMEL/NOAA) for providing cruise equipment and GC–MS use; E. M. Thurman for instruction on XAD use; B. Clark (NWFC/NOAA) for logistical support; Rainier Brewing Company for donating kegs which were crucial to our work; and the officers and crew of the NOAA ship *Discoverer* for cooperation and help. This research was supported by NSF grants OCE-821-9294 and OCE-842-1023. This is contribution no. 1613 from the School of Oceanography, University of Washington.

Received 25 September 1985; accepted 12 February 1986.

1. Likens, G. E., Bormann, F. H. & Johnson, N. M. in *Some Perspectives of the Major Biogeochemical Cycles—Scope 17* (ed. Likens, G. E.) 93–112 (Wiley, New York, 1981).
2. Meybeck, M. *Am. J. Sci.* **282**, 401–450 (1982).
3. Hedges, J. I. & Parker, P. L. *Geochim. cosmochim. Acta* **40**, 1019–1029 (1976).
4. Hedges, J. I. & Mann, D. C. *Geochim. cosmochim. Acta* **43**, 1809–1818 (1979).
5. Ertel, J. R. & Hedges, J. I. *Geochim. cosmochim. Acta* **48**, 2065–2074 (1984).
6. Ertel, J. R. thesis, Univ. Washington (1985).
7. Ertel, J. R., Hedges, J. I., Devol, A. H., Richey, J. E. & Ribeiro, N. *Limnol. Oceanogr.* (in the press).
8. Williams, P. M., Oeschger, H. & Kinney, P. *Nature* **224**, 256–259 (1969).
9. Mantoura, R. F. C. & Woodward, E. M. S. *Geochim. cosmochim. Acta* **47**, 1293–1309 (1983).
10. Pempkowiak, J. & Pocklington, R. in *Aquatic and Terrestrial Humic Materials* (eds Christman, R. F. & Gjessing, E. T.) 371–386 (Ann Arbor Science, Ann Arbor, 1983).
11. Lee, C. & Bada, J. L. *Earth planet. Sci. Lett.* **26**, 61–68 (1975).
12. Gagosian, R. B. *Geochim. cosmochim. Acta* **39**, 1443–1454 (1975).
13. Mopper, K. *Mar. Chem.* **5**, 585–603 (1977).
14. Thurman, E. M. in *Organic Geochemistry of Natural Waters* (eds Kramer, C. J. M. & Duinker, J. C.) (Martinus Nijhoff/Dr W. Junk, Dordrecht, 1985).
15. Stuermer, D. H. & Harvey, G. R. *Nature* **250**, 480–481 (1976).
16. Gagosian, R. B. & Stuermer, D. H. *Mar. Chem.* **5**, 605–632 (1977).
17. Harvey, G. R., Boran, D. A., Chesal, L. A. & Tokar, J. M. *Mar. Chem.* **12**, 119–132 (1983).
18. Stuermer, D. H. & Payne, J. R. *Geochim. cosmochim. Acta* **40**, 1109–1114 (1976).
19. Wilson, M. A., Philp, R. P., Gillam, A. H., Gilbert, T. D. & Tate, K. R. *Geochim. cosmochim. Acta* **47**, 497–502 (1983).
20. Sarkanen, K. V. & Ludwig, C. H. (eds) *Lignins* (Wiley, New York, 1971).
21. Crawford, R. L. (ed.) *Lignin Biodegradation and Transformation* (Wiley, New York, 1981).
22. Ertel, J. R., Hedges, J. I. & Perdue, E. M. *Science* **223**, 485–487 (1984).
23. Hedges, J. I., Ertel, J. R. & Leopold, E. B. *Geochim. cosmochim. Acta* **46**, 1869–1877 (1982).
24. Thurman, E. M. & Malcolm, R. L. *Envir. Sci. Technol.* **15**, 463–466 (1981).
25. Degens, E. T. in *Organic Geochemistry* (eds Eglinton, G. & Murphy, M. T. J.) 304–329 (Springer, New York, 1969).
26. Hedges, J. I. & Ertel, J. R. *Analyt. Chem.* **54**, 174–178 (1982).
27. Horning, M. G., Moss, A. M. & Horning, E. C. *Analyt. Biochem.* **22**, 284 (1968).
28. Gillam, A. H. & Wilson, M. A. *Org. Geochem.* **8**, 15–25 (1985).
29. Eadie, B. J., Jeffrey, L. M. & Sackett, W. M. *Geochim. cosmochim. Acta* **42**, 1265–1269 (1978).
30. Williams, P. M. & Gordan, L. *Deep Sea Res.* **17**, 19–27 (1970).

Fluorescently labelled Na^+ channels are localized and immobilized to synapses of innervated muscle fibres

Kimon J. Angelides*

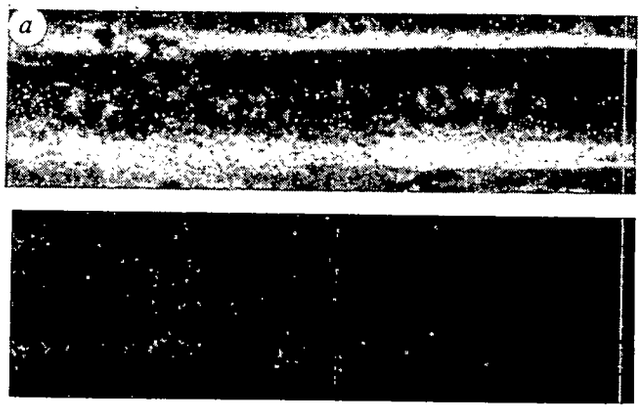
Department of Neuroscience and Center for Neurobiological Studies, University of Florida College of Medicine, Gainesville, Florida 32610, USA

Segregation of voltage-dependent sodium channels to the hillock of motoneurones and nodes of Ranvier in myelinated axons is crucial for conduction of the nerve impulse[1,2]. Much less is known, however, about the distribution of voltage-dependent Na^+ channels on muscle fibres. Recently, Beam *et al.*[3] have shown that Na^+ channels are concentrated near the neuromuscular junction. To determine the topography and mechanisms governing the distribution of voltage-dependent Na^+ channels on muscle, microfluorimetry and fluorescence photobleach recovery (FPR) have now been used to measure the density and lateral mobility of fluorescently labelled Na^+ channels on uninnervated and innervated muscle fibres. On uninnervated myotubes, Na^+ channels are diffusely distributed and freely mobile, whereas after innervation the channels concentrate at neuronal contact sites. These channels are immobile and co-localize with acetylcholine receptors (AChRs). At extrajunctional regions the Na^+ channel density is lower and the channels more mobile. The results suggest that the nerve induces Na^+ channels to redistribute, immobilize and co-localize with AChRs at sites of neuronal contact.

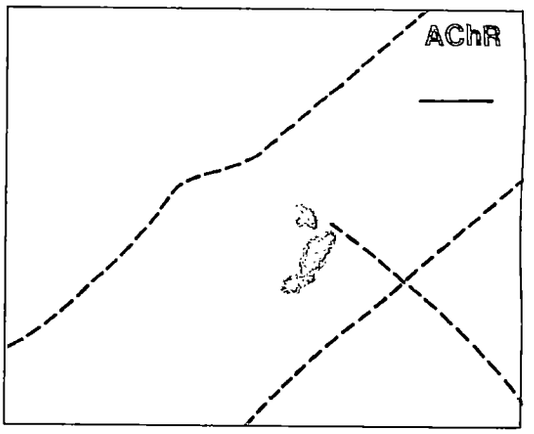
Sodium channels were fluorescently labelled by exploiting the high affinity of fluorescent derivatives of toxin V from *Leiurus quinquiestriatus* (Lqq V), toxin II from *Centruroides suffusus* (Css II) and tetrodotoxin (TTX)[4–6]. Topographical mapping and lateral diffusion coefficients (D_L) of labelled Na^+ channels on aneurally cultured embryonic chick myotubes, chick spinal cord neurone–muscle co-cultures and mouse diaphragm muscle were measured using the spot photobleaching technique[7].

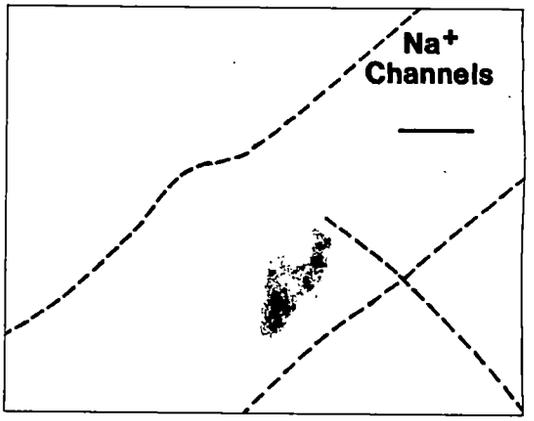
Figure 1 shows the fluorescence labelling of voltage-dependent Na^+ channels by 5-(6-)carboxytetramethylrhodamine-Lys-Lqq V) (TmRhd-Lqq V) on aneurally cultured chick myotubes and myotubes co-cultured with spinal cord neurones. Fluorescence staining of non-innervated myotubes was faint and diffusely distributed over the cell surface (Fig. 1*a*) whereas in the nerve–muscle co-cultures (Fig. 1*b*), more localized and patchy fluorescence was observed at regions which appeared morphologically identifiable as neuronal contact regions and which coincided with fluorescein 5-isothiocyanate (FITC)-α-bungarotoxin fluorescence[8,9]. Comparison of Na^+ channel and AChR distribution showed that the two channels occupy contiguous regions (lower panel to Fig. 1*b*). In most fibres, Na^+ channel and AChR staining appeared as single fluorescent patches that co-localized at neuronal contact sites, although Na^+ channel fluorescence was characteristically less intense than the AChR fluorescence. AChR patches were occasionally found in regions not associated with the neurite. Patches of fluorescently labelled Na^+ channels did not co-localize with these neurite-free AChR clusters.

* Present address: Dept. of Physiology and Molecular Biophysics, Baylor College of Medicine, 1 Baylor Plaza, Houston, Texas 77030, USA.









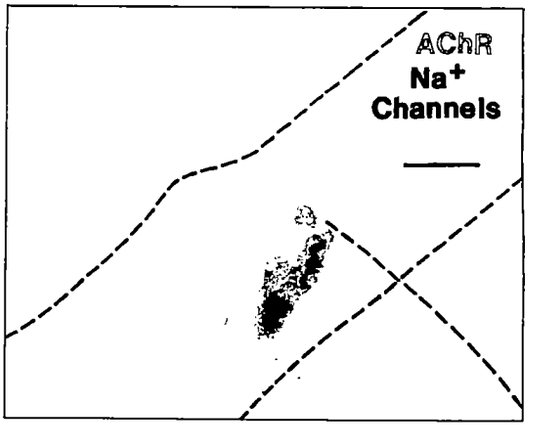


Fig. 1 Fluorescence labelling of Na^+ channels by TmRhd-Lqq V in 11-day-old chick myotubes (*a*) and chick myotubes innervated by spinal cord neurones (*b*). TmRhd-Lqq V binds reversibly to these cells with a K_d of 16 nM. The half-time for dissociation is 65 min at 22 °C. The upper micrographs are phase-contrast images of portions of the TmRhd-Lqq V-labelled myotubes and spinal cord neurone–muscle cell co-cultures. The lower micrograph is fluorescence labelling of Na^+ channels on 11-day-old chick myotubes. In *b* AChRs were visualized on the same fibre after labelling with 10^{-7} M FITC–α-bungarotoxin followed by washing. The bottom panel in *b* is a colour overlay of the AChR and Na^+ channel staining patterns on the same fibre. Scale bar, 10 μm. **Methods.** The cells were incubated with 40 nM TmRhd-Lqq V for 30 min at 22 °C in a buffer composed of 130 mM choline chloride, 50 mM HEPES adjusted to *p*H 7.4 with Tris base, 5.5 mM glucose, 0.8 mM $MgSO_4$, 5.4 mM KCl, to which 2 μM TTX was added to block any ion movement through the Na^+ channels that would lead to membrane depolarization and dissociation of TmRhd-Lqq V (ref. 4). The cultures were rapidly washed five times with ice-cold buffer before photography. Nonspecific binding of ^{125}I-Lqq V to these cells was 15% after depolarization by replacing the external medium with 150 mM external K^+ or by competitive displacement with 200 nM unlabelled Lqq V. The photographs were taken on Ektachrome film pushed to 1,200 ASA using a Nikon UFX automatic exposure attachmeent through a ×40 water immersion, 0.75 numerical aperature objective or a ×100 glycerin immersion, 1.4 numerical aperature objective.

To obtain a detailed profile of Na^+ channel distribution, fluorescently labelled Na^+ channels were mapped with a laser microbeam at various distances from the site of nerve contact using the AChR cluster identified by FITC–α-bungarotoxin as the origin. Figure 2 shows the distribution of these channels. Na^+ channel density in such cultures is much higher at the site of innervation. Within 20 μm of this region the fluorescence intensity doubles and at 200 μm it falls to ~15% of that of the synaptic region. Examination of AChR distribution shows that within the same region the drop in FITC–α-bungarotoxin fluorescence is three- to fivefold greater than the drop in TmRhd-Lqq V fluorescence. When FITC–succinyl concanavalin A (FITC–sCon-A) or tetramethylrhodamine phosphatidylethanolamine (TmRhD-PE) receptors were examined, no pattern in the fluorescence intensities was observed, indicating that the steep gradient observed for Na^+ channels is not due to local invaginations of the membrane at the nerve–muscle junction. Furthermore, this suggests that, compared with the Na^+ channel protein, the general classes of phospholipids and glycoproteins are more homogeneously distributed on the muscle cell surface. The absence of patches or a steep concentration gradient of FITC–sCon-A receptors co-localizing with Na^+ channels or AChRs shows that the innervated sarcolemma forms and maintains a distinct distribution of different membrane proteins. Beam *et al.*[3] and Roberts and Almers[10] have shown that on adult innervated skeletal muscle fibres, Na^+ channels congregate at the neuromuscular junction. Using the loose patch-clamp technique, they observed that immediately adjacent to the endplate the Na^+ current density, which they associated with voltage-dependent Na^+ channels, was 5–10-fold higher than at regions away from the endplate. Although the increased Na^+ conductance at the synapse could arise from channels possessing a high single-channel conductance, this now seems unlikely because our independent measurements by fluorescence methods using probes specific for the voltage-dependent Na^+ channel confirm that Na^+ channels are concentrated at synapses.

To gain insight into the mechanisms that organize Na^+ channels at the synapse and the elements maintaining this distribution, the lateral mobility of fluorescently labelled Na^+ channels was measured by FPR at several locations on the muscle cell. Figure 3 shows representative fluorescence recovery curves obtained from uninnervated myotubes (Fig. 3*a*) and myotubes

Table 1 Lateral diffusion coefficient (D_L) and mobile fraction (f) of sodium channels, FITC-sCon-A receptors and TmRhd-PE on muscle fibres

Cell type and distance from AChR cluster (μm)	Sodium channel* $<D_L>\pm D_L$ $\times10^{-10}$ cm^2 s^{-1}	$<f>\pm f$	N	FITC-sCon-A $<D_L>\pm D_L$ $\times10^{-10}$ cm^2 s^{-1}	$<f>\pm f$	N	TmRhd-PE $<D_L>\pm D_L$ $\times10^{-8}$ cm^2 s^{-1}	$<f>\pm f$	N
Myotube	8.9±2.5	1.04±0.14	14	1.1±0.20	0.57±0.13	14	0.81±0.15	0.93±0.11	14
Spinal/muscle									
0	IM	0.02±0.02	7	2.4±0.37	0.11±0.08	4	0.50±0.08	0.91±0.13	4
14	IM	0.073±0.05	7	1.8±0.11	0.12±0.06	4	0.70±0.08	0.96±0.08	4
	(NBD-TTX:IM)	0.05±0.05	2						
20	0.22±0.09	0.11±0.06	9	2.4±0.26	0.08±0.04	4	0.68±0.09	0.67±0.23	4
54	0.39±0.08	0.34±0.1	7	1.6±0.17	0.27±0.11	4	0.72±0.11	0.73±0.17	4
112	1.71±0.53	0.39±0.08	7	1.3±0.27	0.37±0.10	4	0.91±0.11	0.83±0.15	4
	(Css:1.31±0.43)	0.42±0.10	3						
240	2.3±1.2	0.42±0.06	11	1.89±0.39	0.39±0.14	4	0.86±0.09	0.76±0.09	4
Adult muscle fibres									
Endplate	0.039±0.019	IM	6	IM	0.057±0.05	6	0.82±0.07	0.74±0.04	6
200 μm	2.81±0.42	0.55±0.24	6	1.64±0.11	0.41±0.17	8	0.91±0.09	0.75±0.07	6

$<D_L>$, Lateral diffusion coefficient $\pm D_L$, s.d.; $<f>$, mobile fraction $\pm f$, standard deviation. IM, immobile on FPR timescale, $D \leq 10^{-12}$ cm^2 s^{-1}. N, number of measurements.

* Measured with TmRhd-Lqq V, unless otherwise noted using NBD-TTX or TmRhd-Css II.

innervated by spinal cord neurones (Fig. 3*b*, *c*). The recovery curves show that on uninnervated myotubes all Na^+ channels are relatively unrestricted in their lateral mobility, with diffusion coefficients of 8.9×10^{-10} cm^2 s^{-1} (Fig. 3*a*) whereas Na^+ channels clustered at synapses are immobilized, with diffusion coefficients of $\leq10^{-12}$ cm^2 s^{-1} (Fig. 3*b*). However, not all Na^+ channels are immobile. For example, at 240 μm from the site of neuronal contact, which is a region of lower channel density, 40% of the Na^+ channels are mobile, with lateral diffusion coefficients of 2.3×10^{-10} cm^2 s^{-1} (Table 1).

A general trend emerged from these experiments. Those channels located at and close to neuronal contact sites are immobile, while the rate of lateral motion and fraction of Na^+ channels able to move increase with increasing distance from the synapse. Similar observations were made on adult mouse diaphragm muscle, so these observations do not seem to be restricted to the culture system. The use of three Na^+ channel probes which bind to the Na^+ channel protein at independent and topologically remote sites[4–6], and the demonstration that the diffusion coefficients are independent of the probes themselves, eliminate any biasing or artefactual contribution from the probes. As an additional control, the fluorescent phospholipid derivative TmRhd-PE diffuses freely in all membrane regions with diffusion coefficients of $7\text{–}10\times10^{-9}$ cm^2 s^{-1} (Table 1). *t*-tests of the data show that there is no statistical difference between these regions. Therefore, inhomogeneities in membrane lipid viscosity cannot account for the different channel diffusion rates observed at locations on and away from the neuronal contact site.

Although the diffusion coefficient for FITC-sCon-A receptors does not change over the muscle cell surface, the mobile fraction increases somewhat in parallel with the Na^+ channel distribution (Table 1). The immobility of many FITC-sCon-A receptors at the synapse may be due in part to the high density of AChRs and Na^+ channels, both of which are glycoproteins and sCon-A receptors[11–13]. However, this region contains a small but important group of sCon-A receptors, besides AChRs or Na^+ channels, which are mobile. This indicates that not all proteins in this region are immobile and that Na^+ channels experience still stronger restrictions in lateral mobility.

The results using these probes demonstrate that the heterogeneous distribution and differential mobility of Na^+ channels are not a characteristic of all sarcolemmal proteins, the result of differences in membrane fluidity created by partitioning of particular phospholipids[14], or domains created by the aggregation and clustering of general classes of intrinsic membrane proteins. Our FPR results using nerve–muscle cocultures and Na^+ channel-specific fluorescent probes differ slightly from those of Stuhmer and Almers[15], for they found, using ultraviolet photobleaching and electrophysiological techniques, that on frog muscle all Na^+ channels were immobile.

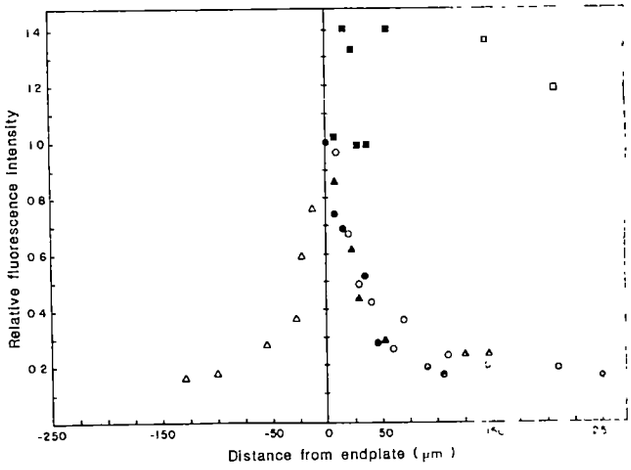


Fig. 2 Profile of fluorescently labelled Na^+ channel (●, ○, △, △) and FITC-sCon-A receptor (■) distribution on myotubes innervated by spinal cord neurones *in vitro*. Typically, a nerve process from a large multipolar neurone was visualized as it passed on top of, adjacent to, or terminated on the muscle fibre by phase or interference contrast illumination. Regions which appeared morphologically identifiable as neuronal contact sites were then examined for the localization of AChRs with FITC-α-bungarotoxin[8,9]. The monitoring beam of an argon ion laser was used to excite a small spot (1.7 or 3.6 μm diameter) on the cell membrane at various regions of the muscle and the fluorescence was accumulated at a photon counting interval of 40 ms. The beam diameter and a reticuled eyepiece were used to record the position of the microbeam relative to the nerve–muscle junction. Within each experiment no change in neutral density filters or in the optical arrangement was made. The neurite-associated ACh receptor patch at the junctional region was defined as the origin (zero distance). Photon counts were normalized to the value obtained at the neurite-associated ACh receptor patch at the junctional region, which was 1,254 counts per 40 ms for specific TmRhd-Lqq V binding and 990 counts per 40 ms for FITC-sCon-A. The absolute photon count levels, however, cannot be compared between FITC-sCon-A and TmRhd-Lqq V because a higher neutral density was required to reduce FITC-sCon-A pre-bleaching. Four representative muscle fibres are shown by the open and closed circles and triangles. The nonspecific binding was measured by displacing TmRhd-Lqq V with 200 nM unlabelled Lqq V and re-measuring the fluorescence intensities under identical counting conditions. The nonspecific binding (15%) was subtracted from the total binding to yield the specific binding to Na^+ channels[4]. The absence of a steep gradient in the fluorescence profile of FITC-sCon-A receptors demonstrates that the high fluorescence intensity observed for Na^+ channels is not due to localized foldings of the membrane which could enhance the fluorescence intensity by increasing the effective surface area.

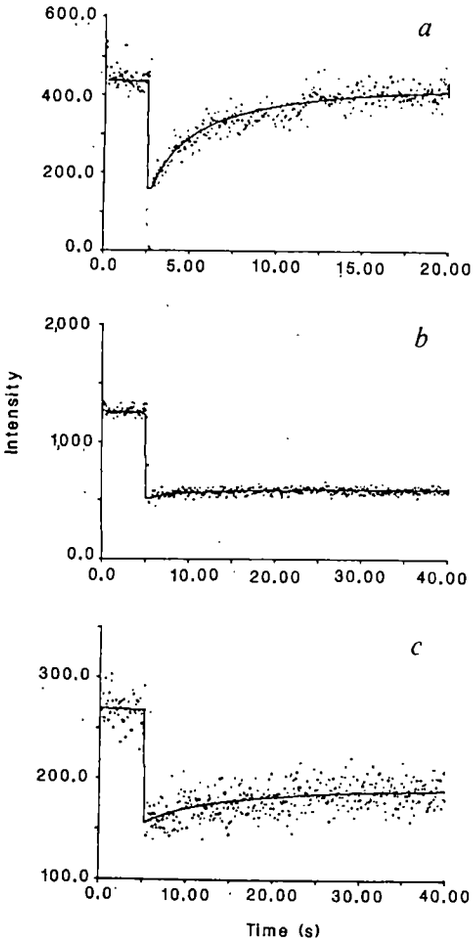


Fig. 3 Typical fluorescence recovery curves demonstrating Na^+ channel mobility on myotubes (*a*), immobility at the neuromuscular junction (*b*) and slow mobility 240 μm from the neuromuscular junction (*c*) in spinal cord neurone–muscle co-cultures. Curves *b* and *c* were obtained on the same muscle fibre. D_L and *f* were determined by curve-fitting procedures[7]. Values for D_L ($cm^2\ s^{-1}$) were determined using the expression $w^2/4T_D$ in which *w* is the e^{-2} radius of the beam profile and T_D is the half-time for recovery. Incomplete fluorescence recovery was interpreted as an indication that a fraction of labelled channels is immobile on the timescale of the experiment; $D_L \leq 3\times10^{-12}\ cm^2\ s^{-1}$ was considered to indicate immobility. The radius of the bleaching spot for the ×100 oil immersion objective used in this figure was 0.85 μm. Analysis of the curve in *a* yields a diffusion coefficient of $8.9\times10^{-10}\ cm^2\ s^{-1}$ and a recoverable fraction of 1.00. In *b*, $D_L \leq 10^{-12}\ cm^2\ s^{-1}$, and in *c*, $D_L = 2.3\times10^{-10}\ cm^2\ s^{-1}$ and $f = 0.37$.

In addition to the possibility of species differences, differences in the maturity of the tissue may contribute to the results observed. The nerve–muscle cultures may be at a stage early in development in which channels at extrajunctional regions still have some lateral mobility.

The sequelae of Na^+ channel accumulation at newly formed synapses is reminiscent of AChR cluster formation, where diffusely distributed AChRs cluster and become immobilized to the neuromuscular junction[16]. However, in contrast to AChRs, there do not appear to be regions of preexisting, dense, immobile Na^+ channel patches on uninnervated myotubes. Rather, all Na^+ channels are diffusely distributed and very mobile before innervation. The factors that specifically control the reorganization and subsequent immobilization of Na^+ channels are unknown. Apparently AChR clustering *per se* does not induce Na^+ channel clustering. Further, the specific recruitment of Na^+ channels and the conspicuous absence of Na^+ channels co-localizing with all AChR hotpsots suggest that the factors governing Na^+ channel cluster formation show some degree of temporal and molecular specificity. However, it is not clear whether the redistributed Na^+ channels originate from areas of diffuse Na^+ channel distribution on the uninnervated myotube or from an endogenous intracellular pool of newly synthesized Na^+ channels which preferentially appear at the synapse during the time of neuronal contact.

The localization and immobilization of Na^+ channels to the synapse is unexpected, for in muscle the action potential is propagated throughout the length of the fibre. The functional role of the high Na^+ channel density at the synapse is unclear but it has been proposed to raise the safety factor for impulse transmission[3]. Further experiments are required to elucidate the mechanisms by which the nerve induces the redistribution of Na^+ channels and the specific intra- and extracellular elements that maintain the elevated Na^+ channel density at the synapse.

I thank Dr Elliot Elson and David Loftus for use of the FPR equipment and for helpful discussions, the laboratory of Dr G. Fischbach, Washington University, for supplying some of the co-cultures, and Dr John Caldwell for careful reading of the manuscript and for invaluable comments. This work was supported by grants from the NIH (NS 18268) and the Muscular Dystrophy Association.

Received 7 October 1985; accepted 10 March 1986.

1. Coombs, J. S., Eccles, J. C. & Fatt, P. *J. Physiol., Lond.* **130**, 291–325 (1955).
2. Waxman, S. G. & Ritchie, J. M. *Science* **228**, 1502–1507 (1985).
3. Beam, K. G., Caldwell, J. H. & Campbell, J. T. *Nature* **313**, 588–590 (1985).
4. Angelides, K. J. & Nutter, T. J. *J. biol. Chem.* **258**, 11948–11957 (1983).
5. Darbon, H. & Angelides, K. J. *J. biol. Chem.* **259**, 6074–6084 (1984).
6. Angelides, K. J. *Biochemistry* **20**, 4107–4118 (1981).
7. Axelrod, D. A., Koppel, D. E., Schlessinger, J., Elson, E. L. & Webb, W. W. *Biophys. J.* **16**, 1055–1069 (1976).
8. Ravdin, P. & Axelrod, D. A. *Analyt. Biochem.* **58**, 585–592 (1977).
9. Role, L. W., Matossian, V. R., O'Brien, R. J. & Fischbach, G.-D. *J. Neurosci.* **5**, 2197–2204 (1985).
10. Roberts, W. M. & Almers, W. *Biophys. J.* **47**, abstr. 189 (1985).
11. Brockes, J. P. & Hall, Z. W. *Biochemistry* **14**, 2100–2106 (1975).
12. Cohen, S. & Barchi, R. L. *Biochim. biophys. Acta* **645**, 253–261 (1981).
13. Elmer, L. W., O'Brien, B., Nutter, T. J. & Angelides, K. J. *Biochemistry* **24**, 8128–8137 (1985).
14. Klausner, R. D., Kleinfeld, A. M., Hoover, R. L. & Karnovsky, M. *J. biol. Chem.* **255**, 1286–1295 (1980).
15. Stuhmer, W. & Almers, W. *Proc. natn. Acad. Sci. U.S.A.* **79**, 946–950 (1983).
16. Stya, M. & Axelrod, D. A. *Proc. natn. Acad. Sci. U.S.A.* **80**, 449–453 (1983).

Single cyclic GMP-activated channel activity in excised patches of rod outer segment membrane

L. W. Haynes, A. R. Kay & K.-W. Yau

Department of Physiology and Biophysics, University of Texas Medical Branch, Galveston, Texas 77550, USA

The plasma membrane of retinal rod outer segments contains a cyclic GMP-activated conductance[1–6] which appears to be the light-sensitive conductance involved in phototransduction[7]. Recently, it has been found that this conductance is partially blocked by Mg^{2+} (refs 3, 8, 9) and Ca^{2+} (refs 3, 4, 8–11) at physiological concentrations, thus possibly accounting for the absence of observable single-channel activity in excised membrane patches[1,3,8] and for the unusually small apparent unit conductance deduced from noise measurements on intact cells[4,10,12,13]. We now report that, as expected from this idea, single cGMP-activated channel activity can be detected from an excised rod membrane patch in the absence of divalent cations. The most prominent unitary current had a mean conductance of ~25 pS. Both individual channel openings (mean open time ~1 ms) and short bursts of openings (mean burst duration of about a few milliseconds) were observed. In addition, there were smaller events which probably

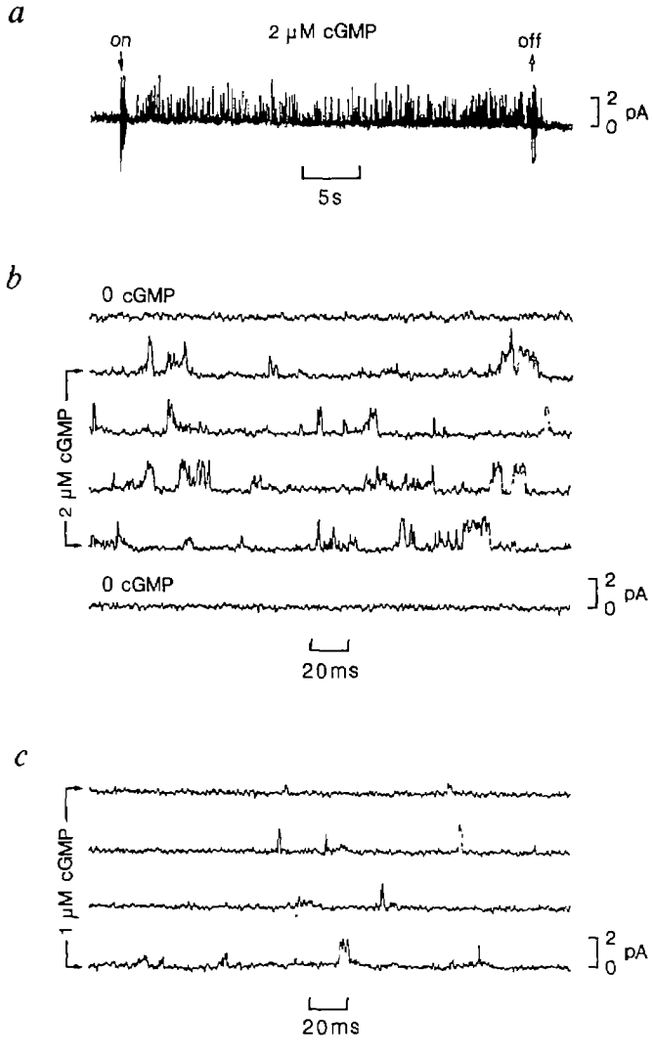


Fig. 1 Single cGMP-activated channels recorded from an inside-out membrane patch excised from a toad rod outer segment (ROS). Isotonic NaCl solution (118 mM NaCl, 0.1 mM Na-EGTA, 0.1 mM Na-EDTA, 5 mM Na-HEPES, *p*H 7.6) was present on both sides of the membrane. The holding potential was +60 mV (that is, interior of pipette being negative). All records were low-pass-filtered at 2 kHz (8-pole Bessel). *a*, Activation of single-channel activity by 2 μM cGMP. The 'on' and 'off' arrows indicate the times when tap movements were made to admit cGMP into the bath and to remove it. The ringing transients immediately following the on and off time markers were caused by vibrations from the tap movements. *b*, Samples of the same recording shown at a higher time resolution. Top trace, control recording before the admission of cGMP; bottom trace, control recording after removal of cGMP. The middle four traces, obtained in the presence of 2 μM cGMP, were not continuous in time, but were selected to illustrate various features associated with openings and closings of the cGMP-activated channels (see text). *c*, Recordings from the same patch at 1 μM cGMP.

Methods. All experiments, except for that in Fig. 4, were performed on ROS from the toad, *Bufo marinus*. The experiment in Fig. 4 was performed on a rod from the larval tiger salamander (*Ambystoma tigrinum*), simply because for a time we failed to obtain stable gigaohm seals from toad rods; other control experiments have indicated that the cGMP-activated channels in the salamander rod have properties similar to those in the toad rod. A piece of retina from a dark-adapted animal was incubated in the dark for 1 h in Ringer's solution containing 1 mg ml^{-1} hyaluronidase (Sigma type I-S), then finely chopped to yield many isolated rod outer segments[8]. The outer segments were then transferred to the experimental chamber and washed thoroughly with isotonic NaCl solution (see above) before recordings began. All recordings were made in visible light at room temperature (23–25 °C). The patch pipette, containing isotonic NaCl solution, was made of thick-walled borosilicate glass capillary and had a lumen diameter at the tip of ≤0.5 μm. The exterior of the pipette tip was coated with Sylgard to reduce electrical noise[30]. Current was measured with a List EPC-7 patch-clamp system in the voltage-clamp mode. Gigaohm seals were made on the plasma membrane of an outer segment near its tip, and the patch was then excised in the inside-out configuration by a gentle tap on the micromanipulator supporting the pipette[2,3,8]. The signals were stored on analog tape and subsequently digitized for analysis.

represented other states of the conductance. The mean current increased with the third power of cGMP concentration, suggesting that there are at least three cGMP-binding sites on the channel molecule. With 0.2 mM Mg^{2+} in the cGMP-containing solution, a flickering block of the open channel was observed; the effect of Ca^{2+} was similar. The results resolve a puzzle about the light-sensitive conductance by demonstrating that it is an aqueous pore rather than a carrier.

All experiments were done in visible light, with an isotonic NaCl solution (see Fig. 1 legend) present on both sides of the membrane. Figure 1*a* shows the current recorded from an excised, inside-out rod membrane patch held at +60 mV. With 2 μM cGMP in the bath, there were fluctuations which resembled the openings and closings of individual ion channels. The effect of cGMP was rapidly reversible. Figure 1*b* shows sample records at a higher time resolution. The most prominent unitary currents, which occurred both singly and in short bursts, had a mean amplitude of ~1.5 pA (see Fig. 2*a*), corresponding to a conductance of ~25 pS. Apart from the large unit currents there were also small events, but these were more difficult to analyse because their amplitudes were not significantly above background noise. The relationship between the small and the large events is not clear at present, though they probably represent different states of the same conductance. In Fig. 1*c*, the same patch was exposed to a lower concentration of cGMP: the frequency of events was lower, and the bursts of openings also seemed to be briefer.

Figure 2*a* shows probability density histograms of current amplitude obtained from the recordings illustrated in Fig. 1*a* and *b*. The solid profile is the histogram obtained in the presence of 2 μM cGMP, while the dashed profile is the control histogram scaled to the same height. The former histogram has two identifiable peaks: one centred at zero and the other at ~1.5 pA. As judged from the raw records, the non-zero peak appears to correspond to the mean amplitude of the large unitary events. The distribution centred at 0 pA overlapped with the control histogram quite well at negative current values, but at positive values there was excess probability density which reflected the contribution of the small events. From the histogram, we estimated that the probability of occurrence for the small events was roughly the same as that for the large events.

We have examined the kinetics of large events selected by a window, as indicated by the arrows in Fig. 2*a*. The open times of the events (low-pass-filtered at 1 kHz; see Fig. 2 legend) showed a roughly exponential distribution, with a time constant of 1.5 ms (Fig. 2*b*, left); the true value, however, was estimated to be ~1.0 ms after correcting for low-pass filtering[14]. The burst times (Fig. 2*b*, right) were also roughly exponentially distributed, with a time constant of 3.3 ms. A similar analysis of the single-channel activity at 1 μM cGMP (that is, Fig. 1*c*) gave a comparable channel open time (uncorrected time constant = 1.3 ms) but a shorter burst time (time constant = 2.4 ms). The significance of this concentration-dependent difference is unclear. It should be emphasized that even though there was little stacking of events at the low concentrations of cGMP used, the successive events did not necessarily reflect activity from the same channel molecule, because many channels were gen-

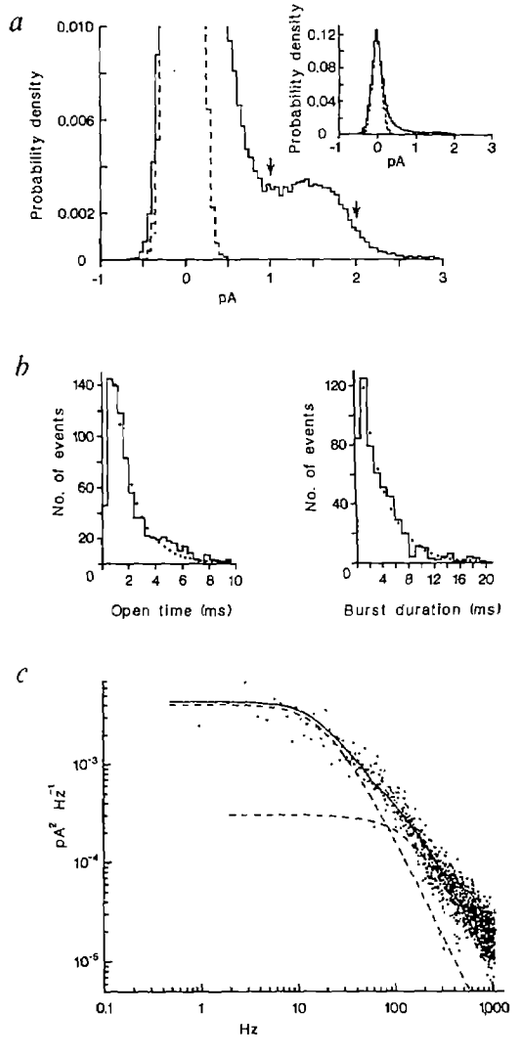


Fig. 2 Analysis of the single-channel records illustrated in Fig. 1*a* and *b*. The automated single-channel analysis program of Sachs *et al.*[31], implemented by Lingle (Florida State University) for the IBM PC, was used to produce the plots shown in *a* and *b*. Before analysis, the data were first filtered at 2 kHz with an 8-pole Bessel filter and digitized at 5 kHz, then further filtered at 1 kHz with a digital Gaussian filter to reduce background noise. *a*, Probability density histrogram of current amplitude (continuous profile) in the presence of 2 μM cGMP. The dashed profile indicates the control histogram obtained after the removal of cGMP; it has been scaled to the same height as the one with cGMP. To compute each histogram, the entire stretch of recording was divided into consecutive sections each 102.4 ms long. The baseline for each section (corresponding to 0 pA on the histograms) was located using an algorithm that maximizes the number of crossings through a horizontal line, and the probability density distribution (bin width 0.05 pA) was then determined. The control histogram was fitted well by a Gaussian distribution with a standard deviation of 0.12 pA. A similar control histogram obtained before the application of cGMP was also fitted by a Gaussian distribution with a standard deviation of 0.15 pA. The non-zero peak of the histogram obtained at 2 μM cGMP is situated at −1.5 pA, and corresponds to the mean amplitude of the large unitary events (see text). The arrows indicate the amplitude window used for computing the time histograms for the large events (see *b*). Inset, the same plots at reduced scales. The probability density histogram for the recordings at 1 μM cGMP (that is, Fig. 1*c*) was similar to the histogram for 2 μM shown here; the non-zero peak was in the same place, but the overall probability for non-zero amplitudes was less, as expected from the relative paucity of events. *b*, Histograms of open times and burst durations for the large events. The amplitude window chosen for analysing these large events (1.0–2.0 pA) also served to minimize the inclusion of stacked events. A burst was defined as either a single-channel opening or a collection of consecutive openings separated by closed periods ≤2 ms. This value was deduced from the closed-time distribution, which could be fitted by the sum of two exponentials, with the shorter time constant (~2 ms) representing the intra-burst closures. The dots in each plot indicate a single exponential fitted to the histogram. The time constant was 1.5 ms for the open time distribution and 3.3 ms for the burst-time distribution. The fall in probability density for short times in each histogram was due to low-pass filtering. *c*, Power density spectrum for the records in Fig. 1*b*. The raw records in this case were low-pass-filtered at 1 kHz (8-pole Butterworth) and digitized at 2 kHz. The control spectrum obtained in the absence of cGMP has been subtracted. The dashed curves indicate Lorentzians with corner frequencies of 20 Hz and 150 Hz respectively, corresponding to time constants of 8 and 1 ms. The continuous curve is the sum of the two Lorentzians.

erally present in a patch (see below). Therefore, the closed-time distribution was of limited usefulness and will not be described here.

Figure 2*c* shows the power spectrum for the current records at 2 μM cGMP. It can be fitted approximately by the sum of two Lorentzians, with characteristic time constants of ~1 ms and 8 ms respectively. The short time constant is comparable in value to the mean open time of the large events, while the long time constant is probably related to the burst times. Interestingly, the short time constant is rather similar to values obtained by others from noise measurements on intact cells[4,10,12,13]. It is difficult, however, to make an exact comparison between the power spectral analysis and the kinetic analysis because, among other reasons, both large and small events contributed to the power spectrum.

An analysis similar to those in Fig. 2*a*, *b*, performed on data from three other patches (all at +60 mV and 1–2 μM cGMP), gave comparable mean unit amplitudes (1.4–1.5 pA) and time constants (event open time 1.4–1.6 ms, burst duration 1.6–3.3 ms, 1-kHz filter). As a comparison, the power spectra obtained from four experiments (1–5 μM cGMP, +60 mV) gave a short time constant of 0.9–1.5 ms and a long time constant of 7–11 ms. At frequencies ≥1 kHz, the power spectra often showed some residual power density which could not be accounted for by just two Lorentzians. In experiments where channel openings were also studied at −60 mV (see, for example, Fig. 3*c*), the events were inverted in polarity and had shorter open times (see legend to Fig. 3*c*). Nevertheless, the latter events had amplitudes similar to those at +60 mV. Thus, the current-voltage relation for the unitary conductance seems to be roughly linear, which agrees with our previous conclusion from macroscopic current measurements—that is, a large part of the outward rectification observed in physiological solutions is the result of a voltage-dependent block by divalent cations[3,8,9].

One advantage of removing divalent cations from the solutions is that a much larger cGMP-induced current is obtained[3,8,9]; this permits the activation of current by cGMP to be studied at very low concentrations of the activator. Figure 3*a* shows one such experiment performed at −30 mV. As the cGMP concentration increased, the single-channel events gradually summed to give a noisy, steady current. No obvious desensitization was evident even after prolonged (>1 min) applications of cGMP. The large amplitude of the saturated current compared with the single-channel current indicated that many channels must be present in the membrane patch, a conclusion arrived at for all the experiments that we analysed. We have attempted to estimate the channel density on the membrane, but this was complicated by the finding that the saturated current amplitude showed large variations (up to almost 100-fold) in different experiments, with little correlation to the apparent patch size (as judged visually). Assuming an average patch size of 0.2 μm^2 (as estimated from the pipette tip lumen) and assuming that at saturating cGMP concentrations each channel molecule is conducting current about half the time, the high and low estimates for the channel density would be 3,000 and 30 μm^{-2}, respectively (average ~1,000 μm^{-2}, 18 patches). Taking a rhodopsin density on the surface membrane of 30,000 molecules μm^{-2}, the channel/rhodopsin mole ratio

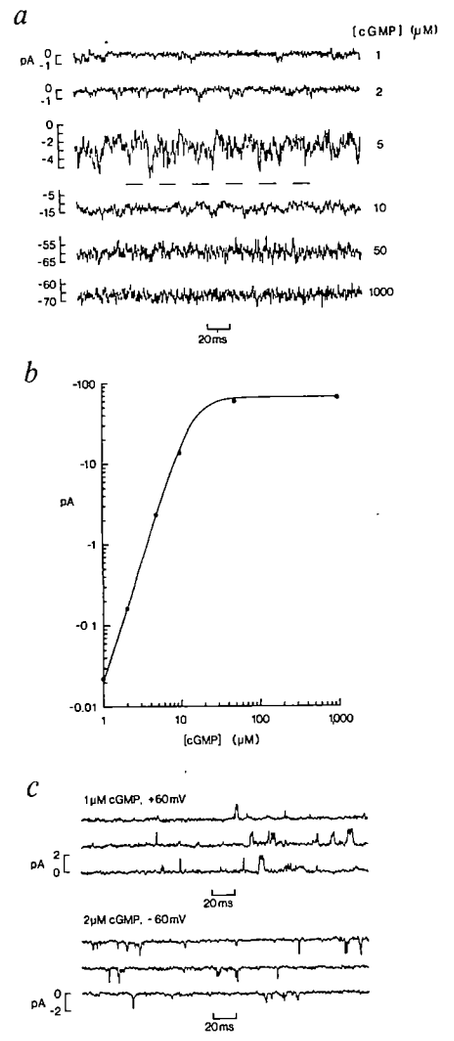


Fig. 3 *a*, Activation of current in toad rod patch at different concentrations of cGMP. Holding potential −30 mV. Records were filtered at 1 kHz. The top three and bottom three traces have different amplitude scales. Note the sustained current fluctuations even at a saturating cGMP concentration. In addition, at 50 μM and 1,000 μM cGMP, there were also slow fluctuations which are not apparent in the records shown here because of the fast time scale. Total current variances (d.c. to 1 kHz) at the different cGMP concentrations were: 0.01 pA^2 (1 μM), 0.08 pA^2 (2 μM), 1.15 pA^2 (5 μM), 6.33 pA^2 (10 μM), 14.56 pA^2 (50 μM) and 13.60 pA^2 (1 mM). *b*, log–log plot of mean current against cGMP concentration. The mean currents were computed from the records shown in *a*. Smooth curve is drawn according to the Hill equation: $j(C) = -67\ pA \times [C^3/(C^3+15^3)]$, where C is the cGMP concentration mean current. *c*, Effect of membrane potential on current activation by cGMP. Different toad rod patch from that in *a* and *b*. Only sample records are shown. Low-pass-filtered at 2 kHz. Analysis of the complete recordings indicated that the frequency of channel activation was about 2.5 times higher for 1 μM cGMP/+60 mV than for 2 μM cGMP/−60 mV. Open time constant (1-kHz filtering) was 1.4 ms at +60 mV and 0.8 ms at −60 mV.

would be between 1:10 and 1:1,000 (average ~1:30). The wide range of channel density estimates suggests that there may be a local clustering of channels on the plasma membrane. Previous estimates based on noise measurements from intact cells were between 100 and 200 channels per μm^2 (refs 10, 13). It is interesting that the current fluctuations remained high even at saturating cGMP concentrations (Fig. 3*a*); this perhaps suggests that the binding of cGMP molecules to the channel is an event separate from (though causally related to) the opening and closing of the channel. In other words, a channel molecule can

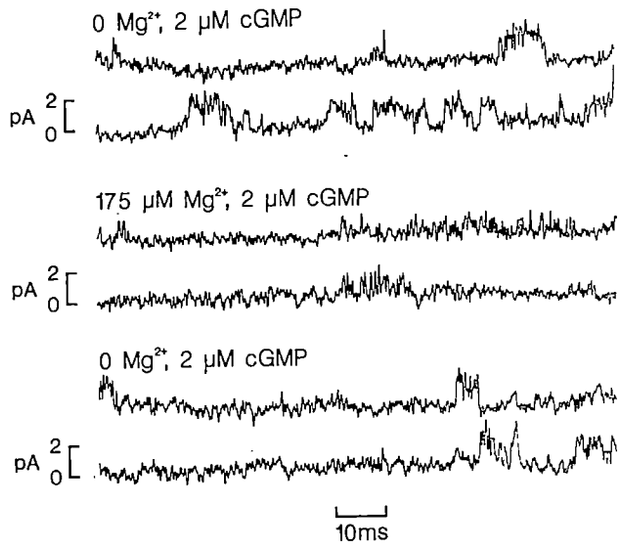


Fig. 4 Flickering block of the open-channel current by Mg^{2+}. Mg^{2+} was added only to the cGMP-containing solution in the bath, while the pipette solution still contained no divalent cations. Holding potential +60 mV, salamander rod patch (see Fig. 1 legend). Top two and bottom two traces were obtained with 0 Mg^{2+}; middle two traces with 175 μM $MgCl_2$ (no Na-EGTA or Na-EDTA; see Fig. 1 legend). To show the flickering blockade more clearly, the records have been low-pass-filtered at 5 kHz instead of the usual 2 kHz.

open and close repeatedly while still binding cGMP; this same mechanism may also explain the burst phenomenon[15]. Figure 3*b* shows the relation between mean current and cGMP concentration based on the records of Fig. 3*a*. The current increased with the third power of cGMP concentration (that is, the Hill coefficient, n, was 3), with a half-saturating cGMP concentration ($K_{1/2}$) of ~15 μM. Collected results gave an n of 2.9 ± 0.4 (mean ± s.d., 15 experiments) and $K_{1/2}$ of 14–45 μM at −30 mV (6 experiments). The n value here is higher than previous measurements made in the presence of divalent cations[1,3,6,7], but is probably more reliable because the current could be resolved down to lower cGMP concentrations. Still, an influence of divalent cations on the Hill coefficient cannot be ruled out. The $K_{1/2}$ values, on the other hand, are broadly consistent with previous measurements[1,3,6,7]. There was also an effect of membrane potential on current activation, in that at depolarizing voltages it took a lower concentration of cGMP to elicit a comparable frequency of events (Fig. 3*c*). This voltage effect, however, was not very large, with $K_{1/2}$ decreasing by only ~40% between −40 mV and +40 mV (2 experiments), or an estimated e-fold reduction over ~160 mV. The Hill coefficient, on the other hand, did not show any obvious voltage dependence. These observations are similar to previous results in cone patches[8].

Figure 4 shows an example of the effect of divalent cations on the current. With 175 μM Mg^{2+} in the bath, the prominent step changes in the current induced by cGMP were no longer observed. Instead, there were clusters of relatively high-frequency flickers, which most probably reflected blockage of the open channel[16]. In other experiments we found that Ca^{2+} had a similar effect, though a higher concentration was required (at least at depolarizing voltages). A flickering block by divalent cations has been observed previously for the glutamate-activated channel in mouse brain[17], as well as for the Ca-channel[18] in conditions where the current is carried by monovalent cations[19–21]. Indeed, the cGMP-activated (or light-sensitive) conductance has certain properties in common with Ca-channels, in that besides the blockade by divalent cations of current carried by monovalent cations, it is also highly permeable to divalent cations[22–28]. Both the blockade and the ion selectivity

can perhaps be explained, as has been proposed for the Ca-channel[21,29], by the presence of binding sites in the channel with different affinities for monovalent and divalent cations.

Thus our results demonstrate that the light-sensitive conductance is a pore rather than a carrier; this confirms a recent inference from noise measurements on intact cells[10]. As the Hill coefficient for current activation is near 3, there must be at least three cGMP binding sites per channel molecule. At present, however, we do not know the details of the kinetic scheme governing the channel activation by cGMP.

We thank Dr Kei Nakatani for invaluable help, Drs Philip Palade and Robert Wong for encouragement and for loaning equipment, and Drs Denis Baylor, Malcolm Brodwick and Philip Palade for discussions. Dr Chris Lingle provided us with an implementation (for the IBM PC) of the single-channel analysis program developed by Dr Frederick Sachs and co-workers. L.W.H. was supported in part by a Fight For Sight Inc. (New York) Research Fellowship; the work was supported by the US National Eye Institute and the Retina Research Foundation, Houston, Texas.

Received 13 December 1985; accepted 4 March 1986.

1. Fesenko, E. E., Kolesnikov, S. S. & Lyubarsky, A. L. *Nature* **313**, 310–313 (1985).
2. Nakatani, K. & Yau, K.-W. *Biophys. J.* **47**, 356a (1985).
3. Yau, K.-W., Haynes, L. W. & Nakatani, K. in *Membrane Control of Cellular Activity* (ed. Lüttgau, H. Ch.) (Gustav Fischer, Stuttgart, in the press).
4. Matthews, G. *Soc. Neurosci. Abstr.* **11**, 1130 (1985).
5. Stern, J. H., Kaupp, U. B. & MacLeish, P. R. *Soc. Neurosci. Abstr.* **11**, 1130 (1985).
6. Zimmerman, A. L., Yamanaka, G., Eckstein, F., Baylor, D. A. & Stryer, L. *Proc. natn. Acad. Sci. U.S.A.* **82**, 8813–8817 (1985).
7. Yau, K.-W. & Nakatani, K. *Nature* **317**, 252–255 (1985).
8. Haynes, L. W. & Yau, K.-W. *Nature* **317**, 62–65 (1985).
9. Yau, K.-W. & Haynes, L. W. *Biophys. J.* **49**, 33a (1986).
10. Bodoa, R. D. & Detwiler, P. B. *J. Physiol., Lond.* **367**, 183–216 (1985).
11. Lamb, T. D., Matthews, H. R. & Torre, V. *J. Physiol., Lond.* **369**, 34P (1985).
12. Gray, P. & Attwell, D. *Proc. R. Soc.* **B223**, 379–388 (1985).
13. Zimmerman, A. L. & Baylor, D. A. *Biophys. J.* **47**, 357a (1985).
14. Roux, B. & Sauve, R. *Biophys. J.* **48**, 149–158 (1985).
15. Colquhoun, D. & Sakmann, B. *Nature* **294**, 464–466 (1981).
16. Neher, E. & Steinbach, J. H. *J. Physiol., Lond.* **277**, 153–176 (1978).
17. Nowak, L., Bregestovski, P., Ascher, P., Herbet, A. & Prochiantz, A. *Nature* **307**, 462–465 (1984).
18. Lansman, J. B., Hess, P. & Tsien, R. W. *Biophys. J.* **47**, 67a (1985).
19. Kostyuk, P. G., Mironov, S. L. & Shuba, Y. M. *J. Membrane Biol.* **76**, 83–93 (1983).
20. Almers, W., McCleskey, E. W. & Palade, P. T. *J. Physiol., Lond.* **353**, 565–583 (1984).
21. Hess, P. & Tsien, R. W. *Nature* **309**, 453–456 (1984).
22. Capovilla, M., Caretta, A., Cervetto, L. & Torre, V. *J. Physiol., Lond.* **343**, 294–310 (1983).
23. Yau, K.-W., McNaughton, P. A. & Hodgkin, A. L. *Nature* **292**, 502–505 (1981).
24. Hodgkin, A. L., McNaughton, P. A., Nunn, B. J. & Yau, K.-W. *J. Physiol., Lond.* **350**, 649–680 (1984).
25. Yau, K.-W. & Nakatani, K. *Nature* **309**, 352–354 (1984).
26. Yau, K.-W. & Nakatani, K. *Nature* **311**, 661–663 (1984).
27. Hodgkin, A. L., McNaughton, P. A. & Nunn, B. J. *J. Physiol., Lond.* **358**, 447–468 (1985).
28. Yau, K.-W. & Nakatani, K. *Nature* **313**, 579–582 (1985).
29. Almers, W. & McCleskey, E. W. *J. Physiol., Lond.* **353**, 585–608 (1984).
30. Sakmann, B. & Neher, E. *Single-Channel Recording* (Plenum, New York, 1983).
31. Sachs, F., Neil, J. & Barkakati, N. *Pflügers Arch. ges Physiol.* **395**, 331–340 (1982).

Cyclic GMP-sensitive conductance of retinal rods consists of aqueous pores

A. L. Zimmerman & D. A. Baylor

Department of Neurobiology, Stanford University School of Medicine, Stanford, California 94305, USA

The surface membrane of retinal rod and cone outer segments contains a cation-selective conductance which is activated by 3′,5′-cyclic guanosine monophosphate (cGMP)[1–4]. Reduction of this conductance by a light-induced decrease in the cytoplasmic concentration of cGMP appears to generate the electrical response to light (reviewed in refs 5, 6), but little is known about the molecular nature of the conductance. The estimated unitary conductance is so small[1,7–9] that ion transport might occur via either a carrier or a pore mechanism. Here we report recordings of cGMP-activated single-channel currents from excised rod outer segment patches bathed in solutions low in divalent cations. Two elementary conductances, of ~24 and 8 pS, were observed. These conductances are too large to be accounted for by carrier transport, indicating that the cGMP-activated conductance consists of aqueous pores. The dependence of the channel activation on the concentration of cGMP suggests that opening of the pore is triggered by cooperative binding of at least three cGMP molecules.

The cGMP-activated conductance of excised patches from salamander rod outer segments was greatly increased when both sides of the patch were bathed in solutions containing a very low concentration of divalent cations. For five patches in low concentrations of divalent cations (total less than 1 μM) the maximal agonist-induced conductance at +50 mV was 15.9 ± 2.1 nS (mean ± s.e.m.), while for 13 patches prepared similarly but studied in solutions with normal levels of divalent cations (external Mg^{2+} concentration ($[Mg]_o$) 6 mM; internal Mg^{2+} concentration ($[Mg]_i$) 3 mM; 1.5 mM $[Ca]_o$) it was 194 ± 27 pS. These results indicate that decreasing the concentration of divalent cations increased the cGMP-sensitive conductance by roughly two orders of magnitude.

Figure 1 shows dose–response relations for the cGMP-sensitive current of patches in 'low divalent' solutions. The cGMP-activated current of each patch is expressed relative to the maximal value; cGMP concentrations were normalized by the estimated half-saturating concentration, $K_{0.5}$, which ranged from 5.3 to 12 μM, with an average value of 9.6 μM. The solid curve was drawn according to the Hill equation: $r/r_{max} = G^3/(1+G^3)$, where r/r_{max} is the normalized response and G is the concentration of cGMP divided by $K_{0.5}$. This equation would apply if opening of a channel required the binding of at least three molecules of cGMP, and if the binding were strongly cooperative. The dashed curve, which gives a poorer fit, was drawn according to $r/r_{max} = (G/[1+G])^3$; this relation is expected if opening requires binding to three independent sites of equal affinity. Somewhat smaller power exponents have been reported from experiments with higher concentrations of divalent cations[1,3,10,11], where the smaller size of the agonist-induced currents prevented measurement of the foot of the dose–response relation.

Figure 2 shows the current obtained from an excised patch at a holding potential of +50 mV. Application of 0.5 or 1 μM cGMP to the cytoplasmic side of the patch caused outward current pulses, which were much more frequent at the higher dose. Removal of cGMP abolished the pulses, demonstrating that they did not result from disruption of the membrane or seal.

Selected records from the experiment of Fig. 2 are plotted on an expanded time base in Fig. 3*A*, which shows unitary outward currents with a mean amplitude close to 1 pA and widely variable durations. For the patch potential of +50 mV the underlying conductance change is 20 pS. In some traces there was a suggestion of smaller events of amplitude ~0.3 pA (conductance = 6 pS). Such smaller events are better resolved in the experiment of Fig. 4. Similar experiments on a total of nine patches gave, for the large and small transitions, mean conductance changes of 23.7 ± 4.1 and 7.7 ± 1.4 pS (mean ± s.d.), respectively. In one experiment the amplitude of the single-channel currents varied approximately linearly with holding potential between −100 and +50 mV.

Figure 3*B* presents further evidence for the quantal nature of the current transitions in the experiment of Fig. 2. The control amplitude histogram (Fig. 3*B*, *a*) is approximately gaussian, with a width at half height of 0.3 pA. The histogram for 0.5 μM cGMP (Fig. 3*B*, *b*) shows a small additional hump between 0.3 and 1 pA. In 1.0 μM cGMP (Fig. 3*B*, *c*) there are two peaks centred at amplitudes of 0 and 0.8 pA, with a smaller hump at ~1.6 pA. The form of the three histograms is consistent with quantal agonist-induced currents of ~0.8 pA, like those in

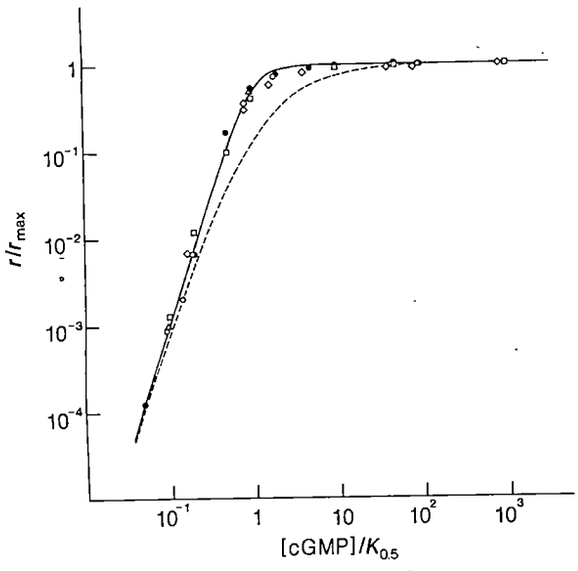


Fig. 1 Dose-response relation for activation of the cGMP-sensitive conductance of excised rod outer segment patches in low divalent solutions. Results from five patches, each plotted using a different symbol. The ordinate is the cGMP-activated current (r) relative to the maximal value (r_{max}), while the abscissa is the cGMP concentration relative to the estimated half-saturating concentration $K_{0.5}$. The curves were calculated from equations described in the text. Saturating currents and values of $K_{0.5}$ for each patch were as follows. ○: 1,021 pA, 5.3 μM; △: 116 pA, 10.5 μM; ◇: 834 pA, 12 μM; □: 774 pA, 10.0 μM; ●: 1,234 pA, 10.0 μM.

Methods. Patches were excised from the distal tip of isolated salamander rod outer segments, which were prepared in the light[1] and cleaned by exposure for 5 min to ~0.5 mg ml^{-1} hyaluronidase (Cooper, HSEP, 5474). Patches were studied in symmetrical solutions consisting of either nominally 0 divalent Ringer's, containing (in mM): NaCl 111, KCl 2.5, EDTA 0.02, *p*H 7.6 HEPES buffer 3.0, dextrose 10, sucrose 22.5 (solution A); or NaCl 128.5, *p*H 7.6 HEPES buffer 2.0, $MgCl_2$ 0.02, EDTA 0.20 (solution B), calculated to give a free Mg concentration of 10^{-7} M and a free Ca concentration $<10^{-7}$ M. cGMP was applied to the cytoplasmic side of the patches by perfusion through the recording chamber. The patch potential was held at +50 mV (cytoplasmic side positive), and the cGMP-activated current determined as the difference between the currents in the presence and absence of cGMP.

Fig. 3*A*. Analysis of histogram *c* in Fig. 3*B* showed that the valley between the main peaks was higher than expected from the summation of two gaussians, perhaps because of the presence of the smaller events. Furthermore, the histogram was not well fitted by a Poisson distribution constructed on the assumption that there were only large events and that they summed linearly; based on this model more samples are expected near an amplitude of $2 \times 0.8 = 1.6$ pA, given the small magnitude of the peak near 0 pA.

Analysis of the fluctuations in the macroscopic cGMP-activated current provided evidence that single-channel currents like those described above sum to produce the current at higher concentrations of cGMP. In four experiments the apparent single-channel current amplitude $\bar{a}$ was estimated from the slope of the relation between the mean response r and the scaled cGMP-induced variance, $\sigma^2 r_{max}/(r_{max} - r)$, which was determined over a bandwidth of only 100 Hz in order to minimize high-frequency noise arising from fast conductance fluctuations in activated channels. For values of r up to half-saturating, $\bar{a}$ was 0.46 ± 0.07 pA (mean ± s.d.) at +50 mV. This value of $\bar{a}$ falls between the mean amplitudes of the large and small transitions that were measured directly at low cGMP concentrations.

Single-channel currents of 0.3 or 1 pA are 100 times larger than those mediated by a variety of membrane carriers[12], sug-

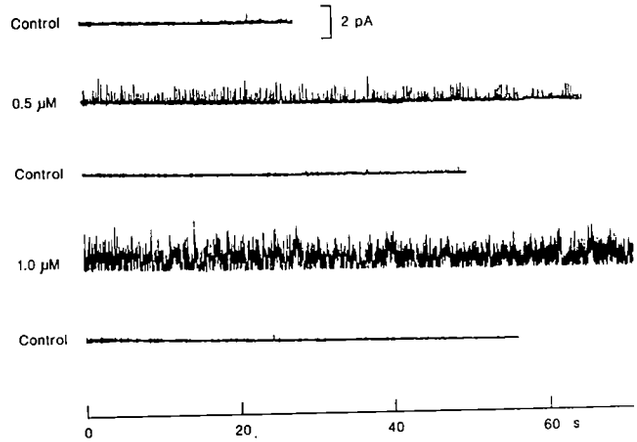


Fig. 2 Currents from an excised patch during application of low concentrations of cGMP to the cytoplasmic side. The patch was in the low divalent solution (A) of Fig. 1 legend. The recording is continuous except for interruptions at the ends of the traces, where the chamber was perfused for solution changes. Patch potential +50 mV, outward change in membrane current plotted upward. Bandwidth 0–100 Hz, temperature 21.8 °C, leakage resistance 10 GΩ.

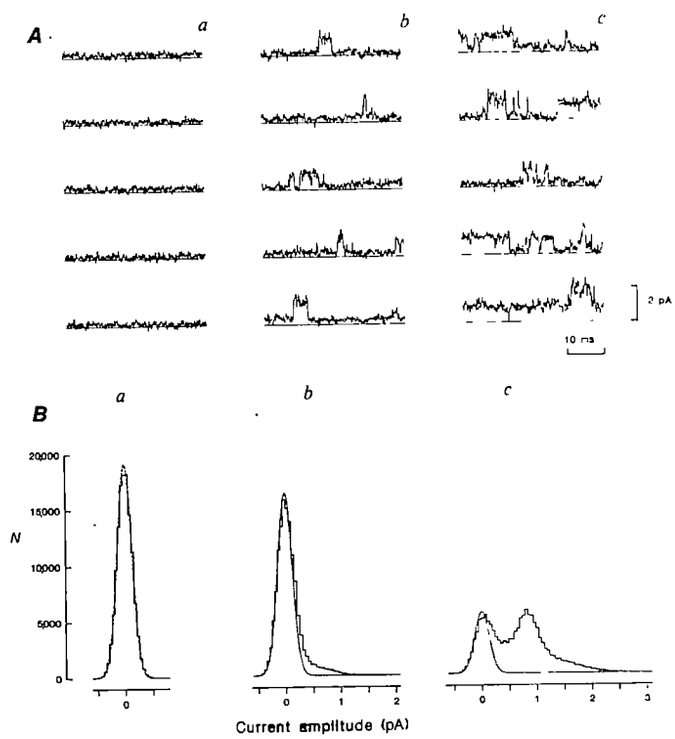


Fig. 3 Characteristics of the cGMP-induced patch currents from the experiment of Fig. 2. *A*, Sample patch currents from control, 0.5 μM cGMP and 1.0 μM cGMP runs (*a*–*c*, respectively). Lines beneath the traces were drawn at the same absolute current level. Recordings were high-pass-filtered with a single pole filter of time constant 10 s to remove a steady d.c. drift of 0.003 pA s^{-1}. Low-pass filtering was at 2 kHz (−3 dB point, 8-pole Bessel filter; Frequency Devices). Each sweep consists of 512 points acquired at a sampling rate of 10 kHz. *B*, Amplitude histograms from the experiment of Fig. 2 (*a*–*c* same as for *A*). Each histogram was prepared from 250 sweeps filtered and sampled as in *A*. The control histogram (*a*) was constructed from 50 sweeps from the initial control run and 100 sweeps from each of the later control runs of Fig. 2. Dashed curves are gaussian distributions with standard deviation $\sigma = 0.134$ pA, the measured value of r.m.s. noise in the control sweeps. The scaling of the gaussians corresponds to baseline probabilities, P_0, of 0.855 (0.5 μM) and 0.289 (1 μM). The average number of open channels, calculated from $-\ln P_0$, was 0.157 (0.5 μM) and 1.24 (1.0 μM).

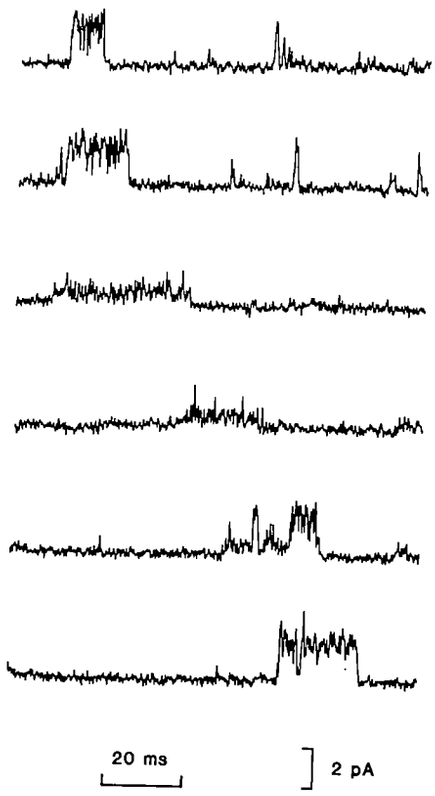


Fig. 4 Evidence for two activated states having different mean conductances. The currents are from an excised patch exposed to 0.5 μM cGMP; holding potential +75 mV, bandwidth 0–2 kHz, sampling rate 10 kHz. The patch was in solution B of Fig. 1 legend. Leakage resistance 10 GΩ.

gesting a pore mechanism of conduction. The effect of divalent cations in reducing the conductance might be explained by assuming that ions move through the channel in single file and encounter one or more binding sites with a high affinity for divalent cations. Divalent cations would pass through the channel[13–15], but with a long transit time, giving a very small time-averaged single-channel current under normal conditions[8].

The total number of channels in a patch can be estimated from the ratio of the current at saturating cGMP concentration to the single-channel current. In the experiments of Fig. 1, the saturating currents averaged 800 pA (range 116–1,234 pA). Taking the single-channel current as 1 pA and the patch area as roughly 2 μm^2, the apparent channel density is ~400 μm^{-2}. A channel density of 200 μm^{-2} was estimated from an analysis of the light-sensitive current noise of whole rods[9]. These rough estimates seem to be in satisfactory agreement, supporting the identity of the light-sensitive and cGMP-sensitive channels.

The large and small conductance states are illustrated in the records of Fig. 4, obtained from a patch held at +75 mV. The upper two traces show outward currents of ~1.9 pA mean amplitude (conductance 25 pS), while the middle two traces show smaller events with a mean amplitude of ~0.7 pA (conductance 9 pS). Both types of currents were noisy, suggesting that there were conductance fluctuations so fast that the method did not resolve them. The two lower traces in Fig. 4 illustrate events suggestive of transitions between the small- and large-conductance states: the highest current level is comparable to the large amplitude alone, rather than to the sum of the large and small amplitudes. It remains to be determined whether the two states have the same peak instantaneous conductance.

We conclude that the cGMP-activated channel of retinal rods is an aqueous pore which has a very small effective conductance in the presence of physiological concentrations of divalent cations. The small conductance is appropriate to give low quantizing noise in the small, stereotyped signals that encode photon absorption[16]. The cubic dependence of channel opening on cGMP concentration makes the channel an efficient molecular switch which is very sensitive to the local cGMP concentration.

We thank Dr K.-W. Yau for suggestions on divalent cation effects, Drs L. Stryer and R. Aldrich for discussions, and Mr R. Schneeveis for technical help. This work was supported by grant EY01543 from the National Eye Institute, USPHS.

Received 4 December 1985; accepted 6 March 1986.

1. Fesenko, E. E., Kolesnikov, S. S. & Lyubarsky, A. L. *Nature* **313**, 310–313 (1985).
2. Nakatani, K. & Yau, K.-W. *Biophys. J.* **47**, 365a (1985).
3. Yau, K.-W. & Nakatani, K. *Nature* **317**, 252–255 (1985).
4. Haynes, L. & Yau, K.-W. *Nature* **317**, 61–64 (1985).
5. Altman, J. *Nature* **313**, 264–265 (1985).
6. Stryer, L. *A. Rev. Neurosci.* **9**, 87–119 (1986).
7. Gray, P. & Attwell, D. *Proc. R. Soc.* **B223**, 379–388 (1985).
8. Bodia, R. D. & Detwiler, P. B. *J. Physiol., Lond.* **367**, 183–216 (1985).
9. Zimmerman, A. L. & Baylor, D. A. *Biophys. J.* **47**, 357a (1985).
10. Koch, K.-W. & Kaupp, U. B. *J. biol. Chem.* **260**, 6788–6800 (1985).
11. Zimmerman, A. L., Yamanaka, G., Eckstein, F., Baylor, D. A. & Stryer, L. *Proc. natn. Acad. Sci. U.S.A.* **82**, 8813–8817 (1985).
12. Hille, B. *Ionic Channels of Excitable Membranes*, 202 (Sinauer Associates, Sunderland, Massachusetts, 1984).
13. Yau, K.-W., McNaughton, P. A. & Hodgkin, A. L. *Nature* **292**, 502–505 (1981).
14. Capovilla, M., Caretta, A., Cervetto, L. & Torre, V. *J. Physiol., Lond.* **343**, 295–310 (1983).
15. Hodgkin, A. L., NcNaughton, P. A. & Nunn, B. J. *J. Physiol., Lond.* **358**, 447–468 (1985).
16. Baylor, D. A., Lamb, T. D. & Yau, K.-W. *J. Physiol., Lond.* **288**, 613–634 (1979).

Neural control of the forms of acetylcholinesterase in slow mammalian muscles

Josephine Lai*, Jolanta Jedrzejczyk†, John A. Pizzey‡, David Green & Eric A. Barnard§

Department of Biochemistry, Imperial College of Science and Technology, London SW7 2AZ, and MRC Molecular Neurobiology Unit, MRC Centre, Hills Road, Cambridge CB2 2QH, UK

The 'heavy', collagen-tailed form of acetylcholinesterase (AChE), having a $s^{\circ}_{20,w}$ of 16S in mammals, occurs at vertebrate muscle endplates and has been widely regarded as a marker of neuronal influence on muscle *in vivo*[1–5]. However, an interesting exception has been described by Bacou *et al.*, in a previous report in *Nature*[6]. They found, in a slow-twitch muscle of the rabbit, that after denervation the 16S form of AChE increases markedly, rather than disappearing. Such a phenomenon would modify current concepts of neuromuscular regulation. We report here, however, that this exception is apparent rather than real in terms of endplate AChE regulation.

The rabbit semimembranosus muscle was described by Bacou *et al.*[6] as containing an 'external region I' composed of fast-twitch glycolytic muscle (type IIB), surrounding an 'internal conoidal region II' containing only slow-twitch (type I) fibres. In fact, these prominent rabbit leg muscles have previously been named, respectively, as the semimembranosus accessorius (SA) and the semimembranosus proprius (SP) muscles[7,8]; the SA has been shown in rabbits to contain 86% type IIB, 12% type IIA and 2% type I fibres[9], while the SP contains 100% type I fibres. These values hold in our rabbits.

The AChE concentration in the normal rabbit SP (Fig. 1*a*) differs in our analyses from that reported[6]. The 16S form is major, not minor, and the light forms are mainly the 6S (dimeric),

* Present address: Laboratory of Neurophysiology, NINCOS, NIH, Bethesda, Maryland 20205, USA.
† Permanent address: Department of Histology, Academy of Medicine, Warsaw 02-004, Poland.
‡ Present address: Biophysics Department, KQC Kensington Campus, London W8 7AH, UK.
§ To whom correspondence should be addressed at Cambridge.

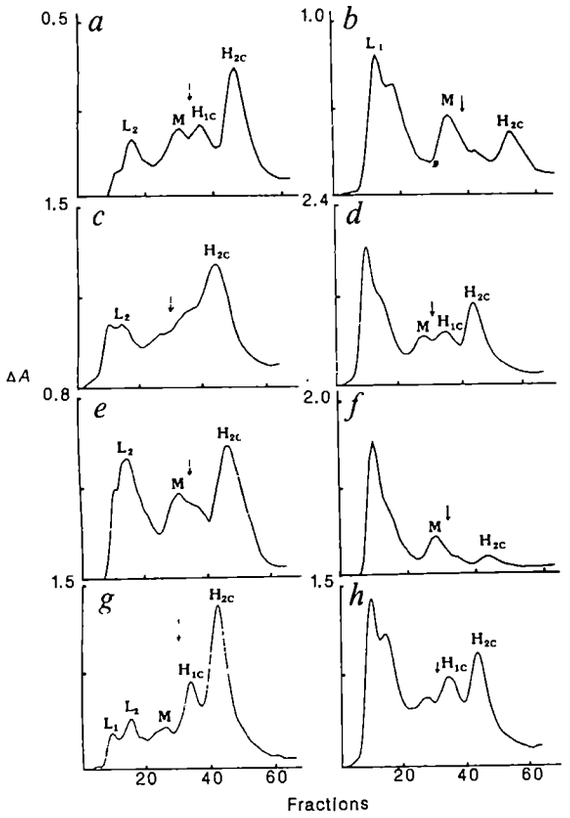


Fig. 1 Sucrose density gradient profiles of AChE in control and chronically denervated (4 weeks) muscles. Right-hand panels show denervated muscles, left-hand panels show control muscles. *a*, *b*, Rabbit SP; *c*, *d*, guinea pig SP; *e*, *f*, rabbit soleus; *g*, *h*, guinea pig soleus. The amounts of control tissue taken were 1.3–1.7 times those of the denervated tissues. M denotes the presumed tetrameric, globular form and H_{1c} the smaller collagen-tailed form, ~13S, which has fewer catalytic units than the maximum in the H_{2c} (~16S) form[1]. L_1 and L_2 denote, respectively, the ~4S and ~6S forms. AChE activity is in units of absorbance change (ΔA)[1] (note the different scales). The total centrifugal force used varied: arrows show the catalase (11.4S) internal marker.

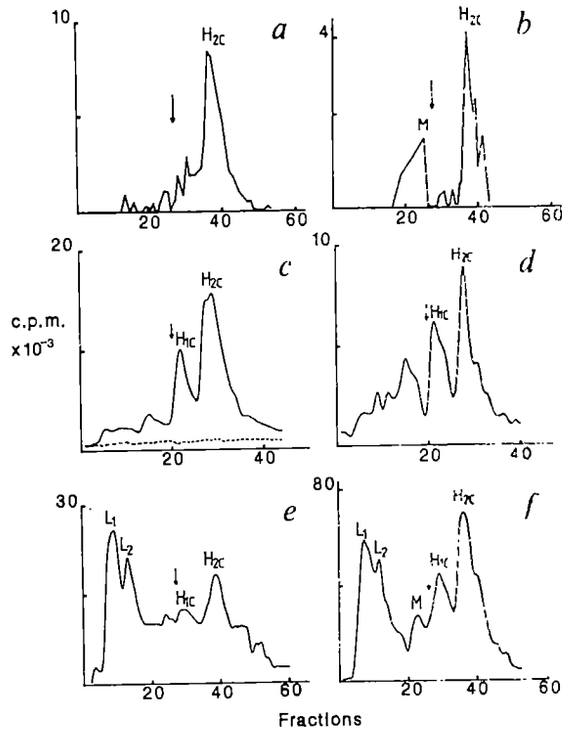


Fig. 2 Sucrose density gradient analysis of AChE (fractions assayed on ^{3}H-acetylcholine)[15] in the endplate (left-hand panels) and the non-endplate (right-hand panels) regions of slow-twitch muscles. *a*, *b*, Rabbit SP; *c*, *d*, guinea pig soleus; *e*, *f*, denervated guinea pig soleus. Endplates and non-endplate segments were microdissected[15] from the same fibres; 20–50 endplates (with the minimum of underlying fibre) or the same number of non-endplate segments (the latter about five times the length of an endplate and cut transversely across the whole fibre) were extracted for 60–90 min at room temperature in 0.25 ml of the extraction buffer described in Table 1 legend and all was applied. A blank was run in parallel with an identical extract, and was assayed in the presence of 10^{-4} M isooctamethyl pyrophosphoramide and 5×10^{-5} M BW284C51 (see ref. 15) to inhibit all cholinesterases: this is illustrated by the broken line in *c*, while in *a*, *b*, *e*, *f* the blank has already been subtracted throughout. The total force and the fraction size used varied, the arrow shows the catalase marker, and only the horizontal pairs can be compared in the amounts. Labelling of peaks is as in Fig. 1. Note that the smaller collagen-tailed form, H_{1c}, is also prominent in the guinea pig muscle both in and outside the endplate. Similar profiles were found when repeated on other guinea pigs and rabbits: see Table 1 for the means of the contributions of the L and H_{2c} peaks in all the experiments.

not the 4S (monomeric), AChE. Equivalent differences in the SA were also found (Table 1). We attribute these differences to our use of more antiproteases (see Fig. 1 legend) and to particularly rapid processing. When these precautions were relaxed, profiles similar to those reported[6] were obtained. High 4S AChE in mature muscles is generally a marker of proteolytic breakdown[1,4,10]. Hence, the starting concentration of SP 16S AChE was much higher than that (only 9.5% of the total AChE) found previously[6]. After complete denervation (see below) for 2–4 weeks, the contribution of the 16S form to the total AChE declined greatly in both muscles (Fig. 1*b*, Table 1). Similar behaviour was observed in other denervated slow-twitch muscles, that is, the SP of the guinea pig (which we have identified as being similar anatomically and in fibre types to rabbit SP), as well as rabbit and guinea pig soleus muscles (Fig. 1*c*–*h*).

It has been frequently reported that mammalian muscles lose nearly all of their 16S AChE when the maximum effect of denervation is attained[3,5,11]. We found, however, that although there was a decline in the 16S form, some persisted throughout, with higher concentrations remaining in certain slow-twitch muscles (Fig. 1, Table 1). Further, on chronic denervation, the AChE concentration (and the AChE content per entire muscle) may either decrease (the most usual case) or increase, depending on the species; rabbit[12] and chicken[10] were previously known to behave exceptionally in increasing their muscle AChE. We find that the guinea pig is also in that group. In those three species a long-lasting increase of severalfold occurred in the AChE concentration in both fast and slow muscles after denervation, and despite the muscle weight loss (to the order of one-half, at the maximum here) the total content of AChE per muscle did not decline but increased further. Nevertheless, the proportion of 16S AChE in the slow muscles was much reduced, while the 16S AChE per entire muscle remained about constant or again decreased (Table 1). The overall increase in AChE was contributed by the lighter forms. In the fast fibres the 16S AChE per entire muscle always declined greatly on denervation.

Another technical reason for the difference in findings may be the surgical procedure involved. We fully denervated both SP and SA, by cutting all relevant branches of the sciatic and obturator nerves (a branch of the latter giving an additional

Table 1 Changes in AChE activities in slow- and fast-twitch muscles on denervation

Species	Muscle	Control [AChE] (U g^{-1})	n	Ratio of denervated to control (basis)	all forms	L	16S	L (%)	16S (%)
Rabbit	SP (100% slow)	0.6±0.07	7	(total)	1.7±0.3	2.7	1.2	55(16)	19(54)
				(conc.)	4.4±0.7	7.0	3.0		
	Soleus (96% slow)	0.6±0.07	6	(total)	1.3±0.3	3.1	0.4	72(33)	10(42)
				(conc.)	2.5±0.4	5.8	0.7		
	SA (98%) fast)	0.5±0.03	7	(total)	1.6±0.1	4.4	0.3	73(26)	10(44)
				(conc.)	3.7±0.8	10.3	0.8		
Guinea pig	SP (100% slow)	0.7±0.04	5	(total)	1.7±0.2	3.0	1.0	48(27)	25(43)
				(conc.)	3.5±0.3	6.2	2.0		
	Soleus (100% slow)	0.5±0.05	6	(total)	1.5±0.3	2.0	0.7	44(17)	25(71)
				(conc.)	3.0±0.4	4.0	1.3		
	SA (99% fast)	0.6±0.01	5	(total)	1.2±0.1	2.8	0.4	60(32)	13(44)
				(conc.)	2.7±0.4	6.2	1.0		
	EDL (94% fast)	0.8±0.02	3	(conc.)	1.3±0.2	2.2	0.4	62(30)	14(51)

Values given are the ratios of the activity of specified AChE forms in the denervated muscles relative to that of the corresponding activity in the contralateral control muscles: the ratio of the activities is expressed either on the basis of per gram (wet weight) of muscle ('conc.') or (for the same specimens) on the basis of the entire muscle content ('total'). The mean ±s.e.m. for n denervated animals sampled is given for each muscle type. (Where s.e. is not shown, it was of the same relative order as given for that muscle or ratio.) The last two columns show the % of the muscle AChE of the denervated muscle (or, in parentheses, of the control muscle) contributed by all the L (~4S and ~6S) forms, or by the 16S form. The difference of their sum from 100% is all accounted for by the forms sedimenting in the region of the M (10S) and H_{1c} (13S) peaks (see Fig. 1), whose poor resolution frequently prevents accurate computation. The fibre typing noted shows the % of type I fibres (slow) or type II fibres (fast) in these muscles. The soleus or extensor digitorum longus (EDL) muscles of New Zealand White rabbits (~3 kg) or Dunkin–Hartley guinea pigs (2 months old) were denervated by sectioning the lower branch of the sciatic nerve. The SP of the rabbit was fully denervated by sectioning the branches of the sciatic nerve, the cutaneous caudal femoral nerve and the obturator nerve to that muscle[8]. Similarly, the guinea pig SP was denervated by cutting the branches of the sciatic nerve, the cutaneous caudal femoral nerve, the femoral nerve and the saphenous nerve to that muscle. The rest of the limb remained mobile in each case. The control (contralateral) and denervated muscles were analysed for their AChE content 4 weeks later. Changes in the same direction, but to a lesser extent, were seen in other cases analysed after 2 or 3 weeks of denervation. For AChE analysis, muscle crude extracts were processed rapidly at 4 °C: the entire muscle was carefully excised, weighed, minced rapidly, mixed and aliquots were homogenized in 10 vol. of 5 mM EGTA, bacitracin (1 mg ml^{-1}), benzamidine-HCl (2 mM), N-ethylmaleimide (5 mM), chicken ovomucoid inhibitor (0.2 mg ml^{-1}), soybean trypsin inhibitor (0.1 mg ml^{-1}), leupeptin (0.04 mg ml^{-1}) and pepstatin (0.02 mg ml^{-1}). The homogenates were centrifuged at 43,500g for 15 min, and aliquots of the extracts thus obtained were used immediately for sucrose density gradient analysis (Fig. 1) or AChE assays[1]. The proportions of the molecular forms were obtained from computer-assisted analysis of the peaks in the profile.

motor supply). Bacou *et al.*[6] cut only the sciatic nerve. When we did this, only partial denervation occurred; a twitch of the semimembranosus could still be elicited by stimulating the obturator nerve. Whether denervation was partial or total, the morphological changes were similar and as illustrated by Bacou *et al.*[6]: the SA was more affected than the SP muscle, with marked fibre atrophy in both, and similarly in other denervated slow muscles such as rabbit and guinea pig soleus. Despite the similar histology, partial denervation may produce increased activity or terminal sprouting[13].

Further, we localized the various AChE forms, using microdissection[14,15] of individual endplates (Fig. 2). In the innervated slow-twitch fibres, the endplate contained essentially only collagen-tailed (16S and a little 13S) AChE (Fig. 2*a*,*c*). However, the extrasynaptic regions of innervated slow-twitch muscles studied also contained most of their AChE in these heavy forms (Fig. 2*b*,*d*). Although at a much lower concentration than at the endplate, when summed over the very great total surface this forms a large contribution to the whole muscle AChE. This extrasynaptic collagen-tailed AChE (also seen in non-endplate segments of rat diaphragm[11], where 40% of fibres are type I, and in hamster slow-twitch fibres) is much lower or absent in fast-twitch fibres[4,14]. The microdissected extrasynaptic regions of the denervated slow-twitch fibres of the SP and soleus showed a large increase in the light forms but also clear retention of the heavy forms (Fig. 2*f*); their endplates showed much loss of the 16S and the appearance of 4S and 6S AChE (Fig. 2*e*).

We conclude that denervation always produces a decline in the proportion of the muscle collagen-tailed AChE and in its amount at the endplates. However, in slow-twitch fibres there is, interestingly, another population of extrasynaptic 16S AChE which does not require neural contact. In a few species where AChE production increases on denervation, this extrasynaptic 16S AChE increases with the rest; this gain is nevertheless balanced or exceeded by the loss from the endplates, and the percentage contribution of this form to the total AChE of the muscle invariably declines markedly.

J.L. held a Croucher Foundation Graduate Studentship and J.J. held a Wellcome Trust Fellowship. We thank the Muscular Dystrophy Group of Great Britain for additional support.

Received 27 January; accepted 10 March 1986.

1. Lyles, J. M., Silman, I., Di Giamberardino, L., Couraud, J. Y. & Barnard, E. A. *J. Neurochem.* **38**, 1007–1021 (1982).
2. Massoulié, J. M. & Bon, S. *A. Rev. Neurosci.* **5**, 57–106 (1982).
3. Hall, Z. W. *J. Neurobiol.* **4**, 343–361 (1973).
4. Randall, W. R., Lai, J. & Barnard, E. A. in *Molecular Basis of Nerve Activity* (eds Changeux, J.-P., Hucho, F., Maelicke, A. & Neumann, E.) 595–618 (de Gruyter, Berlin, 1985).
5. Vigny, M., Koenig, J. & Rieger, F. *J. Neurochem.* **27**, 1347–1353 (1976).
6. Bacou, F., Vigneron, P. & Massoulié, J. *Nature* **296**, 661–664 (1982).
7. Kerr, N. S. *Anat. Rec.* **121**, 481 (1955).
8. Narone, R., Pavaux, C., Blin, P. C. & Cuq, P. *Atlas D'Anatomie du Lapin* (Masson, Paris, 1973).
9. Peter, J. B., Barnard, P. J., Edgerton, V. R., Gillespie, C. A. & Stempel, K. E. *Biochemistry* **11**, 2627–2633 (1972).
10. Silman, I., Di Giamberardino, L., Lyles, J. M., Couraud, J. Y. & Barnard, E. A. *Nature* **280**, 160–162 (1980).
11. Collins, P. L. & Younkin, S. G. *J. biol. Chem.* **257**, 13638–13644 (1982).
12. Tennyson, V. M., Kremzner, L. T. & Brzin, M. *J. Neuropath. exp. Neurol.* **36**, 245–275 (1977).
13. Betz, W. J., Caldwell, J. H. & Ribchester, R. R. *J. Physiol., Lond.* **303**, 265–280 (1980).
14. Jedrzejczyk, J., Silman, I., Lyles, J. M. & Barnard, E. A. *Biosci. Rep.* **1**, 45–51 (1981).
15. Jedrzejczyk, J., Silman, I., Lai, J. & Barnard, E. A. *Neurosci. Lett.* **46**, 283–289 (1984).

Cloning of the gene and cDNA for mammalian β-adrenergic receptor and homology with rhodopsin

Richard A. F. Dixon*, Brian K. Kobilka†, David J. Strader‡, Jeffrey L. Benovic†, Henrik G. Dohlman†, Thomas Frielle†, Mark A. Bolanowski†, Carl D. Bennett§, Elaine Rands*, Ronald E. Diehl*, Richard A. Mumford‡, Eve E. Slater‡, Irving S. Sigal*, Marc G. Caron†, Robert J. Lefkowitz† & Catherine D. Strader‡

Departments of *Virus and Cell Biology Research and §Medicinal Chemistry, Merck Sharp and Dohme Research Laboratories, West Point, Pennsylvania 19486, USA
† Howard Hughes Medical Institute, Department of Medicine, Biochemistry and Physiology, Duke University Medical Center, Durham, North Carolina 27710, USA
‡ Department of Biochemistry and Molecular Biology, Merck Sharp and Dohme Research Laboratories, Rahway, New Jersey 07065, USA

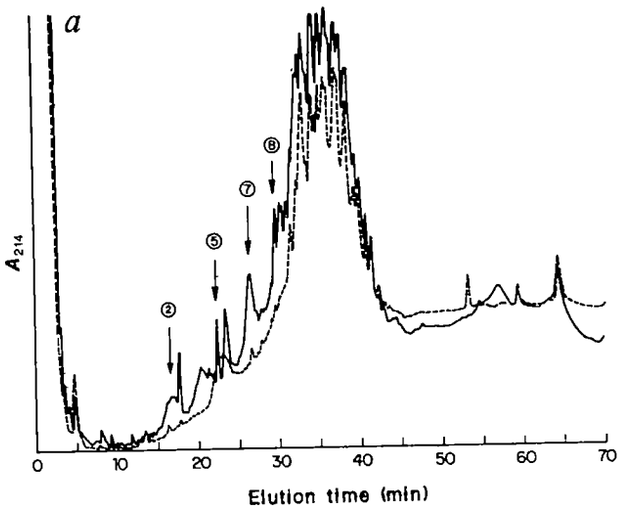
The adenylate cyclase system, which consists of a catalytic moiety and regulatory guanine nucleotide-binding proteins, provides the effector mechanism for the intracellular actions of many hormones and drugs[1]. The tissue specificity of the system is determined by the particular receptors that a cell expresses. Of the many receptors known to modulate adenylate cyclase activity, the best characterized and one of the most pharmacologically important is the β-adrenergic receptor (βAR). The pharmacologically distinguishable subtypes of the β-adrenergic receptor, β_1 and β_2 receptors, stimulate adenylate cyclase on binding specific catecholamines[1]. Recently, the avian erythrocyte β_1, the amphibian erythrocyte β_2 and the mammalian lung β_2 receptors have been purified to homogeneity and demonstrated to retain binding activity in detergent-solubilized form[1–5]. Moreover, the β-adrenergic receptor has been reconstituted with the other components of the adenylate cyclase system *in vitro*[6], thus making this hormone receptor particularly attractive for studies of the mechanism of receptor action. This situation is in contrast to that for the receptors for growth factors and insulin, where the primary biochemical effectors of receptor action are unknown. Here, we report the cloning of the gene and cDNA for the mammalian β_2AR. Analysis of the amino-acid sequence predicted for the βAR indicates significant amino-acid homology with bovine rhodopsin and suggests that, like rhodopsin[7], βAR possesses multiple membrane-spanning regions.

Hamster lung βAR was purified to homogeneity by sequential affinity chromatography and molecular-sieve HPLC as described previously[2,5]. The purified receptor bound ligand with theoretical specific activity and migrated on SDS-polyacrylamide gel electrophoresis as a single broad band at a relative molecular mass (M_r) of 64,000 (64K). Initial attempts to obtain N-terminal sequence data on intact βAR failed, presumably because the N-terminus of this protein was blocked. Therefore, peptide fragments generated by CNBr cleavage of pure βAR were isolated by reverse-phase HPLC.

Figure 1*a* (solid line) shows a peptide map generated from 1 nmol of pure receptor; the broken line shows the HPLC profile resulting from CNBr treatment of the detergent alone. The βAR-derived peptides produced at least nine specific absorbance peaks which were reproducibly observed in five separate βAR preparations. The most prominent of these peptides (marked with arrows in Fig. 1) were subjected to N-terminal sequence analysis, yielding the amino-acid sequences in Fig. 1*b*.

To confirm that the determined amino-acid sequences were those of the βAR polypeptide, we raised anti-peptide antibodies against peptide 7. Peptide 7 was expressed in *Escherichia coli* as a C-terminal peptide fused to the N-terminal domain of the yeast *RAS*^{sc1} protein SC1N (ref. 8). Rabbits injected with the isolated fusion protein produced antibodies which reacted with ^{125}I-labelled immunogen as well as pure ^{125}I-labelled βAR or pure ^{125}I-cyanopindolol-labelled (^{125}I-CYP) βAR. Figure 2*a* shows an immunoprecipitation titration curve of this antibody against ^{125}I-CYP-labelled solubilized βAR from hamster lung, hamster heart, A431 epidermoid carcinoma cells and turkey erythrocytes. No immunoprecipitation of counts above background was observed in control experiments when ^{125}I-CYP was incubated with the antibody in the absence of receptor.

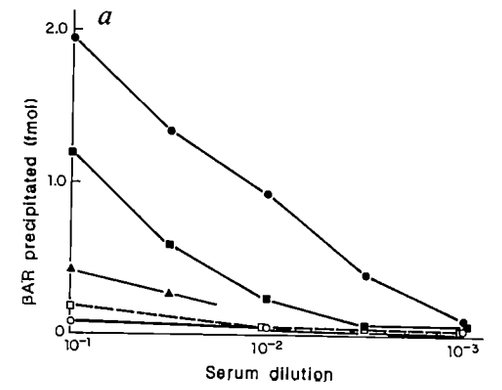
Antibody to the hamster lung βAR-derived peptide was capable of recognizing the human βAR from the A431 line, albeit with a slightly lower sensitivity (50%) (Fig. 2*a*). The antibody also cross-reacted slightly with hamster heart βAR, a tissue containing a β_1 subtype of receptor, but did not immunoprecipitate the β_1AR of turkey erythrocytes. These differences in antibody sensitivity could reflect differences in either primary sequence or the conformation of this region of the protein within the various receptor subtypes and receptors from different species. To confirm that the antibody was recog-



b

Peptide 2	GPPGXXSXFLLTTXGS
Peptide 5	GLAVVPFGAS
Peptide 7	VFVYSRVFQVAKRQLQKIDKSEGRF HSPNLGQVE
Peptide 7a	GEASGSQLG
Peptide 8	VWIVSGLTSFLPI

Fig. 1 Amino-acid sequence of peptides derived from CNBr-treated β-adrenergic receptor. *a*, Absorbance profiles represent CNBr treatment of pure βAR (solid line) or digitonin (dashed line). The arrows indicate the peptides that were sequenced. *b*, Amino-acid sequences identified by HPLC following each cycle of the sequenator. Two of the four blank cycles (X) in the amino-acid sequence for peptide 2 are presumed to be due to *N*-linked glycosylation. Peptides 7 and 7a were located within the same peak. **Methods.** βAR was purified to homogeneity from hamster lung membranes by the method of Benovic *et al.*[5], using affinity chromatography followed by molecular-sieve HPLC. Binding of ^{125}I-CYP to intact cells or to solubilized βAR was determined according to Caron and Lefkowitz[22]. For peptide preparation, ~1 nmol of pure βAR was treated with CNBr (0.4 mM) in 70% formic acid at 23 °C for 20 h. After lyophilization, the sample was resuspended in 20 mM trifluoroacetic acid (TFA) and the peptides separated by reverse-phase HPLC on a Synchropak C-4 column, eluted with a 10–70% acetonitrile gradient containing 20 mM TFA. The N-terminal sequence analysis was performed by the method of Hewick *et al.*[23], using a gas-phase sequenator (Applied Biosystems). The phenylthiohydantoin (PTH) amino acids produced at each step were separated and quantitated by HPLC[24].



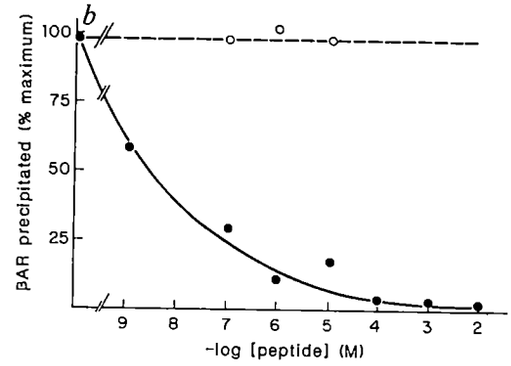




Fig. 2 Immunoreactivity of β-adrenergic receptor. *a*, Immunoprecipitation of ^{125}I-CYP-βAR from hamster lung (●), hamster heart (▲), A431 cells (■) or turkey erythrocytes (○) by serum from rabbits immunized with βAR peptide 7. □, Immunoprecipitation of hamster lung receptor by preimmune serum. *b*, Immunoprecipitation of ^{125}I-CYP-labelled hamster lung βAR with anti-βAR peptide 7 antibody following preincubation with a synthetic peptide containing a portion of the sequence for peptide 7 (●), or with an unrelated peptide, atrial natriuretic factor (○). *c*, Protein immunoblotting of the βAR. Protein samples were separated on a 10% polyacrylamide gel[25], transferred to nitrocellulose and treated sequentially with antibodies and ^{125}I-protein A (10^6 c.p.m. per 25 ml) as described elsewhere[26,27]. Lane 1, pure hamster lung βAR (5 pmol); lane 2, A431 cell lysate from 4×10^5 cells; lane 3, RPMI 1846 lysate from 10^5 cells.

Methods. The immunogen for induction of anti-peptide antibodies was expressed in *E. coli*. Two oligonucleotides encoding the 19 amino acids of peptide 7 (QVAKRQLQKIDKSEGRFHS) were synthesized (see Fig. 1 legend), annealed and ligated[28] into the *Acc*I and *Hin*dIII sites of plasmid pSC1N[8] to give the plasmid pβP1. *E. coli* transformed with pβP1 overexpresses a protein of apparent M_r 23K, while *E coli* containing pSC1N overexpresses a protein of apparent M_r 21K (data not shown). This observed difference in relative molecular mass of the two proteins is consistent with the encoded fusion protein containing 19 additional amino acids. To prepare antigen, plasmid-containing cells were grown in L-broth containing ampicillin and isopropylthiogalactoside at 37 °C for 16 h, harvested by centrifugation, lysed by sonication and the soluble proteins removed by centrifugation at 40,000*g*. The cell pellet was seqentially extracted with 1 M NaCl, 1% Triton X-100 and 1.75 M guanidinium-HCl. The SC1N βAR fusion protein was extracted from the cells with 3.25 M guanidinium-HCl, dialysed against phosphate-buffered saline and used directly as an immunogen. Approximately 100 mg of fusion protein of 90% purity was obtained from 1 litre of starting culture. Antibodies were detected in serum from injected rabbits by incubation of the serum with ^{125}I-CYP-labelled soluble βAR in 10 mM Tris-HCl, 0.1 M NaCl, 0.1% digitonin, 0.5% bovine serum albumin (BSA) *p*H 7.4. After 2 h at 25 °C, the antibody was precipitated by addition of either $(NH_4)_2SO_4$ to 50% or *Staphylococcus aureus* protein A, followed by incubation in ice for 30 min. The precipitated protein was collected by centrifugation, and the radioactivity contained in the antibody pellet measured. For the peptide blocking experiment, the peptide YAKRQLQKIDKSEGR was synthesized[29] using a SAM II peptide synthesizer (Biosearch), and purified on a Whatman C-18 Magnum column in a H_2O/acetonitrile gradient containing 0.2% TFA. The resulting product was judged to be pure by amino-acid sequencing and mass spectral analysis. Increasing concentrations of this peptide were added to a 1:100 dilution of anti-peptide 7 antiserum and incubated for 2 h at 23 °C. The treated antiserum was then mixed with ^{125}I-CYP-labelled βAR and assayed as above.

nizing the amino-acid sequence of peptide 7, a chemically synthesized peptide was used as a specific inhibitor of antibody–receptor interactions. At concentrations ≥100 μM, this synthetic peptide completely prevented the immunoprecipitation of ^{125}I-CYP-labelled βAR by the antibody (Fig. 2*b*). An unrelated peptide, atrial natriuretic factor[9], had no effect on the immunoprecipitation.

The specificity of the antibody for the βAR was demonstrated further by protein immunoblotting. As shown in Fig. 2*c* (lane 1), the antibody reacted specifically with pure hamster lung βAR; a single protein of the same relative molecular mass (64K) was also observed in human A431 and hamster melanoma RPMI 1846 cells (Fig. 2*c*, lanes 2, 3), both of which were found to contain βAR on the basis of ^{125}I-CYP binding[10] (data not shown). This specific immunoreactive band was not observed on prior treatment of the antibody with the synthetic peptide and was not present when normal rabbit serum was substituted for the anti-peptide 7 antibody (data not shown).

To facilitate cloning of the βAR gene, oligonucleotides complementary to the DNA encoding the amino-acid sequence of peptide 7 were synthesized for use as hybridization probes (see Fig. 3 legend). In hybridization experiments performed at high stringency on blots of hamster genomic DNA, a single hybridizing band of 5.2 kilobases (kb) was observed in *Eco*RI digests and a band of 1.3 kb was observed in *Hin*dIII digests (data not shown). When a complete hamster genomic library was screened under the same conditions, five clones were isolated. Restriction analysis of the phage DNA revealed that all these clones contained a 1.3-kb *Hin*dIII and a 5.2-kb *Eco*RI fragment which hybridized to the probes (data not shown). Mapping of the phage DNA indicated that these clones overlap to give a total of 30 kb of contiguous genomic DNA. Figure 3 shows the restriction map of the genomic DNA containing the βAR-related sequences. Sequencing of the 1.3-kb *Hin*dIII fragment revealed a continuous open reading frame encoding 435 amino acids; the sequences of all the CNBr peptides shown in Fig. 1 were contained within this putative polypeptide.

Using the 1.3-kb *Hin*dIII gene fragment as a probe, seven clones were obtained from an unamplified hamster cDNA library (2×10^6 recombinants). Two of these cDNAs hybridized to oligonucleotide probes specific for the N-terminal, middle and C-terminal portions of the βAR gene. The nucleotide sequence of these two cDNA clones (Fig. 4) extends from 210 nucleotides (nt) 5′ to the open reading frame encoding the βAR

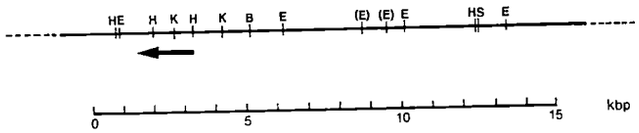
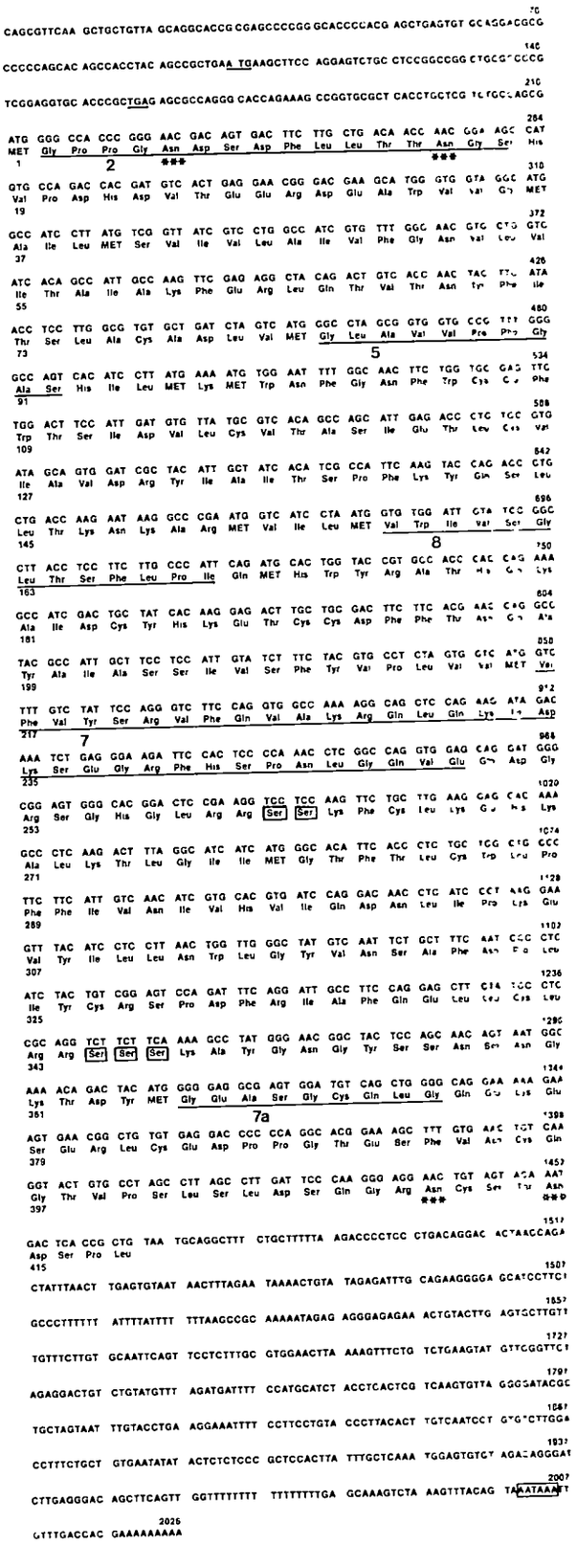


Fig. 3 Restriction map of the hamster βAR gene. A portion of the hamster DNA is shown. The 1.3-kb *Hin*dIII fragment which hybridizes to oligonucleotides specific for peptide 7, is underlined with an arrow indicating the direction of transcription of the βAR gene. The restriction enzyme sites are: B, *Bam*HI; E, *Eco*RI; H, *Hin*dIII; K, *Kpn*I; S, *Sal*I. Those sites shown in parentheses have not been unequivocally ordered.

Methods. All restriction enzymes, *E. coli* DNA polymerase I, T_4 DNA ligase and T_4 polynucleotide kinase were purchased from New England Biolabs. Radiolabelled nucleotides were purchased from Amersham. λ EMBL3A phage arms[30] and λ *in vitro* DNA packaging extracts were purchased from Vector Cloning Systems. Standard recombinant DNA and microbiological procedures were used throughout[28]. Genomic libraries were constructed using high-M_r genomic DNA isolated from hamster lung cells in the vector λ EMBL3 (refs 6, 30). Probes for peptide 7 coding sequences, oligonucleotides ON225(5′ pCTCCACCTGGCCCAGGTTGGG-AGAGTGGAACCTGCCCTCAGACTTGTCGAT) and ON229(5′ pAGGCAGCTGCAGAAGATCGACAAGTCTGAG) and ON168 (5′ pTTCCAGGTGGCCAAGCGGCAGCTGCAGAAGATCGA-CAA) and ON169(5′ pATGGTCTTTGTCTACTCCCGGGTCT-TCCAGGTGGCCAA), were synthesized on an Applied Biosystems Model 3A DNA synthesizer. The oligonucleotides were labelled by either a fill-in reaction (ON225, ON229) using Klenow DNA polymerase and all four [α-^{32}P]dNTPs[31] or by phosphorylation using T_4 polynucleotide kinase and [γ-^{32}P]ATP[28]. Phage libraries were screened by the method of Benton and Davis[32] using the hybridization conditions of Ullrich *et al.*[33]. DNA was isolated from CsCl-banded phage as described elsewhere[28]. For restriction analysis, DNA was digested with the appropriate enzyme and electrophoresed on 0.8% agarose gels. DNA was transferred to nitrocellulose by the procedure of Southern[34] and hybridized as above.

Fig. 4 (Right) Nucleotide and deduced amino-acid sequence of the βAR cDNA. The nucleotides are numbered on the right-hand side of each line beginning with the first nucleotide of the most 5′ cDNA clone. The translated amino-acid sequence is shown beneath the corresponding nucleotide sequence and is numbered to the left of each line. Underlined amino acids represent the CNBr peptides whose sequences are given in Fig. 1. All predicted amino acids agree with those determined by peptide sequencing, with the single exception of a cysteine for serine substitution in peptide 7a. All derived peptide sequences are preceded by a methionine, consistent with CNBr cleavage. The underlined nucleotides preceding the βAR sequences denote the first methionine codon and an in-frame termination codon. The boxed nucleotides at the 3′ end of the sequence represent the polyadenylation signal. Postulated glycosylation sites (Asn-X-Ser/Thr) are indicated by asterisks. Putative protein kinase A phosphorylation sites are boxed.

Methods. Reverse transcriptase was purchased from Seikagaku-America. RNase H was from Pharmacia and λ gt10 arms were from Vector Cloning. Total cellular RNA was isolated from growing cultures of DDT1-MF2 cells by the guanidinium isothiocyanate–CsCl method[47]. Poly(A)$^+$ RNA was purified by chromatography on oligo(dT)–cellulose. Double-stranded cDNA was synthesized by oligo(dT)-primed reverse transcription of the poly(A)$^+$ RNA, followed by treatment with *E. coli* DNA polymerase and RNase[48]. The ends of the cDNA were blunted with T_4 DNA polymerase[28]. Following protection of the *Eco*RI sites with *Eco*RI methylase, *Eco*RI linkers were added[28]. *Eco*RI-digested cDNA was size-fractionated by agarose gel electrophoresis to obtain cDNAs between 2 and 7 kb long. The cDNA was ligated to the vector λ gt10 (ref. 49) and packaged *in vitro*. The resulting library was screened unamplified as described in Fig. 3 legend. The 1.3-kb *Hin*dIII fragment was labelled using [α-^{32}P]dCTP by nick-translation for use as a hybridization probe[28]. The cDNA inserts contained in the positive phage were subcloned into pUC13 or M13 mp19 for DNA sequence analysis[35–37]. Both strands of the clones were sequenced with no discrepancies.



peptides to 560 nt 3′ to the termination codon. A hexanucleotide AATAAA occurs near the 3′ end, followed by a poly(A) stretch. The nucleotide sequence of the genomic clones is identical to that of the cDNA clones up to but not including the poly(A) tail. These data demonstrate an absence of introns within the coding and 3′-untranslated regions of the βAR gene but the possibility of introns in the untranslated region 5′ to the sequence isolated cannot be ruled out. While the lack of introns is unusual, it is not unprecedented in that sea urchin histone genes[38] and mammalian α- and β-interferon genes[39,40] are also uninterrupted. Previous studies with simian virus 40 and β-globin indicate that introns are necessary for efficient expression of those genes[41,42], so the lack of introns within the hamster βAR gene may account in part for its low level of expression.

Whereas most eukaryotic genes are translated using the first AUG encountered in the messenger RNA[43], the open reading frame (ORF) encoding the βAR peptides begins at the second AUG. The first AUG is followed by a termination codon after only 19 amino acids. This open reading frame is in-frame with the AUG codon beginning the βAR polypeptide. A similar situation has recently been reported for the oestrogen receptor, where the reading frame of that receptor is preceded by a short 20-amino-acid ORF[44]. Note that the DNA sequence around the AUG codon for the second ORF agrees well with the consensus eukaryotic translation initiation sequence[43] (CAGCGAUGG compared with CCGCCAUGG), whereas the sequence surrounding the first AUG does not.

Translation beginning with the second AUG as the initiation site would produce a polypeptide of 418 amino acids, with a M_r (46K) in close agreement with the apparent M_r of the deglycosylated βAR (49K)[11]. The protein sequence immediately following the initiator methionine residue is identical to the sequence determined for peptide 2. Apparently, like several other integral membrane proteins—for example, bovine opsin[45]—the βAR does not contain a cleavable signal sequence and may use internal signals for the insertion of the protein into the membrane. The receptor has been shown to have two sites of *N*-linked glycosylation (R.J.L. *et al.*, in preparation). Both sites are present in peptide 2, consistent with the results of peptide sequencing. The presence of two consensus protein kinase A and C sites[46] within the coding region (Fig. 4) agrees with *in vitro* phosphorylation results[20].

Hydropathicity profiles of the predicted βAR amino-acid sequence were produced using the analyses of Hopp and Woods[12] and of Kyte and Doolittle[13], with similar results. As shown in Fig. 5*a*, the βAR sequence should encode a largely hydrophobic polypeptide, with the N-terminal region of the receptor being predominantly hydrophobic and the C-terminal region of the molecule being hydrophilic. The βAR hydropathicity profile is remarkably similar to that of the rhodopsins (Fig. 5*b*), of which bacteriorhodopsin[7] is known to contain seven membrane-spanning helices. Not only does a similar pattern of repeating hydrophobic sequences 20–25 residues long occur in the predicted βAR sequence, but also the amino-acid composition of these postulated helices is similar to that of the rhodopsins, having a high proportion of proline and aromatic amino acids. The exact number of transmembrane regions remains to be determined. Amino-acid homology was apparent when the sequences corresponding to the postulated helices V, VI and VII of bovine opsin[14], which comprise the retinal binding site[15], were aligned with those for the analogous regions of βAR (Fig. 5*c*).

The sequence homology between βAR and rhodopsin parallels similarities in their function: both rhodopsin and βAR are involved in signal transduction mechanisms that involve interaction with the guanine nucleotide regulatory proteins transducin[16] and G_s (ref. 17), respectively. Moreover, it seems that phosphorylation has an important role in the regulation of both rhodopsin and βAR[18,19]. Rhodopsin is multiply phosphorylated at its C-terminus, which contains seven serine

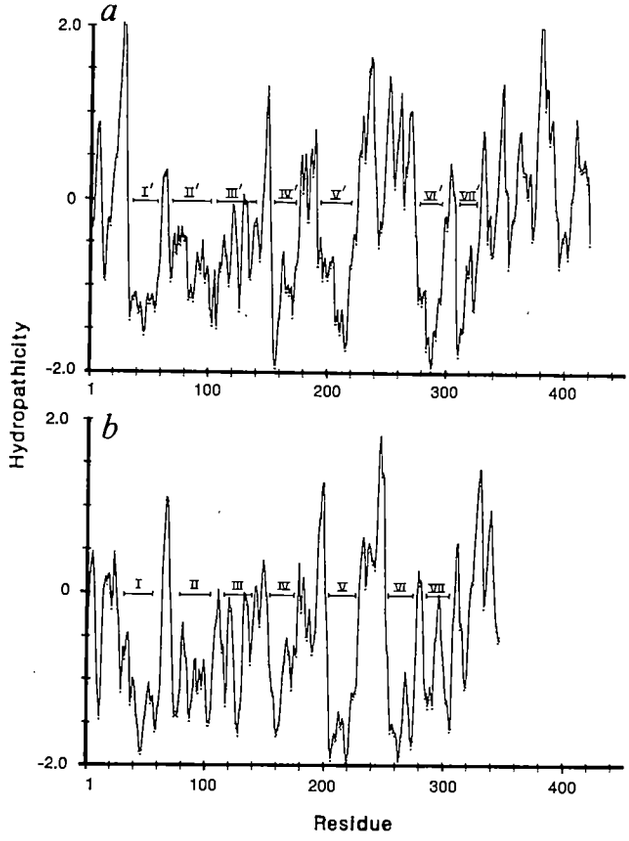


Fig. 5 Structure and sequence homology for hamster βAR and bovine opsin. Hydropathicity profiles are shown for hamster βAR (*a*) and bovine opsin[14] (*b*). Values were calculated by the method of Hopp and Woods[12]. Hydrophobicity increases with decreasing values. Horizontal lines indicate hydrophobic peptide regions 20–25 residues long. The putative transmembrane helices of bovine opsin are numbered as in ref. 14. We have designated the proposed transmembrane helices of βAR based on the analogous hydropathicity patterns of βAR and opsin. *c*, Amino-acid sequence homologies between the hamster βAR and bovine opsin (OPS). Positions of amino-acid identities are designated by asterisks. The underlined lysine residue (296) of bovine rhodopsin is involved in a Schiff base with retinal[15].

and threonine residues[18]. The C-terminus of the postulated sequence for βAR contains several serine and threonine residues that could serve as sites for phosphorylation[19].

The similarity in both the amino-acid sequence and proposed structure for the retinal binding site of rhodopsin and the analogous region in βAR suggests a specific mode of action for the ligands that modulate βAR function. We propose that these compounds interact with the βAR in a manner similar to that by which retinal interacts with opsin[21]; that is, they intercalate among the hydrophobic transmembrane helices and thereby determine whether the receptor is in its active or inactive conformation. According to this model, agonists and antagonists would mimic the action of photoactivated and native retinal. The generality of this hypothesis will be tested once the genes for similar membrane-bound receptors, such as those for leuko-

trienes, prostaglandins, dopamine and histamine, have been isolated. Our proposed model for the structure of βAR and its interaction with pharmacologically important ligands should, together with the biochemical and genetic studies now possible, provide a rational basis for a new approach to the development of more selective drugs.

We thank Lenora Davis, Jill D'Alonzo, Ester Hou, Tong Sun Kobilka, John Rodkey, Claudia Staniszewski, H. Vincent Strout Jr and Barbara Zemcik for technical assistance, Jeanne White and Lynn Tilley for manuscript preparation, and Drs Eugene Cordes, Ronald Ellis, Russell Kaufman, Paul Keller, Pete Kniskern, Richard Lebovitz, Mark Riemen and Michael Rosenblatt for helpful discussions. We particularly thank Dr Edward Scolnick for continued support and direction.

Received 10 March; accepted 11 April 1986.

1. Lefkowitz, R. J., Stadel, J. M. & Caron, M. G. *A. Rev. Biochem.* **52**, 159–186 (1983).
2. Shorr, R. G., Lefkowitz, R. J. & Caron, M. G. *J. biol. Chem.* **256**, 5820–5826 (1981).
3. Shorr, R. G., Strohsacker, M. W., Lavin, T. N., Lefkowitz, R. J. & Caron, M. G. *J. biol. Chem.* **257**, 12341–12350 (1982).
4. Homcy, C. J., Rockson, S. G., Countaway, J. & Egan, D. A. *Biochemistry* **22**, 660–668 (1983).
5. Benovic, J. L., Shorr, R. G. L., Caron, M. G. & Lefkowitz, R. J. *Biochemistry* **23**, 4510–4518 (1984).
6. Cerione, R. A. *et al. J. biol. Chem.* **259**, 9979–9982 (1984).
7. Engelman, D. M., Goldman, A. & Steitz, T. A. *Meth. Enzym.* **88**, 81–88 (1982).
8. Temeles, G. L., Gibbs, J. B., D'Alonzo, J. S., Sigal, I. S. & Scolnick, E. M. *Nature* **313**, 700–703 (1985).
9. Seidah, N. G. *et al. Proc. natn. Acad. Sci. U.S.A.* **81**, 2640–2644 (1984).
10. Delavier-Klutchko, C., Hocheke, J. & Strasberg, A. D. *FEBS Lett.* **169**, 151–155 (1984).
11. Stiles, G. L., Benovic, J. L., Caron, M. G. & Lefkowitz, R. J. *J. biol. Chem.* **259**, 8655–8663 (1984).
12. Hopp, T. P. & Woods, K. R. *Proc. natn. Acad. Sci. U.S.A.* **78**, 3824–3828 (1981).
13. Kyte, J. & Doolittle, R. F. *J. molec. Biol.* **157**, 105–132 (1982).
14. Nathans, J. & Hogness, D. S. *Cell* **34**, 807–814 (1983).
15. Hubbell, W. L. & Bownds, M. D. *A. Rev. Neurosci.* **2**, 17–34 (1979).
16. Stryer, L. *A. Rev. Neurosci.* **9**, 87–119 (1986).
17. Gilman, A. G. *Cell* **36**, 577–579 (1984).
18. Hargrave, P. A. *Prog. Retinal Res.* **1**, 1–51 (1982).
19. Benovic, J. L., Strasser, R. H., Caron, M. G. & Lefkowitz, R. J. *Proc natn. Acad. Sci U.S.A* (in the press).
20. Benovic, J. L. *et al. J. biol. Chem.* **260**, 7094–7101 (1985).
21. Thomas, D. D. & Stryer, L. *J. molec. Biol.* **154**, 145–157 (1982).
22. Caron, M. G. & Lefkowitz, R. J. *J. biol. Chem.* **251**, 2374–2384 (1976).
23. Hewick, R. M., Hunkapiller, M. W., Hood, L. E. & Dreyer, W. J. *J. biol. Chem.* **256**, 7790–7797 (1981).
24. Spiess, J., Rivier, J. E., Rodkey, J. A., Bennett, C. D. & Vale, W. *Proc natn. Acad. Sci U.S.A.* **76**, 2974–2978 (1979).
25. Laemmli, U. K. *Nature* **117**, 680–685 (1970).
26. Towbin, H., Staehelin, T. & Gordon, J. *Proc. natn. Acad. Sci. U.S.A.* **76**, 4350–4356 (1979).
27. Johnson, D. A. & Elder, J. H. *J. exp. Med.* **159**, 1751–1756 (1983).
28. Maniatis, T., Fritsch, E. F. & Sambrook, J. *Molecular Cloning, A Laboratory Manual* (Cold Spring Harbor Laboratory, New York, 1982).
29. Merrifield, R. B. *J. Am. chem. Soc.* **85**, 2149–2154 (1963).
30. Frischauf, A. M., Lehrach, H., Paustka, A. & Murray, N. *J. molec Biol.* **170**, 827–842 (1983).
31. Lauffer, L. *et al. Nature* **318**, 334–338 (1985).
32. Benton, W. D. & Davis, R. W. *Science* **196**, 180–182 (1977).
33. Ullrich, A., Berman, C. H., Dull, T. J., Gray, A. & Lee, J. M. *EMBO J* **3**, 361–364 (1984).
34. Southern, E. M. *J. molec. Biol.* **98**, 503–517 (1975).
35. Maxam, A. M. & Gilbert, W. *Proc. natn. Acad. Sci. U.S.A.* **74**, 560–565 (1977).
36. Vieira, J. & Messing, J. *Gene* **19**, 259–268 (1982).
37. Sanger, F., Nicklen, S. & Coulson, A. R. *Proc. natn. Acad. Sci. U.S.A.* **74**, 5463–5467 (1977).
38. Schaffner, W. *et al. Cell* **14**, 655–671 (1978).
39. Nagata, S., Mantei, N. & Weissman, C. *Nature* **287**, 401–408 (1980).
40. Lawn, R. M. *et al. Nucleic Acids Res.* **9**, 1045–1052 (1981).
41. Volckaert, G., Feunteun, J., Crawford, L. V., Berg, P. & Fiers, W. J. *J. Virol.* **30**, 674–682 (1979).
42. Hamer, D. H. & Leder, P. *Cell* **18**, 1299–1302 (1979).
43. Kozak, M. *Nucleic Acids Res.* **12**, 857–872 (1984).
44. Green, S. *et al. Nature* **320**, 134–139 (1986).
45. Friedlander, M. & Blobel, G. *Nature* **318**, 338–343 (1985).
46. Feramisco, J. L., Glass, D. B. & Krebs, E. G. *J. biol. Chem.* **255**, 4240–4245 (1980).
47. Chirgwin, J. M., Przybyla, A. E., MacDonald, R. J. & Rutter, W. J. *Biochemistry* **18**, 5294–5299 (1979).
48. Gubler, U. & Hoffman, B. J. *Gene* **25**, 263–269 (1983).
49. Huynh, T. V., Young, R. A. & Davis, R. W. in *DNA Cloning a Practical Approach* Vol 1, 49–78 (IRL, Oxford, 1985).

In vitro osteoclast generation from different bone marrow fractions, including a highly enriched haematopoietic stem cell population

Ben A. A. Scheven*, Jan W. M. Visser† & Peter J. Nijweide*

* Laboratory of Cell Biology and Histology, University of Leiden, Rijnsburgerweg 10, 2333 AA Leiden, The Netherlands
† Radiobiological Institute TNO, Lange Kleiweg 151, 2288 GJ Rijswijk, The Netherlands

It is well established that the osteoclast is formed by fusion of post-mitotic, mononuclear precursors[1] derived from circulating progenitor cells[2]. However, the precise haematopoietic origin of the osteoclast is unknown. We have investigated this here by fractionating mouse bone marrow and isolating haematopoietic stem cells using a three-step method combining equilibrium density centrifugation and two fluorescence-activated cell sortings (FACS)[3], and have tested the ability of each bone marrow fraction, including highly purified haematopoietic stem cells, to generate osteoclasts during co-culture with preosteoclast-free embryonic long bones[4,5]. The osteoclast-forming capacity was found to increase with increasing stem cell purity. On the other hand, the culture time needed for osteoclast formation also increased with purification, suggesting the presence of progressively more immature progenitor cells. The pluripotent haematopoietic stem cell fractions with the highest purity needed preincubation with a stem cell-activating factor (interleukin-3) to activate the predominantly quiescent stem cells *in vitro*.

Embryonic long bones stripped of the endogenous osteoclast precursor pool (the periosteum) were used to induce the development of osteoclasts from different bone marrow cell populations. When stripped long bones are co-cultured with cell populations containing osteoclast progenitors, osteoclasts develop which thereby give rise to the formation of a marrow cavity. Culture of stripped bones alone does not lead to appearance of osteoclasts[4,5]. Total bone marrow cell population and both high-density ($1.100 < \rho < 1.078$ g cm^{-3}) and low-density ($\rho < 1.078$ g cm^{-3}) bone marrow fractions, obtained by equilibrium density centrifugation on a discontinuous metrizamide gradient, gave rise to osteoclast formation (Table 1). Autoradiography using continuous ^{3}H-thymidine labelling indicated that the osteoclasts were derived from progenitor cells which had proliferated during co-culture. The osteoclasts exhibited tartrate-resistant acid phosphatase activity, which is specific for these cells. Some mononuclear cells and an occasional multinucleated cell present in the plasma clot surrounding the bones also displayed this osteoclastic enzyme activity. Mature granulocytes accumulated in the developing marrow cavity following the invasion of osteoclasts. With time, other cell types such as megakaryocytes, macrophages and undifferentiated cells were observed in the expanded cavity.

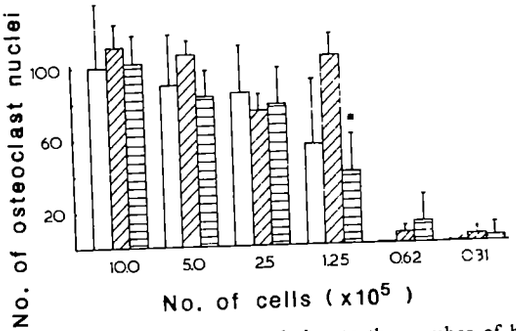


Fig. 1 Osteoclast formation in relation to the number of bone marrow cells (per plasma clot per bone) after 8 days of co-culture. Means ± s.d. of the number of osteoclast nuclei in five axial sections of four to six cultures are shown. □, Unfractionated bone marrow cells; ▨, low-density bone marrow cells; ▤, high-density bone marrow cells. Statistically significant ($P < 0.05$) compared with low-density cells.

Dilution experiments were performed to assess the relationship between the number of cells added to the bones and the

Table 1 Osteoclast formation from different bone marrow fractions

	No. of osteoclast nuclei per bone							
	0	1–5	6–20	>20	(n)	No. of cells added per bone ($\times 10^5$)	No. of day-12 CFU-S per 10^5 cells	Culture time (days)
Unfractionated bone marrow cells				26	26	2.5–10.0	51±5	7–8
Low-density cells				22	22	2.5–10.0	ND	7–8
High-density cells			5	17	22	2.5–10.0	ND	7–8
Total WGA^+ cells	2			12	14	2.0–3.0	ND	7
Total WGA^- cells	14	1			15	2.0–3.0	ND	7
WGA^+ low-density cells		1		4	5	0.40–0.50	ND	9–11
WGA^- low-density cells	8	1			9	0.40–0.50	ND	9–11
WGA^+ and H-$2K^+$ low-density cells (−SAF)	7	1			8	0.0125	690±840	14–17
WGA^+ and H-$2K^+$ low-density cells (+SAF)	1		1	10	12	0.0250	2,900±510	2+8

Metatarsal bones of 17-day-old mouse embryos were dissected and stripped of surrounding periosteum using the collagenase and mechanical treatment of Burger *et al.*[4]. The stripped cartilaginous bone rudiments consisted of a central calcified area (without (pre)osteoclasts and marrow cavity) with a thin bone collar and two uncalcified epiphyses. The bone marrow cell preparation and separation procedures were performed as described elsewhere[3]. The cells were first separated by density using a discontinuous metrizamide gradient and simultaneously labelled with WGA and fluorescein isothiocyanate (FITC), and then collected at the interfaces between the 1.100 and 1.078 g cm^{-3} solutions (high-density fraction) and the 1.078 and 1.055 g cm^{-3} solutions (low-density fraction). Cells from unfractionated bone marrow and the low-density cells were analysed for WGA–FITC binding by a modified fluorescence activating cell sorter (FACS II, Becton Dickinson). All WGA–FITC-positive cells with medium forward light scatter and low perpendicular light scatter were sorted. WGA–FITC was removed from the sorted cells by treatment with 0.2 M *N*-acetyl-D-glucosamine for 15 min at 37 °C. The cells were then labelled with biotinylated anti-H-2K followed by avidin–FITC. The most brightly fluorescent cells were selected by FACS. The low-density cells comprised ~15% of all nucleated bone marrow cells. About 30–40% of the total bone marrow was WGA^+, compared with about 4–6% of the low-density cells. The H-$2K^+$ fraction comprised ~0.3% of all nucleated bone marrow cells. SAF (10 U) was used for preincubation of the isolated H-$2K^+$ cells for 2 days before co-culture with stripped embryonic bones. 1 U of SAF is the amount needed for 50% proliferation of the interleukin-3-dependent cell line DA-1. The isolated cell suspensions of known cell number were diluted with 10% rat serum and 10% chicken embryo extract in HEPES-buffered Hanks' balanced salt solution and centrifuged to collect the cells. Then 10 μl of cock plasma was added to the cells to make a weak plasma clot. The clot was divided into equal parts of ~1 mm^3 and placed along both sides of the stripped bones. Co-culture was performed on a semi-solid medium, composed of 60% Eagle's α-minimal essential medium, 10% rat serum, 10% chicken embryo extract and 20% cock plasma, at 37 °C in a humidified 5% CO_2 atmosphere. The numbers of osteoclast nuclei in the marrow cavity were counted in five axial histological sections of bone rudiments. Recipient mice for the CFU-S assay[10] received 9.5 Gy total body irradiation (^{137}Cs, 0.85 Gy min^{-1}) 4–6 h before transplantation. Spleen colonies were counted on day 12. ND, not determined.

number of osteoclasts formed, and to determine the minimum number of cells needed for osteoclast formation (Fig. 1). At high cell concentrations the number of osteoclast nuclei reached about the same plateau level for all three bone marrow fractions. However, at a cell dose of 1.25×10^5 cells per clot, the low-density cells showed a significantly greater potency for osteoclast formation than the unfractionated and high-density bone marrow cells. The experiments were repeated twice at this critical cell dose, resulting in 89.3±25.0 and 17.3±11.2 osteoclast nuclei for the low- and high-density cells, respectively (means±s.d. of five axial sections, $P < 0.001$, $n = 6$). Lower cell doses led to an abrupt decline in the number of osteoclasts developing during culture from these three fractions.

Examination of the co-cultures using a diavert microscope revealed that resorption of the calcified centre generally started earlier when the bones had been co-cultured with the high-density bone marrow cells than with the low-density cells. To quantitate this, osteoclastic mineral resorption was determined by measuring the release of ^{45}Ca from prelabelled bones during co-culture. These experiments were carried out using high cell doses so as to exclude possible cell concentration effects (Fig. 1). Figure 2 convincingly demonstrates that the high-density cells indeed gave rise to an initial, significantly higher release of ^{45}Ca. However, from day 6 onwards the relative ^{45}Ca release was equal in all groups.

Our results indicate that the different bone marrow density fractions contain subpopulations of osteoclast progenitor cells which differ in maturation stage. The low-density fraction apparently contains more immature progenitor cells which have a greater proliferation capacity (Fig. 1) but need a longer time to differentiate into mature, fusable preosteoclasts (Fig. 2). This is consistent with the finding that the primitive progenitors, type 1 granulocyte–macrophage colony-forming units (GM-CFU-1) and spleen colony-forming units (CFU-S), can be separated from the more mature haematopoietic cells by their low buoyant density[6–9]. At increasing buoyant densities the proliferation potency of the culture colony-forming units (CFU-C) decreases, whereas the maturation rate increases[7,8]. The earlier ^{45}Ca release induced by the high-density cells correlates with the earlier maturation of agar colonies from GM-CFU-2 and -3, while the late osteoclast formation from the low-density cells may be compared to colony formation from GM-CFU-1.

Sorting on the basis of labelling of unfractionated bone marrow cells by wheat germ agglutinin (WGA) resulted in a distinct separation between an osteoclast-forming (WGA^+) and a non-osteoclast-forming (WGA^-) fraction (Table 1). The total WGA^+ cell population comprised cells belonging to the granulocyte series, including the mature forms, immature cells of the monocyte–macrophage lineage and early haematopoietic progenitor and stem cells. The WGA^- cell population, on the other hand, consisted of erythrocytes, lymphocytes, megakaryocytes and their immediate precursors, and mature macrophages and osteoclasts.

The WGA^+ fraction of the low-density cells consisted mainly of early haematopoietic progenitor and stem cells with 60-fold enrichment of CFU-S[8]. Only the WGA^+ low-density cells were able to induce osteoclast development (Table 1). This, however, took a longer co-culture period (8–10 days) compared with the

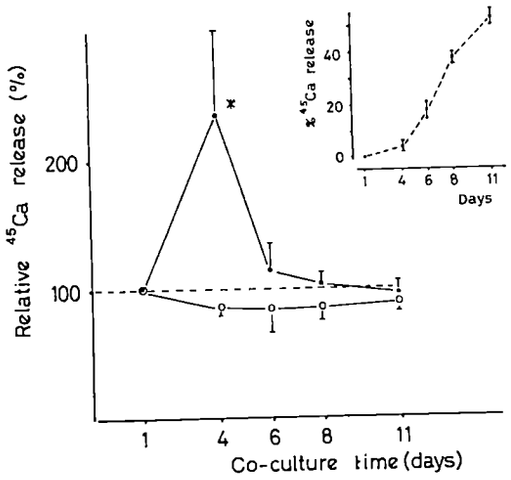


Fig. 2 Osteoclastic mineral resorption during co-culture with high (●)- or low (○)-density bone marrow cells. At each time point the release of ^{45}Ca from prelabelled metatarsal bones is expressed as a percentage of the average ^{45}Ca release obtained during co-culture with unfractionated cells. Inset, cumulative release of ^{45}Ca during co-culture with unfractionated bone marrow cells shown as a percentage of total incorporated ^{45}Ca per bone.
Methods. Pregnant mice were injected with 50 μCi ^{45}Ca on day 16 of gestation. The next day the ^{45}Ca-labelled metatarsal bones were dissected, stripped, explanted on a semi-solid medium and co-cultured with clots containing unfractionated, low-density or high-density bone marrow cells (see Table 1 legend). Medium was changed after 1, 4, 6 and 8 days. After a total culture period of 11 days the co-cultures were fixed in a mixture of 5% glacial acetic acid, 85% ethanol and 10% formaldehyde for 24 h, then decalcified in a 5% formic acid/5% formaldehyde solution. The semi-solid media were digested overnight with 0.1% trypsin and the digested culture media, fixation and decalcification fluids analysed for ^{45}Ca radioactivity on a Beckman LS 1800 liquid scintillation counter. The release of ^{45}Ca during the first culture day, which represents physicochemical exchange, was discarded. The values shown are means ± s.e.m. of seven or eight co-cultures. * Statistically significant ($P < 0.05$) compared with low-density cells.

cell populations described above. This phenomenon is probably due to the lower number of cells per bone and the occurrence of predominantly very immature cells in this fraction which needed more time to mature into preosteoclasts.

H-2K sorting of the WGA$^+$ low-density fraction produced a highly enriched pluripotent haematopoietic stem cell population. Intravenous injection of 100 sorted cells per lethally irradiated mouse resulted in 6.9–9.3 colonies per spleen 12 days later (day-12 CFU-S; refs 3, 10). As the seeding efficiency of transplanted haematopoietic stem cells to the spleen is between 0.05 and 0.10 (refs 3, 11, 12), this indicates that at least 69–93% of the sorted cells were pluripotent stem cells.

The osteoclast-forming capacity of these sorted cells, however, was minimal (Table 1), perhaps because of the lower number of cells present per clot and/or the absence of suitable factors for activating the mainly quiescent stem cells. A stem cell-activating factor (SAF = interleukin-3)[13] was therefore used to stimulate the sorted stem cells. Preincubation of cells with 10 U SAF for 2 days resulted in a doubling of the total number of cells, concomitantly with maintenance of day-8 CFU-S and a slight decrease in the number of day-12 CFU-S per culture. Subsequent co-culture with stripped metatarsal bones led to a burst of haematopoietic cell growth (granulocytes and macrophages) and abundant osteoclast formation. This indicates either that SAF triggers the pluripotent haematopoietic stem cells into a state in which they are responsive to the growth factors in the plasma clot, or that the pluripotent stem cells, because of SAF, differentiate into committed progenitors which are then stimulated by the clot. The plasma clot itself apparently does not contain SAF. When, in another experiment, we added recombinant SAF (10 U ml^{-1}) to a co-culture of purified stem cells and stripped metatarsal bones on day 0 and removed the SAF on day 2 by washing, we observed extensive haematopoietic cell growth and abundant osteoclast formation similar to that in the above experiment. Without SAF no osteoclast formation was observed in this experiment either.

Our results with purified stem cells provide direct, although not yet conclusive, evidence for the hypothesis that osteoclasts are derived from the pluripotent haematopoietic stem cell[14–17]. In addition, the data indicate that SAF is needed to initiate the proliferation and differentiation of the pluripotent stem cell. The evidence presented cannot exclude the possibility that the osteoclast progenitor co-purifies with the CFU-S population, although we consider this highly unlikely. It is not very probable that a distinct osteoclast stem cell would behave exactly like the haematopoietic stem cell during the isolation procedure, causing a >100-fold enrichment of the latter cell, for it would mean the possession of similar cytochemical (WGA, H-2K) and physical (density, light-scattering) properties, and the ability to react in a similar manner to SAF.

The first part of the pathway along which osteoclasts differentiate may very well coincide with the monocyte differentiation lineage, as granulocyte and macrophage precursors are also found among the WGA$^+$ bone marrow cells[18]. However, as we have shown earlier[19], the direct precursors of the osteoclast are not monocytes. The formation of osteoclasts from isolated haematopoietic stem cells in the *in vitro* model used here should facilitate the elucidation of the osteoclast differentiation lineage and its relation to other blood cell lineages.

We thank Dr L. Dorssers for supply of (recombinant) SAF, Mrs A. M. Wassenaar, E. W. M. Kawilarang-de Haas and M. Hogeweg-Platenburg for technical assistance and Professor J. P. Scherft for critically reading the manuscript. This study was supported by the J. A. Cohen Institute, IRS, Leiden.

Received 3 February; accepted 6 March 1986.

1. Scheven, B. A. A., Burger, E. H., Kawilarang-de Haas, E. W. M., Wassenaar, A. M. & Nijweide, P. J. *Lab. Invest.* **53**, 72–79 (1985).
2. Marks, S. C. Jr *J. oral Path.* **12**, 226–256 (1983).
3. Visser, J. W. M., Bauman, J. G. J., Mulder, A. H., Eliason, J. F. & de Leeuw, A. M. *J. exp. Med.* **159**, 1576–1590 (1984).
4. Burger, E. H. *et al. J. exp. Med.* **156**, 1604–1614 (1982).
5. Thesingh, C. W. & Burger, E. H. *Devl Biol.* **95**, 429–438 (1983)
6. Bol, S., Visser, J. & Van den Engh, G. *Expl Hemat.* **7**, 541–553 (1979)
7. Bol, S. & Williams, N. *J. cell. Physiol.* **102**, 233–243 (1980).
8. Visser, J. W. M. & Bol, S. J. L. *Stem Cells* **1**, 240–249 (1981)
9. Baines, P., Bol, S. J. L. & Rosendaal, M. *Leukemia Res.* **6**, 81–88 (1982)
10. Till, J. E. & McCulloch, E. A. *Radiat. Res.* **14**, 213–222 (1962)
11. Lahiri, S. K., Keizer, H. J. & van Putten, L. M. *Cell Tissue Kinet.* **3**, 355–362 (1970)
12. Monette, F. C. & DeMello, J. B. *Cell Tissue Kinet.* **12**, 161–175 (1979)
13. Dorssers, L., Burger, H. & Wagemaker, G. *Expl Hemat.* **12**, Suppl. 13, abstr. 3 (1984)
14. Kahn, A. J. & Simmons, D. J. *Nature* **258**, 325–327 (1975).
15. Walker, D. G. *J. exp. Med.* **142**, 651–663 (1975).
16. Ash, P., Loutit, J. F. & Townsend, K. M. S. *Nature* **283**, 669–670 (1980)
17. Loutit, J. F. & Nisbet, N. W. *Immunobiology* **161**, 193–203 (1982)
18. Visser, J. W. M., Bol, S. J. L. & Van den Engh, G. J. *Expl Hemat.* **9**, 644–655 (1981)
19. Scheven, B. A. A., Kawilarang-de Haas, E. W. M., Wassenaar, A. M. & Nijweide, P. J. *Anat. Rec.* (in the press).

Epidermal growth factor-dependent phosphorylation of lipocortin

R. Blake Pepinsky & Lesley K. Sinclair

Biogen Research Corporation, 14 Cambridge Center, Cambridge, Massachusetts 02142, USA

Lipocortin-like proteins are a family of steroid-induced inhibitors of phospholipase activity with potential anti-inflammatory activity (for reviews see refs 1, 2). Related proteins have been detected in a variety of tissues and species[3–7]. The best characterized form is a protein of relative molecular mass (M_r) ~ 40,000 (40K), which is phosphorylated *in vivo* by protein tyrosine kinases and by protein

serine-threonine kinases[8,9]. It has been proposed that the phospholipase inhibitory activity of lipocortin can be regulated by its phosphorylation[5]. In the A431 cell line, a protein of ~35K is phosphorylated by the protein tyrosine kinase activity of the epidermal growth factor (EGF) receptor[10]. Here we report that human lipocortin is phosphorylated near its amino terminus by the EGF receptor/kinase. By peptide mapping and immunological analyses, we show that lipocortin and the endogenous 35K substrate for the EGF receptor/kinase from A431 cells are the same protein.

Recently, the human gene for lipocortin was cloned and expressed in *Escherichia coli*[11]. The gene encodes a 38.5K protein that inhibits phospholipase A_2 activity. The inhibitory activity was readily detected in crude bacterial lysates, but only from cells transformed with the human gene. Lipocortin was found in cell types of diverse origin, including macrophages, fibroblasts and epithelial cells[4], and levels of expression in these preparations represented 0–0.5% of total cell protein. Figure 1 shows the results of gel filtration analysis of the recombinant human protein. On chromatography, the inhibitor yields a single peak with an apparent M_r of ~40K. The elution profile of phospholipase A_2 inhibitory activity (Fig. 1*A*) and the profile of the protein when subjected to SDS-polyacrylamide gel electrophoresis (SDS-PAGE) (Fig. 1*B*) coincide exactly. The inhibitory activity is trypsin-sensitive, destroyed by boiling and inactivated by treatment with heparin (not shown). Like natural lipocortin, the recombinant protein has a specific activity of 6,000–10,000 units per mg of protein, where 1 unit inhibits 15 ng of phospholipase A_2.

The EGF receptor (170K) is a protein tyrosine kinase that is activated by EGF[12,13]. The enzyme is membrane-associated and retains its activity in preparations of isolated cell membranes[14,15]. Two prominent phosphorylation products of the EGF-dependent kinase are the receptor itself and an endogenous 35K substrate. In the A431 cell line the receptor/kinase is overproduced[16], leading to the frequent use of this human line as a source of the kinase. When membranes from A431 cells are incubated with [γ-^{32}P]ATP and the phosphorylated products analysed by SDS-PAGE, the receptor and the 35K protein are both phosphorylated[14,15]. The degree of phosphorylation is greater if the kinase is prepared from EGF-treated cells. Using the A431 membrane-derived kinase activity, we observed similar results: both the receptor and the endogenous 35K protein were prominent phosphorylation products in the sample derived from EGF-treated membranes (Fig. 2*b*) and were present as minor species in the corresponding untreated sample (Fig. 2*a*).

When membranes from A431 cells were first treated with lipocortin and then subjected to phosphorylation and SDS-gel analysis, the recombinant protein was phosphorylated (Fig. 2*c, d*). Whereas in the absence of EGF, lipocortin was barely detected (Fig. 2*c*), it was the major phosphorylated protein in the EGF-treated preparations (Fig. 2*d*). The incorporation of phosphate into lipocortin varied as a function of the concentration of protein added (Fig. 2*e–h*). The dilution series tested ranged from concentrations where no effect was observed (5 nM lipocortin, Fig. 2*e*) to those where the phosphorylation reaction was saturated (5 μM lipocortin, Fig. 2*h*). The increase in phosphorylation of lipocortin coincides with a decrease in phosphorylation of the EGF receptor. We found that human lipocortin and the endogenous 35K substrate have similar electrophoretic mobilities by SDS-gel electrophoresis. The 4K discrepancy between the predicted and apparent M_rs for lipocortin presumably results from its unusually charged amino-acid composition, as charged amino acids affect the electrophoretic mobility of proteins in SDS-gels[17].

We have shown by peptide mapping analysis that lipocortin and the endogenous 35K protein from A431 cells are the same protein. We incubated gel slices containing phosphorylated lipocortin and phosphorylated 35K protein with CNBr, then separated the cleavage products by SDS-PAGE. Radioactive products were visualized by autoradiography. As shown in

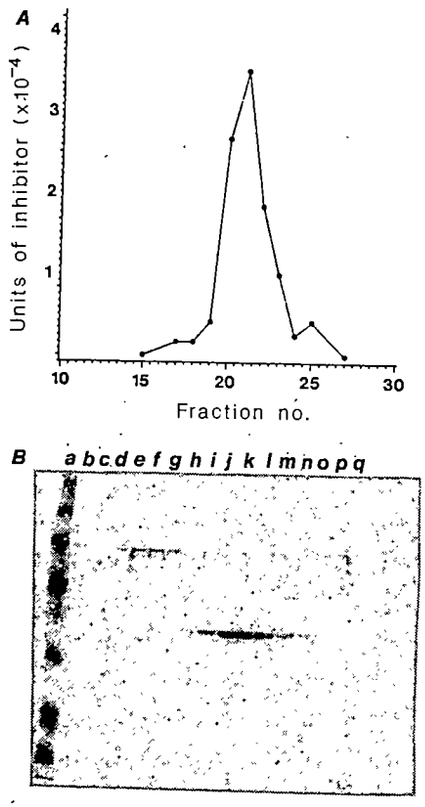


Fig. 1 Gel filtration analysis of recombinant lipocortin. Recombinant human lipocortin produced in *E. coli* was chromatographed on a P150 column (2.5 cm diameter × 45 cm). Aliquots from each 5-ml fraction collected were analysed for phospholipase A_2 inhibitory activity (*A*) and by SDS-PAGE (*B*). Proteins were separated electrophoretically in SDS-gels (15% acrylamide, 0.18% methylene bisacrylamide)[25] and stained with Coomassie brilliant blue R-250. Stacking gels contained 7.6% acrylamide and 0.21% bisacrylamide. *a*, Pre-stained M_r markers (BRL): myosin, 220K; phosphorylase B, 100K; bovine serum albumin, 65K; ovalbumin, 47K; α-chymotrypsinogen, 30K; β-lactoglobulin, 18K; lysozyme, 15K. Lanes *b–q* correspond to column fractions 10, 12, 14, 16–27 and 29, respectively. For inhibitory activity, samples were assayed with porcine pancreatic phospholipase A_2, using autoclaved ^{3}H-oleic-acid-labelled *E. coli* as substrate[4].

Fig. 3*b, c*, phosphate-labelled CNBr fragments from the two protein preparations were identical. The six phosphorylated fragments formed a distinct subset of the total digestion products of lipocortin, which consists of 22 fragments (Fig. 3, lane *a*). This series of fragments is a mixture of complete and partial cleavage products, which we have characterized by CNBr mapping analysis. Although the relative intensities of the cleavage products vary as a function of the CNBr concentration, no additional products were generated when preparations were treated with CNBr at 7–21 mg ml^{-1}, spanning the range of concentrations used routinely for analysis of lipocortin.

To localize the site of phosphorylation within lipocortin, we first identified the fragment composition for each of its 22 digestion products by CNBr mapping and then used this information to identify the subset of fragments that were phosphorylated. This type of procedure has been described in detail previously[18,19] and is based on the fact that each CNBr fragment is represented by a distinct subset of the digestion products. The mapping information for lipocortin is summarized on the left of Fig. 3; however, the actual cleavage maps will be presented elsewhere. Based on the map of lipocortin, the pattern of phosphorylated fragments suggests a modification within fragment 1. The series of radioactive spots corresponds to fragment 1 and each of the fragment 1-containing partial digests. Thus, the

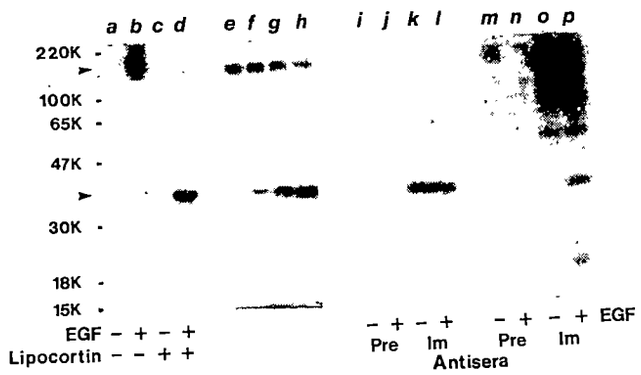


Fig. 2 EGF-dependent phosphorylation of lipocortin. A431 cells were grown at 37 °C in Dulbecco's modified Eagle's medium supplemented with 10% calf serum. *In vitro* phosphorylation reactions using isolated A431 cell membranes (lanes *a–h*) and immune precipitations from metabolically labelled cells (^{35}S-methionine-labelled, lanes *i–l*; ^{32}P-phosphate-labelled, lanes *m–p*) were analysed by SDS-PAGE and radioactive products visualized by autoradiography. Arrowheads denote the positions of the EGF receptor and the 35K protein. *e–h*, *In vitro* phosphorylation products generated when membranes from EGF-treated cells were treated with various concentrations of lipocortin: 0.2, 2, 20 and 200 μg ml^{-1} of lipocortin, respectively.

Methods. For *in vitro* phosphorylation reactions, confluent monolayers of A431 cells in T75 flasks were washed with Dulbecco's medium without serum and incubated at 37 °C for 1 h in 7 ml of serum-free medium without (−) and with (+) 200 ng ml^{-1} EGF (Sigma). Monolayers were rinsed with 2.5 ml of ice-cold hypotonic buffer (10 mM HEPES *p*H 7.5, 0.5 mM $MgCl_2$) and the cells scraped into 1.5 ml of the same buffer. After 30 min on ice, the cells were disrupted with a Dounce homogenizer (20 strokes with a type A pestle), and large particulate debris was removed by centrifugation (2,000*g*, 5 min). The resultant supernatants were centrifuged at 10,000*g* for 10 min and the membranous pellets suspended in 300 μl of phosphorylation buffer (20 mM HEPES *p*H 7.5, 2 mM $MgCl_2$, 10 μM ammonium vanadate). EGF-treated membranes were suspended in buffer plus 2 μg ml^{-1} EGF. 60-μl reactions, each containing 30 μl of a given membrane preparation, were held on ice for 10 min in the presence of 30 μCi [γ-^{32}P]ATP per tube. Reactions were stopped by adding 20 μl of 5× electrophoresis sample buffer. Samples were heated at 55 °C for 10 min, and then subjected to SDS-gel analysis. For the metabolic labelling experiments, A431 cells were grown in 6-well microtitre dishes. Cells were labelled with ^{35}S-methionine (100 μCi per well) in methionine-free medium and with ^{32}P-phosphate (1 mCi per well) in phosphate-free medium. In both cases cells were cultured for 4 h in serum-free medium without and with 200 ng ml^{-1} EGF. Labelled cells were disrupted with 1 ml of lysis buffer (50 mM NaCl, 20 mM Tris-HCl *p*H 7.3, 0.5% Nonidet P-40, 0.5% sodium deoxycholate, 4 mM iodoacetic acid, 1 mM ammonium vanadate), and lysates were subjected to vortex mixing for 30 s and clarified by centrifugation for 5 min in an Eppendorf centrifuge. The appropriate antisera were added (Pre, preimmune serum; Im, immune serum) and the samples were incubated for 2 h at 4 °C. The immune complexes were collected by adsorption to protein A–Sepharose for 1 h at 4 °C with continuous mixing. The adsorbed immune precipitates were washed four times (each with 0.5 ml lysis buffer), suspended in 50 μl of electrophoresis sample buffer, heated at 60 °C for 10 min, and subjected to SDS-PAGE. To prepare anti-lipocortin serum, rabbits were immunized with recombinant human protein produced in *E. coli*. Native protein was emulsified with Freund's complete adjuvant and administered by intramuscular injection; 5 weeks after the primary injection, the rabbits received a booster injection of protein emulsified with incomplete adjuvant.

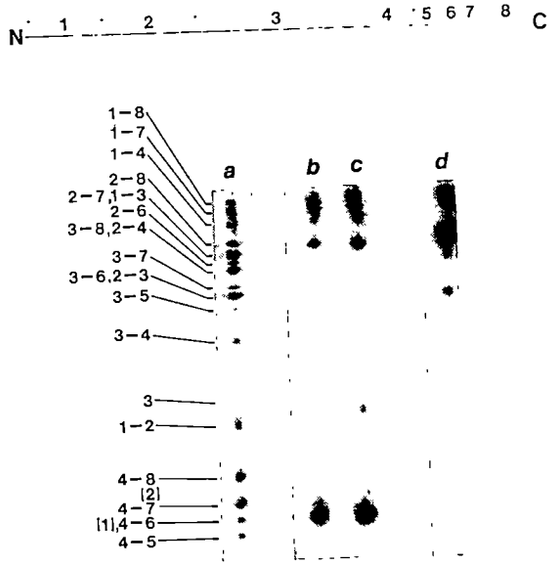


Fig. 3 Cyanogen bromide mapping of phosphorylated lipocortin. *a*, Unlabelled lipocortin; *b*, phosphorylated lipocortin (EGF receptor/kinase); *c*, phosphorylated endogenous 35K protein (EGF receptor/kinase); *d*, phosphorylated lipocortin (protein kinase A). Numbers on the left correspond to CNBr fragments of lipocortin: fragment 1 refers to the amino-terminal fragment and fragment 8 the carboxy-terminal fragment. The distribution and relative sizes of all the fragments are indicated in the schema shown at the top. The fragmentary compositions of cleavage fragments are based on CNBr mapping[18]. Although fragments 1 and 2 are not visualized by this particular silver staining procedure[26], their positions in cleavage profile are indicated. Other cleavage products were not identified because either they were below the size limit of detection of this particular gel system or they were minor cleavage products and could not be analysed.

Methods. Gel slices containing either unlabelled lipocortin or *in vitro* phosphorylated products were incubated with CNBr (10 mg ml^{-1}) for 1 h at room temperature in 0.1 M HCl plus 0.1% 2-mercaptoethanol. The CNBr-treated gel slices were washed twice for 5 min each with water, once for 5 min in 0.25 M Tris-HCl *p*H 6.8, and once for 10 min at 37 °C in electrophoresis sample buffer. The slices were loaded onto SDS-gels and the cleavage products separated by SDS-PAGE using the Laemmli discontinuous buffer system (main gel: 15% acrylamide, 0.4% methylene bisacrylamide).

phosphorylation site is near the amino terminus of lipocortin. The positions of serine, threonine and tyrosine residues within fragment 1 place further boundaries on this site. Recombinant lipocortin also can be phosphorylated *in vitro* by the catalytic subunit of protein kinase A. The cleavage profile of protein kinase A-phosphorylated lipocortin (Fig. 3*d*) suggests a modification within fragment 3.

In addition to the *in vitro* experiments, we have evaluated the phosphorylation state of lipocortin in metabolically labelled A431 cells. Figure 2*i–p* shows the results of an analysis in which crude lysates from labelled cells were treated with either anti-lipocortin serum or preimmune serum, and the immune complexes analysed by SDS-PAGE. In lysates of ^{35}S-methionine-labelled cells, the anti-lipocortin serum recognized a single protein of 35K which was not detected with preimmune serum from the same rabbit. Metabolic labelling of the 35K protein was independent of EGF treatment. The 35K protein was also detected in immune precipitates from ^{32}P-phosphate-labelled cell lysates (Fig. 2*m–p*), but only for preparations derived from EGF-treated cells. Similar results for metabolic labelling of the endogenous 35K protein have been described previously[10]. Using conditions that enrich for tyrosine phosphate (that is, the gel is treated prior to autoradiography with 1 M KOH for 1 h at 55 °C; ref. 20) we observed that the phosphorylated 35K protein was enhanced relative to background radioactivity (not shown).

Here we have presented data demonstrating that the endogenous 35K substrate for the EGF receptor/kinase from A431 cells is lipocortin, and therefore presumably a potent phospholipase A_2 inhibitor. This result was deduced from both

structural and immunological analyses. The relevance of the phospholipase inhibitory activity to the cellular function of these proteins remains to be established. Peptide mapping and the use of the anti-lipocortin antiserum should allow us to clarify rapidly the relationships between the 35K substrate for the EGF-dependent kinase[15,21,22], the 34–40K substrate for *src*-like kinases[21,23,24] and the 35K G-protein β-subunit[22], which to date remain controversial. The role of the 35K protein as a phospholipase A_2 inhibitor probably represents an important biological activity in EGF transduction.

We thank Barbara P. Wallner for the JA221 strain of *E. coli* transformed with plasmid LipTrc155A, a strain producing recombinant human lipocortin; and John Smart, Vicky Sato, Richard Flavell and Jeff Browning for critical reading of the manuscript. This work was funded by Biogen Research Corporation and by Yamanouchi Pharmaceutical Company.

Received 6 February; accepted 20 March 1986.

1. Flower, R. J., Wood, J. N. & Parente, L. *Adv. Inflamm. Res.* 7, 61–69 (1984).
2. Hirata, F. *Adv. Inflamm. Res.* 7, 71–78 (1984).
3. Blackwell, G. J. *et al. Br. J. Pharmac.* 76, 185–194 (1982).
4. Pepinsky, R. B. *et al. J. biol. Chem.* 261, 4239–4246 (1986).
5. Hirata, F. *J. biol. Chem.* 256, 7730–7733 (1981).
6. Rothhut, B., Russo-Marie, F., Wood, J., DiRosa, M. & Flower, R. J. *Biochem. biophys. Res. Commun.* 117, 878–884 (1983).
7. Gupta, C., Katsumata, M., Goldman, A. S., Herold, R. & Piddington, R. *Proc. natn. Acad. Sci. U.S.A.* 81, 1140–1143 (1984).
8. Hirata, F. *et al. Biochem. biophys. Res. Commun.* 118, 682–690 (1984).
9. Hirata, F., Matsuda, K., Notsu, Y., Hattori, T. & DelCarmine, R. *Proc. natn. Acad. Sci. U.S.A.* 81, 4717–4721 (1984).
10. Sawyer, S. T. & Cohen, S. *J. biol. Chem.* 260, 8233–8236 (1985).
11. Wallner, B. P. *et al. Nature* 320, 77–81 (1986).
12. Ushiro, H. & Cohen, S. *J. biol. Chem.* 255, 8363–8365 (1980).
13. Cohen, S., Ushiro, H., Stoscheck, C. & Chinkers, M. *J. biol. Chem.* 257, 1523–1531 (1982).
14. King, L. Jr, Carpenter, G. & Cohen, S. *Biochemistry* 19, 1524–1528 (1980).
15. Fava, R. A. & Cohen, S. *J. biol. Chem.* 259, 2636–2645 (1984).
16. Fabricant, R. N., DeLarco, J. E. & Todaro, G. J. *Proc. natn. Acad. Sci. U.S.A.* 74, 565–569 (1977).
17. Tung, J.-S. & Knight, C. A. *Analyt. Biochem.* 48, 153–163 (1972).
18. Pepinsky, R. B. *J. biol. Chem.* 258, 11229–11235 (1983).
19. Pepinsky, R. B. & Vogt, V. M. *J. Virol.* 52, 145–153 (1984).
20. Cooper, J. A., Sefton, B. M. & Hunter, T. *Meth. Enzym.* 99, 387–402 (1983).
21. Glenney, J. R. & Tack, B. F. *Proc. natn. Acad. Sci. U.S.A.* 82, 7884–7888 (1985).
22. Valentine-Braun, K. A., Northup, J. K. & Hollenberg, M. D. *Proc. natn. Acad. Sci. U.S.A.* 83, 236–240 (1986).
23. Gerke, V. & Weber, K. *J. biol. Chem.* 260, 1688–1695 (1985).
24. Erikson, E. & Erikson, R. L. *Cell* 21, 829–836 (1980).
25. Laemmli, U. K. *Nature* 227, 680–685 (1970).
26. Wray, W., Boulikas, T., Wray, V. P. & Hancock, R. *Analyt. Biochem.* 118, 197–203 (1981).

Ha-*ras* hypervariable alleles in myelodysplasia

S. L. Thein*, D. G. Oscier†, J. Flint* & J. S. Wainscoat‡

* MRC Molecular Haematology Unit, Nuffield Department of Clinical Medicine, and ‡ Department of Haematology, John Radcliffe Hospital, Headington, Oxford OX3 9DU, UK
† Department of Haematology, Royal Victorian Hospital, Boscombe, Bournemouth BH1 4JG, UK

The somatic mutation of one of the *ras* oncogenes is now considered to be a critical step in the pathogenesis of many tumours[1,2]. Circumstantial evidence also suggests that some individuals may be genetically predisposed to malignancy[3] and a general method used to analyse such disease susceptibility is the study of restriction fragment length polymorphisms (RFLPs) at particular loci[4,5]. The Harvey *ras* (Ha-*ras*) locus includes a hypervariable region (HVR) which consists of a series of 28-base-pair (bp) tandem repeats 3′ to the gene[6]. This arrangement gives rise to alleles of a wide range of sizes, making such genetic analysis possible. A previous study reported that white blood cell DNA from cancer patients frequently showed allelic restriction fragments at the Ha-*ras* locus which were found only rarely in normal unaffected individuals, and it was concluded that the inheritance of such unusual alleles may be linked to a susceptibility to cancer[7]. As this conclusion has major implications we sought to investigate whether this association could be confirmed in patients with myelodysplasia, a common haematological malignancy reported to have the highest frequency of rare alleles[7]. The Ha-*ras* alleles were characterized in normal healthy individuals and compared with those found in patients with myelodysplasia (MDS). Our results, reported here, show that the distribution of Ha-*ras* alleles in myelodysplastic patients is not significantly different from that in normal individuals.

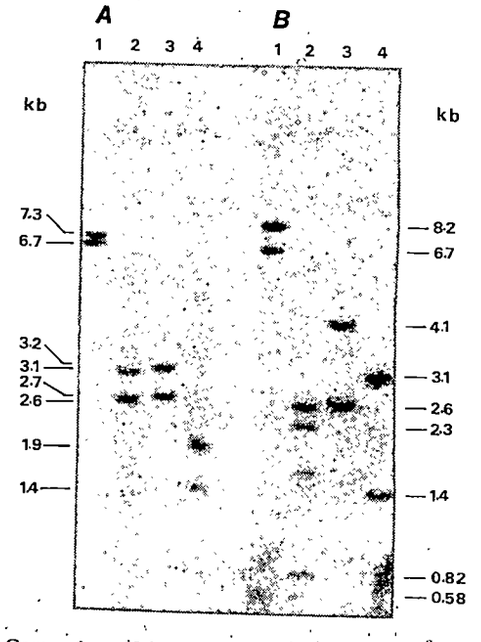


Fig. 1 Comparison of the Ha-*ras* alleles generated by four restriction endonucleases. DNAs from two individuals (*A* and *B*) were digested with *Bam*HI (lane 1), *Taq*I (lane 2), *Hin*fI (lane 3) and *Ava*II (lane 4). The digested DNA was hybridized to the 2.5-kb *Bam*HI–*Sst*I fragment containing the T24/EJ bladder oncogene[6]. *A*, An individual with the *a*/*b* Ha-*ras* alleles corresponding to the *Bam*HI 6.7/7.3-kb fragment and the *Taq*I 2.6/3.1-kb, *Hin*fI 2.7/3.2-kb and *Ava*II 1.4/1.9-kb fragments. *B*, An individual with two *Taq*I site polymorphisms. Corresponding sizes for the *a* allele were seen with *Bam*HI (6.7 kb); *Taq*I (2.6 kb), *Hin*fI (2.7 kb) and *Ava* II (1.4 kb) digests. *Bam*HI, *Hin*fI and *Ava*II digests gave appropriate corresponding sizes (8.2, 4.1 and 3.1 kb respectively) for the '*d*' allele but a pattern of three fragments (2.3 kb, 820 bp and 580 bp) was obtained for the *Taq*I digests. Further investigations suggested the presence of two *Taq*I site polymorphisms within the HVR. All alleles with the *Taq*I site polymorphisms were characterized by the *Ava*II '*d*' (3.1 kb) alleles, which suggests that these *Taq*I site polymorphisms are linked to a particular HVR allele.

Methods. DNA was prepared from peripheral blood buffy coat cells by digestion with proteinase-K and phenol–chloroform extraction as described previously[10] DNA (5 μg) was digested with 25 units of each restriction enzyme, separated by electrophoresis on a 0.8% agarose gel and transferred to nitrocellulose membrane by Southern blotting. The *Bam*HI–*Sst*I fragment of plasmid pEJ[6] containing the Ha-*ras* HVR was purified and nick-translated to a specific activity of $\sim 1.0 \times 10^8$ c.p.m. μg^{-1}. Pre-hybridization, hybridization and washing of the membranes were done as described previously[10]. Autoradiography was at −70 °C.

Fifty-two normal healthy individuals and 53 patients with MDS were studied. The diagnosis of MDS fulfilled the criteria of the FAB classification[8]. DNA was extracted from peripheral blood leukocytes, digested with appropriate restriction enzymes, Southern-blotted and hybridized to the *Bam*HI–*Sst*I fragment of plasmid EJ containing the HVR~1.5 kilobases (kb) from the 3′ terminus of the coding sequences of the Ha-*ras* gene. The first objective was to choose the most appropriate restriction enzyme to give maximal resolution of the different HVR alleles.

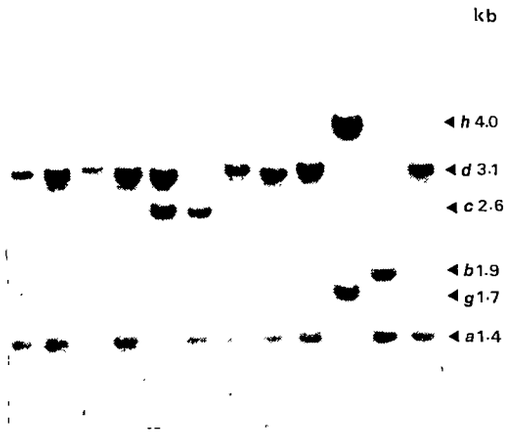


Fig. 2 Microheterogeneity of the common Ha-*ras* allele. DNA (5 μg) was digested with *Ava*II, electrophoresed on a 0.8% agarose gel, and transferred to nitrocellulose membrane by Southern blotting. Hybridization and autoradiography were as described in Fig. 1 legend. Microheterogeneity between the '*d*' alleles could only be visualized when the DNA samples were run in adjacent tracks. However, the differences between the various '*d*' alleles were too small to be measured reliably. There was no obvious microheterogeneity among the different '*a*' alleles.

Table 1 Distribution of the *Ava*II Ha-*ras* alleles

Allele	Size (kb)	Normal individuals	Myelodysplastic individuals	Total
Common				
a	1.4	71 (68%)	66 (62%)	137 (65%)
b	1.9	6 (6%)	15 (14%)	21 (10%)
c	2.6	9 (9%)	14 (13%)	23 (11%)
d	3.1	13 (13%)	8 (8%)	21 (10%)
Rare				
e	2.0	0 (0%)	0 (0%)	0 (0%)
f	1.5	3 (3%)	3 (3%)	6 (3%)
g	1.7	1 (1%)	0 (0%)	1 (<1%)
h	4.0	1 (1%)	0 (0%)	1 (<1%)
Total		104	106	210

DNA was prepared from peripheral blood buffy coat cells and the allele sizes determined as described in Fig. 1 legend. The numbers of particular *Ava*II Ha-*ras* alleles are given with the frequencies in parentheses.

DNAs from 10 unrelated individuals were digested with a panel of restriction enzymes and resolution of the different bands was found to be greatest with the enzyme *Ava*II, which cleaves just outside the HVR. In addition to *Ava*II, all DNAs were digested with *Bam*HI and *Taq*I to ensure that variation in allelic fragment sizes was directly related to the HVR length rather than to restriction enzyme site polymorphisms (see Fig. 1).

Although optimal resolution was obtained with *Ava*II digestion, it was difficult to compare similar-sized Ha-*ras* alleles between different gels. To overcome this problem, all DNAs with apparently similar-sized alleles were re-electrophoresed in adjacent tracks against control DNA samples (Fig. 2). Nine measurably different *Ava*II Ha-*ras* alleles were found, of which four were common and five rare. Microheterogeneity of fragment sizes was observed within the four common allele classes in both groups of indviduals. However, the degree of microheterogeneity was so small that it could be visualized only by examination of the autoradiographs when alleles of the same size class were in adjacent tracks; these small differences cannot be measured reliably. The degree of microheterogeneity was greater within the three classes of common, larger-sized alleles than within the smallest common allele class. This phenomenon probably relates to the greater likelihood of misalignment occurring during recombination between larger HVR alleles. This result is in accord with the observation in a study of the hypervariable minisatellite regions that those probes with the longer HVRs detected more allele sizes[9]. There was no observable difference in the degree of microheterogeneity in the allele sizes between the two groups of individuals.

Table 1 shows the numbers of the different Ha-*ras* alleles found in the two groups of individuals. The frequencies of the four common *Ava*II alleles are not significantly different between the two groups and are very similar to those previously reported using *Bam*HI. The rare alleles were found sporadically in both groups: 5/104 in normal chromosomes and 3/106 in MDS chromosomes. Therefore, there is no significant increase in the frequency of rare alleles in the MDS patients compared with normal individuals. The frequency of the rare alleles in our group of normal individuals (4.8%) was not significantly different from that in the group of normal individuals observed previously (3.9%)[7]. The patients reported previously as having the highest proportion of rare alleles had MDS, 6/7 patients having rare alleles[7]. Here we studied 53 patients with MDS of which only three had rare alleles. Therefore, our finding that the MDS patients do not have an increased frequency of rare alleles is in striking contrast to the previous study, although the reasons for this difference are not clear. Thus, we have found no evidence to suggest that the inheritance of rare HVR alleles at the Ha-*ras* locus prediposes to myelodysplasia.

We thank Liz Gunson for typing the manuscript; Drs D. R. Higgs and A. J. Jeffreys for critical comments on the manuscript; and Dr F. G. Bolton and Professor D. J. Weatherall for their support and encouragement.

Received 3 February; accepted 7 March 1986.

1. Bos, J. L. *et al. Nature* **315**, 726–730 (1985).
2. Bos, J. L. *et al. Nucleic Acids Res.* **12**, 9155–9163 (1984)
3. Burt, R. W *et al. New Engl. J. Med.* **312**, 1540–1544 (1985)
4. Gusella, J. F. *et al. Nature* **306**, 234–239 (1983)
5. Thein, S. L. & Wainscoat, J. S. *Disease Markers* (Wiley, New York, in the press)
6. Capon, D. J., Chen, E. Y., Levinson, A D., Seeburg, P. H & Goeddel, D V *Nature* 302, 33–37 (1983).
7. Krontiris, T. G., Di Martino, N. A., Colb, M. & Parkinson, D R *Nature* 313, 369–373 (1985)
8. Bennet, J. M. *et al. Br. J. Haemat.* **51**, 189–199 (1982)
9. Jeffreys, A. J., Wilson, J. & Thein, S L. *Nature* **316**, 67–73 (1985)
10. Old, J. M. & Higgs, D. R. in *Methods in Haematology*, vol 6, 74–102 (Churchill Livingstone, Edinburgh, 1983).

Spectrin assembly in avian erythroid development is determined by competing reactions of subunit homo- and hetero-oligomerization

Catherine M. Woods & Elias Lazarides

Division of Biology, California Institute of Technology, Pasadena, California 91125, USA

Erythroid differentiation entails the biogenesis of a membrane skeleton, a network of proteins underlying and interacting with the plasma membrane[1–3], whose major constituent is the heterodimeric protein spectrin, composed of two structurally similar but distinct subunits[4], α (relative molecular mass (M_r) 240,000) and β (M_r 220,000), which interact side-on with each other to form a long rod-like molecule[1,3,5–10]. Interaction of this network with the membrane is mediated by the binding of the β subunit to ankyrin[1,6,11–14], which in turn binds to the cytoplasmic domain of the transmembrane anion transporter (also referred to as band 3)[1,15–19]. Purified α and β subunits of spectrin from the membrane of mature red blood cells will spontaneously

heterodimerize[13,14,20–23], suggesting that assembly of the spectrin-actin skeleton is a simple self-assembly process, but *in vivo* studies with developing chicken embryo erythroid cells have indicated that assembly *in vivo* is more complex[24–29]. We now present evidence that newly synthesized spectrin subunits *in vivo* or *in vitro* rapidly adopt one of two competing conformations, a heterodimer or a homo-oligomer. These competing reactions seem to determine the overall extent of spectrin assembled during erythroid development by determining which conformation will assemble onto the membrane-skeleton (the heterodimer) and which conformations are targeted for degradation (the homo-oligomers).

When chicken erythroid cells are pulse labelled with ^{35}S-methionine and lysed hypotonically, excess unassembled ankyrin, β-spectrin and α-spectrin remain soluble[29]. We characterized the unassembled polypeptides by chromatographing hypotonically soluble fractions through an Ultrogel Ac22 gel filtration column, and found that unassembled β- and α-spectrin eluted as distinct species (Fig. 1*A*), well ahead of the fractions where globular proteins of their size would be expected to appear. β-Spectrin was only just included in the column, eluting with the purified adult red blood cell $\alpha\beta$-spectrin heterotetramers used as a standard eluate. Most of the α-spectrin migrated behind β-spectrin, at the position of the heterodimeric red blood cell spectrin standard. Ankyrin eluted in a manner that would be predicted for a globular monomeric protein of its size, slightly ahead of haemoglobin and the bulk of the other polypeptides.

Immunoprecipitation of unassembled β-spectrin, α-spectrin and ankyrin across the column after a pulse-labelling period as short as 5 min showed clearly that the three polypeptides eluted as distinct peaks, with most β- and α-spectrin eluting respectively with the $\alpha\beta$-heterotetramer and $\alpha\beta$-heterodimer standards (Fig. 1*E*). The high mobility of the unassembled β-spectrin was not the result of association with organelles because these should have eluted in the void volume and this β-spectrin species was clearly included in the column. Also, pretreatment of the hypotonically soluble fraction with puromycin, to release nascent polypeptides from ribosomes, or inclusion of 0.5% Triton X-100 in the elution buffer, to disrupt membranous organelles, had no effect on the elution pattern of either α- or β-spectrin (data not shown). Furthermore, neither unassembled α- or β-spectrin sedimented after centrifugation at 150,000*g* for 30 min (see Table 1). Thus, β-spectrin seems to be associated in a species of relative molecular mass equivalent to that of a spectrin tetramer and α-spectrin to that of a spectrin dimer.

Further evidence that the unassembled β- and α-spectrin subunits were indeed separate homo-oligomeric species was obtained by analysing fractions off the column by two-dimensional non-denaturing followed by SDS-polyacrylamide gel electrophoresis (PAGE). The two spectrin species clearly did not co-migrate even in fractions where the β- and α-spectrin peaks overlapped; β-spectrin consistently migrated close to the position of adult red blood cell spectrin $\alpha\beta$-heterotetramers and α-spectrin with spectrin $\alpha\beta$-heterodimers (Fig. 2*A*,*B*). Furthermore, no other protein co-migrating with either spectrin homo-oligomeric species was observed (Fig. 2*A*) even after labelling

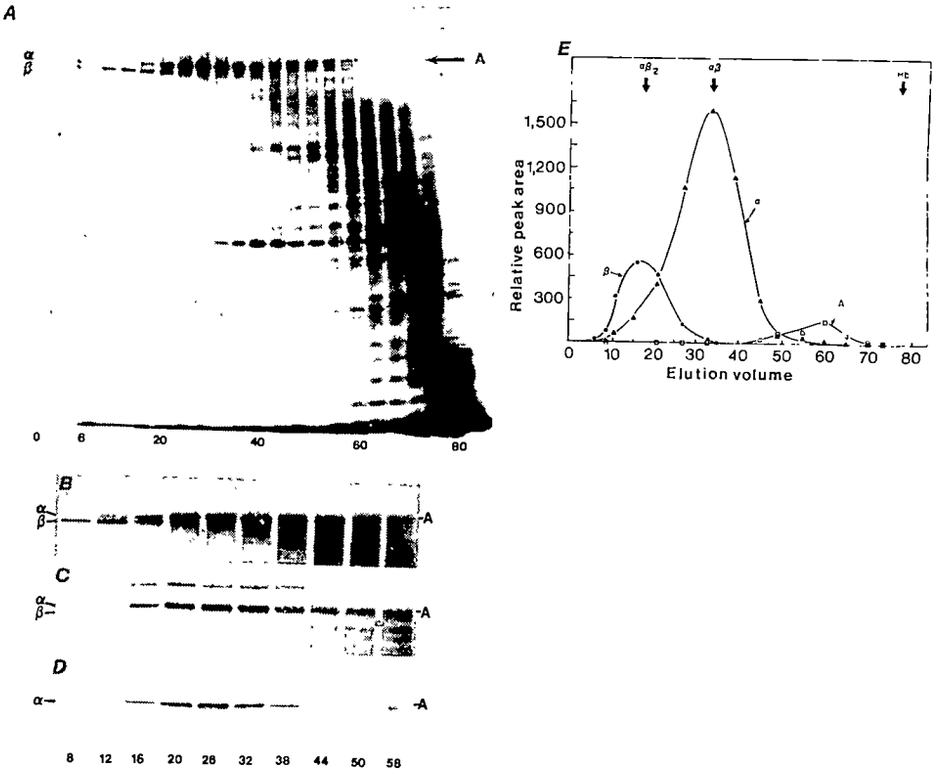


Fig. 1 Gel-filtration elution profiles of the hypotonically soluble fraction of pulse-labelled erythroid cells from 10-day chick embryos. Results shown are for lysates from erythroid cells lysed immediately after 10 min labelling with ^{35}S-methionine (*A*), after 10 min pulse-labelling followed by 30 min chase (*B*), after 1 h chase (*C*), or 4 h chase in the presence of cold methionine (*D*) and quantitation of β-spectrin, α-spectrin and ankyrin in fractions across the column by immunoprecipitation (*E*). *A*–*D* Show autoradiograms after exposure for 48 h. α = α-spectrin; β = β-spectrin; A = ankyrin. The numbers beneath the lanes represent V_e, that is, volumes eluting after the void volume. *E*, Quantitation by immunoprecipitation of β-spectrin (β), α-spectrin (α) and ankyrin (A) across the column shown in *A*. *B* The arrows indicate the peak fractions of the rabbit spectrin $(\alpha\beta)_2$-tetramer and $\alpha\beta$-dimer, respectively, and also the fraction where haemoglobin beings to appear (Hb).

Methods. Samples (0.75 ml) of packed, washed erythroid cells isolated from 10-day chick embryos as described previously[29] were preincubated in methionin e-free minimal essential medium (MEM) supplemented with 5% dialysed fetal calf serum (FCS) labelled for 10 min with 300 μCi ^{35}S-methionine (specific activity 11,000–13,000 Ci mmol^{-1}) and chased for various time intervals in fresh MEM-FCS media containing 2 mM unlabelled methionine all at 38 °C in a humidified atmosphere. Aliquots of cells were collected by centrifugation in ice-cold choline chloride (155 mM), HEPES (5 mM) buffer *p*H 7.2, then lysed in 4 vols ice-cold hypotonic lysis buffer (5 mM Tris-HCl *p*H 7.2, 5 mM $MgCl_2$, 0.1 mM dithiothreitol (DTT), 1 mM EGTA, 1 mM *p*-tosyl-L-arginine methyl ester (TAME) 1 mM phenylmethylsulphonyl fluoride). After centrifugation of the cell lysate at 13,000*g* for 10 min in an Eppendorf centrifuge, the supernatant was recentrifuged for 10 min before being layered on a 2.5 × 50 cm Ac22 Ultrogel gel filtration column (exclusion limit 3×10^6 daltons) and eluted with Tris-buffered saline (125 mM NaCl, 10 mM Tris-HCl *p*H 7.2, 1 mM $MgCl_2$, 1 mM EDTA, 1 mM NaN_3, 0.1 mM DTT; identical elution patterns of the spectrins and ankyrin were obtained whether or not Mg^{2+} or DTT was included) at a flow rate of 15 ml h^{-1}. Beginning at the void volume, the eluate was collected in 2-ml fractions and alternate fractions were assayed by SDS-PAGE using the modified Laemmli gel system described by Hubbard and Lazarides[36]. After processing in 20% diphenyloxazole (PPO) in dimethyl sulphoxide, dried gels were autoradiographed with Kodak XAR film at −80 °C. The levels of β-spectrin, α-spectrin and ankyrin were quantitated by immunoprecipitation using method B of Blikstad *et al.*[23], except that deoxycholate was omitted from the buffer for ankyrin immunoprecipitation, followed by SDS-PAGE. The gels were processed for autoradiography, dried and exposed to pre-flashed Kodak XAR film long enough to give bands of intensity within the linear range of intensity versus amount of ^{35}S. The bands were then scanned with a Quick Scan (Helena Laboratories) and the peaks integrated by computer. Values represent arbitrary relative units. Rabbit spectrin $\alpha\beta$-heterotetramers and heterodimers were isolated from rabbit erythrocyte ghosts by the method of Ungewickell and Gratzer[20]. Their elution profiles through the column were assayed by SDS-PAGE followed by densitometry of the Coomassie-stained gels.

periods of 3–4 h (data not shown). Crosslinking experiments with dithiobis(succinimidyl)propionate provided further evidence that unassembled α-spectrin existed as a homodimer, for it could be efficiently converted to a species of $M_r \simeq 0.5 \times 10^6$, while β-spectrin existed as a homotetramer since an additional product of $M_r \simeq 10^6$ was observed on one-dimensional SDS gels in non-reducing conditions (Fig. 2*C*).

These elution patterns of the unassembled pulse-labelled spectrins and ankyrin persisted until the polypeptides had been turned over (Fig. 1*B–D*), the rates of disappearance of the β-spectrin, α-spectrin and ankyrin peaks matching the individual rates of turnover previously described for these polypeptides ($t_{1/2}$ = 15–20 min, 2 h and 1 h, respectively[29]). Together, our observations indicate that, unlike the assembled polypeptides, unassembled β-spectrin, α-spectrin and ankyrin behave as independent kinetic species and exhibit no obvious association with each other.

Isolated α- and β-spectrin subunits purified from adult red blood cell heterodimeric spectrin after denaturation with urea or SDS reassociate spontaneously into heterodimers upon renaturation[13,14,20,30]. Any α- and β-homo-oligomeric species that might form as the separated subunits are renatured have been considered to be metastable species that will spontaneously convert into heterodimers. The unassembled β-homotetramer and the α-homodimer behaved quite differently in this respect, as there was no evidence of interconversion to an $\alpha\beta$-heterodimer or tetramer even after incubation of an approximately stoichiometric mixture of the β- and α-spectrin peak fractions for 1 h at 37 °C and analysis by sieving chromatography. However, if such a mixture was first denatured with 3 M urea or 0.5% SDS and allowed to renature before chromatography[20], α- and β-spectrin co-eluted. Analysis by two-dimensional-PAGE confirmed that hetero-oligomerization occurred only after the two spectrin homo-oligomers had been previously denatured (data not shown). These results suggest that the homo-oligomeric forms assumed by the newly synthesized α- and β-spectrin subunits represent alternative, but stable, conformations to the normal $(\alpha\beta\text{-heterodimer})_n$ form of assembled spectrin. Similar association experiments showed no evidence of association between the unassembled homotetrameric β-spectrin and unassembled ankyrin (data not shown).

We next tested whether the unassembled forms of spectrin could bind to the erythroid plasma membrane, and whether binding would alter their capacity to interact with each other, by using spectrin- or ankyrin-depleted erythrocyte inside-out membrane vesicles (IOVs), which have been shown to bind chicken spectrin in a similar manner to rabbit spectrin[31]. The β-spectrin homo-tetramer was found to bind selectively to spectrin-depleted IOVs and this binding was inhibited by prior removal of ankyrin or prior trypsinization of the vesicles (Table 1*a*). In contrast, the α-spectrin homodimer did not bind to IOVs, whether added alone or in the presence of stoichiometric amounts of the β-spectrin homotetramer (Table 1*a*). The possibility that filtration through the Ultrogel column had somehow affected the membrane-binding properties of these unassembled spectrin forms was discounted because similar results were obtained with membrane-binding studies on the hypotonically soluble fraction immediately after cell lysis (Table 1*b*). Some binding of the unassembled ankyrin was also detected but this was often accompanied by proteolysis. The inability of the α-spectrin homodimer to bind to spectrin-depleted IOVs, even in the presence of the β-spectrin homotetramer, eliminates the possibility that heterodimerization occurs by nucleation of homo-oligomers by the membrane.

Previous kinetic analysis has indicated that the unassembled pools of the two spectrin subunits represent ~50% of the β-spectrin and 85% of the α-spectrin synthesized after a 10-min pulse-labelling period[24,25]. The rest assembles rapidly with the stoichiometry (1:1) observed at steady state (refs 24, 25 and

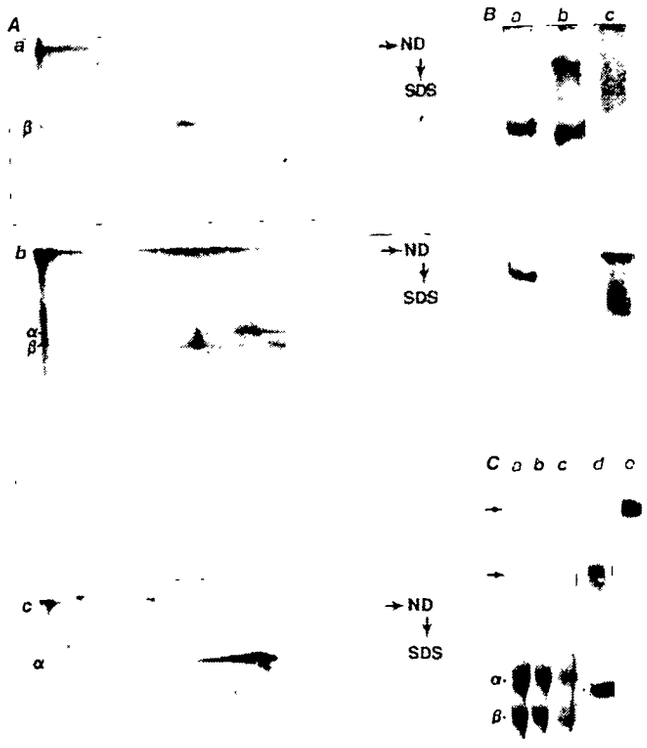


Fig. 2 *A*, *B*, Analysis of the β-spectrin and α-spectrin species from the β-peak fraction (*Aa*, *Bb*), the intermediate fraction (*Ab*) and the α-peak fraction (*Ac*, *Bc*) by non-denaturing PAGE in the first dimension (*B*) followed by SDS-PAGE in the second dimension (*A*), showing that the soluble unassembled α-spectrin and β-spectrin are distinct and separate species. Aliquots identical to those fractions eluting at 8 ml, 18 ml and 28 ml in Fig. 1*A* were analysed by PAGE on a 2.5–5% gradient, polyacrylamide gel under non-denaturing conditions (ND) as described by Morrow and Marchesi[22] in the first dimension, with duplicate lanes being excised and run in a second dimension on 10% SDS-PAGE (*Aa*, *b*, *c*, respectively). Gels were stained with Coomassie blue and then destained before being processed for autoradiography (PPO for the SDS gels, En^{3}HANCE for the non-denaturing gels), dried and exposed to Kodak XAR at −80 °C for 5 days (non-denaturing gels) or 18 days (second-dimension SDS gels). Lane *a* in panel *B* is the Coomassie-stained lane of rabbit spectrin heterotetramers and heterodimers run as standards on the nondenaturing gel. Lane *b* represents the β-spectrin peak fraction (V_e = 8 ml) and lane *c* the α-spectrin fraction (V_e = 28 ml). The smear running diagonally down to the right-hand side from the α-spectrin spot represents α-spectrin breakdwon products and/or nascent chains, since they react with α-spectrin-specific antibodies under stringent conditions but not with β-spectrin antibodies. Some aggregation occasionally occurs in both rabbit spectrin standards and the radioactive chicken spectrin species on electrophoresis in the first (native) dimension and is seen as material at the top of the gel. *C*, The unassembled α-spectrin and β-spectrin species can be crosslinked to a species of $M_r \simeq 0.5 \times 10^6$ and $\sim 1 \times 10^6$, respectively. Rabbit spectrin heterodimer standards (*a–c*) and aliquots from the peak fractions of hypotonically soluble β-spectrin (*d*) and α-spectrin (*e*), partially purified by gel filtration, were incubated in 10^{-3} M dithiobis(succinimidyl)propionate for 0 min (*a*), 10 min (*b*) or 30 min (*c–e*) at 25 °C. The samples were then denatured by addition of 1/5th volume 5% SDS sample buffer in the absence of any reducing agent and boiled for 5 min before loading onto a 3.5–10% polyacrylamide gradient SDS gel. After electrophoresis the gel was stained with Coomassie brilliant blue, destained and processed for autoradiography. Lanes *a–c* represent Coomassie-stained lanes, lanes *d* and *e*, autoradiograms after 48 h exposure. The arrows mark crosslinked products.

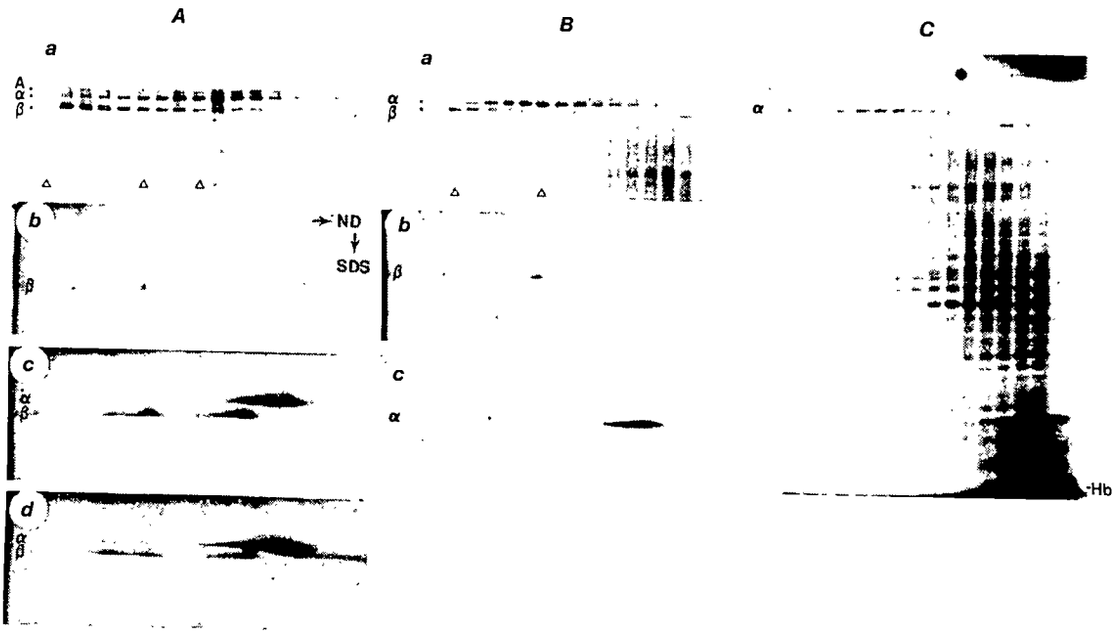


Fig. 3 Products of *in vitro* translation from pre-existing polyribosomes isolated from erythrocytes from 9-day chick embryos. Autoradiograms of the elution profiles of the soluble products of *in vitro* translation carried out in the absence (*Aa*) or presence of 40 μg ml^{-1} of rabbit erythrocyte spectrin-depleted, inside-out vesicle (IOVs; *Ba*) or 330 μg ml^{-1} of rabbit IOVs (*C*). Autoradiograms of the two-dimensional non-denaturing, SDS-PAGE analysis of the fractions, designated by Δ under the elution profiles, are depicted below their corresponding elution profiles in sequence. The smear running diagonally to the right-hand side from the main α-spectrin spot (most prominent in *Ad*) seems to represent nascent α-spectrin chains.

Methods. Erythrocytes from 9-day chick embryos were collected into sterile choline chloride (155 mM), HEPES (5 mM, *p*H 7.2) buffer on ice, concentrated by centrifugation and washed through sterile cotton wool to remove any contaminating white blood cells and platelets with 135 mM NaCl, 5 mM KCl, 10 mM HEPES (*p*H 7.2), 10 mM glucose and recentrifuged. Cells were then lysed in 1.8 vol of sterile distilled H_2O on ice and after 10 min, with periodic gentle mixing, were spun for 10 min at 13,000*g* in an Eppendorf centrifuge. The resultant supernatant was primed for *in vitro* translation as described for rabbit reticulocyte lysates[38] together with 300 μCi ^{35}S-methionine per 475 μl of primed lysate. After incubation at 30 °C for 45 min, rabbit spectrin-depleted IOVs were added at 0 (*A*), 40 (*B*) or 330 (*C*) μg ml^{-1}. After a further 30 min of incubation at 30 °C, the translation mixtures were centrifuged for 30 min at 150,000*g* in a Beckman airfuge with the vesicles pelleted through a 0.6 M sucrose pad. Aliquots (250 μl) of the supernatans were applied to a 1×17 cm Ac22 gel filtration column and fractions of 200 μl collected. Alternative fractions after the void volume were analysed by SDS-PAGE followed by autoradiography as described for Fig. 1.

The fractions designated by Δ were further analysed by two-dimensional non-denaturing followed by SDS-PAGE as described for Fig. 2.

Woods and Lazarides, personal observations). These observations, together with the above results, suggest that the fractions that assemble must exist in an alternative form to the homo-oligomeric conformations that accumulate in the unassembled pools. To approach this issue, we uncoupled synthesis from assembly onto the membrane and analysed any intermediates formed during assembly by a series of *in vitro* polysomal run-off experiments using hypotonic lysates made from erythroid cells isolated from 9–10-day chick embryos[31]. The Ac22 Ultrogel elution profile of the proteins synthesized *in vitro* was similar to that obtained with the *in vivo* labelled soluble proteins (Fig. 3*A*). In this case, however, there was a greater overlap of the β-spectrin with the α-spectrin peak, while a small subset of both proteins also eluted as monomers. Analysis of different fractions across the column by two-dimensional PAGE revealed that whereas there was no evidence for spectrin heterodimers in the soluble pool after *in vivo* labelling, close to 50% of the β-spectrin synthesized *in vitro* existed in the form of heterodimers with α-spectrin; the remainder of β-spectrin existed predominantly as homotetramers (Fig. 3*A*). Similarly, a fraction of the α-spectrin synthesized *in vitro* existed as heterodimers with β-spectrin, with the remainder existing mainly as homodimers (Fig. 3*A*). The proportion of β-spectrin in the form of heterodimers was remarkably close to that of newly synthesized β-spectrin which assembles on the membrane skeleton *in vivo*[25].

The heterodimeric spectrin produced *in vitro* bound to rabbit erythrocyte spectrin-depleted IOVs but not to right-side-out vesicles, ankyrin-depleted or acetic acid-stripped IOVs, similarly to the homotetrameric β-spectrin (Table 1*c*). Binding studies at different IOV concentrations revealed preferential binding of the heterodimeric over the β-homotetrameric species at sub-saturating concentrations of IOVs. At a concentration of IOVs equivalent to 330 μg membrane protein per ml, both β-spectrin-containing forms bound effectively to the IOVs (Fig. 3*C*, Table 1*c*). With 40 μg membrane protein per ml, all of the heterodimeric spectrin bound to the membrane whereas most of the β-homotetramer remained in the soluble fraction (Fig. 3*B*, Table 1*c*). Such experiments suggest that these heterodimers constitute the fraction that rapidly assembles on the membrane *in vivo*, and that their assembly occurs too rapidly for detection after *in vivo* labelling of erythroid cells from 10-day-old chick embryos.

In conclusion, the data presented here indicate that newly synthesized α- and β-spectrin monomers rapidly assume one of two configurations, an αβ-heterodimer or a homo-oligomer (β_4 or α_2). Interestingly, only newly synthesized spectrin polypeptides can assume a stable homo-oligomeric conformation, suggesting that the folding of the nascent polypeptide may begin from the NH_2- towards the COOH-terminus in parallel with synthesis. The diffusion–collision theory of protein-folding dynamics predicts that native secondary structure is achieved within each microdomain of a polypeptide by random events and is stabilized by subsequent interactions between micro-domains[32,33]. Human α- and β-spectrin polypeptides are known to consist of multiple homologous non-identical repeating triple helical segments, each 106 amino acids long[4,7]. as has also been observed in chicken α-spectrin[34,35]. If this model is correct, these

Table 1 Membrane-binding ability of unassembled β- and α-spectrin

a, Partially purified by gel filtration

Membranes added	% Pelleted β-Spectrin	α-Spectrin	Mixture of α+β-spectrin α	β
0	5	5	5	6
ROVs	14	11	19	11
IOVs	97	10	18	92
Acetic-acid stripped IOVs	16	22	21	15
Trypsinized IOVs	8	12	10	3

b, Total lysate

Membranes	β-Spectrin	α-Spectrin
0	9	9
ROVs	11	8
IOVs	97	19
Acetic-acid stripped IOVs	12	11

c, Products of *in vitro* translation

Addition of IOVs (μg ml^{-1} membrane protein)		
330	97	46
124	93	42
40	52	41
4	31	27
0	14	16

Aliquots of the peak fractions of pulse-labelled β-spectrin and α-spectrin, partially purified by gel-filtration chromatography as described in Fig. 1*A* legend. (*a*), total soluble hypotonic lysate, prepared immediately after a 10-min pulse of erythroid cells from 11-day chick embryos (*b*) or the products of *in vitro* translation as described for Fig. 4 (*c*) were incubated either alone or in the presence of rabbit erythrocyte ROVs, spectrin-depleted IOVs, acetic-acid-stripped, ankyrin-depleted IOVs or trypsinized IOVs prepared by the protocol described by Bennett and Branton[37]. Equal aliquots of ghost erythrocyte membranes were used for the preparation of each of these types of vesicles and the resultant vesicles suspended in identical volumes. The volumes added to the soluble spectrin fraction gave concentrations of IOV membrane protein equivalents of 330 μg ml^{-1}. After a 20-min incubation at 38 °C, the vesicles were pelleted through a 0.6 M sucrose cushion in Tris-HCl (5 mM, *p*H 7.2) for 20 min at 150,000*g* in a Beckman airfuge. The relative amounts of α- and β-spectrin in the supernatants and pellets were analysed by SDS–PAGE followed by autoradiography and densitometry of the resultant autoradiograms. The values represent the mean values from three separate experiments; variability was less than 7%.

helices will presumably begin to form as each 106-amino-acid segment is synthesized. The fact that the two spectrin molecules are so long (~4,000 amino acids each) probably increases the chances of coiled-coil interactions occurring between adjacent nascent chains before synthesis is complete. Therefore, the formation of stable spectrin homo-oligomeric species *in vivo* may result from the greater chance of coiled-coil interactions occurring between like rather than unlike spectrin subunits, even though the αβ form may be thermodynamically favoured.

It has been proposed (ref. 25) that spectrin and ankyrin assembly occurs through a cascade of limiting steps, where the extent of α-spectrin assembled is limited by the amount of β-spectrin assembled, which in turn is limited by the amount of ankyrin bound. The data presented here suggest instead that the limiting factor is the extent of heterodimerization. Furthermore, homo-oligomerization prevents the unassembled spectrins from reacting with each other or with ankyrin and in the case of α-spectrin also from binding to the plasma membrane. Although β-homotetramers can bind to spectrin-depleted plasma-membrane vesicles, presumably to ankyrin, they appear to bind with lower affinity than heterodimers. The difference in membrane affinity, coupled with the fact that unassembled β-spectrin (β_4-spectrin) is degraded extremely rapidly and selectively[29], makes it feasible that if any β-homotetramers do bind to the membrane *in vivo*, they are displaced by αβ-heterodimers and then degraded rapidly, thereby ensuring the correct stoichiometry of assembled spectrin.

Finally, it is interesting to note that the β-homotetramer appears to bind to preassembled ankyrin, yet no association can be detected with the unassembled ankyrin that accumulates transiently in the soluble pool. This paradox suggests that this unassembled ankyrin must also exist in some modified form unable to interact with β-spectrin.

We thank Drs Horst Hinssen, John Cox and John Ngai for their valuable comments on the manuscript. This work was supported by grants from the NIH, NSF and the Muscular Dystrophy Association. C.M.W. was also supported by a grant from the Camille and Henry Dreyfus Foundation.

Received 20 September 1985; accepted 4 February 1986.

1. Branton, D., Cohen, C. M. & Tyler, J. *Cell* **24**, 24–32 (1981).
2. Sheetz, M. P. *Semin. Hemat.* **20**, 175–188 (1983).
3. Yu, J., Fischman, D. A. & Steck, T. *J. supramolec. Struct.* **1**, 233–248 (1973).
4. Speicher, D. & Marchesi, V. T. *Nature* **311**, 177–180 (1984).
5. Shotton, D., Burke, B. & Branton, D. *Biochim. biophys. Acta* **536**, 303–329 (1978).
6. Cohen, C. M. *Semin Hemat.* **20**, 141–158 (1983).
7. Marchesi, V. T. *A. Rev. Cell Biol.* (in the press).
8. Ungewickell, E., Bennett, P., Calvert, R., Ohanian, V. & Gratzer, W. B. *Nature* **280**, 811–814 (1979).
9. Fowler, V. & Taylor, D. L. *J. Cell Biol.* **85**, 361–376 (1980).
10. Pinder, J. C. & Gratzer, W. B. *J. Cell Biol.* **96**, 768–775 (1983).
11. Bennett, V. & Stenbuck, P. J. *J. biol. Chem.* **254**, 2533–2541 (1979).
12. Luna, E. J., Kidd, G. H. & Branton, D. *J. biol. Chem.* **254**, 2526–2532 (1979).
13. Calvert, R., Bennett, P. & Gratzer, W. B. *Eur. J. Biochem.* **107**, 355–361 (1980).
14. Litman, D., Hsu, C. J. & Marchesi, V. T. *J. Cell Sci.* **42**, 1–22 (1980).
15. Bennett, V. & Stenbuck, P. *Nature* **280**, 468–473 (1979).
16. Bennett, V. & Stenbuck, P. *J. biol. Chem.* **255**, 6424–6432 (1980).
17. Hargreaves, W. R., Giedd, K. N., Verkleij, A. & Branton, D. *J. biol. Chem* **255**, 11965–11972 (1980).
18. Anderson, R. A. & Lovrien, R. E. *Nature* **307**, 655–658 (1984).
19. Pasternak, G. R., Anderson, R.A., Leto, T. L. & Marchesi, V. T. *J. biol. Chem* **260**, 3676–3683 (1985).
20. Yoshino, H. & Marchesi, V. T. *J. biol. Chem.* **259**, 4496–4500 (1984).
21. Ungewickell, E. & Gratzer, W. B. *Eur. J. Biochem.* **88**, 379–385 (1978).
22. Morrow, J. S. & Marchesi, V. T. *J. Cell Biol.* **88**, 463–468 (1981).
23. Liu, S.-C., Windisch, P., Kim, S. & Palek, J. *Cell* **37**, 587–594 (1984).
24. Blikstad, I., Nelson, W. J., Moon, R. T. & Lazarides, E. *Cell* **32**, 1081–1091 (1983).
25. Moon, R. T. & Lazarides, E. *J. Cell Biol.* **98**, 1899–1904 (1984).
26. Cox, J. V., Moon, R. T. & Lazarides, E. *J. Cell Biol.* **100**, 1548–1557 (1985).
27. Granger, B. L. & Lazarides, E. *Nature* **313**, 238–241 (1984).
28. Weise, M. J. & Chan, L.-N. L. *J. biol. Chem.* **253**, 1892–1897 (1978).
29. Woods, C. M. & Lazarides, E. *Cell* **40**, 959–969 (1985).
30. Davies, J. & Bennett, V. *J. biol. Chem.* **258**, 7757–7766 (1983).
31. Moon, R. T. & Lazarides, E. *Nature* **305**, 62–64 (1983).
32. Karplus, M. & Weaver, D. L. *Nature* **260**, 404–406 (1976).
33. Harrison, S. C. & Durbin, R. *Proc. natn. Acad. Sci. U.S.A.* **82**, 4028–4030 (1985).
34. Wasenius, V.-H., Saraste, M., Knowles, J., Virtanen, I. & Lehto, V.-P. *EMBO J.* **4**, 1425–1430 (1985).
35. Birkenmeier, C. S. *et al. Proc. natn. Acad. Sci. U.S.A.* **82**, 5671–5675 (1985).
36. Hubbard, B. & Lazarides E. *J. Cell Biol.* **80**, 166–182 (1979).
37. Bennett, V. & Branton, D. *J. biol. Chem.* **252**, 2753–2763 (1977).
38. Jackson, R. T. & Hunt, T. *Meth. Enzym.* **96**, 50–73 (1983).

Template-free RNA synthesis by Qβ replicase

Christof K. Biebricher, Manfred Eigen & Rüdiger Luce

Max-Planck-Institut für Biophysikalische Chemie, D-3400 Göttingen, FRG

In the absence of extraneously added template, standard preparations of Qβ replicase spontaneously synthesize RNA *in vitro*, possibly as a result of RNA contamination[1]. Using special enzyme purifications, Sumper and Luce[2] presented evidence that self-replicating RNA not present *ab initio* can grow out of 'template-free' incorporation mixtures. In contrast to DNA polymerase I and RNA polymerase, which also show *de novo* synthesis[3–5], the products synthesized 'de novo' by Qβ replicase are RNA species containing nonrepetitive sequences of defined lengths which differ between experiments, even when synthesized under identical condi-

tions, in fingerprints, chain lengths and kinetic parameters[6]. Kinetic analysis of the *de novo* processes[7] distinguished it from template-instructed synthesis and excluded an assumption of self-replicating RNA contamination. These conclusions were questioned recently by Hill and Blumenthal[8], who claimed to show that highly purified Qβ replicase preparations cannot produce RNA *de novo*. We now present evidence that, under the conditions required for *de novo* synthesis, Qβ replicase prepared according to their method is also capable of *de novo* synthesis. Furthermore, we show that Qβ replicase condenses nucleoside triphosphates to more or less random oligonucleotides.

Hill and Blumenthal[8] presented kinetic profiles of RNA synthesis for standard Qβ replicase preparations, for which RNA synthesis was detectable after about 30 min, and for specially purified R(−S1) Qβ replicase, for which no RNA synthesis was detected over a 4 h; addition of heat-treated standard enzyme preparations restored nucleotide incorporation in a way they claimed to be "kinetically indistinguishable from *de novo* synthesis". None of their data show the characteristics of what we called *de novo* synthesis. Instead, their Figs 1 and 3 identify the underlying process as template-instructed, with much shorter lag times than necessary for amplification of a single strand of self-replicating RNA to macroscopic appearance (see Table IV of ref. 7). Their finding that "the length of the lag period" was "inversely proportional to the concentration of nucleoside triphosphates" is also typical of template-instructed reactions, quite in contrast to the process we called *de novo* synthesis, which depends on the 2.8 th power of nucleotide and 2.5 th power of enzyme concentrations. (Both exponents represent lower bounds.) Hence, their incorporation products indeed did not result from *de novo* synthesis but rather from template-instructed amplification of RNA impurities present in their standard enzyme preparations.

Using enzyme purified by a different method, they detected no incorporation up to 4 h without added template. At R(−S1) enzyme concentrations as low as used in their experiments (68 nM), we also observed no *de novo* synthesis[7] over this time. Other groups have performed experiments with Qβ replicase[9–11] without reporting interference by *de novo* synthesis, and examination of the conditions used by these groups shows in each case that no *de novo* synthesis would be expected.

Unfortunately, Hill and Blumenthal were unable to cooperate in an effort to determine whether their purification procedure yields an enzyme unable to synthesize RNA *de novo* (T. Blumenthal, personal communication). We therefore repeated their experiments independently as well as was possible using the sparse data given in their report. Our results are:

(1) Enzyme prepared according to Blumenthal's standard procedure[12], despite being electrophoretically ~90% pure, contained RNA at optically detectable levels, part of which was self-replicating as macroscopic RNA synthesis started after short lag times. The products were defined RNA species reproducibly selected under identical conditions. However, even minor changes in conditions often resulted in different electrophoretic patterns of the products.

(2) Although phosphocellulose–urea purification step introduced by Hill and Blumenthal indeed removed the RNA, the acidic enzyme subunits S1, and later elongation factors (EFs) Tu and Ts, eluted slowly from the column under their conditions. Depending on the wash volume and time of the urea step, only 10–50% of the input viral β-subunit was recovered. Resulting preparations still contained 10% S1, but excess EF Tu and Ts.

(3) Excess EF Tu.Ts and residual holoenzyme could be removed in the next step if the described stepwise elution was replaced by gradient elution[2,13]. SDS-gel electrophoresis combined with silver staining revealed no impurities in the resulting preparation or in our standard preparations (see Fig. 3 in ref. 14). However, the low synthesis rate found by Hill and Blumenthal (1.6×10^{-3} s^{-1} compared with our $3.3–6.5\times10^{-3}$ s^{-1}) led us to suspect that the concentration of active enzyme in their preparation was overestimated.

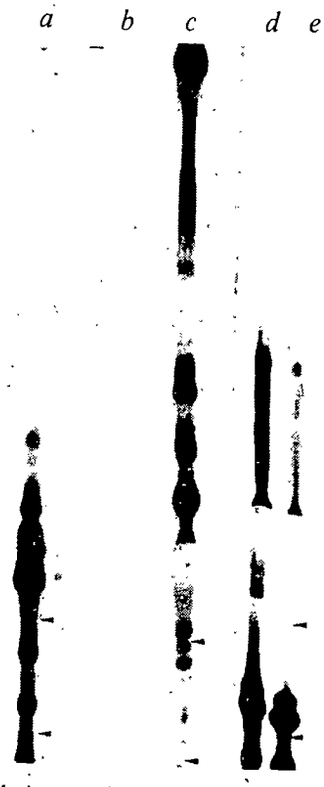


Fig. 1 Electropherograms showing condensation of triphosphates to oligonucleotides by Qβ replicase. The incorporation mixtures contained in Qβ buffer (0.05 M Tris-HCl buffer *p*H 7.5, 0.2 mM dithiothreitol, 10 mM $MgCl_2$, 20% glycerol) were: lane *a*, 500 μM[α-^{32}P]ATP, 200 μM GTP, 50 μM PP_i, 500 nM replicase; lanes *b*, *c*, 200 μM GTP, 50 μM ATP, 1.5 μM[α-^{32}P]CTP, 20 μM PP_i, 200 nM replicase; lane *d*, 800 μM ATP, 800 μM GTP, 20 μM PP_i, 600 nM replicase; lane *e*, 800 μM ITP, 800 μM GTP, 20 μM PP_i, 600 nM replicase.
Methods. Incubations were for 5 min (*b*), 68 h (*a*, *c*) or 16 h (*d*, *e*) at 30 °C. The oligonucleotides from incubations *d* and *e* were treated with phosphatase, isolated on QAE-Sephadex-A25 and labelled with polynucleotide kinase and [γ-^{32}P]ATP before loading onto the gel. The incubation mixtures were analysed on sequencing gels (12% acrylamide). The arrows give the positions of the dyes bromophenol blue (mobility of the undecamer) and dinitrophenol (mobility of the pentamer). Electrophoresis was from top to bottom. The material eluted from the gels was degradable by alkali or snake venom phosphodiesterase.

(4) Using conditions appropriate for observing *de novo* synthesis, we found that replicase purified by their method has about the same ability to synthesize RNA *de novo* as was observed with our preparations. The essential point is to choose sufficiently high enzyme (and nucleoside triphophate) concentrations to utilize the strong concentration dependence of lag times (see Fig. 4 of ref. 7). Concentration of the enzyme on QAE-Sephadex (step VIII of ref. 2) was therefore required for the *de novo* experiments. In accordance with earlier reports[6], the products were different even when synthesized under identical conditions.

(5) Enzyme preparations isolated by the standard purification method[2] from uninfected *Escherichia coli* containing a plasmid carrying the structural gene of the viral replicase showed the same enzyme concentration threshold for *de novo* synthesis and the same product characteristics as found with preparations from Qβ-infected bacteria.

We conclude that the experiments of Hill and Blumenthal do not support their interpretation. Our original kinetic analysis was, as reported[7], an adequate method to disprove a template-instructed process resulting from RNA impurities. Although the molecular mechanism behind this process is unknown, a

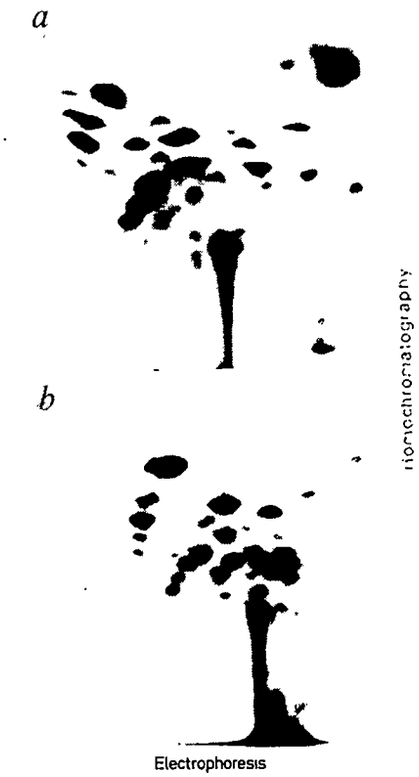


Fig. 2 Fingerprinting of the oligonucleotides. Incorporation mixture (100 μl): 200 μM GTP, 200 μM ATP, 200 μM UTP, 10 mM $MgCl_2$, 1 mM $MnCl_2$, 400 nM holoreplicase in Qβ-buffer. *a*, No addition; *b*, 400 nM yeast 5.8 S RNA.
Methods. The mixture was incubated for 21 h at 30 °C. The enzyme was denatured for 1 min at 100 °C and removed by centrifugation. The soluton was diluted with 500 μl 0.02 M Tris base and treated with 8 U alkaline phophatase (calf intestine, Boehringer, Mannheim) for 1 h at 37 °C. The products were isolated by loading the mixtures on 1-ml columns of QAE-Sephadex-A25 Cl^--form. The column was washed with 0.05 M Tris buffer (*p*H 7.5) and the oligonucleotides eluted with 0.5 M NaCl, desalted on BioGel P2, lyophylised twice and dissolved in 20 μl H_2O. The yields were 0.08 A_{260} (80 μM nucleotide incorporated) in the absence of RNA and 0.21 A_{260} (210 μM nucleotide, 35% incorporated) in the presence of yeast 5.8 S RNA. 500 pmol oligonucleotides were labelled at the 5′ ends with [γ-^{32}P]ATP and polynucleotide kinase (1 h, 37 °C), isolated on BioGel P2 and fingerprinted according to ref. 18. Analysis of the 5′ end of the oligonucleotides: The incorporations were with 5.8 S RNA as described above. Yield of 5′ ends, 43 μM: the 5′-labelled oligonucleotide material was degraded with 10% piperidine and the products separated on polyethyleneimine-impregnated thin layer plates. *pGp was found to be the only labelled product and its radioactivity was measured. Incorporation of [γ-^{32}P]GTP, 48 μM: incubation as in *a* except that [γ-^{32}P]GTP was used. The material was separated on Biogel, degraded with piperidine followed by treatment with snake venom phosphodiesterase to destroy GTP. The degradation products were separated by electrophoresis on DEAE paper in 7% formic acid. The *pppGp spot was cut out and the yield measured by counting the radioactivity. Yield of pppGpA-ends, 29 μM: analysis was as for [γ-^{32}P]GTP, except that [α-^{32}P]ATP was used and the pppGp* spot was counted. The degradation products also included Gp*, Ap*, *pA and Up*. The quantitation method was checked by measuring template-instructed incorporation of [γ-^{32}P]GTP into MNV-11, isolating the products and analysing them as for [γ-^{32}P]GTP.

hypothesis agreeing with the experimental data has been presented[4,6,7], and consists of two phases. In the first, polymerase slowly catalyses random synthesis of oligonucleotides, and in the second, once a suitable template is formed by chance, rapid evolution and autocatalytic amplification to macroscopic appearance occur. It is not surprising that the *de novo* products of DNA polymerase I and RNA polymerase are so different from those of Qβ replicase. The slipping homo- or co-polymer products of DNA polymerase I are indeed the only templates it can amplify autocatalytically, whereas they cannot be amplified autocatalytically by Qβ replicase, because RNA with high internal stabilization of its single-stranded structure is required to escape double-strand formation with replica[15]. It is doubtful whether the first phase can be realized at all with DNA polymerase I, which is unable to initiate a new chain, as the lag times suggest autocatalytic amplification of preexisting impurities[3,16]. The latter possibility, however, is excluded by the kinetic analysis for Qβ replicase[7], whose two nucleotide binding sites would provide, in principle, for slow condensation of nucleotide triphosphates to oligonucleotides.

Under normal conditions, template-instructed nucleotide incorporation proceeds much too rapidly for observable accumulation of the initial *de novo* synthesis products[6]. We blocked RNA amplification by omitting one triphosphate, and were successful when one or both of the pyrimidine nucleotides were omitted; however, ATP and GTP were both required for nucleotide condensation to oligonucleotides. Pyrimidines, if present, were also incorporated. The rate of phosphodiester formation under these conditions was four or five orders of magnitude below that of the template-instructed process. The chain lengths of the oligonucleotides that accumulated to larger concentrations ranged from 5 to 20 (Fig. 1); the fingerprints suggest that there is little sequence preference (Fig. 2), although the 5′ end was always pppGpR- (Fig. 2 legend). Elongation of preexisting oligonucleotides by Qβ replicase therefore did not occur under these conditions. The presence of 5.8S yeast RNA, but not transfer RNA, doubled the incorporation rate. The screening of oligonucleotides synthesized with 5.8 S RNA present showed no biases (Fig. 2), as would be expected if there was any instruction by the RNA.

For RNA synthesis in the absence of extraneously added template, we find: (1) The self-replicating RNA species produced in each template-free experiment differ from each other in sequence and chain length even in experiments performed under identical conditions. (2) Kinetic analysis of the *de novo* synthesis process[7] reveals fundamental differences from the well-understood kinetics of template-instructed replication[17]. (3) When replication is inhibited by omitting one triphosphate, many different oligonucleotides accumulate. (4) Highly purified preparations of Qβ replicase isolated from uninfected *E. coli* cells containing plasmids carrying the structural gene of the viral replicase show the same *de novo* synthesis characteristics as those isolated from infected bacteria.

No alternative has been presented to our original interpretation of these results, that Qβ replicase, in the absence of self-replicating RNA templates, is able to synthesize them in a non-instructed way by trial and selection.

We thank Dr M. A. Billeter for supplying us with the bacterial strain carrying a plasmid with the replicase gene of Qβ, and Dr W. C. Gardiner for critical reading of the manuscript.

Received 20 February; accepted 5 March 1986

1. Weissmann, C., Billeter, M. A., Goodman, H. M., Hindley, J. & Weber, H. *Ann. Rev. Biochem.* **42**, 303-328 (1973).
2. Sumper, M. & Luce, R. *Proc. natn. Acad. Sci. U.S.A.* **72**, 162-166 (1975).
3. Radding, C. R. & Kornberg, A. *J. biol. Chem.* **237**, 2877-2882 (1962).
4. Kornberg, A., Bertsch, L. L., Jackson, J. F. & Khorana, H. G. *Proc. natn. Acad. Sci. U.S.A.* **51**, 315-323 (1964).
5. Krakow, J. S. & Karstadt, M. *Proc. natn. Acad. Sci. U.S.A.* **58**, 2094-2101 (1967).
6. Biebricher, C. K., Eigen, M. & Luce, R. *J. molec. Biol.* **148**, 369-390 (1981).
7. Biebricher, C. K., Eigen, M. & Luce, R. *J. molec. Biol.* **148**, 391-410 (1981).
8. Hill, D. & Blumenthal, T. *Nature* **301**, 350-352 (1983).
9. Palmenberg, A. & Kaesberg, P. *Proc. natn. Acad. Sci. U.S.A.* **71**, 1371-1375 (1974).
10. Kramer, F. R., Mills, D. R., Cole, P. E., Nishihara, T. & Spiegelman, S. *J. molec. Biol.* **89**, 719-736 (1974).
11. Mills, D. R., Peterson, R. L. & Spiegelman, S. *Proc. natn. Acad. Sci. U.S.A.* **58**, 217-224 (1967).
12. Blumenthal, T. *Meth. Enzym.* **60**, 628-638 (1979).
13. Cole, P. E., Sawchyn, I. & Guerrier-Takada, C. *J. biol. Chem.* **257**, 12929-12934 (1982).
14. Biebricher, C. K. *Evol. Biol.* **16**, 1-52 (1983).
15. Biebricher, C. K., Eigen, M. & Gardiner, W. C. *Biochemistry* **23**, 3186-3194 (1984).
16. Kornberg, A. *DNA Replication* (Freeman, San Francisco 1980).
17. Biebricher, C. K., Eigen, M. & Gardiner, W. C. *Biochemistry* **22**, 2544-2559 (1983).
18. Volckaert, G., Min Jou, W. & Fiers, W. *Analyt. Biochem.* **72**, 433-446 (1976).

Applied Biological Sciences

Use of Small Fish Species in Carcinogenicity Testing. Monograph 65. KAREN L. HOOVER (ed.). *U.S. Department of Health and Human Services:1984. Pp.409. Np.*

Veterinary Immunology. By P.M. OUTTERIDGE. *Academic:1985. Pp.280. ISBN 0-12-531130-3. $45, £36.*

Veterinary Microbiology: Molecular and Clinical Perspectives. R. PANDEY (ed.). *Karger:1985. Pp.222. Hbk ISBN 3-8055-4067-1. SwFr.148, DM177, £46.30, $63.*

Sociology

Circulation in Population Movement: Substance and Concepts from the Melanesian Case. By MURRAY CHAPMAN and R. MANSELL PROTHERO. *Routledge & Kegan Paul:1985. Pp.483. ISBN 0-7102-045105. £30.*

Home Environments: Human Behaviour and Environment. IRWIN ALTMAN and CAROL M. WERNER (eds). *Plenum:1985. Pp.339. ISBN 0-306-41976-9. £39.50.*

Reproductive Change in Developing Countries: Insights from the World Fertility Survey. JOHN CLELAND and JOHN HOBCRAFT (eds). *Oxford University Press:1985. Pp.301. ISBN 0-19-828465-9. £15.*

Archaeology

The Cambridge Field Guide to Prehistoric Life. By DAVID LAMBERT. *Cambridge University Press:1985. Pp.256. ISBN 0-521-26685-8. Hbk £17.50; pbk £6.95.*

Contributions to the Archaeology and Ethnohistory of Greater Mesoamerica. WILLIAM J. FOLAN (ed.). *Southern Illinois University Press:1985. Pp.334. ISBN 0-8093-1123-2. $28.95.*

General

The Cape Cod National Seashore: A Landmark Alliance. By CHARLES H.W. FOSTER. *University Press of New England:1985. Pp.125. Pbk ISBN 0-87451-346-4. Pbk £8.60, $10.75.*

Do You Think . . . By HAROLD VAN COLLE. *Harold van Colle, 9 Mayfields Close, Wembley Park, Middlesex HA9 9PP, UK:1985. Pp.54. Pbk £3.*

European Brewery Convention. Proceedings of the 20th Congress, Helsinki 1985. *IRL Press:1985. Pp.784. Hbk ISBN 0-947946-42-X. £50, $90.*

Forest Products: Advanced Technologies and Economic Analyses. By DAVID A. TILLMAN. *Academic:1985. Pp.283. ISBN 0-12-691270-X. $36, £36.*

The Geography of Peace and War. DAVID PEPPER and ALAN JENKINS (eds). *Basil Blackwell:1985. Pp.222. ISBN 0-631-13559-6. Hbk £24.50; pbk £7.95.*

Handbook of Discourse Analysis, Vol.2: Dimensions of Discourse. TEUN A. VAN DIJK (ed.). *Academic:1985. Pp.279. ISBN 0-12-712002-5. $53.50, £45.50.*

Histoire de ma Jeunesse. By FRANCOIS ARAGO. *Christian Bourgois Editeur:1985. Pp.189. Pbk ISBN 2-267-00426-7. Np.*

A History of British Atomic Tests in Australia. By J.L. SYMONDS. *Australian Government Publishing Service:1985. Pp.593. ISBN 0-644-04118-8. Np.*

ICSU Short Reports, Vol. 3: Third European Bioenergetics Conference. GÜNTER SCHÄFER (ed.). *Cambridge University Press:1985. Pp.745. ISBN 0-521-30813-5. £50.*

The Ins and Outs of Peg Solitaire. By JOHN D. BEASLEY. *Oxford University Press: 1985. Pp.275. ISBN 0-19-853203-2. £12.50.*

The International Primate Trade, Vol. 1. DAVID MACK and RUSSELL A. MITTERMEIER (eds). *World Wildlife Fund: 1985. Pp.185. Pbk $20.*

Islands of History. By MARSHALL SAHLINS. *University of Chicago Press:1985. Pp.180. ISBN 0-226-73357-2. £21.50.*

Just Health Care. By NORMAN DANIELS. *Cambridge University Press:1985. Pp.245. ISBN 0-521-23608-8. Np.*

Language Learnability and Language Development. By STEVEN PINKER. *Harvard University Press:1985. Pp.435. ISBN 0-674-51054-2. $29.50, £26.95.*

Learn to Paint Wildlife. By MARTIN KNOWELDEN. *Collins: 1985. Pp.64. Pbk ISBN 0-00-411970-3. Pbk £4.95.*

Living with the Bomb. Can We Live Without Enemies? By DOROTHY ROWE. *Routledge & Kegan Paul: 1985. Pp.243. Pbk ISBN 0-7102-0477-9. £4.95.*

Machine Independent Organic Software Tools (MINT), 2nd Edn. By M.D. GODFREY. *Academic:1985. Pp.375. ISBN 0-12-286983-4. $30, £25.*

MCDM: Past Decade and Future Trends: A Source Book of Multiple Criteria Decision Making. MILAN ZELENY (ed.). *JAI Press: 1985. Pp.337. ISBN 0-89232-439-2. $57.50.*

Medical Rehabilitation. LAURO S. HALSTEAD and MARTIN GRABOIS (eds). *Raven Press:1985. Pp.354. ISBN 0-88167-085-5. $65.*

Methodes de Datation par les Phenomenes Nucleaires Naturels, Applications. ETIENNE ROTH, BERNARD POTY and MARIE THÉRÈSE MENAGER. *Masson:1985. Pp.631. Hbk ISBN 2-225-80674-8. Np.*

Metropolitan Desegregation. ROBERT L. GREEN (ed.). *Plenum:1985. Pp.234. ISBN 0-306-41964-5. Np.*

Money into Light: The Emerald Forest, A Diary. By JOHN BOORMAN. *Faber:1985. Pp.229. Pbk ISBN 0-571-13772-5. Pbk £4.95.*

Nemesis: The Death-Star and Other Theories of Mass Extinction. By DONALD GOLDSMITH. *Walker:1985. Pp.166. ISBN 0-8027-0872-2. $15.95.*

New Methods and Techniques for Publishers and Learned Societies. M. FEENEY (ed.). *Primary Communications Research Centre, University of Leicester: 1985. Pp.288. Pbk ISBN 0-906-083-29-X. Np.*

The Nuclear Confrontation in Europe. JEFFREY D. BOUTWELL, PAUL DOTY and GREGORY F. TREVERTON (eds). *Croom Helm:1985. Pp.247. ISBN 0-7099-2481-X. £22.50.*

On the Frontiers of Science: Strange Machines You Can Build. By G. HARRY STINE. *Atheneum: 1985. Pp.111. Pbk ISBN 0-689-11562-8. Pbk $8.95.*

Operating Systems: Structures and Mechanisms. By PHILIPPE A. JANSON. *Academic:1985. Pp.267. ISBN 0-12-380230-X. $29.50, £19.50.*

Passing Farms: Enduring Values. California's Santa Clara Valley. By YVONNE JACOBSON. *William Kaufmann:1984. Pp.240. ISBN 0-86576-045-4. $39.50.*

Pharmacological and Chemical Synonyms, 8th edn. Compiled by E.E.J. MARLER. *Elsevier: 1985. Pp.545. Hbk ISBN 0-444-90359-3. Dfl.245, $94.25.*

Philosophy Through the Looking Glass: Language, Nonsense, Desire. By JEAN JACQUES LECERCLE. *Hutchinson:1985. Pp.206. Pbk ISBN 0-09-161371-X. £5.95.*

The Politics of Nuclear Defense: A Comprehensive Introduction. By GREVILLE RUMBLE. *Polity Press, Cambridge, UK:1985. Pp.285. Hbk ISBN 0-7456-0194-4; pbk ISBN 0-7456-0195-2. Hbk £19.50; pbk £6.95.*

The Pond. By GERALD THOMPSON, JENNIFER COLDREY and GEORGE BERNARD. *Collins:1985. Pp.256. Pbk ISBN 0-00-219287-X. Pbk £9.95.*

Principles of Phase Conjugation. By B.Y. ZEL'DOVICH, N.R. PILIPETSKY and V.V. SHKUNOV. *Springer-Verlag:1985. Pp.250. ISBN 3-540-13458-1/0-387-13458-1. DM 140.*

Quality Control in the Food Industry, Vol. 1, 2nd Edn. S.M. HERSCHDOERFER (ed.). *Academic: 1985. Pp. 469. ISBN 0-12-343001-1. $45, £45.*

Random Graphs. By BELLA BOLLOBAS. *Academic:1985. Pp.447. Hbk ISBN 0-12-111755-3. £52, $58.50.*

Reflexivity: The Post Modern Predicament. By HILARY LAWSON. *Hutchinson:1985. Pp.132. Pbk ISBN 0-09-160-861-9. £5.50.*

Risk Analysis in the Private Sector. CHRIS WHIPPLE and VINCENT T. COVELLO (eds). *Plenum: 1985. Pp. 506. ISBN 0-306-41924-6. Np.*

Risk Quantification and Regulatory Policy. Banbury Report 19. DAVID G. HOEL, RICHARD A. MERRILL and FREDERICA P. PERERA (eds). *Cold Spring Harbor Laboratory, New York, USA:1985. Pp.368. Hbk ISBN 0-87969-219-7. $67.*

Science and Technology for International Development: An Assessment of U.S. Policies and Programs. By ROBERT P. MORGAN. *Westview Press:1985. Pp.160. ISBN 0-86531-838-7. £17.50.*

The Second Self: Computers and the Human Spirit. By SHERRY TURKLE. *Simon & Schuster:1985. Pp.362. Pbk ISBN 0-671-60602-6. Pbk $8.95.*

Seven Ideas That Shook the Universe. By NATHAN SPIELBERG and BRYON D. ANDERSON. *Wiley:1985. Pp.291. ISBN 0-471-81477-6. £19.95.*

Short Term Bioassays in the Analysis of Complex Environmental Mixtures IV. MICHAEL D. WATER *et al.* (eds). *Plenum:1985. Pp.384. ISBN 0-306-42015-5. Np.*

Should the Baby Live? The Problem of Handicapped Infants. By HELGA KUHSE and PETER SINGER. *Oxford University Press: 1985. Pp. 228. Hbk ISBN 0-19-217745-1; pbk ISBN 0-19-286062-3. Hbk £12.50; pbk £3.95.*

Space Law in the United Nations. By MARIETTA BENKO *et al. Martinus Nijhoff: 1985. Pp. 256. ISBN 90-247-3157-7. Dfl. 115, $38.*

Statistics for Land Managers. By FRANK FREESE. *Paeony Press, Allerley Brae, Oxnam Road, Jedburgh, Roxburghshire TD8 6JL, UK:1984. Pp.176. ISBN 0-946941-00-9. £6.50.*

Striking a Balance: National Security and Scientific Freedom. First Discussions. HAROLD C. RELYEA (ed.). *American Association for the Advancement of Science, 1333 H Street, NW, Washington DC 20005, USA: 1985. Pp. 133. Np.*

Supersymmetry. K. DIETZ *et al.* (eds). *Plenum:1985. Pp.708. ISBN 0-306-42012-0. Np.*

Surveying Subjective Phenomena, Vol. 1. CHARLES F. TURNER and ELIZABETH MARTIN (eds). *Russell Sage Foundation, 112 East 64th Street, New York:1985. Pp.495. Hbk ISBN 0-87154-882-8. $37.50.*

Surveying Subjective Phenomena, Vol. 2. CHARLES F. TURNER and ELIZABETH MARTIN (eds). *Russell Sage Foundation, 112 East 64th Street, New York:1985. Pp.617. Hbk ISBN 0-87154-883-6. $47.50.*

Technology, Economic Growth and the Labour Process. By PHIL BLACKBURN, ROD COOMBS and KENNETH GREEN. *Macmillan Press:1985. Pp.239. ISBN 0-333-37496-7. £25.*

To Whom It May Concern: An Investigation of the Art of Elephants. By DAVID GUCWA and JAMES EHMANN. *W.W. Norton:1985. Pp.269. Hbk ISBN 0-393-02240-4. $14.95.*

The Travelling Salesman Problem: A Guided Tour of Combinatorial Optimization. E.L. LAWLER *et al.* (eds). *Wiley:1985. Pp.465. ISBN 0-471-90413-9. £39.95.*

Twenty Years Before the Mast. By CHARLES ERSKINE. *Smithsonian Institution Press:1985. Pp.311. Pbk ISBN 0-87474-415-6. $4.95.*

Understanding Language: Man or Machine. By JOHN A. MOYNE. *Plenum:1985. Pp.357. ISBN 0-306-41970-X. $49.50.*

The Urban Edge: Where the City Meets the Sea. JOSEPH E. PETRILLO and PETER GRENELL (eds). *William Kaufmann:1985. Pp.108. ISBN 0-86576-078-0. Np.*

Water Law. By WILLIAM GOLDFARB. *Ann Arbor Science: 1985. Pp. 233. Hbk ISBN 0-250-40627-6. £48.00.*

The Wildlife Parks of Africa. By NICHOLAS LUARD. *Michael Joseph: 1985. Pp. 240. Hbk ISBN 0-7181-2485-5. Hbk £14.95.*

Women in the Scientific Search: An American Bibliography 1724–1979. By PATRICIA JOAN SIEGEL and KAY THOMAS FINLEY. *Scarecrow Press, 52 Liberty St, PO Box 656, Metuchen, NJ 08840, USA: 1985. Pp.399. ISBN 0-8108-1755-1. $32.50.*

Computer-assisted model building

from W.C. Ripka

Developments in computer graphics and distance geometry have provided important tools for comparative model building of protein structures.

THE explosion in the number of available protein sequences derived from gene sequence information has created a wealth of opportunities for molecular modellers. Ideally one would like to use only these amino acid sequences and some set of structure-based rules to arrive at accurate secondary and tertiary structures. Recent efforts using an artificial intelligence rule-based system have shown promise for one structural class, the α-β proteins. Accurate structures were found within families generated by this approach[1]. In the general case, however, even secondary structure predictions are often less than 60 per cent accurate. The problem of protein folding, that is, the determination of a protein's tertiary structure from its amino acid sequence, is one of the major unsolved problems of molecular biology.

The problem becomes more manageable, however, if a few assumptions are made. The few hundred protein structures that have been solved by X-ray crystallography show that proteins may be classified in a relatively small number of structural classes. From one of these classes an appropriate homologous member can sometimes be chosen for comparative model building. This assumes that the protein structure to be determined is not too different from the known example, and that changes in side chains and residue insertions and deletions can be considered relatively minor perturbations of the structure as a whole. Such a model can then be used to direct synthetic efforts in drug design and protein engineering.

Model building, particularly of structures as complicated as proteins, has been greatly aided by the increasing number of commercially available computer graphics programs that allow interactive, real-time three-dimensional manipulations of complex molecules[2] [Some of the available software packages: Mogli (Evans and Sutherland), Insight (Biosym), Biograph (Biodesign), Chemmovie (Chemical Design), Midas (Univ. of Cal., San Francisco), Frodo (Rice Univ.) MMS (Univ. of Cal., San Diego), Syble (Tripose)]. These programs can perform bond rotations, on-line calculations of contact distances, side-chain alterations and residue substitutions. Both solvent-accessible and van Der Waals surfaces can be generated to display the space-filling properties of the molecules. Since these surfaces can be selectively coloured to represent partial atomic charges of the atoms that contribute to each surface element, these models also give an indication of charge distributions.

In addition to the increase in available software, the rapid fall in computer hardware prices has made these facilities available to both industrial and academic laboratories.

Bases for structure

Comparative model building can offer insight into the relationship between amino acid sequences and three-dimensional structure, but its ultimate promise lies in its ability to elucidate the molecular basis of enzyme-substrate and protein ligand recognition and specificity. Such knowledge would provide the basis for rational and productive drug design. Although model building should be most effective when the protein of interest is closely related to the macromolecule for which detailed structural information is available, successful examples of molecular modelling have ranged from very qualitative models to very precise, comprehensive models.

At one extreme, Ondetti *et al.*[3] used primarily chemical and biochemical considerations to suggest a qualitative relationship between the active sites of carboxypeptidase A, whose structure was known, and angiotensin converting enzyme (ACE), for which no structural information was available. A number of potential enzyme inhibitors of ACE were designed, one of which, captopril, proved to be a potent inhibitor and an effective antihypertensive agent. At the other extreme, Beddell *et al.*[4] used the X-ray crystal structure of human haemoglobin to design compounds for that molecule. Their modelling suggested an allosteric site at which compounds designed for this site would modulate the protein's oxygen affinity. These compounds are now in clinical trials as anti-sickling agents.

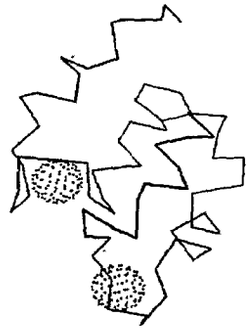


Fig. 1 A computer graphics representation of the ICB protein which provided the starting point for calmodulin modelling. The dot surfaces show calcium locations.

Comparative model building addresses the cases in between these extremes, by constructing useful models of structures from limited information. For example, using the three-dimensional structure of homologous aspartic proteinases and the primary structure of human renin, Blundell and co-workers[5,6] have employed interactive computer graphics to propose a tertiary model of human renin. This model may prove of value in the design of specific renin inhibitors.

Greer[7] has compared the structures of chymotrypsin, trypsin and elastase to allow the construction of 'new' serine proteases based on structually-conserved and variable regions of these proteins. Using computer graphics, coordinates for the main chain atoms of the model are taken from the conserved region, while side chains are substituted to fit the new protein. Modelling of variable regions is considerably more difficult since these areas involve insertions and deletions for which there is no exact correspondence. In these cases, main chain reconformations are required, rather than simple side-chain substitutions. Feldman *et al.* have suggested some simple techniques using interactive computer graphics to approach these problems.

Distance geometry

A potentially more powerful approach for modelling both side-chain and variable region conformations resides in the methodology of distance geometry[8], which allows the construction of random conformations that meet selected distance constraints. These constructs can then be evaluated according to energetic considerations and other geometric criteria.

O'Neil and De Grado have used distance geometry methods[9] along with interactive computer graphics to construct a model of calmodulin based on the structually related intestinal calcium binding (ICB) protein (Fig. 1). In this study, distance geometry was used to construct one of the calcium binding loops by holding the main-chain atoms of the model fixed to the coordinates of the known ICB protein and allowing the side chains to adopt numerous conformations; ligand oxygen atoms were constrained to those positions required in the approximate octahedral geometry of the coordination sphere of calcium. A number of conformers were generated, from which the lowest energy

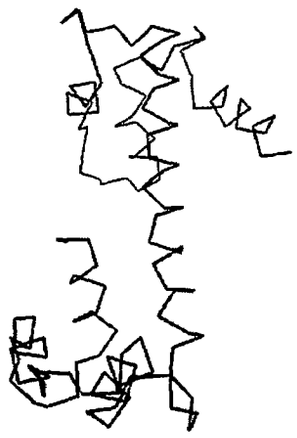


Fig.2 O'Neil and De Grado's calmodulin model.

examples (calculated by molecular mechanics) were selected. Of these, only one could be modelled into the proposed calmodulin structure while maintaining reasonable contacts with the rest of the protein (Fig. 2).

Limitations

Although protein models are useful, they may fall short in detailed structural interpretations. The success of comparative modelling depends on correct sequence alignment of the proposed structure with the known example. Even a single mistake can lead to an incorrect result. James and co-workers[11] have evaluated the types and sizes of errors in such model building based on a comparison of two proposed models for *Streptomyces griseus* trypsin with the experimentally-determined structure. A second sobering report comes from a study of the structures of bovine and porcine phospholipase A2, in which a single residue change from valine to phenylalanine in an otherwise extended homologous chain, leads to a major reconformation of the chain[12]. Whether those kinds of changes are predictable remains to be determined. □

W.C. Ripka is at the Biomedical Products Department, Medicinal Chemistry Division, E.I. DuPont DeNemours Co, Wilmington, Delaware 19898, USA.

1. Cohen, F.E., Abarbanel, R.M., Kuntz, I.D. & Fletterick, R.J. *Biochemistry* **22**, 4894–4904 (1983).
2. Langridge, R., Ferrin, T.E., Kuntz, I.D. & Connolly, M.L. *Science* **211**, 661–666 (1981).
3. Ondetti, M.A., Rubin, B. & Cushman, D.W. *Science* **196**, 441–444 (1977).
4. Beddell, C.R., Goodford, P.J., Norrington, F.E., Wilkinson, S. & Wootton, R. *Brit. J. Pharmac.* **57**, 201–209 (1976).
5. Blundell, T., Sibanda, B.L. & Pearl, L. *Nature* **304**, 273–275 (1983).
6. Sibanda, B.L. *et al. FEBS Letters* **174**, 102–111 (1984).
7. Greer, J., *J. molec. Biol. Biol.* **153**, 1027-1042 (1981).
8. Feldman, R.J. *et al.* in *Macromolecular Structure and Specificity* (eds Venkataraghavan, B., Feldman, R.J.) 12-43 (New York Academy of Sciences, New York, 1985).
9. Crippen, G.M. in *Chemometric Research Studies Series* Vol. 1 (ed. Baudan, D.) 1–58 (Wiley, New York 1981).
10. O'Neil, K.T. & DeGrado, W.F. *Proc. natn. Acad. Sci. U.S.A.* **82**, 4954–4958 (1985).
11. Read, R.J., Brayer, G.D., Jurasek, L. & James, M.N.G. *Biochemistry* **23**, 6570–6575 (1984).
12. Dijkstra, B.W., Weijer, W.J. & Wierenga, R.K. *FEBS Lett.* **164**, 25–27 (1983).

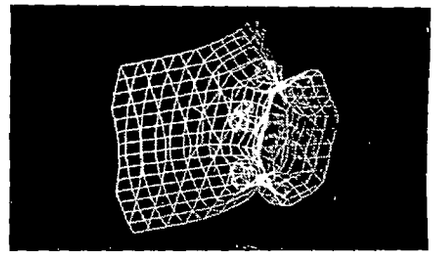
Chemical design takes to the terminals

Software packages for chemists turn ordinary microcomputers into tools for molecular modelling, structural analysis and reaction planning.

DEMONSTRATION kits for Molecular Design Ltd's series of PC software provide a low-cost indoctrination into **chemical database programs**. Beginning last month, MDL now offers their ChemBase database manager, designed for IBM PC's in a $50 (US) demo version that allows the user to experiment with features such as custom table editing, chemical drawing templates, and multi-condition data searching (Reader Service No. 100). ChemText, a chemical wordprocessor package, and the mainframe hook-up ChemTalk/ChemHost, are also available as demo kits. These programs give graphical representations of molecules and reactions in the same format as MDL's mainframe database REACCS (a reaction access system) and MACCS (a molecular access system). CHEMLAB-II, a computational chemistry package, completes MDL's mainframe threesome. The microcomputer demo kits' cost will be deducted from the price of PC software purchased within 30 days of the demo package.

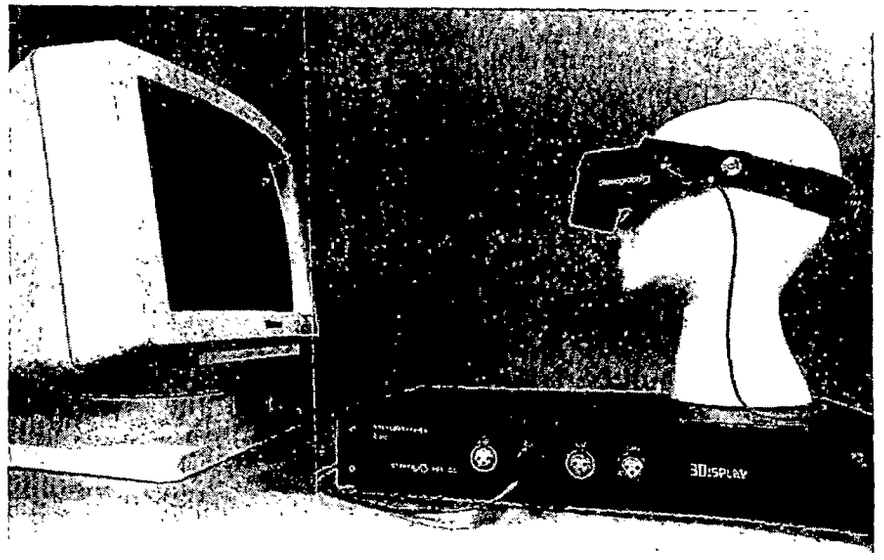
A California company has taken the lead in **three-dimensional molecular modelling** that is both useful and entertaining. Stereographics Corp. has a $20,000 (US) graphics display system that uses alternating viewpoints and visors with liquid crystal shutters to create a convincing 3-D image (Reader Service No. 101). Stereographics' 3Display accepts output from any computer and works with all 3-D graphics software packages. Its imagery provides insight into hidden surfaces with twice the number of fields per second that previous stereoscopic viewers have afforded, reducing irritating flicker effects. A 3-Display system includes a display controller, a 120 Hz RGB monitor and viewing visors.

Chemical Design has a **molecular modelling system** that will run on DEC VAX

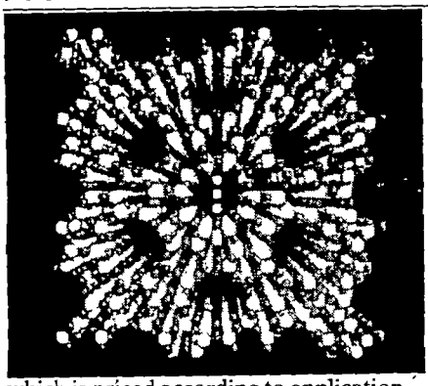


Modelling by Chemical Design. See oppostie for other examples.

computers under the VAX/VMS operating system. Chem-X integrates five specialized modules for design, manipulation and analysis (Reader Service No. 102). The system has a user-friendly front end and interfaces to Quantum Chemistry Program Exchange (QCPE) software (see below) as well as MACCS and CHEMLAB-I. Standard supported graphics terminals or PCs with graphics options can run Chemical Design's 4-megabyte program. Chem-X can be incorporated in a combined hardware/software package called MicroGRAF-2,



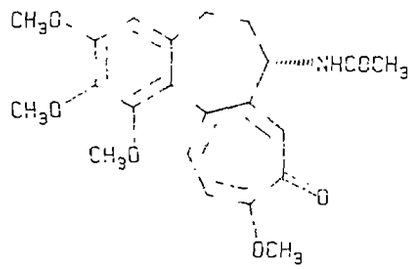
Head-up display in 3-D from Stereographics.



which is priced according to application.

The most affordable **modelling system** for IBM desktops comes from Xiris Corp. in the form of the $1,000 (US) XICAMM software (Reader Service No. 103). XICAMM can perform many of the tasks of much more expensive systems (albeit more slowly) including molecule comparisons, bond angle determinations, structure rotation and generation of QCPE's MOPAC- or MM2-compatible input data files. An evaluation system with full documentation is also available for users who want to gauge XICAMM's merits for themselves. Xiris provides any or all of the hardware needed to run their system, which is based on the same algorithms used in certain mainframe and super-mini computers.

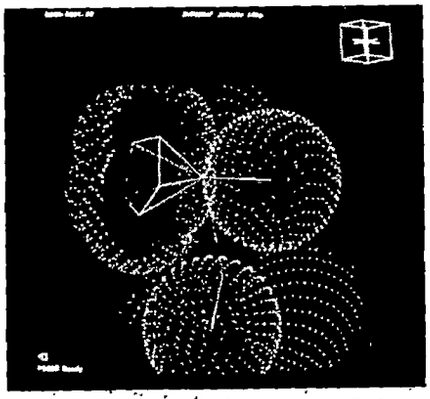
An unconditional 30-day money-back guarantee accompanies Molecular Pre-



A plot straight from the HP 7470 plotter.

sentation Graphics, the **chemical drawing package** from Hawk Scientific Systems (Reader Service No. 104). Hawk's $225 (US) package is compatible with the IBM PC and Hewlett-Packard-150, among others, and excels at the speedy generation of quality diagrams for research texts. MPG is not a modelling system, but can supplement one or stand on its own as a useful aid at the write-up stage of research projects. The menu-driven software gives clear drawing instructions, and diagrams can be printed on Epson or HP LaserJet and ThinkJet printers via MPGLASER, a Hawk option that merges text and diagrams.

Chemdata Ltd makes **molecular graphics packages** for Apple II/IIe and BBC model B/Master 128 microcomputers. Their integrated hardware/software unit, including a graphics display processor unit and (for the Apple series) a hard-wired multiplier card, gives 512 by 512 pixels displays in eight colours (Reader Service No. 105). A structure file editor, model builder, graphics module and library of structure files comprise the software for these units. By merging Chemdata's structure files, two chemical structures can be manipulated together. Chemdata's hardware/software duo costs £890 (UK); in addition, software files with file editors, graphics modules and structure libraries are also available for BBC Master 128 and Apple machines. The Master 128 version, at £75, is priced slightly higher than the £45 Apple series package, but offers sevearl options, such as file merging and model building on a double-buffered four-colour graphics mode, that the less expensive Apple software lacks.

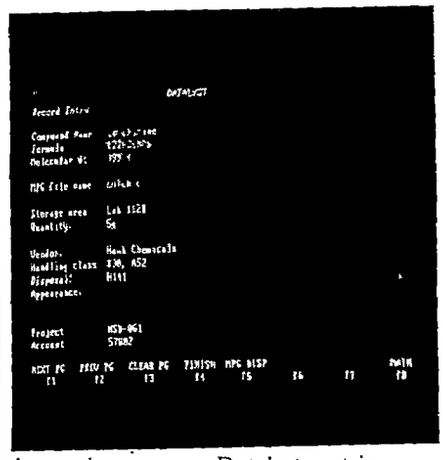


The chemistry department at Indiana University runs a **'library' of chemical analysis software** for IBM and compatible computers called the Quantam Chemistry Program Exchange (QCPE) (Reader Service No. 106). Most of QCPE's offerings are molecular mechanics packages adapted from mainframe programs, which the exchange distributes free of charge to non-profit institutions. Manager Richard Counts conceived the program only a few years ago, since when it has amassed 10 varieties of software for the chemist, including the well-known MOPAC, MM1, MM2 and Galsien 80. Counts plans to expand the program to include a broader range of chemical design packages.

Disks over index cards

The final component of ISI's Sci-Mate version 2.0 software system has now joined the fleet. The editing function for **bibliographic formatting** rounds out Sci-Mate's search and management functions for researching journal literature, building text files and preparing manuscipts (Reader Service No. 107). ISI's package comes in MS-DOS or CP/M 80 formats and cost $399 (US), with volume discounts available.

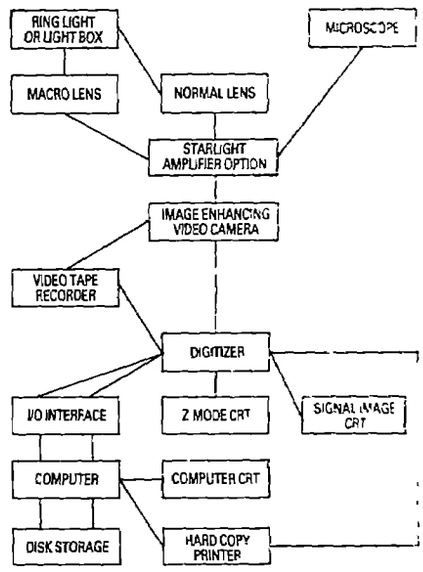
Autoscribe Ltd. distributes a **chemical filing system** for IBM PCs or Hewlett-Packard-150s with a minimum of 256K of



internal memory. Datalyst entries can store compound names, molecular formulas, chemical formulas, vendor information, laboratory storage location, quantity in stock and details of handling requirements (Reader Service No. 108). The £295 (UK) program will also calculate molecular weights and access chemical structure files from Molecular Presentation Graphics systems (see above). Demonstration disks are available.

Software branches out

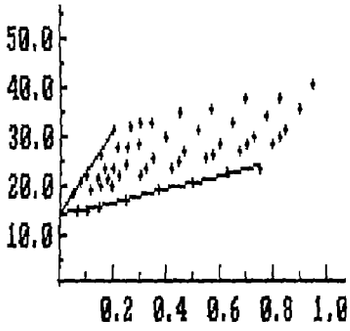
Five new **image analysis programs** from Darwin Instruments, Inc. link Colorado Video's 270A vido digitizer with Apple II+ and IIe PCs. The programs were designed for "researchers limited by budget constraints," says Colorado Video (Reader Service No. 109). A scanning densitometer program will perform sum-averaging and multi-scan, baseline addition or subtraction, noise elimination, area integrations and peak identification. A topography program allows Darwin's system to count the total number of objects in a scan field, determine the area and perimeter of each object, calculate the total area of all objects, and delete



Darwin's route to analysed images.

objects based on size class or object number. Darwin also offers an area program for individual object or total area calculation, a program for automating growth curves for plants and sessile animals and a tracking program which can monitor the rate and direction of an object's movement.

In less than 1 minute, software from Wyatt Technology can generate a Zimm plot and **calculate molecular weights** using data from DAWN laser light scattering



Wyatt's Zimm plot.

instruments. Wyatt's package has a menu which allows users to choose different order polynomials for extrapolating the Zimm plot curves (Readear Service No. 110). Instead of being limited to linear extrapolation, the program can handle quadratics, cubics and higher-order expressions. Wyatt's $1,000 (US) software was developed for IBM PCs, XTs and ATs. Several user inputs, such as the number of concentrations, solvent refractive index and scaling factors for the graphics, must be manually entered for the program to go to work.

Varian Associates put two programs together in a software package that facilitates **automatic data transfer** between atomic absorption spectrometers and a variety of computer systems. With Varian's $2,000 (US) data communications package, the user can specify how much information needs to be transferred, and send data on-line or as a summarized report (Reader Service No. 111). An external communications module accepts information and instructions from a remote keyboard or disk file, then transmits results through an IEEE or Centronix port or to remote computers via either or two RS-232C channels. The other half of Varian's package is the public domain program KERMIT, which can transfer files from the spectrometer to micro- or mainframe computers operating with appropriate versions of the program. IBM PC, DEC VAX and Rainbow, HP-110 and HP-150 and WANG PC are among the compatible computers for these data communications.

ADVERTISEMENT

SINGER INSTRUMENTS

Xenopus Oocytes injection?



SINGER MKI MICROMANIPULATOR

We also offer a Microsyringe Kit.

Write to:
Singer Instrument Co. Ltd.
Treborough Lodge
Roadwater, Watchet
Somerset TA23 0QL
England. Tel. (0984) 40226
Telex: 337492 Comcab G

Reader Service No.9

Microbore tubing up for grabs

Elkay Products' latest catalogue contains $100 (US) worth of coupons for new products including autoclavable pipette tip racks, 1.5 ml microcentrifuge tubes and 50 ml sterile centrifuge tubes (Reader Service No. 112). In 48 colour pages, *Elkay 86* presents a complete line of plas-



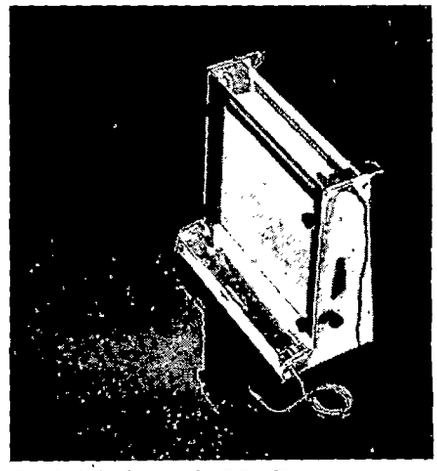
Elkay's latest.

tic disposables for laboratories. General reference material, such as an equipment/consumables compatibility chart, accompanies technical specifications and performance data for Elkay's products.

Elkay is also giving away samples of their extruded microbore tubing (Reader Service No. 113). Sample packages permit inspection of tubing material quality and standards for flow, physical dimensions, durometer and resilience, which Elkay says they carefully control. One package contains six different kinds of tubing for a variety of applications including pump, transmission and bellow forms.

Gel sequels

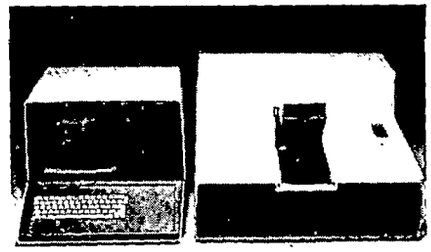
A **sequencing gel electrophoresis system** from Bethesda Research Laboratories promises precision with 48 lanes of read-



Barely $10 a lane in the BRL S2.

able date for less than $500 (US). The model S2 apparatus has an aluminium plate for even heat distribution and 0.4 mm side spacers that won't interfere with gel polymerization (Reader Service No. 114). A removable tray allows easy buffer disposal, and the entire unit is constructed of chemical-resistant, unbreakable plastic. BRL's system comes with an accessory package.

Ciba Corning's **scanning densitometer** can analyse up to 64 samples at a time without operator attendance. The model 780 fluorometer/densitometer is pre-programmed for Ciba Corning procedures, but the protocol can be altered for additional tests (Reader Service No. 115). The system's editing function allows the addition or deletion of minima, baseline adjustment, peak deletion or magnification and repositioning of minima. If used in conjunction with Ciba's 16-track agarose gels, the 780 can analyse all 64 samples in less than 12 minutes. An alphanumeric keyboard, 12-inch CRT and fluorescent pre-viewer have been built in to Ciba's unit. All types of electrophoretic media



Sixty-four samples a time in the model 780.

can be accommodated, and the operator can select the units in which results should appear.

Narrowing the scope to **DNA sequenc-**



ing, Bio-Rad's Gene-Master has been designed for speed and convenience in one particular application (Reader Service No. 116). The system includes an IBM PC AT microcomputer that stores and analyses sequences entered via a digitizing pen. Bio-Rad's model also uses a voice synthesizer to call out bases as the pen records them, so that sequences can be verified without looking away from the autoradiogram. Lane and band curvature doesn't throw the Gene-Master off track, and the menu does not require pen activation which Bio-Rad has deemed distracting. As with most pen-operated readers, the reading process is accelerated when the user can keep an eye on the gel.

Patrons of Shandon's Electrafor products for electrophoresis can now **order supplies by phone** with the Cheshire company's free telephone order service (Reader Service No. 117). A rapid delivery service, combined with the direct-dial

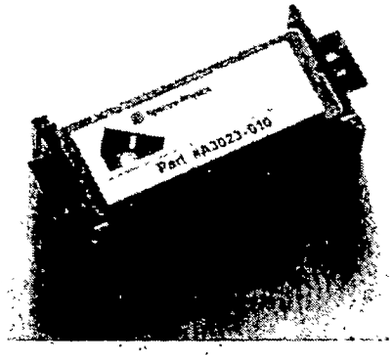


ordering system, helps speed up restocking of the cellulose acetate membranes, buffers and stains in the Elecrafor range. First-time customers will get free samples from Shandon, and all customers get a free box of Electrafor membranes with every 10 purchased. Until the end of May, buffers and stains ordered with membranes will also be discounted 10 per cent.

A New York-based mail-order company has moved into the scientific arena. Transcat Inc. has published its first issue of **Laboratory & Scientific Instruments,** a 274-page catalogue that describes the products of over 200 manufacturers (Reader Service No. 118). Companies featured include Bausch & Lomb, Beckman, Corning, Ohaus, Orion Research, Techne, Thermolyne and Wallace & Tiernan, and products range from microscopes to hot plates. Transcat gives prices, ordering information and a toll-free number to facilitate inquiries.

Tomorrow's program

Spectra-Physics has put a program for **automated stop-flow UV-Vis scanning** on a chip that plugs into their SP4200 computing integrator (Reader Service No. 119). The integrator is attached to a Kratos Spectroflow 783 detector through a current loop serial connection. The program, on the $1,500 (US) 783 SCAN chip, will perform background subtraction, peak ratioing and time-programmed wavelength changes for selected liquid chromatography components; scanning parameters can be set via the integrator.



Three new **software utility programs** now complement IBM Instruments' CAP 2 software for their chromatography workstation (Reader Service No. 121). One of the programs, a utilities library, can aid in the analysis and display of chromatography data. Another, called Touch & View, manages screens, keyboards and key pad functions to allow up to seven programmes to run concurrently. GC/9630 Emulation, the third program, was designed to replace the standard VDU control terminal component of IBM's GC/9630 chromatograph: it provides comprehensive instrument control during data acquisition. IBM Instruments sells the programs for $250, $400 and $200 (US) respectively. □

These notes are compiled by Karen Wright from information provided by the manufacturers. To obtain further details about these products, use the reader service card bound inside the journal.

Data acquisition by word of mouth

In over 2,500 laboratories across the United States, microcomputers that once turned deaf ears to their surroundings may soon be called on to perk up and listen. Laboratory Technologies, makers of the data acquisition package LABTECH NOTEBOOK, recently agreed to develop a scientific vocabulary for their software commands that would enable the package to respond to voice commands. LT's arrangement with Kurzweil Applied Intelligence will link the Kurzweil Voicesystem (KVS), a 1,000-word speech recognition system, with the IBM PCs that run LABTECH NOTEBOOK (Reader Service No. 120).

LT is hoping that setting up and controlling LABTECH NOTEBOOK will be much easier using simple spoken words. The operator talks into a telephone handset or a lightweight headset microphone, and the NOTEBOOK software does the rest: the PC channels will automatically gather information from attached sensors, instruments or gauges, and pass it on for analysis, control and monitoring. A KVS with an IBM PC AT interface costs $6,500 (US); the $895 (US) LABTECH NOTEBOOK package can integrate with Lotus 1–2–3, Symphony and RS/1 for detailed statistial analysis and display. □

Copies of articles from this publication are now available from the UMI Article Clearinghouse.

UMI Article Clearinghouse

Mail to: University Microfilms International
300 North Zeeb Road, Box 91 Ann Arbor, MI 48106

Bringing home the technology

from Richard Pearson

New technology is now enabling more people to work from home rather than in the traditional workplace.

EMPLOYMENT and working patterns are constantly changing in response to economic and social and technological developments. In the United Kingdom, the recession of the early 1980s has been seen as a watershed in terms of patterns of working, with employers restructuring their workforces and making greater use of temporary and part-time staff.

Since 1983, the main areas for new employment have been for part-time work, where there has been an increase of more than 300,000 jobs, and self-employment, where the number of people has also increased by over 300,000 to total over 2.5 million. Self-employment has been helped by employers, who are increasing their sub-contracting of work activities such as catering, transport and legal work to concentrate on what they are good at. New technology, in the form of cheaper telecommunications and computing, is also enabling more people to work from home, again showing more opportunities for flexible employment patterns.

In theory, the technology offers the opportunity for vast numbers of office-based



workers and others to carry out their work at home using computer links. Jobs in computer programming, word processing, accounting, statistical analysis and management information processing are all amenable to distance working. In the United States, AT&T estimates that up to half of its executive jobs could be carried out from home by 1990, while in San Francisco it has been estimated that one in five commuters could stay at home to work. But such distance working need know no boundaries. American Airlines moved its data entry operation from Oklahoma to Barbados in the West Indies, where 200 keyboard operators now process tickets, using a satellite link to receive the work from the US data-processing centre. Another US company with a similar operation claims "we can do the work in St Michaels, Barbados for less than it costs us to pay for the floor space in New York". Yet another company flies its paper work to Singapore, where it is keyed in, and then beams the finished work by satellite to its data-processing centre in Australia.

In the United Kingdom, homeworking is not new; cottage industries in light manufacturing and clothing have been around for generations, although such workers are now a minority of the "homeworkers". Much more common are white-collar workers doing clerical work, or working in occupations such as selling or writing where the home is used as the base. There are estimated to be more than 650,000 homeworkers in the United Kingdom.

There are now a number of initiatives in the United Kingdom aimed at allowing and encouraging traditional office-based professional workers to work from home, becoming the 1980's homeworker or "teleworker". The largest and longest running is the operation of 'F' International, a computer consultancy which employs some 900 people, predominantly women, to work from their homes. The staff, computer programmers, systems analysts and project managers, take on assignments for clients of 'F' International and operate as high-tech cottage workers, working in part from home and in part in the clients' premises. A small core of permanent staff organizes and manages the work, but the 800 or so self-employed workers are able to combine domestic flexibility with a career. They are of course aided in gaining regular work to fit in with their own availability by having skills in short supply.

Another scheme that has attracted a lot of publicity is that started by Rank Xerox, which has cut the number of staff employed in its expensive central London offices. Originally some 20 staff, mainly managers and professionals, were helped to hive themselves off from the company and to sell their services back to Rank Xerox instead of being employees. As well as being paid special bonuses and provided with training and low-cost equipment, the "networkers" as they were called, were guaranteed two days' work per week at consultancy rates for two years. The company saved significant sums on office rental and services, payment of support staff, canteen facilities, pension, company cars and the like. It also freed itself of a long-term commitment to employing those staff. The networkers gained a sheltered transition to self-employment and starting their own businesses, and flexibility to work in the way they wanted. Many have been able to achieve much higher levels of output, without for example the interruptions of working in a major office complex, and thus to boost their earnings. Other companies also have hybrid schemes of networkers, freelancers and teleworkers although the technology, other than the telephone, has assumed a less important role than many had first imagined.

There are of course problems. Many people look to the work place to provide social interaction and a structure for their lives, and not all homes and families' lives are conducive to working at home. There is also the uncertainty for the individual in working in a new and uncertain way. For the employer, there are new skills to be acquired in "managing" such people and setting payment systems where it is difficult to measure the output. With a traditional employee, this is easier because the relationship is one of buying the individual's time for, say, forty hours per week.

The productivity gains benefit both sides, and while the individual gains flexibility of working pattern the employer gains flexibility over controlling labour inputs and transferring many of the overheads and "risks" to the individual. The homeworkers gain most when skills are in short supply, and if the pattern is to develop in the future a key issue will be "who pays for the training and development of new skills as they are needed?".

Distance and homeworking will increase in the future as more workers and employers seek part-time and flexible employment relationships. The increasing numbers of women seeking work, and the shift away from manufacturing-based employment to services will also facilitate this trend. The rate of expansion will probably not, however, be as quick as some of the publicity suggests. While the lower costs of technology will aid the process, economic and social factors will be the prime determinants of its development, while the main beneficiaries will be those whose skills are in scarce supply. □

Richard Pearson is at the Institute of Manpower Studies, Mantell Building, University of Sussex, Brighton BN1 9RF, UK.

nature

The long shadow from Chernobyl

Last week's reactor accident in the Soviet Union is an historic event that will change the course of the remainder of the twentieth century. But the clouds may also have a silver lining.

EUROPEAN governments' attempts to deal with the consequence of the reactor accident at Chernobyl have been seriously impeded by the lack of data from the Soviet Union. Information bearing on two crucial issues has been withheld. At least for the first week after the accident, the Soviet side had nothing to say about the composition of the radioactive material from the damaged reactor. And there has been no serious attempt to estimate what quantities of radioactivity were released. Even allowing for the difficulty of making considered judgement while the graphite moderator of the reactor was still on fire, for the need to protect the local population from serious long-term consequences and for national pride, there is no excuse for having kept silent on these issues for so long.

That is why the Soviet Union may have only itself to blame for the indecently gleeful way in which Western observers of this tragic accident, especially some in the United States, have given currency to wild speculations about the scale of the damage near Chernobyl. In reality, there is no reason to disbelieve the Soviet statement that only two people were killed by the explosion that appears to have marked the onset of the release of radioactivity; the more important questions are whether local fallout has caused potentially fatal radiation sickness among the neighbouring population, and what will be the longer-term load of increased cancer in a wider population.

When the dust has almost literally settled, there will be other international issues on which a fuller degree of Soviet understanding of other people's problems will be required. Who will meet the cost of the trouble which the Scandinavian governments have had to take? What if events in the next few months suggest that some people outside the Soviet Union have been acutely damaged? And what happens twenty or thirty years from now if people die from cancers which may be caused by radioactive effluent from the Chernobyl reactor, but which are most probably due to natural causes? Will those affected have a suit against the government of the Soviet Union? Or merely grounds for a lasting grudge? On past form, the Soviet Union will be grudging with helpful information, perhaps because it is unwilling to admit to its own people that its domestic arrangements are not by definition unalloyed benefits. On this occasion, the pressure for openness from outside may happily coincide with what Mr Mikhail Gorbachev has been advocating domestically.

The consequences of the accident for Soviet plans for the further development of nuclear power will nevertheless be substantial. It is unthinkable that the Soviet government will push forward with the construction of reactors of the type that caught fire at Chernobyl until it fully understands the risks of a repetition of the accident. The essential weakness of the design is its assumption that two mutually energetically reactive materials (graphite and steam) can be rigorously separated from each other by means of welded steel tubes; the assumptions are obviously no better than the quality of the welds. The obvious difficulty now for the Soviet government is that its plans for the generation of electricity hang crucially on the construction of nuclear reactors. Luckily, most of the plants now being built are the more rigorously tested pressurized-water reactors. But it will serve nobody's interests if the Soviet economy, and its refreshing new leader, are set back a decade or so in their expectations for the years ahead.

The consequences of Chernobyl for the nuclear industry elsewhere will be devastating. Mr Saul Steinberg, the US financier, has made something of a splash in the past few weeks by buying a substantial proportion of the shares of the Long Island Lighting Company, the owner of the Shoreham nuclear power plant which has lacked an operating licence for the past several years. His envious competitors had been admiring his flair for making wagers that cannot fail; either Shoreham would be allowed to produce electricity, or the utility that owns it would be nationalized (by the state of New York). But now, Mr Steinberg will be seen to be betting on a single horse, one that hobbles a little. In the adversarial process by which the public good is balanced against the private interest in the United States, the dice will now be further weighted against those who may wish to build the odd nuclear reactor. Even in Britain, where the government is likely to be told in September by the Roskill Commission that it would be safe to allow the nationalized electricity utility to build a pair of pressurized water reactors, there will be a temptation to postpone the decision. In short, whatever the explanation of the Chernobyl accident, the event will reinforce the general prejudice against even the sensible use of civil nuclear power.

The trouble is the public understanding of the concept of probability. Nobody disputes that a substantial release of radioactivity into the atmosphere can damage people and that reactors are a potential source of large quantities of activity. Most designers of nuclear power stations have taken to calculating the chance that the plants they build will suffer a catastrophic accident; the usual outcome is that the chance of catastrophe is one in a million or more per year of operation. Put simply, reactors would not be built if the chance that they would go seriously wrong were much greater, for then utility systems operating several reactors would imply to their taxpayers that there is a chance that a catastrophe would arise within a human lifespan or thereabouts. But this average time does not exclude much shorter intervals, or excuse carelessness.

What side-benefits can there be in such a sombre litany of trouble? Much depends on how serious the local consequences of the accident have been. But even if, as must be hoped, there is no serious loss of life in the immediate neighbourhood of the reactor, there is bound to be a moral obligation on the Soviet Union to acknowledge the trouble and even damage it has caused elsewhere. For what it is worth, the Soviet Union is not a signatory of the 1963 Vienna Convention on the regulation of nuclear accidents, but the past few years have shown clearly that international conventions have a moral force that non-signatories cannot shrug off. Similarly, within the Soviet Union, there is bound now to be built-in pressure on the authorities to be more open about the risks of nuclear power, and of some of the other schemes on which the Soviet Union is engaged. And of course, if the accident has been as serious as it might have been, the internal pressures may be even greater — perhaps even greater than those needed to blow the lid off an isolated nuclear reactor. □

Chernobyl

Anxiety about reactor accident subsides

LAST week's panic in Western Europe and elsewhere about the explosion and subsequent graphite fire at the Soviet nuclear plant north of Kiev was in retreat earlier this week, as the scanty data available outside the Soviet Union were pieced together. While it is plain that the accident at Chernobyl on 26 April was the world's most serious nuclear accident so far, there is no reason to dispute the Soviet statement that only two people at the plant were killed, perhaps a consequence of the initial explosion. The longer-term consequences, including cases of radiation sickness which will become apparent in the next few weeks, and excess cancer deaths, which will be delayed by decades, cannot yet be estimated.

Part of the basis for this reassuring conclusion is the examination of members of the party of British students from Kiev and Minsk, who returned via Moscow last week. Although some of the party's clothing was contaminated with local fallout, ingestion of airborne radioactivity was apparently not sufficient to cause risk of thyroid cancer. An account of the fallout over Poland during the past week, given by a group of Polish experts in Vienna, has led the Polish authorities to the conclusion that there is "no significant risk to the health of any person".

Other estimates of the total quantity of radioactivity released from the Chernobyl reactor have been derived from computer models normally used in the assessment of the risks of nuclear accidents. These suggest that the release from the plant may have been upwards of two orders of magnitude greater than from the British accident at Windscale in 1957, previously the worst nuclear accident on record.

The Swedish measurements, the first clue (on 28 April) to the accident at Chernobyl, suggest that airborne activity over Scandinavia peaked on Tuesday last week at about 10 to 20 times the normal level, mostly because of iodine-131 and caesium-137.

Fallout in the neighbourhood of the plant has been much more serious. Close on 50,000 people have been evacuated from a 30 km radius. Soviet spokesmen visiting the West have spoken of radiation doses at the plant which were initially 200 roentgens an hour, falling to 100 roentgens an hour after a week. In this light, the Soviet statement that 200 people were hospitalized (of whom a quarter were discharged) probably refers to those showing symptoms of radiation sickness.

The cause of the accident remains a matter for speculation. The most common suggestion is that a leak in the steam-raising water circuit which contains the fuel elements and interpenetrates the 1,000-tonne graphite moderator would have produced water gas (carbon monoxide and hydrogen), which might then have caused the explosion that destroyed the roof of the reactor building. It is not known whether Soviet statements that "human error" was responsible for the accident refers to the execution of an improper operation or to an inadequate response to warning signals.

Another possibility is that the accident arose during an operation to anneal the graphite moderator in the reactor to remove structural defects accumulated during prolonged neutron irradiation, and which entails heating the graphite above the normal operating temperature for more than a day.

Although the Chernobyl accident may have been less serious than first reports in Western Europe suggested, most Western governments have been indignant that so little information has been available from Soviet sources to suggest how governments elsewhere might best deal with the fallout from the plant. More detailed information about conditions at Chernobyl began appearing only earlier this week. On Tuesday *Pravda* carried a long article describing conditions around the reactor site.

Perhaps more significantly, an apparently painful interview last Wednesday between the director-general of the International Atomic Energy Agency, Hans Blix, and the Soviet envoy in Vienna had led, by Sunday, to an invitation for Blix to visit Moscow. He left the same day, accompanied by Maurice Rosen, the agency director of nuclear safety.

According to a spokesman of the agency on Tuesday this week, the intention is that the visitors will have full access to what information there is available in Moscow, although it is not known whether the party will be able to visit the reactor site. Blix's companions may stay in the Soviet Union for several days.

Within the Soviet Union, a commission of enquiry under a deputy prime minister is said to be hard at work on an investigation of the causes of the accident and into its aftermath. On the assumption that the reactor building can itself eventually be made safe, the most haunting problem will be that of managing the health of the population in the neighbourhood of the accident over the next three decades. □

Soviet nuclear reactors

Ambitious plans with red tape

UNTIL 26 April, the Soviet Union had a nuclear generating capacity of 28 GW, 11 per cent of total electricity output, but the new five-year plan (1986–90) includes the commissioning of a further 41 GW of nuclear capacity.

Guarded comments by Soviet officials last week suggest that there will be no change in these plans, even though it has for the first time been admitted that the use of nuclear power, even for peaceful purposes, cannot be totally safe. Previously, the Soviet line has been that incidents such as Three Mile Island were the result of corner-cutting by capitalists bent on profit.

Soviet plans specifically suppose the construction of nuclear stations close to major cities. Although, a few years ago, a leading party monthly carried an article suggesting that nuclear stations should be confined to the remoter areas of Siberia, they are now considered so safe that they can serve as thermal generators for city district heating systems, but with a green belt of 1–3 km radius around each station, which would be used for recreational purposes and allotments.

Current plans call for several such "atomic-thermal-power" stations to be commissioned during the next five years, including Gor'kii, Voronezh, Odessa and Minsk, while the construction of several more is to be started. If the Chernobyl accident has any effect on Soviet nuclear policy, it is in this sphere that it is most likely to be felt.

The resiting of at most 10 or 12 power stations (and the quiet dropping of the district heating part of the programme) would be far less difficult, both logistically and politically, than a total reversal of Soviet commitment to nuclear energy. There is likely, too, to be an increased impetus to the fusion energy research programme, which for years has been formally hailed as the ultimate solution to Soviet energy problems.

The Chernobyl station had four RBMK reactors with a fifth under construction. This is a light-water-cooled uranium-graphite channel system, with zirconium alloy fuel cans. As a number of commentators have noted, this type of design has been rejected in Western countries as unsafe, and the presence of the earliest example of this type near Leningrad has, during the past few days, evoked considerable concern in Finland.

The Soviet designers seem to have relied on the regular ultrasonic and acoustic monitoring of the metal coolant loops, which, it was claimed in the technical journal *Atomnaya Energiya* (**50**,

253; 1981) "guaranteed that sudden rupture of the pipes could not occur" and, as a measure of last resort, the incorporation of an automatic emergency water cooling system. This was designed to cope with the worst possible case foreseen, the transverse fracture of a 900-mm turbine pressure collector. On 26 April, however, this system clearly failed to work.

If the Soviet atomic energy commission preserves the reticence it has shown so far, it may be difficult to discover not only what caused the initial fault but also why the emergency system failed to operate. (Earlier this year, the daily *Sovetskaya Rossiya* called for greater openness in the reporting of natural disasters, but the atomic energy commission could well reply that the Chernobyl accident was not "natural".) One possible explanation, however, may lie in Soviet construction procedures which are prone to produce shoddy and hazardous results, in spite of the fact that there is no "capitalist" profit motive.

The Soviet practice of laying down quarterly, annual and five-year production targets (with pay and bonuses dependent on their fulfilment), coupled with a highly bureaucratic supply system and a transport network too overloaded to ensure prompt deliveries, has led to the practice of "storming" — last-minute speed-ups and overtime to catch the target date.

Hasty construction is further exacerbated by the emphasis placed on fulfilling targets ahead of plan, and, in particular, the making of "voluntary" pledges by the workers to reduce their target time in honour of major patriotic events. Although, in 1976, a glowing description of the construction work at the Chernobyl site merited front-page treatment in *Pravda*, an article that appeared in the weekly *Literaturna Ukrayina* just a month before the accident gave a very different picture.

According to the author, Lyubov Kovalevs'ka from the town of Prypyat', building standards have from the very beginning been neglected. The construction of a project such as a nuclear power station, she says, must be "a continuous flow on the basis of the strictest adherence to building technology. But this did not happen here."

The various problems that arose with the first unit (Kovalevs'ka does not specify what they were) were never properly solved, but simply "transferred" to the second, and then to the third and fourth units.

What this meant in practice is seen from her description of current construction work on the fifth unit. The project, she says, is beset by constant shortages; materials are delivered in inadequate quantities and are frequently substandard, yet the planned construction time has been cut from three years to two. The workforce therefore has no option but to try to fulfil its targets by neglecting the specifications and "stretching" such materials as there are as far as possible, and accepting defective supplies even when so vital an item is concerned as the case she cites, the roof-plate for the spent fuel bunker. Quality and inspection of the finished construction moreover, seems to connive at the situation which, Kovalevs'ka warned a month ago, will have to be "paid for over the course of decades". Has this bill yet been paid? **Vera Rich**

Nuclear prognostications

Estimating gravity of problem

ALTHOUGH several agencies in the West have been hard at work during the past week trying to estimate the seriousness of the accident at the Soviet nuclear reactor north of Kiev, nobody is confident of the outcome of their calculations. As part of the now-standard process of calculating the consequences of hypothetical nuclear accidents, several computer models have been developed for estimating what happens to radioactivity released from a damaged reactor. But, as one modeller explained last week, "usually we start with something that we know".

Part of the problem is meteorological. One of the team at the British Radiological Protection Board, an independent government agency based at Harwell, Oxfordshire, explained last week that there is relatively little experience of even models of the spread of radioactive materials from sources remaining active for several days, and that the calculation of the consequences of Chernobyl have been complicated by the rapidly changing wind patterns.

Data from Sweden and elsewhere in Europe have thrown some light on the composition of the fallout from the Soviet reactor. It seems to be agreed that the concentrations of volatile materials such as radioactive iodine and caesium are in the proportions to be expected from fresh fission products. The modellers are, however, unable to estimate with any certainty what proportion of the total emission from the damaged plant will have been deposited in its immediate locality.

This uncertainty bears most directly on the difficulty of estimating the damage that may have been done to the population in the immediate vicinity of the plant, which will become apparent there only in the next few days and even weeks. One of those concerned says the uncertainties are such that the data from outside the Soviet Union are consistent both with the assumption that many people will have been exposed to damaging doses of radiation and that there will be no casualties from radiation sickness even in the neighbourhood of the plant.

There is, however, general scepticism about some of the estimates of Soviet casualties such as that given to a congressional committee by Dr Kenneth Adelman, director of the US Arms Control and Disarmament Agency. It is pointed out that calculations of the consequences of releases of radioactivity from pressurized water reactors, such as the estimates prepared for the public inquiry into the British plan to build such a plant at Sizewell in Suffolk, suggest that acute deaths (within a few weeks) would be counted in hundreds, not thousands. The longer-term consequences — excess cancer deaths — would usually be greater in number.

The generalized effects of the radioactivity observed in Sweden will be much smaller. If atmospheric radioactivity was last week six times greater than the natural background for two or three days, the result will be increased exposure to radiation by a few per cent of the annual dose arising naturally. But this reassuring yardstick does not exclude the possibility that some people may ingest exceptional amounts of artificial radioactivity by the accumulation and concentration of particular radionuclides in foodstuffs.

Attempts to estimate the total amount of radioactivity released at Chernobyl are similarly uncertain. The source of the estimate that a total of 10^{18} bequerel were released at Chernobyl was most of all anxious that the uncertainties, which must be several orders of magnitude, should be clearly appreciated. By this yardstick, the Chernobyl accident may be 100 times potentially more damaging than that at Windscale in 1957, when an air-cooled graphite reactor caught fire. That accident was in turn much more serious, as measured by the total quantity of radioactivity released, than the accident at Three Mile Island eight years ago.

Among those with military and arms control interests, some importance is attached to the likelihood that reactors of the "Leningrad" type such as those at Chernobyl would have been a useful source of military plutonium.

According to the International Atomic Energy Agency's survey of the world's reactors published at the end of last year, there were 26 light-water-cooled graphite-moderated reactors in operation in the Soviet Union at the end of 1984, producing between them a total of 13.7 GW of electricity. A further nine reactors of this type were being built at that stage, although the bulk of the reactors now under construction in the Soviet Union are pressurized-water reactors.

France in Tokyo

Two heads better than one?

FRANCE has had two heads at the economic summit in Tokyo, one of them gung-ho for technological cooperation, and the other apparently lukewarm. The future of French policy in this increasingly important area of politics, which covers matters from the Strategic Defense Initiative (SDI) to joint industrial development and the mobility of scientists, is thus becoming somewhat murky.

At previous summits, President François Mitterrand, head of state and a socialist, has blown the trumpet for technology. His ministers, until the March election which threw them out, energetically pursued at least European cooperation in high technology and research. He launched Eureka, a kind of European civil answer to SDI. From the new Prime Minister, the right-wing Jacques Chirac, who is accompanying Mitterrand in Tokyo, little has been heard on these matters, apart from his proposing a candidate for foreign minister who was highly favourable to French government participation in SDI. Mitterrand vetoed the appointment: he believes out-and-out French participation will lead to a brain-drain, and a loss of French control of important new industrial technologies.

If this was a negative step (in the sense of international cooperation in technology), Chirac has also taken negative steps in his major reduction of the French research budget (see *Nature* **321**, 8; 1986) — which will reduce the capacity of French bodies to join international collaborations — and in a sweeping reduction in the powers of the research ministry, which has lost control of technology policy as well as a number of technological programmes (such as space and energy) to the traditionally inward-looking ministry of industry.

Meanwhile other major divisions seem likely to plague the house of French international cooperation. A highly competent official, Robert Chabbal, ex-director of science for the North Atlantic Treaty Organisation (NATO), has been appointed coordinator for international research affairs, but he will reside in the weakened ministry of research. The ministry's links with the Elysée, President Mitterrand's palace and office across the Seine, were originally strong and well-used in the development of Eureka, but they must now seem somewhat redundant as both parties have lost influence.

The demise of the ministry of research was clear in the new government's attributions of power and budget: the decline of the Elysée is less easy to identify.

When before the election Mitterrand was discussing the possible "cohabitation", as the French like to call it, between himself and a potential right-wing prime minister, he made it clear that he would hold on to one thing: foreign policy. This area of action for the President would of course include his dreams of a "technological Europe", driven by France.

Since the election, however, Chirac, apart from losing his first choice of foreign minister, who might anyway have been a symbolic sacrifice, has made it clear that he, not the President, will determine French foreign policy. Chirac had made four foreign tours before the visit to Tokyo to establish his links with French Africa, and the British, German and Italian Prime Ministers, while President Mitterrand has remained at home. Moreover, Chirac has established a private foreign policy advisory unit in his offices in the Hôtel Matignon, and it seems clear now that French foreign policy is being run by Chirac and the foreign ministry at the Quai d'Orsay. Links between the Elysée, where the Eureka programme originated, and the ministry of research are therefore unlikely to have the importance they once did; in Tokyo, Mitterrand is little more than a constitutional monarch, and his past presidential pronouncements on a new world of technology merely echoes.

What everyone is waiting for, however, is to see where the new power, Chirac, moves in this area. His new foreign policy advisers have a strong industrial slant. Their chief is François Bujon de l'Estang (not to be confused with ex-President Giscard d'Estaing), a past international relations director of the French atomic energy agency (CEA), head of the US subsidiary of the nuclear fuel company COGEMA and chief cabinet adviser to Giscard d'Estaing's minister of industry, André Giraud. Moreover, Chirac's ministry of industry is as strong as the ministry of research is now weak. However, with the appointment as his science adviser of Yves Durant, an advocate of the freedom of research from state interference, who will be counselling Chirac to reduce the power of the ministry of research and its organizations still further, the chance of a renewed campaign by France for a research-led, high-technology future seems small.

Robert Walgate

Good week for Pasteur institute

THE Institut Pasteur, the biological and medical research institute in Paris founded by Louis Pasteur in the nineteenth century, has learned from a US court that it may, after all, be granted priority in its patent dispute with the US National Institutes of Health over who first invented blood tests for AIDS (acquired immune deficiency syndrome).

Millions of dollars could be involved in the argument, which dates back to September 1983, when the Pasteur filed a patent based on the discovery by its researcher Luc Montagnier of the virus that causes AIDS ("HIV", according to the recommended new nomenclature). Robert Gallo of NIH filed a similar patent based on his own work many months later, and was awarded his while the French application is still pending.

Now, the US Patents and Trademakers Office has announced "an interference" between the applications, in terms which, according to the Pasteur, mean that the institute will be awarded the patent rights unless Dr Gallo can prove prior discovery of HIV. Here Pasteur scientists feel on firm ground, but recent statements by Gallo (see p. 119) may give cause for doubt.

Moreover, all is not yet jubilation in Paris, as a final judgement in the US courts will take two years, and any redistribution of royalties on tests will take place only from the date of the judgement and will not be retroactive. Meanwhile, attempts to achieve a negotiated end to the dispute continue, and at the Pasteur (already heartened by a bequest from the Duchess of Windsor) they now feel they have a trump card.

Robert Walgate

ESF joins Ocean Drilling Program

Washington

THE European Science Foundation (ESF) has signed on as the seventh member of the Ocean Drilling Program (ODP), an international project for ocean basin exploration. ESF has been interested in joining for some time, but the $2.5 million membership price tag was a stumbling block that has only recently been overcome.

As an ODP member, ESF can send two scientific representatives on each ODP cruise, and one co-chief scientist each year. ESF will also participate in mission planning and site selection.

Representatives of ESF and the National Science Foundation signed the memorandum of understanding sealing the deal at a meeting in Annapolis, Maryland, last week of the ODP executive committee. ESF joins France, West Germany, the United Kingdom, Japan, Canada and the United States as members of ODP. A representative of the Soviet Union attending the Annapolis meeting indicated that his country is seriously considering rejoining ODP, but has not yet made a decision on that score.

Joseph Palca

US technology

Parallel computer unveiled

Cambridge, Massachusetts

JUST two and a half years after setting out to build the world's first "fifth generation" computer, Thinking Machines Corporation (TMC) of Cambridge, Massachusetts, last week unveiled the Connection Machine (CM), a massively parallel computer with 65,536 individual processors. TMC has already developed some remarkable applications for the new machine but the company consultant, Richard Feynman of California Institute of Technology, says the problems have yet to be dreamed up that will make full use of CM's unique abilities.

While a graduate student at Massachusetts Institute of Technology (MIT) in Cambridge, CM's spiritual father Danny Hillis came up with the blueprint for a data-level parallel processing computer. Using data-level processing leads to a more natural way of thinking about certain problems, says Hillis. For example, organizing a visual image by examining one small section at a time makes less sense than processing all the information in the image simultaneously. Data-level processing works best on problems with large amounts of data, whereas control-level parallel processing machines are most effective when the ratio of program to data is high. But control-level parallelism involves the difficult task of developing algorithms for asynchronous control of operations.

Communication among processors is the key to CM. Locally, this is done by interconnections among neighbouring processors. For general communications and dynamic reconfiguration, CM uses routers to send messages to the 64K processors arranged in a 16-dimensional hypercube at speeds of up to 3,000 megabits per second.

CM consists of a front-end computer, either a VAX or a Symbolics 3600, that sends instructions to the parallel processors. Each processor contains 4K of memory, so a fully configured CM has 32 megabytes of memory. Even with a $3 million price tag, or $1 million for a CM with 16K processors, prospective buyers are lining up to get hold of the new machine. TMC has so far delivered only one CM, to the Defense Advanced Research Projects Agency (DARPA), but in two months machines will be heading to MIT (2), Yale, Perkin Elmer Corporation and a second machine to DARPA.

In 1983, Hillis teamed up with Sheryl Handler to form TMC. Handler wanted to find a product that would provide a "fundamentally new way of computing". The new company quickly brought on board top scientists as consultants: Hillis's adviser Marvin Minsky and Thomas Poggio of MIT, Stephen Wolfram of the Center for Advanced Study at Princeton and Caltech's Feynman. With $16 million in equity capital and a $4.7 million DARPA contract early on, TMC was able to take the risks Handler felt necessary to leapfrog the competition.

A major advantage of CM for new users is its ability to run in familiar operating environments. Extensions to C and LISP computer languages designed by TMC allow immediate access to CM's parallel capabilities. TMC has already come up with applications packages that show off CM's power. A search for key words in a 16,000-document database takes only 30 milliseconds, much faster than conventional searches. Image processing, very large scale integrated (VLSI) circuit design, and fluid flow problems all take advantage of CM by assigning one processor to each element of the problem's dataset. CM can achieve operating speeds up to 7,000 MIPS (million instructions per second) on certain applications, faster than the fastest computer utilizing more conventional architecture.

Although CM's initial capabilities are impressive, Wolfram believes that a new computer language is needed to take full advantage of it. CM is well suited to cellular automata, and Wolfram predicts that almost all problems now being solved using differential equations will be done in future by constructs like cellular automata.

Another plus for CM is its expandability. While traditional computers using principles developed 40 years ago by von Neumann are inherently limited by a single central processing unit, an arbitrarily large number of processors can in theory be linked together using CM's design. TMC scientists have already written simulations of a machine with one million processors that can run on current CM computers.

Hillis says TMC's next goal is to develop a true learning system. In a small way, the interconnecting processors of the CM resemble the interconnections of individual neurones of the brain. Hillis hopes that this type of architecture will encourage the development of learning algorithms that more closely resemble biological processes.

Other groups around the world are working on new computers using parallel architecture, but Poggio points out that CM has one obvious advantage over other projects: "It works". **Joseph Palca**

AIDS in India

Pool of infected women?

New Delhi

THE Indian Council of Medical Research (ICMR) is expanding its network for surveillance on acquired immune deficiency syndrome (AIDS) following the detection of six cases in Madras, capital of the southern state of Tamilnadu.

All those concerned are female prostitutes aged between 20 and 30. Two of them have disappeared and are being sought by the state government and the other four are under observation. Professor V. Ramalingaswami, director-general of ICMR and chairman of the AIDS task force that has been set up, says that none of the women showed clinical manifestations of AIDS except one who lost weight. The women were among 102 prostitutes whose sera were subjected to enzyme-linked immunosorbent assay (ELISA) at the ICMR centre at the Christian Medical College in Vellore.

The findings were confirmed by scientists at the Centers for Disease Control in Atlanta, Georgia, where the sera were analysed by Western blot technique.

ICMR fears that more AIDS cases may be detected once the male contacts of the prostitutes are traced, but this is an almost impossible task. The women have told social workers that they usually had ten partners a day, mostly truck drivers; they all denied having foreigners among their customers.

It is not yet known if the virus is HTLV-III or a related virus recently found in Senegal, West Africa. As there is no experience in India of isolating or characterizing the virus, ICMR has sent three scientists to the United States and West Germany for training.

Meanwhile, ICMR is launching a programme to train physicians and technicians in the diagnosis of AIDS. Twenty-five thousand test kits have so far been imported. It is proposed to set up surveillance centres in each district, and to test donations from professional blood donors. Imported blood and blood products now have to be accompanied by certificates testifying that they are free from AIDS, and a requirement for health certificates from visiting foreigners is being seriously considered.

A separate section is being created in the health ministry to implement the AIDS detection and control programme. Ramalingaswami says this will put an extra strain on the health budget, half of which at present goes towards control of malaria. "We have our priorities and there is not much money for AIDS observation", says Ramalingaswami, but he admits that the detection of AIDS must be a priority if it is not to become widespread. **K.S. Jayaraman**

Archaeology congress

US to attend or stay away?

New Orleans

ATTENDANCE at the 1986 World Archaeology Congress at Southampton, England, has become a "moral litmus test" for US archaeologists. But there was no consensus among potential participants at the meeting here last month of the Society for American Archeology (SAA).

The congress, planned over several years with special attention to the participation of scientists from developing countries, has been controversial ever since the British organizing committee sent letters of "disinvitation" to South African and Namibian scientists. In the aftermath, the international parent body, the International Union of Prehistoric and Protohistoric Sciences (IUPPS), withdrew its recognition of the Southampton meeting; a conference to be held in Mainz, West Germany, in September 1987 is now recognized as the official 11th World Archaeology Congress (see *Nature* **320**, 3; 1986).

Opinion at New Orleans seems to have been that it is for scientists individually to decide how to balance the principle of a stand against apartheid and that of free international exchange between scientists.

Thus one would-be participant said that he wanted nothing to do with a meeting that would exclude such noted scientists and opponents of apartheid as Professor Phillip Tobias (University of the Witwatersrand), but that "I don't go along with some colleagues' wish to ostracize those who may attend".

On the other hand, Thomas Patterson (Temple University), a co-founder of Archaeologists Against Apartheid, urged colleagues to attend the Southampton congress to avoid giving the impression that US archaeologists, "consciously or unconsciously", are in favour of apartheid. According to Ian Hodder (University of Cambridge), some 22 per cent of registrants from the United States have already cancelled.

The large number of participants from developing countries expected at Southampton adds another side to the question. Hodder says that many of them would either be prevented by their governments from attending, or would abstain on their own if South Africans were to be present.

Some at the SAA meeting raised the further question of whether an international congress is possible at all. "What guarantee is there that the same problems will not recur in Mainz?", one archaeologist asked. Hodder says that anti-apartheid groups in West Germany are mobilizing to protest at that meeting.

Meanwhile, in Berkeley, California, a symposium held in mid-April to honour anthropologist J. Desmond Clark upon his retirement, with the participation of several scholars from South Africa, passed without incident, because the existence of the symposium was not made known to anti-apartheid groups there (see *Nature* **320**, 562; 1986).

One project scheduled for discussion at Southampton is the establishment of a truly international body, to correct what is generally conceded to be a European bias in the present make-up of the international union. A more broadly based coalition, it is hoped, could better ensure the free assembly of its members.

James Sacket (University of California, Los Angeles) urged that the United States should bring more weight to bear in future actions of IUPPS, where its role is small although it contributes a large proportion of the world's practising archaeologists. He suggested that one step towards the greater internationalization desired by all would be to hold the 12th World Archaeology Congress, scheduled for 1991, in the United States.

A member of the IUPPS executive committee, Sacket had made several attempts to reconcile the position of the British national committee with the requirements of IUPPS, proposing for example that participants should have the option of registering simply as individuals and not in the name of their country, but was unable to effect a compromise. "I was told that 'We do not want interference from the great powers'", he said. Thus, at this point, the future role of the United States in the international union seems problematic. **Sandra Ackerman**

Biotechnology

DNA fingerprints go commercial

BY early next year, and for something like £250, it will be possible to obtain a DNA fingerprint from a blood or tissue sample sent to a testing centre in Britain. The initial demand is expected to be for paternity testing, but the test has already proved invaluable in proving relationships that are doubted by immigration authorities and has considerable potential in forensic testing too.

The centre is to be operated by the diagnostics group of Imperial Chemical Industries (ICI), the British chemical and pharmaceutical giant, which is in an advanced stage of negotiation with the Lister Institute for the exclusive rights to a test devised by Dr Alec Jeffries of the University of Leicester. Royalties from the tests, which are likely to be substantial, will be shared by the University of Leicester, Dr Jeffries and the Lister Institute, of which he is a research fellow.

It requires considerable expertise to carry out the test, which types individuals in terms of a set of highly variable DNA sequences on human chromosomes. At the heart of the test is a process of hybridization between the individual's DNA and radioactive DNA probes. Before the hybridization can be carried out, however, the DNA has to be extracted and cut by enzymes into fragments which are separated according to size. Even after hybridization, it is not a simple matter to interpret the "result", a series of radioisotopic bands on a gel.

Although such techniques are routine in molecular genetics laboratories, they are much too demanding for any routine diagnostic laboratory. That is why the DNA fingerprinting test will not be marketed as a kit but offered as a service. (There is one commercial kit based on DNA hybridization which is used for the detection of salmonella, and its manufacturers, Integrated Genetics, plan others. But none of these tests will require other than crude sample preparations and they only detect the presence or absence of a DNA sequence that identifies the organism.)

Demand for the test seems certain to be considerable, with estimates that many thousands of immigration disputes worldwide could be settled each year. Dr Jeffries has been able to cope with only a few per cent of the requests that he has received in the wake of the initial publications that illustrated the potential of DNA fingerprinting (*Nature* **314**, 67; **316**, 76; **317**, 818 and **318**, 577 (1985)).

Forensic testing is likely to be more problematic because of the need for prosecution and defence to have recourse to independent tests. There is therefore considerable uneasiness about there being only one centre to which samples can be sent. One solution in Britain would be for the Home Office Forensic Science Service, which has been evaluating the test, to carry out its own DNA fingerprinting, presumably for the police, while the defence made use of the ICI centre. Another solution would be to allow separate scientists, acting for the two sides, to have independent access to a single facility, as they sometimes do now in forensic science laboratories.

Further demand for testing may come from the armed forces. In the United States, at least, there have already been discreet enquiries about the possibility of having all military personnel DNA fingerprinted to make it possible to identify from tissue fragments the victims of air disasters or bombings. **Peter Newmark**

Research planning

UK needs a forum for decision

THERE should be a mechanism in Britain for directing public investment in research towards areas likely to yield economic benefit, according to a report of the Advisory Committee on Applied Research and Development (ACARD), published this week (HMSO, £4.90). But the report does not live up to its title, *Exploitable Areas of Science*, in that it fails to pick winners in which the government might invest, concentrating instead on the considerations it believes should determine investment in research.

The report is the work of a committee under Dr C.H. Reece, the director of research at Imperial Chemical Industries, which includes both academic and industrial scientists. The starting point for the study is the British view (which the committee denies) "that research cannot be organised to deliver economic returns". One of the chief conclusions is that, in the allocation of research funds, the public research councils should be more sensitive to estimates of the kinds of research that might yield economic benefit.

Like other such committees, the ACARD group wrings its hands over Britain's economic performance in recent years. Recognizing that the flow of oil from the North Sea has been one of the influences leading to the decline of British manufacturing industry and that oil will be a declining resource in the future, the committee says that research planning now should be aimed at the development of technology that will allow the maintenance of living standards when the North Sea is less prolific.

The committee says its chief task has been to decide whether deliberate research planning is feasible; it concludes that it is. But, according to the report, there is at present no forum in which these questions can be discussed and decided. ACARD asks for a process of continuing consultation with "researchers (new and established), research allocation organisations . . . and the industrial research community".

To these ends, the committee says, there should be a more systematic approach to the collection of data on the patterns of research in Britain. This echoes a growing concern that the data available on the conduct of research in Britain, even as now gathered in the annual review published by the Cabinet Office, are incomplete, unreliable and out of date.

The committee also asks that its new mechanism for research planning should include a means by which "relevant opinions and information" can be "evaluated". The committee would rely on informed discussion to reach conclusions, but it skirts around the question of who would be involved in such a process. Thereafter, the committee says, there should be a process for allocating funds to priority areas (at least at one point, the report uses the verb "to prioritise") and a "commitment to exploit the results of science to UK benefit".

If the government follows the committee's recommendations, there will be no change in the present arrangements for channelling funds towards research, but more resources will be spent on the gathering and evaluation of data. The report says that "there should be a small management group" to steer the process.

The committee acknowledges that its proposals would entail "changes in emphasis" of the present work of the research councils, but says that the result should be "a more rational allocation of resources to those science areas of prime national interest". On industrial research, the committee pleads for more foresight by industrial companies with the objective of defining "potentially useful fields in which to work." □

AIDS in California

State aid offered for vaccine

Washington

LEGISLATION that would "shut the door" on strict product liability for vaccines against AIDS (acquired immune deficiency syndrome) is working its way through the California State Assembly, with the blessing of the two biotechnology companies closest to vaccine development. In addition to its shield from liability, the bill provides $6 million in aid for clinical testing and $20 million for state purchase of the vaccine to guarantee a million-dose market. Genentech and Chiron, eager to see the bill made law, say it would remove economic obstacles to vaccine development; California hopes it would induce these companies to triple their development efforts.

California ranks second in the United States for diagnosed cases of AIDS, with over 4,600 reported, and a study released last month by the state's Department of Health Services (DHS) predicts the disease will have struck 30,000 Californians by 1990. Feeling both the pressure of a public health threat and the promise of engineered immunization from companies virtually in the legislative backyard, assemblyman John Vasconcellos last year met with Genentech and Chiron to discuss ways to accelerate vaccine development.

The companies outlined the reasons that hormones and growth factors grab most of the attention in their laboratories, while investment in AIDS vaccine research remains modest. They said they were deterred by the uncertainty of the market size, the costs of clinical trials, and the threat of litigation once the vaccine reaches the public.

Vasconcellos and other California assemblymen drew up a bill to answer these concerns. The measure would permit the state to grant each of three companies up to $2 million to defray the costs of clinical testing, the most expensive phase of drug development. If companies sold less than one million doses, California would buy the difference. And the state would also accept responsibility for injuries proved to have resulted from vaccine use, with recovery limited to $250,000 per case. The bill applies to California companies only, and they would still be held liable for cases involving negligence.

Most of California's legislators appear to favour the bill, which was introduced in January and heard in the Assembly judiciary committee last week. However, opposition may emerge next week, when the legislation goes before the Assembly's ways and means committee. But supporters can point to the DHS report, which expects medical costs for AIDS of $3,500 million by 1990, and a California Manufacturers Association estimate that each employee who contracts AIDS costs his employer $250,000. Faced with these figures, state-subsidized vaccines may seem like a bargain to Californians. **Karen Wright**

Degrees by consent

HIGHER degrees in Poland will in future be subject to party approval, according to a Polish scientist who emigrated last month. The PhD *Doctor Habilitatus* degrees can be conferred both by the universities and by the Academy of Sciences, but since 1982, there have been almost no formal doctoral studies in the universities (see *Nature* 320, 693; 1986), and graduates wishing to proceed to a higher degree can best do so by obtaining a research post in one of the institutes of the Academy of Sciences.

Until now, decisions on higher degrees awarded by the academy have been taken by the research council of the relevant institute. Some six weeks ago, however, Dr Zdzislaw Kaczmarek, the Learned Secretary of the academy, announced that from now on, he will decide, on the basis of a confidential report on the candidate from the party organization in the institute; this report will not be accessible to the members of the research council of the institute.

Vera Rich

Future of UK observatory

SIR—Your views on the future of the Royal Greenwich Observatory (RGO) (*Nature* **320**, 384; 1986) cannot be allowed to go unchallenged.

It is quite untrue that British astronomers are unperturbed by the announcement by the Science and Engineering Research Council (SERC) that RGO is to move; stunned would be a better word to describe our reaction to the extraordinary suggestion of a merger with the Royal Observatory, Edinburgh (ROE). But there is a growing ground swell of protest which will begin to surface as more people realize that they cannot this time leave action to somebody else.

I must also take issue with your use of the phrase "surplus observatory" in the heading. To put it at its lowest, if one observatory is surplus, why should it automatically be assumed that it is RGO? The telescopes at ROE are no more used for research than those at RGO. Moreover, I do not believe that either observatory is surplus to the needs of British astronomy. The two royal observatories are the major centres of research in optical astronomy in this country and it is healthy to have rivalry between them, just as it is good to have two major radio observatories and two major X-ray groups.

Each observatory runs large overseas facilities, which are complementary, and so no great benefit would accrue from administering them from the same site. A research council with vision would realize that developing the instruments for these facilities is only the first step in exploiting the overseas sites and that, far from their usefulness diminishing, both observatories can continue to play vital roles by collaborating with university astronomers to obtain the best results from the new instruments. It should not be assumed that the observatories' natural role is just to support university research; they will do that job far more effectively if they also collaborate actively in the research, as they do now.

RGO differs from ROE in not being actually on a university campus. (Actually, ROE is not quite on the campus either, but it is closer.) But that does not mean that it does not collaborate with university groups. Indeed, there has been very active collaboration with the University of Sussex for some twenty years, and we do not understand why the chairman of SERC feels that this connection is "not the kind of interaction we are looking for" (*Nature* **320**, 297; 1986). There are many places where related institutions on the same campus have far less interaction. Propinquity is no guarantee of interaction nor does separation preclude it.

In addition to the connection with its nearest university, RGO also collaborates with 12 British and European university groups on astronomical instrumentation and with more than 50 groups internationally on research projects. It is hard to see how a move to a particular university would increase this collaboration. As you say in your Opinion column, the benefits of an academic partnership are indeed huge, but they are already being realized. The danger of moving RGO from its present site is that the accompanying reduction of resources will be larger than the reductions already threatened at Herstmonceux and that universities as a whole will end up losing some of the valuable resources that they currently enjoy.

In short, the diffidence that you mention in deciding what to do about RGO arises simply from the fact that there is no obvious reason to do anything. RGO is doing a good job where it is and no serious scientific case has been made for moving it. The only conceivable reason for a move would be to save money, and there is no sign that that is possible without a massive reduction in resources which would defeat the claimed object of the move.

R.C. SMITH
Astronomy Centre, Physics Building, University of Sussex, Falmer, Brighton BN1 9QH, UK

Sexist ads

SIR—In the issue of *Nature* for 3 April 1986, organic life forms were represented in your advertisements in the following proportions: four men, all wearing lab coats and engaged in "serious" scientific pursuits; one unisex doctor treating a female patient; one unisex mouse in a laboratory; one woman, dressed in tight-fitting jeans and denim jacket, exposing a portion of her lower back, smiling inanely and apparently advertising a product involved in DNA detection.

Unfortunately, the predilection of your advertisers to portray men (and in some cases animals) as serious-minded scientists, and women as dumb decorative objects, is not confined to this one issue. A notable feature of the back cover of past issues of *Nature* has been a dripping, apparently unclad blonde emerging from a lake and trying to sell air.

Please instruct your advertisers to take into account the fact that many of your readers are professional women, and are not responsive to the type of advertisement normally associated with the darker recesses of the tyre and car parts trades.

KATHLEEN WESTON, ALISON COZENS, HILLARY C.M. NELSON, LOUISE FAIRALL, LINDA AMOS, LAUREL MENGLE-GAW, FLEUR-ANGE LEFEBVRE, MELANIE J. CLARK, CYNTHIA KENYON, MARIANN BIENZ, LINDA BREEDEN, HEINKE SCHNABEL, MARGARET ROBINSON, DONNA ALBERTSON, IVA GREENWALD, MARIA LEPTIN, DANIELA RHODES, MARTINE VERHOEYEN, LYNETTE TIGHE, CLAUDIA BEREK, SANDRA SATCHWELL, C. JANE MITCHELL, CARLOS V. CABRERA, ROB WHITE, HUGH PELHAM, SEAN MUNRO, COLIN WATTS, R.J. BAER, ANDREW J.H. SMITH, ANDREW J. NEWMAN, KIYOSHI NAGAI, ALAN FORSTER, GREG WINTER, DAN BROWN, JEFFERSON FOOTE, LUIS MARTIN, PETER SORGER, GARETH WILLIAMS, GRAHAM COOK, ANDREW FIRE, VICTOR TYBULEWICZ, STEPHAN BECK, RICHARD TURNER, HORACE DREW, TOBY J. GIBSON, TONY KOUZARIDES
MRC Laboratory of Molecular Biology, Hills Road, Cambridge CB2 2QH, UK

SIR—A recent series of advertisements in *Nature* shows us women in jeans or half-naked. Is it not a bit silly for a scientific journal to feature such silent propaganda for feminist and so-called liberal attitudes? Why not give women their dignity back by presenting them in skirts?

A. BRADBURY
F. VAN STRAATEN
MRC Laboratory of Molecular Biology, Hills Road, Cambridge CB2 2QH, UK

MRC unit closure

SIR—We are writing in response to the report (*Nature* **320**, 478; 1986) on the proposed closure of the Medical Research Council (MRC)'s Mammalian Genome Unit in Edinburgh. We find it disturbing that the MRC secretary, Sir James Gowans, should be unable to explain the failure to find a "suitable" director for a molecular biology unit of international reputation.

The reduction in funding of MRC, imposed by the government, is no doubt the root cause of the closure. Financial uncertainty from year to year, together with the greater rewards to be attained elsewhere, produces a decline in morale that increases the rate at which scientists leave the country.

We would have expected that the closure of a molecular biology unit of high calibre would have merited rather more than a "small decision" by MRC. If it cannot find a director deemed "suitable" by its present criteria, we suggest that those criteria may need re-examining. The loss of the Mammalian Genome Unit will be yet another nail in the coffin of British science in a field which is receiving encouragement and increased financial support from more farsighted nations.

MEMBERS OF THE UNIT
MRC Mammalian Genome Unit, Department of Zoology, University of Edinburgh, West Mains Road, Edinburgh EH9 3JT, UK

Hanover highlights all the latest developments and industrial applications in the field of biotechnology

From its very inception BIOTECHNICA Hanover has established itself as Europe's leading forum for research, development and practical applications in the field of biotechnology. The basis for the unprecedented success of BIOTECHNICA is two-fold. Firstly, the excellent program of symposia, workshops and lectures held by internationally renowned experts. And secondly, the user-oriented exhibition presented by leading manufacturers and research institutes.

The international congress – a meeting-place for experts

On three successive days, 16 internationally renowned experts will deliver papers on the application of biotechnology in the following fields:

Medicine/pharmacology
e. g. diagnostics and various approaches to therapy following cardiac infarction

Food production/ agriculture
including the optimization of agricultural produce and quality control in foodstuffs

Environmental protection
from biological methods of combating air pollution to the treatment of sewage

Seminars and workshops – a spotlight on research and its practical application

Research institutes, universities and leading manufacturers will utilize the comprehensive parallel program of talks, symposia and workshops in order to present their latest research findings, products and processes. Hanover illustrates how research findings can be transformed into marketable industrial processes and products.

In a series of special seminars organized by the European Community, BIOTECHNICA '86 will also present the most important results of the biotechnological research projects funded by the EC.

The 3rd US Seminar for Biotechnology, organized by the US Foreign Commercial Service, will also be held on all three days of BIOTECHNICA '86.

The exhibition – geared to industrial applications

Over 200 research institutes and commercial firms will exhibit at BIOTECHNICA '86. The exhibition will highlight biotechnological processes and products, the latest developments in laboratory equipment and techniques, as well as new production technology. It's no surprise, therefore, that in 1985 some 3,500 professional visitors from 27 countries attended this comprehensive display.

At BIOTECHNICA Hanover '86 you can find out all you want to know about every major aspect of biotechnology.

If you require more information please contact:
Deutsche Messe- und Ausstellungs-AG
Abtlg. "Neue Projekte"
Messegelände, D-3000 Hannover 82
Tel.: (0) 511/89-2720

23rd–25th September 1986
2nd International Exhibition + Congress for Biotechnology

BIO Technica'86 Hannover

Reader Service No.10



STILL FIRST WITH THE BEST IN SCIENCE

STILL AVAILABLE AT HALF PRICE!

A PERSONAL SUBSCRIPTION is now something *you* can afford... each week crucial research results and the most important scientific news at your door... keeping you fully informed and right up-to-date – all for just £1 a week, that's £52 a year and **half** the current institutional price.

There's *never* been a better time for you to subscribe. All 51 weekly issues will be delivered to the address of your choice. You can start your annual subscription with any issue you choose. And you will receive six bi-monthly author indexes, together with the annual index of subject and author.

COMPLETE THIS ORDER FORM TODAY 7B64

SPECIAL HALF PRICE RATE OF £52.00

☐ Please send me a personal subscription to Nature for one year (51 issues) at the SPECIAL HALF-PRICE RATE of £52.00

☐ I enclose my personal cheque for £52.00 made payable to Nature. (Note: Institutional cheques cannot be accepted at this special rate).

☐ Please charge to my credit card account: Access/American Express/Visa/Diners Club.

Account No. _____

Card Expiry Date _____ Signature _____

Name _____

Address _____

_____

_____ Date _____

Please return this form to: Circulation Manager, Nature, Brunel Road, Houndmills, Basingstoke, Hants RG21 2XS

This offer applies to UK only.

Please allow approximately 4 weeks for delivery of first issue

Mechanizing cellular automata

Whether or not it is possible to represent hydrodynamical systems by autonomous entities on the vertices of a lattice threatens to become an unreal issue.

THE news this week (see p. 103) of the new parallel architecture computer developed by Thinking Machines of Cambridge, Massachusetts, should be read in conjunction with two unusually contradictory papers in *Physical Review Letters* for 15 April. Both are stimulated by an as yet unpublished paper by J. Salem and Stephen Wolfram.

Wolfram is the Princeton-based physicist who carries a torch for von Neumann's model of the cellular automaton, the microscopic entity in an array whose state at any time is determined by its own state at some previous time and by those of its immediate neighbours.

Steven A. Orszag and Victor Yakhot first set out to show that cellular automata cannot be adapted in the real world to solve the problems of fluid dynamics (*ibid.*, **56**, 1691; 1986). The next paper (Margolus, N., Toffoli, T. and Vichniac, G., *ibid.*, **56**, 1694; 1986), based on the same unpublished paper, purports to reach the opposite conclusion. What is the innocent reader to conclude?

There is nothing startlingly novel about the model of the cellular automaton. Fill accessible space with microscopic cells, most simply of the same size. Then let each be occupied (or empty of) a physical entity which can be in only one of several states (most simply, finite in number), and then allow that future generations of this system will evolve, with the passage of time, according to rules applying equally to all of them (see Wolfram, S., *Nature* **311**, 419; 1984).

Such a system can obviously be a model for various aspects of the real world. If the entities occupying separate cells are members of a population, the evolution of the arrangement as time goes on may be a model of how a living population evolves. But if the cells are occupied by tiny magnets allowed to point in one direction or the opposite (for example), the system is a model for a ferromagnet.

Such systems are also capable of modelling the behaviour of ordinary dynamic systems such as those forever cropping up in physics. Anybody who doubts that has merely to recall that systems of differential equations can be approximated to by finite difference equations which may be more conveniently soluble, but which are in any case a convenient way of writing a computer program to simulate the original set of equations.

So why not think of using networks of cellular automata as means of solving real problems in applied physics? A few simple systems are easily imagined. Suppose, for example, that the objective is to follow the time course of a plucked violin string or of a bent beam; one might approximate the system by a one-dimensional array of cellular automata whose individual states might represent the displacement of the string from a reference datum. If the evolution of the system is then described simply in terms of the instantaneous state of each element and its nearest neighbours, the approximation is certainly no worse than that familiar in the simple textbooks of applied mathematics, where only first and second derivatives seem to matter.

The argument that has now arisen stems from what must be the most ambitious goal of all, how to use networks of cellular automata to stimulate the motion of fluids with real thermodynamic properties, heat capacity, vorticity and friction, for example. This, it seems, is what Salem and Wolfram have been up to, in a paper with the title "Thermodynamics and Hydrodynamics with Cellular Automata", which it is said is "to be published".

Orszag and Yakhot are against the conclusions of that unpublished paper, Margolus and his colleagues show that the arguments are valid. A curious almost-ethical point arises at this stage. It is rare that journals publish disputatious accounts of a paper that has not yet been made accessible to readers. The issue is only nearly ethical; readers who do not care for having to read between the lines can always read some other journal.

Reading between the lines, what Salem and Wolfram have done is to argue that it should be possible to represent a real thermodynamic fluid by a system of cellular automata in the sense that the space and time averages of the properties of cellular automata will follow the behaviour of incompressible fluids which are described by the Navier–Stokes equations. Friction enters, producing heat (and robbing the system of kinetic energy).

A crucial part of the Salem and Wolfram argument (again between the lines) is that the coming of computers with parallel architecture should make these simulations more accurate and also more real.

Orszag and Yakhot do not dispute the virtues of computers made from, say, 64,000 microprocessors strung together (who could?). Their quarrel is with the underlying physics and the computational economy of the cellular automata models Reading between the lines, one can conclude that Salem and Wolfram represent continuous variables such as the velocity (of the fluid) in a velocity field by means of averages over groups of neighbouring cells carrying separate cellular automata. Questions then arise about the efficacy of the representation; either there are so few cells in the group over which average values represent dynamical variables in the real world that the calculation is inaccurate, or the group is large enough to be realistic but the computational work is enormously increased. The essence of the argument is that tractable networks of cellular automata will usually be unrealistic, but that realistic networks will be less easily soluble than the equations to which they are an approximation.

Margolus *et al.* write in a quite different vein. "Surprisingly enough, cellular automata can faithfully model continuum systems such a fluids . . . [but] are poorly supported by conventional scientific computers . . . more appropriate architecture can easily gain a performance factor of at least 10,000 . . ." Part of the trick (to be revealed in the unpublished paper by Salem and Wolfram) is to devise the generation rules for the automata so that microscopic reversibility is assured. Margolus and his colleagues show, among other things, some pretty diagrams in which a central blob of fluid on a two-dimensional plane spreads outwards in a growing concentric ring. The authors surprisingly boast that one simple system (a two-dimensional lattice gas) is macroscopically as well as microscopically reversible.

Quite what the dispute is about can be read only between the lines, but there is an obvious and simple resolution of it: simply build computer systems with as many microprocessors as there are atoms whose behaviour must be simulated, and make sure that they respond at least as quickly. Then the objections of the Orszags and Yakhots of this world will melt away. As it happens, Margolus and his colleagues say that it should be possible to deal with 10^{7} elements (the square of the cube root of Avogadro's number) within a decade, and to "span the gap between the microscopic and the macroscopic world" soon afterwards. That may be possible, but the question will remain of whether it is science.

John Maddox

Protein translocation

A common mechanism for different membrane systems?

from Gottfried Schatz

ALL cells transport specific subsets of their own proteins across membranes in order to segregate metabolic pathways, to communicate with other cells or to build new membranes. Because each of the different membrane types poses the same problem — how to transport a large hydrophilic protein across a hydrophobic phospholipid bilayer — it has been tempting to suppose that cells have evolved a universal solution. Until recently, however, most of the experimental evidence seemed to argue otherwise[1]. Although the endoplasmic reticulum of eukaryotes seemed to translocate proteins only while they were still being synthesized (that is, by co-translational translocation), all other membrane types studied — bacterial, mitochondrial, glyoxysomal and chloroplast — can translocate completed protein chains post-translationally. Reports from several laboratories[2-8] now suggest that these differences are more apparent than real, and that the mechanism of translocation may indeed be fundamentally similar, or even the same for all membrane systems.

The co-translational model of protein translocation, derived from pioneering studies on the mammalian endoplasmic reticulum[9], is as follows. Proteins destined to be translocated into or across the endoplasmic reticulum membrane contain a specific signal sequence, usually located at the extreme amino terminus. As this sequence emerges from the large ribosomal subunit, it binds to a cytoplasmic ribonucleoprotein complex (the signal recognition particle) which stops further elongation of the polypeptide chain. Binding of the blocked ribosomal unit to a proteinaceous receptor on the cytosolic face of the endoplasmic reticulum releases the elongation arrest and causes the growing polypeptide to move across the membrane. Soon after the amino-terminal signal peptide has traversed the membrane, it is removed by a signal peptidase located in the lumen of the endoplasmic reticulum.

This model rests on several key findings[1,9]. First, attempts to translocate completed polypeptides into microsomes (isolated vesicular fragments of endoplasmic reticulum) have always failed: translocation occurred only while the polypeptide was still being synthesized. Second, the signal sequence was removed by the luminal peptidase before the carboxy-terminal domain of the protein had been synthesized; uncleaved, full-length precursors were thus undetectable in pulse-labelled intact cells. Finally, the signal-recognition particle arrested the elongation of secreted, but not of cytosolic proteins; the arrest of elongation could be abolished by adding mammalian microsomes, whereupon the growing secreted proteins were translocated into the microsomes. This tight coupling between synthesis and translocation seemed to be an elegant mechanism for ensuring that proteins destined to be inserted into or across the membrane were not released into the cytosol.

The co-translational model is purely operational and does not invoke an obligate mechanistic coupling between polypeptide elongation and translocation. It has, however, often been interpreted to imply that translocation is driven by chain elongation which is in turn powered by the hydrolysis of high-energy phosphate bonds. This interpretation is difficult to prove or refute: by its very nature, a co-translational mechanism makes it impossible to probe the energy requirement of translocation independently from that of protein synthesis. Moreover, it is clear that in other membrane systems there can be no such mechanistic coupling: all other membrane systems can translocate polypeptide chains post-translationally. For example, mitochondria efficiently import pre-synthesized precursor polypeptides, both *in vitro* and *in vivo*. Import across the inner membrane requires an electrochemical potential across that membrane[10]. Post-translational uptake of proteins is also observed with chloroplasts[11] and glyoxysomes[12]. With chloroplasts, uptake is dependent on ATP rather than a transmembrane potential[13]. Finally, bacteria can translocate proteins across their plasma membrane post-translationally in a process requiring an electrochemical potential across that membrane[14,15]. Although post-translational movement of proteins across bacterial membranes has long been controversial[1], it is now accepted by most workers in the field[16]. For a while it seemed, therefore, that nature had devised two distinct mechanisms for moving proteins across membranes, one coupled to protein synthesis and the other not.

Last year, however, obligate coupling between protein synthesis and translocation across the endoplasmic reticulum began to look less certain. For example, elongation arrest by the signal recognition particle was not detectable with all secretory proteins[17], or when protein-synthesizing systems from mammalian sources rather than from wheat germ were used[18]; this raised the possibility that elongation arrest was an artefact limited only to some secretory proteins, and only if these were synthesized in the heterologous wheat-germ system. Similarly, signal-recognition particles from which a segment of the RNA chain and/or two protein subunits had been removed no longer stopped elongation of secretory proteins, yet still mediated their translocation across the endoplasmic reticulum[8,19]. Finally, a signal sequence engineered into an internal location could effect translocation of both flanking domains into microsomes[20]. In this case, at least the amino-terminal domain had to be translocated after it had been synthesized. Still, there was no direct proof that a completed protein could be translocated into microsomes.

Such proof is now available. Hansen, Garcia and Walter[2]; Rothblatt and Meyer[3-5]; and Waters and Blobel[6] find that the precursor to α-factor (a secreted yeast mating hormone) can first be synthesized in a messenger RNA-dependent protein synthesizing system from yeast and then be translocated into yeast microsomes. Taken together, these experiments show that post-translational uptake into yeast microsomes can be as efficient as co-translational uptake, is insensitive to uncouplers and ionophores, and requires ATP. It will be interesting to see whether post-translational uptake into yeast microsomes can occur with proteins other than the α-factor precursor.

Energy-dependent post-translational uptake into microsomes is not unique to yeast: Mueckler and Lodish report[4] that dog pancreas microsomes can post-translationally incorporate the human glucose transporter, a glycoprotein of relative molecular mass 54,000 containing as many as 12 membrane-spanning segments. Even though post-translational uptake in this system is at least one order of magnitude less efficient than co-translational uptake, it is increased threefold

1. Kreil, G. *A. Rev. Biochem.* **50**, 317 (1981).
2. Hansen, W., Garcia, P.D. & Walter, P. *Cell* **44**, 397 (1986).
3. Rothblatt, J.A. & Meyer, D.I. *Cell* **44**, 619 (1986).
4. Mueckler, M. & Lodish, H.F. *Cell* **44**, 629 (1986).
5. Rothblatt, J.A. & Meyer, D.I. *EMBO J.* (in the press)
6. Waters, G.M. & Blobel, G. *J. Cell Biol.* (in the press).
7. Mueckler, M. & Lodish, E.F. *Nature* (in the press).
8. Siegel, V. & Walter, P. *Nature* **320**, 81 (1986).
9. Walter, P., Gilmore, R. & Blobel, G. *Cell* **38**, 5 (1984).
10. Schatz, G. & Butow, R.A. *Cell* **32**, 316 (1983).
11. Highfield, P.E. & Ellis, R.J. *Nature* **271**, 420 (1978).
12. Zimmermann, R. & Neupert, W. *Eur. J. Biochem.* **112**, 225 (1980).
13. Grossman, A., Bartlett, S. & Chua, N. *Nature* **285**, 625 (1980).
14. Date, T., Zwizinski, C., Ludmerer, S. & Wickner, W. *Proc. natn. Acad. Sci. U.S.A.* **77**, 827 (1980).
15. Randall, L.L. *Cell* **33**, 231 (1983).
16. Wickner, W.T. & Lodish, H.F. *Science* **230**, 400 (1985).
17. Anderson, D.J., Mostov, K.E. & Blobel, G. *Proc. natn. Acad. Sci. U.S.A.* **80**, 7249 (1983).
18. Meyer, D.I. *EMBO J.* **4**, 2031 (1985).
19. Siegel, V. & Walter, P.J. *J. Cell Biol.* **100**, 1913 (1985).
20. Perara, E. & Lingappa, V.R. *J. Cell Biol.* **101**, 2292 (1985).
21. Ferro-Novick, S., Novick, P., Field, C. & Schekman, R. *J. Cell Biol.* **98**, 35 (1984).

when an amino-terminal fragment of the glucose transporter is synthesized off a truncated messenger RNA that encodes the first 340 amino acids of the protein and lacks the stop codon. Uptake of this amino-terminal fragment is insensitive to various ionophores, but requires cleavage of high-energy phosphate bonds[7].

These new findings do not contradict the previous view that movement of proteins into the endoplasmic reticulum is, in fact, co-translational. But they do show that co-translational translocation is not obligatory. As this excludes a strict mechanistic coupling between elongation of a polypeptide chain and its movement across the endoplasmic reticulum, it is now a distinct possibility that proteins move through different membranes by fundamentally the same mechanism. This mechanism is still a mystery, but efforts to unravel it will benefit from the newly developed cell-free endoplasmic reticulum translocation systems from yeast[2,3,6]. As these systems should allow the molecular analysis of yeast mutants defective in early steps of secretion (see, for example, ref. 21), biochemists have been handed a sharp new scalpel for dissecting the machinery which moves proteins across the endoplasmic reticulum. □

Gottfried Schatz is in the Biochemistry Department, Biozentrum, University of Basel, Klingelbergstrasse 70, CH-4056 Basel, Switzerland.

Archaeology

Late Saxon ceramic utensils

from Richard Hodges

POTSHERDS — the tableware, cooking pots and storage containers of ancient times — appear at first sight to be the least attractive component of archaeological excavations. But the study of ancient ceramics turns out to be surprisingly useful, providing detailed information about past societies (see ref. 1). The significance of this approach is well illustrated by the recent work of Alan Vince[2] on the mediaeval pottery of London.

The sheer bulk of potsherds unearthed in modern open-area excavations (for example, several tons from the tenth century Viking dig at York in the United Kingdom[3]) has resulted in a shift of emphasis in ceramic studies away from distinguishing pottery in terms of its shape and decoration and towards a system based on pottery fabrics — the clay matrix used by the potters. This fabric series can distinguish between the workshops responsible for the pottery production. The approach necessitates identifying the macroscopic features of the clay; if these features are unclear or can be assigned more precisely to a specific source, a microscopic analysis is performed. The commonest technique in this second stage of analysis is ceramic petrology, in which thin sections of the fabric are examined under a petrological microscope. In some cases the exact provenance of the clay is apparent from its mineralogical character; more often the clay has been taken from some indistinctive riverine source and only the potter's 'recipe' can be identified.

There are tons of pottery in the excavations of the Department of Urban Archaeology at the Museum of London, making a typological listing impractical. Therefore, the fabric series was classified using macroscopic and microscopic principles[2]. Each fabric embraces forms which vary according to its date of manufacture. Potsherds discarded in the Middle Ages offer fascinating patterns of the history of the potter's craft and how and where these low-grade utensils were sold.

The Late Saxon ceramics from London illustrate this point vividly. It is highly debatable whether London was a significant community before King Alfred's time, but with the explosion of urban development in the tenth century London grew rapidly, so by the end of the century it was engaged in international trading. The ceramic history puts some interesting flesh on this skeleton. First, there was no Middle Saxon (pre-Alfredian) potter serving the community; the pots were made only primitively on a hand-rotated wheel. But, with what I have recently described in *News and Views* as the first English industrial revolution[4], the role of the potter changed. Vince shows that the well-dated tenth century groups are dominated by so-called shelly wares (see figure). Petrological analysis of this fabric shows that it contains abundant calcareous inclusions typical of clays in the Oxford region. Pit-groups dated dendrochronologically (tree-ring analysis of their timber content) to the first half of the eleventh century demonstrate a marked change in the type of pottery being discarded. The amount of shelly ware was halved and replaced by other 'imported' pots from areas such as East Anglia, and lead-glazed pitchers made in the town of Stamford also appear in eleventh century contexts in London. A distinctive local fabric, Early Mediaeval Ware, shows abundant sand-grains in thin sections and is one of various recipes used by potters operating near the city. By the end of the tenth century the products of as many as a dozen workshops had broken a virtual monopoly. Thereafter, the rise and fall of industries follows an inexorable pattern, punctuated by a succession of imported wares that reveals London's overseas connections.



Museum of London

A group of Late Saxon shelly ware vessels from various sites in London. Vessels of this type were made from a clay containing abundant fragments of the fossil *gryphaea*, characteristic of the Jurassic clays of midland England but not of the Thames Basin.

The definition of fabrics has made it possible to chart the history of England's earliest craftsmen. Vince's study of London ceramics, like his earlier studies of mediaeval pottery in the Midlands, reveals the rapid development of workshops and their adaptive attitudes to widening their range of products. The scale of the industry and its fast expansion also sheds light on the customers of these potters. The large quantities of tenth century pottery from lower-ranking urban dwellings in sites like London and York, as well as from many villages, reflects a voracious demand for mass-produced commodities.

It has previously been suggested that the peasantry of Late Saxon and Mediaeval England, in common with many traditional nineteenth and twentieth century peasant societies, had minimal access to commodities[5]. In the opinion of some historians, feudal arrangements meant that rural populations had little opportunity to take advantage of urban industrial output. It is still too early to generalize definitively from these studies of mainly urban pottery assemblages, but a picture of a highly integrated, prosperous community is emerging. Potsherds provide details of industrial and commercial connections beyond the scope of the written sources. In many ways these fragments constitute a new form of historical epigraphy and to judge from Vince's results in particular, the collection and processing of archaeology's seemingly least interesting objects is well justified. □

1. Van der Leeuw, S.E. & Pritchard, A. (eds) *The Many Dimensions of Pottery* (University of Amsterdam, 1984)
2. Vince, A.G. *Medieval Archaeol.* **29**, 25 (1985).
3. Hall, R. *The Viking Dig* (Bodley Head, London, 1984)
4. Hodges, R. *Nature News and Views* **316**, 211 (1985).
5. Hilton, R. *J. Peasant Stud.* **4**, 271 (1978)

Richard Hodges is a Lecturer in the Department of Archaeology, University of Sheffield, Sheffield S10 2TN, UK.

Macroevolution

Predation by drilling gastropods

from Michael J. Benton

PREDATION is an important agent of natural selection, and it is regarded by many as an important driving force of evolution[1]. There is growing evidence that the fossil record can offer unique information on the history of particular predator–prey systems, and thus complement the work of ecologists on living forms. Gastropod molluscs (limpets, winkles and other molluscs with 'coiled' shells) are major marine predators on other shelled animals, and they use various mechanical and chemical means to drill or bore through the shell (see figure). Evidence of this activity has been found in the fossil record, although until recently, the oldest precisely identified gastropod borings dated from the early Cretaceous Blackdown Sands of Southern England — about 100 million years (Myr) ago. But new evidence shows that drilling by gastropods occured much earlier and suggests that these early gastropods had a different form from their present-day counterparts[2].

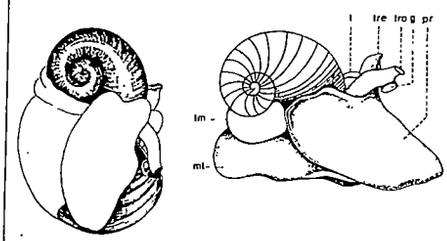
Gastropod drill holes are readily identifiable in fossils or recent specimens of shells. They are round, perpendicular to the shell surface, cylindrical or conical in cross-section, generally pass right through the shell at its thinnest point[3] and are produced by the mechanical action of tooth-like structures on the gastropod radula and by the chemical action of acids.

Certain families of gastropods produce quite distinctive holes. For example, naticid gastropod drill holes are tapered inwards, forming a broad parabolic section on the outside (countersunk) and are 0.2–3.1 mm in diameter; there is a central boss in incomplete holes where the animal has stopped before reaching the flesh inside.

The fauna from the early Cretaceous Blackdown Sands of Southern England[3,4] contains naticid gastropods and other boring forms, as well as various bivalve species. Of the 83 species of bivalves, 43 show gastropod borings, 11 of which account for 73 per cent of the attacks. One species, *Corbula elegans*, accounts for 28 per cent of the attacks. The naticids also bored into the shells of other gastropods. In general, for the Blackdown fauna, prey preference tends to vary with the relative abundance of the prey species, although some particularly thick-shelled oysters (which were quite common) were not drilled very much and some quite rare gastropod prey species were heavily attacked. The naticids selectively attacked medium-sized shells, avoiding very small ones (not enough meat inside) and very large ones (too thick to make the effort worthwhile)[5].

The siting of drill holes is also fairly constant — there seem to be preferred locations that depend on the way the predator grasps the prey shell in its fleshy foot, and on the size, shape, ornamentation and behaviour of the prey species[4,5].

The Blackdown Sands fauna, with its evidence of extensive naticid gastropod predation, forms part of the Mesozoic marine revolution[6], a phase marked by the simultaneous evolution, from the early Cretaceous onwards, of powerful, relatively small, shell-destroying predators such as teleost fishes, stomatopods, decapod crustaceans and drilling gastropods. In response, prey animals took to burrowing and evolved stronger, thicker shells that often had heavy sculpture, spines and narrow apertures[1,4–6]. After the Cretaceous, the shell-drilling gastropods became more efficient — in the Blackdown fauna, about 4 per cent of all bivalve specimens contain drill holes, and this rose to 5–26 per cent afterwards. The numbers of drilled gastropod prey rose from 5 per cent in the Cretaceous to 11–26 per cent afterwards[4].



Right, *Natica josephina*. Feeding apparatus: g, 'foraging gland' secreting acid; t, tentacle) tre, respiratory tube; tro, proboscis containing radula system. pr, lm, mt comprise the hinged foot. (From Ankel, W.E. *Veh. dt. zool. Ges.* **40**, 223; 1938.) Left, *N. josephina* eating a bivalve.

There are several examples of predation by naticid gastropods before the Cretaceous. Newton[7] reported examples from the late Triassic of North America (about 220 Myr ago) and Fürsich and Jablonski[8] described some slightly older late Triassic cases from Italy (about 225 Myr ago). The latter bore holes show all the typical naticid characteristics, and coincide in age with the oldest known naticid gastropods. It had been assumed previously that these gastropods were initially non-drillers, and that they acquired this skill only 125 Myr later in the early Cretaceous.

Fürsich and Jablonski[8] argue that naticid drilling ability evolved twice but became successfully established only the second time. The evidence for this assumption is the absence of naticid bore holes in the intervening Jurassic period. In evolutionary terms, Fürsich and Jablonski view the late Triassic drillers as well enough adapted, but afflicted by bad luck — they may have had low speciation rates, or may have been wiped out in a chance extinction event. When the drilling habit was reinvented by their close relatives in the Cretaceous, it was associated with high rates of diversification, and the habit persisted to the present day in a wide range of naticid species.

But Smith and colleagues now report an even older occurrence of drilling[2] from the middle Devonian of North America (about 380 Myr ago). The holes are indistinguishable from those made by naticid gastropods, but they pre-date the oldest known naticid shells by 155 Myr. The bore holes were made in articulate brachiopods, and the predators show all the features of modern naticid behaviour: the drill holes are highly prey-specific in all localities sampled; they are concentrated over the 'meaty' part of the shell; and the brachiopods were attacked while still alive. As many as 44 per cent of preferred prey species were drilled, but the predators were relatively inefficient — in one locality nearly half of the drill holes were incomplete. This case forms part of the mid-Palaeozoic revolution[9] during which several groups of predators became adapted to shell-crushing and boring (placoderm and chondrichthyan fishes, shrimp-like arthropods and possibly naticid gastropods) and the prey species evolved stronger shells with ribbing and spines in tandem.

In evolutionary terms Smith and colleagues propose that their sample documents a third origin of the naticid-like drilling habit in the Devonian, but they argue that is was not chance that terminated the first attempt at drilling. In the Devonian, there are no known naticids, nor are there any relatives that are fossilized. Smith *et al.* argue that the Devonian driller was a shell-less form (thus not fossilizable) that had evolved the physical and chemical means of drilling. Drilling is a slow process, and the predator was vulnerable itself while going about its business (hence the high number of abandoned drill holes which indicate that the predator may have been disturbed, or

1. Stanley, S.M. *Macroevolution* (Freeman, San Francisco, 1979).
2. Smith, S.A., Thayer, C.W. & Brett, C.E. *Science* **230**, 1033 (1985).
3. Bromley, R.G. *Acta Geol. Hispan.* **16**, 55 (1981).
4. Taylor, J.D., Cleevely, R.J. & Morris, N.J. *Palaeontology* **26**, 521 (1983).
5. Kitchell, J.A., Boggs, C.H., Kitchell, J.F. & Rice, J.A. *Paleobiology* **7**, 533 (1981).
6. Vermeij, G.J. *Paleobiology* **3**, 1977).
7. Newton, C.R. *Geol. Soc. Am. Abstr. Prog.* **15**, 652 (1983).
8. Fürsich, F.T. & Jablonski, D. *Science* **224**, 78 (1984).
9. Signor, P.W., III & Brett, C.E. *Paleobiology* **10**, 229 (1984).
10. Miller, R.H. & Sundberg, R.H. *Lethaia* **17**, 185 (1984).
11. Liljedahl, L. *Lethaia* **18**, 53 (1985).
12. Stridsberg, S. *Fossils Strata* **18**, 1 (1985).
13. Sheehan, P.M. & Lesperance, P.J. *J. Paleont.* **52**, 812 (1978).

indeed eaten, before it could withdraw its drilling equipment). In either case, Smith *et al.* argue that the two 'failures' of the naticid-like shell-drilling habit in the Devonian and the Triassic were the result of poor adaptation. Only in the Cretaceous did the naticids evolve the necessary drilling techniques and the means of self-protection.

Many older examples of predatory bore holes in shells are known — for example from the late Cambrian of the United States (about 510 Myr ago)[10], from the Silurian of Sweden (about 420 Myr ago)[11,12] and from the early Devonian of Canada (about 400 Myr ago)[13]. The predators could have been gastropods in some of these cases[12,13] but the holes are either much smaller than those produced by living naticids[10,11] or they lack the central boss and the inwards taper[12,13]. The holes could have been produced by cephalopods[3,11,12], or by unknown forms[3,11]. Whatever the answer, these studies offer much scope for further work on the history of marine predation, on the modelling of predator–prey interactions[5] and on establishing the role of predation in macroevolution. □

Michael J. Benton is in the Department of Biology, The Queen's University of Belfast, Belfast BT7 1NN, Northern Ireland.

Astrophysics

Unravelling fates of black holes

from Don N. Page

EVER since S.W. Hawking's remarkable theoretical discovery of thermal radiation emitted from black holes[1,2], it has been clear that these objects cannot be the stable final states of gravitational collapse they were once believed to be. But what happens during the last stages of black-hole evaporation has remained uncertain, leaving unanswered several important conceptual issues such as the fundamental predictability of the ensuing state[3-5]. Now M.J. Bowick, L. Smolin and L.C.R. Wijewardhana argue[6] that superstring theories[7,8] can help unravel the answer.

Black holes allow nothing to escape, according to classical (that is, non-quantum) physics in which each particle has a definite position and a definite velocity, which must not exceed c, the speed of light. However, in quantum physics the uncertainty principle prevents a particle from definitely being confined to the space inside the hole and simultaneously definitely having a velocity $\leq c$. In this way quantum mechanics allows a particle to tunnel out from a black hole. Hawking[1,2] calculated this black-hole emission process in a semiclassical approximation in which quantum mechanics was applied to the particles being emitted, but not to the black hole itself, which was instead assumed to have a definite classical gravitational field.

Conservation of energy requires the black hole to lose mass, and hence shrink, as particles carry away its energy. Eventually it evaporates to such a small size that the semiclassical approximation becomes invalid, and quantum mechanics must be applied to the gravitational field of the black hole itself. It is not known how to do this in a completely consistent manner, hence the uncertainty of what happens in the last stages of black-hole evaporation. It has been variously suggested that a black hole stops radiating and shrinking when it reaches a positive-mass stable remnant; that it continues radiating until its mass becomes negative; or that it completely disappears.

There is also the question of whether the quantum evolution of the state is deterministic, or whether there is a new breakdown of predictability beyond the ordinary limitations of the uncertainty principle[3-5]. If the black-hole emission is precisely thermal, with no correlations between different modes (as is predicted by the semiclassical approximation), then its evaporation results in a loss of information or an increase in entropy even without any coarse graining of the final state. Furthermore, in a classical description of the gravitational field, the disappearance of a black hole would be accompanied by a so-called naked singularity (a visible edge to space-time), at which unpredictable information might enter the Universe.

Bowick, Smolin and Wijewardhana[6] now offer a preliminary analysis of these questions in the context of superstring theories[7,8], exciting new candidates for a consistent quantum 'theory of everything' (unification of the fundamental forces, including gravity; see ref. 9 for review). If one of these theories is indeed correct, it should in principle be able to explain what happens when a black hole evaporates. Unfortunately for our curiosity (but perhaps fortunately for the continuation of our careers), our understanding of superstring theories is still far too meagre to say definitely what they imply about black-hole evaporation. Bowick *et al.* readily admit this limitation, but investigate what can be said from our present knowledge of superstring theories.

By a thermodynamic analysis of perturbative (linearized) string modes, Bowick *et al.* conclude that it is statistically probable for a black hole to turn into a massive string when it gets sufficiently small. The string itself then decays into ordinary radiation (massless particles). The authors suggest that this allows the black hole to disappear completely (yet without the accompaniment of a naked singularity) because the gravitational field is only part of the superstring field.

This conclusion is eminently reasonable, although it must be admitted that the paper of Bowick *et al.*[6] is hardly a rigorous derivation of the result. Even before superstring theories, one could have postulated that a sufficiently small black hole turns into a suitable spectrum of massive particles without having a classical gravitational field that would lead to a naked singularity. Superstring theories give hints as to how this could conceivably happen, but so far they are just hints.

On the question of whether there is a breakdown of predictability in black-hole evaporation, Bowick *et al.* admit that they do not see how superstring theory will resolve the problem. Indeed, one would need a method for correctly calculating the enormous number of multi-particle correlations between the different black-hole emission modes. Each one of these correlations is likely to be very small and hence individually close to the semiclassical approximation that it is zero, but cumulatively it is conceivable that the correlations could gradually restore to the exterior all the information that enters the hole during its formation and evaporation process. It is still too early to say whether or not superstring theory will show this possibility to be the case. □

1. Hawking, S.W. *Nature* **248**, 30 (1974)
2. Hawking, S.W. *Commun. Math. Phys.* **43**, 199 (1975)
3. Hawking, S.W. *Phys. Rev.* D**14**, 2460 (1976)
4. Page, D.N. *Phys. Rev. Lett.* **44**, 301 (1980)
5. Wald, R.M. *Phys. Rev.* D**21**, 2742 (1980)
6. Bowick, M.J., Smolin, L. & Wijewardhana, L.C.R. *Phys. Rev. Lett.* **56**, 424 (1986).
7. Green, M.B. & Schwarz, J.H. *Phys. Lett.* B**149**, 117 (1984)
8. Green, M.B. & Schwarz, J.H. *Phys. Lett.* B**151**, 21 (1985)
9. Green, M.B. *Nature* **314**, 409 (1985)

Don N. Page is Associate Professor of Physics at The Pennsylvania State University, University Park, Pennsylvania 16802, USA.

Erratum

Consensus sequence		Lys–Gly–fob–Gly–Thr–Asp–Glu–var–var–Leu–Ilu–fil–Ilu–Leu–Ala–fil–Arg
Lipocortin residues	56 72	Met–Val–Lys–Gly–Val–Asp–Glu–Ala–Thr–Ilu–Ilu–Asp–Ilu–Leu–Thr–Lys–Arg
Lipocortin residues	128–144	Lys–Gly–Leu–Gly–Thr–Asp–Glu–Asp–Thr–Leu–Ilu–Glu–Ilu–Leu–Ala–Ser–Arg
Lipocortin residues	287 303	Lys–Gly–Val–Gly–Thr–Arg–His–Lys–Ala–Leu–Ilu–Arg–Ilu–Met–Val–Ser–Arg

In the article by Robert H. Kretsinger and Carl E. Creutz "Consensus in exocytosis" (*Nature News and Views* 17 April, page 573), two of the amino-acid residues that should have been included in the figure were omitted. The correct figure is shown above.

Steroid receptors

Oncogenes as hormone receptors

from J. Michael Bishop

THE district of Hades most feared by scientists is that ignominious corner called neglect[1]. This is the fate that until recently threatened v-*erb*-A, an oncogene with modest biological effect and no known function. Now however, with the discovery of structural kinship between the v*erb*-A gene and the genes encoding the receptors for steroid hormones[2-4], the oncogene assumes its rightful place among a family of genes whose actions help to orchestrate the specialization of cellular function that typifies metazoan organisms.

Like other retroviral oncogenes, v-*erb*-A arose by transduction of a cellular proto-oncogene (c-*erb*-A)[5]. But v-*erb*-A is unusual in that it shares the genome of the avian erythroblastosis virus (AEV) with another oncogene, the more prominent v-*erb*-B, transduced from the gene that encodes the cell surface receptor for epidermal growth factor[6]. AEV causes erythroleukaemia in chickens and transforms haemopoietic cells of the erythroid lineage in cell culture[7]. The principal responsibility for neoplastic transformation by AEV rests with v-*erb*-B[8,9], whose action impedes the maturation of erythroid precursor cells[7,10]. But when v-*erb*-B acts alone, the transformed cells tend to escape the blockade and mature spontaneously[8]. The leukaemia is consequently sluggish. The cooperative action of v-*erb*-A tightens the leukaemogenic grip on the cell: spontaneous maturation becomes rare, and the leukaemia becomes correspondingly more aggresive.

What is the mechanism of this effect? Our only clues come from the structure of v-*erb*-A. The deduced amino-acid sequence of the v-*erb*-A product reveals a frail resemblance to the enzyme carbonic anhydrase[11]. We still do not know what — if anything — that resemblance signifies; but in the face of what else has now emerged, neglect may be its fate. Our story leads instead, and unexpectedly, to steroid hormones.

The structures of steroid hormones are too simple to embody much information. The cellular receptors for the hormones must therefore serve as molecular adaptors to mount a signal of considerable complexity[12]. Steroids apparently enter cells by diffusion through the plasma membrane and then combine with specific receptor proteins inside the cell. The binding of ligand 'arms' the receptor so that it in turn binds with increased affinity to select sites in cellular DNA — sites that are thought to be enhancers of transcription whose activity requires the hormone–receptor complex. By these means a steroid hormone can induce the expression of a substantial battery of genes.

Each step in this remarkable sequence is clouded by controversy. But matters should soon become clearer because we now have molecular clones and amino-acid sequences for the glucocorticoid receptors of humans[13], mice (G. Ringold, personal communication) and rats (K. Yamamoto, personal communication) and for the oestrogen receptors of humans[3,4] and of chickens[14]. What these results make clear, first and foremost, is that all of the receptors named — and the product of v-*erb*-A for good measure — share an ancient progenitor. The structural similarities that this kinship engenders permit some powerful arguments by analogy.

There are in the receptors several domains whose conservation or other features bespeak important contributions to function. The first of these comprises approximately the amino-terminal half of the receptor molecules. Two functions have been attributed to this domain[12]: it may mediate the effect of the receptor on gene expression by interacting with the enzymatic apparatus for transcription; and it is reputed to exert allosteric influence over the remainder of the receptor. This region of the glucocorticoid receptor also commands attention because it carries prominent antigenic determinants[12,15], and because it contains two short stretches of very limited homology with proteins encoded by the homoeotic genes of the fruitfly *Drosophila melanogaster*[2]. These homologies are not found in the oestrogen receptors and involve no more than six identities among amino-acid residues, so it is a tribute to the communal esteem for homoeotic genes that the homologies are given any mention at all — either here or in the original publication.

The second recognizable domain of the receptors resides near the middle of the proteins, is the most intensely conserved and harbours the site that binds DNA (refs 2–4; K. Yamamoto, personal communication). The third domain includes the carboxy ends of the receptors and extends a still-uncertain distance upstream. That this portion of the receptor binds hormone has been suspected for some time and has now been substantiated in two ways. First, two versions of the glucocorticoid receptor have been found that may arise from alternative splicing (or experimental artefact)[13]. They differ only by short substitutions of amino-acid sequence at their carboxy termini. One version binds glucocorticoids, the other does not. The drastic effect of this small difference in structure, and the means by which similar domains of protein are nevertheless able to distinguish between glucocorticoids and oestrogens pose marvellous puzzles for the crystallographer. Second, mutations have been fashioned in the putative hormone-binding region of both the oestrogen and the glucocorticoid receptors: the fabricated mutants do not bind hormone (ref.14; K. Yamamoto, personal communication).

All of the domains within a receptor molecule may therefore have discrete functions, but they constitute a cascade, and each component may contribute to specificity in the action of steroid hormones: the ligand-binding domain is a trigger that can be thrown only by the correct hormone; the DNA-binding domain recognizes specific nucleotide sequences, whose elements of consensus are beginning to emerge[12]; and the amino-terminal half of the receptor may selectively interact with the transcriptional machinery. Cooperative division of labour of this sort within protein molecules has been elucidated in great detail with examples from bacteria and yeast.

The topographies of steroid receptors again evoke the popular scheme in which complex genes are said to have been cobbled together by genetic recombination, recruiting constituent domains from diverse parts of the evolving genome. The most adventuresome proposal is that the hormone-binding domains arose from primitive enzymes once devoted to the metabolism of steroids[12].

Whatever the origins of steroid receptors, they are apparently similar to those of the protein encoded by v-*erb*-A, which is now seen to contain domains analogous to those that in the receptors bind DNA and hormone[2-4,14]. There is, however, no analogue in the v-*erb*-A protein for the amino-terminal half of the receptors. Instead, v-*erb*-A is fused to a portion of the viral gene *gag* that encodes virion proteins[7]. The topography of c-*erb*-A, from which the viral gene is transduced, has yet to be described. Presumably a

1. Watson, J.D. *The Double Helix* (Atheneum, New York, 1968).
2. Weinberger, C., Hollenberg, S.M., Rosenfeld, M.G. & Evans, R.M. *Nature* **318**, 670 (1985).
3. Green, S. *et al. Nature* **320**, 134 (1986).
4. Greene, G.L. *et al. Science* **231**, 1150 (1986).
5. Vennstrom, B. & Bishop, J.M. *Cell* **28**, 135 (1982).
6. Ullrich, A. *et al. Nature* **309**, 418 (1984).
7. Graf, T. & Beug, H. *Cell* **34**, 7 (1983).
8. Frykberg, F. *et al. Cell* **32**, 227 (1983).
9. Sealy, L. *et al. Virology* **130**, 155 (1983).
10. Graf, T., Ade, N. & Beug, H. *Nature* **275**, 496 (1978).
11. Debuire, B. *et al. Science* **224**, (1984).
12. Yamamoto, K.R. *A. Rev. Genet.* **19**, 209 (1985).
13. Hollenberg, S.M. *et al. Nature* **318**, 635 (1985).
14. Krust, A. *et al. EMBO. J.* (in the press).
15. Lin, P.-F. *et al. Proc. natn. Acad. Sci. U.S.A.* **79**, 4260 (1982).
16. King, W.J. & Greene, G.L. *Nature* **307**, 745 (1984).
17. Welshons, W.V., Lieberman, M.E. & Gorski, J. *Nature* **307**, 747 (1984).
18. Sluyser, M. & Mester, J. *Nature* **315**, 546 (1985).
19. Bishop, J.M. *Nature News and Views* **316**, 483 (1985).

region that encodes an amino-terminal component has been shorn from c-*erb*-A in the course of transduction from the gene that gave rise to v-*erb*-A. So far, there is no hint as to what the ligand for the truncated v-*erb*-A protein may be — if one indeed exists.

But the analogies we do have bring the product of v-*erb*-A into a new light: until now there was nothing to suggest that this protein might interact with nucleic acid; or that it might be activated by natural ligand; or that it might spend part of its functional life-span in the nucleus. This last point raises a question still vigorously debated by students of steroid receptors. It was once thought that the receptors in their inactive form loiter in the cytoplasm, entering the nucleus only after activation by the binding of ligand; more recent evidence places the receptors in the nucleus even in the absence of hormone[16,17]. In either case, the subcellular location of the v-*erb*-A protein — until now thought to be the cytoplasm — deserves careful reappraisal.

What do these new findings suggest about the mechanism by which v-*erb*-A contributes to neoplastic transformation? Perhaps the simplest hypthesis is that v-*erb*-A is a transcriptional regulator run amok — a dangerously constitutive version of c-*erb*-A[2,18]. This hypothesis ignores the possibility that the v-*erb*-A protein may lack a structural domain required for enhancement of transcription. Moreover, there are two forms of mutant glucocorticoid receptors whose properties suggest other mechanisms[12]. The first of these mutant receptors binds ligand and DNA, yet fails to muster any physiological response. These 'increased nuclear transfer' or nt^i mutants (the designation reflects increased affinity of the mutant receptors for the nucleus) bear a striking resemblance to the protein encoded by v-*erb*-A: both contain only the carboxy-terminal half of the archetypal receptor molecule, including the regions that are thought to bind hormone and DNA. For the moment, we can only speculate that v-*erb*-A has structural and functional defects similar to those of the nt^i mutants. But were that speculation correct, the v-*erb*-A protein might occupy sites on DNA in a sterile manner, competing with the product of c-*erb*-A and preventing the activation of genes that would otherwise come into play during erythroid differentiation. The hypothesis demands that c-*erb*-A play a part in erythroid differentiation and that v-*erb*-A be expressed in substantial excess of c-*erb*-A; both are reasonable possibilities, but neither has yet been tested experimentally.

The second pertinent form of mutant receptor (nt^-) binds glucocorticoid, but not DNA. An nt^- mutant has now been sequenced, to reveal (among other abnormalities) substitution of glycine for glutamic acid at a position that might account for the defect in DNA binding (G. Ringold, personal communication). The v-*erb*-A protein has glycine at the analogous position. If the protein were similarly unable to bind DNA, it might represent an inactive 'sump' that could compete with the product of c-*erb*-A for ligand. The physiological effect would be the same as that envisioned for the nt^i mutants: a sufficient excess of the v-*erb*-A protein would nullify the action of c-*erb*-A.

I have previously argued[19] that it may be fallacious to deduce the physiological functions of proto-oncogenes from the properties of their progeny oncogenes. The present instance may be an exception. If the product of v-*erb*-A does indeed act by nullifying the action of c-*erb*-A, then the genes and cells that v-*erb*-A affects are salient clues to the function of c-*erb*-A — clues that moreover deserve the attention of anyone who is interested in normal erythropoiesis.

So once again the study of tumour viruses has conjoined with other disciplines to enrich our knowledge of cell biology, and the obscure v-*erb*-A (or more accurately, its cellular counterpart c-*erb*-A) has acquired new lustre by its accession to a gene family whose members contribute mightily to homeostasis. As one oncogene after another is equated to a previously known determinant of normal cellular phenotype, a brash question comes to mind. Might all the major devices that control the growth of vertebrate cells already be in view? Prudence forbids an answer. □

J. Michael Bishop is in the Department of Microbiology and Immunology and the Hooper Research Foundation, University of California Medical Center, San Francisco, California 94143, USA.

Animal locomotion

Three kinds of flying in animals

from R. McNeill Alexander

JEREMY Rayner and his colleagues report in this issue (*Nature* **321**, 162; 1986) their work on bats that are trained to fly through clouds of helium-filled soap bubbles. These bubbles have the same density as air, so their images in multiple-flash photographs show how the air is set in motion as the bat passes through. As wings generate forces by giving momentum to the air the new results give information about the forces on the wings and allow comparison with the flight of birds.

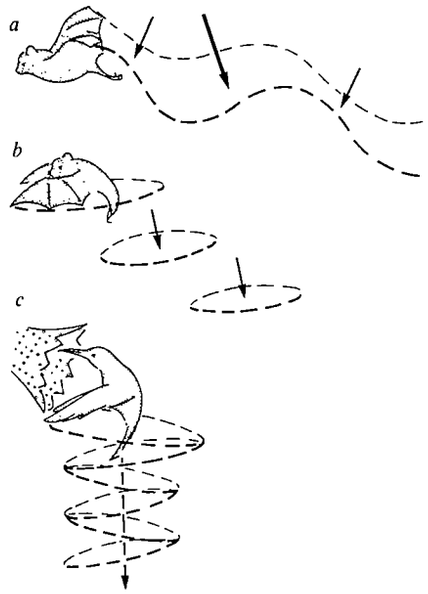


Fig. 1 Diagrams of air movements produced by *a*, kestrels and bats flying fast; *b*, pigeons and bats flying slowly and *c*, hummingbirds hovering. The broken lines represent vortices and the arrows show directions of air movements.

The experiment had been done previously with birds and gave two kinds of result (Spedding, G.R. thesis, Univ. Bristol; 1982). Pigeons produced a downward puff of air in each downstroke, and little air movement in the upstroke. Thus the downstroke produced the force that supported the animal's weight, and the upstroke was passive. Kestrels, which flew faster in the conditions of the experiment, produced downward airflow during the upstroke as well as the down-stroke. Now it has been shown that Noctule bats use both techniques. In slow flight, only the downstroke is active, but at higher speeds both strokes are active. It seems likely that the two techniques are characteristic of slow and fast flight of birds and bats generally. They can be thought of as gaits, the aerial equivalents of walking and running.

Puffs or jets moving through stationary air set up vortices. Smoke rings consist of smoke trapped in the vortex around a puff of air. Vapour trails behind the wing tips of aircraft also mark vortices: the air between the two trails is moving downwards. The two flying gaits of birds and bats produce distinctive patterns of vortices, which were made visible in the experiments of Rayner *et al.* by the helium bubbles. The fast gait produces a pattern like the vapour trails of aircraft, with an important difference. The wing tips are brought closer to the body in the upstroke than in the downstroke, so the vortices undulate in and out instead of remaining parallel (Fig. 1*a*). The slow gait produces a series of vortex rings, one for each downstroke (Fig. 1*b*).

Both aircraft and flying animals need

forces to support their weight and to drive them forward through the air. Aircraft get support from their wings and thrust from their engines, but birds and bats get both from their wings, by flapping them. These mechanisms can help us to understand the difference between the gaits.

Air is driven roughly at right angles to the path of the wing through it. The downstroke drives air downwards and backwards, providing weight support and thrust. The upstroke of fast flight (Fig. 1*a*) drives downwards and forwards, tending to cancel out the thrust of the downstroke. To prevent this, the forces produced by the upstroke must be reduced, either by reducing the wingspan so that less air is moved by the wings, or by weakening the vortices so that the air is driven less fast. (This can be done by adjusting the angle of incidence of the wings.) Rayner has argued (*Biona Rep.* **5**, 27; 1986) that it is most economical to reduce wing span and keep vortex strength (circulation) constant as kestrels and bats seem to do.

Figure 1*c* shows a possibility for hovering and very slow flight, when the wings can be flapped so as to move backwards (relative to the air) in the upstroke. Circulation may be reversed at the end of each stroke so that the wake is a series of linked vortex rings, a ring for each downstroke and one for each upstroke. Hummingbirds seem to do this, but the vortices have not been demonstrated. Many insects apparently are able to do the same (Ellington, C.P. *Phil. Trans. R. Soc.* **B305**, 1; 1984).

The slow gait (Fig. 1*b*) is intermediate between the other two. Circulation is eliminated but not reversed in the upstroke, so vortices (and useful forces) are produced only in the downstroke. There is scope for an optimization theory that would predict the speed at which the change should be made between the slow and the fast gaits. □

R. McNeill Alexander is Professor of Zoology at the University of Leeds, Leeds LS2 9JT, UK.

Circadian rhythms

Benzodiazepines set the clock

from A. T. Winfree

THE time will come when a traveller leaving for the airport, having frantically searched for and found his ticket, will still not be ready: it will be necessary to dash to the medicine cabinet to rummage for the inevitably misplaced bottle of jet-lag pills. Elsewhere in this issue (*Nature* **321**, 167; 1986) Fred Turek and Susan Losee-Olsen, in a simple, straightforward experiment with triazolam and hamsters, provide the strongest hint yet that the elusive jet-lag pill is within reach.

Like any other mammal, humans have a persistent strong tendency to regularity in the ups and downs of diverse physiological functions, such as core temperature and the alternation of sleep and waking. The latter regularity has a native circadian periodicity close to 25 hours, and is usually synchronized by the 24-hour alternation of day and night, so it is called the biological clock. The mechanism of this clock seems rooted in the central nervous system, particularly in the suprachiasmatic nucleus of the hypothalamus. A gene whose alleles determine the periodicity of the circadian clock of the fruitfly has recently been sequenced: it appears to be a proteoglycan (Jackson, F.R. *et al. Nature* **320**, 185; 1986).

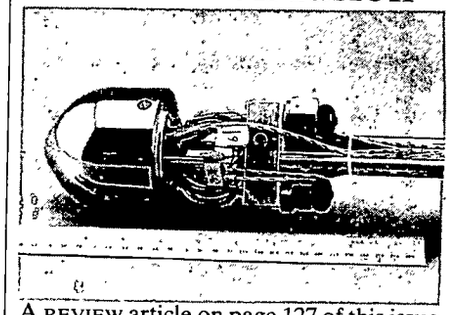
Little more is known of the mechanism of circadian clocks, but their pharmacological sensitivity has recently provided us with some powerful hints about phase shifts such as those one encounters during east–west travel. Ionophores, brain hormones and neurotransmitter analogues are conspicuous among agents capable of permanently shifting the phase of the clock, much as visible light has long been known to do. Alternating light and darkness is the leisurely agent of synchronization that normally guides plants, invertebrates and mammals (including humans) to a standard phase relationship with the environment after a shift of phase. But gradual entrainment to local time requires exposure to cycle after cycle of the synchronizer; would it not be better if we could abruptly set our internal clocks in advance, much as we set our watches? My own favoured procedure involves exposure to bright sunlight at a carefully planned hour (Daan, S. & Lewy, A.J. *Psychopharm. Bull.* **20**(3), 566; 1984), but this is not necessarily convenient if, for example, it is snowing or it is night-time. Pharmaceutical assistance towards synchronization has long been sought; one need only stand in the aisle of any intercontinental jetliner to hear many superstitions about, for example, coffee, diet, alcohol and sleeping pills.

Turek and Losee-Olsen seem to have found a real effect — that of benzodiazepines — although the results of clinical trials have not yet been reported. Benzodiazepines, used for several years in the management of insomnia and related mental disorders, may act by potentiating the action of the inhibitory neurotransmitter γ-aminobutyric acid, which is known to be present in the suprachiasmatic nucleus. But its impact on circadian rhythms has never before been tested in the standard experimental protocol used by Turek and Losee-Olsen. These authors recorded the activity rhythm of a hamster for two weeks (so that the rhythm could be reliably extrapolated to the following days), then injected the animal intraperitoneally with a dimethyl sulphoxide vehicle at any one of eight equally spaced 'times of day' in its circadian cycle. The rhythm continued as anticipated. But if the vehicle carried a benzodiazepine (2.5 mg of triazolam, equivalent to about 5 times a heavy dose for an adult human) then the timing of subsequent activity was disrupted, causing an immediate phase advance or phase delay of about one hour. The exact amount of the delay depends dramatically and quite reproducibly on the timing of the dose, a dependency unlike that caused by stimulation of the retinohypothalamic pathway for phase-shifting by light. Hence Turek and Losee-Olsen have found a new avenue of entry into the clock mechanism.

The potential practical interest of their results lies in the hope that the same or a related fast-acting, quickly eliminated chemical without conspicuous side-effects may also abruptly reset the circadian clock in humans. If so then we may soon find ourselves carrying pills and a schedule whenever we cross time zones at a pace much in excess of one per day. The schedule will prescribe when and what dose of pills to take to achieve an immediate advance or delay appropriate to the foreseen change of longitude.

The result of Turek and Losee-Olsen raises another intriguing question — in three or four of the eight recordings shown not only is there an abrupt phase shift, but also the periodicity of the clock is substantially altered for at least a week. Yet the

Forward on fusion



A REVIEW article on page 127 of this issue describes experiments that provide new optimism for the possibility of generating power from nuclear fusion. The picture above shows the target capsule used to hold the deuterium-tritium mixtures for muon-catalysed fusion experiments at the Los Alamos Meson Physics Facility in 1984. The target was electrically heated to 800 K and then cooled to 14 K with liquid helium. Up to 150 fusions per muon (average) were observed with this apparatus.

drug, if metabolized as it is in humans, should have been eliminated within several hours. Does this mean that hamsters retain much of the large dose of triazolam, or that the clock mechanism has resettable periodicity as well as resettable phase?

The experiment also raises questions about the unforseen circadian side-effects of medications containing psychotropic compounds. David Earnest and Turek recently demonstrated (*Proc. natn. Acad. Sci. U.S.A.* **82**, 4277; 1985) that cholinergic neurotransmission centrally mediates the effect of light on the circadian clock of the hamster. This might lead one to wonder about over-the-counter 'sleeping pills' that contain belladonna and scopolamine: do they also have an impact on circadian coordination? □

A.T. Winfree is at the Institute for Nonlinear Science at the University of California San Diego, La Jolla, California 92093, USA.

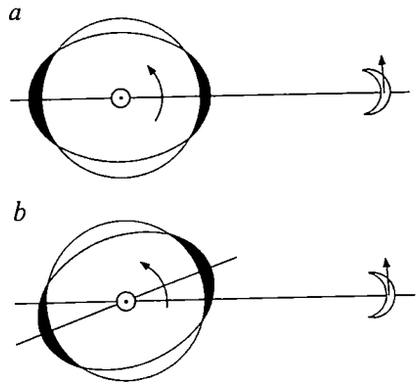
Geophysics

Is there coherence between Earth tides and earthquakes?

from Paul W. Burton

Do tides in the Earth cause earthquakes? Are some types of earthquakes or regions of the Earth more susceptible to earthquakes triggered by tides than others? And is this relevant to the prediction of earthquakes? There has not yet been much success in answering these questions, although the thorough studies of T.H. Heaton[1,2] did demonstrate that some types of shallow earthquakes that have magnitudes greater than 3 are more easily triggered than are smaller events. But his later, more rigorous approach did not confirm his earlier hypothesis — much seems to be ambiguous or inextricably tangled in this subject. A. Palumbo is now trying to provide answers to some of the questions[3]. He finds that earthquakes most likely to be triggered by tides are those with magnitudes higher than 5 and that shallow earthquakes and their foreshocks in the Appennine Mountains are significantly more frequent when stretching in the crust caused by tides in the Earth is at a maximum.

Under consideration are stresses or tides in the solid Earth caused by the action of the Sun or the Moon on the deformable Earth. (Tides in the ocean and in the atmosphere are caused by the same actions but in more mobile and fluid media.) Stress and strain changes in the Earth caused by the varying proximity of the Sun and the Moon are accompanied by variations in the acceleration caused by gravity, g, at the surface of the Earth. Thus, g is not constant at 9.81 m s^{-2} but fluctuates both daily and over longer periods. This may be visualized simply (see figure) as deformation of the Earth's surface, and can amount to a semi-diurnal movement of the ground of as much as 0.1 m up or down. These motions are damped by friction in the Earth and so maximum strain lags behind the response expected in a totally elastic Earth; some parts of the Earth being stretched while others are compressed. Compression is maximum with the Moon or Sun on the horizon (morning earthquakes?), and some earthquake fault systems may be susceptible to compressional perturbations. Tensional regimes across fault zones may be susceptible when the Moon or Sun are overhead (midday earthquakes?).



Earth tides caused by lunar action. *a*, Without friction, Earth strain would cause an upward motion of the ground along a line joining the centres of the Earth and the Moon. With the Moon on the horizon the strain would cause a downward and inward motion of the ground. *b*, With friction, the tidal bulge in the Earth is carried forward by rotation of the Earth causing a phase delay with respect to the action of the Moon on the Earth. These small periodic strains may perturb strain energy stored in the Earth and trigger release of that energy as an earthquake. (Adapted from ref. 6.)

When the Earth acts gravitationally on the Moon (a larger body acting on a smaller body), it is an acceptable interpretation that tidal effects trigger moonquakes. The reverse situation, when the Moon acts gravitationally on the Earth, is riddled with complexity and ambiguity: for example, the perturbations to strain are not so large; the Earth has mobile oceans and an atmosphere which varies the surface loading; and earthquake catalogues are rarely homogeneous and complete. When many globally distributed earthquakes are considered no significant effect is discernible — presumably any effect is blurred by a multiplicity of unidentified fault orientations and stress regimes. Palumbo has deliberately isolated a relatively small region of the Earth, in Italy, and, largely rejecting Fourier spectral analysis, used the Chapman–Miller method to detect lunar daily variations (for an up-to-date account of the method with minimum mathematics, see ref. 4). Palumbo's results are clearer than his discussion and analysis: no tidal term is discernible in the Alpine or southern Calabrian areas but there is a lunar tidal term for major earthquakes and related foreshocks in the Appennines. He suggests that the tidal terms in the frequency of earthquakes are linked with extensional tidal stresses in the east–west direction.

Although hardly being on the level of prognostication associated with a 'Jupiter' effect, this suggestion is fascinating in relation to Appennine earthquakes. It will be interesting to see if the resolution of coherency achieved by Palumbo will improve when seismic moment tensor solutions (giving a full description of seismic fault orientations and slip vectors) for earthquakes in the Appennines can be combined with local tidal strain tensors.

Palumbo certainly seems to have identified one geographical region where tidal variations in the frequency of earthquakes are discernible despite the inevitable problems obscuring potential coherency between Earth tides and earthquakes. The relevance to earthquake prediction is another matter. Although much is known about Earth tides[5] and global and local seismicity, coherency between the two is usually within the noise of any analysis; certainly earthquake disasters do not show the sort of semi-diurnal or diurnal variation which would prompt an actuary to take cover at dawn or dusk.

The problem remains largely unresolved and confused from a statistical viewpoint. But instruments used to measure Earth tides and strain changes will also be sensitive to the volume increases that are thought to accompany changes in rocks before brittle failure. Here there may be a practical link between the two sciences; otherwise coherency between tides and earthquakes appears highly localized, where it merits further study, but elsewhere, given the present state of knowledge and the resolution of this coherency, these studies appear to be rather an esoteric pursuit. □

1. Heaton, T.H. *Geophys. J. R astr Soc* 43, 307 (1975).
2. Heaton, T.H. *Bull. seism. Soc. Am* 22, 2181 (1983).
3. Palumbo, A. *Geophys. J. R. astr Soc* 84, 93 (1986).
4. Malin, S.R.C. & Chapman, S *Geophys J R astr Soc.* 19, 15 (1970).
5. Melchior, P. *The Tides of the Planet Earth* (Pergamon, Oxford, 1978).
6. Kopal, Z. in *Understanding the Earth* (eds Gass, I G., Smith, P.J. & Smith, R.C L.) 97 (Artemis Horsham, Sussex, 1971).

Paul W. Burton is at the British Geological Survey, Murchison House, West Mains Road, Edinburgh EH9 3LA, UK.

Immunology

Development and modification of the lymphocyte repertoire

from Malcolm Gefter and Philippa Marrack

ALTHOUGH recent advances in the understanding of the genes encoding the antigen receptors of T and B lymphocytes have allowed new approaches to some of the traditional problems of immunology, they have not, as quickly became apparent at a recent meeting*, yet provided much in the way of answers. The question addressed at the meeting was that of what determines which particular T- and B-cell receptors from the extraordinarily large potential repertoire will actually be represented in the repertoire of a given animal. Some of the most lively discussion, however, (which the meeting was organized to maximize) concerned genes that are not yet known to contribute to the receptor repertoire at all.

Holes in the idiotype net

One of the most elegant attempts to explain the mechanisms underlying the control of antibody and effector T-cell production was devised some fifteen years ago by Niels Jerne. He argued that what limits and modifies the receptor repertoire is the existence of interactions — which can be either stimulatory or inhibitory — between cells recognizing antigenic determinants called idiotypes on the antigen receptors of other cells of the immune system. Thus, for example, anti-idiotype antibodies may be able to recognize antibodies produced by B cells and the antigen receptors of T cells, and may stimulate or suppress the proliferation of the cells that bear them. This results in an interacting network of cells and products (the idiotypic network) that influences the available repertoire before the organism is ever exposed to environmental antigen.

Although evidence in support of the theory has since accumulated, proof has been difficult to obtain, partly because the theory, although elegant and provocative, is not specific enough to allow definitive experiments to be done. With the introduction of molecular biology into immunology, it has become possible to define both the potential repertoire and the available repertoire. Moreover, much has been learned about the mechanisms whereby the receptor repertoire is expressed.

Above all, it is now known that both antibodies and T-cell receptors for antigen are encoded by genes that are assembled by somatic recombination from separate gene segments drawn from gene pools which for some of the segments (the 'variable', or V, segments in particular) is very large and diverse. Directly or indirectly, an understanding of the molecular mechanisms by which the repertoire is generated may provide alternative explanations for some of the phenomena attributed to the operations of the network.

This applies, for example, to the recent discoveries made by Robert Kleinfeld from Martin Weigert's laboratory (University of Pennsylvania) and Michael Reth (University of Cologne). These two groups demonstrated that the genes encoding the variable region of the heavy chain of antibodies (the V_H gene segments) can undergo secondary intrachromosomal recombinations resulting in the expression of a new variable region, and thus a new recognition specificity, in an apparently already committed B cell. The mechanism of the recombination event is believed to be related to that of the normal mechanism of immunoglobulin-gene rearrangement, which depends on a conserved heptamer sequence; the site of the inter-V_H recombination appears to be a conserved heptamer within the coding region of the V_H genes. But to date, somatic inter-V_H recombination has only been seen in two B-cell lines, and it remains to be determined how general this observation will be.

Secondary recombination between V_H segments may help to explain an apparent paradox in B-cell repertoire expression: namely, that during fetal life it seems that the joining (J_H)-proximal V_H genes are preferentially rearranged (G. Yancopoulos, Columbia University), but by adulthood, all V_H segments appear to be relatively equally expressed. Perhaps the genes that undergo rearrangement early are substrates for further recombination events, the results of which shape the adult immunoglobulin repertoire.

This in turn might provide an explanation for the phenomenon of idiotype dominance — in which in certain mouse strains most of the antibodies produced in response to a particular determinant carry a specific idiotype. This phenomenon has been explained by network theorists as the consequence of amplification by anti-idiotypic interactions. For example, in the case of the T15 idiotype associated with the response of some mouse strains to phosphoryl choline, John Kearney (University of Alabama, Birmingham) provided convincing evidence for the operation of regulatory events involving cascades of anti-idiotypic antibodies. (Unexpectedly, this could only be demonstrated when antibodies were administered *in utero*: in the classical network experiments, anti-idiotypic antibodies administered in adults will affect the repertoire.) Norman Klinman (Scripps Clinic Research Foundation) however suggested that the dominant idiotype phenomenon might be explained just as well by preferential gene rearrangement to the V_H gene responsible for the T15 idiotype.

It is possible that similar phenomena can also account for the provocative observations reported by Tereza Imanishi-Kari (Massachusetts Institute of Technology) on transgenic mice harbouring an immunoglobulin heavy-chain gene bearing the idiotype associated with the response to nitrophenol (NP). B cells in such mice spontaneously express antibodies bearing the idiotype carried by the product of the introduced gene — but these antibodies are not encoded by the introduced gene. Moreover, this pattern of idiotype expression can be transferred to other mice by inoculation with T cells from the transgenic animals. On the face of it, this is strong support for an idiotype network in which the major perturbation consequent on the introduction of the transgene is reflected in a skewing of the repertoire by regulatory T cells that are part of the net and have themselves been elicited by the (presumed) overabundance of the idiotype encoded by the transgene early in ontogeny.

In the lively discussion that followed this presentation, participants at the meeting suggested that preferential V_H rearrangement might explain these results as well; clearly direct evidence on this, and further data from other transgenic mice, are needed.

In the meantime, other recent experiments suggest that antigen alone could account for the selection of a skewed repertoire. In most immune responses, the antibodies produced are very heterogeneous and diverse, and no two animals will be the same. But the response to some antigens seems to draw selectively on a very limited set of V regions which may be identified as the basis of the dominant idiotype. This initial selection is followed by somatic mutation of the V regions. Experiments designed to analyse the responses to the ars idiotype (Malcolm Gefter, MIT), the NP idiotype (Klaus Rajewsky, Cologne) and the Ox-1 idiotype (K. Berek, University of Cambridge) suggest that selection by antigen may be sufficient explanation for their dominance, as in all cases so far the somatic mutations increase the affinity of the antibodies for antigen. The acceptance of non-Jernian explanations for idiotypic phenomena however will undoubtedly require more time.

The most elegant postulate of the net-

* The winter workshop on T- and B-repertoire development, organized by Eli Sercarz and Alex Miller, was held at Lake Tahoe on 22-25 January 1986.

work theory — that idiotypes shared between T and B cells result from a shared genetic pool of *V* segments for B- and T-cell receptors for antigen — has already been excluded by molecular biology. How the cloning of the receptor genes has advanced the understanding of the T-cell receptor repertoire was the other main topic of the meeting.

T-cell receptor

Unlike B cells, T cells are able to respond to antigen only when it is presented to them in association with a cell-surface protein, a product of the major histocompatibility complex (MHC) of the animal in question, a phenomenon called MHC restriction. There has been much debate concerning whether such a feat requires one receptor or two, the bulk of the evidence strongly suggesting that a single T-cell receptor, made up of an α/β heterodimer, is sufficient (see Robertson, M. *Nature News and Views* **317**, 768; 1985). M. Steinmetz (Basel) presented further evidence from transfection experiments to support this point of view (Dembic, Z. *et al. Nature* **320**, 232; 1986). He and his collaborators have used α- and β-chain genes from a cytotoxic T cell specific for the hapten, fluorescein (FL) in association with the MHC product D^d, to transfect a T cell specific for a different hapten and MHC product and with this transferred the specificity for FL/D^d of the donor. This supports the earlier evidence that no clone-specific, variable molecule besides α and β contributes to the specificity of these cells.

The precise contribution of the α- and β-chains to the recognition of MHC and antigen, however, remains unclear. Several investigators reported the results of sequencing α- and β-chain genes from collections of T cells with related specificities for antigen and MHC, in the hope of discovering some correlation between the sequences and the specificities. S. Hedrick (University of California at San Diego) and A. Winoto (California Institute of Technology), for example, had used T-cell clones specific for a pigeon cytochrome C peptide, and with well-defined MHC reactivities (Fink, P.J., Matis, L.A., McElligott, D.C., Bookman, M. & Hedrick, S.M. *Nature* in the press). But although there were suggestions of some correlation between antigen specificity and a region of the β chain around the diversity (D) region (Fink, P.J. *et al.* and Winoto, A.), or the J region (A. Iwamoto, Toronto), J_β regions may also contact MHC (Iwamoto; K. Eichmann, Freiburg), so no general rules are yet apparent.

Gamma revisited

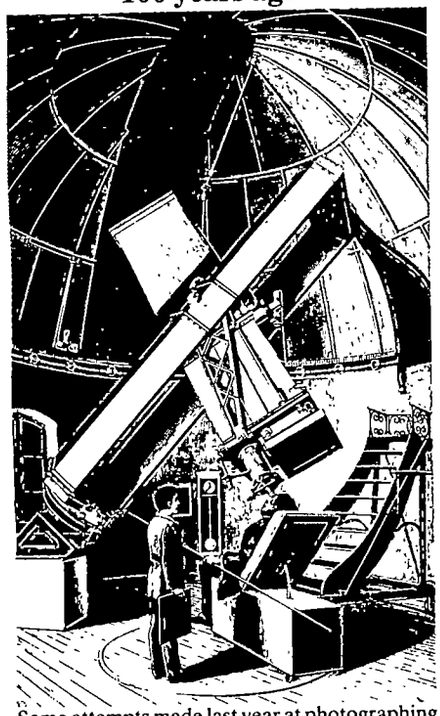
Such experiments still leave unresolved one of the major current T-cell mysteries; the problem of the role of γ chains. About eighteen months ago, Susumu Tonegawa and his colleagues at MIT reported the existence of a T-cell receptor-like complementary (c) DNA clone, the genes for which rearrange and are expressed only in T cells. Because the sequence and glycosylation patterns of the polypeptide predicted from the cDNA sequence did not match known α- or β-chain properties, the predicted protein has been named γ; it has yet to be identified as an entity. Much is known from cDNA and genomic sequences, however. Gamma products, which were at first though to be relatively invariant, are becoming more variable: T. Mak (University of Toronto) and D. Raulet (MIT) respectively, described a new constant (*C*) region and three new *V*-region genes in this complex, bringing the total number of known γ-chain genes in most mouse strains to four *C* regions (three of which cross-hybridize), each with a *J*, and six *V* regions (three of which cross-hybridize with each other). As in the mouse immunoglobulin λ locus, each *V* seems to rearrange to a particular *J–C* pair. Some *V* and *J* segments seem to be intrinsically non-functional.

The additional variability in the gene family implies that the product may play some part in specific recognition, and it has been suggested that it is essential for the function of mature cytotoxic T cells, the cells with which it was originally associated by Tonegawa, because of higher messenger (m) RNA expression in these cells than in helper-T cells. This possibility seems to be excluded, however, not only by the experiment of Steinmetz's group, but also because most rearranged γ-chain genes in peripheral T cells are non-functional, often because they contain termination codons consequent on out-of-frame joining of *V* to *J* regions. E. Reilly, from H. Eisen's group at MIT (Reilly, E.B. *et al. Nature* in the press), for example, has sequenced 11 different cDNA clones from three cytotoxic T-cell clones and found all to be non-functional, and similar examples are available from other laboratories.

The more recently discovered non-cross-hybridizing C_γ genes and the three new non-cross-hybridizing V_γ genes leave open the possibility that the functional γ-chain cDNA in these peripheral T cells has yet to be sequenced. Alternatively, functionally rearranged γ-chain genes may be present at an early stage in the history of the T cell and be lost before maturity. In support of this notion, Raulet (MIT) showed that rearrangement and mRNA involving two particular γ-chain *V* regions gradually disappear from thymocytes and peripheral T cells as the animal ages. He suggested that these *V* regions lie downstream (3′) of a third *V* region. A functional rearrangement to one of the 3′ regions could be deleted during maturation by the subsequent rearrangement of an upstream *V* by a mechanism similar to that described above for V_H genes.

If γ chains do play a part at a particular stage in the life of T cells, when is this likely to be? The γ mRNA is expressed at high levels in early fetal thymocytes illustrated at this meeting by the work of R. Snodgrass (Basel) and D. Pardoll (National Institutes of Health, NIH). It is not clear that these high levels of mRNA imply that there will be high levels of protein, however, because γ-chain rearrangements are rare in hybridomas prepared from early fetal thymocytes (W. Born, Denver) and not universal in adult 'early' thymocytes (M. Davis, Stanford University). Moreover, much of the fetal thymocyte mRNA, as in mature T cells, turns out on sequencing to contain frameshifts making it non-functional (Snodgrass). The cDNA may be overrepresented in non-functional transcripts, as Raulet reported that five out of six rearranged genomic DNA γ clones prepared from day 17 mouse fetal thymuses turned out to have open reading frames. The implications of all this, that γ proteins may be used only in small numbers for a short time during thymocyte development, and that the protein may down-regulate gene expression, are very intriguing in the light

100 years ago



Some attempts made last year at photographing the heavens by means of an instrument quite rudimentary having yielded good results, the director of the Paris Observatory gave orders for the construction of a special apparatus, the design of which is shown in the figure. This new instrument is composed of two telescopes in juxtaposition inclosed in a single metallic tube in the form of a parallelopiped, and separated from each other along their whole length by a narrow partition.

From *Nature* **34**, 34; 13 May 1886.

of a role for the putative γ chain suggested by Tonegawa and Raulet.

These authors hypothesized that the γ protein is important in one of the two critical events in the control of T-cell repertoire which occur in the thymus: the selection of cells bearing receptors that recognize antigen preferentially in association with MHC products expressed in that thymus (the phenomenon of self-restriction); and in the imposition on thymocytes of tolerance to self-MHC proteins themselves. Raulet and Tonegawa propose that immature thymocytes express receptors composed of β-and γ-chains, and that those recognizing self-MHC on thymus cells are selected. Later the γ chain is replaced by the α chain of mature T cells and the affinity of the receptor for self MHC thereby eliminated except in the presence of antigen.

The feeling at the meeting was that this theory is rather unlikely to be correct, at least in its baldest form. For example, there is no evidence in the structure/function experiments described by Hedrick, Winoto, Iwamoto, Eichmann and others (see above) that a particular β chain would predictably impose specificity for a particular MHC product on receptors in which it was first combined with one chain, γ, and then with a completely unrelated polypeptide, α. But although the theory is probably not completely correct, the data dealing with expression are becoming increasingly intriguing, and they do indicate the direction which future investigations will probably take.

Events in the thymus

Further elucidation of the events of thymic maturation will depend on the definition of the pathways of thymocyte differentiation, and these were therefore the focus of considerable interest at the meeting. The thymus contains several cell populations that have been well defined phenotypically but whose exact lineage relationships are only now becoming clear. A minimal outline of these populations and their relationships is shown in the figure.

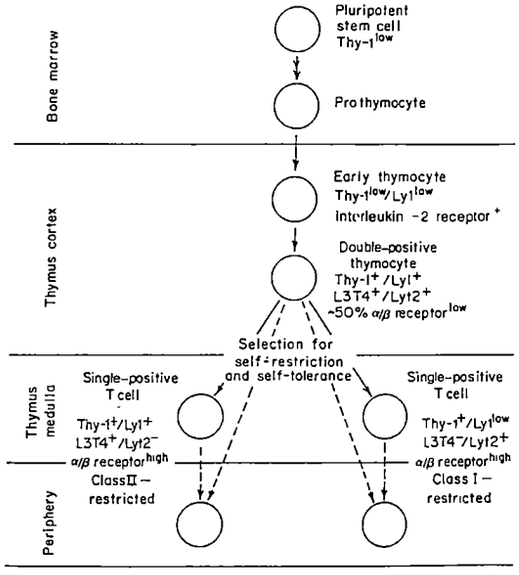
There was general agreement that thymocytes become tolerant to MHC antigens expressed by bone marrow-derived cells (probably dendritic cells) and perhaps also epithelial cells in the thymus (R. Jordan, Newcastle University; E. Jenkinson, Birmingham University; J. Sprent, Scripps Clinic) and that they learn to recognize antigen in association with MHC molecules expressed by thymic epithelial cells (Sprent), although the experiments of D. Longo (NIH) stand in direct contradiction to this. If self-restriction is controlled by cortical epithelial cells, then receptors on cortical thymocytes must be involved in the process. One should therefore be able to learn something about this process, or perhaps tolerance induction (although the site where this occurs is less well understood), by examining receptors on cortical cells.

Complexes of cortical thymocytes and other thymus cells have been isolated by several investigators. For example, a recent paper by A. Farr (University of Washington) (Farr, A. *et al. Cell* **43**, 543; 1985) demonstrated by electron microscopy that cortical thymocytes bind epithelial cells, and that the α/β receptor is 'capped' on that part of the thymocyte surface which is in contact with the epithelial cells. This suggests that the receptor is binding some ligand, perhaps an MHC molecule, on the epithelial cell and that the process of self-restriction or tolerance induction can be seen in the micrographs.

At the meeting, A. Kruisbeek (NIH) reminded us of her past experiments showing that anti-Ia antibodies blocked the appearance of mature, L3T4$^+$, class II-restricted thymocytes, but had no effect on immature 'double-positive' cells, or on Lyt2$^+$ mature thymocytes (see figure). In analogous experiments, Born showed that anti-receptor antibodies also have no effect on double-positive thymocytes (although a portion of them bears receptors) but block completely the appearance of mature cells bearing receptors with which the antibody could react. Taken together, these experiments suggest that an important event involving thymocyte receptors and MHC occurs when immature double-positive cells turn into mature thymocytes and T cells. These are the first indications of the stage of thymocyte development at which self-restriction or tolerance is induced.

Jonathan Sprent summarized what is perhaps the consensus view on thymocyte maturation. Precursor cells enter the thymus, proliferate and rearrange and express their T-cell receptor and receptor-like genes α, β and γ. These cells also become double-positive L3T4$^+$ and Lyt2$^+$. From these cells a few are selected, by interaction of their receptors or γ-chain products with MHC products on epithelial cells, to become mature, single-positive cells. At some stage, cells that react with self-MHC, perhaps on dendritic cells at the cortico–medullary junction, are eliminated and fully mature selected cells are allowed to enter the periphery.

The participants left the meeting as they had come, with the feeling that many useful reagents and methods had become available for the study of lymphocyte repertoire, and with the hope and expectation that these new tools would clarify rather than confuse the situation. □



Thymocyte development. Like all haematopoietic cells in adult animals, thymocytes arise from bone marrow precursors. At the meeting C. Muller-Seiburg and G. Spangrude (Stanford University) showed that the so-called primordial stem cell in bone marrow bears low levels of Thy 1. After colonization, the earliest cells found in the thymus bear little Ly1 and are positive for neither of the surface molecules that characterize mature helper or cytotoxic T cells, L3T4 or Lyt2 (T4 or T8 in man). These cells, which can repopulate an irradiated thymus, are not self-renewing, but give rise to all thymocytes sequentially, being replaced themselves eventually by new precursors from the bone marrow (B.J. Fowlkes, NIH; B. Mathieson, Frederick Cancer Research Facility; F. Jotereau, Nantes). In elegant reconstitutions of thymus organ cultures, E. Jenkinson (Birmingham) showed that a single precursor cell could give rise to all types of thymocytes. Receptors for interleukin-2 on these cells may be important in the generation of later stage thymocytes, particularly the mature L3T4$^+$ or Lyt2$^+$ cells (A. Kruisbeek, NIH).

Later stage cells include L3T4$^+$; Lyt2$^+$ blasts and non-dividing cells; and cells bearing only L3T4 or Lyt2 (like peripheral T cells). There has been considerable argument about the pathways that lead to each of these cell types. Some have suggested that the L3T4$^+$, Lyt2$^+$ double-positive population which comprises the bulk of thymocytes is a compulsory intermediate between the double-negative precursor and single-positive mature cell. Others believe that double-positive cells are all destined to die in the thymus. Mathieson presented at the meeting the first direct evidence for the existence of the former pathway. She selected Lyt2-bearing blast cells composed mostly of double-positive cells, and showed that after intrathymic injection, they could give rise only to cells bearing L3T4.

Malcolm Gefter is in the Biology Department, Massachusetts Institute of Technology, 77 Massachusetts Avenue, Cambridge, Massachusetts 02139, USA; Philippa Marrack is in the Department of Medicine, National Jewish Hospital, Denver, Colorado 80206, USA.

First isolation of HTLV-III

SIR—We wish to address several points raised in a recent commentary in *Nature*[1] regarding HTLV-III/LAV (human T-lymphotropic virus type III/lymphadenopathy-associated virus), the aetiological agent of acquired immune deficiency syndrome (AIDS). It was mentiond that the CEM cell line infected with HTLV-III/LAV may be a better source of antigen for testing HTLV-III/LAV in patients with AIDS and AIDS-related complex (ARC).

The transmission of HTLV-III isolates in several T4⁺ permanent cell lines, including CCRF-CEM, was reported first by our laboratory[2-4]. The transmission of HTLV-III isolates into those T4⁺ cell lines, including CEM, was the subject of a patent application made in early 1984 and now pending.

The fact that we had in our possession electron microscopic pictures of transiently transmitted LAV in Hut-78 and Ti7.4 cell lines should not be surprising. The LAV sample was obtained as a tissue culture supernatant from Dr Montagnier with the express understanding that it could be used for biomedical, biological and molecular biological studies. In accordance with this understanding, we had transiently transmitted LAV into the Hut-78 and Ti7.4 cell lines. Prior to the development of specific reagents for the detection of HTLV-III, the presence of retroviruses other than HTLV-I and HTLV-II could be detected in cultures from AIDS or ARC patients only by reverse transcriptase assay and electron microscopic examination.

Table 1 Summary of the chronological isolation of HTLV-III from patients with AIDS and ARC

No.	Patient samples	Date rec'd	Source	RT	EM	Immunological reactivities HTLV-I p19	HTLV-I p24	AIDS sera	HTLV-III p19	HTLV-III p24
1	G.W./AIDS	12/23/82	Gutterman, Houston, Texas	+	ND	−		ND	ND	ND
2	C.C./AIDS*	2/15/83	Leibowitch, Paris	+	+	±	±	ND	ND	ND
3	M.A./AIDS	2/15/83	Leibowitch, Paris	+	ND	−	−	ND	ND	ND
4	B.U./AIDS	2/15/83	Leibowitch, Paris	+	ND	−	−	ND	ND	ND
5	S.N./AIDS	9/23/83	Haynes, N. Carolina	+	ND	−	−	•	ND	ND
6	R.F./AIDS	10/18/83	Hoxie, Philadelphia	+	+	−	−	•	ND	ND
7	R.R./AIDS	2/4/84	Redfield, WRAIR, Washington, DC	+	+	−	−	+	•	•
8	S.S./ARC	2/4/84	Redfield, WRAIR, Washington, DC	+	+	−	−	•	•	•
9	K.E./ARC	2/4/84	Redfield, WRAIR, Washington, DC	+	+	−	−	•	•	•
10	S.B./ARC	2/4/84	Redfield, WRAIR, Washington, DC	+	+	−	−	•	•	•

Abbreviations used: G.W., C.C., M.A., etc., patients' initials; RT, reverse transcriptase; EM, electron microscopy; ND, not done.
*Patient C.C. was infected with both HTLV-III and HTLV-I.

At the time we obtained LAV it was the contention of several experts on virus morphology that the particles shown in the electron micrograph published in *Science*[5] by Barre-Sinoussi *et al.* was an arena virus. Naturally we wanted to check the material received from Dr Montagnier by electron microscopy to check this contention. Before receipt of LAV, we had detected reverse transcriptase activity in a number of cultures from AIDS and ARC patients which showed no cross-reaction with HTLV-I or HTLV-II reagents, thus indicating the presence of a new retrovirus. In a number of cases electron microscopic examination showed the presence of virus particles with a cylindrical core, characteristic of HTLV-III (Table 1, Fig. 1). A chronological identification of some of these virus particles from cultures obtained from AIDS and ARC patients by our laboratory beginning in December 1982 is summarized in Table 1 and Fig. 1.

The experimental results shown were obtained shortly after receipt of the samples, usually a matter of weeks. We had evidence for the presence of a new retrovirus in AIDS and ARC patients long before the LAV particles were sent to us and even before the publication of the results by Barre-Sinoussi *et al.* in 1983. Since we considered the mere detection of virus particles in cultures from AIDS and ARC patients to be insufficient to confirm scientifically our hypothesis that such particles were implicated in the aetiology of the disease, we decided first to obtain specific reagents against the new virus in order to publish definitive results concerning AIDS aetiology. The results presented in our four papers provided clearcut evidence that the aetiology of AIDS and ARC was the new lymphotropic retrovirus, HTLV-III[2,3,6,7]. In addition, for the first time the virus was produced in large quantities, specific reagents to the virus were made, and a reliable blood test to protect the blood supply and prevent blood transfusion-associated AIDS was now available.

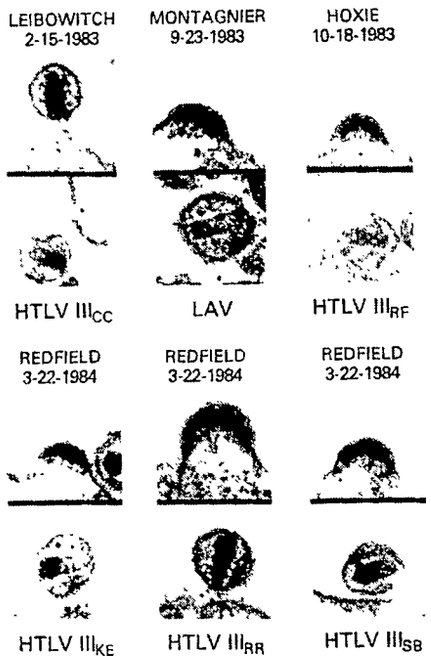


Fig. 1

ROBERT C. GALLO
PREM S. SARIN
BERNARD KRAMARSKY*
ZAKI SALAHUDDIN
PHILIP MARKHAM†
MIKULAS POPOVIC

Laboratory of Tumor Cell Biology, National Cancer Institute, Bethesda, Maryland 20892, USA

**Electronucleonics, Inc., Silver Spring, Maryland 20904, USA*

†*Bionetics Research, Inc., 1330-A Piccard Drive, Rockville, Maryland 20850-4373, USA*

1. Beardsley, T. *Nature* **320**, 563 (1986)
2. Gallo, R.C. *et al. Science* **224**, 500–503 (1984)
3. Popovic, M. *et al. Science* **224**, 497–500 (1984)
4. Popovic, M., Read-Connole, E. & Gallo, R.C. *Lancet* ii, 1472–1473 (1984).
5. Barre-Sinoussi, F. *et al. Science* **220**, 868–870 (1983)
6. Shüpbach, J. *et al. Science* **224**, 503–505 (1984)
7. Sarngadharan, M.G. *et al. Science* **224**, 506–508 (1984)

SIR—I wish to take issue with a comment by Tim Beardsley on the LAV/HTLV-III controversy[1]. Gilden *et al.* clearly state in their correction letter to *Science*[2] that I am not responsible for the erroneous mixing up of LAV and HTLV-III electron micrographs that appeared as part of a composite electron micrograph picture in my paper to *Science*[3]. Nevertheless, the first paragraph of Beardsley's comment evokes the impression that I am to be blamed for this embarrassing error. In fact, my work described in that *Science* paper dealt exclusively with serological and biochemical aspects of the new retrovirus. My drafts did not contain the controversial composite and neither R.V. Gilden nor M.A. Gonda were proposed as

co-authors. It was solely R.C. Gallo's decision that the composite be shifted from another paper to mine.

J. SCHÜPBACH
Swiss Retrovirus Reference Laboratory,
Institut für Immunologie und Virologie,
Universität Zürich,
Gloriastrasse 30,
Postfach CH-8028 Zürich,
Switzerland

1. Beardsley, T. *Nature* **320**, 563 (1986).
2. Gilden, R.V. *et al. Science* **232**, 307 (1986).
3. Schüpbach, J. *et al. Science* **224**, 503–505 (1984).

Keeping supercomputers under control

SIR—The Purdue Water Resources Reseach Center in conjunction with the Office of Health and Environmental Research of the US Department of Energy recently co-sponsored a meeting on the current uses of, and future needs for, supercomputers in hydrology. 'Supercomputers in Hydrology: Future Directions', the first meeting of its kind, aimed to evaluate the need for large-scale vector and parallel processing machines and their peripherals in the hydrologic sciences, especially in subsurface hydraulics. While the charge of the seminar was to specifically deal with hydrologic applications of supercomputers, the conclusions drawn at the meeting apply equally well to many other fields of science and technology.

Almost all technical issues involving the use of supercomputers were presented either by a computer scientist, a programmer or an applied mathematician. Because the architecture of most supercomputers is radically different from scalar processing machines, this is no surprise. The real importance of this observation is the implied increase in the need for multidisciplinary research teams to solve major ecological problems. Unfortunately, in the United States, many of the larger supercomputer funding initiatives do not address this issue at all.

This defect in the supercomputer initiatives leads to two major problems: scientists not doing 'science' and the inefficient use of supercomputers. If funds were available to support programmers with expertise on a machine of a certain architecture, the scientist would only need to communicate effectively with the programmer. The projected changes in architecture affect the programmer and not the scientist; hence the scientist is free to do science.

An alternative to long-run funding of programmer-consultants is for the initiatives to increase their effort in the development of very high level languages. Rice of Purdue's Computer Science Department gave a talk on projected advances in hardware and software over the next 10 years. From 1975 to 1985 computing speed increased by a factor of 25. Between 1985 and 1995 the speed is projected to increase by a factor of 2,000. On the other hand, from 1975 to 1985, computer languages have been improved by a factor of only 1.4. Unless more funding is made available for the development of high-level languages, improvement in ease of coding is not expected to increase nearly as fast as machine computational power. In fact, because of radical changes in architecture, programming may well become more difficult.

Another important point brought out at the seminar is that advances in science should not be overpowered by advances in computational capability. Do we really improve our fundamental understanding of science by looking at larger and larger computational problems? Many would argue that the understanding of complex chemical and physical interactions in the subsurface and the ability to estimate parameters is so poor that the large supercomputer models may in fact be totally incorrect. In this instance, supercomputer modelling efforts may turn out to be a greater obstacle to real progress than no model at all.

So there is clearly a role for supercomputers, but the extent of this role will depend on the availability of high level languages, expert programmer consultants working closely with multidisciplinary teams, exposure to different computational systems, and a judicious choice of problems with the aim of advancing our understanding of science.

JOHN H. CUSHMAN
Water Resources Research Center,
Lilly Hall of Life Sciences,
Purdue University,
West Lafayette,
Indiana 47907, USA

FRANK J. WOBBER

US Department of Energy,
Office of Energy Research,
OHER (ER-75),
Washington, DC 20545, USA

Are light head loads carried free?

SIR—Geoffrey Maloiy and his colleagues (*Nature* **319**, 668; 1986) have shown conclusively that experienced African women can carry head loads at remarkably low energy cost. However, I cannot accept their conclusion that loads of less than 20 per cent of body mass are carried free, on the basis of the evidence they present. They performed no measurements in the load range 0 to 20 per cent: their conclusion is based on the backward extrapolation of a straight regression line fitted to the range of about 24 to 70 per cent of body mass. Extrapolation of a regression line always is risky, and in their case particularly so, because other data they present clearly show that the energy cost to army recruits of carrying a back pack is not a linear function of load.

Maloiy and his colleagues suggest that an explanation for the low cost is that the women achieve a gait such that the load makes little movement against gravity during the walking cycle. Though proof of this theory using accelerometers, as R. McNeill Alexander proposes in his *News and Views* piece on the paper (*Nature* **319**, 623; 1986), would be elegant, my observations of African women carrying head loads leads me to believe that they are right. Many South African women can carry small objects like individual oranges or bottles on their heads with grace and ease; some do so by choice even when their hands are free. While it is possible to carry a metastable object like a bottle on one's head even when one's head is moving up and down, the women appear to reduce or eliminate all vertical and transverse head movements when doing so. Given the human anatomy, I think that stabilizing the head necessarily must stabilize the centre of gravity of the whole body too. Since fuelling of cyclic vertical movements of the centre of gravity constitutes one component of the energy cost of walking, elimination of such movements should reduce the energy cost. Thus, the cost of walking with a light load on the head, in people experienced in the skill, might be less than the cost of walking with no load.

We need the missing measurements.

DUNCAN MITCHELL
Department of Physiology,
University of the Witwatersrand
Medical School,
Johannesburg 2001,
South Africa

SIR—As supporting evidence for Maloiy *et al.*'s suggestion (*Nature* **319**, 668; 1986) about the steadiness of a head load, I cite the observation that even small children can carry liquid loads on their heads without spilling from the container. A woman carrying a bucket of water home from the well is surely one of the commonest sights; and I would think a good substitute for the suggested experiment of attaching an accelerometer to the head load.

It is interesting that it is possible to carry a much heavier load on the head than the bearer can lift unaided. It is normal to see two people lifting a burden and settling it comfortably on the head of a third, who then walks off with it. One of the most impressive, if macabre, sights I ever saw was when a farmer had died in the field, and another carried the corpse, by then rigid, to the village on his head.

D.A.H. TAYLOR
Department of Chemistry and Applied
Chemistry,
University of Natal,
Durban 4001,
South Africa

State of preservation of the Dead Sea Scrolls

SIR—The article "Dead Sea Scroll parchments: unfolding of the collagen molecules and racemization of aspartic acid"[1] is of interest since any method which will improve on our knowledge of vellum fragments is important. The study on the condition and deterioration of vellum which is known to be approximately 2,000 years old is interesting in itself, although the identification into goat, calf or sheep as to origin of the material examined[2,3] would improve the information resulting from their tests. This could be accomplished by a comparison made from samples of the scrolls known to be of goat skin and that of modern goat skin prepared as we believe the scrolls to have been prepared[3]. In this way Weiner *et al.* could make a column to their Table 1 identifying the skin of each scroll as well as the patches and other additions. As the authors state in their paper[1] "Using different skins in one scroll and/or various parchment preparation treatments could conceivably influence the C:G index and the D/L aspartic ratios".

If, however, any relationship is to be drawn to the age of the samples and the agents of deterioration, then the tests they carried out gave insufficient evidence, as we have seen even within the scrolls there is variation. There must be a more comprehensive sampling to form a basis for comparison, which Weiner *et al.* acknowledge. A modern rat tail and a seventeenth century book cover do not provide a varied series, though the authors use them as comparative materials to the scroll samples. An adequate sample basis must be developed on a wider range of material both ancient and modern; this could be accomplished by application of the tests on samples which have a known documentation between the first and sixteenth centuries AD which would include changes in parchment preparation both in Europe and the Near East[1-4].

When considering the condition of materials found in the Qumran caves, it may be of interest that most scholars, given the methods of examination at the time, believed the two scrolls offered to the British Museum in the 1880's by M.W. Schapira to be forgeries based partly on the fact that their condition was throughout so superlative compared to known fragments[5]. There is now little doubt that the Schapira Scrolls came from the Dead Sea caves[6].

It is unfortunate that Weiner *et al.* did not examine the agents of deterioration of vellum to gelatin by controlled testing, and then subject their samples to the collagen/gelatin and D/L testing. Such testing of modern and ancient samples (combined with accelerated aging tests) would give information of a positive and precise nature on the causes of the variations found on Dead Sea Scroll samples (some on the same fragments) which undermine their study. As the authors note, we know damage has occurred, but its cause, and when it occurred are unknown. Plenderleith[7] found during the unrolling of Dead Sea Scroll fragments of cave 1 that certain fragments were permeated with a black bituminous substance which he identified as a decomposition product of the skin. During the unrolling he found it necessary to dampen the Scrolls which caused this substance to become sticky. This black substance apparently was gelatin. This incident brings up a very important topic, that of the interventions made necessary by the fragile and rolled nature of the scrolls. Careful identification of the location from which each sample was taken should have been presented by Weiner *et al.* This information could have been correlated with published data on the condition of the fragments as they were found and treated. Both Plenderleith[7] and Cross[8] report extensive treatments with moisture and oils to remove clay and/or relax the skins[9]. The materials used in the treatments and the originally adherent substance could have altered analytic results.

This consideration of the condition of each fragment and their individual histories, including methods of skin preparation of which Stambolov[10] has prepared a thorough survey and Poole and Reed[3] a precise analysis, is of great importance. Some of the skins were found in the same cave, some scattered on the surface, others buried and some appear to have been discovered several centuries ago and been exposed to quite varied climatic conditions[11-13].

Others were preserved for longer periods as whole scrolls rolled in linen and placed in jars encased in tar. Varied histories of the fragments should be listed and referred to when discussing the results of testing. Rapid deterioration can occur in organic material transferred from one environment to another. Fragments taken from the dry conditions in the caves to a humid environment or one with rapid or frequent variation could cause severe and immediate damage. It is of interest to note that the authors are continuing their research with specific attention to the climatic effects of the transition of collagen to gelatin (S. Weiner, personal communication).

Given the problems with amino acid dating, especially the variation with regard to radiometric methods[15-17], examination of rates of decay from amino acid D/L values should be considered very relative, especially with regard to natural and human interventions. Nevertheless, its use as a source of approximate time during which collagen has changed to gelatin may prove to be of great value

T.B KAHLE
Capricornus School of Book Binding and Restoration,
Berkeley,
California 94701, USA
NICCOLO CALDARARO
Fine Arts Museums of San Francisco, and Tiburon Archaeological Research Group,
1600 Holloway Avenue,
San Francisco State University,
San Francisco, California 94132, USA

1. Weiner, S., Kustanovich, Z., Gil Av, E. & Traub W. *Nature* **287**, 820–823 (1980).
2. Ryder, M.L. *Nature* **182**, 781–783 (1958).
3. Poole, J.B. & Reed, R. *Technol Cult* **3**, 162–176 (1962).
4. Burton, D., Poole, J.B. & Reed R. *Nature* **184**, 353–354 (1958).
5. Allegro, J.M. *The Shapira Affair* (Doubleday, Garden City, 1965).
6. Reed, R. *Ancient Skins, Parchments and Leather* (Seminar Press, London, 1972).
7. Plenderleith, H.J. *Discoveries in the Judean Desert I Qumran Cave Vol I* (eds Barthelemy, D. & Milik, J.T.) 39–40 (1955).
8. Cross, F.M. Jr *Biblical Archaeol* **17** (1954).
9. Araldite as an aid to Archaeology (Ciba Tech. Note No. 218, 1961).
10. Stambolov, T. *Manufacture Deterioration and Preservation of Leather. A Literature survey of theoretical aspects and ancient techniques* (Central Research Laboratory ICOM, Amsterdam, 1969).
11. Kahle, P.E. *The Cairo Geniza* 2nd ed (Blackwell, Oxford 1959).
12. Yadin, Y. (ed.) *The Temple Scroll* Vols 1–3 (University of Jerusalem, 1984).
13. Vermes, G. *Times Lit. Suppl. 3 May*, 50, 501 (1985).
14. Protsch, R.R. *Catalogue of Fossil Hominids of North America* (Fischer, New York, 1978).
15. Hedges, R.E.M. & Wallace, C.J.A. *J. Archaeol Sci.* **5**, 377–388 (1978).
16. La Joie, K.R., Peterson, E. & Ortiz, B.V. in *Biochemistry of Amino Acids* (ed. Hare, P.E.) 477–498 (Wiley, New York, 1980).
17. Kessels, H.J. & Dungworth, G. in *Biochemistry of Amino Acids* (ed. Hare, P.E.) 527–541 (Wiley, New York, 1980).

WEINER *et al.* reply—In our study, we reported the development of a new method for assessing the extent to which collagen has transformed to gelatin in ancient parchments and we tried to estimate the approximate time that elapsed since the transformation took place. We applied these methods to the analysis of some 40 parchment fragments from the Dead Sea Scrolls. We agree with Kahle and Caldararo that a thorough study, which includes more background information on the pieces analysed as well as controlled studies of parchments of different ages, prepared in various ways and subjected to a range of temperature and humidity conditions, would be the most helpful. Incidentally, some of the background information can be ascertained from the literature using the information supplied in our Table 1. We took care to emphasize in our original publication that the transformation of collagen to gelatin may be only one of several different degradative processes that occur in ancient parchments. Thus caution must be exercised when correlations between some parchment property and collagen:gelatin proportions and/or D/L ratios are made, as Kahle and Caldararo are suggesting. We also noted that the

wide range of D/L aspartic acid ratios, even from a single parchment fragment probably precludes the use of this technique for absolute age determination of parchment.

STEPHEN WEINER*
ZINA KUSTANOVICH†
EMANUEL GIL-AV†
WOLFIE TRAUB‡
* *Isotope,* † *Organic Chemistry and* ‡ *Structural Chemistry Departments, Weizmann Institute of Science, Rehovot, Israel*

Nuclear winter and the greenhouse effect

SIR—Ever since its original publication[1], the nuclear winter concept has been in dire need of some form of experimental verification. So great has its need for independent corroboration been, in fact, that when challenged on this point[2,3], the concept's creators responded by grasping at some very strange straws. For one thing, they stated that the climate model they used to develop the concept was only partly calibrated, and that this calibration was accomplished by means of the possible collision of an asteroid or cometary nucleus with Earth at the time of the Cretaceous/Tertiary transition and by research on martian dust storms[4]. To my mind, a much more timely and down-to-earth phenomenon to use as a means of calibration is the CO_2 greenhouse effect; for it pertains to our own planet, is supposed to be happening now, and is itself predicted by the same climate models that produced the nuclear winter concept.

What are the fruits of such a calibration exercise? From data and equations in the US National Research Council's most recent review of the CO_2/climate connection[5], it can be calculated[6] that between 1880 and 1980 the northern third of the Earth (the most climatically sensitive region) should have warmed by about 3°C due to atmospheric CO_2 increases experienced over that period. However, the true model-predicted warming over this time span is actually 6°C; for an important study of the past year[7] has clearly demonstrated that increases in other trace gases over the past 100 years should have had just as great an effect on the Earth's climate as did increases in CO_2 during that time.

So how does this 6°C warming prediction compare with reality? Recent studies of Arctic and Northern Hemisphere temperature trends of the past century[8-10] show that the prediction is fully an order-of-magnitude too large, so it is logical to assume that the nuclear winter prediction is similarly overestimated.

Additional support for this conclusion comes from several climate modelling studies of the past two years, which have shown that when more realistic parameterizations of several real-world processes are included in the models, the climate sensitivity of the Earth is greatly reduced. Somerville and Remer[11], for instance, have introduced a cloud liquid water content effect which halves climate sensitivity; while Spelman and Manable[12] and Wang *et al.*[13] have improved upon the treatment of feedbacks from meridional and vertical dynamical heat fluxes, including ocean currents, reducing it by a factor of four. Finally, Ou and Liou[14] have improved on the treatment of cumulus convection, reducing the climate sensitivity by another 40 per cent. Taken together, these independent model improvements lead to the same order-of-magnitude reduction in the strength of the CO_2 greenhouse effect that is suggested by the temperature history of the Earth.

Why do we not see reference to these developments in the public dialogue over the CO_2/climate question? Is it because their acknowledgement would cast doubt on the nuclear winter hypothesis? These are questions that all who are truly concerned about mankind's future on our fragile planet must ask themselves. As Maddox[3] has rightly said with respect to the effort to avert nuclear war, "by clouding the case with disputable predictions, they [the nuclear winter protagonists] are in danger of weakening it".

S.B. IDSO
US Water Conservation Laboratory, 4331 E. Broadway, Phoenix, Arizona 85040, USA

1. Turco, R.P., Toon, O.B., Ackerman, T.P., Pollack, J.B. & Sagan, C. *Science* **222**, 1283–1292 (1983).
2. Maddox, J. *Nature* **307**, 107 (1984).
3. Maddox, J. *Nature* **308**, 11 (1984).
4. Turco, R.P., Toon, O.B. Ackerman, T.P., Pollack, J.B., & Sagan, C. *Nature* **311**, 307–308 (1984).
5. Carbon Dioxide Assessment Committee, US National Research Council *Changing Climate* (National Academy Press, Washington, DC, 1983).
6. Idso, S.B. *J. environ. Sci.* **27** (3), 19–22 (1984).
7. Ramanathan, V., Cicerone, R.J., Singh, H.B. & Kiehl, J.T. *J. geophys. Res.* **90**, 5547-5566 (1985).
8. Jones, P.D., Wigley, T.M.L. & Kelly, P.M. *Mon. Weath. Rev.* **110**, 59-70 (1982).
9. Kelly, P.M., Jones, P.D., Sear, C.B., Cherry, B.S.G. & Tavakol, R.K. *Mon. Weath. Rev.* **110**, 71–83 (1982).
10. Raper, S.C.B. *et al. Nature* **306**, 458-459 (1983).
11. Somerville, R.C.J. & Remer, L.A. *J. geophys. Res.* **89**, 9668-9672 (1984).
12. Spelman, M.J. & Manabe, S. *J. geophys. Res.* **89**, 571-586 (1984).
13. Wang, W-C., Molnar, G., Mitchell, T.P. & Stone, P.H. *J. geophys. Res.* **89**, 4699–4711 (1984).
14. Ou, S.S. & Liou, K-N. *J. geophys. Res.* **90**, 2223–2232 (1985).

Competition amongst desert perennials

SIR—In his *News and Views* article on regularity in the desert shrub *Larrea tridentata*, Silvertown[1] ignores some areas of current debate and seems to draw spurious analogies between intra-specific competition in plants and inter-specific competition in animals. Intra-specific interactions amongst animals may sometimes create regular spacing[2,3].

King and Woodell[4] explicitly stated how the competition hypothesis could account for regularity in desert perennials. The elimination of small individuals by root competition with neighbours could convert a clumped population first to a random and then to a regular pattern. Silvertown not only ignores this hypothesis but also states that no hypothesis was provided to explain regularly-spaced clumps. King and Woodell[4] added that some regular patterns may have originated during long droughts, when intra-specific competition for water would be at its most intense. This is not 'acknowledging the importance of other factors'[1] as drought will inevitably intensify competition for water.

Larrea tridentata populations develop over such long time spans[5] that the hypothesis that regularity is largely due to competition for water will be difficult to disprove. Genets of *Larrea* can live for up to 11,000 years[6], the shrub grows slowly, and intense droughts are sporadic. Thus the lack of major change in the patterns of *L. tridentata* over 45 years in an area of fairly high rainfall[7] is unremarkable and provides no evidence for or against any of the hypotheses which suggest how regular patterns might arise.

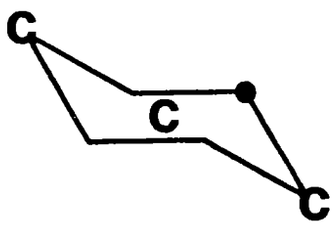
The effects of factors other than competition for water on pattern in *Larrea*, such as allelopathy[8] and run-off[9], have been discussed for a long time. Nevertheless, there is regularity in single-species populations of other dryland perennials[10]. It has been shown that adjacent shrubs of *L. tridentata* compete for water[11,12]. Any refinement of the hypothesis must include (1) the clonal growth pattern of *L. tridentata* in certain sites, (2) the possibility that seedlings become preferentially established on mounds remaining after clumps have died, thus perpetuating existing patterns[13,14] and (3) protection of young plants by older plants against freezing[14].

At some sites clumps which consist of mixtures of genets may have been classified as individuals. The regularity of the clumps still needs an explanation, however, whether a clump consists of one genet or several.

T.J. KING
S.R.J. WOODELL
Department of Plant Sciences, South Parks Road, Oxford OX1 3RB, UK

1. Silvertown, J.W. *Nature* **316**, 298 (1985).
2. King, T.J. *J. Ecol.* **65**, 235 (1977).
3. Nelson, J.B. *The Sulidae* (Oxford University Press 1978).
4. King, T.J. & Woodell S.R.J. *J. Ecol.* **61**, 761 (1973).
5. Sternberg, L. *Madrono* **23**, 408 (1976).
6. Vasek, F.C. *Am. J. Bot.* **67**, 246 (1980).
7. Schlesinger, W. & Jones, C. *Bot. Gaz.* **145**, 116 (1984).
8. Knipe, D. & Herbel, C.H. *Ecology* **47**, 775 (1966).
9. Anderson, D.J. *J. Ecol.* **59**, 555 (1971).
10. King, T.J. & Woodell, S.R.J. *J. Ecol.* **72**, 295 (1984).
11. Fonteyn, P.J. & Mahall, B.E. *Nature* **275**, 544 (1978).
12. Fonteyn, P.J. & Mahall, B.E. *J. Ecol.* **69**, 883 (1981).
13. Wright, R.A. *Arizona Acad. Sci.* **6**, 58 (1970).
14. MacMahon, J.A. & Schimpf, P.F. in *Water as a Factor in the Biology of North American Desert Plants* (eds Evans D.D. & Thomas, J.L.) 114 (Dowden, Hutchinson & Ross, Stroudsberg, Pennsylvania, 1981).

COMPLEX CARBOHYDRATE CORPORATION



"Let us help you with your complex carbohydrate science"

We have determined the structures of the complex carbohydrates of:

- glycoproteins
- glycolipids
- glycosaminoglycans
- cell wall polysaccharides
- extracellular (capsular) polysaccharides
- lipopolysaccharides

Analyses we can now provide:

- glycosyl composition
- glycosyl-linkage composition
- glycosyl sequence
- identification of non-glycosyl substituents
- points of attachment of non-glycosyl moieties
- absolute configuration
- anomeric configuration
- conformations in solution
- complete primary structure

In addition to consulting, the following services are offered:

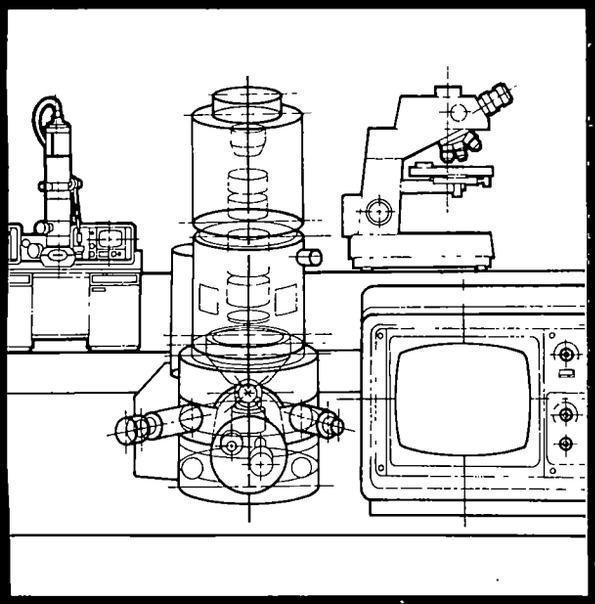
- gas chromatography
- liquid chromatography
- combined g.c.-m.s. (e.i. and c.i.)
- combined l.c.-m.s. (thermospray direct inlet, moving belt)
- high-mass f.a.b.-m.s.
- ultra-high-field ^{1}H– and ^{13}C-n.m.r. spectroscopy (all 1-D and 2-D techniques
- metabolic profiling

For more information, call (404) 546-3153, or write

COMPLEX CARBOHYDRATE CORPORATION, Suite 512
2351 College Station Road
Athens, GA 30605, U.S.A.

Reader Service No.1

MICRO·86 EUROSEM·86



ROYAL MICROSCOPICAL SOCIETY IN ASSOCIATION WITH NATURE

MICRO 86 MICROSCOPY EXHIBITION

Modern Microscopes and ancillary equipment at the Bloomsbury Crest Hotel, Coram Street, WC1.

7th JULY–11th JULY 1986

Tickets and details from: Royal Microscopical Society, 37-38 St. Clements, Oxford OX4 1AJ, England.
Telephone: Oxford (0865) 248768/721081

Reader Service No.150

New volumes from

Handbook of Experimental Pharmacology

Volume 79

New Neuromuscular Blocking Agents

Basic and Applied Aspects

Editor: **D. A. Kharkevich,** Moscow
1986. 128 figures. XXIV, 741 pages. Hard cover DM 780,–
ISBN 3-540-15771-9

This volume is devoted to the applied and fundamental aspects of the studies of new neuromuscular blocking agents. It contains valuable data that until now has been insufficiently reviewed or not elucidated at all, and reflects the up-to-date state of the art of the field together with promising indications of further developments.

Volume 78

The Tetracyclines

Editors: **J. J. Hlavka,** Pearl River; **J. H. Boothe,** Ocean Gate
1985. 77 figures. XIV, 451 pages. Hard cover DM 490,–
ISBN 3-540-15259-8

The editors have compiled a comprehensive review of the tetracyclines, ranging from their discovery to the present and including all the major subdivisions of these chemically important and clinically useful antibiotics.

Volume 77

Chemotherapy of Gastrointestinal Helminths

Editors: **H. Vanden Bossche, D. Thienpont,** Beerse; **P. G. Janssens,** Schilde
1985. 62 figures. XXI, 719 pages. Hard cover DM 660,–
ISBN 3-540-13111-6

In this volume the editors and authors have critically evaluated the immense amount of data on anthelmintic drugs that is scattered throughout the literature. This review is not limited to an evaluation of the therapeutic efficacy of the more important anthelmintics, but also includes information on their pharmacology, pharmacokinetics, toxicity, and mode of action.

Volume 76

Clinical Pharmacology of Antianginal Drugs

Editor: **U. Abshagen,** Mannheim
1985. 81 figures. XVI, 552 pages. Hard cover DM 460,–
ISBN 3-540-13110-8

This volume reviews the epidemiology, pathophysiology and treatment of coronary heart disease. The emphasis placed on clinical pharmacology and research is of immediate relevance for therapeutics. Thus, the volume provides not only the pharmacological basis for treatment, but also the principles of therapy and the rational methods for its assessment.

Prices are subject to change without notice

3307/4/2h

Springer-Verlag Berlin Heidelberg New York Tokyo

Heidelberger Platz 3, D-1000 Berlin 33
175 Fifth Ave., New York, NY 10010, USA
37-3, Hongo 3-chome, Bunkyo-ku, Tokyo 113, Japan

Springer

Reader Service No.11

SCIENCE AND TECHNOLOGY

Whatever the subject... refer to

MACMILLAN DICTIONARIES

DESIGNED FOR STUDENTS

The paperback *Macmillan Dictionary Series* combines new and established works of teaching and reference with an attractive series format.

* authoritative definitions and explanations of all current terminology written by experts
* lucidly written entries with thorough cross referencing
* regular new editions keep the student up to date with the latest research, practice and technology
* a clear layout for easy reference
* prices range from just £7.95 to £9.95

NEW IN 1986...

MACMILLAN DICTIONARY OF BIOTECHNOLOGY
JIM COOMBS March 1986 320pp 0 333 40875 6 £9.95

MACMILLAN DICTIONARY OF THE HISTORY OF SCIENCE
Edited by W. F. BYNUM, E. J. BROWNE and ROY PORTER
March 1986 528pp 0 333 34901 6 £8.95

MACMILLAN DICTIONARY OF PERSONAL COMPUTING AND COMMUNICATIONS DENNIS LONGLEY and MICHAEL SHAIN
August 1986 320pp 0 333 42170 1 £8.95

MACMILLAN DICTIONARY OF PHYSICS
MARY P. LORD August 1986 320pp 0 333 42377 1 £8.95

MACMILLAN DICTIONARY OF IMMUNOLOGY
FRED ROSEN, LISA STEINER and EMIL UNANUE
August 1986 256pp 0 333 39248 5 £8.95

RECENTLY PUBLISHED...

MACMILLAN DICTIONARY OF LIFE SCIENCES *Second Edition*
E. A. MARTIN 1985 400pp 0 333 38647 7 £9.95

MACMILLAN DICTIONARY OF THE ENVIRONMENT
Second Edition
MICHAEL ALLABY 1985 536pp 0 333 37951 9 £8.95

MACMILLAN DICTIONARY OF INFORMATION TECHNOLOGY
Second Edition DENNIS LONGLEY and MICHAEL SHAIN
1985 392pp 0 333 37261 1 £8.95

MACMILLAN DICTIONARY OF MICROCOMPUTING *Third Edition*
CHARLES SIPPL 1985 544pp 0 333 37082 1 £8.95

MACMILLAN DICTIONARY OF DATA COMMUNICATIONS
Second Edition
CHARLES SIPPL 1985 544pp 0 333 37083 X £8.95

MACMILLAN DICTIONARY OF ENERGY
Edited by MALCOLM SLESSER
1985 314pp 0 333 36867 3 £7.95

MACMILLAN DICTIONARY OF ASTRONOMY
VALERIE ILLINGWORTH 1985 320pp 0 333 39243 4 £9.95

Macmillan Press, Houndmills, Basingstoke, Hants RG21 2XS, UK

Not available in USA.

MACMILLAN PRESS

Growth into smallness

Nicholas Kemmer

Inward Bound: Of Matter and Forces in the Physical World. By Abraham Pais. *Oxford University Press:1986. Pp.637. £20, $24.95.*

Inward Bound is an account of how, since the beginning of this century, physicists have progressed towards the understanding of natural phenomena in ever-decreasing dimensions of space. The author, Abraham Pais, can look back on a long and creative career in theoretical physics, towards the end of which his biography of Einstein (*Subtle is the Lord*, published by Oxford University Press in 1982) revealed that he is a remarkably gifted writer. Now he has presented us with a book in which even more varied talents are in evidence.

Pais's mastery of the whole field of elementary particle physics is manifest on every page. In addition, his insight into the personalities of the actors in the story is remarkable. In the case of the earliest of these there is evidence of deep study of the widest range of relevant literature, but it may surprise younger readers that so many persons, whom they only know as famous names from the past, were real people in Pais's life. In particular he had the good fortune to work beside Niels Bohr in Copenhagen *and* Albert Einstein in Princeton. The many personal facts — sometimes of real relevance, sometimes just anecdotal — are a feature of the book, which is also enlivened by occasional spurts of impish humour. (Just one example: early on Pais tells us of speculations that radioactivity might be a property of *all* matter, and writes, "... the conjecture was not heard of again until... the 1970's..., see Chapter 22, which the reader will have time to reach without fear of prior disintegration".)

The scope and level of *Inward Bound* are clearly and extensively stated in its opening chapter, entitled "Purpose and Plan". No reader should skip it. All the chapters are divided into sections, and Section (a) of Chapter 1 is headed "From X to Z"; X is the X-ray and Z is the particle discovered by CERN in 1983, the two objects that are the termini of Pais's inward-bound journey. He explains here why that journey is broken into "A History" (*c.* 400 pages) and "A Memoir" (*c.* 175 pages). With the pace and volume of physics research increasing so enormously over the near-century covered in the book, it is hardly surprising that it was necessary to change the nature of the presentation at a particular moment. No break could be more natural than the end of the Second World War, which also happened to coincide with the start of the author's own career in the United States. Thus the first part covers all that for Pais was there at the start, while the second is what he witnessed and helped to shape.

Even with this break, it is quite astonishing how, in spite of the explosive growth of the subject, Pais has managed to knit events into a unified flow of narrative. This is to a large part due to the way he has chosen to unfold his story. It is not chronological, but rather topic by topic. Each of these is a strand, usually a single section, in a chapter that binds several strands together. Some of these are quite short — one might be on instrumentation, another on some general topic peripheral to the main narrative (there are for instance a few pages on physicists during the First World War) — but others are parts of long threads that can be traced almost right through the whole book, the puzzles of β-decay being an outstanding example. It is as if Pais were guiding the reader's eye along the colours in the weave of a beautiful tapestry. (I am tempted to misapply the current jargon word *fibre-bundle* to what I am trying to describe!) A feature of this particular tapestry is, of course, how it widens and thickens as one looks along it; at one end it displays all the physics that then existed, while at the other all we are following is a single, narrow strip in a huge field of activity.



From *Inward Bound*

Talk of physics: (left to right) Robert Oppenheimer, Paul Dirac and Abraham Pais.

In illustration, a closer look at Chapter 2 may be useful. Section (a) focuses on Roentgen in his environment at Würzburg, on how his accidental discovery came about in the wake of the introduction of cathode rays by Hertz and Lenard, on how his discovery was received and on its impact on the very private and shy discoverer. Section (b) then concentrates on Becquerel, or rather the Becquerel dynasty, to start with. H. Becquerel's discovery is described against this background, and with it Chapter 2 ends. However, Chapter 3 carries this second strand further, in the story of the Curies linked to that of Rutherford and his α- and β-rays. These relatively short chapters are followed by a longer fourth, entitled "The First Particle", in which the figure of J.J Thomson naturally enters, but not at the start. The previous, accidental discoveries (with Rutherford's work taken no further than the analysis of α- and β-*radiation*) did not need a great deal of background. Here, when the notion of elementary particles moves from speculation into physics, Pais needs to present more prehistory. So the first strand deals with the experimental tools that Thomson (not primarily an experimenter) owed to Geissler and Rühmkorff, and the next two with the ideas that were in the air for Thomson to bring to fruition. Section (b) is entitled "Faraday, Maxwell and the Atomicity of Charge", and Section (c) "Of Rowland, Zeeman and Lorentz". Only then does Section (d) get on to Thomson by way of Wiechert and Kaufmann. This still doesn't terminate this particular strand of narrative; Section (e), "β-rays are Electrons", ties it to what we learnt about before, and then, finally, as a link with what is to come, we have Section (f), "Relativistic Kinematics".

At this point one might well ask how a book of this size can say anything meaningful about Faraday, Maxwell, Lorentz and Einstein, all in a few pages? The answer is in part that the exposition is a model of how clarity can be combined with brevity, but also — and this is an outstanding strength of the whole book — that every section ends with a detailed set of references to books, review articles and papers, positively inviting further study

Having described the early chapters in such detail, I must be brief with the rest We hear of the struggle to understand radioactivity before the picture of the nuclear atom had been thought of. Then the first piece of the story of β-decay is presented, followed by a chapter entitled "Atomic Structure and Spectral Lines" where Rutherford, Bohr and the nucleus enter the scene. A short chapter then looks briefly at how the failure of classical mechanics brought confusion into the minds of physicists, and how a generation of young men emerged, poised to sort things out. Then quantum mechanics arrives. In a chapter labelled "An Essay", Pais states emphatically that here the reader should turn to good textbooks for

complete guidance, but this does not prevent him from writing a brilliant account in which the central ideas — and equations — are presented in the midst of much on the personal side.

This is the point where the split of physics into many branches began. The narrative narrows, but an enormous amount of material nevertheless remains to be covered in the closing five chapters of the "History". It could not have been done with greater artistry. The interwoven strands tell us about quantum electrodynamics and the positron, about the continuing mystery of β-decay, leading up to the neutrino, about the merging concepts of fields and of particles that are born and die, and how a deepening understanding of symmetries has proved to be the most reliable guide to progress. In all this Pauli and Dirac, among others, are most vividly portrayed.

Inevitably, much prominence has to be given to the great shadow cast on physics by the knowledge that the theoretical structures used at the time were quite unsound mathematically, and that the necessarily approximate calculations were completely unreliable. The "History" was bound to end on such an unhappy note, but Pais has waited to its last chapter to pick up a final, more optimistic theme, going back to 1932 and the discovery of the neutron. At last there was then a convincing picture of nuclear structure to develop, into which Fermi managed to inject an at least provisionally acceptable description of β-decay. It was from there that the search for an account of nuclear forces started and, to close the story, we hear how Anderson's discovery of the muon and Yukawa's theory of the pion (as they were later to be called) seemed to open new vistas. It is left to the subsequent "Memoir" to tell us how wrong our ideas at that time were. I say "our" because this last episode of the "History" is the first of what might have been "Memoir" for me. I can vouch for the complete authenticity of the story.

The "Memoir" starts with the entirely new situation in physics after the Second World War. Many techniques, many young trained minds and large resources become available, in particular in the United States. Having survived years of danger and tragedy in his native Netherlands, Pais is there to take part in the explosive growth of his subject. The "Memoir" is the story of his life in physics and with physicists, in the centre of unprecedented developments in both experiment and theory. These Pais manages to absorb and to reproduce for the reader, still vividly but inevitably in a more technical manner than many readers (including trained physicists not on the inward-bound track) will only be able to follow in detail thanks to the extensive references.

There are just four chapters in the "Memoir" and it would be difficult to enumerate everything in them. The "strand" structure is as before, the first three chapters telling the story up to 1960. We learn of the transformation of theoretical thinking with the arrival of the idea of renormalization and its success in explaining observed facts in electrodynamics; of the impact of the big machines and of their characteristics; of the discovery of many new particles and of the new symmetries that help to put some order into the picture; of the shock when long-cherished old symmetries turn out to be violated; and of many other avenues that are explored, some fruitlessly.

How Pais manages to fit in an account of the still-more-turbulent developments from 1960 onwards into one chapter of a mere 70 pages (with eight pages of references to end with) is almost miraculous. He shoots the discoveries and ideas at the reader with machine-gun rapidity — but it is still the same author writing, keeping the human side up with the technical.

If I who have lived through the whole period of the "Memoir", but with far less first-hand experience of the great events, ever attempt to get my bearings on these modern things, from quarks to the Z particle, with the description of things like colliders thrown in, I know I shall turn to Pais, both his narrative and his references. It is an inimitable work. □

Nicholas Kemmer, 35 Salisbury Road, Edinburgh EH16 5AA, UK, is Emeritus Professor of Mathematical Physics at the University of Edinburgh.

Membrane steps

Miles Houslay

Reconstitutions of Transporters, Receptors, and Pathological States. By Efraim Racker. *Academic: 1985. Pp. 271. Hbk $28, £24.50; pbk $12.95, £12.*

EFRAIM Racker is one of the founding fathers of membrane reconstitution, and the prospect of reading his book on the subject rather intrigued me. What would be his perception of the past, present and future of membrane biology? In the preface Racker says that the book is based on a lecture series he was used to giving, which sounds promising. Each of the lectures (12 in all) is dedicated to putting over a series of 34 "lessons" varying from good general advice to homespun philosophy. A certain amount of sound advice is indeed to be welcomed by the aspiring "reconstitutor", as taking membranes apart and putting them back together is like gardening, and requires the equivalent of green fingers and a certain feel for the subject.

Lectures 1 and 2 have the central theme of "how to solubilize the protein that you've chosen". Here Racker makes the important point that what works for one protein may well not succeed for another (that is, you often have "to suck it and see"), and lists a variety of parameters of which one has to be aware. He makes it abundantly clear that there is no self-evident set of rules to follow: there are too many parameters and we have too little basic appreciation of how individual membrane proteins are glued into bilayers.

However, having said all this, the reader is then offered little or no constructive help. We are advised to take account of "critical micellar concentrations" and hydrophil–lipophil balances, but without even being told what they are, never mind how such values may be of use to tease proteins out of their membrane home. Purification of membrane proteins, which is after all the main goal of many people interested in this field, gets a desultory page without any references to different ways of coping with this key problem. A series of general methods for reconstitution then follows, with lists of some reconstituted systems and their "activities". These lists (again innocent of references) are of little use except to give a broad view of the variety of systems that the author has got hold of and stuck back into liposomes, though the accompanying, anecdotal text does convey some idea of the principles involved.

The succeeding chapters all suffer from similar drawbacks. The section headings identify important points that should be investigated or considered, but the monologue that follows is superficial and jumps haphazardly from one system to another. One can have a degree of sympathy with such an approach in the introduction, but after three chapters one finds oneself desperately hoping to come across a logical presentation of hard facts. As it is, over the next seven chapters we are led a merry dance around a variety of membrane systems. The penultimate lecture is about cancer; it raises a few interesting points about glycolysis but is largely an indulgence, as is the final lecture centring on the author's current predilections.

I am afraid to say that after having had such high hopes for this book I found it difficult to read to the end; it lacks both substance and cohesion. Further, although Racker apologizes for all those people he has not mentioned, the number of self and selective citations in places leads to history being re-written. I would not recommend the book to students, but lecturers running courses on membranes, or sociologists of science, might find it of some interest. □

Miles Houslay is Gardiner Professor in the Department of Biochemistry, University of Glasgow, Glasgow G12 8QQ, UK.

Illusion in ascent

Peter J. Bowler

Taking Darwin Seriously: A Naturalistic Approach to Philosophy. By Michael Ruse. *Basil Blackwell: 1986. Pp.303. £22.50, $24.95.*

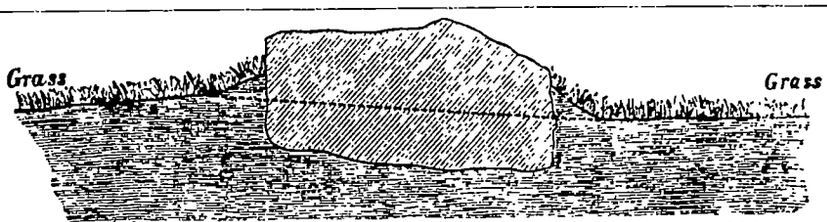
MICHAEL Ruse believes that scarcely anyone *has* taken Darwin seriously up to now. Efforts to apply evolutionism to the problems of philosophy have failed, largely because of a refusal to acknowledge the central tenet of Darwinism: the non-progressive character of natural selection. Whatever one's opinion of Darwinism (Ruse, of course, accepts it as the basis of all legitimate evolutionary thinking), the claim that the theory has seldom been taken seriously can certainly be endorsed by the historian. To depict the growth of evolution theory as a simple ascent from Darwinism to the Modern Synthesis is to fall into the worst kind of Whig history, ignoring the large number of thinkers, including scientists, who have found the principles of natural selection unacceptable. As Ruse points out, modern Darwinists from Julian Huxley to E.O. Wilson have also found it difficult to accept the non-progressionist character of the theory.

Ruse's purpose here is to address the philosophical, not the historical issues. He criticizes evolutionary approaches to the problem of knowledge, from Herbert Spencer to Karl Popper. Drawing a simple analogy between evolution and the growth of science does not work, he says, because science is progressive and evolution is not. He looks instead at the kind of reasoning that we might expect natural selection to have programmed into our ancestors so that they could deal successfully with the real world. We believe that an effect *must* follow its cause, because any of our ancestors who did not have this mental reinforcement to back up their perception of causal regularities would soon have disappeared. The intellectual ancestor of this approach is David Hume, who realized that we read necessity into nature even though we have no philosophically satisfactory guarantee that there is anything corresponding to that necessity "out there". If the analytical philosophers are not satisfied with this, Ruse tells them that they will have to go away disappointed. The philosophers will presumably not be happy with a viewpoint that threatens to put them out of work, but anyone who has lost patience with the apparently endless wrangling of academic philosophy can only applaud.

On the question of morality, Ruse is critical of "social Darwinism" and other efforts to deduce ethical standards from evolution, precisely because they invariably assume that nature is progressing towards some ultimate good. His own approach starts from the principles of sociobiology, but attempts to purge the remnants of progressionism from the work of Wilson and others. Natural selection will have endowed us with epigenetic rules inclining us to behave in a socially responsible manner, when this is to our (reproductive) advantage. The special status we accord to moral laws is nature's way of ensuring that we have a strong tendency to obey them even when they violate our immediate preferences. As a result, we *feel* that moral laws are objective — and our desire to live in an orderly society ensures that we have no interest in rejecting the laws even when we realize that this feeling is an illusion. Once again, Ruse identifies Hume as the philosophical progenitor of this position.

It will be interesting to see how the opponents of sociobiology respond to this book. Far from justifying a harsh social policy, Ruse explains why we feel so strongly about traditional moral values. Those who wish to argue that human beings are infinitely malleable by culture will object to this — but in so doing they will have to accept that we have no built-in moral values at all. If we concede that our evolutionary heritage may have imposed at least some constraints on how we think and behave, Ruse offers us a way of trying to understand the character of such restraints. As we move into a world that differs ever more radically from that in which our ancestors evolved, such insights may help us to come to terms with the philosophical problems that confront us. □

Peter J. Bowler is a Lecturer in the Department of History and Philosophy of Science, Queen's University of Belfast, Belfast BT7 1NN, UK.



Work of worms — section through a fallen Druidical stone at Stonehenge, indicating how much it has sunk into the ground through the undermining action of earthworms. Depth of the stone is c. 30 cm. The illustration is taken from a new paperback edition of *Charles Darwin's* The Formation of Vegetable Mould, through the Action of Worms *(1881), published by University of Chicago Press. Price is $12, £10.25. For review see* Nature *24, 553–556 (1881).*

New journals review



On 25 September *Nature* will publish the sixth annual review supplement devoted to science journals.

Criteria for inclusion of a journal in the 1986 issue are that:

(i) the first number appeared, or the journal was retitled, *between June 1984 and May 1985* (the second cut-off date allows at least three issues of a journal to have been published, the minimum number on which a reasonable judgement can be based).

(ii) it is published at least three times a year;

(iii) the main language used is English

Publishers and learned societies are invited to send *four different issues of each suitable periodical, including the first and most recent numbers* (if from outside the United Kingdom, by air mail) to The Review Editor, *Nature*, 4 Little Essex Street, London WC2R 3LF, England. Subscription details for both 1986 and 1987 should be included.

RÖNNELLS
Scientific Books & Periodicals
For current catalogues:
No. 55
HISTORY OF MEDICINE
No. 56
AMERICANA
and other subjects
write:
RÖNNELLS
Birger Jarlsg. 32
114 29 Stockholm
Reader Service No 12

Parallel promises in computing

Igor Aleksander

The Connection Machine. By W. Daniel Hillis. *MIT Press:1986. Pp.190. $22.50, £22.50.*

THE jacket of this book heralds "the connection machine" as "the second state in the evolution of digital computers"; the first sentence reads "Someday, perhaps soon, we will build a machine that will be able to perform the functions of the human mind, a thinking machine". It must be said immediately that while the concept of the connection machine is intriguing, and the book tells us a lot about the engineering behind it, any reference to "thinking machines" is thoroughly misleading.

The primary characteristic of the connection machine is parallelism. The prototype discussed by Hillis contains approximately 64,000 simple processors that may be linked in large parallel groups, and it is one of the strengths of the book that the author discusses his design decisions with great clarity. The main attraction of the machine is that it allows a user to research the behaviour of different "shapes" of parallel machines; for example, the properties of processors connected in a ring are very different from those of processors connected in a matrix, and the connection machine may be configured into these structures and many more. It almost becomes possible to believe the claim that the machine marks a new era in digital computing, as the possibility of working with different "shapes" of parallel structure is awkward (that is, slow) on conventional computers.

Hillis's main problem, in common with that of designers of similar machines, was to devise schemes that allow processors to be selected from a pool, and then to provide a sufficiently rich set of pre-defined connections so that the user's desired structure can be realized. Clearly, alternatives had to be found to the obvious solution of connecting every processor to every other one: that would require just too many connections, most of which would be unused during the execution of a particular task. Hillis lucidly reviews the various options and describes why he settled on a "Boolean n-cube topology" (the details of which might interest the topologist as an engineer's choice among theoretical alternatives). The end result of the parallel/serial compromise is an achievement of 1,000 million instructions per second (Mips) — the average modern machine in a research laboratory probably delivers about *one* Mip. Another achievement is that this machine may be programmed by means of an extension of LISP, easily mastered by those who use the language anyway. Hillis goes to some pains to argue that this is an arbitrary choice and advanced features of the machine could equally be applied to other languages.

But what scientific advances are likely to follow from the application of the connection machine? As is often the case with innovators in engineering, Hillis is less comfortable with the answer to this question than he is with the technical description of his machine. He points principally to questions arising in research on artificial intelligence, and suggests that image-processing could benefit by arranging the processors into two-dimensional arrays. Although this is true, and possibly useful, processor arrays have been built for some time; for example, Michael Duff's CLIP machines at University College London have been doing workmanlike tasks in practical image-processing for about 15 years, and those who have used them have probably discovered most of the principles that such methodology is likely to reveal.

Closer to the heart of AI, Hillis suggests that the connection machine might implement knowledge stores called "semantic networks". Here, two processors might have respective labels such as "lemon" and "sour", with a connection leading from the former to the latter and labelled as "tastes". The methodology was first introduced by Patrick Winston in 1970 and it is a matter of debate whether the lack of applications of such schemes in more recent research is solely due to the lack of a sufficiently parallel machine. Away from AI, Hillis proposes that the connection machine might be used to simulate silicon circuits (very large scale integrated systems), but at the rate of one processor (containing thousands of transistors) for each simulated transistor this has an air of overkill about it.

All this talk of application only occupies a few pages in the first chapter and is evidently not central to the author's interest. Hillis perhaps gets closer to the real potential for the connection machine in the last two pages of the book, where he suggests that through such "granular" computers of ever-decreasing grain-size, computational theory will extend its explanational powers to an increasing number of natural phenomena. This is where the payoff may really be found. The natural phenomena which, in my opinion, are most in need of attention are those concerning brain-like networks of cells, and the connection machine is an ideal simulation tool for such work. But despite the references to "thinking machines", Hillis does not actually discuss this possibility. The bibliography, although extensive, mostly bears little relation to the text and is notable for its omissions. The most serious of these is notice of the modelling of brain-like systems that has been pursued by Geoffrey Hinton at Carnegie Mellon University since the late 1970s. Exciting discoveries are being made about the way in which cellular learning systems can learn to "understand" concepts such as the shape of objects "seen" through a television camera, or build internal representations of "Italian name" against "English name" in a telephone directory database *without* having been programmed to do so directly. Investigations of this kind have much to do with what is meant by the word "thinking" and, if carried out through the connection machine, will contribute a great deal to understanding the functions of the brain. Indeed, simulations of Hinton's work are clumsy and counter-productive on conventional machines, and it is in this sense that the connection machine provides a useful tool with which "thinking" may be researched. To confuse this with the creation of a "thinking machine" is a category mistake of textbook quality. Moreover, despite the author's implication that the MIT-associated connection machine is unique, it must be seen as taking its place among a number of similar developments such as the "Non-Von" machine at Columbia University and John Darlington's ALICE machine at Imperial College, London.

The Connection Machine will be appreciated best by those who require a lucid description of a computer design that is truly ingenious and indicative of the trend in computer science hardware research towards massive parallelism. It is not for those with no knowledge of computer engineering at all, nor for others who hope to be enlightened on what a "thinking machine" might be. □

The real Frederick Soddy*



*As a number of people have pointed out, the photograph supporting the review of the collection of essays on Soddy (*Nature* **320**, 691; 1986) was in fact of Ernest Rutherford.

Igor Aleksander is Kobler Professor of Information Technology, Department of Computing, Imperial College, University of London, London SW7 2BZ, UK.

Muon-catalysed fusion revisited

Steven Earl Jones

Department of Physics and Astronomy, Brigham Young University, Provo, Utah 84602, USA

Muons introduced into relatively cold, dense deuterium–tritium mixtures can replace the atomic electrons and form muonic molecules which participate readily in nuclear fusion reactions. Catalysis yields of ~150 fusions per muon have been achieved, renewing interest in muon-catalysed fusion as a possible source of energy.

MUON-CATALYSED fusion can be viewed as a series of reactions induced by negative muons in cold hydrogen leading to nuclear fusion and a release of energy. For example, when a negative muon enters a mixture of deuterium and tritium (heavy isotopes of hydrogen):

$$\mu + t + d \tag{1}$$

The muon replaces an electron to form a $t\mu$ atom:

$$\rightarrow t\mu + d \tag{2}$$

A molecule bound by the muon may then form:

$$\rightarrow dt\mu \tag{3}$$

which leads to deuteron–triton (d–t) fusion, freeing the muon to repeat the cycle:

$$\rightarrow \alpha + n + \mu \tag{4a}$$

Occasionally the muon is captured by the α-particle following fusion:

$$\rightarrow \alpha\mu + n \tag{4b}$$

The key to this remarkable sequence of reaction lies in the large mass of the muon, which is 207 times that of the electron. A negative muon admitted into a high-density mixture of deuterium and tritium gases (step 1) quickly replaces the lighter electron to form a muonic atom (step 2). The reaction is energetically favourable and rapid because the muon greatly outweighs the electron. The same holds true for the succeeding step (3), formation of a $dt\mu$ molecule held together by the muon. The muonic molecule is ~200 times smaller than an ordinary heavy hydrogen molecule (such as DT, bound by electrons). Thus, the muon confines the d–t nuclei to a very tiny volume. Although the rest of the gas may be near room temperature, conditions inside the muonic molecule are similar to those found inside a white dwarf star[1]. In such conditions nuclear fusion (step 4) will occur, just as it does in stars. Indeed, d–t fusion occurs in $\sim 10^{-12}$ s in the $dt\mu$ molecule[2].

Without the use of external magnetic fields or lasers, we can thus achieve local star-like conditions by simply adding negative muons to a mixture of hydrogen gases. Each muon can spontaneously induce a number of fusion reactions, so that it serves as a catalyst for nuclear fusion.

In his 1968 Nobel prize acceptance lecture, Luis Alvarez[3] described the excitement generated by the first observation[4] in 1956 of this fascinating phenomenon for muons stopped in liquid hydrogen (H) plus deuterium (D):

> "We had a short but exhilarating experience when we thought we had solved all of the fuel problems of mankind for the rest of time. A few hasty calculations indicated that in liquid HD a single negative muon would catalyse enough fusion reactions before it decayed to supply the energy to operate an accelerator to produce more muons, with energy left over after making the liquid HD from sea water. While everyone else had been trying to solve this problem by heating hydrogen plasmas to millions of degrees, we had apparently stumbled on the solution, involving very low temperatures instead."

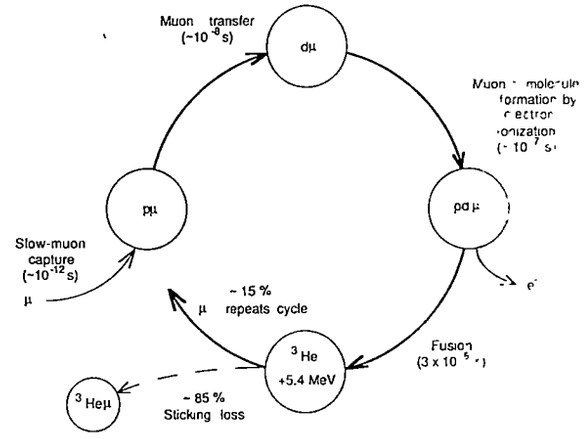


Fig. 1 The muon catalysis cycle for liquid hydrogen containing 1% deuterium. Approximate reaction times are shown[8,9]. Because the mean time required for muon-induced fusion to occur in the $pd\mu$ molecule (3 μs) exceeds the mean muon lifetime (2.2 μs), the muon usually decays before it can repeat the $pd\mu$ fusion cycle

Excitement quickly waned, however, following theoretical predictions that very few fusions could be catalysed by a single muon. Indeed, in experiments performed by Alvarez and others using hydrogen and deuterium, only rarely was a muon observed to induce more than one fusion reaction.

In mixtures of deuterium and tritium, the situation is strikingly different, for reasons which are as yet only partially understood. Within the past few years, we have demonstrated that a single muon can complete the reaction sequence (1)–(4) many times, catalysing many d–t fusions. It is fitting on this thirtieth anniversary to announce the achievement at the Los Alamos Meson Physics Facility of 150 fusions per muon (average) in dense deuterium–tritium mixtures[5]. These yields exceed theoretical expectations, and have stimulated speculation regarding muon-catalysed fusion as a source of energy.

Muon-catalysed fusion research encompasses many disciplines, including atomic, molecular, nuclear and particle physics, chemistry, accelerator technology, and possibly fusion energetics. This review, which is intended to be accessible to scientists in diverse fields, highlights the most recent discoveries which have stimulated renewed interest in muon-catalysed fusion.

Muon-catalysed p–d fusion

The first type of muon-catalysed fusion to be discussed theoretically[6,7] and observed experimentally[3,4] was proton–deuteron (p–d) fusion:

$$\mu + p + d \rightarrow {}^3He + \mu + 5.4\ \text{MeV} \tag{5}$$

The first observation of muon-induced fusion came as a great

surprise[3,4]. Alvarez and his colleagues at Berkeley noticed in their liquid-hydrogen bubble chamber a number of mysterious muon tracks having a characteristic 1.7-cm length. Furthermore, a gap frequently appeared between the 1.7-cm track and the stopping point of the incoming muon.

Unaware of earlier theoretical work by Frank[6], A. D. Sakharov and P. N. Lebedev[54] and Zel'dovich[7], the Berkeley physicists inferred the phenomenon of muon-catalysed fusion from their data. The principal clue was the 1.7-cm range of the muons, which corresponds to an energy of 5.4 MeV—just the energy released in proton-deuteron fusion. It was quickly realized that a muon could form a muonic ($d\mu p$) molecule, and then, "in such a 'molecule', the proton and deuteron would be brought together in such a close proximity for such a long time that they would fuse into ^{3}He, and could deliver their fusion energy to the muon by the process of internal conversions"[3].

The mystery of the observed gap between the stopped and ejected muons was solved by Edward Teller[3,4]. He correctly surmised that the muon would be initially captured by a proton, the nucleus of the predominant isotope of hydrogen in the bubble chamber, to make a muonic $p\mu$ atom. Although the fraction of deuterons in naturally occurring hydrogen is only 1 in 5,000, the muon could transfer rapidly and irreversibly to a deuteron to make a $d\mu$ atom:

$$p\mu + d \rightarrow d\mu + p \qquad (6)$$

because the binding energy for the ground-state $d\mu$ atom is 135 eV greater than that of the $p\mu$ atom. The neutral $d\mu$ atom could then recoil some distance, producing the observed gap, followed by $d\mu p$ molecule formation and fusion. The ability of the $d\mu$ atom to travel a few millimetres in liquid hydrogen before stopping (that is, before becoming thermalized) provides an interesting example of the Ramsauer-Townsend effect[8].

The sequence of reactions just discussed is shown in Fig. 1, along with some observed reaction times[8,9]. A major limiting factor in the process is the likelihood that the negative muon will be captured by the positive ^{3}He ion synthesized during proton-deuteron fusion; another is the long time spent by the muon in the $pd\mu$ molecule before fusion occurs. These factors limit the number of muon catalysis cycles in liquid hydrogen containing ~1% detuterium to an average of less than one fusion per muon.

Muon catalysis in pure deuterium

The Alvarez group and others[8] extended the study of muon catalysis to the case of pure liquid deuterium, observing the reactions

$$\mu + d + d \rightarrow d\mu d \rightarrow {}^3\mathrm{He} + n + \mu + 3.3\ \mathrm{MeV} \qquad (7)$$

and

$$\mu + d + d \rightarrow d\mu d \rightarrow t + p + \mu + 4\ \mathrm{MeV} \qquad (8)$$

Experimental results, shown in Fig. 2, were consistent with expectations based on studies of hydrogen-deuterium mixtures. The relatively slow formation rate of the muonic molecule and the loss of muons due to ^{3}He ion capture limited the average number of fusions per muon to less than one. It thus appeared that muon-catalysed fusion reactions in hydrogen isotopes were rather well understood and quite useless as an energy source[8,10,11].

Persistent research in the Soviet Union, however, led to a revival of interest in muon catalysis[12]. Dzhelepov *et al.*[13] first showed experimentally that the rate at which $dd\mu$ muonic molecules form depends strongly on temperature. In fact, the $dd\mu$ formation rate in deuterium at room temperature was found to be 10 times greater than the rate at liquid-deuterium temperatures (~30 K). That the deuterium temperature could strongly affect the formation rate of $d\mu d$ molecules came as a complete surprise.

In 1967, following an earlier suggestion of Zel'dovich[7],

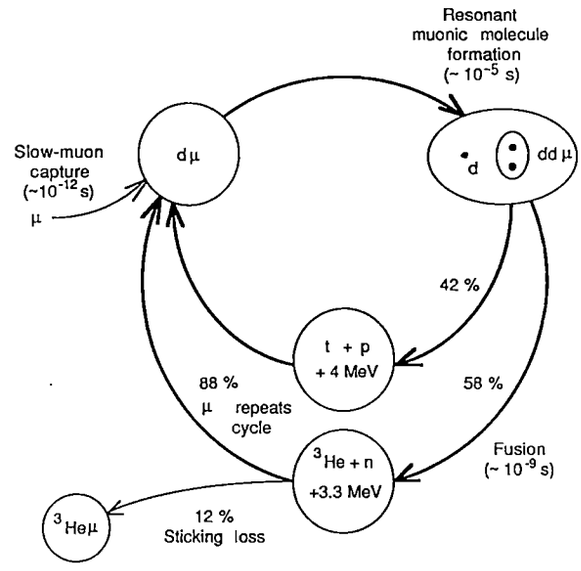


Fig. 2 The major reactions which occur when a muon is admitted into liquid deuterium. Resonant formation of a $dd\mu$ molecular ion within an electronic molecule (without emission of an electron) can occur when a $d\mu$ atom penetrates a D_2 molecule. However, the $dd\mu$ molecular formation process is slow relative to the muon lifetime so that the muon often does not survive to repeat the $dd\mu$ catalysis cycle.

Vesman[14] advanced the notion that the muonic $d\mu d$ molecule could form within a D_2 host molecule, as shown in Fig. 2. Note that the $(d\mu d)^+$ ion serves as one of two nuclear centres in the complex new molecule. For this process to occur, the energy released as the muonic molecule forms ($d\mu d$ binding energy, E_b, plus the initial kinetic energy of the $d\mu$ atom, E_K) must be small enough to be absorbed in the vibrational and rotational excitation ΔE of the host molecule:

$$E_b + E_k = \Delta E \qquad (9)$$

Because the energy levels of the complex molecule are quantized, equation (9) expresses a resonance condition; that is, the muonic molecule forms most rapidly when equation (9) is exactly satisfied. The temperature dependence of the process derives from the E_k term.

Precise calculations showed that there exists an excited state of the muonic $d\mu d$ molecule that has a binding energy of only 1.9 eV, which is small enough to be absorbed by the electronic molecule without causing it to break apart. Furthermore, the temperature dependence of the $d\mu d$ formation rate could be accounted for by the resonance requirement[15,16].

A startling prediction followed from this theoretical model: the formation of muonic $dt\mu$ molecules should also be resonant, and resonant $dt\mu$ formation at 540 K (the expected optimum temperature) should exceed the fastest $d\mu d$ formation rate by two orders of magnitude[17]. In addition, muon capture by the helium ion synthesized during deuteron-triton fusion had been predicted to be ~0.9%[10], much less than the corresponding loss term for proton-deuteron or deuteron-deuteron fusion. Thus, in late 1977 Gershtein and Ponomarev[17] declared:

> "It means that every μ^- meson in the mixture deuterium and tritium can produce ~10^2 of the nuclear fusion reaction and release ~2 GeV which is 20 times the rest mass of muon. We leave the question open about the possibilities of practical applications of the phenomenon discovered...
>
> The reactions [in deuterium plus tritium] are not yet studied experimentally. We hope that such experiments will soon be performed despite the technical difficulties involved."

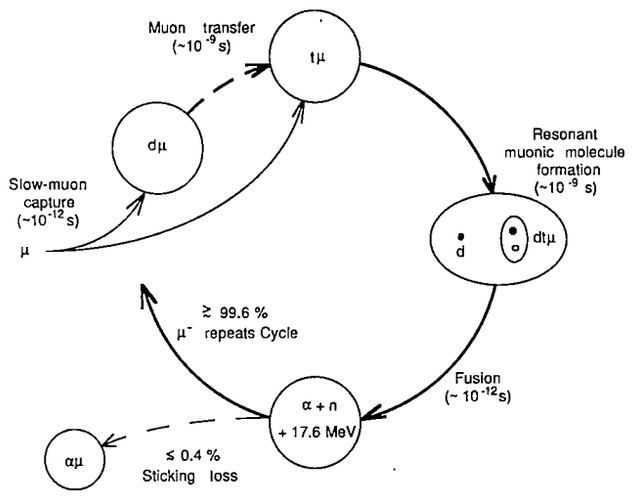


Fig. 3 The major processes which occur when a muon stops in a liquid mixture of deuterium and tritium in roughly equal proportions. The reaction times are very short, compared with the muon lifetime (2.2 μs). In addition, the probability of muon retention by the α-particle synthesized during d-t fusion is small. Thus, the muon-catalysed d-t fusion cycle can easily be repeated more than 100 times.

Experiments were soon mounted. As we shall see, some results were as startling as the predictions. Muon-catalysed fusion was not a closed subject after all.

Muon catalysis in D–T mixtures

Resonant dtμ formation. Bystritsky *et al.*[18,19] set out in 1979 to test predictions that the dtμ molecule could form in ~0.5% of the muon lifetime and that this formation rate would increase with increasing deuterium–tritium (D–T) gas temperature. They showed that dtμ molecules may form at least as fast as predicted by the new resonance model (shown in Figs 2 and 3), and four orders of magnitude faster than expected from the electron-emission process (shown in Fig. 1). The experiment allowed only a lower limit to be set for the dtμ formation rate.

However, no temperature dependence of the dtμ formation process was detected, even though the D–T gas was cooled to 93 K and heated to 613 K. Rapid dtμ formation appeared consistent with the resonance model, but where was the expected temperature dependence? Unfortunately, the Dubna accelerator was closed for refurbishment in 1979 and the Soviet experimenters were unable to pursue their research. (The machine is expected to return to operation soon. Related experiments recently began at the Gatchina facility of the Leningrad Nuclear Physics Institute.)

An experiment was begun in 1982 at the Los Alamos Meson Physics Facility (LAMPF) by our group, with the intention of exploring in depth the muon catalysis cycle in D–T mixtures[5,20–23]. Vessels capable of holding deuterium and tritium gases at pressures up to 1,000 atm (later, 3,000 atm) were developed at the Idaho National Engineering Laboratory (INEL) to allow near-liquid-hydrogen densities to be maintained over a broad temperature range (13–800 K). The experimental team consists of scientists from Brigham Young University (BYU), INEL and the Los Alamos National Laboratory (LANL).

Early one morning in November 1982, we cooled a target containing equal amounts of deuterium and tritium from room temperature to 100 K: the number of fusion neutrons decreased significantly as the gas was cooled. Although in qualitative agreement with the resonance model prediction, the result was surprising because no temperature dependence had been detected in the earlier Dubna experiment. The rest of the night was spent checking the electronics for a malfunction, but nothing was wrong. As the D–T mixture was heated the following day, the fusion yield grew larger. Resonance model predictions of temperature dependence enunciated by Ponomarev and colleagues were finally confirmed.

However, virtually no temperature dependence was seen when a target composed of 10% tritium and 90% deuterium was used. This result was consistent with the Dubna experiment, in which the D–T mixture contained ≤8% tritium. The experiments soon demonstrated that for low tritium fractions, the muon catalysis cycle was dominated by the muon transfer reaction

$$d\mu + t \rightarrow t\mu + d \qquad (10)$$

This reaction, analagous to reaction (6), is nearly independent of temperature. These two facts explain why no temperature dependence was seen in the low-tritium-fraction experiments at Dubna. For tritium fractions ≥30% at LAMPF, the temperature-dependent dtμ formation rate became evident[5,20–23].

With several hundred million muon-catalysed fusion events now recorded in the continuing BYU/INEL/LANL experiments, along with continued theoretical efforts, a consistent picture of the resonant formation of dtμ molecules is emerging. The important features are:

(1) The dtμ-formation rate rises with increasing temperature, as expected[20–23].

(2) The rate does not peak at ~540 K as predicted[15,16]. Instead, it continues to climb at 800 K, the highest temperature reached to date. There are now theoretical reasons to expect the rate to reach a maximum near 1,200 K[24]. Note that the resonance process depends on the presence of intact molecules to host the $(dt\mu)^+$ ion (see Fig. 3). As hydrogen molecules begin to decompose into atoms at temperatures ≥5,000 K, the resonance formation mechanism becomes unavailable so that dtμ formation must decline precipitously. Moreover, muon-catalysed fusion cannot be used in conjunction with plasmas; in particular, it cannot be used for thermonuclear weapons. The term 'cold fusion' is therefore quite appropriate for the process.

(3) The dtμ formation rate depends on whether the host is a D_2 or DT molecule[5,20–23]. In particular, the reaction

$$t\mu + D_2 \rightarrow [(dt\mu)d2e]^* \qquad (11)$$

proceeds more rapidly over a broad range of density and temperature than does the reaction

$$t\mu + DT \rightarrow [(dt\mu)t2e]^* \qquad (12)$$

This host-dependence arises from the different energy levels which are available in the two compound molecules, in keeping with the resonance model[24].

(4) While the rate of reaction (12) scales linearly with density as anticipated, the rate of reaction (11) increases faster than linearly with density[5]. The resonance model implies that $t\mu + D_2$ collisions are special, in having their strongest resonances just below threshold. A third body can allow these resonances to contribute by absorbing some kinetic energy in a reaction such as

$$t\mu + D_2 + T_2 \rightarrow [(dt\mu)d2e]^* + T_2' + \Delta E \qquad (13)$$

Thus, the density dependence of reaction (11) observed at LAMPF provides evidence for significant resonant dtμ formation involving three-body collisions[5,25], although other explanations for the phenomenon cannot be ruled out[26].

Muon capture by the fusion α-particle. Experiments thus demonstrate that dtμ molecules do form extremely rapidly, nearly three orders of magnitude faster than pdμ or ddμ molecules. In fact, owing to the extraordinary resonance in dtμ formation, a muon could catalyse many hundreds of d–t fusions during its lifetime, were it not for muon capture by the synthesized helium nucleus (see equation (4b)). We have seen that muon loss in this way constitutes a dead-end in the p–d and d–d catalysis

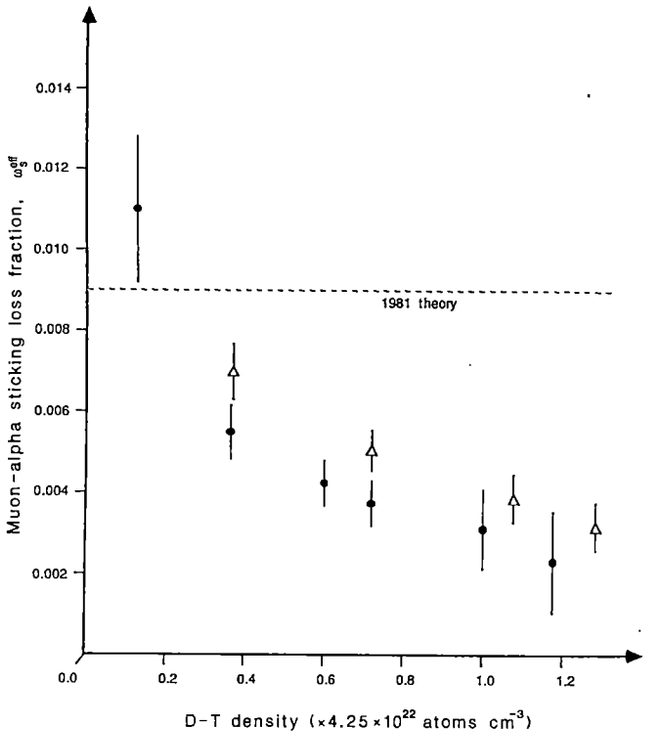


Fig. 4 Data from LAMPF showing the decrease in the deduced μ–α sticking fraction as the density of the duterium–tritium mixture is increased, for 50% tritium/50% deuterium (dots) and 30% tritium/70% deuterium (triangles). At high target densities, the μ–α sticking probability is clearly much lower than was predicted before the experiments were performed.

cycles (Figs 1 and 2); does this feature persist in d-t fusion?

Before 1985, theorists[1,10,27] predicted that the muon would be captured by the fusion-synthesized α-particle in $\omega_s^0 \simeq 1.2\%$ of muon-induced fusion reactions. Then, as the $\alpha\mu$ ion moves rapidly through the surrounding gas, there is a probability $R \simeq 24\%$ that the muon will be collisionally stripped from the α particle and thereby freed to continue the cycle. Thus, after slowing down in the gas, the muon would remain bound to the α-particle with probability $\omega_s = \omega_s^0(1-R) \simeq 0.9\%$. Muon loss due to capture by the synthesized α-particle is cumulative, so that the maximum number of d-t fusions which a muon could possibly catalyse would be $1/\omega_s \simeq 110$ (ref. 10). This limit would apply even if the muon were stable. Thus, the μ–α sticking probability ω_s was perceived to be the ultimate limit on the fusion yield from the muon catalysis cycle[1,10,17].

The only published measurements of ω_s are from the BYU/INEL/LANL experiments[5,20–23]. The deduced quantity ω_s^{eff} (expected to represent ω_s (ref. 5)) is shown in Fig. 4; the results were totally unexpected. Note the striking dependence of the apparent μ–α sticking loss fraction on the density of the D-T mixture. Moreover, the magnitude of ω_s at high gas density is approximately one-third the theoretical prediction of 0.9%. A possible dependence on tritium fraction is also suggested by the data but is statistically inconclusive.

Neither the smallness of ω_s nor its apparent density dependence is understood. Perhaps the muon stripping fraction R depends strongly on density and attains large values for dense D-T mixtures. Then $\omega_s = \omega_s^0(1-R)$ could become small for high densities. Although theorists are now re-examining muon stripping probabilities, this explanation does not appear promising. Or perhaps ω_s^0 itself varies with density; for example, ω_s^0 may depend on the state of the dtμ molecule from which fusion occurs (C.-Y. Hu, in preparation), which in turn could depend on density. It has also been suggested that a certain fraction of muons may be significantly delayed as the dtμ molecule cascades down from the excited state in which it is formed, thus increasing ω_s^{eff} above a small initial value[28]. Two years after the initial observation of this phenomenon at LAMPF, the puzzle persists. It is appropriate to emphasize that no independent confirmation of the LAMPF results has yet been published.

Interestingly, theoretical estimates of values ω_s have decreased significantly since small ω_s values were reported in 1984[21,23]. Jackson, who first calculated ω_s^0 using the Born–Oppenheimer approximation in 1957[10], estimated that corrections to that approximation would reduce ω_s^0 by ~25%[29]. In agreement with this estimate, a precision Monte Carlo calculation by Ceperley and Alder[30] yielded $\omega_s = 0.6\%$. These recent calculations are, however, still larger than the (high-density) experimental values. Mueller and Rafelski[31] argue that the (resonant) nuclear d–t interaction, neglected in other calculations, is capable of affecting the wave function describing the three-body dtμ system. This may have the effect of reducing the initial sticking to $\omega_s^0 \simeq 0.1\%$—a remarkably small value.

Although not yet understood, the BYU/INEL/LANL results clearly point to small ω_s values (Fig. 4). Thus, >300 fusions per muon may be possible in deuterium–tritium mixtures. In the past few years there has been a steady rise in the average number of d–t fusions per muon achieved at LAMPF: 20 in 1982, 80 in 1983 and 150 in 1984. Each step reflects an increased understanding of the rich physics underlying muon-catalysed fusion.

Hyperfine effects. In addition to the research in the Soviet Union and the United States, an experiment on muon-catalysed d–t fusion is in progress at the Swiss Institute for Nuclear Research (SIN). The work by Breunlich *et al.*[32] has so far focused on the fascinating possibility of hyperfine-structure effects.

It was recognized long ago that the reactions in muon catalysis could be influenced by the spin states of muonic atoms and molecules. Indeed, experiments at Columbia University[33] in the early 1960s showed that hyperfine transitions take place in muonic atoms, according to the reaction

$$d\mu(\uparrow\uparrow) + d(\downarrow) \rightarrow d\mu(\downarrow\uparrow) + d(\uparrow) \qquad (14)$$

By increasing the deuterium concentration in a liquid hydrogen target from 0.7 to 25%, Lederman and collaborators enhanced the population of $d\mu(\downarrow\uparrow)$ atoms. This in turn increased the population of those pdμ molecules in which fusion is most rapid, and the number of proton–deuteron fusions per muon increased by ~17% (Wolfenstein–Gershtein effect)[33]. Of course, the average yield was still less than one p–d fusion per muon.

Interest in hyperfine effects, as in muon catalysis generally, was stimulated by the discovery of the resonant formation of ddμ and dtμ molecules discussed above. Breunlich and coworkers repeated studies of hyperfine effects in hydrogen–deuterium mixtures[9], and then observed hyperfine effects in pure deuterium[34]. In particular, they found that the rate of resonant ddμ formation in $d\mu + D_2$ collisions depends strongly on the hyperfine state of the dμ atom. The experimental results can be described within the framework of the resonance formation model for ddμ molecules. Indeed, a rather complete picture of the energy levels of the muonic ddμ molecule, including hyperfine splitting, is anticipated from these experiments.

However, results of experiments conducted at SIN with mixtures of deuterium and tritium appeared to contradict theory. Time spectra of the fusion neutrons gave evidence of two distinct dtμ formation rates[32]. (This effect is also reported in the LAMPF experiments[22].) When the SIN experimenters interpreted their data in terms of hyperfine effects, the results were contrary to theoretical expectations. For instance, the evaluated rate of the spin-flip reaction

$$t\mu(\uparrow\uparrow) + t(\downarrow) \rightarrow t\mu(\uparrow\downarrow) + t(\uparrow) \qquad (15)$$

was much smaller than predicted and displayed an unexpected and strong dependence on temperature. Moreover, very little

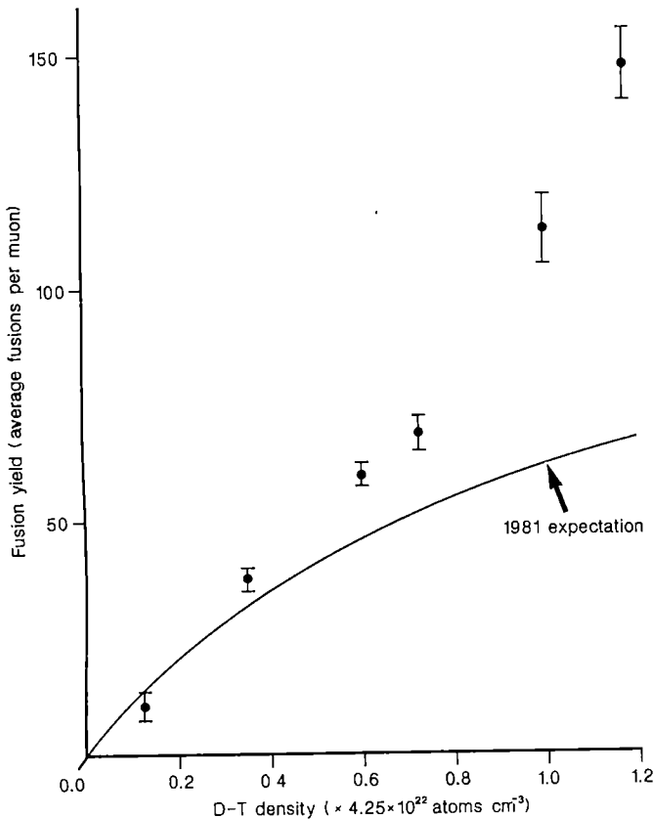


Fig. 5 The average number of muon-catalysed d-t fusion cycles observed by the BYU/INEL/LANL collaboration as a function of target density for cold ($T \lesssim 100$ K), equimolar deuterium-tritium mixtures. The solid line is based on experimental data[18,19] and theoretical predictions[37] as of 1981.

temperature dependence of the dtμ formation rate emerged from the analysis of the SIN data[32].

An alternative explanation has been recently advanced[24,35]: perhaps the data reflect different dtμ formation rates for thermalized or 'stopped' tμ atoms than for 'hot' recoiling tμ atoms. This is reminiscent of the way in which the recoil of dμ atoms accounted for the peculiar gaps observed in the Alvarez experiments. In the present case, a strong resonance for 'hot' tμ atoms colliding with D_2 or DT molecules would account for a very large dtμ formation rate. (This suggests the interesting possibility that if the gas were heated to ~1,200 K, dtμ formation would occur extremely rapidly[24].) The 'hot atom' model accounts for the observed density dependence of the neutron time spectra[22], among other features, and is now generally favoured over the hyperfine-effects interpretation. With this explanation, the fusion-neutron time spectra observed at LAMPF and SIN appear consistent with the resonant dtμ molecule formation model. Clearly, hyperfine effects will be more difficult to extract in dtμ catalysis than in ddμ and pdμ catalysis. In any case, only the lower-energy hyperfine state t$\mu(\uparrow\downarrow)$ should be significantly populated for tritium fractions $\geq$10% and densities $\geq 0.1 \times$ liquid-hydrogen density, because of the rapidity of the spin-flip reaction (15)[36].

Summary. The physics of muon catalysis in mixtures of deuterium and tritium is unexpectedly rich. The major processes and experimental values now thought to describe muon-catalysed d-t fusion are displayed in Fig. 3. By comparing Figs 1–3, one sees why the fusion yield for the muon-catalysed d-t fusion cycle greatly exceeds fusion yields in the p-d and d-d catalysis cycles. The average number of d-t fusion cycles per muon measured at LAMPF by the BYU/INEL/LANL collaboration is shown in Fig. 5. The observed yields at high D-T mixture densities exceed even the optimistic (resonance model) predictions[37], reflecting the discovery of a very small μ-α sticking probability[5].

Other reactions

Can muons induce fusion reactions involving elements heavier than hydrogen? The following reactions, for example, are appealing because there are no neutrons in the final state:

$$d + {}^3He \rightarrow {}^4He + p + 18.3\ MeV \quad (16a)$$

$$d + {}^6Li \rightarrow {}^4He + {}^4He + 22.4\ MeV \quad (16b)$$

A muonic molecule must form before muon catalysis can proceed[8,10] and the rates for d$\mu{}^6$Li and d$\mu{}^3$He formation have been calculated to be rapid relative to muon decay[38–40]. However, Coulomb repulsion in such cases is large, as is the nuclear separation, so the fusion rate is small[10,37]. The normal fate of the muon is to become irretrievably bound to the heavier isotope as the molecules dissociate in picoseconds[38–40].

Muon catalysis experiments involving hydrogen isotopes contaminated with ^{3}He (refs 20–23) or ^{4}He (refs 41, 42) provide a test of these predictions. Helium isotopes, are, in fact, observed to scavenge muons rapidly, thus poisoning the muon catalysis cycle. Consequently, it is desirable to keep helium and other non-hydrogen impurities at a low level[8]. It is intriguing that muon-catalysed fusion proceeds rapidly only for deuterium tritium mixtures.

Energy applications

In experiments performed by the BYU/INEL/LANL collaboration at LAMPF, an average fusion energy release of ~3 GeV per muon has been achieved and larger yields are expected[5]. The achieved fusion energy yield is 25 times greater than the total energy of the muon which drives the fusion reactions. However, muon-catalysed fusion as an energy source suffers from the lack of an efficient way to generate the muon catalysts. It appears that ~5 GeV must be invested to produce one negative muon by advanced techniques[43–48].

In 1980, Petrov[43,44] presented a clever scheme for a power reactor based on muon-catalysed fusion combined with nuclear fission processes and found that a commercial reactor would require ~100 fusions per muon. Others have examined and amplified the fusion/fission hybrid scheme and concluded that 100–300 fusions per muon would suffice for a power plant[45,46]. The LAMPF experiments demonstrate that such yields are indeed possible (see Fig. 5). A pure fusion reactor might require 1,000 fusions per muon, based on current ideas for efficient muon generation[51].

Figure 6 shows a schematic outline of a conceptual muon-catalysed fusion system based on the recent work of Eliezer *et al.*[50]. The first step is to form a beam of high-energy tritium nuclei using an efficient particle accelerator; the development of the radio-frequency (r.f.) quadrupole during the last decade represents a relative advance in accelerator technology. Grid-to-beam power conversion efficiencies as high as 60% appear achievable, along with high beam intensities (~200 mA)[53]. Dramatic progress in superconducting r.f. cavities for particle accelerators[52] may also find application here.

The high-energy (~1 GeV/nucleon) triton beam enters one or more pressurized D-T gas targets. Negative pions are copiously produced in ensuing nuclear collisions and these rapidly decay into muons. (The ratio of negative-to-positive pions and muons is enhanced through the use of neutron-rich tritium nuclei in the beam and the target[43,44,49].) Eliezer *et al.*[50] calculate pion/muon production and stopping rates in the D-T gas; a magnetic mirror effectively confines the charged particles to a small volume (~0.1 m^3). The muons are produced and stopped in the D-T fuel itself, which proves to be much simpler and more efficient than forming intermediate pion and muon beams as is conventionally done at accelerator laboratories, even

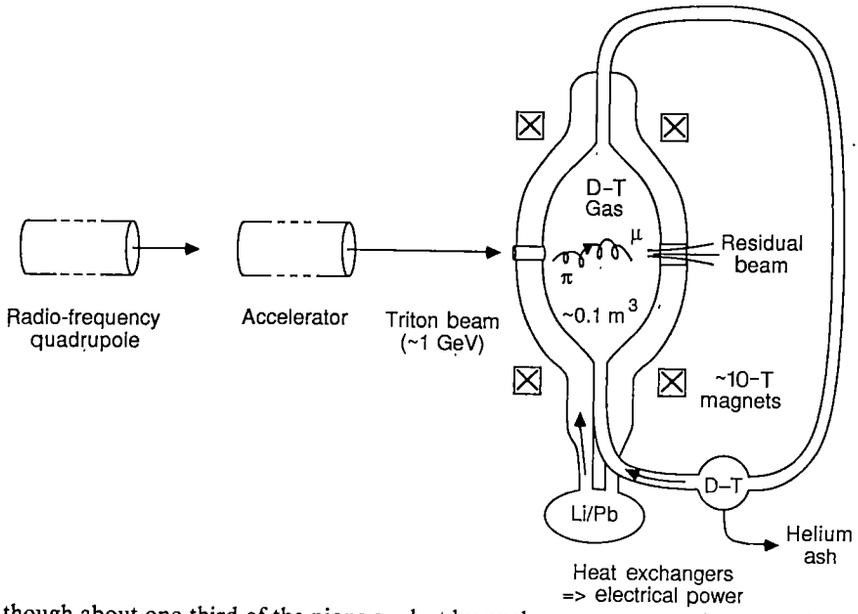


Fig. 6 A conceptual muon-catalysed fusion system, showing detail of a modular reaction vessel where muon-catalysed d-t fusion occurs.

though about one-third of the pions are lost by nuclear capture processes in the D-T gas.

Muons then spontaneously and rapidly catalyse fusion reactions in the D-T fuel as we have discussed, producing energetic α-particles and neutrons. The α particles stop within ~1 mm in the dense gas which protects the vessel walls from α-bombardment. The gas must be circulated to extract heat and ^{4}He, the inert product of the fusion reaction. Note that in a reactor environment, thermal neutrons would consume ^{3}He arising from tritium decay by the reaction (^{3}He+n→p+t)[53].

The energetic neutrons enter a lithium-lead eutectic melt, where they deposit heat and produce tritium by the reactions (n+^{6}Li→α+t) and (n+^{7}Li→n+α+t). A fertile isotope such as thorium could be used in the blanket to greatly amplify the energy gain from the muon-catalysed fusion neutrons[43–50].

A few researchers have studied ways of recovering the significant energy remaining in the form of energetic protons and neutrons following muon production[43–50]. One approach is to use the residual beam to breed fissile fuel; for example, spent fuel rods from fission reactors could be renewed without chemical reprocessing. Alternatively, the energy of charged particles could be recovered directly; neutrons would first produce energetic protons through inelastic collisions (G. Chapline, personal communication). Alvarez (personal communication; see also ref. 49) and Eliezer *et al.*[50] have independently suggested that beam particles which do not interact strongly with the target could be collected, re-accelerated and re-circulated into the reaction chamber.

The scheme of Fig. 6 can be characterized as a power amplifier, with input power to the accelerator ultimately driving the muon-catalysed fusion reactor. There is neither plasma to heat nor danger of thermal runaway. However, it is clear that for such a scheme to succeed: (1) hundreds of fusions per muon must be achieved; (2) muons must be produced cheaply (<10 GeV per muon); and (3) many engineering problems must be solved. Research now centres on the first issue: we are surprised to observe so many catalysed d-t fusions per muon (see Fig. 5) and we are exploring the limits of the process. A better understanding of the physics may suggest ways to further enhance the cold fusion process. The research could thus lead to the serious consideration of muon-catalysed fusion as an energy source.

Conclusion

A resonance which allows muonic dtμ molecules to form in less than one-thousandth of the muonic lifetime is indeed a remarkable phenomenon. The resonant process has been observed when negative muons are stopped in 'cold' mixtures of deuterium and tritium gases and leads to rapidly induced nuclear fusion reactions. This effect could hardly have been predicted from the studies of muon reactions in liquid hydrogen and deuterium 30 years ago. The discovery of this resonance in the last few years has reawakened interest in muon-catalysed fusion.

On top of this surprise comes another: the retention of muons by α-particles synthesized during d-t fusion is much less severe than expected. Muon catalysis research now focuses on confirming and understanding this discovery. Together these phenomena imply that each muon may catalyse hundreds of d-t fusion reactions, releasing a great deal of fusion energy. Not surprisingly, these discoveries, along with advances in accelerator technology, have renewed interest in muon-catalysed fusion as a potential energy source. One might say that muon-catalysed fusion is an idea whose time has come—again.

My colleagues deserve recognition for years of dedicated effort: Alan Anderson, James Bradbury, Gus Caffrey, James Cohen, Peter Gram, Mel Leon, Richard Maltrud, Michael Paciotti, Clinton Van Siclen and Kenneth Watts. I particularly acknowledge also the support of early pioneers in muon catalysis research, Luis Alvarez, David Jackson, David Judd, and Leon Lederman, and of recent bold thinkers such as Leonid Ponomarev, Johann Rafelski and Marshall Rosenbluth. Finally, I thank Ryszard Gajewski of the US Department of Energy, Division of Advanced Energy Projects, for financial support and encouragement.

Note added in proof: Results of the SIN experiment[55] confirm that μ–α sticking is small: $\omega_s^0 = (0.45 \mp 0.05)\%$ for liquid D-T mixture, in good agreement with LAMPF result (Fig. 4).

1. Bracci, L. & Fiorentini, G. *Phys. Rep.* **86**, 169 (1982).
2. Bogdanova, L. *et al. Soviet Phys. JETP* **34**, 662 (1981).
3. Alvarez, L. W. *Adventures expl Phys.* α, 72–79 (1972).
4. Alvarez, L. W. *et al. Phys. Rev.* **105**, 1127 (1957).
5. Jones, S. E. *et al. Phys. Rev. Lett.* **56**, 588 (1986).
6. Frank, F. C. *Nature* **160**, 525 (1947).
7. Zel'dovich, Ya B. *Dokl. Akad. Nauk SSSR* **95**, 493 (1954).
8. Gershtein, S. S. & Ponomarev, L. I. in *Muon Physics* Vol. 3 (eds Hughes, V. W. & Wu, C. S.) 141 (Academic, New York, 1975).
9. Bertl, W. H. *et al. Atomkernergie-Kerntechnik* **43**, 184 (1983).
10. Jackson, J. D. *Phys. Rev.* **106**, 330 (1957).
11. Zel'dovich, Ya. B. & Gershtein, S. *Soviet Phys. Usp.* **3**, 593 (1961).
12. Rafelski, J. in *Exotic Atoms '79* (eds Crowe, K. & Duclos, E.) 177 (Plenum, New York, 1980).
13. Dzhelepov, V. P. *et al. Soviet Phys. JETP* **23**, 820 (1966).
14. Vesman, E. A. *Zh. éksp. teor. Fiz. Pis'ma Redapt.* **5**, 113 (1967).
15. Vinitsky, S. I. *et al. Soviet Phys. JETP* **47**, 444 (1979).
16. Vinitsky, S. I. *et al. Soviet Phys. JETP* **52**, 353 (1980).
17. Gershtein, S. S. & Ponomarev, L. I. *Phys. Lett.* **72B**, 80 (1977).
18. Bystritsky, V. M. *et al. Phys. Lett* **94B**, 476 (1980).
19. Bystritsky, V. M. *et al. Soviet Phys. JETP* **53**, 877 (1981).
20. Jones, S. E. *et al. Phys. Rev. Lett.* **51**, 1757 (1983).

21. Caffrey, A. J. *et al. Pap. presented at Muon-Catalysed Fusion Workshop*, Jackson, 7-8 June (1984).
22. Anderson, A. N. *et al. Pap. presented at Muon-Catalysed Fusion Workshop*, Jackson, 7–8 June (1984).
23 Jones, S E. in *Atomic Physics 9* (eds Van Dyck, R. S. Jr & Fortson, E. N.) 99–115 (World Scientific, Singapore, 1984).
24. Cohen, J. S. & Leon,, M. *Phys. Rev. Lett.* **55**, 52 (1985).
25. Menshihov, L. I. & Ponomarev, L. I. *Zh. éksp. teor. Fiz. Pis'ma Redakt.* (submitted).
26. Petrov, Yu. V. Preprint no. LNPI-1058 (1985).
27. Gershtein, S. S. *et al., Soviet. Phys. JETP* **53**, 872 (1981).
28. Cohen, J. S. & Leon, M *Phys. Rev.* A33, 1437 (1986).
29 Jackson, J. D. in *Proc. Muon-Catalysed Fusion Workshop* (ed. Jones, S. E.) (1984).
30. Ceperley, D & Alder, B. J. *Phys. Rev.* A31, 1999 (1985).
31. Mueller, B. & Rafelski, J *Phys. Lett.* 164B, 223 (1985).
32. Breunlich, W. H. *et al. Phys. Rev. Lett.* **53**, 1137 (1984)
33 Bleser, E. J. *et al. Phys. Rev.* **132**, 2679 (1963).
34. Kammel, P. *et al. Phys. Rev.* A28, 2611 (1983).
35. Kammel, P. *Lett. Nuovo Cim.* **43**, 349 (1985).
36. Ponomarev, L. I. *Atomkernenergie-Kerntechnik* **43**, 175 (1983).
37. Gershtein, S. S. *et al. Soviet Phys. JETP* **51**, 1053 (1980).
38. Kravtsov, A. V. *et al. JETP Lett.* **40**, 877 (1984)
39. Aristov, Yu, A. *et al. Yad. Fiz.* **33**, 1066 (1981) [*Soviet J. nucl. Phys.* 33, 564 (1981)]
40. Kravtsov, A. V. *et al.* Preprint no. LNPI-998 (1984).
41. Bystritsky, V. M. *et al. Soviet Phys. JETP* **57**, 728 (1983).
42. Balin, D. V. *et al. Phys. Lett.* 141B, 173 (1984).
43. Petrov, Yu. V. *Nature* **285**, 466 (1980); *Atomkernenergie-Kerntechnik* 46, 29 (1985).
44. Petrov, Yu. V. & Shabelski, Yu, M. *Soviet J. nucl. Phys.* **30**, 66 (1974)
45 Takahashi, H. *et al. Atomkernenergie-Kerntechnik* **36**, 195 (1980)
46. Watts, K. D. in *Proc. Muon-Catalysed Fusion Workshop* (ed. Jones, S E.) (1984)
47. Miller, R. C. & Krakowski, R. A. in *Proc. Muon-Catalysed Fusion Workshop* (ed. Jones S. E.) (1984).
48. Chapline, G. Jr & Moir, R. Preprint no. UCRL-93611 (1986)
49. Jones, S. E. *Fusion Technol.* **8**, 1521 (1985); Preprint no. EGG-SE-6290, Idaho National Engng Lab. (1983).
50. Eliezer, S., Tajima, T. & Rosenbluth, M. N. Preprint no DOE-ET-53088-221, Inst. Fusion Studies (1986).
51. Jackson, J. D. Preprint no. LBL-18266 (1984).
52. Schwarzschild, B. *Phys. Today* **39**, 18 (1986).
53. Zweig, G. *Science* **201**, 973 (1978).
54. Sakharov, A. D. & Lebedev, P. N. *Physics Inst. Rep.* (1948).
55. Petitjean, C. *Pap. presented at Am. Phys. Soc. Meet.*, Washington, DC, 29 April (1986)

ARTICLES

Splice-site selection by a self-splicing RNA of *Tetrahymena*

Richard B. Waring*§, Paul Towner*, Stephen J. Minter*† & R. Wayne Davies°†‡

* Department of Biochemistry and Applied Molecular Biology, University of Manchester Institute of Science and Technology, PO Box 88, Manchester M60 1QD, UK

† Allelix Inc., 6850 Goreway Drive, Mississauga, Ontario, Canada L4V 1P1

5′ Splice-site selection by the self-splicing Tetrahymena *ribosomal RNA precursor requires the formation of a particular RNA helix by base pairing between an intron 'guide sequence' and bases surrounding the 5′ splice junction. Part of the guide sequence subsequently holds and positions the 3′ end of the cut 5′ exon to attack the 3′ splice junction.*

THE way in which splice sites are selected so precisely is a central question for all systems in which RNA splicing occurs, for a particular phosphodiester bond must be singled out from thousands of bonds that are chemically nearly identical. This specificity can be conferred only by higher-order molecular structure. The intron of the large ribosomal RNA precursor of *Tetrahymena thermophila* is excised, and the flanking exons ligated together in the absence of proteins[1,2]. In this case, the splice junctions are defined, and catalysis carried out, by elements of RNA structure only. The capacity to form a particular set of RNA helices, including several involving distant RNA sequences, is conserved throughout the class of introns to which the *Tetrahymena* intron belongs[3]. Davies *et al.*[3] showed that the capacity for exon sequences near the 5′ and 3′ splice junctions to base pair with an intron 'internal guide sequence' was also conserved, and proposed that these RNA helices could be important for defining the splice junctions and bringing both ends into the active site. We have used second-site suppression as a genetic tool to investigate the roles of these RNA structural elements in this RNA-catalysed RNA splicing reaction.

The RNA self-splicing reaction can be regarded as consisting of two subreactions, one at the 5′ and one at the 3′ splice junction—a simultaneous cleavage and ligation reaction in which phosphodiester bond energy is conserved—occurring via *trans*-esterification (phosphoester transfer)[1,2]. The intron RNA takes up a very specific structure[3-9], binds a guanosine cofactor[10] and can then catalyse the RNA splicing reaction if magnesium ions are present[1]. The intron is excised as a unique linear molecule with the guanosine added to the 5′ end, and subsequently autocyclizes[11-15]. All genetic[16-20] and biochemical[21] evidence is consistent with an RNA secondary structure closely related to that shown in Fig. 1*A*[3,5]. The *Tetrahymena* ribosomal RNA intron is the biochemically best-studied member of a widespread class of introns (class I of fungal mitochondria) all of which are potentially self-splicing and have this RNA structure[5,6,8]. Two mitochondrial introns of this class have been shown to be self-splicing[22,23].

Each subreaction involves an attacking hydroxyl group and a target phosphodiester bond. We show that the formation of a short RNA helix involving an intron '5′ guide sequence' and bases around the 5′ splice junction is essential for 5′ splicing. The structure of this helix and its position within the complete RNA structure define which phosphodiester bond is the 5′ splice site. Part of the 5′ guide sequence has a further role, positioning the attacking hydroxyl group in the 3′ subreaction, which can be separated from the 5′ subreaction. We are thus able to begin to dissect the RNA splicing reaction, and provide the first direct evidence that identifies elements of the mechanism by which a splice junction is selected.

Role of base pairing

A definitive way of demonstrating that interaction occurs between distant portions of RNA (or protein) molecules is to obtain second-site revertants of mutations that affect function. If, in an RNA molecule, the suppression of the original mutant phenotype by the second-site mutation is correlated with the restoration of the capacity to form a base pair disrupted by the first mutation, it follows that the capacity to form this base pair is important for the function that is altered in the mutant phenotype. The base-paired region may be a semi-permanent feature of the RNA structure, or may form transiently but still

‡ To whom correspondence should be addressed at Allelix Inc.
§ Present address: Department of Pharmacology, UMDNJ, Rutgers College of Medicine, PO Box 101, Piscataway, New Jersey 08854, USA.

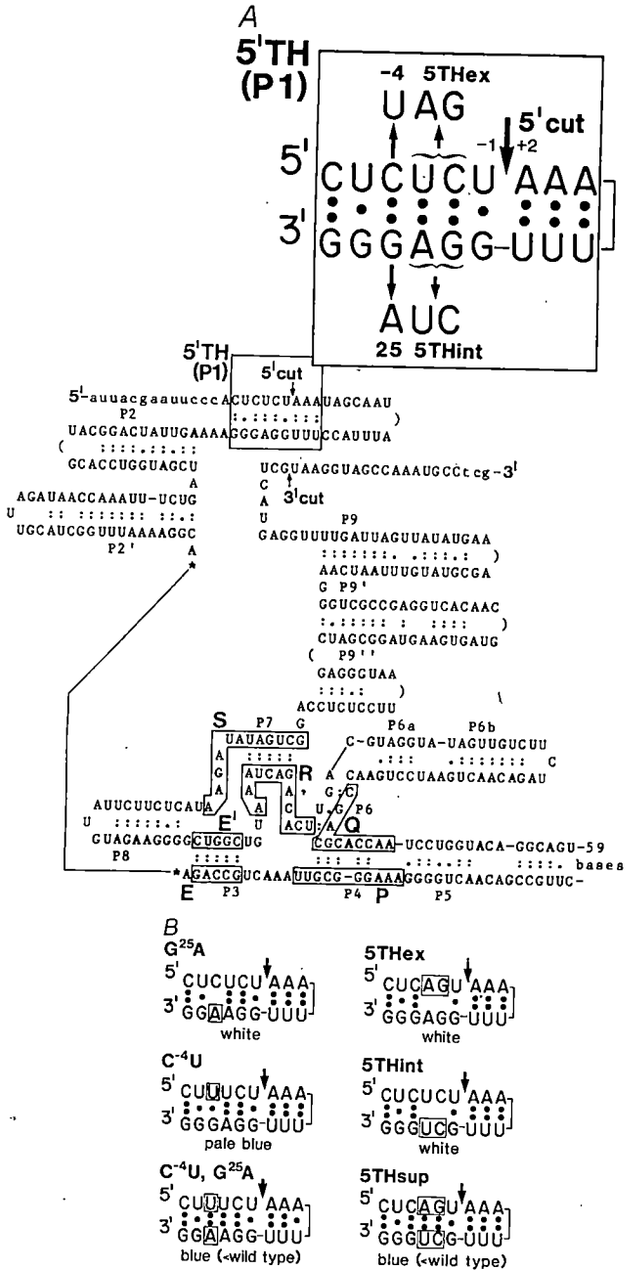


Fig. 1 Wild-type and mutant forms of the *Tetrahymena thermophila* rRNA intron. ***A***, RNA secondary structure of the wild-type intron[5] according to the model of Davies *et al.*[3] as given in ref. 34, showing mutations introduced into the P1 (5′TH) structure. *Tetrahymena* sequence is in upper-case letters and β-gal and M13 polylinker sequence derived from the constructions of Waring *et al.*[18] are in lower-case letters. M.TET.14 (ref. 18) contains 17 *Tetrahymena* exon bases in the 3′ exon. Splice sites are indicated by arrows and all features have been described previously[3,5,8]. P, Q, R and S are conserved sequences found in all introns of this class[3,8]. 'P' in P2–P9 indicates a pairing region; only a part of each conserved sequence is involved in base pairing (P4 for P–Q; P7 for R–S). The P10 pairing[3] between the internal guide sequence and 3′ exon bases is not found in all introns of this class[8], and is therefore not shown here. Its role in RNA self-splicing by the *Tetrahymena* RNA intron will be discussed separately (R.B.W. and R.W.D., in preparation). E and E′ are non-conserved sequence elements that are always able to form a conserved long-range pairing (P3). Genetic evidence for the functional importance of the P–Q, E–E′ and R–S pairings are described in refs 18–20, respectively. The P2′, P9′ and P9″ stem–loop structures are not found in typical class I introns[8], which only have single P2 and P9 stem–loops. Asterisks indicate the point where the structure has been broken in order to be able to display all key base-paired regions. Bases are numbered by taking the 5′ cut site as 0, numbering 5′ exon bases in the 3′ to 5′ direction starting with −1 next to the 5′ cut site, and numbering intron bases in 5′ to 3′ order as in the excised intron, so that base 1 (5′) is the G derived from the guanosine cofactor and is not present in the non-excised intron in the RNA precursor. G^{25} is thus seen as the 24th base 3′ to the 5′ cut site in ***A***. ***B***, Model 5′ splicing target helix structures for the mutant introns. Oligonucleotide site-directed mutagenesis was performed as described by Zoller and Smith[35]. All mutants were sequenced from the *Eco*RI to the *Hin*dIII sites[18] of M83.TET.14 to ensure that no other mutations were obtained during the mutagenesis procedure. Mutant phenotypes were scored from at least four independent mutations.

be functionally important. Davies *et al.*[3] noted that a particular region of RNA near the 5′ end of class I introns[8], including the *Tetrahymena* rRNA intron (the internal guide sequence), is always capable of base pairing with both exon and intron bases flanking the 5′ splice junction, and usually[8] can also use adjacent bases to base pair with 3′ exon bases near the 3′ splice junction. The pairing of the internal guide sequence with bases at the 5′ end of the intron and at the 3′ end of the 5′ exon would form a particular RNA helix called P1, with the phosphodiester bond that is the target for 5′ cleavage in one strand within the helix. Our starting point was the hypothesis that the formation and structure of this helix provide the information that identifies the 5′ splice junction.

We have made two sets of mutations in the short RNA helix named P1, which we now refer to as the 5′ splicing target helix (5′TH) (see Fig. 1). Mutations affecting splicing were easily identified using the system of Waring *et al.*[18]. M83.TET.14 is an M13mp8.3 bacteriophage derivative, with the *Tetrahymena* intron (and short sections of the flanking exons) inserted so that the synthesis of the β-galactosidase α-fragment is prevented unless the intron excises itself *in vivo* in *Escherichia coli*. Phages carrying wild-type introns, which self-excise, make β-galactosidase and give blue plaques on Xgal-containing medium, whereas phages carrying introns defective for RNA splicing produce white plaques. One mutation in the 5′ exon component of 5′TH was picked up as a pale blue plaque in screening phage M83.TET.14[18] for spontaneous splicing-deficient mutants. This $C^{-4}U$ mutation (see Fig. 1 legend for the numbering convention) would form a 5′TH that has lost one of its three key G·C base pairs, but still has a weak U·G base pair rather than no base pair at all at this site. This mutation produces a Phe-to-Ser exchange in the extreme amino-terminal region of the β-galactosidase α-fragment. The steady-state level of excised intron in M83.TET.14$C^{-4}U$-infected *E. coli* is approximately 10% of that found in M83.TET.14-infected *E. coli*, showing that intron excision in this mutant is impaired.

Oligonucleotide-directed *in vitro* mutagenesis was used to generate the intron mutation $G^{25}A$. The $G^{25}A$ mutant itself gives a white plaque on minimal medium (Fig. 2) and is therefore more defective than the $C^{-4}U$ mutant. The double mutant $C^{-4}U$,$G^{25}A$ has a plaque colour phenotype sightly less blue than that of the wild type (Fig. 2), indicating that the $C^{-4}U$ mutation

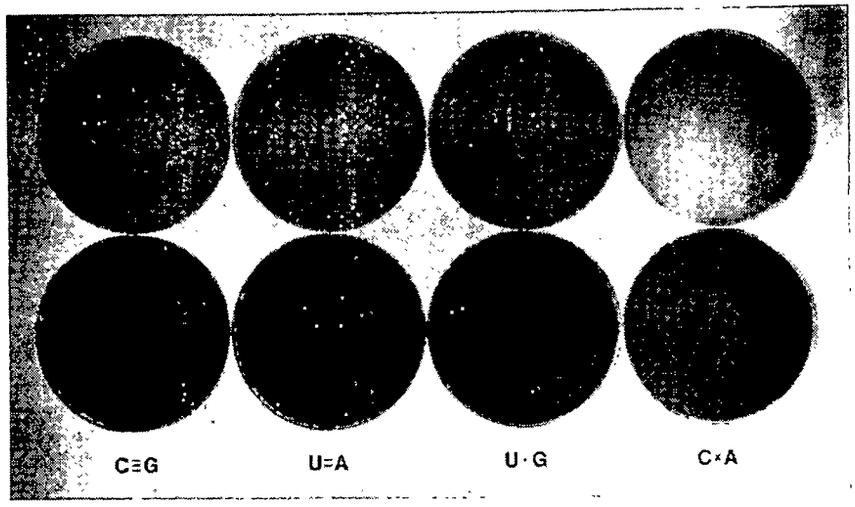


Fig. 2 Plaque phenotypes of M83.TET.14 and M83.TET.14 carrying mutants in the 5′ splicing target helix. The base pair present at position −4 in 5′TH (P1; Fig. 1) is given in each case to show the corelation between phenotype and the stability of 5′TH. From left to right, the phages are M83.TET.14 (C≡G), $C^{-4}UG^{25}A$ (U=A), $C^{-4}U$ (U·G) and $G^{25}A$ (C/A). The top row of plates are of minimal medium, the lower row of YT medium. More intron excision is needed on YT than on minimal medium to produce the same plaque phenotype, which helps to distinguish between partial mutations[18]. For example, $C^{-4}U$ and $C^{-4}UG^{25}A$ are both a fairly similar pale blue on minimal medium, but $C^{-4}U$ is virtually white on YT and $C^{-4}UG^{25}A$ still pale blue.

suppresses the phenotype of the $G^{25}A$ mutation and vice versa; the only reasonable explanation for this is that C^{-4} and G^{25} are normally base paired, that $C^{-4}U$ and $G^{25}A$ weaken or destroy this base pair, and that $C^{-4}U,G^{25}A$ replaces the original C·G base pair with a U·A base pair. The plaque phenotypes of these four phages, and therefore the efficiency of intron excision, are precisely in the order of the known strength of the base pair that each phage has in the −4 position of 5′TH—C≡G> U=A>U·G>C/A (Fig. 2)—as would be expected if base pairing underlies the function affected.

A second set of mutations (Fig. 1*B*) affecting different bases also predicted[3] to be involved in forming 5′TH was made by *in vitro* mutagenesis, with two adjacent bases being altered for generating more extreme phenotypes, so as to facilitate *in vitro* RNA splicing analysis. The mutant phages are M83.TET.14 $U^{-3}A$, $C^{-2}G$ (5THex; Fig. 1*B*) and $G^{23}C$, $A^{24}U$ (5THint; Fig. 1*B*), both of which give white (intron excision-defective) plaques on minimal medium. The predicted second-site revertant combination (5THsup; Fig. 1*B*) would have a 5′TH containing the same base pairs as the wild type, in the same order, but with the purine–pyrimidine positions reversed (Fig. 1*B*). 5THsup plaques are almost as blue as wild-type plaques. Therefore, the pairs of double base-changes suppress each other's effects on intron excision. The occurrence of second-site suppression shows that any effects due to alteration of the β-galactosidase sequence by the exon mutants are not of primary importance, and that the capacity of the affected sequences to base pair is essential for normal intron function.

The phenotypes of these mutants were examined further in *in vitro* RNA splicing assays. Introns (with flanking exons as in Fig. 3*A*) carrying 5THex, 5THint or 5THsup mutations were subcloned into pSP65 (Fig. 3*A*) and transcribed *in vitro*; RNA was prepared and *in vitro* RNA splicing reactions were performed. Figure 3*B* shows the results of a typical *in vitro* RNA splicing experiment. The relevant data here are the levels of excised intron (IVS) and ligated exons (5E3E) produced; the origin of the novel products Y and Z is described below. The 5THex mutant is completely defective, producing no excised intron at all; clearly, this mutant is blocked in the very first step of RNA splicing. The 5THint mutant is slightly less defective, producing a very low but detectable amount of excised intron only in the presence of GTP; the GTP dependence of this reaction shows that the excised intron RNA is produced by the standard splicing reaction, and not by some side reaction. 5THsup produces a significant amount of excised intron in a GTP-dependent reaction, showing that the splicing defects of 5THex and 5THint are suppressed *in vitro*. The level of intron excised is not fully that of the wild type, and significant amounts of the novel products Y and Z generated by the 5THint mutant are still made by 5THsup, so that suppression is not total.

These results show that if we alter the capacity of a particular intron sequence—which we refer to as the 5′ guide sequence (5′GS:5′UUUGGAGGG3′; Fig. 1*A*)—to base pair with the exon sequence adjacent to the 5′ splice junction, RNA splicing is severely blocked. As all the base pairs affected are precisely those that would be centrally located in 5′TH (Fig. 1*A*), it follows that the capacity to form 5′TH is crucial for at least the 5′ cleavage and ligation reaction. There is corroborative *in vivo* genetic evidence from yeast mitochondrial class I introns, as splicing-defective 5′ exon mutations that would affect the 5′THs of cytochrome *b* introns 4 (refs 16, 24) and 5 (P. S. Perlman, personal communication) have been isolated, and one of the classes of revertants of the *cobI4* mutation is in 5′GS and would restore base pairing in 5′TH.

Factors influencing splicing rate

To determine the extent of phenotypic suppression in the 5THsup intron, a time course of the *in vitro* splicing reactions of wild-type and mutant introns (Fig. 4) was carried out. If the base pairing in 5′TH is restored, the splicing defect is suppressed, but splicing is still slow *in vitro*, reaching in 48 min less than half the level of excised intron produced by wild type in 1 min. This is not a result of depletion of the precursor by the reaction yielding Y and Z, as the generation of these products is particularly favoured in RNA transcripts generated from *Pvu*II-cut pSP65 (see below), and RNA splicing of 5THsup in transcripts from *Hin*dIII-cut pSP65, which produce very little Y, occurs at much the same rate (data not shown). The number of hydrogen bonds that can be formed between bases in the wild-type and 5THsup 5′ splicing target helices is the same, so that it is the alteration in the sequence of base pairs in 5′TH that changes the rate of RNA splicing. Moreover, 5THint produced some excised intron and ligated exons but 5THex did not.

Separable 5′ and 3′ reactions

A striking property of the 5THint mutant is the production of large amounts of two completely new RNA species, bands Y and Z, in a GTP-independent reaction. Because the guanosine cofactor is required[1] for the nucleophilic attack that initiates the 5′ cutting reaction, Y and Z must be produced by a reaction that bypasses 5′ cutting, such as a novel version of the 3′ cleavage–ligation reaction. Also, the function affected by the 5THint mutant is a function of the intron strand involved in the formation of 5′TH, and not of the exon strand of 5′TH or 5′TH itself. Both 5THint and 5THex mutations (Fig. 1*A*) disrupt the same two base pairs of 5′TH, yet 5THint makes large amounts of Y and Z, whereas wild-type and 5THex make no Z and very little Y (Fig. 3*B*). The structure of Y and Z reveals the nature of the bypass reaction. Y behaves as a linear molecule in different gel conditions, and is 437 nucleotides long, which corresponds

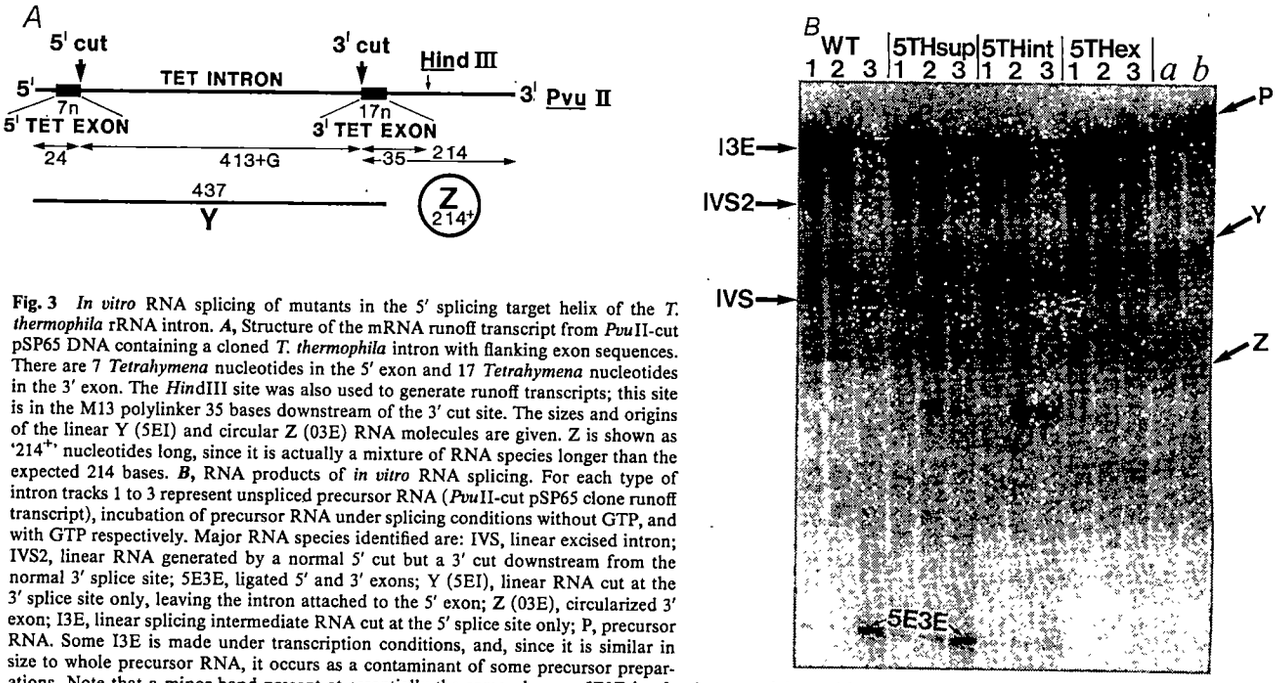


Fig. 3 *In vitro* RNA splicing of mutants in the 5′ splicing target helix of the *T. thermophila* rRNA intron. ***A***, Structure of the mRNA runoff transcript from *Pvu*II-cut pSP65 DNA containing a cloned *T. thermophila* intron with flanking exon sequences. There are 7 *Tetrahymena* nucleotides in the 5′ exon and 17 *Tetrahymena* nucleotides in the 3′ exon. The *Hin*dIII site was also used to generate runoff transcripts; this site is in the M13 polylinker 35 bases downstream of the 3′ cut site. The sizes and origins of the linear Y (5EI) and circular Z (03E) RNA molecules are given. Z is shown as '214^{+}' nucleotides long, since it is actually a mixture of RNA species longer than the expected 214 bases. ***B***, RNA products of *in vitro* RNA splicing. For each type of intron tracks 1 to 3 represent unspliced precursor RNA (*Pvu*II-cut pSP65 clone runoff transcript), incubation of precursor RNA under splicing conditions without GTP, and with GTP respectively. Major RNA species identified are: IVS, linear excised intron; IVS2, linear RNA generated by a normal 5′ cut but a 3′ cut downstream from the normal 3′ splice site; 5E3E, ligated 5′ and 3′ exons; Y (5EI), linear RNA cut at the 3′ splice site only, leaving the intron attached to the 5′ exon; Z (03E), circularized 3′ exon; I3E, linear splicing intermediate RNA cut at the 5′ splice site only; P, precursor RNA. Some I3E is made under transcription conditions, and, since it is similar in size to whole precursor RNA, it occurs as a contaminant of some precursor preparations. Note that a minor band present at essentially the same place as 5E3E is of unknown origin, and is present in precursor preparations. The low levels of 5EI (Y) which occur in wild type (WT) and the 5THex mutant probably result from the known tendency of this intron to undergo hydrolysis at the 3′ splice junction at a low rate[15]. The two tracks on the far right are *in vitro* RNA splicing with precursors of mutant 29 (track *a*) which produces more 5EI/03E than wild type, but has a wild-type 5′TH (R.B.W. and R.W.D., unpublished), and the 5THex mutant (track *b*), incubated under splicing conditions with no GTP and 4 mM spermidine, showing stimulation of 5EI and 03E production by spermidine, which can stabilize weak RNA helices[26,27].

Methods. The 458-bp *Eco*RI–*Hin*dIII fragments from M83.TET.14 mutants were purified and shuttled into the pSP65 transcription vector[25]. pSP65 clones were linearized with *Pvu*II, phenolized and ethanol-precipitated. RNA was synthesized by incubating 2 μg of DNA in the recommended buffer[25] including 4 mM spermidine (which promotes transcription, but partially inhibits splicing[1]), bovine serum albumin (100 μg ml^{-1}), RNasin[25] and 5 U of SP6 RNA polymerase at 37 °C in a final volume of 50 μl. ^{32}P-GTP (20 μCi, 400 Ci mmol^{-1}; Amersham) in the presence of 20–50 μM GTP was used to label the RNA, which was then phenolized, ethanol-precipitated, resuspended in water and loaded onto a 7 M urea/5% polyacrylamide gel after the addition of at least 1 vol. of loading dye (deionized formamide containing 40 mM EDTA, 0.1% bromophenol blue). The gel was made and run exactly as a DNA sequencing gel[36]. *Hin*fI-digested M13mp8 was used as a size marker. RNA was located by autoradiography. Acrylamide strips were cut out, crushed and the RNA eluted overnight in 0.3 M Na-acetate, 20 mM Tris *p*H 8.0, 1 mM EDTA at 4 °C. Gel fragments were removed by centrifugation or filtration through siliconized glass wool and the RNA was then ethanol-precipitated twice at −20 °C. Attempts to clean RNA preparations using a variety of affinity chromatographic media, reverse-phase chromatography and Sephadex G-50 did not increase the initial rate of splicing and frequently reduced yields. RNA was stored frozen at −20 °C in 10 mM Tris *p*H 7.4, 0.1 mM EDTA. Unless otherwise indicated, splicing reactions[1] were performed in siliconized 0.5-ml Eppendorf tubes in 10 mM $(NH_4)_2SO_4$, 30 mM Tris *p*H 7.5, 5 mM $MgCl_2$ and 0.2 mM GTP at 37 °C for 30 min. Splicing was stopped by addition of at least 1 vol. formamide loading dye[36]. Samples were run on polyacrylamide gels as described above. Gels were fixed and usually exposed at room temperature without an intensifier screen.

precisely to the size of molecule consisting of the joined 5′ exon and intron, '5EI'. The presence of the 5′ exon in Y was confirmed by generating a complementary DNA runoff transcript of the expected size using an oligonucleotide that primes only 18 bases downstream of the 5′ splice junction within the intron. The mobility of Z varies with the strength of the polyacrylamide gels, as is typical of circular molecules. Purified Z, when nicked, gives two linear molecules 215 and 216 nucleotides long in roughly equal proportions, corresponding to the expected length (Fig. 3*A*) of the 3′ exon plus one or two nucleotides respectively. As sequencing (Fig. 5) established that the 3′ end of the precursor transcript had been joined to the first base of the 3′ exon, Z must be the circularized 3′ exon, '03E'. 03E contains either one or two extra nucleotides at the circularization point which are not in the DNA template. The runoff transcript itself (and all derivatives of it which contain the 3′ exon) is an approximately equal mixture of RNA molecules with one or two additional nucleotides which must be at the 3′ end and are presumably added spontaneously by SP6 polymerase, an effect observed previously[25]. Thus, the bypass reaction is a cleavage and ligation reaction involving cleavage at the normal 3′ splice site, with ligation of the free 3′ end of the RNA precursor to the 5′ end of the cut 3′ exon, producing a circular 3′ exon (Z, 03E) and a linear molecule comprising the intron joined to the 5′ exon (Y, 5EI).

The generation of 5EI and 03E by the 5THint mutant is 1/10th to 1/20th as rapid as normal splicing by the wild-type intron, and thus 5THint RNA carries out a rapid 3′ splicing reaction analogue while it is almost completely blocked for 5′ cleavage and ligation. 5EI molecules, which lack the 3′ exon, also undergo 5′ cleavage in the absence of a 3′ reaction, and the relative rates of 5′ cleavage for molecules with wild-type, 5THint, 5THex and 5THsup sequences are as expected from the above results (data not shown). The 5′ and 3′ cleavage and ligation reactions are separable, and 5′TH is involved only in the 5′ subreaction.

Positioning of attacking group

The fact that the high 03E and 5EI production results from the 5THint mutation means that the intron sequence altered by this mutation must be involved. In the runoff transcript from *Pvu*II-cut template, the RNA precursor should end in 5′CCAG3′ (actually it ends with 5′ CCAGN(N′)3′; Fig. 5), which can pair precisely with the sequence 5′CUGG3′ containing the double base change (GA→CU) of 5THint compared with wild type. The 3′ end of the transcript can then substitute for the cut 5′ exon. This hypothesis predicts that the phenomenon will be specific to DNA transcripts containing a *Pvu*II end, since sequences adjacent to other restriction enzyme sites will not pair as well with the 5′TH intron strand of 5THint. Table 1 shows that this is the case; the reaction generating 5EI and 03E is much less frequent using runoff transcripts from templates containing *Hin*dIII, *Hpa*II or *Hin*fI ends. The amounts of 5EI and 03E produced actually correlate well with the strength of potential pairing between the end of the RNA transcript and the key region of intron RNA (Table 1), and their amounts are increased

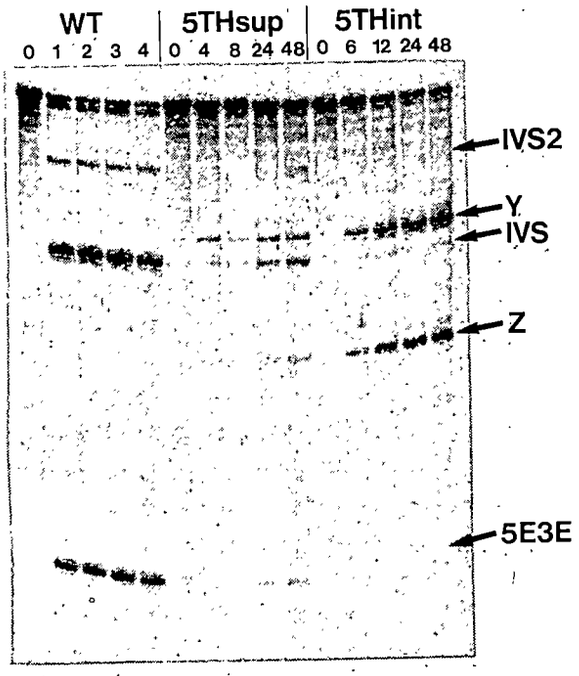


Fig. 4 Time course of *in vitro* RNA splicing of mutant and wild-type *Tetrahymena* rRNA introns. Numbers above each track indicate the time in minutes at which samples were taken. Runoff transcripts from *Pvu*II-cut pSP65 clones were generated, purified and incubated under splicing conditions as described for Fig. 3*B*, except that splicing was performed at 30 °C, rather than 37 °C. Major RNA species are labelled as in Fig. 3*B*.

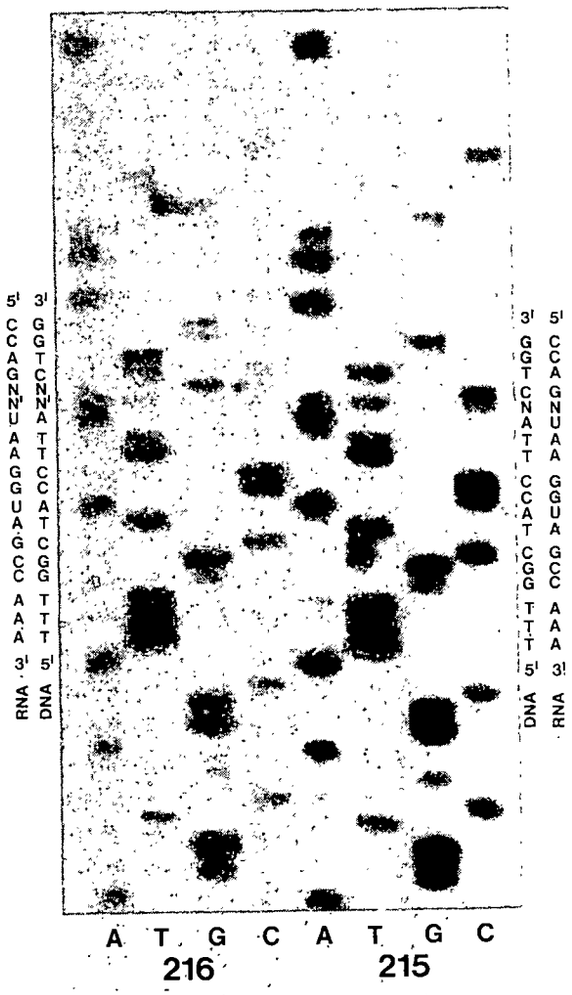


Fig. 5 Nucleotide sequencing of the circularization site of the circular 3′ exon (03E). The two 03E bands (215 and 216 nucleotides long) were separated, and the sequences of both are shown side by side; note that the sequences run parallel until the circularization site, where they shift 1 base out of phase. DNA sequences read directly from the gels are shown alongside, together with the RNA complement which is the true sequence of the 03E molecule in this region. The sequence appears to become unclear after the circularization point; this is because the two 03E species could not be obtained completely without cross-contamination, and their sequences are, of course, shifted by 1 base relative to each other after the circularization point. The 215 03E has one extra base at the circularization site, the 216 03E has two. In the RNA, N is A > U > G ≫ C in the 215-nucleotide 03E. In the 216-nucleotide 03E, N is C > A, U, G, N′ is U > A ≫ C ≥ G.

Methods. RNA was purified as described for Fig. 3. Sequencing was carried out using the dideoxy procedure with reverse transcriptase at 42 °C and priming from ^{32}P-end-labelled M13 reverse sequencing primer (Amersham), which pairs with the downstream exon. The reaction mixes were treated with RNase before boiling and loading onto gels. 03E RNA was produced in sufficient amounts for this experiment by incubating precursor transcript from a pSP65 clone of the 5THint mutant intron under splicing conditions for 1 h. More than 90% of the precursor was converted to 5EI and 03E in this time.

in the presence of spermidine, which stabilizes weak RNA helices[26,27].

Our experiments identify the binding site within the catalytic RNA molecule for the nucleotide sequence (normally the 3′ end of the cut 5′ exon) that carries the 3′ hydroxyl attacking group for the second (3′) step in the RNA splicing reaction; we will refer to the binding site as the 3′ attack site (3′AS). The nucleotides making up 3′AS are a subset of those in the 5′ guide sequence. In the 5THint mutant the sequence of 3′AS is 5′(G)CUGG3′; the wild-type equivalent is 5′(G)GAGG3′. Figure 6 outlines the role of 3′AS in the generation of 5EI and 03E. The reaction described here ('3′ end invasion') is intramolecular, but a clear prediction is that any RNA fragment or oligonucleotide that can pair with the bases 5′[G]GAGG[G]3′ to place a 3′ hydroxyl end correctly will be used as an alternative to the cut 5′ exon if provided in sufficient concentration ('oligonucleotide invasion'). This is consistent with the recent results of Cech and co-workers[28]. Mutants with a weak, unstable 5′TH will be particularly susceptible to oligonucleotide invasion, which would lead to *trans* activity of this RNA catalyst.

Conclusions

Our results lead us to draw three major conclusions about the mechanism of RNA splicing for self-splicing class I introns: (1) the formation, at least transiently, of a short RNA helix (5′TH; 5′ splicing target helix) between an intron 5′ guide sequence and bases surrounding the 5′ splice junction, is essential for the selection of the 5′ splice site and for 5′ cleavage and ligation; (2) the 5′ and 3′ cleavage and ligation reactions are completely separable; (3) a subset of the intron bases in the guide sequence (those that pair with 5′ exon bases) serves to retain and position the cut 5′ exon, or any externally supplied partner sequence with a free 3′ OH end, to attack the 3′ splice junction. In Fig. 6 these conclusions are incorporated into the present understanding of the RNA-catalysed splicing reaction.

As the 3′ splicing bypass reaction occurs at a significant rate (1/10th that of normal splicing), some detailed inferences concerning the structures involved can be drawn. First, the nature of the last base of the cut 5′ exon is not crucial for 3′ cutting, as this base is highly variable on the 3′ end of the precursor transcript due to the semi-random addition of nucleotides by SP6 RNA polymerase. Also, the hydroxyl that attacks the 3′

Table 1 Alternative base pairing by an intron sequence involved in structures essential for 5′ or 3′ cleavage and ligation

		3′AS/RNA 3′ End	5EI(Y)	03E(Z)	I/5E3E
	5′TH ↓ PvuII				
5THint	5′ACUCUCUAAA	5′UGCCAGN(N)			
	: : : : : : : : :	: : : : :	+++++(+++++)	+++++(+++++)	+
	AGGGUCGUUU	AGGGUCGUUU			
	↓ PvuII				
5THsup	5′ACUCAGUAAA	5′UGCCAGN(N)			
	: : : : : : : : :	: : : : :	+++(+++)	+++(+++)	+++
	AGGGUCGUUU	AGGGUCUUU			
	↓ PvuII				
wt	5′ACUCUCUAAA	5′UGCCAGN(N)			
	: : : : : : : : :	: : :	+(+)	-(+)	+++++
	AGGGAGGUUU	AGGGAGGUUU			
	↓ PvuII				
5THex	5′ACUCAGUAAA	5′UGCCAGN(N)			
	: : : : : : : : :	: : :	+(++)	-(++)	-
	AGGGAGGUUU	AGGGAGGUUU			
	HpaII				
	AGCCGN(N)				
5THint	: : :		+(+)	-(+)	+
	AGGGUCGUUU				
	HinfI				
5THint	UUAAUGAAUN(N)				
	: : : : :		+(+)	-(-)	+
	AGGGUCGUUU				

The potential to form 5′TH or 3′AS-RNA 3′ end structures is correlated with the production of normal splicing products (I/5E3E) and unusual RNA molecules derived by 3′ cleavage and ligation only (5EI, Y; 03E, Z) in *in vitro* RNA splicing reactions. 5′TH, 5′ splicing target helix (P1 in refs 3, 5, 8, 9); 3′AS, 3′ attack site; 5EI, linear fused 5′ exon and intron; 03E, circular 3′ exon; I, excised intron; 5E3E, ligated 5′ and 3′ exons. 5′TH is essential for 5′ cleavage–ligation, and the 3′AS–RNA 3′ end pairing is proposed as the basis of the 3′ end invasion reaction that generates 5EI and 03E. The strongest base pairing possible is given in all cases, whether or not such a pairing is potentially stable. The arrow in 5′TH indicates the 5′ splice junction. The 3′ end of the RNA transcript is shown with one or two semi-randomly added nucleotides, as described in Fig. 5 legend. 5THint, 5THex and 5THsup mutants are described in the text; bases differing from wild type are underlined. *Pvu*II, *Hpa*II and *Hin*fI refer to the restriction enzymes used to cut the pSP65 clone DNA template, which determines the end of the runoff transcript. The lengths of the 3′ exons, not including bases added by SP6 polymerase, are: *Hin*dIII, 35; *Hpa*II, 110; *Pvu*II, 214; *Hin*fI, 228. Data for transcripts from *Hin*dIII-cut DNA are not included here, as the very small 03E from this reaction was not identified clearly. Production of various RNA molecules is scored semi-quantitatively on a scale of 0(−) to 5(+++++), based on data obtained under standard splicing conditions. Symbols in parentheses refer to data obtained in the presence of 4 mM spermidine under normal splicing conditions. The production of 03E is the crucial indicator of the 3′ end invasion reaction, as low background levels of 5EI are produced by spontaneous scission at the 3′ splice site[15]. The relative success of the normal 5′ splicing and 3′ end invasion reaction depends on: (1) the potential for base-pairing between the 3′ end of the transcript and 3′AS; (2) the relative stability of 5′TH, the 3′AS–5′ exon pairing, and the 3′AS–RNA 3′end pairing. With 5THint in a transcript from *Pvu*II-cut DNA, normal splicing is rare because of the defective 5′TH, but the bypass reaction is frequent because of the pairing of the 5′CUGG3 sequence with the 3′ end of the RNA transcript. In wild type, 5′TH is strong and the alternative pairing with the end of the transcript is weak so that the bypass reaction rarely if ever occurs; in 5T-ex, which has a wild-type intron strand, 03E production is detectable when the weak alternative pairing is stabilized by spermidine (Fig. 3*B*). 5THsup can form as good a pairing with the transcript's 3′ end as 5THint, but has a much stronger 5′TH, so that 5EI/03E generation is reduced and normal splicing increased in 5THsup over 5THint. Note that the presentation of the 3′ attacking group is achieved adequately by two very different short helices in the wild-type/cut 5′ exon and 5THint/RNA 3′ end combinations. In the role of 3′AS the 5′GGAGGG3′ sequence primarily determines the position of the 3′ hydroxyl group, placing it in close proximity to its target, the 3′ splice junction, and is thus truly acting as an internal guide sequence as proposed by Davies *et al.*[3].

splice junction can be at least one base beyond the usual position, since the '+2' transcript directs 3′ splicing. Finally, the U carrying the hydroxyl that attacks the 3′ splice junction in the 'normal pathway' (Fig. 6) need not be paired with G as in 5′TH because the '+1' structure has a 3′A^{OH} that is unpaired yet gives good 3′ splicing.

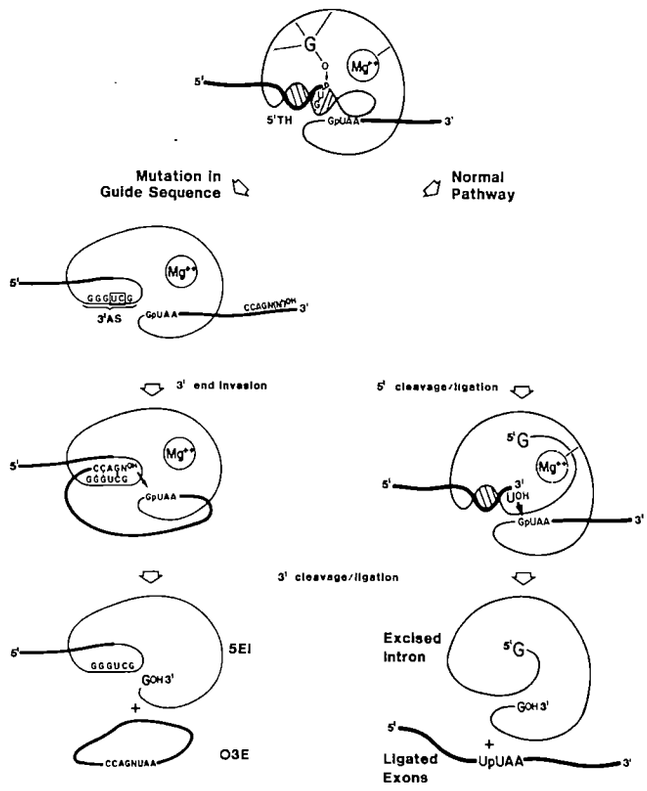


Fig. 6 Diagram of the steps in the RNA splicing reaction catalysed by the intron of the rRNA precursor of *T. thermophila*, and the events leading to the generation of 5EI and 03E by the 3′ end invasion reaction in mutants that alter the sequence of the 5′ guide sequence, such as 5THint. The boxed bases are the mutated bases in the guide sequence of the 5THint mutant, 5′CU3′ replacing the 5′GA3′ of wild type. The RNA precursor shown is an *in vitro* transcript from *Pvu*II-cut DNA of a clone of the 5THint mutant *T. thermophila* rRNA intron. Exon RNA is shown as a thick line, intron RNA as a thin line. 3′AS, 3′ attack site; 5′TH, 5′ splicing target helix; G, guanosine cofactor. The figure is based on conclusions from the present paper and the experiments of T. R. Cech and co-workers[1,2,10,15].

The formation of 5′TH is necessary but not sufficient for effective 5′ splicing, since particular series of base pairs in this helix allow much more rapid reaction than others. It seems unlikely that the difference in stacking energy between the wild-type 5′TH and the 5THsup 5′TH is actually significant enough to account for the difference in behaviour of 5THsup and wild type in terms of stability of 5′TH. The sequence of 5′TH may be a factor in positioning the helix via tertiary interactions between exposed groups on bases in 5′TH and other parts of the RNA catalyst, and/or in determining the susceptibility to cleavage of the phosphodiester bond at the 5′ splice site. Recent work on the crystal structure of A-form DNA helices containing T·G base pairs[29] suggests that U·G base pairs may introduce novel features into RNA helices, changing the availability of groups for tertiary interaction and altering local stacking. A U·G base pair is found in 5′TH next to the 5′ splice site in all but one class I intron[8]. The purine–pyrimidine asymmetry of the *Tetrahymena* 5′TH, which switches strands precisely at the 5′ splice site, may also be significant for this intron, but is not a general feature of class I introns. Either of these features could influence the lability of the bond at the 5′ splice junction, and would be affected by local alterations in the structure of 5′TH.

Pairing of the 3′ end of the RNA precursor with the 3′AS in 5THint would be regarded as unstable on the basis of the rules generally used to establish the stability of RNA structures[30].

Also, in some introns of this class, noticeably the third and fourth introns of the yeast cytochrome oxidase gene and the fourth intron of the yeast apocytochrome *b* gene, 5′TH is very short[3,8], consisting of 4,3 and 4 base pairs (bp), respectively. A role for protein factors such as maturases[31] in stabilizing or directing the folding of RNA can be envisaged; indeed, the intron specificity of maturases could be explained if they stabilize guide sequence-exon interactions rather than other parts of the molecule where conserved sequences underlie the structure. In addition, the RNA structure must be viewed as being dynamic rather than static. The 5THsup mutant RNA is a clear example of this; during the long interval that elapses before a significant proportion of the molecules are cut at the 5′ splice junction (due to the aberrant nucleotide sequence in 5′TH), the 3′ end of the RNA transcript is able to find the intron strand of 5′TH unpaired often enough to generate a considerable level of the 3′ cleavage bypass reaction. Interactions involving only 3 bp have been shown to result in 'reverse cyclization' of the excised intron[32], and CpU can act as a 5′ exon[28], presumably by pairing with the 5′ end GG of 3′AS. In a dynamic, rather than a static, RNA structure, the concept of stability must be used more flexibly, and the establishment of classical 'stable pairings' should not necessarily be used as a prerequisite when seeking to determine the structural elements important in dynamic processes such as RNA splicing or ribosome function.

We have presented here the first direct evidence concerning the mechanism of splice-site selection in a ribosomal or messenger RNA precursor, identifying key elements of RNA structure involved in 5′ and 3′ cleavage and ligation. These elements, within the context of the whole RNA molecule, provide the information that defines particular phosphodiester bonds as the targets for cleavage and ligation. The sequence of 5′TH and its position relative to the attacking guanosine 3′ hydroxyl and the Mg^{2+} ion determines the 5′ splice junction. The 3′AS/cut 5′ exon helix positions the attacking hydroxyl group at the end of the 5′ exon correctly relative to the Mg^{2+} ion and the 3′ splice junction. Similar elements of RNA structure may define splice junctions in nuclear mRNA precursors. An intact 5′ end of the RNA moiety of U1snRNA is essential for splicing[33], and this RNA sequence can pair with bases near 5′ splice junctions to produce a structure similar to 5′TH. Precise understanding of splice-site selection requires crystal structures of 5′TH and the whole RNA.

This work was supported by a grant from the MRC to R.W.D. and Dr C. Scazzocchio. We thank Heather Erfle of Allelix Inc. for assistance in the synthesis of oligodeoxyribonucleotides, and Dr C. Scazzocchio for his contribution to the initiation of this work, as well as for constant support and helpful discussion.

Received 5 December 1985; accepted 18 March 1986.

1. Kruger, K. *et al. Cell* **31**, 147-157 (1982).
2. Cech, T. R., Zaug, A. J. & Grabowski, P. J. *Cell* **27**, 487-496 (1981).
3. Davies, R. W., Waring, R. B., Ray, J A., Brown, T. A. & Scazzocchio, C. *Nature* **300**, 719-724 (1982).
4. Michel, F., Jacquier, A. S. & Dujon, B. *Biochemie* **64**, 867-881 (1982).
5. Waring, R. B., Scazzocchio, C., Brown, T. A. & Davies, R. W. *J. molec. Biol.* **167**, 595-605 (1983).
6. Michel, F. & Dujon, B. *EMBO J.* **2**, 33-38 (1983).
7. Cech, T. R. *et al. Proc. natn. Acad. Sci. U.S.A.* **80**, 3903-3907 (1983).
8. Waring, R. B. & Davies, R. W. *Gene* **28**, 227-291 (1984).
9. Davies, R. W. *Biosci. Rep.* **4**, 707-727 (1984).
10. Bass, B. L. & Cech, T. R. *Nature* **308**, 820-826 (1984).
11. Grabowski, P. J., Zaug, A. J. & Cech, T. R. *Cell* **23**, 467-476 (1981).
12. Brehm, S. L. & Cech, T. R. *Biochemistry* **22**, 2390-2397 (1983).
13. Zaug, A. J., Grabowski, P. J. & Cech, T. R. *Nature* **301**, 578-583 (1983).
14. Zaug, A. J., Kent, J. R. & Cech, T. R. *Science* **224**, 574-578 (1984).
15. Zaug, A. J., Kent, J. R. & Cech, T. R. *Biochemistry* **24**, 6211-6218 (1985).
16. De La Salle, H., Jacq, C. & Slonimski, P. P. *Cell* **28**, 721-732 (1982).
17. Netter, P., Jacq, C. & Slonimski, P. P. *Cell* **28**, 733-738 (1982).
18. Waring, R. B., Ray, J. A., Edwards, S. W., Scazzocchio, C. & Davies, R. W. *Cell* **40**, 371-380 (1985).
19. Weiss-Brummer, B., Holl, J., Schweyen, R. J., Rödel, G. & Kaudewitz, F. *Cell* **33**, 195-202 (1983).
20. Holl, J., Rödel, G. & Schweyen, R. J. *EMBO J.* **4**, 2081-2085 (1985).
21. Inoue, T. & Cech, T. R. *Proc. natn. Acad. Sci. U.S.A.* **82**, 648-652 (1985).
22. Garriga, G. & Lambowitz, A. M. *Cell* **38**, 631-641 (1984).
23. Van der Horst, G. & Tabak, H. F. *Cell* **40**, 759-766 (1985).
24. Perea, J. & Jacq, C. *EMBO J.* **12**, 3281-3288 (1985).
25. Melton, D. A. *et al. Nucleic Acids Res.* **12**, 7035-7056 (1984).
26. Holbrook, S. R. *et al. J. molec. Biol.* **123**, 631-642 (1978).
27. Quigley, G. J., Teeter, M. M. & Rich, A. *Proc. natn. Acad. Sci. U.S.A.* **75**, 64-[illegible] (1978).
28. Inoue, T., Sullivan, F. X. & Cech, T. R. *Cell* **43**, 431-437 (1985).
29. Brown, T., Kennard, O., Kneale, G. & Rabinovitch, D. *Nature* **315**, 604-606 (1985).
30. Tinoco, I. Jr, Uhlenbeck, O. C. & Levine, M. D. *Nature* **230**, 362-367 (1971).
31. Jacq, C. *et al.* in *Mitochondrial Genes* (eds Slonimski, P. P., Borst, P. & Attardi, G.) 155-183 (Cold Spring Harbor Laboratory, New York, 1982).
32. Sullivan, F. X. & Cech, T. R. *Cell* **42**, 639-648 (1985).
33. Krämer, A., Keller, W., Appel, B. & Luhrmann, R. *Cell* **38**, 299-307 (1984).
34. Davies, R. W., Waring, R. B., Brown, T. A. & Scazzocchio, C. in *Mitochondria 1983 Nucleo-Mitochondrial Interactions* (eds Schweyen, R. J., Wolf, K. & Kaudewitz, F.) 179-189 (de Gruyter, Berlin, 1983).
35. Zoller, M. J. & Smith, M. *DNA* **3**, 479-488 (1984).
36. Davies, R. W. in *Gel Electrophoresis of Nucleic Acids: A Practical Approach* (eds Rickwood, D. & Hames, B. D.) 117-172 (IRL Press, Washington, DC, 1982).

LETTERS TO NATURE

High-resolution imaging from Mauna Kea: the triple quasar in 0.3-arc s seeing

J. Patrick Henry & J. N. Heasley

University of Hawaii at Manoa, Institute for Astronomy, 2680 Woodlawn Drive, Honolulu, Hawaii 96822, USA

The 'triple' quasar, PG1115+08 (which actually contains at least four objects: A_1, A_2, B and C) was the second gravitational lens object to be found[1]. But because of its small angular scale (<2.5 arc s separation between components) and lack of detectable radio emission, which precludes the use of high-resolution interferometric radio techniques, not much is known about this object. In particular, the lensing object(s) have not been identified. Here we report imaging observations made on a night of exceptional seeing, as well as spectroscopy of two galaxies near the quasar. We find that there is a galaxy centred approximately midway between the two A components. The properties of this galaxy are consistent with it being the brightest member of a small group at a group redshift of 0.305. Although detailed modelling is required, it is likely that the galaxy and its group are the lenses.

Previous imaging of PG1115+08 has been either by direct photography or speckle interferometry[2-6]; in all cases components B and C have been unresolved. Component A is resolved into two subcomponents (termed A_1 and A_2, north and south, respectively) separated by ~0.5 arc s at a position angle of ~20°. The intensity ratio is ~1. All observations have failed to detect a lens galaxy, which must be fainter than $V = 22$ (visual magnitude) or be ≤1 arc s from a component. Furthermore, there is no cluster in the field brighter than a Thuan-Gunn *r* magnitude of 25 (ref. 2). The only objects previously known to be near PG1115+08 are three galaxies 12-24 arc s to the south-west, whose redshifts have not been measured until now.

We made direct imaging observations of PG1115+08 on 9 April 1983 UT (Universal Time) at an airmass of between 1.02 and 1.07. These observations were obtained with an RCA C33063 image intensifier mounted behind a Barlow lens and a Schott GG 475 filter at the Cassegrain focus of the University of Hawaii 2.2-m telescope on Mauna Kea. This combination yielded a bandpass of ~4,750-6,000 Å and a scale of 4.1 arc s per mm. The data were recorded on a roll of IIa-O film which was mounted in a camera capable of taking many sequential exposures of specified length while automatically advancing the film. From a previous run we determined that 2 s was the minimum exposure time that would record the faintest (B) component. We obtained 285 2-s exposures, 105 3-s exposures and 230 10-s exposures. The sky was well exposed on the 10-s exposures. Only the 2-s exposures were used for imaging because the seeing was noticeably worse on the 3-s exposures.

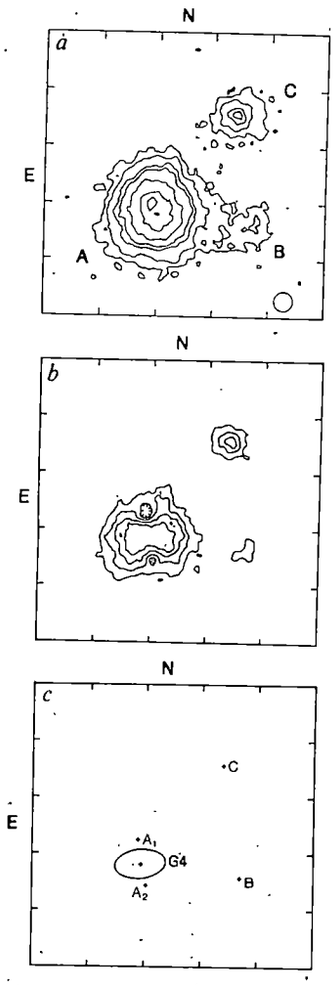


Fig. 1 Diagrams of the PG1115+08 field. The tick marks along the axes are at 1 arc s intervals. *a*, Contours of surface brightness in the 9 April 1983 summed image (see text for details). The contours are at 0.9, 0.8, 0.6, 0.4, 0.3, 0.15 and 0.07 of the peak. If component C did not vary during the one month between our observation and that of ref. 4 (our crude photometry verifies this assumption to 0.2 mag), then the peak surface brightness is $\mu_V = 16.8$ mag (arc s)$^{-2}$. The resolution of this image is shown by the circle at the lower right which indicates the FWHM; it is slightly larger than that of the raw data because of the light smoothing to attenuate the high-frequency noise. *b*, Contour diagram after subtracting the best-fitting point sources in the two point source + galaxy model. The contours are at 0.8, 0.6, 0.4 and 0.2 of the galaxy brightness peak, which, under the assumptions given in *a*, is $\mu_V = 17.1$ mag (arc s)$^{-2}$. Contours with tick marks indicate local minima in the surface brightness at the locations of the imperfectly subtracted point sources. *c*, Schematic diagram of the objects in the PG115+08 field. The outline of the galaxy (G4) is at one core radius.

We examined all the exposures and selected the best 19 for further analysis. These images were scanned on a PDS 1010A microdensitometer; the aperture used was 12 × 12 μm, scanned in 12-μm steps; that is, a pixel size of 0.049 arc s. The maximum density anywhere in the field was only 1.2 density units. The digitized images were then converted to intensities using a calibration curve derived from a step exposure through the image tube onto the same roll of film, developed at the same time as the imaging data. We determined the full width at half maximum (FWHM) of component C in each of these 19 images. The best five were co-aligned and summed to produce our final data set.

During times of extremely good seeing at Mauna Kea, the image consists of a tiny spot dancing within a circle of diameter

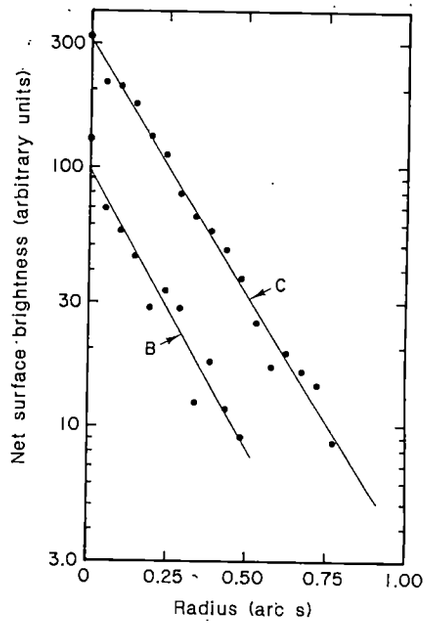


Fig. 2 Azimuthally averaged surface brightness of the B and C components.

~1 arc s; the above procedure was designed to remove the image jitter, leaving only the tiny spot. We show a contour diagram of the final image (slightly smoothed) in Fig. 1*a*.

Azimuthally-averaged profiles for components B and C are shown in Fig. 2. Fitting an exponential to the data yields a point spread function proportional to $\exp(-\theta/0.23 \text{ arc s})$ (C) and $\exp(-\theta/0.21 \text{ arc s})$ (B), implying FWHMs of 0.31 and 0.29 arc s, respectively. In what follows we adopt the point spread function determined from C because it has a higher signal-to-noise ratio. As the two point spread functions are virtually the same, it seems reasonable to assume that the same function will also be applicable to the region of component A. Although most previous descriptions of the seeing function have used a gaussian distribution, at least at small radii (see, for example, ref. 7), such a function does not fit our data, probably because we have eliminated the image motion. Integrating over such motion probably produces a gaussian point spread function by way of the central limit theorem.

The parameters of a nonlinear least-squares fit to a two-dimensional array of data around components B and C yielded the results given in Table 1, which also includes the results of previous measurements. The only significant difference is in the intensity (flux) ratios; in particular, there is a change in the ratio f_B/f_A on a timescale of a month between our data and those of ref. 4. Crude photometry, using the sky as a zero point, indicates that the B component weakened by ~0.5 mag during that time.

Figure 1*a* shows that A must be more complicated than the two equal-intensity point sources separated by 0.5 arc s detected previously. The intensity is approximately constant in an area 0.5 arc s in diameter at the peak, yet we should easily resolve the point sources if they were the only contributors to A. To quantify these statements, and also to better understand the structure of the A component, we have fitted a variety of models to our data. Our intensity data are unlikely to have a Poisson distribution, because of the nonlinearity of the photographic process; therefore, the usual goodness-of-fit tests cannot be used. Yet we need to know when to stop adding free parameters to the models. We adopt the following criterion, which seems reasonable, but is certainly not rigorous: A model for the A component will be considered acceptable if the root-mean-

Table 1 Parameters of PG1115+08B, C

Date	Sep(AB)* (arc s)	PA(AB)* (° E of N)	f_B/f_A†	Sep(AC)* (arc s)	PA(AC)* (° E of N)	f_C/f_A†	Ref.
9 April 1983	1.74 (5)‡	263 (1)	0.074 (5)	2.16 (5)	323 (1)	0.171 (6)	This work
7 March 1983	1.77 (2)	266 (2)	0.12 (2)	2.29 (3)	322.3 (8)	0.19 (2)	4
30 April 1981			0.12 (2)			0.17 (2)	4
17 June 1980	1.77 (3)	265.8 (7)	0.110 (6)	2.28 (2)	322.3 (4)	0.180 (4)	2
3 June 1980	1.9 (1)	263 (5)	0.113 (2)	2.4 (1)	317 (5)	0.174 (8)	3

* Separation (Sep) and position angle (PA) calibrated from those of star S given in ref. 2.
† The flux for component A (f_A) comes from the best-fitting two point+galaxy model described below. Other models change its value by about ±10%.
‡ Number in parentheses is the error in the last digit.

Table 2 Parameters of PG1115+08A

Model	Sep(A_1A_2) (arc s)	PA(A_1A_2) (° E of N)	f_{A1}/f_{A2}	a (arc s)	ϵ	PA(G4)* (° E of N)	Sep(A_1G4) (arc s)	PA(A_1G4) (° E of N)	f_{G4}/f_A	Residual (r.m.s.)
2 points	0.57 (5)†	20 (1)	1.04 (2)	—	—	—	—	—	—	84
2 points+galaxy	0.80 (5)	10 (1)	0.85 (5)	0.47 (1)	0.38 (2)	97 (1)	0.43 (5)	193 (1)	0.46 (2)	56

* The position angle of the galaxy (G4) is that of its semimajor axis.
† Number in parentheses is the error in the last digit.

square (r.m.s.) sum of residuals from it is of the order of the mean of the fluctuations in the A peak (72) and the background (30); that is, 50.

Table 2 contains the results of fits of two models to the A component data. As expected, a model containing just two point sources has unacceptably large residuals, although the best-fitting parameters are virtually identical to those given in refs 4-6. We then tried a model with two point sources and a galaxy. The galaxy was modelled as having an elliptical surface brightness of major axis a, and ellipticity $\epsilon = 1-$(minor axis/major axis). The surface brightness was assumed to fall off as $(1+r^2/a^2)^{-1}$ along the major axis and correspondingly at other position angles. This form accurately approximates a King[8] model in the core. Since the integrated surface brightness of this model diverges logarithmically, we give the light within the core when describing the galaxy brightness. Best-fitting parameters are given in Table 2. The residuals to this second model are acceptably small, although they do exhibit some systematic trends, such as the negative-going contours at the location of A_1 and A_2, shown in Fig. 1*b* (tick marks). A schematic diagram of the various objects in the field is shown in Fig. 1*c*, where the galaxy is labelled 'G4'.

Several tests can be made of the existence of G4. First, do other simple models substantially reduce the residuals? We have tried four additional models: three point sources, three point sources and a galaxy, and two 2 point+galaxy models with broader point spread functions (0.4 and 0.5 arc s). The lowest r.m.s. residual from these four models was 50 (3 points+galaxy). This reduction in the residuals is not large compared with that achieved by going from 2 points to 2 point+galaxy models, so we consider the latter to be a reasonble representation of the data. Second, will a broader point spread function eliminate the galaxy? We find that in order to decrease the galaxy intensity to near zero, it is necessary to increase the FWHM of the point response to 0.5 arc s, which certainly does not fit the data of B and C (see Fig. 2). Third, with a galaxy as bright as we claim, why was it not detected previously? We have better spatial resolution, which facilitates the detection, but in addition our observations were made when the quasar was significantly fainter (by 0.6 mag, according to ref. 4). From the fraction of galaxy light that we observe in the A component ($f_{G4}/f_A = 0.46$, Table 2), we calculate that the corresponding fraction was only 0.26 in 1980 and 1981. Fourth, why are the colours of A not redder than those of B or C? The best constraint is from ref. 2, which gives the $g-r$ of A as 0.05 ± 0.06 mag bluer than that of C. An Scd galaxy at a redshift of 0.3 (see below for this choice of redshift), contributing 26% of the total light of A (the measurements of ref. 2 weremade in 1980) would make A 0.09 mag redder than C in $g-r$. Similar contributions would arise from earlier type galaxies at smaller redshifts. We regard these colour data as the most stringent requirement that the putative galaxy must meet, but given the dispersion of ~0.1 mag in the colours of a galaxy as a function of its Hubble type, such a galaxy is not ruled out by existing data.

In addition to the fitting procedures described above, we have attempted to detect the imaging galaxy directly, by removing the effects of the seeing in the data using a nonlinear deconvolution procedure. The deconvolution procedure used was the Jansson-Van Cittert algorithm as described by Heasley[9]. The results of the deconvolution are shown in Fig. 3. Although A_1 and A_2 are resolved from each other for the first time, there is only a hint of structure aligned with the major axis of G4 (compare Fig. 1*c*). The emission between components A and B, visible in the raw data (Fig. 1*a*), remains after the deconvolution, possibly indicating yet another object.

We made spectroscopic observations of galaxies G1 and G2 (ref. 2) on 25 March 1985 UT with the Hawaii grism (grating/prism) spectrograph and Galileo/IFA CCD (charge-coupled device) mounted at the Cassegrain focus of the Canada-

Table 3 Rest-frame properties of G4 and M104

Galaxy	$\mu_V(0)$ (mag (arc s)$^{-2}$)	Core radius (kpc)	M_V	ϵ	Type
M104*	15.3	1.1†	−23.2	0.3	Sa
G4 ($z=0.3$, $q_0=0$)	15.2‡	$1.4/h$§	$-23.3+5\log_{10}h$‡§‖	0.4	?

M_V, absolute visual magnitude; q_0, deceleration parameter.
* All properties from ref. 13.
† Derived from a de-Vacouleurs-law effective radius of 14.2 kpc using core radius = effective radius/13.2 (ref. 14).
‡ Assuming the brightness of component C was unchanged from ref. 4 (our crude photometry using the sky as a zero point shows this assumption to be true to within 0.2 mag) and using a k-correction appropriate to an Sab galaxy of 0.76 mag.
§ Hubble constant $H_0 = 100\,h$.
‖ Core light only.

France-Hawaii Telescope. Exposures of 57 and 31 min were made of G1 and G2, respectively, through holes in thick clouds. The spectra are normal. Reshifts derived from spectral lines Ca II H, K, Hδ and G for G1 and the 4,000-Å break for G2 are 0.306 ± 0.002 and 0.304 ± 0.005, respectively. Thus these galaxies form a small group at redshift 0.3, which may also contain G3.

It is possible that G4 is the brightest member of this group. Table 3 lists the properties of G4 if it is at redshift $z = 0.3$ and compares those properties with those of M104, a massive spiral galaxy. From the simulations presented by Schweizer[10], the seeing corrections to the core radius and central surface brightness are ~20% if G4 follows a King model and the point spread function is gaussian. We have not applied these corrections to our data because our point spread function is not gaussian, and corrections of this order will not affect our conclusions. G4 and M104 are very similar. Of course, the redshift of G4 may not be the same as that of G1 and G2, but until a spectrum can be obtained, this is a reasonable assumption.

It is obvious that G4 will contribute substantially to the gravitational focusing. If it is the brightest member of the group, it is a massive galaxy. However, the rest of the group must also make some contribution. The only quantitative models[11] of the gravitational focusing explain PG1115+08 using a single flattened galaxy roughly equidistant from all four components, rather than midway between A_1 and A_2. However those models did not incorporate the galaxy group, so it is as yet unclear whether their combined effects can produce the observed configuration. A spectrum of G4 and additional lens modelling, particularly incorporating a possibly nonspherical group, are required for further progress.

After this paper was written we received a preprint from Shaklan and Hege[12] in which they report a flux excess above

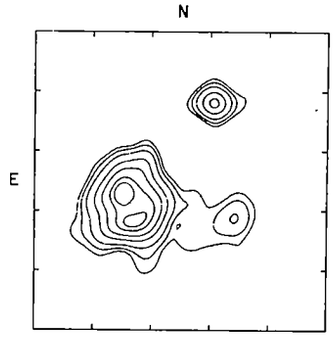


Fig. 3 Contour diagram of the PG1115+08 field after image deconvolution. The tick marks along the axes are at 1 arc s intervals. Contours are at 0.9, 0.8, 0.6, 0.4, 0.2, 0.1 and 0.05 of the peak.

that from the four usual components that is located at ~65% of the distance between A and B and closer to B. We can apparently confirm this report, (see Fig. 3), although our nominal brightness is greater by at least 1 mag. Our resolution of the component may explain the small value of f_B/f_A that we observe.

This research was supported in part by University of Hawaii Research and Training Fund grants to Alan Stockton to adapt the rapid-exposure film camera for use with the image intensifier, and to J.P.H. for observing expenses. We thank John MacKenty for writing the PDS scanning programs, and Robert Hlivak for keeping our CCD in good condition. J.P.H. was a Visiting Astronomer at the Canada-France-Hawaii Telescope, operated by Canadian NRC, the French CNRS and the University of Hawaii.

Received 9 December 1985; accepted 25 February 1986.

1. Weyman, R. J. *et al. Nature* **285**, 641-643 (1980).
2. Young, P. *et al. Astrophys. J.* **244**, 723-735 (1981).
3. Hege, E. K., Angel, R. P., Weyman, R. J. & Hubbard, E. N. *Nature* **287**, 416-417 (1980).
4. Vanderriest, C. *et al.* in *Quasars and Gravitational Lenses, Proc. 24th Liege astrophys. Colloq.* (1983).
5. Hege, E. K., Hubbard, E. N., Strittmater, P. A. & Worden, S. P. *Astrophys. J. Lett.* **248**, L1-L3 (1981).
6. *Foy, R., Bonneau, D. & Blazit, A. Astr. Astrophys.* **149**, L13-L16 (1985).
7. King, I. R. *Publs astr. Soc. Pacif.* **83**, 199-201 (1971).
8. King, I. R. *Astr. J.* **71**, 64-75 (1966).
9. Heasley, J. N. *Publs. astr. Soc. Pacif.* **96**, 767-772 (1985).
10. Schweizer, F. *Astrophys. J.* **233**, 23-34 (1979).
11. Narasimha, D., Subramanian, K. & Chitre, S. M. *Mon. Not. R. astr. Soc.* **200**, 941-950 (1982).
12. Shaklan & Hege, E. K. Preprint no. 609, Steward Observatory, Tucson, Arizona.
13. Boroson, T. *Astrophys. J. Suppl. Ser.* **46**, 177-209 (1981).
14. Kormedy, J. *Astrophys. J.* **218**, 333-346 (1977).

An apparent gravitational lens with an image separation of 2.6 arc min

Edwin L. Turner*, Donald P. Schneider†, Bernard F. Burke‡, Jacqueline N. Hewitt‡, Glen I. Langston‡, James E. Gunn*, Charles R. Lawrence§ & Maarten Schmidt§

* Princeton University Observatory, Princeton, New Jersey 08544, USA
† Institute for Advanced Study, Princeton, New Jersey 08540, USA
‡ Department of Physics, Massachusetts Institute of Technology, Cambridge, Massachusetts 02139, USA
§ Department of Astronomy, California Institute of Technology, Pasadena, California 91125, USA

We report here observations which confirm Paczynski's speculation[1] that the previously known[2] pair of 19th magnitude quasars 1146+111B,C are actually two images of a single object produced by a gravitational lens. The image splitting is 157 arc s, more than 20 times greater than any previously reported[3], thus indicating an exceptionally massive lensing object. The data supporting the lens hypothesis are remarkably similar, high signal-to-noise, moderate-resolution spectra of the two components. Both spectra show strong Mg II λ2,798 emission at $z = 1.012 \pm 0.001$ with indistinguishable redshifts ($\Delta v = 126 \pm 309$ km s^{-1}), widths (FWHM = 64 ± 4 Å) and detailed profile shapes. Both spectra also show broad troughs at λ6,180 and several weaker continuum features. Neither object exhibits the [O II] λ3,727 line which is frequently strong in Mg II emission objects. If the foreground galaxy clustering apparent in a deep R band charge-coupled device (CCD) image proves insufficient to explain the large image splitting, other possibilities such as massive dark objects (for example, a ~10^{15} $M_\odot$ black hole) or a cosmic string may be indicated.

In 1979, Hazard *et al.*[4] reported a 'concentration' of quasars in a field at $\alpha = 11$ h 46 min 14 s and $\delta = 11°11'42''$ (1950). Subsequently, Arp and Hazard[2] gave redshifts based on slit spectra for nine confirmed quasars in the field. Among these, two quasars (B and C) were determined to have redshifts of 1.01, equal within their measuring errors. Arp and Hazard[2] dismissed the possibility that these were a pair of gravitational lens images on the grounds of an implausibly large image separation. Recently, Paczynski[1] again called attention to this system along with four others as possible examples of large splitting gravitational lenses and noted that such systems might result from an intervening cosmic string[5,6].

We obtained spectra of 1146+111B and C on the night of 5 March 1986 UT with the Cryogenic Camera[7] and the R-C spectrograph on the Kitt Peak National Observatory 4-m telescope of the National Optical Astronomy Observatories (NOAO). A 2.5 arc s × 4.4 arc min slit was used to illuminate a 300-line per millimetre grism (grating/prism). An 800 × 800 TI CCD camera recorded the first-order spectra through a GG420 filter giving 15 Å resolution in the λλ4,600-7,800 range with a 4.3-Å per pixel sampling. Two 1,800-s exposures of each object

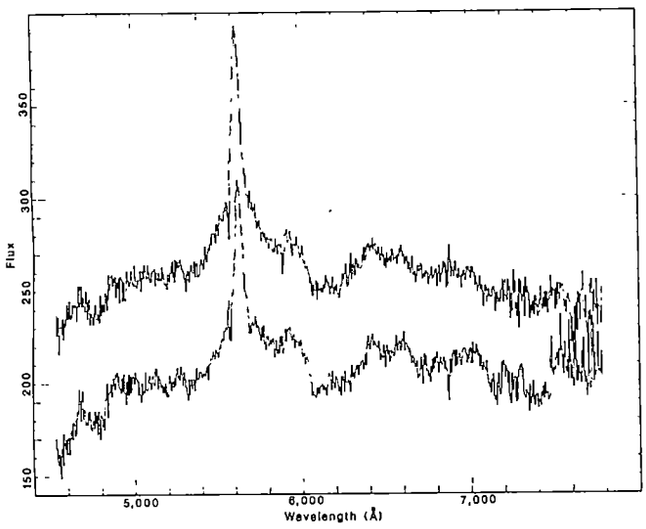


Fig. 1 The spectra of 1146+111B and C. The vertical axis is a linear flux scale in arbitrary units. The upper spectrum is of object B; the lower, of object C (70 counts per channel were added to B to displace it from C). The identification of the strong emission feature as Mg II λ2,798 is primarily based on Arp and Hazard's[2] detection of C III λ1,909. Note the correspondence of the emission feature, the deep trough, and several weaker continuum dips and bumps in the two spectra.

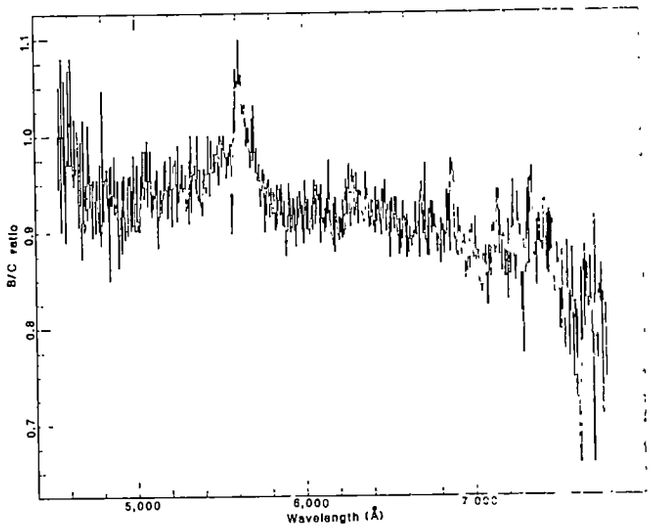


Fig. 2 The ratio of the spectrum of 1146+111B to that of 1146+111C. The feature in this ratio at the wavelength of the Mg II emission indicates that the line-to-continuum ratio in the two objects is slightly different. The smooth variation in the ratio from blue to red indicates that C has a redder detected continuum than B. The absence of other significant features in this ratio demonstrates the detailed match in shape and amplitude between respective emission and absorption features in the two spectra.

were obtained along with interspersed quartz lamp flat fields and He-Ne-Ar comparison arcs. A spectrum of the flux calibrator GD 140 was also obtained to remove the instrumental response function and atmospheric absorption bands. The data frames were reduced individually using the CASSANDRA image processing package and the resulting spectra of each object were then combined. They are shown in Fig. 1.

These two spectra agree precisely in their significant features. Figure 2 gives the ratio B/C of the two spectra. The Mg II line ratio is ~1.02 while the continuum ratio varies from roughly 0.96 at the blue end to around 0.83 at the red end. These small variations do not mitigate against a lens interpretation as similar small differences in line strengths and continuum slopes are observed in such confirmed lens cases as 0957+561 (ref. 8) and 2016+112 (ref. 9). They may be accounted for by a variety of explanations including source variability plus differential time delays, gravitational mini-lensing events[10], extinction by intervening material, contamination of the source spectrum by light from the lens, and systematic observational errors resulting from differential refraction effects. Overall, the spectroscopic similarity of 1146+111B and C is as strong as for any of the known (few arc second separation) lens systems.

On 7 March 1986 UT we obtained six direct images of the 1146+111B, C field, each exposed for 300 s using the TI2 CCD camera at the prime focus of the same telescope. The average of these six images is shown in Fig. 3. Profile fits to stellar images indicate a FWHM seeing of 1.2 arc s. Although accurate calibration of this image was not attempted due to non-photometric observing conditions, we believe that it reaches 23rd to 24th magnitude in the R band.

Analysis of this image shows: (1) an image separation of 156.8±0.5 arc s, (2) an R-band B/C brightness ratio of 0.93± 0.01; (3) a possible very distant rich cluster of galaxies between the two quasar images; and (4) an unusual number of fairly bright ($R \sim 18$ to 19), apparently low redshift ($z \lesssim 0.2$) galaxies in the field including one roughly between B and C. The quasar images themselves show no signs of resolution.

The importance of 1146+111B, C lies in its unprecedented large image separation and the questions and possibilities thus raised.

The first question is that of the nature of the lensing object. The most conventional candidate would be a very massive rich cluster of galaxies. If such a cluster lay at the most probable redshift of 0.32 and had an isothermal sphere mass distribution, the required one-dimensional velocity dispersion would lie near 2,200 km s^{-1} (depending weakly on q_0). If the cluster instead lay at a redshift of 0.81, which would minimize (for a constant M/L value) its visibility (assuming an elliptical galaxy k correction[11]), the requirement would be ~4,500 km s^{-1}. The former value is extreme but not entirely beyond the observed range for rich clusters[12]. Nevertheless, such a cluster would be easily detectable in deep CCD images at any redshift less than 1, so this candidate lens is subject to direct observational test. If no suitable rich cluster can be located, more exotic possibilities such as $\sim 10^{15}\ M_\odot$ black holes and cosmic strings will need to be considered. Indeed, lens systems much like 1146+111B, C are a predicted consequence of cosmic strings[1,5,6]. Of course, the possibility of a physically distinct (not lensed) pair of objects with astonishingly similar spectroscopic properties is not logically excluded by the data.

Second is the possibility that additional objects in the 1146+111 field may be multiply imaged. The large angular splitting of the B, C pair implies a large multiple imaging cross-section for most reasonable lens scenarios. Some of the other known[2] quasars in the field could well have additional, so far undetected images; D, E and K are particularly likely candidates. Even if they are not multiply imaged, lens magnification and hence flux enhancement could account for the statistically unlikely 'concentration' of quasars which originally called attention to the field. In any case, discovery of additional multiply-imaged objects would offer the opportunity to model the lens mass distribution more precisely than for other known lenses and, should this distribution prove simple, to carry out powerful cosmological tests.

Third is the large differential time delay expected for large splitting image pairs. For reasonable lens models, the 1146+111B, C time delay is of the order of 10^3 years. This offers the opportunity of observing variations in the lensed object(s) taking place over time periods well in excess of those usually accessible. If the lensing geometry is highly symmetrical, as the roughly

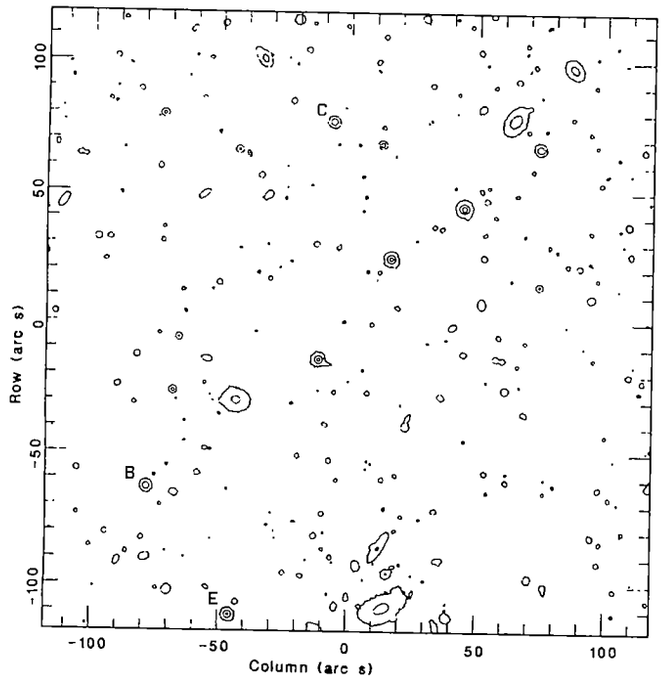


Fig. 3 A contour diagram of the R-band CCD frame of the 1146+111 field. North is at the top, east at the left. The image is 4 arc min on a side. The first contour level is 2.5 times the r.m.s. sky noise with additional contours at 3-magnitude intervals. Dots corresponding to single high pixels are probably noise in many cases; however, larger objects are likely to be real. It is estimated that the faintest objects visible are between 23rd and 24th *R* magnitude. Object B is at column, row coordinates −77.4 arc s, −61.9 arc s while object C is at −6.0 arc s, 77.7 arc s. Note that there are several bright galaxies scattered across the frame including one at −42.5 arc s, −28.7 arc s (roughly between B and C) and a concentration near the centre of the south edge of the field. Also note the arc of faint galaxies, possibly a distant cluster, extending from about −5 arc s, 26 arc s towards −74 arc s, −10 arc s.

equal brightnesses of B and C might suggest, the time delay will be substantially smaller than this 'natural' value.

1146+111B, C and the surrounding field warrant further study, and some attempts in this direction are under way. Verification of the spectral similarity of B and C at other wavelengths and searches for additional, multiply-imaged objects are of particular interest. Other candidate large splitting lenses should also be examined more carefully.

We thank B. Paczynski for a preprint and for discussions, the Kitt Peak staff for assistance with the observations and J. Ostriker for useful comments on the manuscript. D.P.S. acknowledges the support of an Exxon Fellowship. This work was supported by NSF grants AST84-20352 and AST83-14134 and NASA grants NAGW-765 and NAS5-29225. The NOAO is operated by the Association of Universities for Research in Astronomy, Inc., under contract with the NSF.

Received 24 March; accepted 10 April 1986.

1. Paczynski, B. *Nature* **319**, 567–568 (1986).
2. Arp, H. & Hazard, C. *Astrophys. J.* **240**, 726–736 (1980).
3. Turner, E. L. *IAU Symp.* No. 117, 209–218 (1986).
4. Hazard, C., Arp, H. & Morton, D. C. *Nature* **282**, 271–272 (1979).
5. Vilenkin, A. *Astrophys. J. Lett.* **282**, L51–L53 (1984).
6. Gott, J. R. *Astrophys. J.* **288**, 422–427 (1985).
7. DeVeney, J. *An Observer's Manual for the Cryogenic Camera* (Kitt Peak National Observatory, Tucson, 1985).
8. Young, P., Gunn, J. E., Kristian, J., Oke, J. B. & Westphal, J. A. *Astrophys. J.* **241**, 507–520 (1980).
9. Lawrence, C. R. *et al. Science* **223**, 46–49 (1984).
10. Paczynski, B. *Astrophys. J.* **301**, 503–516 (1986).
11. Schneider, D. P., Gunn, J. E. & Hoessel, J. G. *Astrophys. J.* **264**, 337–355 (1983).
12. Mushotzky, R. F., Serlemitsos, P. J., Smith, B. W., Boldt, E. A. & Holt, S. S. *Astrophys. J.* **225**, 21–39 (1978).

Structures in the coma of comet Halley

E. Grün*, U. Graser†, L. Kohoutek‡, U. Thiele§, L. Massonne*‖ & G. Schwehm¶

* Max-Planck-Institut für Kernphysik, D-6900 Heidelberg 1, FRG
† Max-Planck-Institut für Astronomie, D-6900 Heidelberg-Königstuhl, FRG
‡ Hamburger Sternwarte, Gojenbergsweg 112, D-2050 Hamburg 80, FRG
§ German–Spanish Astronomical Center, Calar Alto, Apartado Correos 511, 04080 Almeria, Spain
‖ ESOC/ECD, Robert-Bosch-Str. 5, D-6100 Darmstadt, FRG
¶ ESTEC/SSD, Postbox 299, 2200 AG Noordwijk, The Netherlands

Dense dust jets are expected to be encountered by the spacecraft penetrating the coma of comet Halley in March 1986. At the time of encounters, remote observations of the global distribution of coma constituents will complement the detailed *in situ* measurements. Here we report ground-based measurements of the optical brightness distribution of the coma, made in November 1985, when the comet was at a distance of 1.75 AU from the Sun. From the total brightness we deduce a dust production rate of 1.5×10^6 g s^{-1}, but our results show that cometary dust and gas production, which seem to be correlated, are strongly anisotropic and time-variable. Structures in the coma can be revealed by comparison with a physical model of the coma, but astrometry of the comet nucleus is adversely affected by the anisotropic brightness distribution in the coma.

The coma morphology and dust emission pattern of comet Halley, as revealed on photographic plates taken during the 1910 apparition[1], have been used to determine the nucleus spin vector[2]. A verification of this result and the location of active regions on the nucleus is important for the space probe missions Giotto[3] and Vega[4] currently approaching the comet. An efficient computational method has been developed[5] to analyse images of the coma and to model the dust distribution in it. Repeated observations of coma structures are necessary to determine the rotational state of the nucleus and the distribution of active regions on it.

The observations were performed using the 80-cm Schmidt telescope and the 2.2-m telescope at the German–Spanish Astronomical Center at Calar Alto, Spain. Sixteen Schmidt plates were taken during the period 9–21 November 1985, in order to study the brightness distribution of the outer coma. The following emulsion–filter combinations were used: Kodak IIIa-J plus Schott UG1 or GG495, IIIa-F plus RG610, or 103a-E without filter.

A large, curved, jet-like structure extending 21 arc min to the south of the cometary nucleus was photographed on two plates on the night of 12/13 November; the U-plate image is shown in Fig. 1. The observed structure was nearly perpendicular to the projected antisolar direction; although the projection angle is unknown, this deviation seems too large to be only a projection effect. The brighter inner part of the jet (visible on Fig. 1) is narrow and consists of three 'beams'; its wide and faint outer part looks like a fan. The U-plate (IIIa-J+UG1) has shown that this ejection very probably contained not only dust particles but also CN molecules. Jockers[6] observed a southward-pointing ion tail (CO^+) during the same night: it is thus highly likely that ion emissions contribute to the total brightness observed by us. The coma photographed 3 days earlier was symmetrical, and had a diameter of ~10 arc min (at the isophote level corresponding to the sky background). In addition to the jet, some radial rays are visible on the U-plate at the west side of the coma. On 18.0 November the outer coma appeared symmetrical again, but had expanded to ~15 arc min. In addition to the increase of the cometary brightness due to its decreasing distance from both the Earth and the Sun, the activity observed on 12/13 November

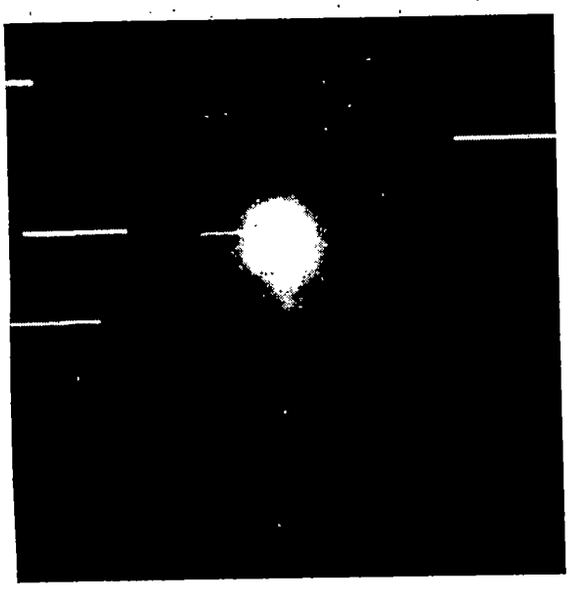


Fig. 1 Jet structure of the coma of comet Halley, observed on 13.0 November 1985 UT (Universal Time) with the 80-cm Schmidt telescope at Calar Alto. The 50-min exposure was taken on Kodak IIIa-J emulsion through a UG1 filter. The field of view is 20 × 20 arc min; north is up, east is left.



Fig. 2 Isophote representation of a CCD image taken with the 2.2-m telescope at Calar Alto on 12.9 November 1985 UT. A continuum filter at 703 nm was used. The field of view is 2 × 2 arc min; north is up, east is left.

probably increased the total brightness of the comet during the subsequent days. On plates taken on 21.0 November two jets are visible to the east (position angles 63° and 90°; the latter is the tail direction), at a distance of ~9 arc min from the nucleus.

More than 100 CCD (charge-coupled device) images have been taken with the 2.2-m telescope. The detector used was a thinned, backside-illuminated RCA CCD (type SID 510-EX), with 512 × 320 pixels. The pixel size is 30 × 30 μm, which corresponds to 0.35 arc s at the Cassegrain focus. The filters used were Johnson R, V and B and the IHW filters at 703 nm ($\Delta\lambda = 22$ nm), 684 nm ($\Delta\lambda = 9$ nm), 514 nm ($\Delta\lambda = 10$ nm) and 485 nm ($\Delta\lambda = 6$ nm). The filter at 514 nm covers a major C_2 emission; the other narrow ones are continuum filters.

Optimum pre-perihelion observation conditions (small zenith distance, large brightness and long observation intervals from a single site) occurred in November 1985. During this time the comet was ~0.7 AU from the Earth, in approximately the anti-solar direction. The comet was close to its ascending node. The required high offset speed of up to 400 arc s h^{-1} was achieved with an accuracy of better than 3 arc s h^{-1}. The exposure times to reach near-saturation in the centre ranged from 15 to 1,000 s for the wide-band and narrow-band filters, respectively.

Figure 2 shows an isophote representation of a CCD image of the coma. The image was taken on 12.9 November. The outer part of the image is elongated towards the south, whereas the centre part is more symmetrical. An image taken ~3.5 h after that shown in Fig. 2 shows that the direction of strongest emission had shifted by 10° to position angle 190°. A similar shift was observed for the jet seen on the Schmidt plates which were taken at about the same times.

To determine photometric magnitudes for Halley's central coma, a set of standard star measurements were taken in the same (photometric) night (~12 stars per waveband with magnitudes between 8.8 and 17. The sky background (per pixel and second) in the Halley frames was determined by averaging the background of three field exposures taken at about the same zenith distance, shortly before or after the respective Halley exposure. Coma magnitudes were measured by flux integration in circles of 10 and 30 arc s diameter around the brightness maximum. The measured values are $B = 12.6$ and 11.3, $V = 11.6$ and 10.4 and $R = 11.4$ and 10.2, respectively. A conservative estimate of the root-mean-square deviation of one observation is ±0.1 mag. The magnitudes were measured on 13.1 November.

Assuming that most of the coma brightness in R can be attributed to sunlight scattered by dust, one can derive the dust production rate. For the measured brightness in R of 11.4 mag we find a mean dust production rate of $\sim 1.5 \times 10^6$ g s^{-1}. We adopt an effective geometric albedo of 0.03, a grain size distribution with an exponent −4.2 in the coma and the effective emission velocity of 150 m s^{-1} according to the standard Halley model parameters proposed by Newburn and Reinhard[7]. Note, however, that the uncertainties in the assumed parameters result in an uncertainty of a factor of ~2 in the production rate.

Taking an average dust-to-gas ratio of 0.3 and a mean molecular mass of 22.3 AMU (ref. 7) we derive a gas production rate of $\sim 1.3 \times 10^{29}$ molecules s^{-1}. This is ~3 times higher than the value predicted by Newburn[8] on the basis of 1910 Halley observations and recent cometary models.

Figure 3 shows radial and azimuthal brightness profiles of the Halley coma. The radial brightness profiles at different wavelengths were obtained by averaging the surface brightness around concentric circles centred on the brightness maximum. Inside $\rho \simeq 5$ arc s (ρ being the distance from the centre) the brightness first rises more steeply than the average increase, then flattens off at $\rho < 3$ arc s. This inner part of the coma represents the seeing disk of the central brightness peak. During the observation period the seeing ranged from 2 to 5 arc s. Outside this radius the coma brightness in the continuum wavelengths decreases roughly as $1/\rho$, as would be expected from a steady stream of particles emitted isotropically at constant speed from the surface of the nucleus. In the outer part of the brightness profile, the effect of the constant sky background is recognized. The radial profiles of the C_2 brightness fall off as $\rho^{-\gamma}$, $\gamma = 0.6$–0.75. This is in good agreement with the C_2 scale length calculated for the inner coma region[9].

The azimuthal brightness profile at continuum wavelengths (Fig. 3*b*) shows deviations of up to 30% from the mean brightness at a given distance from the centre. The C_2 brightness varies azimuthally in the same way, with a smaller amplitude.

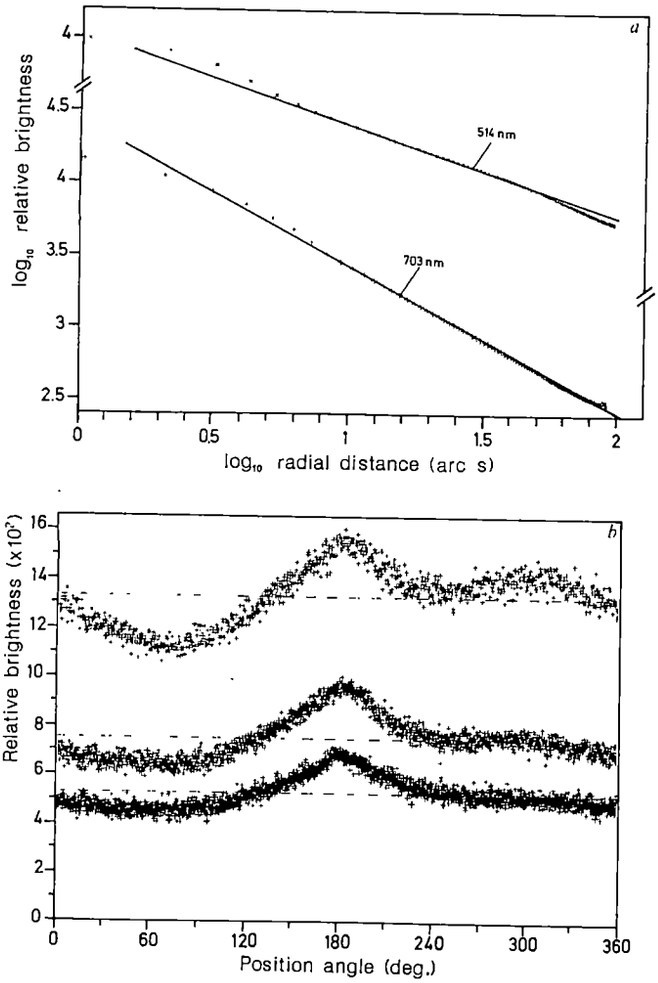


Fig. 3 Brightness profiles of CCD images of the Halley coma, taken on 12.9 November 1985 UT. *a*, Radial profiles of the continuum brightness (703 nm) and C_2 brightness (514 nm). The solid lines have slopes of −1.0 and −0.63, respectively. *b*, Azimuthal profiles of the brightness at 703 nm at radial distances of 21, 37 and 53 arc s from the brightness centre. The dashed lines represent mean brightness values at these distances.

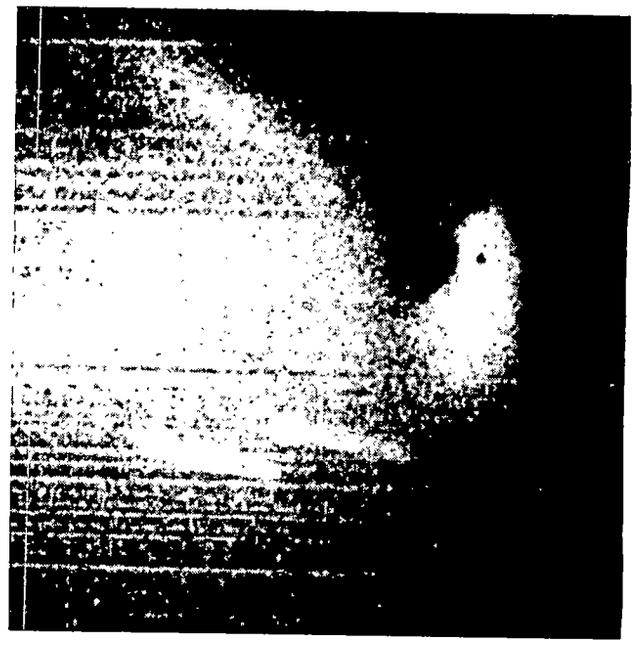


Fig. 4 Jets in Halley's inner dust coma on 21.1 November 1985 UT. This picture (at 703 nm) was obtained by normalizing the observed brightness distribution to the distribution which would be expected for an isotropically expanding coma. The centre of the original brightness distribution is marked by a dark spot in the right-hand part of the image. A major jet can be seen to the south, which bends over to the east. Another jet is visible at position angle 63°. Two star trails can be recognized in the lower part of the image. The east-west striation originates from a defect in the CCD, which could not be corrected for in all portions of the picture. The field of view is 2×2 arc min; north is up, east is left.

The strong overall radial brightness gradient hinders the recognition of local variations in brightness. To enhance the visibility of local inhomogeneities, and hence the variations in dust density, we have compared the images with a simple physical model of the dust coma. After subtraction of a constant background level the images were normalized to a $1/\rho$ brightness distribution centred on the apparent nucleus. Thus, the seeing disk is represented by a low-intensity central part and a bright ring around it. Outside this artefact the brightness distribution represents the deviation from an isotropic expanding dust emission. These deviations are due to non-isotropic emissions and bending of trajectories caused by dynamical effects. A similar method can be used to show structures in the gas coma.

Figure 4 shows a processed image, taken on 21.1 November. It also shows the main dust emission from the nucleus in the southerly direction. This time, however, it bends over to the east, which is the general tail direction. The enhancement of the outer coma in the easterly direction became increasingly dominant during the latter part of the observation period. At position angle 63°, a narrow jet is visible which continues for several arc minutes and has been simultaneously observed on Schmidt plates as described above.

We have found several independent indications that enhancements in the inner dust coma are correlated with enhancements in the gas coma, as well as with jets and perhaps even ion tails outside the coma. This observation indicates that the interaction between dust and gas, and perhaps ions, is more complicated than previously expected.

On nearly all images taken with continuum filters, a prominent emission feature is visible within ~10° of south. This feature shows no periodic orientation changes, such as are generally expected from an active area on a rotating nucleus. We suggest, therefore, that it is caused by increased gas and dust emission at the constantly sunlit rotational pole of the nucleus. Each observation then defines a plane in which the spin vector must be located. All of these planes should intersect in a common line, which is the spin vector. For three representative observations on 12/13 November and three others on 20/21 November these planes have been computed. Their common spin vector lies in the region $\phi = 0$–10° and $I = 30$–55°, following the notation of Sekanina and Larson[2]. This differs by ~40° from the direction recently proposed by Sekanina[10] on the basis of 1910 observations.

The anisotropic brightness distribution of the coma affects the determination of the nucleus position. On some images we have observed elongated seeing disks, suggesting that the deviation of the brightness centre from the nucleus position may be as large as one-third of the mean seeing-disk radius. Local dust density enhancements by about two orders of magnitude—as required to produce visible structures, according to jet simulations[5]—are also expected to occur during the space probe encounters with the comet. The observations cannot tell us whether hazardous large particles (>1 mg) are entrained in the jets, because the observed brightness is mainly due to 1–10-μm-sized particles for all reasonable size distributions.

Remote ground-based observations of the coma, similar to

those presented here, will be of great value during the spacecraft encounters with comet Halley. The remote coma observations will determine the overall structure, while *in situ* measurements provide the absolute calibration.

We thank T. A. Morley, ESOC, for providing exact Halley ephemeris data. E.G. and L.K. are visiting astronomers, German-Spanish Astronomical Center, Calar Alto, operated by the Max-Planck-Institut für Astronomie jointly with the Spanish National Commission for Astronomy.

Received 13 January; accepted 10 March 1986.

1. Larson, S. M. & Sekanina, Z. *Astr. J.* **89**, 571–578 (1984).
2. Sekanina, Z. & Larson, S. M. *Astr. J.* **89**, 1408–1425 (1984).
3. Reinhard, R. *Adv. Space Res.* **2**, 97–107 (1983).
4. Sagdeev, R. Z. *et al. Adv. Space Res.* **2**, 83–90 (1983).
5. Massonne, L., Fertig, J., Grün, E. & Schwehm, G. in *Asteroids, Comets, Meteors* II (eds Lagerkvist, C.-I., Lindblad, B. A., Lundstedt, H. & Rickman, H.), 407–410 (in the press).
6. Jockers, K. & Geyer, E. H. *The ESO Messenger* No. 42, 9 (1985).
7. Newburn, R. L. & Reinhard, R. *Eur. Space Ag. spec. Publ.* SP-174, 19–24 (1981).
8. Newburn, R. L. *ESA Eur. Space Ag. Spec. Publ.* SP-174, 3–18 (1981).
9. Cochran, A. L. *Astr. J.* **90**, 2609–2614 (1985).
10. Sekanina, Z. *IAU Circ.* No. 4151 (1985).

Nitrogen dioxide emitted from space shuttle surfaces and shuttle glow

Ulf von Zahn* & Edmond Murad†

* Physikalisches Institut, Universität Bonn, 5300 Bonn 1, FRG
† Air Force Geophysics Laboratory, Hanscom AFB, Massachusetts 01731, USA

Photographs taken on early space shuttle flights have indicated the presence of a surface glow in the ram direction[1]. Examination of airglow data from the AE and DE satellites has shown the presence of a similar glow[2], suggesting that the phenomenon is general to spacecraft in low Earth orbit, with the emission being concentrated in the ram direction. Several explanations have been offered for the glow: (1) OH formed by surface reactions of fast O atoms[3]; (2) plasma discharge mechanism[4]; (3) surface-induced decomposition of N_2 followed by recombination into an excited state[5]; (4) surface emission by impact of O_2 and O (ref. 6); and (5) near-continuum emission (at a resolution of ~3.4 nm) in the region 400–800 nm from electronically excited NO_2 (ref. 7). With reference to the last hypothesis we discuss here data on the number density of NO_2 measured inside the payload bay of the shuttle orbiter. We also derive fluxes of NO_2 near shuttle surfaces. Our data are shown to be consistent with the hypothesis of the glow being caused by NO_2 emission.

Number densities of NO_2, $[NO_2]$, were measured with a neutral mass spectrometer aboard flight 41-B of the space shuttle. The instrument and its performance have been described in detail by Wulf and von Zahn[8]. The instrument was mounted near the middle of the payload bay. The data discussed here were obtained at the beginning of day 6 of the mission, when the ion source opening was pointing towards the pressure bulkhead of the astronaut cabin. Figure 1 shows the motion of the orbiter and the position of the mass spectrometer sampling orifice. Incoming ambient species bombarded the cabin bulkhead directly; however, the mass spectrometer observed only species reflected or desorbed from the shuttle surfaces, mostly from the pressure bulkhead. The orbiter maintained the attitude shown in Fig. 1 for 11 min, enough time for the signals measured in the mass spectrometer to reach a steady state. The following data were obtained at the end of this period at 290 km altitude and 27° latitude, near 03:45 LT (Local Time). $[NO_2]$ is derived

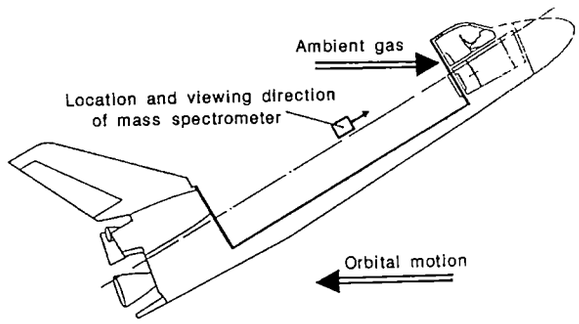


Fig. 1 Observational geometry for measurement of NO_2 density in the payload bay of the shuttle orbiter. The ambient gas strikes the orbiter surfaces with a velocity of 7.3 km s^{-1}, but the ion source of the mass spectrometer receives only species reflected or desorbed from orbiter surfaces.

from the peak at 46 AMU in the mass spectrum, after correcting for the contribution by $^{12}C^{16}O^{18}O$ (heavy CO_2), deduced from the peak at 44 AMU. We find that 43% of the observed 46 AMU peak is due to heavy CO_2. The remaining 57% we assign to NO_2 (the contribution of monomethylhydrazin to the mass 46 peak is considered to be negligible, mainly because of the strong dependence of the observed mass 46 peak on the angle of attack). To derive an absolute value for $[NO_2]$, we use the absolute sensitivity of the mass spectrometer for CO_2, as calibrated in the laboratory, multiplied by the ratio of cross-sections for electron impact ionization of NO_2 and CO_2 (refs 9, 10). This yields the NO_2 density inside the ion source of the mass spectrometer, $[NO_2]_s = (2.7 \pm 1.0) \times 10^7$ cm^{-3}. With an ion source temperature of 315 K, the flux $\Phi(NO_2)_O$ out of the ion source opening becomes $(2.5 \pm 1) \times 10^{11}$ cm^{-2} s^{-1}. The error bars reflect our estimate of an upper bound for potential contributions to the mass 46 peak from gases other than NO_2 and CO_2.

In the presumed steady-state conditions, the flux into the ion source, $\Phi(NO_2)_i$, equals the flux out of it, $\Phi(NO_2)_O$. Because of the observation geometry, $\phi(NO_2)_i$ is only ~40% of $\phi(NO_2)_b$, the flux leaving the cabin bulkhead; hence, $\Phi(NO_2)_b \simeq (6 \pm 3) \times 10^{11}$ cm^{-2} s^{-1}.

To relate this flux to a density $[NO_2]_b$ near the bulkhead we consider two extremes which have been suggested by other studies of the shuttle glow. First, NO_2 desorbs from the bulkhead with the mean thermal velocity(0.37 km s^{-1}). This results in $[NO_2]_b = 6 \times 10^7$ cm^{-3}. Second, NO_2 desorbs with a velocity of 2.5 km s^{-1} (corresponding to a kinetic energy of 1.5 eV), as suggested by Swenson *et al.*[7], based on a calculated *e*-folding distance of 20 cm (ref. 11) for the shuttle glow and a radiative lifetime of NO_2* of 80 μs (ref. 12). This velocity would lead to a considerable thermal accommodation factor for $[NO_2]$ inside the ion source, and for these circumstances $[NO_2]_b \simeq 1 \times 10^7$ cm^{-3}.

We now consider the requirements of the shuttle glow intensities, assuming that the glow arises solely from NO_2 as suggested by Swenson *et al.*[7]. The most recent estimate of the glow intensity is 10–100 kR (1R = 10^6 photons cm^{-2} s^{-1}), viewed normal to the surface[13]. This translates into a flux of excited NO_2, $\Phi(NO_2^*)$, of 10^{10}–10^{11} molecules cm^{-2} s^{-1}. The surface above which this glow is calculated consists of the shuttle tiles, which are made of silica fibres doped with a variety of materials[14]. On the other hand, a large part of the NO_2 observed by our mass spectrometer originates from the bulkhead surfaces, which are covered by Teflon-coated glass[15]. Mende and Swenson[13] reported a study of the relative glow intensities of different materials aboard shuttle mission 41-D at ~300 km altitude. Their study indicated that the glow intensity was weakest above a polyethylene sample and brightest above a material designated Z302, overcoated with silicon. If this latter material is close to that of the shuttle tiles, one would have to

draw the conclusion that the NO_2 flux close to the shuttle tiles is considerably enhanced over that near the bulkhead. Assuming that the conditions for the two flights are the same (mass spectrometer data from flight 41-B and glow data from flight 41-D), and that the glow intensity of the shuttle tiles is the same as that of Si-coated Z302, we deduce that $\Phi(NO_2^*)/\Phi(NO_2) \simeq 0.01$–$0.1$. Thus the mass spectrometer data indicate that NO_2 desorbed from the surface is present in sufficient amount to further consider NO_2 a viable candidate for causing the glow.

To pursue this analysis, let us assume that NO is present on the surfaces of the space shuttle (from the ambient, from surface reaction between N and O (ref. 16), from chemical reaction of fast O with the shuttle materials, or from contamination caused by attitude thruster firings[8]), and that O atoms striking the surface recombine with the adsorbed NO to yield NO_2^*:

$$\text{NO (adsorbed)} + \text{O (fast)} \rightarrow \text{NO}_2^* \text{ (fast)} \quad (1)$$

This is an example of the Eley-Rideal mechanism in catalysis (see ref. 17 for a discussion of this and the Langmuir-Hinshelwood mechanism). In this mechanism, the desorbed molecule is expected to carry the evolved heat of the reaction as rotational, vibrational, electronic or kinetic energy (or a mix of all these). A summary of work relevant to the shuttle glow problem is given in ref. 18. For the case under discussion, reaction (1), the excess energy is enormous: kinetic energy of O (4.5 eV, corresponding to a velocity of 7.3 km s^{-1}) + D_O(NO-O) (3.1 eV), or a total of 7.6 eV. The short wavelength cutoff of the glow is ~430 nm (ref. 7), corresponding to 2.9 eV in the form of electronic excitation. If the desorbed NO_2^* has a kinetic energy of 1.5 eV, as has been suggested[13], then the remainder (3.2 eV, or ~40% of the excess energy) must be partitioned between vibrational/rotational excitation of NO_2 and surface deposition of the excess energy. Results from beam experiments[18] and theoretical calculations[19] indicate that the amount of energy deposited into the surface is quite small. For example, in a theoretical study of the reaction of O with adsorbed carbon on platinum at 0 and 500 K, it was found that >90% of the energy released in the reaction appears in the product, CO. If the case of $O + NO_{ads}$ is analogous, then most of the remaining energy would appear in vibrational/rotational excitation of NO_2 (~2.8 eV); ~5% of the excess energy would be deposited in the surface (~0.4 eV). The implication of this argument is that the glow emitted by NO_2 may be more intense in the infrared than in the visible. The problem becomes even more serious if the velocity of the desorbed NO_2^* is less than that used above. In any case, the prediction from this mechanism is that the rate of desorption of NO_2 will increase with increasing [O], until a plateau is reached.

Another model is provided by the Langmuir-Hinshelwood mechanism, whereby fast O atoms are thermalized on the surface and then react with adsorbed NO to form NO_2:

$$\text{NO (adsorbed)} + \text{O (adsorbed)} \rightarrow \text{NO}_2 \text{ or } \text{NO}_2^* \quad (2)$$

Again, the NO_2 or NO_2^* would be expected to contain the excess energy, which is now considerably smaller than in the Eley-Rideal mechanism, namely only D_O^0(NO-O), 3.1 eV. Since the short-wavelength threshold is ~430 nm (2.9 eV), the remainder, 0.2 eV, is kinetic energy; this corresponds to a velocity of 0.9 km s^{-1} for the desorbed NO_2. If we again use a radiative lifetime of 80 μs, then the e-folding distance becomes ~7 cm, which is not far from the observed distance. If both NO and O are strongly adsorbed on the surface and if the adsorption energies are comparable, then the rate of reaction (2), and therefore the glow intensity, will go through a maximum as [O] is increased. If, on the other hand, both NO and O are weakly bound to the surface, then the reaction will be second-order in [O] (ref. 17). We cannot yet choose between the two mechanisms, although the Langmuir-Hinshelwood mechanism seems easier to reconcile with the observations. Finally, the energies and lifetimes used above represent most probable values. In reality, there will be a distribution (perhaps maxwellian) of interaction energies, which will in turn, lead to a distribution of excitation energies in the products. For the qualitative nature of this discussion, however, it is sufficient to consider the most probable values.

The question of the origin of the surface NO merits some discussion. The four sources mentioned above are all possible, and all can provide the required [NO]. We note that, for example, semi-empirical models of the thermosphere[20] predict ambient densities [O] and [N] of 5.3×10^8 cm^{-3} and 6.5×10^5 cm^{-3}, respectively, during our observational period. Hence, fluxes of ambient species onto the cabin bulkhead have been $\phi(O) = 3.4 \times 10^{14}$ cm^{-2} s^{-1} and $\Phi(N) = 4.1 \times 10^{11}$ cm^{-2} s^{-1}. $\Phi(N)$ seems only just able to balance $\phi(NO_2)_b$. However, due to local-time and latitudinal/seasonal variations in the global N distribution, $\phi(N)$ went through a local minimum at the location and time of our observation and the orbital average of $\phi(N)$ is considerably higher.

The data reported here are consistent with a glow hypothesis based on NO_2 emission. However, they do not prove this hypothesis, and a number of questions remain, concerning NO_2 as the source of the radiation.

We thank E. Wulf for support and I. Kofsky for helpful comments. This work was supported by the German Bundesministerium für Forschung und Technologie under grant 01 QV 239.

Received 29 October 1985; accepted 4 March 1986.

1. *Aviat. Week Space Tech.* **116**, 19, 14 (1982).
2. Yee, J. H. & Abreu, V. *J. Geophys. Res. Lett.* **10**, 126–129 (1983).
3. Slanger, T. G. *Geophys. Res. Lett.* **10**, 130–132 (1983).
4. Papadopoulos, K. *Radio Sci.* **19**, 571–577 (1984).
5. Green, B. D. *Geophys. Res. Lett.* **11**, 576–579 (1984).
6. Prince, R. H. *Geophys. Res. Lett.* **12**, 453–456 (1985).
7. Swenson, G. R., Mende, S. B. & Clifton, K. S. *Geophys. Res. Lett.* **12**, 97–100 (1985).
8. Wulf, E. & von Zahn, U. *J. geophys. Res.* **91**, 3270–3278 (1986).
9. Stephan, K., Helm, H., Kim, Y. B., Seykora, G., Ramler, J. & Grössl, M. *J. chem. Phys.* **73**, 303–308 (1980).
10. Märk, T. D. & Hille, E. *J. chem. Phys.* **69**, 2492–2496 (1978).
11. Yee, J. H. & Dalgarno, A. in *Proc. AIAA Meet. Shuttle Environment and Operations*, Washington (1982).
12. Schwartz, S. E. & Johnston, H. S. *J. chem. Phys.* **51**, 1286–1302 (1969).
13. Mende, S. B. *et al. J. Space Rock.* **23**, 189–193 (1986).
14. Korb, L. J., Morant, C. A., Calland, R. M. & Thatcher, C. S. *Bull. Am. ceram. Soc.* **60**, 1188–1193 (1981).
15. NASA Handbook, *Space Shuttle System Payload Accommodations* Vol. XIV (Rev. H, JSC-07700, 1983).
16. Engebretson, M. J. & Mauersberger, K. *J. geophys. Res.* **84**, 839–844 (1979).
17. Glasser, R. P. H. *An Introduction to Chemisorption and Catalysis by Metals* 190–197 (Oxford University Press, New York, 1985).
18. Kofsky, I. & Barrett, J. L. *Planet. Space Sci.* (in the press).
19. Tully, J. C. *J. Chem. Phys.* **73**, 6333–6342 (1980).
20. Köhnlein, W. *Planet. Space Sci.* **28**, 225–243 (1980).

Atmospheric CH_4, CO and OH from 1860 to 1985

Anne M. Thompson

Applied Research Corporation, Landover, Maryland 20785, USA

Ralph J. Cicerone

National Center for Atmospheric Research, Boulder, Colorado 80307, USA

Atmospheric methane, CO and the gaseous OH radical are interdependent: if CH_4, CO or OH is perturbed, background concentrations of the other two constituents are affected. Perturbations to OH alter photo-oxidation rates of numerous natural and anthropogenic trace gases and affect lifetimes of those species that pass from the Earth's surface to the free troposphere and stratosphere. It is now known that global atmospheric methane con-

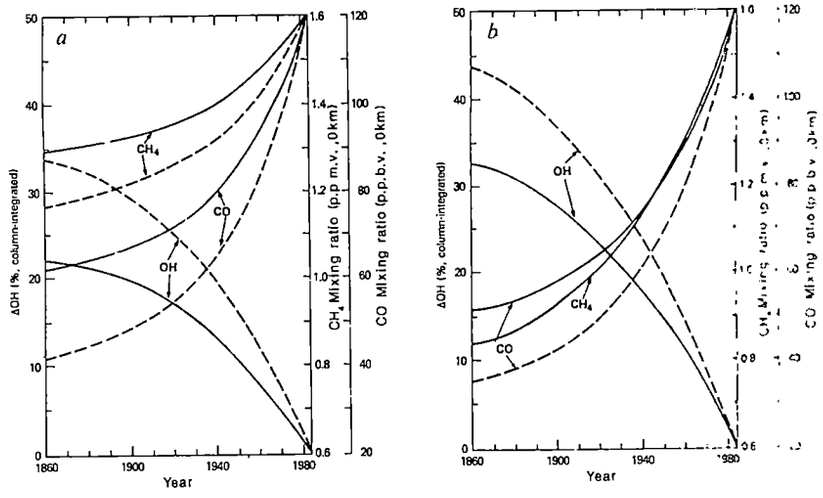


Fig. 1 Calculated ground-level methane and CO mixing ratios and per cent changes in column-integrated tropospheric OH from 1860 to 1985. Model conditions are appropriate for the mid-altitude Northern Hemisphere with low background NO_x (20–25 p.p.t.v). Calculations for low-latitude conditions (higher photolysis rates, lower O_3 and CO mixing ratios) show trends of similar magnitude, implying that the OH changes illustrated here are typical of unpolluted environments. Calculations with higher NO_x levels also show similar trends, but the magnitude of OH change is about half the increase shown here. *a*, Results from models 1 and 2 (Table 1). Methane flux is constant at all times; the calculated CH_4 increase is due solely to CO and OH changes. The solid line is from model runs with a largely anthropogenic upward flux of CO at 35% of the CO source in 1985; the dashed line assumes $flux_{CO}$ (1985) produces 65% of present-day CO. In both cases additional CO derives from CH_4 and C_2H_6 oxidation by OH and from an explicit source, S_S, representing non-methane hydrocarbon oxidation. $flux_{CO}$ and S_S vary in time as described in Table 1. *b*, Results from models 3 and 4 (Table 1). Fixed CH_4 mixing ratios follow ref. 13. Solid and broken lines as in *a*.

centrations are increasing[1–6]; less definite data suggest that carbon monoxide is also increasing[1,7–9]. Even before the measurements of refs 1–9 were made, modelling studies of CH_4–CO–OH coupling had led to predictions[10–12] of future temporal increases of CH_4 and CO. Here we look backwards in time, using a photochemical model to simulate the trace-gas composition of the unpolluted troposphere at the start of the industrial era (taken as 1860), and at intervals up to 1985. We find that the OH concentration in the background troposphere has decreased significantly and O_3 has increased due to increases of CH_4 and CO; calculated changes depend on temporal trends of NO_x ($NO_x = NO + NO_2$), for which no historical data are available. The calculations allow recent trace-gas trends affecting background chemistry and climate to be viewed in a longer-term context.

In modelling the photochemistry of the pre-industrial atmosphere it is essential to specify past concentrations of NO_x and the more stable species CH_4, CO and O_3. Before ~1960, few ambient measurements were made of these trace species, so the input to our model is based on current mixing ratios or source flux estimates extrapolated backwards in time. A summary of key species follows.

CH_4 and CO. We take two extreme methane cases: one with a minimum difference in CH_4 mixing ratio between 1860 and 1985 and one with a maximum difference. Similarly, we assume minimum and maximum temporal changes in CO and combine alternate sets of CH_4 and CO constraints to obtain four model types (Table 1). Models 1 and 2 assume a uniform CH_4 flux (constant sources) at all times, yielding 1.2–1.3 p.p.m.v. (parts per 10^6 by volume) in 1860 and 1.60 p.p.m.v. in 1985 in the models. Models 3 and 4 are based on the assumption that large differences between modern CH_4 and that extracted from ice cores[13–15] represent real changes in atmospheric composition over the past hundred years, rather than diffusive losses of trapped gases[5]. This is consistent with recently published spectroscopic measurements of past CH_4 (ref. 6). Thus, in models 3 and 4, CH_4 is present at a concentration of only 0.82 p.p.m.v. at ground level in 1860.

Choosing model input for CO is complicated because ground-level CO concentrations vary greatly, owing to the short lifetime of CO and uneven geographical distribution of CO sources[7,8]. We take 120 p.p.b.v. (parts per 10^9 by volume) CO at ground level as typical for the 1985 mid-latitude Northern Hemisphere; Southern Hemisphere CO concentrations are lower because there are fewer local sources[16,17]. Uncertainties in CO sources are treated by parameterizing two components in the model representation of the total source, $S^{total,CO}$: S_S (a surrogate for the oxidation of non-methane hydrocarbons besides C_2H_6) and $flux_{CO}$ (representing directly injected surface sources). Both S_S and $flux_{CO}$ include natural and anthropogenic contributions as described in Table 1. In ascribing 82% of present-day S_S to natural hydrocarbon sources, we follow Logan *et al.*[17], recognizing that this apportionment is still uncertain. Model runs for years before 1985 assume that natural sources contributing to S_S and $flux_{CO}$ are unchanged and anthropogenic ones scale with population or fossil-fuel usage[18]. Thus, S_S changes little in time and $flux_{CO}$ is strongly time-dependent.

Table 1 Model characteristics

Input	Model 1	Model 2	Model 3	Model 4
Past CH_4	High CH_4:constant 1985 flux		CH_4 specified from ice-core data[13]	
Past CO	Type 1-CO	Type 2-CO	Type 1-CO	Type 2-CO
Output				
1985 O_3 (0 km)	30.0 p.p.b.v.	29.8 p.p.b.v.	30.0 p.p.b.v.	29.8 p.p.b.v.
1860 O_3 (0 km)	27.7 p.p.b.v.	26.4 p.p.b.v.	25.4 p.p.b.v.	27.1 p.p.b.v.

Type 1-CO: 35% of $S^{total,CO}$ (1985) is $flux_{CO}$; type 2-CO: 65% of $S^{total,CO}$ (1985) is $flux_{CO}$. The total CO source in year t is:

$$S^{total,CO}(t) = Q_{CO}(t) + flux_{CO}(t) + S_S(t)$$

where Q_{CO}, the *in situ* photochemical formation from CH_4 and C_2H_6 oxidation, is derived from the model [$Q_{CO}(z, t)$, integrated from $z = 0$ to 15 km]; S_S (also column-integrated) explicitly represents photo-oxidation of non-methane hydrocarbons (NMHC) besides C_2H_6:

$$S_S(z, t) = S_S(z, 1985)\,[f_{NMHC,N} + r^{ff}(t) f_{NMHC,A}(1985)]$$

where $f_{NMHC,N}$ (0.82) and $f_{NMHC,A}$ (0.18 in 1985) are fractions of S_S due to oxidation of natural and anthropogenic NMHC[17]. $r^{ff}(t)$ is the ratio of fossil-fuel usage[18] in year t relative to 1985. $S_S(z, t)$ is proportional to the product of the OH number density and an exponential function with the latitude dependence of a typical OH+alkane reaction. $flux_{CO}(t)$, the model lower boundary condition for CO, signifies direct surface-injected CO sources:

$$flux_{CO}(t) = flux_{CO}(1985)\,[f_{flux,N} + r^{ff}(t) f_A^{ff}(1985) + r^{pop}(t) f_A^{nf}(1985)]$$

where $r^{pop}(t)$ is the ratio of the population in year t relative to that in 1985. f values are based on a budget[17] for Northern Hemisphere CO sources; $f_{flux,N} = 0.13$ is the natural fraction of $flux_{CO}$ (oceanic flux, emissions from plants and lightning-induced wildfires); f_A^{ff} and f_A^{nf} are fossil-fuel and non-fossil-fuel (wood fuel and biomass burning) combustion components of anthropogenic $flux_{CO}$. In all models C_2H_6 at 0 km was increased from 1.0 to 1.5 p.p.b.v. between 1860 and 1985. This has negligible effect on OH and CO changes.

O_3. Ozone concentrations vary so much in time and space, even on a short timescale, that a realistic determination of tropospheric O_3 in 1860 is impossible. For simplicity we assume identical boundary conditions for O_3 in current and past-year models: these conditions are fixed stratospheric input and fixed deposition velocity[19].

H_2O, NO_x. These species and other model parameters, for example ultraviolet and visible radiation and rainout rates, are critical in determining O_3 and OH concentrations. Water vapour, radiation fluxes and rainout rates for soluble species are fixed at constant levels[19] in all model runs. Boundary conditions for odd nitrogen (NO_x) are assumed to be uniform at all times; a stratospheric odd-nitrogen source controls NO_x in the upper and mid-troposphere and a small upward flux of NO gives 20–25 p.p.t.v. (parts per 10^{12} by volume) NO_x in the boundary layer. Although NO_x sources include a large anthropogenic component that has increased during the past century, it seems reasonable to suppose that the low levels of NO_x that determine O_3 and OH in the background troposphere are supplied by non-anthropogenic sources[20,21] (for example, stratospheric injection, lightning, weak oceanic and soil fluxes of NO) which have not changed appreciably with time.

Details of the model used in the present paper and profiles of tropospheric O_3, NO_x and OH are reported in ref. 19. The model solves for a standard complement of odd O, H, N species; CO, CH_4 and species derived from CH_4 and C_2H_6 oxidation, including peroxyacetylnitrate (PAN). Simulations are performed with a steady-state model at 10–30-yr intervals. CH_4 and CO can exhibit slower transients than would be predicted from their respective 10-yr and 2-month lifetimes[11], depending on the mix of CO sources.

Figure 1 shows ground-level CH_4 and CO mixing ratios and changes in column-integrated OH (0–15 km) from 1860 to 1985. Figure 1*a* shows results assuming minimum CH_4 change between 1860 and 1985 (models 1 and 2), and Fig. 1*b* assumes maximum CH_4 change (models 3 and 4). Tropospheric OH decreases as CO and CH_4 increase, with the greatest change occurring when both CO and CH_4 undergo maximum change (model 4). In that case CH_4, CO and fractional OH increases in 1950 (relative to 1985) are similar to those presented by Levine *et al.*[22], although our NO_x level is much lower. When we calculate perturbed CH_4–CO–OH cycles at higher NO_x levels (1 p.p.b.v. at 0 km) we find that increased CH_4 and CO cause near-surface OH to increase, but total tropospheric OH decreases as in Fig. 1 (although by only half as much).

Changes in atmospheric lifetimes of hundreds of trace gases, for example, reactive hydrocarbons, sulphur and nitrogen compounds, may have occurred since 1860 as a consequence of OH perturbations. Figure 1*a* (models 1 and 2), for which no change in surface CH_4 emissions is assumed, shows that CO increases and OH decreases could have caused background-level CH_4 to increase by 24–37% from 1860 to 1985. Figure 1*b*, however, implies that CH_4 doubling since 1860 requires a change in CH_4 fluxes as well as altered background OH in response to CO changes.

Changes in CO–CH_4–OH chemistry affect climate because O_3, CH_4 and CO_2 (to which CO converts by OH oxidation) are 'greenhouse' gases. Increases in CH_4 and CO cause tropospheric ozone to increase because CH_4 and CO contribute to photochemical O_3 production[23–25]. The temporal changes shown in Fig. 1 imply an 8–18% tropospheric O_3 increase from 1860 to the present (Table 1); observations point to a recent temporal increase in tropospheric O_3 (refs 26, 27). O_3 perturbations instantaneously alter the Earth's infrared radiative forcing. If there has been sufficient time for a temperature response, this could have caused a small rise in global temperature, depending on the altitude profile of the O_3 increase[28,29]. Atmospheric CO increases affect radiation by supplying CO_2 (provided that OH remains at adequate levels), and by suppressing OH and allowing O_3 and CH_4 to accumulate, even if CH_4 emissions do not increase. For example, atmospheric CO_2 formed from the reaction OH+CO in 1860 ($8–16\times10^{10}$ molecules cm^{-2} s^{-1}, integrated through the troposphere) exceeded the direct fossil-fuel source of CO_2, that is, 2.6×10^{10} molecules cm^{-2} s^{-1} (ref. 18). Approximately 75% of this CO was natural in origin (Table 1).

A.M.T. acknowledges partial support from the NASA Tropospheric Chemistry Office. The National Center for Atmospheric Research is sponsored by NSF.

Received 25 November 1985; accepted 17 February 1986.

1. Graedel, T. E. & McRae, J. E. *Geophys. Res. Lett.* **7**, 977–979 (1980).
2. Rasmussen, R. A. & Khalil, M. A. K. *J. geophys. Res.* **86**, 9826–9832 (1981).
3. Blake, D. R. *et al. Geophys. Res. Lett.* **9**, 477–480 (1982).
4. Rasmussen, R. A. & Khalil, M. A. K. *J. geophys. Res.* **89**, 11599–11605 (1984).
5. Ehhalt, D. H., Zander, R. J. & Lamontagne, R. A. *J. geophys. Res.* **88**, 8442–8446 (1983).
6. Rinsland, C. P., Levine, J. S. & Miles, T. *Nature* **318**, 245–249 (1985).
7. Seiler, W., Giehl, H., Brunke, E. & Halliday, E. *Tellus* **36B**, 219–231 (1984).
8. Khalil, M. A. K. & Rasmussen, R. A. *Science* **224**, 54–56 (1984).
9. Rinsland, C. P. & Levine, J. S. *Nature* **318**, 250–254 (1985).
10. Chameides, W. L., Liu, S. C. & Cicerone, R. J. *J. geophys. Res.* **82**, 1795–1798 (1977).
11. Sze, N. D. *Science* **195**, 673–674 (1977).
12. Hameed, S., Pinto, J. P. & Stewart, R. W. *J. geophys. Res.* **84**, 763–768 (1979).
13. Khalil, M. A. K. & Rasmussen, R. A. *Atmos. Envir.* **19**, 397–407 (1985).
14. Stauffer, B., Fischer, G., Neftel, A. & Oeschger, H. *Science* **229**, 1386–1388 (1985).
15. Craig, H. & Chou, C. C. *Geophys. Res. Lett.* **9**, 1221–1224 (1982).
16. Seiler, W. *Tellus* **26**, 116–135 (1974).
17. Logan, J. A., Prather, M. J., Wofsy, S. C. & McElroy, M. B. *J. geophys. Res.* **86**, 7210–7254 (1981).
18. Keeling, C. D. *Tellus* **25**, 174–198 (1973).
19. Thompson, A. M. & Cicerone, R. J. *J. geophys. Res.* (submitted); **87**, 8811–8826 (1982).
20. Levy II, H., Mahlman, J. D. & Moxim, W. J. *Geophys. Res. Lett.* **7**, 441–444 (1980).
21. Liu, S. C., McFarland, M., Kley, D. & Zafiriou, O. C. *J. geophys. Res.* **88**, 1360–1368 (1983).
22. Levine, J. S., Rinsland, C. P. & Tennille, G. M. *Nature* **318**, 254–257 (1985).
23. Fishman, J., Solomon, S. & Crutzen, P. J. *Tellus* **31**, 432–446 (1979).
24. Fishman, J. & Seiler, W. *J. geophys. Res.* **88**, 3662–3670 (1983).
25. Chameides, W. L. & Walker, J. C. G. *J. geophys. Res.* **78**, 8751–8760 (1973).
26. Bojkov, R. *Spec. Envir. Rep.* no. 16 (World Meteorological Organization, Geneva, 1984).
27. Logan, J. A. *J. geophys. Res.* **90**, 10463–10482 (1985).
28. Fishman, J., Ramanathan, V., Crutzen, P. J. & Liu, S. C. *Nature* **282**, 818–820 (1979).
29. Ramanathan, V., Cicerone, R. J., Singh, H. B. & Kiehl, J. T. *J. geophys. Res.* **90**, 5547–5566 (1985).

Spreading direction in the central South China Sea

Guy Pautot*, Claude Rangin†, Anne Briais‡, Paul Tapponnier‡, Paul Beuzart*, Gilles Lericolais*, Xavier Mathieu§, Jinlong Wu‖, Shuqiao Han‖, Hengxiu Li‖, Yingxian Lu‖ & Jicheng Zhao‖

* IFREMER, Centre de Brest, BP 337, 29273 Brest Cedex, France
† Université de Paris 6, Département de Géologie Structurale, 4 Place Jussieu, 75252 Paris Cedex 05, France and Institut Français du Pétrole, l'Avenue de Bois-Préau, 92500 Rueil Malmaison, France
‡ Institut de Physique du Globe, Laboratoire de Tectonique et Mécanique de la Lithosphére, Université de Paris 6, 4 Place Jussieu, 75252 Paris Cedex 05, France
§ Université de Bretagne Occidentale, 615 "Océanologie et Géodynamique" 6, Avenue Le Gorgeu, 29283 Brest Cedex, France
‖ First Institute of Oceanography, National Bureau of Oceanography, PO Box 98, Qingdao, China

Recent work[1,2] indicates that the South China Sea is an 'Atlantic-type' marginal basin of late Tertiary age. Magnetic anomalies in the eastern part of the sea are consistent with seafloor spreading directed approximately north–south[1,2]. We present here a new morphostructural study based on coupled seabeam mapping and single-channel seismic reflection profiling, which reveals dominant normal fault scarps, striking N50° E between 113 and 119° E longitude near the axis of this basin. Such a structural fabric implies a NW–SE spreading direction, at least in the 150–200-km-wide axial region of the South China Sea, and places new constraints on geodynamic models for the formation of this basin in the tectonic and palaeogeographic framework of South-East Asia and the South-West Pacific.

The South China Sea (Nanhai), largest of the marginal basins of the western Pacific, is bounded by the continental margins

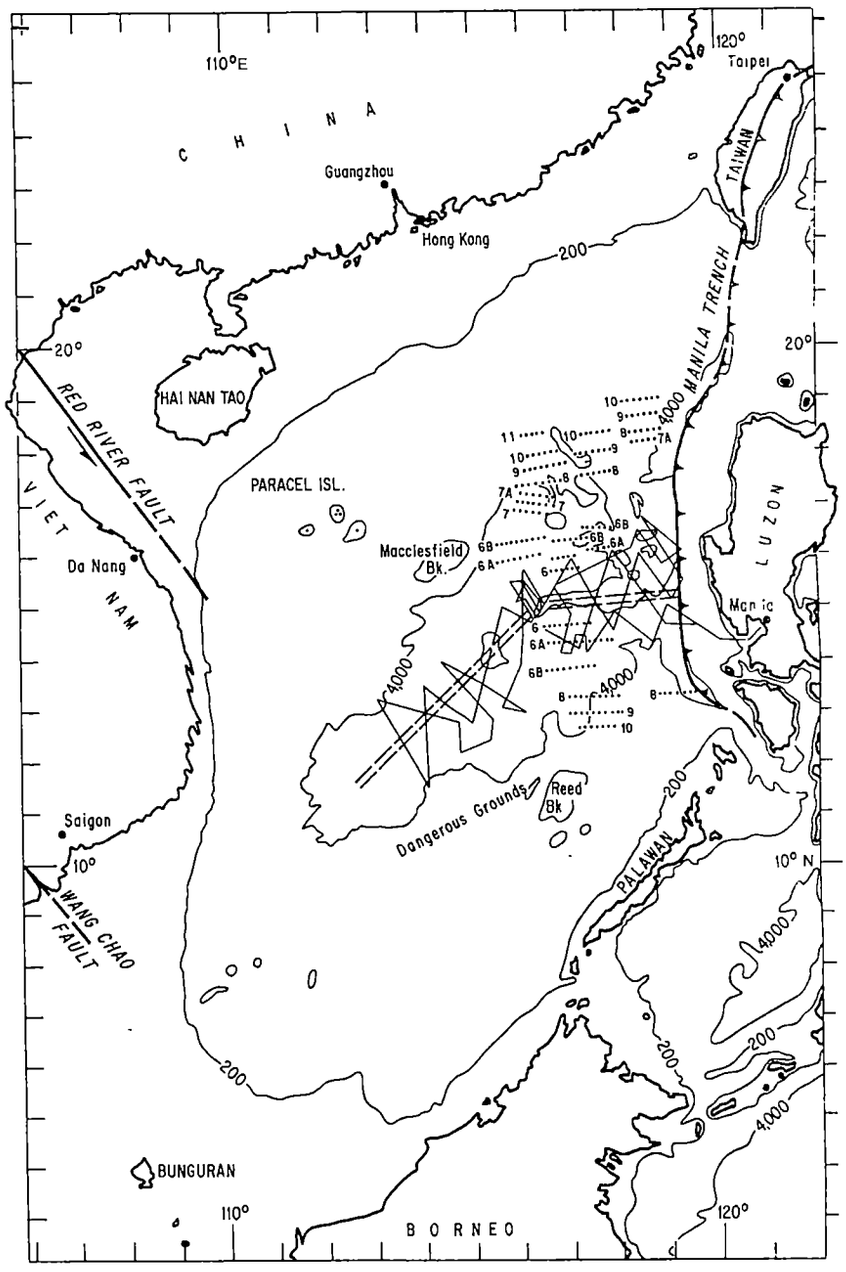


Fig. 1 Bathymetry of the South China Sea. Tracks of RV *Jean Charcot* during the Nanhai survey are reported. Also shown are major structures such as the Red River Fault and Manila Trench. Dashed parallel lines indicate inferred position of ridge axis[1,2]. Magnetic anomalies are from ref. 2.

of South China, Vietnam and Borneo, and by the Manila Trench, where its crust is now being consumed by eastward-dipping subduction (Fig. 1). East of 115° E, its ~700-km-wide oceanic floor, where east-west-trending magnetic anomalies 11 to 5e have been identified[1-3], appears to have formed mostly between 32 and 17 Myr (refs 1, 2). The east-west-trending Scarborough Seamounts probably mark the location of the spreading axis in this part of the basin[1,2]. West of 115° E, the abyssal plain divides into two wedge-shaped basins which narrow westwards, respectively north and south of the Macclesfield-Paracels high[1]. Magnetic anomalies have not yet been identified in these basins, although the deeper crust appears to be of oceanic nature[1], and the axis of the larger, southern basin, trending N50° E, is marked by a −30-mgal gravity low[1,2] (Fig. 1). The difference between the latter NE-SW structural trend and the more nearly east-west orientation of magnetic anomalies east of 115° E has been the source of conflicting interpretations. While Bowin *et al.*[3] inferred a roughly NE-SW fabric extending into the entire eastern basin, other reconstructions[1,2,4,5] imply oblique, north-south spreading in the southwestern sub-basin. Alternatively, the complexity of the South China basin could result from two (or more) distinct phases of spreading[4].

In order to obtain a clearer view of the morphology and structure of the axial floor of the South China Sea, RV *Jean Charcot* performed, between 113 and 119° E, a survey comprising 74 profiles in which seabeam mapping was coupled with single-channel seismic, magnetic and gravity recording (Figs 1, 3). The combination of seabeam with seismic reflection allowed the correlation of faults identified on the seismic sections with morphological scarps outlined by steep gradients or rectilinear bathymetric contours on the sea floor (Fig. 4). The width of the seabeam swaths (2-3 km in most of the survey area) allowed the direct determination of fault orientations, so that the kinematics of spreading could be constrained more tightly than in previous studies[1-3].

Major normal faults observed on seismic profiles (Figs 3, 4) are shown in Fig. 2, with the corresponding seabeam-derived scarp orientations. The rather thin sedimentary cover near the spreading axis does not hide the morphological expression of the faults (Figs 3, 4). Along most of the length of the ridge, we

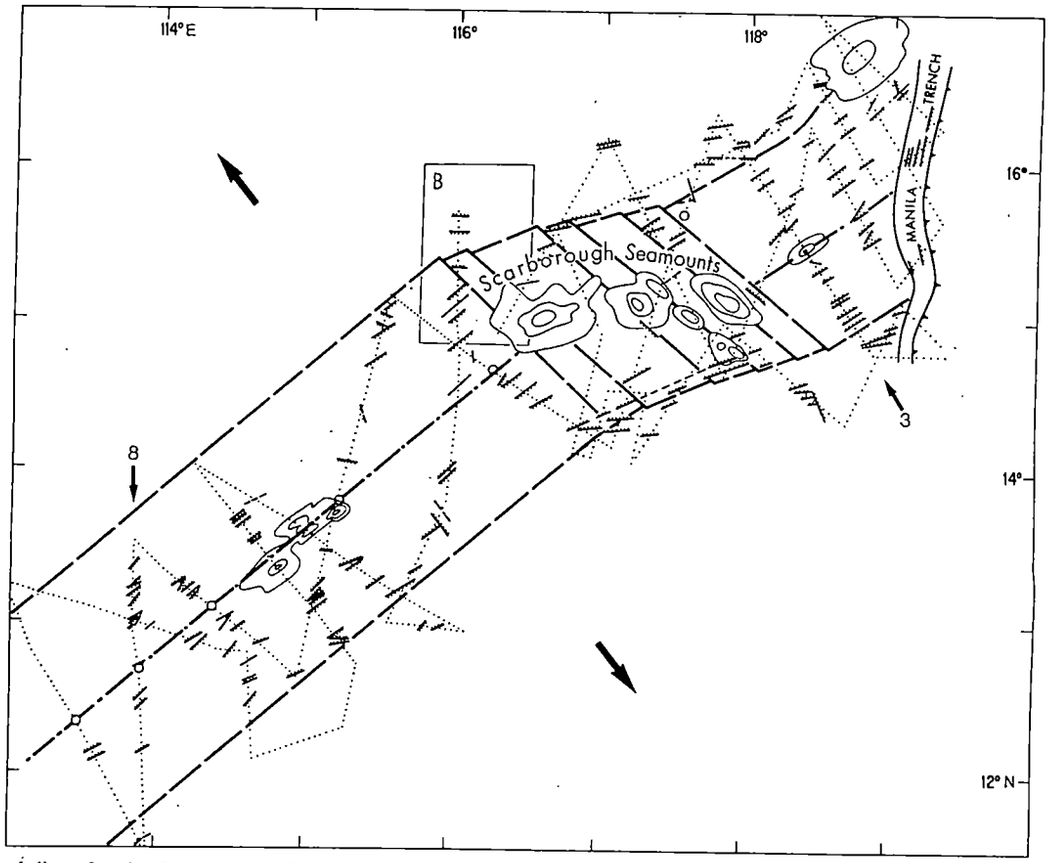


Fig. 2 Strikes and dips of major faults derived from combined analysis of seabeam and seismic reflection records. Dotted lines represent RV *Jean Charcot* profiles. Profiles 3 and 8 (Fig. 3) are indicated. Box B marks an area with denser seabeam coverage. Thin contours represent major seamounts (Scarborough chain). Thick dashed lines indicate outer limit of zone with predominant N50° E-trending scarps, and inferred transverse fault zones between 116 and 118° E. Dash-dot line outlines probable location of spreading axis.

can identify the spreading axis itself by the inwards-facing of the fault scarps and the outwards-tilting of blocks. As shown in Fig. 2, most of the normal faults strike N50 ± 10° throughout the axial region of the South China Sea, implying that the most recent spreading direction was roughly orthogonal (N140° E). Outside the central 150 km, scarps oriented N70–80° E are found, particularly between 116 and 119° E, north and south of the Scarborough Seamounts (Fig. 2).

At a more detailed level, it is possible to subdivide the axial region of the South China Sea into three distinct segments:

(1) A southwestern segment, which extends linearly from about 116° E towards the south-west, with a width of at least 150 km. The rather smooth oceanic acoustic basement, with outward-tilted blocks, is here covered by 1–2 s (seismic two-way travel time) of sediments. To the south, it appears to be bounded by structural highs trending N50–70° E, characterized by deeper reflectors, which may correspond to faulted blocks of attenuated continental crust (Fig. 3, profile 8).

(2) A northeastern segment, between about 118° E and the Manila Trench, with a NE–SW trend comparable to that of the southwestern segment. Inward-facing fault scarps striking N50° E are particularly clear up to ~75 km from the axis (Fig. 2), which is here marked by a gravity low. Farther away from the axis, major fault scarps still face mostly inwards but have more varied orientations, predominantly N70–80 E. To the north, near the Manila Trench, a large seamount masks the area in which fault scarp orientations may change.

(3) A central segment, between about 116 and 118° E, with a more complex structure and morphology. Many of the seamounts of the Scarborough chain have formed along the axis of this segment. These large submarine volcanoes dominate the fabric of the sea floor in the axial region. In addition, the sediment cover in this area is thicker than in the adjacent segments. Despite the coating of the sea floor by sediments and late volcanic products, however, scarps trending N50–60 °E are observed close to the inferred axis. They appear to be dissected by scarps trending N125–140 °E which are more numerous in this segment of the ridge than elsewhere. Moreover, the Scarborough Seamounts and minor volcanic constructions near them are elongated in these two nearly orthogonal directions (particularly the NW–SE one), which thus appear to have controlled the ascent of late basaltic volcanism. This N50° E, N135° E seafloor structural fabric is especially clear in the area near 15°30′ N, 116° E in which a dense seabeam coverage was obtained (box B in Fig. 2). At distances on the order of 80 km from the axis, scarps trending N70–80 °E are observed.

The *Jean Charcot* survey provides new insights into the latest stages of spreading in the South China Sea. Between 113 and 119° E, the 150–200-km wide axial region of the ridge appears to be composed of two rather linear, continuous, north-east-trending segments, separated by a central, east–west-trending segment where the predominant fabric of normal faults striking N50° E and bounding outward-tilted blocks is disrupted by transverse faults striking N135° E, and where the axis has been the site of late intrusions along these dominant fault trends.

Both the small- and large-scale geometries suggest that seafloor spreading took place throughout the axial region in a NW–SE direction. The offset of the northeastern and southwestern segments of the ridge, and the presence of NW–SE-striking fault scarps and elongated volcanic highs in the central segment is easily reconciled with the above spreading direction if such scarps and highs are interpreted to mark left-lateral transform fault zones. Progressive left-lateral displacement of the spreading axis across such transform zones would thus

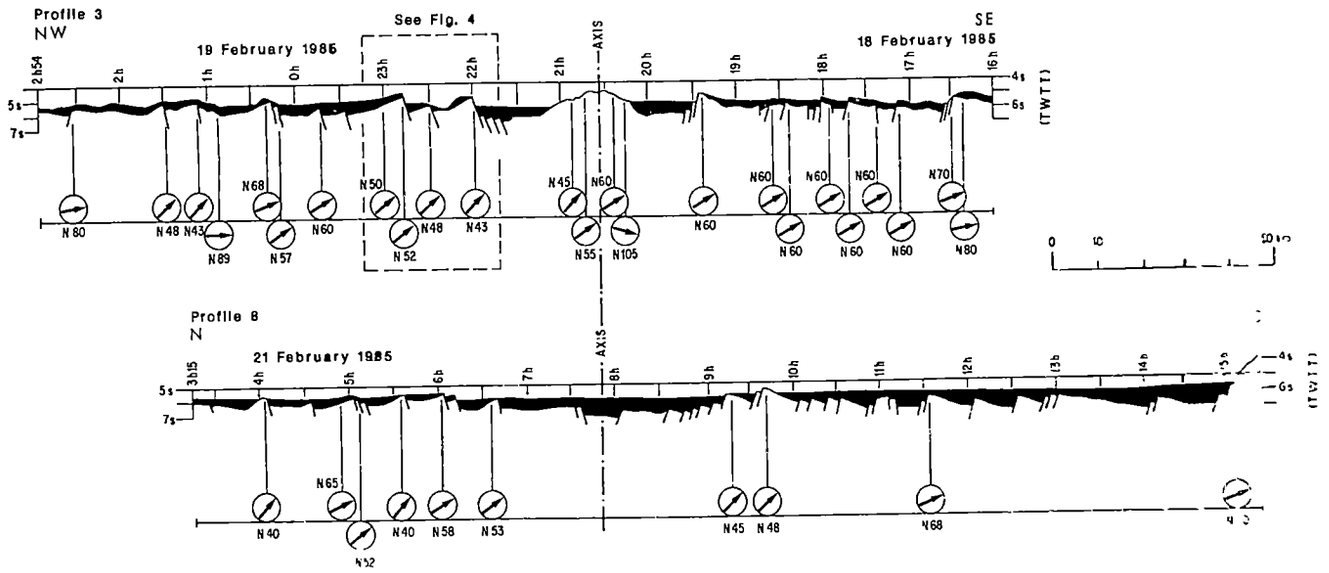


Fig. 3 Schematic sections drawn from single-channel seismic profiles 3 and 8 (sediment cover in black), and orientation of fault scarps (arrows) seen on corresponding seabeam records. TWTT, two-way travel time.

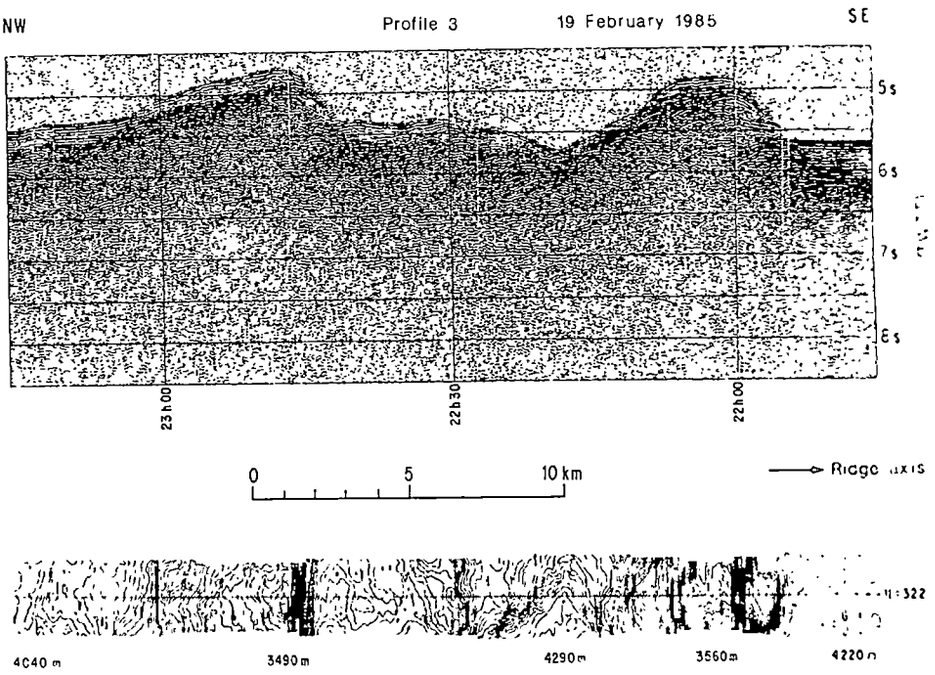


Fig. 4 Coupled single-channel seismic reflection profile (vertical exaggeration = 3) and seabeam record along part of profile 3 (box in Fig. 3). Horizontal scale is the same. Note clear northwestward-tilted blocks and southeastward-dipping normal faults. Steep gradients in bathymetric contours outline fault scarps striking N43–52° E (Fig. 3).

account for the roughly east-west average trend of the central ridge segment. This more densely fractured, and hence particularly weak crustal zone would have been a favoured injection site for basaltic magmas, allowing the formation of the Scarborough seamount chain which now outlines the ridge axis between 116 and 118° E at 15° N (Fig. 2).

The *Jean Charcot* 'Nanhai' survey discussed here was mostly confined within the area bounded by magnetic anomaly 6a[1,2] (Fig. 1), which, along with anomaly 6, was clearly identifiable on profiles made near 116° E, 16° N during a second survey to the north of the axial zone (A.B. and P.T., in preparation). Therefore, in a strict sense, the geometry and kinematics outlined above concern only the sea floor generated after about 20 Myr (that is in the most recent 3–4 Myr of spreading[1,2,4]), at a rate comparable to that estimated by Taylor and Hayes[2] (~5 cm yr^{-1}). Although the NW–SE spreading direction inferred here appears to remain approximately constant along strike, the youngest oceanic floor may have formed in two distinct, crustal environments, east and west of 115° E. West of 115° E this floor was perhaps emplaced within stretched continental crust[1,2,4], the average orientation of fault scarps and faulted blocks north of the southwestern inner basin being apparently compatible with a similar NW–SE extensional regime (A.B. and P.T., in preparation). East of 115° E, on the other hand, the inner oceanic floor formed in the centre of a 500-km-wide area already floored by oceanic crust, perhaps with a different structural fabric[1,3].

The difference between the interpretation presented here and those of previous workers[1–4] follows mostly from the first use of the seabeam imaging technique in exploring the floor of the South China Sea. In establishing the identity of a NW–SE spreading regime in the entire axial region of the sea, this interpretation is in keeping with that of Bowin *et al.*[1], and appears to contradict the north–south direction of spreading inferred by Taylor and Hayes[1,2] from nearly east–west-trending magnetic anomalies, all the way into the axis of the eastern basin. Since such anomalies are clearest outside the area of our

seabeam survey, however, it is now important to determine whether the pattern of faulting observed near the axis extends outside the 150–200-km inner part of the eastern basin. The presence of N60–80° E scarps in the outermost sections of the seabeam profiles between 116 and 119° E (Fig. 2) suggests that it may not. On the other hand, seabeam profiles made well north of the 200-km-wide axial zone, albeit west of 116°30′ E during a shorter survey following 'Nanhai' (A.B. and P.T., in preparation) also reveal N50° E-striking normal fault scarps.

A change from N50° E to N80° E in the strikes of normal faults ~100 km away from the axis could indicate a major anti-clockwise rotation of the spreading direction ~20 Myr ago. Such a major kinematic change appears to be noticeable on land in Taiwan and in the Philippines, where incipient subduction along the Manila Trench is apparently marked by new (late Oligocene–Lower Miocene) volcanism and intrusion in the western cordillera of Luzon[6,7], immediately followed by obduction of middle Oligocene ophiolites in Mindoro[8]. That change could represent the response of the spreading centre to new kinematic constraints along the nearest plate boundary and resembles that documented at about the same time within the Shikoku Basin (N. Chamot-Rooke, V. Renard and X. Le Pichon, in preparation).

Conversely, as suggested by close comparison of Figs 1 and 2, the orientation of the magnetic isochrons (N80° E) could be distinct from that of normal faulting (N50° E) in the inner as well as the outer part of the eastern South China Sea. One way to reconcile magnetic anomalies trending N80° E with normal fault scarps striking N50° E and a NW–SE spreading direction is implicit in the geometry of the disrupted central ridge segment in Fig. 2: magnetic isochrons may smooth out left-lateral offsets on closely spaced NW–SE transform faults (A.B. and P.T., in preparation). In this event, the near-parallelism between the NW–SE spreading direction, the left-lateral transform faults in the central South China Sea, and the large, left-lateral, Tertiary strike-slip faults of South China and Sundaland (Red River, Wang Chao, Three Pagodas)[9,10] could imply, in keeping with the tenets of 'rigid' plate tectonics, that the opening of that sea was driven by the southeastwards extrusion, forced by the India–Asia collision, of different parts of Sundaland along those faults[9–12].

This survey was carried out within a Cooperative Program (Nanhai project) between the National Bureau of the Sea (Beijing) and IFREMER (Paris). We thank all particpants, particularly Commandant Hubert Guidal and the crew, for collaboration on board RV *Jean Charcot*. This is IFREMER contribution 65 and IPGP contribution 902.

Received 31 January; accepted 24 February 1986.

1. Taylor, B. & Hayes, D. E. in *The Tectonic and Geologic Evolution of Southeast Asian Seas and Islands* Pt 1 (ed. Hayes, D. E.) (American Geophysical Union, Washington, DC, 1980).
2. Taylor, B. & Hayes, D. E. in *The Tectonic and Geologic Evolution of Southeast Asian Seas and Islands* Pt 2 (ed. Hayes, D. E.) (American Geophysical Union, Washington, DC, 1983).
3. Bowin, C., Lu, R. S., Lee, C. S. & Schouten, H. *Bull. Am. Ass. Petrol. Geol.* **62**, 1645–1672 (1978).
4. Holloway, N. *Bull. Am. Ass. Petrol. Geol.* **66**, 1355–1383 (1982).
5. Hayes, D. E. *Energy* **10**, 373–382 (1985).
6. Bachman, S. B., Schweller, W. J. & Lewis, S. D. *Bull. Am. Ass. Petrol. Geol.* **67**, 1143–1162 (1982).
7. Wolfe, J. A. *J. geol. Soc.* Philipp. **35**, 1–30 (1981).
8. Rangin, C., Stephan, J. F. & Muller, C. *Geology* **13**, 425–428 (1985).
9. Tapponnier, P., Peltzer, G., Le Dain, A. Y., Armijo, R. & Cobbold, P. *Geology* **10**, 611–616 (1982).
10. Tapponnier, P., Peltzer, G. & Armijo, R. in *Collision Tectonics* (eds Coward, M. P. & Ries, A. C.) 115–157 (Geological Society Special Publication, London, 1986).
11. Zhao, W. L. & Morgan, W. J. *Tectonics* **4**, (4) 359–269 (1985).
12. Peltzer, G., Taponnier, P. & Cobbold, P. *C. r. hebd. Séanc. Acad., Sci., Paris* **294**, 1341–1348 (1982).

Propagation of internal tides from the upper slopes of the Bay of Biscay

R. D. Pingree, G. T. Mardell & A. L. New

Institute of Oceanographic Sciences, Brook Road, Wormley, Godalming, Surrey GU8 5UB, UK

The shelf-break region of the Celtic Sea (north of the Bay of Biscay) is characterized by a reduced sea-surface temperature (~1 °C) throughout the summer months[1]. The cool region stretches for ~300 km along the slopes and exhibits enhanced levels of surface phytoplankton abundance. It has been postulated[2] that physical mixing creates this favourable environment for phytoplankton growth by mixing inorganic nutrients from below the seasonal thermocline, allowing the plant cells to grow more favourably in the well-illuminated surface waters. One possibility is that the mixing is due to the production and propagation of internal tides[3–6]. The present study was undertaken to detect and observe the nature of the internal tide at the Celtic Sea shelf break. We show here that internal tides, generated at spring tides close to the 200-m contour[7–9], propagate simultaneously both on shelf and into the ocean as distorted progressive waves, and when this happens, nutrients are mixed towards the sea surface.

In 1982 and 1983, the RV *Frederick Russell* studied internal waves and tides propagating on-shelf across the Celtic Sea[9,10], whereas in 1984 and 1985 more attention was focused on the off-shelf propagating waves. The September 1985 results were obtained during the participation of the RV *Frederick Russell* in the French *ONDINE* exercise, which examined internal motions and mixing in the stratified surface waters of the Bay of Biscay (to the west of France) and neighbouring shelf regions. The characteristic shelf-break cooling and associated increases in surface levels of chlorophyll *a* (with respect to neighbouring shelf and oceanic waters) were evident (Fig. 1) and at spring tides repeated runs, in a narrow section covering a 300-km extent normal to the shelf break, were made using the SeaSoar to identify the structure of the internal tide. The SeaSoar is a towed undulating conductivity–temperature–depth/fluorometer system[11,12] which allows vertical profiles of temperature, salinity and chlorophyll *a* to be obtained while steaming at 8 knots. Some typical examples of on-shelf and off-shelf waves measured with the SeaSoar are shown in Figs 2 and 3. The internal tide (period 12.4 h) is often characterized by structures of higher frequency (period ~20 min relative to a fixed observer) and higher wavenumber (wavelength ~1 km)[10] which appear mainly in the troughs of the internal tide. Some increase in amplitude of the shorter-period waves in this position would be expected due to compressional straining of the higher-wavenumber structures by the internal tide. In addition, the shorter-period internal waves may be generated locally near this position because the leading slope of the internal tidal trough steepens initially as it propagates from the shelf-break region. The more slowly propagating shorter waves may be partially trapped in the internal tidal trough, where a favourable current structure effectively advects them along. The sea-surface signatures of the higher-wavenumber structures could be observed visually, and ship radar observations[13,14] showed that these waves propagated in a direction (020–200°) normal to the shelf break. The internal tide has an asymmetric structure, where dispersion due to nonlinearity is balanced by that due to Earth's rotation[9], and the characteristic of deeply penetrating troughs together with the associated higher-wavenumber structure has been used to identify all the longer waves encountered on the SeaSoar run. A travel-time graph can be obtained by plotting the position (distance from the 200-m contour) and time (with respect to high water at Plymouth) of each wave. The results are shown in Fig. 4*a*, where the slope of the line represents the speed of travel of the internal tides from the shelf break. The variable speed across the shelf is caused by the barotropic tidal currents alternately

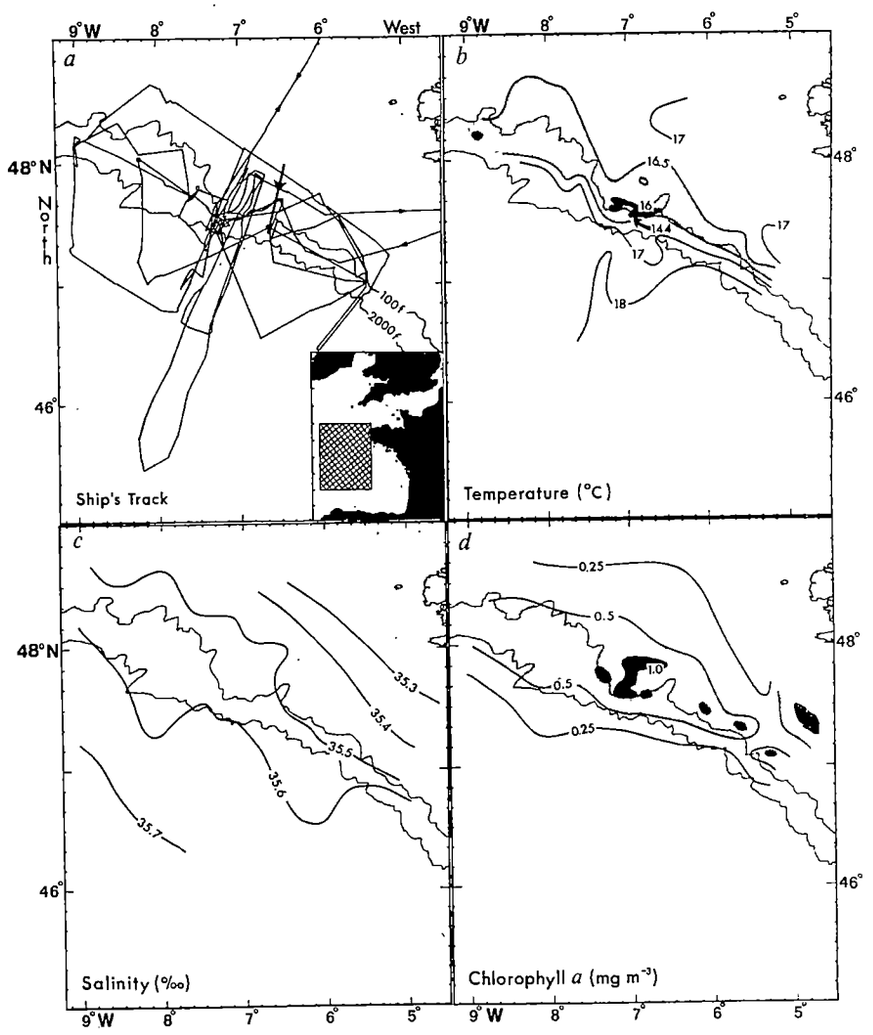


Fig. 1 *a*, Map of the region showing the cruise track of the RV *Frederick Russell* for the period 7–25 September 1985. Also shown (bold line) is the track and direction for the SeaSoar run (30 August 1984) illustrated in Fig. 2. Dots indicate positions of current-meter moorings. *b*, Mean sea-surface temperature contours for the period 13–25 September 1985. *c*, Mean sea-surface salinity contours (‰) obtained while steaming along the track shown in *a*. *d*, Mean surface levels of chlorophyll *a* (mg m^{-3}) obtained while steaming along the track shown in *a*.

assisting and opposing the on-shelf progress. Apart from an initial assistance by the barotropic tidal currents, the off-shelf propagating tide has a steadier oceanward progress since the barotropic tidal currents are only a few cm s^{-1} in the deeper (4,500 m) water regions. Scatter of the points about an idealized line is to be expected as the waves may be refracted by varying density structure[15], propagate through oceanic eddies[16–18], and originate from irregular topography in the upper slope region where there are also variations in the timing of maximum off-shelf tidal streaming in an along-slope direction.

Two interesting points that emerge from the travel graphs concern the generation times of the internal tidal troughs and the differences in mean phase speed for the on- and off-shelf waves. Both the on- and off-shelf travelling troughs seem to be generated near the 200-m contour at about the same tidal state, that is, ~2–4 h after high water at Plymouth, which corresponds to the off-shelf streaming phase for the barotropic tide (maximum off-shelf tidal streaming in a direction normal to the slope occurs ~2 h after high water at Plymouth in this region), ruling out the possibility that they propagate alternately on-shelf and off-shelf due to some form of simple lee-wave mechanism[19]. Although the actual physical mechanism has not been estab-

Table 1 Estimates of phase speeds for internal tides

Internal tide	h_1 (m)	h_2 (m)	$\Delta\rho/\rho \times 10^3$	Phase speeds (m s^{-1}) Using equations (1) and (2)	Numerical studies†	Observations
Shelf	48	122	0.74	0.77	Mode 1 0.70 2 0.26	0.70
Ocean	55	4,500	1.1	(1.2)*	Mode 1 3.5 2 1.6 3 1.2 4 0.95 5 0.73	1.03

* Equations (1) and (2) not valid for the deep ocean.
† Assumes a flat bottom.

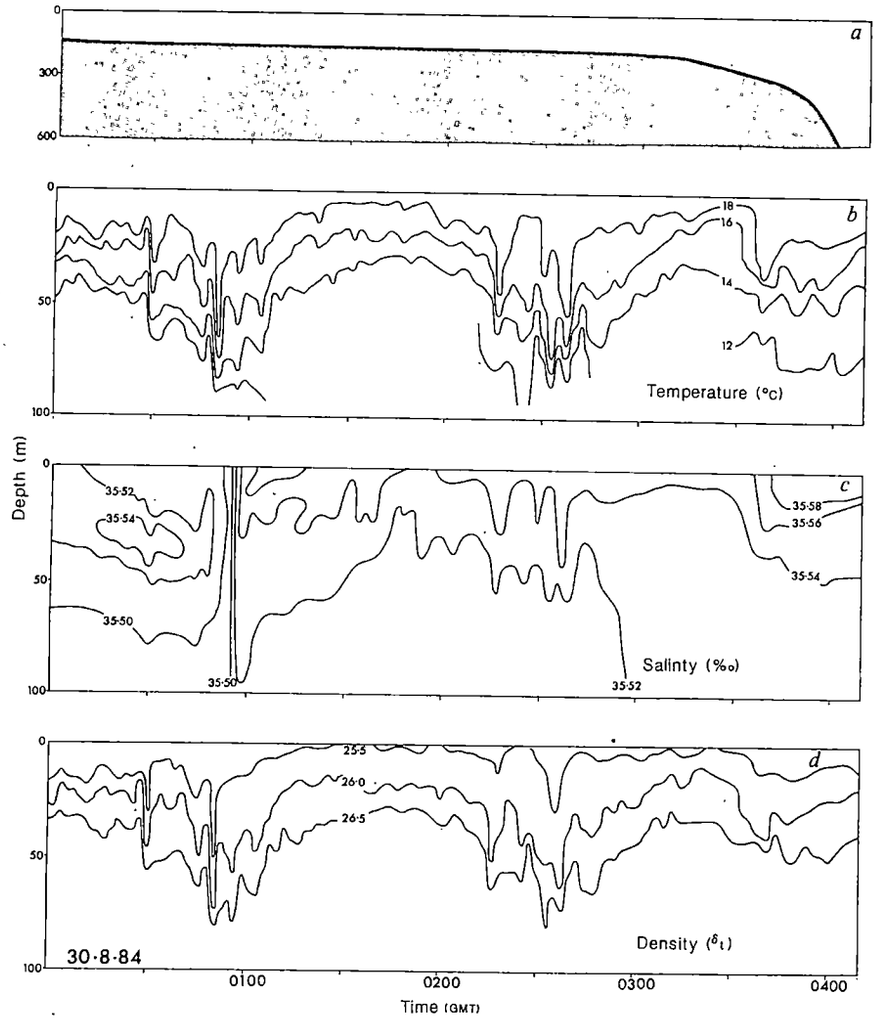


Fig. 2 Simultaneous vertical profiles of water depth (*a*), temperature (*b*), salinity (*c*) and density (*d*) obtained along the SeaSoar run shown in Fig. 1*a*. The temperature, salinity and density profiles were contoured from 100 individual profiles and show two deeply penetrating internal tidal troughs travelling on-shelf. Note the asymmetric structure of the long waves and the higher-wavenumber structures in troughs of the internal tide.

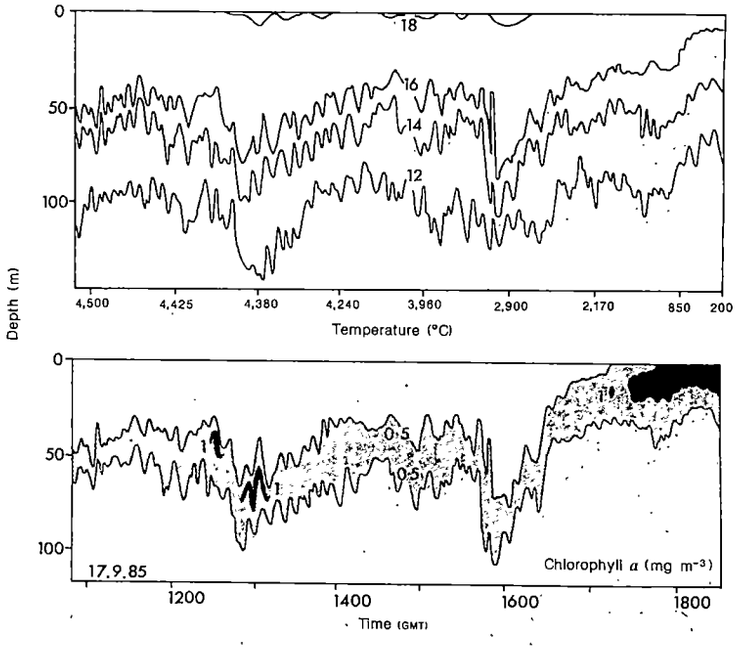


Fig. 3 Simultaneous SeaSoar profiles of temperature and chlorophyll *a*, showing two ocean propagating internal tidal troughs. The section was contoured from 180 vertical profiles and the run was made while the ship was heading towards the shelf. The two troughs at ~1300 and 1600 GMT can be identified in Fig. 4*a* and *b* as numbers 10 and 11. The total water depth (m) is indicated below the temperature section. The surface chlorophyll *a* increases at the shelf break (200 m), as depicted in Fig. 1*d*.

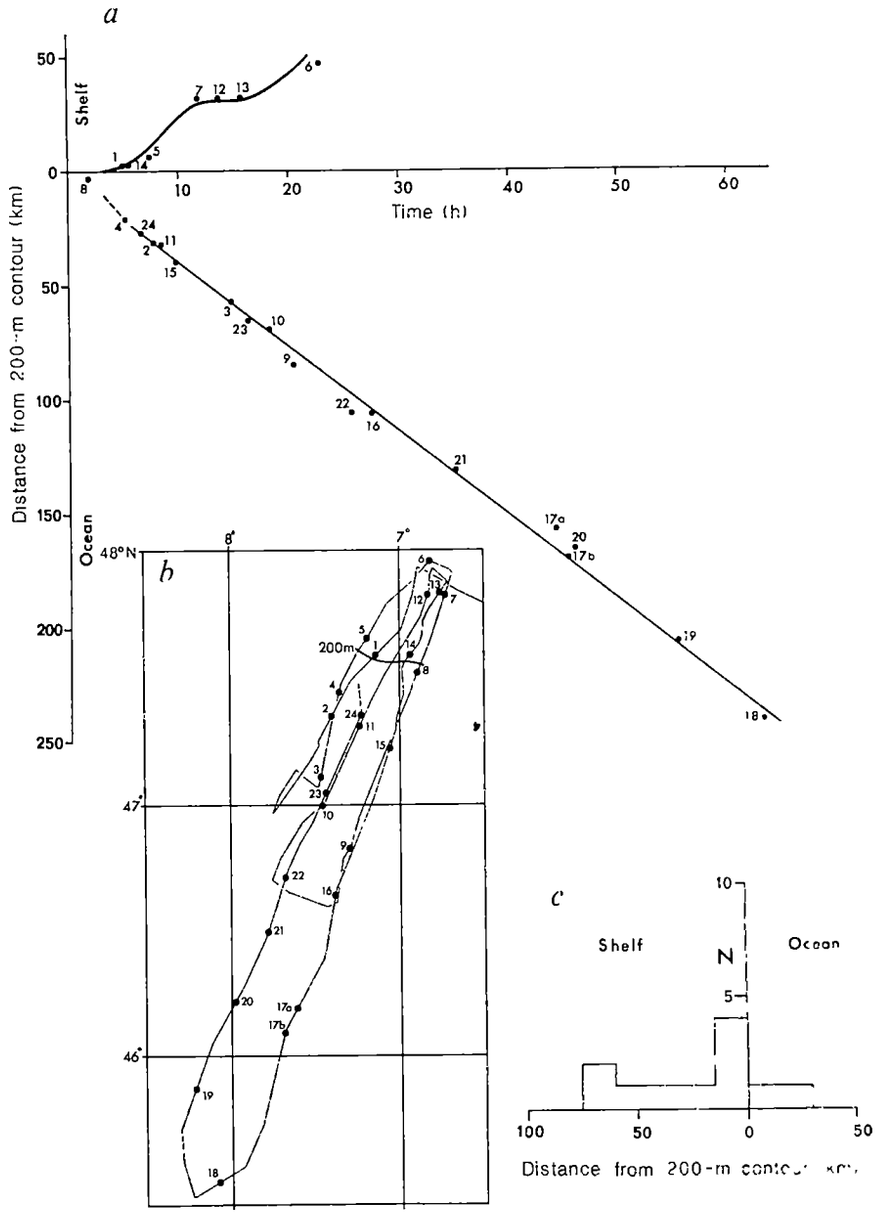


Fig. 4 *a*, Travel-time graphs for all the on-shelf and off-shelf internal tidal troughs identified in the SeaSoar records as the ship progressed along the track shown in *b*. The arbitrary time origin corresponds to high water at Plymouth and distances are measured normally from the shelf break (200-m contour) in kilometres. Individual internal tidal troughs were not followed and so at increasing distance from the shelf break the travel time, t, was determined from $t = T + n\tau$ where T is the time (in h) after the most recent high water (Plymouth) at which a trough was encountered, τ is the semidiurnal tidal period (in h) and n is an integer. Each trough has been numbered in the order in which it was observed and some individual waves were measured subsequently at increasing distances from the shelf break. For example, numbers 11, 16 and 20 represent different encounters with the same tidal trough. Note that the waves are Doppler-shifted, that is, the frequency of encounter is greater when the ship is steaming towards the generating region near the shelf break (compare the observed relative positions of waves 19, 20, 21, 22, 23 and 24 measured when the ship is heading in the direction from which the waves are coming, with the relative positions found for waves 15, 16, 17 and 18 measured as the ship is catching up and overtaking successively older internal tides). Wave 17 appeared to have two troughs and is plotted as 17a and 17b. The on-shelf travel-graph (thick line) represents a steady phase speed of 0.70 m s^{-1} travelling in a medium which is itself oscillating at ~0.70 m s^{-1} due to the barotropic tidal currents. The off-shelf travel graph is more steady at ~1.03 m s^{-1} except near the shelf break where the straight line is assumed to have an increased slope (dashed line) to take account of the increased barotropic tidal current measured on the slopes and an assumed approximate mode-1 oscillation. Errors in positioning the internal tidal troughs in space and time are generally <3 km and <10 min respectively so large deviations from the idealized line represent real variability. *c*, Frequency distribution of the number (N) of surface nutrient pulses observed within 15-km intervals from the 200-m contour. The distribution is biased towards the shelf, showing that surface nutrient levels increase at the shelf break faster than over the slopes and oceanic regions as the thermocline is eroded by internal tidal mixing.

lished, and clearly the real situation is more complex, these preliminary results suggest that during the off-shelf streaming phase of the barotropic tide the isotherms in the upper slope region descend and that this depression separates as the on-shelf and oceanward internal tidal troughs propagate from the generating zone[9,20]. At large spring tides the crest-to-trough height of the internal tide is ~50–60m in the generating region and the decay scale (the travel distance over which the amplitude falls to e^{-1} of its initial amplitude) is ~200 km for the faster ocean-going waves[8] and ~70 km for the more slowly propagating shelf internal tide. The more rapid decay rate (double) of the on-shelf tide can be partially attributed to increased dissipation due to the addition of the internal tidal currents to the barotropic tidal currents in the presence of quadratic friction[21].

Linear theory[22] indicates that in a two-layer fluid the phase speed, c, for internal tides with crests that are parallel and horizontal (Sverdrup waves), and whose wavelengths are long compared with the depth of the ocean and whose periods are long enough to be influenced by Earth's rotation, is given by

$$c = (gh_e)^{1/2} \tag{1}$$

where g is the acceleration due to gravity and h_e, the effective depth for the baroclinic mode, is defined as

$$h_e = \frac{\delta\rho}{\rho}\frac{h_1 h_2}{H(1-f^2/\sigma^2)} \quad \text{with } H = h_1 + h_2 \tag{2}$$

where $\delta\rho$ is the density difference between the upper layer of thickness h_1, and the lower layer of thickness h_2, with density ρ. The ratio of the Corolis parameter, f, at the latitude $\phi = 47°$ N, to the tidal frequency σ, is $f/\sigma = 0.76$.

The energy contained in these waves propagates at the group velocity, c_g, defined as

$$c_g = \frac{\partial\sigma}{\partial k} = c\left(1 - \frac{f^2}{\sigma^2}\right) = 0.43c \tag{3}$$

where $k = 2\pi/\lambda$ is the wavenumber, indicating that maximum internal tides (spring tides for the internal tide) will tend to occur at a distance l from the shelf break at a time $t \sim 2.3l/c$ after spring tides for the barotropic tides.

Mean values of h_1 and h_2 are estimated in Table 1, where $\Delta\rho$ now refers to the density difference that occurs over an arbitrary

50-m interval centred across the seasonal thermocline. Numerical studies showed that nonlinearity had only a small effect on the phase speed and that if the full density structure was taken into account[23-26] then the shelf situation was well represented by the first baroclinic mode, as indicated in Table 1. For the oceanic situation, the density below the thermocline increases slowly with increasing depth, and a two-layer approximation with $\Delta\rho$ estimated as above is not valid. The third and fourth modes give the most realistic phase speeds for the oceanic region. On the upper slopes, in water depths of ~1,500–500 m, the peak-to-trough amplitude of the internal tide increases to ~200–400 m (respectively) at mid-depth and towards the bottom during spring tides. There are some differences of phasing between the upper and lower layers in the deeper regions, and near the bottom in ~500 m depth the currents are intensified at some locations[19], reaching 80–90 cm s^{-1} at times. Thus, the oceanic situation differs from the shelf situation in that the full density structure results in a generation and conversion of internal tidal energy into higher internal modes and allows rays to penetrate the ocean at an angle given by the internal wave characteristic[8,19]. The theoretical estimates of the phase speeds for the internal tides are in reasonable agreement with observed values (Fig. 4) of 1.03 m s^{-1} for the ocean propagating internal tide and 0.7 m s^{-1} for the on-shelf tide, giving corresponding wavelengths of 46 and 31 km respectively, which supports the interpretation of the data obtained from the sea programme.

During the neap tide period immediately before the observations illustrated in Figs 3 and 4 there was little evidence of any internal tidal activity and the sea-surface levels of inorganic nitrate were uniformly low (<0.1 μM). During the spring tide period, nutrient pulses (where the surface values increased by >0.1 μM above background) were detected at the sea surface and their frequency distribution with respect to the 200-m contour is indicated in Fig. 4*c*. The distribution suggests that most mixing events occur near the 200-m contour but spread well on-shelf (~50 km). Although two nutrient pulses were observed on the slopes the indications are that surface nutrient pulses due to internal waves and tides are rare events in the open ocean at this time of year[6]. The distribution bias towards the shelf, the reduced vertical density structure on the shelf (Table 1) and the more rapid decay of the on-shelf propagating internal tide are consistent with increased mixing on the shelf. Some nutrient pulses are completely mixed to the surface and are detectable on successive passes, others do not persist at the surface and collapse back as the crest of the internal tide (or the crest of a structure of higher wavenumber) passes by. No new nutrient pulses were observed in the region during the next period of neap tides from 20 September to the end of the cruise (26 September).

In the present study, we have established that the thermocline is forced near the shelf break of the Celtic Sea during spring tides. In this process, mixing takes place as the internal tides and higher-wavenumber structures are generated and propagate away from the forcing region. Although a causal relationship between internal tides, nutrient renewal and increases in phytoplankton abundance in the vicinity of the shelf break has been indicated, further studies are required to quantify the nutrient flux and phytoplankton response arising from the internal tidal activity.

We thank EPSHOM and especially Yves Camus for coordinating our participation in *ONDINE*, also John Smithers, Ian Waddington, Bob Longmore and the Research Vessel Services Computing Group for assistance at sea. A.L.N. is supported by an ARE contract with NERC.

Received 5 December 1985; accepted 24 February 1986.

1. Pingree, R. D. *J. mar. biol. Ass. U.K.* **59**, 689–698 (1979).
2. Pingree, R. D. & Mardell, G. T. *Phil. Trans. R. Soc.* **A302**, 663–682 (1981).
3. Pingree, R. D., Mardell, G. T., Holligan, P. M., Griffiths, D. K. & Smithers, J. *Continent. Shelf Res.* **1**, 99–116 (1982).
4. Sandstrom, H. & Elliott, J. A. *J. geophys. Res.* **89**, 6415–6426 (1984).
5. Briscoe, M. G. *Nature* **312**, 15 (1984).
6. Holligan, P. M., Pingree, R. D. & Mardell, G. T. *Nature* **314**, 348–350 (1985).
7. Rattray, M. Jr Tellus **12**, 54–62 (1960).
8. Baines, P. G. *Deep Sea Res.* **29**, 307–338 (1982).
9. Pingree, R. D., Griffiths, D. K. & Mardell, G. T. *J. mar. biol. Ass. U.K.* **64**, 99–113 (1983).
10. Pingree, R. D. & Mardell, G. T. *Prog. Oceanogr.* **14**, 431–441 (1985).
11. Collins, D. S., Pollard, R. T. & Suchen, Pu. *Inst. Oceanogr. Sci. Rep.* **148**, 1–75 (1983).
12. Fasham, M. J. R., Pugh, P. R., Griffiths, D. & Wheaton, J. E. G. *Radio electr. Engnr.* **53**, 21–24 (1983).
13. Haury, L. R., Wiebe, P. H., Orr, M. H. & Briscoe, M. G. *J. mar. Res.* **41**, 65–112 (1983).
14. Kerry, N. J., Burt, R. J., Lane, N. M. & Bagg, M. T. *J. phys. Oceanogr.* **14**, 1419–1423 (1984).
15. Sabinin, K. D., Nazarov, A. A. & Serikov, A. N. *Izv. atmos. Oceanic Phys.* **18**, 317–323 (1982).
16. Madelain, F. & Kerut, E. G. *Oceanol. acta* **1**, 159–168 (1978).
17. Dickson, R. R. & Hughes, D. G. *Oceanol. acta* **4**, 43–46 (1981).
18. Pingree, R. D. in *Remote Sensing of Shelf Sea Hydrodynamics* (ed. Nihoul, J. C. J.) 287–315 (Elsevier, Amsterdam, 1984).
19. Huthnance, J. M. *Prog. Oceanogr.* **10**, 193–226 (1981).
20. Mazé, R. thesis, Univ. Bretagne Occidentale (1983).
21. Hunter, J. R. *Estuar. coast. Shelf Sci.* **3**, 473–479 (1975).
22. Proudman, J. *Dynamical Oceanography* (Methuen, Oxford 1953).
23. Bell, T. H. Jr *Naval Res. Labs, Washington, Rep.* No 7294 (1971).
24. James, I. D. *Deep Sea Res.* **29**, 1099–1111 (1982).
25. Pereskokov, A. I. & Schulepov, V. A. *Oceanology* **24**, 565–569 (1984).
26. Pingree, R. D. & Morrison, G. K. *J. phys. Oceanogr.* **3**, 280–285 (1973).

Carbonate recrystallization in basal sediments: evidence for convective fluid flow on a ridge flank

Miriam Kastner, Joris M. Gieskes & Jine-Yu Hu

Scripps Institution of Oceanography, La Jolla, California 92-93, USA

In many Deep Sea Drilling Project (DSDP) drill holes, chalks and/or limestones and even dolomites overlie oceanic basement rocks. These occurrences have often been interpreted as the result of increased calcium carbonate dissolution and reprecipitation as cement and overgrowths (recrystallization) at higher prevailing temperatures, either near an oceanic ridge system or at greater burial depths (burial diagnesis). We report here detailed chemical and isotopic analyses of carbonate sediments recovered from a drill hole on the western flank of the East Pacific Rise during Leg 92 of DSDP. This hole was drilled on 4.6-Myr old oceanic crust and recovered chalks directly overlying oceanic basement at a depth as shallow as 8 m below the sediment/water interface. Oceanic basement was not reached in this hole because of the hardness of deeper chalks, or, more likely, limestones. The chemical and isotopical evidence, detailed below, shows that considerable calcite recrystallization did occur in an aqueous medium similar to normal seawater and at relatively low temperature. This suggests that the observed recrystallization of calcareous ooze to chalk and limestone took place not as a result of burial diagenesis at higher temperatures, but as a result of extensive advective pore water flow through the sediments, which would allow recrystallization of calcium carbonate to take place. This process was, and apparently still is, widespread in the south-east Pacific Ocean.

The sediments of Hole 600C (18°55.70′ S, 116°50·45′ W) at a water depth of 3,398 m, are at least 11.8-m thick, and consist of mixtures of two components: calcite ($CaCO_3$) and red to yellow-brown semi-opaque oxyhydroxides[1], typically observed in this area of the East Pacific Rise[2-4]. The calcite appears in two forms: as biogenic components and as secondary inorganic precipitates. The relative content of $CaCO_3$ decreases with depth (Fig. 1). Some basaltic glass and altered basaltic fragments and traces of terriginous material are also present. At a subbottom depth of 10.25 m a basaltic glass layer occurs which is strongly altered to palagonite and poorly crystalline smectite.

The heat flow at this site is 580 mW m^{-2} (almost 14 heat flow units)[5], with the theoretically expected value being significantly lower[6] (~245 mW m^{-2}). The full spreading rate is ~17 cm yr^{-1}. Interstitial water analyses[7] indicated only small changes in Ca^{2+} and Mg^{2+} with depth as well as increases in dissolved NO_3^-. This suggests little influence of recent upward advection in this hole, although in the vicinity of this hole advective flow has been inferred to occur in certain zones of high heat flow[8].

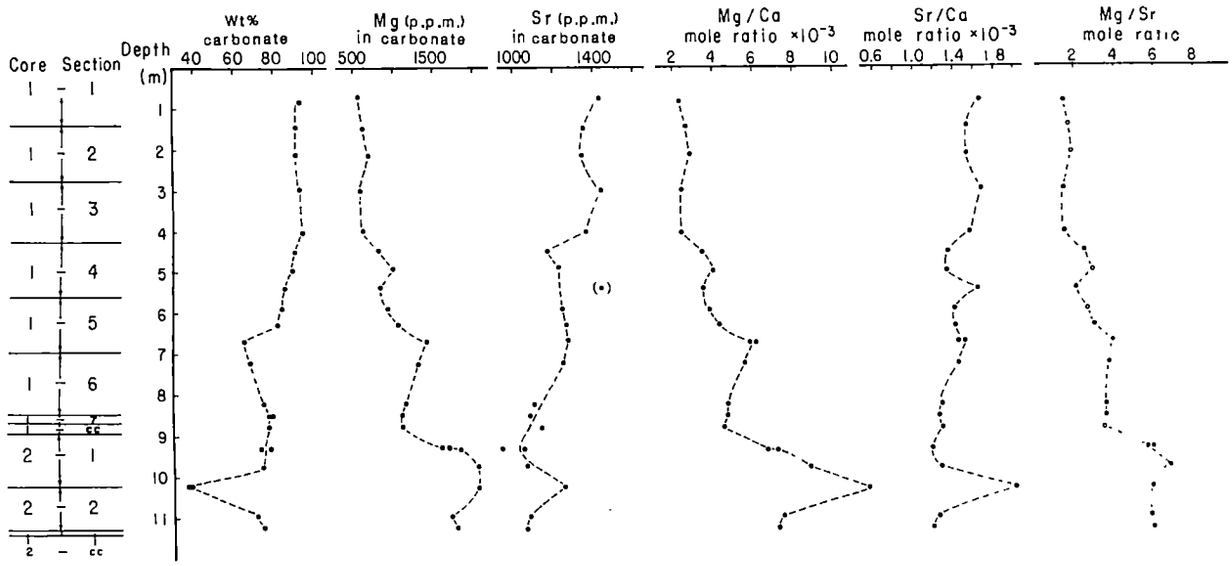


Fig. 1 Weight per cent $CaCO_3$, Mg, and Sr concentrations, and Mg/Ca, Sr/Ca, and Mg/Sr mole ratios in carbonate fraction of sediments of DSDP Hole 600C. Age boundaries: 600C-1-1 (145–150), Pleistocene; 600C-1-2 (145–150), early Pleistocene; 600C-1-4 (145–150), early Pliocene (N 20); 600C-2CC, early Pliocene (N 19).

The boundary between Pleistocene and Pliocene is located close to the top of Core 1, Section 4 (Fig. 1), at about 4.5 m sub-bottom depth[9]. A rather abrupt change in sediment colour is observed below this boundary from brownish yellow to dark brown, associated with a decrease with depth in carbonate contents. About 3 m above the base of the Hole calcareous ooze gives way to chalk.

At present, and throughout its history, the sediments of Hole 600C were deposited above the carbonate compensation depth (CCD)[4,10–13] Preservation of planktonic foraminifera, however, is only moderate to good in the younger samples and moderate to poor in the Pliocene section[14]. The presence of a basal Pliocene chalk layer of at least 3 m thickness in such a thin and young calcareous section cannot be explained by the well documented rates and processes of diagenetic reactions in pelagic calcareous oozes. In this section scanning electron microscopy (SEM) observations revealed extensive calcite dissolution, overgrowth and cement (Fig. 2)[1].

To understand the unexpectedly low degree of preservation of biogenic calcite in the lower two-thirds of Hole 600C, the calcareous fraction was analysed chemically in great detail (Fig. 1). Submarine biogenic calcite recrystallization is generally reflected in chemical, isotopical, and often also in mineralogical changes[15–17].

No important changes in chemical composition are observed in the upper 4–4.5 m, but below this systematic changes do occur, not only in the Sr contents (decreases from ~1,400 to ~1,000 p.p.m. (parts per 10^6)), but particularly in the Mg contents (increases from ~570 to ~2,000 p.p.m.). Sample 2-2 (4–6 cm) at 10.25 m, that is, volcanic glass layer, is unusual. $CaCO_3$ content is only ~37%, and both Sr and Mg increase in the recrystallized carbonate, presumably as a result of special conditions associated with reactions involving volcanic glass alteration. In this thin layer, a small fraction of the calcite cement may have originated in conjunction with low-temperature alteration of the volcanic glass[18].

Below 4–4.5 m burial depth changes in Sr/Ca and Mg/Ca ratios appear systematic, as is also demonstrated in Fig. 3, which, in addition, contains information on a sample of a basal limestone recovered from a Lower Miocene sample of DSDP Site 598 of Leg 92. The Sr/Ca ratio in the latter sample (Sr/Ca $\sim 0.63 \times 10^{-3}$) is close to the equilibrium value at ~2 °C in conditions of normal seawater Sr^{2+}/Ca^{2+} ratios[16,19]. We suggest

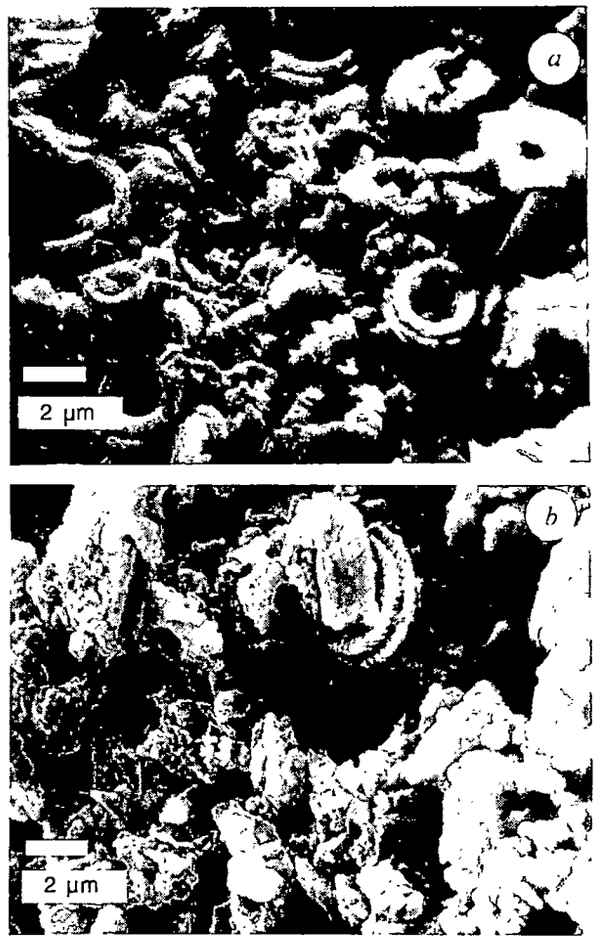


Fig. 2 Scanning electron microscopy photographs of Hole 600C carbonates: *a*, calcareous ooze at 0.8 m depth, and *b*, chalk at 11.2 m depth. Note considerable overgrowth and cementation in chalk but not in the calcareous ooze.

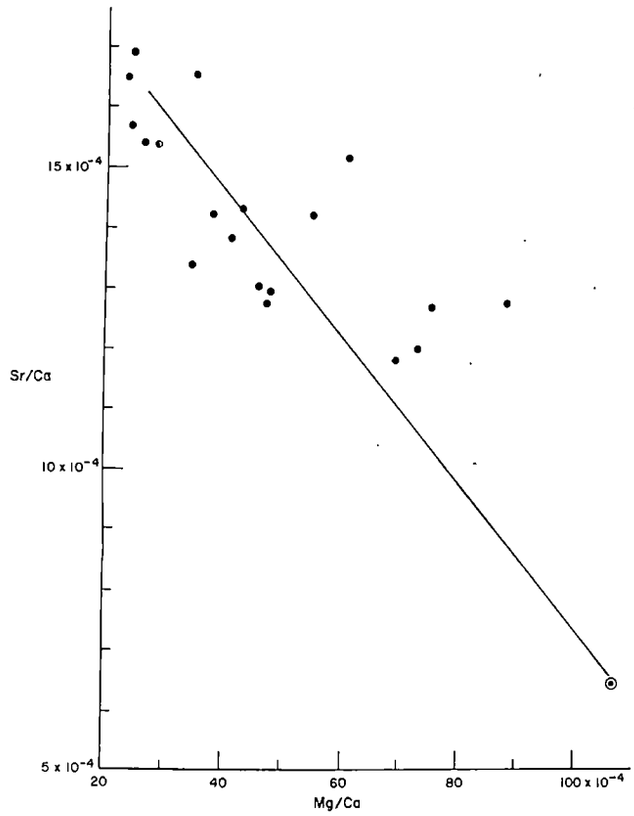


Fig. 3 Correlation between Sr/Ca and Mg/Ca mole ratios in carbonate fraction, DSDP Hole 600C. The circled point is from a basal limestone of nearby DSDP Site 598.

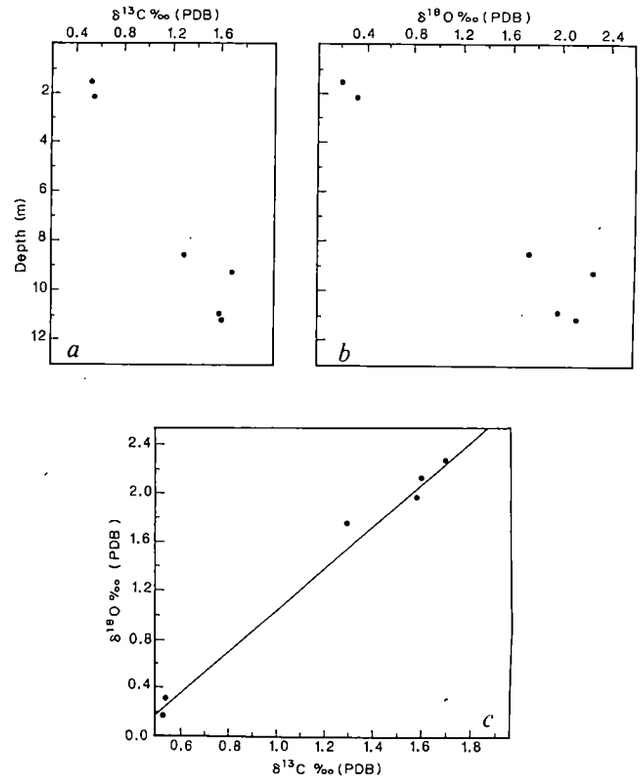


Fig. 4 DSDP Hole 600C: *a*, $\delta^{13}C$ (PDB) in carbonates versus depth; *b*, $\delta^{18}O$ (PDB) in carbonates versus depth; *c*, correlation between $\delta^{13}C$ and $\delta^{18}O$ in carbonate fraction.

that the negative slope in Sr/Ca versus Mg/Ca ratios in Fig. 3 indicates a trend of progressive calcite recrystallization.

Values of $\delta^{18}O$ and $\delta^{13}C$ of the bulk carbonate fraction and of the fraction of coccoliths increase significantly with depth (Fig. 4*a*,*b*). These trends are not expected from the known Pliocene–Quaternary palaeotemperatures[20–23]. Instead, dissolution of planktonic foraminifera and coccoliths and calcite reprecipitation as overgrowth and cements (recrystallization) at lower than surface water temperatures must be responsible for the observed increases in the $\delta^{18}O$ values. The $\delta^{18}O$ value of calcite precipitated from sea water at 2 °C and $\delta^{18}O_w = -1‰$ (SMOW), is 1.9‰ (PDB) and at 2 °C and $\delta^{18}O_w = 0‰$ is 2.9‰ (ref. 24). As for the carbon isotopes, the $\delta^{13}C$ of dissolved CO_2 in surface waters is higher than in the deep and bottom waters[25]. Because of the relatively low ΣCO_2 concentration in seawater (~2,300 μmoles kg^{-1} in Pacific Deep Water), in a sea water–$CaCO_3$ system in which $CaCO_3$ is being dissolved and reprecipitated, the $\delta^{13}C$ of the ΣCO_2 will be controlled by the solid carbonate phase. At 25 °C and in conditions of slow rates of precipitation, the carbon of the solid $CaCO_3$ will be between 1.8 and 2.3‰ heavier than that of dissolved HCO_3^- (refs 26, 27). Up to 60 °C the temperature effect is small, for example, at 20 °C + (0.035 ± 0.013)‰ $°C^{-1}$ (ref. 26). Thus, during recrystallization at low to moderate temperatures, the $\delta^{13}C$ value of reprecipitated $CaCO_3$ will increase. There is a strong positive correlation between the changes in $\delta^{18}O$ and $\delta^{13}C$ (Fig. 4*c*) which again suggests that recrystallization of carbonate is the underlying factor.

On the basis of palaeo-oceanographical and the above documented textural, chemical, and isotopical evidence, we conclude that the processes responsible for the observed extensive calcite dissolution and secondary inorganic reprecipitation and chalk formation in the sediments of Hole 600C, occurred at low temperatures, presumably close to bottom water temperatures, and in solutions similar in composition to bottom sea water. Indeed, Ca^{2+} and Mg^{2+} concentrations in fluids suggesting upward advective flow in this area are similar to sea water[8]. There is little doubt that the recrystallization occurred at an early age. We propose that observed occurrences of chalks and limestones directly overlying oceanic basement generally form at an early age and that special circumstances are needed to explain their early recrystallization. Furthermore we suggest that the most important cause of this process is advective fluid flow through the sediments on the flanks of midocean ridges. In such conditions, recrystallization reactions are greatly enhanced when compared with diffusion controlled systems in which fluid flow is essentially absent. Thus, our observations in Hole 600C suggest that, at least during the first 1–1.5 Myr of the existence of this sediment section, substantial advective flow must have occurred through the sediments. Increasing degrees of recrystallization with depth presumably imply upward flow from underlying basalts, involving low temperature, relatively unaltered sea water. This cementation will lead to eventual sealing of the basement limiting further advective flow. Much of the oceanic basement in the southeastern Pacific Ocean may be covered by similar limestone or chalk layers, which locally restrict convective fluid flow between sea water and oceanic basement.

We thank all cruise participants of Leg 92 for lively discussions. This research was supported by NSF grants OCE-8300692 (M.K.) and OCE-8218539 (J.M.G.).

Received 4 November 1985; accepted 4 March 1986.

1. Kastner, M., Hu, J.-Y. & Gieskes, J. M. *Init. Rep. DSDP* **92** (in the press).
2. Quilty, P. G. *et al. Init. Rep. DSDP* **34**, 779–794 (1976).
3. Bass, M. N. *Init. Rep. DSDP* **34**, 611–624 (1976).
4. Rea, D. K. & Leinen, M., *Init. Rep. DSDP* **92** (in the press).
5. Hobart, M. *Init. Rep. DSDP* **92** (in the press).
6. Sclater, J. G., Anderson, R. N. & Bell, M. L. *J. geophys. Res.* **76**, 7888–7915 (1971).
7. Geiskes, J. M. & Boulegue, J. *Init. Rep. DSDP* **92** (in the press).
8. Bender, M. L. *et al. Earth planet Sci. Lett.* **76**, 71–83 (1985/1986).
9. Knuttel, S. & Romine, K. *Init. Rep. DSDP* **92** (in the press).
10. Berger, W. H. & Winterer, E. L. *Int. Ass. Sedim. Spec. Publ.* **1**, 11–48 (1974).

11. van Andel, Tj. H., Heath, G. R. & Moore, T. C. *Geol. Soc. Am. Mem.* **143** (1975).
12. Broecker, W. S. & Broecker, S. *Soc. Econ. Paleont. Miner. Spec. Publ.* **20**, 44–57 (1974).
13. Berger, W. H., Adelseck, C. G. & Mayer, L. A. *J. geophys. Res.* **81**, 2617–2627 (1976).
14. Romine, K. *Init. Rep. DSDP* **92** (in the press).
15. Schlanger, S. O. & Douglas, R. G. *Int. Ass. Sedim. Spec. Publ.* **1**, 117–148 (1974)
16. Baker, P. A., Gieskes, J. M. & Elderfield, H. *J. Sedim. Petrol.* **52**, 71–82 (1982).
17. Killingley, J. S. *Nature* **301**, 594–597 (1983).
18. Garrison, R. E., Hein, J. R. & Anderson, T. F. *Sedimentology* **20**, 399–410 (1973).
19. Katz, A., Sass, E., Starinsky, A. & Holland, H. D. *Geochim. cosmochim. Acta* **36**, 481–496 (1972)
20. Douglas, R. G. & Savin, S. M. *Init. Rep. DSDP* **17**, 591–605 (1973).
21. Douglas, R. G. & Savin, S. M. *Init. Rep. DSDP* **32**, 509–520 (1975).
22. Savin, S. & Yeh, H. W. in *The Sea* Vol. 7 (ed. Emiliani, C.) 1521–1554 (Wiley-Interscience) (1981).
23. Berger, W. H., Vincent, E. & Thierstein, H R. *Soc. Econ. Paleont. Miner. Spec. Publ.* **32**, 489–304 (1981).
24. O'Neil, J. R., Clayton, R. N. & Mayeda, T. K. *J. chem. Phys.* **51**, 5547–5558 (1969).
25. Kroopnick, P., Weiss, R. F. & Craig, H. *Earth planet. Sci. Lett.* **76**, 103–110 (1972).
26. Emrich, K., Ekhalt, D. H. & Vogel, J. C. *Earth planet. Sci. Lett.* **8**, 363–371 (1970).
27. Turner, J. V. *Geochim. cosmochim. Acta* **46**, 1183–1191 (1982).

Mutual diffusion in a miscible polymer blend

R. A. L. Jones, J. Klein* & A. M. Donald

Cavendish Laboratory, University of Cambridge, Madingley Rd, Cambridge CB3 0HE, UK

Self-diffusion in polymer melts has been extensively studied and is reasonably well understood in terms of the reptation model[1–4]; the related phenomenon of mutual diffusion in miscible blends of chemically different polymers has received little attention, despite its practical relevance and implications for physical processes, such as phase separation kinetics. In such blends, attractive interactions between the monomers, when summed over a polymer chain, may lead to large enthalpic driving forces favouring the mixing; this in turn results in a mutual diffusion rate which is rapid compared with the entropically driven self-diffusion[5], and which is strongly composition-dependent[6]. We have measured mutual diffusion as a function of composition in one such binary blend, polyvinyl chloride (PVC)/polycaprolactone (PCL), and report here that the mutual diffusion coefficient is strongly enhanced in the middle of the composition range. This result is qualitatively, though not quantitatively, in accord with the results of some recent theoretical treatments[5–8].

The molecular characteristics of the polymers used are given in Table 1. Diffusion coefficients were determined by measuring the broadening with time of an initially step-like concentration profile. A sharp interface was set up between blends of PVC and PCL differing in concentration by 10%; the sample was then held at a temperature of 91.5 ± 0.5 °C in a vacuum oven for known times (8 h to 7 days). The final distribution of the two polymer species after diffusion-broadening across the interface was then determined using X-ray microanalysis in a scanning electron microscope, in which X rays from inner-shell transitions excited by the electron beam, and characteristic of the element producing them, are counted by a detector. In this case we measured the concentration of chlorine atoms in the PVC across the sample; the spatial resolution of this technique is 3 μm, and with careful sample preparation a concentration resolution of 1% is possible. The resulting broadened profile was analysed using the standard Fick's law solutions to the diffusion equation, to yield directly the value of $D(c)$, the mutual diffusion coefficient at the average concentration c of the diffusion couple. Examples of concentration profiles before and after broadening are given in Fig. 1. Previous workers have used a similar technique[9,10], but in these earlier studies pure materials were allowed to interdiffuse; this does not give satisfactory information about the concentration dependence of the diffusion coefficient for the polydisperse polymers used in experimental

* Permanent address and address for correspondence: Department of Polymer Research, Weizmann Institute, Rehovot 76100, Israel.

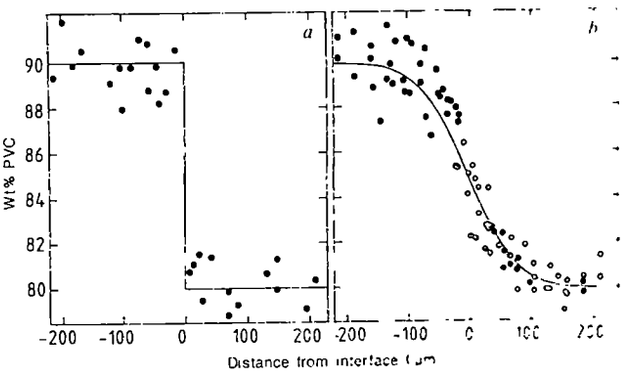


Fig. 1 *a*, Initial concentration profile between two blends (80% PVC/20% PCL, 90% PVC/10% PCL) as revealed by X-ray microanalysis immediately after joining. *b*, Concentration profile after annealing under vacuum for 114.2 h at 91.5 °C. The solid curve is an error-function fit corresponding to $D = 7.42 \times 10^{-11}$ cm^2 s^{-1}, obtained by least-squares analysis. The figure is a composite of five individual profiles measured from different sections of the same diffusion couple. The scatter of each point is ~2–3 times that expected due to counting statistics.

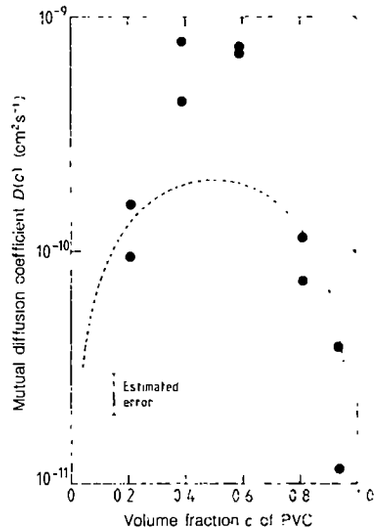


Fig. 2 The measured variation of $D(c)$ with blend composition for the miscible polymer blend PVC/PCL at 91.5 °C. The concentration plotted is the mean volume fraction of PVC in the diffusion couple. Each point corresponds to a value of $D(c)$ taken from a composite concentration profile such as that in Fig. 1, made up of several different profiles for the same diffusion time. Points for a given c correspond to runs carried out over times differing by a factor of ~3. The broken line shows the concentration dependence predicted by equation (1), assuming D_0 to be constant and neglecting the difference in degree of polymerization of the polymers. The actual value chosen for D_0 is arbitrary.

Table 1 Relative molecular masses (M_rs) of polymer samples

Polymer	M_w	M_n	M_w/M_n
PVC	83,500	37,400	2.2
PCL	33,000	10,700	3.1

The polymers used in this study were purchased from Aldrich Chemical Co., and were used as supplied. The M_r characterizations, supplied by Aldrich, were obtained by light scattering and gel-permeation chromatography. M_w, weight-averaged M_r: M_n, number-averaged M_r.

work, as the standard methods for obtaining this information from diffusion profiles apply only to strictly binary systems[11].

Figure 2 shows the measured variation of $D(c)$ with concentration, based on profiles such as that in Fig. 1. A marked maximum in $D(c)$ towards the centre of the concentration range is apparent.

A prediction for the concentration dependence of $D(c)$ is provided by some recent analyses. As in the case of small molecules, the mutual diffusion coefficient may be written as the product of a mobility term and a thermodynamic term expressing the departure from ideality of mixing[12]. The thermodynamic term may be evaluated using the Flory–Huggins theory for the free energy of mixing of a polymer blend; for polymers of identical chain lengths this gives[6–8]

$$D(c) = D_0[1 - 2\chi Nc(1-c)] \quad (1)$$

where c is the volume fraction of one polymer, D_0 is a coefficient expressing the mobility of the components (if the two materials have identical mobilities this would correspond to their self-diffusion coefficient), and χ is an interaction parameter (for polymers to be miscible χ must be $<1/2\ N$). For this sytem χ has been estimated by melting-point depression, and is expressed per monomer unit of PCL ($\chi = -0.38$)[13]. The presence of the polymerization index N ensures that the second term in equation (1) dominates for all but the smallest concentrations; that is, the diffusion is driven by enthalpy rather than by entropy. It is this that leads to the characteristic observed concentration dependence. For polymers with differing molecular masses the thermodynamic term is slightly different[8]; this introduces a skewing of the curve towards the region rich in the longer polymer.

The measured concentration dependence in the system we have studied is rather stronger than the simple quadratic relation given in equation (1) (compare with broken line in Fig. 2). Quantitative agreement with this result is not to be expected, because of the simplifications in the model used. In particular, no microscopic theory exists for the average mobility term D_0 when the polymers have different mobilities. In this system it is clear that there are large differences between the mobilities of the pure components; this is reflected in the large variation of glass transition temperature with composition[14]. Nonetheless, the present study shows directly for the first time that in a miscible polymer blend the mutual diffusion coefficient does indeed vary strongly with blend composition; a maximum is indicated near the middle of the blend composition range, in qualitative agreement with recent theoretical treatments.

We thank Dr F. Brochard, Professor E. J. Kramer and Dr R. C. Ball for useful discussions. R.A.L.J. holds an SERC CASE studentship with ICI PLC.

Received 30 December 1985; accepted 27 February 1986.

1. de Gennes, P. G. *J. chem. Phys.* **55**, 572–579 (1971).
2. Doi, M. & Edwards, S. F. *JCS Faraday Trans. II* **74**, 1789–1801 (1978).
3. Klein, J. *Nature* **271**, 143–145 (1978).
4. Tirrell, M. *Rubber Chem. Technol.* **57**, 523–548 (1984).
5. de Gennes, P. G. *C. r. hebd. Séanc. Acad. Sci., Paris* **292**, 1505–1508 (1981).
6. Brochard, F., Jouffroy, J. & Levinson, P. *Macromolecules* **16**, 1638–1643 (1983).
7. Kramer, E. J., Green, P. F. & Palmstrom, C. J. *Polymer* **25**, 473–479 (1984).
8. Sillescu, H. Die Makromolekulare Chemie, Rapid Communications **5**, 599–603 (1984).
9. Price, F. P., Gilmore, P. T., Thomas, E. L. & Laurence, R. L. *J. Polym. Sci. Polym. Symp.* **63**, 33–44 (1978); *Macromolecules* **13**, 880–886 (1980).
10. Chalykh, A. Ye., Sapozhnikova, I. N. & Aliyev, A. D. *Polymer. Sci. USSR* **21**, 1835–1840 (1980).
11. Crank, J. *Mathematics of Diffusion* 2nd edn (Oxford University Press, 1975).
12. Prigogine, I. *Thermodynamics of Irreversible Processes*, 3rd Edn (Wiley, New York, 1967).
13. Woo, E. M., Barlow, J. W. & Paul, D. R. *Polymer* **26**, 763–774 (1985).
14. Koleske, J. V. & Lundberg, R. D. *J. Polym. Sci.* Pt A-2 **7**, 795–807 (1969).

Vortex flow visualizations reveal change in upstroke function with flight speed in bats

Jeremy M. V. Rayner, Gareth Jones & Adrian Thomas

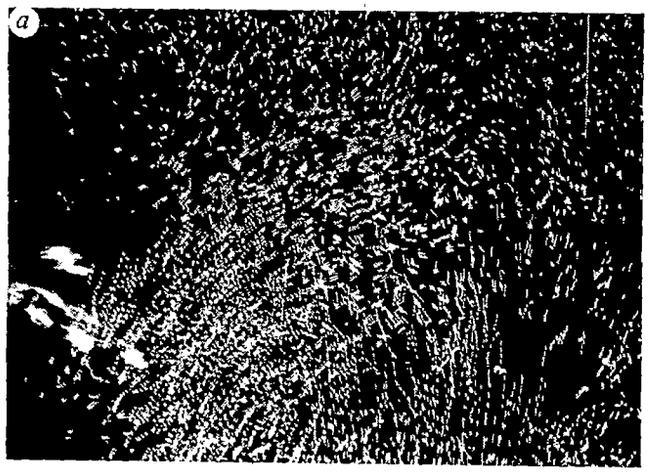
Department of Zoology, University of Bristol, Woodland Road, Bristol BS8 1UG, UK

The flapping wings of flying birds and bats generate complex, unsteady air movements. These consist of well-defined vortex structures which are a necessary result of the aerofoil action of the wings, and which transport momentum below and behind the animal in reaction to the lift force which both balances weight and provides thrust[1]. Visualization of the vortex patterns enables the aerodynamic function of the flapping wings to be determined[2–6]. Here we present the results of experiments with small vespertilionids which allow the first description of the vortex wake of bats. The aerodynamics of flapping flight is similar between birds and bats: thrust is always generated during the downstroke, but wingbeat gait (the cyclic pattern of wing movements) and the mechanical function of the upstroke are determined by wing morphology. We present the first evidence from aerodynamic experiments that in an individual bat or bat species, upstroke function and wingbeat gait also vary with flight speed, with aerodynamic lift being generated during the upstroke at high speeds but not during slow flight. This result confirms that flapping gaits are not species-specific, but are selected according to the mechanical conditions experienced by the animal.

We trained long-eared bats (*Plecotus auritus* L.) and noctules (*Nyctalus noctula* L.) to fly through a cloud of neutrally buoyant helium-filled soap bubbles, and recorded wake airflows by photographing the movements of the bubbles in stereo; illumination by four electronic flash guns fired successively at short intervals (8–12 ms) enabled vortex-induced air speeds to be determined, since speed is proportional to the distance between bubble images. Discrete vortices are identified by localized high flow velocities and pronounced rotational flows. This method has been applied to various species of birds[3,4,6], but has not been used previously with bats. Figures 1–3 show typical photographs from a total of about 250 of the two species, together with sketches, drawn from stereo pairs, of the associated discrete vortex patterns.

Wake photographs should be interpreted in relation to the balance of forces on the flying animal. The lift on the flapping wings acts horizontally as a thrust as well as vertically supporting the weight. If weight support alone were required the wings would not need to be flapped (a fixed gliding wing can generate sufficient lift to equal weight), but flapping of the wings must serve also to balance frictional and vortex drag forces: in gliding flight drag is uncompensated, and the animal has no alternative but to descend or decelerate relative to the air. The wake vortices transport momentum, the mean reaction of which in flapping flight is experienced as a lift force acting on the wings and providing *both* thrust and weight support. In the downstroke the wings move forwards and downwards relative to the air, and lift has the required forwards and upwards action[1,5,7,8]. In the upstroke, however, the wings move primarily upwards; at high flight speeds they also travel forwards, the air flow meets the ventral side of the wing as in the downstroke, and if lift is to contribute to weight support it cannot also give thrust, but must retard the animal[5–7]. In slow flight the wings may move slightly backwards relative to the air; lift forces are likely to be small or absent[1,7], but it has been suggested that if in bats the air flow strikes the dorsal surface of the wing, the resulting weak lift may act as both thrust and weight support[5,7,8].

Thus, upstroke function is the main mechanism of differentiation between flapping flight gaits in flying vertebrates, and the upstroke may be expected to act in different ways at different flight speeds. Experiments with birds have confirmed that gaits are constrained by wing morphology[2–6]: an active, lifting



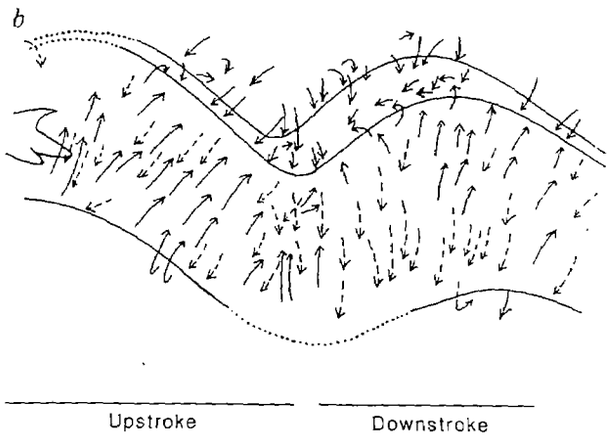


Fig. 1 Flow visualization for the noctule *N. noctula* in steady forward flight at ~7.5 m s^{-1}. *a*, Flow visualization photograph (one half of a stereo pair). *b*, The wake vortices and induced air movements as drawn from stereo pairs. (Bubble direction can be inferred from the photographs as the light intensity is not constant during each flash[3,4]; broken arrows indicate air movements between the vortex cores.) The wake is formed from a pair of continuous vortex tubes which follow the path of the wings; the spacing of the core centres is ~75% of the distance between the wingtips. The cross-sectional diameter of the cores is greater than that commonly seen in birds[2-4] owing to the relatively small size of the bat. The bat is climbing slightly, but this does not substantially distort wingbeat action compared with level flight. Flash interval 10 ms.

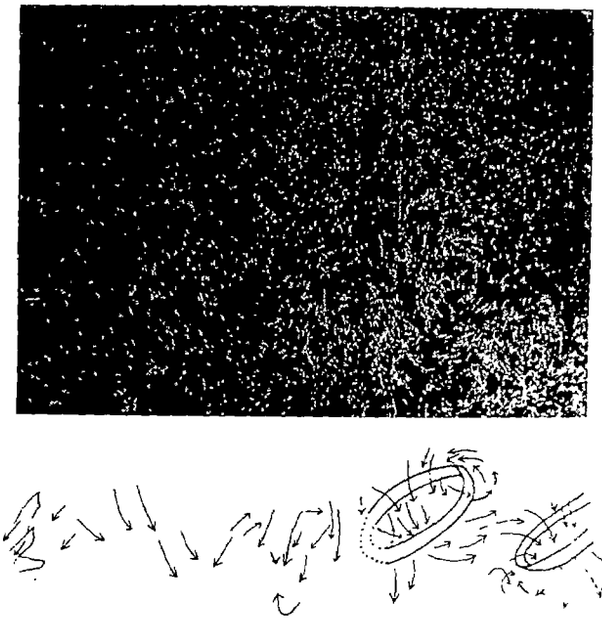


Fig. 2 Flow visualization for noctule in slow flight (3 m s^{-1}), together with the transition to faster flight as the bat accelerates. Two vortex rings are visible to the right; no trailing vorticity is shed during the upstroke, and there is a strong momentum-transporting flux of air through the centres of the rings. These are followed by a weak, continuous tube vortex closer to the bat. Flash interval 10 ms; only three flash guns were used in taking this photograph.

upstroke is more common in long-winged species (typically in fast flight at ~8 m s^{-1} in the kestrel *Falco tinnunculus*[3,6], with above-average aspect ratio and pointed wings), but is absent in small finches[2], which have shorter, rounded wings. During an active upstroke (that is, with aerofoil action generating a lift force) the effective wingspan must be reduced by flexing or sweeping back the wing to reduce retardation from lift and so ensure a mean positive thrust. Theoretical models predict that in an individual animal the upstroke should be active at higher flight speeds, while in slow flight it should be inactive and the wingtips should be brought close to the body to minimize friction drag and inertial forces[1,5,7]. The experiments reported here provide the first direct aerodynamic evidence for such changes in upstroke function.

The wakes of flying microbats have much in common with those of birds. When the wings are actively generating lift, the vortex sheets shed from the trailing edges roll rapidly into a pair of discrete vortex lines or tubes behind the wingtips. In fast flight (7–9 m s^{-1}—normal cruising speeds) the noctule's wake is a continuous, undulating vortex pair (Fig. 1); this indicates that the upstroke is active in the way described above, and confirms an earlier prediction[5] based on wingbeat kinematics. The vortex structure is similar to that seen for the kestrel[3,6]. The marked absence of transverse vorticity leads to the remarkable conclusion that in both animals the strength (circulation) of the bound wing vortex does not vary during the wingstroke; this conveys certain mechanical advantages[5,7]. Both noctule and kestrel have wings of above-average aspect ratio, and use similar wingbeat kinematics which are fully consistent with this form of wake[5]. The wingtip is swept back in the bird, while the arm wing is flexed in the bat; but, in both, the wingtip moves towards the body during the upstroke.

At lower speeds (3 m s^{-1}) the noctule wake is rather different (Fig. 2): prominent transverse vortices are shed at the top and bottom of the downstroke, and the upstroke is flexed and inactive. Circulation can no longer remain constant, although it may be nearly so during the downstroke. This 'vortex ring' wake is similar to that of small finches[2] and slow-flying pigeons[3,4,6]. Noctules are fast-flying bats which rarely fly sufficiently slowly to show an inactive upstroke, but together our results (as illustrated by Figs 1 and 2) provide the first evidence that upstroke function is variable and is not in general species-specific; moreover, an individual animal changes its gait optimally as flight speed increases. In slow flight (1–2 m s^{-1}) in the long-eared bat (which has rather large wings of low aspect ratio) the wake is similar to that of the slow-flying noctule (Fig. 3), with a clear vortex ring corresponding to aerodynamic lift during the downstroke. Our flow visualizations provide no evidence that the upstroke is active in *P. auritus* at any speed, although Norberg concluded from wingbeat photography that in this species at low speeds a weak lift acts as thrust[8]. In slow flight the wingbeat kinematics of both species show considerable flexure and twisting of the wings during the upstroke[5,7-10], and any lift generated then is weak. It has been suggested[5,8,9] that the rapid 'flick' phase at the top of the upstroke in this and similar bats[8-10] may

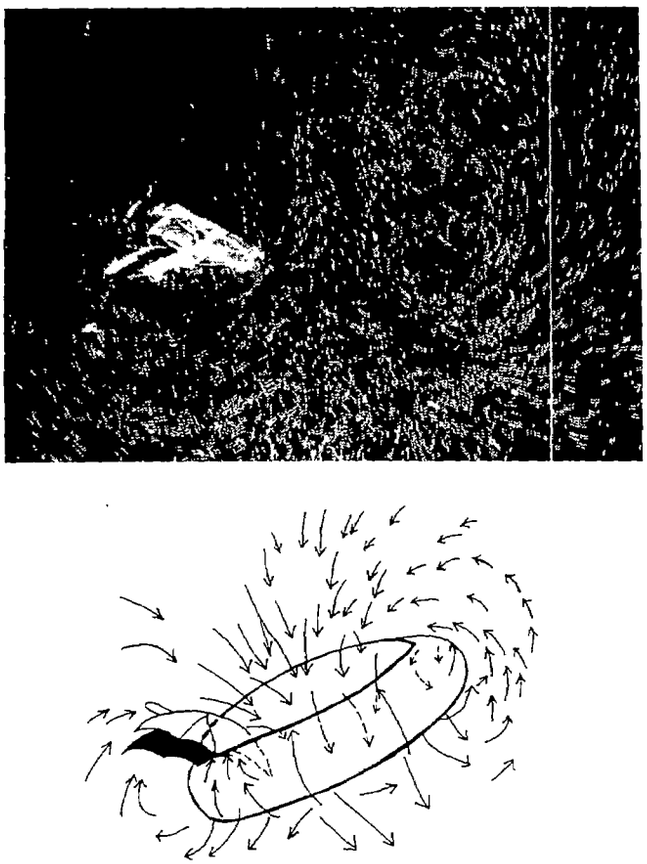


Fig. 3 Flow visualization for long-eared bat *P. auritus* in slow flight (1.5 m s^{-1}). Intense rotational flows induced by a vortex ring generated during the downstroke are visible; at the time of the photograph the wings were at the bottom of the downstroke, and ring generation was still in progress. No vorticity had been shed during the predeeding upstroke, but a similar ring was generated by the preceeding downstroke. The wake in this species is similar to that recorded previously in finches[2] and pigeons[3,4]. Flash interval 8 ms. The matching stereo pair of this photograph is shown on the front cover.

generate thrust; this would entail generation of a concentratated transverse vortex at the start of the flick, approximately midway through the upstroke. We found no trace of such vortices in any of our photographs, although as any lift would necessarily be small, they might have been obscured by the more dominant forces and vortices associated with the downstroke. Although unsupported by the present experimental evidence, we cannot exclude the possibility of weak upstroke lift in at least some bat species.

Despite obvious morphological differences, the flapping-wing aerodynamics of birds and bats show considerable similarities. In both groups gaits are defined by upstroke function, which has been shown to vary with wing morphology. Gait changes with flight speed similar to those reported here in bats have been inferred in birds from analysis of wingbeat kinematics[1,5]; similarly, in bats these changes are likely to be reflected in generation of upstroke lift and the structure of the wake vortices.

We thank H. D. J. N. Aldridge, M. A. Rezende and G. R. Spedding for advice, and U. M. Norberg for comments on the manuscript. This work was supported by grants from the Royal Society, NERC and SERC.

Received 6 February; accepted 20 March 1986.

1. Rayner, J. M. V. *J. exp. Biol.* **80**, 17–54 (1979).
2. Kokshaysky, N. V. *Nature* **279**, 146–148 (1979).
3. Spedding, G. R. Thesis, Univ. Bristol (1982).
4. Spedding, G. R., Rayner, J. M. V. & Pennycuick, C. J. *J. exp. Biol.* **111**, 81–102 (1984).
5. Rayner, J. M. V. in *Biona Report 5* (ed. Nachtigall, W.) 27–74 (Gustav Fischer, Stuttgart, in the press).
6. Rayner, J. M. V. in *Konstruktionsprinzipien lebender und ausgestorbener Reptilien. Konzepte SFB 230 4* (eds Riess, J. & Frey, E.) 89–118 (University of Tübingen, 1985).
7. Rayner, J. M. V. in *Recent Advances in the Study of Bats* (eds Fenton, M. B., Racey, P. A. & Rayner, J. M. V.) (Cambridge University Press, in the press).
8. Norberg, U. M. *J. exp. Biol.* **65**, 179–212 (1976).
9. Eisentraut, M. *Z. wiss. Zool.* **148**, 159–188 (1936).
10. Aldridge, H. D. J. N. Thesis, Univ. Bristol (1985).

Genetics and evolution of female choice

M. E. N. Majerus, P. O'Donald, P. W. E. Kearns & H. Ireland

Department of Genetics, University of Cambridge, Downing Street, Cambridge CB2 3EH, UK

Fisher's theory of the evolution of sexual selection by female choice depends crucially on the premise that the preference of females to mate with males of a specific genotype is itself genetic[1]. In the polymorphic ladybird *Adalia bipunctata*, a genetically determined, non-assortative female preference for melanic males has been demonstrated[2]. Models of the evolution of female choice show that the rate of evolution and the final outcome of this selection depend critically on the exact mode of inheritance of both the preferred character and the preference[3]. Here we describe experiments in which the level of preference has been raised by artificial selection over 14 generations. Resultant estimates of heritability are consistent with models in which one or a small number of genes control the preference. Analysis of the levels of preference in isofemale lines derived from the high preference stock shows a quadrimodal distribution in preference. These results are entirely consistent with the deduction that a single dominant gene controls female choice. We conclude that this complex behavioural strategy is based on simple genetics. Furthermore, the demonstration of a simple genetic basis to female mating preferences in *A. bipunctata* implies that sexual selection by female choice is not only important in the evolution of male sexual adornments in sexually dimorphic species, but may also maintain polymorphisms that are not sex-limited.

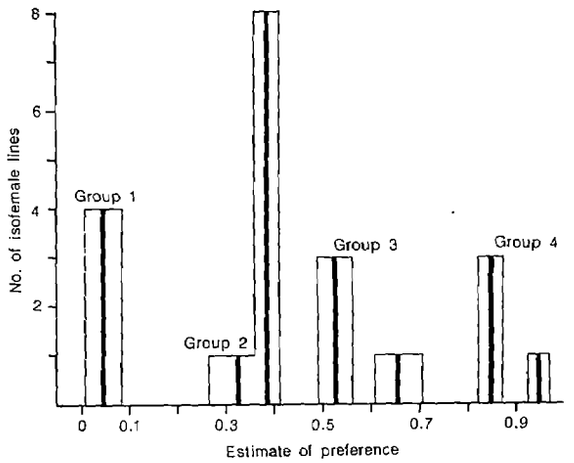


Fig. 1 Isofemale lines shown divided into four distinct groups. The solid black bar shows the position of the estimated preference in the given number of lines, open bars, the standard error. In groups 2, 3 and 4, the preference is also shown for the line most divergent from the others in the group. When groups are considered separately, each of groups 1, 2 and 3 is found to be statistically homogeneous. Group 4 is heterogeneous, with line Z35 having a significantly higher preference. In later population cage experiments, however, Z35 did not show a higher preference. The total χ^2 for heterogeneity within all groups is not significant (Table 2).

Table 1 Matings of males in experiments to select for increased preference in favour of melanic Q males

No. of matings and estimates of preference

Generation	No. of matings Q♂♂	No. of matings T♂♂	Estimates of preference $\hat{\gamma} \pm \sqrt{\text{var}(\hat{\gamma})}$
1	76	98	0.195 ± 0.054
2	47	39	0.352 ± 0.077
3	67	53	0.369 ± 0.065
4	73	48	0.433 ± 0.064
5	132	94	0.406 ± 0.047
6	129	87	0.425 ± 0.048
7	117	63	0.500 ± 0.051
8	125	48	0.604 ± 0.049
9	125	41	0.647 ± 0.048
10	96	55	0.480 ± 0.056
11	118	49	0.581 ± 0.050
12	153	77	0.522 ± 0.044
13	130	61	0.544 ± 0.048
14	118	41	0.632 ± 0.050

Analysis of χ^2 of variation in preference

Component of variation	χ^2	Degrees of freedom	P
Regression on generations	47.2017	1	—
Residual	22.8445	12	0.0291
Total for 2×14 table	70.0462	13	—

Q represents the four-spot melanic *A. b. quadrimaculata* and T the two-spot non-melanic *A b. typica*. The numbers of matings are the combined numbers in two replicate lines. $\hat{\gamma}$, is the estimated proportion of preferential matings for Q males, shown with the standard error[15]. At generations 5 and 10, the replicates were allowed to mate together without artificial selection. Two new lines were then formed from the unselected generations 5 and 10 to give selected generations 5 and 10 for each of the new replicates. The data shown are those for the selected generations 5 and 10 only. The drop in preference at generations 5 and 10 suggests that there may have been some natural selection against the high preference. The latter drop is the main source of the heterogeneity that gives rise to the significant residual χ^2.

In ladybirds, sexual selection takes place because females exercise a genetically determined preference for melanic males. In a natural population of the two-spot ladybird, *A. bipunctata*, at Keele, UK, melanic males gain a mating advantage over non-melanic males. About 20% of matings take place preferentially with melanic males[4]. Majerus, O'Donald and Weir[2] selected increased female preference, raising the proportion of preferential matings from 20% to more than 50% in four generations. Reciprocal matings between males and females from the selected, high preference line and the unselected, original Keele stock showed that female preference, and not male competitiveness, had indeed been selected. The preference was genetic, in accordance with the premise of Fisher's theory.

We have now repeated this experiment, but have selected for both increased and reduced preference, producing high and low preference lines. The experimental protocol follows that of our previous selection experiment[2]. The results of selecting for increased preference are shown in Table 1. At generation 10, single pairs were selected at random from the high line. Each batch of eggs was laid by each female in a separate Petri dish and the larvae thus reared separately to avoid larval cannibalism. In this way, large numbers of progeny, up to 600 from some females, have been produced for measurement of the female preference within each 'isofemale line'. In initial, formal mating tests, 10 males and 10 females each consisting of 5 *A. bipunctata quadrimaculata* melanics (Q) or 5 *A. bipunctata sexpustulata* melanics (S) and 5 *A. bipunctata typica* non-melanics (T) were placed in containers and allowed to mate. At 30-min intervals, mating pairs were removed and replaced with individuals of similar phenotypes. In each 30-min interval, therefore, matings took place without replacement. The results are shown in Table 2. Since as many as five or six matings might take place in each interval, the sampling without replacement creates a very difficult problem for the statistical estimation of the preferences Nevertheless, a general test of significance based on the null hypothesis of no preference shows wide variation between the isofemale lines. Female progeny from some lines mate almost solely with melanics, while those from others mate at random or show intermediate levels of preference (between lines $\chi^2_{39} = 387.08$; $P \sim 0$). No significant differences were found when Keele males or males from other lines were used instead of males from the same line as the females ($\chi^2_4 = 6.01$; $P = 0.198$). The variation in preference is thus produced entirely by genetic differences contributing to the female choice. Lines showing high, intermediate and low levels of preference were chosen for further genetic analysis. We have now tested the preference in some of these lines using large numbers in population cages, with replacement of males as in our original experiments[2]. Table 3

Table 2 Initial formal mating tests on mating preferences in isofemale lines

Frequencies of matings with males

Group	Line	Mated males Q	Mated males T	Total males Q	Total males T	Estimate of preference
1	Z4	51	48	210	210	0.033 ± 0.088
	Y4	218	204	815	815	0.038 ± 0.042
	Z33	49	45	220	220	0.046 ± 0.091
	Y12	57	52	245	245	0.050 ± 0.084
	Totals	375	349	1,490	1,490	0.041 ± 0.032
2	Y18	134	73	395	395	0.324 ± 0.055
	Y14	149	74	435	435	0.367 ± 0.052
	Z36	141	69	400	400	0.375 ± 0.053
	Y13	223	107	700	700	0.380 ± 0.043
	Z17	212	102	620	620	0.381 ± 0.044
	Z34	141	66	420	420	0.393 ± 0.054
	Z20	68	33	125	125	0.398 ± 0.067
	Y15	154	70	395	395	0.411 ± 0.049
	Z32	74	32	200	200	0.430 ± 0.072
	Totals	1,296	626	3,690	3,690	0.381 ± 0.018
3	Z13	218	79	590	590	0.501 ± 0.042
	Y9	150	50	360	360	0.537 ± 0.048
	Z16	80	26	200	200	0.544 ± 0.067
	Y3	153	36	335	335	0.654 ± 0.044
	Totals	601	191	1,485	1,485	0.553 ± 0.024
4	Y19	272	34	575	575	0.801 ± 0.028
	Z37	91	6	240	240	0.887 ± 0.040
	Z40	102	5	200	200	0.918 ± 0.031
	Z35	203	7	385	385	0.942 ± 0.018
	Totals	668	52	1,400	1,400	0.872 ± 0.015

Analysis of χ^2

Component of variation	χ^2	Degrees of freedom	P
Between groups	362.39	3	—
Within groups	24.69	17	0.102
Within replicates of lines	20.35	19	0.374
Total	407.43	39	—

In this analysis of χ^2, the data for replicates of tests on individual lines have not been included. Totals over replicates within lines are shown. The analysis of χ^2 is based on the null hypothesis of random mating of male phenotypes: it is an analysis of the values of χ^2 for interaction in the $2 \times 2 \times N$ table of numbers of mated and unmated phenotypes of males in tests on the isofemale lines. Note that the same males and females may be used several times in successive series of tests.

gives the results obtained so far.

The distribution of levels of preference in the isofemale lines suggests that female preference for melanic males may be largely under the control of one or a very few major genetic loci. The isofemale lines can be divided into four groups according to their preference (see Table 2, Fig. 1). Group 1 females show no significant preference, group 2 females have levels of preference between 0.32 and 0.43, group 3 females have levels of preference of 0.50–0.65, and group 4 females have the highest levels of preferences, between 0.80 and 0.94. There is overall homogeneity within the groups ($\chi^2_{17} = 24.69$; $P = 0.102$), and highly significant differences between groups ($\chi^2_3 = 362.39$; $P = 1.8 \times 10^{-9}$).

The population cage experiments on progeny from the isofemale lines corroborate this apparent discontinuity in the preference distribution (Table 3). Matings were observed in cages in which melanic males and non-melanic males were maintained at the ratio 3Q:7T as in previous experiments[2,4]. If matings take place with males at this ratio, no preference has been exercised and mating has been random. An excess of Q males in mating indicates preference. A simple model yields an estimate of the proportion of females mating preferentially

$$\hat{\gamma} = \frac{n_Q(1-v) - n_T v}{(1-v)(n_Q + n_T)}$$

where v is the frequency of Q males ($v = 0.3$ in these experiments), and n_Q and n_T are respectively the numbers of Q and T males observed to mate. Again, some lines show high levels of preference (lines Y19, Z28, Z35, Z37 and Z40), while others show no preference at all (lines Y12, Z4, Z33) or intermediate levels of preference (lines Y9, Y14, Z13, Z34).

The pattern of preference levels can be easily explained by a single dominant gene. In the population at Keele, females would either carry the preference gene and hence show the high level of preference at about $\gamma = 0.85$ or lack the gene and show no preference at all. If about one-quarter of the females have the preference, this would give the observed level of 20% preferential mating in the unselected Keele population. After selection has raised the preference to around 50% as in our high line, the preference gene would then have a frequency of $P = 0.36$. At this gene frequency, 24% of matings should only produce females with the preference ($\gamma = 0.85$), 21% should produce females of which three-quarters have the preference ($\gamma = 0.64$) and 38% of matings should produce females of which half have the preference ($\gamma = 0.43$). Females from the rest of the matings should all mate without preference, for none of them would carry the preference gene. The isofemale lines follow this pattern closely, as Fig. 1 shows, with groups 1–4 represented by 4, 9, 4 and 4 isofemale lines respectively ($\chi^2_3 = 0.453$, $P = 0.93$ for test of goodness-of-fit).

We have thus shown that female ladybirds are highly polymorphic in their preference for melanic males. This polymorphism is genetic. Single-gene models, such as those of O'Donald[3] and Kirkpatrick[5], may therefore be sufficient to explain the evolution of female choice as a mating strategy.

In the ladybirds, natural and sexual selection apparently act to maintain a stable polymorphism of melanic and non-melanic phenotypes[6]. However, unlike the most obvious and widely quoted examples of evolution by sexual selection—such as the breeding plumage of male peacocks, pheasants, ruffs and birds of paradise—the sexes of the ladybirds are alike: they both show the same polymorphism of melanic and non-melanic phenotypes.

The theory of sexual selection may thus apply more widely than has generally been supposed. It may explain not only the evolution of highly developed display characters in males but also the evolutionary stability of simple genetic polymorphisms in which no sexual dimorphism is present. Sexual selection has been implicated in the maintenance of other non-sex-limited polymorphisms, in scarlet tiger moths[7], snow geese[8,9], arctic skuas[10], and even in the polymorphism of electrophoretic allozymes in the milkweed beetle *Tetraopes tetraophthalamus*[11]. However, the genetic basis of the mating preference has not been demonstrated in any of these cases. That female mating preference can be controlled by a simple genetic system could allow for the appearance and rapid evolution of a frequency-dependent mechanism that would maintain such polymorphisms.

In the wider context of the sociobiological interpretation of animal behaviour, we have shown that a single gene may determine behaviour as complex as the alternative mating choices that an animal might make. This has been a point of great controversy. Models in sociobiology have been based on the assumption that alternative strategies—for example whether to be a 'hawk' or 'dove' in conflicts—are genetic polymorphisms[12,13]. This simple genetic model of complex behaviour has been challenged by opponents of sociobiology[14], but female choice behaviour in *A. bipunctata* is certainly both genetic and polymorphic.

This work was funded by a SERC research grant to P.O'D. and was carried out in a laboratory built in 1984 with a grant from the Wolfson Foundation for research in population genetics.

Table 3 Female preferences from population cage experiments on isofemale lines

Tests on lines producing both Q and T males

Lines used in tests		No. of matings		Estimate of preference
Females	Males	Q/S	T	$\hat{\gamma} \pm \sqrt{\text{var}(\hat{\gamma})}$
Y9(Q, T)	Y9(Q, T)	67	39	0.474 ± 0.067
Y14(Q, T)	Y14(Q, T)	58	52	0.325 ± 0.068
Z13(Q, T)	Z13(Q, T)	75	40	0.503 ± 0.063
Z28(S, T)	Z28(S, T)	100	6	0.919 ± 0.032
Z34(Q, T)	Z34(Q, T)	52	57	0.253 ± 0.068
Z37(Q, T)	Z37(Q, T)	89	13	0.818 ± 0.047
Z37(Q)	Keele(Q, T)	92	8	0.886 ± 0.039
Z37(T)	Keele (Q, T)	86	16	0.776 ± 0.051

Analysis of χ^2

Component of variation	χ^2	Degrees of freedom	P
Between lines	124.8885	5	—
Between males in line Z37	1.5329	2	0.465
Total	126.4214	7	—

Tests on lines producing only one phenotype

Lines used in tests		No. of matings		Estimates of preference
Females	Males	Q	T	$\hat{\gamma} \pm \sqrt{\text{var}(\hat{\gamma})}$
Y12(T)	Keele(Q, T)	26	73	0.053 ± 0.063
Y19(T)	Keele(Q, T)	86	19	0.741 ± 0.054
Z4(T)	Keele(Q, T)	33	66	0.048 ± 0.068
Z33(Q)	Keele(Q, T)	38	59	0.131 ± 0.071
Z33(Q)	Keele(Q, T)	34	69	0.043 ± 0.066
Z35(T)	Keele(Q, T)	94	8	0.888 ± 0.038
Z40(T)	Keele(Q, T)	89	9	0.869 ± 0.042

Analysis of χ^2

Component of variation	χ^2	Degrees of freedom	P
Between lines	220.3729	5	—
Within line Z33	0.7744	1	0.379
Total	221.1473	6	—

S represents the six-spot melanic *A. b. sexpustulata*, which occurs in line Z28. 'Keele' means the original unselected stock from Keele, U.K. Letters in parentheses show the phenotypes used in the test.

Received 20 December 1985; accepted 12 March 1986.

1. Fisher, R. A. *The Genetical Theory of Natural Selection* (Clarendon, Oxford, 1930).
2. Majerus, M. E. N., O'Donald, P. & Weir, J. *Nature* **300**, 521-523 (1982).
3. O'Donald, P. *Heredity* **22**, 499-578 (1967); *Genetic Models of Sexual Selection* (Cambridge University Press, 1980).
4. Majerus, M. E. N., O'Donald, P. & Weir, J. *Heredity* **49**, 37-49 (1982).
5. Kirkpatrick, M. *Evolution* **36**, 1-12 (1982).
6. O'Donald, P., Derrick, M., Majerus, M. E. N. & Weir, J. *Heredity* **52**, 43-61 (1984).
7. Sheppard, P. M. *Heredity* **6**, 239-241 (1952).
8. Cooke, F. & Cooch, F. G. *Evolution* **22**, 289-300 (1968).
9. Cooke, F., Mirsky, P. J. & Seiger, M. B. *Can. J. Zool.* **50**, 529-536 (1972).
10. O'Donald, P. *The Arctic Skua* (Cambridge University Press, 1983).
11. Eanes, W. F., Gaffney, P. M., Koehn, R. K. & Simon, C. M. *Lect. Notes Biomath.* **19**, 49-64 (1977).
12. Dawkins, R. *The Selfish Gene* (Oxford University Press, 1976).
13. Maynard-Smith, J. *Evolution and the Theory of Games* (Cambridge University Press, 1982).
14. Lewontin, R. C. *Nature* **266**, 283-284 (1977).
15. O'Donald, P. & Majerus, M. E. N. *Heredity* **55**, 401-412 (1985).

A benzodiazepine used in the treatment of insomnia phase-shifts the mammalian circadian clock

Fred W. Turek & Susan Losee-Olson

Department of Neurobiology and Physiology, Northwestern University, Evanston, Illinois 60201, USA

Between 5 and 20% of the adult population in Western countries suffer from insufficient and/or unsatisfying sleep[1,2], often associated with certain psychiatric disorders or with certain types of professional activities (for example, shift workers) and travel schedules (for example, jet lag)[1,3,4]. The benzodiazepines are at present the drug treatment of choice for the management of anxiety and stress-related conditions as well as insomnia[5]. Benzodiazepines are thought to act by potentiating the action of the neurotransmitter γ-aminobutyric acid (GABA), a widely distributed transmitter in the central nervous system[6]. The circadian system has a key role in the regulation of the sleep–wake cycle[7–12], and at least some forms of insomnia may be the result of a disorder of the circadian sleep–wake rhythm[8,9]. Similarly, at least some forms of depression may also involve disruption of normal circadian rhythmicity[13,14]. A central pacemaker for the generation of many circadian rhythms in mammals, including the sleep–wake cycle, appears to be located in the suprachiasmatic nucleus[15], and recent research indicates that both cell bodies and axons containing GABA are present within the bilaterally paired suprachiasmatic nuclei[16,17]. These findings raise the possibility that the benzodiazepines, commonly prescribed for sleep and mental disorders, may have an effect on the central circadian pacemaker. Here we report that the acute administration of triazolam, a short-acting benzodiazepine[18] commonly prescribed for the treatment of insomnia, induces a phase-shift in the circadian rhythm of locomotor activity in golden hamsters. This suggests a role for GABA-containing neurones in the mammalian circadian system.

A useful approach in determining whether a specific pharmacological agent can influence a circadian clock is to follow an easily measured pacemaker property, such as the phase of a rhythm driven by the clock, during acute administration of the drug[19]. We have examined the potential phase-shifting effects of triazolam on the circadian rhythm of wheel-running behaviour in golden (Syrian) hamsters. Nine-week-old outbred adult male golden hamsters (*Mesocricetus auratus*, Lakeview Hamster Colony, Newfield, New Jersey) were initially housed in groups and placed under a light/dark (LD) regime of 14:10 (14 h of light per 24-h day) for 1–3 weeks. The animals were then moved to individual cages equipped with a running wheel to allow for the continuous recording of locomotor activity[20]. The animals were transferred 2 to 3 weeks later to either constant light (LL; $N = 40$) or constant darkness (DD; $N = 40$) and were kept under these constant environmental conditions for at least 2 weeks before receiving an intraperitoneal injection of vehicle or 2.5 mg of triazolam dissolved in 0.5 ml of dimethyl sulphoxide at various circadian times. All injections were timed to occur 0, 3, 6, 9, 12, 15, 18 or 21 h after the onset of activity, with onset of activity being designated as circadian time (CT) 12. Thus CT 6 and 21 represent phase points occurring respectively 6 h before and 9 h after the onset of locomotor activity. The hamsters were injected with vehicle or triazolam at least once, and up to four times, with an interval of at least 2 weeks between consecutive injections. The phase-shifting effects of triazolam on the circadian rhythm of locomotor activity were assessed by comparing the onsets of activity before and after drug treatment. The precise nature of the onset of wheel-running activity in the golden hamster makes it easy to detect phase-shifts as small as 15 min (Fig. 1).

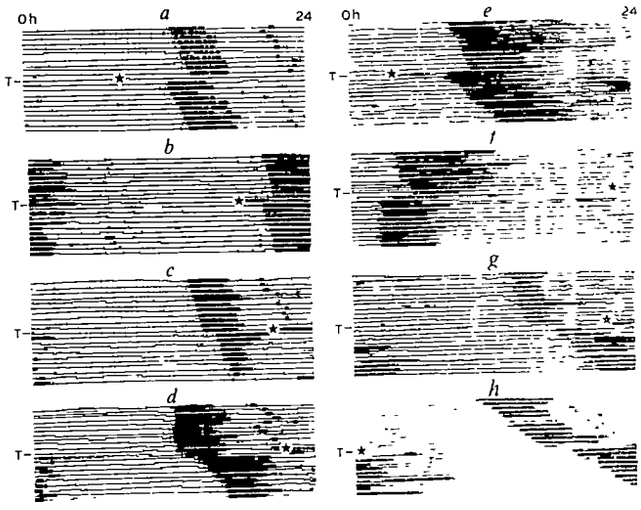


Fig. 1 Representative sections from the activity records of eight hamsters for a 10–12-day period before and after they were injected with 2.5 mg of triazolam at various circadian times. Each line represents a single 24-h period and successive days are plotted from top to bottom in each record. The four animals depicted on the left (*a–d*) were exposed to constant darkness while the four animals shown on the right (*e–h*) were exposed to constant light throughout the study. The day of the triazolam injection is noted by the letter 'T' to the left of each record, and the exact time of the injection on that day is indicated by the star. Using the daily onsets of activity for the 5 days preceding the injection as phase reference points for the pre-injection rhythm, a time of activity onset on the succeeding day was graphically projected. In addition, the daily onsets of activity for 2–7 days after the injection (once a new steady state was achieved) were used as phase reference points for the post-injection rhythm, and a time of activity onset for the first circadian day following the injection was projected backwards. The subtraction of the estimated phase of the rhythm after the treatment from the projected phase of the rhythm before treatment yields the magnitude of the phase-shift induced by the injection of vehicle alone or triazolam. Thus, a negative value indicates a delay in the onset of activity; a positive value indicates a phase advance. Using the onset of activity as representing circadian time (CT) 12, the CT of each injection and the resulting phase shift ($\Delta\phi$) in minutes were calculated to be: *a*, CT = 6, $\Delta\phi = +150$; *b*, CT = 9, $\Delta\phi = +90$; *c*, CT = 18, $\Delta\phi = -60$; *d*, CT = 21, $\Delta\phi = -85$; *e*, CT = 6, $\Delta\phi = +110$; *f*, CT = 6, $\Delta\phi = +180$; *g*, CT = 18, $\Delta\phi = -120$; *h*, CT = 21, $\Delta\phi = -100$. On 32 different occasions, vehicle alone was injected at various circadian times. No clear phase-shift (>10 min) was observed in the activity rhythm following any of these injections.

While injections of vehicle alone had no effect on the rhythm of locomotor activity, injections of 2.5 mg of triazolam induced phase-shifts in the activity rhythm that were dependent on the circadian time of administration in animals exposed to either

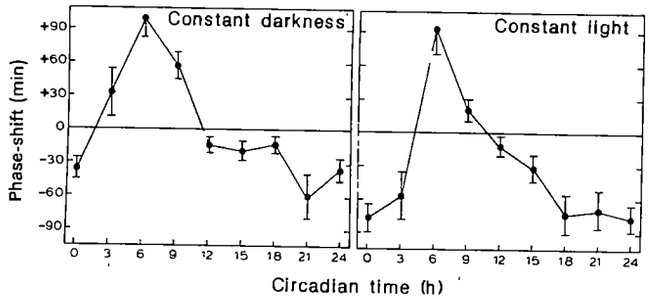


Fig. 2 Mean (±s.e.m.) phase-shifting effect of a systemic injection of triazolam at various circadian times on the free-running rhythm of locomotor activity in hamsters exposed to constant darkness (left, 9 animals per time point) or constant light (right, 7–9 animals per time point). A point above the solid line indicates an advance in the onset of activity, a point below the line indicates a delay in activity onset. The onset of locomotor activity represents CT 12. The values presented for circadian times 0 and 24 represent the same data.

DD or LL (Fig. 1). Phase-shifts induced by triazolam were usually completed within one or two cycles. Injection of as little as 0.1 mg of triazolam has also been found to phase-shift the circadian rhythm of activity (F.W.T., unpublished results). A plot of the phase-shifts induced by triazolam as a function of the circadian time of administration revealed that the general shapes of the 'phase response curves' in DD and LL were similar, with triazolam injections at CT 6 and 9 inducing phase advances while injections between CT 12 and 24 induced phase delays (Fig. 2). The major difference between the phase response curves is that while the mean response to an injection of triazolam at CT 3 was an advance of the activity rhythm for animals exposed to DD, a delay in the activity rhythm was observed in the animals exposed to LL that were injected with triazolam at this circadian time.

The phase response curves generated by injections of triazolam are radically different from those generated by light pulses (on a background of constant darkness) in hamsters and in other mammalian species[20,21]. Light pulses, as well as carbachol, a cholinergic agonist that mimics the phase-shifting and entraining effects of light pulses, induce phase delays early in the subjective night (for example CT 12–14) and phase advances late in the subjective night (for example CT 18–22)[19]. The region CT 3–12 is referred to as a 'dead zone' because light does not induce any phase-shift at these circadian times[21]. In contrast, triazolam induces clear phase advances during the dead zone for light and induces phase delays at a time when light induces phase advances. These results, together with the fact that the phase response curves for triazolam are similar under either LL or DD conditions, indicate that the phase-shifting effects of triazolam do not involve an activation of light input pathways to the biological clock.

Because the effects of triazolam are probably mediated by the GABAergic system[6], the present results suggest a role for GABA-containing neurones in an input pathway to a central biological clock regulating the circadian rhythm of locomotor activity (and presumably many other circadian rhythms) and/or in the clock system itself. The finding that GABA neurones are located within a central circadian pacemaker in rodents—the suprachiasmatic nucleus[16,17]—raises the possibility that the phase-shifting effects of triazolam occur at the level of the suprachiasmatic nucleus itself. Further support for a role of GABA in the circadian organization of mammals is the observation that bicuculline, a selective antagonist of GABA, can block the phase-delaying, but not the phase-advancing effects of light pulses on the circadian rhythm of locomotor activity in hamsters[22].

While triazolam treatment (0.5 m.g) of patients suffering sleep disturbances is effective in improving sleep following a shift in the sleep–wake schedule[23,24], triazolam did not appear to facilitate the re-entrainment of the sleep–wake cycle to the new schedule[24]. However, as the results of the present study demonstrate, the phase-shifting effects of triazolam on the biological clock are dependent on the circadian time of administration. Therefore, any attempt to design an appropriate drug regime that will enhance sleep, as well as shorten the time needed for re-entrainment of the circadian system following a shift in the sleep–wake cycle, must take into account both the direction of the phase shift and the circadian time of drug administration. Drugs which can induce phase-shifts in the circadian system may be useful in the treatment of various physical and mental illnesses that have been associated with a disorder in circadian time-keeping[25].

This work was supported by NIH research grant HD-09885, the Whitehall Foundation and the Upjohn Company, which also provided the triazolam for this study. We thank Dr Eve Van Cauter for critical comments and Dr Kenneth Starz for assistance in the preparation of this paper.

Received 13 January; accepted 10 March 1986.

1. Akerstedt, T. *Experientia* **40**, 417–422 (1984).
2. Mellinger, G. D., Balter, M. B. & Uhlenhuth, E. H. *Archs gen. Psychiat.* **42**, 225–232 (1985).
3. Moore-Ede, M. C., Czeisler, C. A. & Richardson, G. S. *New Engl. J. Med.***309**, 530–536 (1983).
4. Desir, D. *et al. J. clin. Endocr. Metab.* **52**, 628–641 (1981).
5. *J. Am. med. Ass.* **251**, 2410–2414 (1984).
6. Müller, W. E. in *Neuroreceptors* (ed. Hucho, F.) 3–13 (de Gruyter, Berlin, 1982).
7. Aschoff, J. & Wever, R. *Fedn Proc.* **35**, 2326–2332 (1976).
8. Czeisler, C. A., Weitzman, E. D., Moore-Ede, M. C., Zimmerman, J. C. & Kronauer, R. E. *Science* **210**, 1264–1267 (1980).
9. Weitzman, E. D. *et al. Archs gen. Psychiat.* **38**, 737–746 (1981).
10. Winfree, A. T. *Am. J. Physiol.* **245**, R497–R504 (1983).
11. Daan, S., Beersma, D. G. M. & Borbely, A. A. *Am. J. Physiol.* **246**, R161–R178 (1984).
12. Folkard, S., Hume, K. I., Minors, D. S., Waterhouse, J. M. & Watson, F. L. *Nature* **313**, 678–679 (1985).
13. Linkowski, P. *et al. J. clin. Endocr. Metab.* **61**, 429–438 (1985).
14. Wehr, T. A. & Goodwin, F. K. (eds) *Circadian Rhythms in Psychiatry* (Boxwood, Pacific Grove, California, 1983).
15. Turek, F. W. *A. Rev. Physiol.* **47**, 49–64 (1985).
16. Card, J. P. & Moore, R. Y. *Neuroscience* **13**, 415–431 (1984).
17. Van den Pol, A. N. & Tsujimoto, K. L. *Neuroscience* **15**, 1049–1086 (1985).
18. Eberts, F. S., Philopoulos, B. S., Reineke, B. S. & Vliek, R. W. *Clin. Pharmac. Ther.* **29**, 81–93 (1981).
19. Earnest, D. J. & Turek, F. W. *Proc. natn. Acad. Sci. U.S.A.* **82**, 4277–4281 (1985).
20. Ellis, G. B., McKlveen, R. E. & Turek, F. W. *Am. J. Physiol.* **242**, R44–R50 (1982).
21. Daan, S. & Pittendrigh, C. S. *J. comp. Physiol.* **106**, 253–266 (1976).
22. Ralph, M. R. & Menaker, M. *Brain Res.* **325**, 362–365 (1985).
23. Seidel, W. F., Roth, T., Roehrs, T., Zorick, F. & Dement, W. C. *Science* **224**, 1262–1264 (1984).
24. Walsh, J. K., Muehlbach, M. J. & Schweitzer, P. K. *Sleep* **7**, 223–229 (1984).
25. Van Cauter, E. & Turek, F. W. *Perspectives Biol. Med.* (in the press).

Replication of the neurochemical characteristics of Huntington's disease by quinolinic acid

M. Flint Beal, Neil W. Kowall, David W. Ellison, Michael F. Mazurek, Kenton J. Swartz & Joseph B. Martin

Department of Neurology, Massachusetts General Hospital and Harvard Medical School, Boston, Massachusetts 02114, USA

Huntington's disease (HD) is an autosomal dominant neurological disorder characterized by progressive chorea, cognitive impairment and emotional disturbance[1]. The disease usually occurs in midlife and symptoms progress inexorably to mental and physical incapacitation. It has been postulated that an excitotoxin is involved in the pathogenesis of HD[2,3]. Schwarcz and colleagues have shown that quinolinic acid (QA) can produce axon-sparing lesions similar to those observed in HD[4–7]. The lesions result in a depletion of neurotransmitters contained within striatal spiny neurones, for example γ-aminobutyric acid (GABA), while dopamine is unaffected. Recently, we and others have demonstrated that in HD striatum there is a paradoxical 3–5-fold increase in both somatostatin and neuropeptide Y which is attributable to selective preservation of a subclass of striatal aspiny neurones in which these peptides are co-localized[8–12]. In the present study we demonstrate

that lesions due to quinolinic acid closely resemble those of HD as they result in marked depletions of both GABA and substance P, with selective sparing of somatostatin/neuropeptide Y neurones. Lesions produced by kainic acid (KA), ibotenic acid (IA) and *N*-methyl-D-aspartate (MeAsp) were unlike those produced by QA, as they affected all cell types without sparing somatostatin/neuropeptide Y neurones. These results suggest that QA or a similar compound could be responsible for neuronal degeneration in HD.

Although the HD gene has been localized to the short arm of chromosome 4, the pathogenesis of the disease remains unknown[13]. The excitotoxin hypothesis was advanced following the demonstration that KA lesions reproduce many of the neurochemical and neuropathological features of HD[2,3]. These lesions, however, proved to be an imperfect model of HD as they did not spare somatostatin/neuropeptide Y neurones[14-16]. Furthermore, KA is not known to exist in mammalian tissues. It was subsequently shown by Schwarcz and colleagues that QA, an endogenous metabolite of tryptophan present in human brain, could produce excitotoxin lesions in striatum[4-7]. We therefore examined the ability of this compound to reproduce both the neurochemical and histological features of HD in rat striatum.

Male Sprague–Dawley rats (175 g) were anaesthetized with Nembutal (50 mg per kg intraperitoneal, i.p.) and positioned in a David Kopf small-animal stereotaxic apparatus. A 30-gauge blunt-tipped Hamilton syringe needle was inserted into the left striatum at the coordinates 8.4 mm anterior, 2.6 mm lateral and 4.5 mm ventral to the dura[17]. Drugs dissolved in 1 μl of phosphate-buffered saline (PBS) were infused over a period of 2 min; the needle was left in place for an additional 2 min and then slowly withdrawn. Two weeks after the injection the animals were killed and their brains were removed and sectioned at 2-mm intervals as described previously[10]. Both striata, the frontal cortex dorsal to the lesion and hippocampus caudal to the lesion were dissected and placed in a solution of chilled 0.1 M HCl containing 1 mM EDTA and 4 mM sodium metabisulphite. The tubes containing the tissues were frozen and thawed three times, then an aliquot of supernatant was taken for analysis of catecholamines and amino acids using HPLC with electrochemical detection[18,19]. The remaining tissue was boiled for 10 min to inactive peptidases, and the supernatant lyophilized before reconstitution in radioimmunoassay buffer. Radioimmunoassays for somatostatin-like immunoreactivity (SLI), neuropeptide Y-like immunoreactivity (NPYLI), substance P-like immunoreactivity (SPLI) and vasopressin-like immunoreactivity (VLI) were done as described previously[20-23]. Proteins were measured by fluorimetric assay[24].

In an initial experiment control animals were injected with PBS alone, while experimental animals received increasing doses of QA (8 animals per dose). The right (unlesioned) striatal values did not differ from control values by one-way analysis of variance (ANOVAR); these values were therefore averaged with control values to provide a 100% control mean. The left (lesioned) striatal values were expressed as a per cent of the control mean. Control striatal concentrations of neuropeptide (per mg protein) were: SLI, 2.63 ± 0.37 pM; NPYLI, 3.47 ± 0.51 pM; SPLI, 357 ± 54 fM; GABA, 31.2 ± 5.3 nM. Increasing doses of quinolinic acid resulted in significant dose-dependent reductions in both SPLI and GABA (Fig. 1). Not until the highest dose of QA had been reached was SLI or NPYLI affected. (The highest dose was hyperosmolar and might therefore have caused nonspecific damage.) Nevertheless, even at this dose, SLI and NPYLI were preserved relative to SPLI and GABA. In contrast, increasing doses of kainate induce a graded loss of both SLI and SPLI[11]. Dopamine concentrations were unaffected, as expected for a transmitter contained within afferent terminals. There was no significant alteration in SLI, NPYLI or SPLI in frontal cortex or hippocampus with any of the lesions.

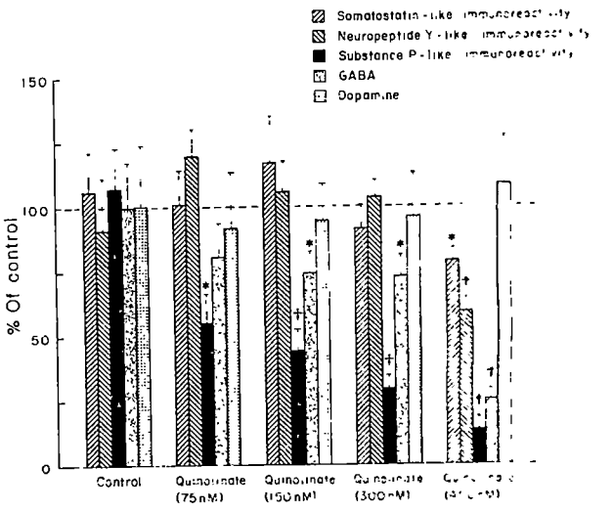


Fig. 1 Increasing doses of quinolinic acid injected into rat striatum resulted in a dose-dependent reduction in both GABA and substance P-like immunoreactivity, but somatostatin and neuropeptide Y were unaffected until the highest dose was applied. $*P < 0.05$, † $P < 0.01$ compared with controls (by ANOVAR).

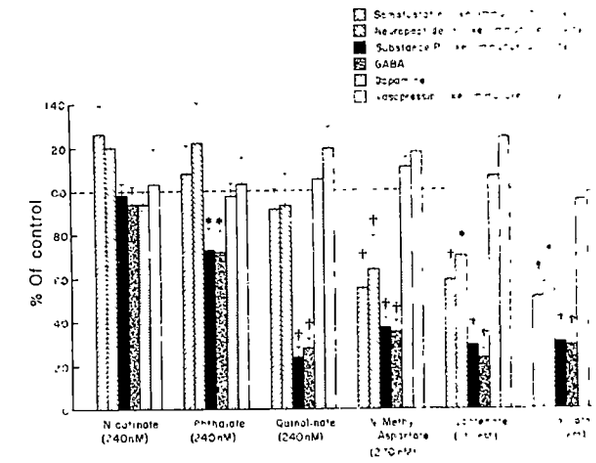


Fig. 2 Quinolinic acid (QA)-induced striatal lesions produced reductions in GABA and substance P comparable to those seen with *N*-methyl-D-aspartate, ibotenic acid and kainic acid, but only QA spared somatostatin and neuropeptide Y. Phthalic acid, which is structurally related to QA, produced similar but less potent changes than QA. $*P < 0.05$, † $P < 0.01$ compared with controls (by ANOVAR).

In a second experiment control animals received nicotinic acid (NA), while experimental animals received phthalic acid (PA), QA, MeAsp, IA or KA (Fig. 2). Nicotinic acid is structurally identical to QA except for the absence of a carboxylate group at position 2 on the pyridine ring. Eight animals in each group were killed 3 weeks after the injection and analysed as in the initial experiment. There was no significant alteration of SLI, NPYLI or SPLI in frontal cortex or hippocampus. Quinolinic acid, MeAsp, IA and KA produced comparable reductions in both SPLI and GABA but only QA lesions spared SLI and NPYLI. Dopamine and VLI (markers of striatal afferents) were unaffected by any of the lesions. Phthalic acid, which is structurally identical to QA except for a substitution of carbon for the nitrogen in the pyridine ring, was less potent than, but qualitatively similar to, QA in its toxicity. Somatostatin and neuropeptide Y were not depleted to the same extent as substance P or GABA by any of the lesions, but this probably reflects

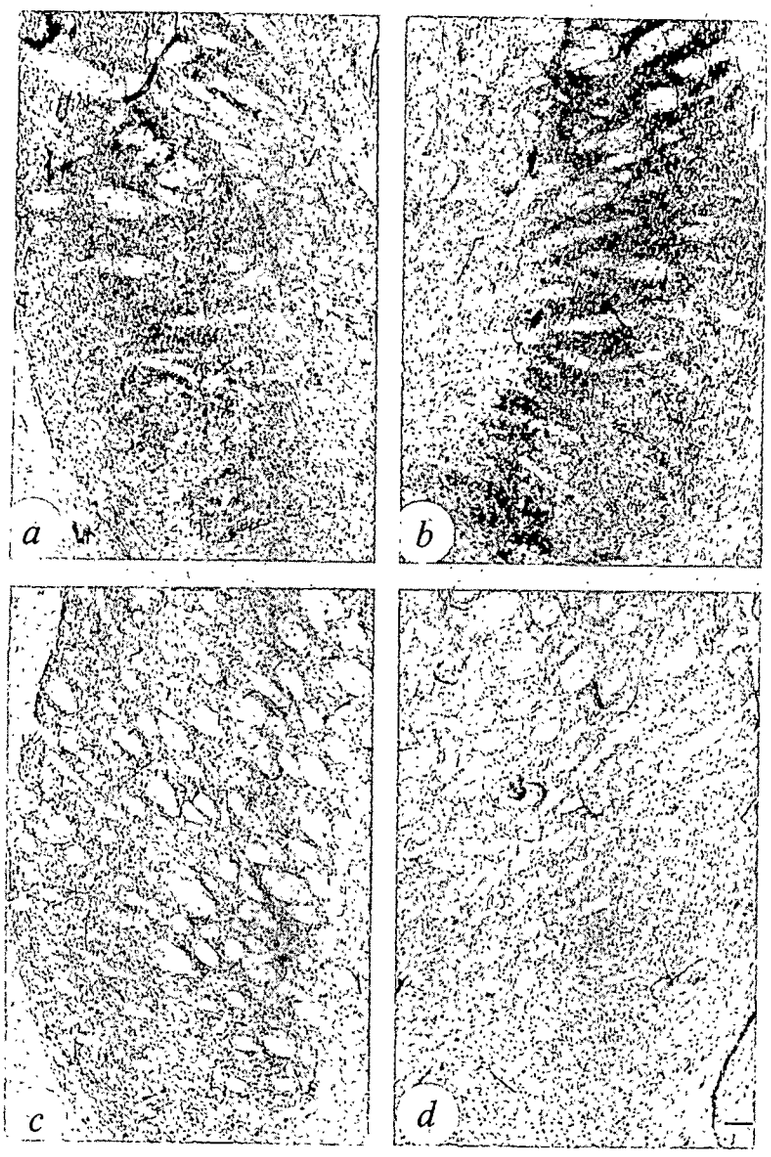


Fig. 3 *a*, *b*: Control (*a*; non-injected) and quinolinate-lesioned (*b*) striatum from the same section stained for NADPH-diaphorase and counterstained with cresyl violet. *c*, *d*: Control (*c*) and kainate-lesioned (*d*) striatum stained as for *a*, *b*. Both sections are equidistant from the injection sites and the lesioned sides show decreased (cresyl violet-stained) neuronal density, but this is difficult to discern because of gliosis. The diaphorase-containing neuronal population (darkly stained neurones) is resistant to the effects of quinolinate (*b*) but is depleted in concert with total neuronal loss in kainate-induced lesions (*d*).

the presence of these neuropeptides in striatal afferents as well as in intrinsic striatal neurones[25,26]. Previous work has suggested that 25–40% of striatal somatostatin may be contained in striatal afferents[10,25–27].

Lesions intended for histological analysis were made identically to those in experiment 2, except that the dosage was halved by administering the drug in 0.5 μl of saline. Five animals were studied per group. Three weeks after the lesions, the rats were pretreated with diisopropyl fluorophosphate (2 mg per kg intramuscular, i.m.) and atropine (5 mg per kg i.p.) 18 h before they were killed. Brains were immersion-fixed in 4% paraformaldehyde in 0.1 M phosphate buffer (*p*H 7.4) at 4 °C. Sections 50 μm thick were cut and processed for diaphorase and cholinesterase histochemistry as described previously[28,29]. Striatal neurones that stain for diaphorase also contain both SLI and NPYLI[30,31].

Nicotinate injections produced no histologically identifiable striatal lesions. In contrast, quinolinate, kainate, ibotenate and phthalate all produced a zone of necrosis surrounded by an area of total neuronal loss at the injection site; neuronal counts made in adjacent sections showed neurotoxic effects, as demonstrated by decreased neuronal density. Diaphorase neurones were resistant to the neurotoxic effects of quinolinate but were more sensitive than cholinesterase neurones to the neurotoxic effects of both kainate and ibotenate (Fig. 3, Table 1). The latter finding is consistent with a previous report[32]. Cholinesterase neurones were equally vulnerable to all neurotoxins examined. The histological observations indicate that preserved concentrations of both SLI and NPYLI are attributable to selective preservation of somatostatin/neuropeptide Y neurones in the face of QA neurotoxicity. Phthalic acid showed qualitatively similar effects but to a lesser degree.

As QA-induced striatal lesions spare somatostatin/neuropeptide Y neurones, they are a better model of the neurochemical and histological features of HD than lesions produced with other excitotoxins. Several other features make QA an attractive candidate for an aetiological agent of HD. It has been shown that neonatal animals are resistant to QA toxicity while mature animals are susceptible[5]; this agrees well with the typical onset of HD in middle age. In addition, it has been shown that striatum, globus pallidus and hippocampus are particularly vulnerable to quinolinic acid neurotoxicity while cerebellum, substantia nigra, amygdala, septum and hypothalamus are less susceptible[5]; many of these regions are affected in HD although the most marked pathology is seen in striatum, which suggests that other factors, such as glutamate input, may influence the topography of the pathology.

Selective sparing of somatostatin/neuropeptide Y neurones could conceivably be related to an ability of these neurones to metabolize quinolinic acid. All striatal somatostatin/neuropep-

Table 1 Quantitative analysis of diaphorase and cholinesterase neuronal populations in double-stained sections

Neurotoxin	Ratio of diaphorase cell counts (control/lesion)	Ratio of cholinesterase cell counts (control/lesion)	Fractional diaphorase/ cholinesterase counts (control/lesion)
Quinolinate	0.97±0.07*	2.04±0.26	0.53±0.03†
Kainate	1.52±0.15	1.59±0.25	1.26±0.10
Ibotenate	1.39±0.14	1.82±0.27	1.30±0.17
Phthalate	1.15±0.06	1.86±0.27	0.71±0.08

Sections at several striatal levels were counted and the cell counts on control and lesioned sides are expressed as a ratio (control striatum cell counts/lesioned striatum cell counts). A ratio of >1 indicates fewer neurones in the lesioned striatum than in the control; this is true in all cases except for diaphorase neurones in the quinolinate-injected cases, where diaphorase cell count ratios are ~1 (that is, unchanged). This proportional sparing of diaphorase neurones is shown further by comparing the numbers of diaphorase and cholinesterase neurones (expressed as the fractional diaphorase counts, calculated by dividing the diaphorase count by the cholinesterase count) (final column). The greater number of diaphorase neurones compared with cholinesterase neurones (which are depleted) in the quinolinate-lesioned striatum results in a ratio of <1. Ratios of >1 suggest that diaphorase neurones are more sensitive than cholinesterase neurones to kainate and ibotenate.

* The value obtained with quinolinate is significantly less than that for kainate ($P<0.01$) or ibotenate ($P<0.05$) by the Kruskal-Wallis multiple-comparison test.

† The quinolinate value is significantly less than that for kainate ($P<0.004$) or ibotenate ($P<0.001$) by the Kruskal-Wallis multiple-comparison test.

tide Y neurones also contain the enzyme NADPH-diaphorase[30,31], and it has been shown that QA can act as a precursor of NADH or NADPH in mammalian liver[33–35]. It is possible, therefore, that these neurones are able to take up and metabolize quinolinic acid; this might explain the relative sparing of the nucleus accumbens in HD[36,37], as concentrations of both somatostatin and neuropeptide Y as well as the density of NADPH-diaphorase neurones and terminals are 2–3-fold higher in nucleus accumbens than in the remainder of the striatum[9,10,31]. It would also explain the paradoxical susceptibility of these neurones to MeAsp yet their resistance to QA, as both compounds are thought to act at the same receptor[5]. Some evidence, however, suggests differential effects which might implicate separate receptors[38,39]. It has been suggested that NADPH-diaphorase neurones are resistant to a variety of neurotoxins[39]; however, the present data suggest that this is not the case with excitotoxins, except for quinolinic acid.

Various therapeutic strategies are suggested if QA proves to be of aetiological significance in HD. Quinolinic acid neurotoxicity is dependent on cortical (presumably glutamatergic) input and can be blocked with kynurenic acid, 2-amino-5-phosphonovaleric acid and 2-amino-7-phosphonoheptanoic acid[5,38,40,41]. It is therefore possible that early diagnosis using molecular genetics could be followed by therapeutic intervention in an attempt to retard the neurodegenerative process.

We thank Linda Lorenz for technical assistance and Ms JoAnn Forti for secretarial assistance. This work was supported by Huntington's Disease Center Without Walls (NINCDS grant NS16367) and the JulieAnne Dorn fund. M.F.B. is supported by a Young Investigator Award (IR23NS19867-1), N.W.K. and M.F.M. are Fellows of the MRC of Canada, and D.W.E. is a Fellow of the Wellcome Trust.

Received 29 January; accepted 11 March 1986.

1. Martin, J. B. *Neurology* **34**, 1059–1072 (1984).
2. Coyle, J. T. & Schwarcz, R. *Nature* **263**, 244–246 (1976).
3. McGeer, E. G. & McGeer, P. L. *Nature* **263**, 517–519 (1976).
4. Schwarcz, R., Whetsell, W. O. & Mangano, R. M. *Science* **219**, 316–319 (1983).
5. Schwarcz, R. *et al. Life Sci.* **35**, 19–32 (1984).
6. Wolfensberger, M. *et al. Neurosci. Lett.* **41**, 247–252 (1983).
7. Kohler, C., Okuno, E. & Schwarcz, R. *Neurosci. Abstr.* **11**, 820 (1985).
8. Aronin, N. *et al. Ann. Neurol.* **13**, 519–526 (1983).
9. Beal, M. F. *et al. Neurology* **34**, 663–666 (1984).
10. Nemeroff, C. B. *et al. Science* **221**, 972–975 (1983).
11. Ferrante, R. J. *et al. Science* **230**, 561–563 (1985).
12. Dawbarn, D., Dequidt, M. E. & Emson, P. C. *Brain Res.* **340**, 251–260 (1985).
13. Gusella, J. F. *et al. Nature* **306**, 234–238 (1983).
14. Beal, M. F. & Martin, J. B. *Brain Res.* **266**, 67–73 (1983).
15. Beal, M. F. *et al. Brain Res.* **361**, 135–145 (1985).
16. Allen, Y. S. *et al. Neurosci. Abstr.* **10**, 813 (1984).
17. Konig, J. F. R. & Klippel, R. A. *The Rat Brain* (Williams & Wilkins, Baltimore, 1963).
18. Beal, M. F. & Martin, J. B. *Neurosci. Lett.* **44**, 271–276 (1984).
19. Lasley, S. M., Greenland, R. D. & Michaelson, I. A. *Life Sci.* **35**, 1921–1933 (1984).
20. Arnold, M. A. *et al. J. Neurosci.* **2**, 674–680 (1982).
21. Beal, M. F. *et al. Neurosci. Lett.* (in the press).
22. Mroz, E. A. & Leeman, S. A. in *Methods of Hormone Radioimmunoassay* (eds Jaffee, B. & Behrman, J.) 121–137 (Academic, New York, 1978).
23. Kasting, N. W. *et al. Can. J. Physiol. Pharmac.* **61**, 427–431 (1983).
24. Bohlen, P. *et al. Archs Biochem. Biophys.* **155**, 213–220 (1973).
25. Beal, M. F., Domesick, V. B. & Martin, J. B. *Brain Res.* **278**, 103–108 (1983).
26. Beal, M. F., Domesick, V. B. & Martin, J. B. *Brain Res.* **330**, 309–316 (1985).
27. Sperk, G. & Widmann, R. *J. Neurochem.* **45**, 1441–1447 (1985).
28. Kowall, N. W., Beal, M. F., Ferrante, R. J. & Martin, J. B. *Neurosci. Lett.* **59**, 61–66 (1985).
29. Vincent, S. R. *et al. Neurosci. Lett.* **35**, 111–114 (1983).
30. Vincent, S. R. *et al. J. comp. Neurol.* **217**, 252–263 (1983).
31. Kowall, N. W., Ferrante, R. J., Beal, M. F. & Martin, J. B. *Soc. Neurosci. Abstr.* **11**, 209 (1985).
32. Araki, M., McGeer, P. L. & McGeer, E. G. *Neurosci. Lett.* **53**, 197–202 (1985).
33. Henderson, L. M. & Hirsch, H. M. *J. biol. Chem.* **181**, 669–675 (1949).
34. Henderson, L. M. & Ramasarma, G. B. *J. biol. Chem.* **181**, 687–692 (1949).
35. Gholson, R. K. *et al. J. biol. Chem.* **239**, 1208–1214 (1964).
36. Vonsattel, J. P. *et al. J. Neuropath. exp. Neurol.* **44**, 559–577 (1985).
37. McCaughey, W. T. E. *J. nerv. ment. Dis.* **133**, 91–103 (1961).
38. Foster, A. C., Vezzani, A., French, E. D. & Schwarcz, R. *Neurosci. Lett.* **48**, 273–278 (1984).
39. Perkins, M. N. & Stone, T. W. *Expl Neurol.* **88**, 570–579 (1985).
40. Thomas, E. & Pearse, A. G. E. *Acta neuropath.* **3**, 238–249 (1964).
41. Schwarcz, R. & Meldrum, B. *Lancet* **ii**, 140–143 (1985).

Channel properties of an insect neuronal acetylcholine receptor protein reconstituted in planar lipid bilayers

W. Hanke & H. Breer

Universität Osnabrück, Fachbereich Biologie/Chemie, D-4500 Osnabrück, FRG

A pentameric membrane protein composed of four types of polypeptide has been identified as the minimal structural unit responsible for the electrogenic action of acetylcholine on electrocytes and muscle cells[1–3]. Because many populations of central and peripheral neurones also have nicotinic acetylcholine receptors (AChRs), considerable effort has recently gone into identifying the neuronal receptor[4,5]. The central nervous tissue of insects contains very high concentrations of nicotinic AChRs[6,7], and we have recently purified an α-toxin binding protein, a putative AChR, from neuronal membranes of locusts[8,9]. It is a component of high relative molecular mass, clearly composed of identical subunits, a structure predicted for an ancestral AChR protein[10,11]. To verify that the purified polypeptides not only represent ligand binding sites but that they are indeed functional receptors, we have now reconstituted the isolated protein in a planar lipid bilayer. We show that in this system cholinergic agonists activate functional ion channels, that have properties comparable to those exhibited by the peripheral AChRs in vertebrates; thus, for the first time a functional acetylcholine receptor channel has been indentified in nerve cells.

The purified receptor protein was first reconstituted into lipid vesicles produced from asolectin and cholesterol by dialysis[12]. These proteoliposomes were then fused with the intact bilayer[13] to incorporate the purified receptor polypeptides. Both sides of the membrane were bathed in solution containing 100 mM NaCl, 1 mM $CaCl_2$ and 10 mM HEPES *p*H 7.2. Receptor-containing vesicles and agonists were added to the *cis* side, and membrane potentials are given with respect to virtual ground on the *trans* side.

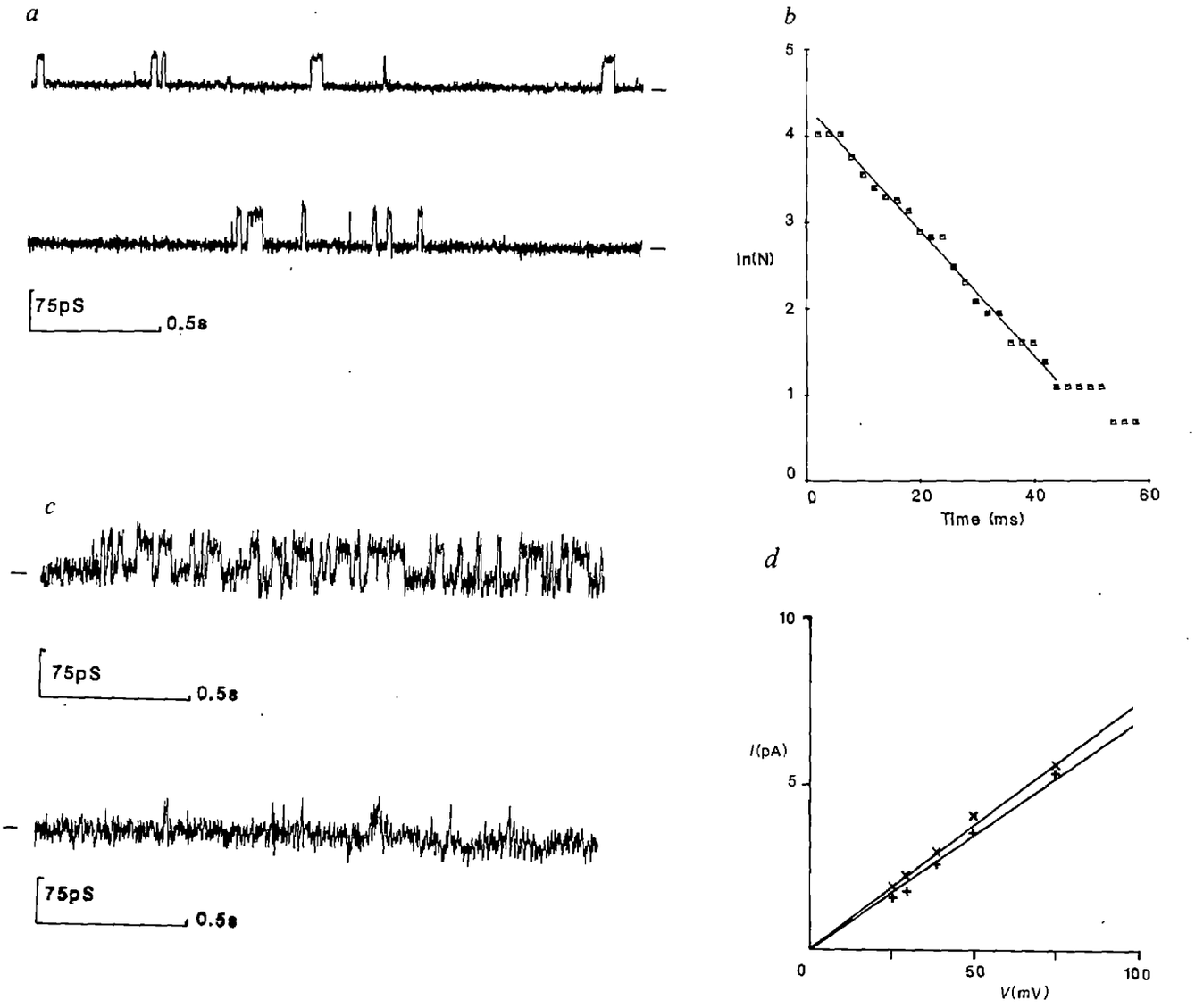


Fig. 1 Cholinergic agonist-induced fluctuations of cationic channels in planar lipid bilayers containing reconstituted α-toxin binding proteins isolated from the nervous tissue of locust. *a*, Current fluctuations of the AChR channel in the presence of 0.5 μM suberyl dicholine at an applied potential of 50 mV. *b*, Evaluation of the lifetime of current events ($n = 78$). Experimental conditions as in *a*. Mean lifetime, 14 ms. *c*, Current fluctuations of the AChR, channel in the presence of two different concentrations of carbamyl choline in aqueous solution: upper trace, 50 μM; lower trace, 0.5 μM. Both traces were obtained from the same bilayer, starting with the lower concentration. $P(o) = 0.75$ and 0.05 in the presence of 50 μM and 0.5 μM carbamyl choline, respectively. The closed state of the channel is indicated at each trace separately (bars on left-hand side). *d*, Current-voltage (I–V) relation for a single channel under conditions given in *a*. ×, Current in the presence of 100 NaCl (75 pS); +, current in the presence of 100 KCl (70 pS). In these and subsequent traces, an upward deflection of the current trace corresponds to opening of a membrane channel.

Methods. Bilayers were made from 1-palmitoyl-2-oleoyl-glycero-3-phosphatidylcholine (Avanti), phosphatidylethanolamine purified from egg yolk by column chromatography in our laboratory, and dioleoyl phosphatidylglycerol (Avanti) in a 40:60:20 molar ratio. 10 mg of lipid mixture was dissolved in 1 ml hexane and 50 μl of this solution was spread on each side of a hexadecane-pretreated hole of about 150 μm diameter. Bilayers were folded onto this hole after the solvent had been allowed to evaporate quantitatively. The lipid bilayer used was virtually solvent-free[18] and generated as described previously[12]; it was shown to be electrically stable and did not respond to cholinergic agonists. Aqueous solutions on both sides of the bilayer contained 100 mM NaCl, 1 mM $CaCl_2$, 10 mM HEPES at *p*H 7.2. The aqueous solutions of the vesicle preparations added were identical except that each contained additionally 200 mM sucrose. The lipid composition of the vesicles was asolectin/cholesterol in a 15:2 molar ratio. The vesicles contained the purified native AChR protein isolated from neuronal membranes of locusts[9]. The vesicle preparation was stored on water/ice and kept there for a maximum of 3 days. 50 μl of the vesicle preparation was added to the *cis* side of the bilayer. The *trans* side was defined to be at virtual ground potential. The receptor-containing lipid bilayer was stable and no resolvable ion channel fluctuation was detected in the absence of any agonist. Agonists were added as indicated and the *cis* side was stirred until first channel fluctuations occurred. Current fluctuation traces were filtered at 300 Hz (−3 dB point, low pass) for better amplitude resolution and stored on an FM-tape recorder for later analysis. Several ($n > 5$) independent experiments were performed for each condition.

Figure 1*a* shows the current flowing through individual agonist-activated channels after addition of 0.5 μM suberyl dicholine to the *cis* side; the size of the current indicates a channel conductance of 75 pS (Fig. 1*a*, *d*). Evaluation of the current duration under these conditions (Fig. 1*b*) showed a distribution with a single exponential indicating a mean lifetime (τ_0) of 14 ms. Figure 1*c* shows the effect of various concentrations of carbamyl choline on the same receptor channel. Again, fluctuations of a channel showing a conductance of 75 pS were observed. With 50 μM carbamyl choline, the current fluctuations

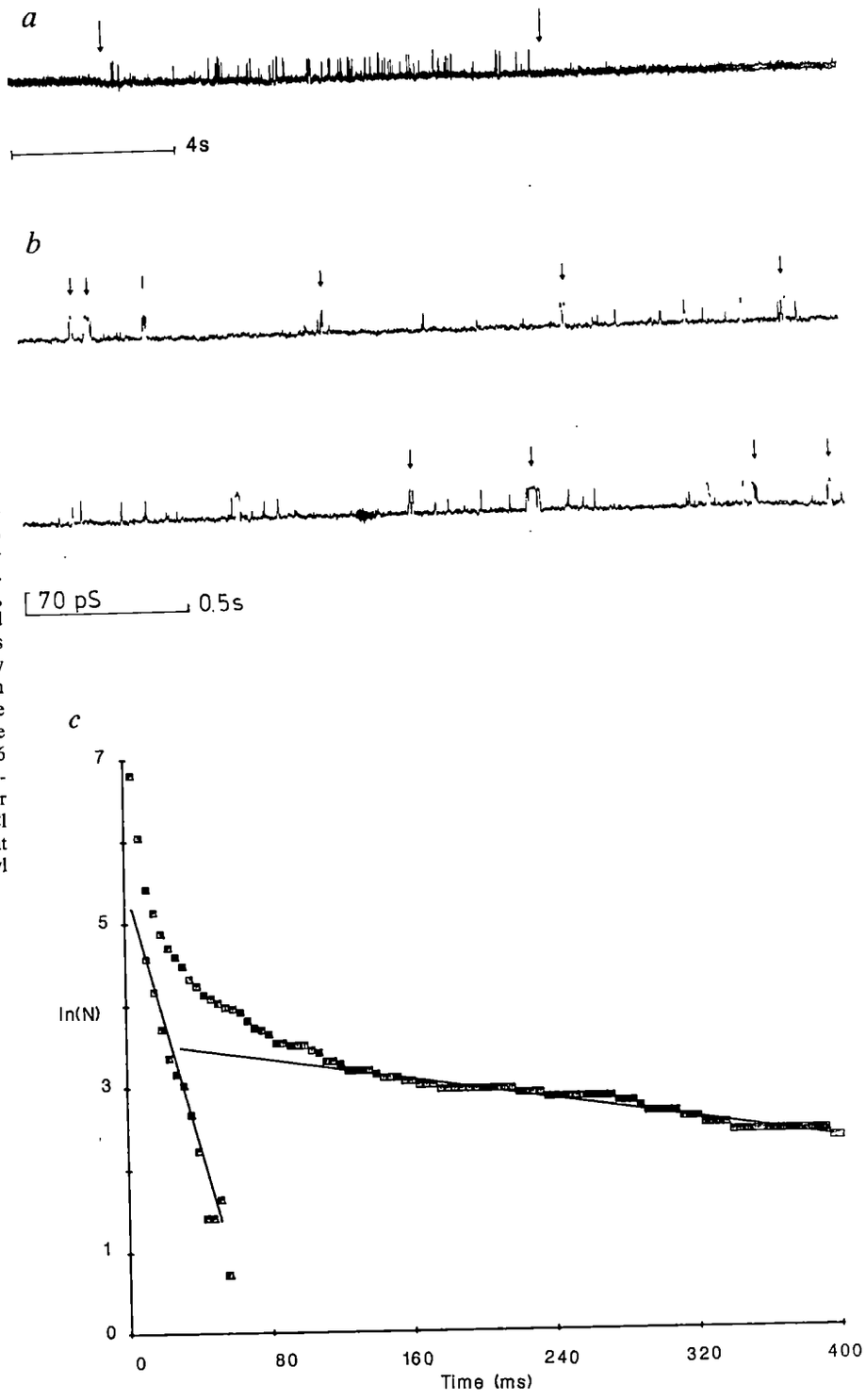


Fig. 2 Structural details of the kinetics and conductance of the neuronal AChR channel. *a*, Bursting of the channel at 25 mV. Arrows indicate the beginning and end of the burst shown. *b*, Occurrence of the multiple gating events, indicated by arrows as in *a*, on an expanded timescale. *c*, Distribution of closed time events plotted at half log scale. The graph clearly demonstrates two different components, with decay constants of $\tau_s = 315$ ms (closing time between bursts) and $\tau_f = 25$ ms (closing time within bursts). Of the 904 events evaluated, 36 were classified as belonging to the slow component. Experimental conditions were similar to those of Fig. 1, except that 100 mM NaCl was replaced by 100 mM KCl. All current fluctuations were induced by 1 μM suberyl dicholine.

had a mean duration of about 15 ms and a high probability of being in the open state ($P(o) = 0.75$), while with 0.5 μM carbamyl choline the channel lifetime was only 3–5 ms and the probability of the channel being in the open state was close to zero ($P(o) \leq 0.05$). These results suggest that the α-toxin binding protein, purified from the nervous tissue of insects, behaves like a functional AChR; although quite different in its molecular organization, its response to agonist application was comparable to that of AChRs from electrocytes in lipid bilayers[13,14].

Comparison of agonist action at the same concentration (compare Fig. 1*a* and *c*, lower traces) shows clearly that suberyl dicholine induced significantly greater current durations (14 ms) than did carbamyl choline (3–5 ms). A similar agonist dependency has been observed on muscle receptors[15] and electrocyte receptors in lipid bilayers[13,14]. A current–voltage curve of single channels obtained with 0.1 M NaCl on both sides of the bilayer showed that the channel behaved ohmically over the voltage range studied (±100 mV). The conductance decreased only slightly if potassium (70 pS) was substituted for sodium (75 pS), indicating that the channel is not significantly selective for sodium over potassium (Fig. 1*d*), and conductance was unchanged when chloride was replaced by sulphate, indicating that the channel is impermeable to chloride.

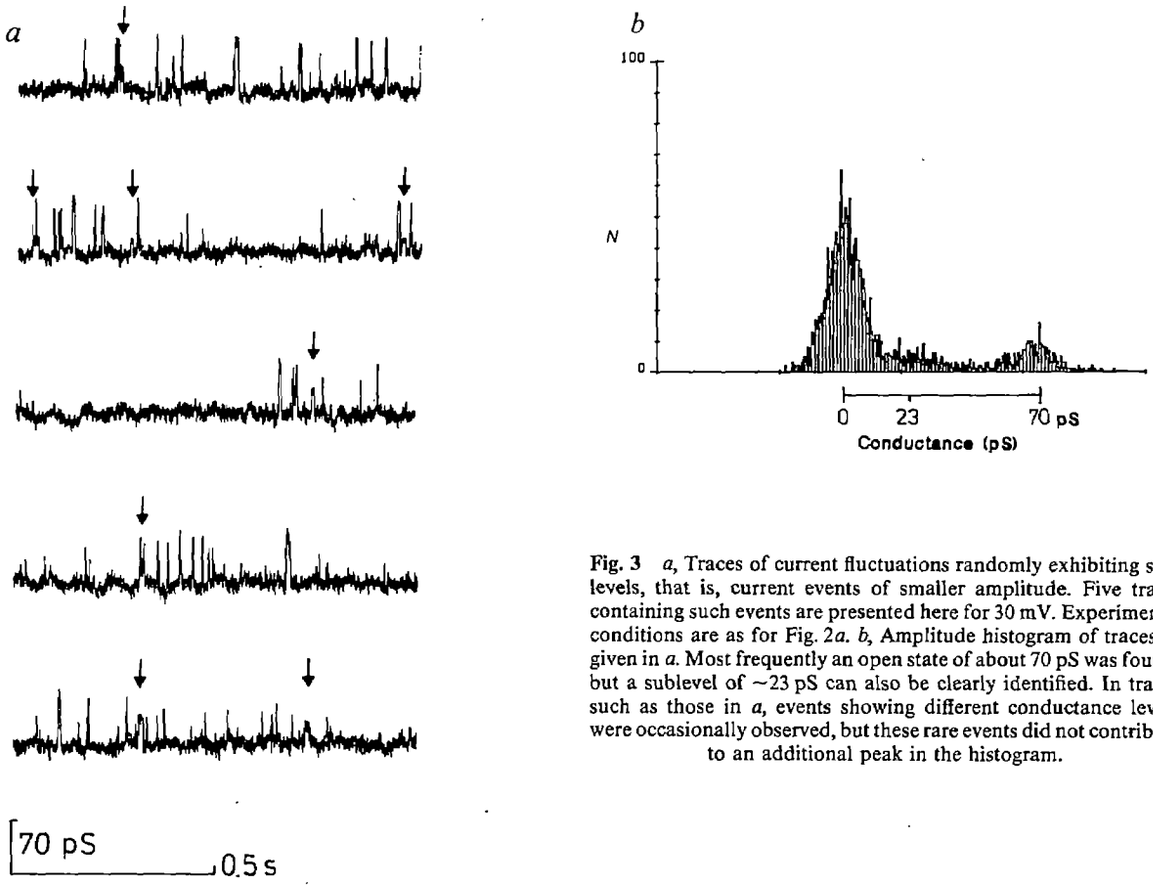


Fig. 3 *a*, Traces of current fluctuations randomly exhibiting sublevels, that is, current events of smaller amplitude. Five traces containing such events are presented here for 30 mV. Experimental conditions are as for Fig. 2*a*. *b*, Amplitude histogram of traces as given in *a*. Most frequently an open state of about 70 pS was found, but a sublevel of ~23 pS can also be clearly identified. In traces such as those in *a*, events showing different conductance levels were occasionally observed, but these rare events did not contribute to an additional peak in the histogram.

Figure 2 shows details of the neuronal receptor channel fluctuations. All current traces in this figure were obtained in the presence of 1 μM suberyl dicholine and an aqueous solution containing symmetrical 100 mM KCl. In Fig. 2*a* the occurrence of bursts of channel activity is shown on a compressed timescale. Within these bursts channels did not open randomly, but rather, multiple gating events occurred, as shown in Fig. 2*b* on an expanded timescale. In addition to isolated single-channel openings, we found blocks of two to five or even more openings. Figure 2*c* evaluates the distribution of channel closed times under the conditions of Fig. 2*a*. The distribution is fitted by two exponentials, indicating a mean closed time between bursts (τ_s) of 300 ms and a mean closed time within bursts (τ_f) of 25 ms.

We also resolved conductance details of the ion channels created by the neuronal AChR protein (Fig. 3) and found currents indicating openings of channels with a conductance lower than the predominant channel type. These channels usually had a conductance of about 23 pS. Selected stretches of recordings show a few of these events (Fig. 3*a*), while Fig. 3*b* shows an amplitude histogram of current fluctuations to quantify this phenomenon. The agonist-induced increase in the bilayer conductance could be completely inhibited by low concentrations of (+)tubocurarine; thus, single-channel currents induced by 1 μM suberyl choline were blocked after the addition of 5 μM (+)tubocurarine. The antagonist did not affect the conductance of the channel, but rather reduced the frequency of occurrence of current events.

These features of the neuronal receptor—the occurrence of bursting multiple gating events and the (+)tubocurarine-induced reduction of the probability that the channel will be in the open state—have also been described for the muscle AChR of vertebrates[16,17]. Our study shows that the purified α-bungarotoxin binding protein isolated from insect central nervous tissue displays the properties of a chemically gated ion channel, thus representing a functional receptor. Experiments are in progress to determine the primary structure of the insect neuronal receptor protein using gas-phase microsequencing and recombinant DNA techniques; such information will allow us to estimate the structural and functional relatedness of insect and vertebrate receptors; this aspect is of particular interest in view of the fact that the complete sequence of a possible neural AChR polypeptide from rat has recently been reported[5].

This work was supported by the Deutsche Forschungsgemeinschaft, SFB 114 and SFB 171. We thank Professor G. Boheim for helpful discussions, Miss G. Hinz for technical assistance and Dr B. Sakmann for constructive comments during the revision of the manuscript.

Received 23 December 1985; accepted 10 March 1986.

1. Conti-Tronconi, B. M. & Raftery, M. *A. Rev. Biochem.* **51**, 491–530 (1981).
2. Popot, J.-L. & Changeux, J.-P. *Physiol. Rev.* **64**, 1162–1239 (1984).
3. Maelicke, A. *Angew. Chem.* **96**, 193–219 (1984).
4. Conti-Tronconi, B. M. *et al. Proc. natn. Acad. Sci. U.S.A.* **230**, 707–717 (1985).
5. Boulter, J. *et al. Nature* **319**, 368–374 (1986).
6. Breer, H. *Neurochem. Int.* **3**, 43–52 (1981).
7. Sattelle, D. B. *Adv. Insect Physiol.* **15**, 215–315 (1980).
8. Breer, H., Kleene, R. & Benke, D. *Neurosci. Lett.* **46**, 323–328 (1984).
9. Breer, H., Kleene, R. & Hinz, G. *J. Neurosci.* **5**, 3386–3392 (1985).
10. Raftery, M. A., Hunkapiller, M. W., Strader, C. D. & Hood, L. E. *Science* **208**, 1454–1457 (1981).
11. Noda, M. *et al. Nature* **302**, 528–532 (1983).
12. Hanke, W. & Miller, C. *J. gen. Physiol.* **82**, 25–45 (1983).
13. Boheim, G. *et al. Proc. natn. Acad. Sci. U.S.A.* **78**, 3586–3590 (1981).
14. Labarca, P., Lindstrom, J. & Montal, M. *J. gen. Physiol.* **83**, 473–496 (1985).
15. Katz, B. & Miledi, R. J. *J. Physiol., Lond.* **230**, 707–717 (1973).
16. Neher, E. & Sakmann, B. *Nature* **260**, 799–802 (1976).
17. Hamill, O. P. & Sakmann, B. *Nature* **294**, 462–464 (1981).
18. Montal, M. & Mueller, P. *Proc. natn. Acad. Sci. U.S.A.* **69**, 3561–3565 (1972).

Potentiation of synaptic transmission in the hippocampus by phorbol esters

Robert C. Malenka, Daniel V. Madison & Roger A. Nicoll

Departments of Pharmacology and Physiology, University of California, San Francisco, California 94143, USA

Protein kinase C (PKC), a calcium-dependent phospholipid-sensitive kinase which is selectively activated by phorbol esters, is thought to play an important role in several cellular processes[1,2]. In mammalian brain PKC is present in high concentrations[1] and has been shown to phosphorylate several substrate phosphoproteins[3–6], one of which may be involved in the generation of long-term potentiation (LTP)[7,8], a long-lasting increase in synaptic efficacy evoked by brief, high-frequency stimulation. Since the hippocampus contains one of the brain's highest levels of binding sites for phorbol esters[9] and is the site where LTP has been most thoroughly characterized, we examined the effects of phorbol esters on hippocampal synaptic transmission and LTP. We found that phorbol esters profoundly potentiate excitatory synaptic transmission in the hippocampus in a manner that appears indistinguishable from LTP. Furthermore, after maximal synaptic enhancement by phorbol esters, LTP can no longer be elicited. Although the site of synaptic enhancement during LTP is not clearly established, phorbol esters appear to potentiate synaptic transmission by acting primarily at a presynaptic locus since changes in the postsynaptic responses to the putative transmitter, glutamate, cannot account for the increased synaptic responses induced by phorbol esters. These findings, in conjunction with previous biochemical studies, raise the possibility that, in mammalian brain, PKC plays a role in controlling the release of neurotransmitter and may be involved in the generation of LTP.

The details of the rat hippocampal slice preparation have been described elsewhere[10]. For all experiments, orthodromic stimulation of fibres in stratum radiatum was adjusted to evoke a 1–2-mV population spike recorded in the CA1 region of stratum pyramidale while another recording electrode placed in stratum radiatum recorded a population excitatory postsynaptic potential (e.p.s.p.) field. A variety of phorbol analogues known to activate PKC were used including 4β-phorbol-12,13-dibutyrate (PDBu), 4β-phorbol-12,13-diacetate (PDAc), and 12-deoxyphorbol-13-isobutyrate[11], all of which elicited similar responses. We also applied 4β-phorbol and 4α-phorbol-12,-13-didecanoate, analogues which do not activate PKC[11]. These drugs were applied by superfusion to over 50 slices. Standard techniques were used for intracellular recording.

Application of phorbol esters caused a pronounced and long-lasting increase in the amplitude of the population spike and decreased its latency (Fig. 1*a*,*b*). Concomitantly the initial slope and amplitude of the population e.p.s.p. increased (Fig. 1*a*,*b*), even at low stimulus strengths when the reflection of the population spike did not appear in the late phase of the population e.p.s.p. Washing the slice with control solution for up to 2 h did not reverse the effects of the phorbol esters. This may be due to the difficulty in completely washing out of the slice the highly lipid soluble phorbol esters. Concentrations of phorbol ester as low as 100 nM (the lowest tested) were effective although higher doses had more rapid and larger effects. Intracellular recordings corroborated these findings ($n = 9$; Fig. 2*b*). The increase in the e.p.s.p. often occurred in the absence of any change in membrane potential or input resistance. Application of phorbol analogues which have been shown not to activate PKC in other systems did not enhance synaptic responses (Fig. 1*c*). This suggests that the potentiation of synaptic transmission by phorbol esters may be due to the activation of PKC, although these physiological experiments cannot entirely rule out an action of phorbol esters independent of PKC.

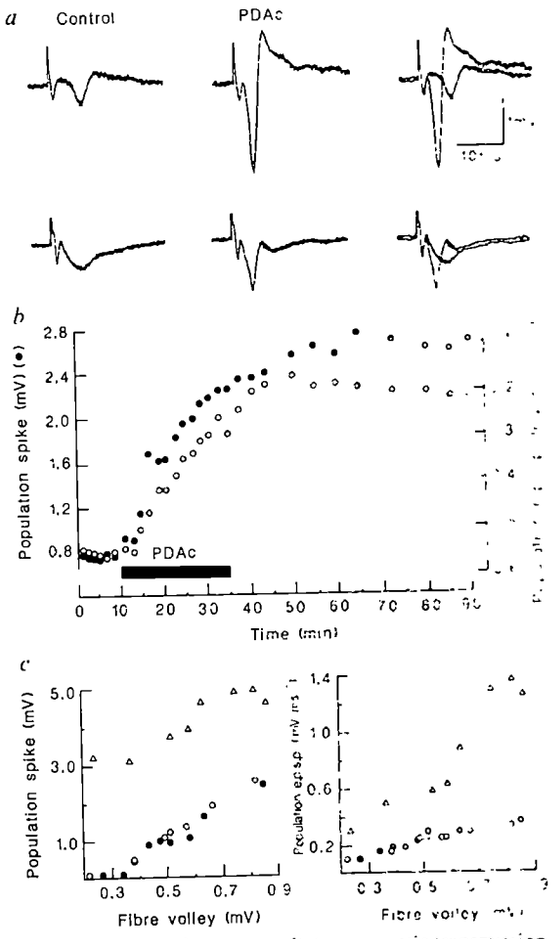


Fig. 1 Phorbol esters increase excitatory synaptic transmission in the hippocampus. *a*, The population spike (top row) and population e.p.s.p. (bottom row) are shown from an experiment in which 2 μM phorbol-12-13-diacetate (PDAc) was applied to the hippocampus for 25 min. The responses in the PDAc column were taken 20 min after returning to drug-free solution. The responses are shown superimposed in the right-hand column. *b*, The changes in the population spike amplitude and population e.p.s.p. initial slope during this experiment; each point is the average of four responses. *c*, The population spike amplitude and population e.p.s.p. initial slope are plotted as a function of presynaptic fibre volley amplitude. Responses were obtained by varying stimulation strength in control media (●), following a 30-min exposure to a solution containing 10 μM 4β-phorbol (○) and also following a 20-min exposure to 5 μM phorbol-12,13-dibutyrate (△), all in the same slice. Sample traces in this and all subsequent figures are averages of four responses.

Methods. The population spike corresponds to the synchronous activation of pyramidal cells. Its amplitude was determined by the method of Alger and Teyler[35]. The initial slope of the population e.p.s.p. was measured as an indication of dendritic synaptic responses because the peak amplitude is often contaminated by the reflection of the population spike. All responses were digitized for later data analysis using a Nicolet 4094 digital oscilloscope

One mechanism which could account for the increased size of the e.p.s.p. is that more presynaptic fibres are activated in the presence of phorbol esters than in control. To control for this variable we compared the population e.p.s.p. with the presynaptic fibre volley by constructing input-output curves (Fig. 1*c*). Application of inactive phorbol analogues had no effect on this input-output function while application of active phorbol ester to the same slice shifted this curve so that a presynaptic fibre volley of the same size elicited a much larger postsynaptic response. These results indicate that changes in presynaptic axonal excitability cannot account for the actions of phorbol esters on synaptic transmission.

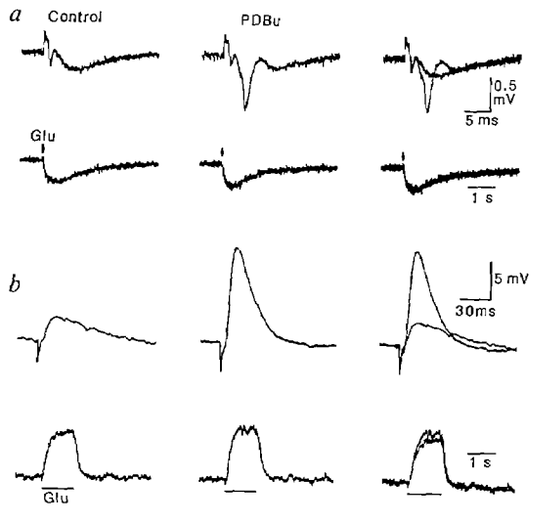


Fig. 2 Phorbol esters have minimal effects on the responses to glutamate at a time when synaptic responses are greatly increased. *a*, The population e.p.s.p. (top row) and response to pressure application of glutamate (5 mM, 40 ms, 50 p.s.i.) (bottom row) recorded with the same extracellular microelectrode are shown before and following application of 5 μM phorbol-12,13-dibutyrate (PDBu). The responses are superimposed in the right-hand column. *b*, The intracellularly recorded e.p.s.p. (top row) and responses to iontophoretically applied glutamate (0.5 M, 20 nA) (bottom row) recorded from the same cell before and following application of 5 μM PDBu. Responses are superimposed in the right-hand column.

Methods. For the field potential experiment, an electrode (tip diameter 2–5 μm) attached to a Picospritzer (General Valve Corp) and filled with 5 mM glutamate in Ringer solution was positioned close to the recording microelectrode in stratum radiatum. Short pulses of glutamate (10–50 ms; 50 p.s.i.) were applied to the slice to elicit small field responses of approximately the same amplitude as the population e.p.s.p. For the intracellular experiments, standard iontophoretic techniques were used. The iontophoretic pipette was filled with 0.5 M glutamate and placed in the mid-apical dendritic zone.

Recently, phorbol esters have been shown to have significant direct postsynaptic effects on hippocampal pyramidal cells[12,13]. To examine the possible locus of phorbol ester's actions on synaptic transmission, we compared the effect of PDBu on the population e.p.s.p. and the field potential elicited by extracellular pressure application of glutamate[14], the putative neurotransmitter at the synapse under study[15]. PDBu caused the usual increase in the population e.p.s.p. but failed to alter the glutamate field response (Fig. 2*a*, $n = 4$). This strongly suggests that any phorbol ester-induced change in postsynaptic parameters (for example, membrane potential) cannot account for the increase in the population e.p.s.p. While intracellularly recorded glutamate responses were often increased, this increase could account for only a small fraction of the increase in the monosynaptic e.p.s.p. recorded from the same cell (Fig. 2*b*) (mean per cent increase in the e.p.s.p. = 135 ± 30 ($n = 4$); per cent increase for the glutamate response = 18 ± 8 ($n = 4$)). Thus it appears likely that the enhancement of synaptic transmission caused by phorbol esters is due primarily to a presynaptic action.

Comparison of synaptic enhancement during phorbol ester application and following a presynaptic tetanus which evokes LTP reveals a precise mimicry. During both conditions, the size of the population spike and e.p.s.p. increase, the population spike latency decreases, and the relationship between the fibre

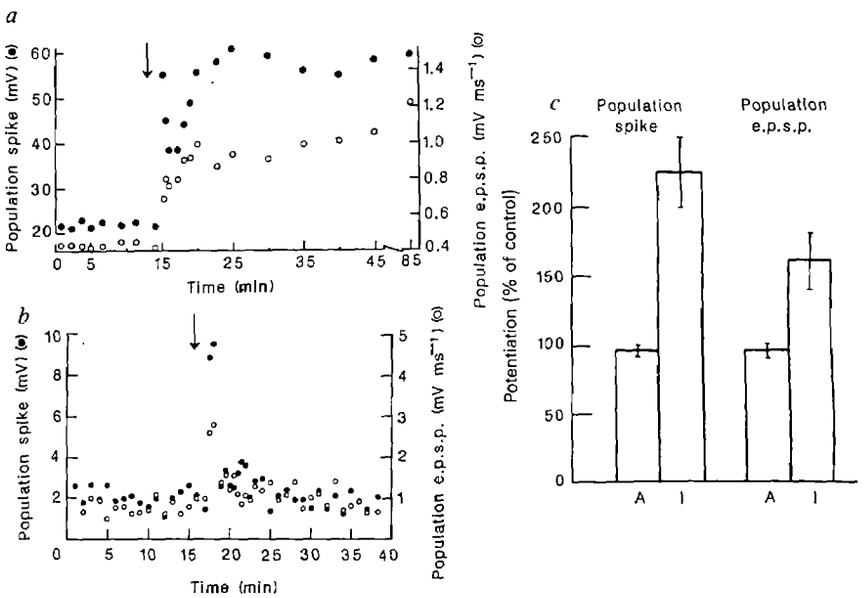


Fig. 3 Increase in synaptic transmission during LTP and its blockage by phorbol esters. *a*, Changes in synaptic responses after high-frequency stimulation (arrow; two 100-Hz/1-s stimulation trains separated by 30 s) from a slice bathed for 20 min with 10 μM of the inactive phorbol ester, 4α-phorbol-12,13-didecanoate. Note that responses are still potentiated more than 80 min after the stimulation. *b*, The changes in synaptic responses from a slice washed for 20 min with 10 μM PDBu are plotted following an identical stimulation as given in *a* (arrow). The responses exhibit post-tetanic potentiation but not long-term potentiation. *c*, Application of phorbol esters which activate PKC prevents LTP. Active or inactive phorbol esters were applied in a blind study. The mean (±s.e.m.) potentiation of the population spike and e.p.s.p. from two groups of slices, one (A; $n = 10$) exposed for 20 min to 10 μM PDBu, an activator of protein kinase C, and the other (I; $n = 10$) exposed for 20 min to 10 μM 4α-phorbol-12,13-didecanoate, an inert phorbol analogue. Highly significant differences between the two groups of slices (A and I) were found (population spike, $P < 0.001$; population e.p.s.ps, $P < 0.01$; Mann–Whitney *U*-test).

Methods. For the blind study, slices were placed in the recording chamber and bathed for 20 min either with 10 μM PDBu or with 10 μM 4α-phorbol-12,13-didecanoate. The experimenter did not know which randomly chosen solution had been applied until after all data analysis was completed. Only those slices meeting the minimum criterion of being able to generate a population spike of at least 5 mV were kept. Following exposure to phorbol esters, a 1–2-mV population spike was elicited every 15 s and responses recorded until a stable 20-min baseline was obtained. A tetanus was then given consisting of two, 100-Hz/1-s stimulus trains separated by 30 s using a voltage twice that used for control responses. Following the tetanus, stimulus voltage was returned to the control value and responses were recorded every 15 s for an additional 30 min. All responses taken during the 5 min prior to the tetanus were averaged and compared with the average of all responses recorded between 25 and 30 min following the tetanus. LTP was considered to have occurred if 30 min after the tetanus the population spike amplitude and/or the population e.p.s.p. initial slope were greater than 125% of control. Since the protocol for this study involved obtaining a control population spike of a fixed amplitude, lower-stimulus voltages would be used in slices exposed to PDBu. To control for this, in four additional slices we first obtained control responses before applying PDBu and for the tetanus used a stimulus voltage two times this pre-phorbol control value. Again we never observed LTP. This demonstrates that possible differences in the stimulus parameters during the tetanus cannot account for the blockade of LTP by phorbol esters.

volley and postsynaptic responses shifts in an identical manner[16]. If activation of PKC is involved in the generation of LTP it should be possible to occlude its generation by maximally activating this enzyme. In a pilot study we found that in seven out of seven slices treated with active phorbol esters we were unable to generate LTP while in seven out of eight control slices LTP was elicited. Based on these findings, we undertook a more rigorous blind study (see Fig. 3 legend) to test this hypothesis. Figure 3 compares the results of high-frequency stimulation in two slices from the blind study, one bathed in an inactive phorbol analogue (Fig. 3*a*) and the other bathed in PDBu (Fig. 3*b*). When stimulated with a tetanus, slices bathed in the inactive phorbol exhibited a brief post-tetanic potentiation (PTP) followed by LTP (Fig. 3*a*), while slices bathed in PDBu exhibited only PTP (Fig. 3*b*). Figure 3*c* summarizes the findings of the blind study. Of the 10 slices exposed to the inactive phorbol analogue, 8 exhibited LTP whereas none of the 10 slices exposed to PDBu exhibited LTP. However, since PDBu did not prevent PTP (Fig. 3*b*) the actions of phorbol esters appear to be specific to the long-lasting form of synaptic potentiation. Consistent with our results is the recently reported preliminary finding that phorbol esters prolong the decay of LTP *in vivo*[17].

The mechanisms underlying synaptic plasticity have generated a great deal of discussion. The most common site responsible for alterations in synaptic strength has been reported in a variety of systems to be the presynaptic terminal[18–21]. Based on our experiments examining glutamate responses and input–output curves, we propose that the enhancement of synaptic transmission induced by phorbol esters is also caused by an action localized to the presynaptic terminal. Consistent with this proposal are several biochemical studies performed in brain tissue which have demonstrated that PKC is present in presynaptic nerve terminals[22], is activated during depolarization of the presynaptic nerve terminal[3], and phosphorylates proteins found in presynaptic terminal membrane[3–6]. Furthermore, phorbol esters have been shown to enhance calcium-dependent neurotransmitter release from both rat brain synaptosomes[23] and cultured brain neurones[24].

The precise mechanism underlying the enhancement of neurotransmitter release induced by phorbol esters is unknown. Phorbol esters have been shown to block a calcium-activated potassium current in hippocampal pyramidal cells[12,13] and similar channels have been shown to exist in rat presynaptic nerve terminals[25]. Blockage of these channels might prolong the action potential in the terminal, thus increasing transmitter release. A similar mechanism involving a different type of potassium channel has been proposed to account for the enhanced transmitter release which underlies behavioural sensitization in the marine mollusc, *Aplysia*[26]. Phorbol esters have also been shown to directly enhance calcium currents in an invertebrate neurone[27]. Alternatively, phorbol esters may sensitize the secretory process to calcium as has been shown in other cell types[2]. A presynaptic locus may also account for the generation of LTP since increases in glutamate release have been demonstrated during LTP in the hippocampus[28,29]. However there are also several experiments consistent with significant postsynaptic modifications[30,31].

Several proteins have been shown to be phosphorylated following the generation of LTP in the hippocampus[7,8,32,33]. One of these, F1 (possibly the same as the synaptically associated B50), also appears to be a substrate for PKC[7,8] although its anatomical localization and function are as yet unknown. If PKC activation is necessary for the induction of LTP, one possible sequence of events for the induction of LTP could be that the high-frequency stimulation raises intracellular calcium concentration to a level that results in a significant activation of PKC. In fact, a recent report has demonstrated that in erythrocyte vesicles small increases in calcium concentration can cause a translocation of PKC from a soluble to a membrane-bound compartment[34]. An alternative hypothesis would be that high-frequency stimulation causes the release of some extracellular messenger capable of stimulating inositol phospholipid turnover. This would result in the generation of diacylglycerol and the subsequent activation of PKC.

This work was supported by NIH grants MH-38256, RCDA MH-00437, the Klingenstein Fund (to R.A.N.), NS-07495 (to R.C.M.) and the Scottish Rite Schizophrenia Research Program NMJ, USA.

Note added in proof: Recently a report has appeared[36] demonstrating translocation of PKC from soluble to membrane fractions following LTP in the hippocampus, thus supporting a role for PKC in LTP.

Received 7 November 1985; accepted 6 March 1986.

1. Nishizuka, Y. *Nature* **308**, 693–698 (1984).
2. Baker, P. F. *Nature* **310**, 629–630 (1984).
3. Wu, W. C.-S., Walaas, S. I., Nairn, A. C. & Greengard, P. *Proc. natn. Acad. Sci. U.S.A.* **79**, 5249–5253 (1982).
4. Sorensen, R. G., Kleine, L. P. & Mahler, H. R. *Brain Res. Bull.* **7**, 57–61 (1981).
5. Kristjansson, G. I., Zwiers, H., Oestreicher, A. B. & Gispen, W. H. *J. Neurochem.* **39**, 371–378 (1982).
6. Aloyo, V. J., Zwiers, H. & Gispen, W. H. *J. Neurochem.* **41**, 649–653 (1983).
7. Nelson, R. B. & Routtenberg, A. *Expl Neurol.* **89**, 213–224 (1985).
8. Akers, R. F. & Routtenberg, A. *Brain Res.* **334**, 147–151 (1985).
9. Murphy, K. M. M., Gould, R. J., Oster-Granite, M. L., Gearhart, J. D. & Snyder, S. H. *Science* **222**, 1036–1038 (1983).
10. Alger, B. E. & Nicoll, R. A. *J. Physiol., Lond.* **328**, 105–123 (1982).
11. Castagna, M. *et al. J. biol. Chem.* **257**, 7847–7851 (1982).
12. Baraban, J. M., Snyder, S. H. & Alger, B. E. *Proc. natn. Acad. Sci. U.S.A.* **82**, 2538–2542 (1985).
13. Malenka, R. C., Madison, D. V., Andrade, R. & Nicoll, R. A. *J. Neurosci.* **6**, 475–480 (1986).
14. Harris, E. W., Ganong, A. H. & Cotman, C. W. *Brain Res.* **323**, 132–137 (1984).
15. Cotman, C. W. & Nadler, J. V. in *Glutamate: Transmitter in the Central Nervous System* (eds Roberts, P. J., Storm-Mathisen, J. & Johnston, G. A. R.) 117–154 (Wiley, Chichester, 1981).
16. Andersen, P., Sundberg, S. H., Sveen, O., Swann, J. W. & Wigström, H. *J. Physiol., Lond.* **302**, 463–482 (1980).
17. Lovinger, D., Colley, P., Linden, D. J., Murakami, K. & Routtenberg, A. *Soc. Neurosci. Abstr.* **11**, 927 (1985).
18. Kandel, E. R. *Nature* **293**, 697–700 (1981).
19. Briggs, C. A., McAfee, D. A. & McCaman, R. E. *J. Physiol., Lond.* **363**, 181–190 (1985).
20. Koyano, K., Kuba, K. & Minota, S. *J. Physiol., Lond.* **359**, 219–233 (1985).
21. Baxter, D. A., Bittner, G. D. & Brown, T. H. *Proc. natn. Acad. Sci. U.S.A.* **82**, 5978–5982 (1985).
22. Girard, P. R., Mazzei, G. J., Wood, J. G. & Kuo, J. F. *Proc. natn. Acad. Sci. U.S.A.* **82**, 3030–3034 (1985).
23. Nichols, R. A., Haycock, J. W., Wang, J.K.-T. & Greengard, P. *Soc. Neurosci. Abstr.* **11**, 846 (1985).
24. Zurgil, N. & Zisapel, N. *FEBS Lett.* **185**, 257–261 (1985).
25. Bartschat, D. K. & Blaustein, M. P. *J. Physiol., Lond.* **361**, 441–457 (1985).
26. Kandel, E. R. & Schwartz, J. H. *Science* **218**, 433–443 (1982).
27. DeRiemer, S. A., Strong, J. A., Albert, K. A., Greengard, P. & Kaczmarek, L. K. *Nature* **313**, 313–316 (1985).
28. Dolphin, A. C., Errington, M. L. & Bliss, T. V. P. *Nature* **297**, 496–498 (1982).
29. Bliss, T. V. P., Douglas, R. M., Errington, M. L. & Lynch, M. *J. Physiol., Lond.* **361**, 50P (1985).
30. Lynch, G., Larson, J., Kelso, S., Barrionuevo, G. & Schottler, F. *Nature* **305**, 719–721 (1983).
31. Wigström, H. & Gustafsson, B. *Nature* **301**, 603–604 (1983).
32. Browning, M., Dunwiddie, T., Bennett, W., Gispen, W. & Lynch, G. *Science* **203**, 60–62 (1979).
33. Bär, P. R., Schotman, P., Gispen, W. H., Tielen, A. M. & Lopes da Silva, F. H. *Brain Res.* **198**, 478–484 (1980).
34. Wolf, M., LeVine, H. III, May, W. S. Jr, Cuatrecasas, P. & Sahyoun, N. *Nature* **317**, 546–549 (1985).
35. Alger, B. E. & Teyler, T. J. *Brain Res.* **110**, 463–480 (1976).
36. Akers, R. F., Lovinger, D. M., Colley, P. A., Linden, D. J. & Routtenberg, A. *Science* **231**, 587–589 (1986).

Platelet activation—a role for a 40K anti-phospholipase A_2 protein indistinguishable from lipocortin

Lhousseine Touqui, Bernard Rothhut, Angus M. Shaw, Armel Fradin, B. Boris Vargaftig & Françoise Russo-Marie

Unité associée Institut Pasteur/Inserm No. 285, Institut Pasteur, 28 rue du Dr Roux, 75015 Paris, France

Stimulus–response (S–R) coupling in platelets requires an intermediary other than an elevation in cytosolic free calcium ($[Ca^{2+}]_i$)[1,2]. While an increase in $[Ca^{2+}]_i$ is essential in S–R coupling, effecting phosphorylation of myosin of relative molecular mass (M_r) 20,000 (20 K)[3], platelet activation is also associated

with phosphorylation of a 40K protein[4], which can occur in the absence of changes in $[Ca^{2+}]_i$ (ref. 5). The 40K protein is the substrate for protein kinase C (PKC)[6,7]. Mounting evidence suggests that activation of PKC by diacyglycerol is the other signal involved in S–R coupling[6,8–10]. Although phosphorylation of the 40K protein is associated with certain platelet functional responses[4,6,8,11,12], no precise role has been accredited to it. Recently, we and others have described several proteins (collectively known as lipocortin) which inhibit phospholipase A_2 (PLA_2)[13–19]. One of the most conspicuous proteins of this group is a 40K peptide whose inhibitory activity can be suppressed by prior phosphorylation[18,20]. We hypothesized that the 40K protein described in platelets may possess anti-PLA_2 activity and that phosphorylation by PKC, suppressing its inhibitory activity, may represent the mechanism underlying mobilization of arachidonic acid, the precursor of prostaglandins. The results of the present study strongly support this hypothesis.

Agonist-induced platelet activation is closely associated with phosphorylation of a 40K protein[4,6,8,10–12] which is the substrate for PKC. Although activators of PKC such as phorbol myristate acetate (PMA) or 1-oleyl-2-acetylglycerol (OAG) can induce some platelet responses, such as aggregation and degranulation[9], no specific function has been reported for the 40K protein. Recent studies have shown that activators of PKC, such as PMA, enhance the activity of PLA_2 in calcium ionophore-stimulated platelets [21], suggesting a possible role for PKC/40K protein in the regulation of PLA_2 activity. Further support for such a role derives from studies[18] which demonstrated, in peritoneal neutrophils, the existence of an anti-phospholipase A_2 protein with a M_r of 40K whose anti-PLA_2 activity can be reduced by prior phosphorylation. The phosphorylation of this protein, originally named lipomodulin and now termed lipocortin[16], in neutrophils parallels the release of arachidonic acid during stimulation by a chemo-attractant. Subsequent investigations[20] demonstrated that in murine thymocytes this protein is phosphorylated by a PKC-dependent mechanism.

On the basis of these observations, we hypothesize that the platelet 40K protein may have anti-PLA_2 activity and that this activity may be regulated by phosphorylation, in a manner similar to that described for lipocortin in neutrophils[18]. Thus, by altering the anti-PLA_2 activity of the 40K protein, activation of PKC may have an important role in the regulation of PLA_2 activity in platelets. To substantiate this hypothesis, we extracted platelet proteins before and after activation of PKC and assayed the extracted proteins for PLA_2 inhibitory activity.

Plasma-free platelet suspensions were prepared from whole blood obtained from the central ear artery of adult New Zealand White rabbits, as described elsewhere[22]. Platelets were lysed by glycerol loading[23] and homogenized in the presence of a membrane solubilizer, Tween-20 (0.5% v/v). Proteins were separated by HPLC using a TSK G2000 SW Ultropac column. The mobile phase, adjusted to a flow rate of 0.2 ml min^{-1}, consisted of Tris-NaCl (0.1–0.15 M, *p*H 7) containing 2 mM EDTA. The activity of each HPLC fraction (0.4 ml) was assessed by monitor-

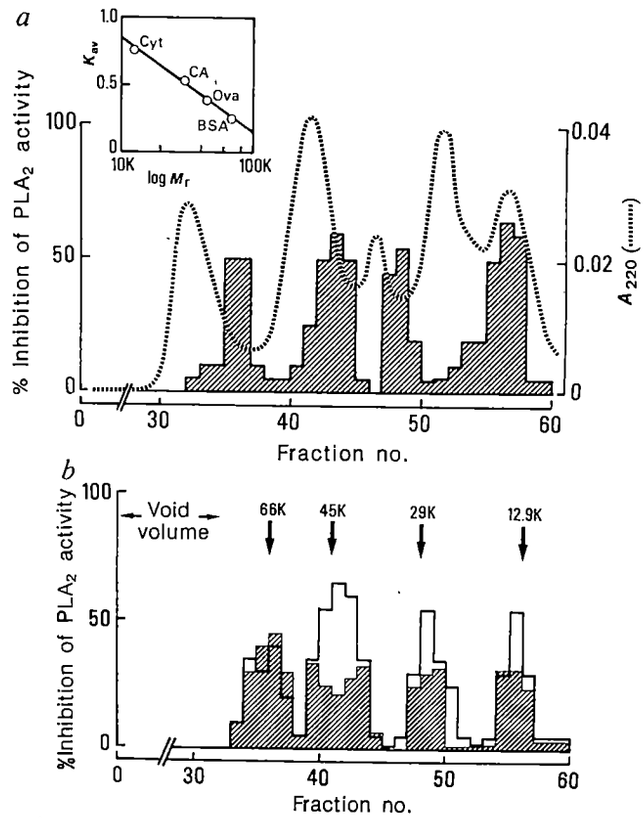


Fig. 1 Anti-phospholipase A_2 activity of HPLC fractions. *a*, Estimation of the M_rs of inhibitory fractions from untreated platelets. *b*, Anti-PLA_2 activity of fractions from thrombin-stimulated platelets. Washed platelets (2×10^9 cells ml^{-1}) were suspended in Tyrode's–gelatin (TG) buffer containing (1 mM) $MgCl_2$, 2 mM $CaCl_2$ and 0.25% (w/v) gelatin (*p*H 7.4). *a*, Aliquots (3 ml) of the platelet suspension were lysed by glycerol loading, then 1 ml of Ca^{2+}-free TG buffer was added to each aliquot to induce osmotic shock. Lysates were then homogenized in the presence of a membrane solubilizer, Tween 20 (0.5% v/v). Ca^{2+}-free TG buffer was added to the homogenates to attain a final protein concentration of 4 mg ml^{-1}. These mixtures were stored in aliquots at −60 °C until required. Aliquots of homogenates containing 0.2 mg protein were subjected to HPLC and the proteins separated on a TSK G 2000 SW Ultropac column using Tris-NaCl buffer (0.1–0.15 M, *p*H 7) as the mobile phase. The M_rs of the resolved proteins were determined by referring to a calibration curve (inset) derived using protein standards [bovine serum albumin (BSA), ovalbumin (Ova), carbonic anhydrase (CA) and cytochrome *C* (Cyt)]. The anti-PLA_2 activity of each fraction was assessed by monitoring its ability to inhibit the release of porcine pancreatic PLA_2-induced ^{3}H-oleic acid from a suspension of labelled *E. coli* membranes[31]. Briefly, 0.1-ml aliquots from each HPLC fraction were each added to 0.25 ml of Tris buffer (100 mM, *p*H 8) containing 10 mM $CaCl_2$ and preincubated with porcine pancreatic PLA_2 (50 ng) for 10 min at 4 °C. In controls, protein fractions were substituted with HPLC buffer. Reactions were initiated by adding *E. coli* substrate (25 μl, 250,000 c.p.m.) and terminated 5 min later by the addition of 50 μl 2 M HCl. The released oleic acid was trapped in the supernatant by the addition of excess BSA (100 mg ml^{-1}), and after centrifugation (10,000*g*, 5 min) to remove particulate material, an aliquot of supernatant was counted for radioactivity by liquid scintillation spectrophotometry. In the absence of any inhibitor, 50 ng PLA_2, over a period of 5 min, induced the release of 8–12% of incorporated oleic acid, a value which represented between 40 and 60% of the maximum response. The inhibition of the anti-PLA_2 activity of the various fractions from one typical experiment is expressed as a percentage of the release evoked in the absence of an inhibitor. The dotted line, representing the profile of the resolved proteins, was determined by measuring the optical absorbance of the eluate at 220 nm. *b*, Aliquots (3 ml) of the platelet suspension were challenged with thrombin (1 U ml^{-1}) (or saline in the case of controls) for 1 min at 37 °C. Reactions were stopped by adding ice-cold EDTA (5 mM final concentration). Thereafter, cells were lysed, homogenized and anti-PLA_2 activity determined (following lysis control cells received 1 U ml^{-1} thrombin). The cumulative results from five experiments are shown; error bars have been omitted for clarity. Compared with controls (open blocks), thrombin treatment (hatched blocks) decreased the inhibitory activity of the fractions containing the 40K, 30K and 15K proteins by 54.7±5.2% ($P<0.001$), 31.0±5.5% ($P<0.01$) and 10.0±2.2% (not significant), respectively (mean±s.e.m.). When thrombin was replaced by PMA (10 nM) a marked decrease in the anti-PLA_2 activity of the 40K fraction was observed (see text).

ing its ability to inhibit porcine pancreatic PLA_2-induced ^3H-oleic acid release from a suspension of labelled *Escherichia coli* membranes (see Fig. 1 legend).

Four fractions, with apparent M_rs of 15K, 30K, 40K and 60K, were found to possess anti-phospholipase activity (Fig. 1*a*), suggesting that rabbit platelets contain proteins which are similar to those now referred to as lipocortin[16]. The principle M_rs reported for the lipocortin proteins are 15K, 30K and 40K. The inhibition associated with the 60K fraction has been reported previously[17] and appears to be due to a nonspecific effect of albumin. The 30K and 15K peptides are considered to be active proteolytic fragments of the 40K protein as in the presence of protease inhibitors (which were omitted in the present study) only the 40K fraction is recovered from the cells[24].

To determine whether the 40K protein extracted from rabbit platelets was similar to lipocortin, we examined the effect of a monoclonal antibody (BF26)[25] raised against renocortin—a lipocortin from rat renomedullary interstitial cells[15,25]—on the ability of the protein fractions to inhibit PLA_2 activity in an *in vitro* assay (see Fig. 1 legend). Fractions containing the 40K protein were incubated with various dilutions of antibody for 1 h at 37 °C and for 24 h at 4 °C. The anti-PLA_2 activity following incubation with a 1:50 dilution of BF26 was reduced from 28.3±3.5% to 6.0±0.7% (mean±s.e.m. of six observations, $P<0.001$). Controls, in which antibody alone was incubated with HPLC buffer, had no effect on PLA_2 activity. This result demonstrates that the 40K protein is immunologically identical to lipocortin.

We further questioned the role of lipocortin in platelets by observing the effect of thrombin, a potent activator of PKC[4], on the anti-phospholipase activity of the extracted proteins. Following treatment of intact platelets with this agonist, the inhibitory activity of the 40K, 30K and 15K fractions was reduced (Fig. 1*b*), the predominant effect being observed with the 40K fraction; no effect on the 60K fraction was observed. In addition, when these fractions were pretreated with alkaline phosphatase, their anti-phospholipase activities were restored (Table 1), suggesting that the effect of thrombin on lipocortin

Table 1 Effect of alkaline phosphatase on HPLC fractions from thrombin-treated platelets

Fraction	% Inhibition of PLA_2 activity	
	Control	Alkaline phosphatase-treated
40K	38.9±7	64.3±4.0*
30K	22.8±6.5	42.8±2.9*
15K	21.7±5.1	51.3±5.1*

The homogenate from thrombin-treated platelets was subjected to HPLC and 0.3-ml aliquots from fractions corresponding to M_rs of 40K, 30K and 15K were each incubated with 1.2 U of insoluble alkaline phosphatase (AP) (*p*H 10) at 20 °C for 90 min. The enzyme was then recovered by centrifugation (5,000*g*, 5 min) and the anti-PLA_2 activity of these and time-matched controls, which received AP buffer alone, was assayed as already described. Values are the mean±s.e.m. of 7–8 observations.

* Significant difference compared with the control ($P<0.001$).

(that is, a reduction of its anti-PLA_2 activity) was linked to a phosphorylating event. This notion was subsequently confirmed using ^{32}P-labelled platelets treated with thrombin or PMA and subjected to SDS-polyacrylamide gel electrophoresis (SDS-PAGE). There was increased incorporation of ^{32}P in two major bands, one corresponding to myosin light chain (20K) and another corresponding to 40K (Fig. 2*b*,*c*). To establish whether the 40K protein was in fact lipocortin, aliquots of homogenates from thrombin- or PMA-stimulated, ^{32}P-labelled platelets were incubated with the monoclonal antibody BF26. Immunoprecipitated proteins were pelleted and subjected to SDS-PAGE; the

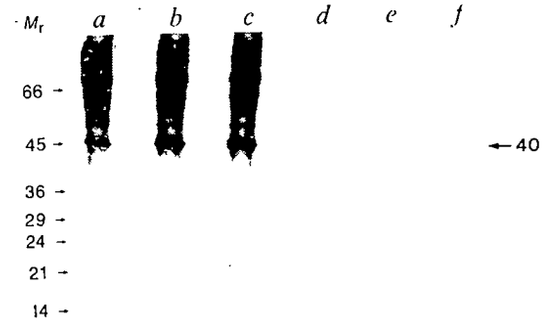


Fig. 2 Immunoprecipitation and SDS-PAGE of ^{32}P-labelled proteins from platelets. The figure shows the autoradiogram of proteins from control (*a*), thrombin-treated (*b*) and PMA-treated (*c*) platelets before immunoprecipitation. *d*, Immunoprecipitation of proteins from thrombin-treated platelets by nonspecific antibody. *e*,*f*, Immunoprecipitation with specific antibody (BF26) of proteins from thrombin(*e*)- or PMA(*f*)-treated platelets. The arrow indicates the 40K protein immunoprecipitated by the specific antibody. **Methods.** Washed platelets were incubated with ^{32}P (0.5 mCi ml^{-1}) for 1 h at 22 °C and aliquots (100 μl) were incubated with thrombin (1 U ml^{-1}), PMA (10 nM) or vehicle alone. After 1 min, reactions were stopped by adding 50 μl of RIPA buffer (*p*H 7.2) containing 140 mM NaCl, 10 mM Tris-HCl, 10 mM EDTA, 1% Nonidet P-40, 0.1% SDS, 1 mM phenylmethylsulphonyl fluoride, 200 IU ml^{-1} aprotinin, 30 mM nitrilotriacetic acid and 30 mM sodium fluoride. Aliquots (15 μl, each containing 100,000 c.p.m.) of homogenates obtained from thrombin- or PMA-treated platelets were incubated at 4 °C with protein A–Sepharose (60 mg ml^{-1}) for 30 min and nonspecific protein binding was subsequently eliminated by centrifugation (5 min at 5,000*g*). Then, 90 μl of supernatant were incubated with anti-renocortin antibody BF26 (26.7 mg protein ml^{-1}) at 37 °C. In the case of the control, aliquots (90 μl) from thrombin-treated platelets received an equivalent amount of nonspecific antibody of the same class (IgG1) as BF26. After 1 h, rabbit anti-mouse antiserum (1:10 dilution) was added to increase specific binding; 30 min later, protein A–Sepharose (60 mg ml^{-1}) was added and the mixture incubated for 18 h at 4 °C. The antibody-bound proteins were pelleted by centrifugation then subjected to SDS-PAGE as described in ref. 32 and radioactivity visualized by autoradiography. Total ^{32}P incorporated into proteins, determined by trichloroacetic acid precipitation, was increased 2–3-fold in thrombin-treated platelets. The radioactivity immunoprecipitated by BF26 (316±38 c.p.m.) in proteins from control platelets increased by 3.7-fold (to 1,168±160 c.p.m.) in proteins from thrombin-treated platelets. In contrast, no significant radioactivity was immunoprecipitated by the nonspecific antibody. Similar results were obtained with proteins from PMA-treated platelets (data not shown).

resultant autoradiograms showed a distinct band corresponding to a M_r of 40K (Fig. 2*e*,*f*), demonstrating that at least part of this protein is immunologically identical to lipocortin. The 30K and 15K fractions (proteolytic fragments of 40K) did not appear in the autoradiograms, as protease inhibitors were present in these experiments.

The present study shows that rabbit platelets contain a 40K anti-phospholipase protein which is recognized by a specific anti-lipocortin antibody (from renomedullary cells), indicating that this protein is immunologically indistinguishable from lipocortin. As shown in Fig. 2, the radioactivity associated with the immunoprecipitated band does not represent all of the phosphorylated 40K protein observed after stimulation with thrombin or PMA; one possible explanation for this is that the 40K protein is not unique but consists of various different proteins, as reported by Imaoka *et al.*[7], and that lipocortin is one of these proteins.

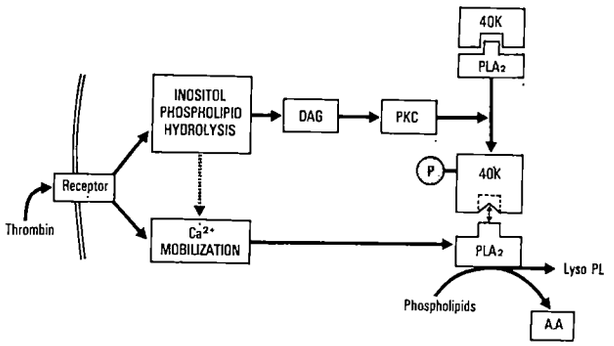


Fig. 3 Synergistic action of protein kinase C (PKC) activation and Ca^{2+} mobilization for eliciting full PLA_2 activation in thrombin-stimulated platelets.

Previous studies[20] have shown that the anti-PLA_2 activity of lipocortin from murine thymocytes can be regulated by PKC-dependent phosphorylation. Here we have shown that, in response to thrombin, the anti-PLA_2 activity of the 40K protein is decreased and that this reduction appears to be associated with phosphorylation of the 40K protein. A role for PKC in suppressing the anti-PLA_2 activity of the 40K protein is therefore suggested. Indeed, when thrombin was replaced by 10 nM PMA, a specific activator of PKC, the anti-PLA_2 activity of the 40K protein was reduced from $71.6 \pm 9.9\%$ in dimethyl sulphoxide (DMSO)-treated control platelets to $16.6 \pm 10.6\%$ after PMA treatment (mean ± s.e.m. of eight observations $P < 0.01$), further suggesting that the anti-PLA_2 activity of the 40K protein in platelets is regulated by PKC.

It has been proposed[26] that two intermediaries—diacylglycerol (DAG) and an elevation in $[Ca^{2+}]_i$—are involved in S–R coupling in various cell types. Here we propose that phospholipase A_2 is also regulated by these two intermediaries to achieve optimal activity. The regulation of PLA_2 by Ca^{2+} and DAG is summarized in Fig. 3. In this scheme, receptor activation leads to an increase in $[Ca^{2+}]_i$ and the concomitant formation of DAG, from the hydrolysis of inositol phospholipids[26]. Activation of PKC, by DAG, phosphorylates the 40K lipocortin, suppressing its anti-PLA_2 activity. In the presence of an agonist-induced elevation in cytosolic $[Ca^{2+}]_i$ (PLA_2 enzymes have an absolute dependency on ionic Ca^{2+}; ref. 27) optimal activity is evoked.

In preliminary experiments, we have observed that the PKC activator PMA, at concentrations that induce phosphorylation of the 40K protein, does not cause the release of ^{3}H-arachidonic acid (^{3}H-AA) from labelled platelets. However, the release of AA induced by the Ca^{2+} ionophore A23187 (250 nM) was enhanced from $15 \pm 4\%$ to $38 \pm 5\%$ (mean ± s.e.m. of four experiments, $P < 0.05$) by pretreating the platelets with PMA (10 nM), which further lends credence to our proposed scheme. A similar PMA-mediated potentiation of ionophore-induced AA release and of thromboxane B_2 formation in rabbit neutrophils and human platelets has been reported elsewhere[21,28]. More recently, both PMA and DAG have been shown to potentiate the release of AA from ionophore-stimulated human platelets[29].

The nature of the interaction between lipocortin and PLA_2 has not yet been elucidated. In Fig. 3 we have shown lipocortin, in its unphosphorylated state, bound to and inactivating PLA_2, rather like the non-enzymatic subunit of crotoxin in snake venom[30]. Phosphorylation of lipocortin dissociates the complex, allowing, in the presence of an elevation in cytosolic calcium, optimal activity of PLA_2.

Received 25 November 1985; accepted 5 March 1986.

1. Knight, D. E., Hallam, T. J. & Scrutton, M. C. *Nature* **296**, 256–257 (1982).
2. Rink, T. J., Smith, W. S. & Tsien, R. Y. *FEBS Lett.* **148**, 21–25 (1982).
3. Lyons, R. M. & Shaw, J. O. *J. clin. Invest.* **65**, 242–255 (1980).
4. Lyons, R. M., Stanford, N. & Majerus, P. W. *J. clin. Invest.* **56**, 924–936 (1975).
5. Yamanishi, J. *et al. Biochem. biophys. Res. Commun.* **112**, 778–786 (1983).
6. Sano, K., Takai, Y., Yamanishi, J. & Nishizuka, Y. *J. biol. Chem.* **258**, 2012–2013 (1983).
7. Imaoka, T., Lynham, J. A. & Haslam, R. J. *J. biol. Chem.* **258**, 11404–11414 (1983).
8. Kajikawa, N. *et al. Biochem. biophys. Res. Commun.* **116**, 743–750 (1983).
9. Rink, T. J., Sanchez, A. & Hallam, T. J. *Nature* **305**, 317–319 (1983).
10. Haslam, R. J. & Davidson, M. L. *Biochem. J.* **222**, 231–361 (1984).
11. Haslam, R. J. & Lynham, J. A. *Biochem. biophys. Res. Commun.* **77**, 714–722 (1977).
12. Haslam, R. H. *et al.* in *Platelets: Cellular Response Mechanisms and their Biological Significance* (eds Rothman, A., Meyer, F. A., Gliter, C. & Silberg, A. 213–231 (Wiley, New York, 1980).
13. Blackwell, G. J. *et al. Nature* **287**, 147–149 (1980).
14. Hirata, F., Schiffmann, E., Venkatasubramanian, K., Salomon, D. & Axelrod, J. *Proc. natn. Acad. Sci. U.S.A.* **77**, 2533–2536 (1980).
15. Cloix, J. F., Colard, O., Rothhut, B. & Russo-Marie, F. *Br. J. Pharmac.* **79**, 313–321 (1983).
16. Di Rosa, M., Flower, R. J., Hirata, F., Parente, L. & Russo-Marie, F. *Prostaglandins* **28**, 441–442 (1984).
17. Blackwell, G. J. *et al. Br. J. Pharmac.* **76**, 185–194 (1982).
18. Hirata, F. *J. biol. Chem.* **256**, 7730–7733 (1981).
19. Wallner, B. O. *et al. Nature* **320**, 77–81 (1986).
20. Hirata, F., Matsuda, K., Notsu, Y., Hattori, T. & Del Carmine, R. *Proc. natn. Acad. Sci. U.S.A.* **81**, 4717–1421 (1984).
21. Mobley, A. & Tai, H. H. *Biochem. biophys. Res. Commun.* **130**, 717–723 (1985).
22. Ardlie, N. G., Packham, M. A. & Mustard, J. F. *Br. J. Haemat.* **19**, 7–17 (1970).
23. Barber, A. J. & Jamieson, G. A. *J. biol. Chem.* **245**, 6357–6365 (1970).
24. Hirata, F. *et al. Proc. natn. Acad. Sci. U.S.A.* **78**, 3190–3194 (1981).
25. Rothhut, B., Russo-Marie, F., Cousin, M. & Lando, D. in *Proc. IUPHAR* Vol. 2, 43–50 (Macmillan, London, 1984).
26. Nishizuka, Y. *Nature* **308**, 693–698 (1984).
27. Van Den Bosch, H. *Biochim. biophys. Acta* **604**, 191–246 (1980).
28. Volpi, M., Molski, T. F. P., Naccache, P. H., Feinstein, M. B. & Sha'afi, R. L. *Biochem. biophys. Res. Commun.* **128**, 594–600 (1985).
29. Halenda, S. P., Zavoico, G. B. & Feinstein, M. B. *J. biol. Chem.* **260**, 12484–12491 (1985).
30. Habermann, E. & Breithaupt, H. *Toxicon* **16**, 19–30 (1978).
31. Rothhut, B., Russo-Marie, F., Wood, J., Di Rosa, M. & Flower, R. J. *Biochem. biophys. Res. Commun.* **117**, 878–884 (1983).
32. Laemmli, U.K. *Nature* **227**, 680–685 (1970).

Equivalence of intracellular *p*H of differentiating *Dictyostelium* cell types

David I. Ratner

Department of Biology, Amherst College, Amherst, Massachusetts 01002, USA

During the development of the cellular slime moulds, spore and stalk cells arise from vegetative amoebae. The intracellular *p*H (pH_i) of the developing cells has been postulated to be important in the choice of morphogenetic programmes[1]. This hypothesis stems from the observation that the addition to the culture medium of weak (membrane-permeable) acids or bases favours the differentiation of pre-stalk or pre-spore cells respectively[1–3]. Similarly, compounds that are known to inhibit a *Dictyostelium* plasma membrane proton pump induce preferential pre-stalk development[1,4,5]; and a stalk-specific *Dictyostelium* morphogen, 'DIF', has been suggested to act via intracellular acidification[6,7]. However, in these studies the pH_i values of pre-spore and pre-stalk amoebae were unknown, and the actual effects of the various agents mentioned above on pH_i were also unknown. By monitoring the intracellular fluorescence of a *p*H-sensitive dye, I have measured the relative intracellular *p*H of pre-spore compared with pre-stalk amoebae. I report here that, contrary to the above hypothesis, there is no significant difference in the pH_i of the two cell types.

The cytoplasmic *p*H of vegetative *Dictyostelium discoideum* amoebae has recently been measured as 6.5–6.7 on the basis of ^{31}P-NMR spectroscopy[8,9] (though the spectra may be open to other interpretations[10]). Unfortunately, NMR measurements require more material than can be obtained as purified precursor cell types. In contrast, *p*H measurements based on the fluorescence of intracellular probes are rapid and highly sensitive. Permeant derivatives of fluorescent dyes readily cross the plasma membrane; negatively charged dye molecules, liberated by intracellular esterases, then accumulate within the cytoplasm. Jamieson *et al.*[11] studied changes in pH_i during *Dictyostelium* development by monitoring the fluorescence of cells labelled

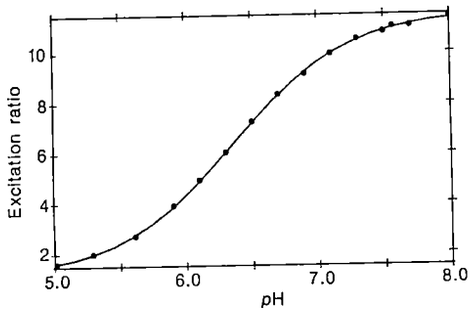


Fig. 1 *p*H-dependence of the excitation ratio of fluorescein in phosphate buffer. Values plotted are the ratio: fluorescence intensity at 489 nm illumination/fluorescence intensity at 438 nm illumination, as a function of the buffer *p*H. Experimental values represent the average of two spectral determinations, which were generally found to agree within 1%. The smooth curve is a theoretical fit derived from the observed *p*K and the fluorescence parameters at the extremes of *p*H.

Methods. Fluorescein (MCB) was dissolved at 0.2 μM in 20 mM phosphate buffers (mixtures of Na_2HPO_4 and KH_2PO_4) of varying *p*H. *p*H determinations, using an Orion 601A meter, and fluorescence spectra were obtained at 0–2 °C. Fluorescence measurements were made with a dual-beam Spex Fluorolog 2 spectrometer controlled by a Datamate, model DM1. Excitation bandwidth 0.9 nm, integration time 1 s, scanning increment 1 nm, emission monochrometer set at 510 nm. All spectra were recorded in a ratio mode to correct for the spectrum due to lamp output.

with fluorescein. The following comparison of the pH_i of prespore and pre-stalk cells was made using a modification of their method.

The fluorescence excitation spectrum of fluorescein is highly *p*H-dependent, the major effect being on the relative fluorescence intensities resulting from illumination at the excitation maximum (489 nm) compared with illumination at a shorter wavelength (438 nm)[11–13]. Figure 1 shows a standard curve, used to calibrate pH_i measurements, of the excitation ratio of fluorescein in phosphate buffer. Sensitivity is excellent over the *p*H range 5.8–7.0 (fluorescence $pK = 6.4$), a range well suited for examination of *Dictyostelium* amoebae.

When amoebae (vegetative or developing) are incubated with a relatively high concentration (100 μM) of fluorescein diacetate, intense but diffuse labelling of the cytoplasm results (ref. 11 and my unpublished results); this indicates that the major contribution to the fluorescence of intracellular dye is cytoplasmic, hence the pH_i reported is expected to be essentially that of the cytoplasm. Figure 2*a* shows the excitation spectrum of fluorescein-loaded vegetative *D. discoideum* amoebae. Despite its negative charge over the entire physiological range, fluorescein is lost from *Dictyostelium* (and mammalian[13]) cells at an appreciable rate. Therefore, measurements were performed quickly, at low temperature, and correction made for any loss of dye from the cells. Figure 2*a* includes the spectrum of the cell suspension, that of the cell-free filtrate taken immediately thereafter, and the calculated difference spectrum corresponding to intracellular fluorescein. The pH_i of the vegetative amoebae in Fig. 2*a* is 6.94. The average pH_i in 14 such measurements was 6.93 ± 0.21. These measurements were obtained in phosphate buffers spanning 2.5 *p*H units (*p*H 5.0–7.5); the intracellular *p*H was unaffected by such changes in the fluorescence buffer (see also refs 8–10).

The fluorescence procedure is also applicable to pre-spore and pre-stalk cells. The two cell types, obtained from migrating slugs, were purified by gradient centrifugation, and fluorescence

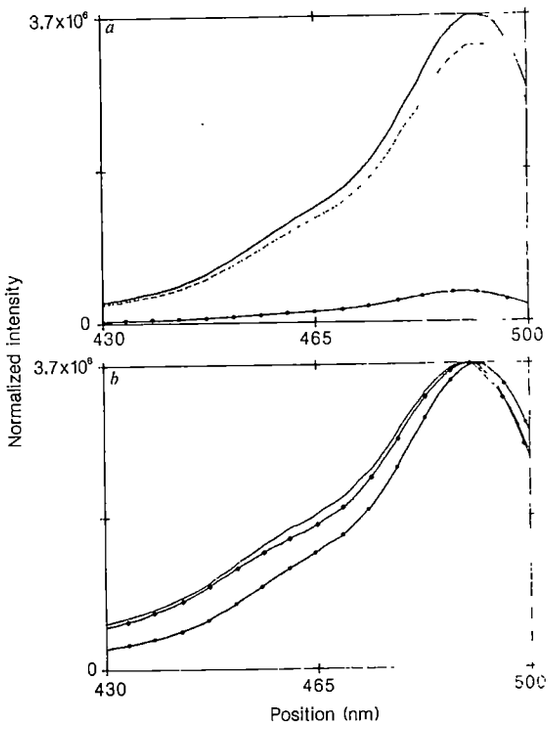


Fig. 2 Fluorescence excitation spectra of vegetative (*a*) and developing (*b*) amoebae. *a*, Spectra for a vegetative cell suspension (—), for the cell-free filtrate (●—●) dye loss 10%, and for intracellular fluorescein calculated as the difference spectrum of the first two (·····) pH_i 6.94. *b*, Normalized, filtrate-corrected spectra for three cell types: pre-spore, pH_i 6.08 (—), pre-stalk, pH_i 6.12 (◆–◆) and a concurrent vegetative cell preparation, pH_i 6.94 (●–●). The pH_i values were determined from the excitation ratio of intracellular fluorescence according to the calibration curve of Fig. 1. Cellular autofluorescence is negligible: the intensity of unlabelled cells is $<10^{-4}$ that of cells containing probe. Note that the difference in pH_i between vegetative and differentiating cells does not result from the choice of strains, as vegetative NC4 amoebae (not shown) have a pH_i equal to that of vegetative AX3 cells.

Methods. Vegetative cells of *D. discoideum* strain AX3 were harvested from axenic medium[18], washed in cold buffer and incubated at 2×10^6 ml^{-1} in 10 mM PO_4 *p*H 6.0 (prepared from Na_2HPO_4 and KH_2PO_4), 9 mM NaCl, 9 mM KCl, 2 mM $CaCl_2$ and 100 μM fluorescein diacetate (Sigma) added from a 100-mM stock solution in dimethyl sulphoxide. After incubation at 22 °C for 15 min, with shaking, cells were washed three times in cold buffer, the final wash immediately preceding the fluorescence measurement. Prespore and pre-stalk amoebae were obtained from migrating slugs of strain NC4, mechanically dissociated in the presence of EDTA, and purified by density gradient centrifugation[19]. Labelling of the precursor cells differed from that of vegetative amoebae only in that the incubation period was increased to 25 min. Vegetative amoebae were resuspended at 10^6 ml^{-1} in 20 mM PO_4 *p*H 7.0; differentiating amoebae were resuspended at 2×10^6 ml^{-1} in buffer of *p*H 6.0. Excitation spectra were obtained from 4 ml of cells as in Fig. 1, except that the integration time was reduced to 0.5 s. Immediately after scanning, each cell suspension was filtered through a 0.45-μm membrane filter (Millipore) under gentle suction. The time between the final washing of the suspended cells and the completion of filtration was <4 min. Leakage of dye during this interval was quantitated by determining the relative fluorescence intensities of the filtrate and cell suspension measured at 440 nm. Dye loss generally accounted for 10–15% of the total fluorescence. Suspension buffers were customarily chosen with a *p*H approximating that of the cells (as revealed in earlier measurements) to ensure that any imprecision in the dye loss correction would have a negligible effect (on the order of 1%) on the calculated intracellular excitation ratio. Because of the small redshift of intracellular fluorescein relative to free dye (the excitation maximum averaging 491 nm rather than 489 nm), the cellular excitation ratio was computed from intensity values at 491 and 440 nm.

measurements were performed as for vegetative amoebae. Figure 2*b* compares filtrate-corrected excitation spectra for pre-spore, pre-stalk and vegetative amoebae. Although the spectra obtained for the differentiating cells differ from that obtained for the vegetative cells, they are very similar to one another. Indeed, as summarized in Table 1, there is no significant difference in the pH_i of the two precursor populations. As is true of vegetative cells, the measured intracellular pH is independent of that of the surrounding medium (Table 1). However, differentiating

Table 1 Identity of pH_i of pre-spore and pre-stalk amoebae

		Pre-spore		Pre-stalk	
Expt	pH_0	Excitation ratio	pH_i	Excitation ratio	pH_i
1	6.85	4.78	6.07	5.52	6.20
		3.97	5.92	5.37	6.18
2	6.0	5.65	6.22	5.51	6.20
		4.80	6.08	5.06	6.12
3	6.0	5.47	6.19	5.16	6.14
		5.52	6.20	5.11	6.13
		Mean $pH_i = 6.11 \pm 0.11$		Mean $pH_i = 6.16 \pm 0.04$	
		Mean of all pH_i values $= 6.14 \pm 0.08$			

Experimental methods and data manipulation were as described in Fig. 2 legend. For each of the three experiments shown, pre-spore and pre-stalk spectra were taken alternately. There is no significant difference between the pH_i values of the pre-spore and pre-stalk groups. Similarly, the pH of the cell suspension buffer ($pH_0 = 6.85$ as opposed to 6.0) and the length of time for which cells were held at 0 °C prior to spectroscopy had no effect on pH_i. The excitation ratio is explained in Figs 1 and 2 legends.

slug cells give the somewhat acidic value for pH_i of 6.14 ± 0.08. The acidification may be the result of accumulation of metabolic acids produced during prolonged slug migration[14], given that the pH_i of amoebae developing in suspension or on pads for shorter periods of time is similar to that of vegetative cells (my unpublished observations; see also refs 8, 10). Because cells within migrating slugs continue to interconvert between pre-spore and pre-stalk (evident immediately in bisected slugs[15] and inferred for undisturbed slugs[16,17]), the acidic pH_i is, for this reason alone, unlikely to be determinative of the differentiated cell state.

Several controls argue that the fluorescence measurements are a valid indication of relative pH_i values. It is conceivable that the production and accumulation of relatively high concentrations of fluorescein within cells (reaching values in excess of 10^{-4} M; ref. 13 and my unpublished observations) might alter the normal pH_i. However, measurements of the pH_i of vegetative amoebae by the independent criterion of ^{31}P-NMR showed no difference between the pH of highly fluorescent cells and that of control cells ($pH_i = 6.7$ for both; C. Thompson and D.R., unpublished observations). The small disparity between the pH_i of vegetative cells determined by fluorescence (pH_i 6.9) and that determined by NMR spectroscopy (pH_i 6.7) may reflect the particular calibration method used here, or a possible mitochondrial contribution to the fluorescence. With slug cells, varying the degree of labelling suggested that there might be a slight acidification attributable to fluorescein, but the effect was small (<0.2 pH units) and not cell-type-specific (data not shown). Finally, the observed pH_i of total slug cells was found to be identical (pH_i 6.15) whether or not the cells were subjected to gradient centrifugation.

Despite any uncertainty in absolute pH, it is clear that the pH_i values of pre-spore and pre-stalk amoebae are, within experimental error, identical. Thus the hypothesis of a more acidic pH within pre-stalk than pre-spore cells is untenable. This hypothesis has been suggested primarily by the established effects on cell proportioning of weak acids and bases, and of known or presumed proton pump inhibitors[1-7]. However, recent measurements using both NMR and fluorescence spectroscopy (ref. 10; C. Town, personal communication; and my unpublished observations) have failed to detect the predicted effects of these compounds on pH_i. Rather, the treated amoebae maintain their pH_i; in so doing, they may perhaps perturb the concentration of some other metabolite(s) whose flux across the plasma membrane is coupled, positively or negatively, to that of protons. Such a metabolite might be the physiological regulator of precursor differentiation in *Dictyostelium*.

This research was supported by NSF grant PCM 8202833. I thank C. Thompson for performing NMR spectroscopy and Dr R. Blankenship for an introduction to fluorescence methods.

Received 24 December 1985; accepted 13 March 1986.

1. Gross, J. D., Bradbury, J., Kay, R. R. & Peacy, M. J. *Nature* **303**, 244-245 (1983).
2. Town, C. D. *Differentiation* **27**, 29-35 (1984).
3. Gross, J. D. *et al. Phil. Trans. R. Soc.* **B295**, 497-508 (1981).
4. Pogge van Strandmann, R., Kay, R. R. & Dufour, J. P. *FEBS Lett.* **175**, 422-442 (1984).
5. Serrano, R., Cano, A. & Pestana, A. *Biochim. biophys. Acta* **812**, 553-560 (1985).
6. Kay, R. R. & Jermyn, K. A. *Nature* **303**, 242-244 (1983).
7. Kopachik, W. J., Dhokia, B. & Kay, R. R. *Differentiation* **28**, 209-216 (1985).
8. Jentoft, J. & Town, C. *J. Cell Biol.* **101**, 778-784 (1985).
9. Satre, M. & Martin, J. B. *Biochem. biophys. Res. Commun.* **132**, 140-146 (1985).
10. Kay, R. R., Gadian, D. G. & Williams, S. R. *J. Cell Sci.* (in the press).
11. Jamieson, G. Jr, Frazier, W. & Schlesinger, P. *J. Cell Biol.* **99**, 1883-1887 (1984).
12. Ohkuma, S. & Poole, B. *Proc. natn. Acad. Sci. U.S.A.* **75**, 3327-3331 (1978).
13. Thomas, J. A., Kolbeck, P. C. & Langworthy, T. A. in *Intracellular pH: Its Measurement, Regulation and Utilization in Cellular Functions* (eds Nuccitelli, R. & Deamer, D. W.) 105-123 (Liss, New York, 1982).
14. Kelly, P. J., Kelleher, J. K. & Wright, B. *Biochem. J.* **184**, 581-588 (1979).
15. Gregg, J. & Karp, G. *Expl Cell Res.* **112**, 31-46 (1978).
16. Tasaka, M. & Takeuchi, I. *Differentiation* **23**, 184-188 (1983).
17. Devine, K. M. & Loomis, W. F. *Devl Biol.* **107**, 364-372 (1984).
18. Watts, D. J. & Ashworth, J. M. *Biochem. J.* **119**, 171-174 (1970).
19. Ratner, D. I. & Borth, W. *Expl Cell Res.* **143**, 1-13 (1983).

Copies of articles from this publication are now available from the UMI Article Clearinghouse.

For more information about the Clearinghouse, please fill out and mail back the coupon below.

UMI Article Clearinghouse

Yes! I would like to know more about UMI Article Clearinghouse.
I am interested in electronic ordering through the following system(s):

☐ DIALOG/Dialorder ☐ ITT Dialcom
☐ OnTyme ☐ OCLC ILL Subsystem
☐ Other (please specify)_____
☐ I am interested in sending my order by mail.
☐ Please send me your current catalog and user instructions for the system(s) I checked above.

Name_____
Title_____
Institution/Company_____
Department_____
Address_____
City_____ State_____ Zip_____
Phone (____)_____

Mail to: University Microfilms International
300 North Zeeb Road, Box 91 Ann Arbor, MI 48106

nature

NATURE VOL. 321 22 MAY 1986

What future for nuclear power?

The outlook for civil nuclear power has blackened everywhere in the aftermath of the Chernobyl accident. Here is what governments other than the Soviet should now do.

WHATEVER went wrong at Chernobyl, that accident has not done much for the job prospects of nuclear engineers outside the Soviet Union. To be sure, there may be a little short-term employment to be had in Austria, where the government decided last week that it will now dismantle the country's only nuclear power station, which has been waiting on the brink of full operation for several years. The Swedish government, which had already decided to build no more reactors, and to close down its nuclear industry when the dozen reactors now operating reach the end of their useful lives in 2010, now says that it may bring forward that deadline. Even in France, Western Europe's most bullish nuclear operator, discontent with the nuclear policy the new government has inherited is being demonstrated in the usual way, with huge crowds gathering around the perimeter of some nuclear plants. At least until the Soviet report of the Chernobyl accident is published, the operators of nuclear plants in Western Europe and elsewhere will find themselves on tenterhooks.

In its broadest sense, the question whether communities should make electricity from uranium is political. Voters have a right to decide whether they wish their governments to sponsor the generation of electricity by means that can cause social disruption and damage on the scale on which it has been caused in the Ukraine. Electorates have a right to know, for example, whether their governments have arrangements that will allow communities to survive serious nuclear accidents without bringing civic administrations to the point of collapse. But in at least three Western European countries, nuclear safety is bound to be an issue in general elections in the coming months. In Britain and West Germany, where pro-nuclear governments must go to the polls quite soon (Britain within two years, West Germany next spring), doubts on nuclear safety will be exploited by the opposition parties. In the Netherlands, where there are elections this week, the government has thought it prudent to sidestep the issue by saying that it will not now plan to add to the two reactors now operating, as had been intended in the 1990s. In the United States, it is inevitable that Chernobyl will reinforce the opposition to plans for nuclear construction; the chance must have markedly diminished that the Long Island Lighting Company will be given a licence to operate the Shoreham plant, which is ready to operate but which has been held up for lack of a convincing plan to evacuate the locality in case of a nuclear accident. What should public utilities and their often timorous governments do now?

Decisions

The first maxim is an old one: do not panic. There is no need, for there is no evidence that nuclear accidents are catching. Probably the opposite is the truth. An accident on the scale of that in the Ukraine will, if anything, make reactor operators elsewhere even more vigilant. Quick decisions are usually costly decisions. The decision of the government of the Netherlands to scrap plans for nuclear development on the eve on this week's elections may be electorally prudent, but may cost Dutch taxpayers money in the coming decade and will not contribute one jot to the safety of the two reactors now operating. And the same is even more true elsewhere. Many communities (in France and Japan, for example) could not turn their backs on nuclear power without giving up some of their present use of electricity. Even those inclined to follow such a course must pay at least as much attention to the safe operation of existing plants during the remainder of their operating lives.

Utilities, governments and their taxpayers should also remember that nothing has happened in the past three weeks to diminish the economic prize to be won by the safe operation of nuclear energy. In very round numbers, a kilogram of uranium can now be bought on the open market for $100, but will yield thermal energy worth $1,000 if used as fuel in a thermal reactor. In a fast reactor designed for breeding fissile material, the value of the thermal energy from a kilogram of uranium may be a further 1,000 times as much. The endless argument about the economics of nuclear power turns on the question of how much of this huge economic rent must be spent on building reactors, on making them safe and on disposing of the radioactive waste materials. Even though uranium would not be as cheap if its exploitation in nuclear energy were more fashionable, the sheer size of the economic benefit cannot be ignored even now. If a country such as Britain were to replace its present annual consumption of 100 million tonnes of oil by the equivalent in uranium, the economic gain would far exceed the government's annual borrowing requirement. It would be foolhardy to ignore the size of this potential economic benefit simply because a reactor in the Ukraine went out of control last month.

Plans

Equally, however, it would be wrong for governments elsewhere to pretend that what happened at Chernobyl is irrelevant to their domestic power policies. In the litany of the hazards of civil nuclear power, the possibility of a serious reactor accident has always been the most awesome. Quite apart from the tragic loss of life in and around the Chernobyl reactor, and the social and economic disruption that the accident has caused, the consequences for the communal psychology of the region around Kiev can only be guessed at. It is natural that people elsewhere should now say that they would pay quite a high price to avoid such accidents on their doorsteps. Prudent governments will pause and reassess their plans to build reactors by some process so public that their constituents will be confident in whatever decisions emerge. Access to a full explanation of what happened at Chernobyl, promised last week by Mr Mikhail Gorbachev, will be an essential starting point for that.

In the West, the process will be complicated by the degree to which civil nuclear power has already been turned into a public and political issue by a gaggle of environmental movements whose motives are rarely as innocent or even respectable as advertised. The West German Greens, for example, likely to emerge from next year's election in a government coalition with the Social Democrats, are as fierce about the supposed evils of the corporatist state as about those of nuclear power. In countries such as Britain, the bubbling opposition to the search, by the public agency responsible for radioactive waste disposal (Nirex), for sites at which to bury low-level waste springs not

from a realistic assessment of the hazards but from the more familiar reluctance of those who enjoy the benefits of modern industry to put up with inconvenient side-effects. Deciding on rational policies for nuclear energy will require that those with an inner certainty that nuclear energy is an abomination should be restored to the pathways of rationality. The gravity of the accident at Chernobyl may, paradoxically, help by showing level-headed people that there are serious arguments on both sides of the question.

Research

Most governments will also recognize that it is a misfortune that so many of them have deliberately allowed research and development programmes in nuclear energy to shrink. In the design of thermal nuclear reactors for example, there has been hardly any research that matters for close on a quarter of a century, since most governments and their construction companies took the view (early in the 1960s) that they knew enough about the subject to make a go of it. The result is that the technology of nuclear power has been immovable for far too long, and in particular since before the potential seriousness of loss-of-coolant accidents (part of the trouble at Chernobyl) was recognized by studies carried out in the United States in the early 1970s. It is as if the technology of air transport had been fixed at the outbreak of the Second World War. Hopes by some of the laboratories with continued interest in reactor design, the Argonne National Laboratory for example, to attract funds for projects aimed at inherently safe reactor systems, have not been conspicuously successful.

Much the same is true of research on waste disposal. People either worry about the isolation from the rest of the environment of entire irradiated fuel elements or they worry about storing the mixed fission products from separation plants; in each case, there is a huge amount of radioactivity at the beginning, but it is also necessary to isolate some low-activity components (actinides) for millennia on end. Technically, the problem would be simplified if the wastes were separated chemically, but the only serious studies made of this possibility are desk studies purporting to show that such sophistication would be uneconomic on the basis of assumptions valid in the 1970s, not now when people may be prepared to spend more for safety. However they decide to generate electricity in the years ahead, governments have a responsibility to breathe new life into more imaginative research. It would be appropriate if they did so collaboratively. In Western Europe, Euratom is still looking for a function after 30 years. The International Atomic Energy Agency, which has played a valuable role in the response to Chernobyl, could become the vehicle for a research programme that would show more convincingly which are the safest ways to go.

Technical developments by themselves will not suffice. There must also be a better public understanding of the nature of the risks. So much has been plain since long before Chernobyl. But the well-meaning attempts of public authorities at general education have been ineffectual because of their failure to distinguish between enlightenment and reassurance. Reactor accidents apart, it is probable that the people most seriously affected by the routine operations of the nuclear industry in the few places at which it flourishes are the workers at nuclear plants, reactors and reprocessing plants. Radioactive waste and routine discharges from reactors (neutron irradiation of atmospheric argon produces beta-active argon-41) have much smaller effects when measured by the yardstick of the radiation dose to a population as a whole. The obvious difficulty is that public authorities cannot go about insisting that even small doses of radiation can cause trouble (delayed cancer induction, genetic defects) without unsettling those who work for them. Much easier to behave as if these risks do not exist or to pretend that they are negligible.

The truth is that (reactor accidents apart) the risks of radiation are for most members of a population small, much smaller than the effects of cosmic rays (a comparison valid only if there is no damage threshold) but not negligible to people who have become convinced that radiation risks, however small, are important. Sadly, the acute radiation deaths at Chernobyl (11 so far) may make ordinary people more receptive to the orders of magnitude of the different risks. Certainly, governments and public authorities cannot leave the task of public education to those now most active in the field, the environmentalists whose interest is to confuse the issue (as well as to confuse civil with military nuclear power).

None of this will, for the time being, persuade ordinary people not to fear what they have now come to fear most, the risk of a reactor accident. The fact that other reactors may differ in design from that at Chernobyl will cut no ice when the world knows that most accidents in the nuclear industry have been caused not so much by errors of design as by personal folly or incompetence, for which the euphemism is "human error". There was nothing in the design of the Brown's Ferry (Tennessee) reactor from which outsiders could infer that it would be set on fire by a man looking for a gas leak with a lighted candle. The long sequence of minor discharges of radioactivity from the British separation plant at Windscale (now Sellafield) has rightly raised in the public mind the question whether people who cannot be trusted to avoid small mishaps will ensure that large mishaps never happen.

So how are the nuclear establishments to re-establish public confidence in their competence? They could help themselves substantially by paying more attention to the design of reactors and their instrumentation with the objective of making them "user friendly", not user hostile as they tend to be at present. Whatever the technical defects of the Three Mile Island reactor that went wrong in 1978, there is no doubt in retrospect that an impending accident required the operators to behave in ways that seemed in the heat of the moment to be unreasonable. It is not surprising that they chose not to follow the instruction manual. The general technical question is that of how to design complicated machines in such a way that the human beings asked to supervise their operation are able to intervene constructively. The problem is by no means novel. Aircraft designers have grappled with it for years. Is it not time that nuclear engineers took a leaf out of this now well-read book?

Ambiguity

A further difficulty arises from the amibiguity of responsibility that afflicts those who are in charge of these complicated machines. The Challenger disaster in January seems clearly to have shown that trouble would have been avoided if it had been easier for unwelcome news to reach the top management of the US National Aeronautics and Space Administration. It will almost certainly emerge that part of the trouble at Chernobyl is that the local management was reluctant to admit to Moscow (especially on the eve of the May Day celebrations) that it had a nasty accident on its hands. What these and other accidents have shown is that there is an urgent need that technical people ostensibly in charge of complicated pieces of machinery should have more freedom in deciding how they should be operated safely, and a more direct responsibility for making sure that this is done. Their situation is not very different from that of the masters of merchant ships, who are still the ultimate arbiters of, for example, whether they should put to sea in rotten weather.

These are only some of the issues that governments and their agencies must face. All of them require a degree of flexibility and a habit of frankness that comes awkwardly to public authorities everywhere. The temptation will be to funk them. But the only course that people will respect will be to face them openly, accepting the promise of nuclear power for what it is, a potential boon that will be attainable only if people at large acknowledge that it is also safe. The task is not impossible, but will require more of governments than they have recently been inclined to show in this cause. □

Chernobyl

US physician tells heroic tale of Moscow

THE medical problems of dealing with the victims of the Chernobyl accident hospitalized in Moscow have turned out to be unexpectedly difficult, according to Dr Robert Gale, the Los Angeles physician who had been working at Moscow's Hospital No. 6 until a brief respite last weekend. Dr Gale, speaking on the telephone from Los Angeles earlier this week, said that the 299 patients at the hospital appear all to have received a damaging dose of radiation while working at or near the reactor damaged on 26 April.

According to Dr Gale, typical doses exceeded 2 Gy (1Gy=100 rad) with the doses received by the most seriously injured workers exceeding 5 Gy. Although most of the radiation exposure appeared to have been caused by gamma rays, Dr Gale explained that the difficulty of treating the patients in Hospital No. 6 arose from the variety of the means by which radiation doses had accumulated. Some people had breathed substantial doses into their lungs, others had ingested radioactive materials while other cases were complicated because the radiation appeared to have come from only one side of the body.

While emphasizing that he had no information about those in or near Chernobyl at the time of the accident apart from those in hospital in Moscow, Dr Gale thought if probable that between 50,000 and 100,000 people among the local population now evacuated would have received doses of radiation or of radioactivity large enough to warrant annual examinations.

Among those acutely injured by radiation, Dr Gale explained, the most common symptoms were gastrointestinal disturbance, liver toxicity and depression of haematopoiesis (blood-cell formation). One of the unexpected difficulties of planning to treat severely injured patients by bone-marrow transplantation had been that of tissue-typing in circumstances where blood-counts were falling rapidly.

Dr Gale's presence in Moscow apparently came about as a consequence of approaches to the Soviet authorities through Dr Armand Hammer, chairman of the Occidental Petroleum Company, and Dr Vincent de Vita, director of the US National Cancer Institute. His offer of help was apparently accepted within 24 hours. He speaks highly of the informality with which he, his colleagues and their equipment were allowed into the Soviet Union. With Dr Gale are two colleagues from the University of California at Los Angeles, Dr Paul Terasaki and Dr Richard Champlin, and Dr Yair Reissner from the Weizmann Institute in Israel.

Much of the activity in Moscow has been concerned with identifying potential donors from among those covered worldwide by the international transplant registry, which is a listing of people with known histocompatibility characteristics. He said it was impressive that it had been possible to identify donors and to deliver tissue for transplantation to Moscow in between 48 and 72 hours. Even so, he said, most of the 35 transplants performed in recent days had used marrow taken from relatives.

Some of the Moscow patients have also received transplants of fetal liver. He takes the view that the experience gathered in the past few weeks in Moscow will be invaluable in responding to future nuclear catastrophes, accidental or otherwise, and says that he is delighted that the Soviet authorities have agreed to full publication of the data now being gathered. He says that the information becoming available will at least double the extent of the pre-existing database.

On the preparedness of his Soviet colleagues, Dr Gale says it is plain that Soviet physicians had "given thought in advance" to the problems that would be posed by a nuclear accident on the scale of Chernobyl.

He also drew attention to the way in which the nuclear accident had stretched the resources of the international transplant registry. Matching tissue for 35 patients had had to be sought in 15 different countries. The problem of dealing with a larger accident could well be beyond present resources, he said.

Tim Beardsley & Vera Rich

SDI

Academics pledge opposition

Washington

LEADERS of a drive to discourage academic scientists and engineers from participating in research on the Strategic Defense Initiative (SDI) brought their case to Washington last week. They delivered a pledge to the White House, signed by more than 3,700 science and engineering professors, not to accept or solicit SDI funds. In addition, 2,800 graduate students signed a similar pledge not to participate in SDI-related projects.

The boycott pledge began early last summer on the campuses of Cornell University and the University of Illinois at Urbana–Champaign. Advocates of the pledge argue that it is fruitless to do research on a project that is "not technically feasible".

Furthermore, they suggest that treating SDI as a partial defence rather than a total nuclear shield against Soviet attack will make SDI merely a new weapon system guaranteed to escalate the arms race. At a press conference held in Washington last week, John Kogut, a physics professor at the University of Illinois at Urbana–Champaign and one of the instigators of the pledge, emphasized that SDI would jeopardize existing arms control agreements, such as the Anti-Ballistic Missile Treaty, and make future agreements more difficult to achieve.

Another consequence of a large funding effort for SDI, according to James Melcher, director of the electromagnetic and electronic system laboratory at Massachusetts Institute of Technology (MIT), is a gradual strangling of the US economy. Melcher sees more and more physicists, engineers and computer scientists being drawn into weapons-related research. At the same time, he fears that corporations are placing less emphasis on developing commercially viable technologies, choosing instead to take a "quick fix" from readily available defence funds.

Although spending on SDI research has increased dramatically in the three years since President Reagan announced the programme, only a small portion of that money has actually arrived at academic institutions. According to figures compiled by the Federation of American Scientists (FAS) for a forthcoming report on SDI spending, teaching institutions have received between two and four per cent of total expenditure on SDI. In 1985, for example, SDI payments to universities totalled $49.1 million, compared with total SDI expenditures of $1,464.8 million. The SDI Organization has provided funds to 69 US universities so far, with Utah State leading the list, having received £27.5 million since 1983. Frank Redd, associate director for Utah State's space engineering centre, says that the bulk of that money comes from existing defence contracts, and was only recently changed to come under the SDI umbrella.

Similarly, Robert Byers, a spokesman for Stanford University, the fourth leading recipient of SDI funds according to FAS figures, explains that the bulk of that money comes from a pre-existing Air Force contract for research on free-electron lasers. But support for the pledge drive was low among physicists at Stanford, only eight of twenty-one faculty members signing the pledge. **Joseph Palca**

Particle accelerators

US agency accused of bad costing

Washington

THE US Congress is likely to scrutinize more closely costs of building particle accelerators following the publication last week of a highly critical report accusing the Department of Energy (DoE) of providing only "fragmented and incomplete" cost estimates in its budget submissions. The report*, prepared by the US General Accounting Office (GAO), recommends that congressional appropriations committees direct DoE to provide full and timely cost estimates, as well as details of technical uncertainties, of current projects.

The GAO study was requested by Senator Bennett Johnston, a Louisiana Democrat on the Senate Appropriations Committee who has made no secret of his scepticism of big accelerator projects.

Prospects of an early start on the construction of the Superconducting Supercollider (SSC) have been dealt a blow by the report, which estimates the total cost of SSC to be 60 per cent higher than DoE has hitherto indicated. DoE has made a point-by-point rebuttal, but the GAO inspectors have seen fit to make only minor changes in the light of the DoE response.

The GAO report examines DoE's six largest high-energy and nuclear accelerator physics projects and finds that DoE consistently understated total and preconstruction costs in its formal budget submissions. Preconstruction research and development for these is, according to GAO, likely to amount of $440 million; only $88 million has so far been formally reported in budget documents.

Preconstruction work for SSC, for example, will cost $62 million more than the $58 million identified in budget submissions to Congress. The Tevatron I and II projects at Fermilab will, according to GAO, cost $180 million more than the $16 million that has been reported. Other projects likely to cost more than indicated are the Stanford Linear Collider and the Continuous Electron Beam Accelerator Facility at Newport News, Virginia, as well as the planned Brookhaven relativistic heavy-ion collider and the Los Alamos Meson Physics Facility II (LAMPF II).

The DoE response to the charges is that much accelerator research is generic in nature, and so need not be identified with a particular project until construction is approved by Congress. GAO disagrees, saying that formal "mission-need statements" should be prepared at an earlier stage than is DoE's practice. The essence of the disagreement is the uncertain definition of the start of a project.

GAO is equally critical of DoE when it comes to estimating total costs associated with a project, however. The total cost of SSC, according to GAO, will be $4,900 million, $1,900 million more than DoE estimated in testimony to Congress a year ago. GAO observes that full cost estimates for this and other projects are not presented to Congress in a coherent form before projects are approved; as a result, Congress gets no clear idea of the cost of a project until it is too late. The Stanford Linear Collider and Tevatron projects are given as examples for which Congress could have been better informed. And GAO specifically criticizes DoE for not fully explaining technical uncertainties in some projects. For Tevatron I the uncertainties led to a $71 million cost overrun.

DoE protests that some estimates have been presented at individual committee hearings, and disagrees with GAO's inclusion of ancillary equipment (for example, dedicated computing facilities) in project costs. But whichever way the issue is decided, the pressures of the Gramm–Rudman deficit reduction law suggest that Congress will want to look much harder at DoE's big science proposals in future. The administration's proposed budget for high-energy and nuclear physics in 1987 is $771 million, an increase of 17 per cent over this year's figure, but it is already clear that Congress is unlikely to countenance an increase on that scale.

Tim Beardsley

**Nuclear Science: Information on DoE accelerators should be better disclosed in the budget.* General Accounting Office, April 1986.

British research

Signs of a silver lining appear

IN a week in which it seemed as if the British government would relax its policy to enforce the continued contraction of universities, a committee of interested parties has produced a telling criticism of public policy on civil research. These developments coincide with a general feeling in the research community that the pressures on the British government to pursue a less rigorous policy on public spending cannot fail to benefit research.

Precisely how the universities will benefit cannot be foreseen from the events of this week. On Tuesday, however, the University Grants Committee (UGC) was due to send to all British universities a notice of payments of recurrent grants to be expected in the academic year beginning on 1 August. This is the year in which the first effects are apparent of UGC's new policy of concentrating resources on the universities with the best records in research. Although, for this year, there is a "built-in safety net" which will ensure that no university is more than 1.5 per cent worse off than the average university (in a total budget that is reduced by 2 per cent in real terms), universities destined for sharper reductions in later years are identifiable from the letters.

The government's concession, due to be announced by the Secretary of State for Education and Science, Sir Keith Joseph, on Tuesday, is that extra financial help will be provided outside the UGC budget for institutions threatened with hardship which are able to meet certain criteria, such as the demonstration of centres of excellence in fields to which insufficient attention has been paid. This broad formula is a means by which the government could avoid the prospect of particular universities being threatened with closure in advance of the next general election. It is understood that no decision has been made about the scale on which extra funds would be made available.

Meanwhile, criticism of government policy on civil research has come from a committee of the Advisory Board for the Research Councils (ABRC) under P. Mathias, professor of economic history at the University of Oxford, which was set up in 1984 to assess the potential importance of private funds as a means of supporting research at academic institutions and research institutes.

The committee says that in spite of the wide discussion of research policy in Britain during the past few years, it is impressed by the sharp contrast between British spending on civil science and that elsewhere. British civil science receives 1.6 per cent of gross domestic product (GDP), compared with 2.0–2.5 per cent in the United States, West Germany and France, according to the report, which notes that British spending is declining while that in other countries is growing.

The report also says that defence research and development consumes a higher proportion of total spending, and of government spending, in Britain than elsewhere, and that industrial companies in Britain account for a smaller proportion of total research spending than in other countries. The committee makes a particular point of the apparent decline of spending on research by private industry in the recession years of 1981–1983 (when the volume of research appears to have fallen by 6 per cent). It notes that the same trend appears to have continued in 1984 (for which final figures are not available) and wryly remarks that if the disinclination of British companies to spend money on research is a permanent phenomenon, this is hardly the best climate in which academic institutions might hope to raise more support from companies. □

Human genome

Department of Energy on the map

Washington

UNTIL recently, sequencing the human genome seemed an impossibly large project, almost like counting all the grains of sand on all the world's beaches. But today the Department of Energy (DoE) is giving serious consideration to a project to sequence all of the estimated 3,500 million base pairs making up the human genetic material. Initial estimates put the cost of the entire project at $1,800–$3,600, or about $1 per base pair.

Early in March, DoE held a conference in Santa Fe, New Mexico, to discuss the feasibility of undertaking the sequencing project. The conference, hosted by DoE's Los Alamos National Laboratory, produced a report outlining a strategy for accomplishing the task. According to David Smith of the Office of Health and Environment Research (OHER) at DoE, the department is expected to decide in a matter of weeks how and whether to proceed with the monumental project.

DoE has historically had an interest in the human genome, and has been supporting research into genetic damage from energy sources for some time. Together with Lawrence Livermore National Laboratory, Los Alamos has been involved in the National Laboratory Gene Library Project, an effort to construct a chromosome-specific gene library. So far, the small insert library — containing fragments of 5,000–10,000 base pairs — is complete, and work on the large insert library for fragments of up to 50,000 base pairs has begun. Los Alamos has also developed flow cytometry technology capable of rapidly separating large amounts of DNA by chromosome, a capability that Los Alamos senior fellow Mark Bitensky sees as important to the success of the project.

Bitensky is coordinating Los Alamos' effort to make the gene sequence a reality. He says the project will "require many laboratories, many funding agencies, and many technologies", but he believes it can be done, and that the time is right to do it.

Although DoE may seem like an unlikely agency to handle such a project, Bitensky and OHER head Charles DeLisi feel that DoE is well placed to take a lead role. In addition to the gene library project, DoE has the computational facilities necessary for such a large-scale project. And DoE believes it has the know-how to undertake large-scale scientific projects, pointing to the DoE-run Fermi National Laboratory as an example of its expertise.

Current plans call for a decentralized programme, with one coordinating facility organizing the work of many centres around the country. The organizers hope the sequence can be a multinational effort. Bitensky says European interest in the project is already high.

Two theoretical approaches to the sequencing project were considered at the Santa Fe meeting. One involved randomly sequencing fragments from the genome, and trying to determine the order of the fragments on a *post hoc* basis (see below). This was rejected in favour of a scheme where the genome is first sorted by chromosome, then digested with a restriction enzyme like *Sfi* I that will produce a relatively small number of relatively large fragments. The first task would be to order these large fragments by chromosome, with a small, pilot sequencing effort started while the ordering task was being completed. Having ordered fragments not only breaks the sequencing down to a size more easily managed conceptually, but will also provide a useful tool for investigating genetic diseases, Bitensky believes.

Critics of the sequencing project do not deny that the information would be useful. Rather they worry that spending so much money on such a large project may be an inefficient use of funds. George Church of the University of California at San Francisco, a participant at the conference, echoed the widely held concern that such a large project could draw money away from other research projects. Church is working on new DNA sequencing techniques, and would like to see the project proceed. Others, including Fred Blattner of the University of Wisconsin, feel that a complete sequence from a smaller organism would yield a great deal of information about cellular processes at a small fraction of the cost. Blattner is currently working on sequencing the *Escherichia coli* genome, and others are working on the yeast and nematode genomes. Another option would be to sequence just part of one human chromosome, providing a window into human genetic control without devoting so many resources to such a major project.

Still unresolved is what to use as a starting material for the sequence project. One possibility is the DNA from a hydatiform mole. Such DNA can be produced in large quantities, but may be inappropriate as it has aberrant genetic properties. A second possibility would be to use material from a variety of different sources, perhaps a different individual for each chromosome. But critics worry that any choice will necessarily exclude information on the diversity of human genetic material.

Bitensky says that one possible method for selecting the DNA to use mentioned at the Santa Fe meeting was to hold a competition among the world's men and women. The person coming up with the largest contribution to the project would have his or her DNA sequenced.

A major player in the sequencing project could be the Howard Hughes Medical Institute, which is already supporting restriction mapping work by Raymond White at the University of Utah Medical School and Frank Ruddle at Yale University. The institute's president Donald Fredrickson confirms that there is interest in the DoE project, but wonders if the time is right to begin such an endeavour.

DeLisi, described as the driving force behind DoE's efforts on this project, says nobody gave serious thought to the idea of sequencing the entire genome as little as five years ago. Now, it is technically feasible; all that is required is the will and the money.

Joseph Palca

The numbers game

Washington

SEQUENCING the estimated 3,500 million base pairs in the human genome is a mammoth undertaking. But Fred Blattner of the University of Wisconsin came away from the Department of Energy's March meeting on the sequence project optimistic about the prospects for completing the task in a reasonable length of time.

The approach that encourages Blattner does not require ordered clones or restriction maps. Instead, sequencing starts on random pieces of DNA. Sorting out repeating sequences may not be possible using this approach, but all the unique sequences would be uniquely assembled.

To show this approach is possible, Blattner presents the following scenario: Work-stations would be set up around the country to carry out the project. Each station would consist of two technicians and four automated sequencing machines. The machines would have 40 lanes, with each lane capable of recording 750 residues. Running the work stations in two eight-hour shifts five days per week gives: 750 residues × 40 lanes × 4 machines × 2 shifts × 5 days = 1.2 million base pairs per week, or 60 million per year.

To make sure the entire genome is covered, Blattner figures it will be necessary to calculate 10 times the number of residues in it, or 35,000 million base pairs. Using this scenario, 580 work-stations could complete the job in a year. With each station costing $500,000, the project would cost $290 million.

Automated sequencers with such capabilities will soon be on the market, says Blattner. Although the information produced by this random sequencing approach would not be as rich as a complete ordered sequence, it would still be extremely useful. A later step could be to put all the unique segments in order.

Despite the organizational problem of coordinating the work of so many laboratories, Blattner believes it can be done.

Joseph Palca

US research costs

White House to back down?

Washington

A STUDY by the White House Science Council calling for substantially increased federal support for university-based research met a favourable reception both in the White House and on Capitol Hill last week, amid signs that the administration may be moving towards modifying highly unpopular proposed changes to indirect cost reimbursement.

Allan Bromley, vice-chairman of the science council study, met officials of the Office of Management and Budget (OMB) and said later that he was "optimistic" that new proposals on indirect costs would be forthcoming. But there was still no word from the administration on how exactly it proposed to defuse the row over OMB's proposal to fix administrative cost reimbursement for university research at 26 per cent of direct costs in the current year (the national average), with reductions in years to come. Revised proposals are expected within the next few weeks, in time for implementation at the beginning of July.

The science council study, chaired by David Packard, is unambiguous about the need for an increase in support for university research without taking money from research elsewhere (see below). It was given an enthusiastic welcome by members of the House of Representatives' Science Policy Task Force last week, and President Reagan was said to be writing to David Packard accepting its principal recommendations.

The study proposed adopting a uniform percentage for indirect cost reimbursement as one of several measures designed in aggregate to benefit the universities. Packard has previously spoken out publicly against the OMB decision earlier this year to adopt the recommendation on indirect cost reimbursement while ignoring recommendations to reduce amortization periods for facilities and equipment. Bromley also pointedly told the task force last week that OMB's proposal was "not at all our recommendation" and that it could lead to "substantial hardship" for universities.

John McTague, acting science adviser to the President, made clear his personal support for the panel's report last week, telling a press conference that he would expect an increase in federal support for university research of a few tens of per cent in the President's proposed budget for 1988. And McTague reminded reporters that President Reagan, presenting awards during National Science Week last week, had said "...we understand the need to increase our investment in basic research".

McTague himself will not, however, be in the administration to see the completed 1988 budget: he is to leave the White House shortly to become chief of research at the Ford Motor Company. **Tim Beardsley**

US space

NRC board urges no skimping

Washington

THE Space Science Board of the National Research Council (NRC) has entered the debate over the future of the US space programme, calling for a "balanced fleet of launch vehicles", and urging a clarification of the goals of the manned and unmanned elements of the national effort.

In a statement released yesterday, the space science board concludes that by failing to identify accurately the resources needed by the manned and unmanned space programme, both have suffered. Thomas Donahue, chairman of the board and principal author of the report, says the country must decide how committed it is to a pioneering space programme. Donahue argues that if sufficient funds are not provided to carry out such a programme with "style and precision", then it should be abandoned. The space programme being a highly visible effort, failures brought on by inadequate funding or poor management are all the more glaring and devastating.

The space science board has been critical in the past of the decision to abandon the procurement of expendable launch vehicles before the shuttle became a proven, reliable system. The decisions not to pursue new unmanned launch sytems and to commit the shuttle to carrying major scientific missions made space science unduly dependent on manned spaceflight. Had the shuttle lived up to its expectations, space science would not have suffered too badly, according to Donahue. But the Challenger accident underscores the fact that there has been no unmanned launch vehicle for major scientific missions for almost a decade, a "devastating" situation for space science.

There are seven scientific missions that were supposed to be launched in the next two years. Of these, only the Hubble Space Telescope and the Gamma-ray Observatory specifically require the lift capacity of the shuttle. The Galileo mission to Jupiter would have required the shuttle with its original trajectory, but may be able to achieve its objectives using a fuel-saving trajectory and a combination of the Titan 34D-7 rocket and Centaur G-prime upper stage, both soon to be available. While the shuttle provides a powerful launch vehicle and the possibility of in-orbit repairs, Donahue questions the wisdom of having a manned spacecraft carry a fully fuelled satellite booster rocket.

The space science board produced its statement following meetings last month and this. Board members felt that the Challenger accident made it imperative for NRC to make suggestions on the course of the space programme. According to Donahue, the board's statement went through the NRC report review process in "world record time". **Joseph Palca**

Strident report

Washington

THE White House panel's report, released in draft form on 17 January but published formally last week, is strident in tone.

Universities now represent only $8,000 million of the $100,000 million in total national research and development, and the proportion is declining. After noting that "in any ranking of priorities for allocating R & D support... universities must come first", it declares that the federal government must make substantially greater investments in universities than it has in recent years. It also proposes a major new initiative to establish university interdisciplinary research centres.

Federal policies must, the panel says, recognize the cost of university research facilities. It proposes that the amortization period of buildings should be reduced from 50 to 20 years, while that for equipment should be reduced from 15 to 5 years. Recognizing widely felt alarm about the poor state of university buildings, it proposes a special facilities fund to be administered by the National Science Foundation, to disburse a total of $10,000 million over 10 years. All proposals to the fund would be peer-reviewed and made on a 50–50 matching basis with non-federal funds. Tax incentives for industrial sponsorship of university research are also proposed.

The study panel also makes the now-infamous recommendation that reimbursements for administrative costs should be fixed at a uniform percentage, rather than being allowed to vary from one institution to another. This is the only recommendation that has been acted upon so far. It also proposes that grant durations should be increased to three or even five years, and makes other recommendations aimed at reducing administrative burdens on universities and, especially, researchers. New "portable" scholarships for the most talented 1 per cent of undergraduates and national merit-based multi-year graduate fellowships are also urged.

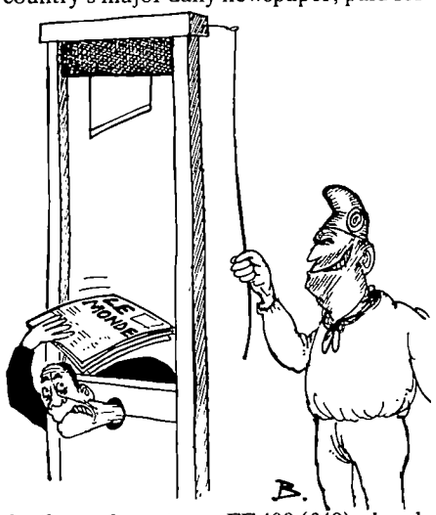
Tim Beardsley

French science

Research directors form lobby

SOME 280 French directors of research — and the number is increasing daily — are making a public appeal to the government over what they consider to be swingeing cuts applied to science by the new Prime Minister, Jacques Chirac.

Last week, this new and spontaneous French pressure group published a half-page advertisement in *Le Monde*, the country's major daily newspaper, paid for



by themselves at over FF 400 (£40) a head, lambasting the government for applying over half the recent cuts in total government spending to one ministry, that for research. A further advertisement is planned in *Le Figaro*, an important right-wing paper read by many of Chirac's supporters, if further funds can be raised.

The petition's organizers, Paris astrophysicists Jean Audouze and Pierre Encrenaz, said last week that the response of the country's leading scientists to their hastily-organized appeal had been "very encouraging". Some 50–60 per cent of those polled had responded within a week with sums from FF 100 to FF 1,000 to support the campaign.

"It really means that the directors have been shocked by this government's actions", said Encrenaz. In terms of cuts in "*autorizations de programme*", a strong indicator for future budgets as it represents sums which may be planned to be spent next year and beyond rather than actual cuts in current spending, 54 per cent of the government's recent savings fell on research and development, even though that represents only 2.3 per cent of the country's gross national product. This was enough to stir researchers into action. But worse may be to come.

Chirac has now told ministers that he will quadruple the present cuts, when the 1987 budget is announced in September. It is not clear whether research will suffer further, but Chirac did say in a letter to his ministers last week that the "overriding necessity" to make major savings in government spending meant that "it will be impossible to satisfy the many sectional interests, however legitimate their arguments, that will certainly protest".

It is difficult to see this statement as anything but a mandate to the already powerful ministry of finance and budget to ignore all pleas, including those made in the form of advertisements in *Le Monde*. However, French scientists continue to hope for a softening of the government's line, even though Chirac's frosty embrace will include, he says, a cut of 1.5 per cent in all civil service positions (except education). This will strike a blow at scientists just like those who, unaware of the new policy, signed the new petition: researchers from the "*grandes organismes*" research councils, the Centre National de la Recherche Scientifique (CNRS), the Institut National de la Santé et de la Recherche Médicale (INSERM), and the Institut National de la Recherche Agronomique (INRA) who recently became civil servants after a great political battle.

Some scientists, indeed, see this winning of civil servant status as the prime cause of their present trouble, for some of the principal and hardest opponents of the deal were the senior officials of the ministry of finance. Only an intervention by the now virtually powerless President François Mitterrand secured researchers their cherished "security". Now the enlarged finance ministry is wreaking its revenge, the story goes.

Whether or not this particular story is merely paranoia among the scientists, there is certainly considerable evidence that research is now being singled out for harsh treatment in France, after a few years of exactly the reverse. Only university researchers outside the research council system seem to have been relatively protected in posts (as teachers) and budget; but this research sector, by common consent, represents the weakest part of French science. Even Chirac's most extreme scientific advisers before his election last March argued that the universities had to be reformed and strengthened before the research council system was attacked (their criticism was that the latter was too centralist); but even their caveats now seem to be being bypassed.

"There seems to have been very little thought behind these new policies — they are very hasty policies", says Audouze. "We hope our campaign will convince ministers that these decisions are jeopardizing French research." **Robert Walgate**

SDI

Abounding hypotheses floated

Washington

To students at the California Institute of Technology, satire has seemed the best way to express opposition to the Strategic Defense Initiative (SDI). Last month they held a competition for the most "destabilizing, unworkable or incredibly expensive" proposal to achieve SDI's goals.

The winner is planetary science graduate Greg Ojakangas. His proposal, estimated to cost $457 million, involves developing a genetically engineered strain of pygmy hippopotamus. Hippos would be fed on a diet enriched with suitable radioactive materials and kept in cages with cathodes embedded in the walls. A continuous flow of electrons neutralizes the alpha particles emitted by the hippos' radioactive diet, forming helium and making the hippos lighter than air.

In the event of missile attack, an "optically thick cascade of buoyant hippos" rises to form a shield. Upon reaching the "hippopause", the height at which the mean hippo density (MHD) equals the atmospheric density, the hippos would fan out, forming a protective ROOPH (Readily Operative Overhead Protection by Hippos). In his proposal, Ojakangas reckons the hippos will remain buoyant for two days. After that, they will float gently to earth where they can be collected.

Second prize went to physics graduate student David Palmer, whose proposal calls for splitting the Earth into hemispheres at the Equator. A large bearing allows the two hemispheres to be rotated. When radar detects a flight of missiles heading over the pole, large motors rotate the two hemispheres 180 degrees in opposite directions.

After this manoeuvre, the eastern and western hemispheres have changed places, and the missiles will land on the country from which they were originally launched.

Other less serious scenarios suggested putting everyone in the United States aboard dirigibles (since "no dirigible has been shot down in 20 years"); erecting a cardboard shield as the final layer of a multilayer defence (cardboard is lighter than plexiglass); and using a series of lenses to focus the ability of the Bermuda Triangle to make things disappear.

The Caltech competition was inspired by a similar effort at Cornell University last fall. The winning entry at Cornell proposed using a particle beam of tachyons, the particles arising in certain superstring theories which travel backwards in time. This would provide a pre-launch destruction capability even after an attack had been initiated. **Joseph Palca**

Supercomputers

India resents US strings

New Delhi

THE United States has imposed certain conditions on the sale of supercomputers to India. The offer was made by President Reagan ten months ago at the height of Indo-US cooperation, but the Pentagon subsequently raised objections.

Acting US Science Advisor Dr John P. McTague, who was recently in India, says the offer still stands but India must comply with a safeguards regime that has just been finalized by the US Departments of Commerce, State and Defense. According to McTague, the United States has not sold supercomputers outside the Western bloc, hence the safeguards. The conditions have been communicated to New Delhi and the ball is now in India's court.

The United States has simplified the procedures for the export of high-technology items since the two countries signed a memorandum of understanding in May 1985. Under the memorandum, the United States agreed to speedy clearance of high-technology equipment for civil and defence needs subject to assurances about its end use and a guarantee by the Indian government that such equipment would not be used for nuclear programmes or allowed to fall into the hands of the Soviets.

But the conditions for the sale of supercomputers go further. The United States is seeking assurance that a computer will be used for the specific purpose for which it is bought and not diverted for military or nuclear research. Programs to be run on the computer must have US approval, as must personnel with access to it. As well as the right of periodic inspection, the company supplying the supercomputer will have control over maintenance and repair and Indians will not be allowed to remove any part of the hardware or software.

Indian officials are studying the implications of the safeguard conditions and it is likely that they will be found unacceptable. "It would be demeaning to purchase a supercomputer under these conditions", one official said: "Inspection means that an American will be sitting at the computer centre checking every program we run. We should not accept this."

Indians have been interested in acquiring supercomputers for medium-range weather forecasting and monsoon research and possibly for computer-aided design of a light combat aircraft.

India has already entered into a $26 million deal with Control Data Corporation (CDC) under which the state-owned Electronics Corporation of India will manufacture 600 units of Cyber-810 and Cyber-830 mainframe computers during the next nine years. India awarded the contract to CDC against stiff competition from the French computer company Bull in the hope that CDC would also sell Cyber-205 supercomputers. Even if India accepts the safeguards, it is believed in India that the United States would be reluctant to supply the supercomputers because of India's opposition to the US bombing of Libya.

If the United States does refuse to sell supercomputers, India will turn to Japan or the Soviet Union. The Department of Electronics has already purchased four S-1000 supercomputers from NEC of Japan for its nationwide information network. And the Soviet Union has agreed to sell, without strings, its Elbrus parallel processing machine as soon as it leaves the factory early in 1987. **K.S. Jayaraman**

Japan Prize

Dutch winner attacks US policy

Tokyo

AT a memorial lecture on artificial organs by one of this year's winners of the Japan Prize, Japan's answer to the Nobel Prize, would one expect to see pictures of aircraft carriers and Trident submarines along with cartoons of star wars and the effects of nuclear winter? Dr Willem Johan Kolff, 1986 Japan Prize laureate for medical technology, apparently felt his lecture in Kyoto and Tokyo last month was a fitting occasion to lambast US defence policy and appeal for support for the anti-nuclear movement. But how does one turn a talk from kidney machines to killer satellites?

Kolff's speech began normally enough, with a historical review of the kidney machine he developed from 20 metres of artificial sausage skin in the Netherlands during the Second World War. With more than 66,000 Japanese now dependent on dialysis and the number doubling about every five years, there are many in Japan grateful for Kolff's invention and few would dispute his eligibility for a major international award.

From kidney machines, Kolff quickly switched to graver topics and a Rubens' picture was compared to the "life and death committees" that sprang up in the United States in the 1960s, when there were too few dialysis machines to go round and those to be saved had to be selected on the basis of age, occupation, number of children and so on. Then came a warning that the life and death committee is raising its ugly head again in the United States under the guise of "cost containment".

And why is cost containment necessary? In sailed slides of aircraft carriers and Trident submarines, along with the message that the United States is spending too much on defence and too little on treating its fellow citizens. In contrast, Kolff portrayed Japan as a haven where low defence spending allows high industrial productivity and where all who need kidney machines get them. But with kidney transplants virtually unobtainable, Japan is hardly a paradise for patients with renal disease (see *Nature* **313**, 338; 1985). And what of the defence the United States has provided for Japan for 40 years?

Kolff then turned to the membrane oxygenators developed from the artificial kidney after it was noticed that blue blood passing through the dialyser turned red. Who needs oxygenators? The 50,000 victims of nuclear war with scorched lungs. But, asserted Kolff, nobody would be interested in artificial lungs because they would all die anyway from the effects of nuclear winter. The stage now set, Kolff leapt back and forth from artificial hearts to nuclear fire power and star wars to artificial eyes and ears. In his abstract he threw in the greenhouse effect for good measure, but his listeners were spared the assertion that "the polar ice caps will melt" and "the coastal plains of Japan will be flooded". Kolff closed by urging the audience to join anti-nuclear movements such as International Physicians for the Prevention of Nuclear War, the controversial winners of last year's Nobel Peace Prize, and ended by asking "what good will an aritificial heart do us if we are all vaporized?".

The Japan Prize is awarded by the Science and Technology Foundation of Japan, a non-profit organization under the direction of the Japanese Prime Minister's office, and is intended to recognize significant and original achievements in science and technology that contribute to peace and prosperity for mankind. The foundation's dedication to peace provided Kolff with the platform for his anti-nuclear appeal, and as Japan is edging towards a decision to participate in the Strategic Defense Initiative under the enthusiastic backing of Prime Minister Yasuhiro Nakasone, Kolff's speech was timely. But will this lecture help elevate the Japan Prize to a comparable level of recognition with the Nobel Prize, one of the unstated aims of its founders? **David Swinbanks**

Correction

IN the article "Making radiation understood" (*Nature* **321**, 195; 1986), the relative value of curies and becquerels is incorrectly given: it should read 1 Ci = 3.7×10^{10} Bq. □

Japan's forests

Welshman begs respect for trees

Tokyo

C.W. NICOL must be Japan's most famous Welshman — indeed perhaps the only Welshman the average Japanese has ever heard of. A string of popular books on the natural world published in Japanese plus, at 45, an autobiography which includes words like "Pwllheli" which no Japanese (or Englishman) will ever be able to pronounce have made his name. Most recently, he has been in the public eye with an impassioned plea to the Forestry Agency to spare the forests that surround his home deep in the mountains of central Japan. The white paper (policy document) recently released from the Forestry Agency, which is assiduously cutting down the forests around Nicol's home, reveals that even without an infuriated Welshman to deal with, the Forest Agency, Japan's forests and the forestry industry are in dire straits.

Trees take a long time to grow and it is not easy to keep forestry policy in tune with a rapidly changing world. Some sympathy must thus go to the Forestry Agency. But there are many who have been telling the agency that its policies are mistaken for at least the past fifteen years.

The Forestry Agency found itself at the end of the Second World War with many mountains denuded of timber. Plantations, largely of *sugi*, the Japanese cedar, were begun. Then Japan entered its high-growth era and it seemed that the demand for timber would never stop growing. Clearance of natural forests began on a massive scale and huge numbers of cedar were planted.

Long before any of this timber was ready for the market, very much cheaper timber began to pour in from abroad. At the same time, new materials began to be used to build houses. Then Japan's growth began to slow; the Forestry Agency and private landowners found themselves with huge tracts of forest on their hands that may never be sold at a profit. Much the greater part of that forest is still young enough to need regular thinning and care to remain healthy. But instead, with no profit in sight, huge areas have been left to rot. The white paper admits that 40 per cent of man-made forests that need thinning are not being attended to.



Natural forest left along water courses in the national park near Tokyo.

Part of the reason why home-grown timber is expensive is that it is difficult to take out trees from Japan's steep mountain sides. Roads capable of carrying heavy timber lorries must be built and aerial ropeways set up. That adequate, cheap technology is not available is something critics have been saying for years. Nor, critics say, was adequate thought given to the suitability of cedar in the rush to plant forests.

Plantations in poor locations have been hit by mice, frost and insects, while too much reliance may have been placed on cedar. There is still plenty of demand for broad-leaved trees. The white paper argues for diversification, which critics have been demanding for years. Meanwhile, profits are being made by cutting existing natural broad-leaved forests, including trees hundreds of years old. That is what angers Nicol.

Letters of protest to the government from individuals do not normally evoke much response, but whether out of respect for a foreign "guest" or from sensitivity to foreign criticism, or because Nicol's letter was also published in the *Yomiuri* newspaper, the Forestry Agency director-general personally promised (according to *Yomiuri*) that the beeches and birches on the mountains around Nicol's home would not be cut. But this, it seems, was too good to be true. Forestry officials who visited Nicol's home revealed plans for cutting the forest on a scale beyond his worst imaginings. The only thing they appeared to take note of, he says, was not to litter the forest with discarded chain-saw blades.

But Nicol has discovered he is not alone in his love of the forest. Hundreds of letters of support and telephone calls have come to his home. The burgeoning enthusiasm for forests is also clearly recognized in the white paper, as it was in an advisory report to the agency published last August. Many Japanese have of course been proclaiming for years that they have a unique sensitivity to nature, but what they mean is cherry blossoms in parks, pot plants outside their homes and cut flowers impaled on spikes in vases and twisted into miniature imitations of nature. Love of nature in the raw, complete with the mosquitoes, snakes and bears that inhabit Japanese forests, is a very new phenomenon. Many new organizations concerned to protect forests and town greenery have sprung up recently, reflecting a change in Japan's society away from pure economic growth to concern for the quality of life. Gradually they are beginning to join forces but none is yet big enough to exert a powerful influence. The Forestry Agency has responded by decreasing the area of forest that can be cut at one time and by increasing emphasis on the selective cutting of forests so that natural regeneration can follow.

Catering for this new interest in forests would not be so difficult were it not that the Forestry Agency is expected both to be financially self-supporting and also to ensure the stability of mountain villages whose only source of income is from forestry. It is not surprising then that the white paper proposes that "the people bear some of the financial burden to improve the nation's woodland". A tax on water resources has been suggested as a way of financing protection forests planted to prevent flash floods. The tax is opposed by industry.

For all the letters he has received, Nicol is not going to try and join in public protest movements. He intends instead to charter a plane and photograph the forests near his home from the air and then from the ground and use his pen and the pictures to publicize the forest's plight. For changes in forest policy there is still time, for Japan is lucky in that large areas of natural forest do still remain — any European country with such forests would consider itself blessed indeed. Whether public awareness of the immense value of the forests will grow fast enough to prevent them disappearing remains the real question. And on top of that there may be some other problems — the white paper is the first to admit that acid rain may be causing forest damage in Japan.

Alun Anderson

Widespread forest

JAPAN'S total land area is 378,000 km². Of this, 250,000 km² is forest: by no coincidence this is a figure very close to the area that is mountainous, 268,000 km², and cannot be used for agriculture or habitation. Almost a third of the forest is owned by the state and a little over a third is man-made, nearly half of it Japanese cedar and a quarter *hinoki*, Japanese cypress. Various kinds of national park and nature park account for a remarkable 54,000 km² of land, an extremely high percentage. But only a small fraction of the park area is completely protected from interference; in other regions, permission can be given for selective cutting, or clear cutting, of forests. □

Safety of French nuclear plant

SIR—The safety record of COGEMA's reprocessing plant UP-2 at La Hague may be better than that of British Nuclear Fuel Limited's Sellafield plant in Britain (*Nature* **320**, 204; 1986), but is it really that much better?

In 1984, collective radiation exposure was the highest in the history of the La Hague plant (728.1 men-rem), surpassing the figure of 1981, when a fire in a waste silo caused significant contamination (and one of the exposed workers caught a dose of 5.7 rem).

The radiological situation on and around the site is anything but stable. The average tritium content in the water of a stream in the area increased 13-fold between May and December 1984, and average β-activity in another stream by a factor of 60 in the last four months of 1984. The official explanations for the presence of unusual quantities of tritium (seasonal rainfalls and air humidity) and β-activity (mainly cobalt-60 washed off the spent fuel cask storage site) are meagre.

There have been several other leaks and incidents in the past few years. The most recent was what COGEMA called a mini-leak in November 1985, when 400 m^3 of "slightly radioactive liquid" was spilled into the environment.

COGEMA's flexible approach to the "nominal capacity" of the plant is significant. In 1976, the official *Revue Générale Nucléaire* says of the processing of fuel from light-water reactors (LWR) that France had completed the UP-2 plant at La Hague by an oxide headend called HAO (Haute Activité Oxydes) which would reach its nominal capacity of 800 tonnes of oxide a year around 1979–80. In 1979, the actual throughput of the plant was 79.4 tonnes of oxide fuel and, in 1980, 104.9 tonnes were reprocessed, 10 per cent and 13 per cent respectively of the "nominal capacity".

In 1978, the optimistic goal of 800 tonnes a year was abandoned and the "new" nominal capacity was fixed at only 400 tonnes a year. In 1982, the Castaing commission, which was asked by the minister of industry to analyse the situation at La Hague, stated that it was more likely that HAO's capacity would be limited to 250 tonnes a year, and COGEMA said in its 1983 annual report that "UP-2 will be capable of reprocessing 250 tonnes a year of LWR fuel, once the reprocessing of other fuel types has been discontinued".

Since 1984 COGEMA has returned to the figure of 400 tonnes a year, as if there had never been anything else. COGEMA proudly announced that 418 tonnes had been reprocessed between November 1984 and November 1985, a performance "beyond its normal capacity". In other words, it took COGEMA ten years to reach 52 per cent of its initial design capacity.

Most of the LWR fuel reprocessed at La Hague was not French but foreign. By June 1982 only 11.5 tonnes (2.6 per cent of the total) were irradiated in a French reactor (Fessenheim). Two years later (June 1984) 82.3 tonnes of EDF (Electricité de France) fuel had been reprocessed and, by the end of 1985, the total quantity had reached 290 tonnes, 22 per cent of the 1,338 tonnes of oxide fuel reprocessed at HAO by the end of 1985, according to Maurice Delange, head of COGEMA's reprocessing branch.

The foreign fuel came from West Germany, Japan, Belgium, Switzerland, the Netherlands and Sweden. COGEMA argues that there was not enough French fuel available, although EDF has a contract with COGEMA for the reprocessing of 5,344 tonnes of LWR fuel; its continuing hesitation to commit itself fully to the reprocessing strategy of the Commission à l'Energie Atomique (CEA) made COGEMA look for additional contracts with foreign clients. According to M. Delange, COGEMA's offer of an additional 1,000 tonnes of capacity for 1986–90 on the international market led to some possible new contracts with the same clients.

The time has passed when CFDT union workers were "not slow to report accidents to their union", as Walgate puts it. Until 1981, CFDT used to be by far the strongest union in La Hague. But after the socialists came to power, it lost many members and half their votes at the elections of union representatives, to the profit of the conservative pro-nuclear FO (*Force Ouvrière*). The union's critical point of view has been turned against it. To be against foreign reprocessing contracts and in favour of the development of alternative waste management strategies has been regarded as "destroying the working tool", as a CFDT worker explained. The "chantage à l'emploi", literally employment blackmailing (threat of redundancy), has been used extensively by the reprocessing lobby, including competing unions. It works well in an area of high unemployment (8,000 people are registered unemployed in Cherbourg), where the only two important employers are the French Navy and COGEMA.

In France, independent information on the nuclear industry and especially on reprocessing is less easily available than ever. The nuclear lobby can give a more "open" appearance and its efforts to "inform" the public, over the past ten years, have indeed been enormous. Workers keep their mouths shut; nobody wants to lose his job.

One of their problems is the lack of strong national support; the national CFDT nuclear branch was "decapitated" in 1981, when highly qualified leaders took over the management of the Agence Française pour la Maîtrise d'Energie, a state energy management agency. For the CFDT section at La Hague this was a second blow. They had had to find new leaders when the organizers of the 1976 strike (to protest against existing safety conditions) left La Hague when COGEMA (100 per cent owned by CEA) took over the management of the plant; they feared repression from a new management which, unlike CEA, was not exempt from private law.

Today, union workers do not want to be telephoned for fear of telephones being tapped, letters stay unanswered and they prefer not to be mentioned in public at all. The few who remained active are gradually giving up; "If they want to eat plutonium, I can't help it", as one stated sarcastically. Another could not find anyone to help write, print and distribute an internal flyer. And nobody wants me to talk about all this...

MYCLE SCHNEIDER
World Information Service on Energy, 4 rue Dunois, 75013 Paris, France

Pre-embryos

SIR—Anne McLaren (*Nature* **320**, 570; 1986) states that the human product of conception before the 14th day of intrauterine life should not be called an "embryo" because the cells are destined to develop into both the fetus and the placenta. By implication, experimenting with or throwing away a conceptus less than 14 days old does not constitute ill-treatment of a human embryo. It is maintained that the use of such terms as "pre-embryo" for these earliest stages of development is not euphemistic or "cosmetic", but scientifically valid terminology.

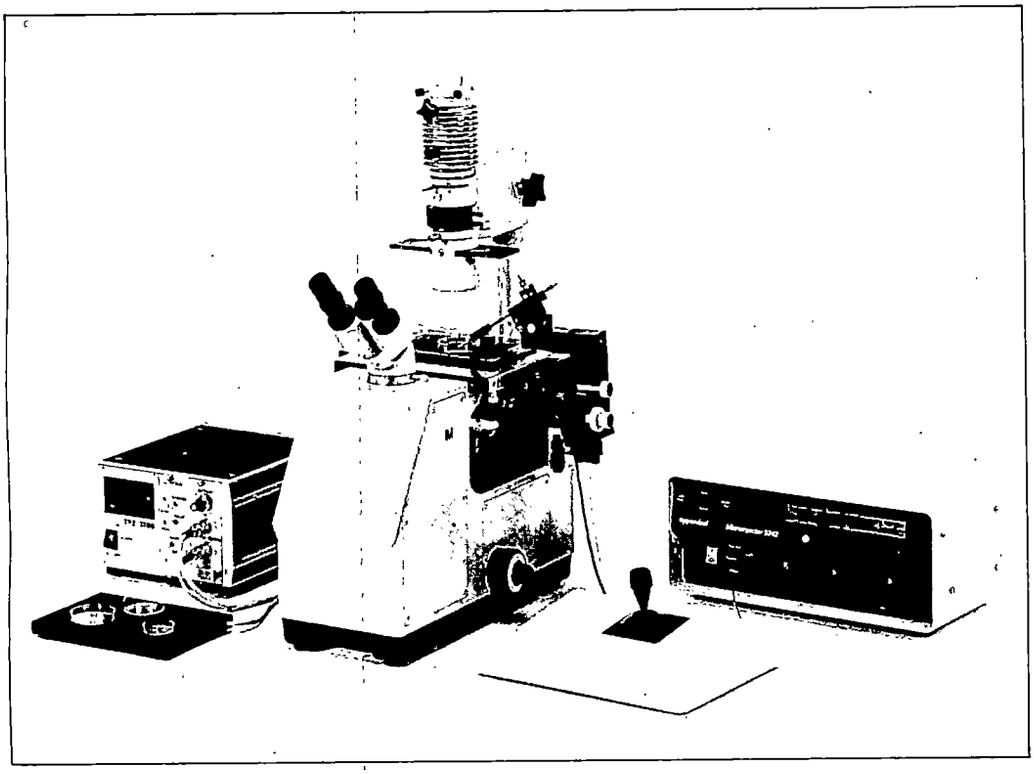
Later in intrauterine life, when obstetricians and perinatologists strive to save a life at risk, the togetherness of the baby and its placenta is emphasized by the currently fashionable term "feto-placenta unit". The placenta is then an essential organ that is discarded only when the baby can manage without it. It happens that before and immediately after implantation the cells that will form the placenta outnumber those that will form the baby, and one cannot look at an individual cell and recognize the organs that will be derived from its progeny.

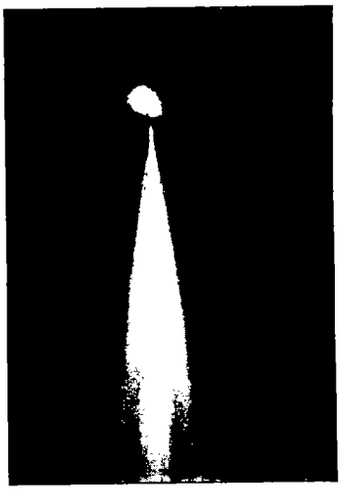
Words like "pre-embryo" may have scientific precision, but they should not be used to foster the delusion that those few cells are anything less than a young feto-placental unit.

J.A. KIERNAN*
Department of Anatomy, University of Western Ontario, London, Canada N6A 5C1

*Present address: Department of Anatomy and Cell Biology, University of Sheffield, Sheffield S10 2TN, UK

For your success in biology, molecular biology and medicine: the Inverted Microscopes from Zeiss.





The Inverted Microscopes IM, IM 35 and ICM 405 from Zeiss offer important advantages:

- large free working space
- extraordinary stability
- the superior quality of Zeiss optics for all optical contrast-enhancement methods
- 35 mm and large-format photomicrography and TV.

Zeiss sets the standards in optics, precision engineering, electronics.

ZEISS

West Germany

Carl Zeiss
Geschäftsbereich
Mikroskopie
Postfach 1369/1380
D-7082 Oberkochen

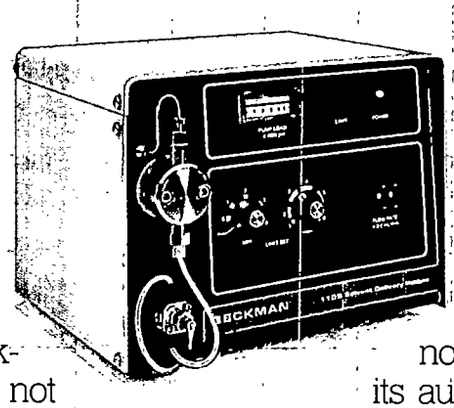
For these practical microscopes Zeiss is now supplying:
Heatable microscope stage and thermostable hotplate for temperature control of cell cultures
Micromanipulator MR for precise positioning of the microinjector
Microinjector eppendorf 5242 for the injection into living cells of minute amounts of liquids down to the picoliter

info-coupon NATURE 5/86

Please send brochures on
☐ Inverted Microscopes IM, IM 35 and ICM 405 for biology, molecular biology and medicine to:

Optimal Chromatography

THE HPLC



Call our 334 HPLC gradient system rugged, hard working, low cost and you'd still not describe it fully.

Take our big 12" CRT display. It's designed to put in a full day's work. To allow real time system control, multiple windows, and a degree of user interaction smaller displays simply can't match.

Or consider our world renowned 110B pump. Known for its auto prime feature and ability to handle bubbles. It uses pressure sensors to maintain flow. Not shut-off switches that encourage mobile phase precipitation.

The fine breeding of the 334 system is also reflected in our microprocessor controlled 160 detector. It combines

CLONES WANTED

We are an international genetic engineering company looking to demonstrate the range of our gene expression technology.

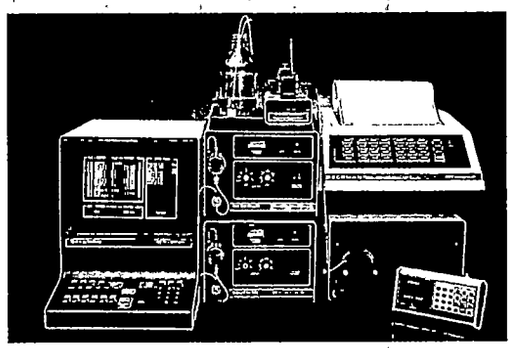
If you have a clone for a natural or designed protein product — for example, human or animal hormones or lymphokines; useful or interesting enzymes; or novel factors (blood, colony, necrosis) — we'd like to talk to you about using it in our systems.

Please send the clone specifications and your requirements to:

C/o Nature Publishing
Display Advertising
Box #22
65 Bleecker Street
N.Y. N.Y. 10022

No. 10 IN A SERIES

WORKHORSE



extreme sensitivity, digital filtration and peak detection algorithms to reduce baseline noise. Without distorting true peak heights.

The point is this. You won't find more dependable performance for your hard earned budget. So why horse around with anything else?

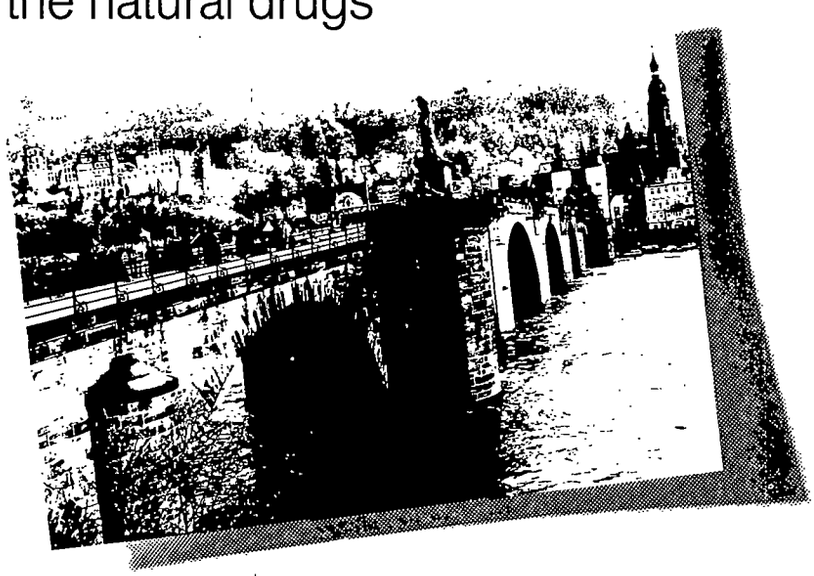
The Beckman 334 HPLC Workhorse. Call your local Beckman office. In the U.S. (800) 742-2345. Or write Beckman Instruments, Inc., Altex Division, 2350 Camino Ramon, San Ramon, CA 94583. Telephone (415) 866-0511. Offices in major cities worldwide.

See us at Analytica

BECKMAN Reader Service No.25

© 1986 Beckman Instruments Inc AX 86-8035

PEPTIDES
the natural drugs



Heidelberg, world-famous for its castle, its ancient city, the bridge, and its 600-years-old university

ORPEGEN, the young company whose start constituted a bridge towards the creation of the TECHNOLOGY PARK HEIDELBERG

ORPEGEN, the bridge between basic research and industrial application of peptide drugs.

ORPEGEN develops, produces, and tests peptides as immunoregulators, hormones, neurotransmitters, antigens, and vaccines.

Our customers come from pharmaceutical industries, as well as from universities, research institutions, and hospitals

We, the bridge between basic research and industries.

® **Analytica 86**

Halle 9, Stand C 21

organic · peptidic · genetic

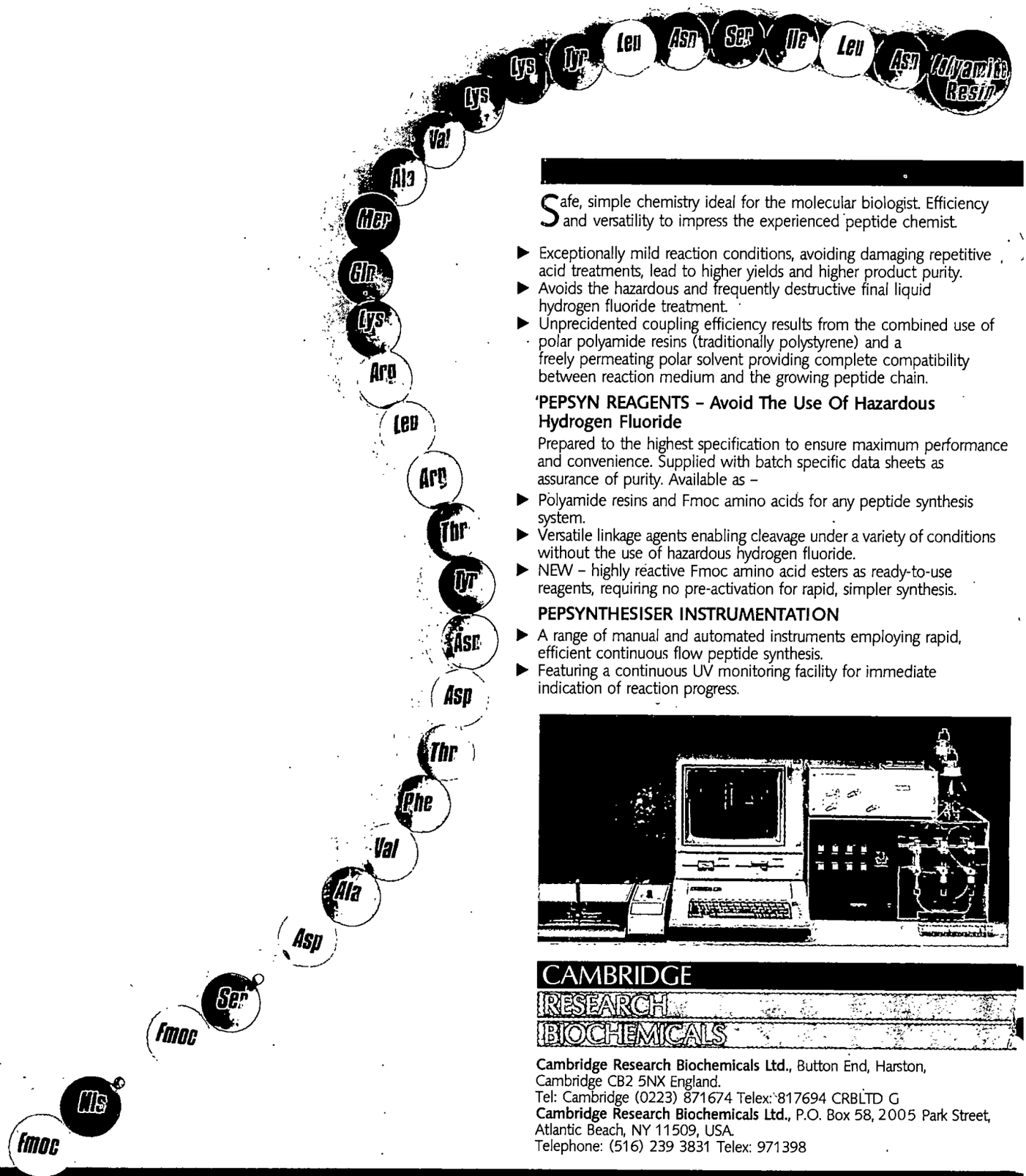
ORPEGEN

Medizinisch-Molekularbiologische Forschungsgesellschaft m.b.H.

Czerny-Ring 22
D-6900 Heidelberg, F.R.Germany
Telephone (0 62 21) 2 70 82 -85
Telex 461362 orgen

CRB

PEPSYN REAGENTS FOR FMOC POLYAMIDE PEPTIDE SYNTHESIS. THE SIMPLER, MILDER ROUTE TO PURER PEPTIDES.



Safe, simple chemistry ideal for the molecular biologist. Efficiency and versatility to impress the experienced peptide chemist.

- Exceptionally mild reaction conditions, avoiding damaging repetitive acid treatments, lead to higher yields and higher product purity.
- Avoids the hazardous and frequently destructive final liquid hydrogen fluoride treatment.
- Unprecidented coupling efficiency results from the combined use of polar polyamide resins (traditionally polystyrene) and a freely permeating polar solvent providing complete compatibility between reaction medium and the growing peptide chain.

'PEPSYN REAGENTS – Avoid The Use Of Hazardous Hydrogen Fluoride

Prepared to the highest specification to ensure maximum performance and convenience. Supplied with batch specific data sheets as assurance of purity. Available as –

- Polyamide resins and Fmoc amino acids for any peptide synthesis system.
- Versatile linkage agents enabling cleavage under a variety of conditions without the use of hazardous hydrogen fluoride.
- NEW – highly reactive Fmoc amino acid esters as ready-to-use reagents, requiring no pre-activation for rapid, simpler synthesis.

PEPSYNTHESISER INSTRUMENTATION

- A range of manual and automated instruments employing rapid, efficient continuous flow peptide synthesis.
- Featuring a continuous UV monitoring facility for immediate indication of reaction progress.

CAMBRIDGE RESEARCH BIOCHEMICALS

Cambridge Research Biochemicals Ltd., Button End, Harston, Cambridge CB2 5NX England.
Tel: Cambridge (0223) 871674 Telex: 817694 CRBLTD G
Cambridge Research Biochemicals Ltd., P.O. Box 58, 2005 Park Street, Atlantic Beach, NY 11509, USA.
Telephone: (516) 239 3831 Telex: 971398

CRB·THE LEADER IN FMOC POLYAMIDE PEPTIDE SYNTHESIS

Disappointment over double quasar

There now seems a high chance that what seemed, two weeks ago, to be a particularly interesting double-quasar image may simply be a record of two independent objects.

Two articles elsewhere in this issue (pp. 419 and 420) provide what appear to be plausible explanations of the remarkable report by E.L. Turner *et al.* (*Nature* **321**, 142; 1986) of the apparent identity of two quasar images separated from each other on the sky by more than two minutes of arc (2.6 minutes, to be precise). The significance of this report was quickly appreciated not merely by its authors but by many others. Although there has accumulated since the first observation in 1979 a handful of cases in which the image of a single quasar is split into two or even three by the interposition of a massive galaxy along the line of sight to the distant object, the angular separations previously reported have been very much smaller than that of the pair of images measured by Turner *et al.*, a few seconds of arc rather than a few minutes.

This week's authors, both Princeton colleagues of Turner, explore the possibility that the very large separation may be caused by the interposition either of a very massive black hole or, alternatively, of one of the galactic structures called a cosmic string. Readers will note that their calculations, interesting in their own right, are at once tentative and suffused with a sense of what good luck it must be that observations should have led so simply to such striking inferences. Now, unfortunately, it appears that these endeavours may have been misplaced.

In a field where it is never easy to be sure that quasar images have been accurately identified with each other, it is too soon for certainty. But stimulated by the report of Turner *et al.*, others have looked at the components of the supposed double quasar in spectral regions other than that on which the original identification was based, and they find enough discrepancies to suggest that the apparent identity of the two objects is in doubt.

Before jumping to the conclusion that Turner *et al.* are in some way to blame for having published their data too quickly, or that they have made an elementary mistake that might have been avoided by taking greater care, readers should consider carefully what is involved in the identification of a gravitationally split quasar image. That an intervening massive object can split one image into two or more follows from the way in which, in relativity, the gravitational field of a massive object distorts the usual straight-line paths open to light. The magnitude of the effect and the apparent separation of the two images depend on the mass of the intervening object. The known cases of split quasar images require intervening masses comparable with those of galaxies. Turner's separated images would require more massive objects, whence the speculation about black holes and cosmic strings.

To establish that a close pair of quasar images has indeed been generated by the interposition of a gravitational lens is, in reality, quite difficult. The first test is that the two images should have the same measured red-shift (which is not affected by the bending of the gravitational lens). One difficulty is that the red-shifts are usually so large that it is hard to tell which atomic transitions are ultimately responsible for the spectral lines observed in the emission from the quasar. Another is that the lines, even if accurately identified, may be so broad that the accuracy of inferences about their displacement is bound to be limited. Turner's two images were reported to have a red-shift defined by $z = 1.012$ on the strength of an emission line from magnesium which, while normally in the ultraviolet, has been displaced by the recession of its source to the middle of the visible light spectrum.

Those who search for double-quasar images also pay close attention to the general characteristics of the spectra of the two candidate images, but there are some important complications. Thus the spectra of quasars can vary rapidly on quite short timescales. Most of the variations show up in the continuum flux, but there may also be substantial variations in the strength of emission lines in the spectra. Because one of the consequences of the effect of a gravitational lens is that different images of the same quasar may reach the observer by paths which differ considerably in the traverse-time of light, there is room for some latitude in the comparison of the spectra of two images. In Turner's case, the two light paths may have differed by as much as 1,000 light years, ample to account for the spectral differences he and his associates reported in the two quasar images.

The new development is a set of measurements by P.A. Shaver and S. Christiani of the European Southern Observatory in a part of the spectrum extending towards the infrared from the longer wavelength limit of the range covered by Turner *et al.* An article describing these measurements will appear in *Nature* two weeks from now. In this previously unexplored region of the spectrum of the Turner quasar, there appear to be pronounced differences in the intensity of certain hydrogen lines. Readers will have to judge for themselves, when this evidence appears, whether the quasar images are indeed produced by a gravitational lens from the same single distant object. Advance notice of these measurements is being provided now, with the consent of its authors, merely because of the excitement generated by the original measurements.

If Turner *et al.* were unlucky in their choice of a spectral range in which to carry out measurements of the components of the double quasar, there will be a widespread sense of disappointment that a potentially fascinating phenomenon has so quickly vanished. But that does not imply that the two quasar images concerned are without interest. The supposition that they might be gravitationally split images of the same object seems first to have been raised by Paczynski (*Nature* **319**, 567; 1986) on the basis of measurements originally due to C.H. Hazard.

If the two images are now gravitational artefacts, then they are most probably distinct quasars (with nearly identical red-shift) which are also members of a distinct galactic cluster. But the measured difference between the velocities of the two images is less than 200km s^{-1}, which is less than the spread of velocities found in typical galactic clusters, and which may therefore suggest some special relationship between the two quasars. That would be an interesting if less spectacular development in its own right, one that would no doubt bring comfort to those who, like H. Arp, have long argued for some systematic relationship between the positions of quasars in the sky.

Meanwhile, the urgent need is further to test the relationship between the two images of Turner's quasar. Detailed study of the relative intensity of the iron and magnesium lines in the two images will no doubt persuade most people one way or the other. When all this has been done, there will remain one logical ambiguity. If the travel times of widely split quasars may be of the order of 1,000 years, and very much greater than the timescale of substantial variability of individual quasars, will it ever be possible to prove (or disprove) that such widely split images are caused by gravitational lenses, however massive or peculiar?

AIDS virus

More and better *trans*-activation

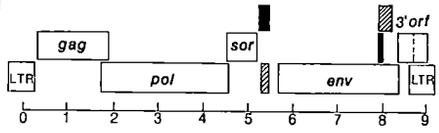
from A. Burny

THE virus that causes acquired immune deficiency syndrome (AIDS) is a sophisticated weapon aimed at the human T4 lymphocyte, a key cell of the immune response. This highly cytopathic virus, called HTLV-III, LAV or, most recently, HIV (see ref. 1), is endowed with the means to stimulate its own replication in an infected cell. One gene involved in this autostimulation is *tat III* (refs 2–4), a bipartite gene encoding a protein that interacts with receptor sequences near the upstream (5′) end of the viral messenger (m)RNA. On page 412 of this issue[5], Bill Haseltine and his colleagues describe the discovery of a new bipartite gene, *art*, of HIV that is also involved in autostimulation. The product of the gene activates the expression of the *gag* and *env* genes of HIV (encoding, respectively, the capsid and envelope proteins) and thereby regulates virus replication.

The discovery of *art* (for anti-repressor translation) is an intellectual and technical achievement. Haseltine's group recently investigated[4] the mechanism of *trans*-activation by the *tat III* gene product and observed that elevation of long terminal repeat-directed gene expression in cells expressing the tat III protein reflects an increase in protein synthesis without a comparable rise in the steady-state level of the respective mRNAs. Deletion analysis of the HIV long terminal repeat demonstrated that the sequence necessary for *trans*-activation (the TAR sequence) is located between nucleotides −17 and +80, that is, 3′ (downstream) from the mRNA initiation site (the cap site). Taken together, the lack of effect of *tat III* on viral mRNA concentration and the presence at the 5′ side of viral mRNAs of nucleotide sequences responsive to tat III protein regulation prompted Haseltine and co-workers to establish experimentally that *trans*-activation by *tat III* is mediated via a post-translational mechanism[6].

Continuing their deletion analysis of the HIV proviral genome, Haseltine and colleagues have now identified a seventh viral gene. Their approach consists of the transfection of matched cell lines with intact or deleted proviral DNA constructs and determination of the amounts of virus and viral antigens produced. It became obvious that a new gene was involved when deletions located in the 3′ region of the first exon of the *tat III* gene, but not extending into the *env* gene, prevented virus production even in the presence of a functional tat III product supplied in *trans*. A second set of mutations (insertions and deletions) located further down the proviral DNA to the 3′ side of the second exon of *tat III* and overlapping *env* yielded proviruses that failed to express viral gag and env proteins. Finally, new plasmids designed to express the putative new open reading frame but not *env* were demonstrated to allow *env* production by proviruses containing mutations in the new open reading frame. As the phenotypes induced by both sets of mutations performed are similar, Haseltine and colleagues conclude that they have identified a new gene.

The protein product of the gene, 116 amino acids long, has no effect on viral



Map of the genes encoding the AIDS virus. Black boxes, the two coding exons of the *tat* gene; hatched boxes, those of the *art* gene; *pol, sor,* genes for other viral proteins; *orf,* open reading frame. Scale, kilobases.

mRNA concentrations but is required for expression of the HIV gag and env proteins. The inescapable conclusion of these experiments is that the *art* gene product specifically allows translation of HIV *gag* and *env* mRNAs, thus unlocking the block imposed on virus expression. The discovery of *trans*-activation of retroviral long terminal repeats or mRNAs will be important for understanding virus persistence and latency, cell killing and cell transformation.

The *tat* and *art* gene products are clearly potent regulators of viral gene expression, and are most probably involved in the successive cycles of latency and expression that characterize the life-span of the AIDS virus. Fine tuning of *tat* and *art* genes must allow silent accumulation of *gag* and *env* mRNAs. Expression of tat and art proteins switches on a burst of expression of *gag* and *env* components that initiates virus production. Such a mechanistic design predicts that *tat* and *art* mRNAs must be translatable in conditions that preclude translation of *gag* and *env* mRNAs. Detailed analysis of the 5′ end of the corresponding mRNAs, and identification of the tat and art protein interactions with their target nucleic acids, are urgent tasks.

As Haseltine and co-workers point out, the new data are highly suggestive of the existence of an early–late switch in HIV infections and in infections mediated by similar agents such as visna virus and caprine arthritis encephalitis virus. The two latter systems are characterized by persistence and latency[7–9], and *trans*-activation has been demonstrated in visna virus-infected cells[9].

Retroviruses, DNA viruses and other systems involving production of a lethal product obey the biological paradigm that production of the product is best achieved if delayed to late stages of the life-span of the cell. Regulation of translation of accumulated mRNAs is an elegant manner of complying with this requirement. □

1. Coffin, J. *et al. Nature* **321**, 10 (1986).
2. Arya, S.K., Guo, C., Josephs, S.F. & Wong-Staal, F. *Science* **229**, 69 (1985).
3. Sodroski, J.G., Patarca, R., Rosen, C.A., Wong-Staal, F. & Haseltine, W.A. *Science* **229**, 74 (1985).
4. Rosen, C.A. *et al. Nature* **319**, 555 (1986).
5. Sodroski, J.G. *et al. Nature* **321**, 412 (1986).
6. Rosen, C.A., Sodroski, J.G. & Haseltine, W.A. *Cell* **41**, 813 (1985).
7. Brahic, M., Stowring, L., Ventura, P. & Haase, A.T. *Nature* **292**, 240 (1981).
8. Geballe, A.P., Ventura, P., Stowring, L. & Haase, A.T. *Virology* **141**, 148 (1985).
9. Narayan, O., Kennedy, F., Stoskopf, S., Sheffer, D., Griffin, D.E. & Clements, J.E. *Infect. Immun.* **41**, 67 (1983).
10. Hess, J.L., Clements, J.E. & Narayan, O. *Science* **299**, 482 (1985).

A. Burny is in the Department of Molecular Biology, University of Brussels, 67 Rue des Chevaux, 1640 Rhode-Saint-Genèse, and at the Faculty of Agronomy, Gembloux, Belgium.

Gravitational waves

Observatories of the future

from M.G. Edmunds

THE direct observation of gravitational waves, the ripples in space-time generated by the motions of masses, is one of the last-known windows that remains to be opened on the Universe. Although detections have been promised within five years for at least the past fifteen years, it does at last seem that the hopes will develop into real data within six years from now, as concluded at a recent meeting* by members of groups working on the problem. This optimism springs from a consensus on the theoretical estimates of the expected strength of cosmic sources of gravitational radiation, as well as growing confidence that the technological advances required for interferometric detectors of sufficient sensitivity can be made.

An interferometric gravitational-wave detector (see Fig. 1) basically consists of three suspended masses arranged at the corners of an L. The two arms of a Michelson interferometer formed with mirrors attached to the masses measure the rel-

*The Interferometric Gravitational Wave Detectors meeting was held at Cardiff University on 17 February 1986.

ative lengths of the two sides of the L. When a gravitational wave passes the detector it moves the masses on one arm apart and the masses on the other arm closer together, resulting in a shift of the interferometer fringe pattern. A parameter h is used to characterize the magnitude of the wave's interaction, defined as the induced difference in length of the two arms divided by the length of a single arm. Just to begin to see sources, values of h as small as 10^{-20} will probably need to be

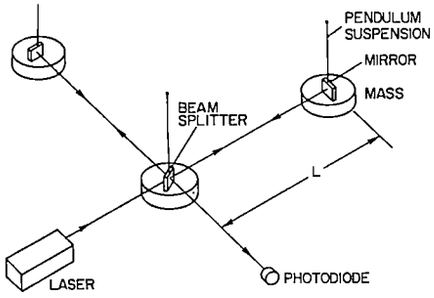


Fig. 1 Basic principle of the laser interferometer.

detected. Really useful astrophysical information will come when h can be measured at the 10^{-22} level. Because even the former of these limits implies measuring length changes of 10^{-2} fermi (about 1/100 the radius of a nucleus) in an interferometer with an arm length of 1 km, it is clear that the technological problems are considerable. Interferometric detectors work at wave frequencies within about a decade of 1,000 Hz, and are limited to optical or near-infrared light by consideration of the optic surface, the noise source and the photon detector.

As summarized at the meeting by Kip Thorne (California Institute of Technology; Caltech) the sources most likely to be seen as single events involve collapse of the core of a single star in a supernova explosion or coalescence of a close binary system of compact stars. Generation of gravitational waves is a strong function of the deviations from spherical and axial symmetry occuring during the collapse to form a neutron star or black hole, and the uncertain magnitude of these deviations leads to uncertainty in the predicted wave fluxes. A sensitivity of h of the order of 10^{-22} may allow collapsing black holes of 100 solar masses to be seen throughout the entire Universe accessible within the light-travel time since the Big Bang. Non-axisymmetrical neutron-star collapses may be seen out as far as galaxies in the Virgo cluster, yielding an expected several events per year. An advantage of interferometric detectors over resonating solid-bar detectors is the spectral information that can be deciphered. Recent numerical collapse calculations suggest very characteristic waveforms for both black-hole and neutron-star collapse; indeed detection of the wave 'signature' of a black-hole collapse may be our only way of unambiguously demonstrating the existence of black holes. If the supernova generating the waves is also detected visibly, the relative arrival times of the light and gravitational waves are a strong test of gravity theories. General relativity predicts the same speed of propagation, while some rivals predict differences of the order of one part in 10^6; the observations should place limits of the order of one part in 10^{10}.

Two neutron stars spiralling into each other should certainly be visible in gravitational waves at the Virgo distance if h limits are pushed to 10^{-22}. The stochastic background of gravitational waves left over from the early Universe may also be detected, perhaps allowing some probing back to the Planck era ($t \sim 10^{-43}$ s) where some estimates place the decoupling of gravitational radiation, or to later eras when the perturbations in density that eventually gave rise to galaxies were generated. Present-day regular periodic sources (such as fast-spinning pulsars) may be observed to much smaller h than 10^{-22} by integrating over many periods.

R.W.P. Drever (Caltech and Glasgow University) outlined some of the neat experimental techniques that have made the interferometric detectors a practical proposition since the first experimental prototype built at the Hughes Aircraft Corporation in 1971. The sensitivity of the detector increases with the arm length. The effective length of the arms is increased either by using multiple reflections to give multiple parallel paths along the arms or by making the arms into resonant cavities, effectively bouncing the light backwards and forwards many times within the period of a gravity wave. The programme in Germany (like that at Massachusetts Institute of Technology, and described by W. Winkler, Max-Planck Institute, Garching) uses a multiple path design of total path length 100 km, possibly in a three-arm triangle configuration. The current experimental rig in Glasgow has an arm length of 10 m, and the rig at Caltech a length of 40 m, both rigs using the resonant cavity approach in preparation for much larger instruments. The development of a servo-loop system by Drever's group to stabilize the laser frequency in these interferometers has led to a standard technique for laser stabilization in many other applications — surely an object lesson for those who doubt the technological advantages of pursuing 'pure' science.

A new technique to use a phase-modulation system to recycle the light used in the interferometer in such a way as to reinforce the laser light feed may reduce the required laser power by a factor of 100, which will require single-mode powers of perhaps 20 or 30 W — a not unreasonable target. Particularly useful in reducing the requirements of laser power is the reported development of robust mirrors with reflectivities of the order of 0.99995. In the more distant future there are real hopes of reducing the effects of photon noise by using a technique termed squeezed states, recently demonstrated experimentally at Bell Laboratories, which attempts to circumvent some of the limitations imposed by the uncertainty principle by careful choice of exactly what quantities are measured.

The practical realization of a working gravitational-wave observatory (see Fig. 2) is most likely to come first from the US and the Glasgow groups. The US project for a laser interferometer gravity-wave observatory should result in two 4-km instruments, one in Maine and one in California. The UK proposal is for a 1-km instrument in Scotland, to be fully operational in its first stage within about six years. These would be true 'observatories',

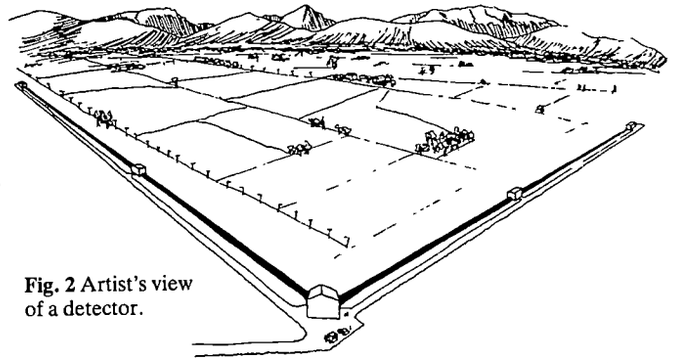


Fig. 2 Artist's view of a detector.

as most of the cost is in the provision of kilometre-length high-vacuum pipes for the interferometer arms. The pipes would be about 1 m in diameter and would work at vacuua of better than 10^{-7} Torr. These pipes will be able to carry several interferometers simultaneously, providing useful coincidence tests against seismic or other instrumental disturbances.

The value of international collaboration in gravitational-wave research was unanimously agreed. Apart from economies resulting from shared technology, there is a real need for several detectors both to obtain directional information and to eliminate spurious signals by correlation of data from different sites. The gravitational waves sweep past and through the Earth, and (as emphasized by B.F. Schutz, Cardiff University) the four principal detectors proposed can be optimally oriented to give good sky coverage and will maximize the rate of detection of the (initially) few events per year. □

M.G. Edmunds is in the Department of Applied Mathematics and Astronomy at University College, PO Box 78, Cardiff CF1 1XL, UK.

Developmental biology

Embryology goes fishing

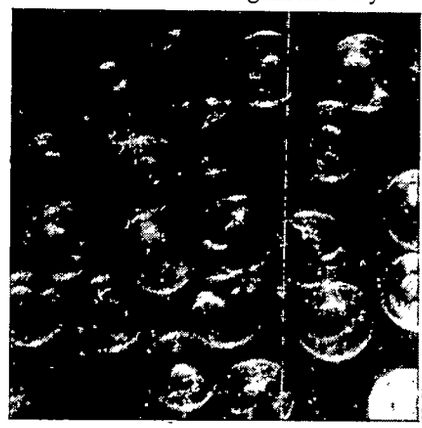
from David Marcey and Christiane Nüsslein-Volhard

In all multicellular organisms, embryonic cells with different developmental potentials arise from a series of cleavage divisions that begin with the first division of the nucleus of the fertilized egg. In some animals, for example the nematode worm *Caenorhabditis elegans*, the developmental fate of a particular embryonic cell is strictly tied to its ancestry, whereas in other systems (for example, the fruitfly *Drosophila melanogaster*), positions and/or cell interactions are instrumental in determining initial restrictions in developmental potential, although these restrictions can be inherited by daughter cells through subsequent cell divisions. But the relationship between embryonic cell fate and cell lineage has been examined extensively in few vertebrates, so the recent report by Kimmel and Warga[1], describing some early cell lineages in the zebra fish *Brachydanio rerio* (a long-time aquarium favourite), is therefore welcome.

Although the various organisms examined to date differ in the degree to which embryonic cell determination is linked to cell lineage, there is no reason to expect that, at the cellular level, fundamentally different determination mechanisms are used during the embryogenesis of diverse taxa. Significant increases in our understanding of development in different species are required before such comparative problems can be addressed. Recently, progress in elucidating embryonic cell-determination mechanisms has been more rapid for invertebrate systems (especially flies and nematodes) than for vertebrate systems. This is partly because of the higher complexity of, say, mouse than worm development, but has also resulted from the lack of a suitable vertebrate system in which the power of a genetic approach to ontogeny can be brought to bear.

In *Drosophila* and *Caenorhabditis*, the discovery of developmentally important genes by the recovery of mutations, followed by their molecular analysis, is permitting significant glimpses into the mechanisms responsible for pattern generation, including those involving cell-lineage restrictions. Are these mechanisms also operative in vertebrates? Two approaches are likely to help answer this question. One involves the analysis of vertebrate DNA sequences that show significant sequence homology with genes known to figure importantly in fly and/or worm development. The other is to perturb development genetically in a vertebrate, to screen systematically for embryonic defects and then to compare the classes of mutant phenotypes obtained with those available in other organisms. Such comparative, genetic embryology should provide valuable information about the evolution of developmental systems.

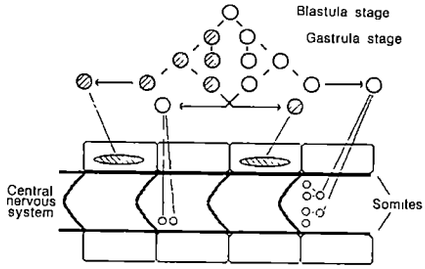
Fortunately, some of the genetic techniques devised by George Streisinger[2] (Fig. 1), coupled with the features of the zebra fish that provide for superb embryological analysis, make this species an ideal vertebrate for the genetic analysis of development. Mutagenesis screens, together with embryological analyses like those of Kimmel and Warga, promise to advance our knowledge of vertebrate ontogeny.



H. Howard, University of Oregon.

Fig. 1 Cloned zebra fish embryos.

Fig. 2 Schematic, simplified representation of sample cell lineages in the zebra fish embryo (the numbers of cell divisions shown are not necessarily real). Striped cells are of a muscle lineage, dotted cells are of a neural lineage. A blastula cell may give rise to both muscle and neural cells, but at the gastrula stage, separation of these lineages occurs. Subsequent divisions produce cells which can separate (arrows) and populate different levels along the anteroposterior axis. In the case of some neural cells, further divisions yield cells that lie on both sides of the nervous system midline.



Taking advantage of the transparency, small size and speedy development of zebra fish embryos, Kimmel and Warga[1] injected a conjugate of the fluorescent label rhodamine and the histochemical marker horseradish peroxidase (or fluorescent label alone) into single cells of the blastula and followed the subsequent fate of their descendants in both living and sectioned material. Confirming previous marker-injection[3] and genetic mosaic[4] studies, progeny of single blastomeres were seen to disperse throughout the embryo and to participate in the development of diverse tissues such as muscle, neural and epidermal tissue. In contrast, a detailed analysis of individual gastrula-stage lineages within a marked clone revealed that, with few exceptions, progeny of gastrula cells are confined to a particular tissue.

These observations fit well into the classical embryological framework for fish development. In teleosts such as *Brachydanio*, pronounced cellular mixing takes place during the spreading movements of the embryonic disk over the yolk that preceed and accompany gastrulation, termed epiboly. A result of this epibolic spreading is the juxtaposition in the blastula of cells having different origins. During and after this mixing, formation of both germ layers and the rudiments of primary organs occurs. Thus, although not surprising, Kimmel and Warga's new result helps to define the stage at which initial segregation of tissue-specific lineages occurs. The observed clonal restrictions might not simply be caused by spatial constraints because the authors have found that separate tissue-specific lineages sometimes produce cells that are near neighbours; gastrula-stage lineages are segregated into tissue types even when there is substantial cell mixing and division throughout the period of observation. These segregations could then reflect heritable choices in cell fate made by individual gastrula cells (see below).

Several clonal patterns in the central nervous system deserve special comment. Kimmel and Warga observe that cells arising from a common neuronal precursor can populate disparate axial levels. Data from one embryo show extensive anteroposterior movement of the descendants from sibling mid-gastrula neural progenitors such that clonal relatives are present as four clusters separated by as many as seven segment widths in the 24-hour-old embryo. One possible interpretation of this result is that the segmental identity of individual neural cells is assumed after a commitment to make nervous tissue. A test of this interpretation would involve making appropriate lesions to prevent the normal migration of neuronal precursors and then following the fate of thwarted cells. Kimmel and Warga found marked, if somewhat variable, periodicity in the clustering of clonal relatives in the spinal cord; sometimes relatives in adjacent segments differentiate into morphologically similar neurones. Another striking observation was the dispersal of some sibling

neural progenitor cells across the embryonic midline after migration of parental cells to a particular axial level. Judged by their morphology and rostro-caudal position within a particular segment in the spinal cord, these neurones appear homologous. The intriguing observations that clonal relatives in different segments and in separate halves of the embryo can differentiate similarly demands thought on the relationship of this differentiation to lineage.

Based on their analyses, Kimmel and Warga suggest a sequence of diverging lineages associated with cell-fate determinations in zebra fish (Fig. 2): although blastomeres mix extensively and are pluripotent with respect to the fate of their descendants, the first divisions of the early gastrula produce tissue-specific lineages; the next divisions produce cells that contribute to different axial levels; and subsequent divisions, at least in the central nervous system, yield sibling cells that form the bilateral halves of the brain and spinal cord. The tracing of cellular pedigrees with injectable markers[5] clearly yields much information about the embryonic fates of clonally related cells, but it must be stressed that cell lineage studies alone cannot establish connections between ancestry and fate. As with the *Xenopus* (clawed toad) central nervous system[6], tests of these relationships must wait for experiments in which particular lineages are challenged to produce derivates normally made by different clones, as has been accomplished in birds with ectopic grafts[7], in *Drosophila* with cell-autonomous growth-rate mutants[8] and in the grasshopper[9], nematode[10] and leech[11] with cell-ablation methods. Molecular probes for special developmental programmes, such as those for some sea-urchin embryonic lineages[12] would also be useful. □

1. Kimmel, C.B. & Warga, R.M. *Science* **231**, 365 (1986).
2. Streisinger, G. *et al. Nature* **291**, 293 (1981).
3. Kimmel, C.B. & Law, R.D. *Devl Biol.* **108**, 94 (1985).
4. Grunwald, D. *et al. J. cell. Biochem.* **9b**, 270 (1985).
5. Weisblat, D.A. *et al. Science* **209**, 1538 (1980).
6. Jacobsen, M. *J. Neurosci.* **3**, 10119 (1983).
7. LeDouarin, N. *The Neural Crest* (Cambridge University Press, 1982).
8. Garcia-Bellido, A. *et al. Devl Biol.* **48**, 132 (1976).
9. Doe, C.Q. & Goodman, C.S. *Devl Biol.* **111**, 206 (1985).
10. Sulston, J.E. & Horvitz, H.R. *Devl Biol.* **65**, 110 (1977).
11. Weisblat, D.A. & Blair, S.S. *Devl biol.* **101**, 326 (1984).
12. Angerer, R.C. & Davidson, E.H. *Science* **226**, 1153 (1984).

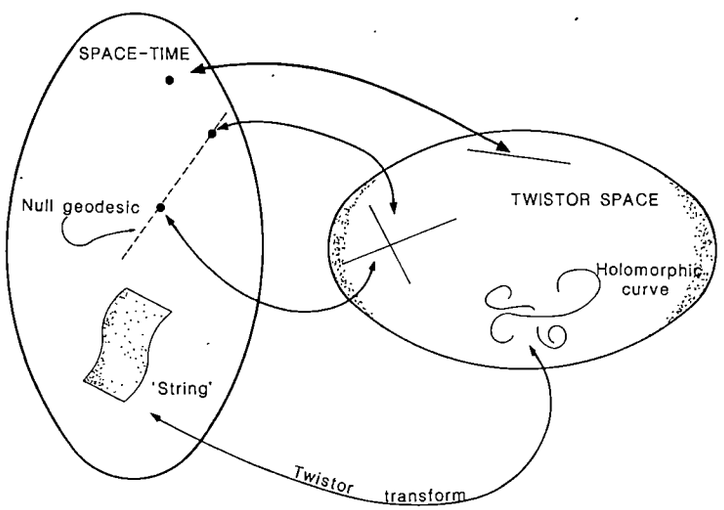
David Marcey is a fellow of The Helen Hay Whitney Foundation and Christiane Nüsslein-Volhard is at the Max-Planck Institute for Developmental Biology, Spemannstrasse 35, 7400 Tübingen, FRG.

Theoretical physics

Supertwistors and superstrings

from L.P. Hughston

ROGER Penrose's 'twistor' method[1] has been fashionable for about a decade among mathematicians and mathematical physicists as a powerful technique for analysing certain classes of partial differential equations and the manifolds or spaces that are naturally associated in various ways with them. The systems of differential equations to which the method is applicable are those arising in relativistic field theories, and thus there is a deep vein of interest in the theory which links these developments with advances in our understanding of elementary particles and gravitation. Although the method was originally devised with space-time modelled as a classical four-dimensional manifold, it has become increasingly clear that the theory can in several instances be developed in higher-dimensional spaces, and can be set up so as to admit supersymmetric degrees of freedom.



Points in space-time correspond to extended structures (complex projective lines) in twistor space. Space-time points which are null-separated correspond to lines which intersect. A relativistic string corresponds, in twistor space, to a type of holomorphic curve.

In particular, G.A.J. Sparling, on page 417 of this issue[2], formulates in simple terms the field equations of no less than five distinct important theories: the classical Einstein gravitational equations; the classical Einstein–Maxwell equations; the bosonic equations of eleven-dimensional supergravity; the curvature and torsional field equations of supergravity in dimension four; and the equations of graded Einstein–Maxwell theory in dimension four.

Sparling shows in each case that the relevant field equations correspond to the 'splitting' of a certain bundle structure (the bundle of local twistors or supertwistors). This characterization of field equations by means of a splitting condition is sufficiently compelling that we may view it in effect as providing an alternative to the time-honoured 'principle of least action'.

In his early work on twistor theory[3,4], Penrose showed how insight could be gained into the nature of the geometry of space-time by consideration of a second manifold, twistor space, which is related to space-time via an intricate transformation (see figure). The points of space-time correspond to extended structures (complex projective lines) in the associated twistor space; intersection of a pair of these lines corresponds in space-time to null-separation (that is, connectedness along a light-like trajectory). Penrose and others were able to demonstrate how the elementary linear equations of non-interacting relativistic fields in space-time could be solved, remarkably, by use of essentially 'free' holomorphic data specified on appropriate regions of twistor space.

A significant step forward came about ten years ago with the discovery of the so-called 'non-linear graviton' construction[5], which showed how certain classes of coupled non-linear partial differential equations could be solved by a kind of non-linear variant of the earlier ideas which had worked for linear theories.

Shortly thereafter it was shown by Atiyah and Ward[7,8], Yasskin and Green[9], Witten[10], and others how, with slight modifications of the basic ideas, theories of the Yang–Mills type could also be treated by twistor methods. Witten[10] played a key part in subsequent developments because, following on from the ideas of Ferber[11], he was the first systematically to wed supersymmetry techniques to the geometrical methods of twistor theory.

Since then there has been widespread activity in generalizing the Penrose transform and related ideas to higher-dimensional systems and to systems of interact-

ing fields. Witten, in particular, recently devised a supersymmetric twistor-like transform in ten dimensions[12], motivated by the possibility that such a transform may be "the proper starting point for understanding the geometrical meaning of superstring theory".

Sparling, following to some extent the prototype of C. R. LeBrun[13], now extends these investigations along a promising new line of enquiry, asking, via consideration of the geometry of twistor bundles, for a general characterization of the most significant field equations of relativistic physics.

As for the future, as both Witten and Sparling point out, an important line of development may be to establish further the links between superstring theory and twistor theory. In this connection another recent step forward is relevant: W.T. Shaw has shown[14] that the dynamical equations of classical string theory in four dimensions can be solved by means of a twistor transform. According to Shaw's scheme a string corresponds in twistor space to a type of holomorphic curve, specified essentially arbitrarily (see figure). Again here the physical object (the relativistic string) is described in terms of free data on the twistor space — the challenge which follows is that of constructing a consistent quantum theory from this essentially classical picture. □

1. Penrose, R. & Rindler, W. *Spinors and Space-Time* Vol.2: *Spinor and Twistor Methods in Space-Time Geometry* (Cambridge University Press, 1986).
2. Sparling, G.A.J. *Nature* **321**, 417 (1986).
3. Penrose, R. *J. math. Phys.* **8**, 345 (1967).
4. Penrose, R. *Int. J. theor. Phys.* **1**, 61 (1968).
5. Penrose, R. & MacCallum, M.A.H. *Phys. Rep.* **6**, 241 (1972).
6. Penrose, R. *Gen. Rel. Grav.* **7**, 31 (1976).
7. Ward, R.S. *Phys. Lett.* **A61**, 81 (1977).
8. Atiyah, M.F. & Ward, R.S. *Comm. Math. Phys.* **55**, 117 (1977).
9. Isenberg, J., Yasskin, P.B., & Green, P.S. *Phys. Lett.* **B78**, 462 (1978).
10. Witten, E. *Phys. Lett.* B77 394 (1978).
11. Ferber, A. *Nucl. Phys.* B132 55 (1978).
12. Witten, E. *Nucl. Phys.* B266, 245 (1986).
13. LeBrun, C.R. *Class. Q. Grav.* **2** 555 (1985).
14. Shaw, W.T. *Class. Q. Grav.* **2** L113 (1985).

L.P. Hughston is Fellow and Tutor in Applied Mathematics at Lincoln College, Oxford OX1 3DR, UK.

Molecular pharmacology

Structure and function of acetylcholine-receptor ion channels

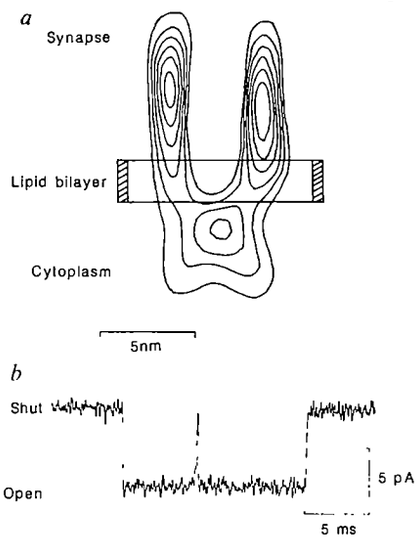
from David Colquhoun

FOR much of this century pharmacologists have been saying that once they knew the structure of the cellular receptor, as well as that of the agonists and antagonists that combine with it, then it would be possible to understand the mechanisms of action of neurotransmitters, drugs and hormones. This dream is now being realized, thanks in no small part to the beautiful work of a group at Kyoto University on structure and of a group at the Max-Planck Institute, Göttingen on function of the acetylcholine receptor. In the latest work from these groups, reported elsewhere in this issue (Mishina, M. *et al. Nature* **321**, 406; 1986), Numa, Sakmann and their colleagues elucidate the structural basis of the difference between the fetal and adult forms of the acetylcholine receptor in bovine muscle.

The nicotinic acetylcholine receptor from electric fish is a pentameric protein, $\alpha_2\beta\gamma\delta$, made from four types of subunit which are arranged around a central ion channel; that from mammalian muscle is almost certainly similar. The primary sequences of all four subunits have now been found using recombinant DNA methods. The subunits span the cell membrane (*a* in the figure); when two acetylcholine molecules combine with sites on the extracellular parts of the α subunits, the ion channel opens for a millisecond or so, resulting in chemical synaptic transmission from nerve to muscle fibre of such rapidity and reliability that it allows us (well, a few of us) to play the Waldstein sonata.

Before the motor nerve reaches embryonic muscle fibres, the acetylcholine receptors are widely distributed over the whole surface of the developing myotube, but following innervation some remarkable changes take place (for a review see Dennis, M.J. *A. Rev. Neurosci.* **4**, 43; 1981). Around the time of birth (in the rat) the rapid turnover of the fetal acetylcholine receptors is slowed, the receptors become highly concentrated over a very small area of the muscle fibre immediately at the junction with the motor nerve ending, and the density of extrajunctional receptors becomes much lower. During the immediate post-natal period the characteristics of the acetylcholine-receptor ion channel change from the fetal to the adult form: the mean duration of an individual opening of the ion channel induced by acetylcholine is shorter by a factor of 3 or 4, and the conductance of the open state is about 50 per cent larger in the adult relative to the fetal form. It is thought that these changes are brought about by some substance released by the motor nerve and/or muscular activity. When the motor nerve of an adult fibre is cut, receptors reappear throughout the length of the muscle fibre membrane, and these new extrajunctional channels are remarkably similar to the fetal receptors in their turnover time, single-channel conductance properties and mean open lifetime.

There has been much discussion about whether the change from fetal to adult receptor during development results from modification of existing fetal-type receptors, for example by phosphorylation, or from synthesis and insertion into the membranes of new adult-type molecules. Some work has suggested that the turnover rate (and rate of insertion of new receptors) is too slow for the latter mechanisms to be correct. But the new work of Mishina *et al.* shows with beautiful clarity that the adult and the fetal receptors are different molecules. The adult protein contains, in place of the γ subunit found in the fetal protein, the recently discovered ε subunit which has a different primary sequence (Takai, T. *et al. Nature* **315**, 761; 1985). The ε subunit has rather more acidic, and fewer basic, amino acids than the γ subunit and it has only 53 per cent homology with the γ-subunit sequence (although this is greater than its homology with the α, β or δ sequences). Furthermore the messenger (m)RNA encoding the γ subunit is found mainly at the early fetal stage whereas the mRNA for the ε subunit becomes predominant after birth (contrary to the report of Takai *et al.*) A particularly nice feature of the new work is the direct com-



Static structure and rapid function. *a*, Electron image map of a cross section of the receptor-ion channel, perpendicular to the plane of the cell membrane; the wide mouth of the channel is clearly resolved (redrawn from Brisson, A. & Unwin, P.N.T. *Nature* **315**, 474; 1985). *b*, A single activation of the ion channel by acetylcholine causes rapid transition to the open state (downward deflection); this channel opening lasts for about 14 ms but the current is interrupted by a brief closure that lasts for about 100 μs (from Colquhoun, D. & Sakmann, B. *J. Physiol., Lond.* **369**, 501; 1985).

parison between the functional properties of the receptors (made in oocytes following injection of mRNAs encoding the pure subunits) and the receptors in their natural environment in fetal and adult muscle membranes. The properties are astonishingly similar — perhaps, after all, the environment of the receptor is not very important.

It now seems likely that during development the motor nerve somehow switches on expression of the gene encoding the ε subunit while stopping expression of the gene encoding the γ subunit. A few problems remain: it is just possible that the nerve might control expression of an enzyme that selectively breaks down the mRNA encoding one type of subunit; and it is conceivable that the γ subunit of an existing fetal-type receptor could be exchanged for an ε subunit while it is in the membrane, although neither of these possibilities seems very likely. There is some evidence to suggest that more than two sorts of channel can exist during development and after denervation. Perhaps this is why the variability of the mean open time of the channel for the fetal type receptor in oocytes is much greater than that of the adult type.

The work by Mishina *et al.* greatly improves our understanding of the relationship between structure and function at the relatively gross level of distinct receptor subtypes. Next, we would like to elucidate the molecular behaviour of a channel when an agonist binds to it. What are the structures of the 'discrete' states inferred from kinetic analysis — for example, what are the structures of the open and shut states; why is it that some agonists can hold the channel open for longer than others; and what is the structural explanation of the brief interruptions in channel openings? These events occur on a timescale of milliseconds or microseconds, whereas our picture of structure is still static (see figure).

Parts of the receptor molecule have already been changed by site-directed mutagenesis (Mishina, M. *et al. Nature* **313,** 364; 1985) and the function of subunit hybrids examined (Sakmann, B. *et al. Nature* **318,** 538; 1985). But clearly the substitution of one amino acid in the sequence could change the conformation of the whole subunit, or even that of adjacent subunits. Attempts to assign discrete functions to parts of the molecule will inevitably be ambiguous unless new methods of assessing the higher-order structure can be devised. Judging by experience with other molecules such as haemoglobin, it could be some time before clear answers emerge — but at least now the light is visible over the horizon. □

David Colquhoun is Professor of Pharmacology at University College London, Gower Street, London WC1E 6BT, UK.

Ocean Drilling Program

A microcosm of ocean basin evolution in the Mediterranean

*from the Leg 107 shipboard scientific party**

THE Tyrrhenian is a small triangular sea surrounded by mainland Italy, Sicily, Sardinia and Corsica (Fig. 1). Leg 107 of the Ocean Drilling Program was the third scientific drilling study in the Mediterranean Sea, following the pioneering Deep Sea Drilling Project legs 13 and 42A in 1970 and 1975. The Leg 107 cruise had three main ojectives: to consider the Tyrrhenian Sea as a back-arc basin; as a young passive margin; and as a stratigraphic type locality.

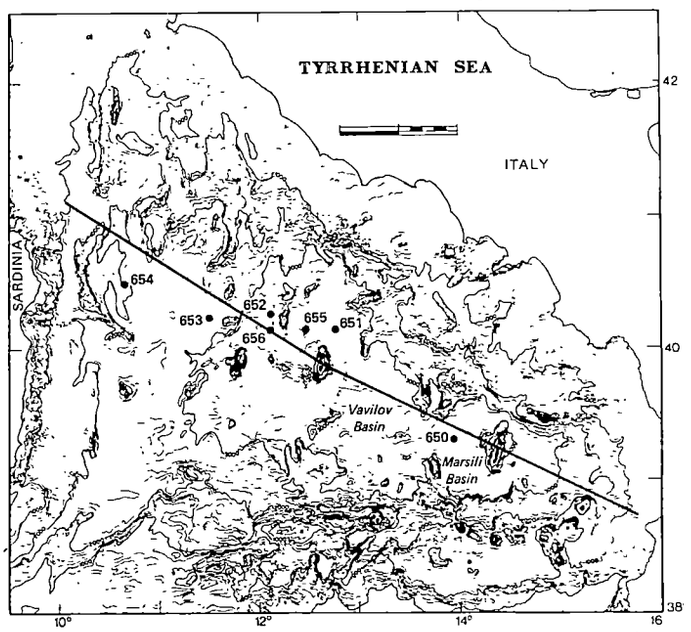


Fig. 1 Tyrrhenian Sea. Leg 107 drilled a north-west/south-east transect of seven sites (650–656) from the Sardinian passive margin (left) across two small deep oceanic basins. (Bathymetry after International Bathymetric chart of the Mediterranean; contour interval, 200 m; scale bar, 100 km).

The Tyrrhenian Sea is a small oceanic back-arc basin that has opened behind a volcanic arc and above a subduction zone. Widespread volcanism and frequent earthquakes indicate that the subduction plate boundary is still active and that the back-arc basin is still evolving. Leg 107 investigated how such a basin evolves in space and time. At the south-easternmost drill site (site 650; Fig. 2), we found evidence that the basin is geologically very young (less than 2 million years old). The basalt recovered at site 650 is very vesicular (full of gas bubbles) which implies that the basalt was erupted into water much shallower than its present 4,100-m depth below sea level. Thus, the eastern part of the Tyrrhenian Sea has subsided markedly since it was formed. At site 655, further north-west, Leg 107 recovered 110 m of basalt flows overlain by sediments that are about 3.5 million years old, and at site 651 the basement is unexpectedly complex — a cap of basalt flows overlies peridotite, a rock type normally associated with the Earth's upper mantle. Sampling the igneous basement and dating the overlying sediment at sites 650, 651 and 655 shows that the locus of oceanic accretion shifted through time from north-west to south-east, that is, towards the subduction zone.

The western Tyrrhenian Sea is a young, passive continental margin that was formed by stretching, faulting and subsidence of the continenetal crust. At site 654, we recovered a textbook example of a sequence of rock types that indicates a progressive transition through time from a continental to a marine environment. The rocks recovered from the bottom to the top of the hole are subaerial conglomerates overlain first by sandstone with oyster shells and then by open marine sediments. Subaerial, shallow-water and then deep-water environments ensue as the site sank relative to sea level. Lower on the continental margin, at sites 652 and 656, we again encountered evidence of significant subsidence within the oldest sediments drilled that appear to have been deposited

Co-Chief Scientists, Kim Kastens (Lamont-Doherty Geological Observatory) and Jean Mascle (Univ. Pierre et Marie Curie). ODP Staff Scientist, Christian Auroux (Texas A&M Univ.). Also Enrico Bonatti (Lamont-Doherty Geological Observatory), Christina Broglia (Lamont-Doherty Geological Observatory), James Channel (Univ. Florida), Pietro Curzi (Ist. di Geologia Marina Bologna), Kay Christian Emeis (Texas A & M Univ.), Georgette Glaon (Univ. de Provence), Shiro Hasegawa (Tohoku Univ.), Werner Hieke (Technische Univ. München), Georges Mascle (Univ. de Grenoble), Floyd McCoy (Lamont-Doherty Geological Observatory), Judith McKenzie (Univ. Florida), James Mendelson (MIT), Carla Muller (Univ. Frankfurt/Main), Jean-Pierre Rehault (Univ. Pierre et Marie Curie), Alastair Robertson (Univ. Edinburgh), Renzo Sartori (Ist. di Geologia Marina), Rodolfo Sprovieri (Ist. di Geologia, Palermo), Massimo Torii (Kyoto Univ.).

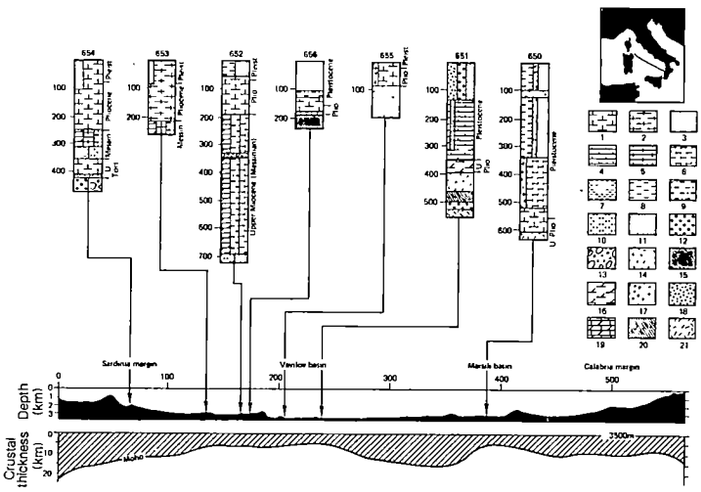


Fig. 2 Simplified lithological columns for each site are projected onto a bathymetric and crustal thickness cross-section of the Tyrrhenian Sea (cross-section after Steinmetz, L., Ferrucci, F., Hirn, A., Morelli, C. & Nicolich, R. *Geophys. Res. Lett.* **10**, 428; 1983). The position of the transect is shown in the insert. Symbols for lithological columns of sites 650–656: (1) nannofossil ooze; (2) nanno–foram or foram–nanno ooze; (3) calcareous ooze; (4) nannofossil chark; (5) nanno–foram or foram–nanno chalk; (6) calcareous chalk; (7) clay/claystone; (8) mud/mudstone; (9) sandy mud/sandy mudstone; (10) silt-siltstone; (11) sand/sandstone; (12) gravel; (13) conglomerate; (14) basic igneous; (15) pebbles and red carbonate mud matrix; (16) dolomite; (17) volcanic ash; (18) volcanic lapilli; (19) gypsum; (20) complex transition zone; (21) peridotite.

in a lake. Slumps, debris flows and small faults are common in the sediments deposited during subsidence and stretching of the crust. Subsidence seems to have occurred 1–2 million years later in the south-east (site 652) than further west (site 654).

The geological stages for the past 5 million years were all originally defined on the basis of outcrops around the Tyrrhenian Sea. These stages are now widely used outside the Mediterranean, but some doubt remains about the calibration between the boundaries of stratigraphic zones recognized in the Mediterranean Sea and the biozones of open oceans such as the Atlantic and Pacific oceans or Caribbean Sea. Thus, the third goal of Leg 107 was to recover nearly continuous sediment successions and to calibrate the various techniques used to date marine sediments. Such techniques are based on microfossils, reversals of the Earth's magnetic field, correlations of volcanic ash layers and ratios of stable isotopes contained in the sediments. Drilling at site 653, where we have successfully obtained two nearly continuous sequences of open marine sediments down to 5 million years old, should be suitable for this purpose.

Leg 107 has touched on many other geological subjects, including evidence for crustal heterogeneity, protrusion of upper mantle material, the chronology of volcanic ash layers, cyclic deposition of Messinian evaporites, the origin of organic-rich and metalliferous sediments, the definition of biostratigraphic boundaries and variation of heat flux through the sediment column. The Tyrrhenian Sea is clearly one of the best places for the study of many geological processes. Other areas of the Mediterranean Sea appear to hold similar promise. □

Parasitology

Spurious *Babesia* antigens

from F. E. G. Cox

A PROMISING approach to the development of a vaccine that would protect cattle against babesiosis has suffered a serious setback with the discovery that what seemed to be the dominant proteins recognized by the serum of babesiosis-infected animals merely reflect a host response to an inflammatory reaction[1]. Worse still, this discovery is a warning to parallel programmes of vaccine development against other parasitic diseases.

Babesiosis is an important tick-borne protozoal disease of erythrocytes in cattle, affecting several hundred million animals worldwide. Routine immunization can be achieved by vaccination with attenuated strains of the parasite[2] and there is also evidence that fractionated parasites can confer some protection[3]. The search for more satisfactory vaccines is currently following the procedures pioneered for malaria parasites — the identification of major antigens by immunoblotting techniques using immune sera, the isolation of the relevant messenger RNA, transcription to DNA and eventual cloning[4]. This kind of approach has attracted considerable attention and Australian scientists at the CSIRO laboratories at Indooroopilly in Queensland have over the past few years identified several antigens associated with *Babesia bovis*-infected erythrocytes that they now believe may be of host rather than parasite origin[1].

Calves with no history of babesiosis and with no detectable antibodies against the parasite were injected with turpentine to induce an acute inflammatory response. At the same time sera were collected from cattle immune to *B. bovis*. Nitrocellulose blots of *B. bovis* antigens treated with anti-babesial antisera from immune animals give rise to numerous reaction bands. The dominant bands revealed were of relative molecular mass 120,000–240,000 and were absent in similar antigen blots treated with control sera. But a similar test with sera from the turpentine-treated animals revealed the same bands. Precautions were taken to ensure that these reactions were not artefacts and the authors conclude that what are apparently *B. bovis* antigens can be detected by sera from animals experiencing a non-specific inflammatory reaction.

The conclusion from these experiments is that these dominant antigens recognized by specific immune sera cannot be of babesial origin, and furthermore that differences in their size range is consistent with their being isoantigens in genetically diverse cattle. Alternatively, these results may indicate interactions between babesias and naturally occurring autoantibodies. The authors suggest that, at the height of parasitaemia, the inflammatory reaction results in the release of acute-phase proteins simultaneously with the depression of the immune response to parasite antigens. Thus, the antigens recognized at this stage are those associated with inflammation and not infection.

These results also explain earlier findings that sera from uninfected cattle sometimes produce a positive immunofluorescence in the indirect fluorescence antibody test in which both *B. bovis*-infected erythrocytes and the parasites themselves fluoresce[5]. Overall, the significance of these findings is twofold. First, they pinpoint possible errors in immunodiagnosis; second, and most important, they suggest that immunoblotting techniques may identify spurious candidate antigens for the possible development of vaccines. This warning must be heeded in fields other than babesiosis for there have been reports that sera from uninfected animals react with various antigens of protozoan and helminth origin[6]. □

1. Goodger, B. V., Wright, I. G. & Waltisbuhi, D. J. *Experientia* **41**, 1577 (1985).
2. Callow, L. L. in *Blood Parasites of Animals and Man* (eds Miller, L. H. Pino, J. A. & McKelvey, J. J.) 121 (Plenum, New York, 1977).
3. Mahoney, D. F., Wright, I. G. & Goodger, B. V. *Prevent. vet. Med.* **2**, 401 (1984).
4. Godson, G. N. *Sci. Am.* **252**(5), 32 (1985).
5. Johnson, L. A. Y., Pearson, R. D., & Leatch, L. *Aust. vet. J.* **49**, 373 (1979).
6. Grogl, M. & Kuhn, R. E. *Fed. Proc.* **43**, 1421 (1984).

F. E. G. Cox is a Professor in the Department of Biophysics, Cell and Molecular Biology, King's College, Strand, London WC2R 2LS, UK

Predicting that comet Halley is dark

SIR—As I write this letter in early March only the scantiest information has come out of the Giotto mission. One of the most interesting preliminary findings was that comet Halley appeared to be quite dark. This may seem to be inconsistent with the high degree of reflectivity one might expect from an icy comet nucleus[1], implying that something extra is required to blacken the surface. I should like to show that a very low reflectivity is a predicted[2] and natural consequence of the comet nucleus being a fluffy aggregate of small solid intersteller particles[2] each of which is largely water ice and at least moderately reflecting. The reflectivity of the comet is low because it is an open structure and light which penetrates it is internally absorbed by being scattered many times by the individual small particles which are its components.

The first stage of interstellar particle coagulation in the presolar nebula which is assumed to lead ultimately to the comet nucleus is shown schematically in Fig. 1 by a model containing 91 individual particles. Each particle is a mean representative of a size distribution of interstellar grains which have fully accreted all the condensable molecules from the dense molecular cloud out of which the solar system was born. It consists of a silicate core, an inner mantle of complex organic refractory material which has evolved by ultraviolet photoprocessing over hundreds of millions of years before comet coagulation, and an outer mantle of volatile ices in which H_2O is dominant[3] and which contains S_2 molecules which could only have been produced in the interstellar dust before coagulation[4]. These particles are typically ~ 0.5 μm thick and at least three times as long[5]. Imbedded in the outer mantle are many small (~ 0.01 μm radius) particles (some strongly absorbing) which show up in space as blocking the ultraviolet radiation of stars[6].

The porosity shown in Fig. 1 was derived by comparing the density of comet dust with the mean density of meteors which are known to be comet debris. Although the mean density of the non-volatile silicate core–organic refractory mantle interstellar grains (no outer icy mantle) is about 1.9 g cm^{-3}, a characterisitic mean meteor density of 0.2 g cm^{-3} is observed[7]. This obviously implies a high degree of porosity. The organic refractory component is the largest part of the comet dust after the volatiles evaporate. Taking into account the volume of volatile ices in the precometary dust (and thus in the original comet matter) one arrives[2] at a mean packing factor for the comet of no more than about 0.4 (60% empty space). This is what has been pictured for the 4 μm aggregate in Fig. 1. An even fluffier comet nucleus structure is probable since the meteor particles must undergo some collapse after evaporation of the volatile components[8].

It is therefore reasonable to approximate the light scattering by a comet as if it were a cloud of small particles each of which is characterized by an albedo α and a scattering asymmetry factor g. The individual particle albedo is defined as the ratio of the light scattered by the particle to the light it both absorbs and scatters (no absorption: $\alpha = 1$; total absorption: $\alpha = 0$). The asymmetry factor, defined as the mean value of the cosine of the scattering angle, is essentially the difference between the forward scattered and the backward scattered light (spherically symmetric scattering: $g = 0$; no back scattering: $g = 1$). At visual wavelengths the normal interstellar grains (no icy coating) have an albedo $\alpha = 0.6 \pm 0.1$ and an asymmetry factor $g = 0.8 \pm 0.1$ (ref. 9). It is a well known property of the scattering of light by small particles that in the size to wavelength range of interstellar dust, a further increase of particle size by the addition of icy mantles leads to an increase in the asymmetry factor up to $g = 0.9$ (ref. 10). The very strongly forward directed scattering implies that light impinging on a particle at the comet surface mostly continues inward where it may be absorbed by repeated scatterings within the body.

Let the forward and backward scattering fractions be F and B so that $F + B = 1$. Using $g = F - B$ the backward scattered fraction is $B = (1-g)/2$. Since only a part, α, of the incident radiation per particle is scattered and, since we shall assume that all the forward scattered radiation is lost, the net back scattering by the sum of the individual particles filling the surface of the comet is the total reflected light. This gives a reflectivity of $A = \alpha\,(1-g)/2$. So for $\alpha = 0.6$ and $g = 0.9$ only about 3% of the light is reflected. This simple but physically reasonable approximation for the reflectivity matches remarkably closely the value $A = 0.028$ obtained from very accurate calculations of Van De Hulst[11].

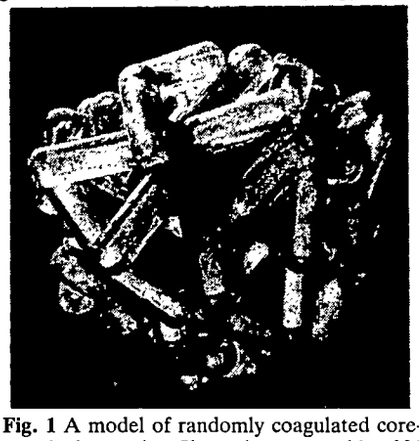


Fig. 1 A model of randomly coagulated core-mantle dust grains. Shown is an ensemble of 91 particles incorporating within their outer icy mantles the very small particles of the interstellar dust population accreted in the final stages of condensation. The degree of volumetric packing is 0.4 (60% open space) and the overall dimension is scaled to about 4 μm.

For the same reason, large comet dust particles should similarly exhibit low reflectivities, as may have been detected in comet Crommelin[12]. Judging by the high infrared emissivity of interplanetary particles well beyond the Earth's orbit (S.S Hong, personal communication) they too, as young comet debris, are highly absorbing because of their fluffy character.

Other critical predictions of this model of the nucleus are: (1) A preponderance of the organics C, O, N relative to the rocky elements Si, Mg, Fe by a factor of five or greater in comet dust grains because of the initially high ratio of the organic refractory to silicate volume in the interstellar core-mantle grains[2]. (2) Individual core-mantle particles of order 0.15 μm radius and mass about 3×10^{-14} g resulting from aggregate breakup. (3) A very large number of *very* small (~ 0.01 μm) particles of mass of about 2×10^{-17} g released from the evaporating icy material[13]. (4) A very low comet heat conductivity leading to high surface heating and a concomittant high vaporization rate due to the very porous surface area.

Should the Giotto and Vega missions confirm these predictions we may well be able to say that comets provide a direct observation of the interstellar dust as it existed 4.5×10^9 years ago and that a comet-nucleus-sample-return mission will accomplish what no amount of remote sensing of the interstellar medium will ever make possible.

J. MAYO GREENBERG

Laboratory of Astrophysics,
University of Leiden,
Wassenaaresweg 78, Postbus 9504,
2300 RA Leiden, Netherlands

1. Whipple, F. in *Cosmic Dust* (ed. McDonnell J. A. M.) 1–73 (Wiley, New York, 1978).
2. Greenberg, J.M. in *Comets* (ed. Wilkening L. L.) 131–163 (University of Arizona Press, Tucson, 1982), in *Asteroids Comets, Meteors* Vol. II (eds Lagerkvist, C.-I. Lindblad, B.A., Lundstedt, H. & Rickman, H.) 221–223 (Uppsala University Press, 1986).
3. Greenberg, J.M. in *Submillimetre Astronomy* (eds Beckman, J.E. & Phillips, J.P.) 261–306 (Cambridge University Press, 1982).
4. A'Hearn, M.F. & Feldman, P.D. in *Ices in the Solar System* (eds Klinger, J., Benest, D., Dollfus, A. & Smoluchowski, R.) 463–471 (Kluwer, Dordrecht, 1985).
5. Greenberg, J.M. in *Stars and Stellar Systems* Vol. VII (eds Middlehurst, B.M. & Aller, L.H.) 221–364 (University of Chicago, 1968).
6. Greenberg, J.M. & Chlewicki, G. *Astrophys. J.* 272, 563–578 (1983).
7. Verniani, F. *Space Sci. Rev.* 10, 230–261 (Reidel, Dordrecht, 1969).
8. Mukai, T. & Fechtig, H. *Plant. Space Sci.* 31, 655–658 (1983).
9. Savage, B.D. & Mathis, J.S. *A. Rev. Astron. Astrophys.* 17, 73–111 (1979).
10. Martin, P.G. *Cosmic Dust* (Clarendon, Oxford 1978).
11. Van de Hulst, H.C. *Multiple Light Scattering* Vol. 2, 369 (1985).
12. Hanner, M.S., Knacke, R., Sekanina, Z. & Tokunaga A.T. *Astron. Astrophys.* 152, 177–181 (1985).
13. Greenberg, J.M. *Adv. Space Res.* 4, 211–212 (1984).

Multiple sclerosis, viruses and glycolipids

SIR—For many years now, and again recently in *Nature* (**318**, November 1985 p101, p104, p154), there has been speculation as to the role of viruses in multiple sclerosis (MS). MS is often considered to be an autoimmune disease initiated by infection; the question has always been and remains, which of the many viruses implicated causes the disease? One possibility, which has perhaps not received sufficient attention, is that MS could be caused not by just one virus but by many enveloped viruses acting together or individually.

All the viruses that have been implicated in MS are capable of infecting the nervous system, and all are enveloped viruses. The membrane of an enveloped virus reflects that of the cell from which it has budded. Indeed it has been suggested that such viruses may be able to trigger autoimmune reactions by the incorporation of host protein into their viral envelope but, with a few possible exceptions, the budding virus takes only the virally-coded proteins which have been inserted into the cell membrane, and the lipid molecules surrounding them. It is the host-cell derived lipid molecules that could be the key to the problem.

The lipid molecules of cell membranes have suffered for too long by being represented as the homogeneous tadpole-like molecules of the cell membrane. In fact they are far from being homogeneous in either their biochemistry or their distribution. Neither are these molecules immunologically inert, they are haptens and can under the right circumstances induce an immune response.

In recent years it has been shown that antibodies to glycolipids are detectable in MS patients[1], that such antibodies can demyelinate cerebellar tissue cultures[2], that T-cell reactivity to glycolipids is present in MS patients[3], and relatively specific to this disease[4], and that rabbits inoculated with glycolipids succumb to a demyelinating encephalomyelitis[5]. Thus it is clear that anti-glycolipid activity is of importance in demyelinating disease.

The question is, how does this anti-glycolipid activity arise? One possibility, as we have suggested previously[6], centres on the possibility that budding viruses can initiate an immune response to glycolipids. We have shown that infection of mice with the budding, avirulent RNA, Semliki Forest virus induces a T-cell dependent demyelinating encephalomyelitis[7], although it is not yet clear whether the T-cells responsible for the demyelination react against viral or self antigens on the surface of central nervous system (CNS) cells and myelin. The virus replicates in CNS cells including oligodendrocytes, host-cell glycolipids are incorporated into the viral envelope[8], and these glycolipds are accessible to antibodies[9]. Infection with the virus and inoculation of inactivated brain derived virus both give rise to anti-glycolipid antibody (S. Amor and H.E.W., unpublished observations).

It is possible that several neurotropic budding viruses have the ability to replicate in the same CNS cell-type (for example oligodendrocytes) and on budding from this cell incorporate into their viral envelope the same host-cell glycolipid (for example galactocerebroside). It is possible that such a glycolipid (normally a hapten), associated on the surface of the virus with the 'foreign' carrier antigens of the viral proteins could be antigenic. In an MS susceptible individual, infection of the CNS with one of the many possible enveloped viruses could trigger an anti-glycolipid immune reaction, leading to demyelination and a first attack of MS. Subsequent relapses in MS, already known to have an association with intercurrent infection, could result from restimulation of the same anti-glycolipid autoimmune response following CNS infection with other enveloped viruses.

Perhaps in the search for the cause of MS, more attention should be given to the possibility that viral envelope glycolipids could induce an immune mediated demyelination, and by the immunologists to the possibility that this may trigger an autoimmune encephalomyelitis.

J.K. FAZAKERLEY
H.E. WEBB

Neurovirology Research Unit,
The Rayne Institute,
St Thomas' Hospital,
London SE1 7EH, UK

1. Arnon, R. *et al. J. neurol. Sci.* **26**, 179 (1980).
2. Dubois-Dalcq, M., Niedieck, B. & Buyse, M. *Path. eur.* **5**, 331 (1970).
3. Offner, H., Konat, G. & Sela, B.A. *J. neurol. Sci.* **52**, 279 (1981).
4. Ilyas, A.A. & Davison, A.N. *J. neurol. Sci.* **59**, 85 (1983).
5. Konat, G. *et al. Acta neurol. Scand.* **66**, 568 (1982).
6. Webb, H.E. & Fazakerley, J.K. *Neuropathol. appl. Neurobiol.* **10**, 1 (1984).
7. Fazakerley, J.K., Amor, S. & Webb, H.E. *Clin. exp. Immun.* **52**, 115 (1983).
8. Webb, H.E., Mehta, S., Leibowitz, S. & Gregson, N.A. *Neuropathol. appl. Neurobiol.* **10**, 77 (1984).
9. Evans, N.R. & Webb, *J. neurol. Sci.* (in the press).

Ventral activation process in insect oocytes

SIR—In a recent *News and Views* article Woodland and Jones reviewed genetic evidence of an active ventral region in establishing the dorsoventral polarity and hence pattern in *Drosophila* eggs[1]. In particular, various recessive — and presumably loss of function — genes are all dorsalizing: not only the genes so lucidly discussed by Woodland and Jones but also the remarkable *K10* gene. Unlike the other dorsal mutants, *K10* acts on the growing oocyte so as to largely symmetrize the early movements of its follicle cells. Thus it produces an egg largely devoid of dorsoventral asymmetry in its shape and shell as well as dorsalizing its embryo[2,3]. Thus lack of *K10* function seems to disable the mechanisms for establishing a dorsoventral gradient. Since it does so by disabling some ventrally localized process, it acutely raises the question of just what this ventral process is.

A clue to this was provided by Kunkel in a study of an analogous growth stage of the cockroach oocyte[4]. He has discovered the presence of large, steady electrical (and thus ionic) currents entering its ventral region. Comparable steady currents rather generally enter regions of developmental action, and in the best studied case — that of the fucoid egg — they seem to establish this region by raising free calcium there[5,6]. So Kunkel's observations suggest that a key early event in *Drosophila* pattern formation is an influx of cations into its ventral region which raises free calcium there, activating gene products like those of *Toll*.

This hypothesis also suggests an explanation for the rather puzzling fact that *Toll*$^+$ cytoplasm from *anywhere* in the egg nevertheless induces a ventral region near the site of injection. Perhaps the *Toll*$^+$ precursor postulated by Anderson *et al.*[7] is artificially activated *during transfer* by contact with the high calcium found in the perivitelline fluid of the *Drosophila* egg[8]. This subsidiary hypothesis predicts that the ability of *Toll*$^+$ cytoplasm to rescue *Toll*$^-$ eggs would be greatly reduced if it were transferred in a way which somehow avoided any transient rise in its free calcium concentration. This postulated artefactual rise would be analogous to the rise in calcium which can destroy the so-called primary cytostatic factor in the cytoplasm of frog eggs[9].

In any case, the main hypothesis predicts the presence of a free calcium gradient across the dorso-ventral axis of the growing insect oocyte with free calcium high along its ventral face. This predicted ventral high calcium zone would be analogous to that already seen — with the aid of aequorin — at the vegetal pole of the early medaka fish egg.[10].

L.F. JAFFE

Marine Biological Laboratory,
Woods Hole,
Massachusetts 02543, USA

1. Woodland, H.R. & Jones, E.A. *Nature* **319**, 261 – 262 (1986).
2. Wieschaus, E. in *Cell Lineage, Stem Cells and Cell Determination* (ed. Le Douarin, N.) 291 – 302 (Elsevier, Amsterdam, 1979).
3. Haenlin, M., Stellar, H., Pirrotta, V. & Mohier, E. *Cell* **40**, 827 – 837 (1985).
4. Kunkel, J.G. in *Ionic Currents in Development* (ed. Nuccitelli, R.) 165 – 172 (Liss, New York, 1986).
5. Jaffe, L.F. in *Membrane Transduction Mechanisms* (eds Cone, R.A. & Dowling, J.E.) 199 – 231 (Raven, New York, 1979).
6. Brownlee, C. & Woods, J.W. *Nature* **320**, 624–626 (1986).
7. Anderson, K.V., Jurgens, G. & Nusslein-Volhard, C. *Cell* **42**, 799-789 (1985).
8. Van der Meer, J.M. & Jaffe, L.F. *Devl Biol.* **95**, 249 – 252 (1983).
9. Masui, Y., Meyerhof, P.G. & Miller, M.A. *Symp. Soc. dev. Biol.* **38**, 235 – 256 (1980).
10. Jaffe, L.F. *CIBA Symp.* **122** (in the press).

The hungry sheep look up

Walter Gratzer

How to Obtain Biomedical Research Funding. Edited by J.T. Dingle.
Elsevier Applied Science: 1986. Pp.56. Pbk £5.95, $10.

A NEW cottage industry appears to have established itself around the sleazier fringes of science in America, and I take it for an omen of the times: announcements have been appearing on notice-boards around the country proclaiming one- and two-day seminars ($200 a throw seems about average) on how to write successful grant applications. Now it must surely occur to all takers that the performers at these events have entered the business of explaining to other people how to get grants only because they have not lately managed it themselves. They are bald men selling hair-restorer. Successful scientists will in general be too busy insuring against failure the next time round. And besides, as Logan Pearsall Smith observed, "few things are more shocking to those who practice the arts of success than the frank description of those arts".

So what have we here? This appears to be the first guide to working the British grant market, and let me quickly add that I have no doubt the three highly respected scientists, who have contributed to this slender paperback (4 mm in its covers), all have abundant grant support, and no idle half-hours to fill for pecuniary gain. What then has motivated their endeavour? Not, for the most part, any unusual luminosity of insight. Slim this volume may be, but there are still indications of a certain desperation in the efforts to give value. The kind of advice that the editor, Dr J.T. Dingle, dispenses is too often along the lines of ". . . it must be concise, to the point and interesting". How so? Why, doctor, because "a dull and repetitive introduction, a turgid summary and incomprehensible experimental detail will not improve the chances of even the most original idea being accepted". Four pages on we are enjoined to "try to be concise and organise one's arguments in short but cohesive sentences", and on the next page, "the summary should state precisely and clearly the objectives of the study". Well, you could have knocked me down with an RG2A application form!

Dr J.L. Gordon from the Clinical Research Centre weighs in with a chapter about the referee's view of grant applications. "What", he asks, "determines whether a referee will agree to review an application?". And he has the answer: "he has to ask himself two questions: first, is this my field? And secondly . . ."; but there, I shall not spoil the impact of the narrative by giving away any more. You must buy the book.

Matters look up with the eruption onto the scene of Professor Jack Lucy, who gives a wholly convincing and distinctly diverting account of how the deliberations of a Medical Research Council Grant Committee might go, confronted with a typical (though imaginary) application. Here are two of the eleven evaluations by the committee members. Number 7 opines that

The applicant has worked in this field for many years but of late there have been diminishing returns. It seems highly likely, unless a new approach is developed, that there is little prospect of this research yielding any observations of significance, and it is suggested that the applicant might be advised that the most likely way of obtaining a further insight into this problem is by gene cloning.

And Number 8:

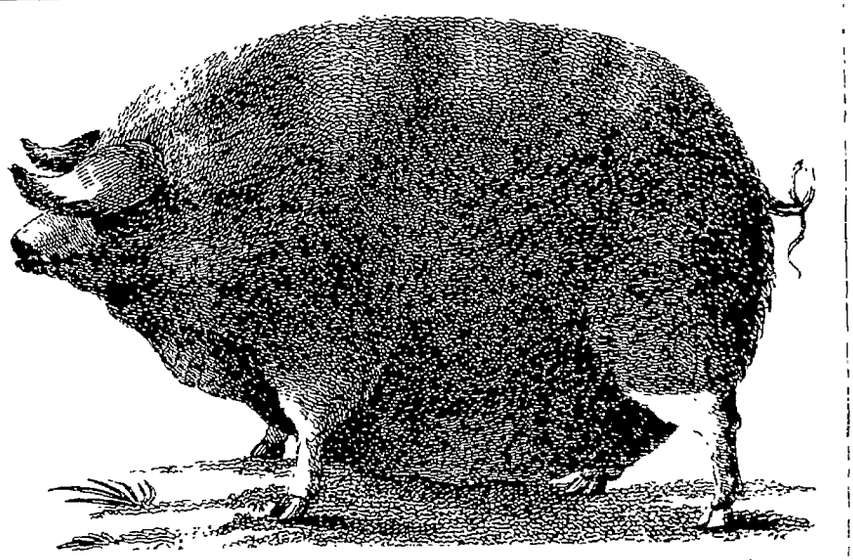
The applicant has a good record of many years of research in this field but now, quite correctly, judges that — if much further progress is to be made in this area — the newer techniques of recombinant DNA technology and site-directed mutagenesis need to be employed. Unfortunately, the applicant has no experience at all in the use of these techniques . . .. I therefore have serious reservations regarding the viability of this otherwise potentially-interesting project.

The ring of truth is unmistakable. This is much more the kind of thing one is looking for.

The last twenty pages of the book are by administrators, and there are no laughs but lots of information. They explain how the MRC and the private charities operate their grant systems, and an appendix lists eighty organizations that will disburse the moola when appropriately stimulated.

This small book then could with advantage have been even smaller, but it will have its uses. One question lingers in the mind: allow for the moment that such a publication as this might contain the key that will unlock the strong-room. Will it then work for the common weal? The Law of Conservation of Matter must surely operate: what each purchaser of the book collects will be snatched from you and me, and have we not all seen the undeserving flourish, yea, as the green bay tree in fact? I would incline to the view that those who cannot work out for themselves that the summary should be clear, concise and fit into the box provided, would do better selling stock in biotechnology, or even explaining to anxious young scientists How to Obtain Biomedical Research Funding.

Walter Gratzer is in the Medical Research Council's Cell Biophysics Unit, King's College London (KQC), 26–29 Drury Lane, London WC2B 5RL, UK.



Fat pig — the illustration, from an agricultural survey of Staffordshire in 1796, is of an animal that was 802lb liveweight at the age of 2½ years. It was by no means the largest recorded. The tendency towards breeding pigs that became excessively fat at a relatively young age began in the late eighteenth century with the introduction of early-maturing foreign breeds to Britain. Because of the demands of the show-ring and the lard industry, the problem became progressively worse through the nineteenth century: one judge at the Royal Show in 1881 felt obliged to comment that "it is painful to see the prostrate masses of fat grunting and sweating under a weary life in the heat". Such opinions went unheeded, many breeds became extinct and the British pig industry suffered accordingly. The picture and historical details are taken from Julian Wiseman's entertaining and informative book A History of the British Pig, *newly published by Duckworth. Price is £12.95.*

Crystallographers' proteins

Kenneth C. Holmes

Diffraction Methods for Biological Macromolecules, Parts A and B. Methods in Enzymology Vols 114 and 115. Edited by Harold W. Wyckoff, C.H.W. Hirs and Serge N. Timasheff. *Academic: 1985. Part A pp.588, $70.50, £59. Part B pp.485, $66.50, £50.50.*

THE structural investigation of protein crystals by X-ray diffraction started in 1934, when J.D. Bernal and Dorothy Crowfoot Hodgkin first successfully photographed a crystal of pepsin. The resulting X-ray diffraction patterns contained so many Bragg reflections that they resisted all known methods of interpretation for 20 years, until Max Perutz was able to show that the small changes in X-ray intensities induced by binding two mercury atoms per molecule of haemoglobin were enough to determine the phase of each reflection. With phases, the electron density can be calculated, albeit by evaluating a Fourier series of around 10,000 terms at each of 100,000 lattice points! Another five years elapsed before John Kendrew's team could carry out a Fourier synthesis for myoglobin to atomic resolution, revealing for the first time the intricacies of the three-dimensional structure of a protein.

Kendrew used programs devised to run on the Cambridge Mathematical Laboratory's EDSAC II. Without such a machine the calculation of the electron density of myoglobin would have been virtually impossible; indeed, the growth of protein crystallography is intimately entwined with the development of the computer.

In the 1950s, because of the influence of Sir Lawrence Bragg and the activities of Perutz and Kendrew, protein crystallography was synonymous with the Medical Research Council unit in the Cavendish Laboratory. (Later, other centres appeared, but even these, in most cases, trace back in apostolic succession to Bernal or Bragg.) In the late 1950s and 1960s, then, a stream of (mostly American) post-doctorate students descended on the MRC unit and worked feverishly to turn protein crystallography into an established science worthy of associate professorships. Now they and their acolytes, and some converts, have written it all down.

The articles in the resulting two volumes are rather technical or mathematical. They are also somewhat uneven in type, ranging from user's guides for various program packages to some thoughtful review papers. Thus, while specialists will find a wealth of useful detail here, those less familiar with the field could have trouble finding their way around. The contributions are grouped in sections: history (an engrossing article by Perutz); crystallization (the nearest we get to wet biochemistry); data collection; phasing; model building; and presentation of results.

Michael Rossmann, who was in at the start on EDSAC II, contributes a detailed and informative chapter on oscillation photography. Other mandarins also make interesting contributions: Fred Richards concerns himself with the problem of defining protein surfaces and, besides, reviews his folly. David Stuart and David Phillips present an excellent analysis of thermal motion and its relationship to molecular dynamics — otherwise hardly mentioned. Hal Wyckoff, also an editor, has provided a definitive review of diffractometry. Jane Richardson's stylized drawings of proteins are truly beautiful, while Lynn Ten Eyck deserves a prize for the most concise account of X-ray diffraction. A summary of the least-squares method has been contributed by Robert Sparks, though this is somewhat out of place in the "phasing" section. No less than 12 articles use the least-squares method and the consistent adoption of Sparks's notation throughout the book would have helped clarity.

The article by Joel Sussman on constrained least-squares refinement reawakened my memories of 1963, when Carl Branden and myself battled with an IBM 7090 for 16 hours to achieve one cycle of constrained refinement of myoglobin. Progress indeed! Once or twice elsewhere I experienced *déjà vu*; for example, mirror benders turn up attributed to all and sundry, but not to Tony Woollard who actually developed the present design in Cambridge. This reflects the fact that in the heady years of the 1960s the rate of innovation outstripped the rate of publication. The present volumes redress the balance with a little to spare. □

Kenneth C. Holmes is Chairman of the Max-Planck-Institut für Medizinische Forschung, Jahnstrasse 29, 6900 Heidelberg, FRG.

The common quest

A.R. Rees

Growth Factors and Transformation. Edited by James Feramisco, Brad Ozanne and Charles Stiles. *Cold Spring Harbor Laboratory: 1985. Pp.450. Pbk $70.*

IN its application to the study of oncogenic transformation, the inductive approach to science has perhaps come under closer scrutiny than in any other area of biology. While it is generally agreed that cancer is not a single disease, this has not prevented researchers from assuming that common mechanisms will emerge if we just look long enough and hard enough. This is by no means obvious. For example, that tyrosine phosphorylation is a causal event in transformation was and remains an attractive hypothesis; but there is still not a single example in which specific substrates of tyrosine kinases can be said to play a key role in the transformation process, although the presence of the kinase itself is often sufficient to transform the target cell. Even if plausible mechanisms for oncogenic transformation were to emerge, we are still left with the problem of how they would relate to transformation *in vivo* — despite the fact that some 30 oncogenes have been characterized that originate within the cell and 10 or so others from within oncogenic viruses.

It was against this background that, in the autumn of 1984, Cold Spring Harbor Laboratory organized its meeting on growth factors and transformation. The subject matter in the resulting book is arranged loosely into chapters, the first five of which survey the properties of growth factors (epidermal growth factor, transforming growth factors, insulin and the related insulin-like growth factors, platelet-derived growth factor and its oncogenic relatives, and, finally, the lymphokines). The second half of the proceedings is devoted to oncogenes and kinases, with a concluding chapter entitled "Futures". In the main each author provides an integrated account of the interplay between growth factors and oncogenes, but the existence of genes for which a growth factor connection (or in some instances, function) has not been established necessitated their collection into the separate chapter on oncogenes. For a number of these oncogenes (E1A, Ha-*ras*-1, c-*fos*, c-*myb*, for example) this biological apartheid would still be necessary.

There are always things to be said for and against conference proceedings, even up-market productions such as those emanating from Cold Spring Harbor. In a fast moving field like this, speed is crucial. Unless the proceedings appear within six months they are generally of dubious value to research workers, though they may be useful as background reading for those at the periphery. *Growth Factors and Transformation* appeared in Britain almost a year after the conference. This delay would have mattered less if some of the chapters had not been quite so repetitive. And this criticism might have been redundant if the meeting itself had not been so parochial — only four papers were contributed by groups working wholly outside the United States.

The repetitive element is at one of its high points in the opening chapter on epidermal growth factor, and is also a feature

of the three c-*fos* papers in the "Oncogenes" chapter. For all that, the discussions of the manner in which some transformed epithelial cell lines and their *in vivo* analogues seem genetically predisposed towards either aberrant or overexpression, or both, of EGF receptor transcripts suggest a potentially important correlate of epidermoid malignancy. The more mechanistic aspects of the action of EGF and other growth factors are presented in the "Kinases" chapter. Here the particular role of tyrosine kinases is explored, alone and in their relationship to that possible arbiter of tumour promotion, protein kinase C. It is here also that an organizational eccentricity placed the second of the two related accounts of phosphorylation of 40S ribosomal protein S6, the first being in the opening chapter on EGF.

If we are to take the "Futures" title of the concluding chapter literally, then we are faced with the prospect that studies of certain phenomena — Na^+/H^+ exchange, mitochondrial responses to growth factors, and growth factor effects in systems such as embryonal carcinoma and the developing nervous system — are the subjects of the future. In fact the manner in which growth control signals are developmentally regulated is an undeniably important area of research. But with the exception of the first paper in this chapter (which explores the thesis that "in the future it is likely that the level of biochemistry of cell proliferation, not as well developed now, will become ever more important"), the conclusion is a rather mixed bag of topics that the organizers obviously could not easily fit in elsewhere.

Many of the presentations in this volume are well worth reading, and the book should certainly be in every library pretending to cover the literature on cancer. Whether individuals in the field will find it of much value, I doubt, because most of the data it contains have now been published or even superseded. Non-specialists, however, may find the book a helpful summary of current problems in oncogene research and of the type of experimental approaches that are available to pursue the search for that elusive Holy Grail — the common mechanism. □

A.R. Rees is a Lecturer in the Laboratory of Molecular Biophysics, Department of Zoology, University of Oxford, South Parks Road, Oxford OX1 3QU, UK.

New in paperback

- *The Musical Mind*, by John A. Sloboda. Publisher is Clarendon, price is £9.95, $17.95. For review see *Nature* **315**, 696 (1985).
- *The Computer Comes of Age*, by R. Moreau. Publisher is MIT Press, price is $9.95, £9.95. For review see *Nature* **312**, 572 (1984).
- *The Stars and the Stones: Ancient Art and Astronomy in Ireland*, by Martin Brennan. Publisher is Thames & Hudson, price is £7.95. For review see *Nature* **306**, 516 (1983).

Down to the bones

Bernard Wood

The Human Skeleton. By Pat Shipman, Alan Walker and David Bichell. *Harvard University Press:1986. Pp.343. $27.50, £23.50.*

THE very word "skeleton" has macabre, if not sinister, associations, and its colloquial use also betrays our perceptions of the human frame; we have all experienced privations in hotels which have been excused by muttered references to the "skeleton" staff. Traditional (by which I mean old-fashioned) medical courses did little to enhance the image. Students were drilled in detailed osteology and every bony lump, bump, nook, cranny and crevice had a name which had to be memorized. Such minutiae provided aggressive examiners with the necessary ammunition to trip up even the most nimble student, but had few other merits for a general undergraduate education in anatomy. It is not surprising that the efforts of physiologists and biochemists to enliven teaching on the skeleton by reference to its metabolic relevance made little headway against this type of introduction.

The image of the skeleton is changing, and this book will help hasten the process. Research on the structure and function of hard tissues, at the levels of cell biology and whole animal studies, are invigorating our attitude to both bone and bones. The authors are particularly well-qualified to provide an applied and broad biological perspective on their subject matter. Pat Shipman has pioneered rigorous methods for assessing the implications of marks on bones found at archaeological sites, while Alan Walker has carried out innovative analyses of primate behaviour and has made important contributions to palaeoanthropology and palaeopathology. Their colleague, David Bichell, is an artist who is trained in anatomical drawing.

The book is in three sections. The first deals with the components and organization of bone and discusses its physical properties. The central, and largest, section is a series of regionally-based descriptions of the form of the normal skeleton, augmented by succinct, but useful, presentations of integrated activities such as breathing, walking and chewing. The third section covers the ways in which the skeleton, and its components, can be used in forensic and anthropological research. Predictably, the chapter on skeletal pathology is a strong one, and it was sensible to include an account of the structure and identification of teeth.

In terms of scientific content, the authors have wisely eschewed the exotic. One of the book's strengths is that it presents sound skeletal biology in a way that will stimulate students to learn more for themselves. The style is such that quite complex principles and ideas are introduced and discussed without intimidating the reader. There is little doubt that this volume will have a long life, and in any new edition the authors might consider setting the vertebrate skeleton in an even broader context than they have done. Their classification of joints is traditional and, for all its apparent complexities, they might consider making more explicit reference to MacConaill's analysis of joint surfaces.

For those of us who bemoan the demise of Le Gros Clark's *Tissues of the Body*, this new book provides a helpful account of hard tissues and the skeleton. Other textbooks and reference works will be needed to provide extra detail, but few are likely to offer a more stimulating introduction to the subject than that set out by Shipman, Walker and Bichell. □

Bernard Wood is Derby Professor of Anatomy at the University of Liverpool, PO Box 147, Liverpool L69 3BX, UK.

New journals review



On 25 September *Nature* will publish the sixth annual review supplement devoted to science journals.

Criteria for inclusion of a journal in the 1986 issue are that:

(i) the first number appeared, or the journal was retitled, *between June 1984 and May 1985* (the second cut-off date allows at least three issues of a journal to have been published, the minimum number on which a reasonable judgement can be based);

(ii) it is published at least three times a year;

(iii) the main language used is English.

Publishers and learned societies are invited to send *four different issues of each suitable periodical, including the first and most recent numbers* (if from outside the United Kingdom, by air mail) to The Review Editor, *Nature*, 4 Little Essex Street, London WC2R 3LF, England. Subscription details for both 1986 and 1987 should be included.

Newts and nuclear winters

John H. Lawton

The Machinery of Nature. By Paul R. Ehrlich. *Simon & Schuster: 1986. Pp.320. $18.95.*

I MUST confess to breaking the law by catching great-crested newts, lovely, ugly creatures with orange bellies, warty backs and crests like those of a dragon. Under the British Wildlife and Countryside Act, catching great-crested newts even to admire them is now illegal, because they are rare, declining in numbers and endangered. So you need a permit to fish for them, and I didn't know. I do now, and promise to behave myself in future. But it is very sad; as a schoolboy I caught "water dragons" easily and kept them for a time in an old sink. There is nothing like having a dragon in the kitchen for learning about biology. Now it is illegal.

So what? Book reviews do not usually start with confessions of guilt, even of little crimes. There is however a purpose in my confessions, because these muddy little creatures symbolize the problems that confront conservationists as we struggle to hold back mankind's creeping extermination of thousands of endangered species throughout the world. We do not even know how many species of plants and animals there are, nor exactly how many have already been lost through human activities. We do know that the pace of exterminations is rising and that we need to take ever-more drastic steps to stop it. Laws against catching newts are a drop in the ocean compared with the action that needs to be taken. Which brings me logically, if indirectly, to Ehrlich's book.

The Machinery of Nature has several themes. One is an eloquent plea for a halt to the inexorable, blind destruction of the species of plants and animals that are the newt's and our fellow travellers on this planet, because some of them are beautiful and others are useful. But most are neither; we must conserve them simply because they are there, and because we do not know what they do and have only the sketchiest idea about how the machinery of nature really works. Once we have taken the machine to pieces and lost some of the bits, we should not gamble on being able to put it back together again. The biggest immediate threat comes from the growing human population, rising expectations and grubby, creeping degradation of all that is varied and beautiful in nature. But instant, cataclysmic destruction in the inconceivable horror of a nuclear war and the freezing terror of a nuclear winter is also a stark possibility, and is a second, recurring theme of the book. A third is the excitement and uncertainty of doing science, mixed with a passionate love of natural history — the newts-in-the-kitchen syndrome. Last is a plea for more funding for ecological research. How can we possibly understand the machinery of nature on miniscule budgets that are a direct result of government indifference to environmental science?

The components of the machinery as Ehrlich sees them are the usual mix of population ecology and evolution, sociobiology, "two-species" interactions (predation and so on), biogeography and the dynamics of communities and ecosystems, constrained by the physical environment. However this is no ordinary ecology textbook. What it aims to do is explain the science of ecology to the layman and to our political masters. The intention is fundamentally to change attitudes about what we can and cannot do to the planet and get away with; it is a scientific manifesto for the Green Party, written by a first-class scientist.

The book is certainly well written, although it does have some distracting features. One is Ehrlich's tendency to describe his friends, associates and graduate students as brilliant, and by default mark everybody else beta minus. It is clearly done to enliven and humanize the science; I found it mildly irritating. Also the chapters are too long and sometimes lack a sense of direction; basically they are walks through natural history and the science of ecology, with the path frequently deflected in unexpected, albeit interesting directions. My preference is to know where I am going, and why.

One criticism is more substantial. Ehrlich is American and the book is directed explicitly at his fellow countrymen. Yet the problems it addresses are global and concern everybody. It makes no sense to talk just to Americans, even though (for several reasons) that may be a good place to start.

Will the message have any effect? I hope so, but fear not. It has been preached many times before to little or no avail. For example, by coincidence I recently came across this:

> It is very certain that the earth is not the chief body in the material universe, and that the world is not subordinate to man's use. It is even more certain that nature is the expression of a definite order with which nothing interferes, and that the chief business of mankind is to learn that order and govern themselves accordingly.

The writer was Thomas Henry Huxley in 1880.

One hundred years later the message is the same but much more urgent. Whether the majority of mankind understand it well enough to respond is another matter. It takes time and effort even to start to understand the machinery of nature, and most decision-makers and politicians do not have that time, or care too little to find it. But the problem goes deeper than that. It is one thing to educate lay people about ecology, even assuming that they might be interested. It is quite another to translate that knowledge into a workable political philosophy, and even harder to put it into practice. Indeed, one reason why the great surge of environmental consciousness that swept through the 1960s fizzled out was because it was politically naive. With millions out of work in Europe, still more starving in Africa, grinding poverty, social unrest, terrorism and super-power confrontation, who cares about newts? The problem is getting decision-makers to understand enough of the machinery of nature to realize that we are slowly degrading the life-support systems of the planet, without being able to predict when things might start to go badly wrong (assuming that they haven't already) and to take a longer view about what is important. We also have to translate environmental science into practical, realistic political policies and, in Huxley's words, govern ourselves accordingly. Ehrlich's book is an attempt to educate, but it has nothing to say about welding science to practical politics.

Of course there is general agreement about some issues. Only lunatics want a nuclear war. Yet the body politic is conspicuously unable to reduce, let alone get rid of nuclear weapons. So we pass laws protecting newts, fiddling quietly whilst Rome teeters on the edge of the holocaust. Worse, we do not even take the laws that we have to protect nature as seriously as we should. It is irritating to have to change your behaviour or, worse, abandon a road-building project for the sake of a newt. Yet if rich, developed nations cannot look after their remnants of wild nature, how on Earth can we expect some of the poorest countries in the world to conserve great rain forests, coral reefs or swamps? Who is going to pay to keep the lions wild, and the deserts at bay?

The forces ranged against conservation are formidable. Some of them are evil, some greedy, some both. But most are simply ignorant of the dangers, and too preoccupied with the problems of today to care about the next generation. I do not pretend for a minute that Ehrlich's book will transform the picture overnight, or even over the next decade. But it will help to educate the growing number of people who want to know about the machinery of nature, and about the stark choices that confront mankind between now and the end of the century. Whether you are concerned about newts or nuclear winters, there must be a better way to manage the planet. The price of failure doesn't bear thinking about. □

John Lawton is a Professor in the Department of Biology, University of York, York YO1 5DD, UK.

Space observations of comet Halley

from John C. Brandt

Following the encounters by Soviet, Japanese and European spacecraft, the International Cometary Explorer took measurments of comet Halley on 22 March. The comet has also been observed by the Solar Maximum Mission, the International Ultraviolet Explorer, the Pioneer Venus Orbiter, the Dynamics Explorer 1, and by sounding rockets.

FOR several days before and after its encounter with comet Giacobini–Zinner on 11 September 1985, the International Cometary Explorer[1] (ICE) measured disturbances in electric and magnetic fields and energetic ions. Because the total gas production rate of comet Halley was expected to be 10 times higher than comet Giacobini–Zinner, direct measurements of comet Halley became plausible (see Fig. 1). This expectation was realized on 22 March 1986 at a distance of $\sim 35\times10^6$ km. Thus, ICE, the sixth spacecraft to measure comet Halley (the Giotto encounter occurring on 14 March), both opened and closed the first chapter in the direct exploration of comets.

Measurements of magnetic field fluctuations clearly associated with the comet are shown in Fig. 2. The data are from the plasma wave experiments on ICE (principal investigator F.L. Scarf, TRW, Inc). Evidence for detection of the comet was also obtained by the energetic particle anisotropy spectrometer on ICE (principal investigator R. Hynds, Imperial College, UK). Direct measurement of ion beams chanelled to the spacecraft from the comet by the interplanetary magnetic field lines at times later than closest approach is also a possibility (Fig. 1). The exact dates of measurement for comet Halley require data processing which is in progress.

Scarf also reports a possible detection of disturbances from comet Halley by the plasma wave experiment of the Pioneer Venus Orbiter (PVO) around the time of the comet's closest approach to Venus in early February 1986.

Visual wavelength observations

Ground-based images of comet Halley could not be obtained during an interval of some 6 weeks near perihelion when the comet was in angular proximity to the Sun. This gap was filled by the coronograph/polarimeter (C/P) experiment on the Earth-orbiting Solar Maximum Mission (SMM) (principal investigator R.M. MacQueen, High Altitude Observatory, Boulder, Colorado; the comet observations were obtained under the auspices of an SMM guest investigation headed by M.B. Niedner). The goal was to obtain a record of the comet's overall structure during the interval when no other visible-light imaging of the comet would be possible.

Because of its design as a solar instrument, the C/P's strong rejection of stray light permitted observations of the comet down to solar elongation of 10°. In principle, a gap of only 10 or 11 days would result when the comet penetrated the limit on 1 February and re-emerged on 11–12 February; Halley's perihelion was on 9 February. The original *C/P* timeline included comet observations starting on 10 January and ending in early March. These start and finish dates were set by spacecraft constraints established during 1985 engineering tests at a series of large offpoint angles for which SMM was not designed. Several days before the first scheduled observations two of the on-board computer memory cells failed, probably as a result of a cosmic-ray hit. Alternative operational procedures were implemented by the SMM operations team and only two and a half weeks of observations were lost.

Comet Halley observations began on 26 January, and the images taken through the 'wide-band blue' filter showed an extended coma elongated approximately in the anti-solar direction. The best of the pre-perihelion observations appear to have been taken on 28 January, and in these images there is definite evidence for both a plasma and a dust tail. The angular extent of the plasma tail was not large, around 0.5°, but the tail direction was strongly foreshortened at this time, resulting in a detected linear length of millions of kilometres. Detailed statements on structures and dimensions require full image processing which has not yet been completed.

The post-perihelion observations were degraded by the loss of the SMM high-gain antenna system. As a result of this second operational setback, it was not possible to carry out the comet observations using the tracking and data relay satellite (TDRS) in the normal manner. Reliance was on ground-station contacts. Many of the images show a plasma and a dust tail, similar in quality to the 28 January images; these should prove useful in correlative studies of the solar wind and comets. The last observation of the comet was made on 28 February 1986. Thus, the SMM observations should be useful in

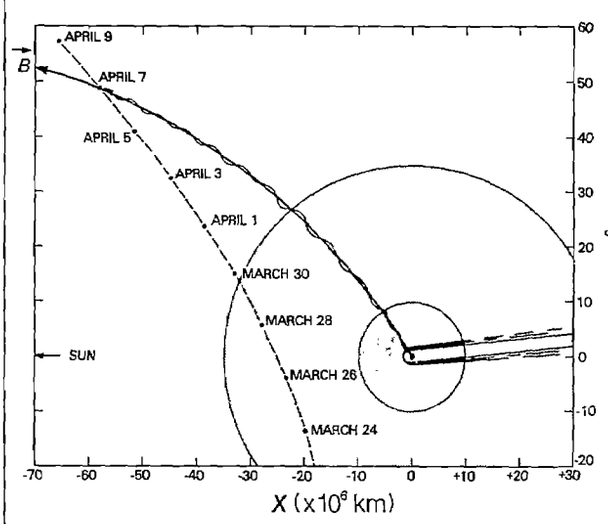


Fig. 1 The trajectory of the ICE spacecraft at closest approach to comet Halley. The distances are plotted in the comet's orbital plane. During the time interval shown, the spacecraft's distance above the orbital plane was 16.6–5.5×10⁶ km. The inner circle around the comet is 10×10^5 km in radius, representing the hydrogen cloud. The outer circle is 35×10^6 km in radius, representing the total comet/solar-wind interaction region based on measurements from Vega and ICE. The arc between the comet and ICE on 7 April illustrates the possibility of particle beams being channelled to the spacecraft. The connection shown is for a steady solar wind at 475 km s^{-1}.

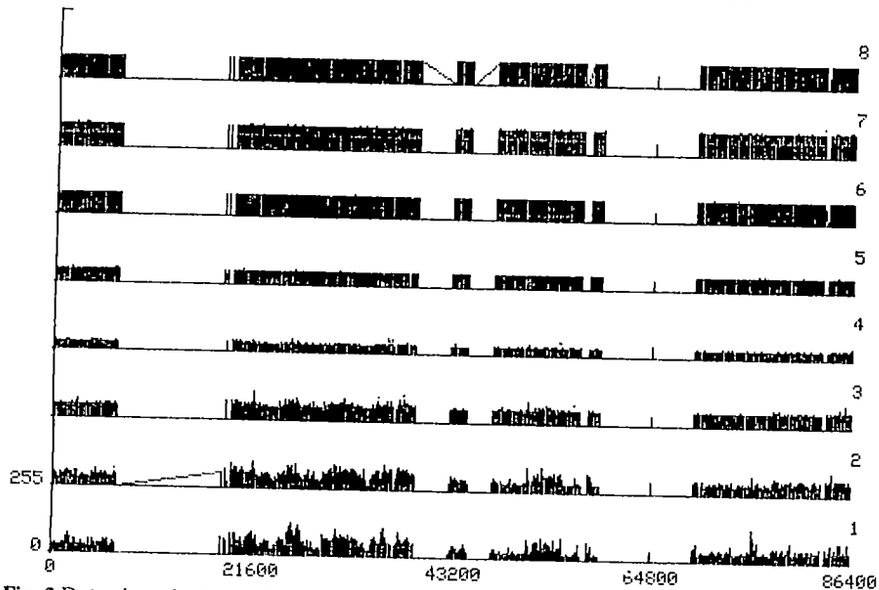


Fig. 2 Detection of enhanced magnetic wave levels on 26 March 1986, indicating traversal of the vast pickup region where cometary ions interact with the solar wind. The frequency sampled varies from 17.8 Hz for channel 1 to 1 kHz for channel 8, and the minimum to full scale spans 80 dB (0 to 255) for each channel. The abscissa is time on 26 March in s. (Courtesy: F.L. Scarf, TRW, Inc.)

providing a record of the structure and evolution of the comet during the last two weeks of February. Ground-based observations will be used to continue the record into March.

Additional visual-wavelength imaging was planned for encounter week from the Astro 1 observatory. The scheduled 6 March launch was cancelled after the loss of Challenger.

Ultraviolet observations

The first IUE star-tracker image of comet Halley was obtained on 11 September 1985, and the ultraviolet spectrum, which showed OH emission, was recorded on 12 September 1985. These are believed to be the first observations of comet Halley from space. The comet was observed every month during the rest of 1985. Due to the comet's angular proximity to the Sun in January and February 1986, it was not observed with IUE. The observations were not scheduled to resume until 13 March when they would support the Giotto encounter. However, when Astro 1, NASA's primary mission to study Halley in the vacuum ultraviolet, was cancelled due to the loss of Challenger, additional IUE observations (requiring new operational techniques) were added. The result was an intensive programme during the week of the Vega and Giotto encounters. Observations are planned to monitor the comet through mid-July 1986; IUE has scheduled 280 hours of observation for comet Halley, more than the telescope has devoted to any previous target in the past year.

Ultraviolet observations provide a means of determining the temporal behaviour of the primary constituents of the gaseous coma. Observations were made from the Goddard Space Flight Center by both the US team (P.D. Feldman, M.F. A'Hearn, H.A. Weaver and L.A. McFadden) on 9, 11, and 16 March, and by members of the European team (M.C. Festou, C. Arpigny and A.C. Danks) on 12, 13, and 14 March. A sample spectrum obtained on 11 March 1986 is shown in Fig. 3. The IUE fine error sensor, used for target acquisition and tracking, was used in a photometer mode to provide nearly continuous light curves over an 8-hour observing shift, a unique capability. During the encounter week, variations in brightness of a factor of two (in a region $\approx$ 7,000 km in radius projected at the comet) were found in a 24-hour period. At the time of the Giotto encounter, this activity was seen to be near a minimum. Preliminary analysis of the ultraviolet spectra, which are qualitatively similar to those of other comets observed by IUE during the past 6 years, shows similar day-to-day variations in both the gaseous emissions and in the continuum of sunlight reflected by cometary grains. The ultraviolet data can also be used to derive an estimate of the total gas production rate (assuming the gas to be primarily H_2O) even though the models generally used for this purpose assume a steady-state gas production. This is clearly not the case for Halley. At the time of the Giotto encounter, the gas production range was 5×10^{29} molecules^{-1}, with an uncertaintly of about a factor of 2. Additionally, the IUE data provide column abundances of carbon, oxygen, sulphur, OH, CO, CS, C_2, and CO^+ to compare with the *in situ* measurements of these species by Vega 2 and Giotto.

The hydrogen cloud surrounding comet Halley has been observed by the ultraviolet spectrometer orbiting Venus on PVO (principal investigator, I.A.F. Stewart, University of Colorado). Detailed observations were made for about 5 weeks in February and March 1986. The spectrometer was used as a spin-scan photometer to build up a Lyman-α image of the entire comet. A unique capability of PVO lies in the fact that, when the comet was behind the Sun near perihelion as seen from Earth, the view from Venus was unobstructed.

The data indicate an extensive hydrogen cloud extending to well over 10×10^6 km from the nucleus, as illustrated in Fig. 4. The derived water production rate for the comet showed very large changes around the time of perihelion, in contrast to a relatively quiescent period in late December 1985 and early January 1986. The trend of the measurements indicated that the total water molecule production rate would be $\approx 1\times10^{30}$ s^{-1} during encounter week. The last PVO observations of comet Halley were made on 7 March 1986.

The VUV-wavelength imaging photometer on DE 1 (in Earth orbit) has been used to map the comet's hydrogen cloud in Lyman-α emission were observed in January 1986. Extensive observations

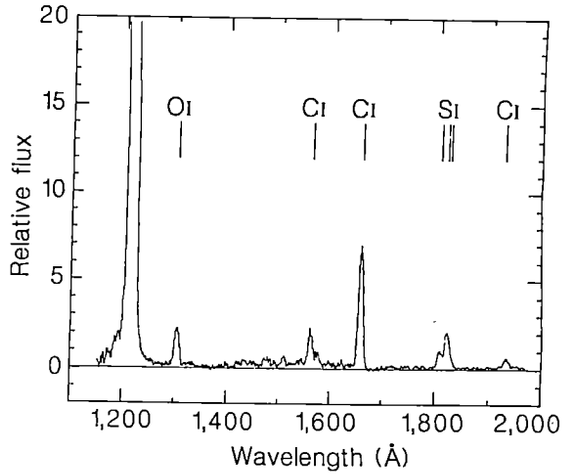


Fig. 3 Preliminary IUE spectrum of comet Halley on 11 March 1986. The saturated feature at 1,216 Å is hydrogen Lyman-β. (Courtesy: P.D. Feldman, Johns Hopkins University.)

were made from 27 February to 20 March 1986 and a last observing period is scheduled for 22 April into June, if possible.

Rocket observations

A sounding rocket experiment specifically designed for ultraviolet spectroscopy of comets and other extended astronomical sources was successfully flown to observe comet Halley from White Sands Missile Range on 26 February at 5:02 MST (12:02 UT). The scientific payload was recovered, refurbished in the field, and reflown on 13 March 1986 at 4:20 MST (11:20 UT), some 13 hours before the encounter of Giotto with comet Halley. The payload, designed and built at the Johns Hopkins University (P.D. Feldman, T.N. Woods, K. Dymond, and D. Sahnow) consists of a 40-cm diameter Dall-Kirkham telescope and Roland circle spectrograph with an ellipsoidal grating. The two-dimensional photon counting detector provides long-slit spectra of the comet with a projected slit length of 5×10^5 km and a resolution of 10^4 km and a spectral range from 1,200 to 1,750-Å, with 10Å spectral resolution. The primary objective of the experiment was to study carbon chemistry in the gaseous coma by measuring the spatial distribution of CO, C and C^+, all of which are detected by resonance fluorescence in this spectral region. Furthermore, by using the Earth's limb to occult the Sun, the rocket observation was possible near perihelion when the comet is most active and the effects of solar photodissociation and photoionization (which vary as the inverse square of the distance from the Sun) are most pronounced. Both rocket flights produced excellent quality data clearly showing, in addition to the strong H I (Lyman-β) O I, and C I emissions, several CO fourth positive bands and the C II emission at 1,335 Å extended into the tail. Also present in the spectra are several weak features, some probably due to atomic carbon, not identified in previous cometary spectra.

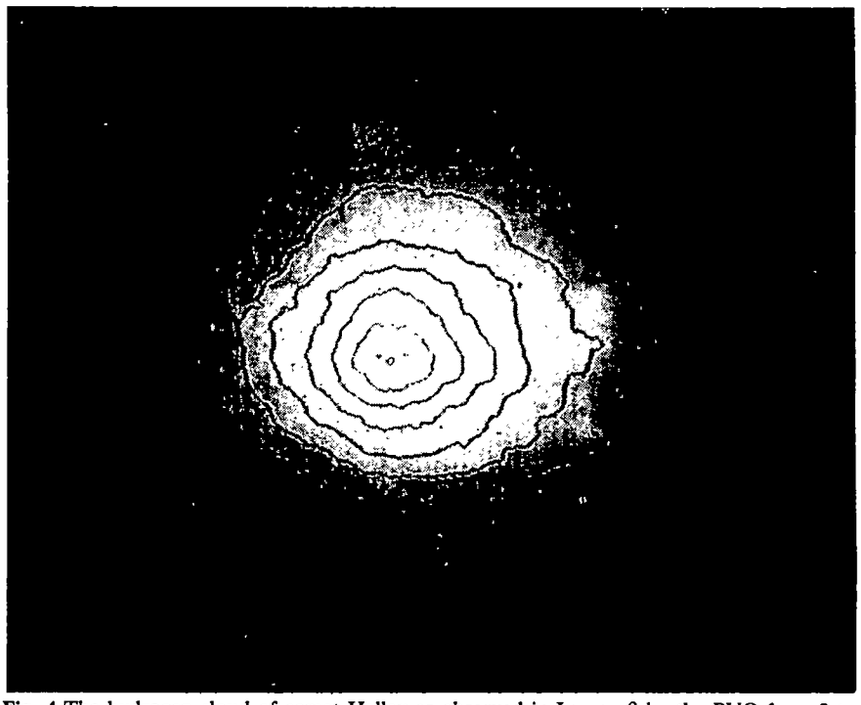


Fig. 4 The hydrogen cloud of comet Halley as observed in Lyman-β by the PVO from 2 to 6 February 1986. The solar direction is to the lower left; the size of the image shown is 0.15×0.15 AU. The crowding of the isophates on the solar side, and their separation on the anti-solar side, clearly show the effects of solar radiation pressure on the escaping hydrogen atoms; for quiet solar conditions this pressure produced an anti-sunward acceleration. The linear 'edge' near the top is an artefact of the image processing due to a large data gap on 3 February. (Courtesy I.A.F. Stewart, University of Colorado.)

An experiment to obtain images and objective spectra of comet Halley was developed by a team consisting of R.P. McCoy, G.R. Carruthers and R.R. Meier (Naval Research Laboratory), C.P. Opal (University of Texas), and M. Silbert (NASA/Goddard Space Flight Center-Wallops). One electrographic camera obtains images at Lyman-β with a 20° field-of-view and 3 arc min resolution. The second camera points at a grating and obtains objective spectra with a 12° field of view and 1 arc min resolution.

The experiment was successfully flown from White Sands Missile Range on 24 February 1986 at 4:53 MST (11:53 UT) and on 13 March 1986 at 3:54 MST (10:54 UT). Sample results are shown in Fig. 5.

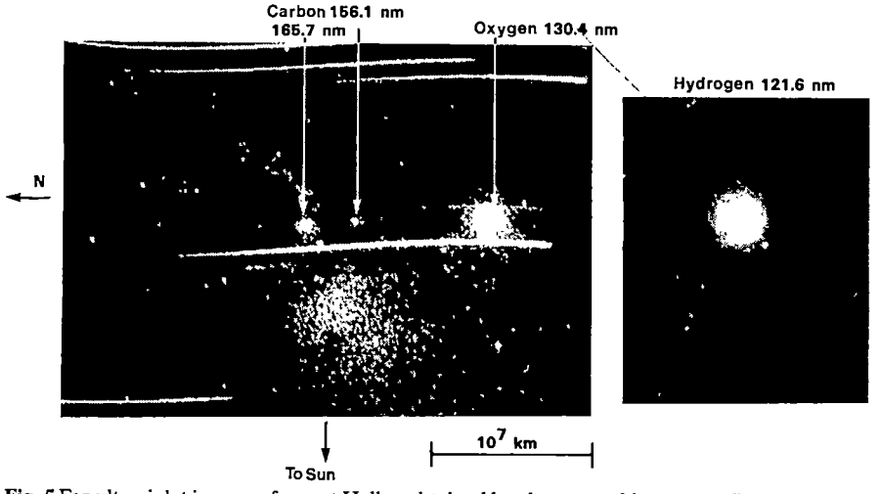


Fig. 5 Far-ultraviolet images of comet Halley obtained by electrographic cameras flow on a rocket launched 24 February, 1986. On the right is a direct image of hydrogen Lyman-β. It shows an extensive coman of hydrogen surrounding the nucleus of the comet and extending out a few million kilometres. On the left, to the same scale, is an objective spectro-gram showing images of the resonance line of atomic oxygen at 130.4 nm and the carbon resonance lines at 156.1 nm and 165.7 nm. The horizontal streaks in the image are the spectra of bright ultraviolet stars. North is to the left, and the Sun is below the images. (Courtesy R.P. McCoy, Naval Research Laboratory).

Conclusions

These diverse measurements and observations of comet Halley should greatly contribute to our physical picture of the comet as it appeared during the 1985–86 apparition. Detailed results will be published by the investigators. Additional contributions will come from a comparison with the results obtained by ICE[1] on the tailward side of comet Giacobini–Zinner during the 11 September 1985 flyby.

The excellent cooperation of the inves-tigators mentioned, demonstrated by their rapid communication of results, is gratefully noted. □

Laboratory for Astronomy and Sola Physics, NASA-Goddard Space Flight Center, Greenbelt, Maryland 20771, USA.

1. von Rosenvinge, T.T., Brandt, J.C. & Farquhar, R.W. *Science* **232**, 353-356 (1986).
2. Craven, J.D., Frank, L.A., Rairden, R.L. & Doering, M.R. Preprint, University of Iowa (1986)

Chaos in light

Robert G. Harrison

Physics Department, Heriot-Watt University, Edinburgh EH14 4AS, UK

Dhruba J. Biswas

MDRS (Physics Group), Bhabha Atomic Research Centre, Bombay 400 085, India

Chaos is an inherent feature of many nonlinear systems. In particular, the transition from a steady to chaotic state occurs independently of the physical properties of the system. Such behaviour occurs in optics, both in lasers and in nonlinear optical devices. Such devices, which are fundamentally simple both in construction and in the mathematics that describes them, provide excellent opportunities for investigating nonlinear phenomena as well as for technological innovation.

MATHEMATICAL discoveries have revolutionized our understanding of nonlinear science. The preconception that physical systems, in general, behave in a predictable manner is seriously in question. Rather than yielding regular and repeatable behaviour, many nonlinear systems also exhibit unstable, even chaotic, solutions. Furthermore, the transition from stable to chaotic behaviour, which may occur when varying a control parameter of the system, follows specific, well-defined routes which are universal in the sense that they are independent of the physical properties of the system they describe. It is these signatures which have been a major impetus to experimentalists in the subsequent search for physical systems that exhibit these phenomena. Such behaviour has now been observed in many branches of science and the number is rapidly growing.

The most recent exciting development is the discovery that such phenomena exist in optics. Here we are concerned, in general, with the nonlinear interaction of light with media contained in optical resonators; the physical properties of the medium, such as absorption and refractive index, being modified by the intensity of the incident radiation.

There are two major areas. The first are lasers or active systems, in which the optical signal is derived from stimulated emission generated within an optical cavity containing a gain medium. The second are passive systems for which the optical signal is but the transmission of an input light signal through an optical cavity containing, for example, an absorptive medium.

Instabilities in laser emission, notably in the form of spontaneously coherent pulsations, have been observed almost since the first demonstration of laser action. However, subsequent theoretical efforts towards understanding these phenomena have been at a modest level, due in part to the wide variety of alternative areas of investigation provided by lasers. It is only with the new mathematical discoveries that these instability phenomena have been investigated to give a deeper insight into the mechanisms of laser action and its deterministic chaotic behaviour. Re-examination of many of these systems show that such effects are quite abundant; the operating window for conventional stable emission in some systems often proving surprisingly small while in some cases, the instabilities are found to prevail just where the lasing emission is optimum.

On the other hand, passive systems which are being increasingly recognized for their potential application as bistable all-optical logic elements, may give rise to similar phenomena. It may, nevertheless, be possible to take advantage of the periodic instabilities that precede chaos in the development of ultra-high frequency all-optical modulators.

Of the variety of physical systems that exhibit deterministic instability phenomena, optical systems, both lasers and passive devices, provide nearly ideal systems for quantitative investigation due to their simplicity both in construction and in the mathematics that describe them, enriched by the possibility of a quantum description. Notable also is the very short timescale (nanosecond to microsecond) over which optical instabilities occur which, in contrast to many other systems, ensures essentially constant environmental conditions during data acquisition. This is particularly important since even small extraneous perturbations, such as noise, may dramatically alter the form of the subsequent temporal evolution of the instability process. These features are fundamental to the rapid establishment of optical systems in this multidisciplinary field.

Universality in chaos

In considering deterministic behaviour, one is tempted into the misconception that such behaviour must be regular since successive states evolve continuously from each other. However, as early as 1892 Poincare showed that particular mechanical systems, where time evolution is governed by hamiltonian equations, could display chaotic behaviour. The subsequent discovery by Lorentz[1] in 1963 that even a simple set of three coupled first-order, nonlinear differential equations can lead to completely chaotic trajectories is recognized as a landmark. This work is fundamental to our understanding of laser instabilities.

At first sight, such behaviour appears alien to our conception of many problems in physical science. This prejudice stems from the dominance of mathematical theory pertaining to linear systems and its subsequent successful application to many fundamental linear problems in the physical sciences. Unfortunately, however, this has led to a narrow vision of the physical world where nonlinear behaviour is the rule and linear behaviour the exception.

Unlike linear systems, nonlinear systems must be treated in their full complexity, and so there is no general analytical approach for solving them. The advances made in understanding many previously intractable nonlinear problems can largely be attributed to the power of contemporary computers, where simulated solutions of nonlinear equations have provided insights into their behaviour and suggested directions for future research.

The temporal evolution in the behaviour of a system can be characterized when presented as a trajectory of a point in the phase space of its dynamical variables. In this representation, consider a familiar dynamical system such as a periodically-forced pendulum in a frictional environment. Such a dynamical system is characterized by the fact that the rate of change of its variable is given as a function of the value of the variable at that time. The space defined by the variables is called the phase space. The pendulum's behaviour can be described by the motion of a point in a two-dimensional phase space whose coordinates are the position and velocity of the pendulum. In

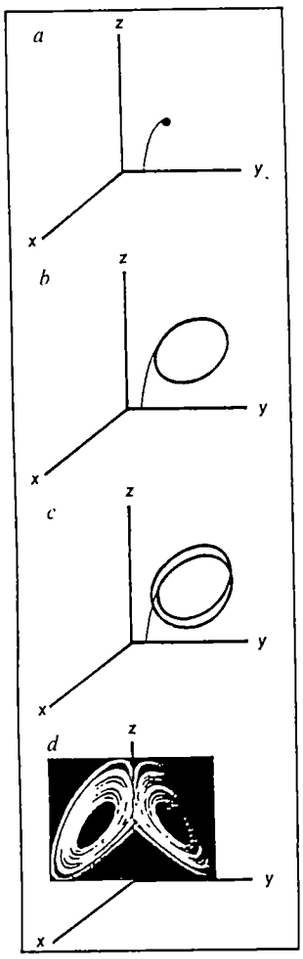


Fig. 1 Phase space portraits of the attractor for the dynamical variables x, y and z. *a*, Stable point corresponding to a steady state in time after initial transients have died out shown as the thin continuous line. *b*, Period-one limit cycle corresponding to a periodic solution in time of single frequency. *c*, Bifurcation to period-two limit cycle; a periodic solution in time with double the period of that in *b*. Successive period doubling bifurcations lead to an eventual chaotic colution. *d* Shows the strange or chaotic attractor for a Lorenz–Haken system describing a single mode laser with a homogeneously broadened two-level gain medium.

more complicated systems, involving many variables, the dimension of the phase space will, however, be considerably larger. If an initial condition of a dissipative dynamical system, such as the pendulum, is allowed to evolve for a long time, the system, after all the transients have died out, will eventually approach a restricted region of the phase space called an attractor. A dynamical system can have more than one attractor in which case different initial conditions lead to different types of long-time behaviour.

The simplest attractor in phase space is a fixed point. The system is attracted towards this point and stays there. This is the case for a simple pendulum in the presence of friction; regardless of its initial position, the pendulum will eventually come to rest in a vertical position. When the pendulum is under the influence of an external periodic driving force, the system is then fully nonlinear and leads to strikingly different behaviour. Irrespectively of the initial conditions the pendulum always ends up making a periodic motion. The limit or attractor of the motion is a periodic cycle called a limit cycle. However, when the driving force exceeds a certain critical value, the periodic motion of the pendulum breaks down into a more complex chaotic pattern which never repeats itself. This motion represents a third kind of attractor in phase space called a chaotic or strange attractor (see Fig. 1).

A trajectory on a chaotic attractor exhibits most of the properties intuitively associated with random functions, although no randomness is ever explicitly added. The equations of motion are purely deterministic; the random behaviour emerges spontaneously from the nonlinear system. Over short times, the trajectory of each point can be followed, but over longer periods small differences in position are greatly amplified making the predictions of long-term behaviour impossible. As such arbitrarily close initial conditions can lead to trajectories which after a sufficiently long time diverge widely; even for the simplest of systems in which all the parameters are determined exactly, long-term prediction is, therefore, impossible. This behaviour is in marked contrast to that of the fixed point and limits cycle attractors for which, irrespective of starting conditions, the system always settles down to the same solutions.

Irratic and aperiodic temporal behaviour of any of the systems' variables implies a corresponding continuous spectrum for its Fourier transform which is, therefore, also a further signature of chaotic motion. However, other factors including noise, can lead to continuous spectra, and distinguishing chaos from noise is one of the major problems of the field. Hence, although time series, power spectra and routes to chaos collectively provide strong evidence of deterministic behaviour further signatures are desirable for its full characterization and in discriminating it from stochastic behaviour. Here analysis of trajectories of a point in the phase space of its dynamical variables is required. However, for a system with, say, N degrees of freedom it seemed that it would be necessary to measure N independent variables; an awesome if not impossible task for complex system. Consequently mathematicians have long tried to develop practical techniques for extracting specific finite dimensional information from the limited output provided by experiment; typically the time record of a specific physical observable; that is, one variable of the system. Here embedding theorems[2] have been recently used to reconstruct phase portraits from which Lyapunov exponents may be determined that measure the average rate of exponential separation or contraction of nearby points on the attractor. These measure intrinsically dynamical properties, unlike power spectra, and provide quantitative measures by which chaotic motion may be distinguished from stochastic behaviour.

The discoveries that deterministic chaos proceeds through a limited number of specific routes when a control parameter of the nonlinear system is varied is profoundly significant as such behaviour is not restricted to a particular model description of a particular physical system. Rather, nonlinear physical systems in all branches of science which may be formally described by the same set of mathematical equations will give solutions that evolve identically in time through one or other routes to chaotic motion. The unique effect of such unification between many separate scientific diciplines forms the basis for the foundation of synergetics[3,4]. There are at least three common routes by which a nonlinear system may become chaotic. These are referred to as period doubling, intermittency and two-frequency scenarios.

Period doubling. From considering various difference equations, many of which can be reduced to simple one-dimensional maps, solutions have been found to oscillate between stable values, the period of which successively doubles at distinct values of the external control parameter[5,6,7]. This continues until the number of fixed points becomes infinite at a finite parameter value, where the variation in time of the solutions becomes irregular (see Fig. 1). One example showing such behaviour is the simple logistic map

$$X_{n+1} = rX_n(1 - X_n)$$

Perhaps the most popular application of this map is in describing

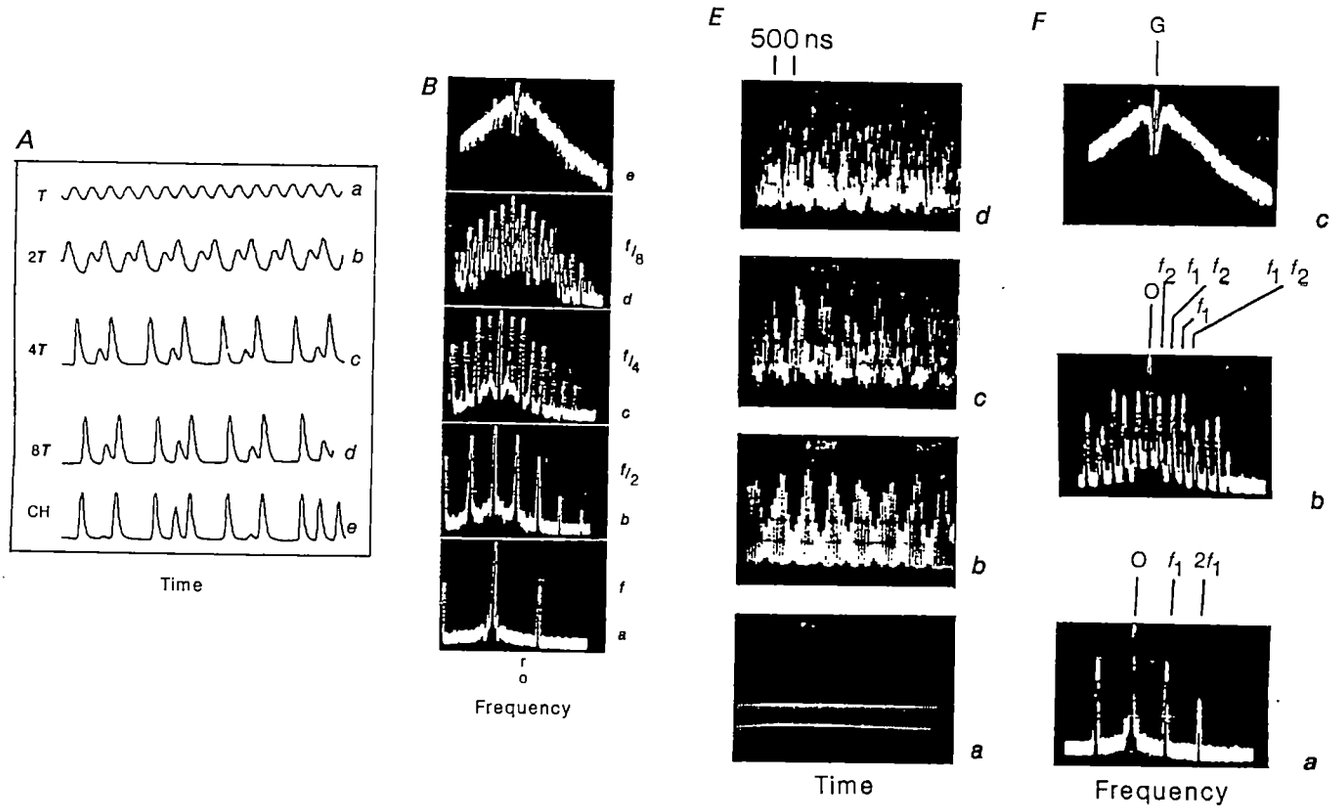


Fig. 2 *A, B* Examples of period doubling route to chaos for laser systems. The time recordings shown in *A* are for a CO_2 laser in which cavity length modulation is used as a control parameter for the generation of chaos (after ref. 20) and *B* shows a spectral recording of the lasing emission for an optically pumped far-infrared ammonia laser with cavity length tuning as a control parameter (after ref. 49). The steady-state solution as in Fig. 1*a* are not shown in these recordings. As seen initial oscillation (*Aa* and *Ba*) undergoes successive period doublings (*Ab–d*) or frequency halving (*Bb–d*) before culminating in chaos where in time the output is aperiodic (*Ae*) and in frequency is a broad continuum (*Be*). *C, D*, Examples of intermittent route to chaos in lasers. The time recordings shown in *C* are for a He–Ne laser in which cavity mirror tilt is used as the control parameter (after ref. 50, and *D* shows a spectral recording of the lasing emission for a He–Xe laser with laser gain as a control parameter (after ref. 25). Steady-state solutions are not shown in the recordings. The initial instability here is characterized by a narrow spectral peak in frequency and periodic pulsation in time. On varying the control parameter the intermittent bursts of chaos become increasingly frequent in time with a corresponding steady broadening of the peaks in the frequency followed by fully chaotic motion. *E, F*, Examples of Ruelle–Takens route to chaos in lasers. The time recordings shown in *E* are for a multimode CO_2 laser in which cavity length tuning is used as a control parameter (after ref. 51) and *F* shows a spectral recording of the lasing emission for a He–Ne laser with cavity mirror tilt as a control parameter (after ref. 50. Steady-state solutions are not shown in the recordings. Initial instability (periodic pulsation, *Ea*; one frequency and its harmonics, *Fa*) develops into quasiperiodic motion with two incommensurate frequencies (*Eb* and *Fb*) as the control parameter is varied before going into eventual chaos (*Ed* and *Fc*).

changes in population ($X_n \rightarrow X_{n+1}$) of an organism or species from year to year ($n \rightarrow n+1$) where there is no overlap between successive generations. The first term in the brackets describes population growth by birth and the second term, population decline due, for example, to preditorial or other environmental conditions. Dependent on the increase in the value of the control parameter r the population may be steady, oscillatory or chaotic the transition following a period doubling scenario (see refs 8, 9). More generally many complex physical systems, often described by large numbers of coupled differential equations, may be reduced in some conditions to the form of this or similar maps. Period doubling bifurcation to chaos has been experimentally observed in numerous systems (see Fig. 2*A*, *B*).

Intermittency. Intermittency[10] means that a signal which behaves regularly in time becomes interrupted by statistically-distributed periods of irregular motion. The average number of these intermittent bursts increases with the external control parameter until the condition becomes completely chaotic (see Fig. 2*C*, *D*).

Two frequency. Turbulence in time was originally considered as a limit of an infinite sequence of instabilities (Hopf bifurcation) evolving from an initial stable solution each of which creates a new basic frequencies[11,12]. However, it has been recently shown[13,14] that after only two or perhaps three instabilities in the third step the trajectory becomes attracted to a bounded region of phase space in which initially closed trajectories separates exponentially; as such the motion becomes chaotic (see 2*E*, *F*).

Chaos in lasers

Chaotic behaviour in lasers may exist in even the simplest of systems: one in which population inversion is established between two discrete energy levels of the medium and where the lasing transition between these two levels is homogeneously broadened. A variety of practical lasers may be controlled to operate in these conditions. A further simplification is that the laser cavity, a Fabry–Perot or ring resonator system surrounding the gain medium, be sufficiently short so that only one resonant frequency of the cavity lies within the bandwidth of the gain medium and that this mode be resonantly tuned to the gain centre frequency. The frequency spacing ($\Delta\nu$) between cavity modes for a Fabry-Perot cavity is given by:

$$\Delta\nu = cn/2L$$

where c is velocity of light, n the refractive index of the lasing medium and L the cavity length. Typical examples of single mode and many mode operation, for short and long cavity lengths respectively, are shown in Fig. 3. In conditions in which the gain or population inversion is maintained at a constant level by, for example, constant electrical or optical excitation, and for the single mode system, lasing occurs with a constant output power at the frequency of the single cavity mode. In this condition, the gain is reduced to a threshold level equal to the cavity losses. Note that even for a multimode system and in the absence of spatial hole burning, lasing is still restricted to a single mode, because the mode with highest gain, here at nor near gain centre, grows at the expense of all other modes. Such behaviour is the accepted operating characteristics of these systems.

However, the discovery[15] that for certain operating conditions emission could be periodic or even chaotic implies that the signal comprises more than one frequency, contrary to the accepted understanding of single mode operation. Prediction of such behaviour were initially identified by Haken through the mathematical equivalence of the equations describing laser action, the Maxwell–Bloch equations, and those derived earlier by Lorenz to describe chaotic motion in fluids. If we consider the trajectory of the Lorenz strange attractor (see Fig. 1*d*) where in the equivalent laser system the dynamic variables x, y and z are the field amplitude (E), polarization of the medium (P),

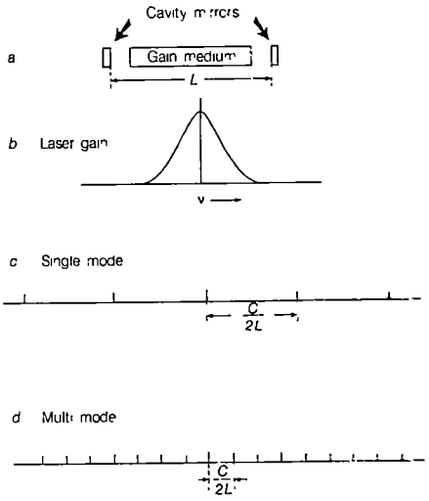


Fig. 3 *a*, A Fabry–Perot laser cavity system with a partially transmitting mirror for coupling out the laser emission; *b*, lorentzian gain profile for a simple two-level homogeneously broadened lasing medium for which each and every atom/molecule emits identically. *c*, Relative position of the cavity modes for a short optical cavity. Here only one mode lies within the gain bandwidth resulting in a single mode emission, *d*, Corresponding position of the modes for a long cavity for which several modes lie within the gain bandwidth.

and the population inversion (D), a point (x, y, z) circles in one region for a while, but then suddenly jumps into another region, where it moves for a while until it jumps, seemingly randomly, back into the first region, and so on; the trajectory never intersects. For the laser, such behaviour not only requires a cavity with high transmission but also a gain of at least nine times that required to produce lasing, making the experimental realization of such operation rather impracticable for most lasers of this simple type. A notable exception are optically-pumped far-infrared molecular lasers[16] which will probably become an important research area.

General prerequisites for the onset of deterministic chaos include: that apart from nonlinear interaction there is a sufficiently large phase space; the minimum requirement being that the system possesses at least three degrees of freedom. For example, the simple pendulum possesses only two degrees of freedom and exhibits at most periodic behaviour. In a two-dimensional phase space, described by the variables, velocity and displacement, it is then impossible for the trajectory to be restrained within a basin of attraction without intersecting itself; repetition of trajectory points resulting in only periodic or quasiperiodic solutions. The addition of one further degree of freedom, through the imposition of a modulated external force, leads to the possibility of a non-overlapping trajectory still in a limited phase space but now described by three variables; the so-called strange attractor (see ref. 17).

The Maxwell–Bloch equations described above for the special case of a single-mode laser with field tuned to the centre of the gain line such that both field and polarization are real quantities, satisfy the minimum condition of three independent variable equations, each of which has its own relaxation.

$$\frac{dE}{dt} = -\kappa E + \kappa P$$

$$\frac{dP}{dt} = \gamma_\perp ED - \gamma_\perp P$$

$$\frac{dD}{dt} = \gamma_\parallel(\lambda + 1) - \gamma_\parallel D - \gamma_\parallel \lambda EP$$

where κ is the cavity decay rate, $\gamma_\perp$ is the decay rate of atomic

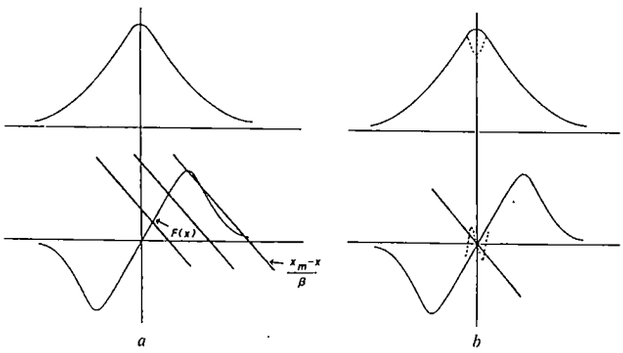


Fig. 4 Graphical solution of the equation of active cavity mode: $F(x) = (x - x_m)/\beta$. Top traces represent gain profile and the corresponding dispersion features associated with these is shown in the bottom traces. *a*, Graphical solution is illustrated for different detunings of the cavity mode. As seen only when the mode is tuned sufficiently away from the line centre, intersection on more than one point is possible resulting in the splitting of the mode into different frequencies all of which fill the same number of half-wavelengths between the cavity mirrors; spontaneous or passive mode splitting. *b*, When the oscillating cavity mode burns a spectral hole into the gain, the associated dispersion takes just the shape required for giving rise to more than one intersection point. As seen, the gain at the split frequencies are indeed higher than that at the original frequency; induced or active mode splitting.

polarization, $\gamma_\parallel$ is the decay rate of population inversion, λ is the pumping parameter, E is the field inside the cavity, D is the population inversion, and P is the atomic polarization.

However, if one variable relaxes faster than the others the stationary solution for that variable may be taken, so resulting in a reduced number of coupled differential equations; commonly termed adiabatic elimination of the fast variables[3,4] In many systems, polarization and population inversion have relaxation times much shorter than the cavity lifetime and both variables can be adiabatically eliminated. With just one variable describing the dynamics, the laser must show a stable behaviour (fixed point in phase space; see Fig. 1*a*). This group of lasers, comprises many common systems such as He-Ne, Ar^+, Dye and lasers. In some cases, only polarization is fast and hence two variables describe the dynamics. In this class, we find ruby, Nd and CO_2 lasers which exhibit oscillating behaviour in some conditions, although ringing is always damped.

Since many lasers are not described by the full set of Maxwell-Bloch equations normally chaotic behaviour from these systems cannot be obtained. For these systems with less than three variables the addition of independent external control parameters to the system, as for the pendulum considered above, have been extensively considered[18] as a means to provide the extra degrees of freedom. Active modulation of a parameter such as population inversion, field, or cavity length as well as injection of a constant field detuned from the cavity resonance and also the use of intracavity saturable absorbers have all been considered[19-21]. For multimode rather than single-mode lasers intrinsic modulation of inversion (or photon flux) by multimode parametric interaction ensures additional degrees of freedom[18]. When the field is detuned from gain centre the field amplitude, polarization and population inversion are complex, providing (in the absence of adiabatic elimination) five rather than three nonlinear equations for single mode systems which is more than sufficient to yield deterministic chaos for suitable parameter values[22]. Also of significance is the remarkably low threshold found for the generation of instabilities and chaos in single mode inhomogeneously broadened laser systems[23-25]. Compared with homogeneously-broadened systems this is attributed to the increased number of independent gain packets available in inhomogeneous systems. Pulsating instabilities and routes to chaos have also been reported for Raman lasers[26] where the instability threshold is again found to be reduced. Significantly, it is also found that instabilities are greatest in conditions for which the laser produces maximum output.

Physical mechanism

A transition from a steady laser output to an oscillatory and subsequently chaotic emission implies the generation of further oscillating frequencies to that of the original stable emission. That this should occur even for a so-called single frequency (single mode) laser seems to be a contradiction in terms. The explanation is in the phenomena of mode splitting[27,28]. This occurs in a region of rapidly varying dispersion when the oscillating cavity mode splits into more than one frequency all of which fill the same number of half-wavelengths between the cavity mirrors. Coupling between these several frequencies having common mode index is a prerequisite for single-mode pulsating instabilities. Dispersion changes its value rapidly near the wings of the gain curve and the splitting that occurs in this region is known as passive mode splitting. An oscillating cavity mode can also induce large variation in dispersion if it can locally saturate the gain curve, hence this splitting is termed induced mode splitting.

To understand spontaneous mode splitting we consider the equation of the oscillating active cavity mode

$$\frac{mc}{2L} = \nu n(\nu) \tag{1}$$

where, m is the mode index and $n(\nu)$ is the index of refraction at the laser oscillation frequency ν. In terms of the empty resonator mode frequencies, $\nu_m = mc/2L$ obtained by putting $n(\nu) = 1$ the above equation may be re-written as,

$$\nu_m - \nu = \nu[n(\nu) - 1] \tag{2}$$

When the value of $n(\nu)$, either for a lorentzian or gaussian gain profile which are common to most lasers, is substituted this equation may be re-expressed as,

$$x_m - x = \beta F(x) \tag{3}$$

where x and x_m are respectively the laser oscillation frequency and empty cavity resonant frequency normalized as a detuning from the atomic resonance. $F(x)$ has the same functional dependence with x as $n(\nu)$ has with ν and it depends on whether the gain is gaussian or lorentzian. The mode splitting factor, β, is dimensionless and is given by

$$\beta = K\frac{cg}{(\Delta\nu)} \tag{4}$$

where g is the peak small-signal incremental gain, $\Delta\nu$ is the FWHM (full width at half maximum) value of gain-width, c is the velocity of light in vacuum and K is a numerical factor equal to $\pi^{-3/2}\sqrt{\ln 2}$ for gaussian gain profile and π^{-1} for lorentzian gain profile. Equation (3) has been graphically solved for different detunings for a gaussian gain profile in Fig. 4*a*. Under certain detuning (near the wings of the gain) the equation is simultaneously satisfied by more than one value of x. Physically this means that the cavity mode is split into more than one frequency and all of which correspond to the same number of half-wavelengths within the resonator cavity. Such effects occur spontaneously at the wings of the gain curve and hence the name spontaneous mode splitting.

Induced mode splitting may be explained in terms of distortions in the dispersion caused by hole burning in the gain profile by a single mode operating above lasing threshold (see Fig. 4*b*). The dispersion may be so distorted that several new frequencies satisfy the boundary conditions. The onset of these sideband frequencies (the gain at which can be more than that at the parent oscillating frequency; see Fig. 4*b*) gives rise to pulsations

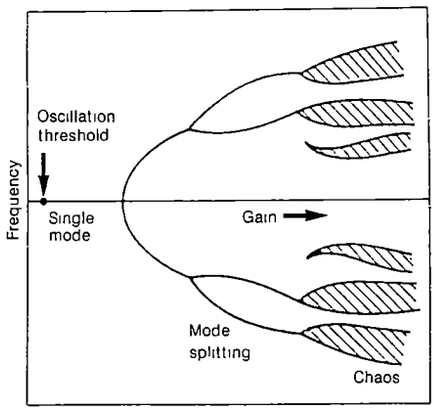


Fig. 5 Mode splitting sequence in which an initially single mode (single frequency lasing oscillation) successively bifurcates on varying gain to generate emission with increasing complex frequency context culminating in a broad band (chaotic) spectrum (after ref. 52).

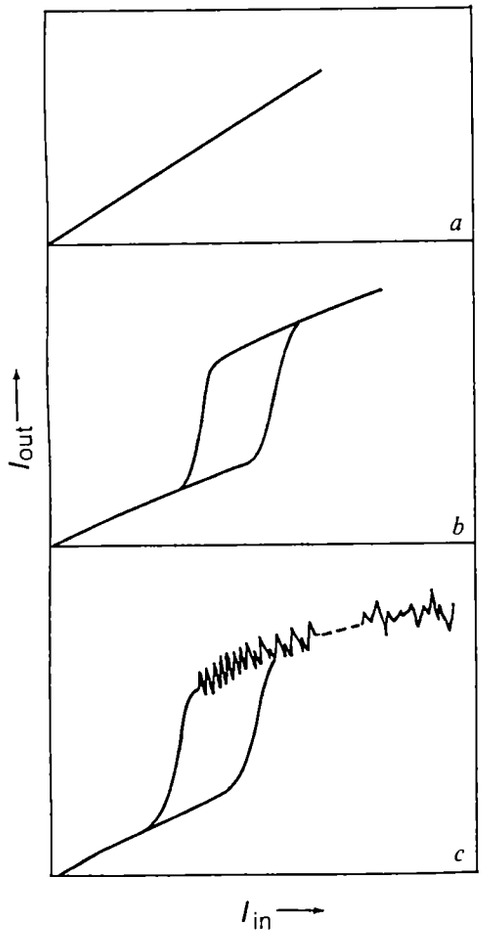


Fig. 6 Transmitted intensity as a function of input intensity for a simple optical resonator, for example, Fabry–Perot or ring cavity. *a*, An empty cavity showing characteristic linear behaviour; *b*, a characteristic optical bistable action and associated hysteresis; *c*, appearance of periodic and chaotic behaviour in the transmitted signal, on increasing the input signal intensity, that may occur in the form of trace *b* for different parameter conditions of the nonlinear cavity.

in the intensity output of the laser. Because the dispersive effects are caused by the oscillating mode itself, this splitting is termed 'induced mode splitting'. This effect should be strongest at line centre and probably exists over much of the lasing tuning range. In view of these effects we may now consider two line broadening situations common to most lasers—homogeneous and inhomogeneous broadening.

The saturating characteristics of an inhomogeneously broadened gain medium is ideal for the realization of mode splitting. In such a medium, unlike the homogeneously broadened case more than one frequency may naturally oscillate since independent sets of atoms/molecules are responsible for lasing at different frequencies across the gain-bandwidth and thus passive mode splitting may be readily observed. The oscillating frequency may also burn a spectral hole into the gain medium thus favouring induced mode splitting. Furthermore, the side bands split again as they again burn spectral holes. This process will continue and may eventually lead to chaos (see Fig. 5). On the other hand, when a homogeneously-broadened gain medium saturates, all the atoms or molecules actually contribute at the oscillating frequency thereby making the possibility of spectral hole burning almost impossible. In such a system, therefore, only the frequency with highest gain would eventually grow. However, for the Haken–Lorentz system, in an extremely high-gain medium survival of more than one frequency is possible.

Chaos in nonlinear optical devices

In parallel with work on laser instabilities, Ikeda predicted oscillation and chaos in passive optical systems[29]. In these systems, the cavity contains a medium whose refractive index is modified by the intensity of the input light signal. This may be expressed as

$$n(I) = n_0 + n_2 I \tag{5}$$

where n_0 and n_2 are respectively the ordinary and nonlinear contribution towards the refractive index and I is the light intensity.

To understand this phenomena we must consider how the light field within the cavity changes, according to the intensity dependent nonlinear phase shift produced by this refractive index, with successive round trips. The simplest case is one in which the intensity-dependent refractive index immediately responds to changes in intensity and where the cavity is of low finesse. The intensity of the signal inside the cavity, here a ring resonator, for successive round trips then obey the one-dimensional mapping rule[30]

$$I_{n+1} = I_{in}\left\{1 + C\cos\left[\frac{2\pi}{\lambda}(n_2 I_n)L + \phi_0\right]\right\}$$
$$= F(I_{in}, C, I_n) \tag{6}$$

where $\phi_0 = (2\pi/\lambda)n_0 L$, is the normal round trip optical phase shift experienced by the input signal in the cavity in the absence of nonlinearity, C is a constant for the particular cavity and we assume that the nonlinear medium fills the whole cavity of length L. The stationary solution of this mapping, denoted by I_s, occurs when $I_{n+1} = I_n$ and yields the relation

$$I_s = I_{in}\left\{1 + C\cos\left[\frac{2\pi L}{\lambda}(n_2 I_s) + \phi_0\right]\right\} \tag{7}$$

where the transmitted signal (I_T) is then simply given by $I_T = I_s T$, where T is the transmission of one of the cavity mirrors.

In the limit of low intensity, the nonlinear term is negligible and the transmitted signal of the ring cavity reduces to the standard expression

$$I_T = I_{in}\{1 + C\cos\phi_0\}T \tag{8}$$

for this optical cavity. Here the intensity of transmitted signal scales linearly with that of the input signal (see Fig. 6*a*) its

magnitude depending on the degree to which the input signal frequency is resonant with the cavity. Tuning the length of the cavity, thereby varying the phase ϕ_0, leads to the familiar resonant transmission peaks characteristic of optical cavities. Returning to the nonlinear equation a corresponding plot of transmitted intensity as a function of input intensity is shown in Fig. 6*b*. The nonlinear form of this curve is the signature of optical bistability, of interest because of its application to all optical logic elements. For example, this particular curve shows switching action and memory in which at a critical input intensity the output signal switches to a higher value but on the return cycle switches down for a reduced input intensity due to optical hysteresis. A stable and reproducible operation is required for such application. However, there are parameter conditions, for the input intensity, and cavity finesse for these systems for which the transmitted signal exhibits a behaviour far from this ideal, manifesting not only pulsating instabilities but also full chaotic characteristics. Such regions are schematically indicated on the bistability curve (Fig. 6*c*).

To understand this behaviour we need to examine more closely the mapping behaviour of equation (6) as shown in Fig. 7*a*. Intersection of this curve with the line $I_{n+1} = I_n$ gives the stationary solution to the mapping. Starting from an arbitrary value of I_n, the corresponding value of I_{n+1} (vertical intersection with $F(I_{in}; C; I_n)$) is then the new value of I_n (horizontal intersection with line $I_{n+1} = I_n$). Successive iteration generates a spiral of successively decreasing steps which converge to a single point intersection shown. This is then a stable single point solution. In time, the iteration steps are then transients which die out to this steady-state solution. Similar constructions are shown in Fig. 7*b* and *c* for two higher values of C; the input intensity could, of course, be used as an alternative control parameter. As seen in equation (6) this is manifested as an increase in amplitude of the map. In Fig. 7*b*, successive iterations, do not converge to a single point but stabilize to a two-point solution; shown by the intersection of the iterations with the mapping function $F(I_{in}; C; I_n)$. The corresponding signal in time, therefore, shows that after transients have died out the transmitted signal exhibits periodic oscillation or limit cycle behaviour. For further increase in C, the oscillatory signal successively bifurcates to yield oscillations which are each double the period of the preceeding ones; the so-called period doubling sequence, as shown in Fig. 2 for laser systems. Ultimately for sufficiently high C a chaotic solution is obtained for which, as seen in Fig. 7*d*, successive bifurcations never converge to fixed points. This figure also shows that a small change in the starting conditions, value of I_n, will soon result in wildly different iterative steps; unlike the stable and periodic solutions such behaviour which characterizes deterministic chaos is often referred to as being sensitive to initial conditions. As such a small difference in the initial condition is amplified by many operations. Mathematically, this is quantified by the Lyapunov exponent λ which for this sytem is

$$\lambda = \log \frac{I_{in} C}{2} \qquad (9)$$

In general, a positive Lyapunov exponent implies exponential separation of nearby trajectories, the signature of deterministic chaos, while a negative exponent implies exponential contraction, the signature of an attracting fixed point. For chaotic behaviour one, therefore, requires $I_{in}C/2 > 1$, whereas bistable action without the presence of instability requires $I_{in}C/2 < 1$. Evidently a transition to chaos may then occur on increasing the input intensity or the value of the parameter C. For convenience, we have assumed that the medium responds instantaneously to the field or more precisely the relaxation time of the medium is much shorter than the cavity round trip time of the field. For systems in which the converse situation applies bistable operation is favoured although even here sideband instabilities may arise.

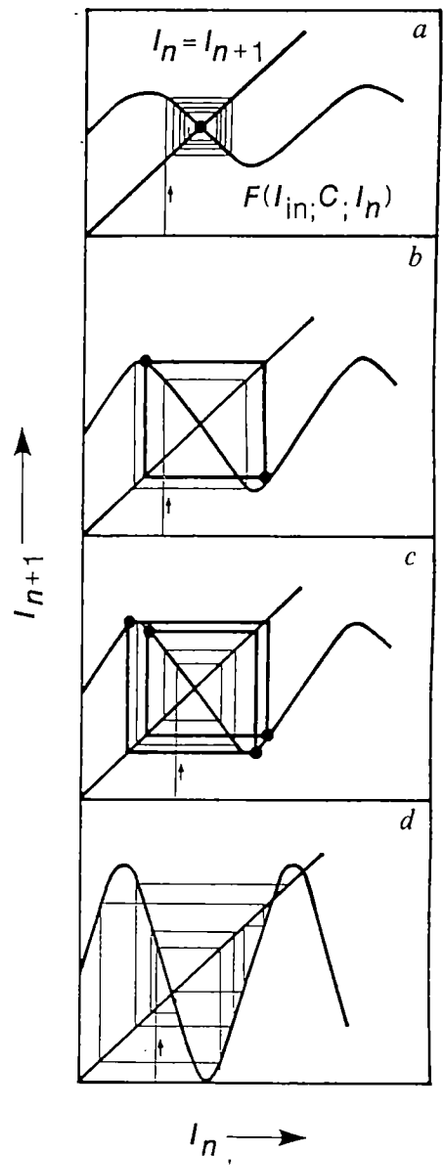


Fig. 7 Graphical solutions of one dimensional map $I_{n+1} = F(I_{in}, C, I_n)$ for various values of control parameter C. The line $I_n = I_{n+1}$ is the condition when the transmitted signal does not change with successive iterations. *a*, A fixed point or steady-state solution I_s for the field in the cavity since successive iterations converge to the single intersection point of the two curves. *b*, An increased value of C, shows the iterations to stabilize on a two-point solution corresponding to a periodic output in time. For further increase in the value of C, a four-point solution is obtained (*c*); that is iterations here have to cycle twice before repeating themselves so corresponding to a periodic oscillation of twice that for the trace *b*. This period doubling behaviour repeats as the control parameter C is further increased until a value is reached when iterations no longer repeat themselves. This is shown in the trace *d* which characterizes an example of chaotic behaviour. We note that the stable and periodic solutions (traces *a*–*c*) are invariant with the starting value of I_n. In contrast, the chaotic trajectory of trace *d* is very sensitive to this initial condition; following a very different path for even the smallest change. The time series of Fig. 2*A* are representative of the behaviour described here.

Observations of these phenomena, although still limited, have been made in various optical systems such as hybrid bistable devices, and all optical bistable systems. In the hybrid system, nonlinearity in a transparent dielectric medium is caused by an externally-applied voltage rather than by the laser signal itself. The impressed voltage is coupled to the transmitted light signal

through a controllable electronic delay with variable gain which serves as the control parameter of the system. On increasing the feedback gain the transmitted optical signal undergoes a period doubling bifurcation though only up to period eight before becoming chaotic. Here[31] as in many other systems, both passive and active, the effect of external noise[32] interrupts the otherwise infinite series of period doublings to create what is termed a bifurcation gap.

The first observation of bifurcation to periodic and chaotic states in an all optical bistable system was made with a single mode optical fibre as the transparent nonlinear medium in a ring cavity[33], the refractive index here being directly modified by the input intensity through the Kerr effect. Here, the high intensities required to induce sufficient nonlinearity precluded the use of a continuous wave (cw) input source and instead a mode-locked train of intense short pulses, separated in time by an amount equal to the round trip time of the ring cavity, was used. Each pulse is, in effect, an iterative step in which the signal of one pulse in circulating the ring cavity adds to the signal of the next incoming pulse, the process repeating for the whole train. Since bifurcations are caused by the interference between the incident field and cavity field which, suffers a nonlinear phase shift in each round trip of the cavity (see equation (6)), the transmitted signal is evidently modified by the intensity of the pulses. With this system period doubling followed by chaos was observed.

The most fundamental of all nonlinear optical systems is nevertheless, one containing a two-level medium as originally analysed by Ikeda for a ring cavity[33]. Near resonant excitation of the medium will, for a sufficiently intense incident signal, cause saturation of the absorption which thereby modifies the associated anomalous dispersion feature of the two-level transition. The mechanism is, in many respects, equivalent to that which gives rise to mode splitting in lasers described earlier for a two-level gain rather than absorptive medium. As for the laser, the intensity dependent change in refraction (dispersion) is resonantly enhanced resulting in considerably reduced power requirements to those used in the fibre experiments. Both atomic and molecular gases are potentially useful media for investigation here, providing discrete levels many of which are in near resonance with available laser lines and approximate reasonably closely to two-level systems. The first corroboration of period doubling routes to chaos in such systems were made in both ring and Fabry-Perot cavities containing ammonia gas near resonantly-excited by pulsed CO_2 radiation[34,35] Recently, experiments have been extended to cw pump laser conditions[36] in which sodium vapour was used as the nonlinear medium. Preliminary results show evidence of period doubling with additional instabilities yet to be fully characterized.

Recognizing the problems that chaotic behaviour may pose for fast all-optical bistable elements, yet, operated in the period doubling window and, in particular, period two oscillation, for which the operational parameter window is largest, they offer the attractive prospect of high-frequency all-optical modulators. But such an operation requires that the relaxation time of the nonlinear medium be much faster than the cavity round trip time, then for small devices (<1 mm in length) the frequency of modulation may, in principle, be in the THz range provided that nonlinear materials may be found with sufficiently short relaxation times. The search for fast large nonlinearities is one of the main efforts in this area.

Conclusions

Nonlinear optics is proving valuable to the fields of nonlinear dynamics and deterministic chaos. On one hand, basically simple optical systems can be constructed exhibiting the most interesting classes of chaotic behaviour enriched by the possibility of a quantum description. On the other hand, lasers and related nonlinear otical devices have a large and growing technical application, and the understanding, control and possible exploitation of sources of instability in these systems has considerable practical importance.

Experimental findings are, in general, not yet sufficiently comprehensive to permit the quantitative analysis necessary to fully test the theoretical models. More carefully controlled experiments are forthcoming from which, along with time series, power spectra and identification of routes to chaos, embedding procedures may be implemented to the attractors describing the dynamical behaviour of these systems.

More detailed discussions of points in this review can be found elsewhere. For laser instabilities see refs 37-39 and also refs 40, 41 which cover both active and passive systems. For passive systems see ref. 42. Comprehensive treatments on the more general principles of deterministic chaos can be found in refs 3, 4. See the recent text on deterministic chaos by Schuster[43]. See refs 8, 9, 44–46 for articles on the general aspects of deterministic chaos, and refs 47 and 48 for discussions on the device application of optical bistable systems.

1. Lorenz, E. N. *J. atoms. Sci.* **20**, 130 (1963).
2. Whitney, H. *Annls Math.* **37**, 645 (1936).
3. Haken, H. *Synergetics—An Introduction* (Springer, Berlin, 1983).
4. Haken, H. *Advanced Synergetics* (Springer, Berlin, 1983).
5. Grossman S & Thomae, S. *Z. Naturforschung.* **32A**, 1353 (1977).
6. Feigenbaum, F. J. *J. Stat. Phys.* **19**, 25 (1978).
7. Coulett, P. & Tresser, J. *J. Phys. Paris* **C5**, 25 (1978).
8. May, R. M. *Nature* **261**, 459 (1976).
9. Feigenbaum M. J. *Physica* **7D**, 16 (1983).
10. Manneville, P. & Pomeau, Y. *Phys. Lett.* **75A**, 1 (1979).
11. Landau, L. D. *Acad. Sci. USSR* **44**, 311 (1944).
12. Landau, L. D. & Lifshitz, E. M. *Fluid Mechanics* (Pergamon, Oxford, 1959).
13. Ruelle, D. & Takens, F. *Commun. Math. Phys.* **20**, 167 (1971).
14. Newhouse, S., Ruelle, D. & Takens, F. *Commun. math. Phys.* **64**, 35 (1978).
15. Haken, H. *Phys. Lett.* **53A**, 77 (1975).
16. Hogenboom, E. H. M. Klische, W., Weiss, C. O. & Godone, A. *Phys. Rev. Lett.* **55**, 2571 (1985).
17. Arecchi, F. T., Lippi, G. L., Puccioni, G. P. & Tredicce, J. R. *Opt. Commun.* **51**, 308 (1984).
18. Scholz, H. J., Yamada, T., Brant, H. & Graham, R. *Phys. Lett.* **82A**, 321 (1981).
19. Arecchi, F. T., Meucci, R., Puccioni, G. P. & Tredicce, J. R. *Phys. Rev. Lett.* **49**, 1217 (1982).
20. Midavaine, T., Dangisse, D. & Glorieux, P. *Phys. Rev. Lett.* **55** 1989 (1985).
21. Lugiato, L. A., Narducci, L., Bandy, D. K. & Pennise, C. A. *Opt. Commun.* **46**, 64 (1983).
22. Mandel, P. & Zeglache, H. *Opt. Commun.* **47**, 146 (1983).
23. Casperson, L. W. *Phys. Rev.* A **21**, 911 (1980).
24. Abraham, N. B. *et al.* Lecture notes in Physics, Vol. 182, 107 (Springer, Berlin, 1983).
25. Gioggia, R. S. & Abraham, N. B. *Phys. Rev. Lett.* **51**, 650 (1983).
26. Harrison, R. G. & Biswas, D. J. *Phys. Rev. Lett.* **55**, 63 (1985).
27. Casperson, L. W. & Yariv, A. *Appl. Phys. Lett.* **17**, 259 (1970).
28. Hendow, S. & Sargent, M. III, *J. opt. soc. Am.* B **2**, 84 (1985)
29. Ikeda, K. *Opt. Commun* **30**, 257 (1979).
30. Ikeda, K. & Daido, H. *Phys. Rev. Lett* **45**, 709 (1980).
31. Gibbs, H. M., Hopf, F. A., Kaplan, D. L. & Shoemaker, R. L. *Phys. Rev. Lett* **46**, [illegible] (1981)
32. Crutchfield, J. P & Huberman, B. A. *Phys. Lett.* **77A**, 407 (1980).
33. Nakatsuka, H., Asaka, S., Itoh, H., Ikeda, K. & Matsuoka, M. *Phys. Rev. Lett* **50**, 109 (1983)
34. Harrison, R. G., Firth, W. J., Emshary, C. A. & Al-Saidi, I. A. *Phys. Rev. Lett.* **51**, 362 (1983)
35. Harrison, R. G., Firth, W. J. & Al-Saidi, I. A. *Phys. Rev. Lett.* **53**, 258 (1984)
36. Gibbs, H. M. *et al. Proc. OSA Topical Meet. on Instabilities and Dynamics of Lasers and Nonlinear Optical Systems*, Rochester (1985).
37. Abraham, N. B *Laser Focus* 73 (May 1983).
38. Harrison, R. G. & Biswas, D. J. *Progress in Quantum Electronics* **10**, 147 (Pergamon, Oxford, 1985).
39. *J. Opt. Soc. Am. B, Spec. Iss. Instabilities in Active Optical Media* **2**, 1-272 (1985)
40. Ackerhalt, J. R., Milonni, P. W. & Shih, M. L. *Phys. Rep.* **128**, 205 300 (1985)
41. Arecchi, F. T. & Harrison, R. G. (eds) *Instabilities and Chaos in Quantum Optics* (Springer, Berlin, in the press).
42. Gibbs, H. M. *Optical Bistability: Controlling Light with Light* (Academic, New York, 1985)
43. Schuster, H. G. *Deterministic Chaos* (Physik, Berlin, 1984)
44. Eckmann, J. P. & Ruelle, D. *Rev. Mod. Phys.* **57**, 617 (1985).
45. Swinney, H. L. *Physica* 7D, 3 (1985).
46. Farmer, J. D., Ott, E. & Yorke, J. A. *Physica* 7D, 153 (1985).
47. Miller, D. A. B. *Laser Focus* **18**, 79 (1982).
48. Smith, S. D. *et al. Opt. Engn* **24**, 569 (1985).
49. Weiss, C. O., Klische, W., Ering, P. S. & Cooper, M. *Opt. Commun* **52**, 405 (1985)
50. Weiss, C. O., Godone, A. & Olafsson, A. *Phys. Rev. A* **28**, 892 (1983)
51. Biswas, D. J. & Harrison, R. G. *Phys. Rev. (Rap. comoun.)* A **32**, 3835 (1985)
52. Minden, M. L. & Casperson, L. W. *J. opt. Soc. Am.* B **2**, 120 (1985).

Observation of an unexplained event from a magnetic monopole detector

A. D. Caplin, M. Hardiman*, M. Koratzinos & J. C. Schouten*

Blackett Laboratory, Imperial College, London SW7 2BZ, UK

A single event was recorded by our 0.18 m^2 inductive magnetic monopole detector, in a total effective observation time of 8,242 hours. None of the monitoring channels that record vibration, radiofrequency interference, and so on, indicated any extraneous cause for this event. An astrophysical estimate of the maximum number flux of monopoles suggests that the chances of a monopole having caused the event are less than 1 in 10^3. Alternative explanations for the candidate are considered, but none of them seem likely.

GRAND unification theories (GUTs) suggest that massive magnetic monopoles (mass $\sim 10^{16}$ GeV) were created profusely during the very early stages of the formation of the Universe, while it was still extremely hot. These electrically neutral monopoles should carry magnetic charge h/e, as do the magnetic monopoles introduced by Dirac[1] more than 50 years ago, or perhaps a small integer multiple of the Dirac charge. The question of how many monopoles are still to be found is much less certain[2]; at one extreme, theories of inflation[3] require that there is at most one monopole in our Universe. There is general agreement that any surviving GUTs monopoles should be moving rather slowly compared with the velocity of light, and consequently interact very weakly with matter; for this reason they are expected to be highly penetrating. The observation 4 years ago by Cabrera[4] of a candidate cosmic magnetic monopole, using a small (10 cm^2) inductive detector, stimulated considerable experimental and theoretical activity[2]. An immediate problem was that Cabrera's candidate, if genuine, implied a number flux of monopoles far higher than astrophysical estimates appeared to allow. This 'Parker' bound[5] arises from considering the outflow of energy from galactic magnetic fields to magnetic monopoles accelerated by passing through them, and comparing it with the rate at which the fields can be regenerated. Although there are some uncertainties[6], the limit seems to be $\sim 10^{-15}$ cm^{-2} sr^{-1} s^{-1}, equivalent, on average, to ~ 1 monopole per 10^6 yr through Cabrera's original detector.

Inductive detectors

The attractive feature of inductive detectors is that they are specific to magnetically-charged particles, and do not respond to electric charges or magnetic dipoles. A magnetic charge traversing a closed conducting loop induces a current, by Faraday's law of induction, that generates magnetic flux equal in magnitude to that carried by the magnetic charge. The magnetic flux associated with a Dirac monopole is 4.1×10^{-15} Wb, equal to $2\Phi_0$, where Φ_0 is the flux quantum of superconductivity. The size of the induced current is independent of monopole speed, and, for an isolated loop, of monopole trajectory. In practical detectors, the loop is made superconducting, so that the induced current is permanent and more easily measurable. The required current sensitivity of nA or better can be attained, non-dissipatively, with SQUIDs (superconducting quantum interference devices). One further use of superconductors in monopole detectors is the incorporation of a superconducting shield around the detector loops, which screens them from external field changes that would otherwise also induce currents. However, the presence of the shield complicates the response of the detector loop to a monopole: the size of induced current is then affected by trajectory, to a degree that depends on relative sizes of loop and shield. It is usual to include also some room temperature magnetic shielding (mu-metal or similar), to reduce the field acting on the superconducting shield.

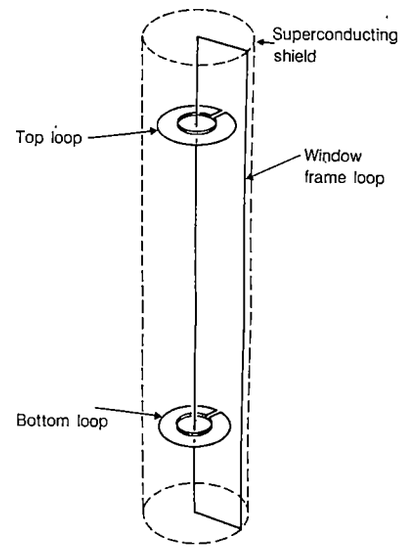


Fig. 1 Configuration of the three independent loops in the Imperial College monopole detector. The superconducting shield, indicated by the dashed line, is 960 mm high and 234 mm in diameter. For clarity, the SQUIDS (positioned near the top of the shield), calibration coils and other details have been omitted.

The design of recent inductive searches[7-10] (none of which reported any candidate monopoles) has been directed towards: (1) greatly enlarged detector area; (2) eliminating, or at least monitoring, as many as possible potential causes of spurious monopole-like events, and (3) the provision of multiple detector loops. Our detector[9,11], designed soon after Cabrera's original report, has three independent detector loops (Fig. 1). The two circular loops (the B and T loops) each has area averaged over 4π of 100 cm^2; if the number flux of magnetic monopoles were to be, for some reason, many orders of magnitude above the Parker limit, the B and T loops would detect events (relatively) frequently. Also, the presence or absence of coincident signals in the B and T loops would provide a limited degree of directional information. The third 'window-frame' (WF) loop serves two purposes: any monopole passing through one of the circular loops would give a confirmatory coincident signal in the WF loop. The other role of the WF loop is to maximize the effective detector area within the available low-temperature and magnetically-shielded volume; it is arranged so that any monopole track through the superconducting shield, even one that has not intersected the WF loop itself, gives a signal. However, the signal

* Present addresses: School of Mathematical and Physical Sciences, University of Sussex, Falmer, Brighton, Sussex, BN1 9QH, UK (M.H.); Oxford Instruments Ltd, Osney Mead, Oxford OX2 0DX, UK (J.C.S.).

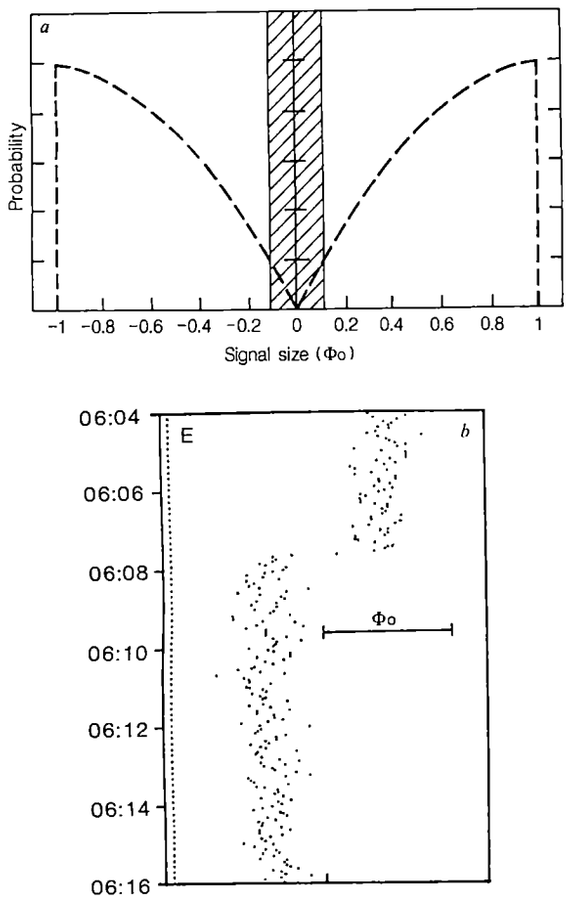


Fig. 2 *a*, The probability distribution of signal sizes in the WF loop, calculated for an isotropic influx of monopoles. Signals within the hatched region are too small to activate the event trigger. *b*, Section of the detailed high-frequency (20 samples per second) record, showing event-160 recorded at 07.06 h (BST) on 11 August 1985. Time is shown in minutes and seconds. The bar indicates the offset corresponding to a change in flux of Φ_0.

size in the WF loop does depend on monopole trajectory, and ranges between 0 and 1 Φ_0 (Fig. 2*a*), and less than half of all trajectories give a measurable coincident signal in the B or T loops[11].

We anticipated three main causes of spurious events: mechanical shock, radiofrequency (r.f.) interference and magnetic field changes. As far as possible, the detector design incorporated isolation from these factors, and in addition we included relevant monitors (accelerometer, r.f. detector and magnetometer). The detector was tested with deliberate external disturbance, at levels of at least two orders of magnitude greater than ambient, and found to be totally insensitive to r.f. interference and changes in external magnetic field. However, it did respond to pressure fluctuations within the helium cryostat, arising from other users of the helium return line; isolation was improved and a pressure monitor added.

The detector loop currents are amplified with a bandwidth of 10 Hz, chosen so that the peak-to-peak noise approaches Φ_0 in magnitude, and thus maximizing the amount of significant information that is collected. A computer controlled data acquisition system (DAS) samples each detector and monitor channel 20 times per second. Shifts in any one of the detector outputs of more than a fraction of a Φ_0 occurring in a period of <100 s trigger storage of the data on floppy disc; this record covers 300 s before the trigger and 100 s after it. Digital filtering of the recorded data allows the bandwidth to be narrowed to $\sim 10^{-2}$ Hz, and the r.m.s. noise to be reduced to $\sim 10^{-2}$ Φ_0. In addition, less detailed data, the maxima and minima in each channel for every 100-s period, are available as a permanent printed record. As a further precaution, the three detector outputs are recorded also on conventional chart recorders.

The detector became fully operational in September 1984, and we have reported previously[9] on its first half-year of operation. During that period, there were about 110 putative events recorded by the DAS; most had immediate and obvious causes, such as low helium level, or cryostat pressure fluctuations. However, there were 12 'non-trivial' events, of which eight were in the T loop (almost certainly caused by a 'weak-link' in the superconducting circuit), three in the WF loop (associated with preceding mechanical shock), and one in the B loop (at a time when that channel was unstable); thus, detailed examination of the record allowed all 12 'non-trivial' events to be discarded as candidate monopoles[9]. The detector continued to run until 30 September 1985, accumulating a total of 8,242 h of active observation. In the second half-year, there were a further 60 putative events, but apart from the one event considered here, there were none in the 'non-trivial' category.

Detailed analysis of the total 170 putative events will be published elsewhere[11], but note that not one of them could be ascribed to two of the anticipated sources of interference: r.f. spikes and external magnetic field changes (r.f. interference in our laboratory is substantial, with capacitor bank discharges in nearby rooms, and a powerful short-wave transmitter at a distance of 50 m; the local magnetic field fluctuates by about 10^{-6} T, with the largest contribution from nearby lifts). This immunity is consistent with the tests on the detector mentioned above. In July 1985, the magnetometer became needed urgently elsewhere, and was removed from the experiment.

11 August 1985 event

At 07.06 h BST on Sunday 11 August 1985, event-160 occurred (Fig. 2*b*), of magnitude $0.83 \pm 0.04\ \Phi_0$ (the uncertainty is primarily that in the calibration of the detector loop), close to the maximum in the calculated distribution of signal sizes in this loop (Fig. 2*a*).

At the time of event-160, the two other detector channels, the B and T loops, showed no obvious coincident offsets; detailed analysis of the data puts limits of 0.01 ± 0.04 (standard deviation, s.d.) and 0.02 ± 0.06 (s.d.) Φ_0 on the signals in those channels. The noise levels in all three detector channels had their usual magnitudes, and application of a range of statistical tests to the data revealed no anomalies. Nor was any obvious abnormal behaviour to be seen in the channels monitoring vibration, r.f. interference and cryostat pressure.

Inspection of the less detailed monitoring record and of the conventional chart records for the days before and after event-160 revealed nothing unusual. The weekly liquid helium refill had been on 6 August, with a moderately noisy period on 7–8 August which always occurs after a refill, and is probably caused by differential thermal expansion within the cryostat. From 11.00 h on 10 August to 09.00 h on 12 August conditions were very quiet, but not unusually so for a weekend. As soon as possible after the event occurred, the detector system, including the monitoring devices, was checked thoroughly for normal operation.

The detector was allowed to continue running normally until 30 September, and then subjected, while still at helium temperatures, to tests. Finally, it was warmed slowly to room temperature, so that an internal inspection could be made.

Later, detailed statistical analysis of the data for event-160 turned up one feature that had no immediate explanation: in quiet (night-time and weekend) conditions the output of the r.f. monitor has a characteristic pattern, with a mean of 5V and peak-to-peak fluctuations of 2V. The r.f. record for event-160 showed the usual pattern, but superimposed on it was a small,

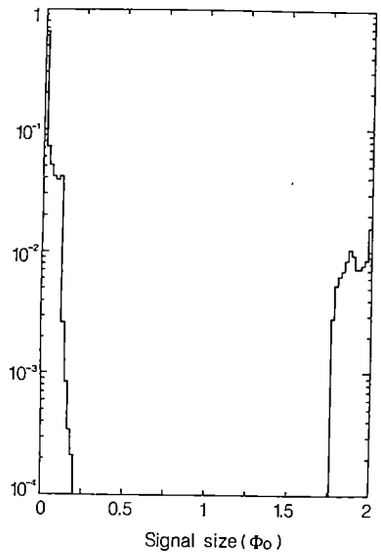


Fig. 3 The probability distribution of signal sizes in the B and T loops, calculated for those monopole trajectories, selected from an isotropic influx, that give a WF signal in the range 0.78–0.88 Φ_0. Positive and negative signals are equally likely.

though statistically highly significant, increase of 100 mV in the mean level, coincident in time with the event itself. We believe this shift to be a consequence of the offset in the WF channel, and it is, therefore, simply an instrumental artefact. The essence of the mechanism linking the two channels is as follows: in quiet conditions, ~90% of the recorded r.f. interference is self-generated, by the digital pulses transmitted between the DAS and its controlling computer. Thus, the pattern of binary digits representing the signals in the various channels is itself the prime determinant of the r.f. level. Event-160 caused a sign change in the output of the WF loop, and the sign is read by the DAS as the most significant bit. The sign bit was always positive before the event, and negative afterwards, and thereby altered the radiated r.f. interference in a systematic fashion. In practice, the mechanism so far described is complicated by the presence in the r.f. monitor of a peak sample- and-hold amplifier with 0.1 s time constant (its function is to ensure that fast r.f. spikes are recorded properly), so that there is in effect a convolution of the r.f. radiated over a period of a few tenths of a second. This complication removes the straight one-to-one relationship between the digit pattern in the WF channel, say, and the recorded r.f. level. However, a simple statistical test on the data for event-160 demonstrated that such an effect was present: because the mangetometer was at that time disconnected, its channel to the DAS was digitized as a small number fluctuating about zero. A correlation with the r.f. channel showed that the consequent alternation of sign sometimes produced changes in the r.f. level of ~150 mV in the correct sense. That the effect was not always present, and that when it was there it gave an offset slightly larger than the 100 mV increase associated with event-160, is understandable in terms of the effect of the peak sample-and-hold amplifier. An experimental test was then made in quiet nightime conditions, using a square-wave oscillator at about 0.5 Hz connected to the WF channel of the DAS. Again, a response in the r.f. channel could be produced.

Thus all our checks show that event-160 took place at a time when the detector was functioning properly, and in the absence of any indication of external interference.

The record of event-160 meets the 'risetime' criterion that can be imposed: relic monopoles, if they exist, are believed to be moving rather slowly, $v/c \sim 10^{-3}$, but it is unlikely that their speed is orders of magnitude less than that[2]. Consequently, the transit time of a monopole through our detector should be of the order of microseconds. The 10-Hz bandwidth of the amplified detector loop outputs is equivalent to a 65 ms risetime (0–90%) for a step input; the record of event-160 shows that its risetime is less than two sampling periods (100 ms), and is certainly consistent with a step input, as would be given by a monopole.

We have calculated the distribution of event sizes in the B and T channels for monopole trajectories giving WF signals in the range 0.78–0.88 Φ_0 (Fig. 3). About 70% of such tracks give signals that are $<0.1\ \Phi_0$, which would be below the noise level, so that the absence of a signal in either the B or T channels coincident with event-160 in the WF channel is consistent with that event being caused by a monopole. Furthermore, if some signal of improbable size had been seen in either of those two channels, it would have indicated the presence of a spurious cause for event-160.

Possible explanations

Unauthorized interference. Appropriately sized offsets can be induced manually, by adjusting the SQUID control unit, but our attempts to do so were not fast enough to be recorded as risetime limited events. Also, tests showed that it was practically impossible to enter and leave the laboratory without there being some trace on the accelerometer. On these two counts, we believe that this explanation can be discounted.

Electronic fault. An offset generated in the WF loop SQUID control unit could mimic a monopole. On one occasion we have had such a fault, which produced temporary offsets of $\sim 20\ \Phi_0$ that lasted for a few minutes, and recurred several times in a month. Faults of this kind could have any size up to $\sim 10^3\ \Phi_0$, and would be likely to recur, particularly if the control unit is given some mechanical shock. After event-160, none of these symptoms were apparent. At the end of our observation period, all three SQUID control units were examined for evidence of electrical and mechanical failure. None was found, apart from some mild corrosion on a printed circuit board in the WF unit; that particular board was remote from the section of the unit that could easily produce offsets.

A fault in the data acquisition system can be excluded because of the 'back-up' chart recorder which showed an appropriate offset corresponding to event-160.

Mechanical shock. As described previously[9], we have seen several events, particularly in the WF loop, that have been induced by mechanical shock; sometimes these have been accompanied by small offsets in the B loop. The mechanism for this response to shock is, we believe, small movements and distortions of the detector loop assembly within the superconducting shield, which alter slightly the coupling of residual flux into the loops; the design of the B and T loops makes them intrinsically less sensitive than the WF loop to this effect.

The accelerometer is mounted at the top of the cryostat, and responds to accelerations in a single direction (in directions perpendicular to its axis, the sensor response is down by about two orders of magnitude). Consequently, no quantitative correlation can be expected between the size of an event induced by this mechanism, and the recorded shock amplitude. However, we found a well-defined trend linking the two (Fig. 4).

Throughout the 400 s detailed record of event-160, the vibration level was $<5\times10^{-4}\ g$, and for the previous 20 h had not exceeded $2\times10^{-3}\ g$ (weekday peak levels are up to $10^{-1}\ g$). The low level of vibration at the time of event-160, and for an extended period before and after, sets it well away from the trend of Fig. 4, suggesting that the event was not caused by mechanical shock.

Motion of trapped flux in the shield. When it was cooled down, the superconducting shield surrounding the detector loops trapped the residual magnetic flux, estimated to correspond to a field of about 10^{-9} T (the field inside the room temperature

nagnetic shields). In principle, this flux is thermodynamically netastable, and if it were to move, it could simulate the passage of a monopole. Because the WF loop is coupled strongly to the shield, whereas the B and T loops are effectively decoupled, such flux motion would be likely to generate a larger signal in the WF loop than in the other two channels.

Movement of pinned flux can be activated thermally (although it may be possible to induce motion with mechanical shock, and in other ways), and so after the initial cooldown we followed the standard procedure of 'annealing' the shield, by maintaining it for some time above its usual operating temperature. Since then, there have been several occasions on which refilling with liquid helium has been delayed, and in consequence the shield has warmed slightly. Thus, any flux that was prone to move would most probably have done so during those periods. Also, the probability of flux depinning declines slowly (logarithmically[12]) with time.

Our detector is certainly much less stable when the helium level is low (and we, therefore, exclude such periods from the total of active observation time), but the data indicate that causes other than flux motion in the shield, such as mechanical movement arising from thermal expansion, are the main culprits. In any case, in those periods of low helium level, the offsets in the WF channel were usually $<0.2\,\Phi_0$; on just one occasion there was an offset of $0.4\,\Phi_0$.

Thus, even when the superconducting shield, which is made from 3-mm thick lead, is warmer than usual, we have seen no clear-cut evidence of flux moving in it. Our experience is similar to that of others (B. Cabrera, and H. Frisch, private communications), that low densities of trapped flux in thick superconducting shields are extremely stable.

While we cannot exclude flux motion in the shield as the cause of event-160, the empirical evidence is that it is unlikely.

Flux motion in SQUID sensor. The SQUID sensors are fabricated from blocks of superconductor (niobium), so that they also trap metastable magnetic flux.

Experiments have been carried out on SQUID sensors with short-circuited input terminals (so as to avoid confusion with effects generated external to the SQUID)[13], and it has been demonstrated that mechanical shock, either from the outside or internal shocks from thermal expansion, can induce offsets. These have been interpreted as arising from flux motion within the SQUID. However, those experiments were carried out in trapped fields of $\sim 10^{-4}$ T (ambient field), whereas our sensors are within the magnetic shields and in a field of only $\sim 10^{-9}$ T. There is some evidence (B. Cabrera, personal communication) that such offsets are larger and more frequent the higher the field.

In both the Stanford[7] and the Chicago[8] inductive detectors several offsets were seen, mostly soon after initial cool down, that were attributed tentatively to this cause (the absence of coincidence and also the signal sizes excluded those events as candidate monopoles). However, in those two experiments, the fields at the SQUIDs are respectively 2 and 3 orders of magnitude greater than in our detector, making them substantially more sensitive to this problem.

The evidence from our experiment indicates that mechanical shock from whatever source affects primarily the detector loops, rather than the SQUID sensors themselves: the WF channel responds most to mechanical shock, with occasional associated smaller offsets in the B and T channels; if it were the SQUID sensors that were being affected, we would expect to see uncorrelated offsets occurring at random in all three channels. As at Stanford and Chicago, our detector was much noisier in the first few days after initial cooldown (for example, events 0, 1 and 16, Fig. 4), and we believe that this was associated with relaxation of mechanical strain, in both the detector assembly and the cryostat, rather than in the SQUID sensors. The evidence of a year's experience with the detector, coupled with the reported behaviour of other experiments, gives us no reason to attribute event-160 to flux motion within the SQUID sensor.

Inadvertent excitation of calibration coils. Each detector loop is fitted with a toroidal calibration coil which can be energized externally. Event-160 could be simulated by a small current, of the order of 100 nA, being induced in the WF calibration coil. For example, if the insulation between the leads to the coil had broken down, thermoelectric voltages, which are invariably present at the microvolt level, could have generated sufficient current. When checked later, the insulation to these coils was in perfect condition, so we can exclude this possibility.

Mechanical fault in detector. When all other checks had been completed, the detector was warmed slowly to room temperature and examined carefully. Some small lead shavings, typically 1-mm in size, were found on the detector loop formers. Presumably, when the detector was originally assembled, and the close-fitting lead shield was pulled over the formers, these particles were scraped off. Because the particles would be quite strongly diamagnetic when superconducting, the flux coupled into a detector loop would alter if a particle were to move. However, an order of magnitude calculation shows that even in the worst possible case, with the particle adjacent to the wire of the detector loop, the particles would need to be at least 10^2 larger in volume to give an offset of the size required. Consequently, we can rule out this mechanism.

In all other respects, the detector assembly was found to be in pristine condition.

Cosmic rays. We consider the likely effect of cosmic ray radiation on both the detector electronics and the SQUID sensor. At sea level, the total flux of neutrons produced by cosmic-ray primaries is $\sim 4\times10^{-2}\,\mathrm{cm^{-2}\,s^{-1}}$ for energies >100 keV, and $\sim 3\times10^{-3}\,\mathrm{cm^{-2}\,s^{-1}}$ for energies above 50 MeV (ref. 14); the proton fluxes at those energies are much lower. In the interaction of cosmic ray particles with solid state electronics, the reaction n (or p) + Si → α + heavy nucleus is thought to be the important mechanism[14]. Both reaction products can generate large numbers of electrons, up to 10^6, by ionization, leading to 'soft errors' (spontaneous changes in logic state) in memory circuits. Recently, Nicholls *et al.*[15] have found that, as the incident

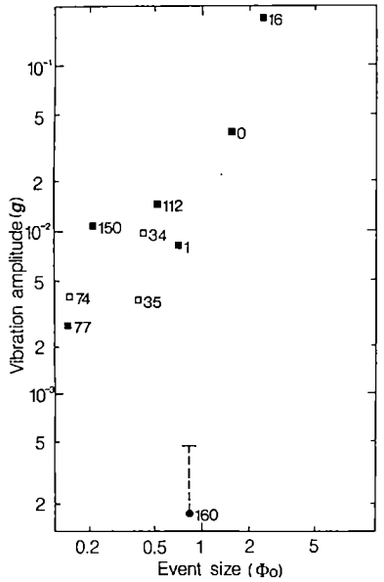


Fig. 4 Correlation between mechanical shock and event size in the WF channel. The shock is that measured at the top of the cryostat and the events are numbered in chronological order. ■, Events with simultaneous (within the 50-ms time resolution of the data acquisition system) shock and event; □, events with preceding shocks, as discussed in ref. 9. ●, Event-160 (the attached bar indicates the maximum shock during the entire 400 s detailed record of the event).

particle energy increases from 20 to 50 MeV, the soft error rate in a variety of devices rises sharply.

Ziegler *et al.*[16] have subjected a small superconducting inductive magnetic monopole detector (with identical SQUID electronics to ours) to bombardment with neutrons of energies 10–16 MeV, and a total dose of 8.6×10^8 neutrons cm^{-2} (equivalent to seven centuries of cosmic-ray dose), and observed no offsets in the detector output. However, in the light of Nicholls *et al.*'s most recent data on energy dependence[15], Ziegler has suggested (personal communication) that their experiment on a monopole detector should be repeated at higher neutron energies.

Our detector would have been subjected to a total flux of cosmic-ray neutrons with energies above 50 MeV of $\sim10^5$ cm^{-2}. The active area of semiconductor devices in significant sections of the circuitry is not more than 10^{-1} cm^2; in Si about 10^{-6} α particles are generated per cosmic-ray neutron[14], so we estimate the probability of a soft error type of charge burst as $\sim10^{-2}$ y^{-1}. However, the mechanism by which such an event might affect the SQUID electronics is unclear: any change in the SQUID control logic circuitry would almost certainly lead to offsets orders of magnitude larger than event-160. Another possibility is that defects created during a soft error type of event could change sufficiently the operating point of a device in the analogue section of the circuitry, and so induce an offset.

The behaviour of Josephson junctions under α-irradiation has been studied also[17]. Near the critical current of the junctions, the 'upset' rate per α particle approaches unity. The rate at which α particles are produced by cosmic-ray neutron bombardment is not strongly target dependent, so we may estimate the α-particle flux (generated by neutrons with energies above 50 MeV) incident on our SQUID sensors as 0.3 cm^{-2} yr^{-1}. The SQUID weak link has area $\sim10^{-6}$ cm^2, so that the probability of a cosmic-ray induced SQUID offset is no more than 10^{-6} yr^{-1}. Were such an offset to occur, we would again expect it to be much larger than event-160.

Although the probabilities of these cosmic-ray mechanisms are low, they are finite and cannot be discounted entirely.

Conclusions

So far, we have no obvious explanation for event-160. The total area-time product of our experiment corresponds to 400 'Cabreras', the unit of exposure equivalent to that of Cabrera's original experiment. The exposure of the three other large detectors now totals 800 'Cabreras' (refs 7, 8, 10 and B. Cabrera, personal communication), so that of itself, our candidate is not statistically at odds with the absence of events in the other experiments. At 90% confidence level, the three other experiments taken together give an upper bound on the cosmic monopole flux of 2×10^{-12} cm^{-2} sr^{-1} s^{-1}; if our experiment and its candidate event are included, there is a lower bound (at 90% confidence level) on the flux of 5×10^{-14} cm^{-2} sr^{-1} s^{-1}, which is still two orders of magnitude above the Parker limit. None of the alternative explanations that we have discussed here for event-160 seem particularly likely, and it is clearly possible that some yet unidentified cause was responsible for it. The results from the larger inductive detectors that are now under construction should help to resolve the puzzle.

We thank A. Cayless, A. Chhabra, W. G. Jones, D. Podger, W. S. Steer and D. Websdale for assistance. Financial support was received from the Particle Physics Committee of SERC and from Imperial College.

Received 6 February; accepted 26 March 1986.

1. Dirac, P. A. M. *Proc. R. Soc.* A133, 60-72 (1931).
2. Groom, D. E. *Phys. Rep.* (in the press).
3. Guth, A. H. *Phys. Rev.* D 23, 347-356 (1981).
4. Cabrera, B. *Phys. Rev. Lett.* 48, 1378-1381 (1982).
5. Turner, M. S., Parker, E. N. & Bogdan, T. J. *Phys. Rev.* D 26, 1296-1302 (1982).
6. Wasserman, I., Shapiro, S. L. & Farouki, R. *Commts Astrophys.* 10, 257-265 (1985).
7. Cabrera, B., Taber, M., Gardner, R. & Bourg, J. *Phys. Rev. Lett.* 51, 1933-1966 (1983).
8. Incandela, J. *et al. Phys. Rev. Lett.* 53, 2067-2070 (1984).
9. Caplin, A. D., Guy, C. N., Hardiman, M., Park, J. G. & Schouten, J. C. *Nature* 317, 234-236 (1985).
10. Bermon, S. *et al. Phys. Rev. Lett.* 55, 1850-1853 (1985).
11. Schouten, J. C. *et al. J. Phys.* E. (submitted).
12. Kim, Y. C., Hempstead, C. F. & Strnad, A. R. *Phys. Rev. Lett.* 9, 306-309 (1962).
13. Fickett, F. R., Cromar, M. & Clarke, A. F. in *Monopole 83* (ed. Stone, J. L.) 477-484 (Plenum, New York, 1984).
14. Ziegler, J. F. & Lanford, W. A. *J. appl. Phys.* 52, 4305-4312 (1981).
15. Nicholls, D. K., Price, W. E. & Andrews, J. L. *IEEE Trans. nucl. Sci.* 29, 2081-2084 (1982).
16. Ziegler, J. F. *et al. Phys. Rev.* D28, 1793-1795 (1983).
17. Magno, R., Nisenoff, M., Shelby, R., Kidd, J. & Campbell, A. B. *IEEE Trans. nucl. Sci.* 29, 2090-2094 (1982).

Molecular distinction between fetal and adult forms of muscle acetylcholine receptor

Masayoshi Mishina, Toshiyuki Takai, Keiji Imoto, Masaharu Noda, Tomoyuki Takahashi* & Shosaku Numa

Departments of Medical Chemistry and Molecular Genetics and * Physiology, Kyoto University Faculty of Medicine, Kyoto 606, Japan

Christoph Methfessel & Bert Sakmann

Max-Planck-Institut für biophysikalische Chemie, D-3400 Göttingen, FRG

Distinct classes of acetylcholine receptor channels are formed when Xenopus *oocytes are injected with combinations of the bovine α-, β-, γ- and δ- or the α-, β-, γ- and ε-subunit-specific messenger RNAs. The conductance and gating properties of the two classes of channels, in conjunction with the developmental changes in the muscular contents of the mRNAs, suggest that replacement of the γ-subunit by the ε-subunit is responsible for the functional alteration of the receptor during muscle development.*

DIFFERENT forms of the nicotinic acetylcholine receptor (AChR) occur in mammalian skeletal muscle during development. The AChR is present predominantly at the neuromuscular junction in adult muscle, whereas in fetal muscle, as well as in denervated adult muscle, the AChR is also found in the non-junctional membrane. The junctional and non-junctional types of AChR channels differ in conductance and gating properties[1-3]. During formation of the neuromuscular contact, two classes of AChR channels coexist in the same muscle fibre[4-7]. Some reports suggest that the different forms of the AChR are

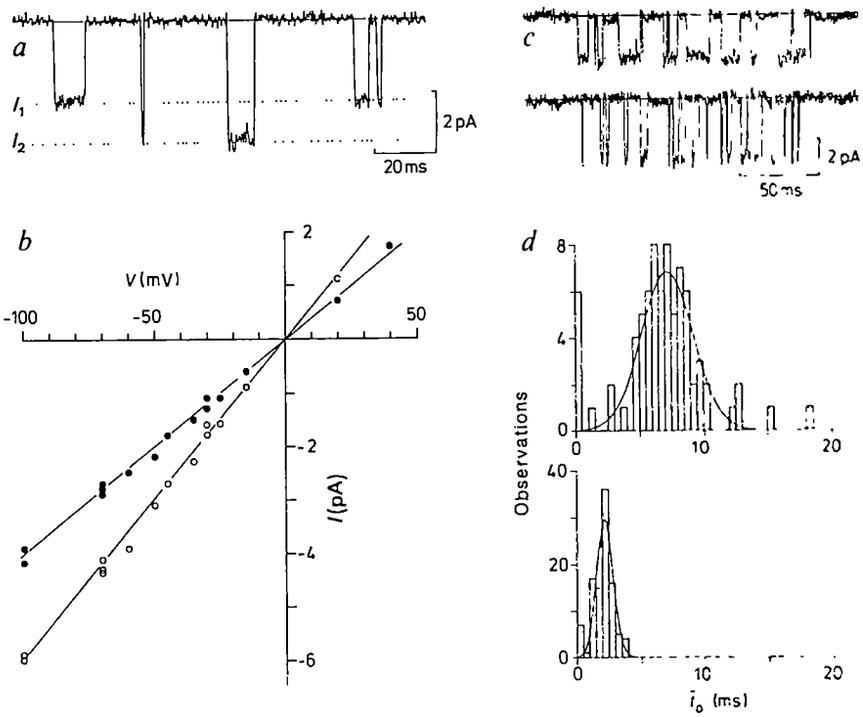


Fig. 1 Properties of ACh-activated single-channel currents in oocytes injected with the calf AChR α-, β-, γ-, δ- and ε-subunit-specific mRNAs. *a*, Single-channel currents activated by 0.5 μM ACh. Outside-out patch. Inward current downwards. Membrane potential, −60 mV. Low-pass filtering at 1 kHz (−3 dB). The short interruptions of the elementary currents occurring in the time range of tens of microseconds are largely attenuated. Two classes of elementary currents are observed and are marked by I_1 and I_2 (dotted lines). *b*, Single-channel I-V relations. Each point is the mean amplitude of at least 20 elementary currents. Data from four outside-out patches. Straight lines are linear regression lines and indicate channel conductances of 40 pS (filled symbols) and 60 pS (open symbols). Interpolated current reversal potentials are 0.6 mV and 0.5 mV, respectively. *c*, Bursts of single-channel currents activated by 10 μM ACh. Cell-attached patch recording. Two bursts recorded on the same patch are shown. Note that current pulses in the two bursts have different mean amplitudes of 2.3 pA and 3.4 pA. Membrane potential of −70 mV was estimated using single-channel conductances of 40 pS and 60 pS and the mean reversal potential of single-channel currents. In three experiments, the oocyte resting membrane potential was measured during patch current recording using an intracellular microelectrode. The reversal potential determined by interpolation of inward and outward currents was −10 ± 2 mV. *d*, Distribution histograms for the average durations of elementary currents during single bursts. Each entry represents the mean of the durations of all elementary currents occurring in a single burst ($\bar{t}_o$). Upper graph represents measurements on 40-pS conductance channel (77 bursts), lower graph on 60-pS conductance channel (101 bursts). Continuous lines are single gaussians. The left-most bins in both graphs and the two right-most bins in the upper graph were not taken into account. Means of the two distributions are 7.2 ± 2.0 ms (n = 69) and 2.3 ± 0.6 ms (n = 94). Cell-attached patch. Estimated membrane potential was −70 mV (that is, −60 mV driving potential). A burst was defined as any sequence of elementary currents separated by a closed interval longer than 50 ms. This value was chosen after inspection of the distribution of the closed intervals of the whole current record. It was characterized in both cases by a short component (5.4 ms and 6.4 ms average duration, >95% of the total area of the distribution in both cases) and two much longer components with durations of several hundreds of milliseconds. Bursts consisting of less than five current pulses were excluded.

Methods. The calf AChR α-, β-, γ-, δ- and ε-subunit-specific mRNAs were synthesized *in vitro*[25,28], combined in a molar ratio of 2:1:1.1:1 and injected into *Xenopus laevis* oocytes (total mRNA concentration, 160 ng μl^{-1}; average volume injected per oocyte, ~50 nl). Whole-cell current measurements[27,28] were made on oocytes after incubation[26] for 2–3 days. Single-channel current measurements were made on oocytes after 2–5 days' incubation followed by removal of the follicular cell layer and the vitelline membrane[28,36]. All single-channel current recordings were carried out at 21 ± 1 °C. In experiments with outside-out patches, pipettes[28] were filled with a solution of the following composition (in mM): KCl, 20; KF, 80; $MgCl_2$, 1; EGTA, 10; HEPES (*p*H 7.2), 10. The extracellular solution had the composition (in mM): NaCl, 115; KCl, 2.5; $CaCl_2$, 1.8; HEPES (*p*H 7.2), 10. Patch membrane potentials of outside-out patches were obtained by correcting the pipette potential by −5 mV for liquid junction potentials[37]. In records from cell-attached patches, the pipette was filled with extracellular solution with ACh added at 0.5–1 μM or 10 μM. Patch-clamp currents were stored on magnetic tape, filtered at 1 kHz (−3 dB), digitized at 0.2-ms intervals and analysed in a PDP 11/73 computer by a semi-automatic procedure to compute distributions of current amplitudes and durations[38]. Distributions of amplitudes were fitted with one or two gaussians and distributions of durations by one or two exponential components; those with two components were made by maximizing the likelihood function[39].

structurally distinct[8]. The mammalian muscle AChR is thought to have a subunit structure of $\alpha_2\beta\gamma\delta$, as is the case for the *Torpedo* electroplax AChR[9–11]. The primary structures of all four subunits of fish[12–17] and mammalian AChRs[18–24] have been elucidated by recombinant DNA techniques. In addition, a novel subunit, termed the ε-subunit, has been discovered by cloning and sequencing the DNA complementary to the calf muscle messenger RNA encoding it[25]. cDNA expression studies with *Xenopus* oocytes[25–27] have indicated that the calf ε-subunit, which shows higher sequence homology with the γ-subunit than with any other subunit, can replace the *Torpedo* γ-subunit to form the functional receptor in combination with the *Torpedo* α-, β- and δ-subunits. Single-channel current measurements have indicated that hybrid AChRs composed of subunits from the two species form channels possessing different gating behaviour[28]. These findings raise the intriguing possibility that the different forms of the AChR observed during muscle development may arise from different combinations of the subunits.

One approach to this issue would be to produce AChR channels in *Xenopus* oocytes by microinjection of various combinations of the subunit-specific mRNAs and to compare the conductance and gating properties of these channels with those of native AChR channels in fetal and adult muscle. We report here that oocytes injected with mRNAs specific for the α-, β-, γ-, δ- and ε-subunits of the calf muscle AChR yield two distinct classes of AChR channels. In contrast, only one of these two channel classes is formed in oocytes injected either with the α-, β-, γ- and δ-subunit-specific mRNAs or with the α-, β-, δ- and ε-subunit-specific mRNAs. The two classes of channels, designated $AChR_\gamma$ and $AChR_\varepsilon$ respectively, differ in conductance and gating behaviour; $AChR_\gamma$ is similar in single-channel properties to the AChR in fetal calf muscle, whereas $AChR_\varepsilon$ resembles the AChR in adult bovine muscle. This finding, together with the developmental changes observed in the contents of the γ- and ε-subunit mRNAs in bovine muscle, suggests that the different properties of the fetal and adult muscle AChRs are a result of the γ-subunit being replaced by the ε-subunit during muscle development.

AChR channels from five subunits

The mRNAs specific for the α-, β-, γ-, δ- and ε-subunits of the calf muscle AChR were synthesized by transcription *in vitro* of the respective cDNAs as described previously[25,28]. The five subunit-specific mRNAs were combined and injected into *Xenopus* oocytes. Figure 1*a* shows a record of acetylcholine (ACh)-activated single-channel currents from an outside-out membrane patch isolated from an oocyte implanted with the five AChR subunits. The distribution of current amplitudes is characterized by two well-separated peaks of mean amplitude 2.6 pA and 3.9 pA (at −60 mV membrane potential). The single-channel current–voltage (I–V) relations of both classes of

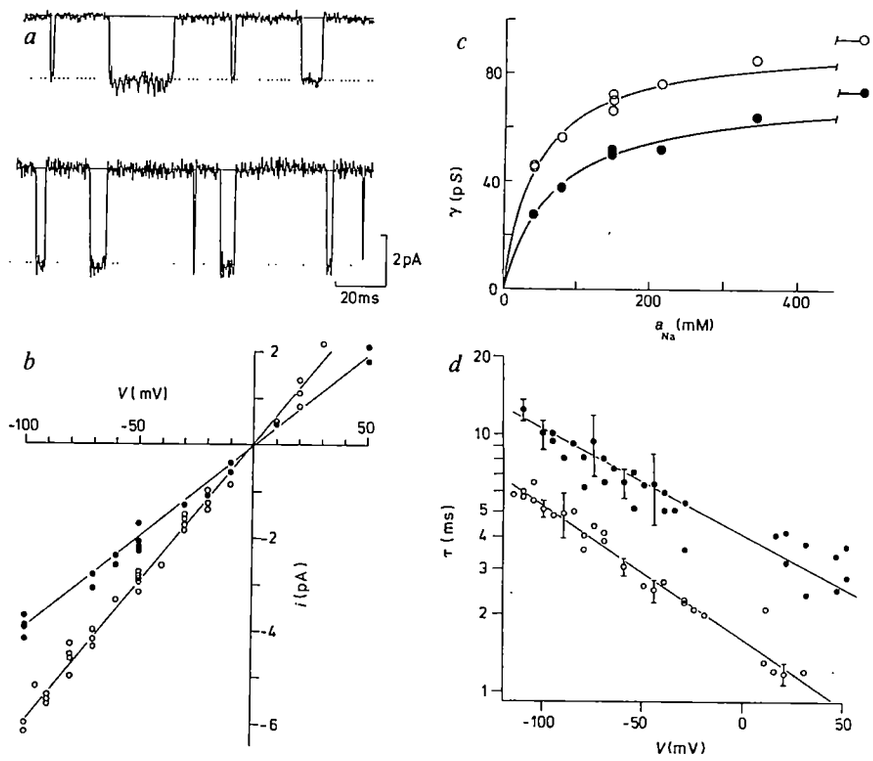


Fig. 2 Properties of ACh-activated single-channel currents in oocytes injected with the α-, β-, γ- and δ-subunit-specific mRNAs ($AChR_\gamma$) or with the α-, β-, δ- and ε-subunit-specifit mRNAs ($AChR_\varepsilon$). *a*, Single-channel currents activated by 0.5 μM ACh. Outside-out patches. Inward current downwards. Upper trace, recording from an oocyte with $AChR_\gamma$. Mean current amplitude, 2.4 pA. Lower trace, recording from an oocyte with $AChR_\varepsilon$. Mean current amplitude, 3.6 pA. Membrane potential, −60 mV in both experiments. Low-pass filtering at 1 kHz (−3 dB). *b*, Single-channel I-V relations of the $AChR_\gamma$ (filled symbols, 7 outside-out patches) and the $AChR_\varepsilon$ channel (open symbols, 6 outside-out patches). Straight lines are linear regression lines. Their slopes are 39 pS and 59 pS for the $AChR_\gamma$ and $AChR_\varepsilon$ channels, respectively. Interpolated current reversal potentials are 1.3 mV and −0.2 mV. *c*, Conductance (γ) versus Na^+ activity (a_{Na}) for $AChR_\gamma$ (filled symbols) and $AChR_\varepsilon$ (open symbols). Slope conductance was measured at −20 to −100 mV driving potential on outside-out patches. The I-V relations in this region were fitted by linear regression lines. The pipette solution was as described in Fig. 1 legend. The extracellular solution contained 50–500 mM Na^+ and 1.8 mM $CaCl_2$. The Na^+ activities are those for pure NaCl solutions[39]. No correction for the differences in osmolarity of various extracellular solutions was made. Continuous lines represent hyperbolas according to $\gamma = \gamma_{max} a_{Na}/(a_{Na} + K_m)$, where γ_{max} is the limiting conductance and K_m is the Na^+ activity at which the channel conductance is half-maximal. Limiting conductances of 75 pS for $AChR_\gamma$ and 93 pS for $AChR_\varepsilon$, obtained by a nonlinear least-squares fit, are indicated by the symbols on the right. Half-saturating Na^+ activities were 73 mM for $AChR_\gamma$ and 46 mM for $AChR_\varepsilon$. *d*, Average duration (τ) of elementary currents versus membrane potential in semilogarithmic coordinates. Filled symbols, $AChR_\gamma$ channel; open symbols, $AChR_\varepsilon$ channel. Data are from seven (filled symbols) and six (open symbols) cell-attached patch recordings. Each point represents a determination of τ from the distribution of single-channel currents or from noise analysis of the single-channel current record (see Methods). Bars indicate 1 s.d. from 3–7 patches. Lines represent linear regression fits as specified in Table 1.

Methods. To avoid slight contamination by aberrant AChR channels resulting from injection of the α-, β- and δ-subunit-specific mRNAs (see text), oocytes were injected either with the α-, β-, γ- and δ-subunit-specific mRNAs or with the α-, β-, ε- and δ-subunit-specific mRNAs in a molar ratio of 2:1:10:1 (total mRNA concentration, 6.4 ng μl^{-1}; average volume injected per oocyte, ~50 nl). Patch current recording as described in Fig. 1 legend. In cell-attached recordings, the oocyte membrane potential was usually measured with an intracellular microelectrode (filled with 3 M KCl, 10–20 MΩ d.c. resistance) during the patch current recording. In some experiments, the oocyte membrane potential was estimated from the channel slope conductance and an assumed reversal potential of −10 mV. The average slope conductances were 40 ± 1 pS ($n = 9$) for the $AChR_\gamma$ and 59 ± 2 pS ($n = 7$) for the $AChR_\varepsilon$ channel. Current reversal potentials from whole-cell I-V relations were −11 ± 2 mV ($n = 5$) for the $AChR_\gamma$ and −9 ± 4 mV ($n = 3$) for the $AChR_\varepsilon$ channel. Current reversal potentials from single-channel I-V relations were −9 mV and −10 mV (mean of two patches) for the two channels. The average duration of elementary currents was estimated in two ways. In recordings with low channel opening frequency, where few superpositions (<5%) of elementary currents occured, τ was estimated as the longer of the decay constants fitted to the distribution of current durations[28]. In recordings where elementary currents superimposed more frequently, τ was estimated using standard techniques of noise analysis[31]. Segments of current record were low-pass filtered (0.8 kHz, 4-pole Butterworth) and digitized at 0.5- or 1-ms intervals. Power spectral densities were calculated on 512-point data sections by an integer Fast Fourier Transform routine on a PDP 11/34 computer; 30–80 such spectra were averaged. For the single-channel records close to the reversal potential, control spectra obtained at the current reversal potential were subtracted. Single lorentzians were fitted by eye to the difference spectra. τ was calculated from the corner frequency, f_c, of the lorentzian as $\tau = 1/(2\pi f_c)$.

currents were linear, and their reversal potentials were close to 0 mV (Fig. 1*b*). These observations suggest that the two classes of ACh-activated currents reflect the opening of two distinct AChR channels coexisting in the oocyte membrane. Their conductances were 40 ± 1 pS and 60 ± 2 pS (mean ± s.d., $n = 4$).

The two classes of currents were clearly distinguishable from each other when activated by desensitizing concentrations of ACh (>5 μM). Figure 1*c* shows two examples of ACh-activated currents recorded from the same cell-attached membrane patch in the presence of 10 μM ACh. The currents occurred in bursts that lasted for hundreds of milliseconds and were separated by silent intervals of much longer duration. This pattern is comparable to that of ACh-activated currents observed in frog and rat muscle at high ACh concentrations (>5 μM)[29,30]. It reflects fluctuations of single AChR channels between long-lived inactive states (inter-burst intervals) and active states (bursts) where a given channel switches repeatedly between open and closed states. Within a given burst, all resolved elementary currents had a similar amplitude. However, bursts fell into two classes with respect to current amplitude. The average sizes of elementary currents in 178 bursts, measured in this patch at about −60 mV driving potential, were 2.3 pA and 3.4 pA, respectively, corresponding to the two current amplitudes observed at low ACh concentrations. A similar separation of bursts into two classes of amplitudes was observed in nine other patches examined at high ACh concentrations, the average ratio of large to small current amplitudes being 1.5 ± 0.04 ($n = 10$). The occurrence of two separate classes of bursts thus indicates that two populations of AChR channels characterized by differing conductances were formed in oocytes injected with the five subunit-specific mRNAs.

The relative frequency of occurrence of each class of currents varied with different oocytes and with different patches from a given oocyte. In every patch, however, the 40-pS conductance channel was observed more frequently than the 60-pS conductance channel. In records from 10 patches, 73 ± 10% of all currents were openings of the 40-pS conductance channel. This may be due to a higher density of the 40-pS conductance channel or to different activation kinetics of the two AChRs.

The two classes of AChR channels also differ in their gating properties. Figure 1*d* shows the distributions of average durations of elementary currents measured from one patch during bursts of the 40-pS (upper graph) and the 60-pS conductance channel (lower graph). The average duration was 7.2 ms for the 40-pS conductance channel and 2.3 ms for the 60-pS conductance channel.

AChR channels from four subunits

Oocytes were injected with various combinations of four of the five subunit-specific mRNAs and then tested for response to

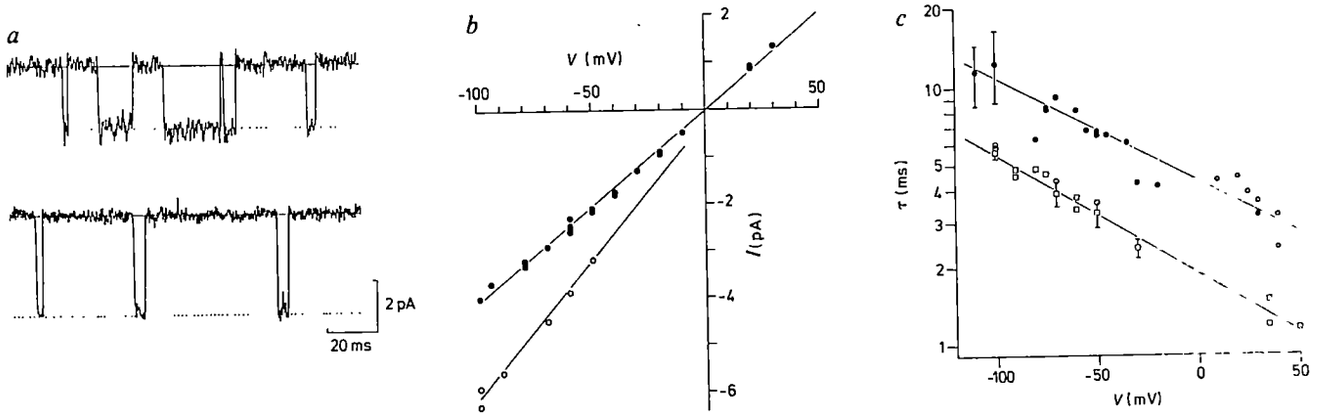


Fig. 3 Properties of ACh-activated single-channel currents in fetal and adult bovine muscle. *a*, Single-channel currents activated by 1 μM ACh in fetal (upper trace) and adult (lower trace) muscle. Outside-out patches. Inward current downwards. Membrane potential, −60 mV. Low-pass filtering at 1 kHz (−3 dB) Mean current amplitudes are 2.5 pA and 3.9 pA. *b*, Single-channel *I-V* relations of ACh-activated currents in fetal (filled symbols, four outside-out patches) and adult (open symbols, two outside-out patches) muscle. The regression lines indicate slope conductances of 40 pS and 59 pS for AChR channels in fetal and adult muscle, respectively. Interpolated current reversal potential is 1.2 mV for fetal muscle. Extrapolated reversal potential is 7 mV for adult muscle. *c*, Average duration of elementary currents against membrane potential in semilogarithmic coordinates from fetal (filled symbols) and adult (open symbols) muscle. In fetal muscle, the τ values were derived from four cell-attached patches as described in Fig. 2 legend. In adult muscle, the τ values were estimated from distribution of single-channel current durations (two outside-out patches, open circles) or from the m.e.p.c. decay time constant (four endplates, open squares). Bars indicate 1 s.d. from three or four different experiments. Lines represent linear regression fits as specified in Table 1.

Methods. Recordings of ACh-activated currents through fetal calf AChR channels were made on myoballs maintained in cell culture. Muscle tissue from the leg of a calf fetus (3–4 months gestation), obtained from a local abattoir, was minced, plated and maintained in cell culture as described for fetal rat muscle[40]. After 4–5 days, elongated myotubes had formed and were exposed to colchicine (10^{-7} M) for 12 h, resulting in the formation of rounded myoballs. All experiments were done 5–9 days after plating. Outside-out patches were isolated from myoballs using conventional patch pipettes containing either the same solution as described in Fig. 1 legend or with K^+ replaced by Na^+. This was necessary in experiments on myoballs maintained in culture for more than 6 days because outward currents carried by K^+ were activated at membrane potentials more positive than −60 mV. The membrane potential in cell-attached recordings was estimated from the slope conductance (40±2 pS, $n=4$), assuming a current reversal potential of −10 mV. ACh-activated single-channel currents in adult bovine muscle were measured on sacro-coccygeal tail muscle of cows (*Bos taurus*, 2–5 yr old) at 20±1 °C. Muscles were removed from the region of the last 10 coccygeal vertebrae (S10–S18)[41] and consisted of many bundles of 50–100 fibres. Such bundles were dissected to 'sheets' of 10–20 fibres each and incubated with 1 mg ml^{-1} collagenase (Sigma type I) at 18–22 °C for 3–4 h in Ringer's solution of the following composition (in mM): NaCl, 140; KCl, 4; $CaCl_2$, 1; $MgCl_2$, 1; HEPES (pH 7.2), 10. This was followed by a 10-min exposure to Ringer's solution containing 0.05 mg ml^{-1} protease (Sigma type VII). Myelinated nerves and nerve terminals still attached to the endplate were then visible in edge fibres viewed with Nomarski optics (×16 objective). Single-channel current recordings were made in the perijunctional region (within a distance of 20–30 μm of the endplate) of four fibres from two muscles. Patch pipettes had a tip diameter of 0.5–0.8 μm. Pipette and extracellular solutions were as described in Fig. 1 legend, except that 80 mM glucose was added to give the same osmolarity as Ringer's solution (290 mOsm). M.e.p.cs were measured in sacro-coccygeal muscle bathed in Ringer's solution at 20±1 °C, using a conventional two-microelectrode voltage-clamp circuit[2]. The placement of the two microelectrodes within 50 μm of the endplate was verified after each measurement by staining the endplate acetylcholinesterase[42] while the microelectrodes were left in place. M.e.p.cs were low-pass filtered (2 kHz, −3 dB) and digitized at 100-μs intervals. M.e.p.c. decay time courses were fitted by eye with single exponentials. In each fibre, 20–60 m.e.p.cs were measured at each membrane potential. In all experiments, the distribution of the decay time constants had a single peak. The τ values shown in Fig. 3*c* represent means of such distributions.

ACh. Whole-cell current measurements showed that omission of the α-, β- or δ-subunit-specific mRNA virtually abolished the ACh response, whereas omission of either the γ- or the ε-subunit-specific mRNA did not appreciably affect the response as compared with oocytes injected with all five subunit-specific mRNAs. Figure 2*a* shows records of ACh-activated single-channel currents from outside-out patches isolated from oocytes injected with the α-, β-, γ- and δ-subunit-specific mRNAs (upper trace) or with the α-, β-, δ- and ε-subunit-specific mRNAs (lower trace). These oocytes, in contrast to those injected with all five subunit-specific mRNAs, each exhibited only a single class of AChR channels ($AChR_\gamma$ or $AChR_\varepsilon$). The conductance and gating properties of the channels formed in a given oocyte depended on the mRNA combination with which it was injected. The distribution of current amplitudes for the AChR, as well as the $AChR_\varepsilon$ channel was characterized by a single peak at all membrane potentials. The *I-V* relations for both channels in outside-out patches were linear in the potential range of −100 mV to +50 mV (Fig. 2*b*). The average conductance, obtained from both outside-out and cell-attached patches, was 40±1 pS ($n=16$) for the $AChR_\gamma$ and 59±2 pS ($n=13$) for the $AChR_\varepsilon$ channel (Table 1).

The conductance sequence of the two AChR channels for monovalent metal cations was $K^+ > Cs^+ > Na^+ > Li^+$, the respective channel slope conductances, measured in cell-attached patches at low extracellular Ca^{2+} (ref. 28), being 72± 4 pS, 61±3 pS, 50±2 pS and 21±2 pS ($n=3$) for the $AChR_\gamma$ channel and 110±4 pS, 90±5 pS, 60±4 pS and 30±2 pS ($n=3$) for the $AChR_\varepsilon$ channel. Thus, the conductance ratios determined for the four cations were nearly identical for the two AChR channels.

With respect to their conductances, the $AChR_\gamma$ and $AChR_\varepsilon$ channels resemble the AChR channels in fetal and adult rat muscle, respectively[3]. This resemblance is further supported by the conductance–activity curves for Na^+ of the $AChR_\gamma$ and $AChR_\varepsilon$ channels (Fig. 2*c*). These curves were fitted by hyperbolic relations, indicating that the $AChR_\varepsilon$ channel has a larger limiting conductance (93 pS) than the $AChR_\gamma$ channel (75 pS).

The $AChR_\gamma$ and $AChR_\varepsilon$ channels differed not only in their conductance but also in their gating properties. The average duration of elementary currents was estimated from the distribution of current durations[28] and from power density spectra[1,31] of single-channel current records (Fig. 2*d*). In both channels, the average current duration decreased exponentially with more positive membrane potentials, but at all membrane potentials the average duration of $AChR_\varepsilon$ channel currents was shorter by a factor of two to three than that of $AChR_\gamma$ channel currents.

The results described above suggest that oocytes injected with all five subunit-specific mRNAs produce two types of AChR molecules which have different functional properties and are composed of the α-, β-, γ- and δ-subunits and of the α-, β-, δ- and ε-subunits, respectively. We also observed that oocytes injected with no more than the α-, β- and δ-subunit-specific mRNAs exhibited a strong response to ACh. Preliminary

analysis of the AChR channels formed in these oocytes indicates that their conductance and gating properties differ markedly from those of the $AChR_\gamma$ and $AChR_\varepsilon$ channels (our unpublished results).

AChR channels in muscle

To compare the two classes of AChR channels produced in *Xenopus* oocytes with the native bovine AChR channels, we examined the conductance and gating properties of ACh-activated channels in fetal and adult bovine muscle. The upper and lower traces in Fig. 3*a* show ACh-activated currents from outside-out patches isolated from fetal and adult muscle fibres, respectively. The distributions of current sizes in the two experiments were characterized by a single peak with different average values of 2.5 pA (fetal muscle) and 3.9 pA (adult muscle) at −60 mV membrane potential. The I-V relations were linear (Fig. 3*b*), and the average conductance was 40 ± 1 pS ($n = 8$) for the fetal AChR channel and 59 pS (mean of two patches) for the adult AChR channel (Table 1).

Table 1 Single-channel properties of two forms of bovine AChRs expressed in *Xenopus* oocytes and in muscle

AChR channels from	Conductance γ (pS)	Average duration $\tau(-100)$ (ms)	H (mV)
Oocytes with $AChR_\gamma$	39 (7)	10.4 (7)	106
Oocytes with $AChR_\varepsilon$	59 (6)	5.3 (6)	83
Fetal muscle	40 (4)	11.0 (4)	108
Adult muscle	59 (2)	5.6 (6)	93

Regression analysis of i-V and τ-V measurements is shown. Numbers in parentheses refer to numbers of patches, except that two patches and four endplates were used for adult muscle. γ represents the slope of i-V relations measured on outside-out patches. $\tau(-100)$ represents the calculated duration of elementary currents at −100 mV membrane potential obtained from the τ-V relation plotted in semilogarithmic coordinates and fitted by the equation $\tau(V) = \tau(0)\exp(-V/H)$, where $\tau(0)$ is the τ value at 0 mV membrane potential. H represents the shift in membrane potential that causes an e-fold change in the average duration of elementary currents. The $\tau(0)$ values were 4.0 ms ($AChR_\gamma$) and 1.6 ms ($AChR_\varepsilon$) in Fig. 2*d* and 4.4 ms (fetal muscle) and 1.9 ms (adult muscle) in Fig. 3*c*. The correlation coefficients, r^2, were 0.88 and 0.96 (Fig. 2*d*), and 0.92 and 0.98 (Fig. 3*c*). The averages of individual slope conductances, measured between the current reversal potential and −100 mV driving potential in both outside-out and cell-attached patches, were 40 ± 1 pS ($n = 16$) and 59 ± 2 pS ($n = 13$) for the $AChR_\gamma$ and $AChR_\varepsilon$ channels in oocytes, and 40 ± 1 pS ($n = 8$) and 59 pS (mean of 2 patches) for AChR channels in fetal and adult muscle, respectively. The averages of measured τ values at −100 mV membrane potential were 10.2 ± 1.4 ms ($n = 4$) and 5.2 ± 0.4 ms ($n = 3$) for the $AChR_\gamma$ and $AChR_\varepsilon$ channels in oocytes, and 12.5 ± 3.8 ms ($n = 4$) and 5.7 ± 0.4 ms ($n = 6$) for AChR channels in fetal and adult muscle, respectively.

The conductance sequence of the AChR channel in fetal muscle for monovalent metal cations was $K^+ > Cs^+ > Na^+ > Li^+$, with slope conductance values (measured in cell-attached patches at low extracellular Ca^{2+}) of 79 pS, 65 pS, 55 pS and 20 pS (one patch). For the AChR channel in adult muscle, the sequence was $K^+ > Cs^+ > Na^+$ with conductance values of 110 pS, 90 pS and 60 pS, respectively (one patch).

The average duration of ACh-activated elementary currents in fetal as well as adult muscle decreased exponentially with more positive membrane potentials (Fig. 3*c*, filled and open circles). The currents were shorter in adult muscle than in fetal muscle. For example, the average duration at −100 mV membrane potential was 12.5 ± 3.8 ms ($n = 4$) in fetal muscle and 6.0 ms (mean of two recordings) on the perijunctional region of adult muscle. The latter duration is considerably longer than that inferred for junctional channels in adult rat muscle from miniature endplate current (m.e.p.c.) decay times[4–6,32]. We therefore measured m.e.p.c. decay time constant in adult bovine muscle (Fig. 3*c*, open squares). At −100 mV membrane potential, it was 5.6 ± 0.4 ms (four endplates), in good agreement with the average duration determined directly from single-channel current recordings. The voltage dependence of the m.e.p.c. decay time constant was similar to that of the duration of elementary currents (Fig. 3*c*). Thus, the estimates of the size and duration of elementary currents and their voltage dependence in bovine muscle indicate that the AChR channel in fetal muscle is similar

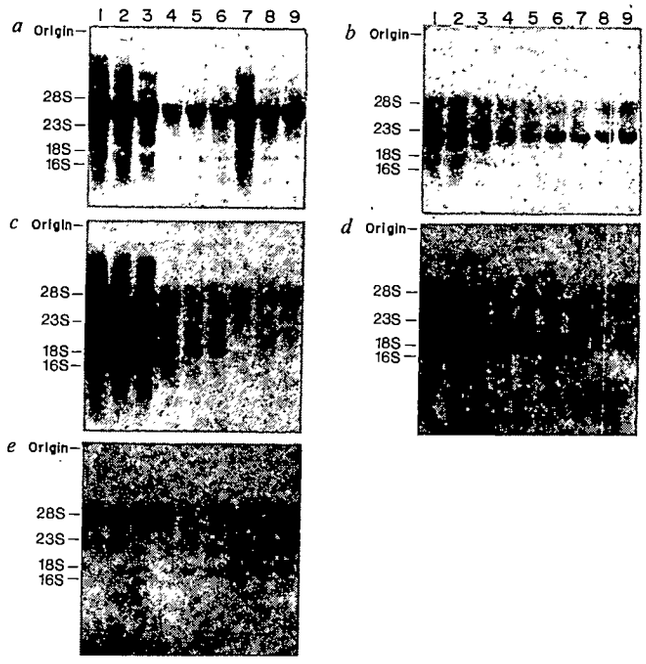


Fig. 4 Autoradiograms of blot hybridization analysis of total RNA from bovine diaphragms at various developmental stages using calf AChR α- (*a*), β- (*b*), γ- (*c*), δ- (*d*) and ε-subunit (*e*) cDNA probes. Bovine diaphragms obtained from a local abattoir were frozen quickly in liquid nitrogen and stored at −70 °C. Fetal age was estimated by fetal body length[43]. Total RNA was extracted by the guanidine thiocyanate method[44]. Samples of total RNA (30 μg each) from diaphragms at various fetal (lanes 1–6) and postnatal (lanes 7–9) stages were denatured with 1 M glyoxal and 50% dimethyl sulphoxide[45], electrophoresed on an 1.5% agarose gel and transferred[46] to a Biodyne nylon membrane (Pall); the ages of the animals were 3.4 months (lane 1), 4.4 months (lane 2), 5.3 months (lane 3), 5.7 months (lane 4), 7.1 months (lane 5) and 8.3 months (lane 6) of gestation and 5 h (lane 7), 25 days (lane 8) and ~2 yr (lane 9) after birth. The hybridization probes used were the 786-base-pair (bp) *BglII*/*ClaI* fragment from clone pcACRα18 (ref. 18; specific activity, 4.6×10^8 c.p.m. μg^{-1}) (*a*), the 1,791-bp *BanI* fragment from pSPcβ (ref. 28; 6.6×10^8 c.p.m. μg^{-1}) (*b*), the 980-bp *HinfI*/*AccI* fragment from pcACRγ5 (ref. 20; 8.4×10^8 c.p.m. μg^{-1}) (*c*), the 1,565-bp *EcoRI*/*XbaI* fragment from pSPcδ (ref. 28; 9.3×10^8 c.p.m. μg^{-1}) (*d*) and the 1,533-bp *BamHI*/*EcoRI* fragment from pSPcε (ref. 25; 8.1×10^8 c.p.m. μg^{-1}) (*e*); the probes were labelled by nick translation[47] with [α-^{32}P]dCTP. After prehybridization, the blots were incubated at 42 °C for 21 h in a solution containing 50 mM sodium phosphate buffer (*p*H 6.5), 5 × SSC (SSC: 150 mM NaCl, 15 mM trisodium citrate), 50% formamide, 0.1% polyvinylpyrrolidone, 0.1% Ficoll 400 (Pharmacia), 0.1% bovine serum albumin, 250 μg ml^{-1} sonicated salmon sperm DNA, 0.1% SDS and 10 ng ml^{-1} ^{32}P-labelled probe. The blots were washed three times, for 5 min each, in 2 × SSC containing 0.1% SDS at room temperature and twice, for 15 min each, in 0.1 × SSC containing 0.1% SDS at 50 °C. Autoradiography was performed at −70 °C for 70 h (*a*, *b*) or 140 h (*c*, *d*, *e*) with an intensifying screen. The size markers used were bovine and *Escherichia coli* ribosomal RNA. The estimated sizes of the α-, β-, γ-, δ- and ε-subunit mRNAs were ~4,500 (ref. 18), ~3,200 (ref. 19), ~2,000 (ref. 20), ~2,200 (ref. 21) and ~1,900 nucleotides, respectively. The ~1,900-nucleotide ε-subunit mRNA was found in both diaphragm and leg muscle RNA. Our previous failure to detect this mRNA species[25] can be ascribed to the use of nitrocellulose filter, which yields weaker hybridization signals than Biodyne nylon membrane; the previous observation of the ~4,200-nucleotide RNA species[25] in poly(A)$^+$ RNA from leg muscle from a fetal calf (4 months gestation) was not reproducible.

to the $AChR_\gamma$ channel expressed in oocytes, whereas the AChR channel in adult muscle and the $AChR_\varepsilon$ channel produced in oocytes share similar properties (Table 1).

AChR subunit mRNAs in muscle

We examined developmental changes in the contents of the five AChR subunit mRNAs in bovine muscle. Total RNA was extracted from diaphragms at various stages of fetal and postnatal development and subjected to blot hybridization analysis using the respective cDNA probes (Fig. 4). One major hybridizable RNA species was observed with the α- (Fig. 4*a*), β- (*b*) or ε-subunit (*e*) cDNA probe, whereas two (or three) major RNA species hybridized with the γ- (Fig. 4*c*) or δ-subunit (*d*) cDNA probe, especially at earlier fetal stages. The larger RNA species hybridizable with the γ- and δ-subunit cDNA probes, as well as the minor, larger RNA species hybridizable with the other cDNA probes, presumably represent incompletely spliced RNA[20,21]. At all the developmental stages studied, significant amounts of the α- (Fig. 4*a*), β- (*b*) and δ-subunit (*d*) mRNAs were found, although the content of the δ-subunit mRNA was smaller at postnatal stages (especially 25 days and ~2 yr) than at fetal stages. In contrast, the contents of the γ- and ε-subunit mRNAs varied markedly during muscle development, showing reciprocal changes. The γ-subunit mRNA was found abundantly at earlier fetal stages (3–5 months gestation), but was hardly or not detectable after birth (Fig. 4*c*). Conversely, considerable amounts of the ε-subunit mRNA appeared only at postnatal stages, and it was not detectable at earlier fetal stages (3–4 months gestation) (Fig. 4*e*). At later fetal stages (7–8 months gestation), appreciable amounts of the γ- and ε-subunit mRNAs coexisted. Analogous experiments with poly(A)$^+$ RNA from bovine leg muscles at different fetal and postnatal stages showed generally similar developmental changes in the contents of the five subunit mRNAs. These results support the notion that replacement of the γ-subunit by the ε-subunit in the AChR complex is responsible for the changes in the properties of the AChR that occur during muscle development[4–6]. The reason for the low content of the δ-subunit mRNA observed at postnatal stages is not known. The possibility that replacement of the δ-subunit may also occur during muscle development cannot be excluded.

Conclusions

Two classes of AChR channels, defined by different conductances and gating properties, are formed in *Xenopus* oocytes injected with the five bovine AChR subunit-specific mRNAs. Only one of these two classes of AChR channels ($AChR_\gamma$) is produced by injection of the α-, β-, γ- and δ-subunit-specific mRNAs, whereas only the other class ($AChR_\varepsilon$) is produced by injection of the α-, β-, δ- and ε-subunit-specific mRNAs. These results suggest that $AChR_\gamma$ and $AChR_\varepsilon$ represent a complex of the α-, β-, γ- and δ-subunits and of the α-, β-, δ- and ε-subunits, respectively.

The two classes of channels, $AChR_\gamma$ and $AChR_\varepsilon$, formed in oocytes have functional properties similar to those of the native bovine AChR channels present in fetal and adult muscle, respectively. This finding, in conjunction with the reciprocal changes in the contents of the γ- and ε-subunit mRNAs observed during muscle development, suggests that the AChR channel in fetal muscle is assembled from the α-, β-, γ- and δ-subunits, whereas the endplate channel in adult muscle is assembled from the α-, β-, δ- and ε-subunits. This conclusion is supported by the observation that the junctional AChR is slightly more acidic than the non-junctional AChR[33]: the bovine ε-subunit contains more acidic residues and less basic residues than does the bovine γ-subunit[25].

The relative contents of the two classes of AChR channels, for example in rat muscle, depend on innervation of the muscle by spinal motoneurones[4,34,35]. Before innervation, the fetal class of channels predominates; during synapse formation, the two AChR classes coexist in the muscle; at later stages of synapse formation, the fetal class is fully replaced by the adult class[5–7,33]. Thus, the shift of the two AChR classes may occur concurrently with the reciprocal changes in the contents of the γ- and ε-subunit mRNAs. It seems plausible to postulate that the nerve terminal exerts control over the synthesis of the γ- and ε-subunits by switching the expression of their genes or by modulating some post-transcriptional events.

We thank Dr R. Eckert for reading the manuscript. This investigation was supported in part by research grants from the Ministry of Education, Science and Culture of Japan, the Mitsubishi Foundation and the Japanese Foundation of Metabolism and Diseases.

Received 17 March; accepted 8 April 1986.

1. Katz, B. & Miledi, R. *J. Physiol., Lond.* **224,** 665–699 (1972).
2. Neher, E. & Sakmann, B. *J. Physiol., Lond.* **258,** 705–729 (1976).
3. Sakmann, B., Bormann, J. & Hamill, O. P. *Cold Spring Harb. Symp. quant. Biol.* **48,** 247–257 (1983).
4. Sakmann, B. & Brenner, H. R. *Nature* **276,** 401–402 (1978).
5. Michler, A. & Sakmann, B. *Devl Biol.* **80,** 1–17 (1980).
6. Fischbach, G. D. & Schuetze, S. M. *J. Physiol., Lond.* **303,** 125–137 (1980).
7. Vicini, S. & Schuetze, S. M. *J. Neurosci.* **5,** 2212–2224 (1985).
8. Fambrough, D. M. *Physiol. Rev.* **59,** 165–227 (1979).
9. Karlin, A. in *Cell Surface Reviews* Vol. 6 (eds Cotman, C. W., Poste, G. & Nicolson, G. L.) 191–260 (North-Holland, Amsterdam, 1980).
10. Changeux, J.-P. *Harvey Lect.* **75,** 85–254 (1981).
11. Conti-Tronconi, B. M. & Raftery, M. A. *A. Rev. Biochem.* **51,** 491–530 (1982).
12. Noda, M. *et al. Nature* **299,** 793–797 (1982).
13. Noda, M. *et al. Nature* **301,** 251–255 (1983).
14. Noda, M. *et al. Nature* **302,** 528–532 (1983).
15. Claudio, T., Ballivet, M., Patrick, J. & Heinemann, S. *Proc. natn. Acad. Sci. U.S.A.* **80,** 1111–1115 (1983).
16. Sumikawa, K. *et al. Nucleic Acids Res.* **10,** 5809–5822 (1982).
17. Devillers-Thiery, A., Giraudat, J., Bentaboulet, M. & Changeux, J.-P. *Proc. natn. Acad. Sci. U.S.A.* **80,** 2067–2071 (1983).
18. Noda, M. *et al. Nature* **305,** 818–823 (1983).
19. Tanabe, T. *et al. Eur. J. Biochem.* **144,** 11–17 (1984).
20. Takai, T. *et al. Eur. J. Biochem.* **143,** 109–115 (1984).
21. Kubo, T. *et al. Eur. J. Biochem.* **149,** 5–13 (1985).
22. Shibahara, S. *et al. Eur. J. Biochem.* **146,** 15–22 (1985).
23. LaPolla, R. J., Mayne, K. M. & Davidson, N. *Proc. natn. Acad. Sci. U.S.A.* **81,** 7970–7974 (1984).
24. Boulter, J. *et al. J. Neurosci.* **5,** 2545–2552 (1985).
25. Takai, T. *et al. Nature* **315,** 761–764 (1985).
26. Mishina, M. *et al. Nature* **307,** 604–608 (1984).
27. Mishina, M. *et al. Nature* **313,** 364–369 (1985).
28. Sakmann, B. *et al. Nature* **318,** 538–543 (1985).
29. Sakmann, B., Patlak, J. & Neher, E. *Nature* **286,** 71–73 (1980).
30. Hamill, O. P. & Sakmann, B. *Nature* **294,** 462–464 (1981).
31. Anderson, C. R. & Stevens, C. F. *J. Physiol., Lond.* **235,** 655–691 (1973).
32. Colquhoun, D., Large, W. A. & Rang, H. P. *J. Physiol., Lond.* **266,** 361–395 (1977).
33. Nathanson, N. M. & Hall, Z. W. *Biochemistry* **18,** 3392–3401 (1979).
34. Brenner, H. R. & Sakmann, B. *J. Physiol., Lond.* **337,** 159–171 (1983).
35. Schuetze, S. M. & Vicini, S. *J. Neurosci.* **4,** 2297–2302 (1984).
36. Methfessel, C. *et al. Pflügers Arch. ges. Physiol.* (submitted).
37. Fenwick, E., Marty, A. & Neher, E. *J. Physiol., Lond.* **331,** 577–597 (1982).
38. Colquhoun, D. & Sigworth, F. J. in *Single Channel Recording* (eds Sakmann, B. & Neher E.) 191–263 (Plenum, New York, 1983).
39. Robinson, R. A. & Stokes, R. H. in *Electrolyte Solution* 2nd edn, 481–492 (Butterworth, London, 1959).
40. Hamill, O. P., Marty, A., Neher, E., Sakmann, B. & Sigworth, F. J. *Pflügers Arch. ges. Physiol.* **391,** 85–100 (1981).
41. Sisson, S. & Grossman, J. D. in *The Anatomy of the Domestic Animals* 4th edn, 251–252 (Saunders, Philadelphia, 1964).
42. Karnovsky, M. J. *J. Cell Biol.* **23,** 217–232 (1964).
43. Arthur, G. H. in *Wright's Veterinary Obstetrics* 3rd edn, 64–69 (Bailliere, Tindall & Cox London, 1964).
44. Chirgwin, J. M., Przybyla, A. E., MacDonald, R. J. & Rutter, W. J. *Biochemistry* **18,** 5294–5299 (1979).
45. McMaster, G. K. & Carmichael, G. G., *Proc. natn. Acad. Sci. U.S.A.* **74,** 4835–4838 (1977).
46. Thomas, P. S. *Proc. natn. Acad. Sci. U.S.A.* **77,** 5201–5205 (1980).
47. Weinstock, R., Sweet, R., Weiss, M., Cedar, H. & Axel, R. *Proc. natn. Acad. Sci. U.S.A.* **75,** 1299–1303 (1978).

A second post-transcriptional *trans*-activator gene required for HTLV-III replication

Joseph Sodroski, Wei Chun Goh, Craig Rosen, Andrew Dayton, Ernest Terwilliger & William Haseltine*

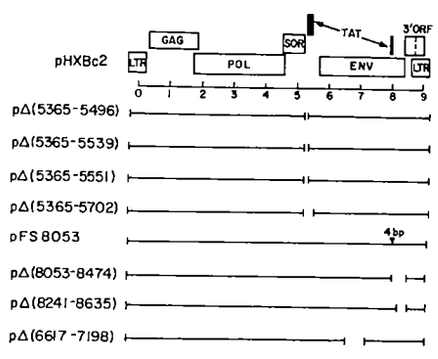
Dana-Farber Cancer Institute, Department of Pathology, Harvard Medical School, and *Department of Cancer Biology, Harvard School of Public Health, Boston, Massachusetts 02115, USA

Evidence is provided for the existence of a seventh gene in the genome of human T-lymphotropic virus type III/lymphadenopathy-associated virus. The gene is necessary for replication and acts post-transcriptionally to relieve negative regulation of the messenger RNA for the virion capsid and envelope proteins. These observations suggest mechanisms for regulating both the latent and lytic phases of the virus life cycle.

THE retrovirus human T-lymphotropic virus type III/lymphadenopathy-associated virus (HTLV-III/LAV) is the primary aetiological agent of AIDS (acquired immune deficiency syndrome) and associated disorders[1-6]. The clinical consequences of HTLV-III infection range from prolonged asymptomatic states to severe depletion of $T4^+$ helper lymphocytes, characteristic of frank AIDS, and profound degeneration of the central nervous system[1-7]. The variable course of HTLV-III-related disease may reflect the complex life cycle of the virus, now thought to include both latent and lytic states in $T4^+$ lymphocytes as well as a state of limited replication in monocytes and macrophages[8].

To analyse viral factors affecting the HTLV-III life cycle, the effects of defined mutations of the viral genome on the replication and cytopathic potential of the virus have been studied. The HTLV-III genome, like that of other retroviruses, contains three open reading frames, *gag*, *env* and *pol*, which encode, respectively, the capsid proteins, the envelope proteins and non-structural proteins necessary for replication[9-17]. In addition, the HTLV-III genome contains other open reading frames that encode at least three additional proteins not common to most retroviruses[9-12,18,19]. Mutations in two of these open reading frames, the *sor* gene which encodes a protein of relative molecular mass (M_r) 23,000 (23K)[20,21] and the 3′ *orf* gene which encodes a 27K protein[22], do not eliminate the ability of the virus to replicate in and kill T lymphocytes[20]. The *trans*-activator (*tat*-III) gene encodes a 14K protein[23] that post-transcriptionally[24] stimulates HTLV-III long terminal repeat (LTR)-directed gene expression[18,19,25] via an interaction with specific target sequences in the leader of viral messages[26]. Mutations in the 5′ portion of the first coding exon of the bipartite *tat*-III gene destroy the ability of the virus to efficiently synthesize structural proteins and to replicate[27]. These mutations can be complemented in *trans* in cell lines that constitutively express the *tat*-III protein[27].

During these experiments, we found that an additional set of



	Jurkat–*tat*–III				Raji				
	Replication		Protein Production		RNA	Protein Production			
	MIF	CPE	gag	env		gag	env	tat	TA
	4	6	+	+	+	+	+	+	41.2
	4	6	+	+	+	–	–	–	0.2
	ND	ND	+	+	ND	–	–	–	0.2
	>30 days		–	–	ND	–	–	–	0.2
	>30 days		–	–	ND	–	–	–	0.2
	>30 days		–	–	+	–	–	+	39.3
	>30 days		–	–	+	–	–	+	35.6
	7	9	+	+	ND	ND	ND	ND	27.1
	>30 days		+	–	ND	ND	ND	ND	43.5

Fig. 1 Structure and properties of the HTLV-III proviral mutants. The complete HTLV-III provirus on plasmid pHXBc2 (ref. 28), together with the known genes, is shown at the upper left. The solid boxes represent the two coding exons of the *tat*-III gene. The vertical broken line in the 3′ *orf* gene represents a stop codon present in the pHXBc2 provirus[20]. The scale beneath the viral genes represents kilobases. Numbers correspond to those in ref. 9, where the RNA cap site is designated +1. For proviral deletion mutants, the numbers in the plasmid name correspond to the endpoints of the corresponding deletion. All plasmids were made using restriction and modification enzymes, according to manufacturers' suggestions. The 4-bp insertion in the pFS8053 plasmid resulted from treating a *Bam*HI-digested provirus with the large fragment of DNA polymerase I in the presence of nucleotide triphosphates and re-ligating prior to transfection of *Escherichia coli*. Replicative potential of the proviruses was tested by transfection of CsCl-banded DNA into Jurkat (*tat*-III) cells[29] using the DEAE-dextran technique[31]. The values for membrane immunofluorescence (MIF) and cytopathic effect (CPE) represent the number of days after transfection that >95% HTLV-III-specific membrane immunofluorescence and >95% cytopathicity, respectively, were noted in a typical experiment. These values were assessed as described previously[20]; >30 days indicates that no more than 2% HTLV-III-related membrane immunofluorescence or cytopathic effect was observed in the cultures, even up to 30 days after transfection. Reverse transcriptase assays[32] of cell supernatants in these cases did not rise above background during the observation period. ND, not done. Production of viral RNA was assessed as described in Fig. 2 legend. Viral protein production was assessed by transfecting cells with 10 μg of plasmid DNA using the DEAE-dextran procedure[31] and labelling with ^{35}S-cysteine at 48–72 h post-transfection. Labelled cell lysates were precipitated using antisera from patients (RV119 for Jurkat (*tat*-III) cells and 38-1 for Raji cells) and assessed for *gag*, *env* and *tat*-III protein production on SDS-polyacrylamide gels[33]. + Indicates detectable *gag* (p55, p38, p24 and/or p17), *env* (gp160/120) or *tat*-III (p14) bands; – indicates no detectable level of these proteins above background. *Trans*-activating ability (TA) was assessed by co-transfecting 10 μg of the proviral plasmid with 10 μg of plasmid pU3R-III, containing HTLV-III LTR sequences from −457 to +80 5′ to the chloramphenicol acetyltransferase gene (*cat*), into Raji cells[34,35]; 48 h after transfection, cell lysates were assayed for *cat* enzyme activity as described. Values represent the percentage conversion of chloramphenicol to acetylated forms in 1 h using equivalent amounts of protein lysate in a typical experiment. No effect on *cat* activity directed by the pSV_2cat plasmid, containing the simian virus 40 (SV40) early region promoter 5′ to *cat*[35], was observed with any of the mutant proviruses tested (data not shown).

mutations near the two coding exons of the *tat*-III gene dramatically attenuated the ability of the virus to express *gag* and *env* proteins. The observation that these mutations could not be complemented by the *tat*-III gene product alone led to the discovery of a second post-transcriptional control pathway governing HTLV-III expression. This pathway is controlled by a *trans*-acting product specified by a novel gene that partly overlaps the *tat*-III and *env* genes.

Replication of proviral mutants

To identify HTLV-III genomic regions important for viral replication, mutations were introduced into the pHXBc2 plasmid, which contains a complete HTLV-III provirus[28]. On transfection of either primary lymphocytes or $T4^+$ lymphocyte lines with this plasmid, infectious cytopathic virus is produced[20,27,28]. The recipient cell used for these experiments is the Jurkat (*tat*-III) cell line, designed to express constitutively the *tat*-III protein[29]. This cell line was chosen as it functionally complements deletions in the 5′ coding exon of the *tat*-III gene and because it is highly sensitive to the cytopathic effects of HTLV-III[27]. By 5 days after transfection with the pHXBc2 plasmid, Jurkat (*tat*-III) cells express HTLV-III proteins in addition to *tat*-III, exhibit cytopathic changes leading to demise of the culture, and produce extracellular virion particles detectable by electron microscopy or reverse transcriptase assays[27]. A similar result with approximately the same time course was obtained after transfection with plasmid pΔ(5365–5496), which contains a deletion in the 5′ portion of the *tat*-III first coding exon (Fig. 1). By contrast, no evidence of virus production was observed after transfection of the Jurkat (*tat*-III) cells with plasmid pΔ(5365–5551) or pΔ(5365–5702); these plasmids contain deletions in the *tat*-III gene which have the same 5′ boundary as that of plasmid pΔ(5365–5496), but extend farther in the 3′ direction. These deletions do not extend into the *env* gene. Apparently a region between nucleotides 5,496 and 5,551 is required for HTLV-III replication, even in the presence of a functional *tat*-III product supplied in *trans*.

Mutations of the pHXBc2 plasmid in the region near the unique *Bam*HI site (position 8,053), including a 4-base pair (bp) insertion at this site, also inactivate viral replication in the Jurkat (*tat*-III) cells (Fig. 1). By contrast, a virus that contains a deletion in the 3′ *orf* gene extending to within 188 nucleotides 3′ to the *Bam*HI site retains the ability to replicate, albeit at a reduced rate compared with wild-type virus (plasmid pΔ(8241–8634) in Fig. 1). This observation suggests that a function necessary for viral replication is located very near the *Bam*HI site, 5′ to nucleotide 8,241. Thus, mutations affecting two separate regions of the HTLV-III genome result in the inability of the provirus to replicate, even in the presence of the *tat*-III gene product.

RNA and protein synthesis of mutants

To investigate the nature of the mutations that could not be complemented by the *tat*-III product, the levels of virus-specific RNA and proteins synthesized by the proviral mutants were measured. The human B-lymphocyte cell line, Raji, was chosen for these experiments as previous experience demonstrated that significant levels of both virus-specific RNA and protein could be detected after transfection of this cell line with the HTLV-III proviral DNA[24].

For these experiments, RNAs and proteins were isolated 48 h after transfection of a single culture. Virus-specific RNA was measured using radiolabelled DNA complementary to HTLV-III RNA. The amount of globin RNA produced by the plasmid

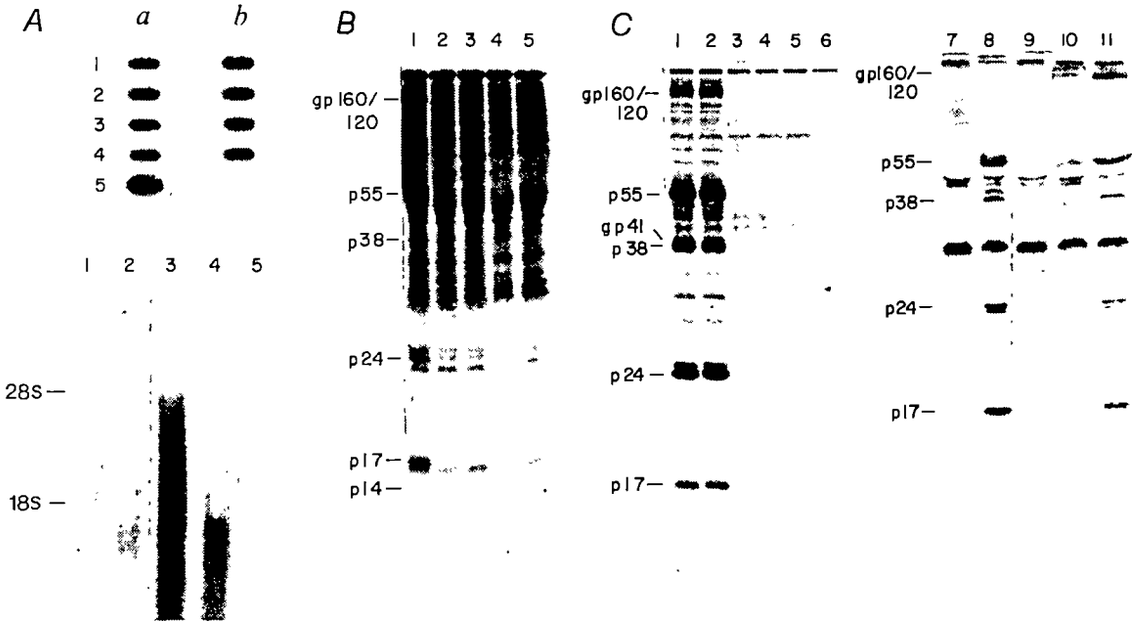


Fig. 2 RNA and protein production following transfection. Approximately 5×10^7 Raji cells were transfected with 10 μg of test plasmid DNA and 10 μg of $pSV_2\beta$-globin DNA using the DEAE-dextran technique[31]; 48 h after transfection, half of the cells were labelled with ^{35}S-cysteine and immunoprecipitated with patient antiserum 38-1, as described elsewhere[33]. The other half of the cells was used for total RNA isolation using the guanidine thiocyanate–CsCl method[36]. *A*, RNA (5 μg) was slot-blotted onto duplicate nitrocellulose filters and 10 μg was size-separated on formaldehyde gels and transferred to nitrocellulose[37]. One slot blot was hybridized to a probe derived from the complete β-globin complementary DNA sequence (*a*); the other slot blot (*b*) and the Northern blot (lower figure) were hybridized to a probe made from a pooled collection of *Bgl*II internal proviral fragments derived from the plasmid pHXBc2. Filters were washed as described elsewhere[37] prior to autoradiography. *B*, Proteins immunoprecipitated from the Raji transfectants. Transfected test plasmids for the Northern blot, slot blots and protein gel were: lane 1, pHXBc2; 2, pΔ(8053–8474); 3, pFS8053; 4, pΔ(5365–5496); and 5, a plasmid, pCR1, containing an incomplete HTLV-I provirus. The control lanes (1 and 4) have been published as part of a separate study[24]. *C*, Immunoprecipitates of Jurkat (*tat*-III) cells transfected with proviral plasmids using patient antiserum RV119, as described in Fig. 1 legend. Transfected plasmids were: lanes 1, 11, pHXBc2; lane 2, pΔ(5365–5496); 3, pΔ(5365–5702); 4, pΔ(8053–8474); 5, pFS8053; 6, 7, pIIIβ-globin, containing an HTLV-III LTR 5′ to rabbit β-globin cDNA sequences[24]; 8, pΔ(6617–7198); 9, pΔ(5365–5551); and 10, pΔ(5365–5539).

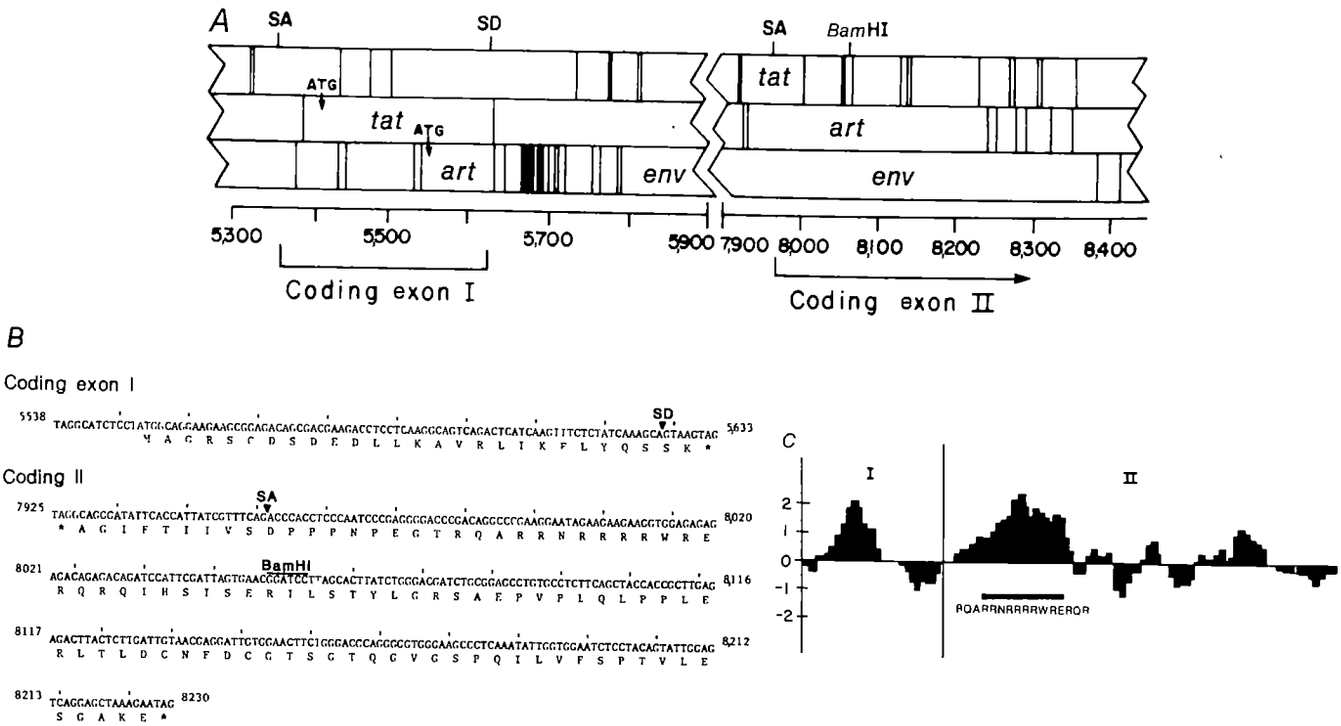


Fig. 3 Structure of the product of the alternative HTLV-III reading frame. The open reading frame in the HTLV-III genome, based on the sequence of Ratner *et al.*[9], is shown in *A*. The vertical lines represent the positions of stop codons. The open reading frames for the *tat*-III, *env* and alternative reading frame (*art*) are indicated. The positions of known splice acceptor (SA) and donor (SD) sites[12] as well as the *Bam*HI site used for mutagenesis (position 8,053) are shown. The putative initiator methionine codons for the *tat*-III and alternative reading-frame products are indicated by arrows labelled ATG. The putative coding exons of the *tat*-III gene and the alternative reading frame are delineated beneath the figure. *B*, DNA sequence of the two open reading frames that constitute the alternative reading frame, with the positions of the probable splice donor (SD) and acceptor (SA) sequences[12] shown. The predicted amino-acid sequence of the potential product of the open reading frame is shown beneath the DNA sequence. If the given splice donor and acceptor sites are used, the amino-acid sequence encoded by the sequence near the splice site would be LYQSNPPPNP. *C*, Hydrophilic (positive)–hydrophobic (negative) profile of the predicted alternative reading-frame product, based on the program of Hopp and Woods[38]. Protein domains specified by the first coding exon (I) are separated by a vertical line from those specified by the second coding exon (II). The amino-acid sequence of a strongly hydrophilic, basic domain is shown beneath the profile.

$pSV_2\beta$-globin[30], which was included in the transfection, was used as an internal standard for RNA synthesis in these experiments. Figure 2 shows that the amount, as well as the size distribution, of the virus-encoded RNA was the same for the pHXBc2 plasmid and for all the mutant HTLV-III proviruses tested, as judged by slot-blot and Northern blot analyses. Evidently the mutations that eliminate the ability of proviruses to produce infectious virus do not affect the synthesis of viral messenger RNA in the Raji cells.

The pattern of HTLV-III proteins produced in the transfected cells differed among the plasmids. Raji cells transfected with the pHXBc2 plasmid expressed HTLV-III-specific proteins of 160K and 120K (the *env* gene products), 55K, 38K, 24K and 17K (the *gag* gene products) and a faint band at 14K (the *tat*-III gene product) (Fig. 2*B*, lane 1). The pHXBc2 provirus used in these studies does not synthesize a complete 27K 3′ *orf* product[20]. Raji cells transfected with HTLV-III provirus containing *tat*-III gene deletions do not express detectable levels of viral protein, as reported previously[24] (Fig. 2*B*, lane 4). To our surprise, Raji cells transfected with pΔ(8053–8474) or pFS8053 failed to express HTLV-III *gag* or *env* gene products, but did synthesize the 14K *tat*-III product in amounts comparable to that seen after transfection with the pHXBc2 plasmid, as judged by radioimmune precipitation (Fig. 2*B*, lanes 2, 3). This observation suggested that mutations at or near position 8,053 attenuate the ability of the provirus to synthesize *gag* and *env* proteins, but do not affect synthesis of the *tat*-III protein.

To determine whether these mutant proviruses produced a functional *tat*-III gene product, the ability of the mutant proviruses to activate the HTLV-III viral LTR in *trans* was measured. Figure 1 shows that the proviruses containing mutations in the 3′ portion of the *env* gene are able to stimulate HTLV-III LTR-directed gene expression to approximately the same extent as is observed for the intact pHXBc2 provirus. We conclude that the mutations that affect *gag* and *env* gene expression do not significantly affect *tat*-III gene expression.

Non-complementation of the defect

Proviruses containing deletions in *tat*-III cannot synthesize detectable levels of viral proteins on transient transfection into cell lines that do not express the *tat*-III product[24]. Therefore, the Jurkat (*tat*-III) cell line was used to test the ability of mutant proviruses to synthesize virion proteins. Immunoprecipitation of Jurkat (*tat*-III) cells 48 h after transfection with the parental pHXBc2 plasmid revealed the presence of *gag* (p55, p38, p24 and p17) and *env* (gp160 and gp120) gene products (Fig. 2*C*, lane 1). HTLV-III *gag* and *env* proteins were also detected after transfection with the plasmids that contained deletions in the 5′ portion of the *tat*-III first coding exon [pΔ(5365–5496) and pΔ(5365–5539) in Fig. 2*C*, lanes 2 and 10, respectively]. By contrast, no *gag* or *env* products were detected in Jurkat (*tat*-III) cells transfected with provirus containing deletions that extend at least 12 nucleotides farther 3′ [pΔ(5365–5551) and pΔ(5365–5702) in Fig. 2*C*, lanes 9 and 3, respectively]. Similarly, none of the proviruses mutated near the *Bam*HI site (position 8,053) that failed to make viral *gag* and *env* proteins in Raji cells yielded detectable levels of these proteins in Jurkat (*tat*-III) cells (Fig. 2*C*, lanes 4, 5). The provirus with a deletion in the

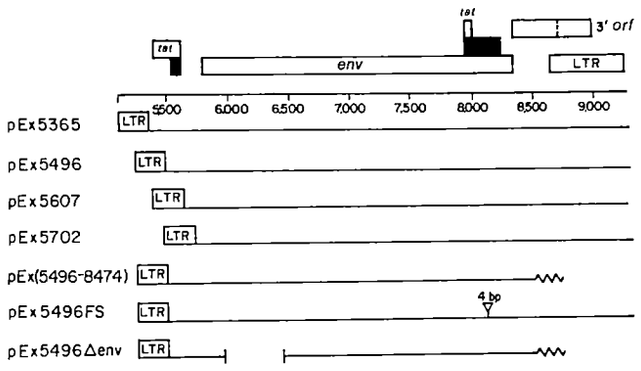


Fig. 4 Structure of plasmids containing the alternative reading frame. The structure of the 3′ half of the HTLV-III genome, based on the sequence of Ratner *et al.*[9], is shown together with the positions of the *env* gene, LTR, 3′ *orf* gene, two *tat*-III coding exons and the putative alternative reading-frame coding exons (here depicted as solid boxes). The position of a stop codon in the 3′ *orf* gene of the parental pHXBc2 plasmid[20,28] used in these studies is denoted by a vertical broken line. In all the plasmids shown, HTLV-III LTR sequences from −167 to +80 are positioned at the nucleotide denoted in the plasmid name. The zig-zag lines represent signals for polyadenylation and splicing derived from the SV40 early region[30]. The 4-bp insertion in plasmid pEx5496FS was constructed as described for plasmid pFS8053 in Fig. 1 legend. pEx5496Δenv was constructed by digesting pEx(5496–8474) with *Stu*I, ligating to 8-bp *Kpn*I linkers, digesting to completion with *Kpn*I, and ligating prior to *E. coli* transfection. All plasmids were constructed using DNA modification and restriction enzymes, by standard procedures.

3′ *orf* gene on plasmid pΔ(8241–8635) synthesized both *gag* and *env* proteins after transfection into Jurkat (*tat*-III) cells (Fig. 1). These experiments suggest that a region having a 5′ boundary between nucleotides 5,539 and 5,551 and a 3′ boundary between 8,053 and 8,241 is necessary for efficient expression of viral *gag* and *env* proteins, even in the presence of a functional *tat*-III product.

A seventh open reading frame

The similarity in the phenotype of mutations located both 5′ to the *env* gene and within the 3′ portion of the *env* gene suggested that these mutations might affect a single gene product. That mutation of the *env* gene product is not alone responsible for the effects observed is demonstrated by the ability of the proviruses on plasmids pΔ(6617–7198) and pΔ(8241–8635) to produce *gag* proteins on transfection into Jurkat (*tat*-III) cells (Figs 1 and 2*C*, lane 8). Plasmid pΔ(6617–7198) contains a deletion-frameshift mutation near the middle of the *env* gene, while plasmid pΔ(8241–8635) contains a deletion involving the 3′ 132 nucleotides of the *env* gene.

We note the existence within the HTLV-III genome of a sequence that could encode a protein and that would be affected by both sets of mutations affecting *gag* and *env* expression. The postulated coding exons of this gene would use alternative reading frames of the first and second coding exons of the *tat*-III gene (Fig. 3). Beginning with a methionine codon at position 5,550, the first coding exon of the putative gene extends to a known splice donor site at position 5,625 (ref. 12). The corresponding splice acceptor, located at nucleotide 7,956, precedes an in-frame open reading frame ending in a stop codon at position 8,227. The splicing events needed to produce this alternative reading-frame product are the same as those used for the *tat*-III gene and are known to occur in the mRNA of HTLV-III-infected cells[12,18,19].

The potential product of the alternative reading frame is 116 amino acids long, and contains stretches of highly basic hydrophilic residues similar to those found in the *tat*-III gene product and in nucleic acid-binding proteins[18,19]. Note that the vectors used for the construction of the Jurkat (*tat*-III) and Raji (*tat*-III) cells are truncated at the *Bam*HI site (position 8,053) and are unable to synthesize the alternative reading-frame product.

A novel *trans*-activator

The hypothesis that a protein encoded by the alternative reading frame described above is necessary, in addition to the *tat*-III product, for efficient HTLV-III *gag* and *env* protein synthesis, would explain the phenotype of the proviral mutants. This hypothesis predicts that plasmids designed to express the alternative reading-frame product should complement the defect of mutants with respect to the synthesis of the *gag* and *env* gene products. To test this prediction, HTLV-III LTR sequences from position −167 to +80 were placed at various positions with respect to the putative initiation codon for the alternative reading frame (Fig. 4). Following co-transfection of these plasmids with plasmids containing mutant proviruses into Jurkat (*tat*-III) cells, viral protein expression was assessed by immunoprecipitation of labelled cell lysates using antiserum from an AIDS patient.

Figure 5 illustrates that placing the HTLV-III LTR 54 nucleotides 5′ to the ATG codon of the alternative reading frame (and downstream of the *tat*-III initiation codon) results in a plasmid (pEx5496) that provides in *trans* a function required for *gag* gene expression by the pFS8053 plasmid (Fig. 5*B*, lane 3 and *C*, lane 4). The *env*-encoded gp160/120 proteins are produced by the pEx5496 plasmid itself on transfection into Jurkat (*tat*-III) cells (Fig. 5*A*, lane 3). The ability of the pEx5496 plasmid to complement the pFS8053 mutation and to synthesize envelope proteins is eliminated by a frameshift mutation within the alternative reading frame (plasmid pEx5496FS; Fig. 5*C*, lane 7 and *D*, lane 3). Plasmids in which the HTLV-III LTR is located 3′ to the ATG codon of the alternative reading frame do not complement the pFS8053 mutation and do not synthesize *env* gene products (plasmids pEx5607 and pEx5702 in Fig. 5*A*, lanes 4, 5 and *B*, lanes 4, 5). By contrast, deletions within the *env* or 3′ *orf* gene of plasmid pEx5496 do not eliminate the ability of the plasmid pFS8053 to activate *gag* gene expression (see plasmids pEx5496Δenv and pEx(5496–8474) in Fig. 5*C*, lanes 5, 6 and *D*, lane 5). HTLV-III *gag* gene expression directed by the plasmid pΔ(8053–8474) can also be activated by pEx5496 (data not shown). We conclude that plasmids capable of producing an alternative reading-frame product can activate, in *trans*, *gag* gene expression by proviruses containing mutations in the alternative reading-frame sequence.

We also note that *gag* gene expression by the plasmid pFS8053 can be activated in Jurkat (*tat*-III) cells by a plasmid that contains the HTLV-III sequences located 5′ to the initiation codon of the *tat*-III gene. The plasmid pEx5365 produces a functional *tat*-III activity as well as providing in *trans* the functions required for *gag* gene expression by plasmid pFS8053 (Fig. 5*B*, lane 2). However, the extent of *gag* gene expression observed in this experiment was less than that observed in the experiments in which pEx5496 was used. pEx5365 does not produce detectable levels of the *env* gene product (Fig. 5*A*, lane 2). One possible explanation for the low level of expression of the complementing activity and of *env* gene products by plasmid pEx5365 is the presence of a strong *tat*-III initiation codon 5 to both genes.

Activation of *env* gene expression

A plasmid designed to express the alternative reading frame but not the *env* gene was tested for the ability to allow *env* gene production by HTLV-III proviruses containing mutations in the alternative reading-frame sequences. The plasmid pEx5496Δenv, which contains a deletion-frameshift mutation in the portion of the *env* gene encoding the exterior glycoprotein gp120, did not yield detectable levels of the *env* protein on transfection into Jurkat (*tat*-III) cells (Fig. 5*D*, lane 2). Co-transfection of this plasmid into Jurkat (*tat*-III) cells with pΔ(5365–5551) allowed the latter plasmid to produce both *gag*

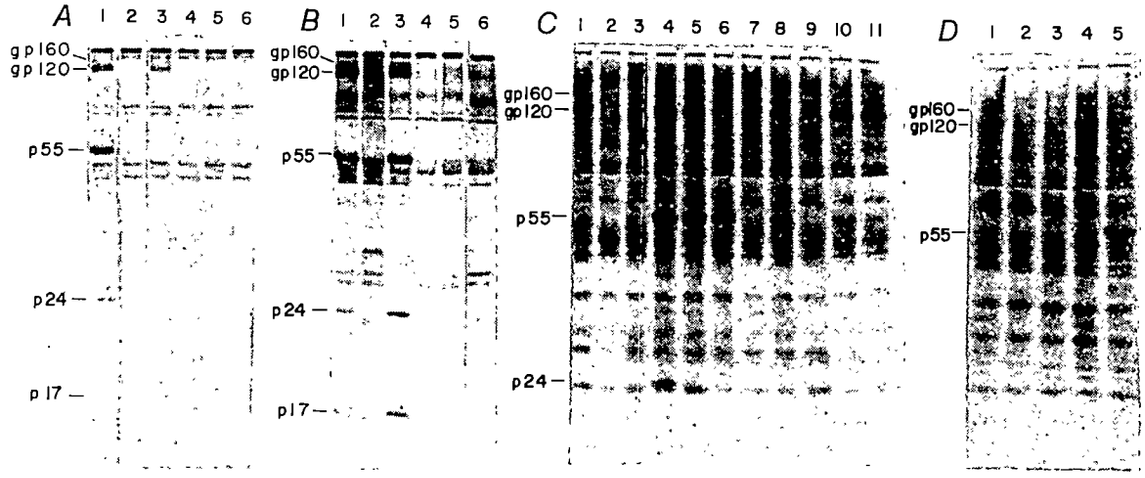


Fig. 5 Complementation of mutations in HTLV-III proviruses by plasmids designed to express the alternative reading-frame product. Jurkat (*tat*-III) cells were transfected by the DEAE-dextran procedure[31] using 10 μg of the proviral mutant to be complemented and 10 μg of the plasmid to be tested for ability to complement the mutation. Forty-eight hours after transfection, cells were labelled with ^{35}S-cysteine and cell lysates were immunoprecipitated using an AIDS patient serum, RV119 (ref. 33). The positions of the gp160 and gp120 *env* proteins and of the p55, p24 and p17 *gag* gene products are indicated. Transfected plasmids in *A* were pΔ(5365–5496) (lane 1), pEx5365 (lane 2), pEx5496 (lane 3), pEx5607 (lane 4), pEx5702 (lane 5) and pIII*β*-globin (lane 6); those in *B* were pΔ(5365–5496) (lane 1), pFS8053 plus pEx5365 (lane 2), pFS8053 plus pEx5496 (lane 3), pFS8053 plus pEx5607 (lane 4), pFS8053 plus pEx5702 (lane 5), and pFS8053 alone (lane 6); and those in *C* were pEx(5496–8474) (lane 1), pEx5496Δenv (lane 2), pEx5496FS (lane 3), pFS8053 plus pEx5496 (lane 4), pFS8053 plus pEx(5496–8474) (lane 5), pFS8053 plus pEx5496Δenv (lane 6), pFS8053 plus pEx5496FS (lane 7), pΔ(5365–5551) plus pEx5496Δenv (lane 8), pΔ(5365–5551) plus pEx5496FS (lane 9), pΔ(5365–5539) plus pEx5496Δenv (lane 10), and pΔ(5365–5539) plus pEx5496FS (lane 11). Transfected plasmids in *D* were pEx(5496–8474) (lane 1), pEx5496Δenv (lane 2), pEx5496FS (lane 3), pEx5496Δenv plus pEx5496FS (lane 4), and pEx5496Δenv plus pFS8053 (lane 5). The predicted *env* gene product synthesized by the pEx5496FS plasmid is 47 amino acids shorter than the wild-type HTLV-III envelope, because of the frameshift mutation.

and *env* proteins (Fig. 5*C*, lane 8). No viral proteins could be detected in Jurkat (*tat*-III) cells transfected either with pΔ(5365–5551) alone (Fig. 2*C*, lane 9) or with plasmids pΔ(5365–5551) and pEx5496FS (Fig. 5*C*, lane 9). pEx5496Δenv also activated the synthesis of the gp160/120 *env* products by plasmids pEx5496FS (Fig. 5*D*, lane 4) and pEx5702 (data not shown). No *env* gene products were detected on transfection of Jurkat (*tat*-III) cells with either pEx5496FS alone (Fig. 5*D*, lane 3) or pEx5702 alone (Fig. 5*A*, lane 5). This result suggests that the inability of these plasmids to synthesize envelope proteins is the result of disruption of the alternative reading-frame sequences rather than of *cis*-acting sequences required to produce envelope proteins.

We conclude that a product encoded by the alternative reading frame can activate, in *trans*, *env* gene expression directed by proviruses mutated in the alternative reading frame.

Discussion

Here we have presented evidence for a novel *trans*-acting function required for efficient synthesis of HTLV-III *gag* and *env*, but not *tat*-III, proteins. In the absence of this second *trans*-acting factor, HTLV-III *gag* and *env* protein synthesis is markedly attenuated, without an apparent change in viral mRNA production. This finding, together with the observation that *tat*-III expression is not dependent on the *trans*-acting function, indicates that the factor exerts its effect at a post-transcriptional level.

The region of the genome required for this second *trans*-acting function is distinct from, but partly overlaps, the *tat*-III and *env* genes. This bipartite region contains an open reading frame that, on splicing, could synthesize a 116-amino-acid, highly basic protein similar to the *tat*-III product. This open reading frame is conserved in all HTLV-III variants sequenced[9–12].

The novel *trans*-acting function defined here activates HTLV-III *gag* and *env* protein expression; this might occur via a positive stimulation of post-transcriptional events affecting utilization of *gag* and *env* mRNA. Alternatively, the second *trans*-acting factor might derepress *cis*-acting negative-regulatory sequences present on viral messages encoding *gag* and *env* products. We favour the latter explanation based on our observations regarding the expression of heterologous genes under the control of the HTLV-III LTR.

We have demonstrated previously that the *tat*-III product alone is sufficient to stimulate HTLV-III LTR sequences (−167 to +80) to direct high-level synthesis of bacterial chloramphenicol acetyltransferase or murine dihydrofolate reductase[24,25]. By contrast, plasmids that contain the same HTLV-III LTR sequences located 5′ to the HTLV-III *env* gene (pEx5486FS or pEx5702) yield no detectable envelope protein in the absence of the alternative reading-frame product, even in the presence of an active *tat*-III gene product. Only after the alternative reading-frame product is supplied in *trans* do the levels of envelope production by these plasmids approximate those of heterologous genes under the control of the HTLV-III LTR in Jurkat (*tat*-III) cells. These observations imply that in the plasmids pEx5496FS and pEx5702 sequences 3′ to +80 inhibit *env* gene expression, and that such inhibition can be relieved by the *trans*-acting function. That the second *trans*-activator is required for *gag* gene expression suggests that *gag* mRNA may contain negative-regulatory sequences in addition to those found in *env* mRNA. We suggest the name *art* (anti-repression *trans*-activator) for the gene that encodes the second *trans*-activator, consistent with the proposed role of this gene in negating the effects of *cis*-acting negative-regulatory sequences present on viral mRNA encoding the HTLV-III structural proteins.

Detectable levels of the *tat*-III gene product but not of the *gag* and *env* gene products are synthesized by proviral mutants defective for the *art* function; therefore whatever inhibits the expression of the *gag* and *env* gene products does not affect *tat*-III gene expression. Sequences encompassing the entire *gag* gene and most of the *env* gene are removed by splicing from the *tat*-III mRNA[12,18,19]. Removal of *art*-responsive *cis*-acting negative-regulatory sequences located in the regions spliced out of *tat*-III messages would explain the independence of *tat*-III expression from the requirement for the *art* product. The *art* product itself should be independent of such negative-regulatory sequences as it should be synthesized from messages that also lack these *gag* and *env* sequences.

The expression of HTLV-III structural genes is governed post-transcriptionally by the *tat*-III product, which acts as a positive regulatory factor[18,19,24], and by the *art* product, which apparently counteracts *cis*-acting negative-regulatory sequences located in or near the *gag* and *env* genes. Two possible roles for this complex regulatory scheme can be considered. HTLV-III is reported to establish a latent state of infection in T cells that are not activated[8]. Lack of *tat*-III or *art* function would lead to a state of infection characterized by accumulation of viral RNA without synthesis of virus structural proteins. Rapid release from such a latent state could be achieved in the absence of new RNA synthesis if the *tat*-III or *art* function were reconstituted. A dependence of *tat*-III and *art* activity on the state of cell differentiation could explain the relationship between HTLV-III latency and T-cell activation.

Alternatively, post-transcriptional regulators may play a part in the lytic cycle of the virus. An early stage of infection characterized by accumulation of viral RNA but not of virion proteins might precede a late phase in which viral proteins toxic to T4 cells are produced. The switch from an early to a late stage of infection would reflect activation of either one or both of the *tat*-III and *art* gene functions. Such an early–late switch would permit accumulation of the mRNAs for toxic virion components before such components themselves are produced. There is some evidence that modulated *tat*-III activity may result in increased production of infectious virus. The yield of virus particles on lytic infection of the Jurkat cell line that constitutively produces high levels of the *tat*-III gene is much lower than that observed on infection of the Jurkat cell line itself, despite the observation that the cytopathic effect of infection is accelerated in the Jurkat (*tat*-III) cells[27]. Premature cell death attributed to high constitutive levels of the *tat*-III gene might explain the decreased virus titres. Temporal regulation of virus gene expression is important in the life cycle of other lytic viruses. The postulated roles of the *tat*-III and *art* genes in the latent and lytic cycles of HTLV-III infection are not necessarily exclusive.

A flexible, multi-tiered regulatory pathway linked to host cell differentiation and proliferation could account for much of the variability observed in victims of AIDS[6]. Similar pathways involving both positive and negative elements may also apply to post-transcriptional regulation of gene expression in the course of normal cellular development. Note also that both the *tat*-III and *art* products provide attractive targets for antiviral agents, as both operate at a post-transcriptional level and are required for viral replication[24,27].

We thank Drs George Shaw, Beatrice Hahn, Flossie Wong-Staal and Robert Gallo for the gift of the pHXBc2 provirus, Mary Fran McLane, Myron Essex, David Ho and Martin Hirsch for gifts of antisera; Kathryn Campbell, Judith Lippke, Renee Zaya and Dennis Perkins for technical assistance; Patricia Baldacci for help with some of the experiments; Roberto Patarca and Daniel Celander for helpful discussions; and Tanya Parks for manuscript preparation. W.H. is supported by a State of Massachusetts contract and by NIH grant CA21082. J.S. is a Special Fellow of the Leukemia Society of America and is also the recipient of NIH grants CA40658 and CA42597. C.R. is a recipient of NIH postdoctoral fellowship CA07580. E.T. was supported by a NIH Virology Training Grant.

Received 20 February; accepted 2 April 1986.

1. Barre-Sinoussi, F. *et al. Science* **220**, 868–871 (1983).
2. Broder, S. M. & Gallo, R. C. *New Engl. J. Med.* **311**, 1292–1297 (1984).
3. Gallo, R. C. *et al. Science* **224**, 497–500 (1984).
4. Popovic, M., Sarngadharan, M. G., Read, E. & Gallo, R. C. *Science* **225**, 497–500 (1984).
5. Sarngadharan, M. G., Popovic, M., Bruch, L., Shupbach, J. & Gallo, R. C. *Science* **224**, 506–508 (1984).
6. Seligman, M. *et al. New Engl. J. Med.* **311**, 1286–1292 (1984).
7. Shaw, G. M. *et al. Science* **227**, 177–182 (1985).
8. Zagury, D. *et al. Science* **231**, 850–853 (1986).
9. Ratner, L. *et al. Nature* **313**, 277–284 (1985).
10. Wain-Hobson, S., Sonigo, P., Danos, O., Cole, S. & Alizon, M. *Cell* **40**, 9–19 (1985).
11. Sanchez-Pescador, R. *et al. Science* **227**, 484–492 (1985).
12. Muesing, M. A. *et al. Nature* **313**, 450–458 (1985).
13. Robey, W. G. *et al. Science* **228**, 593–596 (1985).
14. Veronese, F. *et al. Science* **229**, 1402–1405 (1985).
15. Kitchen, L. *et al. Nature* **312**, 367–370 (1984).
16. Schupbach, J. *et al. Science* **228**, 503–505 (1984).
17. Allan, J. S. *et al. Science* **228**, 1091–1093 (1985).
18. Arya, S., Guo, C., Josephs, S. F. & Wong-Staal, F. *Science* **229**, 69–74 (1985).
19. Sodroski, J., Patarca, R., Rosen, C., Wong-Staal, F. & Haseltine, W. A. *Science* **229**, 74–77 (1985).
20. Sodroski, J. *et al. Science* **231**, 1549–1553 (1985).
21. Lee, T. H. *et al. Science* **231**, 1546–1549 (1985).
22. Allan, J. S. *et al. Science* **230**, 810–812 (1985).
23. Goh, W. C., Rosen, C., Sodroski, J., Ho, D. & Haseltine, W. A. *J. Virol* (in the press)
24. Rosen, C. A. *et al. Nature* **319**, 555–559 (1986).
25. Sodroski, J. G. *et al. Science* **227**, 171–173 (1985).
26. Rosen, C. A., Sodroski, J. G. & Haseltine, W. A. *Cell* **41**, 813–823 (1985).
27. Dayton, A., Sodroski, J. G., Rosen, C. A., Goh, W. C. & Haseltine, W. A *Cell* **44**, 941–947 (1986).
28. Fisher, A. C., Collati, E., Ratner, L., Gallo, R. C. & Wong-Staal, F. *Nature* **316**, 262–265 (1985).
29. Rosen, C. A., Sodroski, J. G., Campbell, K. & Haseltine, W. A. *J. Virol.* **57**, 379–384 (1986)
30. Mulligan, R. C., Howard, B. H. & Berg, P. *Nature* **277**, 108–114 (1979).
31. Queen, C. & Baltimore, D. *Cell* **33**, 741–748 (1983).
32. Rho, H. M., Poiesz, B. J., Ruscetti, F. W. & Gallo, R. C. *Virology* **112**, 355–360 (1981)
33. Lee, T. H. *et al. Proc. natn. Acad. Sci. U.S.A.* **81**, 3856–3860 (1984).
34. Sodroski, J., Rosen, C. & Haseltine, W. *Science* **225**, 381–384 (1984).
35. Gorman, C. M., Moffat, L. F. & Howard, B. H. *Molec. cell. Biol.* **2**, 1044–1051 (1982)
36. Chirgwin, J. M., Przybyla, A. E., MacDonald, R. J. & Rutter, W. J. *Biochemistry* **18**, 5294–5299 (1979).
37. Thomas, P. *Proc. natn. Acad. Sci. U.S.A.* **77**, 5201–5202 (1980).
38. Hopp, T. P. & Woods, K. R. *Proc. natn. Acad. Sci. U.S.A.* **78**, 3824–3825 (1981)

LETTERS TO NATURE

Towards the geometrization of physics

George A. J. Sparling

Department of Mathematics and Statistics, University of Pittsburgh, Pittsburgh, Pennsylvania 15260, USA

The concept of symmetry breaking may be expressed mathematically by the reduction of a structure group, for example, choosing a point on a sphere reduces its symmetry group from the group of all rotations to the subgroup of rotations fixing that point. A systematic analysis of Penrose's twistor equation[1,2] has revealed that twistor theory embodies a truth of nature: that interactive gravitational field theories in space-time correspond to such a symmetry breakdown—a breakdown that occurs, not in space-time, but in twistor space–the space of null geodesics of space-time. In particular, twistor theory lies at the heart of supergravity.

The Penrose transform[3,4] provides the necessary algorithm linking space-time and twistor concepts. Applied to bundles, it encodes the information of bundles with connection, on space-time, in bundles without connection, on twistor space. This is possible because null geodesics, which are local in twistor space (points), are extended in space-time. The information stored in parallel propagation along geodesics is completely used in building the geometry of the twistor bundle.

Remarkably, one can construct a bundle with connection, in space-time, the bundle of local twistors, such that: (1) the reduction of its structure group, combined with, (2) the simultaneous reduction of the connection, give the relevant field equations. Applying the Penrose transform, the field equations are expressed by a reduction of the structure group, in twistor space: the breakdown of symmetry.

For Dirac spinor fields ω and π, the twistor equation is:

$$\nabla_a \omega - \gamma_a \pi = 0 \qquad (1)$$

Here ∇_a is a spin connection; the indices are abstract; γ_a obeys the Clifford algebra: $\gamma_{(a}\gamma_{b)} = g_{ab}$ (g_{ab} is the metric).

Equation (1) is invariant under the replacements:

$$\nabla_a \to \nabla'_a \equiv \nabla_a + \gamma_a \tau, \quad \omega \to \omega' \equiv \omega, \quad \pi \to \pi' \equiv \pi + \tau\omega$$

This structure creates a short exact sequence of bundles:

$$0 \to \Pi \xrightarrow{i} T \xrightarrow{j} \Omega \to 0 \tag{2}$$

where Π, Ω and T are, in turn, the bundles of spinors π, ω and of local twistors $\binom{\omega}{\pi}$; also $i(\pi) \equiv \binom{0}{\pi}$ and $j\binom{\omega}{\pi} \equiv \omega$.

It is fundamental that the integrability conditions of equation (1) allow one, for space-time dimension $m > 2$, to express the derivative $\nabla_a \pi$ linearly in terms of ω and π: $\nabla_a \pi = T_a \pi + R_a \omega$ (T_a is determined by $\nabla_a \gamma_b$ and by the torsion of ∇_a); in terms of the curvature R_{ab} of ∇_a, R_a is given by:

$$R_{ab} \equiv C_{ab} - \gamma_{[a} R_{b]}, \qquad \gamma^a C_{ab} = 0 \tag{3}$$

Accordingly, one obtains a canonical connection D_a on T:

$$D_a \begin{pmatrix} \omega \\ \pi \end{pmatrix} \equiv \begin{pmatrix} \nabla_a \omega - \gamma_a \pi \\ \nabla_a \pi - T_a \pi - R_a \omega \end{pmatrix} \tag{4}$$

giving a one to one correspondence between solutions of the twistor equation and parallelly propagated local twistors.

Next two maps $t: \Omega \to T$, $p: T \to \Pi$ split the sequence (2) if they obey $jt =$ identity, $pi =$ identity, $pt =$ zero. The connection D_a also splits, inducing connections on Ω and Π, provided the fundamental splitting equation holds:

$$pD_a t = 0 \tag{5}$$

One says that D_a splits directly if the induced connection on Ω is ∇_a. This amounts to the requirement, in equation (4), the twistors of the form $\binom{\omega}{0}$ are preserved by D_a. From equation (4) this is just the equation $R_a = 0$. Let ${}^L\nabla_a$ be the Levi-Civita connection. Then for ∇_a given successively by:

(i) for $m > 2$, $\quad \nabla_a \equiv {}^L\nabla_a$,

(ii) for $m = 4$, $\quad \nabla_a \equiv {}^L\nabla_a - (F_a{}^b \gamma_b - \frac{1}{4}\gamma_a F_{bc}\gamma^b\gamma^c)\gamma_5$,

(iii) for $m = 11$, $\quad \nabla_a \equiv {}^L\nabla_a - F_a{}^{bcd}\gamma_b\gamma_c\gamma_d + \frac{1}{12}\gamma_a F^{bcde}\gamma_b\gamma_c\gamma_d\gamma_e$,

(where F_{ab} and F_{abcd} are completely skew), then the condition of direct splitting of the local twistor connection gives: (i) the Einstein vacuum equations[5]; (ii) the full Einstein-Maxwell equations; (iii) the full equations of classical 11-dimensional supergravity[6].

Example (iii) strongly suggests that there should be a supersymmetric generalization of the above formalism, since after all the construction of the equations of (iii) was first made using supersymmetry. To see how to achieve this, consider the original twistor equation of Penrose, the equation for a Weyl spinor ω^A:

$$\nabla_{A'}{}^{(A}\omega^{B)} = 0 \tag{6}$$

In classical supergravity the derivative $\nabla_{AA'}$ factorizes[7]:

$$\nabla_{AA'} = \bar{\nabla}_A \wedge \nabla_{A'} \equiv \bar{\nabla}_A \nabla_{A'} + \nabla_{A'} \bar{\nabla}_A \tag{7}$$

(Here $\wedge$ is the graded commutator: an anti-commutation for a pair of operators with an odd number of spinor indices; otherwise it is a commutation). Equation (6) now becomes:

$$\nabla_{A'}(\bar{\nabla}^{(A}\omega^{B)}) + \bar{\nabla}^{(A}\nabla_{A'}\omega^{B)} = 0 \tag{8}$$

This immediately suggests that the correct generalization of equation (6) should be the graded twistor equations:

$$\bar{\nabla}^{(A}\omega^{B)} = 0 \tag{9}$$

$$\nabla_{A'}\omega^B = 0 \tag{10}$$

Remarkably, this first guess works. In Table 1, the algebra generated by $\bar{\nabla}_A$ and $\nabla_{A'}$ is given, for the theory of minimal classical supergravity[7]. $\bar{\nabla}_{AB}$ and $\nabla_{A'B'}$ generate the Lorentz algebra. Using Table 1, one now analyses the integrability of equations (9) and (10). First rewrite equation (9):

$$\bar{\nabla}_A \omega^B = \delta_A{}^B \pi, \tag{11}$$

for some π. Define the spinor $\pi_{A'}$ in terms of π: $\pi_{A'} \equiv \nabla_{A'}\pi$. Then it is routine to establish that all derivatives of the *graded twistor* $(\omega^B, \pi_{B'}, \pi)$ may be computed linearly in terms of $(\omega^B, \pi_{B'}, \pi)$. This gives immediately the definition of the *graded twistor connection* on GT, the bundle of graded twistors. The definition is presented in Table 2.

Table 1 The minimal classical supergravity algebra

$$\bar{\nabla}_{AB} \wedge \bar{\nabla}_{CD} = 4\varepsilon_{(A(C}\bar{\nabla}_{D)B)} \qquad \bar{\nabla}_{AB} \wedge \nabla_{C'D'} = 0 \qquad \bar{\nabla}_{AB} = \bar{\nabla}_{BA}$$

$$\bar{\nabla}_{AB} \wedge \nabla_{CC'} = -2\varepsilon_{C(A}\nabla_{B)C'} \qquad \bar{\nabla}_{AB} \wedge \bar{\nabla}_C = -2\varepsilon_{C(A}\bar{\nabla}_{B)} \qquad \bar{\nabla}_{AB} \wedge \nabla_{C'} = 0$$

$$\bar{\nabla}_A \wedge \bar{\nabla}_B = 2Q\bar{\nabla}_{AB} \qquad \bar{\nabla}_A \wedge \nabla_{A'} = \nabla_{AA'}$$

$$\bar{\nabla}_A \wedge \nabla_{BB'} = \varepsilon_{AB} Q_{B'} + R_{ABB'}$$

$$\nabla_{AA'} \wedge \nabla_{BB'} = \varepsilon_{AB} Q_{A'B'} + \varepsilon_{A'B'} \bar{Q}_{AB} + \varepsilon_{AB} R_{A'B'} + \varepsilon_{A'B'} \bar{R}_{AB}$$

$$Q_{B'} \equiv 2Q\nabla_{B'} + Q^B_{B'}\bar{\nabla}_B$$

$$Q_{A'B'} \equiv (\nabla_{(A'}Q^B_{B')})\bar{\nabla}_B + 2Q^{C'}_{A'B'}\nabla_{C'} + 2(\nabla_{(A'}Q)\nabla_{B')} + Q^B_{(A'}\nabla_{B')B}$$

$$R_{ABB'} \equiv -(\nabla_{B'}Q)\bar{\nabla}_{AB} + \varepsilon_{AB}(-\tfrac{1}{2}(\bar{\nabla}^{(C}Q^{D)}_{B'})\bar{\nabla}_{CD} + Q^{C'D'}_{B'}\nabla_{C'D'})$$

$$R_{A'B'} \equiv -\tfrac{1}{2}(\nabla_{(A'}\bar{\nabla}^{(C}Q^{D)}_{B')})\bar{\nabla}_{CD} + (\nabla_{(A'}Q^{C'D'}_{B')})\nabla_{C'D'} - \tfrac{1}{2}(\bar{\nabla}_C\bar{\nabla}^C\bar{Q} - 8Q\bar{Q})\nabla_{A'B'}$$

$$Q_{AA'} + \bar{Q}_{AA'} = 0 \qquad Q_{A'B'C'} = Q_{(A'B'C')} \qquad \bar{\nabla}_A Q_{A'B'C'} = 0$$

$$\bar{\nabla}_A Q = 0 \qquad \bar{\nabla}_A Q^{ABC} = \tfrac{1}{2}\nabla^{(B}_{A'}Q^{C)A'} \qquad \bar{\nabla}_A Q^A_{A'} + 2\nabla_{A'}Q = 0$$

The defining property of the connection is that there be a one-to-one correspondence between solutions of the graded twistor equations and covariantly constant graded twistors. There is now a split exact sequence of graded bundles:

$$0 \to G\Pi \xrightarrow{i} GT \xrightarrow{j} G\Omega \to 0 \tag{12}$$

generalizing equation (2);

$$\text{here} \quad i\begin{pmatrix} \pi_{B'} \\ \pi \end{pmatrix} \equiv \begin{pmatrix} 0 \\ \pi_{B'} \\ \pi \end{pmatrix}, \qquad j\begin{pmatrix} \omega^B \\ \pi_{B'} \\ \pi \end{pmatrix} \equiv \omega^B .$$

The graded analogue of the direct splitting is the condition that the graded twistors $(\omega^B, 0, 0)$ are preserved by the graded connection.

By inspection of Table 2, one immediately finds the equations:

$$Q = 0, \qquad \bar{\nabla}_{(A}Q_{B)B'} = 0 \tag{13}$$

Given equation (13) the induced connection on $G\Pi$ itself splits, preserving spinors of the form $\binom{0}{\pi}$, if and only if the slightly stronger system of equations holds:

$$Q = 0, \qquad Q_{BB'} = 0. \tag{14}$$

Equation (13) gives the standard curvature field equations of classical supergravity. Equation (14), the second level of splitting, gives the standard torsion field equations[7].

Finally, if equation (10) is generalized to the equation:

$$\nabla_{A'}\omega^B = \bar{F}^B\bar{\omega}_{A'} \tag{15}$$

then the two levels of broken symmetry provide the graded version of the Einstein-Maxwell equations[7]:

$$\bar{\nabla}_C\bar{F}^C = 0, \qquad \nabla_{C'}\bar{F}^C = 0, \qquad Q = 0, \qquad Q_{BB'} + \bar{F}_B F_{B'} = 0 \tag{16}$$

Thus, one sees that the graded Penrose transform, first envisaged by Witten[4,8], provides an interpretation of the field equations in terms of the breaking of graded symmetry in graded twistor space. In all existing supergravity theories, it is the torsional constraints that allow for the existence of graded null geodesics and for the construction of the transform.

It is tempting to speculate that the simplest supergravity theory, containing a complete spectrum of helicities, from -2 to 2, derived along the above lines, may be physically viable at

Table 2 The definition of graded twistor transport

$$\bar{D}_A\begin{pmatrix}\omega^B\\ \pi^{B'}\\ \pi\end{pmatrix}\equiv\begin{pmatrix}\bar{\nabla}_A\omega^B-\delta_A{}^B\pi\\ \bar{\nabla}_A\pi_{B'}+Q_{AB'}\pi+(\nabla_{B'}Q)\omega_A+(\bar{\nabla}_{(A}Q_{B)B'})\omega^B\\ -\bar{\nabla}_A\pi+2Q\omega_A\end{pmatrix}$$

$$D_{A'}\begin{pmatrix}\omega^B\\ \pi_{B'}\\ \pi\end{pmatrix}\equiv\begin{pmatrix}\nabla_{A'}\omega^B\\ \nabla_{A'}\pi_{B'}-2\bar{Q}\varepsilon_{A'B'}\pi\\ -\nabla_{A'}\pi+\pi_{A'}\end{pmatrix}$$

$$D_{AA'}\begin{pmatrix}\omega^B\\ \pi_{B'}\\ \pi\end{pmatrix}\equiv\begin{pmatrix}\nabla_{AA'}\omega^B-\delta_A{}^B\pi_{A'}\\ \nabla_{AA'}\pi_{B'}+Q_{AB'}\pi_{A'}+X_{AA'B'}\pi+X_{ABA'B'}\omega^B\\ \nabla_{AA'}\pi+Q_{AA'}\pi-(\nabla_{A'}Q)\omega_A+(\bar{\nabla}_{(A}Q_{B)A'})\omega^B\end{pmatrix}$$

$$X_{AA'B}\equiv\nabla_{(A'}Q_{B')A}-\varepsilon_{A'B'}\bar{\nabla}_AQ$$

$$X_{ABA'B'}\equiv\nabla_{(A'}\bar{\nabla}_{(A}Q_{B)B')}+\tfrac{1}{6}\varepsilon_{A'B'}\nabla_{C'}\bar{\nabla}_{(A}Q_{B)}^{C'}+\varepsilon_{AB}\varepsilon_{A'B'}(4QQ-\tfrac{1}{2}\nabla_{C'}\nabla^{C'}Q)$$

some energy scale. If so, there would be widespread consequences for cosmology.

Finally, a point of philsophy. Local twistors survive in the superstring arena, through the theory of two-surface twistors of Penrose[9]: as the two-surface shrinks to a point, one recovers the local twistor. Is there a place in the superstring theory for a full blown twistor theory? Twistors, being fundamentally spinorial, form a 'square root' for space-time. 'Stringy' twistors ought to provide a square root for superstrings. At the quantum level they should give a 'fermionization' of the superstring theory (the reverse of bosonization)[10,11]. Perhaps the above work should be taken as a small piece of evidence that such a theory exists.

I thank Ted Newman, Roger Penrose and John Porter for their continuing support. Supported in part by grants from the NSF and from the Alfred P. Sloan Memorial Foundation.

Received 11 September 1985; accepted 6 March 1986.

1. Penrose, R. in *Quantum Gravity, An Oxford Symposium* (eds Isham, C. J., Penrose, R. & Sciama, D. W. (Clarendon, Oxford, 1975).
2. Dighton, K. *Int. J. theor. Phys.* **11**, 31-43 (1974).
3. Eastwood, M. G., Penrose, R. & Wells, R. O. Jr *Commun. math. Phys.* **78**, 305-351 (1981).
4. Witten, E. *Phys. Lett.* **77B**, 394-398 (1978).
5. Le Brun, C. R. *Class. Quantum Gravitat.* **2**, 555-563 (1985).
6. Cremmer, E., Julia, B. & Scherk, J. *Phys. Lett.* **76B**, 409-412 (1978).
7. van Nieuwenhuizen, P. *Phys. Rep.* **C68**, 189-398 (1981).
8. Crispin-Romão, J., Ferber, A. & Freund, P. G O. *Nucl. Phys.* B **182**, 45-51 (1981).
9. Penrose, R. *Proc. R. Soc.* **A381**, 53-63 (1982).
10. Carey, A. L. & Hurst, C. A. *Commun. math. Phys.* **98**, 435-448 (1985).
11. Sugawara, H. *Phys. Rev. Lett.* **56**, 103-106 (1986).

Is there a black hole in the sky?

Bohdan Paczyński

Princeton University Observatory, Princeton University, Princeton, New Jersey 08544, USA

The recent discovery[1] that the two quasars, Hazard 1146+111B,C, separated by 157 arc s, are in fact two images of the same quasar raises the question: what massive object is responsible for gravitational lensing? Ultimately, the answer will be provided by observations of a few more pairs of images of other sources when it will be possible to analyse the mass distribution of the lens. One of the imaginable candidates is a supermassive black hole. No observational or theoretical argument can be presented in favour of this possibility at present. Should the future observations point to a compact supermassive lensing object, the presence of a black hole could be established by the unique property that it would appear against the microwave background as a black spot with a diameter of ≳0.1 arc s.

Various candidates for a gravitational lens whose images are split by a few minutes of arc have been proposed[1], including an unusually dense cluster of galaxies, a cosmic string or a black hole. As yet there is no observational evidence for the cluster of galaxies, and it is worthwhile exploring the consequences of the hypothesis that the lensing object is a supermassive black hole.

The angular distance between two objects with redshifts z_1 and z_2 in a universe with dimensionless density $\Omega=1$ and cosmological constant $\Lambda=0$ is given as[2]

$$D_{\rm ang}(z_1,z_2)=\frac{c}{H_0}\frac{2}{1+z_2}[(1+z_1)^{-1/2}-(1+z_2)^{-1/2}] \quad (1)$$

where H_0 is the Hubble constant. This formula may be used to calculate the angular distance between the observer and the deflector, $D_{\rm d}$, between the observer and the source, $D_{\rm s}$, and between the deflector and the source, $D_{\rm ds}$, as well as the effective distance to the lens, $D\equiv D_{\rm d}D_{\rm ds}/D_{\rm s}$. If the source, the point-mass deflector, and the observer are perfectly aligned, then the image forms a ring with radius r_0 in the deflector's plane. This may be calculated from

$$r_0^2=4\,GMD/c^2=2\,r_{\rm g}\,D \quad (2)$$

The angular radius of the ring as seen by the observer would be

$$\alpha_0=r_0/D_{\rm d} \quad (3)$$

If the lensing object is a black hole then it might be seen as a dark spot against a bright background. For a Schwarzschild black hole, the dark spot is a circle with a diameter $3^{3/2}\,r_{\rm g}\simeq 5.196\,r_{\rm g}$. For a Kerr black hole, the dark spot is almost the same size, but it looks like a distorted circle[3]. The angular diameter of the dark circle as seen by the observer is

$$d_{\rm BH}=3^{3/2}\,r_{\rm g}/D_{\rm d} \quad (4)$$

Combining equations (1)-(4), we obtain for the observed diameter of the black hole

$$d_{\rm BH}=\frac{3^{3/2}}{2}\alpha_0^2\frac{D_{\rm s}}{D_{\rm ds}} \quad (5)$$

The angular separation between the two images of a source gravitationally lensed by a point mass is always larger than the diameter of the ring-like image, $2\alpha_0$. However, as the two images of 1146+111 are almost equally bright, the lens and the source may be reasonably well aligned, and I shall adopt $\alpha_0=157$ arc s$/2=3.81\times10^{-4}$ rad. Therefore, the expected diameter of the black spot in the microwave background becomes

$$d_{\rm BH}=0.078\;D_{\rm s}/D_{\rm ds}\;\text{arc s} \quad (6)$$

If the black hole is a relatively nearby object then $D_{\rm s}\approx xD_{\rm ds}$, and $d_{\rm BH}=0.078$ arc s. If the black hole is at a cosmological distance, then $D_{\rm s}>D_{\rm ds}$, and the black spot is larger than 0.078 arc s.

Another interesting quantity is the black hole mass. For a given radius of a circular image, α_0, it may be calculated as follows:

$$r_{\rm g}=\frac{\alpha_0^2\,D_{\rm d}D_{\rm s}}{2D_{\rm ds}} \quad (7a)$$

$$M=2.3\times10^{15}\,M_\odot\,h_{100}^{-1}\frac{[(1+z_{\rm s})^{-1/2}-1][(1+z_{\rm d})^{-1/2}-1]}{(1+z_{\rm d})[(1+z_{\rm s})^{-1/2}-(1+z_{\rm d})^{-1/2}]} \quad (7b)$$

where h_{100} is the Hubble constant in units of 100 km s^{-1} Mpc^{-1}. Note that at a very small observer-deflector distance $D_{\rm d}$, the black hole mass is simply proportional to that distance:

$$M_{\rm BH}=8\times10^5\,M_\odot\times D_{\rm d}/1\;\text{pc} \quad (8)$$

A black hole captures microwave background radiation with a cross-section of $27\pi r_{\rm g}^2$, and therefore it may appear as a 'source' with a negative luminosity

$$L_{\rm BH}=-27\pi r_{\rm g}^2\sigma[2.7\times(1+z)]^4 \quad (9)$$

The redshift of 1146+111 is $z_{\rm s}=1.012$ (ref. 1). The redshift of the lens is not known. The values of the black hole mass, the

Table 1 Variation of the apparent diameter of the black spot, the black hole mass and the negative black hole luminosity as a function of the black hole redshift

z	d (arc s)	log M ($M_\odot$)	log $-L$ ($L_\odot$)
0.001	0.078	12.36	0.98
0.01	0.079	13.35	2.99
0.1	0.092	14.36	5.15
0.2	0.11	14.67	5.92
0.3	0.13	14.87	6.45
0.4	0.16	15.02	6.90
0.5	0.20	15.17	7.30
0.6	0.27	15.31	7.70
0.7	0.37	15.47	8.13
0.8	0.57	15.67	8.63
0.9	1.1	15.97	9.33
1.0	10.8	16.97	11.41

diameter of the black spot and the black hole negative luminosity are given in Table 1 for various assumed values of its redshift, z_d, and for $H_0 = 100$ km s^{-1} Mpc^{-1}.

The only bright background that is present everywhere is the microwave background. The only instrument capable of either resolving the black spot, or at least noticing it as a negative luminosity source is the Very Large Array (VLA). In fact, the black-spot detection might be feasible with the present VLA instrumentation (E. L. Turner, personal communication). It would be very interesting to look for this spot if future analysis indicates the existence of a very compact supermassive object.

I thank Dr E. L. Turner for information about the discovery of the new gravitational lens before publication, and for very many stimulating discussions. Discussions with Dr M. Sikora are also acknowledged. This research was partly supported by NASA grant NAGW-765.

Received 25 March; accepted 16 April 1986.

1. Turner, E. L. *et al. Nature* **321**, 142–144 (1986).
2. Weinberg, S. *Gravitation and Cosmology* (Wiley, New York, 1972).
3. Bardeen, J. M. *Black Holes* (eds De Witt, C. & DeWitt, B. S.) 215–240 (Gordon & Breach, Edinburgh, 1972).

Is QSO1146+111B,C due to lensing by a cosmic string?

J. Richard Gott III

Department of Astrophysical Sciences, Princeton University, Peyton Hall, Princeton, New Jersey 08544, USA

A predicted consequence of cosmic strings is that they should produce equal-brightness double-lens images of distant quasars (QSOs), with separations of up to several minutes of arc (see refs 1, 2). Here I discuss a newly discovered lens candidate[3–6]: QSO1146+111B,C which appears to consist of two images of equal brightness (B is 1.02 times as bright as C, with virtually identical spectra over the observed range) of a quasar at redshift $z = 1.01$, which are separated by 2.6 arc min. If this is produced by a cosmic string, its mass per unit length is $\mu \geq 4.0 \times 10^{23}$ g cm^{-1}, a value large enough to be interesting for string-assisted galaxy formation[7–9] and near the upper limits implied by the isotropy of the cosmic microwave background[2,10] and constraints on gravitational radiation[11]. But note that four other QSOs, also close enough to be double-imaged, have thus far not been detected. Searches for these and for the microwave background temperature shift across the string[2,10] would be useful.

The exact metric for a straight cosmic string has been given elsewhere[2]:

$$ds^2 = -dt^2 + dz^2 + dr^2 + (1-4\mu)^2 r^2 d\phi^2 \quad (1)$$

where μ is the mass per unit length in Planck masses per Planck length, and t, z, r and ϕ are the usual cylindrical coordinates. This is a conical space with angle deficit $D = 8\pi\mu$. Because the space-time is locally flat there is no image magnification. For convenience we adopt a value of $\Omega = 1$ for the cosmic density parameter, and the Hubble constant $H_0 = 50$ km s^{-1} Mpc^{-1}. The low-peculiar-velocity string produces double-lens images of equal brightness with separations[2]:

$$\Delta\theta = D\left[\cos\alpha - \frac{1-(1+z_s)^{-1/2}}{1-(1+z_q)^{-1/2}}\right] \quad (2)$$

where α is the angle between the string and the plane of the sky, z_q is the redshift of the QSO, and z_s is the redshift of the string at its point of closest approach. The formula applies only for those values of α, z_s, z_q which make the term in brackets positive. If 1146+111 is produced by a string, $\Delta\theta = 2.6$ arc min and the minimum value of μ is obtained in the limit $\cos\alpha = 1$, $z_s \ll 1$:

$$\mu \geq 3.0 \times 10^{-5} = 4.0 \times 10^{23} \text{ g cm}^{-1} \quad (3)$$

If this string is moving relativistically with a velocity V_s perpendicular to its own length and to the line of sight, this will produce a temperature shift

$$\Delta T \simeq 2.7\, DV_s/c \text{ K} \simeq 2.0\, V_s/c \text{ mK} \quad (4)$$

in the microwave background across the string[2,10]. A detailed map to look for this effect would be invaluable. This effect will also cause a velocity shift $\Delta V \simeq V_s D$ between the two spectra. The observations[6] indicate $\Delta V \simeq 126 \pm 309$ km s^{-1} in the rest frame of the QSO. A velocity shift $\simeq 120$ km s^{-1} could be produced by a perpendicular string velocity $V_s \simeq 0.5\,c$. The value $\mu \geq 3 \times 10^{-5}$ already pushes the allowed[2,10,11] upper limits so $\cos\alpha$ cannot be small and over the region of $1° \times 1°$ near 1146+111 $\cos\alpha \simeq$ constant. Thus, without loss of generality we shall adopt $\cos\alpha = 1$ in what follows.

Figure 1 shows where we should look for additional multiple QSO images. With a low-peculiar-velocity straight string as the lensing object, any QSO with redshift larger than 1.01 which has an image in the strip between the two horizontal lines must have a second image. The string itself must lie in this strip and any point within the strip must lie within 2.6 arc min of the string. Any QSO lying within 2.6 arc min of the string with $z_q > 1.01$ will be double-lensed (see equation (2)). For $0.2 \leq z_s \leq 0.6$ we would expect four of the other QSOs in the field to be double-lensed. No equal-brightness images of these QSOs have been seen. Thus, if this lensing event is caused by a string, it is surprising that there are no other easily detectable double-lensed QSOs in the field. One reason may be because of time delays between images[2]:

$$t_2 - t_1 = H_0^{-1}(\theta_1 - \theta_2) D[1-(1+z_s)^{-1/2}] \quad (5)$$

where θ_1 and θ_2 are the distances of the two images from the string. If the string passes directly down the middle of the strip then $t_1 - t_2 = 0$ for 1146+111B,C and we are guaranteed seeing them at equal brightness. The time delays for the other pairs of QSO images are, for $z_s = 0.2$ and $z_s = 0.6$ respectively: 190 yr and 6,000 yr for the quasar at $z_q = 2.22$; 240 yr and 3,900 yr for the quasar at $z_q = 2.12$; 450 yr and 1,800 yr for the quasar at $z_q = 1.10$; 300 yr and 6,500 yr for the quasar at $z_q = 1.93$. These delays are sufficient that the quasars could have varied considerably in brightness. Mini-lensing could also affect the brightness of the different images and as most of the string length is in the form of closed loops[8,12] it is always possible that the string is significantly curved, so that it misses making images of some of these other QSOs.

If the lensing object were a black hole or cluster of galaxies (singular isothermal sphere) then the QSOs at $z_q = 2.12$ and $z_q = 1.10$ would be more likely candidates for double imaging than those at $z_q = 2.22$ and $z_q = 1.93$. As B and C are of equal brightness (B is 1.02 times as bright as C in the emission lines

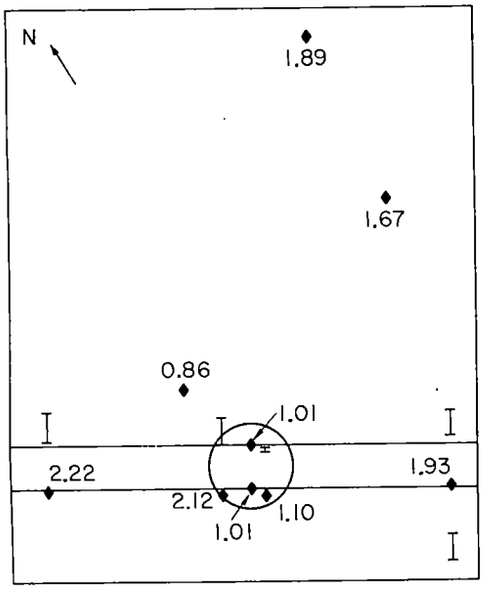


Fig. 1 Map of the known QSO images[4] (with redshifts) in the field of 1146+111B,C. Images B,C are the lower and upper images respectively, with redshifts of 1.01. If the lensing object is a low-peculiar-velocity, straight cosmic string, any QSO image with $z_q > 1.01$ lying in the strip (of width 2.6 arc min) between the two horizontal lines must have an accompanying second image. If $\cos\alpha = 1$ and $0.2 \leq z_s \leq 0.6$, the possible locations for second images of four of the QSOs are shown as vertical bars. The QSO at $z_q = 1.93$ has two sets of second-image locations because the string may pass either above or below it in the figure. If the string moves with a velocity V_s perpendicular to its length and to the line of sight, the two horizontal lines, pivoting on the two QSO images at $z = 1.01$, will be rotated (A. Vilenkin, personal communication) by an angle χ, where $\tan\chi = (v_s/c)\tan\alpha$, so that over some limited ranges of χ it is possible to find solutions which require no additional QSO images. Because, as we have argued, α must be small so that μ is not too large, it is likely that this rotation is relatively small. The lower limit for μ obtained in equation (3) is uncertain (A. Vilenkin, personal communication) by a factor $K = (c - V_{s\parallel})(c^2 - V^2)^{-1/2}$, where V is the velocity of the string and $V_{s\parallel}$ is its velocity parallel to the line of sight,which may be either positive or negative. If the lensing object is a singular isothermal sphere (cluster of glaxies with the requirement that its line-of-sight velocity dispersion $\sigma > 1{,}650\ \mathrm{km\ s^{-1}}$ to produce the observed 2.6 arc min splitting[14]) any QSO image with $z_q > 1.01$ lying inside the circle must have an accompanying second image. If the lensing object is a black hole, any QSO image with $z_q > 1.01$ lying inside the circle must have an accompanying second image at least 1/16th as bright as it is. A failure to find any additional images in this field could be perhaps equally embarrassing for all these lensing scenarios.

which are the most likely to remain constant over a significant period of time) the black hole or singular isothermal sphere cluster must be located approximately midway between the two images, and the critical lensing angle[13,14] is $\beta_{crit} = 1.3$ arc min for a QSO at $z = 1.01$. For quasars at larger redshift β_{crit} will be larger. For the singular isothermal sphere case any QSO image closer than $2\beta_{crit}$ to the centre will have an accompanying secondary image; for the black hole case any QSO image closer than $2\beta_{crit}$ to the centre will have an accompanying secondary image at least 1/16th as bright as itself. (The circle in Fig. 1 for these cases has a radius of $2\beta_{crit} = 2.6$ arc min (refs 13, 14). A supercluster seen edge-on, parallel to the strip and causing some image magnification is another interesting possibility as this might help to account for the unusually large number of QSOs seen[4] in this field.

To differentiate between these lensing models and the possibility that B and C are just too different QSOs, additional spectra of B and C and searches for additional images are essential.

I thank Ed Turner for discussion results before publication. This work was supported by NASA grant NAGW-765.

Received 28 March; accepted 18 April 1986.

1. Vilenkin, A. *Phys. Rev.* D23, 852–857 (1981).
2. Gott, J. R. *Astrophys. J.* **288**, 422–427 (1985).
3. Hazard, C., Arp, H. & Morton, D. C. *Nature* **282**, 271–272 (1979).
4. Arp, H. & Hazard, C. *Astrophys. J.* **240**, 726–736 (1980).
5. Paczynski, B. *Nature* **319**, 567–568 (1986).
6. Turner, E. L. *et al. Nature* **321**, 142–144 (1986).
7. Zeldovich, Ya. B. *Mon. Not. R. astr. Soc.* **192**, 663–667 (1980).
8. Vilenkin, A. *Phys. Rev. Lett.* **46**, 1169–1172 (1981).
9. Turok, N. & Schramm, D. N. *Nature* **312**, 598–599 (1985).
10. Kaiser, N. & Stebbins, A. *Nature* **310**, 391–393 (1984).
11. Hogan, C. & Rees, M. *Nature* **311**, 109–114 (1984).
12. Turok, N. *Phys. Lett.* **123B**, 387–390 (1983).
13. Gott, J. R. & Gunn, J. E. *Astrophys. J. Lett* **190**, L105–L108 (1974).
14. Turner, E. L., Ostriker, J. P. & Gott, J. R. *Astrophys. J.* **284**, 1–22 (1984).

Relation between solar narrow-band decimetre-wave bursts and associated X-ray bursts

Shinzo Enome* & Larry E. Orwig†

* Toyokawa Observatory, Nagoya University, Toyokawa 442, Japan
† Code 682, NASA Goddard Space Flight Center, Greenbelt, Maryland 20771, USA

Theoretical models have been proposed, stimulated by a successful account of the jovian decametric radiation[1], for a maser mechanism, or a normal relativistic cyclotron resonance mechanism, operating in solar flares, and for transport of energy across magnetic fields to the electron gas by maser-amplified radio waves[2]. Much effort has been directed towards observations of solar-flare radio spike bursts[3–8]. Here we compare solar narrow-band decimetre-wave spike bursts with corresponding X-ray events for 25 solar flares. We find that decimetre spike bursts are 10^2–10^3 times stronger than normal impulsive microwave bursts for the same observed amount of hard X-ray emission. This feature, along with the observation of 100% circular polarization, strongly supports a maser origin for the decimetre spike bursts.

A previous study[8] compared narrow-band decimetre (DCM) bursts with X-ray radiation observed by the hard X-ray (HXM) and soft X-ray (FLM) detectors aboard the spacecraft Hinotori[9,10]. In the work described here, we have taken advantage of the larger data recording capacity of the SMM spacecraft to achieve more homogeneous sampling with respect to flare intensity. We have chosen to compare the hard X-ray data at energies above 30 keV from the SMM hard X-ray burst spectrometer, HXRBS[11], with the radio data from the polarimeters at Toyokawa Observatory[12]. The former provides hard X-ray count rate and 15-channel spectral data in the energy range 30–500 keV with 0.128-s resolution, and the latter provides radio data at four frequencies, 9.4, 3.75, 2 and 1 GHz, at a sampling rate of 0.5 s. The narrow-band DCM events treated here, for which emission is strongly polarized and is seen or strongly enhanced only at 1 GHz, are likely to be a subgroup of the fine-structure radio bursts studied by Droege[3], with additional information on polarization, or part of classical DCM type IV[13], but are probably different from the 2.65-GHz spikes investigated by Slottje[4,5] and from blips[6].

The data sets used in the present analysis were obtained during a period of common observations from 12 to 14 November 1981 during a so-called DCM storm. A portion of this storm is shown in Fig. 1, where the total solar radio emission is plotted against time at four frequencies for 13 November 1981. A typical spike burst is illustrated in Fig. 2, in which the 1-GHz data (*a*) and hard X-ray data above 30 keV (*b*) are plotted against the same timescale for comparison.

For each of the events studied we have obtained the peak intensity of hard X rays above 30 keV and in the radio emission at 1 GHz (Table 1). Figure 3 shows the resulting peak intensity correlation diagram for radio and X-ray events, revealing that

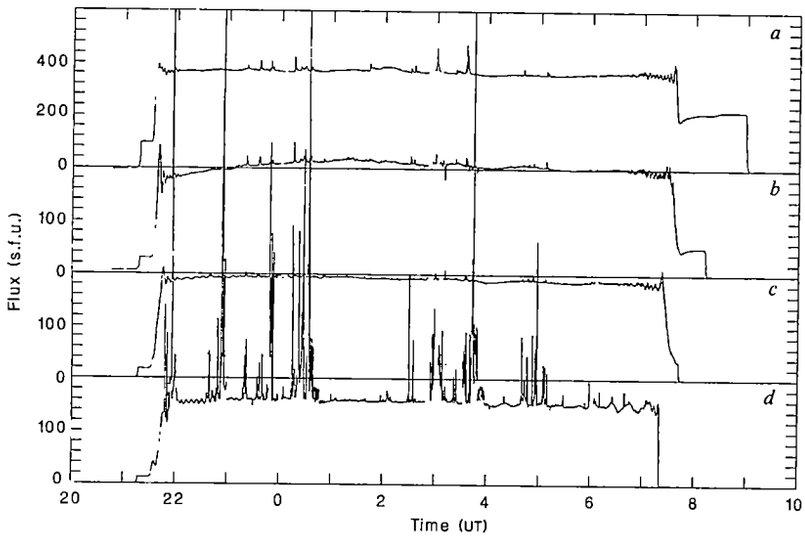


Fig. 1 Time profiles of flux at four frequencies (*a*, 9.4; *b*, 3.75; *c*, 2; and *d*, 1 GHz) observed at Toyokawa on 13 November 1981. Data gaps at 00:00, 03:00, and 06:00 UT (Universal Time) are calibration signals erased.

Table 1 Decimetre-wave events

No.	Date	Universal Time	1-GHz peak flux (s.f.u.)	HXR peak rate (counts per s)	Time delay (HXR−radio)
1	12 Nov. 1981	00:06:50	140	—	—
2		00:59:12*	877	61	−2
3		01:53:30†	74	270	25
4		02:09:19	396	—	—
5		02:32:49	15	—	—
6		03:38:20†	956	1,680	1
7		03:46:56	1,040	—	—
8		04:50:06†	40	87	2
9		06:49:32	157	—	—
10		07:08:09	154	—	—
11	13 Nov. 1981	00:15:18*	480	115	−3
12		00:32:46*	9,220	75	4
13		01:37:48†	12	58	3
14		01:38:20	20	—	—
15		01:40:16	25	—	—
16		01:58:02	30	—	—
17		03:08:32	225	—	—
18		03:22:22†	132	33	−1
19		03:24:50†	122	31	−3
20		03:34:13†	186	1,430	5
21		03:43:34*	19,300	175	8
22		04:40:27†	178	44	1
23	14 Nov. 1981	03:34:56	125	—	—
24		05:09:03	29	—	—
25		06:17:40	69	—	—

Events with no entry in the HXR peak rate column (hard X-ray peak rate above background, in the range 30–500 keV) were not observed above instrument background by the HXRBS. s.f.u. are solar flux units.
* Spike burst; † impulsive burst.

there are two distinct classes of events. One is a group of radio events for which there is very weak, if any, hard X-ray emission above 30 keV. In the second group, the radio events are associated with X-ray events of appreciable size. We will call the first group 'coherent' events and the second group 'incoherent' events. The radio bursts of the first group have the following characteristics: (1) all bursts are strongly polarized, ~100% at 1 GHz; (2) all show very spiky structure on timescales of a few seconds or less; (3) all are intense only at 1 GHz; that is, they have a narrow-band spectral character. These characteristics are a common feature of maser-associated phenomena.

The characteristics of incoherent events are almost entirely opposite to those of coherent events. Thus, the spectra of incoherent bursts are not narrow-banded in character, time profiles are less spiky, with typical time constants of ≥10 s, and the degree of polarization is not high. Some incoherent bursts are almost unpolarized, and for those that are polarized the degree of polarization is much less than 100%, even at 1 GHz. It is important to note that for the incoherent events there is a linear relation between the microwave and hard X-ray intensities, reflecting the well-established proportionality between microwaves and hard X rays[14,15]. We should mention that there are three events (18, 19 and 22 in Table 1) which, while being classified as impulsive events, do show a slight mixture of impulsive and spike characteristics.

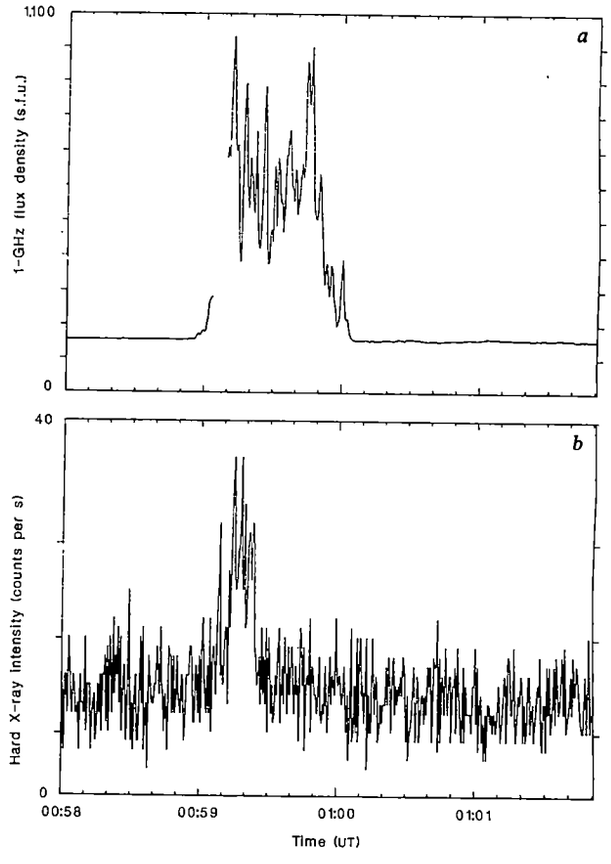


Fig. 2 High-time-resolution profiles of the 1-GHz radio burst (*a*) and X-ray burst (*b*) at 00:59:12 UT on 12 November 1981. The hard X-ray intensity is the raw count rate observed between 30 and 86 keV (including background).

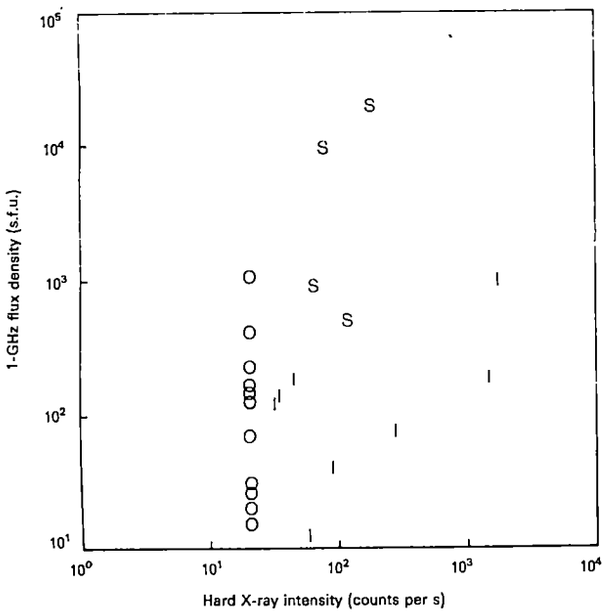


Fig. 3 Correlation diagram between peak flux at 1 GHz and X-ray intensity above 30 keV for the 25 flares studied. 'S' and 'I' indicate spike bursts and impulsive bursts, respectively. Open circles correspond to radio bursts with no observable X-ray enhancement above the background noise, so that the plotted hard X-ray intensity is a 3σ upper limit.

When one considers the above characteristics, the most striking feature of coherent events is the fact that they exhibit unusually weak X-ray emission, almost below the detection limit of the HXRBS. For the events studied here, the ratio of radio to X-ray intensity is larger by a factor of 10^2–10^3 for the coherent events than for the incoherent events. This enhancement factor has thus been determined observationally for the first time, and provides convincing evidence for the existence of a coherent radiation mechanism operating in these events. Its value is indispensable when one considers the saturation mechanism in the maser effect. The factor of 10^2–10^3 should be considered as a lower limit, because the bandwidth and the temporal structure of narrow-band coherent spike bursts might be much smaller and finer than our observational limits of 10 MHz and 0.5 s, respectively. Such bursts, if they exist, could be observed with more sophisticated instruments[3–7,13].

The temporal relation between the two radiations has been examined for both classes of events. Such a comparison is difficult due to the complex structure in both types of radiation. For example, detailed consideration of the event shown in Fig. 2 reveals that the identification of corresponding spikes in each data set for this burst is complicated, and a unique one-to-one correspondence cannot be specified. The results in Table 1 indicate that for those flares for which a comparison can be made there are time delays observed between the main peaks in radio and X-ray emission. In the coherent events the time delays are distributed from −3 to 8 s. Note, however, that radio bursts of the incoherent type are always delayed in time relative to the associated X-ray bursts.

Received 1 October 1985; accepted 26 February 1986

1. Wu, C. S. & Lee, L. C. *Astrophys. J.* **230**, 621–626 (1979).
2. Melrose, D. B. & Dulk, G. A. *Astrophys. J.* **259**, 844–858 (1982); **259**, L41–L45 (1982); **282**, 308–315 (1984).
3. Droege, F. *Astr. Astrophys.* **57**, 285–290 (1977).
4. Slottje, C. *Nature* **275**, 520–521 (1978).
5. Slottje, C. *IAU Symp.* No. 86, 195–203 (1980).
6. Benz, A. O., Bernold, T. E. X. & Dennis, B. R. *Astrophys. J.* **271**, 355–366 (1983).
7. Zhao, Ren-Yang Adv. Space Res. **2**, 177–180 (1983).
8. Enome, S. *Sol. Phys.* **86**, 421–426 (1983).
9. Kondo, I. in *Proc. Hinotori Symp. Solar Flares* (eds Tanaka, Y. *et al.*) 1–12 (Institute of Space and Astronautical Science, Tokyo, 1982).
10. Tanaka, Y. *Sol. Phys.* **86**, 3–6 (1983).
11. Orwig, L. E., Frost, K. J. & Dennis, B. R. *Sol. Phys.* **65**, 25–37 (1980).
12. Torii, C. *et al. Proc. Res. Inst. Atmos. Nagoya Univ.* **26**, 129–132 (1979).
13. Wiehl, H. J., Benz, A. O. & Aschwanden, M. J. *Sol. Phys.* **95**, 167–179 (1985).
14. Kane, S. R. *IAU Symp.* No. 57, 105–141 (1974).
15. Kai, K., Kosugi, T. & Nitta, N. *Publs astr. Soc. Japan* **37**, 155–162 (1984).

Bottom-current pathways in the Argentine Basin revealed by mean silt particle size

Michael T. Ledbetter

Moss Landing Marine Laboratories, PO Box 450, Moss Landing, California 95039-0450, USA

Regional circulation patterns in the deep sea are very difficult to determine because of time constraints on the acquisition of large physical-oceanographic data sets from abyssal depths; in addition, the large number of long-term (≥1 yr) current-meter arrays needed to delineate bottom-current pathways are extremely costly. An alternative method for inferring benthic flow patterns, described here, is to map the mean size of the silt fraction of sediment on the sea floor. Because of the availability of a large number of core samples in the Argentine Basin, the particle-size approach provides a useful method for determining bottom-current pathways in that deep basin.

The mean particle size of the non-biogenic silt fraction of sediment from seafloor (gravity-core-top) samples has been used to delineate deep western boundary undercurrents (DWBUCs) in the Vema channel[1–3], Amirante Passage[4] and the lower continental rise of eastern North America[5,6]. In those cases, however, the method was used only to identify the depth range of a high-velocity DWBUC and was not applied to an entire basin, which would include areas of low bottom-current velocity. The Argentine Basin in the south-west Atlantic Ocean provides a unique opportunity to test the particle-size technique in a basin where bottom-water velocity ranges from high-velocity DWBUCs to low velocities on the lower flank of the Mid-Atlantic Ridge[7,8]. Another useful factor is the availability of a large number of core-top samples in the region.

The mean silt particle size was determined for the non-biogenic fraction of seafloor samples obtained from gravity core tops deeper than 4,000 m, in which there is no evidence of graded bedding or sedimentary structures indicative of turbidites. The bottom-current velocity inferred from particle-size data is contoured to divide the relative velocity into five divisions, arbitrarily classified from highest to lowest velocity (Fig. 1). The boundary between moderate and high relative velocity was chosen at a mean silt particle size $\phi = 6.0$ (16 μm), the mean size which delineates the top of the DWBUC in both North and South Atlantic studies[1–6]. The contour interval for relative velocity (Fig. 1) represents a difference of 0.2 in silt mean ϕ, which is analysed with a precision of 0.05 (refs 2, 3).

The inferred relative bottom-current velocity in the Argentine Basin reveals a benthic flow pattern which is controlled principally by geostrophy and bathymetry (Fig. 1). Antarctic Bottom Water (AABW) enters the South Sandwich Basin through the newly discovered Bullard Fracture Zone[9], which has served as a bottom-water conduit throughout the Quaternary[10]. On encountering the South Sandwich Ridge, AABW is diverted north, where the main branch flows as a DWBUC into the Georgia Basin while a minor branch flows around the eastern flank of the Islas Orcadas Rise. The two branches rejoin near a gap in the Falkland Fracture Zone[11], where the flow intensifies as it follows approximately the 4,000–5,000-m contour interval through the southwestern and western Argentine Basin.

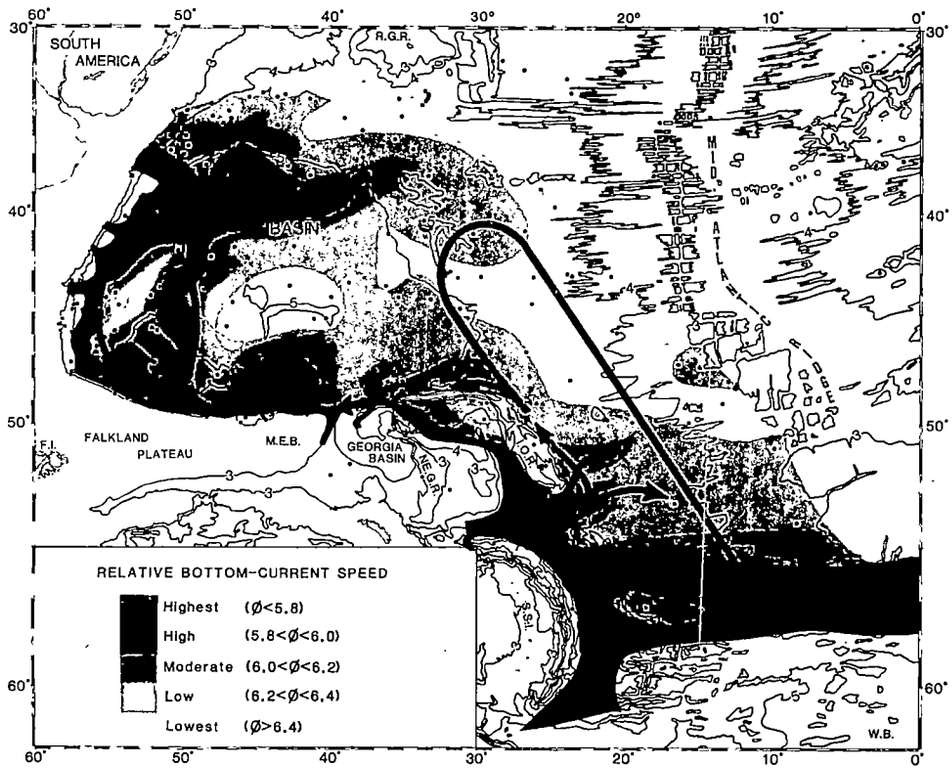


Fig. 1 The relative bottom-current velocity in the Argentine Basin region is inferred from contours of mean silt particle size, $\phi(=-\log_2$ particle size in mm) in gravity core-top samples (dots) deeper than 4,000 m. Benthic oceanography determined from hydrocasts[8] is shown by black arrows (width of arrow volume transport).

Bottom water leaves the Argentine Basin through the Vema and Hunter Channels[12], which have sill depths considerably shallower than the abyssal floor of the basin, with the result that the denser component of AABW, Weddell Sea Bottom Water[7], is diverted east at depths greater than the sill depth of the outlets (Fig. 1). The axis of this flow is at depths slightly greater than 5,000 m, but water as shallow as ~4,500 m is incorporated into a broad return flow which is detectable on the lower flank of the Mid-Atlantic Ridge.

In addition to the main DWBUC flow pattern, the particle-size data reveal several abyssal gyres, or return flows (Fig. 1). A series of small gyres break away from the DWBUC adjacent to rises and ridges in the south-west part of the study area. A large gyre is seen north of the Maurice Ewing Bank and may be controlled by, or be responsible for, the topography of the crescent-shaped Zapiola Ridge[11]. The major return-flow gyre delineated by the particle-size data is found in the western basin to the east of the DWBUC, at a depth of ~5,500 m (Fig. 1). The position of the axis of this return flow corresponds to a zone of eastward-dipping isotherms below 4,000 m which is consistent with a return flow in the hydrographic data[8].

The particle-size data on the South American continental margin have a complex pattern (Fig. 1) resulting from the input of terrigenous material by down-slope processes through the many canyons on the slope. Some of the sources for the input of coarse silt can be seen in the seafloor data map (Fig. 1). It is possible, in principle, to change the particle-size distribution at source or to have different sources of silt particles, so that the regional pattern of particle size represents either source or bottom-current velocity variations, or both. The Argentine Basin is an excellent basin in which to test this hypothesis because of the multiple sources along the Argentine continental margin, the Falkland Plateau, and material transported by deep currents from the Weddell Sea. Despite these numerous sources, the dominant pattern of a high-velocity DWBUC with major return-flow gyres is obvious in the pattern inferred from particle-size data. Therefore, in this basin, the major factor controlling particle-size distribution appears to be the velocity of the current in which the material is deposited.

Because each geological sample represents decades to hundreds of years of sedimentation controlled by flow conditions, the relative bottom-current velocity charted in Fig. 1 represents the long-term bottom-current circulation. It is interesting to note, however, that the bottom-water circulation below 4,000 m determined from hydrocast data[8] on a timescale of years correlates with the long-term geological evidence (decades to hundreds of years) of benthic circulation (Fig. 1). All of the major, high-velocity current patterns are mirrored in the particle-size data, including the small return-flow gyres. The only area of high current velocity which is not predicted by the oceanographic data[8] is the broad eastward-flowing current in the northern basin (Fig. 1), but that study[8] did not extend north of ~40° S and may have missed the eastward-flowing arm of the major gyre in the northern Argentine Basin.

The other disparity between particle-size and hydrographic data lies in the weaker eastern gyre (Fig. 1) predicted from hydrographic data[8]. The particle-size data reveal a large gyre system, with the weakest return flow in the eastern basin, but does not delineate a northern arm of eastward-flowing water in the eastern gyre.

Therefore, the major circulation pattern of long-term bottom-water flow in the Argentine Basin region can be delineated from the particle size of seafloor samples. The pattern revealed by the particle-size approach differs in only one major aspect from that obtained from hydrocast data: the predominant flow pattern includes a basin-wide return-flow gyre to the north and east rather than two separate, smaller gyres[8]. The results are consistent with a major, contour-following DWBUC in the south-western and western Argentine Basin. Because the particle-size method may be applied to existing core-top samples, it should be possible to map the major bottom-current pathways in the abyssal ocean in other areas of dense core coverage. The resulting patterns, when combined with other sediment data, should provide a necessary component for describing the sediment dynamics in areas of current-controlled sedimentation.

Research was supported by ONR contract N00014-84-C-0313 and NSF grant DPP-8316992. Curation of cores at Lamont-Doherty is provided by NSF grant DES72-01568 and ONR

Contract N00014-75-C-0210. Curation of cores at the Antarctic Core Storage Facility is provided by an NSF grant from the Division of Polar Programs. I thank F. McCoy, R. Lotti and D. Cassidy for help in obtaining samples.

Received 21 November 1985; accepted 6 February 1986.

1. Ledbetter, M. T. & Johnson, D A. *Science* 194, 837-839 (1976).
2. Blaeser, C. R. & Ledbetter, M. T. *J sedim. Petrol.* 52, 755-768 (1982).
3. Ledbetter, M. T. *Mar. Geol.* 58, 137-149 (1984).
4. Ellwood, B. B., Ledbetter, M. T. & Johnson, D A. *Mar. Geol.* 33, M51-M55 (1979).
5. Bulfinch, D. L., Ledbetter, M. T, Ellwood, B. B. & Balsam, W. L. *Science* 215, 970-973 (1982).
6. Bulfinch, D. L. & Ledbetter, M. T. *Geo-Mar. Lett.* 3, 31-36 (1984).
7. Reid, J. R., Nowlin, W. D. Jr & Patzert, W. C. *J. phys. Oceanogr.* 7, 62-91.
8. Georgi, D. T. *Deep Sea Res.* 28A, 959-979 (1981).
9. Lawver, L. A. & Dick, H. J. B. *J. geophys. Res* 88, 8192-81022 (1983).
10. Ledbetter, M. T. & Ciesielski, P. F *Palaeogr., Palaeoclimatol., Palaeoecol.* 52, 185-214 (1986)
11. Le Pichon, X., Eittreim, S. L. & Ludwig, W. J *Phys. Chem. Earth* 8, 3-28 (1971)
12. Johnson, D. A., Ledbetter, M. & Burckle, L. H *Mar. Geol.* 23, 1-33 (1977).

Ubiquitous occurrence of 2-nitrofluoranthene and 2-nitropyrene in air

Thomas Ramdahl*, Barbara Zielinska, Janet Arey, Roger Atkinson, Arthur M. Winer & James N. Pitts Jr

Statewide Air Pollution Research Center, University of California, Riverside, California 92521, USA

Several nitrated polycyclic aromatic hydrocarbons (nitro-PAH) are direct-acting mutagens[1,2] and/or carcinogens[2-4], and are important constituents of combustion emissions and ambient air. These nitro-PAH are emitted from various combustion sources including gasoline and diesel engine exhaust[5-8], aluminium smelting effluent[9], coal fly ash[10], wood smoke[6], and cigarette smoke condensates[11]. Of these, diesel engine exhaust is the best characterized[6-8], more than 50 nitrated polycyclic aromatic compounds having been identified by Paputa-Peck *et al.*[8], including 1-nitropyrene (1-NP) as the single most abundant nitro-PAH. However, nitro-PAH may also be formed during source–receptor transport by atmospheric reactions of adsorbed or gas-phase PAH with oxides of nitrogen, nitric acid and other atmospherically important species such as the OH radical[1,12-14]. Evidence for the atmospheric formation of nitro-PAH has come only recently, from observations that 2-nitropyrene (2-NP)[15-17] and 2-nitrofluoranthene (2-NF)[16,17] neither of which has been reported to be emitted from combustion sources, are among the major nitro-PAH present in ambient air. We present here data from several locations which demonstrate that these two atmospherically formed nitro-PAH are ubiquitous in tropospheric ambient air.

Ambient particulate matter was sampled by three different methods. An ultra-high-volume 'mega-sampler'[18], with a 50% cutoff point of 20 μm and typically 6-h sampling periods, was used at Claremont, California, a site ~40 km east of downtown Los Angeles. In Aurskog, Norway, a rural residential area, an electrostatic precipitator (ESP)[19] with an impact stage designed for a 15-μm cutoff was used to collect particulate matter during several weeks in the winter of 1984. The other urban-air particulate matter samples analysed were the US National Bureau of Standards (NBS) Standard Reference Materials (SRMs) No. 1648 and 1649 (refs 20, 21). These samples were collected by means of specially designed filter baghouses over a period of more than a year in St Louis, Missouri (SRM 1648) and Washington DC (SRM 1649).

High-resolution gas chromatography/mass spectrometry (GC/MS) is required to distinguish between 2-NF and the very closely eluting 3-nitrofluoranthene (3-NF) isomer[16,22], as discussed below, because of this near-equality of GC retention times 2-NF has been misidentified as 3-NF in several previous studies[15,23,24]. Our identification of 2-NF is based on the observed GC retention time, along with its characteristically low m/z 217 $[M-NO]^+$ fragment-ion abundance (~4% compared with ~46% relative abundance for this fragment ion in 3-NF)[16,22].

Figure 1 shows that the nitro-PAH fractions of the samples from St Louis, Claremont and Aurskog all contain 2-NF, 1-NP and 2-NP. The concentrations of these three nitro-PAH in the particles analysed from the various locations studied are given in Table 1. Unfortunately, for the NBS SRM baghouse and the Aurskog ESP samples, the actual ambient air concentrations cannot be determined because the sample air volumes are unknown. However, from our present measurements at Claremont and earlier measurements[15,16], these nitro-PAH are typically present in the low pg m^{-3} range. In all of the samples analysed, 2-NF was the most abundant nitro-PAH, with 1-NP and 2-NP being present in lesser amounts.

Due to the small difference in the GC retention times for 2-NF and 3-NF, the 2-NF present in SRM 1648 and in samples from Philadelphia, Pennsylvania, and a rural site in Denmark in winter were originally reported as 3-NF in refs 23, 24 and 15, respectively. These samples have since been re-analysed, with the result that 2-NF, and not 3-NF, has been shown to be present in all cases[17,25,26]. These and our present observations show conclusively that 2-NF and 2-NP are ubiquitous in ambient particulate organic matter (POM). Although Jäger[27] reported the presence of 3-NF in ambient air in Prague, Czeckoslovakia, it is possible that the nitrofluoranthene isomer identified from the thin-layer chromatography–fluorescence quenching measurements was actually 2-NF, as it is not clear that this method[27] could distinguish between 2-NF and 3-NF. Additionally, Morita *et al.*[28] have reported an unidentified nitrofluoranthene or nitropyrene isomer more abundant than 1-NP in an urban air sample in Japan; this could also be 2-NF.

Table 1 Concentrations of nitro-PAH and BeP (μg g^{-1}) in air particulate matter samples at different locations in the USA and Norway

Compound	Claremont*	St Louis†	Washington‡	Aurskog§
2-NF	2.8	0.56	0.60	0.56
1-NP	0.36	0.16	0.20	0.15
2-NP	0.08	0.06	0.05	0.17
BeP	3.4	5.2‖	4.6	44
Concentration ratios				
2-NF/BeP	0.8	0.1	0.1	0.01
2-NP/BeP	0.02	0.01	0.01	0.004

* Combined sample from four 6-h sampling periods from 14 to 15 September 1985.
† NBS SRM 1648.
‡ NBS SRM 1649.
§ Sampled during February and March 1984.
‖ From ref. 24.

Indeed, the only well-documented report of the presence of 3-NF in ambient air is that of Pitts *et al.*[16], in which a small amount of 3-NF, together with a much greater amount of 2-NF, was detected in one sample collected during morning hours in Riverside, California. Based on literature data, the 1-NP and 3-NF observed in ambient POM probably originate from combustion sources[5-11], atmospheric transformations[1,12,13] and/or reactions during collection[1,29]. However, 2-NF and 2-NP have not been observed in combustion emissions, nor from any nitration reactions of adsorbed fluoranthene or pyrene in the dark[1,29-31], although Wu and Niki[32] have recently tentatively identified 2-NP as a product of the reaction of NO_2 with monodisperse pyrene on silica particles in nitrogen in the presence of light.

* Current address: Norsk Hydro A.S., PO Box 4313, S013 Nygaardstangen, Norway.

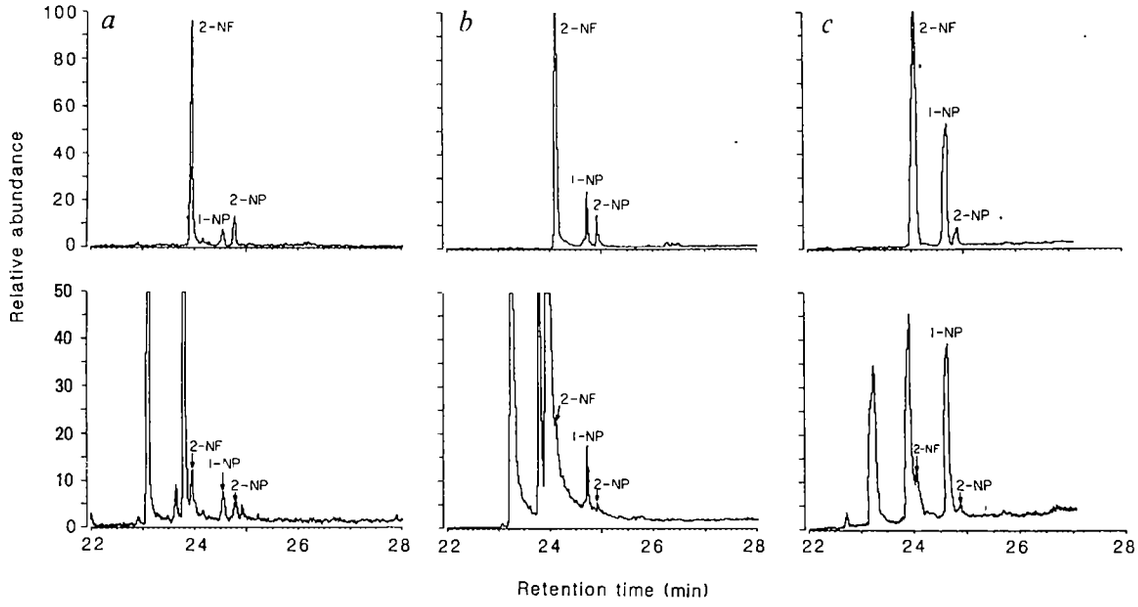


Fig. 1 GC/MS multiple ion detection (MID) mass chromatograms (top, molecular ion M^+; bottom, fragment ion $[M-NO]^+$) of enriched nitro-PAH fractions of extracts of air particulate matter from: *a*, Aurskog, Norway; *b*, St Louis, Missouri and *c*, Claremont, California (see Table 1). Note the characteristically low $[M-NO]^+$ fragment-ion relative abundances for 2-nitrofluoranthene (2-NF, 4%) and 2-nitropyrene (2-NP, 8%), in comparison with that of 1-nitropyrene (1-NP, 39%)[16,22]. The samples were Soxhlet-extracted for 18 h with dichloromethane. 2-Nitrofluoranthene-d_9 and 1-nitropyrene-d_9 were added to the extracts as internal standards. The extracts were pre-cleaned by open-column silica (5% H_2O) chromatography to remove aliphatic hydrocarbons and polar material. The fractions of interest were further fractionated by normal-phase high-performance liquid chromatography (HPLC) using a semi-preparative silica column. The HPLC fractions containing nitro-PAH were analysed by GC/MS MID using a Finnigan model 3200 mass spectrometer operating in the electron impact mode. The samples were chromatographed on a 30-m DB-5 fused silica capillary column (J&W Scientific), directly eluting into the ion source. On-column injection was made at 50 °C, followed by a temperature program at 8 °C min^{-1} to 350 °C. The data were calibrated by comparing the ratios of the areas of the molecular ion (m/z 247) peaks to those of the deuterated internal standards (m/z 256)[16].

Thus, 2-NF and 2-NP observed in ambient POM seem to be formed from their parent PAH during atmospheric transport[15,16]. Table 1 lists the concentrations of 2-NF and 2-NP relative to that of benzo[*e*]pyrene (B*e*P), a fairly non-reactive[33] PAH of similar volatility. Although the same nitro-PAH are observed at all of the locations studied, the extent of the formation of 2-NF and 2-NP from the parent PAH varies (assuming that the ratios of emitted fluoranthene and pyrene to B*e*P are similar at all locations), with that for 2-NF varying much more (by a factor of ~80) than that for 2-NP (a factor of ~5). This suggests that different reaction pathways may be responsible for the formation of 2-NF and 2-NP. Table 1 also shows that the ratios 2-NF/B*e*P and 2-NP/B*e*P exhibit the same trend as the ambient temperatures; that is, Claremont > St Louis ≃ Washington > Aurskog, consistent with the occurrence of gas-phase reactions as formation pathways for these nitro-PAH. Indeed, 2-NF is formed from the gas-phase reaction of fluoranthene with N_2O_5 (ref. 17), and this may be one reaction pathway under atmospheric conditions. Other reaction pathways which could form 2-NF and 2-NP include OH-radical-initiated reactions[15,16] and, for 2-NP, photoinduced reactions with NO_2 (ref. 32).

Summer conditions are not necessary for the formation of 2-NF and 2-NP, as these nitroarenes are present in the winter air samples from Aurskog and Denmark[15,26]. Indeed, the Aurskog sample contains the highest absolute amount (wt/wt particles) of 2-NP of all the samples for which data are given in Table 1. The main sources of PAH in this area of Norway are emissions from residential heating by wood and kerosene, which results in high atmospheric levels of PAH in winter (stagnant air) conditions[34], and as expected (Table 1), the ambient air at this location contains ~10 times more PAH (as indicated by the concentration of benzo[*e*]pyrene) than do the other samples analysed.

Thus, atmospherically formed 2-NF and 2-NP are observed in conditions ranging from Claremont in summer (high temperature, high radiation flux) to Aurskog in winter (low temperature, low radiation flux). Of the known reactions of PAH under atmospheric conditions[17,35,36], the gas-phase reactions with N_2O_5 and/or with OH radicals followed by NO_2 addition are candidates for the formation of these NO_2-PAH. Laboratory and ambient atmospheric measurements intended to resolve these questions are in progress.

We thank the California Air Resources Board (contract no. A4-081-32; Dr Jack K. Suder, project monitor) for financial support. The collection of the Aurskog sample was made possible by support from the Nordic Council of Ministers, through the MIL-2 project. The technical assistance of Mr Travis M. Dinoff (SAPRC) and Mr Adler Mikalsen (Norwegian Institute for Air Research, Aurskog particulate sampling) is acknowledged. T.R. thanks the Royal Norwegian Council for Scientific and Industrial Research for a 1985 Research Fellowship.

Received 30 January; accepted 10 March 1986.

1. Pitts, J. N. Jr *et al. Science* **202**, 515-519 (1978).
2. Rosenkranz, H. S. & Mermelstein, R. *Mutat. Res.* **114**, 217-267 (1983).
3. Poirier, L. A. & Weisburger, E. K. *J. natn. Cancer Inst.* **62**, 833-840 (1979).
4. Ohgaki, H. *et al. Carcinogenesis* **5**, 583-585 (1984).
5. Tejada, S. B., Zweidinger, R. B. & Sigsby, J. E. Jr *S.A.E. Pap.* No. 820775 (Society of Automotive Engineers, Pittsburgh, 1982).
6. Gibson, T. L. *Atmos. Envir.* **16**, 2037-2040 (1982).
7. Schuetzle, D., Lee, F. S.-C., Prater, T. J. & Tejada, S. B. *Int. J. envir. analyt. Chem.* **9**, 93-144 (1981).
8. Paputa-Peck, M. C. *et al. Analyt. Chem.* **55**, 1946-1954 (1983).
9. Oehme, M., Manø, S. & Stray, H. *J. high Resolut. Chromat. Chromat. Commun.* **5**, 417-423 (1982).
10. Harris, W. R., Chess, E. K., Okamoto, D., Remsen, J. F. & Later, D. W. *Envir. Mutagen.* **6**, 131-144 (1984).
11. McCoy, E. C. & Rosenkranz, H. S. *Cancer Lett.* **15**, 9-13 (1982).
12. Nielsen, T., Ramdahl, T. & Bjørseth, A. *Envir. Hlth Perspect.* **47**, 103-114 (1983).
13. Pitts, J. N. Jr *Envir. Hlth Perspect.* **47**, 115-140 (1983).
14. Pitts, J. N. Jr, Zielinska, B., Sweetman, J. A., Atkinson, R. & Winer, A. M. *Atmos. Envir.* **19**, 911-915 (1985).
15. Nielsen, T., Seitz, B. & Ramdahl, T. *Atmos. Envir.* **18**, 2159-2165 (1984).
16. Pitts, J. N. Jr, Sweetman, J. A., Zielinska, B., Winer, A. M. & Atkinson, R. *Atmos. Envir.* **19**, 1601-1608 (1985).
17. Sweetman, J. A. *et al. Atmos. Envir.* **20**, 235-238 (1986).
18. Fitz, D. R., Doyle, G. J. & Pitts, J. N. Jr *J. Air Pollut. Control Ass.* **33**, 877-879 (1983).

19. Steen, B. A. *Envir. Int.* **11**, 105–109 (1985).
20. May, W. E., Chesler, S. N., Hertz, H. S. & Wise, S. A. *Int. J. Envir. Analyt. Chem.* **12**, 259–275 (1982).
21. May, W. E. *et al.* in *Identification and Analysis of Organic Pollutants in Air* (ed. Keith, L. H.) 197–230 (Butterworth, Woburn, 1984).
22. Ramdahl, T. *et al. J. high Resolut. Chromat. Chromat. Commun.* **8**, 849–852 (1985).
23. Ramdahl, T., Becher, G. & Bjørseth, A. *Envir. Sci. Technol.* **16**, 861–865 (1982).
24. Wise, S. A. *et al. Envir. Int.* **11**, 147–160 (1985).
25. Nishioka, M. G., Howard, C. C. & Lewtas, J. *Pap. presented at 10th Int. Symp. Polynuclear Aromatic Hydrocarbons*, Columbus, 21–23 October (1985).
26. Nielsen, T. & Ramdahl, T. *Atmos. Envir.* (in the press).
27. Jäger, J. *J. Chromat.* **152**, 575–578 (1978).
28. Morita, K., Fukamachi, K. & Tokiwa, H. *Eisei Kagaku* **29**, 199–205 (1983).
29. Brorström-Lunden, E. & Lindskog, A. *Envir. Sci. Technol.* **19**, 313–316 (1985).
30. Jäger, J. & Hanus, V. *J. Hyg. Epidem. Microbiol. Immun.* **24**, 1–12 (1980).
31. Tokiwa, H., Nakagawa, R., Morita, K. & Ohnishi, Y. *Mutat. Res.* **85**, 195–205 (1981).
32. Wu, C.-H. & Niki, H. *Environ. Sci. Technol.* **19**, 1089–1094 (1985).
33. Nielsen, T. *Envir. Sci. Technol.* **18**, 157–163 (1984).
34. Ramdahl, T. *Nature* **306**, 580–582 (1983).
35. Pitts, J. N. Jr, Atkinson, R., Sweetman, J. A. & Zielinska, B. *Atmos. Envir.* **19**, 701–705 (1985).
36. Biermann, H. W., Mac Leod, H., Atkinson, R., Winer, A. M. & Pitts, J. N. Jr *Envir. Sci. Technol.* **19**, 244–248 (1985).

Influence of Saharan dust on the rain acidity and atmospheric input to the Mediterranean

M. D. Loÿe-Pilot, J. M. Martin & J. Morelli

Institut de Biogéochimie Marine, UA CNRS 386, Ecole Normale Supérieure, 46 rue d'Ulm, 75230 Paris Cedex 05, France

It has long been recognized that Saharan dust may be transported a long way from its sources, particularly over the ocean[1], and especially over the tropical North Atlantic, as far as the Caribbean[2–7], and over various areas of the Mediterranean[8–10]. The eolian transport of desertic aerosols is a major contribution to oceanic sedimentation[11–13] and may have important climatic implications[14]. This phenomenon is responsible for episodes of so-called 'red rain' or 'red snow' which have been identified in various areas of the European continent[15–17]. Numerous red rains and red dust falls have been observed in Corsica. From 1984 data on the chemistry of precipitation collected in South Corsica, we show here that due to its $CaCO_3$ content, Saharan dust significantly increases the *p*H of rain water. This may counteract the effects of acidic rain. An assessment of African dust deposition indicates that, compared with the sediments discharged by the Rhône river, atmospheric input to the northwestern Mediterranean contributes significantly to sedimentation in that region.

Data were taken from our sampling station located in a clean area near the Bavella Pass (41°50′ N, 9°10′ E), at 1,200 m above sea level. Systematic observations on rain chemistry have been made since 1980 at this station, using a plastic gauge of 400 cm^2 aperture. According to the intensity of precipitation, its frequencies, duration and the accessibility of the site in winter, the sampling times ranged from several hours to one week. Generally, samples represent bulk deposition (wet plus dry), although some samples were taken within precipitation episodes and were thus not mixed with dry deposition. More rarely, in some periods without rain, dry deposition was collected separately, by rinsing the plastic gauge with distilled water. The liquid samples, which were sometimes produced from melting snow, were filtered indoors close to the field, using 0.4-μm Nuclepore filters, to evaluate the particulate matter content. The *p*H was measured using a potentiometric method; Na^+, K^+, Ca^+ and Mg^{2+} by atomic absorption spectrometry; and Cl^-, SO_4^{2-}, NO_3^- and NH_4^+ by a colorimetric method.

Only 1984 data will be discussed here, attention being focused on the magnitude of the load of red dust in rainwater samples and its influence on dissolved calcium enrichment and *p*H. Indeed, it is only the latter two parameters that are systematically affected by the incorporation of red dust in rain water. Figure 1 concerns 60 successive rain samples of 1984, including 19 'red rains'. The represented weights of solid matter relate only to 'red rains', the other values being generally <2 mg per filter. The calcium enrichment, which can be considered as an index of non-marine calcium sources, is defined by the relation E_{Ca} = (Ca/Na) rain water/(Ca/Na) sea water.

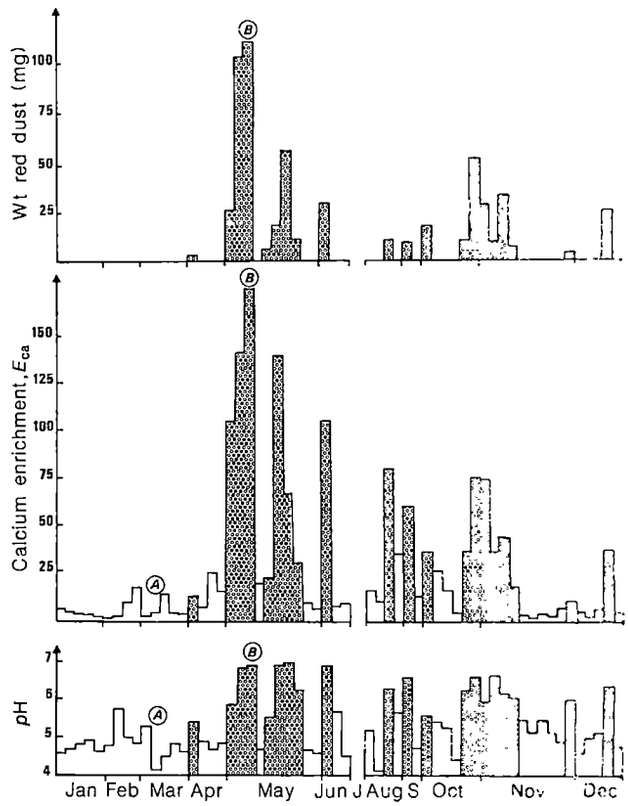


Fig. 1 Simultaneous variations in the red dust content of rainwater samples, their calcium enrichment and their *p*H during 1984. A and B refer to episodes for which air-mass trajectories are given in Fig. 2.

Figure 1 reveals seasonal variations of the input of red dust, with sporadic episodes. A maximum is observed in spring, for example, in May when seven rainfalls account for ~60% of the annual deposition of red particulate matter, with a contribution of 40% for the two events of 5 and 10 May only. Moreover, the two observed episodes of red dust dry fallout occurred in May and June; they account for 10 and 33 mg of red dust and contribute to 8% of the bulk annual red dust input. Compared with the annual total deposition of solid particulate matter, red dust represents 84% of this flux.

Careful study of the back trajectories of the 700- and 850-mbar air masses arriving on the sampling zone confirms that this red dust originates from arid regions in the north of Africa. The incorporation into rain of desert particulate matter is accompanied by a strong increase in the dissolved calcium content. This agrees with the similar evolution of the collected load of red dust and calcium enrichment in rainwater samples. E_{Ca} is maximal and higher than 100 for some May episodes and reflects the strong influence of continental sources. Mineralogical analysis by X-ray diffraction shows that the incoming Saharan dust contains 5–30% of calcite and sometimes gypsum, although this is generally <2%. These $CaCO_3$ contents fit the composition of wind-blown Saharan dust collected in various regions[18–21]. The partial dissolution of this component accounts for a significant increase in rainwater *p*H. During situations without input of Saharan dust, the *p*H varies from 4.1 to 5.6, corresponding to E_{Ca} of often lower than 10 and rarely higher than 20. Such calcium enrichments can be related to the influence of the European continental environment but it is difficult to specify whether they are due to natural sources (soils) or to industrial

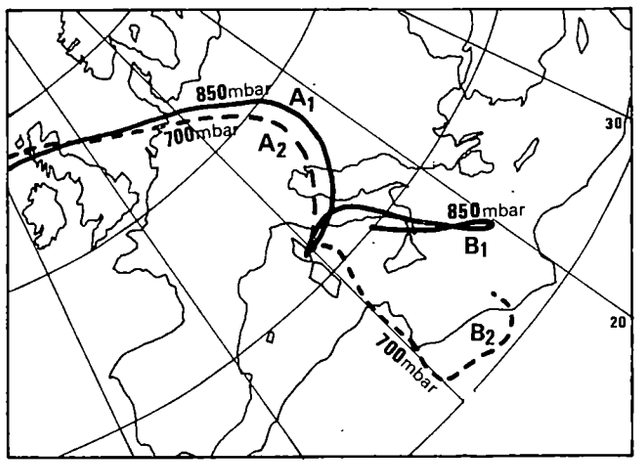


Fig. 2 Back trajectories (4 days) of air masses arriving in the sampling zone for an acidic episode (trajectories A_1 and A_2 correspond to 8 March 1984 at 18.00 UT) and for an episode with a maximal input of Saharan dust (trajectories B_1 and B_2 correspond to 10 May 1984 at 06.00 UT).

emissions (such as cement works). The influence of a residual Saharan aerosol background cannot be excluded.

The *p*H values increase to 6 or 7 during 13 of the 19 Saharan dust episodes. In considering the origin of the more acidic values, we must remember that rain water may be naturally acidic[24]. In the Mediterranean Basin, the Italian volcanoes represent a major natural source of atmospheric sulphuric acidity, especially the SO_2 emissions of Etna, which constitute 1,000–2,000 tonnes day^{-1} on average[25–28]. Nevertheless, for the lower *p*H values, black particulate matter is often recovered after rain filtration. This is in agreement with the relatively high sulphate content of rain water: 5–10 mg l^{-1} after correction of marine sulphate from bursting bubbles. According to the origin of incoming air masses, such a result could be explained by the spreading of atmospheric pollution over the northwestern Mediterranean.

The antagonistic effects of Saharan dust and other natural and industrial sources of aerosols on the acidity of the collected rain samples is supported by the data in Fig. 2. For example, we show back trajectories of 700- and 850-mbar air masses for two well-differentiated kinds of meteorological situations. The first corresponds to an episode of relatively acidic rain with a *p*H of 4.1 (trajectories A, 8 March), the second to a *p*H of 6.8 observed for the maximal input of Saharan dust (trajectories B, 10 May). Taking into account the possible atmospheric impact of long-range transport of pollutants,[29–31], the acid episode could be related to emissions from various European industrial regions and where there is no atmospheric mixing with African aerosols. In this case, the neutralization of rain acidity by incoming Saharan dust must occur later, after deposition, and this may have pedological and ecological implications. On 10 May, there is a more complex situation with the superposition of air masses, which could have passed over volcanic and industrial Italian regions, with air masses of African origin. Thus, the collected rain scavenged atmospheric components of different origins, and the acidity might have been neutralized within cloud and rain.

Finally, we shall consider the geochemical consequence of atmospheric deposition of Saharan material in the Mediterranean environment. If the contribution from dry fallout is included, results from 1984 at Bavella Pass indicate a red dust flux of 14 tonnes $km^{-2}\,y^{-1}$, which represents an annual deposit of ~10 μm assuming a density of 1.25–1.65[32]. This value accounts for about 10% of the Western Mediterranean pelagic sedimentation: 100 μm yr^{-1} [33], which could be greatly influenced by marine biogenic material. How representative this flux is when evaluating atmospheric input into the Mediterranean is questionable, in that rainfall is relatively high in the mountainous areas of Corsica. With respect to the complex removal processes of aerosols[34–35], this effect of relief may enhance the scavenging of atmospheric particulate matter and consequently its deposition rate compared with the corresponding flux for marine-adjacent regions. However, in the case of red dust, we observed that the first rain droplets contributed to the major part of its deposition. Moreover, data from Bavella Pass (1,200 m) and the neighbouring station of Arza (700 m) show similar values for red dust deposition, collected simultaneously for 11 of the 19 red rains of 1984. For these episodes, which represent 80% of the annual red dust wet fallout in Bavella station, the input was 11% higher in Arza where the rainfall was 17% lower. Thus, the altitude effect does not seem to be very important for the removal of airborne desert material. It is, therefore, not unrealistic to extrapolate the above red dust deposition rate to sea level for the northwestern Mediterranean Basin, that is, 277,000 km^2. This leads to an input of 3.9×10^6 tonnes yr^{-1}, which is of the same order as the average annual downstream flow of solids in the Rhône (4.3×10^6 tonnes; ref. 36). A more precise evaluation would have to take into account regional geographical variability in the atmospheric deposition of Saharan dust. Despite the inaccuracy of the present assessment, it appears that this phenomenon must play an important part in the geochemistry and sedimentology of the marine zone considered.

This work was carried with the financial support of the CNRS Land–Sea Interactions Coordinated Group (GRECO–ICO) and ATP Aerosols désertiques and of ENSJF, Biologie-Géologie Laboratory. Air-mass trajectories were established by Météorologie Nationale. We thank Dr R. Chester for useful comments and J. A. Lefèvre and N. Kielbasa for technical assistance.

Received 5 December 1985; accepted 5 March 1986.

1. Darwin, C. *Q. Jl geol. Soc. Lond.* **2**, 26 (1846).
2. Delany, A. C. *et al. Geochim. cosmochim. Acta* **31**, 885–909 (1967).
3. Prospero, J. M., Bonatti, E., Schubert, C. & Carlson, T. N. *Earth planet. Sci. Lett.* **9**, 287–293 (1970).
4. Chester, R. & Johnson, L. R. *Nature* **229**, 105–107 (1971).
5. Buat-Menard, P., Morelli, J. & Chesselet, R. *J. rech. Atmos.* **8**, 661–673 (1974).
6. Hoffman, G. L. *et al. J. rech. Atmos.* **8**, 745–759 (1974).
7. Rahn, K. A., Borys, R. D., Shaw, G. E., Schutz, L. & Jeanicke, R. in *Saharan Dust, Scope 14* (ed. Morales, C.) 243–266 (Wiley, New York, 1979).
8. Ganor, E. & Mamane, V. *Atmos. Envir.* **10**, 1079–1084 (1979).
9. Tomadin, L., Lenaz, R., Landuzzi, V., Mazzucotelli, A. & Vannucci, R. *Oceanol. Acta* **7**, 13–23 (1984).
10. Chester, R., Sharples, E. J., Sanders, G. S. & Saydam, A. C. *Atmos. Envir.* **19**, 929–935 (1984).
11. Buat-Menard, P. & Chesselet, R. *Earth planet. Sci. Lett.* **42**, 399–411 (1979).
12. Chester, R. *Bull. Inst. Géol. Bassin d'Aquitaine (Bordeaux)* **31**, 325–335 (1981).
13. Prospero, J. M. in *The Sea*, Vol. 7 (ed. Emiliani, E.) 801–874 (Wiley, New York, 1981).
14. Junge, C. in *Saharan Dust, Scope 14* (ed. Morales, C) 49–60 (Wiley, New York, 1979).
15. Clement, R., Ricq de Bouard, M. & Thomas, A. *La Météorologie (Paris)* **24**, 65–83 (1972).
16. Prodi, F. & Fea, G. *J. geophys. Res.* **84**, C11, 6951–6960 (1979).
17. Bücher, A. & Lucas, C. *La Météorologie (Paris)* **33**, 53–69 (1975).
18. Game, P. M. *J. sedim. Petrol.* **34**, 355–359 (1964).
19. Chester, R. *et al. Mar. Geol.* **24**, 201–217 (1977).
20. Glaccum, R. A. & Prospero, J. M. *Mar. Geol.* **37**, 295–321 (1980).
21. Ganor, E. & Mamane, Y. *Atmos. Envir.* **16**, 581–587 (1982).
22. Bücher, A., Dubief, J. & Lucas, C. *Rev. Géol. Dyn. Géog. Phys. (Paris)* **24**, 153–165 (1983).
23. Paquet, H., Coudé-Gaussen, G. & Rognon, P. *Rev. Géol. Dyn. Géog. Phys. (Paris)* **25**, 257–265 (1984).
24. Charlson, R. J. & Rodhe, H. *Nature* **295**, 683–685 (1982).
25. Haulet, R., Zettwoog, P. & Sabroux, J. C. *Nature* **268**, 715–717 (1977).
26. Malinconico, L. L. *Nature* **278**, 43–45 (1979).
27. Faivre-Pierret, R., Martin, D. & Sabroux, J. C. *Bull. Volcan.* **43**, 473–485 (1980).
28. Jaeschke, W., Berresheim, H. & Georgii, H. W. *J. geophys. Res.* **87**, C9 7253–7261 (1982).
29. Lannefors, H. O. *et al. Tellus* **32**, 548–557 (1980).
30. Rahn, K. A. *Atmos. Envir.* **15**, 1447–1455 (1981).
31. Morelli, J. *et al. J. rech. Atmos.* **17**, 259–271 (1983).
32. Yaalon, D. H. *Contr. NATO Advanced Study Institute on Physical and Chemical Weathering in Geochemical Cycles*, Aussois, France (NATO 1, Paris, 1985).
33. Chamley, H. *Sci. Géol (Strasbourg)* **35** (1971).
34. Twomey, S. *Atmospheric Aerosols* (Elsevier, Amsterdam, 1977).
35. Pruppacher, H. R. & Klett, J. D. *Microphysics of Cloud and Precipitation* (Reidel, 1980).
36. Savey, P. & Deleglise, R. in *Ass. Int. Hydrol. Scient. Publ. 75*, 462–476 (1967).

Amino-acid sequence of the β-subunit of the $(Na^+ + K^+)$ATPase deduced from a cDNA

Gary E. Shull*, Lois K. Lane† & Jerry B. Lingrel*

Departments of * Microbiology and Molecular Genetics and of † Pharmacology and Cell Biophysics, University of Cincinnati College of Medicine, 231 Bethesda Avenue, Cincinnati, Ohio 45267-0524, USA

The sodium/potassium-dependent ATPase [$(Na^+ + K^+)$ATPase], which establishes and maintains the Na^+ and K^+ gradients across the plasma membrane of animal cells, consists of two subunits, α and β. Complementary DNA clones encoding the catalytic (α) subunit of sheep kidney[1] and *Torpedo californica* electroplax[2] enzymes have previously been isolated and characterized. However, there is little information concerning the primary structure of the β-subunit, a glycoprotein of unknown function and relative molecular mass (M_r) ~55,000 (ref. 3). Here we describe the isolation and characterization of a cDNA clone containing the entire coding region of the β-subunit of the sheep kidney $(Na^+ + K^+)$ATPase. We also discuss structural aspects of the protein and present evidence for a possible evolutionary relationship with the KdpC subunit of the *Escherichia coli* K^+-ATPase[4].

Tryptic peptides of the β-subunit of the sheep kidney $(Na^+ + K^+)$ATPase were isolated and the amino-acid sequences of three peptides determined (Table 1). The N-terminal amino-acid sequences of both sheep[5] and dog[6] kidney β-subunits are included in Table 1. A 26-base oligonucleotide probe, derived from the 9-amino-acid N-terminal sequence shared by the sheep and dog enzymes, was used to screen a sheep kidney cDNA library (see Fig. 1 legend). Eight cDNAs, with inserts ranging in size from 1.8 to 2.6 kilobases (kb), were isolated. Restriction endonuclease mapping and blot hybridization analysis demonstrated that all eight cDNAs were related (data not shown). The identity of these cDNAs was confirmed by analysis of the nucleotide sequence in the region containing homology to the oligonucleotide probe. The N-terminal sequence of the sheep enzyme was identified, and of the 26 amino acids determined for the N-terminus of the dog enzyme, there was only a single mismatch, at residue 28.

The nucleotide sequence of the largest clone, pβNKA1, was determined and the amino-acid sequence of the β-subunit deduced (Fig. 1). The cDNA consists of a 528-base-pair (bp) 5′-untranslated region, a 909-bp open reading frame and a 1,142-bp 3′-untranslated sequence. There is no polyadenylation signal[7] or poly(A)$^+$ tract at the 3′ end of the cDNA; however, restriction analysis of the other cDNAs suggests that pβNKA1 lacks approximately 50 bp at its 3′ end. Three potential polyadenylation signals (AATAAA) occur earlier in the 3′-untranslated sequence (at residues 1,888, 2,408 and 2,433), and restriction endonuclease mapping suggests that two of the cDNAs are polyadenylated following the site at residue 1,888. The 5′-untranslated region, like that of the α-subunit mRNA[1], is G+C-rich (75%). The initiation methionine codon, located at residue 529, is the first ATG triplet in the cDNA, lies in a perfect 9-bp consensus sequence for the initiation of translation[8], and is preceded by an in-frame stop codon at residue 517. The initiation methionine is immediately followed by the N-terminal sequence of the mature sheep β-subunit[5]. Therefore, the β-subunit, like the α-subunit[1], does not contain a hydrophobic N-terminal signal peptide. The amino-acid sequences determined for the three tryptic peptides are located at residues 3–17, 71–90 and 150–156, respectively. The mature protein consists of 302 amino acids and has a M_r (minus the carbohydrate groups) of 34, 937.

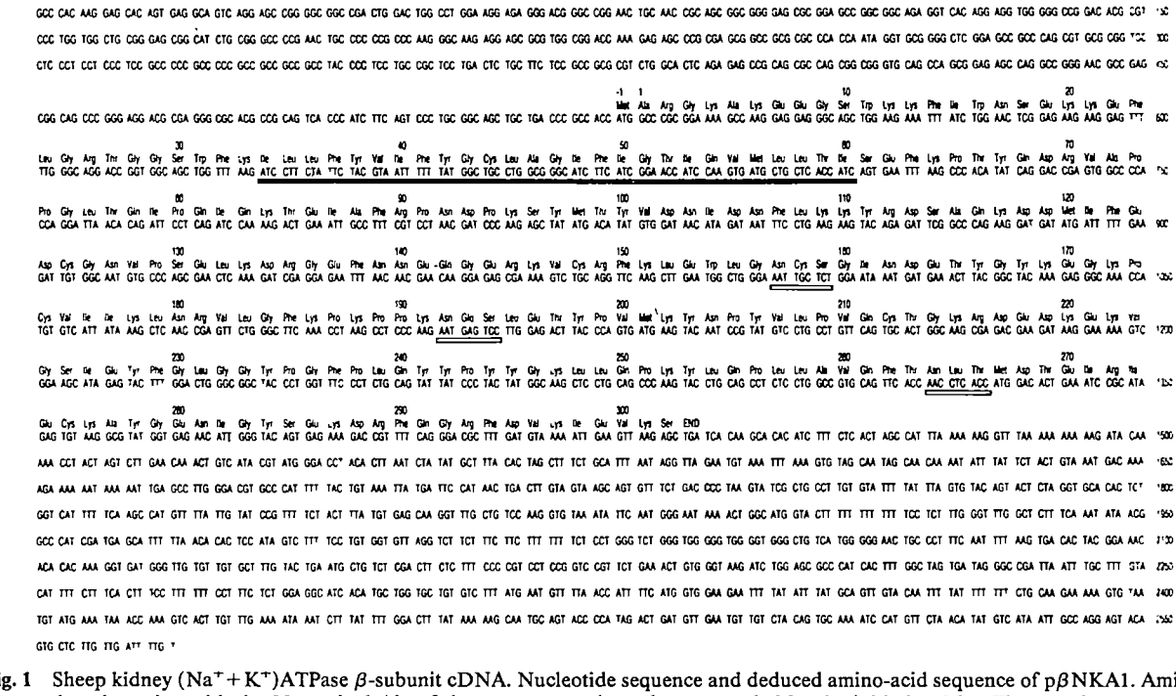


Fig. 1 Sheep kidney $(Na^+ + K^+)$ATPase β-subunit cDNA. Nucleotide sequence and deduced amino-acid sequence of pβNKA1. Amino acids are numbered starting with the N-terminal Ala of the mature protein and are preceded by the initiation Met. The putative transmembrane domain is indicated by the black bar and potential *N*-linked glycosylation sites by open bars.

Methods. A 50,000-colony sheep kidney cDNA library was constructed in the vector pBR322 using size-selected cDNA (800–3,500 bp) as described previously[1]. A 26-base deoxyinosine-containing oligonucleotide probe[24], 5′-GC(I,C)(C,A)G(I,C)GG(I,C)AAIGC(I,C)-AAIGAIGAIGG-3′, was derived from the 9-amino-acid N-terminal peptide (Table 1) and the library was screened as described earlier[1]. Plasmid DNA was isolated from 26 colonies that gave strong hybridization signals and analysed by restriction mapping and blot hybridization analysis. During blot hybridization, high-stringency washes were performed in the presence of tetramethylammonium chloride[25]. Under these conditions eight related cDNAs, including pβNKA1, retained their hybridization signals. DNA sequence analysis of both strands was performed using the Maxam–Gilbert procedure[26].

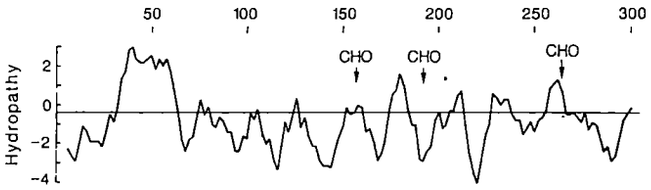


Fig. 2 Hydropathy plot of the $(Na^+ + K^+)$ATPase β-subunit. Nine-residue averages have been plotted using a hydropathy program based on the procedure of Kyte and Doolittle[12]. The locations of potential *N*-linked glycosylation sites (CHO) are indicated.

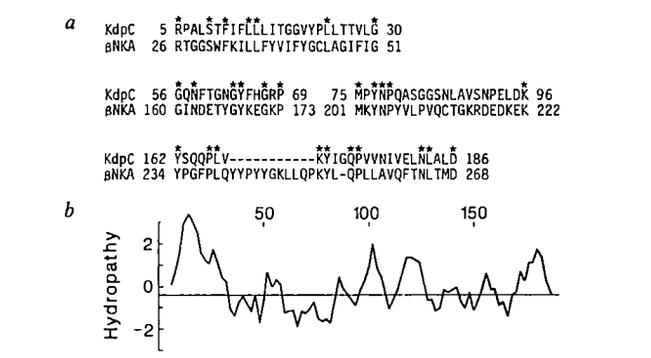


Fig. 3 Similarity between the KdpC subunit of the *E. coli* K^+-ATPase[4] and the $(Na^+ + K^+)$ATPase β-subunit. *a*, Amino-acid homology between KdpC and the β-subunit (βNKA). Homologous residues are indicated by an asterisk; gaps have been added to maximize homology. *b*, Hydropathy plot of KdpC using a 9-amino-acid window as in Fig. 2.

Photochemical labelling[9,10] and immunochemical[11] procedures have led to the suggestion that the β-subunit has one or more transmembrane domains. Hydropathy analysis[12] (Fig. 2) of the deduced amino-acid sequence indicates that the protein has one transmembrane domain (residues 34–60; see Fig. 1), located near the N-terminus. Electron microscopy[13] studies suggest that a large proportion of the β-subunit is located on the extracellular side of the membrane and Geering *et al.*[14] have demonstrated that only a small cytoplasmic domain of ~2,000 daltons is removed by trypsin. Thus, the hydrophilic N-terminal domain (residues 1–33) would appear to be located on the cytoplasmic side of the membrane whereas residues 60–302 probably lie on the extracellular side. Following limited papain digestion of the dog kidney enzyme, Chin[6] determined the partial sequence of a peptide located on the extracellular side of the membrane and approximately 9,000 daltons from the N-terminus. This sequence, Ile-?-Phe-Ile-Pro-?-?-?-Ile, shares partial homology with the sheep sequence beginning with Ile 87, which we have assigned to the extracellular side.

The presence of three *N*-linked oligosaccharide chains has been indicated by studies on the biosynthesis of chicken skeletal muscle $(Na^+ + K^+)$ATPase[15] and by endoglycosidase F treatment[16] of rat kidney and axolemma $(Na^+ + K^+)$ATPase. The deduced primary structure contains three potential *N*-linked glycosylation sites[17] (Asn-X-Ser/Thr), all located in the predicted extracellular regions of the protein (Asn residues 157, 192 and 264). The sequence of tryptic peptide T3 (Table 1), which begins at residue 150, could not be determined beyond residue 156 even though the quantities of the preceding amino acids in the sample being analysed were well above the limit of detection. Asparagine 157 was apparently blocked, as would be expected if it were a site for carbohydrate attachment.

It is of interest to know which transmembrane domains of the α-subunit are in contact with that of the β-subunit. Electron microscopy studies of two-dimensional crystals[18] suggest that

Table 1 $(Na^+ + K^+)$ATPase β-subunit peptides

Tryptic peptides

T1: G K A K E E G S W K K F I W N
T2: V A P P G L T Q I P Q I Q K ? E I A F R
T3: F K L E W L G

N-terminal peptides

Sheep Kidney: A R G K A K E E G
Dog Kidney: A R G K A K E E G S ? K K F I ? N
S E K ? E F L G ? T D ? ? ? F K

$(Na^+ + K^+)$ATPase was purified from the outer medulla of frozen lamb kidneys as described previously[22]. The enzyme (68 mg) was solubilized in 7% SDS, 1% 2-mercaptoethanol and two 34-mg aliquots were applied to a Bio-Gel A-5m column (2.5 × 190 cm) and eluted with 25 mM Tris-HCl *p*H 7.5, 0.1% SDS, 0.02% NaN_3 and 1 mM 2-mercaptoethanol. The β-subunit peaks of the two column runs were pooled and lyophilized. The β-subunit (~10 mg) was dissolved in H_2O and passed through a Sephadex-G 25 column (1.5 × 90 cm) in 10 mM sodium phosphate *p*H 7.5, 0.1% SDS. The void volume fractions containing the β-subunit were adjusted to 5 M urea and 144 mg of solid succinic anhydride was added slowly while maintaining the *p*H at 7.5 ± 0.5. After 30 min the total reaction volume was applied to a Sephadex-G25 column and eluted with 50 mM NH_4HCO_3. Fractions containing succinylated β-subunit were pooled, adjusted to 2 M urea and concentrated by ultrafiltration to ~1 mg ml^{-1}. TPCK-treated trypsin (255 μg; Cooper Biomedical) was added to 4 mg of succinylated β-subunit, incubated for 2 h at room temperature and lyophilized. Aliquots (2 mg) of the digest were dissolved in 0.3 ml of 1 mM dithiothreitol in HPLC grade H_2O and after 15 min adjusted to 0.1% trifluoroacetic acid (TFA) in a final volume of 0.5 ml and injected onto the HPLC system described previously[23]. Peptide peaks detected by absorbance at 280 nm were partially purified on a 15-cm Vydac C_{18} column with monitoring at 220 nm and then purified on a 15-cm Vydac C_4 column using the same solvent system (0.1% TFA in H_2O/0.1% TFA in acetonitrile). The tryptic peptides were sequenced, without prior amino-acid analysis, using an Applied Biosystems 470A gas phase sequencer; phenylthiohydantoin-amino acids were analysed on a Waters Nova-PAK C_{18} HPLC column. Lysine was identified as succinylated lysine. The N-terminal sequences of three tryptic peptides of the β-subunit are shown. Sheep kidney N-terminal peptide data are from ref. 5, dog kidney data from ref. 6.

cleavage of the α-subunit at trypsin site 3 (see ref. 19) removes a substantial portion of the protein which is located well away from the β-subunit. The location of trypsin site 3 at Arg 262 of the α-subunit has been confirmed by amino-acid sequence analysis (L.K.L., unpublished observations). As the first and second hydrophobic domains of the α-subunit occur in the peptide that is removed, they cannot be associated with the β-subunit. It also seems unlikely that the third and fourth hydrophobic domains (H3 and H4) are in contact with the β-subunit; H3 is in close proximity to Arg 262[1] and, because of its length, H4 is likely to be located inside the transmembrane shaft and cytoplasmic stalk. Therefore, one or more of the C-terminal hydrophobic domains of the α-subunit, which begin at residue 780, are likely to be in contact with the β-subunit.

As an evolutionary relationship between the α-subunit of the $(Na^+ + K^+)$ATPase and the KdpB protein of the *E. coli* K^+-ATPase has been clearly demonstrated[1,2,4], we compared the amino-acid sequence and hydropathy plot of the β-subunit with those of the KdpC protein, a 190-amino-acid subunit of the K^+-ATPase[4]. (An additional subunit, KdpA, is exceptionally hydrophobic and is clearly unrelated to the β-subunit.) The results suggest a possible relationship between the two proteins, although this is by no means as clear as that between the α-subunit and KdpB protein. Although there are four blocks of amino-acid homology between the two proteins (Fig. 3*a*), the homology is not extensive and in order to align these sequences it is necessary to postulate a number of large insertions

or deletions. Although this is reasonable considering the evolutionary time separating the two ATPases, such a procedure could also produce an apparent relationship between unrelated proteins (see ref. 20). There are also similarities between the hydropathy profile of KdpC (Fig. 3*b*) and that of the β-subunit (Fig. 2). KdpC has a hydrophobic domain near its N-terminal end which is likely to be a transmembrane domain, and the remainder of the protein lacks any obvious transmembrane domains. Thus, it is possible that the orientation of the KdpC protein in the membrane is the same as that of the β-subunit. Although there is insufficient evidence to conclude that these proteins have evolved from a common ancestor, the similarities suggest such a possibility. This may have important implications for other cation transport ATPases, particularly the $(H^+ + K^+)$ATPase[21] of the gastric mucosa which, like the $(Na^+ + K^+)$ATPase and the K^+-ATPase, transports K^+.

We thank Dr Terence Kirley and Greg Kelso of the Peptide/Protein Chemistry Core Facility of the University of Cincinnati for analysis of peptide sequences, Jeannette Greeb and Kelly Coyne for technical assistance, Michael Hughes for synthesis of the oligonucleotide probe, Greg Wernke for DNA sequence analysis, and Gwen Kraft for preparing the illustrations. This work was supported by NIH grants PO1 HL22619 (Mission I and core 2), RO1 HL25545 and NSF Instrument Grant DMB 8414251.

Received 3 February; accepted 19 March 1986.

1. Shull, G. E., Schwartz, A. & Lingrel, J. B. *Nature* **316**, 691-695 (1985)
2. Kawakami, K. *et al. Nature* **316**, 733-736 (1985).
3. Craig, W. S. & Kyte, J. *J. biol. Chem.* **255**, 6262-6269 (1980).
4. Hesse, J. E. *et al. Proc. natn. Acad. Sci. U.S.A.* **81**, 4746-4750 (1984)
5. Collins, J. H. & Zot, A. S. *IRCS med. Sci.* **11**, 799 (1983).
6. Chin, G. J. *Biochemistry* **24**, 5943-5947 (1985).
7. Proudfoot, N. J. & Brownlee, G. G. *Nature* **263**, 211-214 (1976)
8. Kozak, M. *Nucleic Acids Res.* **12**, 857-872 (1984).
9. Girardet, M., Geering, K., Rossier, B. C., Kraehenbuhl, J. P. & Bron, C. *Biochemistry* **22**, 2296-2300 (1983).
10. Jørgensen, P. L. & Brunner, J. *Biochim. biophys. Acta* **735**, 291-296 (1983)
11. Girardet, M. *et al. Biochemistry* **20**, 6684-6691 (1981).
12. Kyte, J. & Doolittle, R. F. *J. molec. Biol.* **157**, 105-132 (1982).
13. Vogel, F., Meyer, H. W., Grosse, R. & Repke, K. R. H. *Biochim. biophys. Acta* **470**, 497-502 (1977).
14. Geering, K., Meyer, D. I., Paccolat, M. P., Kraehenbuhl, J. P. & Rossier, B. C. *J. biol. Chem.* **260**, 5154-5160 (1985).
15. Fambrough, D. M. *Cold Spring Harb. Symp. quant. Biol.* **48**, 297-304 (1983)
16. Sweadner, K. J. & Gilkeson, R. C. *J. biol. Chem.* **260**, 9016-9022 (1985).
17. Hubbard, S. C. & Ivatt, R. J. *A. Rev. Biochem.* **50**, 555-583 (1981)
18. Mohraz, M. & Smith, P. R. *J. Cell Biol.* **98**, 1836-1841 (1984).
19. Jørgensen, P. L., Skriver, E., Hebert, H. & Maunsbach, A. B. *Ann. N.Y. Acad. Sci.* **402**, 207-225 (1982).
20. Doolittle, R. F. *Science* **214**, 149-159 (1981).
21. Sachs, G. *et al. J. biol. Chem.* **251**, 7690-7698 (1976).
22. Lane, L. K., Potter, J. D. & Collins, J. H. *Prep. Biochem.* **9**, 157-170 (1979)
23. Kirley, T. L., Wallick, E. T. & Lane, L. K. *Biochem. biophys. Res. Commun.* **125**, 767-773 (1984).
24. Ohtsuka, E., Matsuki, S., Ikehara, M., Takahashi, Y. & Matsubara, K. *J. biol. Chem.* **260**, 2605-2608 (1985).
25. Wood, W. I., Gitschier, J., Lasky, L. A. & Lawn, R. M. *Proc. natn. Acad. Sci. USA* **82**, 1585-1588 (1985).
26. Maxam, A. M. & Gilbert, W. *Meth. Enzym.* **65**, 499-560 (1980).

Isolation of cDNA clones encoding the 20K non-glycosylated polypeptide chain of the human T-cell receptor/T3 complex

Daniel P. Gold, Jennifer M. Puck*, Carolyn L. Pettey, Mildred Cho, John Coligan†, James N. Woody‡ & Cox Terhorst

Laboratory of Molecular Immunology, Dana-Farber Cancer Institute, Harvard Medical School, Boston, Massachusetts 02115, USA
* Department of Pediatrics, University of Pennsylvania Medical School, Joseph Stokes, Jr Research Institute, and Wistar Institute, Philadelphia, Pennsylvania 19104, USA
† Laboratory of Immunogenetics, National Institute of Allergy and Infectious Diseases, and ‡ Transplantation Research Branch, Naval Medical Research Institute, Bethesda, Maryland 20814, USA

The antigen receptor on human T lymphocytes consists of two variable immunoglobulin-like glycoproteins, α and β, which occur in association with three invariable T3 membrane proteins[1-3]. In humans two of these proteins, T3-γ and T3-δ, are glycoproteins of relative molecular mass (M_r) 25,000 (25K) and 20,000 (20K), respectively, while the third, T3-ε, is a 20K non-glycosylated protein[4-6]. On the surface of murine T cells, a non-glycosylated protein dimer composed of 17K subunits (T3-ζ) is found associated with the T-cell receptor α and β chains and the three T3-like polypeptide chains[7,8]. It is generally accepted that major histocompatibility complex-restricted antigen recognition is a function of the α–β heterodimer. This has led to the postulation that the proteins of the T3 complex are involved in the signal transduction that immediately follows antigen recognition via the antigen receptor[9]. Events believed to be involved in early T-cell activation, such as rapid increases in phosphatidylinositol turnover and free intracellular calcium[9,10], can be triggered by antibodies directed against either the T3 complex or the clonotypic receptor. We have previously reported our findings on the cloning of the complementary DNA and genomic structure encoding both the human and murine 20K glycoprotein, T3-δ (refs 11–13). We now present our results on the cloning of the cDNA encoding the human 20K non-glycosylated chain, T3-ε.

Complementary DNAs encoding the non-glycosylated T3-ε chain were isolated using a high-titre rabbit antiserum, I3, directed against both T3-δ and T3-ε proteins. A λgt11 library constructed from poly(A)$^+$ RNA derived from pokeweed mitogen-activated peripheral blood T lymphocytes was screened for the presence of bacteriophages synthesizing β-galactosidase fusion proteins immunoreactive with I3. From the $\sim 1 \times 10^6$ plaques screened, 4 were isolated which remained positive in their reactivity with I3 throughout all further purifications.

To eliminate potential bacteriophages encoding T3-δ, DNA was isolated from the four purified plaques and analysed on a Southern blot. All four inserts were of identical size on *Eco*RI digestion and gel electrophoresis (~1.0 kilobase (kb)), and all hybridized with relatively equal intensity to a ^{32}P-labelled probe prepared from one of them (data not shown). Significantly, the T3-δ cDNA insert of clone pPGBC-9 (ref. 11) showed no hybridization with this probe. We therefore concluded that these four isolates were related clones, and since none coded for T3-δ, it was likely that they encoded T3-ε.

To confirm that the isolates were coding for the T3-ε protein, the β-galactosidase-containing fusion protein was analysed by Western blotting using monoclonal antibodies specific for T3-δ or T3-ε[14]. The results (Fig. 1) demonstrated that bacteria containing DNA from one of the four isolates, 5a.2, synthesize a protein slightly larger than β-galactosidase which reacts only with the T3-ε-specific monoclonal antibody and not with the T3-δ-specific antibody. Hence, the cloned cDNA insert contained nucleotide sequences that coded for (part of) the T3-ε polypeptide chain.

A series of immunohistological and immunochemical analyses have led to the conclusion that the T3-ε polypeptide chain is expressed exclusively in T lymphocytes[14]. As judged by Northern blot analyses (Fig. 2*a*), a 1.4-kb messenger RNA hybridizes to the *Eco*RI insert of 5a.2 (subcloned into pBR322, pDJ1) only in human cells of T-cell lineage. Recent data suggest that proteins analogous to the human T3 polypeptides are associated with the murine T-cell receptor α- and β-chains[7,8]. Figure 2*b* demonstrates that murine T3-ε mRNA, ~1.5 kb in size, was also found exclusively in cells of T-cell lineage. Moreover, mRNA hybridizing with the T3-ε cDNA has been found in all T-cell leukaemias tested so far[15,16].

The nucleotide sequence of pDJ1 was determined by the dideoxy chain termination inhibition method of Sanger *et al.*[32].



Fig. 1 Immunoblot analysis of human T3-ε β-galactosidase fusion protein. A λgt11 bacteriophage isolate, 5a.2, containing a putative T3-ε coding region, was selected using a rabbit anti-T3-δ and -T3-ε antiserum. An SDS extract of 5a.2-infected *Escherichia coli* strain Y1089, synthesizing a human T3-ε β-galactosidase fusion protein (lane 1), and immunopurified T3 proteins (lane 2) were separated by SDS-PAGE under reducing conditions on a 7.5% gel. The proteins were transferred to nitrocellulose[25]. The strips were first blocked with 1.5% gelatin followed by either monoclonal anti-human T3-δ antibody SP64 (left panel) or monoclonal anti-human T3-ε antibodies SP6 and SP10 (ref. 14) (right panel). Nitrocellulose strips were developed with ^{125}I-labelled sheep F(ab')$_2$ anti-mouse immunoglobulin (Amersham) followed by autoradiography. 'M' denotes radioactive M_r markers whose sizes are indicated ($\times 10^{-3}$). Lower arrows indicate positive reactivity of both anti-T3-δ and anti-T3-ε antibody populations with purified T3 proteins. The upper arrow indicates the presence of a T3-ε fusion protein slightly larger than the 116K β-galactosidase marker which was detected only by the anti-T3-ε antibodies.

Methods. The λgt11 cDNA isolates were obtained as follows. The cells used for isolation of RNA were normal human peripheral blood lymphocytes that had been cultured with pokeweed mitogen for 5 days. At this time the cells were >90% T3$^+$ as judged by immunofluorescence[26]. Total mRNA was extracted in guanidine hydrochloride[27] and poly(A)$^+$ RNA was isolated by selective retention to oligo(dT)-cellulose. Synthesis of cDNA and addition of *Eco*RI linkers for cloning into the *Eco*RI site of the β-galactosidase-encoding *lacZ* gene of λgt11 was performed as described elsewhere[28,29]. Before ligation into λgt11, the cDNA was digested with *Eco*RI and fragments >800 bases were isolated from low-gelling agarose. A total of 1.2×10^6 recombinants were obtained. After amplification in *E. coli* strain Y1088, the library was grown up in *E. coli* strain Y1090 for screening with antibody. For isolation of human T3-ε cDNAs, an antiserum, I3, was prepared in rabbits that had been immunized with both T3-δ and T3-ε proteins purified as described previously[20]. Antibody screening was performed essentially as described in ref. 29. Nitrocellulose filters were blocked in 1.5% gelatin and then incubated with the I3 rabbit anti-T3-δ and -T3-ε antiserum. The filters were developed with ^{125}I-labelled donkey F(ab')$_2$ anti-rabbit immunoglobulin (Amersham). Four positive bacteriophages were plaque-purified and the DNA was isolated[30]. To produce stable β-galactosidase fusion proteins, bacteriophage particles from one of the four λgt11 isolates, 5a.2, were used to infect *E. coli* strain Y1089 at a multiplicity of infection of 5. Infected bacteria were grown at 30 °C on nitrocellulose filters and replicate filters were prepared[30]. The filters were baked for 2 h at 80 °C, prehybridized and hybridized in 50% formamide, 5×SSC, 50 mM sodium phosphate *p*H 6.5, 250 μg ml^{-1} sonicated salmon sperm DNA, 0.1% bovine serum albumin, 0.1% Ficoll, 0.1% polyvinylpyrrolidone, and 0.1% SDS. The *Eco*RI insert of isolate 5a.2 was ^{32}P-labelled to a specific activity $>10^8$ c.p.m. μg^{-1} by the random hexadeoxyribonucleotide priming method[31] and used to probe the filters. The filters were hybridized at 42 °C overnight, then washed several times in 2×SSC, 0.1% SDS at room temperature followed by two successive washes in 0.2×SSC, 0.1% SDS at 65 °C. Filters were exposed to Kodak XAR-5 film at −70 °C using an intensifying screen. Positive colonies were selected and grown at 32 °C. Induction of the *lacZ* fusion products with isopropyl β-D-thiogalactopyranoside was performed as described by Huynh *et al.*[29].

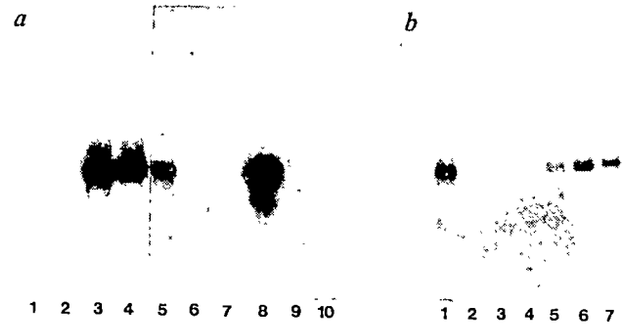


Fig. 2 Northern blotting analysis of human and murine mRNA. Total cellular RNA from the following sources was analysed by Northern blotting to determine the tissue distribution of T3-ε mRNA: *a*, lane 1, human umbilical vein endothelium; lane 2, human B-lymphoblastoid line BL; lane 3, human T-leukaemic cell line HPB-ALL; lane 4, human T-leukaemic cell line Jurkat; lane 5, a human T4$^-$T8$^+$ cell line; lane 6, a human Epstein–Barr virus-transformed B-cell line; lane 7, normal human bone marrow; lane 8, T-leukaemic cells from a Sézary syndrome patient (T3$^+$, T4$^+$, T8$^-$); lane 9, human promyelocytic leukaemic line HL60; lane 10, human fetal brain. *b*, Lane 1, human T-leukaemic cell line HPB-ALL; lane 2, normal murine brain; lane 3, murine Ltk$^-$ fibroblasts; lane 4, murine B-lymphoma cell line A20; lane 5, murine T–T hybridoma (T-helper cell) B8C3; lane 6, normal murine lymph node cells; lane 7, murine thymoma line BW5147.

Methods. Total mRNA was extracted from cells in guanidine hydrochloride[27]. mRNA (20 μg total) was denatured by heating to 65 °C in 50% formamide and separated by electrophoresis in a 1% agarose formaldehyde gel. The RNA was transferred to Biodyne filters (ICN) and the filters were baked for 2 h at 80 °C. Prehybridization, hybridization and washing steps were done exactly as described for Fig. 1 using the ^{32}P-labelled *Eco*RI insert from pDJ1 as probe.

Clone pDJ1 consisted of an insert of 995 base pairs (bp) with an open reading frame of 554 bp. As this clone was not full length, a second library which had been prepared from mRNA of a human T4$^+$T8$^-$ T-cell clone according to the method described by Okayama and Berg[17,18] was screened using the insert from pDJ1 as a probe. From this library, pDJ4 containing an insert of ~1.4 kb, was selected for sequencing.

Figure 3*b* shows the complete nucleotide sequence of the T3-ε cDNAs. The first in-frame AUG was found at position 55 of the nucleotide sequence. There was only one long open reading frame which continued until a termination signal at position 754. A consensus poly(A) addition site, AATAAA, was found at position 1,294 followed by a poly(A) tail 14 nucleotides downstream. The relative molecular mass of T3-ε predicted from the protein sequence in Fig. 3*b* is 23,153. A hydropathicity plot of the coding segment (Fig. 3*c*) predicted the presence of a putative N-terminal signal peptide containing an 11-amino-acid hydrophobic core[19]. This signal peptide is followed by a hydrophilic domain 104 amino acids long. A 26-amino-acid hydrophobic segment, beginning at position 105, delineated a putative hydrophobic transmembrane region. The segment between residues 131 and 190 is hydrophilic, whereas the C-terminus (191–211) is uncharged. The absence of potential sites for *N*-linked glycosylation in the translated amino-acid sequence was consistent with our observation that T3-ε contains no *N*-linked oligosaccharides[5,20].

To compare the amino-acid sequence predicted from the nucleotide sequence with that of the mature T3-ε protein, we performed partial N-terminal radiosequencing of purified T3-ε tryptic fragments. As this protein has the same M_r and almost the same isoelectric point as T3-δ, classic protein separation techniques failed to yield pure T3-ε. Because T3-δ is a glycoprotein and T3-ε is not, treatment with endoglycosidase F followed by preparative SDS-polyacrylamide gel electrophoresis (PAGE) had been used to obtain pure T3-δ[5,20]. Since Endo-F treatment does not always result in complete deglycosylation, the material that remained after digestion is often impure and can give rise to incorrect amino-acid sequences. In these experiments, therefore, we have used a different approach to obtain

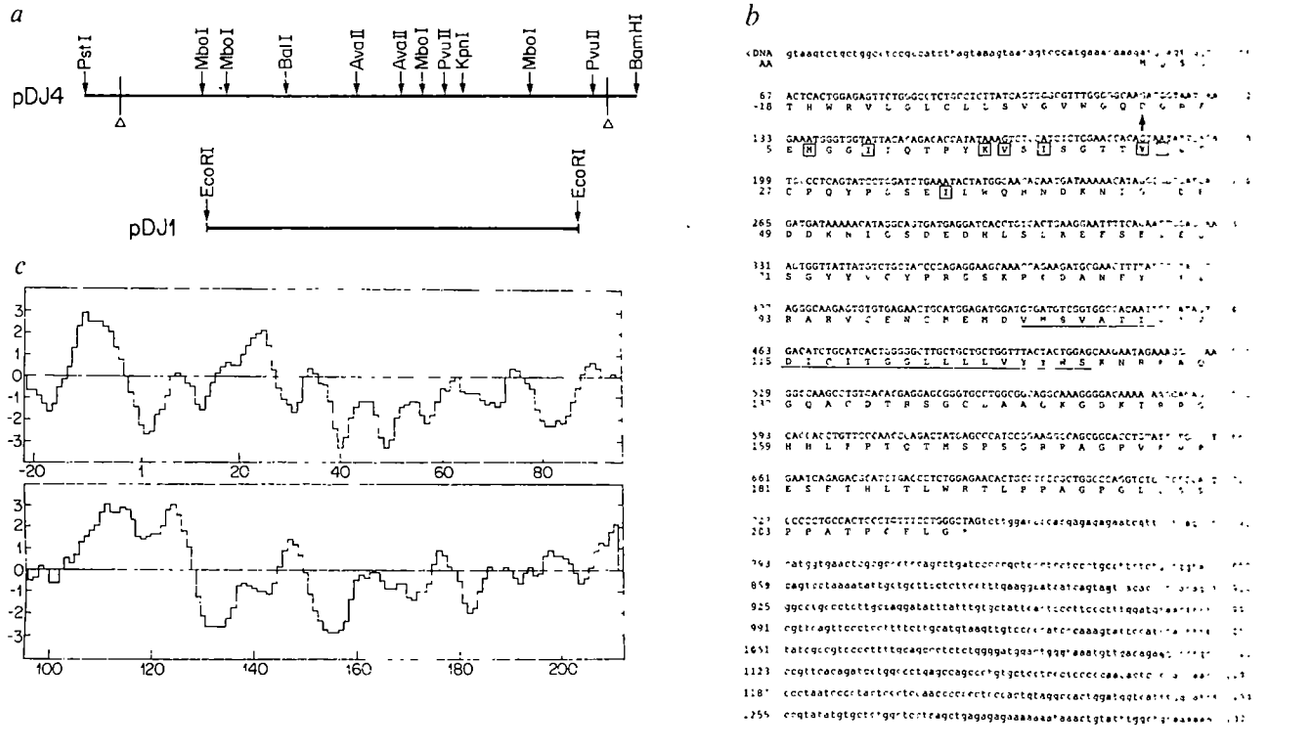


Fig. 3 Analysis of the nucleotide sequence of the human T3-ϵ chain. *a*, Partial restriction map of T3-ϵ cDNA pDJ4 containing restriction endonuclease sites used to determine nucleotide sequences. The open triangles beneath pDJ4 represent the insert boundaries. The 5′ *Pst*I and 3′ *Bam*HI sites are derived from the cloning vector. The *Eco*RI sites in pDJ1 are derived from linkers added during cDNA synthesis. *b*, The combined nucleotide sequence of pDJ1 and pDJ4 was determined by the dideoxy chain termination method of Sanger[32] using bacteriophage M13 mp18 or mp19 (ref. 33). Isolated restriction fragments were either ligated directly into the appropriate M13 vector restriction site or made blunt-ended by treatment with the large fragment of *E. coli* DNA polymerase I before ligation into the *Sma*I site of the appropriate M13 vector. The deduced amino-acid sequence of the only long open reading frame is shown below the nucleotide sequence, beginning with the initiation methionine at position −22. The arrow indicates amino acid 1 of the mature protein. Boxed amino-acid residues 6, 9, 15, 16, 18, 23, 24 and 35 correspond to those residues determined by amino-acid sequencing (see Fig. 4*c*). *c*, Plot of the relative hydropathicity of T3-ϵ. The hydropathicity values of each amino acid have been determined using the weight system of Kyte and Doolittle[34]. The average hydropathicity value at residue i is calculated across 6 residues from $i-3$ through to and including $i+2$. Positive values indicate hydrophobic regions and negative values represent hydrophilic segments.

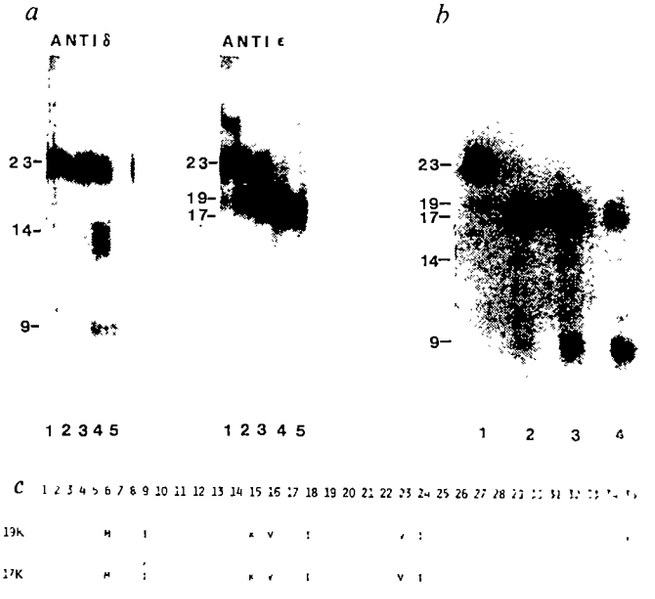


Fig. 4 Isolation and partial amino-acid sequences of the large tryptic fragments of the T3-ϵ protein. *a*, Western blot analyses of the trypsinization products of purified T3-δ and T3-ϵ proteins using monoclonal anti-T3-δ antibodies (left panel) or monoclonal anti-T3-ϵ antibodies (right panel). Lanes 1–5 represent titration of trypsin: lane 1, no trypsin; lane 2, 0.0015 μg ml^{-1}; lane 3, 0.0060 μg ml^{-1}; lane 4, 0.03 μg ml^{-1}; lane 5, 0.15 μg ml^{-1}. *b*, Analysis of ^{35}S-cysteine and ^{35}S-methionine metabolically labelled trypsinization products of T3-δ and T3-ϵ proteins. Lane 1, no trypsin; lane 2, 0.0015 μg ml^{-1}; lane 3, 0.0060 μg ml^{-1}; lane 4, 0.03 μg ml^{-1}. *c*, N-terminal amino-acid assignments for the 19K and 17K tryptic fragments of T3-ϵ.

Methods. Isolation of purified T3-δ and T3-ϵ proteins was as described previously[20]. For metabolic labelling, ^{35}S-cysteine, ^{35}S-methionine and ^{3}H-isoleucine, ^{3}H-lysine or ^{3}H-valine were used. Trypsinization of samples at the appropriate trypsin concentration was carried out at 37 °C for 4 h in the presence of 20 μg sperm whale apomyoglobin (Beckman). Trypsinization was terminated by the addition of trichloroacetic acid to a final concentration of 10%. For Western blot analysis, proteolytic fragments were separated by SDS-PAGE under reducing conditions on a 15% gel. Conditions for Western blotting were exactly as for Fig. 1. For radiosequencing, proteolytic fragments were separated by SDS-PAGE under reducing conditions on a 14–20% gradient gel. The 19K and 17K bands were eluted[35] and radiosequenced on a Beckman protein sequenator with a cold trap modification using the Beckman 0.1 M Quadrol program 121078. Identification of the phenylthiohydantoin-amino acids was as described by Coligan *et al.*[36].

T3-ϵ amino-acid sequences and we believe this explains the differences between the sequence we now report and the earlier published sequence[20]. First, both 20K T3 proteins (T3-δ and T3-ϵ) were isolated after immunoadsorbent column chromatography and SDS-PAGE. The mixture of these two proteins was subjected to limited trypsinization and large tryptic fragments (9K, 14K, 17K and 19K) were separated by SDS-PAGE. Using anti-T3-δ and T3-ϵ monoclonal antibodies in a Western blotting experiment, we determined that the two larger fragments were derived from T3-ϵ and the smaller ones from T3-δ (Fig. 4*a*). The 17K and 19K fragments isolated from metabolically labelled HPB-ALL cells (Fig. 4*b*) had identical N-terminal amino-acid sequences (Fig. 4*c*). As shown in Fig. 3*b*, the predicted amino-acid sequence agrees with the assignment of residues 6, 9, 15, 16, 18, 23, 24 and 35 of the tryptic fragments. Therefore, the cDNA pDJ4 must encode the complete T3-ϵ protein. Since it

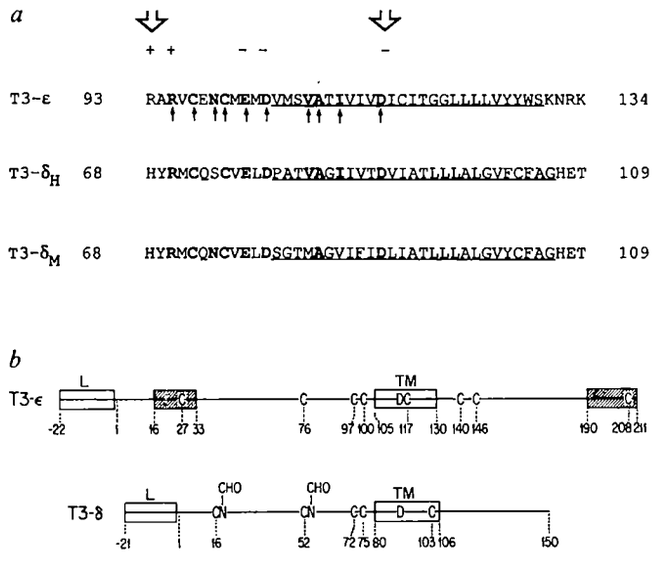


Fig. 5 Comparison of the T3-δ and T3-ε polypeptide chains. *a*, Homology region (see text) of T3-ε, including the entire transmembrane domain, compared with the human (T3-δ_H) and murine (T3-δ_M) T3-δ chains. Residues shared between T3-ε and human or murine T3-δ are shown in bold type and denoted by solid arrows. Boundaries of the homology region are indicated by open arrows. The transmembrane region of each chain is underlined. *b*, General features of the organization of the human T3-ε and T3-δ chains. L, leader sequence; TM, transmembrane region; C, cysteine; N, asparagine; CHO, *N*-linked glycosylation sites. The shaded areas in T3-ε denote the N-terminal and C-terminal uncharged regions. Numbering refers to the relative position of residues in the mature protein.

is unlikely that trypsin would have cleaved a Gln–Asp peptide bond (residues −1, 1; Fig. 3*b*), this sequence must represent the N-terminus of the mature T3-ε protein. We therefore conclude that the 17K and 19K tryptic fragments contain the N-terminus of the mature T3-ε protein and that amino acids −22 to −1 predicted from the cDNA sequences of pDJ4 represent the T3-ε signal peptide.

A search of the Los Alamos National Laboratory DNA database and the National Biomedical Research Foundation (NBRF) protein database using the NUCALN and PRTALN programs revealed no strong homologies between the T3-ε sequences and any other sequence. Although no strong overall homology existed between T3-ε and T3-δ, an interesting feature was noted. As was observed in the case of the T3-δ chain[11], the T3-ε protein contains an Asp residue in the transmembrane region at position 115. Starting from this transmembrane Asp residue in T3-ε and going towards the N-terminus, there is a stretch of 23 amino acids which contains 6 charged residues. Nine of the 23 amino-acid residues are shared between T3-ε and T3-δ, while the remaining 14 residues contain mostly conservative changes. In addition, 5 of the 6 charged residues as well as the 2 Cys residues are shared between T3-ε and both the human and murine[12] T3-δ chains. In particular, the negatively charged Asp residue in the transmembrane region is of great interest because of the association of the T3 proteins with the T-cell receptor heterodimer. Both the α and β chains of the T-cell receptor contain a Lys in their respective transmembrane regions[21–24]. The negatively charged Asp residues in T3-ε and T3-δ could form salt bridges with these charged residues of the heterodimer α and β chains, and such an interaction is likely to be significant because of the hydrophobic milieu of the plasma membrane. The 23-amino-acid homology region of T3-δ and T3-ε may also be important for the interaction with the α and β chains.

Based on the homology between T3-δ and T3-ε, we postulate that the region between residues 105 and 130 is a transmembrane segment and thus that the T3-ε protein is oriented in a fashion similar to the T3-δ chain, that is, the N-terminal domain is extracellular and the C-terminal domain cytoplasmic. Note that there are two relatively long uncharged regions, residues 16–33 and 191–211 (see Figs 3*c*, 5*b*). Although these regions neither form an α-helix nor consist of a strongly hydrophobic nucleus, they may be inserted in the plasma membrane. Further protein chemical studies will clarify this issue. Because the T3-ε cytoplasmic domain is considerably larger than that of the previously described α, β and δ chains, we predict that the ε protein must be involved in some signal transduction property of the T3 complex which is activated on engagement of the associated T-cell receptor heterodimer.

We thank Dr Ken-Ichi Arai (DNAX) for making available to us the cDNA library used to isolate pDJ4, Drs Peter van den Elsen and David Ucker for advice throughout this study, Drs C. T. Caskey and G. Rovera for help in cDNA library synthesis and screening, Sharon McGrath for preparation of this manuscript, and the DFCI/Harvard School of Public Health NIH-supported Molecular Biology Research Resource for assistance with computer analysis. This work was supported by NIH grants AI-15066 and AI-17651. D.P.G. was supported by a fellowship from the Cancer Research Institute/Eleanor Naylor Dana Charitable Trust. J.M.P. was supported by a Physician Scientist Award.HD00657-01. C.L.P. is a Fellow and C.P.T. is a Scholar of the Leukemia Society of America.

Received 13 January; accepted 13 March 1986.

1. Oettgen, H. C., Kappler, J., Tax, W. J. P. & Terhorst, C. *J. biol. Chem.* **259**, 12039–12048 (1984).
2. Meuer, S. C., Acuto, O., Hercend, T., Schlossman, S. F. & Reinherz, E. L. *A. Rev. Immun.* **2**, 23–50 (1984).
3. Brenner, M. B., Trowbridge, I. S. & Strominger, J. L. *Cell* **40**, 183–190 (1985).
4. Borst, J., Alexander, S., Elder, J. & Terhorst, C. *J. biol. Chem.* **258**, 5135–5141 (1983).
5. Borst, J., Prendiville, M. A. & Terhorst, C. *Eur. J. Immun.* **13**, 576–580 (1983).
6. Kanellopoulos, J. M., Wigglesworth, N. M., Owen, M. J. & Crumpton, M. J. *EMBO J.* **2**, 1807–1814 (1983).
7. Samelson, L. E., Harford, J. B. & Klausner, R. D. *Cell* **43**, 223–231 (1985).
8. Oettgen, H. C., Pettey, C., Maloy, W. L. & Terhorst, C. *Nature* **320**, 272–275 (1986).
9. Oettgen, H. C., Terhorst, C., Cantley, L. C. & Rosoff, P. M. *Cell* **40**, 583–590 (1985).
10. Imboden, J. B. & Stobo, D. J. *J. exp. Med.* **161**, 446–456 (1985).
11. van den Elsen, P. *et al. Nature* **312**, 413–418 (1985).
12. van den Elsen, P., Shepley, B.-A., Cho, M. & Terhorst, C. *Nature* **314**, 542–544 (1985).
13. van den Elsen, P., Georgopoulos, K., Shepley, B.-A., Orkin, S. & Terhorst, C. *Proc. natn. Acad. Sci. U.S.A.* (in the press).
14. Pessano, S., Oettgen, H. C., Bhan, A. & Terhorst, C. *EMBO J.* **4**, 337–344 (1985).
15. MacLeod, C. L., Minning, L., Gold, D. P., Terhorst, C. & Wilkinson, M. *Proc. natn. Acad. Sci. U.S.A.* (submitted).
16. Furley, A. J. *et al. Cell* (in the press).
17. Okayama, H. & Berg, P. *Molec. cell. Biol.* **2**, 161–170 (1982).
18. Yokota, T. *et al. Proc. natn. Acad. Sci. U.S.A.* **81**, 1070–1074 (1984).
19. von Heijne, G. *J. molec. Biol.* **184**, 99–105 (1985).
20. Borst, J. *et al. Nature* **312**, 455–458 (1984).
21. Hedrick, S. M., Cohen, D. I., Neilsen, E. A. & Davis, M. M. *Nature* **308**, 149–153 (1984).
22. Yanagi, Y. *et al. Nature* **308**, 145–148 (1984).
23. Chien, Y. *et al. Nature* **312**, 31–35 (1984).
24. Saito, H. *et al. Nature* **312**, 36–40 (1984).
25. Towbin, H., Staehelin, T. & Gordon, J. *Proc. natn. Acad. Sci. U.S.A.* **76**, 4350–4354 (1979).
26. Puck, J. M. & Rich, R. R. *J. Immun.* **132**, 1106–1112 (1984).
27. Woods, D., Crampton, J., Clark, B. & Williamson, R. *Nucleic Acids Res.* **8**, 5157–5168 (1980).
28. Young, R. A. & Davis, R. W. *Proc. natn. Acad. Sci. U.S.A.* **80**, 1194–1198 (1983).
29. Huynh, T. V., Young, R. A. & Davis, R. W. in *Practical Approaches in Biochemistry* (ed. Glover, D.) (IRL, Oxford, 1984).
30. Maniatis, T., Fritsch, E. F. & Sambrook, J. *Molecular Cloning, A Laboratory Manual* (Cold Spring Harbor Laboratory, New York, 1982).
31. Feinberg, A. P. & Vogelstein, B. *Analyt. Biochem.* **137**, 266–267 (1984).
32. Sanger, F., Nicklen, S. & Coulson, A. R. *Proc. natn. Acad. Sci. U.S.A.* **74**, 5463–5467 (1977).
33. Yanisch-Perron, C., Vieira, J. & Messing, J. *Gene* **33**, 103–119 (1985).
34. Kyte, J. & Doolittle, R. F. *J. molec. Biol.* **157**, 105–132 (1982).
35. Hunkapiller, M. W., Lujan, E., Ostrander, F. & Hood, L. E. *Meth. Enzym.* **91**, 227–231 (1983).
36. Coligan, J. E., Gates, F. T., Kimball, E. S. & Maloy, W. L. *Meth. Enzym.* **91**, 413–417 (1983).

Isolation of an HTLV-III-related retrovirus from macaques with simian AIDS and its possible origin in asymptomatic mangabeys

Michael Murphey-Corb*, Louis N. Martin*, S. R. S. Rangan*, Gary B. Baskin*, Bobby J. Gormus*, Robert H. Wolf*, W. Abe Andes†, Melanie West‡ & Ronald C. Montelaro‡

* Delta Regional Primate Research Center of Tulane University, Covington, Louisiana 70433, USA
† Department of Medicine, Tulane University Medical Center, New Orleans, Louisiana 70118, USA
‡ Department of Biochemistry, Louisiana State University, Baton Rouge, Louisiana 70803, USA

Acquired immune deficiency syndrome (AIDS) has become a worldwide epidemic[1–6], so the development of vaccines and antiviral agents effective against the causative agent, human T-lymphotropic virus type III (HTLV-III), is vital. This work would be greatly simplified if a suitable animal model could be developed. Here we report the isolation of an HTLV-III-related retrovirus, STLV-III/Delta, from rhesus macaques (*Macaca mulatta*) with transmissible simian AIDS (SAIDS) and from asymptomatic sooty mangabeys (*Cercocebus atys*). SAIDS was initially diagnosed in several macaques previously inoculated with tissue homogenates of mangabey origin. Western blot analysis of both the mangabey and macaque sera demonstrated the presence of antibody cross-reactive primarily with the HTLV-III proteins p24 and p61. In a related experiment, analysis of these same sera revealed simian antibody to STLV-III/Delta proteins similar, but not identical, to those of HTLV-III with estimated relative molecular masses (M_rs) of 16,000 (16K), 26K, 35K, 45K, 60K and 110K. Infection of the mangabey, an African primate, with an HTLV-III-related virus may provide a clue to the origin of HTLV-III in humans. The apparent difference in susceptibility to SAIDS-like disease between infected macaques and mangabeys suggests that these species may respond differently to STLV-III infection.

Beginning with four macaques which had been inoculated with homogenates of a cutaneous lepromatous leprosy lesion from a sooty mangabey[7], we have transmitted SAIDS and/or lymphoma by inoculation of tissue homogenates in 11 of 14 recipient macaques[8]. Co-culture of lymphoid tissue from six of these animals with the human H9 cell line led to the isolation of a retrovirus morphologically similar to HTLV-III (Fig. 1*a*). This retrovirus, STLV-III/Delta, induced the formation of syncytia in H9 cells and displayed a Mg^{2+}-dependent reverse transcriptase activity.

STLV-III/Delta and HTLV-III are also related antigenically. An enzyme-linked immunosorbent assay (ELISA) for HTLV-III antibodies performed longitudinally on sera from the four inoculated macaques revealed a rise in antibody titre for three of the monkeys (Fig. 2). The rise in antibody titre after inoculation suggests that these macaques may have acquired STLV-III/Delta from the mangabey. Antibody cross-reactive with HTLV-III was detected by ELISA in sera from 3 of 39 mangabeys (Fig. 3). In addition, STLV-III/Delta was isolated from several mangabeys by co-culture of peripheral lymphocytes with H9 cells (Fig. 1*b*).

Western blot analysis of simian antisera using detergent-disrupted HTLV-III virions confirmed the presence of HTLV-III-cross-reactive antibody in all ELISA-positive samples. Antibody specific for STLV-III/Delta was also detected in the serum of 2 macaques and 10 mangabeys that were ELISA-negative. In total, anti-STLV-III/Delta antibody was detected in sera from 5 of 11 macaques from the SAIDS transmission study and in 13 of 44 mangabeys.

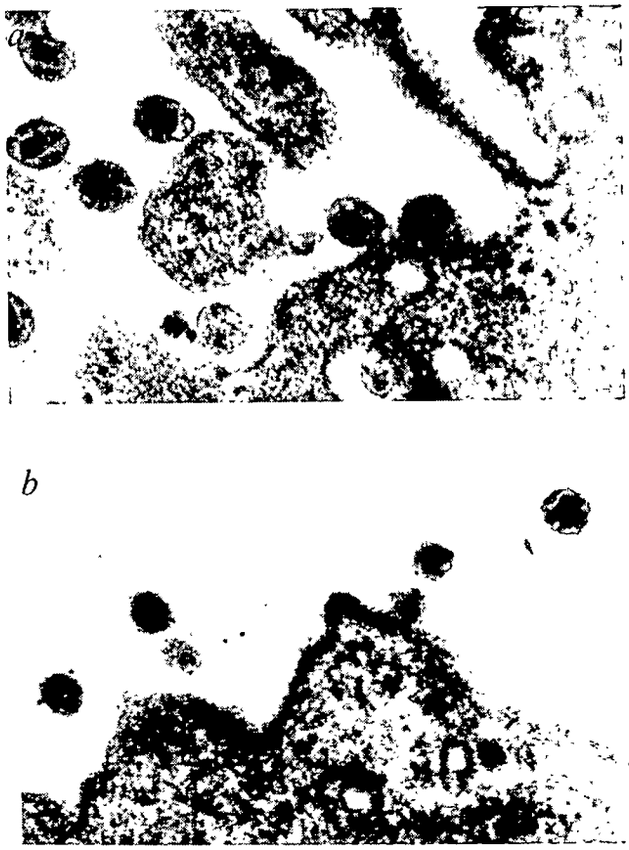


Fig. 1 Electron micrographs of the H9 human T-cell line infected with STLV-III/Delta cultured from a macaque with SAIDS (*a*) and from an asymptomatic mangabey (*b*). Ficoll gradient-purified peripheral lymphocytes from macaque B670 (*a*) and mangabey E038 (*b*) were cultured at 5×10^6 cells ml^{-1} in 7% CO_2 with 10 μg ml^{-1} phytohaemagglutinin (PHA) for 72 h in RPMI-1640 medium supplemented with 15% fetal calf serum (FCS). The PHA was subsequently removed by washing and culturing was continued in RPMI-1640 supplemented with 15% FCS and 10 half-maximal units per ml of human interleukin-2. At 3- and 7-day intervals, H9 cells (5×10^4 ml^{-1}) were added to duplicate cultures and the cells were monitored for syncytia formation. STLV-III infectivity was verified by fixed-cell indirect immunofluorescence using rhesus reference serum and electron microscopy. Infected cells were fixed in glutaraldehyde, embedded in Epoxy resin, and sectioned. Tissue sections were stained with uranyl acetate and lead citrate and photographed in a Siemens transmission electron microscope. Final magnification: *a*, ×83,000; *b*, ×45,000.

Figure 4 shows Western blot results for representative sera. The predominant immunoreactive HTLV-III proteins recognized by sera from both macaque (lanes *d, f*) and mangabey (lanes *h, j, l*) were the p24 core protein and a larger protein of $M_r\sim61$K. Additional proteins ranging in size from 35K to 50K were also variably recognized by these sera. Simian sera reacted with STLV-III/Delta proteins which were of similar, but not identical, M_rs to those of HTLV-III (Fig. 4, lanes *c, e, g, i, k*). The STLV-III/Delta proteins most commonly recognized by both macaque and mangabey sera were of M_r 110K and 26K; these probably correspond to the 120K *env* and 24K *gag*-related proteins of HTLV-III. Additional proteins of estimated M_r 60K, 45K, 35K and 16K also were variably recognized by the different antisera tested. Sera obtained from 50 healthy macaques and from 31 of 44 mangabeys from the Delta Regional Primate Research Center (DRPRC) colony, however, did not react with protein determinants of either virus.

The cross-reactivity of these simian antisera with both STLV-III/Delta and HTLV-III virion preparations suggests that these

two viruses have common immunoreactive epitopes. This observation was confirmed by the ability of STLV-III/Delta virions to adsorb HTLV-III-cross-reactive antibody (data not shown). STLV-III/Delta and HTLV-III are distinct, however, since in the reciprocal Western blot, a pool of human AIDS sera did not react with any of the simian virion proteins (Fig. 4, lanes *m*, *n*). In addition, Southern blot analysis of STLV-III-infected H9 cell DNA using radiolabelled sequences complementary to HTLV-III[9] failed to reveal genetic homology between the two viruses, even under conditions of low stringency (data not shown).

STLV-III/Delta is antigenically distinct from the HTLV-I-related simian virus STLV-I[10]. Analysis of mangabeys for anti-HTLV-I antibodies by ELISA specific for the viral p24 core protein detected significant antibody in 14 of 32 monkeys tested (Fig. 3), whereas sera from sick macaques were uniformly negative for anti-HTLV-I antibody (data not shown). Antibody cross-reactive with HTLV-III was detected in several healthy mangabeys as well as in sick macaques. However, there was individual variation, with several mangabeys being seropositive for a single virus. Thus, Western blot analysis of serum from mangabey A015, which is seropositive for HTLV-I but seronegative for HTLV-III by ELISA, did not detect antibody to STLV-III/Delta viral proteins (data not shown).

A macaque retrovirus similar to STLV-III/Delta, STLV-III_{Mac}, has been identified in association with experimentally induced SAIDS at the New England Regional Primate Research Center (NEPRC)[11,12]. The putative *env*- and *gag*-related proteins of this virus, however, have identical M_rs to those of HTLV-III; antibody cross-reactive with the NEPRC virus was also detected in human AIDS serum. The disparity in cross-reactivity observed between that study and our own may reflect differences in the techniques used. The difference observed in the M_rs of the putative core proteins, however, may be significant, particularly as in both studies the simian viral proteins were normalized to those of HTLV-III. In our hands, Western blot analysis also detected other STLV-III/Delta proteins which

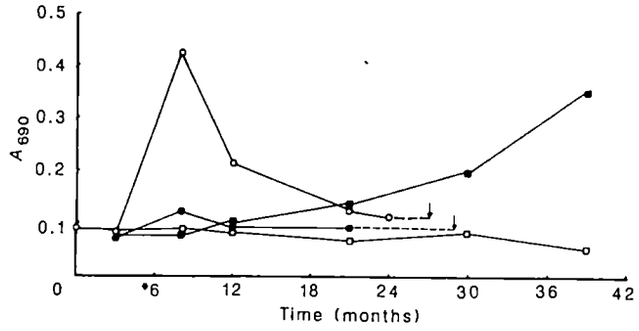


Fig. 2 Presence of HTLV-III-cross-reactive antibody in macaques inoculated with lepromatous mangabey tissue homogenates. Four macaques were inoculated as described elsewhere[15] with tissue homogenates prepared from lepromatous leprosy lesions at the time designated by the asterisk. Serum was obtained from these animals at various times post-inoculation and assayed for HTLV-III-cross-reactive antibody by ELISA using the manufacturer's instructions (Litton Bionetics). The arrows mark the time of death due to SAIDS of two of the animals; two animals remained alive at this time. Monkeys are designated as follows: ○, B988; ●, 8664; ■, B845; □, 745.

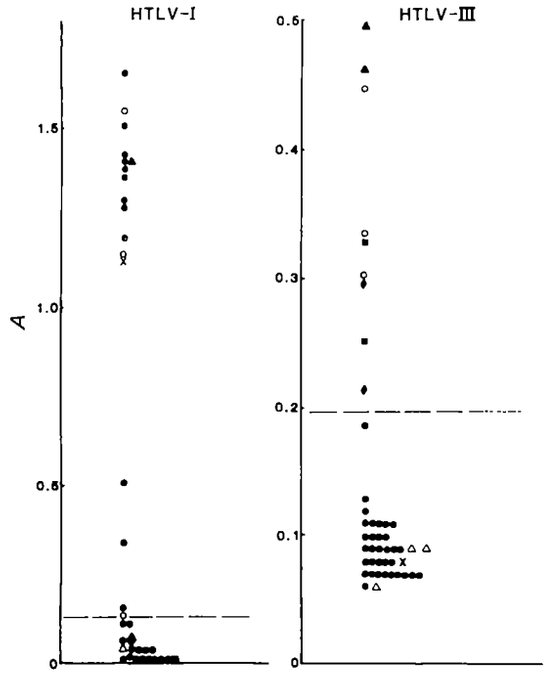


Fig. 3 Prevalence of HTLV-I- or HTLV-III-cross-reactive antibody in the DRPRC mangabey monkey colony. Random sera obtained from mangabey monkeys at the DRPRC were assayed by ELISA (Litton Bionetics) for antibodies to either HTLV-I or HTLV-III. The dashed lines designate the cut-off point for significant positive values calculated for human samples as described in the assay. Individual samples of interest are designated as follows: ○, positive human control sera; △, negative human control sera; ●, representative mangabey sera. The rest are sera obtained at various time intervals from mangabey monkeys A015 (×), D089 (▲), E038 (■) and D178 (◆).

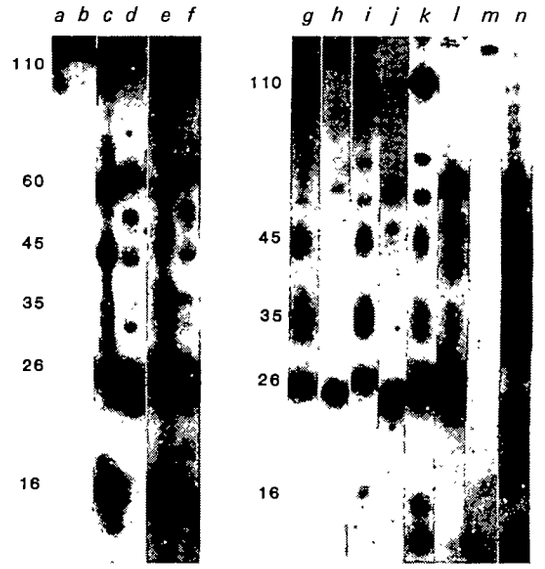


Fig. 4 Western blot analysis of the reaction of primate antisera with detergent-disrupted STLV-III/Delta and HTLV-III virion proteins. STLV-III/Delta virions were purified from infected H9 cell culture supernatants as described elsewhere[16-18]. HTLV-III virions were obtained on a contractual basis from the NIH. STLV-III/Delta (lanes *a*, *c*, *e*, *g*, *i*, *k*, *m*) and HTLV-III (lanes *b*, *d*, *h*, *j*, *l*, *n*) virions were treated with SDS and 2-mercaptoethanol, boiled briefly and subjected to electrophoresis through a 10% polyacrylamide gel containing SDS as described elsewhere[18]. Size-fractionated proteins were electroblotted onto nitrocellulose and the transferred immunoreactive proteins detected by incubation with primate antiserum. Antigen-antibody complexes were detected by subsequent incubation with ^{125}I-labelled *Staphylococcus* protein A, followed by autoradiography. Lanes *a*, *b*, an over-exposure of normal rhesus control sera; lanes *c*, *d*, rhesus B988 serum; *e*, *f*, rhesus B845 serum; *g*, *h*, mangabey E038 serum; *i*, *j*, mangabey D178 serum; *k*, *l*, mangabey D089 serum; *m*, *n*, pool of human AIDS sera.

had similar, but not identical M_rs to those of HTLV-III. Taken together, these data suggest that STLV-III/Delta is related to, but distinct from, STLV-III_{Mac}. Resolution of this discrepancy will require a direct comparison of the two viruses.

An HTLV-related virus endemic in our mangabey colony in the apparent absence of SAIDS is notable. SAIDS at DRPRC has been confined to a single series of transmissions which originated with a mangabey tissue inoculum. This fact, coupled with the prevalence of the virus in mangabeys, suggests that STLV-III/Delta in our macaques with SAIDS is of mangabey origin. Although STLV-III appears to be endemic in our mangabey colony, the characteristic SAIDS pathology has not been observed among these animals. These observations suggest that virus transfer from an African (mangabey) to an Asian (macaque) species may result in significant differences in pathogenicity. A comparison of host responses to infection in the two species may prove useful in understanding the pathogenesis of human AIDS.

STLV-III has also been reported in the African green monkey[13,14]. The presence of HTLV-III-related retroviruses in at least two African primates, the African green monkey and the mangabey, is consistent with the hypothesis that HTLV-III emerged in humans as a result of an early trans-species transfer in Africa.

We thank N. Meiners, C. Wall and P. Eddy for technical assistance. This work was supported in part by a grant from the Division of Research Resources, NIH, and by USPHS grants from the NCI.

Received 2 December 1985; accepted 13 March 1986.

1. Gottlieb, M. *et al. New Engl. J. Med.* **305**, 1425-1430 (1981).
2. Masur, H. *et al. New Engl. J. Med.* **305**, 1431-1438 (1981).
3. Siegal, F. *et al. New Engl. J. Med.* **305**, 1439-1444 (1981).
4. Lane, H. *et al. New Engl. J. Med.* **309**, 453-458 (1983).
5. Ziegler, J. *et al. New Engl. J. Med.* **311**, 565-570 (1984).
6. Goldsmith, M. F. *J. Am. med. Ass.* **253**, 3369-3384 (1985).
7. Wolf, R. H. *et al. Science* **227**, 529-531 (1985).
8. Baskin, G. B. *et al. J. natn. Cancer Inst.* (in the press).
9. Hahn, B. H. *et al. Nature* **312**, 166-169 (1984).
10. Saxinger, C. *et al.* in *Human T-Cell Leukemia/Lymphoma Virus* (eds Gallo, R. C. *et al.*) 323-330 (Cold Spring Harbor Laboratory, New York, 1983).
11. Kanki, P. J. *et al. Science* **228**, 1199-1200 (1985).
12. Daniel, M. D. *et al. Science* **228**, 1201-1204 (1985).
13. Kanki, P. J. *et al. Lancet* ii, 1330-1332 (1985).
14. Kanki, P. J., Alroy, J. & Effex, M. *Science* **230**, 951-954 (1985).
15. Martin, L. N. *et al. Adv. vet. Sci. comp. Med.* **28**, 201-236 (1984).
16. Montelaro, R. C., Lohfey, N., Tarekh, B., Blakeney, E. & Issel, C. *J. Virol.* **42**, 1029-1038 (1982).
17. Montelaro, R. C., Tarekh, B., Orrego, A. & Issel, C. *J. biol. Chem.* **259**, 10539-10544 (1984).
18. Burnett, W. N. *Analyt. Biochem.* **112**, 195-203 (1981).

Mechanism of activation of *HuBlym*-1 gene unresolved

Joan M. Devine*

Dana Farber Cancer Institute, 44 Binney Street, Boston, Massachusetts 02115, USA

The *HuBlym*-1 gene has been isolated from Burkitt's lymphoma DNA on the basis of its reported ability to produce foci of cells when NIH 3T3 cells are transfected with it[1,2]. The sequence of *HuBlym*-1 has been reported[1] but it has not been established whether the sequence of the transforming gene differs from that of the gene in normal tissue, as might be expected from the common observation of mutational activation of proto-oncogenes into oncogenes. I report here that there are no differences between the sequences of three recombinant DNA clones that were isolated from Burkitt's cell lines and that cross-hybridize to *HuBlym*-1 but do not induce foci when transfected into NIH 3T3 cells, and the reported sequence of Burkitt's lymphoma *Blym*[3]. Also there is no obvious or consistent increase in the transcription of the *HuBlym*-1 gene in Burkitt's lymphoma cell lines of the type that might otherwise have accounted for its transforming activity even in the absence of a mutation. How the *HuBlym*-1 gene is activated therefore remains a mystery.

Total genomic DNAs isolated from six Burkitt's lymphoma cell lines have been reported to induce foci with an efficiency of between 0.1 and 1.0 transformants per μg DNA when transfected into NIH 3T3 cells[2]. The gene responsible for this transforming ability, *HuBlym*-1, has been cloned from the Burkitt's lymphoma cell line CW678 (ref. 2). This cloned gene transforms NIH 3T3 cells with high efficiency and has the same pattern of restriction enzyme sensitivity in a transfection assay[2,4] as the genomic DNA from all six Burkitt's lymphoma cell lines[2]. The biologically active transforming gene is contained within a 1.0-kilobase(kb)*Eco*RI fragment of the clone[2]. This fragment has been subcloned into a plasmid, pHuBlym-1, and its nucleotide sequence determined[3]. The gene is 600–700 nucleotides long and is apparently interrupted by a single intervening sequence, yielding a predicted polypeptide of 58 amino acids[3]. Previous, though not extensive, studies indicate that the *HuBlym*-1 gene is neither amplified nor rearranged in Burkitt's cell lines[3], therefore other possible mechanisms of activation of the *HuBlym*-1 gene have to be considered. It is known that *ras* genes can be activated to a transforming phenotype by a single base mutation at position 12 or 61 (refs 5, 6), or by coupling to a viral long terminal repeat (LTR) which gives enhanced transcription of the gene[7,8]. Thus, two possible mechanisms for the activation of the *HuBlym*-1 gene are changes in its nucleotide sequence and changes in the level of transcription of the gene.

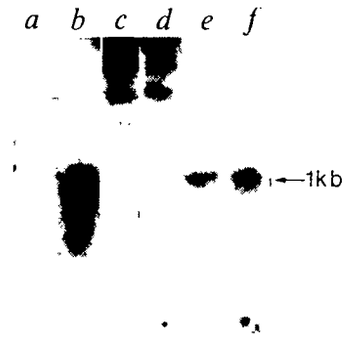


Fig. 1 Southern transfer of DNA clones isolated from λ clones and probed with *HuBlym*-1. *a*, The λ marker, which does not hybridize to the probe. *b*, λHuBlym-1 DNA digested with *Eco*RI. A 1-kb fragment hybridizes to the 1-kb probe which is its exact homologue. *c–f*, *Eco*RI-digested DNAs from clones isolated from the λ libraries constructed in EMBL3: *c*, *d*, DNAs from the EW36 λ library. The DNA in *c* did not transform NIH 3T3 cells whereas that in *d* did. *e*, *f*, DNA from Raji λ library. The DNA in *e* did not transform NIH 3T3 cells; that in *f* did. DNAs were isolated, digested with *Eco*RI, run on a 0.3% agarose gel and then transferred to nitrocellulose. The filter was probed with the ^{32}P-labelled 1-kb *Eco*RI fragment from pHuBlym-1. The 1-kb fragments in *c–f* were subcloned into pBR322 and their nucleotide sequences determined.

During the original isolation of λHuBlym-1, a number of other clones were isolated which hybridized to the *ChBlym*-1 probe[2,9]; these clones were screened together with λHuBlym-1 in a transfection assay. λHuBlym-1 was selected because it transformed NIH 3T3 cells whereas 14 other clones did not (A. Diamond, personal communication). As these other clones could contain the non-transforming counterpart of the *HuBlym*-1, they have now been analysed by digestion with *Eco*RI, gel electrophoresis and Southern blotting to identify those that contain a DNA insert similar to that in λHuBlym-1.

DNAs from six of the clones showed restriction enzyme digestion patterns similar to that of λHuBlym-1, including the presence of a 1.0-kb *Eco*RI fragment which in λHuBlym-1 contains the active transforming HuBlym-1 gene[2] (Fig. 1*b*). The 1.0-kb fragment from one of the clones was subcloned in pBR322 and the nucleotide sequence of both strands was determined, using a combination of the dideoxy chain termination method[10]

* Present address: Celltech Ltd, 250 Bath Road, Slough SL1 4EN, Berkshire, UK.

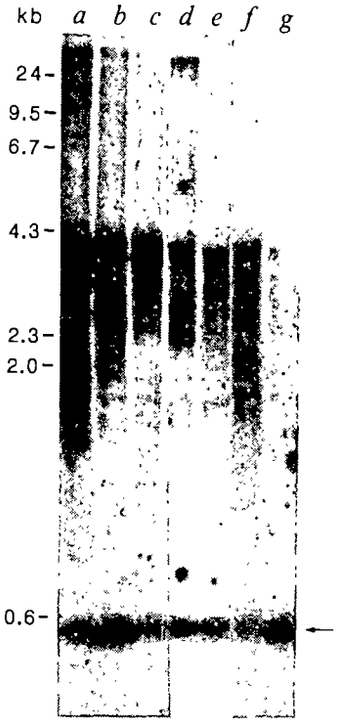


Fig. 2 Hybridization of *HuBlym*-1 probe to poly(A)$^+$ RNA. *a–c*, RNAs isolated from Burkitt's lymphoma cell lines CW678, EW36 and Raji, respectively. *d*, *e*, RNAs isolated from the EBV-immortalized cell lines LAZ φ156 and LAZ 388. *f*, RNA from a pre-B-cell line; *g*, RNA from a myeloma cell line. The size markers shown are λ DNAs digested with *Hin*dIII. The arrow indicates the *Blym* band at ~600 bases. Total RNA was isolated, poly(A)$^+$ RNA selected and samples (10 μg) of poly(A)$^+$ RNA run on a 1.5% formaldehyde gel. The RNA was then transferred to a nitrocellulose filter, which was hybridized to ^{32}P-labelled plasmid pHuBlym-1.

and chemical sequencing[11]. The nucleotide sequence observed was exactly the same as that already determined for *HuBlym*-1. This result was completely unexpected. In order to confirm it, recombinant DNA libraries were constructed from the DNAs of two other Burkitt's cell lines: EW36, an American Epstein-Barr virus (EBV)-negative line[12], and Raji, an African EBV-positive line[13]. These lines were chosen as they represent both associated and non-associated EBV lines[14] and because they are clearly of different origin. Both have been shown to transform NIH 3T3 cells[2]. The DNAs of these cells were partially digested with *Mbo*I, size-fractionated and ligated into the *Bam*HI site of the λ vector EMBL4. After *in vitro* packaging, the library was screened with the 1.0-kb *Eco*RI fragment from pHuBlym-1 and plaques hybridizing to this probe were selected. Both intact phage and DNA were separately used to transfect NIH 3T3 cells. Two subsets of clones were picked from each of the libraries: those that induced transformation of NIH 3T3 cells and those that did not. DNAs from the two groups were then screened for the presence of a 1.0-kb *Eco*RI fragment (Fig. 1*c–f*). Four clones which contained a 1.0-kb *Eco*RI fragment were selected: one from each of the two Burkitt's libraries that transformed NIH 3T3 cells and one from each of the two that did not transform NIH 3T3 cells. The 1.0-kb fragment from each clone was subcloned into pBR322. In this case also, the nucleotide sequence of the two transforming and one of the two non-transforming clones were shown to be identical to the sequence of the original transforming *HuBlym*-1 (approximately 60% of the other non-transforming gene was sequenced and found to be identical).

All the genes described and sequenced so far in this paper were isolated from DNA obtained from Burkitt's lymphoma cell lines. It was therefore important to clone and isolate the corresponding DNA sequence from a recombinant DNA library prepared from a non-Burkitt's lymphoma cell line. DNA was therefore isolated from the IMR 90 cell line[15], which is a human embryo fibroblast line that is not immortalized but which grows well for 20–30 passages[15]. The recombinant DNA library was prepared and screened as above except that the lambda vector used was λ47.1. Two clones homologous to the 1.0-kb *Eco*RI fragment probe isolated from pHuBlym were selected, their 1.0-kb *Eco*RI fragments were subcloned and the nucleotide sequences of both strands determined for one of the subclones. Again, the sequences were identical to that of *HuBlym*-1.

The level of transcription of *HuBlym* in several Burkitt's lymphoma cell lines and in several other human cell lines was investigated by Northern transfer analysis (Fig. 2). In all the lines examined, a messenger RNA of ~600 bases was detected at a similar level, indicating that the induction of foci by DNA from Burkitt's lymphoma cell lines is not a consequence of increased transcription of the *HuBlym*-1 gene.

The nucleotide sequences of the three non-transforming alleles of *HuBlym*-1 described here are identical to the sequence reported for the allele that induced focus formation in NIH 3T3 cells[3]. The results of the mRNA analysis demonstrate that increased levels of *HuBlym* mRNA are not detected in Burkitt's lymphoma cell lines, however there is always a problem in knowing what to use to make a proper comparison. The way in which the *HuBlym*-1 gene is activated therefore remains an open question.

I thank Dr Geoffrey Cooper for his hospitality during this work and for his willingness to read the assays for focus formation that were part of these experiments. I also thank Dr John Cairns for stimulating discussions and helpful comments on the manuscript. J.M.D. was supported by a Travelling Fellowship from the ICRF, London and by a special Fellowship from the Leukaemia Society of America.

Received 5 November 1985; accepted 28 February 1986.

1. Graham, F. V. & van der Eb, A. J. *Virology* **52**, 456–467 (1973).
2. Diamond, A., Cooper, G. N., Ritz, J. & Lane, M. A. *Nature* **305**, 112–116 (1983).
3. Diamond, A., Devine, J. M. & Cooper, G. M. *Science* **225**, 516–519 (1984).
4. Lane, M. A., Sainten, A. & Cooper, G. M. *Cell* **28**, 873–880 (1982).
5. Taparowsky, E. *et al. Nature* **300**, 762–765 (1982).
6. Capon, D. J., Chen, E. Y., Levinson, A. D., Seeburg, P. H. & Goeddel, D. V. *Nature* **302**, 33–37 (1983).
7. De Feo, D. *et al. Proc. natn. Acad. Sci. U.S.A.* **78**, 3328–3332 (1981).
8. Chang, E. H., Furth, M. E. Scolnick, E. H. & Lowry, D. R. *Nature* **297**, 479–483 (1982).
9. Goubin, G., Goldman, D. S., Luce, J., Neiman, P. E. & Cooper, G. M. *Nature* **302**, 114–119 (1982).
10. Sanger, F., Nicklen, S. & Goulson, A. K. *Proc. natn. Acad. Sci. U.S.A.* **74**, 5463–5467 (1977).
11. Maxam, A. M. & Gilbert, W. *Meth. Enzym.* **65**, 499–560 (1980).
12. Magrath, I T. *et al. J. natn. Cancer Inst.* **64**, 465–470 (1980).
13. Epstein, M. A. *et al. J. natn. Cancer Inst.* **37**, 547–559 (1966).
14. Epstein, M. A. & Achong, B. G. (eds) in *The Epstein Barr Virus*, 322–337 (Springer, New York, 1979).
15. Nichols, W. W. *et al. Science* **196**, 60–63 (1977).

COOPER AND DIAMOND REPLY—The work reported by Dr Devine was in part performed in this laboratory and was to have been completed here following her departure in October 1984. At that time, transfection experiments were to be performed on the clones isolated from normal human DNA and the sequence of the clone from normal human DNA required completion to resolve several existing ambiguities and gaps. However, we found that all of the clones from the Raji and EW36 Burkitt's lymphoma libraries used by Devine contained cellular inserts whose restriction endonuclease cleavage patterns were indistinguishable from each other and from the original isolate of λ HuBlym-1. Since these clones were isolated from libraries constructed with DNAs partially digested with *Mbo*I, these results strongly indicated the possibility of contamination of Devine's isolates with the original transforming clone. In addition, transfection assays performed and read by Devine before she left the laboratory indicated that the clones designated by her as "non-transforming" from the CW678 and EW36 Burkitt's lymphoma libraries induced transformation with efficiencies comparable to the clones designated "transforming". Restriction digests of the clones isolated from a random library of normal human DNA were also found to be identical to the original λ HuBlym-1 isolate, again raising concerns about contamination. We therefore concluded that a bona fide normal copy of the gene had to be isolated and analysed in order to exclude the possibility of contamination of the clones on which Devine has reported.

A clone of the 5-kilobase (kb) *Hin*dIII fragment containing *Blym*-1 was therefore reisolated from normal human DNA. The restriction map of this clone is different from other *Blym*-1

clones in the laboratory, ruling out the possibility of cross-contamination. The 1-kb *Eco*RI fragment of this clone induces transformation of NIH 3T3 cells with efficiencies comparable to that of the 1-kb *Eco*RI fragment of the original λ HuBlym-1 clone. Both of these clones have also displayed comparable activities in assays of transformation of primary human foreskin fibroblasts to anchorage independence and transformation of BALB.3T3 cells to platelet-derived growth factor-independent growth. Further, the nucleotide sequences of the 1-kb *Eco*RI fragments of the normal and Burkitt's lymphoma clones are identical.

We therefore conclude that activation of transforming potential does not require a mutation within the minimal 1-kb transforming region of *Blym*-1. These results suggest the hypothesis that flanking sequences may regulate transforming activity and experiments are now in progress to test this possibility. The notion that regulatory changes may be involved in activating transforming genes is not inconsistent with the fact that there are no significant increases in the total level of expression of *Blym*-1 in Burkitt's lymphomas compared with Epstein-Barr virus-immortalized cell lines. In fact this situation is similar to that observed with *myc*, where its activation by translocation appears to result in de-regulation of gene expression rather than in a significant increase in *myc* RNA levels in most Burkitt's lymphomas and plasmacytomas[1-4].

GEOFFREY M. COOPER
ALAN DIAMOND

Dana-Farber Cancer Institute,
and Department of Pathology,
Harvard Medical School,
Boston, Massachusetts 02115, USA

1. Hann, S. R. & Eisenman, R. N. *Molec. cell. Biol.* 4, 2486-2497 (1984).
2. Keath, E. J., Keleker, A. & Cole, M. D. *Cell* 37, 521-528 (1984).
3. Ramsay, G., Evan, G. I. & Bishop, J. M. *Proc. natn. Acad. Sci. U.S.A.* 81, 7742-7746 (1984).
4. Taub, R. *et al. Cell* 36, 339-348 (1984).

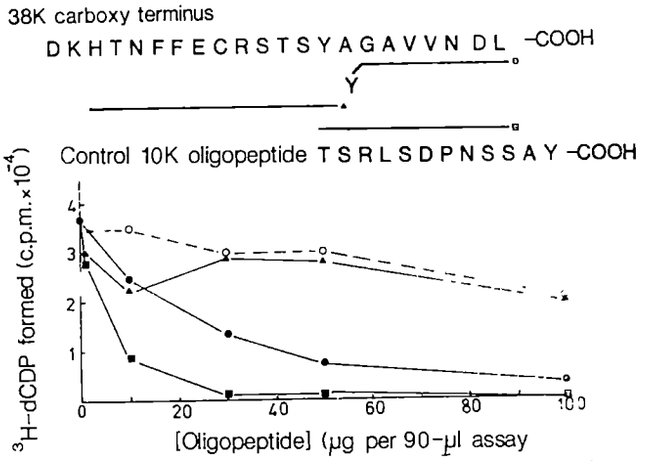


Fig. 1 Effect of synthetic oligopeptides on ribonucleotide reductase activity in an extract of HSV-1-infected baby hamster kidney (BHK) cells. The figure shows the effects of increasing concentrations of peptides 1-4 (●, ○, ■ and ▲, respectively). DK···DL—COOH represents the 22 amino acid sequence of the 38K carboxy terminus. Horizontal lines indicate the amino acid sequences of peptides 1, 3 and 4.

Methods. Synthetic oligopeptides were obtained from Cambridge Research Biochemicals (Cambridge, UK) and Peptide and Protein Research Consultants (Windsor, UK). Crude extracts were obtained from virus-infected cells as described elsewhere[6] and partially purified by precipitation with 45% ammonium sulphate. Ribonucleotide reductase was assayed by determining the amount of cytidine diphosphate (CDP) converted to deoxycytidine diphosphate (dCDP) in a 90-μl reaction (for 1 h at 31 °C) containing 100 μg partially purified extract, 200 mM HEPES *p*H 8.2, 10 mM dithiothreitol (DTT), 100 μM CDP and 1 μCi ^{3}H-CDP (10-30 Ci mmol^{-1}). The nucleotides were converted to the corresponding nucleosides by digestion with snake venom phosphodiesterase and the resulting cytidine and deoxycytidine separated by reverse-phase HPLC (B.M.D., in preparation). In the conditions of this assay, the host cell enzyme is inactive and only the viral enzyme contributes to the measured activity.

Specific inhibition of herpesvirus ribonucleotide reductase by synthetic peptides

Bernadette M. Dutia*, Margaret C. Frame, John H. Subak-Sharpe, William N. Clark & Howard S. Marsden†

MRC Virology Unit, Institute of Virology, University of Glasgow, Church Street, Glasgow G11 5JR, UK

Ribonucleotide reductase is an essential enzyme for DNA synthesis in all prokaryotic and eukaryotic cells; it catalyses the reductive conversion of ribonucleotides to deoxyribonucleotides. Several herpesviruses including herpes simplex virus type 1 (HSV-1)[1], HSV-2[2], pseudorabies virus (PRV)[3], equine herpesvirus type 1 (EHV-1)[4] and Epstein-Barr virus (EBV)[5] have been found to induce novel ribonucleotide reductase activities. There is evidence that the HSV-1 ribonucleotide reductase activity is virus-encoded[6] and essential for virus replication[7]. This makes herpesvirus ribonucleotide reductases potential targets for antiviral chemotherapy. The HSV-1-encoded enzyme consists of two subunits[8,9,18]: V136, the large subunit of relative molecular mass (M_r) 136,000 (136K) (RR_1), which has been shown to be essential for enzyme activity[7], and V38, the small subunit (RR_2) which forms a complex with the large subunit and is also likely to be essential for enzyme activity[9]. Two particular features of the enzyme make it an attractive antiviral target. First, there is evidence for a common, highly conserved herpesvirus ribonucleotide reductase and second, the interaction between the large and small subunits may itself be exploitable. Here we identify a synthetic peptide which specifically inhibits the activity of virus-induced enzyme. We deduce that the mechanism of inhibition involves interference with the normal interaction between the two types of subunit.

The discovery of an oligopeptide which inhibits ribonucleotide reductase activity arose from experiments designed to show that both RR_1 and RR_2 were necessary for enzyme activity. To this end, RR_2 was removed from an enzyme extract of HSV-1-infected cells by immunoaffinity chromatography using IgG from serum raised against the synthetic octapeptide NH_2-Tyr-Gly-Ala-Val-Val-Asn-Asp-Leu-COOH (YGAVVNDL, using the one-letter code). This peptide corresponds to the carboxy-terminal seven amino acids of RR_2 plus an amino-terminal tyrosine added to facilitate linkage to a carrier protein[9]. Immunoaffinity chromatography was performed by first adsorbing the enzyme extract with immune anti-peptide IgG immobilized on Sepharose 4B. After stringent washing, bound RR_2 was eluted with the synthetic peptide. However, attempts to reconstitute the enzyme activity by adding back purified RR_2 were unsuccessful at least because the synthetic peptide necessarily present with eluted RR_2 inhibits enzyme activity (see below). Frame *et al.*[9] had previously obtained indirect evidence that the carboxy terminus of RR_2 is masked by the large subunit; this suggested that the synthetic peptide might correspond to a region

* Present address: Department of Veterinary Pathology, Royal (Dick) School of Veterinary Studies, Edinburgh EH9 1QH, UK.
† To whom correspondence should be addressed.

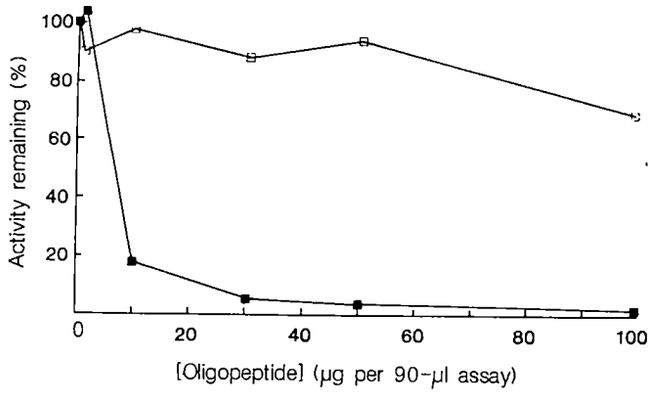


Fig. 2 Inhibition by the synthetic peptide 3 (see Fig. 1 and text) is specific for the viral and not the cellular ribonucleotide reductase. Partially purified extracts were obtained from either HSV-1-infected (■) or uninfected (□) BHK cells, and HSV-1-infected ribonucleotide reductase activity was assayed as described in Fig. 1 legend. The assay was modified to measure mammalian enzyme activity and contained 100 mM HEPES *p*H 7.6, 2.7 mM ATP, 2.7 mM magnesium acetate, 10 mM DTT, 55 μM CDP and 1 μCi ^{3}H-CDP (10–30 Ci mmol^{-1}). The enzyme activity is expressed as a percentage of that found in the absence of oligopeptide. The 100% values correspond to 51,806 and 17,064 c.p.m. of ^{3}H-dCDP formed by the infected and uninfected cell extracts, respectively.

of the small subunit involved in interacting with the large subunit. We suspected that the synthetic peptide might compete for a site on the large subunit and displace the small subunit.

Ribonucleotide reductase activity in extracts of HSV-1-infected and mock-infected cells was assayed in the presence of various concentrations of the synthetic oligopeptide YGAVVNDL (peptide 1). The results show that peptide 1 inhibits virus-specific activity (Fig. 1). Peptide 2 (NH_2-Thr-Ser-Arg-Leu-Ser-Asp-Pro-Asn-Ser-Ser-Ala-Tyr-COOH, TSRLSDPNSSAY), which corresponds to the amino-terminal sequence of the 10K protein product of the HSV-1 gene US9 (ref. 10), was included in the experiment as a control and did not inhibit activity.

A comparison of the predicted amino-acid sequences of ribonucleotide reductases from HSV-1, HSV-2, EBV, *Escherichia coli*, clam and sea urchin[11–15] and varicella zoster virus (VZV)[16] shows that the tyrosine residue at position 9 from the carboxy-terminal end of the herpesvirus RR_2 is conserved in all species[17]; this led us to speculate that this tyrosine was particularly important for enzyme function. We therefore tested two further oligopeptides, one corresponding to the carboxy-terminal nonapeptide NH_2-Tyr-Ala-Gly-Ala-Val-Val-Asn-Asp-Leu-COOH (YAGAVVNDL, peptide 3) and differing from peptide 1 by the inclusion of an alanine residue between the tyrosine and glycine residues, and the other a tridecapeptide NH_2-Ser-His-Thr-Asn-Phe-Phe-Glu-Cys-Arg-Ser-Thr-Ser-Tyr-COOH (HTNFFECRS-TSY, peptide 4), which corresponds to the conserved tyrosine residue and the adjoining 12 amino acids on the amino-terminal side. Figure 1 shows that peptide 3 is a more effective inhibitor than peptide 1 whereas peptide 4 is at best only marginally inhibitory. In this experiment the concentration of peptide giving 50% inhibition of enzyme activity was 4.5 μg per assay for peptide 3 and 21 μg per assay for peptide 1, which shows that peptide 3 is approximately five times more inhibitory than peptide 1.

To test whether the inhibition of ribonucleotide reductase activity by peptide 3 was specific for the virus-induced enzyme, we investigated the effect of the peptide on the viral and cellular enzymes. Figure 2 shows that the inhibition is specific for the virus-induced enzyme and has little effect on the cellular enzyme.

The highly conserved carboxy-terminal amino-acid sequence of HSV-1 and HSV-2 (refs 12, 13), EBV[15] and VZV[16] led us to test whether the antigenic domain(s) recognized by the anti-peptide 1 serum described above is also conserved in other herpesviruses. Extracts from cells infected with HSV-1, HSV-2, VZV, PRV and EHV-1 were made and immunoprecipitations performed as described elsewhere[9]. In those experiments no immunoprecipitation of any cellular proteins was observed. Figure 3 shows that RR_2 is specifically immunoprecipitated from extracts of cells infected with any of these herpesviruses and that RR_1 is co-precipitated from cells infected with HSV-1, HSV-2 and PRV but not VZV and EHV-1. This result suggests that PRV, like HSV-1 and HSV-2, has two types of interacting ribonucleotide reductase subunits and that their site of interaction is likely to be a common target for the inhibitory oligopep-

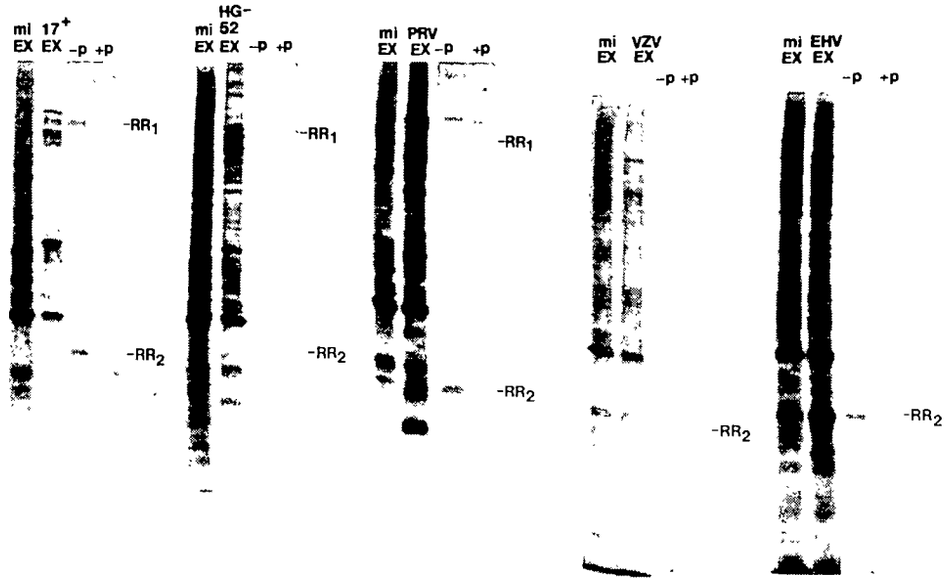


Fig. 3 Immunoprecipitation of polypeptides from extracts of cells infected with herpesviruses HSV-1 (strain 17 syn$^+$), HSV-2 (strain HG52), PRV, VZV and EHV-1, using IgG purified from an antiserum (14119) raised against the carboxy-terminal seven amino acids of the small ribonucleotide reductase subunit (RR_2) of HSV-1 and HSV-2. ^{35}S-methionine-labelled extracts of BHK cells infected with HSV-1, HSV-2 and PRV were prepared as described elsewhere[9]. Rabbit kidney (RK) cells were infected with EHV-1 in a similar manner. HFL cells were infected with VZV by co-culturing confluent monolayers with VZV-infected HFL cells. Immunoprecipitations were carried out as described elsewhere[9] in extraction buffer containing 0.5% SDS. IgG was purified from antiserum 14119 by ion-exchange chromatography and used in immunoprecipitations with (+p) and without (−p) 100 μg of the synthetic peptide 1, against which the antiserum was raised[9]. Lanes designated mi EX, 17$^+$ EX, HG52 EX, PRV EX, VZV EX and EHV EX show ^{35}S-methionine-labelled polypeptide profiles for mock-infected, HSV-1 (strain 17 syn$^+$), HSV-2 (strain HG52), PRV, VZV and EHV-infected cell extracts, respectively. RR_1 and RR_2 are, respectively, the large and small herpesvirus ribonucleotide reductase subunits.

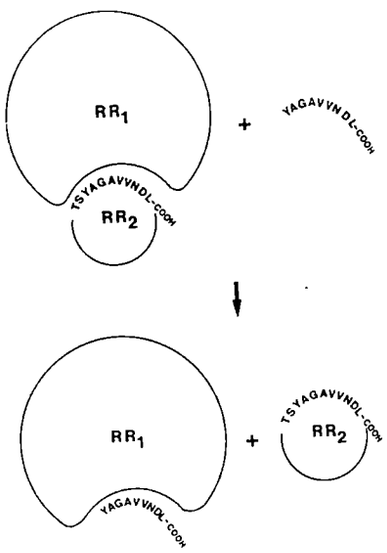


Fig. 4 Possible mechanism for inhibition of the herpes virus ribonucleotide reductase by the synthetic peptide 3.

tides. For EHV-1 and VZV the situation is less clear—different conditions may well be necessary to co-precipitate RR_1 with RR_2 from cells infected with these viruses.

Figure 4 presents a model to explain the inhibition of enzyme activity based on evidence indicating that the two subunits interact via the carboxy terminus of RR_2 (ref. 9). The model proposes that the inhibitory nonapeptide prevents the association of the two subunits by competing for the subunit binding site on RR_1, displacing RR_2. The model is not intended to imply that only one large and one small subunit combine to form the active enzyme, or that the carboxy-terminal region is the only site involved in the interaction between the small and large subunits.

The potential therapeutic implications of specific inhibition of the subunit interaction are being investigated. Exposure of infected cell monolayers to various concentrations of the nonapeptide (peptide 3) did not reduce the yield of infectious virus; this is probably because the peptide is too large to enter the cell unaided. Present efforts are directed towards identification of smaller peptides which specifically inhibit ribonucleotide reductase activity both *in vitro* and *in vivo*.

We thank Mrs M. Murphy, Mrs A. Orr and Mr G. Hope for technical assistance; Dr J. B. Clements, Dr A. J. Davison and Dr J. McLauchlan for helpful discussions; and Ms A. Cullinane for providing the stock of EHV. We also thank Miss F. Conway and Mrs A. Simpson for typing the manuscript.

Received 23 December 1985; accepted 18 March 1986.

1. Cohen, G. H. *J. Virol.* **9**, 408–418 (1972).
2. Cohen, G. H., Factor, M. N. & Ponce De Leon, M. *J. Virol.* **14**, 20–25 (1974).
3. Lankinen, H., Graslund, A. & Thelander, L. *J. Virol.* **41**, 893–900 (1982).
4. Cohen, J. C., Henry, B. E., Randall, C. C. & O'Callaghan, D. J. *Proc. Soc. exp. Biol. Med.* **155**, 395–399 (1977).
5. Henry, B. E., Glaser, R., Hewetson, J. & O'Callaghan, D. J. *Virology* **89**, 262–271 (1978).
6. Dutia, B. M. *J. gen. Virol.* **64**, 513–521 (1983).
7. Preston, V. G., Palfreyman, J. W. & Dutia, B. M. *J. gen. Virol.* **66**, 1581–1587 (1984).
8. Cohen, E. A., Charron, J., Perret, J. & Langelier, Y. *J. gen. Virol.* **66**, 733–745 (1985).
9. Frame, M. C., Marsden, H. S. & Dutia, B. M. *J. gen. Virol.* **66**, 1581–1587 (1985).
10. McGeoch, D. J., Dolan, A., Donald, S. & Rixon, F. J. *J. molec. Biol.* **181**, 1–13 (1985).
11. Standart, N. M., Bray, S. J., George, E. L., Hunt, T. & Ruderman, J. V. *J. Cell Biol.* **100**, 1968–1976 (1985).
12. McLauchlan, J. & Clements, J. B. *J. gen. Virol.* **64**, 997–1006 (1983).
13. McLauchlan, J. & Clements, J. B. *EMBO J.* **2**, 1953–1961 (1983).
14. Carlson, J., Fuchs, J. A. & Messing, J. *Proc. natn. Acad. Sci. U.S.A.* **81**, 4294–4297 (1984).
15. Gibson, T., Stockwell, P., Ginsberg, M. & Barrell, B. *Nucleic Acids Res.* **12**, 5087–5099 (1984).
16. Davison, A. J. & Scott, J. E. *J. gen. Virol.* (in the press).
17. Sjoberg, B.-M. *et al. FEBS Lett.* **183**, 99–102 (1985).
18. Bachetti, S., Evelegh, M J & Muirhead, B. *J. Virol* **57**, 1177–1181 (1986).

Specific inhibition of herpesvirus ribonucleotide reductase by a nonapeptide derived from the carboxy terminus of subunit 2

E. A. Cohen*, P. Gaudreau†, P. Brazeau† & Y. Langelier*

* Institut du Cancer de Montréal and † Laboratoire de Neuroendocrinologie, Centre de Recherche de l'Hôpital Notre-Dame, Centre Hospitalier Notre-Dame, 1560 rue Sherbrooke est, Montréal, Québec, Canada H2L 4M1

Ribonucleotide reductase, an essential enzyme for the synthesis of deoxyribonucleotides, is formed by the association of two non-identical subunits in almost all prokaryotic and eukaryotic cells[1]. The same model probably holds for the herpes simplex virus (HSV)-encoded ribonucleotide reductase[2–6]; two polypeptides of relative molecular mass 136,000 (136K; H1) and 40K (H2) (referred to elsewhere as RR_1 and RR_2; see for example, Dutia *et al.*[26]) have been associated with the viral enzyme by both genetic[7,8] and immunological[9–11] studies. Furthermore, DNA sequence analyses have shown significant stretches of amino-acid homology between these viral polypeptides and those of, respectively, subunit 1 (ref. 12) and subunit 2 (ref. 13) of the *Escherichia coli* and mammalian enzymes. To assess the involvement of the 40K polypeptide in reductase activity, we synthesized a nonapeptide corresponding to the sequence of its carboxy terminus with the intention of raising neutralizing antibodies specific for the viral activity (E.A.C. *et al.*, in preparation). We report here the unexpected finding that the nonapeptide itself specifically inhibits the HSV ribonucleotide reductase activity in a reversible, non-competitive manner, and we suggest that it does this by impairment of the correct association of the two subunits. This phenomenon emphasizes the potential usefulness of synthetic peptides in probing critical sites involved in macromolecular interactions.

The nonapeptide NH_2-Tyr-Ala-Gly-Ala-Val-Val-Asn-Asp-Leu-COOH, corresponding to the carboxy-terminal nine amino acids of the HSV type 1 (HSV-1) 40K and HSV-2 38K polypeptides (as predicted from the DNA sequences[14,15]), was synthesized by the solid-phase technique of Merrifield[16] and its primary structure verified by quantitative amino-acid analysis after acid hydrolysis and digestion with leucine aminopeptidase. The preparation was 99% pure as determined by HPLC. HSV-1 or HSV-2 ribonucleotide reductase was partially purified from quiescent BHK-21/C13 cells infected respectively with strain F and strain HG-52 at 20 plaque-forming units (PFU) per cell, whereas the cellular enzyme was obtained from exponentially growing BHK-21/C13 cells or hydroxyurea-resistant 96-V-2(600) cells. The latter cells exhibit high ribonucleotide reductase specific activity owing to overproduction of the two enzyme subunits (ref. 17 and our unpublished observations for subunit 1).

Figure 1 shows the effect of the synthetic peptide on the HSV-1 enzyme: 50% inhibition was observed with 22 μM nonapeptide and total inhibition was obtained with a concentration of 400 μM. The curve obtained for the HSV-2 enzyme was almost identical (data not shown). The cellular enzyme extracted from 96-V-2(600) (Fig. 1) or BHK-21/C13 cells (data not shown) was completely insensitive to the presence of the peptide in the assay up to a concentration of 1 mM. To show that this specific effect was due to the nonapeptide rather than attributable to some trace contaminants, we used an anti-nonapeptide rabbit serum with specific neutralizing activity against the HSV ribonucleotide reductase activity (E.A.C. *et al.*, in preparation). Purified IgG (5 μg, which gave 60% neutralization in the absence of peptide) was pre-adsorbed with increasing concentrations of nonapeptide

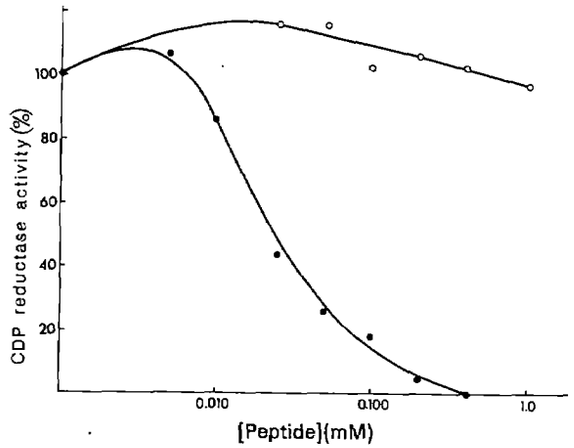


Fig. 1 Effect of the synthetic nonapeptide on viral (●) and cellular (○) ribonucleotide reductase activities. One unit (U) of ribonucleotide reductase activity is defined as the amount of enzyme generating 1 nmol of dCDP per h under the standard assay conditions. The results are expressed as a percentage of the activity obtained in the controls without nonapeptide.

Methods. Viral and cellular ribonucleotide reductases were, respectively, partially purified from HSV-1 (strain F)-infected confluent BHK-21/C13 cells and exponentially growing 96-V-2(600) cells by precipitation of the cell extract with ammonium sulphate as described elsewhere[6]. Aliquots of the viral (50 μg; specific activity 30 U mg^{-1}) or cellular (40 μg; specific activity 34 U mg^{-1}) enzyme preparation were mixed with increasing concentrations of nonapeptide, and ribonucleotide reductase activity was assayed by monitoring the reduction of CDP as described previously[6]. Briefly, the standard reaction mixture, in a final volume of 60 μl, contained: 50 mM HEPES *p*H 7.8, 4 mM $MgCl_2$, 4 mM ATP, 4 mM NaF, 6 mM DTT, 54 μM CDP and 0.25 μCi ^{3}H-CDP. For the viral activity, $MgCl_2$ and ATP (which are non-essential for this activity) were usually omitted and 20 mM DTT was used instead. These changes did not affect the inhibition by the nonapeptide. After 30 min of incubation at 37 °C, the reaction was stopped by immersing the tube in boiling water for 4 min and the precipitate removed by centrifugation. Nucleotides in the supernatant were converted to nucleosides by enzymatic hydrolysis. The deoxyribonucleosides were subsequently separated from the ribonucleosides by ascending polyethyleneimine-cellulose chromatography.

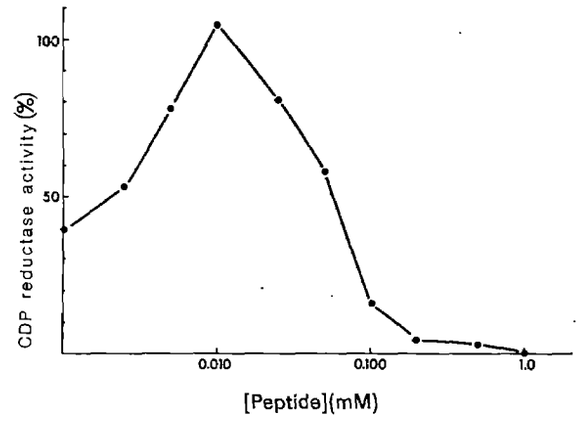


Fig. 2 Effect of the nonapeptide on the neutralizing activity of an anti-nonapeptide antiserum. The anti-nonapeptide antiserum (P9) was obtained by immunizing a rabbit with the nonapeptide conjugated to methylated bovine serum albumin, as described elsewhere[25]. IgGs were purified from the P9 serum by adsorption to a column of protein A-Sepharose CL-4B (Pharmacia), followed by elution with 0.1 M glycine *p*H 2.5. After incubation of 5 μg of P9 IgGs with increasing concentrations of nonapeptide for 30 min at 20 °C, 50 μg of partially purified HSV-1 ribonucleotide reductase (specific activity 30 U mg^{-1}) was added to each sample. After a second incubation of 30 min at 20 °C, ribonucleotide reductase activity was assayed as outlined in Fig. 1 legend.

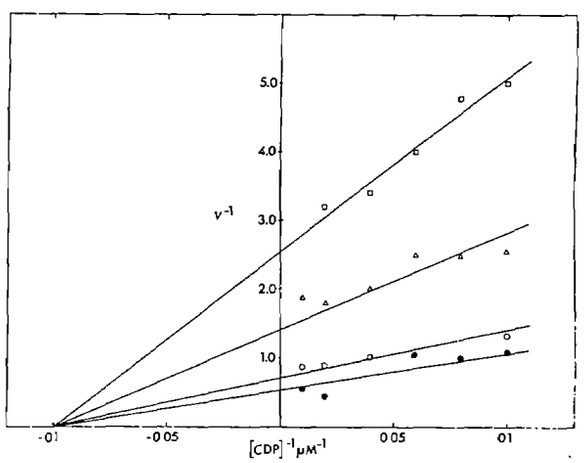


Fig. 3 Double-reciprocal plot of velocity (v) versus CDP concentrations at different nonapeptide concentrations. Aliquots of partially purified HSV-1 enzyme preparation were mixed with the following nonapeptide concentrations: 0 μM (●), 15 μM (○), 25 μM (△), 50 μM (□), and assayed using the standard reaction mixture as described in Fig. 1 legend, except that CDP was added at the appropriate concentrations.

and preincubated with 50 μg of viral enzyme before the ribonucleotide reductase assay. At low nonapeptide concentrations, the ability of the IgG to neutralize the enzyme activity was progressively eliminated until equivalence was reached at 10 μM (see Fig. 2). Subsequently, the activity was inhibited but the curve was displaced to the right relative to that in Fig. 1, as expected if the nonapeptide is responsible for the inhibition.

As further controls for the specificity of the inhibition, we also examined the effect of the nonapeptide on other HSV-encoded enzymatic activities involved in DNA metabolism: thymidine kinase, DNA polymerase and DNase. These viral enzymes were specifically measured respectively by phosphorylation of ^{3}H-bromodeoxycytidine[18], ^{3}H-dGTP incorporation in activated DNA in the presence of 150 mM ammonium sulphate[19], and solubilization of ^{3}H-thymidine from *in vivo* labelled DNA assayed at *p*H 9.0 (ref. 20). None of these enzymatic activities was affected by the presence of 1 mM of the nonapeptide (data not shown), indicating that the action of the inhibitor was specific to the HSV ribonucleotide reductase activity.

We next investigated the mechanism of action of this inhibitor. As HSV ribonucleotide reductase activity could be completely restored when the nonapeptide was removed by dialysis from a preparation of enzyme preincubated with 1 mM nonapeptide, we concluded that the inhibition was reversible. Preincubation of the peptide with the viral enzyme did not change the degree of inhibition observed at given peptide concentrations. Measurement of the initial rate of product formation in the presence of inhibitor revealed that the change in the velocity (v) of the reaction was very rapid, being already established after 2 min. These results suggested that the peptide did not need any modification by a factor present in the extract to become active. The nature of the inhibition was determined by varying the CDP concentration at several fixed concentrations of nonapeptide. By means of a double reciprocal plot, we demonstrated that the nonapeptide behaved as a non-competitive inhibitor with respect to CDP (Fig. 3). The K_i, calculated by re-plotting $1/v$ against the inhibitor concentration, gave a value of 15 μM. By using the same type of analysis, we determined that this inhibitor also does not compete with the reducing agent dithiothreitol (DTT).

To explain the unexpected inhibitory activity of the nonapeptide, we hypothesize that the carboxy terminus of the presumptive subunit 2 (H2) of the HSV ribonucleotide reductase

is directly involved in binding with subunit 1 (H1). Thus, the carboxy-terminal nonapeptide would compete with H2 for some critical binding site and effectively prevent the formation of the active holoenzyme; this notion is supported by the observed specificity of the inhibition for the viral enzyme, as the nonapeptide does not share significant amino-acid homology with subunit 2 of the cellular enzyme[13] and thus presumably does not interact with the cellular subunit 1. Our findings that the inhibition is reversible and non-competitive with respect to the substrate and the reducing agent are also in agreement with this hypothesis. However, at present we cannot exclude other possibilities such as the inhibition by the nonapeptide of some essential interaction between viral subunit 2 and other cellular protein(s) or constituent(s). These hypotheses should be testable by crosslinking studies using radiolabelled nonapeptide.

Here we report that a synthetic peptide derived from the amino-acid sequence of an enzyme behaves as a specific inhibitor of the enzyme, adding another area of research in which synthetic peptides have proved useful. Synthetic peptides have been used largely to examine the interactions between proteins and receptors[21-24]. We predict that the use of such synthetic peptides, derived from amino-acid sequences implicated in the association of proteins with receptors, membranes, DNA, RNA or enzyme subunits, will be of prime importance in elucidating macromolecular interactions. Moreover, it is tempting to speculate that synthetic peptides could have potential in antiviral chemotherapy. In this respect, we are testing the effect of our nonapeptide on replication of HSV.

We thank Claire Guilbault for technical assistance and Lucille Beaudet for the assays of HSV thymidine kinase, DNA polymerase and DNase. We also thank W. H. Lewis for his gift of the 96-V-2(600) cell line and V. Bibor-Hardy and W. E. C. Bradley for critical reading of the manuscript. This work was supported by grants from NCI (Canada) to Y.L. and from MRC (Canada) to P.B. E.A.C. is the recipient of a studentship from La Société de Recherche sur le Cancer and P.G. of a postdoctoral fellowship from FRSQ (Québec).

Received 23 January; accepted 10 March 1986.

1. Thelander, L. & Reichard, P. *A. Rev. Biochem* **48**, 133-158 (1979)
2. Ponce de Leon, M., Eisenberg, R. J. & Cohen, G. H *J. gen Virol* **36**, 163-173 (1977)
3. Huszar, D. & Bacchetti, S. *J. Virol.* **37**, 580-588 (1981)
4. Langelier, Y. & Buttin, G. *J. gen. Virol.* **57**, 21-31 (1981).
5. Averett, D. R., Lubbers, C., Elion, G. B. & Spector, T. *J. biol. Chem* **258**, 9831-9838 (1983)
6. Cohen, E. A., Charron, J., Perret, J. & Langelier, Y. *J. gen Virol* **66**, 733-745 (1985)
7. Dutia, B. M. *J. gen. Virol.* **64**, 513-521 (1983).
8. Preston, V. G., Palfreyman, J. W. & Dutia, B. M. *J gen. Virol.* **65**, 1457-1465 (1984)
9. Huszar, D., Beharry, S. & Bacchetti, S. *J. gen. Virol.* **64**, 1327-1335 (1983)
10. Bacchetti, S., Evelegh, M. S., Muirhead, B., Sartori, C. S. & Huszar, D. *J. Virol.* **52**, 491-501 (1984).
11. Frame, M. C., Marsden, H. S. & Dutia, B. M. *J. gen. Virol.* **66**, 1581-1587 (1985)
12. Caras, I. W., Levinson, B. B., Fabry, M., Williams, S. R. & Martin, D. W. Jr *J. Biol. Chem.* **260**, 7015-7022 (1985).
13. Sjöberg, B. M *et al. FEBS Lett.* **183**, 99-102 (1985).
14. Draper, K. G., Frink, R. J. & Wagner, E. K. *J. Virol.* **43**, 1123-1128 (1982)
15. Galloway, D. A. & Swain, M. A. *J. Virol.* **49**, 724-730 (1984)
16. Merrifield, B. *J Am. chem. Soc.* **85**, 2149-2154 (1963)
17. Lewis, W. H. & Srinivasan, P. R. *Molec. cell. Biol* **3**, 1053-1061 (1983)
18. Summers, W. C. & Summers, W. P. *J. Virol.* **24**, 314-318 (1977)
19. Weissbach, A., Hong, S.-C. L., Aucker, J. & Muller, R *J. biol. Chem* **248**, 6270-6277 (1973)
20. Francke, B. & Garrett, B. *Virology* **116**, 116-127 (1982).
21. Akiyama, S. K & Yamada, K. M. *J. biol. Chem.* **260**, 10402-10405 (1985)
22. Gartner, K. T. & Bennet, J. S. *J. biol. Chem.* **260**, 11891-11894 (1985)
23. Ferreto, P., Guidotti, A., Conti-Tronconi, B. & Costa, E. *Neuropharmacology* **23**, 1359-1361 (1984)
24. Gillespie, L. L. *et al. J. biol. Chem.* **260**, 16045-16048 (1985).
25. Benoit, R. *et al. Proc. natn. Acad. Sci. U.S.A.* **79**, 917-921 (1982).
26. Dutia, B. M., Frame, M. C., Subak-Sharpe, J. H., Clark, W. N. & Marsden, H. S. *Nature* **321**, 439-441 (1986).

Re-routing of a secretory protein by fusion with human growth hormone sequences

Hsiao-ping H. Moore* & Regis B. Kelly†

* Department of Physiology-Anatomy, University of California, Berkeley, California 94720, USA
† Department of Biochemistry and Biophysics, University of California, San Francisco, California 94143, USA

Cells with electron-dense secretory vesicles use them to store only specialized secretory products such as peptide hormones; other types of secreted proteins are externalized by an alternative, constitutive route[1]. One possible mechanism for such segregation is that proteins destined for dense secretory vesicles contain unique 'sorting domains'[2] that allow for selective targeting. Here, we set out to determine whether a constitutively secreted protein could be diverted to the dense secretory vesicles by attachment to a peptide hormone sequence. We made use of the ability of the mouse pituitary tumour cell line, AtT-20, to correctly sort exogenous secretory proteins introduced into them by DNA transfection[3]. We constructed a plasmid encoding a hybrid protein in which a constitutively secreted viral protein was fused to the carboxy terminus of human growth hormone (hGH). Cells expressing the hybrid protein were found to target it to dense secretory vesicles with an efficiency close to that observed for the parental hGH. These results support the hypothesis that sorting domains on peptide hormones direct their packaging into dense secretory vesicles. The results also suggest that proteins secreted by the constitutive pathway either do not contain any sorting domain, or their sorting signals can be overridden by those which direct peptide hormones.

Generation of fusion proteins is a useful means of studying the targeting of nuclear, mitochondrial, vacuolar and membrane proteins to their correct destinations[4-9]. To construct a hybrid between a constitutively secreted protein and a protein destined for dense secretory vesicles (that is, destined for the regulated pathway), we fused the hGH sequence to the truncated vesicular stomatitis virus (VSV) G sequence (Fig. 1*a*). The truncated G protein (designated TG) contains an intact 432-amino-acid luminal region of the G protein but lacks the entire membrane-spanning and cytoplasmic domains (79 amino acids from the carboxy terminus)[10]. When transfected separately into AtT-20 cells, hGH was found to be transported to the regulated pathway while TG was exported efficiently by the constitutive pathway[3]. Figure 1*b* illustrates the strategy for constructing a precise in-frame fusion between the two coding sequences. An hGH complementary DNA including 35 bases of the 5'-untranslated sequence[11] was first inserted in the appropriate orientation between the Rous sarcoma virus (RSV) long terminal repeat (LTR) promoter and the TG coding sequences in an expression vector (step 1 in Fig. 1*b*). A fragment containing the hGH-TG sequences was subcloned into an M13 vector, and a 200-base pair (bp) sequence at the junction of hGH and TG was deleted by oligonucleotide-directed mutagenesis (steps 2, 3 in Fig. 1*b*). As shown in Fig. 1*a*, the resulting sequences encode a hybrid protein in which the last amino acid of hGH is joined directly to the first amino acid of the mature TG protein, which lacks its signal peptide. We found that ~2% of the M13 phage plaques had incorporated the desired mutation. To ensure that no other mutations had been introduced during the mutagenesis procedure, we sequenced the entire insert, including regions outside the mutated area, before cloning it back into the RSV-LTR expression vector (step 4 in Fig. 1*b*).

Figure 2 shows immunoprecipitation analyses of cellular and secreted proteins from an AtT-20 cell line that had been stably transformed with the chimaeric plasmid described above. As neither hGH nor TG is normally processed from larger precursor propeptides, it was predicted that the fusion protein would be a single polypeptide with a relative molecular mass (M_r) equal to the sum of those of hGH (22,000; SSK) and TG (54-56K). The transformed cells synthesized a protein with an apparent

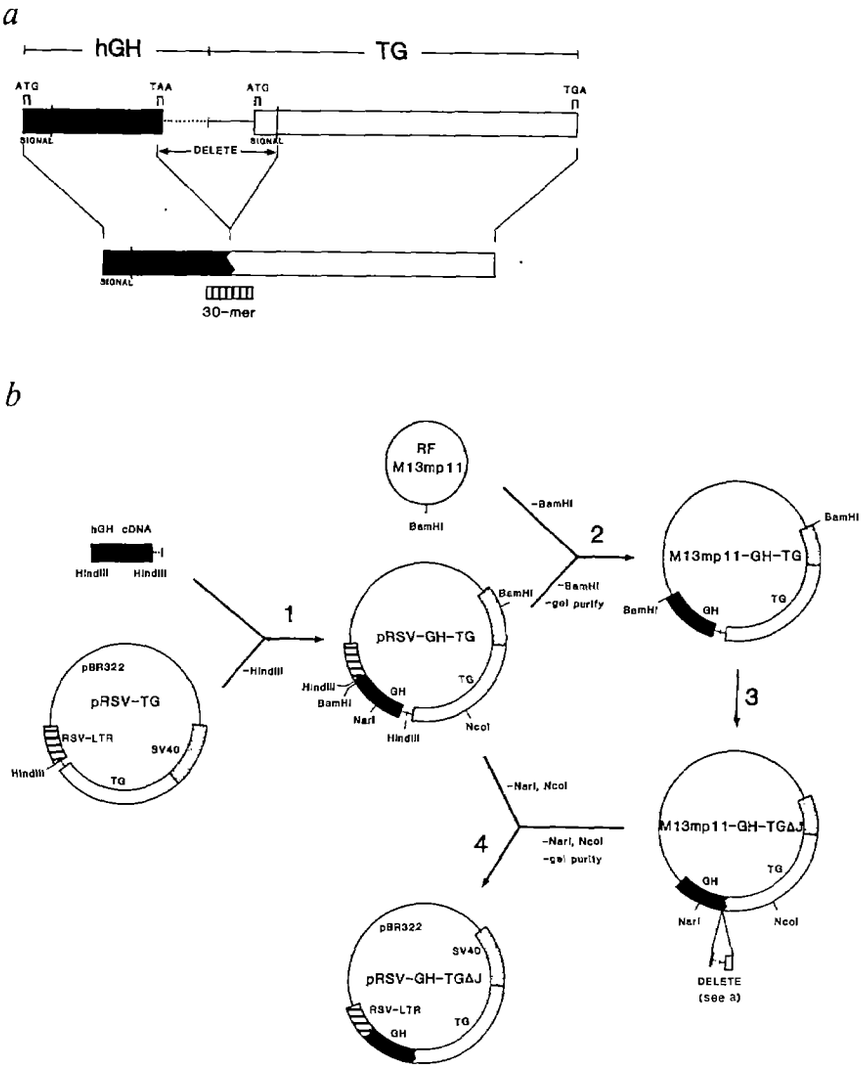


Fig. 1 *a*, Structure of a hGH-TG hybrid created by oligonucleotide-directed mutagenesis. A 30-mer mutagenic primer was used to delete the hGH-TG junctional region, including the stop codon and the 3′-untranslated sequences of hGH, and the 5′-untranslated sequences and the 16-amino-acid signal peptide of the truncated G protein. Half of the primer is complementary to the 15-base sequence immediately downstream from the signal peptide of TG; the other half is complementary to the last 15 bases of the mature hGH coding sequences. *b*, Construction of an expression vector containing the hGH-TG hybrid. The full-length hGH cDNA, carried on a *Hin*dIII fragment (chGH800/pBR322; ref. 11), was inserted in the *Hin*dIII site of pRSV-TG, the plasmid vector used previously to express a truncated VSV G protein in AtT-20 cells[3] (step 1). A 3.0-kilobase (kb) *Bam*HI fragment spanning the entire hGH and truncated G sequences was then subcloned into M13mp11 (step 2). The fusion junction was modified by site-directed mutagenesis using the single-stranded M13 DNA as a template (step 3; see *a*). An 814-base pair (bp) fragment emcompassing the modified fusion junction was then cloned back into the expression vector pRSV-hGH-TG as a *Nar*I/*Nco*I fragment (step 4). ▨, RSV LTR; ■, hGH sequences; □, TG sequences; ▩, simian virus 40 splice junction and polyadenylation site; —, pBR322 sequences; ▥, mutagenic primer.

Methods. pRSV-TG (100 ng) was digested with *Hin*dIII, treated with phosphatase and then ligated to 100 ng of an 803-bp *Hin*dIII fragment which had been excised from chGH800 and purified on agarose gels. Plasmids with the hGH sequences inserted in the same orientation as TG were isolated and digested with *Bam*HI. The 3.0-kb fragment was purified on agarose gels, ligated to *Bam*HI-digested, phosphatase-treated M13mp11 vector, and used to transform *Escherichia coli* JM101. Single-stranded phage DNA was prepared and sequenced by the dideoxy method[18] to ensure the correct orientation of the insert. One pmol of the single-stranded template was annealed simultaneously to 20 pmol of 5′ phosphorylated mutagenic primer and 20 pmol of a second, 15-base primer. The latter anneals to sequences 180 bp away from the mutagenic primer, in the TG coding region. After *in vitro* synthesis in the presence of DNA polymerase large fragment (Klenow) and T_4 ligase, the reaction mixture was used to transform *E. coli* JM101. Phage plaques carrying the desired mutation were identified by hybridization to [5′-^{32}P]-labelled mutagenic primer, followed by washing under conditions of appropriate stringency. DNA from the purified plaque was sequenced by dideoxy sequencing to confirm the mutation. The *Nar*I/*Nco*I fragment was then excised from the M13 vector, gel-purified, and ligated to pRSV-GH-TG, which had been digested with *Nco*I and *Nar*I and treated with phosphatase.

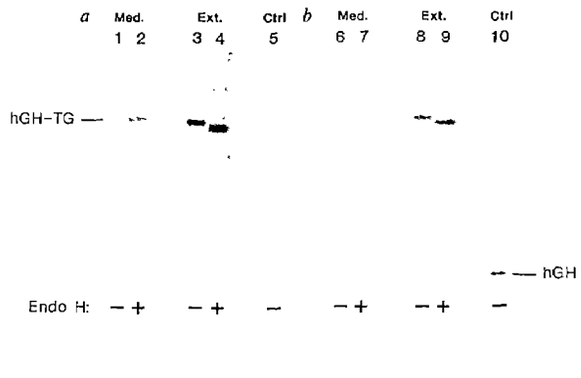


Fig. 2 Transformed AtT-20 cells synthesize and secrete a glycosylated hGH-TG hybrid protein. An AtT-20 cell line stably transformed with the plasmid pRSV-GH-TGΔJ was radiolabelled with ^{35}S-methionine for 13 h. Cellular and secreted proteins were then analysed by immunoprecipitation with anti-VSV (*a*) or anti-hGH (*b*) antisera, followed by SDS-polyacrylamide gel electrophoresis (SDS-PAGE). Lanes 1, 2, 6 and 7 are autoradiograms of immunoprecipitates from samples of medium, and lanes 3, 4, 8 and 9 are from cell extracts. As a control, samples of medium from cells expressing hGH protein not fused to TG were analysed in parallel (lanes 5, 10). Samples in lanes 2, 4, 7 and 9 were digested with Endo H before electrophoresis.

Methods. A 10-cm dish of AtT-20 cells was transfected with 120 μg of pRSV-GH-TGΔJ and 24 μg of pSV2-neo by the calcium phosphate procedure[3]. Clones surviving the G-418 selection were picked and screened by hGH radioimmunoassay (Hybritech). Cells from a positive clone, I17, were labelled, and medium and extract samples were prepared and analysed according to published procedures[3].

M_r of ~72–75K that could be precipitated by both anti-VSV (Fig. 2, lane 3) and anti-hGH (Fig. 2, lane 8) antisera. The specificity of the immunoprecipitation reaction was demonstrated by the fact that authentic hGH could be precipitated only by the anti-hGH (Fig. 2, lane 10), not the anti-VSV (lane 5) antiserum. The fusion polypeptide was secreted into the culture medium by the transformed cells (Fig. 2, lanes 1, 6), and the secreted form exhibited similar immunoreactivity with both antisera. The fusion protein could also be detected by a hGH radioimmunoassay (Hybritech, La Jolla, California) (data not shown); by this assay, the rate of synthesis of the hybrid protein was estimated to be 0.3 pmol per h per mg cell protein. As this is much less than the level of the endogenous hormone, adrenocorticotropic hormone (ACTH; 18 pmol per h per mg cell protein), it is unlikely to perturb the sorting machinery.

The glycosylation pattern of the fusion protein suggests that it traverses the normal secretory compartments before secretion. VSV G has two *N*-linked oligosaccharide addition sites whereas hGH is not glycosylated. The fusion protein acquires post-translational glycosylation similar to that of the truncated G protein. The predominant intracellular form of the fusion protein bears oligosaccharides of the high mannose type and is sensitive to endoglycosidase H (Endo H) digestion (Fig. 2, lanes 3,4 and 8, 9). A minor band with a slightly slower mobility, not apparent in the exposure of Fig. 2, was also detected in the cell extracts, especially after 1–2 h of chase (not shown); this form bears oligosaccharides of the complex type and is resistant to Endo H digestion. In contrast, the secreted fusion protein is exclusively Endo H-resistant (Fig. 2, lanes 1, 2 and 6, 7). Almost identical patterns were also found for ACTH (not shown).

The above results suggest that the conformation of the two parent proteins has not been drastically altered in the hybrid protein. First, the hGH moiety of the hybrid preserved sufficient antigenicity for measurement by radioimmunoassay and immunoprecipitation (note that a monoclonal antibody and two different polyclonal antibodies were used). Similarly, the TG portion retained sufficient antigenicity to be recognized by an anti-VSV-specific antiserum. Furthermore, the glycosylation sites on TG were still available.

To determine whether the hGH sequences could divert TG to the dense secretory vesicles, we examined the effects of secretagogues on the secretion of the hybrid protein. As we have shown previously, secretagogues stimulate the secretion of only those proteins that are packaged in dense secretory vesicles[12], thereby providing a simple test for the secretory pathway taken by the hybrid protein. Cells were labelled with ^{35}S-methionine for 16 h and then chased for 6 h to reduce the background contributed by constitutive secretion[3]. We then determined the effect of the secretagogue 8-bromocyclic AMP (8-Br-cAMP) on the rate of secretion. We have demonstrated previously that secretagogue-stimulated cells show enhanced secretion of hGH but not of TG, indicating that only the former is packaged into the regulated secretory vesicles. Those results were confirmed here (Fig. 3*b*). Under the same conditions, secretion of the hGH–TG fusion protein was clearly stimulated (Fig. 3*a* (lanes 3, 4) and *b*). To quantitate the extent to which the hybrid protein is sorted into the regulated pathway, we calculated the increase in the amount of secretion induced by 8-Br-cAMP and normalized it to the steady-state rate of secretion. The 'sorting indices' obtained by such quantitation (described in detail in ref. 3) indicate that the hGH–TG hybrid enters the regulated secretory vesicles with ~50% the efficiency of hGH (0.43 for hGH compared with 0.22 for hGH–TG; see legend to Fig. 3*b*). This extent of sorting is at least comparable to, if not better than, that of the endogenous hormone ACTH (0.14; see Fig. 3*b*). Thus, because of the attachment of hGH sequences, the truncated G protein has acquired the ability to be packaged into regulated secretory vesicles.

Conceivably, sorting of proteins into the two pathways could be achieved by means of sorting domains present on either the

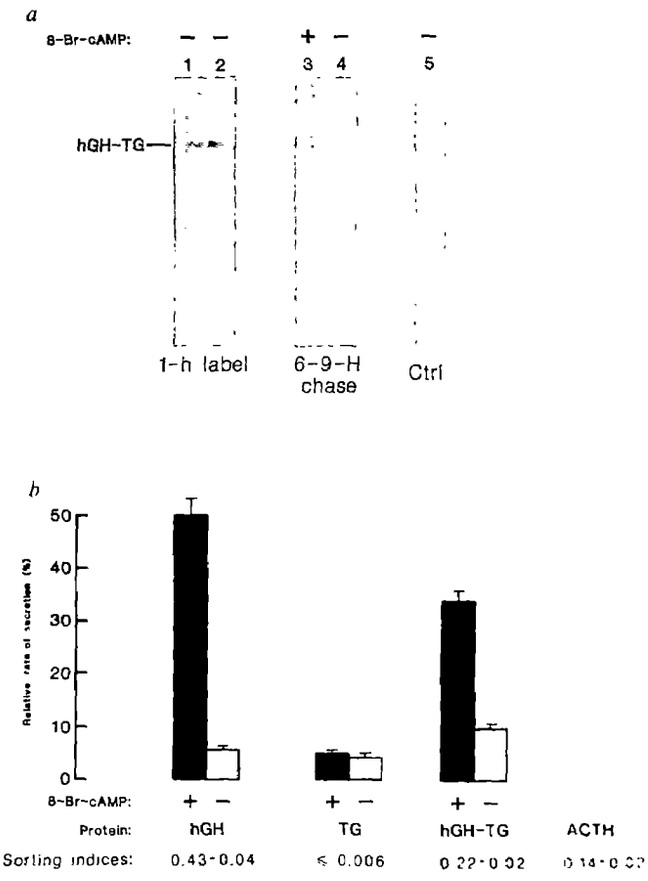


Fig. 3 The hGH–TG hybrid protein is secreted by a secretagogue-dependent, regulated pathway. *a*, Lanes 1 and 2, secretion of ^{35}S-methionine-labelled hybrid proteins from two identical dishes before stimulation. The amount represents total secretion during 1 h of continuous labelling. Lanes 3 and 4, secretion from stimulated and unstimulated cultures, respectively, during a 3-h chase period. Lane 5, control medium collected from untransfected AtT-20 cells. *b*, Comparison of the effects of the secretagogue 8-Br-cAMP on the secretion of hGH, TG and the hGH–TG hybrid protein. For each protein, the rate of secretion in the presence (+) or absence (−) of 5 mM 8-Br-cAMP was measured after cells had been radiolabelled for 16 h and chased for 6 h as in lanes 3 and 4 of *a*. Radioactivity associated with each protein was quantitated by scanning the autoradiograms, and was corrected for the duration of stimulation. Values plotted have been normalized to the rate of secretion measured immediately before the chase (lanes 1 and 2 in *a*). Sorting indices were calculated as described previously[3]. **Methods.** Two 10-cm dishes of I17 cells were each incubated with 0.5 mCi ^{35}S-methionine for 15 h to approach steady-state labelling. For normalization, proteins secreted into the medium during the ensuing hour were collected in the continuing presence of the radiolabel (lanes 1 and 2 in *a*). To test the effect of 8-Br-cAMP on secretion, the labelled cells were first chased for 6 h. During the next 3-h chase, one dish was stimulated with 5 mM 8-Br-cAMP and the other was not. Samples of medium were collected and immunoprecipitated with excess anti-VSV antiserum (lanes 3 and 4 in *a*). For controls, cells synthesizing unfused hGH or TG protein[3] were analysed in parallel using anti-hGH or anti-TG antiserum, respectively. Immunoprecipitation was carried out with the following modifications. Samples were incubated with excess antiserum and precipitated with *Staphylococcus aureus* cells, then the immunoprecipitates were eluted from the cells in 1% SDS at 37 °C for 20 min. The supernatant was diluted to 0.2% SDS and additional antiserum added. After further precipitation with *S. aureus* cells, the immunoprecipitates were eluted from the cells by boiling in Laemmli gel sample buffer. Under these conditions, the specific binding was not significantly altered but the background was drastically reduced[17].

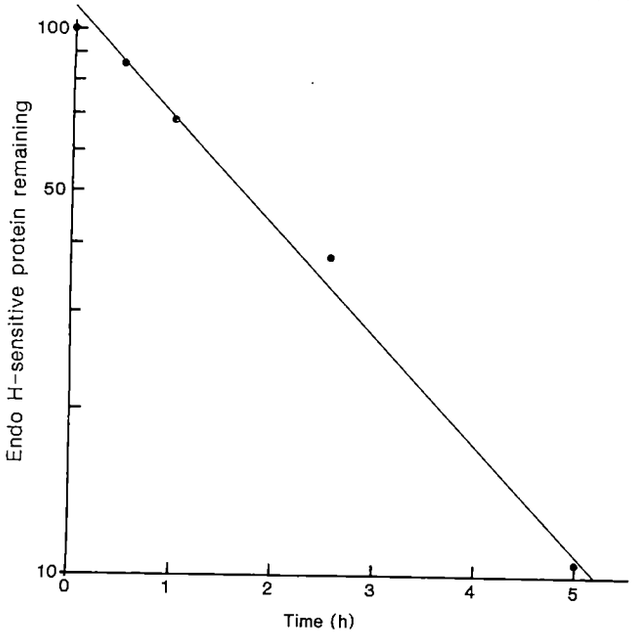


Fig. 4 hGH-TG hybrid protein exits from the RER at a rate characteristic of the TG protein. Cells were pulse-labelled with ^{35}S-methionine and chased for the times indicated. At each time point, the fraction of hybrid protein remaining sensitive to Endo H digestion was calculated from the total hybrid protein recovered in the cell extract and in the medium. Linear regression analysis shows a $t_{0.5}$ of 100 min for the conversion of Endo H-sensitive to Endo H-resistant forms.

Methods. Identical wells of I17 cells were pulse-labelled with ^{35}S-methionine for 10 min, then chased for 30 min, 1 h, 2.5 h and 5 h. At each time point, medium was collected and cells were extracted with detergents[3]. Forty per cent of the extract samples and 100% of the medium samples were immunoprecipitated with an anti-VSV antiserum, digested with Endo H, and analysed by 15% SDS-PAGE. The radioactivity associated with each form was quantitated by scanning the bands and correcting for the amount analysed.

constitutive or the regulated secretory proteins. The other class of proteins would then be transported to the second pathway by a nonspecific, bulk-flow process. Alternatively, both classes may contain sorting signals. Our data support the idea that sorting is effected by active signals on proteins destined for the regulated pathway. The constitutively secreted TG protein may lack any sorting signal, or its sorting domain may be subordinate to those of the peptide hormones. The suggestion that sorting domains are not a mandatory requirement for proteins to exit via the constitutive pathway is consistent with several earlier observations. Under conditions where intracellular targeting is perturbed by drug treatment[13], genetic disorder[14] or overproduction of the transported proteins (T. H. Stevens, G. Payne and R. Schekman, in preparation), the mis-localized proteins from the dense secretory vesicles, lysosomes or vacuoles do not accumulate within the cells, but are secreted continuously into the medium. The constitutive pathway thus appears to be a default route for any soluble protein that cannot find another destination. Therefore, the effective diversion of TG by hGH sequences probably reflects a lack of sorting signals on the VSVG fragment.

While the hGH domain appears to dominate the post-Golgi sorting of the fusion protein, its rate of movement out of the rough endoplasmic reticulum (RER) resembles more closely that of the truncated VSV G protein. In all cell lines examined previously, hGH is transported rapidly out of the RER, the half time ($t_{0.5}$) of RER export in transfected AtT-20 cells being less than 20 min (J. Rose, personal communication, and H.-P.H.M., data not shown). In contrast, TG leaves the RER much more slowly[3,10], with $t_{0.5}$, as measured by the acquisition of Endo H-resistant terminal glycosylation, being 90–100 min. Using similar criteria, we found that conversion of the hGH–TG hybrid from the Endo H-sensitive to the Endo H-resistant forms occurred at a rate comparable to that of TG (Fig. 4): 50% conversion occurred at ~100 min after the chase. Thus the slow movement of the hybrid protein from the RER appears to predominate over the fast movement.

Cellular carriers or receptors have been proposed to explain the different rates at which secreted proteins move from the RER to the Golgi apparatus[15,16]. If such carriers recognize features of newly synthesized proteins, the fusion protein strategy should be equally suited to identifying such features. It is noteworthy, therefore, that the rate at which the fusion protein exits from the RER is determined by a different region from that which determines its sorting into secretory vesicles. If export from the RER were indeed carrier-mediated, it would involve a receptor different from that which effects targeting to the secretory vesicles. An alternative, perhaps more attractive, hypothesis consistent with our observations is that movement out of the RER does not involve specific carriers. In this case, export of TG (and therefore of its fusion product) is retarded simply as a result of its delayed folding as an abnormal secretory protein in the RER.

This work was supported by NIH grant AM 33937 (to R.B.K.), and by Juvenile Diabetes Career Development Award 284087 and NIH grant GM 35239-01 (to H.-P.H.M.). We thank Dr Steve Gardell for assistance in the mutagenesis techniques; Dr Kevin Moore, Dr Peter Walter and Ms Sharon Powell for critical reading of the manuscript; and Mr David Quinn for the graphic work.

Received 6 January; accepted 14 March 1986.

1. Kelly, R. B. *Science* **230**, 25-32 (1985).
2. Blobel, G. *Proc. natn. Acad. Sci. U.S.A.* **77**, 1496-1500 (1980).
3. Moore, H.-P. H. & Kelly, R. B. *J. Cell Biol.* **101**, 1773-1781 (1985).
4. Hall, M. N., Hereford, L. & Herskowitz, I. *Cell* **36**, 1057-1065 (1984).
5. Emr, S. D., Bankaitis, V. A., Garrett, J. M. & Douglas, M. G. in *Protein Transport and Secretion* (ed. Gething, M.-J.) (Cold Spring Harbor Laboratory, New York, 1985).
6. Hurt, E. C., Pesold-Hurt, B. & Schatz, G. *EMBO J.* **3**, 3149-3156 (1984).
7. Silhavy, T. J. & Beckwith, J. *Meth. Enzym.* **97**, 11-40 (1983).
8. Doyle, C., Roth, M., Sambrook, J. & Gething, M.-J. *J. Cell Biol.* **100**, 704-714 (1985).
9. Guan, J.-L., Machamer, C. E. & Rose, J. K. *Cell* **42**, 489-496 (1985).
10. Rose, J. K. & Bergmann, J. E. *Cell* **30**, 753-762 (1982).
11. Martial, J. A., Hallewell, R. A., Baxter, J. D. & Goodman, H. M. *Science* **205**, 602-607 (1979).
12. Moore, H. P., Gumbiner, B. & Kelly, R. B. *J. Cell Biol.* **97**, 810-817 (1983).
13. Moore, H.-P. H., Gumbiner, B. & Kelly, R. B. *Nature* **302**, 434-436 (1983).
14. Neufeld, E. F., Lim, T. W. & Shapiro, L. J. *AZ. Rev. Biochem.* **44**, 357-376 (1975).
15. Lodish, H. F., Kong, N., Snider, M. & Strous, G. J. A. M. *Nature* **304**, 80-83 (1983).
15. Lodish, H. F., Kong, N., Snider, M. & Strous, G. J. A. M. *Nature* **304**, 80-83 (1983).
16. Fries, E., Gustafsson, L. & Peterson, P. A. *EMBO J.* **3**, 147-152 (1984).
17. Firestone, G. L. *J. biol. Chem.* **258**, 6155-6161 (1983).
18. Sanger, F., Nicklen, S. & Coulson, A. R. *Proc. natn. Acad. Sci. U.S.A.* **74**, 5463-5467 (1977).

Expression of biologically active viral satellite RNA from the nuclear genome of transformed plants

David C. Baulcombe*, Graham R. Saunders*, Michael W. Bevan*, Michael A. Mayo† & Bryan D. Harrison†

* Department of Molecular Genetics, Plant Breeding Institute, Maris Lane, Trumpington, Cambridge CB2 2LQ, UK
† Department of Virology, Scottish Crop Research Institute, Invergowrie, Dundee DD2 5DA, UK

The particles of cultures of cucumber mosaic virus (CMV) contain the three genomic species of single-stranded RNA and a subgenomic species that acts as messenger RNA for CMV particle protein. Some cultures also contain a single-stranded linear RNA molecule that is typically ~335 nucleotides long[1,2]. This extra molecule, termed satellite RNA, does not share appreciable nucleotide sequence with CMV genomic RNA[3] but replicates only in

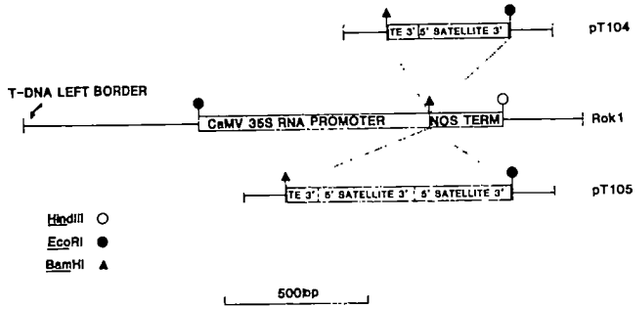


Fig. 1 Structure of the CMV satellite cDNA molecules in the binary Ti plasmid expression vectors. The cloning and nucleotide sequence of the CMV satellite RNA will be presented elsewhere. Briefly, at the 5′ end of the 104 construction there are 51 nucleotides from the polylinker of plasmid pT7-2 extending from the transcriptional start point and including polylinker sequences of pT7-2 and other vectors used in the construction of pT104. On the 3′ end of this, as shown in the diagram, there are 108 nucleotides extending from position 227 of the satellite sequence through to the 3′ nucleotide of the satellite unit at position 335 (TE 3′). Immediately 3′ of this there is a complete satellite unit, in the same orientation as the incomplete unit, flanked at the 3′ end by 16 nucleotides extending between the *Sma*I site and the *Eco*RI site of vector plasmid pT7-2 (ref. 22). The 105 construction is as 104, except that two complete satellite units, in the same orientation, are present. The insertions from 104 and 105 were excised by digestion with restriction endonucleases *Bam*HI and *Eco*RI, rendered blunt-ended by DNA polymerase (Klenow fragment) and inserted into the *Bam*HI site of binary Ti plasmid Rok1. The *Bam*HI site of Rok1 was rendered flush-ended by DNA polymerase (Klenow fragment). Rok1 is a derivative of the binary vector Bin19, described previously[11], containing additionally an expression cassette inserted into the polylinker site. The expression cassette comprised the promoter of cauliflower mosaic virus 35S RNA[23] and the terminator fragment of the nopaline synthase (*nos*) gene of *Agrobacterium* T-DNA[24] (NOS TERM). It is essentially similar to the expression cassette described for the expression of tobacco mosaic virus coat protein gene[12], except that the promoter fragment was deleted back to 6 bp 3′ of the cap site of the 35S transcript using *Bal*31 nuclease. The unique *Bam*HI site was inserted between the promoter and terminator fragments. Transcripts derived from this cassette would contain 10 nucleotides from the promoter and 200 nucleotides from the terminator[24] in addition to the sequence inserted at the *Bam*HI site. The figure shows only the region adjacent to the cDNA insert of pT104 and pT105 and the expression cassette region of Rok1.

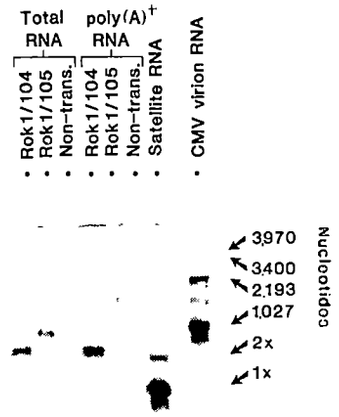


Fig. 2 Northern blot analysis of RNA from transformed plants. Total RNA (20 μg) or poly(A)$^+$ RNA (1 μg) was isolated from leaves of non-transformed plants (non-trans.) or plants transformed with Rok1/104 and Rok1/105 and fractionated on formaldehyde/agarose gels. The transcribed satellite RNA sequences were detected by blotting the gel onto nitrocellulose and hybridization with nick-translated insert from pT105. Total RNA from cells infected with CMV which contained satellite RNA was included as a reference for satellite RNA unit length (1×) and dimer length (2×) molecules. The size markers were virion RNA of CMV, which was detected with a cDNA clone (C20) of CMV genomic RNA (D.C.B., unpublished). This hybridized with CMV RNA-3, CMV RNA-4 and faintly with CMV RNA-1 and RNA-2. The size values given are those of Gould and Symons[25].

Methods. The constructions of pT104 and pT105 in Rok1 were mobilized into *Agrobacterium* strain LBA 4404 using *Escherichia coli* strain HB101 harbouring pRK2013 in a triparental mating, as described previously[11]. The resultant *Agrobacterium* strains containing the binary vector constructions were then used to infect leaf disks from axenically grown *N. tabacum* (cv. Samsun NN). The infected and transformed cells were regenerated into plants by culturing the disks successively on a layer of tobacco feeder cells and then on shoot- and root-inducing medium as described by Horsch *et al.*[26]. The shoot- and root-induction media contained kanamycin at 100 μg ml^{-1} to select for cells expressing the neomycin phosphotransferase gene contained in the T-DNA region of Rok1 (from Bin19)[11]. Transformed plants were propagated by transfer of stem cuttings into root induction medium. RNA isolations were as described by Apel and Kloppstech[27] and electrophoresis and blotting analysis as described by Goldberg[28] and Thomas[29].

plants[1] or protoplasts[4] that are infected with CMV. CMV isolates that do not contain satellite RNA can be cultured repeatedly in plants in a satellite-free state, but when satellite RNA is added to such cultures it is synthesized and persists as a component of the virus isolate[5]. The effect of satellite RNA on CMV infections depends on the strain of satellite: in many cases the usual symptoms of CMV are suppressed and as a result the infected plants show few symptoms of infection[6–8]. However, the presence of other strains of satellite RNA leads to the production of severe symptoms that are quite distinct from those of CMV[8]. Here we describe the transformation of tobacco plants with DNA copies of CMV satellite RNA, the production of satellite RNA transcripts by such plants and the acquisition of satellite RNA by CMV cultures grown in them. These results suggest a means of protecting plants against the effects of CMV and also suggest a method by which satellite RNAs may have evolved.

The satellite RNA used in this work was isolated from CMV strain $I_{17}N$ (ref. 7) and was cloned as complementary DNA. The nucleotide sequence of the cDNA clone was very similar to that of other strains of CMV satellite[2,9,10] and will be presented elsewhere, together with the construction of two head-to-tail concatemer satellite cDNA molecules. These comprised one (pT104) or two (pT105) complete satellite RNA sequence units with incomplete units at the 5′ end (Fig. 1) and were intended to mimic multimeric satellite RNAs that are thought to be replication intermediates (D.C.B., M.A.M., B.D.H. and G.R.S., unpublished results). To achieve expression of these satellite sequences in transformed plants, the cDNA molecules were transferred into an expression vector (Rok1) based on the binary Ti plasmid system of *Agrobacterium tumefaciens*[11,12]. The resultant plasmids are referred to as Rok1/104 and Rok1/105.

Transformed tobacco plants (cv. Samsun NN) were regenerated from *Agrobacterium*-infected leaf disks and were assayed for the presence of the satellite sequence in DNA and RNA by Southern and Northern blot analysis, respectively. The Southern blot analysis showed that the DNA of transformed plants contained the equivalent of 1–3 copies of the satellite cDNA per haploid genome, and also that the cDNA sequence, the promoter site and the RNA termination site had not been rearranged or deleted. The Northern blot analysis (Fig. 2) showed transcripts of ~700 nucleotides (Rok1/104) or 1,000 nucleotides (Rok1/105), which are the approximate sizes predicted from the location of promoter and terminator sequences in the original constructions (Fig. 1) and allowing for the presence of a 3′ polyadenylate tract. These RNA molecules were readily detected in total RNA or in polyadenylated RNA. No virus-like

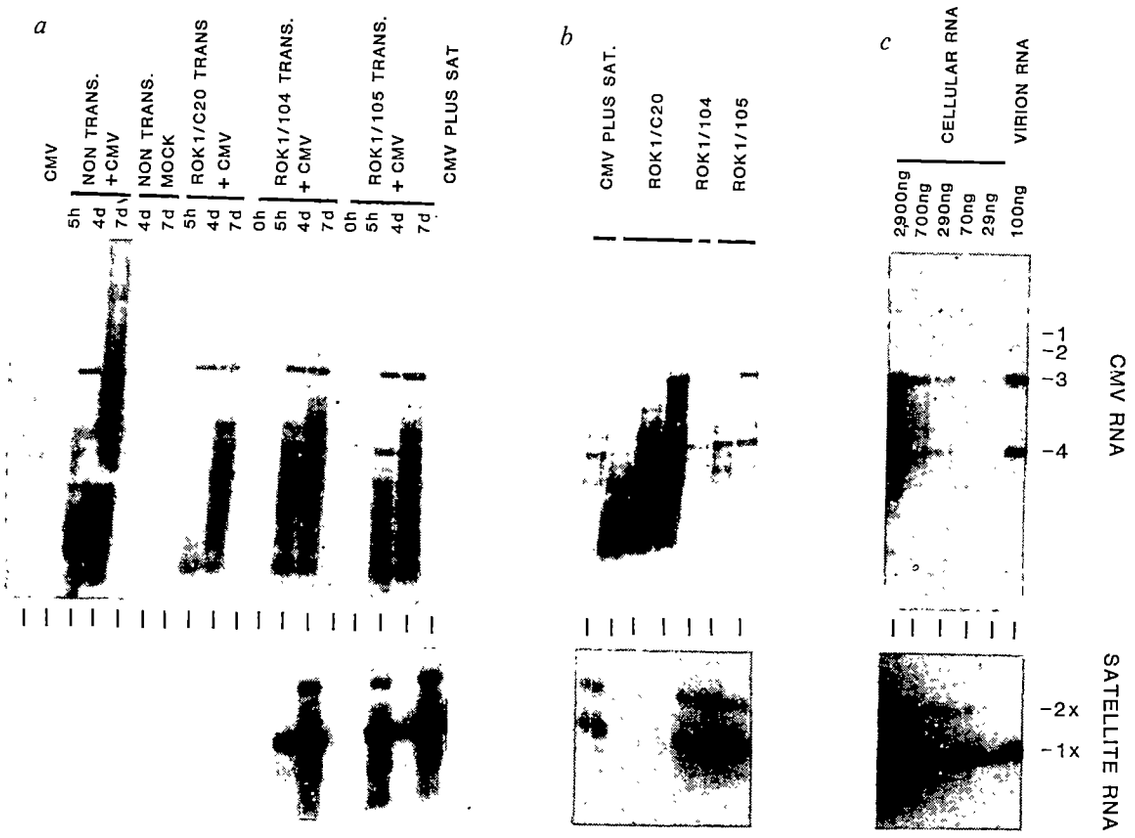


Fig. 3 Effect of CMV infection on the satellite RNA in transformed plants. Leaves of transformed or non-transformed *N. tabacum* (var. Samsun NN) were inoculated with CMV strain R76B and 35-mm disks were cut 5 h later. Batches of five disks were floated on SPS medium (10 g l^{-1} sucrose, 0.2 g l^{-1} Ca $(H_2PO_4)_2 \cdot H_2O$, 0.3 g l^{-1} sulphanilamide). Total RNA (1 μg) was isolated from these samples, or as indicated below, and analysed by Northern blotting as described for Fig. 2 using as probes the insert of pT105 (satellite RNA, lower panels) or C20 (CMV RNA, upper panels). The size markers were RNA of tissue infected with CMV alone or CMV plus satellite to show CMV RNA-1, CMV RNA-2, CMV RNA-3 and CMV RNA-4 or satellite monomer (1×) or dimer units (2×). *a*, RNA in primary infections. RNA was isolated from disks of non-transformed plants or from disks of plants transformed with the indicated derivatives of Rok1 at 5 h, 4 days or 7 days after inoculation with CMV R76B (+CMV) or buffer (mock). In some cases RNA was also isolated before inoculation (0 h). The Rok1/C20 construction was similar to Rok1/104 (Fig. 1) except that the insertion at the *Bam*HI site of Rok1 was a cDNA (C20) of the CMV coat protein mRNA. *b*, RNA in secondary infections. Extracts of CMV-infected leaf disks, similar to those described for *a*, were inoculated onto *N. clevelandii* and RNA was isolated from the systemically infected tissue after 10 days. The RNA (1 μg) was isolated from plants inoculated with extracts of disks of plants transformed with Rok1/C20, Rok1/104 or Rok1/105. *c*, RNA in CMV particles. Disks from CMV (R76B)-infected plants transformed with Rok1/105 were extracted at 7 days after inoculation and the inoculum passaged through non-transformed *N. clevelandii* and re-inoculated onto *N. clevelandii*. After 10 days of infection, CMV particles were isolated from systemically infected leaves[30] and the viral RNA extracted by addition of SDS to 1% and treatment with phenol. Total cellular RNA was also isolated from this tissue for comparison. The samples shown are 100 ng virion RNA or the indicated amounts of total cellular RNA.

symptoms or other abnormalities in growth, flowering or seed production were observed in the transformed plants.

To determine the biological activity of these transcribed RNA molecules, the transformed plants were infected with CMV strain R76B, a satellite-free isolate of CMV obtained originally from a naturally infected raspberry plant in Scotland[13]. In one such test, disks were cut from leaves 5 h after inoculation. RNA was isolated from the disks, either at that time, or after floating the disks on SPS medium for 4 or 7 days. Northern blot analysis of the RNA with a probe for CMV (C20) (Fig. 3*a*) showed that by 4 days the CMV genomic RNAs had accumulated in disks from both the transformed and the non-transformed plants. Many small RNA species which may represent subgenomic RNA species[14] also accumulated over the same period (Fig. 3*a*). Satellite RNA was detected by Northern blot analysis after 4 and 7 days but only in the disks from plants transformed with Rok1/104 or Rok1/105 (Fig. 3*a*). This RNA was present in large amounts and was primarily of unit satellite RNA length although, as is normal for an infection containing satellite, some dimers were also detected (Fig. 3*a*). At the loading of RNA and autoradiographic exposure of Fig. 3*a*, the transcribed satellite RNA molecules of ~700 and 1,000 nucleotides were not detectable. Similar results were obtained from analysis of inoculated leaves of intact plants.

Further tests showed that the satellite produced in transformed plants could be acquired as a permanent feature of the CMV culture. In one such test, sap from leaf disks in the experiments described above was inoculated to *Nicotiana clevelandii* and RNA isolated from the systemically infected leaves after 10 days. The RNA was analysed by Northern blotting and found to contain satellite RNA in monomeric and dimeric forms, at levels typical of natural satellite RNA, when the inoculum had been obtained from disks of plants transformed with Rok1/104 or Rok1/105 (Fig. 3*b*). *N. clevelandii* plants inoculated with CMV which had been passaged through disks of Rok1/C20-transformed plants contained only CMV genomic RNA (Fig. 3*b*).

These experiments also showed that the production of symptoms in *N. clevelandii* was markedly reduced when the inoculum contained satellite RNA acquired from transformed

plants. This was observed in all 12 plants inoculated with CMV R76B that had been passaged through plants transformed with Rok1/104 or Rok1/105 (M.A.M. and B.D.H., unpublished data). The effect of satellite RNA on symptom production could not be assayed in the actual transformed plants as CMV R76B produces very mild symptoms in *Nicotiana tabacum*.

The incorporation of satellite RNA from the transformed plants into virions of CMV was confirmed by Northern blot analysis of RNA isolated from CMV particles. These were isolated from a secondary infection of CMV R76B in *N. clevelandii* following passage of the virus culture through Rok1/105-transformed plants (Fig. 3*c*). Both unit length and dimeric satellite RNA was detected, although there was less satellite RNA per unit of CMV RNA than in cellular RNA from the same plants (Fig. 3*c*). This effect was more marked with the dimer than the monomer satellite.

We also found that monomeric and dimeric satellite RNA accumulated to high levels in systemically infected leaves of CMV (R76B)-inoculated plants which had been transformed with Rok1/104 and Rok1/105 (D.C.B., G.R.S., M.A.M. and B.D.H., unpublished data). Satellite RNA was not detected in the systemically infected leaves of non-transformed or Rok1/C20-transformed plants. Further investigation will determine whether satellite produced in the transformed plants affects CMV replication and accumulation.

Clearly the transcribed satellite RNA in transformed plants can be processed to unit-length molecules following CMV infection and subsequently acquired and perpetuated as a new part of the virus culture. We believe this provides the first proof of the acquisition by a plant virus of genetic material from its host, a process that may be important in the evolution of plant viruses and their satellites. Indeed, although there is no evidence for the occurrence of CMV satellite-like sequences in DNA of non-infected tobacco plants[15], sequences resembling those of the satellite RNA of turnip crinkle virus are reported to occur in the DNA of non-infected turnip plants[16].

The fact that plants infected with CMV cultures containing a benign satellite RNA show milder symptoms than plants infected with satellite-free cultures[8] suggests that satellite RNA might be used to protect crop plants against the effects of CMV infection. Preliminary experiments have shown that pre-infection with a CMV strain containing such a satellite RNA gave protection against CMV symptoms[17] and led to increased yield of pepper plants[18]. It has also been shown that infection of tomato plants with CMV strain containing a benign satellite RNA results in protection against the effects of a CMV culture containing a virulent satellite RNA[19,20]. However, the use of an avirulent virus culture as the prophylactic agent may cause several problems[21]. The protecting strain may itself have adverse effects on growth and yield or spread to other, more sensitive, plant species. It is also possible that the avirulent strain may mutate to virulence or interact with other viruses to cause severe symptoms. However, some of these difficulties may be eliminated by the strategy demonstrated here in which biologically active satellite RNA is maintained in the plant by transcription from the nuclear genome.

We thank Suzanne Mason for technical help and Dr M. Jacquemond (Montfavet, France) for providing strains of CMV. This work was supported in part by the Rockefeller Foundation.

Received 27 January; accepted 26 March 1986.

1. Kaper, J. M., Tousignant, M. E. & Lot, H. *Biochem. biophys. Res. Commun.* **72**, 1237–1243 (1976).
2. Richards, K. E., Jonard, G., Jacquemond, M. & Lot, H. *Virology* **89**, 395–408 (1978).
3. Diaz-Ruiz, J. R. & Kaper, J. M. *Virology* **80**, 204–213 (1977).
4. Linthorst, H. J. M. & Kaper, J. M. *J. gen. Virol.* **66**, 1839–1842 (1985).
5. Gould, A. R., Palukaitis, P., Symons, R. H. & Mossop, D. W. *Virology* **84**, 443–455 (1978).
6. Mossop, D. W. & Francki, R. I. B. *Virology* **95**, 395–404 (1979).
7. Jacquemond, M. & Lot, H. *Agronomie* **1**, 927–932 (1981).
8. Waterworth, H. E., Kaper, J. M. & Tousignant, M. E. *Science* **204**, 845–847 (1979).
9. Gordon, K. H. J. & Symons, R. H. *Nucleic Acids Res.* **11**, 947–960 (1983).
10. Collmer, C. W., Tousignant, M. E. & Kaper, J. M. *Virology* **127**, 230–234 (1983).
11. Bevan, M. *Nucleic Acids Res.* **12**, 8711–8721 (1984).
12. Bevan, M. W., Mason, S. E. & Goelet, P. *EMBO J.* **4**, 1921–1926 (1985).
13. Jones, A. T. *Rep. Scott. Crop Res. Inst. 1983*, 197–198 (1984).
14. Gordon, K. H. J. & Symons, R. H. *Virology* **142**, 144–157 (1985).
15. Mossop, D. W. & Francki, R. I. B. *Virology* **94**, 243–253 (1979).
16. Altenbach, S. B. & Howell, S. H. *Virology* **134**, 72–77 (1984).
17. Tien, P. & Chang, X. H. *Seed Sci. Tech.* **11**, 969–972 (1983).
18. Tien, P. & Chang, X. H. *Proc. 6th int. Congr. Virol., Sendai* (abstr.), 379 (1984).
19. Jacquemond, M. *C.r. hebd. Séanc. Acad. Sci., Paris III* **294**, 991–994 (1982).
20. Jacquemond, M. & Lot, H. *Agronomie* **5**, 84 (1985).
21. Gibbs, A. & Harrison, B. *Plant Virology: The Principles*, 227 (Arnold, London, 1976).
22. Tabor, S. & Richardson, C. C. *Proc. natn. Acad. Sci. U.S.A.* **82**, 1074–1078 (1985).
23. Guilley, H., Dudley, R. K., Jonard, G., Balazs, E. & Richards, K. E. *Cell* **30**, 763–773 (1982).
24. Bevan, M., Barnes, W. M. & Chilton, M.-D. *Nucleic Acids Res.* **11**, 369–385 (1983).
25. Gould, A. R. & Symons, R. H. *Eur. J. Biochem.* **126**, 217–226 (1982).
26. Horsch, R. B. *et al. Science* **227**, 1229–1231 (1985).
27. Apel, K. & Kloppstech, K. *Eur. J. Biochem.* **85**, 581–588 (1978).
28. Goldberg, D. A. *Proc. natn. Acad. Sci. U.S.A.* **77**, 5794–5798 (1980).
29. Thomas, P. S. *Proc. natn. Acad. Sci. U.S.A.* **77**, 5201–5205 (1980).
30. Lot, H., Marrou, J., Quiot, J.-B. & Esvan, C. *Ann. Phytopath.* **4**, 25–38 (1972).

Sequence-directed curvature of DNA

Paul J. Hagerman

Department of Biochemistry, Biophysics and Genetics, University of Colorado School of Medicine, Denver, Colorado 80262, USA

DNAs from both prokaryotic[1–4] and eukaryotic[5–8] organisms have yielded restriction fragments which manifest markedly anomalous electrophoretic behaviour (reduced mobility) when run on polyacrylamide gels. We have shown previously[9] that the abnormal electrophoretic behaviour of one such fragment is a consequence of stable curvature of the helix axis in solution. The molecules involved tend to contain oligo(dA)–oligo(dT) runs which are approximately in-phase with the helix repeat[7,8,10]; however, the precise structural elements responsible for DNA curvature have not been identified. One popular model[11,12] for curvature invokes a non-coplanar 'wedge-like' conformation of ApA/TpT dinucleotide pairs. Despite a lack of direct evidence in support of this model, it has been used to provide quantitative estimates of curvature[4,13,14]. To critically evaluate the ApA wedge model, we have performed an electrophoretic analysis of a series of closely related DNA polymers in which oligo(dA)–oligo(dT) runs of different polarity were compared. We conclude that ApA dinucleotide wedges cannot account for DNA curvature. Therefore, quantitative estimates for ApA wedge deformations, based solely on apparent curvature, cannot be correct.

DNA sequences displaying apparent curvature have been found at both the site of integration[1] and the origin of replication[4] of bacteriophage λ as well as in regions of conserved sequence in trypanosomatid kinetoplast DNA[7]. Disruption of a region of curvature upstream from the histidine transfer RNA gene in *Salmonella* appears to be associated with down-regulation of $tRNA^{His}$ transcription[3]. However, the functional significance of curvature *per se* remains obscure, as does its molecular origin.

Marini *et al.*[12] invoked the notion of non-coplanarity of APA/TpT dinucleotide pairs, proposed earlier by Trifonov and Sussman[11], as a possible basis for the observed curvature. Other workers[4,13,14] have attempted to provide a quantitative relationship between the hypothetical ApA wedge angle and the overall curvature of the helix axis. We have therefore attempted to test the hypothesis that an inherent non-coplanarity of ApA/TpT dinucleotide residues determines the contour of the helix axis in solution. In testing this hypothesis, one can invoke the following simple symmetry argument: for curvature arising solely from ApA wedges, the angle-of-transit of the helix axis through the sequence $5'\text{-}A_nT_n\text{-}3'$ (one strand shown) will be equivalent to the corresponding angle-of-transit through $5'\text{-}T_nA_n\text{-}3'$. Should the angles-of-transit through these two sequences prove to be different, one cannot relate apparent curvatures (for example based on gel mobilities) to ApA dinucleotide non-coplanarity. We have shown recently[10] that certain DNA oligomeric

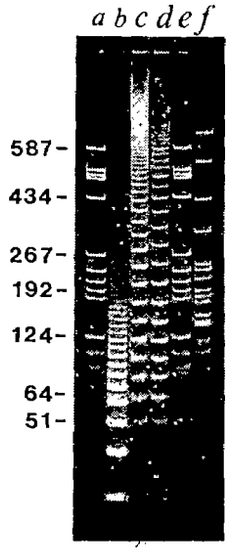


Fig. 1 Demonstration of the anomalous electrophoretic behaviour of certain repeating-block copolymers of DNA. Lane *b* contains polymers of the form $[G_3TCGAC_3]_N$ where $2 < N < 25$. The electrophoretic mobilities of all members of this set are normal *c*, $[G_2A_3T_3C_2]_N$; *d*, $[GA_4T_4C]_N$. The members of the latter two series show distinctly abnormal electrophoretic mobilities for $N > 5$. Lanes *a* and *e* contain DNA molecules derived from pBR322 by *Hae*III digestion; *f*, *Hpa*II digest of pBR322.

Methods. Representative fragment sizes are specified to the left of the gel. All gels used for this study were 12% polyacrylamide (37:1 monomer/bis) and were run at 24±2 °C (running buffer: 40 mM Tris-acetate, 20 mM sodium acetate, 1 mM Na-EDTA, *p*H 7.9). Polymers of varying *N* were constructed from synthetic decamers by phosphorylation and subsequent ligation (with T_4 DNA ligase in 0.5 mM ATP, 50 mM Tris-HCl, 10 mM $MgCl_2$ *p*H 8.0, at 12–15 °C). Ligase concentrations and reaction times were varied in order to produce informative gels; the gel patterns do not represent maximum extents of polymerization. Ligation reactions were stopped by adding Na-EDTA to a final concentration of 20 mM, followed by extraction with phenol/ether. Oligodeoxynucleotides were synthesized manually using the phosphite triester chemistry of Caruthers[15,16]. Oligomer sequences were verified by (1) using the chemical sequencing technique of Maxam and Gilbert[17], with minor modifications for short oligomers, and (2) complete digestion of the polymerized decamers with the appropriate restriction endonucleases.

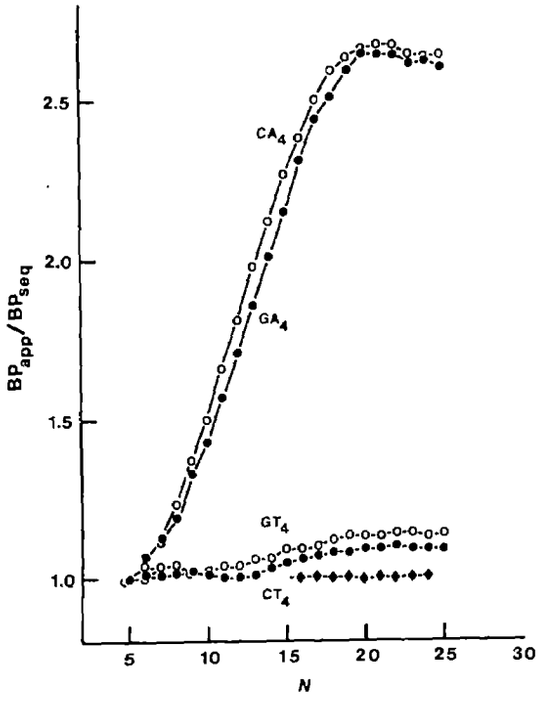


Fig. 2 Gel electrophoretic behaviours of duplex polymers having a repeating decamer motif. CA_4, $[CA_4T_4G]_N$; GA_4, $[GA_4T_4C]_N$; GT_4, $[GT_4A_4C]_N$; CT_4, $[CT_4A_4G]_N$. Mobilities of the various polymers, represented as the ratio of the apparent number of base pairs (BP_{app}) to the true number of base pairs (BP_{seq}), are plotted as a function of the degree of polymerization, *N*. The two curves plotted with solid circles represent sequence inversions of one another; the same applies to the two curves with open circles. ◆, $[G_3TCGAC_3]_N$ (lane *b* of Fig. 1, displaying a normal electrophoretic pattern for a decamer-based series).

sequences, when propagated approximately in-phase with the helix repeat, give rise to significant macroscopic curvature of the helix axis. That study exploited the fact that curved molecules migrate more slowly through polyacrylamide gels than do their linear counterparts (Fig. 1). Figure 2 compares the behaviour of the polymer series 5′-$[GA_4T_4C]_N$-3′ with its counterpart 5′-$[GT_4A_4C]_N$-3′. As the only difference between these polymers is the polarity of the A-T block, they would have to display identical electrophoretic behaviour if ApA/TpT dinucleotide wedges were determining the contour of the helix axis; clearly, this is not the case, as the 5′-T_4A_4-3′-containing polymers display nearly normal electrophoretic behaviour, in stark contrast to the 5′-A_4T_4-3′-containing species. This analysis does not rule out any participation of wedge-like deformations in generating curvature; however, such wedges, if present, do not determine curvature. Hence, it is incorrect to relate macroscopic curvature to an apparent ApA wedge angle. Note that the G and C residues flanking the A–T runs do not appear to influence the degree of curvature, since interchange of these residues (Fig. 2) has essentially no effect on the relative electrophoretic mobilities.

This research was supported by NIH grant GM28293.

Received 12 August 1985; accepted 20 March 1986.

1. Ross, W., Shulman, M. & Landy, A. *J. molec. Biol.* **156**, 505–529 (1982).
2. Stellwagen, N. C. *Biochemistry* **22**, 6186–6193 (1983).
3. Bossi, L. & Smith, D. M. *Cell* **39**, 643–652 (1984).
4. Zahn, K. & Blattner, F. R. *Nature* **317**, 451–453 (1985).
5. Simpson, L. *Proc. natn. Acad. Sci. U.S.A.* **76**, 1585–1588 (1979).
6. Challberg, S. S. & England, P. T. *J. molec. Biol.* **138**, 447–472 (1980).
7. Kidane, G. Z., Hughes, D. & Simpson, L. *Gene* **27**, 265–277 (1984).
8. Wu, H.-M. & Crothers, D. M. *Nature* **308**, 509–513 (1984).
9. Hagerman, P. J. *Proc. natn. Acad. Sci. U.S.A.* **81**, 4632–4636 (1984).
10. Hagerman, P. J. *Biochemistry* **24**, 7033–7037 (1985).
11. Trifonov, E. N. & Sussman, J. L. *Proc. natn. Acad. Sci. U.S.A.* **77**, 3816–3820 (1980).
12. Marini, J. C., Levene, S. D., Crothers, D. M. & Englund, P. T. *Proc. natn. Acad. Sci. U.S.A.* **79**, 7664–7668 (1982).
13. Levene, S. D. & Crothers, D. M. *J. biomolec. Struct. Dyn.* **1**, 429–435 (1983).
14. Ulanovsky, L., Bodner, M., Trifonov, E. N. & Choder, M. *Proc. natn. Acad. Sci. U.S.A.* **83**, 862–866 (1986).
15. Caruthers, M. H. *et al. Cold Spring Harb. Symp. quant. Biol.* **47**, 411–418 (1982).
16. Sproat, B. S. & Gait, M. J. in *Oligonucleotide Synthesis, A Practical Approach* (ed. Gait, M. J.) 83–114 (IRL, Washington, DC, 1984).
17. Maxam, A. M. & Gilbert, W. *Meth. Enzym.* **65**, 499–560 (1980).

Errata

Danish Basin subsidence by Triassic rifting on a lithosphere cooling background

K. Sørensen

Nature **319**, 660–663 (1986)

ON page 662, Figures 2 and 3 have been transposed. The figure legends are correct.

An *Agrobacterium* transformation in the evolution of the genus *Nicotiana*

I. J. Furner *et al.*

Nature **319**, 422–427 (1986)

ON pages 424 and 425, the figures and their legends were labelled incorrectly: Figure 3 should be Figure 4 and vice versa.

CONVENIENT-INFORMATIVE-TIMELY-PROVOCATIVE

FOUR DYNAMITE REASONS WHY YOU SHOULD SUBSCRIBE TO BIO/TECHNOLOGY NOW . . .

1 ■ You'll save time. Because you don't have time to read every journal in the field, BIO/TECHNOLOGY is written and edited to give you all the information you need in ONE convenient source. BIO/TECHNOLOGY is the only journal to give you news. Features. Original research. Product evaluations. Industrial applications. Job openings. Book and product reviews. And more. If it's important to your work, you'll find it between the covers of BIO/TECHNOLOGY.

2 ■ You'll learn new ways to improve your on-the-job skills and run a more successful operation. Each month BIO/TECHNOLOGY gives you the scoop on invaluable start-up information . . . the latest instrumentation . . . marketing breakthroughs . . . funding sources . . . new technologies . . . patents and licences . . . profiles on how others are avoiding the pitfalls and reaping the rewards. In fact, just one practical tip from BIO/TECHNOLOGY can be worth many times the cost of your subscription.



3 ■ You'll be up-to-date on all major industry developments. With correspondents all over the world, BIO/TECHNOLOGY delivers the inside story on who's doing what, where. You'll get the latest word on changing government regulations and tax law, and how they affect your work.

Plus you'll read original research papers by bench scientists, engineers, and biologists that will help keep you in the forefront of every new discovery worth knowing about.

4 ■ You'll get new ideas you can put to use immediately. BIO/TECHNOLOGY lets you rub elbows with eminent scientists, tour new facilities and learn how new processes work in every field from genetic engineering to molecular biology. Each month, BIO/TECHNOLOGY helps spark ideas for your own research, for new industrial applications and for getting along in the increasingly competitive financial arena.

If you're not already subscribing to BIO/TECHNOLOGY, don't delay the moment any longer - return the coupon below and we will send you twelve issues. You risk nothing. If for any reason BIO/TECHNOLOGY doesn't live up to your highest expectations, just let us know and you'll receive a full refund on all unmailed copies. Remember too, that your subscription may be tax deductible

TO START RECEIVING YOUR SUBSCRIPTION, FILL OUT THE COUPON BELOW AND RETURN WITH PAYMENT TO:

U.S.A.: BIO/TECHNOLOGY
Subscription Order Dept., P.O. Box 1543
Neptune, New Jersey 07754-1543 U.S.A.

ENGLAND: BIO/TECHNOLOGY
Subscription Order Dept., Macmillan Journals, Ltd.
Brunel Road, Houndmills, Basingstoke
Hampshire RG21 2XS, England

To speed up your subscription in the U.S.A., call toll free 1-800-524-0328.

☐ YES! Please send me one year of BIO/TECHNOLOGY (12 issues). I understand that I may cancel my subscription at any time and receive a full refund on all unmailed issues.

☐ U.S.A.-$59.00* ☐ Australia-A$130**
☐ U.K.-£70** ☐ Elsewhere-U.S.$112**

Japan Publications Trading Company Ltd
2-1 Sarugaku-cho 1-chome
Chiyoda-ku, Tokyo, Japan Tel: (03) 292 3755

Note: *Represents 24% off Basic Subscription Price of U.S. $78.00
**All other prices quoted are "Air Speed"

☐ My payment is enclosed at the price checked.
☐ Please charge my credit card account:
☐ American Express ☐ Mastercard ☐ Visa

Card No.: _____ Exp. Date: ____ ____ __

Signature: _____ __ _

Name: _____ __ _

Company: _____ ____

Address: _____ __ _

City/State/Postal Code: _____ __ __

Country: _____ ____ __

7AUS

The Division of Cancer Etiology

National Cancer Institute

Announces To The Scientific Community The Availability of the Following Resources/Services For Cancer Related Research As Noted Below:

Biological Resources

Avian Myeloblastosis Virus Reverse Transcriptase—2,000 Unit Minimum Order

Contact: Dr. G.E. Houts
Molecular Genetic Resources
6201 Johns Road, Suite 8
Tampa, Florida 33614
(813) 886-5338

Citing Contract #N01-CP-51007

Cost: $0.05/Unit
(Plus Shipping Outside Contiguous United States)

Goat Antisera Against: Avian, Bovine, Feline, Murine, and Primate Intact Viruses and Viral Proteins; Antibodies to Immunoglobulins for a number of species. Preimmune Sera available for some Virus Antisera.

Contact: Ms. P. Massagee
BCB Repository
Microbiological Associates, Inc.
5221 River Road
Bethesda, MD 20816
(301) 657-8169

Citing Contract #N01-CP-11000

Cost: $50.00/5 ml.
25.00/5 ml. (Preimmune Sera)
Plus Shipping
(Frozen Material)

Human Tissues: Carcinomas, Sarcomas, Lymphomas, Leukemias, Benign Tumors, and other Non-Malignant Disorders.

Human sera from donors with: Carcinomas, Sarcomas, Melanomas, Lymphomas, Leukemias, Benign Tumors, Normal Individuals, Family Members of Leukemics, Hematological Diseases, and other Non-Malignant Disorders.

Contact: Coordinator for Research Resources
Biological Carcinogenesis
Branch, DCE, NCI, NIH
Landow Bldg., Room 9A22
Bethesda, MD 20892
(301) 496-1951

Cost: Shipping Charges Only

Cell Culture Identification Service, Using Isozyme Analysis, Immunofluorescence and Karyotypic Analysis (Chromosome Banding)

Contact: Dr. Ward Peterson
Children's Hospital of Michigan
3901 Beaubien Boulevard
Detroit, MI 48201
(313) 494-5705

Citing Contract #N01-CP-21017

Cost: $200/Analysis

Monoclonal Antibodies are available with specificities for synthetic peptides representing the amino acid sequences of the left end, right end and active site of the oncogene products of avian and mammalian retroviruses. Blocking peptides are also available, as are a limited number of cell lines producing the monoclonal antibodies.

Contact: Ms. P. Massagee
BCB Repository
Microbiological Associates, Inc.
5221 River Road
Bethesda, MD 20816
(301) 657-8169

Citing Contract #N01-CP-11000

Cost: Peptides —$20.00/mg.
Ascites Fluid— 35.00/ml.
Cell Culture — 75.00/culture
(Plus shipping)

Cotton-Top Marmosets *(S. oedipus)* for Use as Models for Carcinogenesis—Holding, Inoculation, Observation, and Pathology Services are Available.

Contact: Dr. Neal Clap
Marmoset Research Program
Oak Ridge Associated Universities
P.O. Box 117
Oak Ridge, TN 37831
(615) 576-4103

Citing Contract #N01-CP-51006

Cost: $10.00 per diem (or higher for procedures involving additional care, etc.) $10.00 per blood sample

---

Viruses: Avian, Feline, Murine, and Primate Viruses Prepared in Tissue Culture

Contact: Ms. P. Massagee
BCB Repository
Microbiological Associates, Inc.
5221 River Road
Bethesda, MD 20816
(301) 657-8169

Citing Contract #N01-CP-11000

Cost: Inquire

Sera from Primates which were housed in the U.S. and inoculated with material from Sukumi, USSR, Baboons with Malignant Lymphoma.

Contact: Coordinator for Research Resources
Biological Carcinogenesis
Branch, DCE, NCI, NIH
Landow Building, Room 9A22
Bethesda, MD 20892
(301) 496-1951

Cost: Shipping Charges Only

Resource materials are available from bovine leukemia virus-infected cattle and sheep and control animals. These include blood, serum, plasma, bone marrow, leukocytes, bone marrow smears and virus-producing lymphocytes.

Contact: Jorge F. Ferrer, M.D.
Chief, Section of Viral Oncology
New Bolton Center
University of Pennsylvania
382 West Street Road
Kennett Square, PA 19348
(215) 444-5800
Extension 286

Citing Contract #N01-CP-51003

Cost: Inquire

Chemical Resources

Analytical resources for the collection, separation, and elucidation of the components of cigarette smoke and cigarette smoke condensates: A contractor with experience in the development of analytical methods for the determination of constituents of cigarette smoke and of specialty instrumentation for inhalation toxicology is available to assist qualified investigators with particular interest in studies on human and animal model exposure to environmental and sidestream smoke. A large inventory of reference experimental cigarettes, Standard Low Yield Reference Cigarettes, and an extensive chemical data base on smoke and smoke condensate components is available.

Contact: Thomas B. Owen, Ph.D.
Chemical and Physical Carcinogenesis Branch, DCE, NCI
Landow Building, Room 9C-18
Bethesda, Maryland 20892
(301) 496-5471

Cost: Inquire

Chemical Carcinogen Reference Standard Repository: Reference quantities of over 700 compounds are available. In addition to the newer Fecapentaenes and food mutagens, numerous representatives of the following classes of compounds are available; polynuclear aromatic hydrocarbons (PAH), PAH metabolites, radiolabeled PAH metabolites, nitrogen heterocycles, nitrosamines/nitrosamides, aromatic amines, aromatic amine metabolites, radiolabeled retinoids, azo/azoxy aromatics, inorganics, nitroaromatics, pesticides, pharmaceuticals, natural products, dyes, dioxins, chlorinated aliphatics and miscellaneous groups. Data sheets provided with the compounds include chemical and physical properties, analytical data, hazards, storage, and handling information. Catalog available upon request.

Contact: Coordinator for Chemical Research Resources
Chemical and Physical Carcinogenesis Branch, DCE, NCI
Landow Building, Room 9B-10
Bethesda, MD 20892
(301) 496-5471

Cost: Subject to chemical class code and quantity (see catalog) plus handling and shipping charges.

Environmental Cancer

NCI's Chemical Carcinogenesis Research Information System (CCRIS) database will be available online through the National Library of Medicine's new Toxicology Data Network (TOXNET) system beginning January, 1986. Through an interagency agreement between NCI and NLM, the CCRIS database will be built, maintained and updated in TOXNET's sponsored databases in the broad areas of chemistry, toxicology, and hazardous waste information. The CCRIS database contains evaluated data and information on carcinogens, mutagens, tumor promoters, cocarcinogens, metabolites of carcinogens and carcinogen inhibitors derived from published review articles, ongoing current awareness survey of primary literature, NCI/NTP's short- and long-term bioassay studies the IARC Monographs on the Evaluation of Carcinogenic Risk of Chemicals to Man, and special studies and reports

Contact: Dr. Thomas P. Cameron
Office of the Director
Division of Cancer Etiology
National Cancer Institute
Landow Building, Room 1D34
Bethesda, MD 20892
(301) 496-1895

Cost: Inquire

The Special Assistant for Environmental Cancer, Office of the Director, announces the availability of a limited number of copies of the following reports, which have been prepared under contract to NCI:

Survey of Compounds Which Have Been Tested for Carcinogenic Activity PHS 149 1974-1975, 1976-1977, 1979-1980, and a Cumulative Index

Monographs on Organic Air Pollutants

Species-to-Species Comparison of Carcinogen Metabolism

Survey of Organic Drinking Water Contaminants: Carcinogens, Mutagens, and T[illegible] Promoters

Inhibitors of Chemical Carcinogenesis

Contact: Ms. I C. Blackwood
Office of the Director
Division of Cancer Etiology
National Cancer Institute
Landow Building, Room 1D34
Bethesda, MD 20892
(301) 496-1625

Cost: Free to investigators interested in environmental cancer

---

Monographs on Human Exposure to Chemicals in the Workplace
(Not included in free distributions)

Monographs on 68 chemicals will be for sale by the

National Technical Information Service
U.S. Department of Commerce
Springfield, VA 22161
(703) 487-4650

Cost: Inquire

Epidemiology Resources

The Immunodeficiency—Cancer Registry (ICR) is a unique registry of cancer cases that occur in patients with naturally occurring immunodeficiencies. Case material collected by ICR comes from case reports appearing in scientific literature and voluntary reporting by physicians. Criteria for inclusion in the registry are clinical or laboratory evidence of a primary immunodeficiency syndrome prior to the onset of malignancy. Data contained in the ICR are available to the extramural research community for the planning, design, and conduct of research efforts. Limited assistance is available to investigators interested in utilizing the registry.

Contact: Dr Alexandra H. Filipovich
Immunodeficiency—Cancer Registry
Box 610 Mayo
University of Minnesota
Minneapolis, MN 55455
(612) 376-2174

Citing Contract #N01-CP-31011

The Tumor Virus Epidemiology Repository (TVER) contains sera and other biological samples from more than 13,000 patients and controls obtained in 12 different countries. The TVER was established primarily to support collaborative research on the role of Epstein-Barr virus (EBV) in Burkitt's lymphoma, nasopharyngeal carcinoma, and related diseases. Part of the collection includes sera that were obtained from nonhuman primates inoculated with EBV.

The TVER is able to adjust its collection to facilitate the development of new collaborative studies. In addition, some samples are available for reagents and independent research. The most extensive collections are serum samples from patients with Burkitt's lymphoma (sera from more than 1,000 patients).

Contact: Dr. Paul H. Levine
Environmental Epidemiology Branch, DCE, NCI, NIH
Landow Building, Room 3C25
Bethesda, MD 20892
(301) 496-4375

Cost: Free to Collaborating Investigators; Others, Shipping Charges Only

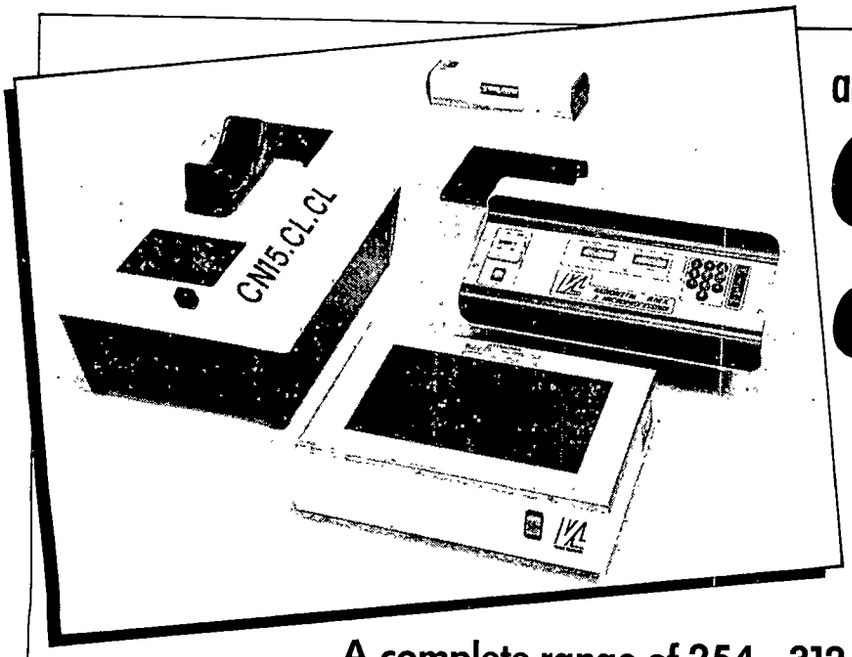
The National Institute of Allergy and Infectious Diseases and the National Cancer Institute have developed a repository of biological specimens from homosexual men. The specimens were collected through contracts with five major U.S. universities for studies of the natural history of acquired immune deficiency syndrome (AIDS).

Information about applying for collaborative use of these specimens and pertinent epidemiological data is now available from the Project Officer or the NCI Co-Project Officer. For further information, write to Project Officer, AIDS Repository, Epidemiology and Biometry Section, National Institute of Allergy and Infectious Diseases, Westwood Building Room 739, National Institutes of Health Bethesda, MD 20892 or to Dr. A R. Pater, Extramural Programs Branch, EBP, Division of Cancer Etiology, NCI, Landow Building Room 8C-16, Bethesda, MD 20892

Human fibroblast cultures from individuals at high risk of cancer, members of cancer-prone families, and normal family members

Contact: Dr. Margaret Tucker
Family Studies Section EEB
DCE, NCI, NIH
Landow Bldg. Room 3C29
Bethesda, MD 20892
(301) 496-4375

Cost: Free to collaborating investigators
Others: $60/cell line



any **U.V.** problems ?

Call upon our lights

254 - 312 - 365 nm lamps
Portable lamps
U.V. darkrooms
Fluorescent tables
U.V. radiometers
Eprom erasers

A complete range of 254 - 312 - 365 nm U.V. Generators for your FLUORESCENT ANALYSIS (DNA - RNA - TLC...)

CI DX PARIS

LOOKING FOR EXPORT AGENTS

VILBER LOURMAT

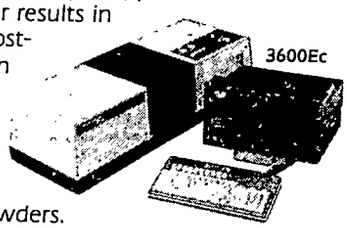
BP 66 - Torcy - Z.I. Sud - 77202 Marne-la-Vallée Cedex 1
France - Tél. : (1) 60.06.07.71 + - Télex VILBER 691062 F

Reader Service No.23

The New Dimension in Particle Technology...

Droplet and Particle Size Analysers 0.5-1800 microns

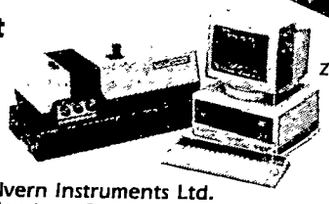
Fast, easy to use instruments for plant and laboratory applications. All with new 16-bit computer/processor giving full graphical and tabular results in 32 size classes. Compact and cost-effective **3600Ec** for powders in suspension up to 560 microns.



SERIES 2600c modular systems for pulsed or continuous sprays and suspensions up to 1800 microns and dry powders.

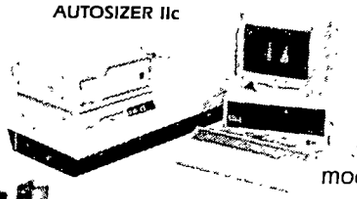
Zeta Potential Measurement

Zetasizer IIc laser based particle electrophoresis system. Automated, rapid, eliminates user fatigue and bias. Also measures submicron particle size.



Submicron Particle Size Analysers

Advanced **SYSTEM 4700c** incorporating Malvern's 8-bit correlator with up to 264 data channels and eight sample times. Measures particle size 0.001-5 microns, molecular weight by PCS or Zimm plot methods, diffusion coefficients etc.



AUTOSIZER IIc also features 8-bit correlator for fast, routine particle sizing 0.003-3 microns, with full mono- or multi-modal size distribution data.

MALVERN INSTRUMENTS at ANALYTICA 86 on the Mütek stand
Hall 11 Stand C12

MALVERN

Malvern Instruments Ltd.
Spring Lane South, Malvern,
Worcestershire WR14 1AQ, England.

Malvern Instruments Inc.
200 Turnpike Road,
Southborough, MA 01772, USA.

Reader Service No.21

Please send me details of

Droplet and Particle Size Analysers ○ **Zeta Potential Measurement** ○
Submicron Particle Size Analysers ○ **Laser Particle Counters** ○

Particle Size Range .....

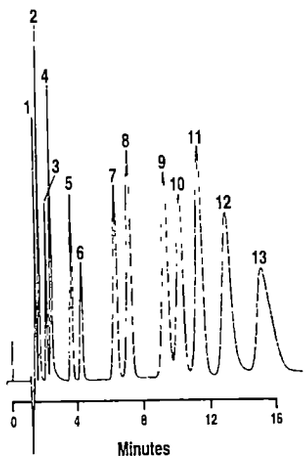
Name ..... Position .....
Company .....
.....
..... Code ..... Telephone .....

Carbohydrate detection gains potential

from Dennis C. Johnson

Combined with liquid chromatography, pulsed amperometric detection extends the capabilities of carbohydrate analysis. The method allows direct electrochemical detection.

THE promise of analytical organic liquid chromatography (LC), enhanced over the past decade by improvements in hardware and methodology, has stimulated the search for new detection concepts to permit greater exploitation of LC capabilities. Detection based on UV-vis photometry (absorbance and fluorescence) has been most common in organic LC; however, photometric detection yields significant results only with unsaturated and aromatic molecules. For aliphatic analytes, photometric detection suffers from poor sensitivity unless aromatic functional groups are attached to the aliphatic molecules using tedious chemical derivatizations.



	Sugar	ppm
1.	Inositol	20
2.	Xylitol	20
3.	Sorbitol	20
4.	Mannitol	40
5.	Fucose	50
6.	Deoxyribose	100
7.	Rhamnose	100
8.	Arabinose	50
9.	Galactose	50
10.	Glucose	50
11.	Xylose	100
12.	Fructose	100
13.	Sucrose	300

Fig.2 Separations of carbohydrates using anion-exchange chromatography with electrochemical detection. The column and detection are as in Fig 1, the mobile phase was 8.0 mM $Ba(OH)_2$/0.5 mM acetic acid. (Provided by W.T. Edwards, Dionex Corp.)

EC detection

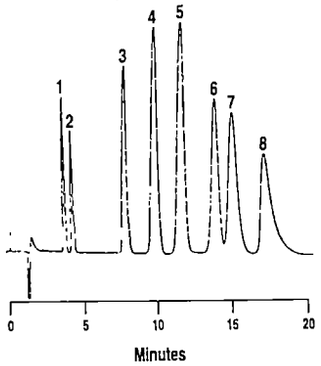
Oxidative electrochemical (EC) detection has also proved useful for aromatic organic molecules such as phenols and biogenic amines and metabolites[1,2]. In contrast, direct anodic detection of underivatized aliphatic organic molecules under constant (d.c.) applied electrode potentials is essentially unknown. Thermodynamic data predict oxidations in aqueous and mixed solvents. Hence, the apparent electroinactivity of aliphatic molecules at constant potential originates from kinetics problems, for instance the lack of resonance-stabilized free-radical reaction products.

Aliphatic molecules frequently generate transient anodic signals at noble metal electrodes, with the magnitude of the temporary signal and speed of its attenuation being a function of the electrode material. Because the electrode surface appears to interact with analyte molecules and/or reaction products, the reaction mechanisms are characterized as electrocatalytic[3-5].

The example of aliphatic molecule electrochemistry that is best understood is the oxidation of simple alcohols at noble-metal electrodes[3-5]. The standard potential (E^0) for the conversion of methanol to CO_2 in aqueous solutions is predicted to be 0.0V versus NHE (normal hydrogen electrode). Electrode potentials many hundreds of millivolts more positive than this E^0 can be applied at common anode materials without causing decomposition of the aqueous solvent. It follows that all alcohols should be easily detected by electrochemical oxidation reactions.

However, the oxidations of alcohols are not 100 per cent efficient and free-radical intermediates are adsorbed strongly at the noble-metal anode surfaces, thereby eliminating further activity of those surface sites. Electrode currents for alcohols at noble metal anodes fall to zero within a few seconds in acidic or alkaline media[3-5].

The adsorbed hydrocarbon materials which foul Pt and Au electrode surfaces can be eliminated by oxidative desorption when a large positive potential pulse is applied[6,7]. A subsequent negative potential pulse cathodically dissolves surface oxides, restoring the full activity of the metal electrode surfaces.



	Sugar	ppm
1.	Fucose	25
2.	Deoxyribose	25
3.	Arabinose	25
4.	Galactose	25
5.	Glucose	25
6.	Xylose	25
7.	Mannose	50
8.	Fructose	50

Fig.1 Separation of common monosaccharides by anion-exchange chromatography with electrochemical detection. A Dionex HPIC AS-6 column with a 1.0 mM $Ba(OH)_2$/0.125 mM acetic acid mobile phase was used, followed by detection with a Dionex pulsed amperometric detector. (Provided by W.T. Edwards, Dionex Corp.)

Cleaning pulses for analytical anodic potential are under the control of multistep potential waveforms[8]. Each application of the detection potential, with measurement of electrode current, is followed by the positive and negative pulses for surface reactivation. Typically, the waveform is applied with a cycle frequency of about 1 Hz (1 cycle per second). The analytical technique has become known as pulsed amperometric detection (PAD).

PAD and chromatography

Response to PAD has been verified for all carbohydrates tested at Pt[6,7] and Au[8] electrodes: sugar alcohols (such as sorbitol), aldoses (glucose), ketoses (fructose), polysaccharides (sucrose) and aminosaccharides.

Because of the electrocatalytic basis of PAD for carbohydrates, the potential dependence of the anodic response is virtually independent of the identity of the molecule. The technique cannot distinguish between different types of carbohydrate in a mixture. Therefore PAD is applied as a general electrochemical detector for carbohydrates in the chromatographic effluent stream.

Among the possible designs for LC electrochemical flow-through detectors[9,10] the most popular is the thin-layer cell. In this design, the fluid stream is confined to a narrow channel cut into a thin Teflon sheet (< 0.2 mm) separating two flat plastic plates (Kel-F). For PAD of carbohydrates, the indicating electrode (Au) and counter electrode (Au, Pt or carbon) are the flat end surfaces of rods (about 1 to 2 mm diameter) pressed into holes drilled

in one plastic plate. The Ag–AgCl reference electrode, mounted in the opposite plate, is separated from the fluid stream by a cation-exchange membrane.

Any chromatographic system designed for carbohydrate LC-PAD must recognize the requirement for a supporting electrolyte and the desirability of maintaining a high *p*H to maximize sensitivity. It is preferable that the buffered supporting electrolyte serve as the chromatographic mobile phase. Low-capacity anion exchange columns, such as those used in ion chromatography[15–17], have been successful in this application[11,12,18]. Cation exchange columns in the Ca^{2+}-form are also effective where pure H_2O is the mobile phase, provided an appropriate electrolyte/buffer solution is mixed with the column effluent stream prior to detection[9].

Separation of a mixture of common monosaccharides is shown in Fig. 1; Fig. 2 shows the separation of a more complex mixture of carbohydrates. The retention mechanism apparently operates by ion exchange of the weakly ionized alcoholic groups under the conditions of moderately high *p*H. Sugar alcohols have low retention under these chromatographic conditions, and oligosaccharides are retained more strongly than the monosaccharides. Detection limits are approximately at the part-per-million (p.p.m.) level.

Analysis by LC-PAD has already been applied to fruit juices and alcoholic beverages[9,18] and other food products[15]. In the future, clinical laboratories may use LC-PAD to obtain carbohydrate profiles of physiological specimens. Ultimately the analytical potential of LC-PAD may reveal the physiologial function of many carbohydrates. □

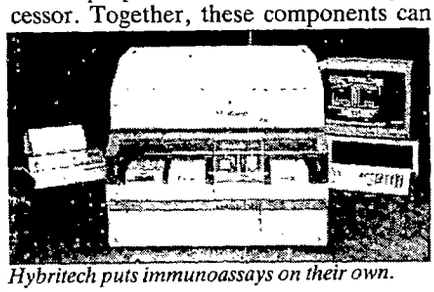
Dennis Johnson is in the Department of Chemistry, Iowa State University, Ames, Iowa 50011, USA.

1. Kissinger, P.T., Bruntlett, C.S. & Shoup, R.E. *Life Sci.* **28**, 455-465 (1981).
2. Shoup, R.E. *Recent Reports on Liquid Chromatography/Electrochemistry* (BAS Press, West Lafayette, Indiana, 1982).
3. Breiter, M.W. *Electrochim. Acta.* **8**, 973-983 (1963).
4. Giner, J. *Electrochim. Acta.* **9**, 63-77 (1964).
5. Bloom, H & Gutman, F. (eds) *Electrochemistry. The Past Thirty and the Next Thirty Years.* (Plenum, New York, 1977).
6. Gilman, S. in *Electroanalytical Chemistry* Vol.2 (ed Bard, A.J.) 111-192 Dekker, New York, 1967).
7. Austin, D.S. *et al. J. Electroanalyt. Chem.* **168**, 227-248 (1984).
8. Hughes, S., Meschi, P.L. & Johnson, D.C. *Analyt. chim. Acta* **132**, 1-10 (1981).
9. Hughes S. & Johnson, D.C. *Analyt. chim. Acta* **132**, 11-22 (1981); **149**, 1-10 (1983).
10. Polta, J.A., Johnson, D.C. & Merkel, K.E. *J. Chromatogr.* **324**, 407-414 (1985).
11. Edwards, P. & Haak, K.K. *Amer. Lab.* April, 78-87 (1983).
12. Rocklin, R.D. & Pohl, C.A. *J. Liq. Chromotogr.* **6**, 1577-1590 (1983).
13. Kissinger, P T. *Analyt. Chem.* **49**, 447A-456A (1977).
14. Weber, S.G. & Purdy, W.C. *I&EC Prod. Res. Dev.* **20**, 593-598 (1981).
15. Small, H., Stevens, T.S. & Bauman, W.C. *Analyt. Chem.* **47**, 1801-1809 (1975).
16. Fritz, J.S., Gjerde, D.T. & Pohlandt, C. *Ion Chromatography* (Hüthig, Heidelberg, 1982).
17. Small, H. *Analyt. Chem.* **55**, 235A-242A (1983).
18. Hughes, S. & Johnson, D.C. *J. Agric. Food Chem.* **30**, 712-714 (1982).

Analytica instrumentation

Munich comes alive this June with chemical technology to count, size and analyse.

HYBRITECH's new fully **automated immunoassay analyser** will be on display at Analytica. The Photon-Era can perform most of the manual laboratory procedures associated with Tandem-E immunoenzymetric assays, including precisely-timed pipetting, aspirating, washing and quenching (Reader Service No. 100). The machine measures samples by way of a fixed- or discrete-wavelength spectrophotometer. Equipped with an IBM-PC XT system, Photo-Era's processing unit is comprised of two independent sections: the sample processor and the reaction processor. Together, these components can



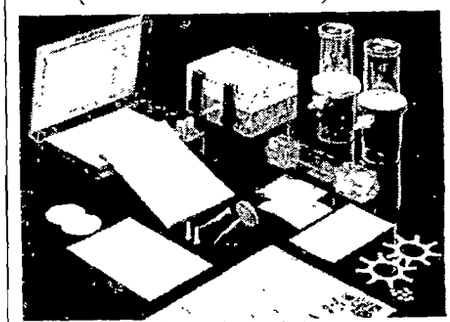
Hybritech puts immunoassays on their own.

process up to 100 samples per hour, and can serve as general automated pipettor/diluters or spectrophotometer/spectroflourometers as well.

A **bench-top liquid scintillation counter** for bioresearch, biotechnology and clinical laboratories fills out Beckman's LS 5801 series. Beckman has designed the LS 1701 for quick and simple routine analyses (Reader Service No. 101). The standard instrument features three independently programmable user files, with preset isotope settings for tritium, carbon-14, phosphorous-32, sulphur-35 and iodine-125, as well as automatic isotope endpoint determination so that the system can adjust itself to any isotope selected. Beckman's machine can provide accurate d.p.m. data regardless of the scintillation cocktail or counting vials being used, and it retains its accuracy throughout changes in volume, quench types or isotope pairs and ratios.

Using protein pigments that occur naturally in algae and cyanobacteria, Biomeda Corp. has developed **immunofluorescent probes** that exhibit 10 to 30 times the fluorescent intensity of conventional fluorescein conjugates. Bound covalently to specific antibodies, these phycobiliproteins can combine recognition with fluorescence emission that is uniform over a wide *p*H range, and in the presence of most biological compounds (Reader Service No. 102). Biomeda's latest addition to their offerings, Phycoprobe-PE (for phycoerythrin) antibodies, can be excited at the same wavelength as fluorescein-labelled compounds, although the Phycoprobe's maxima is at 575 nm. The higher wavelength transmission can translate into a clearer signal, because it creates a larger Stoke's shift.

Schleicher and Schuell, showing in hall 3 at stand B4, plan to present several new products at Analytica including an **electroelution system** for the purification and concentration of electrically-charged biopolymers. Underlying the Biotrap's efficacy is a novel membrane which, when subjected to an electrical field, retains only charged molecules of molecular weights ≥ 5,000 — without adsorbing them (Reader Service No. 103). With Bio-



Schleicher and Schuell's Analytica array.

trap, DNA/RNA and protein samples can be eluted from gels, concentrated by dialysis and separated by isoelectric methods. Disposable filter units, DNA purification chromatography columns and transfer media will also adorn Schleicher and Schuell's exhibit area.

Filter and ferment

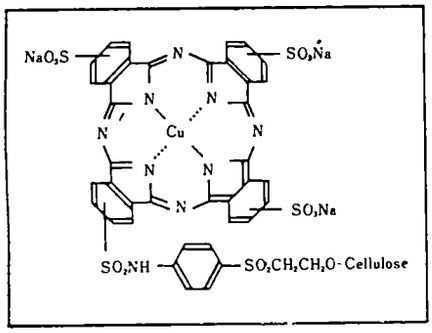
The star of Elga's show in hall 14 stand B16 is the Elgastat UHQ laboratory **water purification unit.** Incorporating five different purification techniques, the Elgastat unit yields high quality water for use in HPLC, fluorescence analysis, atomic absorption and ion chromatography (Reader Service No. 104). Water processed through Elga's system conforms to the following specifications: inorganics, 18 MΩ cm^{-1} at 25°C; organics, 0.0001 absorbance at 254 nm; TOC, 20 parts per 10^9; bacteria, 1 CFU ml^{-1} and particles, 0.2 μm absolute filtration.

In hall 2 stand B14/D, a variety of **fume filtration cupboards** from ASTEC Environmental Systems Ltd will grab the spotlight. All ASTEC's cupboards can be installed without ducting or building work, or mounted on trolleys for the

greatest flexibility (Reader Service No. 105). And 13 types of filters are available to combat the effects of solvents, acids, alkalies, ammonia, H_2S, SO_2, formaldehyde, resins and so on. ASTEC's latest cupboard series, called Condor, has powder handling and cytotoxic drug preparation facilities and can be used as a glove box as well. It features high- and low-level extraction vents, a floor-level filtration system and a 1,200 mm × 600 mm epoxy resin dished work surface. Also exhibited in ASTEC's stand are the Astecair filtration fume cupboards and Mystaire scrubber.

A fermenter family from Infors AG will be making its world premier at Analytica this year, in hall 11 stand B15. Infors says it set out to build fermenters that were easier to handle, maintenance-free, more versatile and safer to operate (Reader Service No. 106). How well they have achieved their purposes can be judged first-hand. Compact ISF-fermenters can use top or bottom drive, selected at sight without tools or service engineers. The bottom valve, with high current flow, is combined with a sampling port which allows the extraction of very small probes. Infors guarantees sterilization *in situ*; when the sterilization procedure is initiated, the air inlet and outlet lines automatically separate from the vessel and can then be sterilized apart from the vessel. Peripheral measurement, together with control and regulation modules, complete Infors's ISF-fermenter package.

Aqueous and organic solutions can be **cleansed of mutagens in minutes** with a new adsorbent from Pierce, hall 14 stand



Mutasorb's formula for nabbing mutagens.

E17. Called Mutasorb, Pierce's agent consists of adsorbent cotton bearing covalently linked trisulpho-copper-phthalocyanine residues (Reader Service No. 107). This ligand enables Mutasorb to adsorb mutagens containing more than three fused aromatic rings, such as mutagenic polycyclic aromatic hydrocarbons, mutagenic heterocyclic amines, polycyclic antibiotics and dyes such as ethidium bromide and crystal violet. One gram of the adsorbent contains approximately 10 μM of copper phthalocyanine; about 5 mg of Mutasorb per ml of solution can remove 1 μM of ethidium bromide. Pierce's product can be added directly to aqueous solutions, whilst solid materials have to be extracted with water or organic solvents.

Next on the bench

Earlier this year, Sartorious brought a new line of **analytical balances** to the market with capacities up to 12,000 g, readabilities from 0.00001 g to 0.1 g and full-range electronic taring. Now at Analytica, Sartorious will show most of these balan-

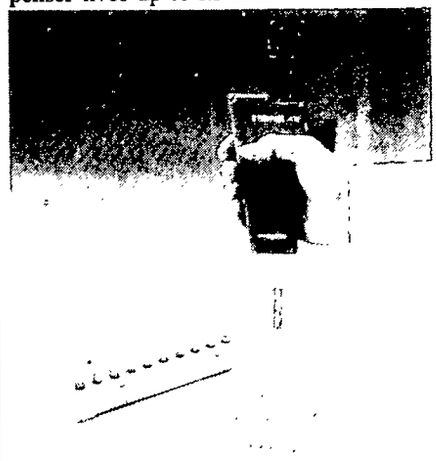


The A200S balance has clear advantages.

ces; and of these, the Analytic balance A200S may capture the most attention (Reader Service No. 108). Sartorius's top-loading A200S, with a 200 g capacity, features a weighing chamber housed in glass all around for 'five-sided' viewing. All balance functions can be controlled with up-front, one-finger formatting. One touch calibrates the balance, which then automatically returns to the weighing mode and displays sample weight. The Sartorious A200S has a 0.1-second update speed and an RS232C data output option that permits interfacing with printers, computers and Sartorious keyboards.

Carl Zeiss's **research microscopes** have just emerged from a design overhaul, and the results will be exhibited at Analytica. The Axioplan and Axiophot microscopes incorporate two design changes that should make switching between microscopic techniques more convenient (Reader Service No. 109). What Zeiss calls infinity colour-correlated system optics, or ICS optics, gives all objectives an infinite image distance so that a range of techniques including brightfield, darkfield, phase contrast, qualitative polarized light, differential interface contrast and fluorescence can be accommodated without additional lenses or loss of image quality. ICS optics also maintains a large consistent field of 25 mm and a contrast magnification factor, regardless of the method employed. System-integrated, or SI, design enables permanent or modular optical components to be integrated into the microscope housing without impairing image quality or field of view. Components for either reflected or transmitted light microscopy fit the system equally well.

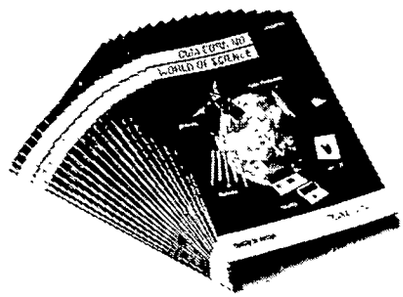
The **adjustable volume repetitive dispenser** lives up to its name: with this de-



Wheaton's dispenser: a cure for the common aliquot.

vice, up to 74 repetitive deliveries of preset microlitre volumes can be made without refilling the syringe. The dispenser is the brainchild of Wheaton Instruments (Reader Service No. 110). Filling the dispenser involves inserting a disposable syringe into the device's housing and raising the piston. A volume knob indicator can be rotated to the desired setting. Three sizes of disposable syringes effect total deliveries from 10 μl to 5,000 μl, with an accuracy of ± 1 per cent above 20 μl, ± 1.5 per cent at 20 μl and less.

As a primer for Ciba-Corning's Analytica exhibit, their 1986 laboratory instruments catalogue *World of Science* describes in full their Delta *p*H meters and ion analysers, their 410 digital flame photometers, carbon dioxide analysers, chloride analysers and colorimeters. The 20-page colour brochure gives individual specifications and information on accessories for Ciba's instruments (Reader Service No. 111). The catalogue also has lists of charts and brochures available on speci-



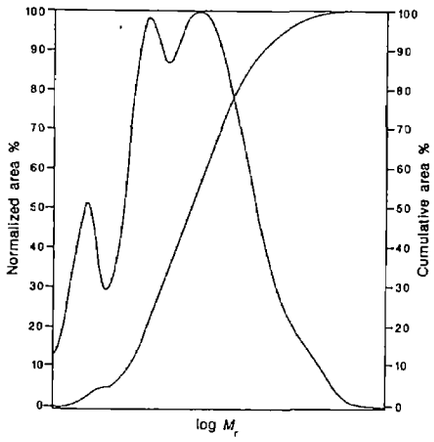
Essentials and accessories in Ciba-Corning's catalogue.

fic application methods should the reader wish to pursue a particular application in further detail.

Perkin-Elmer, in cooperation with the biotechnology company Cetus, have produced a **computerized pipetting system** specifically intended for biological procedures in microtitration assays. The Pro/Pette automated liquid handling instrument can be programmed, using a hand-held controller, in 1-μl increments throughout a 1- too 200-μl range (Reader Service No. 112). With interchangeable pipette heads, Perkin-Elmer's device can perform serial dilutions, plate-to-plate transfers of samples, aspiration, filling and mixing of well contents. The ability to alternate between single- or multi-channel pipetting is another aspect of the Pro/Pette's flexibility. Perkin-Elmer plan to display their product in hall 5, stands A6/B3.

Software schemes

In conjunction with Heyden & Son's Chromatochart software, their new **gel permeation chromatography (GPC) software** for Apple II microcomputers can perform molecular weight distribution calculations. Consisting of two modules, calibration and analysis, GPC enhancement software is linked to Chromatochart's menu structure (Reader Service No. 113). The Software combines information from its parent's method, baseline and data files with calibration coefficients created by the calibration module. The GPC analysis module ties coefficient calculations together with Chromatochart's capabilities to correct for baseline drift and to define peak start and stop positions. Molecular weight distributions for the sample as a whole, or for individual peaks in a sample, can be obtained from Heyden's software package. Heyden can provide additional information on GPC software at their Analytica stand.



Heyden MW distribution straight from the chart.

Two-dimensional gas chromatography, which can be built into any capillary GC system, just got its own microprocessing controller from Chrompack. At Analytica Chrompack will demonstrate the advantage of MUSIC, or multiple switching intelligent controller (Reader Service No. 114). MUSIC analysis begins by using a short 0.53 mm fused silica column to effect pre-separation of chromatography samples. Then, eluting peaks are trapped on a CO_2-cooled cold trap and injected into a narrow-bore fused silica column with a different polarity, to achieve further separation. MUSIC's microprocessor allows fully automated operation and controls all flows, pressures, oven and trap temperatures.

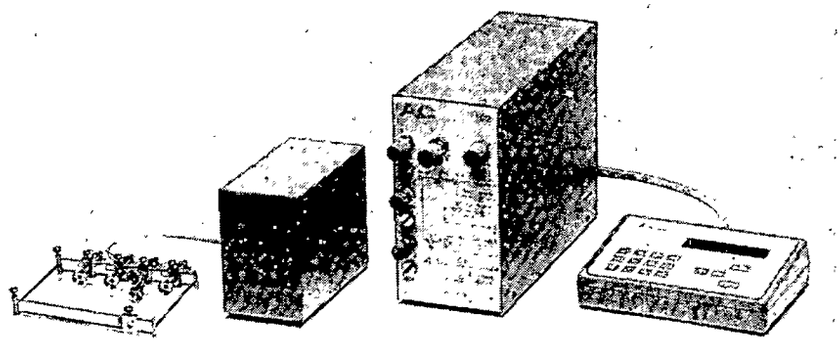
Membranes, media and midgets

As an alternative to conventional cellulose dialysis sacs, Millipore is now offering V series membranes which can prepare microvolumes of proteins or nucleic acids for analysis via the **drop dialysis technique**. With this method, the V series membrane is floated on a Petri dish filled with dialysate, and the sample added to the membrane with a micropipette (Reader Service No. 115). The 0.05- or 0.025-μm pore structure of Millipore's membranes accelerates salt diffusion, and sample additions of 5 μl to 100 μl are probably less time-consuming than procedures used with cellulose bags. At Analytica Millipore can answer questions on their dialysis procedure. The company cites recovery rates in excess of 98 per cent with the drop dialysis technique.



Dialysis with a difference from Millipore

Gold Label **dehydrated culture media** from BBL Microbiology Systems are the result of improved formulations that BBL says will provide superior test results. Currently BBL sell five varieties of the media (Reader Service No. 116). TSA II is BBL's improved general-purpose bacterial culture medium base for preparation with 5 per cent sheep blood. The critical components in another medium, Mueller Hinton II, are controlled to give consistent results in lot-to-lot susceptibility tests. BBL's third Gold Medal culture, MacConkey II, improves the inhibition of *Proteus* swarming so as to give other Gram-negative pathogens room to breath. GC II agar was developed in combination with BBL's IsoVitaleX enrichment and haemoglobin to facilitate the growth of *Neisseria gonorrhoeae* and other fastidious microorganisms. Finally, BBL has a grade A agar that, used as an ingredient, may improve growth and test reaction results.



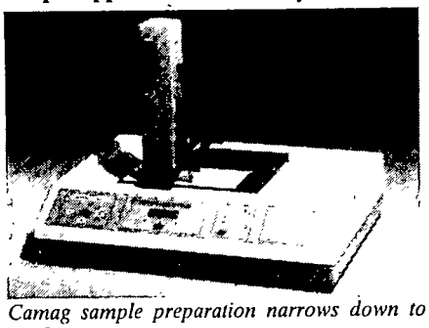
Chrompack will bring MUSIC to chromatography at this year's exhibit.

In the race to catch up with Pharmacia's Phastsystem, LKB has introduced a **miniature electrophoresis system** that completes an analysis from gel-casting to scanning in under two hours. On display at Analytica, LKB's 2050 Midget system can perform screening of small samples by high-resolution techniques such as zone, disc, gradient, SDS and 2D electrophoresis (Reader Service No. 117). The complete Midget package includes multiple gel casting units, an electrophoresis tank, an electrophoretic transfer unit, a laser densitometer, digital power supply and accessories. The system can cast up to 14 gels at one time and run two gels with 5, 10 or 15 samples each in less than 45 minutes;

LKB claims the time savings can cut running costs by 90 per cent.

Newcomers in instruments...

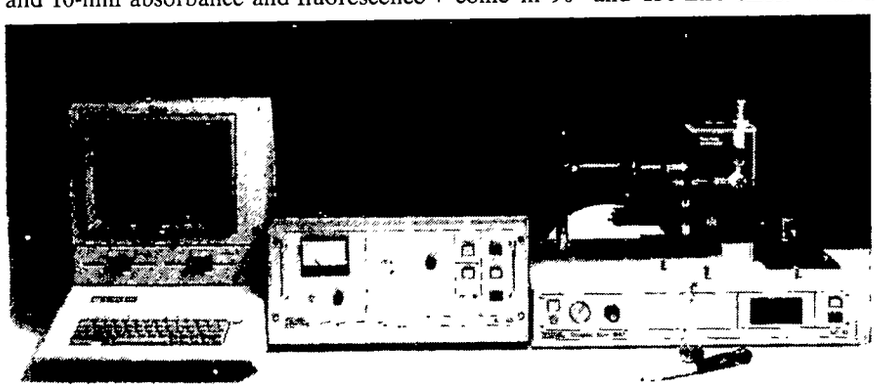
Automation has won over Camag's Linomat spray-on techniques for **narrow-band sample application** in thin-layer chroma-



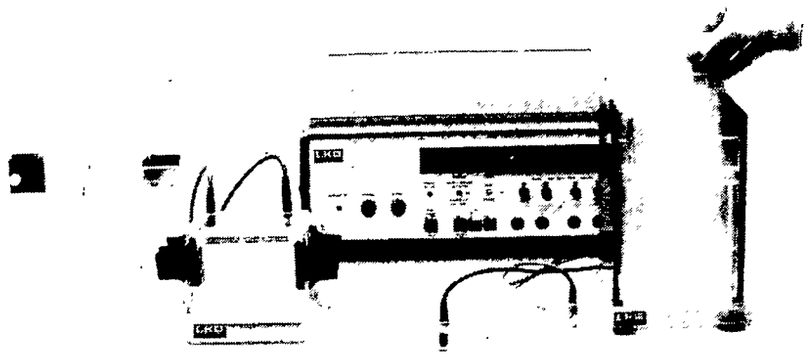
Camag sample preparation narrows down to TLC

tography. The Linomat IV is a microprocessor-controlled, programmable instrument with keyboard parameter entry that automates the same spray-on technique, using nitrogen as the carrier gas, that previously bore the Linomat title (Reader Service No. 118). Camag's latest version, exhibited in stand C8/D7, hall 2, computes the number of available tracks from information on band length, distance between samples, edge space and plate width. Linomat IV then indicates the tracks by means of light-emitting diodes, and sample deliveries from the syringe proceed automatically.

A **stopped-flow spectrophotometer** from Hi-Tech Scientific can generate five runs from 500 µl of each reagent. Hi-Tech intended their instrument for work with precious biological materials, and minimized the quantities required to fill the flow circuit, which is totally thermostatted, chemically inert and readily aerobicized (Reader Service No. 119). Their spectrophotometer features a two-tier design consisting of an upper sample handling platform and lower optical platform. The optical cell itself uses an integral ball-mixer and has four optical windows for 2- and 10-mm absorbance and fluorescence



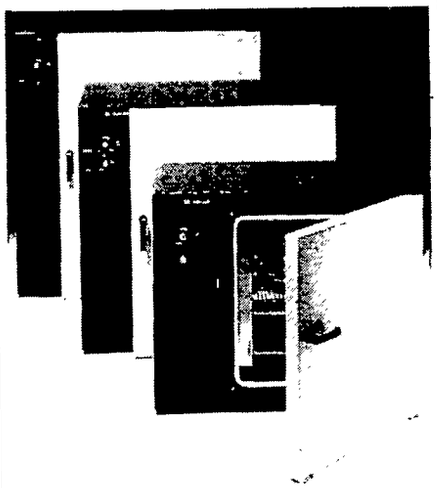
A stopped-flow spectrophotometer from Hi-Tech gets the most out of small samples.



LKB's Midget runs high-resolution separations in less than an hour.

work. At Analytica, Hi-Tech will be located in stand B14, hall 7.

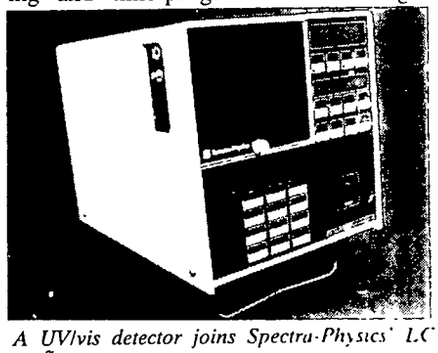
The display at Gallenkamp's stand B3 hall 9 will reveal a rounded-out collection



Gallenkamp ovens in all shapes and sizes.

of **laboratory and light industrial ovens**, from standard 23-litre units to large 586-litre units, and from vacuum to humidity oven environments. Gallenkamp's most recent arrivals are the standard ovens sized up to 200 litres, in gravity-convected and fan-circulated versions (Reader Service No. 120). General-purpose ovens, which specialize in temperature control, come in 90- and 150-litre sizes. With a temperature range of 40°C to 240°C, Gallenkamp's large-capacity ovens (340 and 586 litres) were designed for large loads or awkwardly-shaped items. And two large-capacity vacuum ovens in 90- and 260-litre volumes have joined Gallenkamp's 30-litre vacuum variety. The company will also have their incubator line, including the Gallenkamp Orbital models, at Analytica this week.

Bent on expanding the possible system configurations of their LC instruments, Spectra-Physics has added a **scanning UV-vis detector** to its product list. The SP8480XR connects with the Spectra-Physics computing integrators, SP4270 or SP4290, via a plug-in PROM chip installed by the user (Reader Service No. 121). The SCAN chip enables the integrator to perform automatic stop-flow peak scanning with background subtraction, peak ratioing and time-programmed wavelength



A UV/vis detector joins Spectra-Physics' LC outfit.

changes for selected peaks within a chromatogram. The detector itself has a drift measured at less the 1/10,000th of an absorbance unit per hour. Baseline zeroing can be carried out manually or automatically. Spectra-Physics will have the scanning detector on display at their Analytica stand.

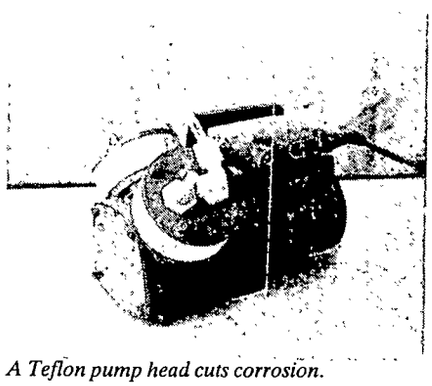
...and accessories

A **wideline solids accessory** (WSA) for use in biophysical research can expand the capabilities of Varian's VXR series of NMR spectrometers to include the examination of samples in solid states. With

Varian's new solids NMR instrumentation, researchers can obtain detailed structural and dynamic information about molecules and investigate molecular motion (Reader Service No. 122). WSA has a 1 kW high-power pulse amplifier that generates the short radio-frequency pulses needed to cover the wide spectral widths associated with solid protein NMR spectra. Likewise, the WSA receiver bandwidth has been increased to 2 MHz. Varian can also demonstrate the software included in WSA that performs specific wideline NMR experiments on Varian's spectrometers.

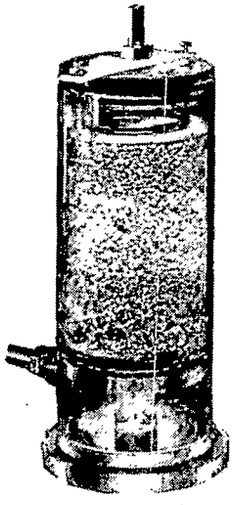
A **sealed rotor** for middle-capacity benchtop and under-bench refrigerated centrifuges helps contain blood samples and other infectious materials during centrifugation. Heraeus Separationstechnik has engineered the 3360 rotor with a stainless steel shield and transparent polycarbonate lid to replace their 3350 rotor (Reader Service No. 123). The tightly-closing lid keeps infectious agents from getting into the centrifuge or surrounding areas in the event of aerosol formation or glass breakage, and breakage can be identified immediately because the lid is clear. Heraeus Separationstechnik's rotor also uses a racking system which caters to tubes of capacities from 7 to 100 ml, and has decanting and incubation facilities. More information will be available at Analytica from Heraeus Separationstechnik.

KNF Neuberger have machined a **vacuum pump head** from solid Teflon, resulting in a pump with strong chemical resistance to corrosive vapours. The inlet and outlet valves in KNF's pump are also made from Teflon, and the diaphragm is produced from rubber laminated to a thick layer of Teflon (Reader Service No. 124). Teflon protection means that the pumps can be used with all kinds of chemical vapours without inevitable pump failure. KNF's series of corrosion-resistant pumps spans flow rates from 18 to 32 litres per minute, with vacuum levels down to 10 mbar.



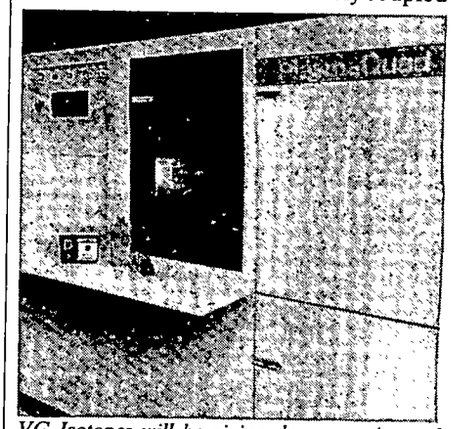
A Teflon pump head cuts corrosion.

Savant Instruments, in stand D4, hall 7, take another approach to vapour corrosion in vacuum pumps. Their **chemical trap**, the model SCT120, removes acidic, alkali, organic and inorganic vapours that can condense in the pump system and wreak corrosive havoc (Reader Service No. 125). Savant's plexiglass cylinder measures 5 inches in diameter by 11 inches in height, with a removeable top for cleaning and re-charging. In operation, the SCT120 should be placed between the concentrator/evaporator and the vacuum pump; standard ½-inch tubing will make adequate connections. □



Savant traps vapours before damage begins.

A computer-assisted **data acquisition and analysis** system for VG Isotope's VG 9000 glow discharge mass spectrometer (GDMS) will make its debut at VG Isotopes' stand A10, hall 11 at Analytica (Reader Service No. 126). The system offers multipaging of screen memory for access to menu-driven utilities such as current status readouts, real-time data acquisition displays, peak information and graphic analysis of old or current data. Graph scaling, peak identification and selection, baseline setting and other parameters are controlled from soft keys. VG Isotopes claim this package enhances the performance and convenenience of their VG 9000, a GDMS instrument which has achieved detection limits below 10 parts per 10^9. Also at the company's Analytica stand, VG Isotopes scientists will be operating the PlasmaQuad inductively coupled mass spectrometry system (ICP-MS), a machine that gives detection limits better than 0.1 parts per 10^9 for most elements.



VG Isotopes will be giving demonstrations of their ICP-MS at Analytica.

Baird & Tatlock's motorless stirring technique has some new followers. The Flatspin 2 range of **stirrers**, on view in Analytica at stand B3 hall 9, has a 'spin-off' feature that provides a warning if the magnetic follower loses capture while stirring (Reader Service No.127). Baird & Tatlock have developed two types of Flatspin 2 products; the new immersion stirrer and a hotplate stirrer. The immersion stirrer has an encapsulated head that can withstand temperatures up to 100°C; the hotplate stirrer now includes an external probe for monitoring temperature suspended in solution. □

These notes are compiled by Karen Wright from information provided by the manufacturers. To obtain further details about these products, use the reader service card bound inside the journal.

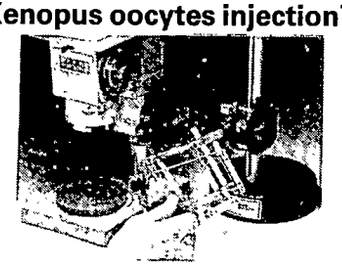
Erratum: VCA/AIDS ELISA test kit

THE product review for Cellular Products' Retro-Tek AIDS test, published in the 10 April 1986 issue of *Nature*, incorrectly stated that "direct absorbance readings [generated by the test kit]... indicate the progress of the disease". In fact, these readings can only be used to monitor the concentration of the AIDS viral antigens in tissue culture samples or the presence of AIDS antigens in isolation and purification schemes. □

ADVERTISEMENT

SINGER INSTRUMENTS

Xenopus oocytes injection?



SINGER MKI MICROMANIPULATOR

We also offer a Microsyringe Kit.

Write to:
Singer Instrument Co. Ltd.
Treborough Lodge
Roadwater, Watchet
Somerset TA23 0QL
England. Tel. (0984) 40226
Telex: 337492 Comcab G

Reader Service No.50

nature

NATURE VOL. 321 29 MAY 1986

The changing of the old guard

The British government seems to have sensed that its policy on education could be an electoral liability, which is correct. But throwing printed money at the problem will not help.

MR Kenneth Baker, the new Secretary of State for Education and Science in the British government, has with enthusiasm taken on an impossible task. After two years of bruising labour troubles in the schools, he has implicitly undertaken to restore the morale of the dwindling band of able teachers, to modernize the school curriculum and to produce results (better examination results). He has to do the same in higher education, somehow persuading academics and their institutions that the government's reduction of their budgets by more than 20 per cent in five years is in reality a measure of its high esteem for them. Harder still, he must persuade researchers (for the government has not taken this golden chance to split off the administration of research) that his predecessors have caused institutes to close, and cohorts of bright young people to find posts elsewhere, so that the remainder will have better pearls to look for. All this has to be done in less than eighteen months.

Mr Baker's enthusiasm is his strongest suit. It won him notable success when, as minister of information technology five years ago, he persuaded the British government and many of its electors that the time had come to "cable Britain", putting umpteen channels of cable television into every home. He had fortunately been promoted from that post by the time it became apparent that he had not persuaded that section of the community with funds sufficient to launch commercial cable that there could be no better place for their money. It would nevertheless be a great misfortune if the transformation now planned for British education follows the pattern of the cable revolution that never happened. Education is too important.

The most chilling sentence in last week's letter from the University Grants Committee to its constituents is the statement that there is now no prospect of being able to increase the proportion of university students following courses in the government's special engineering and technology programme by more than 14 per cent over 1984–85 by the end of the decade because of "early specialization and staffing" in the schools. Similar constraints apply elsewhere across the educational spectrum, and governments are not entirely to blame. British universities have been chiefly influential in requiring that school-leavers should have so thoroughly rehearsed at school what they will learn at university that students are at once bored (because they know it all already) and ill-educated (because they know nothing else). The universities have now changed their tune.

So how should Mr Baker best blend his endearing personal enthusiasm with the long-term character of the problem of education and research? Here are a few maxims he might follow. Most parts of his new intellectual empire have been through a long period of change, which has accelerated in the past few years. The schools had hardly survived the intense curriculum development of the 1960s when they were required to change again, for largely social reasons. Higher education began that period by being expected to grow quickly and was then asked to stand still until the time came to contract. The same has happened in research. People are sick and tired of it. A moratorium on organizational revolution would be a blessing.

An end to upheaval does not however require stagnation. Mr Baker would do himself and his constituents a power of good if he allowed that, within a framework of stability, it would be in the public interest if people or institutions who wish to change were allowed to do so. There would be some schools keen on taking up new bits and pieces of curriculum, even some universities anxious to break out in new directions, not to mention a small army of academic researchers who would eagerly do new things. Inspection might even discover that the Royal Greenwich Observatory, about to be moved for largely administrative reasons, might usefully be left where it is on the understanding that its professional astronomers should compete for research grants with their colleagues in the universities.

To whom should even an enthusiastic new minister turn for advice on matters like these? The trouble with the British enterprise in education and science is that its managers have been tainted by the failures of the past. All honourable men and women, they are the same who have failed to defend their institutions from internal weaknesses and from the malevolence of Mr Baker's predecessors. They have lost the allegiance of their younger and more creative colleagues. Mr Baker, if his intentions are serious, had better get out and about, off the beaten tracks of the corridors of administrative tidiness. While on his journeys, he might make the speech or two suggesting that he is someone who knows what the enterprise is for. □

What yellow peril?

The British government has said it has not found mycotoxins in samples of yellow rain.

THE notion that the people of Laos and Cambodia were attacked by their Vietnamese neighbours by means of a chemical toxin sprayed from aircraft had become a bit of a joke even before Dr Matthew Meselson turned it into pastiche by remarking that most of what appears to be yellow rain consists of the excrement of bees. The allegation was first made by Mr Alexander Haig during his brief spell as US Secretary of State, but on the flimsiest of evidence. Trichothecene toxins, produced naturally by *Fusarium* fungi, are undeniably lethal in appropriate circumstances, but less quickly so than cheaper modern chemical warfare agents.

As time has passed, the case has been less easy to sustain. People's capacity to analyse for trichothecenes is one of the marvels of mass-spectrographic assay. The fact that Britain's Porton laboratory has looked for trichothecenes in yellow rain and failed to find them does not imply that all samples of yellow rain are free from mycotoxins, or that no yellow rain has ever been so contaminated deliberately. But it does give the lie to the notion that all yellow rain is lethal, which is not surprising since most of it is known and admitted to be the excrement of bees. So now there are two choices; either the State Department must acknowledge that the Vietnamese were even more devilishly clever than had been supposed in concealing their use of an improbable chemical weapon behind the cloak of a previously ill-recognized biological phenomenon, or the State Department should allow that it may have been mistaken □

Genetic regulations

US to settle dispute over agency jurisdiction

Washington

AFTER months of inter-agency wrangling, the new federal government policy statement on biotechnology research is expected to be published in the *Federal Register* by the end of the month. Its supporters believe it will make clear the complex maze of regulatory jurisdictions among federal agencies. But even its authors acknowledge that the new document, which is two-and-a-half inches thick, will be a challenge to general understanding.

The framework is the next step in the process begun in December 1984 to coordinate government policy regulating biotechnology (see *Nature* **313**, 85; 1985). Since last November, when an index of relevant statutes appeared in the *Federal Register,* the Domestic Policy Council (DPC) Working Group on Biotechnology has been conducting an intensive effort to arrive at an inter-agency consensus on how those statutes are to be applied.

"The goal was to get coordination and consistency", says David T. Kingsbury, National Science Foundation (NSF) Assistant Director for Biological, Behavioral and Social Sciences and chairman of the DPC working group. The effort attempts to get away from a process approach to regulation, and move toward a product oriented approach.

The DPC working group felt that placing all products created by recombinant DNA techniques under the same regulatory umbrella was misguided. As an example, the pseudorabies vaccine developed by Saul Kit at Baylor College of Medicine uses a modified virus missing a part of its genome. Because it incorporates no new genetic material, it may reasonably be treated just like any other altered vaccine. The working group takes the approach that it is only when genetic material from organisms of different genera are combined that special attention needs to be paid to the potential hazards of a new organism.

The new document, the Coordinated Framework for Regulation of Biotechnology, contains policy statements by all the major regulatory agencies involved in biotechnology. Because of the "mosaic" of statutes covering biotechnology issues, "the potential for confusion is enormous," says Kingsbury. To ameliorate this problem, the new framework proposes two new definitions as a basis for coordinating new regulations.

The Biotechnology Science Coordinating Committee (BSCC), made up of senior policy officials of agencies involved in biotechnology research and products, took responsibility for coming up with the definitions. An "intergeneric organism (new organism)" is one formed by "deliberate combination of genetic material from sources in different genera". A "pathogen" is defined to include microorganisms that "belong to a pathogenic species or that contain genetic material from source organisms that are pathogenic." Specifically excluded from both these definitions are organisms that are "well characterized and contain only noncoding regulatory regions." BSCC is considering expanding these exemptions, as well as defining more formally an environmental release.

A key accomplishment of the new framework is to sort out the overlapping jurisdications of the various federal agencies involved in biotechnology regulations. The framework attempts where possible to identify the single agency having responsibility for a single product, but where overlapping jurisdictions arise, the lead agency is identified. Kingsbury, as chairman of BSCC and DPC working group, will be the *de facto* arbiter of disputes over jurisdiction.

While sorting out overlapping jurisdictions between agencies was a major accomplishment for the DPC working group, jurisdictional issues also cropped up within the agencies. At the US Department of Agriculture (USDA), disputes arose between the science and education division and the marketing and inspection services over review issues.

One upshot of the disputes was the creation of an Office of Agricultural Biotechnology to keep track of all items either reviewed for licence or proposed as research. In addition, the Agriculture Recombinant DNA Committee (ARC) is being disbanded; an Agricultural Biotechnology Recombinant DNA Advisory Committee will now assume responsibility for review of all research projects.

Although the new framework represents a step forward in coordinating federal policy, some worry that the regulatory system is still chaotic. Quick to acknowledge the magnitude of the task Sue Tolin, co-chair of the USDA ARC, is unconvinced that the new framework will sort out all the regulatory tangles now confronting biotechnology research firms. She points to a discouraging catch-22 situation; to prove organisms are safe, they must be tested, but before they can be tested they have to be proven safe.

Meanwhile, the first attempts at actually field-testing a genetically engineered organism are still running into problems. The Environmental Protection Agency declined to issue an experimental use permit to Monsanto to test two strains of *Pseudomonas fluorescens* containing a gene insertion of a toxic gene from the microbial insecticide *Bacillus thuringiensis*. The agency wants to see additional data on the organisms' environmental impact and short-term pathogenicity.

Joseph Palca

Chernobyl

British embassies turn monitors

AN attempt at comprehensive monitoring of the radioactive fallout from the Soviet nuclear accident at Chernobyl has been carried out by British embassies in European capitals bordering the Soviet Union. A statement put out last week by the National Radiological Protection Board and by the Foreign and Commonwealth Office (FCO) suggests that contamination is greatest in north-east Poland, Czechoslovakia and Hungary.

The FCO statement says, however, that the contamination of local foodstuffs is nowhere high enough to suggest that travellers to those parts of Europe would receive "more than a fraction" of the annual dose limit for members of the general population. The statement adds that travel to Kiev and the western Ukraine, and to Minsk and Byelorussia, should be avoided if possible, but that simple precautions (such as the avoidance of fresh milk and leaf vegetables) would be sufficient elsewhere in the Soviet Union and Eastern Europe.

The use of the network of British embassies as a means of monitoring fallout from Chernobyl was made possible by the supply of simple equipment immediately after the accident. According to figures accompanying the statement, the dose-rate at Kiev, south of Chernobyl, had fallen from 30 to 2 microsieverts an hour between the period immediately after the accident and 14 May. Elsewhere in Eastern Europe, the highest dose rates recorded by British embassies were in north-east Poland (4.5 microsieverts an hour) and Romania (3.6 microsieverts an hour), but these had fallen to 0.8 and 0.9 microsieverts an hour by 14 May.

By comparison, the estimated radiation dose rate due to natural causes (cosmic rays, radon and internalized natural radioactive species) is generally taken to be 2 millisieverts a year at normal altitude and in mid-latitude, roughly the equivalent of 0.5 microsieverts an hour. □

British universities

Further contraction ahead?

BRITISH universities were last week divided in their estimation of what the future holds. The replacement as Secretary of State for Education and Science of Sir Keith Joseph, who has retired from the government, by Mr Kenneth Baker, previously Secretary of State for the Environment, was generally regarded as a sign that the government may change course on the continued contraction of the university system. But the letter to universities from the University Grants Committee (UGC) has confirmed others in the belief that deprivation will continue.

Mr Maurice Shock, chairman of the Committee of Vice-Chancellors and Principals (CVCP) and vice-chancellor of the University of Leicester, in a fierce statement after the publication of the UGC letter, said that the present gap between the universities' needs and the total recurrent grant from UGC amounts to 4 per cent of the total budget, not merely the 2 per cent of annual income estimated by UGC. That estimate, he said, had been made in "far-off, happy, dreaming days". Now, "you can forget about 2 per cent".

The worsening of the immediate financial prospects for the British universities has come about for several reasons, most of them outside the control of the universities themselves. One is the unexpected increase in the amounts universities have to pay as rates (local authority taxes), which have risen for the university system as a whole by 13 per cent as a consequence of government policies on central subventions for local government.

The cost in the present financial year amounts to £15 million for all the universities, roughly 1 per cent of their total cost. Shock said last week that if the British government wished to give an earnest of its intention to deal more generously with the universities (see *Nature* **321**, 370; 1986), as promised by Sir Keith Joseph in his pre-retirement statement to the House of Commons, it should make good this shortfall.

Academic salaries (which account for 70 per cent of academic costs) have become another issue between the universities and the government, chiefly because the university budget for the coming year has been drawn up on the assumption that salaries would increase only in line with inflation, itself supposed to be 4 per cent a year, while the government has just concluded a pay settlement with its civil servants that will give them more than 6 per cent a year.

CVCP's pessimism is borne out by the details given in the UGC letter of subventions for universities in the year 1986-87 (which begins on 1 August). By that time, UGC says, it will have become apparent that the university system will have fallen back during the year, relative to inflation, by about 3.5 per cent and that in future the shortfall will exceed 2 per cent in each year.

This year's letter to universities is of particular interest in that it is the first in which UGC has based its allocations on a deliberate assessment of the quality of individual institutions both in research and in quality of teaching. Over the succeeding three years, the proportion of the total UGC budget (£1,213 million in 1986-87 after deduction of rates and other special amounts) likely to be redistributed between institutions to allow for differences in research output is expected to amount to 15 per cent. But in this first year of the new regime, the consequences of these judgements have been limited to variations of between 1 and 3 per cent in the grant to individual universities.

The result is that it is not possible to tell from the figures published last week which universities are likely to prosper in the coming years and which will be in danger of extinction. Two newer universities (Warwick and Bath) do best out of the allocation, with grant increases between this year and next of 4.0 per cent and 3.6 per cent respectively. Oxbridge marks time (the Cambridge budget goes up by 0.7 per cent between this year and next, that of Oxford is unchanged). Universities such as Essex and Hull, the business schools and the Welsh university colleges will have their budgets cut by 0.5 per cent between this year and next, but a full explanation will be apparent only when individual letters are sent to universities early this week.

The prospects for an improvement of the situation turn entirely on a proposal in Sir Keith Joseph's final statement that there should be talks between the universities and the government on the financial situation, and the promise that extra funds would be made available to universities able to demonstrate that they had met certain objectives, not yet clearly defined. Will Mr Baker be able to put flesh on the bare bones of this promise?

Yellow rain

British analyses find no toxin

THE British government last week disclosed that attempts to find traces of mycotoxins in samples of yellow rain from South-East Asia have yielded negative results. In reply to a question from Mr Leo Abse, Member of Parliament for Pontypool, on 19 May, the Ministry of Defence acknowledged what has been widely rumoured for some time, that the British work so far has failed to confirm reports from US laboratories of the presence of trichothecene mycotoxins collected from Laos and Cambodia.

It is understood that the British investigations have been carried out at the Chemical Defence Research Establishment of the British defence ministry at Porton in Wiltshire. Samples of yellow rain collected from South-East Asia were supplied by the US authorities. The British laboratory was involved in a collaborative study of the composition of yellow rain after the first allegations in 1981 by the US State Department that yellow rain was an agent of chemical warfare were followed by reports of mycotoxins, notably by Dr J. Mirocha of the University of Minnesota.

The British government said last week that the Porton laboratory has analysed a number of "environmental and biomedical samples" from South-East Asia "to see whether trichothecene mycotoxins could be detected". Noting that the absence of positive results is "not necessarily incompatible" with positive findings elsewhere from different samples, the statement nevertheless says that "we are confident" that the techniques used at Porton would have detected mycotoxins had they been present in the "alleged chemical warfare" samples available.

The statement by Mr John Stanley, Minister of State for the Armed Forces at the Ministry of Defence, went on to say that, in spite of the negative findings in the analysis is at Porton, the British government believes that "chemical warfare attacks probably did take place in South-East Asia" on the basis of "epidemiological evidence". He added that the British government is unable to say what agent may have been used in those attacks, or who may have supplied it.

In reply to one of the points raised by Mr Abse, the British government said its investigations "neither support nor contradict" the suggestions made chiefly by Dr Matthew Meselson of Harvard University that drops of yellow rain of the kind reported from South-East Asia are indeed the faeces of bees.

The British government's statement is important because of repeated suggestions from the United States that the British measurements confirm the positive findings in some US laboratories. The "epidemiological evidence" referred to in the government statement presumably refers to reports of mycotoxins in the blood of members of the Hmong population of Laos and Cambodia who have reported being attacked by chemical agents in the form of yellow rain.

US research control

Professional societies still at sea

Washington

DESPITE the attention given in recent years to restrictions imposed by the US Department of Defense (DoD) on foreigners' access to technical meetings, professional societies still differ widely in their policies on the sponsorship of closed or restricted sessions.

According to the committee on scientific freedom and responsibility of the American Association for the Advancement of Science (AAAS), many societies apparently deal with DoD in an *ad hoc* fashion. Fewer than half of 45 technical societies affiliated to AAAS that responded to a questionnaire have adopted policies dealing with the question, but those that have generally favour prohibiting restricted-access sessions.

Government policy on open communication has been subject to several revisions in recent years. Recently, controversy has focused not so much on security classification as on export controls used to prevent access by foreigners to unclassified research results. Last October, the White House issued a security directive stating that the administration intended to use only security classification to control access to fundamental research data, to the general approval of the research community. But the imposition of export controls on meeting sessions for limiting access to applied research remains contentious.

Several important scientific societies, including the Institute of Electrical and Electronic Engineers (IEEE), have said they will not sponsor such sessions under any circumstances. Foreigners sometimes voice the suspicion that such controls are imposed more to give US industries a competitive advantage than to protect national security.

The 45 affiliated societies responding to the questionnaire were selected for their interest in subjects likely to be militarily important. Forty per cent had adopted policies on restricted sessions, almost half of them within the past five years; two-thirds of those with explicit policies restricted or closed meetings. The report concludes that if more societies were to adopt formal policies, these would probably prohibit closed sessions.

A total of four societies had actually experienced "problems" with access by foreign participants in the past three years, one of them more than five times. A separate survey of 24 technical societies not affiliated with AAAS drew only 8 responses; 5 of these societies had experienced problems with access by foreigners to meetings. The AAAS report suggests that the response rate of the non-affiliated societies was poor because the subject is politically sensitive.

DoD's most recent proposal on the subject was in a *Federal Register* notice on 12 February (p.5210). DoD responded to professional societies' concern by undertaking to complete security reviews of the research it sponsored in not more than 30 days, except in "rare and exceptional" cases. DoD also informally undertook in meetings organized by IEEE to ensure that security reviews would be conducted by scientifically qualified personnel, rather than by security inspectors who would "see one key word on a page and classify the whole thing", according to one IEEE negotiator.

The February statement did, however, stir already muddy waters by appearing to contradict the October White House directive on fundamental research, declaring that DoD policy is to allow the publication of unclassified fundamental research only "to the maximum extent possible". But the October security directive definitely still stands, according to Leo Young, director of research and laboratory management in the Pentagon's office of research and advanced technology.

Young said his office had erred in not making this clear in the February statement, but, he said, the great majority of responses from societies to the proposed policy had been favourable. Young said he hoped societies could avoid holding export controlled sessions, but that some, such as the Society of Photo-optical Instrumentation Engineers, were likely always to be in sensitive areas, and that it was up to them whether or not to restrict sessions at their meetings by the use of the export controls. **Tim Beardsley**

Ethiopia

Brief respite from famine

Addis Ababa

IT is now raining in Ethiopia, and much of the country has turned green as a variety of arable crops and pasture have begun to grow again. But this has not chased away the general belief that Africa is a continent in crisis. Dr Mostafa Tolba, executive director of the United Nations Environment Programme (UNEP) based in Nairobi, Kenya, is planning to use the special meeting of the United Nations in New York from 27 to 31 May as a chance to emphasize that the current problems of Africa stem from the underlying deterioration of the African environment.

In Ethiopia, the drought and subsequent famine of 1984–85 has been the focus of attention, but the underlying question is why the ill-effects of the drought were so serious. There were at least eight serious droughts earlier this century, but none of them had such disastrous consequences.

The rapidly expanding population concentrated in the highlands of the east is one of the most conspicuous problems. The traditional pattern of settlement is that of a regular distribution of homesteads across the cultivated areas, but the density is now so high that the marginal land on the steep slopes of the mountains and precipitous river gorges has also been cleared and settled.

One consequence is that the loss of traditionally dense forest to firewood and building lumber has been enormous. In twenty years, the proportion of wooded land has fallen from 16 per cent to about 3 per cent. The result is increased erosion of the soil whose capacity for water retention is itself reduced. At the same time, UNEP officials say, the productivity and drought resistance of the land is falling, which puts pressure on subsistence farming especially when the preferred crop (teff) is lower yielding, less drought-resistant and requires more work than near-equivalents such as millet.

The vulnerability of the land to drought is made worse by poor communications and the preoccupation of the government with rebellions in at least three regions. Referred to as "structural problems" by Commissioner Tadesse of the Government Relief and Rehabilitation Commission, their significance is not underestimated. But the continuing internal conflicts make the outcome for the next drought look bleak.

Similar environmental problems in other African countries led governments to attend the first African Environment Conference, organized by UNEP, the Organization for African Unity and the Economic Commission on Africa, held last December. The outcome has been an increased awareness of the seriousness of environmental deterioration and a strong commitment to cooperation in obtaining the best possible assessment of problems such as desertification and water use to provide a reliable basis for appropriate development.

Although the piles of wheelbarrows now accumulating in the distribution centre of the aid agency, Worldvision, in Wallo region attest to the changing emphasis as the current crisis passes, any major reversal in the trend of environmental deterioration will require an awareness at all levels of the importance of the problems and the enormous collaborative effort required to tackle them. **Nigel Williams**

Japan

Another academic city planned

Tokyo

PLANS are being laid for a large-scale academic city in the Kansai area of Japan. It is hoped that the city will be approved as the region's next giant construction project following the completion of the new international airport at Osaka. Its proponents do not see it as a rival to Tsukuba Science City near Tokyo; it will aim more at basic research and cultural activities than Tsukuba, which is dominated by government research laboratories.

Two thousand five hundred hectares of land have been set aside for the city where the prefectures of Kyoto, Osaka and Nara meet. The location is within 30 km of Kansai's major cities of Kyoto, Osaka and Kobe with their large state universities, and the ancient capital of Nara.

The region also contains the headquarters of a number of Japan's high-technology companies, including several of those involved in research in biotechnology and new materials, and many are proud of being "Kansai" as against "Kanto" (Tokyo zone) companies. Contributions from companies and relocation of their research institutes could very significantly help construction of the new academic city.

The nucleus of the city is at present contained in the "International Institute for Advanced Studies", the only part of the city that has passed from a dream to a reality. The institute was set up, in name at least, in 1984 on the initiative of two former presidents of Kyoto University, Professor Azuma Okuda and Professor Michio Okamoto, a member of the Prime Minister's Council for Science and Technology and head of the Extraordinary Reform Council for Educational Reform.

Since then, the institute has successfully passed through its "phase one": raising a capital of 133 million yen ($830,000), largely from Kyoto-based companies, to establish a foundation and open an administrative office. Now it is well into "stage two" in which 3,000 million yen ($18.7 million) is being raised to endow the foundation and to allow construction work to begin. With luck the institute will be built and running in five years' time. It was conceived after the study of succesful advanced studies institutes elsewhere, notably those at Aspen and Princeton and the Rockefeller Institute, as well as other unique research institutions, including the Research Triangle Park of North Carolina and the Cavendish Laboratory (*Nature*'s issues of 1874 providing a record of its establishment).

As in other advanced studies institutes, the aim will be to invite "the foremost scholars of the world" to come and work there for periods of a few years at a time. Early plans for the institute suggest it will provide an exceedingly pleasant environment: Japanese-style buildings containing guest houses, seminar rooms and dining halls are to be laid out in parkland and connected by the covered corridors found in temples and traditional houses.

The Advanced Studies Institute has in fact already begun activities with the sponsorship of international seminars in Kyoto on artificial intelligence and biosciences. More seminars, centred on scholars invited from abroad, will take place until the institute can assume its full functions.

Several other new facilities may serve as kernels for the academic city. Among them are a new branch of the National Library; a new graduate university, linked to the joint-use university research facilities like those at Okazaki; and a new laboratory for basic research in electrocommunications to be run jointly by the Ministry of Posts and Telecommunications and the newly privatized Nippon Telegraph and Telephone Corporation. These are, at least, possibilities that are being pursued; whether they can be turned into realities remains to be seen.

Those supporting plans for the new academic city believe it will be complete within 15 years. But there remain differences of opinion about its final form. There are some in the universities nearby who see it as a chance to relocate existing departments requiring expansion or renewal, or to bring together related institutes from different universities in the areas.

Others see the creation of a new academic city as a chance to break free from restrictions in the Japanese university system and to create a new style of institute, where deficiencies perceived in Japan's basic research contribution can be rectified.

Alun Anderson

Synchrotron sources

Stanford versus Argonne?

Washington

WITH pressure on the big science budget likely to increase in coming years, gentlemanly competition seems imminent over a proposal by the Stanford Synchrotron Radiation Laboratory (SSRL) to expand material research facilities at one of its electron storage rings. Recent experiments with the ring have been so successful that adding more beam lines might reduce the need for a future 6 GeV synchrotron coveted by Argonne National Laboratory.

The PEP (Positron Electron Project) ring at Stanford, generally agreed to have been something of a disappointment, was originally used for high-energy physics experiments, but with the impending completion of the Stanford Linear Collider (SLC), particle physicists have rather lost interest in it. In its heyday, PEP had five beam ports for high-energy physics experiments, but this figure is now down to one.

PEP might, however, be ideal for materials science measurements with synchrotron radiation if suitable beam ports and insertion devices were installed. For this purpose, the ring has to be run in a low-emittance mode. Although not designed for such a purpose, the machine excelled itself when low trials were conducted in March this year, reaching emittances close to those intended for the planned 6 GeV machine. It can reach energies of up to 8 GeV at low emittance, and if it were turned over exclusively for synchrotron radiation studies, 20 or more beam lines could be installed, according to Arthur Beinenstock, director of SSRL.

The Department of Energy (DoE) is indeed this week reviewing a proposal from SSRL to add three more beam lines to PEP, bringing the total to five. The proposal observes coyly that the existing beam lines have demonstrated "an emittance and dynamic aperture comparable to other potential storage rings presently being evaluated". The ring's long straight sections make it ideal for adding insertion devices such as undulators and wigglers.

The proposal to build a 6 GeV synchrotron radiation facility at Argonne by 1992 at an estimated cost of $300 million has not yet received the offical go-ahead from DoE, although its 1987 federal budget request includes some funds for preconstruction research and development. For the time being, extending the radiation facilities at PEP is being considered just as a means of paving the way for the dedicated 6 GeV machine, according to Lou Ianniello of DoE's office of basic energy sciences.

But Don Stevens, deputy associate director, adds that "it's a valid question" to ask whether an expanded PEP might not now be able to do all that the 6 GeV machine could do and one that "will have to be addressed".

Others are not so impressed. Ken Kliewer, who heads the 6 GeV project at Argonne, says that a dedicated above-ground machine could have up to 60 beam lines, and "Stanford can't match that". Kliewer thinks it unlikely that DoE will approve adding 20 or even 10 beam lines at PEP, in part because of the expense of necessary underground tunnelling.

Tim Beardsley

French reactors

Near-catastrophe at Le Bugey

A FRENCH pressurized water reactor (PWR) at Le Bugey on the Rhône river, not far from Geneva, came very close to a serious nuclear accident in 1984 after the failure of a single electrical component, a rectifier, it was claimed last week in the French satirical weekly, *Le Canard Enchainé*. The French national utility, Electricité de France (EDF), and the atomic energy commission, the Commissariat à l'Energie Atomique (CEA), immediately held press conferences and admitted that the satirists were right.

There had been no cover-up, insisted Pierre Tanguy, head of safety at EDF, in a telephone call from Paris; a press release had been issued at the time, but "there had been no Chernobyl incident" to sensitize the media to nuclear issues.

What took place on the night of 14 April 1984 on the five-reactor site at Le Bugey, however, showed how a "very minimal failure" in a control circuit can give rise to a major incident, said Tanguy.

The event began with the failure of the rectifier supplying electricity to one of the two separate 48-V direct-current control circuits of the 900-MW reactor, which was on full power at the time. Instantly, a battery pack switched in to maintain the 48-V supply, and a warning light began to flash at the operators in the control room.

Unfortunately, the operators ignored the light (if they had not they could simply have switched in an auxiliary rectifier). According to Tanguy, the same light served three warning systems (to save space on the control panel). The installation on one of these other circuits had proved faulty a few days before, and the light had been flashing intermittently. It was marked down for repair, and ignored when it began correctly to signal the rectifier failure.

What then happened was something which had been completely ignored in the engineering risk analysis for the PWR. The emergency battery now operating the control system began to run down. Instead of falling precipitously to zero, as assumed in the "all or nothing" risk analysis, the voltage in the control circuit steadily slipped down from its nominal 48-V to 30-V over a period of three hours. In response, a number of circuit breakers began to trip out in an unpredictable fashion until finally the system, with the reactor still at full power, disconnected itself from the grid.

The reactor was now at full power with no external energy being drawn from the system to cool it. An automatic "scram" system then correctly threw in the control rods, which absorbed neutrons and shut off the nuclear reaction. However a reactor in this condition is still producing a great deal of heat — 300 MW in this case. An emergency system is then supposed to switch in a diesel generator to provide emergency core cooling (otherwise the primary coolant would boil and vent within a few hours). But the first generator failed to switch on because of the loss of the first control circuit. Luckily the only back-up generator in the system then did switch in, averting a serious accident.

A report of the whole sequence of events was distributed through the Organisation for Economic Cooperation and Development (OECD) "incident reporting system", said Tanguy, and PWR constructors and operators got together to consider the implications of the incident. "It drew everyone's attention to the possibility of a complete blackout of a nuclear plant", and was probably "the most significant event in relation to safety in a PWR" that has occurred.

The Three Mile Island incident, where operator error led to the venting of primary coolant and the ultimate collapse of the core of the reactor, realerted utilities to the well-known dangers of "loss of coolant accidents", or LOCAs; and so much attention has been paid to those that the danger is now minimized, according to Tanguy. But the Le Bugey incident shows that a whole new class of possible events had been ignored — those where electrical systems fail gradually. It shows that "risk analysis must not only take into account a yes or no, working or not working, for each item in the reactor, but the possibility of working with a slightly degraded system".

Such analysis, involving continuous in place of discrete variables, is very difficult. The French reaction had been to undertake such studies where possible, but also to introduce voltage monitors on critical circuits, to make sure that electrical values stayed within the ranges assumed in the discrete risk analysis.

Other measures taken since Le Bugey have been to introduce a single gas turbine generator that can be started up "within minutes" on each reactor sites, to maintain power to control and safety circuits, and to lay physical cable connections to allow a rapid emergency interconnection of generators between one reactor and another on each site if this proved essential. The critical "three warning system" lights in the control room have also been separated into multiple lights and circuits.

The occurrence of the unpredicted Le Bugey and Three Mile Island incidents had led to a lower probability of such events occurring again Tanguy's view is that accidents were inevitable, but with experience they become less and less likely. Which is why it is essential to learn every detail about what happened at Chernobyl. **Robert Walgate**

Biotechnology companies

T cells' turn to ride high

Washington

ONE of the more unusual new biotechnology companies, T Cell Sciences of Boston, made its first public stock offering last week, raising $12.6 million to continue its development of diagnostics and therapeutic agents focusing on T-cell receptors, in particular the T-cell antigen receptor. The company, founded two years ago by Dr Patrick Kung, has sewn up collaborative research agreements with many of the most prominent US research groups working on T-cell receptors, a remarkable feat given that basic understanding of the subject has been achieved only in the past two years.

The company, which now has about 30 employees, has centred its efforts on developing monoclonal antibody-based products that exploit the correlation of T-cell receptors and disease states. Its one current product (for research only) is ACT-T-SET, which is intended to distinguish chronic and acute immune disorders by assessing immune system activation through expression of very late antigen and interleukin-2 receptor.

Diseases that might be diagnosed through characterization of T-cell structures include various leukaemias, autoimmune diseases such as rheumatoid arthritis and systemic lupus and, perhaps, some cancers and acquired immune deficiency syndrome. Monitoring of the immune system for transplant rejection is another area where the company hopes to develop products. Later still, therapeutic products may be devised that would activate and control the immune system.

T Cell Sciences has a $4.7 million research contract with Syntex Corp, and has licensing agreements with Ontario Cancer Institute, California Institute of Technology, Dana-Farber Cancer Institute and Stanford University, among others. Jim McCamant, editor of *Medical Technology Stock Letter*, comments that T Cell Sciences seems to be typical of a trend in which biotechnology companies are increasingly basing themselves on more speculative ideas and basic science, as the obvious technologies have already been adopted by the larger companies. Nevertheless, according to McCamant, the degree to which T Cell Sciences has established collaborations with major research groups makes it unusual, and means "you have to take it seriously". **Tim Beardsley**

East European nuclear power

Bloc countries think again

THE Soviet Union's Comecon partners have responded to the Chernobyl disaster, predictably, by endorsing the Soviet line that Western commentators have overdramatized the danger of nuclear power for political motives. While, as a result of the accident, Finland has cancelled its fifth and Yugoslavia its second nuclear power plant, the Comecon allies have spoken up firmly in favour of nuclear power. Czechoslovakia, Cuba and East Germany have been particularly vocal.

Within the bloc, the only indirect official criticism of Soviet and Comecon nuclear policy came from Hungary's chief spokesman on Foreign Affairs, Mr Matyas Szueroes, who publicly urged the "inalienable right" of all people to knowledge in all matters which concern them, and the duty of all concerned with science and technology to respect public fears and concern, whether or not those fears were justified, a statement widely interpreted as a hit at Soviet reticence on the consequences of Chernobyl.

Poland, which caught the first phase of fallout from Chernobyl and which is at present building its first nuclear power station at Zarnowiec, is a special case. Clearly, after implementing a mass distribution of iodine pills to under-16s, ordering cows to be kept indoors and destroying contaminated vegetables, the authorities could hardly proclaim that nuclear power was without any hazard. Official statements have therefore urged that the Chernobyl accident will make the Polish authorities "additionally aware of improvements to all safety measures", and that in any case, the Zarnowiec reactor will be of the pressurized water type, quite different from that at Chernobyl, and will have, unlike reactors in the Soviet Union, a containment building. These assurances have clearly not been sufficient. Three thousand citizens of Bialystok, close to the eastern frontier of Poland, the area most affected by the initial fallout, have signed a petition to the Sejm (parliament) asking for the Zarnowiec plant to be cancelled, and five scientists working in nuclear physics and related fields have sent an open letter to the Minister of Energy, General Czeslaw Piotrowski, calling for more stringent safety tests at Chernobyl. At his regular press conference last week, government press spokesman Jerzy Urban said that he knew nothing of these documents.

Dissident opinion in Eastern Europe has been somewhat divided on the issue of Chernobyl. In Poland, some small anti-nuclear protests took place on 1 May and 3 May (Constitution Day), and underground Solidarity newsletters have attacked the reluctance of the Soviet and Polish governments to publish sufficient details. (The Polish government, in fact, has been fairly open with contamination statistics, at least at the international level.) In Czechoslovakia, the Charter-77 movement likewise put out a statement urging the public's right to be fully informed. But in Hungary, the "green" dissidents of the Danube Circle declined to comment, noting only that the hazard of accidents at nuclear power stations was in their opinion less of a threat to the environment than the Gabcikovo-Nagymaros hydroelectric project which would disrupt the ecological balance even when it was working properly. And in the Soviet Union itself, although there was some attempt to organize an anti-nuclear protest last week in Moscow, no less a person than Academician Andrei Sakharov has backed up the official Soviet line. Sakharov, whose place of enforced residence, Gor'kii, will be the site of the first joint power/district heating nuclear plant in the Soviet Union, said last week, in a message to his relatives in America, that he still viewed nuclear power as inherently the best option. Western reporting in Chernobyl, he said, echoing the official Soviet statements, has been considerably exaggerated. **Vera Rich**

Correction

IN last week's News item about Dr Robert Gale's treatment of patients from the Chernobyl nuclear accident (*Nature* **321**, 369; 1986), the number of patients who received bone marrow or fetal liver transplants was incorrectly given as 35; the figure should have been 19. The estimated average radiation dose of the 35 patients Dr Gale examined is 2 Gy or more; the estimated average dose of the 19 who received transplants was 5 Gy or more. □

Chernobyl

Improvising against radiation

THE Chernobyl clean-up has demanded "non-standard" and "unexpected" solutions, Academician Evgenii Velikhov, Vice-President of the Soviet Academy of Sciences, told the Moscow journal *Ogonek* last week. But what are these solutions? The accounts in the Soviet press, which concentrate more on the heroism involved than the technical details, give the impression of a series of improvisations worked out after the accident.

According to Ivan Silaev, one of the deputy prime ministers of the Soviet Union, the cost of a Swedish decontamination fluid at $18.5 a kilogram was so high that a rush effort by Soviet scientists was necessary. By 14 May, production had reached 30 tonnes a day, allowing 300,000 m^2 of contaminated area a day to be coated with the material. Silaev also said, in an interview in *Izvestia*, that exposed surfaces of buildings were being coated with sodium silicate solution to prevent rainwater carrying contamination into the groundwater and to the river Pripyat.

Operations around the damaged reactor itself have been organized in typical Soviet style, with planned targets and campaigns to beat them. The miners drilling under the reactor have a target of five reinforcement rings installed per shift (giving a nominal rate of progress of 14 to 15 m a day, twice that of normal mining operations). Engineers from the Ministry of Transport are installing a liquid-nitrogen cooling system.

The damaged reactor seems to be cooling very slowly; on 6 May, the Ukrainian Prime Minister Aleksandr Lyashko said that the temperature had fallen to around 300°C, but ten days later, Academician Velikhov cited the same figure. Also, the "sarcophagus" being built around the damaged reactor is not a simple casing, but, according to Silaev, is a "complex engineering structure", which will "fully control the internal heat and release any excess".

Not only the damaged reactor, No.4, will be entombed in this way. According to Prime Minister Lyashko, the unfinished reactor No.5, where shoddy building operations had caused concern before the accident, is also to be buried.

Away from the reactor site, but still within the 30-km evacuation zone, some measures have been implemented to safeguard agriculture. By 13 May, barrages had been built to stop effluent or rainwater reaching the river Pripyat. The main problem is the contaminated soil, which is being dealt with mechanically, by digging it out, and by planting with crops that "neutralize harmful elements in the soil".

To deal with long-term contamination further afield, an aerological monitoring station has been established, some 50 km from Chernobyl, which will make round-the-clock measurements of the radioactive contents of the air, and relay aggregate figures to the International Atomic Energy Agency in Vienna daily.

Little has emerged about radiation levels near the plant. By mid-May, according to transport construction minister Vladimir Brezhnev, radiation was still too high to work more than a four- or at most five-hour shift near the reactor, while the youth Party daily *Komsomolskaya Pravda* spoke of the emergency workers receiving a year's maximum permissible dose in two weeks. **Vera Rich**

SERC failing astronomers?

SIR—As a senior member of the research staff of the Royal Greenwich Observatory (RGO), I found your News article "Observatory move stirs passions" (*Nature* **321**, 4; 1986) most interesting. At RGO I am somewhat of a "dove" about the move because I am concerned that a refusal to accept the decision of the Science and Engineering Research Council (SERC) in this matter, particularly on political grounds, could in the long term be bad for UK science. It may be better to accept a bad decision made by scientists now, in the hope of good decisions by scientists in the future, than to give ourselves over to overtly political decisions for ever.

Why does the decision seem so bad and arouse so much passion? Primarily because the stated reasons make no sense and are widely perceived to be a cover for a cost-cutting exercise. Placing RGO in a more stimulating academic environment is a worthy goal, but it would command more credibility if the actions of SERC over the past few years (an overall rundown at RGO, a further cut of our research in favour of a support role and failure to support efforts to strengthen the existing link with the University of Sussex) were consistent with this objective.

The expectation that the move can be self-financing also seems questionable. How can it be self-financing compared, for example, to the unexplored option of selling the castle and grounds at Herstmonceux while retaining the observatory, which is mostly in a modern office block in one corner of the property?

Thus most people believe that the move is an administrative device to cut costs in optical astronomy to free funds for new activities. They are reinforced in this belief by the rundown of RGO over recent years and the failure of SERC to place any of its New-Blood positions in university departments specializing in optical astronomy (only fifteen went to astronomy as a whole).

Thus, as an optical astronomer who believes in the importance and intellectual validity of my subject, I was opposed to the decision for exactly the same reasons as it seems to be attractive to SERC.

I do not believe that there is any wickedness involved in the decision or the under-appreciation of optical astronomy; simply muddle. Two more examples of SERC's confusion appear in your article. First, the publication of the results of the poll of staff in RGO about the move: the survey was co-sponsored by the RGO staff side who had the privilege of seeing them for the first time in your pages. Second, the gymnastics by Harry Atkinson as portrayed in your final paragraph suggest that political considerations (at least of a regional nature) are indeed part of SERC's desiderata.

I am sorry to say that all this makes my stated support of SERC's decision pretty thin. What is needed to get SERC off the hook is an independent review as sought by the East Sussex County Council and preferably along scientific lines. I propose as chairman of this review the vice-chancellor of the University of Sussex, Sir Denys Wilkinson, who should be joined by a world-renowned foreign optical astronomer and a leading representative of our own (non-political) astronomical community. Such a group might have the moral authority to persuade everybody to accept its decision.

It is clear to me, however, that the organization most in need of serious investigation is the Swindon headquarters of SERC. It has shown itself much more eager to control the minutiae of activities in its laboratories, such as RGO, than to try to bring new resources into (in particular) a pure science like astronomy. From my perspective, they have singularly failed me, and other active scientists whether in universities or in their own laboratories, in this regard.

MICHAEL PENSTON

Rose Lodge,
Magham Down,
Hailsham,
E. Sussex, BN27 1PR, UK

SIR—As representatives of the staff of the Royal Greenwich Observatory (RGO), we read with interest your analysis (*Nature* **321**, 4; 1986) of the current debate on the future location of the Observatory. Even though it is our lives and careers that will be affected by the outcome of this debate, we feel we are but pawns in the Science and Engineering Council (SERC)'s game. For example, SERC has refused to allow the report of the Kingman panel to be circulated among RGO staff, although it is obvious that members of the press and others have had copies. We also learnt of the results of the survey of RGO staff for the first time in your columns, and although this has been traced to an administrative bungle rather than a deliberate act, it demonstrates SERC's scant regard for the people who will be most involved. Staff have been asked to state their preferences, but in view of all that has gone before they wonder how much notice will be given to their opinions.

We have now received the results of the staff survey but interpret the numbers very differently from your informant. In the first place, the questions did not even mention the possibility of remaining at Herstmonceux. Almost all staff are strenuously opposed to *any* move and have said so consistently and vociferously from the outset. Had you been present when the chairman of SERC, Professor E.W.J. Mitchell, met staff at Herstmonceux on 1 May, you too would have been in no doubt of their views. Second, the apparently high percentage who preferred Cambridge accounts for only 40 of the 119 "mobile" staff (out of the present total staff of 190 or so): replies from "mobile" staff who said they would resign rather than move anywhere and from "non-mobile" staff who face redundancy as a result of any move, were excluded. Staff who said they would follow the observatory wherever it went were added to the Cambridge-first-choice group. Fifty-five of the 119 did not reply at all to the questionnaire (many because they were fearful that the results would be misused). What price statistics?

Our strong desire to remain in Sussex is not blindly reactionary. If we could be convinced that there were clear and quantifiable benefits to be gained from moving to a different environment, we would welcome the proposal and consider the arguments on their merits: instead we are offered grounds which the council's officers themselves describe as a "matter of judgement" and "intangible" which to us as scientists is just not good enough. RGO staff wish to participate fully in the bright future for ground-based astronomy which the present facilities offer. A futile move would place this future in jeopardy and we urge our many supporters in the astronomical community to convey their views to SERC before it is too late.

JANET DUDLEY
(Chairman, RGO Staff
Trades Union Side)
Royal Greenwich Observatory,
Herstmonceux,
Hailsham, Sussex BN27 1RP, UK

Ageism

SIR—Jürgen Neffe (*Nature* **320**, 295; 1986) writes: "Although now 74, von Weizsäcker's opinion is still influential in West Germany." The probably unintentional pejorative use of "Although now 74...." implies that the influence of an opinion should diminish with advanced age of the opiner.

This is an outdated, incorrect ageist myth. It is out of place in any publication intended to be a modern journal of science. I believe that an apology is due to Professor von Weizsäcker.

ARTHUR CHERKIN
Geriatric Research, Education,
and Clinical Center,
VA Medical Center,
Sepulveda, California 91343, USA

• The form of words correctly complained of was not that used by Jürgen Neffe but was introduced in the editing. — Editor, *Nature*.

Paranormal theories

SIR—While accepting Marks' general remarks about the standing of research into the paranormal (*Nature* **320**, 119; 1986), I should like to comment upon some of his statements.

It is not true that there are "no theories to account for paranormal effects". In Bell's theorem and its refinements, in physics, we are confronted with a universe where local causality might not apply (for an entertaining discussion see Zukav, R. *The Dancing Wu Li Masters;* Fontana, London, 1984). This allows Jung's "synchronicity" and *psi* phenomena to be placed within a theoretical framework, although not suggesting a mechanism.

Theories such as those above are at the same time physical and metaphysical, as they question our basic concept of reality. It is not surprising that "believers" in the paranormal are resistant to change in their core constructs, and it seems trite to add that they have "significantly higher neuroticism scores". What does that prove? Is it Marks' view that these "millions of people throughout the world" are psychologically abnormal? One would assume that the whole review could be rewritten, with relevant changes, to cover "investigating God". Believers would, no doubt, react in a similar way, based on a similar "dearth of hard evidence".

In summary, I agree with Marks' conclusion that there have been no significant discoveries made by parascience, but I think that he need not have looked for psychological reasons for belief in the paranormal. As far as I can see (adjusting one of his phrases), scientific ideas will have little chance of affecting the magical thinking from which science itself evolved, because the fundamental mysteries remain.

M. COUCH
Department of Human Metabolism and Clinical Biochemistry, University of Sheffield Medical School, Sheffield S10 2RX, UK

SIR—In his Commentary, Marks[1] misrepresents the area he purports to review. A large part of the paper refers to religious and neurotic motives as explanation for the belief in the paranormal. However, similar psychiatric explanations are used to account for the need to deny these phenomena[2,3]. *Ad hominem* arguments lead nowhere.

As for Marks' more straightforward claims, they are indirectly based on a sample of works that is by no means representative. He relies on two reviews[4,5] that do not address themselves to the question of repeatability in general, but rather to the specific question of whether parapsychological research involving altered states of consciousness constitutes a repeatable paradigm. Thus, these reviews deal with a narrow group of experiments. For example, Akers[4] excluded all studies of highly selected subjects, thus considerably decreasing the overall significance of the results. Moreover, Hyman's[5] analysis is flawed, as Honorton has demonstrated in a response which followed Hyman's paper[6], and his methods were shown by a statistician to commit the very error that he criticized in the parapsychological studies[7].

Marks is quite right in pointing out that parapsychology has so far failed to produce a repeatable experiment. But it is misleading to use this as an argument against the credibility of parapsychological research. Marks fails to mention highly significant results of experiments that are characterized by extraordinary instrumental sophistication and methodological rigour, as exemplified by the recent work of R.G. Jahn of Princeton University[8], and the Maimonides Hospital dream researches[9–13]. These works, although not yet replicated, pose a serious challenge to the sceptic.

There are four counterhypotheses by which parapsychological findings can be explained away: (1) coincidence; (2) artefact; (3) self-deception; and (4) deliberate fraud. Now, the growing sophistication and rigour of modern psi research[14] is gradually ruling out the first three counterhypotheses. The fraud hypothesis (or, considering the present number of scientists involved in the field, the conspiracy hypothesis) remains as the only resort for the sceptic.

Psi or fraud? This is the real issue. Yet it is seldom presented unambiguously. Recently, Child[15] has thoroughly analysed the ways in which the above parapsychological works have been treated in the sceptical literature. He has shown that they were either ignored or grossly misrepresented, and that the resort to the accusation of fraud was often made implicitly. It is deplorable that Marks' review, written after Child's grave charges have been issued, commits the same errors.

AVSHALOM C. ELITZUR
15 Margolin St, Rehovot 76225, Israel

1. Marks, D.F. *Nature* **320**, 199 – 124 (1986).
2. Greyson, B. *J. nerv. ment. Dis.* **165**, 184 – 200 (1977).
3. Eisenbud, J. *Parapsychology and the Unconscious* (North Atlantic Books, Berkeley, 1983).
4. Akers, C. in *Advances in Parapsychological Research* Vol. 4 (ed. Krippner, S.) 112 – 164 (McFarland, Jefferson, North Carolina, 1984).
5. Hyman, R. *J. Parapsychol.* **49**, 3 – 49 (1985).
6. Honorton, C. *J. Parapsychol.* **49**, 51 – 91 (1985).
7. Saunders, D.R. *J. Parapsychol.* **49**, Appendix B (1985).
8. Jahn, R.G. *Proc. IEEE* **70/2**, 136 – 170 (1982).
9. Krippner, S. & Ullman, M. *J. nerv. ment. Dis.* **151**, 394 – 403 (1970).
10. —, Honorton, C. & Ullman, M. *J. Am. Soc. psychosom. ment. Med.* **20**, 9 – 17 (1973).
11. Ullman, M. *Exp. Med. Surg.* **27**, 19 – 38 (1969).
12. —, Krippner, S. & Feldstein, S. *Int. J. Neuropsychiat.* **2**, 420 – 437 (1966).
13. — & Krippner, S. *Biol. Psychiat.* **1**, 259 – 270 (1969).
14. Wolman, B.B. (ed.) *Handbook of Parapsychology* (Van Nostrand Reinhold, New York, 1977).
15. Child, I.L. *Am. Psychol.* **40**, 1219 – 1230 (1985).

Pesticide dangers

SIR—J. Gordon Edwards (*Nature* **320**, 391; 1986) has misunderstood Lord Ashby's review of *Pesticides and Nature Conservation: The British Experience 1950–1975* by John Sheail (*Nature* **318**, 21; 1985); I cannot believe that he has read the book.

I agree that members of the "loony left" of the conservation movement deserve J. Gordon Edwards' strictures, and I have myself criticized them for the past 30 years. But John Sheail's book describes the way in which scientific work in pesticides in Britain generally resulted in collaboration between industry, government and responsible conservation bodies, to introduce sensible controls of potentially dangerous chemicals. As director of the Nature Conservancy's Monks Wood Experimental Station at the time, I know that my colleagues certainly did not "resort to such unscientific methods as deliberately distorting or omitting all the data that refuted their allegations". The work has, of course, been published in reputable scientific journals.

Lord Ashby in his review implies that Rachel Carson's *Silent Spring* alerted the authorities and the public to the dangers of pesticides. That danger was already fully recognized, at least among scientists. In fact, in Britain the most important controls of pesticides that had been shown to have harmful ecological effects were introduced, with the fullest cooperation of the chemical industry, some months before *Silent Spring* was published.

KENNETH MELLANBY
Monks Wood Experimental Station, Huntingdon PE17 2LS, UK

Ling defended

SIR—The ill-natured and unnecessary sideswipe at Gilbert Ling (*Nature* **320**, 318; 1986) by Peter Newmark needs to be answered. Ling, "a physiologist... who remains a voice in the wilderness", is the man whose pioneer work with Gerard on intracellular potentials initiated just about all the advances in neurophysiology of the past fifty years. Is it possible that Ling knows something about cell interiors that his critics are missing?

As for the sodium pump, Newmark could consult our papers in *Nature*[1] which by some miracle escaped the greater excommunication. To my knowledge, no other papers critical of the peculiar and unlikely hypothesis of active transport "powered" by metabolic pumps have ever been accepted and published by either *Nature* or *Science*. Such unanimity in science is unreal.

H. R. CATCHPOLE
110 West Oak Street, Chicago, Illinois 60610, USA

1. Joseph *et al. Nature* **191**, 1175 (1961); **203**, 931 (1964); **206**, 6 (1965); **209**, 398 (1966).

Prehistoric ecology from pollen record

SIR—A "settlement gap" implied by the Weser estuary pollen records circa AD 500–700 does not pose "a fresh problem"[1], rather it supports an old conclusion. This is a protohistoric period significantly called the Migration Period (*Völkerwanderungszeit*) and virtually every settlement and cemetery in the western half of the Weser–Elbe "triangle" was abandoned in the first half of the fifth century, while those in the eastern half continued into the sixth century[2]. Mass emigration brought many of these people, who called themselves Saxons, to eastern and southern Britain. The artefacts buried in their new settlement and cemeteries here link directly back to the Weser–Elbe homeland.

There is no need to invoke plagues or other sudden catastrophes, for a steadily rising sea level left the coastal marshland settlements on their *Wurten*, for example Feddersen Wierde[3], without sufficient agricultural land and the inland settlements on the *Geest*, for example Flögeln[4], appear to have reached a point of marginal returns from their over-cultivated soils. The Venerable Bede summarized the historical basis for all this in the eighth century AD in Book I Chapter 15 of his *Ecclesiastical History of the English Peoples* and both archaeology and the environmental sciences appear to confirm his account.

MARTIN G. WELCH
Detartment of History (Medieval Archaeology),
University College London,
Gower Street, London WC1E 6BT, UK

1. Moore, P.D. *Nature* **319**, 361–362 (1986).
2. Böhme, H.W. in *Führer zu vor-und frühgeschichtlichen Denkmälern* 29: *Das Elb-Weser-Dreieck*, pt.1, 205–225 (Philipp von Zabern, Mainz, 1976) esp. map on p. 223.
3. Schmid, P. in *Lowland Iron Age Communities in Europe* (eds Cunliffe, B. & Rowley, T.) 123–145 (Oxford, 1978).
4. Zimmerman, W.H. in *Lowland Iron Age Communities in Europe* (eds Cunliffe, B. & Rowley, T.) 147–163 (Oxford, 1978).

Nuclear risks

SIR—After reading your leading article (*Nature* **320**, 384; 1986), the persecuted employees of the nuclear power business must wonder what they have to do to satisfy journalists and broadcasters. As I understand it, their industrial accident record, both in respect of injuries to their own operators and to the public at large, is among the best in either the fuel industries or the chemical industries, to which their activities have perhaps the closest similarity. What can you mean therefore by your reference to the "poor safety record of Sellafield"?

As to the supposed poor public relations activities, I am not sure that you and the press generally give them much attention. What can your victims do in the face of a persistent campaign based upon the supposed occurrence of dangerous accidents for which there appears to be no evidence, when that same lack of evidence is the basis for claims of secrecy and "cover-ups".

Is it not clear that the employee of the nuclear power business is, while at work, far less liable to accident or death than you are at the wheel of your car? Indeed, are not members of the public more at risk from you at the wheel of your car than they are from the nuclear power business? Drivers kill about 5,000 people each year in the United Kingdom, whereas handling radioactive products for nuclear fuels appears to kill nobody (not even, I believe, the shellfish living comfortably by that waste water outlet from Sellafield into the Irish Sea).

A.E. ROUT
73 Cambridge Road,
Middlesbrough,
Cleveland, TS5 5NL, UK

• The article complained of was intended to be ironical, as should have been apparent from the last sentence — Editor, *Nature*.

Sexist ads

SIR—I would like to protest at a number of recent advertisements that have appeared in *Nature* depicting members of the male sex as colourless white-coated individuals. Surely you must realize that many of your readers are men and take exception to this unfair treatment, especially when, in the same issue, several women are illustrated wearing fashionable clothing, doing interesting things like swimming and looking as if they are having a good time?

I am afraid I shall have to cancel my subscription forthwith.

M. CLARK
75 Agarose Grove,
London NW3, UK

Velikovsky's evidence?

SIR—Your more perceptive readers may have been surprised to read in C. Leroy Ellenberger's letter (*Nature* **318**, 204; 1985) the statement, attributed to me, that "if a formerly very bright comet periodically altered the sky's brightness, then the dates of appearances and disappearances for Venus would be affected". Venus is such a brilliant object that variations in the brightness of the sky would make little difference to its setting and rising dates. "The debris from the disintegration of comet Encke 4700 years ago" might, of course, act indirectly by filling the stratosphere with enough dust to prevent Venus being seen near the horizon line. This would produce longer invisibility periods; but only in one year, or perhaps two separated by an interval corresponding to the period of the comet. It would not explain all the anomalies of the Venus Tablets.

With regard to the Velikovsky theory, archaeological evidence from Babylonian clay tablets has not verified the "Comet Venus" identification; but a large comet other than Venus, as deduced by Clube and Napier in their "Cosmic Serpent", is a possibility.

JOHN D. WEIR
72 Baronscourt Terrace,
Edinburgh EH8 7EP, UK

Plasma — the fourth state of matter?

SIR—J.N. Goldschvartz (*Nature* **320**, 302; 1986) basically asks "what is the fourth state of matter?". There is no debate about the first three phases of matter[1] — solid, liquid and gas. When a solid is heated, a liquid is formed, and when a liquid is heated it is transformed into a gas; a commonplace example is the progression from ice to water to steam.

When a gas is heated, that is, when additional energy is provided to the atoms or molecules, some of the electrically neutral particles can be split into electrons and positive ions. Such an electrically charged gas, a partially ionized gas, which overall is electrically neutral, is termed a plasma if it exhibits "collective" (jelly-like) behaviour[2] due to the long-range (on an atomic scale) electromagnetic forces acting between the charged particles.

Clemmow and Dougherty[3] say on page 1 that "the state in which there is an appreciable degree of ionization has indeed been called the fourth state of matter". Surely plasma should, unequivocally, be termed the fourth state of matter.

MICHAEL J. RYCROFT
British Antarctic Survey (NERC),
Madingley Road,
Cambridge CB3 0ET, UK

1. Walton, A.J. *Three Phases of Matter* (McGraw-Hill, Maidenhead, UK, 1976).
2. Chen, F.F. *Introduction to Plasma Physics* (Plenum, New York, 1974).
3. Clemmow, P.C. & Dougherty, J.P. *Electrodynamics of Particles and Plasmas* (Addison-Wesley, London, 1969).

South Africa

SIR—In suggesting that South African scientists be required to sign a statement of political beliefs before their articles are considered by international journals or they themselves be allowed to attend overseas conferences (*Nature* **320**, 486; 1986), Masters, Caithness and Rayner respect neither science nor scientists. The quality of a work of science exists entirely within the work. Other requirements for publication or conference-attending are inherently corrupt and corrupting. And a man's political beliefs are nobody else's business unless he is a politician.

C.W. MCCUTCHEN
5213 Acacia Avenue,
Bethesda, Maryland 20814, USA

A child's guide to radiobiology

The view that radiobiology (made fashionable by the accident at Chernobyl) is unknown territory is belied by the vast literature on the subject. But uncertainties persist.

FEW subjects can have been given as much attention in the past thirty years as that of the biological consequences of radiation. The explanation is simply that governments have felt it necessary to make independent assessments of the consequences for their populations of the bulk production of large amounts of artificial radioactivity, which became a live issue in the late 1950s with the testing of nuclear weapons in the atmosphere. The result is that there is no shortage of information. Public reaction outside the Soviet Union to the consequences of the Chernobyl accident has nevertheless provided further proof that to publish is not necessarily to spread understanding.

That radiation may be damaging has been plain for more than half a century, most vividly by the evidence of the damage accidentally done to occupational groups such as the sad cohort of workers in the US watch-making industry employed to paint the luminous dials of watches and who kept their paint-brushes moist by licking them. In the 1920s, the liability to injury of people working with X rays used for medical diagnosis and therapy was recognized by the fixing of a supposed safety limit for exposure, defined as ten per cent of the dose (in roentgens) required to cause a disorder of the blood-forming process in adults.

Now, as the limits have been steadily reduced for the allowable exposure to radiation for occupational and other groups, there is also a reductionist framework to explain the rationale of the dose-fixing regulations. But that does not mean that the uncertainties have been banished.

The agents of the biological damage are, microscopically, a mixed bag, whose effects are best described in language more familiar in high-energy physics. Charged particles such as alpha-particles are stopped in matter of all kinds, living or dead, by the ionization they cause, although there may be occasional nuclear collisions as well. X rays and more energetic gamma rays are also chiefly sources of ionization. Electrically neutral particles, neutrons for example, interact to a comparatively negligible degree with the electrons in the outer shells of the atoms through which they pass, but are capable of colliding with nuclei, which is the simple reason why neutrons are relatively more damaging, by the yardstick of the amount of energy deposited in irradiated material, than most other kinds of radiation.

Inanimate matter is not permanently damaged by radiation except to the extent that ionization of atoms and molecules may catalyse chemical reactions (which is why radiation may cause organic materials to polymerize) or that atoms may be displaced from their required positions by nuclear collisions (which is why irradiated graphite requires annealing).

Living cells are obviously more vulnerable. The mere deposition of external energy in the form of ion-pairs is an assault that may affect essential processes, killing damaged cells or, alternatively, like nuclear collisions at the wrong places in a vital molecule, causing mutations that, in somatic cells, may lead to cancer and, in germline cells, to genetic defects.

By what yardsticks should the potential of radiation for causing damage be assessed? In an ideal world, there would be two quite different bodies of information: first, a set of what physicists would call cross-sections to determine the chance that the passage of a particle (or photon) would set in train each possible biochemical process; and, second, a body of information about the biological consequences. Instead, there are two largely empirical sets of rules of thumb.

The equivalent of the set of cross-sections is the assumption that the damage done to a tissue by irradiation is proportional to the amount of energy deposited within it, whence the unit called the rad. The different components in a mixed source of radiation are weighted according to their "quality factors" to allow for the biological damage they do, by which process rads are translated into rems (for which the unit is the sievert).

Present practice will probably in due course seem crude. Because cross-sections are functions of energy, one would expect the quality factors of the same particles to be functions of energy as well. This point has emerged from analysis during the past few years of the incidence of genetic defects among the children of the survivors of the two bombs at Hiroshima and Nagasaki. Ultimately, no doubt, there will be different quality factors for the causation of genetic defect, cancer and more acute effects, and new units in which to measure them.

The other side of this coin, the numerical relationship of biological damage to its causes, measured as radiation doses, is inevitably more crude. Part of the trouble is simply biological: a genetic defect may show up as a fetus that dies *in utero*, and the biological consequences may be negligible in a population living within its reproductive potential. That is why the working yardstick since the Second World War has been the assumption that, whatever the quantitative relationships may be, the natural dose of radiation to which we are exposed is, by definition, one with which a species must expect to be able to live.

The assumption is natural but its form has changed. Thirty years ago, cosmic rays were supposed to be the chief source of natural radiation; most of the components of cosmic rays, being fast, penetrate the whole body and deliver a reliably calculable dose of radiation, 0.30 millisieverts a year. The effects of naturally occurring radioactive species such as those of potassium-40, have always been recognized as important, but radon-222 now accounts for as great a general radiation dose as the other two put together. On the average, individual exposure to radiation for people living near sea-level is 2 millisieverts a year.

To use natural exposure as a measure of the risks to which people are artificially exposed, it would clearly be necessary that there would be quantities (not necessarily constants of proportionality) relating damage to dose. But it seems unlikely that simple numbers will ever be found. Different kinds of cancer may be induced by radiation with differing efficacy; some genetic defects may be more likely than others.

Complications such as these already have a bearing on some practical problems, especially where internally ingested radioactivity is involved. Although claims that the rate of genetic malformation among the children of people living near nuclear test sites in the United States, put forward by Dr David Sternglass of the University of Pittsburgh in the 1960s, have been shown to be statistically invalid, there is always a possibility that certain radionuclides may have biological consequences that are systematically underestimated by the measure in rems of the dose they deliver, perhaps because they concentrate in particular places. The difficulty here is that each investigation is a major undertaking, and that there are simply not enough people to go around.

John Maddox

Biomechanics

The flight of the dipteran fly

from H.C. Bennet-Clark

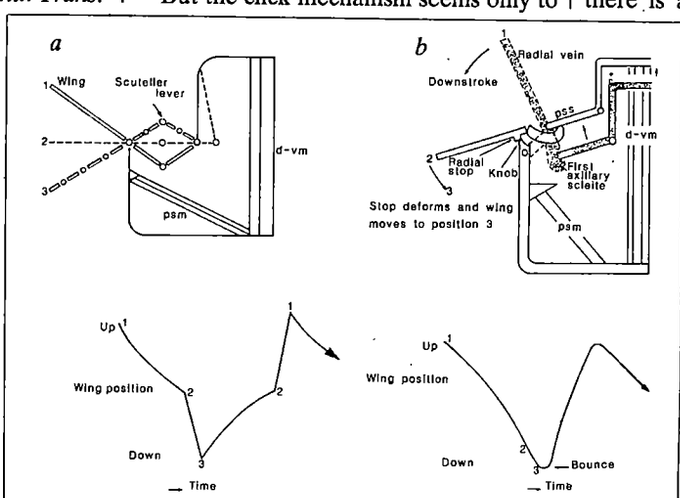
THE wing-beat frequency of flies in the order Diptera varies from 120 Hz in the larger species to more than 500 Hz in the smallest midges. These frequencies are far faster than can be maintained by conventional muscle, where there is one impulse per contraction. The flight muscles of dipteran insects are not excited synchronously in this way (Pringle, J.W.S. *J. Physiol., Lond.* **108**, 226; 1949) but vibrate at a far higher frequency. Attempts to model the processes in the dipteran thorax that cause flight have been based on a 'click' mechanism which can be elicited in anaesthesized flies. But recent experiments indicate that the click mechanism is an artefact and that the flight of flies *in vivo* involves a quite different mechanism (Miyan, J.A. & Ewing, A.W. *Phil. Trans. R. Soc.* B**311**, 271; 1985).

Early experiments by Pringle and others demonstrated that, when insect flight muscle is activated and subjected to rapid elongation, the subsequent response is a contraction after a brief delay and over a short distance. Thus, these muscles are stretch-activated and must be inserted in a skeletal system of considerable stiffness, with kinematics that provide an appropriate stretch to activate the antagonistic wing levator and depressor muscles at appropriate phases in the wing-beat cycle of the insect.

When flies are anaesthesized with CCl_4 they 'go under' with the wings either abnormally elevated or depressed. In this condition, with the wings in the raised position, the thorax can be squeezed longitudinally between forceps and the wings will then start to depress until, at about mid-position, they suddenly click into the fully depressed position. If the thorax is squeezed dorso-ventrally, the opposite slow movement occurs, followed by the click. This model mechanism (Boettiger, E.G. & Furschpan, E. *Biol. Bull. mar. biol. Lab., Woods Hole* **102**, 200; 1952) has two attractive features; it provides, at approximate phases in the wing stroke, stretch-activation for the major flight muscles; and, because of the geometry of the wing base, it automatically alters the angle of attack of the wing between the downstroke and the upstroke.

One snag with this model is that the wing should behave like a toggle switch (*a* in the figure). In such a switch, force on either upstroke or downstroke opposes movement until approximately mid-stroke and then reverses to act in the same direction as movement, to complete it with a snap. In practice, this is only seen in the CCl_4-anaesthetized flies: in normal flight, the wings of Diptera only decelerate near the top and bottom of the wing beat instead of in the mid-downstroke and again in the mid-upstroke. This simple click model has the deficiency that it does not take account of the force caused by the flight muscles, which tends to be maximal in the part of the stroke where maximal force has to be produced to overcome that resulting from the click mechanism.

But the click mechanism seems only to appear under CCl_4 anaesthesia, according to the recent work of Miyan and Ewing (*J. exp. Biol.* **116**, 313; 1985). In this special circumstance, the muscle that tenses the side of the thoracic box (psm in the figure) goes into such strong tetanus that the normal action of the sclerites of the wing base cannot occur — the click mechanism thus appears to be an abnormal artefact of the anaesthetic.



Wing mechanisms of a fly. The upstroke is provided by contraction of the dorso-ventral muscles (d-vm). *a*, In the classic click mechanism model, the wing is driven like a toggle switch and is stable in positions 1 and 3 and metastable at position 2. The spring force required for the click of the toggle is provided by the pleurosternal muscle (psm) stressing the elastic skeleton of the thorax. The movement expected from this mechanism is shown below: at mid up- and downstroke (2) the wing suddenly accelerates in the direction of movement. *b*, With the new radial wing stop mechanism, in the downstroke (1 to 2) the stop engages near the bottom of the stroke (2), slowing the downward movement and raising the top of the thorax via the first axillary sclerite and the parascutal shelf (pss). The wing then bounces off the elastic stop (3). The movement expected from such a mechanism is a slowing at the bottom of the stroke, with a subsequent rapid reversal of movement: that is what is observed in normal flight (see below).

What then does happen during the normal action of the dipteran thorax? In their new work, Miyan and Ewing studied in detail the thoraces of a dozen dipteran species, many of which were literally frozen in flight by being tipped into liquid nitrogen. They describe a stop under the base of the principal vein, the radius, which can engage on a knob at the crest of the side of the thorax (*b* in the figure). In the downstroke, when the wing stop engages, the inertia of the wing causes the outer part of the wing to bend downwards (seen in high-speed films of flight in many species) and, in addition, through the action of the first axillary sclerite and parascutal shelf in the wing base, causes a sharp lifting of the dorsal part of the thorax (*b* in the figure) which, in turn, stretches the dorso-ventral muscles to activate them for the ensuing upstroke. The wing is accelerated upwards only at the very start of the upstroke, probably because of the elastic recoil off the radial wing stop, and thereafter swings with nearly constant angular velocity, as would be expected if there is a steady torque caused by the flight muscles (but which is against the predictions of the click mechanism) until the wing decelerates at the top of upstroke and then starts the downstroke (*b* in the figure). Vortex shedding at the bottom of the wing stroke will be enhanced by the rapid change of wing direction and angle of attack that the radial wing stop allows, which is compatible with the analysis of the unsteady-state aerodynamics in the flight of small insects made by T. Weis-Fogh (*J. exp. Biol.* **59**, 169; 1973). It is not clear whether there is a special mechanism at the top of the upstroke to snap-stretch and activate the muscles involved in the downstroke.

The older click mechanism model also allows the amplitude and/or frequency of the wing beat to be increased by contraction of the pleurosternal muscle (psm in the figure) increasing the spring force produced between the side of the thorax (at the outer wing hinge) and the inner, complex, wing hinge attached to the dorsal part of the thorax. The prediction from the click mechanism model is that this would act symmetrically on both the upstroke and the downstroke, but what is in fact observed is an asymmetrical effect, mainly affecting the downstroke, which can now be explained partly by the larger size of the dorsal-longitudinal wing depressor muscles compared with that of the dorso-ventral wing depressor muscles.

Miyan and Ewing also address the prob-

lems of control of the plane and form of the wing beat by the various skeletal and muscular elements. Their description of the action of the sclerites in the wing base allows both the continued beating of one wing when the other is folded back, as seen in the rapid turning of bluebottles, and also fine control of wing twisting, neither of which is easy to explain using the old model. These manoeuvres are effected by contraction of various of the 17 distinct, normally activated, non-fibrillar muscles in each side of the thorax. The system is amazingly complex: the wing base is the region at which the stresses are highest but it allows both control of the wing beat and the wing to be folded back, both when the insect is at rest and when the other wing is beating. □

H.C. Bennet-Clark is Lecturer in Invertebrate Zoology in the Department of Zoology, University of Oxford, South Parks Road, Oxford OX1 3PS, UK.

Nuclear magnetic resonance

Protein structure determination

from Wolfgang Kabsch and Paul Rösch

ONE of the most fruitful areas of biophysics is the elucidation of the three-dimensional structures of biologically active molecules such as proteins and nucleic acids in atomic detail. These investigations have brought a wealth of new information on the structural design principles of these molecules and their functions and interactions. Two papers published in the 20 May issue of the *Journal of Molecular Biology*[1,2] report the three-dimensional structure of the 75-amino-acid-long α-amylase inhibitor by two different methods: Pflugrath *et al.*[1] used the classical method of X-ray crystallography, whereas Kline, Braun and Wüthrich[2] derived the three-dimensional structure of the protein entirely from proton nuclear magnetic resonance (^{1}H-NMR) measurements in solution. The overall features of the X-ray structure and the NMR structure seem to be very similar, confirming that NMR gives an accurate measure of protein structure.

Until recently, the only method for determining macromolecular structure at atomic resolution was X-ray crystallography. For this technique to be applicable, single crystals of the molecules have to be grown to linear dimensions of at least 0.2 mm. In addition, to resolve the phase ambiguity of the scattered X-rays, isomorphous heavy-atom derivatives of these crystals are required. For proteins up to a relative molecular mass (M_r) of about 50,000, structure determination is a straightforward application of standard techniques as long as the amino-acid sequence is known. Unfortunately, it turns out that not all biologically interesting molecules can be obtained in crystalline form. Although new methods are constantly being developed, crystallization and selection of suitable heavy-atom derivatives remain an art in themselves.

The paper by Kline *et al.* is a remarkable step forward in the biochemical application of NMR. Since the 1950s, ^{1}H-NMR has delivered structural information of small molecules predominantly by its main parameter, the chemical-shift value. Even in the mid-1970s it was generally thought that structural information on biological macromolecules could be obtained, if at all, only by retrieving the information hidden in the shift values of the proton resonances, as for technical reasons no other parameter seemed directly available from the NMR spectra. An obstacle which had to be surmounted anew for each protein molecule was the assignment of resonances to the chemical groups of the individual amino-acid residues in the protein. This task is formidable, considering that even a small protein of $M_r \sim 10{,}000$ (corresponding to about 90 amino acids) already gives approximately 500 different resonance lines. In addition, most of these lines are split into multiplet structures. Thus it seemed that what was needed for ^{1}H-NMR to become generally useful in structure determinations was first, a method for the sequence-specific assignment of resonances; and second, a method for the retrieval of structural information from chemical-shift information. Ten years ago the possibility of achieving at least the first goal, let alone the second, seemed remote. The gradual improvement in available magnetic field strength brought about no substantial change — nor did anybody seriously expect it to do so.

Thus, an entirely new approach was needed. It originated in 1971, when Jeener[3] supplied a basic idea seemingly remote from practical applications in the general NMR laboratory. In Fourier NMR (today the standard way of obtaining NMR spectra) the decay of nonequilibrium magnetization after application of a high-frequency pulse is observed as a function of time. This function yields, after Fourier transformation, the desired spectrum, that is, the absorbance of the sample as a function of frequency. Jeener's idea was to substitute the single high-frequency pulse with two pulses of variable pulse separation, thus introducing a second time parameter. Two-dimensional Fourier transformation then yields a matrix with two frequency axes. Resonances on the diagonal correspond to the normal one-dimensional spectrum and off-diagonal resonances originate from the mutual interactions of protons; lines parallel to the two frequency axes through an off-diagonal resonance connect the two on-diagonal resonances originating from the two protons whose interactions gave rise to this off-diagonal peak. It was the achievement of Ernst and co-workers[4] to recognize the great practical importance of this technique. His group and that of Freeman, among others, developed a wealth of new experiments based on this basic idea (see, for example, ref. 5).

What change did this bring about for biochemical applications? The advantage of two-dimensional over one-dimensional spectroscopy is twofold: first, the basic two-pulse two-dimensional experiment (later termed COSY, from correlated spectroscopy) allows resolution of connectivities of resonances belonging to groups covalently connected with a spacing of only a few bonds. The off-diagonal peaks are generated by 'through-bond' interaction of two protons — in general, a distance of not more than three bonds between the protons is required. This yields, at least in principle, the assignment of all resonances to types of amino-acid residues with one single experiment, because each amino acid is characterized by a specific fingerprint of proton connectivities. In practice, some additional information from other types of two-dimensional experiments may be required. Second, a three-pulse variant of the basic COSY experiment (termed NOESY, from nuclear Overhauser effect spectroscopy) yields information on spatial distances of groups closer than about 0.5 nm via the dipolar 'through-space' interaction of those groups. Thus, the resonances in a two-dimensional spectrum originating from directly neighbouring NH and $C_\alpha H$ groups and $C_\alpha H$-CO-NH groups in the peptide bond are connected via off-diagonal resonances generated by the through-space interaction of those protons. The backbone resonances may then be traced according to the chain of amino acids in the protein by following the chain of -NH-$C_\alpha H$-CO-NH- backbone proton resonances. The corresponding side groups are then identified in the COSY spectrum or via the NH-$C_\beta H$ dipolar interaction in the NOESY spectrum. In addition, the distances between protons belonging to groups closely spaced in the three-dimensional structure — but not necessarily in the sequence — can be estimated. This yields information in the three-dimensional folding of the protein. Unfortunately, the spread of the correlation times for chemical groups in proteins prevents accurate determination of these distances via the nuclear Overhauser

effect. Thus, in general, only upper bounds on distances may be obtained by this method.

Thus, a set of two-dimensional spectra of a small protein generates a set of distance constraints for neighbouring groups. If a nuclear Overhauser effect is detected, the interproton distance is judged to be closer than, say, 0.4 nm. If no such effect is detected, the interproton distance can have any value. The potential of this method for structure determination of proteins was first realized by Wüthrich and co-workers[8], but the methods for structure calculations from the knowledge of a set of proton–proton distance constraints are by no means trivial, and much work went into setting-up computer programs to this end. Evaluation of NMR data with the aid of programs such as those introduced recently by Havel and Wüthrich[6] and Braun and Go[7] may finally result in the elucidation of a few possible tertiary structures.

Kline, Braun and Wüthrich[2] have now gone one step further in the interpretation of their experimental results by grouping their measured nuclear Overhauser effects into three categories: large, medium and small proton–proton separations. They then assigned numerical values to these categories by comparison with the magnitude of the effects observed for protons with covalently fixed distances. As their result shows, the approach works for the α-amylase inhibitor structure, and will thus probably work for most other protein structures.

In the past five years the secondary structures of several polypeptide strands have been determined by these ^{1}H-NMR methods[9,10]. As an example of a larger unit, secondary structure elements have been determined for the DNA-binding *lac*-repressor headpiece and a low-resolution model of its tertiary structure has been suggested[11]. Of course it helped that the tertiary structures of other DNA-binding proteins, such as the CAP of *Escherichia coli*, were known from the start[12]. The *lac*-repressor headpiece was until now the best example of a protein structure determined at low resolution by NMR methods, although the structural model has so far not been verified directly by X-ray studies. For the *lac*-repressor headpiece, extensive use has been made of molecular dynamic calculations as a further method of secondary structure refinement[13], a method that could also strongly influence protein structure determination by NMR methods in the future.

The paper by Kline *et al.*[2] is a step forward in the application of NMR to three-dimensional protein structure determination, but too much enthusiasm would be premature. The conditions under which NMR studies can reveal secondary structures or complete tertiary structures of proteins are rather restrictive: the protein must be sufficiently small ($M_r < 10{,}000$) to allow assignment of most resonances; soluble to high concentrations (several millimolar) to yield sufficiently good signal-to-noise ratios; available in compa large amounts (tens of milligran stable in solution for several day vated temperature and preferably (less than 6) to allow observatio changeable NH backbone prot present, the determination of structures by X-ray analysis is st more straightforward as long crystals are available. Neverthe expect NMR to become a powerfu the foreseeable future for determi structure of small- to medium-siz tides and hormones, which are in very sensitive to heavy-atom sub and are often not crystallizable at a

Wolfgang Kabsch and Paul Rösch a Department of Biophysics, Max-Pla tute for Medical Research, 6900 Hei FRG.

1. Pflugrath, J.W., Wiegand, E. Huber, R & Vertesy, L. *J. molec. Biol.* **189**, 383 (1986).
2. Kline, A.D., Braun, W. & Wüthrich, K. *J. molec. Biol.* **189**, 377 (1986).
3. Jeener, J. *Ampere International Summer School II* (Basko Polje, Yugoslavia, 1971).
4. Aue, W.P., Bartholdi, E. & Ernst, R.R. *J. chem. Phys.* **64**, 2229 (1976).
5. Bodenhausen, G. *Progr. NMR* **14**, 137 (1981).
6. Havel, T. & Wüthrich, K. *Bull. Math. Biol.* **46**, 673 (1985).
7. Braun, W. & Go, N. *J. molec. Biol.* **186**, 611 (1985).
8. Wüthrich, K., Wider, G., Wagner, G. & Braun, W. *J. molec. Biol.* **155**, 311 (1982).
9. Williamson, M.P., Marion, D. & Wüthrich, K. *J. molec. Biol.* **173**, 341 (1984).
10. Wemmer, D. & Kallenbach, N.R. *Biochemistry* **22**, 1901, (1983).
11. Zuiderweg, R.J.P., Kaptein, R. & Wüthrich, K. *Proc. natn. Acad. Sci. U.S.A.* **80**, 5837 (1983).
12. McCray, D.B. & Steitz, T.A. *Nature* **290**, 744 (1981).
13. Kaptein, R., Zuiderweg, R.J.P., Scheek, R.M., Boelens, R. & van Gunsteren, W.F. *J. molec. Biol.* **182**, 179 (1985).

Rock mechanics

Luminous phenomena and th relationship to rock fracture

from John S. Derr

INVESTIGATIONS of earthquake lights are moving from the gathering of anecdotal sightings into the laboratory, and in the process gaining a measure of respectability. Most recently, Brady and Rowell report on page 488 of this issue[1] that breaking rocks in the dark produces lights whose spectra are those of the ambient atmosphere. The experimental design is intended to help discriminate among several possible mechanisms for the lights, including frictional heating to incandescence; sparks caused by the piezoelectric effect; or charge separation, plasmas and charged particle bombardment. The authors show, for example, that rock fracturing under water produces spectra of both atomic and molecular hydrogen, and for this and other reasons conclude that earthquake lights are caused by exo-electron excitation of the ambient medium rather than by any of the other suggestions.

One of the early giants of seismology, Perry Byerly, enjoyed telling students that the subject of earthquake lights was the darkest area of seismology. The reason for its neglect was probably that most observations have been highly anecdotal in nature, made by untrained observers and contain little or no 'hard' data. To make matters worse, sightings of clear examples of earthquake lights and ball lighting are generally confused with even more controversial subjects like UFOs. Typical reports of earthquake lights can be found in the 'grey' literature and the popular press — no wonder scientists have been reluctant to touch the subject!

The phenomena have been reported for centuries. George Frederick created an imaginative rewrite of lical passages for his oratorio " Egypt"

> He gave them hailstones
> for rain: fire mingled
> with the hail ran along
> upon the ground.

This is probably a description of l ning, but is typical of common m tions which read religious or interpretations into the sighting examples include a recent sig luminous phenomena along faul the United Kingdom which was ted as "luminous beings"[2]. Tibet have considered regularly mountain-top lights to be a manif of the Bodhisattva[3]. These acco of course, subject to many in tions, but I find them at least c with the hypothesis that these pe astonished at the sight of phenomena and gave the unknov ious interpretation.

There is a very graphic Japan of unknown origin and time:

> The earth speaks softly
> To the mountain
> Which trembles
> And lights the sky

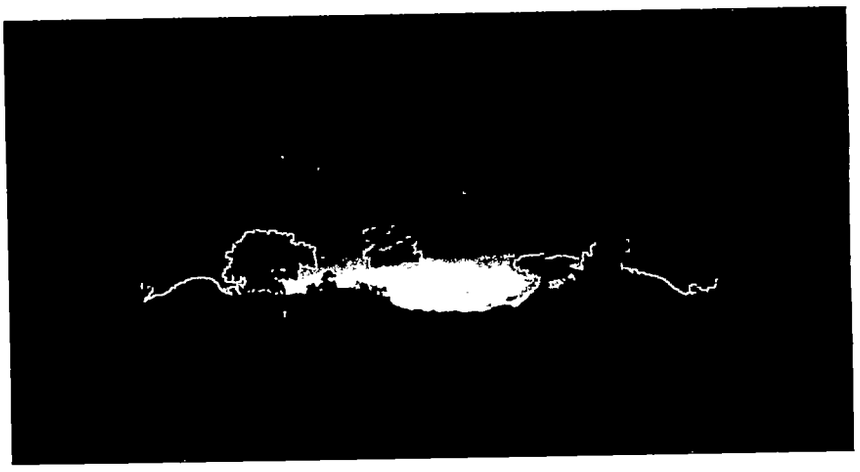
This suggests a general awaren phenomenon which may have Japanese seismologists, Ter Musya, to initiate the modern earthquake lights in the early 19 immediate stimulus was certa ficient: the Idu peninsula earthqu November 1930 was accompa lights brighter than moonlight[4]

descriptions came from the great Tangshan earthquake in China on 27 July 1976: people were woken up, thinking that someone had turned the lights on[5]. Other typical descriptions of earthquake lights include a glow at sea like a ship on fire; small, sequential flashes from different, random places on a hillside; fireballs or meteors; and auronal streamers diverging from a point on the horizon[4].

Probably closely related to the lights are sightings of luminous phenomena which have many of the same characteristics and occur in the same areas as earthquakes, but not at the same time. The best-documented examples come from the Yakima Indian Reservation, Washington[6], where photographs and extensive written records permit statistitical analysis. A typical description compares the luminous phenomena with a bright white light the size of a baseball floating among the tree tops. The results in that study support the hypothesis that the lights are associated with tectonic strain in active seismic areas and tend to accompany increases in earthquakes. Thus, earthquake lights and luminous phenomena may be related phenomena with slightly different time relationships to the associated earthquakes, or else luminous phenomena may, in fact, be earthquake lights for very small, high stress-drop earthquakes that have not been detected because of a lack of instrumentation.

The work of Brady and Rowell is a significant step because it discriminates between several proposed mechanisms and demonstrates that luminosities can be produced by any instrumentally recorded earthquake, even of the lowest magnitude. It strongly suggests that luminous phenomena are indeed earthquake lights produced by microearthquakes. Before this work, it was supposed that rock fracture produced plasmas which would generate easily detected microwave emissions. However, only a low frequency ($\sim 10^3$ Hz) was detected in these experiments[7], a result which agrees with general observations during earthquakes. (Microwave emissions across the fault plane are consistent with this theory, but very little should be observable at the surface.) Also, it was not possible to explain earthquake lights at sea, except by invoking the help of legions of excited, phosphorescent plankton. By actually generating lights underwater, Brady and Rowell have advanced a reasonable mechanism for these sightings. This work is, therefore, the first fully successful laboratory demonstration of a possible mechanism for this phenomenon.

If microwave interference could be detected from an earthquake, a different mechanism involving spark discharge would be required. King and Freund[8] show that nominally anhydrous minerals which dissolve small amounts of OH



Earthquake lights from Matsushiro, Japan, near Mount Kimyo on 26 September 1966 at 0325 JST. The luminosity lasted for 96 s. Direction, due north. Photograph by T. Kuribayashi.

during crystallization eventually develop peroxy anions (O_2^-) and hydrogen molecules (H_2). With heat of decompression, unbound O charge carriers can be generated. Extremely high local electric fields would result, with dielectric breakdown of air and strong microwave emissions if the density of O ions exceeds about 20 parts per million. The dielectric breakdown and exoelectron mechanisms can be differentiated by the presence or absence of significant microwave radio noise, although both mechanisms can produce lights and should generate radiation in the 900- to 5,000-Hz range[7].

Laboratory investigations of earthquake lights are just beginning, and the work of Brady and Rowell suggests many areas for investigation. Both exoelectron and dielectric breakdown mechanisms can explain the lights only if cracks extend to the surface in the area of the actual sightings. If a fault break does not reach ground level, one would require either a continuous series of cracks to provide a path for gas flow; or sufficient secondary fracturing at the surface to generate lights away from the primary fault. There is also a problem of timescale: to date, no experiment has produced any luminosity lasting even as long as one second. All laboratory tests should include broadband electromagnetic spectrum analysers to detect frequencies from ~10 Hz to X ray (10^{17} Hz).

Similarly, field investigations are in their infancy — there are great gaps in our knowledge. No one has tried to obtain pictures of earthquake lights triggered by nearly simultaneous signals from both a seismometer and photometer, or pictures and other measurements of lights in mine tunnels crossing faults. We do not know how exoelectron bombardment could produce a stationary light of relatively constant luminosity for as long as one hour, nor, as observed in the field, can we explain what would cause an image on infrared film that was not visible to the eye when the picture was taken[9]. Further study may reveal luminous phenomena to be a useful geophysical prospecting tool if they are related to mineralized bodies, or for earthquake prediction if we can understand the relationship between the area of sightings and subsequent earthquakes. Very preliminary correlations suggest that stress propagates across a geological terrane, causing luminous phenomena in the strong areas as it moves and earthquakes at the weaker boundaries[10]. In general, however, we remain ignorant of the necessary and sufficient conditions for generation of luminous phenomena and earthquake lights.

Brady and Rowell also suggest that their work has implications for biogenesis. It would be interesting to perform a Miller–Urey experiment using rock fracture as the electrical source to see if amino acids can be generated from primeval components under water or otherwise independent of atmospheric electricity.

Hence, a new, challenging area of geophysics is just opening. Previous studies have been criticized as statistical analyses without contributing towards finding a physical explanation. Brady and Rowell's work is a significant step to finding one such mechanism for the production of geophysical luminosities. But investigations in other areas are still required because we may be looking at several phenomena which sometimes share a common appearance and name. □

1. Brady, B.T. & Rowell, G.A. *Nature* **321**, 488 (1986).
2. Devereaux, P. *Earth Lights* (Turnstone, 1982).
3. Govinda, A. *The Way of the White Clouds* (Shambhala, 1970).
4. Derr, J.S. *Bull. seism. Soc. Am.* **63**, 2177–2187, 1973.
5. Lomnitz, C. & Lomnitz, L. (reported by Malcolm, A.H. *New York Times* 2 June 1977).
6. Derr, J.S. & Persinger, M.A. *Experientia* (in the press).
7. Cress, G.O., Brady, B.T. & Rowell, G.A. *Geophys. Res. Lett.* (in the press).
8. King, B.V. & Freund, F. *Phys. Rev.* **B29**, 5814 (1984).
9. Wiedenmann, C.L. *Vestgia Newslett.* **2**, 1 (1977).
10. Persinger, M.A. & Derr, J.S. *Perceptual and Motor Skills* **61**, 807 (1985).

John S. Derr is at the Geological Survey, US Department of the Interior, Box 25046, Denver Federal Center, Denver, Colorado 80225, USA.

Pattern formation

Segmentation genes and the distributions of transcripts

from Douglas Coulter and Eric Wieschaus

RESEARCH on the fruitfly *Drosophila* during the past five years shows that much of the global character of the insect's segmental pattern, as well as its finer details, depends on gene activity in the embryo. One of the attractions of segmentation as a system for studying pattern formation is that most of these zygotically active genes have been identified and their phenotypes characterized in mutant embryos[1]. In the past year several of the genes have been cloned, so it is now possible to compare the actual patterns of gene expression at the blastoderm stage with the altered segmentation observed in mutant embryos. Recent results, reported on page 493 of this issue[2], suggest that mutant phenotypes and transcript distributions do not always match.

The common feature of all the mutations isolated so far is that they cause reductions in the overall pattern. In what is perhaps the most relevant class (the 'pair-rule' mutations) the pattern deletions are about one segment in size and are repeated at double-segment intervals along the length of the animal (see figure). Although each of the nine pair-rule loci is associated with its own precise deletion pattern, the domains affected by different genes overlap. A given element of the final pattern thus requires a defined subset of pair-rule gene activities for its formation. The deletion phenotypes observed in mutant embryos apparently arise because in the absence of any one of these activities, the cells that make those pattern elements die or assume alternate fates.

If wild-type genes for each locus are required only to form specific subsets of the final pattern, one might expect that at the blastoderm stage the respective gene activities would be found only in the precursor cells for those pattern elements. After the first pair-rule gene, *fushi tarazu* (*ftz*), was cloned[3,4], the distribution of transcripts was determined by using *in situ* hybridization to sectioned blastoderm embryos[5]. The transcripts were localized in seven stripes which seemed to correspond to the seven deletions observed at double-segment intervals in mutant embryos (see figure). This very exciting result suggested that the patterning mechanism in *Drosophila* might be decipherable strictly in terms of localized gene activity at the blastoderm stage.

Because each of the nine pair-rule loci produces its own pattern of deletions, it is difficult to argue that any mutant domain defines a unit more fundamental than any other domain. This is contrary to what one would expect if the repeating pattern was established immediately as a series of units or 'compartments'[6], because, if this were true, realms of gene expression would be expected to coincide with compartment boundaries. At first glance, it seems that the range of phenotypes is more compatible with some combinatorial or hierarchical model assigning fates to individual cells[7] rather than to cell groups or polyclones[8]. Compartments could then be established later in response to the identities assumed by individual cells. Inherent to any of these models, however, is the assumption that one can actually extrapolate from the overlapping phenotypes in mutant embryos to actual gene requirements at the blastoderm stage.

This could only be tested when a second pair-rule gene, *hairy*, was cloned. Transcripts from *hairy* were shown to be localized in stripes with a width and periodicity similar to that of *ftz*[9], but the phasing of the stripes was different for the two loci. When embryos were simultaneously hybridized with probes from both genes, four regions could be identified in each double-segment interval: cells which contained either *hairy* or *ftz*; cells which contained neither transcript; and cells which contained both. This overlapping distribution of transcripts appears to be analogous to the overlapping pattern deletions observed in some mutants at each locus[7], suggesting that domains of gene expression at blastoderm correspond to domains of gene requirement in the final pattern.

Because the double segment is at most eight cells wide at the blastoderm stage, all seven of the remaining pair-rule gene products would not be required to specify unique identities to each cell within the double segment. It follows that not all pair-rule genes would play exactly the same part in the process (see below) — yet no one anticipated the surprising result (reported in this issue by Kilchherr *et al.*[2]) obtained when another pair-rule gene, *paired*, was cloned.

This gene is almost the archetypal pair-rule mutation; the deletion patterns in mutant embryos define seven stripes with the standard double-segment spacing. But analysis of the final pattern of transcripts at late blastoderm revealed fourteen stripes rather than the expected seven, indicating a periodicity corresponding to single-segment primordia. Interestingly, this single-segment mode of expression is preceded at a slightly earlier stage by seven broad stripes; it is (presumably) the subsequent 'splitting' of these stripes caused by elimination of transcripts from cells in the middle which gives rise to the final pattern. Although the stripes in this transient double-segment mode are too broad to correspond exactly to the more limited deletions observed in *paired* mutants, it is possible that this earlier pattern is the one most relevant to the establishment of the final pattern. In any event, the exact relationship between the relatively simple deletion pattern observed in mutant embryos and the more complicated pattern of transcription remains a mystery.

As we have described above for the *paired* pattern, a static description of the final or most stable pattern of striped transcripts from a given pair-rule gene is likely to yield an incomplete picture of a complex, dynamic process. An understanding of how segments are established and maintained requires an understanding of how the patterns arise, how these transcript patterns relate to translational expression and, ultimately, determination of the functions of the gene products. Ideally, such analyses will be extended to all the segmentation genes; meanwhile, most work has focused on the pair-rule gene *ftz*, and on another gene, *engrailed*, which is required later during development in the posterior compartment of each segment[10], but also reveals a pair-rule phenotype in mutant embryos and is transiently expressed in a double-segment mode during the blastoderm stage.

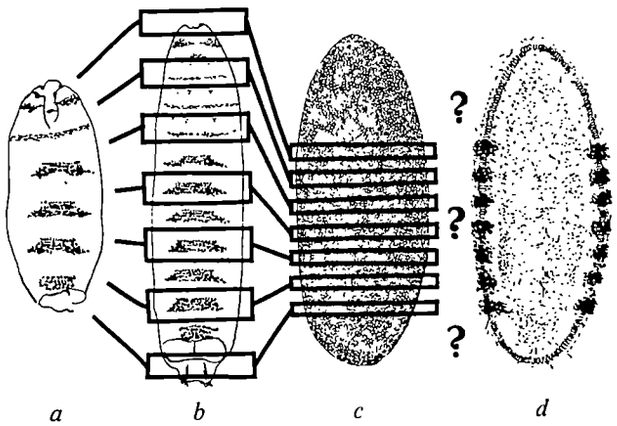
The establishment of a periodic, segmental pattern along the length of the embryo is thought to be initiated by the zygote in response to some maternally derived factor(s) present in the egg, but the nature of this global mechanism is not understood. One approach to studying this problem has been careful reconstructions of transcript distributions during the stages when the pattern is being formed. In general, transcripts arise in a defined sequence, with stripes in anterior regions becoming apparent before posterior ones. This sequence provides the first indication that the segmental pattern may be established progressively, possibly analogous to the gradual addition of the more posteriorly situated somites observed during vertebrate development. Furthermore, Weir and Kornberg[11] show that *engrailed* and *ftz* arise with even broader bands of specificity than the double segment. In pre-cellular stages, the transcripts are spaced at four-segment and even broader intervals, suggesting that the final segment pattern arises by progressive subdivision of larger units into smaller ones.

When fluorescently labelled antisera to the ftz and engrailed proteins were obtained, it was shown that in those cells which express either gene, the protein is

ocalized in the nucleus[12,13]. This presumably reflects the postulated DNA-binding activity conferred by the homoeobox domain present in each protein, and is consistent with a postulated regulatory role in programming cells for specific patterns or fates. The use of antisera has also provided more detailed information on the spatial patterns of gene expression and how they are achieved, while confirming most of the general features inferred from transcript distributions. The distribution observed with the ftz antiserum suggests that the final stage of the patterning process involves two clear phases, with the initially broad stripes tightening up into narrower bands as gastrulation begins. This contrasts with the patterning of engrailed stripes, which are generally a single cell wide at the time they arise.

The transition in the blastoderm patterns of *ftz* suggests that establishment of the final pattern of that gene is not a direct response to maternal cytoplasmic cues, but instead involves some kind of fine-tuning among zygotically active loci. This possibility is currently being investigated in several laboratories by analysis of the striping patterns in mutant embryos. Howard and Ingham[14] have recently analysed transcripts of *hairy*, *ftz* and *engrailed* in embryos mutant for either *hairy* or *ftz*. The pattern of *engrailed* expression is altered in either pair-rule mutant, with the usual pattern of fourteen stripes reduced to seven in each case, reflecting the deletion of alternating segmental repeats. These results are gratifying, but not entirely unexpected, because *engrailed* and other genes that are required later in every segment are likely to be regulated in response to the pattern established by the pair-rule genes at the blastoderm stage.

A more surprising result is that the pattern of *ftz* expression is altered by mutations in *hairy*, whereas the *hairy* pattern appears normal in *ftz* blastoderms. Thus, the two pair-rule genes seem to play different parts in the process of segmentation, with hairy somewhow acting to regulate *ftz* (and possibly other pair-rule genes). Because the *ftz* stripes become much broader, apparently extending further into the domain where *hairy* is normally expressed, *hairy* might at first glance seem to be a simple repressor of *ftz* transcription; the existence of overlapping domains of transcription observed in wild-type blastoderms (see above), however, suggests that the nature of the interaction is more complex. Also, it is not clear whether the only role of *hairy* is to regulate some subset of the pair-rule genes, or whether it also acts together with these genes to regulate processes further downstream. An understanding of segmentation will require the elucidation of all such hierarchical regulatory relationships, both within each 'class' and between classes of segmentation genes.



Relationship between segmentation phenotypes and transcription patterns at the blastoderm stage. Embryos homozygous for *ftz* differentiate as larvae with an abnormal segmentation pattern (*a*) in which the odd-numbered denticle bands have been eliminated (*b*). The cells in the wild-type embryo that would normally make those pattern elements are located in the blastoderm stage as seven parallel stripes (*c*), each of which is about four cells wide. When sectioned, blastoderms (*d*) are hybridized with labelled *ftz* DNA to determine the normal location of ftz transcripts, the transcripts also occurring in seven stripes. The positions of the stripes seem to correspond to the locations of those cells which normally make the pattern elements deleted in *ftz* mutant embryos. Recent results suggest that this correspondence is not maintained for other segmentation loci (see text).

An interesting question which arises from the early *ftz* and *engrailed* transcript patterns (see above) is that the deletions in the corresponding mutant embryos give no clear indication of a requirement at any stage earlier than the double segment. The earlier striping patterns, as well as the localization of *paired* transcripts to fourteen rather than seven stripes, argue that the relationship between phenotypes and transcript distributions must be re-examined. How can such discrepancies be resolved? In some cases, it could be argued that the differences observed are artefactual; or that the patterns of transcription at the blastoderm stage can never be described with absolute accuracy within the eight-celled double-segment interval because of the scarcity of gross morphological landmarks at the stage and the scatter of grains in the emulsion above each stripe. Moreover, the exact deletion domain in a given phenotype is difficult to define because the patterns vary slightly from one mutant individual to the next, even when the genotype is kept constant. But all these inaccuracies are relatively small compared with the differences we outlined earlier in this article, and it is unlikely that the discrepancies will be resolved by more detailed examinations of the phenotype or transcript patterns.

A more likely explanation is that the discrepancy reflects some fundamental difference between molecular and genetic approaches. Transcript analysis determines where RNAs accumulate, independent both of their role in development and of whether they are ever translated (although experiments with the appropriate antisera should resolve that point). Mutations, on the other hand, will only detect gene products if they are needed. They provide no direct indication of where in the embryo those products are made. These differences in techniques provide two classes of explanation for the discrepancy between molecular and genetic results. In the genetics version, *ftz* and *engrailed*, for example, may be transcribed in broader patterns during pre-blastoderm stages not because those transcripts are required, but because whatever condition controls their expression at the double-segment stage is already present and distributed with a broader spacing at earlier stages. In this view, the early transcripts provide a valuable assay for understanding how *ftz* or *engrailed* transcription is controlled, although the elimination of those transcripts does not block the segmental pattern in the larger (earlier) modes and the early transcripts have no obvious function. Similarly, one could assume that only every other stripe of transcripts observed in the fourteen-stripe *paired* pattern is required, or that only the earlier, seven-stripe mode is key to the functioning of the gene.

Alternatively, in the molecular view, gene products are made only in the cells where they are required. In this explanation, the molecular patterns at the blastoderm stage would give the best indication of the actual role of the gene product during development. Unexpected features of the phenotype of mutant embryos could be explained as secondary interactions between the cells once an abnormal pattern has been established at the blastoderm stage. Explanations of this kind demand that mutant phenotypes be

1. Nüsslein-Volhard, C. & Wieschaus, E. *Nature* **287**, 795 (1980).
2. Kilchherr, F. *et al. Nature* **321**, 493 (1986).
3. Weiner, A. *et al. Cell* **37**, (1984).
4. Kuroiwa, A. *et al. Cell*, **37**, 825 (1985).
5. Hafen, E. *et al. Cell* **37**, 833 (1984).
6. Garcia Belido, A. *Ciba Fdn Symp.* **29**, 161 (1975).
7. Gergen, J.P. *et al. Symp. Soc. dev. Biol.* (in the press).
8. Crick, F. & Lawrence, P. *Science* **189**, (1975).
9. Ingham, P.W. *et al. Nature* **318**, 439 (1985).
10. Kornberg, T. *et al. Cell* **40**, 45, (1985).
11. Weir, M.P. & Kornberg, T. *Nature* **318**, 433 (1985).
12. Carroll, S.B. & Scott M.P. *Cell* **43**, 47 (1985).
13. DiNardo, S. *et al. Cell* **43**, 59 (1986).
14. Howard, K. & Ingham, P. *Cell* **44**, 949 (1986).
15. Gergen, J.P. & Wieschaus, E. *Devl Biol.* **109**, 321 (1985).

at least partially non-autonomous in genetic mosaics.

Although large-scale non-autonomy has not been observed in the analysis of segmentation phenotypes, the sample of loci tested so far is relatively small[15]. Also, it is not clear whether the techniques presently available for marking cells in *Drosophila* are sufficiently accurate to exclude the limited non-autonomy needed to explain the discrepancy between the phenotypes and transcript distributions. However, genetic mosaics ultimately provide the most direct technique for relating phenotypes to individual cell requirements, and the variety of mosaic techniques available in *Drosophila* should provide a better understanding of the relationship between the gene products and the patterning process. □

Douglas Coulter and Eric Wieschaus are in the Department of Biology, Princeton University, Princeton, New Jersey 08544, USA.

Mathematics

The class number problem

from Ian Stewart

SOME of the deepest mathematical theories have been built from very humble raw materials, and a classic case is number theory, which studies properties of ordinary whole numbers 1,2,3,... . It has long been remarked that, although it is easy to observe patterns in the behaviour of whole numbers, it can be astonishingly hard to prove that these patterns are generally valid. Number theorists have long been interested in the arithmetic of 'imaginary quadratic fields', systems of numbers in the form $x+y\sqrt{-D}$, where D is a whole number and x,y are rational.

Any whole number can be factorized into primes, and there is an analogous concept for such fields. For whole numbers, the prime factorization can be achieved in only one way. This is not always true for imaginary quadratic fields; and in his *Disquisitiones Arithmeticæ* of 1801, the fount of all modern number theory, Carl Friedrich Gauss in effect conjectured that unique factorization holds precisely when $D = 1, 2, 3, 11, 19, 43, 67$ and 163. This conjecture was proved more than a hundred years later by A. Baker (*Mathematika* **13,** 201; 1966) and independently by H.M. Stark (*Michigan Math. J.* **14,** 1; 1967). But Gauss also stated a more general conjecture, the class number problem, the solution of which by D.M. Goldfeld, B. Gross and D. Zagier has recently been described in a masterly survey by Goldfeld (*Bull. Am. Math. Soc.* **13,** 23; 1985).

The classic example of non-unique factorization occurs in the case $D = 5$. Here $6 = 2.3 = (1+\sqrt{-5})(1-\sqrt{-5})$ exhibits two distinct prime factorizations. (Each of the numbers 2, 3, $1+\sqrt{-5}$ and $1-\sqrt{-5}$ is prime in this particular number field.) The extent to which factorization is not unique can be measured by a quantity called the class number, h: when $h=1$, factorization is unique, and for larger values of h it is not unique. In some sense the larger h becomes the less unique factorization is. For a given D it is relatively easy to calculate the class number (for example, if $D = 5$ then $h = 2$) but the list of values so obtained varies in a very irregular way with D. This makes it hard to solve the inverse problem: given a value for h, find which Ds have that class number. And this is what Gauss's conjectures are about. The conjecture on unique factorization asks for a determination of all D such that the class number is 1, with the guess that they are precisely the 9 values listed above. The general class number problem is to prove that for any given class number h, the list of D having that value for h is finite.

Gauss actually phrased his conjectures in a slightly different setting, the theory of quadratic forms. This goes back to the time of Pierre de Fermat, who stated theorems of the following kind: "Every prime of the form $6n+1$ can be written as x^2+3y^2 for integers x and y." For example, 31 is such a prime, and $31 = 1^2+3.3^2$. The connection with quadratic fields is that $x^2+3y^2 = (x+y\sqrt{-3})(x-y\sqrt{-3})$, a factorization in the field corresponding to $D = 3$. So theorems about quadratic fields carry implications for quadratic forms, and conversely.

Gauss, and Joseph-Louis Lagrange before him, realized that it is not necessary to study all possible quadratic forms, because changes of variable can be used to turn one form into another. For example, if x and y are replaced by $x+2y$ and $x+y$, respectively, then the form x^2+3y^2 becomes $4x^2+10xy+7y^2$. Therefore, the numbers that can be represented in the form x^2+3y^2 are precisely those that can be represented in the form $4x^2+10xy+7y^2$, even though at first sight these are different questions. This led Gauss to the idea of 'equivalent' forms (transformable into each other by such changes of variable). He proved that there is only a finite number of distinct classes of equivalent forms, which is the class number of the associated quadratic field.

H. Heilbronn and E.H. Linfoot (*Q. Jl Math.* **5,** 293; 1934) showed that, apart from the nine known cases, at most one further field has class number 1. In 1952 Kurt Heegner claimed a proof that no such tenth field exists, which would solve the class number 1 problem. But as Goldfeld remarks: "Heegner's paper contained some mistakes and was generally discounted at the time. He died before anyone really understood what he had done."

Baker's proof uses new results from the theory of transcendental numbers (numbers that do not satisfy any polynomial equation with rational coefficients), whereas Stark's proof is much closer in spirit to Heegner's attempt. Then M. Deuring (*Inventiones Mathematicæ* **5,** 169; 1968) showed that the 'gap' in Heegner's attempted proof can be filled relatively painlessly. In 1971 Baker (*Ann. Math.* **94,** 139) and Stark (*Ann. Math.* **94,** 153), again independently, solved the class number 2 problem, finding exactly 18 values of D for which $h = 2$.

Although these results represent enormous progress compared with what was previously known, it is clearly not feasible to tackle the general problem one class number at a time, because the process will never end. The interest of such partial answers is that they suggest new methods. Goldfeld (*Astérisque* **41–42,** 219; 1976) exploited a connection between the class number problem and an elliptic curve, a type of cubic equation. He showed that if just one elliptic curve can be found with a particular property, then the class number problem is solved. Unfortunately, no such elliptic curve was then known. But later, Gross and Zagier (*C.r. hebd. Séanc. Acad. Sci., Paris* **297,** 85; 1983) established the necessary property for the elliptic curve $-139y^2 = x^3+4x^2-48x+80$. By such roundabout methods was Gauss's conjecture on the finiteness of the list of imaginary quadratic fields of given class number demonstrated.

Soon afterwards, J. Oesterlé (*Séminaire Nicolas Bourbaki* 631; 1984) obtained a specific estimate for the size of the largest D with given class number h, making is possible in principle to select values of h and find all possible Ds. As a result, the class number 3 problem (precisely which D gives $h = 3$?) has been solved, and many long-standing problems in number theory begin to appear tractable. For example, a solution of the class number 4 problem would answer a famous question: which integers can be expressed as a sum of three squares in exactly one way? The powerful and beautiful ideas laid bare by a 180-year assault on Gauss's conjecture strikingly attest to the quality of his insight into the deep properties of ordinary whole numbers. But the sad story of Kurt Heegner shows that genius is still not always appreciated during its lifetime. □

Ian Stewart is at the Mathematics Institute, University of Warwick, Coventry CV4 7AL, UK.

Evolution — the struggle continues

SIR—In an interesting and provocative article, Halstead[1] rejected the anti-darwinian views of the Japanese biologist Imanishi. His rejection is apparently based on his negative impressions of Japanese society. Halstead remarked that: "the ordinary Japanese [is] condemned... to the rigid authoritarian feudal society that masquerades as one of the advanced nations of the world."

Halstead sees the world as "demonstrably... [one]... of competition, struggle and disharmony". This is not surprising when one considers that the concept of competition is inherent to Neo-Darwinism and that Halstead is a staunch supporter of this theory. However, while Halstead may see the world in this way, the question remains — is there any evidence for the reality of what he sees?

Halstead states: "Recent research... [has]... demonstrated that interspecific competition takes place in 90 per cent of all cases studied". On the contrary, a critical review of a large number of cases by Underwood[2] suggests that this statement is grossly inaccurate. This also suggests that Halstead's claim that "the informational foundation of Imanishi's theory no longer stands" is incorrect. Irrespective of this, the conclusive demonstration of competition is unlikely to deter the Japanese public from supporting Imanishi's theory. As suggested by Brady[3], there may be more than one reason for accepting a theory. This is not an attribute unique to the Japanese scientific community, as suggested by Halstead, but a characteristic of the development of theories in general.

We agree with Imanishi that the selectionism of Darwin has its roots in Western society. In the same way Imanishi's theory has been influenced by Japanese society. However, while the theory was developed by a Japanese, it is not necessarily uniquely Japanese in concept and therefore judgement of the theory on the basis of the values of the society in which it was developed cannot be feasible. After reading Halstead's article, one is left with the distinct impression that this is exactly what he has done.

C. D. MILLAR
N. R. PHILLIPS
D. M. LAMBERT
Evolutionary Genetics Laboratory, Department of Zoology, University of Auckland, Private Bag, Auckland, New Zealand

1. Halstead, B. *Nature* **317**, 587-589 (1985).
2. Underwood, A.J., Anderson, D.J. & Kikkaw, J. (eds) *Community Ecology-Pattern and Process* (Blackwell, Oxford, 1984).
3. Brady, R.H. *Biol. J. Linn. Soc.* **17**, 79 (1982).

SIR—Halstead's commentary "Anti-darwinian theory in Japan" (*Nature* **317**, 587; 1985) introduces the theory of evolution advanced by Imanishi, at the same time rejecting it. We feel, however, that Halstead rejected Imanishi's theory of evolution without fully understanding it, and we wish to comment on the theory on purely scientific grounds.

First, Halstead introduces Imanishi's concept of habitat segregation and comments that this is but a "dream" attractive to members of Japanese society, which is actually extremely competitive. Leaving aside the rather meaningless discussion as to whether or not Japanese society is more competitive than that of Europe or America, we would like to know whether Halstead will recognize habitat segregation as a principle on which a wholly different theory of evolution could be built. We consider habitat segregation to be a real biological phenomenon.

Second, if Halstead recognizes habitat segregation as propounded by Imanishi as a possibility, he ought either by explaining habitat segregation by means of Darwinism, include it in Darwinism or clearly recognize Imanishi-ism as a view of evolution which is independent of Darwinism. Interestingly, Halstead does not attempt this but tries to give a "sociological" explanation of Imanishi's theory. We think that there is a relationship between the competitive exclusion principle of Gause[1] and Hardin[2] and Imanishi's concept of habitat segregation.

Third, Imanishi strongly refutes Darwin's hypothesis of the survival of the fittest and asserts that: "Survival is in most cases purely accidental. It is a matter of luck rather than selection". Darwin considers the struggle for existence to be fierce among individuals of the same species as well as between different species, but Imanishi is critical of this idea. Imanishi, as Halstead stresses several times, understands evolution as being a transformation only occurring to the species, and not to the individual. In contrast to Darwinism, which considers the individual to be the unit of evolution and expends great energy in explaining how the transformations of this individual are magnified in the transformations of the species, Imanishi asserts that the unit for explaining evolution is not the individual but the species.

We believe this idea of the species as a unit to be the essence of Imanishi's assertion that "all the individuals of a species change at once when the time to change comes" will be understood. Concerning this unit of evolution, we support Imanishi's ideas. In the case of the law of movement of heavenly bodies, the Earth and the Moon are considered the units regardless of their components. The minute examination of brain cells probably will not be able to tell us how humans think. Building theories to explain natural phenomena requires an appropriate unit. The originality of Imanishi's theory of evolution is the idea of the species as its unit. We would like to ask what Halstead's opinions are upon this point.

We consider that Darwinism and Imanishi's theories are two separate views of evolution. If Halstead feels that Imanishi's theory of evolution is unscientific, that it could not even stand as a hypothesis, he should give scientific reasons, and not literary or sociological explanations.

HIDEOMI NAKAHARA
Department of Environmental Health, Medical University of Yamanashi, Yamanashi, Japan
TAKASHI SAGAWA
TAKASHI FUKE
Institute of Human Sciences, Tokyo, Japan

1. Gause, G.F. *The Struggle of Existence* (Hafner 1934)
2. Hardin, G. *Science* **131**, 1292-1297 (1960)

Kenyan finds not early Miocene *Sivapithecus*

SIR—In his recent commentary in *News and Views* questioning the assignment of the new Miocene hominoid specimens from Buluk, Kenya[1] to *Sivapithecus*, Delson[2] referred to a paper of ours in which we discuss the hominoid genus *Ouranopithecus* from Ravin de la Pluie, Greece[3]. As he states, we suggested a link with "hominines", but one based upon a particular assumption about character state polarities drawn from several alternatives, any of which, as we stated, might be correct.

He failed to note another argument in that paper which goes to the heart of the issue of the generic status of the Buluk specimens. As others have done, we argue for a *Sivapithecus*–orangutan clade based on a set of facial characters worked out by Ward[4] and Andrews[5] relating to the premaxilla and palate. As the clade is defined by these presumed shared derived features, any species included in *Sivapithecus* must also possess these character states. By these criteria, only *Sivapithecus* species from the Siwaliks of Indo-Pakistan and *S. meteai* from the Sinap series in Turkey are definitely included in *Sivapithecus*. *Ouranopithecus* from Ravin de la Pluie[3,6], *Rudapithecus* or *Dryopithecus* from Rudabanya, Hungary[7], *Kenyapithecus* from Nachola, Kenya[8], and the large hominoid from Lufeng, China (personal observation) clearly are not. The status of other thick-enamelled hominoid samples which lack specimens with the critical nasopalatal morphology, such as that from Buluk, must remain open, although in some other features Buluk specimens differ markedly from Asian *Sivapithecus*.

We have provided a specific diagnosis

of *Sivapithecus* based upon a set of character states that most now accept as being derived features showing phyletic affinity with the orangutan. It is a framework in which neither the definition nor the species inclusivity of *Sivapithecus* is as ambiguous as Delson suggests.

JAY KELLEY
Division of Biology and Medicine, Brown University, Providence, Rhode Island 02912, USA
DAVID PILBEAM
Department of Anthropology, Harvard University, Cambridge, Massachusetts 02138, USA

1. Leakey, R.E.F. & Walker, A. *Nature* **318**, 173-175 (1985).
2. Delson, E. *Nature* **318**, 107-108 (1985).
3. Kelley, J. & Pilbeam, D. *Am. J. phys. Anthrop.* **66**, 188 (1985).
4. Ward, S.C. & Kimbel, W.H. *Am. J. phys. Anthrop.* **61**, 157-171 (1983).
5. Andrews, P. & Cronin, J.E. *Nature* **297**, 541-546 (1982).
6. de Bonis, L. & Melentis, J. *C. r. hebd. Séanc. Acad. Sci., Paris* **300**, 429-432 (1985).
7. Kelley, J. & Pilbeam, D. in *Comparative Primate Biology* Vol. 1 (ed Swindler, D.R.) (Liss, New York, in the press).
8. Pickford, M. in *Hominid Evolution: Past, Present and Future* (ed. Tobias, P.V.) 107-112 (Liss, New York, 1985).

Quantum behaviour of superconducting rings

SIR—In a recent *Nature* (**319**, 726; 1986), U. Eckern discussed the applicability of quantum mechanics to macroscopic objects, for which superconducting rings incorporating weak link constrictions are considered to be very strong candidates. To set this in context, we wish to point out that there are modes of operation of weak link rings other than the one considered by Eckern. For these, experimental results already exist which are very strong evidence for the fact that such rings do indeed behave as macroscopic quantum objects.

The magnetic flux threading the superconducting ring ϕ and the electric charge localized at the weak link Q are the conjugate variables for a weak link ring. If it is a quantum object a Heisenberg relation for the flux and charge uncertainties $\Delta\phi\Delta Q \geq \hbar/2$ exists. Eckern addressed only the limit where the flux is exceedingly well defined compared to the quantum unit of flux ϕ_0 ($\phi_0 = \hbar/2e$ where $\hbar$ is Planck's constant and e the electric charge), so $\Delta\phi << \phi_0$, and thus $\Delta Q >> 2e$, $2e$ being the charge on a Cooper pair of electrons in the superconductor. Our experimental and theoretical work over the past few years has considered two other limits: (1) where the flux is quite well defined $\Delta\phi << \phi_0$, and the charge is fairly uncertain $\Delta Q >> 2e$. (2) Where the charge is quite well defined $\Delta Q << 2e$, and the flux is fairly uncertain $\Delta\phi >> \phi_0$. We have accumulated a large amount of experimental data which are in accord with the predictions made theoretically by considering weak link rings as quantum objects, and which to date have no alternative explanation.

Readers who are interested in the quantum mechanics of macroscopic objects but are unfamiliar with the published literature on superconducting weak link rings are referred, for example, to *Helv. phys. Acta* **56**, 789 (1983) and *Phys. Lett.* **104**, 375 (1984); **107**A, 133 (1985); **111**A, 199 (1985); **115**A, 125 (1986).

TIMOTHY P. SPILLER
T.D. CLARK
Physics Division, School of Mathematical and Physical Sciences, University of Sussex, Brighton BN1 9QH, UK

The stability of zoological nomenclature

SIR—The long letter on this subject by Erzinclioglu and Unwin (*Nature* **320**, 687; 1986) reveals some fundamental misunderstandings. But if they, or others prompted by their letter, will make constructive suggestions then a valuable purpose will have been served.

As stated in its introduction, the *International Code for Zoological Nomenclature* (3rd Edn, 1985) "provides guidance for zoologists needing to establish new names, and rules to determine whether any name, previously proposed, is available and with what priority..." It is a do-it-yourself manual and like any must be used with commonsense for the desired results, in this case stability coupled with taxonomic freedom.

The purpose of the International Commission on Zoological Nomenclature is the very opposite of that portrayed in the situation graphically described by Erzinclioglu and Unwin: "taxonomists... are kept in place by the tyranny of the Commission: the Code must be obeyed". Their statements that "[in some circumstances] a name must still be changed in spite of the confusion that will be caused" and "there is only one course open to us if sanity is to be restored and that is that some sections of the code must be consistently ignored" are not accurate and overlook the basic function of the Commission.

Some code of zoological nomenclature, internationally recognized, must clearly exist, and like any other set of 'rules' the existing one is imperfect and could not be otherwise. The number of zoological names runs into millions, and naturally rigid adherence to the code's prescriptions will sometimes cause confusion. Individual zoologists (in the widest sense of the word) cannot follow the recommendation of Erzinclioglu and Unwin and "consistently ignore some sections of the Code", because in the nature of things they would be inconsistent. The International Commission, at present of 25 scientists from 15 countries, exists largely to overcome this problem.

Anyone encountering a difficulty, for example a conflict between the priority of one name and the established usage of another (the blood-sucking maggot mentioned by Erzinclioglu and Unwin is a case), should submit the matter to the Commission. This does not then act in any tyrannical manner, but solicits the comments of zoologists by publishing the problem in the quarterly *Bulletin of Zoological Nomenclature*, and also by notifying appropriate journals. The Code (Article 80) provides that existing usage should be maintained meanwhile. Comments adding any new facts are published in the *Bulletin*, and in every case are brought to the attention of the Commission. After at least six months (commonly two years, although this is being reduced) the members of the Commission vote by postal ballot, and a two-thirds majority will suffice to set aside the provisions of the Code if appropriate. The outcome is published as an 'Opinion' in the *Bulletin*. Of course there is no power to enforce anybody either to approach the Commission or to abide by its conclusions, but it is in the common interest that they should do so.

The 1985 Code is a carefully considered result of very numerous contributed suggestions, although none were proposed as "devices to ensure unnecessary name changes"! Of course it needs amendments. One is proposed by Erzinclioglu and Unwin (although they are not the first), and concerns the requirement that the gender of generic and specific names should agree. This was clear in the past when naturalists knew Latin and classical Greek, but many feel it unsuited to the present day of computer information retrieval (see p.xix of the Code's introduction). The Commission invites views on this and on any matters concerning zoological nomenclature.

P.K. TUBBS
International Commission for Zoological Nomenclature, c/o British Museum (Natural History), London SW7 5BD, UK

In the eye of the beholder

SIR—T. Nash (*Nature* **320**, 402; 1986) believes that the patches he sees in the out-of-focus image of a light point originate from individual light receptors in his retina. If he set about measuring their angular subtense, he would discover that they are about an order of magnitude larger than those of retinal cones. And how does he think he gets to "see" the spaces between the "receptors"? In fact, Nash is viewing entoptically the quality of his eye's optics and the transparency of his crystalline lenses.

GERALD WESTHEIMER
University of California, Berkeley, California 94720, USA

Error rates in prenatal cystic fibrosis diagnosis

SIR—Pembrey and Malcolm[1] state that if a prenatal diagnosis is based on an empirical correlation between an amniotic fluid protein and fetal genotype, an attempt should be made to confirm diagnosis on the abortus after termination of pregnancy. This is certainly standard practice for α-fetoprotein-based diagnosis of neural tube defects, and has become part of our procedure for microvillar enzyme-based prenatal diagnosis of cystic fibrosis[2]. Apart from providing a continual updating of the sensitivity and specificity of the test, such procedures are useful for monitoring the inevitable errors of sample handling which creep into even the best-regulated laboratories.

What puzzles us is why Pembrey and Malcolm should feel that diagnosis based on linked DNA probes should be excluded from such quality control. The accuracy of such diagnosis is dependent on recombination frequencies. The derivation of recombination frequencies is a form of empirical correlation and only as good as the most recent set of data. In fact, because the total number of informative meioses observable can be quite small, recombination fractions may be subject to dramatic fluctuations. The linkage between the G8 probe and the Huntington's disease gene was initially very tight[3], but recombinants appeared with the acquisition of new family data[4,5]. The same is true for linkage between the cystic fibrosis gene and the probes, pJ3.11 and met[6,7]. Recombination fractions are usually stated as lying within a given confidence interval, to indicate the uncertainties inherent in their estimation.

There is also the question of genetic heterogeneity. Pembrey and Malcolm suggest that careful linkage studies in a large number of families from different populations will allow exclusion of significant non-allelic heterogeneity. But what do they mean by significant? An average non-allelic heterogeneity level of 5 per cent would be very significant if it meant that a similar proportion of prenatal diagnoses were wrong. It is difficult to see how this figure can go much below 5 per cent when the error rate in diagnosing cystic fibrosis is believed to be of this order[8].

The point that we were making in our earlier letter[9] is that the whole edifice of quality control is not based on pedantry but on the realization that laboratories do make mistakes. It is possible that, as first-trimester prenatal diagnosis becomes more widely available, the standard procedure of confirmation of diagnosis on abortuses will have to be abandoned. We should, nonetheless, continue to collect and analyse the outcomes of as many of these pregnancies as is possible, since it will improve the reliability of the linkage data. And let us be clear what we are doing, and not imply — as do Pembrey and Malcolm — that we have acquired new procedures which are now error-free.

DAVID J.H. BROCK
Human Genetics Unit,
University of Edinburgh,
Edinburgh, UK

VERONICA VAN HEYNINGEN
MRC Clinical and Population Cytogenetics Unit,
Western General Hospital,
Edinburgh EH4 2XU, UK

1. Pembrey, M.E. & Malcolm, S. *Nature* **320**, 114 (1986).
2. Brock, D.J.H. *et al. Lancet* **1**, 1175 (1985).
3. Gusella, J.F. *et al. Nature* **306**, 234 (1983).
4. Folstein, S.E. *et al. Science* **229**, 776 (1985).
5. Youngman, S. *et al. J. med. Genet.* **21**, 299 (1984).
6. White, R. *et al. Nature* **318**, 382 (1985).
7. Wainwright, B. *et al. Nature* **318**, 384 (1985).
8. Denning, C. *et al. Pediatrics* **66**, 752 (1980).
9. Brock, D.J.H. & van Heyningen, V. *Nature* **319**, 184 (1986).

Homology of trichosanthin and ricin A chain

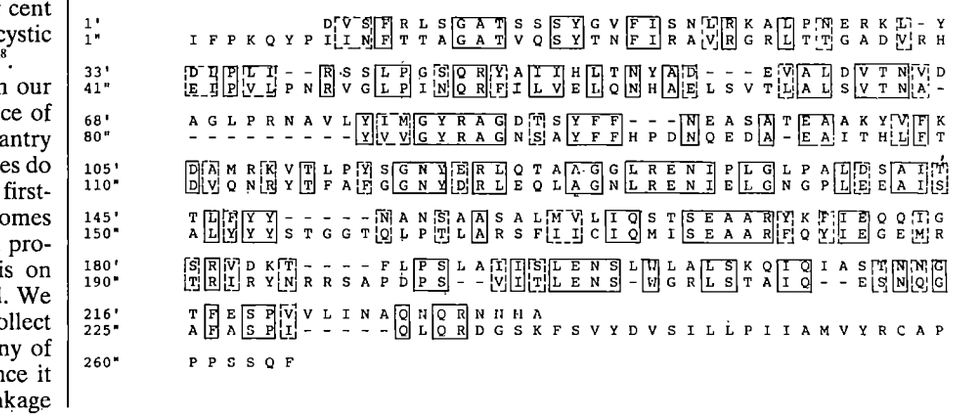
SIR—Trichosanthin is a plant protein extracted from a Chinese herbal medicine, the root tuber of *Trichosanthes kirilowii maxim,* Cucurbitaceae. It has been shown to bind to the trophoblastic syncytial layer killing the cells quite selectively. It can therefore be used clinically to terminate pregnancy and inhibit trophoblastic tumours[1]. This basic single-chain protein consists of 234 amino acid residues. Its sequencing has recently been completed[2,3] and a molecular model has been derived from the X-ray analysis[4]. Here we report a striking degree of sequence homology between trichosanthin and subunit A of ricin-D (ricin A for short). It is the first example of the complete sequence comparison between a ribosome-inactivating protein and cytotoxin.

In recent years, much attention has been paid to cytotoxins and the like for theoretical reason and because of their potential as immunotoxins to treat cancers. Many cytotoxins consist of two kinds of subunits. The toxic action is associated exclusively with subunit A which enzymatically inhibits protein synthesis of eukaryotes, whereas one or more B subunits have the ability to bind to cell surfaces and aid subunit A penetration into cytosol. Among others, typical protein cytotoxins are diphtheria toxin, cholera toxin (from bacteria), ricin and abrin (from plants). However, it has also been found that many plants contain single chain proteins which are very similar to the toxic subunit A of the above cytotoxins in having the ability to inhibit protein synthesis. Pokeweed antiviral protein (PAP), momorcharin, wheat germ inhibitor and gelonin are good examples (for review see ref 5). *Momordica* and *Trichosanthes* are taxonomically closely related and all belong to the Cucurbitaceae family. It has been reported that momorcharin and trichosanthin have similar biological functions[6]. It led us to think that trichosanthin may also fall into the same group. To test for this possible relatedness, we therefore carried out sequence comparison studies. Sequence comparisons between short pieces of N-terminal segments of some ribosome-inhibiting proteins (RIPs) and cytotoxins have been recently reported[7,8]. Here we report the complete sequence comparison by computer analysis between trichosanthin and ricin A.

Figure 1 demonstrates our alignment of trichosanthin and ricin A, in which 91 residues are identical and 42 conservative. In our analysis, substitutions are taken as conservative only if two conditions are met — a minimum base change of one and that the two side-chain's physico-chemical properties are similar, as with Ser and Thr or Asp and Glu. The identical and conservative residues comprise at least 56 per cent of the trichosanthin sequence.

Further inspection shows that the identical and conservative residues are rather concentrated and that very little deletion needs to be assumed. In particular, there is no deletion at all from residues 97 to 149 in trichosanthin. We therefore believe that the sequence similarity between trichosanthin and ricin A is by no means a random event. It has been reinforced by the probability estimation of the alignment.

It is reportedly very rare for an identical pentapeptide to appear in different chains[9], the probability is estimated to be about 1×10^{-6}. One may then expect the



frequency of appearance of any identical pentapeptide in both trichosanthin and ricin A to be only about 0.05. In fact, three identical pentapeptides have been found. One is GYRAG in residues 80–84 of trichosanthin and 83–87 of ricin A. The second is LRENI in residues 128–132 of trichosanthin and 133–137 of ricin A. And the third is SEAAR in residues 166–170 of trichosanthin and 176–180 of ricin A. Thus the remarkable sequence homology between trichosanthin and ricin A seems not to be coincidental, and may well be of biological significance.

There is a pool of evidence indicating that it is an enzymatic process by which the toxic subunits of cytotoxins affect the host cell metabolism. For diphtheria toxin and cholera toxin, the subunit A acts on the elongation factor EF2 and GTP-binding protein respectively. Nevertheless they share a common mechanism — ADP= ribosylation. For plant toxins such as ricin and abrin, in spite of considerable efforts, the nature of their enzymatic activity is obscure. It is known, however, that they inactivate the 60S subunit of ribosomes (for review see ref. 5). It is likely that different cytotoxins may not use the same mechanism, but the sequence homology between trichosanthin and ricin A shown here strongly suggests that these two do act by similar mechanisms. Taxonomically, *Ricinus* belongs to the Dicotyledoneae Archichlamydeae Euphorbiaceae *Ricinus* L. and *Trichosanthes* belongs to the Dicotyledoneae Sympetalae Cucurbitaceae Trichosanthea L. They are not closely related. But the possibility can not be ruled out that they originate from a common ancestor.

There is a speculation[7] that in the ancient plants there was a special defensive protein which could inactivate eukaryotic ribosomes. In the evolution process, the gene coding for this toxic chain might have fused with the gene for some sort of sugar-binding proteins, resulting in cytotoxins with two different types of subunits as found in species like *Ricinus*. However, in some plants, such as pokeweed, the toxic chain remains independent and has been termed the ribosome-inactivating protein (RIP). The overall sequence homology between trichosanthin and ricin A strongly supports this hypothesis.

We thank Professor Wang Yu and his colleagues for their kindness in showing us the sequence of tricosanthin before publication. This work was supported by a special grant from the State Commission of Science and Technology of China.

ZHANG XUEJUN
WANG JIAHUAI

Biophysics Institute,
Academia Sinica,
Beijing, China

1. *Acta zoologica sinica* (Chinese) **22**, 126 – 136 (1974).
2. Gu Ziwei *et al. Acta chemica sinica* (Chinese) **43**, 943–945 (1984).
3. Wang Yu *et al.* (*International Symposium on Organic Chemistry of Medicinal Natural Products*) at Shanghai, China, November 1985.
4. Pan Kezhen *et al. Supplement of Proc. of China-Japan Bilateral symposium on Biophysics*, May, 1985, Wuxi, China.
5. Olsnes, S. & Pihl, A. in *Molecular Action of Toxins and Viruses*, 51-105 (Elsevier, Amsterdam, 1982).
6. Chan, W.Y., Tam, P.P. & Yeung, H.W. *Contraception* **29** (1), 91-100 (1984).
7. Ready, M., Wilson, K., Piatak, M & Robertus, J.D. *J. biol. Chem.* **259** (24), 15252-15256 (1984).
8. Lappi, D.A., Esch, F.S., Barbieri, L., Stirpe, F. & Soria M. *Biochem. biophys. Res. Comm.* **129**, 934-942 (1985).
9. Kabsh, W. & Sander, C. *Proc. natn. Acad. Sci. U.S.A.* **81**, 1075-1078 (1984).

Putting a charge on a quark

SIR—The magnitudes of the quark electric charges raise the perplexing question: what is the magnitude of the unit electric charge? When the proton and electron were thought to be the elementary particles of nature, it appeared quite acceptable to take the electronic charge as the unit and to express all other charges in terms of it but, if quarks are elementary particles, it is meaningless to speak of a unit charge in any unambiguous way; only charge ratios are meaningful.

It is thus sensible to ask why the charge on the *u* (*up*) quark is minus twice that on the *d* (*down*) quark and why the latter is one third that of the electron, but it is not meaningful to ask which of these is the unit charge. If it is desirable to work with integral charges, the *d*-charge should be taken as he unit; the *u*-charge is then −2 units and the electronic charge is +3 units. That the latter is universally accepted as the unit charge is merely a matter of a bias which perpetuates the belief that the electron is an elementary particle for which, at present there is no conclusive evidence.

Nothing in current particle theories even begins to answer the question why only two elementary charges exist in nature and why their ratio is −2. Nor can these theories indicate how the answer is to be found. Quantum chromodynamics confuses things even more for it raises the additional question as to why all colours of a given quark flavour have the same electric charge.

If the three quarks in a nucleon form a linear structure, with one of the quarks always at the centre, as I have already proposed in my gravitational linear rotator model of the nucleon, then a simple variational principle answers the questions about quark charges.

In a series of papers I have proposed a linear rotator model of baryons in which the constituent particle triplets are gravitationally bound unitons, particles of mass $m \simeq (\hbar c/G)^{1/2}$, where G is the universal gravitational constant. The gravitational binding force between any two such particles is thus larger than the electrostatic force by a factor of the order of 137. Accepting this model one sees that the overall dynamical configuration is determined essentially by the gravitational field and that the electromagnetic field plays only a minor role in it; that is, the linear arrangement of three unitons, with one at the centre, is a consequence of the large masses of the unitons and would persist if the three unitons were electrically neutral. Nevertheless, the assignment of electric charges to the unitons does matter, for only one such assignment among the various possibilities is preferred by the energetics of the problem.

I now show that one obtains this unique uniton charge distribution by imposing the condition that the electrostatic potential energy of the linear triplet be a minimum. I have assumed here that gravity is the dominant force in this linear nucleon model, but any strong force field that gives the same linear arrangement will do.

If Q is the charge on the nucleon and q_1, q_2, q_3, are the three quark charges, we have:

$$q_1 + q_2 + q_3 = Q \qquad (1)$$

where q may be positive or negative. Placing q_1 at the centre of the linear configuration and q_2 and q_3 at the ends, the electrostatic potential energy is:

$$E = \frac{1}{r}(q_1q_2 + q_1q_3 + \frac{1}{2}q_2q_3) \qquad (2)$$

where $2r$ is the length of the structure; or,

$$rE = q_1(q_2 + q_3) + \frac{1}{2}(q_2q_3)$$

$$= q_1Q - q_1^2 + \frac{1}{2}Qq_2 - \frac{1}{2}q_1q_2 - \frac{1}{2}q_2^2 \qquad (3)$$

where I have used (1) to eliminate q_3. Varying this with respect to q_2, keeping Q and q_1 fixed, leads to the condition that $d(rE)/dq_2 = 0$ if, and only if, $q_2 = q_3$.

In other words, regardless of the value of Q and which uniton is at the centre of the configuration, the charges on the two ends must be equal in magnitude and in sign. Moreover, from (1), $q_2 = \frac{1}{2}(Q - q_1)$ or $q_2 = \frac{1}{2}(1 - q_1)$ if Q is the unit charge of the proton.

If, now, quark q_2 is at the mid point of this configuration, $q_2 + 2q_1 = Q'$, where Q' is another value of the total charge, to be identified with that of the neutron, so that $q_2 = -2q_1$. But from the equivalent information for the proton $-2q_1 = \frac{1}{2}(1 - q_1)$, or $(1 + 3q_1) = 0$ or $q_1 = -1/3$ hence $q_2 = 2/3\, q_1$.

This is as far as one can go with this simple type of analysis, but its simplicity and its seeming meagreness hide its importance, for it clearly points to the linear rotatore with a uniton (quark) at its centre as the correct model of the nucleon. We are ineluctably led to this conclusion by the coefficient $-\frac{1}{2}$ in front of q_2 in equation (3); if it were numerically different, we would not obtain the important equality $q_2 = q_3$.

LLOYD MOTZ

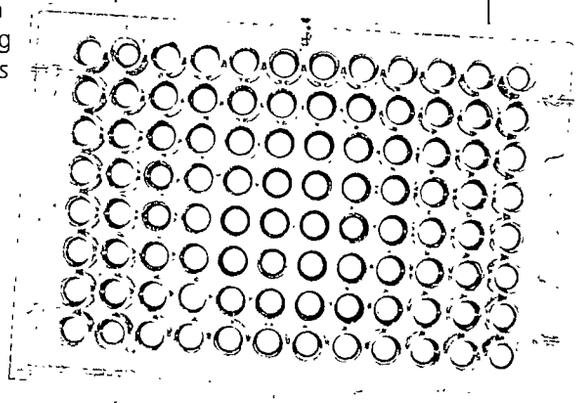
Department of Astronomy,
Columbia University,
New York 10027, USA

Everything For ELISA

From Bio-Rad, The Quality Choice

Monoclonal Antibody Screening Kits

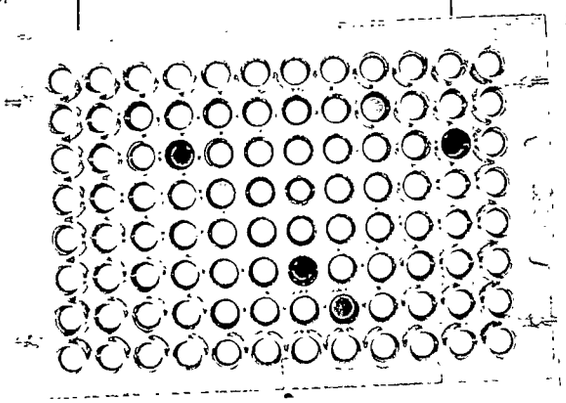
Bio-Rad's mouse, human, and rat Clone Selector™ kits provide an efficient EIA method for selecting monoclonal antibodies. All 3 kits use high activity alkaline phosphatase labeled second antibodies which are highly antigen specific and are guaranteed to react with the most common monoclonal subclasses and isotypes. The anti-mouse and anti-rat reagents are cross-adsorbed to remove unwanted cross-reactivities. Each Clone Selector kit contains enough conjugate to screen 30,000 mouse, 5,000 human, or 5,000 rat supernatants and comes with everything required for fast, sensitive, and reproducible ELISA assays.



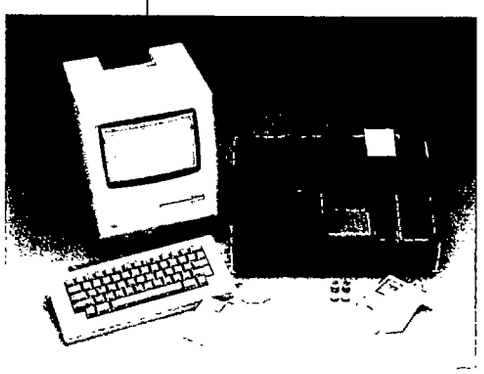
Hybridoma screening using Bio-Rad's Clone Selector system.

Mouse EIA Subtyping Kit

Bio-Rad's Mouse-Typer™ kit provides the most accurate ELISA method for identifying mouse Ig class and subclass. Monoclonal subtypes are identified quickly and easily by utilizing an ultra pure panel of rabbit anti-mouse typing reagents (IgG_1, IgG_{2a}, IgG_{2b}, IgG_3, IgM, and IgA). This method depends on antibody-antigen interaction, not antibody-antibody immunoadsorption, so background-free assays are guaranteed. The included protocol assures accurate typings, with positive wells having absorbances 3-6 times those of negatives. Each kit comes with all the essential reagents for 600 tests (100 typings).



Subtyping of mouse monoclonals using Bio-Rad's Mouse-Typer Kit.



Model 2550 EIA plate reader and Macintosh Computer.

EIA Grade Affinity Purified Antibody Conjugates and Substrates

Bio-Rad offers a broad selection of EIA grade antibodies conjugated to either horseradish peroxidase (HRP) or alkaline phosphatase (AP). These conjugates exhibit a high degree of specific enzyme activity, and most are cross-adsorbed to remove cross-reactivities. The high quality HRP and AP substrates specially formulated for use with the enzyme conjugates are safe, stable, 100% soluble reagents that produce chromophores with high extinction coefficients.

EIA Reader and Applications Software Speed Data Analysis

MacReader™ ELISA software, a complete data analysis package for the Model 2550 EIA reader, provides statistical analysis and data reduction of ELISA results in seconds. The combination of the speed and sensitivity of the EIA reader and the computing power of Apple's Macintosh™ computer produces a high performance ELISA system which reduces analysis time from hours to minutes.

MacReader™ is a trademark of Bio-Rad Laboratories
Macintosh™ is a trademark of the Apple® Computer Co

BIO-RAD

2200 Wright Avenue
Richmond, CA 94804
800-4-BIORAD
In California, (415) 234-4130

Also in Rockville Centre, N.Y., Australia, Austria, Canada, England, Germany, Italy, Japan, The Netherlands and Switzerland.

Reader Service No.170

New in Current Communications.....
from Cold Spring Harbor Laboratory

Computer Graphics and Molecular Modeling

Edited by Mark Zoller, *Cold Spring Harbor Laboratory;* **Robert Fletterick,** *University of California School of Medicine, San Francisco*

COMPUTER GRAPHICS AND MOLECULAR MODELING summarizes work presented at a December 1985 Cold Spring Harbor Laboratory Banbury Center meeting at which a diverse group of researchers addressed issues such as protein sequence homology, three-dimensional structure homology in proteins, molecular design of functional, macromolecules, X-ray crystallography, hardware and software for displaying and analyzing three-dimensional macromolecules, and software for the analysis of the energetics and dynamics of proteins.

Molecular biologists, crystallographers, and computer specialists will find COMPUTER GRAPHICS AND MOLECULAR MODELING a useful collection of extended abstracts indicating directions for integrating the various approaches to the study of protein structure and function.

March 1986, 150 pp. (approx.), illus., colorplates, appendix
Paper $29 **ISBN 0-87969-193-X**

Translational Control

Edited by Michael B. Mathews,
Cold Spring Harbor Laboratory

Control of gene expression at the level of protein synthesis is a widespread phenomenon that has enjoyed a recent upsurge of interest, with great progress being made in explaining regulation at the initiation step. TRANSLATIONAL CONTROL is a collection of extended abstracts presented by some of the leading practitioners in this field at a small conference held at the Banbury Center of Cold Spring Harbor Laboratory in November 1985. Topics at the meeting ranged from the regulation of initiation factor activity and the influence of RNA structure to the effects of virus infection, heat shock, and interferon in organisms as diverse as *Volvox* and man. Mechanistic aspects of the problem were emphasized. Cell and molecular biology investigators and students and biochemists will find TRANSLATIONAL CONTROL an interesting survey of the latest developments in this field.

March 1986, 194 pp. (approx.), illus.
Paper $27 **ISBN 0-87969-191-3**

Plant Cell/Cell Interactions

Edited by Ian Sussex, *Yale University;*
Albert Ellingboe, *University of Wisconsin;*
Martha Crouch, *Indiana University;*
Russell Malmberg, *University of Georgia*

In much of plant growth and development, there is no new contact between cells that have not arisen together as clones after cell division. The rigid structure of the plant cell wall usually prohibits the sort of morphogenetic movements that are commonplace in animal development. This book, the result of an October 1985 Cold Spring Harbor Banbury Center meeting, presents current research aimed at analyzing exceptions to this rule. Converging from several quite diverse fields, the areas of research covered have in common the bringing together of plant cells with the consequent interactions of two distinct cellular genomes and developmental potentials.

The majority of the work presented focuses on two topics—plant self-incompatibility and host/pathogen interactions. Both the formal and molecular genetic approaches are discussed, as well as attempts to study the biochemical reactions that are subsequent to the interactions of the plant and pathogen phenotypes. In addition, discussions of plant cell/cell interactions during normal and graft chimeral development and in the mating-type biology of some fungi and algae are included.

Workers in the fields of plant pathology, plant development, and plant molecular biology will find much in this volume of current interest.

1985, 151 pp. illus.
Paper $27 **ISBN 0-87969-189-1**

PREVIOUS TITLES IN SERIES

Immune Recognition of Protein Antigens
July 1985. 197 pp., illus.
Paper $30 ISBN 0-87969-185-9

Eukaryotic Transcription: The Role of *cis*- and *trans*-acting Elements Initiation
August 1985. 200 pp., illus.
Paper $30 ISBN 0-87969-186-7

Plant Infectious Agents
1983. 230 pp., illus., appendix
Paper $28 ISBN 0-87969-159-X

Protein Transport and Secretion
1985 215 pp., illus.
Paper $30 ISBN 0-87969-183-2

FORTHCOMING TITLES IN/86

Microbial Energy Transduction
Mechanisms of Yeast Recombination
Applications of DNA Probes



Cold Spring Harbor Laboratory
P.O. Box 100
Cold Spring Harbor, NY 11724

Reader Service No.41

THE MANAGEMENT OF AIDS PATIENTS

Edited by DAVID MILLER, JONATHAN WEBER and JOHN GREEN

The Management of AIDS Patients is the first comprehensive guide to the practical clinical management of patients with AIDS or HTLV III infections. The book avoids the sensational aspects of the disease, offering solid advice and information for all people involved in patient care.

The editors and many of the contributors come from St Mary's Hospital, London one of the foremost centres in Britain for the treatment of AIDS patients. The knowledge and experience of these experts has been combined to provide a much-needed book for doctors, nurses, dentists and indeed for health-care professionals everywhere.

January 1986

200pp	Hardback	0 333 40465 3	£30.00
	Paperback	0 333 40466 1	£10.95

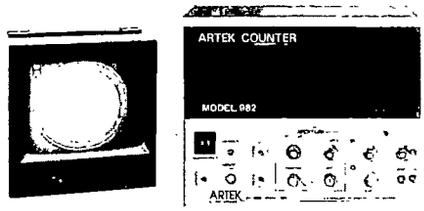
Please order this title from your bookseller – or in case of difficulty from Judy Chappell, Macmillan Press, Houndmills, Basingstoke, Hants RG21 2XS.

MACMILLAN PRESS

THE IMAGE OF PERFECTION

Artek's New 982B Image Analyzer. It's the perfect addition for your lab. Using a unique combination of hardware and software, the Artek 982B provides highly accurate, reproducible total counts as well as aperture or object area in less than one second. Change simultaneously from edge to density detection. Select circular, square and rectangular apertures. Set size detection thresholds (down to increments of .025mm in the macro mode). And/or switch from positive to negative images. All without interrupting statistical software routines. The Artek 982B is ideal for all kinds of micro and macro applications, from analyzing petri dishes to counting 96 well micro plates. It's also available with an X,Y stage mover. For more information, write or call Artek today.

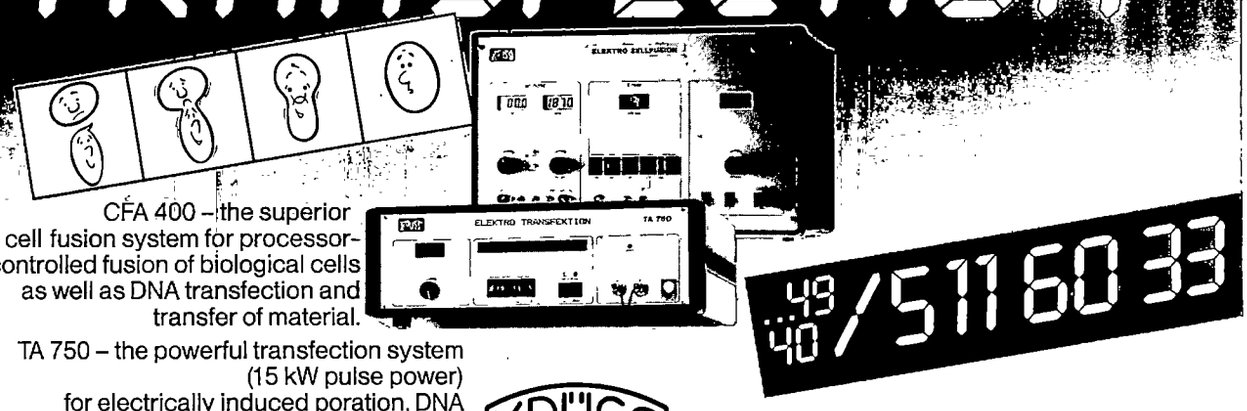
ARTEK®
SYSTEMS CORPORATION
SUBSIDIARY OF DYNATECH CORPORATION
170 Finn Ct., Farmingdale, N.Y. 11735 USA
Tel: 516-293-4420 Telex: 221219 ARTKUR
FAX: 516-293-4461



Reader Service No.15

ART-POWER HH

ELECTRO-CELL FUSION / TRANSFECTION



CFA 400 – the superior cell fusion system for processor-controlled fusion of biological cells as well as DNA transfection and transfer of material.

TA 750 – the powerful transfection system (15 kW pulse power) for electrically induced poration, DNA transfection and for fusion using pellet or bio-linkage techniques.

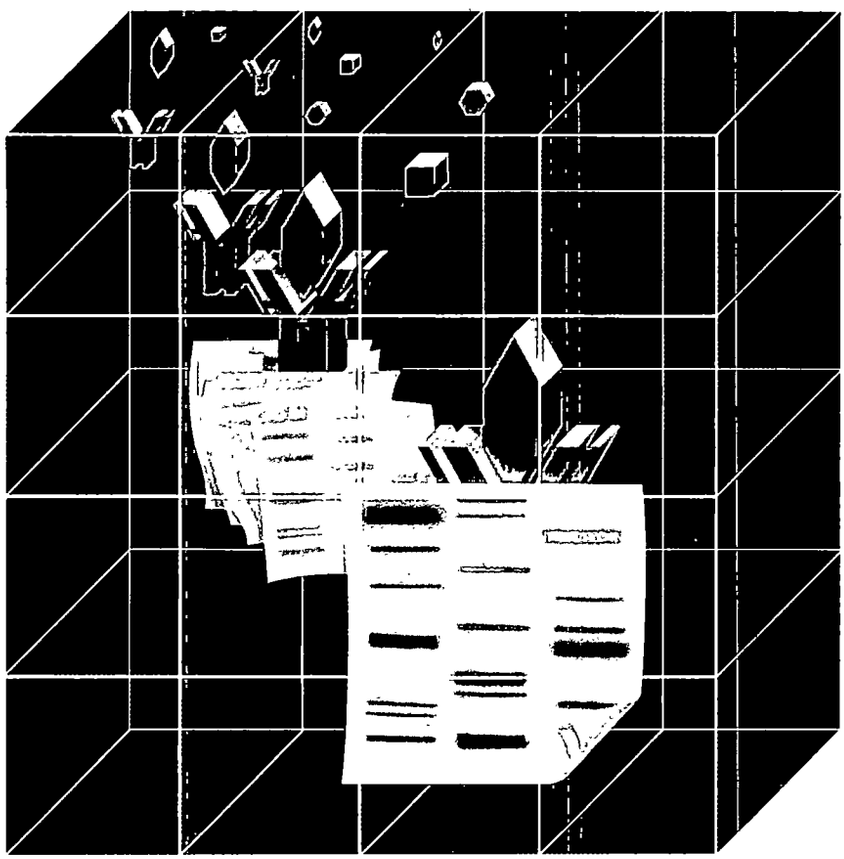
KRÜSS

Ask for our comprehensive system- and literature-information.

KRÜSS GmbH · Wissenschaftliche Laborgeräte · Borsteler Chaussee 85 – 99 · D-2000 Hamburg 61 · Telex 2174898 krue

Now-A Superior Western Blotting System from Promega Biotec

ProtoBlot™ Immunoblotting System



- Alkaline Phosphatase-base detection system:
  - Eliminates the need for radioactive isotopes
  - Provides greater sensitivi than Protein A or HRP-based systems
- Reproducible, reliable performance
- Protein detection in as little as two hours
- Systems available for the detection of Mouse, Rabbi and Human antibodies
- All essential components plus easy-to-use protocols-Promega-Qualified for Western blotting
- Call toll-free to place an order or to receive additional information on the ProtoBlot Immunoblotting System

Ordering Information	Cat. #
Each system contains enough reagents to process at least ten 15×15cm filters	
ProtoBlot Immunoblotting System, Human	P3910
ProtoBlot Immunoblotting System, Mouse	P3920
ProtoBlot Immunoblotting System, Rabbit	P3930

Promega Biotec

800-356-9526

Call toll-free to receive our catalog and more information about our complete selection of molecular biological products.
United States: Products may be ordered from either Promega Biotec or your Fisher Scientific Branch.
Canada: BIO/CAN SCIENTIFIC INC.,

Promega Biotec
2800 S. Fish Hatchery Road
Madison, WI 53711 U.S.A.

Toll Free	800-356-9526
Telephone	608-274-4330
TWX/Telex	910-286-2738

Consent — or compulsion?

Eric Ashby

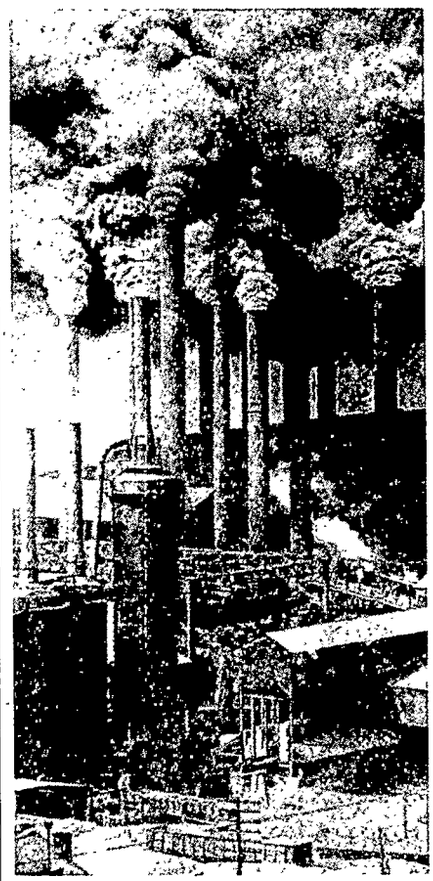
National Styles of Regulation: Environmental Policy in Great Britain and the United States. By David Vogel.
Cornell University Press: 1986. Pp.325. Hbk $39.95; pbk $14.95.

IT WAS Winston Churchill who is reputed to have said: "The English never draw a line without blurring it". This comment would be a fair summary of David Vogel's verdict on the regulation of environmental policy in Britain: guidelines rather than rigid standards, persuasion through advisory committees rather than compulsion through the courts, "best practicable means" for the abatement of pollution rather than "best available technology". Behind this policy there is an important assumption, namely that the concept of zero risk is a mirage but acceptable risk is a reality. Politicians rely on this reality when they make regulations to control the exploitation of land, air and water. The result, to a non-British observer, is piecemeal policy which its supporters call pragmatic and its critics call sloppy. And, as David Vogel concludes after a scholarly examination of the evidence, it works quite well.

In the United States the policy for regulating the state of the environment is set out in sharp lines, no blurring. "The 1972 amendments to the Clean Water Act required all [*sic*] of the nation's waters to become 'fishable and swimmable by July 1, 1983'." Section 112 of the Clean Air Act amendments of 1970 required the Federal Environmental Protection Agency to regulate particularly hazardous pollutants to zero risk, with an "ample margin of safety" and regardless of cost. This policy, to a non-American observer, seems unrealistic, impracticable, and to offer a picnic to lawyers. But this policy, too, David Vogel concludes, works quite well. By "works quite well", I mean that there are better safeguards for health and amenity in Britain and the United States than there are in many other industrial societies. Risks are abated to what are, on the whole, levels acceptable to the public (though, when one considers the horrible harvest of road accidents in these countries, one is alarmed at the public perception of what constitutes "acceptable").

Vogel considers in detail the politics of control of pollution and land-use-planning in Britain and the United States. But his book is much more than a prosy "compare-and contrast" essay. He uses his material to examine a much deeper issue, namely how governments in democratic countries can control the Externalities — the economist's technical word — produced by autonomous industry. And this again is part of an even deeper issue: how to control the social behaviour of corporations. Both in Britain and the United States there has been progress in this policing of behaviour, but there are extraordinary contrasts in style. What is the reason for these contrasts? Why are there so few signs of convergence in means to achieve what are essentially the same ends?

Part of the answer to these questions is to be found in history. Britain suffered from the social misbehaviour of industry long before it affected the United States. By the year 1900 no fewer than 21 bills had been put before parliament for the abatement of smoke. Most of them failed because it could not be proved that smoke was actually a hazard to health, and in any case smoke-abatement would have been difficult and costly. But Britain was learning how to control the social behaviour of industry: in 1863, when the Alkali Act was passed to control the emission of hydrochloric acid from alkali works, it had the support not only of conservationists and landowners, but of the alkali industry itself. This was because the hazards of hydrochloric acid were evident and conrol was easy and cheap. The Act was administered by consensus, rarely by compulsion, although the Alkali Inspector had punitive powers. It would be an oversimplification to say that this set the pattern for regulation in Britain; what is more likely is that this pattern reflected the style of British politics over some — though not all — social issues, a style that seeks to persuade, to generate a willing compliance from the very people who are prone to unsocial behaviour. It is often criticized as a cosy consensus between the gamekeeper, paid to protect the environment, and the poacher, bent on exploiting it for his own profit. There is some justice in this criticism, but in the long run — perhaps because Britain is a small country where the leaders of industry belong to the same class as the leaders in politics — many industries do behave in a socially responsible way, induced to do so by desire to keep a bright public image fortified by fear of punishments held in reserve for intractable anti-social behaviour. What the critics call collusion between government and industry over industry's social behaviour is in fact sometimes genuine cooperation; the issues are settled over lunch in the club and subsequently validated by the issue of some regulation or guideline.



Pollution past — industrial smokestacks in Pittsburgh in 1906. The picture is taken from Introduction to Environmental Science, 2nd Edn, *by Joseph M. Moran* et al., *recently published by W.H. Freeman. Price is $29.95, £29.95.*

This is in striking contrast to the adversarial style of control in the United States where the impression is one of antagonism between the legislator and the industries against which he is legislating. The wrangles end up in the courts of law. At any one time there are hundreds of prosecutions going on. And no wonder. If the line is blurred its exact position can be a matter for compromise between non-lawyers. If the line is sharp and, as for the 1972 amendments to the Federal Clean Water Act, utterly unrealistic (it was estimated that it would have cost the entire gross national product of the United States for a year to achieve its declared intention), then of course there is hostility from industry and recourse to the courts. Vogel discusses one of the many difficulties that arise from this: that policy-making on environmental problems, which in Britain is still greatly influenced by scientific and technological experts, is, in the United States, in the hands of lawyers, who are less familiar with the scientific uncertainties and unsympathetic towards ambiguity. Hence some of the decisions of the courts in the United States are not the kind that would be made if

experts in environmental sciences had been in control.

Vogel does not pronounce judgement on the relative merits of the two systems of control. The American system is more time-consuming and expensive in legal costs. The British system relies on flexibility which can become mere laxity. Perhaps the secret of a successful policy is to be inflexible over principles (for example over the environmental quality standard ultimately desired) but flexible in the manner and pace at which one proceeds toward the desirable goal. Doubtless, on the statute book, the United States has the best-protected environment in the world; but the words of the statute book have not reached many of the rivers nor much of the atmosphere. The British statute book is more modest in its aspirations for the environment; but it does not often prescribe what could not be enforced without constant applications to the courts. Transferred to Vogel's larger canvas, this shows an interesting and (I suspect) controversial picture. Are the mild British regulations, the preference for self-disciplined industry, signs of weakness in Westminster, or of a strong and respected government which can afford to rely on voluntary compliance? And is the American "reliance on rule-oriented enforcement" a sign that Washington can bring to heel unsocial behaviour in industry, or is it a sign of weakness in a government which does not command the loyalty of its industrial corporations?

It is no mere academic exercise to reflect on these questions. Expand Vogel's theme from environmental control to the control of trade-unions, corporation-cartels and local government, and you see its significance. Upon the answers to these questions depend the patterns of government Britain and the United States will have in the twenty-first century. □

Lord Ashby is a Fellow of Clare College, Cambridge CB2 1TL, UK. He was Chairman of the Royal Commission on Environmental Pollution from 1970 to 1973, and sometime member of the House of Lords Select Committee which deals with environmental directives from the European Economic Community.

Fuss over nothing

W.D. Hackmann

Leviathan and the Air-Pump: Hobbes, Boyle, and the Experimental Life. By Steven Shapin and Simon Schaffer. *Princeton University Press:1986. Pp.440. $60, £43.*

THE air-pump, more than any other scientific instrument, was the emblem of the revolution in physics that took place in the mid-seventeenth century. Other devices, such as the telescope, microscope, thermometer and barometer, preceded it, and all of them had a dramatic impact on how scientists conducted research and viewed the world. But the air-pump was the first mechanical device which made it possible for experiments to be carried out in a controlled laboratory environment — in this case, inside a glass bell-jar. It was also the seventeenth-century equivalent of "Big Science": very expensive, difficult to manufacture and temperamental to operate. Only a handful were made and each one was a prototype. The pump did become commercially available in the late 1670s, but it remained a costly instrument affordable only by wealthy virtuosi.

Until the middle of the seventeenth century, vacuum experiments were done in the small space above the mercury in the Torricellian barometer tube. Then, in about 1654, Otto von Guericke captured the public imagination with a startling performance of his "Magdeburg hemispheres"; two teams of burly horses could not pull the hemispheres apart after the air within them had been exhausted by the first mechanical air-pump ever constructed. Robert Boyle's interest was aroused after reading about von Guericke's device in a book published in 1659, by the Jesuit Kaspar Schott, a prolific writer on scientific subjects. Boyle, and his assistant Robert Hooke, immediately set to work to develop a better pump. More significantly, Boyle began an experimental programme to delineate the properties of the vacuum inside the bell-jar of his pump. The results and conclusions were published in *New Experiments Physico-Mechanical Touching the Spring of Air* (1660), where Boyle consolidated his ideas about what he considered to be the proper experimental method (upon which much of our present-day science is based). *New Experiments...* touched off a series of controversies in the 1660s and 1670s that went far beyond what we would conventionally consider to be the realms of science. It is these controversies that are the subject of Shapin and Schaffer's impressive book.

The chief protagonists were Boyle and the philosopher Thomas Hobbes, one-time mathematics tutor to Prince Charles (Charles II). While Hobbes became best known for his political philosophy, expressed in *Leviathan* (1651), he also took a deep interest in science. The fullest statement of his philosophy of science is to be found in *Dialogus physicus* (1661), written in response to Boyle's experiments on the spring of air and here appearing for the first time in English translation.

Boyle distinguished between "obvious experiments" — simple observations of naturally occurring phenomena — and "unobvious" or "elaborate experiments" in which artificial phenomena were produced by apparatus, in this case the air-pump. The difficulties faced by Boyle are not unfamiliar to the modern experimental scientist: problems with the physical integrity of his pump (leakage, for example), with standardizing or calibrating the phenomena, and with replication. All these matters led to disputes with his fellow scientists but, as Shapin and Schaffer demonstrate, the confrontation with Hobbes was much more profound and went to the heart of the experimental method. For Hobbes not only rejected the existence of the vacuum in nature but (to borrow from Wittgenstein) he played a different "language-game", arguing that only reason or philosophy, not Boyle's "engine philosophy", could yield reliable knowledge.



Public display — a demonstration of Otto von Guericke's air-pump in Germany, in the mid seventeenth century, reproduced from Technica curiosa sive mirabilia artis *(1687).*

According to Shapin and Schaffer, this controversy was not so much about science as about social order. They examine the social conventions established for producing knowledge, and Boyle's techniques for making his experimental results acceptable to the scientific community. Thus (as the authors put it), the book is an exercise in the "sociology of scientific knowledge" and is written primarily for the community of scientific historians. Scientists may find this community's particular language-game at times rather off-putting, with its terms such as "literary technology" and "boundary-speech", and they will not find out how Boyle discovered the gas law (for which his air-pump was not necessary). But they should gain some thought-provoking insights into the complex relationship between experiment, theory, and the political and intellectual community. □

W.D. Hackmann is Assistant Curator at the Museum of the History of Science, University of Oxford, Broad Street, Oxford OX1 3AZ, UK.

Brain failure after eighty years

T.J. Crow

Normal Aging, Alzheimer's Disease and Senile Dementia: Aspects on Etiology, Pathogenesis, Diagnosis and Treatment. Edited by C.G. Gottries. *Editions de l'Université de Bruxelles, Avenue Paul Heger 26, Bruxelles, Belgium:1985. Pp.308. FB 992.*

In 1907, Alois Alzheimer described the thickening and tortuosity of fibrils within the neuronal cytoplasm of almost every fourth cell of the cerebral cortex of a 51-year-old woman who had been suffering from dementia. At that time he can have had little conception of the growth of interest in the phenomenon 80 years later. What may then have seemed an isolated pathological curiosity now appears as but one manifestation of an ubiquitous process whose relevance to ageing itself is the centre of discussion. What has become known as "Alzheimer-type dementia" is now generally agreed to include not only the unusual cases of presenile dementia (onset before 65 years of age) such as Alzheimer described, but also the great mass of dementias of old age. The prevalence of this condition is 5–8 per cent of the population at the age of 65, rising to 20 per cent at age 80 and 40–50 per cent above the age of 90 years.

The neuropharmacological aspects of the subject have been one of the features of recent research, and these proceedings record the contributions to two symposia at the Collegium Internationale Neuro-Psychopharmacologicum in Florence in 1984. Since 1976 it has been recognized that the cholinergic projections to the cerebral cortex are lost, giving rise to hopes that cholinergic replacement therapy might ameliorate some part of the psychological deficit. Such hopes are as yet unfulfilled. One problem, well documented in this volume, is that the cholinergic losses are far from isolated—there is evidence of loss of adrenergic and serotonergic projections as well. Whether the primary change occurs in the cell bodies of origin of the ascending systems, or whether these systems are affected secondarily to changes in the cortex itself (the temporal areas being a probable site of early change), is still a matter of debate, although opinion is swinging towards the latter possibility. Whichever viewpoint is correct, the anatomical and chemical selectivity of the process is surprising; in the cortex, for example, somatostatin-containing neurones are affected and cholecystokin and vasoactive intestinal polypeptide-containing cells are spared (see *Nature* **314**, 92–94; 1985). This may yet provide a clue to the origin of the Alzheimer process.

Contributions to the book are not confined to neuropharmacology. They touch also on aetiology, both with respect to the enigmatic role of aluminium and to genetic factors (Alzheimer's disease shares with two other neurodegenerative conditions, Parkinson's disease and amyotrophic lateral sclerosis, a tendency to an earlier age of onset when there is greater incidence of familial cases). Aluminium is now known to be present in high concentration in the amyloid plaque, the structure which, together with the neurofibrillary tangle described by Alzheimer is the hallmark of the disease. Whether the element accumulates as a secondary effect or plays a pathogenic role remains unclear. In a short chapter, D.R.C. McLachlan speculates that aluminium could interact with calcium to contribute to the pathology. That electrolyte changes may be relevant to the aetiology of neurodegenerative disease is also suggested by Gajdusek and Garruto; they attribute the high incidence of amyotrophic lateral sclerosis and Parkinson's disease on Guam, the Kii peninsula of Japan and an area of New Guinea to low concentrations of calcium and magnesium in the soil, and the subsequent decline in incidence to correction of these mineral deficiencies. Such secular changes challenge the therapeutic nihilism which may be generated by the suspicion that these diseases, along with Alzheimer's dementia, are inseparable from the molecular genetic mechanisms of ageing.

This volume thus deals with a number of aspects of recent progress on Alzheimer's disease. There is relatively little reflection of the current interest in the protein structure of the plaques and tangles, but drug treatment strategies, although as yet of little practical value, are well covered. □

T.J. Crow is in the Division of Psychiatry, Clinical Research Centre, Northwick Park Hospital, Watford Road, Harrow, Middlesex HA1 3UJ, UK.

New editions

- *Microbes and Man, 2nd Edn*, by John Postgate (Penguin; pbk £4.95, $6.95).
- *Methods in Plant Ecology, 2nd Edn*, edited by P.D. Moore and S.B. Chapman (Blackwell Scientific; hbk £34.80, $57, pbk £23.80, $36).
- *Statistics and Data Analysis in Geology, 2nd Edn*, by John C. Davies (Wiley; hbk $52.55, £40.35, pbk $24.95, £18.95).
- *Superfluidity and Superconductivity, 2nd Edn*, by D.R. Tilley and J. Tilley (Adam Hilger; hbk £36, $60, pbk £18, $25).
- *Partition of Cell Particles and Macromolecules, 3rd Edn*, by Per-Åke Albertsson (Wiley; $59.95, £61.85).
- *Chromatographic Methods, 4th Edn*, by A. Braithwaite and F.J. Smith (Chapman & Hall; hbk £29, $65, pbk £12.95, $27).
- *The Colour Science of Dyes and Pigments, 2nd Edn*, by K. McLaren (Adam Hilger; £19.50, $35).

Plenum: Making It Happen

Forthcoming ...

CHEMISTRY BY COMPUTER
An Overview of the Applications of Computers in Chemistry
by **Stephen Wilson**
In this wide-ranging survey, Dr. Wilson covers the techniques of computational chemistry and shows how they may be applied to problems ranging from interstellar chemistry to molecular biology.
0-306-42152-6/approx. 200 pp./Jul./1986

DIGITAL RADIOGRAPHY
Selected Topics
edited by **James G. Kereiakes, Stephen R. Thomas,** and **Colin G. Orton**
Many of the significant developments resulting from the applications of physics and engineering to digital radiography are described here by noted authorities in the field.
0-306-42188-7/approx. 200 pp./Jul./1986
$39.50 ($47.40 outside US & Canada)

PRINCIPLES OF ENDOCRINE PHARMACOLOGY
by **John A. Thomas** and **Edward J. Keenan**
Thomas and Keenan discuss a wide range of drug induced alterations in glandular secretions, drug-hormone interactions, and effects of drugs on clinical chemistry tests. Advances in recombinant DNA technologies are covered as they pertain to endocrine pharmacology, especially revolving recombinant human insulin and recombinant human growth hormone.
0-306-42129-1/hardcover/310 pp./Jul./1986
$39.50 ($47.40 outside US & Canada)
0-306-42143-7/paperback/310 pp./Jul./1986
$22.50 ($27.50 outside US & Canada)

PHARMACEUTICAL RESEARCH
Official Journal of the American Association of Pharmaceutical Scientists
Editor: **Wolfgang Sadee**
Pharmaceutical Research provides excellent research in all areas of pharmaceutical science including:
- drug delivery
- computer-aided drug design
- biotechnology in drug development
- novel methods of drug analysis

Subscription, Volume 3 1986 (6 issues)
Institutional rate
$89.50 in US/$102.50 elsewhere
Personal rate
$45.00 in US/$53.00 elsewhere

Plenum Publishing Corporation
233 Spring Street
New York, N.Y. 10013
In the United Kingdom
88/90 Middlesex Street
London E1 7EZ England

Reader Service No. 13

Copies of articles from this publication are now available from the UMI Article Clearinghouse.

Yes! I would like to know more about UMI Article Clearinghouse. I am interested in electronic ordering through the following system(s):

☐ DIALOG/Dialorder ☐ ITT Dialcom
☐ OnTyme ☐ OCLC ILL Subsystem

☐ Other (please specify)_____
☐ I am interested in sending my order by mail.
☐ Please send me your current catalog and user instructions for the system(s) I checked above.

Name_____
Title_____
Institution/Company_____
Department_____
Address_____
City_____ State_____ Zip_____
Phone (____)_____

UMI Article Clearinghouse

Mail to: University Microfilms International
300 North Zeeb Road, Box 91 Ann Arbor, MI 48106

NUCLEAR POWER AND ITS ENVIRONMENTAL EFFECTS

For the Layman, Nuclear Technician, Manager

Places the effects of possible nuclear radiation in perspective. Meets the need for a better understanding of radiation and its consequences especially after the TMI accident.

All vital aspects of nuclear power generation are considered, from fundamental principles to plant licensing, from uranium mining to disposal of waste. The safe operation of nuclear power plants, to prevent the escape of dangerous amounts of materials in case of an accident, is fully covered.

By Samuel Glasstone
Walter H. Jordan
American Nuclear Society
555 No. Kensington Ave.
La Grange Park, IL 60525
USA

408 pages
ORDER TODAY
$18.95 Softbound
$26.95 Hardbound

The source for the latest knowledge in Nuclear

Reader Service No.38

On common ground in Scandinavia

Chris Stillman

The Caledonide Orogen — Scandinavia and Related Areas. Edited by D.G. Gee and B.A. Sturt. *Wiley:1986. Two volumes, pp.1,266. £150, $214.50.*

LIKE most scientists, geologists work within a paradigm, and their main paradigm for the past quarter-century has unquestionably been the theory of plate tectonics. One of the fundamental concepts of this theory involves the formation of orogens — mountain belts — by the spreading and closing of ocean basins. The Caledonide Orogen evolved through the Palaeozoic period by the movements of North American, Baltic and European continents around a proto-Atlantic ocean; a full understanding of its development thus requires correlation of the rock units and their history throughout these extensive and now widely separated regions.

The decade 1974–1984 saw the flowering of one of the International Geological Correlation Programme's most successful ventures. This was Project 27, "The Caledonide Orogen", the objective of which was to establish a geological frame of reference for the whole orogen by encouraging researchers to get together and pool their knowledge. A series of annual meetings was arranged in each of the participating countries in turn, at which all concerned could meet, compare notes, deliver papers and visit the actual geological locations. In August 1981, Uppsala was the venue for the meeting at which the Scandinavian Caledonides were displayed, and the papers read there form the basis for this beautifully presented two-volume work.

This is a fine example of the book-maker's art — a lavish production, with excellent illustrations and extremely useful maps (the best being a 1:2,000,000 tectono-stratigraphic map of the Scandinavian Caledonides) — but its main value lies in the fact that it is the first major compilation of modern work on the Scandinavian Caledonides to become widely accessible. Rocks belonging to this orogen dominate Norway and much of Sweden; traditionally, the view taken on their geological history was determined by the perspective from either side of the national boundary (a point effectively made by the cartoon from 1896 illustrating the nappe controversy, here used to preface the section on regional geology). Until recently, publication in national and local journals tended to perpetuate the differences, hence the need for a comprehensive, integrated review. It is our good fortune that the review arose from an international meeting, the proceedings of which could be published in clear English and made widely available to geologists throughout the world. We are doubly fortunate in that the editors represent both traditions; they have succeeded in pulling together a stylistically uniform and coherent review, and have produced a major step forward in Scandinavian geology.

Nevertheless, for all that the two volumes are a thorough and accurate reflection of how things stood in 1981, time has moved on. The whole style of approach to the problem has begun to change. Even before the publication of these books, awareness was growing of the logical improbability of achieving the orogen-wide correlation that was the *raison d'être* of the Project. Many now favour a way forward by applying terrane analysis, a strong hint of which is given in a short contribution by Duncan Keppie entitled "The Appalachian Collage". This, perhaps, increases the value of the books — in a subject which changes its ground rules so frequently, it is often difficult to achieve a correct perspective for judging the publications of previous years, but through the consistency of direction applied by the editors this compilation has a built-in spirit level.

The volumes are properly focused on Scandinavia, with 62 contributions dealing with the geology of the Scandinavian Caledonides, but the regional context is not forgotten and 22 other papers add wider-ranging though not particularly representative reviews. Indeed, while Greenland and Britain are obviously related areas, the addition of Sardinia, Kazakhstan and Mongolia is bizarre. The main body of the Scandinavian contributions is arranged with regional reviews followed by sets of papers on stratigraphy, structure, igneous rocks and metamorphism, each with introductory chapters. A final section includes various interpretations of the general tectonic evolution of the mountain belt. The reader wishing to obtain an overview need do little more than read the regional reviews and the introductory contributions to the subsequent sections. For the specialist, there is ample material in many of the individual papers, which are not just bare outlines of conclusions but properly present the supporting data. Access to the contents is greatly facilitated by the excellent subject index.

Those wondering whether or not to purchase this work should bear in mind that although the cost is great, so are the rewards. The coverage is high and wide, and the books themselves are handsome. Geologists around the world can learn much from them, and they may yet provide the seed for many more ideas on Caledonide orogenesis. □

Chris Stillman is an Associate Professor in the Department of Geology, Trinity College, Dublin 2, Ireland.

FEBS LETTERS

An International journal established for the most rapid possible publication of essentially final short papers in the fields of biochemistry, biophysics and molecular biology

Published by Elsevier Science Publishers B.V.
on behalf of the Federation of European Biochemical Societies

One of the world's leading journals in biochemistry, FEBS Letters is renowned both for its quality of content and speed of production. Bringing together the most important developments in biochemistry, biophysics, molecular and cellular biology, FEBS Letters provides an international forum for minireviews, research results, commentaries, meeting reports and hypotheses which merit urgent publication.

FEBS Letters' annual **Index of Biochemical Reviews** lists titles, authors and sources of reviews and lectures from a large range of publications in related biological sciences. Entries are indexed under subject headings to serve the research and teaching interests of all biochemists, biophysicists and molecular biologists.

Cited in: Current Contents/Life Sciences; Chemical Abstracts; Biological Abstracts; Excerpta Medica; Index Medicus; PASCAL M

- Direct submission to editors
- Referees' decision within 3 weeks
- Publication within 6 weeks
- Distribution before cover date
- Fifty free reprints per article
- No submission charges
- No page charges

Editors
H. R. V. Arnstein, *London (Reviews Editor)*
B. A. Askonas, *London*
J. E. Celis, *Aarhus*
F. Chapeville, *Paris*
S. P. Datta, *London (Honorary Chairman)*
P. L. Dutton, *Philadelphia PA*
A. L. Haenni, *Paris*
J. Hanoune, *Créteil*
A. Mirzabekov, *Moscow*
Y. Nishizuka, *Kobe*
O. B. Ptitsyn, *Pushchino*
P. J. Randle, *Oxford*
T. A. Rapoport, *Berlin-Buch*
G. C. K. Roberts, *London*
M. L. Salas, *Madrid*
G. Semenza, *Zurich (Managing Editor)*
N. Sharon, *Rehovot*
A. Trebst, *Bochum*
M. Wikström, *Helsinki*
B. Witkop, *Bethesda MD*

1986 - *Vols. 193-207 (15 volumes in 30 issues)*
Subscription price:
US $ 1055.00/Dfl. 3060.00 including postage and handling
ISSN 0014-5793

Reduced personal subscription rates are available for members of FEBS National Societies, the American Society of Biological Chemists and Japanese Biochemical Society. Please apply to the publisher for details.

ELSEVIER

For further information and/or free sample copy please write to:

In the U.S.A. and Canada:
Journal Information Center
ELSEVIER SCIENCE PUBLISHERS
52 Vanderbilt Ave., New York, NY 10017, U.S.A.

In all other countries:
ELSEVIER SCIENCE PUBLISHERS
P.O. Box 211, 1000 AE Amsterdam,
The Netherlands

Please send your orders to the Amsterdam address

The Dutch guilder price is definitive, US $ prices are subject to exchange rate fluctuations. Prices are excl. B.T.W. for Dutch customers

Reader Service No.34

FL37A419

The latest titles from
CAMBRIDGE

PHYSICAL SCIENCE

Introduction to Experimental Particle Physics

RICHARD C. FERNOW

Written for nuclear physicists and graduate students in high-energy physics, this book gives a brief but balanced overview of the most important topics in experimental particle physics over the last forty years.

431 pp. 0 521 30170 X **£32.50 net/$44.50**

Now in paperback

Remote Sounding of Atmospheres

J.T. HOUGHTON, F.W. TAYLOR and **C.D. RODGERS**

This book describes how measurements can be made of the Earth's and other planets' atmospheres using the techniques of remote sounding. It includes descriptions of the scientific principles, technical implementation, mathematical methods and discussions of the phenomena that have been found.

351 pp. 0 521 31065 2 **Paperback £12.95 net/$24.95**

GENETICS/PHYSIOLOGY

Regulation of Gene Expression – 25 Years On

Edited by **IAN R. BOOTH** and **C.F. HIGGINS**

This volume deals firstly with regulation of gene expression in the context of cellular physiology and then examines the major new developments in our understanding of the molecular basis of gene control. The authors primarily discuss bacterial systems, but some consideration is also given to lower eukaryotes.

Society for General Microbiology Symposium 39
309 pp. 0 521 32201 4 **£32.50 net/$59.50**

The Biotechnological Challenge

S. JACOBSSON, A. JAMISON and **H. ROTHMAN**

The socio-economic implications for developing countries of various biotechnologies are analysed in this unique volume, which discusses both the technologies themselves and case studies of their application in the Third World.

181 pp. 0 521 30775 9 **£22.50 net/$34.50**

Receptors in Tumour Biology

Edited by **C.M. CHADWICK**

This book discusses the phenomenon of recognition at the molecular level, examining specifically its relevance to metastatic disease. The contributors emphasise various aspects of cancer that can be traced to changes in the cell surface.

Intercellular and Intracellular Communication 2
257 pp. 0 521 32117 4 **£30.00 net/$49.50**

An Introduction to the Mathematics of Neurons

FRANK HOPPENSTEADT

This book suitable for students studying mathematical biology, introduces some mathematical methods that can help us to understand how neurons work, and in particular it aims to uncover the frequency-response properties of neurons.

Cambridge Studies in Mathematical Biology 6
175 pp. 0 521 30566 7 **Hc £27.50 net/$49.50**
0 521 31574 3 **pb £9.95 net/$7.95**

BOTANY/ECOLOGY

The European Garden Flora Volume I

A Manual for the Identification of Plants Cultivated in Europe, Both Out-of-doors and Under Glass

Edited by **S.M. WALTERS** *et al*

Volume I is the first in a series of six; it contains accounts of the ferns and their allies, the conifers and 16 families of Monocotyledons, including the Liliaceae, Amaryllidaceae and Iridaceae. Volume II, which has already been published, completes the Monocotyledons, including the popular Orchidaceae.

430 pp. 0 521 24859 0 **£55.00 net/$99.50**

Now in paperback

Ecological Implications of Body Size

ROBERT HENRY PETERS

'Here is a treasure house of information.... by blending physiology and ecology and by looking at problems with a fresh eye, Peters yields new insights and opens up new questions.' *Nature*

Cambridge Studies in Ecology
352 pp. 0 521 28886 X **Paperback £12.50 net/$16.95**

Pests and Parasites as Migrants

Edited by **ADRIAN GIBBS** and **ROGER MEISCHKE**

From an Australian perspective, this book discusses the scientific, social and legal aspects of the migration of plants, animals and microbes. It considers both the rise to pest proportions of migrants such as the rabbit and prickly pear and the use of other introduced species as control agents of these pests.

192 pp. 0 521 30163 7 **Paperback about £20.00 net/$39.50**
Forthcoming (June)

HISTORY OF SCIENCE/ PHILOSOPHY

Now in paperback

Dimensions of Darwinism

Themes and Counterthemes in Twentieth-Century Evolutionary Theory

Edited by **MARJORIE GRENE**

'The book is well-produced and clearly laid out, and illustrates the diversity of evolutionary thought from the morphological 'metaphysic' of Riedl to the 'neo-Darwinian orthodoxy' of Maynard Smith.' *The Naturalist*

336 pp. 0 521 31021 0 **Paperback £9.95 net/$14.95**
Co-publication with the Maison des Sciences de l'Homme, Paris

Templets and the Explanation of Complex Patterns

MICHAEL J. KATZ

Where does the particular form or configuration of a pattern come from, and how is it propagated from pattern to pattern? This book provides a natural language for analysing such questions.

127 pp. 0 521 30673 6 **£12.50 net/$24.95**

John Ray

Naturalist: His Life and Works

The late **CHARLES E. RAVEN**
With an introduction by **S.M. WALTERS**

Charles Raven's biography of the seventeenth-century English naturalist, John Ray, is one of the great works in the history of science. The publication of this *Cambridge Science Classics* edition coincides with the tercentenary of the publication of Ray's *Historia Plantarum* in 1686.

531 pp. 0 521 31083 0 **Paperback £15.00 net/$24.95**

For further details of these titles please write to Annette Duggan or Paul Wehn at the Cambridge and New York offices respectively.

Cambridge University Press
The Edinburgh Building, Shaftesbury Road, Cambridge CB2 2RU England
32 East 57th Street, New York, NY 10022

Reader Service No 18

BURN YOUR REFERENCE CARDS

REF-11 ™

Computerizes your REFERENCES and prepares your BIBLIOGRAPHIES

- ☐ Maintains a data base of references
- ☐ Searches for any combination of authors, years of publication, reference title (or any words in the title), and topics covered by the reference
- ☐ Formats bibliographies exactly as you want them
- ☐ Alphabetizes references
- ☐ Menu driven dialogue
- ☐ Abbreviates journal titles
- ☐ Compact storage format
- ☐ Runs on any video terminal and printer
- ☐ 20 lines of comments for each reference

IBM PC/XT/AT, MS-DOS, CP/M 80 ... $195.00

RT-11, TSX-Plus; RSX-11, P/OS $250.00

VAX/VMS (native mode) $350.00

DG SYSTEMS ™

ANY MANUAL $15.00 — ANY MANUAL & DEMO $20.00

322 Prospect Ave., Hartford, CT 06106
(203) 247-8500

Connecticut residents add 7½% sales tax

Reader Service No.39

SCIENCE AND TECHNOLOGY

Whatever the subject... refer to MACMILLAN DICTIONARIES

DESIGNED FOR STUDENTS

The paperback *Macmillan Dictionary Series* combines new and established works of teaching and reference with an attractive series format.

- * authoritative definitions and explanations of all current terminology written by experts
- * lucidly written entries with thorough cross referencing
- * regular new editions keep the student up to date with the latest research, practice and technology
- * a clear layout for easy reference
- * prices range from just £7.95 to £9.95

NEW IN 1986...

MACMILLAN DICTIONARY OF BIOTECHNOLOGY
JIM COOMBS March 1986 320pp 0 333 40875 6 £9.95

MACMILLAN DICTIONARY OF THE HISTORY OF SCIENCE
Edited by W. F. BYNUM, E. J. BROWNE and ROY PORTER
March 1986 528pp 0 333 34901 6 £8.95

MACMILLAN DICTIONARY OF PERSONAL COMPUTING AND COMMUNICATIONS DENNIS LONGLEY and MICHAEL SHAIN
August 1986 320pp 0 333 42170 1 £8.95

MACMILLAN DICTIONARY OF PHYSICS
MARY P. LORD August 1986 320pp 0 333 42377 1 £8.95

MACMILLAN DICTIONARY OF IMMUNOLOGY
FRED ROSEN, LISA STEINER and EMIL UNANUE
August 1986 256pp 0 333 39248 5 £8.95

Macmillan Press, Houndmills, Basingstoke, Hants RG21 2XS, UK
Not available in USA.

MACMILLAN PRESS

ACADEMIC PRESS

TITLES FOR THE BIOLOGICAL CHEMIST . . .

MAMMALIAN PROTEASES:

A Glossary and Bibliography

Volume 2 **Exopeptidases**

J. K. McDonald and **A. J. Barrett**

May 1986, 373pp., $34.00/£21.00 (UK only), ISBN 0 12 079502 7

As an effective key to the literature for the study of exopeptidases this book will be invaluable to those working in biochemistry, medicine, biology, physiology and pathology, from undergraduates to researchers and teachers

Contents: Preface. Contents of Volume 1 Introduction *A Brief History of the Study of Mammalian Exopeptidases* Aminopeptidases Tripeptidases Dipeptidyl Peptidases. Tripeptidyl Peptidases Carboxypeptidases Peptidyl Dipeptidases. Dipeptidases. Omega Peptidases Index

Volume 1 **Endopeptidases**

August 1980, 435pp., $48.50/£35.50 (UK only), ISBN 0 12 079501 9

ESSAYS IN BIOCHEMISTRY

Volume 21

Edited by **R. D. Marshall** and **Professor K. Tipton**

December 1985, 162pp., $19.50/£12.00 (UK only), ISBN 0 12 158121 7

CHEMISTRY AND TOXICOLOGY OF PYRROLIZIDINE ALKALOIDS

A. R. Mattocks

March 1986, 367pp., $88.00/£55.00 (UK only), ISBN. 0 12 480570 1

Contents: Structures and Plant Sources of Pyrrolizidine Alkaloids Extraction, Separation and Analysis of Pyrrolizidine Alkaloids Syntheses of Necines, Pyrrolizidine Alkaloids and Analogues and Pyrrolic Derivatives Physical Properties and Spectroscopy of Pyrrolizidine Alkaloids and Related Compounds. Chemical Properties of Pyrrolizidine Alkaloids and Their Dehydroderivatives Metabolism, Distribution and Excretion of Pyrrolizidine Alkaloids. Toxicology of Pyrrolizidine Alkaloids in Animals Further Toxic and Other Biological Actions of Pyrrolizidine Alkaloids, Analogues and Metabolites. Effects of Pyrrolizidine Alkaloids in Humans Mutagenic Antimitotic and Other Cell-damaging Effects of Pyrrolizidine Alkaloids. Pyrrolic Derivatives and Analogues. Carcinogenicity and Antitumour Activity of Pyrrolizidine Alkaloids and Plants Containing Them Relationships between Structure, Metabolism and Toxicity. References Index

EXPERIMENTAL MODELS IN ANTIMICROBIAL CHEMOTHERAPY

Edited by: **O. Zak** and **M. A. Sande**

Volume 1, May 1986, 380pp., $63.50/£39.50 (UK only).
ISBN: 0.12.775401.6
Volume 2, June 1986, 416pp., $65.00/£38.00 (UK only).
ISBN: 0.12.775402.4
Volume 3, June 1986, 424pp., $67.50/£39.50 (UK only).
ISBN: 0.12.775403.2

Set price for all 3 volumes $166.50/£99.50 (UK only)

Contents: Volume 1: *Introduction* · *The Role of Animal Models in the Evaluation of New Antibiotics*, **O. Zak and M. A. Sande.** *Principles of Animal Care*, **H. Bruhin.** *Use of Serum Bactericidal Titers in Animal Studies* **Y. Van Laethem and J. Klastersky.** *Ex Vivo Models for Studying Adherence of Bacteria/Fungi to Host Tissues*, **C. H. Ramirez-Ronda and Z. Z. Fuxench-Chiesa.** *Studies on the Morphology of Bacteria in Vivo Techniques and Chemotherapeutic Implications*, **D. M. Ryan.** *Tissue Fluid Pharmacokinetic Models in Humans and Animals*, **M. G. Bergeron and L. Brousseau.** *The Selbie or Thigh Lesion Test*. **P. Acred.** *The Granuloma Pouch*, **A. Dalhoff.** *Experimental Animal Models of Bacterial Meningitis* **W. M. Scheld.** *Animal Models in the Evaluation of Chemotherapy of Ocular Infections*, **M. Barza.** *Animal Models of Otitis Media*. **G. S. Giebink, W. L. Meyerhoff and E. I. Cantekin.** *Use of Animal Models to Evaluate Antimicrobial Therapy for Bacterial Pneumonia*. **J. E. Pennington.** *Experimental Endocarditis*, **T. A. Drake and M. A. Sande.** *The Use of Animal Models in Studying Vascular Graft Infection*. **R. Rutledge, S. J. Burnham and G. Johnson, Jr.** *Models of Foreign Body Infections*. **W. Zimmerli and F. A. Waldvogel.** *Urinary Tract Infections. Pyelonephritic Scars, and Chemotherapy*, **M. P. Glauser, R. Ransley and J. Bille.** *A Model System for Experimental Infections of the Female Genital Tract* **P. J. Hartigan.** *Animal Models of Experimental Gonococcal Infection*. **R. J. Arko and A. Balows.**

Prices subject to change without notice.

24-28 OVAL ROAD, LONDON NW1 7DX, ENGLAND • ORLANDO, FLORIDA 32887 U.S.A.

Keep up to date with

CANCER SURVEYS

Editor: L M **Franks,** *Published for the Imperial Cancer Research Fund by Oxford University Press*

Brings you critical and comprehensive reviews of the latest research. For clinicians, cell and molecular biologists and epidemiologists.

JUST PUBLISHED —

GROWTH FACTORS AND MALIGNANCY *Volume 4 No. 4*
Edited by **Anita B Roberts** with **Michael B Sporn,** National Cancer Institute, National Institute of Health, Bethesda, Maryland, USA.

Contents

Introduction: autocrine, paracrine and endocrine mechanisms of growth control **Michael B Sporn and Anita B Roberts**

Platelet-derived growth factor: roles in normal and *v-sis* transformed cells **Thomas F. Deuel, Akiro Kimura, Shuji Maehama and Benton D Tong**

Transient induction of *c-fos* and *c-myc* is an immediate consequence of growth factor stimulation **Tom Curran, Rodrigo Bravo and Rolf Müller**

Transforming growth factors **Anita B Roberts and Michael B Sporn**

Autocrine growth factors in human small cell lung cancer **Frank Cuttitta, Desmond N Carney, James Mulshine, Terry W Moody, Joseph Fedorko, Adam Fischler and John D Minna**

Modulation of the epidermal growth factor receptor by mitogenic ligands: effects of bombesin and role of protein kinase C **Ian Zachary and Enrique Rozengurt**

The EGF receptor: structure, regulation and potential role in malignancy **David M Thompson and Gordon N Gill**

The colony-stimulating factors and myeloid leukaemia **Nicos A Nicola and Donald Metcalf**

Cancer Surveys focuses on a new topic every quarter. Each edition provides a definitive and up-to-date account of the present state of knowledge in the chosen area. Guest Editors, with specialist knowledge of that field, provide general assessments. Contributors review the areas where they have made important contributions, include research which may not have been published elsewhere and relate epidemiological and laboratory research to clinical problems.

Each issue costs £13.50(UK), US $29 (N. America), £15.50 (Elsewhere) or take out a year's subscription: £47 (UK), US $95 (N. America), £53 (Elsewhere). Cancer Surveys is published quarterly.

All Previous issues are available. Details on request.

ORDER FORM Please complete the order form and return (with remittance enclosed) to Journals Subscription Department, Oxford University Press, Walton Street, Oxford OX2 6DP UK

☐ Please send me **Growth Factors and Malignancy—Vol 4 No 4 of Cancer Surveys**
☐ Please record my subscription to **Volume 5 of Cancer Surveys**
☐ Please send me details of previous issues
☐ I enclose my remittance of .....

Name .....

Address .....

.....

☐ I wish to pay by Visa/Access/Diners/American Express

My card number is ☐☐☐☐☐☐☐☐☐☐☐☐☐☐☐☐

Expiry date ..... Signature .....

If address registered with credit card company differs from that given above please give details

Half-price to members of recognised cancer societies. Apply to OUP for details

OXFORD JOURNALS

Journals Subscription Department, OUP, Walton Street, Oxford OX2 6DP, UK

Reader Service No.27

New and Forthcoming Titles from Springer

Cadmium

Editor: **E. C. Foulkes,** University of Cincinnati
1986. 59 figures. XIV, 400 pages (Handbook of Experimental Pharmacology, Volume 80). Hard cover DM 490,-
ISBN 3-540-16025-6

Contents: The Estimation of Cadmium in Biological Samples. – Cadmium in the Environment and its Entry into Terrestrial Food Chain Crops. – Absorption of Cadmium. – The Chronic Toxicity of Cadmium: Influence of Environmental and Other Variables. – Effects of Cadmium Exposure in Humans. – The Nephropathy of Chronic Cadmium Poisoning. – Cadmium and the Cardiovascular System. – Role of Metallothionein in Cadmium Metabolism. – Immunotoxicity of Cadmium. – The Effect of Dietary Selenium on Cadmium Cardiotoxicity. – Cellular Resistance to Cadmium.

New Neuromuscular Blocking Agents

Basic and Applied Aspects
Editor: **D. A. Kharkevich,** Moscow
1986. 128 figures. XXIV, 741 pages (Handbook of Experimental Pharmacology, Volume 79). Hard cover DM 780,-
ISBN 3-540-15771-9

This volume contains data on the relationship between chemical structure and neuromuscular blocking activity in some series of compounds. Chapters dealing with the structure of endplate acetylcholine receptors, pre- and post-synaptic action of the agents considered, and their effects on the autonomic and central nervous systems are included.

Medical Informatics Europe 85

Proceedings, Helsinki, Finland, August 25–29, 1985
Editors: **F. H. Roger,** Brussels; **P. Grönroos,** Tampere; **R. Tervo-Pellikka,** Helsinki; **R. O'Moore,** Dublin
1985. XXVII, 823 pages. (Lecture Notes in Medical Informatics, Volume 25). Soft cover DM 118,-. ISBN 3-540-15676-3

From the contents: Hospital Information Systems. – Departmental Patient Data Systems. – Decision Support and Expert Systems. – Medical Record Management and Classification Problems. – Application Development and Software Tools. – New Technology. – National Policy and Management. – Privacy and Data Protection. – Medical and Clinical Research and Epidemiology.

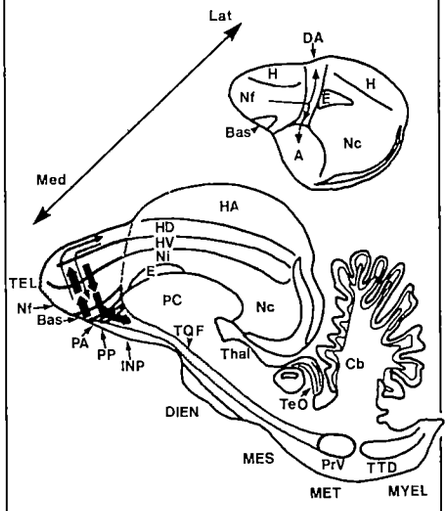
Advances in Anatomy, Embryology and Cell Biology

Volume 96
C. L. Veenman, K.-M. Gottschaldt, University of Göttingen

The Nucleus Basalis-Neostriatum Complex in the Goose (Anser anser L.)

1986. 41 figures. VIII, 85 pages. Soft cover DM 68,-. ISBN 3-540-15338-1

This work provides insight into telencephalic sensor-motor aspects in Anserformes and other birds possessing a similar system, which can be compared with the corresponding circuit in mammals. This comparison will help researchers gain a better understanding of the principles governing the organization of higher vertebrate central nervous systems.



Volume 98
K. Hinrichsen, University of Bochum

The Early Development of Morphology and Patterns of the Face in the Human Embryo

1985. 82 figures. VII, 79 pages. Soft cover DM 68,-. ISBN 3-540-15848-0

The morphological changes accompanying the development of the human face are studied here for the first time in a consecutive series of photographs of embryos by Scanning Electron Microscopy (SEM) technique. The changes documented occur in the embryo between stage 12 and stage 23. This unique presentation with SEM photographs offers a new morphological basis for research into malformations.

The Influence of Antibiotics on the Host-Parasite Relationship II

Editors: **D. Adam,** University of Munich, **H. Hahn,** Free University of Berlin; **W. Opferkuch,** University of Bochum
1985. 98 figures, 60 tables. XIV, 298 pages
Hard cover DM 124,-. ISBN 3-540-15843-X

Contents: The Influence of Antibiotics on the Morphology and the Surface of Bacteria. – The Influence of Antibiotics on Immunogenicity. – The Influence of Antibiotics on the Interaction of Bacteria with Host Defence Mechanisms. – The Influence of Antibiotics on the Pathogenicity Factors and Virulence.

Advances in Forensic Haemogenetics

11th Congress of the Society for Forensic Haemogenetics
Editors: **B. Brinkmann,** Münster; **K. Henningsen,** Copenhagen
1986. 126 figures, 119 tables. Approx. 535 pages. Soft cover DM 98,-
ISBN 3-540-16500-2

This book offers a survey of the latest results in forensic haemogenetics. The topics covered include formal genetics, population genetics, and the biochemistry and serology of nearly all hereditary blood group polymorphisms, with several reviews of isolated subjects such as the HLA system, enzyme polymorphisms, protein polymorphisms and DNA polymorphisms. Legal considerations are also discussed.

Skin Models

Models to Study Function and Disease of Skin
Editors: **R. Marks,** Cardiff; **G. Plewig,** Düsseldorf
1986. Approx. 217 figures, approx. 87 tables
Approx. 385 pages. Soft cover DM 178,-
ISBN 3-540-15330-6

Considerable information on the physiological disturbances of disorders such as psoriasis and atopic dermatitis has accumulated, which permits a rational approach to treatment. Here the successful use of antimitotic agents, immunomodulators and retinoids may be cited as examples. This book provides specialists with the models of skin that have proven particularly helpful.

11/1/1

Prices are subject to change without notice

Springer-Verlag Berlin Heidelberg New York Tokyo

Heidelberger Platz 3, D-1000 Berlin 33
175 Fifth Ave., New York, NY 10010, USA
37-3, Hongo 3-chome, Bunkyo-ku, Tokyo 113, Japan

Springer

Reader Service No. 29

NEW JOURNAL – Issue one to be published June 3rd 1986 by Macmillan Press

BONE MARROW TRANSPLANTATION

Editor:
John Goldman
MRC Leukaemia Unit, Hammersmith Hospital, London

Co-Editor (USA and Canada)
Robert Peter Gale
Division of Hematology and Oncology, UCLA School of Medicine, Los Angeles

Associate Editors:
Elaine Gluckman, *Paris*
Alberto Marmont, *Genoa*
Tohru Masaoka, *Osaka*
George Santos, *Baltimore*
Don Thomas, *Seattle*
Jon van Rood, *Leiden*

Contents of Issue One

Short editorial comment – Goldman (Hammersmith)
Review of the contribution of the International Bone Marrow Transplant Registry – Gale (Los Angeles)
Bone marrow transplant for thalassaemia – Slavin (Jerusalem)
Bone marrow transplant for myeloma – Tura (Bologna)
Results of second transplants after graft failure – Bolger (Seattle)
Soy-bean lectin fractionation of marrow for prevention of graft versus host disease - Slocombe (London Hospital)
Comparison of cyclosporin and methotrexate for prevention of GVHD – Ringden (Stockholm)
Campath-1 for T-depletion before BMT for chronic myeloid leukaemia – Apperley (Hammersmith)
Toxoplasmosis after bone marrow transplant – Derouin (Paris)
Bone marrow transplant for ALL in second CR – Bacigalupo (Genova)
Bone marrow transplant for lymphoma – Ernst (Copenhagen)
Race as prognostic factor after BMT – Klingerman (Seattle)
Porphyria cutanea tarda revealed by bone marrow transplant – Dopfer (Tubingen)

THIS IMPORTANT NEW JOURNAL WILL INCLUDE:

- clinical results in man and experimental results with animals
- allografting and autografting
- HLA determination and other methods of selecting donors
- aspects of graft-versus-host disease, its prevention and treatment
- many other topics associated with bone marrow transplantation
- correspondence section for exchange of topical and controversial ideas
- stimulating editorials and book reviews

Announcement: XIII Annual Meeting European BMT Group, Interlaken, 1-5th March 1987. Further details from Dr A. Gratwohl Division of Haematology, Kantonsspital, Basel, Switzerland.

SUBSCRIPTION DETAILS

Frequency quarterly, commencing 1986
ISSN 0268 3369
Language English

Subscription price

UK and Eire	£48
USA	$99 (accelerated post)
	$125 (airmail)
Rest of the World	£68 (accelerated post)
	£80 (airmail)

Two year subscriptions are *guaranteed against price increase:* simply double the payment sent.

ORDER FORM

☐ Please enter my subscription to Bone Marrow Transplantation for one year/two years. Please despatch copies by accelerated surface post/airmail (overseas customers please delete as applicable).

☐ Please invoice me.

Name _____

Address _____

_____

Return to: Alison Baverstock, Macmillan Press, Houndmills, Basingstoke, Hants RG21 2XS, UK. Sample copies are also available from this address.

Macmillan Press Scientific & Medical

Ecological consequences of nuclear war

from S.J. McNaughton, R.W.Ruess and M.B. Coughenour

Simulations of the ecological effects on grassland ecosystems projected from the proposed climatic changes that would follow a nuclear war indicate that temperature and light reductions below ambient mean levels exceeding 10°C and 28%, respectively, are required for severe ecosystem deterioration to occur and that thresholds between promotion and decline are very abrupt.

ESTIMATES of the mass of smoke particles that would be injected into the atmosphere by fires following a nuclear war indicate that the resultant attenuation of light by suspended elemental carbon could substantially increase the optical depth of the atmosphere, producing major, rapid reductions of temperature and incident radiation at the Earth's surface[1], a phenomenon termed nuclear winter[2]. Climatic models using various degrees of structural and dynamic detail have provided diverse predictions of the global climatic effects of atmospheric soot loading, but all are in general agreement that fires of the extent and intensity now reasonably projected to follow a nuclear war that included significant targeting of urban centres would lead to major falls in surface light intensities, temperature and, less certainly, precipitation[3-5]. More complex models have tended to predict both a longer duration and a broader geographical scale of climatic effects[6]. Transitory surface temperature reductions of more than 40°C and extended reductions of 20°C below mean ambient levels and light reductions to 0.01 and 0.1 of normal have been predicted. To place these estimates in perspective, the seventeenth century 'little ice age' is believed to have been caused by only a 1°C decline below mean ambient temperature[7], and major glacial and interglacial periods may involve only 10–15°C peak-to-trough changes[8]. The potential biological and ecological consequences of the climatic changes projected to follow nuclear war could obviously be devastating[9,10].

Initial evaluations of the potential ecological effects of nuclear winter have been, of necessity, largely qualitative[9,10]. Here we present quantitative results obtained by applying a wide range of the climatic effects currently predicted to result from atmospheric soot loading after a nuclear war to a documented, detailed, mechanistic simulation model of grassland ecosystem processes[11-13].

Procedures

We used nuclear winter climatic predictions to modify climatic sub-models of the Grassland Research and Serengeti Systems Model[11-13], hereafter referred to as GRASS. It combines plant physiological processes; plant growth processes; plant morphometry; shoot demography; and grazing, with carbon, nitrogen, radiation and water sub-models. The principal focus or our research is the grazing ecosystem in the Serengeti region of Tanzania and Kenya[15-18], so both biotic and abiotic parameters were drawn from studies of that ecosystem.

Experimental studies leading to parameter values have previously been documented[19-21]. Because the productivity of cultivation agriculture would probably be severely reduced after a nuclear war, forage agriculture and particularly non-subsidized rangelands, might be major food production systems for human survivors in non-combatant countries, many of which might be located in tropical-to-subtropical locations[19].

We parameterized the GRASS simulations described here for mid-height grasses with a terminal canopy height of 50–150 cm, growing in an equatorial location at an elevation of 1,500 m with a mean annual rainfall of 793 mm and a rainfall-determined growing season of 296 days. We produced rainfall events probabilistically by GRASS and included all microclimatic parameters that might reasonably be modified by decreased light, lower temperatures and modified rainfalls. We ran diurnal variables at 2-h time steps and all others at 2-day time steps. For grazing simulations, we harvested the canopy uniformly to a height of 4 cm above the soil surface every 50 days, the optimum defoliation level for maximum mass yield to grazers in previous simulations[12].

The climatic predictions that have resulted from modelling nuclear war scenarios can be applied to ecological modelling in various ways. We chose the imposition of fixed changes on normal seasonal progression for the entire courses of growing seasons as we wanted to saturate a reasonable climatic factor space with ecological simulations that would produce response surfaces over as broad a range of conditions as was relevant, feasible and interesting.

We ran 90 full growing-season simulations, 45 each under grazed and ungrazed conditions, and modified precipitation by applying fixed percentages of −50, −30, −10, + 10 and + 30 to each rainfall generated by the weather simulator sub-model of the model. We simulated both increased and decreased rainfall because of the uncertainty of precipitation predictions from climatic modelling[6]. Because light intensity and temperature co-vary upon the injection of smoke into the atmosphere[1-6], we coupled values for those variables down to near freezing night-time temperatures, which terminated growth. Tropical pasture species are both chilling-sensitive and frost-intolerant, although species with ranges that extend outside the equatorial belt often have cold-tolerant populations in cooler habitats[22-24]. We did not simulate mean temperature reductions lower than 13°C once initial screening indicated that these temperatures produce periodic night-time frosts.

In addition to control conditions, we performed temperature- and light-intensity reductions at °C/% light combinations of −1°C/−6%; −2°C/−12%; −3°C/−16%; −5°C/−22% and −10°C at light reductions of −28%, −50%, −65% and −88%. The last two light reductions simulated atmospheric optical depths near 1 and 2, which might be widely distributed during post-war periods in non-combatant geographical locations[1-6]. Although we did not apply a time-varying post-war trajectory to climatic variables, the typical seasonal patterns of GRASS were preserved, producing characteristic seasonal progression of precipitation, humidity, cloud cover and other normal weather variables. Control mean temperature was 21°C with a mean diurnal range from 28°C daytime highs to 14°C night-time lows. A given temperature reduction reduced maximum, minimum and intervening 2-h interval temperatures by that fixed amount. We superimposed radiation reductions on diurnal patterns and the cloud cover simulator and then fed them into sub-models of radiation and water balances to affect their performance and the resultant temperatures of plant tissues and

soils. Hence, we simulated total productivity, both above- and below-ground.

Baseline validation

Published data on below-ground primary productivity are scarce and our model produces reasonable outputs when compared with the available data[11]. More widely available are data on above-ground productivity of ungrazed grasslands. We used three such data sets for a model validation internal to the simulations presented here. Data sets of above-ground primary productivities of ungrazed grasslands have been fit to regressions on annual rainfall for the Serengeti ecosystem[18], eastern and southern Africa[25] and the world[26]. There are many similar fitted curves in the literature but we used these three for baseline comparisons because they are both extensive, relevant to the ecosystem modelled, and have no data overlap.

The most complete data set for 52 worldwide sites[26] produces a best fit (r^2 = 0.51)-line of ANP = 0.5 (rain) − 29, where ANP is above-ground net primary productivity in g m^{-2} yr^{-1} and rainfall is in mm. A Serengeti dataset for 20 locations subject to neither excessive drainage nor runoff water influx[18] produces a best fit (r^2 = 0.48) line of ANP = 0.69(rain)−102 and the other African dataset of 33 values[25] produces a line (r^2 = 0.67) of ANP = 0.85(rain)−20.

Simulated above-ground productivities of ungrazed grasslands at ambient light and temperatures, and rainfalls less than 900 mm, above which both simulated and measured[27] productivities become asymptotic to the abscissa, produces a line (r^2 = 0.97) of ANP = 0.48(rain)−48, as similar to the empirical lines as they are to each other. Together with previous comparisons of model performance with published empirical results[11–14], these results indicate that GRASS produces realistic grassland performance over a wide environmental range. Still, the application of post-war climatic predictions, themselves of uncertain surety, to any ecological model is a venture into uncharted predictive realms unamenable to experimental verification. But, where verification is feasible, GRASS performance is in good accord with empirical datasets and the climatic projections considered here deal mainly with conditions close to normal climatic variation, rather than extremes of extended cold, dark conditions.

Aftermath simulations

Our control conditions for simulations are 793 mm of rain at normal light and temperature; our baseline is the rainfall span at unreduced light and temperature. The total, above- and below-ground, simulated productivities of ungrazed grasslands are very sensitive to rainfall near

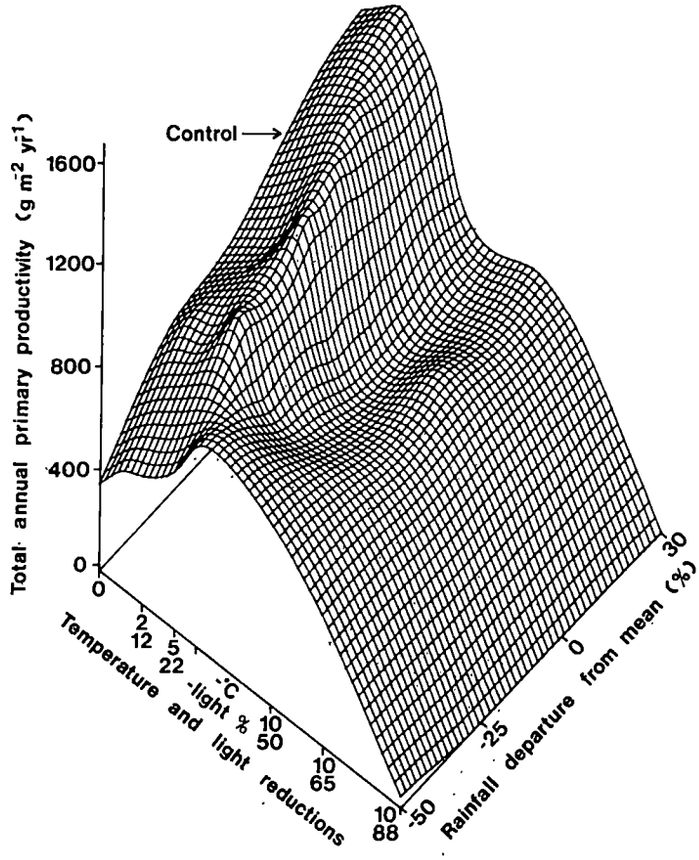


Fig. 1 Simulated total primary productivity in g m^{-2} yr^{-1} of ungrazed grasslands in relation to deviations of precipitation and temperature-radiation environments from the long-term mean condition, the indicated by arrow labelled control. Note that the *y*-axis is linear in light intensity and non-linear in temperature. Data were fitted with the bivariate spline interpolation and graphed with the PROC 3D procedure of the 82.2 enhancements and update release of SAS/ GRAPH (SAS Institute, Cary, North Carolina, 1982). Tilt, 60°; rotation, 50°.

normal light and temperature conditions, but are resistant to light and temperature departures from normal until mean reductions approach 28% and 10°C, respectively, below mean ambient levels (Fig. 1). This results in a substantial shelf where primary productivity is near or above control values for moderate climatic changes projected to follow a nuclear war. The upper level of the response surface is twisted by the tendency for cooler, darker conditions to compensate for reduced rainfall.

At the lowest rainfall level, in fact, primary productivity continues to increase at light-temperature reductions that significantly reduce production at higher rainfall levels. Therefore, reduced light and temperature have much greater water-conserving effects at low rainfalls than at higher rainfalls. These environmental interactions were expressed, in part, through compensatory changes in plant water potential, averaged over all shoots. Midway during the growing season, plant water potentials increase from −1.73 MPa at control light/temperature to −0.49 MPa at the 10°C/28% reduction under the lower rainfall conditions. At the highest rainfall conditions, the increase is only from −1.03 to −0.17 in this range.

Plant water potential regulates productivity by influencing net photosynthetic rates and tissue growth rates, and these compensatory interactions are propagated through GRASS performance. In addition, greater rainfalls increase leaf longevity, producing greater average ages of active canopy tissues, which are accompanied by declines in leaf nitrogen content and resultant rates of net photosynthesis. So no simple explanation suffices to explain the twisted response surface; rather, it is a complex consequence of plant growth and metabolic responses to interacting environmental variables. Because of the diagonal crest, productivity at high rainfall levels drops much more precipitously as the more severe region of the factor space is penetrated. The greatly reduced light levels indicate that the grasslands have a broad ability to compensate for light reductions after the initial drop, producing a shelf extending to the light

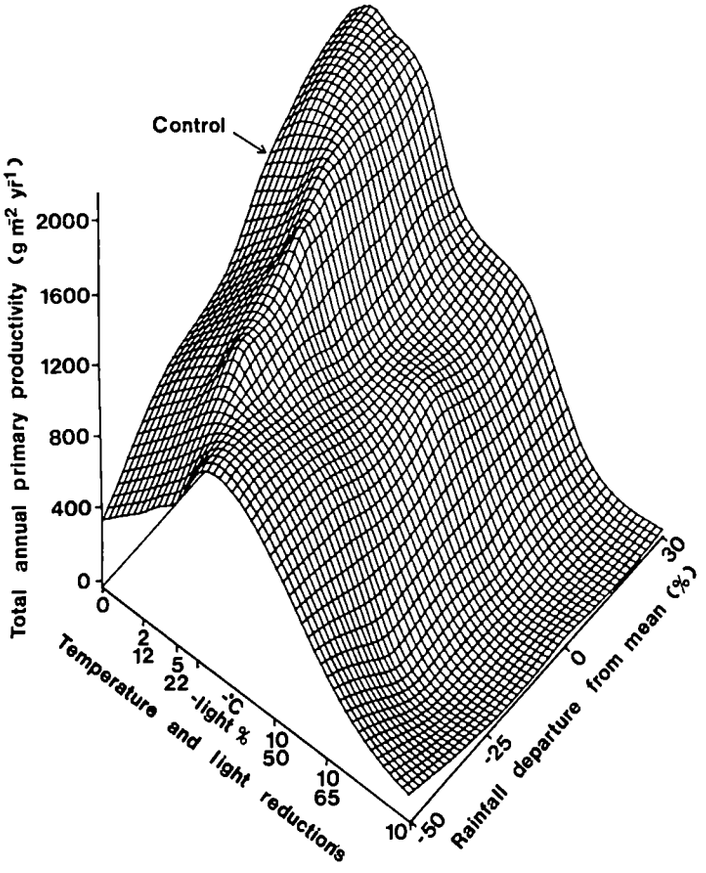


Fig. 2 Simulated total primary productivity in g m^{-2} yr^{-1} of grazed grasslands in relation to deviations of precipitation and temperature-radiation environements from the long-term mean condition, indicated by an arrow. Note that the *z*-axis scale differs from Fig. 1 if comparing the two response surfaces. Data were fitted and plotted as described in Fig. 1 legend. Aspect as in Fig. 1.

intensities produced by an atmospheric optical depth of one. At that optical depth, productivities are 79% of baseline at low rainfall levels, 61% at normal levels, and 46% at the highest simulated rainfall. Beyond an optical depth of 1, however, productivity again plunges precipitously to near zero at an optical depth of 2 and this surface of steeply decreasing primary productivity was rainfall-independent.

More interesting than the obvious fact that severe temperature and light reductions will drive production to zero is the finding that productivities are increased by most simulated post-war light and temperature reductions of moderate extent at a broad range of rainfalls. The minimum productivity on the upper response shelf, equivalent to 41% of control, is produced by the 50% rainfall reduction with no changes in temperature and light. The maximum productivity of the ungrazed simulations, 44% above control, occur at the highest simulated rainfall level accompanied by temperature and light reductions below ambient of 2°C and 12%, respectively. The diagonal crest is produced by the tendency for very minor light/temperature reductions to produce maximum productivities at higher rainfall levels, whereas low rainfall systems continued to exhibit increased productivity at substantial light/temperature reductions. Beyond this crest productivity in low rainfall simulations declined steadily to zero levels, lacking the shelf that occurs at higher rainfalls. These results have important implications for potential yields from water-limited ecosystems in post-war environments.

Grazing stimulates the primary productivities of grasslands at higher rainfall levels but not at low rainfalls; as a consequence, the overall grazed response surface has simpler but much steeper contours (Fig. 2). Primary productivity has a more convex shape under grazed than ungrazed conditions because of higher peaks, steeper contours and more abrupt thresholds. The diagonal crest on the upper shelf is more pronounced because of the tendency for primary production at high rainfall to decline after a slight rise with minor light/temperature reductions and an extension of the ameliorating range of those reductions at the lowest simulated rainfalls. Net primary productivity is stimulated a maximum of 38% above control conditions by the combination of highest rainfall with a light/temperature reduction of just 1°C and 6%. At baseline conditions, the lowest simulated rainfall reduces the productivity of grazed grasslands to only 28% of the value at control conditions. There is little evidence of a shelf of resistance to light reductions at temperatures above freezing.

Grazed grasslands are generally able to maintain reasonable levels of primary productivities down to a light reduction of 50% below normal, but they are severely inhibited by the reductions produced by an atmospheric optical density of 1. At that level, primary productivities are 19% of baseline at low rainfalls, 12% at normal rainfalls, and 9% at the highest rainfall simulated. Compared with the ungrazed simulation, this result suggests that the trophic web would collapse under conditions still allowing significant primary productivities in ungrazed grasslands.

The ameliorating effects of light and temperature reductions produce steeper responses under grazed conditions over the upper productivity shelf. For example, at control rainfall the productivity of ungrazed systems is 17% below normal at the 10°C/28% temperature/light reduction. In the grazed ecosystem, in contrast, net primary productivity under those conditions is still 13% above baseline. As a consequence, the descent of productivity as the limiting factor space is penetrated is much more precipitous for grazed than for ungrazed ecosystems.

As grasses must be converted into animal products for uncultivated vegetation in grassland climates to support human populations, secondary productivity is of particular importance to consideration of the potential consequences to humans of climatic changes that might follow a nuclear war. There are two fundamentally different approaches to estimating secondary productivity from model output. The simplest, but perhaps least revealing, is to convert the plant mass consumed by grazers to animal biomass by assuming some conversion efficiency based on animal feeding trials[27]. That approach assumes that forage quality does not vary across the range of conditions simulated and has the virtue of converting forage consumption per unit area directly into animal yield per unit area.

When we applied a 10% conversion efficiency[28,29] to animal forage consumption output from GRASS, with that output varying according to both forage amount and its availability due to canopy geometry[12], we found (r^2 = 0.87, $P < 0.001$)

that secondary productivity = 0.052 × total primary productivity, the units of productivity are in mass area^{-1} yr^{-1} for the 40 environmental combinations above zero. Secondary productivity then, under this assumption, would reproduce the response surface of Fig. 2, but with absolute values 95% lower on a mass density basis.

A second and, we believe, more realistic approach to estimating secondary productivity is to account for differences in forage quality. Both wild[30] and domestic[31] ungulates, particularly in tropical locations, are more often limited by forage quality than by its quantity. Higher mass productivities produced by GRASS are generally accompanied by lower forage quality because nutrients such as nitrogen are diluted by carbon accumulation in plant tissue, consistent with real ecosystems[32]. Over the range of non-zero conditions simulated here, the relationship between the nitrogen content of forage consumed and the mass of carbon that is consumed is

$$\%N = 1.93 - 0.00386\,gC$$

where $r^2 = 0.92$, $P<0.001$ and gC is grams of carbon consumed per square metre of land surface per year.

As a consequence of this negative relationship between forage quality and mass availability, the amount of N consumed was asymptotically related to the amount of forage carbon consumed ($r^2 = 0.86$, $P<0.001$) with gN = (2.27 ln gC) −5.2 where units are masses of N and C m^{-2} yr^{-1}. This conundrum relating forage quality and quantity of further exacerbated by a positive relationship between forage nitrogen content and the digestibility of that nitrogen (ref. 33). Therefore, as a more realistic approach to estimating potential secondary productivities of post-war ecosystems, we multiplied N yield to grazers in gN M^{-2} yr^{-1} by the digestibility of that N predicted from the linear relationship between forage N content and digestibility of N (ref. 33). This yielded digestible gN m^{-2} yr^{-1} consumed by grazers. Additional assumptions that we are unwilling to make at this stage would be required to convert the areal yield of digestible N to animal production, but the shape of the response surface is more likely to reflect the secondary productivity potentials of post-war ecosystems than the simple conversion from Fig. 2.

The quality-based secondary productivity response surface produced by GRASS varies markedly from both primary productivity surfaces (Fig. 3). Maximum secondary productivity, 38% above the control value, is produced at moderate drought and no reduction of ambient light and temperature. Minimum secondary productivity potential outside the severe factor space is at the highest rainfall with temperature-light reductions of 5°C/22%, where the value is only 36% of the control. This response surface is caused by a greater reduction in plant-carbon assimilation than of nutrient assimilation by mild environmental stress, a phenomenon documented empirically[34,35] and that GRASS reproduces. As a consequence, there was a pronounced peak of secondary productivity potential at a rainfall reduction to 30% below normal in baseline light and thermal environments. Values drop precipitously around this optimum, particularly at lower rainfall levels and no light/temperature reduction. But the surface is convoluted with folds and pockets, especially as severely limiting conditions are approached. Reduced light levels at non-freezing temperatures produce a broad secondary shelf of slightly increasing secondary productivity potential with a reversal of the rainfall field leading to higher potentials at higher rainfalls. At light intensities above half normal, potential secondary productivity drops sharply to zero. Compared with control conditions, all higher rainfall simulations and all reduced light and temperature conditions under the normal rainfall regime result in secondary productivity potential lower than the control. But many of the climatic conditions predicted to follow a nuclear war, that is, combinations of reduced rainfall with cooler, darker conditions, result in significant enhancements in the yield of digestible N to herbivores.

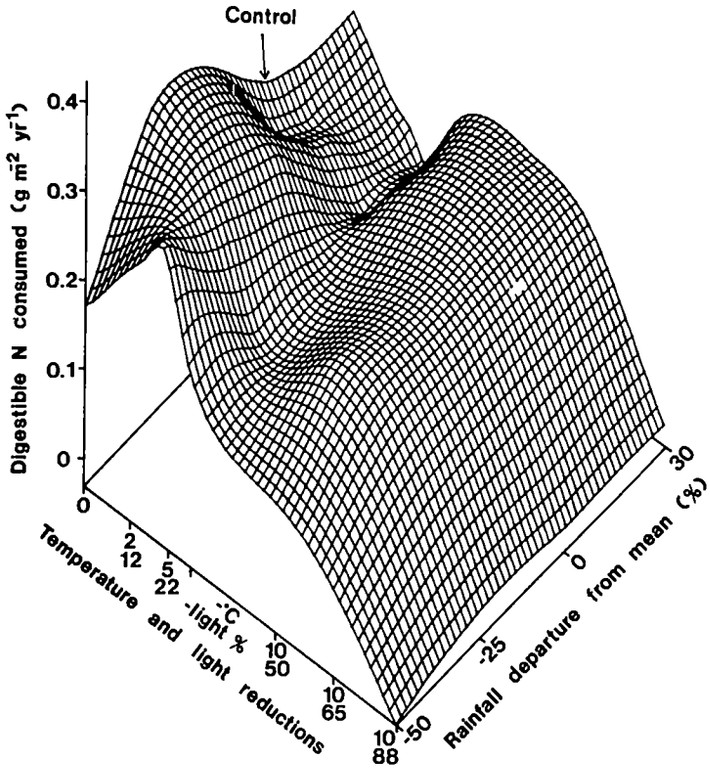


Fig. 3 Simulated yield of digestible N to grazers in g m^{-2} yr^{-1} in relation to deviations of precipitation and temperature-radiation environments from the long-term mean condition, indicated by an arrow. Data were fitted and plotted as described in the legend for Fig. 1. Aspects as in Fig. 1.

When compared with the primary productivity simulations and simple extrapolations of secondary productivity from them, these simulations highlight two significant features of ecosystems. First, countervailing processes make it difficult, if not impossible, to optimize all performance standards simultaneously. Second, simple extrapolations are incapable of providing meaningful estimates of the effects of complex biological responses to environmental variation.

Implications

We make no claim for the ultimate accuracy with which GRASS simulations could predict the ecological aftermath of a nuclear war. But we do believe that those projections are fundamentally realistic; that they provide reasonable boundary conditions for severe declines in ecosystem carrying capacity; and that they prudently reflect the ecological conditions that could be expected to occur in many grassland and other water-limited ecosystems following such a war. Primary productivities under both grazed and ungrazed conditions, and secondary productivity potentials, are stimulated by cli-

matic conditions that would be relatively severe under normal conditions, although they can be characterized as mild compared with the more extreme nuclear winter conditions predicted by some models. The abrupt interfaces between stimulatory and degradative effects emphasize the hazards associated with deductions from imprecise climatic predictions.

The sensitivity of our simulations to the countervailing effects of precipitation and radiation-temperature changes within the non-severe factor space indicates that it would be profitable to devote more effort in climatic modelling to precise definitions of the coupling between precipitation and radiation-thermal regimes, perhaps at the sacrifice of global spatial scales where the models are in general, if not precise, agreement. Because climatic effects have post-war meaning only through their ecological effects, more attention to ecological modelling is clearly also warranted.

Our simulations indicate several areas where additional empirical research could contribute fruitfully to a better understanding of both the potential ecological consequences of nuclear war and basic ecological knowledge. We terminated temperature reductions at levels just above those producing periodic nighttime frosts as tropical pasture plants are both chilling sensitive and frost intolerant[22–24]. However, strains of a widely cultivated tropical grass, *Cynodon dactylon*, have been produced that are tolerant of winter conditions to near 40° N in central North America[36], and tropical species with ranges extending outside equatorial locations have frost tolerant genotypes[22,23]. This suggests that there is sufficient genetic variability in tropical grasses to produce freeze-tolerant genotypes, and natural selection accompanying severe nuclear winter would be intense. If some tolerant genotypes survived as either dormant individuals or as seeds, ecosystem recovery might be possible following even the most severe nuclear winter. We know of no extensive evidence on the freeze tolerance of drought-dormant rather than actively growing tropical grasses. Nuclear winter during the tropical dry season might not result in extensive plant mortality if drought-hardened individuals are also cold tolerant; information on the relationships between these adaptive traits would allow more realistic estimates of the expected recovery potentials of tropical and subtropical ecosystems if severe nuclear winter penetrated those geographical regions. Information is also limited on the seed banks of tropical soils and the freeze tolerance of those seeds[23]. Nuclear winter would expose seeds to cold, dry, dark environments, which in many cases are optimal for increasing seed longevity.

Secondary productivities can also be influenced by many factors in addition to the limitations imposed by food quantity and quality. Radiant heat load[37], availability of water, wind speed[28], mineral nutrient availability[31,33] and the shield of veterinary practices protecting both wild and domestic ungulates from potentially epidemic disease[38,38] could all be modified by post-war conditions. In addition, cold rains accompanying periodic smoke cover and chilling that precipitates water out of the atmosphere might have devastating effects on tropical animals. Realistic estimates of such ecological effects would add precision to estimates of the post-war carrying capacity of ecosystems.

But even with the many uncertainties, we believe that the results of simulations with GRASS have three principal implications for the carrying capacities of ecosystems were a nuclear war to modify climate in the directions now envisaged. First, mild (by the standards of nuclear winter) climatic changes tending to reduce heat loads and evaporative demands of the atmosphere might increase the productivities of many water-limited ecosystems. Such ecosystems occupy major expanses of Earth's surface.

Second, distinctly different conditions lead to performance optima at different levels in the trophic web. Those optima, therefore, cannot be attained simultaneously. Grain production, for example, would probably track the response surface that we obtained for primary productivities of ungrazed vegetation. Because grassland climates are centres of grain production, increases in precipitation and/or reduced evaporative demands could tend to increase substantially the grain production potential of post-war ecosystems. Animal production, on the other hand, would probably be inhibited by the same conditions.

Third, and, we believe most important, the transition between non-catastrophic (even favourable) environmental changes and those that are calamitous may be extremely abrupt. The presence of those thresholds in all three simulation results suggests that the ecological effects of a nuclear war are very unpredictable and may change drastically over narrow environmental ranges. A population of human survivors in tropical-to-subtropical locations might encounter an increased carrying capacity for certain climatic perturbations only to be plunged into destruction by a seemingly minor drift away from those conditions. Overall, our results emphasize the uncertainty that must be attached to any predictions about the ecology of a post-war Earth, and suggest that ecological unpredictability itself could be one of the most damaging consequences of post-war climatic effects.

Development of GRASS was funded by the US National Science Foundation's Ecosytem Studies Program. Its application here was funded by Syracuse University. That application was prompted by two workshops sponsored by the ENUWAR unit of SCOPE, University of Essex (attended by S.J. McN.) None of those organizations necessarily endorses the conclusion of the research reported. □

S.J. McNaughton and R.W. Ruess are at the Biological Research Laboratories, Syracuse University, 130 College Place Syracuse, New York 13210, USA; and B.M. Coughenour is at the Natural Resources Ecology Laboratory, Colorado State University, Fort Collins, Colorado 80523, USA.

1. Crutzen, P.J. & Birks, J.W. *Ambio* **11**, 114–125 (1982).
2. Turco, T.P., Toon, O.B., Ackerman, T.P., Pollack, J.B. & Sagan, C. *Science* **222**, 1283 (1983).
3. Covey, C., Schneider, S.H. & Thompson, S.L. *Nature* **308**, 21–25 (1984).
4. Crutzen, P., Galbally, I.E. & Bruhl, C. *Climatic Change* **6**, 323–364 (1984).
5. Thompson, S.L. *et al. Ambio* **12**, 236–243 (1984).
6. Pittock, A.B. *et al. Environmental Consequences of Nuclear War* Vol. 1 (Wiley, Chichester, 1986).
7. Parker, G. *Europe in Crisis 1598–1648* (Harvester, Sussex, 1980).
8. Heusser, C.J., Streeter, S.S. & Stuiver, M. *Nature* **294**, 65–67 (1981).
9. Ehrlich, P.R. *et al. Science* **222**, 1293–1300 (1983).
10. Harwell, M.A. & Hutchinson, T.C. *Environmental Consequences of Nuclear War*, Vol. 2 (Wiley, Chichester, 1985).
11. Coughenour, M.B., McNaughton, S.J. & Wallace, L.L. *Ecol. Modelling* **23**, 101–134 (1984).
12. Coughenour, M.B., McNaughton, S.J. & Wallace, L.L. *Ecol. Modelling* **26**, 177–201 (1984).
13. Coughenour, M.B. *Ecol. Modelling* **26**, 203–220 (1984).
14. Coughenour, M.B. *Ann. Mo. Bot. Gard.* **72**, 852–963 (1985).
15. McNaughton, S.J. *Science* **191**, 92–94 (1976).
16. McNaughton, S.J. *Am. Nat.* **113**, 691–703 (1979).
17. McNaughton, S.J. *Ecol. Monogr.* **53**, 291–320 (1983).
18. McNaughton, S.J. *Ecol. Mongr.* **55**, 259–294 (1985).
19. McNaughton, S.J., Wallace, L.L. & Coughenour, M.B. *Ecology* **64**, 307–318 (1983).
20. Ruess, R.W., McNaughton, S.J. & Coughenour, M.B. *Ocecologia* **59**, 253–261 (1983).
21. Coughenour, M.B., McNaughton, S.J. & Wallace, L.L. *Afr. J. Ecol.* **23**, 179–194 (1985).
22. Clements, R.J. & Ludlow, M.M. *J. appl. Ecol.* **14**, 551–566 (1977).
23. Humphreys, L.R. *Environmental Adaption of Tropical Pasture Plants* (Macmillan, London, 1981).
24. Larcher, W. & Baurer, H. in *Physiological Plant Ecology I, Encyc. Plant Phys.* Vol. 12A (eds Lange, O.L., Nobel, P.S., Osmond, C.B. & Ziegler, H.) 403–437 (Springer, New York, 1981).
25. Deshmukh, I.K. *Afr. J. Ecol.* **22**, 181–186 (1984).
26. Lauenroth, W.K. in *Perspectives in Grassland Ecology* (ed. French, N.) 3–24 (Springer, New York, 1979)
27. Sims, P.L. & Singh, J S *J. Ecol.* **66**, 573–597 (1978)
28. Garrett, W.N., Bond, T.E. & Kelly, C F *J Anim Sci* **19**, 60–66 (1960).
29. Lodge, G.A. & Lamming, G E *Growth and Development of Mammals* (Butterworths, London, 1968)
30. Sinclair, A.R.E. *J. Anim. Ecol* **44**, 497–520 (1975)
31. McDowell, L.R., Conrad, J H., Ellis, G L & Loosli, J K. *Minerals for Grazing Ruminants in Tropical Regions* (Univ. Florida, Gainesville, 1983)
32. Vitousek, P. *Am. Nat.* **119**, 553–572 (1982)
33. McDonald, P., Edwards, R.A & Greenhalgh, J F D. *Animal Nutrition* (Longman, London, 1973)
34. White, T.C.R. *Oecologia* **22**, 119–134 (1976)
35. Mattson, W.J. *A. Rev. Ecol. Syst* **11**,119–161 (1980)
36. Beard, J.B. *Turfgrass: Science and Culture* (Prentice-Hall, Englewood Cliffs, New Jersey, 1973).
37. Garrett, W.N., Givens, R.L., Bond, T E & Hull, J L. *Proc. Western Sect Am. Soc. Anim Sci* **17**, 349–355 (1966).
38. Rossiter, R.B. *et al. Vet. Rec* **113**, 459–461 (1983)
39. Rossiter, P.B. *et al. Prev. Vet. Med.* **1**, 257–264 (1983)

Laboratory investigation of the electrodynamics of rock fracture

B. T. Brady & Glen A. Rowell

Denver Research Center, US Department of the Interior, Bureau of Mines, Denver, Colorado 80225, USA

Light produced by the failure of rocks subjected to uniaxial compression in various atmospheres has been analysed spectroscopically in the visible and near-infrared. In each case, the observed spectrum was unique to the ambient atmosphere. Spectrographical and electromagnetic investigations support an exoelectron bombardment mechanism to explain the observed light emission. Several implications of this result are discussed.

OBSERVATIONS of light emissions and other lower-frequency electrical phenomena associated with rock fracture in mines and earthquakes have been reported for several centuries[1-4]. These reports did not attract serious scientific attention until photographs of light emissions were obtained during the 1965 Matsushiro, Japan, earthquake swarm[1]. Although many theories as to the source(s) of these light emissions have been presented[1-6], it is only within the past few years that serious attempts have been made to conduct laboratory investigations of this phenomenon[7-12]. Due to the absence of precise experimental data, the lack of consensus regarding the possible explanations of the light-producing mechanism(s) from fracturing rock is understandable. The mechanisms most commonly proposed[5] include: (1) rock fragments frictionally heated to incandescence; (2) electrostatic discharge produced by the deformation of piezoelectric minerals or due to charge separation on fractured surfaces; (3) plasmas produced by rapid and intense heating of rock material; and (4) excitation of the ambient atmosphere by particle (electron and/or positive or negative ion) bombardment.

As each of the above mechanisms produces an optical spectrum having characteristic features, spectroscopic analysis in the visible region (10^{14}–10^{15} Hz) offers an experimental means of elucidating the process by which the light is produced. For example, rock fragments frictionally heated to incandescence would produce a continuous spectrum approximating that of a black-body radiator at a temperature corresponding to that of the heated rock. An electrostatic discharge caused by deformation of piezoelectric minerals would normally produce line spectra characteristic of the excited elements: little or no background continuum would be observed, and transitions from both neutral and ionized states might occur. In addition, because this type of excitation can be best categorized as 'spark-like', microwave emantions would be expected. A plasma originating from the rock sample during catastrophic failure would produce a background continuum closely approximating that of a black-body radiator. Atomic emission lines, characteristic of electromagnetic interactions occurring within the plasma, would be superimposed on this spectrum. Transitions from neutral as well as ionized species might also be observed. The plasma temperature could be inferred from the ratio of the line-to-background intensities[13]. Finally, excitation of the ambient atmosphere by particle bombardment would produce molecular and atomic line spectra. The spectrum would be determined by the chemical properties of the atmosphere as well as by the energy, mass and charge of the particles. Spectroscopic examination and characterization of the emitted light should determine which, if any, of the above models are valid.

Experimental philosophy

Experimental conditions and materials were chosen to enable positive differentiation between the four proposed light causing mechanisms. Five ambient atmospheres were chosen: argon, helium and air at atmospheric pressure; water and a vacuum of 1×10^{-6} torr.

The monatomic rare gases, argon and helium, were selected because of their relatively simple atomic line spectra[13]. These gases have been the subject of extensive spectroscopic investigations and the energy levels of both neutral and ionized species are well established. Because the first ionization potentials for argon and helium are 15.8 and 24.6 eV, respectively, the minimum energy available to the excitation process can be deduced from the observed transitions.

The high-vacuum ($\sim 10^{-6}$ torr) experiments were designed to determine whether the emitted light originated in the ambient atmosphere or in the rock material. Since the mean free path of nitrogen and oxygen is $\sim 10^{4}$ cm at 10^{-6} torr and 25 °C, vacuum conditions would seem to preclude the production of light from collisional excitations[14]. Should light be observed during rock fracture in the vacuum experiments, then either the ambient atmosphere (gas remaining in the vacuum chamber) is being excited by a mechanism other than an electric field or the rock material itself (including any excited gases that might exist within the rock pores) is the source of the light.

Water was chosen as an ambient fluid because a liquid has a much higher density than does a gas, an important consideration if collisional processes cause the light emission. Additionally, tap water is a relatively good conductor (~ 200 μS)[14] and would minimize the possibility of any capacitive charge buildup caused by piezoelectric minerals present on the sample surface.

A fine-grained granite from Salida, Colorado, and a fine-grained basalt from Table Mountain near Golden, Colorado, were the two rock materials chosen for the tests. Basalt was chosen specifically because of the absence of quartz or other strongly piezoelectric minerals. All rock samples except those used in the high-speed movies were drill cores, of diameter 2.2 cm and length 5 cm. All samples were prepared to ASTM standards.

Preliminary experimental results

Figure 1 illustrates the typical fracture behaviour of a 5.4-cm-diameter × 10.8-cm-long specimen of Salida Granite from high-speed movies (3,000 frames s^{-1}). Several observations are noteworthy. First, the dust cloud (composed of finely ground rock particles) forms during the main shock ($t = 0$) and not as a result of frictional sliding along crack (fault) surfaces. Second, the loading platens exhibit no significant motion until the sample has disintegrated; that is, the stiffness of the loading system may be irrelevant to the fracture process in brittle materials. Third, the process of fracture in brittle materials, such as rock, is explosive. Implications of these observations will be discussed elsewhere (in preparation).

Figure 2 illustrates typical light emission from rock fracture. This photograph was obtained using a night-vision scope. Generally, light produced by rock fracture can be viewed only in

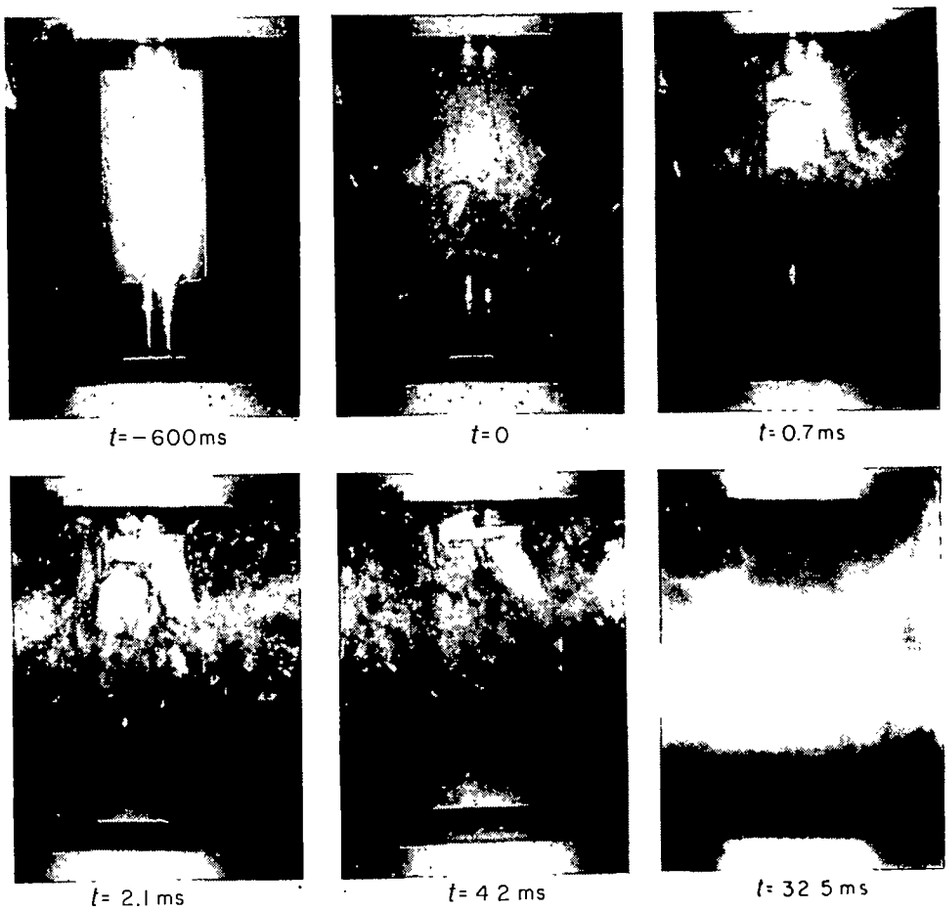


Fig. 1 Sequence of high-speed (3,000 frames s^{-1}) photographs illustrating fracture of Salida Granite.

darkness by an observer with night-adapted vision. Photodiode experiments show that the light emission is composed of a few discrete pulses, each persisting for only ~100 μs. Figure 3 illustrates typical photodiode and applied load outputs versus time for the two rock types studied in this investigation. (Note that the response time of the PIN (positive/insulated/negative) diode and recording system is ~1 μs, and the fall time is much slower because of the amplifying electronics.) Therefore, the major problem of this investigation was low light intensity of short duration. This point is amply shown in Fig. 4*a*, *b*. Figure 4*a* shows a sample of Salida Granite photographed during catastrophic failure and illustrates the formation of the 'dust' plumes and other larger pieces of rock in the process of spalling. Of particular interest is the nature of the 'dust' plumes emanating along fracture surfaces. In several fractures, the plumes occur only along discrete segments, with no plumes occurring elsewhere along the fracture surface. Figure 4*b*, taken through a single-stage image intensifier, illustrates the light emission emanating from a different sample of Salida Granite and supports the observation that the light duration is short ($<10^{-3}$ s); if the light duration were greater than several milliseconds, discrete emissions would be smeared. In addition, the discrete nature of the light emissions along selected fracture surfaces is evident and similar to the plume distribution shown in Fig. 4*a*.

Experimental procedures

The final design of our spectrographic system resulted from these preliminary tests and much trial and error. Because of the low light intensity and short duration, priority was given to optical speed, with resolution a secondary consideration. A variable slit prism spectroscope with a two-stage image intensifying system (two night-vision scopes mounted in series) was used to observe spectra. The image formed by the spectroscope was focused on the photocathode tube of the first stage intensifier. The final image was then viewed directly on the screen of the second stage or recorded photographically.

Because light emission from rock failure has been the subject of considerable controversy, it was important to acquire photographic spectra. In addition to the short time duration and low intensity of the light produced by rock fractures, the problem

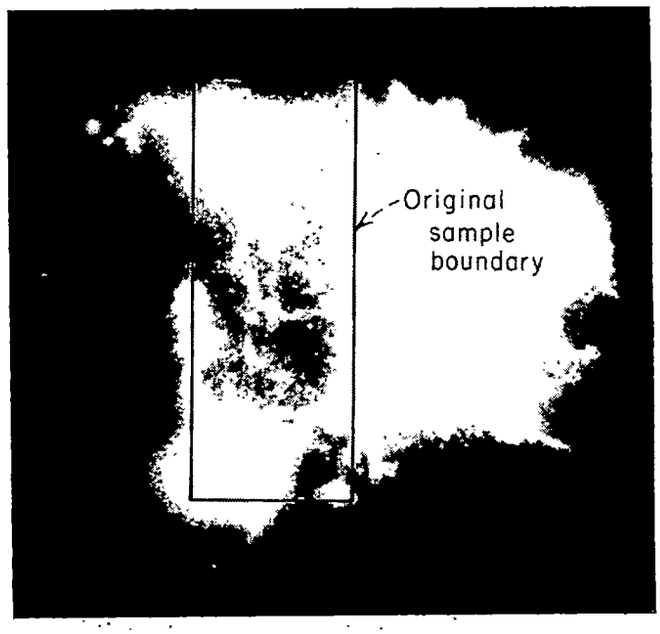


Fig. 2 Typical light emission observed from fracture of Salida Granite.

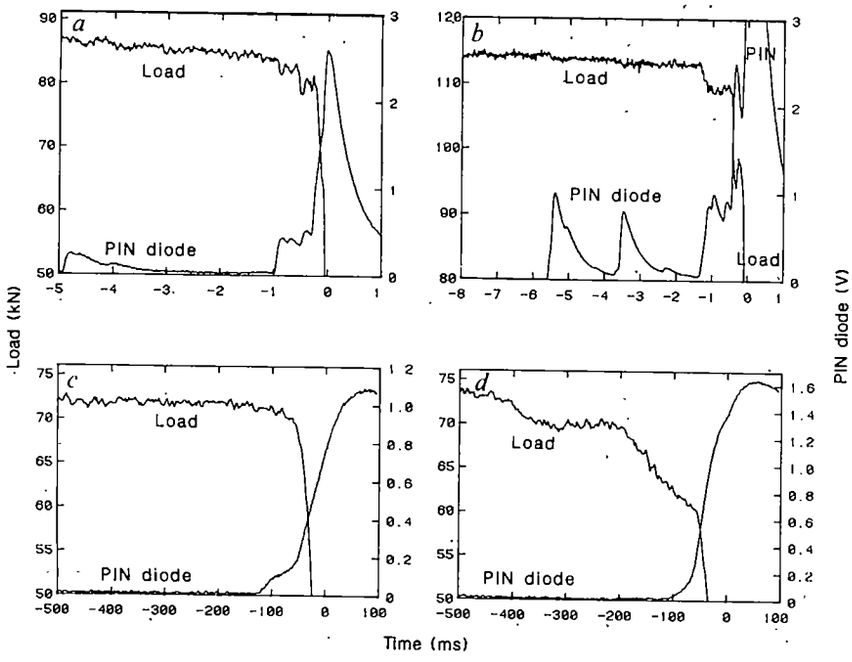


Fig. 3 Typical photodiode and applied load outputs versus time for Salida Granite (*a*, *b*) and Table Mountain Basalt (*c*, *d*).

of photographing a spectrum was complicated by inexact knowledge of when the rock sample would fail and the unfavourable signal-to-noise ratio of operating both image intensifiers at maximum gain. On the other hand, operating the system at less than maximum gain produced images too faint to photograph.

The spectra were finally recorded on Polaroid type 612 film, with an ASA rating of 20,000. The ultra-high speed of this high-contrast black and white film made it ideally suited to our experiment. Accordingly, an XL Graflex camera with a Polaroid back was placed at the exit of the second image intensifier to take photographs. With both image intensifiers set at maximum gain, 1/10 s at $f/5.6$ was the longest exposure able to produce acceptable images compared with the background noise. Output from a load cell was used to activate a digital oscilloscope which sent a pulse to a circuit which activated a low-mass solenoid which triggered the camera shutter. This 'Rube Goldberg'-type system afforded a probability of ~0.5 of the camera lens being open during rock failure to record the spectra of any light emission.

The rock specimens were isolated in a cylindrical (7.6 cm inner diameter) Lexan chamber to prevent damage to the spectroscope. To maintain a gas-tight seal, a sliding steel disk at each end of the chamber was fitted with O-rings. Brass platens were placed between the rock sample and the steel disks. The chamber assembly was then placed in the press and a slight force applied to align the components. Next, gas was introduced into the chamber through one port, and the end of a tube from the exit port was placed under water to maintain a slight positive pressure within the chamber. The laboratory was then darkened and the spectrum from a reference lamp recorded on film. The camera shutter and solenoid were reset, the oscilloscope trigger was armed, and the image intensifiers were turned to maximum gain. By this time, the chamber had been sufficiently flushed of air, and the sample was loaded rapidly (strain rate $\dot{\varepsilon} \simeq 10^{-2}\ s^{-1}$) to failure. The photographic print was removed from the film pack and developed.

Results

Figure 5*a* is the spectrum resulting from the fracture of Salida Granite in argon. The reference spectrum at the top of the photograph was produced by a low-pressure argon lamp. Several prominent lines are identified. Of particular importance is the observation that no spectral lines are produced by the failure of Salida Granite in argon other than the lines present in the reference spectrum. All lines observed are produced by neutral atomic argon. No transitions from ionized states are observed. The 7,635-Å line is prominent, and the fact that the upper state of this transition lies 13.2 eV above the ground state indicates that at least this much energy is available for the excitation process. Finally, there is no evidence of a background continuum. The random dots in Fig. 5*a*–*e* adjacent to the spectral lines are caused by Johnson noise in the image intensifier system.

Figure 5*b* is the spectrum produced by the fracture of Salida Granite in helium. The apparent broadening of the 7,065-Å line in the top reference spectrum was caused by overexposure. As in the case of argon, this spectrum shows only neutral atomic transitions. The upper state of the 7,065-Å transition lies 22.7 eV above the ground state. There is no evidence of a background continuum.

Figure 5*c* is the spectrum of Table Mountain Basalt (no piezoelectric minerals) in argon. This spectrum is similar in every feature to that produced by the failure of Salida Granite in argon. Again, the 7,635-Å line is prominent, and no lines are present other than those of the argon spectrum. There is no evidence of a continuum background.



Fig. 4 *a*, Photograph of Salida Granite during failure. Maximum load at failure was 300 MPa. Load during photograph was 205 MPa. *b*, Light emission from failing Salida Granite. Note discrete emissions along failure surfaces. Samples shown in *a* and *b* are different.

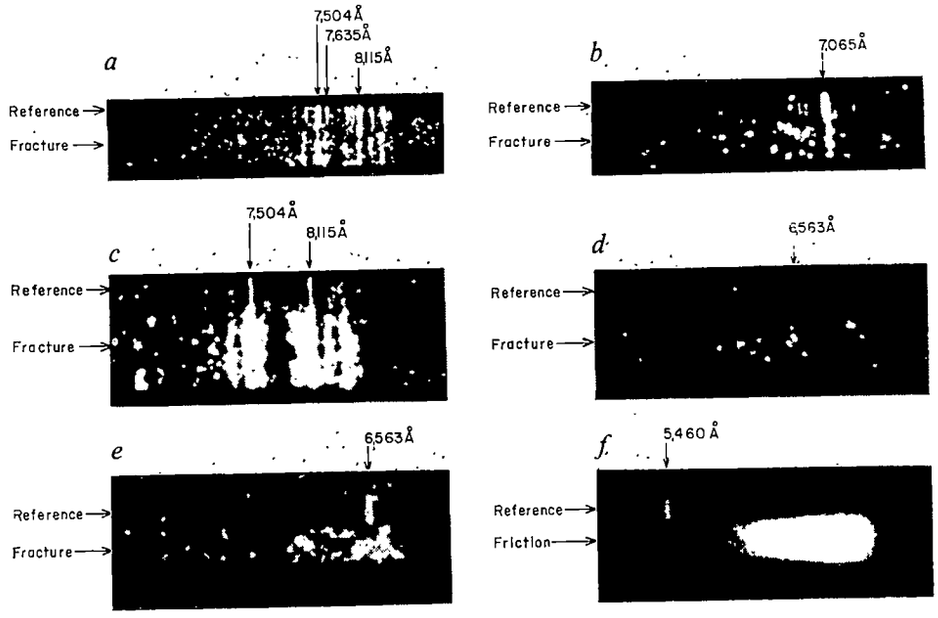


Fig. 5 *a*, Spectrum from Salida Granite fracturing in argon atmosphere. Top spectrum is the reference gas spectrum. *b*, Spectrum from Salida Granite fracturing in helium atmosphere, *c*, Spectrum from Table Mountain Basalt fracturing in argon atmosphere. *d*, *e*, Spectra from Salida granite fracturing in water. Top reference spectra are Hα. *f*, Spectrum produced by frictional heating of two pieces of bulk quartz in air atmosphere. The reference line (5,460 Å) appears at top. No image intensifier used.

Figure 5*d* and *e* are spectra from Salida Granite being fractured in water. The single line in the top reference spectrum is hydrogen α (Hα), 6,563 Å (12.1 eV). The spectra have several important features. First, as seen in Fig. 5*d* and, in particular, visually through the spectrometer, radiation occurring at the 6,563-Å position can be positively identified as being Hα, produced by atomic hydrogen. In Fig. 5*e*, radiation centred around the Hα position has been broadened into a band. This spectral broadening is attributed to perturbation of the atomic hydrogen energy levels by potential interactions in the liquid water. A second band of radiation extends from ~5,700 to 6,200 Å. This is identified as unresolved structure of the molecular hydrogen spectrum[13]. No other transitions are observed, and no background continuum is present. Thus, the spectra from Salida Granite being fractured in water indicate that both atomic and molecular hydrogen are produced during fracture.

Figure 5*f* is the spectrum produced from rubbing (frictionally heating) two pieces of quartz in air. No image intensifier was used in this experiment. A mercury reference spectrum appears at the top, with the 5,460-Å line prominent. The spectrum is a continuum. It is characteristic of a black-body radiator at a temperature of ~1,500 K, inferred from the spectral energy distribution. No line or band features are observed.

Regrettably, the photographic spectra from the fracture of Salida Granite in 10^{-6} torr vacuum are even less clear than those already discussed; therefore, only the results of visual observation are reported. The spectra observed exhibited typical molecular band structure. Comparison of the best photographic spectrum with that produced by a 10^{-3} torr air Geissler tube indicated that the spectrum was that of air. No line structure was detected visually or photographically and, consistent with the other experiments, no continuum radiation was observed.

Figure 6 is a photograph of the light emissions from fracturing a core of Salida Granite in an air atmosphere. The photograph was taken with ASA 400 film by turning out the room lights, opening the camera shutter, breaking the core, and then closing the shutter. The light source was determined to result from burning chips of steel scoured from the steel platens by the exploding rock fragments. The spectrum produced from this light is a continuum representative of oxidizing steel. That the light source was oxidizing steel was demonstrated in two ways. First, an increase in the oxygen content of the ambient atmosphere dramatically increased the light intensity, and second, by covering the upper platen with a thin piece of rubber, this comparatively bright light disappeared, even in a 50% oxygen atmosphere.

Discussion

An important and surprising result of this investigation is the complete lack of spectroscopic evidence for continuum radiation. Continuum radiation would be produced by material heated to incandescence by frictional sliding. That such a continuum is produced by frictionally heated rock material and is easily detectable is confirmed by Fig. 5*f*. Other experiments were performed in which drill cores of various rock types were lightly ground together, and similar continuum radiation spectra were produced. The lack of continuum radiation from fracturing rock indicates that frictional heating does not produce the light observed during fracture and provides corroborative evidence of the explosive character of fracture shown in Figs 1 and 4*a*. Furthermore, the lack of continuum radiation also indicates that the finely ground dust material produced during rock fracture is not formed by frictional sliding, as is commonly believed. Microscopic examination of the rock dust shows euhedral surfaces with no apparent smoothing or roughening characteristic of frictional grinding. Thus, our results suggest a tensional origin for these fine-grained particles, such as could be produced by shock waves propagating through the rock structure during catastrophic failure.

An additional feature common to all recorded spectra is the absence of emission lines from ionized species. The absence of both continuum radiation and emission lines from ionized species eliminates the possibility that a plasma is a source of emitted light. However, note that the most significant argon (II) lines are located towards the ultraviolet end of the visible spectrum.

The absence from all the spectra of lines produced by the elemental constituents of the rock material is significant. Although the strongest silicon lines are in the ultraviolet region[13], highly sensitive calcium, sodium and potassium lines occur in the visible and would have been readily detectable had they been present. There is no evidence of excitation of the constituent rock minerals. The spectra in all cases are those of the ambient atmosphere.

The piezoelectric excitation model[1,3,7] has been seriously considered as a light-producing agent because many rock materials contain minerals known to be piezoelectric. In terms of an excitation mechanism, a piezoelectric discharge is best charac-

terized as spark-like, that is, a high-voltage differential with low current in which the excitation is due primarily to a high electric field. No ionized line spectra, such as typically produced by a spark discharge, were detected. The spectrum of basalt broken in an argon atmosphere is of interest in this case. Petrographic analysis confirmed that the basalt was free from any strongly piezoelectric minerals. Yet the spectrum of basalt in argon is identical to that produced by granite in argon. While deformation of piezolelectric minerals does occur during fracture of rocks, our evidence is that a piezoelectric mechanism is not responsible for the observed excitation of the ambient atmosphere. Finally, the absence of microwave emanations during the time interval in which the light is observed confirms the observation that a piezoelectric discharge is not the source of visible light[11].

Although most of our experimental evidence is indirect, there is substantial support for an excitation mechanism entailing electron bombardment. The tendency of a particle to produce ionizing events is a function of the particle's energy, mass and charge. An α-particle will typically produce 10^3 times more ionizing events in a medium than a β-particle of the same energy. The absence of spectra from ionized species argues against the excitation of the ambient atmosphere by α-particles or heavier nuclei. The fracture of Salida Granite in water produced both atomic and molecular hydrogen. The formation of these gases is similar to their generation when water is irradiated by β-particles (electron bombardment).

We conclude that exoelectron excitation of the ambient atmosphere is the mechanism responsible for the light emissions observed during rock fracture. For this mechanism to explain light emissions produced during massive failures in mines or earthquakes, it would be necessary for the fracture to reach the surface to allow exoelectron excitation of the ambient atmosphere. Recent observations have shown that light emissions, coincident with acoustic emissions resulting from rock spalling off the surface, have occurred along highly stressed drifts on the 5,400-ft level of the Consolidated Silver venture near Osburn, Idaho (J. Suveg, personal communication). Here the light emission is probably due to exoelectrons emitted from fresh fracture surfaces exciting the air. Of course, for this mechanism to be a source of light when the fracture does not reach the surface, as in deep crustal earthquakes where surface cracking does not occur, would require that sub-surface stress changes induced by the earthquake preparation process cause cracks on the surface which could then emit electrons. Note that surface cracking was observed in earthquakes where light emissions were reported, such as the 1965 Matsushiro earthquake swarm[15,16] and the 1976 Tangshan earthquake (T. K. Tan, personal communication). Resolution of the light problem in mines and earthquakes will require spectroscopic analysis. An exoelectron excitation type of illumination is not likely to cause isolated light sources to appear several hundred metres above the Earth's surface, as is reported to occur in some earthquake-prone regions.

Last, our study shows that energy levels of the observed atomic and molecular transitions indicate a minimum of 23 eV is available from the exoelectron excitation mechanism. The molecular dissociation of water by rock fracture producing atomic and molecular hydrogen suggests that fracture might produce interesting chemical effects within a fluid or gas-saturated rock mass. For example, we speculate that exoelectron emission occurring within fracturing coal or potash rock masses may result in dissociation of methane, thereby producing hydrogen gas which could, in suitable conditions, be of importance in igniting a gas outburst. We believe that insufficient consideration has been given to the role of rock fracture in fluid (H_2O) and gas (CH_4, CO_2, H_2S, and so on) saturated rock masses in promoting molecular dissociations by exoelectrons and the role of this process in initiating chemical reactions of geological and biological interest. This problem needs to be thoroughly investigated.

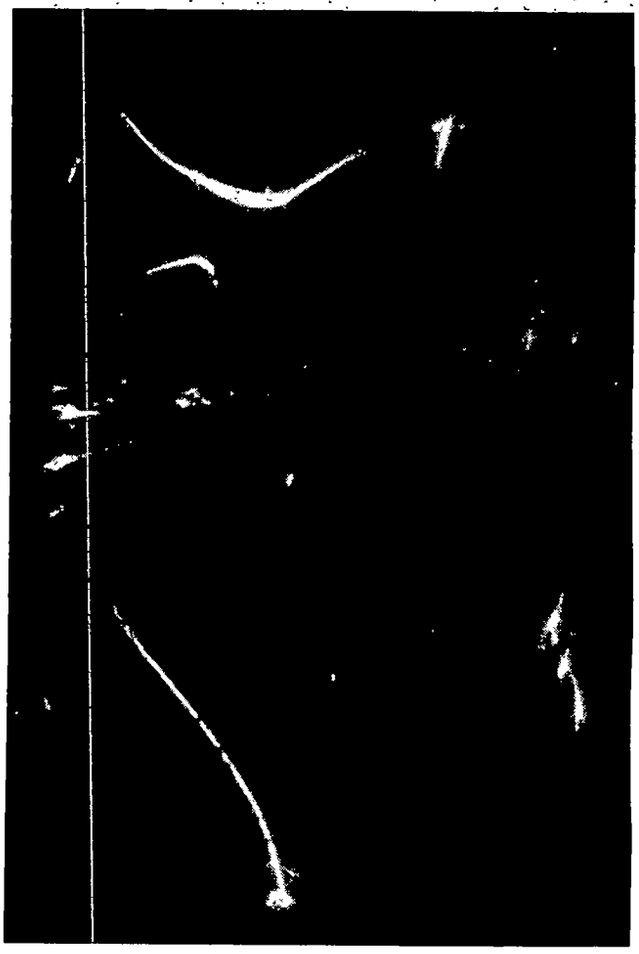


Fig. 6 Light emissions (discrete) from failing Salida Granite in air. Steel platens used in test. Light emissions are produced by oxidation of steel particles abraded from platens by high-velocity ($v \simeq 2 \times 10^3$ cm s^{-1}) rock dust.

We thank Stuart Hoenig, Tom Dickinson, John Derr, Michael Persinger, and Glynn Cress for conversations; Glen and Karen Winters (Winter Productions, Los Angeles, California), for exciting our interest in examining light emissions from fracturing rock and their role in explaining the occurrence of such emissions before earthquake-related phenomena; and last the research staff at the Denver Research Center for aid with the difficult experimental procedures.

Received 11 November 1985; accepted 12 March 1986.

1. Derr, J. *Bull. seis. Soc. Am.* **63**, 2177–2187 (1973).
2. Derr, J. & Persinger, M. A. *Experientia* (in the press).
3. Dmowska, R. *Geophys. Surv.* **3**, 157–174 (1977).
4. Paul, W. *Mining Lore* (Morris Printing Co., Portland, 1970).
5. Hoenig, S. A. & Cole, M. A. preprint, Univ. Arizona (1980).
6. Lockner, D. A., Johnston, M. J. S. & Byerlee, J. D. *Nature* **302**, 28–33 (1983).
7. Powell, J. R. & Finkelstein, D. *Am. Scient.* **58**, 262–280 (1970).
8. Dickinson, J. T., Donaldson, E. E. & Park, M. K. *J. Mater. Sci.* **16**, 2897–2908 (1981).
9. Hoenig, S. A. & Itani, F. S. *4th int. Congr. on Rock Mechanics*, Montreux, Switzerland (1979).
10. Parkhomenko, E. U. *Electrification Phenomena in Rocks* (Plenum, New York, 1971).
11. Cress, G. O., Brady, B. T. & Rowell, G. A. *Geophys. Res. Lett.* (submitted).
12. Wollbrandt, J., Linke, E. & Meyer, K. *Phys. stat. Sol.* **A27**, K53–K55 (1975).
13. Pearse, R. W. B. & Gaydon, A. G. *The Identification of Molecular Spectra* (Wiley, New York, 1941).
14. Weast, R. C. (ed.) *Handbook of Chemistry and Physics*, 53rd edn (Chemical Rubber Co., Cleveland, 1972–73).
15. Hamada, K. & Hagiwara, T. *Bull. Earthq. Res. Inst.* **44**, 1239–1268 (1966).
16. Nakamura, K. & Tsurneish, Y. *Bull. Earthq. Res. Inst.* **44**, 1371–1384 (1966).

Isolation of the *paired* gene of *Drosophila* and its spatial expression during early embryogenesis

François Kilchherr, Stefan Baumgartner, Daniel Bopp, Erich Frei & Markus Noll

Department of Cell Biology, Biocenter of the University of Basel, Klingelbergstrasse 70, CH-4056 Basel, Switzerland

We have cloned the paired *gene of* Drosophila melanogaster, *a pair-rule gene required for the establishment of proper segmentation. The transcriptional pattern in young embryos shows developmental polarities along the antero-posterior and dorso-ventral axes. Transcripts, initially expressed with a double-segment periodicity, switch to a single-segment repeat during syncytial blastoderm.*

SEGMENTATION, an important process of animal development, is the most conspicuous event of compartmentalization. A systematic search for mutations affecting segmentation in the fruitfly *Drosophila* has revealed that it is governed by ~30 genes which can be divided into four classes according to their mutant phenotypes[1,2]. In the first class, the gap mutants, various overlapping non-terminal subregions of the larva are deleted. The second class contains the segment-polarity mutants which exhibit defects that are reiterated in every segment; whereas in the third class, the pair-rule mutants, structures are deleted at a two-segment periodicity (Fig. 1). These three classes of mutants suggest that segmentation involves three different units of spatial organization: one of a single-segment periodicity; one of a two-segment periodicity and a third comprising groups of adjacent segments and exhibiting no obvious periodicity. Mutants of the fourth class, the coordinate mutants, are all maternal and show global effects on the segmentation pattern. Their phenotypes have been explained by a defect in the expression of maternal components that regulate the genes of the three other classes[1,2].

In *Drosophila*, segmentation becomes visible as early as 1 h after the onset of gastrulation[1]. Even earlier, however, during cellular blastoderm, cell lineage may already become restricted to segments[3-7]. At the molecular level, this is probably reflected by the spatially restricted expression of the pair-rule gene *fushi tarazu* (*ftz*) at cellular blastoderm, which shows a repetitive pattern of seven evenly spaced bands[8] that correspond to the primordia of the regions deleted at a two-segment periodicity in homozygous *ftz* mutants[1,2]. More recently, another pair-rule gene, *hairy*(*h*), has been cloned[9,10]. Its expression, as analysed by *in situ* hybridization to blastoderm sections, exhibits a pattern of the same periodicity as *ftz* but is shifted anteriorly with respect to *ftz*, by slightly more than one segment primordium[10]. In addition, *h* transcripts are found in a band of the anterior dorsal blastoderm, extending from 85 to 95% of the egg length (EL)[10].

Here we report the isolation of the pair-rule gene *paired* (*prd*) whose mutant phenotype is shown in Fig. 1. Transcripts of *prd* exhibit a pattern of seven evenly spaced bands during late syncytial blastoderm, reflecting a double-segment periodicity similar to the previously analysed pair-rule genes *ftz* and *h*. However, in contrast to the patterns of *ftz* and *h*, this pattern of *prd* transcripts is expressed only transiently and changes during cellularization of the blastoderm to a pattern with a single-segment repeat length of 14 regularly spaced bands. In addition, *prd* transcripts are detected in a dorsal band close to the anterior pole at a position similar to that seen for *h* transcripts[10] and corresponding to 87 to 93% of EL.

Chromosomal walk from *esc* to *prd*

Recently, we cloned and identified the *extra sex combs* (*esc*) gene from DNA sequences at the cytogenetic locus 33B1,2 on the left arm of chromosome 2 (refs 11, 12). The initial clones, obtained by microdissection of salivary gland chromosomes[13], were spread over a region of 500 kilobase pairs (kb) comprising the entire deletion *Df(2L)esc*[10]. The most proximal clones, 1b.1 and 1b.8, were located just to the right of the deficiency *esc*[10] and at the left end of a deficiency of *paired*, *Df(2L)prd*[1 7 20] (ref. 1). The *prd* gene has been mapped previously by the deficiency

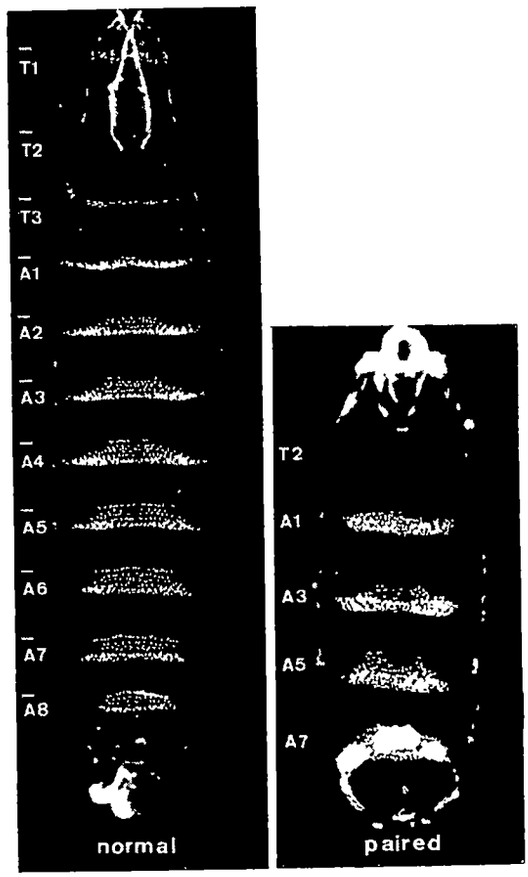


Fig. 1 Ventral cuticular pattern of a wild-type and a homozygous *prd*⁻ *Drosophila* larva. In the wild type the three thoracic (T) and eight abdominal (A) segments are indicated. In *prd*⁻, a pair-rule mutant, analogous portions of segments are deleted at a two-segment periodicity, giving rise to only half the normal number of segments[1]. Because the missing portions include every other segment boundary, the segments are of a composite nature[1]. For example, in the A1/A2 segment the anterior part is derived from A1, the posterior part from A2. Accordingly, the designation of segments in the *prd* mutant refers to the character of the anterior parts of the composite segments[2]. Courtesy of C. Nüsslein-Volhard (from ref. 1).

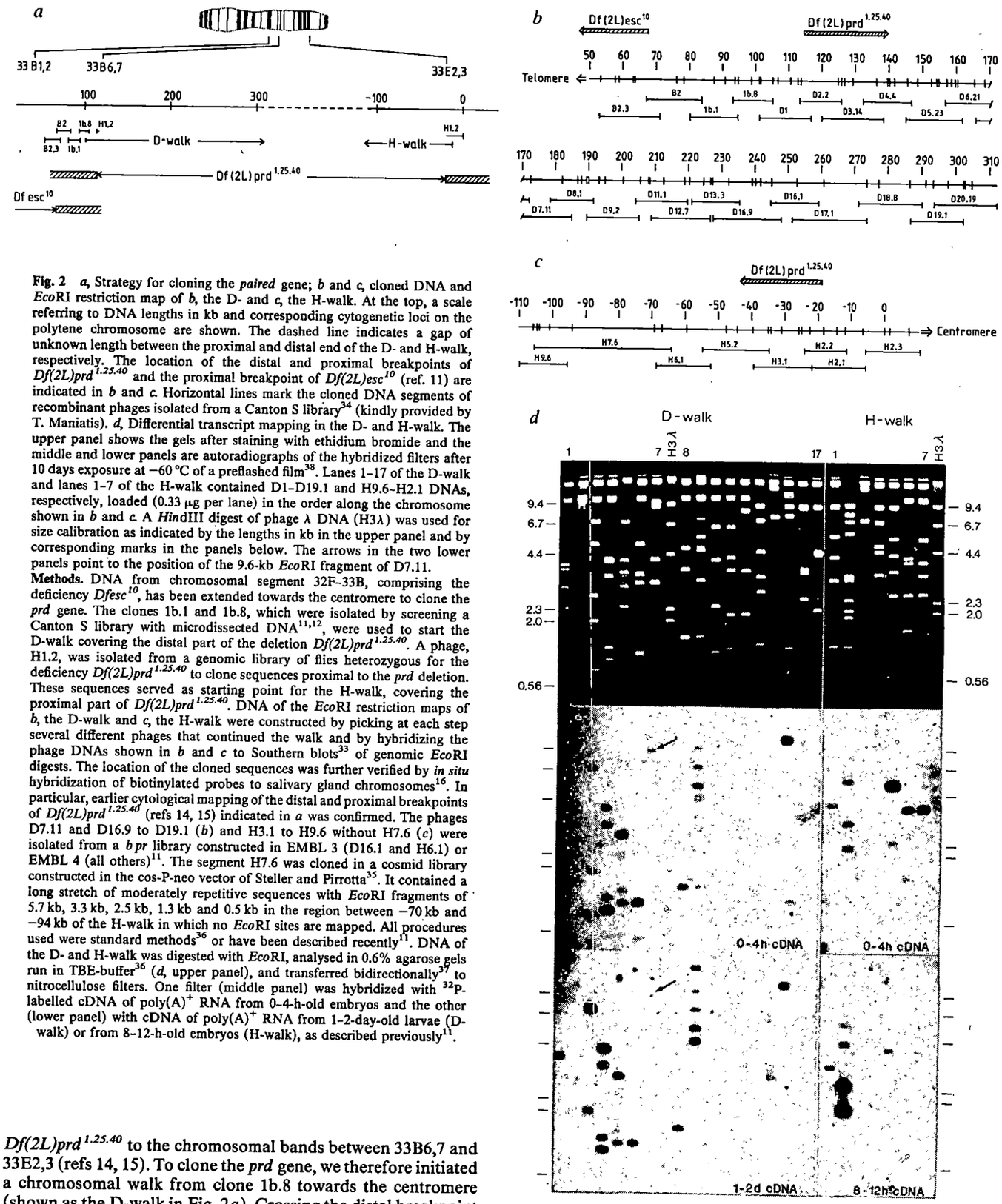


Fig. 2 *a*, Strategy for cloning the *paired* gene; *b* and *c*, cloned DNA and *Eco*RI restriction map of *b*, the D- and *c*, the H-walk. At the top, a scale referring to DNA lengths in kb and corresponding cytogenetic loci on the polytene chromosome are shown. The dashed line indicates a gap of unknown length between the proximal and distal end of the D- and H-walk, respectively. The location of the distal and proximal breakpoints of *Df(2L)prd*$^{1.25.40}$ and the proximal breakpoint of *Df(2L)esc*^{10} (ref. 11) are indicated in *b* and *c*. Horizontal lines mark the cloned DNA segments of recombinant phages isolated from a Canton S library[34] (kindly provided by T. Maniatis). *d*, Differential transcript mapping in the D- and H-walk. The upper panel shows the gels after staining with ethidium bromide and the middle and lower panels are autoradiographs of the hybridized filters after 10 days exposure at −60 °C of a preflashed film[38]. Lanes 1–17 of the D-walk and lanes 1–7 of the H-walk contained D1–D19.1 and H9.6–H2.1 DNAs, respectively, loaded (0.33 μg per lane) in the order along the chromosome shown in *b* and *c*. A *Hin*dIII digest of phage λ DNA (H3λ) was used for size calibration as indicated by the lengths in kb in the upper panel and by corresponding marks in the panels below. The arrows in the two lower panels point to the position of the 9.6-kb *Eco*RI fragment of D7.11.

Methods. DNA from chromosomal segment 32F–33B, comprising the deficiency *Dfesc*^{10}, has been extended towards the centromere to clone the *prd* gene. The clones 1b.1 and 1b.8, which were isolated by screening a Canton S library with microdissected DNA[11,12], were used to start the D-walk covering the distal part of the deletion *Df(2L)prd*$^{1.25.40}$. A phage, H1.2, was isolated from a genomic library of flies heterozygous for the deficiency *Df(2L)prd*$^{1.25.40}$ to clone sequences proximal to the *prd* deletion. These sequences served as starting point for the H-walk, covering the proximal part of *Df(2L)prd*$^{1.25.40}$. DNA of the *Eco*RI restriction maps of *b*, the D-walk and *c*, the H-walk were constructed by picking at each step several different phages that continued the walk and by hybridizing the phage DNAs shown in *b* and *c* to Southern blots[33] of genomic *Eco*RI digests. The location of the cloned sequences was further verified by *in situ* hybridization of biotinylated probes to salivary gland chromosomes[16]. In particular, earlier cytological mapping of the distal and proximal breakpoints of *Df(2L)prd*$^{1.25.40}$ (refs 14, 15) indicated in *a* was confirmed. The phages D7.11 and D16.9 to D19.1 (*b*) and H3.1 to H9.6 without H7.6 (*c*) were isolated from a *b pr* library constructed in EMBL 3 (D16.1 and H6.1) or EMBL 4 (all others)[11]. The segment H7.6 was cloned in a cosmid library constructed in the cos-P-neo vector of Steller and Pirrotta[35]. It contained a long stretch of moderately repetitive sequences with *Eco*RI fragments of 5.7 kb, 3.3 kb, 2.5 kb, 1.3 kb and 0.5 kb in the region between −70 kb and −94 kb of the H-walk in which no *Eco*RI sites are mapped. All procedures used were standard methods[36] or have been described recently[11]. DNA of the D- and H-walk was digested with *Eco*RI, analysed in 0.6% agarose gels run in TBE-buffer[36] (*d*, upper panel), and transferred bidirectionally[37] to nitrocellulose filters. One filter (middle panel) was hybridized with ^{32}P-labelled cDNA of poly(A)$^+$ RNA from 0–4-h-old embryos and the other (lower panel) with cDNA of poly(A)$^+$ RNA from 1–2-day-old larvae (D-walk) or from 8–12-h-old embryos (H-walk), as described previously[11].

Df(2L)prd$^{1.25.40}$ to the chromosomal bands between 33B6,7 and 33E2,3 (refs 14, 15). To clone the *prd* gene, we therefore initiated a chromosomal walk from clone 1b.8 towards the centromere (shown as the D-walk in Fig. 2*a*). Crossing the distal breakpoint of the *Df(2L)prd*$^{1.25.40}$ deletion allowed us to clone the DNA fragment H1.2, containing sequences from both sides of the deletion (Fig. 2*a*), by screening a genomic library constructed from flies heterozygous for the deficiency *Df(2L)prd*$^{1.25.40}$. From proximal sequences of the clone H1.2, a second walk was then started into the *Df(2L)prd*$^{1.25.40}$ deletion (shown as the H-walk in Fig. 2*a*). The D- and H-walks are shown in Fig. 2*b*, *c*. Together they cover ~300 kb of the *Df(2L)prd*$^{1.25.40}$ deletion.

Screening for the *prd* gene

Although the converging sequences of the D- and H-walk had not joined, a screen for possible candidates of the *prd* gene by differential transcript mapping was carried out, similar to the screen that proved successful when the *esc* gene was identified[11,12]. Radioactively labelled complementary DNAs of poly(A)$^+$ RNA isolated from egg follicles, 0–4- and 8–12-h-old

embryos and 1-2-day-old larvae were hybridized to Southern blots of *Eco*RI digests of the D- and H-walk (Fig. 2*d*). We screened for DNA fragments that were labelled with cDNA from 0-4-h-old embryos (middle panel of Fig. 2*d*) but remained unlabelled when hybridized to cDNA from later stages of development (lower panel of Fig. 2*d*) or egg follicles (not shown). This expectation was based (1) on experiments with a temperature-sensitive *prd* allele showing zygotic expression during the blastoderm stage[1] and (2) on the absence of a maternal effect of the *prd* gene[15]. In the D-walk, only one such fragment was found, a 9.6-kb *Eco*RI fragment of phage D7.11 (arrows in Fig. 2*d*). In the H-walk, two regions at the proximal end, the 3.9-kb *Eco*RI fragment of H2.2 and the 2.6-kb *Eco*RI fragment of H3.1 (which comprises the 1.6-kb left terminal fragment of H2.2) were transcribed in 0-4-h-old embryos but not in 8-12-h-old embryos (Fig. 2*d*). However, these fragments of the H-walk are unlikely to harbour the *prd* gene because they are also heavily labelled by cDNA of poly(A)$^+$ RNA from follicles (data not shown). Therefore, if the *prd* gene was located within the 300 kb of the *Df(2L)prd*$^{1.25.40}$ that had already been cloned, the most likely location was the 9.6-kb *Eco*RI fragment of D7.11, at about 170-180 kb in the D-walk or 240 kb to the right of the *esc* gene[11,12].

Mapping the mutant *prd*$^{2.45.17}$

To test whether the *prd* gene was contained within the cloned 300 kb, and specifically within the 9.6-kb *Eco*RI fragment of D7.11, the D- and H-walk DNA of an X-ray-induced *prd* mutant, *prd*$^{2.45.17}$, was compared with that of its parent strain by whole genome Southern analysis of *Eco*RI digests. No differences were detected except for a 1.1-kb insertion into the 9.6-kb *Eco*RI fragment of D7.11 in the *prd*$^{2.45.17}$ mutant (data not shown). The mutated DNA was isolated from a λ phage library of the heterozygous *prd*$^{2.45.17}$ mutant, and the 4.0-kb *Bam*HI fragment containing the 1.1-kb insert was subcloned. We compared its restriction map with that of the corresponding 2.9-kb BamHI fragment of the *prd*$^+$ DNA to locate the insertion more precisely. As shown in Fig. 3, in *prd*$^{2.45.17}$ a 1.1-kb DNA sequence has been inserted into a 0.41-kb *Sma*I fragment of the *prd* DNA. When a biotinylated probe consisting of the 1.5-kb *Sma*I fragment from *prd*$^{2.45.17}$ (Fig. 3) was hybridized to salivary gland chromosomes[16] of an Oregon R strain, it labelled more than 100 bands scattered over all chromosome arms (not shown).

Developmental profile of the *prd*$^+$ transcript

Although both differential transcript mapping as well as whole genome Southern analysis suggested that the *prd* gene was located in D7.11, the possibility remained that a gene with a developmental profile similar to that of *prd* was present in D7.11 and that the 1.1-kb insert was fortuitous and did not result in an altered gene expression at its location. This objection was excluded by Northern analysis of the *prd*$^{2.45.17}$ mutant in this region. As shown in Fig. 4, two poly(A)$^+$ RNAs of 2.5 and 3.6 kb were detected in embryos of heterozygous *prd*$^{2.45.17}$ parents whereas only a single RNA species of 2.5 kb was found in *prd*$^+$ embryos. Hence, the insert in the mutant DNA is located within a transcript that exhibits the developmental profile expected for the *prd* gene. The *prd* mRNA, while absent in oocytes, accumulates to a sharp peak in 2-4-h-old embryos (blastoderm and early gastrula), followed by a precipitous decline (Fig. 4). Essentially no 2.5-kb transcripts were detectable after 12 h of embryonic development (stages after 18 h are not shown) which is consistent with the results obtained with a temperature-sensitive allele of the *prd* gene[1].

Spatial transcription pattern

Genetic analysis[1] and the developmental profile shown in Fig. 4 suggest that the main period of *prd*$^+$ activity occurs around cellular blastoderm. In addition, inspection of the cuticular pattern of homozygous *prd*$^-$ larvae (Fig. 1) reveals that the

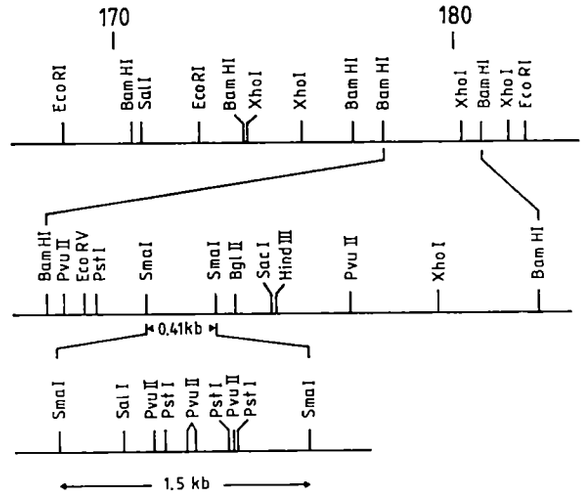


Fig. 3 Restriction map of DNA containing the *paired* gene and of *prd*$^{2.45.17}$ mutant DNA. A restriction map of the *paired* region, obtained from D7.11, is shown at the top. Below, the 2.9-kb *Bam*HI fragment, subcloned from D7.11, has been mapped in more detail. At the bottom a restriction map of the *prd*$^{2.45.17}$ mutant DNA, containing the 1.1-kb insertion of a repetitive element, is illustrated. This region was mapped by isolating the mutated DNA from a *prd*$^{2.45.17}$/*prd*$^+$ library according to standard methods[36] and mapping a subclone of the corresponding 4.0-kb *Bam*HI fragment containing the inserted DNA.

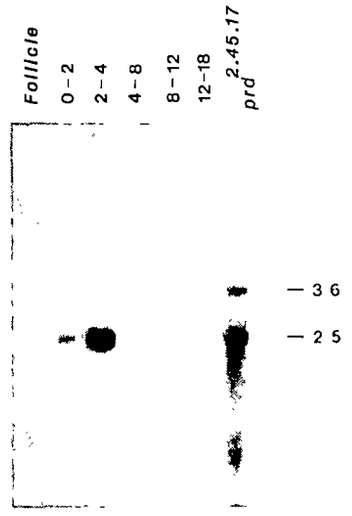


Fig. 4 Northern analysis of the *prd*$^+$ and *prd*$^{2\,45\,17}$ transcripts. For size calibration, end-labelled fragments of a partial *Rsa*I digest of pBR322 (4.36 kb, 3.68 kb, 2.80 kb, 2.25 kb, 2.12 kb, 1.57 kb and 0.68 kb) were used (data not shown).

Methods. Poly(A)$^+$ RNA (2 μg each), isolated from wild-type egg follicles and 0-2-h, 2-4-h, 4-8-h, 8-12-h and 12-18-h-old embryos and from 0-4-h-old embryos of heterozygous *prd*$^{2.45.17}$/*prd*$^+$ parents, as previously described[11], were run in a 1.1% agarose gel containing formaldehyde[39]. The RNA was transferred in 20× SSC to a nitrocellulose filter according to Southern[33] and hybridized with a cDNA fragment, c73.2, nick-translated[40] with [α-^{32}P]dATP (3,000 Ci mmol^{-1}) and consisting of 400 base pairs (bp) at the 3′ end of the *prd*$^+$ transcript located to the immediate left of the 0.9-kb *Bam*HI fragment (Fig. 3). The same 2.5-kb RNA was observed after hybridization with the genomic 0.9-kb *Bam*HI fragment and with the genomic fragments to its left (*Xho*I-*Bam*HI) and right (*Pvu*II-*Pvu*II), whereas no RNA was detected in a region of at least 2 kb to the right of the *Xho*I site at 180 kb (Fig. 3). A 2.3-kb cDNA clone, c7340.6, isolated from a cDNA library constructed from poly(A)$^+$ RNA of 0-4-h-old embryos, spanned the same region, labelling only DNA within the 4.7-kb *Xho*I fragment between 175 and 180 kb on the genomic map (Fig. 3).

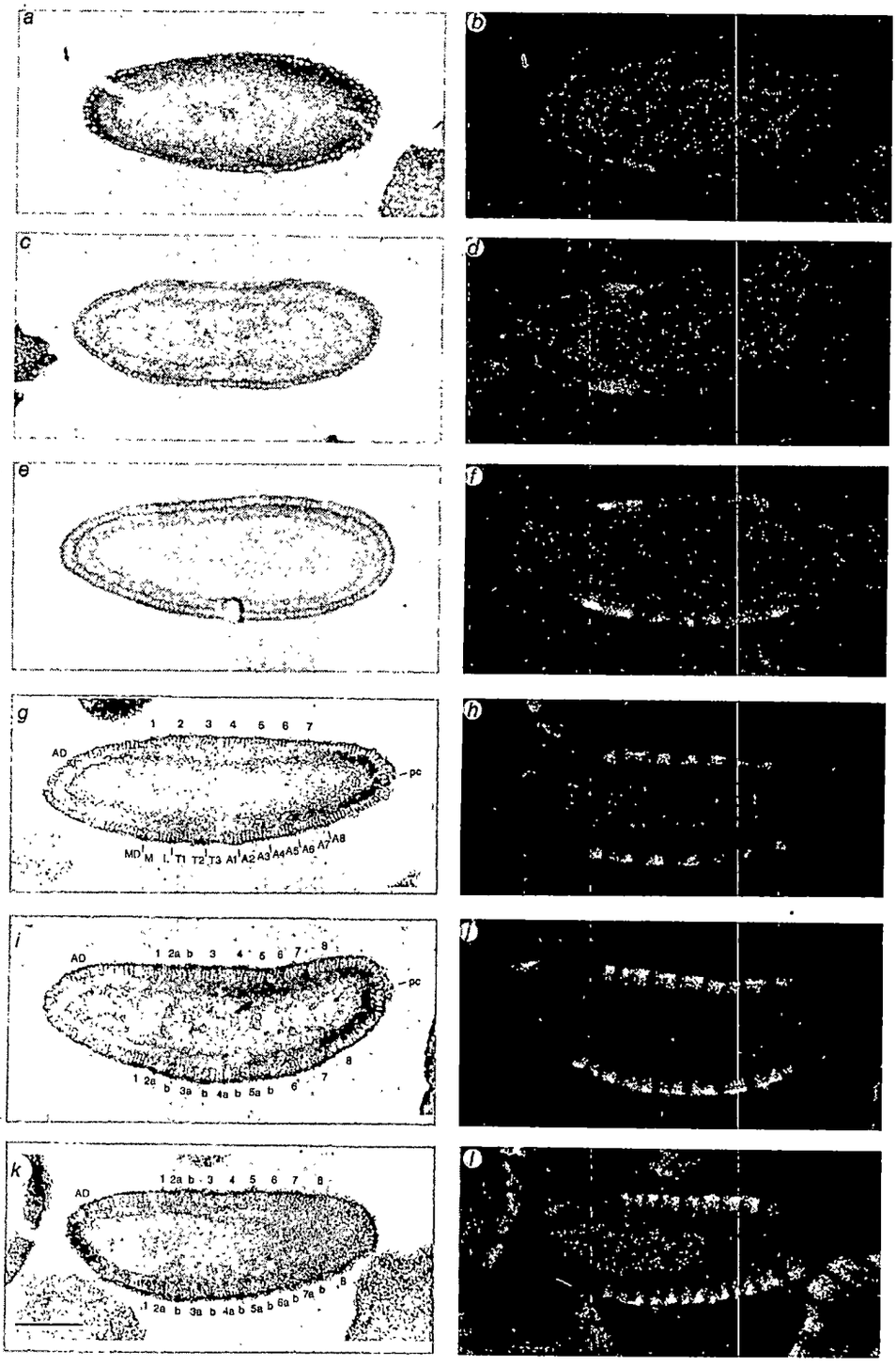


Fig. 5 Localization of *prd* transcripts in tissue sections of embryos at syncytial and cellular blastoderm. The panels show photomicrographs of the same embryos taken under phase contrast (left) or dark-field illumination (right). Sagittal or parasagittal sections through embryos during the 12th (*a*,*b*), 13th (*c*,*d*) and 14th nuclear cycle (*e*–*j*) of syncytial blastoderm, or at cellular blastoderm (*k*, *l*), are shown. Tissue sections are oriented with their dorsal side up and their anterior end to the left. The orientation was determined by morphological markers such as pole cells (pc) visible in other sections exhibiting very similar labelling. The presumptive locations of thoracic (T1–T3), abdominal (A1–A11), as well as labial (L), maxillary (M), and mandibular (MD) head segment primordia are indicated. The bands are labelled AD (anterior dorsal), 1–7 at early, and 1a–7b and 8 at late cellular blastoderm. The horizontal bar in *k* indicates a length of 0.1 mm. **Methods.** Tissue sections through young embryos were prepared, hybridized *in situ* with ^{3}H-labelled 2.2-kb *prd* cDNA, c7340.1 and exposed according to Hafen *et al.*[41]. Autoradiographic exposure was for 29 days except in *f*, which shows a 20-day exposure.

equivalent of one segment is missing for every two segments[1,2]. From previous studies on the pair-rule genes *ftz* (ref. 8) and *h* (ref. 10), in which the structures deleted in the mutants correspond approximately to the wild-type primordia in which the genes are transcribed, we would expect *in situ* hybridizations of embryonic tissue sections with ^{3}H-labelled *prd*-cDNA to show a double-segment periodicity expressed at cellular blastoderm. Surprisingly, we do not observe such a strict correlation between the mutant phenotype of *prd* and the spatial distribution of its transcripts in the wild-type embryo (Fig. 5).

Localized *prd* transcripts are first observed during syncytial blastoderm (nuclear cycle 12; ref. 17) in a band 6 nuclei wide which is stronger on the ventral than on the dorsal side and located at a distance of approximately 13 nuclei from the anterior end; that is, between 63 and 77% of EL (Fig. 5*a*, *b*). During the following nuclear cycle, the band widens to ~12–16 nuclei on the ventral and 8–10 nuclei on the dorsal side (Fig. 5*c*, *d*). It is separated by ~16–20 nuclei from the anterior pole and thus extends between 60 and 75% of EL, corresponding to the location of the primordial head segments[6,18]. The nuclei in the anterior portion of the band are labelled more strongly than those in the posterior half. The transcripts clearly accumulate in the cortical part of the cytoplasm surrounding the nuclei, as has been observed previously for transcripts of *ftz* (ref. 8) and *h* (ref. 10). During the fourteenth nuclear cycle, at late syncytial blastoderm when nuclei begin to elongate, five additional bands

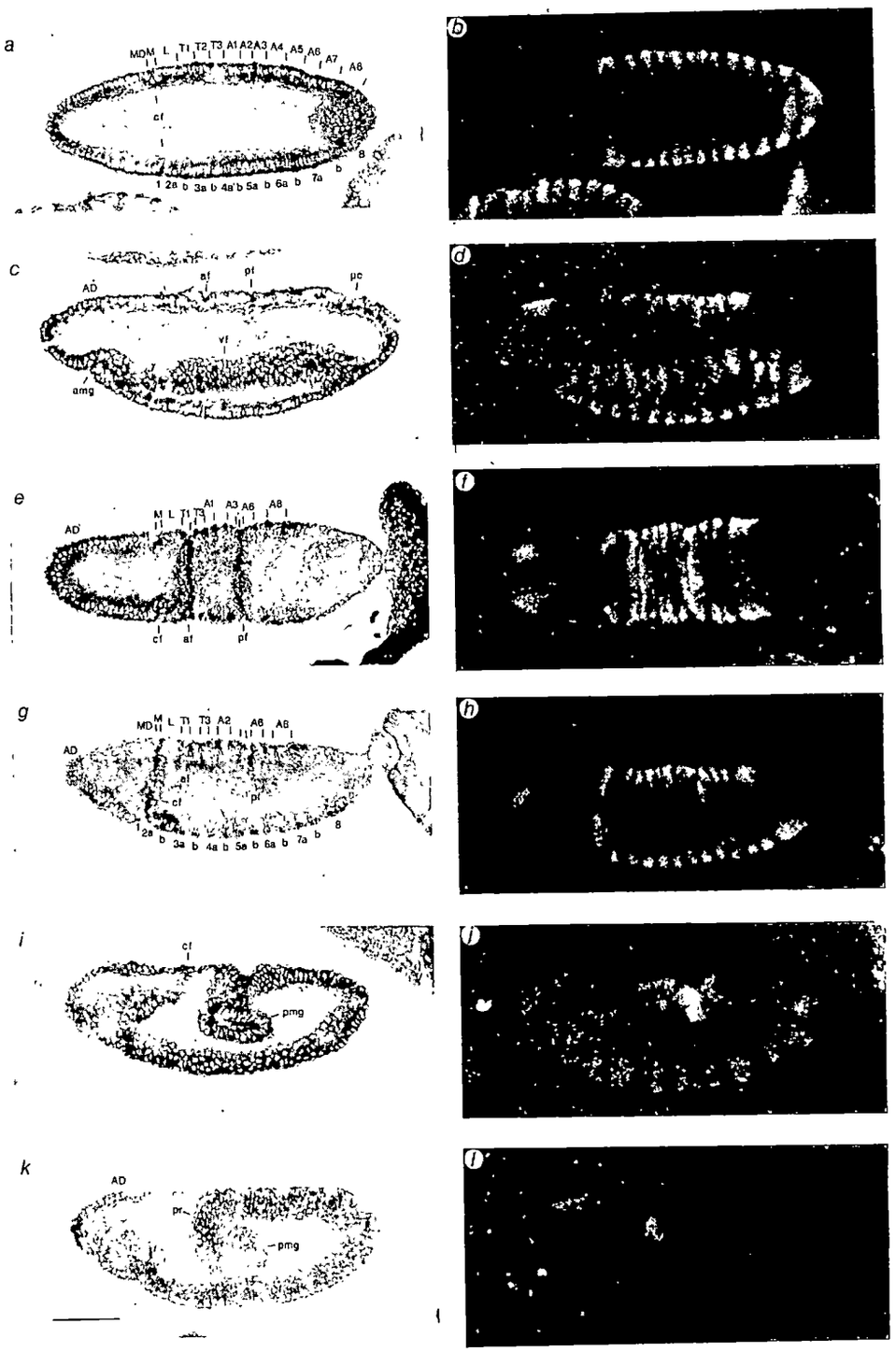


Fig. 6 Localization of *prd* transcripts in gastrulating embryos. Photomicrographs of embryonic tissue sections, prepared and treated as in Fig. 5, were taken under phase contrast (left) or dark-field illumination (right). The following developmental stages are shown: *a, b*, formation of the cephalic furrow; *c, d*, formation of the ventral furrow; *e–h*, beginning of germ-band extension at 3.5–4 h; *i, j*, germ-band extension at 4–4.5 h; *k, l*, end of germ-band extension at ~5 h development at 25 °C. The sections chosen were *a, b*, midventral and *e, f*, superficial dorsal horizontal sections; *c, d, g–l*, median or lateral sagittal sections. The anterior end is oriented to the left and, in sagittal sections, the dorsal side up. Autoradiographic exposure was for 20 days (*a–d, i–l*) or 29 days (*e–h*). The probes used for hybridization in Figs 5 and 6 comprise two short regions of the *prd* gene that are homologous with sequences elsewhere in the genome (G. Frigerio and M.N., unpublished results). However, the same patterns of hybridization are observed when a probe is used from which these *prd*-cDNA sequences have been deleted. Bands and primordial segments are labelled as in Fig. 5. The horizontal bar in *k* indicates a length of 0.1 mm. Abbreviations: af, anterior transverse fold; amg, anterior midgut; cf, cephalic furrow; pc, pole cells; pf, posterior transverse fold; pmg, posterior midgut invagination; pr, proctodeum.

of transcripts appear at approximately equal intervals. These bands are located posterior to the first band and extend to ~20% of EL, that is, to the eighth abdominal segment primordium[6,18]. At the same time, the early anterior band splits into two bands equal in width to the five posterior bands (Fig. 5*e, f*). At this stage, therefore, *prd* transcripts occur in seven bands located between 20 and 75% of EL. The spacing of the bands is regular but closer on the dorsal than on the ventral side, and the signal intensity of the newly formed five posterior bands is again weaker dorsally than ventrally, indicating a dorso-ventral polarity of pattern development (Fig. 5*e, f*). These seven bands increase in intensity as the nuclei elongate and plasma membranes grow inwards (Fig. 5*g, h*). While the width of the posterior six bands remains unchanged at 5–7 cells, the most anterior band is reduced in width to about four cells. This results from an elimination of transcripts in the cells of the anterior portion of the first band. In each of these six posterior bands, however, the labelling intensity is skewed in such a way that cells of the anterior half exhibit less *prd* transcripts than cells of the posterior half. The cells transcribing the *prd* gene are separated by gaps of ~2–3 cells in which no *prd* transcripts are detectable. At the same time transcripts begin to accumulate in cells located close to the anterior pole of the embryo, forming a band six cells wide (Fig. 5*g, h*) which extends between 87 and 93% of EL (Fig. 5*i, j*). In contrast to the other bands, this new band covers only the dorsal half of the embryo (Fig. 5*g–j*).

At a slightly later time, shortly before the completion of cellular blastoderm, two conspicuous events take place (Fig. 5*i, j*). First, an additional band (8) appears posterior to band 7, extending the banding pattern to ~13% of EL. Second, bands 2 to 7 begin to split into an anterior and a posterior band, a process that moves from the anterior to the posterior pole. At the stage shown in Fig. 5*i, j*, the splitting of band 2 is nearly complete whereas that of bands 6 and 7 is barely visible. This band splitting is accomplished by elimination of the transcripts in the two middle cells of each band. As a result of this process, band 2 is split into an anterior band 2a and a posterior band 2b, band 3 into 3a and 3b, and so forth. By the time of cellular blastoderm, the splitting of bands 2–7 is complete, and the width of band 1 has been further reduced from 4 to its two most posterior cells (Fig. 5*k, l*). Thus, when cellularization of the blastoderm is nearly complete, 13 bands have arisen that are about two cells wide and are separated by gaps of about two cells on the ventro-lateral side. Dorsally, splitting of the bands occurs later and is complete only in band 2 at the stage illustrated in Fig. 5*k, l*. In addition, the intensity appears to be skewed in that more transcripts accumulate in the posterior than in the anterior band. The most posterior band (8) remains unsplit and is about five cells wide. Thus, both the formation of the transcript pattern exhibiting a double-segment periodicity and its transition to one with a single-segment repeat are oriented in an anterior–posterior as well as in a ventral–dorsal direction.

Transcript distribution and morphology

To assess the morphological significance of these transcription patterns, we have attempted to relate the spatial distribution of the label to morphological features that are well known from microscope studies[19–21]. This required an extension in time to gastrulation when such features are beginning to appear. Initially, gastrulation is marked by the formation of the ventral and cephalic furrows. As evident from Fig. 6*a, b*, the first two bands (1 and 2a) migrate into the anterior and posterior part of the cephalic furrow. In a similar manner, as the ventral furrow forms, giving rise to the mesodermal germ band, cells transcribing *prd* migrate into it. This is evident from the persistence of the banding pattern in register across the ventral furrow (Fig. 6*c, d*). Similarly, at a slightly later stage when the dorsal transverse folds appear, cells of bands coinciding with the locations of these folds move into them (Fig. 6*e–h*). At this stage, the dorsal portions of the bands have also completed their splitting (Fig. 6*e–h*). From the end of cellular blastoderm to this stage no dramatic change in band intensities is observed. However, during the next stage of germ-band extension, all bands fade with the exception of the anterior dorsal band (Fig. 6*k, l*) and the unsplit band 8, located at the proctodeal invagination (Fig. 6*i, j*). The intensity with which these two bands persist is remarkable. Only after germ-band retraction, shortly before the beginning of head involution, have these bands disappeared (data not shown).

ftz transcripts and segment primordia

Previous determinations of the positions of the *ftz* bands in the blastoderm embryo[8,22] allow us to identify the blastoderm primordia expressing the *prd* gene. When hybridizing three consecutive sections with probes for either *prd* or *ftz*, or with both probes, we found that the pattern of *prd* transcripts is shifted to the anterior of the *ftz* bands. Whereas band 1 of *prd* does not overlap with *ftz* signals, the anterior borders of bands 2–7 (2a–7a) and band 8 of *prd* coincide with the anterior borders of bands 1–7 of *ftz* (Fig. 7). As the *ftz* bands are only about four cells wide and are spaced by gaps of about four cells[8,10,22,23], cells between the seven *prd* bands at late syncytial blastoderm (Fig. 5*g* and *h*) also remain unlabelled by *ftz* (data not shown). At the later stage of cellular blastoderm, when the repetitive pattern of *prd* transcripts consists of 14 bands (Figs 5*k, l*; 7*a*),

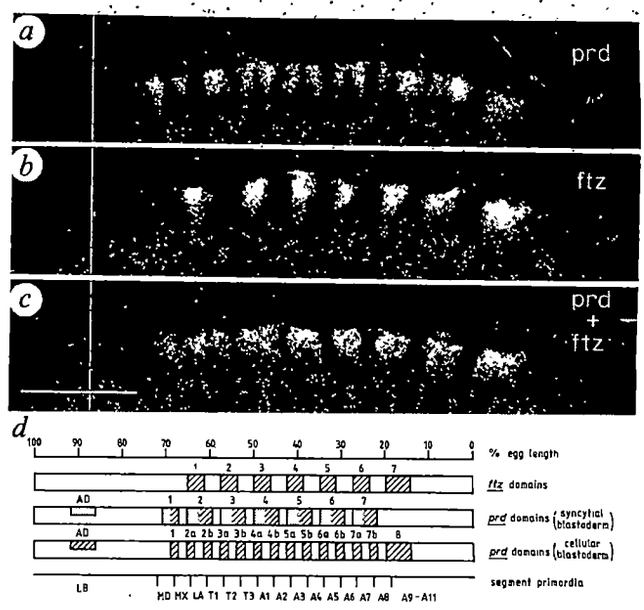


Fig. 7 Localization of *prd* relative to *ftz* transcripts. Three consecutive ventral horizontal sections through an embryo at cellular blastoderm were hybridized with *a*, ^{3}H-labelled c7340.1 *prd* cDNA; *b*, p523B *ftz* DNA[8,42,43]; *c*, the two probes combined and exposed for 29 days according to Hafen *et al.*[41]. Only one lateral side of the embryo is shown under dark-field illumination. The anterior end is oriented to the left. In *d*, the domains of *ftz* and *prd* expression are illustrated schematically relative to each other and the segment primordia. Stippled and hatched areas indicate blastoderm regions showing low and high numbers of transcripts, respectively. The *ftz* domains represented are those seen at syncytial blastoderm when they are about four nuclei wide and regularly spaced by gaps of about four nuclei[8,22]. By the time of cellular blastoderm (*b*), *ftz* domains have been reduced in width to about three cells[22]. The most posterior *ftz* domain is broader and about six cells wide, as previously noted[10]. The horizontal bar in *c* indicates a length of 0.1 mm.

the cells of every second gap still express *ftz* (Fig. 7*b*). Thus, in the combined pattern of *prd* and *ftz* transcripts, we still observe a narrow anterior band two cells wide, consisting only of *prd* transcripts, and seven wide posterior bands, about six cells wide, separated by gaps of about two cells (Fig. 7*c*). Because the third *ftz* band covers the posterior compartment of the metathoracic and the anterior compartment of the first abdominal segment primordium[8,22,24], we conclude that band 4a of *prd* transcripts spans the T3/A1 segment boundary, as indicated in Figs 6*a, b* and 7*d*. If we assume that the four-cell repeat length of the *prd* banding pattern observed at this stage corresponds to the length of one segment primordium, we find that the most anterior *prd* band (1) crosses the boundary between the mandibular and maxillary segment primordia and that band 7b crosses the boundary between the seventh and eighth abdominal primordial segments (Figs 6*a, b*; 7*d*). Accordingly, the most posterior band (8) would cover the posterior compartment of A8 and probably the segment primordia of A9–A11 (Figs 6*a, b*; 7*d*). Our interpretation of the positions of the *prd* bands relative to those of *ftz* is confirmed by their relative positions with respect to the cephalic furrow. Whereas the most anterior band of *ftz* labels the posterior portion of the cephalic furrow[8], bands 1 and 2a of *prd* are situated at its anterior and posterior edge (Fig. 6*a, b, e–h*).

Knowing how the banding pattern of *prd* RNA at early gastrula (Fig. 6*a, b*) develops from that at late syncytial blastoderm (Fig. 5*g, h*), we may trace back the location of *prd* transcripts with respect to the primordial segments at blas-

toderm. Thus, we find that the more strongly labelled posterior portions of bands 1–7 cross the boundaries between mandibular and maxillary, labial and first thoracic, second and third thoracic segment primordia, and so on, as indicated in Figs 5*g*, *h*, 7*d*. Similarly, we may identify segment primordia and relate them to morphological markers during later developmental stages by following the fate of cells labelled with *prd* transcripts. Accordingly, the prothoracic segment gives rise to the anterior transverse fold while the fourth and fifth abdominal segments coincide with the posterior transverse fold (Fig. 6*e–h*).

Discussion

Our analysis of the spatial distribution of *prd* transcripts during embryogenesis has revealed a more complex pattern than anticipated on the basis of results from previous studies with the pair-rule genes *ftz* (ref. 8) and *h* (ref. 10). Transcripts of *prd* appear first during the twelfth nuclear cycle in the region where the primordial head segments form. During subsequent nuclear divisions of the syncytial blastoderm, a pattern of seven bands builds up posteriorly along the antero-posterior axis and dorsally along the ventral–dorsal axis. At the end of this process, the *prd* pattern is similar to that of *ftz* (ref. 8) or *h* (ref. 10), showing a periodicity corresponding to two primordial segments. However, in contrast to the *ftz* and *h* patterns, the seven *prd* bands are wider and hence each covers more than one segment primordium. Thus, no simple correlation of the location of *prd* transcripts with the *prd* phenotype[1,2] (Fig. 1) exists. To derive such a correlation, as has been possible for *ftz* (ref. 8) and *h* (ref. 10), it might be postulated that only those portions of segments are deleted in the mutant that exhibit strong transcription of the *prd* gene in the corresponding wild-type primordial segments during late syncytial blastoderm. As evident from Fig. 5*g*, *h*, these are the posterior parts of each of the seven *prd* bands, corresponding to the posterior mandibular plus anterior maxillary segment, posterior labial plus anterior first thoracic segment and so on (Fig. 7*d*). That this pattern of transcripts corresponds reasonably well to that of fused and deleted segments in the mutant[1,2] (Fig. 1) may indicate that determination of segments and segment boundaries occurs already at this early stage and hence would not depend entirely on a cell-autonomous expression of *prd*.

The pattern of seven *prd* bands exists only transiently and develops during late syncytial blastoderm into a regular pattern of 13 bands of equal width and spacing. This transition of the pattern exhibiting a two-segment periodicity into one of a single-segment repeat occurs again in an anterior to posterior direction and spreads from the ventral towards the dorsal side. Such polarities of pattern development have been observed also for *engrailed* (*en*) and *ftz* transcripts[23] and may suggest a common control mechanism. It is interesting that the pair-rule gene *prd*, initially transcribed with a two-segment repeat, is later switched to be expressed with a single-segment periodicity. Spatial expression patterns of *en* (refs 23, 25) and *ftz* (ref. 23) are also switched from longer to shorter periodicities. A switch in the pattern of *ftz* expression occurs also at a later developmental stage, as shown by the finding that the *ftz* gene product is detected in neuroblasts and ganglion cells of every segment[26,27]. Such changes in patterns would be expected if regulatory interactions among segmentation genes occur and we anticipate that, as more of these genes are studied, more examples of such temporal changes in pattern will be discovered.

The patterns of *en* (refs 23, 28, 29) and *prd* transcripts are very similar at the end of cellular blastoderm. The two most anterior bands of both *en* (ref. 23) and *prd* label the anterior and posterior portion of the cephalic furrow. The two patterns may even coincide as *en* is probably expressed in posterior compartments of each segment[23,28–31] and our spatial assignments of the *prd* bands are based on those of the *ftz* bands, which may be off by one cell. Thus, although *prd* and *en* are initially under different controls, as apparent from their distribution of transcripts, such a spatial and temporal coincidence of the expression of these two genes during cellular blastoderm might indicate that their control becomes at least partly coordinated at this stage.

Two additional groups of cells begin to express the *prd* gene during late syncytial blastoderm. First, transcripts appear in a dorsal band of cells close to the anterior pole at a location similar to that of *h* expression[10]. As has been argued previously[10], these cells may represent the primordium for the labrum[32]. It remains to be shown, however, whether all of these cells express both *h* and *prd*. Second, a wide posterior band of *prd* transcripts that appears in the posterior region of A8 (and possibly in the primordia for A9, A10 and A11) migrates to the proctodeal invagination during germ-band extension. This band, together with the anterior dorsal band, are the last cells to exhibit *prd* expression during embryogenesis.

We thank Maya Burri for technical assistance, Christiane Nüsslein-Volhard for the *prd* mutant strains and discussions, Michael Levine for the *ftz* clone p523B, Hermann Steller for the cos-P-neo vector and Hans Noll for comments on the manuscript. This work was supported by Swiss NSF grants 3.180-0.82, 3.600-0.84 and 3.600-1.84 and by the Canton of Basel.

Received 1 October 1985; accepted 2 April 1986.

1. Nüsslein-Volhard, C. & Wieschaus, E. *Nature* **287**, 795–801 (1980).
2. Nüsslein-Volhard, C., Wieschaus, E. & Jürgens, G. *Verh. dt. zool. Ges.*, 91–104 (1982).
3. *Wieschaus, E. & Gehring, W. Devl Biol.* **50**, 249–263 (1976).
4. Steiner, E. *Wilhelm Roux Arch. dev. Biol.* **180**, 31–46 (1976).
5. Lawrence, P. A. & Morata, G. *Devl Biol.* **56**, 40–51 (1977).
6. Lohs-Schardin, M., Cremer, C. & Nüsslein-Volhard, C. *Devl Biol.* **73**, 239–255 (1979).
7. Szabad, J., Schüpbach, T. & Wieschaus, E. *Devl Biol.* **73**, 256–271 (1979).
8. Hafen, E., Kuroiwa, A. & Gehring, W. J. *Cell* **37**, 833–841 (1984).
9. Holmgren, R. *EMBO J.* **3**, 569–573 (1984).
10. Ingham, P. W., Howard, K. R. & Ish-Horowicz, D. *Nature* **318**, 439–445 (1985).
11. Frei, E., Baumgartner, S., Edström, J.-E. & Noll, M. *EMBO J.* **4**, 979–987 (1985).
12. Frei, E. *et al. Cold Spring Harb. Symp. quant. Biol.* **50**, 127–134 (1986).
13. Scalenghe, F., Turco, E., Edström, J.-E., Pirrotta, V. & Melli, M. *Chromosoma* **82**, 205–216 (1981).
14. Nüsslein-Volhard, C., Wieschaus, E. & Kluding, H. *Wilhelm Roux Arch. dev. Biol.* **193**, 267–282 (1984).
15. Nüsslein-Volhard, C., Kluding, H. & Jürgens, G. *Cold Spring Harb. Symp. quant. Biol.* **50**, 145–154 (1986).
16. Langer-Safer, P. R., Levine, M. & Ward, D. C. *Proc. natn. Acad. Sci. U.S.A.* **79**, 4381–4385 (1982).
17. Foe, V. E. & Alberts, B. M. *J. Cell Sci.* **61**, 31–70 (1983).
18. Underwood, E. M., Turner, F. R. & Mahowald, A. P. *Devl Biol.* **74**, 286–301 (1980).
19. Sonnenblick, B. P. in *Biology of* Drosophila (ed. Demerec, M.) 62–167 (Wiley, New York, 1950).
20. Poulsen, D. F. in *Biology of* Drosophila (ed. Demerec, M.) 168–274 (Wiley, New York, 1950).
21. Turner, F. R. & Mahowald, A. P. *Devl Biol.* **57**, 403–416 (1977).
22. Martinez-Arias, A. & Lawrence, P. A. *Nature* **313**, 639–642 (1985).
23. Weir, M. P. & Kornberg, T. *Nature* **318**, 433–439 (1985).
24. Akam, M. E. & Martinez-Arias, A. *EMBO J.* **4**, 1689–1700 (1985).
25. DiNardo, S., Kuner, J. M., Theis, J. & O'Farrell, P. H. *Cell* **43**, 59–69 (1985).
26. Carroll, S. B. & Scott, M. P. *Cell* **43**, 47–57 (1985).
27. Hiromi, Y., Kuroiwa, A. & Gehring, W. J. *Cell* **43**, 603–613 (1985).
28. Kornberg, T., Sidén, I., O'Farrell, P. & Simon, M. *Cell* **40**, 45–53 (1985).
29. Fjose, A., McGinnis, W. J. & Gehring, W. J. *Nature* **313**, 284–289 (1985).
30. Kornberg, T. *Proc. natn. Acad. Sci. U.S.A.* **78**, 1095–1099 (1981).
31. Kornberg, T. *Devl Biol.* **86**, 363–372 (1981).
32. Jürgens, G., Lehmann, R., Schardin, M. & Nüsslein-Volhard, C. *Wilhelm Roux Arch. dev. Biol.* (in the press).
33. Southern, E. *J. molec. Biol.* **98**, 503–517 (1975).
34. Maniatis, T. *et al. Cell* **15**, 687–701 (1978).
35. Steller, H. & Pirrotta, V. *EMBO J.* **4**, 167–171 (1985).
36. Maniatis, T., Fritsch, E. F. & Sambrook, J. *Molecular Cloning: a Laboratory Manual* (Cold Spring Harbor Laboratory Press, New York, 1982).
37. Smith, G. E. & Summers, M. D. *Analyt. Biochem.* **109**, 123–129 (1980).
38. Laskey, R. A. & Mills, A. D. *FEBS Lett.* **82**, 314–316 (1977).
39. Lehrach, H., Diamond, D., Wozney, J. M. & Boedtker, H. *Biochemistry* **16**, 4743–4751 (1977).
40. Rigby, P. W. J., Dieckmann, M., Rhodes, C. & Berg, P. *J. molec. Biol.* **113**, 237–251 (1977).
41. Hafen, E., Levine, M., Garber, R. L. & Gehring, W. J. *EMBO J.* **2**, 617–623 (1983).
42. McGinnis, W., Levine, M. S., Hafen, E., Kuroiwa, A. & Gehring, W. J. *Nature* **308**, 428–433 (1984).
43. Kuroiwa, A., Hafen, E. & Gehring, W. J. *Cell* **37**, 825–831 (1984).

Latitude and depth variation of solar rotation

T. L. Duvall Jr*, J. W. Harvey† & M. A. Pomerantz‡

* Laboratory for Astronomy & Solar Physics, NASA/Goddard Space Flight Center, Greenbelt, Maryland 20771, USA
† National Solar Observatory, National Optical Astronomy Observatories, Tucson, Arizona 85726, USA
‡ Bartol Research Foundation, University of Delaware, Newark, Delaware 19711, USA

Measurements of the frequencies of various modes of trapped acoustic waves provide information about rotation and structure within the Sun. Previous work dealt with observations of wave modes confined near the solar equator, which provided some information about the depth variation of rotation without resolving a possible latitude variation[1,2]. Recent work extended measurements to modes covering various latitude ranges from which the variation with latitude of solar rotation can be studied[3–5]. Since these measurements were restricted to modes with spherical harmonic degrees less than 50, they provide averages of rotation over great depth ranges that do not resolve the convective envelope. We now present new results for degrees up to 98 which allow the convective envelope to be isolated. For degrees between 20 and 98 we find no evidence that internal rotation differs significantly with depth or latitude from the rotation of surface magnetic field patterns. Modes covering a wide latitude range have systematically lower frequencies than those confined near the equator, indicating the existence of a structural asymmetry within the Sun.

Modal patterns of trapped acoustic waves are described by the number of nodes of the wave pattern in the radial direction, n, the indices of the spherical harmonic function that characterizes the lateral wave pattern, l (degree) and m (azimuthal order) and cyclic oscillation frequency, ν. Slow rotation causes the frequency to depend on m approximately as[4]

$$\nu(n, l, m) - \nu(n, l, 0) = -m \frac{\int_{-1}^{1} \bar{\Omega}(\theta)[P_l^m(\cos\theta)]^2 \, \mathrm{d}\cos\theta}{\int_{-1}^{1}[P_l^m(\cos\theta)]^2 \mathrm{d}\cos\theta} \quad (1)$$

where θ is the colatitude, $\bar{\Omega}(\theta)$ is an appropriate average of the rotation frequency over the depth range sampled by the particular mode and P_l^m is the associated Legendre function. One may represent a general frequency variation with m as a series

$$\nu(n, l, m) - \bar{\nu}(n, l) = L \sum_{i=0}^{i=N} a_i P_i(-m/L) \quad (2)$$

where $\bar{\nu}$ is the frequency averaged over m, P_i are the Legendre polynomials of degree i and $L = \sqrt{l(l+1)}$. The argument m/L minimizes the innate l dependence of the coefficients. Unlike power series expansions in m used previously, equation (2) produces coefficients that are independent of each other and of the value of N. Expressed in terms of equation (2), the surface differential rotation measured by the motion of magnetic features[6] (or spectroscopically[7]) yields even-indexed coefficients equal to zero and odd-indexed coefficients (nHz sidereal) $a_1 =$ 442.8 (435), $a_3 = 21.7$ (21) and $a_5 = -2.5$ (−4) with negligible l dependences for $l > 20$.

We observed from the geographic South Pole in December 1981 and January 1982, in an effort to obtain sequences of sufficient length to resolve the oscillation spectrum freed from spurious features caused by diurnal interruptions. For the present investigation we used a set of observations started on 24 December 1981 having a duration of 50 h with one 4-h interruption. These data are the best 1/3 of the total collected. The instrument and observing programme have been discussed elsewhere[8,9]. Briefly, we recorded full-disk intensity images in a spectral band (±0.6 nm) centred on the Ca II line at 393.3 nm.

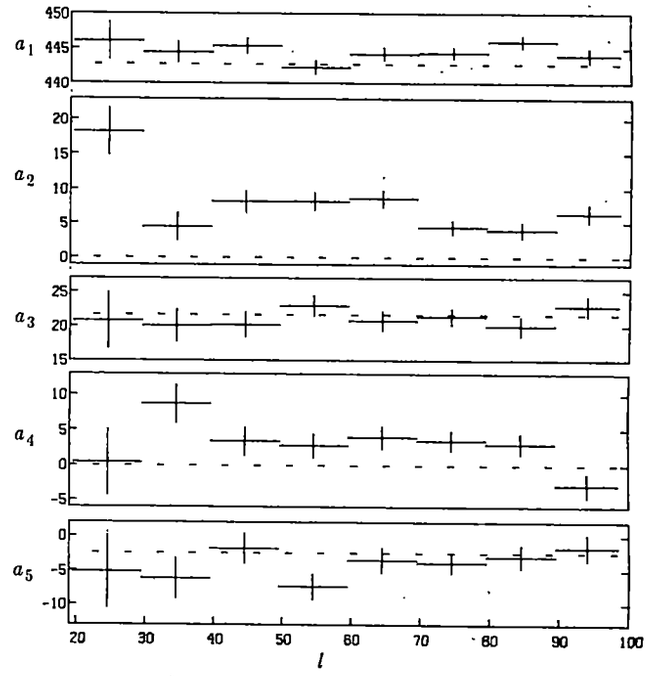


Fig. 1 Averaged coefficients from equation (2) and 1σ random errors as a function of l (nHz). The dashed lines are computed from measurements of the surface differential rotation based on observations of magnetic fields[6].

This spectral region shows intensity oscillations due to trapped acoustic modes which are several times stronger than adjacent continuum regions[10,11]. An advantage of intensity observations over the usual Doppler shift observations is a lack of signal weakening near the limb due to projection effects. A disadvantage of intensity observations is greater noise from solar and terrestrial sources[12]. Exposures were made with a telescope and a charge-injection-device camera which provided 226 pixels along the solar equator and 178 pixels along the solar rotation axis. Integrations were digitally recorded on magnetic tape cartridges every 90 seconds. After correction of the images for various characteristics of the camera, each image of the visible hemisphere was interpolated onto a longitude, sine latitude grid consisting of 512 by 421 elements. In the manner described by Brown[3,4], a Fourier transform in longitude was followed by a transformation by associated Legendre functions in sine latitude and then a Fourier transform in time to produce a spectrum of the solar oscillations with independent variables $l = 0(1)250$, $m = 0(2) \pm l$ and $\nu = 0(5.43)5556$ μHz. To save computation time and because higher resolution is not justified unless the entire surface of the Sun can be observed at once, the spectrum was computed only for even values of m.

The spectra show tens of thousands of modes. It has not yet been possible to assign the frequency of each mode in order to evaluate equation (2). Instead we used a cross-correlation procedure in a manner similar to Brown[3,4]. For each l, trial assumptions of $a_1 = 450$ nHz and $a_3 = 0$ were used for modes between

Table 1 Average rotation coefficients and standard deviations (nHz)

l range	a_1	a_2	a_3	a_4	a_5
20–29	446.1±2.7	18.2±3.4	20.8±4.1	0.4±4.7	−5.2±5.3
30–39	444.5±1.5	4.5±2.0	20.1±2.4	8.7±2.7	−6.2±3.0
40–49	445.4±1.1	8.2±1.5	20.2±1.8	3.4±2.0	−1.8±2.2
50–59	442.3±1.0	8.2±1.3	23.0±1.5	2.8±1.7	−7.4±1.9
60–69	444.2±0.9	8.6±1.2	20.8±1.4	4.0±1.6	−3.5±1.8
70–79	444.4±0.8	4.4±1.0	21.4±1.2	3.5±1.4	−3.9±1.5
80–89	446.0±0.9	4.0±1.1	20.0±1.4	3.0±1.5	−3.0±1.7
90–98	444.0±1.0	6.4±1.3	22.9±1.5	−2.9±1.7	−1.7±1.9

2.4 and 4 mHz to produce a frequency spectrum averaged over m that estimated the spectrum for a non-rotating Sun. This estimate was cross-correlated with the spectrum for each value of m. The frequencies of the peaks of the cross-correlations were then used to improve estimates of $a_{1,3}$. The improved mean spectrum was then cross-correlated with each m-value spectrum to provide values for the solution of equation (2) with $N=5$. Results for $l<20$, $l>98$ were too noisy to be useful. The remaining results were averaged in groups of ten l values and are tabulated in Table 1. The uncertainties in the means are derived from the individual l uncertainties by normal error propagation rules. Individual uncertainties were based on the assumption that the frequency estimation error is independent of m at a given l. The values of a_0 were all less than 1 nHz and are not included in Table 1.

The results are shown in Fig. 1 together with values derived from the measured rotation of surface magnetic field patterns[6]. The odd-indexed coefficients carry information about rotation. There appears to be no significant variation of the rotation coefficients with changing l value. The slight difference between magnetic rotation coefficients and our results is within the range of variation of surface rotation during the solar activity cycle. Thus one may conclude from our results that the rotation averaged over the outer half of the Sun, probed by modes with $l>20$, is essentially identical with that of the surface. This conclusion requires verification by a formal inversion to deduce the range of possible rotation variations with latitude and depth admitted by the data. Pending such an inversion, we conjecture that differential rotation with latitude persists at least through most of the convection zone.

The even-indexed coefficients provide information about the latitude variation of sound speed versus depth. If the internal structure of the Sun were independent of latitude the even coefficients should be zero. Centrifugal distortion of the Sun would produce a negative value of a_2 (ref. 13). There appears to be a significant, positive difference from zero in the sense that apart from rotation, near-zonal modes have lower frequencies than near-sectoral modes of the same degree. Brown[3,4] also found a systematic, positive quadratic frequency dependence with m but attributed no significance to it. Transformed to the same basis, his values are about 1/3 of our values. We believe that the effect is genuine and indicates that the structure of the convection zone is different near the equator compared with higher latitudes.

The present measurements may be used to compute the frequency difference to be expected from prograde and retrograde sectoral modes. These calculated frequency differences agree with direct observations of sectoral mode frequencies[1]. Brown's[4] calculated sectoral mode frequency differences also agree with the present results. Unfortunately our results for the latitude dependence of rotation significantly disagree with those of Brown[3,4]. His values of a_3 for $l=20$–29, 30–39, 40–49 are 4.6 ± 1.2, 9.1 ± 1.4 and 4.1 ± 2.7 respectively, or roughly 1/3 of our values. Brown's rotation results indicate much less differential rotation with latitude than we find.

We have examined many possible sources of this discrepancy without identifying a satisfactory explanation. Some possibilities which have been examined and are now considered unlikely are: (1) simple numerical error, (2) different frequency ranges used in the analyses, (3) the different spatial responses of intensity and velocity, (4) the cross-correlation technique responding to (in the intensity observations) the solar background signal rotating at the surface rate and (5) the Sun changing with time. Some more likely possibilities which have been considered and which require additional evaluation include: (1) the different frequency resolution, (2) the different temporal sidelobe structure and (3) the surface pattern of intensity modulating the oscillations and changing the spatial response functions. Further observations should reveal the source of the systematic error. Although Libbrecht's observations[5] do not cover the degree range that we observed, his measurements substantially agree with those of Brown[3,4] at l values less than 20.

This work was done while T.L.D. was a visiting astronomer at the National Solar Observatory in Tucson. R. Aikens of Photometrics, Ltd and R. Pfeiffer of Bartol greatly assisted the success of our observations from the South Pole. R. Nagel of NOAO designed and assembled the data recording system. We appreciate discussions with T. Brown aimed at resolving the discrepancy between our separate results. P. Goode pointed out an error in the original version of equation (2). This work was supported in part by NSF grant DPP78-22267. The National Optical Astronomy Observatories are operated by the Association of Universities for Research in Astronomy, Inc. under contract with NSF.

Received 18 February; accepted 26 March 1986.

1. Duvall, T. L. Jr & Harvey, J. W. *Nature* **310**, 19–22 (1984).
2. Duvall, T. L. Jr *et al. Nature* **310**, 22–25 (1984).
3. Brown, T. M. *Nature* **317**, 591–594 (1985).
4. Brown, T. M. in *Seismology of the Sun and the Distant Stars* (ed. Gough, D. O.) 199–214 (Reidel, Dordrecht, 1986).
5. Libbrecht, K. G. *Nature* **319**, 753–755 (1986).
6. Snodgrass, H. B. *Astrophys. J.* **270**, 288–299 (1983).
7. Snodgrass, H. B. *Solar Phys.* **94**, 13–31 (1985).
8. Harvey, J., Pomerantz, M. & Duvall, T. Jr *Sky Telesc.* **64**, 520–523 (1982).
9. Pomerantz, M. A. Harvey, J. W. & Duvall, T. Jr *Antarctic J.U.S.* **17**(5), 232–233 (1982).
10. Jensen,, E. & Orrall, F. Q. *Astrophys. J.* **138**, 252–270 (1963).
11. Duvall, T., Livingston, W. & Mahaffey, C. in *Nonradial and Nonlinear Stellar Pulsation* (eds Hill, H. A. & Dziembowski, W. A.) 237–240 (Springer, Berlin, 1980).
12. Harvey, J. in *Future Missions in Solar Heliospheric & Space Plasma Physics* (eds Rolfe, E. & Battrick, B.) 199–208 (ESA, Noordwijk, 1985).
13. Gough, D. O. & Taylor, P. P. *Mem. Soc. Astron. Ital.* **55**, 215–226 (1984).

Superparamagnetic component in the Orgueil meteorite and Mössbauer spectroscopy studies in applied magnetic fields

M. B. Madsen*, S. Mørup*, T. V. V. Costa†‡, J. M. Knudsen† & M. Olsen†

* Laboratory of Applied Physics II, Technical University of Denmark, DK-2800 Lyngby, Denmark
† Physics Laboratory I, H. C. Ørsted Institute, University of Copenhagen, DK-2100 Copenhagen Ø, Denmark

The Orgueil meteorite is a carbonaceous chondrite of group CI. Wdowiak and Agresti[1] have recently shown that very small magnetic particles, which exhibit superparamagnetic relaxation below 80 K, are present in this meteorite. They suggested that these small particles consist of magnetite. Using Mössbauer spectroscopy in external magnetic fields we have found that the Orgueil meteorite does not contain superparamagnetic magnetite in any appreciable amount. The meteorite contains another, as yet unidentified iron (III) compound which exhibits superparamagnetic behaviour below 80 K.

The sample of the carbonaceous chondrite Orgueil was ground into a powder and a Mössbauer absorber was prepared in a plexiglass absorber holder. Mössbauer spectra were obtained at various applied magnetic fields and temperatures.

Figure 1 shows a series of Mössbauer spectra of the meteorite recorded at various temperatures without applied magnetic fields. The spectra obtained at 298 and 125 K show the presence of magnetically split components due to iron in the tetrahedral (A) and octahedral (B) sites of magnetite[2]. The area ratio of

‡ Permanent address: Departamento de Física, UFC POBox 3004, 60000 Fortaleza, Brazil

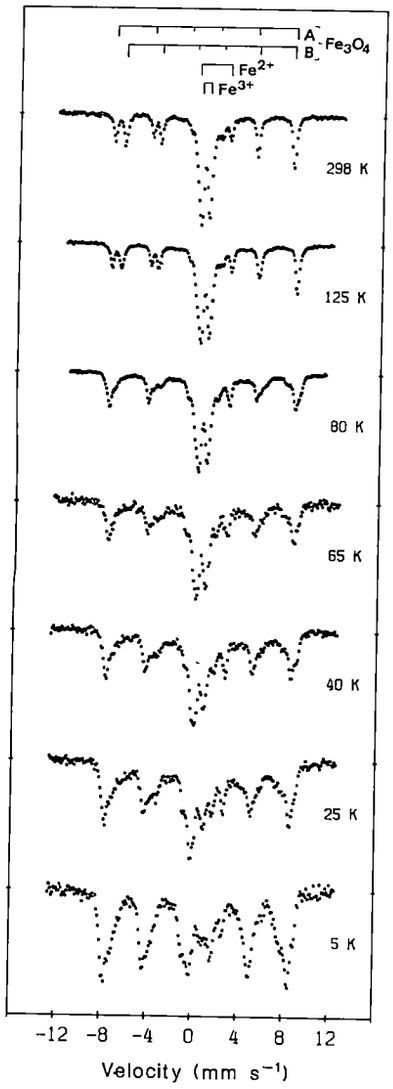


Fig. 1 Mössbauer spectra of the Orgueil meteorite obtained at different temperatures. The bar diagram indicates the tetrahedral (A) and octahedral (B) sites of the magnetite and the Fe^{2+} and Fe^{3+} doublets.

the A and B components indicates that the magnetite is slightly more oxidized than ideal stoichiometric magnetite, in which this area ratio is approximately 1:2. The spectra also contain quadrupole doublets due to paramagnetic Fe^{2+} and Fe^{3+}. At room temperature the Fe^{3+} doublet has a quadrupole splitting $\Delta E_Q = 0.73 \pm 0.03$ mm s^{-1} and an isomer shift relative to α-Fe, $\delta_{Fe} = 0.37 \pm 0.02$ mm s^{-1}. The line width is $\Gamma = 0.46 \pm 0.02$ mm s^{-1}. For the Fe^{2+} component we find $\Delta E_Q = 2.75 \pm 0.08$ mm s^{-1}, $\delta_{Fe} = 1.13 \pm 0.04$ mm s^{-1}, $\Gamma = 0.33 \pm 0.02$ mm s^{-1}. The Mössbauer parameters of the Fe^{2+} components are in accordance with Fe^{2+} ions in a hydrated silicate[3,4].

Below the Verwey transition temperature (~119 K)[5] the Mössbauer spectrum of magnetite is very complex and as many as six sextets may be required to fit the spectrum adequately[6]. The spectra of Fig. 1 reveal that the relative area of the iron (II) doublet remains nearly constant, at least down to 25 K. However, below 65 K, the relative area of the iron (III) doublet gradually decreases with decreasing temperature, whereas the total area of the magnetically split components increases. The observed behaviour is typical for a system containing superparamagnetic microcrystals with a distribution of particle sizes[7,8]. Thus the spectra indicate that Fe^{3+} ions are present in a compound which exhibits superparamagnetic relaxation in this temperature range. On the basis of similar spectra Wdowiak and

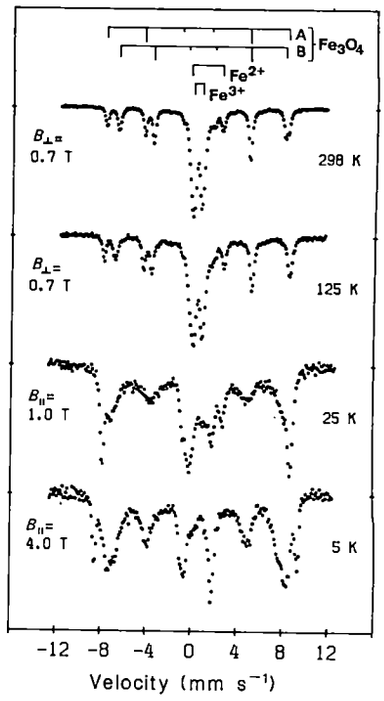


Fig. 2 Mössbauer spectra of the Orgueil meteorite obtained at different temperatures with the absorber in external magnetic fields. The intensity and direction of the external field, B, with respect to the γ-rays is indicated.

Agresti[1] concluded that the Orgueil meteorite contains superparamagnetic magnetite particles.

Because of the overlap of many different magnetically split components in the low-temperature spectra, it is difficult to determine the exact Mössbauer parameters of the six-line component which appears at low temperature at the expense of the Fe^{3+} doublet. Mössbauer studies in applied magnetic fields may, however, give supplementary information on superparamagnetic microcrystals and, in particular, such studies can give information on the magnetic moments of the microcrystals[7,8].

Therefore, to clarify whether the mineral that exhibits superparamagnetic relaxation above 5 K and contributes the Fe^{3+} doublet above 80 K has any net magnetic moment, Mössbauer spectra were obtained with external magnetic fields applied to the sample. The spectra are shown in Fig. 2. At 298 and 125 K a magnetic field of 0.7 T was applied perpendicular to the γ-ray direction. This leads to a change in the area ratios of the magnetite sextet lines from ~3:2:1:1:2:3 to 3:4:1:1:4:3, indicating alignment of the magnetization direction parallel to the applied field. The doublets are only slightly affected by the magnetic fields; that is, the width of their lines increases.

Comparing the parameters with those of the spectrum obtained in zero field, it was found that the relative areas of the doublets and the sextets do not change significantly on application of the external field. Previous studies[7,8] of samples of superparamagnetic magnetite particles with average particle diameters down to 4 nm have shown a substantial splitting of the spectra when similar magnetic fields were applied. This is due to the fact that the Zeeman energy is comparable with, or larger than, the thermal energy even at room temperature and, therefore, the particles are significantly magnetized by the external field. The present results, therefore, show that the quadrupole doublet is not due to superparamagnetic magnetite particles, as was suggested by Wdowiak and Agresti.

Further information about the nature of the superparamagnetic phase can be obtained from the spectra measured at 25 and 5 K with applied magnetic fields parallel to the γ-ray direction, shown in Fig. 2. From these spectra it is seen that the

magnetization direction of the magnetite aligns parallel to the applied magnetic field. This alignment leads to the disappearance of the $\Delta m = 0$ lines, that is, the lines 2 and 5 of the magnetite sextets. Some broad lines remain, however, at velocities where the magnetite should not give absorption lines. The broad lines at about -4 and $+5$ mm s^{-1} thus indicate the presence of an iron-containing compound with no significant net magnetization. This is the compound that gives rise to the iron(III) doublet at higher temperatures. The magnetic hyperfine fields of this compound are about 47 T at 25 K and 49 T at 5 K. The large line widths (>1 mm s^{-1}) of this compound suggest that it is a poorly crystallized or perhaps amorphous iron (III) compound. The low net magnetization of the compound could be due to antiferromagnetic ordering.

From our results we conclude that the superparamagnetic component in the Orgueil meteorite is not due to magnetite particles. The meteorite contains particles of another iron (III) compound that has a negligible net magnetization, but exhibits a superparamagnetic behaviour below 65 K.

The carbonaceous chondrites of group CI have an elemental composition closely resembling that of the Sun, if we disregard the most volatile elements. These meteorites are believed to have condensed in the very early phase of the formation of the Solar System. Even if the carbonaceous chondrites are partially altered, for example by aqueous activity, their chemical composition may still have some similarity to interstellar, and circumstellar, dust[9]. If this is so, the findings of Wdowiak and Agresti[1] and the results of the present work indicate that superparamagnetism is a much more common phenomenon in the Universe than hitherto believed.

The sample of the meteorite was supplied by the Mineralogical Museum of Copenhagen. The project is supported by the Danish Natural Science Research Council. T.V.V.C. is supported by the Brazilian Agency CAPES.

Received 23 December 1985; accepted 7 March 1986.

1. Wdowiak, T. J. & Agresti, D. G. *Nature* **311**, 140–142 (1984).
2. Häggström, L. *et al. Hyperfine Interactions* **5**, 201–214 (1978).
3. Nagy, B. *Carbonaceous Meteorites* (Elsevier, Amsterdam 1975).
4. Coey, J. M. D. in *Mössbauer Spectroscopy Applied to Inorganic Chemistry* (ed Long, G. J.) 443–509 (Plenum, New York, 1984).
5. Verwey, E. J. W. & Haayman, P. W. *Physica* **8**, 979–987 (1941).
6. Rubinstein, M. & Forester, D. W. *Solid State Commun.* **9**, 1675–1679 (1971).
7. Mørup, S., Dumesic, J. A. & Topsøe, H. in *Applications of Mössbauer Spectroscopy*, Vol. II, 1–53 (ed. Cohen, R. L.) (Academic, New York, 1980).
8. Mørup, S., Topsøe, H. & Clausen, B. S. *Phys. Scr.* **25**, 713–719 (1982).
9. Cameron, A. G. W. & Pine, M. R. *Icarus* **18**, 377–406 (1973).

Gaseous ammonia and ammonium ions in the free troposphere

H. Ziereis & F. Arnold

Max-Planck-Institut für Kernphysik, Postfach 103980, D-6900 Heidelberg, FRG

Ammonia, the most important alkaline compound commonly found in the atmosphere, has a key role in aerosol chemistry. Gaseous ammonia is released at the Earth's surface primarily through the decomposition of organic material and, due to its extremely large solubility in water and reactivity with acid aerosol components, is efficiently removed by interaction with aqueous and acid aerosols. While the presence of ammonium ions (NH_4^+) in aerosols and rain water is well established, there have been few studies of gaseous ammonia and its abundance is not well established, particularly in the free troposphere[1]. This is probably due to the difficulty in developing sufficiently sensitive analytical methods, which are not affected by interference of ammonium-containing aerosols. Due to its large proton affinity or gas-phase basicity, ammonia vapour is expected to react also with atmospheric gaseous positive ions leading to gaseous NH_4^+ 'core ions'. Detection of the gaseous NH_4^+ core ions, which have not yet been observed in the free atmosphere, may provide sensitive means of detecting atmospheric ammonia vapour[2,3,4]. We report here on the first measurements of this ion in the free atmosphere at altitudes from 4,000 to 8,000 m. Ammonia vapour abundances inferred from these data are very low suggesting efficient heterogeneous ammonia removal and very low ammonia saturation pressures over aerosols.

Due to its large proton affinity (204.0 kcal mol^{-1}), ammonia vapour reacts with most atmospheric positive ion species[2]. This is particularly true for $H^+(H_2O)_n$ clusters, which are quickly formed from primary positive ions created in the troposphere by cosmic rays and radioactivity and react with ammonia vapour:

$$H^+(H_2O)_n + NH_3 \rightarrow NH_4^+(H_2O)_{n-1} + H_2O \qquad (1)$$

(rate coefficient: $k = 1.8 \times 10^{-9}$ cm^3 s^{-1} for $n = 3$; (ref. 5)).

Also $H^+CH_3CN(H_2O)_n$ clusters, which were recently found in the middle and lower stratosphere[6], undergo reactions analogous to (1) and the rate coefficients, as recently measured in our laboratory[7], are 1.8×10^{-9} cm^3 s^{-1} ($n = 0$), 1.8×10^{-9} cm^3 s^{-1} ($n = 1$) and 1.2×10^{-9} cm^3 s^{-1} ($n = 2$). Reactions (1) involving proton hydrate ions with n around 8 are also fast, having rate coefficients around 1×10^{-9} cm^3 s^{-1} as we have recently found by creating large $H^+(H_2O)_n$ clusters in ambient air and letting them react with ambient ammonia vapour. Using this active chemical ionization (ACIMS) method and taking the above $k = 1.8 \times 10^{-9}$ cm^3 s^{-1}, we obtained a ground-level ammonia vapour mixing ratio of 3.2 p.p.b.v. (parts per 10^9 by volume) which falls well inside the range of previous ammonia measurements employing denuder, chemical filter, and condensation collection techniques (0.5–10 p.p.b.v.; see refs 8, 9). Thus, it seems fairly well established that NH_4^+-containing clusters should be found in the Earth's atmosphere provided that ammonia vapour is sufficiently abundant.

We have used an improved aircraft-borne ion mass spectrometer with high mass resolution and sensitivity to search for NH_4^+-containing cluster ions. This instrument was similar to one used previously[10–14] and so will not be described here. It has three modifications: (1) A larger quadrupole mass spectrometer (rod diameter: 1.6 cm) providing higher mass resolution and sensitivity; (2) a larger cryopump (liquid neon-cooled) adding to the improved sensitivity; (3) an ECA (electric field-induced collisional activation) mode used for fragment ion studies facilitating ion identification and adding to an improved overall sensitivity.

Three flights of the modified ion mass spectrometer were carried out aboard a twin-jet research aircraft of the DFVLR (Deutsche Forschungs- und Versuchsanstalt für Luft- und Raumfahrt). The flights (F11, F12, F13), which took place on 11, 14, and 15 May 1985 over the FRG, covered a total altitude range from ~4,000 to 10,000 m.

When the ECA mode was used, the major positive ion mass peaks occurred within the mass range 12–25 AMU (atomic mass units). Therefore, this portion of the mass spectrum was preferably scanned to increase the effective sampling time and thereby increase the sensitivity for ion detection which is particularly helpful at high mass resolution. Figure 1*a*, *b*, and *c* show mass spectra as obtained in flight F12 at different altitudes. These mass spectra contain three major peaks at 19, 18, and 15 AMU which are due to H_3O^+, NH_4^+ and CH_3^+. To ensure that the two peaks of 18 and 19 AMU are due to two different ion species and not an artefact resulting from a bad peak shape (peak splitting), an in-flight calibration was carried out. Here, $H^+(H_2O)_n$ clusters were created using the ACIMS mode of the instrument employing a high-frequency glow discharge ion source[13].

A typical ACIMS spectrum as shown in Fig. 1*d* contains

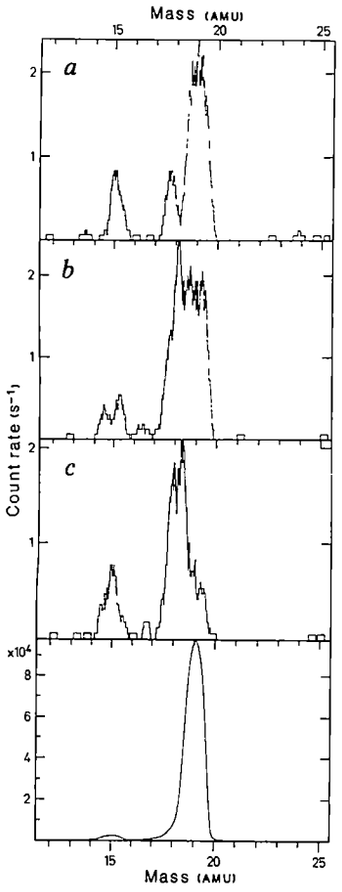


Fig. 1 Portions of positive ion mass spectra as obtained on flight F12 at altitudes of: *a*, 6,900 m; *b*, 6,000 m; *c*, 5,100 m. For comparison an ACIMS spectrum is also shown (*d*), obtained on the same flight at 8,000 m and serving as an in-flight calibration of the mass scale and the peak shape.

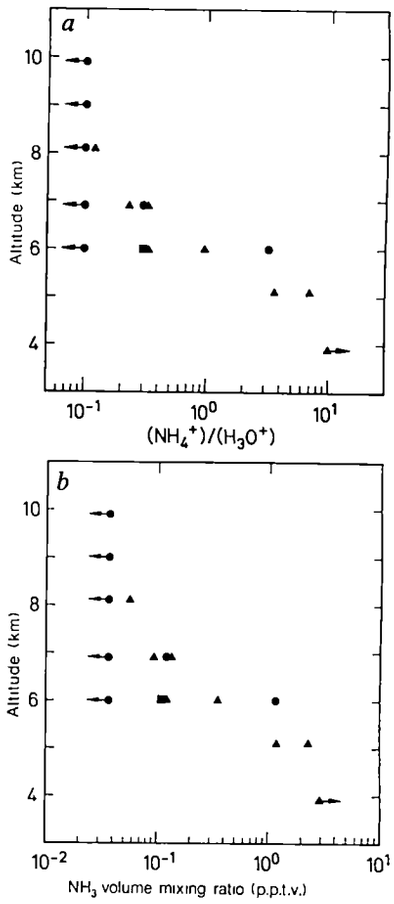


Fig. 2 *a*, Abundance ratios for NH_4^+ and H_3O^+ 'core' ions as measured in the aircraft flights given in the insert. Arrows denote upper or lower limits. *b*, Ammonia vapour volume mixing ratios as inferred from the data given in *a*. ●, F11, 11 May 1985; ▲, F12, 14 May 1985; ■, F13, 15 May 1985.

mainly a peak at mass 19 (H_3O^+). The peak shape of 19 is nominal with no peak splitting present. While H_3O^+ represents a core of ambient cluster ions, CH_3^+ is probably a fragment of core ions made up by a protonated molecule containing a methyl group as, for example, H^+CH_3CN (protonated acetonitrile), $H^+(CH_3)_2CO$ (protonated acetone) or $H^+(C_3H_6)$ (protonated propylene). The spectra shown in Fig. 1*a*–*c* also reveal a marked change of the abundance ratio for NH_4^+ and H_3O^+ taking place around 6,000 m. Figure 2*a* shows the height variation of this ion abundance ratio. It increases from 0.1 (lower limit of measurements) at 10,000 m to 10 (upper limit of measurements) at 4,000 m. At 6,000 m where most data were obtained, a marked variability was also found even during a single flight (F11). The time span between the two extreme F11 measurements at 6,000 m was only about 15 min corresponding to a horizontal distance of about 200 km. Weather conditions were characterized by clouds reaching up to about 3,000 m (F13) and no clouds present (F11, F12). Local tropopause levels were 9,800 m (F11), 11,570 m (F12), and 9,130 m (F13).

The ammonia vapour abundance can be roughly estimated from our ion composition data by assuming that NH_4^+-containing ions are formed from the other observed ions (mainly H_3O^+-containing ions) and lost by ion–ion recombination (typical[15] tropospheric ion–ion recombination lifetime: $t_R = 100$ s). A steady-state treatment yields the following continuity equation:

$$(H_3O^+)k(NH_3) = (NH_4^+)t_R^{-1} \quad (2)$$

(brackets denote number densities). H_3O^+ and NH_4^+ stand for clusters containing these 'cores'. Applying this passive chemical ionization mass spectrometry (PACIMS) method and taking $k = 2\times10^{-9}$ cm^3 s^{-1} (see above) and $t_R = 100$ s, one obtains ammonia vapour abundances as given in Fig. 2*b* ranging between ~0.043 and 3.5 p.p.t.v. (parts per 10^{12} by volume). The uncertainties for k, t_R, and the measured $(NH_4^+)/(H_3O^+)$ ratio are about ±50%, ±50%, and ±30%, respectively. Thus, the uncertainty for the inferred (NH_3) is about ±80%. An additional systematic error may arise if ECA-induced fragmentation of $NH_4^+(H_2O)_n$ clusters

$$(NH_4^+(H_2O)_n)^* \rightarrow NH_4^+(H_2O)_{n-m} + mH_2O \quad (3a)$$

$$\rightarrow H_3O^+(H_2O)_{n-k} + NH_3 + (k-1)H_2O \quad (3b)$$

(the asterisk denotes that the $NH_4^+(H_2O)_n$ cluster is internally highly excited) gives rise not only to H_3O^+ (equation (3*a*)) but also to NH_4^+ (3*b*). As can be judged from our above mentioned laboratory ACIMS measurements, process (3*b*) should be much less efficient than process (3*a*). However, even if there was only a minor side channel leading to H_3O^+ large errors could be induced for ratios of ambient $NH_4^+(H_2O)_n$ and $H^+(H_2O)_n$ ions being much larger than one. In such conditions, the PACIMS and ACIMS methods may underestimate ambient ammonia vapour abundances.

Compared with the two upper tropospheric ammonia vapour measurements of Hoell *et al.*[16], who used an infrared heterodyne radiometer technique (the only upper tropospheric ammonia vapour measurements previously reported) and obtained values between about 0.6 and 2 p.p.b.v., our present data are much

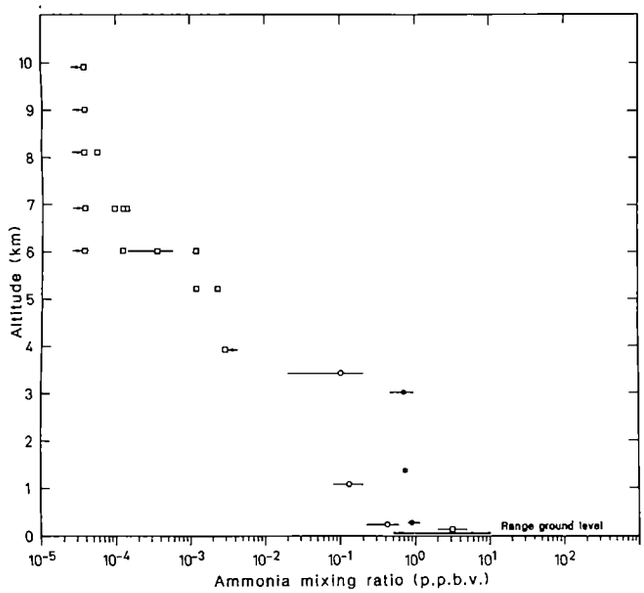


Fig. 3 Comparison of present ammonia vapour data (□) and previous denuder measurements by Lebel *et al.*[17]: ○, March 1983; ●, September, 1983. A typical range for previous ground level measurements at continental sites[8,9] is also given (△). Also shown is a typical ground level value obtained from active chemical ionization mass spectrometry during tests of the present method (see text).

lower. All other ammonia vapour measurements previously reported are restricted to heights below about 3,500 m and, therefore, a direct comparison with the present data is not possible. Recent aircraft-borne denuder measurements by Lebel *et al.*[17] (Fig. 3). extending up to 3,500-m range between about 0.1 and 1 p.p.b.v. Ground-level values, as mentioned before, typically fall into the range between about 0.5 and 10 p.p.b.v. (Fig. 3) being mostly much larger than free tropospheric values.

The observed decrease with height of the ammonia vapour volume mixing ratio suggests that an efficient sink for this gas must be operative throughout the troposphere. This sink can probably be identified as ammonia vapour interaction with aerosols of various sorts ultimately followed by washout and rainout of the aerosols. Even in fair weather conditions, the surface area densities of continental background aerosols are sufficiently large to make the lifetime t_c of a gaseous ammonia molecule against collision with aerosols much smaller than typical timescales t_{vT} for tropospheric vertical transport. Consequently, a very steep decrease with height of the ammonia vapour volume mixing ratio should be expected if ammonia reevaporation was negligible. On average, the aerosol content decreases with increasing height and therefore t_c increases. Considering typical aerosol abundances[1] and sizes, one estimates tropospheric t_c values to be much less than typical timescales for tropospheric vertical transport ($\sim 2\times10^4$–2×10^6 s km^{-1}). Thus, in many conditions, a local equilibrium between ammonia absorption by and re-evaporation from aerosols may be established depending sensitively on the aerosol composition. In reality, ambient aerosols are complex systems whose chemical and physical states are governed by atmospheric conditions and often vary with time and location. Depending on the extent of neutralization and atmospheric relative humidity, they may exist in a completely dissolved, partially dissolved or crystalline state as pure or mixed salts. For example, solid NH_4NO_3, a relatively simple aerosol, would have ammonia vapour equilibrium saturation volume mixing ratios[19] (ammonia equilibrium saturation pressures converted to volume mixing ratios) of about 0.37 p.p.b.v. (4,000 m), 0.15 p.p.b.v (5,200 m), 0.06 p.p.b.v (6,100 m), 0.03 p.p.b.v. (7,000 m), and 0.003 p.p.b.v. (8,200 m) if atmospheric temperatures as measured in F12 are considered. Compared with our measured ammonia abundances, these are generally larger by factors around 10–100. For NH_4HSO_4 and $(NH_4)_2SO_4$ aerosols the equilibrium saturation abundance for ammonia vapour may be much smaller than for NH_4NO_3 depending sensitively on the molar ratio NH_4^+/SO_4^{2-} and relative humidity[20]. At ground level (temperature of 25 °C and a relative humidity of 85%) for example, the equilibrium ammonia vapour pressure over ammonium sulphates (molar ratio $NH_4^+/SO_4^{2-}=1$) is about 50 times lower than over NH_4NO_3.

We conclude that it is at least conceivable that our measured ammonia vapour abundances represent equilibrium abundances over ambient aerosols. If so, they may contain valuable information on the chemical nature of aerosols. Future measurements should focus on variations of ambient ammonia vapour abundances with atmospheric temperature which should be very pronounced if ammonia reevaporation was in fact important. An attempt should be made to carry out combined measurements of ammonia vapour and other relevant parameters including H_2SO_4, HNO_3, and H_2O vapours as well as atmospheric temperatures.

We thank E. E. Ferguson and C. Brosset for helpful discussions, and the technical staffs of the Max-Planck-Institut für Kernphysik, particularly K. Oberfrank and W. Dann and of the Deutsche Forschungs- und Versuchsanstalt für Luft- und Raumfahrt (Flugbereitschaft), for their support. Part of this project was funded by the Bundesministerium für Forschung und Technologie through Gesellschaft für Strahlen- und Umweltforschung.

Received 13 November 1985; accepted 10 March 1986.

1. Graedel, T. E. & Weschler, C. J. *Rev. Geophys. Space Sci.* **19**, 505–539 (1981).
2. Ferguson, E. E. & Fehsenfeld, F. C. *J. chem. Phys.* **59**, 6212 (1973); *Gas phase Chemistry* (ed. Bowers, M. T.) (Academic, New York, 1979).
3. Arnold, F. *Proc. Dahlem Workshop on Atmospheric Chemistry* (ed Goldberg, E. D.) 273 (1982).
4. Arnold, F. in *Chemical Events in the Atmosphere and their Impact on the Environment* (Pontificiae Academiae Scientarum Scripta Varia, 1985).
5. Bohme, D. K., Mackay, G. I. & Tanner, S. D. *J. Am. chem. Soc.* **101**, 3724 (1979).
6. Arnold, F., Böhringer, H. & Henschen, G. *Geophys. Res. Lett.* **5**, 653–xxx (1978).
7. Schlager, H., Fabian, R. & Arnold, F. *Proc. 3rd Swarm Seminar, Innsbruck*, 257–262 (1983).
8. Dawson, G. A. & Farmer, J. C. *J. geophys. Res.* **89**, 4779–4787 (1984).
9. Ferm, M. *Atmos. Envir.* **13**, 1385–1393 (1979).
10. Heitmann, H. & Arnold, F. *Nature* **306**, 747 (1983).
11. Arnold, F., Heitmann, H. & Oberfrank, K. *Planet. Space Sci.* **12**, 1567 (1984).
12. Hauck, G. & Arnold, F. *Nature* **311**, 547 (1984).
13. Arnold, F. & Hauck, G. *Nature* **315**, 307 (1985).
14. Knop, G. & Arnold, F. *Planet. Space Sci.* (submitted).
15. Arnold, F., Knop, G. & Ziereis, H. *Nature* (in the press).
16. Hoell, J. M., Harward, C. N. & Williams, B. S. *Geophys. Res. Lett.* **7**, 313–316 (1980).
17. Lebel, P. J., Hoell, J. M., Levine, J. S. & Vay, A. *Geophys. Res. Lett.* **12**, 401–404 (1985).
18. Liu, S. C. & McAffee, J. R. *J. geophys. Res.* **89**, 7291–7297 (1984).
19. Brandner, J. D., Junk, N. M., Lawrence, J. W. & Robina, J. *J. Chem Engng Data* **7**, 227–228 (1962).
20. Tang, I. N. *Atmos. Envir.* **14**, 819–828 (1980).

Acetone measurements in the upper troposphere and lower stratosphere—implications for hydroxyl radical abundances

F. Arnold, G. Knop & H. Ziereis

Max-Planck-Institut für Kernphysik, Postfach 103 980, D-6900 Heidelberg, FRG

Atmospheric acetone serves as a precursor of PAN (peroxyacetyl nitrate) which represents a temporary reservoir for reactive nitrogen and has a potential to form aerosols. Acetone has recently been detected in the atmosphere by Penkett[2], using ground-level flask sampling and gas chromatography/mass spectrometry (GC/MS) analysis in the laboratory finding an average volume mixing ratio of 470 p.p.t.v. (parts per 10^{12} by volume) in Atlantic

air. Very recently, acetone was for the first time detected in the free atmosphere, at heights around the tropopause, by Arnold and his colleagues[3,4] using aircraft-borne chemical ionization mass spectrometry (CIMS). We report here on the first measurements of atmospheric acetone abundances over an extended altitude range (5,900–11,300 m) covering the lowermost part of the stratosphere and the upper troposphere. The measured upper tropospheric abundances (average 120 p.p.t.v.) are substantially lower than the average values (470 p.p.t.v.) measured at ground level. Above the tropopause, a marked decrease of the acetone mixing ratio was observed. Our present data have interesting implications for the chemistry of non-methane hydrocarbons and possibly also hydroxyl radical abundances.

Aircraft-borne CIMS, used for the present measurements, is similar to the experimental method previously employed by our group[3–7] and will only briefly be reviewed here. It involves a flow reactor through which atmospheric air is passed and within which ions created in the air stream by a high-frequency glow discharge ion source undergo ion molecule reactions with atmospheric trace gases. Precursor and product ions are then mass analysed using a cryogenically-pumped quadrupole mass spectrometer. Abundances of reactant trace gases can be determined from measured ion abundance ratios and independently measured ion residence times.

The present CIMS-instrument has several modifications to the previous model including a larger quadrupole mass spectrometer (quadrupole rod diameter: 1.6 cm) and an ECA (electric field-induced collisional activation) mode. The larger quadrupole provides a larger sensitivity and mass resolution while the ECA mode is used for fragmented ion mass spectrometry studies, which greatly facilitates ion identification. A detailed description of the modified instrument will be given elsewhere.

Six flights (F6, F8, F9, F11, F12, F13) were carried out over the FRG using a twin-jet research aircraft (type: FALCON 20) of the Deutsche Forschungs- und Versuchsanstalt für Luft- und Raumfahrt. The flights, which all took place during daytime, covered a total altitude range from 5,900 to 11,300 m.

The acetone volume mixing ratios measured during these flights are shown in Fig. 1*a* along with the single data point of our first CIMS-flight (F5 (ref. 4)). Some of the data were obtained at altitudes above the local tropopause levels. Figure 1*b* shows the same data, but replotted as a function of the vertical separation from the local tropopause level. These data exhibit substantial scatter, but a trend also seems to exist towards lower values above the tropopause which is particularly pronounced for F6 and F8 where altitude profiles were obtained covering both the uppermost part of the troposphere and the lowermost part of the stratosphere. Our stratospheric data (obtained at heights at least 500 m above local tropopause levels) range between ~20 and 50 p.p.t.v. (average: 31 p.p.t.v.) whereas our tropospheric data range between ~50 and 250 p.p.t.v. (average: 120 p.p.t.v.).

Compared with the ground-level average of 470 p.p.t.v. our upper tropospheric average of 120 p.p.t.v. is substantially lower which, if both values were representative, would imply that efficient tropospheric acetone sinks must exist. Known sinks include photolysis and OH-attack of which the former process appears to be dominant. The photodissociation frequency J is about $1\text{–}2\times10^{-6}\ s^{-1}$ at the 10-km level[8] which implies an acetone lifetime of about 10 to 20 days (diurnal average). The reaction coefficient[1] for OH-attack is $2\times10^{-13}\ cm^3\ s^{-1}$ which implies a typical lifetime of about 53 days (diurnal average) in summer at middle latitudes (here a typical diurnal average OH-concentration of $1\times10^6\ cm^{-3}$ as given by the model of Crutzen[9] was taken). By comparison, the timescale for vertical mixing[10] between ground level and the 10 km level is about 10–100 days mostly exceeding the photochemical lifetime of acetone. Consequently, substantial upward mixing of acetone originating from the planetary boundary layer has to be expected. Taking a lower limit to the photochemical lifetime of acetone of 10 days, assuming a ground-level mixing ratio of 470 p.p.t.v., and neglecting photochemical acetone production above the ground, average winter and summer volume mixing ratio profiles as shown in Fig. 1 would be expected. Here, recent vertical eddy diffusion coefficients as given by Liu *et al*[10] were considered. Compared with our data (Fig. 1*a*), the model curves are gen-

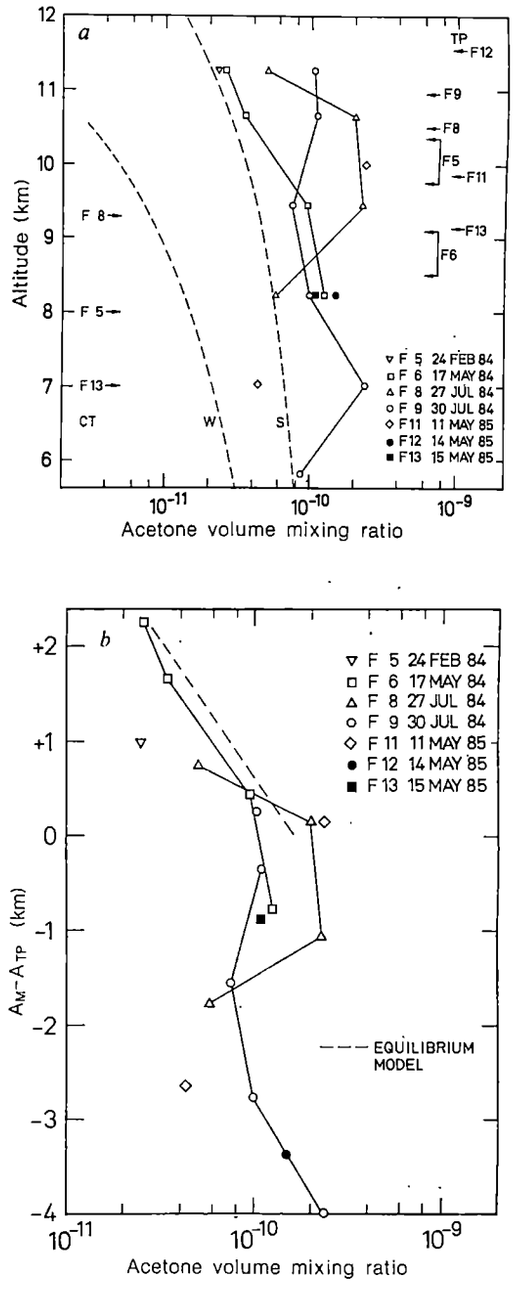


Fig. 1 *a*, Acetone volume mixing ratios as measured during the aircraft flights (F6, F8, F9, F11, F12, F13; see inset) along with the single data point of our previous flight (F5; ref. 4). Also given are local tropopause (TP) and cloud top (CT) levels. Model curves for a gas with a surface source, a 10-day lifetime and a ground-level mixing ratio of 470 p.p.t.v. are also shown for winter (W) and summer (S) conditions. *b*, As *a* with vertical separation from local tropopause level (A_M is the altitude of the measurement and A_{TP} the local tropopause level) instead of geometric altitude as the *y*-coordinate. A model curve assuming local photochemical equilibrium in the stratosphere between acetone formation by propane photooxidation and loss by photolysis is also shown (dashed curve).

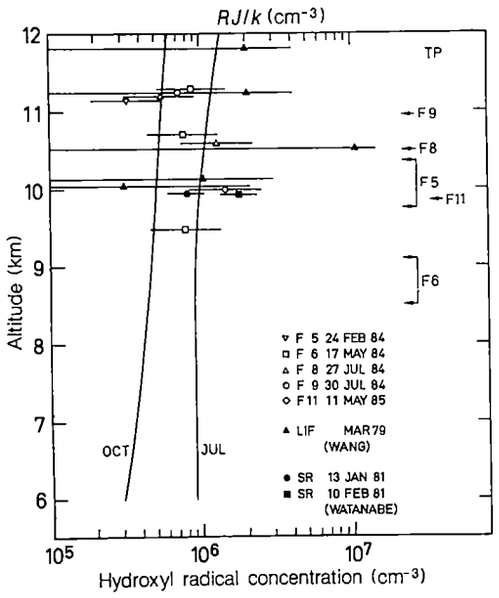


Fig. 2 Inferred stratospheric RJ/k values (see text), which would be equal to OH-concentrations (diurnal averages) for local photochemical equilibrium of acetone formation by C_3H_8+OH and acetone formation by C_3H_8+OH and acetone destruction by photolysis. For comparison, previous OH-measurements using laser-induced resonance fluorescence[15] (Wang) and spin trapping[16] (Watanabe), and the photochemical model calculations (diurnal averages for July and October at mid-altitudes) of Crutzen[9] are shown.

erally lower, particularly for the only winter data point (F5). This discrepancy may be due to a longer photochemical lifetime or faster vertical transport. The latter may occur during strong convective events of deep penetration like a mid-latitude storm when vertical transport may eventually occur within about 1–3 days[11]. However, it seems unlikely that all of our measurements were influenced by such events. An additional potential cause for the observed discrepancy is local photochemical production of acetone by photooxidation of hydrocarbons. It has been proposed by Singh and Hanst[1] that acetone may be formed by photooxidation of propane through the reaction chain:

$$C_3H_8 \xrightarrow{OH} CH_3CHCH_3 \xrightarrow{O_2} CH_3(O)CH_3 \longrightarrow$$
$$\xrightarrow{NO} CH_3CH(O)CH_3 \xrightarrow{O_2} CH_3COCH_3 \qquad (1)$$

which is initiated by the OH-radical and also involves nitric oxide as a reactant. Propane is emitted at ground level mainly as a result of natural gas losses and biomass burning[12] and reaches the upper troposphere and even the lower stratosphere since it has a photochemical lifetime of about 6–12 days which is mainly determined by OH-attack. Propane measurements[12,13] give free tropospheric volume mixing ratios at middle latitudes of about 50–1,000 p.p.t.v. (most values ranging between 100 and 300 p.p.t.v.) and rapidly decreasing values above the tropopause. At ground level[13], propane volume mixing ratios range between about 600–1,000 p.p.t.v. at middle latitudes being substantially higher than the upper tropospheric average of about 120 p.p.t.v.. It is conceivable that photooxidation of other, possibly even more reactive atmospheric hydrocarbons may contribute to the formation of acetone. In the stratosphere, the situation is different. Here vertical mixing becomes much slower having a typical timescale[10] of 100–200 days km^{-1} which is much longer than the photochemical lifetime of acetone. Therefore, the acetone concentration may be determined by local photochemical production and destruction by photolysis. However, here only relatively long-lived hydrocarbons like propane serve as potential precursors. Considering only photooxidation of propane one obtains the following continuity equation:

$$[C_3H_8]k[OH] = (CH_3)_2CO]\,J^{-1} \qquad (2)$$

Taking stratospheric propane volume mixing ratios as measured by Rudolph and Ehhalt[12], an OH-reaction coefficient k of $1.82\times10^{-11}\exp(-675/T)$ $cm^3\,s^{-1}$ as measured by Darnall and coworkers[14], and OH concentrations for summer conditions at middle latitudes as given by the theoretical model of Crutzen[9] (see Fig. 2, curve Jul), one obtains a photochemical equilibrium volume mixing ratio profile as shown in Fig. 1*b*. It is in reasonably good agreement with our stratospheric data. However, this agreement may be fortuitous since substantial temporal and spatial variations of lower stratospheric propane abundances may occur. Combined measurements of acetone and propane at the same time and location are required to investigate the local photochemical acetone production.

Finally, we consider the potential role of acetone as a tracer for hydroxyl radicals. In conditions where local photochemical equilibrium is established, which may be the case in the lower stratosphere, combined measurements of acetone and propane may allow to estimate the OH-concentration by applying the continuity equation (2). To illustrate the kind of information, which may be obtained, we have inferred the quantity RJ/k ($R=((CH_3)_2CO)/(C_3H_8)$), which should be equal to the OH-concentration (diurnal average) for local photochemical equilibrium conditions, from our data using propane volume mixing ratios as above (same as those taken for calculating the theoretical curve in Fig. 2). Resulting stratospheric RJ/k values are given in Fig. 3 along with published OH-measurements previously made in the tropopause region using laser-induced fluorescence[15] (only measurements with no O_3-interference are included) and spin trapping[16]. While our data represent diurnal averages, the above previous data were obtained during daytime, mostly at large solar elevations. As OH should be absent during the nightime, diurnal average values should be smaller than daytime values by about a factor of two to three. Considering this fact, our inferred values are roughly consistent with previous data. Theoretical model calculations (diurnal averages) by Crutzen[9] are also shown in Fig. 2.

We thank E. E. Ferguson, D. Ehhalt, P. Crutzen, and R. Chatfield for helpful discussions. Support by the technical staffs of the Max-Planck-Institut für Kernphysik, in particular K. Oberfrank and W. Dann, and of the Deutsche Forschungs- und Versuchsanstalt für Luft- und Raumfahrt (Flugbereitschaft) is gratefully appreciated. Part of this project was funded by the Bundesministerium für Forschung und Technologie through Gesellschaft für Strahlen- und Umweltforschung.

Received 18 November 1985; accepted 11 March 1986.

1. Singh, H. B. & Hanst, P. L. *Geophys. Res. Lett.* **8**, 941–944 (1981)
2. Penkett, S. A. in *Atmospheric Chemistry* (ed. Goldberg, E. D.) (Springer, Berlin, 1982)
3. Hauck, G. & Arnold, F. *Nature* **311**, 547–550 (1984).
4. Arnold, F. & Hauck, G. *Nature* **315**, 307–309 (1985).
5. Heitmann, H. & Arnold, F. *Nature* **306**, 747–751 (1983).
6. Arnold, F., Heitmann, H. & Oberfrank, K. *Planet. Space Sci.* **32**, 1567–1576 (1984)
7. Knop, G. & Arnold, F. *Planet Space Sci.* **33**, 983–986 (1985).
8. Gardner, E. P., Ranmali, D., Wijayaratne, R. D. & Calveri, J. G. *J. phys. Chem.* **88**, 5069 (1984).
9. Crutzen, P. in *Atmospheric Chemistry* (ed. Goldberg, E. D.) 313–328 (Springer, Berlin 1982)
10. Liu, S. C., McAfee, J. R. & Cicerone, R. C. *J. geophys. Res.* **89**, 7291 (1984).
11. Chatfield, R. B. & Crutzen, P. J. *Geophys. Res.* **89**, 7111 (1984).
12. Ehhalt, D. H. & Rudolph, J. *KFA Rep.* ISSN 0366-0885 (July 1984).
13. Rudolph, J. & Ehhalt, D. H. *J. geophys. Res.* **86**, 11959 (1981)
14. Darnall, K. R., Atkinson, R. & Pitts, J. N. Jr *J. Phys.* **82**, 1581 (1978).
15. Wang, C. C., Davis L. I. Jr & Selzer, P. M. *J. geophys. Res.* **86**, 1181–1186 (1981)
16. Watanabe, T. *et al. Analyt. Chem.* **54**, 2470–2474 (1982).

Precipitation scavenging of aerosol particles over remote marine regions

Patrick Buat-Ménard* & Robert A. Duce†

* Centre des Faibles Radioactivités, Laboratoire Mixte CNRS-CEA, BP 1, 91190 Gif-sur-Yvette, France
† Center for Atmospheric Chemistry Studies, Graduate School of Oceanography, University of Rhode Island, Kingston, Rhode Island 02881, USA

There is increasing evidence that the deposition of atmospheric particulate material has a significant influence on the chemistry of trace elements in many oceanic regions[1–4]. One significant but unknown parameter is the efficiency of in-cloud and below-cloud scavenging processes as a function of aerosol particle size. Studies in continental regions have indicated that the largest particles are scavenged most efficiently by rain[5]. We report here, for the first time, an evaluation of particle scavenging by tropical showers, based on data obtained at Eniwetok Atoll and American Samoa in the tropical Pacific Ocean. We find no clear evidence of a particle size dependence for scavenging in this remote marine region. This indicates that estimates of global atmospheric deposition over the ocean based on extrapolation of measurements made on land may be invalid.

Because of the regional variability of both the atmospheric and oceanic cycles of some trace elements, especially trace metals, an assessment of the impact on ocean chemistry of the deposition of atmospheric particulate material from natural or man-made sources must go beyond simple estimates of global mass balances. The need for accurate data on net air-to-sea particulate fluxes requires a precise assessment of the importance of both dry and wet deposition processes. Such data are extremely difficult to obtain, especially over remote marine regions.

Wet deposition appears to be the dominant removal process for particulate material from the remote marine atmosphere[3,6]: there is thus a need to understand how the concentrations of trace elements in rain are related to their concentrations in the atmosphere. The investigation of the relationship between particle size and scavenging efficiency over remote marine areas is of crucial importance, because the various sources contributing to the marine atmospheric burden of particulate trace elements generate aerosol particles with different mass-size functions.

The data reported here were obtained during the SEAREX Program experiments in 1979 at Eniwetok Atoll (11°20′ N, 162°20′ E) in the Marshall Islands, and in 1981 at American Samoa (14°15′ S, 170°34′ W). Both sites are >5,000 km from the nearest continent. Trade-wind rain-shower and atmospheric particulate samples were collected from the top of an 18-m-high tower on the windward shore of the islands. Samples were collected only during sustained on-shore winds, using ultra-clean procedures. Rain was collected on an event basis, whereas aerosol particle samples were generally collected over 2–5 days. Two different data sets are presented here which allow us to investigate the precipitation scavenging efficiency for aerosol particles as a function of particle size.

The first data set[4,7] consists of results of chemical analyses of 14 pairs of rain and air samples for trace elements at Eniwetok Atoll. These samples were analysed by neutron activation analysis and atomic absorption spectrometry. The air samples were obtained with high-volume cascade impactors, which separate aerosol particles into six different size ranges. Because the elements analysed are partitioned differently among particles of different size[7], we can examine the dependence of element concentrations in rain and air on aerosol particle size. Elements have been characterized by the mass median diameter (MMD) of the particles containing them. Although the aerosol samples were collected over intervals of several days, whereas the rain samples represent aerosol scavenging on a timescale of minutes to hours, the aerosol trace-metal size distributions were found to be quite consistent over a period of several months at Eniwetok. Comparison of rain and aerosol chemistry is thus justified.

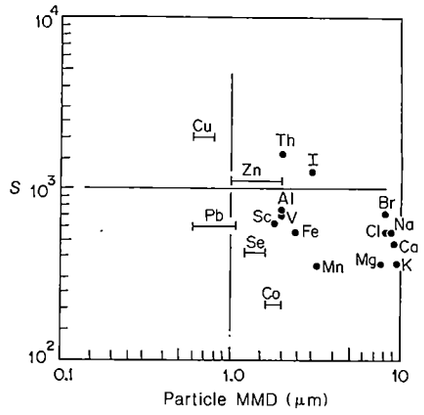


Fig. 1 Scavenging ratio, S, plotted against marine airborne particle size (mass median diameter) for various trace elements at Eniwetok Atoll.

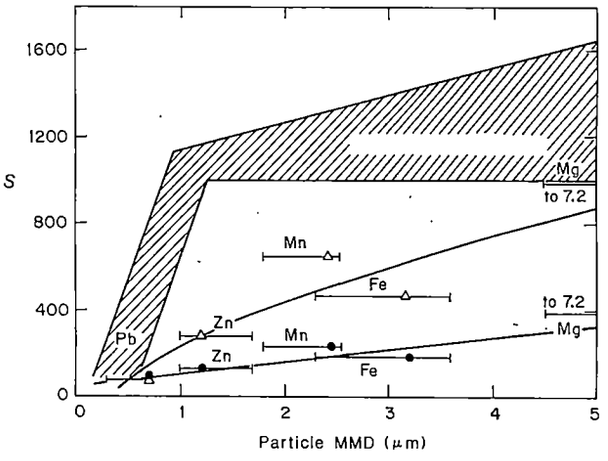


Fig. 2 Scavenging ratio, S, plotted against particle size for various trace elements in urban areas (adapted from ref. 5). The shaded area indicates the relationship observed in Chilton, UK[10]; the solid lines are for two sites near St Louis, USA[9].

The second data set[8] was obtained by means of scanning-electron-microscopic examinations of individual aluminosilicate dust particles in air and rain samples at Eniwetok and American Samoa. Such particles are nearly insoluble in rain water; therefore, these data should provide a direct estimate of wet removal efficiencies as a function of particle size.

The precipitation scavenging efficiency for a given substance is commonly expressed as a dimensionless number, the scavenging ratio (or washout factor) S, given by $S = C_{rain}\,\rho / C_{air}$, where C_{rain} is the concentration in rain in g kg^{-1}, C_{air} is the concentration in air in g m^{-3} and ρ is the density of air (1.2 kg m^{-3}) at standard conditions.

In Fig. 1, the mean scavenging ratios for elements in rain samples from trade-wind showers at Eniwetok Atoll are plotted against the mass median diameter of the aerosol particles containing them. There is no statistically significant correlation between scavenging ratio and particle size ($r = -0.39$, not significant at $P = 0.1$). This result is corroborated by the data

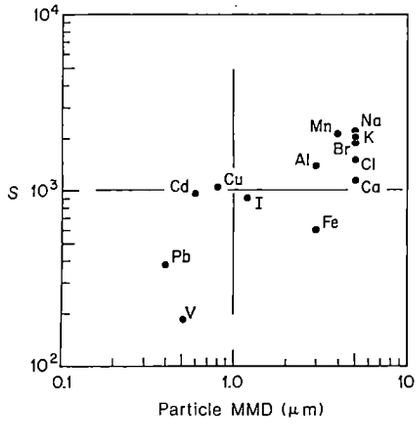


Fig. 3 Scavenging ratio, S, plotted against particle size for various trace elements in the Florida Keys (adapted from ref. 11).

Table 1 Scavenging ratios for mineral aerosols, Eniwetok and American Samoa

Particle diameter (μm)	S
0.1–0.5	940 ± 1,100
0.5–1	800 ± 620
1.0–1.5	500*
1.5–3	310 ± 250
3.0–6	270 ± 170
6–15	320 ± 120

Scavenging ratio S is given as arithmetic mean $\pm 1\sigma$, based on five air samples and three rain samples. Details of the particle counting statistics can be found in ref. 8. 100–400 particles were examined from each sample. The size distributions were found to be log-normal. Scavenging ratios were then calculated from the idealized log-normal distributions of the particles in air and rain samples. The stated uncertainties relate only to the variability of the particle size distribution from one sample to another.

* Assumed value (see text).

presented in Table 1 for aluminosilicate particles collected at Eniwetok and American Samoa, which show no statistical difference (at the 1σ level) among the values of S for the different size fractions. The data presented in this table indicate only the relative variation in S, because the data have been normalized to $S = 500$ for aerosol particles in the size range 1–1.5 μm.

If what we have observed is representative of the trade-wind regime, it can be inferred that over tropical marine areas the elemental concentration ratios in near-surface air and rain may be similar. This conclusion may also apply to the westerlies regime of the South Pacific, as indicated by recent analyses of individual aluminosilicate particles in air and rain samples collected during the SEAREX Program experiment in 1983 at Ninety-Mile Beach, New Zealand (P.B.-M., unpublished data).

The results presented here, which are to our knowledge the first of this type obtained over remote marine regions, contrast markedly with data obtained over continental and coastal areas. For example, Scott[5] has shown that S increases with MMD for metals collected in St Louis[9], USA, and Chilton, UK[10] (Fig. 2), and Duce *et al.*[11] have found similar results in the Florida Keys (Fig. 3) ($r = 0.76$, significant at $P = 0.01$). These results may be explained by the lower collection efficiency of raindrops for the smaller particles (down to perhaps a few tenths of a micrometre in radius) present over the continents[5,12]. These authors also note that differing chemical properties, particularly the solubility, of particles of different size may also play a role. Over remote marine regions, the absence of a particle size dependence of scavenging ratios is as yet unexplained. Slinn[12] has suggested that in truly remote marine regions, where there are relatively few cloud condensation nuclei (<200 cm^{-3}), essentially all particles are activated in clouds regardless of their size or chemical composition. This suggestion deserves further investigation, but there are other possible causes which might explain the results reported here.

Indeed, it can be argued that such a continental–marine comparison should result in differences, because for a given element the vertical distribution of its atmospheric concentration may be quite different over land from that over the sea. For example, elements (such as sodium) associated with atmospheric sea-salt particles exhibit a marked negative concentration gradient between the sea surface and the top of the marine boundary layer[13,14], whereas such a gradient is much less pronounced or non-existent over land. The reverse is generally observed for materials attached to aerosol particles over the ocean which are derived from land-surface sources[14,15]. Such differences in vertical distribution may generate large uncertainties in the calculation of S, because S values are estimated from near-surface air concentrations, which can be quite different from those at the altitude of cloud scavenging. However, such uncertainties should affect S values similarly for materials during their atmospheric transport from land to sea or from sea to land. That this is not observed is clear from Figs 1–3, which show that for elements derived from continental sources the shift of S values from continental or coastal regions to remote oceanic areas is not uniform for a given element, and seems to be related to the mass–size distribution of the element. Indeed, this shift is much more pronounced for elements (such as aluminium) attached to large aerosol particles than for those (such as lead) attached to smaller aerosol particles.

Another possible cause for the continental–marine difference is related to precipitation patterns over land and sea. Differences in the vertical and horizontal extent of cloud systems and in the duration, intensity and droplet size of the precipitation will certainly affect the precipitation scavenging efficiency of aerosol particles and the relationship between S and the mass–size distribution of the materials associated with these particles. As shown by Scott[5], large variations in S can be expected at different latitudes. For example, smaller scavenging ratios would be expected in 'cold clouds', where a much greater fraction of the precipitation occurs as a result of vapour-phase growth rather than droplet coalescence. The latter apparently dominates in 'warm' rains, that is, those not containing ice particles or supercooled droplets. This obviously implies that our limited data set may not apply to high-latitude oceanic areas.

The data presented here suggest strongly that the particle-size-dependent rain scavenging relationships observed in continental regions do not apply in tropical marine regions, where precipitation is often dominated by trade-wind showers. These apparent differences in scavenging processes must be evaluated more fully before accurate models can be made of the wet deposition of aerosol trace constituents into the ocean. Such modelling will become increasingly necessary in response to the growing interest in the use of new oceanic tracers[16,17], especially those (such as heavy metals) which are derived from aeolian inputs of anthropogenic origin.

We thank R. Arimoto and G. Ayers for helpful discussion and criticism. This research was supported by the NSF Division of Ocean and Atmospheric Sciences under grants OCE77-13071, OCE77-13072, OCE81-11895 and OCE 84-05605. This is CFR contribution no. 724.

Received 18 November 1985; accepted 7 January 1986.

1. Cambray, R. S., Jeffries, D. F. & Topping, G. *U.K. atom. Energy author. Publ* no. AERE-R7733 (HMSO, London, 1975).
2. Buat-Menard, P. & Chesselet, R. *Earth planet. Sci. Lett.* 42, 399–411 (1979).

3. Settle, D. M. & Patterson, C. C. *J. geophy. Res.* **87**, 8857-8869 (1982).
4. Arimoto, R., Duce, R. A., Ray, B. J. & Unni, C. K. *J. geophys. Res.* **90**, 2391-2408 (1984).
5. Scott, B. C. *Atmospheric Pollutants in Natural Waters* (ed. Eisenreich, S. J.) 3-21 (Ann Arbor Science, 1981).
6. Uematsu, M., Duce, R. A. & Prospero, J. M. *J. atmos. Chem.* **3**, 123-138 (1985).
7. Duce, R. A., Arimoto, R., Ray, B. J., Unni, C. K. & Harder, P. J. *J. geophys. Res.* **88**, 5321-5342 (1983).
8. Buat-Menard, P., Ezat, U. & Gaudichet, A. *Precipitation Scavenging, Dry Deposition and Resuspension* Vol. 2, 1259-1270 (Elsevier, New York, 1983).
9. Gatz, D. F. *Precipitation Scavenging—1974* (eds Beadle, R. W. & Semonin, R. G.) 71-87 (U.S. Energy Res. Dev. Ag., Washington, DC, 1975).
10. Cawse, P. A. *U.K. atom. Energy Auth. Publ.* no. R7669 (HMSO, London, 1974).
11. Duce, R. A. *et al.* in *Abstr. IAMAP/CACGP Symp. Budget and Cycles of Trace Gases and Aerosols in the Atmosphere* (University of Colorado Press, Boulder, 1979).
12. Slinn, W. G. N. *Air-Sea Exchange of Gases and Particles* (eds Liss, P. S. & Slinn, W. G. N.) 299-405 (Reidel, Dordrecht, 1983).
13. Blanchard, D. C. & Woodcock, A. H. *Ann. N.Y. Acad. Sci.* **338**, 330-347 (1980).
14. Delaney, A. C., Pollock, W. H. & Shedlovsky, J. P. *J. geophys. Res.* **78**, 6249-6268 (1973).
15. Gillette, D. A. & Blifford, I. H. *J. atmos. Sci.* **28**, 1199-1210 (1971).
16. Gwinn, E. & Sarmiento, J. L. *A Model for Predicting Strontium-90 Fallout in the Northern Hemisphere* (1954-1974) (Ocean Tracers Lab., Princeton University, 1984).
17. Sarmiento, J. L. & Gwinn, E. *J. geophys. Res.* (in the press).

Calcium-free pumpellyite, a new synthetic hydrous Mg–Al-silicate formed at high pressures

W. Schreyer, W. V. Maresch, O. Medenbach & T. Baller

Institut für Mineralogie, Ruhr-Universität Bochum, D-4630 Bochum, FRG

The mineral pumpellyite, $W_4X_2Y_4Z_6O_{(20+t)}(OH)_{(8-t)}$ where W = Ca, Mn; X = (Mg, Fe^{2+}, Mn)$_{2-t}$ (Fe^{3+}, Al)$_t$; Y = Fe^{3+}, Al; Z = Si (ref. 1) is a well-known constituent of very low-grade metamorphic rocks, especially of metabasic compositions. Schiffmann and Liou[2] have synthesized the ideal Fe-free endmember 'Mg–Al' pumpellyite', $Ca_4MgAl_5Si_6O_{21}(OH)_7$, and found its upper thermal stability to lie near 375–400 °C in the range of 5–8 kbar water pressure. Here we report the high-pressure synthesis of a pumpellyite-type phase in which the position W of the above formula is solely occupied by magnesium. This 'Mg–Mg–Al pumpellyite', which is chemically nearly equivalent to pyrope + H_2O, crystallizes at 40–55 kbar, 700–850 °C. Therefore, it qualifies as a potential hydrous mantle phase in a subduction zone regime.

During a recent high-pressure investigation of the system $MgO-Al_2O_3-SiO_2-H_2O$ (MASH) aimed at synthesizing a Ti-free ellenbergerite[3], reflections were encountered in the powder X-ray diffraction pattern that did not fit any of the known crystalline phases of the MASH system, nor could they be related to an ellenbergerite variety. In a run with a gel of the composition $4MgO \cdot 2Al_2O_3 \cdot 5SiO_2$ plus excess water at 700 °C, 50 kbar water pressure, for 5 days, these unknown peaks became dominant, while only small amounts of talc could be identified in addition. A comparison of the unknown peaks with those of potentially related silicate phases suggested a pumpellyite-type crystal structure. This was confirmed by successful indexing of more than 40 observed reflections below 70° 2θ CuKα, on the basis of a monoclinic cell. The refined cell dimensions, using an internal *F*-phlogopite standard, are given in Table 1. Observed diffraction data for the most prominent reflections of the new phase to a *d*-spacing of 2,000 are given in Table 2. Compared with the synthetic Ca-bearing 'Mg–Al pumpellyite' of Schiffmann and Liou[2], also listed in Table 1, the unit cell volume of the synthetic Ca-free phase is ~9% smaller. Under the microscope, the new phase forms small tabular crystals (4 × 10 × 40 μm) with negative elongation for all orientations. The refractive indices listed in Table 1 are appreciably higher than those of the synthetic Ca-bearing phase.

The crystal structure of pumpellyite[4,5] has Ca in sevenfold coordination with respect to oxygen and relatively short Ca—O distances of ~2.43 Å. Following the straightforward rule of increasing coordination number with pressure, it is most likely that, at the high pressure of synthesis, Mg is able to substitute for Ca in the sevenfold positions. Thus a general formula of the synthetic MASH pumpellyite can be expected to be

$$Mg_4(Mg_{2-t}Al_t)Al_4Si_6O_{20+t}(OH)_{8-t}$$

Since t can vary only between zero and 2, we can define the following theoretical compositions of Ca-free pumpellyites, which are here called 'Mg–Mg–Al pumpellyites':

Pu 1: $Mg_4Mg_2Al_4Si_6O_{20}(OH)_8$ (for $t = 0$)

Pu 2: $Mg_4(MgAl)Al_4Si_6O_{21}(OH)_7$ (for $t = 1$)

Pu 3: $Mg_4Al_2Al_4Si_6O_{22}(OH)_6$ (for $t = 2$)

In Fig. 1, these three compositions are plotted in the MAS compositional triangle and connected through the line of mutual theoretical substitution Mg + H = Al. Note that in this projection Pu 1 plots together with pyrope, $Mg_3Al_2Si_3O_{12}$. Pu 2 and 3 can be represented, for example, by the three-phase assemblage pyrope + SiO_2 + Al_2SiO_5.

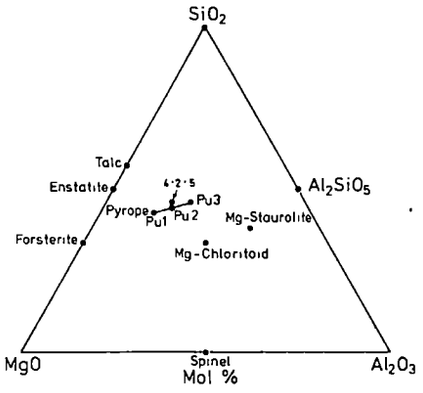


Fig. 1 Projection from H_2O of the $MgO-Al_2O_3-SiO_2-H_2O$ system, showing the possible extent of solid solution of the Ca-free pumpellyite phase (Pu 1 to Pu 3), as well as the bulk composition 4:2:5 of the critical run discussed in the text.

Figure 1 also shows the projection point of the gel composition 4:2:5 used as starting material for the successful synthesis. This composition lies very close to the theoretical 'Mg–Mg–Al pumpellyite' Pu 2. Indeed, the observed products of synthesis, 'Mg–Mg–Al pumpellyite' plus small amounts of talc, seem to indicate that this new pumpellyite phase has a composition close to that of Pu 2 and may even be identical to it. Note that in the system $CaO-MgO-Al_2O_3-SiO_2-H_2O$, 100% yield of Mg–Al pumpellyite could only be achieved with a bulk composition having $t = 1$ as in Pu 2 (ref. 2).

No reliable information is available as to the thermodynamic pressure/temperature (P/T) stability of the new pumpellyite-type phase. In other MASH synthesis runs at 40 kbar/700 °C, some of the characteristic X-ray powder diffraction lines were discerned as well. In addition, these reflections were observed, together with others, in chemically similar mixtures of the system $MgO-BeO-Al_2O_3-SiO_2-H_2O$ run in the P/T range 45–55 kbar, 700–850 °C (ref. 6). Nevertheless, all these products could be metastable. Seeded runs are required to resolve this problem.

The geoscientific importance of the high-pressure synthesis reported here lies in the fact that 'Mg–Mg–Al pumpellyite' is, as a first approximation, chemically equivalent to pyrope garnet + water. As this garnet is one of the minerals making up the Earth's mantle at depths ≥60–80 km, the question arises as to whether or not this garnet can be replaced in the mantle

Table 1 Physical properties of synthetic Ca-bearing pumpellyite and the new Ca-free pumpellyite phase

Parameter	$Ca_4MgAl_5Si_6O_{21}(OH)_7$*	Ca-free phase†
a (Å)	8.825(8)	8.540(1)
b (Å)	5.875(5)	5.712(1)
c (Å)	19.10(1)	18.481(2)
β (°)	97.39(7)	97.71(1)
V (Å^3)	982.1	893.4(1)
n_x		1.674(2)
n_y	Average	1.6825(10)
n_z	1.624	1.699(2)
$2V$ (°)	—	72(1)
D_x (g cm^{-3})	3.04	~3.3

* Synthetic; † data from this paper.

Table 2 The most prominent reflections of Ca-free pumpellyite observed for $d > 2.000$

d(Å)	I^{rel}	hkl	d(Å)	I^{rel}	hkl
9.18	7	002	2.728	12	022
8.51	3	100	2.651	48	$20\bar{6}$
4.67	24	$11\bar{1}$	2.548	58	$31\bar{1}$
4.58	33	004	2.463	3	311
4.50	22	111	2.423	37	024
4.23	6	200	2.367	100	220
4.05	3	$20\bar{2}$			$11\bar{7}$
3.891	3	$11\bar{3}$	2.252	31	222
3.659	62	202	2.244	28	313
3.410	16	$21\bar{1}$	2.225	4	$30\bar{6}$
3.339	21	$20\bar{4}$	2.208	5	$31\bar{5}$
2.918	28	204	2.170	11	$22\bar{4}$
2.856	15	020	2.137	55	$20\bar{8}$
2.846	41	213	2.125	39	$40\bar{2}$
		300	2.086	23	026
2.798	84	$30\bar{2}$	2.041	23	224
		115	2.027	18	$40\bar{4}$

material by the new pumpellyite phase, provided water is available and the temperatures are sufficiently low for hydration. If 'Mg-Ag-Al pumpellyite' were stable, for example, at 40 kbar and 800 °C, this phase could be a constituent of a mantle plate which is being subducted along a low geothermal gradient of ~7.5 °C km^{-1} to ~120 km. Such low geothermal gradients and subduction to at least 100 km were recently inferred even for crustal rocks[7]. The water required for the formation of the pumpellyite phase would be readily available in the serpentinized upper portions of an oceanic mantle. This model becomes even more attractive when one considers the possibility of solid solution in the pumpellyite phase, involving both Mg and Ca in the W-position of the structure, with concomitant stabilization towards lower water pressures. The new phase is also of interest in relation to a series of hydrous synthetic high-pressure phases in the system MgO-SiO_2-H_2O (refs 8, 9) which have largely unknown structures, and are also discussed as possible receptacles of water in the Earth's mantle.

Received 13 January; accepted 2 April 1986.

1. Coombs, D. S., Nakamura, Y. & Vuagnat, M. *J. Petrol.* **17**, 440-471 (1976).
2. Schiffman, P. & Liou, J. G. *J. Petrol.* **21**, 441-474 (1980).
3. Schreyer, W., Baller, T. & Chopin, C. *Terra cognita* **5**, 327 (1985).
4. Galli, E. & Alberti, A. *Acta crystallogr.* **B25**, 2276-2281 (1969).
5. Yoshiasa, A. & Matsumoto, T. *Am. Miner.* **70**, 1011-1019 (1985).
6. Hölscher, A., Schreyer, W. & Lattard, D. *Contr. Miner. Petrol.* **92**, 113-127 (1986).
7. Chopin, C. *Contr. Miner. Petrol.* **86**, 107-118 (1984).
8. Ringwood, A. & Major, A. *Earth planet. Sci. Lett.* **2**, 130-133 (1967).
9. Yamamoto, K. & Akimoto, S. *Am. J. Sci.* **277**, 288-312 (1977).

A new ^{36}Cl hydrological model and ^{36}Cl systematics in the Jordan River/Dead Sea system

M. Paul*, A. Kaufman†, M. Magaritz†, D. Fink*, W. Henning‡, R. Kaim§, W. Kutschera‡ & O. Meirav*

* Racah Institute of Physics, The Hebrew University, Jerusalem, Israel 91904
† Isotope Department, Weizmann Institute of Science, Rehovot, Israel 76100
‡ Argonne National Laboratory, Argonne, Illinois 60439, USA
§ Nuclear Physics Department, Weizmann Institute of Science, Rehovot, Israel 76100

The recent breakthrough in our ability to detect the radioactive isotope ^{36}Cl (half-life $T_{1/2} = 301{,}000$ yr) at natural levels by accelerator mass spectrometry[1] allows the processes of salination of water systems to be studied in a new way by distinguishing the chloride content originating in young rainwaters and their subsequent evaporation from that generated by the leaching of ancient rocks. Results for the Jordan River/Dead Sea system show that the amount of chloride leached from rocks ranges from ~70% in source springs to >90% in water bodies downstream. Furthermore, the amount of water left after evaporation decreases from ~50% in the source springs to 20% in the intermediate Lake Kinneret. In the terminal Dead Sea, 99% of the stable chloride originates from ancient rocks and evaporite formations while ~80% of its ^{36}Cl content is of meteoric origin. Using ^{36}Cl measurements, we estimate the accumulation time of the Dead Sea salt to be 19,000–25,000 yr.

Meteoric ^{36}Cl enters the hydrological cycle together with stable chloride from aerosols when they are both washed out of the atmosphere by precipitation. The evaporation and evapotranspiration (through vegetation) of surface and soil water, which follow soon after, are not expected to alter significantly the chlorine isotopic ratio, although they increase the chloride concentration. In contrast, the addition of chloride leached from rocks with a ^{36}Cl/Cl ratio generally much lower than that of precipitation, reduces this isotopic ratio. The chloride concentration is further increased by the evaporation which occurs in rivers and lakes after ground water emerges in springs.

It is extremely difficult to distinguish between the processes of evaporation (including evapotranspiration) and of rock leaching by means of standard hydrological methods, as both processes result in concentration increases. But independent measurement of ^{36}Cl/Cl ratios and of stable chloride concentrations permit the quantitative determination of the extent to which each of the two processes has occurred in a given system.

We denote the chloride concentration of a water body and of precipitation by C_W and C_P, respectively (in mg l^{-1}), their respective ^{36}Cl/Cl ratios as R_W and R_P, and the ^{36}Cl/Cl ratio in the rock leachate by R_L. The fraction of the total chloride in the water body which originated in the rock leachate is then given by:

$$f_L = (1 - R_W/R_P)/(1 - R_L/R_P) \quad (1)$$

The evaporation factor (EF), defined as the ratio of the volume of the water body to the volume of the precipitation from which it originated, may then be calculated from:

$$EF = (C_P/C_W)/(1 - f_L) \quad (2)$$

These equations demonstrate how the processes of evaporation and rock chloride addition may be distinguished by measuring the quantities C_P, C_W, R_P, R_W and R_L. If $R_L/R_P \ll 1$ (as expected in leachates of old rocks), equation (1) reduces to $f_L = 1 - R_W/R_P$.

Table 1 Results of ^{36}Cl measurements in samples from the Jordan River/Dead Sea System

Map location no.	Sample origin and collection date	$^{36}Cl/Cl$* (10^{-15})	$^{36}Cl/Cl$† (10^{-15})	Cl (mg l^{-1})	^{36}Cl (10^6 atoms l^{-1})	F_L‡	EF‡	EF§ (hydro.)
1	Mount Hermon Snow (January 1983)	1,470±250 1,425±300 1,630±250 1,680±350 1,400±300 2,075±350	1,580±120	1.50	40±5			
2	Banias River (July 1983)	440±140 430±80 310±140 340±150	400±60	11.9	80±15	0.74	0.50	0.40
3	Snir River (July 1983)	400±175 460±180	430±125	11.0	80±20	0.72	0.50	
4	Dan River (July 1983)	725±140	725±140	10.5	129±25	0.54	0.31	
5	Lake Kinneret (April 1983)	49±15	49±15	252	210±65	0.97	0.20	0.25
6	Yarmuq River (July 1983)	186±48	186±48	137	431±110	0.88	0.09	0.16
7	Jordan River (February 1982)	137±35 114±22	121±19	646	1,320±210	0.92	0.03	0.15
8	Dead Sea 10 m depth (March 1977)	16±7 27±9 13±7	17±4					
	80 m depth (March 1977)	26±7 21±6 13±4 14±3 48±12 12±12	17±2	2.30×10^5	$(6.6\pm0.8)\times10^4$	0.99		
	310 m depth (March 1977)	13±5 29±10 38±10	20±4					
9	Ashlag Spring‖ (August 1982)	4±2	4±2	2.6×10^5				
10	Mount Sedom¶ 2,000 m depth	3±3 6±3 7±5	5±2					

* Results of independent measurements for samples of same origin are given when available. Quoted errors include statistical counting errors or random instrumental errors. The error in the absolute value is ±15%.

† Weighted mean of the independent measurements (column 3). Quoted error is the variance of the mean.

‡ See text for definition.

§ Ref. 7; see text.

‖ Hypersaline spring near Dead Sea shore.

¶ Rock salt core.

The physical meaning of the above equations is illustrated in Fig. 1. In the case of a closed system (no evaporation), all analytical results plotted in the $^{36}Cl/Cl$ versus (1/Cl) plane fall on a straight line PL. The value of the rock leachate fraction f_L determines the location of a given point on the line. Evaporation will shift a point horizontally to the left of the line PL by an amount related to the evaporation factor EF. Any additional source of ^{36}Cl (such as ^{36}Cl from the nuclear test pulse) will shift results of measurements in the vertical direction above the line PL.

The estimation of the salt accumulation age in a water body from ^{36}Cl measurements was first attempted by Bonner *et al.*[2]. This age t(yr) satisfies the equation:

$$N_{36} = \frac{I_{36}}{\lambda}(1 - e^{-\lambda t}) \qquad (3)$$

where λ(yr^{-1}) is the decay constant, N_{36} the total number of ^{36}Cl atoms present in the water body and I_{36} the annual input of this isotope. We assume that the amount of salt precipitated from the water is negligible. If the water body, as is often the case with saline lakes, receives in addition to the ordinary observable chloride input a significant sub-lacustrine input (from springs emerging below the lake surface and hence difficult to observe) of chloride originating from the leaching of old rocks, then the salt accumulation time of the water body may be determined by combining its ^{36}Cl balance with its stable chloride balance, even if the only information known about the sub-lacustrine source is its $^{36}Cl/Cl$ ratio. In this case, the annual ^{36}Cl input to the water can be shown to be the sum of two components: the annual ^{36}Cl input of meteoric origin and that of rock leachate origin. The accumulation age then satisfies the following equation:

$$N_{36} = C_W V_W R_W = \frac{Q_I C_I (R_I - R_L) + C_W V_W R_L / t}{\lambda}(1 - e^{-\lambda t}) \qquad (4)$$

where Q is the annual water discharge, V the water body volume, the subscript 'I' designates the input to the water body and the other symbols are as defined above.

To illustrate these applications of ^{36}Cl as a hydrological tracer, we consider the waters of the Jordan River/Dead Sea systems. This system (Fig. 2) is located in the northern part of the Syro-African rift and is composed primarily of the upper Jordan river,

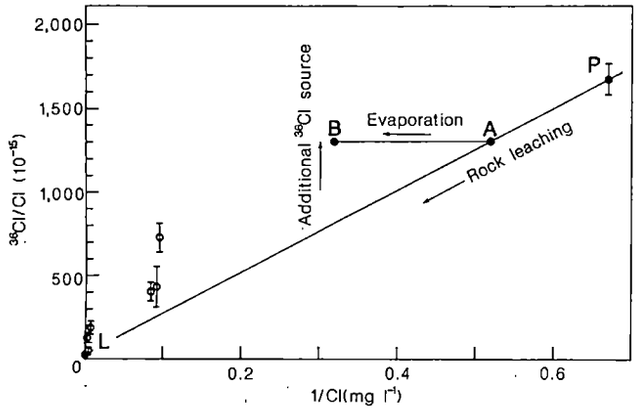


Fig. 1 Variation of the ^{36}Cl/Cl isotopic ratio versus the reciprocal (1/Cl) of the stable chloride concentration and schematic representation of different effects on the isotopic ratio. The straight line PL represents a hypothetical closed system (no evaporation) in which all samples are admixtures of precipitation (P) and rock leachate (L); as the latter contribution increases, the result moves down along line PL (A). Line AB reflects the effect of evaporation, which does not change the ^{36}Cl/Cl ratio. Results may lie above the line also due to an additional source of ^{36}Cl (for example, the ^{36}Cl nuclear test pulse). Also shown are results of measurements (open circles and vertical bars) for the Jordan River/Dead Sea system. The fact that all data points lie above the mixing line is mostly explained by evaporation processes (see text).

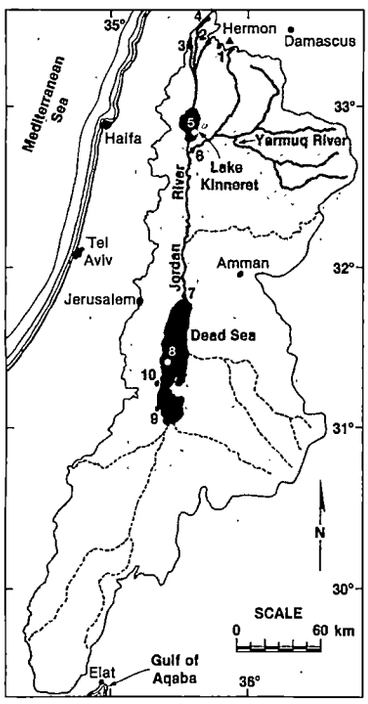


Fig. 2 Map showing the Jordan River/Dead Sea catchment basin (light shading) and the localities (numbered 1-10) sampled for ^{36}Cl measurements. The sample locations and their numbers are listed in Table 1.

Lake Kinneret, the Yarmuq river, the lower Jordan river and the Dead Sea terminal lake. The three important tributaries of the upper Jordan river—the Dan, Snir and Banias rivers—arise as springs which derive their waters from precipitation on Mount Hermon, with an underground residence time of a few years[3]. These waters collect large quantities of salt from the many saline springs that enter the system during their flow to the Dead Sea. This extremely saline lake acquired its present shape about 15,000 yr ago[4] as a result of the shrinking of its less saline predecessor, Lake Lisan. This 15,000 yr age is distinct from the

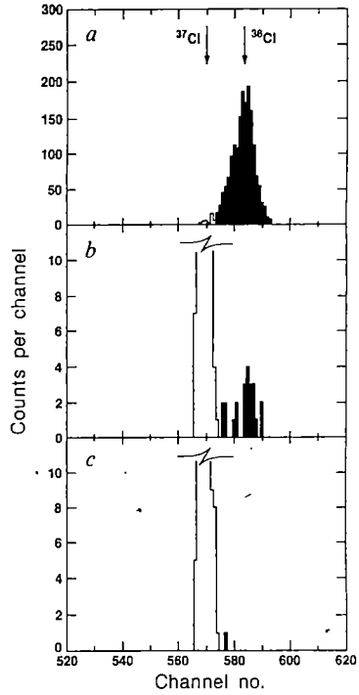


Fig. 3 Identification spectra of chlorine ions for: *a*, reference sample with ^{36}Cl/Cl = 3.5×10^{-12}; *b*, Dead Sea water; *c*, rock salt from Mount Sedom. The spectra were obtained after a software filtering of events to reject background (^{36}S isobaric and contaminant) ions. ^{37}Cl ions shown result from a tail of ^{37}Cl$^-$ injected into the accelerator. They are further discriminated from ^{36}Cl ions by time-of-flight measurements. See ref. 5 for details of the identification scheme.

age of the salt, discussed below. The high salinity of the Dead Sea results partly from intense evaporation and accumulation of the salt discharged by the Jordan River and smaller rivers, and partly from extremely saline springs which emerge at the lake shore and at its bottom.

The water samples on which the present study is based were collected from the localities indicated in Fig. 2. After removing SO_4^{2-} ions with Ba^{2+}, Cl^- was precipitated with Ag^+ and purified by dissolution in NH_3 before the final reprecipitation as AgCl. The ^{36}Cl/Cl ratio was measured using the accelerator mass spectrometry system set up at the Rehovot 14UD Pelletron tandem laboratory[5]. Figure 3 shows examples of ^{36}Cl spectra. The stable chloride concentrations in the same water samples were determined by titration with $AgNO_3$.

The results of our measurements are shown in Table 1 and Fig. 4. The consistent downstream decrease in ^{36}Cl/Cl in Fig. 4*a* reflects the progressive dilution of the meteoric ^{36}Cl input, represented by the Mount Hermon snow sample, with the chloride leached from rocks. Samples representing essentially pure rock chloride, whose meteoric ^{36}Cl component is expected to be extinct, were obtained from materials near the Dead Sea: rock salt from an old formation (Mount Sedom) and brine from a hypersaline spring. These samples yielded the two lowest ^{36}Cl/Cl values in our measurements. These values are, however, higher than ratios determined in some old salt deposits[6]; they may result from natural radioactivity[6], but at such low levels, experimental effects such as cross-contamination during sample preparation or ion source operation cannot be excluded. The downstream increase in the ^{36}Cl concentration (Fig. 4*b*), is attributed to evaporation processes. This is also illustrated in Fig. 1 where, in agreement with important evaporation effects, all data points lie above the rock leachate-precipitation mixing line. Extensive evaporation and accumulation are believed to

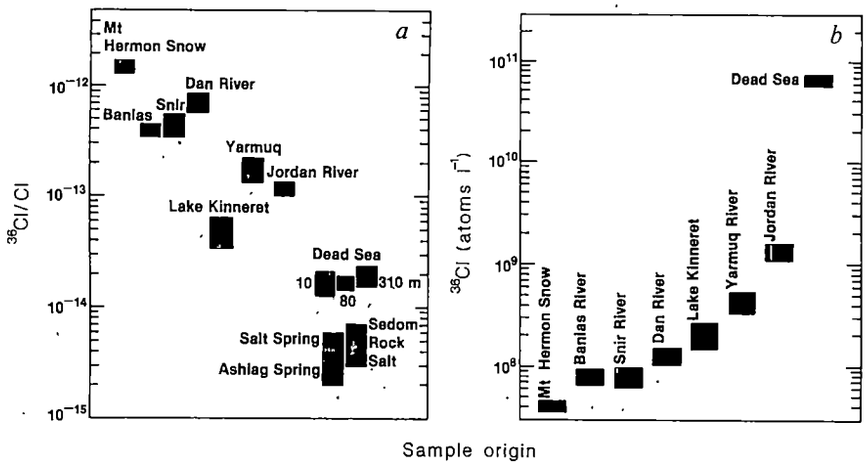


Fig. 4 Systematic variation of ^{36}Cl levels in waters from the Jordan River/Dead Sea system, arranged in downstream order. The distances along the horizontal axis are arbitrary. Also shown are a rock salt sample from a 2,000-m-deep core in the Mount Sedom area and a brine sample from the hypersaline Ashlag spring which is believed to be representative of the sub-lacustrine saline springs: *a*, ^{36}Cl/Cl isotopic ratios measured by accelerator mass spectrometry; *b*, ^{36}Cl concentrations in waters obtained from the ^{36}Cl/Cl ratios and measurements of the stable chloride concentrations. The monotonous downstream enrichment is attributed mainly to evaporation.

be responsible for the particularly high ^{36}Cl concentration in the terminal lake.

The rock leachate fraction f_L and the evaporation factor EF relative to Mount Hermon snow, calculated using equations (1) and (2), are shown for the various waters of the Jordan River/Dead Sea system in Table 1. The last column in Table 1 shows, for comparison, the available EF values obtained by hydrological methods[7]. Except for the Jordan River, the agreement between the two sets of estimates is surprisingly good. The agreement with independent measurements of the evaporation factors indicates that the additional ^{36}Cl source from the nuclear test pulse, known to have been important around 1960 (ref. 8), does not significantly affect our results. Substituting for example the hydrological estimates (EF(hydro.), Table 1) for Lake Kinneret and the Yarmuq River in equation (2), we derive expected values for the ^{36}Cl/Cl ratio of 38×10^{-15} and 108×10^{-15} respectively, only marginally different from the measured values, considering the uncertainties in the ^{36}Cl/Cl and EF(hydro.) values. The discrepancy for the case of the Jordan River may be due in part to such a contribution but is most probably caused also by an increase of evaporation following the great reduction in the flow of the Jordan river (presently <10% of the 1964 flow)which has resulted from the diversion of both Lake Kinneret and Yarmuq River waters for irrigation purposes.

The considerable amount of chloride contributed by rocks, even in the very dilute Jordan river tributaries, could not have been determined previously because it was not possible to distinguish between the effects of evaporation and of rock chloride addition. The relatively high evaporation factors for these tributaries are almost entirely caused by evapotranspiration, whereas the much lower values for the Yarmuq River must result from the intense evaporation which occurs along the long desert route between its source and the sampling point. Finally, the high rock leachate fraction for both Lake Kinneret and the Dead Sea undoubtedly reflect the well-known salt contributions by sub-lacustrine springs[9]. Note that an added advantage of the present method of determining the rock leachate fraction and the evaporation factor over the standard hydrological methods is that the former can be applied to any element of a river system and related directly to precipitation without making any measurements on other water bodies in the system.

Turning now to the determination of the salt accumulation age of the Dead Sea, we first use equation (3). But, as explained above, because of man-made changes in the hydrological system, the ^{36}Cl input of the natural system before 1964 cannot be directly measured. The annual ^{36}Cl input ($I_{36}=3.9\times10^{20}$ ^{36}Cl atoms yr^{-1}) may be estimated using the annual rainfall over the entire Dead Sea basin (9.8×10^{12} l yr^{-1}, ref. 7) and the ^{36}Cl concentration measured in the Mount Hermon snow (Table 1), assuming that it is representative of the whole basin. The number of ^{36}Cl atoms in the Dead Sea, as calculated by the expression $N_{36}=V_W C_W R_W$, is 9.4×10^{24} ^{36}Cl atoms, using both the Dead Sea volume ($V_W=1.43\times10^{14}$ l, ref. 10) and our measured Cl concentration and ^{36}Cl/Cl ratio (Table 1). The accumulation time of ^{36}Cl in the Dead Sea thus obtained is 25,000 yr. A value of 20,000 yr is obtained if one uses actual measured contributions of the two main inputs, Lake Kinneret and the Yarmuq River (0.5×10^{12} and 0.44×10^{12} l yr^{-1}, respectively, ref. 7) to estimate the annual ^{36}Cl input; to these contributions we added the annual ^{36}Cl input from precipitations over the rest of the basin (5.1×10^{12} l yr^{-1}, ref. 7), estimated as was done above for the entire basin.

The above calculations assume that the sub-Dead Sea saline springs derive their salt from very old deposits ($R_L=0$). If we assume that the measured ^{36}Cl/Cl value of 4.5×10^{-15} in Ashlag Spring and Mount Sedom (Table 1) is a representative value of the rock leachate fraction, we obtain, solving equation (4) by iteration, a range of slightly lower accumulation ages, 19,000–21,000 yr. For this calculation, an effective value of the ^{36}Cl/Cl ratio of the input waters from the various sources ($R_I=35$–44×10^{-15}) was derived by dividing the annual ^{36}Cl input, estimated above, by the Cl discharge (using $Q_I=1.4\times10^{12}$ l yr^{-1}, ref. 7 and $C_I=474$ mg l^{-1}, ref. 10). This range of R_I values, lower than the ^{36}Cl/Cl values measured in Lake Kinneret and the Yarmuq River, shows the effect of the known important salt addition in the lower Jordan River basin. The ratio of the ^{36}Cl contributions from meteoric input to that of rock leachate in the total ^{36}Cl content of the Dead Sea water can be estimated to be ~4:1 by using equation (4) and the calculated accumulation age. The contribution of the increase in the ^{36}Cl content of the atmosphere during the nuclear test period[8] is quite small compared with the amount of ^{36}Cl accumulated in the Dead Sea. The correction to the above accumulation times can be estimated by using the measured integral ^{36}Cl bomb pulse[8] to be ~500 yr. Furthermore, the contribution of ^{36}Cl produced by the capture of cosmic-ray neutrons by ^{35}Cl in the Dead Sea can be shown to be negligible.

Note that the present ages, although not very much higher than the 12,100 yr geochemical age derived by Bentor[10], were obtained without making any assumptions as to the detailed chemical nature of the saline springs. A comparison of these age estimates with the ~15,000 yr age of the present Dead Sea basin[4] may indicate that some of the salt now in the Dead Sea was inherited from its predecessor Lake Lisan.

This work was supported in part by the US-Israel Binational Science Foundation and by the Minerva Foundation.

Received 23 December 1985; accepted 21 March 1986.

1. Elmore, D. *et al. Nature* **277**, 22-25 (1979).
2. Bonner, F. T. *et al. Geochim. cosmochim. Acta* **25**, 261-266 (1961).
3. Simpson, B. & Carmi, I. *J. Hydrol.* **62**, 225-242 (1983).
4. Vogel, J. C. & Waterbolk, H. T. *Radiocarbon* **14**, 6-110 (1972).
5. Fink, D. *et al. Nucl. Instrum. Meth.* **B5**, 123-128 (1984).

6. Bentley, H. W., Phillips, F. M. & Davis, S. N. in *Handbook of Environmental Isotope Geochemistry*, Vol. 2 (eds Fritz, P. & Fontes, J. C.) (Elsevier, Amsterdam, in the press).
7. Dalin, Y. *Proc. Symp. Hydrological Activities Dictated by the Energy Crisis*, 5 (Israel National Council for Research and Development, Rehovot, Israel, 1981) (in Hebrew).
8. Elmore, D. *et al. Nature* **300**, 735-737 (1982).
9. Mazor, E., Mero, F. *J. Hydrol.* **7**, 318-333 (1969).
10. Bentor, Y. K. *Geochim. cosmochim. Acta* **25**, 239-260 (1961).

Phosphate pumps and shuttles in the Black Sea

Gary Shaffer

Oceanographic Institute, University of Gothenburg, Box 4038, 400 40 Gothenburg, Sweden

Phosphate distributions in oxic–anoxic ocean basins are related to distributions of total oxygen consumed (mainly from free oxygen, nitrate and sulphate) in the decomposition of organic matter[1,2]. Data from the Black Sea show, however, that phosphate concentrations immediately above and below the redox front are considerably lower and higher, respectively, than would be predicted from such stoichiometric models. This implies extra sinks and/or sources of phosphate and/or total oxygen not associated with organic decomposition. Here, I present two physical–biogeochemical interactions that result in phosphate sinks and sources with the structure needed to explain the observed phosphate anomalies. A phosphate pump based on iron can account for up to 40% of the required sink–source strength. The rest may be caused by a phosphate shuttle based on manganese.

The salinity, temperature, PO_4^{3-}, NO_3^-, O_2, H_2S, Fe^{2+} and Mn^{2+} data analysed here originated from cruise 49 of RV *Atlantis II* in March and April 1969 (refs 3, 4). I chose 18 stations which had a good coverage of the Black Sea and good sampling depth and salinity data. All PO_4^{3-} and sample depth data from these stations have been plotted as functions of salinity (Fig. 1) and fitted with least-mean-square B-splines[5]. The splines, plotted against each other, yield a pseudo-mean distribution with depth ($\overline{PO_4}$, Fig. 2). This procedure is superior to conventional depth averaging[6] or depth averaging relative to an oxygen zero boundary[4,7]. It averages over isopycnal surfaces, where the salinity determines the density below the Black Sea surface layer, and thus should retain maximum information on mean 'vertical' structure[8]. Indeed, the $\overline{PO_4}$ minimum/maximum pair (Fig. 2) reflects a similar structure from detailed, individual PO_4^{3-} profiles from this data set[6,9].

Phosphate distribution can be calculated from organic decomposition, $(PO_4)_{exp}$ (Fig. 2) and be expressed as

$$(PO_4)_{exp} = a\Delta O_2 + b\Delta NO_3 + c\Delta SO_4 + (PO_4)_p \qquad (1)$$

where $\Delta O_2 = O_2(\text{saturation}) - \overline{O_2}$, $\Delta NO_3 = d\Delta O_2 + (NO_3)_p - \overline{NO_3}$, and $\Delta SO_4 = \overline{H_2S}$. The subscript 'p' refers to preformed substances[1,2]. Here the concentrations of $(NO_3)_p$ and $(PO_4)_p$ are 0 and 0.15 μmol l^{-1} respectively. Pseudo-mean distributions are determined as above and a–d are $(138)^{-1}$, $(85)^{-1}$, $(53)^{-1}$ and $(8.6)^{-1}$, respectively[2]. $(PO_4)_{exp}$ over-estimates $(PO_4)_{ox}$ (a 'true' PO_4^{3-} distribution from organic decomposition) above L, the O_2–H_2S boundary (Fig. 2) and under-estimates it below this boundary. In the present-day Black Sea nearly all H_2S-S produced during sulphate reduction below L should reappear, after advection, diffusion and a series of intermediate oxidation steps, as SO_4^{2-}-S above L. This implies extra O_2 and H_2S consumption, above and below L, respectively, without concurrent PO_4^{3-} release. A $(PO_4)_{ox}$ distribution (Fig. 2) based on estimates of this extra O_2 consumption and $(PO_4)_{ox} \rightarrow \overline{PO_4}$ away from L, underlines some inherent weaknesses in using only chemical data. With a knowledge of diapycnal advection and diffusion, rates could be calculated and a stoichiometric model applied directly to them[8]. The large phosphate anomaly dipole pivoted near the O_2–H_2S boundary in the Black Sea, however, needs extra sinks and sources of PO_4^{3-} to be explained.

Iron-oxyhydroxo-phosphates (FeOP) form in oxidizing conditions ($Eh > \sim 200$ mV) and dissolve in reducing conditions ($Eh < \sim 200$ mV)[10,11]. Any combination of physical processes which lead to a net transport of such particles down through the redox front and Fe^{2+} and PO_4^{3-} ions back up through it, would produce an extra sink–source pair for PO_4^{3-} of the type needed to explain the observed anomaly dipole. Two possible cycles containing such combinations are the phosphate pump and the phosphate shuttle (Fig. 3). In the pump, vertical isopycnal displacements sweep the redox front back and forth across a sea-bottom segment B. During the release phase (shallow redoxocline) PO_4^{3-} and Fe^{2+} leave B as FeOP dissolves. Some Fe^{2+} reprecipitates as iron sulphide (FeS). During the retention phase (deep redoxocline) FeS dissolves and FeOP forms on B. PO_4^{3-} is adsorbed from the water column and the pore water. Increased upward diffusion of PO_4^{3-} (caused by its enhanced vertical gradients) closes the cycle. Thus, baroclinic motions near the coast pump PO_4^{3-} down through the O_2–H_2S boundary in oxic–anoxic basins. In the shuttle, Fe^{2+} is advected and diffused up through the redox front to form FeOP, thereby adsorbing PO_4^{3-}. FeOP particles sink through the front, dissolve, and release PO_4^{3-}. Again increased diffusion closes the cycle.

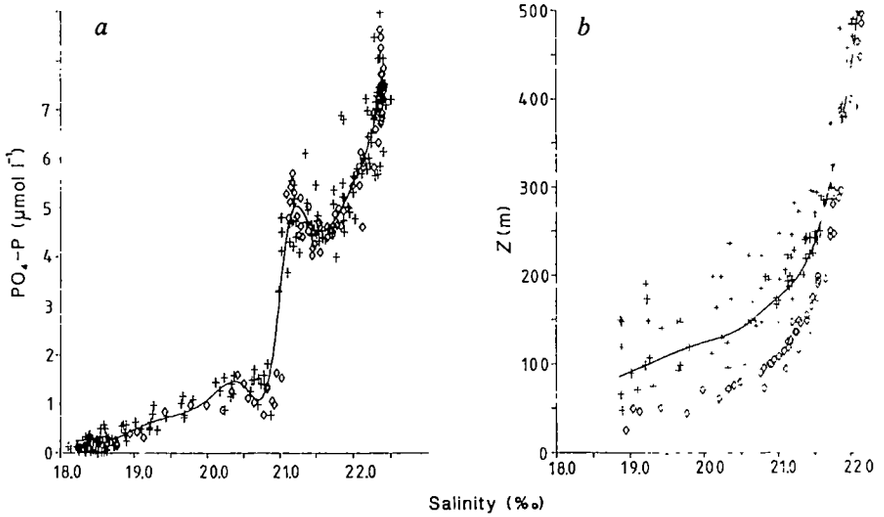


Fig. 1 Phosphate-phosphorus (a) and water sample depth (b) plotted against salinity for 18 stations of the *Atlantic II* cruise 49 to the Black Sea, March–April 1969 (ref. 3). The open sea stations (◇) are numbers 1445, 1446, 1447, 1466, and 1468. The shelf stations (+, water depth <1,800 m) are numbers 1435, 1437, 1439, 1441, 1443, 1447, 1450, 1452, 1454, 1461, 1470, 1473 and 1476. Least mean square B-spline fits[5] are shown for data from all 18 stations. For the water sample depths linear interpolation in salinity space[8] was applied to individual stations before B-spline fitting.

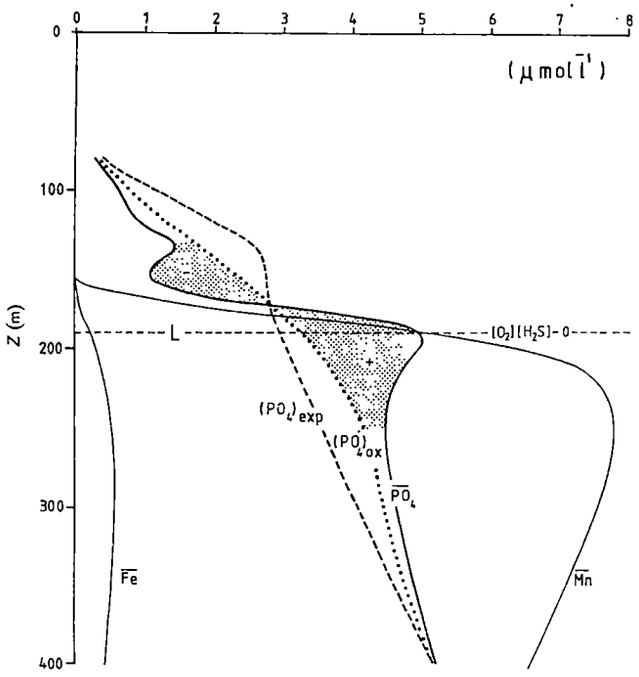


Fig. 2 Pseudo-mean distribution of phosphate-phosphorus with depth, $\overline{PO_4}$, formed by plotting the B-splines in Fig. 1 against each other. This procedure should retain a maximum of 'real' mean vertical structure and gradients. Analogous distributions are shown for dissolved manganese, $\overline{Mn}$, and iron, $\overline{Fe}$, from data of stations 1435, 1439, 1445, 1446, 1452, 1461, 1464 and 1466 (ref. 4). The zero oxygen and hydrogen sulphide concentration level, L, is indicated (taken from $\overline{O_2}$ and $\overline{H_2S}$ distributions calculated as $\overline{PO_4}$ above). Also presented is the phosphate-phosphorus distribution expected from organic decomposition alone, $(PO_4)_{exp}$, as calculated from equation (2). $(PO_4)_{ox}$ is $(PO_4)_{exp}$ 'corrected' for extra O_2 consumption as described in the text. The phosphate anomaly dipole, shaded, is defined by $(PO_4)_{ox}$-$\overline{PO_4}$.

The strength of the extra PO_4^{3-} sinks and sources, $|Q_{PO_4}|$, can be estimated from

$$Q_{PO_4} \approx Ak\mathrm{d}(PO_4)_{anom}/\mathrm{d}z \qquad (2)$$

where A, the cross-sectional area, k, the vertical turbulent diffusion coefficient and the vertical gradient of $(PO_4)_{anom}$ $[=(PO_4)_{ox}-\overline{PO_4}]$; all are evaluated at the $(PO_4)_{ox}$, $\overline{PO_4}$) intersection near level L (Fig. 2). There, $A \approx 3.0\times10^{11}$ m^2 (ref. 12) and $\mathrm{d}(PO_4)_{anom}/\mathrm{d}z \approx 9\times10^{-2}$ mmol m^{-4} (Fig. 2). Previous estimates[4,7] of k of 1.4×10^{-6} m^2 s^{-1} in the Black Sea halocline are probably in error. Salt conservation requires that the vertical velocity, w, be much greater than the w used to obtain this estimate: A salty (35‰) inflow of 190 km^3 yr^{-1} (refs 4, 13) must entrain much 18.5-22.0‰ ambient water before becoming 22.0-22.4‰ deep water; a six to ninefold increase in volume transport (and in the w and k estimates) is implied. Although a constant w and k, one-dimensional model[4,7] is probably not a good one for a system like the Black Sea, for example, entrainment and decreasing cross-section with depth imply a large increase in w with depth, a k from a salt space method can be estimated[14,15] which agrees with the new k above and thus the value $k=1\times10^{-5}$ m^2 s^{-1} is adopted here; then $|Q_{PO_4}| \approx 2.3\times10^{10}$ mmol PO_4^{3-} day^{-1}. A mean cycling time, τ, for PO_4^{3-} ions around the anomaly dipole may be estimated by $|RQ^{-1}_{PO_4}|$ where R is the mean total PO_4^{3-} anomaly. From Fig. 2, $R \approx 1.5\times10^{13}$ mmol and thus, $\tau \approx$ 2 yr. A τ of ~500 yr results for the cycle PO_4^{3-} uptake by phytoplankton followed by PO_4^{3-} regeneration in the deep water.

Isopycnal displacements near the Black Sea coast may be caused by upwelling/downwelling[14], coastal-trapped waves[16] and seasonal changes of the mean circulation[17]. The r.m.s. displacement near level L from these processes may be ~30 m, which implies a typical bottom area swept by the phosphate pump of $\sim1.5\times10^{10}$ m^2 (Fig. 3 and ref. 12) and mean retention-release rates for PO_4^{3-} bound with Fe oxyhydroxides of ~1.5 mmol m^{-2} day^{-1} to explain the anomaly dipole by the pump. Retention-release rates of 0.7-1.5 mmol m^{-2} day^{-1} have been obtained in benthic chamber experiments meant to simulate redox turnovers[18,19]. Such high retention rates, however,

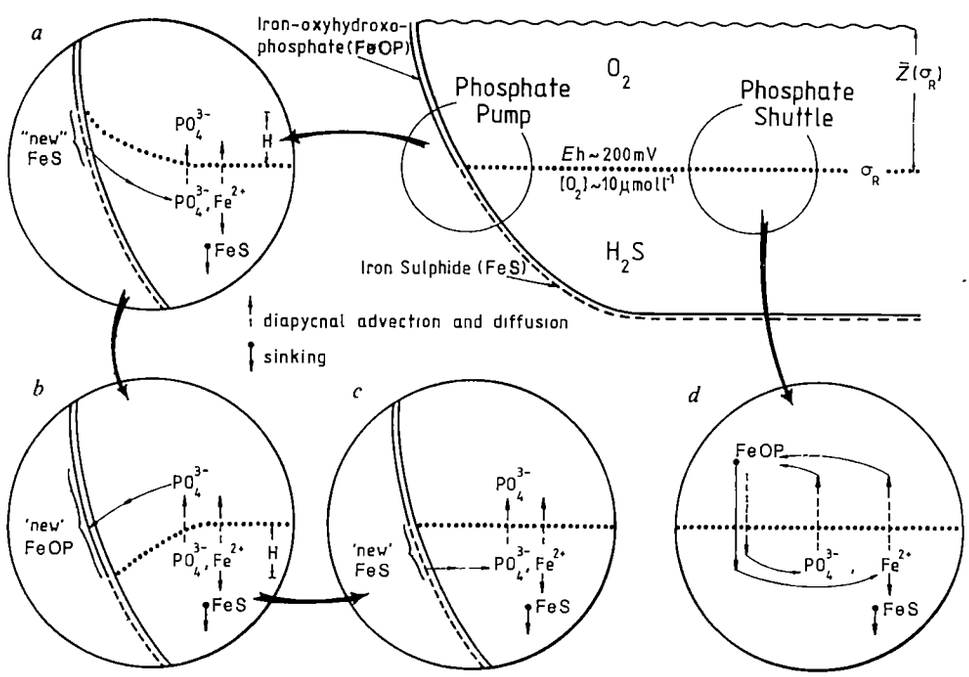


Fig. 3 The basic situation shown in the upper right hand corner is a basin with oxygen in the surface water and hydrogen sulphide in the deep water. The redox front between these two layers is represented by an isopycnal surface σ_R with mean depth $\bar{Z}$, chosen to coincide with $Eh\sim$ 200 mV, the approximate potential of the Fe^{2+}-Fe^{3+} redox pair. Iron-oxyhydroxo-phosphate (FeOP) and iron sulphide (FeS) are found at the sediment surface in contact with the upper and lower layer respectively. In the phosphate pump, isopycnal displacements sweep back and forth across a segment of sea bottom between depths $\bar{Z} \pm H$. The release and retention phases for PO_4^{3-} are illustrated by insets *a*, *c* and *b*, respectively. The + and − anomalies for PO_4^{3-} should have comparable vertical scales, ~2*H*. In the text, it is argued that the efficiency of the pump is limited by its retention phase, also, since some Fe^{2+} is continually lost to the deep anoxic bottoms with FeS, new Fe from runoff is needed to keep the pump primed. In the phosphate shuttle (*d*), the vertical scales of the + and − anomalies depend on the balance between diapycnal advection and mixing and speeds of sedimentation and chemical reactions. Thus, these scales should differ.

were observed at water column $PO_4^{3-} \sim 10$ times greater than the Black Sea ones and in artificial flow conditions. Some PO_4^{3-} retention in the sediment is caused by adsorption from the water column. A likely maximum rate for this would be $D\,[PO_4^{3-}]\,\delta^{-1}$ where D is a molecular diffusion coefficient, $[PO_4^{3-}]$ is the water column PO_4^{3-} and δ is the thickness of the diffusive sublayer at the sediment/water interface. With $D \sim 6\times10^{10}$ m^2 s^{-1} (ref. 20, $T \sim 8$ °C), $[PO_4^{3-}] \sim 2$ μmol l^{-1} and $\delta \sim 2\times10^{-4}$ m (ref. 21, large flow velocities), this rate is ~ 0.5 mmol m^2 day^{-1}. The rest of PO_4^{3-} retention is caused by direct adsorption of PO_4^{3-} released in the sediment during organic decomposition. An estimate of the sedimentation rate of organic P is $[w(PO_4)_{ox} + k\,d(PO_4)_{ox}/dz]_L$ from a physical transport-production balance. With k as before, $[(PO_4)_{ox}, d(PO_4)_{ox}/dz]_L$ from Fig. 2 and $w = 1.2\times10^{-7}$ m s^{-1} in accordance with the discussion earlier, this rate is ~ 0.06 mmol m^{-2} day^{-1}. Thus the efficiency of the phosphate pump seems to be limited by its retention phase and the pump can only explain up to 40% of the Black Sea PO_4^{3-} anomaly dipole.

The strength of the Fe^{2+} sink resulting from precipitation above level L may be estimated from

$$Q_{Fe} \approx A[w\overline{Fe} + k\,d(\overline{Fe})/dz]_L \qquad (3)$$

With A, w, k as above and $[\overline{Fe}]_L$ from Fig. 2, $Q_{Fe} \approx 2\times10^9$ mmol Fe day^{-1}. Thus $Q_{Fe}|Q_{PO_4}|^{-1} < 0.1$ and a phosphate shuttle based on iron probably makes no significant contribution to the observed PO_4^{3-} anomalies. Concentrations of dissolved manganese are ~ 10 times greater than those of iron in the Black Sea (Fig. 2) caused by the greater solubility of Mn salts in reducing conditions[4]. From a calculation like equation (3), $Q_{Mn} \approx 5.2\times10^{10}$ mmol Mn day^{-1} and $Q_{Mn}|Q_{PO_4}|^{-1} \approx 2.3$. Note that, from equations (2) and (3), $\overline{Fe}$ and $\overline{Mn}$, the Q ratios above are insensitive to choices of w and k.

I suggest that manganese, like iron, forms oxyhydroxophosphate and that a shuttle based on Mn explains the rest of the PO_4^{3-} anomaly dipole. This would require a P/Mn ratio of at least 0.3 in the Mn precipitate observed above level L in the Black Sea[22]. The hypothesis is supported by the $\overline{Mn}$, $\overline{Po_4}$ and $(PO_4)_{ox}$ distributions (Fig. 2) which indicate good spatial correlations between Mn^{2+} and extra PO_4^{3-} sinks and sources. For both ions, the scale of the source layer is apparently greater than that of the sink layer. This is consistent with the shuttle scenario (Fig. 3). Also, the PO_4^{3-} anomalies appear more pronounced for open Black Sea stations (Fig. 1), and may indicate an open sea process. The $\overline{PO_4}$ distribution (Fig. 2) and our w and k imply an order of magnitude weaker PO_4^{3-} sink directly below the PO_4 maximum. This has been attributed to bacterial chemosynthesis[7].

Similar large PO_4^{3-} anomalies near the O_2–H_2S zone have been observed elsewhere, for example, in Lake Nitinat[2]. The processes presented here probably also explain these observations, and detailed sampling should reveal similar PO_4^{3-} anomaly dipoles in most other oxic–anoxic basins. Finally, observational and theoretical searches for other possible important effects should be carried out, for instance, on denitrification and sulphate reduction rates, of redox front bottom sweeping due to coastal dynamics. After all, such physical processes not only expose the sediment surface to cyclic changes of O_2 and H_2S concentrations but also may alter the diffusive sublayer thickness in a systematic way through associated currents.

I thank David Dyrssen for help with the data and literature search and for discussions. This research was supported by grants from the geoscience division of the Swedish Natural Science Research Council.

Received 28 October 1985; accepted 7 March 1986.

1. Richards, F. A. in *Proc. 2nd Int. Wat. Pollut. Res. Conf.* Tokyo 1964, 215–243 (Pergamon, Oxford, 1965).
2. Richards, F. A. in *Chemical Oceanography* Vol. 1, (eds Riley, J. P. & Skirrow, G.) 611–645 (Academic, London, 1965).
3. Brewer, P. G. *Woods Hole Oceanogr. Inst. Tech. Rep. Ref. no. 71-65* (1971).
4. Spencer, D. W. & Brewer, P. G. *J. geophys. Res.* **76**, 5877–5892 (1971).
5. Cox, M. G. *J. Inst. Math. Appl.* **10**, 134–149 (1972).
6. Fonselius, S. H. in *The Black Sea—Geology, Chemistry and Biology* (eds Degens, E. T. & Ross, D. A.) 144–150 (American Association of Petroleum Geologists, Tulsa, 1984).
7. Brewer, P. G. & Murray, J. W. *Deep-Sea Res.* **29**, 803–818 (1973).
8. Shaffer, G. & Rönner, U. *Deep-Sea Res.* **31**, 197–220 (1984).
9. Grasshof, K. in *Chemical Oceanography* Vol. 2 (eds Riley, J. P. & Skirrow, G.) 455–563 (Academic, London, 1975).
10. Einsele, W. *Archiv. Hydrobiol. Plankton* **33**, 361–387 (1938).
11. Krom, M. D. & Berner, R. A. *Geochim. cosmochim. Acta* **45**, 207–216 (1981).
12. Deuser, W. G. in *The Black Sea—Geology, Chemistry, and Biology* (eds Degens, E. T. & Ross, D. A.) 133–136 (American Association of Petroleum Geologists, Tulsa, 1974).
13. Merz, A. & Möller, L. *Veröff. Inst. Meeresforsch. Berlin. Neue Folge* **A18** (1929).
14. Shaffer, G. *J. Phys. Oceanogr.* **9**, 847–855 (1979).
15. Walin, G. *Tellus* **29**, 128–136 (1977).
16. Csanady, G. T. *Circulation in the Coastal Ocean* (Reidel, Dordrecht, 1982).
17. Neumann, G. *Z. Ges. Erdk. Berl.* **3**, 92–114 (1944).
18. Balzer, W., Grasshoff, K., Dieckmann, P., Haardt, H. & Petersohn, U. *Oceanol. Acta* **6**, 337–344 (1983).
19. Holm, N. *Ophelia* Suppl. 1, 287–304 (1978).
20. Li, Y.-H. & Gregory, S. *Geochim. cosmochim. Acta* **38**, 703–714 (1974).
21. Santschi, P. H., Bower, P., Nyffeler, U. P., Azevedo, A. & Broecker, W. S. *Limnol. Oceanogr.* **28**, 899–912 (1983).
22. Spencer, D. W., Brewer, P. G. & Sachs, P. L. *Geochim. cosmochim. Acta* **36**, 71–86 (1972).

Mechanosensitivity of mammalian auditory hair cells *in vitro*

I. J. Russell, G. P. Richardson & A. R. Cody

MRC Neurophysiology Group, School of Biology, University of Sussex, Falmer, Brighton BN1 9QG, UK

Intracellular responses recorded *in vitro* from the cochleas of anaesthetized mammals have shown that the mechanoreceptive inner and outer hair cells are sharply tuned, accounting for many of the properties of the afferent fibres in the auditory nerve[1–4]. However, *in vivo* it has not been possible to measure directly the excitatory mechanical input to these cells (the displacement of their mechanosensitive stereocilia)[5,6] and thus to determine the relationship between the receptor potentials and displacement of their stereocilia. As a means of circumventing this technical difficulty, we have developed an organ culture of the mouse cochlea and here we describe the receptor potentials generated by the hair cells in response to direct displacement of their stereocilia.

Cochleas were dissected from mice at days 1–3 postnatal. The capsules surrounding the cochleas, stria vascularis and Reissner's membranes were removed and the organs of Corti, together with the spiral ganglia, were cultured for 2–7 days at 37 °C on collagen-coated coverslips in Maximow slide assemblies using a method similar to that described by Sobkowitz *et al.*[7]. Figure 1*a*, *b* shows the morphology of the hair cells in these *in vitro* preparations. Figure 2 shows the arrangement for making intracellular recordings from the hair cells while displacing their stereocilia. The resting membrane potentials of inner hair cells, outer hair cells and supporting cells measured *in vitro* in HEPES-buffered HBSS (Hanks' balanced salt solution) are very similar to those found *in vivo* for the cells of the guinea pig cochlea: −30 to −70 mV for inner hair cells, −40 to −70 mV for outer hair cells and −60 to −75 mV for supporting cells. In contrast to the situation *in vivo*, there is no endocochlear potential in these cultures and the abneural surfaces of the hair cells are exposed to an ionic environment whose dominant cation is sodium rather than potassium.

In the absence of mechanical stimulation, the resting membrane potentials of the hair cells were remarkably constant and did not exhibit the oscillatory behaviour characteristic of hair cells in the turtle cochlea and frog sacculus[8,9]. The voltage responses of inner and outer hair cells from the same region of the mouse cochlea to sinusoidal displacement of their stereocilia (Fig. 3*a*, *b*) were very similar in shape to those recorded from hair cells in isolated preparations from other species (for example, bullfrog sacculus[5]). The transfer functions in Fig. 3*c*, *d* show that in response to depolarizing displacements of their stereocilia towards the kinocilium, the responses of the inner

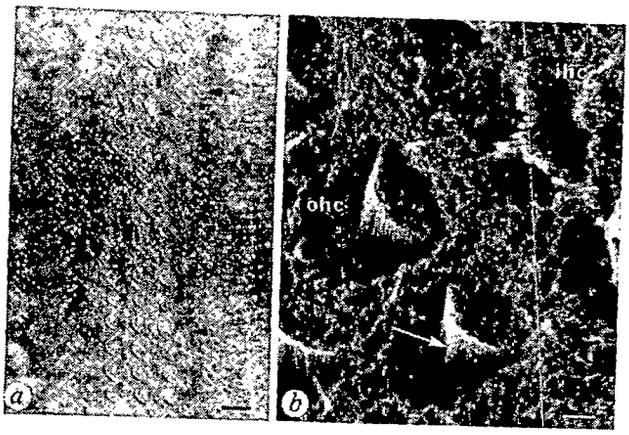


Fig. 1 *a*, Surface view of a 4-day-old culture of a mouse cochlea viewed using Nomarski optics. The stereocilia of the three rows of outer hair cells are clearly visible. The position of the single row of inner hair cells is marked by the arrowheads. The stereocilia of the inner hair cells are positioned slightly higher than those of the outer hair cells and are out of focus in this photomicrograph. The stereocilia of the inner hair cells form palisades while those of the outer hair cells form V-shapes whose internal angles become increasingly acute towards the basal high-frequency turn of the organ of Corti. Scale bar, 10 μm. *b*, Scanning electron micrograph of a 2-day-old organ culture of the mouse organ of Corti, showing the arrangement of the mechanically sensitive stereocilia of the inner (ihc) and outer (ohc) hair cells. The cells still possess a vestigial kinocilium (arrow) which is lost later in development. In scanning electron micrographs the bundles of stereocilia have the appearance of bundles of organ pipes as each row decreases in height with distance from the kinocilium. In these immature hair cells the stereocilia are more numerous than those found in the adult, and the microvilli on the apical surfaces of the intercalated supporting cells are more extensive. Scale bar, 1 μm.

Methods. Cultures were prepared from the cochleas of mice at days 1–3 postnatal. The cartilaginous capsule, stria vascularis, Reissner's membrane and the immature mesenchymal internal spiral lamina were removed by dissection in HEPES-buffered HBSS, leaving the organ of Corti, greater epithelial ridge and attached spiral ganglion as one unit. These tissue pieces were then explanted onto collagen-coated round glass coverslips, fed with ~50 μl of complete medium (8 parts Eagle's minimum essential medium with Earle's salts, 1 part heat-inactivated horse serum, 1 part mouse embryo extract buffered with 10 mM HEPES *p*H 7.2) and maintained in Maximow slide assemblies in the lying drop position at 37 °C for up to 7 days. For scanning electron microscopy the cultures were fixed in 5% glutaraldehyde in 0.1 M sodium phosphate, *p*H 7.2, for 2 h at room temperature, post-fixed in 1% OsO_4, dehydrated in acetone, dried to the critical point from liquid CO_2, sputter-coated with gold and viewed with a Jeol 100C scanning transmission electron microscope.

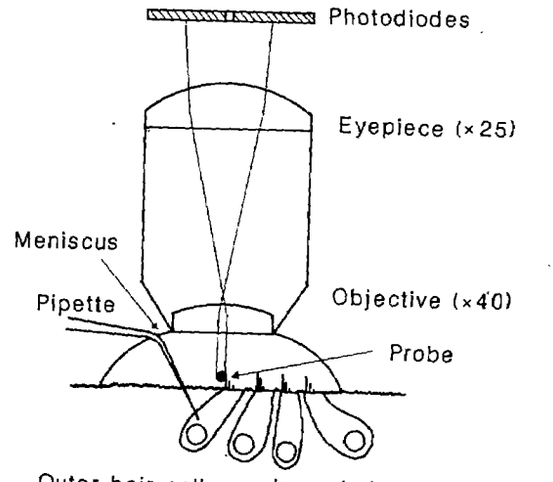


Fig. 2 For the electrophysiological experiments hair cells were maintained at room temperature (20 °C) and observed with the aid of a microscope equipped with a fixed stage, Nomarski optics and a ×40 water immersion lens. The stereocilia of the hair cells were displaced with the tip of a fine glass probe (0.5–1.5 μm diameter) along their axis of greatest sensitivity, that is, towards and away from the kinocilium in a plane parallel to the cuticular plate[17]. The probe was attached to a piezoelectric driver constructed from a short length of Vernitron bimorph (type PZT-5B). The displacement of the tip of the probe was monitored according to a method described elsewhere[18]. With the preparation illuminated in bright field from a battery-driven light source, the secondary image of the microscope was projected onto a screen by a ×25 eyepiece fitted to a trinocular head stage. The focused image of the tip of the probe was adjusted until it was ~0.5 mm wide and thus filled about half the width of a double photodiode array (2×0.5 mm; Centronics Ltd 2–5) mounted at the centre of the screen. The differences between the photocurrents of the two photodiodes was proportional to the displacement of the probe tip over the range 1–500 nm. The absolute displacement of the tip was determined as described by Art *et al.*[19]. The position of the photodiode array (which was mounted on a micropositioner) was adjusted until the difference in photocurrents was zero; the photodiode array was then displaced by a known amount (1–10 μm) and the photocurrent measured. The same photocurrent would have been measured if the tip had been displaced by this amount divided by the magnification of the optical system (~×1,000). Glass micropipettes (resistance 120–300 MΩ) were bent at right angles 200–250 μm from their tips, filled with 4 M potassium acetate, and inserted into the hair cells close to the nucleus. When stable recording conditions were achieved, the vibrating probe was placed against the stereocilia and the static position of the probe adjusted until a maximum response was obtained for a displacement of ~50 nm.

and outer hair cells are about three times greater than the hyperpolarizing and strongly saturating responses to displacements in the opposite direction. In this respect, the receptor potentials of hair cells in the mouse cochlea *in vitro* are similar to the receptor potentials recorded *in vivo* for hair cells from the apical, low-frequency turns of the guinea pig cochlea in response to tones close to their most sensitive frequencies; they are also similar to receptor potentials recorded for inner hair cells from the basal turn in response to low-frequency tones[2,10,11]. They differ from the responses of outer hair cells, however, in the basal high-frequency turn of the guinea pig cochlea to very-low-frequency tones, where the receptor potentials are predominantly hyperpolarizing, except at high intensities when they become depolarizing[12]. We propose that the different transfer functions of outer hair cells in the basal turn of the guinea pig cochlea may result from their mechanical interaction with the tectorial membrane. In the *in vitro* preparations the tectorial membrane does not cover the hair cells because it has not grown over them by the stage at which the organs are explanted. Thus, in the *in vitro* preparation, the outer hair cells do not interact with the tectorial membrane.

Figure 3 shows that the receptor potentials of the outer hair cell saturate at a lower voltage than those of the inner hair cell. Results from a further five outer hair cells showed that the receptor potentials saturate in the depolarizing direction at a mean of 6.5 mV (s.d. = 1.4 mV) above resting membrane potential, while the responses of the inner hair cells studied always saturated at higher levels. Further experiments are needed to determine whether the lower saturating voltage levels in outer hair cells reflect smaller receptor currents. The transfer functions of the hair cells shown in Fig. 3 show that the inner hair cells are most sensitive to stereocilia displacements in the depolarizing direction over the 0–60-nm range whereas the outer hair cells are most sensitive over the 0–30-nm range. This measure of sensitivity and dynamic range is largely dependent on the coupling between the stimulus probe and the stereocilia and is

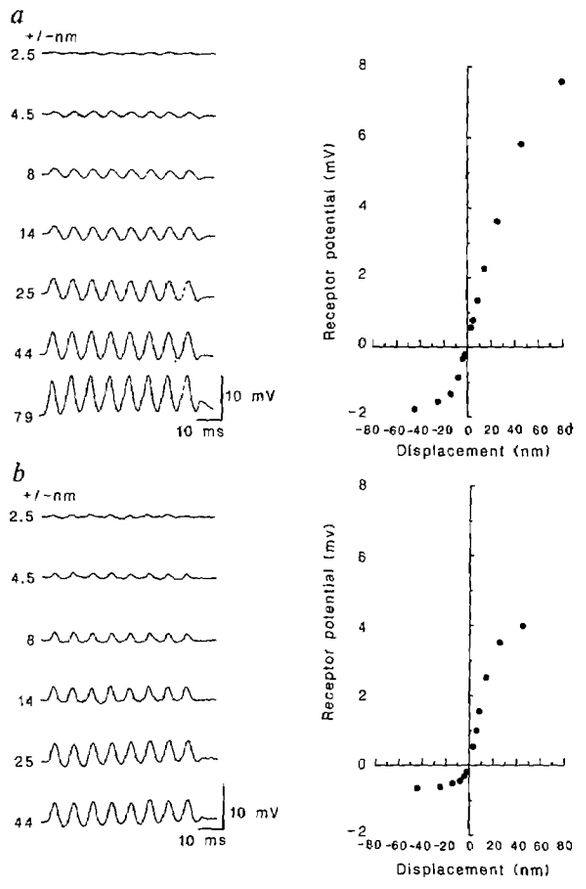


Fig. 3 Intracellular receptor potentials recorded from an inner hair cell (*a*) and an outer hair cell (*b*) from the apical low-frequency turn of the mouse cochlea *in vitro*, in response to sinusoidal displacements of their stereocilia. The peak amplitudes of the displacements are indicated alongside each trace. *c*, *d*, The relationship between peak displacement of the stereocilia and receptor potential for the inner hair cell and the outer hair cell, respectively.

not necessarily an indication that outer hair cells are more sensitive than inner hair cells. The stereocilia are at most 4 μm long, and it is difficult to determine the exact point of contact of the probe along the length of the stereocilia. Obviously, the angular rotation of the stereocilia will be greatest for a given displacement the closer it is to their points of attachment on the abneural surface of the hair cells.

The most sensitive cells recorded from the mouse cochlea *in vitro* are depolarized by ~0.8 mV (mean = 0.53, s.d. = 0.17, n = 18) when their stereocilia are displaced by 2 nm (Fig. 3*c*,*d*). The tallest hair-cell stereocilia in the *in vitro* preparations are 3–4 μm long. Thus the sensitivity of these hair cells is ~30 mV per degree of angular rotation of their stereocilia, or 0.4 mV per nm of displacement. This estimate of hair-cell sensitivity is considerably greater than that of hair cells in the frog sacculus (5–7 mV per μm), based on their responses to displacements of their stereocilia[5,9], but similar to estimates of hair-cell sensitivity reported for the turtle cochlea when the influence of the membrane resonance is disregarded (0.2 mV per nm)[13].

We have compared the mechanosensitivities of hair cells recorded *in vivo* in the basal turn of the guinea pig cochlea with those recorded from the mouse cochlea *in vitro*. Inner hair cells in the basal turn of the guinea pig cochlea are depolarized by 0.8–2 mV in response to tones close to their best frequencies at neural threshold[1]. At this sound level the basilar membrane displacement has been estimated to be ~0.1 nm[14]. In the intact cochlea the tips of the sterocilia are in contact with, or embedded in, the tectorial membrane and they are free to pivot about their bases[15]. This mechanical arrangement amplifies the rotational displacement of the stereocilium caused by the displacement of the basilar membrane by the ratio of the thickness of the organ of Corti to the stereocilium height which, in the basal turn of the guinea pig cochlea, is ~10 (ref. 16). Thus, at neural threshold the displacement of the stereocilia is probably ~1 nm. In comparing the mechanosensitivities of hair cells in the two preparations, it should be remembered that the driving voltage for the receptor current in hair cells recorded *in vivo* is about 2–3 times that of the hair cells *in vitro*, because the driving voltage is provided by the hair-cell membrane potential (−40 to −80 mV; refs 1, 11) and the endocochlear potential (+80 to +90 mV), producing a total of 120–170 mV in the guinea pig cochlea *in vivo*. In the mouse cochlea *in vitro*, the driving voltage is produced solely by the hair-cell membrane potential (−30 to −70 mV). Thus, the measurements of the sensitivity of inner hair cells in the mouse cochlea *in vitro* (0.4 mV per nm displacement of their stereocilia) are similar to the estimates of the mechanosensitivity of inner hair cells in the guinea pig cochlea *in vivo*, if the increased driving voltage due to the endocochlear potential is taken into account. In view of this finding, the *in vitro* preparation offers the opportunity for direct measurements of the electrical and mechanical properties of mammalian cochlear hair cells and for elucidation of the mechanisms of mechano-electrical transduction.

We thank Mrs E. M. Cowley, Mr D. Bowell and Dr J. Thorpe for technical assistance, and the MRC for support.

Received 13 February; accepted 10 April 1986.

1. Russell, I. J. & Sellick, P. M. *J. Physiol., Lond.* **284**, 261–290 (1978).
2. Dallos, P., Santos-Sacchi, J. & Flock, A. *Science* **218**, 582–584 (1982).
3. Goodman, D. A., Smith, R. L. & Chamberlain, S. C. *Hearing Res.* **7**, 161–175 (1982).
4. Brown, M. C., Nuttall, A. R. & Masta, R. I. *Science* **222**, 69–72 (1983).
5. Hudspeth, A. J. & Corey, D. P. *Proc. natn. Acad. Sci. U.S.A.* **74**, 2407–2411 (1977).
6. Hudspeth, A. J. & Jacobs, R. *Proc. natn. Acad. Sci. U.S.A.* **76**, 1506–1509 (1979).
7. Sobkowitz, H. M., Bereman, B. & Rose, J. E. *J. Neurocytol.* **4**, 543–572 (1975).
8. Crawford, A. C. & Fettiplace, R. *J. Physiol., Lond.* **306**, 79–125 (1980).
9. Ashmore, J. F. *Nature* **304**, 536–538 (1983).
10. Dallos, P. *J. Neurosci.* **5**, 1591–1608 (1985).
11. Russell, I. J. & Sellick, P. M. *J. Physiol., Lond.* **338**, 179–206 (1983).
12. Cody, A. R. & Russell, I. J. *Nature* **315**, 662–665 (1985).
13. Crawford, A. C. & Fettiplace, R. *J. Physiol., Lond.* **364**, 359–380 (1985).
14. Sellick, P. M., Patuzzi, R. & Johnstone, B. M. *J. acoust. Soc. Am.* **72**, 131–141 (1982).
15. Lim, D. J. *J. acoust. Soc. Am.* **67**, 1686–1695 (1980).
16. Johnstone, J. R. & Johnstone, B. M. *J. acoust. Soc. Am.* **40**, 1408–1413 (1966).
17. Shotwell, S. L., Jacobs, R. & Hudspeth, A. J. *Ann. N.Y. Acad. Sci.* **374**, 1–10 (1981).
18. Corey, D. P. & Hudspeth, A. D. *J. Neurosci. Meth.* **3**, 183–202 (1980).
19. Art, J., Crawford, A. C. & Fettiplace, R. *J. Physiol., Lond.* (in the press).

NMDA-receptor activation increases cytoplasmic calcium concentration in cultured spinal cord neurones

Amy B. MacDermott*§, Mark L. Mayer†, Gary L. Westbrook†, Stephen J. Smith‡ & Jeffery L. Barker†

* Laboratory of Neurophysiology, NINCDS and † Laboratory of Developmental Neurobiology, NICHD, National Institutes of Health, Bethesda, Maryland 20892, USA
‡ Section of Molecular Neurobiology, Yale University School of Medicine, New Haven, Connecticut 06510, USA

Excitatory amino acids act via receptor subtypes in the mammalian central nervous system (CNS)[1–3]. The receptor selectively activated by *N*-methyl-D-aspartic acid (NMDA) has been best characterized using voltage-clamp and single-channel recording; the results suggest that NMDA receptors gate channels that are permeable to Na^+, K^+ and other monovalent cations[4–7]. Various experiments suggest that Ca^{2+} flux is also associated with the activation of excitatory amino-acid receptors on vertebrate neurones[8–11]. Whether Ca^{2+} enters through voltage-dependent Ca^{2+} channels or

§ Present address: Howard Hughes Medical Institute, Columbia University, CPS, 722 West 168th Street, New York, New York 10032, USA.

through excitatory amino-acid-activated channels of one or more subtype is unclear. Mg^{2+} can be used to distinguish NMDA-receptor-activated channels from voltage-dependent Ca^{2+} channels, because at micromolar concentrations Mg^{2+} has little effect on voltage-dependent Ca^{2+} channels[12] while it enters and blocks NMDA receptor channels[4,5,7,13,14]. Marked differences in the potency of other divalent cations acting as Ca^{2+} channel blockers compared with their action as NMDA antagonists also distinguish the NMDA channel from voltage-sensitive Ca^{2+} channels[5,7]. However, we now directly demonstrate that excitatory amino acids acting at NMDA receptors on spinal cord neurones increase the intracellular Ca^{2+} activity, measured using the indicator dye arsenazo III, and that this is the result of Ca^{2+} influx through NMDA receptor channels. Kainic acid (KA), which acts at another subtype of excitatory amino-acid receptor, was much less effective in triggering increases in intracellular free Ca^{2+}.

Experiments were performed using spinal cord neurones in dissociated cultures prepared from 13–14-day-old mouse embryos as described previously[5–7]. After 1–4 weeks in culture, whole-cell recording was performed using the patch-clamp technique[15] with a high-speed discontinuous voltage-clamp amplifier. The intracellular solution contained 0.8–1.5 mM arsenazo III dissolved in a conventional electrolyte solution for whole-cell recording (see Fig. 1 legend for details). The application of NMDA to spinal cord neurones voltage-clamped at −50 to −60 mV evoked an inward current accompanied by an increase in the intracellular Ca^{2+} concentration ($[Ca^{2+}]_i$) signalled by wavelength-specific changes in the absorbance of arsenazo III (Fig. 1). The inward current activated by NMDA was accompanied by an increase in variance (Fig. 1), and fluctuation analysis (not shown) had the properties characteristic of the 50-pS channel of mean open time 5–6 ms linked to NMDA receptors on mesencephalic, striatal and cerebellar cultured neurones[4,16]. Under the conditions of our experiments, NMDA-evoked increases in $[Ca^{2+}]_i$ similar to that shown in Fig. 1, were recorded in almost all neurones examined ($n = 29$).

In each neurone a depolarizing voltage jump, usually a step from −60 to 0 mV for 0.5–2 s, was used to induce Ca^{2+} influx through conventional voltage-regulated Ca^{2+} channels to check on the adequacy of the optical recording system before application of excitatory amino acids. Voltage-sensitive Ca^{2+} entry in spinal cord neurones, measured using arsenazo III, could be detected with command voltages as negative as −40 mV, depending on the duration of the step. The increase in $[Ca^{2+}]_i$ peaked near +10 mV, and declined in amplitude on further depolarization; at membrane potentials more positive than +80 mV Ca^{2+} entry was too small to measure. The similarity of the arsenazo III voltage–absorbance curve to the current–voltage relationship of neuronal Ca^{2+} currents[17] suggests good voltage-clamp control of the membrane area through which Ca^{2+} influx was measured. Such results are similar to those obtained in larger cells[18,19] and show that arsenazo III can be used to measure Ca^{2+} entry in mammalian spinal cord neurones.

Increases of $[Ca^{2+}]_i$ evoked by excitatory amino acids could be caused by either transmembrane influx of Ca^{2+} or release of Ca^{2+} from intracellular stores. For example, production of inositol trisphosphate ($InsP_3$), one of the second messengers known to stimulate intracellular Ca^{2+} mobilization[20], may increase in response to excitatory amino acids[21]. The fact that ion channels activated by excitatory amino acids allow influx of Na^+ provides another indirect mechanism for the increase in $[Ca^{2+}]_i$ induced by NMDA (that is, Na^+-stimulated Ca^{2+} release from mitochondria[22]). We used two procedures (Fig. 2) to demonstrate that transmembrane ion flux is necessary for the appearance of the arsenazo III signal evoked by NMDA, thus eliminating a major contribution by $InsP_3$ production to the elevation in $[Ca^{2+}]_i$ described here. Figure 2*a* shows the blockade by Mg^{2+} of both the inward current and the increase in $[Ca^{2+}]_i$ evoked by NMDA; as Mg^{2+} ions interfere with ion flux through the NMDA-receptor-activated channel[4,5,7,13,14], without

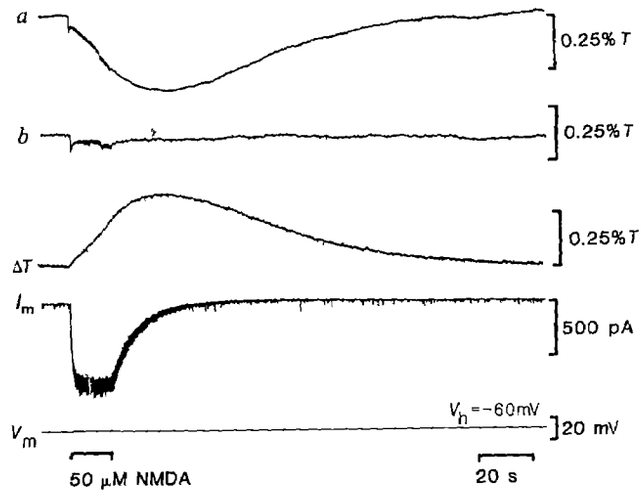


Fig. 1 NMDA increases $[Ca^{2+}]_i$, as measured with the metallochrome indicator dye arsenazo III in mouse spinal cord neurones under voltage clamp. Traces *a* and *b* show optical absorbance signals recorded simultaneously at wavelengths of: *a*, 660 nm (the wavelength at which changes in $[Ca^{2+}]$ evoke maximal increases in absorbance) and *b*, 570 nm (the isosbestic wavelength of arsenazo III, used to control for movement-related artefacts). Application of 50 μM NMDA reduced the transmittance at 660 nm but not at 570 nm, indicating an increase in $[Ca^{2+}]_i$. The trace labelled ΔT shows a differential record, obtained by subtracting the transmittance at 660 nm from that at 570 nm, and detects optical absorbance changes due to arsenazo III binding of Ca^{2+}; an upward deflection reflects an increase in $[Ca^{2+}]_i$. Small deflections in traces *a* and *b* are movement-related artefacts caused by pressure application (90 ms, ≤1 p.s.i., 3.6 Hz) of NMDA; these are subtracted in the third trace, the difference record. I_m, Membrane current; application of 50 μM NMDA evoked an inward current associated with a large increase in variance as described previously[4]. V_m, Membrane potential, voltage-clamped at −60 mV to prevent Ca^{2+} entry through voltage-gated calcium channels. The slow decay of the optical traces probably reflects sequestration and extrusion of calcium ions[19] and is typical of responses recorded using arsenazo III.

Methods. Experiments were performed on the stage of an inverted microscope. Light from a quartz halogen source was focused onto the cell body and an iris diaphragm used to select a field 50 μm in diameter; spinal cord neurones 15–20 μm in diameter were centred in this field for whole-cell recording using patch pipettes containing 0.8–1.5 mM arsenazo III. Light from the microscope objective was focused onto a diffraction grating and photodiodes used to measure the intensity at 570, 610, 660 and 700 nm. $[Ca^{2+}]_i$ signals were recorded differentially as 570–660 nm or 700–660 nm. The change in absorbance at 660 nm was greater than that at 610 nm, as expected for changes in $[Ca^{2+}]_i$ rather than intracellular *p*H. Records are calibrated as changes in transmittance (T) from the pre-stimulus baseline. Calibration of optical signals in terms of the underlying free calcium change was not attempted here, because of uncertainties as to dye behaviour in the cytoplasm, and difficulties in estimating the path length and stray light under our experimental conditions. The intracellular solution contained (in mM): 140 K-gluconate, 2 $MgCl_2$ and 10 HEPES titrated to *p*H 7.2 with KOH; sucrose was added to adjust the osmolarity to 310 mosM. In some experiments CsCl or $CsMeSO_3$ was substituted for K-gluconate. In addition, the intracellular solution usually contained 1.1 mM EGTA without or with 0.1 mM $CaCl_2$, but similar results were obtained with either no EGTA and no $CaCl_2$ (in this solution arsenazo III chelates residual free Ca^{2+} normally present in patch solutions) or with 5 mM EGTA plus 0.5 mM $CaCl_2$. The extracellular solution contained (in mM): 145 NaCl, 2.5 KCl, 2.5 $CaCl_2$, no added Mg^{2+}, 10 glucose, and 10 HEPES titrated to *p*H 7.3 with NaOH; sucrose was added to adjust the osmolarity to 325 mosM. Spontaneous activity and synaptic transmission were reduced by adding 1 μM tetrodotoxin. NMDA, KA and L-glutamic acid were applied to individual spinal cord neurones by miniperfusion using extracellular patch pipettes.

Experiments were performed at room temperature (25 °C).

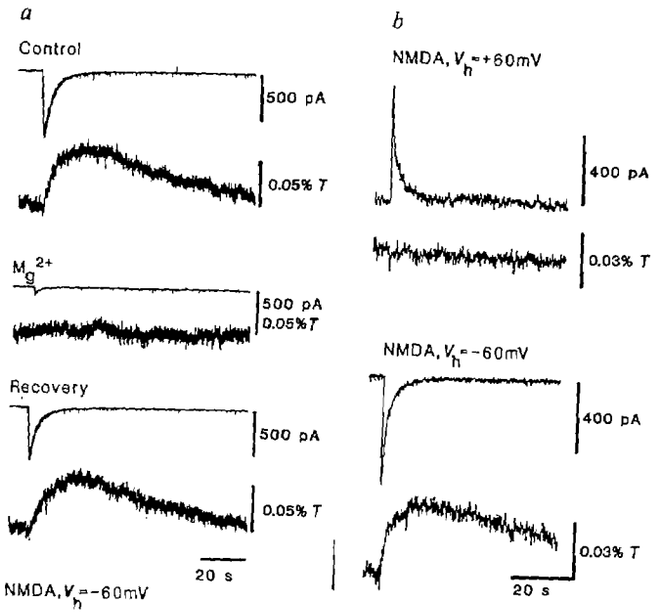


Fig. 2 Increases of $[Ca^{2+}]_i$ result from inward current flow through ion channels activated by NMDA. *a*, Reversible block by pressure application of Mg^{2+} of both the inward current and the increase in $[Ca^{2+}]_i$ evoked by brief application of NMDA (350 ms, 1 mM) to a spinal cord neurone voltage-clamped at −60 mV; an upward deflection represents an increase in $[Ca^{2+}]_i$. The fact that Mg^{2+} ions block the channels activated by NMDA, but do not interfere with agonist binding to the receptor, suggests that ion flux through the NMDA-receptor-activated channel is necessary for the increase in $[Ca^{2+}]_i$. $MgCl_2$ (10 mM) was dissolved in the bathing medium and applied from a patch pipette similar to that used to evoke NMDA responses; the actual concentration of Mg^{2+} at the membrane surface was unknown but dilution by the Mg^{2+}-free bathing medium is expected to have decreased the concentration below that in the pipette. *b*, Responses to pressure application of NMDA (110 ms, 1 mM) recorded at holding potentials of +60 mV and −60 mV (the NMDA reversal potential is ~0 mV); at +60 mV NMDA evokes outward current flow, with no change in $[Ca^{2+}]_i$, whereas at −60 mV NMDA evokes inward current flow associated with an increase in $[Ca^{2+}]_i$. NMDA evokes current flow of similar amplitude at both membrane potentials, suggesting that inward current flow through ion channels activated by NMDA is the source of the increase in $[Ca^{2+}]_i$.

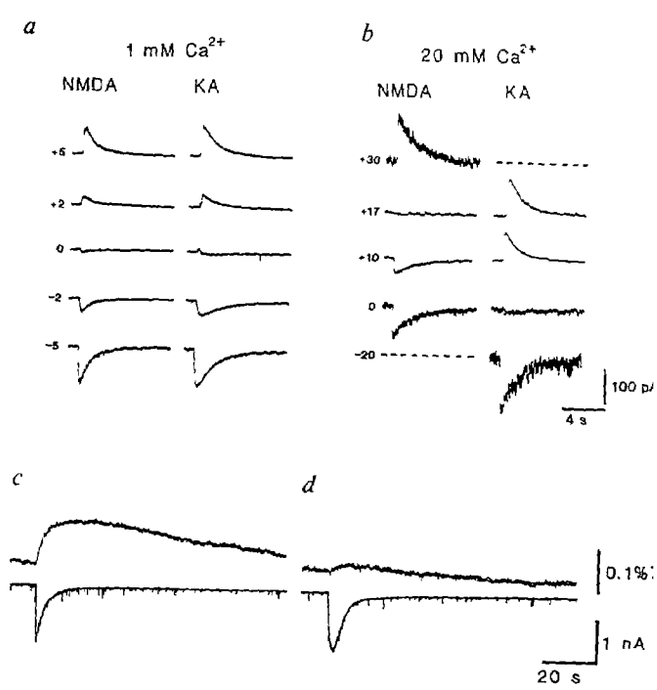


Fig. 3 Measurements of reversal potential suggest that NMDA channels are more permeable to Ca^{2+} than are KA channels. *a*, Current responses of one spinal cord neurone bathed in medium containing 1 mM Ca^{2+}, to pressure application of NMDA (60 ms, 1 mM) and KA (200 ms, 300 μM) as the membrane potential (under voltage clamp) was varied over the range −5 to +5 mV; the reversal potential of the response to both excitatory amino acids is close to 0 mV. *b*, Current responses of a second spinal cord neurone, bathed in medium containing 20 mM Ca^{2+}, to application of NMDA (90 ms, 1 mM) and KA (120 ms, 300 μM) as the membrane potential was varied over the range −20 to +30 mV. The reversal potential to NMDA is shifted to +17 mV, whereas reversal of the response to KA occurs at 0 mV. Assuming equal permeability (P) of monovalent cations through NMDA receptor channels, this result suggests that P_{Ca}/P_{Na} is ~5, which compares with a value of 0.22 for nicotinic acetylcholine receptor channels[33,34]. *c*, *d*, Optical measurements of $[Ca^{2+}]_i$ transients recorded from one spinal cord neurone bathed in medium containing 2.5 mM Ca^{2+} evoked by pressure application of NMDA (*c*: 200 ms, 1 mM) and KA (*d*: 70 ms, 100 μM); the responses were matched for similar peak inward current activation by each of the excitatory amino acids at a holding potential of −60 mV. Note that the increase in $[Ca^{2+}]_i$ evoked by NMDA is much greater than that evoked by KA, a result compatible with the interpretation of the measurements of reversal potential shown in *a* and *b*.

preventing agonist binding[23], this result suggests that $[Ca^{2+}]_i$ is increased by transmembrane ion flux through the NMDA-receptor-activated ion channels. L-Glutamate, a mixed agonist acting at NMDA receptors[2,6,7], also evoked Mg^{2+}-sensitive increases in $[Ca^{2+}]_i$. Figure 2*b* shows the responses to a constant dose of NMDA recorded at two membrane potentials; the inward current activated by NMDA at −60 mV was associated with an increase in $[Ca^{2+}]_i$, whereas the outward current activated by NMDA at +60 mV did not increase $[Ca^{2+}]_i$. In Mg^{2+}-free medium the NMDA current–voltage relationship was linear at membrane potentials more positive than −60 mV[4,5,7], and in the present experiments the increase in $[Ca^{2+}]_i$ evoked by constant doses of NMDA varied with the driving force for inward current over the membrane potential range 0 to −60 mV, suggesting that inward flux of Na^+ or Ca^{2+} through the ion channels opened by NMDA causes the increase in $[Ca^{2+}]_i$. At membrane potentials positive to +10 mV, NMDA did not induce increases in $[Ca^{2+}]_i$ detectable with arsenazo III. These experiments indicate that receptor activation *per se* is insufficient to account for the increase in $[Ca^{2+}]_i$ described here, and suggest that under our experimental conditions the production of $InsP_3$ does not play a major part in the response to excitatory amino acids. Our results do not by themselves exclude the possibility that Ca^{2+} or Na^+ influx through ion channels activated by NMDA triggers the intracellular release of Ca^{2+}, but the results presented below suggest that NMDA channels are indeed permeable to Ca^{2+}.

There is good evidence that the unitary properties of the ion channels linked to NMDA receptors are different from those linked to other excitatory amino-acid receptors in the vertebrate CNS[16,24]. To determine whether these ion channels show differences in their permeability to Ca^{2+}, we measured the reversal potential of responses to NMDA and KA with extracellular calcium concentrations ($[Ca^{2+}]_o$) of 1 and 20 mM (Fig. 3*a*, *b*). A depolarizing shift of the NMDA reversal potential on increasing the $[Ca^{2+}]_o$ provides direct evidence that NMDA channels have a measurable calcium permeability. In contrast, the reversal potential of responses evoked by KA showed little Ca^{2+} dependence. Recently, Ca^{2+} dependence of the NMDA reversal potential[25] has been confirmed using single-channel recording experiments[26]. Arsenazo III measurements also

differed between NMDA and KA (Fig. 3c, *d*), and in individual spinal cord neurones KA-evoked increases in $[Ca^{2+}]_i$ were always much smaller than those evoked by NMDA. These experiments suggest that Na^+ is a poor trigger for inducing an increase in $[Ca^{2+}]_i$, since in several neurones the inward (Na^+) current activated by KA produced no detectable arsenazo III signal. However, our results do not exclude the possibility that Ca^{2+} influx through ion channels activated by NMDA triggers release of Ca^{2+} from intracellular stores[27], contributing further to the NMDA-evoked arsenazo III signals reported here. Although the present results suggest a high Ca^{2+} permeability of NMDA-receptor-activated channels (Fig. 3), the net flux of monovalent cations (that is, conductance) decreases in the presence of Ca^{2+}. This reflects interactions between permeant ions within the channel with Ca^{2+} acting as both a permeant ion and as a blocker of monovalent cation flux[25,26,28].

The experiments reported here provide evidence for an agonist-triggered increase in $[Ca^{2+}]_i$ in mammalian spinal cord neurones. Previously, ion-sensitive microelectrodes were used to measure changes in intracellular ionic activity triggered by excitatory amino acids in frog motoneurones[9]. The latter experiments suggested an increase in both $[Na^+]_i$ and $[Ca^{2+}]_i$ during perfusion with L-glutamate but the results were difficult to interpret clearly as (1) neurones were not voltage-clamped and thus it is difficult to separate the relative contributions of Ca^{2+} influx via voltage-dependent calcium channels and agonist-activated channels, and (2) L-glutamate is a mixed agonist that acts at multiple subtypes of excitatory amino-acid receptor[2,6,7].

The response to NMDA-receptor activation thus provides a second source of calcium flux, distinct from that resulting from conventional voltage-dependent calcium channels, which may have important long-term effects on excitability. Our finding that the ion channels linked to the NMDA receptor subtype are more permeable to Ca^{2+} than those linked to KA receptors, has implications for the role of excitatory amino-acid receptors in CNS function. It is possible that Ca^{2+} influx activated by NMDA receptors underlies the synaptic plasticity generating long-term potentiation, as the latter is prevented by intracellular injection of EGTA to chelate Ca^{2+} (ref. 29), or by blocking NMDA receptors with selective antagonists[30]. For example, Ca^{2+} influx localized at transmitter-operated ion channels could have a role in organizing and regulating postsynaptic structures in an appropriate spatial relation to transmitter-releasing presynaptic terminal boutons, and it is important to consider that Ca^{2+} influx occurring at NMDA receptors located on dendritic spines might produce an especially large but localized elevation in intracellular Ca^{2+} concentration, due to restriction of Ca^{2+} diffusion along the narrow shaft of the spine. In addition, our results have some bearing on the mechanisms of desensitization of NMDA receptors, as the link that has been demonstrated between $[Ca^{2+}]_i$ and desensitization of nicotinic receptors at the neuromuscular junction[31,32] may occur also for other receptor-ionophore complexes. Thus our results may help to explain the similar desensitization evoked by either large doses of NMDA or depolarizing voltage jumps[7], which trigger Ca^{2+} entry through NMDA channels and voltage-dependent calcium channels, respectively.

Received 3 January; accepted 1 April 1986.

1. Krogsgaard-Larsen, P., Honoré, T., Hansen, J. J., Curtis, D. R. & Lodge, D. *Nature* **284**, 64–66 (1980).
2. Watkins, J. C. & Evans, R. H. *A. Rev. Pharmac. Tox.* **21**, 165–205 (1981).
3. McLennan, H. *Prog. Neurobiol.* **20**, 251–271 (1983).
4. Nowak, L., Bregestovski, P., Ascher, P., Herbet, A. & Prochiantz, A. *Nature* **307**, 462–465 (1984).
5. Mayer, M. L., Westbrook, G. L. & Guthrie, P. B. *Nature* **309**, 261–263 (1984).
6. Mayer, M. L. & Westbrook, G. L. *J. Physiol., Lond.* **354**, 29–53 (1984).
7. Mayer, M. L. & Westbrook, G. L. *J. Physiol., Lond.* **361**, 65–90 (1985).
8. Dingledine, R. *J. Physiol., Lond.* **343**, 385–405 (1983).
9. Bührle, C. P. & Sonnhof, U. *Pflügers Arch. ges. Physiol.* **396**, 154–162 (1983).
10. Zanotto, L. & Heinemann, U. *Neurosci. Lett.* **35**, 79–84 (1983).
11. Pumain, R. & Heinemann, U. *J. Neurophysiol.* **53**, 1–16 (1985).
12. Lansman, J. B., Hess, P. & Tsien, R. W. *J. gen. Physiol.* (in the press).
13. Ault, B., Evans, R. H., Francis, A. S., Oakes, D. J. & Watkins, J. C. *J. Physiol., Lond.* **307**, 413–428 (1980).
14. Crunelli, V. & Mayer, M. L. *Brain Res.* **311**, 392–396 (1984).
15. Hamill, O. P., Marty, A., Neher, E., Sakmann, B. & Sigworth, F. *Pflügers Arch. ges. Physiol.* **391**, 85–100 (1981).
16. Cull-Candy, S. G. & Ogden, D. C. *Proc. R. Soc.* **B224**, 367–373 (1985).
17. Hagiwara, S. & Bylerly, L. *A. Rev. Neurosci.* **4**, 69–125 (1981).
18. Smith, S. J., MacDermott, A. B. & Weight, F. F. *Nature* **304**, 350–352 (1983).
19. Gorman, A. L. F. & Thomas, M. V. *J. Physiol., Lond.* **308**, 259–285 (1980).
20. Berridge, M. J. & Irvine, R. F. *Nature* **312**, 315–321 (1984).
21. Sladeczek, F., Pin, J. P., Récasens, M., Bockaert, J. & Weiss, S. *Nature* **317**, 717–719 (1985).
22. Schoffelmeer, A. M. N. & Mulder, A. H. *J. Neurochem.* **40**, 615–621 (1983).
23. Evans, R. H. & Watkins, J. C. *J. Physiol., Lond.* **277**, 57P (1977).
24. Nowak, L. M. & Ascher, P. *Soc. Neurosci. Abstr.* **10**, 23 (1984).
25. Mayer, M. L. & Westbrook, G. L. *Soc. Neurosci. Abstr.* **11**, 785 (1985).
26. Ascher, P. & Nowak, L. *J. Physiol., Lond. Proc.* (in the press).
27. Fabiato, A. & Fabiato, F. *Ann. N.Y. Acad. Sci.* **307**, 491–522 (1978).
28. Nowak, L. M. & Ascher, P. *Soc. Neurosci. Abstr.* **11**, 953 (1985).
29. Lynch, G., Larson, J., Kelso, S., Barrinuevo, G. & Schottler, F. *Nature* **305**, 719–721 (1983).
30. Collingridge, G. L., Kehl, S. J. & McLennan, H. *J. Physiol., Lond.* **334**, 33–46 (1983).
31. Parsons, R. L. in *Calcium in Drug Action* (ed. Weiss, G. B.) 289–314 (Plenum, New York, 1978).
32. Miledi, R. *Proc. R. Soc.* **B209**, 447–452 (1980).
33. Adams, D. J., Dwyer, T. M. & Hille, B. *J. gen. Physiol.* **75**, 493–510 (1980).
34. Edwards, C. *Neuroscience* **7**, 1335–1366 (1982).

Replacing the complementarity-determining regions in a human antibody with those from a mouse

Peter T. Jones, Paul H. Dear, Jefferson Foote, Michael S. Neuberger & Greg Winter

Laboratory of Molecular Biology, Medical Research Council, Hills Road, Cambridge CB2 2QH, UK

The variable domains of an antibody consist of a β-sheet framework with hypervariable regions (or complementarity-determining regions—CDRs) which fashion the antigen-binding site. Here we attempted to determine whether the antigen-binding site could be transplanted from one framework to another by grafting the CDRs. We substituted the CDRs from the heavy-chain variable region of mouse antibody B1–8, which binds the hapten NP-cap (4-hydroxy-3-nitrophenacetyl caproic acid; $K_{NP\text{-}cap} = 1.2\ \mu M$), for the corresponding CDRs of a human myeloma protein. We report that in combination with the B1–8 mouse light chain, the new antibody has acquired the hapten affinity of the B1–8 antibody ($K_{NP\text{-}cap} = 1.9\ \mu M$). Such 'CDR replacement' may offer a means of constructing human monoclonal antibodies from the corresponding mouse monoclonal antibodies.

The three-dimensional structures of several immunoglobulins show that the variable domains consist of two β-sheets pinned together by a disulphide bridge, with their hydrophobic faces packed together[1–3]. The individual β-strands are linked by loops which at one tip of the β-sheet may fashion a binding pocket for small haptens[1,2]. Sequence comparisons among heavy- and light-chain variable domains (V_H and V_L respectively) reveal that each domain has three CDRs flanked by four relatively conserved regions (framework regions—FRs)[4]. As seen in the structure of the human myeloma protein NEWM (Fig. 1), the CDRs include each of the three main loops. Often the CDRs also include the ends of the β-strands, suggesting that side chains at the ends of the β-strands may help to fix the conformation or orientation of the loops. The framework regions form the bulk of the β-sheet, although for example in the V_H domain of NEWM, FR1 includes part of the loop between the two β-sheets and CDR2 not only forms a loop but a complete β-strand (Fig. 1). The structure of the β-sheet framework is similar in different antibodies, as the packing of different side chains is accommodated by slight shifts between the two β-strands[5]. Furthermore, the packing together of V_L and V_H FRs is conserved[6], therefore the orientation of V_L with respect to V_H is fixed. We wondered whether the FRs represent a simple β-sheet scaffold on which new binding sites may be built, and

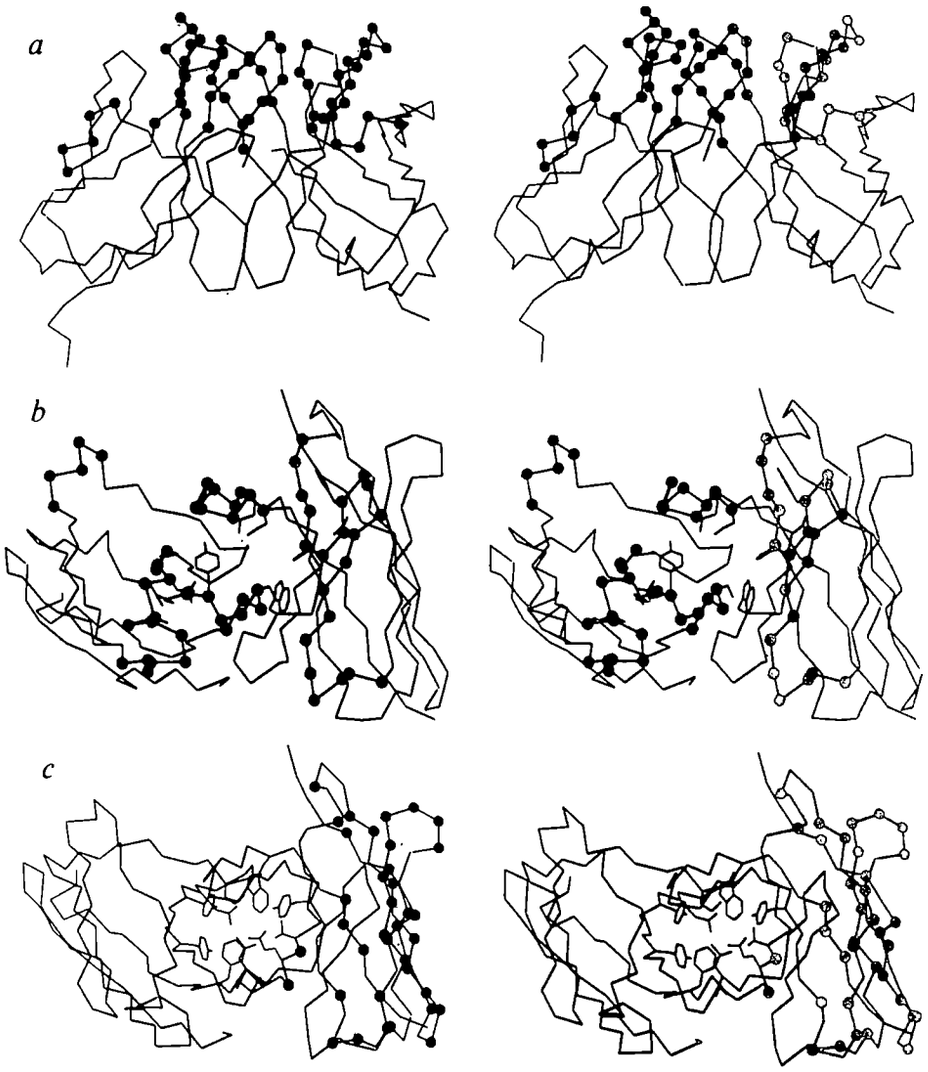


Fig. 1 Stereo pairs of the V_H (right) and V_L (left) domains of the human myeloma protein NEWM[1,8] generated using the computer graphics program FRODO[25]. The tracings indicate the backbone of C^α atoms for the framework regions. *a*, The C^α atoms of the CDRs (●) cluster at the tip of the variable domain. *b*, A view into the hapten binding pocket with the CDRs in the order (clockwise from noon): V_H CDR3, CDR1 and CDR2, and V_L CDR3, CDR1 and CDR2. The side chains lining the binding pocket (V_L A 28, N 30, Y 90, S 93, R 95; V_H W 47, Y 50, F 52, I 100, A 101) lie almost entirely in the CDRs. *c*, The C^α atoms in the NEWM V_H domain are marked (●) where side chains in the mouse B1-8 V_H domain are different. The side chains (V_L Y 35, Q 37, A 42, P 43, Y 86, F 99; V_H V 37, Q 39, L 45, Y 94, W 107) involved in packing V_H and V_L framework regions are traced. In the V_H domain all these side chains are conserved in mouse B1-8.

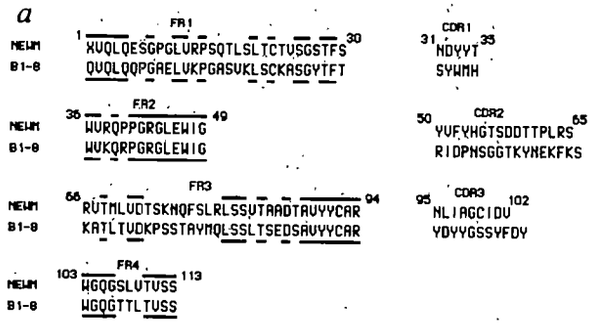
whether the structure of the CDRs (and antigen binding) is therefore independent of the FR context. To answer these questions experimentally, we have grafted the CDRs from one antibody to another, to determine whether antigen binding transfers with the CDRs.

We grafted the CDRs from the V_H domain of the mouse monoclonal antibody B1-8 (ref. 7) into the V_H domain of the human myeloma protein NEWM, whose crystallographic structure is known[1,8]. The V_H domain of the CDR donor (B1-8) is attached to a μ constant region and associated with a mouse λ1 light chain, and the antibody is directed against the hapten NP-cap. Both the V_H and V_L domains seem to have a role in determining the affinity of the antibody for NP-cap as the substitution of either domain by other, often highly related variable domains can destroy hapten binding (refs 7, 9 and M.S.N., unpublished results). In the V_H domain, each of the CDRs has been implicated in NP-cap binding[10], but the class of constant domains attached to V_H does not seem to affect binding of hapten[11,12]. The CDRs from the V_H domain of antibody B1-8 (ref. 13) are longer than the CDRs which they replace in NEWM[4] and this may give rise to a deeper binding pocket.

Most of the residues conserved between the V_H domains of B1-8 and NEWM are located in FR2, FR4 and the carboxy-terminal third of FR3 (Fig. 2*a*) and largely form the region of β-sheet which is packed against the light chain. Therefore, it might be expected that the V_H domain of B1-8 (hereafter abbreviated to MV_{NP}) and the hybrid B1-8/NEWM domain (HuV_{NP}) would dock in a similar manner with the mouse V_L domain to form the antigen-combining site[6]. The more variable FR1 and N-terminal two-thirds of FR3 form the other β-sheet which is exposed to solvent (Fig. 1*c*).

The gene encoding the HuV_{NP} domain was constructed by gene synthesis (Fig. 2*b*). We then constructed a plasmid, pSV-$HuV_{NP}H\varepsilon$, in which the HuV_{NP} domain is linked to a human ε constant region, and cloned into a pSV2gpt-derived vector[14]. The plasmid DNA was introduced into cells of the J558L mouse myeloma by spheroplast fusion. J558L secretes λ1 light chains which have been shown to associate with heavy chains containing a MV_{NP} variable domain, to create a binding site for NP-cap or the related hapten NIP-cap (3-iodo-4-hydroxy-5-nitrophenylacetyl caproic acid)[7]. As the plasmid pSV-$HuV_{NP}H\varepsilon$ contains the *gpt* marker (encoding guanine phosphoribosyltransferase), stably transfected myeloma cells could be selected in medium containing mycophenolic acid[14]; transfectants would be expected to secrete an antibody (HuV_{NP}-IgE) with a heavy chain composed of a HuV_{NP} variable domain and human ε constant regions, and the λ1 light chain of the J558L myeloma. The culture supernatants of several gpt^+ clones were assayed by radioimmunoassay and found to contain NIP-cap-binding antibody. The antibody secreted by one such clone was purified from the culture supernatant by affinity chromatography on NIP-cap–Sepharose, and by SDS-polyacrylamide gel electrophoresis the protein was indistinguishable from the mouse chimaeric MV_{NP}-IgE (ref. 12) (results not shown). The HuV_{NP}-IgE antibody competes effectively with MV_{NP}-IgE for binding to both anti-human ε (Fig. 3*a*) and NIP-cap coupled to bovine serum albumin (NIP-BSA) (Fig. 3*b*).

The affinities of HuV_{NP}-IgE for NP-cap and NIP-cap were



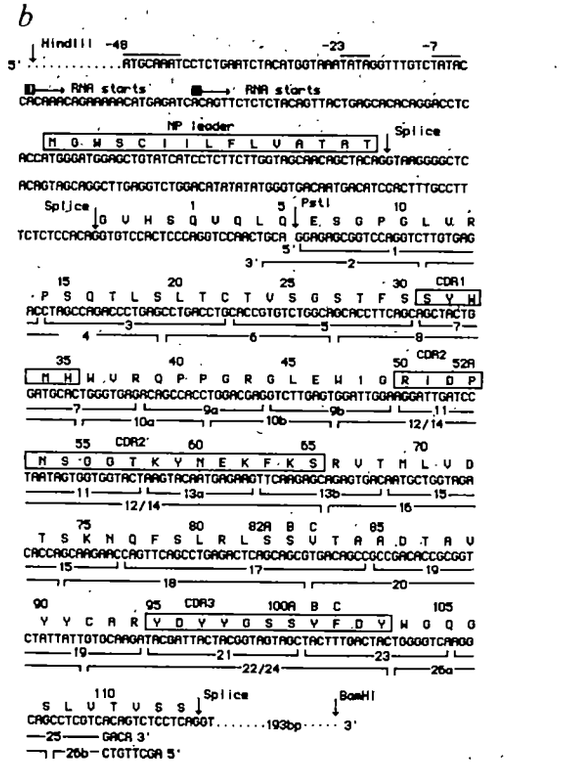


Fig. 2 *a*, Amino-acid sequence of the V_H domain of the human myeloma protein NEWM compared with that of the mouse B1-8 (anti-NP) antibody, and divided into FRs and CDRs according to Kabat *et al.*[4]. Conserved residues are marked with a line above and below the residue. *b*, Amino-acid and nucleotide sequence of the HuV_{NP} gene, in which the CDRs from the V_H domain of the mouse B1-8 antibody alternate with the FRs of human NEWM protein. The gene was constructed by replacing a section of the MV_{NP} gene in the vector pSV-V_{NP} (ref. 12) with a synthetic fragment encoding the HuV_{NP} domain. Thus the 5′ and 3′ noncoding sequences, the leader sequence, the leader–variable region intron, five N-terminal and four C-terminal amino acids are derived from the MV_{NP} gene; the rest of the coding sequence is derived from the synthetic HuV_{NP} fragment. The oligonucleotides are aligned with the corresponding portions of the HuV_{NP} gene. For convenience in cloning, the ends of oligonucleotides 25 and 26b form a *Hin*dII site followed by a *Hin*dIII site, and the sequences of the 25/26b oligonucleotides therefore differ from the HuV_{NP} gene.

Methods. The synthetic gene for HuV_{NP} was constructed as a *Pst*I–*Hin*dIII fragment. The nucleotide sequence was derived from the protein sequence using the computer program ANALYSEQ[26] with optimal codon usage taken from the sequences of mouse constant-region genes. The oligonucleotides used in synthesis (1–26b, 28 in total) vary in size from 14 to 59 bases and were made on a Biosearch SAM or an Applied Biosystems machine, and purified on 8 M urea/polyacrylamide gels[27]. The oligonucleotides were assembled in eight single-stranded blocks (A–D and A′–D′) containing oligonucleotides 1, 3, 5 and 7 (block A); 2, 4, 6 and 8 (block A′), 9, 11, 13a and 13b (block B), 10a, 10b and 12/14 (block B′), 15 and 17 (block C), 16 and 18 (block C′), 19, 21, 23 and 25 (block D); and 20, 22/24, 26a and 26b (block D′). In a typical assembly, for example of block A, 50 pmol of oligonucleotides 1, 3, 5 and 7 were phosphorylated at the 5′ end with T_4 polynucleotide kinase and mixed with 5 pmol of the terminal oligonucleotide which had been phosphorylated with 5 μCi of [γ-^{32}P]ATP (Amersham; 3,000 Ci mmol^{-1}). These oligonucleotides were annealed by heating to 80 °C and cooling to room temperature over 30 min with unkinased oligonucleotides 2, 4 and 6 as splints in 150 μl of 50 mM Tris-HCl *p*H 7.5, 10 mM $MgCl_2$. For the ligation, ATP (1 mM) and dithiothreitol (10 mM) were added, together with 50 units of T_4 DNA ligase (Anglian Biotechnology Ltd), and the mixture was incubated for 30 min at room temperature. EDTA was added to 10 mM, the sample extracted with phenol, precipitated from ethanol, dissolved in 20 μl of water and boiled for 1 min with an equal volume of formamide dyes. Then the sample was loaded onto a thin (0.3 mm) 8 M urea/10% polyacrylamide gel[27] and a band of the expected size detected by autoradiography and eluted by soaking. The two full-length single strands were assembled from A–D and A′–D′ using splint oligonucleotides; thus, A–D were annealed and ligated in 30 μl as above with 100 pmol each of oligonucleotides 10a, 16 and 20 as splints, then incubated overnight (A′–D′ were constructed with oligonucleotides 7, 13b and 17 as splints). After phenol/ether extraction blocks A–D were annealed with blocks A′–D′, small amounts were cloned in the vector M13 mp18 (ref. 28) then cut with *Pst*I and *Hin*dIII, and the gene sequenced by the dideoxy technique[29]. The MV_{NP} gene was transferred as a *Hin*dIII–*Bam*HI fragment from the vector pSV-V_{NP} (ref. 12) to the vector M13mp8 (ref. 30). To facilitate the replacement of MV_{NP} coding sequences by the synthetic HuV_{NP} fragment, three *Hin*dII sites were removed from the 5′ noncoding sequence by site-directed mutagenesis, and a new *Hin*dII site subsequently introduced near the end of FR4. By cutting the vector with *Pst*I and *Hin*dII, most of the V_{NP} coding sequence falls out and the synthetic fragment could be introduced as a *Pst*I–*Hin*dII fragment. The sequence at the *Hin*dII site was corrected to give NEWM FR4 by site-directed mutagenesis. The *Hin*dIII–*Bam*HI fragment, now carrying the HuV_{NP} gene, was excised from M13 and cloned back into pSV-V_{NP} to replace the MV_{NP} gene (and yield the vector pSV-HuV_{NP}). Finally, the heavy-chain constant domains of human IgE (ref. 31) were introduced as a *Bam*HI fragment to yield the vector pSV-$HuV_{NP}H_\varepsilon$, which was transfected into the myeloma line J558L by spheroplast fusion. The sequence of the HuV_{NP} gene in pSV-$HuV_{NP}H_\varepsilon$ was checked by re-cloning the *Hin*dIII–*Bam*HI fragment back into M13mp8 (ref. 30).

Table 1 Affinity of HuV_{NP}-IgE and MV_{NP}-IgE for the haptens NP-cap and NIP-cap

	$K_{NP\text{-}cap}$ (μM)	$K_{NIP\text{-}cap}$ (μM)
MV_{NP}-IgE	1.2 ± 0.1	0.02 ± 0.01
HuV_{NP}-IgE	1.9 ± 0.2	0.07 ± 0.02

The affinity of HuV_{NP}-IgE and MV_{NP}-IgE for NP-cap was determined by fluorescence quenching with excitation at 295 nm and emission observed at 340 nm (ref. 22). Antibody solutions were diluted to 100 nM in phosphate-buffered saline, filtered (0.45 μm-pore cellulose acetate) and titrated with NP-cap in the range 0.2–20 μM. As a control, the mouse D1-3 antibody[23], which does not bind hapten, was titrated in parallel. A decrease in the ratio of the fluorescence of HuV_{NP}-IgE or MV_{NP}-IgE (as appropriate) to that of the D1-3 antibody was taken as being proportional to NP-cap occupancy of the antigen-binding sites. The maximum quench was ~40% for both HuV_{NP}-IgE and MV_{NP}-IgE, and hapten dissociation constants were determined from least-squares fits of triplicate data sets to a hyperbola. The concentration of NIP-cap was varied from 10 to 300 nM, and ~50% quenching of fluorescence was observed at saturation. As the antibody concentrations were comparable to the values of the dissociation constants, data were fitted by least-squares to an equation[24] describing tight binding inhibition.

then measured directly using the fluorescence quench technique, and compared with those of MV_{NP}-IgE (Table 1). The antibodies HuV_{NP}-IgE and MV_{NP}-IgE have similar affinities for either hapten (NP-cap or NIP-cap), and although the affinity of HuV_{NP}-IgE for both haptens is slightly lower than that of MV_{NP}-IgE (2–3-fold, 0.3–0.6 kcal mol^{-1}), the difference in affinity is less than expected for loss of either a hydrogen bond or van der Waals' contact from the active site of an enzyme[15,16]. Thus, it seems that binding affinity and specificity for hapten can be conferred on a human antibody by grafting in the CDRs from an appropriate mouse antibody.

Is this result likely to be general? This would assume (1) that antigen usually binds to the CDRs, and any contacts to the FRs are made to the polypeptide backbone or to conserved side chains, and (2) that substitutions in the FRs do not usually affect the conformation of the CDR loops. These assumptions seem reasonable: thus, in the structure of a complex of the D1-3 antibody with lysozyme (R. A. Mariuzza, S. Phillips and R. J. Poljak, personal communication) most contacts to the lysozyme are made by the CDRs, but there is also a hydrogen bond in FR1 of the V_H domain from the β-OH of Thr 30 (often conserved or replaced by Ser). Similarly, the conformation of CDR loops

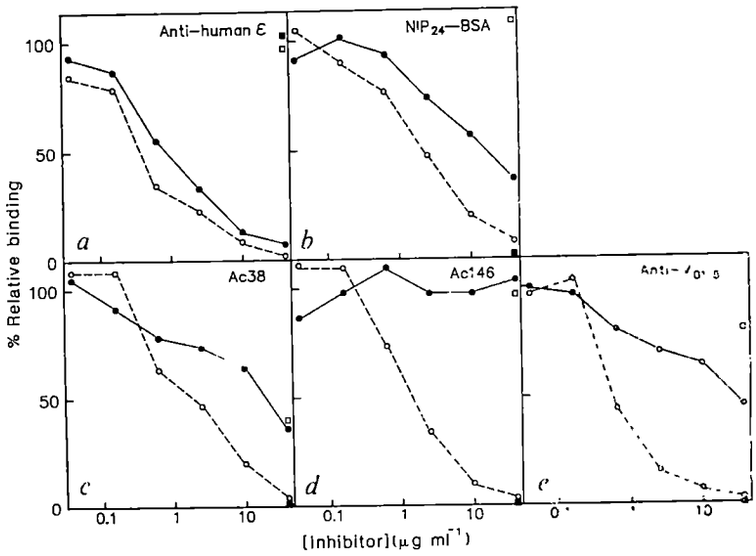


Fig. 3 Comparison of HuV_{NP} and MV_{NP} IgEs in binding inhibition assays. Various concentrations of HuV_{NP}-IgE (●) and MV_{NP}-IgE (○) were used to compete the binding of radiolabelled MV_{NP}-IgE to polyvinyl microtitre plates that had been coated with *a*, sheep anti-human ε antiserum (Seward Laboratory); *b*, $(NIP\text{-}cap)_{24}$-BSA; *c*, Ac38 anti-idiotypic antibody; *d*, Ac146 anti-idiotypic antibody; *e*, rabbit anti-MV_{NP} antiserum. Binding was also carried out in the presence of MV_{NP}-IgM antibody JW1/2/2 (ref. 32) (■) as well as in the presence of JW5/1/2 (□), which is an IgM antibody that differs from JW1/2/2 at 13 residues mainly located in V_H CDR2 (M.S.N., unpublished results). Values of binding are relative to the binding in the absence of inhibitor.

between β-strands depends on loop size and specific interactions of the loop back to the β-sheet. However, in the same class of variable domains (V_H, V_κ or V_λ) these interactions are usually conserved (ref. 5 and A. M. Lesk and C. Chothia, personal communication).

While human monoclonal antibodies have therapeutic potential in human disease, they can be difficult to prepare[17] and treatment of patients with mouse monoclonal antibodies often increases the titre of circulating antibody against the mouse immunoglobulin[18]. As chimaeric antibodies containing human constant domains[12,19,20] and variable domains made by grafting mouse CDRs into human FRs, could have therapeutic potential, we wondered whether the HuV_{NP}-IgE antibody loses antigenic determinants associated with the MV_{NP} variable region (idiotopes). The binding of HuV_{NP}-IgE and MV_{NP}-IgE to both monoclonal and polyclonal anti-idiotypic antibodies directed against the MV_{NP} domain was examined by using inhibition assays. As shown in Fig. 3*d*, the HuV_{NP}-IgE antibody has lost the MV_{NP} idiotypic determinant recognized by antibody Ac146 (ref. 21). Furthermore, HuV_{NP}-IgE also binds the antibody Ac38 (ref. 21) less well (Fig. 3*c*), therefore it is not surprising that HuV_{NP}-IgE has lost many of the determinants recognized by a polyclonal rabbit anti-idiotypic antiserum (Fig. 3*e*). While the loss of idiotypic determinants that accompanies 'humanizing' of the V_H region is reassuring in view of potential therapeutic applications, it does suggest that the recognition of the hapten and of anti-idiotypic antibodies is not equivalent. Thus the HuV_{NP}-IgE antibody retains hapten binding but has lost idiotypic determinants, indicating that the immunoglobulin uses different sites to bind hapten and anti-idiotypic antibodies. It appears, therefore, that both FR and CDR side chains form the binding site for these anti-idiotopes, but mainly CDR side chains interact with hapten.

We thank C. Milstein for suggesting this project, K. Rajewsky and M. Reth for the anti-idiotypic antibodies Ac38 and Ac146, and A. M. Lesk, C. Chothia, R. J. Leatherbarrow and C. Milstein for helpful discussions. J.F. is a Fellow of the Jane Coffin Childs Memorial Fund for Medical Research.

Received 17 February; accepted 17 March 1986.

1. Poljak, R. J. *et al. Proc. natn. Acad. Sci. U.S.A.* **70**, 3305-3310 (1973).
2. Segal, D. M. *et al. Proc. natn. Acad. Sci. U.S.A.* **71**, 4298-4302 (1974).
3. Marquart, M., Deisenhofer, J., Huber, R. & Palm, W. *J. molec. Biol.* **141**, 369-391 (1980).
4. Kabat, E. A., Wu, T. T., Bilofsky, H., Reid-Miller, M. & Perry, H. in *Sequences of Proteins of Immunological Interest* (U.S. Department of Health and Human Services, 1983).
5. Lesk, A. M. & Chothia, C. *J. molec. Biol.* **160**, 325-342 (1982).
6. Chothia, C., Novotny, J., Bruccoleri, R. & Karplus, M. *J. molec. Biol.* **186**, 651-663 (1985).
7. Reth, M., Hämmerling, G. J. & Rajewsky, K. *Eur. J. Immun.* **8**, 393-400 (1978).
8. Saul, F. A., Amzel, M. & Poljak, R. J. *J. biol. Chem.* **253**, 585-597 (1978).
9. Brüggemann, M., Radbruch, A. & Rajewsky, K. *EMBO J.* **1**, 629-634 (1982).
10. Reth, M., Bothwell, A. L. M. & Rajewsky, K. in *Immunoglobulin Idiotypes and Their Expression* (eds Janeway, C., Wigzell, H. & Fox, C. F.) 169-178 (Academic, New York, 1981).
11. Neuberger, M. S. & Rajewsky, K. *Proc. natn. Acad. Sci. U.S.A.* **78**, 1138-1142 (1981).
12. Neuberger, M. S. *et al. Nature* **314**, 268-270 (1985).
13. Bothwell, A. L. M. *et al. Cell* **24**, 625-637 (1981).
14. Mulligan, R. C. & Berg, P. *Proc. natn. Acad. Sci. U.S.A.* **78**, 2072-2076 (1983).
15. Fersht, A. R. *et al. Nature* **314**, 235-238 (1985).
16. Fersht, A. R., Wilkinson, A. J., Carter, P. & Winter, G. *Biochemistry* **24**, 5558-5561 (1985).
17. Boyd, J. E., James, K. & McClelland, D. B. L. *Trends Biotechnol* **2**, 70-77 (1984).
18. Shawler, D. L., Bartholomew, R. M., Smith, L. M. & Dilman, R. O. *J. Immun.* **135**, 1530-1535 (1985).
19. Morrison, S. L., Johnson, M. J., Herzenberg, L. A. & Oi, V. T. *Proc. natn. Acad. Sci. U.S.A.* **81**, 6851-6855 (1984).
20. Boulianne, G. L., Hozumi, N. & Shulman, M. J. *Nature* **312**, 643-646 (1984).
21. Reth, M., Imanishi-Kari, T. & Rajewsky, K. *Eur. J. Immun.* **9**, 1004-1013 (1979).
22. Eisen, H. N. *Meth. med. Res.* **10**, 115-121 (1964).
23. Mariuzza, R. A. *et al. J. molec. Biol.* **170**, 1055-1058 (1983).
24. Segal, I. H. in *Enzyme Kinetics*, 73-74 (Wiley, New York, 1975).
25. Jones, T. A. in *Computational Crystallography* (ed. Sayre, D.) 303-310 (Clarendon, Oxford, 1982).
26. Staden, R. *Nucleic Acids Res.* **12**, 521-538 (1984).
27. Sanger, F. & Coulson, A. *FEBS Lett.* **87**, 107-110 (1978).
28. Yanisch-Perron, C., Vieira, J. & Messing, J. *Gene* **33**, 103-119 (1985).
29. Sanger, F., Nicklen, S. & Coulson, A. R. *Proc. natn. Acad. Sci. U.S.A.* **74**, 5463-5467 (1977).
30. Messing, J. & Vieira, J. *Gene* **19**, 269-276 (1982).
31. Flanagan, J. G. & Rabbitts, T. H. *EMBO J.* **1**, 655-660 (1982).
32. Neuberger, M. S., Williams, G. T. & Fox, R. O. *Nature* **312**, 604-608 (1984).

Regulation of human insulin gene expression in transgenic mice

Richard F Selden*, Marek J. Skośkiewicz†, Kathleen Burke Howie*, Paul S. Russell† & Howard M. Goodman*

Departments of *Molecular Biology and †Surgery, Massachusetts General Hospital, and Departments of *Genetics and †Surgery, Harvard Medical School, Massachusetts General Hospital, Boston, Massachusetts 02114, USA

Insulin is a polypeptide hormone of major physiological importance in the regulation of fuel homeostasis in animals (reviewed in refs 1, 2). It is synthesized by the β-cells of pancreatic islets, and circulating insulin levels are regulated by several small molecules, notably glucose, amino acids, fatty acids and certain pharmacological agents. Insulin consists of two polypeptide chains (A and B, linked by disulphide bonds) that are derived from the proteolytic cleavage of proinsulin, generating equimolar amounts of the mature insulin and a connecting peptide (C-peptide). Humans, like most vertebrates, contain one proinsulin gene[3,4], although several species, including mice[5] and rats[6,7], have two highly homologous insulin genes. We have studied the regulation of serum insulin

levels and of insulin gene expression by generating a series of transgenic mice containing the human insulin gene. We report here that the human insulin gene is expressed in a tissue-specific manner in the islets of these transgenic mice, and that serum human insulin levels are properly regulated by glucose, amino acids and tolbutamide, an oral hypoglycaemic agent.

The human insulin gene that we have used to generate transgenic mice is contained within a 12.5-kilobase (kb) *Eco*RI fragment that was isolated from a genomic library[4]. Of 46 mice born after one series of single-cell embryo microinjections, three contained human insulin gene sequences as detected by Southern hybridization analysis (Fig. 1*a*). A human C-peptide radioimmunoassay (Behringwerke) was used to monitor expression of the human insulin gene in the transgenic mice and their offspring. Several hundred transgenic and control mice have been analysed under a variety of physiological circumstances (see below), and the transgenic mice show variable levels of human C-peptide in their sera, whereas control mice show no such expression.

The tissue specificity of human insulin gene expression in these transgenic mice was examined by both RNA analyses and pancreatic islet function studies. Northern hybridizations using a human insulin complementary DNA probe demonstrated that total pancreatic RNA from both transgenic (Fig. 1*b*, lane 11) and control (lane 1) mice hybridized to the human insulin cDNA probe, whereas RNAs from transgenic spleen, kidney, brain, lung, liver, salivary gland, intestine, heart and muscle (lanes 2–10, respectively) showed no hybridization. Because no transgenic tissues other than pancreas were found to express detectable levels of insulin RNA, insulin expression in both transgenic and control pancreas was studied to determine whether the transgenic pancreas is a site of human insulin expression. Pancreatic islets from six transgenic and six control mice were isolated by collagenase digestion as described previously[8,9] and cultured in groups of 80–100 islets per tissue culture well. The following day, aliquots of media were taken and human C-peptide levels measured. The samples from the transgenic islet wells contained 250–650 ng ml^{-1} of human C-peptide, but the control islet wells contained no detectable human C-peptide. The cultured transgenic islets continued to express human C-peptide for several days. From these experiments, we conclude that the major site of human insulin expression in these transgenic mice is the endocrine pancreas.

Transgenic and control pancreas were stained with immunoperoxidase using a guinea pig anti-porcine insulin antibody and a goat anti-human C-peptide antibody (Fig. 2). The anti-porcine insulin antibody cross-reacted with both human and mouse insulin, and islets from both transgenic (Fig. 2*a*) and control (Fig. 2*b*) mice were stained. The size, distribution and number of islets were essentially the same in transgenic and control mice. The anti-human C-peptide antibody showed little or no cross-reactivity with mouse C-peptide, however, and the transgenic islets (Fig. 2*c*) were stained using this antibody whereas the control islets (Fig. 2*d*) were not. These immunohistochemistry data are consistent with the Northern analysis and islet function studies presented above, and demonstrate that the transgenic islets were specifically expressing human insulin.

Glucose and human C-peptide levels in the transgenic mice were studied under a variety of physiological conditions to determine whether normal glucose homeostasis was being preserved and whether expression of the human insulin gene was being regulated appropriately in these mice. Blood glucose regulation was studied by glucose tolerance tests. Transgenic offspring of mouse 16 and non-transgenic siblings were fasted overnight, given an intraperitoneal (i.p.) injection of glucose, and bled at various times after injection to determine serum glucose levels. The glucose tolerance curve from the transgenic mice was similar to that from the control mice (Fig. 3*a*). Of particular importance is the finding that the fasting and maximally stimulated glucose levels as well as the kinetics of

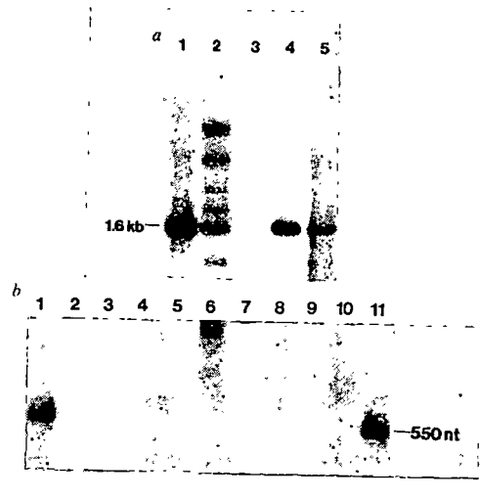


Fig. 1 Characterization of microinjected mice. *a*, Detection of human insulin sequences in total genomic DNA of microinjected mice. DNA samples digested with *Pvu*II are from the following microinjected mice: lane 1, mouse 16, containing 5–10 copies of the human insulin gene fragment per haploid genome; lane 2, mouse 20, also containing 5–10 copies of the human insulin gene fragment per haploid genome; lane 3, mouse 21, negative for human insulin sequences, demonstrating that the endogenous mouse insulin genes do not hybridize significantly to the human insulin genomic probe; lane 4, human control, containing 1 copy of the human insulin gene per haploid genome; lane 5, mouse 38, containing 1–2 copies of the human insulin gene fragment per haploid genome (this DNA sample was analysed in a separate experiment in which the hybridizing band was of comparable intensity to the human control). DNA samples from each transgenic mouse contain a hybridizing band of ~1,600 bp which corresponds to a 1,594-bp *Pvu*II fragment contained within the 12.5-kb human insulin DNA fragment[4] used for microinjection. This result suggests that at least one structurally intact human insulin gene was incorporated into the genome of each transgenic animal, although the presence of multiple hybridizing bands in lane 2 indicates that other integration events are likely to have occurred during the embryogenesis of mouse 20. Mouse 16, a male, was bred to generate a colony of several hundred offspring, and the human insulin gene was transmitted in mendelian fashion, with ~50% of both the F_1 and F_2 offspring inheriting the injected DNA fragment. *b*, Detection of human and mouse insulin messenger RNAs in tissues of transgenic and control mice. Total cellular RNA samples are from transgenic and non-transgenic offspring of mouse 16 as follows: lane 1, non-transgenic pancreas; lane 2, transgenic spleen; lane 3, transgenic kidney; lane 4, transgenic brain; lane 5, transgenic lung; lane 6, transgenic liver; lane 7, transgenic salivary gland; lane 8, transgenic intestine; lane 9, transgenic heart; lane 10, transgenic muscle; lane 11, transgenic pancreas. Neither the mouse insulin cDNA nor gene sequences have been determined, but since the coding regions of the human and rat insulin mRNAs share 81% sequence homology[15], it was expected that both transgenic and control pancreatic RNAs would hybridize to the human insulin cDNA probe.

Methods. A 12.5-kb *Eco*RI fragment containing the human insulin gene[4] was isolated from pBR322 sequences by preparative gel electrophoresis and electroelution[16]. Fertilized mouse eggs for microinjection were recovered *in cumulus* from the oviducts of $(C57\times C3H)F_1$ females that had mated with F_1 males several hours earlier. Approximately 1,000 copies of the human insulin gene fragment were microinjected into the male pronucleus of each fertilized egg. Microinjected eggs were implanted into the oviducts of 1-day pseudopregnant ICR foster mothers and carried to term[17]. Several weeks after the birth of animals that developed from microinjected eggs, total genomic DNA was prepared[18] from mouse tails. For the Southern blot analysis in *a*, 8 μg of total genomic DNA for each mouse were digested with *Pvu*II, subjected to electrophoresis on a 0.9% agarose gel and transferred to nitrocellulose[19]. The filter was then prehybridized overnight, hybridized to a ^{32}P-labelled genomic human insulin probe, washed and exposed to X-ray film. The genomic human insulin probe is a fragment that extends from a *Bgl*II site at −169 with respect to the transcriptional start site of the human insulin gene to an *Ava*I site at +644 (ref. 4). In addition to promoter sequences, this fragment contains the first intervening sequence, the first exon (including sequences encoding the signal peptide, B-peptide and a portion of C-peptide), and a portion of the second intervening sequence. Approximately 75% of the genomic human insulin probe consists of noncoding sequences that are not highly conserved between species, which explains its limited cross-hybridization with the endogenous mouse insulin genes (which can be detected only after long exposures). Total cellular RNA was isolated from tissue samples by the guanidinium isothiocyanate/caesium chloride technique[20]. For Northern blot analysis, 4 μg of total RNA from each sample was subjected to electrophoresis on a 1.2% agarose–formaldehyde denaturing gel and transferred to nitrocellulose filters[16]. The filter was then prehybridized, hybridized to a ^{32}P-labelled human insulin cDNA[15] probe, washed and exposed to X-ray film.

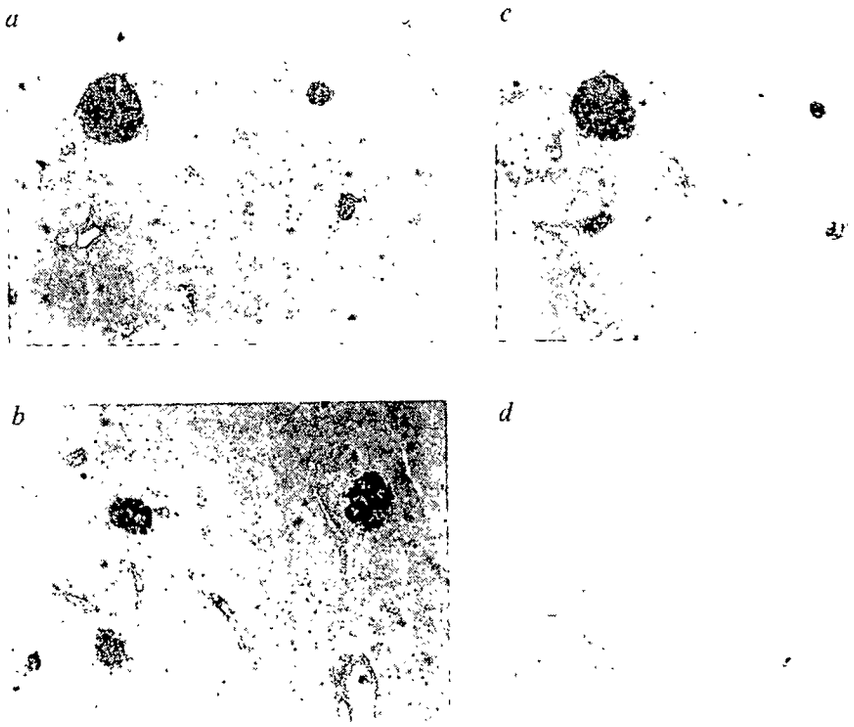


Fig. 2 Immunoperoxidase staining of transgenic and control pancreas. Pancreas samples were immersed in liquid nitrogen and 4-μm tissue sections were prepared using a cryostat. Immunoperoxidase staining of serial sections was performed as described previously[21], using either guinea pig anti-porcine insulin antibody (*a* and *b*) or goat anti-human C-peptide antibody (*c* and *d*). *a*, Transgenic pancreas stained with anti-insulin antibody (Arnel Products). *b*, Control pancreas stained with anti-insulin antibody. *c*, Transgenic pancreas stained with anti-human C-peptide antibody (Behringwerke). *d*, Control pancreas stained with anti-human C-peptide antibody (photographically enhanced to allow visualization of islets). Other transgenic tissues, including liver, adrenal and thyroid, are not stained using the guinea pig anti-porcine insulin antibody (not shown).

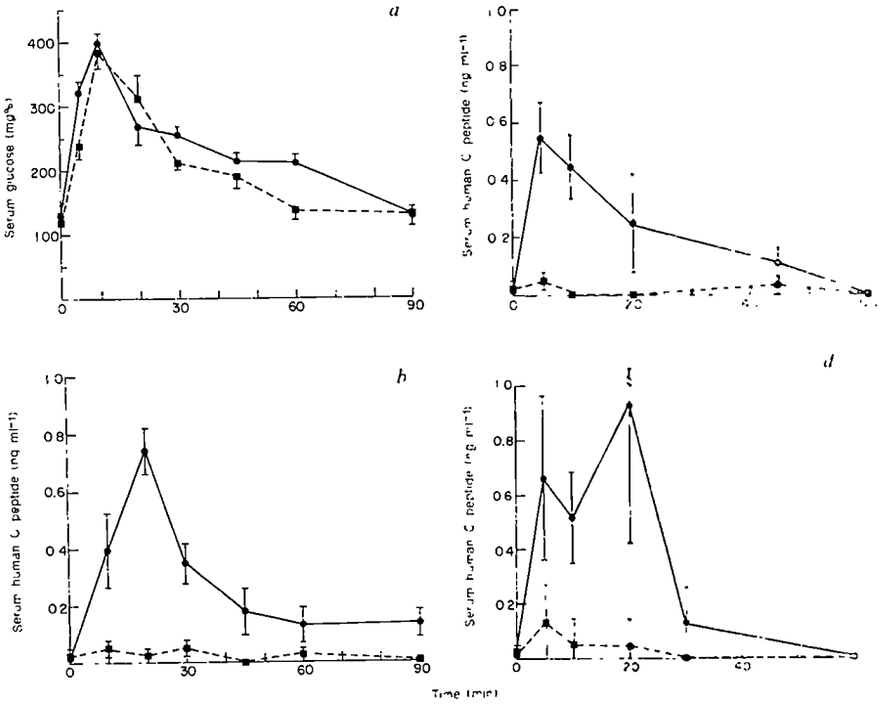


Fig. 3 *a*, Intraperitoneal glucose tolerance test. Transgenic offspring of mouse 16 and non-transgenic siblings were fasted overnight, then given an i.p. injection of glucose (1 mg glucose per g body weight). Each mouse was then arbitrarily assigned to a group of four for serum sampling at 5, 10, 20, 30, 45, 60 or 90 min post-injection. Four mice did not receive glucose and were bled to determine fasting serum glucose levels. Each time point therefore represents an average of values from four animals, and standard deviation half-bars are indicated. Solid line, transgenic mice; dashed line, control mice. Serum glucose determinations were performed using a commercially available kit (Worthington) under the conditions recommended by the manufacturer. Intravenous and oral glucose tolerance tests performed as described above showed no statistically significant difference between the transgenic and control mice (data not shown). *b*, Human C-peptide levels during an i.p. glucose tolerance test. The experiment was performed as described in *a*, with each transgenic point representing an average of values from six animals (i.p. injection of 2 mg glucose per g body weight). Serum human C-peptide levels were measured using a commercially available kit (Behringwerke) under the conditions recommended by the manufacturer. Solid line, transgenic mice; dashed line, control mice. These data are similar to glucose tolerance results previously reported for both mice[22] and humans[2]. Preliminary experiments suggest that mouse 20 also expresses human C-peptide and responds to a glucose tolerance test, and more extensive studies will be performed when mouse 20 and mouse 38 have generated large colonies. An assay specific for mouse C-peptide is not available, and we were unable to compare levels of endogenous mouse C-peptide with levels of human C-peptide. *c*, Human C-peptide levels during an i.v. amino-acid tolerance test. Transgenic and control mice were fasted overnight, infused with a solution containing 0.5 mg arginine and 0.5 mg leucine, and bled at the indicated times for human C-peptide determination. Each time point represents the average of values from four animals. Solid line, transgenic mice, dashed line, control mice. *d*, Human C-peptide levels during an i.v. tolbutamide infusion test. Transgenic and control mice were fasted overnight, infused with a solution containing 0.5 mg of tolbutamide (Upjohn) and bled at the indicated times for human C-peptide determination. Each time point represents the average of values from two animals. Solid line, transgenic mice; dashed line, control mice.

the return to basal glucose levels were similar for the transgenic and control animals. In addition, intravenous (i.v.) administration of glucagon increased serum glucose levels by ~50% within 15 min in both transgenic and control mice. Taken together, these results strongly suggest that serum glucose levels were appropriately modulated in the transgenic mice. The weights of the transgenic mice, growth rates, feeding behaviour, reproductive capability and longevity appeared normal.

The role of human insulin in the regulation of blood glucose levels in transgenic mice was investigated by performing a glucose tolerance test on transgenic and control mice (Fig. 3*b*). No human C-peptide was detected in the sera of fasting transgenic mice, but within 10 min of i.p. administration of glucose, human C-peptide appeared in the serum, and peak levels were attained within ~20 min. By 45 min post-glucose, human C-peptide levels fell to values approaching the pre-stimulation or basal level. This pattern of human C-peptide expression correlates closely with the glucose tolerance curves presented above, and suggests that serum human insulin levels were being appropriately regulated by glucose. The control mice did not express any detectable human C-peptide, indicating that the human gene must have been the source of the human C-peptide in the transgenic animals.

Insulin is regulated by several other factors, including amino acids and certain pharmacological agents. An i.v. amino-acid infusion test was performed on fasting transgenic and control mice and human C-peptide levels in the serum were determined. Peak human C-peptide levels were seen within 5 min of amino-acid infusion and declined gradually over the next 40 min (Fig. 3*c*). Similarly, serum human C-peptide levels responded to tolbutamide, a sulphonylurea derivative known to promote insulin release[10] (Fig. 3*d*). Within 20 min of i.v. tolbutamide administration, serum human C-peptide levels peaked, then decreased rapidly over the next 10 min. Tolbutamide has been used clinically to diagnose insulinomas[11] because in normal subjects serum insulin (or C-peptide) levels rapidly return to normal from their tolbutamide-induced peak, but in insulinoma patients elevated insulin levels persist. That the transgenic mice quickly regained basal serum human C-peptide levels supports the conclusion that their insulin expression was tightly regulated.

We have demonstrated that the human insulin gene is expressed in the pancreas of transgenic mice. Cell-type- and tissue-specific expression of human[12] and rat[12–14] insulin genes has been documented in two other laboratories. A 230-base-pair (bp) region (from −103 bp to −333 bp with respect to the transcriptional start site) of the rat insulin I promoter was reported to be sufficient to allow tissue-specific expression of insulin/chloramphenicol acetyltransferase fusion genes in a hamster pancreatic cell line[12,13]. Similarly, a rat insulin II/simian virus 40 large-T antigen fusion gene has been reported to cause the development of islet cell tumours in transgenic mice[14]. As both of these studies used fusion genes, the regulation of circulating human insulin could not be studied.

Serum insulin levels are regulated by glucose, amino acids, proteins and drugs such as the sulphonylurea derivatives. The human insulin gene in these transgenic mice is regulated appropriately by all of these agents, and serum glucose homeostasis is normal. These transgenic animals can therefore now be used to study several critical aspects of the physiological regulation of insulin gene expression, including the mechanisms controlling serum insulin and total β-cell insulin levels. Because at least one additional insulin gene is being expressed in the transgenic mice and total insulin RNA and protein levels are approximately the same as in control mice, the question of dosage compensation can be investigated. Moreover, our tolbutamide results indicate that drugs thought to affect human insulin metabolism can now be tested in an *in vivo* animal system. In a more general sense, the *in vivo* effects of various pharmacological agents on human gene expression and protein function can therefore be evaluated in a non-human setting.

Finally, it is noteworthy that a 12.5-kb DNA fragment contains sufficient information for the appropriate physiological regulation of insulin levels in these transgenic mice. The organism's ability to modulate foreign DNA sequences and proteins on a minute to minute basis clearly has important implications for both molecular biology and gene therapy.

We thank Dr Tom Wagner for instruction in microinjection, Victoria Roman for technical assistance and Patrick Mattoon for animal care. The human C-peptide assay was the gift of Dr H. H. Schoene and Behringwerke, AG. This work was supported by grants from Hoechst AG and the NIH (AM-07055).

Received 17 December 1985; accepted 18 March 1986.

1. Steiner, D. F. & Tager, H. S. in *Endocrinology* Vol. 2 (eds DeGroot, L. J. *et al.*) 921–934 (Grune & Stratton, New York, 1979).
2. Rubenstein, A. H. in *Endocrinology* Vol. 2 (eds DeGroot, L. J. *et al.*) 951–957 (Grune & Stratton, New York, 1979).
3. Tager, H. *et al. Nature* **281**, 122–125 (1979).
4. Bell, G. I. *et al. Nature* **284**, 26–32 (1980).
5. Lally, P. A. & Chirgwin, J. M. *Cytogenet. cell. Genet.* **37**, 515 (1984).
6. Cordell, B. *et al. Cell* **18**, 533–543 (1979).
7. Lomedico, P. *et al. Cell* **18**, 545–558 (1979).
8. Moskalewski, S. *Gen. comp. Endocr.* **5**, 342–353 (1965).
9. Lacy, P. E. & Kostianovsky, M. *Diabetes* **16**, 35–39 (1967).
10. Ganda, O. P. *et al. Diabetes* **24**, 354–361 (1975).
11. Fajans, S. S. & Conn, J. W. *J. Lab. clin. Med.* **54**, 811 (1959).
12. Walker, M. D., Edlund, T., Boulet, A. M. & Rutter, W. J. *Nature* **306**, 557–561 (1983).
13. Edlund, T., Walker, M. D., Barr, P. J. & Rutter, W. J. *Science* **230**, 912–916 (1985).
14. Hanahan, D. *Nature* **315**, 115–122 (1985).
15. Bell, G. I. *et al. Nature* **282**, 525–527 (1979).
16. Maniatis, T., Fritsch, E. F. & Sambrook, J. *Molecular Cloning: A Laboratory Manual* (Cold Spring Harbor Laboratory, New York, 1982).
17. Wagner, T. E. *et al. Proc. natn. Acad. Sci. U.S.A.* **78**, 6376–6380 (1981).
18. Rogol, A. D. *et al. Pediat. Res.* **19**, 489–492 (1985).
19. Southern, E. M. *J. molec. Biol.* **98**, 503–517 (1975).
20. Chirgwin, J. M., Przybyla, A. E., MacDonald, R. J. & Rutter, W. J. *Biochemistry* **18**, 5294–5299 (1979).
21. Sobel, R. A., Blanchette, B. W., Bhan, A. B. & Colvin, R. B. *J. Immun.* **132**, 2402–2403 (1984).
22. Larkins, R. G. *Diabetes* **22**, 251–255 (1973).

Genetic recombination between RNA components of a multipartite plant virus

Jozef J. Bujarski & Paul Kaesberg

Biophysics Laboratory and Department of Biochemistry, University of Wisconsin-Madison, Madison, Wisconsin 53705, USA

Genetic recombination of DNA is one of the fundamental mechanisms underlying the evolution of DNA-based organisms and results in their diversity and adaptability. The importance of the role of recombination is far less evident for the RNA-based genomes that occur in most plant viruses and in many animal viruses. RNA recombination has been shown to promote the evolutionary variation of picornaviruses[1–4], it is involved in the creation of defective interfering (DI) RNAs of positive- and negative-strand viruses[5–9] and is implicated in the synthesis of the messenger RNAs of influenza virus[10] and coronavirus[11]. However, RNA recombination has not been found to date in viruses that infect plants. In fact, the lack of DI RNAs and the inability to demonstrate recombination in mixedly infected plants has been regarded as evidence that plants do not support recombination of viral RNAs. Here we provide the first molecular evidence for recombination of plant viral RNA. For brome mosaic virus (BMV), a plus-stranded, tripartite-genome virus of monocots, we show that a deletion in the 3′ end region of a single BMV RNA genomic component can be repaired during the development of infection by recombination with the homologous region of either of the two remaining wild-type BMV RNA components. This result clearly shows that plant viruses have available powerful recombinatory mechanisms that previously were thought to exist only in animal hosts, thus they are able to adapt and diversify in a manner comparable to animal viruses. Moreover, our observation suggests an increased versatility of viruses for use as vectors in introducing new genes into plants.

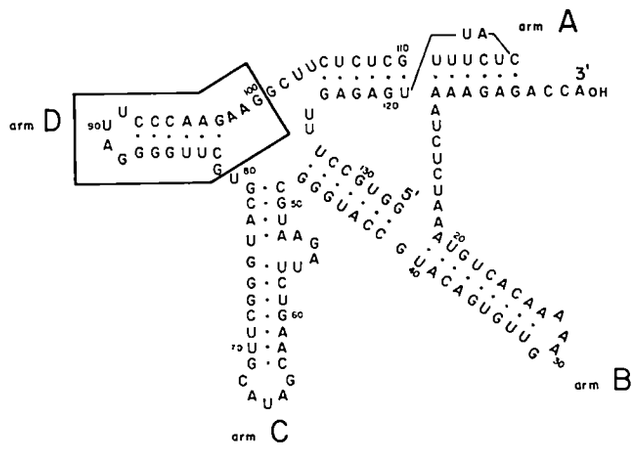


Fig. 1 Schematic representation of the postulated conformation of the tRNA-like structure at the 3′ end of BMV RNA3 (after Rietveld *et al.*[14]). The open box indicates the location of the 20-nucleotide deletion (deletion m4) so that the entire D arm is absent from the resulting structure. This deletion, located between nucleotides 81 and 100, was originally introduced into a cDNA clone comprising the last 200 bases of BMV RNA3 as described in ref. 19 and subsequently transferred into the full-length cDNA clone of BMV RNA3 as described in ref. 21.

To study recombination between the individual BMV RNAs, we used wild-type RNA1 and RNA2 together with an engineered BMV RNA3 in which a sequence located in its 3′-proximal noncoding region had been deleted. The 3′-noncoding region for each of the three BMV RNAs extends for ~300 nucleotides, the last 200 of which are similar in sequence but not identical in the three RNAs[12]. Their 3′-proximal 134 nucleotides are folded into a transfer RNA-like conformation[13,14], which is involved in initiation of BMV RNA replication[15,16], aminoacylation[17] and adenylation[18]. The RNA3 mutant, designated m4, had been constructed previously by S_1 nuclease deletion of a 20-base long, stem-and-loop hairpin corresponding to arm D in its tRNA-like structure[19] (bases 81–100; see Fig. 1).

RNAs 1 and 2, transcribed from cDNA clones of wild type (Madison M1 strain)[20], together with transcribed m4-type RNA3, are infectious to barley plants and progeny virus initially has the m4-type 3′ region in both RNA3 and RNA4 (ref. 21). RNA4 is a subgenomic RNA derived during virus infection from the 5′-proximal one-third of negative-strand RNA3 (ref. 22). However, m4 RNA3 and RNA4 accumulated less well than their wild-type counterparts, probably because of modified activity of the m4-type 3′ region, as determined *in vitro*[19,21]. We therefore decided to test the possibility that, after a prolonged infection, the original m4 RNA3 might be outcompeted by a revertant form of RNA3 which had regained the deleted stem-and-loop region as a result of recombination with wild-type RNA1 or RNA2.

Time-course analysis of progeny viral RNA3 species from successively appearing leaves of plants inoculated with transcribed wild-type RNAs 1 and 2 and m4 RNA3 revealed a stepwise decrease of the m4 RNA3 over days 3–16 after inoculation (Fig. 2). The presence of the m4 deletion near the 3′ end in RNAs 3 and 4 was determined by observation of a readily identifiable, 3′-terminal fragment released by partial digestion with ribonuclease T_1 (ref. 23). The disappearance with time of the 141-base-long m4-type fragment expected for m4 RNA3, and the parallel appearance of a 161-base fragment characteristic of wild-type RNA3 (compare lanes 2 and 4 of Fig. 2) indicated a gradual increase of an RNA3 variant that was more similar to wild-type RNA3.

To delineate the emergent RNA more precisely, we examined progeny RNA3 and RNA4 isolated from three individual barley plants on day 15 post-inoculation. In plant I we found that the variant RNA3 and RNA4 each migrated more slowly on agarose

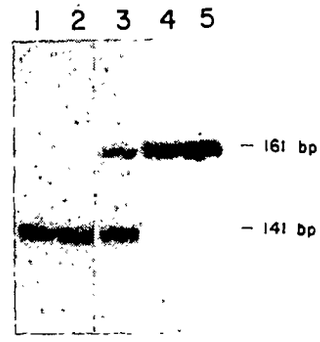


Fig. 2 Analysis by polyacrylamide gel electrophoresis for the presence of the m4 deletion in a 3′-terminal fragment released from progeny BMV RNA3 by limited digestion with RNase T_1. Lanes 5 and 1, standard T_1 fragments obtained from wild-type (161 base pairs (bp) long[23]) or m4-type (141 bp) transcript RNA3, respectively. Lanes 2, 3 and 4, T_1 fragments from progeny BMV RNA3 isolated from the virus at 3, 10 and 16 days post-inoculation, respectively.
Methods. Barley seedlings were inoculated with a mixture of transcribed wild-type BMV RNAs 1 and 2 and the m4 RNA3 following the procedure described in ref. 20. Progeny viral RNA was isolated from virus extracted from 0.1 g of leaves of a single infected plant, as described elsewhere[27]. The BMV RNA3 component was separated by electrophoresis on a low-melting point 1% agarose gel and a 3′-terminal fragment was released from the purified RNA3 by limited digestion with RNase T_1 as described elsewhere[21]. To generate standard 161- and 141-bp T_1 fragments, both wild-type and m4 RNA3 were synthesized by transcription *in vitro* as described in ref. 28, and the fragments were released from transcripts with RNase T_1. After labelling of the 3′ ends with ^{32}P-pCp and T_4 RNA ligase[29], the released RNA fragments were analysed on a 6% polyacrylamide/7 M urea sequencing gel and their positions were determined by autoradiography.

gel electrophoresis than m4-type and also wild-type RNAs 3 and 4 (see Fig. 3, lanes 1 and 2), indicating that they are larger than both m4-type and wild-type RNAs 3 and 4. There was no evidence of m4-type or wild-type RNA3 or RNA4. This pattern was unaltered after two passages of the virus through other barley plants. Sequence analysis of RNA3 from the emergent virus (designated mutant A; see Fig. 4 legend) indicated that the region corresponding to the last 267 bases of wild-type RNA3 had been replaced with the last 307 bases of wild-type RNA2. Thus, mutant A RNA3 had the deleted stem-and-loop region restored plus 39 more bases than wild-type RNA3 and 59 more bases than its m4 RNA3 progenitor.

In plant II, viral RNA3 and RNA4 co-migrated with wild-type BMV RNA3 (Fig. 3, lanes 4 and 5). Electrophoresis on a higher-resolution gel showed that the RNA3 was composed of at least two bands, the lower band containing most of the material (Fig. 3, lane 6, bands 3a and 3b). In plant III, gel electrophoresis revealed two bands each in the regions of RNA3 and RNA4 (compare lanes 7 and 10 of Fig. 3); a similar pattern was present after the first passage of the virus (lane 8), whereas after the second passage the upper band was absent (lane 9). Analysis on a higher resolution gel indicated that the lower band in the region of RNA3, present as a single band in lane 9, in fact consisted of at least two closely migrating bands (lane 11, bands 3c and 3d).

To identify the species present in RNA3 preparations obtained from plants II and III, a complementary DNA library was created and individual clones were sequenced in their 3′-noncoding regions, as described in Fig. 4 legend. Three sequences, corresponding to mutants designated B, C and D, were found in both libraries. In addition, a fourth sequence, corresponding to mutant E, was identified in the library of plant III. While four clones of mutant B, three clones of mutant C, eight of mutant D and one of mutant E were identified, cDNA clones corresponding to neither m4-type RNA3 nor the strictly wild-

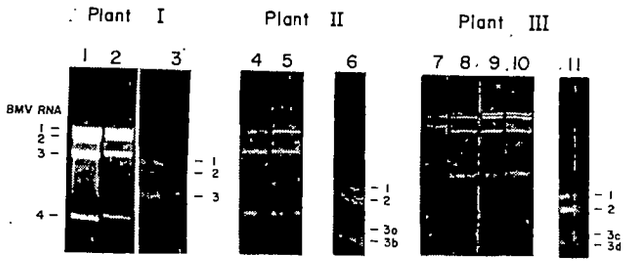


Fig. 3 Electrophoretic analysis of progeny BMV RNA extracted from three independently inoculated barley plants. Barley leaves were infected with transcribed wild-type RNAs 1 and 2 and m4 RNA3. Plants I and II: BMV RNA was extracted from leaves showing symptoms of infection, on day 15 after inoculation, and was analysed on 1.2% agarose gels (either 10 cm long, lanes 2 and 5; or 30 cm long, lanes 3 and 6). Plant III: viral RNA was obtained from leaves 15 days after inoculation with transcribed BMV RNAs (lane 7) as well as on day 15 after the first and second passages through barley (lanes 8 and 9, respectively; 10-cm gels). Lane 11, RNA from lane 9 analysed on a 30-cm gel. Lanes 1, 4 and 10, wild-type BMV RNA.

type 3′ end sequence of BMV RNA3 were found. This last observation tends to exclude the possibility that a causal infection with wild-type BMV RNA3 contaminated the experiments.

The sequences of RNA3 in mutants B, C and D revealed recombination between RNA3 and RNA1 or RNA2 at a site in their homologous 3′ end region. As these RNAs differ in only a small number of bases in this region (see Fig. 4 legend), the exact site of putative recombination could not be specified. We can conclude, however, that mutant B is a combination of RNA3 and RNA1 somewhere between bases 130 and 101, mutant C combines the RNA3 and RNA1 sequences somewhere between bases 175 and 131, and mutant D combines RNA3 and RNA2 somewhere between bases 205 and 101. Similar to mutant A, mutant E had its deleted stem-and-loop region restored and was larger than wild-type RNA3. Sequence analysis showed that the region corresponding to the last 206 bases of the wild-type RNA3 had been replaced by 215 3′-terminal nucleotides from wild-type RNA2 (see Fig. 4).

The structure of these five mutants suggests strongly that one or more recombination events have occurred between the 3′-noncoding regions (within or outside the homologous sequences) of individual BMV RNAs, resulting in the restoration of the deleted hairpin in progeny RNA3. Clearly, that stem-and-loop region is not essential for infectivity but its presence nevertheless confers a selective advantage. In mutants A and E recombination outside the closely homologous region resulted in emergent noncoding regions larger than wild-type RNA3, indicating that a degree of structural variability is permissible there. In mutants B, C and D the recombination event(s) occurred within the homologous region and resulted in sequences of wild-type lengths only.

The results described here demonstrate that recombination between viral RNAs occurs in plant cells at a relatively high frequency and at various positions on the RNA. As with animal RNA viruses, the mechanism of recombination between the BMV sequences is unknown. Two diverse mechanisms have been suggested for RNA genomes: (1) Enzymatic cutting and re-ligation. (2) A 'copy-choice', during replication, between adventitiously proximal templates. The latter mechanism has been favoured for recombination in picornaviruses[24], negative-strand viruses[5,10] and alpha viruses[7].

The recent discoveries of remarkable sequence similarities among encoded proteins of diverse plant RNA viruses[25,26] suggest that recombination may be a common phenomenon during synthesis of plant viruses. Like other processes of natural mutagenesis, recombination between plant viruses may render the progeny more adaptable to new environments or hosts.

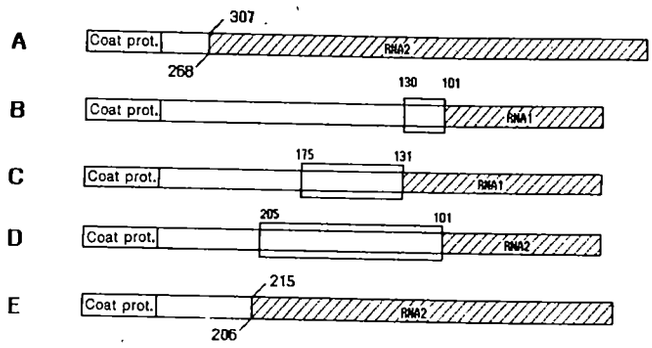


Fig. 4 Schematic representation of BMV RNA3 recombinants identified by sequence analysis of BMV RNA3 preparations obtained from plants I–III. Mutant A was obtained from plant I; mutants B–E were identified in plants II and III. The figure shows the 3′ region of RNA3 for the five mutants downstream to the coat protein open reading frames (ORFs). The open regions adjacent to the ORFs represent wild-type BMV RNA3 sequences. The cross-hatching indicates regions identical to wild-type RNA1 or RNA2, possessing the stem-and-loop region of arm D, and also differing from wild-type RNA3 at the following base positions: RNA1 has distinctive bases at positions 101, 44 and 43 while RNA2 has distinctive bases at positions 101 and 44 and has a point deletion corresponding to base 74 of RNA3 (refs 13, 20). The boxes enclose regions in which the recombination event occurred, assuming a recombination mechanism involving a single event. Sequences of wild-type RNAs 1, 2 and 3 are identical in these regions.

Methods. Mutant A RNA3 was sequenced directly by a chain-temination (dideoxy) technique with RNA-dependent DNA polymerase (reverse transcriptase[30]. Briefly, 2 μg of RNA3, obtained after fractionation on a sucrose gradient[31], was hybridized with 1 μg of either the 15-mer d(GAGATTTTCTCTGGT), complementary to nucleotide positions 1–15, or the 15-mer d(TCTCACAGATCCTCG), complementary to nucleotides 129–143, and these primers were extended with 10 units of reverse transcriptase (Life Science) in the presence of dideoxy nucleoside triphosphates. RNA3 preparations obtained from plants II and III (mutants B–E) were sequenced as cDNA clones in an M13mp19 vector by a chain-termination (dideoxy) technique with a synthetic 17-mer primer (BioLabs) and DNA polymerase large fragment (Klenow)[32,33]. Two cDNA libraries were created for BMV RNA3 preparations obtained either from primary infection in plant II or after a second passage of the virus in plant III. The first cDNA strand was synthesized with reverse transcriptase as described elsewhere[34], using the d(TAGAGATTTTCTCTGGT) primer complementary to the last 17 nucleotides of BMV RNA3. After purification on a 1 × 20 cm Sepharose CL2B column, the second strand was obtained by means of a replacement reaction with RNase H, *Escherichia coli* DNA polymerase and *E. coli* DNA ligase[35]. After treatment with T_4 DNA polymerase (blunt-ending), the resulting double-stranded cDNA preparation was cloned into a *Sma*I restriction site of M13amp19 vector and the sequence of the corresponding single-stranded M13 DNA templates was determined by a chain-termination procedure using the Klenow fragment of *E. coli* DNA polymerase and a synthetic 17-mer (BioLabs) as primer.

Conversely, RNA recombination between plant viral RNAs may be important for the preservation and stabilization of crucial functional sequences of multipartite genome viruses. Because it facilitates the association of unrelated genes, recombination also represents an attractive candidate for the mechanism of origin of viruses and for the insertion of new genes into existing viruses.

We thank Ola Dzianott-Bujarska for technical assistance, and G. Duke, P. Shaklee and P. Ahlquist for valuable advice with respect to cDNA cloning. This work was supported by NIH research grants AI01466 and AI15342 and Career Award AI21942.

Received 21 January; accepted 18 March 1986.

1. Cooper, P. D. *Virology* **35**, 584–596 (1968).
2. King, A. M. Q., McCahon, D., Slade, W. R. & Newman, J. W. I. *J. Virol.* **41**, 66–77 (1982).

3. Tolskaya, E. A., Romanova, L. A., Kolesnikova, M. S. & Agol, V. I. *Virology* **124**, 121–132 (1983).
4. Emini, E. A., Leibowitz, J., Diamond, D. C., Bonin, J. & Wimmer, E. *Virology* **137**, 74–85 (1984).
5. Lazzarini, R. A., Keene, J. D. & Schubert, M. *Cell* **26**, 145–154 (1981).
6. Jennings, P. A., Finch, J. T., Winter, G. & Robertson, J. S. *Cell* **34**, 619–627 (1983).
7. Monroe, S. S. & Schlesinger, S. *J. Virol.* **49**, 865–872 (1984).
8. Stark, C. & Kennedy, S. I. T. *Virology* **89**, 285–299 (1978).
9. Lai, M. M. C. *et al. J. Virol.* **56**, 449–456 (1985).
10. Plotch, S. J., Bouloy, M., Ulmanen, I. & Krug, R. M. *Cell* **23**, 847–858 (1981).
11. Baric, R. S., Stohlman, S. A., Razavi, M. K. & Lai, M. M. C. *Virus Res.* **3**, 19–33 (1985).
12. Ahlquist, P., Dasgupta, R. & Kaesberg, P. *J. molec. Biol.* **172**, 369–383 (1984).
13. Ahlquist, P., Dasgupta, R. & Kaesberg, P. *Cell* **23**, 183–189 (1981).
14. Rietveld, K., Pleij, W. A. & Bosch, L. *EMBO J.* **2**, 1079–1985 (1983).
15. Ahlquist, P., Bujarski, J. J., Kaesberg, P. & Hall, T. C. *Pl. molec. Biol.* **3**, 37–44 (1984).
16. Miller, W. A., Bujarski, J. J., Dreher, T. W. & Hall, T. C. *J. molec. Biol.* **187**, 537–546 (1986).
17. Hall, T. C. *Int. Rev. Cytol.* **60**, 1–26 (1979).
18. Joshi, R. L., Joshi, S., Chapeville, F. & Haenni, A. L. *EMBO J.* **2**, 1123–1127 (1983).
19. Bujarski, J. J., Dreher, T. W. & Hall, T. C. *Proc. natn. Acad. Sci. U.S.A.* **82**, 5636–5640 (1985).
20. Ahlquist, P., French, R., Janda, M. & Loesch-Fries, L. S. *Proc. natn. Acad. Sci. U.S.A.* **81**, 7066–7070 (1984).
21. Bujarski, J. J., Ahlquist, P., Hall, T. C., Dreher, T. & Kaesberg, P. *EMBO J.* (submitted).
22. Miller, W. A., Dreher, T. W. & Hall, T. C. *Nature* **313**, 68–70 (1985).
23. Bastin, M., Dasgupta, R., Hall, T. C. & Kaesberg, P. *J. molec. Biol.* **103**, 737–745 (1976).
24. Cooper, P. D., Steiner-Pryor, A., Scotti, P. D. & DeLong, D. J. *Gen. Virol.* **23**, 41–49 (1974).
25. Haseloff, J. *et al. Proc. natn. Acad. Sci. U.S.A.* **81**, 4358–4362 (1984).
26. Cornelissen, B. & Bol, J. *Pl. molec. Biol.* **3**, 379–384 (1984).
27. Shih, D. S., Lane, L. C. & Kaesberg, P. *J. molec. Biol.* **64**, 353–362 (1972).
28. Ahlquist, P. & Janda, M. *Molec. cell. Biol.* **4**, 2876–2882 (1984).
29. England, T. & Uhlenbeck, O. *Nature* **275**, 560–561 (1978).
30. Zimmern, D. & Kaesberg, P. *Proc. natn. Acad. Sci. U.S.A.* **75**, 4257–4261 (1978).
31. Kiberstis, P. A., Loesch-Fries, L. S. & Hall, T. C. *Virology* **112**, 804–808 (1981).
32. Sanger, F., Nicklen, S. & Coulson, A. R. *Proc. natn. Acad. Sci. U.S.A.* **74**, 5463–5467 (1977).
33. Biggin, M. D., Gibson, T. J. & Hong, G. F. *Proc. natn. Acad. Sci. U.S.A.* **80**, 3963–3965 (1983).
34. Fields, S. & Winter, G. *Cell* **28**, 303–313 (1982).
35. Okayama, H. & Berg, P. *Molec. cell. Biol.* **2**, 161–170 (1982).

A tobacco mosaic virus-induced tobacco protein is homologous to the sweet-tasting protein thaumatin

Ben J. C. Cornelissen, Rob A. M. Hooft van Huijsduijnen & John F. Bol

Department of Biochemistry, State University of Leiden, PO Box 9505, Leiden, The Netherlands

Infection of tobacco plants with tobacco mosaic virus (TMV) results in an increase in the activities of several enzymes and induces the *de novo* synthesis of about 10 proteins that are protease-resistant and soluble at *p*H 3. These proteins accumulate in the intercellular leaf space[1,2]. The appearance of pathogenesis-related (PR) proteins is closely associated with the phenomenon of 'systemic acquired resistance' and it has been suggested that such proteins have an antiviral function[3,4]. Previously, we cloned complementary DNAs to the messenger RNAs for the three smallest PR proteins, PR-1a, -1b and -1c, and these clones were used to show that there is an increase of more than 100-fold in the concentration of PR-1 mRNAs following TMV infection of tobacco[5,6]. Here, we describe the cDNA cloning of another mRNA whose synthesis is induced by TMV infection. Sequencing of the cDNA showed that the encoded protein is highly homologous to thaumatin, the intensely sweet-tasting protein from the fruits of the monocot *Thaumatococcus daniellii* Benth, a West African rainforest shrub. The conservation of a gene encoding a thaumatin-like protein in tobacco suggests that the encoded protein may have a more general function than that of being sweet-tasting.

Poly(A)-containing RNA from TMV-infected Samsun NN tobacco was used as a template to construct a cDNA library; 1,400 transformants were screened by a differential hybridization procedure, using ^{32}P-labelled DNA complementary to poly(A) RNA from healthy or TMV-infected tobacco as probes. Forty transformants were found to correspond to TMV-induced mRNAs and an analysis of their inserts showed that they could be divided into six clusters, with cross-hybridization occurring within but not between the clusters. Details of the cloning and selection procedure will be given elsewhere (R.A.M.H. *et al.*, in preparation).



Fig. 1 Northern blot loaded with poly(A) RNA from healthy tobacco (H), tobacco sprayed with salicylic acid (S) and tobacco infected with TMV (T). The blot was probed with ^{32}P-labelled PROB 12. Samsun NN tobacco plants were sprayed with salicylic acid (5 mM, adjusted to *p*H 7) on three successive days before RNA extraction. RNA was extracted from TMV-infected tobacco plants 7 days after inoculation. The method of extraction, Northern blotting and the cloning of PROB 12 are described in ref. 6.

One cluster was represented by a single clone, PROB 12, which was used to probe the Northern blot shown in Fig. 1. The gel used to make the blot was loaded with poly(A) RNA from healthy tobacco (lane H), tobacco sprayed with salicylic acid (lane S), and tobacco infected with TMV (lane T). Salicylic acid is known to induce the synthesis of several PR proteins, notably proteins 1, 2 and N[2]. The mRNA corresponding to PROB 12 occurs at a low level in healthy tobacco, is not induced by treatment with salicylic acid, but is strongly induced by TMV infection. This mRNA is estimated to be 1,000–1,100 nucleotides long. Sequencing studies showed that the insert in PROB 12 is 845 base pairs (bp) long. As no poly(A) tract was found in the cDNA, the 3′ end of the mRNA is probably not represented in the clone. Figure 2 shows that the insert contains an open reading frame for a protein of 226 amino acids, flanked by 5′- and 3′-noncoding regions of 3 and 164 nucleotides, respectively.

The nucleotide sequence of the insert of PROB 12 was compared, by computer analysis, with plant sequences stored in a databank (Genbank). Extensive homology was found with the mRNA for thaumatin, the sweet-tasting protein that occurs in the arils of *Thaumatococcus daniellii* Benth, a West African shrub[7]. At least five different forms of thaumatin (I, II, III, b and c) can be isolated, all of which are almost 100,000 times sweeter than sucrose on a molar basis[8]. The most abundant forms are thaumatin I and II, polypeptides of 207 amino acids each that differ at only five positions[9]. The mature protein is derived from preprothaumatin by removal of an amino-terminal signal peptide of 22 amino acids and an acidic carboxy-terminal extension of 6 amino acids[7]. In Fig. 3, preprothaumatin II is aligned with protein encoded by PROB 12; the amino-acid sequence homology between the two proteins is 65%. In addition, there are several conserved amino-acid changes; when these are taken into account, the homology is more than 70%. The Ala-Ala sequence, which represents the site of cleavage of the signal peptide, is conserved in both proteins. However, except for their hydrophobic nature, there is little similarity between the signal peptides of the two proteins, and the tobacco protein lacks the C-terminal extension of the thaumatin precursor. Because of its homology to thaumatin, we provisionally refer to the PROB 12-encoded protein as a thaumatin-like (or TL) protein of tobacco.

The alignment shown in Fig. 3 suggests that PROB 12 contains the complete coding region for the precursor of the TL protein. A possible polyadenylation signal in TL mRNA (underlined in Fig. 1) is located 80 bp upstream from the 3′ end of the cDNA insert. There may be additional polyadenylation signals in the TL mRNA sequence that are not represented in PROB 12. Three potential polyadenylation signals have been found in thaumatin mRNA[7].

The relative molecular mass (M_r) of the mature TL protein of tobacco is 21,596. It is unknown whether the TL protein

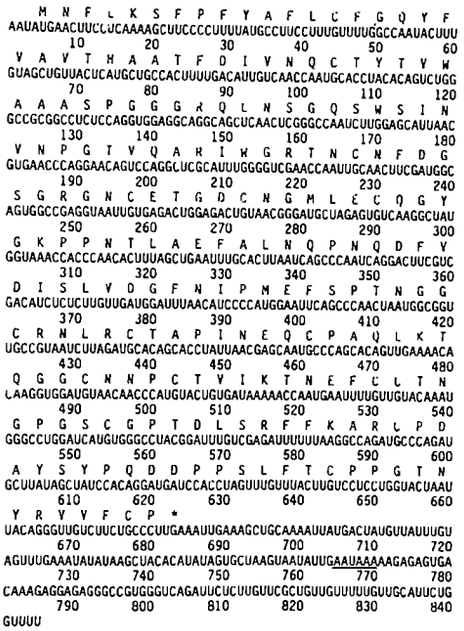


Fig. 2 Nucleotide sequence of the coding strand of PROB 12 cDNA. The amino-acid sequence corresponding to the open reading frame is indicated (one-letter code). The polyadenylation signal in the 3'-noncoding region is underlined.

corresponds to a known PR protein, for example, P or Q (each of estimated M_r ~27,000; ref. 5). In preliminary immunodiffusion experiments, purified PR proteins, or a total protein extract from TMV-infected tobacco, did not react with an antiserum to thaumatin. The PR-1 proteins are derived from their precursors by the removal of a 30-amino-acid signal peptide, probably during excretion into the intercellular space of the tobacco leaf[5,6]. The evidence for a signal peptide in the TL primary translation product also suggests that the TL protein is translocated through a membrane. The thaumatins are known to accumulate in intracellular vesicle-like organelles[10]. If, by analogy, the TL protein is not localized extracellularly in tobacco, it may not belong to the PR class of proteins.

The extreme sweetness of thaumatin, which is only recognized by man and Old World monkeys, may contribute to the spreading of the seeds of *T. daniellii* Benth. The conservation of a thaumatin-like gene in tobacco and possible other dicotyledonous plants suggests that in these plants the encoded protein performs a more general function. Thaumatin ($pI = 12$) has a high proportion of basic residues and modification studies indicate that some lysine residues are important for the sweet taste[11,12]. In the tobacco TL protein there is an excess of acidic residues over basic residues, which may alter its properties with respect to taste perception. Recently, the three-dimensional structure of thaumatin I has been deduced at 3.1 Å resolution[13]. It will be interesting to compare the predicted TL protein structure with the thaumatin backbone.

The presence of two very small introns at different positions in several thaumatin genes has led to the suggestion that the genes encoding thaumatin are structurally similar to those encoding storage proteins such as zein (maize) and glycinin (soybean)[9]. The availability of PROB 12 offers the possibility of monitoring for a tissue-specific expression of the TL gene during the life cycle of tobacco. A model has been proposed in which the burst of ethylene production that is evoked by TMV infection of tobacco, is responsible for the induction of PR proteins and of several enzymes[1]. In this respect it is noteworthy that ethylene production increases considerably during specific developmental processes such as fruit ripening.

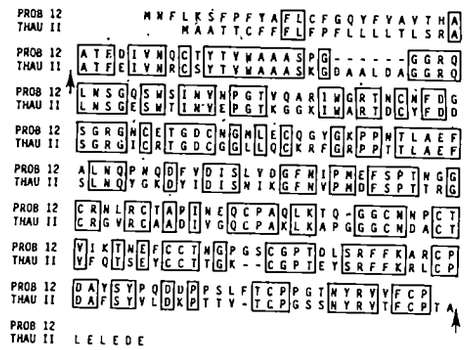


Fig. 3 The amino-acid sequence encoded by the open reading frame in PROB 12, aligned with the preprothaumatin II sequence[7]. Amino acids that are identical in the two sequences are boxed. The arrows indicate the cleavage sites that are used to remove the N-terminal signal peptide and the C-terminal extension from preprothaumatin II.

We thank Dr A. M. Ledeboer (Unilever Research Laboratory, Vlaardingen, The Netherlands) for providing an antiserum against thaumatin. This work was sponsored in part by the Netherlands Foundation for Chemical Research (SON) with financial aid from the Netherlands Organization for the Advancement of Pure Research (ZWO).

Received 26 February; accepted 21 March 1986.

1. Van Loon, L. C. in *Active Defense Mechanisms in Plants* (ed. Wood, R. K. S.) 247–274 (Plenum, New York, 1982).
2. Van Loon, L. C. *Pl. molec. Biol.* 4, 111–116 (1985).
3. Kassanis, B., Gianinazzi, S. & White, R. F. *J. gen. Virol.* 23, 11–16 (1974).
4. Van Loon, L. C. *Virology* 67, 566–575 (1975).
5. Hooft van Huijsduijnen, R. A. M. *et al. EMBO J.* 4, 2167–2171 (1985).
6. Cornelissen, B. J. C., Hooft van Huijsduijnen, R. A. M., Van Loon, L. C. & Bol, J. F. *EMBO J.* 5 37–40 (1986).
7. Edens, L. *et al. Gene* 18, 1–12 (1982).
8. Higginbotham, J. D. in *Developments in Sweeteners-I* (eds Hough, C. A. M., Parker, K. J. & Vlitos, A. J.) 87–123 (Applied Science Publications, London, 1979).
9. Ledeboer, A. M., Verrips, C. T. & Dekker, B. M. M. *Gene* 30, 23–32 (1984).
10. Edens, L. & Van der Well, H. *Trends Biotechnol.* 3, 1–4 (1984).
11. Van der Wel, H. & Bel, W. *Chem. Senses* 2, 211–218 (1976).
12. Morris, R., Cagan, R., Martenson, R. & Deibler, G. *Proc. Soc. exp. Biol. Med.* 157, 194–318 (1978).
13. De Vos, A. M. *et al. Proc. natn. Acad. Sci. U.S.A.* 82, 1406–1409 (1985).

Nature Product Review

MANUFACTURERS and distributors of scientific equipment are reminded that the following special features are appearing in July and August:

3 July: **Microscopy/Image analysis,** covering all aspects of microscope hardware and techniques as well as latest developments in image analysers.

3 July: **Immunology.** Also in this issue, details of exhibits at the Toronto International Congress of Immunology, to be held on 7–10 July.

4 August: **New on the Market:** A selection of recently introduced laboratory equipment with the accent on novelty.

14 August: **Computers in the laboratory:** Information technology and computer services in the modern laboratory.

Press releases, photographs and comments on these features should be addressed to the Editor in *Nature*'s London office or to:
Karen Wright,
Nature,
1134 National Press Building,
Washington, DC 20045, USA

Was there 26-Myr periodicity of extinctions?

HOFFMAN[1] has questioned our claim[2] that extinction events during the past 250 Myr exhibit a 26-Myr periodicity. Hoffman argues that the apparent periodicity originates not from any evolutionary signal but from arbitrariness in the choice of taxonomic level, treatment of data and selection of geologic timescales in our analysis. His letter succeeds in outlining many problems inherent in working with data from the fossil record. However, we find his conclusion unconvincing because there is no hypothesis-testing. In fact, when statistical tests and independent criteria are applied, we find that Hoffman's results support our contention of periodicity better than our initial analyses.

In our initial paper[2] we analysed a set of data on fossil marine families that was highly culled in order to enhance the signal-to-noise ratio. Hoffman implies that this culling may have induced an appearance of periodicity. However, our subsequent analyses[3,4] indicate that this culling had no important consequences and an evident 26-Myr periodicity remains when a variety of extinction metrics (including rate and probability of extinction) are computed from the complete, unculled data set. Indeed, Hoffman's own measures of extinction intensity, summarized in his Table 1, also show this if consistent patterns rather than random noise are sought. Ten of Hoffman's 43 stages exhibit peaks (local maxima) in more than half of the 21 metrics (including the unillustrated regression residuals for number of family extinctions per stage). The ten stages are the Guadalupian, Olenekian, Norian, Pliensbachian, Bajocian, Tithonian, Cenomanian, Maestrichtian, late Eocene and middle Miocene. Of these, all but the Olenekian, Bajocian and middle Miocene have been independently recognized as containing extinction events by palaeontologists using detailed biostratigraphic data on species and genera[3,5], and only one other stage (the Pliocene) in the Guadalupian-to-Recent interval has been so recognized. The probability that the family data would encompass 7 of 8 events in 10 random peaks among 43 stages is <0.00003, strongly indicating that the consistent peaks among Hoffman's metrics result from evolutionary variation rather than artefact. This conclusion is further supported by the good correlation between familial and generic[4,6] extinctions throughout the 43 stages. (For per cent extinction, $r = 0.893$ and for probability of extinction $r = 0.877$.)

Statistical tests similar to those used in our initial paper indicate that the 10 stages listed above exhibit a significant ($p < 0.002$) nonrandomness at a 26-Myr periodicity. Tests of this periodicity result in a standard deviation of differences between observed and expected peaks of 3.28 Myr using the Harland *et al.* timescale[7] and 5.53 Myr using the Odin timescale[8]; both fits are better than those obtained in our original analysis[2]. Fits with even higher significance are obtained if only the four most recent, and therefore most reliably dated[9], stages are tested[4].

Why did Hoffman conclude that the familial data appeared random with respect to extinction? It may have been because he used a necessary but not sufficient criterion for randomness. He argued that if random, the extinction metrics should display an average frequency of one peak in four stages; because our data displayed this frequency, he concluded that they were random. But there is a great difference between an average frequency of occurrence and a regular occurrence. A fair coin will, on average, come up heads once in two flips, but if it comes up heads regularly every other flip, we should suspect its fairness. In our analysis of the extinction data, our randomization test[2] actually converted the data into random walks with the same frequency of maxima as in the observed time series. Yet, when compared to these random walks, we found that the observed distribution of maxima was significantly ($p < 0.01$) more uniform than in the random walks. Thus, we rejected the hypothesis of randomness in favour of periodicity. We suggest that Hoffman might have done the same if he had performed the proper statistical tests.

J. JOHN SEPKOSKI JR
DAVID M. RAUP

Department of the Geophysical Sciences, University of Chicago, 5734 S. Ellis Avenue, Chicago, Illinois 60637, USA

1. Hoffman, A. *Nature* **315**, 659-662 (1985).
2. Raup, D. M. & Sepkoski, J. J. Jr *Proc. natn. Acad. Sci. U.S.A.* **81**, 801-805 (1984).
3. Sepkoski, J. J. Jr & Raup, D. M. in *Dynamics of Extinction* (ed. Elliott, D.) 3-36 (Wiley, New York, 1986).
4. Raup, D. M. & Sepkoski, J. J. Jr *Science* **231**, 833-836 (1986).
5. Sepkoski, J. J. Jr *Spec. Pap. geol. Soc. Am.* **190**, 283-289 (1982).
6. Sepkoski, J. J. Jr in *Patterns and Process in the History of Life* (eds Raup, D. M. & Jablonski, D.) (Springer, Berlin, in the press).
7. Harland, W. B. *et al. A Geologic Time Scale* (Cambridge University Press, 1983).
8. Odin, G. S. (ed.) *Numerical Dating in Stratigraphy* (Wiley, New York, 1982).
9. Maddox, J. *Nature* **315**, 627 (1985).

HOFFMAN[1] and Hoffman and Ghiold[2] recently presented a statistical argument that has been widely regarded[3-5] as casting serious doubt upon Raup and Sepkoski's[6] proposed 26-Myr extinction periodicity. Here I show that their conclusion is false and reflects an incorrect application of their own neutral model. When properly applied, the model actually supports Raup and Sepkoski's position and underscores the need for a causal explanation.

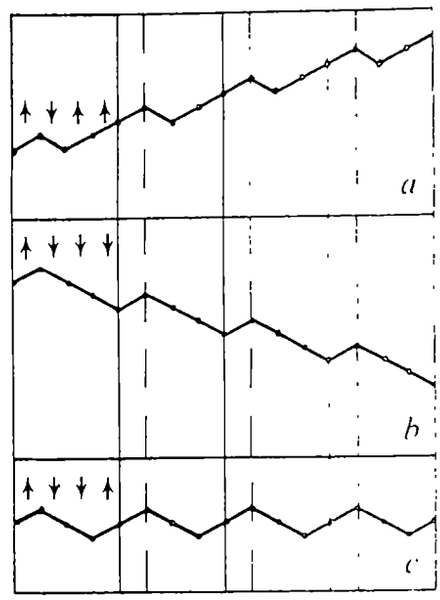


Fig. 1 The leftmost column shows the three ways of producing exactly one local extinction maximum in the second of a sequence of 4 stages. These are the unit sequences referred to in the text. Arrows indicate the direction of change (increase or decrease) in the extinction metric in each unit sequence. The unit sequences are repeated, producing three long periodic sequences of period 4. Although *a*, *b* and *c* each involve repetition of a single unit sequence, any unit sequence may follow any other and still create a periodic series. The magnitudes of the changes in extinction metric are ignored

Hoffman and Hoffman and Ghiold's argument is as follows:

(1) Given Raup and Sepkoski's definition of mass extinction as any local maximum of extinction metric; that is, any increase followed by decrease, and

(2) Given that the probabilities of increase and decrease in extinction metric both equal 0.5, and

(3) Given that the average stage length in the late Phanerozoic is 6.4 Myr, then the following conclusions hold:

(i) The probability that any particular stage is a local extinction maximum is equal to $(0.5)^2 = 0.25$.

(ii) Local extinction maxima are to be expected, on average, every four stages or every $4 \times 6.4 = 25.6$ Myr.

(iii) "The appearance of approximately 26 million year periodicity is inevitable."[2]

Conclusions i and ii are true. However, conclusion iii does not follow from premises 1-3 above and is false. The mistake is clarified by the following: Conclusion ii in more precise language, means that in a large number of samples of four stages, the arithmetic mean number of mass extinctions per sample will be 1. However, for an extinction pattern to be periodic with a period of four stages requires that every fourth and only every fourth stage

be a local extinction maximum. As these two statements are not equivalent conclusion ii does not guarantee an extinction periodicity of 4 stage-lengths, and the neutral model does not predict that a 26-Myr periodicity is "inevitable". Conclusion iii is false.

To calculate the probability of producing an extinction periodicity of 4 stage lengths by a random process under the neutral model, one must determine the number of ways of producing an extinction periodicity of this period that persists for n stages, and multiply this by the probability of generating any sequence n stages in duration. Let us treat a periodic sequence of period 4 and duration n as a series of unit sequences four stages in duration. In order for such a series to be periodic, each unit sequence in the series must have exactly one local extinction maximum, and these maxima must be in the same position. There are only three unit sequences that have the local maximum at the second stage (Fig. 1). Thus there are only three infinitely long periodic sequences of period 4 that can be built by infinite repetition of the same unit sequence. But since the conditions for periodicity allow any of the three unit sequences of Fig. 1 to precede or follow any other, it follows that there are exactly $3^{n/4}$ possible ways of producing a periodicity of period 4 with the extinction peak at the second stage. Because there are actually 4 different positions where the extinction peak may occur, corresponding to shifts of phase, there are a total of $4\times3^{n/4}$ possible periodic sequences of length n and period 4. The probability of generating any particular sequence of length n under the neutral model is 0.5^n; therefore the probability of generating an extinction periodicity of duration n and period 4 is $4\times3^{n/4}\times0.5^n$.

Applying this formula to the 39-stage periodicity reported by Raup and Sepkoski[6], the probability of an extinction event occurring every 4 stages (~26 Myr) under the neutral model is $4\times3^{39/4}\times0.5^{39}=3.3\times10^{-7}$. For a 43-stage periodicity, as proposed more recently[7], the probability is 6.1×10^{-8}. Thus the probability, under the neutral model, of the periodicity being a simple artefact of Raup and Sepkoski's definition of mass extinction and of the average duration of stratigraphic stages is essentially zero.

The neutral model, like all models, is an oversimplification of nature. Thus, even my exact solution is only an approximate assessment of the probability of producing the observed pattern by chance. In fact, the complexities of the real palaeontological record would render an exact analytical calculation of probability extremely complex, if not impossible. Accordingly, Raup and Sepkoski employ a non-parametric randomization technique to allow them to include real-world complexities implicitly in the approximation of a probability value. The neutral model and randomization yield consistent results, and both support the conclusion that the proposed periodicity is real and needs to be explained.

I thank I. J. Good for discussion of the probability calculation.

NORMAN L. GILINSKY
Department of Geological Sciences, Virginia Polytechnic Institute and State University, Blackburg, Virginia 24061, USA

1. Hoffman, A. *Nature* **315**, 569-662 (1985).
2. Hoffman, A. & Ghiold, J. *Geol. Mag.* **122**, 1-4 (1985).
3. Maddox, J. *Nature* **315**, 627 (1985).
4. Lewin, R. *Science* **229**, 640 (1985).
5. *Scient. Am.* **253**(3), 52-53 (1985).
6. Raup, D. M. & Sepkoski, J. J. Jr. *Proc. natn. Acad. Sci. U.S.A.* **81**, 801-805 (1984).
7. Sepkoski, J. J. Jr & Raup, D. M. in *Dynamics of Extinction* (ed. Elliot, D.) Wiley, New York, in the press).

STATISTICAL testing, essential to the effective argument of controversies based on data and hypotheses, depends on distributions of random processes. Raup and Sepkoski[1] present data describing the ratio of marine families believed to have become extinct during each of 39 stratigraphic stages in the past 250 Myr. Ratios record the number of extinct to extant families, per stage, exclusive of families extant today or during the past 11.3 Myr. On the basis of these data, Raup and Sepkoski[1] have suggested that these extinction ratios have varied with regular periodicity. Hoffman[2] proposed a non-periodic random model, which formed the basis of his criticism of the work of Raup and Sepkoski. Hoffman's argument rests on the claim that the empirical mean time between peaks of extinction ratios reported by Raup and Sepkoski is not very different from the mean expected under this random model. However, the variance, and not the mean, tests the hypothesis of periodicity.

To compare the empirical variance with that expected under Hoffman's model, we have simulated the distribution of the statistic used to estimate variance, which should be the basis of Hoffman's criticism. The problem of the expected variance in the spacing of peaks, given this random process, can be restated as follows: what is the variance in waiting time to a reversal from increase to decrease in extinction ratio? For each time interval the extinction ratio either increases or decreases relative to the preceding interval. An interval of increase is recognized as a peak (that is, a local maximum in extinction rate) if the time interval immediately following is an interval of decrease. The number of time intervals between successive peaks (measured by counting the peak at the beginning and all time intervals until but not including the next peak) is the length of time, L, between successive peaks. In the data of Raup and Sepkoski[1] the lengths of these inter-peak times are: 2, 4, 4, 2, 2, 3, 3, 4, 5, 5, 4. The average of these lengths is 3.454, which would be the approximate period of the hypothesized periodicity.

To retain equivalency with the non-periodic random process described by Hoffman, we assumed, as he did, that (1) the probabilities of increase and decrease are equivalent and equal to 0.5, (2) the probabilities are independent, and (3) the time steps are of equal duration. To test whether extinction rate is a periodic function of time, we need to consider the distribution of the random variable L, its mean and variance, and the distribution of estimators of its mean and variance calculated from the sampling procedure used to observe the data of Raup and Sepkoski[1]. The distribution of L is

$$\Pr(L=r)=\sum_{i=1}^{r-1}(1-p)^i\,p^{(r-1)},$$

$$r=2,3,4,\ldots$$

When $p=0.5$, as suggested by Hoffman, the probability of an inter-peak time of r intervals is

$$\Pr(L=r)=\frac{(r-1)}{2^r}$$

The expected mean and variance of L are both equal to 4. Most of this distribution occurs in the inter-peak lengths 2–5, with frequencies of 0.25, 0.25, 0.19 and 0.125, respectively. If the observed inter-peak lengths are more uniform than would be expected under Hoffman's random hypothesis, this would support the idea that extinction rate is a periodic function of time. Thus, if the variance estimated from the data were significantly less than the value of this estimator of the variance of L expected under Hoffman's hypothesis, then periodicity would be supported; otherwise, periodicity would seem less plausible. The observed variance among the inter-peak lengths of the Raup and Sepkoski[1] data is 1.19. To determine its significance, however, we need to know the distribution of the variance estimates according to Hoffman's null hypothesis, based on a sequence of the same length as that observed, namely 40 time intervals (39 stages plus the assumption of a decline following the last datum).

To determine this distribution, we generated 10,000 such sequences with a random number generator. We observed the collection of inter-peak lengths for each sequence, calculated a mean and variance of these lengths, and empirically observed the distribution of these means and variances. The mean of the 10,000 sampled means was 3.966, very close to the mean of L. A non-significant one-sixth of the sampled means were less than the mean (3.454) observed in the data. Hence, Hoffman correctly asserted that the mean of the data is not significantly different from the mean expected under his hypothesis. But the mean of the 10,000

sampled variances (3.580) was less than the variance (4) of *L*. This is because rare, very long lengths are eliminated or made less likely by considering only sequences of 40 intervals and because short lengths are made slightly more common by requiring that the sequence end with a decrease.

The central purpose of this note is to determine the significance of the variance estimated from the data. Only 0.07 of the 10,000 sampled variances of inter-peak length under Hoffman's hypothesis were less than 1.19, the variance observed in the data of Raup and Sepkoski[1]. Our results verify statistically that the average spacing of peaks is not significantly different from the expected from Hoffman's random process, but show that the variance of spacing is sufficiently small to suggest that Hoffman's non-periodic random process is an inadequate explanation. The observed low variance in the Raup and Sepkoski data string can instead by interpreted to indicate that the pattern is more periodic than Hoffman's random model would imply. Our note is intended to show how statistics can better enable this controversy to be argued on the bases of data and hypotheses.

JENNIFER A. KITCHELL*
GEORGE ESTABROOK†

* *Department of Geological Sciences and Museum of Palaeontology, University of Michigan, Ann Arbor,*
† *Division of Biological Sciences, University of Michigan, Ann Arbor, Michigan 48109, USA*

1. Raup, D. M. & Sepkoski, J. J. Jr *Proc. natn. Acad. Sci. U.S.A.* **81**, 801-805 (1984).
2. Hoffman, A. *Nature* **315**, 659-662 (1985).

HOFFMAN REPLIES— Sepkoski and Raup disagree with my view[1] that 26-Myr periodicity of extinctions is only insufficiently demonstrated and may reflect an effect of stochastic processes. They argue that their more recent, as yet unpublished analyses of the complete, unculled data set on marine animal families and genera still indicate a significant 26-Myr periodicity. This result is not surprising, given the nature of their statistical test, the definition of extinction events as local maxima, and the geological timescale with approximately constant stage durations. In fact, it is precisely what should be expected if my arguments about the stochastic nature of the pattern of extinctions are correct. Genus-level data do not avoid the biases of the fossil record and the arbitrariness of taxonomic decisions.

Two other predictions made in ref. 1 appear to be confirmed by these more recent analyses. I suggested, first, that the test developed by Raup and Sepkoski[2] should not reject periodicity even if a few minor peaks are omitted; and second, that 35- to 40-Myr periodicity should appear in the Palaeozoic. As reported by Jablonski[3] and Rampino and Stothers[4], both these predictions have been confirmed by Raup and Sepkoski's new analyses.

Sepkoski and Raup now contend that my illustration of the variety of geological stages that appear to contain extinction events, depending on definition and timescale, in fact provides strong support for 26-Myr periodicity. They reach this surprising conclusion by identifying the stages which consistently (that is, in more than half of the examples I considered) stand out as peaks of extinction, and by subsequently analysing their distribution according to the timescales of Harland *et al.*[5] and Odin[6]. This procedure, however, is inappropriate. The majority of these examples are normalized for duration (and are thus strongly timescale-dependent) and each assumes a different timescale. The periodicity can be validly analysed only if the extinction rate is plotted against the timescale for which it was calculated (as in Fig. 1 of ref. 1). Moreover, my illustration assumes two different extinction processes. If the process of family extinction is viewed as possibly continuous rather than necessarily catastrophic, and hence if time normalization of extinction data is required, then the Coniacian and Rhaetian show up as peaks more consistently than the Cenomanian and Norian. The pattern of variation illustrated in ref. 1 does not represent statistical noise but mutually incompatible assumptions. Therefore, its statistical analysis as a single sample is meaningless.

Sepkoski and Raup's contention is also based on factually incorrect premises. Contrary to their assertion, I did illustrate peaks of the number of family extinctions per stage (*B* in Table 1 of ref. 1). One is therefore left with 20 (instead of Sepkoski and Raup's 21) patterns of extinction. The Barremian and Ladinian show peaks as consistently as the Cenomanian and Norian. These two stages—and also the Pliocene, explicitly acknowledged by Sepkoski and Raup as a major event—should also be included in their list of presumed extinction events. Contrary to their other assertion, this list does not include all events recognized by palaeontologists in the late Permian—Quaternary interval. The Toarcian (rather than Pliensbachian) event was identified by Hallam[7], and Sepkoski[8] cited additional preliminary evidence. The Callovian (ref. 9 and W. Brochwicz-Lewinski, personal communication), mid-Oligocene[10,11], and of course Pleistocene[12] have also been cited as extinction events. On the other hand, the late Eocene event is strongly contested even as regards the marine plankton[13], the only group that, according to Sepkoski[6], experienced at least fairly severe extinction at that time.

Finally, Sepkoski and Raup argue that the pattern of family extinctions deviates significantly from randomness. Their original test, however, involves randomization of the extinction pattern within the constraints of the definition of extinction events as local maxima and the timescale with approximately constant stage durations[2]. That these constraints are not trivial is clearly indicated by the fact that, whether the extinction data were all assigned to the beginnings, the mid-points, or the ends of individual stages, the periodicity was essentially the same[2]. This is possible only with constant stage durations. Otherwise, discordant shifts in the timing of events would affect the pattern of temporal relationships among events. Thus, the random distribution generated by Raup and Sepkoski is inherently biased. It is artificially truncated and its variance is smaller than it would be in a truly random model of the temporal distribution of peaks of extinction. Consequently, it is inadequate for testing my proposed hypothesis of randomness.

It takes only a glance at the pattern of peaks in family extinctions per stage[14] to see that it is not perfectly periodic. Therefore, Gilinsky misses the point of the argument when he calculates the infinitesimally small probability of a random walk yielding a perfectly periodic pattern. Precisely the same mistake was made by Gould[15]. (Gilinsky, however, correctly points out that Hoffman and Ghiold's[14] statement about inevitability of "the appearance of approximately 26 million year periodicity" may suggest an incorrect conclusion; we should have emphasized more strongly the words "appearance" and "approximately".) The question to be addressed is not if a perfect periodicity is likely to be produced by random walk, but rather if the approximate periodicity observed in the fossil record is sufficiently close to perfect regularity that it is unlikely to be produced by random walk. A world of difference distinguishes these two questions. I suggest that available statistical tests are insufficiently

1. Hoffman, A. *Nature* **315**, 659-662 (1985).
2. Raup, D. M. & Sepkoski, J. J. Jr *Proc. natn. Acad. Sci. U.S.A.* **81**, 801-805 (1984).
3. Jablonski, D. *Paleobiology* **10**, 139-145 (1984).
4. Rampino, M. R. & Stothers, R. B. in *The Galaxy and the Solar System* (eds Smoluchowski, R., Bahcall, J. N. & Matthews, M. S.) (University of Arizona Press, Tucson, in the press).
5. Harland, W. B. *et al. A Geologic Time Scale* (Cambridge University Press, 1982).
6. Odin, G. S. (ed.) *Numerical Dating in Stratigraphy* (Wiley, New York, 1982).
7. Hallam, A. *Paleobiology* **3**, 58-73 (1977).
8. Sepkoski, J. J. Jr *Spec. Pap. geol. Soc. Am.* **190**, 283-290 (1982).
9. Fischer, A. G. & Arthur, M. A. *Spec. Publs Soc. econ. Paleont. Miner.* **25**, 19-50 (1977).
10. Keller, G. *Mar. Micropaleont.* **7**, 463-486 (1983).
11. Prothero, D. D. *Science* **229**, 550-551 (1985).
12. Martin, P. S. & Klein, R. G. (eds) *Quaternary Extinctions: A Prehistoric Revolution* (University of Arizona Press, Tucson, 1984).
13. Corliss, B. H. *et al. Science* **226**, 806-810 (1984).
14. Hoffman, A. & Ghiold, J. *Geol. Mag.* **122**, 1-4, (1985).
15. Gould, S. J. *Discover*, November, 89-91 (1985).

sensitive to reject the hypothesis of randomness in this case.

In fact, Kitchell and Estabrook tested in a rigorous fashion the appropriate null hypothesis. Given their result that 7.9% of 10,000 random walks appear more periodic than the actual pattern of extinctions, one may conclude that my model is not unlikely to provide an adequate explanation for the empirical pattern.

As explicitly stated in my original article, there may be periodicity in late Permian to Quaternary extinctions, but the evidence is as yet insufficient. On the basis of my analysis, which is now confirmed by Kitchell and Estabrook's result, I concluded that I could not reject the hypothesis of randomness of the pattern of extinctions. I suggest that Raup and Sepkoski might have done the same if they had considered the appropriate null hypothesis.

ANTONI HOFFMAN
Lamont-Doherty Geological Observatory, Columbia University, Palisades, New York 10964, USA

Endocast morphology of Hadar hominid AL 162–28

ACCORDING to Falk[1], the endocast morphology of the Hadar hominid AL 162-28 is ape-like, contrasting with Holloway's[2] original conclusion that this specimen exhibits important human-like cortical features. We contend that Falk's interpretation is the result of a major error in her orientation of the endocast.

A comparison of Falk's Fig. 1 (redrawn here as Fig. 1*a*) with a photograph of the AL 162-28 calvaria in norma lateralis (Fig. 1*b*) demonstrates Falk's error. In her orientation, the middle arched portion of the squamosal suture, clearly identifiable on the calvaria (SS in Fig. 1*b*; see also ref. 3), lies below the level of asterion, and the planum occipitale faces almost directly superiorly with the planum muchale almost vertical. Clearly, this combination of features does not characterize any normal hominoid cranium (nor is it found in any other hominid crania from Hadar or elsewhere), and it is apparent that the endocast must be rotated some 40° in a clockwise direction to achieve correct anatomical orientation. When this is done, the cerebellar fossae are tucked under (and are rostral to) the occipital poles, as in all hominids and almost all apes. Falk[4] has defended her orientation by citing Kimbel[3] to the effect that the cerebellar fossae are deeper than the cerebral fossae. Correcting the specimen's orientation, the cerebellar fossae are deeper, but certainly not more posteriorally projecting, a position Kimbel never claimed.

Figure 1 indicates Falk's identification of the cortical features on the endocast.

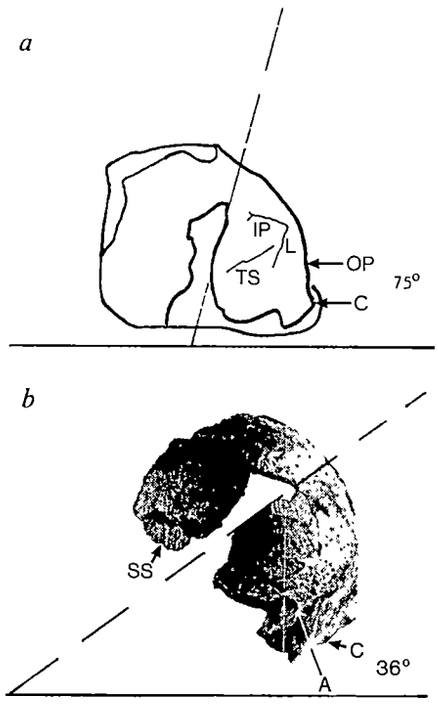


Fig. 1 Diagrams showing the error in Falk's[1] orientation of the Hadar AL 162-28 endocast. *a*, A tracing from Falk's Fig. 1; *b*, a lateral view of the AL 162-28 original cranial fragment correctly oriented. The difference between the two orientations is approximately 39° as measured from the dashed lines intersecting the horizontal planes, using the notch created by the missing bone as a landmark. Falk rotated the endocast 39° in an anticlockwise direction, thereby erroneously positioning the cerebellar lobes posterior to the occipital poles of the cerebrum. SS, squamosal suture; A, asterion; C, cerebellum; OP, occipital pole; IP, interparietal sulcus; TS, the superior temporal sulcus, and L, the lunate sulcus are Falk's designations[1].

The rostral position of the lunate sulcus (L in Fig. 1*a*) is said to be an ape-like condition. When the endocast is correctly oriented, however, L (as identified by Falk) crosses the posterior aspect of the endocast in a more caudal position than on ape brains[5]. The relative caudal location of Falk's L is confirmed by its close proximity to the occipital pole (OP); the distance between L and OP on the AL 162-28 is approximately half that separating these structures in a sample of 10 chimpanzee brain casts (the hominid falls 5.5 s.d. below the ape mean), despite the fact that eight of these brain casts have volumes less that the 375-400 cm^3 estimated for the Hadar endocast, including one chimpanzee infant. (See data in ref. 6, in which the distance from the interparietal sulcus (IP) to OP is the same as the OP-L distance.)

The lambdoidal suture is discernible on the internal aspect of the Hadar calvaria[3], where, on both sides, it is 2 mm (not 5 mm, as claimed by Falk[1]) below the feature corresponding to Falk's L. We suggest that Falk's L may be a manifestation of the lamboidal sutural complex which is frequently reproduced on chimpanzee endocasts as a distinct furrow (feature 'x' in ref. 7). Holloway[2,6] recognized the likelihood that feature 'x' masks the position of L on the AL 162-28 endocast. We do not, therefore, believe that L can be identified unequivocally on this specimen. But if Falk is correct in her identification of the lunate sulcus, and does accept Holloway's[2] identification of the interparietal sulcus, then both the correct orientation of the specimen and metric data[6] confirm that this structure occupies a caudal position on AL 162-28, a major derived hominid condition.

RALPH L. HOLLOWAY
Department of Anthropology, Columbia University, New York, New York 10027, USA

WILLIAM H. KIMBEL
Institute of Human Origins, 2453 Ridge Road, Berkeley, California 94709, USA

1. Falk, D. *Nature* **313**, 45–47 (1985).
2. Holloway, R. L. *Nature* **303**, 420–422 (1983).
3. Kimbel, W. H., Johanson, D. C. & Coppens, Y. *Am. J. phys. Anthrop.* **57**, 453–499 (1982).
4. Bower, B. *Sci. News* **127**, 157 (1985).
5. Connolly, C. J. *External Morphology of the Primate Brain* (Thomas, Illinois, 1950).
6. Holloway, R. L. in *Hominid Evolution: Past, Present and Future* (ed. Tobias, P. V.) 47–64 (Liss, New York, 1985).
7. Le Gros, Clark, W. E., Cooper, D. M. & Zuckerman, S. *J. R. anthrop. Inst.* **66**, 249–268 (1936).

FALK REPLIES—Holloway and Kimbel claim that my interpretation of the sulcal pattern of AL 162-28 is due to an error in the orientation of the endocast because "in her orientation, the middle, arched portion of the squamosal suture, clearly identifiable on the calvaria . . . , lies below the level of asterion . . .". Kimbel *et al.*'s photograph of the left side of the calvaria shows neither the apex of the squamosal suture nor the external (temporal bone) portion of that suture[1]. What it does show is a 13.5 segment of the temporal margin of the parietal bone that is, by their own description, *posterior* to (where) the apex of the squamosal suture (would have been). Furthermore, because of overlap at the squamosal suture, the temporal margin of the parietal bone which is present in AL 162-28 would have been *below* the external (temporal bone) portion of the squamosal suture. Unfortunately, "a long, narrow strip of external table is lost just above the left parietal's temporal margin"[1]. Neither the squamosal suture nor asterion is reproduced on the endocast, and I do not think the calvaria of AL 162-28 is complete enough to allow speculation about where the locations and relative positions of both features would have been on the (whole) endocast. Even if Holloway and Kimbel's SS and A identifications (Fig. 1*b* above) could be

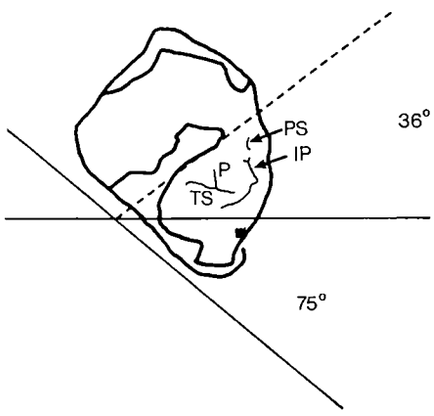


Fig. 2 Holloway and Kimbel's Fig. 1*a* rotated to correspond to their preferred orientation. Such an orientation for the sulci on AL 162-28 is unlike that seen in other primates. On the other hand, the configuration of these sulci oriented as in Fig. 1*a* is common for primates. PS, superior parietal sulcus; P, superior parallel branch of TS; other abbreviations as for Fig. 1*a*.

interpreted and projected onto the endocast as they suggest, given the overlap at the squamosal suture and the variation of its course in hominoids, there is ample room for forward rotation of their calvaria within the normal hominoid range. (Walker *et al.*[2] describe a hominid cranium with a vertically oriented planum occipitale, which is what I believe Holloway and Kimbel meant by the planum occipitale facing almost "directly superiorly".)

More to the point, I have rotated Holloway and Kimbel's Fig. 1*a* to correspond to their preferred orientation, and traced the sulci back on to my original[3] Fig. 1 (see Fig. 2). The angle of the intraparietal sulcus (IP, an identification on which Holloway and I agree) is nearly vertical, whereas the angle of the superior temporal sulcus (TS, not mentioned by Holloway and Kimbel) is nearly horizontal. This combination of sulci does not occur in this orientation for primates[4], but this combination of sulci in the orientation shown in Fig. 1*a* is common for primates[4]. The question of orientation of sulci is not to be dismissed lightly, since Radinsky[5] has shown that the issue of direction and orientation of sulci is fundamentally important for primate brain evolution (especially the origin of anthropoids).

If I am correct in my observations, then Holloway and Kimbel's statistics on distances between points on the endocast are not useful since all of them would depend on an incorrectly identified occipital pole (OP) (if one is used which is consistent with Holloway and Kimbel's orientation of the endocast). The OP which I have identified, on the other hand, does not project as far caudally in this specimen as it does in most hominoids. This alone would account for shortened distances. Furthermore, absolute distances should not be used to refute a chimpanzee-like sulcal pattern; ratios would be better.

Holloway and Kimbel contend that the feature I identify as the lunate sulcus (L) may be a groove cuased by lipping at the lambdoid suture, and they cite LeGros Clark's[6] study of six chimpanzee brains and corresponding endocasts to support their contention. I have shown that the course of the lambdoid suture (determined from its traces and their relationship to ridge X on the endocast that corresponds to the nuchal crest) runs 5 mm caudal to the feature I identify as L on AL 162-28 (Fig. 1 of ref. 3). Holloway and Kimbel say (above) that the lambdoid suture is 2 mm rather than 5 mm below the feature I identify as L. I have repeated my analysis and again find the distance to be 5 mm. How can this feature be due to lipping of a suture that is 5 mm behind it? Furthermore, how can Holloway and Kimbel attribute a 'groove' on an endocast to a skull suture which is so smooth and obliterated that it can be traced only with difficulty[1]?

Both the lunate sulcus and a groove due to the lambdoid suture may be reproduced on endocasts of chimpanzees[6] and presumably on those from early hominids. How are we to decide which of these two features is the disputed feature on endocast AL 162-28? As noted above, the feature in question cannot be due to lipping at the lambdoid suture because that suture is 5 mm away and because the suture does not lip in this specimen, that is, it is so smooth it is almost obliterated.

On the other hand, the feature in question merges with the intraparietal sulcus (IP in Fig. 2), as does the lunate sulcus in *Pan*; it is rostral to the lambdoid suture, as is the lunate sulcus in *Pan*; and has a sulcus-like texture and shape similar to the lunate sulcus in *Pan*. I therefore believe that the feature in question on AL 162-28 is a lunate sulcus that is similar to those seen in brains of chimpanzees, a finding that is consistent with the entire sulcal pattern that is reproduced on the endocast of AL 162-28.

DEAN FALK
Department of Anatomy/Caribbean Primate Research Center, University of Puerto Rico School of Medicine, PO Box 5067, San Juan, Puerto Rico 00936

1. Kimbel, W. H., Johanson, D. C. & Coppens, Y. *Am. J. phys. Anthrop.* **57**, 453-499 (1982).
2. Walker, A., Falk, D., Smith, R. & Pickford, M. *Nature* **305**, 525-527 (1983).
3. Falk, D. *Nature* **313**, 45-47 (1985).
4. Connolly, C. J. *External Morphology of the Primate Brain* (Thomas, Illinois, 1950).
5. Radinsky, L. B. *Am. Sci.* **63**, 656-663 (1975).
6. Le Gros Clark, N. E., Cooper, D. M. & Zuckerman, S. J. *R. anthrop. Inst.* **66**, 249-268 (1936).

Maternal investment in mammals

IN a recent paper Martin and MacLarnon[1] claim to clarify the allometry of neonatal size and gestation period of mammals, attributing particular importance to the distinction between altricial and precocial taxa. In addition, Martin and MacLarnon suggest that maternal investment, as reflected by a fetal growth parameter, is higher for altricial than precocial mammals. Unfortunately, we find that such conclusions are not warranted and propose that other interpretations are possible.

We are confused by Martin and MacLarnon's definition of maternal investment. They suggest that altricial mammals have high maternal investment indicated by high fetal growth "factors", with precocial mammals having the opposite traits. Yet, in mammals bearing altricial young, overall maternal investment at birth actually is low: gestation periods are relatively short[1,2] and neonatal weights are typically low[1]. Hence, it confuses the issue to say that high fetal growth rates are indicative of high maternal investment. Using different measures of parental investment is revealing[3]. However, we maintain that the neonate's developmental status and the time and energy put into it are the most important criteria in evaluating maternal investment at birth.

Also, we cannot accept their definitions of altricial and precocial: precocial mammals are those with a litter size less than 1.5 and eyes open at birth; altricial mammals have litter sizes equal to or greater than 3, and the eyes are closed at birth. Taxa that do not conform to either of these criteria are placed in an "intermediate" group. Even humans, which are highly altricial[4], would be classified as precocial by such standards. We[2] and others[5] have experienced difficulty classifying neonates as altricial versus precocial because these categories are discrete and arbitrary, whereas in reality mammalian species occur along a continuum of developmental maturity at birth. In a previous study of the relationship between maternal investment at birth and mating systems in mammals, we at first used definitions from the literature to classify a species as altricial or precocial. However, because of problems with a simplistic 'either/or' categorization scheme, we subsequently used several relative measures of maternal investment at birth instead[2]. One of these measures, neonate weight/litter size standardized for body weight, is useful as it describes investment in an individual neonate relative to the number of siblings it shares that investment with. Indeed, we found that 78% of mammals with litter sizes of ≤ 2 bear precocial young and 87% of those with at least 3 young have altricial offspring. Yet, this does not imply that

litter size should be a criterion for classification of neonate development.

Classifying species as altricial versus precocial based on differences in litter size introduces a serious confounding effect not discussed by Martin and MacLarnon[1]. In particular, we note that fetal growth parameters for precocial taxa are essentially standardized for constant litter size as most of these taxa have only one young per litter (by Martin and MacLarnon's definition). By contrast, we find a great variability in litter size among altricial species (again, using their definition). That litter size is inversely correlated with adult body size among mammalian species[6-8] confounds Martin and MacLarnon's analysis of how fetal growth relative to body size differs between altricial and precocial species. A larger litter size results in each individual offspring obtaining a relatively smaller fraction of the mother's total parental investment at birth[9]. Growth rates of such offspring might be comparatively high simply to increase survivorship.

If a more rigorous consideration of neonatal status is used[2-4], the discreteness of altricial and precocial taxa is not as great as suggested by Fig. 1 of ref. 1. Related to this, we find the legend to Fig. 2 inappropriate because it is not obvious that an "overall best-fit line of fixed slope 0.1" essentially constitutes a linear discriminant function between the 'altricial' and 'precocial' taxa. Their discriminant function with a 0.1 slope is as effective with a slope of 0; there are about five misclassified points using either slope. This suggests that Martin and MacLarnon's altricial and precocial categories are more explicitly defined as groups of short versus long gestation period. Realization of this leads us to question seriously the relevance of Martin and MacLarnon's use of this 0.1 slope as an allometric coefficient, as in their equations (6) and (8)[1], since it has no biological basis.

Allometric pattern is often presumed to reflect physiological constraints to life history alternatives. Although we recognize that such constraints certainly exist, we caution that sampling bias might be present because the representation of mammals of various body sizes is seldom independent of environmental variation. Large mammal species are most numerous in regions of pronounced seasonality[10]. We suggest that natural selection may favour rapid growth rates in highly seasonal environments to ensure that the young attain adequate size during the limited growth season to enhance survival through the oncoming winter or seasonal drought. This implies that environmental seasonality selects for a suite of life-history attributes which increase survival during periods of resource shortage, but which capitalize on abundant resources during the growth season[11,12]. Such a sampling bias may well account for the positive correlation between "fetal growth factor" and body mass as described by Martin and MacLarnon[1].

SAMUEL I. ZEVELOFF
Department of Zoology,
Weber State College,
Ogden, Utah 84408, USA

MARK S. BOYCE
Department of Zoology and Physiology,
University of Wyoming,
Laramie, Wyoming 82071, USA

1. Martin, R. D. & McLarnon, A. M. *Nature* **313**, 220-223 (1985).
2. Zeveloff, S. I. & Boyce, M. S. *Evolution* **34**, 973-982 (1980).
3. Knapton, R. W. *Can. J. Zool.* **62**, 2673-2674 (1984).
4. Zeveloff, S. I. & Boyce, M. S. *Am. Nat.* **120**, 537-542 (1982).
5. Case, T. J. *Q. Rev. Biol.* **53**, 243-282 (1978).
6. Tuomi, J. *Oecologia* **45**, 39-44 (1980).
7. Eisenberg, J. F. *The Mammalian Radiations* (University of Chicago Press, 1981).
8. Millar, J. S. & Zammuto, R. M. *Ecology* **64**, 631-635 (1983).
9. Smith, C. C. & Fretwell, S. *Am. Nat.* **108**, 499-506 (1974).
10. Zeveloff, S. I. thesis, Univ. Wyoming, Laramie (1982).
11. Boyce, M. S. *Am. Nat.* **114**, 569-583 (1979).
12. Lindstedt, S. L. & Boyce, M. S. *Am. Nat.* **125**, 873-878 (1985).

MARTIN AND MACLARNON REPLY— The points raised by Zeveloff and Boyce indicate the need for further clarification of issues raised by our paper[1], and we are glad of the opportunity to comply.

There is, indeed, potential confusion surrounding the definition of 'maternal investment'. In our paper, we implicitly used this term in relation to the mother's investment per unit time in the growth of an individual fetus. In order to convert this to total investment per unit time during pregnancy, it would, of course, be necessary to multiply each fetal growth factor by litter size for the species. Thus, the distinction between altricial and precocial mammals in this respect is far more marked than indicated in our Fig. 3. However, we recognize that maternal investment could be defined as total investment in individual neonates, regardless of the time over which the investment is spread. By such a definition, mothers clearly invest more in precocial neonates than in altricial neonates. We would defend our definition on the grounds that it relates to the mother's division of her total resources (which are heavily influenced by her body size) between reproduction and other functions during pregnancy. Clearly, accurate calculation of total maternal investment by any definition would require data on lifetime reproductive performance.

The double criterion that we used to define altricial as opposed to precocial mammals (combining time of eye opening and litter size) was a quantitative translation of two features originally emphasized by Portmann[2] in his pioneering studies separating '*Nesthocker*' from '*Nestflüchter*' in both birds and mammals. While we accept that some gradation exists (and, in fact, we allowed for it in our paper—intermediates), the important point is that a clear bimodal distribution among mammals emerges when gestation period is considered in relation to body size, closely matching the distinction between altricial and precocial categories. Incidentally, although human infants are often described as 'altricial', they are precocial both by Portmann's definition and by ours. It has been shown that the relative helplessness of the human neonate is a special condition, unique among mammals, related to an unusual pattern of postnatal brain development[3,4].

The fixed slope value of 0.1 used to derive the histogram in our Fig. 2 was initially determined by the average empirical value for major mammalian groups with a single neonate type (our Table 1). The iterative technique reported was used as an additional approach, primarily to investigate the distributions of residuals generated with different slope values. As Zeveloff and Boyce point out, altricial and precocial mammals (as defined by us) are to a large extent separated by gestation period even without taking maternal body size into account (that is, slope value of 0). This, surely, is one of the most convincing indications that there is an underlying split between altricial and precocial mammals. The histogram of residuals in fact becomes trimodal when a slope value of 0 is used for all gestation periods, as certain large-bodied altricial mammals (for example, some carnivores) overlap with certain small-bodied precocial mammals (for example, some primates, and some hysticomorph rodents). This overlap is largely eliminated when a slope value of 0.1 is used, and an order-by-order analysis of residuals (unpublished) shows that the resulting pattern is entirely in accord with Portmann's interpretation of the altricial/precocial division.

As Zeveloff and Boyce themselves produce a separation of mammals into two groups that are 80% in agreement with our altricial/precocial division, despite an entirely different approach, there would seem to be an underlying biological reality in such distinctions, regardless of any disagreement about finer details. It is important that debate about the details should not obscure this fact.

R. D. MARTIN
A. M. MACLARNON
Department of Anthropology,
University College London,
Gower Street,
London WC1E 6BT, UK

1. Martin, R. D. & MacLarnon, A. M. *Nature* **313**, 220-223 (1985).
2. Portmann, A. *Biomorphosis* **1**, 109-126 (1938).
3. Portmann, A. *Revue suisse Zool.* **48**, 511-518 (1941).
4. Martin, R. D. *Human Brain Evolution in an Ecological Context* (American Museum of Natural History, New York, 1983).

Announcing New U.S. Receiving Center

BIOCHIMICA ET BIOPHYSICA ACTA

BBA is pleased to announce the opening of a new receiving center in the Boston area of the United States. This office will operate in conjunction with the three other receiving centers in Amsterdam, Dundee and Oxford. Using advanced telecommunication links these centers will provide the benefits of a unified administrative system for manuscript processing, and improve manuscript handling efficiency particularly in North America – and also allow potential authors the advantage of more choice when submitting papers. Authors should send their manuscripts (4 copies) to one of the managing editors at the following addresses:

Dr. P. Borst
c/o BBA Editorial Secretariat
P.O. Box 1345
1000 BH Amsterdam
The Netherlands

Dr. P. Cohen
Department of Biochemistry
Medical Sciences Institute
University of Dundee
Dundee DD1 4HN
United Kingdom

Dr. K. van Dam
c/o BBA Editorial Secretariat
P.O. Box 1345
1000 BH Amsterdam
The Netherlands

Dr. L. L. M. van Deenen
c/o BBA Editorial Secretariat
P.O. Box 1345
1000 BH Amsterdam
The Netherlands

Dr. E. P. Kennedy
c/o BBA Editorial Secretariat (Boston)
Box C 9123
Brookline
Massachusetts 02146
U.S.A.

Dr. G. K. Radda
Department of Biochemistry
University of Oxford
South Parks Road
Oxford OX1 3QU
United Kingdom

For instructions to Authors please apply to:
BBA Editorial Secretariat
P.O. Box 1345
1000 BH Amsterdam
The Netherlands

North American authors may apply to.
BBA Editorial Secretariat (Boston)
Box C 9123
Brookline
Massachusetts 02146
U.S.A.

For further information, sample copies and full subscription details please apply to:
Promotion Department
Elsevier Science Publishers B.V.
Biomedical Division
P.O. Box 1527
1000 BM Amsterdam
The Netherlands

ANNOUNCING

MOLECULAR BRAIN RESEARCH

A section of Brain Research devoted to the publication of molecular studies.

Editor-in-Chief:

D. P. Purpura,
Brain Research, Office of the Dean, Albert Einstein College of Medicine, 1300 Morris Park Avenue, Bronx, NY, U.S.A.

The powerful techniques and approaches of molecular biology have greatly enriched brain research in recent years. The wide application of recombinant DNA technology, monoclonal antibody production, molecular analysis of receptor – ligand interactions and ion channel mechanisms have generated a wealth of data bearing upon fundamental processes underlying the structure and function of nervous systems. Indeed it is anticipated that reports dealing with the application of molecular biological techniques will increase greatly over the next few years and require appropriate recognition and organization. Cognizant of the need to make such interpretations available to the readership of **Brain Research,** we are pleased to announce publication of a new section of **Brain Research** entitled **"Molecular Brain Research".** This decision carries with it awareness of the rapid progress in molecular biology of the nervous system as well as the desirability of encouraging the focus of molecular biological research on brain mechanisms.

Editorial Board
E. A. Barnard, Cambridge, U.K.
I. B. Black, New York, NY, U.S.A.
F. E. Bloom, La Jolla, CA, U.S.A.
A. C. Cuello, Montréal, Que., Canada
P. C. Emson, Cambridge, U.K.
S. J. Enna, Houston, TX, U.S.A.
R. M. Evans, San Diego, CA, U.S.A.
D. M. Fambrough, Baltimore, MD, U.S.A.
C. S. Goodman, Stanford, CA, U.S.A.
J. F. Gusella, Boston, MA, U.S.A.
E. Herbert, Portland, OR, U.S.A.
G. A. R. Johnston, Sydney, Australia
B. S. McEwen, New York, NY, U.S.A.
S. Numa, Kyoto, Japan
L. F. Reichardt, San Francisco, CA, U.S.A.
E. Roberts, Duarte, CA, U.S.A.
J. L. Roberts, New York, NY, U.S.A.
M. G. Rosenfeld, La Jolla, CA, U.S.A.
B. Sakmann, Göttingen, F.R.G.
M. Schachner, Heidelberg, F.R.G.
R. H. Scheller, Stanford, CA, U.S.A.
J. H. Schwartz, New York, NY, U.S.A.
E. M. Shooter, Stanford, CA, U.S.A.
P. Siekevitz, New York, NY, U.S.A.
S. H. Snyder, Baltimore, MD, U.S.A.
C. F. Stevens, New Haven, CT, U.S.A
K. Suzuki, Bronx, NY, U.S.A.
L. Terenius, Uppsala, Sweden
A. Ullrich, San Francisco, CA, U.S.A.

Aims and Scope
Molecular Brain Research is a special section of **Brain Research** which provides a medium for the prompt publication of studies of molecular mechanisms of neuronal, synaptic and related processes, that underlie the structure and function of the brain. Emphasis is placed on the molecular biology of fundamental neural operations relevant to the integrative actions of nervous systems.

Subscribers to Brain Research automatically receive this section.

Subscription information:
1986 Volumes 1 and 2 (2 volumes in 6 issues)
Price: US $ 203.25/Dfl. 518.00
including postage and handling
ISSN 0169-328X

ELSEVIER

For further information and/or free sample copy please write to:

In the U.S.A. and Canada:
Journal Information Center
ELSEVIER SCIENCE PUBLISHERS
52 Vanderbilt Avenue, New York, NY 10017, U.S.A.

In all other countries:
ELSEVIER SCIENCE PUBLISHERS
P.O. Box 1527, 1000 BM Amsterdam
The Netherlands

Please send your orders to the Amsterdam address

The Dutch guilder price is definitive. US $ prices are subject to exchange rate fluctuations. Prices are excl. B.T.W. for Dutch customers

Reader Service No.59

IT 37A672

Latest Advances in the Biomedical Sciences

ANALYTICAL BIOCHEMISTRY
Editorial Committee Chairmen: Nathan O. Kaplan and William D. McElroy
University of California — San Diego, La Jolla
Volumes 152–159 (1986), 16 issues ISSN 0003-2697
In the U.S.A. and Canada: $792.00
All other countries: $899.00
In the U.K.: £666.00

ARCHIVES OF BIOCHEMISTRY AND BIOPHYSICS
Chairman of Editorial Committee: R. W. Estabrook
University of Texas Health Sciences Center, Dallas
Co-Chairman of Editorial Committee: S. Udenfriend
Roche Institute of Molecular Biology, Nutley, New Jersey
Volumes 244–251 (1986), 16 issues ISSN 0003-9861
In the U.S.A. and Canada: $792.00
All other countries: $905.00
In the U.K.: £670.50

BIOCHEMICAL AND BIOPHYSICAL RESEARCH COMMUNICATIONS
Editors: Ernesto Carafoli, Pedro Cuatrecasas, I. C. Gunsalus, Osamu Hayaishi, B. L. Horecker, M. Daniel Lane, William J. Lennarz, William D. McElroy, Frederick C. Neidhardt, Claude Paoletti, William D. Phillips, Alberto Sols
Volumes 134–141 (1986), 24 issues ISSN 0006-291X
In the U.S.A. and Canada: $596.00
All other countries: $684.00
In the U.K.: £507.00

BIOCHEMICAL MEDICINE AND METABOLIC BIOLOGY
Editor: S. P. Bessman
University of Southern California, Los Angeles
Volumes 35–36 (1986), 6 issues ISSN 0885-4505
In the U.S.A. and Canada: $184.00
All other countries: $204.00
In the U.K.: £151.50

BIOCHEMISTRY INTERNATIONAL
Editor-in-Chief: A. W. Linnane
Monash University, Clayton, Victoria, Australia
Volumes 12–13 (1986), 12 issues ISSN 0158-5231
In the U.S.A. and Canada: $280.00
All other countries: $280.00
In the U.K.: £200.00

BIOORGANIC CHEMISTRY
Editor: Gordon A. Hamilton
Pennsylvania State University, University Park
Volume 14 (1986), 4 issues ISSN 0045-2068
In the U.S.A. and Canada: $95.00
All other countries: $110.00
In the U.K.: £81.50

BIOTECHNOLOGY AND APPLIED BIOCHEMISTRY
Editor-in-Chief: P. N. Campbell
Courtauld Institute, The Middlesex Hospital, London
Volume 8 (1986), 6 issues ISSN 0885-4513
In the U.S.A. and Canada: $75.00
All other countries: $75.00
In the U.K.: £56.00

MICROCHEMICAL JOURNAL
Editor: Peter N. Keliher
Villanova University, Villanova, Pennsylvania
Volumes 33–34 (1986), 6 issues ISSN 0026-265X
In the U.S.A. and Canada: $164.00
All other countries: $198.00
In the U.K.: £147.00

PROCEEDINGS OF THE SOCIETY FOR EXPERIMENTAL BIOLOGY AND MEDICINE
Editor: M. R. Nocenti
Columbia University, New York City
Volumes 181–183 (1986), 11 issues ISSN 0037-9727
In the U.S.A. and Canada: $97.00
All other countries: $125.00
In the U.K.: £93.00

Personal subscription rates are available for some journals. For more information or a free sample copy, please write or call:

ACADEMIC PRESS, INC.
Journal Promotion Dept.
1250 Sixth Avenue, San Diego, CA 92101, U.S.A.
(619) 230-1840

or

ACADEMIC PRESS, INC. (LONDON) LTD.
Journal Marketing Dept.
24-28 Oval Road, London NW1 7DX, England
01-267-4466



ACADEMIC PRESS, INC.
Harcourt Brace Jovanovich, Publishers

San Diego Orlando New York Austin Boston London Sydney Tokyo Toronto

S6066

Reader Service No.24

Molecular dynamics resolved

from David D. Thomas

Time-resolved optical and magnetic resonance techniques offer complementary views of large-scale cooperative molecular motions within macromolecular assemblies.

ONE of the most exciting trends in biophysical chemistry is the increasing emphasis on understanding, quantitatively, the role of molecular motions in biological function. While much of the study of molecular dynamics has focused on small-scale intramolecular motions on the picosecond or nanosecond time scale, it is increasingly apparent that the large-scale motions within assemblies such as membranes and chromosomes are crucial to the understanding of cellular biophysics. This article presents an overview of recent advances in the technology for probing rotational molecular motions in the microsecond time range. The discussion will address the two most effective techniques: transient optical anisotropy and saturation transfer electron paramagnetic resonance (ST-EPR).

Both of these techniques rely on the use of extrinsic spectroscopic probes with excited-state lifetimes in the microsecond to millisecond time range[1]. The optical probes are mainly derivatives of eosin or erythrosin, organic dyes that have efficiently populated and stable triplet states. The paramagnetic probes are nitroxide spin labels.

Each experiment begins with a pulse of exciting radiation that causes a transient decrease in the number of ground-state probes available for subsequent excitation. This pulse of radiation is delivered so that it selectively excites molecules with a particular orientation in space ('photoselection'), and the sample's absorption or emission is monitored with the same orientational preference. The system re-equilibrates as excited probes return to the ground state; the recovery is accelerated by rotational motion that brings unexcited molecules into the detectable orientation range. Of course, rotational motion is detectable only if it occurs within a time comparable to or less than the excited-state lifetime of the probe — hence the need for μs lifetimes in the study of μs motions.

Optical anisotropy

An example of the optical data for transient absorption anisotropy (TAA) is shown in Fig. 1. The instrument used in this experiment has evolved from those designed by R. Cherry and others in the 1970s[2-4]. In this case, a nitrogen-pumped dye laser excites the sample with an intense vertically polarized 5-ns pulse, and a low-intensity beam from an argon-ion laser is used to monitor the time-resolved recovery of the polarized absorption following the pulse. The fast transient digitizer (LeCroy 2256, 50 ns/time point) permits high time-resolution, while the high-repetition-rate (200 Hz) pulsed laser (Lambda-Physik EMG-53MSC), along with a microcomputer-controlled direct-memory-access (DMA) circuit (LeCroy 3500) permits very rapid data acquisition and signal averaging, minimizing the time required for high-quality data acquisition. Although this particular configuration was constructed of commercially available components[1,5], an instrument that approaches some of its capabilities is available from PRA (London, Ontario).

The function plotted in Fig. 1 is the absorption polarization anisotropy, whose exponential decay constants (rotational correlation times) and amplitudes are related directly to the time constants and amplitudes of molecular rotational motions[1,5,6]. Similar experiments probing emission instead of absorption do not usually achieve the same high time resolution because the laser pulse interferes with detection. But emission studies offer sensitivity sufficient to study extremley small samples, possibly even single cells[7].

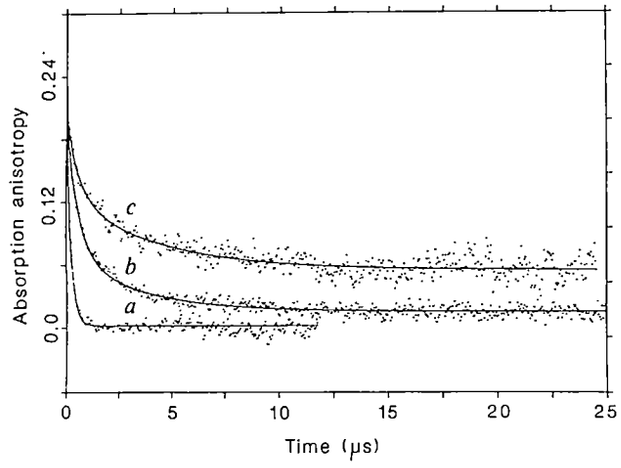


Fig. 1. Transient saturation transfer EPR (saturation recovery) data from maleimide-spin-labelling haemoglobin solutions corresponding to the rotational correlation times τ. The bottom trace in each case is the motion independent recovery, governed by T_1, and the top trace shows the increase in the recovery rate when the effects of rotational motion are included[8].

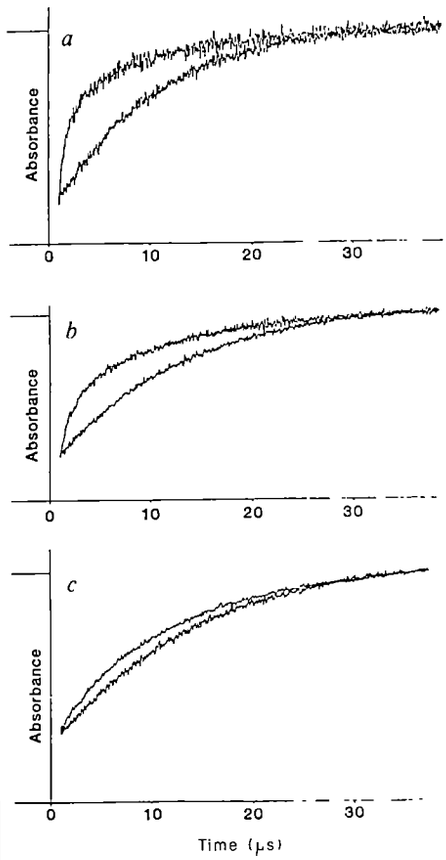


Fig. 2. Transient absorption anisotropy data from eosin-iodoacetamide attached to myosin heads in (*a*) the proteolytically isolated head (S-1), (*b*) the intact myosin monomer, and (*c*) myosin filaments (several hundred myosin molecules self-assembled essentially as in a muscle fibre)[5]. Note that the rate and amplitude of decay are much less in the filaments, indicating that the microsecond segmental protein motions have been restricted in both rate and amplitude.

Saturation recovery EPR

As in optical spectroscopy applications, EPR experiments involve transient absorption, which is often referred to in magnetic resonance as saturation recovery or as pulsed saturation transfer EPR, since rotation transfers saturation away from the irradiated spins.

In EPR the exciting radiation is a microwave pulse from a klystron. Photoselec-

tion arises because spin labels with different orientations absorb at different frequencies[1,7]. This selectivity is more specific than that conferred by optical spectroscopy. Because EPR is an inherently weaker effect than optical absorption, rapid data acquisition and signal averaging (at thousands of transients averaged per second) are even more important[8]. A key element in this instrument is a loop-gap resonator, a device that facilitates the use of intense microwave pulses in EPR spectroscopy[9].

A pulsed EPR spectrometer[8] with increased sensitivity was recently developed which expands the range of biological samples that can be studied. Many of the components of this instrument are now commercially available, but commercial systems (from IBM Instruments/Bruker) still fall considerably short in terms of sensitivity and signal averaging rate. Figure 2 illustrates the sensitivity of pulsed ST-EPR to microsecond rotational motion[10]. When the motion is slow on the microsecond time scale (Fig.2*c*) it has very little effect on the absorption recovery, which occurs with a time constant equal to the relaxation time (excited-state lifetime) T_1. However, sub-millisecond correlation times result in dramatic increases in rate of recovery (Fig.2 *a*,*b*).

In both EPR and optical spectroscopy, time resolution increases the range of motions and systems that can be studied and decreases the ambiguity of data interpretation. While optical spectroscopy has better absolute sensitivity (and can therefore be used to study smaller amounts of material), EPR offers the advantage of orientational resolution[11]. Thus, a pulsed EPR experiment on a macroscopically oriented system (for example, parallel muscle fibres or stacked membranes) offers the potential for unequaled resolution and accuracy in the elucidation of large-scale motions involved in the function of biological assemblies.

David D. Thomas is in the Department of Biochemistry, University of Minnesota Medical School, Minneapolis, MN 55455 USA.

1. Thomas, D.D. in *Techniques for Analysis of Membrane Proteins* (eds Cherry, R. & Ragan, I.) Ch. 13 (Chapman & Hall, London, 1986).
2. Cherry, R.J. in *Membranes and Transport* (ed. Martonosi, A.) 145-152 (Plenum, New York, 1982).
3. Corin, A.F., Matayoshi, E D. & Jovin, T.M. in *Spectroscopy and the Dynamics of Biological Systems* (eds Bayley, P.M. & Dale, R.E.) 53-78 (Academic, London, 1985).
4. Garland, P.B. & Johnson, P. in *Spectroscopy and the Dynamics of Biological Systems* (eds Bayley, P.M. & Dale, R.E.) 95-118 (Academic, London, 1985).
5. Eads, T.M., Thomas, D.D. & Austin, R.A. *J. molec. Biol.* **179**, 55-81 (1984).
6. Kinosita, K.Jr., Kawato, S. & Ikegami, A. *Adv. Biophys.* **17**, 147-203 (1984).
7. Thomas, D.D. *et al.* in *Spectroscopy and the Dynamics of Biological Systems* (eds Bayley, P.M. & Dale, R E.) 239 - 257 Academic, London, 1985.
8. Hyde, J.S., Froncisz, W. & Mottley, C. *Chem. phys. Lett.* **110**, 621-625 (1984).
9. Froncisz, W. & Hyde, J.S. *J. Magn. Reson.* **47**, 515-521 (1982).
10. Fajer, P. Thomas, D.D., Feix, J.B. & Hyde, J.S. *Biophys. J.* (submitted).
11. Cooke, R., Crowder, M.S. & Thomas, D.D. *Nature* **300**, 776-778 (1982).

Biochemists converge at the capital

Washington, DC is the host city for the ASBC meeting this year. Almost 200 exhibitors will be competing for the attention of conference visitors.

TIME-resolved **fluorescence detection** can reveal the dynamics of molecules kept in solution or embedded in membranes and proteins. The GREG 200 from ISS Inc. is a multi-frequency cross-correlation phase and modulation fluorometer with the capability to perform such analyses (Reader Service No. 100). Displayed at booth B32, the instrument uses lifetime measurement ranges from a few picoseconds to one millisecond to unravel complex decay processes. With the aid of a dedicated PC, ISS's fluorometer can solve multi-exponential and non-exponential decays; phase- and modulation-resolved spectra allow the separation of spectral components from a mixture of several emitting species with overlapping bands. The GREG 200 will also provide time-resolved spectra in three dimensions, with time along the *z* axis. ISS can say more about their machine at their ASBC booth.

Pharmacia have filled out their chromatography products with two more additions to the family. The MinoRPC S 5/20 is a **reversed-phase column** designed for the gradient or isocratic separation of small biomolecules, including amino acids and nucleotides (Reader Service No. 101). The bonded phase affords selective recovery of such molecules due to an end-capping process which, Pharmacia claims, also makes column results highly reproducible.

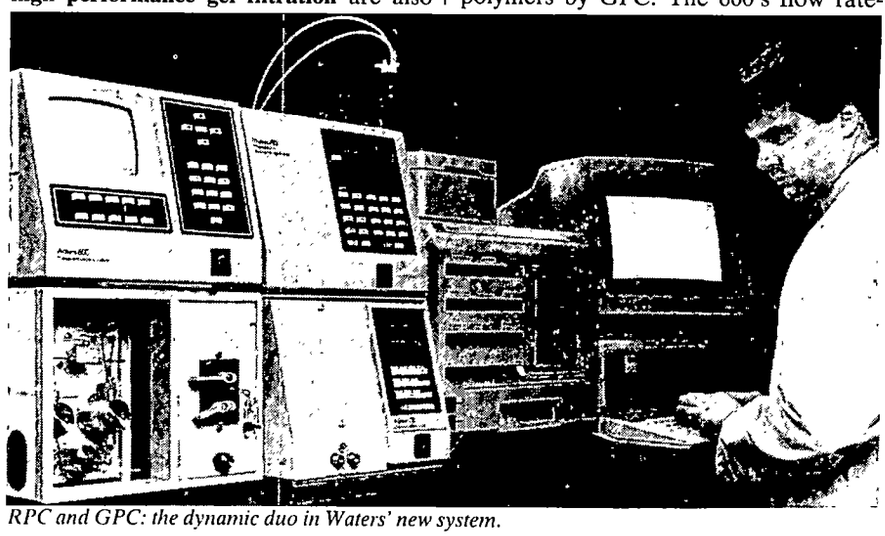
Two preparative-grade matrices for **high performance gel filtration** are also being offered by Pharmacia to scale-up their prepacked Superose 6 HR 10/30 and 12 HR 10/30 columns (Reader Service No. 102). The new, rigid Superose 6 and



Pharmacia's scale-up matrices.

Superose 12 prep grades are based on 30 μm agarose beads, stable from *p*H 2 to 14. With Pharmacia's scale-up grades, preparative separations can be achieved in a few hours. The Pharmacia divisions represented at ASBC will be in the area of booths E46 – F51.

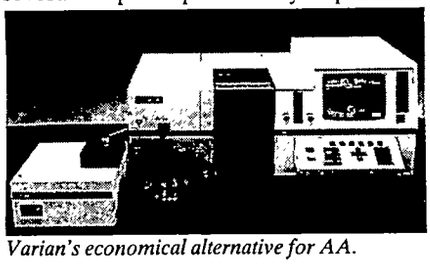
Combining reversed-phase gradient chromatography and detection modules, Waters has created a **gel permeation chromatography** (GPC) system with isocratic or gradient operation, programmable UV detection and stable refractive index (RI) detection (Reader Service No. 103). With the Waters 600 gradient module, the GPC system can analyse additives and low-molecular-weight polymers by gradient RPC, then perform molecular weight determinations for larger polymers by GPC. The 600's flow rate-



RPC and GPC: the dynamic duo in Waters' new system.

control is accurate to ±0.5 per cent, and its gradient composition will conform to specifications within ±0.15 per cent. The two detectors in the GPC III system are the Waters 490, which can optimize spectroscopic information for analyses between 190 and 600 nm, and the 410, which carries out refractive index detection. As an option to their new machine, Waters has the 840 data and chromatography control station with Expert software. The package will provide several types of calibrations, processing and storage of GPC data. Waters are showing in the area between booths G46 and H51.

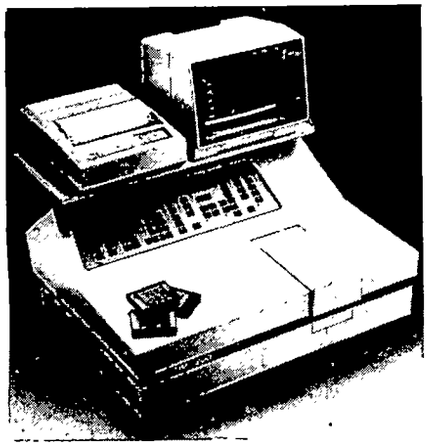
Varian, at ASBC in booths G63 through G70, have recently released several spectrophotometry products



Varian's economical alternative for AA.

including a lower-cost version of their SpectrAA 30/40 series **atomic absorption spectrophotometers.** The new SpectrAA 10 single-beam and the double-beam SpectrAA 20 have retained several automation features of the earlier models, such as centralized control for the automatic sample changer and the GTA-96 graphite furnace (Reader Service No. 104). But the SpectrAA 10/20 series machines can sell for as much as £10,000 (UK) less than the 30/40 series counterparts. A single keyboard ties in to all system components and allows access to the measurement and system control software. Method development and instrument set-up procedures can be stored on the instrument's floppy disk.

Plug-in modules for Varian's latest **UV-vis spectrometer** will make the machine more flexible for individual



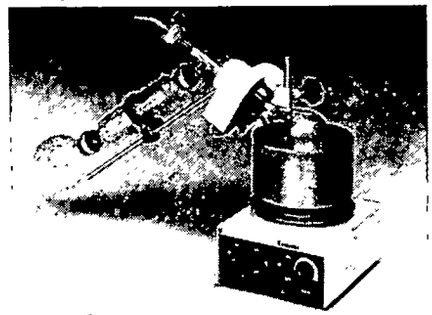
The DMS 200, with more modules in store.

analytical needs (Reader Service No. 105). The first such module offered has a soft-key menu that enables the user to construct data and mathematical routines for calculating final results from raw data. This so-called scan application module includes built-in functions such as spectral subtraction/addition/division, absorbance ratio, peak area and multi-wavelength and dilution correction calculations; stored instrument parameters can be linked with calculation routines to create methods for specific applications. The £8,000 (UK) DMS 200 can then present final results on a high-resolution plotter.

A **compact scintillation counter** from Integrated Genetics fills the niche between low-cost survey meters and high-volume counting instruments that can cost up to $35,000. The Gene-Trak beta detector directly measures beta particle emissions from samples on membrane filters (Reader Service No. 106). The system was designed to complement Integrated Genetics's *Salmonella* hybridization assay, but many researchers working with DNA and ^{32}P may find the Gene-Trak works well in their experimental regime. Gene-Trak's maker says its counting efficiency compares with that of large-scale instruments, yet their instrument costs less to purchase and operate. Integrated Genetics sells Gene-Trak at $3,600 (US).

Biochemical side-kicks

For small-scale evaporation, reflux or off-distillation, Haake Buchler makes a **micro rotary evaporator** with variable speed



Small-scale evaporation with a twist.

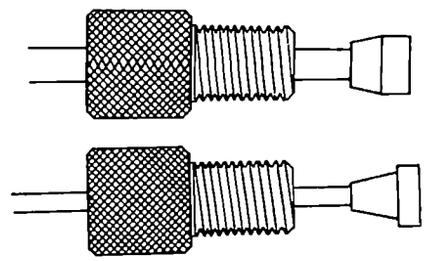
between 80 and 200 r.p.m. (Reader Service No. 107). The adjustable speed allows effective evaporation of viscous liquids; an inlet tube which feeds to the evaporation flask removes the need for operator intervention. Haake Buchler's evaporator comes with a stainless steel bath and complete set of glassware (evaporating flasks in 50, 100 and 250 ml sizes, with corresponding receiving flasks) for less than $1,200 (US). The entire unit measures 200 mm width × 235 mm depth × 165 mm height. At ASBC, Haake Buchler will have more information in booths G16 through G20 even.

Two equipment companies have recently tackled problems with Teflon tubing. Zeus Industrial Products invites custom designs for multi-lumen subminiature tubing (Reader Service No. 108). The company can manufacture **Teflon tubing** with two or more constant-diameter, continuous-length passages in a range of internal and outer diameters. Such tubing is flexible, impervious to most corrosives, inert, non-toxic and heat-resistant up to 500°F. Zeus's prices vary for standard ready-made and customized tubing.



Customized lumen configurations from Zeus

Upchurch Scientific have developed flangeless fittings for Teflon and plastic



Ferrules replace flanging.

tubing that can be directly substituted for all flange-type fittings (Reader Service No. 109). These fittings consist of a Tefzel ferrule, which slides onto the end of the tubing, and a Delrin male nut which must be finger-tightened. Upchurch's fittings are compatible with ¼-28 or metric threads. The ferrule for 1/16-inch tubing holds to over 1,000 p.s.i., and the 1/8-inch ferrule is good for over 500 p.s.i., according to Upchurch. The fittings go for less than $4 (US) each.

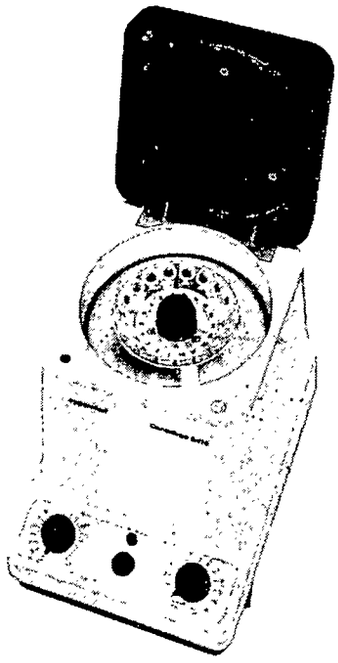
Another brand of **acrylamide** has become available to biochemists: this one, from Serva Fine Biochemicals (Reader Service No. 110). Serva maximize their product's stability by packaging it in nitrogen and storing it at −20°C. Servalyt Precotes, Serva's 0.1 mm precast gels, are made from the same acrylamide, which Serva is now offering for home-made gels at $27 (US) per 100 g bottle.

Hamilton's PB600 **dispenser** can be fitted with syringes of different sizes to yield repeated volumes, each 2 per cent of the syringe capacity (Reader Service No. 111). Depending on syringe size, the instrument's range of volumes extends between 0.5 µl and 200 µl. Fitted with

Hamilton's LT syringes, the dispenser-syringe unit is autoclavable at 121°C; alternatively, the dispenser can be attached to an adaptor that enables standard disposable tips to be used. Hamilton will be located at booth G23 at ASBC to answer questions on this and other products.

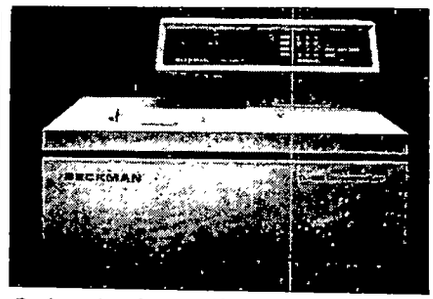
Bench-top varieties

An updated version of the Eppendorf **microcentrifuge** came from Brinkmann this year. The new model 5415 can accommodate up to eighteen 1.5-ml microcentrifuge tubes, or accept adaptors which expand its capabilities to 250, 400 and 500 µl tubes (Reader Service No. 112). The Eppendorf rotor holds tubes at a 45° angle, the ideal inclination for pellet formation. The rotor is also enclosed to reduce air turbulence and noise. Brinkmann's new Eppendorf costs $1,295 (US) and can be operated in a cold room. Its speed tops out a 14,000 r.p.m., and timing, as well as speed, is adjustable. Brinkmann will be in booths E15 through E19 (odd) at ASBC.



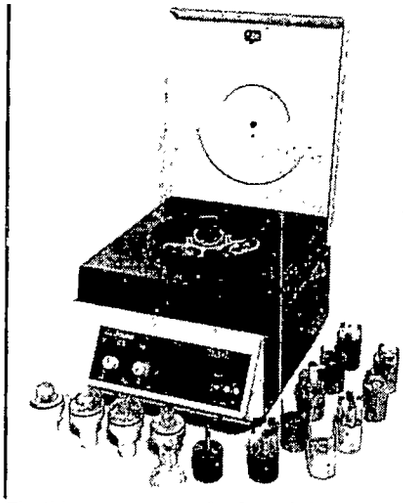
Eppendorf expands its accommodations.

In scores of booths between D4 and F11, Beckman Instruments will be exhibiting their wares, one of which is the TL-100 **table-top ultracentrifuge**. Beckman has brought out another rotor for the $19,590 (US) machine, itself just introduced this spring. The fixed-angle TLA-100.3 rotor spins larger sample volumes than previous varieties could accommodate, in 3 ml open-top or 3.5 ml sealed tubes (Reader Service No. 113). Six tubes at a time can be spun at speeds up to 541,000 g. Beckman's TLA-100.3, with a k factor of 16.5 at top speed, sells for $2,970 (US). With the other rotors available, the TL-100 allows ultracentrifugation of samples as small as 0.2 ml, and can process samples up to four times faster than floor models, says Beckman. It has a controlled temperature environment ideal for applications such as rapid sample clarification, density gradient separation, isolation of plasmid DNA, molecular weight determinations and binding studies.



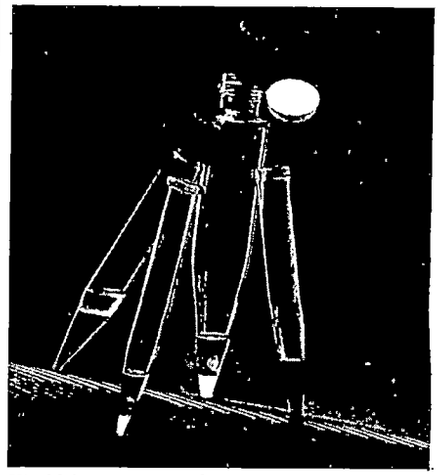
Beckman's ultracentrifuge: smaller, but still speedy.

A **compact bench-top centrifuge** from Jouan will centrifuge up to 48 5 ml tubes at 1,630*g*. The B311, designed for laboratories that do not require high carrying capacities, features closed loop speed control, digital speed readout, dynamic electric braking and an imbalance detection and shutdown system (Reader Service No. 114). In addition, the B311 has several adaptors and options that broaden its usefulness without sacrificing its $1,500 (US) base price. A swing bucket rotor carries tubes ranging from 1.5 ml microtubes through 180 ml bottles. Fifteen and 50 ml conical tubes can also be centrifuged using a different carrier, and aerosol containment covers are available for toxic or pathogenic samples. Jouan will have booths at J37 and J39 in Washington.



Flexible arrangements for Jouan's benchtop.

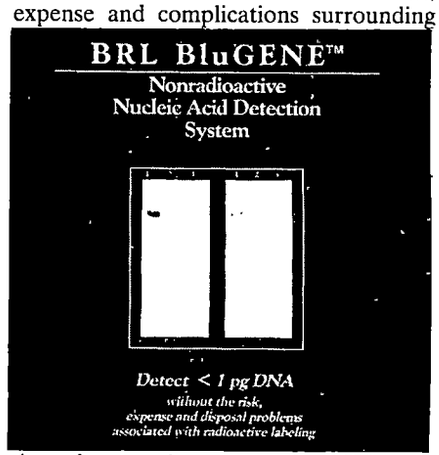
Kimble now manufactures a selection of plain-top and 50 ml screw-top **disposable glass centrifuge tubes** (Reader Service No. 115). The tubes come in 5, 10, 15 and 50 ml sizes, and all but the 50 ml are available with polyethylene snap caps. In screw-thread sizes, the new 50 ml complements an existing array of disposable tubes. These tubes are topped by black phenolic caps with rubber or PTFE/rubber liners. All of Kimble's disposable centrifuge tubes are made from borosilicate glass that resists organic solvents and preserves *p*H-sensitive solutions. Kimble protects its product from contamination in shrink-wrapped low particle trays; costs vary depending on size and quantity.



Kimble's toss-away tubes.

Away from radiation

Bethesda Research Laboratories (BRL) have a **nonradioactive nucleic acid detection system** called BluGENE that they think will turn the heads of autoradiography users (Reader Service No. 116). Using a streptavidin–alkaline phosphatase conjugate developed at BRL, the BluGENE method can detect single-copy genes of genomic DNA in Southern blots in less than one hour. BluGENE's detection levels reach down to the 0.25 pg level. BRL says the system has several advantages over autoradiography, and by circumventing sandwich methods, their conjugate heightens sensitivity and saves time. Biotin-labelled probes, once prepared, are good for at least a year, and signal development is complete in three hours. BluGENE also avoids the risk, expense and complications surrounding

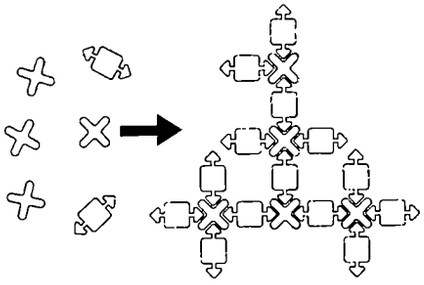


A novel streptavidin conjugate from BRL.

radioactive labelling techniques (as do all nonradioactive methods). BRL prices their BluGENE kit at $75 (US) for 40 assays; they are in booths D31 and D33 at ASBC.

Photo-activatable biotin (PAB) from Clontech has many of the same advantages as BRL's system (Reader Service No. 117). Determined colorimetrically, PAB's detection can be as sensitive as that afforded by ^{32}P, according to Clontech. One μg of PAB will label 1 μg of DNA, and the label sells for $75 (US) per mg or $300 (US) for 5 mg.

Streptavidin, a protein product of *Streptomyces avidinii*, is counterpart to biotin in nonradioactive signal amplification

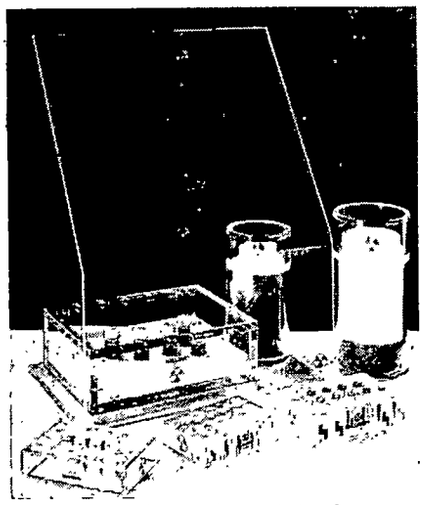


Signal amplification via streptavidin-biotin complexes.

systems. Porton Products Ltd now makes **streptavidin,** purified to X-ray crystallographic standard, for immunological and biochemical techniques (Reader Service No. 118). In comparison to avidin, streptavidin seems to have numerous advantages, including a reduction in nonspecific background effects and improved performance at neutral *p*H. The chemical is available in bulk quantities from Porton for £5 (UK) per 100 mg, the minimum order.

Vector Laboratories have their own version of a **biotin labelling reagent,** called Photoprobe (Reader Service No. 119). With photoactivation, Photoprobe biotin can produce stable hybridization probes that can be detected via a variety of enzymatic of fluorescent detection systems (including avidinbiotin interaction). In addition to this new probe, information and protocols for Southern, Western and Northern blot detection using Vectastain ABC and Vectastain ABC-alkaline phosphatase kits will be at Vector's booth E0 at ASBC. These kits provide a means of localizing hybridized biotinylated nucleic acid probes, biotinylated antibodies and biotinylatd lectins. Photoprobe sells for $120 a milligram, while the kits cost $100 (US) each.

When nonradioactive probe labels can't do the trick, Nalge has **acrylic beta radiation shields** to keep exposure to a minimum (Reader Service No. 120). Although acrylic cannot supply protection against

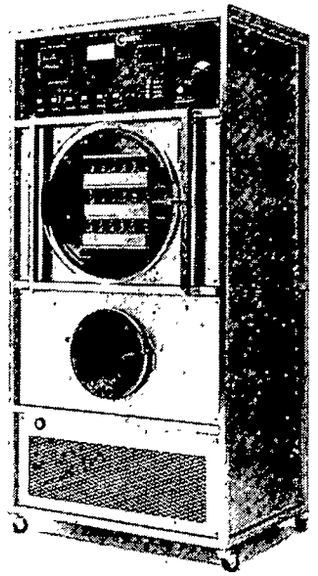


Acrylic shields keep radiation in its place.

gamma radiation or secondary X-rays, Nalge's 3/8-inch-thick layer has been proven effective against the beta emissions from isotopes such as ^{32}P, ^{3}H, ^{14}C and ^{35}S. Nalge's line includes benchtop shields and waste containers, test tube racks and microcentrifuge tube racks. A standard benchtop shield costs about $100 (US).

Freeze-dried and frozen

A dedicated **control system for freeze drying** was recently granted a patent, and the company holding the patent will be at ASBC showing their wares. VirTis Co., in booths H27 and H29, devised the FCP-II microprocessor-based system with electronic circuitry and a three-way mixing

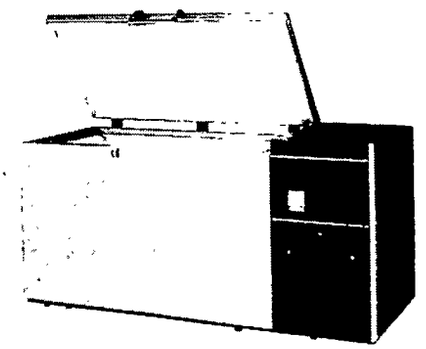


VirTis has freeze drying under control.

valve that can ensure shelf temperature control to 1/10°C (Reader Service No. 121). Their programmer requires no special computer training, has complete manual override capability and provides a hard copy summary (in keeping with FDA requirements) at the end of each run. Any combination of heating, cooling and vacuum level control can be preprogrammed and used repeatedly from memory. The FCP-II takes readings from 14 different probes monitoring product, shelf and condensor; if any sensors become defective, it discounts their readings, and it automatically takes corrective measures if part of the system malfunctions. VitTis's $29,750 (US) software and hardware fits all VirTis SRC sublimators.

Fisher just published a 16-page colour brochure detailing their new Isotemp family of laboratory cold units (Reader Service No. 122). *Fisher Isotemp Refrigerators, Freezers, Ultracold Freezers* describes several acid-and-chemical resistant general-purpose refrigerators, chromatography refrigerators, ultra-cold freezers for research and red cell storage and units approved for whole blood and plasma storage. Also making an appearance, above and beyond the 23 models introduced in the booklet, is a variety of new accessories — and plenty of penguins.

The Supercold 135, a recent addition to Gallenkamp's **freezer** collection, runs

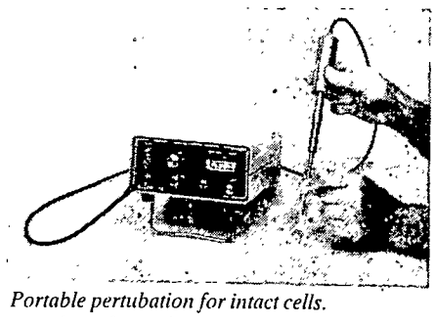


The deathknell for LN, storage?

from a standard wall socket and may jeopardize the popularity of conventional LN_2 storage devices (Reader Service No. 123). The unit is part of a generation of very low temperature freezers posed as an alternative to LN_2 freezing; it combines digital temperature display with a convenient height (37 inches) and a lid that makes opening and closing less of a struggle. For about £10,000 (UK) and potentially less power consumption, the Super-cold 135 might yet beat out liquid nitrogen varieties.

Cells in pieces

An **ultrasonic cell disrupter** that can homogenize, disaggregate, disintegrate and otherwise influence sample integrity will be demonstrated at booth G42, Sonics & Materials' display. The 40 W model VC-40 is compact and portable, designed for processing small laboratory samples from 100 μl to 25 ml (Reader Service No. 124). The functions of S & M's machine are multi-faceted: it can disrupt cells, bacteria, spores or tissue; prepare an emulsion down to 1/100 μm; homogenize liquids; disaggregate particulates; solubilize difficult compounds; and prepare



Portable pertubation for intact cells.

samples for electron microscopy and particle size analysis. S & M says their instrument will also accelerate and catalyse chemical reactions and degas liquids, as well as extract serums, toxins, enzymes and viruses from organic sources. For $1,080 (US), the VC-40 covers all bases.

For biochemists studying cell surface reactions, Genetic Research Instrumentation Ltd. has presented a **compact electrofusion instrument** that punches holes in the cell walls of plant and microbial cells, or the cell membranes of animal cells (Reader Service No. 125). These holes, according to GRI, can facilitate the incision of material into cytoplasm or improve the yields of cell fusion experiments; GRI reports up to 50-fold increases in incision for its electroporation systems. The Labpulse electrofusion/poration apparatus consists of an oscilloscope to determine pulse shape and strength and control circuitry for voltage outputs of 1 to 1,000 V, which generates pulses 5 ms to 150 ms and pulse-by-pulse repetition to 10 Hz. The system is fully integrated, and the electrodes, which fit into 9 ml polypropylene tubes, can be sterilized by autoclaving or methanol washing and flaming. GRI's instrument works by creating a volatage gradient across the cells that is carefully controlled to puncture, rather than rupture, the cells. Labpulse sells for £5,500 (UK).

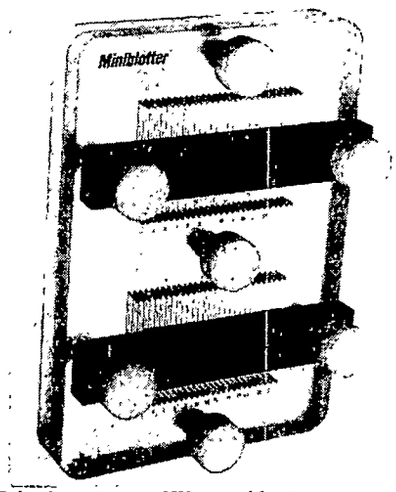
The Artek **dismembrator,** model 301, makes many of the same claims for ultrasonic disruption as do Sonics & Materials for their instrument (Reader Service No. 126). But Artek's model is not compact; this 2-litre 300 W version features a proprietary feedback system to keep the dismembrator working at maximum efficiency, and the percentage of ultrasonic power emitted is indicated by an output meter. Artek will supply a standard 3/4-inch tip, a 5/32-inch diameter microtip or a 3/8 diameter intermediate tip to accompany the model 301. In addition to disintegrating most cells, bacteria, spores and tissue, Artek's 301 will prepare emulsions down to 1/100 μm, homogenize immiscible liquids, accelerate enzymatic and chemical reactions and stimulate bacterial activity, among other things. Artek offers the model 301 at $1,950 (US).



Artek's dismembrator: a disturbing prospect.

Enzymes and antibodies

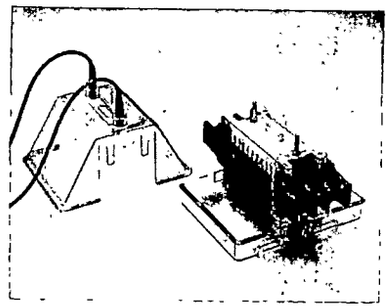
Western blot screening of hybridomas at early stages is made possible by a device recently released by Immunetics that required only 100 μl of an antibody solution to perform an analysis (Reader Service No. 127). The Miniblotter, on booth C29 at ASBC, is effective with both hybridomas and serum antibodies: 28 separate antibodies can be screened against a single blot the size of most minigels. Hybridoma supernatants can be transferred directly from 96-well plates into the Miniblotter's channels using a standard 8-channel automatic pipedtter. The blot, sandwiched between two plates, receives antibody solutions through holes in the upper plate, and the solutions are kept in their respective channels with a simple clamp system. For larger loads, Immunetics also offer a Miniblotter version with 45 channels, which requires 200 μl of antibody solution. Both sizes cost $295 (US).



Take the wait out of Western blotting.

The latest developments at Promega Biotec include an alkaline phosphate-based Western blotting system and ten new restriction enzymes. Promega will

First In Electrophoresis!



Mighty Small II Dual 7cm Slab Unit

Hoefer Scientific pioneered small-gel electrophoresis with its Mighty Small I. The new Mighty Small II can run two 7 x 8 cm gels in as little as 45 minutes—with no smiling. Heat dissipation is outstanding. Gel sandwiches have alumina back plates that conduct heat 40 times faster than glass. Also, there is a serpentine cooling channel sealed between the two vertical upper buffer chambers.

Formerly, Hoefer's Mighty Small I was distributed through Bio-Rad as its Model 360. Hoefer products are no longer available from Bio-Rad. Mighty Small I and II and all parts and accessories are available from the distributors listed below.

AUSTRALIA Narellan, NSW
Edwards Instrument (02)605-6777
AUSTRIA Vienna
Bio-Trade (0222) 88 73 13
BELGIUM Brussels
Van der Heyden S.A. 02/21.20.611
CANADA Mississauga, Ont.
Technical Marketing (416) 826-7752
FRANCE Illkirch Cedex
BIOBLOCK 88 67 14 14
& Vanves Cedex 146 44 46 46
GERMANY Heidelberg
Atlanta GmbH 06221/502144
JAPAN Tokyo
Central Scientific (03) 806 4361
THE NETHERLANDS PJ de Meern
Brouwer Scientific 03406/64'299
SOUTH AFRICA Tokai, Cape
Scientific Associates 53 7400
SPAIN Madrid
Iberlabo S.A. 251 14 91
SWITZERLAND Lucerne
Brouwer Engineering 041/44.44.48
TAIWAN Taipei
Mightek Scientific (02) 721-5482/3
UNITED KINGDOM Luton/Beds
Biotech Instruments 0582 502388

Reader Service No.4

Hoefer Scientific Instruments
P.O. Box 77387, San Francisco, CA 94107
TELEX: 477078

For Nucleic Acid Hybridization Compare With Hoefer's **HYBRID-EASE™** —— The **PLASTIC BAG**

COMPARE RESULTS



Membrane I: 40μg/lane of total cellular RNA blotted to Nylon (NYS) membrane. Membrane was hybridized to a ^{32}P labeled Actin cDNA probe (2 x 10^8 cpm/μg) in Hybrid-Ease.

Membrane II: Similar RNA samples and identical reagents used as in Membrane I. Prehybridized and hybridized in a sealed plastic bag and washed using large volumes and high stringency.

COMPARE EASE OF USE

Simply mount the membrane in the Hybrid-Ease and carry out prehybridization, hybridization and stringency washing without opening the unit again.

Prehybridize in plastic bag. Remove solution. Add solution for hybridization. Reseal bag. After hybridizing, remove solution. Remove membrane and do stringency washing in lab tray.

COMPARE EFFECTIVENESS

In the Hybrid-Ease, solution contacts both sides of the membrane equally. Fluid entering the inner chamber goes through a unique laminar flow induction device that ensures uniform and bubble-free liquid contact with the entire membrane. No shaking necessary.

Contact with plastic bag leaves marks on membrane. Even flow of solution around membrane is nearly impossible. Shaking is necessary. Inside a plastic bag, a membrane is more likely to get damaged.

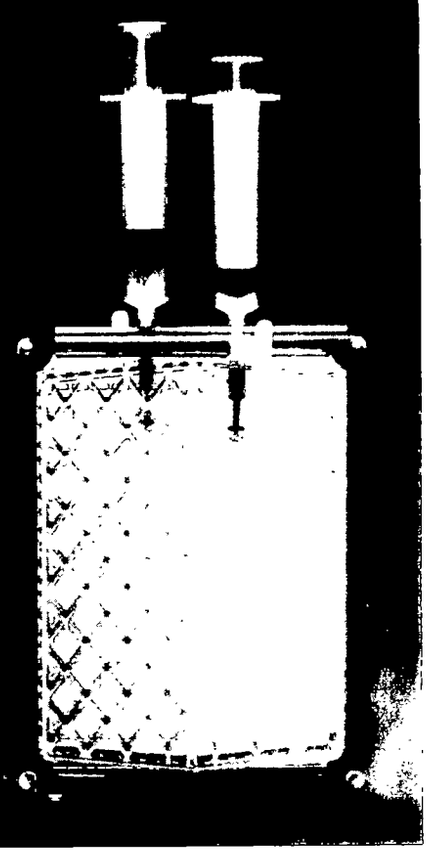
COMPARE SAFETY

Hybrid-Ease reduces the danger from radioactivity. A sturdy, leakproof unit, it uses solutions in small amounts, introduced and withdrawn safely through syringes. In addition, the unit is automatically decontaminated during wash cycles.

Plastic bags can be tricky to seal and open and are prone to leaking. Adding and removing large volumes of radioactive solutions increases the likelihood of spilling.

Reference: Hardy, K.J., et al. Proc. Natl. Acad. Sci., 82, 8173-8177, 1985.

Compare it to the plastic bag...



THERE'S NO COMPARISON WITH HOEFER'S NEW Hybrid·Ease™

First in Electrophoresis!

HOEFER SCIENTIFIC INSTRUMENTS
654 Minnesota St., San Francisco, CA 94107 · Tel. 800-227-4750 · In California 415-282-2307 · Telex 470778

Roland GRÜNBERG - NANCY - FRANCE



DO YOU NEED PEPTIDES?

NEOSYSTEM LABORATORIES

PROVIDE
A COMPLETE SERVICE FOR
PEPTIDE SYNTHESIS
PEPTIDE AND PROTEIN SEQUENCING
PEPTIDE ANTIBODY PRODUCTION

WE PROVIDE ALSO
CONTRACT RESEARCH SERVICES
TO INDUSTRIAL AND ACADEMIC
INSTITUTIONS



NEOSYSTEM LABORATORIES
B.P. n° 309 R8
67008 STRASBOURG Cedex .
FRANCE - Télex 880 088 F
Tél. : 88.36.96.96

Reader Service No.28

Macmillan Press Scientific...

NICHOLAS COPERNICUS

THE COMPLETE WORKS

In 1985 Macmillan were proud to publish the third and final volume of Copernicus' Complete Works. These volumes, published as limited editions, are the result of many years' research and will make a significant contribution to the advancement of scientific scholarship.

VOLUME III: **NICHOLAS COPERNICUS: COMPLETE WORKS**
The Minor Works
Translated by Edward Rosen

This volume contains English translations of all his writings other than on the *Revolution of Heavenly Bodies* which was contained in Volumes I and II. This project was undertaken by the Polish Academy of Sciences and many of his writings have been translated into English for the first time.

Volume III contains astronomical writings – The Commentariolus and the Letter Against Werner – as well as other scientific, economic and administrative documents. These give a fascinating insight into this turbulent period of European history, and into the mind of one of the greatest and most influential of scientists.



Contents of Volume III
Introduction
Editor's Notes on Volume III
Copernicus' Translation of Theophylactus Simocatta
Copernicus' Minor Astronomical Works
Copernicus and the Money Question
Copernicus' Administrative Documents
Letters written by Copernicus
Indexes
Polish Places in Copernicus' Life and Work
Additions and Corrections to Volumes I and II

Volume III 380pp 0 333 14531 3
£60.00 1985

Other volumes in the series:

VOLUME I
This volume is a facsimile copy of Copernicus' autograph the Revolutions.

Volume I 0 333 14034 6 **£40.00** 1973

VOLUME II
Edited by Jerzy Dobrzyki. Translation and Commentary by Edward Rosen.
This volume is a translation of Volume I the Revolutions.

Volume II 0 333 14530 5 **£35.00** 1978

MACMILLAN PRESS

Please order these titles from your bookseller – or in case of difficulty from Judy Chappell, Macmillan Press, Houndmills, Basingstoke, Hants RG21 2XS, UK.

have plenty of information on both of the fledgling products at their ASBC booths GO1 and GO2. The $175 (US) ProtoBlot **immunoblotting system** is a nonradioactive method which Promega claims has greater sensitivity than either protein A or HRP-based systems (Reader Service No. 128). The **restriction enzymes** come with enzyme-specific 10× digest buffer and acetylated nuclease-free bovine serum albumin, both of which have been optimized for reaction efficiency (Reader Service No. 129).

A **recombinant protein A** for the study of cell surface antigens and receptors and for the detection of antibody-secreting cells has emerged from the laboratories at ICN Immuno-Biologicals (previously ICN Biomedicals). The high-affinity protein is just one of the many chemicals for immunology research that ICN will feature at their booths J15 through J19 (odd) (Reader Service No. 130). Other recent introductions, such as monoclonal and polyclonal antibodies for cytoskeletal elements, should be prominent in ICN's display.

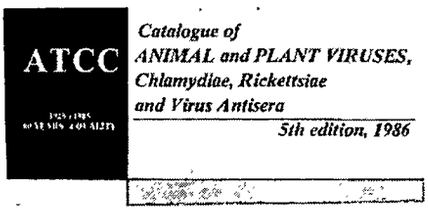
A **neurotransmitter** commonly known as AMPA (and less often called 3-isoxazolol amino acid (*RS*) α-amino-3-hydroxy-5-methylisoxazole-4-propionic acid) is a newcomer to Cambridge Research Biochemicals' cadre of neurotransmitters. AMPA, a synthetic analogue of the less stable natural compound ibotenic acid, is a powerful agonist of a subclass of glutamic acid receptors (Reader Service No. 131).

From the pamphlet file

"Filtration — the separation of materials from a gas or a liquid — is one of the most basic and important laboratory procedures." Thus begins Fisher Scientific's new catalogue, the *Fisher Filtration Catalog* (Reader Service No. 132). In full colour spreads, the brochure follows products for micro, macro and process filtration down avenues of applications in biological, microbiological, clinical and pharmaceutical procedures.

As Bond Elut and Chem Elu **sorbent extraction methods** gain a healthy reputation, keeping track of their potential uses becomes more difficult. Analytichem has published a bibliography listing nearly 500 applications for their two extraction methods as a resource for method development ideas (Reader Service No. 133).

The fifth edition of the American Type Culture Collection's *Catalogue of Animal and Plant Viruses* has now made it to the scientific newstands (Reader Service No. 134). This year's 193-page brochure houses descriptions of over 2,200 strains,



The consummate bug collection.

including molecularly cloned viruses. At ASBC, information on how to obtain a free edition can be had at ATCC's booth C32.

Late in March of this year, BioSciences Information Service (BIOSIS) launched a free sample issue campaign and a discount programme for its *BioResearch Today* publication series (Reader Service No. 135). It may not be too late to catch up with these offers at BIOSIS's ASBC booth A27. BIOSIS describes **BioResearch Today** (BRT) as a 'group of monthly current awareness abstract journals' that covers 14 specific research topics such as addiction, carcinogenesis, human and animal aging and pesticides. Each issue offers between 75 and 250 abstracts selected from the latest two issues of Biological Abstracts, BIOSIS's main publication. □

These notes are compiled by Karen Wright from information provided by the manufacturers. To obtain further details about these products, use the reader service card bound inside the journal.

ADVERTISEMENT

JOURNALS FROM MACMILLAN

SCIENTIFIC AND MEDICAL DIVISION

In 1986 Macmillan are launching two new journals for new fast developing areas of science as well as strongly supporting their established titles. The publication of **Anti-Cancer Drug Design** and **Bone Marrow Transplantation** respond to new developments in scientific research, and will provide a valuable forum for exchange of ideas.

At the same time our already established journals – Postgraduate Medical Journal will shortly be celebrating its 60th anniversary – continue to chart and report new developments. If you are out of touch with our journals – or would like to see sample copies of our new ones as they are published, we would be pleased to send you a sample copy.

ANTI-CANCER DRUG DESIGN

NEW JOURNAL – FIRST ISSUE DUE SOON

Bi-monthly

Editors: Dr S. Neidle, Dr S. T. Crooke

The development of new clinically-useful anti-cancer agents is increasingly dependent on rational scientific principles drawn from a wide range of disciplines. This new journal aims to promote such approaches, providing a common meeting ground for medicinal chemists, pharmacologists, biochemists, biophysicists and oncologists involved in both fundamental and clinically orientated aspects.

This journal is published with the support of The Cancer Research Campaign.

£45 (UK) $95 (USA/Canada) £63 (ROW)

BONE MARROW TRANSPLANTATION

NEW JOURNAL – FIRST ISSUE DUE EARLY 1986

Quarterly

Editor: Dr J. M. Goldsman, Co-Editor: Dr R. P. Gale

A new journal which will publish clinical results in man and experimental results with animals; allografting and autografting; HLA and other methods of selecting donors; graft-versus-host disease and all types of methods to prevent and treat it; and much more.

BRITISH JOURNAL OF CANCER

Monthly

Chairman: Professor D. G. Harnden, Editor: Dr M. Moore

One of the leading cancer journals in the world publishing articles on all the major scientific disciplines. Publishes papers from scientists and researchers throughout the world and the proceedings of meetings of the British Association for Cancer Research and other symposia.

£125 (UK) $275 (USA/Canada) £165 (ROW)

PHARMACEUTICAL MEDICINE

Quarterly

Editor: Dr R. N. Smith, Assistant Editor P. J. Keen

..."a quarterly journal, which includes papers on the validation of new and established methods of testing drugs in man written by investigators both inside and outside the pharmaceutical industry. It also provides a forum for the exchange of ideas about issues affecting drug development. These new developments merit support from all involved in the management, sale and use of drugs." – *Lancet*

£48 (UK) $99 (USA/Canada) £65 (ROW)

BRITISH JOURNAL OF PHARMACOLOGY

Monthly

Chairman: Professor J. F. Mitchell
Secretary to the Editorial Board: Dr G. M. Lees

One of the top five most cited pharmacology journals in the world

A vital source of relevant information for physiologists, immunologists, molecular biologists

£175 (UK) $410 (USA/Canada) £289 (ROW)

POSTGRADUATE MEDICAL JOURNAL

Monthly

Editor: Dr B. I. Hoffbrand

A monthly compendium of current clinical research and practice invaluable to the graduate in training

£68 (UK) $155 (USA/Canada) £85 (ROW)

HUMAN TOXICOLOGY

Bi-monthly

Secretary to the Editorial Board: Professor P. Turner

Covers all aspects of human toxicology embracing both animal research and studies with humans

£80 (UK) $168 (USA/Canada) £120 (ROW)

To receive sample copies, details of rates and how to submit papers indicate the titles you are interested in and contact: Alison Baverstock, Macmillan Press, Houndmills, Basingstoke, Hampshire RG21 2XS. Customers in the United Kingdom may mark their envelope FREEPOST and need not affix a stamp.

Macmillan Press Scientific & Medical

Mathematics

Discrete Mathematics. By NORMAN L. BIGGS. *Oxford University Press:1985. Pp.480. Hbk ISBN 0-19-853252-0; pbk ISBN 0-19-853266-0. Hbk £30.00; pbk £15.00.*

Finite Algorithms in Optimization and Data Analysis. By M.R. OSBORNE. *Wiley:1985. Pp.383. Hbk ISBN 0-471-90539-9. £32.00.*

From Error-Correcting Codes Through Sphere Packings to Simple Groups. By THOMAS M. THOMPSON. *The Mathematical Association of America:1985. Pp.228. Hbk ISBN 0-88385-023-0. £22.*

Hamilton's Principle in Continuum Mechanics. By A. BEDFORD. Research Notes in Mathematics, 139. *Pitman Publishing Ltd:1985. Pp.106. Pbk ISBN 0-273-08730-4. £12.50.*

Introduction to Mathematical Control Theory, 2nd Edn. Oxford Applied Mathematics and Computing Science Series. By S. BARNETT and R.G. CAMERON. *Oxford University Press:1985. Pp.404. Hbk ISBN 0-19-859640-5. £25.00.*

Mathematical Models and Applied Mechanics. By A.B. TAYLOR. *Oxford University Press:1986. Pp.280. Hbk ISBN 0-19-853533-3; pbk ISBN 0-19-853541-4. Hbk £25; pbk £12.50.*

Numerical Analysis of Parametrized Nonlinear Equations. By WERNER C. RHEINBOLDT. *Wiley: 1986. Pp.299. Pbk ISBN 0-471-88814-1. £35.75.*

Numerical Solution of Partial Differential Equations: Finite Difference Methods, 3rd Edn. By G.D. SMITH. *Oxford University Press:1985. Pp.337. Hbk ISBN 0-19-859641-3; pbk ISBN 0-19-859650-2. HBK £20; pbk £10.95.*

Prime Numbers. By WILLIAM and FERN ELLISON. *Wiley:1985. Pp.416. ISBN 0-471-82653-7. Pbk £51.*

Statistical Analysis of Measurement Errors. By JOHN L. JAECH. *Wiley:1985. Pp.293. ISBN 0-471-82731-2. £35.75.*

Astronomy

Armchair Astronomy. PATRICK MOORE. *Norton:1986. Pp.185. Hbk ISBN 0-393-02253-6. $16.95.*

The Astronomer's Software Handbook. By R.A. MACKENZIE. *Sigma Press, 5 Alton Road, Wilmslow, Cheshire, UK:1985. Pp.292. Pbk ISBN 1-85058-024-3. £8.95.*

The Cambridge Astronomy Guide: A Practical Introduction to Astronomy. By BILL LILLER and BEN MAYER. *Cambridge University Press:1985. Pp.176. ISBN 0-521-25778-6. £13.95. $24.95.*

Comet! The Story Behind Halley's Comet. By GREG WALZ-CHOJNACKI. *Astro Media:1985. Pp.64. ISBN 0-918831-51-2. $9.75.*

Comets, Meteors & Asteroids: How They Affect Earth. By STAN GIBILISCO. *Wiley:1985. Pp.208. Pbk ISBN 0-8306-1905-4. Pbk $12.95.*

Cosmic Rays in Interplanetary Magnetic Fields. By I.N. TOPTYGIN. *D. Reidel:1985. Pp.375. Hbk ISBN 90-277-1863-6. NP.*

Data Analysis in Astronomy. V. DI GESU *et al.* (eds). *Penum:1985. Pp.541. ISBN 0-306-42018-X. Np.*

Invitation to Astronomy. By SIMON and JACQUELINE MITTON. *Blackwell:1985. Pp.210. Hbk ISBN 0-631-14699-7. £14.50.*

Supernovae: Their Progenitors and Remnants. G. SRINIVASAN and V. RADHAKRISHNAN (eds). *Indian Academy of Sciences:1985. Pp.178. Np.*

1986 Year Book of Astronomy. PATRICK MOORE (ed.). *Norton.1986. Pp.231. Hbk ISBN 0-393-30254-7. $15.95.*

Chemistry

Advances in Protein Chemistry, Vol.37. C.B. ANFINSEN, JOHN T. EDSALL and FREDERIC M. RICHARDS (eds). *Academic: 1985. Pp.373. Hbk ISBN 0-12-034237-5. £43, $49.*

Asymmetric Catalysis. B. BOSNICH (ed.). *Martinus Nijhoff: 1986. Pp.160. Hbk ISBN 90-247-3259-X. Dfl. 115, £31.95, $45.50.*

Chemical Demonstrations: A Sourcebook for Teachers. By LEE R. SUMMERLIN and JAMES L. EALY Jr. *American Chemical Society: 1985. Pp.190. Pbk ISBN 0-8412-0923-5. Pbk £19.95.*

Chemistry of Coal Conversion. RICHARD H. SCHLOSBERG (ed.). *Plenum: 1985. Pp.336. Hbk ISBN 0-306-41974-2. $52.50.*

Comparison of *Ab Initio* Quantum Chemistry with Experiment for Small Molecules: The State of the Art. R.J. BARTLETT (ed.). *D. Reidel: 1985. Pp.513. Hbk ISBN 90-277-2129-7. Dfl. 210, £58.25, $79.*

Crystal Structure Analysis. A Primer, 2nd Edition. By JENNY PICKWORTH GLUSKER and KENNETH N. TRUEBLOOD. *Oxford University Press: 1985. Pp.269. Hbk ISBN 0-19-503531-3; pbk ISBN 0-19-503543-7. Hbk £29.00; pbk £17.00.*

Crystallographic Computing 3: Data Collection, Structure Determination, Proteins and Databases. G.M. SHELDRICK, C. KRÜGER AND R. GODDARD. *Oxford University Press: 1985. Pp.314. Hbk ISBN 0-19-855211-4. £25.00.*

Environmental Chemistry. By PETER O'NEILL. *George Allen & Unwin: 1985. Pp.232. Hbk ISBN 0-04-551085-7; pbk ISBN 0-04-551086-5. Hbk £8.95, $13.95; pbk £18.00, $25.00.*

Ferrohydrodynamics. By R.E. ROSENSWEIG. *Cambridge University Press: 1985. Pp.344. Hbk ISBN 0-521-25624-0. £45, $69.50.*

Grosse Moleküle. Plaudereien über Synthetische und Natürliche Polymere. By H.-G. ELIAS. *Springer Verlag: 1985. Pp.204. Pbk ISBN 3-540-15599-6. DM 29.80.*

Hydrogenation Methods. By PAUL N. RYLANDER. *Academic: 1985. Pp.193. Hbk ISBN 0-12-605365-0. £40, $48.*

International Tables for Crystallography. THEO HAHN (ed.). *Reidel: 1985. Pp.119. Pbk ISBN 90-277-1964-0. Pbk Dfl. 27.50, $8.50.*

Technology

Detectors and Chromatography. Australian Scientific Industry Association. Proceedings of an International Conference, May 30 to June 3, 1983. A.J.C. NICHOLSON (ed.). *Australian Scientific Industry Association:1986. Pp.198, Pbk ISBN 0-949761-08-7. Np.*

Industrial Adhesion Problems. D.M. BREWIS and D. BRIGGS (eds). *Orbital Press/Wiley:1985. Pp.298. ISBN 0-946193-01-0. £40.*

Industrial Hygiene Aspects of Plant Operations. Vol. 2 Unit Operations and Product Fabrication. LEWIS J. CRALLEY, LESTER V. CRALLEY and JOHN E. MUTCHLER (eds). *Macmillan:1985. Pp.537. ISBN 0-02-949360-9. £65.*

An Introduction to Scanning Acoustic Microscopy. By ANDREW BRIGGS. *Oxford University Press: 1985. Pp.70. Pbk ISBN 0-19-856412-0. £5.95.*

Liquid Phase Sintering. By RANDALL M. GERMAN. *Plenum: 1985. Pp.240. Hbk ISBN 0-306-42215-8. Np.*

Snack Food Technology, 2nd Edn. By SAMUEL A. MATZ. AVI *Reidel:1985. Pp.415. ISBN 0-87055-460-3. Dfl. 180, £49.95.*

Statics and Applied Strength of Materials. By RAYMOND F. NEATHERY. *Wiley:1985. Pp.655. Hbk ISBN 0-471-88811-7. £35.75.*

Techniques for the Automated Optimization of HPLC Separations. By JOHN C. BERRIDGE. *Wiley:1985. Pp.203. ISBN 0-471-90861-4. £22.*

Teleoperation and Robotics: Applications and Technology. Robot Technology, Vol. 3B. By JEAN VERTUT and PHILIPPE COIFFET. *Kogen Page, London, UK:1985. Pp.256. Hbk ISBN 0-85038-962-3. £32.50.*

Computer Science

Compulsive Technology: Computers as Culture. TONY SOLOMONIDES and LES LEVIDOW (eds). *Free Association Books, London, UK:1985. Pp.160 Pbk ISBN 0-946960-20-0. Np.*

Emperical Foundations of Information and Software Science. JAGDISH C. AGRAWAL and PRANAS ZUNDE (eds). *Plenum:1985. Pp.415. Hbk ISBN 0-306-42091-0. Np.*

The Principles of Computer Hardware. By. ALAN CLEMENTS. *Oxford University Press:1985. Pp.454. ISBN 0-19-853704-2. Hbk £25, pbk £12.50.*

Selective Computation. By RICHARD E. BELLMAN. *Wiley:1985. ISBN 9971-966-86-7. £23.85.*

Supercomputers in Theoretical and Experimental Science. JOZEF T. DEVREESE and PIET VAN CAMP (eds). *Plenum:1985. Pp.225. Hbk ISBN 0-306-42107-0. Np.*

Earth Sciences

Advances in Soil Science, Vols 2 & 3. B.A. STEWART (ed.). *Springer-Verlag:1985. Vol. 2 pp.235. ISBN 0-387-96114-3. DM 148. Vol. 3 pp.217. ISBN 0-387-96116-X. DM 138.*

Aspects of the Analysis of Plate Structures. A Volume in Honour of W.H. Wittrick. D.J. DAWE, R.W. HORSINGTON, A.G. KAMTEKAR and G.H. LITTLE (eds). *Oxford University Press:1985. Pp.332. Hbk ISBN 0-19-856168-7. £45.00.*

Down to Earth: One Hundred and Fifty Years of the British Geological Survey. By H.E. WILSON. *Scottish Academic Press:1985. Pp.189. ISBN 0-7073-0473-3. Pbk £9.50.*

Formation Evaluation: Geological Procedures. The EXLOG Series of Petroleum Geology and Engineering Handbooks. ALUN WHITTAKER (ed.). *D. Reidel: 1985. Pp.183. Hbk ISBN 90-277-1978-0. Dfl. 115, £31.95.*

The Future of Geography. R.J. JOHNSTON (ed.). *Methuen:1985. Pp.342. Hbk ISBN 0-416-36690-2. £19.95.*

Gravity Field, Seismicity and Tectonics of the Indian Peninsular and the Himalayas. By R.K. VERMA. *D. Reidel:1985. Pp.213. Hbk ISBN 90-277-1864-4. £36.23, $44.00.*

Improvement of Desert Ranges in Soviet Central Asia. NINA T. NECHAEVA (ed.). *Horwood Academic Publishers:1985. Pp.327. Hbk ISBN 3-7186-0222-9. $130.00.*

Issues in Atmospheric and Oceanic Modeling. Part A, Climate Dynamics. SYUKURO MANABE (ed.). *Academic:1985. Pp.591. Hbk ISBN 0-12-018828-7. £79, $89.50.*

General

Problems in Combinatories and Graph Theory. By IOAN TOMESCU. *Wiley:1985. Pp.335. ISBN 0-471-80155-0. £36.95.*

A Recapitulation of the Lord's Prayer. By J.P. ROSS. *Element Books:1985. Pp.148. ISBN 0-9510274-0-9. £4..95.*

Research in Technical Communication: A Bibliographic Sourcebook. MICHAEL G. MOKRAN and DEBRA JOURNET (eds). *Greenwood Press:1985. Pp.515. ISBN 0-313-23431-0. £63.50.*

Residential Development and the Planning System: A Study of the Housing Land System at the Local Level. By Y. RYDIN. *Permagon:1985. Pp.69. ISBN 0-08-032742-7. Np.*

The Riemann Zeta-Function: The Theory of the Riemann Zeta-Function with Applications. By ALEXSANDER IVIC. *Wiley:1985. Pp.517. ISBN 0-471-80634-X. £57.80.*

Sagamore Army Materials Research Conference Proceedings, Vol. 30: Innovations in Materials Processing. GORDON BRUGGEMAN and VOLKER WEISS (eds) *Plenum:1985. Pp.519. ISBN 0-306-41839-8. Np.*

Scientific Realism. JARRETT LEPLIN (ed.). *University of California Press:1984. Pp.266. Hbk ISBN 0-520-05155-6; pbk ISBN 0-520-05326-5. Hbk $32.75, £29.95; pbk $11.50. £10.50.*

Shall We Make the Year 2000? The Decisive Challenge to Western Civilization. By J.G.DE BEUS. *Sidgwick & Jackson:1985. Pp.183. ISBN 0-283-99221-2. £12.95.*

Speech Science. RAYMOND G. DANILOFF (ed.). *Taylor & Francis:1985. Pp.326. ISBN 0-85066-500-0. £22.*

Structure in Thought and Feeling. By SUSAN AYLWIN. *Methuen:1985. Pp.274. ISBN 0-416-35990.£25.*

Symmetry and Structure. By S.F.A. KETTLE. *Wiley:1985. Pp.330. ISBN 0-471-90705. Np.*

Temporal Order. L. RENSING and N.I. JAEGER (eds). *Springer-Verlag:1985. Pp.325. 3-540-15274-1/0387-15274-1. Np.*

Urban Geomorphology in Drylands. By R.U. COOKE *et al. Oxford University Press: 1985. Pp.324. ISBN 0-19-823258-6. £9.95.*

nature

NATURE VOL. 321 5 JUNE 1986

Scrapping treaties is wrong

The United States seems to be losing patience with the only existing agreement on strategic arms. But the US's tetchy demeanour may prove to be an embarrassment.

PRESIDENT Ronald Reagan's announcement last week that the United States will not necessarily honour the Salt II treaty after September of this year is almost certain to prove more of an embarrassment for the United States than for the Soviet Union. While it is good news that the president has agreed to scrap two Poseidon submarines to make room, within the limits of Salt II, for a new Trident submarine in the US strategic fleet, it is bad news that he has also, for practical purposes, set an arbitrary limit on the time for which the complicated negotiations at Geneva should continue while simultaneously diminishing the chance of their success. The immediate consequence is that the other members of the North Atlantic Treaty Organization (whose foreign ministers were conveniently meeting last week in Canada) have been outspokenly dismayed by what seems to have been a needless provocation in the fragile climate of the arms control process. Much more of this and Europe's inclination towards Gallic ways will be strengthened. Worse still, the United States may find that it has lost the benefit of the charitable doubt it has enjoyed for the past six years. All kinds of people, many in the United States, will now be asking whether the administration can be serious in its protestations that arms control is at the centre of its attention.

The most curious feature of the president's decision is that it appears to have been unprovoked. This is not the first time that a working strategic submarine has had to be laid up so as not to violate Salt II; the same happened last September. Ostensibly, the warning that Salt II may not be kept after September is intended as a riposte to alleged Soviet violations of the treaty, and indeed is conditional on the failure of the Soviet government to mend its ways, yet nothing new has happened in the past few months except that Mr Mikhail Gorbachev has put out a whole string of proposals on arms control, many of which are sensible and well worth talking about.

Change

It is true that much has changed since Salt II was signed (it has not been ratified) just ten years ago. The Soviet Union has broken the spirit but not the letter of the treaty by deploying several hundred SS20 missiles in positions from which targets in Western Europe could be attacked, and has been able to modernize its force of longer range missiles by pretending that the new SS25 missiles are but more modern versions of older rockets. And, in an undisputed violation of the treaty, the Soviet Union has also taken to coding the telemetry from test rockets, thus depriving the United States of one of the most effective means at its disposal of "national verification", acknowledged by the treaty to be necessary. But there is no suggestion that the Soviet Union has broken the chief restriction of its freedom of action — the numerical ceiling on the missiles it may deploy.

Nothing in this list of supposed transgressions justifies the US administration's display of impatience last week. The most substantial complaint, about the encryption of telemetry from Soviet test rockets, is long-standing. Is President Reagan now saying that the United States will withdraw its threat to breach Salt II if Soviet telemetry is no longer encrypted? Or is he asking that the SS25s should be dismantled, which is a much taller and more impractical order, and which would also raise questions from the Soviet Union about the legitimacy, within Salt II, of the development of both the MX and the Midgetman missiles in the United States? Even if last week's statement were intended merely as a piece of public diplomacy, it has the thoroughly unsatisfactory feature that neither the Soviet Union nor the rest of the world can tell what must be done to ensure that the United States does not follow the threatened breach of Salt II.

All these are matters that are capable of being resolved within the framework of the bilateral negotiations of Geneva. Indeed, to the extent that one of the chief objectives of those negotiations is an agreement on strategic weapons at a reduced level (half as many warheads as at present, or thereabouts), the negotiations are plainly also a way of replacing Salt II by a treaty that is not "fatally flawed" — President Reagan's description last week which is ominously borrowed from his rhetoric of the 1980 election campaign. One obvious defect is that it counts missiles rather than warheads (although the calculations of supposed strategic balance are based on the assumption that missiles with multiple warheads are fitted with their full complement). The treaty is also cumbersome, well provided with potential bones of contention. If the United States were now urging the potential benefits of a better treaty, nobody would complain. From the Soviet point of view, there are also good reasons why Salt II is unsatisfactory. It says nothing about the British and French nuclear forces, for example, although the calculations of strategic balance were made by subtracting from the US missile quota an allowance for the European striking forces of a decade ago. Both sides could fairly ask for a better treaty than Salt II. But Salt II is far better than no treaty at all. Moreover, there is no sense in which the present treaty, which allows each side the equivalent of 5,000 nuclear warheads, restricts the freedom to deploy a sufficient retaliatory force.

These are the reasons why last week's announcement that Salt II will not necessarily be considered binding later in the year is bound to unsettle opinion and policy elsewhere. Both parties to the Geneva negotiations have been saying for months that the other is not seriously interested in an agreement, but Mr Mikhail Gorbachev is the one who has been stunning everybody with a string of tangible proposals, some of which may be practical. The US administration seems not to have calculated (or cared?) what the effect will be in, say, Western Europe of presenting itself as the party that will tear up an existing treaty unless the other meets certain vague requirements. The new development seems all the more sombre because it virtually coincides with the curious refusal of the United States at Berne to sign the modest but useful agreement (within the Helsinki treaty framework) on personal and professional freedom to travel. One common reaction will be to wonder whether the time has come for separate agreement with the Soviet Union on the British and French nuclear forces, which would disastrously spell the end of thirty years of planning for the defence of Western Europe. Another, more constructive, will be to ask whether the cause of arms control is not so important that it can no longer be left to the superpowers. One specific issue is likely to become a thorn in Mr Reagan's flesh in the next few months; hitherto, most European

governments have accepted that the time has not been ripe for a comprehensive test-ban treaty, given the US argument that there is a need to develop warheads for the Midgetman, but that position will now almost certainly be eroded.

Where all this will end is anybody's guess. The United States seems to have calculated that, what with one thing and another, its impatience will not dissuade Mr Gorbachev from going to Washington later in the year for a replay of last year's Geneva summit. The calculations may be correct, but the consequences will be that Mr Gorbachev will travel intransigently. But he may decide not to go at all, which will be a greater embarrassment for the United States in its dealings with its friends. □

Who pays for AIDS?

The alarming financial implications of the US epidemic of AIDS creates another social dilemma

ACQUIRED immune deficiency syndrome (AIDS), a haunting source of trouble for the past five years, has become a problem for the US insurance industry. In several states, it is now a matter for vigorous controversy whether insurance companies should be allowed to deny health or life insurance to people who test positively for antibodies against the virus for AIDS, human immunodeficiency virus (HIV). California and Wisconsin have already enacted legislation that forbids the use of HIV antibody tests in this way, and similar proposals are being considered in New York. In the District of Columbia, the council is likely soon to approve a bill that would forbid insurance companies using any type of test for AIDS for the purpose of determining insurability. The insurance industry, aware that similar proposals are likely to be enacted elsewhere, has started an energetic (and expensive) lobbying campaign to oppose legislation of this kind.

The kernel of the problem is that a positive result in a test for HIV antibodies by no means proves that a person will develop AIDS, which in its fully developed form is at present always fatal. Estimates of the proportion of those who test positively who will eventually succumb to the disease vary, and because of the long incubation period of the virus it will be years before this is known with any accuracy. The federal Centers for Disease Control estimate that the proportion is between 5 and 19 per cent, although it could be much higher. As a consequence, and because the hospital costs of an AIDS patient average $147,000, those who test positively are in practice uninsurable.

Recent estimates of the number of people in the United States infected with the virus range from 500,000 to 2 million. The number of AIDS cases may reach 100,000 by 1989 if current trends continue, corresponding to claims under "life" (more accurately, death) insurance policies worth perhaps $5,000 million by the early 1990s. But if the insurance companies are able to deny insurance to those testing positively to the antibodies, many seeking new insurance in most of the United States are liable to find themselves being denied coverage.

AIDS is not unique; similar problems have been raised by other high-risk conditions such as diabetes and cystic fibrosis. A solution that has been adopted in nine states so far is the "high-risk pool", a special state-administered insurance scheme for individuals known to be bad medical risks. The pool is maintained by contributions from insurance companies in approximate proportion to the amount of business they do. Individual premiums are capped, typically at 150 per cent of the standard premium, ensuring that high-risk individuals can buy coverage.

Organizations representing victims of chronic diseases applaud such schemes, which allow their members to get insured. The insurance industry approves because it avoids divisive strains on individual companies. Ultimately, of course, other insurants still pay for the misfortunes of the high-risk groups. Congress should consider legislation that would effectively oblige other states to set up high-risk pools, bringing them into line with those that already have successful schemes. □

Who will pity Africa?

The plight of Africa commands attention, but throwing money in that direction is no solution.

THIS has been a bad week for Africa, but that is not unusual. The number of black Africans killed in the Republic of South Africa (mostly in intra-racial fighting) exceeds the number of those killed by radiation at Chernobyl. The death-toll among students in Nigeria, where most of the universities have been closed, is almost as great. The willingness of perhaps 20 million people elsewhere to run to raise funds for Africa is a moving proof that Africa can still stir the world's compassion; it is only natural that the organizer, Mr Bob Geldof, should be furious that the special session of the United Nations last week failed to echo his runners' enthusiasm. But Geldof's tirade last week against the "politicians", whom he alleges have neglected a golden opportunity to put Africa to rights, is thoroughly misplaced, at least so long as it stems from the assumption that Africa will become a Garden of Eden if only enough money is thrown at it.

The plain truth is that many of Africa's most serious problems have been created in Africa by Africans, and that only palliation of them is possible while these policies persist. The recent history of Africa is a sufficient proof of the validity of that charge. Ghana, relatively prosperous among African countries a quarter of a century ago on the basis of a successful cocoa-growing industry, is now among the poorest. Nigeria, rich more recently at the height of the oil boom, has squandered its brief wealth, becoming one of the world's major debtors. Uganda, already a kind of paradise in the early 1960s, has now settled for inter-tribal violence and the chaos that follows. Ethiopia, sadly ravaged by two years of serious drought, would have found that ecological catastrophe less damaging if the previous food distribution system had not been undermined by the government's ideological conviction that middle-men (admittedly a grasping lot) should be replaced by a public bureaucracy whose efficiency is notoriously below par, and which offers farmers prices that provide no worthwhile incentive to increase production. This same error is the rule elsewhere in Africa, East and West, where governments' attempts to keep their urban populations happy by fixing food prices at unrealistically low levels has contributed powerfully to the decline of agriculture, the hunger of those same urban populations and the dependence of potentially fertile Africa on food imports. Mr George Shultz, the US Secretary of State, was right to say, at last week's meeting of the United Nations, that poor Africa's governments should prudently mend their ways. Geldof and the many who contributed to international fund-raising should understand that as well.

This does not mean that there is nothing to be done. Africa's request of the United Nations last week was for an increase of aid by donor nations amounting to more than $80,000 million over the next four years, together with a moratorium on foreign debts that would cost about half as much. Given the need, the figures are not unreasonable. But there was never a chance that the rich countries would or could respond on such a scale.

Indeed, the years immediately ahead are likely to make the rich countries seem to Africans more skinflint than they have ever been, as the United States struggles to control its budget deficit and cuts its direct contributions to foreign aid in the process. Yet there are now enough illustrations of how development projects can succeed, even in Africa, to suggest that many of Africa's problems could be tackled successfully with much more modest sums of money. What is needed now is not a meeting of the United Nations at which politicians rehearse their government's well-known positions, but a practical clearing-house for the good ideas that have already contributed to the improvement of African conditions on a small scale, and which could, with the imagination and enthusiasm of the Geldofs of this world, be spread more widely. □

US research funds

Defense Department to shed unwanted monies

Washington

A FIGHT is brewing in the US Senate over provisions in a money bill to divert $80 million of defence research funds to support unreviewed research and construction projects at 10 named universities. The Department of Defense (DoD) has refused to allocate funds that Congress has already pressed upon it for the purpose, and support is growing for an amendment that would free the $80 million for competitively awarded research.

The disputed funds were added piecemeal to DoD's appropriations during the legislative process as rewards for political favours by influential members of Congress. None of the 10 named projects has been subjected to competitive merit review, and the favoured institutions are "not the sort of places where one would normally go" to find the best high-tech research, according to one DoD official.

Academic and scientific organizations are uniformly opposed to Congress awarding research and construction funds by political horse-trading. But most of the disputed projects are in the home states of members of Congress who occupy senior positions on key committees, and the effort to block them, to be introduced in the Senate by John Danforth (Republican, Missouri) will be hard fought.

Ten such "pork barrel" projects worth $65 million were provided for in DoD's 1986 appropriations bill, which passed Congress at the end of last year. Several of them, notably the $13.5 million proposal of Northeastern University for a research complex, consist mainly of buildings and look more like campus improvement schemes than defence research.

Defense Secretary Caspar Weinberger refused to spend the $65 million on the grounds that DoD had no legal authority to support construction projects from its research account, and that the sums were recommended, not mandated, in the bill.

DoD also invited the universities in question to submit research proposals that would be subject to normal competitive review; the reviews are still in progress. But Weinberger has also made plain that DoD would oppose non-competitive construction funding even if it had legal authority to spend the money. "It isn't a matter of legality, it's a matter of policy", says Robert Rozenzweig of the Association of American Universities, which has consistently opposed pork-barrelling.

In response to DoD's refusal, seven US Senators last month introduced wording into an emergency supplemental bill approved by the Senate Appropriations Committee that would, if approved by Congress, oblige DoD to spend the money anyway. In addition, the committee introduced a special provision that would allocate an extra $25 million for a proposed Center for Science and Engineering Technologies at Arizona State University. A spokesman for the university explained that the proposal was the consequence of efforts to help the university by Senator Dennis DeConcini (Democrat, Arizona).

A sum of $10 million that had been intended for a Floating Point Systems supercomputer at Cornell University was dropped after Cornell's president, Frank Rhodes, refused on principle to accept the grant unless it had been awarded by competitive review. Cornell's proposal is now being scrutinized by DoD; ironically, one DoD source close to the review process says that of all the original pork-barrel proposals, the supercomputer is the most likely to be successful in the review.

Pork-barrel provision have been used in numerous federal appropriations bills over the years to buy special favours for universities, but there is now alarm in the academic community over the unprecedented scale of the proposals in the 1986 DoD appropriation.

One previous attempt to defeat the pork-barrel provisions, led by Senator William Proximire (Democrat, Wisconsin) was defeated in the appropriations committee. But supporters of Danforth's amendment believe that the bipartisan support now emerging gives it a good chance when it is introduced on the floor of the Senate, probably in the first half of June. Among the supporters of the move is, surprisingly, Senator Barry Goldwater, the Arizona Republican who heads the Senate Armed Services Committee. DoD's stand might carry the day.

Tim Beardsley

Space launchers

Launch failure; boardroom fracas

THE failure of the third cryogenic stage of Ariane, Europe's space launcher, at the weekend, coming after the recent serious setback to the US space programme, has put the West's space launching capacity into jeopardy. It has also thrown into vivid relief the sacking just a couple of days earlier of the president of the company that makes Ariane rocket motors.

Ariane has now lost two out of its last three launches and four out of the past eighteen — the last two as a result of third-stage failure. Last week's launch was aborted with an Intelsat communications satellite aboard. A long investigation by an independent commission of all possible sources of error in the manufacture of the liquid hydrogen–liquid oxygen third stage will now be started, and delays to the programme now seem likely to be months rather than weeks. A complete redesign of the third stage engine might be necessary, so even longer delays are possible.

Strangely enough the president of the company, Roger Lesgards, was precipitately sacked last week in circumstances that suggest that the reasons may have been political rather than commercial.

M. Lesgards had been a close adviser of the previous minister of research and technology, Jean-Pierre Chevènement, and is thought to have been letting his feelings about the recent reductions of research support become widely known. Contracts with the government and government agencies are the chief source of work for SEP (Societé Européene de Propulsion).

Late last week, M. Lesgards had already quit his office and could not be reached at home, but he has made no secret of his anger at his treatment by the board of SEP. The company appears to be doing well commercially, having increased its turnover by 42 per cent in the year to October 1985 and having taken orders worth FF 3,000 million (£300 million) during last year. With half of the company's activity concerned with Ariane, whose commercial prospects have been strengthened since the shuttle disaster and failures of US Titan and Delta rockets, SEP's future seemed bright.

Lesgards' successor is M. Jean Sollier of the aerospace company SNECMA, another supplier for the Ariane programme. SNECMA happens to hold a marginal majority (50.14 per cent) of the shares of SEP, and there has recently been some friction over the rate and regularity with which SEP has been supplying components for Ariane.

Robert Walgate

• Meanwhile, Britain changed its mind last week about which rocket will launch the first Skynet military communications satellite. The Ministry of Defence can get a guaranteed launch date "several months" earlier by using Ariane, rather than the US space shuttle, to launch Skynet 4B, the first satellite in the series. It has therefore cancelled its booking with the shuttle and Ariane will launch Skynet 4B in late 1987 unless the latest setback calls for more changes to the schedule. The shuttle will still carry the next satellite, Skynet 4A, in 1988, and Ariane will carry Skynet 4C in 1989. □

Chernobyl

Fusion may be a better way

ONE lesson to be learned from last month's nuclear accident is that there should be a renewed effort in thermonuclear fusion. This was the opinion offered last week by Academician Evgenii Velikhov, vice-president of the Soviet academy and a member of the investigating commission at Chernobyl, speaking at a press conference in Moscow.

The same point was echoed at an international conference on nuclear technology in Yalta last week. Academician Boris Kadomtsev, director of plasma physics at the Soviet Atomic Energy Institute, called for greater international collaboration in the field. The Soviet Union is a partner in the International Atomic Energy Agency's project for the design of a thermonuclear reactor and also has a number of bilateral agreements on collaboration on fusion work.

The main emphasis of Velikhov's statement was that the clean-up operation at Chernobyl has presented those involved with unprecedented problems. Little had been done in advance, he said, to construct models that would assist in the management of the damaged reactor, while such data as were available were often contradictory. The mound of concrete, lead and boron under which the damaged Number 4 reactor is now buried prevents access, so that it will be necessary to estimate its future behaviour by extrapolation. Even so, it appears that it has been possible to install sensors for temperature and radiation intensity in and around the reactor.

After the burial of the reactor, the main task has been, according to Velikhov, that of trapping airborne particles, for which purpose a special film of polythene has been used. Velikhov added that, in any case, only a "certain percentage" of the fission products in the reactor core has reached the atmosphere.

As the most urgent problems were dealt with, others emerged. As well as the pollution of agricultural land and livestock, the forests of the Polessye region and their wildlife aroused concern. These forests — mostly managed plantations of conifers (although the original tree-cover was deciduous) — appear to have taken the brunt of the pollution. Valerii Brezhnev, deputy minister for forests of the Ukranian SSR, said last week that many plantations will have to be felled and the clearings ploughed up, while veterinary monitoring of wild animals (elk, roe deer, boar and other species) has begun.

Boris Paton, chairman of the Ukranian Academy of Sciences, also said last week that there are plans for establishing "artificial geochemical barriers" on the "migration paths of radionuclides in the groundwater". The river Pripyat' and the Kiev reservoir were mentioned specifically. Paton was presumably referring to techniques more specific than the emergency mechanical barriers thrown up to prevent the run-off of rainwater from Chernobyl into the river Pripyat', and which were said to have been completed two weeks after the accident.

On the future of nuclear energy in the Soviet Union, there seems to be a conflict of opinion. The first deputy minister for electrification of the Soviet Union, Alexsei Makukhin, said somewhat offhandedly last week that the accident at Chernobyl had been a "hitch" in the "mastering of the atom". Velikhov was more cautious, saying that although it is unlikely that reactors of the Chernobyl type will be closed down, "it is unlikely that they will stay in the same form".

Vera Rich

Counting the score on transplants

Washington

PROFESSOR Robert Gale, normally to be found at the University of California, Los Angeles, but who has spent most of the past month in Moscow carrying out bone marrow transplantations on victims of the Chernobyl accident, has contributed an account of the present status of marrow transplantation to a new journal *Bone Marrow Transplantation*, first published this week. Gale estimates that there will be some 2,500 transplantations worldwide during 1986, not many fewer that the 4,000 such operations reported to the International Bone Marrow Registry during the past decade.

Radiation exposure is a comparatively rare cause for transplantation, which is most commonly used in the treatment of leukaemia and other diseases of the blood-forming process. The international registry is meant as a means by which data about the effectiveness of transplant operations can be compiled and compared.

Gale's article, which is the first in the new journal, cannot fail to be widely read by those elsewhere than in the Soviet Union who are concerned to know what part marrow transplantation should have in case of future nuclear accidents.

The new journal, published by Macmillan from the United Kingdom, is meant to be a quarterly in the first instance. The editor is Dr John Goldman from the Medical Research Council's leukaemia unit at the Royal Postgraduate Medical School, London. Dr Gale is the journal's co-editor for the United States and Canada. □

British universities

Reputation by repute

BRITISH academics learned last week a great deal more about the reasons why their institutions had done relatively well or badly in the carve-up of the public subsidy for the impending academic year (see *Nature* **321**, 459; 1986). The explanations are contained in letters sent to the heads of academic institutions by the University Grants Committee (UGC), and together constitute the most detailed survey of the state of British universities ever.

The two successive sheaves of letters are the first steps in UGC's policy of concentrating resources considered to be inadequate on what are deemed to be the institutions of the highest quality. In this first stage, UGC has made relatively modest steps in that direction, but in the autumn a further word-processing exercise will tell universities what they can expect to receive from public funds in the succeeding three academic years (1987–90).

Apart from providing universities individually with a inkling of how the harsher winds will be blowing in the autumn, last week's letters give the university system as a whole warning of far-reaching and unexpected structural changes. In particular, it is now clear that UGC intends to give less on account of the cost of student education to universities (Oxbridge and some others) organized in a collegiate fashion, and that it will in future exercise its right to deal individually with the member institutions of federal universities.

The first change arises because the collegiate universities and the several colleges to which students are required to belong are able to charge separate tuition fees, mostly paid in respect of British students by local education authorities. The universities chiefly concerned are Oxford and Cambridge, but Durham, Kent, Lancaster and York charge similar but smaller fees. By deciding that half the income derived from college fees should be subtracted from the annual recurrent grant, UGC is in the short run releasing funds to spend in universities under greater pressure. With the prospect that the time will come when British students' fees will not automatically be paid by local authorities, UGC is requiring Oxbridge to choose between conformity and the privatization of at least their collegiate functions.

Last week's sheaf of letters also explains why both Oxford and Cambridge were placed below the middle of the previous week's league table, with increases of cash income of zero and 0.7 per cent respectively, compared with the average for the system as a whole of 1.0 per cent.

UGC's decision to circumvent the

federal structure of the University of London by providing its constituent colleges with an account of what the future holds for them (the University of Wales has always been dealt with in this way) is also potentially far-reaching, and could presage the break-up of the university. Imperial College has been able to talk directly to UGC since the early 1960s, but the other member colleges have had to wait on the university court for the reallocation of UGC's grant to the university as a whole. Now that the university has been reorganized into only five general colleges and the number of its medical schools is shrinking by almagamation, the proof of the case for the contiuation of what is widely thought to be an inefficient system will fall to the central organization.

The consequence of last week's letters from UGC which cannot as yet be calculated is the effect of its opinions on student recruitment. All university departments have been categorized on the basis of their research performance as average, below average and above average, while departments whose research attainment is judged to be of international character are singled out for special mention. UGC has said separately that it will attempt to categorize departments by the quality of their teaching when there are tools available for carrying out that task. Meanwhile, however, it must be expected that students will flock to the departments praised by UGC and will shun the others, which may accelerate the selectivity exercise.

Many academics are complaining that the time remaining between now and the autumn is not sufficient for the implications of UGC's judgement to be grasped. A crucial unknown quantity is whether the new Secretary of State for Education and Science, Kenneth Baker, will be able to wring extra funds from the Treasury. Nothing was heard of Baker last week. □

• The grant for 1986–87 for the University of Essex has not been reduced (as reported last week) by 0.5 per cent but, rather, increased by 1.7 per cent.

Chilean physicians

Campaign against torture grows

Philadelphia

CHILEAN physicians are leading a new national movement demanding an end to the dictatorship of General Augusto Pinochet. The Chilean Medical Association (Colegio Medico de Chile, CMC), which has for the past four years been investigating and exposing physicians' cooperation in torture by the security forces, has been joined by 17 other professional organizations in a new national assembly (Asamblea Nacional de la Civilidad) that is calling for immediate national democratic elections. With the expiration last week of the assembly's 31 May deadline for its demands, CMC is likely soon to be at the centre of an escalating series of strikes.

The president of CMC, Dr Juan Luís González, and its general secretary, Dr Francisco Rivas, were in Philadelphia last week at the annual meeting of the American Association for the Advancement of Science (AAAS) to receive on behalf of CMC the AAAS award for scientific freedom and responsiblity. AAAS has been monitoring human rights in Chile since the early 1980s. The award was shared with Dr Victor Paschkis of the United States, who founded the Society for Social Responsibility in Science.

CMC was honoured for its efforts to track down physicians who cooperated in torture of government prisoners during the 1970s. Some 10,000 civilians, including 80 physicians, were murdered by the secret police or disappeared in the period between 1973 and 1978, and the use of torture is said to have been widespread.

CMC represents 14,000 physicians, more than 90 per cent of Chile's total. It was run by puppet officers appointed by the government until 1982, when Pinochet gave in to demands for election of officers in order to avoid a showdown with the profession. González and Rivas, who head a council of 23 members, were elected on a three-point platform of solidarity in the profession, peaceful protest against the government's health policies, and investigation of physicians who participate in torture.

As a result of the torture investigations, two physicians, Luis Losada and Manfred



Jurgensen, have been expelled from the association. They admitted examining and certifying as healthy a government prisoner, Frederico Alvarez, who had been tortured and who died a few hours later from respiratory insufficiency due to multiple rib fractures. Two other members of the association accepted suspension for a year for examining a blindfolded prisoner who was being forced to remain standing, and CMC is continuing investigations of five others.

Rivas suspects that between 70 and 80 CMC members have cooperated in government torture, although in most cases firm evidence is lacking. The association conducts its investigations by examining court records (many of the torture deaths have been examined by the judiciary, although usually to no effect) and by interviewing torture victims or their families. In addition, files left over from the period when CMC was a government organization have provided many clues; the outgoing puppet officials apparently made no attempt to destroy evidence that would help the new CMC council.

Rivas stresses that those under investigation are allowed to retain the lawyer of their choice, at CMC's expense if neccessary. Penalties are recommended by CMC's ethics committee and are decided finally by the full 23-member council.

After the most brutal period of Pinochet's rule in the 1970s, there was a lull in political repression in Chile during the early 1980s. But, according to Rivas, the reemergence of organized opposition parties and the end of a temporary economic boom has increased discontent, so that repression is once again on the rise. Recently the Reagan administration has backed away from its policy of "quiet diplomacy" towards Chile, and spokesmen have started to refer to the administration's opposition to dictatorships both of the left and the right.

CMC has already held one and two-day strikes of its members to protest against the government's summary dismissal of the head of Santiago Medical College, Dr Ricardo Vaccare. According to Rivas, a neurosurgeon in private practice whose work for CMC is unpaid, 85 per cent of members supported the strikes. It is therefore not surprising that CMC's activities have attracted the government's unfavourable attentions. Rivas says that CMC officials frequently receive anonymous death threats to themselves and their families and are often shadowed by secret police. In recent months CMC's headquarters in Santiago has been under constant overt police surveillance.

Among the organizations supporting CMC in calling for a return to democratic rule is the National Association of Academics of Chilean Universities. CMC has received expressions of moral support from most major national medical associations, although representatives of governmental organizations such as the World Health Organization have declined to offer their support for fear of compromising their impartiality. But the medical profession has already become a significant political force in Chile. Supported or not, physicians seem determined to make a still larger impact. **Tim Beardsley**

SDI

Congress embraces restraint

Washington

NEARLY half of the US Senate has signed a letter criticizing the rapid increase of the budget sought by the Reagan administration for the Strategic Defense Initiative (SDI). The administration is asking for a 77 per cent increase in SDI funds for 1987.

The letter was addressed to Senator Barry Goldwater (Republican, Arizona), chairman of the armed services committee, which will be taking up the SDI budget request this month. The 35 Democrats and 9 Republicans say they are concerned that SDI has received "excessive and inappropriate emphasis" in the Department of Defense (DoD) budget request, threatening "vital" military research programmes.

While expressing support for "vigorous" ballistic missile defence research, the senators worry that the SDI research programme is being rushed in an attempt to meet unrealistic deadlines. The administration hopes that a decision about SDI deployment will be made in the early 1990s.

Support for SDI this year is set at $3,050 million, of which $2,760 million comes from DoD and the rest from the Department of Energy (DoE). For next year, the administration is seeking $5,400 million for SDI — $4,800 million to go to DoD and $600 million to DoE. The senators argue that SDI funds have out-paced technological progress, and that a 3 per cent increase, allowing for inflation, will keep the programme going on an even keel.

The House of Representatives may take an even more restrictive approach to the SDI budget. Representative Charles Bennett (Democrat, Florida), a member of the House Armed Services Committee, believes there is backing for a freeze at the present year's level of support. This committee will also be considering the SDI appropriations request this month.

The White House has reacted quickly to this rebuke from the Senate. The President's spokesman Larry Speakes said the administration "disagrees strongly" with the letter's recommendation, and urged Congress to support the President's budget request.

In future, the administration should have a new ally in its battle for support of SDI. The Science and Engineering Committee for a Secure World, comprised of some 77 scientists and engineers, believes SDI deserves the "full support of the scientific community, Congress and the American people". Fred Seitz, president emeritus of Rockefeller University and acting chairman of the committee, says the group was formed in response to recent efforts by academics opposed to SDI (see *Nature* **321**, 369; 1986). Spokesman John Kwapisz says that one of the committee's chief goals is to correct the growing public misconception that all scientists and engineers oppose SDI. But with no financial support and no clear agenda for the future, Seitz says he cannot tell how large a part the committee will play in the debate over SDI.

Joseph Palca

Laser cut down to size

LOCAL residents in the predominantly rural and conservative area of California in which the Lawrence Livermore Laboratory is located have forced the laboratory to modify its plans to build a free-electron laser (FEL) too big to fit within the laboratory fence. A high-level panel under Dr George Dacey, president of the Sandia National Laboratory, has been convened to settle the issue.

The Livermore FEL is part of the development of the Strategic Defense Initiative (SDI) and in its original form would have cost $1,000 million. The device was to have been a 300 MeV induction linac (linear accelerator) designed to produce 1 μm radiation at a power of 100 MW.

Local opposition to the proposal to extend the laboratory's perimeter fence to accommodate such a large machine has led Livermore to propose a new plan for two FELs operating at half the linac voltage (150 MeV), one at the laboratory and one at the army range at White Sands, New Mexico. The second FEL would be capable of being upgraded to 300 MeV.

Enthusiasm at Livermore for free-electron lasers as part of the SDI programme stems from the recent success of the 1.5 MeV induction linac at Livermore, at which 40 per cent of the beam energy is converted into 3 cm radiation. The larger versions would incorporate long tapering "wiggler" sections for generating radiation output by the motion of fast electrons through a corrugated magnetic field.

Among the outstanding problems are the construction of a pair of laser mirrors separated by 4 km so as to match the linac beam. Another problem faces the "second" FEL — apparently neither Livermore nor the US Army will accept responsibility for its maintenance.

Livermore is now the main centre in the United States for military FEL research, with a budget of $80 million a year. As with many other SDI elements, supporters argue that recent developments constitute a major breakthrough; opponents of the ground-based FEL system say it would be, at best, cumbersome and vulnerable. □

Neolithic Jericho

Ancient wall theory teeters

Rehovoth

HEBREW University Professor Ofar Bar-Yosef seems bent on seeing the walls of Jericho come tumbling down again. Bar-Yosef says that the structure identified by the British archaeologist, the late Dame Kathleen Kenyon, as part of a mediaeval city wall, was in fact part of a flood control system used by farmers to control the flow of water from neighbouring wadis. If confirmed, this may mean that Jericho was not the world's first walled city.

This development has emerged from a programme of research that has thrown new light on the first use by farmers of cereals in the Middle East. Bar-Yosef has, for example, excavated from the site of another Neolithic village at the brief settlement of Netiv Hagdud, 15 km to the north of Jericho, samples of carbonized grain which, according to Mordechai Kislev, contain both wild and cultivated barley dating from the period 8,200 BC to 7,500 BC.

The fact that both wild and cultivated barley were found at the same site suggests that both were growing there 10,000 years ago. Bar-Yosef believes that his new find is the earliest record of the use of cultivated cereals, and he believes that wheat as well as barley was part of the Neolithic farming pattern. By the biblical era, the use of cereals was sufficiently well established to support the well-known statement in *Deuteronomy* that "Man doth not live by bread alone...".

Several research groups in Israel are involved with the search for the origin of modern cereals. Since the discovery almost exactly eighty years ago of a surviving primordial wild wheat plant growing out of a crevice in a rock near the village of Rosh, in what was then Turkish Palestine, much has been done to conserve these ancient plants. The agronomist Aaron Aaronsohn who found the first plant, followed by others in Syria and trans-Jordan in succeeding years, had hoped to transfer some of the genetic characteristics of the wild wheat to the commercial strains, but breeding techniques at the time were not good enough. But now Professor Moshe Feldman at the Wiezmann Institute, by manipulating chromosomal segments, claims to have incorporated some of the ancient genes into commercial strains of wheat that yield as much as existing varieties but boast a protein content up to six per cent greater.

Meanwhile, Feldman and his colleagues are asking that the existing fields of wild wheat will be carefully fenced off so as to preserve the pristine genetic constitution of the plants.

Nechemia Meyers

Japanese psychiatry

Fetus research criticized

Tokyo

ARGUMENT over the rights of psychiatric patients in Japan has resurfaced with the release of a report from the Japanese Society of Psychiatry and Neurology's human rights committee. The report censures the conduct of an experiment on a fetus aborted from a schizophrenic woman. The "human experiment", performed at Gifu University, is seen as a test case by those critical of current psychiatric practice, as is spelt out in a letter from one of their representatives in this issue of (see page 556).

There is general agreement only on the bare facts of the Gifu case. The patient concerned was a 34-year-old schizophrenic woman with a long history of mental illness. She was admitted to a Gifu hospital in January 1984 and found to be about five months pregnant. Shortly afterwards she was transferred to Gifu University Hospital where the pregnancy was terminated. The fetus was dissected and its brain examined for the effect of the drugs the woman had been taking.

It was not until May 1985 that the case attracted the attention of the press. It was alleged that the woman had been forced to undergo an abortion simply so that the doctors could experiment on the fetus. Those critical of psychiatric conduct quickly labelled the case as an example of the "research supremism" that leads psychiatrists to view patients merely as opportunities to further their academic careers. Protests over the case grew to such an extent that fear of violence led the Japanese Society for Biological Psychiatry to cancel a meeting that was to have been held at Gifu with doctors involved in the experiment present.

Two invited foreign speakers also had to abandon their talks even though they were moved to a secret venue. Both speakers have expressed their views in *Nature* (**319**, 172; 1986; and **320**, 392; 1986). They had been told that protesters were radical "anti-psychiatrists" who frequently disrupted meetings with violence and that Dr Moriyama of Tokyo University who was their *de facto* leader. Dr Moriyama has clearly rejected the label of "anti-psychiatrist" for himself and denied any violent intent on the part of Gifu protesters (*Nature* **318**, 308; 1986).

Did the Gifu case involve malpractice? On the evidence supplied by the Gifu doctors alone there is no reason to think so. They say that the woman was admitted to hospital because she was showing schizophrenic symptoms; that she freely chose to have an abortion because of the difficulties she would face in bringing up a child; and that the idea of examining the fetus came up only after the woman had decided to have an abortion.

The Society of Psychiatry and Neurology's report does not accept this view of events and raises some fresh ethical issues. In the committee's view there was evidence that the woman wished to have the baby and that she had been pushed into receiving an abortion: "informed consent" had not been properly obtained. There were also suspicions that admission procedures had not been properly observed. Finally, consent to the fetal experiment was not obtained from the patient, only from her mother.

Further problems stem from the experiment. Japan is without clear guidelines for such experiments so criticism was made in the light of foreign guidelines, principally there of Britain's Department of Health. Here it is made clear that a living fetus retains its rights even if it is going to die in an abortion — thus a pregnant patient should not be allowed to take a drug that could harm the fetus, even if an abortion has already been planned and even if the doctors would like to know what the effect of the drug on the fetus would be. It is not clear whether the Gifu doctors agree with this point, and further public discussion of the issues involved is called for in the report.

What is certain is that there is a need in Japan for clear research guidelines for those who perform experiments involving human beings. At least reform is now in the air. The legal rights of psychiatric patients (or the lack of them) has already become a topic of international concern and the Ministry of Health and Welfare has promised to produce changes in the law by next spring. Ethical committees are now appearing in hospitals and increasing numbers of doctors are involved in providing alternatives, such as community care, to the long stays in isolated mental hospitals that are a much criticized feature of the Japanese psychiatric system. Soon, the present controversy may be seen as one step towards an improved psychiatric care system. **Alun Anderson**

***Nature* in Tokyo:** next week (9 June) David Swinbanks takes over from Alun Anderson as *Nature's* Tokyo Correspondent.

Ageing research

Japan faces the old old problem

Tokyo

A NEW study from Japan's Council for Science and Technology tackles the nation's most serious long-term problem — its rapidly ageing population.

At present Japan has relatively few people over 65 compared with those in the working population; European countries and the United States have to divert a far larger percentage of their economic resources to care of the aged. But in 15 years' time the situation will have reversed. By the year 2000, one out of every five Japanese will be more than 60 years old. And by 2025 there will be two and a half times as many elderly people per worker as at present. The trend is a result of the remarkable longevity achieved by the Japanese coupled with a declining birth rate.

The government is already planning changes in health insurance and pension laws to ensure that it is not saddled with a bill it cannot pay in the next century The proposals from the Council for Science and Technology are complimentary changes in the scientific field and are expected to serve as guidelines for the next ten years. The council, directly answerable to the prime minister, is the top government policy body and all government ministries are expected to begin promoting research according to the guidelines. A likely outcome is the establishment of a new research centre for the study of ageing, perhaps equivalent to the US National Institute of Aging.



Senile dementia is likely to be the main research topic. In Japan around 5 per cent of the over-65 age group (more than 600,000 people) suffer from senile dementia, causing serious social problems. This total will double by the end of the century. Some means, the report says, must be found to enable old peole to live healthy and independent lives to maintain the national economy. Some forms of senile dementia are largely due to cerebrovascular disorders and there have already been successes in treatment. Research will focus on finding methods of early diagnosis when chances of recovery are high. The causes of other forms of senile dementia are still unknown. Alzheimer's disease, already a major problem in advanced countries with large populations of the elderly, will be another major research topic, as will improved methods of nursing. **Alun Anderson**

Yellow rain

Another treaty threatened

Washington

THE Canadian government last week reluctantly released new information casting further doubt on charges that the Soviet Union has engaged in biological warfare in South-East Asia. The new data show that trichothecene toxins, claimed to be the toxic agent in yellow rain, can be found in individuals who do not report being exposed to yellow rain attacks.

The data were collected as part of a Canadian effort to monitor the use of biological and chemical weapons. A spokesman for the Canadian Ministry of External Affairs said investigators obtained 272 blood samples in 1984 from different locations in Thailand. By early summer 1985, Agriculture Canada had analysed all the samples using gas chromatography and mass spectrometry. Blood from five individuals in three different locations showed signs of trichothecene toxins T-2 and HT-2 ranging from 2 to 76 parts in 10^9. The analysis also correctly detected 7 of 8 control blood samples that had been spiked with 100 parts of 10^9 of trichothecene toxins.

Although the Canadian government has had the results of the analysis for more than a year, government officials are quick to deny that the information was being supressed. Ron Cleminson for the Ministry of External Affairs explained that the information is for a report to the United Nations on arms-control verification procedures, and was never intended as a study on toxin poisoning.

Officials from the US State Department had no specific comment on the Canadian data. But department official Tom Reich says that the United States still maintains that the Soviet Union engaged in biological warfare in South-East Asia in the early 1980s. Unofficially, however, a government official did say that the new data should have a profound effect on the US position.

The past few weeks have seen a spate of new data on yellow rain. Reports from both Canada and the United Kingdom found insignificant levels of trichothecene toxins in yellow rain samples (*Nature* **320**, 699; 1986 and **321**, 459; 1986) gathered in 1982. Matthew Meselson of Harvard University, a principal author of the theory that yellow rain is not a biological weapon but rather mass bee defecation, believes that the Canadian evidence makes the US position untenable.

The latest controversy comes as the United States is preparing to attend the Geneva conference reviewing the 1972 Biological Weapons Convention. Hailed as the first step on the road to true disarmament, the treaty requires signatories to destroy existing stockpiles of biological weapons. It further prohibits any future development of production of biological agents that have no justification for "prophylactic, protective or other peaceful purposes".

The United States now takes the position that the Soviet Union has violated the terms of that treaty. In addition to charges that the Soviet Union has used biological weapons in South-East Asia and Afghanistan, the US government also believes that the Soviets have a biological weapons programme under way at a research facility near Sverdlovsk. But James Leonard, former US disarmament negotiator who negotiated the 1972 treaty, says the United States has made charges that "cannot be substantiated." To reverse the present climate of mistrust, Leonard recommends steps to encourage communication among the superpowers, such as an international registry of high-containment laboratories and greater participation in international scientific exchanges. While there is no indication that the treaty will collapse, Leonard believes the prospects for strengthening or expanding it in the fall review are nil.

Joseph Palca

French research

Chevènement's expected outburst

JEAN-Pierre Chevènement, the architect of the past administration's buoyant policy on research, last week accused France's new government of "unilateral disarmament in the economic war". He was referring to the cuts on science spending which flow from the conviction of the right-wing Prime Minister, M. Jacques Chirac, that reduced public spending will revitalize the economy by releasing private enterprise from tax burdens.

Chevènement's complaint, published in *Le Monde* last week, stems from his belief that world competition now threatens "whole economic and social systems" and that research is particularly important, and will "more and more decide the winners". So, says Chevènement, the Chirac government's transformation of real growth of four per cent a year in science spending into a four per cent cut was "a grave blow".

Chevènement fears that the new government is allowing the "two conservatisms" against which he had to battle to reestablish themselves. One conservative influence is industry, where only 100 companies employ more than 50 researchers and only 1,500 have any at all. The other is the academic community, which Chevènement fears may abandon its flirtation with industry and retreat to its old ivory towers.

Chevènement has a kind word for General de Gaulle, who he says was the only president before Mitterrand to recognize the importance of research, but who took ten years (1958–68) to make an economic impact with it. But the Mitterrand–Chevènement policies have now been "halted in mid-stream", while power has now returned to those who, under President Pompidou, presided over a steady decline of scientific output. Chevènement quotes Pompidou as saying that, of three ways to lose money "the most agreeable is women, the most rapid gambling, and the most certain research".

Chevènement also credits the new minister of research and higher education, Alain Devaquet, for "courageously defending" the research councils against dismemberment. On the break-up of his own ministry of research and technology, Chevènement said that it would not now be possible to establish joint programmes across research institutions. What Chirac has dismembered is the "ministry of the future".

Robert Walgate

Optical computer in sight

Edinburgh

A GALAXY of stars of European science politicians gathered at Herriott-Watt University in Edinburgh on Monday to celebrate what former French science minister Pierre Aigrain described as a "spectacular" success along the road to the development of an entire optical computer.

EJOB, the European Jount Optical Bistability programme, has cost just 1.8 million ECU (about £1.2 million) over two years but it has stimulated 20 research groups around Europe to produce what was first demonstrated in Edinburgh this week — broad-band optical switching and a basic "classical finite state machine" (the guts of a computing engine) using nothing but lasers and nonlinear optical material. "Massively parallel" optical image processing and new forms of laser-driven television are also just plausible.

Professor Desmond Smith of Herriott-Watt University and leader of the EJOB project, says the programme could absorb a tenfold increase of funding to 10 million ECU per year, but the European Council of Ministers, meeting in Luxembourg next Tuesday, has yet to be convinced of the need for an increase. Parliamentarians at Edinburgh agreed, and pressure is now increasing on European ministers, to divert a small part of the enormous Commission agricultural policy funding to science and technology. Robert Walgate

Beckman anniversary

Analysing profitable research

Fullerton, California

AT the age of 86, Arnold O. Beckman still has his sights set on the future.

Beckman launched his corporate career with the innovation of the *p*H meter in 1935. Many years and many millions of dollars later, the founder and chairman of Beckman Instruments still considers himself more a scientist than a businessman. Today, with his $1,000 million company safely tucked under the Smith Kline Beckman wing, the former chemistry professor from the California Institute of Technology spends most of his time and money supporting programmes that he hopes will shape scientific enterprise in the years to come. He has contributed more than $100 million in the past decade, nearly $70 million in the past year alone.

Last month, at the festivities to mark the company's 50th anniversary, Beckman spelled out his formula for keeping science in the United States alive and well. The key ingredient, he says, is education.

Of the US education system, Beckman says "we've got a big repair job to do". He sees education as a dynamic, rejuvenating escort that directs an individual throughout his or her lifetime, and he feels that the present structure of higher education misrepresents that vision. "This strange idea of dividing education into four-year packages", he says, blurs the mission of college education, which is "to teach people how to learn".

Beckman maintains that degrees awarded at the conclusion of an arbitrary period of time give the impression that education is a static commodity. The one big advantage to be gained from having a PhD, he claims, "is to realize it doesn't mean anything. I've seen PhDs who are nitwits."

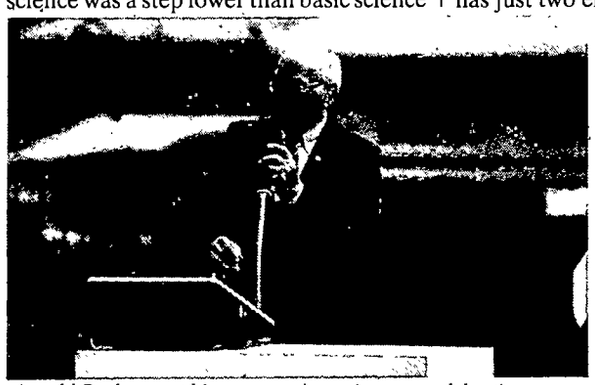
How would he restructure higher education? "Like a department store" that people would patronize whenever the need for a particular item arose, not like a remote citadel whose doors shut firmly behind those who graduate.

Certainly Beckman's own career has been spurred on by insatiable curiosity. A blacksmith's son from Cullom, Illinois, he had built his own chemistry laboratory before he reached his teens. He graduated first in high school class and, within four years, earned both bachelor's and master's degrees in chemistry from the University of Illinois. A brief spell at Bell Laboratories gave Beckman the electronics background he would later exploit in instrumentation design. In 1928, when Beckman received his PhD in photochemistry from California Institute of Technology, the institute invited him to join the faculty.

Beckman and his wife Mabel were settled at Caltech when, late in 1934, one of Beckman's fruit-growing friends asked him to build a device to measure the acidity of lemon juice. Within a few months, Beckman had developed the "acidimeter"; the term *p*H had not yet been established.

By 1939, Beckman's instrument had spawned a business that demanded a full-time manager. Beckman left Caltech, not without considerable deliberation, to pour his energy into National Technical Laboratories, Inc., which eventually became Beckman Instruments. A year later, his company began marketing the model DU quartz photoelectric spectrophotometer, the Helipot potentiometer, and a portable oxygen analyser. These three products guaranteed the company's success, and by 1966, Beckman had received a business statesman award from Harvard Business School of Southern California.

Beckman's philosophy on research echoes his personal experience. "The end result of research is to find out something useful", he says. "The days when applied science was a step lower than basic science are gone." For Beckman, academic research should not be spiked with financial incentives from outside an institution. Unless patent proceeds go to the individual's employer, a researcher will find himself "working for two masters".



Arnold Beckman at his company's anniversary celebration.

Patent royalties aside, Beckman expresses concern over the lack of reliable sources of research support. "We've been too affluent", he laments. "The money (for research) comes from the public, but look at what the public is interested in; look at the salaries they pay someone for throwing a few baseballs over a plate. I'd like to see a small percentage of the GNP automatically devoted to basic research." Beckman also advocates industry support in the form of cooperative arrangements. These are in industry's best interests, he contends, because industry needs academic links.

Since the 1982 merger with Smith Kline Corporation relieved Beckman of many of his executive responsibilities, he has been kept busy practising what he preaches. Last month Caltech students, faculty and trustees gathered for the dedication of a $6.5 million chemistry building established through a Beckman donation. Beckman had previously remembered his alma mater with $7 million for an auditorium and behavioural biology laboratory. A $3.5 million gift created the Beckman Laser Institute and Medical Clinic at the University of California, Irvine and another $3.5 million set up a vision centre at the University of California, San Francisco.

Beckman also donated $10 million to form the City of Hope Beckman Research Institute; Stanford University received $12 million to erect the Arnold and Mabel Beckman Laboratories of Biochemistry. Finally, Beckman outdid himself last October with a $40 million gift to the University of Illinois, the largest amount ever given by any individual to a public university (see *Nature* **317**, 568; 1985).

Although Beckman suggests that he is "not a generous man", this lack of generosity has saddled him, to his dismay, with the label of philanthropist. Today Beckman distributes his beneficence through the Beckman Foundation, which has just two employees, Beckman and his secretary, and which receives 1,300 proposals every year.

Despite Beckman's apparent nonchalance about his benefactions, he shrewdly manipulates his wealth to promulgate his philosophy. He supports only proposals that fit his criteria for the successful research community. Beckman encourages interdisciplinary interaction, which he thinks will become imperative as science becomes more complex. He also looks for a steady "infusion of young brains, people who don't know what you can't do".

Tempering his confidence in the saving powers of science, Beckman is also keenly aware of the thorny problems it thrusts upon society. Last November, Beckman gave the National Academy of Sciences and the National Academy of Engineering $20 million for a west coast headquarters to study and adjudicate the ethical and social challenges posed by scientific advance (see *Nature* **318**, 97; 1985).

Vital to Beckman's action-oriented formula, however, is one component that cannot easily be institutionalized: enthusiasm, which he considers the best motive for any endeavour. "If you're not enthusiastic about what you're doing, you're probably doing the wrong thing", says the spirited octogenarian. By that measure, Arnold Beckman must be doing all the right things.

Karen Wright

State of Japanese psychiatry

SIR—I have read the letters from T.J. Crow (*Nature* **319,** 172; 1986) and D.P. van Kammen (*Nature* **320,** 392; 1986) and greatly appreciate the interest shown by both authors in my letter on the deplorable situation in Japan's psychiatric hospitals (*Nature* **318,** 308; 1986). I should like to repeat once again that the protest action taken against the seventh congress of the Japanese Society for Biological Psychiatry was not directed against either of these visiting scientists.

The reason for the protest was that, in Japan, the scientists responsible for experiments involving humans often refuse to acknowlege criticism. As they remain silent and avoid discussion, concerned people have to resort to protest. Such action is then sensationalized and described as "violent". Protest actions are not illegal and it is regrettable that this is their only response.

This year, on 27 March, we were able to carry out a discussion in the assembly hall of the eighth congress on biological psychiatry held in Kanazawa. We discussed with many members of the society the problem of the previously mentioned experiment on a human fetus carried out by Dr Namba and his colleagues. The doctors actually involved in the experiment did not participate in the discussion. Dr N. Hatotani, the chairman of the board of directors of the society, answered written enquiries supplied beforehand and commented that the experiment of Dr Namba was not to be censured so much. However, the discussion made clear that the investigation carried out by the society into Dr Namba's experiment was inadequate. The society had heard about the experiment from Dr Namba but did not listen to the views of those who had brought up the ethical problems of the experiment. We suggested this was biased and criticized such a method of investigation. Dr Hatotani promised further investigation and discussion.

It seems to us that the measure taken by the society on the ethical problem is quite inadequate. Professor Hidebumi Hazama of Tottori University, a member of the society, has already thrown doubt on the existing ethics of biological psychiatry in Japan and has suggested the need for a system of ethical committees. He had expected the society to take a more positive and serious attitude in this respect (*Seishin igaku* **27,** 118–119; 1985).

We also hear that the president of Gifu University orally admonished Dr Namba and other staff in February 1986 about inadequate procedures in an experiment on a human fetus. In the near future, we expect the *ad hoc* committee of the Japanese Society of Psychiatry and Neurology to make a report on that experiment.

I have previously stated that some of the published summaries of papers that were to have been delivered at the 1985 Gifu congress provided evidence of unethical conduct. As requested, we will send these summaries to Dr Crow and Dr van Kammen along with several articles on ethical issues in Japan. In my opinion, in order to assess these papers, it is necessary to be conversant with the real background of such research in Japan, for example the very low standing of patients compared with that of doctors, the difficulty of peer review owing to the absolutism of some professors, the closed character of psychiatric departments to avoid discussion and investigation of their research and so on. Such a situation is far from that envisaged in the *Proposed international guidelines for biomedial research involving human subjects* (CIOMS/WHO, Geneva, 1982).

I sincerely hope that Dr Crow and Dr van Kammen will understand the actual state of Japanese psychiatry. I would advise them both to investigate especially the experiments carried out by Dr Namba and his colleagues and to refer to the more detailed report of the *ad hoc* committee of the Japanese Society of Psychiatry and Neurology which we will send them as soon as possible.

KIMIO MORIYAMA
(Acting chairman)
Psychiatrists Union
of Tokyo University,
7–3–1 Hongo, Bunkyo-ku,
Tokyo,
Japan 113

Dutch legislation

SIR—Your leading articles have frequently highlighted developments in the United States and the United Kingdom concerning ethical and legal aspects of the use of animals in research. New regulations, based on the 1977 Act of Animal Experimentation, recently became effective in the Netherlands.

From 1 January 1986, institutes in which animal experiments are performed require a government licence, issued only if and when a number of conditions are fulfilled. One of these is that the welfare of the experimental animal must be supervised by a specialist in laboratory animal science. This officer, who is on the payroll of the institute, is a veterinarian or biomedical scientist who has taken a one-year postgraduate course in laboratory animal science and who also has some years' experience in this field. He or she reports to the director of the institute and also to the Inspectorate of Veterinary Public Health. If the animals endure extreme and/or unnecessary discomfort, the inspectorate may advise the Minister of Public Health to withdraw the licence.

A unique provision is that the scientists responsible for animal experiments must have taken an introductory course in laboratory animal science. This applies to all scientists who began animal experimentation after 2 July 1985. Courses in laboratory animal science are now being incorporated into the biomedical education programme of most universities. The course takes three weeks and its contents have to be approved by the Minister of Public Health. It covers topics such as husbandry, gnotobiology and anaesthesiology as well as the ethical aspects of animal experimentation. The primary goal is to set the stage for a justified and humane use of animals for a scientific purpose.

The training programmes are coordinated nationally and commissioned in the department of laboratory animal science at the veterinary faculty in the University of Utrecht.

L.F.M. VAN ZUTPHEN
A.C. BEYNEN
Department of Laboratory
Animal Science,
Veterinary Faculty,
University of Utrecht,
PO Box 80.166,
3508 TD Utrecht, The Netherlands
H. ROZEMOND
Veterinary Public Health Inspectorate,
Animal Experimentation Section,
Ministry of Welfare, Health and
Cultural Affairs,
PO Box 439,
2260 AK Leidschendam, The Netherlands

Search for truth?

SIR—I disagree with Leo Uzych (*Nature* **320,** 480; 1986) that "science involves a search for truth", and with the inference he draws from this, that the orchestration of data in support of a particular point of view is an impediment to scientific advancement. I do not see science as being the gradual excavation of a buried city, but rather as the inspirational formation of structures *de novo*. What one builds is determined by the existing foundations, vision and experimental data. As such, science is not a search for truth but for quality. The extent to which one is justified in advocating individual predilections is therefore a matter for careful judgement based on the consideration that while all constructions are ephemeral, some are more so than others. Unless one is selective with data, all one can hope to produce are bricks for use by others who do not show this restraint.

J. LIEBESCHUETZ
Department of Genetics,
University of Liverpool,
PO Box 147,
Liverpool L69 3BX, UK

Danger of delay for genetic tests

Molecular biology is providing novel means of testing for genetic disease, with the result that researchers are having to spend their time on repetitive testing. Now is the time to make better plans.

THE detractors of molecular biology used to complain that its discoveries might be interesting in an academic fashion, but would have no clinical significance. But recent years have shown that position to be untenable. Indeed, the growing impact of molecular biology on medicine is nurturing a band of clinicians with a deep interest in research while bringing molecular biologists face to face with some of the realities of disease. So much was clear, for example, at the latest International Titisee Conference (24–27 April) on human gene mapping and molecular pathology; progress is rapid, in both the laboratory and the clinic. But it will need a great deal of care, at least in Europe, if present enthusiasms are not to dissipate under the weight of that age-old resentment in which clinicians unthinkingly demand more (and different) diagnostic testing from researchers who believe, rightly or otherwise, that they have better ways in which to spend their time.

The high crest of the common ground between the laboratory and the clinic is undoubtedly, just now, the hunt for the unidentified genes whose defects are responsible for diseases such as cystic fibrosis and muscular dystrophy for which no molecular basis has as yet been determined. The magnitude of this task should not be underestimated, but, as Peter Little explains on page 558, adequate techniques are now available, if not perfected. Each gene has been located in a rather small fragment of a chromosome, but which corresponds to a stretch of DNA which is long by the yardstick of what can now be sequenced. Yet there should not be too long to wait before the first of them is identified.

The molecular probes used in location of these genes are already valuable in the prenatal diagnosis of carriers of defective genes, for the time being only within families in which the disease is known to be present. So long as the genes themselves have not been identified, success depends on a variety of factors — how many independent gene probes there are, how close they lie to the defective gene and whether there are enough close relatives of the two parents of the fetus who are 'informative' in the genetic sense. For some diseases, there is clearly room for improvement, but for many others diagnosis is already reliable. So there is a growing demand, by physicians on behalf of their patients, for tests to be carried out. Already the demand sometimes outstrips the time and people available, not to mention the people's interest in work that may seem routine.

The procedures are far from simple. Obtaining the prenatal samples is often the least of the problems, but may sometimes be limiting. This may be especially so as pressure grows to replace sampling of the amniotic fluid by sampling of the placenta as a means of obtaining fetal material, which in principle allows diagnosis earlier in pregnancy and thus earlier termination (if indicated). Curiously, although chorionic villus sampling of the placenta was originally thought to be more risky (for the fetus) than amniocentesis, experience has tended to reverse that view, although chorionic villus sampling is still relatively uncommon.

Sampling, however done, is for physicians. It is the samples that demand the immediate attention and the experience of the researchers. For the time being, most of them are likely to be eager to devote time and energy to this task, not only for humanitarian reasons but also, where the still-cryptic genetic diseases are concerned, because of the possibility that any new case may turn out to have a particular genetic defect that provides a short cut to the defective gene itself.

For each disease, this captive enthusiasm of the researchers must be a passing phase. The time must come when they want to move on to other problems. When, for example, the defective gene for cystic fibrosis or muscular dystrophy is identified, the laboratory emphasis is certain to shift to the function of the protein encoded by the gene and to the links between that function and the symptoms of the disease. Because these links are likely to lead both to new discoveries in fundamental science and to new approaches to therapy, it is in everybody's interest that they should be investigated. But who will then take over the presumably increased diagnostic load?

Even if prenatal diagnosis is confined to the industrialized countries, the imagination is challenged by the sheer scale on which testing may be required if the potential of the new discoveries is to be as fully exploited as preventive medicine. Tests which are at present complicated will no doubt be simplified as time goes on, but by then there will be other defective genes for which to test.

The problems occasioned by diseases that run in families may be relatively small, requiring as they do the testing only of family (including embryonic family) members, most probably at specialist centres which they attend already, so that there is a persuasive argument that the costs of diagnosis and even of the requested termination that may follow will be more than offset by what is saved in there being fewer afflicted patients to treat. But nobody will be surprised if this argument runs into the hidden buffers that so often hinder the application of preventative medicine.

How much greater will be the problems when it becomes feasible and seems to be desirable to screen whole populations for diseases that most often arise as new mutations, not as inherited genetic defects? Or what happens when the several genetic factors contributing to susceptibility to cardiovascular disease have been identified, a question now at the focus of a great deal of research? It should then be possible to categorize groups of people who are at risk, and who could (and should) take preventive steps, but only by complicated population screening.

At the rate at which this science is progressing, the diagnostic needs occasioned even by the simple single-gene diseases are almost certain to outstrip the creation of new testing facilities within public health-care systems, nowhere expansionist. Will medical charities feel compelled to spend less on research and more on testing? Commercial services will certainly grow to meet the need; in the United States, biotechnology companies seem bent on exploiting an emerging market, while, even in Britain, ICI's investment in a centre for providing DNA fingerprinting tests seems well set for moving to meet the growing demand of sophisticated prenatal diagnostic tests.

But where will that leave those who cannot afford the going commercial cost of tests? Especially when the need, in many industrialized communities, is most evident among immigrant populations? It will be frustrating for those laboratory scientists who have helped to open up this new vein of preventative medicine if they are faced, a few years from now, with the unpalatable choice of devoting themselves to routine analysis of a kind that they alone are able to perform or, alternatively, to see the potential benefits of their research simply run to waste.

Peter Newmark

Restriction fragment length polymorphisms

Finding the defective gene

from Peter Little

CHANGES in DNA sequences that introduce or destroy restriction-enzyme cleavage sites and cause restriction fragment length polymorphisms (RFLPs) are the key to identifying the chromosomal location of genes that cause major human genetic diseases. Here I will discuss how useful the linked RFLPs are as a starting point to isolating the defective gene itself, as this remains an unanswered question. I will then describe some ideas about how this might be achieved and some of the technical problems in reaching this goal.

What is the logic behind the use of RFLPs? Once linkage of a single RFLP with a defective gene has been demonstrated, other RFLPs that straddle the affected gene (G) can be identified. These flanking RFLPs (R_L and R_R to the left and right, respectively, of G) can be ordered by observation of the recombination between R_L and R_R, R_L and G or R_R and G. R_L and R_R then define a stretch of DNA that contains the gene. The distance between R_L and R_R must be small if these elements are to be helpful starting points from which to isolate the gene. The proximity with which R_R or R_L can be mapped to G is fixed by the number of meiotic events that are available for the analysis. Lange *et al.*[1] show that if 100 meiotic events could be studied, and assuming that 1 per cent recombination corresponds to a separation of 10^6 base pairs (bp), then the best resolution that could be achieved for the separation of R_R and R_L would be about $2 \times 10^6 \pm 1.4 \times 10^6$ bp of DNA. Steinmetz and co-workers have shown that the relationship between recombination and physical distance in one such locus, H–2 of mouse, is not linear; 1 per cent recombination can be equivalent to 5×10^5 and at worst, from an experimental point of view, 10^7 bp depending on the location within this gene family[2].

The DNA probe that defines a RFLP provides indirect information about the physical distance between R_R and R_L, because orthogonal[3] or field-inversion[4] gel electrophoresis can be used to fractionate DNA fragments of up to 2×10^6 bp generated by cutting with rare 6-, 7- or 8-base recognition restriction enzymes in combination with Southern blotting.

The RFLPs define a stretch of DNA which is probably 2×10^6 bp in length and located within or near a specific chromosomal band. Three strategies can be used to isolate the defective gene: candidate gene, chromosome rearrangement and cloning strategies.

The candidate-gene strategy involves the isolation of messenger (m)RNAs either from genes that are thought to be involved in the genetic defect (for example, those encoding membrane-associated ion transporters in the case of cystic fibrosis); or using randomly selected mRNAs from normal tissues that are affected by the disease, followed either by screening of somatic cell hybrid lines or by *in situ* chromosomal hybridization to show that the mRNA is encoded within the appropriate chromosomal band. Both approaches are technically feasible, but require a formidable amount of work if the normal transcript of the gene is at low abundance.

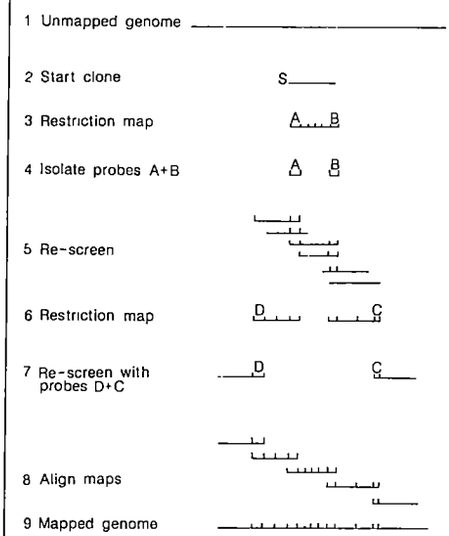


Fig.1 A and B, C and D; probes for each step.

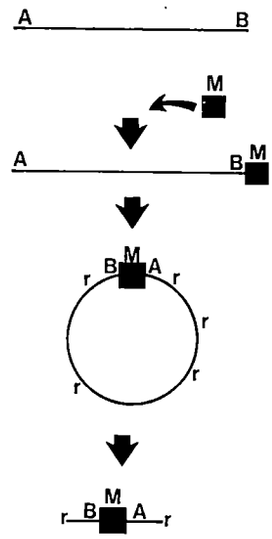


Fig.2 A and B are sequences 200,000 bp apart. M, marker DNA that can be selected in *E. coli*; r, restriction sites. The jumping library consists of many fragments with r sites at each end containing M and different As and Bs.

The chromosome-rearrangement strategy makes use of chromosome deletions, insertions and translocations to provide a marker that must be close to the affected gene[5]. Where these occur, the markers can be used to order the relative position of genes (or DNA probes) within or near the specific chromosomal region. Very little is known about the relationship of cytologically defined bands and their DNA content, but if one assumes a linear relationship (which is not true of the *Drosophila* polytene chromosome[6]) then a single band should contain about 2×10^6 bp of DNA. There are special circumstances where chromosomal rearrangements of known genes into regions of unknown structure or function can help to identify a region implicated in the gene defect[7], but these are generally rare and the precision of mapping of rearrangement breakpoints remains close to the level of the single band — again about 2×10^6 bp of DNA. Where they are available, chromosomal rearrangements will be powerful tools for the analysis of specific gene loci. Duchenne muscular dystrophy, Wilms' tumour of the kidney and retinoblastoma are the diseases that appear to be most tractable to this strategy.

The cloning strategy is based on isolating all the DNA between R_L, R_R and, by definition, the gene, and is itself divided into three approaches: mapping, walking and jumping. Mapping was first used by Steinmetz and co-workers[2,8] who isolated cosmids that contained mouse major histocompatibility complex (MHC) genes by cross-hybridization with MHC class I and II complementary DNA probes. These cosmids were restriction-site mapped and the structure of a substantial portion of the mouse MHC complex was established by aligning cosmids that contained overlapping sequences. The random mapping procedure has been extended by Olson and co-workers (manuscript in preparation) to the yeast genome (10^7bp) and by Sulston and Olson (in preparation) to the nematode genome (8×10^7 bp, which is about the same size as human chromosome 11). Similar techniques could be applied to a human chromosome isolated from a cell hybrid that only contains the required chromosome. It is well known that cosmids containing human DNA can be isolated from these cell lines by hybridization with human-specific repetitive DNA sequences. The mapping of a whole chromosome is a very considerable challenge but one that is technically achievable within the next 5–10 years. The isolation of cell hybrids that contain only a small region of the human genome by chromosome-mediated gene transfer of a naturally or artifically introduced selectable marker has also been achieved[9]. These cell lines generally contain less than 5×10^6 bp of DNA and could be ideal targets for the

mapping approach.

Walking consists of the systematic isolation of a DNA sequence located at the extreme left or right of a starting (S) cloned DNA and the use of this fragment to screen a library of cloned sequences for DNA that must be adjacent and slightly overlapping with S (ref. 10). This process is called a 'step' — a walk proceeds as a linear sequence of steps. Figure 1 shows the complex set of manipulations comprising a step. At present the cloning vectors with the largest capacity are cosmids that can carry 40,000 bp of human DNA. S.H. Cross and I have developed cosmid vectors that are designed to facilitate this procedure (manuscript in preparation). If the markers are separated by 2×10^6 bp, to walk from R_L to R_R would require at least 60 steps (allowing 20 per cent of cosmid overlap per step), which would be a formidable task. An exacerbating factor is that it is not normally possible to orientate R_L and R_R with respect to each other, and thus it is required to walk from R_R and R_L in both directions simultaneously, making the number of steps required twice as large — in the case of our procedure, a total of at least 120. The technique becomes much more attractive where several different 'starts' for the walk are available as well as R_L and R_R. Each walk can then be spread out from four or five starts, considerably reducing these difficulties.

Jumping has been suggested as a method that would reduce the number of steps that are required to walk large distances to an acceptable level — large jumps would be taken rather than individual steps[11]. Consider a 200,000-bp linear DNA molecule (Fig. 2). If it were possible to mark one end of the molecule with a short DNA sequence (M) and then to join the whole molecule into a circle, pieces of DNA (A and B) that were originally 200,000-bp apart would be on either side of the marker DNA. If many such random 200,000-bp circles (representing the whole human genome) could be constructed, and if the marker DNA plus flanking sequences could then be isolated, a 'jumping' library representing all DNA sequences 200,000-bp apart would be produced. We could isolate R_L from the library and 'jump' down the chromosome until we found R_R.

Collins (personal communication) and Lehrach (personal communication) have very recently overcome the considerable technical difficulty involved in constructing statistically complete jumping libraries. Their libraries will allow rigorous testing of the frequency of artefactual joining of sequences by inter- rather than intramolecular fragment joining and of the distance and difficulty of each jump. The use of these techniques, together with orthogonal- or inverting-field gel electrophoresis to locate jump sites, should enormously improve our chances of isolating the defective gene.

I have not approached the obvious question of how one can identify a single, defective gene in 2×10^6 bp of cloned DNA. The answer to this depends very much on the gene and the defect and will prove to be a technical challenge.

One question remains concerning all these approaches: are all human DNA sequences clonable in *Escherichia coli*? The answer is that most are but that some, probably less than 5 per cent, may not be. Wyman *et al.*[12] show that about 5 per cent of human DNA fragments cloned into lambda phage vectors will not propagate on the normal lambda phage *E. coli* hosts but require specific *E. coli* mutant strains for successful growth. The problem will probably be overcome by careful strain construction and testing.

In conclusion, it is certain that RFLPs will lead to the affected gene. Which route is taken in each case depends on the disease pathology, the chromosome location and the tenacity of the investigator, but the search will eventually be successful. It is to be hoped that the good luck which has accompanied some attempts at RFLP mapping will extend to the search for affected genes. □

Peter Little is at the Institute for Cancer Research, Chester Beatty Research Institute, Fulham Road, London SW3 6JB, UK.

1. Lange, K. *et al. Am. J. Hum. Genet.* **37**, 853 (1985).
2. Steinmetz, M. *et al. Cell* **44**, 895 (1986).
3. Smith, C.L. & Cantor, C.R. *Nature* **319**, 701 (1986).
4. Carle, G.F., Frank, M. & Olsen, M.V. *Science* **232**, 65 (1986).
5. Kunkel, L.M. *et al. Proc. natn. Acad. Sci. U.S.A.* **82**, 4778 (1985).
6. Spierer, P. *et al. J. molec. Biol.* **168**, 35 (1983).
7. Ray, P.N. *et al. Nature* **318**, 672 (1985).
8. Steinmetz, M. *et al. Cell* **28**, 489 (1982).
9. Kamarck, M.E. *et al. Expl Cell Res.* **152**, (1984).
10. Bender, W. *et al. J. molec. Biol.* **168**, 17 (1983).
11. Collins, F. & Weissman, S. *Proc. natn. Acad. Sci. U.S.A.* **81**, 6812 (1984).
12. Wyman, A.R. *et al. Proc. natn. Acad. Sci. U.S.A.* **82**, 2880 (1985).

Radiation detectors

Wirechambers in Vienna

from David J. Miller

BOTH 'wirechamber families' are growing; the family of users and the family of radiation detectors which they use. The Vienna meeting* serves as a reunion every three years for a worldwide community of astrophysicists, plasma physicists, medical physicists and biologists as well as the particle physicists who were the first to use proportional chambers and tubes.

The basic principle of all wirechamber devices is multiplication of the electrons released when a gas is ionized by radiation. In true wirechambers multiplication occurs in very high electric fields around fine-sense wires at positive high voltage. In parallel-plate chambers the multiplication is in more uniform fields between plates or grids. Some devices are best adapted to the detection of charged particles, but there are important developments in the detection of photons, especially at ultraviolet and X-ray energies.

Biologists are using multiwire chambers with X-rays from synchrotron sources (A.R. Farouki, MRC Laboratory of Molecular Biology, Cambridge) and with neutron beams (B.P. Schoenborn, Brookhaven National Laboratory). In both cases the chambers were developed by groups with their roots in high-energy physics. The Brookhaven chamber is filled with up to six atmospheres of ^{3}He, one of the few substances which detects slow neutrons. The chamber has a spatial resolution of just over a millimetre, which is close to ideal for resolving the neutron-diffraction patterns from laminated structures from, for example, frog retinas or crystals of complex proteins.

Recent developments in parallel-plate avalanche chambers for X-ray astronomy were discussed in a review by G. Charpak (CERN, Geneva), referring to work from the Mullard Space Science Laboratory of University College London and the University of Leicester. A minority gas (usually acetylene) has been used to enhance the avalanche gain and to reduce statistical fluctuations in measurement of X-ray energies from pulse height. Very simple readout with good position resolution has also been achieved by using fine intersecting patterns of wedges and strips on the anode. A. Breskin (Weizmann Institute, Israel) has achieved a gain of 10^8 in a multistep low-pressure parallel-plate chamber, and plans to use the technique to detect ultraviolet photons from cerenkov rings produced by electrons in a fixed-target experiment at CERN.

'The golden egg of Chicago', a large detector for primary cosmic rays which has been flown on the Space Shuttle (D. Mueller, Emrico Fermi Institute, Chicago), is a beautiful and complex device that contains cerenkov counters, scintillators and special transition-radiation detectors which are read out by xenon-filled multiwire proportional chambers. The detector already has results on the abundances of the lighter nuclei (such as C, N and O) in cosmic radiation, with a clear peak in the iron region, but there is much data still to be analysed. Wirechambers normally need a lot of tuning but these performed perfectly without any maintenance during the flight.

The new generation of storage-ring

*The fourth Wirechamber Conference took place in Vienna on 25–28 February 1986.

experiments in particle physics has generated dozens of new devices with at least two radically different solutions on offer for every problem. Almost every experiment contains a large cylindrical chamber to measure the moments of changed particles, but half of them use time projection chambers (TPCs) and the other half jet chambers. A TPC is a completely clear gas volume with a multiwire detector at one end onto which electrons drift in a uniform electric field. It is, in principle, the ideal three-dimensional detector, but the first big TPC had many teething troubles and has only begun to work well in the past two years (D. Nygren, Berkeley, California). Meanwhile the jet chambers, which use shorter drifts and large numbers of wires stretched throughout their volume, have accumulated a very good record of reliability. Their advocates claim that these chambers can resolve bundles (or jets) of closely correlated tracks much better than TPCs. The conference heard detailed reports on new developments in TPCs from Japan and on two detectors for the large electron–position (LEP) collider at CERN, Geneva. There are new jet chambers for the linear electron– positron collider (SLC) at Stanford, California, for the Cornell University e^+/e^- collider (CESR) and for the other two LEP experiments. Each of these jet chambers has different wire geometry and different electronics. It will be fascinating to see who has guessed right.

Perhaps the most ambitious detectors of all are the ring-imaging cerenkov (RICH) counters for the DELPHI expriment at LEP (J. Seguinot, College de France; M. Turala, University of California, Santa Cruz). As in Breskin's detector, the ultraviolet photons from high-energy tracks ionize an organic vapour (TMAE). Electrons from the ionization process then drift for very long distances before reaching the sense-wires. Apart from the mechanical problems of constructing large-area thin mirrors and windows for these counters, there is a fundamental problem in RICH counters arising from the multiplication process. Electron multiplication releases ultraviolet photons that can interact with the TMAE to produce extra spurious electrons. Test results suggest that this problem can be solved by shielding each sense wire from its neighbours with little 'fences' or tubes.

One of the most exciting potential applications of wirechambers is in positron emission tomography. Good spatial resolution is needed for the 511-KeV γ rays from electron–positron annihilation, with a fast data-collection rate to accumulate a picture of the distribution of the positron-emitting isotope inside an immobilized patient. Charpak thinks it can be done with barium fluoride crystals and parallel-plate avalanche chambers. But there are problems as well as several other competing techniques such as the use of bismuth germanate crystals with solid-state photodetectors. There is a good chance that a successful system will be working before the next family reunion in 1989. □

David J. Miller is in the Department of Physics and Astronomy at University College London, Gower Street, London WC1E 6BT, UK.

Immunology

A common form of killing

From Peter J. Lachmann

IT HAS been established for some years that serum complement kills cells by the insertion of pore-forming molecules (plugs) into the target membrane and the suggestion that lymphocytes kill target cells by an analogous process, discussed in a *News and Views* article[1] some time ago, has been amply confirmed[2,3]. Certain bacterial toxins — for example streptolysin-O and staphylococcal alpha-toxins act in a similar way[4] as does the bee venom toxin, melittin, whose pore-forming activity is rather similar to that of complement[5]. The paper by Young *et al.*[6] on page 613 of this issue extends the role of pore-forming molecules to the eosinophil, a cytotoxic cell of the myeloid series which is known to have important cytotoxic activities both in defence against parasitic infections and in the pathogenesis of the cardiac lesions associated with eosinophilia.

The evidence presented by Young *et al.* is based largely upon electrical potential changes in membranes and lipid monolayers, techniques which have been used by other groups to demonstrate pore formation by complement and by this group to confirm the existence of such molecules in the granules from cytotoxic T cells and natural killer cells[7-9] as well as to demonstrate similar pore-forming molecules in *Entamoeba histolytica*[10]. Marker release from liposomes can be demonstrated and molecular sieving is now being used to find the size of the functional lesion. The ultrastructural appearance of the lesions produced by the membrane attack complex of complement, the final pore-forming components, and by perforins, the leukocyte equivalents, has also been extremely helpful in elucidating their nature and it will be of interest to see what the eosinophil pore looks like when seen under the electron microscope.

That the eosinophil can form pores is of particular interest because, like other granulocytes, the eosinophil has another major killing mechanism available to it — the production of oxygen metabolites producing what may be termed 'burns'. Oxygen metabolites formed by the 'superoxide burst' are known to be the principal intraphagosomal killing mechanism for microorganisms[11]. Oxygen metabolites are also implicated in extracellular cytotoxicity brought about by neutrophils and by macrophages[12]. These reactions produce their membrane damage finally by lipid peroxidation and can characteristically be inhibited by catalase or superoxide dismutase or by iron chelators. Because the eosinophil contains a peroxidase in its granules and is capable of producing a superoxide burst, it is likely that it also uses oxygen metabolites for cytotoxicity in some circumstances. It is therefore a clear example of a cell that has, and seems to use, two of the major cytotoxic mechanisms.

The third major cytotoxic mechanism of eukaryotic cells involves the production of soluble cytotoxic factors, of which tumour necrosis factor and lymphotoxin are the best described. It is clear that monocytes use tumour necrosis factor when they kill nucleated cells by antibody-dependent cellular cytotoxicity[13-15] and although the roles of lymphotoxins in killing by T cells (or B cells) remain to be clearly defined, these cells can certainly produce lymphotoxin, which presumably does function *in vivo*.

It is therefore now becoming clear that these three major mechanisms — plugs, burns and poisons — are used in various combinations by different cell types and in different circumstances. Young *et al.* show that eosinophils can use plugs as well as burns. Lymphocytes use plugs as well as poisons and macrophages certainly use burns as well as poisons. It will be interesting to see if any cell uses all three mechanisms. □

1. Lachmann, P.J. *Nature News and Views* **305**, 473 (1983).
2. Tschopp, J., Masson, D. & Stanley, K.K. *Nature* (in the press).
3. Ward, R.H.P. & Lachmann, P.J. *Immunology* **56**, 179 (1985).
4. Bhakdi, S. & Tranum-Jensen, *Microbial Pathogenesis* **1**, 5 (1986).
5. Esser, A.F. in *Membrane Mediated Cytotoxicity* UCLA Symposia New Series **56** (in the press).
6. Young, J. D-E., Peterson, C.G.B., Venge, P. & Cohn, Z.A. *Nature* **321**, 613 (1986).
7. Young, J. D-E., Young, T.M., Lu, L.P., Unkeless, J.C. & Cohn, Z.A. *J. exp. Med.* **156**, 1677 (1982).
8. Young, J. D-E., Hengartner, H., Podack, E.R. & Cohn, Z.A. *Cell* **44**, 849 (1986).
9. Young, J. D-E., Nathan, C.F., Podack, E.R., Palladino, M.A. & Cohn, Z.A. *Proc. natn. Acad. Sci. U.S.A.* **83**, 150 (1986).
10. Young, J. D-E. & Cohn, Z.A. *J. Cell Biochem.* **29**, 299 (1985).
11. Johnson, W., Pizzo, S.V., Imber, M. & Adams, D.O. *Science* **218**, 574 (1982).
12. Nathan, C.F. & Cohn, Z.A. *J. exp. Med.* **152**, 198 (1980).
13. Matthews, N. *Immunology* **44**, 135 (1981).
14. Espevik, T., Kildahl-Andersen, O. & Nissen-Meyer, J. *Immunology* **57**, 255 (1986).
15. Ziegler-Heitrock, H.W.L., Moller, A., Linke, R.P., Rieber, E.P. & Reithmuller, G. *Cancer Research* (in the press).

Peter J. Lachmann is in the Mechanisms of Tumour Immunity Unit, MRC Centre, Hills Road, Cambridge CB2 2QH, UK.

Physics

Low-dimensional electron movement in a magnetic field

from Paul Chaikin

ELECTRONS in two dimensions in a perpendicular magnetic field move in circular orbits. Quantization of these orbits is responsible for the quantum Hall effect as well as a wealth of oscillatory phenomena in metals. But electrons in one dimension in a magnetic field cannot form such orbits. The discovery of a series of magnetic field-induced phase transitions, oscillations and behaviour like the quantum Hall effect in Bechgaard salts, which act as quasi-one-dimensional organic conductors, has stimulated a flurry of recent experimental[1-5] and theoretical[6-9] work and the discovery of a new form of instability in a two-dimensional system[10,11], as well as many unanswered questions.

The crystal potential has two interesting effects on the states of a two-dimensional system in the field. If the potential is reasonably isotropic (as in a square lattice) the electron orbits are distorted but closed and periodic. The wavefunctions must satisfy both orbital quantization and crystalline symmetry, conditions which are usually incommensurate. The result is a complex hierarchical self-similar energy spectrum with gaps on all energy scales[12,13] (Fig. 1). If the potential is highly anisotropic the motion of the electron may form a zigzag pattern which goes off in the easiest direction and never closes — an open orbit (Fig. 2).

The Bechgaard salts provide a unique system for the study of an interacting two-dimensional electron gas in a magnetic field. They have the formula $(TMTSF)_2X$ where X is PF_6, ClO_4, ReO_4 and so on[1-5], and are variously regarded as quasi-one- or quasi-two-dimensional. They are better known as the first organic superconductors, but they can also have insulating spin-density wave (SDW) ground states depending on the pressure and on the anion X. The band structure has been calculated and measured: the anisotropy in bandwidths in the highly conducting plane is about 10:1, whereas between the planes the bandwith is smaller by a factor of 30.

It is well known that one-dimensional metals are unstable against a Peierl's distortion or SDW which leads to an insulating ground state. For the Bechgaard salts under consideration the band-

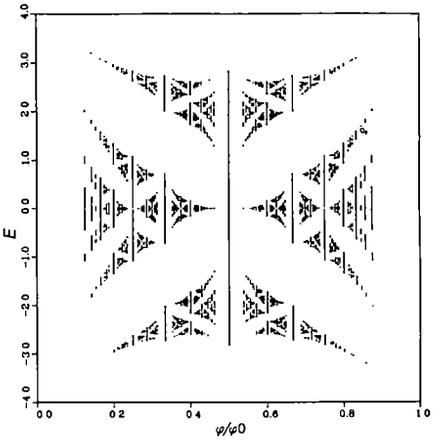


Fig. 1 Energy spectrum of an electron in a square tight binding model in the presence of a magnetic field measured in flux quanta per unit cell (ϕ/ϕ_0). Dark regions, allowed states.

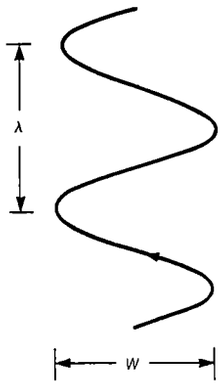


Fig. 2 Electron motion in a magnetic field for an open orbit. w and λ are proportional to the reciprocal of the magnetic field.

width in the second most conducting direction is large, the systems are effectively two-dimensional and they remain metallic to low temperatures. But the anisotropy is sufficient to make all the orbits open at the Fermi surface. In the presence of a magnetic field the electrons undergo the motion illustrated in Fig. 2. As the magnetic field increases the width w of the motion along the x direction and the period λ along the y direction decrease. The effect is to make the electrons more one-dimensional and thus increasingly susceptible to an SDW transition. Strictly speaking, the electron motion and the spectrum of the open-orbit electrons in a magnetic field is always one-dimensional (limited excursions along x and infinite along y). Thus, two-dimensional open-orbit metals cannot exist at zero temperature. An infinitesimal magnetic field will drive them to an insulating Peierl's or SDW state[12,14].

The basic instability leading to the field-induced transition is therefore well established. There are several quasi-classical models that seek to explain the series of phase transitions which allow the wavevector of the SDW distortion to change both continuously and discontinuously to take advantage of the magnetic quantization of carrier pockets which result from the distortion[6-9].

In the usual treatment of the one-dimensional instability a single length is considered — the reciprocal of the Fermi momentum (P_f) — and this sets the wavelength of the distortion at $\hbar/2\ P_f$. In the field-induced phase there at least three lengths, $\hbar/2\ P_f$, the magnetic length λ (Fig. 2), which varies reciprocally with the magnetic field, and the lattice period. In general the lengths are incommensurate with one another. The distortion wavevector results from the competition of the interactions represented by these lengths. The spectrum resulting from incommensurate potentials is often quite complex, as illustrated for a particular case in Fig. 1.

One might expect that the existence of the small gaps in the spectrum are inconsequential, as they are usually smeared out by finite temperature or scattering. The gaps have a profound effect on the Hall conductance, with the most dramatic effects involving large changes in magnitude and sign of the Hall conductance resulting from the smallest gaps[14]. More perfect crystals show an increasing number of field-induced transitions with abrupt sign changes in the Hall voltage[15], suggesting that in these salts an incommensurate spectrum is involved[3]. The existence of oscillations with a different magnetic frequency at high fields also points to a complex spectrum[2].

There are still basic questions left to be answered. The eventual state at high field should be insulating, but so far only semimetallic behaviour has been observed. And what of the quantum Hall effect? Hall measurements indicate steplike structure, but it is temperature dependent and has other dissimilarities[15-17]. The interplane bandwidth is small enough to allow the two-dimensional instability to occur, but is the system two-dimensional enough for the quantum Hall effect? The roles of incommensurability and dimensionality need further investigation. □

Paul Chaikin is Professor of Physics at the University of Pennsylvania, Philadelphia 19104, and is a Research Associate at the Exxon Research and Engineering Co., Annadale, New Jersey 08801, USA.

1. Kwak, J.F. *et al. Phys. Rev. Lett.* **46**, 1296 (1981).
2. Schwenk, H. *et al. Phys. Rev. Lett.* **56**, 667 (1986).
3. Kwak, J.F. *et al. Phys. Rev. Lett.* **56**, 972 (1986).
4. Pesty, F. *et al. Phys. Rev. Lett.* **55**, 2495 (1985).
5. Naughton, M.J. *et al. Phys. Rev. Lett.* **55**, 969 (1985).
6. Montambaux, G. *et al. Phys. Rev. Lett.* **55**, 2078 (1985).
7. Yamaji, K. *et al. Phys. Soc., Japan* **54**, 1034 (1985).
8. Virosztek, A. *et al. Phys. Rev.* A (submitted).
9. Azbel, M. Ya *et al. Phys. Rev.* A (submitted).
10. Gorkov, L.P. & Lebed, A.G. *J. Phys. Lett., Paris*, **45**, L433 (1984).
11. Chaikin, P.M. *Phys. Rev.* **B31**, 4770 (1985).
12. Azbel, M. Ya *Zh. Eksp. Teor. Fiz.* **46**, 939 (1964) [Sov. Phys. JETP 19, 634 (1964)].
13. Hofstadter, D.R. *Phys. Rev.* **B14**, 2239 (1976).
14. Thouless, D. *et al. Phys. Rev. Lett.* **49**, 405 (1982).
15. Ribault, M. *Molec. Cryst. Liq. Cryst.* **119**, 91 (1985).
16. Ribault, M. *et al. J. Phys. Lett., Paris* **44**, L953 (1983).
17. Chaikin, P.M. *et al Phys. Rev. Lett.* **51**, 2333 (1983).

Desert ecosystems

Desertification or xerification?

from N.E. West

'DESERTIFICATION' has become a common term to describe the impoverishment of terrestrial ecosystems induced by man. But the word is much abused, often preventing the realization that deserts occur naturally in certain ecological contexts. Although the impression that deserts are produced by man helps to generate interest, and therefore money, to investigate problems of vegetation diminishment and soil degradation, particularly in regions of semi-arid climates[1,2], it encourages emphasis on treating the symptoms of abuse rather than the causes of the problems.

Deserts vary enormously around the world, with only some of those under the most arid conditions having escaped severe alteration by man[3,4]. Le Hourerou[5] proposed the term 'desertization' to imply the expansion of desert-like landforms and landscapes in arid to semi-arid environments. This word is supposed to avoid issues such as ecological degradation of tropical forests into savanna of forest into maquis, which can still be described as 'desertification'. But the distinction is probably missed by most and, in any case, degradation of terrestrial ecosystems usually does involve drying-out of the previous environment. Water typically enters the biological phases less easily, yet moves through an ecosystem more rapidly, following disturbance introduced by man. If soils are more compacted and organic matter lower, less water can infiltrate and be stored. Accelerated erosion of the soil surface may reduce the depth of the rooting profile as well as removing the most nutrient-rich portions. More xerophytic (drought-tolerant and less water-demanding) plants typically replace the preceding comparatively less xerophytic ones removed by excessive livestock grazing, wood harvest, fire and mechanical damage. This gives the impression that macroclimates must have changed when the major alterations in climate have occurred at soil level. Kovda[6], therefore, proposed the term 'aridization' to describe the drying-out process. The disadvantage of this word is that it can be confused with a permanent change in macroclimate.

I have recently used the term 'xerification' to describe the concomitant diminishment of vegetation and degradation of soils under unsustainable levels of land use in semi-arid areas in western North America[7]. This term could be used in more climatically favourable regions without the value-judgement implicit in



LANDSAT imagery of the boundary between Egypt and Israel as it appeared in 1973. 1, sand, vegetation destroyed; 2, sand occupied by intact vegetation; 3, Mediterrean Sea; 4, shifting sands next to coastal strands; 5, sandy area covered by orchards in southern part of Gaza; 6, fenced area of Sadat and Vetiv ha Asara where grazing and direct plant cutting ceased after 1967. From Danin, A. *Desert Vegetation of Israel and Sinai* (Cana, Jerusalem, 1983). Image provided by NASA.

Albert L. Lehninger (1917–1986)

ALBERT LEHNINGER, who died on 4 March, is known to young and not so young biochemists all over the world as the sole author of the widely used textbook, simply called *Biochemistry*, the first edition of which appeared in 1970. To the older biochemist and to all those engaged in the study of the branch of biochemistry and biophysics called bioenergetics, he is known as one of the founders of their field. He was one of the first to publicize the word bioenergetics in his monograph bearing that name, published in 1965. His first book, *The Mitochondrion*, had appeared a year earlier.

It was his work on this sub-cellular organelle in the late 1940s and the 1950s that first brought him fame. Together with E.P. Kennedy, he showed in 1948 that a particulate fraction of rat liver, identified as mitochondria, catalyses all the reactions of the Krebs cycle and fatty acid oxidation. For this work Kennedy and Lehninger are co-recipients of the 1986 Passano Foundation Award.

Lehninger is perhaps best known for his second classical paper, also published in 1948. In that paper, together with his student Morris Friedkin, he described phosphorylation of adenosine diphosphate by inorganic phosphate, coupled to electron transfer between reduced nicotinamide nucleotide and oxygen (catalysed by the so-called respiratory chain). The phenomenon of oxidate phosphorylation itself had already been established by Engelhardt and Kalckar in the 1930s and before the Second World War Ochoa and Belitzer had made it likely that it was of a fundamentally different type from the only known phosphorylation reaction, linked with anaerobic processes. But the direct demonstration of what became known as respiratory-chain phosphorylation had proved elusive. Lehninger succeeded in two types of experiments, one with reduced nicotinamide-adenine dinucleotide as substrate and the other with 3-hydroxybutyrate, which reduces the nucleotide in a reaction that could not conceivably be associated with phosphorylation.

With the hindsight of nearly 40 years, we now know that the results of the first type of experiment were not as unambiguous as they at first appeared, but the second type remain valid and were sufficient to establish the concept of respiratory-chain phosphorylation. Lehninger was also the first to demonstrate phosphorylation in the terminal reaction of the respiratory chain — the oxidation of reduced cytochrome *c* — once again after failures by others. He was also one of the first to observe the energy-linked uptake of calcium by mitochondria and the first to make a thorough study of its characteristics.

Lehninger was one of a vanishing type: the highly successful research worker who is also a prolific writer. Also unusual is that all his books are monographs. How he was able to face up to the tremendous chore of regularly bringing out new editions of his monumental textbook was a source of wonder to many. Surely the explanation is that he enjoyed writing. That he was a such a lucid writer was no surprise to those of us who used to listen spellbound to his lectures at international meetings, delivered without any notes. The polish of these performances could only have been achieved with meticulous preparation.

Lehninger's early work was done at the University of Chicago where he moved in 1945 after obtaining his Ph.D. at that nursery of American biochemists at that time, the University of Wisconsin. He spent the academic year 1951–1952 at the University of Cambridge, England, and in 1952 was appointed Professor of Physiological Chemistry at Johns Hopkins University, Baltimore, where he stayed until his death. His colleagues at Johns Hopkins had planned a symposium, appropriately called *The Mitochondrion, 1986*, to be held in his honour on 5–7 June. The symposium will still be held, now sadly to his memory as well as in his honour. E.C. Slater

words such as desertification, desertization and aridization.

Irrigated lands in arid to semi-arid climates which have increased water tables and/or direct salt input from the irrigation water eventually support lowered crop production. Even some originally forested lands in southern Australia develop such problems when the high transpiration draw-downs affected by the forest are eliminated after tree removal. The only plants that can grow on some of the most heavily salinized former farm- or forestlands are shrubs normally found in desert regions. The soil moisture is excessive, but the soils are physiologically dry to non-desert species. The term xerification would more usefully describe these processes than the narrow word salinization.

Clearly it will be difficult to distinguish natural xerification from that induced by man. But palaeoecological evidence shows that deserts are relatively young ecosystems on all continents, and thus have arisen naturally. Therefore it is important to elucidate natural, as well as man-made, mechanisms. □

1. Karrar, G. & Stiles, D. *J. Arid Environ.* **7**, 309 (1984).
2. *Nature and Resources* **20** (1984).
3. McGinnies, W.G. *Desert Plants* **6**, 182 (1984).
4. Dregne, H.E. *Desertification of Arid Lands* (Harwood, New York, 1983).
5. Le Hourerou, H.N. *Ann. Alger. Goeg.* **3**, 2 (1965).
6. Kovda, V.A. *Land Aridization and Drought Control* (Westview, Boulder, 1981).
7. West, N.E. *Temperature Deserts and Semideserts.* (Elsevier, Amsterdam, 1983).

N.E. West is Professor of Range Ecology at the College of Natural Resources, Utah State University, Logan, Utah 84322, USA.

Muscle contraction

Crossbridges, force and motion

from Richard T. Tregear

THE basic question that concerns those interested in crossbridges is 'what makes muscle pull?'. Many different answers have been suggested over the years. Some simple and elegant experiments described at a recent workshop* exclude several of them. Other experiments place constraints on the part of the myosin head (or crossbridge) responsible for the generation of force consequent on ATP hydrolysis. The picture which emerges is of a crossbridge (which projects from the thick filament of muscle fibres) that can easily attach and detach from actin (in the thin filament) in the first part of the enzymatic cycle and then 'harden' its attachment and produce force in the later part of the cycle. The contractile process occurs in the middle of the myosin head, does not need the other head of the myosin molecule, much of the tail region of the molecule or even, perhaps, the light chains of the head itself. The process probably involves only a small change in the shape of the head, is reversible and can sometimes couple to a huge interfilament movement. Altogether this picture is not very like the usual undergraduate idea of crossbridge rotation and force production.

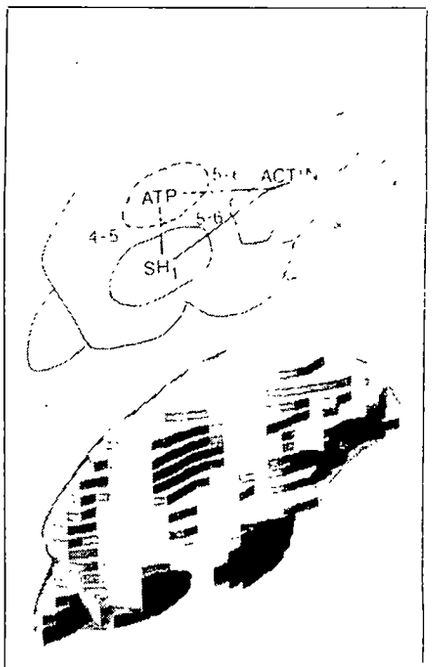
The evidence for these statements comes from a wide variety of approaches. The idea of the rapidly attaching weak-binding crossbridge comes from enzymatic studies (E. Eisenberg, NIH), and fits both with the way in which measurements of crossbridge attachment by X-ray diffraction (H. Huxley, Cambridge; K. Wakabayashi, Osaka) and mechanical stiffness (R. Simmons, London) are seen to rise before tension during activation and with the large number of disorganized myosin heads still seen by electron proton resonance (EPR) when a muscle is contracting strongly (D. Thomas, Minneapolis). On the other hand, the strong-binding, tension-generating state may be best seen by electron microscopy of muscle in rigor (M. Reedy, Duke); at any rate, no regular crossbridge angle other than that of rigor (thought to represent the maximal force-producing state) has been detected by EPR or polarized fluorescence in actively contracting muscle.

The resolution of immuno-electron microscopy is now good enough to divide the myosin head into a regulatory neck and an operative body, and within that body to locate the three regions most likely to transfer energy across it: the nucleotide- and actin-binding regions and the interlinking part close to the active thiol residue (T. Wakabayashi, Tokyo; see figure). Furthermore, both the sequence near the thiol and the purine-binding sequence have turned out to be highly conserved, being invariant from slime mould to rabbit, as if they perform an essential function (J. Spudich, Stanford).

Optical microscopy has now improved to such an extent that one can see the motion of unrestrained actin filaments over myosin, or of particles coated with myosin over actin (Spudich; T. Yanagida, Osaka). Such motion occurs even when the myosin is single-headed or its tail is greatly reduced in length. These experiments appear to eliminate contractile mechanisms dependent on either head–head interaction[1] or a change in tail structure[2].

Chemists have managed to attach a photolysable group to ATP (caged ATP) that can be diffused into muscle before lysis releases the ATP itself[3]. The resultant synchronized events indicate that phosphate release and tension generation occur together and that both processes are reversible (Y. Goldman, Philadelphia). It follows that tension can be regenerated without coupled ATP hydrolysis, which was not envisaged in earlier ideas of the crossbridge cycle[4].

An ingenious argument was presented from a couple of conceptually simple experiments. If actin is proteolytically cut loose in a myofibril or if myosin heads are floated into a brush of actin filaments, they remain still until ATP is added and then they move, quite rapidly. Yanagida measured the speed of motion and the rate of ATP hyrolysis and deduced that each crossbridge stroke using ATP moves the myosin molecule by at least 60 nm, which is too far for the crossbridge to stretch[5,6]. Is there something wrong with Yanagida's logic, or with the crossbridge theory itself? □



Location of the ATP-binding and reactive thiol (SH_1) sites on the surface of the myosin head (top), determined from avidin binding and three-dimensional reconstruction of the actin-myosin head complex (bottom). ATP binds to the back of the head. Units, nm. (Courtesy of M. Tokunaga, A. Tomioka, C. Toyoshima, K. Sutoh, K. Yamamoto & T. Wakabayashi, unpublished observations.)

1. Sydorenko, N.P. *J. Muscle Res. Cell Motility* **5**, 117 (1984).
2. Harrington, W.F. *Proc. natn. Acad Sci U S.A.* **76**, 5066 (1979).
3. Goldman, Y.E., Hibberd, M.G. & Trentham, D.R. *J. Physiol., Lond.* **304**, 577 (1984).
4. Lymn, R.W. & Taylor, E.W. *Biochemistry* **10**, 4617 (1971).
5. Yanagida, T., Arata, T. & Oosawa, F. *Nature* **316**, 366 (1985).
6. Irving, M., *Nature News and Views* **316**, 292 (1985).

Richard T. Tregear is at the AFRC Institute of Animal Physiology, Babraham, Cambridge CB2 4AT, UK.

* Workshop on the interaction between actin and myosin in skeletal muscle held at Alpbach, Austria, 17-22 March 1986. Supported by the European Molecular Biology Organization and the Muscular Dystrophy Association of America.

Neuroscience

Optical mapping of activity in primate visual cortex

from D. Van Essen and H. S. Orbach

MUCH of our current understanding of cortical function has been gained by analysing how different types of information are represented in a systematic fashion within the three-dimensional architecture of the cortex. This is most evident in the case of primary visual cortex (striate cortex) of primates, where cortical architecture is specialized to a notably high degree and where many of these specializations have interesting neurophysiological correlates. In a report on page 579 of this issue, Blasdel and Salama[1] use a relatively new technique involving *in vivo* application of voltage-sensitive dyes to ascertain how selectivity for stimulus orientation is mapped across the surface of striate cortex in the macaque monkey. Their study provides an intriguing and unexpected hint about modular organization of the cortex. In addition, it emphasizes the feasibility of the optical approach for attacking a host of interesting issues concerning cortical function.

It is well known[2] that cells in the striate cortex are arranged in orientation columns, in which aggregates of cells aligned orthogonal to the cortical surface all respond best to the same stimulus orientation (except for cells completely lacking orientation selectivity). Parallel to the cortical surface, orientation preferences tend to shift gradually and smoothly, with only occasional discontinuities in the progression. A major unresolved issue has been the relationship of this orderly array of orientation columns to two other basic features of striate cortex: a system of ocular dominance stripes that is most clearly delineated by a sharp segregation of geniculocortical inputs from the two eyes within layer 4; and a patchwork array of cytochrome oxidase-rich 'blobs', which are aligned with ocular dominance stripes and whose constituent cells generally lack orientation selectivity[3].

What has clearly been needed to sort out these relationships is a means for monitoring the two-dimensional pattern of visually evoked cortical activity with high spatial resolution. The 2-deoxyglucose technique, in which activity-dependent metabolism is measured autoradiographically, has proven helpful in this respect[4]. But it suffers from being a one-shot approach, in which only a single stimulation condition can be tested in any given cortical region. The technique of *in vivo* optical monitoring of neural activity using voltage-sensitive dyes is in principle much more flexible, because it has vastly superior time resolution and allows repeated measurements using various stimuli. First developed and tested on invertebrate preparations by Cohen and collaborators[5], voltage-sensitive dyes have recently been successfully applied to the mammalian somatosensory and visual cortex [6,7].

Several methodological refinements introduced in the study of Blasdel and Salama[1] yield a spectacular increase in the spatial resolution of the technique. Most importantly, the authors used a video camera instead of the standard photodetector array, and monitored a very slow visually evoked response, thereby gaining spatial resolution in exchange for an affordable loss of temporal resolution. In addition, they used a clever combination of stimulation paradigms and image-processing techniques to generate detailed false-colour maps of how orientation preferences are mapped across the surface of the cortex. The basic validity of this analysis was confirmed by direct comparisons between optical and electrophysiological determinations of ocular dominance and preferred orientation at selected sites.

Blasdel and Salama find that regions of similar orientation preference generally occupy small patches in the orientation map. These patches range from nearly circular to highly elongated in shape, with a length typically less than 1 mm. The alignment of iso-orientation domains is not strongly correlated with ocular dominance stripes nor with cytochrome oxidase blobs, an outcome which is consistent with previous deoxyglucose-based results[4]. It runs counter to more organized patterns that have been hypothesized, such as an orthogonality between ocular dominance and orientation stripes[7] or a radial or circumferential arrangement of iso-orientation domains centred around cytochrome oxidase blobs[8].

A particularly striking feature of the orientation maps is a pattern of 'fractures', lines or narrow strips along which the preferred orientation changes very rapidly. The fracture lines form a tightly interlaced network containing numerous loops and rings that are variable in size and shape, but are generally much less than 1 mm across. Blasdel and Salama raise the intriguing suggestion that these fracture lines form the outlines of discrete 'modules' within the cortex. However, they also note several potential complications relating to the fracture lines, and these deserve careful evaluation.

One of the complications arises from the fact that the maps display a well-defined orientation at all points, even in regions which post-mortem histochemistry shows to be superimposed on the cytochrome oxidase blobs. This is surprising in view of the previously mentioned complete absence of electrophysiologically assessed orientation selectivity in most blobs[3]. One possibility is that orientation selectivity might indeed be present in the blobs, but restricted to the most superficial cells (say, in layer 2), which presumably dominate the optical signals. Alternatively, the apparent orientation selectivity within the blobs might arise from spatial blurring of the optical signal, for example, as a result of light scattering within the cortex or as a reflection of the extent of dendritic arborizations. By this hypothesis patches whose cells genuinely lack orientation selectivity would nonetheless show an apparent orientation preference throughout, by virtue of spatial averaging of the orientations of nearby sites within the blur circle. Fracture lines associated with blobs would then no longer represent an abrupt discontinuity in a parameter that has a well-defined value at each point, but rather a mismatch in the extrapolated orientation in going from one side of a blob to the other.

Another puzzling feature is that not all orientations are equally represented within either of the two orientation maps illustrated by Blasdel and Salama. In particular, one oblique orientation (light blue in their false-colour representations) appears to be notably sparse, generally occurring as very narrow strips. Non-linearities in the colour reproduction process may contribute to this impression but are unlikely to provide a complete explanation, because many of the fracture lines run directly along the thin strips associated with the under-represented orientation. There may be pronounced anisotropies in the cortical representation of orientation, analogous to those suggested from electrophysiological recordings[9]. Yet another possibility is that the apparent under-representation was a consequence of slightly reduced efficacy of a particular stimulus orientation, conceivably because of astigmatism of one or both eyes. A final complication to the fracture story is that some of the fracture lines (more than seems likely by chance association) appear by visual inspection to parallel closely the vascular pattern (including some of the smaller blood vessels) that is shown in a figure accompanying the study. This may reflect yet another way in which non-neural factors can subtly bias the orientation estimates derived from optical measurements.

The question of whether striate cortex contains well-defined modules is fundamental to our understanding of cortical organization. Hubel and Wiesel[2,4] laid the

groundwork for this notion with the suggestion that any small region of cortex, about 1–2 mm on a side, contains a set of 'hypercolumns', that is, all the neural machinery needed for the analysis of orientation and ocular dominance in any small portion of the visual field. The idea received a major boost with the discovery of the cytochrome oxidase blobs, which clearly denote an anatomically distinctive two-dimensional repetitive pattern, but which leave open the question of whether hypercolumns have well-defined starting and stopping points.

The orientation fracture lines described by Blasdel and Salama are attractive candidates for hypercolumn boundaries. But the relationship is not entirely straightforward, as most of the modules delineated by fractures fail to enclose a complete set of orientations, and do not all contain a representation of both ocular dominance stripes. A more precise understanding of this relationship must await resolution of the technically based concerns described above about the origins and interpretations of some of the orientation fracture lines.

These concerns are amenable to experimental analysis, and clarification of the key issues should not be long in coming. Further refinements may also be anticipated for dealing with various technical limitations of the optical technique relating to signal-to-noise problems, image blur and the analysis of signal distribution within the third dimension (depth) of the target tissue.

In the meantime there is good reason to celebrate the successful application of voltage-sensitive dyes to basic questions of cortical organization. Blasdel and Salama have made clear that optically based activity monitoring techniques will become a powerful component in the ever-expanding repertoire available to neuroscientists interested in structure–function relationships within the brain. Application of this approach to questions of information processing, development and plasticity in sensory and motor areas of the cortex will keep many laboratories busy for years to come. □

1. Blasdel, G. & Salama, G. *Nature* **321**, 579 (1986).
2. Hubel, D.H. & Wiesel, T.N. *Proc. R. Soc.* B**198**, 1 (1977).
3. Livingstone, M.S. & Hubel, D.H. *J. Neurosci.* *4*, 309 (1984).
4. Hubel, D.H., Wiesel, T.N. & Stryker, M. *J. comp. Neurol.* **177**, 361 (1978).
5. Grinvald, A., Cohen, L.B., Lesher, S. & Boyle, M.B. *J. Neurophysiol.* **45**, 829 (1981).
6. Orbach, H.S., Cohen, L.B. & Grinvald, A. *J. Neurosci.* **5**, 1886 (1985).
7. Grinvald, A., Gilbert, C.D., Hildesheim, R., Lieke, E. & Wiesel, T.N. *Soc. Neurosci. Abstr.* **11**, 18 (1985).
8. Braitenberg, V. & Braitenberg, C. *Biol. Cybern.* **33**, 179 (1979).
9. Mansfield, R.J. *Science* **186**, 1133 (1974).

D. Van Essen and H.S. Orbach are in the Division of Biology, California Institute of Technology, Pasadena, California 91125, USA.

Molecular biology

Why do disused proteins become genetically lost or repressed?

from Jared M. Diamond

ARTICLES in these columns typically focus on recent discoveries. But progress also depends on exposing areas of ignorance. Hence this article concerns our failure so far to resolve a fundamental problem of biology: why disused proteins become phenotypically repressed and are eventually genetically eliminated[1–5].

Evolution consists of the acquisition and loss of traits. Most biologists since Darwin have agreed that the acquisition of functionally significant traits is caused by natural selection. But why do disused, formerly significant traits become lost? (Think of the loss of eyes in cave animals, or the loss of flight in birds on predator-free islands.) Two answers have been suggested, both stemming from Darwin's work: disuse or natural selection. Most mutations destroy a function rather than improve it. Thus, if a character becomes selectively neutral through disuse, mutations will gradually remove the character even in the absence of positive selection to eliminate it. On the other hand, any character costs something to build and maintain. Thus, a disused character may be selectively disadvantageous, not merely neutral; selection may eliminate the character to recoup the wasted costs. The cost most often mentioned in this context is biosynthetic energy.

The traits whose costs could be measured most easily are single enzymes or biosynthetic pathways. Consider auxotrophic mutants, which have lost the ability to synthesize some essential solute and can grow only if that solute is provided exogenously. Lwoff[6] proposed that there should be positive selection for such mutants in the presence of the solute because the mutants save unnecessary biosynthetic costs incurred by the wild strain. Zamenhof and Eichhorn[7] confirmed that His^- and Trp^- auxotrophs of *Bacillus subtilis* are selected over the wild-type strain in the presence of His and Trp, respectively. Similar findings apply to Tyr^- and Trp^- auxotrophs of *Escherichia coli*[1,8]. Few attempts have been made to compare the saved biosynthetic costs of the auxotroph at the molecular level with its selective advantage at the population level, and thereby to decide whether the wasted energy hypothesis suffices to explain this genetic loss of a disused trait. The rare attempts that have been made cast doubt on the energy hypothesis[1,2].

The most detailed comparison is one in which Dykhuizen[1] used a chemostat to study *E. coli* mutants differing from the wild type only in their inability to synthesize tryptophan (Trp). Dykhuizen first calculated the energy needed by wild-type *E. coli* to synthesize various amino acids, assuming maintenance costs to be negligible compared with the costs of growth[9]. Amino-acid synthesis was estimated to cost 40 per cent of the total energy budget, Trp, in particular, 1.25 per cent. In a Trp-containing medium, the synthesis of this amino acid is repressed to a level where it costs only 0.01 per cent of the energy budget. The energy to synthesize the Trp-synthesizing enzymes themselves (in the absence of turnover) was estimated as only 17 per cent of this cost of Trp synthesis. Thus, if the sole advantage of the auxotrophs over the wild type in a Trp-containing medium were the saved synthetic energy, the auxotrophs should have had an insignificantly higher growth rate, by 0.01 per cent per generation (independent of generation time). In fact, their growth rate advantage was far greater — around 10 per cent per generation — and it increased with generation time.

Because these calculations of saved energy involve many assumptions, Dykhuizen next compared the selective advantage (over the wild type) of a mis-sense mutant that makes Trp-synthesizing enzymes but not the protein against a polar nonsense mutant that makes neither the enzymes nor Trp. By the saved energy hypothesis the polar nonsense mutant should have had a 17 per cent greater selective advantage than the mis-sense mutant (because energy savings are 17 per cent greater), but the two mutants were found to have the same advantage. Furthermore, mutants can still synthesize Trp from anthranilate via indole, although at some biosynthetic cost. Hence the selective advantage of the mutants over the wild type should decrease from a Trp to an indole to an anthranilate medium, and Dykhuizen, from the biosynthetic costs of each step, predicted relative advantages of 1.00:0.83:0.67. The actual relative advantages were the same for indole and anthranilate, and were lower than predicted (1.00:0.50:0.50).

Most puzzling of all, the advantage of mutants over the wild type was apparent only when they were grown together; the mutants and wild type had the same growth rates when grown separately. One can think of many uncertainties in these cost estimates: assumptions in the energy calculations that would affect the numbers; features of cell physiology that could

amplify a biosynthetic energy difference; and factors other than biosynthetic energy that should also be considered costs of Trp synthesis (for example, the space that Trp synthesis preempts in the already crowded cytoplasm or membrane[3,10]). But all these considerations still predict incorrectly that the mutants should grow faster than the wild type when grown separately. Thus, the advantage of mutants must instead involve some interaction with the wild type when grown together, such as competition for glucose, the limiting substrate.

Similar doubts concerning the energy hypothesis emerge from experiments on *lac* operon proteins[3,11,12]. For example, Andrews and Hegeman[12] compared five strains of *E. coli* differing in production of *lac* operon proteins (from 0.6 to 3.6 per cent of total cellular protein) growing in media with a substrate other than lactose. The authors observed no significant correlation between selective advantage and percentage of wasted protein.

The traditional explanation in terms of saved biosynthetic energy appears to fail. The familiar observation that synthesis of specific proteins becomes phenotypically repressed in the absence of requirement for the protein is also usually attributed to saved energy. Experiments are needed in which the selective disadvantage of a mutant that cannot repress an enzyme in the absence of its substrate is measured and compared with the saved energy or other postulated costs. □

1. Dykhuizen, D.E. *Evolution* **32**, 125 (1978).
2. Dykhuizen, D.E. & Hartl, D.L. *Microbiol. Rev.* **47**, 150 (1983).
3. Koch, A.L. *J. molec. Evol.* **19**, 455 (1983).
4. Hall, B.G., Yokoyama, S. & Calhoun, D.H. *Molec. Biol. Evol.* **1**, 109 (1984).
5. Li, W.-H. *Molec. Biol. Evol.* **1**, 213 (1984).
6. Lwoff, A. *L'Evolution Physiologique* (Herman, Paris, 1944).
7. Zamenhof, S. & Eichborn, H. *Nature* **216**, 455 (1967).
8. Mason, T.G. & Slater, J.H. *Antonie van Leeuwenhoek, J. Microbiol. Ser.* **45**, 253 (1979).
9. Marr, A.G. *et al. Ann. N.Y. Acad. Sci.* **102**, 536 (1963).
10. Dykhuizen, D. & Davies, M. *Ecology* **61**, 1213 (1980).
11. Novick, A. & Weiner, M. *Proc. natn. Acad. Sci. U.S.A.* **43**, 553 (1957).
12. Andrews, K.J. & Hegeman, G.D. *J. molec. Evol.* **8**, 317 (1976).

Jared M. Diamond is Professor of Physiology at the University of California Medical School, Los Angeles, California 90024, USA.

Earth sciences

Magnetotelluric evidence for subduction of seafloor sediments

from D. Ian Gough

NEW results from magnetotelluric soundings across Vancouver Island reported by R.D. Kurtz, J.M. DeLaurier and J.C. Gupta elsewhere in this issue (*Nature* **321**, 596; 1986) provide the first correlation of high electrical conductivity with a seismic reflector at the top of a subducted plate. The good conductor, at depths of 20–50 km down the sloping plate, is best understood as composed of seafloor sediments and volcanic rocks that contain brine in their pore spaces, and carried on the Juan de Fuca plate as it subducted beneath Vancouver Island. If saline water is thus subducted at many convergent plate boundaries, the implications for the continental crust and the tectonic processes in it are important.

The magnetotelluric profile reported by Kurtz *et al.* forms part of the first of a series of transects across major structures in LITHOPROBE, the Canadian national programme of deep crustal studies. The central discipline of the programme is seismology, supported by other geophysical and geological techniques. In southern Vancouver Island three seismic reflection sections of outstanding clarity have been secured, showing both the subducting plate and much detail in the layered rocks above it (Green, A.G. *et al. Nature* **319**, 210; 1986). The magnetotelluric stations in the study of Kurtz *et al.* were sited along two of the three seismic profiles. At three stations, the top of the good conductor is correlated with a seismic reflector within 10 per cent of depths in the range 23–28 km. The results from all 18 stations in the study can be fitted to a two-dimensional model in which a sloping conductive layer correlates well with a seismic reflector interpreted as the top of the downgoing plate throughout the depth range 23–34 km. Such correlations facilitate recognition and interpretation of structures located in different physical parameters (such as elastic moduli and electrical conductivity). It is planned to obtain magnetotelluric profiles at high station density along future seismic reflection sections of LITHOPROBE on land.

Fluids in the crust are attracting increasing attention. Crustal water is of critical importance in the response of rocks to stress, in particular in the thrusting of rock sheets a few kilometres thick over areas of several thousands of square kilometres in continental collison zones such as the Himalayan, Alpine and Appalachian mountain systems. Crustal water has great economic importance in relation to metallic ore genesis and to maturation and migration of hydrocarbons. Such water is generally a brine (Fyfe, W.S. *et al. Fluids in the Earth's Crust* Elsevier, Amsterdam, 1978); the effects of the chemical reactions of this water with silicate minerals in the lower crust are being explored. A brine is a very good electrolytic conductor, and provided that it fills interconnected pore spaces or fractures it will give high bulk conductivity in the rock (Shankland, T.J. & Ander, M.E. *J. geophys. Res.* **88**, 9475; 1983). This is the interpretation of the conductive layer beneath Vancouver Island offered by Kurtz *et al.*

Saline water probably exists in crustal rocks of all ages. In tectonically active regions close to ocean ridges and subductions the silicate mineral of lowest melting point may provide another fluid that fills cavities between the other silicate crystals, both in the upper mantle and locally in the crust. Such partial melt is generally a good electrolytic conductor, and will produce high bulk conductivity if it is in interconnected spaces (Shankland, T.J. & Waff, H.S. *J. geophys. Res.* **82**, 5409; 1977).

In the interior of British Columbia, 200–600 km north-east of Vancouver Island, a large regional conductive layer is known to exist in the lower crust and uppermost mantle. I have suggested (*J. geophys. Res.* **91**, 1909; 1986) that this Canadian cordilleran regional conductor is caused by partial melt at upper mantle depths and saline water in the crust above. The evidence for subduction of seafloor rocks containing brine presented by Kurtz *et al.* gives one reasonable explanation of the accumulation of brine in the crust of the hinterland of the subduction. If similar evidence is found in other zones of subduction, the new result may lead to better understanding of the mechanisms responsible for the transfer of water into other regions of the continental crust.

It is to be hoped that magnetotelluric soundings will be added to the collection of seismic reflection profiles in other regions so that structures can be sensed in terms both of electrical conductivity and of seismic-wave parameters. Either saline water or partial melt produces contrasts of one to two orders of magnitude in electrical conductivity, whereas the corresponding effects on seismic-wave velocities and attenuations are of the order of 10 per cent. Magnetotelluric soundings should therefore detect fluids of both kinds with much greater sensitivity than can be achieved by seismology. On the other hand, seismology gives better location of velocity interfaces and faults. The two methods are complementary, and much more powerful together than either alone, as demonstrated in recent studies of the crust beneath the Rhenish Massif in Germany (Meissner, R. & Wever, T. *Am. Geophys. Union Geodynamics Ser.* **13**, 31; 1986, and Jödicke, H. *et al.* in *Plateau Uplift* ed. Fuchs, K. Springer, Berlin, 1983), as well as in the Vancouver Island studies of Kurtz *et al.* and of Green *et al.* □

D. Ian Gough is Professor of Physics at the Faculty of Science, University of Alberta, Edmonton, Canada T6G 2J1.

Weather forecasts still tricky

SIR—The recent paper on 'Fractal characterization of inhomogeneous geophysical measuring networks' by Lovejoy *et al.*[1] and a discussion in *News and Views*[2] address the important problem of detectability of sparse atmospheric phenomena and, therefore, of the very feasibility of useful weather forecasting. Now, whatever the difficulty of its detection might be, a sparse phenomenon will exert an influence on the *time course* of a multitude of more systematic phenomena occurring over a wide range of space scales. The main reason for this is the fundamental instability of the atmospheric system[3]: a perturbation arising from an uncontrollable localized event and acting on a larger scale phenomenon pertaining to atmospheric circulation may give rise to an (exponentially) divergent history and to an altogether different regime, or to an aperiodic sequence of regimes perceived by an unaware observer as 'noise'.

Let γ be the precision with which the initial state of the system can be determined in phase space. Assuming that the atmosphere behaves as an unstable dynamical system we obtain the following estimate for the error growth after time t:

$$\gamma(t) = \gamma e^{tK} \qquad (1)$$

where K is the largest positive Lyapounov exponent (or more generally the Kolmogorov entropy).

Since our variables are distributed in physical space, an inadequate spatial resolution l will clearly induce an error in the estimate of the variables. Conversely, if for some reason their values are subject to uncertainty, it will be difficult to locate with precision the region of space from which these variables had initially emanated. We may therefore substitute, in our crude estimate, the phase space uncertainty γ by the precision l with which the initial state of the atmosphere can be determined in the physical space and write, instead of (1)

$$l(t) = le^{tK} \qquad (2)$$

When the size $l(t)$ will reach a value of the order of the dimensions of the entire system, L, predictions concerning individual histories will become meaningless and should be replaced by statistical considerations. The time τ_m for which this will happen is[4]:

$$\tau_m \simeq \frac{1}{K} \ln \frac{L}{l} \qquad (3)$$

This gives a quantitative measure of the limits of predictability of the system. A significant feature of τ_m is its logarithmic dependence on the parameter l, and thus its relative insensitivity to space resolution. Going from a quasi-uniform to a fractal distribution of l or vice versa is not going to change this picture drastically.

So although detection of sparse phenomena is important in its own right, it is worth stressing that even with a considerable improvement of the world detection network the problem of forecasting of the global state of the atmosphere is likely to remain as acute as ever.

C. NICOLIS
Institut d'Aéronomie Spatiale de Belgique, 1180 Bruxelles, Belgium

G. NICOLIS
Faculté des Sciences, Université Libre de Bruxelles, 1050 Bruxelles, Belgium

1. Lovejoy, S. *et al. Nature* **319**,43–44 (1986).
2. Hollingsworth, S. *Nature* **319**, 11 – 12 (1986).
3. Lorenz, E.N. Tellus 36A, 98–110 (1984).
4. Schuster, H.G. *Deterministic Chaos* (Physik, Weinheim, 1984).

Activation of cellular calcium entry

SIR—A recent *News and Views* piece by Baker[1] discusses the mechanisms of intracellular calcium ion (Ca^{2+}) release from the endoplasmic reticulum (ER) but refers briefly to cellular calcium entry from the extracellular fluid as being mediated by Ca^{2+} channels gated either chemically or by voltage. Voltage-activated Ca^{2+} channels that can be modulated by intracellular messengers have been characterized in many systems[2], but are unlikely to be present in a number of different epithelial tissues such as exocrine glands and liver simply because they are unable to fire action potentials and many activating hormones or neurotransmitters evoke membrane hyperpolarization rather than depolarization in these cells[3]. Nevertheless there is clear evidence that hormones and neurotransmitters can increase unidirectional Ca^{2+} flux into, for example, pancreatic acinar cells[4].

The mechanisms underlying this receptor operated Ca^{2+} entry are at present obscure although a link with the increased turnover of phospholipids after stimulation has been suspected for more than ten years[5] with evidence for such a link being particularly clear in relation to Ca^{2+} entry in blowfly salivary glands[6]. A recently formulated hypothesis[7] suggests that receptor operated Ca^{2+} entry is secondary to the emptying of an intracellular Ca^{2+} pool mediated by the action of inositol trisphosphate (IP_3) on an electrogenic Ca^{2+} pathway (channel) in the ER[8,9]. The well-established biphasic nature of agonist-activated Ca^{2+} mobilization is, according to the new hypothesis, explained by an initial emptying of the intracellular (ER) Ca^{2+} pool by IP_3 followed by entry of extracellular Ca^{2+} into the pool and, in the continued presence of IP_3, into the cytosol. On removal of the stimulant, IP_3 is rapidly broken down closing the Ca^{2+} channel in the ER and Ca^{2+} entry from the outside continues only until the content of the ER pool has reached a level that prevents further entry.

In this model[7] intracellular Ca^{2+} release and Ca^{2+} entry are both controlled by the same messenger, IP_3. Ca^{2+} entry is therefore not directly linked to the hormone receptor, but is messenger-mediated. A recent patch-clamp study on pancreatic acinar cells[10] demonstrating an external Ca^{2+} requirement for sustained K^+ channel (Ca^{2+}-activated) opening evoked by a peptide belonging to the cholecystokinin-gastrin group may be relevant in this context since the Ca^{2+}-requirement could be localized at a site separated from the hormone-receptor interaction indicating messenger-mediated rather than receptor-mediated Ca^{2+} uptake. These recent findings[10] appear to be compatible with the hypothesis forwarded by Putney[7].

OLE H. PETERSEN
MRC Secretory Control Research Group, University of Liverpool, Liverpool L69 3BX, UK

1. Baker, P.F. *Nature* **320**, 395 (1986).
2. Reuter, H. *Nature* **301**, 569–574 (1983).
3. Petersen, O.H. & Maruyama, Y. *Nature* **307**, 693–696 (1984).
4. Kondo, S. & Schulz, I. *Biochim. biophys. Acta* **419**, 76–92 (1976).
5. Michell, R.H. *Biochim. biophys. Acta* **415**, 81–147 (1975).
6. Berridge, M.J. & Fain, J.N. *Biochem. J.* **178**, 59–69 (1979).
7. Putney, J.W. *Cell Calcium* **7**, 1–12 (1986).
8. Streb, H., Irvine, R.F., Berridge, M.J. & Schulz, I. *Nature* **306**, 67–69 (1983).
9. Mualem, S., Schoeffield, M., Pandol, S. & Sachs, G. *Proc. natn. Acad. Sci. U.S.A.* **82**, 4433–4437 (1985).
10. Suzuki, K., Petersen, C.C.H. & Petersen, O.H. *FEBS Lett.* **192**, 307–312 (1985).

Beam balance test of weak equivalence principle

SIR—In the recent article by Fischbach *et al.*[1], commenting on a *News and Views* piece[2], a new hypercharge force is postulated as being responsible for various apparently anomalous effects in physics. Although there may not be unanimity in the interpretation of the Eötvös data in terms of this new force[3], its existence would have such far reaching consequences in physics that further experiments are clearly required. As suggested by Fischbach *et al.*, further Eötvös-type or galilean experiments come to mind. Here we propose an experiment using a common balance which would allow the force, if it exists, to be measured with good precision. The experiment would be as follows.

The weights of the two test masses made of materials having different values of (B/μ) (see ref. 1 for notation) are compared using a beam balance at two different sites. The first site is in a tunnel deep inside a mountain where it can be assured that there are some kilometres of solid rock in all directions. Here, in the absence of any net hypercharge force, the test masses are adjusted to have apparently equal masses as measured using the balance. The balance and test masses are then moved out of the tunnel to a second site on the surface of the Earth, preferably

at the same altitude and not too distant. According to Fischbach *et al.* we would expect to find at this second site a difference in apparent weight ΔW:

$$\Delta W = a\,Mg\left(\frac{B_1}{\mu_1} - \frac{B_2}{\mu_2}\right) \qquad (1)$$

Taking a value for a derived from the Eötvös data as given in ref. 1 and masses of one kilogram, the largest value of ΔW that could reasonably be obtained would be for masses of an appropriate stainless steel and lithium hydride (^{6}LiH) respectively, for which $\Delta W \approx 2.5 \times 10^{-7}$ N, equivalent to a 25 μg difference in apparent mass. Replacing the ^{6}LiH by beryllium would reduce the apparent mass difference to 14 μg but would avoid possible dangers involved in the handling of kilogram quantities of ^{6}LiH. If, instead, we take the value of a deduced from the geophysical measurements of G, we find a value of ΔW equivalent to 1.5 μg and 0.9 μg for ^{6}LiH and Be respectively.

The practicality of carrying out such an experiment with a worthwhile accuracy requires first a transportable balance having a reproducibility better than 1 part in 10^9 (equivalent to 1 μg for a 1kg mass). Traditional knife-edge balances, although there are at least two which achieve such reproducibility[4,5], are certainly not transportable so would not be suitable. Such balances are much too delicate and require extreme care in the mounting, handling, and adjustment of the beam and knife edges. However, a flexure-strip balance has recently been described[6] that is much less subject to these constraints. The beam and flexure elements are designed to be assembled without any adjustment and to be relatively robust. Preliminary results indicate that a reproducibility of 5 parts in 10^{10} can be achieved in the comparison of 1 kg masses. A similar performance may eventually also be possible using a hydrostatic balance[7]. Second, we need to be able to construct pairs of appropriate test masses that are not subject to significant differences in air buoyancy or sorption effects. Adequate test masses could be made by enclosing up to about 1.5 kg of the test material (^{6}LiH, Be and stainless steel) in stainless-steel vessels made to have nearly identical external volumes and surface finishes. The stainless steel should be chosen to be one of those already used for stainless-steel mass standards, such as Immaculate V, Nicral D or an equivalent AISI 310 steel, whose magnetic and other properties are suitable. Provided that the external volumes of the test masses differ by only a few parts in 10^4, the differences in their respective air-buoyancy corrections are sufficiently small to be measurable without significant error. Vacuum weighing would of course remove this problem altogether but would, perhaps, introduce further problems due to desorption. It is not difficult to ensure that the values of the masses themselves and the heights of their centres of mass are sufficiently close for the demands placed on the knowledge of g and its vertical gradient to be modest.

Although the quickest tests of the ideas of Fischbach *et al.* could probably be made by repeating the Eötvös experiment using already existing equipment[3], we think it worth while pointing out that an experiment made using a beam balance could give results of ample precision. Indeed, if the force predicted is shown to exist its presence would, among many other things, lead to modifications in high-precision weighing procedures, to say nothing of its implications for the present definition of the kilogram.

C.C. SPEAKE
T.J. QUINN

Bureau International des Poids et Mesures, Pavillon de Breteuil, F-92312 Sevres, Cedex, France

1. Fischback, E., Sydarsky, D., Szafer, A., Talmadge, C. & Aronson, S.H. *Phys. Rev. Lett.* **56**, 1, 3 – 6 (1986).
2. Maddox, J. *Nature* **319**, 173 (1986).
3. Keyser, P.T., Niebauer, T., Faller, J.E. *Phys. Rev. Lett.* (in the press).
4. Almer, H.E. *J. Res. NBS* **76C**, 1 – 10 (1972).
5. *BIPM Com. Cons. Masse:* Document 85/4; *Bull. NRLM* **33**(2), 7 – 18 (1984).
6. Quinn, T.J., Speake, C.C. & Davis, R. *Metrologia* (in the press).
7. Probst, R. & Kochsiek, M. *Metrologia* **19**, 137-146 (1984).

Blym clone could be contaminant

SIR—In their reply to my recent paper[1] Cooper and Diamond[2] raise two points — first, that some of the clones I describe are contaminated by the original *HuBlym*-1 clone and, second, that the results of a single transfection assay, not described in my paper, conflict with other assays reported in the paper.

The original clone described in the paper is one of several isolated and designated as non-transforming (using the transfection assay) and reported by Diamond *et al.*[3]. There has never been any suggestion that this clone, which has the same sequence as *HuBlym*-1, is a contaminant.

It is not possible to exclude the possibility raised by Cooper and Diamond that the other clones described in this paper are indeed contaminants. Unfortunately, the clones, which I left in the laboratory, were disposed after my departure and before the issue of contamination was raised with me. These clones had, however, been designated as transforming or non-transforming in transfection assays read by Cooper and it was precisely because of this classification that they were subsequently selected for sequencing.

Cooper and Diamond cite a transfection assay performed by me in May 1984, when the sequencing of the Burkitt's clones was 90 per cent complete and the cloning and selection of the gene from normal human embryo fibroblast DNA had just started. This particular transfection was carried out at a time when the assay was not working reproducibly and was an exercise in trying to find out what the problem might be. Therefore this result, which conflicted with several other assays carried out previously and read by Cooper, cannot be considered in any way accurate or meaningful.

It is gratifying that Cooper and Diamond confirm my conclusion regarding the nucleotide sequences of *HuBlym*-1.

JOAN DEVINE

Celltech Ltd, 244-250 Bath Road Slough, Berkshire SL1 4DY, UK

1. Devine, J.M. *Nature* **321**, 437–438 (1986).
2. Cooper, G.M. & Diamond, A. *Nature* **321**, 438 – 439 (1986).
3. Diamond, A., Cooper, G.M., Ritz, J. & Lane, M.A. *Nature* **305**, 112–116 (1983).

Writing enzyme units in the correct way

SIR—There seems to be a great deal of ambiguity and a frequent scientific error in the literature when the specific activity of enzymes is reported. Very often, it is expressed as "nmol/min/mg", as "nmol/min per mg" or as "nmol per min per mg". (See, as examples, refs 1–7, but many others could be cited.) Phonetically it seems correct but I believe it to be mathematically incorrect. It should be expressed as "nmol × min^{-1} × mg^{-1}".

The expression "*a*/*b*/*c*" is indeed ambiguous, because

$$(a/b)/c = \frac{a/b}{c} = \frac{a}{b\times c}$$

and

$$a/(b/c) = \frac{a}{b/c} = \frac{a\times c}{b}$$

therefore, in the linear form "*a*/*b*/*c*", the use of parentheses is obligatory.

To express the term

$$\frac{a}{b\times c}$$

it is necessary to write $a\times b^{-1}\times c^{-1}$ or $a/(b\times c)$.

And similarly, to express the term

$$\frac{a\times c}{b}$$

we must write $a\times c\times b^{-1}$ or $a/(b/c)$.

The formula that is derived for enzyme activity is defined correctly as "nmol × min^{-1} × mg^{-1}" or as "nmol/(min × mg)". The common expression "nmol/min/mg" is therefore ambiguous.

The same holds true for other units expressed in a similar formal way, such as mutations/cell/hour and disintegrations/min/tube. I urge the adoption of the correct designation for specific activity of enzymes, and similar units.

MORENO PAOLINI

Istituto di Farmacologia, Università degli, Studi, Via Irnerio, 48–40126, Bologna, Italy

1. Rifkind, A.B. & Muschick, H. *Nature* **303**, 524–526 (1983).
2. West, D.C., Hampson, I.N., Arnold, F. & Kumar, S. *Science* **228**, 1324–1326 (1985).

3. Biron, K.K. *et al. Proc. natn. Acad. Sci. U.S.A.* **82**, 2473–2477 (1985).
4. Daggett, S.G., Gruys, K.J. & Schuster, S.M. *J. biol. Chem.* **260**, 6213–6218 (1985).
5. Ramos, F. & Wiame, J.M. *Molec. gen. Genet.* **200**, 291–294 (1985).
6. Huang, D.P., Cote, G.J., Massari, R.J. & Chiu, J.F. *Nucleic Acids Res.* **13**, 3873–3890 (1985).
7. Inman, R.B. *Biochim. biophys. Acta* **783**, 205–215 (1985).

Gamma-ray spectrum of Chernobyl fallout

SIR—The activity in Oxfordshire due to the plume of radioactive material released from the Chernobyl reactor reached a peak on 2 May[1]. On 8 May we examined the 'Polyfoam' air filters routinely used in our laboratory air supply system and monitored a small but distinct amount of β- and γ-radiation activity. We have measured the γ-ray energy spectrum from the filters using a high-efficiency (40%) germanium detector, shielded from room background.

Figure 1 shows the complex γ-ray spectrum from the filters. The background is due to Compton-scattered γ-rays, which do not deposit their full energy in the detector. An analysis of the full-energy peaks yields a definite identification of 16 radioisotopes, with a further three (weaker) tentatively identified radioisotopes. The activity of each radioisotope is categorized as strong or weak in Table 1. The relative activities for the most prominent isotopes vary significantly from those deduced by Fry *et al.*[1], which serves to emphasise that these coarse filters were not designed to collect fallout products. The measured activity of ~ 2,000 Bq m^{-2} of ^{131}I on each 0.1m^2 filter suggests that ~ 1% of the local iodine activity[1] was deposited by the air flow of 2×10^4 m^3 per day.

Table 1 Relative γ-ray activities of radioisotopes measured in laboratory air filters

Isotope	Relative activity*	Half-life
^{131}I	S	8 d†
^{137}Cs	S	30 yr
^{132}Te	S	3 d
^{132}I	S	2 h
^{103}Ru	S	39 d
^{134}Cs	S	32 yr
^{106}Ru	S	367 d
^{140}Ba – ^{140}La	S	13 d–40 h
^{136}Cs	W	13 d
^{95}Zr – ^{95}Nb	W	64–35 d
^{141}Ce	W	33 d
^{99}Mo	W	3 d
^{144}Ce	W	284 d
^{129}Te^m	W	33 d
[^{127}Sb]	[W]	4 d
[^{105}Rh]	[W]	1.5 d
[^{143}Ce]	[W]	1.5 d

*Identified radioisotopes are listed in order of activity. Isotopes with activities greater than 10% that of ^{131}I are labelled strong (S) and those with activities less than 5% are labelled weak (W). † Days.

All of the identified radioisotopes are ^{235}U fission decay products. The criteria for observing a particular fission product in such a simple γ-decay experiment are: (1) the feeding mass chain should have a lifetime ≥ 1 day and ≤ 500 yr; (2) the fission yield should be ≥ 0.5% for the mass chain; (3) the β-decays should significantly populate excited nuclear states which subsequently γ-decay. Using these simple criteria, we find that all of the expected mass chains are accounted for, except masses 133 and 147, whose identifications are made difficult by the complexity of the spectrum.

Most of the activity (70%) will decay over the next month and the levels will approach those measured normally from the natural thorium and radium background. Air-supply filters with greater air flows or greater capture efficiency will have proportionally greater activity.

D.M. PRINGLE
W.J. VERMEER
K.W. ALLEN
Nuclear Physics Laboratory,
Keble Road,
Oxford OX1 3RH, UK

1. Fry, F.A., Clarke, R.H. & O'Riordan, M.C. *Nature* **321**, 193–195 (1986).

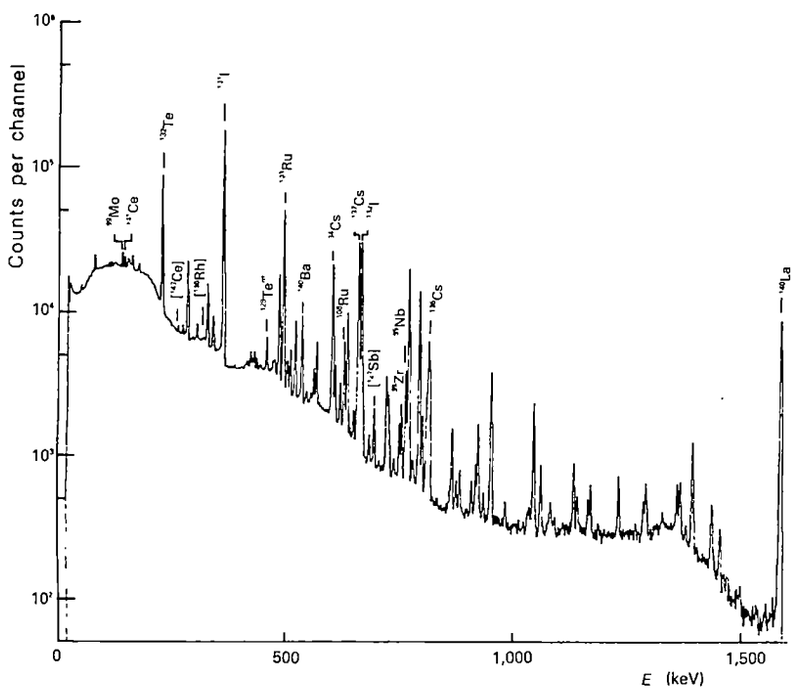


Fig. 1 Part of the γ-ray spectrum obtained with a Ge(Li) detector from a typical air filter. The strongest identified peak of each radioisotope is labelled.

Q1146+111B,C quasar pair: illusion or delusion?

SIR—The quasar pair Q1146+111B,C has been re-observed by Turner *et al.* who argue that it comprises two gravitationally lensed images of a single source. In this letter, we show that we are probably observing two distinct though neighbouring quasars.

Were quasars placed randomly on the sky, the probability of finding another quasar of apparent magnitude m within an angle θ of a given quasar would be $P(\theta, m) \simeq n\pi\theta^2$, where $n(m)$ is the sky density of quasars brighter than magnitude m. For Q1146+111B,C, $\theta = 157$ arc s, $n(18.5) \sim 1$ per deg^2 (ref. 4), giving $P_c \sim 6 \times 10^{-4}$. However, quasars are probably not distributed uniformly throughout the Universe, and there is evidence that they are clustered in much the same way as are galaxies[5,6] (but see ref. 7), so their two-point correlation function is $\xi(r) = (r/r_0)^{-1.8}$, where $r_0 = 5(1+z)^{-1}h^{-1}$ Mpc, h = the Hubble constant $H_0/100$ km s^{-1} Mpc^{-1} and the cosmological density parameter $\Omega_0 = 1$. The probability associated with this excess for a given quasar to have a companion within angle θ brighter than magnitude m is then

$$P_c(\theta,m,z) = 2\pi(1+z)^3 \int_0^m db\, b \times \int_z^\infty dl\, \Phi\, \xi(b^2 + l^2) \qquad (1)$$

where $D(z)$ is the angular diameter distance of the quasar, and $\Phi(L,z)$ is the integral luminosity function for quasars with luminosity $L(m,z)$. Now, $\Phi(L,z) = (dn/dz)/D^2(1+z)^{1.2}$ (ref. 8) and observations[4] indicate that for $0.5 < z < 2$, quasars of a given magnitude are uniformly distributed in redshift with $dn/dz = 0.5n$. Substitution in equation (1) then gives $P_c(\theta,m,z) = 38(1+z)(\sqrt{1+z}-1)\theta^3\xi(\theta D)dn/dz$ for $D\theta \leq 2r_0$, where n is per steradian and θ in radians. Numerically, $P_c \sim 2 \times 10^{-4}$.

Published quasar catalogues[9,10] contain $N(19) \sim 2{,}000$ quasars brighter than $B = 19$. Unpublished surveys probably treble this number. The expected number of random associations with the separation and magnitude of Q1146+111B,C is $NP_r(157 \text{ arc s}, 18.5)/2 \sim 20$, which is roughly what is observed[5,9]. The expected number of closely clustered companions is $NP_c(157 \text{ arc s}, 18.5, 1.0)/2 \sim 1$. Hence we would expect by now to have discovered of the order of one physically associated pair of magnitude 18.5 quasars separated in angle by less than 157 arc s and in velocity by the velocity dispersion of small groups which dominate the correlation function, $\sim 300 \text{ km s}^{-1}$. We should not be unduly surprised if Q1146+111B,C fails tests of the lensing hypothesis[11] — it may be that expected pair.

In conclusion, we suggest that the necessity for lensing in some of the other gravitational lens candidates should be re-examined. This is especially important for faint quasars when there is no independent evidence for lensing (for example, an intervening giant galaxy or distortion of background galaxies) and no sign of common spectroscopic or morphological peculiarities. (Overall spectral dissimilarity need not rule out lensing because quasars can very significantly in the time delay between two images.) The quasar pairs Q2345+007A,B (ref. 12) and Q1635+267A,B (ref. 13) in which the fainter quasars are both roughly magnitude 21 both give $P_c \simeq P_r \sim 2 \times 10^{-4}$, if we assume that the correlation function is valid for proper distances ~ 20 kpc (as it is for the galaxy–galaxy correlation[14]; it has been suggested that the quasar–galaxy correlation function is even higher[15,16]). It is therefore not unreasonable that these two pairs comprise distinct objects; since $P_r \sim P_c$ we should expect to find a few similarly separated quasars with discrepant redshifts, for example, Q1548+114A,B (ref. 17).

We thank Ramesh Narayan for helpful suggestions. We acknowledge support by NSF Presidential Young Investigator grant AST84–51725 and grants from the Exxon Education Foundation and Boeing Company (E.S.P.) and NSF grant AST84–15355 (R.D.B.).

E.S. PHINNEY
R.D. BLANDFORD
Theoretical Astrophysics,
130–33 Caltech,
Pasadena,
California 91125, USA

1. Arp, H. & Hazard, C. *Astrophys. J.* **240**, 726–736 (1980).
2. Turner, E.L. *et al. Nature* **321**, 142–144 (1986).
3. Burbidge, E.M., Burbidge, G.R. & O'Dell, S.L. *Nature* **248**, 568–569 (1974).
4. Marshall, H.L. *et al. Astrophys. J.* **283**, 50–58 (1984).
5. Shaver, P.A. *Astr. Astrophys.* **136**, L9–10 (1984).
6. Kruszewski, A. Princeton Observatory preprint (1986).
7. Webster, A.S. *Mon. Not. R. ast. Soc.* **199**, 683–783 (1982).
8. Weinberg, S. *Gravitation and Cosmology* (Wiley, New York, 1972).
9. Véron-Cetty, M.P. & Véron, P. ESO Scientific Report No. 4 (1985).
10. Hewitt, A. & Burbidge, G.R. *Astrophys. J. Supple.* **43**, 57–158 (1980).
11. Blandford, R.D., Narayan, R. & Phinney, E.S. *Astrophys. J. Lett.* (submitted).
12. Weedman, D.W., Weymann, R.J., Green, R.F. & Heckmann, T.M. *Astrophys. J. Lett.* **255**, L5–L9 (1982).
13. Djorgovski, S. & Spinrad, H. *Astrohys. J. Lett.* **282**, L1–L4 (1984).
14. Lake, G. & Tremaine, S. *Astrophys J. Lett.* **238**, L13–L16 (1980).
15. Stockton, A. *Astrophys. J.* **257**, 33–39 (1982).
16. Hutchings, J.B. & Campbell, B. *Nature* **303**, 584–588 (1983).
17. Shaver, P.A. & Robertson, J.G. *Mon. Not. R. astr. Soc.* **212**, 15p - 20p (1985)

Beware the cups that cheer

SIR—Aluminium toxicity, intoxication or accumulation is associated (not necessarily causally) with several conditions including dialysis encephalopathy[1] and osteomalacia[2], the amyotrophic lateral sclerosis of Guam, and Alzheimer's disease[3] (believed to account for some one third of a million UK sufferers from senile dementia and said to affect over two million people in the United States). Edwardson and his colleagues have recently shown[4] the presence of aluminosilicates in senile plaques in Alzheimer's disease. Dietary intake of aluminium has not generally been regarded as a hazard, though one Swedish study[5] showed that cooking rhubarb in aluminium saucepans mobilized a significant amount of aluminium, presumably complexed by oxalate (ethanedi-oate). We would like to suggest that attention is paid to the high aluminium content of tea leaves and their infusion.

The tea bush (formerly *Thea sinensis*, now *Camellia sinensis*) is grown on acid soil, and tolerates high levels of aluminium, accumulating great quantities[6] of it. Indeed, potassium alum is used as a fertilizer[7]. The only other food plant which tolerates such high aluminium levels is the cranberry. The tea bush accumulates aluminium in the leaves to enable it to overcome a high level of aluminium in the leached acid soils in which it thrives.

We have examined samples of Chinese, Indian and Russian tea bought as packets from a local supermarket. The X-ray powder picture of each dry ash (all of surprisingly good quality) was essentially that of α-alumina (Al_2O_3). Other weak lines were present. The aluminium content (by gravimetric analysis) of these dry ashes varied from 8,700 p.p.m. to 23,000 p.p.m., in line with several reported analyses; up to 20,000 p.p.m. Al/dry weight have been reported in mature leaves[8].

We infused the teas in a teapot for up to 30 minutes using Cardiff tap-water (very soft), then analysed the infused liquids for aluminium with gravimetric references to underpin routine atomic absorption measurements. A typical finding was that the infusion of Russian tea had about 100 p.p.m. aluminium (100 mg dm^{-3}), and the Indian and Chinese typically had 40 and 60 p.p.m. aluminium, respectively.

Since many Britons drink a litre of tea a day, tea is likely to be as great a source of aluminium as any other in the British diet. (The aluminium foil often used for lining tea chests seems unlikely to exacerbate the problem).

Assuming (in the absence of information on the transfer of aluminium from diet into organs) that any source of aluminium is to be avoided at least for those suffering from conditions related to high aluminium levels, the belief that tea is a sovereign remedy under all circumstances may need revision. "The cups that cheer but not inebriate", may not be as true as William Cowper thought in 1785.

A.-M. CORIAT
R.D. GILLARD
Department of Chemistry,
University College,
Cardiff CF1 1XL, UK

1. Alfrey, A.C., Hegg, A. & Creswell, B. *Am. J. clin. Nutr.* **33**, 1509-1516 (1980).
2. Parkinson, I.S. *et al. Lancet.* **i**, 406-407 (1979).
3. Crapper, D.R. McLauchlan, S. & de Boni, V. *Neurotoxicity* **1**, 3-16 (1980).
4. Candy, J.M. *et al. Lancet* **1**, 354-357 (1986).
5. Mattsson, P. *Vår Foda* **33**, 231-236 (1981).
6. Ellis, R.T. *Biologist* **30**, 247-258 (1983).
7. Eden, T. *Tea* (Longmans Green, London, 1958).
8. Talibudeen, O. & Sivasubramanian, S. *J. Sci. Food Agric.* **22**, 325-329 (1971).

Frequency of dizygotic twinning

SIR—I am puzzled by a calculation in J.M. Diamond's article "Variation in human testis size" (*Nature* **320**, 488; 1986). In it he states that a single ovulation with intercourse will result in a live birth with probability ¼ and therefore a double ovulation will result in dizygotic twins with probability 1/16. He concludes that the double ovulation frequency must be 16 times the observed dizygotic twinning rate among births.

This conclusion is incorrect since a large fraction of the double ovulations will not lead to any birth at all. A double ovulation will yield zero births with probability 9/16, one birth with probability 9/16 and two births with probability 1/16. Hence the probability that a double ovulation will yield twins conditioned on there being any birth at all is $(1/16)/(1/16+9/16)=1/7$. Therefore Diamond should conclude that the double ovulation frequency is 7 times the observed twinning rate. Thus, for example, the Yoruba women would have a double ovulation frequency of 34.3% rather than 78%, as stated.

MICHAEL SIPSER
Department of Mathematics,
Massachusetts Institute of Technology,
Cambridge, Massachusetts 02139, USA

SCIENCE AND TECHNOLOGY

Whatever the subject... refer to MACMILLAN DICTIONARIES

DESIGNED FOR STUDENTS

The paperback *Macmillan Dictionary Series* combines new and established works of teaching and reference with an attractive series format.

* authoritative definitions and explanations of all current terminology written by experts
* lucidly written entries with thorough cross referencing
* regular new editions keep the student up to date with the latest research, practice and technology
* a clear layout for easy reference
* prices range from just £7.95 to £9.95

NEW IN 1986...

MACMILLAN DICTIONARY OF BIOTECHNOLOGY
JIM COOMBS March 1986 320pp 0 333 40875 6 £9.95

MACMILLAN DICTIONARY OF THE HISTORY OF SCIENCE
Edited by W. F. BYNUM, E. J. BROWNE and ROY PORTER
March 1986 528pp 0 333 34901 6 £8.95

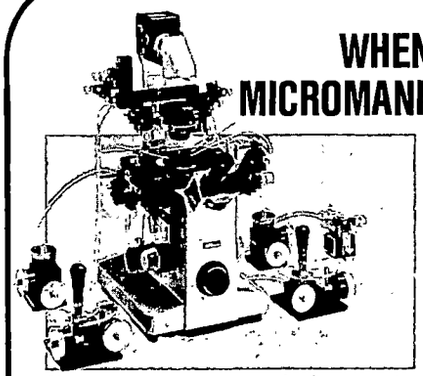
MACMILLAN DICTIONARY OF PERSONAL COMPUTING AND COMMUNICATIONS DENNIS LONGLEY and MICHAEL SHAIN
August 1986 320pp 0 333 42170 1 £8.95

MACMILLAN DICTIONARY OF PHYSICS
MARY P. LORD August 1986 320pp 0 333 42377 1 £8.95

MACMILLAN DICTIONARY OF IMMUNOLOGY
FRED ROSEN, LISA STEINER and EMIL UNANUE
August 1986 256pp 0 333 39248 5 £8.95

Macmillan Press, Houndmills, Basingstoke, Hants RG21 2XS, UK
Not available in USA.

MACMILLAN PRESS



WHEN YOU THINK MICROMANIPULATION...

THINK MEDICAL SYSTEMS CORP.

Now you can mount manipulators onto your inverted microscope. Eliminate stage clutter while enhancing stability for micromanipulation.

Look to Medical Systems Corp.... for all your micromanipulator needs.

For more information, call us or return the coupon.

Send more micromanipulation information to:

Name_____
Institution_____
Address_____
City_____ State_____ Zip_____
Phone ( )_____

Medical Systems Corp.
ONE PLAZA ROAD, GREENVALE, NEW YORK 11548 • 516-621-9190
TELEX: 645031 MEDSYSTEMS • OUTSIDE N.Y. STATE 800-654-5406

Reader Service No.15

CAMBRIDGE *Journals*

Established titles from two leading societies . .

The Journal of Physiology

Chairman of the Editorial Board: **E.S. Petersen**

Published for The Physiological Society, each hardbound monthly volume is concerned with all aspects of research in physiology, especially vertebrate. This includes respiration, circulation, excretion, reproduction, digestion, homeostasis, and particulary neurophysiology and muscular contraction.
Volumes 370-381 (1986) **£410.00** per year in U.K. only; **£435.00/$1030** elsewhere; Airmail **£200.00** extra
ISSN 0022-3751

Quarterly Journal of Experimental Physiology

Chairman of the Editorial Board: **C.R. House**
University of Edinburgh

QJEP was founded in 1908 and has been published by The Physiological Society since 1979.
Volume 71: January, April, July and October 1986
£60.00/$130. Airmail **£20.00** extra
ISSN 0144-8757

Journal of Anatomy

Editor: **Prof. D.B. Moffat** *University College, Cardiff*

Published for the Anatomical Society of Great Britain and Ireland, the journal presents original work and book reviews in anatomy, embryology and histology in six casebound issues each year. Its scope, which includes human and comparative anatomy (functional aspects, neurology, embryology, histology, histochemistry, and electron microscopy), has made Journal of Anatomy the leader in its field.

Forthcoming articles include: Current developments and future directions in autonomic neuromuscular junctions; The granular peripolar cell of the human glomerulus; A Golgi study of the sixth layer of the cerebral cortex; Freeze-fracture observations on human peripheral nerve; Ultrastructural evidence for fibril-to-fibril associations in articular cartilage and their functional implications.
Volumes 144-149: February, April, June, August, October and December 1986 **£188/$440** per year; Airmail **£42.50** extra
ISSN 0021-8782

Write to Lesley Boyle (Cambridge) or Harry Florentine (New York) if you need further information.

Cambridge University Press
The Edinburgh Building, Shaftesbury Road, Cambridge CB2 2RU, England
32 East 57th Street, New York, NY 10022

Reader Service No.18

Journal of Biotechnology

Managing Editor:
A. Fiechter, *Institut für Biotechnologie, ETH–Hönggerberg, CH-8093 Zurich, Switzerland*

Associate Editors:
H. Bungay, *Dept. of Chem. & Environmental Engineering, Rensselaer Polytechnic Institute, Troy, NY 12181, U.S.A.*
S. Fukui, *Kyoto University, Dept. of Industrial Chemistry, Faculty of Engineering, Kyoto 606, Japan*
J. Messing, *Dept. of Biochemistry, University of Minnesota, St. Paul, MN55108, U.S.A.*
E.-L. Winnacker, *Universität München, Chemisches Laboratorium, Institut für Biochemie, Karlstrasse, 23, D-8000 München 2, F.R.G.*

Review Editor:
C. R. Lowe, *University of Cambridge, The Biotechnology Center, Downingstreet, Cambridge CB2 3EF U.K.*

Aims and Scope

The journal provides a medium for the rapid publication of full-length articles as well as short communications on various aspects of biotechnology. Information on new or potential applications of biotechnological relevance in the following areas will be considered for publication:

- molecular biology
- genetics
- biochemical aspects of metabolism and its control, including viral, microbial, plant and animal cell systems
- process development and its control, including computer applications automation and the development of (bio)-sensors as applied to biosystems.

The overriding criteria for publication are originality, high scientific quality and interest to a multidisciplinary audience.

Editorial Board
G. Belfort, *Troy, NY, U.S.A.*
T. Beppu, *Tokyo, Japan*
N.C. Brady, *Washington, DC, U.S.A.*
W. J. Brill, *Middleton, WI, U.S.A.*
N.H. Carey, *Slough, U.K.*
M.H. Caruthers, *Boulder, CO, U.S.A.*
Ch. Cooney, *Cambridge, MA, U.S.A.*
M.W. Fowler, *Sheffield, U.K.*
D.V. Goeddel, *San Francisco, CA, U.S.A.*
H. Heslot, *Paris, France*
J.G. Kuenen, *Delft, The Netherlands*
M.R. Ladisch, *West Lafayette, IN, U.S.A.*
A.I. Laskin, *Piscataway, NJ, U.S.A.*
M. Linko, *Helsinki, Finland*
P.K. Maitra, *Bombay, India*
K. Matsubara, *Osaka, Japan*
K. von Meyenburg, *Copenhagen, Denmark*
B.S. Montenecourt, *Bethlehem, PA, U.S.A.*
H. Okada, *Osaka, Japan*
A.D. Panek, *Rio de Janeiro, Brazil*
U. Pettersson, *Uppsala, Sweden*
P.L. Rogers, *Kensington, N.S.W., Australia*
M. Salas, *Madrid, Spain*
K. Schügerl, *Hannover, F.R.G.*
H. Simon, *Garching, F.R.G.*
H. Yamada, *Kyoto, Japan*

Subscription Information:
1986: Vols. 3-4 (2 volumes in 12 issues).
Price: US $185.50/Dfl. 538.00 including postage and handling.
ISSN 0168-1656

ELSEVIER

For further information and/or free sample copy please write to:

In the U.S.A. and Canada:
Journal Information Center
ELSEVIER SCIENCE PUBLISHERS
52 Vanderbilt Ave., New York, NY 10017, U.S.A.

In all other countries:
ELSEVIER SCIENCE PUBLISHERS
P.O. Box 211, 1000 AE Amsterdam,
The Netherlands

Please send your orders to the Amsterdam address

The Dutch guilder price is definitive, US $ prices are subject to exchange rate fluctuations. Prices are excl. B.T.W. for Dutch customers

Reader Service No.34

FL37A475

All around biotechnology

A.N. Emery and A. Lyddiatt

Comprehensive Biotechnology: The Principles, Applications and Regulations of Biotechnology in Industry, Agriculture and Medicine.
Editor-in-chief Murray Moo-Young.
Pergamon:1985. Four volumes, pp.3,764. £695, $995.

BIOTECHNOLOGY feeds upon many disciplines, and is dependent upon the cross-fertilization of ideas and information from a wide variety of sources. Ready access to the relevant literature is frequently inhibited by its style and format, and it is this drawback that is addressed by *Comprehensive Biotechnology*.

The work has been promoted as an integrated presentation of the basic principles, methods and applications of biotechnology. This is a formidable claim, and the fact that four volumes totalling over 3,500 pages were found to be necessary is a measure of the difficulty of the task that the editors set themselves. Moreover, the editorial board, under the direction of Murray Moo-Young, set out to assemble the work under several self-imposed constraints: they had to coordinate successfully an international team of 150 writers, combine intellectual appeal with comprehensive coverage *and* publish all four volumes at the same time. Such testing goals have been largely met in a work which lives up to its billing.

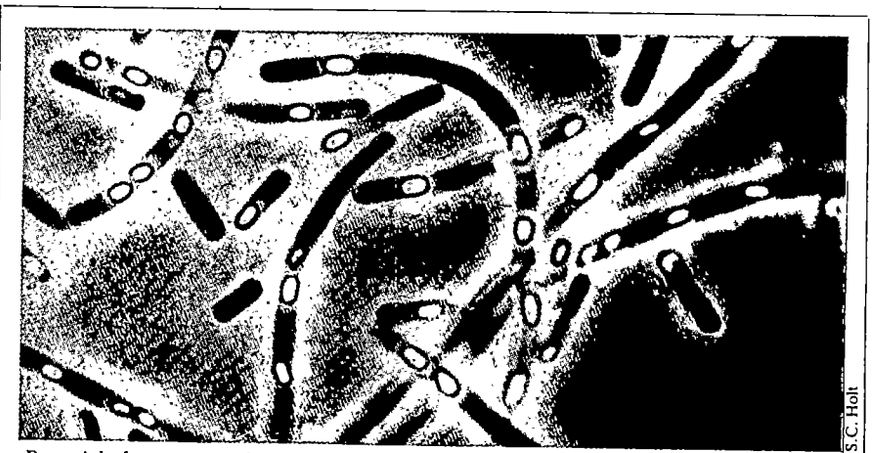
The four volumes are respectively entitled *Scientific Fundamentals, Engineering Considerations, Current Commodity Products* and *Speciality Products and Service Activities*, and each of them is in turn subdivided into either two or three sections. Volume 1, Section 1 covers genetic and biological fundamentals (including isolation methods, nutrition, growth and death of microorganisms as well as their genetic manipulation), while the regulation of cellular metabolism and enzyme evolution, mechanisms and kinetics are dealt with in Section 2. The introduction rightly describes this as a "pedagogic academic coverage" of the scientific disciplines underpinning the field as a whole, but the absence of stuffiness in the prose or inhibitory jargon is a strong incentive for the reader to explore the text rather than merely use it for reference. The relatively low-key coverage of animal and plant cell culture (combined in one lone chapter), however, reflects an emphasis out of keeping with the rapid increase of activity in these areas.

Volume 2 contains sections on bioreactor design, operation and control, and on upstream and downstream processing, written by a varied group of academic and industrial authors. This mix is not wholly successful, because some of the contributors have been allowed to reflect rather too strongly their commercial affiliations. Also, a stricter editorial hand would have avoided the repetition found, for example, in all four chapters on instrumentation, data handling and control, as well as in four chapters on aspects of membrane-based processes. Cross-referencing both between operations described within Vol. 2, and with applications in Vol. 3, would have greatly added to the value of these two components of the work.

Volumes 3 and 4 are described in their introductions as "utilitarian practical account[s] of commercial processes and products". The authorship is truly international (except for Soviet and Eastern European representation), and is largely drawn from industry. Volume 3 gives good accounts of present practices in the development and manufacture of health-care products, food and beverage products, and industrial chemicals, biochemicals and fuels. Volume 4 is much more ill-assorted: the first section, in particular, while aiming to introduce potential applications in biomedicine and chemotherapy, agriculture and other areas, is also left to pick up pieces of instrumentation, detection and containment of biohazards, and even surface thermodynamics. The remaining two sections give, first, an interesting and helpful international comparison of governmental approaches to both support and regulation of biotechnology, and lastly a useful blend of the theory and practice of waste management and pollution control.

It would need a football team of specialists to provide a detailed evaluation of the diverse contents of these four volumes. Instead, we sought to assess *Comprehensive Biotechnology* by making it available in our laboratories for anyone who cared to consult it — academic and research staff, students and industrial collaborators with interests across a wide range of subjects. By and large, their response has been enthusiastic. Specialists have generally judged the treatments of their own areas to be thorough, well illustrated, topical and generously referenced (up to about mid-1983). Venturing into less-familiar areas, we and our colleagues have found ourselves neither patronized by too shallow a text nor left floundering, bereft of explanation or definition. Each volume includes a glossary of terms and is individually indexed, though only Vol. 4 contains a cumulative index to the work as a whole — indeed, a general lack of inter-volume cross-referencing is a weakness. There is surely a strong case for producing a separate cumulative index.

Our personal expertise is in biochemical engineering, so it is inevitable that our more detailed criticisms arise with Vol. 2, and particularly the section on upstream and downstream processing. Here there are some surprising omissions, for example protein precipitation, non-specific adsorption, evaporation and drying. Such operations are now widely used in biochemical recovery, and absence of discussion of them is puzzling. This, however, could well be rectified in the subsequent, "update" volumes which the editors promise will appear at intervals to chronicle the scientific and technical developments of the future. Inclusion of an overview of the integration of unit processes in production and recovery operations would be beneficial, as would coverage of topics such as multiphase mixing,



Bacterial change — a phase-contrast photomicrograph of spores and vegetative cells of Bacillus fastidiosus. *The picture is reproduced from* Developmental Biology of the Bacteria, *by Martin Dworkin, published by Benjamin/Cummings. Price is $31.95, £24.95.*

biosensors, product polishing and quality control.

Finally, we have doubts about the grouping of certain topics and (more importantly) the physical robustness of the volumes. This is unquestionably a work of reference which will have to endure the rigours of usage in both library and laboratory. Two of the books contain over 1,100 pages in bindings likely to surrender to heavy patronage. Division into eight volumes might have inflated production costs but would have guaranteed a prolonged physical life — surely something to be expected from a work costing nearly £700. It would also have permitted a more rational allocation of material, avoiding the uneasy juxtapositions of topics in Vols 2 and 4, and consolidating individual volumes as entities in their own right.

For all that, Murray Moo-Young and his colleagues have brought off a notable success in producing this work and our limited criticism does not diminish this overall view. *Comprehensive Biotechnology* will be an essential purchase for all departments and institutions, academic or industrial, that claim an interest in any aspect of the ill-defined field popularly known as biotechnology. □

A.N. Emery and A. Lyddiatt are in the Department of Chemical Engineering, University of Birmingham, PO Box 363, Birmingham B15 2TT, UK.

HUMOUR THERAPY

in

Cancer
Psychosomatic Diseases
Mental Disorders
Crime
Interpersonal and Sexual Relationships

by BRANKO BOKUN

A NEW THEORY ON THE PART THAT FEAR PLAYS IN OUR MENTAL ACTIVITIES AND BEHAVIOUR

VITA BOOKS (Publisher)
26 Chelsea Square, London SW3

ISBN 0 9510525 0 0

221 pages. £5.00

Controlling disease in the valleys

G. Webbe

Schistosomiasis: The St Lucia Project. By Peter Jordan. *Cambridge University Press: 1985. Pp. 442. £35, $49.50.*

THE aim of the St Lucia schistosomiasis project was to compare the effects of control of the snail intermediate host, chemotherapy (that is, drug treatment) and improving water supplies in reducing transmission of *Schistosoma mansoni*, and thus the incidence, prevalence and intensity of the infection. The project ran from 1966 to 1981. It was based upon an epidemiological model which predicted the relative importance of the three approaches to control, and the experimental programmes were therefore designed for maximum impact in separate valleys which had similar epidemiological characteristics. These programmes are described in Part I of Peter Jordan's book.

In one valley, area-wide molluscicide was directed against snail colonies, detailed research into the dynamics of transmission having been undertaken as a basis for an appropriate snail control strategy. In a second valley, the contamination with schistosome ova was reduced by chemotherapy; treatment was offered to anyone found to be infected at any of the four annual surveys. Water supplies were provided in part of a third valley to reduce exposure to infection in rivers and streams. Piped water was introduced to individual houses in five valleys, together with communal laundries with shower units, and simple pools for recreational purposes.

After four years the effects on transmission of *S. mansoni* through snail control and the improvement of water supplies had been assessed, and chemotherapy was offered to people found to be infected. At this time, too, the area-wide strategy of snail control was changed to one of focal control. Over the next four years different consolidation strategies after therapy were tried out in each of the valleys. Further control schemes (through the provision of latrines or chemotherapy) were also initiated to compare the effect on transmission of reduced contamination with *S. mansoni* ova.

Comparison of the control strategies, based on parasitological findings, showed that the chemotherapy programme resulted in the cheapest, quickest and greatest fall in incidence, prevalence and contamination potential (cost $1.00 per person per year). In the snail control schemes, where area-wide molluscicide and focal control were applied, the overall declines in incidence and prevalence were similar, with intensity being reduced more with area-wide control (cost $3.24 and $2.87 per person per year, respectively). There was substantial reduction in all indices of infection in the water supplies programme (cost $2.99 per person per year). The results of additional chemotherapy were disappointing, however, while the effect of the provision of latrines remained inconclusive because of sporadic water supplies. In the maintenance phase, after chemotherapy in all areas, the best results came from focal snail control or the provision of individual household water supplies and communal laundries and showers.

The overall results of the St Lucia project confirmed the predicted relationship between morbidity and intensity of infection, and it seems that, for rapid disease prevention, chemotherapy will now be the main component of schistosomiasis control. The effectiveness of any drug delivery system must, however, determine the level of residual infection after treatment in a particular area. Moreover, in global terms, the transmission of schistosomiasis is characterized by its variability. While patterns of human contact with water, as well as human–parasite–disease relationships, are similar around the world, the transmission patterns differ greatly according to the ecology of the species of snail concerned. Thus, while it highlighted the relative cost-effectiveness of different control approaches over a limited period, the St Lucia project does not provide a basic protocol which can be applied in all situations. Further, more information is required about different chemotherapy regimens and even about the effects of treatment on acquired immunity, before formulating treatment policy. With such a limited number of effective compounds available, the problem of drug resistance must also be considered when developing long-term maintenance strategies requiring periodic re-treatment campaigns.

Part II of the book contains details of several related studies that were carried out in St Lucia. Among these, the accounts of epidemiological research on human exposure, morbidity and the longevity of adult worms, and of the immunological work, are of special interest.

The book is well illustrated and the data are very clearly presented. Altogether it is an important contribution to the literature on schistosomiasis; it strongly reflects the multidisciplinary nature of the St Lucia project, and it contains a unique wealth of information for parasitologists and all who are concerned with control of this disease. □

G. Webbe is Professor of Applied Parasitology at the London School of Hygiene and Tropical Medicine, Keppel Street (Gower Street), London WC1E 7HT, UK, and was a member of the Rockefeller Foundation Advisory Panel for the St Lucia Project.

Issues of analysis

Paul H. Harvey

Ecology and Natural History of Desert Lizards. By Eric R. Pianka. *Princeton University Press:1986. Pp.208. Hbk $45, £30; pbk $19.95, £13.30.*

FOR the past 20 years Eric Pianka has compared desert lizard communities in America, Africa and Australia, using standardized methods to allow comparisons among study sites within and between continents. The main results of his work are now brought together in a book which is not short on data; in addition to 31 pages of appendices, over 60 pages of the 150-page text are taken up by tables and figures.

Most of the book describes differences in reproductive tactics, activity and feeding habits of the various species, anatomical correlates of ecology, and community structure. The discussions are frequently based on statistical and multivariate summaries of the data. Such analyses can be dangerous, because hidden assumptions often lead to incorrect conclusions. Over the past ten years, there has been particular focus on this issue and Pianka is acutely aware of the pitfalls involved. Indeed, he devotes a full chapter to describing and assessing the methods used in the analysis of community structure. Most of his conclusions seem sound; for example, using a carefully designed "computer transplant experiment" Pianka and Larry Lawlor show that diets of particular species tend to change from site to site in a way that complements the diets of other species with which they are found.

Not all the analyses are as careful as this, however. At one point Pianka identifies what he terms a "transcendent" relationship. Some lizard species thermoregulate more effectively than others. The extent to which lizards thermoregulate can be described by their change in body temperature over a set range of air temperatures. But, at a set air temperature, some lizards are warmer than others. Pianka believes that these two components of the relationship between body and air temperature are not independent of each other, and plots the slopes relating body temperature to air temperature against their respective regression intercepts for a sample of 82 lizard species. He claims that the resulting highly significant negative relationship "represents an innate design constraint imposed by lizard physiology and metabolism". But, for given air and body temperatures, slopes and intercepts are not *expected* to be independent values: if we change the slope, we also change the intercept.

We clearly need to compare Pianka's data with a model in which slopes are independent of the air and body temperatures measured. To set up such a model, I randomly shuffled the empirical slopes among the different species and then calculated new intercepts using the mean external and body temperatures for each species. I repeated this procedure ten times and the correlation between slope and intercept ranged between –0.87 and –0.90, which to some extent describes Pianka's "transcendent" relationship. Pianka's relationship between slope and intercept may be tighter than expected, but he has not demonstrated that it is under a clearly defined null hypothesis. Indeed, his description leads the reader to assume that the expected correlation between slope and intercept is zero.

One chapter deals with reproductive tactics and, here again, I suspect that statistical analyses have missed their mark. Body size effects are either ignored or "removed" by taking simple weight ratios. Since larger species of most vertebrate groups are known to lay disproportionately small eggs (the relationship is one of negative allometry), Pianka's techniques are probably inappropriate and his analyses need to be repeated correctly

Nonetheless, the book has considerable strengths. It is a rich source of unique data; it highlights our ignorance of factors influencing the structure of even relatively simple communities; and it documents excellent natural history observations of particular species. In addition, the text is enlivened by a delightful collection of superbly reproduced colour photographs illustrating the variety of species studied □

Paul Harvey is in the Department of Zoology, University of Oxford, South Parks Road, Oxford OX1 3PS, UK.

Technique in time

D.J. Huntley

Thermoluminescence Dating. By M.J. Aitken. *Academic: 1985. Pp. 359. Hbk £50, $59; pbk £30, $34.95.*

MARTIN Aitken's first book, *Physics and Archaeology*, published in 1961, contained only a page on thermoluminescence dating. This new book presents a stunning contrast.

In 1961 it was thought that thermoluminescence (TL) resulted from radiation damage due to α-particles emitted by naturally occurring uranium and thorium; we know now that it results from electrons becoming trapped at crystal defects as a consequence of their liberation by various kinds of radiation. The general idea of using TL to determine past radiation doses, and hence the ages of samples (using separate measurements of the dose rates), has been around for several decades. It was not, however, until Aitken took up the subject that real progress was made and reliable dates of practical value to archaeologists were obtained. Most advances in the technique originated in Aitken's own laboratory at Oxford, but description of them is spread over such a wide literature that we all welcome having them brought together in a single book.

In the first two chapters the basic principles and methods are outlined in language that anyone with a scientific training should be able to follow. Thereafter the reader will learn that the subject is riddled with complications. The archaeologist who has studied ^{14}C dating knows that here one has to measure only the $^{14}C/^{12}C$ ratio in order to calculate a date. In TL dating, on the other hand, the number and complexity of the problems that have to be taken into account is extraordinary. Non-linear TL response, differing TL sensitivities, inhomogeneous samples, varying water contents, radon escape and a host of other factors have to be coped with, and all of them are discussed in detail by Aitken Some of these complexities can, however, be thought of as simply reflecting the great richness of TL dating, which now subsumes several different techniques (fine-grain, quartz inclusion, subtraction, predose, zircon, etc.). Again, all are described thoroughly. Each chapter includes a page or more of "Technical Notes", where many useful details are given without interrupting the main text, while the book itself ends with 13 appendices, taking up 90 pages. These are an invaluable reference source which TL workers will often have cause to consult.

The shortcomings of the book are minor. Aitken admits to being biased towards research done at Oxford; here the book is naturally strong, but in consequence work done elsewhere receives less thorough treatment. My main criticism, however, is reserved for a lack of rigour at some points and for Aitken's use of units. An "ionized electron" (p.42) is not part of my vocabulary, and reference to the activity of potassium as 89.5 per cent beta and 10.5 per cent gamma will confuse the unwary. "Annual dose" is used where "dose-rate" is meant, R is used for α-particle range in units of length on p.299 and units of mass per unit area on p.300, and a sievert can no more equal a gray than a digested apple can equal a fresh one. These and others like them are not too serious, though they will puzzle those not sure of their science.

This is a book by a physicist for physicists, and an essential acquisition for any TL dating laboratory and library. It will be the standard reference for many years. □

D.J. Huntley is Professor in the Department of Physics, Simon Fraser University, Burnaby, British Columbia V5A 1S6, Canada.

Ways to dispose of radioactive waste

J.L. Knill

Geology and Radwaste. By A.G. Milnes. *Academic: 1985. Pp.328. Hbk £50, $60; pbk £36.95, $39.95.*

EVENTS during the first months of 1986 have placed the nuclear industry in Britain at the centre of public attention. A series of minor incidents at the Sellafield nuclear fuel reprocessing plant, the identification of four possible sites for the shallow disposal of low-level radioactive waste, the publication of the Environment Select Committee's critical report on radioactive waste — all have been greeted with outcries from the various groups opposed to all forms of nuclear proliferation. Now, of course, we have had Chernobyl, and the attacks on the nuclear industry will intensify. The consistent reply from the industry has been that its critics are over-reacting, that technical improvements will continue to be made and that the risks associated with release of nuclides into the environment are overstated. These differences of opinion will not be resolved easily, and will fuel the continuing debate on the sources, and disposal methods, of radioactive waste.

Such waste is traditionally subdivided into four classes: very low, low, intermediate and high-level/heat-generating. However, this classification can be over-simple in that short-lived, intermediate-level waste may be disposed of together with low-level waste, and some argue that α-emitting low-level waste should be grouped with intermediate-level waste.

Because of the long half-lives of the radionuclides it contains, and the daughter products, high-level/heat-generating material will be an environmental hazard for hundreds of thousands of years. For this reason, disposal must be at depth in a geologically stable environment. A British research programme into deep disposal was stopped by the government in 1981, and for the next 50 years high-level waste will be stored on the surface as a fluid, and progressively encapsulated in glass, in order to maximize dissipation of the heat which is less easy to control underground. Deep disposal will then follow.

Since 1981 the responsibility for finding, proving and developing low- and intermediate-level waste disposal sites has rested with UK NIREX Ltd, a company controlled by the energy and nuclear industry. Selection of a deep site for intermediate-level waste in an anhydrite mine at Billingham led to local opposition, and then withdrawal of the site by the government. The choice of Elstow for an engineered low-level disposal site in clay met a similar reaction but, now, three further shallow sites in clay have been named; after detailed investigation, one of them will be selected and the case for development put to a public enquiry.

Against this background, the appearance of *Geology and Radwaste* is timely. Milnes defines his reasons for writing the book in the preface. He notes that the geological uncertainties are inherent, that simple solutions rarely exist and that this field offers much scope for conflict, as did the classic geological controversies of the past. Despite his conviction that the nuclear road is not the one we should take, he recognizes that here is a problem that will not go away, and that radioactive waste disposal is no more of an environmental hazard than the uncontrolled emission of (for example) carbon dioxide, sulphur dioxide and heavy metals.

The book is divided into three parts, the opening chapter of Part I providing a summary of radioactive waste types. As in the remainder of the book, the text here is exceptionally clearly written and well illustrated, meeting the author's objective of being accessible to a wider audience than the specialists involved. Also notable is Milnes's impressive grasp of the literature; much that is published on this subject is unrefereed, and is available only in rather obscure reports and conference proceedings. Each chapter ends with a summary of selected literature, with full references at the back of the book.

The second chapter of Part I covers the alternative methods of disposal of low-level liquid wastes, and the disposal of low- and intermediate-level solid wastes at sea, by shallow burial and in deep, mined cavities. The particular problems of high-level waste are highlighted, attention being drawn to some of the more exotic solutions that have been offered in the past.

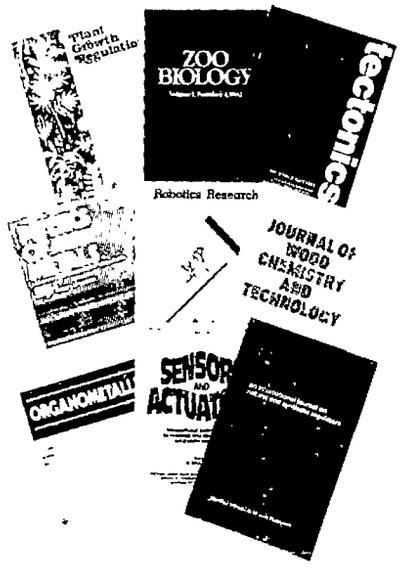
Part II, occupying about two-thirds of the text, gives the geological perspective to radioactive waste disposal by describing the subsurface and surface processes operating through geological time. Much of the material here is familiar, but the author skilfully draws in case histories and examples to illuminate particular points; for instance, rates of denudation are illustrated by reference to the Texas Panhandle and to a mine test site at Mol, in Belgium. The eleven chapters systematically cover the relevant rock-forming, tectonic, geomorphological and fluid processes which provide the potential environments for storage and disposal. These processes are discussed in the context of the time-scale within which hazardous disruption of a repository could occur.

The two final chapters review predictive methods for identifying the disposal system most likely to guarantee that any release to the environment will not exceed regulatory limits. Safety assessment of potential sites demands expertise well beyond geology, and the book does not provide a guide to methods of site selection, site specific investigation or the geological aspects of safety assessment. Within his chosen compass, however, Milnes has produced a lucid and thorough book which should be read by all of those who have involvement with, or interest in, the geological disposal of radioactive waste. In the aftermath of Chernobyl, that is likely to be very many people indeed. □

J.L. Knill is Professor of Engineering Geology in the Department of Geology, Imperial College, University of London, London SW7 2BP, UK, and is a member of the UK Radioactive Waste Management Advisory Committee.

• *Management of Toxic and Hazardous Wastes*, published by Lewis Inc., Chelsea, Michigan, contains the (updated) proceedings of a conference on the subject held in Columbus, Ohio, in 1983. Price is $49.95, £45.95.

New journals review



On 25 September *Nature* will publish the sixth annual review supplement devoted to science journals.

Criteria for inclusion of a journal in the 1986 issue are that:

(i) the first number appeared, or the journal was retitled, *between June 1984 and May 1985* (the second cut-off date allows at least three issues of a journal to have been published, the minimum number on which a reasonable judgement can be based);

(ii) it is published at least three times a year;

(iii) the main language used is English.

Publishers and learned societies are invited to send *four different issues of each suitable periodical, including the first and most recent numbers* (if from outside the United Kingdom, by air mail) to: The Review Editor, *Nature*, 4 Little Essex Street, London WC2R 3LF, England. Subscription details, for both 1986 and 1987 should be included.

Galaxy formation by mock gravity

C. J. Hogan & S. D. M. White

Steward Observatory, University of Arizona, Tucson, Arizona 85721, USA

Absorbing particles in an isotropic radiation field experience an attractive force due to their mutual shadowing. If the pre-galactic universe contained suitable sources of radiation and absorbing material, an instability caused by this effect may have led to the formation of galaxies and galaxy clusters. Other consequences include the segregation of galaxies from dark matter and a strong anisotropic far-infrared background.

RADIATION pressure can have a significant effect in structuring the interstellar medium, dominating gravity for some species and environments by many orders of magnitude[1-5]. As first pointed out by Spitzer[2], absorbing particles in an isotropic radiation field experience 'mock gravity', an inverse-square attraction due to their mutual shadowing. Gamow[6] originally suggested that mock gravity resulting from Compton absorption of the microwave background by free electrons might provide a source of cosmological instability. However, as demonstrated by Field[7], this effect is negligible, both because matter and radiation are very close to thermodynamic equilibrium, and because the temperature is so low at epochs of interest that scattering exceeds absorption by a very large factor. On the other hand, it is possible that conditions in the pre-galactic universe might resemble those in the interstellar medium today, with stars emitting ultraviolet radiation and dust providing significant continuum opacity[8-15]. In this situation, mock gravity can drive a rapidly growing instability which might extend up to scales comparable to those observed in galaxy clustering.

Several non-gravitational mechanisms have been investigated which could, in principle, generate large-scale structure[16,17]. Mock gravity provides another such mechanism, but is unique in several respects. No true instability has previously been demonstrated to occur on such large scales. The gravitational instability usually invoked to explain large-scale structure is just a reflection of energy conservation in pre-existing fluctuations which are left behind as the universe expands around them. Mock gravity can behave like a true instability in that a wide range of scales can grow to nonlinearity in much less than an expansion time. It has a natural scale-length (the photon interaction length) which limits the size of structures, and a natural scale of binding energy determined by the radiation field. Together these scales determine the mass and density of the largest structures produced. Segregation of light and dark matter, and of enriched and unenriched gas, are also natural consequences of mock-gravitational instability. Within this theoretical framework, the development of structures qualitatively like those observed is a natural consequence of certain general conditions in the pre-galactic medium, and has little dependence on the previous large-scale mass distribution.

Our analysis differs from previous discussions[2,3] of mock gravity. Instead of presupposing an isotropic, externally generated radiation field, we introduce a homogeneous density of radiation sources. In linear theory, we are then able to treat the growth of optically thick perturbations. Our analysis includes the expansion of the universe, which was omitted from discussions focusing on the interstellar medium. We make the usual assumptions that the absorbing particles are continuum absorbers such as dust grains, that scattering can be neglected, and that the re-emitted radiation has a negligible interaction with the grains.

Mock gravitational instability

Consider a uniformly radiating background medium with luminosity density l. Within this medium are distributed dust grains with number density n, and frequency-averaged absorption cross-section σ. The sky brightness in a direction $\mathbf{i}$ seen from the origin is

$$S(\mathbf{i}) = \int_0^\infty \mathrm{d}r\, r^2 (l/4\pi r^2) \exp\left[-\int_0^r \mathrm{d}r'\, n(r'\mathbf{i})\sigma\right] \qquad (1)$$

Decomposing n into a uniform and a perturbed part $n_0 + \delta n$, we find the perturbation in brightness

$$\delta S(\mathbf{i}) = (-l/4\pi) \int_0^\infty \mathrm{d}\tau\, \mathrm{e}^{-\tau} \int_0^{\tau/n_0\sigma} \mathrm{d}r'[\delta n(r'\mathbf{i})/n_0] \qquad (2)$$

The net force exerted by radiation pressure on a grain at the origin is then

$$\mathbf{F} = -\frac{\sigma}{c}\int \mathrm{d}\Omega\, \delta S(\mathbf{i})\mathbf{i} = -\frac{l\sigma}{4\pi c}\int_0^\infty \mathrm{d}\tau\, e^{-\tau}\int_0^{\tau/n_0\sigma} \mathrm{d}\Omega \frac{\delta n(r'\mathbf{i})}{n_0}\mathbf{i} \qquad (3)$$

Let us consider the force due to a plane-wave perturbation $\delta n/n_0 = \delta_k\, \mathrm{e}^{i\mathbf{k}\cdot\mathbf{x}}$. Then $\mathbf{F} = F_k\, \mathrm{e}^{i\mathbf{k}\cdot\mathbf{x}}\mathbf{k}/|\mathbf{k}|$ with

$$F_k = -\frac{l\sigma}{c}\frac{\delta_k}{ik}[1 - p^{-1}\tan^{-1} p] \qquad (4)$$

where $p = k/n_0\sigma$. For a static medium the equation of motion of such a linearized plane wave is $\ddot{\delta}_k = -ikF_k/m$, where m is the effectively coupled mass per dust grain. Hence

$$\ddot{\delta}_k = \frac{l\sigma}{mc}[1 - p^{-1}\tan^{-1} p]\delta_k \equiv \omega_k^2 \delta_k \qquad (5)$$

and the fluctuation grows exponentially with growth rate ω_k. For optically thin perturbations ($p \gg 1$) ω_k is independent of wavelength. In the opposite limit, the growth rate decreases with $\omega_k \propto p$.

In an expanding universe filled with well-coupled dust and gas, the equation of motion becomes

$$\ddot{\delta}_k + (2\dot{a}/a)\dot{\delta}_k = (l\sigma/mc)[1 - p^{-1}\tan^{-1} p]\delta_k \qquad (6)$$

where $a(t)$ is the expansion factor, k is a co-moving wavenumber defined so that $p \equiv k/a(t)n_0(t)\sigma$, and gravitational effects have been neglected. The growth rate of the fluctuation relative to the expansion depends on the dimensionless parameter

$$A \equiv (2\omega_k(t)/3H)^2 \equiv A_0[1 - p^{-1}\tan^{-1} p];\ H \equiv \dot{a}/a$$

defined by the coefficients in this equation. For optically thin perturbations in an approximately Einstein–de Sitter universe, $A \cong A_0 = 4l\sigma/9mcH^2$ is independent of time provided the properties of the dust and the sources do not evolve. In this situation, the fluctuations grow as

$$\delta_k \propto t^\alpha, \qquad \alpha = (A_0 + \tfrac{1}{36})^{1/2} - \tfrac{1}{6} \qquad (7)$$

For large A_0, $\delta_k \propto t^{\sqrt{A_0}}$ and growth is rapid. For a given perturbation $p \propto a^2$, and even for large A_0, rapid growth can occur only after a characteristic time $t_c(k)$ defined by $p(t_c, k) = 1$. The equation for δ_k can be written

$$\ddot{\delta}_k + 4\dot{\delta}_k/3t = (A_0/t^2)[1 - (t/t_c)^{-4/3}\tan^{-1}(t/t_c)^{4/3}]\delta_k \qquad (8)$$

The solutions of this equation are shown in Fig. 1 for several values of the parameter A_0. The gravitational mode $\delta_k \propto t^{2/3}$ is also shown for comparison. Rapid growth occurs only after $t = t_c$ and only for $A_0 > 1$. The transition at $t = t_c$ is quite sharp. Note that the initial amplitude of the fluctuation need not result from an enhancement in physical density. Inhomogeneities in the distribution of luminosity sources and of dust production sites will introduce initial white noise fluctuations on all scales greater than those characteristic of these processes. If, however, real density fluctuations are dominant on large scales, mock gravity will take over from normal gravity as soon as the slope of the appropriate curve in Fig. 1 exceeds 2/3.

Astrophysical context

For this instability to be cosmologically interesting, A_0 must be >1 and at the same time fairly large scales must be optically thin. We now investigate the range of astrophysical parameters where this may occur.

It is useful to write the luminosity density in units of the Eddington limit[15]:

$$l_E \equiv \rho c^2 / t_{Sal} \tag{9}$$

where

$$t_{Sal} = c\sigma_T / 4\pi G m' \simeq 4 \times 10^8 \text{ yr} \tag{10}$$

is the Salpeter time, $\sigma_T \simeq 6 \times 10^{-25}$ cm^2 is the Thomson cross-section, and m' is the mean mass of cosmic atoms. Once again ignoring curvature terms in the expansion law, $H^2 = 8\pi G\rho/3$, we obtain

$$A_0 = \frac{t^2 l \sigma}{mc} = \frac{2}{3}\frac{l}{l_E}\frac{\sigma}{\sigma_T}\frac{m'}{m} \tag{11}$$

If the radiation sources are Eddington-limited, it is apparent that the effective cross-section per gas atom $\sigma m'/m$ must exceed the Thompson value in order for rapid growth to occur.

This requirement is found to be generously satisfied in the interstellar medium (ISM) of our own galaxy. Spitzer (ref. 5, p. 162) finds empirically that the sky coverage per gas atom is

$$\frac{\langle n_{dust}\sigma_{dust}\rangle}{\langle n_H \rangle} \simeq 10^{-21} \text{ cm}^2 \tag{12}$$

based on measured selective extinction at 1,000 Å. In Spitzer's model, the corresponding dust-to-gas mass ratio is $X_d = 6 \times 10^{-3}$. In what follows we therefore adopt $\sigma m'/m \equiv f_{ISM}\ 10^{-21}$ cm^2. Because $\sigma \propto \lambda^{-1}$ for wavelengths larger than the typical grain size, the value of f_{ISM} is sensitive to the mass in dust grains but not to their size distribution, provided they are small compared with the characteristic wavelength of the radiation. f_{ISM} is also sensitive to the value of this wavelength. A similar opacity per mass would be expected for large molecules[11–13,18].

In our discussion of mock gravity, we focus exclusively on grain opacity. Although atomic continuum cross-sections in the ultraviolet are large enough to be interesting ($f_{ISM} \simeq 6000$ for Lyman continuum absorption), atoms are quickly ionized in ultraviolet radiation fields strong enough to produce instability unless the gas is concentrated in small, very dense lumps. Line opacity is ineffective both because line widths are less than the systematic Hubble velocity across the structures that interest us, and because only a small fraction of the radiation participates in the instability. Dust grains or large molecules absorb ultraviolet continuum radiation efficiently but are large enough to survive the absorption of an ultraviolet photon. Grains and molecules tend to survive more easily at earlier epochs than they do now, because the dominant destructive process—sputtering by collisions with energetic ions—is suppressed. Gas at redshift $z > 7$ is cooled by Compton interaction of electrons with the microwave background, and does not reach the high temperatures needed for sputtering[5].

Formation of structures

If the effective opacity is too high, scales of interest will be optically thick and structure will not grow. Let us require that the instability operates up to a fiducial wavelength $\Lambda_c = 32\Lambda_{32}h^{-1}$ Mpc. A value of $\Lambda_{32} \simeq 1$ seems necessary to produce galaxy density fluctuations of order unity in spheres of radius $8h^{-1}$ Mpc, as inferred from the observed galaxy autocorrelation function. The optical depth parameter across this characteristic scale is

$$p_c = 2\pi/\Lambda_c n\sigma = 6.5 f_{ISM}^{-1}\Omega_g^{-1}h^{-1}(1+z)^{-2}\Lambda_{32}^{-1} \tag{13}$$

where we have set the gas density to $n_H = 10^{-5}\Omega_g h^2(1+z)^3$ cm^{-3} and the current value of $H = 100h$ km s^{-1} Mpc^{-1}. For the instability to operate efficiently, p_c must exceed unity. Thus for significant growth across Λ_c by $z = 20$, we require $\Omega_g < 0.016 f_{ISM}^{-1}h^{-1}\Lambda_{32}^{-1}$.

Although individual sources might be expected to radiate at the Eddington limit, the mean luminosity density at $t > \varepsilon t_{Sal}$ is likely to be limited by the total efficiency, ε, with which rest mass is converted into radiation (this constraint could be avoided, in principle, by having an intense burst of radiation). For a population of sources which forms at $t = 0$ and burns uniformly until time t_b,

$$l/l_E = \varepsilon(t_{Sal}/t_b) = 6 \times 10^{-4}\varepsilon_{-2}(\Omega h^2)^{1/2}(1+z_b)^{3/2}(\rho_s/\rho) \tag{14}$$

where ρ_s is the density of sources and z_b is the redshift corresponding to t_b, ρ is the total density, and $\varepsilon_{-2} = \varepsilon/10^{-2}$ for the sources. For such a population of sources, the optically thin growth parameter is

$$A_0 = 0.9\varepsilon_{-2}(\Omega h^2)^{1/2}(\rho_s/\rho)(1+z_b)^{3/2} f_{ISM} \tag{15}$$

To obtain rapid growth, structure formation and burn-out must occur at $z_b > 10$. We can eliminate the explicit dependence on the opacity parameter f_{ISM} by requiring $p_c \geq 1$. Then

$$A_0 \leq 6\varepsilon_{-2}\Omega^{1/2}\Omega_g^{-1}(\rho_s/\rho)(1+z_b)^{-1/2}\Lambda_{32}^{-1} \tag{16}$$

where the density parameters Ω and Ω_g refer to the present. This bound is saturated if we identify Λ_c as the wavelength for which $t_c = t_b$. Equation (16) shows that plausible situations exist in which rapid fluctuation growth at $z > 10$ would occur on all scales up to those of galaxy clusters.

What is the efficiency of converting luminous energy to binding energy? Let u_k denote the Fourier coefficient of peculiar

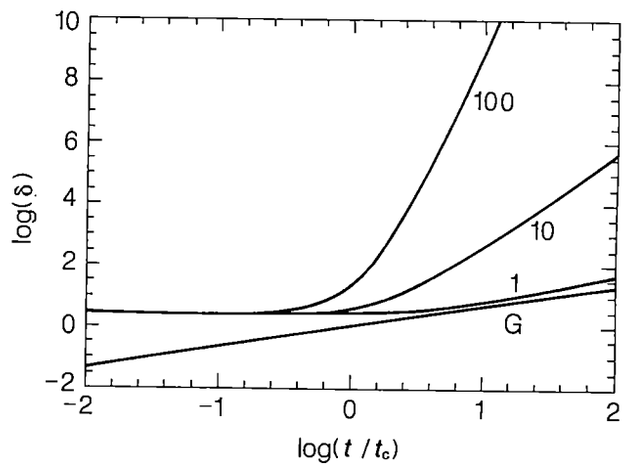


Fig. 1 Growth of perturbations due to mock gravity in the linear approximation. Density perturbation amplitude in arbitrary units is plotted as a function of time, which is expressed in terms of the time t_c when a scale becomes optically thin. The models shown here assume constant opacity and luminosity per mass, and are labelled by the value of their growth parameter A_0. The curve labelled G represents growth by ordinary gravitational instability.

velocity in the gas. Neglecting the expansion, equation (4) gives us the typical velocity attained in an expansion time:

$$v_{\rm gas} \cong |u_k/H| \simeq |F_k/mH| = \frac{l\sigma\delta_k}{kmcH}[1-p^{-1}\tan^{-1}p] \quad (17)$$

From equations (9) and (14), the luminosity density at t_b is given by

$$l = \varepsilon\rho_s c^2/t_b \quad (18)$$

and thus the gas velocity is

$$v_{\rm gas} \simeq 3/2\varepsilon c\delta_k(\rho_s/\rho)p^{-1}[1-p^{-1}\tan^{-1}{\rm p}] \quad (19)$$

Hence, radiation energy is converted to gas motion with maximum efficiency if the scale with $p=1$ goes nonlinear; in this case $v_{\rm gas} \simeq \varepsilon c(\rho_s/\rho_g)$. This corresponds roughly to all the momentum of unidirectional radiation $\varepsilon\rho_s/c$ being imparted to the gas; if $\delta_k = 1$ and $p=1$, the radiation field indeed becomes highly anisotropic (see equation (2)). It is interesting that this degree of coherent structuring of the radiation field occurs spontaneously.

If the evolution after t_b is purely gravitational, the binding energy density is $\sim v_{\rm gas}^2\rho_{\rm gas}$. While the maximum mass scale of structure is determined by the opacity ($f_{\rm ISM}$), the specific binding energy is therefore determined by the radiative efficiency (ε). It is encouraging that we can obtain reasonable results for both simultaneously.

Even during the nonlinear evolution of the instability, radiation pressure acts on optically thin systems exactly like ordinary gravity, but with an effective gravitational constant $3A_0/2\Omega_g$ times larger[2]. As a result, we expect the gas and dust to be swept quickly into a hierarchy of structures. For optically thick systems, the details of the nonlinear evolution driven by mock gravity are complex. Once a system is optically thick, it inhibits the action of mock gravity on both larger and smaller scales. As a result, the growth of structure is coupled on widely disparate scales and is very difficult to treat. Here we discuss two aspects of the optically thin hierarchy: the characteristic masses that emerge and the specific angular momentum generated by mock-tidal torquing.

A characteristic mass scale for nonlinear evolution is defined by the requirements that a contracting clump should become optically thick at the same time as the gas density within it comes to dominate the total background density. Mock gravity then begins to switch off just as normal gravitational effects become nonlinear. This mass M_1 satisfies

$$M_1/\pi r_1^2 = m/\sigma;\ 3M_1/4\pi r_1^3 = \rho_0(1+z)^3 \quad (20)$$

and hence

$$M_1 \cong 2\times10^{16} f_{\rm ISM}^{-3}(\Omega h^2)^{-2}(1+z)^{-6}M_\odot$$
$$r_1 \simeq 30 f_{\rm ISM}^{-1}(\Omega h^2)^{-1}(1+z)^{-3}\ {\rm Mpc} \quad (22)$$

For the plausible parameters $\Omega h^2 = 0.25$, $z=20$, $f_{\rm ISM}=0.5$, these give $M_1 = 4\times10^{10}M_\odot$, $r_1 = 30$ kpc. Thus this mass scale might be identified with individual galaxies.

A consequence of the rapid growth rate is that the specific angular momentum acquired by gas clumps as they form is typically a factor $\frac{3}{2}(\dot\delta/\delta) = \frac{3}{2}\sqrt{A}$ larger than that which similar clumps would acquire if they turned around at the same epoch under the action of normal gravity alone. As a result, the rotational kinetic energy of a gas clump becomes comparable to its normal gravitational binding energy when it is $(9A/4)$ times larger than in the familiar normal-gravity case[19,20]. Thus a system which has virialized at size r from maximum expansion size r_m has typical dimensionless spin parameter $\lambda = |E|^{1/2}J/GM^{5/2} \simeq 0.06\ (9A\Omega r_m/8\Omega_g r)^{1/2}$ if it is gas-dominated. It appears that with little or no collapse, mock gravity can make rotationally supported systems with the parameters of spiral galaxies at a redshift of $\sim$20.

The maximum gas mass over which the instability can operate effectively is larger than M_1 (equation (22)) by a factor Ω_g^{-2}:

$$M_{\rm max} = \frac{4\pi}{3}\bar\rho_g\left(\frac{m^3}{\bar\rho_g\sigma}\right)$$
$$= 4\times10^{16}\Omega_g^{-2}(1+z)^{-6}(\Omega h^2)^{-2}f_{\rm ISM}^{-3}M_\odot \quad (23)$$

This mass is naturally identified with galaxy clusters. For the parameters suggested above together with $\Omega_g = 0.02$, $M_{\rm max} = 2\times10^{14}\ M_\odot$, which is comparable to the total mass of gas and galaxies seen in the largest nonlinear systems known. If the instability is able to drive perturbations on this scale mildly nonlinear ($\delta\rho_{\rm gas}/\rho_{\rm gas}\sim5$) at $z=20$, then systems of total mass $\sim10^{15}M_\odot$ will collapse as a result of normal gravitational instability at $z\simeq1$ and will contain $\sim$10 times as much 'dark' matter as gas and visible stars.

We have made several arbitrary assumptions about the time evolution of luminosity and opacity. If l remained high while the gas density were gradually depleted, the remaining gas would be swept up into ever larger structures, limited by the current optical depth in the remaining gas. Thus, a small fraction of galaxies—those which formed last—might appear in nonlinear structures with a very large coherence length. It might be possible to explain in this way the observed superclustering of Abell clusters, which appears to be coherent over $>50h^{-1}$Mpc. As we have demonstrated, the gravitational binding of these very large-scale structures is not expected to be large. Large-scale peculiar velocities in the gas of order HR occur while the structure is forming but decay thereafter like $a(t)^{-1}$. The coherence length should scale roughly as the inverse fraction of gas remaining.

Astrophysical implications

The notion that gas clustered first by non-gravitational processes and that dark matter followed its gravitational influence leads to several predictions about galaxy–mass segregation. First, the structure of haloes might be expected to correspond to spherical infall models[21,22]. Second, the mass-to-light ratio of many-galaxy systems is expected to be simply related to their crossing times. When mock gravity switches off, a highly clumped gas and galaxy distribution will remain superposed on a relatively uniform background of dark matter. A region where the gas density is $(j+1)\bar\rho_g$ at this time will later collapse to a system with virialized gas density, $\rho_{fg}\sim(j+1)\bar\rho_g(j\Omega_g)^3$, and with a gas-to-total mass ratio, $\rho_{fg}/\rho_f \sim (j+1)\Omega_g$. The crossing time, t_c, of such a system is proportional to $\rho_f^{-1/2}$, and so objects that form at late times should obey the scaling relation $M/L \propto t_c^{2/3}$. If, in addition, we assume that the hierarchical clustering induced by mock gravity leads to a present distribution obeying $\rho_{fg} \propto r^{-2} \propto M_g^{-2}$ as inferred from observed galaxy correlations, we can derive the scaling relations, $M/L \propto L^{1/2}$ and $L \propto V^{1/4}$, where V is the characteristic virial velocity. These relations are in reasonable agreement with observations of galaxy systems.

The stellar population required in our model cannot have the same mass function as that in our Galaxy; normal stars with a large ultraviolet flux and lifetimes $<10^8$ yr eject too large a fraction of their mass in metals to produce the needed light without over-enriching the remaining gas. One promising type of radiation source for our purposes would be a 'very massive object'[8,9] ($M \gtrsim 200M_\odot$), which sends nearly all its metals into a black hole and blows off an envelope of hydrogen and helium. Radiative efficiencies for such objects typically[8,9] exceed 10^{-3}. The effects of the explosions from such objects could possibly dominate over their mock-gravity effects if they formed at sufficiently low redshift ($z<6$). Accreting black holes could also match our luminosity requirements without creating an enrichment problem, and could reach even higher efficiencies.

On the other hand, an appreciable metal abundance ($\lesssim10^{-3}$, depending on luminosity), is necessary in the protogalactic gas to provide sufficient dust opacity for the instability to operate. In this model, it is possible that a significant portion of present galactic dust originated at high redshift; this is a desirable feature

as present dust formation rates seem inadequate[23]. The high metallicity of the intergalactic gas in galaxy clusters may result from sputtering of pre-galactic grains once Compton cooling has turned off at $z \simeq 7$. Observed objects with low metallicity are not a serious embarrassment because mock gravity segregates gas according to its dust content. Initial chemical inhomogeneities thus tend to get amplified, highly enriched regions being brought together while metal-poor gas is left behind. This segregation can occur even though dust and gas may be locally well coupled, because enriched clouds are compressed by radiation pressure and can pass through the unenriched gas with little interaction: some such segregation would be expected even on scales as large as $M_{\max}$, provided the enriched clouds are compressed to $\tau \gtrsim 1$. Thus, the existence of metal-poor systems such as IIZw40 may not be in conflict with our model. We would, however expect such systems to be less strongly clustered than normal galaxies. There are physical reasons why globular clusters may form preferentially from low-abundance clouds in protogalaxies[24], and there is some observational support for just such selective cluster formation[25]. The low metal abundance of clusters in the galactic halo may, therefore, be compatible with the substantial pre-galactic metal formation our model requires. Such relations between metallicity and structure may also explain why Lyman-α absorption systems in quasars are less strongly clustered than metal-line systems, and indeed why there should be a correlation between column density and metallicity.

Perhaps the cleanest prediction of our model—because it is a direct by-product of the fundamental mechanism—is the intensity and anisotropy of the re-radiated emission from the grains. This is expected to produce a cosmic far-infrared background peaked at $200\,\mu\text{m} \lesssim \lambda \lesssim 600\,\mu\text{m}$ (ref. 10). The total present energy density parameter in radiation from sources which burned from $z=\infty$ to $z=z_b$ is

$$\Omega_R = \tfrac{3}{5}(\rho_s/\rho)10^{-2}\varepsilon_{-2}(1+z_b)^{-1}\Omega \qquad (24)$$

Using equation (16) and requiring $A_0 > 6$ so that the instability can operate, we find

$$\Omega_R > 0.6\times 10^{-2}\Omega^{1/2}\Omega_g\Lambda_{32}(1+z_b)^{-1/2} \qquad (25)$$

which should be compared with the total energy density of the cosmic microwave background, $\Omega_R = 2.4\times 10^{-5}h^{-2}$. Even for $z > 10$ and $\Omega_g \simeq 0.01$, the two fluxes are comparable. Such a strong far-infrared background should be easily detectable by the Cosmic Background Explorer Satellite (COBE).

The anisotropy in this background may be estimated as follows[10]. Suppose that the re-radiated infrared luminosity density has variance $(\delta I/I)_{IR} \cong 1$ on the co-moving scale $\Lambda \simeq 32h^{-1}\,\Lambda_{32}$ Mpc of observed clustering. Roughly $N \simeq 100\,\Lambda_{32}^{-1}h^{-1}(1+z_b)^{-1/2}$ such regions contribute to the dust emission integral in any direction, so the r.m.s. variation in observed brightness will be

$$\frac{\delta I}{I} \cong N^{-1/2} \simeq 0.1\Lambda_{32}h^{1/2}(1+z_b)^{1/4}(\theta/\theta_c)^{-1} \qquad (26)$$

for angular scales θ larger than that subtended by Λ_c.

$$\theta_c \simeq 16\Lambda_{32}\Omega \text{ arc min} \qquad (27)$$

Anisotropy with these characteristics should be detectable by the Space Infrared Telescope Facility (SIRTF). The techniques for calculating small-scale anisotropy, and the observational issues, are discussed in ref. 10.

These fluctuations in the dust radiation can generate further inhomogeneities in the matter distribution as a result of coupling by Thomson drag[17]. This effect is negligible for the parameters we prefer here, but it could be significant on large scales if dust and radiation sources were present at $z \gtrsim 200$ in sufficient quantities to generate a small-scale mock gravitational instability. If the mock-gravity instability occurs at high enough redshift or gas density, the Thomson optical depth may exceed unity, suppressing anisotropy on angular scales less than a few degrees[17]. This does not occur, however, for parameters which produce large-scale structure.

Discussion

The model we have presented is radically different from conventional models for galaxy formation. In view of this, it is surprising that many observed facts fall into place quite 'naturally' and that no fatal flaw has appeared. Apparently, the model deserves serious consideration. Unfortunately, however, there is considerable difficulty in sharpening many of its predictions. The nonlinear evolution of the structure in mock gravity is particularly difficult to analyse rigorously, and even numerical simulations are difficult because the force between two gas elements in optically thick systems depends on the global configuration of the system. It may be possible to construct an apparatus in which mock gravity between many particles could be observed directly. This would offer the advantage of representing most aspects of the phenomena in question with a very large number of particles and with high spatial resolution and dynamic range. The acceleration of a grain in an evacuated chamber with $\sigma = 10^{-8}\,r_\mu^2$ cm^2 and $m = 10^{-12}\rho_g r_\mu^3$ g due to a beam of radiation with an energy flux of $100F_{100}$ W cm^{-2} is

$$a = 300 \text{ cm s}^{-2}F_{100}r_\mu^{-1}\rho_g^{-1} \qquad (28)$$

Thus, it may be possible to build an apparatus in which the mock gravitational acceleration exceeds normal terrestrial gravity ($g = 981$ cm s^{-2}), or the mock-gravity instability proceeds so rapidly that the entire apparatus can be dropped briefly to eliminate normal gravity during the experiment. It would be amusing to build an analog computer in the laboratory that might allow us to study the formation of galaxies and galaxy clusters in the real Universe.

This work was supported by NASA Theoretical Astrophysics grant NAGW-763 and by the Theoretical Astrophysics Program of the University of Arizona.

Received 15 January; accepted 2 April 1986.

1. Greenstein, J. L. *Harvard College Observatory Circ.* No. 422 (1937).
2. Spitzer, L. *Astrophys. J.* **94**, 232-244 (1941).
3. Whipple, F. L. *Astrophys. J.* **104**, 1-11 (1946).
4. Chiao, R. Y. & Wickramasinghe, N. C. *Mon. Not. R. astr. Soc.* **159**, 361-374 (1972).
5. Spitzer, L. *Physical Processes in the Interstellar Medium* (Wiley, New York, 1978).
6. Gamow, G. *Rev. mod. Phys.* **21**, 367 (1949).
7. Field, G. in *Galaxies and the Universe* (eds Sandage, A., Sandage, M. & Kristian, J.) 375 (*University of Chicago Press*, 1976).
8. Bond, J. R., Arnett, W. D. & Carr, B. J. *Astrophys. J.* **280**, 825-847 (1984).
9. Carr, B. J., Bond, J. R. & Arnett, W. D. *Astrophys. J.* **277**, 445-469 (1984).
10. Bond, J. R., Carr, B. J. & Hogan, C. J. *Astrophys. J.* **306**, (in the press).
11. Layzer, D. & Hively, R. *Astrophys. J.* **179**, 361-369 (1973).
12. Wright, E. L. *Astrophys. J.* **250**, 1-6 (1981).
13. Wright, E. L. *Astrophys. J.* **255**, 401-407 (1982).
14. Ostriker, J. P. & Heisler, J. *Astrophys. J.* **278**, 1-10 (1984).
15. Rees, M. J. *Nature* **275**, 35-37 (1978).
16. Ostriker, J. P. & Cowie, L. L. *Astrophys. J.* **243**, L127-131 (1981).
17. Hogan, C. J. & Kaiser, N. *Astrophys. J.* **274**, 7-19 (1983).
18. Purcell, E. M. *Astrophys. J.* **158**, 433-440 (1969).
19. Fall, S. M. & Efstathiou, G. *Mon. Not. R. astr. Soc.* **193**, 189-206 (1980).
20. White, S. D. M. *Astrophys. J.* **286**, 38-41 (1984).
21. Gunn, J. *Astrophys. J.* **218**, 592-598 (1977).
22. Fillmore, J. A. & Goldreich, P. *Astrophys. J.* **281**, 1-8 (1984).
23. Aanested, P. & Purcell, E. M. *A. Rev. Astr. Astrophys.* **11**, 309-362 (1973).
24. Fall, S. M. & Rees, M. J. *Astrophys. J.* **298**, 18-26 (1985).
25. Forte, J. C., Strom, S. E. & Strom, K. M. *Astrophys. J.* **245**, L9-L13 (1981).

Voltage-sensitive dyes reveal a modular organization in monkey striate cortex

Gary G. Blasdel & Guy Salama

Departments of Ophthalmology and Physiology and the Centre for Neuroscience, University of Pittsburgh, Pittsburgh, Pennsylvania 15261, USA

Voltage-sensitive dyes allow neuronal activity to be studied by non-invasive optical techniques. They provide an attractive means of investigating striate cortex, where important response properties are organized in two dimensions. In the present study, patterns of ocular dominance and orientation selectivity were obtained repeatedly from the same patch of cortex using the dye merocyanine oxazolone, together with current image-processing techniques. The patterns observed agree with most established features of monkey striate cortex and suggest a new unit of cortical organization; one that is modular in structure and which appears to link the organization of orientation selectivity with that of ocular dominance.

NEURONES in the striate cortex perform several important transformations using visual information[1-8]. They combine inputs from both eyes so that retinal images appear fused, yet they retain information on ocular disparity, so that objects may be viewed in relief. They also respond selectively to edges at certain orientations in visual space. The two response properties most related to depth and edge perception, ocularity and orientation selectivity, are organized systematically across the cortical surface.

The anatomical basis for ocular interaction in the cortex is better understood than that of orientation selectivity because it originates from patterns of terminating geniculate afferents and there are methods to visualize these afferents. The geniculate axon terminals establish a repeating sequence of right-eye/left-eye bands in lamina 4C (refs 5, 8, 9) which, when viewed from the cortical surface, display an average width of 0.5 mm and run vertically into the boundary of area 17 (striate cortex). As information flows radially out of lamina 4C (ref. 10), the monocular responses that these bands establish carry over into, and dominate, the responses of cells lying above and below, creating a system of slab-like columns that extend from pia to white matter.

Orientation selectivity, like ocular dominance, seems to be organized radially (vertically between pia and white matter)[1,2,6,8], but its precise anatomical substrate is unknown, and its organization has thus proved more difficult to define[11]. Using long tangential electrode penetrations, Hubel and Wiesel found that incremental steps through the cortex are accompanied by incremental shifts in preferred orientation[6]. This led them to suggest that orientation selectivity, like ocular dominance, might be organized as a system of parallel slabs, and experiments with 2-deoxyglucose (2DG), a metabolic marker that labels active neurones, seemed to confirm this notion[12]. But these experiments suffer from the fact that 2DG can be used only once (the animal must be killed to visualize the result), and this makes it difficult to determine how the same piece of tissue might respond to a different stimulus (a different orientation, for example). The presence of cytochrome oxidase blobs (identified on the basis of their rich cytochrome oxidase content), at regular intervals in the superficial layers, complicates the issue further since cells within these blobs lack selectivity for orientation and label strongly with 2DG for any orientation that is used. On account of all these difficulties, the evidence for an overall slab-like organization has never seemed quite as compelling for orientation selectivity as it has for ocular dominance[13-15].

A technique that might perhaps allow repeated mapping of cortical activity patterns was reported by Cohen and co-workers, who showed that certain dye molecules function as optical transducers of membrane potential[16-19]. Squid axons stained with merocyanine 540 were found to emit a fluorescence signal that closely followed action potentials measured with an intracellular electrode[16]. The mechanism(s) responsible for these optical signals are not understood completely, but are thought to entail a voltage-dependent transition between monomer and dimer states of membrane-bound dye molecules[19]. Rotations of dye molecules within the membrane[20] or rotations of dipole moments during monomer to dimer transitions may also be involved[19,21].

While voltage-sensitive dyes may seem a complicated way to monitor membrane potentials, they offer great promise in the study of two-dimensional phenomena because surfaces are well suited to optical inspection. Although initially the small amplitude of voltage-dependent optical signals and the phototoxicity of the dyes restricted widespread application of the method[16,18,22], many of these problems have now been overcome[19-22] and it is possible to obtain optical signals from many different neural preparations, including mammalian cortex[23].

We report here results achieved with one such potentiometric dye, merocyanine oxazolone (NK2367)[24], on the organization of the monkey striate cortex. Our approach differed from that of previous investigators in that we used video imaging technology instead of photodiodes[23,25,26] to monitor activity. This sacrificed temporal resolution (which was not needed in the present study as ocular dominance and orientation are stable over time), but allowed us to achieve greater spatial resolution than previously possible. As a result, we observed patterns of activity not visualized before, including direct images of ocular dominance bands in living animals and the first detailed maps of orientation selectivity covering large areas of cortex. Analysis of these patterns revealed that orientation changes continuously within discrete domains, or modules, and that these modules overlie ocular dominance borders in such a way that ocular dominance varies continuously within them.

Monkeys

We used macaque monkeys for these studies because this species has contributed most to our understanding of the striate cortex. Macaque monkeys offer the additional advantage that large areas of striate cortex (corresponding to central and parafoveal parts of the visual field) lie in the relatively flat and exposed operculum directly under the cranium at the back of the head. Three animals that served as subjects in unrelated experiments were used to test and develop the chamber and optical apparatus. However, the results reported here were achieved with only two animals (one *Macaca nemestrina* and one *Macaca fascicularis*). Both were implanted with chronic chambers that allowed us to record from single patches of cortex on successive occasions over a period of eight weeks.

Monkeys were anaesthetized and paralysed according to established procedures[3,27]. Both eyes were refracted and fitted with contact lenses and 3-mm artificial pupils. Preliminary recordings with microelectrodes established visual field locations for the exposed cortex and allowed us to align each eye separately with the centre of a computer-driven 19-inch monitor.

Optical apparatus

Figure 1 shows the apparatus used. Light from a tungsten halogen lamp passes through a collimator, interference filter and diaphragm before being reflected onto the cortical surface. An objective lens (0.1–0.3 numerical aperture) collects the reflected light, passes it to a projection lens to focus an image of the cortex either onto a set of four photodiodes or to a Newvicon television camera (COHU Inc., Model 5300, San Diego, California). Outputs from the photodiodes were fed into conventional current-to-voltage converters, amplified and sampled by an A/D converter. The video signal was fed into an image processor (Imaging Technology Inc., Woburn, Massachusetts) which consisted of a digitizer with a flash 8-bit A/D converter (AP-512), four frame buffers (FB-512-Q) and an arithmetic unit processor (ALU-512-Q). Video images taken under different conditions of visual stimulation were accumulated in separate frame buffers for subsequent manipulation by the processor. Because of the small size of the expected signals (1 part in 1,000 or less) and the limited dynamic range of the A/D converter (256 grey levels), additional circuitry was required: (1) to flatten the signal (to shade the video image so that all parts had roughly equivalent values); (2) to boost the small signal gain (which contains most of the voltage-dependent information); and (3) to eliminate d.c. bias (reduce the apparent white level). This additional circuitry put radiant changes >0.01% within the range of the flash A/D converter; it also introduced and amplified noise which was removed through averaging. Tests with the calibrated emissions of a light-emitting diode indicate that this system detects radiant changes greater than 0.01% if they persist long enough (of the order of seconds) to be averaged. Improvements in the signal/noise ratio at the front end (for example, by cooling the image detector) should shorten the duration of required averaging.

Cortex staining

The dura was removed and the exposed cortex stained by circulating a 0.1% solution of NK2367 (Nippon, Kankoh-Shikiso, Kenkyusho, Ltd., Okayama, Japan) in balanced salt solution over the surface for 0.5–1 h. This solution was then washed out and the inlet and outlet tubes sealed to minimize cortical pulsations. Sections from freshly stained monkey cortex indicate that this procedure allows NK2367 to penetrate ~0.5 mm into the cortex. Because the observed signals strengthen steadily during the first 0.5–1 h after staining, it seems that dye in the more superficial layers (probably in the pia) must be bleached before optical signals from the deeper tissue become visible.

Observations

A set of four photodiodes were placed in the image plane of our optical apparatus (Fig. 1) to monitor optical signals simultaneously from separate patches of cortex (100 μm wide, separated by at least 400 μm). This arrangement allowed us to screen several membrane-permeable cyanine and impermeant merocyanine dyes known to exhibit voltage-dependent optical responses. Several dyes yielded signals, but those achieved with NK2367 stood out to such an extent that we concentrated all subsequent efforts on experiments with this dye.

Figure 1*b* shows the signal from one photodiode averaged over 10 presentations of vertical and horizontal gratings. Movement artefacts associated with heartbeat and respiration were eliminated from this trace by synchronizing each presentation to the animal's electrocardiogram and respiration[23]. In this trace, an increase in absorption (at 700–740 nm) corresponds to the appearance of a drifting vertical grating. A small glitch appears approximately at the time the vertical grating is replaced by a horizontal one, and the signal begins to decay back to baseline

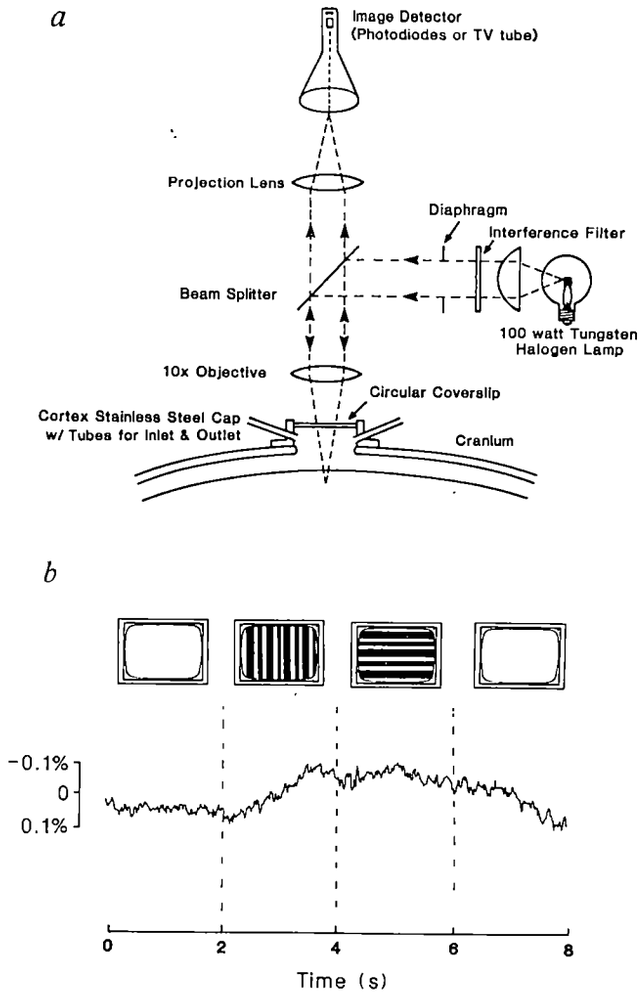


Fig. 1 *a*, Experimental arrangement for monitoring voltage-sensitive dyes in monkey striate cortex. A hole (25 mm diameter) was cut in the cranium, a stainless-steel ring cemented to the skull and the dura removed. The ring had stainless-steel inlet and outlet tubes to bathe the cortical surface with dye solution (0.1% in balanced salt solution). A second ring containing a round glass coverslip was screwed into the first ring to form a water-tight compartment. The position of the glass could be adjusted to dampen cortical pulsations and provide an optically smooth window for viewing the cortex. A condenser lens collimated light from a 100-W tungsten halogen lamp and directed it through an interference filter (720 ± 25 nm, Omega Optical, Brattleboro, Vermont), an aperture, then to the reflective surface of a beam splitter (a 50% half-silvered mirror). Reflected light passed through an objective lens and glass coverslip onto the cortex. Reflected and scattered light from the cortex passed through the coverslip, to the objective lens, through a projection lens, to the image detector (photodiodes or the TV camera). *b*, Averaged response to 10 successive presentations of vertical and horizontal gratings as seen by one photodiode that surveyed a 100-μm^2 patch of cortex. At the onset of a drifting vertical grating, there is a sudden increase in absorption for this part of cortex. A small glitch appears where the grating changes from vertical to horizontal, and the trace returns to baseline when the horizontal grating fades back again into a blank screen. Sequential presentations were synchronized to both the electrocardiogram and the respiration so that movement artefacts produced by these events could be subtracted, as previously described by Orbach *et al.*[23].

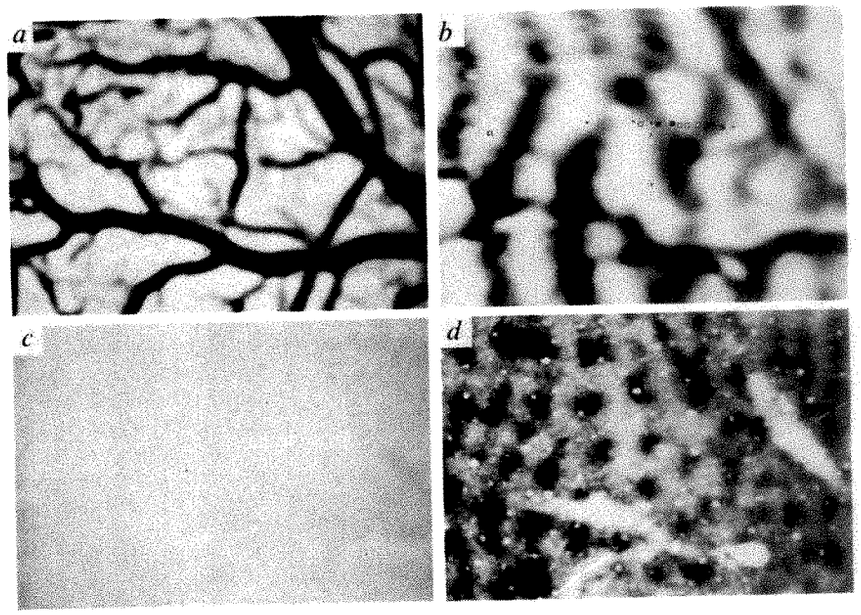


Fig. 2 *a*, Cortical blood vessels viewed under white light. Blood vessels appeared out of focus because the optical system was focused 300 μm below the pial surfaces. This patch of cortex was located just behind the lunate sulcus in the right hemisphere. Posterior, anterior, medial and lateral correspond to the top, bottom, right and left of the image frame, respectively. The border between areas 17 and 18 lies parallel to and just below the lower border of this frame. The height and width of this image corresponds to a 4×5-mm patch of cortex. *b*, The familiar pattern of ocular dominance bands is produced by subtracting images accumulated during visual stimulation of the contralateral eye from images accumulated during stimulation of the ipsilateral eye (all orientations). This produces an intensity difference of ~0.2% (amplified electronically) between the dark and light bands. The bands have an average width of 0.5 mm, run vertically into the area 17/18 border, and correspond to the rows of cytochrome oxidase 'blobs' which appear in *d*. The spots in *b* illustrate the location of 16 electrode penetrations conducted in this region of cortex before and after measurements with voltage-sensitive dyes. Small black dots indicate sites that yielded binocular responses, open squares indicate sites that were dominated by the contralateral eye, and closed squares indicate sites dominated by the ipsilateral eye. In agreement with the photodiode results, the correspondence between the dark bands and closed squares indicated that stained cortical tissue darkens with increased electrical activity (see text). *c*, The result of subtracting two time-averaged images while the monkey viewed a blank screen. The same algorithm was used as in *b*. *d*, At the end of the experiment, the same piece of cortex was sectioned tangentially and stained for cytochrome oxidase[36]. The section image shown here was aligned and expanded (necessary because of tissue shrinkage) according to the positions of blood vessels so that they laid in register with the images in *a*–*c*. Note that during examination of the histological preparations, no evidence was found of tissue damage attributable to repeated applications of the dye over more than eight weeks.

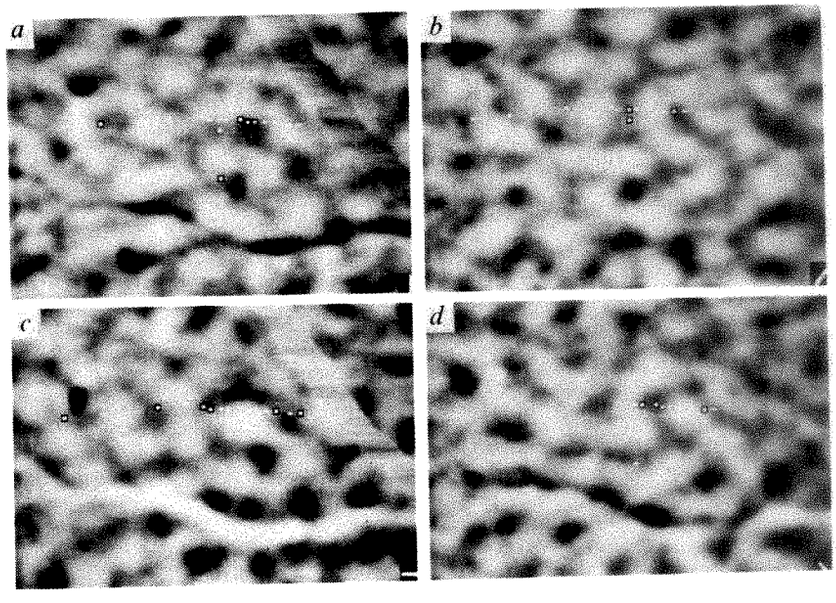


Fig. 3 Iso-orientation activity patterns produced by four separate orientations—vertical, right oblique, horizontal and left oblique. Each image was compiled separately and related to a reference image generated by the orthogonal orientation. This subtraction was necessary to minimize the effects of activity-dependent hyperaemia[28]. For example, images of cortex taken during horizontal presentations were subtracted from images taken during vertical presentations to produce the pattern in *a*. The observation that vertical and horizontal patterns shown in *a* and *c* are complementary merely underscores the consistency of the result. White dots indicate the positions of electrode recording sites. Those outlined in black denote locations where sampled cells preferred orientations within 22.5° of that presented. These correlate with the darker parts of each image and never overlap with the lighter ones. Major blood vessels, which sometimes produce shadows caused by uncontrollable dilation during image acquisition, have been blocked out to prevent unwanted influences on adjacent regions of the same image during subsequent normalization and image processing.

when the horizontal grating disappears. The occurrence of similar responses for horizontal and vertical gratings (increased aborbance in both cases) is probably due to the location and size of the cortical patch surveyed.

The large sizes, stability and long durations of these signals suggested that they might be monitored with higher spatial resolution using a TV camera. Stable signals over a long period made it possible to average many frames during each visual presentation; typically, 1,800 frames (30 frames per s) were summed during a set of 10 presentations. This led to a profound improvement in the signal to noise ratio; and further improvements were achieved through lateral averaging—that is, by dividing the image into squares 4 pixels high and 4 pixels wide, and averaging all the pixel values within each square. As noted above, the paradigm detects radiant changes greater than 0.01%.

Ocular dominance

Figure 2*a* shows a 4×5-mm patch of striate cortex as it appeared under white light. Blood vessels appear out of focus because the focal plane lies 300 μm beneath the pial surface. The lunate sulcus, as well as the accompanying border between areas 17 (striate cortex) and 18, lie parallel to and just below the lower boundary of the image. Blood vessels do not present a problem because they become virtually transparent to light at 720 nm (the wavelength at which we monitor the response of the dye), and disappear altogether (except for a couple of the largest

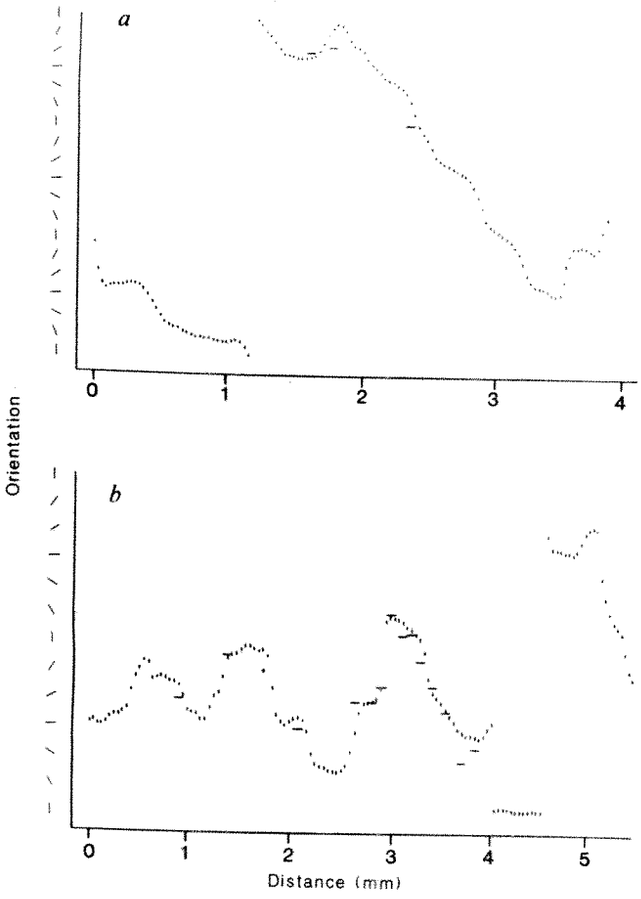


Fig. 4 Orientation values as they would appear along a single, tangential electrode penetration. This is done twice. *a*, Orientation values along a vertical scan line running through the three vertically aligned sites in the centre of Fig. 5*a*. *b*, Orientation values along a single horizontal scan line lying along the 14 horizontally aligned sites in Fig. 5*a*. Short horizontal lines indicate the actual orientation values that we determined (by averaging orientation preferences determined at three different depths) for each of the sites.

vessels) when one cortical image is subtracted from another (Fig. 2*c*). Because of the strong haemoglobin absorption at 430–610 nm it is unlikely that such controls could be obtained at wavelengths below 620 nm.

Figure 2*b* depicts the characteristic pattern of ocular dominance bands produced by subtracting cortical images accumulated during visual stimulation of the contralateral eye from images accumulated during stimulation of the ipsilateral eye. Because cortical tissue darkens with activity once it has been stained with NK2367, the dark bands in Fig. 2*b* correspond to ipsilateral dominance. Comparison of Fig. 2*a* and *b* shows that these bands have little in common with blood vessels. However, there is a tendency for the largest vessels to produce shadows (either light or dark), largely through uncontrollable changes in vascular perfusion during neuronal activity[28].

Besides resembling ocular dominance bands visualized with other techniques[5,8,9], the bands in Fig. 2*b* display several characteristic features: they have the same width as those observed with 2DG, they run vertically into the border of area 17, and every light and dark stripe straddles a row of cytochrome oxidase blobs, as would be expected[13]. The latter correlation is apparent from the aligned image (Fig. 2*d*) of a section from the same patch of cortex which was stained for cytochrome oxidase.

To confirm the identities of these bands independently, direct electrical measurements were made with microelectrode penetrations at 16 separate locations. The spots in Fig. 2*b* indicate ocular dominance values determined (on the basis of recordings at three separate depths) for each location. The round spots (indicating balanced binocular responses) predominate near the edges of bands while the open squares (contralateral dominance) align with the light bands and the closed squares (ipsilateral dominance) with the dark.

Orientation

Initial attempts to visualize orientation selectivity were made by subtracting images obtained during control conditions (equiluminant grey screen) from images obtained while the monkey viewed a drifting vertical grating. This approach was hampered by the previously mentioned vascular changes induced by neuronal activity[28], and by a diffuse, activity-dependent darkening of the cortex which may be the result of generally heightened activity within the stained cortical neuropil.

These problems can be avoided by comparing frames accumulated during stimulation with two orthogonal orientations. Activity remains high for both sets of frames such that perfusion and diffuse changes remain constant, and only events induced by a change in the stimulus orientation are detected.

We used this approach to produce the four images in Fig. 3, all of which resemble patterns achieved with 2DG[12]. The patterns produced by horizontal and vertical gratings complement one another, as do patterns produced with right and left oblique. Although this finding might appear self-evident given our subtraction protocol, the lack of overlap between the patterns reinforces their stimulus-relatedness and stability, and reduces possible concern about spontaneous fluctuations in neuronal activity. The image in Fig. 3*c*, for example, was obtained half an hour (and six intervening scans) after that in Fig. 3*a*.

Small white squares in Fig. 3 indicate the positions of our 16 electrode penetrations. Those revealing an orientation preference within 22.5° of the test stimulus are outlined in black. It is easy to see that the latter predominate within active (darkened) regions of cortex and avoid inactive (light) regions.

To improve our resolution of orientation selectivity, we obtained 12 separate activity patterns from the same patch of cortex taken at 12 separate orientations (that is, at 15° intervals). These allowed us to compare values at each pixel location (for every image) to determine the orientation responsible for the strongest response. Figure 5*a* depicts the colour-coded optimal orientation at each point, and shows that orientation values change continuously in most regions of cortex and that all orientations are represented within fairly small areas (<1 mm^2). It also allows the extraction of orientation values along single scan lines so that they may be plotted directly. This is done in Fig. 4*a* and *b*, which shows orientation values along two orthogonal axes that intersect the sites of electrode recordings (white squares in Fig. 3*a*). These plots resemble qualitatively those of Hubel and Wiesel's tangential electrode penetrations[6], and agree with the results of our own recordings (indicated by short horizontal lines).

Fractures

The colour-coded images in Figs 5*a* and 6*a* highlight the distribution of regions responsive to different orientations in one patch of cortex. This distribution is not one of parallel bands since the image does not have an overall rainbow appearance, but it is possible to find small regions where such an appearance is predominant; these regions are separated from one another by sudden shifts in preferred orientation which break the continuity.

To visualize the pattern of disruption more completely, we applied a gradient operator to the orientation values in Figs 5*a* and 6*a*. This is a simple operator which derives the rate of orientation shift (like a first derivative) in each part of the image. The results appear colour-coded in Figs 5*b* and 6*b*, where the colour sequence orange, yellow, green, blue, red and black

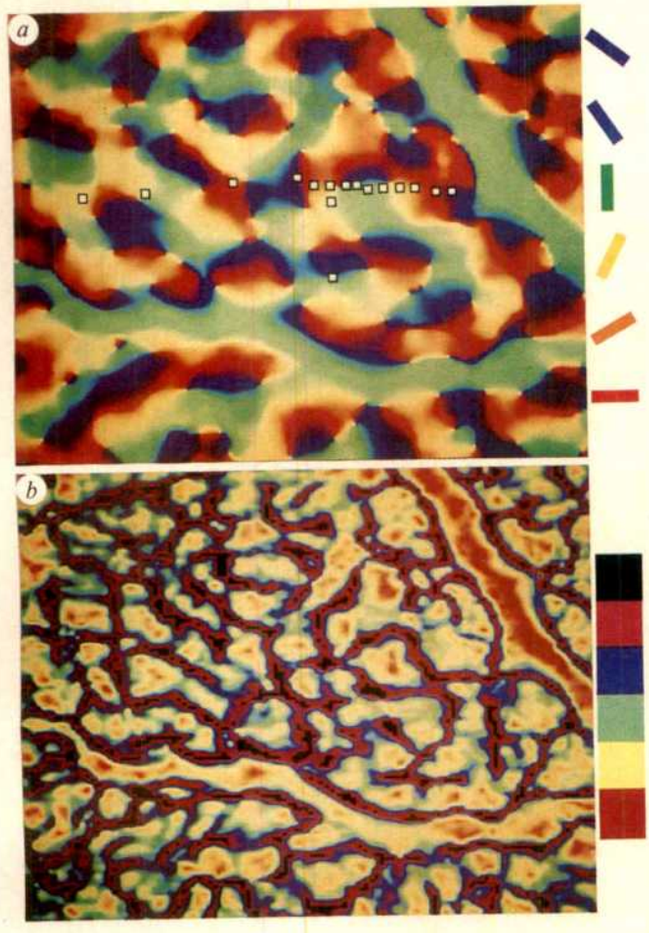


Fig. 5 *a*, Detailed orientation preferences mapped from the same patch of cortex using successive presentations of 12 separate orientations. Like the images in Fig. 3, these patterns were generated by collecting two sets of frames with orthogonal orientations, as the animal viewed bi-directionally moving gratings, and subtracting one from the other. The process was then repeated with different orthogonal pairs. Our computer (LSI 11/73) used the 12 resulting images to analyse orientation selectivity at every point in the image. Every pixel in each image was transformed into a vector; the magnitude of each vector was the pixel value (response intensity), and its angle was twice the orientation of the stimulus grating. This representation ensured that for each pixel, vectors representing equivalent responses at orthogonal orientations would cancel out. The 12 vectorial images were then summed to produce an output image consisting of two parts, one corresponding to vector magnitudes which reflects the degree of orientation selectivity for each part of cortex, and one corresponding to half the vector angle, reflecting orientation preferences. This figure shows colour-coded representations of optimal orientations. Actual orientation values appear graphically in Fig. 4. It is important not to overinterpret areas devoted to any particular orientation as most of the apparent differences derive from nonlinearities in colour processing (particularly with respect to blue). *b*, Gradient of the orientation values presented in *a*, taken so as to visualize the two-dimensional distribution of continuous regions and sudden breaks. The colours orange, yellow, green, blue and red indicate increasingly rapid rates of orientation change; black denotes regions where orientation preference jumps by 45° or more within a distance of 40 μm.

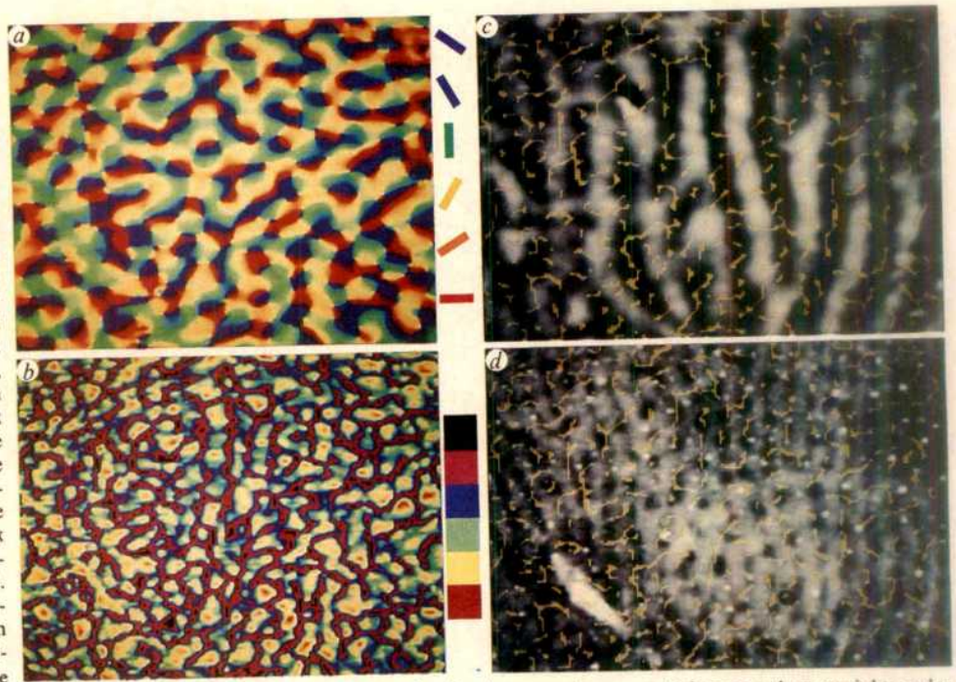


Fig. 6 Low-power view of the striate cortex. The horizontal width of this image corresponds to 8 mm on the cortical surface. As in Fig. 5, the area 17/18 border lies parallel to and just below the lower border of this image. *a*, Colour-coded distribution of orientation, similar to that shown in Fig. 5*a*. If orientation selectivity really were organized into parallel slabs, this image should look like a rainbow, or stacks of rainbows. Such colour distributions are present only on a small scale. *b*, Colour-coded representation of the orientation gradient. At this lower power, modules of continuous orientation domains are even more apparent than in Fig. 5*b*. As in Fig. 5*b*, the most abrupt transitions—those exceeding 45° in 40 μm—are indicated in black. *c*, Ocular dominance pattern for the same part of the cortex (obtained by alternate visual stimulation of the two eyes, as in Fig. 2*b*). Fine yellow lines indicate exceptionally radical shifts in orientation preference and correspond approximately to the black regions in *b*. Note the pronounced tendency for these lines to run down the centres of adjacent ocular dominance columns, or to intersect them at right angles. If we lower the fracture threshold to include slightly less radical jumps in preferred orientation, these lines elongate, becoming more modular in appearance, and eventually converge to form a pattern similar to that in *c*. The fracture-bounded modules are situated between the centres of adjacent ocular dominance columns, an opportune place for receiving balanced inputs from both eyes. This arrangement also establishes a continuous shift in ocular dominance across each module. *d*, Cytochrome oxidase-stained section from the same patch of cortex. Even a casual comparison between this image and that produced in *c* shows the close correspondence between cytochrome oxidase blobs and the centres of optically determined ocular dominance columns (both light and dark). As in *c*, yellow lines indicate the positions of fractures. Due to their pronounced tendency to align with the centres of ocular dominance columns, the fractures also overlap with the cytochrome oxidase blobs, an observation perhaps related to Livingstone and Hubel's finding that orientation tuning weakens and sometimes disappears near blobs[15]. Maps of orientation tuning (derived from the vector magnitude of the operation that produced the images in 5*a* and 6*a*) reveal a

indicates increasingly rapid changes (with respect to distance) in preferred orientation. It is clear from this representation that the most abrupt changes (indicated by red and black) travel along lines similar to fractures in a crystal, and circumscribe small (0.5–1 mm wide) regions of cortex. Within each region, orientation changes continuously along one axis, in a manner consistent with an organization of parallel slabs. Because these regions occupy most of the cortical surface area, and clearly are circumscribed by fractures, one can think of them as modules. The latter appear highly regular in area, and where larger areas are observed they take the form of elongated, module-wide strips, suggesting that smaller domains with mutually confluent maps have merged.

Fractures and ocular dominance

As both orientation selectivity and ocular dominance repeat their representation within short distances (<1 mm), it seems likely that they are related. One possibility, suggested by Hubel and Wiesel[6,7], but which they subsequently disproved[10], is that iso-orientation bands intersect ocular dominance columns at some consistent angle. Our results also reject this notion. But when we compare ocular dominance columns with sudden changes in preferred orientation (that is, with the fractures), we find a marked correlation. As can be seen from the superposition of ocular dominance columns and fracture segments in Fig. 6*c*, the fracture segments that are aligned with ocular dominance columns run down their centres and avoid the edges. Those that intersect the boundaries of two adjacent columns do so at right angles. Accordingly, disruptions in the gradient of preferred orientation tend to coincide with reversals in the gradient of ocular dominance; and orientation and ocular dominance both vary continuously along single but separate axes within each module.

Comments

Our results demonstrate the feasibility of using voltage-sensitive dyes in conjunction with video imaging techniques to study functional organization in the monkey striate cortex. They reveal for the first time a detailed map of cortical regions responsive to different orientations. We will discuss these two very different findings separately.

Dye technology. One important issue concerns the source of our optical signals. Although we have noticed a general, activity-dependent darkening of unstained cortex, we have not found this phenomenon useful in identifying cortical response properties. We believe that changes in dye absorbence underlie the generation of the patterns we see because: (1) these patterns do not become apparent until after the cortex has been stained; (2) they become weaker with exposure to light; and (3) they become stronger when the cortex is restained. These signals could be derived from dye-stained neurones and glia, and although it would be interesting to know the relative contributions of these two populations, this information is not critical as both neurones and glia exhibit preferences for orientation and ocular dominance[29].

A second issue concerns the observation that cortex stained with NK2367 exhibits an increased absorption at 700–740 nm associated with increased activity. The direction of the change is opposite to that reported for NK2367 in studies of invertebrate neurones[30], heart muscle[20], and skeletal muscle[31,32]. However, the voltage-dependent spectral changes of this dye are known to be species-dependent[30], and dye molecules bound to skeletal muscle sarcolemma and transverse-tubule membranes exhibit voltage-dependent absorption changes of opposite direction[32]. Finally, the prolonged staining period required to allow dye to percolate through the pia and upper layer of cortex may alter the dye–membrane interaction such that the action spectrum might invert[21]. In this regard, one reason NK2367 works better than other dyes tested lies in its ability to penetrate pia, which entails some degree of membrane permeability.

By visually inspecting cross-sections of freshly stained monkey cortex we determined that NK-2367 diffuses ~0.5 mm beneath the cortical surface. Cells lying any deeper than 0.5 mm do not stain and so presumably do not contribute to the optical signals. Although cells in the upper zone make some contribution, the amount is difficult to gauge, and vagaries of light scattering further complicate the issue. These uncertainties are not critical as long as the properties under investigation (ocular dominance and orientation selectivity) are aligned in depth and the optical results correlate with electrophysiological recordings.

Orientation selectivity and ocular dominance. Given the newness of the technique reported here it seems inevitable that technical limitations will become more apparent with future developments. It is possible, for example, that our results are affected more than we allow by small blood vessels and by blobs (where orientation selectivity is weak). More work is clearly needed on these issues; and for the moment we can only stress the close correlation between our optical, anatomical, and electrophysiological results. With these limitations in mind, therefore, we present here the best conclusions that we can reach with regard to cortical organization.

The model of Braitenberg and Braitenberg[33] suggests that cortical regions responsive to different orientations might be organized, clockwise and anticlockwise, in a pinwheel fashion about various distributed foci. Although there are many places where this is not seen, in those where it is, the rapid changes in preferred orientation (which we call fractures) might serve merely to make adjustments in the overall map. It is difficult to see, though, how this arrangement could produce the open-looped network of fractures apparent in Figs 5*b* and 6*b*. Given the prominence of these fractures, it seems likely that they would correlate with (and possibly be derived from) some anatomical constraint. Hubel and Wiesel[7] suggested that continuous shifts in orientation might provide an economic means of wiring up many cells with different orientation selectivity and overlapping receptive fields. Along these lines it is easy to envisage a developmental mechanism whereby neurones express some innate tendency to shift orientation preferences in their neighbours. If such a mechanism operated over ranges of 0.5–1 mm, it could lead to the condensation of stable aggregates, each with their own internally consistent map. The space constant of 0.5–1 mm could originate from local dendritic arborizations, which extend about this far.

As a slight variation of this theme, specific connections or neurones might organize the small ordered map wthin each module. These connections might then compete for territory and thereby produce the highly regular size that is apparent for the domains in Fig. 6*b*. This possibility is supported by a striking similarity between the fractures we observe and the lattice-like patterns that Rockland and Lund produced in monkey striate cortex by making large injections of horseradish peroxidase[34]. Given the overlap between fractures and blobs in Fig. 6*d*, this possibility is also suggested by the finding that horseradish peroxidase injected into blobs is transported, sometimes asymmetrically, to other blobs[35]. In this regard, it is perhaps significant that the blobs in macaque striate cortex are not usually circular and frequently extend, like fracture segments, down ocular dominance column centres.

Apart from their involvement in the anatomical and developmental constraints listed above, how might a modular design facilitate image analysis? One appealing notion is that it compartmentalizes visual space. Each module might examine a small part and reach some conclusion regarding depth and edges; the overlap between ocular dominance and orientation gradients within each module underscores this possibility. There is a problem, however, in that most modules are not large enough (by a factor of ~0.3) to accommodate all orientations. It is possible that the compartments either do not need complete sets of orientation, or, if such compartments do exist, that each may contain more than one module. On the basis of receptive field

sizes and scatter, Hubel and Wiesel[7] estimated that a point in visual space affects the firing of cells within a 1-2-mm block of cortex. Needless to say, a block of this size could include several of the continuous domains that are cell modules.

Within a module, orientation changes continuously (to a good approximation, linearly) along a single axis. The simplest explanation for this arrangement is that it satisfies some sort of packing constraint; that is, the need to represent all orientations evenly within a given distance. Given the relatively broad orientation tuning (20–60°) for most cells, it also ensures that cells responding to a particular edge will be grouped together, which might enable some sort of local averaging to improve the reliability of detection. But why should the orientation preference remain constant along the orthogonal axis? Is there really a need for such redundancy, or is there some other response parameter (such as position, edge length or spatial frequency) that varies along this axis? We cannot answer these questions yet, but they should influence the direction of future research and the answers should contribute significantly to our understanding of the striate cortex.

This work was supported by NIH grant EY05403, by American Heart Association grant AHA 82 1231, NIH, NS 18590, and in part by EY0582. G.G.B. is the recipient of a Research Fellowship from the Alberta Heritage Foundation for Medical Research, and G.S. is the recipient of NIH Research Career Development award 5K04 NS 00909. We thank Dr J. S. Lund for enthusiastic support throughout this work, Drs David Hubel, Douglas Bowling, Brian Macvicar, Peter Jones and Ted Famiglietti for comments on the manuscript, and particularly Suzanne Hollbach for technical support, Tom Harper for help with photography, and Shari Berridge for typing the manuscript.

Received 15 January; accepted 16 April 1986.

1. Hubel, D. H. & Wiesel, T. N. *J. Physiol., Lond.* **160,** 106–154 (1962).
2. Hubel, D. H. & Wiesel, T. N. *J. Neurophysiol.* **28,** 229–289 (1965).
3. Hubel, D. H. & Wiesel, T. N. *J. Physiol., Lond.* **195,** 215–243 (1968).
4. Hubel, D. H. & Wiesel, T. N. *Nature* **225,** 41–42 (1970).
5. Hubel, D. H. & Wiesel, T. N. *J. comp. Neurol.* **146,** 421–450 (1972).
6. Hubel, D. H. & Wiesel, T. N. *J. comp. Neurol.* **158,** 295–306 (1974).
7. Hubel, D. H. & Wiesel, T. N. *J. comp. Neurol.* **158,** 267–294 (1974).
8. Hubel, D. H. & Wiesel, T. N. *Proc. R. Soc.* **B198,** 1–59 (1977).
9. LeVay, S., Hubel, D. H. & Wiesel, T. N. *J. comp. Neurol.* **159,** 559–576 (1975).
10. Fitzpatrick, D., Lund, J. S. & Blasdel, G. *J. Neurosci.* **5,** 3329–3349 (1984).
11. Sillito, A. M. in *Cerebral Cortex* Vol. 2 (eds Jones, E. G. & Peters, A.) 91–118 (Plenum, New York, 1984).
12. Hubel, D. H., Wiesel, T. N. & Stryker, M. *J. comp. Neurol.* **177,** 361–380 (1978).
13. Horton, C. H. & Hubel, D. H. *Nature* **292,** 762–764 (1981).
14. Humphrey, A. L. & Hendrickson, A. E. *J. Neurosci.* **3,** 345–358 (1983).
15. Livingstone, M. S. & Hubel, D. H. *J. Neurosci.* **4**(1), 309–356 (1984).
16. Davila, H. V., Salzberg, B. M., Cohen, L. B. & Waggoner, A. S. *Nature new Biol.* **241,** 159–161 (1973).
17. Salzberg, B. M., Davila, H. V. & Cohen, L. B. *Nature* **246,** 508–509 (1973).
18. Cohen, L. B. *et al. J. Membrane Biol.* **19,** 1–360 (1974).
19. Ross, W. N. *et al. J. Membrane Biol.* **33,** 141–183 (1977).
20. Morad, M. & Salama, G. *J. Physiol., Lond.* **292,** 267–295 (1979).
21. Cohen, L. B. & Salzberg, B. M. *Rev. Physiol. Biochem. Pharmac.* **83,** 35–83 (1978).
22. Salzberg, B. M. *Curr. Meth. cell. Neurobiol.* **3,** 139–187 (1983).
23. Orbach, H. S., Cohen, L. B. & Grinvald, A. *J. Neurosci.* **5,** 185–195 (1985).
24. Salzberg, B. M., Grinvald, A., Cohen, L. B., Davila, H. V. & Ross, W. N. *J. Neurosci.* **40,** 1281–1286 (1977).
25. Grinvald, A., Cohen, L. B., Lesher, S. & Boyle, M. B. *J. Neurophysiol.* **45,** 829–840 (1981).
26. Salama, G., Sanger, T. & Cohen, L. B. *Biol. Bull.* **161,** 316 (1981).
27. Blasdel, G. G. & Fitzpatrick, D. *J. Neurosci.* **4,** 880–895 (1984).
28. Sokoloff, L. *CIBA Fdn Symp.* **56,** 171–197 (1978).
29. Kelley, J. P. & Van Essen, D. C. *J. Physiol., Lond.* **238,** 515–574 (1974).
30. Ross, W. N. & Reichardt, L. F. *J. Membrane Biol.* **48,** 343–356 (1979).
31. Nakajima, S. & Gilai, A. *J. gen. Physiol.* **76,** 729–750 (1980).
32. Heiny, J. A. & Vergara, J. *J. gen. Physiol.* **85,** 805–837 (1984).
33. Braitenberg, V & Braitenberg, C. *Biol. Cybernet.* **33,** 179–186 (1979).
34. Rockland, K. S. & Lund, J. S. *J. comp. Neurol.* **216,** 303–313 (1983).
35. Livingstone, M. S. & Hubel, D. H. *J. Neurosci.* **4,** 2830–2835 (1984).
36. Wong-Riley, M. *Brain Res.* **162,** 201–217 (1979).

LETTERS TO NATURE

Test of the gravitational lens hypothesis for the quasar pair 1146+111B,C

P. A. Shaver & S. Cristiani

European Southern Observatory, Karl-Schwarzschild-Str. 2, D-8046 Garching bei München, FRG

It has recently been suggested[1] that the quasars 1146+111B,C, separated on the sky by 2.6 arc min, are actually two images of a single object produced by an extremely massive gravitational lens. The basis for this suggestion is the similarity in redshifts (within 100–200 km s^{-1}) and spectral features. Here we report differences between the two spectra in a hitherto unobserved range, suggesting that the two images are in fact distinct quasars located close together in space.

Close pairs of quasars are of interest in connection with both gravitational lensing, in which case the two images originate from the same object, and physical clustering, when the two images are due to distinct but spatially close quasars with similar redshifts. At separations of several arc seconds it is generally assumed that quasar pairs of similar redshifts and spectra are due to gravitational lenses, although even some of these could be physical pairs: the physical clustering of quasars may be similar to that of galaxies today[2], and separations of 5–10 arc s correspond to 30–60 kpc at redshifts of ~1–3 (for Hubble constant $H_0 = 100$ km s^{-1} Mpc^{-1} and deceleration parameter $q_0 = 0$), not uncommon in clusters and groups of galaxies. Pairs at arc-min separations have generally been thought to be distinct objects, although the possibility of gravitational lensing has occasionally been raised on these distance scales as well, particularly in the context of cosmic strings[3–6].

Distinguishing between the two effects can be difficult for several reasons: redshifts of broad emission lines are difficult to measure accurately and can differ substantially from the true systemic redshifts[7]; spectra of different quasars tend to be broadly similar; and some spectral differences can be present even in gravitationally lensed images, because of differential extinction by intervening material or intrinsic temporal variations combined with differential time delays along the two lines of sight[8]. However, definitive tests of gravitational lensing can be made, for example, by comparing the magnitude variations of the two images, or the redshifts of narrow forbidden lines arising in the host galaxies.

The quasars 1146+111B,C, separated by 2.6 arc min, have been known for several years to have similar redshifts[9] (ΔV = 100–200 km s^{-1}), and they have been included in lists of possible physical pairs[2]. Recently, on the basis of the similarity in redshifts and spectra, it has been suggested that this pair may be produced by a gravitational lens[1]. If so, it would be most unusual, as the large angular separation would imply an extremely large mass for the lensing object.

To test this interpretation, we have observed this pair in the red wavelength region, to look for similarities or differences between corresponding spectral lines in that unexplored range.

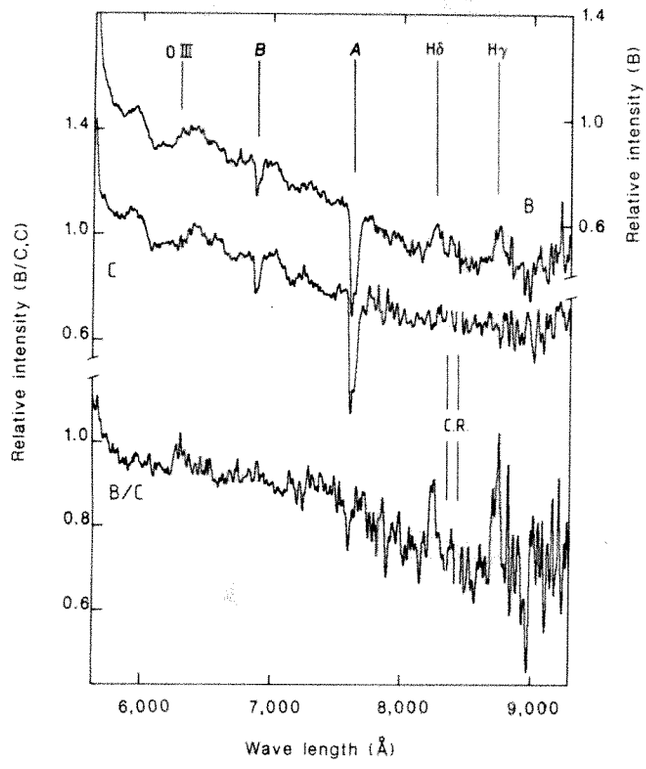


Fig. 1. Spectra of the quasars 1146+111B and C, and their ratio (B/C). The positions of the redshifted ($z = 1.0115 \pm 0.0003$) emission lines of Hγ, Hδ and O III in 1146+111B, the atmospheric *A* and *B* bands, and two cosmic-ray events (C.R.) are indicated.

The observations were made in the period 14–16 April 1986, using the European Southern Observatory faint object spectrograph and camera (EFOSC) on the 3.6-m telescope at La Silla. A red grism providing a dispersion of 270 Å mm^{-1} was used with a slit width of 1.5 arc s, resulting in a spectral resolution of 18 Å (full width at half-maximum) throughout the wavelength range 5,600–9,300 Å. Both objects were observed simultaneously. Standard flat-fielding, sky subtraction, and wavelength and intensity calibration techniques were applied, and the resulting spectra are shown in Fig. 1.

Many features are common to both spectra, particularly the ubiquitous Fe II multiplets[10]. There is, however, a significant difference: the Hγ 4,340 Å and Hδ 4,102 Å emission lines are prominent in the spectrum of B and not seen in that of C (Hγ equivalent widths of ~26 Å in B and <4 Å in C). The ratio of the two spectra reveals a third possible difference, an emission feature in the spectrum of B at 6,301 Å, probably the O III, 3,133 Å Bowen fluorescence line which is sometimes seen in quasar spectra.

In view of these spectral differences, it seems unlikely that the two objects are different images of one quasar. Even allowing for possible intrinsic variations and path-length differences, it is improbable that the hydrogen lines could have varied by a factor of 6–7 relative to both the continuum and the Mg II emission line over the suggested[1] delay time of $\sim 10^3$ yr. The spectra are different, and the most straightforward interpretation is that the objects are two different quasars. The similarity in redshift is not at all surprising for a physical pair: there are enough close pairs (in redshift and projected separation) in the Véron catalogue[11] that the probability of at least one of them having a redshift difference ≤ 100 km s^{-1} is essentially unity. There is another quasar pair, of separation 1 arc min, which was also suggested to be due to a gravitational lens[12], but closer scrutiny revealed significant spectral differences in that case also[13]. In the absence of any compelling evidence to the contrary, therefore, we conclude that 1146+111B,C are simply two separate quasars located close to each other.

We thank John Danziger, Bob Sanders and Joe Wampler for useful comments and discussions.

Received 15 May; accepted 16 May 1986.

1. Turner, E. L. *et al. Nature* **321**, 142–144 (1986).
2. Shaver, P. A. *Astr. Astrophys.* **136**, L9–L10 (1984).
3. Vilenkin, A. *Astrophys. J.* **282**, L51–L53 (1984).
4. Hogan, C. & Narayan, R. *Mon. Not. R. astr. Soc.* **211**, 575–591 (1984).
5. Gott, J. R. III *Astrophys. J.* **288**, 422–427 (1985).
6. Paczynski, B. *Nature* **319**, 567–568 (1986).
7. Gaskell, C. M. *Astrophys. J.* **263**, 79–86 (1982).
8. Young, P., Gunn, J. E., Kristian, J., Oke, J. B. & Westphal, J. A. *Astrophys. J.* **244**, 736–755 (1981).
9. Arp, H. & Hazard, C. *Astrophys. J.* **240**, 726–736 (1980).
10. Wampler, E. J. *Astrophys. J.* **296**, 416–422 (1985).
11. Véron-Cetty, M.-P. & Véron, P. *Eur. south. Obs. scient. Rep.* No. 4 (1985).
12. Surdej, J. *et al.* in *Proc. 24th Liège int. Colloq.* 355 (Institut d'Astrophysique, Liège, 1983).
13. Surdej, J. *et al. Astr. Astrophys.* (in the press).

Natural ventilation of the Paintings Room in the Altamira cave

P. L. Fernández*, I. Gutierrez†, L. S. Quindós†, J. Soto† & E. Villar*

* Fundamental Physics Department, Science Faculty, and †Medical Physics Department, Medicine Faculty, University of Santander, 39005 Santander, Spain

The Altamira cave (Santillana del Mar, Santander, Spain) is famous for the ceiling of one of its chambers, the Paintings Room, which is decorated with palaeolithic paintings. However, the massive influx of visitors resulted in deterioration of these rupestrian paintings and the cave was closed in 1977 to determine both the causes and the maximum number of visitors that could visit the cave without putting the paintings at risk[1–3]. The natural ventilation of the Paintings Room is one of the most important factors in formulating the maximum occupational index for visitors to the cave. The emission of carbon dioxide and water vapour by visitors inside the chamber is directly proportional to the number of visitors and the time spent in the room. By ventilating the room, these components should be removed from the air within a short period of time, thus returning the chamber to the prevailing conditions before visitors were allowed in. We report here variations in the ^{222}Rn concentration in the air of the Paintings Room which we use as a quantitative index of the natural ventilation existing in this chamber. We carried out parallel studies of the temperature at different points in the cave and the evolution of the carbon dioxide concentration in the air of the Paintings Room, and hence established the maximum number of people per hour that should be allowed to visit this chamber.

Radon-222 is a noble gas of the radioactive series of ^{238}U, an element that occurs in rocks in the Earth's crust with a concentration between 2 and 5 p.p.m. (parts per 10^6). Because of its gaseous nature and its greater concentration within the Earth, radon escapes through the interstices of the soil to the atmosphere, with an exhalation rate of ~1 atom c^{-2} s^{-1}. When this exhalation occurs in places with little ventilation, the radon concentration of the air may be high.

The ^{222}Rn concentration of the air of the Altamira cave was measured by scintillation cells with a capacity of 500 cm^3, in which a vacuum had been created down to a pressure of 50 torr. These scintillation cells were made of transparent plastic and

Table 1 Mean monthly ^{222}Rn concentration in the air of the Hall and Paintings Room; and the natural ventilation rate in the Paintings Room

Month	Location	^{222}Rn concentration (pCi/l^{-1})	Ventilation rate ($m^3 h^{-1}$)
February 1983	Hall	47 ± 3	10.3 ± 1.6
	Paintings Room	76 ± 4	
March 1983	Hall	149 ± 8	9.2 ± 1.3
	Paintings Room	159 ± 8	
April 1983	Hall	162 ± 8	6.9 ± 1.0
	Paintings Room	171 ± 9	
May 1983	Hall	159 ± 9	1.0 ± 0.2
	Paintings Room	185 ± 12	
June 1983	Hall	43 ± 4	13.4 ± 2.1
	Paintings Room	67 ± 5	
July 1983	Hall	6 ± 1	20.3 ± 3
	Paintings Room	27 ± 3	
August 1983	Hall	13 ± 2	16.9 ± 2.4
	Paintings Room	37 ± 5	
September 1983	Hall	16 ± 2	17.9 ± 2.6
	Paintings Room	38 ± 5	
October 1983	Hall	37 ± 5	16.4 ± 2.3
	Paintings Room	58 ± 6	
November 1983	Hall	117 ± 7	5.1 ± 0.8
	Paintings Room	143 ± 8	
December 1983	Hall	173 ± 9	5.7 ± 0.8
	Paintings Room	180 ± 9	
January 1984	Hall	177 ± 9	9.3 ± 1.2
	Paintings Room	181 ± 9	

their internal walls were covered with a film of SZn(Ag). The emission of α radiation by the radon ($t_{1/2} = 3.8$ days) contained in the air filling the cell leads to this radiation falling onto the film of SZn(Ag), where it produces fluorescence. The light thus emitted can be detected using a photomultiplier tube and the pulses produced can be recorded.

Because two of the short-lived radon daughters, ^{218}Po and ^{214}Po, are also α emitters, their contribution to the total counting supplied by an air sample increases with time until a radioactive equilibrium is reached between the radon and the two daughters. This equilibrium is reached 3 h after the sample is taken only if, initially, radon gas was present in the air sample. Therefore, to calculate the radon concentration, we carried out a 10-min counting 3 h after the collection of the air sample assuming that there was a radioactive equilibrium between the radon and its daughters. The number of counts obtained from the scintillation cell when empty was subtracted from each measurement resulting from fluorescence of the SZn(Ag).

The ^{222}Rn concentration was measured in two chambers within the cave: the Hall chamber, located at the entrance to the cave; and the Paintings Room (see Fig. 1). Measurements were made three times per week over a period of 1 yr between February 1983 and January 1984. From these results, we calculated the monthly average radon concentrations (Table 1).

To calculate the natural ventilation in the Paintings Room from the radon concentrations, we used the simplified model proposed by Wilkening[4], which is based on the fact that the temporal variation in the radon concentration (C) in the air of this chamber can be expressed as the sum of the production caused by radon exhalation from the rock surfaces, the radioactive decay and the radon loses resulting from the natural ventilation:

$$\frac{dC}{dt} = E\frac{S}{V} - \lambda C - \frac{Q}{V}(C - C_h) \quad (1)$$

where E is the radon exhalation rate, S and V the surface and volume of the Paintings Room, respectively, Q the ventilation rate in this chamber, λ the radon decay constant and C_h the radon concentration in the Hall chamber.

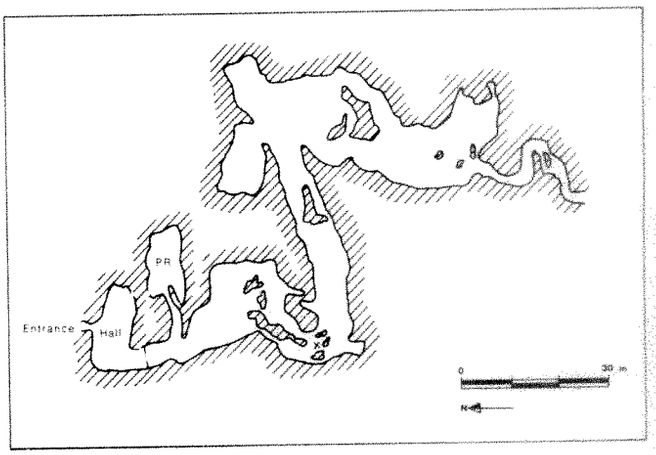


Fig. 1 Map of Altamira cave. PR, Paintings Room.

In stationary conditions, and assuming that $Q \simeq 0$ when the radon concentration reaches its maximum value C_{max} (in our case 196 pCi l^{-1}), then

$$E\frac{S}{V} = \lambda C_{max} \quad (2)$$

We can calculate the ventilation rate as

$$Q = \lambda V\frac{(C_{max} - C)}{(C - C_h)} \quad (3)$$

To apply this model to the experimental values obtained in the Altamira cave, we calculated the natural ventilation in the Paintings Room. Table 1 shows that values obtained for the ventilation rate are low throughout the whole year. Taking into account the volume of the Paintings Room, ~330 m^3, it would take ~16 h to totally renew the air in the chamber by natural ventilation in July, the period of maximum ventilation rate, and ~330 h in May, the period of minimum rate.

At the same time as measuring the radon concentration, we studied two variables that may be related to the ventilation rate: air-temperature differences between the Paintings Room and the Hall chamber and the carbon dioxide concentration in the air of the Paintings Room.

The Altamira cave has a single entrance. In such a static cave, ventilation currents are principally caused by convective air movements that basically depend on the temperature gradients between the different points into the cave. In the Altamira cave, the air temperature differences between the Paintings Room and the other chambers, with the exception of the Hall chamber, are always very small[5]. Temperature differences between the air in the Paintings Room and that in the Hall chamber are appreciably caused by the influence of the outside temperature on the latter so convective interchanges can be expected.

Figure 2 shows the monthly mean values obtained for the ventilation rate in the Paintings Room and the temperature differences between the air of the Paintings Room and the air of the Hall chamber throughout the measurement period. The correspondence can be observed between the annual variations in both ventilation in the Paintings Room is basically determined by convective processes between these two areas.

The carbon dioxide concentration in the air of the Paintings Room has its origin from the gas dissolved in the infiltration waters that flows into this enclosure. In the same way as the radon gas, the carbon dioxide concentration in the Paintings Room is eliminated by natural ventilation as the air interchanges with the outside atmosphere. The experimental measurement of the carbon dioxide concentration was carried out using an infrared analyser connected to a continuous trace graph plotter.

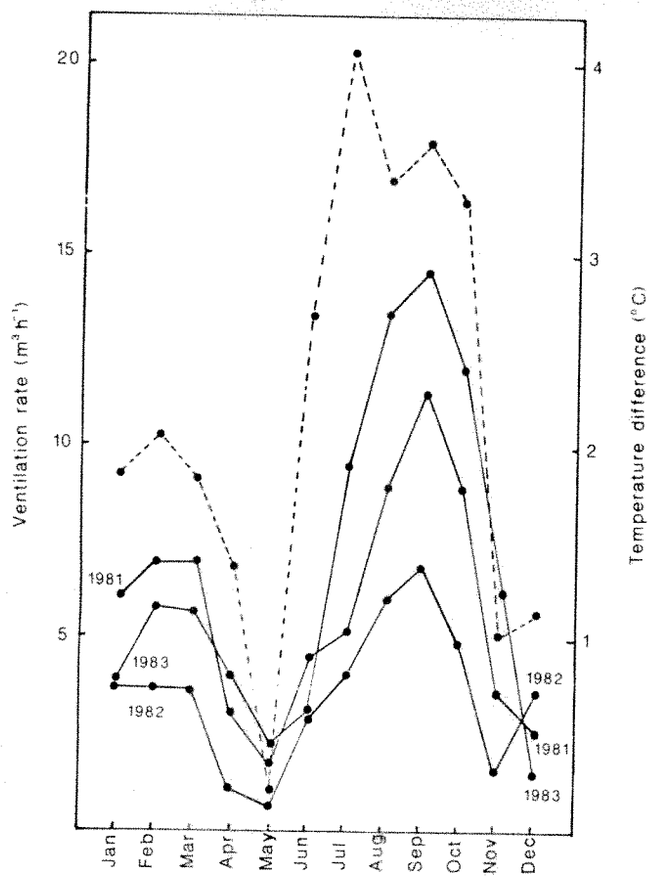


Fig. 2 Variations in the ventilation rate (dashed line) and the temperature differences (solid lines) between the Paintings Room and the Hall chamber.

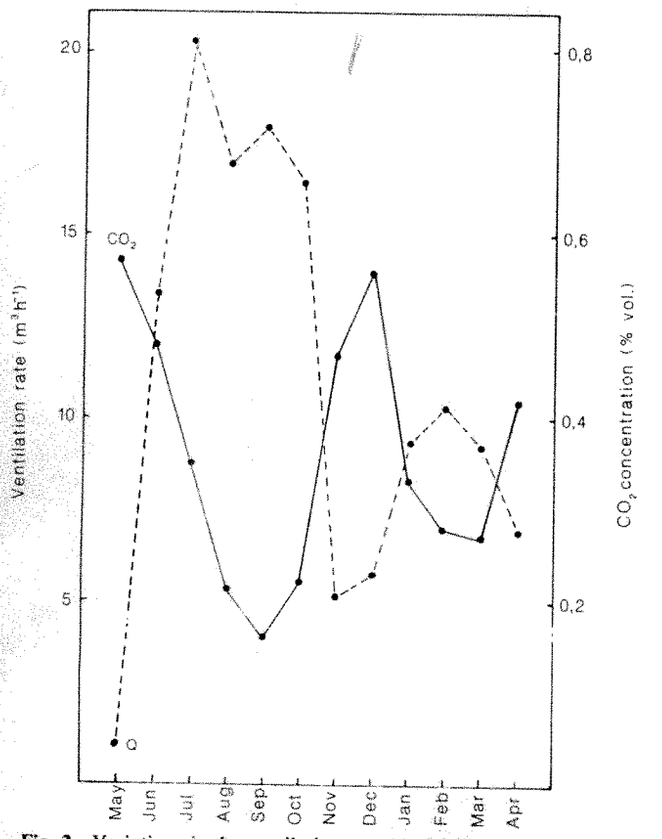


Fig. 3 Variations in the ventilation rate (dashed line) and carbon dioxide concentration (solid line) in the Paintings Room.

Figure 3 shows the ventilation rate calculated previously together with the monthly mean carbon dioxide concentrations measured in the Paintings Room. The inverse relationship between both variables consistent both with the variations in the temperature differences between the Hall chamber and the Paintings Room and with the fact that natural ventilation is the major factor affecting changes in the carbon dioxide concentration.

Taking into account that a person exhales an average carbon dioxide volume of $\sim 17\,l\,h^{-1}$ (ref. 6) our results show that the maximum number of people that could visit the Paintings Room for a period of one hour each day in the summer months without raising the carbon dioxide concentration higher than that seen in May are 43, 74 and 80 visitors in July, August and September, respectively.

Our results indicate a weak natural ventilation in the Paintings Room throughout the whole year. The ventilation rate shows minimum values in May and November and maximum values in the summer months. These results agree with the estimations obtained from the temperature differences between the air of the Paintings Room and that of the Hall chamber and of the carbon dioxide concentration in the air of the Paintings Room. The minimum radon concentration and maximum ventilation rate, found in July, match the maximum absolute value of the temperature difference between the Hall chamber and the Paintings Room and the minimum carbon dioxide content in the air of the latter, found in the same month. In the same way, the maximum radon concentration and minimum ventilation rate recorded in May match the minimum absolute value of the temperature difference between the Hall and the Paintings Room and the maximum carbon dioxide concentration measured in this month.

Received 19 December 1985; accepted 17 March 1986.

1. Villar, E., Fernández, P. L., Quindós, L. S., Solana, J. R. & Soto, J. *Trans. Br. Cave Res. Ass.* **10**, 65–70 (1983).
2. Bonet, A. *et al. Trans. Br. Cave Res. Ass.* **11**, 92–97 (1984).
3. Fernández, P. L., Quindós, L. S., Soto, J. & Villar, E. *Hlth Phys.* **46**, 445–448 (1984).
4. Wilkening, M. H. & Watkins, D. E. *Hlth Phys.* **31**, 139–146 (1976).
5. Villar, E., Fernández, P. L., Quindós, L. S., Solana, J. R. & Soto, J. *Trans. Br. Cave Res. Ass.* **11**, 99–105 (1984).
6. Marion, J. B. *General Physics with Bioscience Essays* (Wiley, New York, 1979).

Global distribution of peroxyacetyl nitrate

Hanwant B. Singh*, Louis J. Salas† & William Viezee†

* NASA-Ames Research Center, Moffett Field, California 94306, USA
† SRI International, Menlo Park, California 94025, USA

Nitrogen oxides (NO_x) have a central role in the chemistry of the atmosphere, especially in key processes relating to ozone, hydroxyl-radical (OH) and acid formation[1–7]. High reactivity of NO_x (lifetime of 0.5–2 days) precludes hemispheric-scale transport and it has been proposed that non-methane hydrocarbons present in the troposphere can transform NO_x into its organic forms principally as peroxyacetyl nitrate (PAN)[8,9]. PAN is highly stable in the colder regions of the middle and upper troposphere and can provide a mechanism for NO_x storage and transport. Once transported, PAN and its homologues can easily release free NO_x in warmer atmospheric conditions. PAN is probably ubiquitous and its concentrations could exceed those of NO_x in clean tropospheric conditions[10–12]. Here we present the first view of the global distribution of PAN based on extensive shipboard and aircraft measurements. PAN is more abundant in the Northern than in the Southern

Hemisphere and in the continental than in the marine troposphere. In contrast to its behaviour in polluted atmospheres, PAN mixing ratios in winter greatly exceed those in summer. These measurements provide a basis for assessing the significance of PAN as a reservoir of NO_x and for extending and validating reactive nitrogen chemistry theory in the troposphere.

Details of the measurement techniques for PAN and light hydrocarbons (LHC) used in the present observational program have been described elsewhere[13,14]. An overall accuracy of ±20% is estimated for the PAN measurements. We determined the hemispheric PAN distribution in surface air aboard the US Coast Guard vessel *Polar Star* while travelling from Seattle, Washington (48° N), southward to Puenta Arenas, Chile (48° S), between 11 November and 28 December 1984. All PAN and LHC measurements were made over the ocean 50 miles or more away from the coast on a daily hourly schedule from 08:00 to 22:00 local time. Figure 1*a* shows the inter-hemispheric PAN profile. PAN levels in the Northern Hemisphere are highly variable, ranging from <10 p.p.t.v. (parts per 10^{12} by volume) to some values >70 p.p.t.v. A sharp decrease towards the Equator is evident. Mean daily surface PAN levels in the Southern Hemisphere are only ~5 p.p.t.v., compared with the average Northern Hemisphere level of 38 p.p.t.v. The relatively high concentrations encountered at latitudes 28° N and 35° S are attributable to air masses of continental origin. Figure 1*b* shows the hemispheric profile of selected light hydrocarbons measured earlier on a similar North–South Pacific track[14]. Figure 1 shows that the PAN latitudinal distribution is similar to that of the alkanes, but is unlike the more uniformly distributed propene. The theoretical assertion that light alkanes (and NO_x) are probably the most important precursors of PAN, and therefore their hemispheric gradient is translatable into a PAN latitudinal gradient, is at least partially supported[8,9]. Although reliable NO_x data are not available, it is possible to conjecture that in the lower marine troposphere, NO_x levels are extremely low (10–30 p.p.t.v.), and probably of comparable magnitude in the two hemispheres[15,16] (also B. Ridley, unpublished data). Although PAN can hydrolyse relatively rapidly in sea water (half-life ≃15 min at $pH = 8.3$)[17], the extremely low partition coefficient suggests that oceans are, at best, a minor sink.

Aircraft measurements to an altitude of 10 km above sea level (~250 mbar) were made aboard the instrumented NCAR/NSF Beechcraft King Air research aircraft. Flights were conducted in the summer of 1984 over the Colorado–Wyoming area (19–28 July; 40° N) and over the eastern Pacific (12–22 August; 40° N); and in the winter of 1985 over the eastern Pacific (12 February to 4 March; 40° N). A total of 130 flight hours were logged. Each flight lasted 5–6 h to allow for reaching ceiling altitude and for collecting a maximum number of data points during ascent and descent. Figure 2 gives examples of typical vertical PAN profiles measured during day (~11:00–17:00) and night (~22:00–04:00) in fair weather conditions. The differences between the profiles measured during ascent (solid line) and descent (dashed line) are indicative of the variability associated with region and time of day. Figure 2 shows that PAN is preserved at night with concentrations that can be comparable to the daytime values. An important feature of these data is the indication that PAN concentrations in stable weather conditions tend to increase with height, which supports the proposed theory for *in situ* PAN synthesis[8]. PAN concentrations along the summer profile in Colorado (Fig. 2*a*) vary between 100 and 200 p.p.t.v., whereas those along the summer profile off the California coast (Fig. 2*b*) are much lower, varying between 20 and 50 p.p.t.v. Observations showed that during unsettled weather (for example, when a cold front passed through the region on 27 July), PAN values over Colorado temporarily approached those measured over the Pacific. There is a great deal of structure and variability in PAN concentration in the atmosphere, especially during winter (Fig. 2*c*). Aircraft observations of temperature and wind obtained during the February 1985 flights

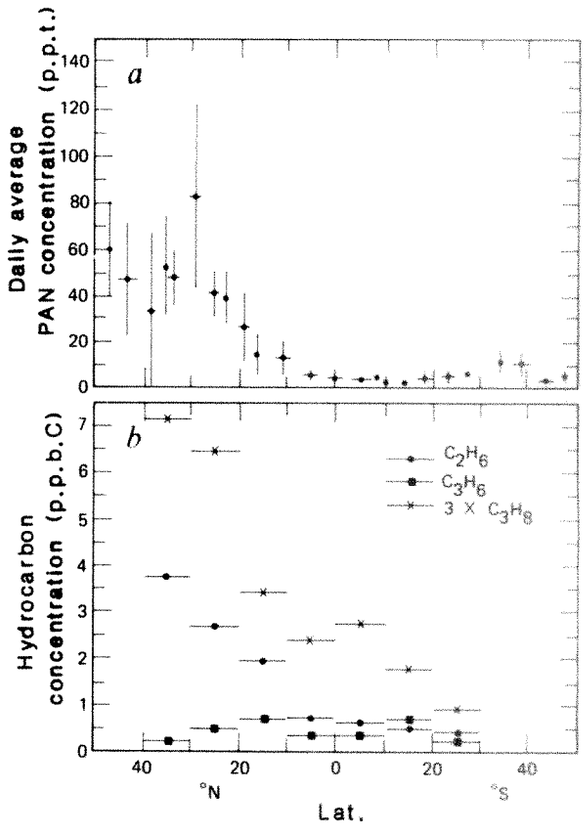


Fig. 1 Inter-hemispheric profile of surface-air concentrations for PAN and selected non-methane hydrocarbons. *a*, PAN data obtained from measurements aboard the US Coast Guard vessel *Polar Star*. The horizontal line segments represent the daily averaged PAN concentration in p.p.t.v. over the latitude (time) interval during which measurements were made. The standard deviation of the daily measurements ($\pm 1\sigma$) is indicated. *b*, Hydrocarbon data from ref. 14 obtained over the eastern Pacific Ocean during the period 30 November–21 December 1981 (p.p.b. C = 10^{-9} v/v carbon). ●, Ethane; ■, propene; ×, 3 × propane.

showed no significant variations in the vertical temperature profiles but did indicate a different wind direction and speed in the lower and middle troposphere for each of the five research flights. For the two profiles of Fig. 2*c*, the winds changed from north-north-west at 35–40 knots (21–22 February) to easterly at 25–30 knots (27 February). More research is needed to explain whether this is attributable to regional anthropogenic effects, to chemistry, meteorology or to all of the above.

Figure 3*a*,*b* shows composite vertical profiles of PAN concentration for the various time periods and geographical locations of the aircraft flights. Composite profiles are obtained by averaging the day and night measurements collected during stable, uniform air mass conditions. In Fig. 3*a*, three salient features of PAN abundance are evident: (1) in the Pacific during summer (August) and winter (February), PAN concentrations in the upper troposphere are higher than in the lower troposphere—this feature may be evident also in the summer (July) profile for Colorado except that the lower troposphere shows relatively large concentrations, possible because of continental or regional anthropogenic influences; (2) during summer, PAN concentrations throughout the continental troposphere are significantly larger than throughout the marine troposphere; and (3) PAN concentrations over the Pacific in winter are considerably higher than in summer.

The relatively high upper tropospheric PAN concentrations are consistent with PAN's extreme stability in this region, due

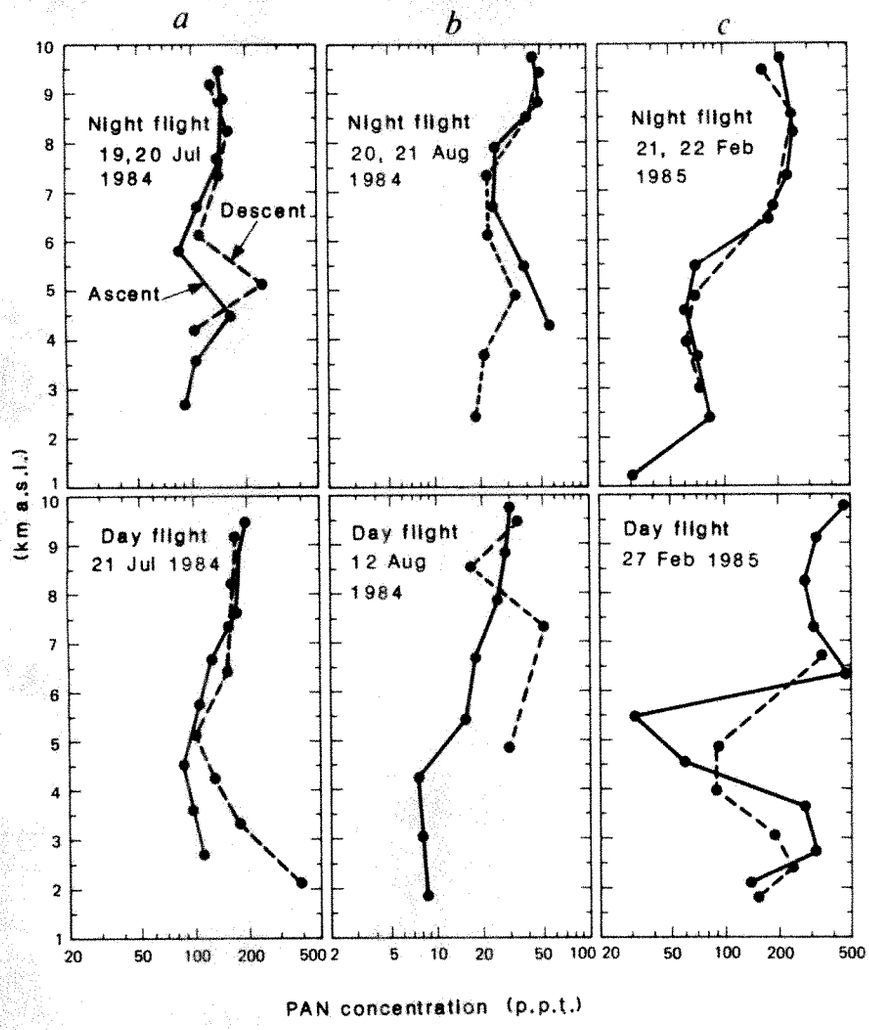


Fig. 2 Ascent (solid) and descent (dashed) vertical profiles of PAN to 10 km above sea level. Night and day profiles are shown for: *a*, the Colorado July 1984 flights; *b*, Pacific August 1984 flights; *c*, Pacific February 1985 flights.

principally to colder temperatures[8,9]. Also, there seems to be a greater free NO_x availability in the upper troposphere[16,18] and this would facilitate PAN formation. The continental PAN abundance of 100–200 p.p.t.v. is almost five times higher than its marine abundance during the same season (summer). This difference is even more significant when one considers that the continental troposphere was observed to be 2–4 K warmer than the marine troposphere. A 4 K increase in temperature can reduce PAN half-life by a factor of two because of the strong temperature dependence of the PAN dissociation rate [$K = 1.95 \times 10^{16} \exp(-13{,}543/T)$ s^{-1}]. A rational explanation must depend on the availability of non-methane hydrocarbons (NMHC) and NO_x precursors. The second feature of interest in Fig. 3*a* is the large increase in PAN concentration off the California coast between August 1984 and February 1985. If these profiles are representative of summer and winter, respectively, PAN levels in winter over the eastern Pacific Ocean could be nearly five times higher than in summer. This wintertime enhancement of PAN abundance is completely out of phase with what is normally encountered in polluted atmospheres, where highest values occur in summer[19]. The temperatures throughout the troposphere during the February 1985 aircraft flights were 8–10 K lower than those in August 1985. This temperature reduction alone could increase PAN stability by a factor of 5–6 and is likely to be an important part of this seasonal behaviour. Figure 3*b* shows measurements for the February 1985 California flights averaged for locations both over the ocean and ~50 km inland from the coastline. In the lower trophosphere, the PAN concentrations over land are consistently higher than over the ocean. In the upper troposphere, the differences are nominal.

In addition to PAN, measurements of PPN (peroxypropionyl nitrate) were also made. PPN was frequently below our detection limit because of its very low abundance. However, during the Colorado flights it was possible to measure PPN along with PAN. Figure 3*c* shows composite profiles for PAN and PPN based on the July 1984 Colorado flights. The shape of the vertical PPN profile is similar to that of PAN, but its abundance is only ~5% of PAN.

Figure 4 shows the composite profile of two surrogate hydrocarbons, propane and ethane, which were measured as part of a C_2–C_5 hydrocarbon analysis conducted during the same flights. Figure 4*a*,*b* shows that although the hydrocarbon abundance over the continental troposphere is greater than that over the marine troposphere, it is so by only a factor of two or less. No reliable NO_x data from these two regions have been published. A comparison of recent NO and NO_2 data from the Pacific troposphere (B. Ridley, unpublished data) and the earlier less reliable NO_x data from this continental tropospheric region[18] suggest that the latter NO_x levels are significantly higher. The concurrent higher abundance of both NO_x and NMHC precursors over the continental troposphere may be responsible for this large PAN gradient. Measurements of PAN along with NO_x and peroxyacetyl radical precursors (such as acetaldehyde and acetone) are required to reconcile adequately the observed PAN distributions. The winter NMHC abundance is also higher (Fig. 4*a*, *c*), probably because of reduced wintertime removal rates (lower OH). Global models which currently do not include NMHC–PAN chemistry point to the possibility of higher winter NO_x for the same reason[5]. However, a great deal of this extra winter NO_x seems to be contained in the form of PAN and is unavailable for photochemical participation[20]. Figure 4*d* shows

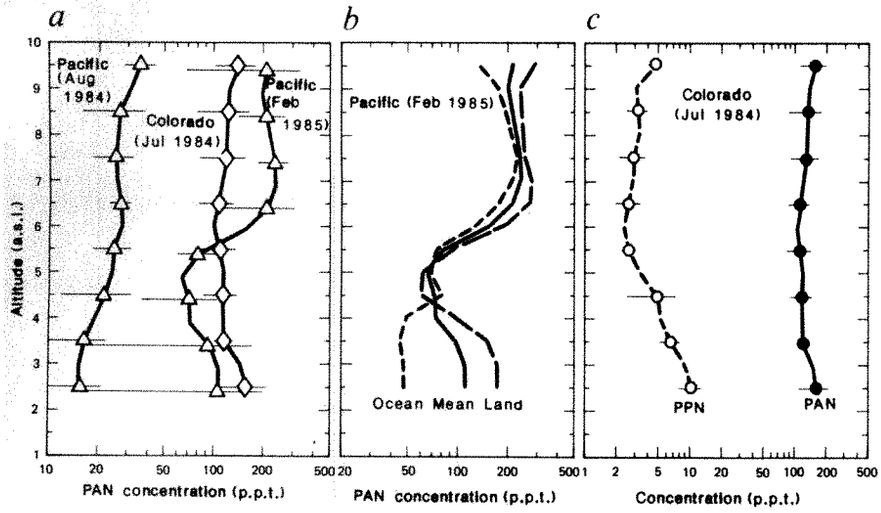


Fig. 3 Composite vertical profiles of PAN and PPN. *a*, Comparison between composite profiles ($\pm 1\sigma$) from Colorado for July 1984, and from the Pacific Ocean off the northern California coast for August 1984 and February 1985. The February profile is shifted slightly in the vertical for clarity. *b*, Mean PAN profiles observed over the ocean and 50 km inland during February 1985. *c*, PPN and PAN profile measured over Colorado.

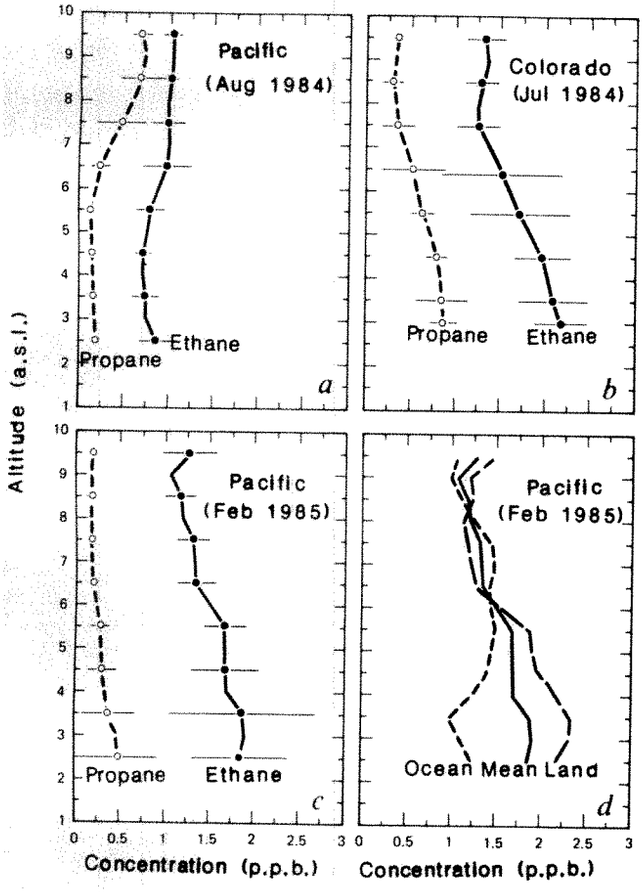


Fig. 4 *a–c*, Composite vertical profiles of ethane and propane. *d*, Ethane concentrations observed over the Pacific Ocean and 50 km inland during the February 1985 flights.

ethane data for the February 1985 California flights averaged for locations over the ocean and over land. These profiles can be compared with those for PAN in Fig. 3*b*. In the lower troposphere, both the ethane and PAN concentrations over land are consistently higher than over the ocean. In the upper troposphere, land/ocean differences are nominal.

Our free tropospheric PAN measurements point to the following important features: (1) PAN concentrations in the Northern Hemisphere are significantly greater and more variable than in the Southern Hemisphere; (2) PAN concentrations show evidence of increase with height; (3) PAN concentrations in winter are higher than in summer; (4) PAN is more abundant in the continental troposphere than in the marine troposphere, at least in the summer; (5) there is a reasonable association between PAN levels and its NMHC precursors; and (6) PAN concentrations in the free troposphere are large and may exceed those of free NO_x. All of these observations are in qualitative agreement with the theory that background NMHC/NO_x precursors can tie up significant quantities of NO_x as PAN, especially in the colder regions of the upper troposphere[8,20]. Preliminary modelling results suggest that photochemical models which do not include NMHC–PAN chemistry may significantly overpredict the availability of free NO_x and HNO_3 in the troposphere, with consequent important implications for tropospheric ozone production[20]. Simultaneous NO_x and carbonyl precursor data are needed to explain the PAN behaviour. Future increases in atmospheric NMHC and NO_x abundance, either due to increased emissions or falling hydroxyl radical concentrations[21], may enhance the role of PAN in the troposphere. Indeed, this may be one of nature's ways of regulating the photochemistry of the troposphere.

This research was funded by NSF grant ATM-8308816 to SRI International. We thank the US Coast Guard for making facilities available aboard the *Polar Star*. The support of the NCAR flight facility personnel is much appreciated.

Received November 1985; accepted 5 March 1986.

1. Haagen-Smit, A. J. *Ind. Engng Chem.* **44**, 1342–1346 (1952).
2. Chamiedes, W. L. *Geophys. Res. Lett.* **5**, 17–20 (1978).
3. Crutzen, P. J. *A Rev. Earth planet. Sci.* **7**, 443–472 (1979).
4. Liu, S. C., Kley, D., McFarland, M., Mahlman, J. D. & Levy, H. *J. geophys. Res.* **85**, 7546–7555 (1980).
5. Logan, J. A., McElroy, M. B., Wofsy, S. C. & Prather, M. J. *J. geophys. Res.* **96**, 7210–7254 (1981).
6. Logan, J. A. *J. geophys. Res.* **85**, 10785–10807 (1983).
7. Stedman, D. H. & McEwan, M. J. *Geophys. Res. Lett.* **10**, 168–171 (1983).
8. Singh, H. B. & Hanst, P. L. *Geophys. Res. Lett.* **8**, 941–944 (1981).
9. Aikin, A. C., Herman, J. R., Maier, E. J. & McQuillan, C. J. *Planet Space Sci.* **31**, 1075–1082 (1983).
10. Singh, H. B. & Salas, L. J. *Nature* **302**, 326–328 (1983).
11. Spicer, W. C., Holdren, M. W. & Keighley, G. W. *Atmos. Envir.* **17**, 1055–1058 (1983).
12. Singh, H. B. *et al. Nature* **318**, 347–349 (1985).
13. Singh, H. B. & Salas, L. J. *Atmos. Envir.* **17**, 1507–1516 (1983).
14. Singh, H. B. & Salas, L. J. *Geophys. Res. Lett.* **9**, 842–845 (1982).
15. MacFarland, M., Kley, D., Drummond, J. W., Schmeltekopf, A. L. & Winkler, R. H. *Geophys. Res. Lett.* **6**, 605–608 (1979).
16. Ridley, Caroll, M. & Gregory, J. *J. geophys. Res.* (submitted).
17. Lee, Y. N. *Pap. BNL-34735 presented at Conf. Gas-Liquid Chemistry of National Waters*, Brookhaven natn. Lab., Upton, N.Y., 1–6 April (1984).
18. Kley, D., Drummond, J. W., McFarland, M. & Liu, S. C. *J. geophys. Res.* **86**, 3153–3161 (1981).
19. Environmental Protection Agency, *Air Quality Criteria for Ozone and Other Hydrocarbons*, 600/8-78-004 (1979).
20. Kasting, J. F. & Singh, H. B. *J. geophys. Res.* (submitted).
21. Levine, J. S., Rinsland, E. P. & Tennille, G. M. *Nature* **318**, 254–257 (1985).

Geometry of accretion and oceanic thrusting of the Spongtang Ophiolite, Ladakh-Himalaya

Ingrid Reuber

Greco Himalaya-Karakorum, CNRS,
Laboratoire de Geologie Stratigraphique et Structurale,
40, ave du Recteur Pinneau, 86022 Poitiers, France

Ductile mylonitic shear zones, which in ophiolitic peridotites overprint high-temperature ductile flow, have been commonly associated with intra-oceanic thrusting, if situated at the base of the peridotites[1,2]. In fewer cases, such shear zones have been related to the vicinity of transform faults cutting the spreading ridge[3–9]. In the Spongtang nappe, one of the few well preserved Himalayan ophiolite slabs, obducted southward from the Indus–Tsangpo suture zone, two successive mylonitic ductile shear events in the peridotites have been observed. The first can be related to a transform fault, the second to intra-oceanic thrusting, resulting in the superposition of two peridotite sheets[10,11]. Poor development of the crustal sequence also indicates the presence of a transform fault, and/or to a very slowly spreading ridge. Here a three-dimensional geometry of the accretional and successive oceanic environment in the context of the eastern Neo-Tethys is proposed.

The peridotites in the high Zanskar mountains[12–14] have been mapped and studied with increasing accuracy in the past decade[10,11,15–20]. The true ophiolitic units overlie tectonically a very heterogenous series of volcanosedimentary mélange[21]. The complete assemblage has been thrust over sedimentary series of the Zanskar unit (Fig. 1*a*)[15–19].

The peridotites are harzburgitic tectonites affected everywhere by high-temperature ductile flow (S1). Two tectonic units are superposed by a mylonitic shear zone. The upper unit consists of lherzolitic harzburgite, whereas the lower one represents more depleted facies expected originally at a higher level of the sub-oceanic upper mantle.

Few cumulates are present at the east end of the lower unit (Fig. 1*b*, *d*). Ultramafics (wherlites with pyroxenitic layers) predominate over gabbros. Two measurements of the magmatic layering show it to be rather flat (Fig. 1*c*).

Pegmatitic gabbro and pyroxenite dykes of decimetric to metric width in the harzburgites just west of the cumulates represent magma from the cumulate magmatic chamber injected into host rock that is still hot.

Dyke swarms with a NW-SE mean orientation for each of the four observed swarms (Fig. 1*b*, *c*) intrude the cumulates. They are the only sheeted dykes observed in the Spongtang nappe.

Isolated diabase dykes a few metres wide with chilled margins, indicating their intrusion into cold host rock (~400 °C, ref. 22) are common throughout the harzburgites of the lower unit (Fig. 1*c*).

The high-temperature plastic flow which is linked to the ascent of the upper mantle and consequent partial fusion below a spreading centre[21], is ubiquious in the peridotites. The kinked olivine grains indicate activation of the (0*kl*) (100) 'pencil glide' of olivine at 1,000–1,200 °C and relatively low deviatoric stress[23,24]. The orientation of measured S1 foliation planes shows a random distribution.

The dunitic banding, gabbroic schlieren as well as all ultrabasic dykelets are affected by this deformation, whereas the diabases, and the pegmatitic gabbro and pyroxenite dykes are not, showing their intrusion in the upper mantle later than the plastic flow.

The dispersion of the plastic flow structures may be explained by: (1) originally random orientation, indicating poorly-developed, slow or irregular mantle flow and the absence of a well defined spreading axis, at least locally; (2) frequent reorientation of the S1 structures by the following deformations, as observed at a small scale (see refs 10, 11 for details).

A second ductile deformation affected the harzburgitic tectonites in distinct shear zones. Mylonitization starts from the grain boundaries of the kinked olivine and lamellar orthopyroxene (Fig. 2*a*), and finally affects the whole rock, leaving only small relict islands of the high-temperature plastic flow (Fig. 2*b*). This mylonite forms under high deviatoric stress and at 700–1,000 °C, together with the amphibolite facies metamorphism frequently observed in the accompanying metamorphic sole[1]. It is also in accordance with the proposed oceanic environment[25].

In the Spongtang peridotites, the chronology of the two successive episodes of mylonitic shearing can be established according to the dykes they affect: the first (S2) deforms the pegmatitic gabbro dykes, coeval with the final crystallization of the cumulates, but not the isolated diabase dykes. In some cases, shear zones develop more intensely in and around these dykes, rather than in the adjacent harzburgite. This has been explained by shearing immediately following the injection of these dykes[4,5,10,11].

The second shear event also affects isolated diabase dykes within the shear zone, and transforms them to foliated green amphibolite, indicating a temperature of ~500 °C. It follows their intrusion into cold host rock, and thus postdates the first mylonitic shear event S2. Deformation textures in the two fine-grained olivine mylonites are very similar, but some serpentine is involved in the S2′ shear zones (Fig. 2*c*), indicating

Fig. 1 (Opposite and page 594) *a*, Location of the Spongtang Klippe in western Zanskar. *b*, Structural map of the Spongtang ophiolite, showing the four major vertical shear zones S2 (1–4) in the west and upper unit with the observed dominating shear sense, some of the minor shear zones in the lower unit (5–7), frequently associated with gabbro dykes, and the intra-peridotitic thrust. For each shear zone the total of the observed lamellar pyroxenes in the dominant direction and in the opposite one is indicated, following the method of Reuber *et al.*[28]. Z, Zanskar unit; VS, volcanosedimentary sole; hbs, serpentinized harzburgite in the mélange; hb1, harzburgites of the lower unit; dun, dunites; cum, cumulates; gab, gabbro dykes; dyk, diabase dyke swarms; hb2, harzburgites of the upper unit; S2′, intraperidotitic thrust; Φ1, thrust of peridotites over mélange series, Φ2, thrust of the whole Klippe over Zanskar units. *c*, Stereogram of the poles of diabase dykes; big dots, dyke swarms (four measurements); small dots, isolated dykes (23 measurements); squares, deformed isolated diabase dykes (two measurements) within the intra-peridotitic thrust, stars = cumulate layering (two measurements). *d*, Simplified cross-section along *a*–*b*, symbols are as in *a*. *e*, Stereograms of the poles of the mylonitic foliations and lineations associated showing the transform shear S2 in the upper unit (measurements of 60 foliations and 24 lineations), the intra-peridotitic thrust S2′ (measurements of 26 foliations and six lineations), and the transform shear in the lower unit (measurements of 47 foliations and 13 lineations). In the upper unit, the squares represent centrimetric zones of especially intense shear, in the lower unit they represent S2 shear associated to the gabbro dykes. *f*, Stereograms of the poles of the pegmatitic gabbro and pyroxenite dykes (gab, 46 measurements: A, six pematitic pyroxenites; B, eight pegmatitic pyroxenites with a gabbroic centre; C, 16 leuco-gabbro dykes; A to C from the section on the west bank of Photang; D, leuco-gabbro dykes from other places between Photang and Central Spong); of the foliations S1 (measurements of 50 foliation planes in the upper, 55 in the lower unit, 22 lineations in the upper, 26 in the lower unit); compare with the early ultrabasic dykes (dun, dunitic banding, nine measurements in the upper, 16 in the lower unit, opx, orthopyroxene dykelets, eight measurements in the upper, 12 in the lower unit; px, websterite dykelets, two measurements in each unit; gb, gabbroic schlieren, one measurement in the upper, four in the lower unit; large symbols, upper; small symbols, lower unit). Stereograms *c*, *e*, *f* are equal angle projections of the lower hemisphere. Localities may be differentiated as follows: 1, west of Spong; 2, central and upper Spong; 3, Spong/Photang ridge; 4, south-east, Photang.

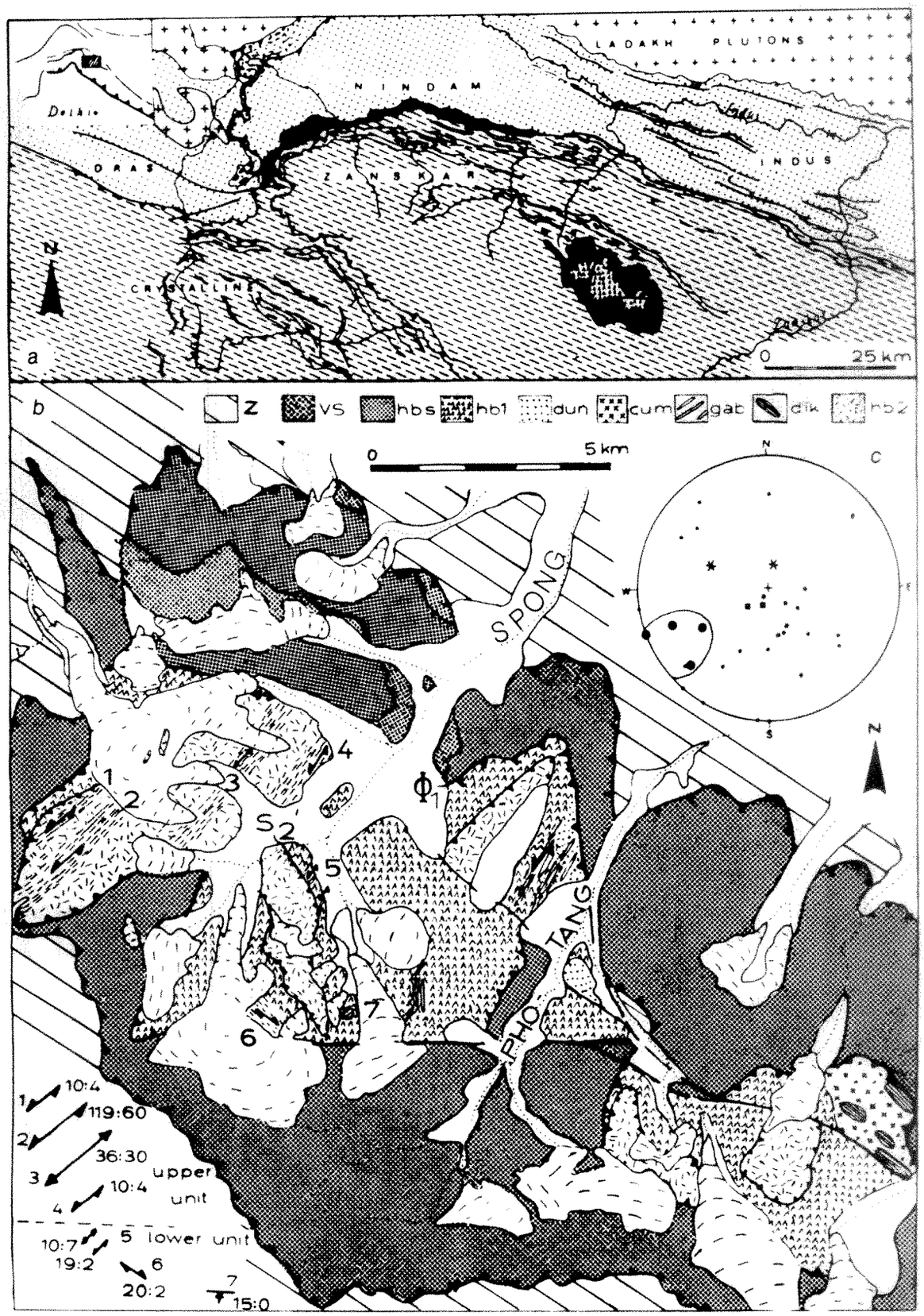

a
LADAKH PLUTONS
NINDAM
ZANSKAR
INDUS
CRYSTALLINE
0 25 km
b
Z
VS
hbs
hb1
dun
cum
gab
dik
hb2
0 5 km
N
C
SPONG
PHO TANG
1
2
3
4
5
6
7
10:4
119:60
36:30
upper unit
10:4
10:7
19:2
5 lower unit
6
20:2
7
15:0

Fig. 1*a/b/c*

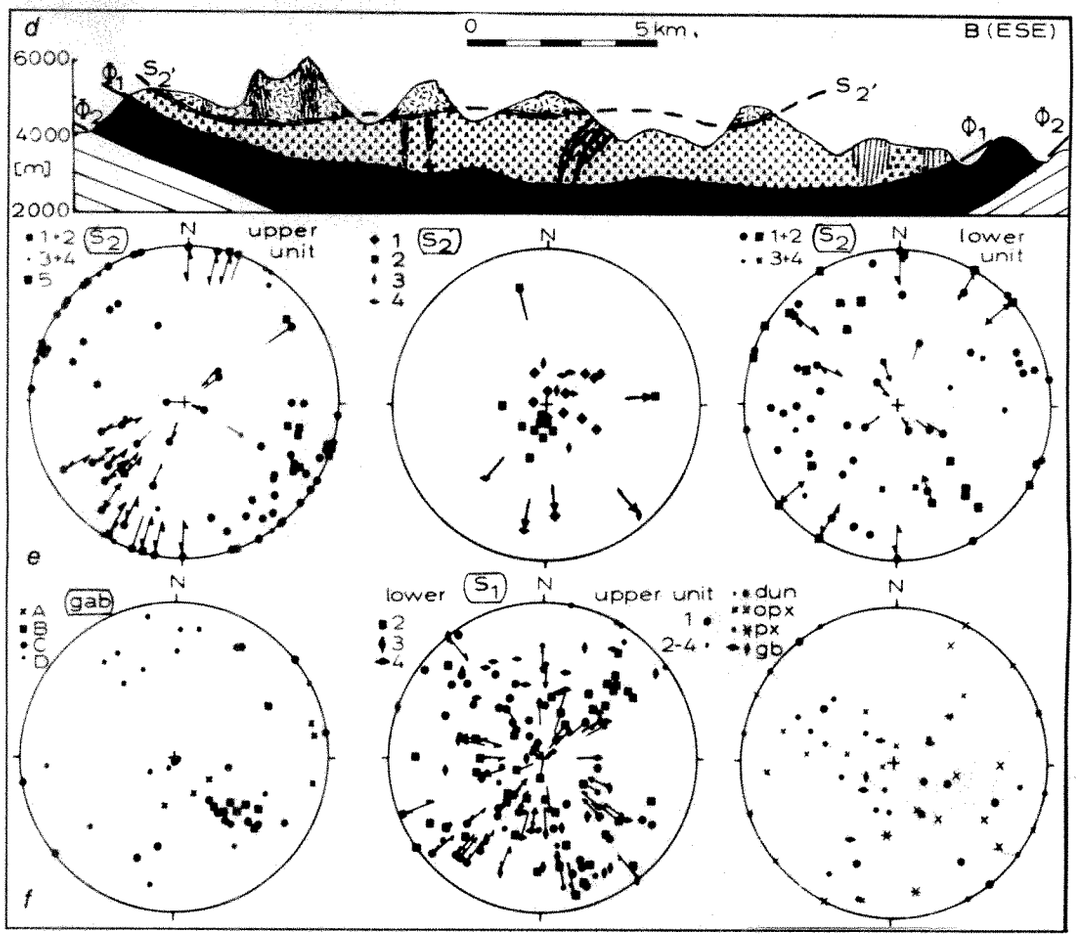


Fig. 1*d/e*

deformation at conditions proximate to the olivine-serpentine transformation, that is again at a temperature around 500 °C. The small temperature increase between dyke injection and shearing, can be produced by shear heating. However, this temperature is at least 200 °C too low for plastic creep in olivine[25], and the deformation involves olivine re-crystallization in a serpentine matrix, rather than olivine creep, a similar result to that obtained by E. Rutter (ref. 26 and personal communication).

The orientation of these shears is different. The first event, constitutes four main vertical shear zones between 50 and 600 m wide, totalling 1.6-km of sheared harzburgite within a 4-km wide zone west of the upper unit. Originally, this zone may have continued farther west beyond the actual outcrop. These main shear zones strike around N 40° E (Fig. 1*b*, *d*), and the associated ductile shear is predominantly sinistral, as shown by lamellar orthopyroxenes, interpreted directly in the field[27,28]. From west to east the sinistral shear is progressively accompanied by pure flattening, as the relative number of orthopyroxenes indicating dextral shear increases (Fig. 1*b*).

In the lower unit, several minor shear zones add up to an additional ~500 m width of sheared harzburgite dispersed over 5 km. Their orientation as well as the observed shear sense become progressively dispersed and less important towards the east (Fig. 1*e*), as expected at the edge of a mega-shear zone.

The second mylonitic shear S2′ is concentrated in one main shear zone of sub-horizontal orientation (Fig. 1*e*), and a width of 20–70 m. This zone, marking the limit between the upper and the lower peridotite units, can be followed throughout the Spongtang Klippe (Fig. 1*e*, *d*). It is most visible in the mountain north of Spong glacier, where a sheared diabase dyke is coated with white magnesite (Fig. 3). The few lineations and the little information available on the shear sense indicate, however, a predominance of south- to southeastward thrusting of the upper unit over the lower one (52: 11 lamellar orthopyroxenes, Fig. 1*e*).

The present data constrain the accretionary geometry of the Spongtang ophiolite. In the absence of palaeomagnetic data, rotation with respect to a vertical axis cannot be traced, and the data are treated as if no such rotation occurred during or after obduction. A small rotation with respect to an horizontal axis will improve the internal kinematic coherence of the model proposed as follows.

The dykes of the dyke complex are, in general, considered to be parallel to the ridge orientation[22]. In the absence of a true dyke complex, the mean orientation of the dyke swarms indicates a NW–SE orientation for a poorly developed ridge (N 140° E).

The S2 vertical shear zones may be linked to a transform fault zone continuing farther west beyond the actual outcrop. The transform fault should be parallel with the major shear zones, thus trending NE–SW (N 40° E).

The flat S2′ shear can be related to intra-oceanic thrusting in a NNW–SSE direction. Thus, for considerations of accretionary geometry, the upper unit can be restored towards the NNW of the lower one.

The proposed ridge and transform orientations are nearly perpendicular, and the predominantly sinistral shear of the transform zone results in a dextral offset of the ridge segments.

This idea is consistent with the poorly-developed cumulates in the vicinity of the transform fault, which limits the cumulate magmatic chamber in the west. This observation does not exclude a normal crustal section farther east beyond the Spongtang Klippe. Predominantly ultrabasic cumulates at the edge of

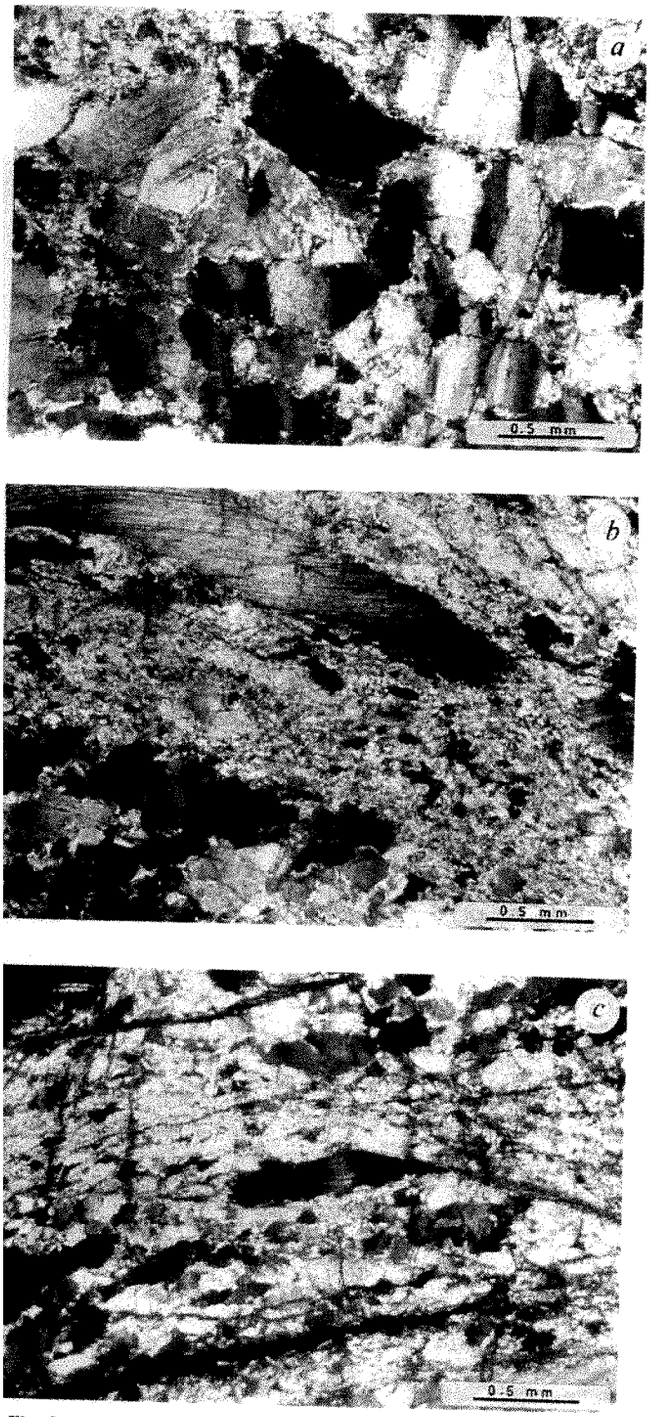


Fig. 2 *a*, Start of mylonitization at the grain boundaries of kinked olivine and lamellar pyroxene porphyoclasts. *b*, Complete mylonitization with few relic porphyroclasts, S2 shear. *c*, Intense mylonitization including some serpentine, of the S2′ shear. All are photomicrographs, cross-polarized light.



Fig. 3 At the Spong glacier the intra-peridotitic thrust is underlined by the white magnesite coating of a deformed diabase dyke.

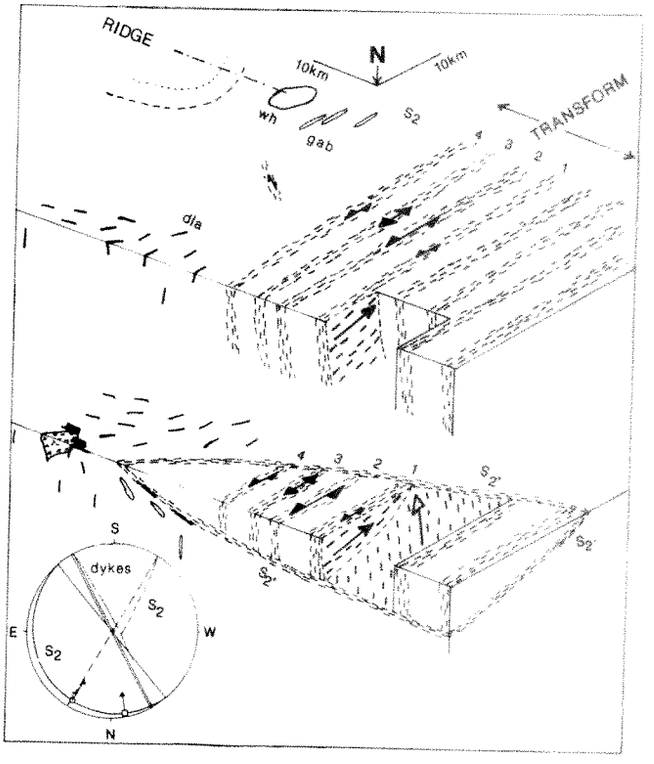


Fig. 4 *a*, Sketch of the oceanic accretion geometry before intra-oceanic thrusting, looking southward. Disposition of the ductile shear zones (1–4) at an approximately median level of the cumulate magmatic chamber (in white) possibly existing farther east of the transform fault. The observed cumulates rather originate in a small magmatic chamber (wh), nearer to the transform zone, where the pegmatitic dykes (gab) are also found, the intrusion of the isolated diabase dykes (dia) is drawn off-axis (not to scale). The true position of L2 is shown in the inset. *b*, Intra-oceanic southward thrusting of the transform zone over the block east of the transform, the inset shows position of L2 and L2′ lineations. *c*, Stereogram showing the circular trace of the mean position of the main planar structures and associated lineations after rotation to their proposed original position as explained in the text.

ransform fault have previously been described in a very similar t-up for the Antalyan ophiolite (Turkey[4,5]). The high content primary clinopyroxene in the harzburgites of the western part ıd the upper unit indicates again little partial fusion as would expected in a compressive transform zone[29].

A rotation of 20°, less than the dispersion of the measurements r S2′ foliation planes, with the azimuth of the mean S2′ plane the axis, is proposed to restore a thrust movement on the S2′ liation planes (Fig. 4*c*). At the same time, the normal com-ıent related to the transform shear S2 becomes inverse (Figs 1*e*, 4*c*), which is in better accordance with the compressive aspect of this transform zone.

This is the first ophiolitic example of intra-oceanic thrusting resulting in the superposition of two peridotite units. The absence of amphibolites of volcanosedimentary origin underly-

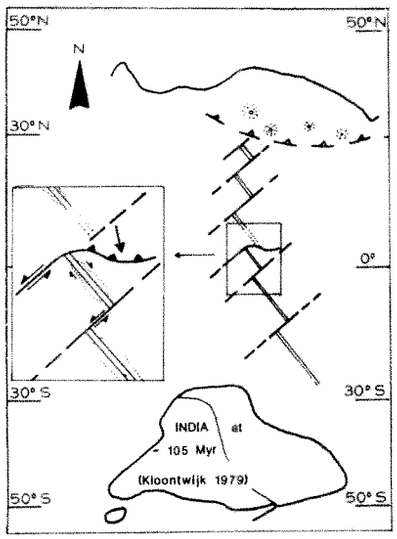


Fig. 5 Sketch of the possible geometric relations between the accretionary ridge, the transform fault and the intra-oceanic thrusting in the context of the beginning northward move of the Indian plate. Its northern boundary is stable at 30° south from the Permian to Middle Cretaceous[33], a time span which should include the phenomena described in the text.

ing the thrusted peridotites[10,11,20,21], can be explained by: the absence of volcanism in the transform zone; the scarcity of volcanosedimentary cover due to thrusting shortly after accretion; Spongtang representing a deep-seated part of the section.

This model, which is concerned with details of the accretionary geometry, does not decide the global geotectonic environment. However, there is a strong preference for the creation of Spongtang ophiolite in the open ocean, because: transform faults and intra-oceanic thrusts are not known in back arc basins; preliminary geochemical results show mid-ocean ridge basalt characteristics for more than half of the studied samples of volcanics of the sole of Spongtang as well as from the Dras area[30,31].

This does not exclude the possibility that such oceanic crust travelled into the arc environment through the combined effects of spreading and subduction, and eventually became overprinted by arc intrusives, volcanics, and associated sediments[32].

Applying this model to the eastern Neo-Tethys, shows us the possibility of maintaining extension along NW-SE oriented ridge segments, associated with minor dextral shear, even under the beginning of NNW-SSE compression. The latter is concordant with sinistral shear on the NE-SW oriented transform faults, possibly even beyond their true transform segment, and may initiate the first intra-oceanic thrusts (Fig. 5).

I thank M. Colchen, E. Gilbert and A. Nicolas for discussions and critical comments, as well as P. Nehlig, E. Reuber, G. Reibel, D. Perret, M. Dabas for company in the field. Financial support from the Greco Himalaya-Karakorum, CNRS is gratefully acknowledged.

Received 11 December 1985; accepted 5 March 1986.

1. Parrot, J. F. & Whitechurch, H. *Rev. Geogr. Phys. Geol. Dyn.* **20**, 153–170 (1978).
2. Boudier, F. & Coleman, R. G. *J. geophys. Res.* **86**, 2573–2592 (1981).
3. Prinzhofer, A. *et al. Tectonophysics* **69**, 85–112 (1980).
4. Reuber, I. *Geol. Soc. Lond. Spec. Publ.* **17**, 319–334 (1984).
5. Reuber, I., Juteau, T. & Whitechurch, H. *Bull. Soc. geol. Fr.* **26**, 945–954 (1984).
6. Casey, J. F. & Karson, J. A. *Nature* **292**, 295–301 (1981).
7. Casey, J. F., Carson, J. A., Elthon, D., Rosencrantz, E. & Titus, M. *Tectonics* **2**, 509–528 (1983).
8. Karson, J. A. *Geol. Soc. Lond. Spec. Publ.* **16**, 63–76 (1984).
9. Karson, J. A. & Dewey, J. F. *Bull. geol. Soc. Am.* **89**, 1037–1049 (1978).
10. Reuber, I., Nehlig, P. & Reibel, G. in *Himalayan Shears* (ed. Saklani, P. S.) (Himalayan Books, New Delhi, 1983).
11. Reuber, I. *Sci. Geol. Strasbourg* (in the press).
12. Lydekker, R. *Mem. geol. Surv. Ind.* 1–344 (1883).
13. La Toucher, D. *Rec. geol. Surv. Ind.* 160–162 (1888).
14. MacMohan, C. A. *Mem. geol. Soc. Ind.* **31**, 303–329 (1901).
15. Frank, W., Gansser, A. & Trommsdorf, V. *Schweiz. Min. Petrogr. Mitt.* **57**, 89–113 (1977).
16. Fuchs, G. *Jb. Geol. B.A. Wien* **122**, 513–540 (1979).
17. Bassoulet, J. P., Colchen, M., Juteau, T., Marcoux, J. & Mascle, G. *C.r. hebd. Séanc. Acad. Sci., Paris* **290D**, 389–392 (1980).
18. Gansser, A. *Tectonophysics* **62**, 37–52 (1980).
19. Srikantia, S. V. & Razdan, M. L. *J. geol. Soc. Ind.* **22**, 227–234 (1981).
20. Reibel, G. & Reuber, I. *C.r. hebd Séanc. Acad. Sci., Paris* **294**, 557–562 (1982).
21. Reuber, I. & Colchen, M. *11th Réun. Sci. Terre*, Clermont Fermond (1986).
22. Nicolas, A. &Ceuleneer, G. *Earth planet. Sci. Lett.* (submitted).
23. Nicolas, A., Boudier, F. & Bouchez, J. L. *Am. J. Sci.* **280A**, 192–210 (1980).
24. Raleigh, C. B. *J. geophys. Res.* **73**, 5391–5406 (1968).
25. Nicolas, A. & Le Pichon, X. *Earth planet. Sci. Lett.* **46**, 397–406 (1980).
26. Brodie, K. H. & Rutter, E. *Can. J. Earth Sci.* (in the press).
27. Darot, M. & Boudier, F. *Petrologie* **1**, 225–236 (1975).
28. Reuber, I., Michard, A., Chalouan, A., Juteau, T. & Jermouni, B. *Tectonophysics* **82**, 231–251 (1982).
29. Boudier, F. & Nicolas, A. *Earth planet. Sci. Lett.* (in the press).
30. Reibel, G. *Mem. D.E.A., Univ. Strasbourg* (1981).
31. Reibel, G. & Juteau, T. *C.r. hebd Séanc Acad. Sci., Paris* **293**, 57–60 (1981).
32. Sutre, F., Reuber, I. & Colchen, N. *11th Réun. Sci. Terre*, Clermont Fermond (1986).
33. Klootwijk, C. T. in *Geodynamics of Pakistan* (eds Farah, A. & De Jong, K. E.) 41–80 (Geological Society of Pakistan, 1979).

A magnetotelluric sounding across Vancouver Island detects the subducting Juan de Fuca plate

R. D. Kurtz*, J. M. DeLaurier† & J. C. Gupta*

* Geological Survey of Canada, Department of Energy, Mines and Resources, 1 Observatory Crescent, Ottawa, Ontario, Canada K1A 0Y3
† Geological Survey of Canada, Department of Energy, Mines and Resources, 9860 W. Saanich Road, Box 6000, Sidney, British Columbia, Canada V8L 4B2

Magnetotelluric[1] (MT) and geomagnetic[2] depth-sounding measurements have been made at 18 sites (7 with remote reference[3]) across Vancouver Island (Fig. 1), beneath which the Juan de Fuca plate is underthrusting[4,5]. Vancouver Island is part of the old accretionary Wrangellia terrane[6] and is located in the central portion of a 350-km forearc region that extends from the sediment-filled trench[7] to the Garibaldi volcanic belt[8]. Gravity[9] and seismic refraction studies[10] suggest that the descending plate has a shallow northeasterly dip of 8°–16° with perhaps higher dips beneath northeastern Vancouver Island. A high-resolution seismic reflection survey[11] along lines 1 and 3 (Fig. 1) located a zone of strong acoustic reflections (the E-horizon[11]) near the top of the subducting Juan de Fuca plate at depths of 23–34 km. Our model of the broad-band MT data defines a sloping, highly conducting zone also near the top of the subducting plate at the same depths as the seismic E-horizon. The high electrical conductivity in this zone (the E-conductor) is the result of saline fluid within the pore spaces of sedimentary and mafic materials of the upper oceanic crust that have been subducted to those depths beneath Vancouver Island. These are the first data which clearly define a dipping conductive layer associated with the boundary region between converging plates; they have significant implications for thrust earthquakes and metamorphic reactions that occur in subduction zones.

The MT data were processed at each field site in real time, to evaluate data quality and, where possible, to maintain standard deviations of $<5\%$ for apparent resistivity and $<\pm1°$ for impedance phase. The upper panels of Fig. 2 show the suite of apparent resistivity curves spanning six decades from 384 Hz to 1,820 s determined in the major and minor axes of anisotropy and grouped for the electric field measured approximately perpendicular (B-polarization mode) or parallel (E-polarization mode) to the strike of the continental margin. The curves in each group are similar in shape and display a decrease in amplitude at periods longer than 1 s, an indication of increasing conductivity at depth. The apparent resistivities for these two modes diverge at the longer periods (>30 s), which is charac-

teristic of data from stations on the resistive side (the crust beneath Vancouver Island) of a boundary adjacent to a more conductive structure (the seawater and oceanic crust). The vertical displacements of up to two decades along the ordinate are caused by near-surface resistive[12] or conductive[12,13] anomalies. The average phase curves, however, have small standard deviations at periods >10 s, indicating a generally laterally uniform resistivity distribution in lower crust beneath southwestern Vancouver Island.

At site 12, the two orthogonal resistivity curves (highlighted in Fig. 2) and phases (not shown) are nearly isotropic for periods <10 s while at sites 10 and 14 the isotropy is moderate for periods <1 s. We have used an inversion procedure[14,15] on the data for these three sites to obtain one-dimensional layered models (Fig. 3). The sedimentary materials covering the valley beneath site 14 are more conductive than the resistive bed rock with little overburden beneath sites 10 and 12. Below depths of several kilometres the crust is moderately resistive, in the range 5,000–15,000 Ωm. All models are characterized by a low-resistivity layer (the E-conductor) at depths of 23–28 km which agree (<10%) with those to the seismic E-horizon (bold bars in Fig. 3). The long period divergence of the data between the two modes precludes a precise determination of the thickness and resistivity of the E-conductor with one-dimensional models. A two-dimensional interpretation is required to explain both polarization modes with the same model.

The two-dimensional model (Fig. 4) was constructed using the known conductivity and thickness of the sea water in the Pacific Ocean and in the Strait of Georgia. The parameters of the accretionary wedge beneath the continental margin west of Vancouver Island are consistent with the two-dimensional geomagnetic depth-sounding model of DeLaurier *et al.*[16]. Their model, as well as the seismic interpretation of Spence *et al.*[10], suggest that the oceanic lithosphere/asthenosphere boundary is near 25 km depth and dips to 55 km beneath the coast of Vancouver Island. The depth to the E-conductor is determined by the one-dimensional inversion models (Fig. 3) and by the seismic E-reflector[11], except for that beneath the very northeastern part of the island where there is an apparent absence of deep seismic reflections. The E-conductor increases in dip from about 10° beneath the three MT sites to about 35° beneath the Strait of Georgia, consistent with gravity models[9] and the down-dip of the tension axis from earthquake focal mechanisms[17]. A conductive region[18,19] is required in the lower crust beneath mainland British Columbia to model the long-period geomagnetic transfer functions and the MT data, although its depth and resistivity are not well determined by a survey limited to Vancouver Island. The thickness and resistivity of the E-conductor were varied until good agreement (<5%) was attained between the model response[20] and measured data at site 12. Since no attempt was made to include the near-surface structures apparent in the models of Fig. 3, a good fit to only the long period (>10 s) phases at sites 10 and 14 was obtained. At all sites, however, the geomagnetic transfer functions were predicted for periods >0.1 s.

The E-conductor near the top of the descending Juan de Fuca plate is 6 km thick with a 30-Ωm resistivity, and extends up-dip to merge with oceanic layers 1, 2 and 3. We have not investigated the response of a very thin conductor, say 1 km, since this necessitates a fine mesh in the model, resulting in unreasonably large matrices to invert. However, even a thin E-conductor must have a conductance (thickness/resistivity = 200 S) close to that in the model. Although our data do not resolve detail in the oceanic crust west of the coast, the conductance of the E-conductor is compatible with those obtained in oceanic layers 1 and 2 from seafloor controlled-source electrical sounding experiments[21,22] and deep-sea drilling resistivity logs[23]. The seismic E-reflection zone is 3–5 km thick, and Green *et al.*[11] suggest several possible sources for this, including layered sediments, intercalated volcanics and sediments, layered igneous basement rocks or tectonic structures induced by underthrusting.

The two-dimensional model (Fig. 4) simulates the subduction of the Juan de Fuca plate beneath the forearc region. Low resistivities in the lower crust or upper mantle have frequently been reported and are attributed to fluids filling the pore spaces[24] or to partial melting[25]. The heat flow pattern is typical of forearc regions[26]; heat flow decays from moderate values on the west coast of Vancouver Island to a minimum east of the Straight of Georgia, increasing to high values over the Garibaldi volcanic belt (T. Lewis, personal communication). Based on heat flow measurements, the temperature beneath Vancouver Island increases to 400 ± 100 °C at the top of the E-conductor; at greater depths, within the young subducting plate, the downward displacement of isotherms suggests that this estimate is a maximum. A temperature of 500 °C is more than a factor of 2 less than is required to give a resisistivity of 30 Ωm for dry granites or gabbros[24]. Furthermore, it is not sufficient to induce partial melting in wet basalts or granites[27]. Consequently, the materials within the E-conductor beneath our sites must be porous and saturated with saline fluid.

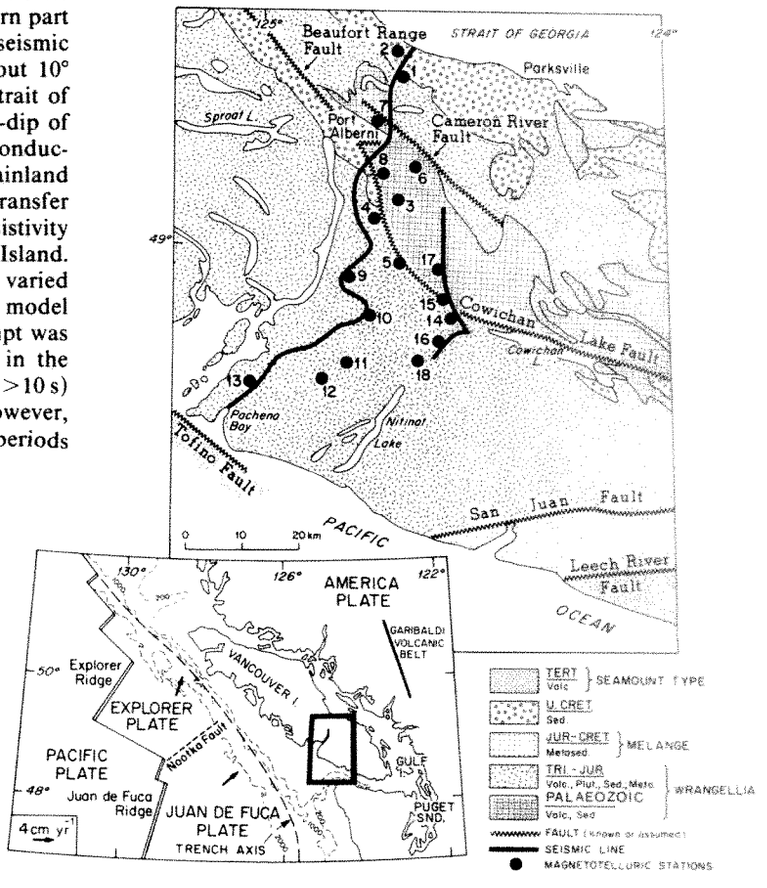


Fig. 1 Simplified geology (adapted from ref. 38) of southwestern Vancouver Island and the locations of the magnetotelluric (MT) sites near seismic reflection lines 1 (west) and 3 (east). The inset shows the location of our survey area with respect to the four plates and the pertinent convergence arrows. Bathymetry is in metres.

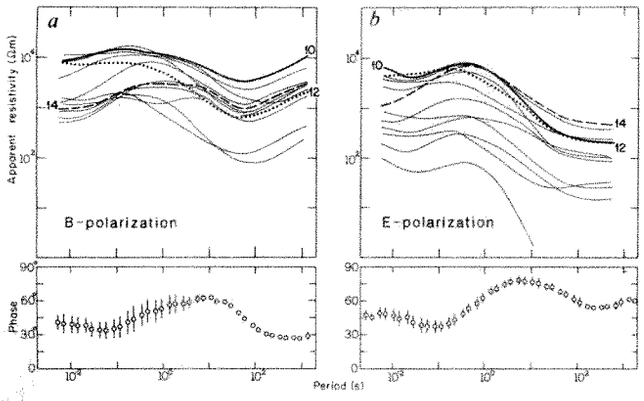


Fig. 2 The apparent resistivity curves for the southern MT sites (including remote reference sites if available). A discussion of the more complex data from the remaining sites will be presented elsewhere. The highlighted curves are for stations 10, 12 and 14 discussed in the text. Lower panels show the averaged phases associated with all the apparent resistivity curves in the corresponding upper panel. Error bars are two standard deviations in length. *a*, B-polarization mode for the electrical field perpendicular to the coast. *b*, E-polarization mode for the electric field parallel to the coast.

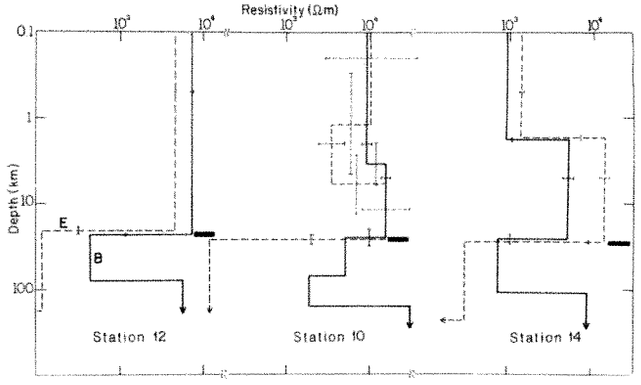


Fig. 3 One-dimensional models obtained by inversion of the apparent resistivity and phase for the E- and B-polarization data from stations 10, 12 and 14. The bold horizontal bars indicate the depths to the top of the seismic reflection zone that originates from the boundary region between the descending Juan de Fuca plate and overriding North American plate. The standard errors are determined from an eigensolution analysis[39].

A simple form of Archie's law expresses the ratio of the fluid resistivity to the bulk resistivity as equal to the square of the porosity[23,28]. If the fluid filling the pore space within the E-conductor has the salinity of sea water (3 wt% NaCl), and its resistivity at 375 °C is 0.04 Ωm (ref. 29), then the bulk resistivity of 30 Ωm leads to a porosity of 3.6%. Salinities higher than that of sea water could be expected since the solubilities of mineral species increase with temperature[30]. Therefore, the porosity can be lower; for example, a 20-wt% NaCl solution at 375 °C has a resistivity of 0.008 Ωm and, with the E-conductor resistivity, the porosity is 1.6%. Pressure effects are negligible, as the load pressure of ~850 MPa (assuming a crust density[9] of 2,920 kg m^{-3}) is more than sufficient to maintain the liquid phase[31] at the expected temperature at the top of the E-conductor. These porosities, an order of magnitude larger than those measured[32] in the laboratory for mafic crystalline rocks, could be supported with fluid pressures equal to lithostatic. This requires impermeable boundaries above or within the E-conductor. If the fluid pressures are hydrostatic, then the rock matrix is supporting the differential pressure. As the pressure and temperature at the top of the E-conductor suggest that metamorphic reactions within the blueschist to greenschist fields[33] are occurring, dehydration[26] may enhance porosity[30] and provide a source for the fluid. The trapping of fluid within the sedimentary and mafic materials of the descending plate is another complementary source.

Our MT depth-sounding data see, beneath Vancouver Island, a highly conducting zone near the top of the subducting Juan de Fuca plate which, at the expected temperatures, suggests that a conductive fluid fills the pore space of the materials within the E-conductor. This result has important geophysical implications for active or exhumed subduction complexes. First, the low level of historic seismic activity compared with the tectonic convergence rate of the Juan de Fuca and American plates[34] suggests aseismic creep on a zone of lubrication, perhaps the result of high pore pressure, although it is possible that strain accumulation occurred over the period of the seismicity data[35]. Second, the variation of the acoustic impedance across fluid-

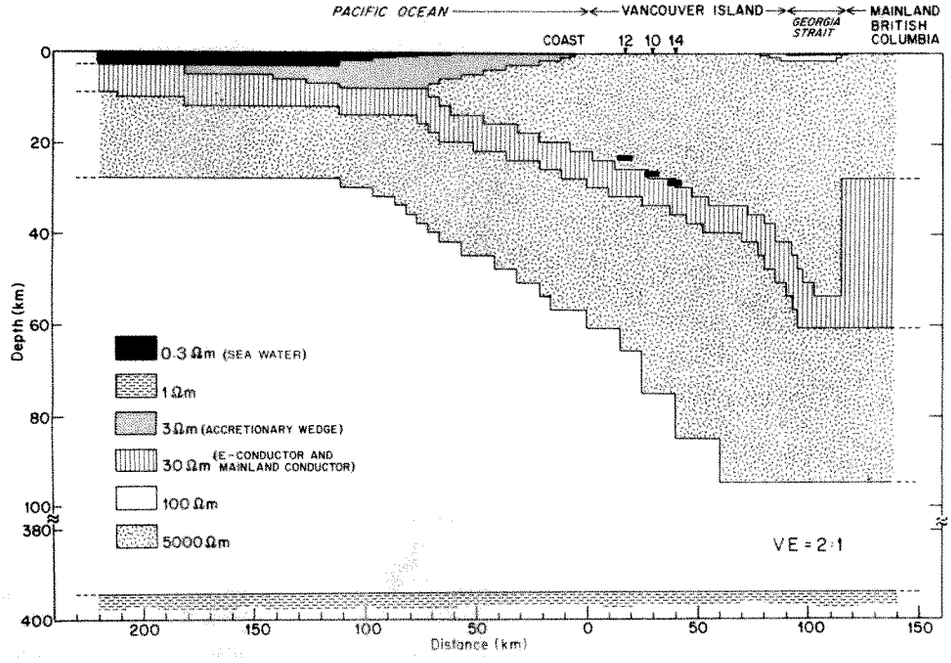


Fig. 4 The two-dimensional electrical resistivity model representing the subduction of the Juan de Fuca plate. The E-conductor (30 Ωm) is near the top of the plate. The bold horizontal bars beneath sites 10, 12 and 14 on Vancouver Island indicate the depths to the seismic E-horizon. The global decrease in resistivity[40] is represented by a 1-Ωm half-space below 390 km.

saturated porous materials[36] could explain the band of multiple, enhanced seismic reflections observed beneath the E-horizon[11]. Third, the conducting zone beneath the western portion of the forearc region suggests a depth of origin for the widespread occurrences of high-pressure/low-temperature metamorphic rocks such as glaucophone schists[37]. All these possibilities seem to necessitate the presence of fluids with pressures near or equal to lithostatic.

We thank Alan Green for reviews and discussions, and R. D. Hyndman, L. K. Law, J. Sweeney and M. J. Berry for reviews and constructive comments. Alan Jones provided analysis programs. This is Lithoprobe paper 14; Geological Survey of Canada contribution no. 11186.

Received 21 January; accepted 6 March 1986.

1. Vozoff, K. *Geophysics* **37**, 98–141 (1972).
2. Schmucker, U. *Bull. Scripts Inst. Oceanogr.* **13**, 1–165 (1970).
3. Gamble, T. D., Goubau, W. M. & Clarke, J. *Geophysics* **44**, 53–68 (1979).
4. McKenzie, D. P. & Parker, R. L. *Nature* **216**, 1276–1280 (1967).
5. Riddihough, R. P. & Hyndman, R. D. *Geosci. Can.* **3**, 269–278 (1976).
6. Jones, D. L., Silberling, N. J. & Hillhouse, J. *Can. J. Earth Sci.* **14**, 2565–2577 (1977).
7. Riddihough, R. P. *EOS* **59**, 836–842 (1978).
8. Souther, J. G. *Geol. Ass. Can. Spec. Pap.* **16**, 1–24 (1977).
9. Riddihough, R. P. *Can. J. Earth Sci.* **16**, 350–361 (1979).
10. Spence, G. D., Clowes, R. M. & Ellis, R. M. *J. geophys. Res.* **90**, 6754–6772 (1985).
11. Green, A. G. *et al. Nature* **319**, 210–213 (1986).
12. Berdichevsky, M. N. & Dmitriev, V. I. *Acta geodaet. geophys. montanist.* **11**, 447–483 (1976).
13. Park, S. K. *Geophysics* **50**, 785–797 (1985).
14. Fischer, G., Schnegg, P.-A., Peguiron, M. & Le Quang, B. V. *Geophys. J.R. astr. Soc.* **67**, 257–278 (1981).
15. Fischer, G. & Le Quang, B. V. *Geophys. J.R. astr. Soc.* **67**, 279–292 (1981).
16. DeLaurier, J. M., Auld, D. R. & Law, L. K. *J. Geomagn. Geoelectr.* **35**, 517–528 (1983).
17. Rogers, G. C. thesis, Univ British Columbia (1983).
18. Caner, B. *J. geophys. Res.* **76**, 7202–7216 (1971).
19. Gough, D. I., Bingham, D. K. & Ingham, M. R. *Can. J. Earth Sci.* **19**, 1689–1690 (1982).
20. Ku, C. C., Hsieh, M. S. & Lim, S. H. *Can. J. Earth Sci.* **10**, 645–656 (1973).
21. Young, P. D. and Cox, C. S. *Geophys. Res. Lett.* **8**, 1043–1046 (1981).
22. Nobes, D. C., Law, L. K. & Edwards, R. N. *Geophys. J. R. astr. Soc.* (in the press).
23. Becker, K. *et al. Nature* **300**, 594–598 (1982).
24. Shankland, T. J. & Ander, M. E. *J. geophys. Res.* **88**, 9475–9484 (1983).
25. Shankland, T. J. & Waff, H. S. *J. geophys. Res.* **82**, 5409–5417 (1977).
26. Anderson, R. N., Uyeda, S. & Miyashiro, A. *Geophys. J. R. astr. Soc.* **44**, 333–357 (1976).
27. Wyllie, P. J. *Trans. geol. Soc. S. Afr.* **84**, 281–291 (1981).
28. Brace, W. F., Orange, A. S. & Madden, T. R. *J. geophys. Res.* **70**, 5669–5678 (1965).
29. Ucok, H. Thesis, Univ. Southern California, Los Angeles (1979).
30. Fyfe, W. S., Price, N. J. & Thompson, A. B. *Fluids in the Earth's Crust* (Elsevier, Amsterdam, 1978).
31. Olhoeft, G. R. *J. geophys. Res.* **86**, 931–936 (1981).
32. Brace, W. F. & Orange, A. S. *J. geophys. Res.* **73**, 5407–5420 (1968).
33. Hyndman, D. W. *Petrology of Igneous and Metamorphic Rocks* (McGraw-Hill, New York, 1985).
34. Hyndman, R. D. & Weichert, D. H. *Geophys. J.R. astr. Soc.* **72**, 59–82 (1983).
35. Heaton, T. H. & Kanamori, H. *Bull. seism. Soc. Am.* **74**, 933–941 (1984).
36. Berry, M. J. & Mair, J. A. *Am. geophys. Un. Monogr.* **20**, 319–348, (1977).
37. Ernst, W. G. *Tectonophysics* **17**, 255–272 (1973).
38. Muller, J. E. *Geol. Surv. Can. Open File Map* 463 (1977).
39. Jones, A. G. *Geophys. J.R. astr. Soc.* **68**, 371–388 (1982).
40. Roberts, R. G. *Geophys. J.R. astr. Soc.* **78**, 547–572 (1984).

Seaward extension of the East African Rift

D. Mougenot*, M. Recq†, P. Virlogeux* & C. Lepvrier†

* Laboratoire de Géodynamique Sous-Marine, CEROV, BP.48, 06230 - Villefranche-sur-Mer, France
† Département de Géologie Dynamique et Département de Géotectonique, Université Pierre et Marie Curie, 4, Place Jussieu, 75252 Paris Cedex 05, France

The continental margin of northern Mozambique is edged by a north–south trending alignment of submarine peaks forming the Davie Ridge (Fig. 1*a*). From earlier studies[1–5], the ridge has been interpreted as a remnant transform fault that controlled the late Jurassic/early Cretaceous drift of Madagascar and the opening of the Somali Basin[6–8]. During MD40–MACAMO cruise (June 1984), 7,500 km of water gun seismic reflexion lines have been implemented throughout the region where two flat-bottomed troughs, the north–south trending Kerimbas and Lacerda deep grabens, interrupt the continental slope alongside the ridge. These grabens cut into Tertiary sediments correspond westward, to a Miocene tilting or a recent normal fault; and eastward, to an old discontinuity several times reactivated and located above an abrupt uplift of the Moho. The two grabens are separated from each other by a rigid region of thickened crust, affected by intense seismicity and supporting volcanoes. We report here that the eastern branch of the East African Rift joins the submerged grabens across the Tanzanian continental shelf (Fig. 1*b*).

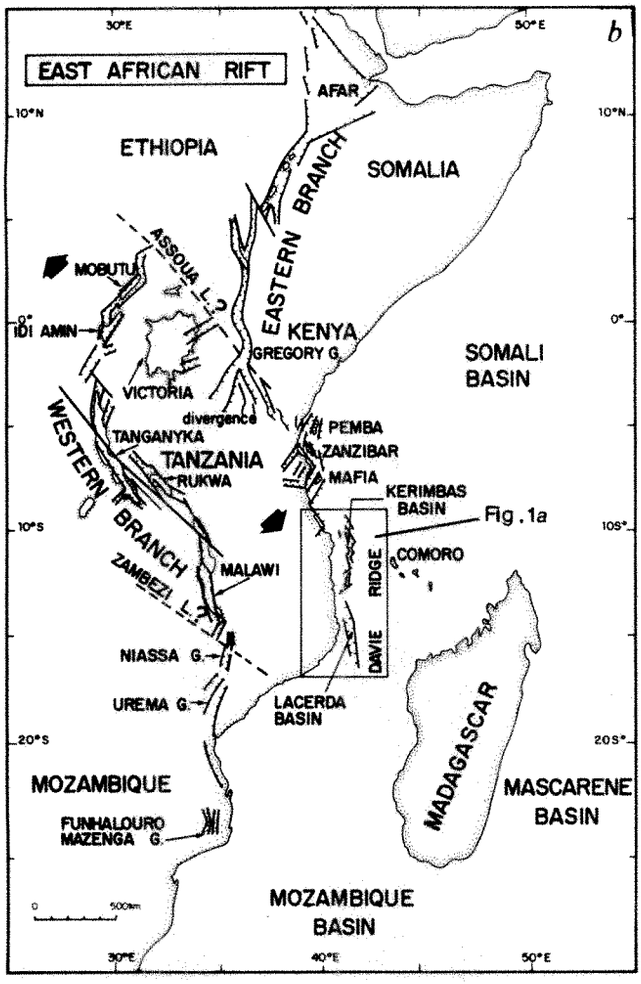
From 9° S to 17° S, the Mozambique margin is split into three domains (Fig. 1*a*). (1) North of the Saint-Lazare Seamount, the continental slope is interrupted downwards by a 250-km long trough known as the Kerimbas Basin[9]. Its 20–30-km wide flat-bottom dips slightly northward (2,400–2,800 m deep). Its asymmetrical edges are cut into four segments directed either north-northwest or north-northeast. The western boundary runs alongside the foot of the uppermost slope of the margin, which is cut by gullies. To the east, the basin is bounded by the western 1,000 m and more high escarpment of the Davie Ridge, sometimes formed by steps. The top of the wide (120 km) Davie Ridge is 1,700 m below sea level and gently dips towards the Somali Basin. (2) The rugged relief is interrupted southward by two circular features: the Saint-Lazare (12° S) and Paisley (14° S) seamounts, between which the slope gently deepens towards the Comoro Basin. (3) South of the Paisley Seamount, the abrupt uppermost continental slope is cut by several canyons that terminate near the shore. The Davie Ridge is bounded by a flat-bottomed 400-km elongated depression, the 2,700-m deep Lacerda Basin. To the south both edges of the trough become more asymmetrical, as the continental slope widens and the Davie Ridge narrows and rises. Thus, the Davie Ridge culminating at 300 m deep below sea level, is rising as much as 2,300 m above the Lacerda Basin.

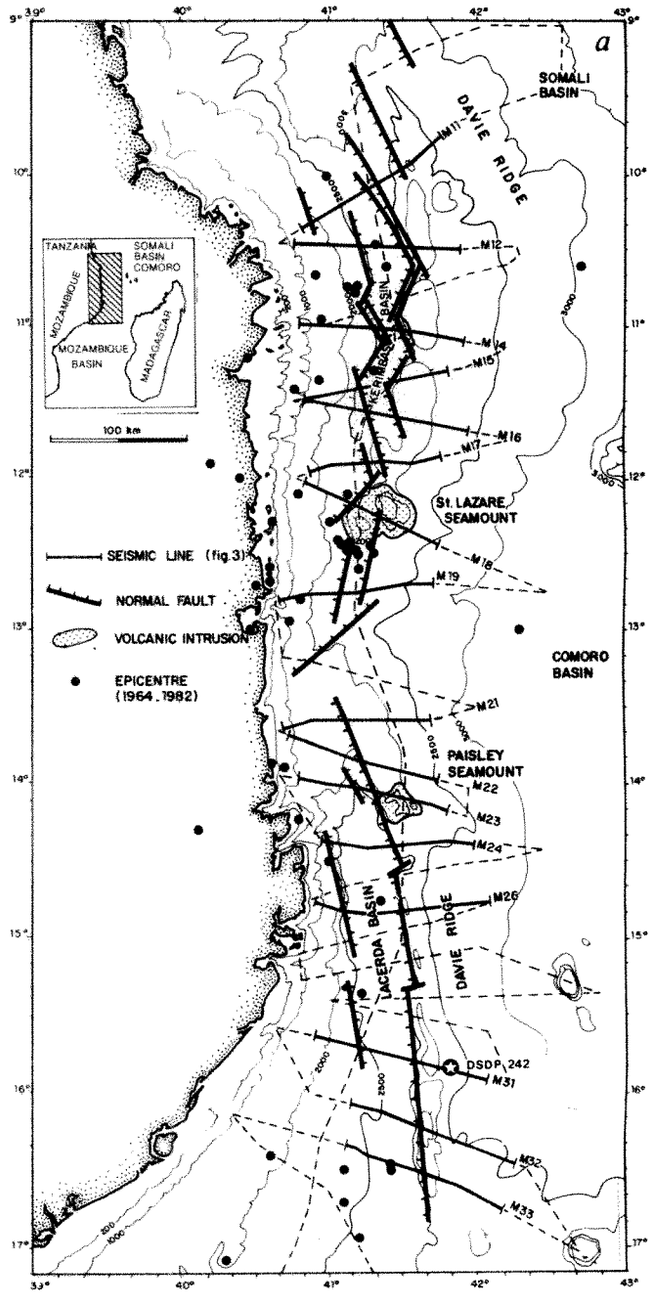
The relief pattern on the continental slope off the northern Moçambique is strongly related to neotectonics. Reflection seismic lines reveal that the steep elevation of the Davie Ridge with respect to both basins, appears to be a scarp produced by a normal fault. East of the Kerimbas Basin, several newly formed staggered faults (Fig. 3) cut the thick well stratified sedimentary layers (2.5 s two-way travel time). The fault scarps decrease at either end of the basin (Fig. 3*a*). East of the Lacerda Basin a nearly linear normal fault edges an horst consisting of probably continental basement that forms the diffracting substratum of the ridge. This horst is part of a north–south trending alignment of three parallel ridges underlain by Tertiary cover[9]. This horst has been remobilized as shown by unconformities (Fig. 3*b*) within the Tertiary cover east of the ridge and by upturning at the fault contact in most of Neogene layers infilling the Lacerda basin.

Within the trough, most of the latest depositions are discordant and onlap the fractured, flexured and even folded older formations (Fig. 3). These deformations are related to probable strike-slip subvertical faults. Both normal and strike-slip fractures may have originated by several breaking tectonic phases and by an oblique opening of these troughs. To the west, the basins are edged by a flexure or a normal fault, at the foot of upper slope of the margin. These troughs are thus interpreted as grabens in the central region and as half-grabens at either end.

Volcanic intrusions occur on both sides and at either end of these grabens. A dyke and a sill (Fig. 3) can be observed where the Kerimbas graben is at its narrowest. Here, an alkaline basalt bearing peridotites nodules sandwiched within middle Miocene (N14) to present (N23) haemipelagic sediments has been dredged (DR03). The size and shape of Saint-Lazare and Paisley seamounts, whose intrusive appearance on seismic lines is associated to a sharp magnetic anomaly, denote their igneous origin. Both features are interpreted as volcanoes contemporaneous with the evolution of the grabens.

Fig. 1 *a*, The northern Mozambique continental margin: the continental slope is discontinued downward by troughs (the Kerimbas and Lacerda basins), except between the Paisley and Saint-Lazare seamounts interpreted as volcanic intrusive bodies. These basins are bounded by normal faults running alongside the foot of the upper continental slope and the western scarp of the Davie Ridge. Most of the epicentres are located west of the ridge beneath grabens, south of the Saint-Lazare Seamount and near the shoreline of Mozambique. Bathymetry in metres drawn by Jean René Vanney. Dashed lines, ship tracks. *b*, The East African Rift: graben (G) and transform faults or lineaments (L) after ref. 14. The eastern branch of the East African Rift is not interrupted with the north Tanzanian divergence but extends southeastward across the Tanzanian continental shelf[20] and the continental slope off Mozambique. With such mapping, both branches of the rift are sigmoïd shaped and of the same length. Arrows, direction of extension derived from microtectonic analysis[14,24] and seismicity[11,25].





The age of Tertiary bedding within the continental margin has been inferred from correlations with DSDP 242 drilling[5] and from core samples. The tilting running alongside the upper-slope and the Davie Ridge, the variation in thickness of sedimentary layer at either side of the ridge fault scarp, and the graben itself are likely to have originated at middle Miocene time. The undisturbed horizontal stratification within the trough, and on the other hand the undulation of seismically transparent layers of the continental rise show that the depression was already differentiated at Plio-Quaternary times. The Lacerda graben is originated from an older structure but it is also of middle Miocene age, as shown by flexures and onlaps observed under the continental rise and under the slope (Fig. 2*b*). But the upturning of Miocene strata by faulting denotes a later deformation occurring at Plio-Quaternary time. Faults and flexures located South of the Saint-Lazare Seamount (Fig. 2) are related to this period of activity, however, their throw is small and have a limited influence on the morphology.

Neogene deformations of the northern Mozambique margin can be explained by the tilting of two domains located at either side of a major discontinuity below the western scarp of the Davie Ridge. Samples from a condensed and decarbonated series of late Cretaceous age have been cored on the ridge, indicating an uplift up to 1,500 m since the Maastrichtian[10]. On the continental shelf, emergent marginal reefs and canyon heads also indicate a period of uplift. So the deepening of troughs and the tilting of the upper slope may explain the instability of this zone where canyons and slumps occur (Fig. 3).

From International Seismological Centre data, we plotted epicentres of earthquakes related to this region and occurring between 1964 and 1982 (Fig. 1*a*). Most of the earthquakes are shallow and of magnitude <5. As already quoted for the East

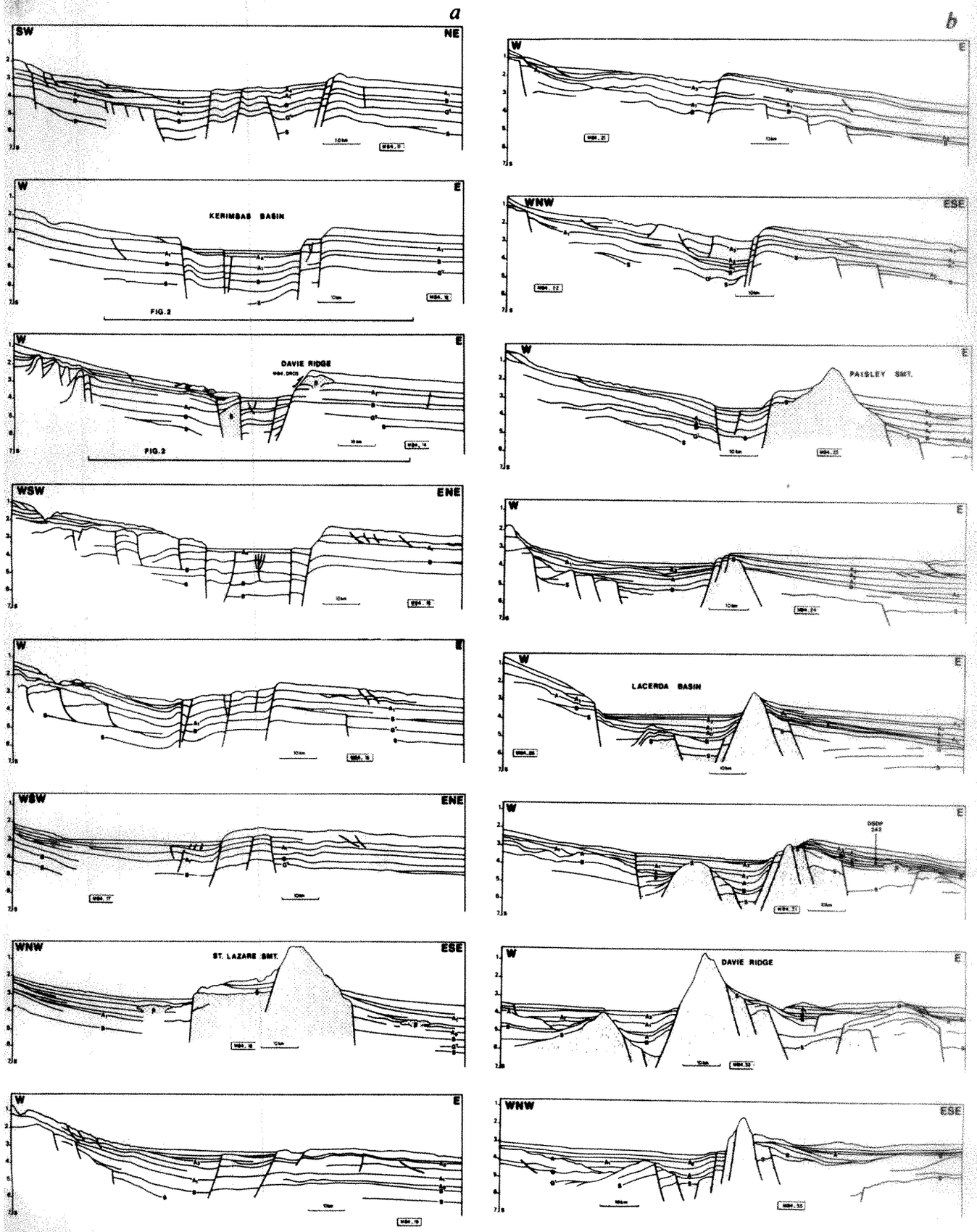


Fig. 2 Two-way travel-time seismic sections (as located on Fig. 1*a*) through the Kerimbas (*a*) and Lacerda (*b*) Basins. The structure formed by symmetrical faults is only shown from the median region of either basin. Only normal faults alongside the Davie Ridge extend towards the ends of the troughs. To the north, the ridge is formed by a thick well bedded sedimentary series; to the south by a horst of diffracting pre-tertiary basement later reactivated. Dotted lines, volcanic intrusive bodies; dashed lines, continental basement; S, acoustic basement; B, Cretaceous/Tertiary boundary; A, Eocene/Oligocene boundary; A_0, Oligocene/Miocene boundary; A_{1-2}, middle Miocene; A_3, late Miocene; A_4, Plio-Quaternary.

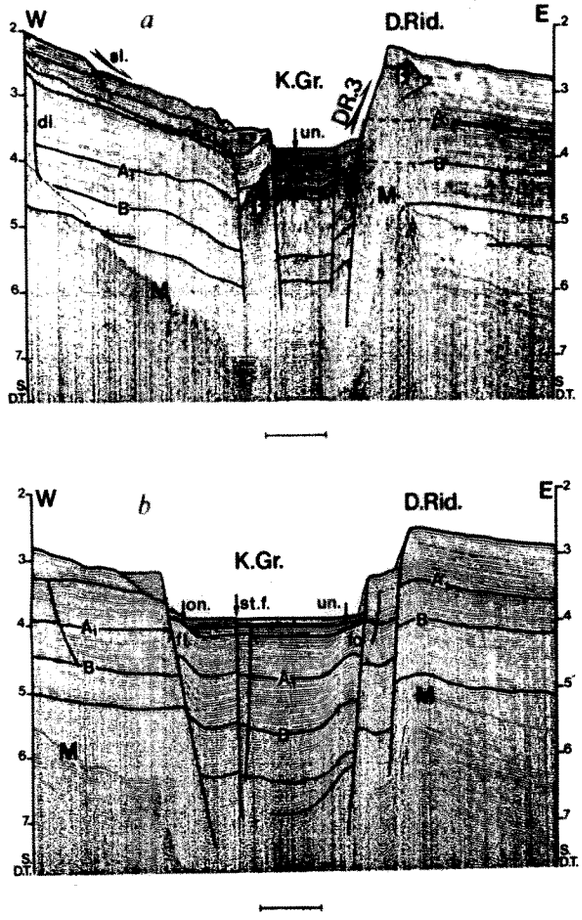


Fig. 3 Single channel watergun seismic profiles: *a*, profile 14; *b*, profile 12. Sections through the Kerimbas graben (K. Gr) and the Davie Ridge (D. Rid) exhibit the asymmetry of the troughs and associated features. β, Volcanic intrusion (dyke and sill); di., diapirism; fl., flexure; fo., fold; on.: onlap; sl. slumping; st. f., strike-slipe fault; un., unconformity; M, bottom multiple. Scale bar, 10 km.

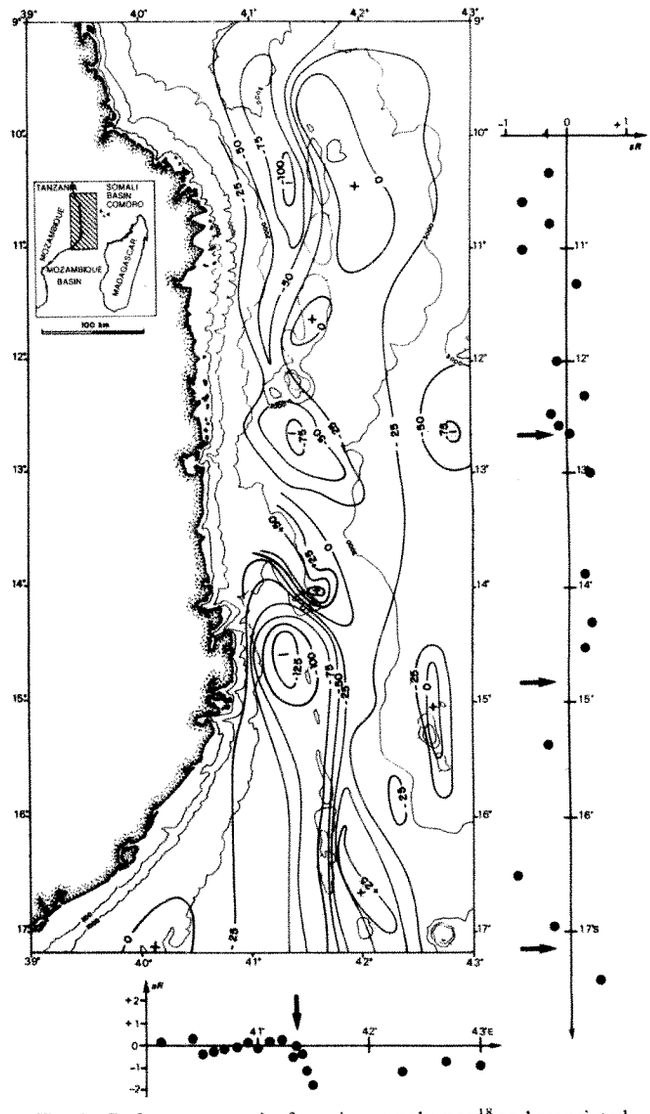


Fig. 4 Bathymetry, gravity free-air anomaly map[18] and associated P-wave residual anomalies[12] alongside the continental margin off northern Mozambique. Across the ridge, the steep gradient between negative and positive gravity anomalies may be correlated with a dramatic advance of P-wave travel-times interpreted on a first step, as a sharp landward thickening of the continental crust, that is roughly superimposed over the westward fault scarp of the ridge. North-west-south-east trending discontinuities are observed between the Paisley and Saint Lazare seamounts, where both earthquake epicentres and volcanic intrusive bodies are clustered. This domain of thickened crust may be one wherein the rift is propagating. *sR* in seconds denote residuals corrected for the structure below the seismological observatories located in Africa and Madagascar.

African Rift[11–14], epicentres are not only located along the grabens, but also extend far away, from the grabens to the shore. Epicentres are clustered south of the Saint-Lazare Seamount where the grabens disappear. Seismicity is poorly active east of the western fault scarp of the Davie Ridge which forms a major discontinuity.

P-wave travel-time anomalies have been computed from residuals (O/C) published in ISC Bulletins (O, observed travel time; C, computed travel time from an Earth model). Having made corrections for the influence of the structure below the seismological observatories located in southern Africa and in Madagascar[15], previous studies[12,13] showed that the variation of residuals with earthquake location suggests at first glance mainly a change in the structure below the epicentre, such as a Moho-deepening of 2 km for 0.15 s residuals. Along the Davie Ridge, residuals are slightly negative (Fig. 4), except between the Saint-Lazare and Paisley seamounts, where grabens are younger or absent. We presume that residuals emphasize the presence of a thickened continental crust below this active zone that may impede the opening of the rift.

From the continent throughout the ridge, a sharp drop of residuals (−1.7 s at 41°30′ E) denotes initially a dramatic eastward shallowing of the Moho from 35 km below Mozambique to 12 km deep below the Comoro Basin. However, the variation of residuals with longitude does not preclude lateral inhomogeneities within the crust and the upper mantle. In the absence of deep refraction lines, some of the results quoted above are not well constrained. This discontinuity is probably inherited from a fossil transform fault[16]. Sandstone and schist samples dredged from the ridge[4] and the lack of significant magnetic anomaly preclude an ocean/continent boundary along the western flank of the ridge and support earlier studies[10,12,17] emphasizing that the Davie Ridge belongs to the African domain with the presence of a sharp intra-continental discontinuity governing the graben pattern and the local seismicity.

The correlation between free-air anomalies[18] and bathymetry is good (Fig. 4). However, short-wavelength anomalies and high gradients may be modelled only by either upright elongated bodies culminating at shallow depth within the crust or by a dramatic change into the crustal structure. Free-air gravity values are negative over Kerimbas and Lacerda grabens, whereas they are positive over the Davie Ridge. Despite a slight eastwards offset, these gravity gradient may be associated with P-wave

travel-time anomalies and support the north–south trending of the crustal discontinuity along the grabens. Although the Kerimbas Basin is newly created, this feature and the Lacerda Basin seem to be generated from an older structure.

Between the Saint-Lazare and Paisley seamounts, north-west–south-east-trending positive and negative gravity anomalies outline transverse structures parallel to the main transform lineaments of the East African Rift[14]. These discontinuities not seen in the shallow fracture pattern, mark the boundaries of the thickened crust zone wherein volcanism activity and most of the earthquakes occur. This area could be a good example of a locked zone[19] to propagating rifts during continental breakup.

Earlier studies[14] quoted that the eastern branch of the East African Rift terminates at the North Tanzanian divergence (Fig. 1*b*). But seismicity[11] suggests the existence of a tensile zone extending the rift, on land in a north-west–south-east direction and seaward from the Tanzanian coastline (7° S) to the northern Mozambique continental slope (17° S). This active zone was not thought to be related to the continuation of troughs observed along the eastern branch of the African Rift[14]. Recently, Neogene basins have been revealed from seismic surveys on the continental shelf off Tanzania[20] and Kenya[21] substantiating the interpretation[22] that Pemba, Zanzibar and Mafia islands (Fig. 1*b*) are remnant horsts, reactivated in Miocene times and edged by subsident Neogene synclines. So, Tanzanian grabens would form a link between the eastern branch of the East African Rift and troughs alongside the northern Mozambique continental margin.

The western branch of the East African Rift extends also southwards as far as Cretaceous southern Mozambique grabens[23], reactivated recently and outlined by a topographic depression. So shaped, both branches of the East African Rift are sigmoïd like and of comparable extent. The distribution of the seismicity[11] and the rift pattern as depicted by this study, support a deformation picture affecting the whole of eastern Africa, rather than well defined boundaries, early stage of an oceanic opening.

MD40-MACAMO cruise would not have reached completion without the logistics and financial support of Terres Australes and Antarctiques Françaises. The seismic sources were provided by IFREMER. We thank the master, officers, the crew of the N/O *Marion Dufresne* and the scientific party, also Carol Williams and Gilbert Boillot for comments and Michel Moullade and Jacques Hernandez for sample study. Additional fundings come from ATP GGO (no. 106) and ATP Transferts (no. 1533) grants. Contribution no. 353 from the Groupe d'Etude de la Marge Continentale (UA718-CNRS).

Received 23 December 1985; accepted 20 March 1986.

1. Heirtzler, J. R. & Burroughs, R. H. *Science* **174**, 488–490 (1971).
2. Lort, J. M., Limond, W. Q., Segoufin, J. & Patriat, P. *Mar. Geophys. Res.* **4**, 71–89 (1979).
3. Fellah, N. thesis, Univ. Paris VI (1981).
4. Leclaire, L. *Courrier Cent Nat Rech. Scient.* **60**, 8 (1985).
5. Simpson, E. S. W. *et al. Init. Rep. DSDP* Leg **25**, 139–176 (1974).
6. Scrutton, R. A. *Earth planet. Sci. Lett.* **39**, 84–88 (1978).
7. Segoufin, J. & Patriat, P. *Bull. Soc. Géol. Fr.* **23**, 603–607 (1981).
8. Rabinowitz, P., Coffin, M. F. & Falvey, D. *Science* **220**, 67–69 (1983).
9. Mougenot, D., Virlogeux, P., Vanney, J. R. & Malod, J. *Bull. Soc. geol. Fr.* (in the press).
10. Segoufin, J., Leclaire, L. & Clocchiatti, M. *Ann. Soc. Geol. Nord* **97**, 309–314 (1978).
11. Fairhead, J. D. & Henderson, N. B. *Tectonophysics* **41**, T19–T26 (1977).
12. Recq, M. *Tectonophysics* **82**, 189–206 (1982).
13. Segoufin, J. & Recq, M. *Bull. Soc. géol. Fr.* **12**, 3, 469–479 (1980).
14. Chorowicz, J. *Bull. Centr. Rech. Expl. Prod. Elf-Aquitaine* **7**, 1, 155–162 (1983).
15. Poupinet, G. thesis, Univ. Grenoble I (1977).
16. Scrutton, R. A., Heptonstall, W. B. & Peacock, J. H. *Mar. Geol.* **43**, 1–20 (1981).
17. Segoufin, J. thesis, Univ. Strasbourg (1981).
18. Talwani, M. & Kahle, O. in *Geological and Geophysical Atlas of the Indian Ocean* (Pergamon, Oxford, 1976).
19. Courtillot, V. *Tectonics* **1**, 239–260 (1982).
20. Kajato, H. K. *Oil Gas J.* 123–131 (1982).
21. Coffin, M. F. & Rabinowitz, P. D. *EOS* **65**, 45, 986 (1984).
22. Kent, P. E., Hunt, J. A. & Johnstone, D. W. *Geophys. Pap. Inst. Geol. Sci., Lond.* **6**, 1–101 (1971).
23. Lafourcade, P. thesis, Univ. Paris VI (1984).
24. Vidal, G. thesis, Univ. Paris VI (1985).
25. Shudofsky, G. N. *Geophys. J. R. astr. Soc.* **83**, 3, 563–614 (1985).

Eutectoid phase transformation of olivine and spinel into perovskite and rock salt structures

J. P. Poirier*, J. Peyronneau*, M. Madon*, F. Guyot* & A. Revcolevschi†

* Institut de Physique du Globe de Paris, 4, place Jussieu 75252 Paris Cedex 05, France
† Laboratoire de Chimie Appliquée, Université Paris Sud, 91405 Orsay, France

The 700-km seismic discontinuity which defines the top of the Earth's lower mantle is generally attributed to the transformation of the upper mantle (Mg, Fe)$_2$ SiO$_4$ spinel into magnesiowüstite (Mg, Fe)O and (Mg, Fe)SiO$_3$ with perovskite structure[1]. Large-volume high-pressure experiments[2] have provided important thermodynamical information on this transition, but its mechanisms and kinetics are still unknown. Here we report microstructural observations of the products of the transformation of (Mg, Fe)$_2$SiO$_4$ olivine and spinel and Ca$_2$GeO$_4$ olivine, effected in a laser-heated diamond anvil cell (DAC). The observations were made by transmission electron microscopy (TEM), a technique that has already proved useful in investigating the olivine–spinel transition in the DAC[3,4]. We find that, in all cases, the transformed product has a eutectoid-like appearance (as in pearlitic carbon steels), with alternating lamellae of the rock salt and perovskite phases. The thickness and spacing of the lamellae increase with temperature until a granular structure forms. These observations suggest that the transformation starts as a eutectoid transformation, whose physical mechanisms might be as effective in the Earth's mantle as in the DAC.



Fig. 1 Olivine in the DAC, transformed into perovskite and magnesiowüstite in the three vertical strips that have been laser-heated.

The starting material powder was placed in the 300-μm-diameter hole of a hardened nickel gasket, 200 μm thick, and pressurized in the DAC to a maximum pressure (P) of ~400 kbar at the centre of the cell. Pressure was measured by calibrated strain gauges on the steel members of the cell[5], to avoid introducing ruby which could react with the material under investigation. A 60-W YAG laser beam was focused on a 30-μm-diameter spot and scanned across the sample at a speed of 100 μm s^{-1}. Three strips of transformed material, each 50 μm wide, were then produced (Fig. 1), allowing analysis of the effects of various pressure and temperature conditions. (The temperature across a strip ranged from the minimum temperature necessary to effect the transformations at the edges of the strip, up to an estimated temperature of 2,000 °C along the axis.) The two strips at the

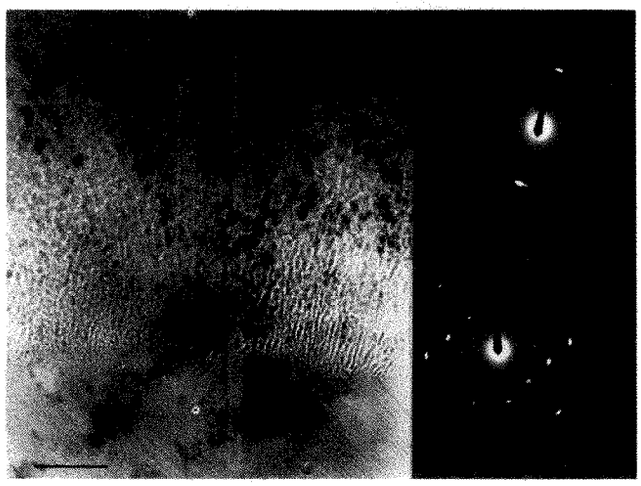


Fig. 2 Contact between sheared olivine–spinel phase (bottom) and eutectoid perovskite–rock salt structure. The dark subvertical lamellae are strongly textured magnesiowüstite (top diffraction pattern at right). Towards the centre of the strip (top) the structure becomes granular. Scale bar, 0.2 μm.

edges of the cell were at pressures too low for the perovskite–rock salt transition, but high enough for the olivine–spinel transition, whereas the centre strip was at the maximum pressure of 400 kbar in the central part of the sample. After heating, the sample was slowly decompressed, ion-beam thinned and examined by TEM at 200 keV.

In the first series of experiments, the starting material was San Carlos olivine (Fo_{88}). Examination of the edge strips confirms previous results[3,4,6,7] on the olivine–spinel transition, showing intercalated olivine and spinel layers at the edge of the strip, giving way to polygonal grains of spinel with stacking faults at higher temperatures towards the strip axis.

At the edge of the central strip, the same sheared olivine–spinel polytype is visible (the superimposed olivine and spinel diffraction patterns show that the (100) plane of olivine and the (111) plane of spinel are parallel); towards the axis of the strip this region is abruptly replaced by another with a very regular lamellar structure (Fig. 2) which becomes coarser and eventually granular at higher temperatures towards the axis. The smallest spacing (and thickness) of the lamellae is ~50–100 Å. The dark lamellae are identified by electron diffraction as magnesiowüstite (Mg, Fe)O; the light lamellae give no diffraction pattern. By continuity, they can be shown to consist of a glass with (Mg, Fe)SiO_3 composition: in the high-temperature region,

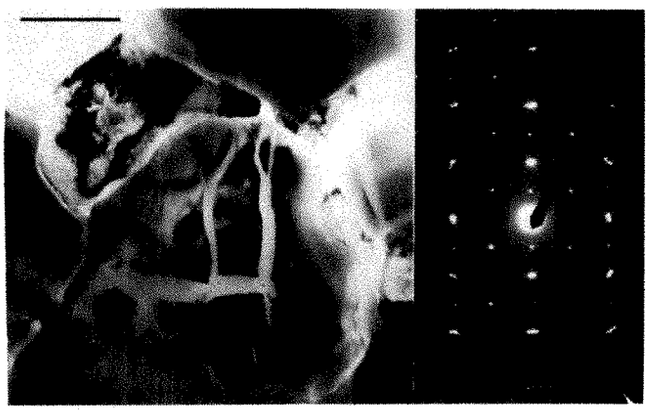


Fig. 3 Rectangular domains of (Mg, Fe)SiO_3 perovskite before amorphization under the electron beam (diffraction pattern at right). In the top left-hand corner a grain of magnesiowüstite with a very high dislocation density is seen. Scale bar, 0.5 μm.

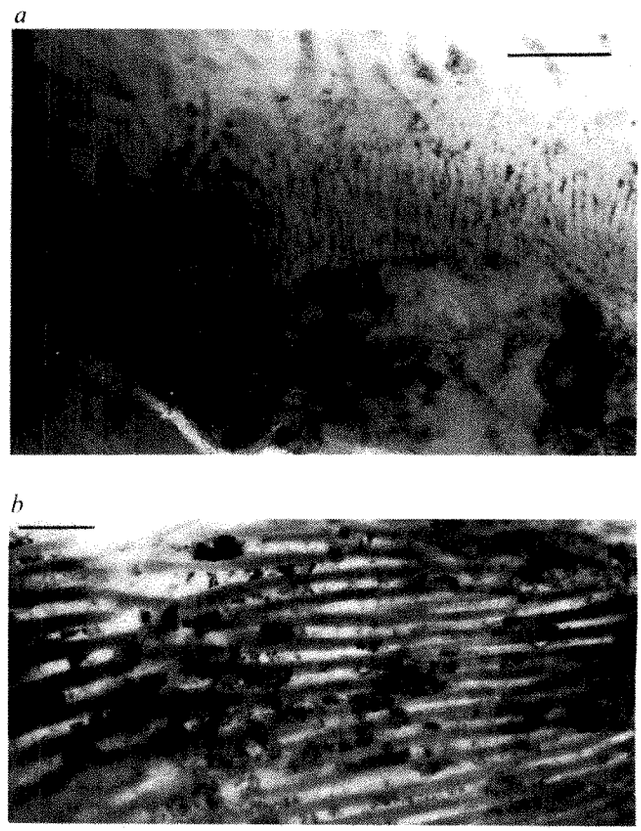


Fig. 4 *a*, Eutectoid structure of the perovskite–rock salt phases formed from *a*, spinel (bottom); *b*, Ca_2GeO_4 olivine. Towards the centre of the strip in *a* (top), the spacing of the lamellae increases. In *b*, dark bands are CaO, light bands are amorphized perovskite. Scale bars: *a*, 0.1 μm; *b*, 0.2 μm.

similar glassy, roughly rectangular grains were produced by amorphization under the electron beam of crystalline (Mg, Fe)SiO_3 perovskite grains (Fig. 3) whose grain boundaries are parallel to (100) planes of the ideal cubic lattice. The grains, without any dislocations, correspond to twinned domains of the $GdFeO_3$-type distorted structure. Magnesiowüstite grains contain a very high density of dislocations, which accounts for the invariably dark contrast of the magnesiowüstite lamellae.

In the second series of experiments the olivine was first transformed to spinel by uniformly scanning the sample, compressed to a maximum pressure of 200 kbar, with the laser beam. The sample was then compressed to 400 kbar and the laser beam drawn across it in strips as previously. TEM examination showed that the starting material then consisted of spinel grains with the usual (110) stacking faults. The transformed material was identical to the previous one and exhibited the same lamellar microstructure (Fig. 4*a*), coarser towards the centre of the strip.

All our observations point to the transformation $(Mg, Fe)_2SiO_4 \rightarrow (Mg, Fe)O + (Mg, Fe)SiO_3$ being of the discontinuous, eutectoid type well known in metallic alloys[8–11]. The lamellar microstructure, typical of the transformed product, is thought to be caused by the growth of nuclei by bulk and grain-boundary diffusion in the direction of grain-boundary migration[10]. From the geometry of our experiments, the reaction seems to start at the centre of the strip, the grain boundaries migrating towards the edges, this direction being favoured by the internal stress arising from the decomposition[9]. The interlamellar spacing decreases as temperature decreases[13]. The mechanism of the formation of nuclei of (Mg, Fe)O or (Mg, Fe)SiO_3 is unclear, but might involve a transient local distortion of the spinel structure into the K_2NiF_4 structure. This structure, denser than spinel, is not stable at any pressure for (Mg, Fe)SiO_4,

but it is stable for Ca_2GeO_4 at pressures greater than 100 kbar (ref. 14); it can be described as an alternate stacking of layers with the perovskite and the rock salt structure. At ~200 kbar, Ca_2GeO_4 transforms into $Ca_3Ge_2O_7 + CaO$ (ref. 15). We performed with Ca_2GeO_4 the same type of experiments as with the silicate olivine, starting with Ca_2GeO_4 powder with olivine structure and compressing it to 300 kbar. TEM examination showed, for the first time, that it eventually decomposes into CaO and $CaGeO_3$ perovskite, also with eutectoid structure (Fig. 4*b*). It is therefore possible that shear and cation shuffling of the spinel structure[16] might produce defects with local K_2NiF_4 structure, thus providing embryos of MgO or $MgSiO_3$ that can grow by diffusion until the grain boundaries start moving and creating the cellular structure.

The DAC and TEM coupled experiments on the perovskite + rock salt decomposition therefore lead to several conclusions: (1) The decomposition in the DAC exhibits all the characteristics of a eutectoid reaction driven by diffusion and grain-boundary reaction, that is, by processes that may be active in the mantle (but leading to different lamellar spacing and thickness). (2) The K_2NiF_4 structure exhibited by Ca_2GeO_4 at moderate pressure decomposes at higher pressure into rock salt and perovskite structures; a transient distortion to the K_2NiF_4 structure may have a role in the post-spinel decomposition of silicates. (3) The high dislocation density of the magnesiowüstite may come from plastic accommodation of the 10% volume decrease on transformation; this could be the first hint that magnesiowüstite could be more deformable than perovskite in the lower mantle.

This work was partly supported by CNRS (UA 734, ATP Physique des Hautes Pressions, RCP Pérovskites à Hautes Températures). This is IPG contribution no. 919.

Received 10 February; accepted 19 March 1986.

1. Liu, L. in *The Earth: its Origin, Structure and Evolution* (ed. McElhinny, M. W.) 177–202 (Academic, New York, 1979).
2. Ito, E. & Yamada, H. in *High Pressure Research in Geophysics* (eds Akimoto S. & Manghnani, M. H.) 405–419 (Reidel, Dordrecht, 1982).
3. Lacam, A., Madon, M. & Poirier, J. P. *Nature* **288**, 155–157 (1980).
4. Boland, J. N. & Liu, L. *Nature* **303**, 233–235 (1983).
5. Peyronneau, J., Madon, M. & Poirier, J. P. *J. Phys.* **45**, C8403–404 (1984).
6. Putnis, A. & Price, G. D. *Nature* **280**, 217–218 (1979).
7. Madon, M. & Poirier, J. P. *Science* **207**, 66–68 (1980).
8. Doherty, R. D. in *Physical Metallurgy* (eds Cahn, R. W. & Haasen, P.) 996–1004 (North-Holland, Amsterdam, 1983).
9. Hornbogen, E. *Metall. Trans.* **3**, 2713–2727 (1972).
10. Fournelle, R. A. & Clark, J. B. *Metall. Trans.* **3**, 2757–2767 (1972).
11. Puls, M. P. & Kirkaldy, J. S. *Metall. Trans.* **3**, 2777–2796 (1972).
12. Livingston, J. D. & Cahn, J. W. *Acta Metall.* **22**, 495–503 (1974).
13. Sundquist, B. E. *Acta Metall.* **16**, 1413–1427 (1968).
14. Reid, A. F. & Ringwood, A. E. *J. Solid State Chem.* **1**, 557–565 (1970).
15. Liu, L. *Phys. Earth planet. Inter.* **17**, P29–33 (1978).
16. Madon, M. thesis, Univ. Paris (1986).

Visualization of the dynamic instability of individual microtubules by dark-field microscopy

Tetsuya Horio & Hirokazu Hotani

Department of Biophysics, Faculty of Science, Kyoto University, Kyoto 606, Japan

It has previously been shown that two populations of microtubules coexist in a dynamically unstable manner *in vitro*: those in one population elongate while those in the other shorten and finally disappear[1,2]. This conclusion was based on changes in the number and length distribution of microtubules after dilution of the microtubule solution. Here, we demonstrate directly that growing and shortening populations coexist in steady-state conditions, by visualization of the dynamic behaviour of individual microtubules *in vitro* by dark-field microscopy. Real-time video recording reveals that both ends of a microtubule exist in either the growing or the shortening phase and alternate quite frequently between the two phases in a stochastic manner. Moreover, growing and shortening ends can coexist on a single microtubule, one end continuing to grow simultaneously with shortening at the other end. We find no correlation in the phase conversion either among individual microtubules or between the two ends of a single microtubule. The two ends of any given microtubule have remarkably different characteristics; the active end grows faster, alternates in phase more frequently and fluctuates in length to a greater extent than the inactive end. Microtubule-associated proteins (MAPs) suppress the phase conversion and stabilize microtubules in the growing phase.

Microtubules, very dynamic structures that can rapidly assemble and disassemble[3,4], form a cytoskeleton that is stable in the interphase of the cell cycle and that disintegrates rapidly into tubulin subunit in the prophase of mitosis. The subunits then completely reorganize to form the mitotic spindle[5]. In the late telophase stage of mitosis the reverse process takes place, that is, the spindle microtubules disassemble and the cytoskeletal microtubules re-form. To determine the mechanism by which microtubules assemble or disassemble without changing the concentration of tubulin subunits, we observed the dynamic behaviour of individual microtubules by dark-field light microscopy. When a single microtubule is monitored, its two ends grow at different rates (Table 1) as described previously[6,7]. However, each end independently stops growing in a stochastic manner, and then immediately begins to shorten at high speed (Fig. 2). After shortening for 1–30 s, the microtubule suddenly stops this process and starts growing again. Each end can thus exist either in the growing phase or in the shortening phase, and can alternate between the two phases in a stochastic manner.

These phase conversions at the two ends of a single microtubule occur independently, and conversions take place without any correlation among the individual microtubules on each slide in the microscope. As a result, some microtubules shorten whereas others elongate within a field of observation (Fig. 1), and no synchronized phase conversion is observed. This excludes the possibility that a cyclic environmental change in a specimen causes the switching between the two phases of microtubules. All the microtubules shown in Fig. 1 exhibit the phase changes, and >90% of the filaments in any particular observation field undergo phase conversions. The filament labelled b in Fig. 1, for example, attached to the glass surface throughout its length while filament e attached at only one point on the filament. As a result, when the direction of flow changed, filament e pivoted about its attached point whereas filament b

Table 1 Kinetic parameters of the dynamic instability

End	Growth rate ($\mu m\ min^{-1}$)	Shortening rate ($\mu m\ min^{-1}$)	Shortening length ($\mu m\ phase^{-1}$)	Duration time: Growing (min)	Duration time: Shortening (min)	No. of samples: Growing phase	No. of samples: Shortening phase
Active	0.63 ± 0.15	7.9 ± 2.2	2.4 ± 1.9	2.9 ± 1.8	0.30 ± 0.23	54	69
Inactive	0.20 ± 0.06	15.2 ± 7.7	0.73 ± 0.35	6.0 ± 4.0	0.05 ± 0.02	32	23

Values, mean ± s.d.

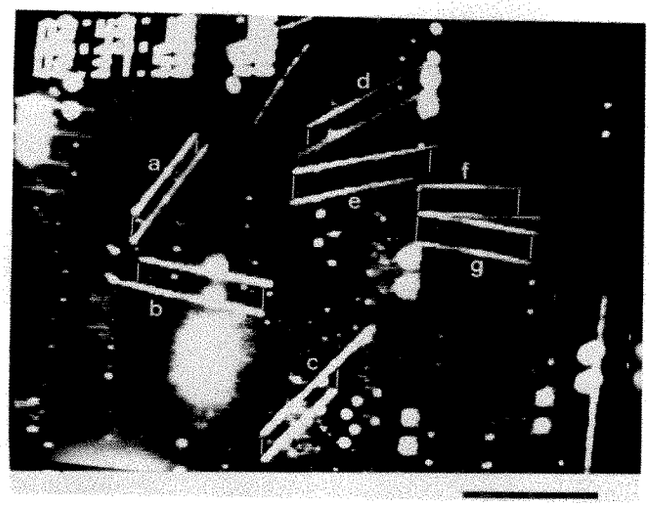


Fig. 1 Instability of microtubules visualized by dark-field microscopy. Several microtubules were attached to a glass surface so that their growing and shortening processes could be monitored continuously. Dynamic images were recorded on videotape. To demonstrate the changes in their lengths, two video images at different times (37 min 53 s and 43 min 18 s) were photographed on the same frame of a film by double exposure. The camera position was moved slightly before the second exposure so that the change in length could be seen. The two ends of a microtubule interconverted a few times between the growing and shortening phases during the time interval between the two exposures. As a result, some ends elongated while others shortened. The white lines show the shift of a corresponding point on a microtubule caused by movement of the camera position. Comparison of the images in pairs shows that the upper end of the microtubule designated as a, has shortened, the upper end of c has elongated, and so on. **Methods.** Tubulin was prepared from calf brains by three cycles of assembly-disassembly as described previously[11]. Further purification of tubulin was performed by phosphocellulose column chromatography[8]. Assembly of a microtubule was initiated by raising the temperature to 37 from 0 °C in the tubulin solution at a concentration of 1.7 mg ml^{-1} in buffer (90 mM PIPES, 1.8 mM EGTA, 0.9 mM $MgSO_4$, 2.7 mM GTP, *p*H 6.9). After incubation for 2 min, 4 μl of the solution was transferred onto a slide glass, mounted with a coverslip (22 × 22 mm) and observed by dark-field light microscopy. Microtubules were illuminated through an Olympus DC dark-field condenser by a Ushio 500-W high-pressure mercury arc lamp and observed with an Olympus Apo ×40 objective lens. The dynamic dark-field images were recorded on videotape using an ultrasensitive Ikegami CTC-9000 SIT video camera as described previously[12]. Scale bar, 10 μm.

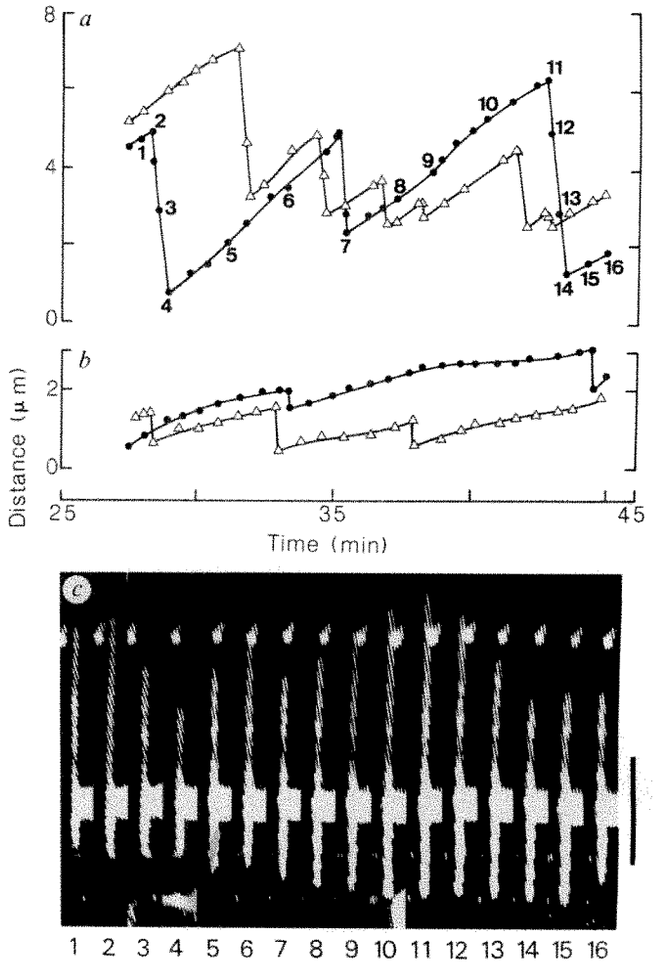


Fig. 2 Interconversions between the growing and shortening phases at ends of a single microtubule. The change in microtubule length at each end was followed by dark-field microscopy and recorded on videotape as described in Fig. 1. The dynamic video images, which were superimposed on the monitor screen of a personal computer (Fujitsu FM 77) with the aid of a superimposer (Fujitsu MB22610), were analysed as a function of time. *a*, *b*, The distance between one of the ends and an arbitrary fixed point on the microtubule was measured so that increase and decrease in the distance correspond respectively to the growth and shortening of the microtubule. The length change at an active (*a*) or inactive (*b*) end of an individual microtubule is shown. The curves were obtained from the microtubules designated as b (●) or e (△) in Fig. 1. *c*, Successive frames were obtained from the video image of the microtubule designated b in Fig. 1. Scale bar, 5 μm. Each numbered datum point in *a* has a one-to-one correspondence with the successive video frames in *c*. The upper and lower ends of the microtubule shown in *c* correspond to the active and inactive ends, respectively.

did not move. Despite the difference in the manner of attachment, the filaments underwent phase conversions in a similar manner (Fig. 2), indicating that the interaction between a microtubule and a glass surface produces only a small, if any, effect on the nature of the phase conversion.

The frequencies of phase interconversion at the two ends of a microtubule are distinct from each other, being 0.63 and 0.23 min^{-1}. We designated the ends which had higher and lower interconversion frequencies as active and inactive ends, respectively. The active end differs from the inactive end not only in interconversion frequency but also in growth and shortening rates. In the growing phase, the active end elongates about three times faster than the inactive end (Table 1); in the shortening phase, it shortens more slowly than the inactive end. In general, at the active end, a microtubule grows quickly, alternating frequently between the two phases and fluctuating greatly in length, while the reverse is true at the inactive end, where growth is slow, phase alternation infrequent and there is a little fluctuation (Table 1).

It is well established that a microtubule has a structural polarity and that the 'plus' end grows about three times faster than the 'minus' end[6,7]. Hence, the active and inactive ends designated in this study must correspond respectively to the plus and minus ends. Despite the independent alternation of phases of the ends which makes the time course of a length change quite unique in each microtubule, similar rates of growth were obtained with active ends and this rate changed very little during the observation period (Fig. 2). This result also holds for the other three kinetic parameters: the shortening rate of the active end, and both the growth and the shortening rates of the inactive end. These homogeneities in rate indicate that each end has a well-defined molecular structure unique to the respective phases and suggests that there is no intermediate phase. The homogeneities also indicate that the concentration of tubulin

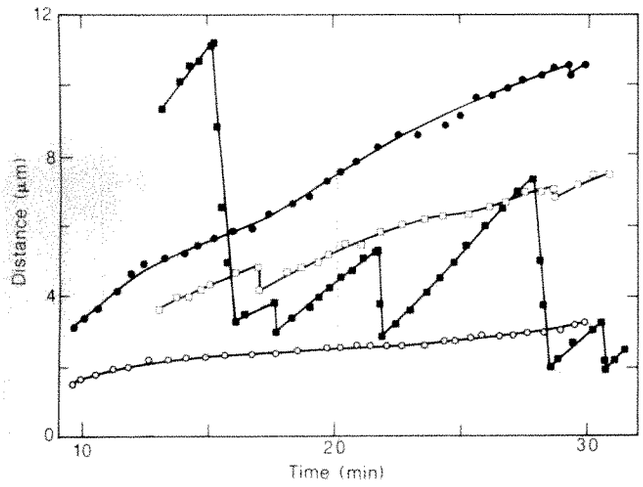


Fig. 3 Effect of MAPs on microtubule instability. Microtubules are formed as described in Fig. 1 except for the presence of MAPs (0.24 mg ml^{-1}). Changes in microtubule length at the active end (●) and the inactive end (○) were measured as described in Fig. 2. In the absence of MAPs, both the active end (■) and the inactive end (□) show the phase conversion in a similar manner to that in Fig. 2. MAPs were purified by phosphocellulose column chromatography as described previously[8].

subunits is constant during the observation period because a change in subunit concentration would cause a change in growth rate. In other words, we observed the phase conversions in an apparent steady-state condition of microtubule assembly and disassembly (see below).

As shown in Table 1, the shortening rate is much higher than the growth rate at both the active and the inactive ends of the microtubules. Hence, once an end switches to the shortening phase, the microtubules often shorten all the way to disappearance. But in practice this is not the case. The active end stays in the growing phase for a period which averages 10 times longer than it stays in the shortening phase (Table 1). As a result, the microtubule length lost in the shortening phase is compensated for by an elongated length in the growing phase. On average, a microtubule loses 2.4 μm during one shortening phase and recovers 1.8 μm during a single growing phase. A similar compensation takes place at the inactive end: 0.7 μm is lost in one shortening phase and 1.2 μm recovered in one growing phase. Therefore, a microtubule does not become so short as to disappear, although its length does fluctuate greatly. This evidence also implies that the net amount of microtubules is almost constant, as it would be in a steady state.

Microtubule filaments are stabilized in interphase cells to maintain the cell shape. How does a microtubule prevent dynamic instability *in vivo*? The purified tubulin used here contained almost no MAPs, whereas in the partially purified tubulin preparation used elsewhere, MAPs make up ~20% of the total protein[8]. Microtubules in the tubulin preparation grow continuously without any shortening phase, and after reaching the steady state they maintain constant length and do not exhibit any dramatic shortening. This suggests that MAPs suppress phase conversion and stabilize microtubules in the growing phase. The results shown in Fig. 3 confirm that MAPs can stabilize both ends of a microtubule as well as their well-known property of nucleation for tubulin polymerization[8]. A detailed description of the effects of MAPs on the stability of microtubules will be published elsewhere.

A GTP cap model has been proposed as the mechanism of phase transition[2,9,13,14]. When tubulin monomers bound to GTP and ligand are incorporated into a microtubule, the GTP is hydrolysed at a constant rate to form a GDP-tubulin lattice. If the polymerization rate is high enough at an adequate concentration of free tubulin, however, the GTP-tubulin lattice will form near the ends of the microtubule because the hydrolysis cannot follow the polymerization[10]. This lattice, or GTP cap, has been proposed as a mechanism to stabilize the growing phase. On the other hand, when the polymerization slows down with a decrease in tubulin concentration, the GTP cap size is predicted to decrease and the GDP lattice to become exposed on the microtubule end. When this happens, rapid depolymerization of the GDP-tubulin takes place which continuously exposes GDP-tubulins at the end until the microtubule disappears or some rare event recaps the microtubule[2].

Our results raise some questions about the GTP cap hypothesis as microtubules can interconvert frequently between the two phases without changing polymerization rate. The active end was frequently in the shortening phase at the tubulin concentration used here. Therefore, if the GTP cap hypothesis is correct, the inactive end may always be in the shortening phase because the polymerization rate at the inactive end is only one-third of that at the active end. To clarify the molecular mechanism of the phase conversion, more detailed studies, especially of the effects of GTP, are necessary.

The cytoskeleton and the mitotic spindle can disintegrate rapidly without decreasing the free tubulin concentration in the cell. These structures can also be formed in a range of tubulin concentrations similar to that at which they disintegrate. These cellular events could be related to our demonstration that growing and shortening microtubules really coexist under steady-state conditions.

We thank Dr Tim Mitchison for helpful comments and Dr M. Yanagida for encouragement. This work was supported by a grant from the Ministry of Education, Science and Culture of Japan.

Received 6 February; accepted 4 April 1986.

1. Mitchison, T. & Kirschner, M. *Nature* **312**, 232-237 (1984).
2. Mitchison, T. & Kirschner, M. *Nature* **312**, 237-242 (1984).
3. Inoue, S. & Sato, H. *J. gen. Physiol.* **50**, 259-292 (1967).
4. Salmon, E. D., Jeslie, R. J., Saxton, W. M., Karow, M. L. & McIntosh, J. R. *J. Cell Biol.* **99**, 2165-2174 (1984).
5. Karsenti, E., Newport, J., Hubble, R. & Kirschner, M. W. *J. Cell Biol.* **98**, 1730-1745 (1984).
6. Summers, L. & Kirschner, M. *J. Cell Biol.* **83**, 205-217 (1979).
7. Bergen, L. & Borisy, G. *J. Cell Biol.* **84**, 141-150 (1980).
8. Sloboda, R. D. *et al.* in *Cell Motility* (eds Goldman, R., Pollard, T. & Rosenbaum, J.) 1171-1212 (Cold Spring Harbor Laboratory, New York, 1976).
9. Hill, T. L. & Chen, Y. *Proc. natn. Acad. Sci. U.S.A.* **81**, 5772-5776 (1984).
10. Carlier, M. F. & Pantaloni, D. *Biochemistry* **20**, 1918-1924 (1981).
11. Sloboda, R. D., Rudolph, S. A., Rosenbaum, J. L. & Greengard, P. *Proc. natn. Acad. Sci. U.S.A.* **75**, 177-181 (1975).
12. Hotani, H. *J. molec. Biol.* **156**, 791-806 (1982).
13. Carlier, M. F., Hill, T. L. & Chen, Y. *Proc. natn. Acad. Sci. U.S.A.* **81**, 771-775 (1984).
14. Chen, Y. & Hill, T. L. *Proc. natn. Acad. Sci. U.S.A.* **82**, 1131-1135 (1985).

Evidence that reserve cells are a source of regenerated adult newt muscle *in vitro*

Jo Ann Cameron, Allen R. Hilgers & Timothy J. Hinterberger

Department of Anatomical Sciences and College of Medicine, University of Illinois, 190 Medical Sciences Bldg, 506 S. Mathews, Urbana, Illinois 61801, USA

Skeletal muscle of adult, metamorphosed urodele amphibians regenerates despite the absence of satellite cells[1], the myogenic reserve cells present beneath the external lamina of muscle fibres in larval urodeles and in other vertebrates[2–9]. Adult-stage muscles of several urodeles examined (*Notophthalmus viridescens*[1,10], *Ambystoma maculatum*[10], *Triturus vulgaris*, *Triturus cristatus*[11], *Hynobius tokyoensis*[12] and *Ambystoma mexicanum*[13]) have instead a unique cell type enveloped in its own external lamina. Several studies suggest that these cells are larval satellite cells that have become completely surrounded by a segment of external lamina

during metamorphosis[10–12]. Although Popiela[10] termed these cells 'pericytes', he suggested that they might function as a myogenic reserve population. Cherkasova, who was the first to recognize these cells as distinct from vascular pericytes, termed them post-satellite cells and also proposed that they might be myogenic[11]. Here, we present evidence that post-satellite cells in adult *N. viridescens* give rise to regenerated myotubes *in vitro*. The myotubes could be stained with MF20, a monoclonal antibody to purified skeletal muscle myosin[14], and also with 22/18, a monoclonal antibody that reacts with an antigen present in newt-limb blastema myogenic cells[15]. The presence of myogenic post-satellite cells in adult newt muscle provides an alternative to the hypothesis that myoblasts in regenerating adult urodele limbs arise through dedifferentiation of mature myofibres[15–17].

Recent results from our laboratory demonstrate that adult newt muscle undergoes repair regeneration *in vivo* even though the original myonuclei degenerate[18], and that it is able to form new myotubes from muscle explants *in vitro*, where it is apparent that mature fibres do not give rise to myogenic cells by dedifferentiation[19]. Those studies supported the idea that adult newt muscle can regenerate from a reserve cell population, whose identity remained unknown.

Post-satellite cells in adult *N. viridescens* limb muscle are similar at the fine structural level to those described in other urodeles, with heterochromatic nuclei and varying amounts of rough endoplasmic reticulum, Golgi and pinocytotic vesicles (Fig. 1). Although post-satellite cells can resemble fibroblasts, their distinctive feature is that each is enveloped in an external lamina. In electron micrographs, we observed only post-satellite cells immediately adjacent to myofibres away from nerves or vascular elements. Light microscopy with serial sections showed that cells in this location usually have basophilic cytoplasm that is sometimes wrapped partially around the adjacent myofibre (Fig. 2*b*). To test our ability to identify post-satellite cells by their location and cytology at the light microscopic level, 11 such cells in thick Epon sections from both uninjured and cultured muscle were re-mounted and examined at the fine structural level. All 11 possessed intact external laminae, which in the cultured muscle often appeared loosened (Fig. 2*a*), possibly due to some rounding up of the cells. Therefore, in the subsequent steps of this experiment, post-satellite cells were identified by serial sectioning and light microscopy alone.

We found that post-satellite cells began synthesizing DNA *in vitro* earlier than did any other cell type present in adult newt muscle. Explants of forelimb muscles were prepared according to methods described previously[19] and exposed to ^{3}H-thymidine for 24 h at 2, 4, 6 or 8 days in culture. Incorporation of the label by post-satellite cells and other cell types was determined autoradiographically for each of those days. Up to day 6, ^{3}H-thymidine incorporation was confined to post-satellite cells; no labelled perivascular cells, endothelial cells, perineural cells, Schwann cells or tendon fibroblasts were observed. By day 8, however, an occasional cell of these types was labelled. Of those cells that met our criteria for identification as post-satellite cells by light microscopy, 29.6% (134 of 452 cells in six explants) were labelled with ^{3}H-thymidine on day 6. Only three labelled cells could not be assigned with certainty to a particular histological type because of their appearance and location in the tissue. Thus, restricting the exposure to ^{3}H-thymidine to just the first 6 days in culture appears to provide a means of selectively labelling post-satellite cells, although not all of them incorporate the label during this period (for example, the cells in Figs 1, 2).

Labelled cells identified as post-satellite cells (on the basis of their location and basophilia in serial-section autoradiographs of newt limb muscle exposed to ^{3}H-thymidine continuously for 48 h on days 4 and 5 in culture) were re-mounted for electron microscopy. Some of these cells could be confirmed as post-satellite cells by the presence of intact external laminae (Fig. 3), but many of them lacked intact laminae. As cells lacking intact laminae were not observed in uninjured muscle, we assume that they are post-satellite cells that lost their external laminae before or shortly after synthesizing DNA, although the steps in this process remain to be elucidated.

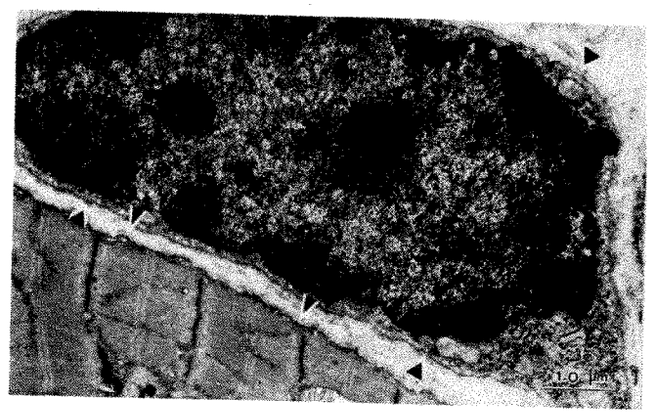


Fig. 1 A post-satellite cell in newt limb muscle after 10 days *in vitro*. Note its external lamina (large arrowheads) and that of the adjacent muscle fibre (small arrowheads). This post-satellite cell did not incorporate tritiated thymidine.
Methods. One μCi of ^{3}H-thymidine was added to cultures on day 5. After 24 h the medium was replaced with medium containing 4×10^{-5} M cold thymidine, and this medium was changed at least three times over the next few hours. The cultures were fixed with 2.5% glutaraldehyde in 0.1 M phosphate buffer at *p*H 7.4, after 6 days *in vitro*. Fixed explants were removed from the plates and either embedded in methacrylate or post-fixed with OsO_4 in 0.1 M phosphate buffer at *p*H 7.4 and embedded in Epon. Serial sections (3 μm) were coated with NTB2 emulsion (Kodak). After exposure for 1 week at 4 °C the autoradiographic preparations were developed, then stained with toluidine blue. Labelled and unlabelled cells in the Epon-embedded muscle tissue were photographed, and selected sections were re-mounted for fine structural analysis.



Fig. 2 *a*, A post-satellite cell in a 10-day explant of newt limb muscle prepared as described in Fig. 1 legend. This cell did not incorporate tritiated thymidine. Note the pinocytotic vesicles along the lower right edge of the post-satellite cell and its loose external lamina (large arrowheads) characteristic of post-satellite cells in injured muscle. Although the two adjacent muscle fibres are degenerating, their external laminae are intact (small arrowheads). *b*, Light micrograph of this cell prior to re-mounting, demonstrating its location with respect to the two adjacent muscle fibres.

Cells labelled with ^{3}H-thymidine *in vitro* as described above were followed until they formed regenerated myotubes in longer-term cultures. When muscle explants labelled with ^{3}H-thymidine for 48 h on days 4 and 5 were maintained for periods of up to 4 weeks, myotubes were observed on the culture plates within 14 days *in vitro*. Following autoradiographic processing, many myotubes were seen to contain ^{3}H-thymidine-labelled nuclei (Fig. 4). Immunocytochemical staining with antibody MF20 (ref. 14) confirmed the myogenic nature of these multinucleated

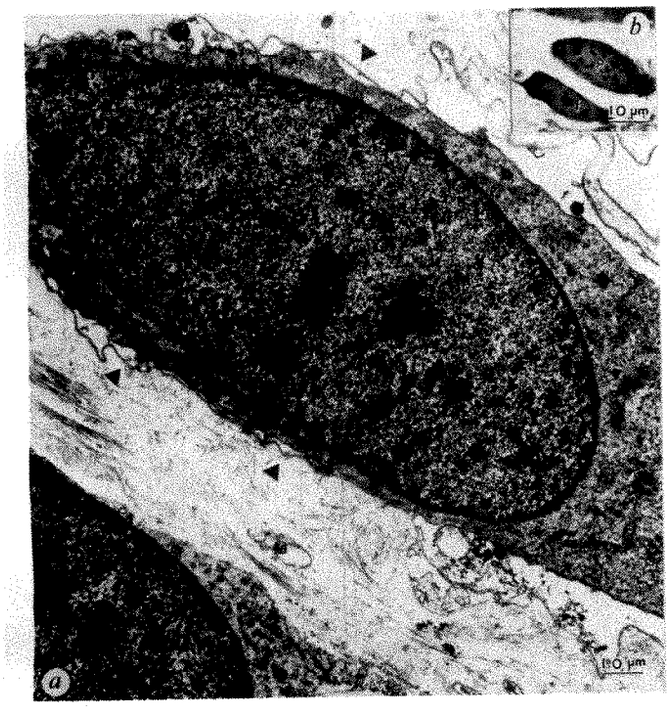


Fig. 3 *a*, A post-satellite cell in a 10-day explant of newt limb muscle labelled with ^{3}H-thymidine on days 4 and 5 and processed as described in Fig. 1 legend. Note the loose external lamina of the post-satellite cell (arrowheads). *b*, Light micrograph of this cell (p) demonstrating its location with respect to an adjacent muscle fibre on one side and a fibroblast (f) on the other. Note the silver grains over the nucleus of the post-satellite cell.

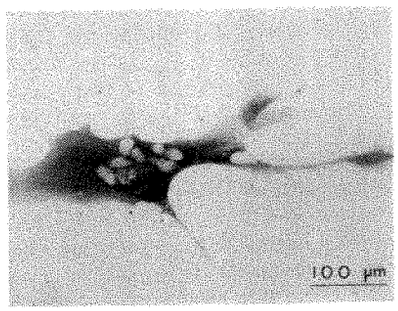


Fig. 4 A myotube in a 14-day culture of newt limb muscle labelled with ^{3}H-thymidine on days 4 and 5 and stained with MF20 on day 14. Note the silver grains over several of the myonuclei; unlabelled myonuclei are also seen.
Methods. Cultures were fixed in 5% neutral formalin and permeabilized with 0.01% Triton X-100 in 0.02 M phosphate-buffered saline (PBS) for 5 min, followed by 95% ethanol for 5 min. Monoclonal antibody MF20, given by Dr Donald Fischman, was raised against purified myosin heavy chain from adult chicken pectoralis muscle[14]. (Immunoautoradiographic analysis of electrophoretically separated adult newt muscle myosin, performed, with slight modifications, according to the protocol of Bader *et al.*[14], demonstrated the specificity of MF20 for a newt muscle peptide of relative molecular mass (M_r) 220,000 (220K) which migrated close to adult chicken myosin (200K) and purified rabbit myosin (220K).) Supernatant containing MF20 was diluted 1:3 in 0.02 M PBS (0.25 M NaCl) *p*H 7.6, and applied to the cultures overnight. After three 5-min rinses in the same buffer, the tissue was reacted with 20 μg ml^{-1} goat anti-mouse IgG (Jackson Immunoresearch Laboratory) for 8 h in the same buffer, followed by three more rinses with buffer. The MF20 was visualized by incubating cultures in a solution of 4 μg ml^{-1} mouse peroxidase/anti-peroxidase (Jackson Immunoresearch Laboratory) in 0.02 M PBS (0.14 M NaCl) plus 1% normal goat serum overnight, followed by three rinses in the same buffer and routine diaminobenzidine treatment. Controls omitting the monoclonal antibody or substituting a known non-reactive primary antibody showed no staining. For autoradiography, culture plates were coated with NTB2 emulsion and processed in the same way as the sectioned material.

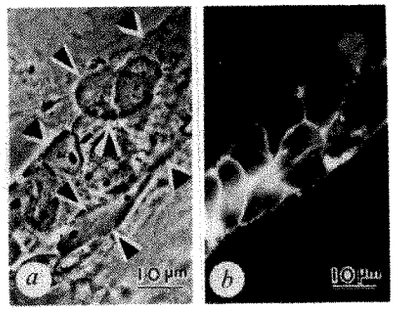


Fig. 5 *a*, A phase-contrast micrograph of a myotube (large arrowheads) in a 21-day culture of newt limb muscle. Two mononucleated cells are also visible (small arrowheads). *b*, The same myotube demonstrating 22/18 immunofluorescence.
Methods. Cultures grown on collagen-coated glass coverslips were fixed in acetone and stained with monoclonal antibody 22/18 (given by Dr Jeremy Brockes) according to the protocol of Kintner and Brockes[15], followed by fluorescein-conjugated rabbit anti-mouse IgG (1:100; Miles). Controls omitting the monoclonal antibody or substituting a known non-reactive primary antibody gave no staining.

cells and in addition allowed some mononucleated cells to be identified as myogenic. Mature fibres within explants were largely degenerated, although they stained weakly with MF20; this is in agreement with our previous conclusion that dedifferentiation of myofibres is not a prerequisite for the regeneration of *N. viridescens* muscle[18,19], and the present study points to post-satellite cells as a source of the myogenic cells *in vitro*.

Recently, Kintner and Brockes[15] examined the possibility of myofibre dedifferentiation being involved in regeneration of *N. viridescens* limbs, by using a monoclonal antibody raised against muscle and a second antibody, named 22/18, raised against blastema tissue. In regenerating limbs 14 days after amputation, cells bearing both the myofibre and blastemal antigens were found only in the region between the blastema and the intact muscles of the stump. Although those authors observed double-labelled cells also in muscle-forming regions of palette-stage blastemas 28 days after limb amputation, they interpreted the appearance of the double-labelled cells in the stump at 14 days as evidence of myofibre dedifferentiation. An alternative explanation for the presence of double-labelled cells in the limb stump at 14 days is that there too it indicates muscle redifferentiation rather than dedifferentiation. Repair myogenesis just proximal to the blastema has been noted at later stages of newt-limb regeneration[17], but we believe it may begin as early as 2 weeks after injury, as it does when newt muscle is injured by mincing *in vivo*[18]. To determine whether 22/18 labelling is associated with muscle regeneration *in vitro*, we prepared cultures as before and exposed them to this antibody after new myotubes had formed. The myotubes and some mononucleated cells stained with 22/18 (Fig. 5); taken together with our other results described above, this demonstrates that 22/18 can label myogenic cells apparently derived from post-satellite cells. If post-satellite cells can give rise to myotubes by 14 days *in vitro*, we hypothesize that they do so in limb stumps *in vivo* and that the multinucleated myofibres labelled with 22/18 observed by

Kintner and Brockes in limb stumps 14 days post-amputation were newly repaired or regenerated.

As we have demonstrated the presence of myogenic reserve cells in adult newt muscle, we believe that electron microscope observations of regenerating newt limbs are open to re-interpretation also. Hay[17] showed that mononucleated cells not present in uninjured muscle appear within myofibre external laminae in adult newt limb stump muscle following amputation. Hay postulated that the mononucleated cells arise from the adjacent fibres, enter the blastema and give rise to myoblasts. But neither the origin of these cells nor their possible role in epimorphic limb regeneration has been established rigorously. Even though in the present study we have described repair myogenesis only *in vitro*, we hypothesize that post-satellite cells are also a source of myogenic cells in the epimorphically regenerating limb; this would be consistent with observations that reserve cells are the source of regeneration myoblasts in other vertebrates and would avoid invoking a unique mechanism for the formation of regeneration myoblasts in newts. It may, however, be impossible to test our hypothesis against that of myofibre dedifferentation until some means becomes available for unambiguously marking either post-satellite cells or the putative viable myofibre fragments.

We thank Bruce Carlson for translating Dr Cherkasova's publications, Donald Fischman and Jeremy Brockes for providing the monoclonal antibodies, Robert Fontaine for conducting the immunoblot tests, and Alex Mauro for encouragement. This work was supported by NSF grant PCM 83-10006.

Received 13 February; accepted 14 March 1986.

1. Hay, E. D. & Doyle, C. M. *Anat. Rec.* **175,** 339 (1973).
2. Mauro, A. *J. biophys. biochem. Cytol.* **9,** 493–495 (1961).
3. Carlson, B. M. in *Muscle Regeneration* (ed. Mauro, A.) 57–81 (Raven, New York, 1979).
4. Kahn, E. B. & Simpson, S. B. *Devl Biol.* **37,** 219–223 (1974).
5. Konigsberg, U. R., Lipton, B. H. & Konigsberg, I. R. *Devl Biol.* **45,** 260–275 (1975).
6. Bischoff, R. *Anat. Rec.* **180,** 645–662 (1975).
7. Bischoff, R. in *Plasticity of Muscle* (ed. Pette, D.) 119–129 (Walter de Gruyter, Berlin, 1980).
8. Snow, M. H. *Cell Tissue Res.* **186,** 535–540 (1978).
9. Campion, D. R. *Int. Rev. Cytol.* **87,** 225–251 (1984).
10. Popiela, H. *J. exp. Zool.* **198,** 57–64 (1976).
11. Cherkasova, L. V. *Dok. Akad. Nauk. SSSR.* **267,** 1235–1236 (1982).
12. Takahama, H., Mizuhira, V., Sasaki, F. & Watanabe, K. *Cell Tissue Res.* **236,** 431–438 (1984).
13. Cherkasova, L. V. *Dokl. Akad. Nauk. SSSR* **273,** 991–993 (1983).
14. Bader, D., Masaki, T. & Fischman, D. A. *J. Cell Biol.* **95,** 763–770 (1982).
15. Kintner, C. R. & Brockes, J. P. *Nature* **308,** 67–69 (1984).
16. Lentz, T. L. *Am. J. Anat.* **124,** 447–480 (1969).
17. Hay, E. D. in *Concepts of Development* (eds Lash, J. & Whittaker, J. R.) 404–428 (Sinauer Associates, Stamford, Connecticut, 1974).
18. Cameron, J. A. in *Limb Development and Regeneration* Pt A (eds Fallon, J. F. & Caplan, A. I.) 491–500 (Liss, New York, 1983).
19. Schrag, J. A. & Cameron, J. A. *J. Embryol. exp. Morph.* **77,** 255–271 (1983).

Stimulation of oligodendroglial proliferation and maturation by interleukin-2

Etty N. Benveniste* & Jean E. Merrill

Department of Neurology, UCLA School of Medicine, Los Angeles, California 90024, USA

There exists considerable evidence that the growth of glial cells can be influenced by T-cell-derived lymphokines and monokines. Astrocytes proliferate in the presence of mitogen- or antigen-stimulated T-cell supernatants[1–3], supernatants from human T-lymphotropic virus (HTLV)-transformed T cells[3], and purified human interleukin-1 (IL-1; ref. 4). Oligodendrocytes proliferate and differentiate when incubated with supernatants from mitogen-activated or HTLV-transformed T cells[3]. In addition, we have recently purified a T-cell-derived lymphokine of relative molecular mass 30,000, termed glial growth promoting factor (GGPF), which specifically stimulates the proliferation of oligodendrocytes[5]. The traditional role of interleukins 1 and 2 is in the initiation, propagation and regulation of the immune response[6]. IL-1, released by a variety of cells including monocytes, stimulates T cells to produce IL-2 (ref. 7); IL-2 in turn induces the expansion of T cells that is critical for immune responsiveness. Recently, IL-2 has been shown to induce B-cell proliferation[8,9] and immunoglobulin secretion[10], indicating that its action is not restricted to T cells. We now report that recombinant human IL-2 influences the growth of glial cells—specifically, the proliferation and differentiation of oligodendrocytes. IL-2 may have a role in the inflammatory neural lesions of multiple sclerosis patients and in the growth of brain glia during injury or disease.

Primary glial cell cultures were established from neonatal rat cerebra by a modification of the McCarthy and DeVellis technique[11]. Meninges were removed prior to culture. After 7–10 days in primary culture, oligodendrocytes were separated by brief mechanical dislodging. (The overnight shaking technique of McCarthy and DeVellis was not used.) Astrocytes (day 10) were obtained by trypsinization. The two cell populations were resuspended in culture media containing 10% fetal bovine serum (FBS)[5]. Oligodendrocytes were seeded in Falcon Microtest II plates at a concentration of 2×10^4 cells per well, while astrocytes were seeded at 2×10^3 cells per well. The IL-2-containing material to be tested was serially diluted, and 0.1-ml aliquots were added to the cells. Assays were performed in triplicate. Cells were cultured for various times at 37 °C, pulsed with ^{3}H-thymidine (TdR, 1 μCi per well), and collected after 17 h with an automated cell harvester (PHD harvester, Cambridge Technology). Cells were monitored for purity by immunofluorescence as described previously[3,5] and by nonspecific esterase staining[12] for contaminating microglia. Oligodendrocyte-enriched cultures were assayed for the presence of the following markers before and after stimulation with IL-2 (see Table 1): galactocerebroside (GalC), a myelin-associated galactosphingolipid that is a surface antigen specific for oligodendrocytes[13]; the A2B5 antigen (which identifies a bipotential glial progenitor cell[14], type II astrocytes[15] and some types of neurones[16]); glial fibrillary acidic protein (GFAP), an astrocyte marker[17]; tetanus toxin receptor (which identifies neurones[18],

Table 1 Composition of oligodendrocyte-enriched cultures

Marker	Pre-stimulation (%)	Post-stimulation (%)
GalC	86	93
A2B5	12	3
GFAP	5	4
Tetanus toxin receptor	0	0
Nonspecific esterase	5	1

Oligodendrocytes were stained on harvesting (day 7–10), and after a 4-day incubation with recombinant IL-2. Surface staining for GalC was performed for 30 min in the cold with rabbit anti-GalC antibody (1:25), followed by fluorescein isothiocyanate (FITC)-conjugated F(ab')$_2$ goat anti-rabbit immunoglobulin (1:20; Cappel) for 30 min; and for A2B5 using mouse monoclonal anti-A2B5 (1:20; Sera Labs) for 30 min, followed by FITC-conjugated goat anti-mouse immunoglobulin (1:20; Tago) for 30 min. Surface tetanus toxin receptors were tested for by staining with tetanus toxin, human antisera to tetanus toxin, and FITC-conjugated rabbit anti-human immunoglobulin (1:25; Accurate). Cytoplasmic staining was performed on fixed cells with rabbit antibody to GFAP (1:20; Dako) for 30 min at room temperature, followed by incubation with FITC-conjugated goat anti-rabbit immunoglobulin (1:20; Cappel). Nonspecific esterase staining was performed as described in ref. 12.

* Present address: Department of Neurology, University of Alabama at Birmingham, University Station, Birmingham, Alabama 35294, USA.

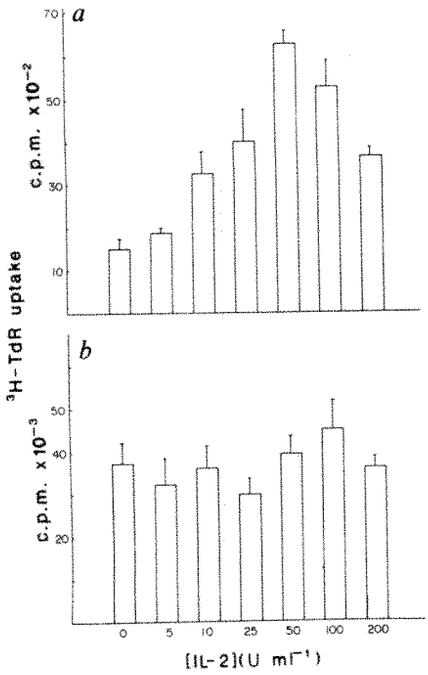


Fig. 1 Effect of recombinant human IL-2 (rIL-2) on oligodendrocyte and astrocyte proliferation. rIL-2 from two sources (Amgen, Thousand Oaks, California and rIL-2 given by Genetics Institute, Boston, Massachusetts) was tested at various concentrations (5–200 U ml^{-1}) on: *a*, oligodendrocytes (2×10^4 cells per well); and *b*, astrocytes (2×10^5 cells per well). The cells were pulsed on day 3 with ^{3}H-TdR, and harvested 17 h later. For oligodendrocytes, three of the experiments were performed with Amgen rIL-2 and three with Genetics Institute rIL-2. The data are expressed as the mean ± s.d. of these six experiments. For the astrocyte experiments, the values represented are the mean ± s.d. of three experiments, all performed with Amgen rIL-2. Control media consisted of 50% Dulbecco's modified essential medium (DMEM), 50% Ham's F-12 medium, 2 mM glutamine, 0.1% gentamycin and 10% FBS. Comparable results for oligodendrocyte proliferation were obtained when the experiments were performed in SFM: DMEM (high glucose formula) supplemented with glucose to a total of 6 g l^{-1}, 0.1 mM non-essential amino-acid mixture, 5 μg ml^{-1} transferrin, 2 mM glutamine and 0.1% gentamycin. Result for experiment using SFM alone = 2,139 ± 222 c.p.m., and for SFM plus 100 U ml^{-1} rIL-2 = 5,494 ± 204 c.p.m.

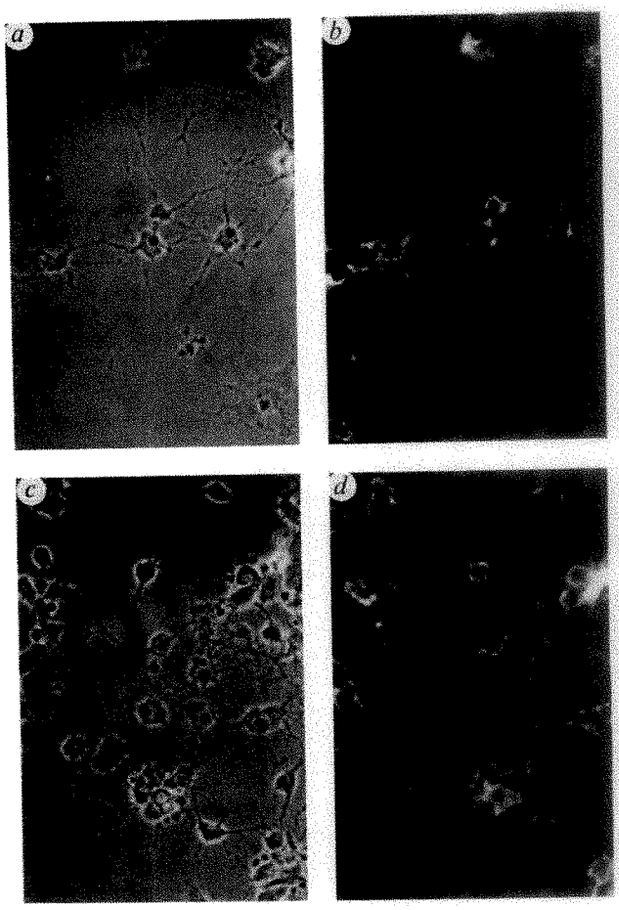


Fig. 2 Photomicrographs of oligodendrocytes after treatment with rIL-2. Phase-contrast microscopy (*a*, *c*) demonstrates the effects of rIL-2 on cultures of rat oligodendrocytes. Cells (2×10^5) were treated for 4 days with either 100 U ml^{-1} of rIL-2 (*c*, *d*) or control media (*a*, *b*). Immunofluorescence staining for GalC demonstrates that rIL-2 stimulated the growth of oligodendrocytes (*d*). Surface staining for GalC was performed for 30 min in the cold with rabbit anti-GalC antibody (1:25), followed by FITC-conjugated F(ab')$_2$ goat anti-rabbit immunoglobulin (1:20; Cappel) for 30 min.

glial progenitor cells[19] and type II astrocytes[15]); and nonspecific esterase, which identifies microglia[12]. Astrocyte populations were more than 95% GFAP-positive before and after stimulation.

We initially tested the ability of partially purified human IL-2 to stimulate enriched populations of both oligodendrocytes and astrocytes. Concentrations of partially purified delectinated IL-2 (Electronucleonics) in the range 0.1–5.0 U ml^{-1} significantly enhanced the proliferation of both cell types, as measured by ^{3}H-TdR incorporation (data not shown). A different pattern emerged when recombinant human IL-2 (rIL-2) was tested. Two different sources of rIL-2 were tested: 99.5% pure recombinant human IL-2 from Amgen and recombinant human IL-2 from Genetics Institute[20]. rIL-2 stimulated the proliferation of oligodendroglial cells (Fig. 1*a*), but not of astroglial cells (Fig. 1*b*). Thus, astrocyte proliferation in response to partially pure IL-2 may result from the presence of other factors or contaminants in the IL-2 preparation. A titration curve demonstrates that oligodendrocytes respond to rIL-2 in a dose-dependent manner: responsiveness begins at 10 U ml^{-1}, with maximal proliferation observed at 50–100 U ml^{-1} (Fig. 1*a*). These rIL-2 concentrations are comparable to those required for human B-cell proliferation[8,9]. Figure 2 shows the oligodendrocyte response to rIL-2: 2×10^5 cells were incubated in 24-well Costar plates with or without rIL-2 for 4 days (previously determined to be the optimal time in culture), after which time the cells were counted and assayed for GalC immunofluorescence. Cell counts were determined by trypsinization of triplicate wells, counting the cells per well, and taking a mean of the three values. The results of three separate experiments indicated that cell numbers were increased in cultures containing rIL-2 (Fig. 2*c*; 5.9×10^5 cells), compared with those without rIL-2 (Fig. 2*a*; 2.5×10^5 cells). Over 90% of the cells in both cultures were positive for GalC (Fig. 2*b*, *d*).

Oligodendrocyte proliferation in response to rIL-2 was confirmed by autoradiography[3,5]. Oligodendrocyte-enriched cultures (89% GalC input cells) were grown for 4 days with or without rIL-2 (100 U ml^{-1}) on sterile coverslips in Costar 24-well plates. The cells were labelled with ^{3}H-TdR (3 μCi per well) for 17 h before collection. After harvesting, the coverslips were washed to remove unincorporated ^{3}H-TdR, and fixed in acetone for 10 s. The slides were then immersed in Ilford K2 nuclear emulsion, exposed for 2 days at 4 °C, and developed. Sister cultures were stained for GalC after stimulation, and were 92%

GalC-positive. In the presence of rIL-2, 60–70% of the cells incorporated ^{3}H-TdR, compared with 10% of cells incubated in control media alone.

At the time of addition of growth factor, oligodendrocyte populations were predominantly GalC-positive. However, there were also 12% A2B5-positive cells, on average (Table 1). The bipotential glial progenitor cell which carries the A2B5 antigen has the ability to differentiate into either an astrocyte or an oligodendrocyte, depending on the culture conditions[14]. To exclude the possibility that our results could be explained by rIL-2 stimulating these progenitor cells instead of exerting a direct effect on GalC-positive cells, the following experiments were performed: oligodendrocyte cultures were treated twice with anti-A2B5 antibody (1:50) plus complement at 37 °C for 30 min to remove progenitor cells[3]. These antibody-treated oligodendrocytes then contained fewer than 4% A2B5$^+$ cells; but they retained the ability to respond to rIL-2 as determined by ^{3}H-TdR incorporation (1,436 ± 449 c.p.m., control media alone; 4,876 ± 222 c.p.m., with rIL-2). This result indicates that rIL-2 directly stimulates the proliferation of GalC$^+$ oligodendrocytes.

Another parameter of oligodendrocyte growth and maturation is the synthesis of myelin basic protein (MBP)[21]. While most oligodendrocytes express the surface antigen GalC[13], the simultaneous expression of GalC and MBP implies a more differentiated state[22]. MBP appears during oligodendrocyte development, and accumulates before the onset of myelination[23]. As determined by double immunofluorescence staining, an increased percentage of GalC$^+$ MBP$^+$ oligodendrocytes (38 ± 5%) was detected in cultures containing rIL-2 for 4 days compared with those in control media alone (11 ± 3%) (Table 2). This finding suggests that rIL-2, in addition to inducing proliferation of oligodendrocytes, enhances and/or accelerates maturation.

Table 2 Immunocytochemical characterization of oligodendrocytes

Total no. of cells counted			% GalC$^+$	% GalC$^+$, MBP$^+$
Expt 1	−IL-2	200	89	14.5
	+IL-2	241	92	32.0
Expt 2	−IL-2	214	89	11.7
	+IL-2	228	91	42.5
Expt 3	−IL-2	170	85	8.0
	+IL-2	168	89	40.5

Double immunofluorescence staining was performed on cultures of oligodendrocytes incubated either in the presence of rIL-2 (100 U ml^{-1}) or in control media alone (−IL-2) for 4 days. Oligodendrocytes (2×10^5) were incubated in Costar 24-well cluster plates on sterile coverslips with or without rIL-2 for 4 days, after which cells were stained for surface (GalC) and cytoplasmic (MBP) markers using indirect immunofluorescence. Surface staining was performed for 30 min in the cold with rabbit anti-GalC (1:25), followed by rhodamine-conjugated F(ab')$_2$ goat anti-rabbit immunoglobulin (1:20; Cappel) for 30 min. The cells were fixed in cold acetone for 10 s, then stained with mouse monoclonal anti-MBP antibody (1:20) for 30 min at room temperature. The cells were then stained with FITC-goat F(ab')$_2$ anti-mouse immunoglobulin (1:20; Accurate). For each experiment, three separate fields (each with a minimum of 150 cells) were counted by phase-contrast microscopy. GalC$^+$ cells were counted using a rhodamine filter, then MBP$^+$ cells were determined with a FITC filter. The values shown are the means of the three fields counted for each individual experiment. Identical experiments performed in serum-free medium (SFM) gave similar results: for SFM alone, 9 ± 1% of cells were GalC$^+$, MBP$^+$; for SFM plus rIL-2, 38 ± 2% of cells were GalC$^+$, MBP$^+$.

Our results demonstrate that rIL-2, a T-cell-derived lymphokine which has previously been shown to influence the growth of T and B cells, is also capable of inducing the proliferation and maturation of rat oligodendrocytes *in vitro*. To our knowledge, this is the first observation of rIL-2 stimulating a non-lymphoid cell, and provides further evidence that the growth of glial cells can be influenced by specific T-cell lymphokines. Our results differ from those of Giulian and Lachman[4], who found that oligodendrocytes did not respond to rIL-2. This discrepancy may be the result of different culture conditions, isolation procedures and age at which the cells were tested. Giulian and Lachman used mixed glial cultures which consisted of both astrocytes and oligodendrocytes. These cells were cultured for 2 days, at which time rIL-2 was added for an additional 3 days. No information was provided as to the number of GalC$^+$ cells or A2B5$^+$ cells present before and after stimulation. In the present study, we used enriched populations of oligodendrocytes obtained after 7–10 days in primary culture. The cells which responded to rIL-2 were predominantly GalC$^+$ oligodendrocytes.

A previous study by Merrill *et al.*[3] indicated that purified human IL-2 stimulated neither astrocytes nor oligodendrocytes. The concentration of IL-2 used in that study was <10 U ml^{-1}, and we now know that oligodendrocyte responsiveness begins at 10 U ml^{-1}, with optimal proliferation at 50–100 U ml^{-1} (Fig. 1*a*). Thus, the concentration of IL-2 used in the previous study was too low to induce oligodendrocyte proliferation.

In the demyelinating disease of multiple sclerosis (MS), there is an astrocytic reaction consisting of hyperplasia and gliosis which results in the formation of brain plaques[24,25]. IL-1 is released in the brain following injury[4], and may mediate inflammation associated with brain injury. In addition, its proliferative effect on astrocytes may promote scar formation in damaged or diseased brain (for example, in MS). The myelin-producing cells, the oligodendrocytes, are to a large extent destroyed during the MS disease process, although a small number do persist and proliferate at the edge of the plaque[26]. The characteristic inflammatory infiltrate in MS consists predominantly of T lymphocytes, with the T-helper/inducer subset being most numerous at the plaque edge, and T-suppressor/cytotoxic cells more abundant within the plaque[27]. Both of these T-cell subsets secrete IL-2 when stimulated[28]. *In situ* lymphoid/mononuclear cells in MS brain secrete immunoregulatory molecules such as IL-2, IL-1 and prostaglandin E_2, which suggests that these cells are activated[29]. In addition, staining with monoclonal antibody to IL-2 is observed in areas of MS brain containing very few lymphoid cells, suggesting that brain cells themselves may provide an endogenous central nervous system source of IL-2 or of an IL-2-like molecule[29]. Astrocytes and glioma cells produce an IL-1-like factor[30,31], which indicates that glial cells are able to secrete immunoregulatory molecules. Oligodendrocytes *in vivo* may encounter IL-2 in the periphery as a result of damage to the blood–brain barrier[32]; alternatively, they may encounter endogenous IL-2 secreted by infiltrating lymphoid cells, or possibly by other brain cells. While we have demonstrated that oligodendrocytes can specifically absorb IL-2 (unpublished observation), it is unknown whether IL-2 acts on oligodendrocytes via the same type of cell-surface receptor as that required for T-cell and B-cell activation. As in the case of IL-1 and insulin, the receptors on different cell types may be distinct. Separate sites on the IL-1 molecule act on fibroblasts and thymocytes[33], while the insulin receptor on rat brain cells is distinct from those on rat liver cells and human lymphocytes[34]. The finding that rIL-2 enhanced MBP expression (Table 2) is particularly intriguing; this may be the result of either accelerated synthesis of MBP or selective proliferation of MBP$^+$ cells. MBP expression in oligodendrocyte cytoplasm precedes myelination[18]. Oligodendrocytes, in the presence of IL-2, may be able to accelerate/enhance their ability to myelinate or remyelinate, which would be beneficial in demyelinating diseases.

We thank Dr Scott Linthicum for the gift of mouse monoclonal anti-MBP antibody, Dr Steve Clark of Genetics Institute for recombinant IL-2, and Richard Burger for preparation of the manuscript. This work was funded in part by USPHS grant NS 19145 and grant JF 2012A3 from the National Multiple Sclerosis

Society (to J.E.M.). E.N.B. is the recipient of a NIH Postdoctoral Trainee Fellowship (CA-09120, NS-07771) and was funded in part by the Joe Gheen Fund.

Received 17 October 1985; accepted 21 March 1986.

1. Fontana, A., Otz, U., DeWeck, A. L. & Grob, P. J. *J. Neuroimmun.* **2**, 73-81 (1982).
2. Fontana, A., Grieder, A., A., Arrenbrecht, S. T. & Grob, P. J. *J. neurol. Sci.* **46**, 55-62 (1980).
3. Merrill, J. E. *et al. Science* **224**, 1428-1430 (1984).
4. Giulian, D. & Lachman, L. B. *Science* **228**, 497-499 (1985).
5. Benveniste, E. N., Merrill, J. E., Kaufman, S. E., Golde, D. W. & Gasson, J. C. *Proc. natn. Acad. Sci. U.S.A.* **82**, 3930-3934 (1985).
6. Gillis, S., Ferm, M. M., Ou, W. & Smith, K. A. *J. Immun.* **120**, 2027-2032 (1978).
7. Larsson, E. L. & Coutinho, A. *Nature* **280**, 239-241 (1979).
8. Boyd, A. W., Fischer, D. C., Fox, D. A., Schlossman, S. F. & Nadler, L. M. *J. Immun.* **134**, 2387-2392 (1985).
9. Mittler, R. *et al. J. Immun.* **134**, 2393-2399 (1985).
10. Kishi, H. *et al. J. Immun.* **134**, 3104-3107 (1985).
11. McCarthy, K. D. & DeVellis, J. *J. Cell Biol.* **85**, 890-902 (1980).
12. Suckling, A. J., Kirby, J. A. & Rumsby, M. G. *Prog. Brain Res.* **59**, 317-322 (1983).
13. Raff, M. C. *et al. Nature* **274**, 813-816 (1978).
14. Raff, M. C., Miller, R. H. & Noble, M. *Nature* **303**, 390-396 (1983).
15. Raff, M. C., Abney, E. R., Cohen, J., Lindsay, R. & Noble, M. *J. Neurosci.* **3**, 1289-1300 (1983).
16. Eisenbarth, G., Walsh, F. S. & Nirenberg, M. *Proc. natn. Acad. Sci. U.S.A.* **76**, 4913-4917 (1979).
17. Bignami, A., Eng, L. F., Dahl, D. & Uyeda, C. T. *Brain Res.* **43**, 429-435 (1972).
18. Mirsky, R. in *Neuroimmunology* (ed. Brockes, J.) 141 (Plenum, New York, 1982).
19. Abney, E., Williams, B. P. & Raff, M. C. *Devl Biol.* **100**, 166-171 (1983).
20. Clark, S. C. *et al. Proc. natn. Acad. Sci. U.S.A.* **81**, 2543-2547 (1984).
21. Sternberger, N. H., Itoyama, Y., Kies, M. W. & Webster, DeF. H. *Proc. natn. Acad. Sci. U.S.A.* **75**, 2521-2524 (1978).
22. Ranscht, B., Clapshaw, P. A., Price, J., Noble, M. & Seifert, W. *Proc. natn. Acad. Sci. U.S.A.* **79**, 2709-2713 (1982).
23. Roussel, G., Labourdette, G. & Nussbaum, J. L. *Devl Biol.* **81**, 372-378 (1981).
24. Adams, C. W. M. *Br. med. J.* **33**, 15-20 (1977).
25. Prineas, J. *Hum. Path.* **6**, 531-554 (1974).
26. Raine, C. S., Scheinberg, L. & Waltz, J. M. *Lab. Invest.* **45**, 534-536 (1981).
27. Traugott, U., Reinherz, E. L. & Raine, C. S. *J. Neuroimmun.* **4**, 201-221 (1983).
28. Meuer, S. C. *et al. J. Immun.* **129**, 1076-1079 (1982).
29. Hofman, F. *et al. J. Immun.* (in the press).
30. Fontana, A., Kristensen, F., Dubs, R., Gemsa, D. & Weber, E. *J. Immun.* **129**, 2413-2419 (1982).
31. Fontana, A., Hengartner, H., de Tribolet, N. & Weber, E. *J. Immun.* **132**, 1837-1844 (1984).
32. Tourtellotte, W. W. & Ma, B. I. *Neurology* **28**, 76-83 (1978).
33. Kimball, E. S., Pickeral, S. F., Oppenheim, J. J. & Rossio, J. L. *J. Immun.* **133**, 256-260 (1984).
34. Hendricks, S. A., Agardh, C.-D., Taylor, S. I. & Roth, J. *J. Neurochem.* **43**, 1302-1309 (1984).

Mechanism of membrane damage mediated by human eosinophil cationic protein

John Ding-E Young*, Christer G. B. Peterson†, Per Venge† & Zanvil A. Cohn*

* Laboratory of Cellular Physiology and Immunology, The Rockefeller University, 1230 York Avenue, New York, New York 10021, USA
† Department of Clinical Chemistry, University Hospital, Uppsala, Sweden S-75014

Recent evidence suggests a role for eosinophil granule proteins in contact-dependent antibody-mediated cytotoxicity[1-3]. Cytolysis may involve a secretory phenomenon whereby granule proteins are released at the site of contact between eosinophil and target cells[1-4]. Several basic proteins have been isolated from eosinophil granules, including the major basic protein[5-7], eosinophil cationic protein[8,9], eosinophil protein-X[10] and eosinophil peroxidase[11]. One of the major granule proteins of human eosinophils is the eosinophil cationic protein (ECP)[3,8,9] which has been shown to damage schistosomula of *Schistosoma mansoni* at concentrations as low as 10^{-7} M (Ref. 12). Here, we describe the formation of functional channels by purified human ECP. The transmembrane pores formed by ECP are relatively voltage-insensitive and non-ion-selective, suggesting a role for channel formation by ECP in target cell damage mediated by eosinophils. Channel formation by granule proteins of immune effector cells[13-20] may represent a general and effective mechanism of target cell killing.

ECP was purified from human eosinophil granules by means of a low-*p*H extraction scheme[8,9]. The purity of the ECP was confirmed by SDS-polyacrylamide gel electrophoresis (Fig. 1*a*) and agarose gel electrophoresis (not shown). Purified ECP showed potent haemolytic activity at submicromolar levels (Fig. 1*b*). Haemolysis by ECP was not dependent on, or enhanced by, the presence of Ca^{2+}, Mg^{2+} or Zn^{2+} but was closely dependent on temperature. Maximal haemolytic activity was observed at 37 °C; below 28 °C haemolysis was decreased several-fold and at 4 °C virtually no haemolysis was observed.

The activity of ECP was also studied using nucleated cells as targets and by monitoring membrane potential changes as a result of incubation with ECP (Fig. 1*c*). All the cells tested (J774 macrophages, CTLL-A11, P388, chicken embryo myotubes) showed rapid and sustained membrane depolarization.

The permeability increase produced by ECP was not restricted to cell membranes. A lipid vesicle-permeability assay, described previously[21,22], was used to study ion fluxes induced by ECP across lipid vesicles (Fig. 1*d*). Vesicles treated with ECP became leaky to monovalent ions (Fig. 1*d*) and also showed some permeability to divalent ions (Ca^{2+}, Mg^{2+}), ^{14}C-sucrose and the fluorescent markers lucifer yellow and carboxyfluorescein.

Voltage-clamped phospholipid planar bilayers[23,24] were used to dissect the permeability properties of ECP. Because of the high impedance of these bilayers, small conductance changes can be measured with better resolution than with other techniques. Planar bilayers formed from egg soybean phospholipids were exposed to nucleus-free homogenates of human eosinophils, derived from three hypereosinophilic patients by means of density gradient centrifugation[25]. Current steps of heterogeneous sizes were immediately observed in the recording, consistent with the incorporation of ion channels into the bilayer (Fig. 2*a*).

Granules from these eosinophils were isolated by centrifugation through a Percoll density gradient[26] and a homogeneous population of granules was obtained, as visualized by electron microscopy (data not shown). Granules were then solubilized in detergent and added to planar bilayers. A significant enhancement of channel activity was observed compared with that obtained with a similar concentration of whole-cell-lysate proteins (Fig. 2*b*). The enhancement of channel activity was even higher when purified ECP was added to lipid bilayers at the same protein concentration (Fig. 2*c*), indicating that ECP is probably responsible for most of the pore-forming activity produced by eosinophil granules. Purified eosinophil protein-X (EP-X) and eosinophil peroxidase produced no channel activity under similar experimental conditions (data not shown).

ECP channels are resistant to closing by high transmembrane potentials. Up to 100 mV, the conductance associated with ECP channels showed little or no relaxation to lower steady-state values in response to voltage pulses (Fig. 3*a*). This is confirmed by a continuous current-voltage (I-V) plot, generated by passing a voltage ramp from −120 to +120 mV (Fig. 3*b*,*c*). As shown in Fig. 3*b*, the current trace became noisy, deviating from linearity only at voltages exceeding 60 mV in either polarity. This region of noise or instability probably represents the closing of individual ECP channels which occurs only at high voltages, as demonstrated with bilayers containing low amounts of ECP channels (Fig. 3*c*). In such bilayers, the voltage-ramp-induced closing of individual channels can be seen as a quantal leap in the current trace (Fig. 3*c*). Thus, human ECP forms stable transmembrane pores which are relatively resistant to the effects of the electrical field, resembling the channels formed by polymerized C9 (unpublished observations) and by the pore-forming protein isolated from granules of cytotoxic T lymphocytes and natural killer (NK)-like cells[16,19,20].

Single-channel fluctuations were observed only at high transmembrane potentials (Fig. 4). In 0.1 M NaCl ECP channels show unit conductances of 120 ± 7 pS ($n = 432$ events; range 95-150 pS). At least two intermediate conductance states were identified, usually observed when channels flickered between open and closed states at high voltages. ECP channels showed

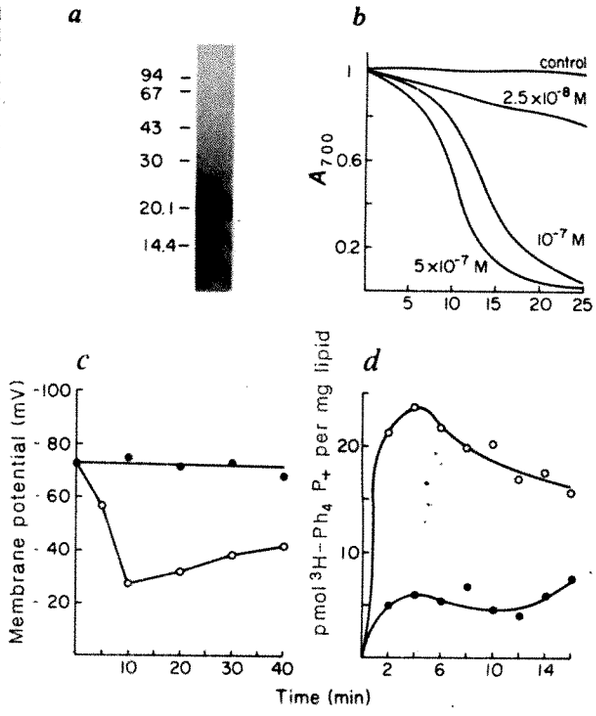


Fig. 1 *a*, SDS-polyacrylamide gel electrophoresis profile of ECP. 10 μg ECP was applied under reducing conditions to a 12.6% polyacrylamide gel slab. The three closely spaced bands migrating with relative molecular mass (M_r) 18,000–21,000 showed cross-reactivity on immunoblotting, using monospecific polyclonal and monoclonal antibodies directed against ECP. The purity of ECP was also ascertained by double immunodiffusion, agarose gel electrophoresis and by radioimmunoassays using a library of polyclonal and monoclonal antibodies directed against several granule proteins from eosinophils and neutrophils. *b*, Kinetics of haemolysis produced by human ECP at 37 °C. Sheep red blood cells (SRBC) were washed and resuspended to 10^6 ml^{-1} in phosphate-buffered saline (PBS) containing 1% Vitrogen (Gibco) with 1 mM $CaCl_2$. ECP in PBS was added in small aliquots (1:100–1:1,000 dilution) to the final concentrations indicated and haemolysis assayed continuously by absorbance reading at 700 nm. Haemolysis curves represent absorbance recordings traced over with continuous lines. *c*, Effect of ECP on cell membrane potential of J774 macrophage-like cells plated on coverslips, as assayed by the uptake of ^{3}H-tetraphenylphosphonium ion (^{3}H-Ph$_4$P$^+$)[16,18,34]. ECP in PBS was added to cells at 37 °C to 10^{-6} M for the indicated periods (○), at which time the medium was aspirated and the coverslips rapidly washed by immersing them four times in separate beakers containing ice-cold PBS and 1 mg ml^{-1} bovine serum albumin (BSA). Cells were lysed in 0.5 ml of 0.05% Triton X-100 and 0.25-ml aliquots assayed for radioactivity. Values for ^{3}H-Ph$_4$P$^+$ trapped in the cells were against background and converted into $\Delta\Psi$ values as previously described[22]. ●), Control: PBS was added to cells. Data points represent average of four experiments. *d*, Ion fluxes in lipid vesicles. The uptake of ^{3}H-Ph$_4$P$^+$ into lipid vesicles was quantitated by filtration[22]. The reaction was initiated by diluting 0.1 ml of lipid vesicles into 0.9 ml of 0.25 M sucrose, 1 ml $CaCl_2$, 10 mM HEPES, *p*H 7.0, containing 50 μM ^{3}H-Ph$_4$P$^+$ and 10^{-6} M ECP (○) or control PBS (●). At intervals, aliquots of the reaction mixture were filtered and washed, and the radioactivity remaining on the filter determined[22]. Data points represent the average of experiments performed in triplicate. All experiments were done at 37 °C.

Methods. ECP used in this study was derived from either normal human blood buffy coat cells or from patients with hypereosinophilia. Leukocytes (~10^{12} cells) were homogenized in 0.34 M sucrose and centrifuged at 800*g* for 15 min to sediment nuclei and large cell debris. The supernatant was then centrifuged at 10,000*g* for 15 min. The enriched granule fraction was extracted with 10 vol. of 0.2 M ammonium acetate buffer, *p*H 4, and centrifuged at 20,000*g* for 30 min. The supernatant was eluted though Sephadex G-75 with 0.2 M ammonium acetate, *p*H 4, and ECP-containing fractions concentrated by ultrafiltration on a Diaflow PM-10 membrane. ECP was further purified by ion-exchange chromatography on Bio-Rex 70 (200–400 mesh; Biorad), equilibrated with 0.09 M ammonium acetate, *p*H 8.4, and 8.7% glycerol and eluted on a 0.09–0.9 M gradient of ammonium acetate, *p*H 8.4–9.3, and 8.7% glycerol. Cells plated overnight on coverslips were washed three times with low-K$^+$ buffer (118 mM KCl, 1.3 mM $CaCl_2$, 0.8 mM $MgSO_4$, 5.5 mM glucose, 20 mM HEPES, 9 mM Na_2CO_3, *p*H 7.4) and incubated with 20 μM ^{3}H-Ph$_4$P$^+$ for 30 min at 37 °C. Lipid vesicles were formed from a mixture of phosphatidylethanolamine/phosphatidylcholine/cholesterol at a wt ratio of 3:2:1 and 25 mM β-D-octylglucoside in 0.05 M Na-isethionate, 0.165 M sucrose, 1 mM $CaCl_2$ and 10 mM HEPES, *p*H 7.0 (buffer A). The mixture was sonicated to clarity and vesicles were formed by a one-step 1:100 dilution with buffer A[21]. Vesicles were sedimented by centrifugation at 100,000*g* for 90 min and resuspended to 10 mg ml^{-1}.

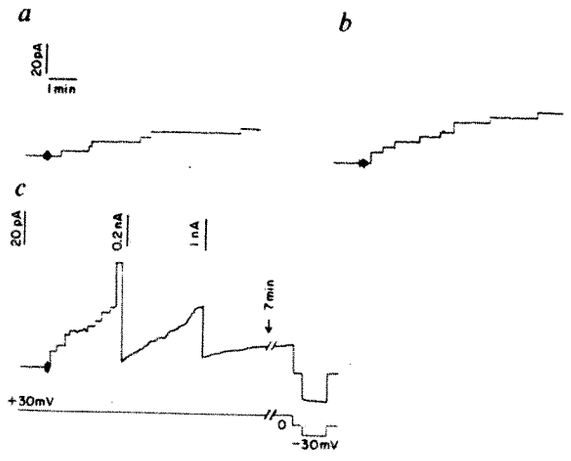


Fig. 2 Effect of eosinophil-derived material and ECP on planar bilayers. Bilayers[22,24] were formed in 0.1 M NaCl, 1 mM $CaCl_2$, 3 mM NaN_3, 10 mM HEPES, *p*H 7.0 (buffer C), and clamped at +30 mV throughout the experiments unless otherwise indicated (the positive side was named the *cis* side). Baseline conductances did not exceed 10 pS. Reagents were introduced into the aqueous phase of the *cis* side, followed by stirring for 15–20 s (which explains the noise in the recording). *a*, Eosinophils were enriched from the blood of a patient with eosinophilia (42% eosinophil count) by density gradient centrifugation[25], resulting in a 94% enrichment, and an aliquot (5 μg protein, 10-μl vol.) containing 0.1% Triton X-100 was introduced into the *cis* side of a bilayer bathed in 4 ml of buffer C. Note the upward deflection of current in steps. Two other patients with eosinophilia were used as sources of cells, yielding comparable results. Time resolution 1 ms; temperature 22 °C. *b*, Granules were obtained from eosinophil lysates by centrifugation, and 5 μg of granule protein in a 10-μl volume containing 0.1% Triton X-100 was added through the aqueous phase of a bilayer (noise). Same scale as in *a*. *c*, 5 μg of ECP, purified from granules as described in Fig. 1 legend and dialysed against buffer C, was added to a bilayer. At the points indicated, the current gain was reduced to accommodate the progressive rise of current. The lower trace shows the applied voltage; the parallel bars represent a lapse of 7 min. Note the many-fold enrichment of channel activity compared with *a* and *b*. The voltage polarity was switched to −30 mV to demonstrate that the amplitude of the current remained unchanged, suggesting that channel activity was not dependent on voltage polarity. ECP incorporated into bilayers in the absence of any detergent. The channel activity from granules could also be incorporated without detergent provided that granules were first ruptured by sonication, freeze-thawing or high-salt extraction.

Methods. Eosinophils, enriched as described previously[25], were washed in relaxation buffer (130 mM KCl, 4 mM NaCl, 1 mM disodium ATP, 2 mM $MgCl_2$, 10 mM HEPES, *p*H 6.8) and resuspended to 5×10^7 ml^{-1}. Cells were cavitated under N_2 (500 p.s.i., 25 min) and collected dropwise in the presence of EGTA, to a final EGTA concentration of 1 mM. After removal of nuclei and unbroken cells (800*g*, 15 min), the cell extract was sonicated for 1 min on ice and dialysed against buffer C. Triton X-100 (0.5%) was added to this cell lysate and the whole mixture was vortexed vigorously. Cell cavitate in relaxation buffer was centrifuged through a pre-formed continuous Percoll gradient[26] (densities 1.02–1.14 g ml^{-1}) at 20,000*g* for 35 min in a Sorvall SS-34 rotor. Granule enrichment was ascertained by β-glucuronidase assay and by ultrastructural examination (not shown). After removal of Percoll[26], granules were sedimented at 13,000*g* for 15 min and resuspended in buffer C to 1 mg protein ml^{-1}.

slow kinetics even at high voltages, with the open channel lifetime persisting for up to several minutes (Fig. 4*c*).

The ion selectivity of ECP channels was determined from the reversal potential necessary to nullify current flow from a 10-fold higher electrolyte concentration (*cis* or positive compartment made more concentrated). The results of such experiments showed permselectivity ratios of 1.00:0.93:0.58:0.21 for $K^+/Na^+/Cl^-/Ca^{2+}$. Similarly, Mg^{2+}, Ba^{2+}, Zn^{2+}, $EGTA^-$, $HEPES^-$, $Tris^-$ and glucosamine (Stokes diameter of 8 Å) also permeated through these channels. Lipid vesicles exposed to ECP for 16 h at 37 °C were examined by negative-contrast electron microscopy. The vesicle interior was stained with uranyl formate, in contrast to control vesicles which excluded the stain (data not shown). These data indicate that the channels formed by ECP are non-ion-selective and of large functional diameter. The relative molecular mass cutoff associated with these pores is being investigated.

No specific lipid requirement for formation of channels by

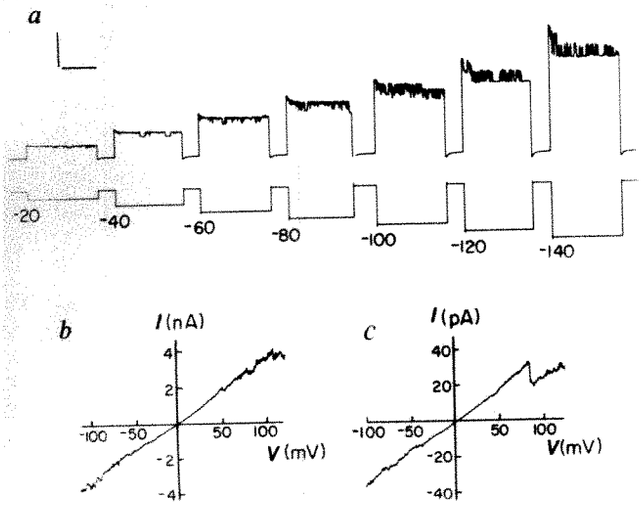


Fig. 3 Effect of electrical field on ECP channels. *a*, A membrane formed in buffer C was treated with 1 μg of ECP for 30 min prior to application of voltage pulses, in 20-mV increments. Upper and lower traces correspond to current (*I*) and voltage (*V*), respectively. Between two pulses, the membrane was allowed to remain at 0 mV for 10 s. Note that the initial capacitative current relaxed to lower steady-state values only at voltages exceeding 80 mV. Increased noise in the recording was associated with current relaxation, corresponding possibly to channel flickering activity at high voltages. Scale bars: 50 pA (vertical) and 20 s (horizontal). *b*, Membrane treated with 1 μg ECP as in *a* and subjected to a continuous voltage ramp running from −120 to +120 mV in 900 ms. The current record became noisy at high voltage but note the relatively small deviation from linearity even at high voltages. *c*, Membrane containing fewer channels after exposure to 0.1 μg ECP and subjected to a voltage ramp as in *b*. The downward deflection of current represents closing of one single ECP channel. This result demonstrates that the increase of noise in a many-channel bilayer induced by high voltages (*a*) can be explained by the voltage-dependent behaviour of each individual channel unit.

ECP was observed. Changing the lipid composition of the bilayer from a mixture of phospholipids to pure phosphatidylethanolamine, phosphatidylcholine or cholesterol membranes did not change the overall characteristics of the channel. At 37 °C, the rate of channel incorporation into planar bilayers was markedly enhanced (data not shown), an observation which is consistent with the temperature dependence of haemolysis.

Pore formation by ECP may represent the mechanism by which this protein damages target cell membranes. The lack of channel-forming activity associated with other granule proteins such as EP-X or peroxidase suggests that pore formation is a function specifically associated with ECP. Preliminary experiments with MBP do not indicate any functional channel formation associated with this protein. MBP has been shown to damage parasites[27,28] and cells[29] but at concentrations exceeding 10^{-5} M. At these concentrations, it is possible that surface charge interaction with negatively charged membranes may result in the increased permeability of target membranes[30,31] without concomitant formation of transmembrane channels.

Pore formation has been associated with a number of different cytolytic proteins in the immune effector system. The prototype of the channel former is the terminal membrane attack complex of complement which appears to be formed mainly by a single protein species, polymerized C9 (ref. 32 and J.D.-E Y., in preparation). A pore-forming protein has also been isolated from granules of cytotoxic T lymphocytes and NK-like cells[16–20], and from the protozoan parasite *Entamoeba histolytica*[21,33] and implicated in cell killing. Pore formation may therefore represent a general and well conserved immunological mechanism by which effector proteins inflict target membrane damage.

We thank S. S. Ko and M. A. DiNome for technical assistance. This work was supported in part by a grant from the Lucille P. Markey Charitable Trust and a Cancer Research Institute grant to J.D.-E Y.; by NIH grants CA 30198 and AI 070122 to Z.A.C., and by funds from the Swedish MRC and the Medical Faculty of the University of Uppsala to P.V. J.D.-E Y. is a Lucille P. Markey Scholar.

Received 8 October 1985; accepted 25 March 1986.

1. Ackerman, S. J. *et al. J. Immun.* **131,** 2977–2982 (1983).
2. D. Dessein, A. J. & David, J. R. in *Advances in Host Defense Mechanisms* Vol. 1 (eds Gallin, J. I. & Fauci, A. S.) 243–268 (Raven, New York, 1982).
3. Venge, P., Dahl, R., Hallgren, R. & Olsson, I. in *The Eosinophil in Health and Disease* (eds Mahmoud, A. F. F. & Austen, K. F.) 131–142 (Grune & Stratton, Inc., New York, 1980).
4. Tai, P. C., Spry, C. J. F., Peterson, C. G. B., Venge, P. & Olsson, I. *Nature* **309,** 182–184 (1984).
5. Gleich, G. J., Loegering, D. A. & Maldonado, J. E. *J. exp. Med.* **137,** 1459–1471 (1973).
6. Gleich, G. J., Loegering, D. A., Kueppers, F., Bajaj, S. P. & Mann, K. G. *J. exp. Med.* **140,** 313–332 (1974).
7. Gleich, G. J., Loegering, D. A., Mann, K. G. & Maldonado, J. E. *J. clin. Invest.* **57,** 633–640 (1976).
8. Olsson, I. & Venge, P. *Blood* **44,** 235–246 (1974).
9. Olsson, I., Venge, P., Spitznagel, J. K. & Lehrer, R. I. *Lab. Invest.* **36,** 493–500 (1977).
10. Peterson, C. G. B. & Venge, P. *Immunology* **50,** 19–26 (1983).
11. Carlson, M. G. Ch., Peterson, C. G. B. & Venge, P. *J. Immun.* **134,** 1875–1879 (1985).
12. McLaren, D. J., McKean, J. R., Olsson, I., Venge, P. & Kay, A. B. *Parasite Immun.* **3,** 359–373 (1981).
13. Millard, P. J., Henkart, M. P., Reynolds, C. W. & Henkart, P. A. *J. Immun.* **132,** 3197–3204 (1984).
14. Podack, E. R. & Konigsberg, P. J. *J. exp. Med.* **160,** 695–710 (1984).
15. Blumenthal, R., Millard, P. J., Henkart, M. P., Reynolds, C. W. & Henkart, P. A. *Proc. natn. Acad. Sci. U.S.A.* **81,** 5551–5555 (1984).
16. Young, J. D.-E, Nathan, C. F., Podack, E. R., Palladino, M. A. & Cohn, Z. A. *Proc. natn. Acad. Sci. U.S.A.* **83,** 150–154 (1986).
17. Masson, D. & Tschopp, J. *J. biol. Chem.* **260,** 9069–9072 (1985).
18. Podack, E. R., Young, J. D.-E & Cohn, Z. A. *Proc. natn. Acad. Sci. U.S.A.* **82,** 8629–8633 (1985).
19. Young, J. D.-E, Hengartner, H., Podack, E. R. & Cohn, Z. A. *Cell* **44,** 849–859 (1986).
20. Young, J. D.-E, Podack, E. R. & Cohn, Z. A. *J. exp. Med.* (in the press).
21. Young, J. D.-E, Blake, M., Mauro, A. & Cohn, Z. A. *Proc. natn. Acad. Sci U.S.A.* **80,** 3831–3835 (1983).
22. Young, J. D.-E, Young, T. M., Lu, L. P., Unkeless, J. C. & Cohn, Z. A. *J. exp. Med.* **156,** 1677–1690 (1982).
23. Montal, M. & Mueller, P. *Proc. natn. Acad. Sci. U.S.A.* **69,** 3561–3566 (1972).
24. Young, J. D.-E, Unkeless, J. C., Young, T. M., Mauro, A. & Cohn, Z. A. *Nature* **306,** 186–189 (1983).
25. Vadas, M. A., David, J. R., Butterworth, A., Pisani, N. T. & Siongok, T. A. *J. Immun.* **122,** 1228–1236 (1979).
26. Borregard, N., Heiple, J. M., Simons, E. R. & Clark, R. A. *J. Cell Biol.* **97,** 52–61 (1983).
27. Butterworth, A. E., Wassom, D. L., Gleich, G. J., Loegering, D. A. & David, J. R. *J. Immun.* **122,** 221–229 (1979).
28. Wassom, D. L. & Gleich, G. J. *Am. J. trop. Med. Hyg.* **28,** 860–863 (1979).

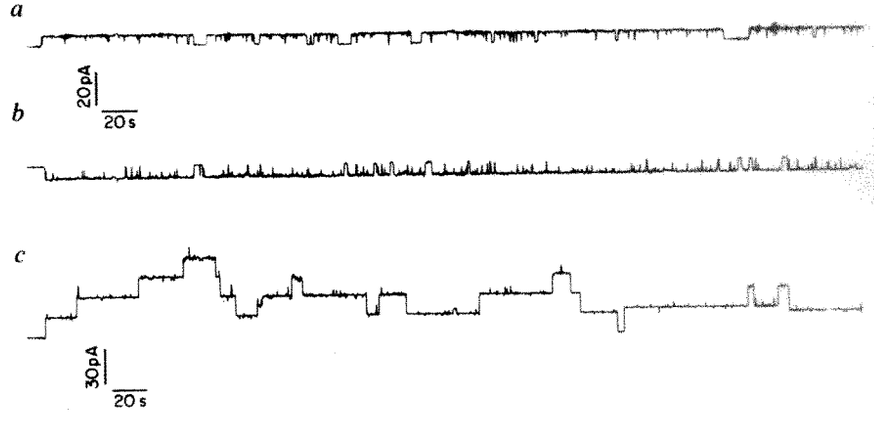


Fig. 4 Single-channel recordings associated with purified ECP. Bilayers, prepared as described in Fig. 2 legend, were treated with 10 ng of ECP. *a* and *b* represent traces from the same bilayer clamped at +50 and −50 mV, respectively. Note the infrequent closing of a single channel (closing represented by downward (*a*) and upward (*b*) deflections) at +50 mV. Same scale for *a* and *b*. *c*, Bilayer treated with 30 ng of ECP and clamped at +120 mV. Note that channel fluctuations are observed more frequently at this voltage.

29. Gleich, G. J., Frigas, E., Loegering, D. A., Wassom, D. L. & Steinmuller, D. *J. Immun.* **123**, 2925-2927 (1979).
30. Montal, M. *J. Membrane Biol.* **7**, 245-266 (1972).
31. Bach, D. & Miller, I. R. *J. Membrane Biol.* **11**, 237-254 (1973).
32. Tschopp, J., Muller-Eberhard, H. J. & Podack, E. R. *Nature* **298**, 534-538 (1982).
33. Lynch, E. C., Rosenberg, I. M. & Gitler, C. *EMBO J.* **1**, 801-804 (1982).
34. Sung, S.-S. J. *et al. J. biol. Chem.* **260**, 13442-13449 (1985).

A novel cell surface molecule on early B-lineage cells

Max D. Cooper*, David Mulvaney*, Antonio Coutinho† & Pierre-André Cazenave†

* Cellular Immunobiology Unit, Department of Pediatrics and Microbiology, and The Comprehensive Cancer Center, University of Alabama at Birmingham, Birmingham, Alabama 35294, USA
† Department of Immunology, Pasteur Institute, Paris Cedex 15, France

B cells and their antibody-secreting progeny represent one of several differentiation pathways that haematopoietic stem cells (HSC) may enter[1,2]. Cells representing intermediate stages between HSC and B cells have been identified in mammalian haematopoietic tissues[3,4] and studied intensively over the past decade. This population of early B-lineage cells, termed pre-B, is characterized by cellular proliferation and an orderly cascade of immunoglobulin gene rearrangements[5-7], a combination of events leading to the generation of clonally diverse B cells which then migrate to peripheral lymphoid tissues. It remains to be determined what elements determine the polyclonal growth of pre-B cells, how immunoglobulin gene rearrangements are regulated, and what happens to pre-B cells undergoing 'non-productive' immunoglobulin gene rearrangements. These issues could be resolved more easily if early B-lineage cells could be identified precisely and isolated. Here, we describe a cell surface glycoprotein that is selectively expressed by pre-B and newly formed B cells in murine haematopoietic tissues. The molecule, a homodimer formed by disulphide-linked chains of relative molecular mass (M_r) 140,000, is identified by a mouse monoclonal alloantibody called BP-1.

Previous attempts to identify cell surface molecules on pre-B cells have involved immunizing rats with mouse pre-B-cell lines, and fusion of the rat spleen cells to form antibody-producing hybridomas. Monoclonal antibodies which identify cell surface molecules on murine pre-B cells have been produced in this manner, but they do not identify differentiation antigens exclusive to early B-lineage cells[8-12]. We have used an alloimmunization strategy to produce such monoclonal antibodies (named BP antibodies to indicate collaboration between our laboratories in Birmingham and Paris) against pre-B and associated cell types.

Mus spretus, a wild mouse captured in Spain (Mus 3 biochemical group[13]), was selected for immunization, and the Abelson murine leukaemia virus-transformed cell line 18.81 was used as the immunogen; this pre-B-cell line is of BALB/c (Mus 1) origin[14]. Following immunization of *Mus spretus* with 18.81 cells, spleen cells were fused with SP2/0 myeloma cells[15]. One resultant hybridoma (G10) produced an IgG2a antibody (BP-1) which reacted with 18.81 cells (Fig. 1*A*) but not BALB/c thymocytes. Immunofluorescence microscopy revealed that crosslinkage of the 18.81 cell surface antigen by the BP-1 antibody (plus a second fluorescein-labelled goat antibody to mouse γ2a heavy chain) induces the formation of fluorescent caps, suggesting that BP-1 reacts with a surface molecule having a transmembrane connection to intracellular contractile elements.

When normal lymphoid tissues from perinatal mice of Mus 1 strains were examined by indirect immunofluorescence, BP-1$^+$ cells were found in the haematopoietic liver and spleen, but not in the thymus. In adult mice, approximately 10% of nucleated cells in bone marrow expressed BP-1 antigen on their surface, but not in the cytoplasm. When bone marrow cells were fixed following surface immunofluorescence staining with BP-1 (fluorescein label)[16] and then stained with anti-μ-chain antibodies (rhodamine label), all cytoplasmic μ^+ cells were BP-1$^+$. The intensity of surface staining of BP-1$^+$ cells from normal haematopoietic tissues was much lower than that of pre-B cells of the 18.81 line (Fig. 1).

Most IgM$^+$ B cells in haematopoietic tissues expressed the BP-1-reactive determinant. In adult bone marrow an average of 61% (s.e. = ±4.6%) of the B cells expressed the BP-1 antigen, as did ~80% of B cells in the neonatal liver. In contrast, BP-1$^+$ cells were not found in non-haematopoietic lymphoid tissues: thymus, spleen, lymph nodes, intestinal Peyer's patches and peritoneal cells from adult mice. None of the cells expressing the Thy-1 (ref. 17), Mac-1 (ref. 18) or BP-2 (an alloantigen on granulocytes; our unpublished observations) antigen markers of T cells and myeloid cells were BP-1$^+$, nor were cells of erythroid, megakaryocytic, endothelial, epithelial or connective tissue lineages.

Table 1 Reactivity of antibodies BP-1 and 14.8 with transformed B-lineage cells

Cell line	Maturational stage	Immunofluorescence intensity* BP-1	14.8
18.81	Pre-B	17.1	20.1
70Z	Pre-B/B	4.0	36.9
38C-13	Immature B	2.9	26.1
4.5	Mature B	1.2	35.5
BCL-1	Mature B	1.0	31.6
WEHI 279	Mature B	1.0	3.2
Ag8.563	Plasmacytoma	1.1	3.3
43.5	Plasmacytoma/pre-B hybridoma	1.0	1.4
56.3	Plasmacytoma/pre-B hybridoma	1.0	1.5

* The ratio of the staining intensities of BP-1 and 14.8 (ref. 5) to the background fluorescence. Methods used for immunofluorescence analyses are described in Fig. 1 legend.

Table 2 Genetic distribution of BP-1 alloantigen expression

Biochemical group	Strain	Geographical origin	Expression of BP-1 antigen
Mus 1	ULA	Palaiseau, France	+
	WLA	Issus, France	+
	DFL	Larzac, France	+
	BNC	Cairo, Egypt	+
	BFM/2	Montpellier, France	+*
	38CH	Chiarello, Italy	+
	WMP	Monastir, Tunisia	+
	WGQ	France	+
Mus 2A	PWK	Prague Zoo, Czechoslovakia	–
	MBT	General Toshevo, Bulgaria	–
	MPW	Varsovia, Poland	–
	MBK	Kranero, Bulgaria	–
Mus 2B	MOL	Japan	–
Mus 3	SPE	Santa Fe, Spain	–
	SEI	Ibiza, Spain	–
Mus 4A	XBS	South Bulgaria	–
Mus 4B	ZBN	North Bulgaria	–
	ZRU	Ukrania, USSR	–
Caroli	KAR	Thailand	–

* Unusual immunofluorescence reactivity pattern characterized by the absence of the discrete micro-immunofluorescence patches noted (by fluorescence microscopy) on bone marrow cells from the other Mus 1 strains.

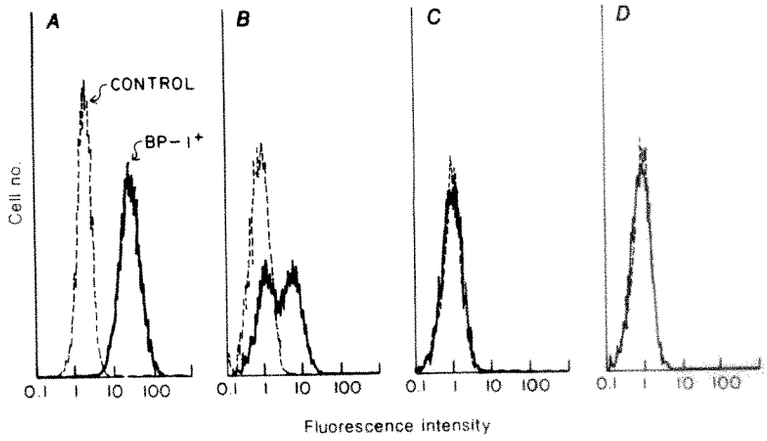


Fig. 1 Immunofluorescence analysis of the reactivity of various cells with the BP-1 monoclonal antibody. The results obtained with cells from different sources (*A*, 18.81 cells; *B*, bone marrow; *C*, spleen; *D*, lymph node) are presented as fluorescence histograms with the relative number of cells plotted on a linear scale and the relative fluorescence intensity on a logarithmic scale, both in arbitrary units. Solid lines indicate the staining intensity of the cell-bound BP-1 antibody (IgG2a) detected by fluorescein isothiocyanate-labelled antibodies to mouse IgG2a. Broken lines indicate staining of the cells with the second antibody alone.

Methods. Viable cells, teased from their tissue sources, were suspended in phosphate-buffered saline (PBS, *p*H 7.4) containing 3% bovine serum albumin and 0.2% sodium azide, filtered through a loose glass wool column, washed by centrifugation and incubated (20 min at 4 °C) with supernatant of hybridoma clone G10-All containing the BP-1 antibody. After extensive washing the cells were incubated with affinity-purified, fluorescein-conjugated goat antibodies to mouse γ2a heavy chains (0.025 mg ml^{-1}; fluorescein/protein molar ratio = 3.9; Southern Biotechnology Associates). The relative fluorescence intensities of individual cells were measured by automated flow cytometry using the FACS IV instrument (Becton Dickinson Immunocytometry Systems) equipped with a 2-W argon laser. Forward-angle light scatter was used to exclude erythrocytes, dead cells and debris from the analysis. In addition, the bone marrow sample was pre-sorted to remove myeloid cells reactive with the BP-2 monoclonal antibody.

BP-1$^+$ and BP-1$^-$ populations of bone marrow cells were separated by fluorescence-activated cell sorting (FACS). Because myeloid cells display considerable autofluorescence and the staining intensity of BP-1$^+$ cells is relatively low, cells of granulocytic lineage were first removed, on the basis of their immunofluorescence staining with the BP-2 monoclonal alloantibody. Residual bone marrow cells were predominantly lymphoid in appearance, and about half expressed μ-chains. Analysis of this population by automated flow cytometry revealed a roughly equal division of BP-1-positive and -negative cells (Fig. 1*B*). When these two subpopulations were separated, ~90% of the BP-1$^+$ population were found to express μ-chains while <10% of the BP-1$^-$ population were positive for μ-chains. Pre-B cells and most of their B-cell progeny in normal haematopoietic tissues can thus be isolated on the basis of their selective expression of the BP-1 antigen.

Various T-cell lines (BW5147, EL4, B6, KGV, PP16, PP17), macrophage lines (A3, P388D) and a mastocytoma cell line (P815) did not react with the BP-1 antibody. Neoplastic representatives of mature B and plasmacytoid cells also did not react with the BP-1 antibody, while transformed cells of pre-B and immature B phenotypes expressed the BP-1 antigen, the relative amounts of which decreased as a function of maturational stage (Table 1). For example, the BP-1 immunofluorescence staining intensity of the 38C-13 B-cell line, which expresses IgM only[19], was approximately three times the background fluorescence level, whereas the IgM$^+$/IgD$^+$ BCL-1 line[20] has no demonstrable BP-1 reactivity. As is the case for normal B-lineage cells, neoplastic B cells exhibited discordant expression of the BP-1 and 14.8 (B220) antigens.

Control of BP-1 expression was examined by immunofluorescence analysis of hybridomas formed by fusion of the non-immunoglobulin producer Ag8.653 plasmacytoma cells with normal pre-B cells from fetal liver. While these hybridomas display the pre-B-cell characteristics of intracytoplasmic heavy-chain expression and non-rearranged light-chain genes[21-23], there was no apparent expression of the BP-1 antigen. Three additional hybridomas formed by fusion of Ag8.563 with the 18.81 pre-B-cell line[24] also failed to express the BP-1 antigen while continuing to express the 14.8 determinant. This suggests a *trans* gene control of down-regulation of BP-1 expression with progression of B-cell differentiation.

Wild mice belonging to the genus *Mus* have been assigned to five biochemical groups based on protein electrophoretic polymorphisms[13]. Our examination of bone marrow samples revealed BP-1-reactive cells in Mus 1 strains, but not in mice representative of other biochemical groups (Table 2). Common laboratory strains of inbred mice (BALB/c, CBA/N, CBA/HeJ, Swiss, DBA/2) also had BP-1$^+$ cells in their bone marrow.

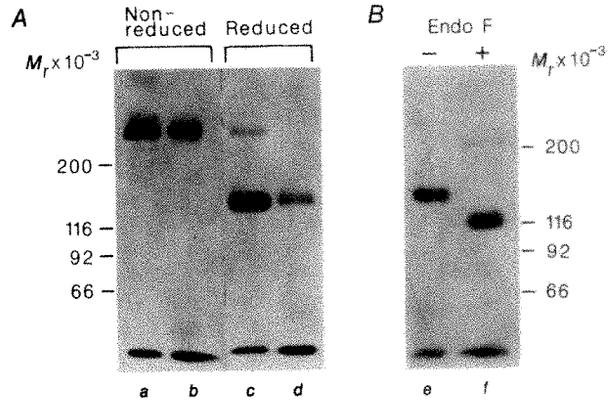


Fig. 2 SDS-polyacrylamide gel electrophoresis (PAGE) of ^{125}I-labelled membrane proteins of 18.81 and bone marrow cells. *A*, The BP-1-reactive molecules in lanes *a* and *c* were derived from 18.81 cells, and those in lanes *b* and *d* from normal bone marrow cells. No bands were seen in control lanes, which consisted of material dissociated from wells coated with irrelevant antibody. *B*, BP-1-reactive molecules examined under reducing conditions and following cleavage of complex sugars by overnight treatment with endoglycosidase F at 37 °C (ref. 29).

Methods. Cells (5.5–7.5 × 10^7) were surface-labelled with 2 mCi of Na^{125}I (Amersham) using the lactoperoxidase-catalysed method[25], washed and lysed in Nonidet P-40 (1% in 0.05 M Tris *p*H 7.5) containing 0.15 M NaCl, 0.02% NaN_3, 50 mM iodoacetamide, 1 mM phenylmethylsulphonyl fluoride, 20 mM ε-amino-*n*-caproic acid and 0.01% soybean trypsin inhibitor at 4 °C for 30 min. The cell lysate was centrifuged at 10,000*g* for 15 min and the supernatant precleared by overnight incubation at 4 °C in a plastic well precoated first with goat antibodies to mouse immunoglobulin, then with a mouse monoclonal antibody to chicken IgM. Precleared cell lysate supernatants were incubated overnight in plastic wells precoated with goat antibody to mouse immunoglobulin and the BP-1 antibody. The wells were washed and BP-1-reactive molecules dissociated from the plate by incubation with 2% SDS without or with 5% 2-mercaptoethanol (reducing conditions) for 1 h at 37 °C. Aliquots of antigens dissociated from the immunocomplexes were examined by SDS-PAGE using 5% polyacrylamide slab gels[27]. Gels were fixed, dried and autoradiographed on Kodak SB-5 film with an enhancing screen.

When surface proteins on 18.81 cells were radiolabelled[25] with ^{125}I and the BP-1-reactive molecules isolated[26] and analysed by electrophoresis in sizing gels (SDS-polyacrylamide, 5–12%)[27],

a band of M_r ~250,000 (250K) was identified under non-reducing conditions. A single band of M_r ~140K was generated under reducing conditions for disulphide bonds (Fig. 2). Internal labelling of 18.81 cells with ^{23}S-methionine, followed by sizing gel analysis of BP-1-reactive material, also revealed a molecule comprising disulphide-linked subunits of ~140K. The 140K band could be detected when the BP-1 antibody was used to identify reactive molecules after electrophoresis of an 18.81 cell lysate (reducing conditions) and transfer of the separated proteins to a nitrocellulose membrane[28], indicating relative stability of the antigenic determinant on individual subunits. When BP-1-reactive molecules on 18.81 cells were isolated, reduced and treated with endoglycosidase F (Endo F) to remove *N*-linked oligosaccharides[29], the M_r of the subunits was reduced to ~115K (Fig. 2*B*).

BP-1-reactive molecules of identical size and composition were also found in normal bone marrow (Fig. 2*A*) and in 18.81, 70 Z and 38C-13 cell lines (data not shown). Immunochemical analysis failed to reveal BP-1-reactive molecules on cells from spleen, brain and kidney or on cell lines representative of later stages in B-cell differentiation.

The restricted expression of the BP-1 alloantigen suggests that it could serve as a cell adhesion molecule for early B-lineage cells, or it could be a receptor for a unique induction signal. Noteworthy in the latter regard is the relatively high expression of BP-1-reactive molecules by transformed as opposed to normal pre-B cells. Whatever the functional role of this surface molecule, the BP-1 antibody provides an incisive probe with which to explore early events in the differentiation of normal and neoplastic B-cell clones. The alloimmunization strategy used to produce this antibody could be useful for identifying a variety of highly conserved molecules involved in cellular differentiation.

We thank Larry Gartland and Lanier Agar for help with the FACS analyses; Chen-lo Chen, Eliane Barbier and Hiromi Kubagawa for help with immunochemical studies; Peter Burrows, John Kearney, Paul Kincade, Ingrid Haas and Carol Gulis for helpful discussions and cell lines; Southern Biotechnology Associates for fluoresceinated antibodies; and Ann Brookshire and Maxine Aycock for help in preparing the manuscript. This work was supported by USPHS grants CA 16673 and CA 13148, and by INSERM and Mission Scientifique.

Received 30 December 1985; accepted 24 March 1986.

1. Cooper, M. D., Peterson, R. D. A., South, M. A. & Good, R. A. *J. exp. Med.* **123**, 75-102 (1966).
2. Moore, M. A. S. & Owen, J. T. T. *Lancet* **ii**, 658-659 (1967).
3. Osmond, D. G. & Nossal, G. J. V. *Cell. Immun.* **13**, 117-131 (1974).
4. Owen, J. J. T., Cooper, M. D. & Raff, M. C. *Nature* **249**, 361-363 (1974).
5. Kincade, P. W. *Adv. Immun.* **31**, 177-245 (1981).
6. Cooper, M. D., Velardi, A., Calvert, J. E., Gathings, W. E. & Kubagawa, H. in *Progress in Immunology V* (ed. Tada, T.) 603-612 (Academic, Tokyo, 1983).
7. Alt, F. W., Blackwell, T. K., DePinho, R. A., Reth, M. G. & Yancopoulos, G. D. *Immun. Rev.* **89**, 5-30 (1986).
8. Coffman, R. L. & Weissman, I. L. *Nature* **289**, 681-683 (1981).
9. Kincade, P. W., Lee, G., Watanabe, T., Sun, L. & Scheid, M. P. *J. Immun.* **127**, 2261-2268 (1981).
10. McKearn, J. P., Baum, C. & Davie, J. M. *J. Immun.* **132**, 332-339 (1984).
11. Paige, C. J., Skarvalt, H. & Sauter, H. *J. Immun.* **134**, 3699-3704 (1985).
12. Pillemer, E., Whitlock, C. & Weissman, I. L. *Proc. natn. Acad. Sci. U.S.A.* **81**, 4434-4438 (1984).
13. Bonhomme, F. *et al. Biochem. Genet.* **22**, 275-303 (1984).
14. Alt, F., Rosenberg, N., Lewis, S., Thomas, E. & Baltimore, D. *Cell* **27**, 381-390 (1981).
15. Shulman, M., Wilde, C. D. & Kohler, G. *Nature* **276**, 269-270 (1978).
16. Gathings, W. E., Lawton, A. R. & Cooper, M. D. *Eur. J. Immun.* **7**, 804-810 (1977).
17. Williams, A. F. *Nature* **314**, 579-580 (1985).
18. Springer, T. G., Galfre, G., Secher, D. S. & Milstein, C. *Eur. J. Immun.* **9**, 301-304 (1979).
19. Bergman, Y., Haimovich, J. & Melchers, F. *Eur. J. Immun.* **8**, 574-579 (1977).
20. Knapp, M. R. *et al. J. Immun.* **123**, 992-999 (1979).
21. Maki, R., Kearney, J., Paige, C. & Tonegawa, S. *Science* **209**, 1366-1369 (1980).
22. Perry, R. P., Kelley, D. E., Coleclough, C. & Kearney, J. F. *Proc. natn. Acad. Sci. U.S.A.* **78**, 247-251 (1981).
23. Burrows, P. D., LeJeune, M. & Kearney, J. F. *Nature* **20**, 838-841 (1979).
24. Burrows, P. D., Beck-Engeser, G. B. and Wabl, M. R. *Nature* **306**, 243-246 (1983).
25. Goding, J. W. *J. Immun.* **124**, 2082-2088 (1980).
26. Chen, C. H., Chanh, T. C. & Cooper, M. D. *Eur. J. Immun.* **14**, 385-391 (1984).
27. Weber, K. & Osborn, M. *J. biol. Chem.* **244**, 4406-4412 (1969).
28. Bordier, C. *J. biol. Chem.* **256**, 1604-1607 (1981).
29. Elder, J. H. & Alexander, S. *Proc. natn. Acad. Sci. U.S.A.* **79**, 4540-4544 (1982).

Chloroquine and ammonium chloride prevent terminal glycosylation of immunoglobulins in plasma cells without affecting secretion

Bernard Thorens & Pierre Vassalli

Department of Pathology, University of Geneva, Centre médical universitaire, CH-1211 Geneva 4, Switzerland

The generation of an acidic *p*H in intracellular organelles is required for several membrane and protein recycling processes. For instance, the internalization of ligands by receptor-mediated endocytosis is followed by the development of an acidic *p*H inside endosomes; this allows dissociation of the ligand, which is then transported to the lysosomes, from the receptor, which is recycled to the cell surface[1-4]. There is evidence that part of this recycling process involves the distal region of the Golgi complex, where terminal glycosylation occurs: when the plasma membrane transferrin receptor is desialylated by neuraminidase treatment, it acquires new sialic acid molecules after endocytosis and before cell-surface re-expression[5]. Golgi membranes have been shown to contain a proton pump[6] and the distal Golgi cisternae appear to have an acidic content[7]. Here, we have studied the effects of chloroquine and ammonium chloride, which raise the *p*H of acidic intracellular compartments[8], on the processing and secretion of immunoglobulins by plasma cells. Sialic acid transfer to terminal galactose residues, a reaction known to occur in the distal Golgi shortly before secretion[9], is completely and rapidly inhibited in the presence of these drugs, without significant modification of the secretion rate. This effect is accompanied by a dilatation of the Golgi cisternae and is not rapidly reversible.

Biosynthetically labelled immunoglobulin μ-chains are secreted in the form of pentameric IgM by mouse plasma cells; when fully reduced and alkylated, they have a retarded mobility on SDS-polyacrylamide gel electrophoresis (PAGE) compared

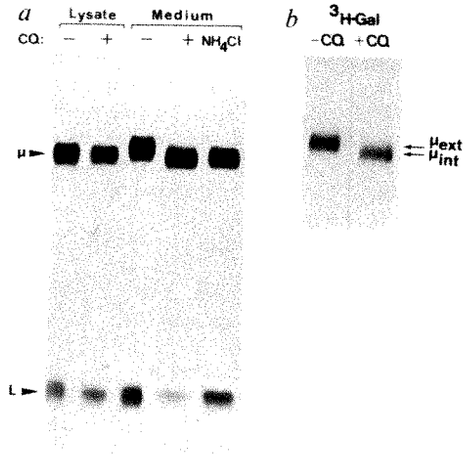


Fig. 1 *a*, Plasma cells, elicited in spleen cell cultures by *Escherichia coli* lipopolysaccharide[18], were labelled biosynthetically with 100 μCi ml^{-1} ^{35}S-methionine for 1 h, the lysates and media were prepared and immunoglobulins were immunoprecipitated and analysed by SDS-PAGE[19] (17.5% polyacrylamide). Chloroquine (CQ) was at 100 μM and ammonium chloride (NH_4Cl) at 10 mM. μ, μ-chains; L, light chains. *b*, Plasma cells were labelled biosynthetically for 1 h with 100 μCi ml^{-1} ^{3}H-galactose in Dulbecco's modified Eagle's medium containing 0.1 mg ml^{-1} glucose and 10% dialysed fetal calf serum, in the presence or absence of 100 μM chloroquine. Secreted μ-chains were on the same gel, analysed as in *a*. μ_{ext}, Mobility of secreted normal μ-chains; μ_{int}, mobility of intracellular incompletely glycosylated μ-chain precursors.

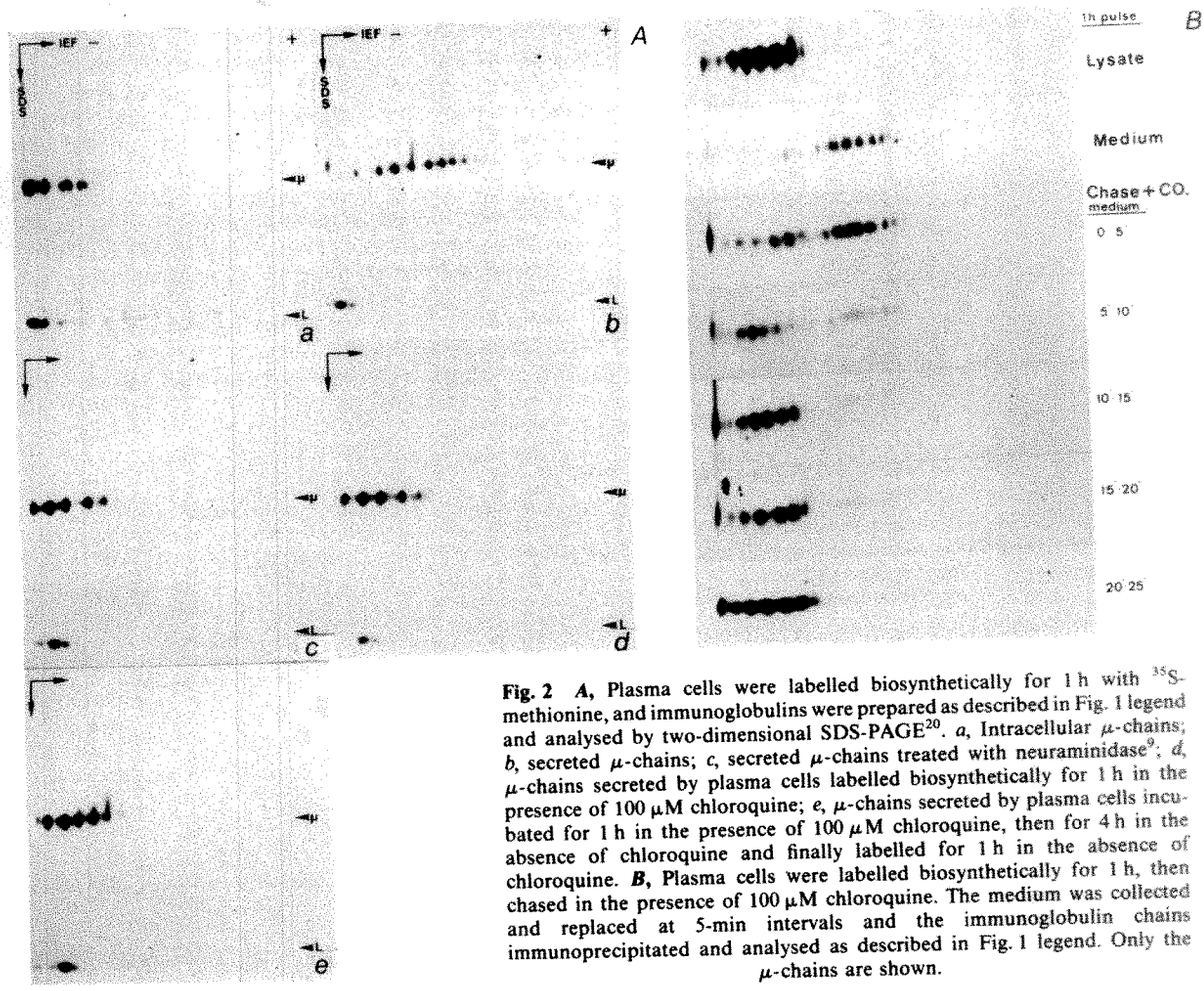


Fig. 2 ***A***, Plasma cells were labelled biosynthetically for 1 h with ^{35}S-methionine, and immunoglobulins were prepared as described in Fig. 1 legend and analysed by two-dimensional SDS-PAGE[20]. *a*, Intracellular μ-chains; *b*, secreted μ-chains; *c*, secreted μ-chains treated with neuraminidase[9]; *d*, μ-chains secreted by plasma cells labelled biosynthetically for 1 h in the presence of 100 μM chloroquine; *e*, μ-chains secreted by plasma cells incubated for 1 h in the presence of 100 μM chloroquine, then for 4 h in the absence of chloroquine and finally labelled for 1 h in the absence of chloroquine. ***B***, Plasma cells were labelled biosynthetically for 1 h, then chased in the presence of 100 μM chloroquine. The medium was collected and replaced at 5-min intervals and the immunoglobulin chains immunoprecipitated and analysed as described in Fig. 1 legend. Only the μ-chains are shown.

with intracellular μ-chains, due to the complete glycosylation of their oligosaccharide side chains (ref. 9 and Fig. 1). When plasma cells were labelled in the presence of chloroquine or ammonium chloride, the secreted μ-chains had the same mobility as their intracellular precursors (Fig. 1*a*), indicating that the glycosylation process was impeded. To determine the nature of the missing sugar residues, plasma cells were labelled biosynthetically in the presence of ^{3}H-galactose, the penultimate sugar residue in complex-type *N*-linked oligosaccharides. Figure 1*b* shows that the presence of chloroquine did not prevent the addition of ^{3}H-galactose to μ-chains and that the galactose-labelled chains secreted by the chloroquine-treated cells also had a higher mobility. The degree of sialylation of μ-chains was then assessed by two-dimensional SDS-PAGE (Fig. 2*A*). Heavy μ-chains secreted by plasma cells have more acidic *p*Is (Fig. 2*Ab*) than do intracellular μ-chains (Fig. 2*Aa*) (the vast majority of which have not undergone terminal glycosylation, topologically and chronologically a very late event in the intracellular pathway[9]). This difference in *p*I was totally suppressed after treatment of secreted immunoglobulins with neuraminidase (Fig. 2*Ac*). Secreted μ-chains synthesized in the presence of chloroquine (Fig. 2*Ad*) or ammonium chloride (not shown) had the same mobility as unsialylated μ-chains.

Pulse-chase experiments showed that the abolition of immunoglobulin sialylation by these drugs is induced very rapidly, but is not rapidly reversible and has no effect on the kinetics of immunoglobulin secretion. Plasma cells were first labelled biosynthetically for 60 min to allow homogeneous labelling of the immunoglobulins present along the secretory pathway, then placed in a chase medium containing chloroquine; the medium was collected and replaced at 5-min intervals. Two-dimensional SDS-PAGE showed that μ-chains lacking sialic acid could be detected within 5 min of chloroquine addition, and that sialylated μ-chains were dramatically reduced after 10 min of chloroquine treatment (Fig. 2*B*). To explore the reversibility of this inhibition, plasma cells were treated for 1 h with chloroquine without labelling, then placed in a medium without chloroquine for 4 h and finally pulse-labelled for 1 h: the secreted μ-chains were still not sialylated (Fig. 2*Ae*), indicating that the effect of the drug is not rapidly reversible. Similar observations were made with ammonium chloride (not shown). That this inhibition of sialylation has no significant effect on the kinetics of immunoglobulin secretion was found by labelling plasma cells for 30 min then chasing for periods of various length, in the absence or presence of chloroquine; analysis of the μ-chains remaining in the cells or secreted in the medium at these various intervals (Fig. 3) showed that the presence of the drug did not significantly modify the secretion rate.

To explore the possibility that the inhibition of sialylation resulted from a greater sensitivity of sialyltransferase than galactosyltransferase to changes in *p*H or to the presence of high concentrations of chloroquine, plasma cell membranes were

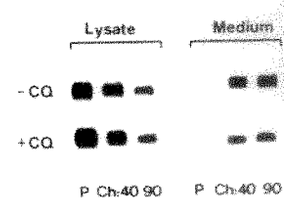


Fig. 3 Plasma cells were labelled biosynthetically with ^{35}S-methionine for 30 min (P), then chased (Ch) for 40 or 90 min, in the presence or absence of 100 μM chloroquine (CQ). The μ-chains present in the lysates of, and secreted by 2×10^{6} cells were immunoprecipitated and analysed by SDS-PAGE.

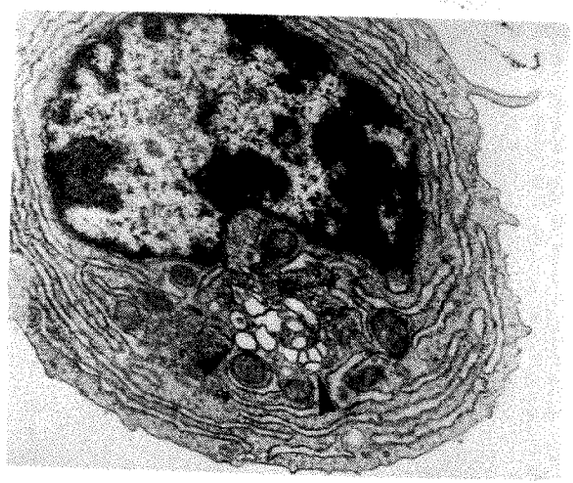


Fig. 4 Electron micrograph of a plasma cell incubated for 1 h in the presence of 10 mM ammonium chloride, showing the dilatation of the Golgi cisternae (arrowheads) (×9,800).

prepared[10] and their sialyl- and galactosyltransferase activities determined[11] at *p*Hs between 5.8 and 7.0, in the presence or absence of 10 mM chloroquine. The activity of neither enzyme was modified within this *p*H range; chloroquine at this high concentration decreased the sialyltransferase activity by 30–40% and the galactosyltransferase activity by 60%. Thus, defective sialylation does not result from a simple differential effect of *p*H or chloroquine on the terminal sugar transferase activities.

Plasma cells incubated for 1 h in the presence of chloroquine or ammonium chloride showed two types of ultrastructural alterations: a dilatation of some of the Golgi cisternae (Fig. 4), which were usually positive for thiamine pyrophosphatase activity (not shown), and the presence of very large, clear vacuoles with a scattered distribution, which were observed only in the presence of 100 μM chloroquine, and which have been described in similar conditions in other cells, such as fibroblasts[12]. Golgi alterations were still present 3 h after removal of the drug, while the large vacuoles observed in 100 μM chloroquine, which are probably swollen lysosomes or endosomes, had disappeared. Thus, only the Golgi dilatation is consistently correlated with the metabolic abnormality.

It is not clear why drugs that raise the *p*H of acidic intracellular compartments, such as ammonium chloride, chloroquine and monensin, induce an irreversible, probably *trans*, dilatation of the Golgi complex. In the case of monensin, a carboxylic membrane ionophore, the perturbations of the Golgi complex are probably both structurally and functionally more complex since, in addition to an extensive vacuolation of the Golgi cisternae, secretion of immunoglobulins by plasma cells is blocked[13]. In the case of ammonium chloride and chloroquine, it is not obvious why the more limited Golgi alteration is accompanied by inhibition of sialic acid addition but not of galactose addition or immunoglobulin secretion, even though it is usually considered that the two transferases share the same cisternal localization[11,14–16]. However, in highly secretory cells such as plasma cells, there is an enormous and very rapid vesicular traffic between the distal Golgi cisternae and the cell surface. Sialyltransferase, being the last enzyme to act in the processing of immunoglobulin carbohydrate side chains, may lie still more distally along the secretory pathway; indeed, it has recently been shown in hepatocytes that sialyltransferase is present not only in the Golgi *trans* cisternae, but also more distally in a complex network continuous with these cisternae[17] and in which no galatosyltransferase has been detected[15]. If a comparable structure exists in plasma cells, it is conceivable that the enzyme should be constantly carried back towards the distal Golgi cisternae, as part of a membrane protein recycling process. This may require the constant generation of a *p*H gradient to allow the persistence of a steady enzyme gradient. Disruption of the *p*H gradient may allow sialyltransferase and perhaps other membrane proteins (for instance, the Golgi proton pump itself) to remain at the cell surface irreversibly, explaining the persistence of the Golgi alterations and of the lack of sialylation seen in the present experiments. Since the *trans* part of the Golgi complex is involved in the intracellular traffic of endocytosed plasma membrane receptors[5], its involvement in the recycling of other membrane-associated proteins may explain the effects of intracellular *p*H-disrupting drugs in highly secretory cells.

We thank Dr J.-D. Vassalli for helpful advice in the preparation of this manuscript.

This work was supported by Swiss National Science Foundation grant 3.614-0.84.

Received 16 January; accepted 8 April 1986.

1. Brown, M. S., Anderson, R. G. W. & Goldstein, J. L. *Cell* **32**, 663–667 (1983).
2. Tycko, B., Keith, C. H. & Maxfield, F. R. *J. Cell Biol.* **97**, 1762–1776 (1983).
3. Schwartz, A. L., Bolognesi, A. & Fridovich, S. E. *J. Cell Biol.* **98**, 732–738 (1984).
4. Harford, J., Wolkoff, A. W., Ashwell, G. & Klausner, R. D. *J. Cell Biol.* **96**, 1824–1828 (1983).
5. Snider, M. D. & Rogers, O. C. *J. Cell Biol.* **100**, 826–834 (1985).
6. Glickman, J., Croen, K., Kelly, S. & Al-Awqati, Q. *J. Cell Biol.* **97**, 1303–1308 (1983).
7. Anderson, R. G. W. & Pathak, R. K. *Cell* **40**, 635–643 (1985).
8. de Duve, C. *et al. Biochem. Pharmac.* **23**, 2495–2534 (1974).
9. Tartakoff, A. & Vassalli, P. *J. Cell Biol.* **83**, 284–299 (1979).
10. Chicheportiche, Y., Vassalli, P. & Tartakoff, A. M. *J. Cell Biol.* **99**, 2200–2210 (1984).
11. Bretz, R., Bretz, H. & Palade, G. E. *J. Cell Biol.* **84**, 87–101 (1980).
12. Basu, S. K., Goldstein, J. L., Anderson, R. G. W. & Brown, M. S. *Cell* **24**, 493–502 (1981).
13. Tartakoff, A. & Vassalli, P. *J. exp. Med.* **146**, 1332–1345 (1977).
14. Dunphy, W. G. & Rothman, J. E. *J. Cell Biol.* **97**, 270–275 (1983).
15. Roth, J. & Berger, E. G. *J. Cell Biol.* **97**, 270–275 (1983).
16. Roth, J., Lucocq, J. & Charest, P. M. *J. Histochem. Cytochem.* **32**, 1167–1176 (1984).
17. Roth, J., Taatjes, D. J., Lucocq, J. M., Weinstein, J. & Paulson, J. C. *Cell* **43**, 287–295 (1985).
18. Anderson, J., Coutinho, A., Lenhardt, W. & Melchers, F. *Cell* **10**, 27–34 (1977).
19. Thorens, B., Schulz, M.-F. & Vassalli, P. *EMBO J.* **4**, 361–368 (1985).
20. O'Farrel, P. H. *J. biol. Chem.* **250**, 4007–4021 (1975).

Structure of DNase I at 2.0 Å resolution suggests a mechanism for binding to and cutting DNA

Dietrich Suck & Christian Oefner

European Molecular Biology Laboratory, Postfach 102209, D-6900 Heidelberg, FRG

Bovine pancreatic deoxyribonuclease I (DNase I), an endonuclease that degrades double-stranded DNA in a nonspecific but sequence-dependent manner[1–4], has been used as a biochemical tool in various reactions, in particular as a probe for the structure of chromatin and for the helical periodicity of DNA on the nucleosome and in solution[5–10]. Limited digestion by DNase I, termed DNase I 'footprinting', is routinely used to detect protected regions in DNA–protein complexes[11]. Recently, we have solved the three-dimensional structure of this glycoprotein (relative molecular mass 30,400) by X-ray structure analysis at 2.5 Å resolution[12] and have subsequently refined it crystallographically at 2.0 Å (ref. 26). Based on the refined structure and the binding of Ca^{2+}–thymidine 3′,5′-diphosphate (Ca-pTp) at the active site[12], we propose a mechanism of action and present a model for the interaction of DNase I with double-stranded DNA that involves the binding of an exposed loop region in the minor groove of B-DNA and electrostatic interactions of phosphates from both strands with arginine and lysine residues on either side of this loop. We explain DNase I cleavage patterns in terms of this model and discuss the consequences of the extended DNase I–DNA contact region for the interpretation of DNase I footprinting results.

In our earlier paper[12] we described the binding of Ca-pTp to DNase I the binding of Ca-pTp to DNase I. The di-*p*-nitrophenylester of pTp is a substrate for DNase I (ref. 13). Similar

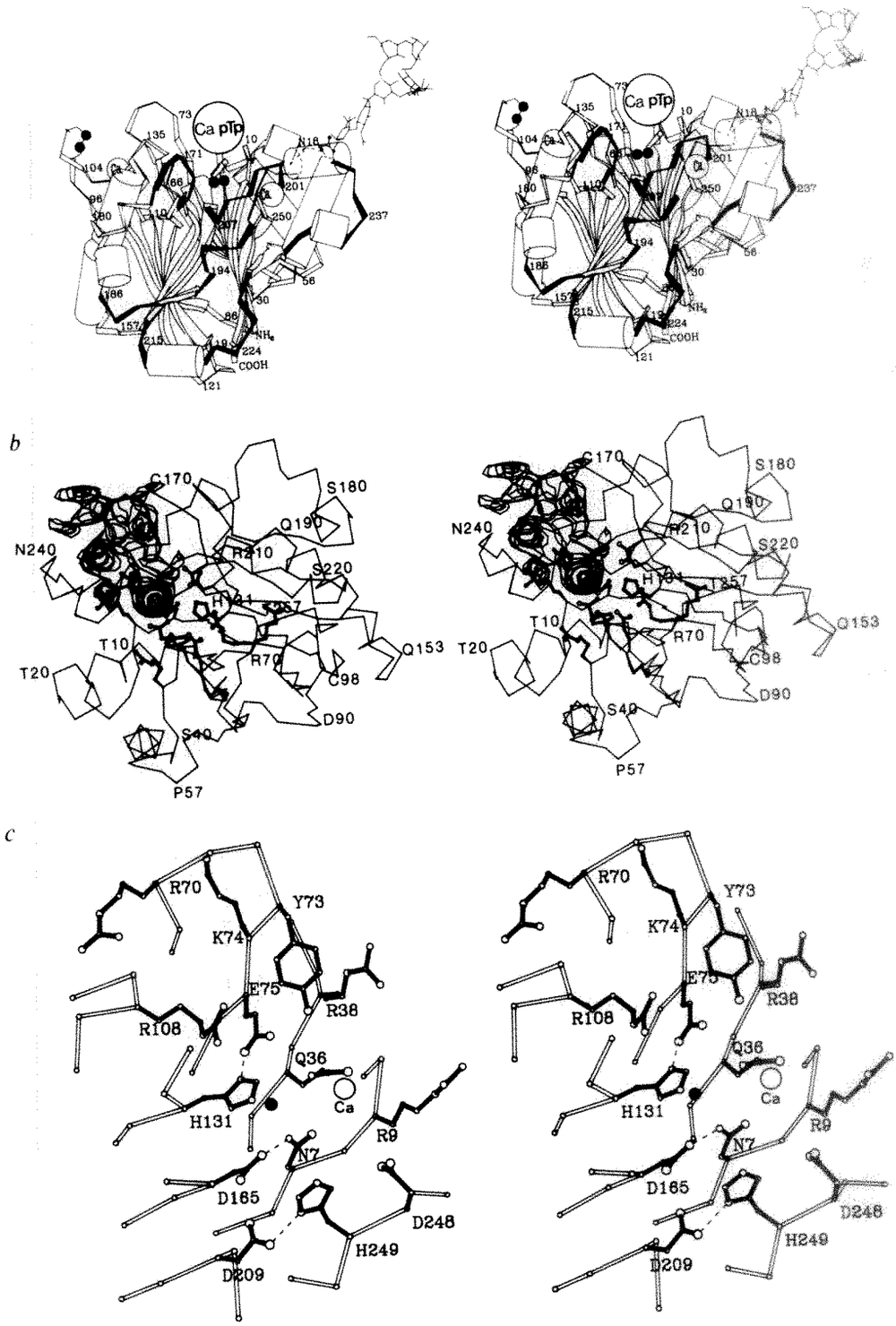


Fig. 1 Three-dimensional structure and active site of DNase I. *a*, Schematic stereo representation of DNase I with the Ca-pTp binding site indicated. DNase I is a sandwich-type structure with two 6-stranded β-sheets (arrows) forming a large hydrophobic core surrounded by helices (cylinders) and loop regions. The carbohydrate unit (drawn in skeletal form) protrudes by ~15 Å from the otherwise compact structure. The disulphide bridges connecting C 170/C 206 and C 98/C 101 are indicated by black dots; the two structurally important Ca^{2+} binding sites, which are distinct from the active-site Ca^{2+}, are marked. *b*, Stereo representation of the C^{α} backbone of DNase I viewed along the *b*-axis with the Ca-pTp difference density superimposed. The position of the Ca^{2+} ion is clearly defined as the point of highest density in the difference map. Some of the side chains at the active site including His 131 are shown as heavy lines. *c*, Stereo view of the active site of DNase I. Indicated are the position of the Ca^{2+} ion as determined from the Ca-pTp complex and the position of water molecule 390 (black dot) which is in hydrogen-bonding contact with N-3 of the essential H 131 and which, according to the proposed mechanism, acts as the attacking nucleophile. The remarkably strong hydrogen bonds between E 75 and H 131 (2.6 Å) and D 209 and H 249 (2.7 Å) are indicated by dashed lines.

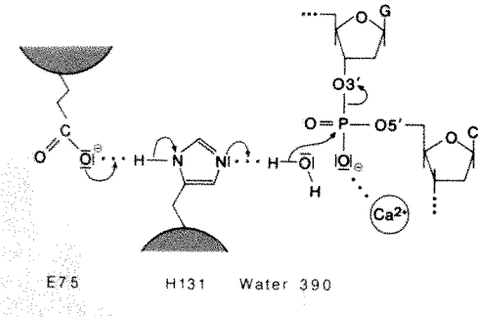


Fig. 2 Proposed mechanism of action. In a general acid–base catalysis, E 75 accepts a proton from H 131, which in turn accepts a proton from a water molecule which then as a nucleophile attacks the phosphorus and cleaves the P–O-3′-bond. The nucleophilic attack of the water hydroxyl is facilitated by the positive charge of the Ca^{2+} ion interacting with the phosphate. This proton acceptor–donor chain Glu-His-water is reminiscent of the catalytic triad Asp-His-Ser found in serine proteases. In agreement with this mechanism, carboxymethylation of H 131 at N-3 as well as protonation by lowering the *p*H inactivates the enzyme.

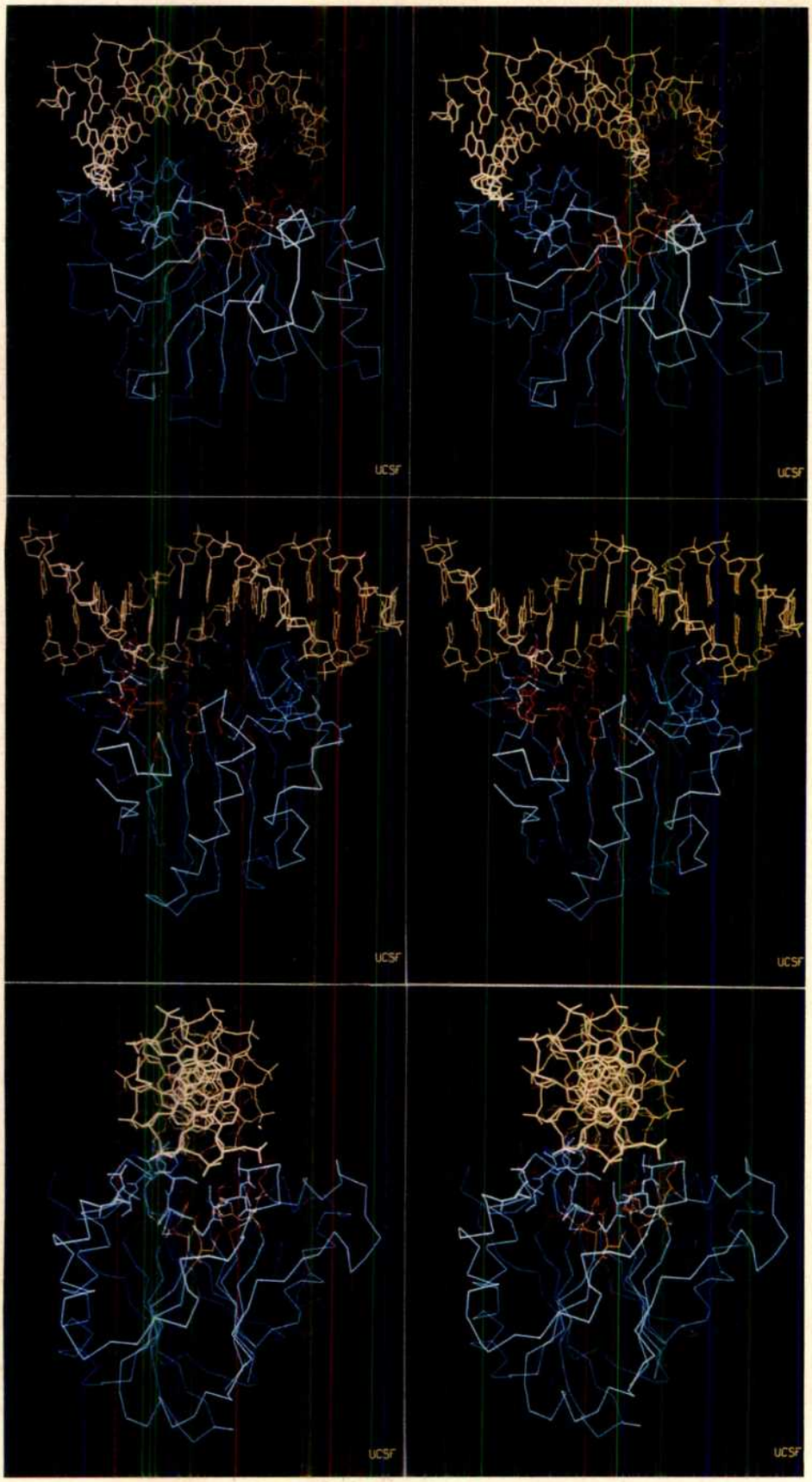


Fig. 3 DNase I–DNA interaction. Three different stereo views are shown, with a piece of B-DNA on top (in yellow) and the DNase I C^{α}-backbone beneath it. The catalytic Ca^{2+} ion, represented by a green dotted sphere, is in contact with the scissile phosphodiester bond (marked in red). Amino-acid side chains directly interacting with the DNA are shown in red and orange, other side chains in the contact region are shown in blue. Y 73, located in the exposed loop R 70-N 71-S 72-Y 73-K 74, is interacting in the minor groove with O-2 of a pyrimidine base. Phosphates from both DNA strands opposing each other in the minor groove make electrostatic interactions with positively charged side chains on either side of the exposed loop (R 9, R 108, R 70 and R 38, K 74). About 5 bp away from the cutting site, additional, mainly van der Waals' type interactions occur in the region of C 170 and T 174. The DNase I contact region extends over approximately one complete turn on one side of the DNA double helix.

to the degradation of DNA, the hydrolysis of this small substrate requires divalent cations and is inhibited by carboxymethylation of the essential residue H 131 (one-letter amino-acid notation). We diffused Ca-pTp into a native crystal and determined its binding site from a 4-Å difference Fourier transform. As expected from the biochemical data, Ca-pTp binds near H 131 at the surface of the protein in a shallow groove between the central β-pleated sheets of DNase I (Fig. 1). (There are two six-stranded β-pleated sheets packed against each other, forming the core of DNase I.) Because of limitations in resolution, the orientation of the nucleotide could not be determined unambiguously but, as we have discussed previously[12], this orientation may not be the same as with DNA. Precisely known from the difference density map, however, is the position of the Ca^{2+} ion bound at the active site in the presence of the nucleotide (see Fig. 1). As described below, we used the position of Ca^{2+} together with the geometry of the active site to derive the model for the DNase I-DNA interaction. The disposition of the Ca^{2+} ion, the amino-acid side chains and the water molecule at the active site is shown in Fig. 1. Note that the assignment of Q 36, which is in contact with the Ca^{2+} ion, has changed compared with our earlier paper[12], because of the insertion of a tripeptide at position 27. (Previously this residue was identified as D 39.) During refinement at 2 Å it became obvious that the chemically determined sequence[14] had to be corrected at several places, the major correction being the insertion of the tripeptide I-V-R at position 27. Remarkably strong hydrogen bonds exist between the carboxylate group of E 75 and the N-1 position of H 131 (2.6 Å) and between D 209 and H 249 (2.7 Å). These salt bridges will shift the pK_a values of the involved histidines to values about one unit higher than expected for a free histidine at the surface of a protein[15]. One of the water molecules found in the active-site region (water 390) is within hydrogen-bonding distance of the N-3 position of H 131. As discussed below, this water molecule is the most probable candidate for the attacking nucleophile in DNA hydrolysis.

Mehdi and Gerlt investigated the stereochemical course of the DNase I reaction by nuclear magnetic resonance techniques using substrates with chiral phosphorus atoms[16]. Their results show that hydrolysis by DNase I is accompanied by an inversion of configuration at the phosphorus, indicating that a single displacement has taken place during the reaction. The most straightforward explanation for such a reaction course is that the enzyme catalyses the direct nucleophilic attack of a water molecule at the phosphorus atom. A second possibility that was discussed by Mehdi and Gerlt is the formation of an acyl-phosphate intermediate with a carboxylate side chain and subsequent hydrolysis of this intermediate by nucleophilic attack of a water at the carboxyl carbon (and not the phosphorus). This reaction route also implies that there is a single displacement at the phosphorus and would therefore lead to inversion of configuration as well. But for stereochemical reasons, this type of mechanism seems unlikely because even with the most accessible candidate, D 248, the necessary close approach between the phosphate group of the DNA substrate and the carboxylate group appears to be impossible. Based on the geometry of the active site and using in particular the positions of the Ca^{2+} ion in the Ca-pTp complex and of the water molecule 390 in contact with H 131, we propose the following mechanism of action for DNase I (Fig. 2): in a general acid-base catalysis the carboxylate anion of E 75 accepts a proton from H 131, which in turn accepts a proton from the water molecule (water 390), which then, as a nucleophile, attacks the phosphorus cleaving the P—O-3′ bond. The Ca^{2+} ion correctly positions the phosphodiester bond with respect to the enzyme and also facilitates the nucleophilic attack of the water hydroxyl through its positive charge. The proton acceptor-donor chain E-H-water of DNase I is reminiscent of the 'catalytic triad' D-H-S found in serine proteases. In agreement with the proposed mechanism, carboxymethylation of H 131 at N-3 (ref. 17) as well as protonation of the histidine by lowering the pH (the pH optimum for DNase I lies between 7.5 and 8.5) inactivates the enzyme. In both cases H 131 can no longer act as a general base and accept a proton from the water molecule.

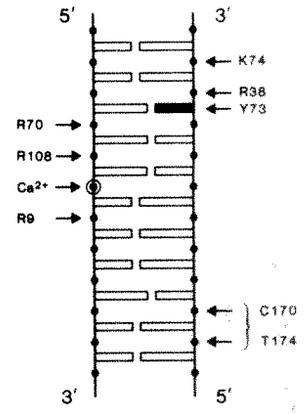


Fig. 4 Schematic drawing of DNase I-DNA interactions. The scissile phosphodiester bond (circle) is anchored by a Ca^{2+} ion to the enzyme. Adjacent phosphates on either side of the cleavage point interact with arginine side chains (R 9, R 70, R 108). Two phosphates of the other strand directly opposite across the minor groove interact with R 38 and K 74. Black rectangle, base interacting with Y 73.

Based on the geometry of the active site and using the crystallographically determined position of Ca^{2+} we have derived a model for the interaction of DNase I with double-stranded DNA in its B-form. Given the constraints imposed by the Ca^{2+} ion, the distribution of the charged residues and the van der Waals' surface of the protein around the active site, the docking was rather straightforward and immediately suggested a starting model similar to the final version shown in Fig. 3. Details of the interaction were elucidated using a colour-graphics display system and the docking program MIDAS (from the University of California at San Francisco). Only the orientations of some exposed side chains of DNase I were altered to optimize the interactions with DNA. The basic features of our model are the rather tight fit of the exposed loop R 70-N 71-S 72-Y 73-K 74 in the minor groove of B-DNA and the electrostatic interactions of phosphates from both DNA strands with positively charged side chains on either side of this loop. The DNA strand being cut is bound at the slightly concave surface between the β-sheets. The scissile phosphodiester bond is anchored to the enzyme through the Ca^{2+} ion, two neighbouring phosphates in the 5′-direction make ionic interactions with R 108 and R 70, the phosphate following in the 3′-direction interacts with R 9 (Fig. 4). Two phosphates of the other DNA strand, directly across the minor groove, are bound to K 74 and R 38. Additionally, mainly van der Waals'-type interactions involving C 170 and T 174 occur 5–6 base pairs (bp) away from the cutting site. The schematic drawing in Fig. 4 shows where the interactions occur on the DNA relative to the point of cleavage. Further ionic interactions, not included in this model, can occur between negatively charged side chains and the phosphate backbone mediated by divalent cations. Possible candidates for this kind of contact are the carboxylate groups of D 248, D 136, E 13 and E 99. The last residue is not visible in the crystal structure because it is located in the flexible loop containing the short disulphide bridge between C 98 and C 101, which, however, is not essential for enzymatic activity[18]. Therefore, it appears that any interactions involving this disordered loop are of only minor importance for DNA binding. It is the combination of these interactions—tight fit of a loop region in the minor groove, ionic interactions of phosphates from both DNA strands and van der Waals' interactions somewhat remote from the cutting site—which provides the precise alignment of the DNA-substrate on

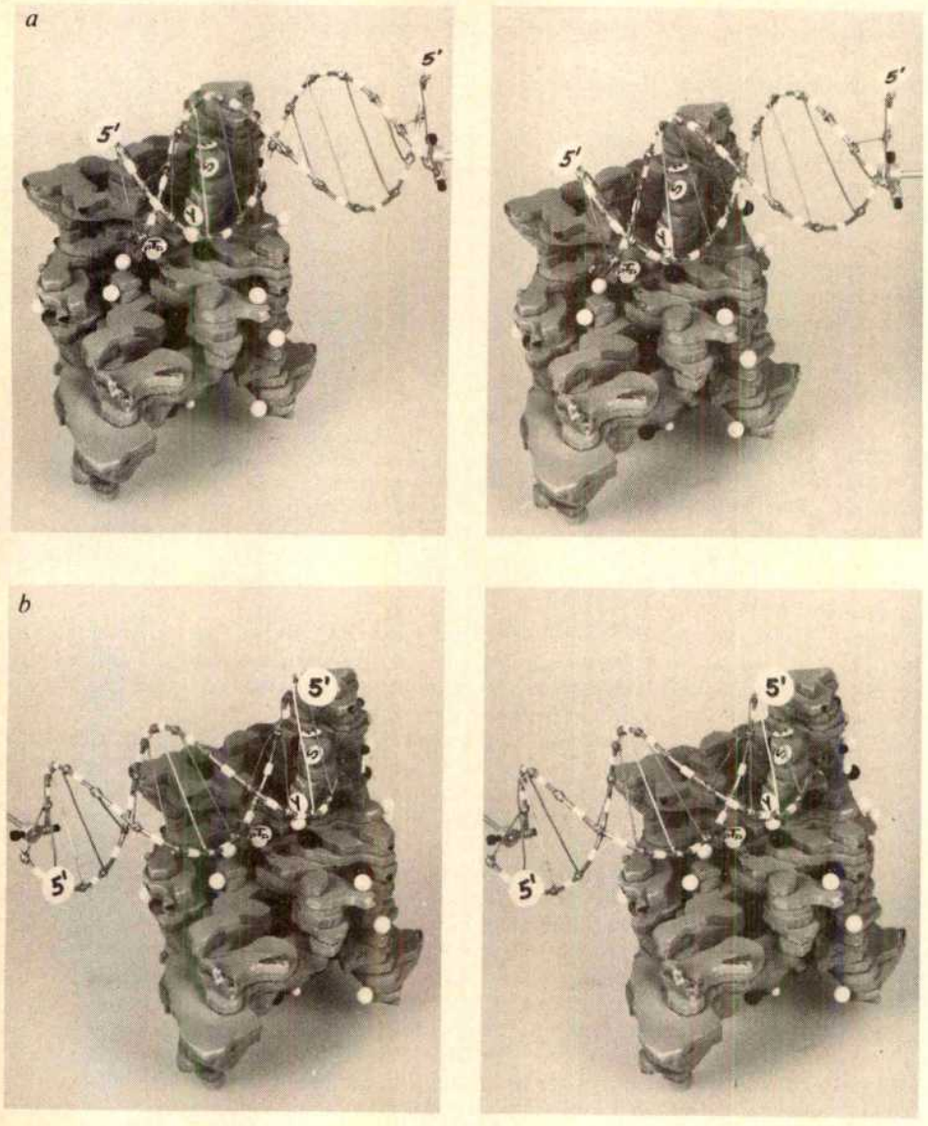


Fig. 5 DNase I cleavage at the 3′ end and near the 5′ end of DNA. Stereo view of the 5-Å balsawood model of DNase I with a piece of B-DNA at the same scale. Charged residues at the surface of DNase I are indicated by black (R, K) and white (D, E) spheres. Active site marked by pTp, residues N 71, S 72 and Y 73 in the exposed loop interacting in the minor groove of DNA are labelled. *a*, Cutting a bond at the 3′ end allows full binding in the minor groove and accurate alignment of the DNA, with R 9, R 108, R 70 interacting with phosphates on the DNA strand to the left of the exposed loop and R 38 and K 74 interacting with phosphates on the other strand. The contacts to R 38 and K 74 to the right of the exposed loop are lost when the cleavage site is 5 bonds away from the 5′ end. This feature of the model nicely explains the observation that oligonucleotides are cut near the 3′ end or the centre but not, or at very low rates, near the 5′ end.

the surface of the enzyme. Y 73, which is located in the exposed loop mentioned above, penetrates into the minor groove of DNA such that its OH-group is in hydrogen-bonding distance from either O-2 of pyrimidines or N-3 of purines. These two atoms are located in equivalent positions relative to the helix axis, so that this interaction in a first approximation will not lead to a purine/pyrimidine discrimination, in agreement with the biochemical results. However, the NH_2 group in position 2 of a G will have a steric effect which could influence the binding (see below).

As shown in Fig. 3, one of the DNA strands follows the direction of the β-sheets and residues at the N- or C-termini of the β-strands or the connecting loop regions participate in the binding or cleavage of DNA. A somewhat similar situation has been found in the *Eco*RI/DNA complex, possibly indicating a general correspondence of β-sheet structure displaying a left-handed twist with a right-handed double helix (J. Rosenberg, personal communication). Whereas the recognition of DNA is different in both cases—major groove interactions in the case of the sequence-specific restriction enzyme, minor groove interaction in the case of the unspecific or better, less-specific DNase I—the catalytic portions of the two enzymes seem to have some resemblance, reflecting the fact that both are endonucleases.

In this context it is interesting to note that DNase I, if present in high concentrations, is able to degrade single-stranded DNA at a rate about four orders of magnitude slower than double strands[1]. The smallest substrate being attacked is a tetranucleotide (NpN↓pNpN) or a trinucleotide carrying a 3′-phosphate group (NpN↓pNp), whereas a trinucleotide (NpNpN) is resistant. In good agreement with our binding model, this shows that phosphate groups on either side of the scissile bond are necessary to align the oligonucleotide on the enzyme for cutting (Fig. 4).

Various biochemical results concerning the enzymatic activity and cleavage patterns observed with DNase I can be explained in terms of our model. Evidence for the involvement of Y 73 in the binding comes from a chemical modification study[19]. The oligopeptide antibiotic netropsin, which is known from X-ray studies to bind in the minor groove at A+T-rich sequences[20], prevents DNase I cleavage at these sites. According to our model, netropsin binding in the minor groove will directly interfere with the binding of the exposed loop R 70 to K 74 of DNase I. Indirect evidence for binding of DNase I across the minor groove stems from a comparison of DNase I cleavage patterns of a hairpin loop structure with a double-stranded piece of DNA of identical sequence[21].

DNase I digestion studies of self-complementary oligonucleotides show that the enzyme cleaves near the 3′ end or the centre of a DNA strand but not, or at very low rates, near the 5′ end[3,21]. The reason for this behaviour is obvious from our model: full binding and accurate orientation of the DNA with respect to the enzyme are only possible with a complete minor groove

allowing for interactions with phosphates from both strands. The situation for binding near the 3′ and the 5′ ends of a DNA strand are illustrated in Fig. 5. In the case of 3′-end cutting, both strands of the DNA interact with the protein, whereas the contacts to R 38 and K 74 are lost when a phosphodiester bond about 4–5 bonds inwards from the 5′ end is cut. One can use this argument to exclude binding across the major groove: exactly the opposite behaviour (cutting all the way to the 5′ end and no cutting near the 3′ end) would be expected from this kind of model.

Figure 3 shows that the fit of the exposed loop R 70 to K 74 in the minor groove is rather tight and therefore the width of the helix grooves will be a critical factor for the binding. X-ray studies on short double-stranded DNA pieces indicate that the groove width can indeed vary with the sequence[22,23]. The sequence-dependent variation of the DNase I cleavage pattern and cutting frequencies can therefore be nicely explained in terms of this model by a variation of the minor groove width that directly affects the binding. Among other factors, variation of helix groove width has been discussed by Drew and Travers as a possible explanation for the DNase I cleavage pattern they observed for a 160-bp DNA fragment[4]. They found that the locally averaged probabilities of cleavage were usually higher in regions with random base sequence than in those with runs of A-T or G-C. In agreement with these digestion data, our model predicts optimal binding for a minor groove width of 12–13 Å, a value occurring in 'normal' (that is, random-sequence) B-DNA. There are, however, considerable variations in cutting frequencies of neighbouring phosphates which cannot be explained by a smoothly varying parameter like the groove width. As mentioned above, Y 73 interacts in the minor groove with N-3 or O-2 of the purine or pyrimidine base on the opposite strand, 3 bp away from the cutting site (Figs 3, 4). If there is a G-C (or C-G) pair at this position, steric hindrance between the NH_2 group in the 2-position of the guanine base and the tyrosine hydroxyl group will force the tryosine into a different orientation compared with the A-T (or T-A) case. Similarly, local changes in the helix twist angle, the base-pair propellor-twist and the roll and tilt angles will have an effect on this interaction. Therefore, it seems probable that the tyrosine interaction in the minor groove has a modulating effect on the cutting frequencies of DNase I.

Another feature of our model is the rather extended binding surface. One side of the DNA double helix is in contact with the DNase I over ~10 bp, that is, over almost a complete turn (see Figs 3, 4). For optimal binding and therefore rapid cutting of DNase I, a piece of DNA of at least this length is required. The well-known fact that the rate of cutting is a function of the length of the DNA fragment[1,3] can be explained by this feature of the model. The fact that DNase I, unlike a chemical probe, has an extended DNA binding surface has important consequences for the interpretation of DNase I footprinting studies: at least 4 bp to the 5′ side and 6 bp to the 3′ side of the cutting site are covered by DNase I on one side of the DNA double helix. In other words, DNase I cutting at a given site implies that the protein whose interaction with DNA is being probed by the footprinting experiment is interacting neither in the minor groove following in the 5′ direction nor in the major groove following in the 3′ direction. Our model nicely explains the difference observed in the size of footprints generated by DNase I and the synthetic DNA cleaving reagent methidiumpropyl-EDTA·Fe(II) (ref. 24). Knowledge of the mode of DNase I–DNA interaction will solve the problem of overestimating the size of DNA binding sites by DNase I footprinting experiments and will therefore significantly increase the accuracy of the method. Another implication of our model is that DNA segments displaying an A- or Z-type conformation will either be resistant to DNase I digestion or will be attacked only after conversion into a B-type conformation. In fact, brominated poly (dG-dC), which was shown by spectroscopic methods to exist as Z-DNA under the conditions used, was degraded to only 10% by DNase I (ref. 25). Finally, our model can be used to predict the accessibility of phosphodiester bonds by DNase I (angle of attack) in the nucleosome.

We thank Graham Frost and Harald Lahm for technical assistance, Dr Wolfgang Kabsch (MPI für medizinische Forschung, Heidelberg) for discussions and the use of his data-reduction and scaling software, Dr Heinz Bosshard and Chris Carlson (EMBL) for advice with the PS2 graphics display system and Drs Arthur Lesk (MRC, Cambridge) and Johann Deisenhofer (MPI für Biochemie, Martinsried) for molecular plotting programs.

Note added in proof: An X-ray structure analysis of a complex between DNase I and a self-complementary octanucleotide proceeding in our laboratory confirms the proposed binding of the exposed loop R 70 to K 74 in the minor groove of DNA.

Received 16 December 1985; accepted 12 March 1986.

1. Laskowski, M. *Enzymes* **4**, 289–311 (1971).
2. Bernardi, G., Ehrlich, S. D. & Thiery, J. P. *Nature new Biol.* **246**, 36–40 (1973).
3. Lomonossoff, G. P., Butler, P. J. G. & Klug, A. *J. molec. Biol.* **149**, 745–760 (1981).
4. Drew, H.R. & Travers, A. A. *Cell* **37**, 491–502 (1984).
5. Moore, S. *Enzymes* **14**, 287–296 (1981).
6. Noll, M. *Nucleic Acids Res.* **1**, 1573–1578 (1974).
7. Sollner-Webb, B. & Felsenfeld, G. *Cell* **10**, 537–547 (1977).
8. Prunell, A. *et al. Science* **204**, 855–858 (1979).
9. Klug, A. & Lutter, L. C. *Nucleic Acids Res.* **9**, 4267–4283 (1981).
10. Rhodes, D. & Klug, A. *Nature* **286**, 573–578 (1980).
11. Galas, J. D. & Schmidtz, A. *Nucleic Acids Res.* **5**, 3157–3170 (1978).
12. Suck, D., Oefner, C. & Kabsch, W. *EMBO J.* **3**, 2423–2430 (1984).
13. Liao, T. H. *J. biol. Chem.* **250**, 3721–3724 (1975).
14. Liao, T. H., Salnikow, J., Moore, S. & Stein, W. H. *J. biol. Chem.* **248**, 1489–1495 (1973).
15. Perutz, M. F., Gronenborn, A. M., Clore, G. M., Fogg, J. H. & Shih, D. T.-b. *J. molec. Biol.* **183**, 491–498 (1985).
16. Mehdi, S. & Gerlt, J. A. *Biochemistry* **23**, 4844–4852 (1984).
17. Price, P. A., Moore, S. & Stein, W. H. *J. biol. Chem.* **244**, 924–928 (1969).
18. Price, P. A., Stein, W. H. & Moore, S. *J. biol. Chem.* **244**, 929–932 (1969).
19. Hugli, T. E. & Stein, W. H. *J. biol. Chem.* **246**, 7191–7200 (1971).
20. Kopka, M. L., Yoon, C., Goodsell, D., Pjura, P. & Dickerson, R. E. *J. molec. Biol.* **183**, 553–563 (1985).
21. Drew, H. R. *J. molec. Biol.* **176**, 535–557 (1984).
22. McCall, M., Brown, T. & Kennard, O. *J. molec. Biol.* **183**, 385–396 (1985).
23. Fratini, A. V., Kopka, M. L., Drew, H. R. & Dickerson, R. E. *J. biol. Chem.* **257**, 14686–14707 (1982).
24. Van Dyke, M. M. & Dervan, P. B. *Science* **225**, 1122–1127 (1984).
25. Möller, A., Nordheim, A., Kozlowski, S. A., Patel, D. J. & Rich, A. *Biochemistry* **23**, 54–62 (1984).
26. Oefner, C. & Suck, D. (submitted).

L1 family of repetitive DNA sequences in primates may be derived from a sequence encoding a reverse transcriptase-related protein

Masahira Hattori*, Satoru Kuhara†, Osamu Takenaka‡ & Yoshiyuki Sakaki*

* Research Laboratory for Genetic Information, Kyushu University, Fukuoka 812, Japan
† Department of Agricultural Chemistry, Faculty of Agriculture, Kyushu University, Fukuoka 812, Japan
‡ Primate Institute, Kyoto University, Inuyama, Aichi Prefecture, Japan

Primate and rodent genomes contain a family of highly repetitive, long interspersed sequences, designated the L1 family or LINE-1 (refs 1–4). Characteristic features of the L1 family sequences such as an A-rich stretch at the 3′ end, a truncated 5′ end, the existence of significantly long open reading frames (ORFs)[5–9] and the presence of L1 family transcripts in various types of cells, including pluripotential embryonic cells[10–15], suggest that the L1 family is derived from a sequence encoding a protein(s) and dispersed in the genome through an RNA-mediated process. These features of the L1 family are believed to be due to reverse transcription

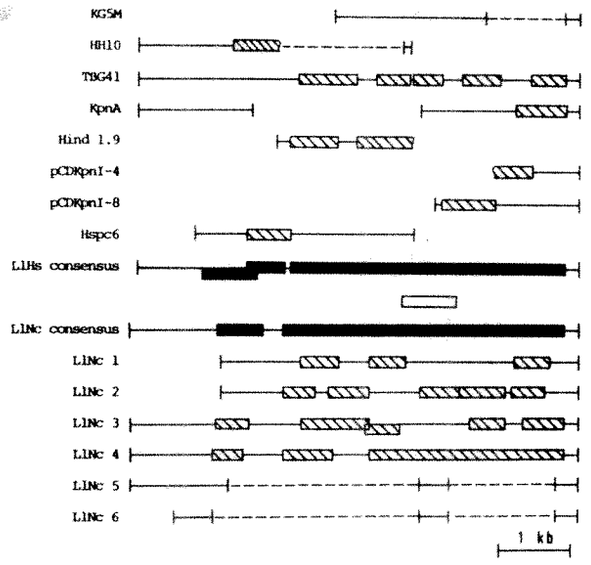


Fig. 1 Schematic representation of the structure of L1 family members and the consensus sequences. The human consensus sequence was deduced from TβG41 (ref. 9), KpnA (ref. 8), Hind1.9 (ref. 5), pCDKpnI-4 and pCDKpnI-8 (ref. 6), HH10 (ref. 25 and K. Yoshioka *et al.*, unpublished), Hspc6 (ref. 26 and K. Yoshioka *et al.*,, unpublished) and KG5M (A. Fujita *et al.*, unpublished). The *N. coucang* consensus sequence was deduced from the sequence data of six members (L1Nc1–L1Nc6) analysed here. Filled bars in the consensus sequences and hatched bars in each member show positions of ORFs over 420 base pairs. An open bar between two consensus sequences indicates the region homologous to reverse transcriptase sequences (see text). Broken lines show the region where the sequence has not been determined.

Methods. *N. coucang* DNA, prepared from liver, was partially digested with *Eco*RI, and 15–20-kilobase (kb) fragments were ligated to *Eco*RI-digested arms of bacteriophage vector Charon 4A. After *in vitro* packaging, the recombinant phages were propagated in *Escherichia coli* LE392. The phage library was screened with ^{32}P-labelled fragments of a human L1 family, TβG41 (refs 9, 27). Positive phage clones were further analysed by the Southern blotting technique[28] and selected DNA fragments subcloned into pUC13 or pUC18 (refs 29, 30). Cloned DNA was subjected to sequence determination by the method of Hattori and Sakaki[31].

beginning at the 3′ end of the L1 transcript and terminating prematurely and to the site duplication caused by the insertion of the complementary DNA (reviewed in refs 3, 4). It is likely that this type of transcript is converted to cDNA and inserted into the chromosome through a process similar to that of the formation of processed pseudogenes[16]. The above model, however, does not necessarily explain why the L1 family should produce the extraordinarily large number of copies (more than 10^4 per haploid genome[17]) seen during evolution. It seems likely that the progenitor of the L1 family itself carries (or carried) a function which promotes the active dispersion of the L1 family sequence. We reasoned that such a function, if present, must be conserved during evolution and may be shown by comparative analysis of L1 family sequences from evolutionarily distant species. We show here that the L1 family sequence contains an ORF possessing significant sequence homology to several RNA-dependent DNA polymerases of viral and transposable element origins. This provides a plausible explanation for the preferential and active dispersion of the L1 family sequence during evolution.

For a comparative analysis, we chose the human and prosimian, which diverged from each other about 70 million years ago. Six 'full-length' or nearly 'full-length' L1 family members were isolated from a genomic DNA library of slow loris (*Nycticebus coucang*) and their complete (L1Nc1–L1Nc4) or partial (L1Nc5, L1Nc6) nucleotide sequences determined. These members showed a homology of 90% or more among each other



Fig. 2 Amino-acid sequences of large ORFs found in human (L1Hs, upper) and prosimian (L1Nc, lower) consensus L1 family sequences. The amino-acid sequences were deduced from the consensus nucleotide sequences and aligned by the program of Wilbur and Lipman[32] in the GENAS system[33] to achieve maximum homology. Colons indicate amino acids identical in both sequences. Only the region homologous between the two sequences is presented. The numbers shown alongside each sequence correspond to those given for the large ORFs. The homology is 65% at the amino-acid sequence level and 71% at the nucleotide sequence level. Underlining indicates amino-acid sequences homologous to reverse transcriptases.

and a very large ORF of 927 amino-acid residues was found in L1Nc4 (Fig. 1). All the large ORFs in other members were found to use the same reading frame as the very large ORF of L1Nc4, and overlapped each other (Fig. 1). From these sequence data, a consensus nucleotide sequence for the prosimian L1 family was deduced and found to be capable of encoding a very large ORF of 1,294 amino acids. Similarly, a consensus sequence of the human L1 family was deduced from family members (the consensus sequences of human and prosimian are available on request). Just as in the case of prosimian, a very large ORF (1,280 amino acids) was identified at a position similar to that of the prosimian ORF (Fig. 1). Figure 2 shows the two ORFs of the consensus sequences. Human and prosimian large ORFs showed a homology of about 65%, and these ORFs, a large ORF in a mouse L1 family member (L1Md4)[7,18] and a partial consensus ORF of rat L1 family[19], were found to be using the same reading frame. Our results provide additional support for the idea that the L1 family is derived from a sequence(s) encoding a protein(s)[7] and, moreover, suggest that the protein is a relatively large polypeptide which is evolutionarily conserved.

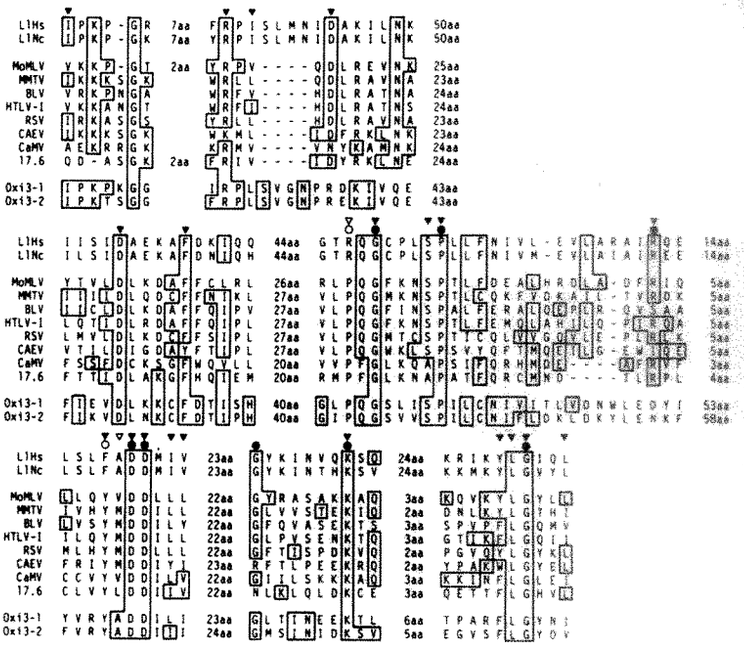


Fig. 3 Homology of amino-acid sequences between L1 consensus ORFs and RNA-dependent DNA polymerases of various origins. The amino-acid sequences were taken from Moloney murine leukaemia virus (MoMLV)[34], murine mammary tumour virus (MMTV)[35], bovine leukaemia virus (BLV)[36], human T-lymphotropic virus type I (HTLV-I)[37], Rous sarcoma virus (RSV)[38], caprine arthritis-encephalitis virus (CAEV)[35], cauliflower mosaic virus (CaMV)[22,39], 17.6 (ref. 40) and the mitochondrial class II introns Oxi 3-1 and Oxi 3-2 (ref. 41). Seven homologous sequence blocks shown by underlining in Fig. 2 are presented here. Amino acids that are common to at least five polymerase sequences and either of the L1 consensus ORFs, and amino acids in polymerase sequences identical to those of either of the L1 consensus ORFs are boxed. Ten invariant amino-acid residues[21] are indicated by circles; the residues conserved in L1 ORFs are shown by filled circles. The 27 identical and chemically similar amino-acid residues reported by Toh *et al.*[22] are indicated by triangles; among these, the residues conserved in L1 ORFs are shown by filled triangles (5 out of 27 amino-acid residues are not included in the region shown here). Using the mutation matrix of Schwartz and Dayhoff[42], the significance of each homologous sequence block was estimated using a computer algorithm[43]. The statistical test showed that the homologies of most of the sequence blocks between L1 ORFs and yeast intron-encoded ORFs are significant with a probability of $\leq 1.3 \times 10^{-3}$ ($>3\sigma$).

To investigate the protein encoded by the progenitor of L1, we searched the Protein Sequence Database of the National Biochemical Research Foundation for amino-acid sequences homologous to ORFs in the human L1 family sequence TβG41; a relatively high homology was found between TβG41 ORF and transferrins[9]. Using the same approach, significant homology was also found between consensus ORFs and some retroviral reverse transcriptases. Alignment of the amino-acid sequences of RNA-dependent DNA polymerases of various origins was then carried out together with those of L1 family ORFs. As shown in Fig. 3, the L1 family ORF is evidently homologous to RNA-dependent DNA polymerases, particularly to that of yeast mitochondrial class II introns (Oxi3-1 and Oxi3-2), which show a high sequence homology to RNA-dependent DNA polymerases[20]. Out of 102 amino-acid residues, 37 were identical between the consensus ORFs and Oxi3-1. Toh *et al.*[21] found 10 invariant amino acids in 5 viral RNA-dependent DNA polymerases, and we found that 8 of these were conserved in human and prosimian consensus ORFs (Fig. 3, filled circles). Toh and his colleagues[22] also noted 27 positions at which identical or chemically similar amino acids occurred in 8 RNA-dependent DNA polymerases. At 20 of the 27 positions, the consensus ORFs were found to possess amino acids common to the polymerases (Fig. 3, filled triangles). A highly conserved sequence, YXDD (one-letter notation), flanked by three hydrophobic residues was described by Toh *et al.*[21,22]. Although L1 consensus ORFs use F (phenylalanine) instead of Y (tyrosine) in the sequence, the RNA-dependent DNA polymerase of the yeast Ty transposable element[23,24] also uses F instead of Y, and the sequence LFADDMI of L1 consensus ORFs is very similar to the sequence LFVDDMI of Ty polymerase. Thus, the L1 consensus ORF shows significant homology to known RNA-dependent DNA polymerases. It is probable that the protein potentially encoded by the L1 family or its progenitor is closely related to reverse transcriptases. If the protein is actually a reverse transcriptase, it is conceivable that the enzyme binds to its own messenger RNA immediately after translation to start cDNA synthesis. This is consistent with a preferential and active dispersion model for L1 family sequences. It will be of interest to test whether a protein carrying the amino-acid sequence of the consensus ORF actually possesses reverse transcriptase activity.

We thank Dr Frederick I. Tsuji for a critical reading of the manuscript, H. Hamada for help in its preparation, K. Yoshioka and A. Fujita in our laboratory for unpublished data and Dr K. Saigo for critical comments. This work was supported by grants from the Ministry of Education, Science and Culture of Japan to Y.S.

Note added in proof: After submission of this paper, we found a report[44] pointing out the homology between the ORF of the mouse L1 family and the reverse transcriptases of retroviruses; the results of that study were consistent with ours.

Received 10 March; accepted 4 April 1986.

1. Adams, J. W., Kaufman, R. E., Kretschmer, P. J., Harrison, M. & Nienhuis, A. W. *Nucleic Acids Res.* **8**, 6113-6128 (1980).
2. Brown, S. D. M. & Dover, G. *J. molec. Biol.* **150**, 441-466 (1981).
3. Singer, M. F. *Cell* **28**, 433-434 (1982).
4. Singer, M. F. & Skowronski, J. *Trends biochem. Sci.* **10**, 119-121 (1985).
5. Manuelidis, L. *Nucleic Acids Res.* **10**, 3211-3219 (1982).
6. DiGiovanni, L., Haynes, S. R., Misra, R. & Jelinek, W. R. *Proc. natn. Acad. Sci. U.S.A.* **80**, 6533-6537 (1983).
7. Martin, S. L. *et al. Proc. natn. Acad. Sci. U.S.A.* **81**, 2308-2312 (1984).
8. Potter, S. S. *Proc. natn. Acad. Sci. U.S.A.* **81**, 1012-1016 (1984).
9. Hattori, M., Hidaka, S. & Sakaki, Y. *Nucleic Acids Res.* **13**, 7813-7827 (1985).
10. Kole, L. B., Haynes, S. R. & Jelinek, W. R. *J. molec. Biol.* **165**, 257-286 (1983).
11. Shafit-Zagardo, B., Brown, F. L., Zarodny, P. & Maio, J. J. *Nature* **304**, 277-280 (1983).
12. Lerman, M. I., Thayer, R. E. & Singer, M. F. *Proc. natn. Acad. Sci. U.S.A.* **80**, 3966-3970 (1983).
13. Schmeckpeper, B. J., Scott, A. F. & Smith, K. D. *J. biol. Chem.* **259**, 1218-1225 (1984).
14. Sun, L., Paulson, K. E., Schmid, C. W., Kadyk, L. & Leinwand, L. *Nucleic Acids Res.* **12**, 2669-2690 (1984).
15. Skowronski, J. & Singber, M. F. *Proc. natn. Acad. Sci. U.S.A.* **82**, 6050-6054 (1985).
16. Sharp, P. A. *Nature* **301**, 471-472 (1983).
17. Grimald, G., Skowronski, J. & Singer, M. F. *EMBO J.* **3**, 1753-1759 (1984).
18. Voliva, C. F., Martin, S. L., Hutchison, C. A. III & Edgell, M. H. *J. molec. Biol.* **278**, 795-813 (1984).
19. Soares, M. B., Schon, E. & Efstratiadis, A. *J. molec. Evol.* **22**, 117-133 (1985).
20. Michel, F. & Lang, B. F. *Nature* **316**, 641-643 (1985).
21. Toh, H., Hayashida, H. & Miyata, T. *Nature* **305**, 827-829 (1983).
22. Toh, H. *et al. EMBO J.* **4**, 1267-1272 (1985).
23. Hauber, J., N.-Hochstetter, P. & Feldmann, H. *Nucleic Acids Res.* **13**, 2745-2758 (1985).
24. Clare, J. & Farabaugh, P. *Proc. natn. Acad. Sci. U.S.A.* **82**, 2829-2833 (1985).
25. Miyake, T., Migita, K. & Sakaki, Y. *Nucleic Acids Res.* **11**, 6837-6846 (1983).
26. Kunisada, T. & Yamagishi, H. *Gene* **31**, 213-223 (1984).
27. Shafit-Zagardo, B., Brown, F. L., Maio, J. J. & Adams, J. W. *Gene* **20**, 397-407 (1982).
28. Southern, E. M. *J. molec. Biol.* **98**, 503-517 (1975).
29. Vieira, J. & Messing, J. *Gene* **19**, 259-268 (1982).
30. Yanisch-Perron, C., Vieira, J. & Messing, J. *Gene* **33**, 103-119 (1985).
31. Hattori, M. & Sakaki, Y. *Analyt. Biochem.* **152**, 232-238 (1986).
32. Wilbur, W. J. & Lipman, D. J. *Proc. natn. Acad. Sci. U.S.A.* **80**, 726-730 (1983).
33. Kuhara, S. *et al. Nucleic Acids Res.* **12**, 89-99 (1984).
34. Shinnick, T. M., Lerner, R. A. & Sutcliffe, J. G. *Nature* **293**, 543-548 (1981).
35. Chiu, I.-M. *et al. Nature* **317**, 366-368 (1985).
36. Sagata, N. *et al. Proc. natn. Acad. Sci. U.S.A.* **82**, 677-681 (1985).

37. Seiki, M., Hattori, S., Hirayama, Y. & Yoshida, M. *Proc. natn. Acad. Sci. U.S.A.* **80**, 3618–3622 (1983).
38. Schwartz, D., Tizard, R. & Gilbert, W. *Cell* **32**, 853–869 (1983).
39. Gardner, R. C. *et al. Nucleic Acids Res.* **9**, 2871–2888 (1981).
40. Saigo, K. *et al. Nature* **312**, 659–661 (1984).
41. Bonitz, S. G. *et al. J. biol. Chem.* **255**, 11927–11941 (1980).
42. Schwartz, R. M. & Dayhoff, M. O. in *Atlas of Protein Sequence and Structure* Vol. 5 (ed. Dayhoff, M. O.) 353–358 (National Biomedical Research Foundation, Washington, DC, 1972).
43. Barker, W.-C. & Dayhoff, M. O. in *Atlas of Protein Sequence and Structure* Vol. 5 (ed. Dayhoff, M. O.) 101–110 (National Biomedical Research Foundation, Washington, DC, 1972).
44. Loeb, D. D. *et al. Molec. cell. Biol.* **6**, 168–182 (1986).

MATTERS ARISING

Physiological relevance of erythroid-potentiating activity or TIMP

WE note the unusual story unfolding in *Nature* concerning the molecular biology of a glycoprotein that acts as a tissue inhibitor of metalloproteinases (TIMP) and has erythroid-potentiating activity (EPA)[1,2]. While the occurrence of two such disparate activities within one molecule would be interesting, the physiological relevance of these data should evoke some caution.

TIMP is a well described entity capable of blocking the action of vertebrate collagenases as well as numerous other neutral metalloproteinases, that is, gelatinases, proteoglycanases and type-specific collagenases. This inhibitor forms a tight ($K_i < 10^{-9}$) enzyme/inhibitor complex and appears to serve as a general tissue anti-proteinase[3]. TIMP is almost ubiquitous in human tissues. Connective tissue fibroblasts of multiple origins synthesize this product[4,5] as do several cell types of haematopoietic origin including alveolar macrophages, HL-60 and platelets[6–8].

In vivo plasma concentrations of TIMP are on the order of 17 nM with a fairly narrow (~25%) standard deviation[5]. TIMP concentrations in amniotic fluid are even higher, averaging 68–102 nM. It is unlikely that the concentrations of this glycoprotein in tissue and bone marrow are significantly different; and these levels are at least 1,000-fold higher than the maximally stimulating concentrations of EPA (10–20 pM)[9]. Although it may be the case that *in vivo* conditions require significantly higher EPA concentrations than the *in vitro* assays, these data suggest that the marrow is saturated with respect to the activity of this modulator.

Thus, the dual role of TIMP/EPA appears incongruous in several respects. This glycoprotein is almost ubiquitous in human tissues and seems to be a common housekeeping product of numerous cell types, perhaps in keeping with its role as a protective agent of the extracellular matrix. While purified EPA demonstrates maximal activity at biologically anticipated concentrations, these are far exceeded by ambient levels of the glycoprotein. It may well be that the erythroid-potentiating activity of TIMP represents a coincidental property of this molecule. Alternatively, it might be best to re-examine the properties of this glycoprotein using both purified natural products and a purified recombinant-derived protein.

GEORGE P. STRICKLIN
Department of Medicine,
Veterans Administration,
Medical Center,
and University of Tennessee, Memphis,
1030 Jefferson Avenue,
Memphis, Tennessee 38104, USA
HOWARD G. WELGUS
Department of Medicine,
Jewish Hospital of St Louis at
Washington University Medical Center,
216 S. Kingshighway,
St Louis, Missouri 63110, USA

1. Docherty, A. J. P. *et al. Nature* **318**, 66–69 (1985).
2. Gasson, J. C. *et al. Nature* **315**, 768–771 (1985).
3. Welgus, H. G. *et al. Collagen Rel. Res.* **5**, 167–179 (1985).
4. Stricklin, G. P. & Welgus, H. G. *J. biol. Chem.* **258**, 12252–12258 (1983).
5. Welgus, H. G. & Stricklin, G. P. *J. biol. Chem.* **258**, 12259–12264 (1983).
6. Welgus, H. G. *et al. J. clin. Invest.* **76**, 219–224 (1985).
7. Bar-Shavit, Z. *et al. Proc. natn. Acad. Sci. U.S.A.* **82**, 5380–5384 (1985).
8. Cooper, T. W. *et al. Proc. natn. Acad. Sci. U.S.A.* **82**, 2779–2783 (1985).
9. Westbrook, C. A. *et al. J. biol. Chem.* **259**, 9992–9996 (1984).

GASSON AND GOLDE REPLY—The description of a single glycoprotein with both protease inhibitor and erythroid-potentiating activity is indeed intriguing. Erythroid-potentiating activity was originally purified using a sensitive bioassay which measures the enhanced growth of normal human erythroid progenitors in semi-solid medium[1]. The purified 28,000-dalton protein was subsequently sequenced, and oligonucleotide probes were generated and used to obtain complementary DNA clones[2]. Both the purified natural and biosynthetic (recombinant) proteins stimulate the growth of primitive and more mature erythroid precursors *in vitro*. In addition, the partially purified EPA and the purified biosynthetic material have direct effects on colony formation by human cell lines[3,4]. The availability of human cell lines as homogeneous target cells has made it possible to pursue the mechanism of action of human erythroid-potentiating activity. Our recent studies using radioiodinated human EPA have demonstrated the presence of specific cell surface receptors on responsive cell lines, but not on other types of primary human cells or cell lines (unpublished observation). It seems that EPA has many of the properties of a haematopoietic growth factor, in that it stimulates primary cells, responsive cell lines, and appears to bind to a specific cell surface receptor which could mediate these biological responses. We doubt whether hormonal potentiation of cellular growth observable at picomolar concentrations on target cells with specific binding sites could be considered "coincidental".

The role of the EPA *in vivo* is, of course, a difficult question to address. Using the cDNA clone as a probe, as well as a sensitive radioimmunoassay to look for the synthesis of EPA messenger RNA and protein, we had arrived at similar conclusions to those reported for TIMP. In other words, EPA appears to be synthesized in many cell types; this is not necessarily unusual for haematopoietic growth factors (for example, colony-stimulating factor, CSF-1 or M-CSF, is produced by most, if not all, tissues examined in the mouse). Our estimate of the circulating EPA concentration in human serum was somewhat lower than 17 nM more in the range of 5–10 nM, although these levels are also high relative to the concentration of EPA required for a maximum growth-promoting effect *in vitro*. As we do not know the site of EPA action *in vivo* nor, as pointed out, do we know the actual concentration required for biological activity *in vivo*, it is hard to interpret these findings in a physiological framework.

Because of the availability of cell culture techniques, it has been possible to purify this erythroid growth factor. Molecular biological approaches have allowed us to produce sufficient material to investigate the effects on responsive target cells at the molecular level *in vitro* and at the organismic level *in vivo*. Ultimately it should be possible to reconcile the enzymatic inhibitory effects and the growth-promoting properties of the molecule. We feel it would be unwise at this point to regard the hormonal properties of this molecule as 'coincidental' or trivial.

JUDITH C. GASSON
DAVID W. GOLDE
Division of Hematology-Oncology,
Department of Medicine,
UCLA School of Medicine,
Los Angeles, California 90024, USA

1. Westbrook, C. A., Gasson, J. C., Gerber, S. E., Selsted, M. E. & Golde, D. W. *J. biol. Chem.* **259**, 9992–9996 (1984).
2. Gasson, J. C. *et al. Nature* **315**, 768–771 (1985).
3. Gauwerky, C., Lusis, A. J. & Golde, D. W. *Blood* **59**, 300–305 (1982).
4. Avalos, B. R., Golde, D. W., Gasson, J. C. & Clark, S. C. in *Recombinant Lymphokines and Their Receptors* (ed. Gillis, S.) (Marcel Dekker, New York, in the press).

CONVENIE..T·INFORMATIVE·TIMELY·PROVOCATIVE

FOUR DYNAMITE REASONS WHY YOU SHOULD SUBSCRIBE TO BIO/TECHNOLOGY NOW . . .

1. You'll save time. Because you don't have time to read every journal in the field, BIO/TECHNOLOGY is written and edited to give you all the information you need in ONE convenient source. BIO/TECHNOLOGY is the only journal to give you news. Features. Original research. Product evaluations. Industrial applications. Job openings. Book and product reviews. And more. If it's important to your work, you'll find it between the covers of BIO/TECHNOLOGY.

2. You'll learn new ways to improve your on-the-job skills and run a more successful operation. Each month BIO/TECHNOLOGY gives you the scoop on invaluable start-up information . . . the latest instrumentation . . . marketing breakthroughs . . . funding sources . . . new technologies . . . patents and licences. . . profiles on how others are avoiding the pitfalls and reaping the rewards. In fact, just one practical tip from BIO/TECHNOLOGY can be worth many times the cost of your subscription.



3. You'll be up-to-date on all major industry developments. With correspondents all over the world, BIO/TECHNOLOGY delivers the inside story on who's doing what, where. You'll get the latest word on changing government regulations and tax law, and how they affect your work.

Plus you'll read original research papers by bench scientists, engineers, and biologists that will help keep you in the forefront of every new discovery worth knowing about.

4. You'll get new ideas you can put to use immediately. BIO/TECHNOLOGY lets you rub elbows with eminent scientists, tour new facilities and learn how new processes work in every field from genetic engineering to molecular biology. Each month, BIO/TECHNOLOGY helps spark ideas for your own research, for new industrial applications and for getting along in the increasingly competitive financial arena.

If you're not already subscribing to BIO/TECHNOLOGY, don't delay the moment any longer - return the coupon below and we will send you twelve issues. You risk nothing. If for any reason BIO/TECHNOLOGY doesn't live up to your highest expectations, just let us know and you'll receive a full refund on all unmailed copies. Remember too, that your subscription may be tax deductible.

TO START RECEIVING YOUR SUBSCRIPTION, FILL OUT THE COUPON BELOW AND RETURN WITH PAYMENT TO:

U.S.A.: BIO/TECHNOLOGY
Subscription Order Dept., P.O. Box 1543
Neptune, New Jersey 07754-1543 U.S.A.

To speed up your subscription in the U.S.A., call toll free 1-800-524-0328.

ENGLAND: BIO/TECHNOLOGY
Subscription Order Dept., Macmillan Journals, Ltd.
Brunel Road, Houndmills, Basingstoke
Hampshire RG21 2XS, England

☐ YES! Please send me one year of BIO/TECHNOLOGY (12 issues). I understand that I may cancel my subscription at any time and receive a full refund on all unmailed issues.

☐ U.S.A.-$59.00* ☐ Australia-A$130**
☐ U.K.-£70** ☐ Elsewhere-U.S.$112**

Japan Publications Trading Company Ltd
2-1 Sarugaku-cho 1-chome
Chiyoda-ku, Tokyo, Japan Tel: (03) 292 3755

Note: *Represents 24% off Basic Subscription Price of U.S. $78.00
**All other prices quoted are "Air Speed"

☐ My payment is enclosed at the price checked.
☐ Please charge my credit card account:
☐ American Express ☐ Mastercard ☐ Visa

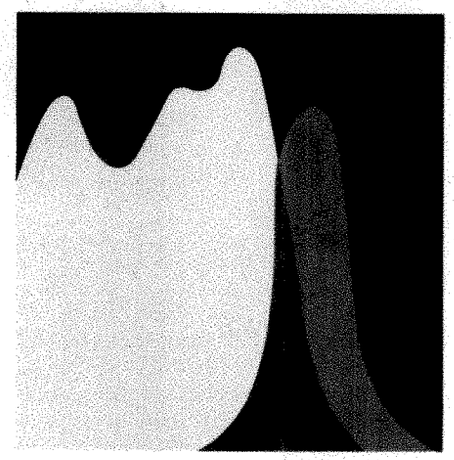
Card No.: _____ Exp. Date: _____
Signature: _____
Name: _____
Company: _____
Address: _____
City/State/Postal Code: _____
Country: _____

7AUS

INTRODUCING

serotec QB·AR

integrated analytical grade reagent conjugates



The QB-AR range meets a variety of assay needs and offers significant practical benefits to the user. The range includes:

Streptavidin conjugates

Streptavidin has significant advantages over Avidin for detection of biotin labelled antibodies – principally that it causes negligible background binding. Biotin should preferably be coupled via a flexible linker arm to minimise reduction of affinity due to steric hindrance.

R-Phycoerythrin* conjugates

R-Phycoerythrin has a strong excitation maximum at the same wavelength as fluorescein; it emits in the orange/red while fluorescein emits in the yellow/green, so two-colour fluorescence is easily accomplished. R-Phycoerythrin is very stable and shows negligible non-specific binding.

Rabbit F(ab')2 anti-rodent antibodies

Rabbit antisera are characterised by high titre and very avid, specific antibodies. Purification of IgG and digestion to F(ab')2 fragments eliminates non-specific binding, and purification of the fragments results in high concentration of antibody seeing multiple determinants on first-stage antibody molecules. This gives a much brighter signal than monoclonal anti-Ig reagents which see only single determinants.

* United States Patent Number 4542104

serotec

serving science

For full details of the Serotec QB-AR range, contact

Serotec Ltd, Station Road, Blackthorn, Bicester, Oxon OX6 0TP England
Telephone: (0869) 243241
Telex: 83683 OLACUK G

Reader Service No.2

JANSSEN BIOCHIMICA

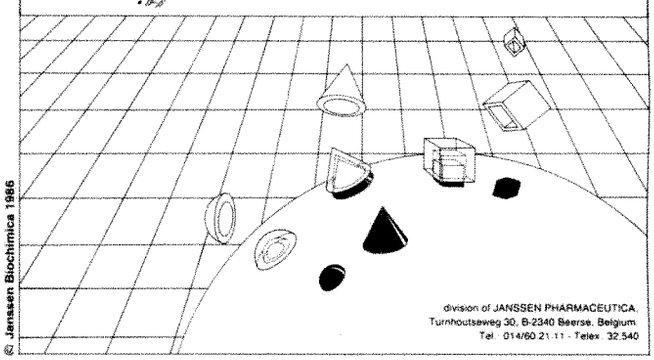
I...mune reagents

- Anti-human proteins including immunoglobulins subclasses
- Anti-ds DNA kits size: large, medium, small
- Immunoglobulins allotype determination
  a) anti G1m (z),(a),(x), (f) G2m (n) G3m (g), (b0), (b1), (b3), (b), (c), (c3), (c5) Km (1), (3)
  b) anti-D for G1m (f) G1m (f) and Km (1) G1m (x), (za) G3m (b), (c3c5), (g), (s) Km (3)

Immunological research:
- Interleukin 2 (recombinant and human source)
- Monoclonal antibodies to
  - IL-2 receptor
  - Transferrin receptor

New:
- H.G.F. (Hybridoma Growth Factor)
- Interleukin 1 (human)
- Interferon α, β and γ
- Monoclonal Antibodies:
  - T-cell antigens
  - IF-β

Special:
- TTX (tetrodoxin)
- TTX-^{3}H-Lysine

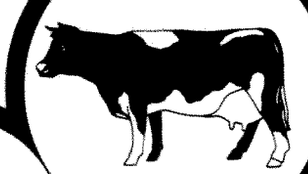


© Janssen Biochimica 1986

division of JANSSEN PHARMACEUTICA
Turnhoutseweg 30, B-2340 Beerse, Belgium
Tel. 014/60.21.11 - Telex 32.540

Reader Service No.33

A complete range of sera, media and reagents for cell culture





Components	F-10 mg L	F-12 mg L
Amino Acids		
L-Alanine	8.91	8.91
L-Arginine HCl	211.00	210.70
L-Asparagine H_2O	15.01	15.01
L-Aspartic Acid	13.30	13.31
L-Cysteine $HCl.H_2O$	35.12	35.12
L-Glutamic Acid	14.70	14.71
L-Glutamine	146.20	146.20
Glycine	7.51	7.51
L-Histidine $HCl.H_2O$	23.00	20.96
L-Isoleucine	2.60	3.94
L-Leucine	13.10	13.1
[illegible]sine HCl	29.30	[illegible]
[illegible]onine	4.48	[illegible]



Sera–Media
Insect media
Plant media

Imperial laboratories

Ashley Road, Salisbury SP2 7DD Telephone 0722 332228

Reader Service No.6

Growth factors spawn new cell cultures

from W.L. McKeehan

Heparin-affinity chromatography allows the isolation and chemical definition of a family of hormone-like polypeptide growth factors that support several important cell types in defined culture conditions.

IMPROVED nutrient media formulas[1] and the discovery that crude serum can be replaced in large part by defined polypeptides[2] have revolutionized regulatory cell biology and opened up subdisciplines of study using isolated cells in culture that can be called cellular nutrition[3] and cellular endocrinology. The commercial availability of high quality chemically-defined preparations of polypeptide growth factors (Table 1)[4] has played a part in the revolution. Despite this progress, many tissue-specific normal cell types and tumour-derived counterparts have resisted routine culture except in the presence of undefined biological fluids, tissue extracts or the medium from cultured cells.

Cultures of tissue-specific cell types are of keen interest as model systems for studying specific organs and their diseases. Fibroblast cells, which arise from many tissues placed in culture, have remarkably similar properties and are unsuitable for such studies. Likewise, the many tumour-derived cell lines that have been adapted to serum-free medium retain few characteristics of the tissues of origin beyond fixed expression of one or more gene products.

Neural tissue extracts

Crude or partially purified extract of neural tissue makes a beneficial additive to many tissue-specific cell cultures, including cell types such as endothelial cells[5], smooth muscle cells[6], keratinocytes[7,8], melanocytes[9], prostate epithelial cells[10,11], breast epithelial cells[12], tracheobronchial epithelial cells[13], intestinal epithelial cells[14] and hepatocytes (H. Hoshi, M. Kan & W.L. McK., unpublished results). To determine whether these cell types are responding to related or different polypeptides, the active species must be isolated to homogeneity and carefully analysed for chemical structure. But isolating these hormone-like factors in quantities sufficient for chemical analysis, which uses cell growth assays, is no light task since the factors are at low concentrations in most tissues and fluids.

Table 1 Commercially available growth factors

Factor	Target cells
EGF, α-TGF	Epithelial/ mesenchymal
PDGF	Mesenchymal
β-TGF	Epithelial/ mesenchymal
Insulin, IGF-I, IGF-II	Epithelial/ mesenchymal
β-NGF	Neurones
IL-2	T-lymphocytes
IL-3	Haematopoietic

Characteristics of these defined polypeptides were recently reviewed[4]. EGF (epidermal growth factor) and α-TGF (α transforming growth factor) act on the same receptor. PDGF, platelet-derived growth factor. β-TGF (β transforming growth factor) is both an inhibitor and growth factor. Insulin and IGFs (insulin-like growth factors) have separate receptors, but act on both at high concentrations. β-NGF, β nerve growth factor. IL = interleukin.

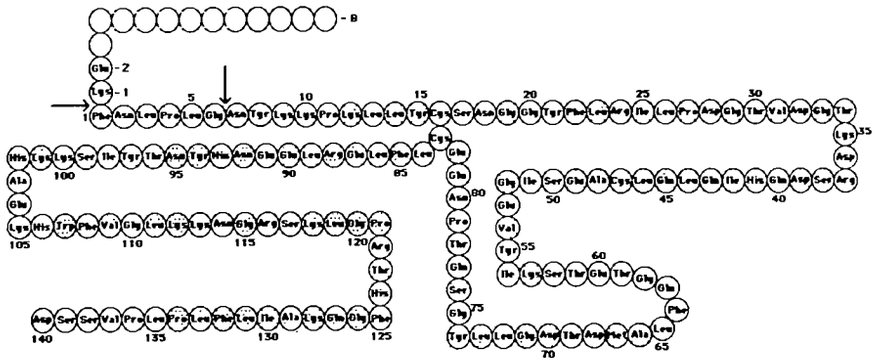


Fig. 1 Primary structure of prostatropin (acidic FGF, acidic ECGF) and homology to basic *p*I heparin-binding growth factor (bFGF). Amino acid residues 1 to 140 are those reported[19] for a truncated form of acidic FGF (M_r = 15,883). Open circles indicate unpublished residues of the 14-amino acid peptide with blocked amino terminus (B)[20,21]. The lysine (residue −1) has been assigned by V8 protease cleavage and the glutamate (residue −2) is inferred from specificity of V8 protease cleavage[20]. Placement of the disulphide bond is tentative, but is present in at least one chromatographic form of prostatropin based on unpublished data from the author's laboratory. Shaded amino acid residues indicate homologies with bFGF[18]. Arrows indicate cleavage points that yield truncated molecular forms of the growth factor.

Purified factors

Heparin-binding growth factors constitute a family of homologous polypeptides in the molecular weight range of 15,000 to 18,000 daltons. The molecular forms fall into two classes based on isoelectric point (*p*I) and amino acid sequence. One class of factor has an apparent *p*I of 8 to 10, and the other, a *p*I of 4.5 to 5.5. The largest sequenced species of the cationic factor contains 146 amino acid residues (M_r = 16,415)[18], and a truncated form, missing amino terminal amino acids 1 to 15, has also been reported.

Three molecular forms of the acidic class of factor have been described in more detail (Fig. 1). One truncated form, consisting of 140 amino acids (M_r = 15,883) and an amino terminal phenylalanine, has been completely sequenced[19]. We have isolated two other forms that are distributed among five chromatographic peaks on reverse phase HPLC. Of these, one form is missing the first six amino terminal amino acids due to cleavage between a glycine-asparagine bond. However, the other, predominant form of the acidic growth factor is longer than the longest truncated form by a 14-amino acid peptide. This predominant form, which can be isolated if proper precautions are taken to limit proteinase activities, has a blocked amino terminus and a molecular weight of 17,400[20,21].

Mitogenic effects

Both the cationic and acidic families of heparin-binding growth factors are potent mitogens for the ubiquitous cultured fibroblasts; hence, their designation as fibroblast growth factors (FGFs)[16,17]. However, these factors have had their largest impact as ECGFs, or endothelial cell growth factors. These factors have angio-

genic activity *in vivo* and are a requirement, in serum or serum-free culture, of cells from a variety of vascular tissues.

Surprisingly, the acidic form of the heparin-binding polypeptides also accounts for the neural extract requirement of normal and tumour rat and human prostate epithelial cell proliferation[10,11,20-22]. All three forms of the acidic factor, called prostatropin in this role, supported half-maximal proliferation rates for normal and tumour prostate epithelial cells at concentrations of 50 and 7 pM, respectively, in chemically-defined medium[20,22]. These findings place at least one epithelial cell type in the target cell spectrum for the heparin-binding family of growth factors.

In summary, this growth factor family enables cell biologists to culture new cell types in defined medium. Until recombinant technologies for factor production are developed, heparin-affinity chromatography can provide purified factors from bovine brain or other tissues in quantities sufficient for commercial distribution. The complete spectrum of target cell types whose maintenance is dependent on these growth factors has not been established. The current spectrum, however, includes both cell types of the human vascular system which are central to understanding heart disease, atherosclerosis and abnormal angiogenesis, and one epithelial cell type important for studying prostate hyperplasia and adenocarcinoma. □

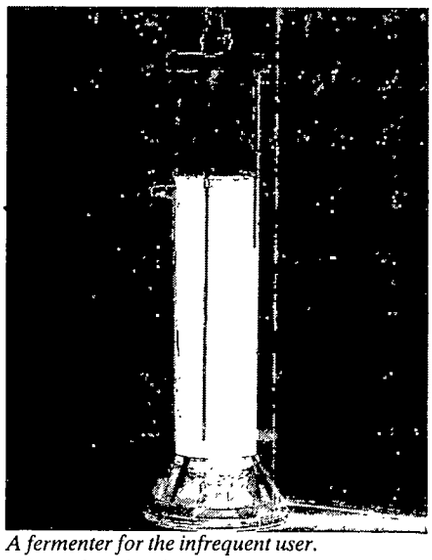
Wallace L. McKeehan is at the W. Alton Jones Cell Science Center, Inc. and president of Upstate Biotechnology, Inc., Lake Placid, New York 12946, USA.

1. Ham, R.G. & McKeehan, W.L. *Meth. Enzym.* **59**, 44–93 (1979).
2. Barnes, D.B. & Sato, G. *Analyt. Biochem.* **102**, 255–270 (1980).
3. Bettgar, W.J. & McKeehan, W.L. *Physiol. Rev.* **66**, 1–35 (1986).
4. Goustin, A.S., Leof, E.B., Shipley, G.D. & Moses, H.L. *Cancer Res.* **46**, 1015–1029 (1986).
5. Maciag, T. *Prog. Thromb. Hemostasis* **7**, 167–182 (1984).
6. Hoshi, H. & McKeehan, W.L. *In Vitro cell. dev. Biol.* **22**, 51–56 (1986).
7. Maciag, T., Nemore, R.E., Weinstein, R. & Gilchrest, B.A. *Science* **211**, 1452–1453 (1981).
8. Tsao, M.C., Walthall, B.J. & Ham, R.G. *J. cell. Physiol.* **110**, 219–229 (1982).
9. Gilchrest, B., Karassik, R.L., Wilkins, L.M., Vrabel, M.A. & Maciag, T. *J. cell. Physiol.* **117**, 235–240 (1983).
10. McKeehan, W.L., Adams, P.S. & Rosser, M.P. *Cancer Res.* **44**, 1998–2110 (1984).
11. Chaproniere, D.M. & McKeehan, W.L. *Cancer Res.* **46**, 819–824 (1986).
12. Hammond, S.L., Ham, R.G. & Stampfer, M.R. *Proc. natn. Acad. Sci. U.S.A.* **81**, 5435–5439 (1984).
13. Lechner, J.F., Haugen, A., McClendon, I.A. & Pettis, E.W. *In Vitro* **18**, 633–642 (1982).
14. Moyer, M.P. & Aust, J.B. *Science* **224**, 1445–1446 (1984).
15. Savage, C.R. & Cohen, S. *J. biol. Chem.* **23**, 7609–7611 (1972).
16. Lobb, R.R., Harper, J.W. & Fett, J.W. *Analyt. Biochem.* **154**, 1–14 (1986).
17. Thomas, K.A. & Gimenez-Gallego, G. *Trends biochem. Sci.* February, 81–84 (1986).
18. Esch, F., *et al. Proc. natn. Acad. Sci. U.S.A.* **82**, 6507–6511 (1985).
19. Gimenez-Gallego, G., *et al. Science* **230**, 1385–1388 (1985).
20. Crabb, J.W., Armes, L.G., Johnson, C.M. & McKeehan, W.L. *Biochem. biophys. Res. Commun.* (in the press).
21. Crabb, J.W., Armes, L.G., Johnson, C.M. & McKeehan, W.L. *6th int. Conf. Methods in Protein Sequence Analysis* (Seattle, 1986).
22. McKeehan, W.L., Adams, P.S. & Fast, D. *Proc. natn. Acad. Sci. U.S.A.* (submitted).

Hi-tech for tissue culture: a growing endeavour

Persuading cells to grow outside of their native surroundings can be a complicated task, demanding elaborate materials and equipment.

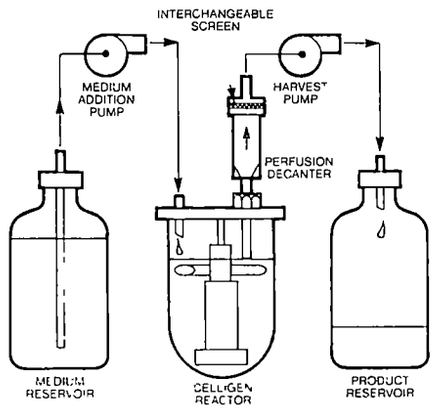
VENTREX makes a **disposable, pre-sterilized airlift fermenter** for one-time use in laboratories that don't routinely perform cell culturing (Reader Service No. 100). Their 650-ml benchtop device, called Cellift, can be used for batch cultures or in continuous feed mode when attached to an infusion instrument. Ventrex also



A fermenter for the infrequent user.

offers a heating jacket as an option to their system. Constructed of polystyrene, Cellift is suitable for bacterial as well as mammalian cell cultures, and it can maintain cultures for up to two months. Positive pressure operation reduces the risk of contamination in the fermentor. Ventrex sells a Cellift starter kit for $225 (US); the Cellift unit alone costs $125 (US).

The design of the aeration cavity on New Brunswick Scientific's **bioreactor** enables large quantities of shear-sensitive cells

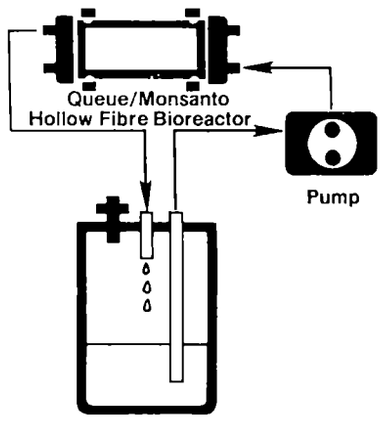


Cell perfusion is a CelliGen option.

to flourish in sparged medium without damage (Reader Service No. 101). By confining the screened cavity to a remote site on the inside of the hollow impeller, the CelliGen system protects microcarriers and suspended cells from sparging turbulence whilst freely circulating culture medium absorbs the gas. NES says that their bioreactor achieves up to 10 times the K_La efficiency of conventional surface-aeration systems that use a gas overlay. Swept-back, rotating impeller ports keep cells or microcarriers evenly dispersed throughout the CelliGen vessel, and a foam elimination chamber coalesces foam into liquid. NBS put a microprocessor in charge of the four-gas control system, which regulates the volumes of air, N_2, O_2 and CO_2 needed to support the desired dissolved oxygen saturation and *p*H. The microprocessor also regulates temperature to within ± 0.025°C, and stirrer speed to ± 1 r.p.m. over a 15- to 225-r.p.m. range. CelliGen comes in 1.5-, 2.5- and 5-litre sizes starting at $9,450 (US), and is available with four types of impeller systems.

Bellco aims to solve similar cell culture dilemmas with a modified shape for its bioreactor (Reader Service No. 102). Their **conical glass culture reactor** requires less vigorous gas flow, thereby providing gentler circulation for suspended cells and microcarriers. Bellco claims their design also eliminates foaming in high-serum media. The 3.5-litre vessel has a sealed water jacket to reduce contamination, and a microprocessor takes care of harvest/feed cycling to minimize supervision. Bellco's reactor, with its nine-port head, can be expanded via accessory panels. The company also offers an optional dispenser that produces macrocarrier alginate gel beads for cell immobilization. With Bellco's machine, batch or perfusion cycling can be specified through programmable cartridges for the bioreactor's microprocessor.

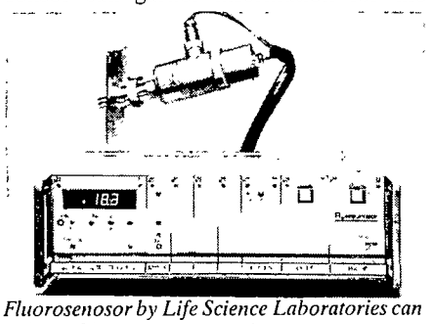
Modelling the *in vivo* environment, a **hollow fibre perfusion bioreactor** developed by a Queue Systems — Monsanto collaboration lets nutrients flow to culture cells whilst carrying waste away (Reader Service No. 103). A pumping system and a media reservoir complete the basic reactor system, but Queue/ Monsanto recommend a more elaborate control system



The Hybrinet low-shear configuration.

(the Queue Mouse, in particular, was mentioned). Hybrinet is composed of biocompatible materials and does not require pre-sterilization methods or wetting agents that could confer toxicity. The Luer-Loc penetrations accommodate a variety of fittings, probes, valves and filters for specialized applications. Queue/Monsanto say they subject Hybrinet units to non-destructive integrity tests following fabrication. The instrument's specifications are geared towards the maintenance of eukaryotic cells in a low-shear environment: fibres measure 9 inches with a 300 Å pore size, and the flow rate can vary between 10 and 40 m min^{-1}. The hollow fibre module can be purchased alone for $375 (US), or with fittings and a support stand at additional cost.

A **fluorescence probe** from Ingold has just been introduced by Life Science Laboratories in the United Kingdom (Reader Service No. 104). The Fluorosensor can garner information for the



Fluorosenosor by Life Science Laboratories can estimate biomass concentration.

control of oxygen supply and substrate feed and can be sterilized along with bioreactor vessels. Proteins, enzymes, coenzymes, pigments and primary or secondary metabolites can all serve as fluorophores, if subjected to the correct excitation wavelengths. The £10,200 (UK) Flurosensor fits into standard DN25 ports. Once proper excitation wavelengths have been determined for a number of biological compounds, the method's flexibility could open up new control and monitoring options for many biotechnological processes.

The first chapter of a technical support publication from LH Fermentation Ltd. gives practical advice on fermenter use in **continuous culture fermentation** (Reader Service No. 105). This issue of *Hints & Tips* also expounds upon the applications of continuous culture, as well as problems frequently encountered with this particular technique. LH Fermentation, which recently expanded their airlift fermenter range with a 10-litre version, expects to continue their *Hints & Tips* series chapter by chapter to build a complete laboratory

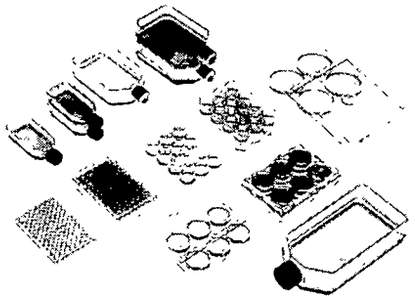


The first in a fermentation series

manual on fermentation. This first issue comes as part of a larger literature package including LH's newsletter and their 1986 price list.

Labware lookout

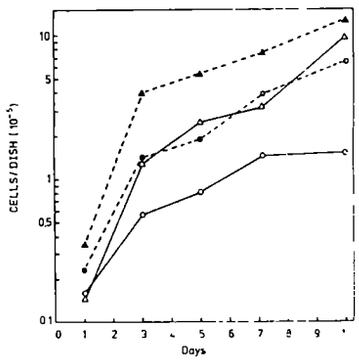
Where tissue culture is concerned, **labware coated with extracellular matrix** is often touted as the next best thing to being there. In Vitro International now produces flasks in 25-, 75- and 150-cm^2 sizes coated with bovine ECM, to complement their existing supply of ECM-coated 4-, 6-, 12-, 24- and 96-well plates (Reader Service No. 106). This labware, used like plastic culture labware but stored at 4°C, owes its origin to the efforts of endothelial cells, which excrete ECM into the labware during proliferation. The matrix adheres



IVI expands their ECM-coated labware selection.

strongly to the plastic, and subsequent removal of the endothelial cells leaves the substratum behind. In Vitro's flasks cost between $20 and $120 (US) in single units or packs of five, and have a shelf-life of four months.

ECM cultured cell lines show reduced requirements for serum supplements and



Cell proliferation on IBT's ECM-coated plates (dotted lines) vs. traditional labware (solid lines).

cellular mitogens while at the same time exhibiting greater attachment, migration, proliferation and in some cases differentiation, than those reared in traditional plastic labware. International Bio-Technologies supplies a wide selection of ECM-coated **tissue culture plastics** and also provides custom-coating services (Reader Service No. 107). One such service is the coating of labware disposables with radiolabelled ECM, tailored to specific customer needs. IBT has compiled technical literature describing the use of their substrate in human amniotic cell and human primary malignant epithelial cell cultures. The main goal is the rapid diagnosis of prenatal disorders and perhaps the *in vitro* study of biologically derived antitumour agents.

Gibco Laboratories, familiar source of cell culture reagents, has taken the plunge into **tissue culture treated labware** (Reader Service No. 108). Gibco has

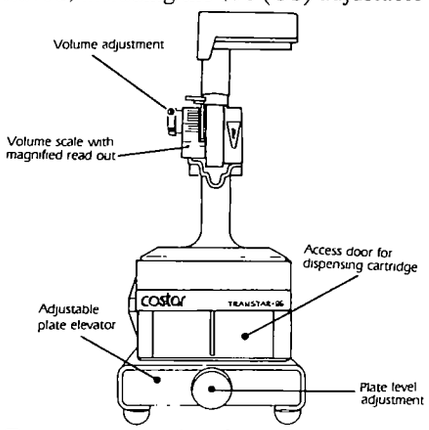


Gibco goes with surface effects.

flasks, dishes, cluster dishes and roller bottles that have been scored with electron beams to improve cell growth. The company tests its labware for growth support; adherent heteroploid cell lines including CHO-K1, BHK-21 and VERO are used in these plating efficiency and monolayer proliferation assays. Pipettes, microtitration plates, freezing vials and

centrifuge tubes are also part of Gibco's labware introduction. A 12-page catalogue gives more information on the new products.

A portable **96-tip dispenser system** from Costar has applications in changing cell culture media, sterile partial removal of media, diagnostic screening assays, and research on and isolation of pathogens (Reader Service No. 109). The 648-gram Transtar will dispense volumes between 25 and 200 µl, under sterile conditions. The entire Transtar unit can be autoclaved, including the $96 (US) adjustable plate elevator that allows plate-to-plate transfers and removal of media without disturbing monolayers. Costar's $496 (US) instrument has a reproducibility of between ±5 per cent at 25 µl volumes and ±2 per cent with 200 µl volumes. It comes with disposable reagent reservoirs having 8 or 12 separated compartments, or with an open reservoir.



Transtar protects microplate and user from contamination.

Chemistry for culture

Techniques for **mononuclear cell separation** must welcome a newcomer: Sepratech Corp. has a system based on continuous density gradient centrifugation using their colloidal silica-based medium, Sepracell-MN (Reader Service No. 110). One to six ml of whole blood, added directly to Sepracell tubes, separates with 10 minutes of centrifugation on the gradient established by the rapid sedimentation of Sepracell-MN particles. The resulting MNC fraction segregates above a wide band of Sepracell-MN, whilst the rest of the components are sequestered beneath this band. Sepratech's technique also entails the use of a 'Seprapette' that makes band recovery simple and more complete. The procedure should only be applied to EDTA and heparin anticoagulated blood. Sepratech's $75 (US) package includes 50 sterile tubes, wash media and 50 Seprapettes; Sepratech also gives free samples.

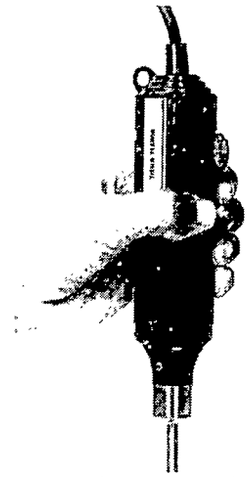
Nearly 500 items for tissue culture are the subject of Sigma's 1986/87 *Cell Culture Reagents Catalogue* (Reader Service No. 111). The brochure's 100 pages cover culture staples such as RPMI-1640 and fetal bovine serum, as well as reagents that only Sigma provides, such as cell culture tested biochemicals.



A culture catalogue with terminology and methodology.

Shear sensitivity

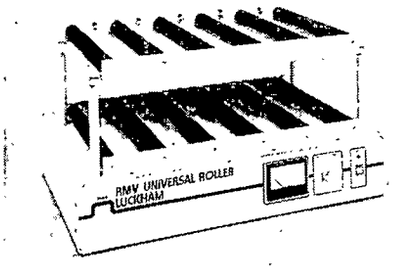
A small volume rotor/stator from Biospec Products can homogenize tissues in less than one minute (Reader Service No. 112). The Tissue-Tearor runs at 28,000 r.p.m. with a 4-inch long probe that draws suspended material into the stator, where the tissue gets repeatedly cycled through six narrow slits. Volumes less than 0.5 ml are fair game for Biospec's device, and samples can be kept cold during the Tissue-Tearor's operation by immersion in an ice bath. The 14-oz instrument can be hand-held or stand-mounted. Speed control allows flexibility: the $388 (US) Tissue-Tearor will mix, emulsify, shred and chop.



Biospec's stainless steel tissue homogenizer.

Roller assemblies for the cultivation of mammalian cells give these fragile cultures gentle treatment (Reader Service No. 113). New Brunswick Scientific has two RollaCell apparatus, RC41 and RC42, that provide precise control of rotation and adhesion for shear-sensitive cells. These units can be expanded from four-place roller assemblies to seven-tiered structures, thereby facilitating mass production. Even larger-scale production models are available, with up to nine tiers and space for 500 mm roller bottles. These systems also incorporate fail-safe devices that signal problems in operation. NBS offers the RC41 and RC42 for £1,231 and £1,425 (UK) respectively.

Luckham Ltd also has a system for continuous **rolling of tissue culture vessels**, with a capacity of up to 25 bottles (Reader Service No. 114). The RMV Universal Roller features a speed meter that fixes rolling speeds up to 60 r.p.m. with a minimum of variation. Luckham's roller will



Luckham Ltd is on a roll.

ADVERTISEMENTS

SINGER INSTRUMENTS
MICROMANIPULATORS & ACCESSORIES
YEAST?
TETRAD ANAYSIS?



Singer MK III Micromanipulator and Precision Elavator.

Write direct to:
Singer Instrument Co. Ltd.
Treborough Lodge
Roadwater, Watchet
Somerset TA23 0QL
England. Tel. (0984) 40226
Telex: 337492 Comcab G

Reader Service No.50

RAW SERUM SPECIALISTS

High Quality Serum for
Cell Culture – Vaccine
Production – Biotechnological Applications

* *Foetal Calf Serum*
* *Newborn Calf Serum*
* *Donor Calf and Horse Serum*
* *U.K.–New Zealand–Australian Sources*

MEDICAL & VETERINARY SUPPLIES LIMITED
Botolph Claydon,
Buckingham MK18 2LR
Tel: 029 671 4555

nature

What happens to NASA now?

This week's report on the shuttle disaster is diagnostic rather than prescriptive. The most urgent need is that NASA should be broken into more manageable pieces.

THE Rogers Commission has at least been swift: it was told to be. While the shuttle catastrophe is still fresh in the mind, there has appeared an intelligent diagnosis of the trouble and a recipe for its avoidance in future. Psychologically, this is what the people of the United States have been yearning for ever since Challenger, with its crew of seven, was destroyed off the coast of Florida in January. The catastrophe was a blow to national self-esteem which has since been made to seem the more cruel by the capture of US citizens as hostages in the Middle East and other assorted insults. Much as it always helps to know the truth, the realism of the Rogers report will persuade people that even if the problems uncovered are serious, they are not insuperable. That is a plus by anybody's reckoning.

The downside is the severity of the criticism directed at the US National Aeronautics and Space Administration (NASA), even if Dr Richard Feynman, a member of the commission, would have preferred a more outspoken report. For several months, it has been clear that the commission would point to errors of two kinds, technical and managerial. The tale of how the different sections of the booster rockets were held together by mechanical joints including rubber seals to prevent the escape of combustion gases has been widely discussed, not least because of the commission's public hearings; these rockets were poorly conceived and their behaviour in exceptional circumstances poorly understood. The managerial errors, for which several senior NASA people have already lost their jobs (the director of the Marshall Space Flight Center in Alabama did well to quit before the Rogers report appeared), have also been apparent for some time. There are many other large organizations in which bad news travels only slowly upwards in the hierarchy, but by the beginning of this year, NASA appears to have been persuaded by the pressure to keep on launching shuttles to devise mechanisms for preserving the innocence among its senior people of the realities of the launching-pad. It is no wonder that the Rogers report is scathing on the subject.

There is every likelihood that the steps recommended by the Rogers Commission will right these faults. The boosters will be redesigned, while there is almost certain for a few months to be a mood in which doubts and criticisms will move freely within the organization and be openly discussed. Given past achievements, there is no reason why NASA should not be able to put these things to rights, so that shuttles will be climbing safely through the atmosphere into Earth orbits a year or so from now. But these are relatively minor and even technical matters, well within NASA's competence. What nobody has considered yet, but what the US administration should take up urgently, is the more teasing question of what NASA is for, and whether its organization is compatible with those goals.

Goals

It tends to be forgotten, but should not be, that NASA as it now is grew out of a federally-supported aeronautical research organization in the United States, and that basic research in the field remains an important part of its function. Much the same is true with rocketry and spacecraft construction. Of necessity, NASA has had to pave the way with these developments. One of its perennial difficulties is that it has been able to shed responsibility for only a small part of its role in technological research and development, mostly the work on satellite design and construction on which the telecommunications companies are engaged. But NASA has also, almost without recognizing it, become an operating agency, continuing to operate satellites that cannot be handed over to commercial interests (which means most of them), launching and recovering spacecraft and so on. That, through the agency of a talented if geographically scattered staff, NASA has also become an essential complement to the academic community, is an uncovenanted benefit.

Defects

NASA's defects, unfortunately, are also many and familiar. Whether it is fair to say, as many newspapers have been doing, that NASA has become arrogant and over-confident is irrelevant. With 15 years of almost unalloyed success in launching well-publicized spacecraft to its credit, it must be tempting to be cocky. But there is plenty of evidence that goes the other way. It is a long time since NASA as an organization behaved as if it were possible to fight the US administration and the Congress for a budget that matched the ambitions with which it had been saddled by public policy. Of necessity always a big spender, NASA has nevertheless become almost a passive spender, willing to cut its coat to suit the cloth the appropriations committees handed out even when this meant abandoning important projects, most often important scientific projects, sometimes projects to which agencies elsewhere (such as the European Space Agency) had been induced to commit funds. Is it possible that NASA's learned behaviour of pleading poormouth and blaming the US Congress for that condition led it also to the view that trouble caused by cutting corners, as in January, could also be blamed on others? The Rogers Commission says the pressure was to run shuttle launches as if by an airline timetable so as to cultivate congressional indulgence. It is a shame that, because this calculation has misled, parts of NASA's operations that are well conceived and imaginatively run may be tainted by the same charge of mismanagement.

The truth is that NASA has acquired too many partially conflicting goals. Space launchers are at best means to a variety of ends, but when the launcher programmes are in trouble, the ends tend to be sacrificed to the means. The solution is to break up the present organization into a few smaller pieces whose objectives would be more coherent. One way of doing this would be to separate technical development (including that of aircraft), the business of running transportation systems and NASA's role as a doer and sponsor of space research (which at present is hurt first when funds are short). Then at least there would be only the budget-people to blame if the parts of the programme swung out of balance. NASA will no doubt protest that the same argument could be used to take high-energy physics away from the Department of Energy, but that is not the case; the department, like its predecessor, the Atomic Energy Commission, has sensibly devised a mechanism by which the high-energy physics community's claims on public funds stand or fall by the good sense of what the High-Energy Physics Advisory

Panel thinks it proper to recommend from time to time.

NASA may also fear that dismemberment into more manageable pieces may complicate its matching of the demand for launching facilities with the supply it has created. That, too, is misplaced. While the vast majority of the projects on which researchers have set their sights could be handled as well by inanimate rockets as by the shuttle, that is not the case for the most valuable of all the projects, the Hubble Space Telescope (which must now languish on the ground for an extra year), while there would be no case against a craft such as the shuttle if it were dependable and cheap. In any case, especially after the latest failure of Ariane two weeks ago, launcher operators are unlikely to have spare capacity for a long time to come.

This is why the best framework in which to solve NASA's problems is quick clean surgery, which will in any case be necessary at some stage in the future, when spacecraft with or without people have ceased to be seven-day wonders. □

Observers in arms

The fate of Britain's oldest observatory will be decided next week. Or will it?

How strong are the nerves of the Science and Engineering Research Council (SERC), the chief sponsor and even manager of Britain's academic research? This is what British astronomers will be asking in the time between now and 18 June, the date fixed for the next meeting of the council and, at SERC's own choice, for a final decision on the future of the Royal Greenwich Observatory (RGO). In the three months since the decision was announced (see *Nature* **320**, 239; 1986) that the observatory would have to move again — forty years have gone since it said goodbye to Greenwich — there has been a fierce rumbling of protest from many of those affected that the decision is mistaken, which message has been blunted and confused by the siren-sounds from those other astronomers with an interest in tempting RGO to some particular place or other. A meeting of astronomers of all kinds in London last Friday seemed to be united in feeling that SERC has somehow mismanaged the whole business. So next week's council meeting becomes a test of SERC's credibility as well as of its good sense.

The reasons why some kind of decision is needed are by now well-known. Because of decisions taken by SERC (then merely SRC) in the 1970s, British astronomers are about to be blessed with a range of what may reasonably be called modern telescopes, and which will also give academic astronomers allocations of telescope time about which they cannot seriously complain. The snag is that the new equipment is a long way from Britain, in the middle either of the Atlantic or of the Pacific. As observers elsewhere know as individuals, geography may be a nuisance but is not an insuperable obstacle to good work. SERC's difficulty is that, having built the new telescopes as part of its terms of reference to foster research at British universities and polytechnics, it discovers on its payroll some 250 people at the two British observatories, RGO and the Royal Observatory Edinburgh. The problem might have been anticipated a decade ago, but was not. Since then, by common consent, the two observatories have done valuable work in supporting the development of instruments for the facilities being built elsewhere and, more recently, have been providing academic users of the new facilities with advice and assistance based on their own experience, frequently much greater. That there will be a continuing need for services of this kind is generally accepted. SERC's problem is three-fold. First, as a consequence of past decisions, it is spending more on astronomy relative to other things than it would if it were starting from scratch (but nothing said about the decision to move RGO suggests immediate savings). Second, without the issue ever having been declared, SERC is seeking (rightly) to effect a shift of responsibility (or opportunity) for observational astronomy from the in-house observatories to the universities, which is why the decision that Greenwich rather than Edinburgh should move was based on SERC's opinion (which RGO disputes) that Greenwich has been the less successful at forming links with universities. Third, at no point during the five years in which the need for reorganization has been apparent, during which time there have been two formal attempts to find an acceptable solution, has there been a serious effort to decide how the now-expanded British effort in astronomy should be managed. There is a sense in which the present council is the victim of its predecessors' neglect which, given collective responsibility, is an explanation but not an excuse. The anger and bitterness that have preceded next week's council meeting have arisen because too little has been said to those whose careers are affected.

What, then, should be done to manage the transition without further exacerbating relations between SERC and important sections of the astronomy community? The first need is for a convincing statement of SERC's strategy for astronomy. To what extent is the long-term aim, that most observers should be academics, desirable, for example? Having made a good if belated beginning on the provision of modern facilities, does SERC intend to follow through when the demands come (as they surely will) for even better equipment? And may it then not act alone, picking up assistance from others as an afterthought (Dutch as well as Spanish astronomers are partners in the La Palma observatory), but by seeking partners from the outset? All three questions should of course be answered yes. But only if they are answered clearly and sympathetically will those at the observatories whose careers will be affected have the stomach to soldier on.

What would such a strategy imply for the immediate future? If the best way of building on past investments in astronomy without jeopardizing science as a whole is to build the next generation of telescopes in collaboration with partners overseas, SERC would recognize more clearly that national support centres are inappropriate. Planning that observers should be distributed among universities, it would conclude that technical support should be similarly spread out. In the long run, neither Edinburgh nor RGO would be needed. The objection to SERC's planned course, amalgamation on the Edinburgh site, is that it would permanently institutionalize the complex. If it were now to say that Edinburgh will in due course follow RGO in being made part of a university, RGO's bitter pill would be easier to swallow. If SERC is not ready to say that, the case for moving RGO diminishes.

SERC should also be more open about its financial plans. It says that present recurrent spending will not increase, but no allowance has yet been made for future capital expenditure. Why not say flatly that SERC needs to save money now on running costs against capital spending in the future? RGO itself will have shrunk to 150 people (of whom 40 will be based in mid-Atlantic) when the present contraction is complete by 1990, but there is a case for going faster and further. The millstone that SERC has made to hang around its successors' necks is the promise that RGO will retain its independence, which will be taken as a promise of constant budgets a decade hence.

There remains the question of how British astronomy should acquire a sense of being led in a recognizable direction. SERC is a benign and well-intentioned organization that has done good works from time to time. Unfortunately, it cannot help but seem part of the civil service: why else have the directors of the two observatories been compelled to say nothing in the past three months about the aspect of their institutions that matters most, their future? Like NASA, which has the more serious problem of the shuttle to accommodate (see previous page), SERC needs a mechanism for helping the community it tries to serve to believe that its true wishes, not some others wished upon it, will be met. If SERC could arrange for that, its difficulties with those at RGO would melt away. If it cannot, its credibility will indeed decline. □

Shuttle catastrophe

Rogers Commission report makes waves all round

Washington

DESIGN flaws, organizational problems and inadequate safety procedures all played a role in the accident on 28 January that destroyed the space shuttle Challenger, according to the presidential commission chaired by William P. Rogers, whose 250-page report was published this week.

The commission concludes that the accident to mission 51L occurred when a gas leak developed at the joint connecting two segments of the right solid rocket booster (SRB). The leak developed within seconds of launch, showing up in photographs as a puff of black smoke. Then it evidently sealed itself, possibly with combustion products from the booster, but after the shuttle successfully passed through severe wind shear, the leak reappeared 58 seconds after lift-off.

Then the slipstream directed the burning gas from the leak onto the external fuel tank, ultimately burning a hole in it. At 72 seconds, the lower strut holding the booster to the fuel tank was severed or pulled away, allowing the booster to pivot, smashing into the external fuel tank and releasing massive amounts of liquid hydrogen. Within milliseconds there was a "massive, almost explosive burning" of the hydrogen spilling from the tank.

The commission concluded that the accident occurred because O-rings supposed to form a seal between two segments of the right solid rocket booster failed to do so. The O-ring seals are designed to be "pressure actuated", only sealing once increased pressure is applied to the joint by the firing of the rocket motor. The commission concluded that the failure was due to "a faulty design".

The commission was also critical of the process that resulted in the decision to launch Challenger. Testimony presented to the commission revealed that the decision to fly was based on "incomplete, and sometimes misleading information". The O-rings had been identified as early as December 1982 as parts whose failure could result in a mission disaster. In July 1985, SRB manager Lawrence Mulloy placed a launch constraint on all shuttle launches, which meant that a waiver had to be signed before each flight could proceed. But neither the constraint nor the waivers were known to the director of the shuttle programme or his senior deputies.

The 24 previous successful launches of the shuttle also contributed to the accident. As commission member Richard Feynman put it, NASA convinced itself that safety standards could be lowered a little bit after each launch "because we got away with it last time".

The commission also investigated the pressures on the shuttle programme caused by NASA's reluctance to relax optimistic schedules. A critical shortage in spare parts forced NASA to turn to cannibalization, borrowing parts from one



orbiter to allow another one to fly. But the accelerated launch schedule meant the shuttle would either be in orbit or preparing for launch, thus not available for supplying spare parts.

The commission's chief recommendation is that the faulty joint and seal of the solid rocket booster should be either eliminated or redesigned. But other recommendations are likely further to increase the cost of bringing the shuttle back into service and to decrease the rate of shuttle launches thereafter.

The booster joints had for several years been suspect. Instead of a complete redesign of the joint, now as seen as necessary, Morton Thiokol Inc. and NASA opted for some retesting and the imposition of "launch constraints", which were then overridden for every launch after 10 July 1985.

The commission is forthright on the need for other safety improvements, landing safety included. Tyres on the landing gear are acknowledged by NASA to be "critical" components, but tyres have shown "excessive" wear during several previous landings. The brakes, which have been damaged on most flights, have "little or no margin".

The commission urges efforts to provide a crew escape system for use during gliding flight. Although early test flights of the shuttle included ejection seats, recent space missions have had no such feature, which would require a major effort, and probably taking up valuable space and weight. "Rocket-assisted extraction" is a possibility.

The commission, impressed that pressure on NASA to maximize launch rates may have contributed to management failures and the accident, says the capabilities of the system stretched "to the limit" to support flight rate in winter 1985–86. In what may be one of the most significant long-term recommendations, the commission urges that the United States should not rely exclusively on the shuttle for launching capacity, a complete reversal of the administration's declared policy.

On management, Rogers says there must be a redefinition of the programme manager's responsibility. Project managers apparently felt more accountable to their particular NASA centre than to the programme as a whole.

Tim Beardsley & Joseph Palca

Other avenues?

Washington

THE Rogers inquiry subdued the natural inclination of Congress to get involved; now that the report is public, both houses of Congress intend to hold hearings on the findings, and on the accident itself.

At least one senator, unable to wait until publication day on Monday, introduced legislation last week following a "recommendation by the Rogers Commission" to revive quality assurance at NASA. Congress has also been impatient with the inability of the White House to decide on buying a new orbiter, and may suggest its own plans for the agency.

The National Research Council (NRC) will also have a future role in the shuttle programme. NRC's standing review committee on NASA's scientific and technological programme will set up a panel to evaluate development and construction of the new solid rocket boosters.

NASA itself is also having to reevaluate its role. The Reagan administration no longer wants NASA to be the sole provider of launch services for commercial satellites, while the Department of Defense has already ordered ten Titan 34D7 rockets capable of launching payloads nearly as large as those carried by the shuttle.

Without the military or industry as steady users, will NASA find itself more interested in the needs of the scientific community? Bruce Murray, professor of planetary science at the California Institute of Technology and former director of the Jet Propulsion Laboratory, says NASA took a procrustean approach, forcing users to fit their projects to the shuttle's capabilities. Murray believes NASA will now have to serve space science and manned exploration of space.

For the time being, with no shuttle and no alternative launch vehicles, space science projects are dead in their tracks. Even if funds for scientific projects are preserved, NASA's chief scientist Frank McDonald says the shuttle's loss will damage the programme. Joseph Palca

Seismic monitoring

Private diplomacy emergent

Washington

A REMARKABLE agreement signed last month would permit a team of US and Soviet seismologists to establish a seismic monitoring station within 200 km of the Soviet nuclear test facility at Semipalatinsk. What makes the agreement all the more unusual, and contentious, is that it was not signed by representatives of the US government.

The agreement came out of a series of meetings between representatives of the Natural Resources and Defense Council (NRDC), a private non-profit organization devoted to protecting the environment, and the Soviet Academy of Sciences. Adrian DeWind, NRDC's board chairman, and E.P. Velikhov, vice-president of the Soviet Academy, signed the agreement in Moscow on 28 May.

Under the agreement, six monitoring stations would be established, three in the Soviet Union near Semipalatinsk and three near the Nevada test site in the United States. All data recorded will be made available to both the US and Soviet governments. NRDC will pay all the travel expenses involved in the project and will take responsibility for obtaining the necessary seismological equipment. DeWind estimates that NRDC will have to raise $500,000 to get the project off the ground. It hopes to establish the first listening post in the Soviet Union by the end of this month, with two more to follow in the fall. The US monitoring posts will be established only when the Soviet posts are in place.

Thomas Cochran, a physicist on NRDC's senior staff, says the idea for the agreement came from discussion last January on the monitoring of US explosions whose occurrence is not made public. Cochran and his colleagues at NRDC felt that monitoring only the Nevada test site might be regarded as "giving away state secrets", so he devised the bilateral plan.

Although the monitoring sites may provide information about the local geology of the Semipalatinsk region useful for evaluating yields of Soviet nuclear tests, that is not the point of the exercise. Rather, says Cochran, it is to show the feasibility of on-site seismic monitoring, proving that verification is not an obstacle to a test-ban treaty. The Soviet Union is currently observing a self-imposed moratorium on tests, but that may expire on 6 August.

Before the plan can go forward, NRDC must obtain export licences for the seismic equipment. A State Department official said last week that no decision had been made on NRDC's request for a licence, but that the agencies responsible for technology transfer issues were considering it. NRDC plans to purchase off-the-shelf equipment for the monitoring stations, according to Charles Archambeau of the University of Colorado who acted as a consultant to NRDC. If the export licences are not granted, Archambeau says the project could still proceed using Soviet-built equipment. But Archambeau says that Soviet equipment is not as sensitive as that from the United States, nor is it digital, making data acquisition and analysis more difficult.

Critics of the agreement believe that it will serve only as a propaganda weapon for the Soviet Union. Misha Tsypkin, Salvatori Fellow in Soviet Studies at the Heritage Foundation, a conservative think-tank, argues that the Soviets are adept at manipulating foreigners to serve Soviet goals. Tsypkin believes that NRDC was "irresponsible and out of order" to proceed with such politically sensitive negotiations off its own bat, without government participation or approval. Archambeau concedes that NRDC's plans may undercut current US government positions on arms control. But according to Cochran, something was needed to "get some movement in the arms control arena".

The agreement comes at a time when the United States has announced it plans to end its observance of the unratified SALT II treaty later this year. The government believes that Soviet unwillingness to abide by the terms of the treaty makes it impossible for the United States to do so. But efforts are under way in Congress to force US compliance with the treaty by eliminating funds for projects that would violate its terms; these are unlikely to succeed, however. Supporters of the Soviet test moratorium are also planning to introduce legislation stopping US nuclear testing, although these efforts also face an uphill struggle.

Accoding to a State Department official, the NRDC agreement "may be encouraging" to the extent that it represents a change in Soviet attitudes on verification of the Threshold Test Ban Treaty, which the United States believes the Soviet Union has been violating. But the State Department believes that negotiations that could have such a great impact on arms control and national security should be conducted only between governments.

Frank Press, president of the National Academy of Sciences, sees the NRDC agreement as an "extraordinary event", but says it is too soon to judge its implications. "Arms control has never been a private sector activity before... When books on arms control are written, this will certainly be included." **Joseph Palca**

Soviet industry

Reformers get the wrong man

IT seems that Mr Mikhail Gorbachev's drive to make Soviet industry more efficient is not without its hitches. Last month, none other than the Central Committee of the Communist Party of the Soviet Union intervened to demand the reinstatement of a person who had earlier been wrongfully demoted from his managerial post at the Irbit Chemical and Pharmaceutical Plant.

The Central Committee's special decree dealing with the state of affairs at the plant is revealing. The plant is supposed to produce high-quality supplies for the Soviet medical services, but is run-down, behind in its modernization programme and provides no scope for the development of new ideas and products. These are precisely the conditions condemned by the plenum of the Central Committee held in April 1985.

The Central Committee now says that, instead of trying to rectify these conditions, the director of the plant, with the support of the local party organization, deprived a certain Vadim Bakharev of his post, in charge of production unit Number 2, on the grounds that "he had ignored the opinion of working teams", shown "crudeness" in dealings with his subordinates and had "consistently failed to fulfil his work obligations". Bakharev accepted his transfer to the lower grade of engineer only because of the threat that he would otherwise be dismissed outright.

Bakharev was demoted on 4 December last year. How and when the higher echelons of the party learned what was going on is not clear, but, on 20 April, the newspaper *Pravda* carried a long account of the affair which claimed that, far from being responsible for the shortcomings at the Irbit plant, Bakharev was a lone hero who had fought neglect and inefficiency, and who had been victimized for his zeal.

According to *Pravda*, Bakharev had in reality combined two previous production units together so as to cut costs by 75 per cent and increased labour productivity by 98 per cent (partly by eliminating 36 jobs) at a saving of 300,000 rubles a year. It was not Bakharev but the plant managers who had "ignored the opinion of the working teams" by demoting such a paragon.

A month later, the Central Committee pronounced. The Ministry of Medical and Microbiological Industry was instructed that Bakharev's demotion had been unjustified, and that he must be reinstated forthwith. The ministry was also told to put matters at the factory right, modernizing and re-equipping the production lines and improving the working and living conditions of the workforce. The party

secretary at the plant has been relieved of his post and other officials disciplined.

The Irbit factory is important in the Soviet Union's plans to build a sophisticated pharmaceutical and specialist chemical industry, and should be at the leading edge of the government's new drive for modernization. The intervention of the Central Committee, and the attention it has been given, may be intended as a warning to plant managers elsewhere that they had better put their affairs in order before the drive for modernization gathers momentum and that a random selection of scapegoats will not suffice.

Vera Rich

AIDS research

New foundation begins work

Washington

SUPPORT for research into acquired immune deficiency syndrome (AIDS) has received a shot in the arm from the American Foundation for AIDS Research (AmFAR). The new foundation handed out 20 grants totalling $1.1 million, mostly for basic research on the biology of the virus assocaited with AIDS, with a smaller number for drug development and epidemiology. AmFAR's scientific advisory committee was looking primarily for projects demonstrating "fresh ideas", according to a spokesman for AmFAR.

The 20 projects receiving grants were chosen from 146 applications. The maximum $60,000 grant is not intended to sustain a major research effort, but will instead provide start-up money for new projects.

AmFAR came into existence last September when the AIDS Medical Foundation, based in New York, merged with the National AIDS Research Foundation of Los Angeles. Actress Elizabeth Taylor serves as AmFAR's national chairman, and has been an active force in fundraising. In future, AmFAR hopes to move its financial base away from special fundraising events to long-term commitments from corporations and philanthropic foundations.

Although the $1.1 million offered by AmFAR is only a small fraction of the $233 million AIDS budget of the US Public Health Service, there is always enthusiasm for a new source of funds. "Any branch I can shake for support is marvellous," says Murray Gardner of the University of California at Davis, who received a $60,000 grant from AmFAR to study the structure of the envelope protein of the AIDS virus.

AmFAR can also move more quickly than the federal government. It solicited proposals in January, and made decisions on them just 4 months later. **Joseph Palca**

Rice breeding

Manipulation of cereal succeeds

Tokyo

THE basic techniques for the genetic engineering of rice have been developed in research institutes in Japan. Several laboratories are racing to draw the techniques together so as to be the first to produce a genetically engineered rice plant. The development is important not only because genetic manipulation has so far been mostly confined to dicotyledonous plants but also because rice is the staple food of half the world's population.

The transfer of genetic material into cereal plants has hitherto been held up because they cannot be infected with the *Agrobacterium* species which have provided a simple route to the transfer of genes in dicotyledonous plants. But two new developments have given rise to optimism that genetic manipulation of rice will be possible in the near future.

The regeneration of whole rice plants from protoplasts (single rice cells stripped of their cell wall) is one way. Success has just been reported in print by Professor Yasuyuki Yamada's group at the Kyoto University Research Center for Cell and Tissue Culture (see *Plant Cell Reports* **5**, 85; 1986). Two industrial laboratories, a joint laboratory run by Mitsubishi Chemical and Mitsubishi Corporation and Mitsui Toatsu's research laboratory have also described regeneration techniques at research meetings. Each group has its own method and it is too early to know which will prove most practical.

Yamada can regenerate tissue from protoplasts by the simple trick of adding calf serum, commonly used in the culture of animal cells, to his medium; after all, he says, a "plant protoplast is almost the same as an animal cell".

From one culture cell line, Yamada has been able to produce calli (undifferentiated tissue) from 10 per cent of protoplasts, many of which formed roots and shoots and developed into whole plants when transferred to regeneration medium. Although other strains produced calli, only one regenerated whole plants and there is evidence that the adult plants, now out in pots and the fields, are not entirely normal. Further work may thus be needed to make the regeneration method of general use.

The Mitsubishi group, led by Dr K. Shimamoto, appears to have had much broader success. It has successfully regenerated whole plants from protoplasts of five different genotypes, two of them major commercial cultivars. More than 300 plants have now been regenerated, and of these 120 are now growing in paddy fields. They can later be studied in detail for differences from the parent stock.

The innovations behind the Mitsubishi group's success is that, instead of making protoplasts from rice cell lines maintained for a long time in culture, they have induced calli from rice seeds. The protoplasts so produced are "young" and have strong morphogenic potential. In the past, this approach has not been favoured because cells in fresh culture from seed do not divide — overcoming this obstacle is the secret of Shimamoto's method.

The second group of advances, for the transfer of foreign genes into protoplasts, has also very recently been reported, and depends on the observation that protoplasts prepared from cultured callus cells and treated with polyethylene glycol will take up foreign DNA. Dr Uchimiya's group at the University of Tsukuba has successfully introduced a chimaeric gene containing an antibiotic resistance gene in experiments of this kind. He was not, however, able to regenerate plants from the transformed cells.

With both regeneration and transformation proved possible, the race is now on to "put both techniques in one hand", as Uchimiya says, and to produce the first genetically engineered rice plants. Judging from reports from the five or so laboratories carrying out similar work, the winner should be declared fairly soon.

The question remains of what useful application can come from the research. In theory, the potential is vast, for rice is the major source of carbohydrate for almost half of the world's population. But rice has been intensively improved by breeders for almost a century, while large increases in production can be expected in the poorer countries of Asia simply through extending irrigation. This makes Japanese companies wary about investing heavily in rice research, for even now rice can be grown in Japan only by maintaining an artificial price several times that of the world market.

Early on, genetic engineering may be used to make things easier for the conventional breeder. Male sterile lines, valuable in breeding new strains of rice, are hard to produce by ordinary methods but should be easily made by protoplast fusion. One protoplast carrying the cytoplasmic male sterility factor but with its nucleus inactivated can be fused with the desired strain of rice.

In the longer term there are the possibilities of transferring genes from other cereal crops that seem to perform more efficiently, introducing viral resistance genes and altering genes to improve the quality of the seed protein. Again, there are ten wild species of rice which present an almost untapped reserve of genetic variability. Protoplast fusion will make it accessible. **Alun Anderson**

Germany and Chernobyl

End of the nuclear programme?

Hamburg

THE cloud whose changing direction carried radioactivity from Chernobyl over Western Europe last month has changed the political climate in West Germany. Fallout has become a national issue which will affect the regional (*länder*) elections due in the next few months and even the federal elections next January.

The general confusion in the days following the accident has left its mark. Chancellor Helmut Kohl, in Tokyo for the economic summit, at first reacted calmly, saying that the accident was characteristic of planned economies and could not have happened in West Germany. By the time, six days after the accident, that fallout reached West Germany, Kohl (still in Tokyo) was urging further expansion of nuclear energy in West Germany even as the first warnings against drinking fresh milk were being published.

Conflicting information was given out from several sources. The Minister of the Interior, Friedrich Zimmermann (CSU), was explaining on television that contamination from a reactor 2,000 miles away could not occur while the first radioactive rain began to fall. Officials of the federal and *länder* governments gave out contradictory advice. In Bavaria, the most affected of the *länder*, the right-wing government played down the problem for the first few days, but in Munich, with its SPD (Social Democrat) city government, people were told to avoid contact with soil or grass.



Police clash with demonstrators at Brokdorf last week

The federal government said that people should not drink milk whose radioactivity was more than 500 Bq per litre, but in some *länder* the limit was only half as much, while Hesse fixed it at 20 Bq per litre. In many cities, kindergartens and playing-fields were closed and the marketing of green salad and spinach forbidden. Farmers were forced by the police to destroy vegetables or, as in Nordrhein–Westfalen, to keep cattle off pasture. Geiger counters were sold out after a few days.

Psychoanalysts claim to have identified a novel fear among the people of West Germany, whose dread has been described by the newspaper *Bild* as "Atom-Angst" (nuclear fear).

The political consequences are signalled by the latest opinion polls, to which the political parties have begun to adapt their nuclear policies. The Greens, who have always wanted an end to nuclear construction, now demand that nuclear plants should be abandoned. The Social Democrats (SPD), conscious of the figures, have adopted the slogan "the beginning of the end" and have appointed a committee under Volker Hauff, a former federal minister of research, to suggest by the summer how the nuclear programme should be run down.

Public opinion has changed dramatically. The percentage of those wanting no further nuclear reactors to be built grew in a few days from 46 per cent to 69 per cent and reached a peak of 83 per cent. In Niedersachsen (Lower Saxony), where there is an election on 15 June, the opinion polls put CDU (Christian Democrats) and SPD almost equal with 43 per cent of popular support, compared with 51 per cent for CDU and only 37 per cent for SPD at the 1982 elections. The same poll gives FDP (Free Democrats) less than the 5 per cent required for representation in the regional parliament. The Greens have increased their support to 10 per cent from 6.5 per cent in 1982.

This week's elections in Niedersachsen could have national consequences. If SDP in coalition with the Greens (as in Hesse) is able to oust the present CDU chief minister, the government coalition could lose its majority in the Bundesrat in Bonn.

SDP is looking further ahead, to the federal elections in January 1987. It has already said that it would probably stop the DM7,000 million fast reactor project at Kalkar, but Johannes Rau, the SDP candidate for the chancellorship next year who is at present chief minister of Nordrhein–Westfalen, where Kalkar is situated, has already ensured that the builders of the project will be forced to give it up by demanding new safety measures.

With the Kalkar reactor apparently doomed, attention has turned to the reprocessing plant at Wackersdorf in Bavaria, the technical need for which turns on the manufacture of plutonium for the fast reactor. There have been violent clashes at the plant between police and demonstrators. The Austrian government has also demanded that West Germany should give up the project, but has been told not to interfere. Both Bonn and the CSU Bavarian government seem committed to the DM6,000 million project, although that may change before the autumn's election in Bavaria, whose farmers have been most affected by fallout.

West Germany's present use of nuclear power is impressive. There are 19 nuclear plants producing 16,000 MW of electricity, or 36 per cent of the total. A further seven plants (including 300 MW Kalkar) are due to be commissioned by 1990, equivalent to 50 per cent of generating capacity. In North Germany, around Hamburg, no less than 70 per cent of electricity generation is nuclear.

Meanwhile, the SDP–Green coalition in Hesse has taken up the question of how to implement the Greens' demand that nuclear generation should be halted. A paper by the first regional environment minister (see *Nature* **321**, 299; 1986), Joschka Fischer, accepts that there would be higher electricity prices and more air pollution during a transitional period, and has been called utopian by most politicians. But it won support last week from a surprising source, the director of the huge energy supplier Preussag Electra: a director, Hermann Kramer, said that the calculations are essentially correct.

Elsewhere, the CDU government of Schleswig–Holstein has delayed the start of the construction of the twentieth reactor planned at Brokdorf, near Hamburg, at least until after this week's elections in neighbouring Niedersachsen, while Ernst Albrecht has announced the creation of a new centre of solar energy research.

The federal government is softening its arguments. Chancellor Kohl is no longer asking for more nuclear power stations, while many SDU and FDP politicians suggest a "pause for reflection", while insisting that a halt to the nuclear programme would go too far and would not in any case make West Germany safe from nuclear accidents because there are at present a total of 66 nuclear plants in surrounding countries.

A reminder of that truth came last week, when the Oko-Institut of Darmstadt announced that there had been a small release of radioactivity from its high-temperature reactor at Hamm-Uentrop, previously thought one of the safest. It seems that the leak was swamped by the fallout from Chernobyl, but the Nordrhein–Westfalen government has ordered the reactor closed until the company produces a full report on the safety of the system.

Meanwhile, the Bonn government has conceded one of the first demands of the Greens, and has appointed Walter Wallmann (CDU) as the federal government's Minister for the Environment, Nature Protection and Reactor Safety. The opposition regards the appointment as a clear admission of the mistakes of recent weeks. No issue has so much stirred West Germany as the fallout from Chernobyl.

Jürgen Neffe

US biotechnology

Row over industry regulation

Washington

CONGRESSIONAL frustration with the White House's delay over its regulation of the US biotechnology industry was plain last week at noisy hearings on Capitol Hill into Congress's own proposals on the subject. But Congress's attempt to act alone to regulate biotechnology was decried by administration officials and by industry representatives alike.

Although the administration's plans for coordinating agencies that deal with biotechnology were promised for early this year, they had not appeared by the end of last week. The legislation proposed in the House of Representatives would upstage the administration's plans and make them irrelevant.

The chief proposals in the Biotechnology Science Coordination Act of 1986 are the establishment of a Biotechnology Science Coordinating Committee to scrutinize government actions, and also of a biotechnology science research programme to be paid for jointly by industry and by the government. The bill would also modify statutes governing the Environmental Protection Agency and the US Department of Agriculture (USDA) to ensure that all environmental releases of genetically modified organisms that include DNA from different genera would be subject to special licensing and permit requirements.

The bill (HR 4452) was introduced by Representative Don Fuqua (Democrat, Florida), the outgoing chairman of the House of Representatives' Science and Technology Committee. Because Fuqua will not be present to lobby for the bill, it has little chance of becoming law in the current Congress. But congressional staff think that if a consensus emerges that new legislation is needed, there might be legislation next year.

The administration's proposals rely on existing statutes, and will exempt from special review those modified organisms whose new DNA includes only non-coding regions (see *Nature* **321**, 458; 1986). The proposals have apparently been held up in the White House domestic policy council. David Kingsbury of the National Science Foundation, who directs the day-to-day business of the working group that drafted the guidelines, told an angry Representative Harold Volkmer (Democrat, Missouri) that he was "as frustrated as you are" over the delay.

The chairman, Representative James Scheur (Democrat, New York), even threatened to postpone the hearing until the administration had announced its plans. That draft copies of the administration's proposals have been leaked to industry spokesmen (admitted by the Industrial Biotechnology Association) did nothing to improve the congressman's temper.

One of the chief objections voiced to the bill was that a statutory Biotechnology Science Coordinating Committee would be less flexible than the existing committee of the same name, which consists only of senior officials of the relevant agencies meeting in private. The proposed new committee would have more open meetings, and industry spokesmen fear that it would be unable to deal with confidential business information in secrecy.

The proposed new biotechnology research programme was more popular, although industry spokesmen were worried that their newer members would be unable to afford such a scheme. The programme as outlined in Fuqua's bill would create a database bearing on regulatory decisions that would also point to projects for research. But witnesses were critical of limitations imposed on agencies' discretion to give special consideration to small environmental releases by research institutions, and said the cost of meeting unmitigated safety requirements might well prove prohibitive. **Tim Beardsley**

Chernobyl

Now for the long haul

THE Soviet government's special commission on the causes of the Chernobyl disaster and its aftermath will shortly be finishing its work, according to Academician Valerii Legasov, first deputy director of the Kurchatov Atomic Energy Institute at a Moscow press conference last week. But it has already been established, he said, that there are no grounds for abandoning the commercial use of RBMK reactors.

Not all participants in the press conference were so sanguine. Deputy Premier Yurii Batulin, in particular, called for "more time" to evaluate the disaster "comprehensively". He said that what was at stake was not simply a specific incident but the reliability of the whole nuclear power industry, a comment that tends to support an earlier statement of Academician Eugenii Velikhov that the safety systems of RBMK reactors still in service may have to be modified in the light of the commission's findings.

Time, however, is something the commission does not have if it is to retain its credibility and satisfy the demands of the planners. The optimistic tone of Soviet reports by engineers and servicemen mining under the reactor, dispersing radioactive rainclouds and spreading special decontaminating film have raised public expectations that life in the contaminated area will be back to normal within a few weeks.

By contrast, the experts are becoming more and more cautious. "Why risk your children's health by a premature return?" they urge. So, although the Ukrainian press has reported that the Chernobyl victims will have their names commemorated in new streets in the towns of Chernobyl and Pripyat, it may be some considerable time before the memorial nameplates are unveiled. Instead of an early return home, the evacuated power-workers and construction workers from the Chernobyl power station are to be rehoused in new prefabricated estates on the outskirts of Kiev and Chernigov.

As far as farmland is concerned, Dr Yuri Israel, the head of the state commission for hydrometeorology and environmental control, says only that the "greater part" of the contaminated territory will eventually be "restored to the economy", implying that some areas may not be. A thorough study is now being made, Dr Israel told the press conference, of the potential doses that are involved in "protracted agricultural activity" in the affected areas.

Although (according to Batulin), the long-term economic effect of the close-down at Chernobyl will be "barely perceptible" in the statistical reports, it seems that the shortfall in power generation has been covered only by using all other Ukrainian power stations at full capacity. This is clearly a short-term solution, and it has been officially stated on several occasions that the three remaining Chernobyl reactors will be back in operation in the autumn.

In spite of the use of robots and remote-controlled machinery, there are still considerable health constraints on prolonged work at the site itself. Moreover, the references last week to a new phase of laying up the damaged reactor and the long-term measures to prevent seepage on contaminated ground water suggest that many of the practical details still remain to be worked out.

Meanwhile, new problems continue to occur. A number of wells in Byelorussia have been found to be contaminated (whether through seepage or rainfall is not clear), while forest fires in Poless'ye have begun recirculating the radioactive dust. In spite of earlier assurances that Kiev would remain safe from water-borne pollution, the public have now been warned against bathing in the Dnieper or relaxing on the river-beaches until further notice. **Vera Rich**

French science

Old guard takes high jump

In a week of long knives, the new right-wing government of France has removed three of the old guard in charge of the major scientific institutions. The development is to say the least surprising, coming as it does just a few weeks before the council of ministers has to decide the distribution of a FF40,000 million (£4,000 million) cut in overall government spending.

Last Wednesday, Pierre Papon, director-general of the Centre National de la Recherche Scientifique (CNRS), with its 20,000 staff and budget of FF9,000 million (£900 million), was sacked. Independently, Jean-Jacques Payan, in charge of the universities, and Bernard Descompes, who had introduced innovative new funding structures designed to improve university research, resigned.

The sacking of the CNRS director-general, who was re-appointed by presidential decree for a three-year term only last December, is unprecedented. Papon had been a key figure in the development of the previous administration's policy on science, and his removal may be symbolic of the new government's determination to have its way. Usually (as with Payan and Descompes) the government is content to provoke the resignation of those among its senior officials with whom it is out of sympathy.

Papon seems to have been determined to hold on to protect the considerable achievements of the old regime, and had been planning in September to present a package of policies designed to achieve that to the new science minister, Alain Devaquet. But the new government seemed unable to wait.

Nevertheless, Papon's replacement should not cause too many shudders in the scientific community, at least if he inherits some of his predecessor's power. The new man, Serge Feneuille, is a reputed physicist who for five years has been chief scientist of the cement makers La Farge Coppée, a company which with Feneuille's help had begun to diversify and take an interest in biotechnology.

Despite the pre-election pressure from the right to dismantle the vast and interdisciplinary CNRS, the feeling at the research council, where Feneuille has worked before, is that he will "protect" the institution. With his background, he should also be interested in continuing to forge links between the scientific community, industry and the public in line with the previous administration's policy.

Such doubts as there are arise because of the government's budget-cutting mood and the apparent political weakness of the research minister Alain Devaquet, a man whom most scientists are willing to embrace as an ally against a larger foe, the finance ministry, which has emerged as the main instrument of Prime Minister Chirac's political philosophy. The outlook for research spending in France looks bleak, with a new CNRS director-general reporting to a minister already in a weak political position and with major budget decisions due in July.

Sacked Papon spoke last week of the need to maintain the integrity of CNRS, and especially, the momentum of the interdisciplinary programmes on which he spent much of his effort. "Feudalities are a permanent temptation in France", Papon said.

He is also anxious that the policy of cooperation between universities and industry should be maintained. "The end of the Ministry of Research and Technology was a mistake", says Papon, because of the separation of "responsibilities for science and technology" which is implied. If the ministry is not strong, "it will be the end of the coherence of the whole programme".

Robert Walgate

US policy

Another new White House man

Washington

President Ronald Reagan last week nominated William R. Graham, deputy administrator of the National Aeronautics and Space Administration (NASA), as his science adviser and director of the White



House's Office of Science and Technology Policy (OSTP). The twin posts had been without a permanent occupant for the past 6 months, since George A. Keyworth II resigned in December to form a private consulting company. The acting director of OSTP since the start of the year, John McTague, resigned two weeks ago to take a position in industry.

The six-month delay in finding a replacement for Keyworth has provoked criticism from the scientific community. Several potential candidates have turned down offers, and many observers felt the difficulty in finding a permanent incumbent was indicative of the diminishing influence of OSTP in the White House. Several other senior OSTP officials have resigned in recent months without being replaced, and the office's proposed budget for 1987 is a hefty cut from this year's level.

Graham's nomination has therefore been greeted with subdued relief by scientific leaders, but some express reservations that his military background and advocacy of the militarization of space made him a less than ideal candidate. Robert Park of the American Physical Society said that the appointment was consistent with Reagan's previous appointments of "technocrats" to the post, rather than of distinguished academic scholars.

William Carey, executive officer of the American Association for the Advancement of Science, who had been vocal in his criticism of the hiatus at OSTP, said he was glad someone was now in place who was familiar with high-technology initiatives. But he admitted to being concerned that Graham's background might lead him to offer advice on investment decisions that would be "tilted in one direction". Asked specifically about Graham's known support for the Strategic Defense Initiative, Carey responded "what's new?". Keyworth was also a staunch defender of the programme.

Graham first came to public attention last year when he stepped in to become acting administrator of NASA after the indictment on fraud charges of NASA's former administrator, James Beggs. With the appointment in May of James Fletcher as permanent NASA administrator, Graham needed somewhere to go, as Fletcher had no special desire to keep Graham on as his deputy. Graham's appointment will need confirmation by the Senate, but because his appointment at NASA was also the subject of a confirmation hearing, no serious opposition is expected.

Before going to NASA, Graham was chairman of the general advisory committee of the Arms Control and Disarmament Agency. He started his career as a research physicist at Stanford University, and subsequently worked on survivability of strategic systems for the Air Force and a National Research Council study of submarine warfare. In 1971 he formed a consulting company, R&D Associates, and he has frequently been a consultant for the Department of Defense. But there was some criticism of his performance at NASA during the admittedly turbulent period of his office as acting administrator.

Tim Beardsley

Laboratory accidents

Inquiry into lab's bone cancers

THE Institut Pasteur in Paris has set up an external commission of inquiry to investigate the occurrence of three cases of bone cancer among workers in the same laboratory at the institute. Two of those affected have died in the past few months, and some colleagues suspect that the cluster of cases may be linked with work on oncogenic viruses being carried out in the laboratory. The outcome of the inquiry will be awaited anxiously by those elsewhere whose research involves mammalian oncogenes.

The Pasteur laboratory is called the genetic toxicology laboratory, and is largely concerned with the molecular biology of oncogenic viruses and of oncogenes. One of those who has died, Dr Françoise Kelly (aged 50), had worked in the laboratory for four years. A close friend of Dr Kelly's says that, before her death, she had come to believe that there should be an investigation of the hazards of the research on which she had been engaged.

Most recently, Kelly had been working on a project to effect the transformation of mouse embryo carcinoma (teratoma) cells by the transfer of genes derived from viruses known to be oncogenic in certain circumstances, simian virus 40 (SV40) and adenovirus in particular.

Specifically, Kelly was attempting to endow the mouse cells with a synthetic gene consisting of the "early T" gene of SV40, the DNA coding for a protein produced early in the viral life-cycle, linked with the promoter region of an early gene from adenovirus.

According to a spokesman at the Pasteur Institute, the experimental manipulations were carried under a hood which, while drawing air from the surrounding experimental area, filtered it through active charcoal. The spokesman added that the procedures followed in the genetic toxicology laboratory were "much more careful" than those common in molecular biology laboratories because members of the same staff were also used to dealing with a stream of potential industrial and environmental mutagens and carcinogens.

Little is known about the mutagens and carcinogens handled in the laboratory, apparently because much of the work is confidential to the commercial companies and other interests by whom it has been commissioned. According to an institute report in 1981, it signs secrecy agreements with clients who commission testing. It is, however known that the laboratory has worked on derivatives of the benzo and naphtho-nitrofuranes, known to be powerful mutagens.

The possibility that the cluster of three bone cancers may be linked with the programme of testing for mutagenicity and carcinogenicity is contradicted by the usual length of the latency period for cancers induced by chemicals.

The second researcher to die, aged under 40, had worked in a laboratory across a corridor from Dr Kelly, but only for a period of six months in 1979–80, before the project to transform mouse embryonic cells had been begun. The third bone cancer patient, who is at present ill, is also under 40, and had worked in the same room as Dr Kelly although on a series of genetic manipulations of *E. coli*. There is no sign of damage to the technicians and the two students who had been assisting Dr Kelly with her last project.

These circumstances lend support to the suggestion by the director of the Pasteur Institute, Raymond Dedonder, that the occurrence of the three cancer cases is probably a statistical coincidence. Dedonder put this view at a private meeting with Pasteur staff earlier this year. And while it seems that one of the bone cancers is a primary osteosarcoma, it appears that Dr Kelly's bone cancer was metastatic, and that the character of the primary cancer has not, in her case, been determined.

The case that the cluster may be statistical in origin is further supported by what is known of the movements of those involved. During the past ten years, between 200 and 400 people have worked in the Pasteur laboratories in which the three cases of bone cancer have now been recognized. Senior members of the Pasteur Institute also point to the occurrence of a similar cluster of cancer cases (brain cancers, characterized as glioblastomas) at a laboratory at Orsay over a period of twelve years; surprisingly, this has been shown to be consistent with chance.

Arguments such as these appear to have dampened most fears at the Pasteur itself, but there remains some concern that the external committee of inquiry set up by Dedonder last month may be inclined to cloud the issues. The commission includes Professor Jean Bernard, who is president of the French national ethical committee which considers issues raised by the new biology, and Professor Maurice Tubiana, director of the Parisian cancer hospital at Villejuif, both respected figures in French medicine. But the commission also includes three members chosen by the Pasteur's safety committee, a long-standing thorn in the flesh of the French nuclear industry.

Robert Walgate

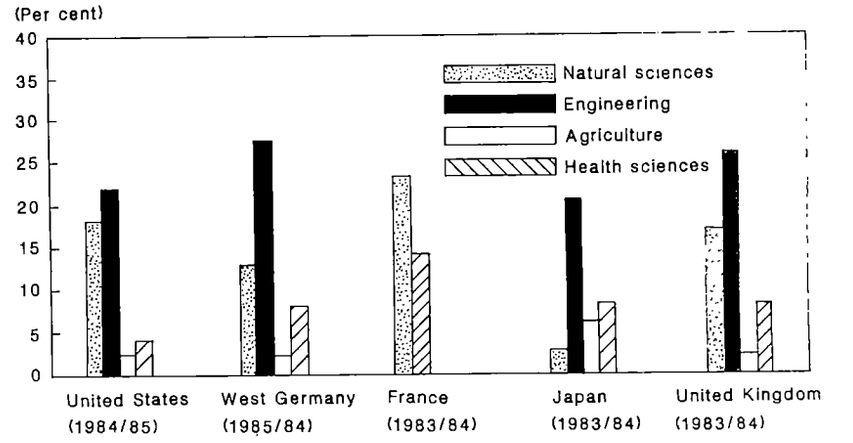
Chernobyl fallout: corrigendum

IN the letter "Initial observations of fallout from the reactor incident at Chernobyl" by L. Devell *et al.* (*Nature* **321**, 192–193; 1986), the inventory figures in the first column of Table 2 are low by a factor of 2.92. The correct column should read:

Nuclide	Inventory (10^{17} Bq)
^{137}Cs	1.52
^{131}I	29
^{103}Ru	41
^{141}Ce	53
^{132}Te	41
^{239}Np	543

Foreign students in science and engineering

OF all technical disciplines, engineering has the highest proportion of foreign students in each of the five countries above. The proportion ranges from 28 per cent in West Germany to 21 per cent in Japan. Japan also has the lowest percentage of foreign students in natural sciences (3 per cent), compared with 18 per cent in the United States. For France in the histogram there are no data available for engineering, and agriculture and natural sciences are combined. From International Science and Technology Data Update 1986, National Science Foundation, Washington, DC. □



AIDS virus nomenclature

SIR—Since July 1984 I have been writing on acquired immune deficiency syndrome (AIDS) for the London weekly free newspaper, *Capital Gay*. In the issue of 11 April I referred to a rumour that "human immune deficiency virus", "HIV" or "HIDV", was about to be proposed as the name for the causative agent. I fear that Robert Gallo is therefore mistaken in attributing first publication of this nomenclature to Luc Montagnier.

Your own objection to "HIV", that the "IV" might be confused with the roman "four", could be resolved by adopting the abbreviation "HIDV", for which there is an obvious precedent in "AIDS" for "acquired immune deficiency syndrome". However, combinations such as "HIV infection", "HIV disease", "HIV brain disease", "HIV lung disease" and "HIV lymphadenopathy" read far better than their "HIDV" equivalents.

As for the idea of "HTLV-III/LAV", fossilized forever, forget it. Are we expected to continue with "HTLV-IV/LAV-3" and "LAV-2/HTLV-V"? What next?

While the name of the virus is totally irrelevant to the needs of those directly affected by it, an agreement to use the new name opens the way to an easily-understood terminology for the whole spectrum of conditions linked to this virus, which would be very useful to the agencies concerned with educating the public and health professionals about it.

JULIAN MELDRUM
Capital Gay,
38 Mount Pleasant,
London WC1X 0AP, UK

SIR—At a meeting on 22 and 23 May 1986, the Executive Committee of the International Committee on Taxonomy of Viruses (ICTV) endorsed the name human immunodeficiency virus, recently proposed by a large majority of the members of a study group of ICTV, headed by Harold Varmus (J. Coffin *et al. Nature* **321,** 10; 1986 and *Science* **232,** 697; 1986), as appropriate for retrovirus isolates implicated as causing acquired immune deficiency syndrome (AIDS). The new name describes the host and a major biological property of the virus, recognizes the difference of the virus from isolates of human T-cell lymphotropic virus types I and II and avoids any controversy regarding priority of discovery of the virus and emotive connections of the virus with AIDS and its methods of transmission.

ICTV is working towards a uniform international nomenclature for viruses based on their taxonomy. Much still remains to be learned about the relationships of the human immunodeficiency virus with other retroviruses and therefore designation of an international name would be premature. However, the committee recommends the use of the name human immunodeficiency virus as the vernacular name to replace HTLV-III and LAV.

F. BROWN
(President, ICTV)
Wellcome Biotechnology Ltd,
Ash Road, Pirbright,
Woking, Surrey GU24 0NQ, UK

French science policy

SIR—France may be one of the richest countries in the world, but prosperity does not uniquely determine a country's scientific potential. The recent developments in science policy in France, and in particular the emphasis on applied sciences, is not a particularly creditable achievement for the policy-makers.

Every laboratory now seems to have been diverted towards applied science. In biology, chemistry, physics and mathematics, it is almost as if those responsible for policy have concluded that France has now done enough in basic science, and the time has come to exploit this knowledge for practical purposes. The result is debilitating for the laboratories previously concerned with basic science, now compelled to work in applied science to conform with the present fashion.

There is also a clear difference between the way in which those supported by the Centre National de la Recherche Scientifique (CNRS) establishment are equipped and the provision for ordinary academic scientists, who often work in the same laboratories. While CNRS groups have by no means everywhere attained the targets they have been set, they are nevertheless pampered with generous grants and sophisticated facilities that do not exist in ordinary university laboratories. Why should there be such a segregation?

In the basic science laboratories of the universities, scientists are to be found working on applied projects simply to earn the funds needed for their survival and to remain among the ranks of active scientists. No thought seems to have been given to this problem.

At the same time, research students are busily accumulating theses, a waste of money and time. These students are better served if they are trained in first-class laboratories instead of being fed a huge bulk of theoretical science. Policy-makers would find that if they abolished the present system, they could save time and money that could be used partly to safeguard French basic science.

NITIN K. SAKSENA
Université Paul Sabatier,
118 Route de Narbonne,
31062 Toulouse Cedex, France

Chernobyl's message

SIR—An important lesson of the Chernobyl disaster is that "probabilistic risk analysis" is a misapplied science. Its irrelevance to decision-making is now amply demonstrated. A core meltdown, designed to be less than a "one-in-a-million" chance in all reactors adopted by members of the International Atomic Energy Agency, has occurred twice within a decade.

Although such mathematical tools have their use in reactor design, they are still being applied uncritically in technology policy. In this respect they are dangerous, as they divert attention from the essential safety issues. These concern the hazard once realized (however improbably): control, and communication with and protection of the affected public. Doubtless misled by their own reassuring probabilistic predictions, Soviet scientists were caught unprepared in all respects, like their US colleagues at Three Mile Island.

British reactors are, on paper, exceptionally safe compared with Soviet reactors. But can the British public now believe that there is no need for detailed and well-rehearsed contingency plans for nuclear disasters? These should include not merely technical procedures on site, but also tested plans for communication with the public, and evacuation procedures for at-risk populations.

Developing such plans would involve scientists, public authorities and communities, in an extensive, open consultative dialogue. In the absence of such a programme, the nuclear industry's credibility will not be rescued by more reassurances couched in statistical rhetoric.

S.O. FUNTOWICZ
J.R. RAVETZ
Research Methods Consultancy Ltd,
158 Western Road, Sheffield S10 1LD, UK

No chance...

SIR—As positive probabilities refer to events that can happen, negative probabilities presumably refer to events that cannot happen. The greater the probability that the event cannot happen (as distinct from being unlikely to happen), the higher the (negative) numerical value.

DAVE E. PARRY
Department of Education,
Bell College of Technology,
Almada Street, Hamilton ML3 0JB, UK

Erratum

IN the letter "Too many fourth states of matter?" by J.M. Goldschvartz (*Nature* **320,** 302; 1986), the second sentence in paragraph 2 should read: "Moreover, physicists should be aware that since 1940 the attribution was used to describe the superfluidity of liquid helium 4 and 3 (refs 3–6)". □

Technetium-99m radiopharmaceuticals are being increasingly used for in vivo diagnosis in nuclear medicine

Our COMPLETE Tc-99m PROGRAM provides the basis for wide routine clinical application

^{99}Mo SODIUM MOLYBDATE	High radiation purity Constant availability
ROTOP-$^{99}Mo/^{99m}Tc$ STERILE GENERATOR	Easy and safe handling High elution yields
ROTOP-^{99m}Tc LABELING KITS	Ease of preparation High in vivo stability Constant availability in connection with a technetium generator

isocommerz

GmbH · Binnen- und Aussenhandelsunternehmen
für radioaktive und stabile Isotope
DDR - 1115 Berlin, Lindenberger Weg 70
German Democratic Republic

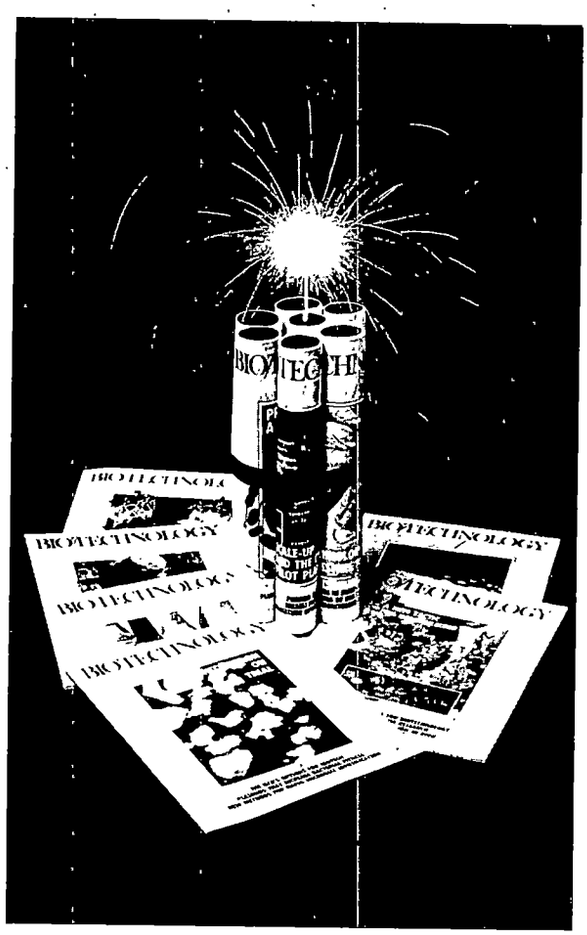
Reader Service No.13

CONVENIENT·INFORMATIVE·TIMELY·PROVOCATIVE

FOUR DYNAMITE REASONS WHY YOU SHOULD SUBSCRIBE TO BIO/TECHNOLOGY NOW . . .

1. You'll save time. Because you don't have time to read every journal in the field, BIO/TECHNOLOGY is written and edited to give you all the information you need in ONE convenient source. BIO/TECHNOLOGY is the only journal to give you news. Features. Original research. Product evaluations. Industrial applications. Job openings. Book and product reviews. And more. If it's important to your work, you'll find it between the covers of BIO/TECHNOLOGY.

2. You'll learn new ways to improve your on-the-job skills and run a more successful operation. Each month BIO/TECHNOLOGY gives you the scoop on invaluable start-up information . . . the latest instrumentation . . . marketing breakthroughs . . . funding sources . . . new technologies . . . patents and licences . . . profiles on how others are avoiding the pitfalls and reaping the rewards. In fact, just one practical tip from BIO/TECHNOLOGY can be worth many times the cost of your subscription.



3. You'll be up-to-date on all major industry developments. With correspondents all over the world, BIO/TECHNOLOGY delivers the inside story on who's doing what, where. You'll get the latest word on changing government regulations and tax law, and how they affect your work.

Plus you'll read original research papers by bench scientists, engineers, and biologists that will help keep you in the forefront of every new discovery worth knowing about.

4. You'll get new ideas you can put to use immediately. BIO/TECHNOLOGY lets you rub elbows with eminent scientists, tour new facilities and learn how new processes work in every field from genetic engineering to molecular biology. Each month, BIO/TECHNOLOGY helps spark ideas for your own research, for new industrial applications and for getting along in the increasingly competitive financial arena.

If you're not already subscribing to BIO/TECHNOLOGY, don't delay the moment any longer - return the coupon below and we will send you twelve issues. You risk nothing. If for any reason BIO/TECHNOLOGY doesn't live up to your highest expectations, just let us know and you'll receive a full refund on all unmailed copies. Remember too, that your subscription may be tax deductible.

TO START RECEIVING YOUR SUBSCRIPTION, FILL OUT THE COUPON BELOW AND RETURN WITH PAYMENT TO:

U.S.A.: BIO/TECHNOLOGY
Subscription Order Dept., P.O. Box 1543
Neptune, New Jersey 07754-1543 U.S.A.

To speed up your subscription in the U.S.A., call toll free 1-800-524-0328.

ENGLAND: BIO/TECHNOLOGY
Subscription Order Dept., Macmillan Journals, Ltd.
Brunel Road, Houndmills, Basingstoke
Hampshire RG21 2XS, England

☐ YES! Please send me one year of BIO/TECHNOLOGY (12 issues). I understand that I may cancel my subscription at any time and receive a full refund on all unmailed issues.

☐ U.S.A.-$59.00* ☐ Australia-A$130**
☐ U.K.-£70** ☐ Elsewhere-U.S.$112**

Japan Publications Trading Company Ltd
2-1 Sarugaku-cho 1-chome
Chiyoda-ku, Tokyo, Japan Tel: (03) 292 3755

Note: *Represents 24% off Basic Subscription Price of U.S. $78.00
**All other prices quoted are "Air Speed"

☐ My payment is enclosed at the price checked.
☐ Please charge my credit card account:
☐ American Express ☐ Mastercard ☐ Visa

Card No.: _____ Exp. Date: _____
Signature: _____
Name: _____
Company: _____
Address: _____
City/State/Postal Code: _____
Country: _____

7AUS

Towards understanding snowflakes

The reasons why the microscopic anisotropy of molecules in crystals is reflected in the shapes of the macroscopic structures which they form have been obscure. Now there is some progress.

THE celebrated symmetrical hexagonal dendritic shapes of snowflakes are so familiar that they should long ago have been explained; that might be everybody's reasonable expectation. But the physics of the problem is not nearly as simple as it seems. The essential difficulty is to account for the way in which anisotropy on the scale of molecules is reflected in the shapes of macroscopic crystals.

The problem is not especially difficult with crystals that form a reasonably compact mass. The crystals grown by the multitude in kindergarten classrooms by suspending a crystal seed by a piece of thread in a supersaturated solution form in regular shapes for energetic reasons, because that is how best to minimize the free energy of the system; provided that the access of extra molecules (or ions) is equally easy from all directions, which requires that in practice the crystal seed should not be too close to the side of the jar in which it is suspended, extra elements will be added in such a way as to form sheets parallel to the planes in the basic unit cell. If access is not independent of direction, the result will be a misshapen crystal, but the underlying symmetry will remain at the level of the unit cell.

Dendritic structures such as snowflakes are more difficult because they combine what often seems a startling gross symmetry with a disconcerting disorderliness on the scale of the dendrites. The simple-minded rules of crystal growth seem not to apply. The article by Johann Nittmann and H. Eugene Stanley (this issue, p.663) goes a long way to explain why some recent attempts at a solution have not succeeded fully. More than that, it embodies the essence of an explanation of the growth of dendritic crystals.

Broadly speaking, there have been two complementary approaches to the problem, the first due to J.S. Langer (reviewed by Langer in *Rev. mod. Phys.* **82**, 1; 1980), who has dealt with the growth of dendritic tips by the diffusion of new material through the surrounding medium. The arguments apply as well to crystallization from a solution as to condensation from a vapour phase. The rate at which material is added to a particular point on a growing surface is determined by the local geometry in the sense that protuberances are more likely than re-entry points to acquire material by diffusion. There may be circumstances in which growth is limited by the need that latent heat should be conducted away from the surface. The fact that growth depletes the local environment of the uncondensed phase of material means that growth will also be limited by the rate of diffusion. The usual upshot is a set of differential equations that cannot usually be solved exactly, but can be used to define the conditions under which a dendritic tip will continue to elongate or, alternatively, split.

The frustrations of this approach have stimulated the more recent phase of computer simulation, of which T.A. Witten was the first exponent (see Witten, T.A. & Sander, L.M. *Phys. Rev. Lett.* **47**, 1400; 1981). In the simplest model of diffusion-limited aggregation, as it is called, extra elements of the material of which a crystal is being constructed are supposed to be added to the system at random points of some distant boundary and are allowed to migrate by means of a random walk along the links of some underlying lattice. If the diffusing element should reach a point on the lattice which is an immediate neighbour of the growing aggregate, it may be supposed captured, but there are a host of ways of defining the aggregation rules, most of which appear to have been tried in the past few years.

The virtue of these simulations is that they yield patterns which indeed resemble those of real aggregates. In particular, they show that aggregates whose growth is limited by diffusion are fractal structures; in two dimensions, for example, the number of elements in an aggregate is not proportional to the square of its dimensions but to some lesser power of them, called the fractal dimension. At some cost in computer time, the simulations can be (and have been) carried out in any number of dimensions.

What Nittmann and Stanley have done is to combine these two approaches or, more accurately, to carry out lattice-based simulations of aggregation in a way that can be made to correspond to equations of the kind that Langer (and, now, many others) formulated. They have overcome the persistently annoying feature of simulations, the difficulty of telling the meaning underlying the patterns produced, by producing a series of patterns corresponding to the variation of some physical parameter over a known range. Their aggregation rules are among the simplest there could be, consisting simply of the requirements that new elements are added at random to the periphery of a growing aggregate, but that their assignment to the sites available is biased to reflect what the macroscopic equations suggest will be the rate of growth there.

One result of consequence to emerge arises from the fact that the simulation model can deal only with the addition of discrete elements to the aggregate. There are, as a consequence, departures from the macroscopic prediction of the regular outward extension of a regular envelope of the growing aggregate, which is fairly described by the authors as noise. The essence of this part of the result is that outward extensions of the surface are quickly smoothed out by the later addition of material, but that inward depressions are less readily filled in, but may instead persist as the apices of what are to become fiords in the pattern as the aggregate grows.

The simulations (see p.664) show that the patterns are typically broken up into a number of radially extended tongues of substance separated by lengthening fiords, while the tips of new fiords repeatedly form at the outer surfaces of the extending tongues. Given that the aggregation rules correspond to the penetration of one liquid into another with which it is immiscible, it is pleasing but not surprising that the fractal patterns formed resemble those found in such experiments. The circumstances correspond to those of practical importance in which oil companies pump water down into the oil wells so as to displace crude oil from its reservoirs.

But the most remarkable result of these simulations stems from the apparently successful attempt to allow for the anisotropy of the real world, which depends on the assumption that not all sites on the surface of a growing aggregate are equally suitable energetically. The criteria used in extending the aggregation rules are strictly microscopic; they depend only on the orientation — some sites are more likely to be occupied than their immediate neighbours.

One outcome is the pattern of an aggregate which is virtually indistinguishable from a fairy-tale snowflake, a feathery collection of dendrites which is plainly hexagonally symmetric overall, but whose smaller-scale structure is far from symmetric, which is the case with real snowflakes. That looks a convincing demonstration that the snowflake problem is on the way to solution.

John Maddox

Molecular biophysics

Energy and signal transduction by transmembrane protein complexes

from Alexander N. Glazer

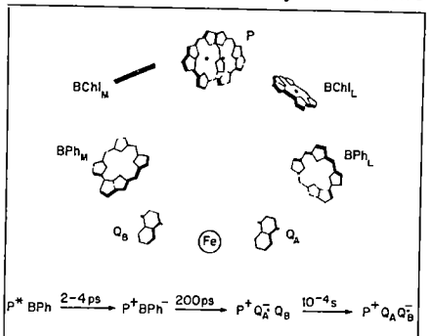
A RECENT conference* brought together molecular biologists, biochemists, X-ray crystallographers and spectroscopists to discuss the structure and function of various transmembrane protein complexes. These molecular machines enable cells as well as intracellular organelles to generate proton and ion gradients, transport metabolites, transduce information from one side of the membrane to the other and to control flagellar motion. But details of the mechanisms whereby these functions are accomplished remain to be discovered.

Approximately two years have passed since the determination of the crystal structure of the reaction-centre complex from the purple bacterium *Rhodopseudomonas viridis*. This achievement provided the first (and to date the only) high-resolution view of an integral membrane–protein complex. The *R. viridis* reaction-centre complex contains four molecules of bacteriochlorophyll-b (BChl), two of bacteriophenophytin-b (BPh), two different quinones (menaquinone, Q_A and ubiquinone, Q_B), a non-haem iron and four haems. All these components are embedded in a complex of four polypeptide subunits. (See Henderson, R. *Nature News and Views* **318**, 598; 1985 for further explanation.)

Electron flow

In principle, it should be possible now to gain a precise understanding of the details of electron flow through the complex, and the first session at the meeting dealt with studies directed towards that end. The formation of the P^+BPh^- state takes place within 4 picoseconds of excitation of the special pair of BChls (see figure). Topological considerations suggest that the electron might flow through the BChl which is between the special pair and the BPh. But P^+BChl^- does not appear to be a resolvable intermediate in the electron-transfer sequence. A P^+BChl^- charge-transfer state facilitates electron tunnelling between P* and BPh (see figure) by mixing electronically with both P* and P^+BPh^- (W.W. Parson, University of Washington).

The protein environment of the prosthetic groups modulates their properties in important ways. For example, electron paramagnetic resonance and electron-nuclear double resonance (ENDOR) data (W. Lubitz, Freie Universität, Berlin) on the *R. viridis* P_{960}^+· radical cation indicate an asymmetrical spin distribution. Moreover, the two BPh groups are spectroscopically distinct — the electron travels selectively down the pathway directed towards the Q_A site. A major feature of the reaction centre is that Q_A accepts one electron whereas Q_B can be doubly reduced. Both semiquinones are bound to the protein through hydrogen bonds. For Q_B^-· these bonds (of length *r*) appear to be symmetrical and fairly long whereas for Q_A^- the ENDOR data clearly indicate two hydrogen bonds of different strengths, about 1.3 and 1.6 Å, respectively. The asymmetrical H bond at the A site might be important in adjusting the redox potentials and locking Q_A as a one-electron gate.



Approximate arrangement of the chromophores in the *R. viridis* reaction centre (modified from Fig. 1 of Woodbury *et al. Biochemistry* **24**, 7516; 1985 and based on Deisenhofer *et al. Nature* **318**, 618; 1985). Abbreviations, P, 'special pair' BChl dimer; L and M, L and M subunits of the reaction centre (see text). The approximate position of the Q_B site is inferred from crystallographic studies of reaction-centre complexes with the competitive inhibitors *O*-phenanthroline and terbutryn.

Attempts to elucidate the biosynthesis, assembly and function of purple bacteria reaction centres and antenna complexes using molecular genetics are also in full swing. Thus far genetic manipulation has been confined to the photosynthetic apparatus of *R. capsulata* (now called *Rhodobacter capsulatus*). Replacement in the L subunit of a special-pair BChl ligand, His 174, by Leu leads to a loss of all three reaction-centre subunits from the membrane. But both the light-harvesting LHI and LHII antenna complexes assemble normally (D.C. Youvan, Cold Spring Harbor Laboratory).

Another surprising result was reported by F. Daldal (Cold Spring Harbor Laboratory). It had been thought that in *R. capsulata* cytochrome c_2 served as an obligate electron carrier between the cytochrome bc_1 complex and the reaction centre. Daldal replaced a portion of the cytochrome c_2 gene encoding the haem-binding domain of the protein with an insert encoding kanamycin resistance. As expected, the mutant cells contain no cytochrome c_2. The unexpected result is that the mutant grows at near wild-type rates under photosynthetic conditions.

Spectroscopic studies of electron transfer in both mutant and wild-type cells prompted by these findings reveal a complex situation (R. Prince, Exxon Corporation). In wild-type cells, the cytochrome c_1 of the bc_1 complex delivers energy directly and rapidly with a half-time of less than 100 μs to about 20 per cent of the reaction centres. A further 20 per cent receive energy rapidly from cytochrome c_2, whereas 30 – 40 per cent receive electrons on a timescale of several milliseconds. The slow transfer is attributed to cytochrome c_2 functioning as a mobile carrier diffusing along the membrane–aqueous interface and shuttling electrons from the cytochrome bc_1 complex to more distant isolated reaction centres.

Cytochrome complex

The ubiquitous cytochrome bc_1 complex was itself much discussed. In photosynthetic organisms, it stands at the crossroads of respiratory and photosynthetic electron flow. Independent of source, the bc_1 complex contains a cytochrome c_1, a cytochrome *b* with two haem centres and an iron–sulphur protein. In the mitochondrial complex described by G. von Jagow (University of Munich), theFe_2S_2 protein of relative molecular mass (M_r) 21,600 (21.6K) is largely polar and is attached to the outside of the mitochondrial cristae membrane by a short anchor at the carboxy terminus. Cytochrome c_1 (M_r = 28K) is also a polar protein with a membrane anchor inserted into the cytosolic surface of the membrane. Cytochrome *b* is a transmembrane protein (M_r = 42.4K) with a haem b_{566} centre (oxidation–reduction midpoint potential E_M = −50 mV) at the cytosolic surface of the membrane and a haem b_{562} centre (E_M = +50 mV) near the centre of the membrane. The iron atoms of the two haem *b* groups are spaced some 20 Å apart. The two haems create a path for electron transfer across the membrane. Six different small subunits, all of unknown function, are associated with the three polypeptides bearing the four redox centres. In contrast, the *Paracoccus denitrificans* bc_1 complex has the simplest composition and one of the highest turnover numbers of any bc_1 complex isolated to date (B. Trumpower, Whitehead Institute). The complex is made up of three polypeptides:

* The Banbury Conference *Microbial Energy Transduction: Genetics, Structure and Function* was held at the Cold Spring Harbor Laboratory on 23–26 February 1986. A summary will be published shortly by the Cold Spring Harbor Laboratory.

cytochrome c_1 (M_r = 62K); cytochrome *b* (M_r = 39K); and the Fe_2S_2 protein (M_r = 20K). The much larger size of the cytochrome c_1 polypeptide suggests that its sequence encompasses some of the components found as individual polypeptides in mitochondrial bc_1.

The notion that bacterial complexes are generally simpler than their mitochrondrial counterparts was supported further by a comparison of *Escherichia coli* cytochrome *d* terminal oxidase (R.B. Gennis, University of Illinois) with the cytochrome oxidase of mitochondria (T.G. Frey, University of Pennsylvania). The former complex is made up of one copy of cytochrome c_1 and two of cytochrome *d*, whereas the mitochrondrial complex contains six to twelve different polypeptides. Structural information on two-dimensional crystals of the mitochondrial complex is available at a resolution of 20 – 30 Å, but the question of whether mitochondrial cytochrome oxidase is a dimer or monomer *in vivo* remains unanswered.

In the examples described above, the distinctive spectroscopic properties of the multiple prosthetic groups provide direct access to information bearing on the consecutive steps in the electrogenic reactions which these complexes perform. Unfortunately, this is not the case with the next group of transmembrane complexes discussed — for example, the H^+-translocating ATP synthases, $(Na^+ + K^+)$ATPase and Ca^{2+}ATPase. Consequently, speculation still occupies centre stage in proposals for the detailed mode(s) of action of these complexes.

Common mechanism

There is increasing evidence that all of the synthases which react with ATP to form a covalent β-aspartyl phosphate (D*) intermediate may share a common mechanism of action. For example, the sequence CSD*KTGTLT (single-letter code) is fully conserved in the H^+ATPase of *Neurospora* and *Saccharomyces cerevisiae*, the $(Na^+ + K^+)$ATPase of sheep kidney and the Ca^{2+}ATPase of rabbit muscle. Moreover, a 15-residue sequence near the carboxy terminus of these enzymes shows variation in only three positions. The sequences of all three enzymes give rise to very similar hydropathy plots (C.W. Slayman, Yale University). In contrast, enzymes of the bacterial phosphotransferase system, enzyme II^{mtl} and enzyme II^{gut}– enzyme III^{gut}, which phosphorylate and transport mannitol and glucitol, respectively, show no significant sequence homology (M. Saier, University of California, San Diego).

R.M. Macnab (Yale University) presented the latest chapter in the continuing saga of studies of the bacterial flagellar motor. Genetic and biochemical studies have focused on five polypeptides which are not integral components of the basal body. Two of these, MotA and MotB, appear to be circumferentially arranged about the basal body and involved in interaction with other components of the motor to transduce proton potential into torque. The rest, Fla AII.2, FlaQ and FlaN, are important for assembly, rotation and switching. Deletion mutants in the corresponding genes do not assemble any detectable flageller structure. Missense mutants, depending on the allele, may be Fla^-, Mot^- or Che^-. The available evidence suggests that these switch proteins form a complex that is peripheral to the membrane and may be associated with the M-ring of the basal body. □

Alexander N. Glazer is in the Department of Microbiology and Immunology at the University of California, Berkeley, California 94720, USA.

Robert Day Allen (1927–1986)

Robert Day Allen, who died at home on 23 March after an intense one-year fight with pancreatic cancer, was one of the modern founders of the field of cell structure and motility, an area that he investigated during his entire career.

After a doctoral dissertation under L.V. Heilbrun on the nature of artificial activation of clam eggs, Allen continued basic studies on the structure of egg cytoplasm and pronuclear movements at the Wenner-Gren Institute, the Kristinebergs Zoological Station in Sweden, followed by a period at the University of Michigan and then at Princeton University. It was during this period that he evolved two major concepts that stayed with him during his entire research career. One concept was that living cells could yield important information about basic biological processes; the other that light optical methods in concert with electronic control and detection devices could yield molecular information in living cells. Allen was clearly one of the pioneers in applying quantitative light microscopy to basic questions in cell and molecular biology.

He next combined the use of biophysical techniques, especially light microscopy, to test the prevailing dogma on the mechanism of amoeboid movement. A combination of studies on living cells and isolated cytoplasm led him to re-examine the tail contraction model. He demonstrated that cytoplasm was not a newtonian fluid and possessed structure as evidenced by its optical polarization properties and ability to transmit applied tension. His observation, in 1955, that isolated cytoplasm from single cells could continue to generate motile forces ultimately led to the preparation of motile cell extracts that continue to yield important biochemical information today.

This early work demonstrated, experimentally, two fundamental concepts that had been discussed previously with much less experimental evidence: first, that cytoplasm can exist as both a medium of weak structural properties (sol) and as a viscoelastic solid (gel); and second, that the elements responsible for the generation of contractile forces exist in the cytoplasm. Allen's research on the structure and motility of cytoplasm led him to propose the frontal contraction model of amoeboid movement, still used as a valuable guide in the design of experiments for testing mechanisms of this type of movement.

In the late 1960s and early 1970s, at the State University of New York at Albany, Allen assembled his first electro-optical microscope. The phase-modulated microspectrophotometer enabled him to measure separately the optical polarization properties of linear birefringence, linear dichroism, optical rotation and circular dichroism in tissue sections, muscle fibres and solutions of proteins.

The last part of Allen's career was probably the most important in that he had a seminal influence on the development and use of video-enhanced contrast microscopy in cell and molecular biology. This method allows large increases in optical contrast which facilitates the detection of structures well below the limit of resolution of traditional optical microscopy. At the Marine Biological Laboratory in Woods Hole, Massachusetts, Allen and his many collaborators investigated fast axonal transport in squid axons and in isolated axoplasm. The fundamental discovery was that particles are transported along single microtubules. Furthermore, individual microtubules can exhibit motility along glass substrates. This exciting discovery has stimulated research in several fields where microtubules have been implicated in motile events.

Robert Allen loved the challenge and thrill of performing basic research and communicating the results. He was particularly interested in seeing the same kind of enthusiasm and drive in students. A major part of his interest in science was in communicating facts and concepts in novel ways. He produced many educational movies and pioneered the use of video disks as a medium for publishing results in the journal *Cell Motility* which he founded. His uncanny intuition in both biological processes and in optical methods was expressed repeatedly in his work on the structure and motility of cytoplasm, organelles and whole cells. The fluid nature of his scientific thought and experimental approach was undoubtedly influenced, in part, by his abilities as a concert cellist. His extraordinary talents will be missed, but his impact will long be felt.

D. Lansing Taylor

Mammalian energetics

Energetic costs of reproduction

from Paul H. Harvey

How expensive is reproduction? The answer depends on how we measure costs. Many evolutionary biologists and behavioural ecologists think in terms of parental investment, which is defined as decrements in a parent's future reproductive success that result from a current reproductive episode[1]. In contrast, ecologists and physiologists tend to focus on energetic costs which can be measured during pregnancy and lactation, either directly as energy allocated to reproduction or indirectly by increases in metabolic turnover or loss of fat reserves. A recent meeting* showed how advances in technology coupled with an ingenious choice of subjects for study provide a useful database which answers some questions but poses many more[2]. One of the most interesting results presented is reported by S.D. Thompson and M.E. Nicoll on page 690 of this issue[3].

Particularly striking contrasts in both reproductive patterns and energy needs are apparent when marsupials are compared with other (eutherian) mammals[4]. Large-bodied mammal species wean large offspring. A head start is given to the young of many eutherians because large species have long gestation length and produce large neonates. This trend is not so evident among the marsupials (gestation length is independent of maternal size, and the increase in neonatal weight with maternal size is much less marked). Furthermore, for their body sizes, marsupials tend to have lower basal metabolic rates than do eutherians, yet they still manage to wean larger offspring. How, then, do marsupials cope with the energy demands of lactation? The simple answer, illustrated by the work of Thompson and Nicoll[3], is that productive females of at least one species of marsupial (and two eutherian mammals with low metabolic rates) increase their resting metabolic rates during gestation and lactation to about the normal eutherian level, whereas the typical eutherian barely increases its higher resting metabolic rate. Which is energetically the more costly mode of reproduction — the short gestation and long lactation of marsupials, or the typical eutherian pattern of long gestation and shorter lactation? We do not yet know.

Size and taxonomic affinity are not the only correlates of basal metabolic rate. For several years, Brian McNab (University of Florida at Gainsville) has been pointing out dietary associations with metabolic rate[5–7]. Among the eutherian mammals, species feeding on invertebrates, fruit, seeds or the leaves of woody plants have low metabolic rates whereas those feeding on vertebrates, nuts and herbs tend to have high rates. McNab postulates cause and effect relationships, arguing that eutherian mammals exhibit the highest metabolic rates that their diet will allow, because high rates permit high reproductive output[6]. Species with low metabolic rates, so his argument runs, live on foods that "limit the rate at which energy is acquired by a mammal". For example, leaves of woody plants and some



Does the mass-specific resting metabolic rate of all marsupials increase during lactation? Bennett's wallaby (*Macropus rufogriseus*) with young, currently being studied at the Zoological Society of London.

invertebrates have low digestibility and often contain chemical deterrants to herbivory or predation. Such arguments may, of course, amount to nothing more than adaptive story telling, and might best be viewed as hypotheses that need testing.

How do the low mass-specific basal metabolic rates of the marsupials fit into McNab's scheme? The alternatives are that marsupials never live on diets which allow high rates of energy acquisition, or that increased metabolic turnover does not result in higher reproductive output among marsupials. Marsupials differ considerably in their diets, and like their eutherian counterparts, frugivorous and folivorous marsupials have low metabolic rates. However, vertebrate- and nut-eating marsupials do not have high metabolic rates. This, McNab claimed at the meeting, is because high basal metabolic rates are not reproductively advantageous for marsupials. His statement is supported by an apparent positive correlation between the maximum rate of population increase and basal metabolic needs in eutherians and the absence of such a correlation in marsupials. McNab's claim needs qualification in the light of Thompson and Nicoll's new work, and does not appear to have a ready explanation.

Metabolic rates like many other physiological and reproductive variables, change with body size. Almost all the work reported at the meeting included routine allometric analyses, which can place many problems into clear perspective. T.H. Kunz, A. Kurta and E.D. Pierson (Boston University) reviewed recent work showing that bats invest heavily in reproduction. Neonates are more than 20 per cent of the mother's body weight in most families, and even reach 38 per cent in the Rhinolophids. Is this unusual for a mammal? It is, but bats are small mammals, and small mammals produce disproportionately large young. When body size is taken into account, bats do produce large neonates but litters are small (generally singletons), so that litter mass is typical for a mammal the size of a bat. Why, then, do bats produce large single young? Bats wean when they are relatively young, perhaps an important feature in such mobile mammals. If the production of large young is an evolutionary tactic to shorten dependence on the parents, a trade-off between prenatal and postnatal development is implied. Yet the opposite pattern is found in primates and birds. Birds with long incubation for their body size also take longer to fledge after hatching[8], whereas those primates with relatively long gestation lengths wean their offspring late[9].

Differences in patterns of reproductive investment found in the primates are also apparent when comparing orders of mammals. For example, primates have longer gestation lengths and slower postnatal development for their body size than do other mammals: gestation is two to four times longer than in other mammals of equivalent weight, whereas milk production per unit time is far lower[10,11]. In this respect, humans turn out to be fairly typical primates, having low daily energetic costs of gestation and lactation. Humans are, however, atypical in one important respect: females have large subcutaneous fat reserves[12] and are thus further protec-

*Reproductive Energetics in Mammals, Zoological Society of London Symposium, 10–11 April 1986. Organized by Andrew Loudon and Paul Racey.

1. Trivers, R.L. in *Sexual Selection and the Descent of Man 1871–1971* (ed. Campbell, B) 136 (Aldine-Atherton, Chicago, 1972).
2. Loudon, A. & Racey, P.A. (eds) *Reproductive Energetics in Mammals* (Zoo. Soc. Lond. Symp., in the press).
3. Thompson, S.D. & Nicoll, M.E. *Nature* **321**, 690 (1986).
4. Russell, E.M. *Biol. Rev.* **57**, 423 (1982).
5. McNab, B.K. *Am. Nat.* **116**, 106 (1980).
6. McNab, B.K. *Ecol. Monogr.* **56**, 1 (1986).
7. McNab, B.K. *J. Zool., Lond.* **A208**, 595 (1986).
8. Lack, D. *Ecological Adaptations for Breeding in Birds* (Methuen, London, 1968).
9. Harvey, P.H. & Clutton-Brock, T.H. *Evolution* **39**, 559 (1985).
10. Martin, R.D. *J. Morph. Anthrop.* **71**, 115 (1980).
11. Martin, R.D. *Symp. Zool. Soc., Lond.* **51**, 87 (1984).
12. Verhaegen, M.J.B. *Med. Hypoth.* **16**, 17 (1985).

ted from short-term energy crises during pregnancy and lactation.

A.M. Prentice and R.G. Whitehead (Cambridge University) presenting their own and others' work, conclude that the costs of reproduction in humans may be even lower than previously estimated. Important and previously unrecognized factors are a drop in basal metabolic rate over the first trimesters of pregnancy (which can be large enough to mean a net saving over the whole of pregnancy) and, for many women, a further drop in basal metabolic rate during lactation. Perhaps we should not be surprised that, under conditions of acute food shortage, birth weight is decreased by no more than 10 per cent, and that lactation capacity appears to be largely unaffected (except perhaps in women with primary protein deficiency). Prentice and Whitehead, however, were at pains to point out that although "human pregnancy and lactation are remarkably resilient to the effects of energy restriction", babies born in the Gambia with a "biologically trivial deficit in birthweight of about 5 per cent" have significantly increased mortality[2].

Energy is a resource that can have a profound influence on reproductive success. Although the importance of energetic limitations have, on occasion, been over-emphasized by biologists, it can be equally unwise to overlook the energetic costs of biological processes. □

Paul Harvey is in the Department of Zoology, University of Oxford, South Parks Road, Oxford OX1 3PS, UK.

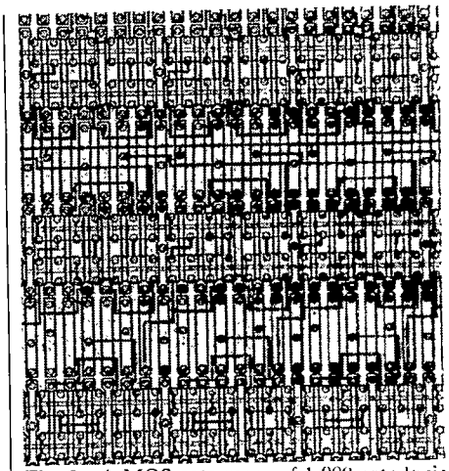


Fig. 2 A MOS gate array of 1,000 gate logic circuits interconnected with laser deposited poly-silicon in a direct-write mode at Lawrence Livermore National Laboratory (courtesy of Bruce M. McWilliams).

Laser technology

Microfabrication of thin films

from Ian W. Boyd and F. Micheli

THERE is a growing realization that laser-beam processing could provide a powerful and versatile technology for manufacturing thin films and surface structures, and this has remarkable implications for microelectronic, optoelectronic and microwave devices. In recent years this realization has stimulated research interest in laser processing of thin films in almost every major semiconductor industry. The many recent publications and international conferences devoted solely to this topic[1-4] show that lasers can accurately and controllably perform etching, doping, alloying, surface cleaning, crystallization, oxidation and deposition — indeed, all the processes required to fabricate microelectronic circuits. Even more excitingly, because of the tunability, high intensity and focusability of the radiation emitted by lasers, completely new regimes of processing can now be attained.

Technological interests in this area are abundant. For example, as very large-scale integration (VLSI) devices shrink towards sub-micron dimensions, reductions in processing temperature become necessary to improve resolution and to minimize defect densities. Lasers offer both a controllable decrease in high-temperature processing times and many alternative low-temperature methods of film and pattern formation. In optical lithography, ultraviolet radiation from excimer lasers is already replacing conventional light sources, thereby maximizing the resolution of the photoresist definition.

Because of the complex nature of energy redistribution within matter, many different routes to laser-initiated reactivity are possible. Often photothermal contributions can be identified in primarily photochemical reactions. There are usually also subtle but important influences on the reaction arising from surface phenomena. Consequently, the area of laser-surface chemistry presents opportunities to observe many new phenomena, but also presents problems in understanding photon-enhanced chemical reactions.

There are two main modes of operation in laser processing, pyrolysis and photolysis, each defining specific bond-breaking mechanisms. In the former, chemical reactions are stimulated by supplying thermal energy to reduce the reaction barrier. This is conventionally achieved by furnace heating, but a stronly absorbed laser beam can also induce the temperature necessary for deposition, alloying, diffusion, oxidation or evaporation

Photolysis involves direct stimulation of a bond through a precise matching of the energy of the individual photons to particular electronic or vibrational levels in the irradiated species. When a sufficient number of photons have been absorbed, selective dissociation occurs, thereby creating reactive species that promote, say, film growth or material removal In this way many types of gas-solid interactions can be initiated.

Laser etching and removal of oxides, nitrides, metals, silicon and gallium arsenide has led to maskless direct patterning, thereby dispensing with conventional photolithographic methods. The delineated pattern is realized by 'drawing' the focused beam across the film through electronic control of positioning stages The etching reaction occurs around the area of substrate illuminated by the laser beam. An alternative technique involves direct imaging of the mask pattern on to the film using the intense processing beam (Fig. 1).

The complementary process of thin-film growth (or deposition) has also been intensively studied. In fact, direct writing, or laser pantography, has been used at Lawrence Livermore National Laboratory successfully to produce the first functional *ab initio* multi-layered MOS (metal-oxide-silicon) transistors. Figure 2 shows a poly-silicon interconnect pattern obtained by the Livermore group written by a computer-controlled laser beam[6]. Patterned deposition by mask imaging has not been studied nearly so extensively.

The technology is clearly still at the investigative stage. Whether it will be

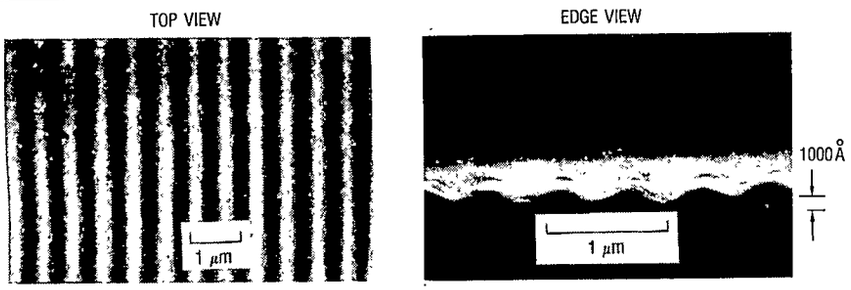


Fig. 1 Pattern-etched molybdenum by projection exposure technique. Conditions: 193-nm laser photolysis of 760-Torr NF_3, fluence 36 mJ cm^{-2}; Ronchi pattern projected with Schwartzchild objective (G.L. Loper and M.D. Tabat, Aerospace Corporation, Los Angeles).

accepted by the microelectronics industry, where present production has been fine-tuned and optimized by a deliberate and complex programme over many years of intensive investigation, depends on several criteria. New methods can only be accepted if they can be fitted succesfully into the production line with minimal disruption. Many laser-processing methods require major redesign of the existing production lines.

Throughput and reliability are also major considerations. We have calculated that it would take almost one month to draw a metallization pattern on a 6-inch wafer using a half-micron diameter laser beam and a rapid deposition rate of one micron per second. For the imaging techniques to be superior in this application, large-area high-power beams would be necessary. Although several years ago the field was somewhat limited by the availability of reliable high-power ultraviolet lasers, there has recently been dramatic progress in excimer laser technology that make this processing mode more realistic.

The essentially 'one-step' maskless processing capability does present a range of modest applications in VLSI that require only discretionary processing, or corrective 'surgery'. Discrete material removal (by etching, ablation or evaporation) filling-in (by deposition), or rerouting (by direct writing) of particular features is possible on a low-volume basis on newly fabricated or prototype masks, thereby dispensing with design correction and costly manufacture.

Similar operations are also feasible on low-volume complex circuitry and on customization of chips using elective interconnection of prefabricated gate arrays or programmable logic arrays. In this way, the development of prototype circuits may be speeded up, through interconnection of predesigned cells on 'generic' chips[8]. Additionally, areas of the circuit that are notoriously difficult to fabricate and that exhibit very low yields can be reproduced many times on the same chip and wired in afterwards using localized metal deposition when one particular cell is found to work satisfactorily.

For the full potential of this emerging technology to be realized, there is a need both for more extensive research into the fundamental aspects and for increased effort in developing more useful precursor compounds and even more powerful and reliable ultraviolet laser systems. □

1. *Beam Induced Chemical Processes* (eds von Gutfeld, R.J., Greene, J.E. & Schlossberg, H.) Extended Abstracts Materials Research Society, Pittsburgh, 1985).
2. *Laser Assisted Deposition, Etchng and Doping* (ed. Allen, S.D.) Vol. 459 (SPIE, 1984).
3. *Laser Processing and Diagnostics* (ed. Bauerle, D.) (Springer, Berlin, 1984).
4. Loper, G.J. & Tabat, M.D. *SPIE EO LASE 86* Los Angeles, 19-24 January 1986 (in the press),
5. Lawrence Livermore National Laboratory Laser Processing Group *SPIE OE LASE 86* Los Angeles, 19-24 January 1986 (in the press).
6. McWilliams, B., Herman, I., Mitlitsky, F., Hyde, R.A. & Wood, L.L. *Appl. Phys. Lett.* 43, 946 (1983).
7. Yasaitis, J.A., Chapman, G.H. & Raffel, J.I. *IEEE Electron Dev. Lett.* 3, 1264 (1982).
8. Ehrlich, D.J. *et al. IEEE Electron Dev. Lett.* 3, 164 (1984).

Ian W. Boyd and F. Micheli are in the Department of Electronic and Electrical Engineering at University College London, Torrington Place, London WC1E 7JE, UK.

Immunology

Approaches to tolerance in man

from Leslie Brent

THE title of a recent meeting* suggests that the immunologist's El Dorado — specific unresponsiveness in man — is within our reach. Alas, this proved not yet to be the case. What emerged clearly enough was that it is now possible to manipulate the immune system of experimental animals, from rodents to non-human primates, in various ways so as to achieve functional tolerance of skin, kidney, heart or bone marrow allografts, and that this is almost invariably accompanied by the appearance of suppressor cells.

There are all manner of difficulties in applying these models to man, for some of them are highly complex and others depend on genetic tricks that can be performed only in experimental animals with a short gestation period, such as rodents, but the miniature swine, too, seems to lend itself to this kind of selective breeding (D. Sachs, National Cancer Institute, Bethesda).

A ray of hope was provided by the technique of total lymphoid irradiation (TLI), pioneered for the treatment of Hodgkin's disease, when followed by bone marrow transplantation. This technique involves the irradiation of the patient's immune system with a series of relatively small doses (150–200 rad) over a period of time while shielding certain parts of the body. It is immensely safer than whole-body irradiation and is now being applied not only to bone marrow and kidney transplantation but also to diseases thought to have an autoimmune origin such as rheumatoid arthritis, systemic lupus erythematosus and multiple sclerosis.

Although the elusive suppressor cell provided a link between many of the very heterogeneous contributions to the conference it is fair to say that, in the context of autoimmunity, TLI has so far merely provided a reasonably safe form of non-specific, although long-lasting, immunosuppression, with tolerance to the offending and unknown autoantigens still to be demonstrated. One interesting spin-off was the observation (B. Bresniham, St Vincent's Hospital, Dublin) that TLI given to rheumatoid arthritis patients appears to retard the rate of radiological change in the joints without in the least affecting the level of rheumatoid factor, thus throwing some doubt on the causative role of the immunoglobulin M factor.

The ray of hope alluded to above was provided by TLI in combination with transplantation of bone marrow cells matched for antigens at the major histocompatibility complex (HLA) and depleted of T cells. This was applied in several protocols (with and without chemotherapy and in one group with additonal fractionated doses of whole body irradiation) to patients suffering from aplastic anaemia and to a small group of β-thalassaemic children (M. Slavin, Hadassah University Hospital, Jerusalem). The clinical results are extremely encouraging. It is, however, questionable whether the tolerance of the donor cells to host antigens can be attributed to the irradiation rather than to the absence of mature T lymphocytes in the transplant and the acquisition of tolerance by newly generated T cells, as happens in both animal and human bone marrow recipients when other forms of immunosuppression are used. Likewise, good survival of cadaveric renal allograft can be obtained by TLI given together with an initial regimen of low cyclosporin and prednisolone (J.A. Myburgh, Unversity of Witwatersrand Medical School). But whereas Myburgh has incontrovertible evidence that TLI leads to donor-specific tolerance in baboons, this has yet to be demonstrated in patients.

The question of whether TLI is good and safe enough to supplant immunosuppressive drugs in routine kidney transplantation is finely balanced and, until further information is provided, I suspect that most transplant surgeons will continue to opt for drug-induced immunosuppression which, in the best centres, is now yielding very good results although side-effects continue to be a problem.

The mechanism preventing graft-versus-host disease after TLI and allogeneic bone marrow transplantation in rodents was the subject of lively debate. S. Strober (Stanford University) reminded the meeting that natural suppressor cells generated by this strategy have a null phenotype, that they can be cloned and that they appear to be closely similar to the natural suppressor cells that Strober's group and others have identified in the spleens of neonatal mice. A subset of neonatal suppressor cells can be cultured in interleukin-3 (M. Jadus, University of

**Approaches to Human Immune Tolerance* Asilomar, California, 9–12 March 1986; organized by S. Strober and R. Hoppe, Stanford University.

South Florida and R. Parkman, Children's Hospital of Los Angeles) and are 'mast cell-like' in that they contain granules that can be shown to cytotoxic.

The nature of the cytotoxicity has yet to be elucidated. M. Slavin described the suppressor cells induced after TLI in rodents as thymus-independent, non-lymphoid, large and immature, and suggested that the effect of TLI is to cause a reversion of the animal's lymphoid system to the neonatal state. Examining the thymus after TLI, Strober found both histological and functional abnormalities in the medulla (failure of cell proliferation after exposure to interleukin-1 and a marked drop in interleukin-2 production when cultured with the lectin concanavalin A), which he explained by the premature departure of cells from the thymus.

There seemed to be some consensus that the suppressor cells in many experimental models are large granular lymphocyte-like cells and K. Singhal (University of Western Ontario) showed that such cells, isolated from normal bone marrow, can regulate *in vitro* immunoglobulin M responses to several non-transplantation antigens. These cells release a heat-stable, low molecular mass glycolipid that is suppressive *in vitro* if antigen is present from an early stage. The view was expressed that the role of natural suppressor cells is primarily to assist with the functional deletion of self-reactive clones, but they could also have great significance in protecting the mammalian fetus against destruction by maternal responses. The study by B. Roser (Institute of Animal Physiology, Babraham, UK) on neonatally induced tolerance was, however, a salutory reminder that suppressor T lymphocytes, in this case anti-idiotypic cells acting together with another, as yet unidentified, cell can be critically important in transplantation tolerance.

In summary, the conference left no doubt that approaches towards human tolerance are varied; that the main objective remains both valid and desirable; and that we still have a long way to go. □

Leslie Brent is in the Department of Immunology, St Mary's Hospital Medical School, London W2 1PG, UK.

Visual information

Do computers need attention?

from Anya Hurlbert and Tomaso Poggio

DESPITE enormous progress in the past few decades, machine vision is still far from achieving the goal that human vision attains with such speed and reliability — in David Marr's words[1], to "know what is where by looking". Recent results on the physiology and psychophysics of visual attention, one example of which is reported on page 693 of this issue[2], accentuate the gap between machines and humans, and provide a first step to understanding why it is so large and what machines must learn to overcome it.

Paradoxically, what appear to be the simplest tasks for humans may be the most difficult for machines. Consider, for example, recognizing your mother in a sketch of her sitting in the kitchen. You could immediately and effortlessly locate her face, match it with your memory and pronounce it a good or a bad likeness. If the sketch were upside-down you could easily right it for a proper view. You would probably expend the most painstaking scrutiny in determining just which feature was slightly off, but even so, your final judgement would be quick. In contrast, a computer, using the most sophisticated face-recognition routine, would perform the task slowly and incompletely, because it would not know where to start. Given the location of the two eyes in a sketch cluttered with dark, round blobs, a computer could be programmed to search for the mouth, nose and chin at the appropriate distances and methodically to match each feature to a virtually identical image in its memory. But failing to find the eyes, the computer could not go on to recognize the face.

Object recognition

The difficulty of the face-recognition problem — and, more generally, object recognition — has called into question one of the main assumptions in the construction of a machine that sees as humans do. The assumption holds that the goal of the first stages in vision is solely to determine 'where' things are, that is, to transform the initial image, an array of intensity values, into a map of the scene which records the distance and orientation of each surface point relative to the viewer (the $2\frac{1}{2}-D$ sketch[1]). In machine vision the $2\frac{1}{2}-D$ sketch may serve to guide a mobile robot around an obstacle or to control its manipulations as it picks up a tool. But, like the raw image from which it is computed, the $2\frac{1}{2}-D$ sketch is itself simply a large array of numbers. Although it may contain preliminary information for object recognition by assigning a colour or texture to each surface point, it does not tell 'what' things are. The critical task in object recognition is therefore to find the object or its crucial part within an array of intensity values or distances. Until now, many attempts to elucidate object recognition (reviewed in refs 3,4) have assumed that the relevant object is already located and isolated in the image.

Unlike machines, humans are adept in spotting the salient features of an object. To understand the mechanisms underlying this ability, psychophysicists have investigated visual attention. Treisman[5] and Julesz[6] have demonstrated that humans are extremely efficient in detecting a part of an image that differs in a single aspect from its background. For example, a red dot pops out in a field of yellow dots, and the same happens for a horizontal line in a field of vertical lines (Fig.1). The time required to detect the unusual item is independent of the number of other items, implying that the search for it occurs in parallel across the entire field. The human visual system obviously possesses a fast, parallel mechanism which can direct attention to salient chunks of the image. (This is sometimes called 'preattentive'. Here, we consider it as part of the entire attention mechanism whose characteristics probably require more complex descriptions than 'serial' or 'parallel'.) Although the possible computational purposes of this mechanism have not been probed by psychophysical experiments, its potential role in object recognition seems critical. For example, in face recognition the attention mechanism may perform two essential steps: first, to locate 'blobs' which could be eyes; and second, to direct processing towards the blobs to verify that they are eyes and thereby to initiate recognition. The role of attention, therefore, may be not only to spotlight distinctive parts of the image but, more importantly, to segment the image into objects or parts of objects, a crucial first step in determining what things are.

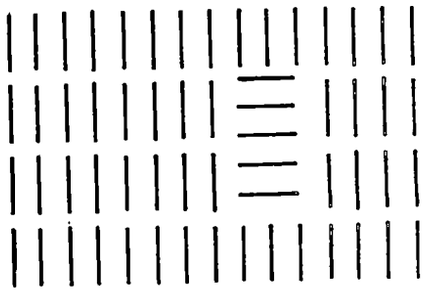


Fig 1. A patch of horizontal line segments pops out in a field of line vertical line segments.

Separable features

An important and still open question is: what are the features or primitives that drive attention? Likely candidates are separable features which, by definition, can be attended to selectively and are processed independently and in parallel. Pop-out and texture-discrimination experiments provide a test for separable features and so far have diagnosed colour, line orientation, line ends (terminators) and possibly crossings among the candidates.

Conjunction experiments test whether two or more separable features can combine to produce a higher-order primitive. For example, when a green T in a field of randomly mixed green Xs and brown Ts is the target, it does not pop out, and the time required to detect it increases linearly with the number of background items. Thus, the detection of a particular conjunction of colour and shape appears to require a search over each item in turn, across the entire field. Conjunction experiments thus reveal another aspect of the attention mechanism, a serial searchlight which appears to operate independently of eye movements and does for feature conjunctions what the parallel mechanism does for features.

Until recently, all conjunctions between known separable features had been shown to require the serial searchlight. The recent results of Nakayama and Silverman[7] reveal a surprising exception to this pattern. In pop-out experiments using fields of small rectangular patterns displayed on a colour television monitor, the authors demonstrate that binocular disparity and motion individually behave as separable features. The conjunction of motion and colour does not; the search for a pattern of blue upward-moving dots is slow and serial across a field of blue-downward patterns and red-upward patterns. Contrary to this trend, conjunctions of binocular disparity and either colour or motion behave as separable features: they are searched for in parallel. (The authors report that when the field splits into two planes, one in front of the other, the search for a conjunction amounts to a pop-out of the unusual item in one plane. Thus, we suggest that it may be possible, using a different kind of motion stimulus, to create separate planes of coherent motion and thereby induce a parallel search for motion-colour conjunctions.)

Experiments

The psychophysical studies on separable features coincide with the recent emphasis on functional localization in visual neurophysiology and neuroanatomy. It is tempting to draw an explicit connection between biology and psychophysics by equating different visual cortical areas with different feature maps; for example, calling area V4 the colour map, MT the motion map and V1 the orientation map. Psychophysics suggests that in a given feature map there exists at each spatial location a collection of neurones each tuned to a different value of the feature (for example, red, green or blue for colour). Although such an organization has not been demonstrated, evidence for segregation of functionally similar neurones in distinct cortical areas is steadily accumulating. From this point of view, the results of Nakayama and Silverman have interesting implications for neurones and feature maps: they preclude the existence of neurones tuned for both motion and colour; predict the existence of neurones tuned to a particular combination of binocular disparity and motion and of neurones tuned to disparity and colour; and suggest that feature maps are replicated at each of several disparity planes. The prediction of disparity–motion-tuned neurones is supported by the recent report[8] of similar neurones in cortical area MT.

Other recent work on visual neurophysiology puts the emphasis on a different aspect of attention. Rather than address computational questions such as 'what are the salient features?' and 'how does the attention mechanism work?' or the psychophysical question 'is feature processing parallel or serial?', the new class of physiological experiments on alert animals seeks to demonstrate the ways in which attention can modulate neuronal responses. In the course of such experiments, insights into the neural circuitry

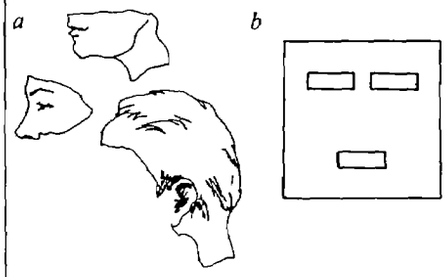


Fig. 2 *a*, each separate set of 'face' features is sufficient to suggest the hypothesis of a face. *b*, It is spatial relation between features and not the features themselves that cue recognition to the face of hypothesis.

and anatomical location of the attention mechanism have emerged. For example, based on studies of attention-mediated modulation in the inferior parietal lobe (area 7), Mountcastle[9] proposed that neurones there are responsible for directing attention to visual targets.

More recent research demonstrates the effects of attention at other levels in the visual pathway. Moran and Desimone[10] have recently shown that, in the monkey, the response of a neurone in V4 or IT to a preferred stimulus (for example, a red horizontal bar) is dramatically reduced when the animal ignores it and instead attends to an ineffective stimulus (such as a green vertical bar) within the same receptive field (which, for IT neurones, may extend at least 12°). The response of the neurone to the preferred stimulus is unaffected when the attended stimulus is outside its receptive field. Thus, V4 and IT neurones are able to filter out an irrelevant stimulus when it competes with a relevant stimulus within the same receptive field. V1 neurones do not have this property, since the monkey cannot even perform the differential attention task when two stimuli are close enough to fit within a single receptive field in V1.

The psychophysical experiment in humans reported in this issue by Sagi and Julesz[2] provides an intriguing complement to the physiological results described above. The authors find that visual attention directed to a random location for an orientation-discrimination task enhances the detection of a test flash presented simultaneously within a certain radius of the target. The area of enhancement, which the authors conjecture to be the area covered by the searchlight of attention, varies from 1.5° at 2° eccentricity to about 3° at 4° eccentricity. Interestingly, these areas are likely to be larger than the average receptive-field sizes in V1.

The above results imply that attention to one region of an image involves both suppression of visual processing in irrelevant domains and enhancement of visual processing in relevant domains. Thus, attention may indeed be responsible for directing a processing focus to specific locations in the initial steps of recognition. Yet although biological research may have found the key to machine vision, it has yet to describe how it opens the lock.

Attention mechanism

Computational results suggest that the attention mechanism is even more complex and powerful than experiments have revealed. Consider again the face-recognition problem. Individual features such as eyes or the curved line of nose and mouth can by themselves lead to the hypothesis of a face (Fig.2*a*). In contrast (Fig.2*b*), features alone cannot be the only cue for recognition. The spatial relationship between the two eye tokens and the closed outer contour can also cue the face-recognition process. Ullman[11] argues that spatial relations must be computed by a mechanism similar to the serial searchlight of attention.

The unravelling of the full complexity of visual attention will clearly involve computational, psychophysical and physiological research. It will influence not only our understanding of visual perception but also the architecture and the control structure of machine vision systems. □

1. Marr, D. *Phil. Trans. R. Soc.* B275, 483 (1976).
2. Sagi, D. & Julesz, B. *Nature* 321, 693 (1986).
3. Besl, P.J. & Jain, R. *Computing Surveys* 17, 74 (1985).
4. Harmon, L.D., Kahn, M.K., Lasch, R. & Ramig, P.F. *Pattern Recognition* 13, 97 (1979).
5. Treisman, A. in *Physical and Biological Processing of Images* (eds Braddick, O.J. & Sleigh, A.C.) 316 (Springer, Berlin, 1983).
6. Julesz, B. *Trends Neurosci.* 7, 41 (1984).
7. Nakayama, K. & Silverman, G.H. *Nature* 320, 264 (1986).
8. Van Essen, D.C. & Maunsell, J. *J. Neurophysiol.* 49, 1148 (1983).
9. Lynch, J.C., Mountcastle, V.B., Talbot, W.H. & Yin, T.C.T. *J. Neurophysiol.* 40, 362 (1977).
10. Moran, J. & Desimone, R. *Science* 229, 782 (1985).
11. Ullman, S. *Cognition* 18, 97 (1984).

Anya Hurlbert and Tomaso Poggio are in the Center for Biological Information Processing, Whitaker College, and at the Artificial Intelligence Laboratory, Massachusetts Institute of Technology, Cambridge, Massachusetts 02139, USA.

Epstein–Barr virus

Infection and tumour induction

from M. A. Epstein

EPSTEIN–BARR (EB) virus, a herpesvirus of man, resembles all other herpesviruses in establishing a persistent carrier state throughout life following initial infection. It has long appeared to infect B lymphocytes exclusively and this specific tropism has been explained by the recent demonstration that the B-lymphocyte C3d receptor CR2 for serum complement also acts as the virus receptor. Infected individuals, however, shed virus into the saliva and the cellular site of viral replication in the epithelium-lined oropharynx has been an enigma. So too has been the oncogenic role of the virus in undifferentiated nasophargeal carcinoma, a tumour whose malignant epithelial cells always carry the viral DNA. The finding of virus receptors on epithelial cells[1] and of a viral transforming gene[2] has now shed the first light on these interrelated problems.

Because only B lymphocytes could be infected experimentally by EB virus it was easy to understand the presence of latent infection readily demonstrable in a percentage of the circulating B cells of infected subjects. For similar reasons, it was assumed that the productive infection responsible for the infectious virions shed into saliva probably arose from infected B cells within the lymphoid tissue of Waldeyer's ring — including tonsils, adenoids, Eustachian cushions and lingual follicles. Hints that epithelial cells might be involved proved difficult to interpret in the absence of a satisfactory mechanism whereby the virus could enter and infect them. But early claims that EB virus replicated in oropharyngeal epithelial cells during primary infection accompanied by infectious mononucleosis were eventually supported and there were also reports that the viral DNA was present in both salivary gland and normal nasopharyngeal epithelial cells. Furthermore, a small proportion of epithelial cells from the human uterine cervix, not usually thought to be associated with EB virus, could apparently be infected after appropriate manipulation *in vitro*.

Striking and unequivocal evidence for EB virus replication in epithelial cells has recently been obtained[3] in the context of the immunological disarray which accompanies the acquired immune deficiency syndrome (AIDS). 'Hairy' leukoplakia of the tongue is a newly described lesion of homosexual males suffering from characteristic immunodepression involving absent or poor responses to antigen skin tests and altered, or frankly inverted, ratios of helper to suppressor T lymphocytes. The patients either have AIDS or are likely to develop it and large numbers of biopsy samples of the tongue lesions have been shown by electron microscopy, specific immunofluorescence tests, and DNA hybridization using EB virus probes in Southern blots, to have EB virus replicating in prickle cells[3]; a papillomavirus was frequently also present, sometimes even in the same cells.

The crucial importance of specific cytotoxic T cells in maintaining the virus-host balance in the life-long EB virus infection has come to be recognized in the past few years. The balance is delicate, and impairment of T-cell surveillance predisposes to virus-induced pathology. It has been demonstrated repeatedly that transplant recipients on immunosuppressive therapy to prevent graft rejection have depressed numbers of cytotoxic T cells and increased amounts of EB virus shed from the mouth; they also have a heightened incidence of EB virus-associated lymphomas. There is thus a clear parallel with certain aspects of AIDS in which cytotoxic lymphocytes are depleted, unusual EB virus production takes place as seen in the epithelial prickle cells of "hairy" leukoplakia[3], and lymphomas carrying EB virus are common. It is of great interest that attacks of falciparum malaria are likewise accompanied by a fall in T-cell numbers and inversion of the ratio of helper to suppressor T cells, since the hyperendemic form of this disease has been recognized for many years as an essential co-factor in the induction of virus-related endemic Burkitt's lymphoma.

Interactions between EB virus and epithelial cells are no longer mysterious. Using two monoclonal antibodies against different epitopes of the complement C3d CR2 EB virus receptor, Young and colleagues[1] show that the receptor molecules are present on the cells of oral and nasopharyngeal squamous epithelia and, in view of the hairy leukoplakia findings, it may be significant that on the tongue the receptors appear to be restricted to the prickle cell layers. All the evidence now supports the view that permissive productive replication of EB virus takes place in oral and pharyngeal epithelial cells, which fits well with the ten-year-old observation that malignant epithelial cells of nasopharyngeal carcinoma, which carry the virus genome, can be readily induced to produce infectious virus both in tissue culture and in nude mice.

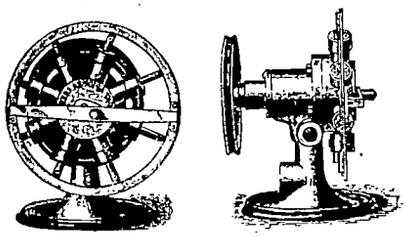
If entry of EB virus into epithelial cells can now at last be understood, what of its role in changing them into cancer cells? As far as nasopharyngeal carcinoma is concerned, nothing has hitherto been clear.

100 years ago

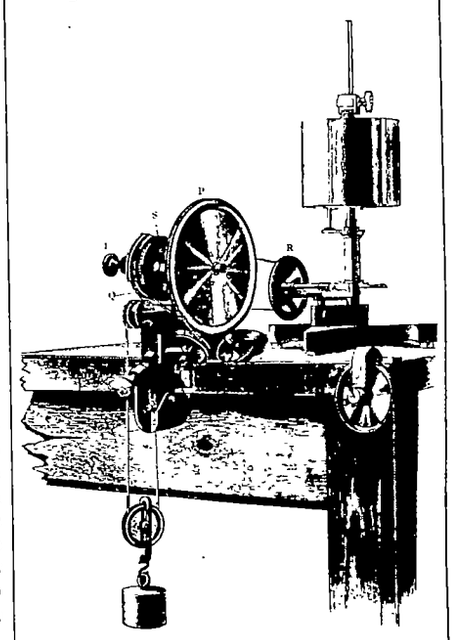
Power in Laboratories

IN connection with the admirable devices for the distribution of driving-power in laboratories, illustrated in *Nature*, vol. xxxiii. p. 248 (shown opposite), the description of a novel and very effective form of water-engine, with which I have been experimenting for several months, will be of interest.

One of these motors is set up in the cellar of our science hall, where it is supplied with aqueduct-pressure of sixty pounds to the square inch, and the power is transmitted from it by means of rubber belting led over



"idle pulleys" to the upper stories of the building, where a small engine-lathe and dynamo are driven. A word will suffice to explain the very simple construction of the motor-system of radial cylinders, with their bases at the centre of the motor, through which runs the driving-shaft. The pistons in these cylinders are single-acting, and the water is admitted to them in succession by the rotary valve which forms part of the main shaft. The pistons, thus, in pressing outward, exert their force against a strong ring, to which is bolted a crossbar which engages the crank of the main shaft. Thus the ring, in turning the shaft, has the vibratory motion of an eccentric, and returns the opposite pistons to the bases of the cylinders, at the same exhausting the water through the interior of the rotary valve.



From *Nature* **34**, 121; 10 June 1886.

although racial, genetic and environmental co-factors are necessary. On the other hand, enough has been learned about EB virus in relation to endemic Burkitt's lymphoma for a persuasive theory to have emerged[5].

Thus, it has been suggested that latently infected B cells undergo unusually abundant virus-driven replication, no doubt because of impaired T-cell control resulting from recurrent attacks of falciparum malaria, such that one or other of three specific chromosomal translocations occurs, each being a cause of c-*myc* oncogene activation. Serious doubts have been raised, however, as to whether cellular oncogenes are relevant at all to the induction of cancer[6], and certainly c-*myc* alone cannot render cells cancerous[7].

New information on a key EB virus gene promises to reconcile these conflicting views. The gene for the virus determined membrane protein of latently infected cells has been identified and cloned, and after transfection into quite alien cells expression of the product has been shown to confer tumorigenicity[2]. This transforming gene explains the ability of EB virus to cause malignant tumours rapidly and directly in susceptible animals[8], and clearly plays a major role in the chain of events leading to the development of endemic Burkitt's lymphoma, whether with or without interaction with an activated c-*myc* oncogene. Discovery of this gene also provides a first and important indication as to how EB virus might be involved in causing nasopharyngeal carcinoma and, indeed, the other epithelial tumours in which preliminary investigations have indentified the viral genome. □

1. Young, L. S., Sixbey, J. W., Clark, D. & Rickinson, A. B. *Lancet* **1**, 240 (1986).
2. Wang, D., Liebowitz, D. & Kieff, E. *Cell* **43**, 831 (1985)
3. Greenspan, J. S. *et al. New Eng. J. Med.* **313**, 1564 (1985).
4. Whittle, H. C. *et al. Nature* **312**, 449 (1984).
5. Klein, G. *Cell* **32**, 311 (1983).
6. Duesberg, P. H. *Science* **228**, 669 (1985).
7. Adams, J. M. *et al. Nature* **318**, 533 (1985).
8. Cleary, M. L. *et al. Science* **228**, 722 (1985).

M. A. Epstein is at the Nuffield Department of Clinical Medicine, University of Oxford, John Radcliffe Hospital, Oxford OX3 9DU, UK.

Plant ecology

Pesticides and pollination

from Peter D. Moore

INTERDEPENDENCE in nature is often regarded as a source of strength and stability, but it can also become a point of weakness when one member of a complex chain of interactions is affected by catastrophe. In the case of insects involved in flower pollination, for example, there are evident evolutionary advantages in specialization that involve interactions between individual plant species and specific vectors, but such relationships may lead to problems if the vector population becomes depleted as a result of catastrophe. And catastrophe in insect populations is a far from unlikely event in these days of broad-spectrum pesticides. This problem is the subject of a recent study on the consequences to the reproductive success of plants in a New Brunswick forest of pesticide spraying (Thomson, J.D., Plowright, R.C. & Thaler, G.R. *Can. J. Bot.* **63**, 2056; 1985).

In the coniferous forests of New Brunswick, the spruce budworm (*Choristoneura fumiferana*), a defoliation agent of balsam fir (*Abies balsamea*), is an economically significant pest. Various pesticides have been sprayed onto the forests in the past 25 years in efforts to control the budworm, but concern has been expressed about the possible effects of spraying on other, non-harmful insect species and even economically beneficial species, such as the bees involved in pollination, and therefore fruit production, in the blueberries (*Vaccinium* spp.) that grow in the same area. P.G. Kevan (*Biol. Conserv.* **7**, 301; 1975), studying the pesticide fenitrothion, provided evidence that such effects can indeed be harmful.

Thomson and his co-workers investigated the effects of spraying Matacil, an anti-budworm agent which, because it is less toxic to bees, has replaced fenitrothion. When they tested the effects of Matacil on the mortality of a range of wild insect species, Thomson *et al.* found that the most pronounced effects occurred among the smaller bees (Andrenidae, Halictidae and Anthophoridae) and one fly family, the Syrphidae. These families are important pollinators of some of the understorey plants such as the Canada mayflower (*Maianthemum canadense*) and the red-osier dogwood (*Cornus stolonifera*). But the question to be answered is whether the spraying influences the populations of these insects to a degree that affects the breeding success of these plants.

By studying fruit sets in *M. canadense*, *C. strolonifera* and the creeping dogwood (*C. canadensis*) both inside the sprayed area and in control plots outside the influence of the spray, Thomson *et al.* obtained an estimate of fecundity, expressed as a percentage of the total flowers on an individual achieving fruit set. In *M. canadense* and *C. stolonifera* they found a significant reduction in fecundity within the sprayed area (means of 4.6 and 8.8 per cent, respectively) compared with the control sites (9.7 and 24.6 per cent). But in *C. canadensis* there was no significant difference (spray mean of 13.1 per cent and control mean of 11.6 per cent). The discrepancy between the two *Cornus* species could be caused by the fact that *C. canadensis* is also pollinated by larger bumblebees (*Bombus* sp.) which are not affected by Matacil spraying. These results add weight to the argument that spraying where the pollinator is sensitive decreases fecundity.

The question of whether the decrease in plant fecundity actually influences its overall population stability still remains unanswered. Much depends on the degree to which the plant requires the seed as a survival and/or dispersal mechanism. If vegetative growth and dispersal are available as alternative strategies for a species, then the decrease may be of little consequence. Although there are exceptions, such as the pin cherry (*Prunus pensylvanica*) (Marks, P.L. *Ecol. Monogr.* **44**, 73; 1974), most woodland understorey species are long-lived perennials with little dependence on their seed set.

Where the effects I have described here are likely to have the most profound impact is in plants which have a limited geographical range, are out-breeding, perhaps dioecious, short-lived, have no capacity for vegetative propagation and are specific in their pollination vectors. A plant which answers to most of the elements in this description is the hop tree (*Ptelea trifoliata*), a rare plant that colonizes shorelines on the northern side of Lake Erie in Canada. J.D. Ambrose, P.G. Kevan and R.M. Gadawski (*Can. J. Bot.* **63**, 1978; 1985) have studied the reproductive biology of this species and conclude that it is dioecious, is entirely dependent on wind-dispersed seeds for its spread and exhibits a rapid population turnover. Its breeding would therefore seem particularly susceptible to any catastophic disruption such as that in the New Brunswick forests. But there is one factor in its favour — a considerable diversity of insect vectors in its pollination system. Ambrose *et al.* found that the flowers were visited by Hemiptera, Coleoptera, Diptera and Hymenoptera, totalling at least 102 species from 37 families. In this particular respect, what seems to be a vulnerable plant has a survival strategy and the ability to withstand the almost inevitable impact of pesticides on its pollination vectors. Perhaps we should give special attention to the conservation of those plant species which lack this key factor in their defences against human environmental disruption. □

Peter D. Moore is Reader in Ecology at the Department of Biology, King's College, 68 Half Moon Lane, London SE24 9JF, UK.

Iodine-131 in human thyroids in Britain following Chernobyl

SIR—On 2 May 1986 raised atmospheric levels of radioactive material were detected in the southern United Kingdom, apparently due to the Chernobyl reactor accident. Some activity persisted subsequently, but at a level considerably lower than the initial peak[1]. One of the most serious consequences believed to result from the accidental release of fission products from irradiated fuel is irradiation of the thyroid gland by ^{131}I (ref. 2). Thus, particularly because a substantial component of the radioactivity detected was identified as ^{131}I, it seemed desirable to carry out some direct measurements of ^{131}I in human thyroids. Between 10 May and 22 May we carried out a series of measurements on the thyroids of adults and children resident in the southern United Kingdom (predominantly South London) during the period of exposure.

Measurements were taken in a chalk-shielded room with a low radiation background, using a high purity germanium detector, collimated to be sensitive mainly to the thyroid region and with an overall counting efficiency for ^{131}I of 0.27%. Of necessity, subjects were chosen on the basis of availability and willingness and consequently consisted predominantly of departmental staff and students, together with five children of staff. None of the individuals for whom data are reported here had been occupationally exposed to ^{131}I in the recent past. However, to check for the possibility of inadvertent contamination in the hospital environment, we carried out identical measurements on three staff employed full time in our clinical radioisotope dispensary and found their ^{131}I levels to be within the range observed for the test group. Measurements were commenced over the weekend of 10–11 May and continued thereafter. Measured values of activity in the test group of subjects, and corresponding dose-rates calculated using data of International Commission on Radiological Protection[3–5], are presented in Table 1. From these data it seems reasonable to conclude that the peak in thyroid activity for most subjects occurred in the period between 14 and 19 May.

To estimate, from the measured activities, the time integral of dose commitments to the thyroid that may be expected to result from these exposures, we have made use of the data from a parallel set of measurements that we have carried out — commencing on 8 May and using similar measurement technique — on ^{131}I concentrations in milk delivered by a local dairy. The results of these measurements are presented in Table 2 and appear to be consistent with those observed at Chilton (some 100 km north-west of Sutton) which peaked on 6 May at 54 Bq l^{-1} and were made on farm-fresh milk[1]. If it is assumed that approximately 0.5 l of milk, ingested in the 24 hours following each day's delivery, was the main source of ^{131}I in the subject group[1,6], then the data are consistent with the ICRP model in which 30% of ingested ^{131}I is deposited in the thyroid, where it remains with half-life of 7.6 days[4,5]. On this basis the appreciable increases in thyroid activity (10–65%) during the week following 10 May further suggest that the peak activity in milk delivered in Sutton did not arrive until some 2 days following that observed for the Chilton farm, coinciding with the start of our own measurements on 8 May.

Accepting these assumptions, and assuming also that dietary activity hence-

Table 2 Iodine-131 activity measured in milk from a Sutton dairy

Date of delivery	Activity (Bq l^{-1})
8 May	41 ± 5
10 May	34 ± 5
12 May	21 ± 5
13 May	13 ± 4
14 May	11 ± 4
15 May	9 ± 4
16 May	8 ± 4
17 May	8 ± 4
19 May	7 ± 3
20 May	5 ± 3

forth decays with the half-life of ^{131}I, it is possible to estimate the time integral of thyroid activity resulting from the incident. Such a calculation, consistent both with our limited measured data on thyroids and also with similar measurements following the Windscale reactor accident in 1957[7] (made later in the time variation in activity), points to a total dose commitment from the incident equivalent to that from the peak dose rate, in each individual, acting over a period of about 26 days. Values derived in this manner (using the highest observed dose rate) are listed in the final column of Table 1. These values can be compared with a figure of approximately 1,000 μSv for the population mean annual dose to the thyroid that arises from natural sources[8]. These values are close to the estimates of ^{131}I dose to thyroid that resulted from the intensive series of nuclear weapons tests in 1961[9].

Prior to the Chernobyl incident, one of the world's most serious reactor accidents appears to have been that at Windscale (subsequently renamed Sellafield) in 1957. On that occasion, ^{131}I measurements were also made for the population centred

Table 1 Iodine-131 radioactivity measured in the neck region (Bq)

Subject	Age(sex)	Measurement date (May 1986)													Assumed mass of thyroid[3]	Highest observed dose	Estimated dose commitment
		10	11	12	13	14	15	16	17	18	19	20	21	22	(g)	(μSv d^{-1})	(μSv)
Adults																	
A1	60(M)		8±4					10±4							20	1.4	40
A2	56(M)	8±4						13±4			7±4		6±3		20	1.8	50
A3	33(M)	21±5					30±5				33±6			26±4	20	4.8	130
A4	36(M)	17±5													20	2.4	60
A5	35(F)												8±3		20	1.1	30
A6	35(M)		27±6				30±5					23±4			20	4.1	110
A7	34(M)		17±5						23±4						20	3.1	80
A8	26(F)	15±5				20±4					13±4		20±5	15±4	20	2.6	70
Children																	
C1	12(M)		8±4												10.2	2.1	50
C2	6(F)	6±5									2±2				4.9	3.3	90
C3	4(M)												8±3		2.5	8.8	230
C4	4(M)												13±4		2.6	14.0	360
C5	2.5(F)		11±6						16±5						2.3	19.1	500

on Sutton (including one of the present subjects) and showed peak levels of ^{131}I thyroid activity at that time ranging up to 300 Bq in adults[7]. The present values are clearly an order of magnitude lower.

It may also be of interest to note that our measurements (made using a simpler, screening procedure) on five UK citizens on their return from residence in Warsaw during the week 28 April–4 May showed levels of ^{131}I in the thyroid (at 4 May) ranging from 40 to 150 Bq. Measurements made on the same date on two individuals returning from residence in Kiev showed thyroid ^{131}I levels of 1,100 and 1,700 Bq. In contrast, the levels in 11 individuals returning from Leningrad and Moscow and two from parts of West Germany were all below the 40-Bq detection limit in our screening measurement.

C.R. HILL
I. ADAM
W. ANDERSON
R.J. OTT
F.D. SOWBY

Institute of Cancer Research,
Royal Marsden Hospital,
Sutton, Surrey SM2 5PT, UK

1. Fry, F.A., Clarke, R.H. & O'Riordan, M.C. *Nature* **321**, 193–195 (1986).
2. Stather, J.W. & Greenhalgh, J.R. *NRPB Publ.* No. R140 (1983).
3. *International Commission on Radiological Protection Publ.* No. 23, (Pergamon, New York 1976).
4. International Commission on Radiological Protection *Ann. ICRP* **2**, (3/4) (1979).
5. Internationl Commission on Radiological Protection *Ann. ICRP* **3**, (1–4) (1979).
6. Harrison, N.T. & Simmonds, J.R. *NRPB Publ.* No. DL3 (1980).
7. Maycock, G. & Vennart, J. *Nature* **182**, 1545–1547 (1958).
8. United Nations Scientific Committee on the Effects of Atomic Radiations *1982 Report to Gen. Assembly with Annexes UN Publ. E.82.IX.8.06300P* (1982).
9. United Nations Scientific Committee on the Effects of Atomic Radiations *UN Records of 17th Session of Gen. Assembly, Suppl. 16 (A/5216)* (1962).

Do mammals need P elements?

SIR—In a recent *News and Views* piece, Andy Flavell describes a way by which the *Drosophila* P element has been engineered to eliminate the germ-cell specificity of synthesis of the P transposase and allow transposition of P elements in somatic cells[1]. As he says, these modified elements may well direct synthesis of transposase in mammalian cells, and cause transposition of P elements around mammalian genomes. Would this then give vertebrate molecular biologists all the advantages given by P elements to *Drosophila* geneticists? The answer, I fear, is no.

The P elements have proved to be yet another powerful addition to the already well-equipped armoury used in solving the problems of developmental biology of *Drosophila*. They provide tools for both isolating and analysing genes. It is the prospect of easy transposon tagging of mutations and a high efficiency of production of transgenic animals that has tempted mammalian developmental biologists and geneticists (myself included) to yearn for a P-like element in mammals. However, sober reflection suggests that even if this were come about, we would be only slightly, if at all, better off.

None can doubt the enormous potential of *Drosophila* biology for adding to our understanding of the genetic control of development of a complex animal. Much of this potential stems from the wealth of mutations which affect development in surprisingly precise ways. With this fount providing the raw material those who work on *Drosophila* can count their further blessings; the use of polytene chromosomes to correlate genetic with physical maps, the small genome which facilitates cloning and chromosome walking and the tricks of the P elements. It is, however, the genetics of *Drosophila* upon which all else hangs, and this genetics in turn has become so well-understood because of two key factors: the small size of the animal and its rapid generation time which permit the analysis of many thousands of individuals and crosses.

Amongst the vertebrates only mice have a comprehensive and manipulatable genetics and are small enough to enable large numbers to be maintained. But the two main benefits brought to *Drosophila* by P elements, transposon-tagging and gene integration, already exist in mouse molecular biology. The rate-limiting steps in the advance of these experiments lie elsewhere, in the handling and analysis of large numbers of animals.

Retroviruses have been used as transposon tags for isolating mouse genes for a number of years. Natural infection of the germ-line has produced at least one coat-colour mutation, and allowed DNA from the region to be isolated[2]. Infection of embryos *in vitro* has been used as a method of generating insertional mutants, and their subsequent isolation[3]. Additionally, a spin-off from producing transgenic mice, which have insertions of foreign DNA, has also been the isolation of mutations caused by the insertion event[4,5]. These methods are all technically difficult and slow. More efficient *in vitro* viral infection of embryos would speed things up and methods have been described which yield about 10% of offspring with new viral inserts in the germ line[6]. *In vivo*, appropriate crosses between Swr and RF mice — in a sense analogous to a dysgenic cross of *Drosophila* — result in 0.35 to 0.67 new retroviral inserts per animal[7], a rate that begins to approach that of P-elements.

Testing carefully for new recessive mutations caused in the mouse by DNA insertion entails a great deal of cross-breeding, DNA preparation and Southern blotting, but there is a good chance of identifying embryonic lethals[4] (rather few of which are likely to be 'developmental' mutations). Setting up sib-crosses without DNA analysis and simply waiting for a new recessive mutation to reveal itself would reduce the work required. Of course this would only allow identification of viable mutations, and is extremely inefficient as even under the best circumstances the vast majority of crosses would be between animals not carrying any inserts. If one were to look for a *specific* mutation caused by an insertion the logistics become daunting to say the least. If one were to take all the offspring of Swr/RF crosses 'blind', and backcross them to a tester stock, assuming a target size for mutation of 20 kilobases and a genome size 100,000 times that, a rate of new insertion of 50% overall would produce the desired mutant once in 200,000 mice. Using a multiple tester stock carrying ten or twenty interesting genes would hardly reduce the scale of the task to one which the average worker would tackle. Few mouse facilities house more than twenty thousand animals in total. Even if only ten thousand crosses were needed (routine in a *Drosophila* lab), this would occupy a good sized room and several animal technicians for a couple of years. We would have to be confident indeed that the gene being tagged was truly interesting to justify such efforts.

Introduction of foreign genes into the mouse genome by microinjection of the embryo is now a widely used method of analysis of gene function. Despite early setbacks it now seems that most intact human or mouse genes will function after microinjection[8]. The efficiency at which injected embryos integrate the foreign DNA varies between 5 and 30%, which is about the same as the efficiency of P-mediated integration after injection. There is, at the moment, no marker which allows identification of transgenic animals, other than DNA analysis. The rate-limiting step, however, is the number of embryos which can be readily handled. It will always be a very skilful task to handle, inject, culture and replace the embryos into foster mothers.

Integration mediated by the P transposase almost always results in only a single integrant. Transgenic mice very frequently have multiple, tandem inserts, although there seems to be no correlation between insert number and expression of the genes[8]. Retroviral vectors can be employed to produce transgenic mice with only single inserts[6] but there are size restrictions on the DNA that can be introduced in this way. It is here that appropriately modified P elements may be most useful, allowing the easy generation of single-insert transgenics.

All this said, even if transposing P elements onto the mouse genome and having them jump around there will not push mouse biology into the same league as *Drosophila* biology, it would be worth-

while and informative. Moreover, it sounds like fun!

IAN J. JACKSON
MRC Mammalian Development Unit,
Wolfson House,
(University College London),
4 Stephenson Way,
London NW1 2HE, UK

1. Flavell, A. *Nature* **320**, 397 (1986).
2. Copeland, N.G., Hutchinson, K.W. & Jenkins, N.A. *Cell* **33**, 379–387 (1983).
3. Jaenisch, R. *et al. Cell* **32**, 209–216 (1983).
4. Wagner, E.R., Covarrubias, L., Stewart, T.A. & Mintz, B. *Cell* **35**, 647–655 (1983).
5. Woychik, R.P., Stewart, T.A., Davis, L.G., D'Eustachio, P. & Leder, P. *Nature* **318**, 36–40 (1985).
6. Van Der Putten, H. *et al. Proc. natn. Acad. Sci. U.S.A.* **82**, 6148–6152 (1985).
7. Jenkins, N.A. & Copeland, N.G. *Cell* **43**, 811–819 (1985).
8. Palmiter, R.D. & Brinster, R.L. *Cell* **41**, 353–345 (1985).

Initiating boiling with ice

SIR—When an observation in the physical world appears to be paradoxical, running counter to one's intuition, experience and learning, it usually provides an opportunity to achieve some valuable scientific insight. Such a case began with the observation by one of us (R.L.D.) that a large spoon that had been kept in the freezer would initiate boiling in water that had been heated in a cup in a microwave oven, which the other one of us (R.E.A.) suggested might occur because crystals of ice initiate boiling in overheated water.

Water is said to be overheated or 'superheated' when its boiling temperature for a given pressure is surpassed without transformation to the vapour phase. This can be brought about by heating a drop of water as it rises in a heated column of oil. Using this technique, water can be heated to as high as 279.5°C at atmospheric pressure before explosive boiling occurs[1]. This extreme superheating occurs because there is no free vapour/liquid interace, the water being immersed in oil. Even if there is a free interface, significant superheating is possible[2] because the internal temperatures can rise above the boiling temperature which occurs at the interface where vaporization occurs. (The true definition of boiling relates to vaporization at a flat liquid/vapour interface, and, therefore, is not defined by the onset of vapour bubbles.) 'Bumping' occurs when clean water is heated and boils unevenly but can be avoided by the presence of a boiling 'chip' or a piece of Teflon, which contains many gas-entrapping crevices.

We found that the temperature that could be achieved by tap water in a beaker heated on an oven-top burner was 100.75 ± 0.25°C, close to the boiling temperature. But when tap water was heated in a microwave oven, the temperature measured by a thermocouple was briefly in excess of 110°C and there were more sustained periods of 105–106°C. To ensure that our thermocouple did not trigger boiling, we put it in a glass well that contained cooking oil. The tip of the glass well was positioned in the centre of the tap water held in a Pyrex beaker. The leads to our thermocouple were not attached to the voltmeter while the microwave was running, because the radiation would cause spurious readings. Our chromel/alumel thermocouple was calibrated with a crushed ice-water bath, and checked at the boiling temperature using water brought to a rolling boil (using a large chunk of Teflon).

Several kitchen objects were used to check the hypothesis that ice crystals nucleate boiling in ordinary tap water. When a stainless-steel or silver serving spoon was used, it would only nucleate boiling when cooled in a freezer (where some ice crystals could form). Glass, a screwdriver, and a plastic utensil behaved in the same way. If small boiling chips were added to the water before it was heated, we could not produce enough superheating, and inserted objects did not stimulate boiling.

Ice cubes themselves triggered a 'rolling' boil if the temperature rose above about 102°C. At a superheat of about 10°C above the boiling temperature, ice could nucleate boiling for 3–4 s. The time of boiling roughly scales to the number of degrees of superheat. Ice made with degassed water behaved in the same way as ice made with tap water saturated with gas.

It is quite clear that the mechanisms of the phenomena we observed are as follows: the microwave oven heats the water directly and the container indirectly, the opposite of what happens when heating by conduction with a burner. Therefore, the internal temperature can rise above the boiling temperature at positions away from the container's surface which tended to provide sites for boiling. Evaporation at the free surface does not occur rapidly enough to cool the bulk of the sample. When an ice cube is introduced, its crevic-ed crystalline structures, which can hold gas or water vapour, stimulate film boiling on local parts of the surface of the ice cube. The vapour film acts as a partial thermal insulation, slowing down the heat transfer between the ice cube (at about −15°C) and the water (at 110°C). When the water temperature immediately around the ice cube drops below 102°C, or so, the observed boiling ceases.

When our experiments are repeated with water in a plastic cup, a much smaller degree of superheat is achieved, primarily because the water wets plastic much more poorly that it does Pyrex glass, and therefore boiling on the surfaces of plastic is much more active, cooling the interior and preventing significant superheating.

One word of caution. We used extremely fine, insulated thermocouple wire, which allowed us to close the microwave oven door and not risk radiation leakage. Similar precautions should be taken by those who desire to repeat our experiments.

ROBERT E. APFEL
Department of Mechanical Engineering,
Yale University,
New Haven
Connecticut 06520, USA
RICHARD L. DAY
Department of Pediatrics,
Yale University School of Medicine,
New Haven,
Connecticut 06510, USA

1. Apfel, R.E. *Nature phys. Sci.* **239**, 63-64 (1972)
2. Harvey, E.N. *et al. J. Cell comp. Physiol.* **24**, 23-34 (1944)

In defence of bacterial phylogeny

SIR—In recent correspondence, Woese *et al.*[1] say that our differences on *Archaebacteria* eocytes and photocytes are semantic. Our differences are fundamental and are based on two contradictory evolutionary trees. If one tree is correct the other is not. These trees are our combined photocyte/eocyte tree[2,3] and the tree of Woese[1]. Each relates all extant organisms.

The most widely used and accepted method for selecting a tree is parsimony analysis[4]. The four prokaryotic groups, halobacteria, eubacteria, methanogens and eocytes, can be topologically connected (by unrooted trees) in only three different ways. These correspond to our photocyte tree, to Woese's tree and to a third alternative, shown in Fig. 1. According to parsimony, a tree relating four taxa is supported if a given molecular property is found in two taxa while an altered version of the property is found in both of the other two. Thus "two-and-two" properties are valid. However, if a property is found only in one of the four groups, then it does not support any tree. Hence "three-and-one" properties are invalid.

All of the photocyte molecular properties listed in Table 1 below support the photocyte tree. All are two-and-two and hence are phylogenetically valid properties by the parsimony criteria. The list includes basic cellular properties such as membrane related components [tetraether lipids[5] and fatty acid esters[6]], biochemical pathways [carotenoid synthesis[7] and arginine deiminase pathways[8]] and bioenergetic components [C_{40} and C_{50} carotenoids[9] and 2Fe-2S ferredoxin[10]] in addition to ribosomal RNA sequences and ribosome structure. Contrary to the implication of Woese *et al.*[1], the eocytic 50S lobes found in ribosomes of eocytes and systematically distributed within the methanogens[2,11,12] are also two-and-two. All molecular characters are the same for halobacteria and eubacteria and for methanogens and eocytes, hence they all support the photocyte tree. Many are

deeply integrated into the molecular fabric of these cells. These are precisely the features expected to be good evolutionary markers.

No properties support the Woese tree, including the "founding" ones upon which both the tree and classification were proposed, "membrane, cell walls, rRNAs and tRNAs"[1]. These "founding" properties are listed in Table 1. For example, 16S rRNA oligonucleotide catalogues indicate that the eubacterial pattern is different, but they do not identify which group the eubacteria are closest to. All of their characters are three-and-one and cannot support any tree. When judged by standard evolutionary procedures and tests, the same "founding" properties which prompted Woese's taxonomic proposal, fail to support his tree.

Ribosomal RNA sequences, as rapidly evolving molecular characters, are subject to artefactual analysis by parsimony. No matter what the correct tree, parsimony and other treeing algorithms can consistently predict a tree which, like Woese's places fast-clock groups (that is, eubacteria and eukaryotes) together[13]. When we analyse the rRNA sequence data using the method of phylogenetic invariants, which is insensitive to this artefact and independent of evolutionary rates, we find support for our eocyte/photocyte trees is significant at greater than the 99% level[14,15].

Woese claims that his proposed classification could be used with any tree. A classification that fits all trees is no classification at all. Consider the arginine deiminase pathway found in the photocytes (eubacteria and halobacteria). We interpret it as having evolved once in the photocytes. Woese's proposed classification, making it a property occurring in two "kingdoms," misdirected others to propose either (1) that it was invented twice, or (2) that it was laterally transferred between "kingdoms"[8]. An incorrect classification has great negative power to obscure and misdirect.

Science and not semantics, then, is the basis of our claims. We see no support for Woese's tree and taxonomic proposal from any molecular properties, whereas deep and fundamental properties support our eocyte and photocyte trees and classification. Viewed through the photocyte tree, membranes, biochemical pathways, and components of biochemical energetics are all natural and logical consequences of evolutionary history. Well integrated molecular biological and metabolic properties support the photocyte and eocyte trees and classifications. In the end, evolutionary connections, and not semantic ones, between organisms give theories true organizational and predictive value.

Table 1 Prokaryotic molecular properties

	Eubacteria	Halobacteria	Methanogens	Eocytes
	VALID BY PARSIMONY (Photocyte)			
Arginine deiminase pathway	+	+	-	-
Tetraether lipid	-	-	+	+
2Fe-2S ferredoxin	+	+	-	-
C40 carotenoids	+	+	-	-
Fatty acid esters	+	+	-	-
C50 carotenoids	+	+	-	-
Similar carotenoid synthesis pathways	+	+	-	-
Ribosomal 50S eocytic lobes	-	-	+	+
rRNA sequences	SEE DISCUSSION			
	IRRELEVANT BY PARSIMONY (Woese's characters)			
Ester lipids	+	-	-	-
Eubacterial cell walls	+	-	-	-
Eubacterial oligonucleotide catalogs	+	-	-	-
F-met initiator tRNA	+	-	-	-

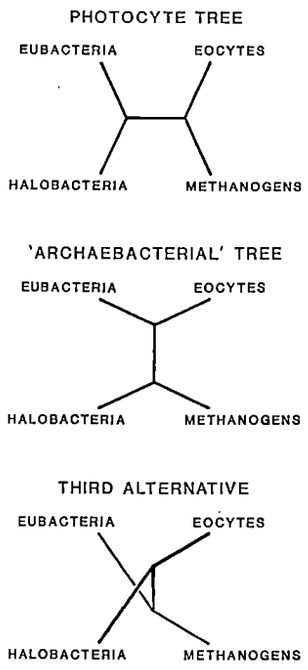


Fig. 1 All alternatives for linking the four prokaryotic evolutionary groups are represented in these three unrooted trees.

JAMES A. LAKE
Molecular Biology Institute and Department of Biology, University of California, Los Angeles California 90024, USA

1. Woese, C. *et al. Nature* **320**, 401 (1986).
2. Lake, J.A. *et al. Proc. natn. Acad. Sci. U.S.A.* **82**, 3716 (1985).
3. Lake, J.A. *et al. Proc. natn. Acad. Sci. U.S.A* **81**, 3786 (1984).
4. Fitch, W.M. *Am. Nat.* **111**, 223 (1977).
5. Langworthy *et al.* in *Archaebacteria* (ed. Kandler, O.) 228 (Fischer, Stuttgart, 1982).
6. Bu'lock, J.D. *et al.* in *Biosynthesis of Isoprenoid Compounds* (eds Porter, J.W. & Spurgeon, S.L.) Ch. 3 (Wiley, New York, 1983).
7. Spurgeon, S.L. & Porter, J.W. in *Biosynthesis of Isoprenoid Compounds* (eds Porter, J.W. & Spurgeon, S.L.) Ch. 1 (Wiley, New York, 1983).
8. Stalon, V. in *Evolution of Prokaryotes* (eds Schleifer, K.H. & Stackebrandt, E.) 277 (Academic, New York, 1985).
9. *Bergey's Manual of Determinative Bacteriology* (eds Buchanan, R.E. & Gibbons, N.E.) (Williams & Wilkins, Boston, 1974).
10. Tsukihara, T. *et al.* in *Molecular Evolution, Protein Polymorphism and the Neutral Theory* (ed. Kimura, M.) (Japan Societies Press, Tokyo, 1982).
11. Stoffler-Meilicke *et al. Science* **231**, 1306 (1986).
12. Oakes, M.I. *et al. System. Appl. Microbiol.* **351** (in the press).
13. Felsenstein, J. *Syst. Zool.* **27**, 401 (1978).
14. Oakes, M. *et al.* in *Structure, Function and Genetics of Ribosomes* (eds Hardesty, B. & Kramer, G.) (Springer, New York, in the press).
15. Lake, J.A. *Origins Life* (in the press).

Testis size and dizygotic twins

SIR—A recent article in *News and Views*[1] discussed R.V. Short's observations[2] on human testis size and dizygotic twin frequency in Asian, Indian, Caucasian and African ethnic groups.

Large testes were the first clinical feature to be associated with fragile X chromosome-linked mental retardation[3,4]. A mean testicular volume of 48 ml (range 15–127 ml, modal volume 35–40 ml) was observed[5] for adult white fragile X males in whom testicular volume was not a factor in ascertainment. The average testicular volume in unaffected Caucasian males is 20 ml. In an ascertainment of fragile X-affected kindred in Hawaii[6], it was noted that the mean testicular volume (22 ml) of pure Japanese males was less than that (39.5 ml) of pure Caucasian males. This reflected a previously observed difference between unaffected males of these ethnic origins.

A recent Belgian study[7] of 144 obligate female carriers of the fragile X led to the conclusion that such carriers have a high fertility, especially in those who are mentally subnormal (30%). An increase in the incidence of twinning was observed in the 642 progeny of 134 obligate carriers. Of 18 pairs of twins, 12 were dizygotic, and, in the remaining 6, the zygosity could not be determined. This incidence (1 in 35 births) is three- to-four-fold that of the expected incidence of twinning in Caucasians (1 in 80 to 1 in 140 births)[8]. This specialist fragile X-bearing population therefore would appear to express parallel variations to those already observed by your contributors.

L.R. WILLATT
D.J. BARTLETT
Department of Clinical Cytogenetics, Addenbrooke's Hospital, Hills Road, Cambridge CB2 2QQ, UK

1. Diamond, J.M. *Nature* **320**, 488 (1986).
2. Short, R.V. in *One Medicine* (eds Ryder, O.A. & Byrd, M.L.) 32 (Springer, Berlin, 1984).
3. Escalante, J.A. *et al. J. gen. Hum.* **19**, 137 (1971).
4. Turner, G. *Med. J. Aust.* **2**, 624 (1978).
5. Sutherland, G.R. *Int. Rev. Cytol.* **81**, 107 (1983).
6. Rhoads, F.A. *Am. J. med. Genet.* **17**, 209 (1984).
7. Fryns. J.P. *Am. J. med. Genet.* **23**, 157 (1986).
8. Sofaer, I.A. in *Principles and Practice of Medical Genetics* (eds Emery, A. & Rimoin, D.L.) 120 (Churchill Livingstone, Edinburgh, 1983).

SCIENCE AND TECHNOLOGY

Whatever the subject... refer to MACMILLAN DICTIONARIES

DESIGNED FOR STUDENTS

The paperback *Macmillan Dictionary Series* combines new and established works of teaching and reference with an attractive series format.

* authoritative definitions and explanations of all current terminology written by experts
* lucidly written entries with thorough cross referencing
* regular new editions keep the student up to date with the latest research, practice and technology
* a clear layout for easy reference
* prices range from just £7.95 to £9.95

NEW IN 1986...

MACMILLAN DICTIONARY OF BIOTECHNOLOGY
JIM COOMBS March 1986 320pp 0 333 40875 6 £9.95

MACMILLAN DICTIONARY OF THE HISTORY OF SCIENCE
Edited by W. F. BYNUM, E. J. BROWNE and ROY PORTER
March 1986 528pp 0 333 34901 6 £8.95

MACMILLAN DICTIONARY OF PERSONAL COMPUTING AND COMMUNICATIONS DENNIS LONGLEY and MICHAEL SHAIN
August 1986 320pp 0 333 42170 1 £8.95

MACMILLAN DICTIONARY OF PHYSICS
MARY P. LORD August 1986 320pp 0 333 42377 1 £8.95

MACMILLAN DICTIONARY OF IMMUNOLOGY
FRED ROSEN, LISA STEINER and EMIL UNANUE
August 1986 256pp 0 333 39248 5 £8.95

Macmillan Press, Houndmills, Basingstoke, Hants RG21 2XS, UK
Not available in USA.

MACMILLAN PRESS

BURN YOUR REFERENCE CARDS!

REF-11™

Computerizes your REFERENCES and prepares your BIBLIOGRAPHIES

- ☐ Maintains a data base of references
- ☐ Searches for any combination of authors, years of publication, reference title (or any words in the title), and topics covered by the reference
- ☐ Formats bibliographies exactly as you want them
- ☐ Alphabetizes references
- ☐ Abbreviates journal titles
- ☐ Runs on any video terminal and printer
- ☐ Menu driven dialogue
- ☐ Compact storage format
- ☐ 20 lines of comments for each reference

IBM PC/XT/AT, MS-DOS, CP/M 80 ... $195.00

RT-11, TSX-Plus, RSX-11, P/OS $250.00

VAX/VMS (native mode) $350.00

DG™ SYSTEMS

ANY MANUAL $15.00 ANY MANUAL & DEMO $20.00

322 Prospect Ave., Hartford, CT 06106
(203) 247-8500
Connecticut residents add 7½% sales tax

Reader Service No.39

THE POLITICS OF CHANGE

How much does your weekly diet of Press, Television and Radio really inform you? How much does it teach you about the true state of British politics? How aware are you of the real options available to government on any policy issue?
Are you satisfied with the current quality of political debate?
Harold Lever, Mary Warnock, Douglas Wass and Ian Gilmour aren't.
That's why they're working for Catalyst, breathing new life into the body politic.

CATALYST

A Journal of Policy Debate
Authoritative Non-Partisan Analysis

The quarterly magazine that's a solid read and a definitive source of reference
It's never too late to improve your reading habits.

'Informative and provocative' – T.H.E.S.

'Indispensable reading for the political commentator' – PEREGRINE WORSTHORNE

'Thank you for helping to get our brains into gear' – AUSTIN MITCHELL

'Deserves to succeed' – DAVID OWEN

'Of great value' – MERLYN REES

'I greatly commend Catalyst' – SIR JOHN HARVEY-JONES

'By far the best discussion that I have seen of the 'British Disease' and its possible remedies' – LORD BLAKE

'Like lighthouse beams into a dark night' – ROY JENKINS

'Quite excellent' – DAVID STEEL

'Absolutely indispensable... difficult to imagine how one got on without it' – STEWART STEVEN

SUMMER 1986 ISSUE, OUT NOW: **CHOICE AND THE ENVIRONMENT.** AVAILABLE FROM: UNIT 8, GROVE ASH, BLETCHLEY, MILTON KEYNES MK1 1BZ. ANNUAL SUBSCRIPTION (4 ISSUES): £15 (UK); £19-50 (EUROPE); £22-50 (USA); £4 (SINGLE ISSUES).

Keep up to date with

CANCER SURVEYS

Editor: **L M Franks,** *Published for the Imperial Cancer Research Fund by Oxford University Press*

Brings you critical and comprehensive reviews of the latest research. For clinicians, cell and molecular biologists, and epidemiologists.

DRUG RESISTANCE *Volume 5 Number 1*

Edited by **G Stark** and **H Calvert,** Imperial Cancer Research Fund, London, and the Institute of Cancer Research, Sutton, UK.

Contents

DNA amplification in drug resistant cells and in tumours **George R Stark**

Multidrug resistance **James H Gerlach, Norbert Kartner, David R Bell and Victor Ling**

Membrane transport alterations as a mechanism of resistance to anticancer agents **D W Fry and R C Jackson**

Biochemical and cellular determinants of bleomycin cytotoxicity **Branimir I Sikic**

Clinical aspects of drug resistance **A Sobrero and J R Bertino**

Circumvention of resistance to anthracycline by calcium antagonists and other membrane-perturbing agents **David Kessel**

In vitro human tumour model systems for investigating drug resistance **Bridget T Hill**

Cancer Surveys focuses on a new topic every quarter. Each edition provides a definitive and up-to-date account of the present state of knowledge in the chosen area. Guest Editors, with specialist knowledge of that field, provide general assessments. Contributors review the areas where they have made important contributions, include research which may not have been published elsewhere and relate epidemiological and laboratory research to clinical problems.

Each issue costs £13.50(UK), US $29 (N. America), £15.50 (Elsewhere) or take out a year's subscription: £47 (UK), US $95 (N. America), £53 (Elsewhere). Cancer Surveys is published quarterly.

All Previous issues are available. Details on request.
The next issue in the series is BIOCHEMICAL MECHANISMS OF ONCOGENE ACTIVITY: Proteins Encoded by Oncogenes, edited by Harold E Varmus and J Michael Bishop

ORDER FORM Please complete the order form and return (with remittance enclosed) to Journals Subscription Department, Oxford University Press, Walton Street, Oxford OX2 6DP UK

☐ Please send me **Drug Resistance—Vol 5 No. 1 of Cancer Surveys**
☐ Please record my subscription to **Volume 5 of Cancer Surveys**
☐ Please send me details of previous issues

I enclose my remittance of .....

Name .....

Address .....

.....

☐ I wish to pay by Visa/Access/Diners/American Express

My card number is ☐☐☐☐☐☐☐☐☐☐☐☐☐☐☐☐

Expiry date ..... Signature .....

If address registered with credit card company differs from that given above please give details

Half-price to members of recognised cancer societies. Apply to OUP for details

OXFORD JOURNALS

Journals Subscription Department, OUP, Walton Street, Oxford OX2 6DP, UK

Unnatural science?

Marie Jahoda

Profiles of Social Research: The Scientific Study of Human Interactions.
By Morton Hunt. *Russell Sage Foundation, New York:1986. Pp.324. Distributed by Basic Books, hbk $17.50, pbk $8.95.*

LONGSTANDING readers of this journal on both sides of the Atlantic may raise their eyebrows at the very title of the book here under review. Natural scientists often deny the legitimacy of using the word "science" in conjunction with social research, a view shared by some people in high places. But surely nobody can doubt that the social world is as much part of nature as the world studied by natural scientists, equally there to be observed, understood, measured, occasionally manipulated in experimental fashion, conceptualized and perhaps even explained.

The denial of scientific status for social research cannot rest on these generally accepted criteria for science. Indeed it does not. The verbal quibble is a substitute for an appreciation of some genuine differences between the natural and the social sciences beyond the unquestioned difference in achievements. There is a distinction between the phenomena in the social and the physical worlds. The regularities social scientists discover are subject to change. Those in the natural sciences are not; they are assumed to hold for all times and through the entire Universe. This has implications for the development of theories on both sides of the fence. In the natural sciences, a new theory should encompass the regularities a previous one has explained. No such demand can be met in the social sciences, because the regularities themselves may have altered. So, while there is no shortage of theories in the social sciences, there are no cumulative explanations, at least not so far. Social scientists must deal with their complex subject matter in an extended "Now", the duration of which is unknown.

The relatively low public prestige of the social sciences is, however, less grounded in this feature of the subject and more in another ineluctable fact: while no lay person can pronounce on the unification of the four forces, not even on a single particle, everybody has daily experience of the social world and holds implicit or explicit theories about it. Depending on such personal views, one and the same social scientific formulation is regarded by some as trivial common sense, by others as false.

Morton Hunt's competent and lively description of several social research projects, their methods, achievements, difficulties and public reception, addresses these issues not directly but by example. The volume was commissioned by the Russell Sage Foundation of New York, in celebration of its 75-years-long support for the social sciences. It deals understandably but regrettably almost exclusively with American research, but social scientists elsewhere will have no difficulty in recognizing their subject, apart from the incomparably greater funding available in the United States. The book is based on published research and interviews on aspects of the research process that are not normally included in the written record. Hunt conveys above all something that should appeal to natural scientists: the intellectual quality and commitment to high standards that outstanding social scientists invest in their efforts.



Popperfoto

Boston, September 1974 — racial hatred erupts as whites protest against the court-ordered integration of public schools through the bussing of students to different parts of the city.

Part I gives an illustrated overview of the standard methods of social research, paying due attention to their assets and shortcomings as well as to the ethical problems that inevitably arise when people are the subject of study. Neither advocacy nor critique, this is a fine presentation of the state of the art in social research.

Part II contains detailed descriptions of five major projects, including their internal histories, costs, methods, results and, in one dramatic case, the wide-reaching public consequences that followed publication. This was James Coleman's famous — according to some, notorious — large-scale survey of school segregation and its effects. Coleman's study was commissioned by the government in 1965, with a budget of $1.5 million, and Hunt describes it by skilfully interweaving the research issues with an account of the social and legal context, an intellectual biography of Coleman and the views of various social scientists on the question of whether social research should remain "pure" by choosing its own topics, or try to answer questions raised by policy-makers. After describing the conceptual and practical problems of conducting a survey of more than 600,000 children in 4,000 schools, Hunt presents the computer-produced results. They shocked the civil rights movement, which had confidently expected they would show that more money spent on desegregated schools would reduce, if not eliminate, the achievement differential between black and white children. Coleman's conclusions were different. For example, he found that parental economic status had more to do with achievement than race or quality of school. Uproar followed: simplified press accounts, congressional hearings, attack and defence in popular journals. At that time the controversial bussing policy was introduced — and failed. White parents took their children from the integrated city schools and moved out into the suburbs, or put them through private education. And Coleman, re-analysing his data after several years, acknowledged publicly that the original data already contained evidence for "white flight" as a result of desegregation.

It is to Hunt's great credit that he presents this confusing story without minimizing the intellectual and political passions it aroused, nor the mistakes made on all sides, and yet shows convincingly the potential power of social research to illuminate controversial issues. One question, however, he leaves unasked: is it in the best interest of social scientists or policy-makers to demand quick answers to immediate problems?

Case histories of two further government-initiated studies allow Hunt to enlarge on the assets and vicissitudes of social research. One was the decade-long, real-world experiment on negative income-tax, better described as income maintenance for the very poor. Economists, statisticians, sociologists and social psychologists cooperated in this complex project. Hunt uses it as a basis for a sophis-

ticated exposition of the research process, its relation to theory and, in this case where time was not pressing, for the demonstration that the amount of thought and expertise invested in such research has its intellectual pay-off and its social uses. The other government-initiated study, the Survey of Income and Program Participation (in social welfare programmes), gives Hunt occasion to trace the history of survey research and indicate what is considered to be current best practice.

A fourth case takes the example of a social psychological laboratory experiment with undergraduates to illustrate the great power of this method, which dominates American social psychology, and its inherent problems: Do the results apply to the world outside the laboratory? Is the desire for experimental precision responsible for all too many elegant trivialities in the literature? A final case exemplifies the methods of longitudinal panel research through analysis of some studies, designed to continue for 20 years, of aging in an originally healthy middle-aged sample.

Altogether this is an engagingly and clearly written book. It presents social science as it is, warts and all. Social scientists could well use it as a textbook. Natural scientists may gain from it insight into the intellectual challenges social scientists face, and respect for their efforts in meeting them. □

Marie Jahoda is Emeritus Professor of Social Psychology at the University of Sussex, Falmer, Brighton BN1 9QG, UK.

Inflamed appeal

Gerry Higgs & Brendan Whittle

The Inflammatory Reaction. By Henry Z. Movat. *Elsevier:1985. Pp.365. Dfl.260.*

THE inflammatory reaction continues to be a centre of interest in the medical sciences, largely because of the high incidence of inflammatory diseases throughout the world. One in three people in the West can expect to suffer from some sort of chronic inflammatory disorder during the course of their life. This book, however, is devoted essentially to the acute inflammatory reaction and here Professor Movat has dealt very thoroughly with the subject. He makes no apology for his somewhat idiosyncratic approach, drawing heavily upon his own research findings to illustrate and explain the events of inflammation. This is not to say that the book lacks objectivity. It is an impressive review of current knowledge, with an extensive bibliography that takes up more than a fifth of the text.

The study of inflammation was for many years considered the province of pathologists and has only recently been hijacked by pharmacologists and immunologists. Professor Movat emphasizes the need for integration of the disciplines concerned, but, as a pathologist himself, he is well placed to lead his readers through the historical developments and on to current ideas. Not surprisingly then, he places inflammation in the context of the structure and function of the tissues affected. Beginning with the anatomy of the microcirculation, he goes on to describe the vascular and lymphatic changes occurring as a result of inflammatory injury. The morphological and functional aspects of leukocyte activation are dealt with in a similar way. This approach provides a good basis for the chapters on mediators and mechanisms.

The longest chapter, occupying almost a quarter of the book, tackles the formidable list of mediators that are known to contribute to the vascular phenomena of acute inflammation. Another chapter deals with substances which stimulate leukocyte emigration. The problem with categorizing inflammatory mediators is that they are rarely involved in discrete functions. For example, the prostaglandins, leukotrienes and complement-derived factors contribute to vascular as well as cellular responses in inflammation. Professor Movat has overcome this difficulty by demonstrating the relative importance of individual mediators in processes such as vasodilation, vascular permeability, chemotaxis and degranulation. This has not been achieved without cross-referencing between chapters, which in places is confusing. The picture that emerges, however, is that inflammatory reactions are initiated and amplified by the actions and synergistic interactions of a large number of mediators.

It is a little disappointing that the mechanisms of chronic inflammation are not touched upon until the penultimate chapter of the book. Also, discussions of the treatment of inflammation or the mechanisms of anti-inflammatory drugs have been deliberately avoided. Nevertheless, this is the most comprehensive and up-to-date text available on the subject of acute inflammation, and as such it will prove useful for reference. A large part of the book is based on experimental findings and this aspect should appeal to the post-graduate and post-doctoral workers in inflammation research. Professor Movat should, therefore, succeed in his objective of stimulating the young investigators to whom this monograph is primarily addressed. □

Gerry Higgs is Head of the Anti-Inflammatory Section and Brendan Whittle Head of the Department of Mediator Pharmacology at the Wellcome Research Laboratories, Langley Court, Beckenham, Kent BR3 3BS, UK.

Engineered viruses out of doors

D.H.L. Bishop

Genetically Altered Viruses and the Environment. Edited by Bernard Fields, Malcolm A. Martin and Daphne Kamely. *Cold Spring Harbor Laboratory: 1986. Pp.362. $63.*

THE use of genetically altered viruses in medicine or veterinary practice is, of course, old hat. Since the late eighteenth century and Jenner's pioneering work on smallpox, attenuated genetic variants of disease-causing viruses have been employed to protect man and domestic animals from infection by virulent viruses.

Such vaccine strains of viruses have been obtained by serendipity. What then is the concern about genetically altered viruses in the environment? With modern technologies and precise knowledge of the genetics of viruses (genome sequences and coding strategies), not only can we now achieve the objectives of earlier scientists by direct and specific genetic engineering, but we can go much further in custom-designing viruses for new purposes. It is against this background that the symposium that spawned this book was organized. The issues raised are both broad and far-reaching, and are of importance not only to scientists but also to the public, especially local and national regulatory authorities.

The initial chapters of the book describe the US legislative and regulatory frameworks pertaining to the use of genetically engineered viruses. Corresponding frameworks in other countries are not considered, limiting the interest of this information to the international audience, though one appreciates from these accounts the problems that have arisen in the United States where regulations are being applied to a subject that goes beyond the concepts involved in originally formulating the legislation.

The development and use of genetically engineered viruses in agriculture and forestry will open up new tracts of science, and will doubtless have irreversible environmental consequences. The question of risk assessment is therefore a central one, but there is only restricted discussion of this subject in the book. It was, for example, a major oversight of the organizers that there is a detailed report neither of the use in Australia of the South American myxomatosis virus to control rabbit populations, nor of the domino effects of the introduction of the virus to continental Europe and the United Kingdom. Likewise our extensive knowledge of the use of viral insecticides to control pests of agriculture and forestry is given

short shrift. Chapters are devoted to the subject of virus spread between hosts by vectors, or water or airborne transmission, topics which bear strongly on potential environmental effects. But there is much more to the issues involved than can be covered in each of these short contributions.

In a section on virus tropisms, the genetic basis of the cell–organ selectivities exhibited by certain viruses is discussed succinctly, as is the role of cellular receptors in determining particular virus tropisms and the penetration processes used by viruses to invade cells. Similarly, the genetic elements involved in the control of virus replication and expression of particular viral phenotypes are well reviewed. The complicated matter of virus–host interactions is covered in four chapters dealing with virus persistence and variation, and host responses to virus infection, with particular reference to genetically altered viruses such as the attenuated virus vaccines. The final section of the book is devoted to accounts of virus vectors that are of value for the expression of foreign genes (vaccinia, bovine papillomavirus, adenoviruses, *Autographa californica* nuclear polyhedrosis virus). This is a topical subject, in that such vectors are being developed by the biotechnology industry for the production of foreign gene products. Again, however, there is little mention of their use (and impact) in the environment.

All in all, it is evident that the original meeting was a thought-provoking and worthwhile exercise. Unfortunately, the resulting book provides only sketchy outlines of selected areas of the subject matter, and I would question its value to either the specialist or the more general reader. □

D.H.L. Bishop is Director of the Natural Environment Research Council's Institute of Virology, Mansfield Road, Oxford OX1 3SR, UK.

A manifold mind

John C. Marshall

The Citadel of the Senses and Other Essays. By Macdonald Critchley. *Raven: 1986. Pp.277. $32.50.*

MACDONALD Critchley is one of our most senior and distinguished neurologists, and a man for whom "retirement" means an opportunity to work harder than ever. His current collection of essays, some reprinted, many previously unpublished, bears witness to an undimmed interest in all aspects of neurological disease and an acute awareness of the rich variety of humankind, its triumphs and its foibles. The volume is appropriately prefaced by a novelist's *bon mot*: "Somerset Maugham regarded old age as the time to undertake those tasks shirked in youth because they would have taken too long".

The title essay, "The Citadel of the Senses: The Nose as its Sentinel", restores to olfaction the high ground usually occupied by the visual and auditory systems. Some brief remarks on the comparative anatomy of the nose introduce a vignette on the role of smell in medical diagnosis; but lest such odours seem unduly fetid, we are also treated to extracts from "Vins et Vignes de France", "La Psychologie du Parfumeur", and the adventures of Flush amidst the redolent aromas of spring in Florence. The protean world of touch is equally well represented in a chapter on haptic perception; here Critchley ranges from the skills of the silk mercer, through the neuropsychology of braille reading, to disorders of tactile discrimination and localization consequent upon damage to the peripheral and central nervous system. Disorders of the visual system likewise provoke a wealth of anecdote and differential diagnosis: in what terms should we describe and explain how some patients with adequate sight nonetheless fail to recognize objects (visual agnosia), or how yet other patients apparently cannot see two objects at the same time (simultanagnosia)? What are we to make of the aurae in migraine or the bizarre visual hallucinations that may precede an attack? Was the terrifying abyss that Blaise Pascal purportedly saw plunging to his left a symptom of ophthalmic migraine? (Neurologists are almost as keen as psychoanalysts to diagnose the famous dead.)

Although most of the papers collected here are essays for the left hand, intended to stimulate thought rather than solve problems, one does occasionally long for a more extended analysis. For example: Critchley claims that "it is a vain pursuit to seek to isolate various subtypes of visual agnosia, e.g., for colours or for faces". Yet there are many well-documented case-reports, with extensive testing and more than adequate controls, that do seem to indicate the existence of high-level perceptual disorder in which an impairment of colour or face recognition is disproportionately severe. What *specifically*, one wants to know, does Critchley find inadequate about the investigation and interpretation of these cases? Similarly, in his discussion of claims that there are subtypes of specific developmental dyslexia, Critchley writes: "To medical men like myself such efforts are not impressive and seem premature and speculative". Those of us who have attempted to provide solid, empirical evidence for a typology of dyslexic impairment would welcome criticism more detailed than the blank assertion that "to make a rigid parcellation within the clinical picture of developmental dyslexia is going too far".

Throughout the volume Critchley wears his prejudices and his enthusiasms on his sleeve. Particularly generous and appealing are his biographical sketches of esteemed neurologists: Hughlings Jackson, Newman Neild and Josef François Babinski. How refreshing it is to discover that the last of these was a person, not merely a reflex. I was especially happy to learn of Babinski's term for "confused, obscure, or imprecise" writing — "chieurs d'encre" (ink-shits, as Critchley forthrightly puts it). The enthusiasms that Critchley recommends for study by the young neurologist include the physiology of laughter and smiling, the transcendental states that music can provoke, and the sensory skills of the blind; on occasion an enthusiasm and a prejudice will interact, as when Critchley advocates the study of aphasias in African, Asian and Amerindian languages, but tells the student to take no notice of "contrastive linguistics"!



From *The Citadel of the Senses*

Sole stimulation — the Babinski sign, reported in C.r. Séanc. Soc. Biol. *in 1896. "Here at last", writes Critchley, "was a clinical shibboleth which would distinguish the organic from the hysteric, the genuine from the counterfeit".*

One final foible: in this, as in most of his collections, Critchley refuses to give references, a habit that is decidedly unhelpful to those whose knowledge and memory cannot match Critchley's own. As it happens, I do have the "original" reference for "Anton's syndrome" (1899), a condition where a cortically-blind patient denies his blindness. But I'd appreciate chapter and verse for the claim that the circumstance "had been described with the utmost lucidity by Seneca centuries ago". □

John C. Marshall is in the Neuropsychology Unit, part of the Neuroscience Group at the Radcliffe Infirmary, Oxford OX2 6HE, UK.

Roland GRÜNBERG - NANCY - FRANCE



DO YOU NEED PEPTIDES?

NEOSYSTEM LABORATORIES

PROVIDE
A COMPLETE SERVICE FOR
PEPTIDE SYNTHESIS
PEPTIDE AND PROTEIN SEQUENCING
PEPTIDE ANTIBODY PRODUCTION

WE PROVIDE ALSO
CONTRACT RESEARCH SERVICES
TO INDUSTRIAL AND ACADEMIC
INSTITUTIONS



NEOSYSTEM LABORATORIES
B.P. n° 309 R8
67008 STRASBOURG Cedex
FRANCE - Télex 880 088 F
Tél. : 88.36.96.96

Whales: transition in translation

Samuel A. McLeod

General Features of the Paleobiological Evolution of Cetacea. By G.A. Mchedlidze. *Balkema:1984. Pp.139 + plates. Dfl. 65, £16.50, $26.*

FOR the general reader there is, surprisingly, still no overview of cetacean evolution to replace Kellogg's 1928 *History of Whales*. Despite its title, Mchedlidze's book will not suffice as a successor to Kellogg's work. Specialists, on the other hand, will find this to be a very useful volume, though they will also need access to Mchedlidze's 1970 monograph (published in Russian) and his 1977 English-language summary of some of his ideas on cetacean evolution. Mchedlidze's monographs are separate publications, not generally available; this translation provides a much-needed introduction to some of the Soviet fossil cetacean faunas (including important Azerbaidzhan and Georgian fossils discovered over the past two decades), together with several rather idiosyncratic essays on particular morphological transformations.

The descriptions of the fossil cetaceans alone make the book invaluable, though a couple of them are confusing. *Oligodelphis azerbajdzanicus* and *Kelloggia barbarus* were both originally described in a 1968 manuscript by Mchedlidze and his erstwhile Russian collaborator, S.M. Aslanova, but by the rules of zoological nomenclature those species names are available only as of 1976. *Kelloggia barbarus* is also said to have "intercostal plates", reminiscent of the now-disproven cetacean "armour" of Kükenthal and Lydekker. In 1970 Mchedlidze described a new genus and species, *Mirocetus riabinini,* but in the 1976 work, and this translation of it, the species name appears as *M. rjabinini.*

The drawbacks of the book for the unwary reader are several. For example, while Mchedlidze cites most of the pertinent Western palaeontological research, he seems unaware of, or ignores, the general systematic literature. His systematic methodology is therefore seriously out of date. Although he uses individual characters to assign species to higher taxa, most of these characters are primitive and the assignments are based on the vague notion that the characters "most closely resemble" those of a higher taxon. His conclusions frequently are not borne out by the anatomy of the specimens in the photographs. Thus he describes *Ferecetotherium kelloggi* and assigns it to the Aetiocetidae (here placed in the Archaeoceti, although the family is now usually classified in the Mysticeti), and considers it transitional to mysticetes. But there is no derived character, beside the supposed lack of a mandibular symphysis (not demonstrable from the plate), that this species shares uniquely with any archaeocete or mysticete. It may be a sperm whale. Many of his interpretations about the origin of mysticetes and the evolution of cetacean dentitions rely heavily on the systematic position of this species.

Mchedlidze initially cites the age of all the Russian fossil cetaceans as Upper Oligocene, but notes they are of different evolutionary stages. Subsequently he mentions that most of the specimens were not found *in situ* and that they may actually be of different ages. This problem also affects his systematic conclusions in terms of which taxa might be ancestral to other cetaceans. A different sort of chrono-evolutionary difficulty appears when Mchedlidze uses the old and extreme gradualistic argument that there was not enough time for the evolution of the various cetacean groups from their closest but more primitive reputed relatives. Most particularly, he believes the direct ancestors of cetaceans are "archaic [presumably Late Cretaceous] placental mammals".

Many of Mchedlidze's essays are adaptive scenarios for the origin and evolution of various cetaceans. This is a thought-provoking approach, but it depends directly on the soundness of the systematic conclusions; these, in my opinion, are the book's greatest failing. Several bizarre ideas, some initially espoused by such zoologists as W. Kükenthal, R. Lydekker and A.B. Howell, are re-cycled. Noteworthy is Mchedlidze's resurrection of the idea that odontocete skull asymmetry evolved because of increased swimming speed. More astounding is his statement that the dorsal position of the external nares allows cetaceans to remain "out of sight of predators for longer periods of time"!

The translator, editor and publisher have done a fine job on the book, correcting some mistakes, adding several text citations not in the original bibliography and, most particularly, reproducing the plates more clearly. The disparity between the number of specimens listed in the legends and those on the plates remains, however, and the genus *Mirocetus* appears in three places instead of the original *Microcetus,* which changes the author's meaning.

This book is indispensable for the specialist. It will also be of interest to Western zoologists more generally, but they should treat its conclusions with great caution. □

Samuel A. McLeod is in the Section of Vertebrate Paleontology, Natural History Museum of Los Angeles County, 900 Exposition Boulevard, Los Angeles, California 90007, USA.

Tip splitting without interfacial tension and dendritic growth patterns arising from molecular anisotropy

Johann Nittmann* **& H. Eugene Stanley†**

* Etudes et Fabrication Dowell Schlumberger, 42003 St. Etienne, France
† Center for Polymer Studies and Department of Physics, Boston University, Boston, Massachusetts 02215, USA

Two growth mechanisms of considerable recent interest are related to a single statistical mechanical model. Tip splitting without interfacial tension occurs when a fluid pushes into another miscible fluid of higher viscosity. Dendritic growth occurs when anisotropic molecules aggregate—a common example is the snowflake. We find that both structures are fractal objects, and can be obtained from a single statistical mechanical model, implying that there is a relation between the underlying physical processes involved.

GROWING structures have fascinated mankind for centuries, and today the field of growth phenonena elicits interest from many disciplines, ranging from medicine and biology to fluid mechanics. Two growth forms that have attracted recent interest are the following:

(1) Dendritic growth[1-9]. No two snowflakes are identical; each is assembled by the random aggregation of water molecules. Yet every child can distinguish a snowflake from other growth forms. The key scientific question is by what mechanism the anisotropy of a water molecule becomes amplified from its weak 'local' effect at the molecular level to its pronounced 'global' effect at the macroscopic level of the snowflake.

(2) Tip splitting[10-20]. A classic experiment in fluid mechanics concerns the splitting of a low-viscosity body of fluid which results when it is forced under pressure into a high-viscosity fluid. If the two fluids are immiscible, then the interfacial tension between them serves to establish a length scale at which tip splitting occurs. When the two fluids are miscible there is no interfacial tension, yet tip splitting nonetheless occurs. Thus an important question concerns the physical mechanism which determines the point at which the finger splits.

The scientific questions in (1) and (2) have been the object of research for many years, in part because our present state of understanding is so incomplete[21] that even a little progress would be valuable. The two categories of growth mechanism (1) and (2) have been considered to be quite different, in the sense that the physical basis for one has no relation to that of the other. Here we develop a statistical mechanical model which incorporates both dendritic growth and tip-splitting, thereby relating two disparate fields of enquiry.

Relation between noise and tip splitting

The model is most clearly explained if we begin with the dielectric breakdown model (DBM) of Niemeyer *et al.*[22] on, for example, a triangular lattice. We first place a seed particle at the origin of a large circular domain of radius R. If we think of this seed particle as being the source of a fluid of infinitesimally small viscosity, which is being forced under pressure to displace a fluid with much higher viscosity[23,24], then the interface must move according to Darcy's law:

$$v_n = -\mathbf{n} \cdot \nabla P \tag{1}$$

Here v_n is the velocity component normal to the interface, $\hat{\mathbf{n}}$ is the normal unit vector and P is the pressure field. P is constant in the less viscous fluid and, because $\nabla \cdot \mathbf{v} = 0$, P satisfies the Laplace equation

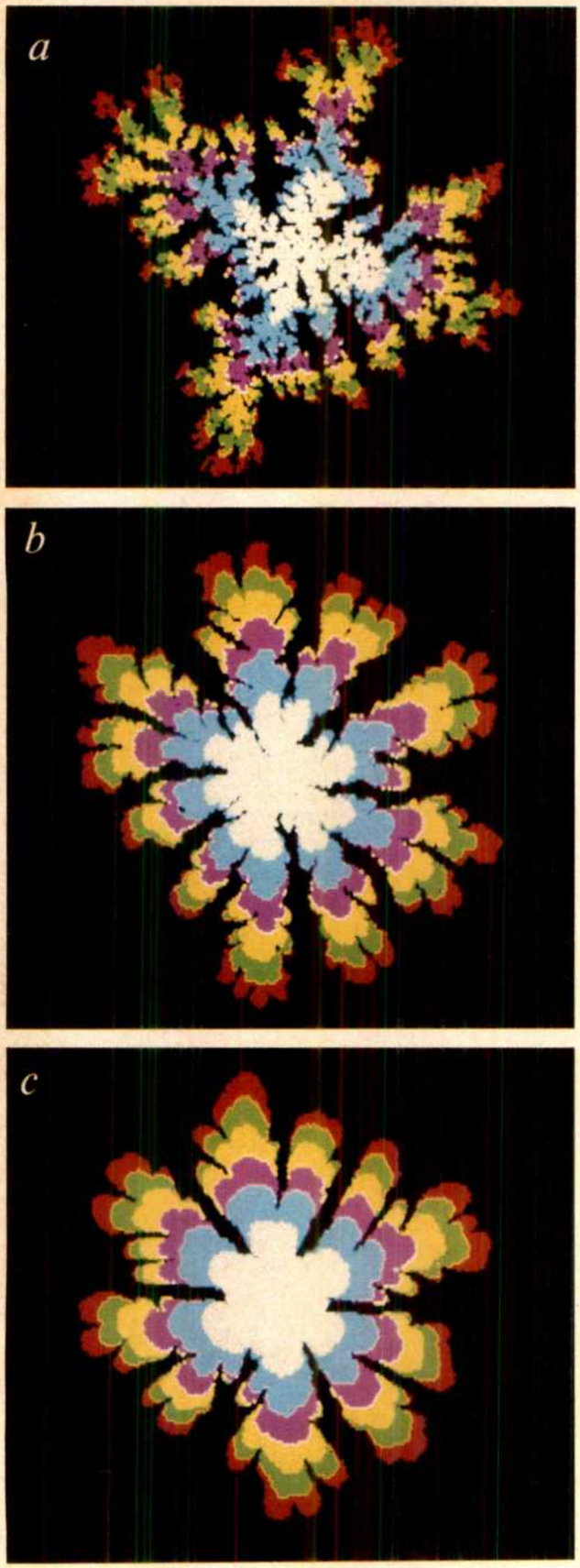
$$\nabla^2 P = 0 \tag{2}$$

in the more viscous fluid. Hence the relevant boundary conditions are $P(r, \theta) = 1$ anywhere in the low-viscosity body of fluid, and $P(R, \theta) = 0$ along a circle of radius R.

In a perfect medium with radial symmetry and no pressure fluctuations, the interface will spread out in concentric circles. However, because there is always some noise in the system, a fluid-dynamical instability[25] will occur and irregularities in the interface will grow. This noise phenomenon is reproduced in the DBM, which includes fluctuations by means of the following algorithm. First, ∇P is calculated at every perimeter site of the cluster; this is done by solving equation (2) with an overrelaxation technique. At step 1 there is a single seed on a triangular lattice with six perimeter sites. As all sites have equal values of ∇P, the first perimeter site is mapped to the numerical interval $[0, \frac{1}{6}]$ the second to $[\frac{1}{6}, \frac{2}{6}]$, the third to $[\frac{2}{6}, \frac{3}{6}]$ and so forth. Next, a random number generator is used to choose a number in the interval $[0, 1]$. Suppose that this random number is 0.2603238: the second perimeter site is then occupied, and the procedure iterated. For this two-site cluster, ∇P is calculated at the eight perimeter sites, the values are normalized to unity, a new random number is chosen, and one of the eight sites occupied. Such a DBM cluster is characterized by a high degree of noise: as each growth step is determined by only one random number, it is always possible that the random number chosen corresponds to a perimeter site with an extremely small value of ∇P, which by equation (1) should almost never grow. Thus the DBM violates the fundamental Darcy law due to the noise inherent in the algorithm.

We now describe a procedure whereby this noise can be systematically reduced in a controllable fashion. Clearly we need an algorithm such that perimeter sites with extremely small values of ∇P are extremely unlikely to be chosen. This is accomplished by advancing to a new perimeter site only after it has been chosen s times, where s is a parameter which can be tuned. Each perimeter site has a counter which registers how many times that particular site has been chosen. As $s \to \infty$, the growth of the interface will approach Darcy-law growth, in which any point of the interface grows according to the true local pressure gradient. In the Darcy 'zero-fluctuation' or 'mean-field' limit[26] ($s \to \infty$), the interface would be a perfect circle if there were no underlying lattice.

Figure 1*a–c* shows the results of calculations for successive values of s. We find that Fig. 1*b* and *c* resemble tip splitting as observed in the viscous fingering of both newtonian (refs 19, 27; J. D. Chen, personal communication; R. Lenormand, personal communication) and non-newtonian[10,12,18] fluids. When $s = 2$ (Fig. 1*a*), the structure resembles the DBM both qualitatively (although the branches look thicker) and quantitatively



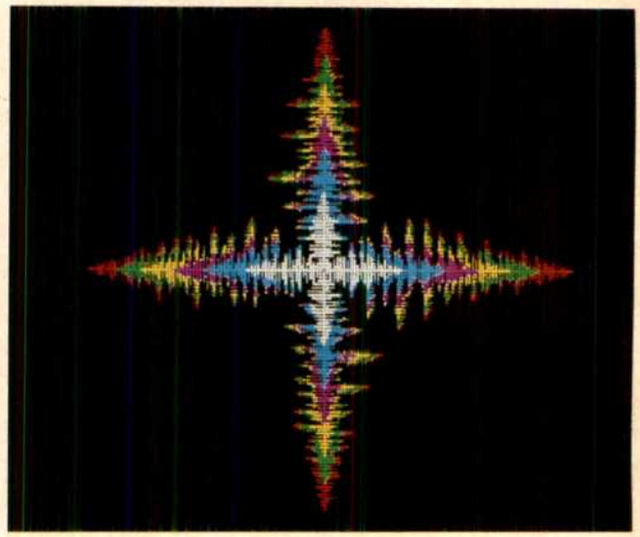


Fig. 2 A typical fractal structure on a square lattice with $s = 50$ and a microscopic anisotropy (defined by equations (6), (7)) of $k - 1 = 10$. The colour coding is the same as in Fig. 1.

($d_f = 1.7$). Here d_f is the fractal dimension obtained, for example, from the slope of a log–log plot of the mass against the caliper diameter. For large s (for example, $s = 20$; Fig. 1*b*), the qualitative appearance appears to differ: the system appears at first sight to cross over to a new 'universality class', with a larger value of d_f. However, when we extrapolate the apparent fractal dimension to large cluster sizes we find that $d_f = 1.7$ for all values of s; that is, the growth forms are quantitatively identical, independent of the degree of noise reduction.

Note that tip splitting always occurs by the same mechanism. First a cluster grows 'smoothly', without tip splitting. However, as the radius of curvature increases, the interface becomes 'rough', with both positive (outward) and negative (inward) fluctuations. The positive fluctuations are not significant, as they are soon damped out; however, the negative fluctuations persist (Fig. 3). This is because, for a charged fractal object, the electric field inside a single notch is very small, and the equation relating the electric field to the gradient of the potential is formally identical to the Darcy law relating growth velocity to the gradient of the pressure. Hence, the tiny notch is not likely to be filled in so quickly as one would expect if interfacial tension were present (Fig. 3*d*). The tiny protrusions on both sides of the notch see a much larger field than does the notch, so they attract mass. The tiny notch thus becomes the terminus of a long fjord (Fig. 3*e*). A fjord is almost perfectly screened, and so is almost never filled in. In Fig. 3, $s = 50$. If $s > 50$ (less noise), then the same tip-splitting mechanism will apply but a negative fluctuation (notch) will decay more efficiently: the system is less susceptible to negative fluctuations and a fjord is formed only when the cluster has reached a larger radius of curvature.

Although the asymptotic fractal dimension d_f is independent of s, the finger thickness W_f clearly increases with s. Moreover, our model explains the existence of a well-defined W_f: the less the noise, the thicker the finger (see Fig. 1). We find the quantitative law:

$$W_f \simeq 4.5 \log s + 2 \qquad (3)$$

Fig. 1 Examples of fractal structures generated when the anisotropy parameter k is held fixed at unity, but the noise parameter $1/s$ is decreased. In *a*, *b* and *c*, $s = 2, 20$ and 200, respectively. For all finite values of s, we find that the fractal dimension is equal to the DBM value, $d_f = 1.7$, providing we take care to extrapolate the apparent mass dependence of d_f to its asymptotic limit. The colour coding is as follows: the first one-sixth of the sites are white, the next sixth are blue, followed by magenta, yellow, green and red.

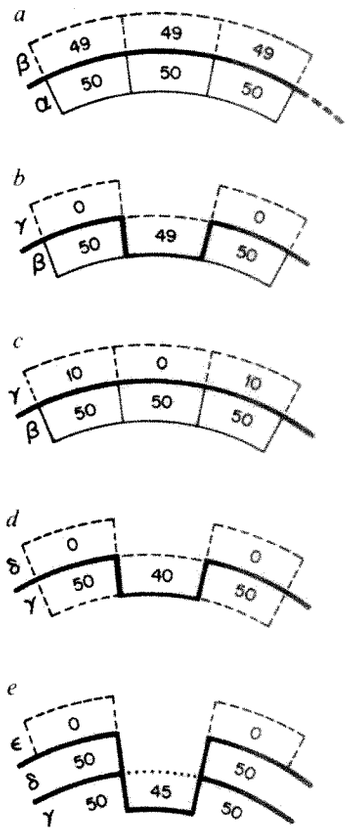


Fig. 3 Schematic illustration of the difference between an outward ('positive') and an inward ('negative') interface fluctuation. A positive fluctuation tends to be damped out rather quickly, as mass quickly attaches to the side of the extra site that is added. On the other hand, a negative fluctuation grows, in the sense that mass accumulates on both sides of the tiny notch. The notch itself has a lower and lower probability of being filled in, as it becomes the end of a longer and longer fjord. This is the underlying mechanism for the tip-splitting phenomenon when no interfacial tension is present. *a* shows the advancing front (row α) of a cluster with $s = 50$. The heavy line separates the cluster sites (all of which were chosen 50 times) from the perimeter sites (all of which have counters registering less than 50). In *a*, no fluctuations in the counters of these three sites have occurred yet, and all three perimeter counters register 49. *b* shows a negative fluctuation, in which the central perimeter site is chosen slightly less frequently than the two on either side; the latter now register 50, and so they become cluster sites in row β. The perimeter site left in the notch between these two new cluster sites grows much less quickly because it is shielded by the two new cluster sites. For the sake of concreteness, let us assume it is chosen 10 times less frequently. Hence by the time the notch site is chosen one more time, the two perimeter sites at the tips have been chosen 10 times (*c*). The interface is once again smooth (row γ), as it was before, except that the counters on the three perimeter sites differ. After 40 new counts per counter, the situation in *d* arises. Now we have a notch whose counter lags behind by 10, instead of by 1 as in *b*. Thus the original fluctuation has been amplified, due to the tremendous shielding of a single notch. Note that no new fluctuations were assumed: the original fluctuation of 1 in the counter number is amplified to 10 solely by electrostatic screening. This amplification of a negative 'notch fluctuation' has the effect that the tiny notch soon becomes the end of a long fjord. To see this, note that *e* shows the same situation after 50 more counts have been added to each of the two tip counters, and hence (by the 10:1 rule) 5 new counts to the notch counter. The tip counters therefore become part of the cluster, but the notch counter has not yet reached 50 and remains a perimeter site. The notch has become an incipient fjord of length 2, and the potential at the end of this fjord is now exceedingly low. Indeed it is quite possible that the counter will never pass from 45 to 50 in the lifetime of the cluster. In our simulations we can see tiny notch fluctuations become the ends of long fjords, and all of the above remarks on the time-dependent dynamics of tip splitting are confirmed quantitatively.

We also find that W_f is independent of the magnitude of the pressure field. To see this, we varied the global pressure gradient by changing the size of our computational grid from 200 to 25 units and found no variation of the finger thickness. This discovery is explained if one considers that the ratio of the local pressure gradient between a site at a finger tip and a site within a fjord does not change if the global pressure gradient is changed: this in turn is a direct consequence of the fact that the pressure field satisfies a Laplace equation.

Previous work on tip-splitting phenomena has focused on explaining the non-zero value of the finger thickness W_f as arising from the presence of interfacial tension σ (ref. 28; see also ref. 29). However this explanation cannot be applied to miscible fluids, such as those used in recent experiments[10,12,18,27,28], because in this case, by definition, $\sigma = 0$. In our model interfacial tension does not exist (that is, σ acts only on the length scale of a single fluid element or 'pixel'); our observed finger thickness is thus related solely to the concept of noise.

Before proceeding further we note that in the limiting case $s = 1$ the DBM is equivalent to diffusion-limited aggregation[30–32] (DLA). The diffusion analogue of the DBM for $s > 1$ is a DLA-type model in which growth occurs only after a perimeter site has been hit by s random walkers. If all the counters are reset to zero after each growth step, then we have the Meakin model[33] or the Kertész–Vicsek model[8], in which growth of the positive fluctuations (the tips) is amplified because a tip of size 1 pixel is more likely to experience the next growth event—so the apparent value of d_f decreases toward unity as the cluster grows. The DLA-type analogue of our DBM-type model in which the counters are not reset to zero after each growth event is the Tang model[26], for which it is not the positive fluctuations (the tips) that display amplified growth but the negative fluctuations (the notches). Amplified growth of negative fluctuations is the characteristic feature of DLA, explaining our result that d_f has its DLA value for all finite values of s.

Thus we conclude that noise reduction—arising from suppression of fluctuations—does not change the overall 'universality class', but does introduce a characteristic finger thickness.

Local anisotropy and dendritic growth

Real growth phenomena are never perfectly isotropic. In fact, anisotropy appears to dominate dendritic crystal growth; thus, for example, a snowflake is recognized by its six-fold anisotropy, although the noise is also reflected in the variability from one snowflake to another[9]. No two are alike, although the eye immediately recognizes the pattern of a snowflake.

The problem of understanding the growth of a snowflake has a rich history. A large class of models has focused on introducing anisotropy in a 'global' or macroscopic fashion by introducing angular variables and assuming that the growth depends sensitively upon these variables[2–4]. Although the resulting patterns have, by virtue of their rules of construction, the requisite six-fold symmetry, their resemblance to real snowflakes is not striking. Moreover, they lack the random variations that seem to characterize real snowflakes and also fractal objects.

A snowflake grows by successive landings of water molecules, and we have therefore focused our attention on how microscopic irregularities in the landing surface can be translated into the macroscopic structure of the snowflake. To reflect the presence of these microscopic irregularities, we must incorporate into our model the essential fact that the landing sites seen by an incoming molecule are not all equivalent. Hence we replace equation (1) by

$$v_n = -\mathbf{n} \cdot (k \nabla P) \tag{4}$$

where the conservation of mass condition $\nabla \cdot \mathbf{v} = 0$ implies that equation (2) is replaced by

$$\nabla \cdot (k \nabla P) = 0 \tag{5}$$

with the same boundary conditions as for $k = 1$. Here the anisotropy parameter $k = k(x, y)$ would be the permeability in a fluid problem.

Consider a square lattice. One simple choice for $k(x, y)$ is (see Fig. 2)

$$k(x, y) = 1 \tag{6}$$

for x or y even,

$$k(x, y) = k > 1 \tag{7}$$

otherwise equations (6) and (7) express mathematically the fact that the surface affinity for incoming water molecules depends on the spatial coordinate: the incoming particles do not see a perfectly smooth and homogeneous 'landing surface'.

Moreover, our anisotropy is fundamentally different from that considered in, for example, refs 4 and 11. Schematically, in these models the interface is moved according to the rule

$$u = f(\kappa) - f(\theta)u_n \tag{8}$$

where u is the growth velocity, $f(\kappa)$ is an interfacial tension term and u_n is essentially the local pressure (or temperature, or concentration) gradient at the interface. The function $f(\theta)$ indicates the extent to which the growth is enhanced along directions separated by an angle θ. In marked contrast, our model assumes that the anisotropy is present on a molecular level at the interface. We assume that along the interface, the affinity for an incoming water molecule alternates from site to site:

$$u = -f(x, y)u_n \tag{9}$$

We believe that our model is more realistic, as an incoming water molecule in snowflake formation cannot possibly sense the angle $\theta = \arctan(y/x)$, but does see a 'landing surface' whose 'attraction' fluctuates from point to point.

Next we consider the effect of tuning the anisotropy parameter k. Figure 5*a–d* shows structures grown with a succession of increasing values of k, ranging from 1.1 to 11. We hold s fixed at the value $s = 50$; if s were too small, then noise effects would complicate visualization of the effect of anisotropy. Figure 5 is for a triangular lattice, for which equations (6) and (7) are replaced by a different rule: we set $k > 1$ for every fifth row of the three principal directions of the lattice (E–W, NE–SW, NW–SE). We see from Fig. 5 that as k increases there is a pronounced change from the isotropic case $k = 1$, and the resulting growth (see, for example, Fig. 5*d*) resembles a 'snowflake' for reasons more subtle than merely the characteristic 6-fold axis of rotation[34]. Using standard methods (for example, all three methods of ref. 18), we measured d_f for this 'snowflake' and found values that decrease with the number of particles used in the calculation. Extrapolating to infinite size, we find[35,36] $d_f = 1.5 \pm 0.1$.

Although the structure at first sight appears to be somewhat ordered, we realize that this is a trick played by the 6-fold axis. In fact, an individual branch is quite disordered, with side branches of all sizes extending from it. The reason $d_f > 1$ is that the side branches occur with many different length scales. This is especially apparent from Fig. 5*d*, where we see from the colour coding that the latest particle to arrive can attach to the side branches as well as to the tip. Figure 5*e* shows real snowflakes with side branches, which show a striking resemblance to the anisotropic simulations of Fig. 5*d*. The differences between Fig. 5*d* and *e* are the subject of current investigation.

We now address the actual structure of the fractal objects in the presence of anisotropy. It is important to note that there are distinct effects that cooperate to generate the final structure obtained. The first effect is the fine structure of the side branches (see Fig. 2), consisting of a set of 'trees' of varying height, as shown schematically in Fig. 4*a*. The trees are mainly without branches, as the anisotropy favours growth only in even-numbered rows or columns of the lattice. However the height of a tree varies widely from one tree to the next, due to the tendency of tall trees to screen shorter trees. An analogous variation in the height of trees has been found by Meakin[37] in his classic studies of DLA on a planar substrate: he found that

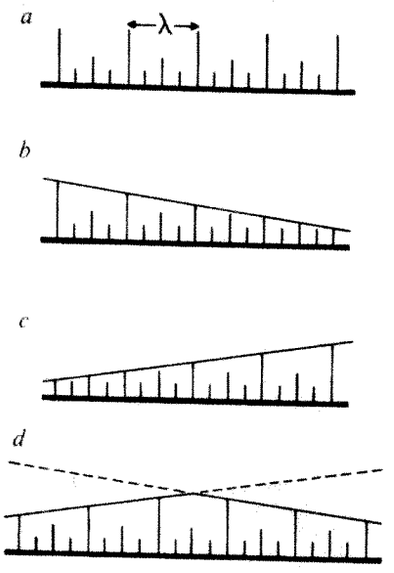


Fig. 4 Schematic illustration to explain the characteristic shape of the four arms of the 'snowflake' cluster in Fig. 2; *a* recalls the fundamental structure of aggregation onto an equipotential surface, first studied by Meakin[37]. For simplicity, the 'trees' are drawn as straight line segments, and the hierachical or fractal distribution of tree height is indicated by a difference of a factor of 2 between successive sizes, together with a spacing, $\lambda(M)$, which increases as M^{1/d_f}, where M is the total cluster mass. *b* shows the modification expected from the fact that the regions of an arm near the centre have more time to accumulate mass than the regions near the tip. *c* shows the effect of the fact that ∇P is much larger near the tip; *d* shows the result of combining *a–c*, and resembles the overall shape observed in Figs 2 and 5*d*.

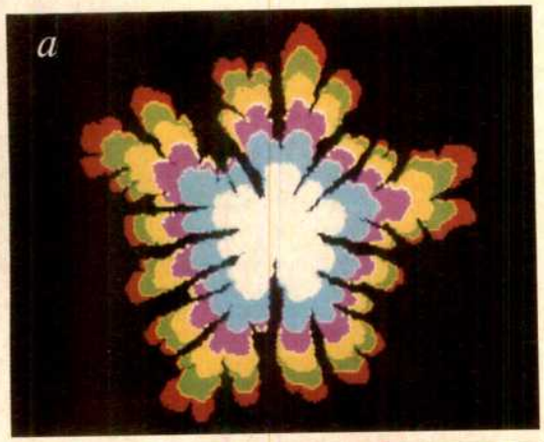
the resulting fractal structure is a 'forest' of trees, with fewer but taller trees surviving at large times due to their tendency to shield the shorter trees.

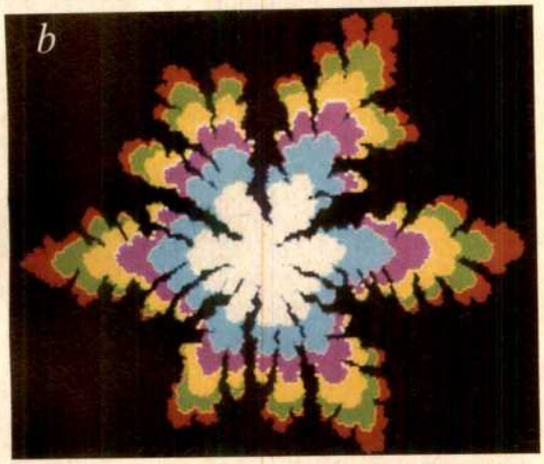
The main difference between our work and the Meakin (planar substrate) DLA simulations is our lattice anisotropy (parameterized by $k - 1$) and our noise reduction (parameterized by $1/s$), which have the effect of making the trees tall and straight instead of ramified. Consider now the overall profile for the height of the trees in the side branches. This profile can be understood mathematically as arising from the product of two functions. The first, a decreasing function from origin to tip, is related to the fact that the regions of the branches that were formed at early times tend to be larger than the regions of the branches that were formed at late times (Fig. 4*b*). The second, an increasing function, is related to 'screening'; that is, to ∇P, which is larger near the tips and smaller near the origin (Fig. 4*c*). As $v \propto \nabla P$, the growth rate is larger near the tips. The product of the increasing and decreasing functions gives the characteristic profile for the height of the trees in the side branches (Fig. 4*d*).

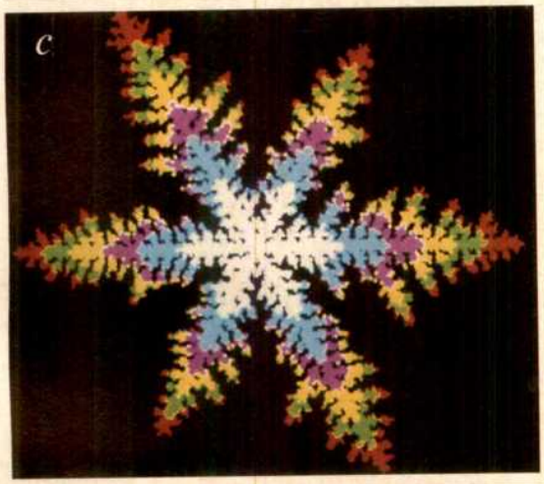
We also measured as a function of cluster mass: (1) the caliper width of the side branches of Fig. 2, and (2) the caliper diameter of the entire cluster. Both log–log plots are parallel, with slope $1/d_f$.

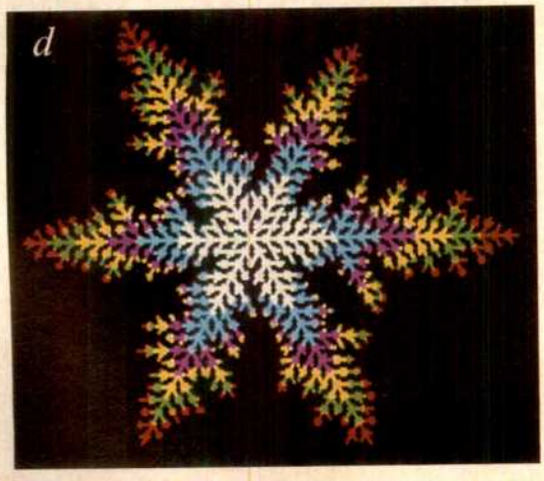
Discussion

We have shown that two fundamental physical phenomena that are not yet understood, dendritic growth and tip splitting in the absence of interfacial tension, can be related in that both arise from the same statistical mechanical model—a generalization of the DBM[22]. This means that there are physical features common to both phenomena: they differ only in parameter values. In our model we can incorporate in a direct and systematic fashion the crucial role played by fluctuation phenomena









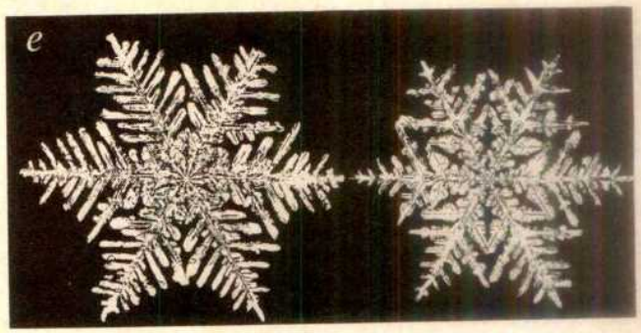


Fig. 5 *a–d*, Examples of fractal structures formed when the noise parameter s is held constant at $s = 50$, but the anisotropy parameter k is chosen to be, respectively, $k-1 = 0.1$, 0.31622, 1.0 and 10.0 (0.31622 interpolates logarithmically between 0.1 and 1.0). The limiting fractal dimension (as mass $\to \infty$) is $d_f \simeq 1.5$, independent of k, for all $k > 1$. The colour coding is the same as in Fig. 1. *e*, Examples of real snowflakes (reproduced with permission from ref. 9) which show a striking resemblance to *d*.

and anisotropy. The physical picture that we have proposed is embodied in two fundamental equations, (4) and (5) (or (1) and (2) for $k = 1$). The second equation describes the spatial change of the pressure field which drives the instability; the first represents the 'growth law', which relates the growth rate of the interface to the pressure field. We have used a generalized Darcy-type law, which enables us to selectively tune both noise and anisotropy.

The overall physical picture that emerges is as follows: Tip-splitting phenomena in the absence of interfacial tension are triggered by microscopic fluctuations (that is, noise). Although positive and negative fluctuations of the interface occur symmetrically, the stability (and hence the subsequent growth) of positive and negative fluctuations are totally different: tip splitting is the direct consequence of this asymmetry in the stability of positive and negative fluctuations. A small protrusion of size 1 pixel is much less long-lived than a small notch of the same size; in fact, it is remarkably difficult to fill even the shallowest notch. Zero noise ($s = \infty$) results in a compact (non-fractal) circular object. A very low noise level (large s) has little effect when a cluster is small, but its effect becomes much more pronounced as the cluster grows larger. In the limit of infinite cluster size, an arbitrarily small but non-zero amount of noise is sufficient to make the cluster fractal. The measured fractal dimension is identical to that of DBM and DLA, two models designed to describe phenomena in the limit in which there is a very high noise level.

The tip-splitting phenomena that occur in the case of zero anisotropy are generalized into a fractal hierachy of side branches in the presence of anisotropy. In the limit of infinite cluster size even a tiny degree of anisotropy changes the fractal dimension from the DLA value of 1.7 to the value 1.5.

Thus, the complete phase diagram has $1/s$ on the abscissa and $(k-1)$ on the ordinate. Asymptotically we find that d_f is constant, at the DBM value of ~1.7, everywhere on the x-axis, and d_f is also constant, at the value 1.5, everywhere else in the phase diagram except on the y-axis (zero noise), where $d_f = 1$. Thus noise reduction is not a sufficient perturbation to change d_f from its DBM value, because the negative fluctuations persist for all values of s, and these negative fluctuations control the value of d_f. On the other hand, anisotropy at the microscopic level does change d_f. Further details of this phase diagram suggest an intriguing analogy to critical point phenomena, and this will be the subject of future investigation.

Finally, we return to the question posed in the introduction, of how a tiny anisotropy can become 'amplified' from its local effect at the molecular level to a global effect at the macroscopic

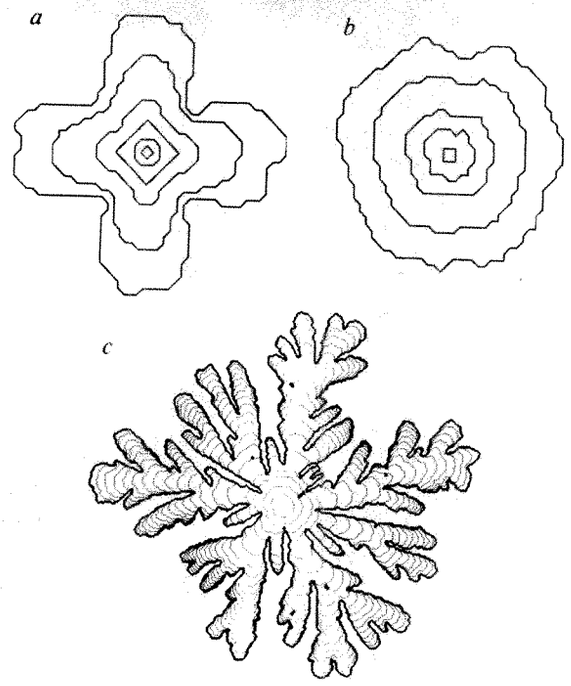


Fig. 6 *a*, Initial growth of an interface on a square lattice for the case $s = 500$. Growth can occur in any of the four space directions (four nearest neighbours). The interface is shown after 5, 21, 85, 200, 500 and 1,000 growth steps. *b*, As in *a*, except that here growth can occur into eight directions (four nearest neighbours and four next-nearest neighbours). The interface is shown after 9, 21, 85, 200, 500 and 1,000 steps. *c*, Viscous fingering structure for $s = 50$, after 15,000 growth steps for eight-fold coordination on a square lattice. The first four contour lines are drawn after 100, 300, 650 and 1,000 steps; subsequent lines are drawn at intervals of 1,000 steps.

level. Our model directly demonstrates this fact: we have shown that in the presence of anisotropy, the resulting fractal dimension is not the DBM value of 1.7, but rather tends asymptotically toward 1.5, a new 'universality class'. Our result is supported by Meakin's very recent calculations for DLA[38] without any local anisotropy, except for that arising from the square-lattice substrate. For this classic and well-studied system, 'pure DLA', Meakin finds the same behaviour that we find in the presence of anisotropy, but only after the cluster size reaches 5 million sites—almost three orders of magnitude larger than the clusters we study! Thus Meakin's local anisotopy, arising solely from the effect of the square lattice itself on the trajectories of random walkers, can lead to a pronounced global effect, altering not only the overall appearance of the cluster but also the fractal dimension itself. As pure DLA is the limit of maximum noise ($s = 1$), we have to wait for an extremely large cluster to see its effect. To support this idea, we systematically reduced s from 50 to 1 while keeping the local anisotropy fixed at the value $k = 2$. When $s = 50$ it is easy to see the snowflake anisotropy pattern, but as s decreases the snowflake vanishes.

To understand better the subtle role played by the anisotropy of the square lattice, we show in Fig. 6*a* the initial growth events for the case $s = 500$, $k = 1$. The early stage of growth is characterized by the competition of 'lattice anisotropy', which attempts to pull the interface into the four principal directions of the plane, and 'interface smoothing' (due to the decay of positive and negative fluctuations), which initially prevents splitting. The competition between these two contradicting tendencies leads to an oscillation of the interface: the structure of the interface alternates between a circle and a diamond-shaped cusp until, eventually, the weak anisotropy of the lattice dominates. As in real systems, no cusp singularities[39] occur: the noise in our systems smooths the sharp corners of the initial cusp as interfacial tension would do. A well-defined finger thickness has developed. The larger the value of s, the smaller is the noise and the larger is W_f. To weaken the lattice anisotropy, which results from the rule that growth is possible only in one of the four space directions (nearest neighbours), we can also allow growth into the four diagonal directions (next-nearest neighbours). Figure 6*b*,*c* shows that such growth is initially almost circular until it reaches a critical radius, after which negative fluctuations are no longer filled in. This gives rise to the characteristic fingering structure shown in Fig. 6*c*. Thus this model seems to represent both qualitatively and quantitatively the viscous fingering phenomenon for the case of miscible fluids (zero interfacial tension).

We thank G. Daccord, R. Lenormand and J. D. Chen for sharing their experimental results with us before publication, and we also thank them and F. Rondelez for helpful discussions. We thank David Kamins for generous and patient assistance with colour computer graphics, and the Boston University Academic Computer Center for generous computer time on the mainframe IBM-3090 computer.

Received 19 December 1985; accepted 21 April 1986.

1. Langer, J. S. *Rev. mod. Phys.* **52**, 1 (1980).
2. Ben-Jacob, E., Goldenfeld, N., Langer, J. S. & Schön, G. *Phys. Rev.* **A29**, 330–340 (1984).
3. Brower, R. C., Kessler, D. A., Koplik, J. & Levine, H. *Phys. Rev.* **A29**, 1335–1342 (1984).
4. Kessler, D. A., Koplik, J. & Levine, H. *Phys. Rev.* **A30**, 2820–2823 (1984).
5. Honjo, H., Ohta, S. & Sawada, Y. *Phys. Rev. Lett.* **55**, 841–844 (1985).
6. Vicsek, T. *Phys. Rev. Lett.* **53**, 2281–2284 (1984).
7. Szép, J., Cserti, J. & Kertész, J. *J. Phys.* **A18**, L413–L416 (1985).
8. Kertész, J. & Vicsek, T. *J. Phys. A* (in the press).
9. Bentley, W. A. & Humphreys, W. J. *Snow Crystals* (Dover, New York, 1962).
10. Nittmann, J., Daccord, G. & Stanley, H. E. *Nature* **314**, 141–144 (1985).
11. Sander, L. M., Ramanlal, P. & Ben-Jacob, E. *Phys. Rev.* **A32**, 3160–3165 (1985).
12. Van Damme, H., Obrecht, F., Levitz, P., Gatineau, L. & Laroche, C. *Nature* **320**, 731–733 (1986).
13. DeGregoria, A. J. & Schwartz, L. W. *J. Fluid Mech.* **164**, 383–400 (1986).
14. Bensimon, D. *Phys. Rev.* **A33**, 1302–1308 (1986).
15. Lenormand, R. & Zarcone, C. *Phys. chem. Hydrodyn.* **6**, 497–506 (1985).
16. Chen, J. D. & Wilkinson, D. *Phys. Rev. Lett.* **55**, 1892–1895 (1985).
17. Måløy, K. J., Feder, J. & Jøssang, T. *Phys. Rev. Lett.* **55**, 2688–2691 (1985).
18. Daccord, G., Nittmann, J. & Stanley, H. E. *Phys. Rev. Lett.* **56**, 336–339 (1986).
19. Ben-Jacob, E. *et al. Phys. Rev. Lett.* **55**, 1315–1318 (1985).
20. Paterson, L. *J. Fluid. Mech.* **113**, 513–529 (1981).
21. Maddox, J. *Nature* **313**, 93 (1985).
22. Niemeyer, L., Pietronero, L. & Wiesmann, H. J. *Phys. Rev. Lett.* **52**, 1033–1036 (1984).
23. Paterson, L. *Phys. Rev. Lett.* **52**, 1621–1624 (1984).
24. Sherwood, J. D. & Nittmann, J. *J. Phys., Paris* **47**, 15–21 (1986).
25. Saffman, P. G. & Taylor, G. I. *Proc. R. Soc.* **A245**, 312–329 (1958).
26. Tang, C. *Phys. Rev.* **A31**, 1977–1979 (1985).
27. Paterson, L. *Physics Fluids* **28**, 26–30 (1985).
28. Chuoke, R. L., Van Meurs, P. & Van der Pol, C. *Trans. Am. Inst. Min. Engrs* **216**, 188–194 (1959).
29. Mullins, W. W. & Sekerka, R. F. *J. appl. Phys.* **34**, 323–329 (1963).
30. Witten, T. A. & Sander, L. M. *Phys. Rev. Lett.* **47**, 1400–1403 (1981).
31. Witten, T. A. & Sander, L. M. *Phys. Rev.* **B27**, 5686–5697 (1983).
32. Meakin, P. in *On Growth and Form: Fractal and Non-Fractal Pattern in Physics* (eds Stanley H. E. & Ostrowsky, N.) (Nijhoff, Dordrecht, 1985).
33. Meakin, P. *Phys. Rev.* (submitted).
34. Mason, B. J. *Scient. Am.* **204**, No. 1, 120–130 (1961).
35. Jullien, R., Kolb, M. & Botet, R. *J. Phys., Paris* **45**, 395–399 (1984).
36. Ball, R. C., Brady, R. M., Rossi, G. & Thompson, B. R. *Phys. Rev. Lett.* **55**, 1406–1409 (1985).
37. Meakin, P. *Phys. Rev.* **A27**, 2616–2623 (1983).
38. Meakin, P. *Pap. presented at int. Conf. Fragmentation, Form and Flow in Fractured Media* Neve Ilan, 6–9 January (1986).
39. Shraiman, B. I. & Bensimon, D. *Phys. Rev.* **A30**, 2840–2844 (1984).

Nodule-specific expression of a chimaeric soybean leghaemoglobin gene in transgenic *Lotus corniculatus*

Jens Stougaard Jensen & Kjeld A. Marcker

Department of Molecular Biology and Plant Physiology, University of Aarhus, DK-8000 Århus C, Denmark

Léon Otten* & Jeff Schell

Max-Planck-Institut für Züchtungsforschung, D-5000 Köln 30, FRG

When a chimaeric soybean leghaemoglobin gene was introduced into the genome of another legume species, Lotus corniculatus, *nodule-specific expression of the chimaeric gene was found in root nodules formed on fully regenerated plants inoculated with the* Lotus *microsymbiont,* Rhizobium loti. *Expression under control of the 5′ upstream region of the soybean gene was regulated at the level of RNA and followed the correct developmental timing. This indicates a conserved induction mechanism for leghaemoglobin genes in legumes.*

THE symbiotic association between soil bacteria of the genus *Rhizobium* and plants of the family Leguminosae results in the formation of a unique specialized plant organ—the root nodule. Fixation of atmospheric dinitrogen by the bacterial nitrogenase enzyme within this organ enables the plant to grow without external supply of reduced nitrogen. The interaction between the symbionts is generally very specific and has been used to subdivide the bacterial genus into species and the legumes into cross-inoculation groups[1]. *Bradyrhizobium japonicum* will thus infect soybean while *Rhizobium loti* infects *Lotus corniculatus.* Normal root nodule formation occurs only after invasion of the plant root by the compatible bacteria. Successful invasion initiates a series of developmental events in the plant. Root cortex cells re-differentiate into meristematic cells that proliferate and differentiate to form the organized tissues[2]. Around 30 different plant encoded-polypeptides ('nodulins') are specifically synthesized or present in higher concentration during this development[3,4]. Biochemical function has been assigned to genes encoding glutamine synthetase[5], uricase[6,7] and leghaemoglobin polypeptides[8].

Four leghaemoglobin proteins, Lbc_3, Lbc_2, Lbc_1 and Lba, are synthesized in soybean nodules[8]. The corresponding genes together with a pseudogene and a truncated gene are organized in two clusters with intergenic regions of some 2 kilobases (kb) separating the individual genes[9,10]. Induction of the four active *lb* genes occurs in a sequential manner during nodule development. Transcription of the lbc_3, lbc_2 and lbc_1 genes starts slightly before the appearance of visible nodules while transcription of the *lba* gene is delayed for another day or two[11]. Later in development, transcription of the *lba*, lbc_3, lbc_1 genes is drastically increased at the same time as several other nodulin genes are activated, indicating common features in the regulation of nodule-specific genes[11]. Typical eukaryotic promoter sequences homologous to sequences required for optimal transcription of a mammalian β-globin gene are located 5′ to each of the coding sequences of the four active genes[12,13], but β-globin gene expression is also dependent on downstream sequences[14]. In order to analyse the role of 5′ upstream and 3′ downstream sequences in the specific regulation of leghaemoglobin genes, we have transferred a chimaeric gene (*lbc_3 5′3′-cat*) with the composition 5′ lbc_3-chloramphenicol acetyltransferase (CAT) coding sequence-3′ lbc_3 to a heterologous legume species, *Lotus corniculatus* (bird's-foot trefoil), using the Ri plasmid of *Agrobacterium rhizogenes* as gene vector.

Here we describe the nodule-specific expression of the chimaeric soybean *lbc_3 5′3′-cat* gene in root nodules formed on fully regenerated plants of a member of the legume family. We further show that the expression is regulated at the level of RNA and that the correct transcription initiation signals are used. Finally it is shown that the chimaeric gene is activated at the correct stage of nodule development.

Transformation system

The minimal requirement for the study of the expression of transferred genes in root nodules is a legume transformation and regeneration system that allows transformed cells to differentiate into roots. Such a system was developed using the capacity of *Agrobacterium rhizogenes* to induce root formation in transformed plant cells. For this particular study an approach leading to the integration of a complete 'intermediate cloning vector'[15] carrying the chimaeric gene in the T-DNA region of the Ri plasmid was chosen. Figure 1*a* shows the two intermediate vectors, pAR29 and pAR30, used to integrate the chimaeric *lbc_3 5′3′-cat* gene into *A. rhizogenes* T-DNA. Homologous recombination through the pRi *Eco*RI fragments 36 and 40 was obtained after conjugation[16] of the two 'intermediate vectors' from *Escherichia coli* to the *A. rhizogenes* 15834 strain[17]. Transconjugants underwent Southern blot analysis to demonstrate the presence of the chimaeric gene and of co-integrate formation through the homologous T-DNA sequences (data not shown). Roots formed after wound site infection of *L. corniculatus* seedlings were cultured *in vitro* and freed from the infecting bacteria by treatment with antibiotics (500 μg ml^{-1} Claforan). Whole plants were regenerated from root cultures through somatic embryogenesis or organogenesis[18]. The structure of the co-integrate T-DNA region transferred to *L. corniculatus* lines L6-23 and L5-9, as deduced from recombinant constructions and confirmed by Southern blot analysis, is given in Fig. 1*b*. Figure 2 demonstrates the presence of the *lbc_3 5′3′- cat* gene in the L6-23 line.

The number of T-DNA inserts in the two plant lines were estimated from the number of *Eco*RI or *Hin*dIII restriction fragments hybridizing to the left T_L-DNA border in genomic DNA Southern blot analysis. An *A. rhizogenes* T_L-DNA-derived probe shown below Fig. 2 was used to recognize the various restriction fragments generated after insertion of the T_L-DNA into the plant genome. Two T-DNA inserts were found in L6-23 while only one insert was present in the L5-9 line. These values reflect the minimum copy numbers for the *lbc_3 5′3′-cat* gene. Regenerated plants were transferred to growth cabinets and

* Present address: Department of Molecular Plant Pathology, Université Louis Pasteur, 67083 Strasbourg, France.

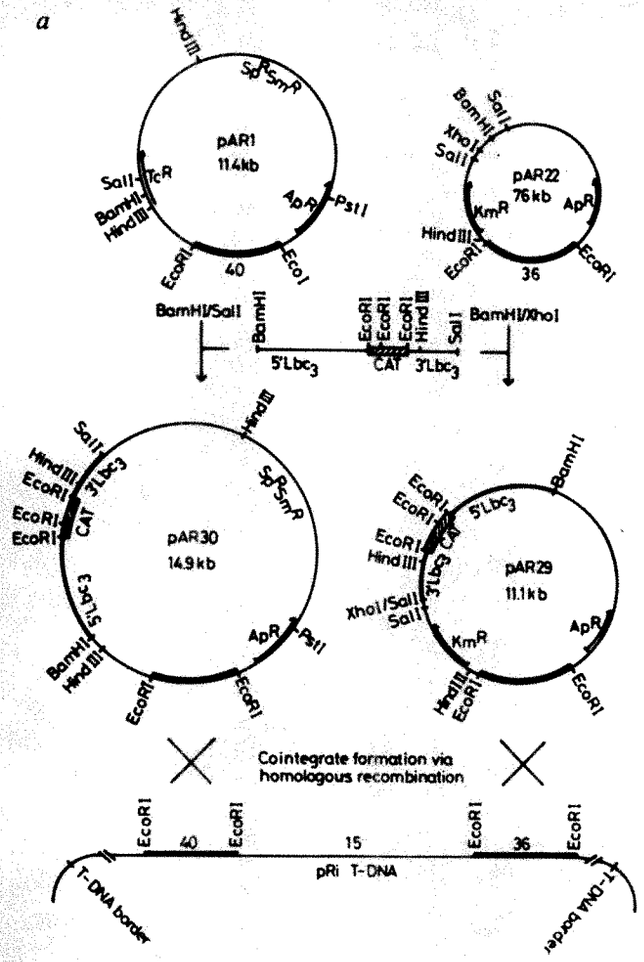
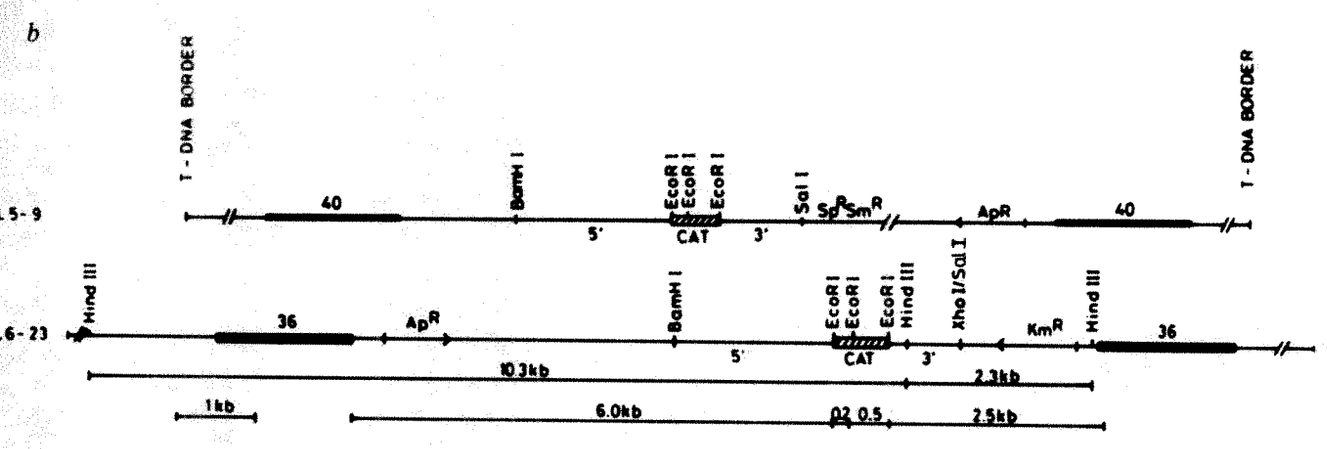


Fig. 1 *a*, Integration of the chimaeric *lbc*$_3$ *5'3'-cat* gene into the *A. rhizogenes* T_L-DNA region. *b*, Structure of the T_L region after integration of the chimaeric *lbc*$_3$ *5'3'-cat* gene.
Methods. *a*, Two *Eco*RI fragments (36 and 40) from the T_L (T-left) T-DNA region of the agropine pRi plasmid 15834 were chosen as integration 'sites'. The ColE1 replicons pAR1, pAR22 J.S.J. unpublished) carrying the corresponding subcloned *Eco*RI fragments were therefore used as 'intermediate cloning vectors'[15] for the *lbc*$_3$ 5'3'-*cat* 3.6-kb *Bam*HI/*Sal*I fragment[37]. The resulting plasmids pAR29, pAR30 were then separately conjugated to a rifampicin-resistant (rif^R) *A. rhizogenes* 15834 using a plasmid helper system[16]. Transconjugants carrying co-integrates were selected on LB medium containing rifampicin (100 μg ml^{-1}) plus spectinomycin (100 μg ml^{-1}) plus streptomycin (100 μg ml^{-1}) or kanamycin (300 μg ml^{-1}). ColE1 plasmids are unable to replicate in *Agrobacterium*. Selection for plasmid resistance markers will therefore select co-integrates formed after homologous recombination through the region offered. The chimaeric *lbc*$_3$-*cat* gene consists of a 2-kb *lbc*$_3$ promoter region terminating 7 bp upstream of the *lbc*$_3$ initiator codon, CAT coding sequence including 5-bp 5' and 31-bp 3' untranslated sequence and 0.9 kb of the *lbc*$_3$ 3' flanking region starting 3 bp after the *lbc*$_3$ stop codon. See ref. 37 for further details. *b*, The presence and orientation of the chimaeric gene within the pRi T-DNA was determined by Southern analysis of total DNA from *A. rhizogenes* co-integrate strains. Integrity of the inserted plasmids and the position of generated restriction sites within the T-DNA was also confirmed. The figure shows the deduced structure of T_L-DNA transferred to the transformed *L. corniculatus* lines L6-23 and L5-9. See *a* for restriction sites not indicated. The lines below the L6-23 structure indicate the fragments generated after *Hin*dIII and *Eco*RI digestion of DNA from transformed plant lines. The same fragments are shown in Fig. 2. Subcloning and plasmid preparation were according to Marcker *et al.*[11]. The procedure of Van Haute *et al.*[16] was used for conjugational transfer of plasmids. Total DNA was extracted and analysed according to Dhaese *et al.*[44].



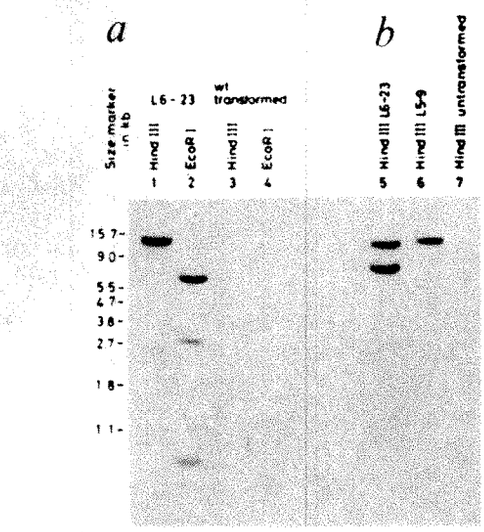
inoculated with the *Rhizobium loti* strain NZP2037[19]. Nodules for analysis were harvested 3–6 weeks later.

Nodule-specific expression

Chloramphenicol acetyltransferase activity was measured in 3–6-week-old nodules excised from the roots of L6-23 and L5-9 transformed *Lotus* lines. Root tissue as well as leaf plus stem fragments derived from the same transformed plant were also extracted and CAT activity measured. Conversion of ^{14}C-chloramphenicol to the acetylated forms followed by thin layer chromatographic separation was used to assay CAT activity. Data from *Lotus* lines L6-23 and L5-9 are presented in Fig. 3, together with data from untransformed *Lotus* plants and from a line transformed with the complete *lbc*$_3$ gene. No CAT activity could be detected in any tissue from untransformed or *lbc*$_3$-transformed plants. High enzymatic activity was, however, expressed from the chimaeric *lbc*$_3$ *5'3'-cat* gene in root nodules of the L6-23 line. Neither root nor leaf plus stem tissue from this same line contained any CAT activity. The *lbc*$_3$ *5'3'-cat* gene is therefore expressed in an organ-specific manner. Similar results were obtained with the L5-9-transformed line. A remarkable result is the lack of expression in any of the other major tissues tested. Even prolonged exposure of the autoradiogram did not reveal any CAT activity in transformed leaf stem or root tissues. The CAT assay conditions used would have detected an activity 5,000 times lower than the activity observed in root nodules.

Expression regulated at RNA level

The nodule-specific expression of CAT from the soybean *lbc*$_3$ *5'3'-cat* gene may be the result of transcriptional, translational or post-translational control. In order to distinguish among these



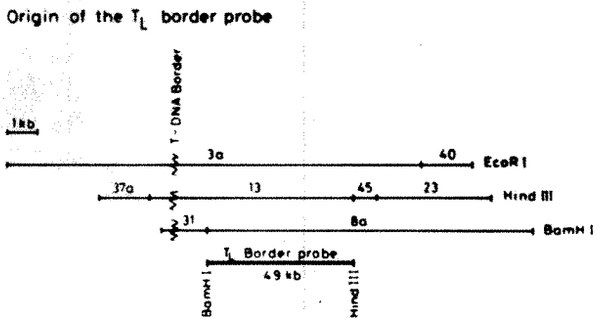


Fig. 2 *a*, Southern hybridization analysis of the transformed *L. corniculatus* line L6-23. Lanes 1 and 2 contain ~10 μg *Hin*dIII or *Eco*RI-digested DNA from leaves of L6-23 plants. Lanes 3 and 4 contain corresponding digests of DNA from *L. corniculatus* plants transformed with the *A. rhizogenes* wild-type strain. The size of the fragments hybridizing to a *lbc*$_3$ *5'3'-cat* probe are indicated below the diagram of the co-integrate structure in Fig. 1*b*. *b*, Estimation of copy number of the *lbc*$_3$ *5'3'-cat* gene in L6-23 and L5-9 *Lotus* lines. A *Bam*HI/*Hin*dIII fragment adjacent to the left T_L border was used in Southern hybridization to visualize the *Eco*RI and *Hin*dIII fragments generated after insertion of the T_L-DNA into the plant genome. The restriction map[45] below shows the exact position of the *Bam*HI/*Hin*dIII restriction fragment used as probe and give the size of *Eco*RI, *Hin*dIII restriction fragments hybridizing to this probe within the pRi plasmid itself. Lanes 5–7 contain *Hin*dIII digests of L6-23, L5-9, and untransformed *Lotus* plants, respectively. Copy numbers were estimated by counting the hybridizing bands. Total plant DNA was extracted and digested according to Dellaporta *et al.*[46].

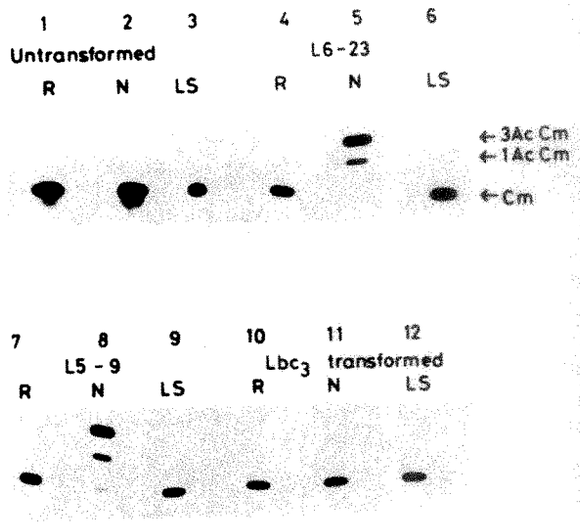


Fig. 3 Expression of the chimaeric *lbc*$_3$ *5'3'-cat* gene in various tissues from transformed and untransformed *Lotus* plants. Equal amounts of tissues were homogenized in a mortar and CAT activity measured by conversion of ^{14}C-chloramphenicol (Cm) to acetylated (Ac Cm) derivatives. Lanes 1–3 demonstrate the lack of CAT activity in root (R), nodule (N), and leaf + stem (LS) tissue of untransformed plants. Lanes 4–6 and 7–9 show the CAT activity in corresponding tissues of the L6-23, L5-9 *lbc*$_3$ *5'3'-cat* transformed lines. Conversion of chloramphenicol in lanes 5 and 8 demonstrate the organ-specific expression of the chimaeric gene in root nodules. Lanes 10–12 show the assays of *lbc*$_3$ transformed control tissues. Reconstruction experiments showed that CAT enzyme from root nodule extracts are stable when mixed with root and leaf plus stem extracts (data not shown).

Methods. Tissue was homogenized with mortar and pestle in 50 mM Tris *p*H 7.5 1 mM EDTA, 400 mM NaCl, 2 mM phenylmethylsulphonyl fluoride buffer (1:1 w/v) at 0 °C. The crude extract (50 μl) was diluted 10-fold into reaction mixture (450 μl) containing 200 mM Tris *p*H 7.5, 0.5 mM acetyl coenzyme A and 0.5 μCi ^{14}C-chloramphenicol and incubated for 1 h at 37 °C. Samples were extracted with 5 ml ethyl acetate and analysed by thin layer chromatography using chloroform/methanol (95:5). The chromatograms were autoradiographed and CAT activities quantitated by counting corresponding regions by liquid scintillation. Standard assays contained 100 μg protein.

possibilities total RNA was extracted from nodule, root and leaf plus stem tissues from L6-23, L5-9 and *lbc*$_3$ transformed control plants. The RNA was separated on agarose gels, transferred to nitrocellulose and hybridized with a probe from the CAT coding sequence. A strong hybridization signal was detected with L6-23 and L5-9 nodule RNA while none of the RNA preparations from any other tissue tested showed hybridization (Fig. 4*a*). Expression of the *lbc*$_3$ *5'3-cat* gene is therefore clearly controlled at the level of RNA. The gene for ubiquitin, a histone-associated protein, is constitutively expressed in a range of eukaryotes including plants[20,21]. Hybridization of a heterologous ubiquitin cDNA to the various RNA preparations was therefore used as an internal standard. Figure 4*b* shows the constitutive expression of endogenous *Lotus* ubiquitin genes in the tissues tested.

Lotus corniculatus plants contain endogenous leghaemoglobin genes, and cross-hybridization with soybean leghaemoglobin sequences was detected in Southern blot DNA hybridizations (data not shown). A hybridization signal was also detected in Northern blots. Figure 4*c* shows the signal obtained with a full-length cDNA probe for the soybean *lba* gene. The steady-state level of transcripts from the chimaeric *lbc*$_3$ *5'3'-cat* gene is more than 200-fold higher than the lowest level detectable with the Northern hybridization technique used here.

The size of the CAT hybridizing transcript is approximately 900 nucleotides, which corresponds well with the 860 nucleotides between the *lbc*$_3$ cap site and the *lbc*$_3$ polyadenylation site on the chimaeric gene. The endogenous soybean *lbc*$_3$ has a cap site 51 nucleotides upstream of the ATG codon[22] (position +1). To test whether the heterologous host *L. corniculatus* recognizes and faithfully utilizes the 5' soybean *lbc*$_3$ promoter, the transcription initiation point of the CAT transcript from L6-23 nodules was determined. Total nodule RNA was subjected to oligo(dT) chromatography and subsequently used in a primer extension assay. An oligonucleotide primer (5'CAACGGTGGTATATCCAGTG3') complementary to nucleotides 15–34 in the CAT coding sequence was used. Figure 5 shows the resulting 85, 86, 87, 88 and 90 nucleotide long cDNA species generated. These sizes correspond well with the distance between the cap site (+1) and the 5' end (+83) of the primer. The cDNA species of 85, 87 and 88 nucleotides correspond exactly to endogenous

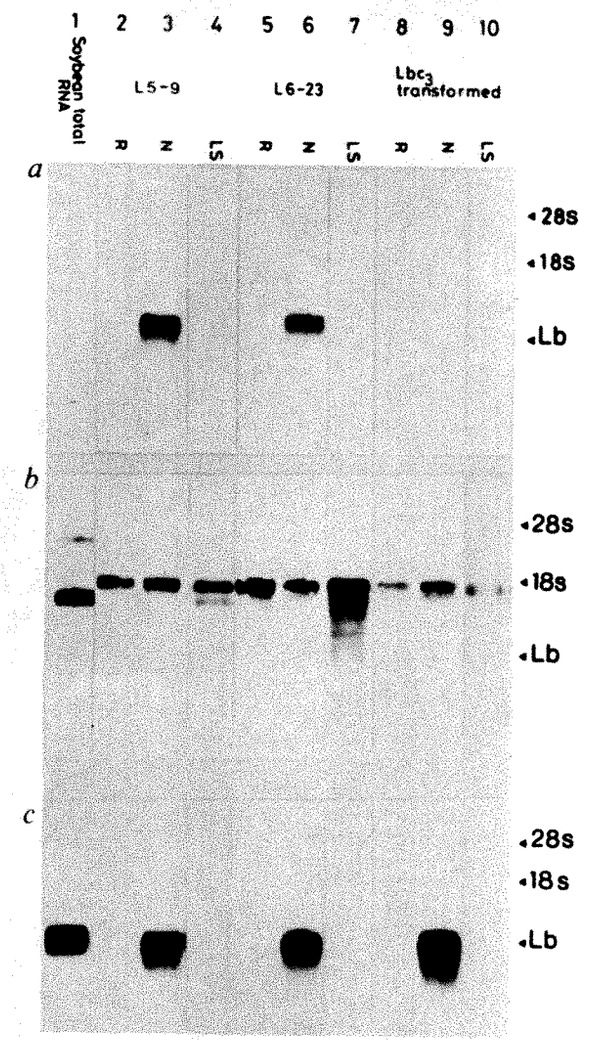


Fig. 4 Northern analysis of transcripts from tissues of *lbc*$_3$ *5'3-cat* transformed and *lbc*$_3$ transformed *Lotus* lines. Five μg of total RNA extracted from root (R), nodule (N) or leaf+stem (LS) tissue was separated in formaldehyde-containing agarose gels and blotted onto nitrocellulose (Gene Screen). Lane 1 contains total RNA from 20-day-old soybean nodules. Lanes 2–4 total RNA from roots, nodules or leaf+stem of the *lbc*$_3$ *5'3'-cat*-transformed L5-9 line. Lanes 5–7 contain total RNA from root nodules, roots or leaf+stem of the L6-23 line while lanes 8, 9 and 10 contain RNA from an *lbc3* transformed line. The complete CAT coding sequence was used as a probe in *a* and demonstrates the presence of the *lbc*$_3$ *5'3'-cat* transcript in L5-9 and L6-23 nodules. In *b* the transcript for the constitutive ubiquitin genes is visualized using a cDNA probe for the human ubiquitin gene[20]. Nodule-specific expression of the endogenous *Lotus lb* genes is shown in *c*. A cDNA probe for the *lba* gene was used in this hybridization. Total RNA was extracted and analysed according to Marcker *et al.*[11] except for leaf+stem RNA which was extracted in 100 mM Tris *p*H 8, 50 mM EDTA, 500 mM NaCl, 5% β-mercaptoethanol, 1.4% sarkosyl at 65 °C for 15 min.

soybean *lbc*$_3$ cap sites determined by S_1 mapping at lower exonuclease concentrations[22].

Developmental regulation

Vertebrate β-globin genes are regulated by a gene-switching mechanism that ensures transcription of only one gene in embryogenic, fetal and adult tissue[23]. The four active leghaemoglobin genes (*lba*, *lbc*$_3$, *lbc*$_2$, *lbc*$_1$) are also induced at different stages of nodule formation, but all four genes remain active throughout the lifetime of the nodule. The *lbc*$_3$, *lbc*$_2$ and *lbc*$_1$ are expressed at a low level immediately before the nodule turns pink. At this developmental stage there is a strong and abrupt increase in transcription of the *lbc*$_3$, *lbc*$_1$ and *lba* genes. A number of 'nodulin' genes are induced at this stage while the bacterial nitrogenase genes are induced even later[11]. CAT activity from the chimaeric *lbc*$_3$ *5'3'-cat* gene in L6-23 was therefore followed throughout nodule development. Figure 6 shows the induction kinetics of the chimaeric gene relative to nodule development and nitrogenase activity. The lack of CAT activity in small white nodules (panel 2 in Fig. 6), the low level of activity in white nodules (panel 3) and the strong increase in activity in pink nodules with high nitrogenase activity follow the kinetics of the native *lbc*$_3$ gene. Correct developmental regulation of the *lbc*$_3$ promoter is thus maintained in the *L. corniculatus* transformants.

Discussion

Agrobacterium Ti plasmids have been used as gene vectors for plant transformation by a number of investigators. Protoplasts[24], leaf disks[25], callus[26] and wounded plants[27] have been infected and transformed tissue was recovered by screening or selection[28]. The transferred genes are functionally expressed and expression in complete regenerated plants has so far been achieved in tobacco[29–34], petunia[31,34–36] and tomato plants[25]. Chimaeric genes consisting of the T-DNA-derived nopaline synthase promoter and coding sequences specifying resistance to chloramphenicol, kanamycin and methotrexate respectively were initially used for transfer and expression in model studies[29,32]. More recently, chimaeric genes derived from genes encoding the chlorophyll *a*/*b* binding protein[33,36] were transferred, organ-specifically expressed and shown to maintain their photoregulation upon transfer.

The transferred *lbc*$_3$ *5'3'-cat* gene is specifically expressed in root nodules of the heterologous *L. corniculatus* host and is regulated at the level of RNA. We therefore infer that the DNA sequences responsible for the nodule-specific expression of the *lbc*$_3$ gene are located on the 2-kb 5'-flanking or 0.9-kb 3'-flanking region of the chimaeric *lbc*$_3$ *5'3'-cat* gene and that interactions at these sequences control the activity of the *lb* promoter. The most reasonable explanation of our results is that the regulation

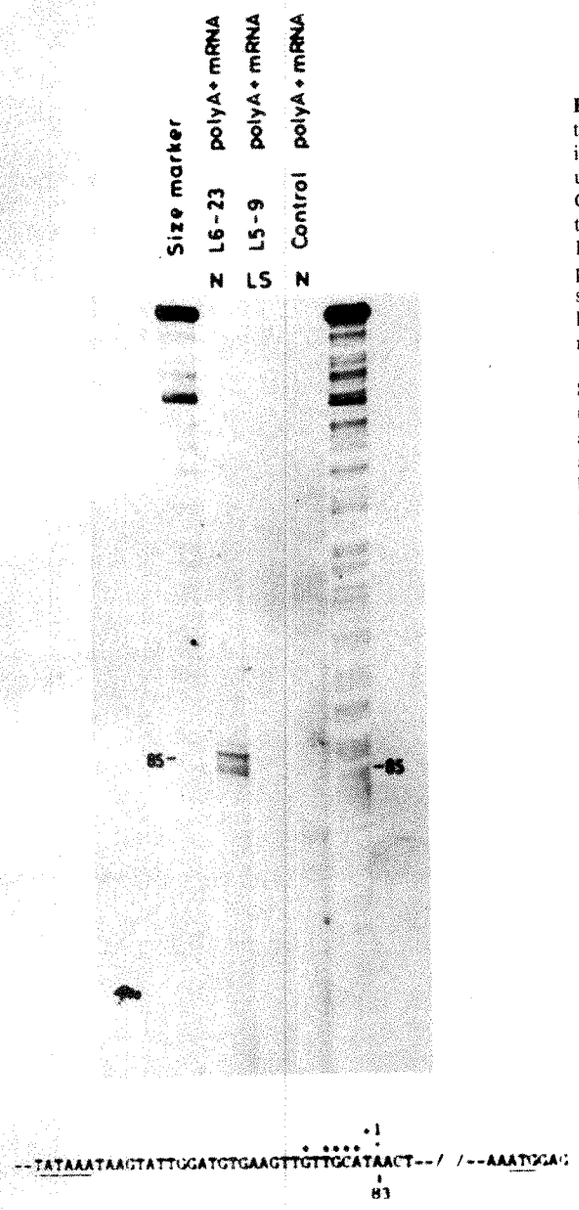


Fig. 5 (Left) Determination of the transcription initiation site for the lbc_3 *5'3'-cat* gene in *L. corniculatus* root nodules. Total RNA isolated from nodules or leaf+stem was oligo(dT) purified and used in a primer extension assay. A synthetic oligonucleotide 5' CAACGGTGGTATATCCAGTG 3' complementary to nucleotides 15 to 34 of the CAT coding sequence was used as primer. Lane 2 shows the cDNA species resulting from extension of the primer on the CAT transcript present in L6-23 nodules. Lane 3 shows the negative control using leaf+stem mRNA from the L5-9 line and lane 4 the negative control with mRNA from untransformed nodules. No other specific cDNA species were detected. Lanes 1 and 5 show the sequence ladder used to size the cDNA. A cDNA 83 nucleotides long would be expected if the soybean cap site at (+1) was used. The cap sites corresponding to the 85, 86, 87, 89 and 90 nucleotide long cDNA species generated are indicated with asterisks on the partial sequence of the lbc_3 *5'3'-cat* 5' region given below. The translation initiation codon of the CAT coding sequence and the TATA box of the lbc_3 promoter are underlined. The primer was end labelled with ^{32}P using polynucleotide kinase and the extension assay was according to Boel *et al.*[47].

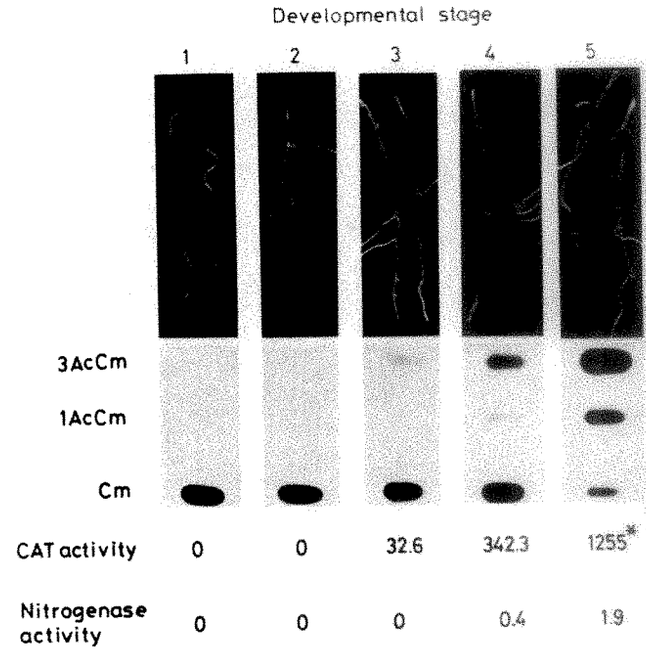


Fig. 6 (Above) Comparison of the lbc_3 *5'3'-cat* gene expression in developing root nodules. CAT and nitrogenase activity were measured on root pieces with nodules in different developmental stages. Stage one shown in panel 1: no visible nodules. Stage 2, panel 2: emerging nodules. Stage 3, panel 3: distinct white nodules. Stage 4, panel 4: small pink nodules. Panel 5 shows nodules in various later states of maturity. The CAT activities and nitrogenase activities follow the developmental control of *lb* gene expression in soybean root nodules. *, This enzymatic activity is only valid for the substrate-limited reaction shown.

Methods. 400 mg root tissue carrying appropriate nodules was analysed for each developmental state. CAT activity was determined in half of this material according to the previously given procedure. The other half was used to measure acetylene reduction capacity of the nodules. Roots and nodules were incubated for 1 h with an atmosphere of 10% acetylene in Suba Seal-stopped 7 ml Bijoux bottles. Ethylene was measured on a gas chromatograph and nitrogenase activity determined as nmol ethylene per μg protein per h. CAT activity is in c.p.m. per μg protein per h.

of the *lb* promoter is exerted on the initiation of transcription, but other models for regulating the level of RNA cannot entirely be ruled out.

Haem, the prosthetic group in globin proteins, controls the efficiency of lbc_3 *5'3'-cat* mRNA translation in yeast[37]. A similar translational control of leghaemoglobin gene expression might therefore also exist in root nodules, but this has not been investigated here.

Sequences required for expression of photoregulated genes are present in 5' flanking regions[33,36,38–40]. A short 33-base-pair (bp) sequence located between the TATA box and the transcription start site is sufficient to confer light induction on the ribulose 1,5-biphosphate carboxylase *rbcS-E9* gene[39] while the *rbcSss3.6* gene has light-responsive and enhancer-type regulatory sequences upstream of the TATA box[41]. Organ specificity and light-induction control regions are both located on a short DNA fragment derived from the pea chlorophyll *a*/*b* binding protein gene[33]. The available evidence, therefore, suggests that DNA sequences controlling organ specificity are closely linked to the promoter. We therefore expect that the regulatory sequences involved in nodule-specific expression are located on the lbc_3 5' flanking region. The correct initiation of transcription and organ-

specific expression of the lbc_3 promoter in the distantly related legume *L. corniculatus* has further implications concerning the control of nodule expressed genes. *Lotus corniculatus* belongs phylogenetically to the tribe Loteae while soybean belongs to the Phaseoleae[42]. The microsymbiont *Rhizobium loti* is a species separate from the soybean symbiont *B. japonicum*[1] and nodulates plants from a different cross-inoculation group. It appears therefore that both a putative bacterial induction signal and DNA sequences involved in nodule-specific expression of plant 'nodulin' genes are conserved in the legume *Rhizobium* symbiosis. Efficient nodulation of different plant species by broad host range isolates of *Rhizobium* and the wide susceptibility of certain host plants, support this idea[1,43].

We thank Dr A. Petit and Professor J. Tempé, Orsay, for introducing us to the *Lotus* system, and A. Kühle and D. Abildsten for technical assistance. This research was supported by the Danish Biomolecular Engineering Programme, EEC contract GBI-4-025-DK and De Danske Sukkerfabrikker A/S. J.S.J. was supported by the Danish Agricultural Research Council and an OECD travel grant.

Received 5 February; accepted 15 April 1986.

1. Vincent, J. M. in *The Biology of Nitrogen Fixation* (ed. Quispel, A.) 265–341 (North-Holland, Amsterdam, 1974).
2. Vincent, J. M. in *Nitrogen Fixation II* (eds Newton, W. E. & Orme Johnson, W. H.) 103–129 (University Park, Baltimore, 1980).
3. Legocki, R. P. & Verma, D. P. S. *Cell* **20**, 153–163 (1980).
4. Bisseling, T., Been, C., Klugkist, J., Van Kammen, A. & Nadler, K. *EMBO J.* **2**, 961–966 (1983).
5. Cullimore, J. V. *et al. J. molec. appl. Genet.* **2**, 589–599 (1984).
6. Jochimsen, B. & Rasmussen, O. in *Abstr. 1st int. Symp. Molecular Genetics of the Bacteria-Plant Interactions*, 83 (Springer, Berlin, 1982).
7. Nguyen, T., Zelechowska, M., Foster, V., Bergmann, H. & Verma, D. P. S. *Proc. natn. Acad. Sci. U.S.A.* **82**, 5040–5044 (1985).
8. Fuchsman, W. H. & Appleby, C. A. *Biochim. biophys. Acta* **579**, 314–324 (1979).
9. Bojsen, K., Abildsten, D., Jensen, E. Ø., Paludan, K. & Marcker, K. A. *EMBO J.* **2**, 1165–1168 (1983).
10. Lee, J. S., Brown, G. G. & Verma, D. P. S. *Nucleic Acids Res.* **11**, 5541–5553 (1983).
11. Marcker, A., Lund, M., Jensen, E. Ø. & Marcker, K. A. *EMBO J.* **3**, 1691–1695 (1984).
12. Grosveld, G. C., de Boer, E., Shewmaker, C. K. & Flavell, R. A. *Nature* **295**, 120–126 (1982).
13. Dierks, P. *et al. Cell* **32**, 695–706 (1983).
14. Wright, S., Rosenthal, A., Flavell, R. & Grosveld, F. *Cell* **38**, 265–273 (1984).
15. Leemans, J. *et al. J. molec. appl. Genet.* **1**, 149–164 (1981).
16. Van Haute, E. *et al. EMBO J.* **3**, 411–417 (1983).
17. White, F. F. & Nester, E. W. *J. Bact.* **141**, 1134–1141 (1980).
18. Chilton, M.-D. *et al. Nature* **295**, 432–434 (1982).
19. Pankhust, C. E. *Can. J. Microbiol.* **23**, 1026–1033 (1977).
20. Wiborg, O. *et al. EMBO J.* **4**, 755–759 (1985).
21. Gausing, K. & Barkardottir, R. *Eur. J. Biochem.* (in the press).
22. Brissan, N. & Verma, D. P. S. *Proc. natn. Acad. Sci. U.S.A.* **79**, 4055–4059 (1982).
23. Nienhuis, A. W. & Benz, E. J. *New Engl. J. Med.* **297**, 1318–1328; 1371–1381, 1430–1436 (1977).
24. Marton, L., Wullems, G. J., Molendijk, L. & Schilperoort, R. A. *Nature* **277**, 129–131 (1979).
25. Horsch, R. B. *et al. Science* **227**, 1229–1231 (1985).
26. Pollock, K., Barfield, D. G., Robinson, S. J. & Shields, R. *Pl. Cell Rep.* **4**, 202–205 (1985).
27. Zambryski, P. *et al. EMBO J.* **2**, 2143–2150 (1983).
28. Herrera-Estrella, L. *et al. EMBO J.* **2**, 987–995 (1983).
29. De Block, M., Herrera-Estrella, L., Van Montagu, M., Schell, J. & Zambryski, P. *EMBO J.* **3**, 1681–1689 (1984).
30. Sengupta-Gopalan, C., Reichert, N. A., Barker, R. F., Hall, T. L. & Kemp, J. O. *Proc. natn. Acad. Sci. U.S.A.* **82**, 3320–3324 (1985).
31. Lamppa, G., Nagy, F. & Chua, N.-H. *Nature* **316**, 750–752 (1985).
32. De Block, M., Schell, J. & Van Montagu, M. *EMBO J.* **4**, 1367–1372 (1985).
33. Simpson, J. *et al. EMBO J.* **4**, 2723–2729 (1985).
34. Nagy, F., Morelli, G., Graley, S. G. & Chua, N.-H. *EMBO J.* **4**, 3063–3068 (1985).
35. Beachy, R. N. *et al. EMBO J.* **4**, 3047–3053 (1985).
36. Jones, J. D. G., Dunsmuir, P. & Bedbrook, J. *EMBO J.* **4**, 2411–2418 (1985).
37. Jensen, E. Ø., Marcker, K. A. & Villadsen, I. S. *EMBO J.* **5** (in the press).
38. Herrea-Estrella, L. *et al. Nature* **310**, 115–120 (1984).
39. Morelli, G., Nagy, F., Fraley, R. T., Rogers, S. G. & Chua, N.-H. *Nature* **315**, 200–204 (1985).
40. Facciotti, D., O'Neal, J. K., Lee, S. & Shewmaker, C. H. *Biotechnology* **3**, 241–246 (1985).
41. Timko, M. P. *et al. Nature* **318**, 579–582 (1985).
42. Polhill, R. M. in *Advances in Legume Systematics* Vol. 1 (eds Polhill, R. M. & Raven, D. H.) (University of Reading, 1981).
43. Trinick, M. J. *J. appl. Bact.* **49**, 39–53 (1980).
44. Dhaese, P., De Greve, H., Decraemer, H., Schell, J. & Van Montagu, M. *Nucleic Acids Res.* **7**, 1837–1849 (1979).
45. Pomponi, M., Spano, L., Sabbadini, M. G. & Costantino, P. *Plasmid* **10**, 119–129 (1983).
46. Dellaporta, S. L., Wood, J. & Hicks, J. B. *Pl. molec. Biol. Rep.* **1**, 10–21 (1983).
47. Boel, E. *et al. Proc. natn. Acad. Sci. U.S.A.* **80**, 2866–2869 (1983).

Fluorescence detection in automated DNA sequence analysis

Lloyd M. Smith, Jane Z. Sanders, Robert J. Kaiser, Peter Hughes, Chris Dodd, Charles R. Connell*, Cheryl Heiner*, Stephen B. H. Kent & Leroy E. Hood

Division of Biology, California Institute of Technology, Pasadena, California 91125, USA
* Applied Biosystems, Inc., Foster City, California 94404, USA

We have developed a method for the partial automation of DNA sequence analysis. Fluorescence detection of the DNA fragments is accomplished by means of a fluorophore covalently attached to the oligonucleotide primer used in enzymatic DNA sequence analysis. A different coloured fluorophore is used for each of the reactions specific for the bases A, C, G and T. The reaction mixtures are combined and co-electrophoresed down a single polyacrylamide gel tube, the separated fluorescent bands of DNA are detected near the bottom of the tube, and the sequence information is acquired directly by computer.

THE structural analysis of DNA has an increasingly important role in modern molecular biology. About 4×10^6 bases of DNA have been sequenced since the introduction of the enzymatic method of rapid sequencing developed by Sanger and co-workers[1,2] and the chemical method developed by Maxam and Gilbert[3]. Typically, four separate reactions are performed on the particular DNA segment to be analysed. In the enzymatic method, these reactions produce DNA fragments terminating in either adenosine (A), cytosine (C), guanosine (G) or thymidine (T). In the chemical method fragments terminating in G, G+A, C+T, or C are typically produced. In both cases the four sets of reaction products are electrophoresed in adjacent lanes of a high-resolution polyacrylamide gel. An autoradiographic image of the gel is produced which can be examined to determine the relative lengths of the DNA fragments generated in each of the four reactions. The DNA sequence is inferred directly from this information. Both these techniques are highly effective but are also very labour-intensive, fairly expensive and involve the use of radioisotopes. For these reasons, and because many genes remain to be sequenced (there are 3×10^9 bases in the human genome alone), we have undertaken the development of an automated and non-isotopic method of DNA sequence analysis.

Strategy

Our approach has two major aims. The first is to acquire, store and analyse sequence information directly by computer. Doing this in real-time during the gel electrophoresis eliminates the

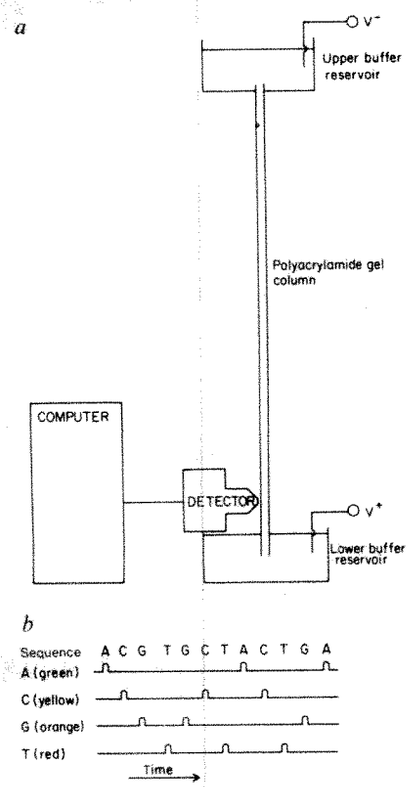


Fig. 1 *a*, Simplified diagram of the automated DNA sequenator. *b*, Idealized output from the automated DNA sequenator.

transfer of information from gel to film (autoradiography), the tedious manual analysis and the need to run several overlapping gels; instead, a single gel can be run for as long as resolvable sequence is obtained. The second aim is to avoid the use of radioisotopes, which are hazardous, costly and unstable.

With these considerations in mind, we have developed a strategy for the automated sequence analysis of DNA which is based on two key points (proposed initially in ref. 4). First, fluorophores are used for detection rather than radioisotopes. Fluorescence provides sufficient sensitivity for real-time optical detection of the small amounts of DNA present in DNA sequencing gels ($\sim 10^{-15}$ mol per band) (see the discussion below). Second, four different fluorophores are used, one for each of the base-specific reactions. The reaction products are combined and co-electrophoresed, and the DNA fragments generated in each reaction are detected near the bottom of the gel and identified by their colour. These fluorescence data are continuously acquired and stored by computer during the electrophoresis. The data may then be analysed by computer to yield the DNA sequence. An idealized version of this process is depicted in Fig. 1.

We applied this strategy to Sanger's enzymatic method of DNA sequence analysis. We use chemically synthesized fluorescent oligonucleotide primers to label the DNA fragments. When these fluorescent primers are used instead of the usual underivatized primer in the enzymatic sequencing reactions, the DNA fragments generated in the reactions are fluorescent.

Chemistry

The first step in implementing this strategy was to develop chemistry for the synthesis of the fluorescent oligonucleotide primers[4,5]. Briefly, we synthesized a derivative of thymidine which contains a phosphoramidite moiety at the 3′ carbon and a protected amino group at the 5′ carbon. When this molecule is used in the final addition cycle of oligonucleotide synthesis by the phosphoramidite method (see ref. 6 for review), the product after deprotection and cleavage from the solid phase is an oligonucleotide containing a single aliphatic amino group

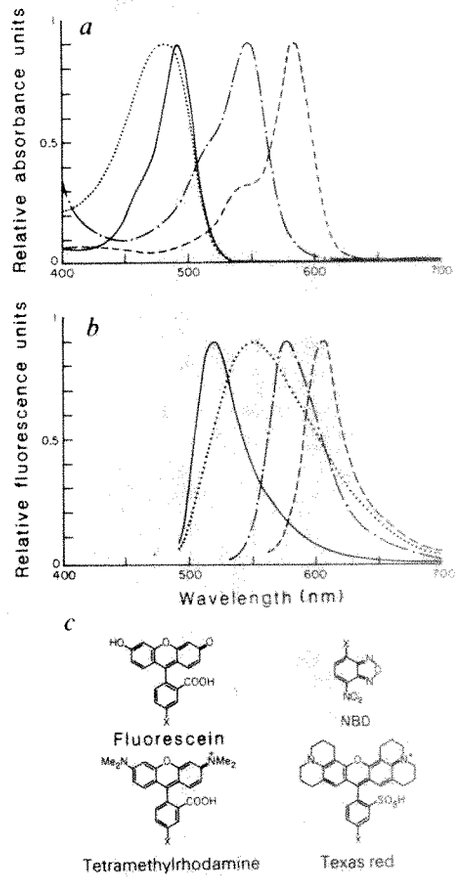


Fig. 2 *a*, Absorption spectra of the four dyes used in the DNA sequenator: ——, fluorescein; ·····, NBD; -·-·-, tetramethylrhodamine; - - - -, Texas Red. *b*, Florescence emission spectra of the four dyes; the same line types as in *a*, are used to denote the dyes. *c*, Chemical structures of the four dyes. X, The moiety to which the dye is bound, for example, an oligonucleotide primer. **Methods.** All spectra were obtained in 10 mM sodium carbonate buffer, *p*H 9.0; absorption spectra were taken on an H/P 8451 spectrophotometer; fluorescence spectra were taken on a Perkin-Elmer MPF4 spectrofluorimeter (uncorrected). The following dye derivatives were used for measurements: fluorescein isothiocyanate (FITC), NBD aminohexanoic acid, Texas Red (all from Molecular Probes, Junction City, Oregon); and tetramethylrhodamine isothiocyanate (Research Organics, Inc., Cleveland, Ohio).

at the 5′ terminus. This material may then be conjugated readily to any of various commercially available amino-reactive fluorescent dyes to yield the corresponding oligonucleotide derivative.

The selection of a set of four fluorophores was central to development of the DNA sequenator. Several criteria were used in the selection of these fluorophores. (1) The absorption and emission maxima had to be in the visible region of the spectrum, as far to the red end as possible, to minimize scattering and fluorescence background. (2) To be able to distinguish between the dyes effectively, their emission maxima had to be well resolved from one another. (3) The dyes had to be highly fluorescent to provide sufficient detection sensitivity. (4) The dyes should not significantly impair the hybridization of the oligonucleotide primer, as this would also decrease the efficiency of synthesis in the sequencing reactions. Finally, the electrophoretic mobility of the DNA fragments should not be distorted unacceptably by the presence of the dyes. The chemical structures and absorption and emission spectra of the four dyes we have chosen are shown in Fig. 2. Their absorption and emission maxima range from 486 nm (4-chloro-7-nitrobenzo-2-oxa-1-diazole (NBD) absorption maximum) to 604 nm (Texas Red emission maximum), well within the visible region of the spectrum. The emission maxima are evenly spaced at 30-nm

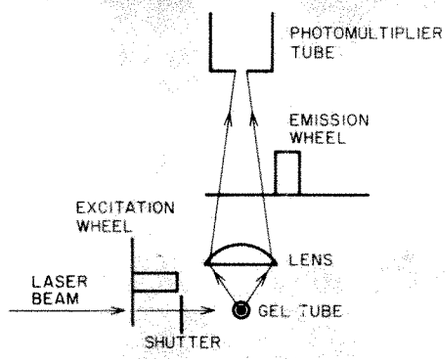


Fig. 3 Diagram of the optical configuration used for within-gel detection of fluorescence at four different wavelengths.

intervals, allowing reasonably good spectral discrimination. All the dyes have good fluorescence sensitivity, and are widely used and readily available. Conjugates of these dyes and an oligonucleotide primer (with the sequence 5′ CCCAGTCACGACGTT 3′, used in the single-stranded M13 phage vectors) were prepared and tested in conventional sequencing reactions using radioisotope detection (see ref. 4 for details). All the dye–primer conjugates were effective in the DNA sequencing reactions. The dyes do, however, affect the electrophoretic mobility of the DNA fragments to which they are bound; this necessitates a mobility correction to the sequence data which is discussed in the section on data analysis. The suitability of these primers in fluorescence-based detection was tested in instrumentation constructed for that purpose, as described below.

Instrumentation

The primary consideration in the design of the fluorescence detection apparatus was sensitivity. We performed preliminary experiments using radiolabelled nucleoside triphosphates of known specific activity to measure the amount of DNA present in a single band of a conventional sequencing gel, and obtained values of the order of 10^{-15}–10^{-16} mol DNA per band. If the DNA is assumed to occupy a volume of 1 mm^3, the DNA concentration is 10^{-9}–10^{-10} M. Therefore, the instrument had to be capable of detecting dye concentrations of that order. This level of detection is readily achieved in commercial spectrofluorimeter systems. However, detection directly within the gel leads to much higher background scatter from the gel and from the circular glass tubing than is normally encountered, leading to decreased sensitivity. We therefore chose to use a laser excitation source in order to obtain maximum sensitivity, and have continued to use the laser source in subsequent work.

Figure 3 shows a schematic diagram of the optics used for detection of the fluorescent bands of DNA in the tube gel. The beam from an argon-ion laser (Lexel 65-0.1) operated in 'multiline' mode is passed through a 1-nm-bandpass interference filter (to select out either the 488-nm or 514-nm laser line for excitation) mounted on a circular 'excitation' wheel and directed into a gel tube (glass or quartz tubing of 1–2 mm internal diameter; typically a 50-cm-long 8% polyacrylamide/6 M urea gel with the laser beam at 40 cm from the top of the gel) suspended between two tanks containing electrophoresis buffer. A single, fast-collection lens (Melles Griot 01 LAG 013, F/0.7) is used to collect the emitted light and focus it through a 10-nm-bandpass filter (Corion S10-*x*-R series, where *x* denotes the bandpass wavelength in nanometres, chosen to match the emission maximum of the dye being used) mounted on a second circular emission wheel, and onto the aperture of a photomultiplier tube (Hamamatsu R928). The optics are mounted on an optical table (MST46 with NN4-28 legs; Newport Research Corporation) enclosed in a dark room which has been painted black, and appropriate baffling is used to prevent stray light from reaching the photomultiplier tube. Four interference filters are mounted at equally spaced intervals on each filter wheel, and a given excitation filter is always used in conjunction with a given emission filter. The filter pairs used are (in the order excitation filter, emission filter) 488, 520; 488, 550; 514, 580; 514, 610. The use of two different excitation wavelengths gives more efficient excitation of the different dyes (tetramethylrhodamine and Texas Red are excited more efficiently at 514 nm, whereas fluorescein and NBD are excited more efficiently at 488 nm) and thereby provides greater detection sensitivity. Neutral-density filters (Melles Griot BK-7 series) are also used in conjunction with the bandpass excitation filters to balance the baseline gel scatter levels obtained in each filter position. Light-emitting diodes and phototransistors are used to sense the position of the wheels. The excitation and emission wheels are accelerated and decelerated between the different filter positions using time intervals between pulses to the stepper motor that have been chosen to yield a constant acceleration. The movement of the wheel from one position to the next took 0.7 s, and the wheel was held stationary at each position for 0.8 s, giving a total time of 1.5 s between data points. A Uniblitz shutter (Vincent Associates) to protect the photomultiplier tube from excess scattered laser light was inserted into the laser beam and appropriate electronics were constructed to close the shutter if the photomultiplier tube (PMT) current exceeded a pre-set limit. Software was written to close the shutter, align both of the wheels into their starting positions, and then to re-open the shutter and commence data acquisition.

Typically, 8,000 points were taken for each of the four filter positions (total of 32,000 points) in a 13-h run; this rate of data acquisition gives 40 or more data points per DNA peak, under the electrophoretic conditions used. Filtering of the data to eliminate high-frequency noise was performed at three levels. First, an analog filter with a 100-ms time constant was used on the phototube output. Second, at each filter position, 200 data points were taken in succession and averaged, to yield a single point which was stored. At the 40-kHz rate of the Tecmar analog-to-digital converter, this required ~5 ms. Finally, the data were smoothed further with a low-pass Fourier filter included in the analysis (see below). Figure 4 shows a set of four-dye data obtained with this system. The raw data are shown in Fig. 4*a*; *b* and *c* show the same data after analysis. The procedures used in data analysis are described briefly below. These data demonstrate the practicality of this four-dye fluorescence approach for automated DNA sequence analysis.

Data analysis

If the raw data obtained with this instrument were as readily interpretable as the idealized data presented in Fig. 1*b*, very little data analysis would be required to determine the DNA sequence. In reality, however, several factors render the analysis of the data more complex. First, the emission spectra of the different dyes overlap substantially (see Fig. 2*b*); because of this, peaks corresponding to the presence of a single dye are seen in more than one channel. To discern the DNA sequence, one must therefore perform a multicomponent analysis to determine the different amounts of the four dyes present in the gel at any given time. The second major factor complicating the analysis is that the different dye molecules impart non-identical electrophoretic mobilities to the DNA fragments (see ref. 4). The fluorescein- and rhodamine-labelled DNA fragments move as if they were approximately one base longer than the NBD-labelled fragments, and the fragments labelled with Texas Red move as if they were approximately $1\frac{1}{4}$ bases longer. These mobility shifts must be compensated for. The third complicating factor in the analysis of the data comes from the imperfections of the enzymatic method of DNA sequence analysis itself. It is well known that the enzymatic method suffers from several anomalous traits, such as substantial variations in the intensity of bands in a given reaction, and occasional areas that prove difficult to sequence (thought to be associated with regions of

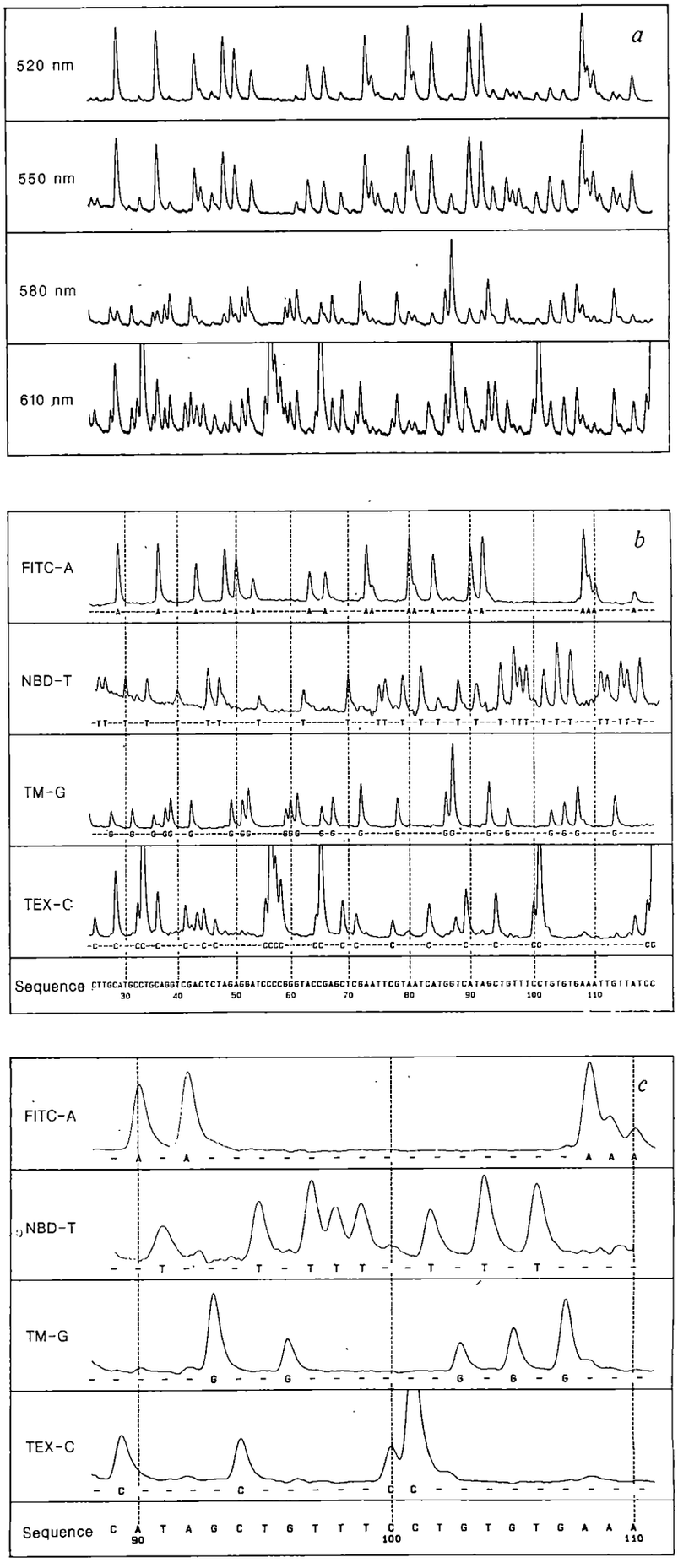


Fig. 4 Fluorescence data (*a*, raw; *b*, analysed) obtained from a mixture of four sequencing reactions. *c*, Expanded plot of 1,000 points of the analysed data. The mixture was applied to a single gel tube (quartz tubing with i.d. 1.3 mm; Heraeus Amersil, Sayreville, New Jersey) and detected using the optical configuration shown in Fig. 3 and described in the text. The relative amounts of each reaction used were chosen to give comparable signal intensities for each dye. This mixture contained 0.025 units of an FITC-A reaction, 0.1 units of Texas Red-C (Tex-C), 0.15 units of tetramethylrhodamine-G (TM-G), and 0.4 units of NBD-T, mixed with one volume of formamide, in a total volume of 14 μl. A unit amount of sequencing reaction contains 0.4 pmol of template DNA and 0.8 pmol of primer DNA. The protocols used in the preparation and loading of the sequencing reactions are given in detail in ref. 6. See text for details of the data analysis.

secondary structure in the DNA itself). These complications must be handled in the analysis.

The procedures we have used in data analysis are described in detail in ref. 5. Briefly, the analysis consists of five steps: (1) High-frequency noise is removed by using a low-pass Fourier filter. (2) The time delay (1.5–4.5 s) between measurements at different wavelengths is partially corrected for by linear interpolation between successive measurements. (3) A multicomponent analysis is performed on each set of four data points; this computation yields the amount of each of the four dyes present in the detector as a function of time. (4) The peaks present in the data are located. (5) The mobility shift introduced by the dyes is corrected for using empirically determined correction factors. Figure 4*b* shows the processed data obtained when these five steps were applied to the raw data of Fig. 4*a*, and Fig. 4*c* shows an expanded plot of a region of 1,000 data points taken from Fig. 4*b*; the DNA sequence is aligned with the data. The correspondence between the sequence and the order of peaks obtained in the different channels is evident.

To date we have successfully executed hundreds of single-dye runs, 20–30 two-dye runs, and about 10 four-dye runs. In single-dye runs we often obtain well resolved and clearly discernible sequence beyond base 400 in ~16 h (data not shown). In four-dye runs we generally have obtained ~200 bases of clear sequence information. Present efforts are directed towards further defining and optimizing the parameters important in obtaining good resolution.

Sensitivity

The question is often raised of how the sensitivity of the fluorescence method compares with the sensitivity of conventional radioactive methods. The comparison is complicated by the fact that in the radioactive detection methods, the signal is integrated (by exposure on film) over long time periods ranging from hours to days. In contrast, the fluorescence approach uses real-time acquisition with integration times of a fraction of a second per data point; sensitivity is naturally much lower when the signal is integrated over such relatively short times. If one ignores this aspect, and simply considers sensitivity to be a measure of the amount of material one can detect over background in either method, the radioactive method clearly has higher sensitivity. The most sensitive of the four dyes we are using is fluorescein, and when small amounts of fluorescein-labelled primers are detected during electrophoresis on short tube gels, we obtain a minimum detectable level (defined here as a signal-to-noise ratio of 1) of ~10 amol (1 amol is 10^{-18} mol). Approximate minimum detectable levels obtained for the other dyes are NBD, 40 amol; tetramethylrhodamine, 20 amol; and Texas Red, 50 amol. These levels are about one order of magnitude less sensitive than those typically obtained with autoradiography[7]. The sensitivity of this method could be increased in several ways (see discussion below), which would be of value for extending the amount of sequence information obtained in a run and increasing the accuracy of the analysis.

Future directions

Here we have demonstrated the practicality of a novel method for the automated non-isotopic sequence analysis of DNA. This work opens up several avenues for further investigation. First, the fluorescence sequencing method that we have described will benefit from optimization of several interacting factors, including (1) the gel itself, including its length, diameter and composition (for example, different acrylamide percentages, gradients), (2) the procedures and reagents used in the sequencing reactions, (3) the electrophoresis conditions (for example, voltage, current and temperature), (4) the optics and electronics used in data acquisition, (5) the chemistry used in fluorescent primer synthesis (for example, attaching multiple dye molecules per primer to increase sensitivity, adding linker arms to the dyes to compensate for their non-identical electrophoretic mobilities, finding new dyes with improved fluorescence characteristics), and (6) the software used in data reduction. We have obtained resolved peaks with good signal-to-noise 400 bases into the sequence in some instances, even with the present relatively unoptimized configuration. It is therefore reasonable to expect that an optimized system would yield sequence information beyond position 500 on a routine basis.

The data analysis methods we have developed to date reduce the raw data into a form which is interpretable by the user. We are presently developing the software to perform the final step of data analysis, the interpretative step of assigning the DNA sequence to the data. This interpretation must take into account the high degree of variability in peak intensity obtained in the enzymatic sequencing reactions (see Fig. 4*b*, particularly the Texas Red–C (Tex–C) reaction), and the possibility of 'false' peaks (see, for example, the false C peaks at base numbers 43, 87 and 116 in Fig. 4*b*). The software will be able to minimize, but not to eliminate, these problems. It is therefore important that bases which cannot be assigned unambiguously are left unidentified, and that the sequence of unknown DNAs is determined on both strands. A reasonable goal for the system accuracy is a 1% error rate for a single strand, which would give a 0.01% error rate or 1 base in 10,000 for the sequence determined from both strands. This level of accuracy is satisfactory for most applications, and is comparable to or better than the accuracies generally obtained in DNA sequence analysis by conventional methods.

It will also be of great value to apply this fluorescence technology to the chemical method of DNA sequence analysis. This is important for several reasons. First, as mentioned previously, there are occasionally regions of DNA that are difficult to sequence by the enzymatic method but which are usually amenable to analysis by the chemical method. Second, whereas the enzymatic method is characterized by significant peak-to-peak variations in intensity, visible in both autoradiograms and in the fluorescence data presented here, the chemical method generates a much more uniform distribution of fragments of different lengths, which would facilitate data analysis. Third, the simple and inexpensive reagents used in the chemical method can be stored easily, and are easier to handle in a machine for automating the sequencing reactions than the delicate reagents (for example, the Klenow fragment of DNA polymerase) used in the enzymatic reactions. Recent advances in solid-phase methods of sequence analysis by the chemical method[8,9] will also be of great value in automating those reactions.

Thus, the practicality of a novel non-isotopic method for automated DNA sequence analysis has been demonstrated. It is our hope that this work will help to eliminate much of the labour associated with the structural analysis of DNA, and thereby allow investigators to focus on the more interesting and important questions of modern biology.

We thank Dr Walter Craig for invaluable advice on the mathematics used in data analysis as well as for critical reading of the manuscript; Dr Steven Fung for helpful advice and discussion; Mr Mike Walsh and Mr Tim Heitzman for technical support in the design and construction of the filter wheel assemblies, as well as much invaluable assistance with hardware; and Mr Frank Ostrander for help in the construction of the instrumentation. The concept of using four different dyes was conceived in conjunction with Mr Tim Hunkapiller of Caltech and Dr Michael Hunkapiller of Applied Biosystems. This research was supported by NSF grant DMB-8500298, the Baxter Foundation, Monsanto Chemical Co. and Upjohn, Inc. L.M.S. was a NIH postdoctoral trainee (HD07257) during part of the work described here.

Received 30 December 1985; accepted 11 April 1986.

1. Sanger, F., Nicklen, S. & Coulson, A. R. *Proc. natn. Acad. Sci. U.S.A.* **74**, 5463–5467 (1977).
2. Smith, A. J. H. *Meth. Enzym.* **65**, 560–580 (1980).
3. Maxam, A. M. & Gilbert, W. *Meth. Enzym.* **65**, 499–559 (1980).

4. Smith, L. M., Fung, S., Hunkapiller, M. W., Hunkapiller, T. J. & Hood, L. E. *Nucleic Acids Res.* **13**, 2399–2412 (1985).
5. Smith, L. M., Kaiser, R. J., Sanders, J. Z. & Hood, L. E. *Meth. Enzym.* (in the press).
6. Atkinson, T. & Smith, M. *Oligonucleotide Synthesis: A Practical Approach* (ed. Gait, M. J.) 35–81 (IRL, Oxford, 1984).
7. Forster, A. C., McInnes, J. L., Skingle, D. C. & Symons, R. H. *Nucleic Acids Res.* **13**, 745–761 (1985).
8. Chuvpilo, S. A. & Kravchenko, V. V. *Sov. J. bioorg. Chem.* **9**, 1694–1697 (1983).
9. Rosenthal, A., Schwertner, S., Hahn, V. & Hunger, H. *Nucleic Acids Res.* **13**, 1173–1184 (1985).

Coordinated Exosat and spectroscopic observations of flare stars and coronal heating

C. J. Butler*, M. Rodono†, B. H. Foing‡ & B. M. Haisch§

* Armagh Observatory, College Hill, Armagh BT61 9DG, UK
† Institute of Astronomy, University of Catania, Italy
‡ European Southern Observatory, Santiago, Chile
§ Lockheed Palo Alto Research Laboratory, Palo Alto, California 94304, USA

The X-ray flux of dMe stars is thought to arise from two distinct mechanisms, one involving a continuous 'quiescent' emission from a high-temperature plasma and the other involving the dramatic flare events which have long been known to occur on these stars. We present here some results of simultaneous monitoring of the two flare stars, UV Ceti and EQ Peg, with Exosat and ground-based optical spectroscopy. We observe short-timescale variability in the 0.1–2-keV emission from both these objects and, in the case of UV Ceti, find a strong correlation between the soft X-ray and Hγ fluctuations. The implication is that much of the low-level X-ray flux previously considered 'quiescent' probably originates from small flare events.

Our understanding of coronal structure and of mechanisms for coronal heating in the Sun and stars has evolved considerably as a result of the solar observations of Skylab and the Solar Maximum Mission (SMM) and the stellar observations of the Einstein Observatory and now Exosat. The Skylab photographs of the Sun showed that the soft X-ray emission originated almost exclusively in active-region loops, in larger loops connecting active regions and in X-ray bright points, which are thought to be unresolved, small-scale loops of newly emerging magnetic flux. In place of the diffuse Parker-type hot corona/wind, the closed magnetic loop is now widely thought of as the basic unit of coronal structure[1–3]. By contrast, regions of open magnetic field, called coronal holes, are dark in X rays and appear to be the primary source of the solar wind. Because many of the Skylab and other images emphasize the higher-temperature and more dense structures (the emission for a collisionally excited line is $\sim n(e)^2$), it may well be that there is a significant diffused coronal component, in addition to coronal loops and coronal holes. Whether or not this is the case, the concept of a 'quiet corona' (be it diffuse or the average state of the quasi-steady loop ensemble) has persisted since the discovery of the solar corona. This concept has recently been extended to 'quiet stellar coronae'[4], the dichotomy being one between the quasi-steady evolution of high-temperature, X-ray-emitting structures, on timescales of hours to days to weeks, and the more obvious variability associated with flares. The heating of the 'quiet corona' and the nature and energetics of solar flares have thus historically been viewed as different and distinct problems.

However, recently, using balloon-borne instrumentation, a significant number of solar hard X-ray microflares have been observed[5], presumably produced by bremsstrahlung of non-thermal electron beams in the solar chromosphere and transition region. It was found that the average rate of energy deposition above 20 keV and above the detection threshold amounted to $\sim 10^{24}$ erg s^{-1}. In addition, the integral number of events appeared to vary as the inverse of the peak flux down to their detection threshold, in which case the total rate of energy release, allowing for low-level events, could begin to approach the total quiescent solar coronal X-ray luminosity[6], $L_x \simeq 5 \times 10^{27}$ erg s^{-1}. The timescales for these microflares ranged from seconds to tens of seconds in duration. Elsewhere in the spectrum, short-lived extreme-ultraviolet bursts of subflare magnitude have been observed on the Sun in several transition-region lines; these bursts probably result from the same electron beaming event that creates the hard X-rays[7]. From a re-analysis of Skylab data[8], frequent subflare-like extreme-ultraviolet brightenings have been found near the foot-points of loops, and using the SMM

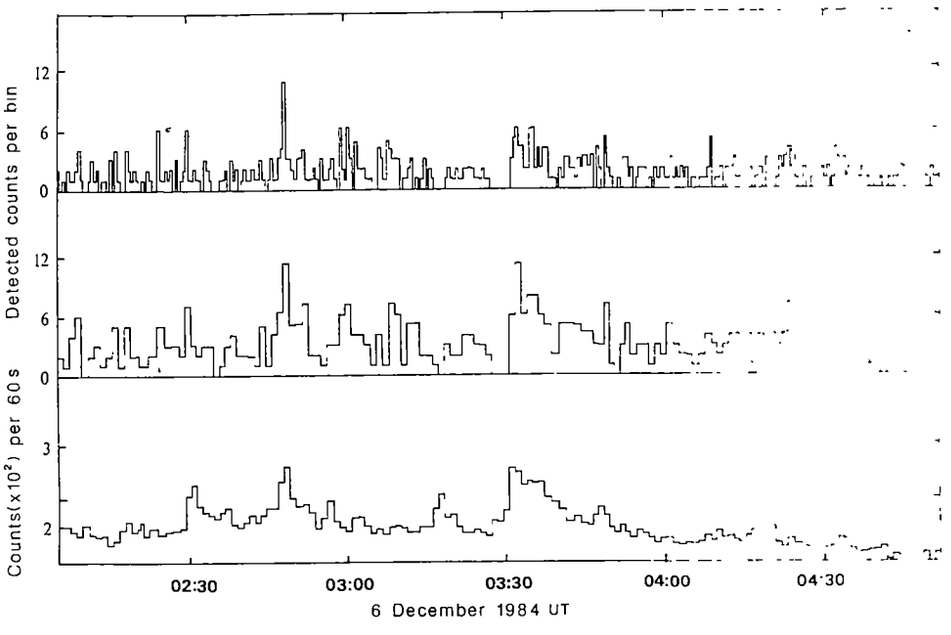


Fig. 1 Soft X-ray flux detected by the CMA on Exosat from UV Ceti, compared with the Hγ peak intensity from the ESO 3.6-m telescope. *a*, X-rays (LE), bin size 30 s; *b*, X-rays (LE), bin size 60 s; *c*, Hγ peak, exposure 60 s.

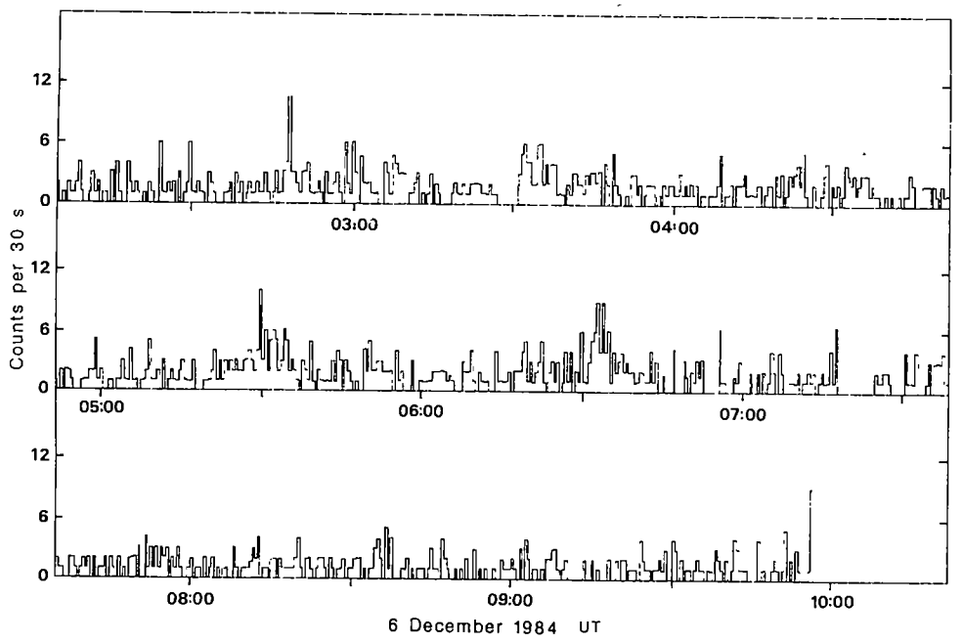


Fig. 2 Soft X-ray flux from UV Ceti for the entire Exosat exposure. The background level is 0.21 counts per 30 s over the source area.

ultraviolet spectrometer polarimeter, almost continual fluctuation has been seen in the Si IV 1,402.8 Å ($T \simeq 60{,}000$ K) and O IV 1401.2 Å ($T \simeq 160{,}000$ K) lines in a solar active region[9,10]. The timescales for these changes are 10–60 s and the brightenings are sometimes more than a factor of two. The timing of these events is such that there must be an almost instantaneous local heating event followed by radiative cooling. In some cases, a secondary brightening is observed after an impulsive burst, which may be the small-scale analogue of the thermal phase of a flare. More importantly, it has been shown[11] that the incidence of extreme-ultraviolet bursts exceeds that of flares by more than two orders of magnitude, which suggests that, in total, they may be as important energetically as flares. These results, together with our own, suggest that heating due to magnetic field reconnection within an active region is proceeding almost stochastically.

The recent studies of correlations between 'quiescent' X-ray fluxes and stellar U-band flare energy rates for dMe stars are of particular interest as they point to a possible equality between total energy released in flaring and the energy requirements of the quiet stellar corona. The relationships between the time-averaged U-band flare luminosity, $\langle L_{\text{flare; U-band}} \rangle$, and coronal X-ray luminosity, L_x (refs 12, 13), are linear over several orders of magnitude, and imply that $L_x/\langle L_{\text{flare; U-band}} \rangle \simeq 10$–$25$. This result appears to hold not only for the dMe stars, from which it was established, but also for non-emission M dwarfs, and possibly even for the Sun[14]. Because the U-band flare (which is the band most easily measured by optical observers) encompasses only a fraction of the flare energy, it is possible that there is an approximate equality between total flare emission and quiescent coronal emission. However, the mean U-band flare energy is dominated by the relatively large and infrequent flares (>1 per 10 h), and if they are to be the source of coronal heating, it is difficult to see how their energy, once it has been released in a flare, could be stored for times of this order. The present new data demonstrate the importance of continual microflaring on the dMe flare stars.

As part of a coordinated campaign of multi-band observations of stellar flares[15], we observed UV Ceti and EQ Peg on 6 and 7 December 1984, respectively, with ground-based optical telescopes and with the two satellites IUE (International Ultraviolet Explorer) and Exosat. Included among several optical telescopes was the 3.6-m of the European Southern Observatory (ESO), with which intermediate dispersion spectroscopy of the region 3,600–4,400 Å was obtained using the image dissector scanner on the Boller and Chivens spectrograph. Exposures were of 60 s duration with a short delay of ~10 s between spectra. Although these data have not yet been fully reduced, it was possible to determine, in real time, an uncalibrated peak flux value at the wavelength of Hγ. The variation of this peak value will be predominantly due to the Hγ emission line itself; however, some continuum variations will also be included.

Because of Exosat pointing restrictions, it is difficult to obtain, from one site, more than ~5–6 h of simultaneous ground-based coverage. In the case of UV Ceti, Exosat observations were made from 02:00 to 10:45 UT on 6 December 1984, but only the first 3 h could be covered from ESO.

The X-ray (0.1–2 keV) photon counts detected by the channel multiplier array (CMA) of the Exosat low-energy imaging telescope (LE) (using the 4,000-Å-thickness Lexan filter) have been analysed using the reduction package at Mullard Space Science Laboratory, University College London. Some gaps are present in the data where data transmission, or small solar flares, have caused the exposure time to fall below 80% of the nominal value. Although small solar flares do not noticeably increase the flux over the area of the CMA detector containing the stellar image, the increase over the entire image area can be sufficient to overload the detector system and cause a reduction in the effective exposure time.

In Fig. 1*a*, *b* the X-ray data have been grouped into 30-s and 60-s bins, respectively, and Fig. 1*c* shows the time variation of the peak Hγ flux. The data in Fig. 1*a* are binned in successive 30-s intervals; however, to allow a better comparison with the Hγ peak flux, the 60-s X-ray data (Fig. 1*b*) have been grouped into 60-s bins that do not follow on from each other immediately, but rather are as nearly as possible coincident with the windows of the Hγ observations. Therefore, the total counts in the two X-ray plots will not be exactly the same.

Figure 1 shows two important features. First, the X-ray emission appears to be quite non-uniform, with frequent rises of a factor of two or three in flux, lasting for periods of a few tens of seconds to several minutes. Second, five or six of the X-ray events correspond to similar rises in Hγ peak flux. We have investigated this correlation statistically and find that the correlation coefficient between the 60-s data points used to construct Fig. 1*b* and *c* is 0.51, or a Student's *t* value of 7.0. For 143 data points this implies a highly significant correlation between the Exosat and Hγ data, with a probability of

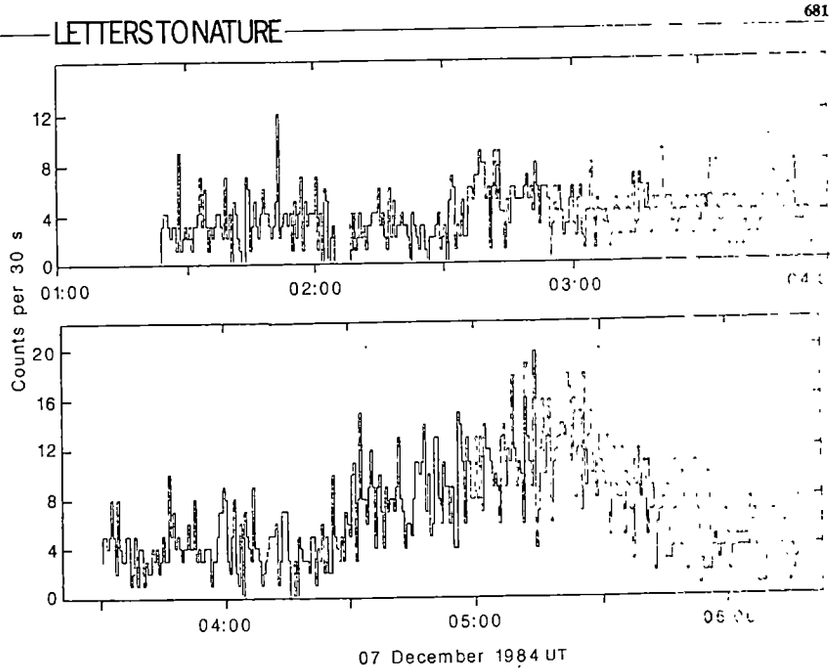


Fig. 3 Soft X-ray flux from EQ Peg. Note the large flare beginning at 04:30 UT. The background level is 0.23 counts per 30 s over the source area.

occurrence by chance of less than 1 in 10^5.

We conclude that the events seen in the X-ray and Hγ fluxes are in fact small flares, which, like flares on the Sun, show increased X-ray emission accompanied by Balmer-line enhancements; the X-rays are presumably due to thermal emission of the flare-heated plasma in one or more loops and the Balmer-line enhancements to chromospheric ablation[16]. While both the soft X-ray events and the Balmer-line enhancements on the Sun last rather longer than these events on UV Ceti, the energies are similar: at a distance of 2.62 pc (ref. 17), the energies in the UV Ceti low-energy X-ray events vary from $\sim$0.5 to 5×10^{30} erg, similar to the energies of compact solar flares.

Figure 2 shows all of the Exosat data for UV Ceti in 30-s bins. Here again we see evidence for an almost continuously variable soft X-ray flux, and to determine whether this variability is statistically significant, we have binned the data with a bin size varying from 10 to 160 s, and compared the observed number of bins with a given population to a Poisson distribution using a χ^2 test. In all cases, the probability of the observed distribution arising from a random arrival of photons from a constant source is $\leq$0.5%. The departure from a poissonian distribution is in the same sense for each trial bin-size, with both more bins with zero or a low number of photons than expected, and more bins with high numbers of photons than expected. The number of bins found with intermediate numbers of photons is correspondingly decreased. This type of distribution could arise from the clumping together of photons from a source which is variable on timescales of 10–160 s.

In Fig. 3, which shows the soft X-ray flux from EQ Peg on 7 December 1984, we again see evidence of continuously variable emission, followed by a substantial LE (soft X-ray) flare, which was also detected by the ME (medium energy) experiment. The flare lasted for $\sim$90 min, with a gradual rise and fall in LE and a more sudden rise in ME. A preliminary analysis of the integrated ME spectral data for the event gave, for effectively zero column density of hydrogen, a best-fit temperature of $\sim2.2\times10^7$ K: this is a typical temperature for the non-impulsive, thermal phase of solar and stellar flares[18,19]. If we adopt the standard calibration of the Exosat detectors[20], and a distance for EQ Peg of 6.41 pc (ref. 17), the total integrated X-ray energy of the flare on EQ Peg is 6×10^{32} erg in LE (0.1–2 keV). This corresponds to the energy of a very large two-ribbon solar flare[21].

Our data for UV Ceti and EQ Peg suggest that the soft X-ray emission of these stars is almost continuously variable, with many surges or microflares lasting from tens of seconds to several minutes. These microflares, which have energies of $\sim2\times10^{30}$ erg in the 0.1–2 keV range, are similar to compact solar flares, but possibly more short-lived. The fact that these microflares occur so frequently in the two dMe stars studied indicates that the concept of a 'quiescent' corona for these stars may be erroneous and that we are seeing, not a quiet, uneventful, low-level emission, but a continuum of flares with energies similar to those of compact solar flares. Most probably, if our detection threshold could be significantly reduced, we could see many even smaller X-ray events. The logical consequence of these results is that what we call stellar coronal emission (the X-ray flux) may be just a succession of microflares.

There are now three other lines of evidence pointing to the possibility that coronal heating in dwarf M flare stars is a direct result of energy input through widespread, low-level microflaring[22,23]: (1) the recently found correlation between time-averaged flare energy release and coronal X-ray luminosity[12,13]; (2) the high-temperature component identified in the two Einstein Observatory solid state spectrometer observations of 'quiescent' coronal emission from the dMe stars[24,25] and in many of the Einstein imaging proportional counter pulse-height spectra of dMe stars which have now been reprocessed (J. Bookbinder, L. Golub, R. Rosner and J. H. M. M. Schmitt, in preparation); and (3) the observed variability on timescales of hundreds to thousands of seconds of practically all reprocessed Einstein coronal X-ray fluxes for dKe and dMe stars (C. Ambruster, S. Sciortino and L. Golub, in preparation).

We thank Drs C. Jordan, C. Ambruster, J. Bookbinder, G. Branduardi Raymont and T. Kiang for useful discussion and the staffs of the ESO and Exosat observatories for their assistance. This work was supported in part by NASA contract NAS5-28409 to the Lockheed Palo Alto Research Laboratory, by a grant from the Piano Spaziale Nazionale of the Italian CNR to the Astronomy Institute of Catania University, and by a grant for International Collaboration in Research from the NATO Scientific Affairs Division.

Received 20 November 1985; accepted 24 March 1986.

1. Jordan, C. *Proc. IAU Symp.* No. 68, 109–131 (1975).
2. Landini, M. & Monsignori Fossi, B. C. *Astr. Astrophys.* **42**, 213–220 (1975).
3. Rosner, R., Tucker, W. H. & Vaiana, G. S. *Astrophys. J* **220**, 643–665 (1978).
4. Rosner, R., Golub, L. & Vaiana, G. S. *A. Rev. Astr. Astrophys.* **23**, 413–452 (1985).
5. Lin, R. P., Schwartz, R. A., Kane, S. R., Pelling, R. M. & Hurley, K. C. *Astrophys. J* **283**, 421–425 (1984).

6. Vaiana, G. S. & Rosner, R. *A. Rev. Astr. Astrophys.* **16**, 393–428 (1978).
7. Mariska, J. T. & Poland, A. I. *Sol. Phys.* **96**, 317–330 (1985).
8. Habbal, S. R., Ronan, R. & Withbroe, G. L. *Sol. Phys.* **98**, 323–340 (1985).
9. Porter, J. G., Toomre, J. & Gebbie, K. B. *Astrophys. J.* **283**, 879–886 (1984).
10. Hayes, M. & Shine, R. A. Preprint, Lockheed Palo Alto Res. Lab. (1986).
11. Athay, R. G. *Sol. Phys.* **93**, 123–131 (1984).
12. Doyle, J. G. & Butler, C. J. *Nature* **313**, 378–380 (1985).
13. Skumanich, A. *Aust. J. Phys.* **38** (1985).
14. Skumanich, A. Preprint, High Altitude Obs., NCAR, Boulder (1985).
15. Rodono, M. *et al. Bull. Eur. s. Obs.* **39**, 9–10 (1985).
16. Gunkler, T. A., Cranfield, R. C., Acton, L. W. & Kiplinger, A. L. *Astrophys. J.* **285**, 835–842 (1984).
17. Pettersen, B. R. *Inst. theor. Astrophys. Blindern* No. 46 (1976).
18. Haisch, B. M. in *Activity in Red Dwarf Stars*, (eds Byrne, P. B. & Rodono, M. 255 (Reidel Dordrecht, 1983).
19. Haisch, B. M. *et al. Astrophys. J.* **267**, 280–290 (1983).
20. *The European X-Ray Astronomy Satellite, EXOSAT Observers Guide* Pt III (Final Observation Tape Handbook ESA) (1984).
21. Svestka, Z. *Solar Flares*, 306 (Reidel Dordrecht, 1976).
22. Haisch, B. M. *Ir. astr. J.* (in the press).
23. Mullan, D. J. *Ir. astr. J.* (in the press).
24. Swank, J. H. in *The Origin of Nonradiative Heating/Momentum in Hot Stars* (NASA Conf. Publ. 2358, 1985).
25. Swank, J. H. & Johnson, H. M. *Astrophys. J.* **259**, L67–L70 (1982).

Metallic ions in cometary comae and plasma tails

W.-H. Ip & W. I. Axford

Max-Planck-Institut für Aeronomie, D-3411 Katlenburg-Lindau, FRG

Ion composition measurements made in the environment of the comet Giacobini-Zinner by the International Cometary Explorer (ICE) spacecraft have shown that H_2O^+ is a major ion species, together with CO^+ ions[1]. The presence of these two cometary ions has long been evident in optical spectra of cometary ion tails[2]. However, the ICE observations were surprising in that they detected ions of mass 23–24 AMU with a relatively high abundance[1]. According to the experimenters, these ions may be either Na^+ or C_2^+, if not both. We suggest here that the ions detected may indeed be in part Na^+ and/or Mg^+ and that these and other metallic ions (especially Si^+ and Fe^+) may be an important component of the cometary ionosphere and central plasma tail. Our reasons are similar, in principle, to those which account for the prevalence of such ions in sporadic E layers in the terrestrial ionosphere, notably the comparatively short timescales for ionization of their neutral parent atoms and the large difference between the rates of dissociative and radiative recombination[3,4].

Because of its strong optical emission, the source strength of C_2 relative to that of H_2O and the scale length for photodissociation and/or photoionization have been well determined. The average values are: $Q(C_2) \sim 4 \times 10^{-3}\, Q(H_2O)$ and $R(C_2) \sim 1.2 \times 10^5$ km, respectively[5]. In comparison, the corresponding scale length for the ionization of the water-group neutrals (that is, H_2O, OH and O) is a factor of 10 larger. It is possible, therefore, that the faster ionization of C_2 radicals in a more limited region could lead to some enhancement of the relative abundance of C_2^+ ions with respect to H_2O^+ ions in a region $<10^5$ km from the tail axis.

Sodium D-line emissions and emissions from other metallic species (Ca, Cr, Co, Mn, Fe, Ni, Cu, V, Si and K) are usually seen most prominently in Sun-grazing comets or bright comets at solar distances <0.5 AU (refs 6, 7). It is often argued that these emissions originate from atoms released by the sublimation of refractory dust grains[8]. At a solar distance of 1 AU, however, the sublimation rate of such dust grains is negligible and essentially no metal atoms should be released. Sodum D-line emissions were detected in comet West (1975n) when it was at a solar distance of 1.4 AU, which gave rise to the suggestion that a component of Na atoms could be embedded in volatile icy grains or matrix in atomic or molecular forms such as NaOH (ref. 9). Although estimates for the production rate of these Na atoms (or their parent molecules) are very uncertain (an upper limit of $Q(\mathrm{Na})/Q(H_2O) \leqslant 10^{-3}$ may be set), such observations, together with the ICE ion composition measurement, call attention to the potential importance of Na^+ ions and metallic ions, in general, in cometary comae and ionospheres. Below, we discuss several implications of metallic ion production in the coma environment and, in particular, emphasize that metallic ions could be a significant component of the central ionosphere and ion tail if their production rates are sufficiently large. The relative (solar) abundances of the most important species concerned are Na (0.06), Mg (1.00), Al (0.08), Si (0.95), Ca (0.07) and Fe (0.85)[10].

Note that, in addition to sublimation from non-volatile dust grains and possibly from volatile material containing their parent molecules, sputtering of dust grains and the nucleus itself by solar-wind protons and the energetic 'pick-up' ion created in the coma should provide a source of secondary neutral atoms (~90%) and ions (~10%)[11]. For a comet with a gas production rate up to that of Halley ($Q = 10^{30}$ molecules s^{-1} at 1 AU) and a dust production rate $\dot{m}_d/\dot{m}_g \sim 1$, the effective cross-sectional area of the dust coma is estimated to be 10^{17} cm^2 assuming a cutoff radius of 1 μm (ref. 12). With a solar-wind flux of 3×10^8 cm^{-2} s^{-1} and a sputtering yield of about unity, the effective sputtering rate of neutral atoms and ions from the dust coma is of the order of 5×10^{24} s^{-1}, which is a factor of 2×10^5 less than the volatile gas production rate. This alone might not be sufficient to account for the relatively high fluxes of ions of mass 23–24 detected by the ICE spacecraft at 2×10^4 km from the tail axis. Nevertheless, secondary ions must be produced by sputtering in the coma and their fluxes may be detectable; there are processes which in any case tend to enhance their fluxes relative to those of molecular ions. Furthermore, the local production rates of sputtered atoms and ions may be larger than we have estimated here if $m_d \gg m_g$ locally (as a consequence of differing expansion speeds of the gas and dust components) and if there is a significant component of dust particles with radii <1 μm.

In general, the solar-wind plasma should not be able to reach the surface of the nucleus but the large gyroradii (~ 1–5×10^4 km) of energetic pick-up ions may allow them to do so. Thus the nucleus and inner coma should be continuously subject to sputtering even when the outgassing rate is large. However, because of the small area of the nucleus ($\leqslant 10^{12}$ cm^2), the production rate of neutral atoms and ions arising from direct energetic particle sputtering is many orders of magnitude less than the sublimation rate of H_2O and other gases. Indeed, only when a comet nucleus is inactive at large solar distances would surface sputtering have a major role in releasing surface material into the surrounding coma region[13,14].

Despite the relatively low production rates of sputtered atoms, it is important to recognize that by virtue of their short photoionization timescales ($\sim 3 \times 10^4$ s at 1 AU (ref. 9) compared with 3×10^6 s for H_2O), together with the fact that a substantial fraction of the sputtered gas is already ionized, metallic ions could become relatively enriched. The very fact that such neutral atomic species as Na appear in the spectra of some comets suggests that their photoions should be abundant. The ionization potentials of these atoms are such that they are photoionized by hydrogen Lyman-α radiation, whereas the more abundant molecules require photons of 12 eV or more for photoionization. In addition to photoionization, metallic ions can be produced by charge transfer reactions such as

$$H_3O^+ + Na \rightarrow Na^+ + H_3O$$

which has a rate coefficient $\leqslant 10^{-9}$ cm^3 s^{-1} (ref. 15); this process may be important in the denser regions of the cometary ionosphere where the H_3O^+ density is $\sim 10^4$ cm^{-3}.

It is difficult to find reactions which can neutralize metallic ions faster than radiative recombination, which with a typical recombination coefficient of 10^{-12} cm^3 s^{-1} is itself unimportant in the present context. To remove metallic ions quickly they

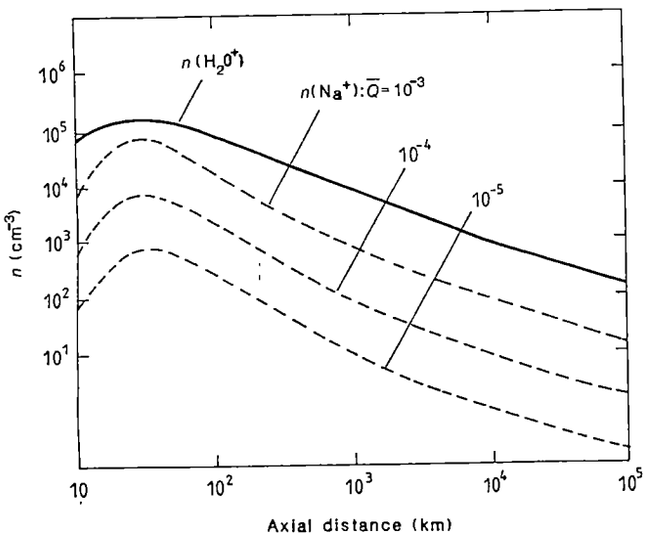


Fig. 1 Comparison of the number density of the H_2O^+/H_3O^+ ions with that of Na^+ (or other metallic ions) for different relative source abundances of the metallic neutrals, $\bar{Q}=Q(Na)/Q(H_2O)$. In the calculation, simulating the free-streaming ionospheric flow along the tail, the flow speed increases linearly from 1 km s^{-1} near the nucleus to 100 km s^{-1} at 3×10^4 km from the nucleus. The metal ion enhancement in this case is entirely the result of the relatively high ionization rate of their atoms in comparison with that of water molecules.

must first be converted to some form of molecular ion so that dissociative recombination is a possibility. However, the rates of formation of such molecular ions are low, except perhaps very close to the nucleus: for example, in the case of Na^+ the process

$$Na^+ + H_2O \rightarrow Na\cdot H_2O^+ + h\nu$$

has a rate coefficient of only $1.6\text{–}6.1\times10^{-16}$ cm^3 s^{-1} at 20 K (ref. 16). This is competitive with radiative recombination in regions where the H_2O density is 10^4 or more (that is, within 3×10^4 km) but provides loss rates for Na^+ ions which are significantly only in regions where the H_2O density exceeds 10^9 cm^{-3} and the electron density is $\geqslant10^2$ cm^{-3}.

In the inner coma, a basic (convective) timescale is determined by the plasma flow characteristics. These are, in turn, controlled by drag which resists motions of plasma relative to the neutrals and by the tension stress created by strongly curved magnetic field lines which pull the plasma inwards towards the nucleus on the upstream side and eventually out along the tail on the downstream side[17]. The flow speeds in the 'ionospheric' region surrounding the nucleus may be quite small, perhaps 10^2–10^3 m s^{-1}, corresponding to convective timescales of 10^4–10^5 s. The tail plasma flow behind the nucleus can be regarded to a first approximation as an expansion of the ionospheric plasma along a quasi one-dimensional tunnel, accelerated by the thermal pressure gradient and magnetic field streams into a region of negligibly small neutral drag. In this manner, flow speeds of 10–30 km s^{-1} may be achieved in $\sim3\times10^4$ km, giving a convective timescale of $\sim10^3$–10^4 s. Detailed calculations are required to analyse these processes fully, involving the ion chemistry as well as the plasma flow dynamics, but the essential features can be demonstrated by a simple approach.

Figure 1 shows results from a model calculation with a range of the relative production rate of the metallic atoms ($Q(Na)/(Q(H_2O)=10^{-5}$, 10^{-4} and 10^{-3}). Ionospheric plasma flow in the tailward direction is simulated here by converting to a one-dimensional geometry with the flow acceleration approximated by assuming $d(\log A)/dx=(2/x)\exp(-x/X_a)$ for the stream-tube area A and an acceleration $dV/dx=(100\text{ km s}^{-1})/X_b$. The scale lengths are taken to be $X_a=3\times10^3$ km and $X_b=3\times10^4$ km. This calculation demonstrates that an enhancement of a factor of ~100 could be introduced into the metal ion abundance simply as a result of more rapid ionization.

There is a second important effect which could enrich the metallic ion component of the cometary plasma: in the sunward region of the ionosphere, which is a region of very low speed flow, metallic ions carried in or produced *in situ* could gradually replace H_2O^+ as the dominant ion as a consequence of their differing rates of recombination (see Fig. 2). The lifetime of ions against recombination is $\tau\sim1/\alpha N_e$, where α is the recombination coefficient and N_e the electron density. For metallic and other atomic ions the (radiative) recombination coefficients are typically of the order of 10^{-12} cm^3 s^{-1}, whereas for molecular ions, which undergo dissociative recombination, $\alpha\sim10^{-6}$ cm^3 s^{-1}. According to magnetohydrodynamic (MHD) simulations (J. A. Fedder, personal communication), ions produced in or brought into the central coma reside for as long as 10^5 s with electron densities of 10^2–10^4 or more; in these circumstances the metallic ions simply accumulate ($\tau\sim10^8$–10^{10} s), whereas molecular ions continually recombine ($\tau\leqslant10^2$–10^4 s). Thus, as plasma is carried through the coma by contraction of the looped magnetic field lines to eventually form the plasma tail of the comet, it should become progressively enriched in atomic, especially metallic, ions to a much greater extent than would be implied by their higher ionization rates alone. The formation of such a metallic ion-rich zone by 'magnetic scavenging' in the neutral atmosphere of a comet is analogous to the occurrence of sporadic E in the Earth's ionosphere, where, following rapid photoionization of metallic atoms, neutral atmospheric wind shears in the presence of the geomagnetic field produce the scavenging effect. This, in turn, leads to the formation of metallic ion-rich layers of high plasma density in which the molecular ions may actually be depleted relative to the surroundings[3,4,18,19].

The ICE spacecraft passed through the tail of comet Giacobini-Zinner along a path very favourable for the detection of metallic ions but unfortunately it was not designed for this purpose and so only a hint of their pesence may have been obtained. However, the Giotto spacecraft has five mass spectrometers of various types which may be able to detect and identify metallic ions. Such ions should be most prevalent in the region immediately surrounding the nucleus ($<10^4$ km) but

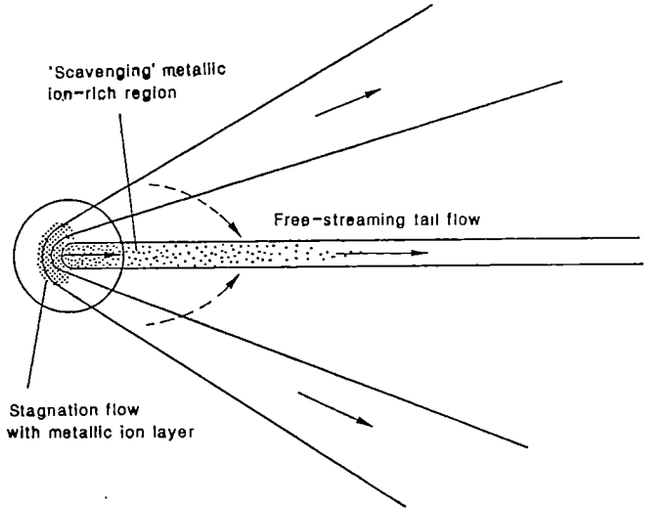


Fig. 2 A schematic view of how the metallic ions might be accumulated in the low-speed flow region of the cometary ionosphere. Metallic ions produced in the coma upstream from the nucleus are carried inwards and concentrated, without suffering recombination losses as do molecular ions, before eventually escaping downstream along the tail.

some should be detectable at larger distances. In some cases, the metallic ions may be submerged beneath large peaks associated with more abundant ions but Fe^+, in particular, may be relatively free of such intereference and hence be more easily identifiable.

Received 9 December 1985; accepted 7 April 1986.

1. Ogilvie, K. W., Coplan, M. A., Bochsler, P. & Geiss, J. *Science* (in the press).
2. Wurm, K. *The Nature of Comets* (Methuen, London, 1963).
3. Whitehead, J. D. *Space Res.* **7**, 90–98 (1967).
4. Axford, W. I. *Space Res.* **7**, 126–134 (1967).
5. A'Hearn, M. F. in *Comets* (ed. Wilkening, L. L.) 433 (University of Arizona Press, 1982).
6. Spinrad, H. & Miner, E. D. *Astrophys. J.* **153**, 355–366 (1968).
7. Lanzerotti, L. J., Robbins, M. F., Tok, N. H. & Neff, S. H. *Icarus* **23**, 618–622 (1974).
8. Huebner, W. F. *Astr. Astrophys.* **5**, 286–297 (1970).
9. Oppenheimer, M. *Astrophys. J.* **240**, 923–928 (1980).
10. Cameron, A. G. W. *Space Sci. Rev.* **15**, 121–146 (1973).
11. Axford, W. I. *Proc. Workshop on Cometary Missions.* Bamberg, *Astr. Inst. Univ. Erlangen-Nürnberg* **12**, 1–12 (1979).
12. Sekanina, Z. & Miller, F. D. *Science* **179**, 565–567 (1973).
13. Lanzerotti, L. J., Brown, W. L., Poate, J. M. & Augustini, W. M. *Nature* **272**, 431–433 (1978).
14. Strazzula, G., Pirronello, V. & Foti, G. *Astrophys. J.* **271**, 255–258 (1983).
15. Aikin, A. C. *Astrophys. J.* **193**, 263–264 (1974).
16. Smith, D., Adams, N. G., Alge, E. & Herbst, E. *Astrophys. J.* **272**, 365–368 (1983).
17. Ip, W.-H. & Axford, W. I. in *Comets* (ed. Wilkening, L. L.) 588 (University of Arizona Press, 1982).
18. Chimonas, W. & Axford, W. I. *J. geophys. Res.* **73**, 111–117 (1968).
19. Zbinden, P. A., Hidalgo, M. A., Eberhardt, P. & Geiss, J. *Planet. Space Sci.* **23**, 1621–1642 (1975).

Gas-like nature of the sodium anion in solution

Ahmed S. Ellaboudy*, Dolores M. Holton*, Nicholas C. Pyper*, Peter P. Edwards*‡, Brian Wood† & William McFarlane†

* University Chemical Laboratory, Lensfield Road, Cambridge CB2 1EW, UK
† Department of Chemistry, City of London Polytechnic, London EC3N 2EY, UK

During the past decade a considerable amount of evidence has accumulated for the existence of an anion of sodium, Na^-, as a stable, long-lived entity in certain non-aqueous solvents[1–7]. The term sodium anion refers to a spherically symmetric diamagnetic species in which, in the orbital model of atomic structure, the two valence electrons are accommodated in the 3*s* orbital of sodium[7]. We report here direct measurements of ^{23}Na nuclear spin–lattice relaxation rates for Na^-, coupled with nuclear magnetic resonance (NMR) chemical shift data, which are used to show that Na^- in solution is almost completely decoupled from its environment, behaving as if it were in the gas phase.

The systems chosen for study were solutions of sodium and mixed sodium/alkali metal samples (Na/M, where M = K, Rb and Cs) in the solvent 1, 4, 7, 10-tetraoxacyclododecane (12-crown-4, 12C4; Fig. 1). This solvent has a powerful and specific ability to complex alkali cations. For example, the dissociation of sodium/potassium alloy proceeds through the disproportionation reaction[8]

$$NaK \rightleftharpoons Na^- + K_s^+$$

where K_s^+ represents a complexed or solvated potassium cation.

Metal solution samples were prepared under stringent high-vacuum conditions[8] and ^{23}Na, ^1H and ^{13}C relaxation rates were measured using established procedures.

The frequency of the $^{23}Na^-$ resonance was found to be unchanged to within 0.5 p.p.m. on examining, over a range of temperatures, about 50 metal/12C4 solutions differing in both concentration and counter cation. All these Na^- resonance frequencies correspond to an increase in the electronic shielding of the ^{23}Na nucleus relative to that in the gaseous sodium atom, Na^0_{gas}, by ~2.5 p.p.m., after allowing for bulk-susceptibility corrections. To within the experimental errors arising from relating the solution measurements to the Na^0_{gas} data, the shift in resonance frequencies is the same as that predicted (2.88 p.p.m.) from an accurate calculation[7] of the shielding of a gaseous sodium anion, Na^-_{gas}, relative to that of Na^0_{gas}. This indicates that both the 2*p* and 3*s* electrons of Na^- in solution interact very weakly, if at all, with their surroundings, the resonance frequency of the Na^- ion being diamagnetically shifted relative to that of Na^0_{gas} by the additional shielding generated by the two, spin-paired 3*s* valence electrons.

The shielding of Na^- relative to Na^0_{gas} should be contrasted with the substantial de-shielding of ~60 p.p.m. of Na^+_s relative to Na^0_{gas}, which is considerably larger than the 5.18 p.p.m. de-shielding[7] of a gaseous sodium cation, Na^+_{gas}, relative to Na^0_{gas}. The additional de-shielding of Na^+ in the solution arises from the Ramsey paramagnetic contribution to the shielding generated by the interaction of Na^+ with the environment. Any such paramagnetic contribution is absent in the gaseous atoms and ions.

A detailed examination[9] of the concentration and temperature dependence of the rates of ^{23}Na nuclear spin–lattice relaxation shows that the dominant, but still extremely inefficient, relaxation arises from the interaction of the nuclear electric quadrupole moment (eQ) of the ^{23}Na nucleus with fluctuating electric field gradients. The relaxation of nuclei with spin (I) $>1/2$ is expected to be dominated by this quadrupolar mechanism[10].

Nuclear spin–lattice relaxation rates (T_{1n}^{-1}) for Na^- in 12C4 are very much less than the value of 3,770 s^{-1} for Na^+ in this solvent. The cation relaxation arises from the very large fluctuations in the electric field gradient caused by the asymmetric environment of the Na^+ ion resulting from its strong complexation by the solvent[11]. The very small relaxation rate for Na^- in the solvent 12C4 is comparable with that reported in Table 1 for Na^+ in H_2O, which experiences an environment, the time average of which is centrosymmetric[10,12,13].

It is therefore of interest to compare the Na^- nuclear relaxation rate with those of other ions which are in a centrosymmetric environment[10,12,13]. Note, however, that the experimental spin-lattice relaxation times of Table 1 are not, at this stage, directly comparable because T_{1n}^{-1} is proportional, among other things, to the square of the nuclear electric quadrupole moment $(eQ)^2$, and depends on a theoretically well-established function of the nuclear spin I. Thus, column (2) of Table 1 reports the suitably scaled T_{1n}^{-1} values that would arise if all the ions had the same eQ and I as the ^{23}Na nucleus. This scaling (from column (1) to (2) in Table 1 uses theory of such firmly established validity[10] that these numbers can be regarded as experimental results.

Table 1 Measured and scaled nuclear spin relaxation rates for ions in various solvents

Ion/solvent	(1) Measured T_{1n}^{-1}* (s^{-1})	(2) Nuclear properties (I, eQ)	(3) T_{1n}^{-1} scaled for: Electronic anti-shielding (β_2)	(4) Viscosity (τ_{solv})
Na^+/H_2O	16.2	16.2	191	7,109
$Na^-/12C4$	3.33	3.33	3.33	3.33
Cl^-/H_2O	25	39	1.66	61.66
Cl^-/C_2H_5OH	1,300	2,047	86	716.7
$Cl^-/12C4$	14,100	22,260	935	935
I^-/H_2O	4,600	346	3.58	133
Cs^+/H_2O	0.075	817	15.5	577

* With the exception of relaxation rates in 12C4 these data are taken from refs 12, 13.

‡ To whom correspondence should be addressed.

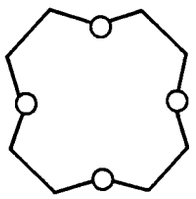


Fig. 1 1,4,7,10-tetraoxacyclododecane (12-crown-4).

The electric field gradient at the ^{23}Na nucleus generated by the environment is magnified by a factor $(1+\beta_2)$, the Sternheimer anti-shielding factor[14], which originates from the additional electric field gradient generated by the electrons belonging to the ion. This additional electric field gradient arises because the external environment distorts the electronic charge distribution away from spherical symmetry. Since T_{1n}^{-1} is proportional to $(1+\beta_2)^2$, the results of column (2) of Table 1 can be scaled to yield the rates that would arise if all the ions had the same Sternheimer anti-shielding factor as Na^-. The resulting data (column (3) of Table 1) are genuine reflections of the differences in strengths of the interactions of each nucleus with its environment external to the ion. Thus, these numbers now reflect the differences in the microscopic structure and microdynamics of the ions in solution.

In any theory of nuclear relaxation in liquids[10], these microdynamics can be characterized by a correlation time, τ_c, defining the rate of fluctuations of the electric field gradient at the nucleus. For all of the ions except Cl^- in 12C4 and Na^+, the molecules in the first solvation shell reorientate independently both of the ion and of each other[12,13]. As this is the first report of the T_{1n}^{-1} data for Cl^- in 12C4, the details of the microdynamics reponsible for this relaxation have not yet been elucidated.

For all of the Na^- solutions, differing in concentration and counter cation, the activation energy (22 ± 1 kJ mol^{-1}) for the process responsible for the Na^- spin-lattice relaxation was found to be essentially identical to that (23 ± 1 kJ mol^{-1}) for the process responsible for the ^{13}C and ^1H relaxation in the pure solvent. As the latter relaxation arises from reorientation of individual 12C4 molecules, our activation energies show that such independent solvent reorientation is the source of the fluctuations in the electric field gradient responsible for the Na^- spin-lattice relaxation. Hence the correlation time governing the Na^- relaxation is the same as that, τ_{solv}, for the reorientation of individual uncomplexed solvent molecules in the neat liquid. This τ_{solv} was derived from the values of T_{1n}^{-1} for nuclei such as ^{13}C and ^1H, whose relaxation is dominated by direct dipolar interactions between the spins. As the correlation time for neat 12C4 thus derived, 130 ps, is much longer than either that (15.6 ps) of C_2H_5OH or that (3.5 ps) of H_2O, the scaled relaxation rates of column (3) in Table 1 for Na^- relaxation in 12C4 would be expected to be much greater than those for the ions in the other two solvents if the strengths of the fluctuating electric field gradients were comparable. The much longer τ_{solv} of 12C4 is consistent with the much greater viscosity[9] (10 cP) compared with that of H_2O (1 cP).

The data in column (4) of Table 1 are derived by scaling those of column (3) by the factor τ_{solv} (12C4), thereby generating the relaxation rates that the ions would have if they all had the same quadrupole moments, nuclear spins and Sternheimer factors as Na^-, and were all in solvents of the same viscosity as 12C4. This scaling markedly increases the rates of column (3) in Table 1, except those for Na^- and Cl^- in 12C4 yielding scaled relaxation rates which illustrate that the strength of the fluctuations of the environment experienced by the Na^- ion is at least an order of magnitude smaller than those for all of the other systems.

Note that the 'raw' experimental relaxation rates of column (1) (which govern the NMR line width) might be incorrectly interpreted to suggest that the interaction of Na^+ with its environment in H_2O is only slightly greater than that of Na^- with its environment in 12C4. However, the present scaled relaxation rates show that this is not the case, and they (column (4)) provide the first conclusive evidence that the sodium anion in these systems is considerably more decoupled from its environment than any of the other common ions. In particular, the interaction of Na^- with its environment is ~280 times smaller than that of the Cl^- ion in the same solvent (12C4).

The chemical shift measurements show that Na^- in 12C4 interacts so weakly with its environment that it behaves essentially as if it were in the gas phase. The nuclear relaxation data also show that Na^- interacts only very weakly with its environment. We have shown not only that this interaction is much smaller than that of halide ions in a variety of solvents, but also that Na^- interacts much more weakly with 12C4 than does the Cl^- ion. It would be inappropriate to attempt to explain here the reasons for this remarkable difference between Na and halide ions.

We thank the SERC for support.

Received 30 July 1985; accepted 13 March 1986.

1. Dye, J. L. in *Progress in Inorganic Chemistry* Vol. 32, (ed Lippard, S. J.) 327 (Wiley, New York, 1984).
2. Dye, J. L., Andrews, C. W. & Ceraso, J. M. *J. phys. Chem.* 79, 3076–3079 (1975).
3. Dye, J. L. *Angew. Chem. int. Edn. Engl.* 18, 587–598 (1979).
4. Edwards, P. P. *J. phys. Chem.* 88, 3772–3780 (1984).
5. Holton, D. M. & Edwards, P. P. *Chem. Br.* 21, 1007–1013 (1985).
6. Edwards, P. P. *Adv. Inorg. Chem. Radiochem.* 25, 135–185 (1982).
7. Pyper, N. C. & Edwards, P. P. *J. Am. chem. Soc.* 108, 78–81 (1986).
8. Edmonds, R. N., Holton, D. M. & Edwards, P. P. *JCS Dalton Trans* 323–327 (1986).
9. Holton, D. M., Ellaboudy, A. S., Pyper, N. C. & Edwards, P. P. *J. chem. Phys* 84, 1089–1095 (1986).
10. Abragam, A. *The Principles of Nuclear Magnetism* (Clarendon, Oxford 1983).
11. Remoortere, F. P. & Boer, F. P. *Inorg. Chem.* 13, 2071–2078 (1974).
12. Hertz, H. G. *Ber. Bunsen. phys. Chem.* 77, 531–540 (1973).
13. Melendres, C. A. & Hertz, H. G. *J. chem. Phys.* 61, 4156–4162 (1974).
14. Sternheimer, R. M. *Phys. Rev.* 84, 244–253 (1951).

Distribution of atoms at the surface of liquid mercury

Scott W. Barton*, Britt N. Thomas*, Frank Novak*, Peter M. Weber*, Jonathan Harris*, Paul Dolmer†, J. Mati Bloch‡ & Stuart A. Rice*

* Department of Chemistry and James Franck Institute, and
† Central Development Shop, The University of Chicago, Chicago, Illinois 60637, USA
‡ NSLS, Brookhaven National Laboratory, Upton, New York 11973, USA

Theoretical studies of the anisotropic distribution of atoms in the liquid/vapour interface have led to two conclusions. First, the density along the normal to the interface (the longitudinal one particle distribution function) has different forms in a liquid dielectric and a liquid metal. In a dielectric[1], the density decreases monotonically as one passes from the liquid to the vapour, while in a metal[2] the liquid/vapour interface is stratified for about three atomic diameters into the bulk liquid, Fig. 1 shows examples. Second, the transverse structure factor at the surface of a liquid (the Fourier transform of the in-plane distribution of pairs of atoms) is very similar to the bulk liquid structure factor except near the origin, the difference arising from long-range correlations in the surface[1]. The very few experiments[3,4] that can be interpreted in terms of the properties of the density along the normal to the liquid surface are in agreement with the first set of predictions. There have been no published reports on the transverse structure factor in the liquid/vapour interface. Here we describe the transverse structure factor of the room temperature liquid/vapour interface of mercury, determined using the method of grazing incidence X-ray diffraction[5]. Our experimental results are consistent with the above predictions.

The experiments were carried out at the Cornell High Energy Synchrotron Source (CHESS) using an apparatus that will be

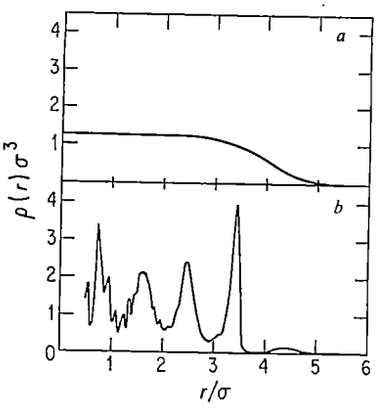


Fig. 1 The density (ρ) along the normal to the surface for: *a*, a typical dielectric liquid; and *b*, liquid Hg as determined in the Monte-Carlo simulations of D'Evelyn and Rice[2]. The density and distance are put in reduced units through the atomic diameter σ. The coordinates chosen assume a free cluster configuration as actually used in ref. 2.

described in detail elsewhere. The geometry used is shown in Fig. 2. The sample is illuminated with X rays of wavelength λ at an angle ϕ which is much smaller than the critical angle for total external reflection, ϕ_c. Given that $\phi_c \propto \lambda$, in our experimental conditions the penetration depth of the X rays, $d \simeq \lambda(2\pi)^{-1}(\phi_c^2 - \phi^2)^{-1/2}$, is independent of wavelength; for Hg it has the value 30 Å. The detector is set with vertical pick-off angle $\phi' \approx \phi_c$ and is scanned as a function of the azimuthal angle 2θ. Let $\mathbf{k}_0$ and $\mathbf{k}_d$ be the wavevectors of the incident and diffracted X rays. Since ϕ' is very small, the scattered wavevector magnitude is given by $|\mathbf{k}| \equiv |\mathbf{k}_0 - \mathbf{k}_d| = 4\pi \sin\theta/\lambda$, the usual Bragg relation. This observation has the important consequence that, since the momentum transfer in the X-ray scattering is parallel to the surface of the liquid, only those atom–atom correlations in planes parallel to the surface are probed in our experiment.

We define the transverse structure factor (excluding polarization and inelastic X-ray scattering effects) by

$$S_{\parallel}(k) = \frac{\int w(\phi, \phi', z) S(k_{xy}; z) f^2(k) \rho(z)\, dz}{\int w(\phi, \phi', z) f^2(k) \rho(z)\, dz}$$

where $w(\phi, \phi', z)$ is a weight factor which describes the X-ray intensity at depth z, $S(k_{xy}; z)$ is the transverse liquid structure factor at z, $f(k)$ is the atomic structure factor and $\rho(z)$ scales as the average number of scatterers at depth z. The normalization is $S_{\parallel}(k) \to 1$ as $k \to \infty$.

Our sample was commercially obtained triply-distilled Hg. It was further purified by hot oxidation of impurities and their subsequent removal by filtering the liquid repeatedly through very long glass capillaries. The Hg was introduced into the beryllium-windowed stainless-steel ultra-high vacuum chamber through a capillary after the base pressure in the chamber had been reduced to 10^{-8} torr or less. Using the same conditions,

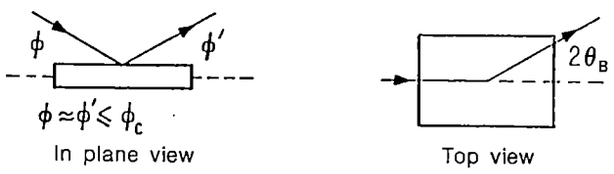


Fig. 2 Geometry of grazing incidence X-ray diffraction experiments.

previous experiments have shown that the liquid Hg surface remains clean for several days[6]. The 8- and 16-keV X rays used were reflected from a double-bounce channel-cut Si(220) crystal and deflected down onto the liquid sample by a Pt-coated float glass mirror, at an angle of incidence of 1.3 mrad. Horizontal slits were used to define the incident beam and the pick-off angle, while vertical Soller slits in front of the detector define the azimuthal angle 2θ to $\pm 0.15°$. An intrinsic germanium energy-dispersive detector was used, which enabled us to separate X-ray fluorescence from X-ray scattering. Corrections for the instrument geometry, and for the decay of incident intensity as the storage ring current decays, were made by scaling the diffraction intensity to the intensity of the 10.1-keV Hg fluorescence line. In our experiment, the intensity of such a fluorescence line is independent of θ. The data were corrected for atomic, anomalous and Compton scattering and polarization (assuming the X-ray beam is plane polarized), and normalized using the Krogh-Moe method[7].

Figure 3 shows the experimentally determined structure factor at 298 K and, for comparison, the structure factor for bulk liquid Hg at 293 K (ref. 8). The error in the bulk structure factor is predicted from counting statistics and is not greater than twice the line thickness in Fig. 3. Note the distinct features: $S_{\parallel}(k)$ for the interface is lower than $S_{bulk}(k)$ in the region from 1 to 2 Å^{-1}; the trough between the first and second peaks in $S_{\parallel}(k)$ is slightly

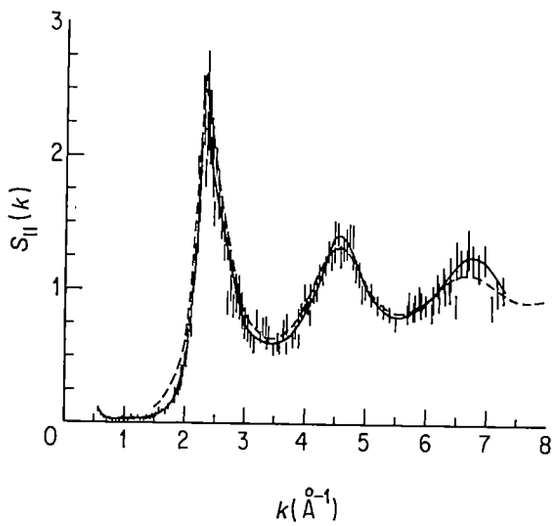


Fig. 3 The transverse structure factor for X-ray scattering from the surface of liquid Hg at 298 K. The vertical lines are out statistical error bars through which we have drawn a solid line to guide the eye. The dashed line is the bulk liquid structure factor at 293 K, from ref. 8.

deeper than in $S_{bulk}(k)$; the second peak amplitude in $S_{\parallel}(k)$ is slightly higher and narrower than the corresponding peak in $S_{bulk}(k)$; there is an apparent increase in $S_{\parallel}(k)$ as $k \to 0$ starting at $k \approx 1$ Å^{-1}.

An examination of the temperature dependences of the structure factors of several bulk liquid metals[7] shows that as the density increases, the low k onset of the first peak decreases and the peak amplitudes are increased. Our results imply that the surface of liquid Hg is more dense than that of the bulk. This further supports the predictions of a stratified liquid/vapour interface density profile; since the total elastic scattering intensity scales as the atomic density, $S_{\parallel}(k)$ will be dominated by the contributions from the high-density strata.

Kalos *et al.*[1] calculated the transverse structure function for the liquid/vapour interface of a model Lennard-Jones system

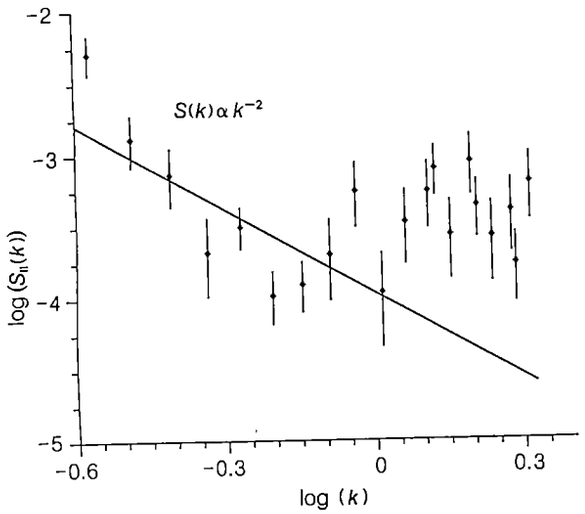


Fig. 4 A log-log plot of $S_{\parallel}(k)$ against k at low k.

with parameters of the potential chosen to describe Ar. They find a divergence in $S_{\parallel}(k)$ as $k \to 0$ with variation as k^{-2}. The theoretical interpretation of this divergence associates it with the existence of long-range correlations in the surface, the absence of any external force acting on the system and the non-vanishing of the derivative of density with respect to displacement along the normal. While our surface transverse factor is different from that of Kalos *et al.*[1] (their factor is given for a thin slice at $z = 0$ and ours is integrated and averaged over a pentration depth), it is assumed that only the first or second uppermost layers will show any long-range transverse correlation; if present, the contribution of such a correlation to $S_{\parallel}(k)$ would overwhelm any contribution to $S_{\parallel}(k)$ from lower layers. Of course, our experiments are carried out in the Earth's gravitational field, which violates one of the conditions used in the theoretical analyses, but that field is so weak that, if everything else is the same, long (but not infinite)-range correlations should still be present.

Although the log-log plot in Fig. 4 shows that some scatter exists for the low k values of $S_{\parallel}(k)$, we believe the k^{-2} dependence of $S_{\parallel}(k)$ is a reasonable fit to our data. At least for the present, there is no reason to disbelieve the predicted k^{-2} dependence of $S_{\parallel}(k)$.

Our results are the first determination of the transverse-structure factor at the surface of a liquid. We expect that the grazing incidence X-ray diffraction technique and its neutron-scattering equivalent will be powerful tools for studying the variation of interface structure when a metal is alloyed, when a liquid supports a film or other structure and, in general, the interaction of a liquid interface and a contact medium.

The research described here was supported by a NSF grant. Some construction funds were provided by a grant from EXXON and we have benefitted from the support of the Materials Research Laboratory at the University of Chicago by the NSF. We thank the support staff at CHESS for valuable assistance. J.H. is an NSF and McCormick Foundation Fellow.

Received 25 November 1985; accepted 4 April 1986.

1. Kalos, M. H., Percus, J. K. & Rao, M. *J. statist. Phys.* **17**, 111–136 (1977).
2. D'Evelyn, M. P. & Rice, S. A. *J. chem. Phys.* **78**, 5081–5095 (1983).
3. Bosio, L. & Oumezine, M. *J. chem. Phys.* **80**, 959–960 (1984).
4. Braslau, A. *et al. Phys. Rev. Lett.* **54**, 114–117 (1985).
5. Marra, W. C., Eisenberger, P. & Cho, A. Y. *J. appl. Phys.* **50**, 6927–6933 (1979).
6. Lu, B. C. & Rice, S. A. *J. chem. Phys.* **68**, 5558–5567 (1978).
7. Waseda, Y. *The Structure of Non-Crystalline Materials* (McGraw-Hill, New York, 1980).
8. Bosio, L., Cortes, R. & Segaud, C. *J. chem. Phys.* **71**, 3595–3600 (1979).

Efficient solar energy conversion with $CuInS_2$

H. J. Lewerenz, H. Goslowsky, K.-D. Husemann & S. Fiechter

Hahn-Meitner-Institut für Kernforschung Berlin, Bereich Strahlenchemie, 1000 Berlin 39, FRG

The high absorptivity associated with a direct energy gap in the optimum range for solar-energy conversion makes $CuInS_2$ a particularly promising material for efficient solar-energy conversion[1]. Achieved solar-to-electrical conversion efficiencies have been limited to ~6% (refs 2–8). We report here a new heterogeneous polycrystalline *n*-$CuInS_2$ based semiconductor which has yielded conversion efficiencies of 9.7% in an electrochemical cell. The high photoactivity is also evident in a Schottky barrier solar cell configuration. The origin of the improved efficiency is attributed to impurity scavenging by In spheres resulting from a modified vapour/liquid/solid (VLS) growth process[9–11] and the influence of the acidic iodine iodide electrolyte on the cell performances.

Samples with increased In excess exceeding the single-phase region in the phase diagram[12] were prepared. $CuInS_2$ was synthesized from the elements (6 N/Ventron) in a mole ratio of 0.95, 1.05 and 2, respectively. In the growth process, the molten Cu–In alloy reacted with S at $T = 1{,}175$ °C to yield the new material. The resulting boule consists of large-grain polycrystalline material and exhibits a comparably porous structure in its interior. The samples with the highest photoactivity are found in this region inside the boule. Sizes range between 1 and 5 mm^2. A typical surface is shown in Fig. 1. The morphology is characterized by extended steps typical for VLS growth[13]. In addition, small In spheres and In_2S_3 and $Cu_{2-x}S$ occlusions are found and extend up to the surface on some samples.

For photoactivity measurements, electrodes were prepared as described earlier[14] using In–Ga alloy as the ohmic back contact. Figure 2*a* shows the current/voltage characteristic under illumination with simulated AM1 direct radiation (85 mW cm^{-2}) (Oriel Solar Simulator) of *n*-$CuInS_2$ in contact with acidic iodine–iodide electrolyte. Because of the comparably small electrode, area determination was done by scanning laser spot analysis[15–17] to measure the photoactive area accurately. In a two-electrode experiment, the cell converts light to electricity



Fig. 1 Electron micrograph of a typical melt grown $CuInS_2$ sample with In excess; note terraces indicative of VLS growth and In spheres. Scale bar 200 μm.

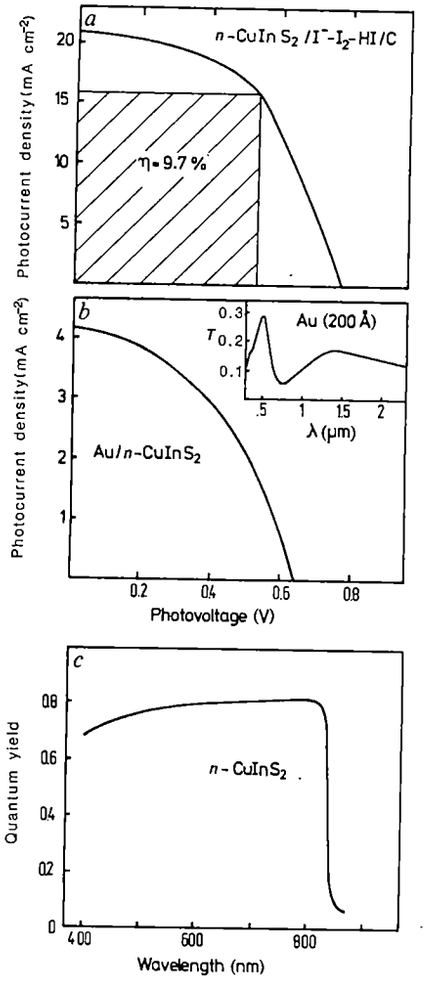


Fig. 2 Photoactivity of heterogeneous $CuInS_2$. *a*, Output power characteristic of the *n*-$CuInS_2$/HI-I^--I_2/C solar cell; electrolyte: 2 M HI, 2.5 M CaI_2, 50 mM I_2; illumination: Oriel Solar Simulator, AM 1 direct (85 mW cm^{-2}). *b*, Output power characteristic of the Au/*n*-$CuInS_2$ solar cell; evaporation of front metal contact after potential cycling in HI-I^--I_2 redox electrolyte; illumination: 64 mW cm^{-2} natural sunlight. *c*, Spectral dependence of the quantum yield; electrolyte: 2 M HI, 2.5 M CaI_2, 50 mM I_2; potential: 0.1 V (SCE).

with an efficiency of 9.7%. The short-circuit photocurrent is stable for ~20,000 Cb cm^{-2}. During the long time testing period no decrease in photovoltage has been found. Figure 2*b* shows the photocurrent/voltage characteristic of a Au/*n*-$CuInS_2$ junction obtained in natural sunlight of 64 mW cm^{-2} (Kipp-Zonen global detector). Before metal evaporation, the sample was polarized in HI-I^--I_2 electrolyte (−0.1 V→ −0.6 V (SCE)) which resulted in an improved cell output compared with untreated electrodes. The spectral dependence of the transmission of the 200 Å thick Au film is displayed in the inset of Fig. 2*b*. The light attenuation for photon energies above the $CuInS_2$ band gap (~830 nm) can be estimated by the area under the transmittivity curve. Since the total transmission is 25% in this energy range, a correction factor of ~4 for efficiency calculation is obtained. This would result in a solar-to-electrical conversion efficiency of ~7.5%.

The spectral dependence of a typical quantum yield is shown in Fig. 2*c*. The experiments were performed in the standard potentiostatic arrangement with a carbon counter electrode and a calomel reference electrode. The quantum yield was obtained by calibrating a photocurrent spectrum with the photon flux of a He-Ne laser at 633 nm. Despite the absorptivity of the iodine-iodide solution and the fact that the distance between electrode and cell window was not optimal, the values exceed 0.8.

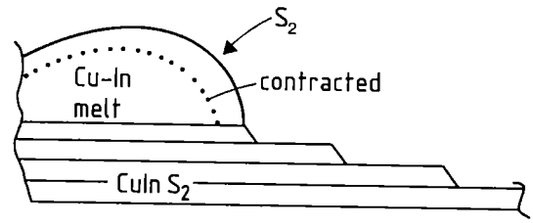


Fig. 3 Schematic representation of VLS growth of highly photoactive $CuInS_2$ (see text).

The photoactivity improvement of the new material can be interpreted based on details of the growth process. An additional advantageous influence of the selected electrolyte is also evident, particularly from the preparation experiments before metal evaporation indicating that surface optimization contributes to the high cell output[18–20]. In VLS (vapour/liquid/solid), growth of $CuInS_2$, a Cu-In melt exists at a given temperature which is supersaturated by gaseous S_2 leading to abrupt contraction of the melt and resulting in the growth of a new terrace[21,22]. This process, schematically shown in Fig. 3, explains the surface morphology shown in Fig. 1. When the growth is interrupted at a time when not all of the remaining sulphur has reacted, the In excess leads to the observed residual In spheres found on these samples (Fig. 1).

The spheres seem to act as a reservoir for impurities, as spark source mass spectrometry (SSMS)[23] and inductively coupled plasma (ICP)[24] analyses show a ~40 times increased Fe content of the metal spheres compared with the neighbouring material[11]. Fe probably substitutes In in the host compound leading to the localized formation of $CuFeS_2$ which acts as a deep trap. Time resolved microwave conductivity (TRMC)[25] and photoluminescence (PL) experiments reveal a drastic reduction in the trap density in the energy gap compared with differently prepared $CuInS_2$ (ref. 10). The prevailing effect of the material heterogeneity thus seems to be the creation of a reservoir for the most deleterious impurities with a material (In) with favourable segregation coefficients, similar to the process of zone refining[26].

We thank Professor H. Tributsch for support and stimulating discussions. The work was in part supported by a BMFT grant No. 03E-8375-A.

Received 23 September 1985; accepted 11 March 1986.

1. Shay, J. L. & Wernick, J. H. in *Ternary Chalcopyrite Semiconductors: Growth, Electric Properties and Application* (Pergamon, Oxford, 1975).
2. Robbins, M. *et al. J. electrochem. Soc.* **125**, 831–832 (1978).
3. Lewerenz, H. J., Goslowsky, H. & Thiel, F. A. *Sol. Energy Mater.* **91**, 159–166 (1983).
4. Cahen, D. *et al. J. electrochem. Soc.* **132**, 1062–1070 (1985).
5. Mirovsky, Y., Tenne, R., Cahen, D., Sawatzky, G. & Polak, M. *J. electrochem. Soc.* **132**, 1070–1076 (1985).
6. Russak, M. A. & Creter, C. *J. electrochem. Soc.* **132**, 1741–1745 (1985).
7. Kazmerski, L. L. & Sanborn, G. A. *J. appl. Phys.* **48**, 3178–3180 (1977).
8. Tell, B. & Thiel, F. A. *J. appl. Phys.* **50**, 5045–5046 (1979).
9. Goslowsky, H., Fiechter, S., Könenkamp, R. & Lewerenz, H. J. *Sol. Energy Mater.* (in the press).
10. Lewerenz, H. J. *et al. J. mater. Sci.* (in the press).
11. Goslowsky, H., Husemann, K.-D., Luck, J., Szacki, W. W. & Lewerenz, H. J. *Mater. Lett.* (in the press).
12. Verheijen, A. W., Giling, L. J. & Bloem, J. *Mater. Res. Bull.* **14**, 237–240 (1979).
13. Wagner, R. S. & Ellis, W. C. *Appl. phys. Lett.* **4**, 89–90 (1964).
14. Goslowsky, H., Kühne, H.-M., Neff, H., Kötz, R. & Lewerenz, H. J. *Surf. Sci.* **149**, 191–208 (1985).
15. Furtak, T. E., Canfield, D. C. & Parkinson, B. A. *J. appl. Phys.* **51**, 6018–6021 (1980).
16. Menezes, S., Schneemeyer, L. F. & Lewerenz, H. J. *Appl. phys. Lett.* **38**, 949–951 (1981).
17. Lewerenz, H. J., Tributsch, H. & Spiesser, M. *J. electrochem. Soc.* **132**, 700–703 (1985).
18. Parkinson, B. A., Heller, A. & Miller, B. *J. electrochem. Soc.* **126**, 954–959 (1979).
19. Heller, A., Lewerenz, H. J. & Miller, B. *Ber. Bunsen. phys. Chem.* **84**, 592–595 (1980).
20. Menezes, S., Lewerenz, H. J., Thiel, F. A. & Bachmann, K.-J. *Appl. phys. Lett.* **38**, 710–712 (1981).
21. Binsma, J. J. M. *thesis*, Univ. Nijmegen (1981).
22. Binsma, J. J. M., Van Enckevort, W. J. P. & Staarnick, G. W. M. *J. crystallogr. Growth* **61**, 138–156 (1983).
23. Ahearn, A. J. (ed.) *Trace Analysis by Mass Spectrometry* (Academic, New York, 1972).
24. Thomson, M. & Walsh, J. N. *A Handbook of Inductively Coupled Plasma Spectrometry* (Blackie, Glasgow 1983).
25. Kunst, M. & Tributsch, H. *Chem. phys. Lett.* **105**, 123–126 (1984).
26. Pfann, W. G. in Solid State Phys. 4: Techniques of Zone Melting and Crystal Growing (New York, 1957).

Vertical profile of lead isotopic compositions in the north-east Pacific

A. R. Flegal*, K. Itoh†, C. C. Patterson‡ & C. S. Wong§

* Institute of Marine Sciences, University of California, Santa Cruz, California 95064, USA
† Kitami Institute of Technology, Kitami, Hokkaido, Japan
‡ California Institute of Technology, Pasadena, California 91125, USA
§ Institute of Ocean Sciences Sidney, British Columbia, Canada V8L 4B2

Ratios of lead isotopes (^{204}Pb, ^{206}Pb, ^{207}Pb and ^{208}Pb) may be used to distinguish leads from different sources in sea water[1–3] in a manner similar to neodynium isotopes[4–8]. The following data from the north-east Pacific include the first vertical profile measurements of lead isotopic compositions in sea water. These preliminary data indicate that lead in offshore (48° N, 141° W) north-east Pacific surface waters (^{206}Pb/^{207}Pb = 1.164) was derived from aeolian inputs of Asian (Japanese) industrial leads (^{206}Pb/^{207}Pb = 1.160) (M. Murozumi, personal communication), but that lead in water immediately (400 m) below it (^{206}Pb/^{207}Pb = 1.211) was derived from North America industrial leads (^{206}Pb/^{207}Pb = 1.222)[9]. This remarkable contrast in isotopic compositions over such a relatively short distance reveals the potential of lead isotopic compositions to resolve the importance of horizontal transport processes on the lead cycle in the oceans, which were recently proposed to partially account for its oceanographic variability in the North Pacific[10].

Seawater collections were obtained along a transect from 48° N, 125° W to 48° N, 141° W in August 1980 (Fig. 1). Surface water samples were obtained from a workboat deployed away from the research vessel, *CSS Parizeau*. Subsurface samples were collected with Caltech 10-1, deep-water samplers[11]. Those samples were then transferred to bottles for storage at 4 °C within a shipboard clean laboratory[12], using trace-metal clean procedures[11].

Isotopic composition measurements by thermal ionization mass spectrometry were made with samples (4 1) after extraction with the dithizone-chloroform procedure described elsewhere[3], as were the lead concentration measurements[11,13]. Coefficients of variation of individual ratios typically were: ^{208}Pb/^{206}Pb ≦ 0.2%; ^{207}Pb/^{206}Pb ≦ 0.01%; and ^{206}Pb/^{204}Pb ≦ 0.3%. Contaminant lead corrections calculated from summations of individually determined contributions of contamination by reagents and containers were ≦2% of the sample lead.

The different sources of lead in north-east Pacific surface waters are established by the differences in their isotopic compositions listed in Table 1, especially the ^{206}Pb/^{207}Pb ratios which are most commonly used as indicators of different lead sources in sea water[2,3]. Isotopic compositions of lead aerosols from industrial sources impacting those waters are also listed in Table 1 for comparison. The ^{206}Pb/^{207}Pb ratios in these north-east Pacific surface waters range from 1.164 in the offshore (48° N, 141° W) waters (Station P-12) to 1.204 in the coastal (48° N, 127° W) waters of the Juan de Fuca Straits (Station P-17). This range in ^{206}Pb/^{207}Pb ratios over 1,900 km in the north-east Pacific is greater than that (1.174–1.196) over 3,300 km in the central (19° N, 158° W to 15° S, 150° W) Pacific[3]. It substantiates reports that the lead in offshore surface waters of the north-east Pacific is primarily derived from Asian industrial lead (^{206}Pb/^{207}Pb = 1.160), and the lead in surface waters of the Juan de Fuca Straits is primarily derived from North American industrial lead (^{206}Pb/^{207}Pb = 1.222)[2,3,11,13]. It is also consistent with ^{210}Pb data from the Pacific, which indicate the predominance of aeolian inputs in oceanic surface waters and of both aeolian and fluvial inputs in coastal waters[14–20].

The vertical gradient in lead isotopic compositions in the

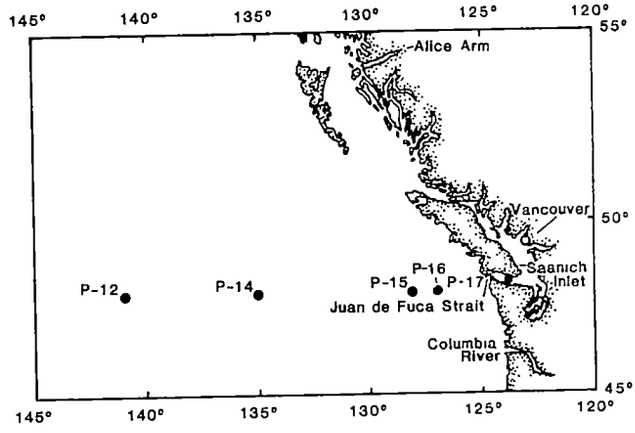


Fig. 1 Sampling locations in the north-east Pacific.

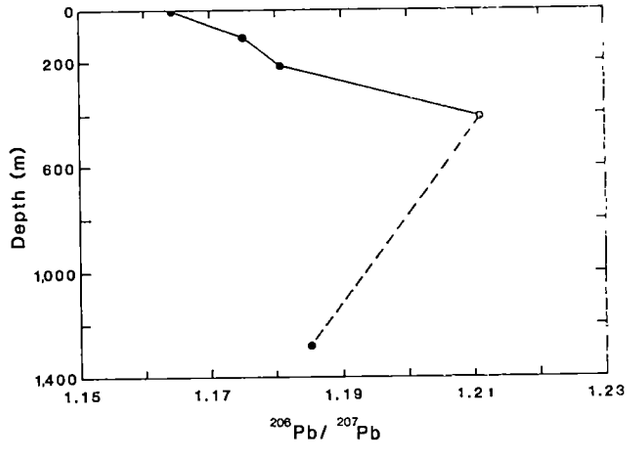


Fig. 2 Lead isotopic ratios (^{206}Pb/^{207}Pb) at 48°N, 141°W in the north-east Pacific.

offshore (48° N, 141° W) waters (Station P-12) is even more pronounced. There the ^{206}Pb/^{207}Pb ratio increases from 1.164 in the surface waters to 1.211 at 400 m, and then decreases to an intermediate value at greater depth (Fig. 2). The relatively large magnitude of this range over the upper 400 m is illustrated by comparison with the previously cited ranges of ^{206}Pb/^{207}Pb ratios in surface waters over 1,900 km in the north-east Pacific and over 3,300 km in the central Pacific. For example, the ^{206}Pb/^{207}Pb vertical gradient (Δ ^{206}Pb/^{207}Pb: Δ km) is more than 19,000 times greater than the horizontal gradient in the central Pacific.

This pronounced vertical gradient in lead isotopic compositions indicates the potential of lead isotope systematics to delineate the element's biogeochemical cycle in the ocean. Specifically, these data indicate that lead isotopic compositions can establish the significance of horizontal transport processes within the ocean, which have been proposed to account for the parallel vertical concentration gradients of lead, bismuth and plutonium in the North Pacific[10]. For example, the subsurface (728 m) lead concentration maximum (68 pmol kg^{-1}) in these subarctic waters is consistent in size and shape with those in more temperate waters of the north-east Pacific[11,13,21,22], but the apparent North American isotopic composition of that lead precludes it from having the western Pacific origins which have been proposed to account for the lead concentration maxima in the more southern waters[10].

Unfortunately, there were neither samples for additional lead measurements nor sufficient oceanographic data obtained on the cruise to resolve adequately the lead inputs at this oceanographically-complex location. Consequently, the subsurface lead may reflect a horizontal input of North American lead

Table 1 Isotopic compositions of lead in the north-east Pacific and in aeolian inputs from industrial sources

	Lat.	Long.	Depth (m)	Isotopic composition 206/207 ($\bar{x}\pm$1s)	206/208 ($\bar{x}\pm$1s)	206/204 ($\bar{x}\pm$1s)	Concentration (pmol kg^{-1})
Seawater samples							
Station							
P-12	141°00′ W	48°00′ N	0	1.164±0.0023	0.4709±0.0022	17.39±0.70	27.0/25.5*
			106	1.175±0.0019	0.4785±0.0010	18.36±0.05	45.4
			216	1.181±0.0005	0.4824±0.0003	—	59.8
			404	1.211±0.0017	0.4965±0.0023	18.98±0.19	62.7
			728	—	—	—	68.0
			1,247	—	—	—	27.0
			1,282	1.185±0.0046	0.4822±0.0025	19.05±0.53	20.7
			1,650	—	—	—	18.8
			1,980	—	—	—	14.4/15.4
			2,714	—	—	—	11.1
			3,249	—	—	—	12.5
			3,945	—	—	—	10.1
P-14	135°00′ W	48°00′ N	200	1.191±0.0048	0.4884±0.0029	18.35±0.09	60.3/60.3*
P-15	128°00′ W	48°00′ N	200	1.180±0.0006	0.4826±0.0005	—	91.7
			400	—	—	—	125.0
P-16	127°00′ W	48°00′ N	0	1.204±0.0005	0.4915±0.0032	—	7.7/13.9*
P-17	124°00.8′ W	48°21.8′ N	0	—	—	—	31.4
Aeolian inputs							
Western USA[9]				1.22	0.496	19.3	—
Asia/Japan USA†				1.16	0.479	17.8	—
Western Canada[2]				1.16	0.480	18.4	—

* Concentrated acid digestion as detailed elsewhere[14].
† M. Murozumi, personal communication.

from a southern incursion of the California Undercurrent, the diagenic mobilization of shelf sediments, the nepheloid transport of unconsolidated shelf sediments, or the subsurface decomposition of plankton in coastal waters. Additionally, that lead may reflect a vertical input from a previous aeolian flux of North American lead to the surface waters. Although those potential inputs cannot be resolved with these preliminary data, their multiplicity illustrates the need for additional isotopic data to distinguish different sources of lead in the ocean.

Therefore, the principal significance of these data is that they demonstrate the potential of stable lead isotopic compositions as geochemical tracers in the ocean. The pronounced $^{206}Pb/^{207}Pb$ gradient in this preliminary vertical profile indicates that those ratios can be utilized to determine the significance of different inputs and transport processes on the oceanic lead cycle. It also indicates that those ratios may be utilized as tracers of water masses, as well as of biogeochemical transformations of lead and its analogues (such as calcium) within those water masses.

Received 22 October 1985; accepted 10 March 1986.

1. Broecker, W. S. & Peng, T. H. (eds) *Tracers in the Sea* (Columbia University, Palisades, New York, 1982).
2. Stukas, V. J. & Wong, C. S. *Science* **211**, 1424–1427 (1981).
3. Flegal, A. R., Schaule, B. K. & Patterson, C. C. *Mar. Chem.* **14**, 281–287 (1984).
4. Piepgras, D. J. & Wasserburg, G. J. *Earth planet. Sci. Lett.* **50**, 128–138 (1980).
5. Hooker, P. J., Hamilton, P. J. & O'Nions, R. K. *Earth planet. Sci. Lett.* **56**, 180–188 (1981).
6. Chyi, M. S., Carlson, R. W. & Crerar, D. A. *Geol. Soc. Am. Abstr.* **14**, 463 (1982).
7. Shaw, H. F. & Wasserburg, G. J. *Geochim. cosmochim. Acta* **49**, 503–518 (1985).
8. Palmer, M. R. thesis, Univ. Leeds (1983).
9. Shirahata, H., Elias, R. W. & Patterson, C. C. *Geochim. cosmochim. Acta* **44**, 957–960 (1980).
10. Lee, D. S., Edmond, J. M. & Bruland, K. W. *Earth planet. Sci. Lett.* **76**, 254–262 (1986).
11. Schaule, B. K. & Patterson, C. C. *Earth planet. Sci. Lett.* **54**, 97–116 (1981).
12. Wong, C. S., Cretney, W. J., Piuze, J., Christensen, P. & Berrang, P. G. *Clean Laboratory Methods to Achieve Contaminant-Free Processing and Determination of Ultra-Trace Samples in Marine Environmental Studies* (National Bureau of Standards Spec. Publ. 464, 1977).
13. Flegal, A. R. & Patterson, C. C. *Earth planet. Sci. Lett.* **4**, 19–32 (1983).
14. Nozaki, Y., Thomson, J. & Turekian, K. K. *Earth planet. Sci. Lett.* **32**, 304–312 (1976).
15. Schell, W. R. *Geochim. cosmochim. Acta* **41**, 1019–1031 (1977).
16. Nozaki, Y., Turekian, K. K. & Von Damm, K. *Earth planet. Sci. Lett.* **49**, 393–400 (1980).
17. Chung, Y. & Craig, H. *Earth planet. Sci. Lett.* **65**, 406–432 (1983).
18. Chung, Y., Finkel, R., Bacon, M. P., Cochran, J. K. & Krishnaswami, S. *Earth planet. Sci. Lett.* **65**, 393–405 (1983).
19. Noriyuki, T., Takeda, Y. & Tsunogai, S. *Geochim. cosmochim. Acta* **47**, 1783–1790 (1983).
20. Nittrouer, C. A., DeMaster, D. J. McKee, B. A., Cutshall, N. H. & Larsen, I. L. *Mar. Geol.* **54**, 201–221 (1984).
21. Bruland, K. W., Coale, K. H. & Mart, L. *Mar. Chem.* **17**, 285–300 (1985).
22. Martin, J. H., Knauer, G. A. & Broenkow, W. W. *Deep-Sea Res.* **32**, 1405–1427 (1985).

Basal metabolic rate and energetics of reproduction in therian mammals

Steven D. Thompson* & Martin E. Nicoll†

Departments of * Zoological Research and † Mammalogy, National Zoological Park, Smithsonian Institution, Washington, DC 20008, USA

Traditionally, the fact that reproduction in eutherian (=placental) mammals tends towards prolonged intrauterine development and short lactation has been interpreted as an evolutionary advance over the metatherian (=marsupial) short gestation and prolonged lactation[1]. However, it has recently been postulated that marsupial reproduction involves low initial energy investment and may be advantageous by minimizing energy loss if conditions necessitate early termination[2–5]. Moreover, because marsupials have basal metabolic rates (BMRs) 30% lower than those of most eutherians[6,7], it has been suggested that daily and total energy expenditures during reproduction may also be lower[8]. We have now tested the predictions that low BMR is maintained during reproduction and that initial investment is lower in marsupials. Using indirect calorimetry, we have made the first longitudinal measurements of energy expenditure during reproduction for a marsupial and for two eutherian species with low BMRs[9]. We find that initial investment is lowest in a eutherian and total energetic expenditures were greatest for the marsupial. We also find that, relative to BMR, all three species have increased mean maternal resting metabolic rates (RMRs) during both gestation and lactation; this is the first evidence that mammals with low BMRs can substantially elevate metabolism for prolonged periods during gestation and lactation.

We measured oxygen consumption ($\dot{V}O_2$) and body temperature (T_b) in five South American short-tailed opossums (*Monodelphis domestica*, Metatheria: Marsupialia: Didelphidae), three elephant shrews (*Elephantulus rufescens*,

Table 1 Comparison of incremental and absolute costs of reproduction among wild mammals

Species	Mass (g)	Litter size	BMR (% expected)	kcal per day	Gestation Duration	Gestation X-cost	Gestation kcal per day	Lactation Duration	Lactation X-cost	Lactation kcal per day	Total kcal total	Total Use per young	Increment kcal total	Increment Use per young	% Increase in mother's % Kleiber Gest	% Increase in mother's % Kleiber Lact.	Ref.
Order Marsupialia																	
Monodelphis domestica	82.0	8	64	6.8495	14	126	8.7	56	316	21.6	1,333	167	853	107	12.5	52 3	
Didelphis virginiana	2,240.0	7	76	97.4941	14	—	—	85	—	—	—	—	—	—	–	15 0	25
Order Macroscelidea																	
Elephantulus rufescens	84.1	1	82	8.9720	57	122	10.9	15	184	16.5	872	872	226	226	31.8	46 7	
Order Insectivora																	
Echinops telfairi	140.6	5	28	4.5043	60	183	8.2	23	539	24.3	1,054	211	681	136	43 9	132 3	
Suncus murinus	30.2	3	139	7.0550	30	—	—	18	248	17.5	—	—	—	—	0.0	0 0	26
Order Rodentia																	
Sigmodon hispidus	125.8	5	95	14.0593	26	154	21.6	12	296	41.7	1,084	217	560	112	0.0	0 0	13
Microtus arvalis	25.0	4	345	15.1968	18	118	17.9	16	255	38.7	941	235	419	105	-7.8	4.0	27
Neotoma floridana	237.0	3	146	34.7450	35	—	—	22	—	—	—	—	—	—	0.0	0.0	28
Reithrodontomys megalotis	7.7	3	127	2.3129	—	—	—	21	—	—	—	—	—	—	–	1.0	*

BMR = per cent of expected as calculated from Kleiber[9]. kcal per day = [resting oxygen consumption (ml h^{-1}) × 0.0048 kcal ml^{-1} oxygen × 24 h] + kcal stored as mass in young. X-cost = incremental cost over BMR, as a multiple of BMR, per day. Total incremental cost = duration × X-cost. Per cent increase in mother's % Kleiber = (mean % Kleiber)/(BMR % Kleiber).

* S.D.T., unpublished data.

Eutheria: Macroscelidea: Macroscelididae) and one tenrec (*Echinops telfairi*, Eutheria: Insectivora: Tenrecidae). Earliest marsupials are thought to have been reproductively similar to small modern didelphids[10] and tenrecs are among the most primitive of extant eutherians[11]. To this extent the comparison reflects the potential for energetic differences having been involved in the evolutionary divergence of the two groups. Respirometry allowed maternal metabolism to be separated from that of the offspring during lactation, avoided the inclusion of activity costs usually included in studies of caloric intake, and thus allowed us to distinguish among net investment (growth of young), the cost of allocating that investment (mother's respiration) and maintenance costs for the growing litter (litter's respiration). Specific basal (or resting) metabolism ($\dot{V}O_2$ g^{-1} h^{-1}) was determined within thermoneutrality for each female before reproduction (BMR), during gestation (RMR_g), during lactation (RMR_l) and after weaning (BMR).

During gestation, females were placed in a Perspex chamber and submerged in a circulating water bath for at least 2 h at a maximum frequency of once weekly; room air was metered through the chamber at 40–150 ml min^{-1}. During lactation, measurements were made first on the mother and young together, then the young were removed and the female was immediately measured alone. $\dot{V}O_2$ was determined using an open-circuit respirometry system with a Beckman G-2 oxygen analyser calibrated using nitrogen gas[12]. Animals were 6–12 h post-absorptive during all measurements and all measurements were made during the inactive phase of the day. We assumed a respiratory quotient of 0.8 in calculating $\dot{V}O_2$ (ref. 12). Because specific metabolism varies with body mass, we expressed the specific basal or resting metabolic rate as a proportion of that predicted by Kleiber[9] for a non-reproductive eutherian of the same body mass. This was intended only to simplify comparisons between individuals and species of different mass. Oxygen consumption was converted to kcal per day assuming 0.0048 kcal per cm^3 O_2 consumed. The energy content of the young was assumed to be 0.87 kcal per g wet body mass[13].

RMR increased throughout reproduction in all three species (Fig. 1). RMR_l of female opossums plus offspring peaked immediately before weaning (50–56 days; M. Roberts, unpublished data) at 189% of Kleiber's predicted rate, when mean maternal T_b increased from 35 to >36 °C. Between 35 days post-partum and weaning, female RMR_l of *Monodelphis* was within 15% of the predicted value, peaking during the last week of lactation, at 106% of Kleiber, before declining to near pre-reproductive BMR. Mean RMR_l of female *E. rufescens* was

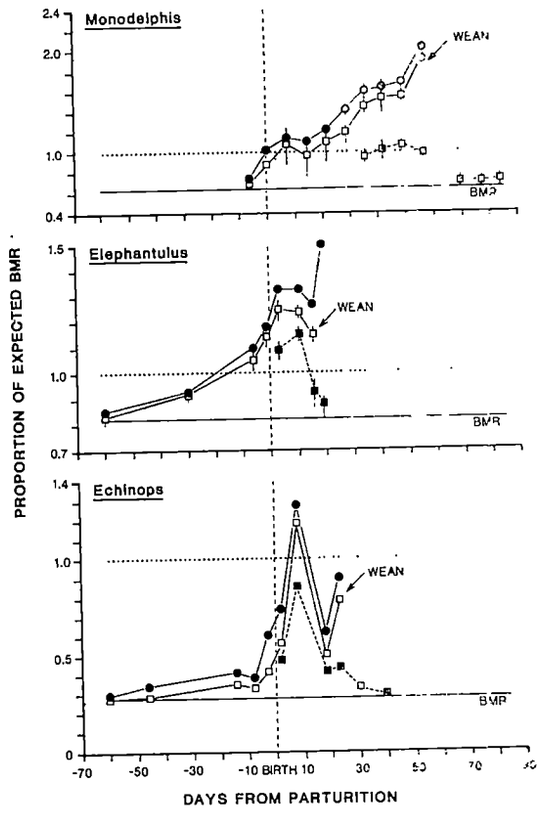


Fig. 1 Mass-independent rates of energy expenditure, expressed as a proportion of that expected from total body mass[9] of mother alone (solid squares), mother with young (open squares), and mother with young with rate of energy storage as growth of litter added to oxygen consumption (solid circles); symbols before birth reflect conception to birth, those after birth reflect birth to weaning. Dotted horizontal line identifies Kleiber's[9] predicted eutherian BMR. Solid horizontal line identifies mean BMR of non-reproductive females. Vertical bars denote ± 1 s.d. of the mean. Values calculated from $\dot{V}O_2$ h^{-1} times 0.0048 kcal per ml O_2 and assuming 0.87 kcal per g wet mass of growing offspring[13]. Values are per 24-h day.

Table 2 Proportion of incremental energy and total incremental energy expended during reproduction as a function of relative and absolute time from conception

	Proportion of CW time					
	0.25	0.50	0.75	0.85	0.90	0.95
Elephantulus						
Days from conception	18	35	53	60	63	67
Proportion of energy	0.029	0.141	0.435	0.638	0.743	0.889
Incremental kcal	7	31	97	145	168	201
Cumulative effort	0.02	0.09	0.202	0.262	0.29	0.327
Echinops						
Days from conception	21	42	62	71	75	79
Proportion of energy	0.044	0.155	0.397	0.712	0.822	0.910
Incremental kcal	30	106	270	484	560	619
Cumulative effort	0.322	0.558	0.953	1.494	1.635	1.719
Monodelphis						
Days from conception	17	35	52	59	62	66
Proportion of energy	0.046	0.166	0.445	0.626	0.730	0.852
Incremental kcal	38	142	381	536	625	729
Cumulative effort	0.339	0.608	1.07	1.321	1.456	1.604

CW, conception to weaning time. Incremental kcal = (RMR kcal per day of mother and young plus kcal stored as growth) − (BMR kcal per day of non-reproductive female). Cumulative effort = (incremental kcal per day/BMR of non-reproductive female) days from conception.

higher than predicted while that of *E. telfairi* was lower than predicted. These increases in specific metabolism were not due to separation anxiety; measurements made on the litters alone added to those for the mother alone were ±6.5% of values for mother and young measured together. Female plus offspring of both eutherians showed a similar increase in RMR over non-reproductive BMR, but peak RMR_l was lower than that of the opossum: 125% of Kleiber's predicted in *E. rufescens* and 118% in *E. telfairi*. Lowest tenrec RMR_l corresponded with maternal hypothermia, paralleling thermoregulatory patterns in resting non-reproductive tenrecs (S.D.T. and M.E.N., unpublished data) and involving a 3–5 °C reduction in T_b from 35–36 °C.

The proportion of total energy expended from conception to weaning, including that stored as growth of the young, which was allocated to pregnancy, reflected relative length of gestation and degree of neonatal development: 0.71 in the precocial *E. rufescens*, compared with 0.47 in *E. telfairi*, and 0.09 in *M. domestica*. Mean RMR_g of *M. domestica* was not significantly greater than the non-reproductive BMR in the same individuals ($U = 40$, d.f. = 16, $P > 0.05$), although $\dot{V}O_2$ rose as female mass increased (~5 g) during pregnancy (Fig. 1).

Comparison of *E. rufescens* and *M. domestica*, with their similar adult body mass and conception to weaning time, revealed that total energy expenditure (kcal) and incremental energy expenditures (exceeding that required for BMR of a non-reproductive female of the same mass) during reproduction were greater in the marsupial. Higher incremental costs in *M. domestica* were related to greater reproductive effort and a comparatively high RMR_l of the female plus offspring during late lactation. Although almost twice as large in size, total energy expenditure during reproduction by *E. telfairi* was lower than in *Monodelphis* (Table 1), reflecting maternal torpor and a slow increase in RMR from an extremely low BMR. Similarly, when *E. telfairi* is compared with a precocial rodent, *Sigmodon hispidus*, which has the same litter size and similar body mass[13], the difference in total energy expenditure during reproduction is surprisingly small given the divergence in duration of maternal care and BMR (Table 1). The similarity stems in part from the compensatory increase in tenrec maternal RMR towards Kleiber's predicted value, which the BMR of *S. hispidus* approximates with no increase in maternal RMR during reproduction[13].

Initial energy investment in reproduction, as defined by the incremental energy expended during the first 25% of parental care, was lower in the two eutherians than in *M. domestica*. Through the first 75% of the duration of parental care, all three species expended about 40–45% of their total energy allocation to reproduction and all deferred over 29% of their energy expenditure until the last 15% of maternal care (Table 2). Despite great differences in energetic effort, all species showed a gradual increase in energy expenditure regardless of allocation of time or energy to either gestation or lactation (Table 2).

Our data reveal no advantages to either marsupial or eutherian reproduction with respect to total, daily or temporal patterning of energy expenditure. Comparison of longitudinal energy expenditure during reproduction suggests a continuum based not on phylogeny but on relative BMR. Thus, our three low BMR species, of diverse phylogeny, show a large increase in mean maternal RMR during reproduction whereas for species with a BMR near that predicted, such as wild eutherians (Table 1), laboratory mice[14] and rats[15,16], mean maternal RMR is virtually the same as BMR. Our calculations from limited data for another marsupial, the North American opossum (*Didelphis virginiana*; Table 1), also show RMR_l values greater than BMR. Because species with high BMRs show little increase in reproductive RMR, we suggest that high RMRs are either advantageous or necessary for mammalian reproduction and that at least some mammals with low BMRs can compensate during reproduction. The increased mean maternal RMRs of our study are distinct from those reported for livestock[15–17], chiefly because most livestock have not been measured when post-absorptive; thus, these elevated maternal RMRs reflect the heat of feeding[17] associated with increased ingestion to support larger body mass during reproduction. Data from post-absorptive livestock agree with those in Table 1: fasted, lactating cows (BMR 87–120% predicted) have RMR_ls equal to BMR and fasted, lactating goats (with low BMRs, 70–75% predicted) have RMR_ls 12–15% above BMR[16]. Humans have BMRs near the predicted value and, whether fasted or fed, show little or no difference between average reproductive and non-reproductive rates of metabolism[15,16,18]. Interspecific variation in both BMR and the ability to elevate RMR during reproduction could be responsible for the wide variation in pre- and postnatal growth rates, and the interaction of reproductive RMR with duration of gestation and lactation could be associated with 'intermediates' along the continuum from altricial to precocial neonates[19,20]. If the latter proves correct, developmental stage (or relative mass) at birth will be more accurately predicted by the interaction of rate of metabolism and duration of gestation. Our study also supports recent suggestions that the predicted BMR reflects an advantageous or essential energetic regime for therian reproduction[21–24], from which deviations represent adaptation to small body size[24] or food habits[21].

R. D. Martin, P. Racey, M. Roberts and O. Oftedal made valuable comments on the manuscript. Dr B. K. McNab loaned the necessary equipment and the NZP's Departments of Zoological Research and Mammalogy provided financial support. DZR animal keepers and interns provided assistance in breeding and maintaining animals.

Received 25 November 1985; accepted 2 April 1986.

1. Lillegraven, J. A. *Evolution* **29**, 707–722 (1975).
2. Parker, P. A. in *The Biology of Marsupials* (eds Stonehouse, B. & Gilmore, D.) 273–286 (University Park Press, Baltimore, 1977).
3. Low, B. S. *Am. Nat.* **112**, 197–213 (1978).
4. Kirsch, J. A. *Am. Scient.* **65**, 276–288 (1977).
5. Kirsch, J. A. *Evolution* **31**, 898–900 (1977).
6. MacMillen, R. E. & Nelson, J. *Am. J. Physiol.* **217**, 1246–1251 (1969).
7. Dawson, T. J. & Hulbert, A. *Am. J. Physiol.* **218**, 1233–1238 (1970).
8. Morton, S. R., Recher, H., Thompson, S. D. & Braithwaite, R. *Am. Nat.* **119**, 120–128 (1982).
9. Kleiber, M. *The Fire of Life* (Wiley, New York, 1961).
10. Lillegraven, J. A. in *Mesozoic Mammals: the First Two-thirds of Mammalian History* (eds Lillegraven, J., Kielan-Jawarowska, S. & Clemens, W.) 259–276 (University of California Press, Berkeley, 1979).
11. Eisenberg, J. F. *The Mammalian Radiations* (University of Chicago Press, 1981).
12. Fedak, M., Rome, L. & Seehrman, H. J. *Appl. Physiol.* **51**, 772–777 (1981).
13. Randolph, P. A., Randolph, J. C., Mattingly, K. & Foster, M. M. *Ecology* **58**, 31–45 (1977).
14. Studier, E. S. *Comp. Biochem. Physiol.* **64A**, 473–481 (1979).
15. Brody, S., Riggs, J., Kaufman, K. & Herring, V. *Res. Bull. Mo. agric. Exp. Stn* **281**, 5–42 (1938).

16. Brody, S. *Bioenergetics and Growth* (Hafner, New York, 1964).
17. Oddy, V. H., Goosen, J. M. & Annison, E. F. *Aust. J. biol. Sci.* **37**, 375-388 (1984).
18. Shutz, Y., Lechtig, A. & Bradfield, R. B. *Am. J. clin. Nutr.* **33**, 892-902 (1980).
19. Martin, R. D. & MacLarnon, A. M. *Nature* **313**, 220-223 (1985).
20. Martin, R. D. *Symp. Zool. Soc. Lond.* **51**, 87-117 (1984).
21. McNab, B. K. *Am. Nat.* **116**, 106-124 (1980).
22. Hennemann, W. *Oecologia* **56**, 104-108 (1983).
23. Hennemann, W. *Oikos* **43**, 363-368 (1984).
24. McNab, B. K. *J. zool. Res.* **199**, 1-29 (1983).
25. Fleming, M., Harder, J. D. & Wukie, J. J. *Comp. Biochem. Physiol.* **70B**, 645-648 (1981).
26. Dryden, G., Gebczynski, M. & Douglas, E. L. *Acta theriol.* **19**, 453-461 (1974).
27. Trojan, P. & Wojciechowska, B. *Ekol. Pol.* **15**, 811-817 (1967).
28. McClure, P. A. & Randolph, J. C. *Ecol. Monogr.* **50**, 199-217 (1980).

Enhanced detection in the aperture of focal attention during simple discrimination tasks

Dov Sagi

Department of Applied Mathematics, Weizmann Institute of Science, Rehovot 76100, Israel

Bela Julesz

AT&T Bell Laboratories, Murray Hill, New Jersey 07974, USA

There is increasing evidence that it is possible to shift an aperture of focal attention to a position in visual space independent of fixation and that this can be done much faster than the eyes are able to move[1-4]. Recently, we showed[4] that such serial scrutiny by the aperture of focal attention is required before an observer is able to tell what a target is (for example, to know whether the orientation of a line segment is horizontal or vertical). Here we considered whether attention directed towards a specific position in the visual field for an orientation discrimination task improves performance on a simple detection task in the area to which attention is directed. We found that a small test flash could be detected when it was positioned near a peripheral line target presented briefly, if the orientation of the target had to be identified. The test flash could not be detected when presented at some distance from the same target or when another target had to be identified. This enhancement implies that even simple identification tasks such as orientation discrimination are not performed passively by the visual system.

Against a dark field, we presented two bright targets each extending 0.7 degrees of arc in length (horizontal or vertical line segments; or the letter L or T), one in the position where the observer was fixating, the other at 4° eccentricity from the fixation marker, but in any random direction from this marker. Observers were asked to identify only one of the targets (either peripheral or central) in a given block of trials, and were told that the peripheral target would always be at the same eccentricity but in any random direction. Presentation time was short (10 ms) to avoid a second fixation on the target by eye movement, and a mask was applied at a specific time, termed stimulus onset asynchrony (SOA), after target onset, in order to limit processing time (see Fig. 1*a*). Simultaneously with this target identification task, we also presented a small test flash with a 4 arc min diameter lasting 10 ms, at various positions across the visual field, and asked observers to report the presence or absence of the test flash, by pressing one of four keys: two for presence or absence of the test flash when target A was identified and another when target B was identified. Detection errors were signalled by ringing of a bell on the computer that ran the experiments. The test flash and the targets were masked at different SOAs so that performance on the two tasks could be controlled independently. The test flash appeared on 66% of the trials, and was presented at positions along two cardinal directions from the peripheral target: on the perimeter of an imaginary circle of the same eccentricity as the peripheral target or on a line running from the central target to the peripheral target and beyond (see Fig. 1*b*). In each block of 50 trials the test flash could appear in any of the four directions and at any of three distances from the discrimination target. As observers had to identify only one of the targets in a given block of trials, we could compare detection rates for the test flash when the peripheral or the central target was identified, thus isolating changes in detection rate caused by the identification processes.

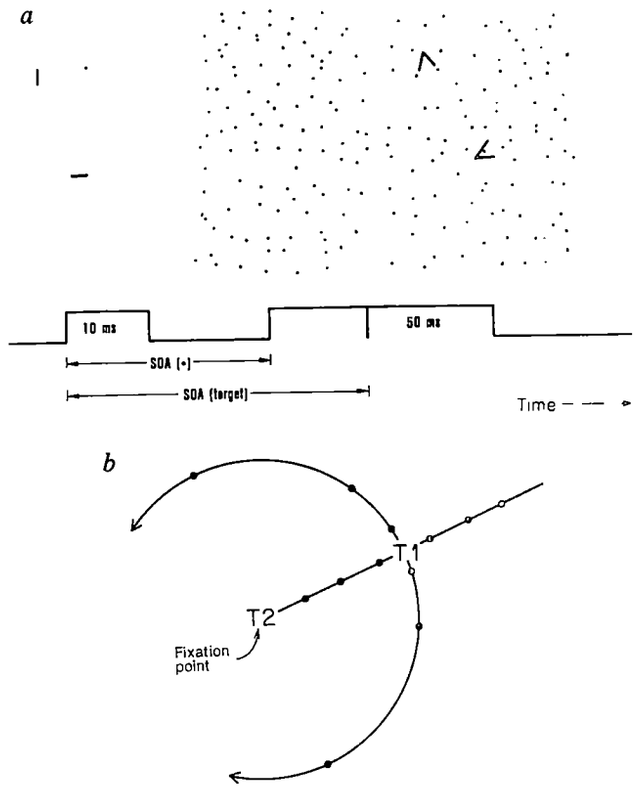


Fig. 1 *a*, The stimulus used in our experiments. The observers were presented first with a pair of targets, one at the fixation point (here a horizontal line) and another at 4° eccentricity. A small dot, the test flash, shown here near the vertical peripheral target, was presented on 66% of the trials. This pattern was presented for 10 ms then masked by random dots after a certain time, SOA(·), and after a longer time, SOA(target), a pair of randomly oriented 'V' symbols were presented at the locations of the targets for 50 ms. A fixation cross was presented at the position of the central target before each trial began, but was removed 50-100 ms (randomized between trials) before the stimulus onset. *b*, Possible locations of the test flash relative to the discrimination target T1. Fixation point is on T2, where the central target was presented. T1 represents the peripheral target; solid lines represent the two cardinal directions from T1 that were used for presenting the test flash. The test flash could be placed in one of 12 positions (indicated by the solid circles). These positions are relative to T1; when T1 appeared in another direction all the possible positions would rotate in this direction. We used the same configuration for experiments involving central and peripheral target discrimination.

The results of experiments in which observers had to identify the peripheral target are shown in Fig. 2*a*. The results are presented as the difference between the frequency of correct detection when the test flash was presented, P(detect), and the false alarm rate, P(FA), representing the frequency of observers falsely reporting the presence of the test flash. As the distances between the test flash and the discrimination target were varied in each block of trials, the same false alarm rate was measured for all distances, so an increase in $[P(\text{detect}) - P(\text{FA})]$ reflects

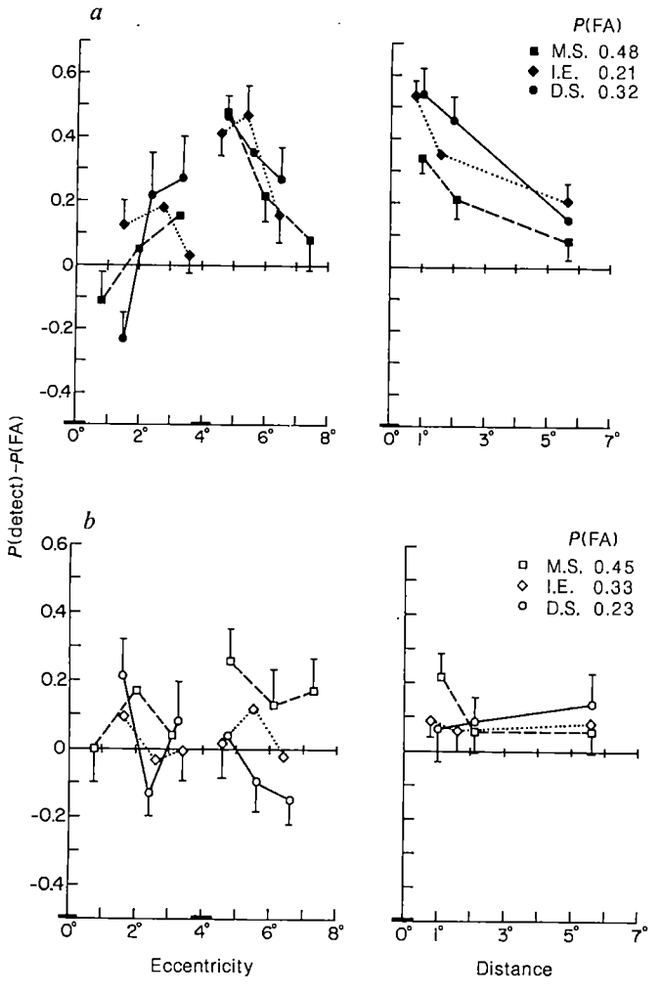


Fig. 2 *a*, Data from experiments in which observers had to identify the peripheral target. Plot on the left shows the dependence of $P(\text{detect}) - P(\text{FA})$ on the radial distance of the test flash from the fixation point, the peripheral target here being at 4° eccentricity. Plot on the right shows the dependence of $P(\text{detect}) - P(\text{FA})$ on the distance from the peripheral target along an equi-eccentricity circle; data for the clockwise and anticlockwise directions were combined. Data shown are for three observers: M.S. and D.S., who performed an orientation discrimination task with SOA(target) = 60 ms for M.S. and 70 ms for D.S. Observer I.E. discriminated between T and L with SOA(target) = 120 ms. For all observers SOA(·) was 60 ms. *b*, Same as *a*, but discrimination was performed on the central target. Target discrimination rates were 0.90 ± 0.01, 0.90 ± 0.02 and 0.89 ± 0.02 in *a* and 0.86 ± 0.02, 0.84 ± 0.02 and 0.83 ± 0.02 in *b* for observers I.E., D.S. and M.S., respectively.

an increase in correct detection for each observer. When examining detection rates for the test flash at different positions in the radial direction, at different eccentricities, a clear enhancement was seen at about 4° eccentricity, where the discrimination target was presented (Fig. 2*a*, left). The same increase in detection rate was seen along the constant eccentricity direction in the vicinity of the discrimination target (Fig. 2*a*, right). To prevent contamination, the test flash was never presented closer than 0.6° from the target centre. To ensure that the increase in detection rate did not originate from trials in which incorrect discriminations were made, we kept the error rate on the discrimination task low by adjusting the masking delay (SOA) for each observer, so that the performance on the discrimination task was ~90% correct (see Fig. 2 legend) for all observers (although one of us served as observer, the other two observers were unaware of the purpose of this study). Surprisingly, the detection rate was lower at positions between the central target (fixation point) and the

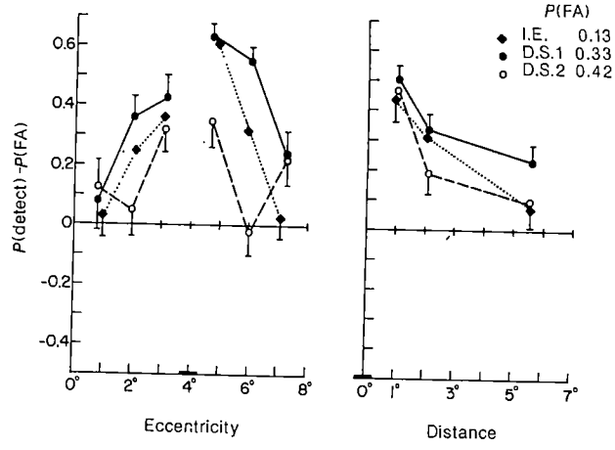


Fig. 3 The same as Fig. 2*a*, but without presentation of the central target. Note that detection at locations between the fixation point and the peripheral target is improved. Data shown are for observers I.E. (T/L discrimination) and D.S. (expt 1, T/L discrimination; expt 2, vertical/horizontal discrimination).

peripheral target than at more peripheral positions. Experiments in which the central target was absent yielded a more symmetrical enhancement around the peripheral target (see Fig. 3). Thus the area of highest detection rate is not around the fixation point, but is shifted to the location of the target being identified; this is demonstrated in a plot of $[P(\text{detect}) - P(\text{FA})]$ isocontours (Fig. 4). The two regions of enhancement were reconstructed from the data of two experiments, a new one with the peripheral target at 2° eccentricity and the one with the peripheral target at 4°, as in Figs 2, 3. The size of the enhancement area is larger at the larger eccentricity, having a diameter about twice that of the enhancement area at 2° eccentricity.

Next we attempted to confirm that this enhancement originated from the discrimination task that our observers were performing, rather than from the presence of the target itself. The presence of the target might cause luminance interaction between itself and the test flash or might bias the observers to detect the test flash when it is located near the target. We performed additional experiments using the same stimuli, but

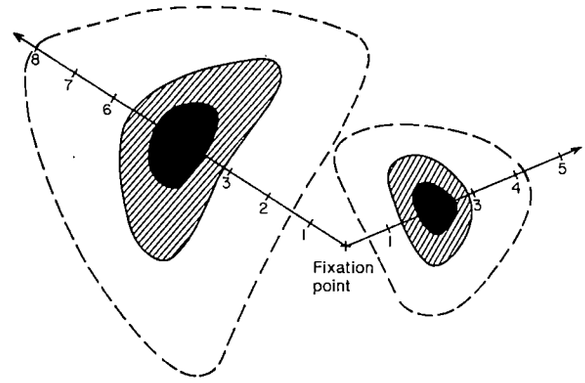


Fig. 4 Test flash detection isocontours plotted at two different eccentricities for observer D.S., in experiments such as those of Fig. 2*a*. The broken lines represent the borders of the enhancement areas where correct detection of the test flash is about the same as without enhancement (Fig. 2*b*), approaching the 'false alarm' rate; within the shaded area the detection rate is more than twice the false alarm rate, and in the solid area about three times the false alarm rate. Note that the linear size of the enhancement area scales linearly with eccentricity, being about twice the size at 4° than at 2°.

asked the observers to perform discrimination on the central target; the results of these experiments are shown in Fig. 2*b*. The enhancement around the peripheral target disappeared, and performance everywhere was close to chance level [P(detect) ~ P(FA)], with about the same false alarm rates as in the previous experiments). There was also no clear improvement at positions close to the central target. This lack of enhancement might be a result of the coarse sampling used, as the size of the enhancement area around the centre of gaze might be smaller than that at the peripheral positions. This decrease in size would be consistent with that seen with decreasing eccentricity (see Fig. 4).

When attention is focused on the discrimination task, does it cause a change of sensitivity or a change of criterion for detection of the test flash? The psychophysical method we used to investigate this question does not allow a direct answer as it was designed to maximize test-flash position uncertainty and to force attention shifts to the discrimination target. To obtain an answer, we would have to present the test flash at known locations on each block of trials, but that might have allowed the observers to shift their attention to the expected location of the test flash, a strategy we wanted to avoid. As a result, the false alarm responses from all locations were combined, thus it is unknown whether there was an increase in false alarm rate in the vicinity of the discrimination target resulting from the discrimination process. However, the false alarm rates measured using the peripheral target were not significantly larger than those for the central target (FA differences of 0.03 ± 0.06, -0.12 ± 0.06, 0.09 ± 0.08 for the three observers; ±s.e.m.).

We conclude, therefore, that visual discrimination involves a process that increases the probability of detecting a nearby test flash. This increase is not due to the presence of the target to be identified nor is it due to any expectation that the test flash will be found at a particular position, cued by the discrimination target, but results from discriminating the target. At present we cannot decide whether the observed visual enhancement is caused by some sensitivity or criterion change, but we find that this enhancement is involved in a task as simple as discriminating between vertical and horizontal lines. This result indicates that even a simple discrimination task cannot be performed passively by the visual discrimination system. The enhancement might be a property of the serial attentive process that is required for discrimination of orientation[4]. According to our finding, the size of the area processed by the attentive system is scaled with eccentricity, having an average diameter of ~3° at 4° eccentricity, and ~1.5° at 2° eccentricity. Interestingly, this area is the same for the two tasks that we used—orientation discrimination (vertical versus horizontal) and positional relationship discrimination (T versus L). It is possible that the area of visual enhancement that we have plotted here is the 'searchlight' of attention.

Received 6 December 1985; accepted 1 April 1986.

1. Posner, M. I. *Q. J. exp. Psychol.* **32**, 3-25 (1980).
2. Treisman, A. & Gelade, G. *Cognitive Psychol.* **12**, 97-136 (1980).
3. Bergen, J. R. & Julesz, B. *Nature* **303**, 696-698 (1983).
4. Sagi, D. & Julesz, B. *Science* **228**, 1217-1219 (1985).

Phorbol esters block a voltage-sensitive chloride current in hippocampal pyramidal cells

Daniel V. Madison*, Robert C. Malenka & Roger A. Nicoll†

Departments of Pharmacology and Physiology, University of California, San Francisco, California 94143, USA

The importance of second-messenger systems in controlling the excitability of neurones and other cells, through modulation of voltage- and calcium-dependent ionic conductances, has become increasingly clear. Cyclic AMP[1-3], acting via protein kinase A[4-6], has been identified as the second messenger for several neurotransmitters, and recent studies have suggested that activation of protein kinase C may have similar modulatory actions on neurones[7-11]. Calcium and potassium currents have so far been shown to be the major ionic conductances modified by kinase activation[4-11]. We now report that hippocampal pyramidal cells contain a previously undescribed voltage-dependent chloride current which is active at resting potential and is turned off either by membrane depolarization or by activation of protein kinase C by phorbol esters. We propose that this current may reside predominantly in the cell's dendritic membrane and thereby may regulate dendritic excitability.

In 53 out of 55 rat hippocampal pyramidal cells in which K^+ currents were blocked (see Fig. 1 legend), voltage clamp recording with Cl^--containing microelectrodes revealed slow inward current relaxations, in response to hyperpolarizing steps from depolarized holding potentials. These current relaxations appeared to be caused by the turning on of an inward current, as the amplitude of the instantaneous current jump at the beginning of a hyperpolarizing step was smaller than that at the end, suggesting an increase in membrane conductance during the step (Fig. 1*a*). In addition, the amplitude of the instantaneous currents produced by short-duration hyperpolarizing voltage steps increased during the inward current relaxation produced by a long hyperpolarizing voltage step, and returned slowly to baseline amplitude when the membrane potential was stepped back to the holding potential (V_H) (Fig. 1*b*). This is in contrast to the M-current (I_M) recorded in conditions where K^+ currents are present, which turns off with similar voltage steps[12]. Also in contrast to I_M, this current was insensitive to muscarinic receptor activation. This slow inward current was voltage-sensitive over a wide range of membrane potentials (Fig. 1*c*). As determined by steady-state conductance measurements, the current was completely inactive at membrane potentials postive to approximately −10 mV, was largely active at the resting potential (−55 to −70 mV in these cells), and was fully activated at potentials negative to −90 mV (Fig. 1*c*). These voltage values could be overestimates of the actual voltage-sensitive range of the current if it was generated at a site electrotonically remote from the recording electrode in the soma (see below). Relaxations caused by this current could also be evoked by holding the cell at relatively hyperpolarized levels and turning it off with depolarizing commands (see Figs 1*e*, 2*b*).

We suspected that the ionic carrier of this current was chloride because currents carried by K^+, Ca^{2+} and Na^+ should be effectively blocked in the medium used in our experiments (see Fig. 1 legend). Indeed, when cells were impaled with electrodes containing the anion methyl sulphate ($MeSO_4^-$), hyperpolarizing steps produced an outward current (Fig. 1*d*(ii), $n = 11$), rather than an inward current as invariably seen in cells recorded with Cl^--filled electrodes (Fig. 1*d*(i), $n = 53$). The reversal potential of this current was determined with both Cl^- and $MeSO_4^-$-containing microelectrodes. With the former, when cells were held at hyperpolarized levels and depolarizing steps of increasing size were applied, a turning off of the current was observed, resulting in outward current relaxations which reversed to inward relaxations at a membrane potential of about +15 mV in the cell illustrated (Fig. 1*e*(i)). The average reversal potential of this current with Cl^- in the recording electrode was

* Present address: Department of Physiology, Yale University School of Medicine, New Haven, Connecticut 06510, USA.
† To whom reprint requests should be addressed.

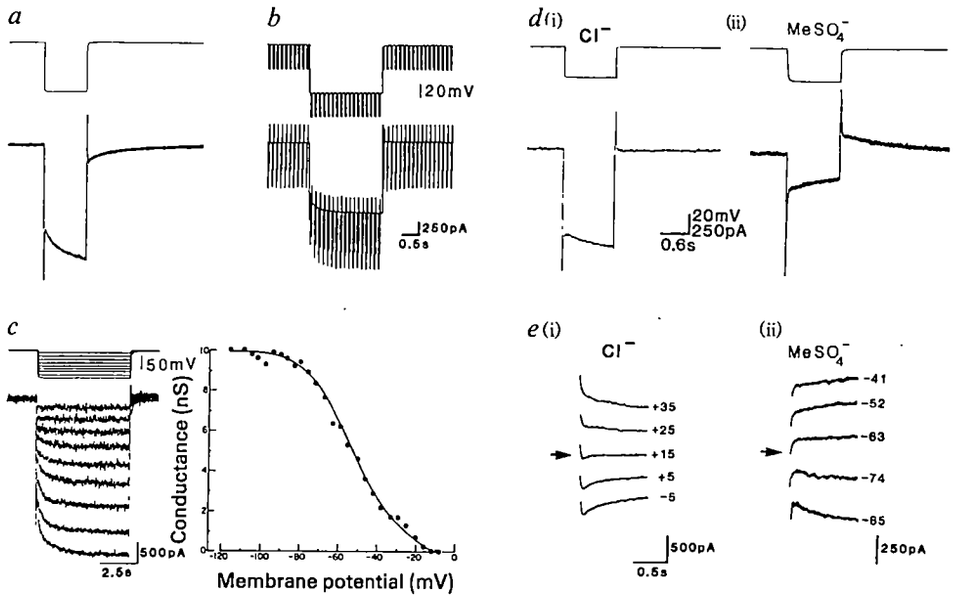


Fig. 1 A voltage-dependent chloride current ($I_{Cl(V)}$) in hippocampal pyramidal neurones. ***a***, A voltage- and time-dependent inward relaxation of membrane current in response to a 1-s hyperpolarizing voltage command from a holding potential (V_H) of −10 mV. An inward tail current follows the return to V_H. This cell was recorded with a CsCl (3 M)-filled microelectrode. ***b***, Short-duration hyperpolarizing pulses superimposed on a long-duration hyperpolarizing voltage step show an increase in membrane conductance during the developing inward current relaxation, and a slow return to resting conductance following return to V_H, although little tail current is visible due to the proximity of V_H to E_{Cl}. CsCl-filled microelectrode, $V_H = +5$ mV. ***c***, Membrane currents resulting from a family of long-duration hyperpolarizing commands from a V_H of −4 mV. A plot of the steady-state membrane conductance during the illustrated voltage commands (value plotted is the steady-state conductance during hyperpolarizing commands minus the steady-state conductance at V_H). CsCl-filled microelectrode. ***d*(i)**, Hyperpolarizing 1-s command from a holding potential of −20 mV in a cell impaled with a KCl-filled microelectrode produces an inward current. ***d*(ii)**, A similar voltage step in a cell impaled with a $KMeSO_4$-filled microelectrode produces an outward current; $V_H = -20$ mV. ***e*(i)**, Tracings of current relaxations produced by depolarizing voltage commands from a holding potential of −50 mV to the voltage indicated at the right of each trace (in mV) in a cell impaled with a KCl-filled microelectrode. ***e*(ii)**, Tracings of current relaxations produced by hyperpolarizing steps from a holding potential of −21 mV to the voltage (in mV) indicated at the right of each trace in a cell impaled with a $KMeSO_4$-filled microelectrode. The arrows indicate the approximate value of the reversal potential. Calibrations in *a* are the same as in *d*. Records in *a*, *b* and *d* were photographed from chart records; those in *c* were digitized on a Nicolet 4094 digital oscilloscope and plotted on a Hewlett-Packard 7470A digital plotter; those in *e* were traced by hand from chart records.

Methods. Rat hippocampal slices were prepared and maintained as described previously[19]. Intracellular recordings were made from the cell bodies of pyramidal neurones. Microelectrodes were made from thin-wall glass capillaries (Omega Dot; 1.2 mm o.d., 0.9 mm i.d.; Glass Company of America) and contained 3 M CsCl, 3 M KCl or 2 M potassium methyl sulphate ($KMeSO_4$). Membrane currents were recorded with an Axoclamp-2 single-electrode voltage clamp (Axon Instruments, Burlingame, California). Electrodes were coated to within ~50 μm of the tip with M-coat D (Measurements Group Inc., Raleigh, North Carolina) and the tips were dipped in mineral oil just before use to electrode capacitance. The voltage-clamp head-stage output was monitored continuously and the switching frequency adjusted to the maximum rate, which still allowed the electrode voltage to settle completely between oscillations, usually between 3 and 7 kHz. The superfusing medium used in most experiments was designed to block K^+, Ca^{2+} and Na^+ currents and consisted of (mM): NaCl, 70; KCl, 2.5; $MgSO_4$, 16; $NaHCO_3$, 26.2; glucose, 11; TEA as chloride, 30; CsCl, 10; and tetrodotoxin (TTX), 0.5 μM. Our standard medium consisted of (mM): NaCl, 119; KCl, 2.5; $CaCl_2$, 2.5; $MgSO_4$, 1.3; NaH_2PO_4, 1; $NaHCO_3$, 26.2; glucose, 11. Phorbol ester solutions were prepared and bath-applied as described previously[8].

+9.5 ± 6.6 mV (mean ± s.d., $n = 10$), which is in the range expected for Cl^--mediated events in Cl^--loaded pyramidal cells[13]. With $MeSO_4^-$ in the recording electrode, the outward current produced by hyperpolarizing steps reversed to an inward current at about −70 mV in the cell illustrated (Fig. 1*e*(ii)), and the average reversal potential was −71 ± 5.2 mV ($n = 8$). The large difference between the reversal potentials in cells recorded with Cl^-- and $MeSO_4^-$-containing electrodes indicates that Cl^- ions are the primary charge carrier for this current.

The evidence presented in Fig. 1 indicates that pyramidal cell membranes contain a voltage-sensitive Cl^- current that is turned off by depolarization. This current, which we will refer to as $I_{Cl(V)}$, resembles in many respects Cl^- currents described in peripheral and invertebrate systems[14–17]. However, $I_{Cl(V)}$ differs from a similar current found in *Aplysia* neurones[15,16] in that it does not require intracellular Cl^- loading for its detection. Like the similar voltage-sensitive Cl^- current found in rat superior cervical ganglion cells[17], $I_{Cl(V)}$ is blocked by cadmium (100 μM, $n = 3$), although it is clearly not dependent on Ca^{2+} influx because it is unaffected by medium containing 16 mM Mg^{2+} and no added Ca^{2+} (see Fig. 1).

The application of the phorbol esters 4β-phorbol-12,13-diacetate (PDAc) or 4β-phorbol-12,13-dibutyrate (PDBu), known to activate protein kinase C[18], caused a near-total abolition of $I_{Cl(V)}$ at all membrane potentials examined in all 11 cells tested (Fig. 2*a*). The blockade occurred regardless of the intracellular anionic composition, as the current relaxations seen with Cl^-- ($n = 7$; Fig. 2*b*(i)) or $MeSO_4^-$-filled microelectrodes ($n = 4$; Fig. 2*b*(ii)) were abolished by phorbol esters. When cells were held at −50 mV, a potential at which $I_{Cl(V)}$ is tonically active (see Fig. 1*c*), the application of phorbol esters to the bathing medium caused opposite shifts in the standing current depending on the anion contained in the microelectrode. When recording with Cl^--containing microelectrodes, phorbol esters caused a marked outward shift in standing membrane current which was associated with a decrease in membrane conductance (Fig. 2*c*(i)), whereas recording with a $MeSO_4^-$-containing electrode not only reversed the direction of the $I_{Cl(V)}$ relaxations (Fig. 2*b*(ii)), but also reversed the direction of the shift in standing current when phorbol ester was applied (Fig. 2*c*(ii)). This is to be expected because when the microelectrode contains the impermeant $MeSO_4^-$, the Cl^- current should be in the outward direction rather than inward as it was when Cl^- was in the electrode. The small size of the inward shift with $MeSO_4^-$ is due to the proximity of the holding potential to the reversal potential of $I_{Cl(V)}$. An analogue of phorbol, 4α-phorbol-12,13-didecanoate (10 μM), which has been shown in other systems not to activate protein kinase C[18], had no effect on $I_{Cl(V)}$ ($n = 5$), suggesting that the blockade of $I_{Cl(V)}$ by PDBu and PDAc results from the activation of protein kinase C. The effect of phorbol esters on $I_{Cl(V)}$ is not mediated synaptically, as these effects

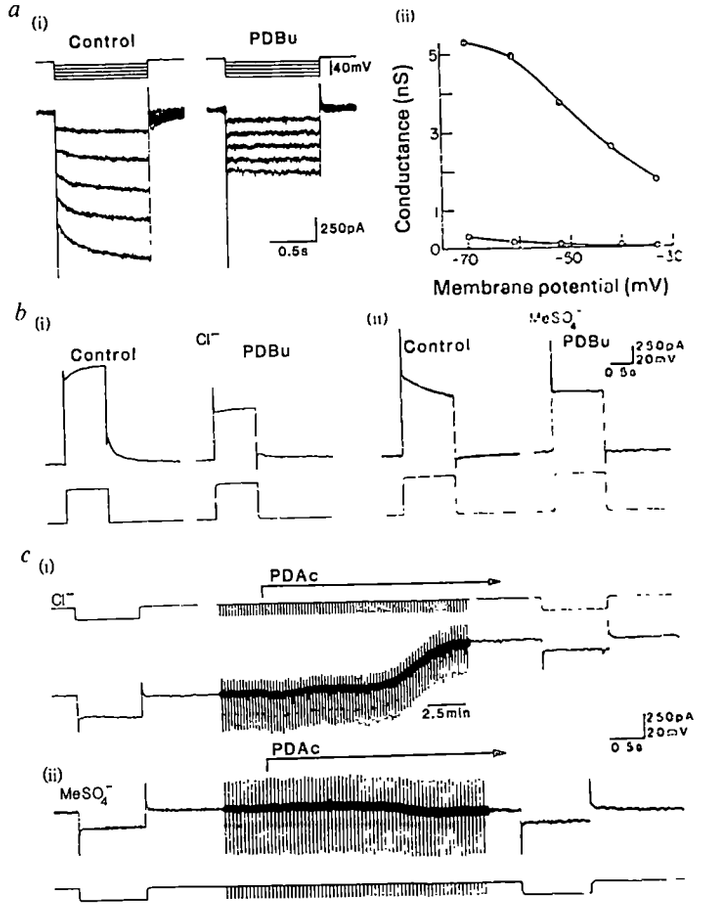


Fig. 2 $I_{Cl(V)}$ is blocked by phorbol esters. ***a*(i),** A family of currents resulting from hyperpolarizing voltage commands from a V_H of −35 mV in a control and 20 min after application of 10 μM 4β-phorbol-12,13-dibutyrate (PDBu). The substantial decrease in resting conductance caused by PDBu was presumably due to the fact that the holding potential of −35 mV was well within the range of $I_{Cl(V)}$ activation (see Fig. 1*c*); CsCl-filled microelectrode. ***a*(ii),** A plot of steady-state membrane conductance against membrane potential corresponding to the traces in *a*(i) (as in Fig. 1*c*) in control medium (closed circles) and in PDBu-containing medium (open circles). ***b*,** Depolarizing steps, which turn off $I_{Cl(V)}$, produce outward current relaxations and an outward tail current in cells impaled with CsCl-filled microelectrodes (i) and inward relaxations and tail currents in cells impaled with $KMeSO_4$-filled microelectrodes (ii) (V_H in both cases −50 mV). These current relaxations and tail currents were abolished by 10 μM PDBu regardless of the recording anion used. ***c*(i),** Effects of 4β-phorbol-12,13-diacetate (PDAc) (10 μM) on the resting membrane conductance and current at a holding potential of −50 mV in a cell impaled with a KCl-filled microelectrode. In this condition, PDAc caused an outward shift in resting membrane current and a decrease in membrane conductance, as measured by the instantaneous current produced by 10-mV hyperpolarizing steps. ***c*(ii),** Same as *c*(i) except in a cell impaled with a $KMeSO_4$-filled microelectrode. In this case PDAc (10 μM) caused an inward shift in resting current and a decrease in membrane conductance. The bathing medium for all experiments was the same as for Fig. 1. Records in *a* were digitized on a Nicolet 4094 oscilloscope; *b* and *c* were photographed from chart records.

occur in medium containing no added Ca^{2+} and high (16 mM) Mg^{2+}.

Although we found no direct evidence for the membrane localization of this current, we were unable to detect $I_{Cl(V)}$ in our somatic voltage-clamp recordings in the absence of K^+-channel blockade. One of several explanations might account for this finding. First, the use of intracellular Cs^+ ions and/or extracellular tetraethylammonium (TEA) or Cs^+ could themselves enhance the size of this current. This seems unlikely as $I_{Cl(V)}$ could be seen clearly after blockade of the M-current and Ca^{2+}-activated K^+ current using bath-applied carbachol (40 μM) in otherwise standard medium ($n = 4$; not shown). Second, prior blockade of K^+ currents may be necessary for the detection of $I_{Cl(V)}$ because K^+ currents with voltage sensitivities and kinetics similar to $I_{Cl(V)}$ may mask the Cl^- current present in the somatic membrane. $I_{Cl(V)}$ present in the somatic membrane should contribute substantially to somatic resting input resistance because this current is active at membrane potentials near the resting potential. However, $I_{Cl(V)}$ does not seem to contribute significantly to the resting conductance measured at the soma, as phorbol esters do not increase somatic input resistance in standard medium and in fact usually cause a small decrease (ref. 8, but see ref. 7). We favour a third possibility, that a substantial portion of this current is generated at a site electrotonically remote from the soma, perhaps in the dendritic membrane. In this case, blockade of resting K^+ currents would lengthen the space constant of the cell and allow voltage steps imposed at a somatic site to be more effective in eliciting changes in $I_{Cl(V)}$ in the dendrites and would also enhance passive propagation of this current back to the recording site at the soma.

Although a physiological role for $I_{Cl(V)}$ remains to be demonstrated, it is active at the resting membrane potential, and therefore should contribute substantially to the resting conductance of the membrane at which it is located. If this current is present in dendritic membranes, its blockade by activation of protein kinase C could, by increasing dendritic membrane resistance, increase the transmission of dendritic excitatory events, such as excitatory postsynaptic potentials, to the spike trigger zone in the soma/initial segment.

We thank Dr B. Lancaster for reading the manuscript. This research was supported by NIH grants MH38256, NS07495, RCDA MH00437, the Klingenstein Fund, and the Scottish Rite Schizophrenia Research Program, NMJ, USA.

Received 18 November 1985; accepted 2 April 1986

1. Cachelin, A. B., dePeyer, J. E., Kokubun, S. & Reuter, H. *Nature* 304, 462–464 (1983)
2. Madison, D. V. & Nicoll, R. A. *J. Physiol., Lond.* 372, 245–259 (1986)
3. Siegelbaum, S. A., Camardo, J. S. & Kandel, E. R. *Nature* 299, 413–417 (1982)
4. Ewald, D. A., Williams, A. & Levitan, I. B. *Nature* 315, 503–506 (1985)
5. Osterrider, W. *et al. Nature* 298, 576–578 (1982).
6. Shuster, M. J., Camardo, J. S., Siegelbaum, S. A. & Kandel, E. R. *Nature* 313, 392–395 (1985)
7. Baraban, J. M., Snyder, S. H. & Alger, B. E. *Proc. natn. Acad. Sci. U.S.A.* 82, 2538–2542 (1985)
8. Malenka, R. C., Madison, D. V., Andrade, R. & Nicoll, R. A. *J. Neurosci.* 6, 475–480 (1986)
9. DeReimer, S. A., Strong, J. A., Albert, K. A., Greengard, P. & Kaczmarek, L. K. *Nature* 313, 313–316 (1985).
10. Rane, S. G. & Dunlap, K. *Proc. natn. Acad. Sci. U.S.A.* 83, 184–188 (1986)
11. Strong, J. A., Fox, A. P., Tsien, R. W. & Kaczmarek, L. K. *Biophys. J.* 49, 430–434 (1986)
12. Halliwell, J. V. & Adams, P. R. *Brain Res.* 250, 71–92 (1982).
13. Collingridge, G. L., Gage, P. W. & Robertson, B. *J. Physiol., Lond.* 356, 551–564 (1984)
14. White, M. W. & Miller, C. *J. biol. Chem.* 254, 10161–10166 (1979)
15. Chesnoy-Marchais, D. *Nature* 299, 357–361 (1982).
16. Chesnoy-Marchais, D. *J. Physiol., Lond.* 342, 277–308 (1983).
17. Selyanko, A. A. *J. Physiol., Lond.* 350, 49P (1984).
18. Castagna, M. *et al. J. biol. Chem.* 257, 7847–7851 (1982).
19. Madison, D. V. & Nicoll, R. A. *J. Physiol., Lond.* 372, 221–244 (1986).

Phorbol ester facilitates ^{45}Ca accumulation and catecholamine secretion by nicotine and excess K^+ but not by muscarine in rat adrenal medulla

Arun R. Wakade, Ravindra K. Malhotra & Taruna D. Wakade

Department of Pharmacology, State University of New York, Downstate Medical Center, 450 Clarkson Avenue, Brooklyn, New York 11203, USA

Several investigators have shown that tumour promoter phorbol esters mimic the effects of endogenous diacylglycerol to activate a second messenger, protein kinase C (refs 1–3). These phorbol esters have proved to be valuable tools for exploring the role of protein kinase C in many cellular functions[3–8]. We demonstrate here that secretion of catecholamines evoked from the rat adrenal gland[9,10] by stimulation of splanchnic nerves, excess potassium (K^+) and nicotine is facilitated by phorbol 12,13-dibutyrate. An inhibitor of protein kinase C, polymixin B, produced concentration-dependent inhibition of the evoked secretion, and the effect was reversed by the phorbol ester. Furthermore, we show that an increase in the accumulation of radioactively labelled calcium (^{45}Ca) obtained in the adrenal medulla after stimulation with nicotinic agonists and excess K^+ is further enhanced by phorbol ester. Muscarine-evoked secretion of catecholamines, which depends on mobilization of intracellularly bound Ca^{2+}, was not associated with an increase in $^{45}Ca^{2+}$ uptake, and phorbol ester did not facilitate either catecholamine secretion or $^{45}Ca^{2+}$ accumulation. We suggest that protein kinase C is involved in the exocytotic secretion of catecholamines by regulating the influx of Ca^{2+} through voltage-sensitive and nicotine receptor-linked Ca^{2+} channels of rat chromaffin cells.

Figure 1 shows that increasing concentrations of phorbol 12,13-dibutyrate (phorbol ester) produce a concentration-dependent increase in catecholamine secretion evoked by stimulation of splanchnic nerves. Secretion increased significantly at 1 nM, more than trebled at 10 nM and was maximal at 30 nM. At 1–30 nM, phorbol ester had no effect on the spontaneous secretion of catecholamines, but 100 nM produced a modest increase in the secretion (16±2 compared with 4±3 ng per 6 min, $n=12$). The inset of Fig. 1*a* shows that phorbol ester facilitated the secretion evoked at 1 Hz and 10 Hz; however, the degree of facilitation was significantly ($P<0.001$) greater at 1 Hz. The most commonly used activator of protein kinase C, 12-*O*-tetradecanoylphorbol 13-acetate (TPA), also enhanced catecholamine secretion evoked at 1 Hz by about fivefold (58±7 compared with 276±31 ng per 6 min, $n=7$). On the other hand, a non-tumour promoter, phorbol 13-acetate, even in high concentrations (up to 1,000 nM), did not modify catecholamine secretion at rest or after stimulation. The enhancing effect of phorbol ester was reversed within 15 min after the washout, whereas that of TPA lasted for at least 2 h after its washout (not shown).

Several compounds inhibit the activity of protein kinase C isolated from pig heart and rat brain[12,13]. As shown in Fig. 1*b*, polymixin B caused concentration-dependent (10–100 μg ml^{-1}) inhibition of the secretion. The inhibitory effect was fully reversible 30 min after washout of the drug (not shown). Furthermore, prior treatment of the adrenal medulla with 50 nM phorbol ester partially reversed the inhibitory effects of 100 μg ml^{-1} polymixin B, almost prevented the inhibitory effects of 30 μg ml^{-1} polymixin B, and produced a significant enhancement in the presence of 10 μg ml^{-1} polymixin B (Fig. 1*b*).

The increased catecholamine secretion described in Fig. 1*a* could be a result of the action of phorbol ester either on splanchnic nerves to release more acetylcholine or on postsynaptic

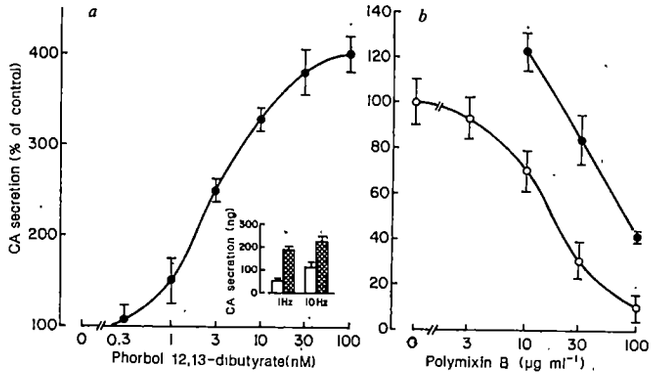


Fig. 1 *a*, Facilitation by phorbol 12,13-dibutyrate of the secretion of catecholamines (CA) evoked by stimulation of splanchnic nerves. *b*, Polymixin B-induced inhibition of catecholamine secretion evoked by nerve stimulation, and its reversal by phorbol ester. In *a*, the left adrenal glands of male rats (300–350 g) were prepared for *in vitro* perfusion as described previously[9]. The perfusion medium was Krebs–bicarbonate solution and the rate of perfusion was 0.35 ml min^{-1} at 37 °C. Ag/AgCl electrodes were used for transmural stimulation of the gland, and the parameters were set to stimulate selectively presynaptic splanchnic nerve terminals[9,10]. Splanchnic nerves were stimulated at 1 Hz (300 pulses), first without phorbol ester and then in increasing concentrations of phorbol ester (●). Each concentration remained in contact with the adrenal medulla for 15 min before collection of samples. Perfusate was collected for 6 min to determine catecholamine secretion in the absence of stimulation, and then for another 6 min, during which the gland was stimulated for 300 s. Amounts of catecholamines secreted during the immediately non-stimulation period have been subtracted from those secreted during stimulation period to obtain net catecholamine secretion, which is expressed either in per cent or in absolute values. In *a* all values are expressed as per cent of the control, which was 64±6 ng, $n=16$. The inset shows the effect of 30 nM phorbol ester on catecholamine secretion evoked by delivering 300 pulses at 1 and 10 Hz. Open columns, control; cross-hatched columns, phorbol ester–Krebs solution. Catecholamine content of the perfusate was measured directly by the fluorometric method as described elsewhere[9,11]. Adrenaline (base) was used as a standard; all values are presented as means with standard errors, and differences were compared using Student's paired *t*-test. Phorbol ester (LC Services, Woburn, Massachusetts) was dissolved in dimethyl sulphoxide and added to Krebs solution. The final dilution of the solvent in the Krebs solution was 500–100-fold. At these dilutions, the solvent alone had no effect on catecholamine secretion when added to Krebs solution. Each dot and column is a mean of four experiments. Vertical lines show s.e.m. In *b*, catecholamine secretion was evoked by stimulation of splanchnic nerves at 10 Hz (300 pulses), first in Krebs solution and then in increasing concentrations of polymixin B (○). The adrenal medulla was pretreated with each concentration for 15 min, and then nerves were stimulated in the presence of the agent. After testing the highest concentration, the adrenal gland was perfused with Krebs solution for 30 min to determine whether the inhibitory effect was reversible. In all the glands tested ($n=5$), secretion was restored to 110±14% of the initial control value. The perfusion medium was then changed over to 50 nM phorbol ester–Krebs solution for 10 min, and in its presence various concentrations of polymixin B were added (●) for 15 min and then samples (spontaneous and stimulated) collected. All values are expressed as per cent of control, which was 103±9 ng ($n=7$). The entire protocol was carried out in the same adrenal gland. Each point, except the control, represents a mean of four experiments. Vertical lines show s.e.m.

chromaffin cells to release more catecholamine from acetylcholine-induced activation of the nicotinic and muscarinic receptors[9,10]. To distinguish between these possibilities, we investigated the effect of phorbol ester on catecholamine secretion evoked by direct stimulation of chromaffin cells with cholinergic agonists as well as excess K^+ (Fig. 2).

Secretion of catecholamines evoked by nicotine, carbamylcholine and excess K^+ was approximately doubled by 30 nM phorbol ester. However, secretion evoked by muscarine, which was of the same order of magnitude as that evoked by nicotine, remained unaffected by phorbol ester. Because of these differential effects of phorbol ester, it was essential to know the role of Ca^{2+} in the secretion evoked by nicotine and muscarine. Perfusion of the adrenal gland with Ca-free and 1 mM EGTA–Krebs solution for 15 min completely blocked the secretion evoked by nicotine and muscarine (Fig. 3), and addition of phorbol ester to this medium had no effect on secretion evoked by either agent. If the same adrenal gland was perfused with 0.1 mM

Table 1 Effects of different stimulatory agents on $^{45}Ca^{2+}$ accumulation and secretion of catecholamine in absence and presence of phorbol ester

Stimulating agent	Catecholamine secretion (ng mg^{-1})		$^{45}Ca^{2+}$ accumulation (pg mg^{-1})	
	Krebs	Phorbol ester* (30 nM)	Krebs	Phorbol ester* (30 nM)
None (control)	2±0.4	2±0.4 (NS)	110±20	123±25 (NS)
Muscarine (30 μg ml^{-1})	38±4.5	41±5.1 (NS)	126±11	124±28 (NS)
Carbamylcholine (4 μg ml^{-1})	39±6.3	68±7.4 ($P<0.001$)	303±34	489±32 ($P<0.001$)
Nicotine (3 μg ml^{-1})	29±0.2	67±8.2 ($P<0.001$)	343±21	463±26 ($P<0.001$)
Excess K^+ (1.5 mg ml^{-1})	48±6.5	91±17.4 ($P<0.001$)	303±25	507±48 ($P<0.001$)

Thirty minutes after perfusion of the adrenal gland with Krebs solution, the medium was changed to Krebs solution containing 0.5 μg ml^{-1} $^{45}Ca^{2+}$ (as $^{45}CaCl_2$, specific activity 23.69 mCi mg^{-1}; NEN) for 10 min. The gland was perfused for a further 30 min with Krebs solution to wash out most of the extracellular $^{45}Ca^{2+}$. Within this time period the radioactivity in the wash fluid approaches a very low and steady-state level (~2% of that in the first 5-min period). An identical protocol was then carried out in further series of adrenal glands, except that the 10-min perfusion with $^{45}Ca^{2+}$-Krebs solution contained various secretagogues. Perfusates collected for 10 min during $^{45}Ca^{2+}$ exposure and stimulatory agents were assayed for catecholamine to ensure the expected effects of these agents on catecholamine secretion. NS, statistically non-significant; other P values show comparison between the data obtained in Krebs solution and in phorbol ester–Krebs solution.

* In another series, the above protocol was carried out, except that before exposure to $^{45}Ca^{2+}$ medium the adrenal gland was perfused with Krebs solution containing 30 nM phorbol ester for 15 min. Phorbol ester was also present during 10 min perfusion with $^{45}Ca^{2+}$ medium alone, or that containing stimulatory agent. After the 30-min wash period, the adrenal gland was removed, and the adrenal medulla separated, weighed, homogenized in 1 ml of 0.05 M perchloric acid; the homogenate was centrifuged and the supernatant (0.5 ml) was counted in a liquid scintillation counter (Beckman, model LS7000). Total counts after correction for dilution and quenching were converted to pg and expressed as pg per mg of the wet weight of the adrenal medulla. Each value represents a mean of four or five experiments.

Ca–Krebs solution and the secretion was evoked by both agents, nicotine-evoked secretion was <20% of that in 2.5 mM Ca medium, but that evoked by muscarine was ~65% of the control value. Phorbol ester increased nicotine-evoked secretion by more than 300% in 0.1 mM Ca medium, but muscarine-evoked secretion was enhanced only 15% in the same medium (statistically not significant, $P>0.5$).

The effect of phorbol ester on $^{45}Ca^{2+}$ accumulation in the adrenal medulla was investigated at rest and after stimulation with different agonists (Table 1). Although muscarine increased catecholamine secretion from a basal level of 2 ng to 38 ng, it was not accompanied by a significant increase in the accumulation of $^{45}Ca^{2+}$ over the control value. More importantly, phorbol ester did not enhance the effect of muscarine on catecholamine secretion and $^{45}Ca^{2+}$ accumulation. Catecholamine secretion evoked by carbamylcholine and nicotine, which was almost identical to that evoked by muscarine, was associated with a marked increase (275%) in $^{45}Ca^{2+}$ accumulation. In the presence of phorbol ester, the secretion was even further enhanced, and that too was associated with an additional increase (400%) in $^{45}Ca^{2+}$ uptake. K^+-evoked secretion was also accompanied by a large increase in the accumulation of $^{45}Ca^{2+}$ and was further enhanced by the phorbol ester. Catecholamine secretion and $^{45}Ca^{2+}$ accumulation under resting conditions were not affected by the phorbol ester.

Phorbol 12,13-dibutyrate significantly enhanced catecholamine secretion evoked by several procedures that activate chromaffin cells, either directly or indirectly, through the splanchnic nerves. We believe this to be the first report in which phorbol ester has produced a clear-cut facilitation of catecholamine secretion after activation of nicotinic receptors and depolarization of chromaffin cells. Furthermore, we show that an inhibitor of protein kinase C, polymixin B (ref. 13), almost completely inhibits catecholamine secretion, and the effect is reversed by the phorbol ester. This is the first example in which phorbol ester was able to overcome the inhibitory effects of an inactivator of protein kinase C to restore the secretory process. Assuming that the major target of action of phorbol ester and polymixin B in the rat chromaffin cells is the protein kinase C, it is tempting to postulate that this second messenger is involved in the exocytotic secretion of adrenal medullary hormones. Knight and Baker first studied the effects of phorbol ester on catecholamine secretion in bovine adrenal medullary cells, and found that Ca^{2+} sensitivity of the secretory process was enhanced by TPA. They therefore concluded that protein kinase C is involved in exocytosis[4]. Other investigators have reached a similar conclusion by studying the effects of phorbol ester in cultured bovine chromaffin cells and phaeochromocytoma (PC12) cells[14–16]. However, in none of these experiments was it possible to show facilitation by phorbol ester of catecholamine secretion evoked by a nicotinic agonist or excess K^+.

The next question is at which step protein kinase C participates in the process of exocytosis. We have found that the net increase in $^{45}Ca^{2+}$ accumulation obtained after stimulation of chromaffin cells with nicotinic agents and excess K^+ was further enhanced by phorbol ester. We therefore propose that protein kinase C may actually control the transport of Ca^{2+} entering through nicotinic receptor-operated and voltage-sensitive Ca^{2+} channels of the chromaffin cells. Recently, it has been reported that

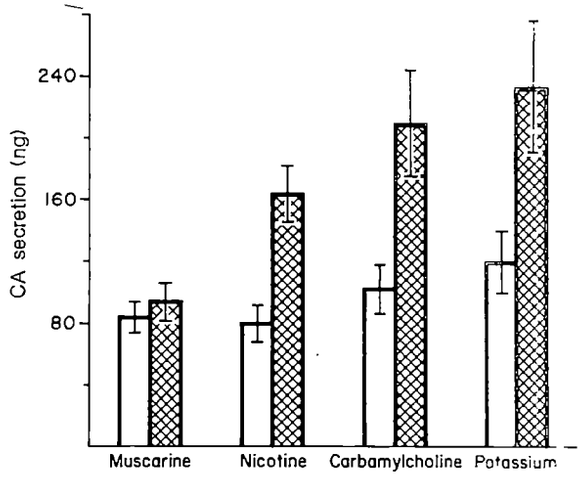


Fig. 2 Effects of phorbol ester on catecholamine secretion evoked by nicotinic agonists, muscarine and excess K^+. Adrenal gland was perfused with Krebs solution and secretion was then evoked by injecting muscarine (30 μg) and nicotine (0.3 μg) (open columns) within 20 min of each other. The perfusion medium was then changed to Krebs solution containing 30 nM phorbol ester for 15 min and in its presence muscarine and nicotine were injected (cross-hatched columns), as described above. The same protocol was carried out in another series of adrenal glands, except that nicotine was replaced with either carbamylcholine (4 μg) or KCl (40 μg) before (open columns) and after (cross-hatched columns) 30 nM phorbol ester. All agents were injected in a total volume of 100 μl saline. Each column is a mean of 5 experiments, except the column for muscarine, which is a mean of 10 experiments. Vertical lines represent s.e.m.

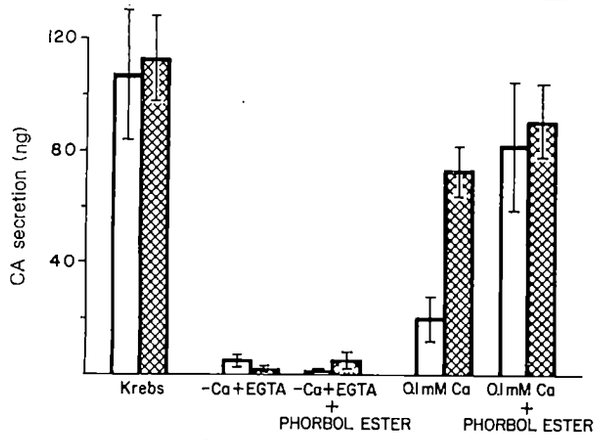


Fig. 3 Role of Ca^{2+} in the enhancement of catecholamine secretion evoked by nicotine and muscarine. Secretion was evoked by nicotine (open column) and muscarine (cross-hatched column), as described in Fig. 2 legend, in Krebs solution, Ca^{2+}-free plus 1 mM EGTA-Krebs solution and 0.1 mM Ca^{2+}-Krebs solution, before and after addition of 30 nM phorbol ester to various solutions. The adrenal gland was perfused with each solution for 15–30 min before sample collection. The entire protocol was carried out in the same adrenal gland. Each column represents a mean of four experiments. Vertical lines represent s.e.m.

injection of purified protein kinase C into *Aplysia* neurones or treatment with phorbol ester enhances the potential-sensitive membrane Ca^{2+} current[17]. It is likely that protein kinase C regulates the activity of Ca^{2+} channels by phosphorylating membrane proteins involved in opening and closing these channels. Protein kinase C-induced phosphorylation of different types of proteins associated with cytosol, cytoskeleton and other unidentified cell organelles of neuronal tissues has been documented[18–22]. Our present work shows that phorbol ester alone does not increase catecholamine secretion and has no effect on $^{45}Ca^{2+}$ accumulation. This means that active protein kinase C itself cannot affect the kinetics of Ca^{2+} channel opening and that their opening depends on other intracellular messengers generated by nicotinic receptor activation and membrane depolarization.

Another important finding leading to our proposal that protein kinase C regulates Ca^{2+} channels was the inability of phorbol ester to increase muscarine-evoked catacholamine secretion and of muscarine to increase $^{45}Ca^{2+}$ accumulation in either the absence or presence of phorbol ester. Note that Ca^{2+} is essential for muscarine-evoked secretion. These results clearly demonstrate the differential modes of Ca^{2+} mobilization by nicotinic and muscarinic agonists in the rat chromaffin cells; nicotine enhances the influx of extracellular Ca^{2+}, whereas muscarine mobilizes intracellularly bound Ca^{2+}. In bovine adrenal medullary cells, muscarine produces a modest rise in intracellular Ca^{2+} that is independent of external Ca^{2+} (ref. 23), however this increase in Ca^{2+} concentration does not lead to catecholamine secretion[24]. In the rat chromaffin cell, muscarine must mobilize large amounts of intracellular Ca^{2+} to raise its levels sufficiently high to initiate secretion. Because muscarine-evoked secretion is unaffected by phorbol ester, it is likely that the role of protein kinase C is restricted to the events regulating the influx of extracellular Ca^{2+} rather than those affecting the steps involved in the utilization of Ca^{2+} in exocytosis.

This work was supported in part by NIH grants HL22170 and HL18601, and NSF grant BNS 8409685. This paper is dedicated to the memory of the late Professor S. M. Kirpekar.

Received 16 December 1985; accepted 18 March 1986.

1. Castagna, M. *et al. J. biol. Chem.* **257**, 7847–7851 (1982).
2. Niedel, J. E., Kuhn, L. J. & Vandenbork, G. R. *Proc. natn. Acad. Sci. U.S.A.* **80**, 36–40 (1982).
3. Yamanishi, J., Takai, Y., Mori, T., Kikkawa, U. & Nishizuka, Y. *Biochem. biophys. Res. Commun.* **112**, 778–786 (1983).
4. Knight, D. E. & Baker, P. F. *FEBS Lett.* **160**, 98–100 (1983).
5. Peterfreund, R. A. & Vale, W. W. *Endocrinology* **113**, 200–208 (1983).
6. Tanaka, C., Taniyama, K. & Kusunoki, M. *FEBS Lett.* **175**, 165–169 (1984).
7. Barban, J. M., Gould, R. J., Peroutka, S. J. & Snyder, S. H. *Proc. natn. Acad. Sci. U.S.A.* **82**, 604–607 (1985).
8. Wakade, A. R., Malhotra, R. K. & Wakade, T. D. *Naunyn Schmiedebergs Archs Pharmak.* **331**, 122–124 (1985).
9. Wakade, A. R. *J. Physiol., Lond.* **313**, 463–480 (1981).
10. Wakade, A. R. & Wakade, T. D. *Neuroscience* **10**, 973–978 (1983).
11. Anton, A. H. & Sayre, D. F. *J. Pharmac. exp. Ther.* **138**, 360–375 (1962).
12. Wise, B. C. *et al. J. biol. Chem.* **257**, 8489–8495 (1982).
13. Wise, B. C. & Kuo, J. F. *Biochem. Pharmac.* **32**, 1259–1265 (1983).
14. Pocotte, S. L. *et al. Proc. natn. Acad. Sci. U.S.A.* **82**, 930–934 (1985).
15. Brocklehurst, K. W., Morita, K. & Pollard, H. B. *Biochem. J.* **228**, 35–42 (1985).
16. Pozzan, T., Gatti, G., Dozio, N., Vicentini, L. M. & Meldolesi, J. *J. Cell Biol.* **99**, 628–638 (1984).
17. De Reimer, S. A., Strong, J. A., Albert, K. A., Greengard, P. & Kaczmarck, L. K. *Nature* **313**, 313–316 (1985).
18. Takai, Y., Kikkawa, U., Kaibuchi, K. & Nishizuka, Y. *Adv. Cyclic Nucleotide Res.* **18**, 119–158 (1984).
19. Wu, W. C. S., Walass, S. I., Nairn, A. C. & Greengard, P. *Proc. natn. Acad. Sci. U.S.A.* **79**, 5249–5253 (1982).
20. Turner, R. S., Chou, C. H. J., Kibler, R. F. & Kuo, J. F. *J. Neurochem.* **39**, 1397–1404 (1982).
21. Wrenn, R. W., Katch, N., Wise, B. C. & Kuo, J. F. *J. biol. Chem.* **255**, 12042–12046 (1980).
22. Streb, H., Irvine, R. F., Berridge, M. J. & Schulz, I. *Nature* **306**, 67–69 (1983).
23. Schneider, A. S. & Kao, L. S. *J. biol. Chem.* **260**, 2019–2022 (1985).
24. Knight, D. E. & Baker, P. F. *J. Membrane Biol.* **68**, 107–140 (1982).

Mediation of mouse natural cytotoxic activity by tumour necrosis factor

John R. Ortaldo, Llewellyn H. Mason, Bonnie J. Mathieson, Shu-Mei Liang*, David A. Flick† & Ronald B. Herberman

Biological Therapeutics Branch, Biological Response Modifiers Program, Division of Cancer Treatment, National Cancer Institute, National Institutes of Health, Frederick Cancer Research Facility, Building 560, Room 31-93A, Frederick, Maryland 21701; USA
* Biogen SA, PO Box 121, Geneva 24, Switzerland
† Department of Immunology and Medical Microbiology, University of Florida College of Medicine, Gainesville, Florida 32610, USA

Natural cell-mediated cytotoxic activity in the mouse has been associated with two types of effector cells, the natural killer (NK) cell and the natural cytotoxic (NC) cell, which seem to differ with regard to their patterns of target selectivity, cell surface characteristics and susceptibility to regulatory factors[1]. During studies on the mechanism of action of cytotoxic molecules, it became evident that WEHI-164, the prototype NC target cell, was highly susceptible to direct lysis by both human and mouse recombinant tumour necrosis factor (TNF). Here we show that NC, but not NK activity mediated by normal splenocytes, is abrogated by rabbit antibodies to recombinant and natural TNF, respectively. Thus, the cell-mediated activity defined as NC is due to release of TNF by normal spleen cells and does not represent a unique natural effector mechanism.

The prototype target for detection of mouse NK activity is the YAC-1 lymphoma cell line[2], whereas WEHI-164 cells are the main targets used to selectively measure NC activity[1,3]. Mouse NK cells have been shown to express asialo-GM_1, and the alloantigens of Ly5, Qa5, NK1 and NK2, on the cell surface[2,4,5]. Some mouse NK cells also express Thy-1 antigen. In contrast, treatment of cells bearing any of these markers with antibody plus complement has little effect on NC activity[1,3,6]. NK activity is quite rapid, with close to maximum levels achieved within 4 h, whereas NC activity usually requires incubation periods of 18 h or longer[1,5]. NK activity has been shown to be strongly augmented by pretreatment of the effector cells with interferon or interleukin-2 (refs 5, 7, 8), whereas NC activity has been shown to be enhanced primarily by interleukin-3 (refs 7, 9). Mouse NK activity, analogous to previous findings with human and rat NK cells[5], has been closely associated with a morphological counterpart, the large granular lymphocyte[5]. In contrast, it has proved difficult to directly associate NC activity with any specific cell type[5,9], raising the possibility that this activity is not a direct cell-mediated event. In addition to the

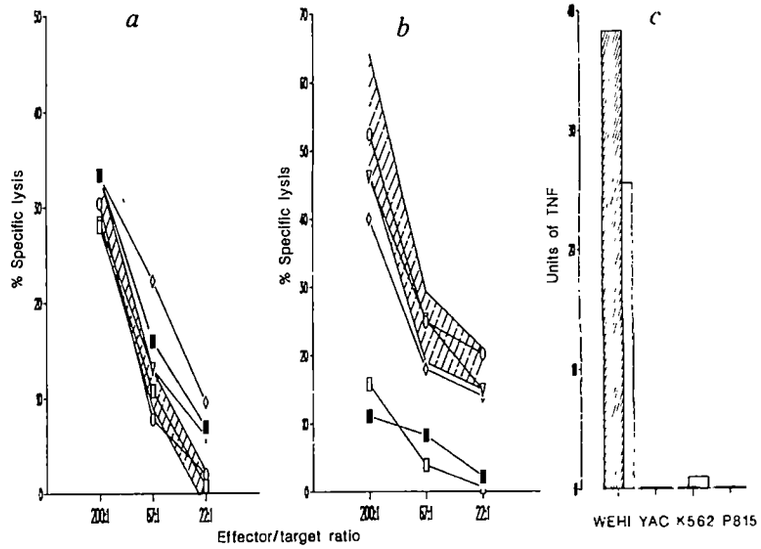


Fig. 1 *a, b,* Effect of antisera or monoclonal antibodies on cell-mediated lysis of YAC-1 (NK) and WEHI-164 (NC) cells, respectively. *c,* TNF stimulation by various target cells. The per cent specific lysis of ^{51}Cr-labelled WEHI-164 and YAC-1 targets in an 18-h or 4-h assay[8,9] is shown in *a* and *b*, respectively. Effector cells from 7-week-old C57BL/6 mice were tested at various effector/target cell ratios (200:1, 67:1 and 22:1, with 5,000 targets per well) in a standard microcytotoxicity assay[8]. The specific lysis above that obtained in control medium is shown. The shaded area represents the control level of cytotoxicity (mean ± s.d.) mediated by untreated spleen cells. A final 1:40 dilution of each antibody was added to the assay. Similar results were seen with a 1:200 final dilution, with approximately 50% inhibition of cytotoxicity seen with antisera to mouse TNF (data not shown). ■, Rabbit anti-TNF-1 antiserum (300 TNF neutralizing units); □, rabbit anti-TNF-2 antiserum (300 TNF neutralizing units); ○, monoclonal anti-human TNF antibody (1,000 TNF neutralizing units); ▽, monoclonal anti-human LT antibody (1,000 LT neutralizing units); ◇, normal rabbit serum (obtained from a pre-bleed for anti-TNF-1 antiserum). Similar results to those for NRS were seen with two other normal rabbit sera (data not shown). *c,* Plot of units per ml of TNF produced during co-culture of nylon-passed C57BL/6 spleen cells (2×10^6) with various targets: NK (K562-human NK; YAC-mouse NK), NC (WEHI) or NK/NC-insusceptible (P815). Supernatants from reactions with effector splenocytes/target cell ratios of 200:1 (▨) or 50:1 (□) were collected after 18 h, filtered and units of mouse TNF determined relative to a recombinant mouse TNF standard curve. Controls consisting of cells alone and targets alone yielded no detectable TNF production (data not shown).

incomplete characterization of the NC effector cells, there is also little information available concerning the mechanism of cytotoxicity of NC cells. In contrast, recent studies have indicated that a highly cytolytic protein in the granules of large granular lymphocytes has a key role in the cytotoxic activity of NK cells[10]. Also, NK cells have been shown to release a soluble cytotoxic factor (NKCF) on interaction with NK-susceptible target cells[11]. Thus, it was of considerable interest to determine whether a similar mechanism of cytotoxicity was used by NC cells.

During re-examination of the spectrum of cytotoxic activity reported for human tumour necrosis factor (TNF)[12], we found that WEHI-164 cells were highly susceptible to the effects of this cytotoxic factor, which raised questions regarding the possible role of TNF in the mechanism of cytotoxicity of NC cells. We have found that WEHI-164 cells are highly susceptible to both recombinant mouse TNF and recombinant human TNF. In addition, NC activity by mouse spleen cells was strongly inhibited by two independently produced rabbit antisera raised against mouse TNF. Thus, the cell-mediated cytotoxicity defined as NC activity appears to be attributable to release of TNF *in vitro* by normal mouse spleen cells. These data also indicate that this cytokine may be produced spontaneously by certain normal cells and thereby contribute to natural cell-mediated cytotoxicity.

Table 1 shows the susceptibility of WEHI-164 cells to lysis by purified recombinant mouse TNF (Biogen SA) and by recombinant human TNF[13] (provided by Dr M. Shepard, Genentech, Inc., South San Francisco). Both recombinant TNFs had cytolytic activity against WEHI-164 cells but had little effect on YAC-1, the classical mouse target cells for NK activity. To confirm that the activities observed were indeed due to TNF,

Table 1 Effect of anti-TNF and anti-LT antibodies on lysis of WEHI-16 cells by recombinant mouse or human TNF

	% Specific lysis in TNF in the presence of various antibodies						
		WEHI-164					
Agent (U ml^{-1})	YAC-1	None	Anti-TNF-1	Anti-TNF-2	Monoclonal anti-TNF	Monoclonal anti-LT	NRS
MuTNF (500)	2.2	68.8	13.3	36.8	78.5	80.4	76.8
MuTNF (50)	2.1	54.6	11.6	33.7	62.5	57.5	52.5
MuTNF (5)	0.5	41.4	NT	NT	NT	NT	NT
HuTNF (500)	3.2	65.3	NT	NT	10.2	68.7	NT
HuTNF (50)	−1.1	56.7	NT	NT	5.4	54.3	NT
HuTNF (5)	0.1	44.3	NT	NT	1.3	40.3	NT

The per cent specific lysis of ^{51}Cr-labelled WEHI-164 target cells in an 18-h release assay is shown[8,9]. The results presented indicate the per cent release of ^{51}Cr above the background of spontaneous release in medium alone. The table shows the effects of rabbit anti-mouse TNF-1 (300 TNF neutralizing units), rabbit anti-mouse TNF-2 (300 TNF neutralizing units), monoclonal anti-human TNF antibody (1,000 TNF neutralizing units), monoclonal anti-human LT antibody (1,000 LT neutralizing units), and normal rabbit serum (NRS) obtained from a preimmunization bleeding of the rabbit used for production of anti-TNF-1. The assay was performed as described previously[8,9]. Recombinant human (Hu) and mouse (Mu) TNF were purified from *Escherichia coli* cells containing HuTNF and MuTNF gene-encoded plasmids. The cells were broken using a Manton-Gaulin press. The TNF in the supernatant was then purified using DEAE-Sepharose CL6B, phenyl-Sepharose CL4B and Sephacryl S-200. The proteins were purified to greater than 97% purity with a specific activity of 3×10^7 U mg^{-1} for MuTNF and 1.5×10^7 U mg^{-1} for HuTNF. One unit of TNF, as defined previously[12], is the amount resulting in 50% inhibition of growth of the L929 cell line. Anti-MuTNF antiserum was produced in a New Zealand White female rabbit by intradermal immunization at multiple sites with a suspension of purified mouse TNF (200 μg ml^{-1} in phosphate-buffered saline, 1 ml) in Freund's complete adjuvant (1 ml); this was followed by a booster injection at 1 month. Serum was obtained 10–14 days after the boost. The rabbit produced satisfactory titres of antibody (<3,000) as determined by enzyme-linked immunosorbent assay. Various concentrations of recombinant mouse or human TNF preparations were added to labelled target cells in the presence of various concentrations of antisera or monoclonal antibodies. A final 1:40 dilution of each antibody was added to the assay. NT, not tested.

we determined the effects of specific anti-TNF antibodies. The cytotoxicity of recombinant mouse TNF for WEHI-164 target cells was inhibited strongly by two different rabbit antisera, raised independently against either the purified natural mouse cytokine (anti-TNF-1) or recombinant mouse TNF (anti-TNF-2). In contrast, monoclonal antibody to human TNF or lymphotoxin (LT), or normal rabbit serum (NRS), had no significant effect on the cytotoxicity of recombinant mouse TNF. However, monoclonal antibody to human TNF blocked human TNF-mediated lysis of WEHI-164 cells (Table 1). The species specificity of this monoclonal antibody suggests that the blocking effect is not dependent on the NC target, but rather on the source of TNF. It is noteworthy that YAC-1 cells were highly resistant to lysis by either human or mouse TNF. Addition of antisera against target cells had no toxic effect on NK or NC targets (data not shown).

To study more directly the possible involvement of TNF in NC activity, the antibodies to mouse TNF were added to a standard NC assay (Fig. 1). Each of these antibodies to murine TNF strongly inhibited the lysis of WEHI-164 cells by normal mouse spleen cells. Based on calculations of the lytic units, derived from the cytotoxicity data at several effector to target cell ratios, greater than 90% of the lytic activity was neutralized by each of the rabbit anti-mouse TNF antibodies. In contrast, no significant inhibition was seen with the NRS controls including sera from preimmunization bleeds, or with monoclonal antibody to human TNF or LT. Parallel experiments were performed to evaluate the possible effects of the antibodies on mouse NK activity against YAC-1 target cells. No significant inhibition of NK lysis was seen with any of the antibodies (Fig. 1). The increase in NK lysis seen at low effector/target cell ratio with selected antisera was not observed in all experiments or at higher dilutions of antisera. Thus, two antisera to mouse TNF (one raised against recombinant and the other against highly purified natural mouse TNF) selectively inhibited cell-mediated cytotoxicity against the NC target cells but had no effect on NK activity. This result further demonstrates a major distinction between these two forms of natural cytotoxicity.

We have demonstrated that NC activity against WEHI-164 target cells appears to be a cytokine-mediated phenomenon, apparently mediated by the spontaneous release of TNF during the cytotoxicity assay. The mediation of NC activity by the release of TNF may explain the prolonged incubation periods required to demonstrate this activity, in contrast to the rapid kinetics of NK activity. This notion is supported by the results in Fig. 1*c*, which demonstrate high levels of TNF production only in co-cultures with WEHI-164, but not in co-cultures with NK or other potential targets. Presumably the extended period of incubation is required for sufficient release, if not also production, of the cytokine. The association of TNF with NC activity also provides new clues as to the nature of the NC cell. TNF has been found to be produced predominantly by macrophages[12,15]. The possible derivation of NC cells from the myelomonocytic lineage would be consistent with previous evidence for adherence properties of NC cells[1,5,9], the resistance of NC activity to treatments which strongly inhibit lymphocyte numbers and functions (for example, a high dose of cyclophosphamide and anti-lymphocyte antibodies plus complement), and the ability of interleukin-3, a cytokine with multipotential colony-stimulating factor effects on monocytic cells as well as other haematopoietic cells, to promote both the growth and cytolytic activity of NC cells[5,7,9].

Our observation that TNF has a key role in NC, but not NK, activity raises the possibility of a new approach to discriminating between NC and NK activities. Although it was initially thought that most solid tumour cells were selectively sensitive to NC cells and that lymphoma cells were preferentially lysed by NK cells[9], it has recently been found that many target cells of both types are susceptible, to a certain extent, to lysis by each category of effector cells[5]. Monoclonal antibody to TNF may help to determine the contribution of NC cells to the natural cell-mediated lysis of various target cells. Also, in analogy to the present results with mouse NC cells, it will be of considerable interest to study the effects of antibodies to human TNF on the recently reported human counterpart to NC activity[14].

Received 31 December 1985; accepted 4 April 1986.

1. Stutman, O., Paige, C. J. & Feo Figarella, E. *J. Immun.* **121**, 1819–1823 (1978).
2. Herberman, R. B. & Holden, H. T. *Adv. Cancer Res.* **27**, 305–319 (1978).
3. Kumar, V., Luevano, E. & Bennett, M. *J. exp. Med.* **150**, 531–534 (1979).
4. Minato, N., Reid, L. & Bloom, R. B. *J. exp. Med.* **154**, 750–755 (1981).
5. Ortaldo, J. R. & Herberman, R. B. *A. Rev. Immun.* **2**, 359–394 (1984).
6. Paige, C. J., Feo Figarella, E., Cuttito, M. J., Cahan, A. & Stutman, O. *J. Immun.* **121**, 1827–1832 (1978).
7. Djeu, J., Heinbaugh, J. A., Holden, H. T. & Herberman, R. B. *J. Immun.* **122**, 175–179 (1979).
8. Ortaldo, J. R. *et al. J. Immun.* **133**, 779–784 (1984).
9. Djeu, J. Y., Lanza, E., Pastore, S. & Hapel, A. J. *Nature* **306**, 788–789 (1983).
10. Henkart, P. A., Millard, P. J., Reynolds, C. W. & Henkart, M. P. *J. exp. Med.* **160**, 75–93 (1984).
11. Wright, S. C., Weitzen, M. L., Kahle, R., Granger, G. A. & Bonavida, B. *J. Immun.* **130**, 1479–1484 (1983).
12. Darzynkiewicz, Z., Williamson, B., Carswell, E. A. & Old, L. J. *Cancer Res.* **44**, 83–90 (1984).
13. Iscove, N. N., Roitsch, C. A., Williams, N. & Guilbert, L. J. *J. cell. Physiol.* Suppl. 1, 65–78 (1982).
14. Rola-Pleszczynski, M. & Lieu, H. *Cell. Immun.* **82**, 326–333 (1983).
15. Somura, K., Nakano, K., Abe, M., Nakata, K. & Yoshida, H. *Gan To Kagaku Ryoha* **12**, 160–162 (1985).

A block to elongation is largely responsible for decreased transcription of c-*myc* in differentiated HL60 cells

David L. Bentley & Mark Groudine*

Fred Hutchinson Cancer Research Center, 1124 Columbia Street, Seattle, Washington 98104, USA and *Department of Radiation Oncology, University of Washington School of Medicine, Seattle, Washington 98195, USA

The c-*myc* gene product is a nuclear protein[1,2] expressed in a wide variety of cell types[3]. It has been implicated in the control of normal cell growth as well as transformation[4–7], but its exact function is unknown. When the human promyelocytic leukaemia cell line HL60 is treated with retinoic acid, the cells differentiate into granulocytes, and there is a reduction in steady state c-*myc* RNA of more than 10-fold[8]. Nuclear runoff assays show that this reduction is caused by a corresponding decrease in the transcription of exon 2. However, only a minor decrease in exon 1 transcription is observed upon differentiation. In undifferentiated HL60 cells there is an approximately 3-fold molar excess of exon 1 transcription over exon 2, and this excess increases to about 15-fold in differentiated cells. This observation suggests that a major component of c-*myc* transcriptional down-regulation in HL60 cells is at the level of elongation rather than at the level of initiation. The position of the elongation block was mapped to the region of the boundary between exon 1 and intron 1. During HL60 differentiation, a DNase I hypersensitive site in the chromatin about 300 bases downstream of the 5′ end of of intron 1 increases in intensity relative to other sites, possibly reflecting events associated with the termination of transcription. Our runoff analysis also revealed transcription of both strands immediately upstream of exon 1 in HL60 cells. The sense strand transcription of this region produces a novel c-*myc* RNA which initiates several hundred bases upstream of the previously defined promoters and is found in a variety of cell types.

Large changes in c-*myc* RNA levels occur during terminal differentiation[8,9] and mitogenic stimulation of quiescent cells[5]. Both transcriptional[10] and post-transcriptional mechanisms[11] have been reported to control the transient increase of c-*myc* expression which follows mitogenic stimulation. In contrast, post-transcriptional destabilization alone has been reported to account for the reduction in c-*myc* RNA level of differentiating

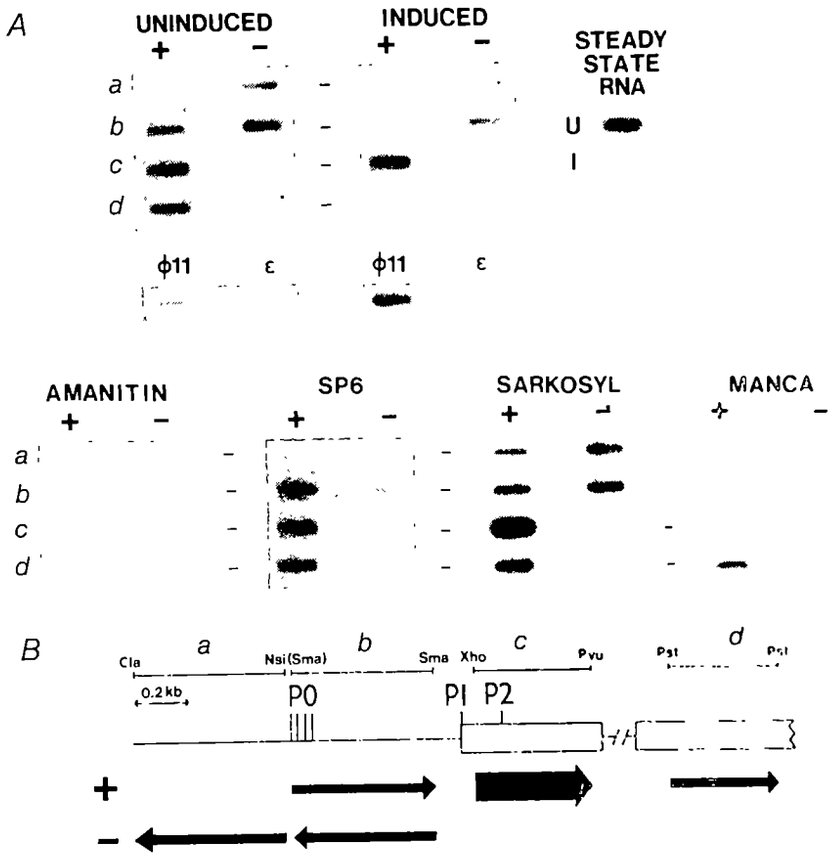


Fig. 1 Runoff transcription of c-*myc* in HL60. *Steady state RNA*: Slot blotted total RNA (4 μg) from the same cell prep used for the run-off assays shown to the left was hybridized to a ^{32}P-RNA exon 3 probe. By Northern analysis, this probe detects only genuine c-*myc* transcripts. *A*, Hybridization of RNA (15×10^6 c.p.m.) from HL60 uninduced or induced for 2.5 days in retinoic acid (1 μM). Probes marked +, detect sense transcripts and − detect anti-sense transcripts. As controls equimolar amounts of the pε 0.7 ε-globin plasmid[18] and the granulocyte specific Φ11 cDNA clone (1.4 kb) were used. *α-amanitin*: Hybridization of RNA from uninduced HL60 synthesized in the presence of 2 μg ml^{-1} α-amanitin. The number of cells used was 33% more than in untreated samples. Under these conditions the amount of rRNA synthesized is as great as in untreated samples (not shown). *SP6*: Hybridization of SP6 RNA from a full length P0 cDNA clone[19]. Transcripts were eluted from a gel and degraded in NaOH prior to hybridization. *Sarkosyl*: Hybridization of RNA from uninduced HL60 synthesized in the presence of 0.5% sarkosyl. *Manca*: Run-off transcripts from the Manca, B-cell lymphoma. *B*, Map of the restriction fragment probes, *a–d*, cloned in M13 vectors and summary of c-*myc* transcription pattern in HL60. The mapping of the P0 promoter will be published elsewhere[19]. The lengths of the probes are: *a*, 586, *b*, 535, *c*, 443, *d*, 414 bases. They were subcloned from the genomic clone pMC41-HE[20] (*a*) or the P0 cDNA clone (*b–d*).

Methods. Preparation of nuclei was as described (15) and equivalent results were obtained from fresh and frozen nuclei. The results shown except for Manca were from nuclei pretreated with 10 μg ml^{-1} RNase A for 30 min on ice[16] but identical results were also obtained with untreated nuclei. (In the latter case ^{32}P-RNA was hydrolysed with 0.3 M NaOH for 10 min on ice.) RNase was inactivated with RNasin (200 U ml^{-1}) and washing once in 500 μl nuclear freezing buffer (NFB; ref. 15) plus RNasin. The nuclei ($\simeq3\times10^7$) were then resuspended in 210 μl of NFB and the runoff reaction performed as in ref. 17. The ^{32}P-RNA was on average 100 bases long. Hybridizations to 0.5 μg of single-stranded M13 DNA slot blotted in 20×SSC were carried out at 0.3 M NaCl and 65 °C for 36–40 h followed by washing in 0.1×SSC, 0.1% SDS at 65 °C (ref. 17). Washing the filters at 72 °C did not alter the signal ratio of the c-*myc* probes. Autoradiographs were exposed for 2 days.

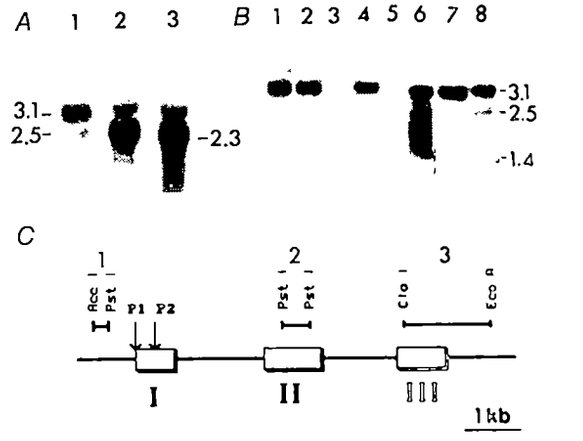


Fig. 2 *A*, Northern blot of c-*myc* RNAs in HL60 cells. Lanes 1–3: Poly (A)$^+$ RNA (10 μg) was analysed by hybridization to the corresponding nick-translated restriction fragments in Fig. 1*c*. Autoradiography was for 20 h, 1 h, and 1 h for lanes 1, 2 and 3 respectively. *B*, P0 transcripts in different cell types. Northern filters containing poly(A)$^+$ RNA (1–5 μg) were hybridized to an antisense strand ^{32}P-RNA of fragment 1 (Fig. 1*c*). as in ref. 24. Autoradiography was for 1–5 days. Lane 1, KG1; 2, KC122; 3, EBV transformed B lymphoblasts; 4, EM3; 5, K562; 6, foreskin fibroblasts, passage 5; 7, COLO-320 neuroendocrine carcinoma; 8, 293 embryo kidney cells. Lanes 1,2 4 and 5 contain RNA from myeloid leukaemia cell lines. *C*, Map of the human c-*myc* gene. The three exons, the P1 and P2 promoters and fragments 1–3 which were used as hybridization probes, are marked.

F9 embryonal carcinoma and mouse erythroleukaemia cells[9]. We have investigated transcription of the amplified c-*myc* genes in HL60 using a nuclear runoff assay. In this assay, short labelled RNAs (approximately 100 bases) are synthesized by polymerases *in situ* and hybridized to an excess of a cloned probe. Assuming a constant elongation rate, the hybridization signals from different probes reflect the number of RNA polymerase molecules present in corresponding regions of the gene. We initially examined transcription in four regions of the c-*myc* gene, labelled *a–d* in Fig. 1, using single-stranded M13 probes for both strands. The cloned restriction fragments were of similar length so as to be approximately equally efficient hybridization targets.

As shown in Fig. 1, transcription of exons 1 and 2 is highly strand-specific, and the amount of exon 1 transcription is greater than that of exon 2 by an average of 3-fold (range 2–5) in uninduced cells and 15-fold (range 9–24) in induced cells. Each of these values is the average of four independent determinations made by densitometry of autoradiograms. Background signal was not subtracted, so the average value of 15 for the ratio of exon 1 to exon 2 transcription in differentiated cells is a minimum estimate. To ensure that the high exon 1 signal is not due to

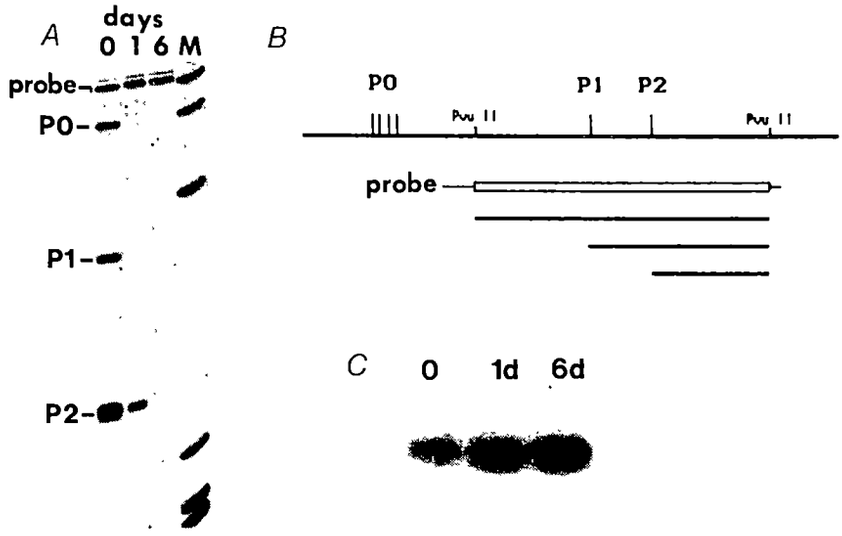


Fig. 3 *A*, S_1 analysis of c-*myc* RNA during retinoic acid induced differentiation of HL60 cells. Markers (*M*) are 1,078; 872; 603; 310; 278 and 271 bases. *B*, Strategy for S_1 mapping. The probe is depicted with thin lines for M13 vector sequence and an open bar for c-*myc* sequence. The solid lines below represent S_1 resistant fragments characteristic of P0, P1 and P2 RNAs. *C*, Northern blot of actin RNA. Samples of 1 μg of the same RNA samples as in Fig. 3*A* were analysed by hybridization to a ^{32}P-RNA probe from the chicken β-actin gene[26] (3 h exposure).

Methods. The probe in *A* was a uniformly labelled single-stranded fragment (prepared as in ref. 25) including 862 bases between two *Pvu*II sites and about 200 bases of M13 vector sequences. Samples of 1 μg poly $(A)^+$ RNA from uninduced cells labelled 0, and from cells treated with retinoic acid for 1 day (21 h) and 6 days were analysed. 0.5 ng of probe (25,000 c.p.m.) was hybridized to RNA in 10 μl of 0.5 M NaCl, 20 mM PIPES, *p*H 6.4, 1 mM EDTA at 65 °C for 3 h, then digested in 100 μl containing 350 mM NaCl, 30 mM Na-acetate, *p*H 4.5, 1 mM $ZnSO_4$, 1,200 U ml^{-1} S_1 nuclease (BRL) for 40 min at 37 °C followed by ethanol precipitation and electrophoresis on a 4.5% acrylamide 7 M urea gel. (2.5 day expsoure).

cross-hybridization with other transcribed sequences in the genome, we analysed runoff transcripts in another human cell line which was expected to have little or no exon 1 transcription. This line was the B-cell lymphoma Manca which has a single active c-*myc* allele that is disrupted in the first intron such that exons 2 and 3 are transcribed from cryptic promoters under the influence of the immunoglobulin heavy chain enhancer[12]. In contrast to HL60, Manca, showed an excess of exon 2 transcription over exon 1 (Fig. 1). This result rules out the possibility of a highly transcribed sequence in the human genome which spuriously hybridizes to our exon 1 probe. In addition, ^{32}P-RNA corresponding to the anti-sense strand of probe C (Fig. 1) hybridizes to a unique band in Southern blots of HL60 and placental DNA (data not shown), thereby eliminating the possibility that the molar excess of exon 1 signal over exon 2 is due to the presence of amplified truncated c-*myc* genes containing exon 1 but not exon 2 sequences in HL60. The unequal signals obtained with exon 1 and exon 2 probes are not the result of differential hybridization efficiency since these two probes hybridized equally well to SP6 RNA from a cDNA clone (Fig. 1). The excess exon 1 transcription also does not represent artifactual initiation resulting from the nuclear isolation and runoff procedures, since the pattern of transcription in both uninduced (Fig. 1) and induced cells (data not shown) is unaffected by concentrations of sarkosyl (0.5%) which block Pol II initiation but not elongation[13]. The slight differences between the 'uninduced' and 'sarkosyl' runoff experiments shown in Fig. 1 are within the normal range of variation between experiments. Transcription of all parts of the gene assayed was sensitive to 2 μg ml^{-1} α-amanitin, demonstrating that these transcripts are synthesized by RNA polymerase II[14] (Fig. 1). The high level of exon 1 transcription is apparently due to a high polymerase density throughout this exon and not a pile up of polymerases at its 5′ end, since an equally high signal relative to probe length was obtained when the 5′ 150 bases of probe C were deleted (data not shown).

Transcription of exon 2 sequences was down-regulated by over 90% when the cells were induced to differentiate for 2.5 days. This transcriptional regulation (Fig. 1) fully explains the reduction in steady state c-*myc* RNA in this cell preparation (see Fig. 1) without the need to invoke post-transcriptional control. Our result confirms a previous report[21] in which a v-*myc* probe homologous to exons 2 and 3 was used to monitor transcription. As a positive control for the transcriptional activity of differentiated cells, we monitored the induction of a gene called Φ11, which was selected from an HL60 cDNA library by a differential screening procedure (D.B., unpublished).

In contrast to exon 2, there was only a 10–20% down regulation of exon 1 transcription during HL60 differentiation in four experiments. At least part of the modest transcriptional down regulation of exon 1 is due to reduced transcription from upstream of the gene (see below). These results suggest that the major c-*myc* promoter, P2, is not turned off during HL60 differentiation. We cannot eliminate the possibility that the P1 promoter is turned off, since it seems to be a minor transcriptional start site based on steady state RNA measurements (see Fig. 3 below). The maintenance of a high transcription rate of exon 1 in differentiated cells while exon 2 transcription declines to background levels suggests that inhibition of elongation between exons 1 and 2 is an important component of the c-*myc* down-regulation in HL-60.

An unexpected result of the runoff assay was the detection of transcription upstream of exon 1 on both strands, at a level almost as great as that of exon 2. The observed hybridization is not due to homology with another part of the genome since nick-translated fragment *b* (Fig. 1) hybridized to a unique sequence in a Southern blot of genomic DNA (data not shown). In addition, the bidirectional transcription signal does not result from a lack of strand specificity of the probes, as demonstrated by asymmetric hybridization of SP6 RNA synthesized from a cDNA clone (Fig. 1). The origin of anti-sense transcripts was mapped to a *Sma*I-*Nae*I fragment that extends from 101 bases upstream of P1 to 49 bases downstream of P2 (data not shown). This fragment contains two TATA box homologies which might promote transcription: a GATAAA at 2,483–2,488 and a TATAAA at 2,298–2,303 of the sequence in ref. 22 as well as the distal element consensus, CCGCCC at 2,531–2,536. Divergent transcription from the area of the major promoter of the mouse dihydrofolate reductase (DHFR) gene has also been observed[23]. Perhaps these two cases of divergent transcription are indicative of a more widespread lack of absolute polarity in promoter function. Anti-sense transcription originating about

100 bases upstream of the major mouse DHFR promoter produces a cytoplasmic, spliced polyadenylated RNA with an open reading frame. We have been unable to detect such a stable anti-sense RNA from the c-*myc* gene in HL60 or human fibroblasts; therefore, we presume that the anti-sense transcripts are very unstable.

In contrast, we did detect sense strand transcripts of the region upstream of P1 in steady-state RNA. Northern blots of HL60 RNA revealed a 3.1-kilobase (kb) c-*myc* RNA which hybridizes to a probe (Fragment 1, Fig. 2*C*) spanning 409–608 bases upstream of the P1 promoter (Fig. 2*A*, lane 1). A minor 2.5-kb RNA is also detected by this upstream probe. The 3.1-kb species also hybridized to exon 2 and exon 3 specific probes (Fig. 2*A*, lanes 2 and 3). Full length cDNAs of both these RNA species have been isolated and characterized, and the 5′ ends of these RNAs were mapped to a promoter called P0 located 550–650 bases upstream of P1[19]. Several human cultured cell lines as well as primary fibroblasts were surveyed by Northern blot hybridization with the upstream probe, and all of them contain the 3.1-kb transcript (Fig. 2*B*), although usually as a lower proportion of c-*myc* RNA than observed in HL60. Thus, transcripts initiating upstream of the first exon appear to be found wherever the c-*myc* gene is expressed.

The regulation of P0, P1, and P2 RNAs during differentiation of HL60 into granulocytes was examined using an S1 protection assay (Fig. 3*B*). The results (Fig. 3*A*) show that steady-state levels of P0, P1 and P2 RNA are coordinately reduced when the cells differentiate. RNA levels declined to less than 10% of their original amounts after 21 hours when there is no overt morphological differentiation, and to undetectable levels after 6 days when differentiation is complete. As a control for the integrity of these RNA samples, a Northern blot was hybridized to an actin probe, and a slight increase in the amount of actin RNA was observed in the differentiated HL60 cells (Fig. 3*C*).

The relative amounts of RNA from the three c-*myc* promoters in HL60 were measured by cutting out the gel bands in Fig. 3*A*, lane 0 and counting them. After compensating for the number of labelled nucleotides in each fragment, it was calculated that P0, P1, and P2 contributed 7%, 12% and 81% of c-*myc* RNA respectively. The small amount of steady-state P0 RNA contrasts with the relatively high transcription rate from this promoter as judged by the nuclear runoff assay. This result implies that the majority of P0 transcripts are less stable than P1/P2 transcripts.

We next examined whether HL60 differentiation was accompanied by a change in the chromatin fine structure of the c-*myc* gene. DNase I hypersensitive sites in the c-*myc* gene of undifferentiated and differentiated HL60 cells were mapped using the indirect end-labelling strategy in Fig. 4*A*. The result demonstrates two major differences in chromatin structure on treatment with retinoic acid for 3 days. Hypersensitive site 2 (II_2 in ref. 28) which is located about 100 bases upstream of the P0 promoter disappears, as previously reported[29], whereas site 4 located in the first intron is enhanced relative to the other sites upon differentiation. Note also that the relative intensities of site 1 (1.85 kb upstream of P1) and site 3 (between P1 and P2) are unchanged after retinoic acid treatment. The disappearance of site 2 correlates with turn-off of the P0 promoter (Figs 1 and 3) which appears to be regulated independently of the major promoters P1 and P2. The persistence of site 3 (III_2 in ref. 28) correlates with maintenance of a high exon 1 transcription rate in differentiated cells (Fig. 1).

The position of hypersensitive site 4 about 300 bases into the first intron, and its induction during differentiation suggest that it may be associated with the block to elongation of transcription between exons 1 and 2. We therefore analysed transcription of the intron 1 sequences around this hypersensitive site in differentiated HL60 cells (Fig. 4*b*). The results show a sharp drop in the transcription downstream of probe A (Fig. 4*b*) which extends to the *Pvu*II site 40 bases upstream of the exon 1 splice donor. The apparent site of the transcriptional block

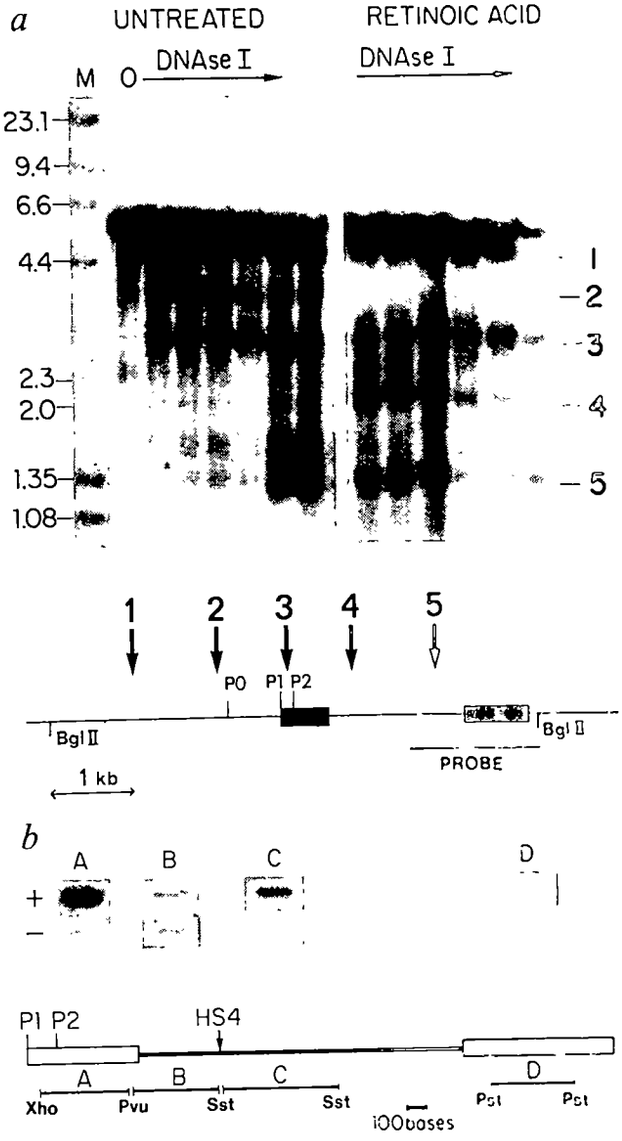


Fig. 4 *a*, DNase I hypersensitive sites in differentiating HL60. *b*, Run-off transcription of HL60 cells induced with retinoic acid for 2.5 days.

Methods. *a*, DNA from DNase I digested nuclei was restricted with *Bgl*II, blotted and hybridized[27] to the nick translated 1.5 kb *Sac*I fragment spanning exon 2. The map shows the 5′ portion of the gene including the first two exons and marks the five hypersensitive sites. (The minor sites II_1 and III_1[28] were not clearly resolved.) Lane M, marker; Lane 0, no DNase I. Arrows indicate increasing extents of DNase I digestion. HL60 was induced with 1 μM retinoic acid for 3 days. Methods for *b* were as in Fig. 1. + and − refer to probes which detect sense and anti-sense transcripts, respectively. Lengths of probes: A, 443; B, 430; C, 606; D, 414 bases.

therefore maps to the 3′ end of exon 1 or the 5′ end of intron 1 several hundred bases upstream of hypersensitive site 4. One testable hypothesis is that sequences near this hypsersenstive site function at a distance to influence the process of termination which occurs upstream. It is of interest that several stretches of T residues occur in the region of the elongation block defined in Fig. 4*b*: T_7, T_4 and T_7 occur 17, 64 and 74 bases downstream of the *Pvu*II site near the end of exon 1. Such sequences have previously been implicated in the termination of transcription. Pol III terminates at the 3′ end of *Xenopus* 5S RNA genes within clusters of four or more T residues[30]. Furthermore, in two cases of termination by Pol II the phage λ 4S gene[31] *in vitro* and the human gastrin gene *in vivo*[32], the 3′ termini map to clusters of

five or more T residues. Similarly, premature termination downstream of the adenovirus 2 major late promoter *in vivo* occurs near a cluster of 5 T residues[33,34]. Further analysis is required to establish whether the T-rich sequence near the exon 1-intron 1 border of the c-*myc* gene also functions as a terminator.

Our nuclear runoff analysis of c-*myc* transcription in HL60 led to the discovery of a novel c-myc RNA initiating several hundred bases upstream of the major promoters. In addition, perhaps the most striking feature of the transcription pattern revealed here is the molar excess of exon 1 over exon 2 transcription observed in HL60 (Fig. 1) and also in HeLa and COLO 320 cells (data not shown). In this respect, our results differ from those of Blanchard *et al.*[11] who concluded that there was equimolar transcription throughout the c-*myc* gene in Chinese hamster lung fibroblasts. The explanation for this discrepancy could be the different cell types used. However, it is possible that the results of Blanchard *et al.* were biased against exon 1 by using non-homologous human probes. Exon 1 sequences have diverged considerably more between human and mouse than have the protein coding sequences of exons 2 and 3[35]. The excess of exon 1 over exon 2 transcription which is accentuated from approximately 3- to 15-fold when HL60 cells differentiate, suggests a block to transcriptional elongation which can be modulated to control synthesis of full-length c-*myc* RNA. We have mapped the site of this block to the region of the boundary between exon 1 and intron 1. Although premature termination at this site seems likely, we cannot rule out the alternative of transcriptional pausing. In either case an elongation block, rather than decreased initiation, seems to account for the reduced exon 2 transcription in differentiated HL60 cells, and hence the reduced steady-state c-*myc* RNA level. Control of gene expression by blocking elongation is a flexible mechanism that allows modulation of transcription without requiring assembly an disassembly of the transcriptional apparatus. It will be of interest to determine whether this mechanism operates in other eukaryotic genes whose transcription is rapidly regulated.

We thank H. Weintraub for encouragement and discussions, H. Devitt for typing, M. Peretz for technical assistance and J. Lewis, J. McDougall, S. Collins, S. Hann and R. Eisenman, for gifts of RNA and cells. D.B. is supported by a Helen Hay Whitney Fellowship. This work was supported by NIH Cancer Institute Grant CA28151 (M.G.) and CA2663 (H.W.), and NSF Grant DCB 8502591 (M.G.). M.G. is a scholar of the Leukemia Society of America.

Received 16 January; accepted 28 March 1986.

1. Alitalo, K. *et al. Nature* **306**, 274-277 (1983).
2. Hann, S., Abrams, H., Rohrschneider, L. & Eisenman, R. *Cell* **34**, 789-798 (1983).
3. Gonda, T., Sheiness, D. & Bishop, *Molec. Cell. Biol.* **2**, 617-624 (1982).
4. Hayward, W., Neel, B. & Astrin, S. *Nature* **290**, 475-480 (1981).
5. Kelly, K., Cochran, B.; Stiles, C. & Leder, P. *Cell* **35**, 603-610 (1983).
6. Land, H., Parada, L. & Weinberg, R. *Nature* **304**, 596-602 (1983).
7. Palmieri, S., Kahn, P. & Graf, T. *EMBO J.* **2**, 2385-2389 (1983).
8. Westin, E., *et al. Proc. natn. Acad. Sci. U.S.A.* **79**, 2490-2494 (1982).
9. Dony, C., Kessel, M. & Gruss, P. *Nature* **317**, 636-639 (1985).
10. Greenberg, M. & Ziff, E. *Nature* **311**, 433-438 (1984).
11. Blanchard, J-M. *et al. Nature* **317**, 443-445 (1985).
12. Hayday, A. *et al. Nature* **307**, 334-340 (1984).
13. Hawley, D. & Roeder, R. *J. biol. Chem.* **260**, 8163-8172 (1985).
14. Lindell, T., Weinberg, F., Morris, P., Roeder, R. & Rutter, W. *Science* **170**, 447-448 (1970).
15. Groudine, M., Peretz, M. & Weintraub, H. *Molec. Cell. Biol.* **1**, 281-288 (1981).
16. Schibler, U., Hagenbuchle, O., Wellauer, P. & Pittet, A. *Cell* **33**, 501-508 (1983).
17. Linial, M., Gunderson, N. & Groudine, M. *Science* **230**, 1126-1132 (1985).
18. Baralle, F., Shoulders, C. & Proudfoot, N. *Cell* **21**, 621-626 (1980).
19. Bentley, D. and Groudine, M. *Molec. cell. Biol.* (in the press).
20. ar-Rushdi, A. *et al. Science* **222**, 390-393 (1983).
21. Grosso, L. & Pitot, H. *Cancer Res.* **45**, 847-850 (1985).
22. Gazin, C. *et al. EMBO J.* **3**, 383-387 (1984).
23. Crouse, G., Leys, E., McEwan, R., Frayne, E. & Kellems, R. *Molec. cell. Biol.* **5**, 1847-1858 (1985).
24. Melton, D. *et al. Nucleic Acids Res.* **12**, 7035-7056 (1984).
25. Bentley, D. L. *Nature* **307**, 77-80 (1984).
26. Cleveland, D. *et al. Cell* **20**, 95-105 (1980).
27. Stalder, J., Groudine, M., Dodgson, J., Engel, D. & Weintraub, H. *Cell* **19**, 973-980 (1980).
28. Siebenlist, U., Hennighausen, L., Battey, J. & Leder, P. *Cell* **37**, 381-391 (1984).
29. Dyson, P., Littlewood, T., Forster, Z. & Rabbits, T. *EMBO J.* **4**, 2885-2892 (1985).
30. Bogenhagen, D. & Brown, D. *Cell* **24**, 261-270 (1981).
31. Hatfield, G., Sharp, J. & Rosenberg, M. *Molec. cell. Biol.* **3**, 1687-1693 (1983).
32. Sato, K., Back, K-H. & Agarwal, K. *Molec. cell. Biol.* **6**, 1032-1043 (1986).
33. Maderious, A. & Chen-Kiang, S. *Proc. natl. Acad. Sci. U.S.A.* **81**, 5931-5935 (1984).
34. Gingeras, T. *et al. J. biol. Chem.* **257**, 13475-13491 (1982).
35. Bernard, O., Cory, S., Gerondaikis, S., Webb, E. & Adams, J. *EMBO J.* **2**, 2375-2383 (1983).

Idealization of the hydrophobic segment of the alkaline phosphatase signal peptide

Debra A. Kendall, Susan Clark Bock & Emil Thomas Kaiser

Laboratory of Bioorganic Chemistry and Biochemistry, The Rockefeller University, New York, New York 10021, USA

Proteins secreted by prokaryotic cells are synthesized as precursors containing an amino-terminal extension sequence or signal peptide[1]. Although these signal peptides share little primary sequence homology, recent studies suggest that they function via common pathways during the transport process[2] and that a common element may reside in their secondary structural characteristics[3–7]. We are investigating the role of an idealized hydrophobic sequence with high potential for α-helix formation in the *Escherichia coli* alkaline phosphatase signal peptide. Here, amino-acid substitutions were made using site-directed mutagenesis to produce a mutant signal sequence containing nine consecutive leucine residues in the hydrophobic core segment. Transport studies with this mutant precursor indicate that mature alkaline phosphatase is correctly targeted to the *E. coli* periplasm and that processing of the precursor to the mature form of the enzyme is extremely rapid. In contrast, processing is slowed when the mutant signal sequence is lengthened by the insertion of five additional leucine residues and one serine.

The alkaline phosphatase signal peptide, like other signal sequences, is characterized by a positively charged amino-terminus, a central hydrophobic core and a cleavage site recognized by the signal peptidase[1]. Previous studies suggest that the hydrophobicity[8] and helix-forming potential[5,6,9] of the residues in the core region are important to signal peptide function. The unambiguous evaluation of the importance of these features has been complicated, however, as these studies often involve peptides of varied amino-acid composition. To optimize the potential to form an α-helical, hydrophobic domain and minimize problems in interpretation due to heterogeneity in amino-acid content, we have designed a mutant alkaline phosphatase signal sequence having a core region consisting of nine leucine residues. Leucine is an ideal amino acid for this approach as it is hydrophobic, has a substantial propensity to adopt an α-helical conformation[10,11] and, fortuitously, already occurs five times in the alkaline phosphatase signal peptide. A similar approach has been used successfully to determine the requirements for amphiphilic secondary structures in peptide hormones, using chemically synthesized analogues[12].

The mutant signal peptide, denoted 13A (see Fig. 1), was constructed by making single amino-acid substitutions during each of four successive rounds of site-directed mutagenesis. In each round, a synthetic oligonucleotide primer containing the DNA sequence for the desired amino-acid substitution was annealed to single-stranded phage DNA from M13mp19 into which the structural gene[13] for alkaline phosphatase (*phoA*) had been cloned. After elongation of the mutagenic primer and a second 'universal' primer[14] located 5′ to it, followed by ligation, the double-stranded phage DNA was used to transform *E. coli* strain AW1043F′ Amp (Δ*lac galU galK* Δ(*leu-ara*) *phoA-E15 proC* : : Tn*5* F′Amp). Mutant phage were identified by screen-

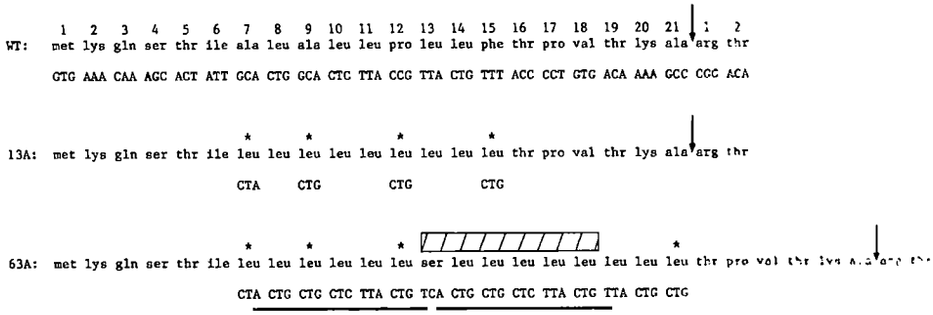


Fig. 1 Amino-acid and DNA sequences of wild-type (WT) and mutant alkaline phosphatase signal peptides. The amino-terminal 23 codons of the precursor DNA are shown in sense-strand polarity, together with the corresponding amino-acid residues and the signal processing site (arrow). Amino-acid substitutions used to construct mutants 13A and 63A are indicated by asterisks. Residues inserted into the hydrophobic core of the mutant 63A sequence are indicated by a hatched bar, and the DNA sequence repeated in this mutant is underlined. The DNA sequences of mutants 13A and 63A are identical to wild type except for the nucleotides shown.

ing plaque lifts with the ^{32}P-labelled oligomer used for mutagenesis, and subsequently verified by direct DNA sequencing[15]. Single-stranded template containing this mutant sequence was then used during the next round of mutagenesis.

During mutagenesis, an additional mutant containing an insertion of six amino-acid residues was isolated. This insertion resulted in a sequence of 14 leucine residues with a serine at the centre of this hydrophobic core (denoted 63A; see Fig. 1). The 63A mutant contains a 17-base-pair direct repeat, and probably arose from DNA replication or repair errors.

For transport studies, 2.5-kilobase DNA fragments containing the mutant *phoA* genes were subcloned into pBR322 between the *Bam*HI and *Hin*dIII sites and the resultant plasmids were used to transform *E. coli* strain AW1043 (Δ*lac galU galK* Δ(*leu-ara*) *phoA-E15 proC* : : Tn*5*). This strain contains a partially deleted alkaline phosphatase gene and a wild-type *phoR* regulatory gene[13,16].

Since a secretion-competent signal peptide directs export of alkaline phosphatase to the *E. coli* periplasm, we analysed the contents of this cellular compartment for the presence of the mature enzyme. Cells that harboured wild-type or mutant plasmids were labelled with ^{35}S-methionine for 1.5 min, washed, then treated with lysozyme to release the contents of the periplasm. Protein from the periplasmic fraction and an aliquot of whole cells were immunoprecipitated with rabbit anti-alkaline phosphatase antiserum, then analysed by SDS-polyacrylamide gel electrophoresis and autoradiography. Analysis of the periplasmic fraction for mutant 13A (Fig. 2) demonstrated that mature alkaline phosphatase was transported efficiently and correctly and localized within the periplasmic space. The protein from this fraction co-migrated with purified bacterial alkaline phosphatase (data not shown). No acccumulation of precursor was observed in the whole-cell sample from this mutant.

Analysis of mutant 63A (Fig. 2) also showed release of mature alkaline phosphatase into the periplasm but, in contrast to 13A, some accumulation of precursor in immunoprecipitates of whole cells was observed. We have found that the precursor form of the 63A mutant has a slightly greater electrophoretic mobility than the wild-type precursor; this may reflect changes in SDS binding caused by the introduction of extra hydrophobic residues rather than aberrant processing. Similar changes of electrophoretic mobility for mutant precursors have been noted in other systems[17].

To assess the effect of the signal mutations on alkaline phosphatase processing, the rate of conversion of the precursor to the mature form was determined in pulse-chase experiments. Cells were radiolabelled with ^{35}S-methionine for 40 s, then chased with cold methionine for the times indicated in Fig. 3. The chase was stopped by adding trichloroacetic acid (TCA), then the cells were extracted with acetone. After extract solubilization, alkaline-phosphatase-immunoreactive material was isolated and analysed by SDS-PAGE and autoradiography. Analysis of the ratio of the precursor to the mature form of alkaline phosphatase in the pulse-chase experiment shown in Fig. 3 indicates that cleavage of the mutant 13A signal peptide was rapid. Within the detection limits of our experiment, there was

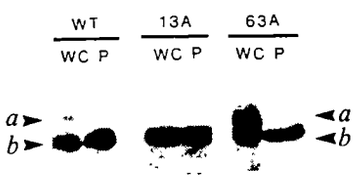


Fig. 2 Localization of alkaline phosphatase in *E. coli* transformed with wild-type, mutant 13A or mutant 63A plasmids. Arrows indicate the positions of the precursor (*a*) and mature forms (*b*) of alkaline phosphatase. WC, whole cell; P, periplasm.
Methods. Cultures of *E. coli* were washed and resuspended in MOPS (morpholinopropanesulphonate) medium[21] supplemented with amino acids at 20 μg ml^{-1}, minus methionine. The cells were labelled with 100 μCi ^{35}S-methionine for 1.5 min. Labelling was stopped by adding ice-cold 200 mM sodium azide, 10 mM dinitrophenol and 200 μg ml^{-1} chloramphenicol as described previously[2]. Half the culture was pelleted and washed with cold acetone. Protein was solubilized with 10 mM Tris *p*H 8.0, 1% SDS, 1 mM EDTA by boiling for 3 min. Following dilution by the addition of 50 mM Tris *p*H 8.0, 150 mM NaCl, 0.1 mM EDTA, 2% Triton X-100, the clarified supernatant was immunoprecipitated essentially as described by Ito *et al.*[22]; this constituted the whole-cell fraction. The remaining portion of the culture was washed with 33 mM Tris *p*H 7.5, 30 mM NaCl, then resuspended in 20% sucrose, 30 mM Tris *p*H 7.5, 1.0 mM EDTA containing 50 μg ml^{-1} lysozyme for 20 min on ice[23]. After centrifugation, the supernatant which constituted the periplasmic fraction was immunoprecipitated[22]. The immune precipitates from whole cells and the periplasm were then analysed by SDS-PAGE under reducing conditions[24].

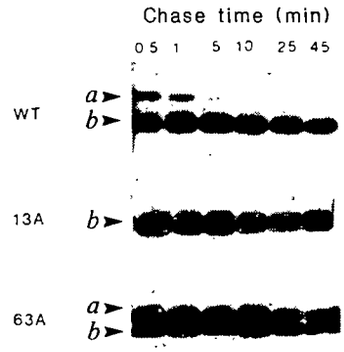


Fig. 3 Kinetics of alkaline phosphatase maturation in *E. coli* strains carrying the wild-type, mutant 13A or mutant 63A plasmids. Arrows indicate the positions of the precursor (*a*) and mature forms (*b*) of alkaline phophatase.
Methods. Cultures were washed and resuspended in MOPS medium[21] supplemented with amino acids at 20 μg ml^{-1}, minus methionine. The cells were labelled with 100 μCi ^{35}S-methionine for 40 s, and the chase was initiated by adding cold methionine to a final concentration of 4 mg ml^{-1}. At the times indicated, an aliquot of cells was precipitated in 5% TCA, then washed with cold acetone. Protein was solubilized, immunoprecipitated[22] with anti-alkaline phosphatase antiserum, and analysed as described in Fig. 2 legend.

no accumulation of the 13A precursor. The accelerated rate of maturation of alkaline phosphatase encoded by the mutant 13A gene relative to that of alkaline phosphtase encoded by the corresponding wild-type gene may reflect optimization of an important recognition element or stabilization of an active conformation. In contrast, the kinetics of maturation of the 63A alkaline phosphatase gene product were slower than those for the wild-type gene and some mutant precursor was observed throughout the experiment. Inclusion of a serine in the hydrophobic core sequence and/or lengthening of this region thus seem to decrease the efficiency of processing and transport of the enzyme.

The above experiments were carried out using bacteria carrying a multi-copy plasmid bearing the wild-type or mutant alkaline phosphatase gene. Cellular transport factors may become limiting in a multi-copy situation where large amounts of a specific, secreted protein are being produced and the extent to which the cellular transport system is overburdened may contribute to the observed differences in processing rates. The wild-type, 13A and 63A plasmids are identical except in the regions encoding the signal peptide hydrophobic core. However, it is possible that, because of their location in the 5′ end of the gene, these signal mutations could have nucleotide sequence-mediated effects on the degree of translation. The predicted minimum-energy structures[18] for the 5′ ends of the wild-type and mutant messenger RNAs were found to differ somewhat. It is possible, therefore, that translation initiation occurs at different rates in the mutants[19,20]. Parallel experiments in single-copy systems will allow definitive examintion of this issue.

The present results demonstrate that a signal peptide containing a polyleucine core region efficiently supports export of alkaline phosphatase to the *E. coli* periplasm. The signal sequence of this mutant (13A) differs from the wild type by four amino-acid substitutions. The complete retention of biological activity despite multiple residue changes in the mutant enzyme underlines the importance of overall structural features as opposed to primary sequence. Furthermore, the interpretation of the effects of individual substitutions can be misleading: for example, we have found that the individual substitution of phenylalanine for leucine (residue 15; see Fig. 1) in the alkaline phosphatase signal sequence retards precursor processing although export does occur (data not shown). The detrimental perturbation produced by this single mutation appears to be eliminated by the complete idealization of the region.

Extending the total length of the signal sequence by six residues may impair the orientation of the cleavage site, leading to the diminished rate of processing of the mutant 63A precursor. In addition, the inclusion of an extra serine, with its polar hydroxyl group, may decrease the effective length of the hydrophobic, potentially helical segment between this residue and the polar amino-terminus. Characterization of several export-defective mutants of maltose-binding protein indicates that the length of an uninterrupted hydrophobic domain is critical to function[5].

In previous studies, correlations have been observed between the predicted secondary structure of signal peptides, transport activity, and the conformation of synthetic peptides corresponding to these sequences[5,6,9]. We have now used a new approach to delineate the relationship between macromolecular structure and the function of signal peptides—that is, we have idealized the core segment to maximize the potential for formation of a hydrophobic α-helix. The results demonstrate that optimization of this structural unit is sufficient for transport and processing, and that specific residues are not required in the hydrophobic domain of the alkaline phosphatase signal peptide. This modelling approach can now be extended to other regions of the signal peptide and the mature protein.

We thank Drs H. Inouye and J. Beckwith for providing the original alkaline phosphatase plasmid and *E. coli* strains used in this work; Dr D. Osterman for suggestions regarding the approach to these studies; Drs S. Ghosh, S. Rokita, K. Strauch, P. Model and M. Russel for helpful discussions; and D. Levitan, J. Marrinan, J. Harris and E. Radziejewska for technical assistance. Support of D.A.K. by NIH postdoctoral fellowship HD06570 is gratefully acknowledged.

Received 13 March; accepted 3 April 1986.

1. Michaelis, S. & Beckwith, J. *A. Rev. Microbiol.* **36**, 435-465 (1982).
2. Bankaitis, V. A. & Bassford, P. J. Jr *J. biol. Chem.* **259**, 12193-12200 (1984).
3. Engleman, D. M. & Steitz, T. A. *Cell* **23**, 411-422 (1981).
4. Reddy, G. L. & Nagaraj, R. *Biochim. biophys. Acta* **831**, 340-346 (1985).
5. Bankaitis, V. A., Rasmuseen, B. A. & Bassford, P. J. Jr *Cell* **37**, 243-252 (1984).
6. Briggs, M. S. & Gierasch, L. M. *Biochemistry* **23**, 3111-3114 (1984).
7. Shinnar, A. E. & Kaiser, E. T. *J. Am. chem. Soc.* **106**, 5006-5007 (1984).
8. Von Heijne, G. *J. Mol. Biol.* **184**, 99-105 (1985).
9. Emr, S. D. & Silhavy, T. J. *Proc. natn. Acad. Sci. U.S.A.* **80**, 4599-4603 (1983).
10. Arfmann, H.-A., Labitzke, R. & Wagner, K. G. *Biopolymers* **16**, 1815-1826 (1977).
11. Chou, P. Y. & Fasman, G. D. *A. Rev. Biochem.* **47**, 251-276 (1978).
12. Kaiser, E. T. & Kézdy, F. J. *Science* **223**, 249-255 (1984).
13. Inouye, H., Michaelis, S., Wright, A. & Beckwith, J. *J. Bact.* **146**, 668-675 (1981).
14. Zoller, M. J. & Smith, M. *DNA* **3**, 479-485 (1984).
15. Sanger, F., Nicklen, S. & Coulson, A. R. *Proc. natn. Acad. Sci. U.S.A.* **74**, 5463-5467 (1977).
16. Ghosh, S. S., Bock, S. C., Rokita, S. E. & Kaiser, E. T. *Science* **231**, 145-148 (1986).
17. Vlasuk, G. P., Inouye, S. & Inouye, M. *J. biol. Chem.* **259**, 6195-6200 (1984).
18. Zuker, M. & Sankoff, D. *Bull. math. Biol.* **46**, 591-621 (1984).
19. Iserentant, D. & Fiers, W. *Gene* **9**, 1-12 (1980).
20. Schwartz, M., Roa, M. & Débarbouillé, M. *Proc. natn. Acad. Sci. U.S.A.* **78**, 2937-2941 (1981).
21. Neidhardt, F., Bloch, P. L. & Smith, D. F. *J. Bact.* **119**, 736-747 (1974).
22. Ito, K., Bassford, P. J. Jr & Beckwith, J. *Cell* **24**, 707-717 (1981).
23. Oliver, D. B. & Beckwith, J. *Cell* **30**, 311-319 (1982).
24. Laemmli, U. K. *Nature* **277**, 680-685 (1970).

Stringent control of initiation of chromosomal replication in *Bacillus subtilis*

Simone J. Séror, Francoise Vannier, Alain Levine & Gilles Henckes

Institut de Microbiologie, Bâtiment 409, University Paris XI, 91405 Orsay, Cedex 05, France

Interconnecting regulatory networks are characteristic of probably all cellular systems. Such 'regulons' allow the cell to respond in a coordinated manner to changes in its environment, including a rapid return to balanced growth after stress[1,2]. A regulon is usually composed of diverse metabolic pathways whose activities are amplified or inhibited by regulatory proteins, through the action of a small molecule, an alarmone[3]. Thus, for example, when the level of any aminoacyl transfer RNA becomes limiting in the bacterial cell, the stringent response is initiated; this is mediated through the nucleotide ppGpp and leads to the inhibition of synthesis of several major macromolecules, including stable RNA[4,5]. Surprisingly, the key control point in the cell cycle, initiation of DNA replication, has not previously been implicated in the stringent response. Using a *Bacillus subtilis* mutant in which the transcriptional step of initiation can be studied independently of any requirement for protein synthesis[6], we now show that initiation of chromosomal replication is indeed subject to stringent control.

The synthesis of a specific RNA–DNA co-polymer containing RNA and DNA sequences has been correlated with the transcriptional step required for initiation in *B. subtilis*[7,8]. Moreover, a ribosomal RNA operon, *rrnO*, has been identified within the origin region of the chromosome[9]. These observations suggested to us that initiation of DNA replication, which may involve the synthesis of a stable RNA, was also likely to be subject to stringent control.

To induce the stringent response, we used *O*-methylthreonine (*O*-MeT), an inhibitor of isoleucyl tRNA synthetase, or an aminoacyl hydroxamate. These drugs promote the accumulation of large amounts of ppGpp and inhibit synthesis of stable RNA in a *relA*$^+$ strain[10,11]. In contrast, in a *relA*$^-$ strain, the rate of RNA synthesis continues relatively undisturbed under these conditions. Figure 1 shows the results obtained with strains OMM242(*dna37, thy*$^-$, *trp*$^-$, *relA*$^+$) and OMM243(*dna37, thy*$^-$, *trp*$^-$, *relA*$^-$).

We tested the effect of the drugs on initiation of chromosomal replication and, for that purpose, replication rounds were synchronized in the temperature-sensitive *dna37* mutant of *B. subtilis*. As described previously[12], after return to the permissive temperature, DNA synthesis is synchronized for at least two rounds of replication. Under these conditions, initiation of the first round proceeds even in the absence of protein synthesis. However, the first round of DNA replication is blocked in the presence of inhibitors of transcription, for example, rifampicin and streptolydigin. Thus, we were able to test the effect of *O*-MeT on the transcriptional step quite independently of any requirement for protein synthesis. When added at the time of initiation, *O*-MeT, completely abolished DNA synthesis in the *relA*$^+$ strain (Fig. 2*a*). To exclude the possibility that the drug was inhibiting elongation of DNA replication or the uptake of the labelled precursor, rather than inhibiting initiation, control experiments were done using exponentially growing cultures in which either the rate of incorporation of ^{3}H-adenine into DNA or the amount of residual DNA synthesis in uniformly labelled cells was measured after the addition of *O*-MeT or chloramphenicol, which also blocks chromosomal initiation. In both cases, the effects of *O*-MeT and chloramphenicol were identical, indicating no major effect of *O*-MeT on uptake or DNA replication *per se*. Moreover, in synchronized cells, when *O*-MeT was added after initiation, substantial levels of DNA synthesis were detected (Fig. 2*a*).

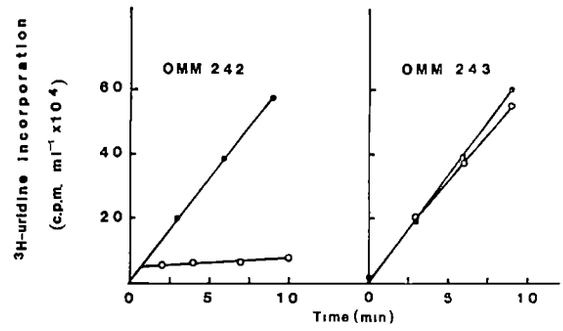


Fig. 1 Effect of *O*-MeT on RNA synthesis in *B. subtilis* OMM242 (*dna37 thy*$^-$*trp*$^-$*relA*$^+$) and OMM243 (*dna37 thy*$^-$*trp*$^-$*relA*$^-$). A derivative of OMM242 carrying the *relA*$^-$ locus was constructed by transformation from strain BR17 (ref. 23). Strains OMM242 and OMM243 were grown at 30 °C in Spizizen medium[24] containing glucose (0.5%), casein hydrolysate (0.02%) and the required supplements. At t_0, cells were labelled with ^{3}H-uridine (24 Ci mmol^{-1}; 10 μCi ml^{-1}) and *O*-MeT (1 mg ml^{-1}) (Sigma) was added to induce the stringent response. At intervals samples were removed and radioactivity in the RNA was determined after precipitation with trichloroacetic acid (TCA). ●, Without *O*-MeT; ○, plus *O*-MeT.

The effect of *O*-MeT was then tested in a *relA*$^-$ derivative of *dna37*. As shown in Fig. 2*b*, initiation of DNA synthesis was in this case largely resistant to the presence of *O*-MeT. Using another inhibitor of tRNA synthetase, arginine hydroxamate, which also induces the stringent response in OMM242, we found that initiation of DNA replication was again blocked in the *relA*$^+$ strain but not in the *relA*$^-$ derivative.

It was important to establish whether DNA synthesis occurring in the *relA*$^-$ strain in the presence of such drugs involved initiation from the normal origin of the chromosome. Therefore, we compared the first fragments to bed replicated after initiation of DNA synthesis in the untreated *relA*$^-$ strain and in the same strain exposed to the drug. Figure 3 shows that the earliest fragments to be replicated were in fact identical in both cases. Moreover, these fragments corresponded exactly to the origin region of the chromosome (ref. 13 and A.L., G.H. and S.J.S., in preparation).

All these results indicate that initiation is subject to stringent control and therefore imply that high levels of ppGpp inhibit chromosomal initiation. One way to test that possibility is to increase the concentration of ppGpp without inducing amino-acid starvation; this can be achieved by adding a drug which inhibits the normal degradation of ppGpp. We used levallorphan[14], which completely inhibited initiation of DNA replication in OMM242 without affecting DNA synthesis. This result is consistent with our hypothesis. However, as the full effects of levallorphan might be quite complex, further work is needed to verify this conclusion.

Here, we have presented evidence that chromosomal initiation is subject to stringent control in *B. subtilis*. Our results also indicate that ppGpp might be involved in this process. Future work will be concerned with identifying the precise step of the initiation process that is regulated by the stringent response.

In a previous study, Orr *et al.*[15] examined the factors required for the expression of initiation potential that accumulated in non-synchronized cultures of the *Escherichia coli dnaA46* initiation mutant. Those workers observed that, although initiation proteins could be expressed during amino-acid starvation in a *relA*$^-$ strain, this was not the case in a *relA*$^+$ strain. These results indicated that normal initiation in *E. coli* might also be subject

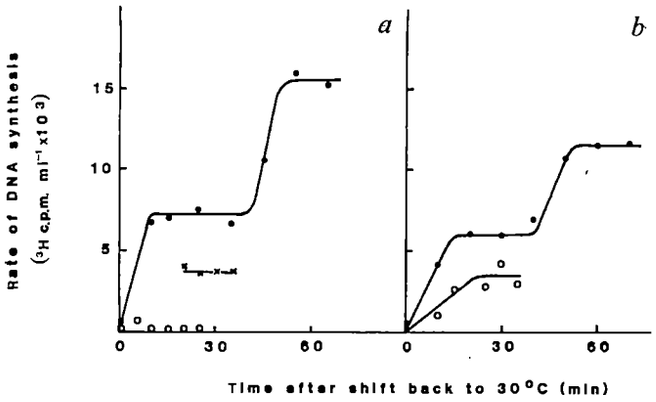


Fig. 2 Effect of *O*-MeT on initiation of DNA synthesis in cultures of *B. subtilis* OMM242 (*a*) and OMM243 (*b*) synchronized for DNA replication. An exponential culture of strain OMM242 and its derivative OMM243 ($A_{570}=0.175$) was shifted to 45 °C for 30 min, diluted three times and shifted back to 30 °C. Under these conditions, DNA replication is synchronized. At intervals, 2.5-ml samples were removed and ^{3}H-adenine (19 Ci mmol^{-1}; 2 μCi ml^{-1} was added. After 10 s, 2 min and 4 min, 0.5-ml samples were withdrawn and incorporation was stopped by adding 0.1 vol. of 1 mM NaN_3. Samples were incubated at 80 °C for 30 min in the presence of 0.4 M NaOH, neutralized by addition of 0.5 ml of 0.5 M HCl and precipitated with TCA. The rate of DNA synthesis is expressed as ^{3}H-adenine counts incorporated per ml of culture. ●, Control cultures; ○, plus *O*-MeT (1 mg ml^{-1}). The drug was added at 45 °C 3 min before the return to 30 °C. X, Addition of *O*-MeT (1 mg ml^{-1}) 15 min after the return to 30 °C.

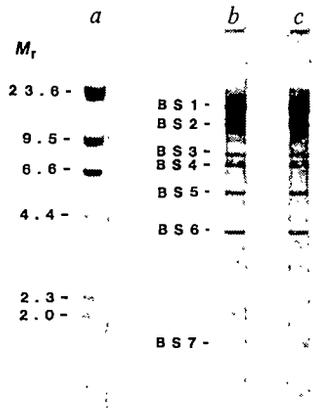


Fig. 3 Identification of the first DNA fragments to be replicated in *B. subtilis* OMM243 in the presence of arginine hydroxamate. A culture of strain OMM243 was shifted back from 45 °C to 30 °C as described in Fig. 2 legend, then pulse-labelled for 3 min with ^{3}H-thymidine (40 Ci mmol^{-1}; 20 μCi ml^{-1}) in either the absence (*b*) or presence (*c*) of arginine hydroxamate (50 μg ml^{-1}); (sigma). The labelled DNA was purified and digested with *Bam*HI and *Sal*I. ^{3}H-labelled first replicating DNA fragments were separated by electrophoresis on a 0.8% agarose gel and detected by fluorography as described elsewhere[25]. BS1–BS7 are fragments numbers from the replication origin of the chromosome. *Hin*dIII-digested λ fragments, indicated in *a*, are relative molecular mass (M_r) markers.

to stringent control, although the authors did not draw this conclusion. In the light of the results with *B. subtilis*, we re-investigated this possibility using an initiation mutant of *E. coli*, under similar conditions to those described in the present paper. Our preliminary results indicate that initiation of chromosomal replication in *E. coli* is also subject to stringent control Interestingly, Hecker *et al.*[16] have reported that the replication of the multi-copy plasmid pBR322 is also negatively controlled by the stringent response in *E. coli*.

In the present work, the effect of the *rel* system on initiation was observed under stress conditions mimicking amino-acid starvation. The question remains as to whether the stringent control system has any part in regulation of initiation under steady-state conditions. Bremer and colleagues[17] have provided evidence that the levels of ppGpp are strictly correlated with ribosomal RNA synthesis in *E. coli* under steady-state growth conditions. Moreover, Van Verseveld *et al.*[18] reported that ppGpp also negatively regulated cell division in *E. coli*, at least at extremely slow growth rates. It is therefore possible that the *rel* system, perhaps mediated through the effect of ppGpp, also has a role in the regulation of initiation during steady-state growth of bacteria.

As the initiation of chromosomal replication must be coordinated with the overall growth of a cell, it seems logical to suppose that this process also forms part of the stringent control system which includes the coordinated control of, for example, stable RNA, nucleotides, carbohydrates, fatty acids and peptidoglycan[19]. In eukaryotes there is evidence that the alarmone Ap4A, rather than ppGpp, is involved in some way in the regulation of DNA replication[20,21] and in cellular proliferation[22]. It would be interesting to determine whether this particular phosphorylated nucleotide is also involved in the coordination of other macromolecular processes in a regulon analogous to the *rel* system, in higher organisms.

We thank Drs I. Barry Holland, Paul Boquet, A. Danchin and Mathias Springer for helpful discussions during this work. These studies were supported by grants from CNRS, ATP 'Biotechnologie', no. 040136.

Received 10 March; accepted 1 April 1986.

1. Gottesman, S. & Neidhart, F. C. in *Gene Function in Procaryotes* (eds Beckwith, J., Davies, J. & Gallant, J. A.) 163-183 (Cold Spring Harbor Laboratory, New York, 1983).
2. Gottesman, S. *A. Rev. Genet.* **18**, 415-441 (1981).
3. Stephens, J. C., Artz, S. W. & Ames, B. N. *Proc. natn. Acad. Sci. U.S.A.* **72**, 4389-4393 (1975).
4. Cashel, M. *A. Rev. Microbiol.* **29**, 301-318 (1975).
5. Gallant, J. A. *A. Rev. Genet.* **13**, 393-415 (1979).
6. Laurent, S. J. *J. Bact.* **116**, 141-145 (1973).
7. Henckes, G., Vannier, F., Buu, A. & Séror-Laurent, S. J. *J. Bact.* **149**, 79-91 (1982).
8. Séror-Laurent, S. J. & Henckes, G. *Proc. natn. Acad. Sci. U.S.A.* **82**, 3586-3590 (1985).
9. Henckes, G. *et al. Nature* **299**, 268-271 (1982).
10. Price, V. L. & Gallant, J. A. *J. Bact.* **149**, 635-641 (1982).
11. Pizer, L. I. & Merlie, J. P. *J. Bact.* **114**, 980-987 (1973).
12. Laurent, S. J. & Vannier, F. *J. Bact.* **114**, 474-484 (1973).
13. Ogasawara, N., Mizumoto, S. & Yoshikawa, H. *Gene* **30**, 173-182 (1984).
14. Boquet, P. L., Devynck, M. A., Monnier, C. & Fromageot, P. *Eur. J. Biochem.* **40**, 31-42 (1973).
15. Orr, E., Meacock, P. A. & Pritchard, R. H. in *DNA Synthesis: Present and Future* (eds Molineaux, I. & Kohiyama, M.) 85-99 (Plenum, New York, 1978).
16. Hecker, M., Schroeter, A. & Mach, F. *Molec. gen. Genet.* **190**, 355-357 (1983).
17. Ryals, J., Little, R. & Bremer, H. *J. Bact.* **151**, 1261-1268 (1982).
18. Van Verseveld, H. W., Chesbro, W. R., Braster, M. & Stouthamer, A. H. *Arch. Mikrobiol.* **137**, 176-184 (1984).
19. Cozzone, A. J. *Biochimie* **62**, 647-664 (1980).
20. Grummt, F. *Proc. natn. Acad. Sci. U.S.A.* **75**, 371-375 (1978).
21. Weinmann-Dorsch, C. *et al. Eur. J. Biochem.* **138**, 170-185 (1984).
22. Rapaport, E. & Zamenick, P. C. *Proc. natn. Acad. Sci. U.S.A.* **73**, 3984-3988 (1976).
23. Swanton, M. & Edlin, G. *Biochem. biophys. Res. Commun.* **46**, 583-588 (1972).
24. Spizizen, J. *Proc. natn. Acad. Sci. U.S.A.* **44**, 1072-1078 (1958).
25. Marsh, R. C. & Worcel, A. *Proc. natn. Acad. Sci. U.S.A.* **74**, 2720-2724 (1977).

Copies of articles from this publication are now available from the UMI Article Clearinghouse.

For more information about the Clearinghouse, please fill out and mail back the coupon below.

Yes! I would like to know more about UMI Article Clearinghouse. I am interested in electronic ordering through the following system(s):

☐ DIALOG/Dialorder
☐ OnTyme
☐ ITT Dialcom
☐ OCLC ILL Subsystem
☐ Other (please specify)_____
☐ I am interested in sending my order by mail.
☐ Please send me your current catalog and user instructions for the system(s) I checked above.

Name_____
Title_____
Institution/Company_____
Department_____
Address_____
City_____ State_____ Zip_____
Phone ( )_____

UMI Article Clearinghouse

Mail to:
University Microfilms International
300 North Zeeb Road, Box 91
Ann Arbor, MI 48106

NEW EDITION

INFORMATION SOURCES IN BIOTECHNOLOGY, *2nd Edition*

Anita Crafts-Lighty

"This book is a model. As such it should be in the hands of every librarian and information officer..." *Process Biochemistry*

"...very useful. No comparable work is available." *Choice*

First Edition—*Choice* Outstanding Academic book 1984-5

Revised and updated throughout, this new edition provides even more practical, incisive evaluations of both the traditional and more elusive sources of information in biotechnology. It will bring you right up to date by systematically and critically reviewing the many different sources available in:

• Trade and research literature • Market surveys • Company directories • Conference Reports • Secondary sources—abstracts, title lists, indexes, bibliographies

PLUS—*Greatly expanded sections on* • Conference proceedings • Reading lists of introductory books • *New information on* • international organizations • Books out of print • How to set up and run information services • What is available for those seeking state-of-the-art coverage

A full index of publishers and addresses is included.

320pp	August 1986
$100.00	£50.00
0-943818-18-4	0-333-39290-6

CONTENTS

1. What is Biotechnology? The Science and the Business
2. Information Sources in Biotechnology—Outline of Types
3. Monographs, Book Series and Textbooks
4. Conferences and Their Proceedings
5. Trade Periodicals and Newsletters
6. Research and Review Periodicals
7. Abstracting and Secondary Sources
8. Computer Databases/Databanks
9. Patents and Patenting
10. Market Surveys
11. Directories of Companies, Products and Research
12. Organizations
13. Providing Library and Information Services in Biotechnology

Publishers' Addresses
Appendices and Tables
Index

Order now on FREE APPROVAL by mail or phone.
We accept all major credit cards.

US/Canada—Mail to:
Stockton Press, 15 East 26th Street, New York, N.Y. 10010. To order by phone, call toll-free 800-221-2123. In N.Y., call 212-481-1334. NYS residents add sales tax. Shipping and handling costs added to billed orders. Prepay and save s/h charges. Place a Standing Order and receive a 5% discount on this and all future editions.

UK/Rest of World—Mail to:
Elaine Coles, Globe Book Services, Ltd., FREEPOST, Brunel Road, Houndmills, Basingstoke, Hants RG21 2BR; England
Telephone: Basingstoke (0256) 26222
Charges for Postage and Packing:
UK: £2.00 per order, Libraries free.
Continental Europe: £2.00 per book.
Rest of World: £3.50 per book.
FREEPOST applies UK only.
Globe Book Services, a division of Macmillan Publishers Ltd

NEW

INTELLECTUAL PROPERTY RIGHTS IN BIOTECHNOLOGY WORLDWIDE

R. Schwaab, D. Conlin, D. Jeffery, S. Bent

The first comprehensive guide to the law governing the protection of new developments in biotechnology

This up-to-date resource will provide valuable guidance on protecting applied biological inventions in a broad range of countries. Covering patent laws, plant breeders' rights, trade secret laws, and relevant international treaties, *it gives you the latest tools with which to develop appropriate protection strategies.*

The book's practical "how-to" approach emphasizes how legal principles differ from country to country, and helps you answer such questions as: What laws can and should I turn to? Does a specific action in one country harm my position in another? What are the implications for research and development, investment and product planning?

Intellectual Property Rights in Biotechnology will prove essential to biotechnologists, business people, attorneys and libraries.

Order your copy now on FREE APPROVAL by mail or phone.
We accept all major credit cards.

320pp	October 1986
$100.00	£50.00
0-943818-15-X	0-333-39288-4

CONTENTS

Part 1.
1. Proprietary Rights in Biotechnology: A Conceptual Framework
2. The Past is Prologue: Development of Proprietary Rights in Plant Varieties
3. Patentability of Biotechnological Inventions
4. Patent Description Requirements for Biotechnological Inventions
5. Bases and Barriers for Protection of Biological Inventions Internationally
6. Scope of Patent Protection for Biotechnology
7. Trade Secret Protection for Biotechnology
8. Proprietary Vehicles for Biotechnology

Part 2.
Summary of Legal Framework for Selected Countries
Australia — Austria — Belgium — Canada — Denmark — Federal Republic of Germany — Finland — France — Hungary — Japan — Luxembourg — The Netherlands — People's Republic of China — Poland — Republic of South Africa — South Korea — Switzerland — United Kingdom — USSR — USA

US/Canada—Mail to:
Stockton Press
15 East 26th St.
New York, N.Y. 10010
Call toll-free 800-221-2123
In N.Y., 212-481-1334

UK/Rest of World—Mail to:
Elaine Coles, **Globe Book Services, Ltd.,**
FREEPOST
Brunel Road, Houndmills
Basingstoke, Hants RG21 2BR, England
Basingstoke (0256) 26222
FREEPOST applies UK only.

Postage & Packing: US/Canada: Added to invoice at cost; prepaid free.
UK/Rest of World: £2.00 per order UK; £2.00 per book Continental Europe; £3.50 per book rest of world. UK libraries free.

Physics

Advances in Nuclear Physics, Vol. 15. J.W. NEGELE and ERICH VOGT (eds). *Plenum: 1985. Pp. 218. Hbk ISBN 0-306-41864-9. Np.*

Applications of Circularly Polarized Radiation Using Synchrotron and Ordinary Sources. FRITZ ALLEN and CARLOS BUSTAMANTE (eds). *Plenum: 1985. Pp. 193. Hbk ISBN 0-306-42087-2. Np.*

Applied Electromagnetics, 2nd Edn. By J.E. PARTON, S.J.T. OWEN and M.S. RAVEN. *Macmillan: 1986. Pp. 288. HBK ISBN 0-333-37101-1. £20.*

Atomic Shell Physics. BERND CRASEMANN. *Plenum: 1985. Pp. 754. Hbk ISBN 0-306-41847-9. Np.*

Concise Dictionary of Physics. *Oxford University Press:1986. Pp.292. Hbk ISBN 0-19-866142-8. £7.95.*

Electronic Excitations in Condensed Rare Gases. Springer Tracts in Modern Physics, Vol. 107. By N. SCHWENTNER, E.-E. KOCH and J. JORTNER. *Springer-Verlag:1985. Pp.239. Hbk ISBN 3-540-15382-9. DM 98.*

Engineering Rheology. Oxford Engineering Science Series 14. By ROGER I. TANNER. *Oxford University Press:1985. Pp.451. Hbk ISBN 0-19-856144-X. £55.*

Frontiers of Nuclear Dynamics. R.A. BROGLIA and C.H. DASSO (eds). *Plenum:1985. Pp.402. Hbk ISBN 0-306-42069-4. Np.*

Group Theoretical Methods in Physics, Vol. 1. M.A. MARKOV, V.I. MAN'KO AND A.E. SHABAD (eds). *Harwood Academic: 1985. Pp. 717. Hbk ISBN 3-7186-0245-8. $250.*

An Introduction to the Linear Theories and Methods of Electrostatic Waves in Plasmas. By W.D. JONES, H.J. DOUCET and J.M. BUZZI. *Plenum: 1985. Pp. 312. Hbk ISBN 0-306-41961-0. Np.*

Laser Spectroscopy VII. T.W. HANSCH and Y.R. SHEN (eds). *Springer-Verlag:1985. Pp.419. Hbk ISBN 3-540-15894-4. DM 82.*

Light in Einstein's Universe. The Role of Energy in Cosmology and Relativity. By S.N. PROKHOVNIK. *Reidel: 1985. Pp. 221. Hbk ISBN 90-277-2093-2. Dfl. 110, £30.50, $39.*

Long Distance Propagation of HF Radio Waves. By A.V. GUREVICH and E.E. TSEDILINA. *Springer-Verlag:1985. Pp.344. ISBN 0-540-15138-7. DM 220.*

The Mathematics of Combustion. JOHN D. BUCKMASTER (ed.). *SIAM/Wiley: 1985. Pp. 254. ISBN 0-89871-053-7. £29.90.*

Methods in the Qualitative Theory of Dynamical Systems in Astrophysics and Gas Dynamics. By OLEG. I. BOGOYAVLENSKY. *Springer-Verlag: 1985. Pp.301. ISBN 0-387-13614-2. DM 144.*

Microcomputer Quantum Mechanics, 2nd edn. By J. P. KILLINGBECK. *Adam Hilger Ltd: 1985. Pp. 187. Hbk ISBN 0-85274-803-5. Np.*

Nuclear Shell Models. MICHEL VALLIERES and BRYAN HOBSON WILDENTHAL (eds). *World Scientific:1985. Pp.754. ISBN 9971-978-23-7. £72.50.*

Picosecond Electronics and Optoelectronics. G.A. MOUROU, D.M. BLOOM and C.H. LEE (eds). *Springer-Verlag:1985. Pp.258. ISBN 0-387-15884-7. DM 84.*

The Picture Book of Quantum Mechanics. By SIEGMUND BRANDT and HANS DIETER DAHMEN. *Wiley: 1985. Pp. 306. Hbk ISBN 0-471-81776-7. £26.50.*

Principles of Optical Disc Systems. By G. BOUWHUIS *et al. Adam Hilger:1985. Pp.277. ISBN 0-85274-785-3. £30, $47.50.*

Rayleigh-Wave Theory and Application. E.A. ASH and E.G.S. PAIGE (eds). *Springer-Verlag: 1985. Pp. 360, Hbk ISBN 3-540-15933-9. DM 89.*

Spectroscopy of Molecular Excitons. By V.L. BROUDE, E.I. RASHBA and E.F. SHEKA. *Springer-Verlag:1985. Pp.271. Hbk ISBN 3-540-12409-8. DM 148.*

Techniques and Concepts of High-Energy Physics III. THOMAS FERBEL (ed.). *Plenum:1985. Pp.436. Hbk ISBN 0-306-42106-2. Np.*

The Thermodynamics of Fluid Systems. By L.C. WOODS. *Oxford University Press: 1985. Pp. 359. Pbk ISBN 0-19-856180-6. £12.50.*

Thermodynamics and an Introduction to Thermostatistics, 2nd Edn. By HERBERT B. CALLEN. *Wiley:1985. Pp.493. ISBN 0-471-86256-8. £34.75.*

Viscoelasticity and Rheology. ARTHUR S. LODGE, MICHAEL RENARDY and JOHN A. NOHEL (eds). *Academic:1985. Pp.445. ISBN 0-12-454940-3. $35, £31.50.*

Biological Sciences

Adenosine: Receptors and Modulation of Cell Function. V. STEFANOVICH, K. RUDOLPHI and P. SCHUBERT (eds). *IRL Press, P.O. Box 1, Eynsham, Oxford, UK: 1985. Pp.520. Pbk ISBN 0-947946-49-7. £36, $65.*

Advances in Animal Conservation. J.P. HEARN and J.K. HODGES (eds). *Oxford University Press: 1985. Pp.282. ISBN 0-19-854002-7. $35.*

Amino Acids. ALAN A. BOULTON, GLEN B. BAKER and JAMES D. WOOD (eds). *Humana: 1985. Pp.281. ISBN 0-85603-077-6. $45.*

Aquatic Microbiology, 3rd Edn. By G. RHEINHEIMER. *Wiley: 1985. Pp.257. Hbk ISBN 0-471-90657-3. £17.95.*

Assessment of Ventricular Function ANGELO RAINERI, ROBERT D. LEACHMAN and JAN J. KELLERMANN (eds). *Plenum: 1985. Pp. 347. Hbk ISBN 0-306-42092-9. Np.*

The BALB/c Mouse: Genetics and Immunology. M. POTTER (ed.). *Springer-Verlag: 1985. Pp.253. Hbk ISBN 3-540-15834-0. DM 126.*

Biochemistry of Macrophages. Ciba Foundation Symposium 118. *Pitman: 1986. Pp.256. Hbk ISBN 0-272-79822-3. $35.*

Biochimie Illustrée. By PETER N. CAMPBELL and ANTHONY D. SMITH. *Masson, Paris: 1985. Pp.240. Pbk ISBN 2-225-80456-7. F 120.*

The Biology of Echinococcus and Hydatid Disease. R.C.A. THOMPSON (ed.). *George Allen & Unwin: 1986. Pp.290. Hbk ISBN 0-04-591020-0. £35, $50.*

Brain Plasticity, Learning, and Memory. B.E. WILL, P. SCHMITT and J.C. DALRYMPLE-ALFORD (eds). *Plenum: 1985. Pp.599. Hbk ISBN 0-306-42063-5. Np.*

Cancer: An Enigma in Biology and Society. By R. NERY. *Croom Helm, London & Sydney: 1985. Pp.436. Hbk ISBN 0-7099-1825-9. £29.50.*

Cell Membranes and Cancer. T. GALEOTTI *et al.* (eds). *Elsevier: 1985. Pp.446. ISBN 0-444-80723-3. Np.*

Ctenostome Bryoans. By P.J. HAYWARD. *E.J. Brill: 1985. Pp.169. ISBN 90-04-07471-6. Pbk Dfl. 56.*

Current Topics in Microbiology and Immunology. Iridoviridae. DAWN B. WILLIS (ed.). *Springer-Verlag: 1985. Pp.173. Hbk ISBN 3-540-15172-9. DM 118.*

Darwin's Metaphor. By ROBERT M. YOUNG. *Cambridge University Press: 1985. Pp.341. Hbk ISBN 0-521-30083-5; pbk ISBN 0-521-31742-8. Hbk £27.50, $44.50; pbk £9.95, $15.95.*

The Flowers Around Us. By MARY PARKER BUCKLES. *Harper & Row: 1986. Pp.118. ISBN 0-8262-0480-5. £23.50.*

Fundamentals of Insect Physiology. MURRAY S. BLUM (ed.). *Wiley: 1985. Pp.598. ISBN 0-471-05468-2. £40.90.*

Handbook of European Sphagna. By R.E. DANIELS and A. EDDY. *Natural Environment Research Council: 1985. Pp.262. Pbk ISBN 0-904282-82-1. £10.50.*

Heavy Metals in Water Organisms. J. SALANKI (ed.). *Akademiai Kiado, P.O.B. 24, H-1363 Budapest: 1985. Pp. 440. Hbk ISBN 963-05-3614-5. £32.50.*

Immune Regulation. MARC FELDMANN and N.A. MITCHISON (eds). *Humana: 1985. Pp.391. ISBN 0-89603-083-0. $55.*

The Insect World. By KEITH PORTER. *Macmillian: 1986. Pp.48. ISBN 0-333-40933-7. £4.95.*

International Review of Neurobiology, Vol. 27. JOHN R. SMYTHIES and RONALD J. BRADLEY (eds). *Academic: 1985. Pp.398. Hbk ISBN 0-12-366827-1. £68.00, $78.50.*

Introductory Microbiology, 2nd Edn. By FREDERICK C. ROSS. *Merrill: 1986. Pp.551. Hbk ISBN 20460-7. Np.*

The Leafhoppers and Planthoppers. L.R. NAULT and J.G. RODRIGUEZ (eds). *Wiley: 1985. Pp.500. Hbk ISBN 0-471-80611-0. £61.35.*

Membranes and Muscle. MERVYN C BERMAN, WIELAND GEVERS and LIONEL H. OPIE (eds). *IRL Press: 1985. Pp.392. Pbk ISBN 0-947946-40-3 £27.00, $50.00.*

Methods in Enzymology. Vol. 18: Glutamate, Glutamine, Glutathione and Related Compounds. ALTON MEISTER (ed.). *Academic: 1985. Pp 723. ISBN 0-12-182013-0. $75, £65.*

Molecular Mechanisms of Transmembrane Signalling. P. COHEN and M.D. HOUSLAY (eds) *Elsevier: 1985. Pp.487. ISBN 0-444-80689-X. Dfl. 315.*

Neurobiology of Arachnids. FREDRICH G BARTH (ed.). *Springer-Verlag: 1985 Pp 385. Hbk ISBN 3-540-15303-9. DM 198.*

Photosynthetic Mechanisms and the Environment. J. BARBER and N.R. BAKER (eds). *Elsevier: 1985. Pp.565. ISBN 0-444-80674-1. Dfl. 375*

Plasma Fibronectin: Structure and Function. JAN MCDONAGH (ed.). *Dekker: 1985 Pp.288. Hbk ISBN 0-8247-7384-5. $59.75 (US and Canada), $71.50 (other countries).*

Recent Advances in Biological Membrane Studies. Structure and Biogenesis, Oxidation and Energetics. LESTER PACKER (ed.). *Plenum: 1985. Pp.554. Hbk ISBN 0-306-42017-1. Np.*

Regulation of Vertebrate Limb Regeneration. RAYMOND E. SICARD (ed.). *Oxford University Press. 1985. Pp.185. ISBN 0-19-503604-2. £40.*

Space, Time and Life: The Probabilistic Pathways of Evolution. By V.V. NALIMOV. *ISI Press: 1985. Pp.110. ISBN 0-89495-048-7. Np.*

Surgical Anatomy of the Orbit. By BARRY M. ZIDE and GLENN W. JELKS. *Raven: 1985. Pp.87. ISBN 0-88167-054-5. $71.50.*

Synopsis of Invertebrate Pathology Exclusive of Insects. By ALBERT K. SPARKS. *Elsevier: 1985. Pp.423. ISBN 0-444-80678-4. Dfl. 325*

Termitologia, Tome III: Comportement, Socialite, Ecologie, Evolution, Systematiques. By PIERRE P. GRASSE. *Masson: 1986. Pp.715. Hbk ISBN 2-225-80368-4. F 465.*

Tratado de Entomologia. By JUAN MANUEL NIETO NAFRIA and MILAGROS PILAR MIER DURANTE. *Ediciones Omega, Plato 26, 08006 Barcelona, Spain: 1985. Pp.599. Pbk ISBN 84-282-0748-8. Np.*

Trichothecenes and Other Mycotoxins. Proceedings of the International Mycotoxin Symposium, Sydney, Australia (1984). JOHN LACEY (ed.). *Wiley: 1985 Pp.571. Hbk ISBN 0-471-90751-0. £55.*

World Perspectives in Apiculture. By EVA CRANE. *International Bee Research Association, Hill House, Gerrards Cross, Bucks SL9 0NR, UK: 1985 Pp.184. Pbk ISBN 0-86098-142-8. Pbk £11.60, $14.*

Applied Biological Sciences

Adenosine Deaminase in Disorders of Purine Metabolism and in Immune Deficiency. Annals of the New York Academy of Sciences, Vol. 451. GEORGE L. TRITSCH (ed.). *The New York Academy of Sciences: 1985. Pp.345. Pbk ISBN 0-89766-297-0 Np.*

Advances in Gene Technology: Molecular Biology of the Immune System. J. WAYNE STREILEIN *et al.* (eds). *Cambridge University Press:1985. Pp.366. ISBN 0-521-30486-5. £30, $59.50.*

Advances in Inflammation Research, Vol. 10. FRANCOISE RUSSO-MARIE, JEAN MICHEL MENCIA-HUERTA and MICHEL CHIGNARD (eds). *Raven Press:1985. Pp.461. Hbk ISBN 0-88167-123-1. $60.50.*

Advances in Microscopy. RONALD R. COWDEN and FREDERICK W. HARRISON (eds). *Alan R. Liss:1985. Pp.362. ISBN 0-8451-5046-4. £38.*

Advances in Nutritional Research, Vol. 7. HAROLD H. DRAPER (ed.). *Plenum 1985 Pp. 273. ISBN 0-306-42213-1. Np.*

Alpha-Fetoprotein and Congenital Disorders. GERALD J. MIZEJEWSKI and IAN H. PORTER (eds). *Academic:1985. Pp.363. ISBN 0-12-501630-1 $35, £31.*

Ataxia-Telangiectasia Genetics, Neuropathology, and Immunology of a Degenerative Disease of Childhood. Kroc Foundation Series, Vol. 19. RICHARD A. GATTI and MICHAEL SWIFT (eds). *Alan R. Liss: 1985. Pp.430. Hbk ISBN 0-8451-0309-1. $79.*

Behavioural Epidemiology and Disease Prevention. R.M. KAPLAN and M.H. CRIQUI (eds). *Plenum: 1985. Pp.450. Hbk ISBN 0-306-41929-7. Np.*

Biochemical Basis of Medicine. By ERIC D. WILLIS. *Wright, Techno House, Redcliffe Way, Bristol, UK:1985. Pp.631. ISBN 0-7236-0722-2. £14.95.*

Biological Responses to Cancer, Vol. 4. ENRICO MIHICH (ed.). *Plenum:1985. Pp.256. Hbk ISBN 0-306-42044-9. Np.*

Burn and Scald Accidents to Children. Report of a Working Party of the Child Accident Prevention Trust. *Bedford Square Press:1985. Pp.65. Pbk ISBN 0-7199-1160-5. £3.95.*

Cancer: A Biological and Clinical Introduction. 2nd Edn. By STEVEN B. OPPENHEIMER. *Jones and Bartlett Publishers Inc., Boston:1985. Pp.262. Hbk ISBN 0-86720-062-6. Np.*

Carbon Nitrogen Sulfur. Human Interference in Grand Biospheric Cycles. By VACLAV SMIL. *Plenum:1985. Pp.459. Hbk ISBN 0-306-42026-0. Np.*

Causation of Cardiovascular Risk Factors in Children: Perspectives on Cardiovascular Risk in Early Life. GERALD S. BERENSON (ed.). *Raven:1985. Pp. 408. ISBN 0-88167-138-X. $76.50.*

21st Century Medicine: A Layman's Guide to the Medicine of the Future. By J. N. KENYON. *Thorsons: 1986. Pp.160. Pbk ISBN 0-7225-1198-1. Pbk £4.99.*

Current Studies in Nephrology, Dialysis and Transplantation. G. D'AMICO and G. COLASANTI (eds). *Karger:1986. Pp.206. Hbk ISBN 3-8055-4141-4. SwFr. 138, DM 165, $58.75.*

Diabetes Mellitus. Recent Knowledge on Aetiology, Complications and Treatment. SHIGEAKI BABA, MICHAEL K. GOULD and PAUL ZIMMET (eds). *Academic:1985. Pp.256. Hbk ISBN 0-12-069450-6. £37.50, $49.50.*

Dietary Fiber: Basic and Clinical Aspects. G. V. VAHOUNY and D. KRITCHESVSKY (eds). *Plenum: 1985. Pp.566. ISBN 0-306-42028-7. Np.*

Diseases of Complex Etiology in Small Populations: Ethnic Differences and Research Approaches. Progress in Clinical and Biological Research, Vol. 194. RANAJIT CHAKRABORTY and EMOKE J.E. SZATHMARY (eds). *Alan R. Liss:1985. Pp.436. Hbk ISBN 0-8451-5044-8. £38.*

Drug Level Monitoring. Analytical Techniques, Metabolism and Pharmacokinetics, Vol. 2. EMIL T. LIN and WOLFGANG SADEE (eds). *Wiley:1986. Pp.364. Hbk ISBN 0-471-80613-7. £61.35.*

Dyslipoproteinaemias and Diabetes. R.W. JAMES and D. POMETTA (ed.). *Karger: 1985. Pp.180. ISBN 3-8055-4139-2. DM 178, £46.60.*

Endocoids. Progress in Clinical and Biological Research, Vol. 192. HARBANS LAL, FRANK LABELLA and JOHN LANE (eds). *Alan R. Liss: 1985. Pp.566. Hbk ISBN 0-8451-5042-1. £60.*

The Endocrine Physiology of Pregnancy and the Peripartal Period. Serono Symposia Publications, Vol. 21. R.B. JAFFE and S. DELL'ACQUA (eds). *Raven Press:1985. Pp. 290. Hbk ISBN 0-88167-096-0. $43.*

The Enzymology of Post-translational Modification of Proteins, Vol. 2. ROBERT B. FREEDMAN and HILARY C. HAWKINS (eds). *Academic:1985. Pp. 374. Hbk ISBN 0-12-266502-3. £81, $95.*

Fetal Liver Transplantation. ROBERT PETER GALE, JEAN-LOUIS TOURAINE and GUIDO LACARELLI (eds). *Alan R. Liss:1985. Pp.373. Hbk ISBN 0-8451-5043-X. £44.*

Gastrointestinal Disorders in Diabetes Mellitus. By S. FORGACS. *Akademiai Kiado, Budapest, Hungary:1985. Pp.104. Hbk ISBN 963-05-3948-9. £8.50.*

Genetic Control of Host Resistance to Infection and Malignancy. Progress in Leukocyte Biology, Vol. 3. EMIL SKAMENE (ed.). *Alan R. Liss:1985. Pp.860. Hbk ISBN 0-8451-4102-3. £75.*

Have Healthy Teeth and Gums. By MERVYN PICHEL and NEIL CURTIS. *Javelin Books, Dorset, UK:1986. Pp.128. Pbk ISBN 0-7137-1431-X. £2.95.*

Homeostasis and Thermal Stress: Experimental and Therapeutic Advances. K. COOPER, P. LOMAX, E. SCHÖNBAUM and W.L. VEALE (eds). *Karger: 1986. Pp.210. Hbk ISBN 3-8055-4228-3. SwFr. 116, DM 139, £36.30, $49.50.*

Hybrid Models of Tropical Infections. Lecture Notes in Biomathematics, 59. By INGEMAR NASELL. *Springer-Verlag:1985. Pp.206. Pbk ISBN 3-540-15978-9. DM 36.*

Immunobiology of Proteins and Peptides-III. Viral and Bacterial Antigens. Advances in Experimental Medicine and Biology, Vol. 185. M. ZOUHAIR ATASSI and HOWARD L. BACHRACH (eds). *Plenum:1985. Pp.280. Hbk ISBN 0-306-42014-7. Np.*

Immunology of Rheumatic Diseases. SUDHIR GUPTA and NORMAN TALAL (eds). *Plenum: 1985. Pp.818. Hbk ISBN 0-306-41987-4. Np.*

Immunopharmacology. Serono Symposia Publications from Raven Press, Vol. 23. P.A. MIESCHER, L. BOLIS and M. GHIONE (eds). *Raven Press:1985. Pp.261. Hbk ISBN 0-88167-093-6. $43.*

Introduction to Drug Metabolism. By G. GORDON GIBSON and PAUL SKETT. *Chapman and Hall:1986. Pp.293. Pbk ISBN 0-412-26400-5. Pbk £12.95.*

An Introduction to Medical Genetics, 8th Edn. By J.A. FRASER ROBERTS and MARCUS E. PEMBREY. *Oxford University Press: 1985. Pp.394. Pbk ISBN 0-19-261409-6. £11.95.*

Ion Measurements in Physiology and Medicine. M. KESSLER, D.K. HARRISON and J. HÖPER. *Springer-Verlag:1985. Pp.336. Pbk ISBN 0-387-15468-X. Pbk DM 120.*

Leukemia: Recent Advances in Biology and Treatment. ROBERT PETER GALE and DAVID W. GOLDE (eds). *Alan R. Liss:1985. Pp.741. ISBN 0-8451-2627-X. £69.*

Logic of Discovery and Diagnosis in Medicine. K.F. SCHAFFNER (ed.). *University of California Press: 1985. Pp. 248. ISBN 0-520-05305-2. Np.*

Macromolecules as Drugs and as Carriers for Biological Active Materials. D.A. TIRRELL *et al.* (eds). *New York Academy of Sciences: 1985. Pp.458. Hbk ISBN 0-89766-286-5; pbk ISBN 0-89766-287-3. Np.*

The Management of AIDS Patients. DAVID MILLER, JONATHAN WEBER and JOHN GREEN (eds). *Macmillan Press:1986. Pp.202. Pbk ISBN 0-333-40466-1. £10.50.*

Mechanisms and Toxicity of Chemical Carcinogens and Mutagens. W.G. FLAMM and R.J. LORENTZEN (eds). *Princeton Scientific Publishing: 1985. Pp.264. Hbk ISBN 0-911131124. £53.35.*

Metabolic and Endocrine Disturbances in Renal Diseases. A. AMERIO, P. CORATELLI, V.M. CAMPESE and S.G. MASSRY (eds). *Karger:1985. Pp.224. Hbk ISBN 3-8055-4143-0. SwFr. 93, DM 111, $39.75.*

Myocardial Revascularization in Acute Conditions: Medico-Surgical Aspects. S.G. DEGRE (ed.). *Karger:1985. Pp.146. Hbk ISBN 3-8055-4142-2. SwFr. 115, DM 138, £36, $49.*

Non-Hodgkin's Lymphomas: New Techniques and Treatments. J.J. SOTTO, C. VROUSOS, M.F. SOTTO and F. VINCENT (eds). *Karger: 1985. Pp. 232. Hbk ISBN 3-8055-4064-7. SwFr. 162, DM 194, £50.70, $69.*

Non-Mammalian Models for Research on Aging. F.A. LINTS (ed.). *Karger:1985. Pp.288. Hbk ISBN 3-8055-4019-1. SwFr. 198, DM 237, $84.25.*

Occlusive Arterial Diseases of the Lower Limbs in Young Patients. P. FIORANI, G.R. PISTOLESE and C. SPARTERA (eds). *Raven:1985. Pp.312. ISBN 0-88167-090-1. $47.*

Patients and Practitioners: Lay Perceptions of Medicine in Pre-Industrial Society. ROY PORTER (ed.). *Cambridge University Press: 1986. Pp.356. Hbk ISBN 0-521-30915-8. £27.50, $49.50.*

Pocket Atlas of Normal Ultrasound Anatomy. By M.D. RIFKIN and L. WALDROUP. *Raven Press: 1985. Pp.70. Pbk ISBN 0-88167-163-0. $14.*

Polymeric Materials in Medication. C.G. GEBELEIN and C.E. CARRAHER Jr. (eds). *Plenum:1985. Pp.302. ISBN 0-306-42115-1. Np.*

The Posterior Pituitary: Hormone Secretion in Health and Disease. PETER H. BAYLIS and PAUL L. PADFIELD (eds). *Marcel Dekker: 1985. Pp.416. Hbk ISBN 0-8247-7359-4. $75 (US & Canada), $90 (other countries).*

Prostaglandins, Leukotrienes and Lipoxins: Biochemistry, Mechanism of Action and Clinical Applications. J. MARTYN BAILEY (ed.). *Plenum:1985. Pp. 705. Hbk ISBN 0-306-41980-7. Np.*

Rabies: the Facts (new edn.). By COLIN KAPLAN, G.S. TURNER and D.A. WARRELL. *Oxford University Press:1986. Pp. 126. Hbk ISBN 0-19-261441-X. £7.50.*

Rapid Detection and Identification of Infectious Agents. DAVID T. KINGSBURY and STANLEY FALKOW (eds). *Academic:1985. Pp.296. Hbk ISBN 0-12-408550-4. £26.50, $29.50.*

Rapid Methods and Automation in Microbiology and Immunology. K-O. HABERMEHL (ed.). *Springer-Verlag:1985. Pp.730. Hbk ISBN 3-540-13695-9. DM 248.*

Recent Developments in Parkinson's Disease. STANLEY FAHN, C. DAVID MARSDEN, PETER JENNER and PAUL TEYCHENNE (eds). *Raven Press:1986. Pp.397. Hbk ISBN 0-88167-132-0. $82.50.*

Renal Tubular Disorders: Pathophysiology, Diagnosis and Management. HARVEY C. GONICK and VARDAMAN M. BUCKALEW (eds). *Marcel Dekker:1985. Pp.640. Hbk ISBN 0-8247-7371-3. $95 (US & Canada), $114 (all other countries).*

Surgery and Support of the Premature Infant. P. PURI (ed.). *Karger:1985. Pp.210. Hbk ISBN 3-8055-4073-6. SwFr. 163, DM 195, £51, $69.50.*

Therapeutic Photomedicine. H.HONIGSMANN and G. STINGL (eds). *Karger:1986. Pp.308. Hbk ISBN 3-8055-4151-1. SwFr 230, DM 276, £71.90, $98.*

Tumor Markers in Cancer Control. HERBERT E. NIEBURGS, J.H. HOLZNER and VICTOR E. VALLI (eds). *Alan R. Liss: 1985. Pp.346. ISBN 0-8451-4201-1. £52.*

Veterinary Viral Diseases: Their Significance in South-East Asia and the Western Pacific. ANTONY J. DELLA-PORTA (ed.). *Academic:1985. Pp.616. Hbk ISBN 0-12-208870-0. Np.*

Virology in Medicine. HENRY ROTHSCHILD and J. CRAIG COHEN (eds). *Oxford University Press:1986. Pp.334. Hbk ISBN 0-19-503559-3. £39.95.*

Vitamin B-6: Its Role in Health and Disease. Current Topics in Nutrition and Disease, Vol. 13. R. D. REYNOLDS and J. E. LEKLEM (eds). *Alan R. Liss: 1985. Pp.526. Hbk ISBN 0-8451-1612-6. £60.*

X-Ray Microanalysis in Electron Microscopy for Biologists. By A.J. MORGAN. *Oxford University Press:1985. Pp.79. Pbk ISBN 0-19-856409-0. £5.95.*

General

Advances in Meat Research. Vol.1 Electrical Stimulation. By A.M. PEARSON and T.R. DUTSON. *AVI:1985. Pp.327. ISBN 0-87055-457-3. Np.*

Applied and Computational Complex Analysis, Vol.3. By PETER HENRICI. *Wiley:1986. Pp.637. Hbk ISBN 0-471-08703-3. £61.35.*

Architecture in Living Structures. G.A. ZWEERS and P. DULLEMEIJER (eds). *Nijhoff:1985. Pp.290. ISBN 90-247-3240-9. £33.25.*

Artificial Seawaters: Formulas and Methods. By JOSEPH P. BIDWELL and STEPHEN SPOTTE. *Jones and Bartlett Publishers Inc., Boston:1985. Pp.349. Hbk ISBN 0-86720-057-X. Np.*

Children Within Environments: Towards a Psychology of Accident Prevention. TOMMY GARLING and JAAN VALSINER (eds). *Plenum:1985. Pp.249. ISBN 0-306-42116-X. Np.*

Countryside Conversation. Resource Management Series 3. 2nd Edn. By B. GREEN. *George Allen & Unwin: 1985. Pp.253. Hbk ISBN 0-04-719005-1; pbk ISBN 0-04-719006-X. Hbk £25, $30; pbk £8.95, $19.95.*

Day of the Bomb. Countdown to Hiroshima. By DAN KURZMAN. *McGraw-Hill:1986. Pp.546. Hbk ISBN 0-07-035683-1. $19.95.*

Deception: Perspectives on Human and Nonhuman Deceit. ROBERT W. MITCHELL and NICHOLAS S. THOMPSON (eds). *State University of New York Press:1986. Pp.388. Hbk ISBN 0-88706-107-9. $44.50.*

The Detoxification and Natural Degradation of Chemical Warfare Agents. SIPRI Chemical and Biological Warfare Studies, Vol.3. By RALPH TRAPP. *Stockholm International Peace Research Institute: 1985. Pp.104. Pbk ISBN 0-85066-309-1. Np.*

Drinking Water Materials: Field Observations and Methods of Investigation. By D. SCHOENEN and H.F. SCHÖLER. *Ellis Horwood:1985. Pp.195. Hbk ISBN 0-85312-929-0. £25.*

Emil du Bois-Reymond (1818–1896) – Anton Dohrn (1840–1909). Briefwechsel. CHRISTIANE GROEBEN and KLAUS HIERHOLZER. *Springer-Verlag: 1985. Pp.322. Pbk ISBN 3-540-15812-X. DM 48.*

nature

Where next with the greenhouse?

The US Congress seems to have taken the threat of catastrophic greenhouse warming under its wing politically. But there is a long way to go before it can decide what to do about it.

Now that the seasonal summer has at last arrived in the Northern Hemisphere, it is natural enough that the US Congress should be in turmoil (see p.714) about the greenhouse effect, a phenomenon that comes to the surface every few years. But it is hard to believe that either of the two representative houses that sit on Capitol Hill in Washington can seriously think they have the means to legislate about this complicated matter when, to tell by recent experience, they cannot bring themselves to do the decent thing by the government of which they are a part, and avoid spoiling the administration's posture on free trade if the result is that they must abandon protection for US printing.

Here are a few homilies on the greenhouse effect that may (but that is unlikely) give Congress pause. They are offered, so to speak, in a spirit of moderation: Congress is indeed worrying about an issue on which the expenditure of anxiety is appropriate and even potentially constructive, but there is a danger that it may pace its anxiety by the timetable laid down for general elections, every two years for mere representatives and six years for grander senators. The time-span of the greenhouse effect is longer than either. And it is incalculable.

Recent past experience shows that well enough. Carbon dioxide absorbs radiation more efficiently in the infrared than in the visible part of the spectrum, so that if it should accumulate in the atmosphere, the result should be that solar energy will the relatively more easily reach the surface of the Earth than escape from it, increasing the surface temperature. This primitive scenario has been current for the best part of half a century. Moreover, it is now plain that carbon dioxide has indeed accumulated in the Earth's atmosphere, by roughly 30 per cent in the past century. So the temperature at the surface of the Earth should be steadily increasing, should it not?

Events have unfortunately taken a more tortuous course. The increase in the concentration of atmospheric carbon dioxide has been substantial and dramatic, but is roughly only a half of what it would have been if all the fossil fuel burned in the past century had produced combustion gases that had stayed in the atmosphere. Where has the rest gone? A general flourishing of vegetation is one possibility, solution in the oceans is another. There is also the curious but surprising conundrum that, the concentration of carbon dioxide having increased, the temperature has not followed by the amount predicted. The difficulty here is that the soothsayers (many of them professional scientists) have made more of their first-approximation models than is proper; they may not, for example, have disclosed that they cannot cope with real clouds in their climatic models or that ocean-atmosphere interactions are accounted for only in the most rudimentary way, but are likely when properly counted to be stabilizing. Even so, the long-term outlook cannot but be gloomy. One day, in the next few decades or so, the greenhouse effect will become reality. That, with its occasional introspections on the subject, is the issue for which Congress is preparing itself.

It might do worse than read the two articles on the remarkable disappearance of ozone from the Antarctic which appear on pp.755 and 759 of this issue. Ozone is an important component of the lower stratosphere because it absorbs solar ultraviolet, heating that layer and protecting the people who live beneath from ultraviolet radiation that might cause skin cancer. What the data show is a quick destruction of atmospheric ozone when the Sun appears above the horizon at the end of the Antarctic night; the assumption that most damage to the stratispheric ozone layer is done by chlorine is on this occasion complemented by the damage done by bromine, another halogen used for the general good in the putting out of fires, whose use is generally applauded by Congress. These phenomena also have an influence on what the greenhouse will do, but in ways that cannot yet be determined. The importance of these components of the upper atmosphere is that their presence has been recognized only recently, that they may in various chemical guises be greenhouse gases like carbon dioxide, but that their influence may also tend in the other direction.

What should Congress do? First it must recognize that the problem is essentially international. Everybody puts carbon dioxide into the air, for reasons that are usually good — keeping warm, cooking food, getting from one place to another. So when the temperature of the Earth's surface begins significantly to increase, some mechanism will have to be invented whereby something that might provisionally be called the World, or the World Community, is empowered to tell smaller parts of itself that they cannot continue doing what they have always done.

While the general principle is generally acceptable, its implementation is beyond the present ken of those who generate carbon dioxide. A host of academic conferences in the past decade has amply illustrated what the difficulties would be. Should carbon dioxide (or other greenhouse gas) quotas be proportional to present GNP? Or to potential GNP? Or to some other index of a country's ambition, such as the size of its population? By what means could such an agreement be enforced? By fines proportional to the disadvantage done to the peoples of countries other than the transgressor's? And should the disadvantaging multiplier be so great that people would find it more profitable to turn to nuclear power than to pay the fines? The enthusiasts for the greenhouse problem now raising the roof in Congress had better take a close look at what lies down the pike before they pin their electoral futures on this scary prospect.

What is to happen to the rest of us? In a world in which legislative bodies, including Congress, are notoriously unwilling to sign binding international agreements, there are two rational attitudes to strike. One is to concentrate on the uncertainties in present calculations, and on the features of most respectable calculations which show that there will be winners as well as losers in the global greenhouse, and to say that the problem is of no significance. The other is to take the line that there will be a greenhouse problem one day, perhaps next decade, perhaps a century from now; in that case, the rational course is now to seek to strengthen international institutions, and the trust that ordinary people put in them, against the time that a durable agreement is needed. Sadly, there is no obvious correlation between the opinions on contemporary international issues among those who have lately rediscovered the greenhouse effect and the small membership that would, for example, do something about arms control. □

Atmospheric greenhouse

US Congress says climate is part of politics

Washington

POLITICAL efforts are under way in Washington to bring into the policy arena the depletion of the atmospheric ozone layer warming due to the greenhouse effect. Declaring that the topics "can no longer be treated solely as important scientific questions", Senator John Chafee (Republican, Rhode Island), chairman of the Senate subcommittee on environmental pollution, last week announced that he would ask the Environmental Protection Agency (EPA) and Congress's Office of Technology Assessment to conduct studies of policy options to stabilize world levels of atmospheric gases.

Chafee's statement was made at the start of two days of hearings at which administration officials and prominent scientists were called to give evidence on the problem and their views of appropriate responses. Chafee also said he would ask the National Academy of Sciences to review gaps in scientific knowledge on the topic, and that he would ask the State Department to bring the issue to international attention.

Although administration officials at the hearings generally stuck to the line that more research is needed before policy options can be considered, EPA administrator Lee Thomas said a working group has been established within the agency to estimate trends in greenhouse gas emissions and to determine possible control options. The working group will also conduct long-term research.

EPA is already considering further controls on the use of chlorofluorocarbons (CFCs), which catalyse the breakdown of the ozone layer; a decision will be made by November 1987. Several witnesses referred to recent measurements showing a 40 per cent reduction in the ozone layer over Antarctica, the causes of which remain unknown but which may be related to human activities.

Concern over the effects of CFCs on the ozone layer led the United States in 1978 to ban their use in non-essential aerosol sprays, but EPA has failed to persuade other nations to follow suit. Thomas said EPA had "stepped back" from those efforts, but it is considering regulations further to limit domestic uses of CFCs, used mainly as refrigerants.

Several witnesses at last week's hearings referred to the need for international cooperation on research, including Thomas and Alvin Trivelpiece, director of the office of energy research at the Department of Energy (DoE). DoE is concluding an agreement on joint climate research with China, to be conducted through the Chinese Academy of Sciences. Other countries are participating in DoE's carbon dioxide research programme.

A scientific view of the problems was provided by James Hansen of the National Aeronautics and Space Administration (NASA)'s Goddard Space Flight Center. Hansen has used a global climatic model to simulate the climatic effect of the transient growth of atmospheric carbon dioxide and other trace gases now thought collectively to be as important.

Among Hansen's results is the conclusion that a large part of the equilibrium warming due to the well-documented carbon dioxide increase since 1850 has probably not yet occurred; the same is true for the other gases. The effect of warming will start to emerge from statistical background noise in the 1990s.

In response to submitted questions, Hansen also prepared estimates of the increased number of days per year over 90 degrees Fahrenheit in Washington DC that would result from a doubling of carbon dioxide. Conclusion: from 35 days (at present) to 85, with 12 of them over 100 degrees. Temperature across much of the United States might rise by an average of 3 degrees Fahrenheit or more by 2020. Local press, sweltering in 90-degree-plus weather, were duly impressed.

Hansen said later in an interview that he was surprised at Chafee's call for immediate studies of policy options; he would prefer to emphasize the need for integrated and long-term studies of climate systems as he thought policy options would not meet political approval in the absence of clearer evidence. Recommendations along these lines have been made in a report to be published by the NASA Earth System Sciences Committee chaired by Francis Bretherton of the National Center for Atmospheric Research. But, while also stressing the need for more research, Bretherton said he approved of Chafee's call for an assessment of policy options.

Although the greenhouse effect is not at present under specific consideration in the White House, a consensus is emerging in the scientific community on the need for coordinated and long-term measurements of climate. An international initiative has been proposed by the International Council of Scientific Unions, and the roles of US federal agencies in a long-term climate study are being considered in the administration by the Senior Inter-agency Group on Space, called SIG-Space. A major international conference on the subject sponsored by the United Nations Environment Programme and EPA takes place this week in Arlington, Virginia.

Tim Beardsley

French universities

One reform too many?

FRENCH university presidents walked out of a meeting with the new research and higher education minister, Alain Devaquet, last week, after hearing that France is to abandon its newly-created PhD degree, much welcomed by natural scientists for its similarities to the research degrees of Britain and the United States. The plan is to return to the old idiosyncratic system of "troisième cycle" and "thése d'Etat" degrees.

This is just one of the reforms promised last week by Devaquet, a physicist, in a new law for the universities to be put before the National Assembly before the summer. Another reform will allow universities to select their own students, the first such selection system allowed in France since the European university revolution of 1968. But the selection will be only nominal: Devaquet, no doubt fearful of the political consequences of avowing selection, has also reaffirmed the right of every school-leaver who passes the coveted "baccalaureate" to gain a university place, just as each of them can do at present. It will be up to local education authorities to square this selective circle.

Other promised reforms include a lightening of the system of the three elective councils by which universities and their departments are managed, in order to give more power to professors ("and less to cleaning staff", according to one supporter), but the present national system for awarding degrees will be retained.

The law thus does not go so far as the promise of Prime Minister Jacques Chirac to return autonomy to the universities both in the selection of students and the awarding of degrees. But it went far enough for the university presidents to walk out of their meeting with Devaquet, which was held just a couple of hours before the minister's previously arranged press conference on the new law. The presidents were protesting at an almost total lack of consultation in the brief preparation of the law since the general elections in March, and at the prospect of yet another long hot summer of discontent as the French university system is yet again lifted up by the roots to see how the fragile plant is growing.

Robert Walgate

US copyright

Will Congress blot US copybook?

Washington

WHILE the US administration bangs the drum of free trade, Congress is busily preparing to muffle its beat. Now, a coalition of 54 major corporations and association is lobbying hard to persuade Congress not to extend legislation requiring non-dramatic works by US authors to be printed in the United States.

The so-called "manufacturing clause" has been declared illegal by the General Agreement on Tariffs and Trade (GATT), and the European Economic Community (EEC) has threatened economic sanctions against the United States if the clause is not allowed to expire at the end of this month. But influential members of Congress want the clause made permanent, and the Senate Finance Committee has approved a bill to do so.

The current manufacturing clause prohibits importing into the United States copyrighted non-dramatic literary material in English unless it is printed and bound there. The effect is to ensure that US copyright material is printed in the United States. The price of books in the United States is consequently estimated to be 12 per cent higher than it would otherwise be. Newspapers are also affected.

Among those most affected by the bill are manufacturers of computers and business equipment; the legislation prevents them from printing instruction manuals and the like abroad, where many of their manufacturing plants are situated. Burroughs, IBM and Xerox are among the corporations that have joined the Coalition to Oppose the Manufacturing Clause. EEC estimates the clause costs it between $300 and $500 million per year and has threatened retaliatory sanctions.

The clause is also opposed by the US Department of Commerce: commerce secretary Malcolm Baldrige told the Senate Finance Committee last week that the clause is "an embarrassment" that undermines the United States' position as it tries to negotiate fair trade practices and strong protection for intellectual property rights overseas. Baldrige said he would advise President Reagan to veto any legislation Congress might pass to extend the clause.

The clause was formerly set to expire in 1982, but Congress voted then to extend it and overturned a presidential veto. It had not by then been declared illegal by GATT, however, and opponents are using the GATT ruling as a major plank for their case. The clause also makes it impossible for the United States to adhere to the Berne copyright convention, which provides international protection for intellectual property rights.

The controversial clause dates back to 1891, when it was enacted to protect the US printing industry. Although it has since been progressively weakened, the printing industry would still like to see the clause extended, and some members of Congress are unwilling to be seen to be increasing foreign competition for the industry. Critics contend, however, that the number of US printing jobs that would be saved if the clause is extended is trivial compared with the number of jobs lost in other export industries. Singapore, thought to be one of several countries that turn a blind eye to piracy of US-copyright trade materials, has tied improvements to its copyright laws to an exemption from the US manufacturing clause, and other countries may follow suit.

Some computer manufacturers have already chosen to forgo US copyright protection on their manuals printed overseas rather than print them in the United States, according to the coalition. Vico Henriques, president of the Computer and Business Equipment Manufacturers' Association, said it was recognized good business practice to print documentation for a product at the point of manufacture so that local alterations and conditions could be included easily.

The legislation approved by the Senate finance committee to extend the clause (S. 1822) would remove the existing exemption for Canada. The exemption allows Canada to export to the United States US-copyright works not printed in the United States. Retaliatory action from Canada would therefore also be on the cards if the legislation were passed.

To placate the opposition, the Senate bill, introducted by Republican Senator Strom Thurmond, includes some compromise provisions. The chief one is that after two years, waivers could be issued allowing imports from countries which the Secretary of Commerce certifies as fair trading partners that respect US copyright laws (among other things). But the US Trade Representative, Clayton Yeutter, told the finance committee that he had "strong doubts that Canada, the European Economic Community or Japan could obtain a waiver" under the "cumbersome" waiver provisions. Yeutter said the ostensible purpose of the clause, protection of US printers' jobs, was unnecessary: total employment in the US printing and publishing sector is projected to grow by 2.2 per cent a year to 1995, creating more than 30,000 jobs each year.

The House of Representatives' Judiciary Committee is soon to consider a bill identical to Thurmond's. Senate floor action on Thurmond's bill is scheduled for next week; the coalition is only cautiously optistic that it will have rallied sufficient votes to defeat it. **Tim Beardsley**

British software

Looking over the shoulder

THE common British conceit that Britain may not be much good at hardware, but has the edge in software, takes a tumble this week with the publication of a report by a committee of the Advisory Council for Applied Research and Development (ACARD) that cries for urgent action from everybody in sight (*Software. A vital key to UK competitiveness*. HMSO. £6.00). It is not true, says ACARD, that British software houses run on an inside track; after the United States, France is next, while even in Europe, West Germany is number two.

Both perceptively and courageously, ACARD sees the British software problem as part of the general decline of British industrial competiveness. While the "man in the street" may still expect that software houses would be among the most rapidly growing and most profitable parts of British industry, the real prospect is quite different.

The committee says that evidence from overseas confirms its own view that the rate of growth of the British software industry will lag behind that of the world leaders, that market shares will decline and that the British market for software will be dominated by overseas suppliers in the 1990s.

The ACARD committee gives several reasons for this gloomy outlook, including the chronic shortage of skilled people in information technology, the failure of companies in the field to spend enough on selling the products they have developed and, latterly, their unwillingness or incapacity to invest in research and development. According to the ACARD report, the chief objective among software houses now is to make software development less labour-intensive, which means investment in the techniques of automation.

The diagnosis is more persuasive than the remedy. Above all, ACARD wants Britain to know there is a problem. Beyond that it has a miscellany of remedies, such as the proposal that government departments should give thought to generic needs when commissioning new developments, that the Science and Engineering Research Council should elevate the information engineering committee of its engineering board to the status of a full board and that the programming language BASIC should be outlawed as soon as it can be replaced by something better.

The committee's theme is that designing a piece of software is like making anything else — a task in engineering in the widest sense. Many British software-users will say amen to that.

Cancer research

Boom in new laboratories

FUNDAMENTAL cancer research in Europe is about to be strengthened by several new privately financed laboratories. One will be in Vienna and is jointly owned by Genentech, the Californian biotechnology company, and the West German chemical and pharmaceutical company Boehringer Ingelheim. The other four, and probably five, laboratories are new branches of the Ludwig Institute of Cancer Research, administered from Zurich.

Despite its commercial backing, the Vienna institute will be concerned only with basic research in the general area of molecular pathology, with a particular focus on oncogenes. First rights on any discovery of commercial interest stemming from the research are shared by Genentech and Boehringer Ingelheim. The German partner will foot the bill for the institute for its first five years, after which costs will be shared equally.

During the initial five-year period, Genentech's contribution is know-how, in terms of both the recruitment of suitable staff and the structure of the research programme. Just over half the cost of building the institute (in Vienna's third district) and 80 per cent of the running costs for the first five years will be met by Boehringer Ingelheim, with the balance coming from the city of Vienna and the Austrian government, eager to counter a Freudian past with a double-helical future. Various relevant university institutes, at present scattered around the city, are likely to be re-sited alongside the new institute.

Building work on what is likely to be called the Institute of Molecular Pathology will begin this summer. Shortly thereafter its director, Dr Max Birnstiel, will leave the University of Zurich for Vienna. Negotiations are already well advanced with some potential group leaders for the institute and enthusiasm for heading east is said to run high.

Those who prefer to head west or north may find positions in four new branches of the Ludwig Institute of Cancer Research. Two of these have begun operation in Sweden (in Stockholm, under Dr Ulf Pettersson and in Uppsala, under Dr Carl-Henrik Heldin) and two will start soon in London (at Middlesex Hospital Medical School, under Dr Michael Waterfield, and at St Mary's Hospital Medical School, under Dr Paul Farrell). Negotiations are under way for another London branch and Dr Webster Cavenee has just begun to direct a new Ludwig in Montreal's McGill University.

As a result, there are now 14 Ludwig branches consuming US$33 million last year. There will now be a period of consolidation with no new branches, according to Mr Hugo Frei, chairman of the board of directors, which is responsible for managing the assets provided by Mr Daniel K. Ludwig in 1974 in such a way as to produce sufficient income to finance the research programme. Each branch, of 20–80 people, is set up in cooperation with a hospital for an initial six-year period and is subject to review every three years. So far, the only branch to be closed was the previous London laboratory at Sutton (see *Nature* **318**, 400; 1985) for reasons that included its location, lack of patients and scientific shortcomings, according to Frei.

To judge by the new branches, Ludwig has little difficulty in attracting good directors despite the lack of guaranteed long-term support and a policy that sets salaries at local levels.

There is, however, some generosity in terms of capital expenditure. A recent board decision means that the US Research Corporation will handle the transfer to commerce of any potentially profitable discovery in a Ludwig laboratory.

Peter Newmark

Soviet education

University shake-up canvassed

A RADICAL reorganization of Soviet higher education is on the cards. In what is called a draft proposal, published last week, the Central Committee of the Soviet Communist Party says the time has come for curricula to be "retuned" and for the administration of higher education to be simplified. There should be more money for equipment and better salaries for professors. If implemented, the proposals will give universities a more prominent place in the pattern of Soviet research, at present dominated by academy and ministry institutes.

The theme of the proposals is familiar outside the Soviet Union, to arrange matters so that higher education contributes more fully to the national economy. But the breadth of what is proposed represents radical reform of many established practices and institutions.

The scale of Soviet higher education, with a total of 894 universities and other institutions of higher education, is huge. But, according to the Central Committee, the system is bedevilled by bureaucracy. Part of the trouble is the division of responsibility between the All-Union and republic governments, but ministries and departments also run their own institutions for training people with special skills, as in agriculture and medicine. Altogether, 74 ministries and departments are in some way involved, but 30 of these run only one or two institutions (called VUZy when they are not universities).

To meet the complaint that many production ministries and departments fail to provide suitable teaching staff and facilities for their institutions, the Central Committee proposes that the Ministry of Higher Education should have more control of VUZy run by other ministries. There would be regular checks of teaching standards and, because sectional interests have often led to the duplication of specialist courses and, sometimes, whole new VUZy, the system would be rationalized so that redundant courses and establishments would be gradually phased out.

Teaching is also to be overhauled. The Central Committee says that the present pay structure discourages the best scholars and scientists from making an academic career. It says that too much emphasis is placed on formal lectures and textbook knowledge, with the result that students are overworked, while the ratio of students to staff is far too high.

What the Central Committee wants to see is more teaching in small seminar groups (not more than 15 people), with more practical and laboratory work. The notion that each student should have an individual timetable and more choice of lecture courses is encouraged, and there is even a tentative suggestion that intending university teachers should spend a probationary period of two years in some part of the national economy in which their students may later work.

Recruitment into graduate programmes will centre on people seconded from industry or with work experience in their chosen field. Research for the degree of Candidate (PhD) will concentrate on "priority fields of science and technology" and efforts will be made to raise the ideological as well as scientific standard of research students. The possibility is canvassed that some universities and VUZy might offer courses leading to the degree of Doctor of Science, at present awarded on the basis of a second dissertation in the course of a professional career.

Apart from the threat of more direct control, the Central Committee's prospectus should be welcomed by Soviet universities and VUZy. More is to be spent on laboratories, libraries and computers. Students are to have better living conditions, and academics better pay. There is even talk of higher aesthetic standards for university buildings. In return, the universities and VUZy have to produce graduates of the type required by the "scientific and technical revolution" and also play a part in the intended "unified state retraining scheme for older generations of scientists".

Vera Rich

Chemical weapons

Binary weapons in trouble

Washington

A GENERAL Accounting Office (GAO) report has given a black eye to Bigeye, the binary chemical weapon the US Department of Defense (DoD) says will give the chemical weapons arsenal a deep-strike capability now said to be lacking. But in spite of the doubts raised by the GAO report, DoD is proceeding with operational tests of Bigeye, and hopes soon to begin initial production at a low rate.

The GAO report focuses on DoD's tests of Bigeye performed since 1982. The Bigeye bomb consists of two non-lethal chemicals carried separately. When mixed, these agents form the persistent lethal nerve agent VX. Originally, DoD planned that high-flying aircraft would drop the bomb after the two chemicals had combined. But lessons learned during the 1976 Yom Kippur War in the Middle East convinced DoD that this approach made planes too vulnerable to anti-aircraft missiles, so that DoD decided that the bomb would have to be carried by aircraft flying at high speed and low altitude.

This plan also has problems. The extra temperature caused by increased air friction at low altitudes raised pressure inside the bomb, causing one to explode during testing. This is why, since 1982, DoD's plans for delivering Bigeye have required mixing the two chemicals only after the bomb has left the plane, and "lofting" the bomb — tossing it upwards from the aircraft — so that the chemicals have time to mix before the bomb's contents are released. The GAO report concludes that this delivery scheme places a heavy burden on pilots and systems software.

Eleanor Chelimsky, one of the report's principal authors, said at a press conference last week that the Bigeye bomb has satisfied neither chemical purity requirements nor system reliability, and is "therefore not ready for production". Pressure build-up inside the bomb after mixing could still result in a premature release of its contents. DoD solved the pressure problem in laboratory tests with a pressure relief valve, but the valve will not be included in working models of the bomb.

Another concern is the potential of the bomb's chemical components to catch fire or "flash", destroying the nerve agent's effectiveness. Also troubling Chelimsky is the way DoD performed tests on the bomb. "DoD seems to be confused about what in fact has been tested and what the results have been", she says. According to the GAO report, DoD changed performance criteria during testing to make Bigeye look better.

DoD is quick to defend Bigeye. John E. Krings, director of DoD's office of Operational Test and Evaluation, agreed that GAO had identified some of Bigeye's initial problems, but said the report was "not totally accurate". Krings denied that the criteria that the weapon had to meet had in any sense been eased, pointing out that all new weapons systems experience modifications in design criteria during testing. The bottom line, says Deputy Assistant to the Secretary of Defense for Chemical Matters Thomas J. Welch, is whether the bomb represents an improvement in combat effectiveness. Welch believes it does. "We understand the shortcomings of Bigeye", says Welch. "We have a handle on fixing them, and the fixes are under way." The logic of binary weapons is that they are safer to store and transport than unitary weapons. But even here Bigeye has problems. VX is formed by mixing QL (ethyl 2-(diisopropylamino) ethyl methyl-phosphonite) with rhombic sulphur. But according to sources at GAO, DoD is aware that if QL were accidentally released near a power plant burning high-sulphur coal, VX could form spontaneously.

Bigeye is just one part of a planned improvement in chemical weapons. By 1994, DoD plans to destroy all existing stocks of unitary weapons, switching over to binary weapons. Besides Bigeye, DoD plans to deploy 155-mm artillery shells carrying the non-persistent nerve agent GB, and a multiple-launch rocket system also carrying GB. But Congress has required that the North Atlantic Council, the political arm of the North Atlantic Treaty Organization (NATO), should approve the United States' "force goals" before production can proceed. Congress has also insisted that NATO's Supreme Allied Commander in Europe must establish plans for how chemical weapons will be used before production funds are released.

To gain European support, President Reagan is said to have struck a deal with West German Chancellor Helmut Kohl to remove existing stockpiles from West Germany in exchange for Kohl's support for binary weapons production. Last month, the NATO Defense Planning Committee endorsed the US plans for new chemical weapons production, a move the administration hopes will allow production to proceed. But congressional opponents argue that North Atlantic Council approval is still needed.

Even if the binary weapons plan is approved, critics worry that not having the weapons actually based in Europe will make them ineffective as a deterrent. DoD plans to airlift the bomb components separately to Europe in the event of an attack. The United States holds to the position that it will never be the first to use chemical weapons. But critics worry that a massive influx of such weapons to Europe at a time of crisis may make it appear that the United States is abandoning that policy, prompting a Soviet first strike.

A report by the specially empanelled Chemical Warfare Review Commission to President Reagan last year concluded that the long-range capability offered by the Bigeye bomb is urgently needed if the United States is to have a credible chemical weapons deterrent. But many in Congress believe the binary bomb is just an expensive mistake. The GAO reports should provide congressional opponents with ammunition when they attempt to shoot down Bigeye. **Joseph Palca**

Estonian protest

A GROUP of Estonian scientists, including members of the Estonian Academy of Sciences, has written an open letter to the West, calling for protests against Soviet plans to build a large oil terminal at Muuga near Tallinn. The terminal, which will be adjacent to the controversial grain harbour, will, the scientists say, be a major source of pollution to north Estonia and to the whole Baltic area. The oil terminal, although necessary to the All-Union plans, is not necessary to the economy of the Estonian republic. Since the plans for the terminal have not been officially announced (the scientists describe their source as a reliable leak from civil servants), they clearly hope that international criticism might induce the central planners to scrap the project quietly, and to deny the report as unfounded.

The area under threat by the proposed terminal includes lake Peipsi, the main water source for Tallinn. It is the only area of the country not already a victim of major pollution from oil-shale and phosphorite mining. (A recent study by the Estonian Academy's Institute of Economics found that the large phosphorite mine now being planned at Toolse will cause extensive seepage of pollution through the ground-water.) A particularly worrying aspect of the problem is that, since January 1986, censorship control has become so strict that it is now virtually impossible to inform the general public about environmental hazards.

The scientists, however, are not concerned only with the pollution threat posed by the oil-terminal, grave though that is. All major construction and engineering projects in Estonia are accompanied by a major influx of Russian labour, which, in its turn, means the gradual linguistic and cultural Russification of the area. If this policy continues, the scientists say, by the end of the century, a broad zone of north-eastern Estonia, comprising about 60 per cent of the population of the republic, will be effectively Russified. Vera Rich

Biotechnology

Insect virus as super-vector?

Washington

AN insect virus that could become a second-generation recombinant vector is gaining a quiet following in biotechnology. The baculovirus is easily engineered and achieves both high synthesis rates and complex processing of recombinant products. Cetus, Eli Lilly, Genentech and 15 other companies are investigating the system, but a three-year-old Connecticut company called MicroGeneSys claims it has already foiled the competition.

Although he heads only 25 employees, founder and president Frank Volvovitz believes MicroGeneSys has invested more time, money and expertise in the use of baculovirus than any other company. Volvovitz culled six virologists from laboratories at the National Institutes of Health, Baylor College of Medicine and Texas A&M for his research team. The company will not disclose the yields it has achieved, but published reports contain examples of recombinant protein production nearing 700 mg per litre of culture within a few days of infection. This rivals the rates of monoclonal antibody production by hybridomas, the most efficient recombinant machinery known.

The system is based on a cell line established in the late 1970s from the pupal ovarian cells of the moth *Spodoptera frugiperda*. When infected with baculovirus carrying a foreign gene, these cells can secrete recombinant products complete with post-translational modifications such as phosphorylation and glycosylation. The system may therefore dispense with costly downstream processing. Mammalian cell cultures offer the same processing advantages, but are not as prolific.

The productivity of the baculovirus derives from the efficiency of the viral promoter of the gene encoding the protein called polyhedron, the sole component of a crystalline matrix that acts as a protective shield for viral particles existing outside their insect host. Caterpillars eat the matrix and release the particles, which then temporarily suspend polyhedron synthesis. When the caterpillar is near death, the virus resumes matrix protein production until roughly 20 per cent of the larval host consists of polyhedron.

MicroGeneSys has already harnessed this productivity for a hepatitis-B vaccine which will enter clinical trials this fall. The company is also developing vaccines against acquired immune deficiency syndrome and malaria infections. Meanwhile, research in Texas A&M and the University of Idaho is generating a network of academic and corporate collaboration on baculovirus technology.

Eli Lilly has been working closely with Max Summers in Texas, who is generally recognized as the technology's pioneer. Summer's laboratory is also working on interleukin-2 with Hoffman–LaRoche. Cetus is building on its preliminary results with colony-stimulating factor, while Genentech assigned a handful of researchers to investigate the system and says merely that it is "very interesting". Genetics Institute (which has just raised $75 million in its first public offering of shares), had originally planned to use baculovirus for making pesticides, but changed the emphasis of its programme on learning more about the system.

There are some sceptics in the field as well. Chiron considers that the baculovirus has only "marginal utility" compared with its own yeast systems. Even the staunchest supporters of baculovirology admit that the analysis of the gene products so far has not been thorough enough to ensure smooth passage through the regulatory process. Little is known, for example, about the characteristics of the insect cell glycosylation, which could affect biological activity. **Karen Wright**

European research

Still hope for budget increase

Luxembourg

RESEARCH ministers of the twelve member states of the European Economic Community (EEC) meeting here last week refused to triple the research budget of EEC, demanding that the European Commission, which administers EEC affairs, be more "realistic" in its requests. The Commission, however, regards its proposal for an ECU (European Currency Unit) 10,350 million (£6,600 million) "framework programme" of international research for 1987–91 as eminently realistic, and indeed vital for the economic future of Europe — and has retired to prepare a new proposal to put before the ministers in October.

But this apparently eyeball-to-eyeball confrontation is not official. It occurred over lunch — when no official minutes are taken. But the British, French and German delegations did not aid Commission digestions with their insistence on only small increases in the ECU 3,750 million five-year research budget of the EEC.

The EEC spend is dwarfed by the ECU 150,000 million or so that the individual nation members of EEC spend on research each five years, and the Commission is arguing, in effect, that a great part of this national spending is wasted, either by duplication of effort or by a failure of research or technological enterprises to reach a critical mass of talent or investment. In its strategy to 1991, the Commission aims to expand existing successful coordination programmes in areas such as information technology and biotechnology, and to turn pilot programmes into fully-fledged actions.

EEC research ministers, particularly in the larger European nations, are apparently holding back this expansion, or — even if the research ministers are more willing to support the Commission — over-zealous finance ministers in the newly monetarist France, in West Germany and the United Kingdom are putting the brakes on. Research ministers at a political level now strongly back the objectives of "improving Europe's technological competitiveness" and of increasing the "cohesion" among individual national research and technology policies, two of the current "buzz phrases" in European science policy, but at an economic level the ministers seem unable or unwilling to back the principles with cash.

Meanwhile, Geoffrey Pattie, the British minister of technology, recommended that the Commission could save money on science, by cutting its energy research by 20 per cent (it is set to remain roughly constant in the new framework programme) or by offering only fractional subsidies (down to 25 per cent on a sliding scale from the current 50 per cent) to university, institutional and industrial projects granted EEC support, thus making a small sum go further. The Chernobyl reactor disaster may make the first unlikely, as projected decreases in nuclear fission safety research may have to be reversed; and according to Commission officials the second is already practised.

Pattie and other "purse-strings" ministers present, including Alain Devaquet from France and Heinz Reisenhuber from West Germany, made it plain that when the Commission returns with new proposals they must be realistic or further delays in agreeing the programme are inevitable. Everything rests on what "realistic" means, but estimates were ranging here from around ECU 4,300 million — the sum estimated to be necessary to keep going with the present programme, to "around half" the proposed programme (some ECU 5,500 million). With these sums it would be possible to go ahead with the planned programme, according to Commission officials, but the number of grants awarded would be nowhere near able to satisfy the demand, the disappointment of good applicants would cause disillusion, and the function of the programme as a real catalyst of European economic and technological transformation would prove more difficult to achieve.

Robert Walgate

Materials research

Europeans wake up

Luxembourg

EUROPE is to launch an ECU (European Currency Unit) 30 million (£20 million) three-year programme of research on new materials, it was agreed here last week, a year after the proposal was first tabled. The programme covers ceramics to the new neodymium-iron-boron high-field permanent magnets which are posted to replace electromagnets and reduce the volume of electric motors by half. The plan has been held up only because the European Parliament demanded more than either the European Commission had proposed or the Council of Ministers, which takes decisions, could accept.

EURAM, (European Research on Advanced Materials), is a belated response to the spending of some $1,000 million (£666 million) by the US Federal Government each year on materials science, to similar spending in Japan and to the relative weakness of European research and industry in new materials. In the new magnetic technologies alone, which were Japanese and American research discoveries just four years ago, General Motors has already begun pilot production of starter motors.

According to the Commission, "there are still excellent materials laboratories in Europe, but their innovative capacity is one the decline". EURAM aims to help reverse the decline, and also to strengthen perennially weak links between universities and industry. Its budget was less than the ECU 38 million the Commission had requested, but much more than what it had been spending in pilot programme.

In the ambitious "framework programme" also debated by ministers here (see p.718), support for materials research would leap to some ECU 200–300 million over five years. Although the ministers declined to back the whole budget, a further expansion of the new materials programme won political support.

With the framework programme to be debated again in October, the Commission can meanwhile get on with implementing EURAM, which already has a detailed list of projects to support in metallic materials, engineering ceramics and composites. The object will be to link existing laboratories in joint programmes of research, with, preferably, an industrial partner. The programme will not be exclusive to the European Economic Community; the Swedish car-makers Volvo and Saab have already shown interest. Officials claim that 90 per cent of the leading European laboratories in the field of magnetic materials are involved in a pilot programme. **Robert Walgate**

US research overheads

Government semi-retreat

Washington

THE Office of Management and Budget (OMB) bit the bullet last week and published, in the *Federal Register* for 9 June, its final revisions to Circular A-21, the document that determines how institutions are reimbursed for the indirect costs associated with research grants. OMB came under a storm of criticism from universities after publishing its initial proposals for revising Circular A-21 earlier this year.

Indirect costs now represent nearly a third of all payments for research grants, according to OMB figures. To control this steady increase, the new revisions set a fixed allowance of 3 per cent of total research costs for the salaries of department heads and faculty attributable to the administrative overhead costs of research. Institutions receiving federal funds will not have to fill in forms to receive the allowance, which will eliminate the need for the much-hated "effort reports" formerly required to justify payments for time spent on administrative activities.

According to Milton Goldberg of the Council on Governmental Relations, this will give a windfall to universities whose costs have been less than 3 per cent. OMB estimates these costs now run between 5.5 and 6 per cent nationwide (see table).

	Deans, chairs	department lab directors	Faculty
Yale University	0.88	5.55	
Boston University	5.74	4.82	
University of California, Berkeley	0.80	1.45	
Harvard University	1.77	2.30	

OMB's first shot at a revision of A-21, first published in the *Federal Register* on 12 February, brought a storm of disapproval from universities and their allies in Congress. The proposal would have capped reimbursements for all administrative costs at 26 per cent for the current fiscal year, a figure that was to drop to 20 per cent for 1987. OMB estimated the government would save $200 million if the original plans had been put into effect. The new plan will save the government only $100 million.

A principal complaint of universities at the time of the initial OMB proposal was that they had not been consulted. Although OMB held numerous meetings with interested parties in the months following publication of the proposal, Goldberg says its final proposal still came as a surprise. Carol Scheman of the American Association of Universities is encouraged that OMB is taking universities' concern seriously, but is unconvinced the new revisions will solve the problem of rising indirect costs. She maintains that such costs will continue to rise as more money is needed for facilities and equipment.

The new regulations must take effect by 1 July 1987, although individual agencies may implement the changes sooner if they wish. The changes will apply only to new federal grants, leaving existing commitments untouched. But a move by Congress may hold up the new rules until October, the beginning of the next fiscal year. Congressman Sidney Yates (Democrat, Illinois) has amended the House version of a supplemental appropriations bill in a manner forbidding government agencies from spending money to implement the new plan.

The original Senate version of the appropriations bill contained a similar form of words. A House/Senate conference will make a decision this week whether to include the provision in the final version of the bill. **Joseph Palca**

Test-tube babies

Tokyo

JAPAN may be on the edge of a test-tube baby boom, according to predictions made by Dr Bob Seamark, an Australian expert in *in vitro* fertilization (IVF), and Dr Masakuni Suzuki, Japan's pioneer of the test-tube baby. Suzuki is so confident of the future that he has built a private hospital near Sendai to deal primarily with infertility problems using IVF techniques. But there are many problems still holding back development of IVF in Japan.

In Japan and Australia the incidence of infertility is similar, with as many as 10–12 per cent of couples unable to produce children. But the number of test-tube babies in Japan stands at only 27 compared with over 1,300 in Australia. Why has Japan lagged so far behind?

The Japanese public and academics are often severe critics of major new medical procedures, as shown, for example, by the outcry against heart transplants and sex selection. But probably more important than this is the lack of government support for IVF research and the cost of IVF treatment. Unlike Australia, IVF is not covered under national health insurance in Japan.

Another major difference between Australia and Japan is the almost complete lack of communication between Japanese scientists involved in reproductive biology research and the clinicians in hospitals who apply IVF techniques. Co-operation between clinicians and scientists, particularly those involved in animal breeding, is, according to Seamark, one of the major driving forces behind the tremendous surge in IVF research in Australia. David Swinbanks

Japanese gynaecology

Gender selection sparks row

Tokyo

A GROUP at Keio University in Tokyo has caused a sensation by claiming a major medical scoop on national television last month, when it announced that six married woman had given birth to baby girls after artificial insemination with X-chromosome sperms separated by centrifugation. But the publicity has back-fired, and the Keio team has come under a barrage of criticism even from within their own university for failing to inform the public of the experiments, and for going ahead without first discussing the ethical questions raised by sex selection.

The ethical committee of Keio University met last week and decided that once the reliability of the method has been established, it should be used only to prevent hereditary diseases. In the meantime, practitioners around Japan have already started using the technique.

Soon after the Keio group made its announcement, a group promoting sex selection headed by Dr Shiro Sugiyama, owner of Sugiyama Gynecology Clinic in Tokyo, revealed that 40 girls had been born around the nation using the Keio technique, and out of 24 women who conceived, 22 gave birth to girls, a success rate of over 90 per cent.

The principle of the technique is simple enough and well known — X-chromosome sperms are marginally more dense than those with Y chromosomes because of the larger size of the former chromosome, and they can, in theory, be separated by centrifugation. Although many claims of successful sex selection based on this principle have been made, no reliable technique has yet emerged. The Keio team, headed by Professor Rihachi Iizuka of Keio University and Professor Hideo Mori of Tokyo University, described their method in 1984 (*Biomedical Research*, **5**, 187; 1984).

The secret lies in the fluid in which the sperm are suspended for centrifugation. A density gradient of Percoll, a modified silica gel, is used and the sperm are separated on the basis of differential velocity sedimentation. After a 20–30-minute spin in a centrifuge at 250*g*, 95–100 per cent of the sperm in the bottom layer carries the X chromosome, while the overlying layer has about 85 per cent sperm containing the Y chromosome. According to Sugiyama, it is then just a simple matter of pricking a hole in the bottom of the centrifuge tube and draining a few drops of the X-chromosome-rich sperm which are used for impregnation.

First treatment in the Sugiyama Clinic costs 50,000 yen (about £170) and, in the case of failure, each subsequent treatment is 20,000 yen. Four or five attempts are usually required for success.

Sugiyama heads the Sex Selection Research Group which was established 7 years ago and which has 770 practising gynaecologist members throughout the nation. In the past they used vinegar-rinsing of the vagina as a technique to promote the conception of girls. But success was "less than 80 per cent".

According to Sugiyama, the new method has been used in most cases to prevent hereditary diseases such as haemophilia which occur in men, but he admitted some parents wanted a girl for personal reasons, such a wanting to raise their child to be a ballerina. It is revelations like this that have raised a furore.

Iizuka also initially claimed that the technique had been applied to avoid hereditary diseases, but many Japanese colleagues questioned this and Professor Yasuo Uemura, head of Keio University ethics committee, criticized the Keio team for applying the technique to couples who simply wanted a girl because they already had boys.

Uemura also though it "regrettable" that Iizuka went ahead without consulting the ethics committee in advance and "imprudent" that some of the members of his team attended meetings of obstetrical practitioners to teach them the sex-selection method.

Immediately after the meeting of the Keio University ethics committee, Sugiyama said he would abide by the committee's decision and limit application of the technique to prevention of hereditary diseases.

But in a complete about-turn a few days later he declared that he would continue to help ordinary parents to select the sex of their babies until advised otherwise by nationwide medical organizations, such as the Japan Medical Association or the Japan Society of Obstetrics and Gynecology. His change of heart came because he was deluged with letters and telephone calls from people asking him to continue the technique, and he felt it was "his duty as medical practitioner" to respect the wishes of such people.

According to a report in *Shukan Bunshun*, a Japanese weekly publication, the Keio group started clinical trials of the technique in May last year, and for the past six months Japan's national broadcasting corporation, Nihon Hoso Kyokai (NHK), has been allowed to cover the research.

But a difference of opinion arose between the Keio group and NHK about when to release the news; NHK felt that the preliminary success of the technique raised important social issues which should be discussed in public while the Keio team wanted to test about 100 women to obtain statistically reliable results.

In the end, NHK was allowed to broadcast after the successful birth of six girls by the Keio technique. **David Swinbanks**

Brown eggs catch on in Japan

Tokyo

FIRST it was the Australian "superpig" and now comes Japan's "biochicken", the next contender in the farmyard biotech race. And what makes biochicken special? She lays brown eggs, lots of them.

That may not sound like much of a feat until one realizes that shiny reddish brown eggs (literally "red eggs" in Japanese) command twice the price of the paler white variety on the Japanese domestic market. The inflated price of brown eggs in Japan can be attributed to limited supply and a belief among the general public that brown eggs are more nutritious.

Quick to spot a potential money-maker, scientists at Nagoya University and the Agricultural Experiment Station of Aichi prefecture have created White Leghorn hens that lay brown eggs instead of their usual white ones. Ths is achieved by false fertilization.

Sperm of a Rhode Island Red rooster, which carries the gene for brown eggs, is first irradiated with gamma radiation to inactivate it. The sperm is then allowed to enter the egg of a White Leghorn, thereby introducing some Rhode Island Red genetic material into the egg which is then fertilized with normal White Leghorn sperm. About 7 per cent of the fertilized eggs result in chickens that lay brown eggs. This technique was developed in New Zealand in 1982 by Pandey, but it had no commercial applications there — in New Zealand brown eggs cost the same as white.

But why go to all this trouble when Rhode Island Reds already lay brown eggs? The answer lies in greater productivity — the White Leghorn is a profuse egg layer. No doubt also, the label "bioeggs" will have commercial appeal in this country where "biolipstick" has swamped the cosmetic market (see *Nature* 314, 395; 1985).

Biochicken, however, is not yet quite living up to expectations; her eggs are only pale brown and are more typical of a hybrid White Leghorn/Rhode Island Red than a true Rhode Island Red.

But by selective breeding the Japanese team is confident that by this autumn it can come up with a hen that lays pure brown eggs, and it has already named this chicken of the future the "Aichi Bio Red".

David Swinbanks

Colombian immunology

More plans for malaria vaccine

Bogotá

COLOMBIA, hitherto best known for its coffee, now seeks to cultivate a reputation in science. As his last act in support of science, outgoing President Belisario Betancur earlier this month announced a



scheme whereby six of Colombia's best science graduates at a time would be awarded fellowships to study at the Research Institute of Scripps Clinic in California.

As the students will be paid from Colombia, they will be obliged to return there after their three-year stints in Richard Lerner's department of molecular biology at Scripps.

The hope is to increase Colombia's abilities in modern biomedical research, now concentrated in Manuel Patarroyo's Institute of Immunology at the San Juan de Dios Hospital in Bogotá.

Patarroyo, with the aid of the presidency and particularly of one of its economic advisers, Diego Pizano, whose support of science stems from a friendship with French virologist Gerard Bricogne while both were studying at the University of Cambridge, together with a gift of several sequencing and synthesizing machines from Arnold Beckman, has set up what is probably the best-equipped biomedical laboratory in South America.

Patarroyo, together with approximately thirty enthusiastic young researchers, is beginning to pursue gene cloning and vaccine development for malaria, leprosy and tuberculosis. They do so against the odds. For example, customs and other delays tend to allow "hot" radioisotopes to become cold and heat-degradable enzymes to warm up before they reach the institute. And there is no adequate postgraduate research programme in Colombia.

On the other hand, Colombians do have the advantage over laboratories in North America and Europe of having easy access to malaria and leprosy patients and to the animal models for the diseases, the *Aotus* monkey and the armadillo, respectively.

The most important outcome of the institute's research so far is the development of a candidate malaria vaccine. Reporting the initial data on the vaccine at a conference entitled Perspectives for Chemistry in Medicine in Bogotá this month, Patarroyo described how the immunization of monkeys with a combination of three synthetic peptides, corresponding to partial sequences of one of the major proteins on the surface of malarial red blood cells, protects the animals against infection with the protozoan *Plasmodium falciparum*, which is the main malaria parasite of humans.

So far the tests have involved only a few monkeys, but up to 50 will be included in an extended trial.

About a thousand scientists and students attended the conference. According to the organizers, Patarroyo and Pizano, the main purpose was to provide a stimulus to Colombian science, which came in the form of 10 speakers from the United States and 4 from Europe.

Four of the speakers, Lerner plus Gobind Khorana of Massachusetts Institute of Technology, David Baltimore of the Whitehead Institute and Peter Perlmann of the University of Stockholm, were awarded the Order of San Carlos in the rank of knight by President Betancur during the conference.

Should an effective malaria vaccine emerge — and even with the first phase of clinical trials of some possible vaccine components about to begin in other countries, nobody doubts that there is a long way to go — Colombia should be well placed to carry out a mass vaccination campaign.

During 1985 and early 1986, several million young children were vaccinated against five common diseases by means of a campaign that involved the newspaper *El Tiempo*, the radio network *Caracol*, UNICEF, the Roman Catholic Church, the armed forces, various government agencies and a host of volunteers.

The only part of the country to be missed out, a strip of inaccessible Pacific coastland, is about to be tackled in a week of action involving 100 helicopters and hundreds of boats. **Peter Newmark**

Catch your monkey

AOTUS monkeys are collected by Indians in the Amazonian basin. With a group of monkeys inside the hollow tree trunks that they live in, the Indians first seal off all the exit holes. They then reopen one hole and as the enraged animals emerge, try to catch them by the tail.

It can take a week to catch a single animal. Captured monkeys are taken to Leticia at the southernmost tip of Columbia, where the malaria trials are carried out. Because the *Aotus* monkey is a protected species, those that succumb to malaria have to be cured with drugs. They are then passed on to a breeding colony elsewhere in Colombia and, sometimes, released back into the wild. □

Coffee benefaction

As coffee is far and away Colombia's main export, it is not surprising that the *Federación Nacional de Cafeteros de Colombia* maintains two laboratories, one that concentrates on the chemistry and the other on the biology of coffee.

The chemistry laboratory in Bogotá under Marco Quijano employs approximately twenty scientists and seventy students to study coffee composition and processing as well as tissue culture and the problems of coffee rust, a fungal disease that reached Colombia only in the past two or three years.

Copper-containing sprays are the main way to defeat the rust fungus but they are expensive to administer, not least because they have to be delivered by hand as aerial spraying would ruin the electricity cables. The chemistry laboratory is conducting a careful study of the effects of copper on the coffee plant, to establish whether it would be possible to treat the soil with copper to inhibit rust disease. In the end, however, Quijano believes that the fungus will develop resistance to copper.

Studies of coffee processing are a particular focus of the laboratory because of the growing demand for decaffeinated coffee in the developed nations. There has been talk of using biotechnology genetically to manipulate the coffee plant so that the beans are caffeine-free. But in economic terms, this makes little sense, because the process of decaffeination is paid for by the sale of the caffeine to the pharmaceutical industry. Cloning of coffee plants, on the other hand, is considered important and 250 plants derived by tissue culture are being studied.

Colombian coffee tends to be sold at a premium price because it is made from ripe beans only. That is possible because the beans are hand-picked rather than mechanically shaken from the plants. This fits with the fact that Colombian coffee is largely grown on small plots owned by a single family which receives a guaranteed price from the coffee growers' association to whom they have to sell their crop. This provides a buffer against bad years, but also means that the farmers are not benefiting from this year's high prices, occasioned by the failure of the Brazilian crop. □

The Paluxy River mystery

SIR—The article "On the Tracks of Men and Money" by Tony Thulborn (*Nature* **320,** 308; 1986) contains many inaccuracies on a subject that cries for clarity. The presumed occurrence of both human and dinosaur tracks in the Lower Cretaceous Glen Rose limestone in central Texas has for over a decade been the favourite illustration of the creation model, while being, as Thulborn personally admitted to me, "the evidence evolutionists feared the most".

It is true, as Thulborn stated, that, at a January 1986 lecture at the University of New South Wales, I called attention to recent changes in the nature of the tracks which bring into question the original interpretations by myself and others. Having been involved in this project for a decade and having written the definitive book on the subject, I did not find this comfortable, but as an empiricist and honest man, I dared not do less. Even though Thulborn calls the present nature of the tracks "embarrassingly obvious" and the process by which they changed "well known", the truth is, evidently, that an unprecedented geological phenomenon has taken place which is, as yet, only poorly studied and less well understood.

Somehow, since 1984, surface stains in the shape of tridactyl dinosaur prints have appeared, surrounding many of the eroded remnants of elongated tracks once interpreted as human-like. In almost all cases, these stains are not associated with any impression in the rock — they are a coloration phenomenon only. In some cases, the stain ingores the "mud up-push" surrounding the human-like impressions.

Neither my two field trips to the Paluxy in the fall of 1985, nor the analysis of samples taken, answer all the questions. There are only two possibilities: (1) an, as yet, undeciphered geological process partially obscured portions of the tracks of a previously unknown dinosaur which walked in an atypical plantigrade fashion, or (2) that someone has fraudulently altered the appearance of the tracks.

I emphasize that I have seen no direct evidence of fraud. I plan to continue my research once water levels are lower, to gain a more complete understanding, but meanwhile I have encouraged creationists to refrain from using the Paluxy as an anti-evolutionary argument.

Thulborn and other evolutionists are rushing to embrace this evidence, relishing the fact that the tracks, once thought to be human, now appear reptilian. But hitherto, the usual evolutionists' explanation has been that the markings were not tracks at all. The 1986 booklet *Creationism, an Australian Perspective* by the Australian Skeptic Society implied that I had carved some of them. Others have claimed they were scour marks, eroded potholes, worm burrows or creationist footprints in the river-bottom mud. After studying both the present nature of the prints and photographs of their nature when first discovered, I am convinced that the original interpretation was not only valid, but arguably the best.

Thulborn, president and founder of the Australian Association for the Protection of Evolution (APE), is also less than objective when he repeats the Skeptics' charge of financial impropriety on the part of the Creation Science Foundation (CSF) of Australia. He claims "CSF still declines to give a detailed explanation" of the whereabouts of $92,000. However, he should know (I was standing next to him when the president of CSF explained it to him) that an employee of the investment company in which the money had been placed had embezzled from many accounts, including that of CSF, and that the authorities had frozen the remaining assets. Court cases are now in progress. So far CSF has received only a portion of its money back.

Likewise, Thulborn repeats the charge that federal money had wrongly been given to CSF in the form of an "export market development grant". My understanding is that the Australian government financially encourages companies and organizations that export products to be sold overseas; CSF has recently begun to publish and print locally a magazine and other publications which are primarily sold in North America and Europe and, as such, is eligible for such an export development grant.

JOHN D. MORRIS
Institute for Creation Research,
10946 Woodside Avenue North,
Santee, California 92071, USA

SIR—Tony Thulborn reports (*Nature* **320;** 308; 1986) that Robert Morris now admits that the "human" footprints on those of big dinosaurs in Cretaceous limestones, Paluxy River, Texas, were those of small three-toed dinosaurs. Additional news is now available from San Diego, California, that the fake exhibit at the Institute for Creation Research, showing an 80-million-year-old human being beside a dinosaur[1], has been "closed for revision", and that the "casts" have been removed. Will there be a revision of *Dry Bones*[1]?

There is more joy, among evolutionists, over one sinner that repenteth than over ninety and nine that are too brazen to repent. Can we hope that other creationist intellectual atrocities may be abjured by their perpetrators? Examples are misrepresentations of the second law of thermodynamics and of isotopic dating, claims for variability of the speed of light, and engagement, by good and bad angels, in their own form of star wars[1].

Many evolutionists will be glad to help the creationists put their house in order, even at the expense of its disappearance into thin air.

THOMAS H. JUKES
Department of Biophysics and
Medical Physics,
University of California,
Berkeley, California 94720, USA

1. Jukes, T.H. *Nature* **308,** 390–400 (1984).

Cometary first

SIR—The magnificent 15 May 1986 issue of *Nature* containing the first results from the spacecraft voyages to comet Halley was marred by an unfortunate lapse in the Editorial (p. 366) by John Maddox entitled "First journey to a comet". For the record, the first encounter took place on 11 September 1985 when the International Cometary Explorer passed 7,800 km tailward of the nucleus of comet Giacobini–Zinner. Of the missions to comet Halley, only Giotto came closer to the nucleus.

The field of cometary research has been advanced in 1985 and 1986 by a massive effort from a variety of disciplines. We applaud the work of the Giotto, Sakigake, Suisei and Vega projects for their pivotal contribution. However, appreciation of this achievement does not require a revision of history.

JOHN C. BRANDT
ROBERT W. FARQUHAR
TYCHO T. VON ROSENVINGE
International Cometary Explorer,
NASA–Goddard Space Flight Center,
Greenbelt, Maryland 20771, USA

Safe nuclear energy

SIR—The important lesson from the Chernobyl disaster is that the best brains in the world are needed urgently to work on developing safe nuclear energy, and that the warnings of these scientists must be heeded even when they say things that their governments and the nuclear power industry do not like. Unfortunately, one of the best brains in the nuclear safety business has been out of the action for several years. Andrei Sakharov has been isolated, harassed and prevented from contributing to this important effort because he says things that his government does not like.

If General Secretary Gorbachev is really serious about the need for a collective world effort to make nuclear energy safe, he should bring this great pioneer of nuclear safety back into the mainstream of nuclear research.

HARRY J. LIPKIN
High Energy Physics Division,
Argonne National Laboratory,
9700 South Cass Avenue,
Argonne, Illinois 60439, USA

When reference means deference

Hoyle and Wickramasinghe protest that none of the contributors to recent accounts of the encounters with Halley's comet have referred to them. But they have only themselves to blame.

WHAT follows is a sad but disturbing tale, which is told not for the sake of making further trouble but in the hope of stilling what there is already. It centres on the recent encounters of the two Soviet Vega spacecraft and the European Giotto spacecraft with Halley's comet in March, the publication of preliminary accounts of the encounters in *Nature* on 15 May, the publication in the succeeding issue (**321**, 385; 1986) of a "prediction" (published after the event) by Professor J.M. Greenburg at the University of Leiden that the surface of the nucleus of Halley's comet would appear black and the complaints of two British scientists, Sir Fred Hoyle and Professor Chandra Wickramasinghe, that their own earlier predictions to the same effect have wilfully and even maliciously been overlooked.

Most readers will not have ready access to the documents in which the complaints surface, which consist chiefly of "preprints" circulated from the Department of Astronomy at University College, Cardiff. The description of this now considerable volume of largely unpublished literature is a misnomer, because much of it is plainly not written with the intention that it should go through the processes that ordinarily precede publication, scrutiny by referees, for example. This is certainly the case with "Cardiff Astrophysics and Relativity preprint No. 125", dated 1 June 1986, under the title *On deliberate misreferencing as a tool of science policy*, which has been artfully contrived to appear as if it were the galley proof of a letter due to appear in *Nature*. (For future reference, the authors of this little joke should know that our type size is known in the trade as "9 on 10", not "9 on 11", and that our wide columns are 20.6, not 20.0 "ems" wide.)

Readers will also know that Sir Fred Hoyle is one of the most talented and ingenious theoretical scientists since the Second World War. With Bondi and Gold, he launched the steady-state theory of cosmology, with a variety of collaborators (W.H. Fowler and the two Burbidges) he laid down the outlines of the theory of nucleogenesis and, almost as if in passing, showed how to calculate the evolution of stars. Latterly, Hoyle has been exploring a question originally posed in urgent form by Wickramasinghe, that of the constitution of interstellar dust. Many readers will know the eccentric direction this work has taken. Hoyle and Wickramasinghe have remarked that carbon is a common constituent of interstellar dust (as it is of gas), that much of this carbon is in the form of sedimentary organic molecules and have then gone on, in a series of mostly *samizdat* publications, to argue that the prevalence of interstellar carbon only goes to support one of the other theories to which they are attached. They say that life as it is known on the surface of the Earth is genetically far too complicated to have arisen by means of darwinian evolution from primordial chemicals, that at least the first steps in the evolution of life are likely to have taken place "out there" and that, as it happens, comets are likely to have been among the means by which the surface of the Earth is from time to time repopulated by external organisms.

Those writing off for a copy of preprint 125 should be sure also to ask for preprint 121, dated 1 March, which put forward a particular model of the constitution of the periodic comets (of which Halley is one). Most of the objects, the argument goes, will have lost volatile material from the outer surface, which will therefore be a loose uncompacted "protective" skin of material with low refractive index and, therefore, low reflectivity for sunlight. The authors are partly concerned to explain the discrepancy between the calculated and observed (only a tenth as many) number of periodic comets; their solution is to suggest that most periodic comets slip by unobserved, but that those with more than one nucleus become visible because the nuclei rub against each other, exposing parts of the volatile interior to solar radiation. Hoyle and Wickramasinghe did not on 1 March say so explicitly, but it may be inferred from their general discussion that the surface of Halley's comet was predicted to appear mostly black.

The complaints in preprint 125 are more entertaining. First, they marvel at Greenberg's "sibylline achievements" in predicting what Halley's comet would seem like after the event, overlooking that Greenberg's model is radically different from their own; in fact the reason for its publication was not that it made a "prediction" but that it is a model of which many readers of *Nature* would not previously have heard. Second, they remark, in sorrow rather than anger, that none of the Halley authors in the issue of 15 May refers to them. They go on to note that, in its time, *Nature* has been guilty of removing a reference to their work from an article written by a third party. Finally, they darkly speculate on the possibility that this neglect may simply have been a consequence of this journal's malign attitude both towards themselves and as a willing "vehicle of propaganda for Darwin's theory". They suspect that it may be a "management condition" that "persons judged to be a threat to Darwinism are to be blotted out from the scientific world".

This lengthy reply to what Hoyle and Wickramasinghe allege stems not so much from the circumstance, attested by preprint 125, that the authors and the present editor of *Nature* are old friends but from a wish that these two talented people should come to see the error of their ways. But in passing, it should be known that the sinister deleted reference was a reference to their panspermiology in D.A. Allen and D.T. Wickramasinghe (*Nature* **294**, 239; 1981), an otherwise helpful measurement of infrared absorption in interstellar space.

Moreover, they may be right about comets. Much of what they have written over the years deserves to be widely read, for example the argument that comets contain polyformaldehyde (Vanysek, V. and Wickramsinghe, N.C. *Astr. Space Sci.* **33**, 19; 1975) or the demonstration (with W.K. Wallis) that comets Cernis and Bowell probably contain organic molecules rather than water-ice (*Earth, Moon and Planets* **33**, 179; 1985). What these authors seem incapable of understanding is that their panspermian convictions sully even their sober contributions to the literature. People who might (and even should) read their articles on comets do not do so for the simple reason that they half expect to find there a rehearsal of the now familiar and widely popularized view that life began in space.

Not that even that is necessarily wrong. Time may yet show that Hoyle and Wickramasinghe have been true prophets crying in the wilderness of disbelief. Yet as things are, there is no evidence but conjecture on their side. Their flimsy account of the origin of life has as its sole foundation their scepticism of the efficacy of natural selection among primordial molecules. It is as if a particle theorist chose to say that, while the Higgs boson remains undiscovered, the only partly successful theory so far must be discarded and all others, however flimsy, must be given more than equal time. They ask a lot, too much for most.

John Maddox

Endocrinology

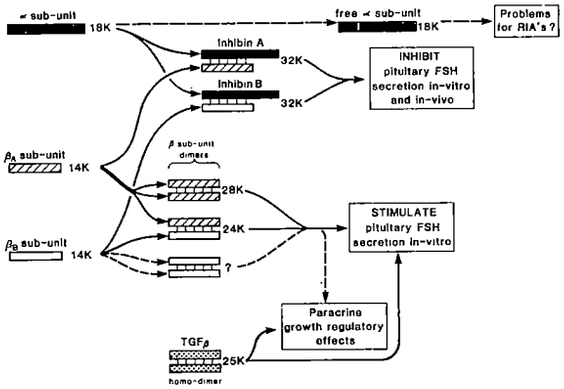
Dual gonadal control of follicle-stimulating hormone

from Con G. Tsonis and Richard M. Sharpe

OF all the reproductive hormones, none has had a more chequered history than inhibin, a glycoprotein produced by the gonads that feeds back to the anterior pituitary gland to decrease specifically the secretion of follicle-stimulating hormone (FSH)[1]. Attempts at the purification of inhibin proved far from straightforward. Reports of molecules with inhibin-like activity ranging in relative molecular mass (M_r) from 10,000 to 100,000, (10K–100K) raised doubts about the authenticity of inhibin. These have recently been resolved by demonstration that is composed of an interlinked α- and β-subunit. Now comes a major surprise. Two reports on page 776 and 779 of this issue[2,3] show that dimers of the β-subunits of inhibin are potent stimulators of FSH synthesis and secretion, raising the possibility of dual control of FSH from within the gonads.

Clarification of the nature of inhibin occurred in two phases. In 1984 a low M_r (14K) form of inhibin, present in human seminal plasma, was purified and sequenced[4], but was later shown to originate from the prostate and not the gonads[5]. It is now known to be structurally unrelated to gonadal inhibin. This probably excludes it as a physiological regulator of pituitary FSH secretion. More importantly, in December 1985 the full sequence of two 32K forms of porcine follicular fluid (pFF) inhibin (inhibin$_A$ and inhibin $_B$) were published[6], and have since been confirmed for bovine inhibin[7]. Each form is composed of two crosslinked subunits (see figure), a larger common α-subunit of M_r 18K and a smaller, distinctive β-subunit of M_r 14K, designated as β_A or β_B according to differences in the amino terminus. As these were the predominant forms of inhibin present in pFF and, as higher molecular mass forms of FF inhibin (for example, 58–108K) can probably be explained by extensions of the α- or β-subunits[7,8], it appeared that inhibin had finally yielded its main secrets.

Two independent laboratories now report the isolation and purification of two inhibin-related factors from pFF which are potent and selective stimulators of pituitary FSH release *in vitro*. These factors are referred to as FRP (ref.2) and activin[3], respectively, by the authors. FRP is a 28K polypeptide composed of two β_A subunits of inhibin and activin is a polypeptide composed of one β_A and one β_B subunit of inhibin held together by disulphide bond(s) (see figure). Although only two β dimers were isolated this does not exclude the possibility of a third factor, a homodimer composed of two β_B subunits. For the β dimers to have biological activity both subunits must be joined together because reduction of the disulphide bonds destroys their bioactivity, as is also the case for inhibin. The β dimers are highly potent stimulators of both the biosynthesis and secretion of FSH but have no effect on luteinizing hormone (LH) or prolactin. The β_A homodimer is reported also to reduce the secretion of growth hormone and adrenocorticotrophic hormone[2].



Diagrammatic representation of how the α- and β-subunits of porcine follicular fluid inhibin can be combined to yield molecules with either FSH-inhibiting of FSH-stimulating activity. ——→ Proven pathways; - - - → possible pathways. Reported relative molecular masses are shown.

The action of the β dimers can be distinguished from those of luteinizing hormone-releasing hormone (LHRH) in several ways. Compared with LHRH, β dimers have no effect on LH secretion, act much more slowly (greater than 4 hours rather than minutes for LHRH) and have greater stimulatory effects on the biosynthesis of FSH. Also, LHRH antagonists, which completely block the LHRH-stimulated release of both FSH and LH *in vitro*, have no effect on the secretion of FSH mediated by the β dimers. These data suggest that the β dimers act through receptors separate from those for LHRH and probably via a different mechanism.

An additional finding of great interest is the striking homology between the β dimers and transforming growth factor-β (TGF-β)[6]; the homology is such that they are considered to be products of the same gene family. TGF-β exists as two 12.5K sub-units linked by disulphide bond(s) to yield a 25K homodimer (see figure) which is also a potent stimulator of FSH release at low concentrations (10^{-10} M)[9].

The discovery that the β dimers are present in follicular fluid together with inhibin suggests that there is a 'push-pull' system operating from within the gonad to control production of FSH. When both inhibin and the β dimers are added to pituitary cells, the effect of inhibin predominates and FSH secretion is decreased. As inhibin is present in follicular fluid in higher amounts than the β dimers this implies that negative control of FSH by the gonad is the principal feedback message, though this does not exclude the possibility that secretion of the β dimers may predominate under different physiological states.

However, before critical evaluation of the role(s) of the β dimers is possible it will be necessary to establish first, whether they are secreted from the gonads into the peripheral circulation; and, second, whether they have local growth effects within the gonads analogous to the effects of TGF-β reported in other tissues[10]. If the β dimers are secreted systemically then problems would arise if they also had TGF-β-like activity because the latter has widespread local effects in various tissues and the β dimers might activate these sites. The structural differences between the β dimers and TGF-β may prevent this.

Alternatively, the β dimers may not be released systemically but the ability of the β dimers (or TGF-β) to increase pituitary FSH release at picomolar concentrations or less *in vitro* suggests strongly that this effect is of some physiological importance. Indeed, if the β dimers are not secreted from the gonads into the blood, then perhaps a molecule resembling the β dimers or TGF-β is secreted by the hypothalamus to modulate pituitary FSH. There are several reports of the existence of a hypothalamic FSH-releasing hormone[11], but these have never been widely accepted and appear to describe a smaller molecule than the β dimers. With respect to the possible local effects of the β dimers, it has been shown recently that TGF-β can enhance FSH-stimulated secretion of oestradiol by rat granulosa cells *in vitro*[12]. This suggests that the β dimers may normally exert a comparable effect within the ovarian follicle. In the same study, 32K inhibin was shown to antagonize FSH-stimulated secretion of oestradiol, raising the possibility of dual local modulation of FSH action within the gonad.

These recent developments have important implications with regard to the measurement of inhibin by radioimmunoassay[13] and bioassay[1]. The relative abun-

dance in the ovary of the messenger RNAs for the α-subunit precursor of inhibin is estimated from Northern blots to be at least 10-fold greater than that for the β_A precursor, and about 20-fold greater than for the β_B precursor[6]. This suggests that there may be secretion of free α-subunit or its precursor. As free α- or β-subunits are devoid of FSH-releasing or inhibiting activity, antibodies directed towards the α-subunit of inhibin may cross-react with the free α-subunit, therefore overestimating the amount of inhibin in a sample. In a preliminary report[8], however, free α-subunit of the hormone could not be detected in bovine follicular fluid.

Antibodies raised against the β-subunits of inhibin (β_A or β_B) may prove even more troublesome in that they may well cross-react with the β dimers as well as with inhibin. This again would lead to an overestimation of the levels of inhibin. Similar problems can be expected with antibodies raised against the β dimers, as these may show major cross-reaction with inhibin. Furthermore, bioassays of inhibin may underestimate the actual level of the hormone in a sample if the β dimers are also present and countering the effects of inhibin.

Until now it has been an accepted principle of endocrinology that gonadal feedback control of FSH secretion is under the dual control of steroids and inhibin. Introduction of β dimers or an equivalent as a third candidate would neccessitate a major rethink about control of the hypothalamic-pituitary-gonadal axis. Finding out how the function of this third factor interacts at the pituitary level with the actions of LHRH and with those of the recently described LHRH-associated peptide (GAP)[14,15] and elucidating the local roles of inhibin and the β dimers undoubtedly presents reproductive endocrinologists with a considerable task but it also promises more surprises. □

1. de Jong, F.H. & Robertson, D.M. *Molec. Cell. Endocr.* **43**, 95 (1985).
2. Vale, W. *et al. Nature* **321**, 776 (1986).
3. Ling, N. *et al Nature* **321**, 779 (1986).
4. Ramasharma, K. *et al. Science* **223**, 1199 (1984).
5. Beksac, M.S. *et al. Int. J. Androl.* **7**, 389 (1984).
6. Mason, A.J. *et al. Nature* **318**, 659 (1985).
7. Forage, R.G. *et al. Proc. natn. Acad. Sci. U.S.A.* (in the press).
8. Miyamoto, K. *et al. Biochem. biophys Res. Commun.* **136**, 1103 (1986).
9. Ying, S.-Y. *et al. Biochem. biophys. Res. Commun.* **135**, 950 (1986).
10. Brown, K.D. & Blakeley, D.M. *Biochem. Soc. Trans.* **12**, 168 (1984).
11. Mizunauma, M. *et al. Brain Res. Bull.* **10**, 623 (1984).
12. Ying, S.-Y. *et al. Biochem. Biophys. Res. Commun.* **136**, 969 (1986).
13. McLachlan, R. I. *et al. Lancet* **i**, 12 (1986).
14. Aldelman, J.P. *et al. Proc. natn. Acad. Sci. U.S.A.* **83**, 179 (1986).
15. Seeburg, P.M. & Aldelman, J.P. *Nature* **311**, 666 (1986).

Con G. Tsonis is in the Department of Obstetrics and Gynaecology and Richard M. Sharpe is in the MRC Reproductive Biology Unit at the Centre for Reproductive Biology, University of Edinburgh, Edinburgh EH3 9EW, UK.

Precambrian geology

The most ancient rocks revisited

from Stephen Moorbath

THREE years ago, a group of workers from the Australian National University surprised the geological world by reporting[1] uranium–lead (U–Pb) dates of between 4,100 and 4,200 million years (Myr) for 4 detrital zircons out of 102 analysed from the Mount Narryer quartzite in Western Australia, which was probably deposited and metamorphosed about 3,600–3,350 Myr ago. On page 766 of this issue[2], W. Compston and R.T. Pidgeon report a further occurrence of such old detrital zircons, identified once again with the ion-microprobe SHRIMP, in a conglomerate from the Jack Hills metasedimentary belt at a site about 60 km north-east of Mount Narryer.

In Compston and Pidgeon's study, 17 zircon grains out of 140 analysed yield U–Pb dates greater than 4,000 Myr. Indeed, one zircon grain registers the exceptionally old date of 4,276±6 Myr, which may still be a minimum value for its original age. The authors regard the 'old' zircon population as either having a single original age close to 4,300 Myr with subsequent early as well as recent Pb loss, or as a mixed-age population that formed during discrete events over an extended time period between 4,100 and 4,300 Myr ago. The age of these ancient minerals constrains the time of the earliest preservation of Earth's solid crust.

As at Mount Narryer, the majority of zircons at Jack Hills register very much younger dates than 4,000 Myr, probably related to igneous and/or metamorphic thermal events 3,100–3,500 Myr ago. In principle, early gain of Pb (or loss of U) followed by recent Pb loss could produce anomalously old apparent U–Pb zircon dates, but although this process has been demonstrated in a zircon from Mount Sones, Antarctica[3], it is not regarded by the Australian workers as a plausible model for Mount Narryer and Jack Hills.

What clearly needs to be done next is to subject the Jack Hills zircon population to conventional solid-source mass spectrometry and isotope dilution analysis of single grains and individual fragments of single grains. Schärer and Allègre[4] performed this type of analysis on 32 single zircon grains from Mount Narryer; they obtained no 4,100–4,200 Myr dates and interpreted the results solely in terms of zircon crystallization 3,800–3,300 Myr ago. From simple statistics, Compston *et al.*[5] countered by postulating that Schärer and Allègre had simply been unlucky in failing to find any zircons more than 4,100 Myr old at Mount Narryer. (The chance of selecting 32 'young' grains in succession was shown to be 27 per cent.) Because the proportion of 'old' zircon grains at Jack Hills is about five times that at Mount Narryer, the conventional analytical approach will be greatly facilitated.

The morphology as well as the U and Th contents of the Jack Hills zircons suggest to Compston and Pidgeon that their source consists of a mafic rock which has undergone granulite-facies metamorphism. In contrast, the source rock at Mount Narryer may have been a felsic igneous rock not recrystallized by granulite-facies metamorphism. Thus, the ancient source terrain of the detrital zircons, not yet found *in situ*, may have had considerable geological complexity although, as I pointed out in a previous *News and Views* article[6], one should be cautious in attributing a truly continental character to the source-region crust. Perhaps the ancient source terrain was more like an early non-continental volcano-sedimentary assemblage of greenstone belt facies, such as the now well-known Isua Belt of West Greenland which, with a well-established age of ~3,800 Myr, is the oldest *in situ* terrestrial rock assemblage known[7,8] and has survived in a relatively pristine condition until the present day. It is highly significant for any model of early crustal evolution that a 4,100–4,300-Myr-old source region should have remained exposed for at least 600–800 Myr at such a very early period of the Earth's history and preserved from recirculation into the mantle by plate tectonics or by any other process.

It may be too much to hope that the source rocks of the oldest Mount Narryer and Jack Hills zircons will actually be found *in situ* and thus become amenable to dating by other isotope methods. In the meantime, I shall try to repress a recurring nightmare that SHRIMP will one of these days come up with zircon U–Pb ages significantly greater than 4,600 Myr, the widely accepted age of the Earth. It would not be the first dating method to have undergone this embarrassing trial, and yet emerged triumphantly. □

1. Froude, D.O. *et al. Nature* **304**, 616 (1983).
2. Compston, W. & Pidgeon, R.T. *Nature* **321**, 766 (1986).
3. Williams, I.S. *et al. Contrib. Mineral. Petrol.* **88** 322 (1984).
4. Schärer, U. & Allègre, C.J. *Nature* **315** 52 (1985).
5. Compston, W. *et al. Nature* **317**, 559 (1985).
6. Moorbath, S. *Nature News and Views* **304** 585 (1983).
7. Moorbath, S., O'Nions, R.K. & Pankhurst, R.J. *Nature* **245**, 138 (1973).
8. Baadsgaard, H. *et al. Earth planet. Sci. Lett.* **68** 221 (1984).

Stephen Moorbath is Reader in Geology at the Department of Earth Sciences, University of Oxford, Oxford OX1 3PR, UK.

Archaeology

Finding the earliest Americans

from Warwick Bray

THE problem of the age and nature of the first human colonization of the New World has divided the archaeological profession for more than a century. Even now, there is general agreement on only two points: that the source of the colonizing population was north-east Asia; and that man was around by 11,500 years before present (BP), when fluted stone spear heads (Clovis points) are documented at several localities in North America. The Chilean site of Monte Verde[1] (13,000 yr BP), and perhaps the Alice Boer locality in Brazil[2] (14,200 ± 1,150 yr BP), push back the threshold by a few millennia, but no material older than 15,000 yr BP has gained universal acceptance. The strong evidence for stone tools dated at 32,000 yr BP at a site in Brazil, reported by Guidon and Delibrias on page 769 of this issue[3], is therefore important to archaeologists and to palaeontologists. The controversial belief that human predation caused the extinction of many large mammals at the end of the Pleistocene (that is, the Clovis point period)[4] is much weakened if large populations of hunters were already present in the Americas some twenty thousand years earlier.

Recently, the proponents of very early dates have suffered two setbacks. Using a corrected calibration, the apsartic acid racemization ages of the California 'Palaeoindian' skeletons have been drastically revised, and all these specimens turn out to be Holocene[5]. Still worse is the revised date for the only undisputed bone tools from the Old Crow Basin in the Yukon. In the 1970s, carbon extracted from the inorganic apatite fraction of a fleshing tool made of caribou rib gave a radiocarbon age of about 27,000 yr BP, but a re-dating of organic proteinaceous material (by the accelerator mass spectrometry method) has reduced this age to 1,350 ± 150 yr BP, though the dates for the redeposited (and possibly flaked) mammoth bones from these gravels remain more or less the same as the original date[6].

In essence, however, the basic dispute is not about individual sites or artefacts, but about what constitutes archaeological proof. It is true, of course, that piling up dubious cases proves absolutely nothing, and that a single unassailable find is enough. In theory, the criteria for acceptability are simple: there must be man-made artefacts (or other signs of human presence, such as hearths or structures) datable either directly or by their occurrence in deposits of known age. The ideal site would have a long stratigraphy, plentiful tools, multiple radiocarbon dates and evidence for evolution within the stone industries. This is exactly what Guidon and Delibrias provide in the work on the Brazilian site of Boqueirao of Pedra Furada[3]. Their oldest carbon-14 date, 32,160 ± 160 yr BP, comes from a fire hearth in a stratum with flaked tools and with spalls of painted rock from the walls of the shelter. Another sixteen radiocarbon dates are scattered at intervals through 3.5 metres of sediments. The validity of their evidence seems beyond doubt, and the excavation also suggests that cave art in the New World began at much the same time as in Eurasia and Africa.

It is to be hoped that Pedra Furada does not suffer the neglect given to Tlapacoya, in the Basin of Mexico, where good artefacts were discovered more than 20 years ago in a long sequence of lacustrine sediments and volcanic ashes dated at about 24,000 yr BP[7]. And there are other reports which, if eventually confirmed, will strengthen the argument for early colonization. At El Cedral, Mexico, stone tools and extinct fauna are provisionally dated at more than 30,000 yr BP[8] and in the deepest strata at Monte Verde, Tom Dillehay (personal communication) has found a split basalt pebble, wood fragments, two modified stones and charcoal dated at about 33,000 yr BP.

Evidence supporting an early colonization is also emerging from other disciplines. A study by Richard Rogers[9] of linguistic diversification in North America suggests that man must have been present south of the ice sheets before the Wisconsin maximum of about 18,000 yr BP, and long before the (post-glacial) incursions of the Na-Dene and Eskimo-Aleut language families.

A parallel study of the dental evidence by Christy Turner II[10] also indicates three separate colonizations, equating with the three major language introductions. He proposes that colonists initially spread outwards from North China around 20,000 yr BP and moved, via the Lena Basin of Siberia, into Beringia and Alaska. By the end of the Pleistocene this same, early Amerindian population had got as far as Tierra del Fuego. The descendants of Turner's proposed original group of immigrants could have filled up the Americas and must have been responsible for all stone industries older than 10,000 yr BP, when microblade tools and Na-Dene languages came to Alaska. In the light of the evidence from Pedra Furada we may now have to push Turner's starting date back by more than ten thousand years. □

1. Dillehay, T.D. *Scient. Am.* **251**(4), 100 (1984).
2. Bryan, A.L. & Beltro, M.C. in *Early Man in America from a circum-Pacific Perspective* (ed. Bryan, A.L.) 303 (Univ. Alberta, Edmonton, 1978).
3. Guidon, N. & Delibrias, G. *Nature* **321**, 769 (1986).
4. Martin, P.S. & Klein, R.G. (eds) *Quaternary Extinctions. A Prehistoric Revolution* (University of Arizona, Tucson, 1984).
5. Bada, J.L. *Am. Antiquity* **50**, 645 (1985).
6. Nelson, D.E., Morlan, R.E., Vogel, J.S., Southon, J.R. & Harington, C.R. *Science* **232**, 749 (1986).
7. Mirambell, L. in *Early Man in America from a circum-Pacific Perspective* (ed. Bryan, A.L.) 221 (Univ. Alberta, Edmonton, 1978).
8. Lorenzo, J.L. & Mirambell, L. *Proc. 10th Congreso UICPYP Mexico, Comision XII*, 112 (1981).
9. Rogers, R.R. *Quat. Res.* **23**, 130 (1985).
10. Turner, C.G. II *Natn. geogr. Res.* **2**, 37 (1986).

Warwick Bray is a Reader in the Institute of Archaeology, University of London, London WC1H 0PY, UK.

Caldesmon

Thin filament regulatory proteins of smooth- and non-muscle cells

from Anthony Bretscher

THE mechanism by which changes in the concentration of cytosolic calcium regulate the contractile machinery of smooth muscle has been a controversial problem. But the situation has now changed dramatically with the emergence of evidence in favour of a Ca^{2+}-calmodulin-mediated filament regulatory system.

The now well-established discovery[1,2] that the interaction of myosin light-chain kinase and Ca^{2+}-calmodulin leads to the phosphorylation of myosin and thereby enhances the actin-activated ATPase of myosin was a major step forward. It led to the common belief that smooth muscle contraction is controlled by the regulation of thick filaments. This mechanism contrasts with that in striated muscle, which is regulated by the classic tropomyosin–troponin thin filament system.

The smooth muscle thick filament regulatory model was extended to non-muscle cells when regulation of some non-muscle myosins via light-chain phosphorylation and dephosphorylation was found[3]. Overwhelmed by the simple elegance of the phosphorylation mechanism of smooth muscle thick filament regulation, scant attention was paid to suggestions of thin filament regulation — that is, thin filaments that activate myosin in the presence, but not in the absence, of Ca^{2+}.

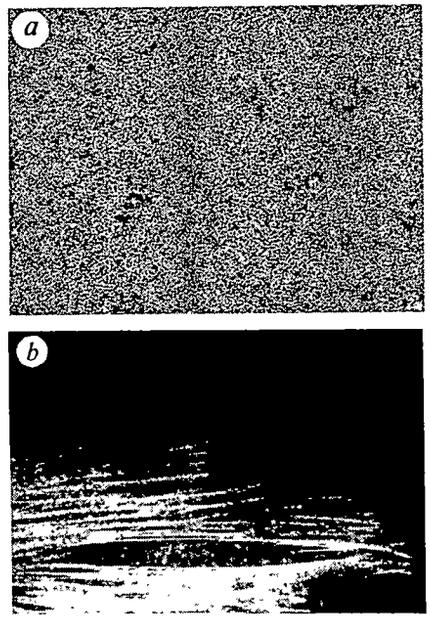
During this period, Ebashi and colleagues[3] suggested that a protein called leiotonin might impart some regulation, although this has not been independently substantiated.

The first evidence that suggested thin filament regulation of smooth muscle contraction was in systems containing activated myosin, but gave no clear indication of the regulatory molecules involved. As these experiments were refined, interest focused on the major components of partially purified thin filaments that retained Ca^{2+} regulation, namely actin, tropomyosin and a polypeptide of high relative molecular mass (M_r) $\simeq$ 120,000 (120 K)[4]. The second line of evidence was the identification in chicken gizzard smooth muscle of a protein that binds both actin filaments (F-actin) and Ca^{2+}-calmodulin[5]. This protein, with an apparent polypeptide $M_r \simeq$ 140 K, was named caldesmon (from a combination of calmodulin and $\delta\varepsilon\sigma\mu o\varsigma$ — bond) because its binding to F-actin can be inhibited in the presence of calmodulin in a Ca^{2+}-dependent manner. Further characterization in a reconstituted contractile system (consisting of desensitized actomyosin, myosin light-chain kinase, tropomyosin and limiting calmodulin) revealed that caldesmon inhibits the phosphorylated actin-activated ATPase of myosin[6]. This system can be regulated by the addition of excess Ca^{2+}-calmodulin which relieves the inhibition imposed by caldesmon (refs 4,6, but see ref. 7 for an alternative view). The two lines of evidence merged when it was found that the 120 K thin filament protein is caldesmon[4]. The inhibitory activity of caldesmon can be inactivated by phosphorylation of the protein by a specific protein kinase, which suggests another level of regulation. This caldesmon kinase activity is activated, like myosin light-chain kinase, by Ca^{2+}-calmodulin[7].

Taken together, these data indicate that smooth muscle is regulated at several levels by Ca^{2+}-calmodulin: first, regulation of myosin by reversible phosphorylation; second, Ca^{2+}-calmodulin binding to caldesmon which relieves the inhibitory effects of caldesmon on the actomyosin interaction; and third, regulation of caldesmon by reversible phosphorylation via the Ca^{2+}-calmodulin-regulated specific kinase and a phosphatase.

So what is known about the molecular properties of caldesmon? The protein appears to be structurally very stable, as it can be boiled in high salt or precipitated with organic solvents, yet retains its characteristic properties. It is a mildly acidic protein that, at least in chicken gizzard, exists as two polypeptide chains of slightly different apparent M_rs that can each be resolved into several isoelectric variants[8]. Hydrodynamic data indicate that caldesmon is highly asymmetrical[8]; low-angle rotary shadow electron micrographs confirm this and reveal that it is a long, flexible molecule (*a* in the figure)[9].

Caldesmon seems to be widely distributed as immunologically related proteins have been found in all smooth and non-muscle cells so far examined (*b* in the figure)[10,11]. Here the story becomes perplexing. There is a great deal of heterogeneity in caldesmon species in different cells: the apparent M_rs of caldesmons from different smooth muscles varies although they are in the region of 140 K (ref. 9). In various non-muscle tissues and cultured cell lines the apparent heterogeneity becomes even more noticeable. Some tissues and all the cell lines so far examined contain two classes of immunoreactive polypeptides: those in the M_r range 120–150 K and those in the range 71–77 K[11]. Because these species all remain soluble after heat treatment and bind F-actin in a Ca^{2+}-calmodulin inhibitable manner[11,12], they are functionally related to smooth muscle caldesmon, but nothing is known about how they are related to one another. Caldesmon is present along stress fibres of cultured fibroblasts in a periodic pattern apparently coincident with the localization of myosin, myosin light-chain kinase and tropomyosin, and complementary to the distribution of α-actinin[11]. In smooth muscle, caldesmon is localized in the actomyosin domain rather than in the apparently non-contractile filamin domain[9]. Thus it is not only capable of regulating the actomyosin interaction *in vitro*, but is also localized in the correct region of the contractile apparatus of smooth and non-muscle cells to perform this function *in vivo*.



a, Low-angle rotary shadow electron micrograph of smooth muscle caldesmon (× 43,000). *b*, Indirect immunofluorescence micrograph of part of a cultured A7r5 smooth muscle cell showing localization of caldesmon (× 530).

How does caldesmon regulate the actomyosin interaction? Is it, together with tropomyosin, a primitive form of the tropomyosin–troponin regulatory system of striated muscle? We do not yet have enough information to answer either of these questions. But any model must take into account the following observations. First, the apparent regulatory properties of caldesmon seem to require the presence of tropomyosin[4,6]. The co-localization of caldesmon and tropomyosin along stress fibres of cultured cells may also indicate a regulatory role for tropomyosin. Tropomyosin has been suggested to stabilize selectively certain classes of microfilaments. In the light of the results I have described here, it seems more likely that caldesmon and tropomyosin are part of a contractile unit that regulates actomyosin interaction.

Second, the molar ratio of caldesmon to actin is surprisingly low for a putative regulatory protein, far below the level of tropomyosin. How can a protein with low stoichiometry to F-actin regulate the actomyosin interaction? Could caldesmon alter the interaction between tropomyosin and F-actin over considerable distances and thereby regulate the interaction? Or is caldesmon perhaps selectively associated with restricted domains of F-actin–tropomyosin filaments involved in contraction? Finally, the ability of Ca^{2+}-calmodulin to inhibit the binding of caldesmon to F-actin requires a large molar excess of calmodulin over caldesmon[12], a level in excess of that reported for chicken gizzard. Perhaps that's just life in a test-tube under the wrong conditions, or missing another component. An alternative explanation may be that caldesmon release from F-actin is not required for relief of the actomyosin inhibition[2]. To explore these questions further, we need to know more about the interaction of caldesmon with calmodulin, F-actin and other (identified or yet to be identified) components. In addition to these questions, the possibility that caldesmon is a 'latch' between the thick and thin filaments needs to be examined.

1. Sobieszek, A. & Small, J.V. *J. molec. Biol.* **112**, 559 (1977).
2. Adelstein, R.S. *Cell* **30**, 349 (1982).
3. Ebashi, S. *Proc. R. Soc.* B**207**, 259 (1980).
4. Marston, S.B. & Smith, C.W.J. *J. Muscle Res. Cell Motil.* **6**, 669 (1985).
5. Sobue, K., Muramoto, Y., Fujita, M. & Kakiuchi, S. *Proc. natn. Acad. Sci. U.S.A.* **78**, 5652 (1981).
6. Sobue, K., Morimoto, K., Inui, M., Kanda, K. & Kakiuchi, S. *Biomed. Res.* **3**, 188 (1982).
7. Ngai, P.K. & Walsh, M.P. *J. biol. Chem.* **259**, 13656 (1984).
8. Bretscher, A. *J. biol. Chem.* **259**, 12873 (1984).
9. Furst, D.O., Cross, R.A., De Mey, J. & Small, J.V. *EMBO J.* **5**, 251 (1986).
10. Owada, M.K., Hakura, A., Iida, K., Sobue, K. & Kakiuchi, S. *Proc. natn. Acad. Sci. U.S.A.* **81**, 3130 (1984).
11. Bretscher, A. & Lynch, W. *J. Cell Biol.* **100**, 1656 (1985).
12. Sobue, K., Tanaka, T., Kanda, K., Ashino, N. & Kakiuchi, S. *Proc. natn. Acad. Sci. U.S.A.* **82**, 5025 (1985).

Anthony Bretscher is in the Section of Biochemistry, Molecular and Cell Biology, Cornell University, Wing Hall, Ithaca, New York 14853, USA.

Cell biology

The fibronectin receptor family

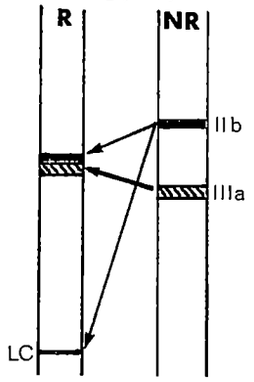
from Maria Leptin

In a developing embryo cells and tissues are constantly on the move. Individual cells migrate over long distances and sheets of cells rearrange during processes such as gastrulation and neural tube formation. During wound healing and metastasis in cancer similar situations are recreated in adult organisms. The extracellular matrix (ECM) provides a guiding substrate for cell movement, and, *in vitro*, its components can serve as an attachment substrate for cells to spread and migrate on plastic surfaces. How do cells bind to the ECM and what is the link between the ECM and the cytoskeletal motor? Do different cells use the ECM to migrate to different places and, if so, how? The properties of a family of recently isolated receptors for fibronectin and other ECM components suggest that a complex system of receptor–ligand interactions governs cell movements.

Two paths led to the identification of fibronectin receptors. One used the cell binding domain of fibronectin to purify proteins from cell lysates by affinity purification. The success of this approach depends on a specific elution of material bound to the column. An obvious candidate for an eluant is the hexapeptide Gly-Arg-Gly-Asp-Ser-Pro (GRGDSP) containing the recognition sequence RGD of the fibronectin cell-recognition domain, especially as the peptide inhibits the binding of cells to fibronectin substrates, and of soluble fibronectin to cells. The second approach was to immunoprecipitate cell surface proteins with antibodies that inhibit cells from binding to fibronectin.

With these two methods similar cell surface proteins, each consisting of at least two subunits, were purified from a diversity of cell types[1-7] including epithelial, erythroid and myogenic cells and thrombin-activated platelets. The subunits of the platelet proteins are the previously identified glycoproteins IIb and IIIa. The RGD-containing domain of fibronectin binds to the IIIa subunit. All these cell surface complexes have the same general rather unusual structure (see figure). On reducing SDS gels the two (or more) subunits run as one band or as a doublet at a relative molecular mass of about 140,000. On non-reducing gels they appear as well-separated bands. This is because the lower band runs more slowly under reducing conditions (typical of proteins containing intramolecular disulphide bonds), while the upper bands (which I shall call IIb-like) run faster under reducing conditions. For the platelet IIb band this behaviour is caused by the release of a small component on reduction[8]; it is likely that all IIb-like components will have such a light chain attached.

What do all these receptors have to do with each other? Their fibronectin-binding activity (shown directly for some and inferred from the adhesion-blocking activities of the antibodies for the others) and their common structure suggest that they are all the same type of receptor. However, the differences between them indicate that there does not seem to be such a thing as *the* fibronectin receptor, but rather a whole family of related but subtly different receptors. They differ in molecular mass, glycosylation and number of components. Until direct comparisons of the proteins are made it is futile to speculate whether the differences in mass simply result from variations in gel conditions, but some are so great, that they probably reflect real differences between receptors from different cells.



Migration of the platelet fibronectin receptor IIb/IIIa on reducing (R) and non-reducing (NR) polyacrylamide gels. LC, light chain. (After ref. 8.)

A family of cell surface glycoproteins in which such cell-specific differences do occur are the PS antigens in the fruitfly *Drosophila*, which have the same unusual structure as the fibronectin receptors[9]. Found in most tissues of the body, these complexes each consist of one IIa-like component and one or more IIb-like components. The IIIa-like component is present in every complex whereas the IIb-like components attached to it vary between tissues[9]. PS antigens are thought to be involved in the segregation of cell populations during development, so it will be interesting to see if they are functionally similar to vertebrate fibronectin receptors.

Most importantly, fibronectin receptors differ in their affinities and fine specificities. In fact, these receptors are only a subset of a larger family of receptors for proteins containing the RGD recognition sequence (for example, vitronectin, laminin and fibrinogen). Cells can carry two separate receptors with different specificities, or they can use one receptor to bind to more than one ligand. The first case is exemplified by osteosarcoma cells[10], which have two different receptors for fibronectin and vitronectin, neither of which binds laminin. The binding of both receptors to their ligands is inhibited by peptides containing the RGD sequence. On the other hand, the receptor on fibroblasts can bind to both fibronectin and laminin[3]. Platelets appear to use a single receptor to bind fibronectin and fibrinogen, because fibrinogen inhibits binding of fibronectin to platelets. Finally, receptors for the same ligand on different cells can differ in their affinities. In contrast to the molecules isolated by affinity purification, the receptor isolated by one of the antibodies is not retained on fibronectin columns, but only retarded (compared with its elution from bovine serum albumin columns)[6]. Such weak binding is not unexpected, as receptors which cells use for migration should bind and be readily detachable from the substrate.

The RGD receptors may use the same trick that is developed to perfection by the immune system and that might be used by olfactory neurones[11], namely to use receptors with constant structure but variable specificities to handle diverse ligands in the environment. If all these receptors bind to the RGD sequence, how is their fine specificity determined? They all consist of more than one component, only one of which seems to bind to the RGD-containing domain, if the finding for the platelet IIIa band can be generalized. Perhaps this subunit mediates the binding to the recognition sequence RGD, while the other associated components determine the fine specifity of the receptor. These components might affect the conformation of IIIa and thereby modulate the binding site, so that RGD is recognized only in some contexts but not in others; they might combine to form different binding sites; or they might themselves carry a second binding site specific for another epitope on the target molecule. Such variation of receptor specificity could provide a guiding and sorting mechanism for cells during morphogenesis. □

1. Pytela, R. *et al. Cell* **40**, 191 (1985).
2. Gardner, J.M. & Hynes, R.O. *Cell* **42**, 439 (1985).
3. Horwitz, A. *et al. J. Cell Biol.* **101**, 2134 (1985).
4. Giancotti, F.G. *et al. Expl Cell Res.* **156**, 182 (1985).
5. Brown, P.J. & Juliano, R.L. *Science* **228**, 1448 (1985).
6. Okiyama, S.K. *et al. J. Cell Biol.* **102**, 442 (1986).
7. Patel, V.P. & Lodish, H.F. *J. Cell Biol.* **102**, 449 (1986).
8. Phillips, D.R. & Agin, P.P. *J. biol. Chem.* **252**, 2121 (1977).
9. Wilcox, M. & Leptin, M. *Nature* **316**, 351 (1985).
10. Pytela, R. *et al. Proc. natn. Acad. Sci. U.S.A.* **82**, 5766 (1985).
11. Chen, Z. & Lancet, D. *Proc. natn. Acad. Sci. U.S.A.* **81**, 1859 (1985).

Maria Leptin is in the Medical Research Council Laboratory for Molecular Biology, Hills Road, Cambridge CB2 2QH, UK.

Stratospheric chemistry

Depletion of Antarctic ozone

from A. F. Tuck

THE total amount of ozone overhead in late winter and early spring at Antarctica has decreased by about 40 per cent during the past decade[1]. Recent analysis of satellite data[2] shows that the phenomenon affects much of the cold, cyclonic vortex found there, and that column abundances are among the lowest recorded anywhere on the globe. A time series of ozonesonde profiles[3] taken in 1982, when compared with data taken in the late 1960s and early 1970s, suggests that much of the decrease occurs in the lower stratosphere, at and below the altitudes where maximum number densities of ozone occur (Fig.1). These experimental findings are a major surprise, and are taxing the theoretical ingenuity of stratospheric researchers. The first calculations of these late winter and spring antarctic ozone reductions appear on pages 755 and 759 of this issue[4,5]. Until an experimentally validated mechanism for these reductions is available, the implications for the global ozone layer are not clear.

The work reported in refs 2,4 and 5 was presented for the first time at a recent meeting*. Some simple numerical model calculations demonstrate the extent of the ozone deficit caused in southern mid-latitudes as poleward motion of ozone-rich air over Antarctica, largely suppressed during winter, occurs in spring and fills in the 'ozone hole' in the cold vortical air by mixing with it (R. Rood, NASA Goddard Space Flight Center). This induced mid-latitude deficit is small; the model calculation is based on simplified large-scale dynamics, with no photochemistry or radiative transfer. The antarctic winter polar vortex in the stratosphere is approaching the radiative equilibrium temperatures computed for air with 'climatological' O_3, CO_2 and H_2O as the gaseous absorbers and emitters; general circulation models indicate that under these circumstances the vortex can be quite sensitive to comparatively weak perturbations (J. Mahlman, NOAA Princeton Geophysical Fluid Dynamics Laboratory). Finally, I reported UK Meteorological Office calculations of radiatively corrected isentropic trajectories over both arctic and antarctic winter polar caps in 1979, which show that over a 10-day period, air parcels starting poleward of 75° latitude in the Arctic tend to encounter sunlight within a few days. In Antarctica, however, most air parcels stay in the dark for the entire 10 days (Fig.2).

At the meeting, results were described of forward and back trajectories initiated by observations of arctic polar stratospheric clouds by the SAM II instrument[6]. Coincident observations of O_3, NO_2, HNO_3 and H_2O by the LIMS instrument[7] on Nimbus 7 in January 1979 are also available. Preliminary results show ozone and nitric acid reductions along the forward trajectories which are fast enough to be consistent with the Antarctic data; the scatter means that the results are barely at the 2σ level. The results depend critically on removing the effects of cloud from the LIMS data.

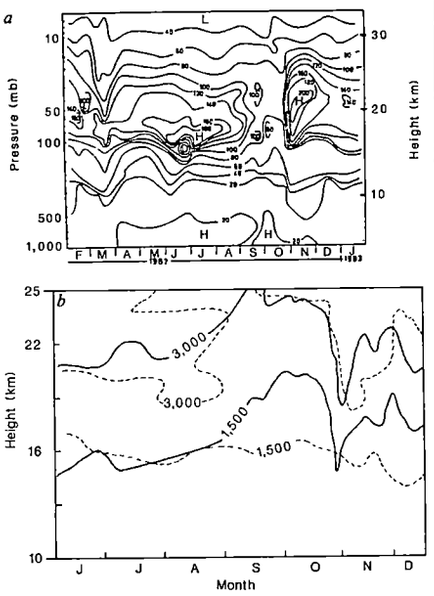


Fig.1 *a*, Partial pressure of ozone over Syowa (69°S, 40°E) during 1982, from 22 ozonesonde ascents. Contours are in nanobars. (Redrawn from ref.3.) *b*, Contours of ozone volume mixing ratio (p.p.b.v.) over Syowa (69°N, 40°E) during the last half of 1970 (broken lines) and 1982 (continuous lines). Note the coherent behaviour of the 1,500 and 3,000 contours in 1982 over the whole period, in contrast to the behaviour in 1970. Redrawn from plots supplied by S. Solomon (personal communication).

There was discussion of the general requirements for a ground-based network for early detection of stratospheric change, particularly in relation to Antarctica. Several techniques for measuring the contrasting conditions in the upper mid-latitude stratosphere and the lower polar stratosphere were discussed, prominent among them ground-based laser radars (lidars) and passive microwave millimetre and sub-millimetre radiometers. One instrument, a high-resolution infrared interferometer that scans the spectrum from 2- to 16-μm wavelength using absorption of solar radiation, offers the possibility of detecting and measuring the column abundances of many different stratospheric molecules.

The planned campaign for austral spring 1986 includes flights of ozone balloon-sondes from the US antarctic stations at McMurdo and Amundsen–Scott. There will be a supply flight (sponsored by the National Science Foundation) into McMurdo on 21 August, and it is hoped to fly in scientists to measure ozone and aerosols (D. Hoffman, University of Wyoming); ClO (P. Solomon and R. de Zafra, State University of New York at Stony Brook); NO_2 and OClO (A. Schmeltekopf, G. Mount and S. Solomon, NOAA Aeronomy, Boulder); and instruments such as a high-resolution absorption FTIR spectrometer (C.B. Farmer, NASA Jet Propulsion Laboratory). There will also be measurements of NO_2 column amounts at three New Zealand stations, and British Antarctic Survey ozone measurements will continue. A more extensive Antarctic campaign, which may include aircraft and balloon experiments in addition to the ground-based instruments, is planned for austral spring 1987. There is clearly a need for a small network aimed at early detection of trends in the key molecules, but there is at present no obvious source of funds for the long-term commitment required.

Several points emerged from the meeting. First, and possibly the most important, is that it is difficult to find any reliable data in the chemical kinetics literature on gas–ice crystal interactions in the atmospheric conditions of the lower antarctic winter stratosphere. It is also true that the relevant homogeneous gas-phase rate coefficients involve a considerable extrapolation to reach the temperature range 165–225 K. We simply cannot be sure of the chemistry in this regime, particularly concerning the larger reservoir species like N_2O_5 and $ClONO_2$, and molecules such as BrO. Therefore, laboratory measurements are as essential as those in the atmosphere.

Second, it is not clear what substituting ice crystals for water vapour (which is what happens as temperature falls below about 192 K) does to the radiative balance, although there has been a calculation of this effect[8].

Third, it seems probable that a reliable calculation of the dynamical-radiative balance is essential, presumably by a yet-to-be developed general circulation model which handles the stratospheric polar night vortex and its low temperature adequately. The coherent behaviour of the 1,500 and 3,000 parts per 10^9 by volume (p.p.b.v.) contours over the entire second half of 1982 at Syowa (Fig.1*b*), a pattern not evident in 1970 or earlier, suggests that attention should not be confined to

*Antarctic Ozone meeting, Boulder, Colorado 4–7 March 1986. Sponsored by National Aeronautics and Space Administration (NASA), National Oceanographic and Atmospheric Administration (NOAA) and the Chemical Manufacturer's Association.

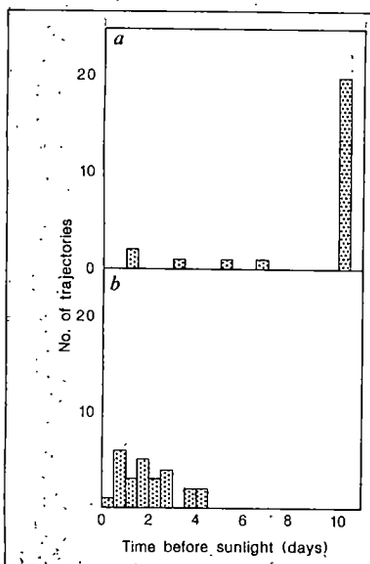


Fig. 2 Numbers of 10-day trajectories starting in the polar caps (75°–90° latitude) and staying in the darkness for differing lengths of time. Twenty-five parcels evenly distributed over the cap were considered, using the quasi-isentropic approach of Austin and Tuck[9]. *a*, Antarctica 18–28 June 1979; *b*, Arctic 12–22 January 1979. Eighty per cent of the antarctic parcels had not experienced sunlight at the end of 10 days, whereas all the arctic ones had done so after 4–5 days.

September and October. It may also mean that the polarization of theories so far, into dynamical and chemical categories, may be premature — it seems likely that both sorts of process are involved. If chemistry on ice-particle surfaces at very low temperatures (−80°C or colder) is important, then it may be worth looking more closely at those locations in the tropical lower stratosphere where large cumulonimbus storms are believed to maintain extensive anvil cirrus sheets at the low temperatures, by moist convection rather than by radiative cooling. The different exposure to solar radiation at the two places may yield important clues.

Finally, it should be apparent from the above that model calculations of this effect are as yet in their infancy, and are no better than the input physico-chemical data. There is a long way to go experimentally before an accepted qualitative, let alone quantitative, explanation is available. □

1. Farmer, J.C., Gardiner, B.G. & Shanklin, J.D. *Nature* **315**, 207 (1985).
2. Stolarski, R.S. *et al. Nature* (in the press).
3. Chubachi, S. *Atmospheric Ozone* (Reidel, Dordrecht, 1984).
4. Solomon, S., Garcia, R.R., Rowland, F.S. & Wuebbles, D.J. *Nature* **321**, 755 (1986).
5. McElroy, M.B., Salawitch, R.J., Wofsy, S.C. & Logan, J.A. *Nature* **321**, 759 (1986).
6. McCormick, M.P., Steele, H.M., Hamill, P., Chu, W.P. & Swissler, T.J. *J. atmos. Sci.* **39**, 1387 (1982).
7. Gille, J.C. & Russell, J.M. III *J. geophys. Res.* **89**, 5125 (1984).
8. Pollack, J.B. & MacKay, C.P. *J. atmos. Sci.* **42**, 245 (1985).
9. Austin, J. & Tuck, A.F. *Q.J. R. Met. Soc.* **111**, 279 (1985).

A.F. Tuck is at the Meteorological Office, London Road, Bracknell, Berkshire RG12 2SZ, UK.

Molecular biology

Globin gene monkey business

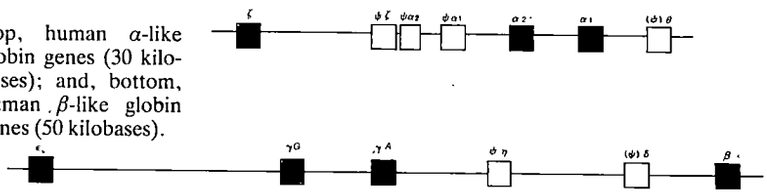
from Nick Proudfoot

THE discovery of a new α-like globin gene in orang utan, reported by Marks, Shaw and Shen on page 789 of this issue[1], and the possibility that a similar gene has until now escaped notice in humans, is an illustration of how there are still many surprises in store even in a well-characterized gene system such as globin. It is, however, possible that the orang utan θ-globin gene is inactive — in other words, a pseudogene — because it may not possess a functional promoter sequence. Although θ-globin could have little significance to the orang utan, it is possible that in other primates, man included, the new globin gene has an important but as yet undetected biological role. The characterization of θ-globin in other primates is therefore eagerly awaited to see whether a new functional θ-globin gene will be identified.

Globin genes were among the first to be mapped and sequenced in eukaryotes[2]. Tidy clusters of either α- or β-like globin genes (see figure) are now familiar in molecular biology textbooks. The human globin gene clusters are especially well characterized as globins at each developmental stage have each been assigned their gene and many mutations from different thalassaemias have been pinned down to specific positions on the globin gene map[3]. In addition to functional genes, there are a surprisingly high number of apparently functionless pseudoglobin genes, particularly in the human α-globin gene cluster. At the last count (see figure), there are three pseudogenes between the embryonic ζ-globin and the two adult α-globin genes. These pseudogenes cover the whole spectrum of gene inactivity. The ψζ gene looks quite healthy and, were it not for a nonsense mutation at codon 6, might be expected to produce ζ-globin[4]. In some human populations, ψζ-globin has a normal codon 6 but surprisingly still fails to produce a gene product[5]. The gene ψα1 is very clearly non-functional, as a whole set of mutations prevent both its translation and its transcription[6,7]. The newly identified pseudogene, ψα2, is so extensively diverged from α that it was only picked up by a computer search for α-like sequences in the recently completely sequenced intergenic regions between ζ and α2 (ref. 8).

To this collection we must add the θ-globin gene at the downstream end of the α-gene cluster that is described in this issue[1]. In the orang utan this gene has the usual arrangement of three exons that would encode a fairly standard α-like globin polypeptide chain. Furthermore, most of the amino acids common to the α-globins of different mammals are found in θ-globin, and those that are not found fit with a β-like globin sequence. Even so, it seems unlikely that this gene can be active because its promoter sequence elements, the CCAAT and ATA boxes, are moved more than 100 nucleotides away from their normal position by the insertion of a GC-rich sequence. Such alterations to the spacing of the θ-globin promoter would be expected to prevent initiation of transcription. Although the θ-globin gene is probably non-functional in orang utan, it may still be active in humans. Indeed, there are possibly a few as yet unassigned embryonic globins, as shown by the recent analysis of very early human embryos[9]. What the new work of Marks *et al.*[1] does show is that θ-globin in orang utan is quite similar to a rabbit α-globin pseudogene, suggesting a very early evolutionary origin for θ-globin.

A similar situation to θ-globin exists in the human β-like globin gene cluster. Here, only one pseudogene, the ψβ1 gene, has been unequivocally identified[10], although the low level of δ-globin gene activity could be taken as an argument that δ is also effectively a ψβ gene[11]. Interestingly, ψβ1 has strongly con-



Top, human α-like globin genes (30 kilobases); and, bottom, human β-like globin genes (50 kilobases).

1. Marks, J., Shaw, J.-P. & Shen, C.-K. *Nature* **321**, 789 (1986).
2. Maniatis, T., Fritsch, E.F., Lauer, J. & Lawn, R.M. *A. Rev. Genet.* **14**, 145 (1980).
3. Weatherall, D.J. *The New Genetics and Clinical Practice* 2nd edn (Nuffield Provincial Hospitals Trust, London, 1985).
4. Proudfoot, N.J., Gil, A. & Maniatis, T. *Cell* **31**, 552 (1982).
5. Hill, A.V.S., Nicholls, R.D., Thein, S.L. & Higgs, D.R. *Cell* **42**, 809 (1985).
6. Proudfoot, N.T. & Maniatis, T. *Cell* **21**, 537 (1980).
7. Whitelaw, E. & Proudfoot, N.J. *Nucleic Acids Res.* **211**, 7717 (1983).
8. Hardison, R.C., Sawada, I., Cheng, J.-F., Shen, C.-K.J. & Schmid, C.W. *Nucleic Acids Res.* **14**, 1903 (1986).
9. Peschle, C. *et al. Nature* **313**, 235 (1985).
10. Jagadeeswaran, P., Pan, J. Forget, B.G. & Weissman, S.M. *Cold Spring Harbor Symp. quant. Biol.* **47**, 1079 (1982).
11. Martin, S.L., Vincent, K.A. & Wilson, A.L. *J. molec. Biol.* **164**, 513 (1983).
12. Harris, S., Barrie, P.A., Weiss, M.L. & Jeffreys, A.J. *J. molec. Biol.* **180**, 784 (1984).

served counterparts in other primates and even in more distant evolutionary relatives such as goat, where it is a functional embryonic globin gene. Indeed Harris *et al.*[12] renamed $\psi\beta$ η-globin to emphasize that it does have a function in some mammalian globin gene systems but that this function has been lost in primates. It may be similar with θ-globin, where the gene is probably functional in some mammals but possibly is not in primates.

What these studies on globin genes and pseudogene in mammals clearly illustrate is that globin gene evolution has produced a very flexible set of genes capable of providing the individual needs of each species for oxygen carriage at each developmental stage. Every newly created globin gene is then randomly mutated and the mutations either selected for functional globin variants or are put on the gene scrap-heap as useless variants. Studies of θ- and η-globin further show that previously useful variants may subsequently cease to be so and thus will end up with other non-functional duplicated globin genes in the scrap-heap. The title of a paper describing the evolutionary path of the δ-globin gene as "the rise and fall of a globin gene"[11] is equally applicable to θ- and η-globin genes and it might turn out to be applicable to other gene families. □

Nick Proudfoot is in the Sir William Dunn School of Pathology, South Parks Road, University of Oxford, OX1 3RE, UK.

Neurobiology

Clues about glues in development

from Colin J. Barnstable

FORMATION of a complex nervous system from a simple neuroepithelium involves many events of regionalization, cell migration, cell death, directional axon growth and specific cell interactions. It has often been proposed that molecules at the cell surface mediate the interactions between the genetic and the epigenetic processes of neural development. It has been thought such molecules can be recognized by their ability to cause adhesion between cells. Several recent papers have suggested ways in which known cell surface molecules might interact with each other and with extracellular matrix molecules to control important events, such as synapse formation, in neural development.

Probably the best-characterized cell adhesion molecule is N-CAM[1,2]. This transmembrane glycoprotein appears after neural induction in the embryo. It is expressed by all neurones, some glia and a few other cell types in the adult and causes cell adhesion by homophilic interactions between domains in the amino-terminal portion of the molecule. It has become clear over the past few years that many other molecules detectable by adhesion assays appear during development of the nervous system but the mechanism of action of many of them remain obscure.

The potential functions of cell adhesion molecules in the outgrowth of axons has been studied intensively. There is now evidence that some aspects of directed axon growth might be controlled through N-CAM. The simplest model for this would be one in which a track of an adhesive molecule such as N-CAM is laid down in the tissue. An immunocytochemical study of the developing chick optic tract suggested that the retinal ganglion cell axons were following a track of N-CAM expressed on the endfeet of radial glia[3]. Although an attractive model, its general applicability to pathway formation is not clear. Other factors are almost certainly operating, as retinal ganglion cells placed in ectopic sites can send axons along very abnormal pathways yet still reach their correct targets[4].

A second class of model has arisen from studies on the innervation and reinnervation of muscle. N-CAM is present on the surface of myotubes in the embryo, but is lost as development proceeds and is almost absent from adult muscle. Denervation or paralysis of adult muscle leads to an increase in N-CAM levels over the whole myotube until synapses are re-established. N-CAM is also associated with interstitial cells between the muscle fibres[5]. But the increase in N-CAM expression over the whole muscle cell does not explain why synapse formation during reinnervation preferentially takes place at the old synaptic sites. In studying the changes in other molecules after denervation, Sanes and co-workers found that fibronectin, a heparan sulphate proteoglycan and an extracellular glycoprotein J1 also accumulated in the interstitial spaces near the denervated synaptic sites[6].

These molecules, particularly J1, have all been shown to mediate adhesion of neurones to other cells or to basement membranes. The findings led the authors to suggest these molecules may act with N-CAM to provide a hierarchy of cues that guide axons towards the old synaptic sites (see Fig.1). McMahan and colleagues have described a molecule in the extracellular matrix that may mark the old synaptic sites and perhaps this type of molecule represents the final step in the hierarchy[7]. Thus, the control of axon growth may involve a generalized interaction mediated by N-CAM and then more specialized interactions mediated by N-CAM plus other molecules. Whether this hierarchy represents quantitative levels of adhesivity or qualitative differences in the signals provided by the different molecules is not yet clear.

Recent reports by Glaser and co-workers suggest that some aspects of such an adhesive hierarchy may be caused by modulations of N-CAM itself. Adhesion

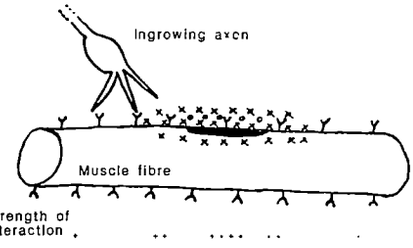


Fig. 1 The growth cone of the ingrowing axon can detect the molecules on the muscle surface and in the interstitial space. Its growth is directed up the gradient of increasing strength of interaction that leads to the old synaptic site. Y, N-CAM; ×, J1 fibronectin and heparan sulphate. ○, synapse-specific molecules; ■, old synaptic site.

100 years ago

The Hong Kong meteorological observatory

THIS first-class meteorological observatory was erected in 1883, and the regular work of observing began on January 1, 1884. Weather Reports appear monthly, and we have now before us the observations and work of Mr Doberck and his staff for the first two years. For the first two months the work was restricted to eye-observations, but meanwhile no time was lost in erecting the barograph, thermograph, anemograph, pluviograph, and sunshine recorder, which are similar to those in use at Kew; and from April 1, 1884, the Monthly Reports include a continuous hourly record of the more important elements of the climate of Hong Kong. The buildings are erected on the peninsula of Kaulung, facing the harbour, on the top of Mount Elgin, a small eminence rising from the plain to a height of about 100 feet above mean sea-level. It may also be noted that the ground has been carefully turfed where the instruments are placed. In addition to the usual tabulations and their averages, the Monthly Report gives a carefully observed log of non-instrumental phenomena, such as dew, fog, unusual visibility, halos, and thunderstorms.

The results show that the amplitude of the daily range of the barometer is greatest from November to February, when the rainfall is least and their air driest, the mean difference during these four months between the morning maximum and afternoon minimum amounting to 0.102 inch. On the other hand, the mean of the four months from June to September when the monthly rainfall nearly equals 12 inches, only amounts to 0.069 inch. The diurnal range of temperature is small, being for the year only 5°.5, the maximum, 7°.2, occurring in December, and the minimum, 4°.0, in February.

From *Nature* **33**, 148; 17 June 1886.

of chick neural retina cells to extracellular matrix material was inhibited by an antibody against N-CAM and by heparan sulphate[8]. It has now been shown that N-CAM itself has a binding site for a heparin-like proteoglycan[9]. Thus binding of neurones, and perhaps neuronal processes, to extracellular matrix may result from a N-CAM–proteoglycan interaction.

As heparan sulphate has been shown to be on the cell surface of retinal cells, Glaser and co-workers asked whether it might also have a role in the N-CAM-mediated cell–cell adhesion. They found that binding of chick neural retina cells to retinal monolayers was inhibited by heparin but not an unrelated proteoglycan[10]. This cell–cell adhesion was also inhibited by the isolated heparin-binding domain of N-CAM and by an antibody that recognizes this domain. As binding of heparin alters the susceptibility of N-CAM to proteolytic cleavage it is thought that the interaction involves a

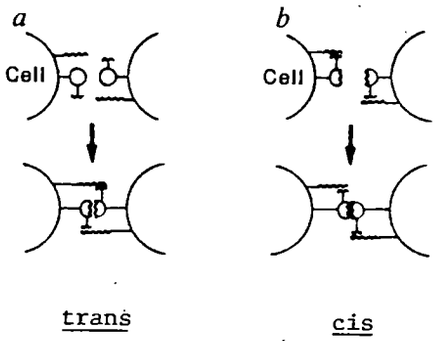


Fig. 2 Possible modes of interaction between heparan sulphate (—) and N-CAM (—○). *a*, In a *trans* interaction the heparan sulphate on one cell can interact with the N-CAM on another cell. *b*, in a *cis* interaction the heparan sulphate binds to and possibly modifies the N-CAM on the same cell. (From ref. 10.)

conformational change in N-CAM. What is not yet clear is whether the proteoglycan on one cell interacts with the N-CAM on another cell, or whether the proteoglycan interacts with N-CAM on the same cell and thus affects the affinity of the N-CAM–N-CAM homophilic interaction between cells (see Fig.2).

These results lead to several conclusions and speculations. One is that the distinction between cell–cell adhesion and cell–substrate adhesion is becoming less distinct. Molecules such as N-CAM may function in both. A second is that

1. Rutishauser, U. *Nature* **310**, 549 (1984).
2. Edelman, G.M. *A. Rev. Neurosci.* **7**, 339 (1984).
3. Silver, J. & Rutishauser, U. *Devl Biol.* **106** 485 (1984).
4. Taghert, P.H. & Lichtman, J.W. *Nature* **320** 111 (1986).
5. Couvalt, J. & Sanes, J.R. *Proc. natn. Acad. Sci. U.S.A.* **82**, 4544 (1985).
6. Sanes, J.R., Schachner, M. & Couvalt, J. *J. Cell Biol.* **102**, 420 (1986).
7. Fallon, J.R. *et al. Nature* **315**, 571 (1985).
8. Cole, G.J. Schubert, D. & Glaser, L. *J. Cell Biol.* **100**, 1192 (1985).
9. Cole, G.J. & Glaser, L. *J. Cell Biol.* **102**, 403 (1986).
10. Cole, G.J., Loewy, A. & Glaser, L. *Nature* **320**, 445 (1986).

events such as cell adhesion formation may require seve molecules, and the affinity o action might be modulated cellular and extracellular Finally, as interactions betwe molecules can lead to co changes in transmembrane gl these molecules may do muc glue cells together. Cell a measured by binding assays be an experimental epi

Ichnology

Sedimentol

from Michael J. Benton

In films and in fictional literat brontosauri are pictured crash the undergrowth, felling tree creating seismic tremors as foot meets the ground. New st silized dinosaur footprints sh can be used by geologists t ancient water depths, currer the slopes of sand dunes. A these studies launches the jou which will be devoted to rese mentological and palaeoec pects of the fossil record.

Dinosaur footprints are k dozens of localities around Most research effort so far h voted to determining the taxo tracks and to identification c makers. Specimens produce kind of dinosaur have been fo from the tiny bird-like footpri small theropods to the vast marks made by sauropods suc *saurus*. Palaeobiological int of these trackways have also In many places, for examp tracks show that herds of din ed in close formation in the tion[1,2]. It has also been possil late how fast the dinosaurs w when they made the tracks. spacing of individual prints wi way give estimates of speed ac simple formula[3]. The fastest 'c saurs could run as fast as 35 whereas *Brontosaurus* would dered along at 12–17 km h^{-1} (

The new work on dinosau focuses on their use in sed Several authors, for example gested that dinosaur tracks largely along the edges of wa close proximity to the strand tracks can even be used to rec exact position of a marine c shoreline by measuring the c locomotion, which are assu roughly parallel to the sho cases, the footprints within a way vary in depth, the dept

Portuguese role in spread of HTLV-I virus

SIR—Having arrived in Tokyo recently, I thought that I had learnt another word to improve my Japanese vocabulary, by reading Gallo *et al.*[1] on the origins of human T-lymphotropic viruses. However, the word *amakawa,* which they inform us is the Japanese word for monkey, is absent in recent reference sources[2] I have checked. Even my Japanese colleagues in the laboratory seem unaware of it as an alternative term for monkey. The popular word for the Japanese macaque monkey is *saru*. The monkey deity in Japanese mythology is known as *sarutahiko,* while a monkey show, once a common street entertainment, is termed *sarumawashi*[3].

Rosenior's comment, "the presence of the HTLV-I virus in the vast expanse of continental Asia cannot be ruled out due to lack of epidemiological studies in the area"[4], seems to have an element of truth, if we believe the historical records of the seafaring adventures of the Portuguese. Figure 1 of Wong-Staal and Gallo[5] neglects (or slightly distorts) the travel routes taken by the Portuguese in the early part of the sixteenth century. Vasco da Gama landed in Calicut, South India in 1498[6] and, in 1505, a Portuguese fleet commanded by Lourenco de Almeida was blown into Colombo, Ceylon, by adverse winds[7]. Malacca fell to the Portuguese in 1511. It was only after establishing contacts in India, Ceylon and Malacca that the Portuguese arrived in Japan, in 1543.

Prior to his arrival in Japan in 1549, Saint Francis Xavier first disembarked in Goa, India, the centre of Portuguese activity in the East in 1542 and spent the next three years on the southeastern coast of India among the Tamil-speaking pearl fishermen, the Paravas[8].

According to Percival Spear[6], in those times the Portuguese relied greatly on sea power based on fortified posts and backed by settlements; however, Portugal, with less than one million people, was desperately short of manpower. Therefore, intermarriage was encouraged between the Portuguese seafaring adventurers and the natives of the Indian subcontinent. That practice was the origin of the mixed population of Luso-Indians (or Goanese) along the western coast of India and in Ceylon.

If it is believed (as mentioned by Gallo *et al.*[1]) that the Portuguese came to Japan with monkeys, it is highly probable that the monkeys would have been from the Malayan region and not from Africa. (South-East Asia is also the endemic zone of apes such as gibbon, siamang and orang utan.) Historical records reveal that Portuguese trade was directed mainly between Japan and China rather than Africa.

Therefore, it is my hypothesis that the dark-skinned people who were taken to Japan by Portuguese were the South Indian Tamils of fishermen caste, and not Africans, as suggested by Gallo *et al.* The linguistic relationship between the Tamil language and Japanese language has been studied by Ohno[9].

SACHI SRI KANTHA
Laboratory of Marine Biochemistry,
University of Tokyo,
Bunkyo-ku,
Tokyo 113, Japan

1. Gallo, R.C. *et al. Nature* **320,** 219 (1986).
2. Imaizumi, Y. *Kodansha Encyclopedia of Japan* Vol. 5, 245 (Kodansha, Tokyo, 1983).
3. Saneyoshi, T. *Kodansha Encyclopedia of Japan* Vol. 5, 245 (Kodansha International Ltd, Tokyo, 1983).
4. Rosenior, J. *Nature* **318,** 100 (1985).
5. Wong-Staal, F. & Gallo, R.C. *Nature* **317,** 395 (1985).
6. Percival Spear, T.G. *Encyclopedia Britannica* Vol. 9, 15th edn 392 (Encyclopedia Britannica Inc. Chicago, 1983).
7. Arasaratnam, S. *Encyclopedia Britannica* Vol. 4, 15th edn 5 (Encyclopedia Britannica Inc. Chicago, 1983).
8. Bireley, R.L. Rev. *Encyclopedia Britannica* Vol. 19, 15th edn 1055 (Encyclopedia Britannica Inc. Chicago, 1983).
9. Ohno, S. *Nihongogo to Tamirugo* (Shinchosha, Tokyo, 1981).

Commercial samples of subtilisin BPN′

SIR—The serine protease subtilisin BPN′ (also known as novo or nagarse) from *Bacillus amyloliquefaciens* has been cloned and expressed on three separate occasions[1-3]. We have found a discrepancy of over a factor of 10 between the activity of the cloned enzyme and the activity of commercial enzyme purchased from Sigma Chemical Company (Protease Type VII, P 5255, from *Bacillus amyloliquefaciens*). The cloned enzyme has identical activity to an authentic sample of nagarse enzyme which was used for the original crystallographic studies[4]. (This sample was given to A.R.F. by Dr C.S. Wright in 1969.) Kinetic and physical properties indicate that the commercial enzyme is probably subtilisin Carlsberg, isolated from *Bacillus licheniformis*. We reported our findings to Sigma who have now conducted their own tests. They have just informed us that they agree with our findings and that, for the past ten years, their subtilisin BPN ′ has not been the authentic enzyme.

The hydrolysis of the synthetic substrate succinyl-L-alanyl-L-alanyl-L-prolyl-L-phenylalanyl *p*-nitroanilide by the cloned enzyme is characterized by values for k_{cat} and K_m of 57 s^{-1} and 0.15 mM respectively (25 °C in 0.1 M Tris-HCl buffer, *p*H 8.6), the enzyme concentration being measured by active-site titration. These are identical to the values for the independently cloned gene[1]. Under the same conditions, the values for the authentic nagarse enzyme are essentially identical at 60 s^{-1} and 0.15 mM. The values of k_{cat} and

ing laser gyro) and such rotation sensors vill undoubtedly find practical application n space vehicles. It is logical to verify vhether the Michelson interferometer can ense translational motion of a space ehicle, once it has moved outside the Earth's influence.

However, the underlying hypothesis of 'simopoulos and Theocharis leaves one vondering how small the ambient field ffects have to be in order not to control he electromagnetic reference frame. In his regard it should be remembered that he Michelson–Morley experiment of 887 antedates Wiener's 1890 discovery of he existence of stationary light waves vhen a ray of light is reflected back upon :self by a mirror. This means that in the Aichelson experiments the incident ray is assing through the field of the reflected ay. We assume that this field does not ffect the speed of the incident ray. If this ssumption is wrong and field energy can resent, in effect, a refractive index odifying the speed of light, then without ppealing to the ambient effects of an Earth field we can even consider that the ptimization of the energy in the standing vave system will determine the local rame of reference for light speed. Indeed, nless the action is to cause the incident ght speed relative to the mirror to be dentical to that of the reflected light peed, there will be an amplitude modu- ation of the standing wave pattern and the nergy will be deployed unevenly along he ray path. It seems possible that the tanding wave energy would adopt the notion of the system and assure uniform- y, thus making the light-speed isotropy a orced condition of the apparatus.

Thus while Psimopoulos and Theo- haris may well be correct in regarding the trong influence of the Earth as the dom- nating consideration, there is a possibility hat a weak ambient field is sufficient. In his case the Michelson–Morley experi- ent cannot give any valid indication oncerning motion through Maxwell's ther and this will hold also for free flight n space. Note also that a wave is not eflected back on itself in the ring laser yro. Here, any standing waves are set up n a non-rotating frame and are not locked nto the rotary motion. Clearly, there- ore, the objectives of the Michelson xperiments have not been met for trans- ational motion until one devises an ptical configuration that works without aving light rays reflected back along the ame path. Such experiments have not yet een performed in the laboratory, but are, n principle, feasible[2].

H. ASPDEN

Department of Electrical Engineering,
Southampton University,
Southampton SO9 5NH, UK

1. Psimopoulos, M. & Theocharis, T. *Nature* **319**, 269 (1986).
2. Aspden, H. *Nuov. Cim.* **38**, 568–572 (1983).

PSIMOPOULOS AND THEOCHARIS REPLY — Aspden gives a valid theoretical objection to our proposal that the Michelson interferometer might detect its translational movement through the assumed electromagnetic ether. This seems to be a sound, though not conclusive, criticism. It is true that, unlike in the Michelson interferometer, in the ring laser gyro a ray is not reflected back on itself by a single mirror. Nevertheless, a ray is indeed reflected back on itself by a combination of optical devices. Thus everywhere in the ring laser gyro, just like in the Michelson interferometer, every ray is passing through the field of a ray propagated in the opposite direction. Therefore standing waves are set up in the ring laser gyro too (in the non-rotating frame), but they have not been observed to be locked into the rotary motion (except perhaps for very slow rotations). Likewise, standing waves are indeed set up in the Michelson interferometer (in the non-moving frame), and we would expect that they will not be locked into the translational motion. Of course the ultimate judge is the experimental test, which however has never been performed.

The practical application of optical *rotation* sensors having been mentioned, we note that such a sensor is in an advanced stage of development: Standard Telecommunication Laboratories have recently announced (*Electronics Power* **32**, 111; 1986) that they expect to have a marketable fibre-optic gyro available within two years. The practical issue which we would like to raise is: Why is there no laboratory in the world working on the development of optical *translation* sensors? The answer is the almost universal acceptance of the special relativistic postulates, and the consequent lack of interest in directly testing them experimentally. It is quite possible that this lack of interest might be preventing not only theoretical advancements, but also, as presently indicated, important technological applications. This is the chief reason why we insist that the fundamental assumptions themselves, rather than their mere inferences, should be directly and constantly tested.

M. PSIMOPOULOS
T. THEOCHARIS

Physics Department,
The Blackett Laboratory,
Prince Consort Road,
London SW7 2BZ, UK

Scientific Correspondence

Scientific Correspondence is intended to provide a forum in which readers may raise points of a rather technical character which are not provoked by articles or by letters previously published (where the Matters Arising section remains appropriate).

NEW BOOKS FROM CHAPMAN AND HALL

Accuracy in Molecular Processes

Its control and relevance to living systems

Edited by D. J. GALAS, T. B. L. KIRKWOOD and R. F. ROSENBERGER

This book provides the first comprehensive review of the study of accuracy in molecular biology and incorporates the latest research by internationally recognised experts. It will provide an excellent introduction for advanced students and an up-to-date source text for all biologists.

Hardback 0 412 26940 6 £48.50
450 pages

CHAPMAN AND HALL
11 New Fetter Lane,
London EC4P 4EE

Wildlife Conservation Evaluation

Edited by M. B. USHER,

This book addresses one of the central issues in conservation – how the best areas are recognised and how areas can be compared. The book explores the approach taken in different parts of the world, different kinds of environment and different kinds of organisms. An essential reference for undergraduate and graduate students in ecology, conservation and natural resources, and all those interested in the scientific basis of conservation biology.

Hardback 0 412 26750 0 £30.00
406 pages
Paperback 0 412 26760 8 £14.95

Dictionary of Scientific Units

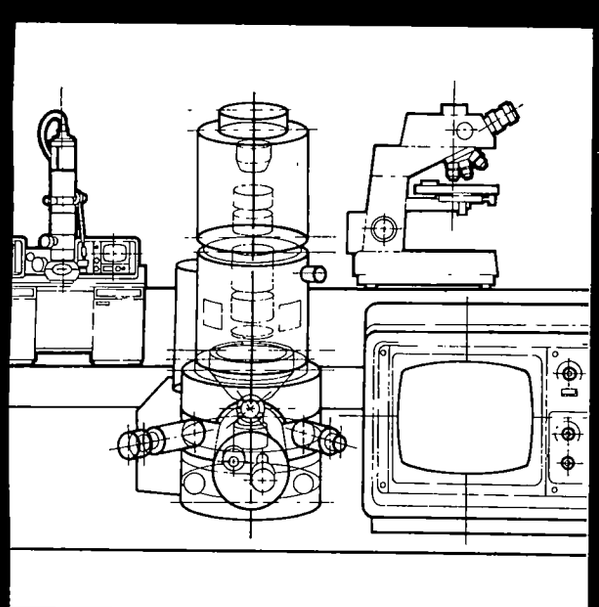
H. G. JERRARD and D. B. McNEILL
Fifth Edition

The most up to date and complete listing of all important units used in science, technology and medicine. This new edition incorporates advances in technology which have led to more precise values for fundamental physical constants, as well as several additional units, now giving a total of more than 850. An invaluable dictionary for scientists of all disciplines.

Hardback 0 412 28090 0 £18.00
232 pages
Paperback 0 412 28100 7 £8.95

Reader Service No.1

MICRO·86 · EUROSEM·86



ROYAL MICROSCOPICAL SOCIETY
IN ASSOCIATION WITH NATURE

MICRO 86 MICROSCOPY EXHIBITION

Modern Microscopes and ancillary equipment at the Bloomsbury Crest Hotel, Coram Street, WC1.

7th JULY–11th JULY 1986

Tickets and details from: Royal Microscopical Society, 37-38 St. Clements, Oxford OX4 1AJ, England.
Telephone: Oxford (0865) 248768/721081

Reader Service No.150

TWO IMPORTANT JOURNALS FROM ELSEVIER

NEW

BONE AND MINERAL

AN INTERNATIONAL JOURNAL OF BONE AND MINERAL RESEARCH

THE OFFICIAL JOURNAL OF THE INTERNATIONAL CONFERENCES ON CALCIUM REGULATING HORMONES, INC.

Editor-in-Chief:
David V. Cohn
Bone and Mineral
Department of Oral Biology,
Health Sciences Center,
University of Louisville,
Louisville, KY 40292 (USA)

Associate Editor:
C. Conrad Johnston Jr.
Indianapolis *(USA)*

Associate Editor (Far East):
Takuo Fujita
Kobe *(Japan)*

Assistant Editor:
(Symposia/Special Features):
Warren K. Ramp
Louisville *(USA)*

Aims and Scope
The Journal will publish basic and clinical papers on the structure and development of bone and other mineralized tissues and on the biochemistry and physiology of factors and hormones that regulate bone metabolism.

Reviews, letters to the editor and editorials will also be published.

Featuring:
- rapid publications
- no page charges
- international editorial representation
- bibliographic alerting service

Subscription Information:
1986: Volume 1 (1 volume in 6 issues)
Institutional Rate: US $ 116.25/Dfl. 314.00 including postage and handling

Members of the ICCRH are eligible for the discounted subscription price of US $ 45.00.
Membership subscription dues (together with US $ 10.00 membership fee for new members) should be addressed to:
Dr. D. V. Cohn, Editor, Bone and Mineral, Department of Oral Biology, Health Sciences Center, University of Louisville, Louisville, KY 40292, USA

ELSEVIER

For further information and/or free sample copy please write to:
In the U.S.A. and Canada:
Journal Information Center
ELSEVIER SCIENCE PUBLISHERS
52 Vanderbilt Ave., New York, NY 10017, U.S.A.
In all other countries:
ELSEVIER SCIENCE PUBLISHERS
P.O. Box 211, 1000 AE Amsterdam,
The Netherlands
Please send your orders to the Amsterdam address
The Dutch guilder price is definitive. US $ prices are subject to exchange rate fluctuations. Prices are excl. B.T.W. for Dutch customers

Reader Service No.11

MOLECULAR AND CELLULAR ENDOCRINOLOGY

An international journal integrating all aspects related to the biochemical effects, synthesis and secretions of extracellular signals (hormones, neurotransmitters, etc.) and to the understanding of cellular regulatory mechanisms involved in hormonal control.

Managing Editor:
B. A. Cooke, Dept. of Biochemistry, Royal Free Hospital School of Medicine, Rowland Hill Street, London NW3 2PF, U.K.

Associate Managing Editor:
E. R. Simpson, Cecil H. and Ida Green Center for Reproductive Biology Sciences, The University of Texas Health Science Center at Dallas, 5323 Harry Hines Boulevard, Dallas, TX 75235, U.S.A.

Aims and scope
Molecular and Cellular Endocrinology was established in 1974 to meet the demand for integrated publication on all aspects related to the biochemical effects, synthesis and secretions of extracellular signals (hormones, neurotransmitters, etc.) and to the understanding of cellular regulatory mechanisms involved in hormonal control. The journal is fulfilling this aim by publishing full-length and short original research papers, invited mini-reviews and book reviews. The scope encompasses all subjects related to biochemical and molecular aspects of endocrine research and cell regulation. These include (1) mechanisms of action of extracellular signals (hormones, neurotransmitters, etc.), (2) interaction of these factors with receptors, (3) generation, action and role of intracellular signals such as cyclic nucleotides and calcium, (4) hormone-regulated gene expression, (5) structure and physicochemical properties of hormones, hormone receptors and other hormone-binding components, (6) synthesis, secretion, metabolism and inactivation of hormones, neurotransmitters, etc., (7) hormonal control of differentiation, (8) related control mechanisms in non-mammalian systems, (9) methodological and theoretical aspects related to hormonal control processes, (10) clinical studies as far as they throw new light on basic research in this field, (11) control of intermediary metabolism at the cellular level, (12) ultrastructural aspects related to hormone secretion and action.

Subscription Information:
1986 - Vols. 44-48 (5 volumes in 15 issues)
Subscription price: US $ 620.00 including postage and handling
ISSN 0303-7207

ELSEVIER

Send your orders to:
Elsevier Scientific Publishers Ireland, Ltd.,
P.O. Box 85, Limerick, Ireland
Requests for free sample copies should be sent to:
In the U.S.A. and Canada:
Journal Information Center
ELSEVIER SCIENCE PUBLISHERS
52 Vanderbilt Avenue, New York, NY 10017, U.S.A.
In all other countries:
ELSEVIER SCIENCE PUBLISHERS
P.O. Box 211, 1000 AE Amsterdam,
The Netherlands
The US $ price is definitive.

37A604

Reader Service No.12

Biologists under control

Sheldon Krimsky

The Politics of Uncertainty: Regulating Recombinant DNA Research in Britain. By David Bennett, Peter Glasner and David Travis. *Routledge & Kegan Paul: 1986. Pp.218. £20, $35.*
Cloning and the Constitution: An Inquiry into Governmental Policymaking and Genetic Experimentation. By Ira H. Carmen. *University of Wisconsin Press: 1986. Pp.223. $22.50, £27.*

In February 1986, eleven years to the month after the international meeting on the risks of recombinant DNA (rDNA) research was convened at Asilomar in Monterey, California, citizens of that county stopped the first federally authorized field test of a genetically modified bacterium. The California biotechnology company Advanced Genetic Sciences had received approval from the US Environmental Protection Agency and the National Institutes of Health (NIH) to spray the bacterium on a strawberry patch as a means of assessing its potential for inhibiting ice-nucleation. Local residents successfully opposed the release on the grounds that the risks were unknown and that no effort had been made to inform the community.

What a strange coincidence! "Asilomar 1975" was the starting point of the first generation of debates on the safety and regulation of rDNA technology. Now, as the technology reaches the stage of agricultural use, a new public controversy has emerged at the same place. This time the issue is over the intentional release of genetically engineered products into the biosphere.

Science and politics are still playing out the legacy of "Asilomar 1975" as gene splicing takes new turns in its journey towards public acceptance. No event since the release of thermonuclear energy, in the form of the atomic bomb, has fostered such intense discussion about the responsibility and accountability of science to society. The questions are twofold. If faced with uncertainties about the safety of their research, will scientists ever again expose their collective anxieties to the public; that is, has Asilomar and its aftermath driven scientists into a shell? And what has the experience of the rDNA controversy taught us about science and democracy?

The two books reviewed here provide a fresh set of perspectives on these matters. *The Politics of Uncertainty* is the first book-length investigation of British policy on rDNA research; cast in a sociological framework, it is rich in historical detail and filled with insightful comparisons of British and American policy-making. *Cloning and the Constitution* examines selected periods of the rDNA debate in the United States through the prism of the author's unique construction of US Constitutional theory. While Bennett, Glasner and Travis are concerned about the public's role in the formulation of science policy, Carmen emphasizes instead the rights of scientists to engage in research. This dichotomy expresses the essential tension underlying the DNA controversy; namely, the struggle between the self-governance and the social control of science.

Recent advances in techniques for the isolation and rejoining of segments of DNA now permit construction of biologically active recombinant DNA molecules in vitro. ...

There is serious concern that some of these artificial recombinant DNA molecules could prove biologically hazardous. One potential hazard in current experiments derives from the need to use a bacterium like E. coli *to clone the recombinant DNA molecules and to amplify their number.* E. coli *strains commonly reside in the human intestinal tract, and they are capable of exchanging genetic information with other types of bacteria, some of which are pathogenic to man. Thus, new DNA elements introduced into* E. coli *might possibly become widely disseminated ... with unpredictable effects. ...*

Warning shot — extract from the letter from Berg *et al.*, July 1974, recommending the deferral of various types of rDNA experiment.

In gathering material for *The Politics of Uncertainty,* the authors were at a considerable disadvantage compared to their counterparts who have studied the corresponding events in the United States. British policy-making essentially took place behind closed doors. In contrast, meetings of the NIH Recombinant DNA Advisory Committee (RAC) were open to the public; moreover, streams of documents, minutes of meetings, internal memoranda and public letters flowed liberally from the committee. Bennett and his colleagues compensated for the lack of a complete published record by relying on interviews with key players in rDNA policy-making, including those involved in the Genetic Manipulation Advisory Group (GMAG). Their book provides a fine-grained analysis of the path towards the formulation of guidelines in Britain and their subsequent relaxation in response to changing perceptions of risk.

At the outset, American and British biologists responded to the 1974 letter from Berg *et al.* according to the two nations' differing recent histories (the letter, published in both *Science* and *Nature,* urged that certain classes of rDNA experiments should be postponed until the risks were better understood). Many American scientists had been sensitized by the debates about atomic weapons and the role of "responsible physics" in a nuclear age, Robert Oppenheimer being the symbol of ambiguity. How can one be true to one's science, true to one's nation and true to one's humanity? When in doubt, which takes precedence? American involvement in Vietnam and the morally dubious roles of science and technology during the war were other factors shaping the consciousness of American scientists. Perhaps going public on gene splicing was the biologists' way of cleansing their consciences and setting themselves apart from the physicists and the chemists. British scientists, on the other hand, faced the rDNA issue in the wake of a widely publicized accident in which two people died after the escape of smallpox virus from a high-containment laboratory at the London School of Hygiene and Tropical Medicine. These backgrounds may explain some of the differences in how the respective political cultures handled rDNA policy-making.

In Britain, organized groups of teachers, civil servants, laboratory personnel and trade unionists were active in the policy process, while in the United States participation came from environmental groups and local communities. Compared to the United States, British rDNA policy was drawn up taking into account diverse interests, but it was all done in greater secrecy. *The Politics of Uncertainty* highlights differences in the way guidelines were established. British policy-makers sought a loose code, preferring general principles to detailed taxonomies of experiments and viewing the American system of strict guidelines as too inflexible. A canonical framework for assessing the potential risks of recombinant DNA experiments, introduced by Sydney Brenner, was an attempt to bring rationality and order to the taxonomy of cloning. When, in 1979, the approach was brought before the RAC for consideration, it was hastily dismissed. Not only did the committee fail to make sense out of it, but, more significantly, the scheme rated NIH containment levels for certain experiments as too low. Tightening up the rules on containment during a period when the US guidelines were on a fixed course of relaxation was too great a price for a dose of British rationalism.

In comparison to the British way of doing things, the American approach to rDNA regulation is legalistic and process-orientated. Typically, this reflects the

adversarial style of resolving environmental policy debates in the United States, where regulatory discretion is a target for litigation. The British regulatory system is more flexible, and thus, in the case of rDNA, was compatible with the adoption of general principles applied by scientific élites.

Notwithstanding these differences, the similarities in outcome were striking. Here were two countries which nourished highly advanced research communities in molecular genetics, which had captured a sizeable share of the Nobel prizes and which faced the prospect that strict regulation of rDNA research might delay the scientific progress of one relative to the other. Out of disparate policy cultures emerged unity of scientific values. The outcome was not coincidental but stemmed from the international and competitive nature of science. Both in Britain and the United States the passage of special legislation was avoided; the guidelines were viewed as an interim measure only, and subject to considerable relaxation; and a multi-tier review process for rDNA research activities was adopted. Even the taxonomies of potential risks varied little.

Overall, *The Politics of Uncertainty* emerges as the leading study of rDNA policy in Britain. The authors' insights about the blending of science and social process, the interplay of scientist and non-scientist in risk analysis, and, more generally, the process of negotiating the control of research also make it a notable contribution to the broader literature of science policy.



"Run for the hills — the recombinant DNA has escaped!"

Cloning and the Constitution arrives at a time when discussion about the rights and responsibilities of scientists has intensified. The US Office of Technology Assessment recently published *The Regulatory Environment for Science,* which examines issues of controls on research, and there are a number of cases where American communities have exercised control over research. On top of the furore over the release of genetically modified bacteria, the city of Cambridge, Massachusetts, recently banned the use of five chemical warfare agents in a testing programme funded by the military, and a farm-worker organization filed a suit against the University of California to stop its research on the mechanization of farming practices.

Carmen's book is made up of three elements: an answer to the question "Is scientific inquiry protected by the Constitution?"; an interpretation of selected periods of the rDNA controversy through a Constitutional perspective; and a report on Carmen's interviews with 52 individuals associated with rDNA research or its regulation. The unifying thread is the author's thesis on scientific inquiry and civil liberties, which is derived from his theory of a living Constitution. Because the US Supreme Court has not decided a case involving the rights of scientists to do research, this thesis is prescriptive only. It can be summarized as follows. Scientific inquiry falls on a continuum; on one end there is pure research, on the other, applied. Both types of research may involve experimentation. Pure research is a form of creative expression and deserves the status of quasi-speech. Once classified as quasi-speech, any research (including experimentation) should be afforded Constitutional guarantees under the First Amendment. To interfere in pure research, the government bears an "extraordinary burden of proof" that it needs to do so. Because much of the early work involving gene splicing was part of basic research, from a Constitutional standpoint federal interference was unjustified.

Under this theory, applied research is treated as conduct or quasi-conduct and, as such, is not guaranteed protection under the First Amendment. For the cases between the extremes, the author suggests a "totality test" to ascertain whether the basic or the applied aspect of the research carries more weight.

Carmen, then, maintains that there is a fundamental right to scientific research (including experimentation) if the research is "pure"; but a rather more useful distinction has been drawn between cognitive/theoretical and experimental inquiry. Under this scheme, scientific work (whether basic or applied) that pertains to generating hypotheses, constructing explanations, propounding theories and the correlative activities of disseminating information, is protected unambiguously as a form of free speech. However, experimental work is a form of action, and it should not make a wit of difference, from the safety and ethical standpoint, whether the experimental programme is basic or applied.

Carmen has constructed a noteworthy thesis but one that I find caught in a web of ambiguity. The dichotomy between pure and applied research is not a sound basis for establishing Constitutional guarantees for science. Curiously, though, this concept has already found a place in the Department of Defense's (DoD) export control regulations on research results, part of a general policy designed to protect the national security and domestic economy of the United States. This goes back to 1984 when the US executive branch issued a draft policy justifying the application of export control regulations to basic research. The policy gave agencies of the government, including DoD, the right to censor any information that "can be used or adapted for use, in the design, production, manufacture, utilization, or reconstruction of articles or materials". In response to vigorous opposition among scientists to *post hoc* censorship of research results, DoD issued a policy clarification stating that export control regulations will not be applied to fundamental research unless that research has been initially classified. More than any other intervention into the scientific enterprise, national policies restricting the open communication of scientific results are the clearest infringement of civil liberties. Regrettably, these policies escape the critical eye of the author. □

Sheldon Krimsky is an Associate Professor in the Department of Urban and Environmental Policy, Tufts University, 97 Talbot Avenue, Medford, Massachusetts 02155, USA, and author of Genetic Alchemy: The Social History of the Recombinant DNA Controversy *(MIT Press, 1982).*

AIDS
Papers from *Science*, 1982–1985

Edited by R. Kulstad with an introduction by M. Essex

108 research papers and reports on acquired immune deficiency syndrome (AIDS) from ***Science*** magazine. This fully indexed collection provides essential experimental results and is an excellent source of references to AIDS research worldwide.

1985; 653 pages
Hardcover **$32.95**
Softcover **$19.95**

Order from AAAS Marketing, Dept. K, 1333 H Street, NW, Washington, DC 20005. Add $1.50 postage and handling.

American Association for the Advancement of Science

Reader Service No.4

Skipping across the waterfront

Robert T. Rubin

Hormones and Human Behaviour. By Bernard T. Donovan. *Cambridge University Press:1985. Pp.223. £25, $39.50.*

On receiving *Hormones and Human Behaviour* for review, I was excited by the prospect that here was a succinct, integrated overview of "psychoneuroendocrinology", written with the consistency of a single author. Such a book would be of great value for students and others interested in acquiring a basic understanding of this complex field. I was further buoyed by the author's statement of purpose in the preface — we are told to expect an exciting, concise and intelligible review of present knowledge, not definitive or comprehensive, but a guide to the literature and of help to those working in the behavioural sciences or studying for a specialist qualification in psychological medicine. After careful reading of the contents, however, I fear that while the book contains a great deal of useful information, it falls short of the mark in several respects.

In writing the book, the author undertook a formidable task, perhaps an impossible one. In a mere 191 pages of text he has attempted to cover a vast range of topics: limbic/hypothalamic/pituitary/target endocrine gland interrelations; all the pituitary and other hormones; the roles of the many neurotransmitters and neuromodulators in endocrine function; patterns of hormone secretion; cellular mechanisms of hormone action; the interrelations of hormones and brain development; and male and female sexual behaviour; aggression; control of food intake; emotion; and learning and memory. To cope successfully with all these subjects would require an economy of concept and of style quite beyond that shown here.

Clearly, Donovan has a broad interest in this field, and he has marshalled a mass of references into an impressive bibliography which is accurately cited in the text. However, he paints his subject with a broad, and occasionally reckless, brush. I should let some quotations speak for themselves: the hypothalamus "integrates almost all higher functions" (p.16); "hypothalamic function is modulated or regulated by the amygdala" (p.19); "The secretion of cortisol is increased in depressive illness" (p.25); the structural similarity between growth hormone and prolactin "gives rise to problems in hormone assay" (p.48); "it has become clear that the locus ceruleus... plays a major role in the control of anxiety" (p.169). While each of these statements may be accurate when accompanied by the appropriate qualifiers, such qualifiers are too often absent or tacked on in desultory fashion at the ends of paragraphs.

In the book, Donovan covers the waterfront of psychoneuroendocrinology. However, the organization of the impressive array of facts he has brought together is often wanting, particularly in conveying the concepts and controversies surrounding behaviour–hormone interactions. The introduction and overview, which, conceptually, ought to be the clearest of the chapters, is a jumble. By contrast the paragraphs on homosexuality (pp.129 and 130) are well-balanced. If only the rest of this volume were consistently so.

In his final chapter, "What Next?", Donovan puts forth some cautions and caveats which he himself has failed to observe earlier in the book. For example: "It is not enough to refer to 'depression' or 'schizophrenia.' The endocrine evidence points to different categories or groups of depressed or schizophrenic patients" (p.188). He further states, "Hormonal disturbances seem to be less common in psychiatric patients than the incautious reader of Chapter 1 might be led to expect" (p.188). We well may ask, especially of a volume intended for beginners, who should be more cautious, the reader or the author?

The subject matter of this book fits in well with the aims of the series, *The Scientific Basis of Psychiatry*, of which it is part. The book also highlights an area of the "mind–body interface" that is growing ever more important (and ever more complex), and it contains an abundance of fascinating material. But it should be read with great caution, especially by the naive reader hoping to find a trustworthy introduction to psychoneuroendocrinology. □

Robert T. Rubin is in the Division of Biological Psychiatry, Department of Psychiatry, Harbor UCLA Medical Center, Torrance, California 90509, USA.

Zeolitic first

William S. Wise

Natural Zeolites. By Glauco Gottardi and Ermanno Galli. *Springer-Verlag:1985. Pp.409. DM 160.*

By various counts, depending on nomenclature and definitions, there are at least 42 different zeolite minerals, some of which have been known since the eighteenth century. In *Natural Zeolites* Gottardi and Galli have provided the first book entirely devoted to the description of them. Writing it must have been difficult, because new physical descriptions and fresh information on occurrences is continually accruing. But, for the moment at least, this book is a valuable addition to the literature.

In an account of this nature the topics that should be included are some sort of classification, and for each species a description of crystallography (morphology and crystal structure), physical properties, chemical compositions (including dehydration and ion exchange data), occurrences (localities and geology), and nomenclature and history. All of these are covered to some extent. As Gottardi and Galli note in their preface, however, no book could satisfy all readers in the completeness of its coverage. Because the authors are structural crystallographers, the emphasis of the book is appropriately upon a new structural classification and upon details of framework geometries, such as ordering.

Certainly, the topic of widest interest beyond mineralogy is the framework arrangements of the various minerals or groups of minerals. In the introductory chapter, these structures are well described and illustrated not with the usual stereographic drawings, but with "tetra-units and spaghetti", a technique developed by Gottardi himself. I found these drawings to be a particularly effective way of depicting most of the three-dimensional arrangements. Other strengths of the book are the detailed comments on the historical development of nomenclature, the critical evaluation of structural crystallography, and the inclusion of newly determined DTA, TG, DTG curves and new x-ray powder diffraction data for most species.

My only disappointment was with the depth of treatment of the occurrences and of paragenesis. For the most part, in this book zeolites are classified as "sedimentary" or "hydrothermal". Actually the first category is the diagenetic alteration of volcanic glass in sediments, while the second pertains to the large crystals found mostly in cavities of volcanic rocks. To be sure, many of these are results of low-temperature (<150°C) hydrothermal alteration of volcanic piles. However, there are also large areas of zeolite occurrence where these minerals grow as a result of diagenetic adjustment of the basalt or andesite to shallow burial and saturation with ground water. □

William S. Wise is in the Department of Geological Sciences, University of California at Santa Barbara, California 93106, USA.

• Newly published by Elsevier is *Zeolites Synthesis, Structure, Technology and Application*, the proceedings of a symposium held by the International Zeolite Association in Yugoslavia in 1984. Editors are B. Držaj, S. Hočevar and S. Pejovnik, price is Dfl. 345, $127.75

For the student or practicing professional

ESSENTIAL ENDOCRINOLOGY
A Primer for Nonspecialists
by C. R. Kannan

A perfect text for medical students studying basic endocrinology and diabetology, this book is also a quick, concise guide for practicing professionals. Kannan stresses standard concepts in a direct and readable style, providing a step-by-step approach to clinically oriented topics of the endocrine system, disorders of sexual differentiation, and diabetes and glucose intolerance.
0-306-42172-0/548pp./ill./1986 $49.50
text adoption price on orders of six or more copies: $29.50

MOLECULAR AND CELLULAR MECHANISMS OF ANESTHETICS
edited by Sheldon H. Roth and Keith W. Miller

This stimulating overview of the molecular and cellular mechanisms of general anesthetics discusses the progress achieved over the last five years, summarizes the present situation, and indicates future areas of research.
0-306-42128-3/510pp./ill./1986 $59.50

ENDOCRINE AND METABOLIC EFFECTS OF LITHIUM
by John H. Lazarus

Opening with a review of the pharmacology of lithium and the psychiatric indications for its use, this extensively referenced monograph gives a full account of the effects of lithium on the physiology and biochemistry of the thyroid gland, brain metabolism, renal function, and the immunological system, among others.
0-306-42057-0/220 pp./ill./1986 $35.00

PRINCIPLES OF ENDOCRINE PHARMACOLOGY
by John A. Thomas and Edward J. Keenan

A splendid overview of the relationships between hormones as they normally exist in the body and as used in therapeutic and diagnostic situations.
0-306-42129-1/hardcover/310 pp. ill./1986/$39.50
0-306-42143-7/paperback/310 pp. ill./1986/$22.50

THE LANGUAGE OF SCIENCE
Plenum
PUBLISHING CORPORATION

Plenum Publishing Corporation
233 Spring Street
New York, NY 10013-1578

Reader Service No.5

Bent for philosophy

H.C. Longuet-Higgins

Mind from Matter? An Essay on Evolutionary Epistemology. By Max Delbrück. Edited by Gunther S. Stent *et al.* *Blackwell Scientific: 1986. Pp.290. Hbk £29.50, $29.95; pbk £14.80, $14.95.*

MAX Delbrück was one of the very few physicists who have ever really made good in biology. A not unusual pattern is for an eminent physicist to distil into a public lecture or a slim volume his or her philosophical reflections on the nature of life and then to rest on his Laureate, leaving younger scientists to fill in the essential details. Fortunately for molecular biology, Delbrück never achieved great distinction in theoretical physics, and wisely decided, in the mid 1930s, to devote himself to the study of bacterial viruses and, later, bacterial resistance to virus infection. In 1969, with Luria and Hershey, he won the Nobel Prize in Medicine or Physiology. But all his life Delbrück was an earnest philosopher of science, having sat as a young man at the feet of Niels Bohr and heard him discourse upon the principle of complementarity and how it might apply to living organisms. Delbrück's 1949 essay *A Physicist Looks at Biology* was his first — somewhat baffling — contribution to the philosophy of science; his posthumous book *Mind from Matter?* he epitomized as "an investigation into human cognitive capabilities, as expressed in various sciences".

Mind from Matter? is a labour of love by a number of Delbrück's friends — most notably Gunther Stent, whose introduction to the book is a model of clarity and insight. Stent evidently shares Delbrück's perplexities about the relations between life and non-life, mind and matter, and appearance and reality, and this makes it possible for him to act as a sympathetic interpreter and expositor of Delbrück's often difficult ideas. As he explains, the book originated as a course of lectures at Caltech on "evolutionary epistemology" — a phrase strongly reminiscent of Jean Piaget's "genetic epistemology", which Delbrück freely acknowledges as a major philosophical influence. Unfortunately, Delbrück's declining health did not permit him to do more than publish a couple of articles summarizing the lectures; the present volume is consequently a heavily restored mosaic of Delbrück's notes and the lectures he based on them, recorded and interpreted by his students and colleagues. It would obviously be ungenerous to criticize too sharply the outcome of their unselfish endeavours.

Delbrück's message is not easy to capture in a few sentences, because the book ends by declaring its own title to be absurd, claiming with no obvious justification that "if we can learn to accept this ultimate absurdity, there may yet be hope for developing a formal approach that will permit a grand synthesis". But it is better to travel hopefully than to arrive, and *Mind from Matter?* supplies much intellectual refreshment along the road. The first half-dozen or so chapters present a matter-of-fact, almost tedious account of cosmic evolution, the origin of life and the ascent of man. Then there is a subtle change of perspective and we find ourselves looking at perceptual and cognitive psychology *from the inside*. In discussing the acquisition of fundamental physical concepts Delbrück leans heavily on the writings of Piaget, and reveals him in his true colours as a philosopher of mind rather than a mere developmental psychologist.

There follows a set of chapters on pure mathematics and the paradoxes which gave birth to modern mathematical logic. Delbrück makes the interesting proposal that our mathematics inevitably suffers from the same limitations as our own minds when we attempt to describe those parts of reality which lie too far outside our day-to-day experience. Delbrück obviously enjoyed airing his wide knowledge of number theory and quantum theory, but all too often the intellectual virtuosity of the book obscures its main theme. Relativity is used as a text for the unreliability of naive physics; quantum theory as a warning against attaching too much objectivity to the outcome of a measurement. The chapter on "the cartesian cut" argues cogently that many of our most acute philosophical problems arise from the misguided attempt to erect a barrier between subjective and objective reality: "Is there not but one reality: the act of seeing what our language makes us call an 'object'?".

Unfortunately the chapter on language is something of a disappointment when it arrives; it is largely taken up, in fact, with a cursory account of artificial intelligence. Perhaps Delbrück felt that AI raises philosophical issues which he hadn't yet had time to think about, but must nevertheless be raised in any serious discussion of the nature of mind.

What the professional philosophers will make of *Mind from Matter?* remains to be seen, but at least it should be required reading for students of the philosophy of science, who so often pronounce on the notions that inform scientific enquiry without acquainting themselves with the considered philosophical positions of real scientists. Max Delbrück may not have been a great philosopher, but he certainly knew his trade as a scientist. □

H.C. Longuet-Higgins is Royal Society Research Professor in the Laboratory of Experimental Psychology, University of Sussex, Brighton BN1 9QG, UK.

Milankovitch climatic origin of mid-Cretaceous black shale rhythms in central Italy

Timothy D. Herbert

Department of Geological and Geophysical Sciences, Princeton University, Princeton, New Jersey 08544, USA

Alfred G. Fischer

Department of Geological Sciences, University of Southern California, Los Angeles, California 90089-0741, USA

The Earth's orbital variations, reflected in Pleistocene ice volume, were also recorded in non-glacial times. Carbonate production in pelagic mid-Cretaceous sediments, quantified by calcium carbonate and optical densitometry time series, reflects the orbital eccentricity and precessional cycles. Minimal eccentricity brought deep-sea anoxia. Most of the sedimentary variability of this 100-Myr-old sequence lies within the Milankovitch (orbital) frequency band.

TIME-SERIES analysis of several parameters of deep-sea sediments (carbonate content[1-3], accumulation rate of aeolian material[4] and oxygen isotope values in carbonates[5-7]) has provided measures of climatic variability during the past two million years, and has demonstrated its sensitivity to periodic changes in the geometry of the Earth's orbit[7-10]. Several studies[11-17] have found sedimentary rhythms in ancient sediments at periods approximating those of the modern orbital parameters, suggesting that Milankovitch (orbitally induced) climatic rhythms have persisted at their modern frequencies throughout a large portion of the geological record. This conclusion raises the possibility of a comparative study of the climate system's response to a continuing series of perturbations under different boundary conditions (continental positions, sea level, extent of continental glaciation, oceanic interconnections and atmospheric CO_2 levels). Most studies of the pre-Pleistocene have relied on somewhat subjective field measures of cyclicity, such as thickness of strata; very few sets of finely sampled, objective measurements allow for a closer comparison with the modern record of astronomical variations. We report here high-resolution data on oxidation-reduction (redox) conditions and carbonate cyclicity during an estimated 1.6 Myr of deep-sea history from the mid-Cretaceous (100 Myr BP) of central Italy, in which the character of the cycles, as well as their estimated periods, clearly link the variability to Milankovitch precessional and eccentricity forcing. The dominance of 100-kyr and 400-kyr cyclic components during a non-glacial era raises questions about the present understanding of climatic change.

Numerous data indicate that Cretaceous climate was significantly different from the present. Oxygen isotope studies imply deep-water temperatures 10–12 °C warmer than at present[18,19]. Large-scale continental glaciation was absent and climate was more equable[20-22]. The warmer global Cretaceous climates seem to require a CO_2-rich atmosphere[21,23]; thus, studies of mid-Cretaceous climate dynamics may furnish a crude analogue to climates of the anthropogenic greenhouse of the future. The questions we shall explore are: what is the evidence of climate change on a thousand- to million-year timescale during the Cretaceous, how does this variability compare with what is known from the Pleistocene climate record, and what mechanisms drove Cretaceous climate oscillations?

The interval analysed comes from part of a core 84 m deep cut through the Scisti a Fucoidi (Fucoid Marls) in Piobbico (Marche), in the central Appennines of Italy, as a joint project by the US National Science Foundation and the Italian Consiglio Nazionale della Ricerche. The core spans most of the Aptian and Albian stages of the Cretaceous and consists of deep-sea foraminiferal-coccolith limestones and marls deposited on the southern side of the narrow Tethyan seaway at a palaeolatitude of ~19° N (ref. 24). The lithology shows spectacular ranges in oxidation state, with intervals of highly oxidized (red), intermediate (white to drab) and highly reduced (black) strata. The mixing of one lithology into another by burrowing organisms indicates that the alternations are of primary origin. Frequent black, finely laminated beds, 2–20 cm thick and containing 1–9% organic carbon, record episodes of seafloor anoxia in a pattern similar to that found in other mid-Cretaceous ocean basins[13,25-28]. The suite of microfacies within black shale bands—a dark, burrow-mottled base, an intermediate black, but unlaminated portion and an upper laminated interval—indicates that these deposits are not turbiditic, and record *in situ* dysaerobic to anaerobic conditions.

Cyclic sedimentation

Outcrop studies of bundled portions of the Umbrian sequence (Barremian[16], Albian–early Cenomanian[14] and late Cenomanian[16]) have led to the suggestions that the bedding couplets reflect the Earth's axial precession cycle (mean period 21 kyr) and that the bundles mirror the short cycle of eccentricity (~100 kyr). In the Piobbico core, a ~8.7-m-thick interval from the upper Albian foraminiferal zone of *Ticinella breggiensis* (subzone *T. praeticinensis*) (I. Premoli Silva, personal communication) was chosen for detailed analysis. Because the core intersected strata dipping at 23°, the data to be presented are plotted against true thickness rather than core thickness. Our initial observations indicated that the sequence represents a repetitive alternation of more calcareous, relatively oxidized beds with more shaly, reduced beds. Stratigraphic variations in this interval were quantified using two techniques. Calcium carbonate content (Fig. 1*a*) was measured by a Coulometrics Inc. coulometer at ~2-cm spacing. Variations in darkness of colour were determined by densitometry: scaled and colour-corrected 35-mm diapositives ('slides') of split-core sections were measured for light transmission in a Perkin-Elmer microdensitometer at a sampling rate of 50 data points per cm of core length, and 25 parallel passes per slide were averaged along bedding and compiled into the curve shown in Fig. 1*b*. Values of transmission are low in dark beds and high in light beds, thus the curve yields a measure of the oxidation state of the sediment. The analysis was discontinued when the core colour changed from drab to dominantly red at 7.5 m depth in the section.

One way of approaching the question of rhythmicity is to

identify the cycles by simple inspection, and to estimate their duration from sedimentation rates; an alternative approach involves spectral analysis. As will be shown, the two approaches yield slightly different results.

A back-to-back or mirror plot of the curves (Fig. 1) expands where carbonate values are high and colour is light, and contracts for lower carbonate values and darker colours. The high-frequency oscillation depicts the bedding couplets, and the curve is segmented by an oscillation of lower frequency: typically two or three couplets with a comparatively carbonate-rich and drab-coloured marl member are succeeded by two to three couplets having marl members of lower carbonate content and darker colour, commonly black and laminated. This segmentation of the mirror-plot is the bundling of couplets so evident to the eye in outcrop. For reference the bundles have been assigned letters (Fig. 1). In addition, the envelope of the mirror plot (dotted line) shows the presence of a longer cycle.

The 8 m length of core contains 74 ± 4 couplets and 17 ± 0.5 bundles (the bundles become poorly defined near the top of the record). Statistics for mean thickness are provided in Table 1. We postulate that these couplets and bundles are the products of rhythmic forcing functions. If so, their periods can be derived from the mean sedimentation rate. The length of the Albian age is variously estimated at 15.5, 12 and 11.5 Myr (refs 29, 30 and 31, respectively); the 65 m of Albian at Piobbico (I. Premoli Silva, personal communication) therefore accumulated at a mean rate (compacted) of 5.0 ± 0.75 m Myr^{-1}, yielding a couplet period of 21–22 kyr and a bundle period of 95–96 kyr (Table 1). The long cycle, which acts as the amplitude-modulating frequency of the bundle cycle, is depicted by the envelope of the mirror curve, and has an apparent wavelength of ~2 m, corresponding to a period of 400 kyr. The three frequencies found thus yield close matches to the means of the present axial precession, the short cycle of orbital eccentricity, and the long eccentricity cycle[10]. Table 1 includes estimated periodicities from ref. 16, derived from other portions of the mid-Cretaceous Umbrian sequence. The consistency of the estimates over ~25 Myr, despite uncertainties in the dating of Cretaceous stages and errors introduced by the use of mean sedimentation rates, argues strongly for the persistence of frequencies of 20–25 kyr and 100 kyr.

Table 1 Lower Cretaceous carbonate cycles in the Umbrian region

	Thickness (cm)	Duration (kyr)
Late Albian, Piobbico (65 m)*		
Couplet	10.8	21.6 ± 20%
Bundle	48	96 ± 20%
Long cycle	200	400 ± 20%
Barremian[16] (80 m)*		
Couplet	28.3	19 ± 50%
Bundle	130	88 ± 50%
Late Cenomanian[16] (36 m)*		
Couplet	21.7	29 ± 25%
Bundle	106	141 ± 25%

Sedimentation rates calculated using refs 29–31, 59.
* Thickness of stage.

The 8-m core segment discussed here appears to record ~1,600 kyr of history. Figure 2 shows a comparison of the 7.2-m carbonate curve with 1,500 kyr of orbital eccentricity variations, calculated from ref. 9 and extending from 1,350 kyr BP to 150 kyr AP (the comparison is intended to be qualitative; no match of absolute values is intended). The core data (Fig. 2*a*) are shown as a smoothed curve obtained by a cubic spline routine, in which the precessional signal and possible high-frequency noise have been eliminated. Curve *a* in Fig. 2 matches the orbital signal (Fig. 2*b*) in number of elements and shows similar changes in

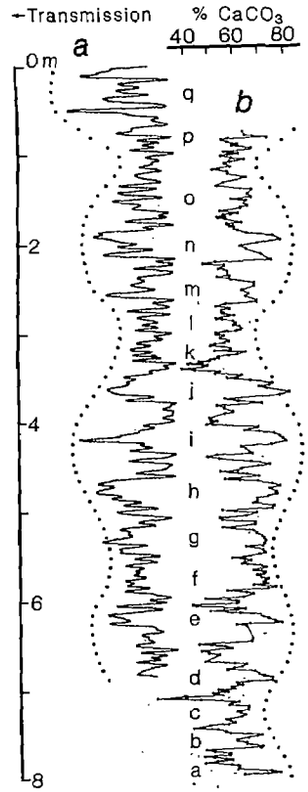


Fig. 1 Transmission (*a*) and carbonate content (*b*) versus thickness in metres for part of Upper Albian section of core (*T. praeticinensis* foraminiferal subzone). Transmission curve is plotted to mirror carbonate data: values of transmission (brightness) increase towards the left, while dark beds plot to the right. Dots indicate carbonate sample points. Individual bundle cycles are lettered.

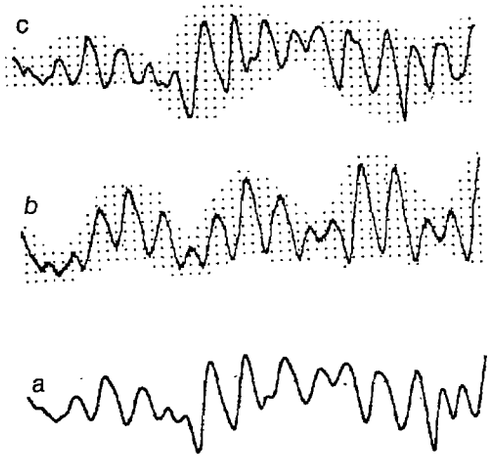


Fig. 2 Piobbico carbonate series (*a*), smoothed by a cubic spline routine, compared with the orbital eccentricity curve[9] (*b*) for the period 1,350 kyr BP to 150 kyr AP. A simple tuning of the carbonate record to constant spacing of peaks and troughs (*c*) results in a good match to the orbital curve (*b*). Stippled pattern emphasizes beating pattern of both records, with nodes of low amplitude coinciding with minima of the 413-kyr eccentricity term in the orbital series.

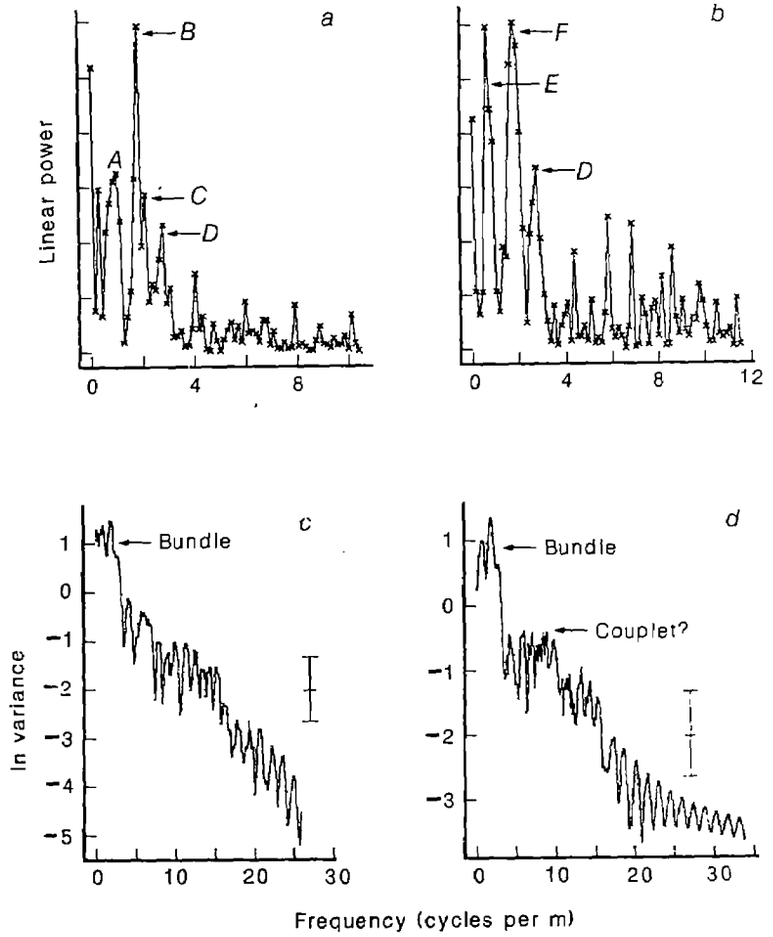


Fig. 3 *a*, Detail of carbonate power spectrum, showing peaks at: *A*, 90 cm (225 kyr); *B*, 53 cm (108 kyr); *C*, 48 cm (98 kyr); and *D*, 36 cm (73 kyr). *b*, Detail of transmission power spectrum, showing peaks at: *E*, 171 cm (347 kyr); *F*, 57 cm (116 kyr); and *D* (as in *a*). In *a* and *b*, higher-frequency peaks, probably harmonics of the ~100-kyr cycle, are not labelled. *c*, *d*, Lower-resolution power spectrum of carbonate (*c*) and transmission (*d*) curves plotted as ln variance. 90% confidence interval and bandwidth (vertical and horizontal error bars) calculated following ref. 60.

amplitude, which waxes and wanes with a 2-m wavelength. However, the peaks and troughs of these curves are not well aligned. The length of bundles (see Fig. 1) varies by a factor of two. If the bundles are of equal duration, then their sedimentation rate has also varied by the same factor, and the stratigraphic dimension departs strongly from time. The fact that the couplet periodicity also narrows during short bundles and lengthens during long ones indicates a coherent shift in apparent frequency which is best explained by changing sedimentation rates. The carbonate-poor bundles, showing low amplitude in Fig. 2*a*, are the short members. A simple tuning which assumes that maxima and minima of the carbonate bundles demarcate approximately constant time increments, and assignment of a periodicity equal to the modern mean value of 95 kyr (compare the 95–96 kyr estimated from the mean sedimentation rate) results in a good match between the core-derived curve (Fig. 2*c*) and the modern orbital cycle (Fig. 2*b*).

Departures from ideal cyclicity shed light on the dynamics of Tethyan deep-sea sedimentation. We consider the record to be the product of forcing functions, periodic in time but stratigraphically distorted by variable sedimentation rate. These distortions are to a large degree a function of the cyclicity itself: where mean carbonate values are high, the redox (bundle) cycle is stretched; where low, it is contracted. This is not a reflection of variable compaction: densities in fact increase with carbonate content, from ~2.45 g cm^{-3} in very marly beds to 2.65 g cm^{-3} in the most limy beds. Analyses in progress indicate that the total clay content per bundle shows much less variability than does carbonate content. Thus, carbonate supply seems to have been the chief variable in sedimentation rate.

Good to excellent preservation of foraminifera suggests little or no seafloor dissolution of calcite and identifies the cycle as one of biogenic carbonate productivity. Black marls, indicative of a dysaerobic to anaerobic sea floor, correspond to episodes of low carbonate productivity. The very modest rates of organic carbon accumulation during anoxic events in the Atlantic and Tethys[14,32] are consistent with the picture of lowered surface fertility that emerges from the Piobbico time series. At the couplet level, variations in carbonate content (31–84%) suggest variations in productivity of up to a factor of 9. The rate of clay supply may have varied at this level, and the couplets may have been enhanced by diagenetic solution transfer of carbonate from marls to limestones[33], but carbonate productivity still appears to be the most variable factor, controlling sedimentation rate in response to orbitally induced climatic change.

Spectral analysis

Figure 3 shows power spectra derived from the carbonate content and transmission time series in Fig. 1. Figure 3*a* (carbonate) and *b* (transmission) show details of the spectra in the frequency range discussed above (wavelengths of 4 m to 10 cm), whereas in Fig. 3*c* (carbonate) and *d* (transmission) the spectra are plotted as the natural log of the variance, and smoothed with a five-point moving average. The frequency range is extended to 25 (Fig. 3*c*) and 30 (*d*) or to ~8- and 7-kyr periods. The detailed spectra show the following large peaks: for the carbonate content at about 90 cm (225 kyr), 53 cm (108 kyr), 48 cm (98 kyr) and 36 cm (73 kyr); for transmission at about 171 cm (347 kyr), 57 cm (116 kyr) and 36 cm (73 kyr).

The low-frequency terms correspond quite well to the estimated periodicities of elements of the present eccentricity cycle. Although resolution is low at this end of the spectrum, the

171-cm peak (*E*, Fig. 3*b*) in the transmission series seems to correspond to the 2-m wavelength visible to the eye. The presence of terms at slightly greater and less than 100 kyr (Fig. 3*a*, *b*, peaks *B–D*, *F*) suggests peak splitting of a ~95-kyr periodicity, and corresponds to the amplitude modulation of the bundle cycle by the 2-m (400-kyr) cycle. An unexplained component is the carbonate peak at ~225 kyr (peak *A*, Fig. 3*a*). At higher frequencies, most peaks seem to correspond to harmonics of the bundle frequency.

The low-resolution spectra (Fig. 3*c*, *d*) demonstrate that virtually all of the sedimentary variance lies within the Milankovitch frequency band (periods ≥12 kyr). There is a general resemblance to the Pleistocene $\delta^{18}O$ spectrum[7–8] in that most of the amplitude is concentrated in a peak near 100 kyr; however, the peaks in the 11–65-kyr range are very weak. The transmission spectrum (Fig. 3(*d*)) shows a broad band of power in the range 8–10 cycles per m range which may match the couplet frequency, but most of the spectrum in this region is dominated by harmonics of the bundle peak. This is to be expected from the sedimentational distortion of the time axis discussed above: variations in the spacing of the bundle cycle, as well as systematic shifts in accumulation rate with the cycle phase (lower accumulation in the troughs) will generate higher-frequency multiples of the dominant peak. The even higher variation in sedimentation rates at the precessional level (21–22 kyr), compounded by the inherent range in the precession period[10], masks the high frequencies. A detailed statistical analysis of the series broken into shorter time windows is in preparation (T.D.H. and J. Park), and shows promise of yielding an objective tuning function to compensate for some of the distortion introduced by variable sedimentation rate.

Cretaceous climate dynamics

Our data have important implications for mid-Cretaceous climatology and the origin of the black shales which were so common during this time. The mid-Cretaceous has been considered to be a time of generally 'sluggish' oceanic and atmospheric circulation due to low Equator-to-pole temperature gradients[21,22], with moribund overturning of the water column leading to the common occurrence of black shales[25,32,34]. The high-frequency excursions in deep-water oxygenation and surface productivity recorded in the Piobbico core indicate that stagnation occurred only episodically and do not imply continuous slow circulation. The prominence of carbonate and redox cyclicity suggests a highly dynamic ocean–climate system, in which wide swings in climatic regime occurred in response to external forcing; there is no evidence of sluggishness on a thousand-year timescale. If carbonate cycles are indeed reflective of Tethyan surface fertility, then large changes in deep-water upwelling rate must have occurred on a geologically rapid timescale.

The lack of spectral amplitude at the 41-kyr obliquity frequency indicates that our data record predominantly low- to mid-latitude climatic effects. Theoretical and empirical work indicates that low-latitude regions are sensitive to the precessional and eccentricity parameters, which control seasonality and intensity of monsoonal circulation[35–37]. Of several climatic mechanisms that might link orbital forcing to oceanic anoxia, perhaps salinity and temperature variations are the most plausible. In a salinity-driven model, abrupt freshening of the surface layer leads to reduced vertical mixing and alters thermohaline exchange of water between ocean basins. These factors are crucial to the nutrient and oxygen balance of an ocean basin, and hence to production of biogenic material and preservation of organic matter. The correlation between orbital cycles, monsoonal intensity and anoxic events in the Pleistocene eastern Mediterranean has been convincingly demonstrated by Rossignol-Strick[35]. Recent model simulations of Cretaceous climate have in fact predicted sensitivity of the monsoonal response along the margins of the Tethys to precessional forcing[38]. Weissert *et al.*[39] have used palynological data from the Lower Cretaceous of Italy to correlate the onset of black shale rhythms with a shift to a more humid climate.

Climatic modulation of deep-water temperatures might also explain the cyclic occurrence of black shales. Brass *et al.*[40] have postulated that intrusions of warm, saline bottom water, capable of holding less oxygen than the normal cooler bottom water, may have episodically pushed already poorly oxygenated Cretaceous deep water over the threshold to anoxia.

Individual anoxic episodes in the Piobbico sequence occur with a 20-kyr period, as did the Pleistocene anoxic events of the eastern Mediterranean. However, the pattern in the Cretaceous seems to have been anti-monsoonal: anoxic events took place during periods of low amplitude of the eccentricity and precessional cycles. In order to match the phases of carbonate and redox cycles with an eccentricity input function, we examine the systematic changes in amplitude of the bundle cycle. Association of high carbonate content and lighter colour with maxima of orbital eccentricity is possible by matching the characteristic nodal pattern of the Berger eccentricity curve[9] to the similar pattern in the Piobbico records. Computation of eccentricity for the past 5 Myr shows that the node of minimum 100-kyr amplitude stays locked into phase with the minima in the 413-kyr term. A decrease in amplitude is also associated with a shift to slightly higher frequency. Minimum-amplitude fluctuations in the Piobbico time series occur during periods of generally low carbonate and oxidation state (for example, bundles l and k, p and o). If the eccentricity phase relationships can be extrapolated into the past, the lows of carbonate and transmission values follow lows in eccentricity. Individual anoxic episodes would then follow precessional minima (lowered monsoonality) during periods of generally low eccentricity.

We prefer to correlate Tethyan anoxic events with periods of minimal seasonal contrast because of the above-mentioned phase match, and because such a mechanism could lead to a relatively simple covariance of surface productivity and deep-water oxygenation. Modulation of seasonal temperature contrast by orbital cycles could be expected to influence thermocline stability, wind stress and rates of deep water formation, resulting in changes in flux of nutrient-rich deep water to the surface over time. For example, Prell[37] has related the record of upwelling intensity off the Arabian coast with the strength of the Northern Hemisphere precessional cycle. We interpret variability in carbonate in our sequence as reflecting climatic control on the rate of upwelling of deep water to the surface ocean. In our model, black shale events occurred as rates of deep water formation slowed due to lessened seasonality. If deep water was formed at the coldest time of the year, then periods of minimal seasonal contrast would produce warmer, less oxygenated bottom water than periods of precessional highs. Anoxia would therefore be linked to lower overturning rates and lowered carbonate productivity.

Implications

The strong eccentricity and precessional power in the Tethyan region indicate that changes in seasonal contrast may leave a distinctive mark in the geological record. The striking similarities of the Piobbico Aptian–Albian sequence with early- to mid-Cretaceous rhythmic deposits in other ocean basins (see, for example, refs 26–28, 33, 41) leads us to expect that time-series analysis of other records will confirm the global signature of climatic rhythms in the mid-Cretaceous deep-sea record. A number of workers consider many of the deep-water black shales to be turbiditic in origin, or unreflective of widespread deep-basin anoxia[42–45]. Detailed sampling such as that reported here may help to establish whether these sequences record external climatic forcing or random local events.

Quantitative understanding of the translation from insolation cycles to palaeooceanographic response remains a major chal-

lenge. Recent theoretical work on climate change during the Quaternary has emphasized the importance of internal mechanisms, associated with ice sheet dynamics, which might enhance what are considered to be the rather weak primary Milankovitch signals[46,47]. Various feedback mechanisms linked to glaciation, such as ice-albedo effects, bedrock response to glacial loading, and the hydrological cycle, seem capable of generating large global temperature and ice volume changes when forced by orbital variations[48-50]. The hypothesis of sluggish Cretaceous circulation has also been based on the supposition of the centrality of polar conditions to world climate dynamics[22,34]. Our data suggest that ice sheet amplification may not be a prerequisite to large-scale climate modulation by cyclic variations in insolation. The carbonate content variations in the interval sampled are comparable to glacial/interglacial fluctuations observed in Pleistocene deep-sea cores; similarly, the high-amplitude redox cycles in our core, and in similar Cretaceous sequences in the North and South Atlantic, argue for significant climatic-oceanographic change on a timescale of 10–100 kyr. These changes were apparently driven by low-latitude (eccentricity and precessional) forcing.

Another intriguing observation is the prominence of the 100-kyr cycle, with its modulation at slightly more than 400 kyr, in the Piobbico core. Although calculated eccentricity variations should not have a significant effect on mean annual insolation[9,51], 100- and 400-kyr peaks are in fact large spectral components of the Pleistocene ice volume[5,6,8], pelagic carbonate[1-3,52,53] and magnetic intensity[51] records. The origin of these spectral peaks is the subject of controversy[6,46,48-50,53-57]. Although many authors have ascribed the 100-kyr period to nonlinearities associated with ice sheet growth and decay[48-50,54,55], 100- and 400-kyr cycles appear to have controlled a large part of the variance in this deep-sea record of the non-glaciated Cretaceous. Several interpretations are possible. Nonlinearities not associated with ice may play, or have played during the Cretaceous, an important part in climatic response to orbital forcing. The 100- and 400-kyr frequencies may thus result from the climate system's nonlinear response to the precessional signal rther than from a direct effect of the 100- and 400-kyr insolation cycles[46,54,57]. Alternatively, evidence from the Pleistocene appears to indicate that eccentricity forcing exerts a major direct control on climate[8]. The strong resemblance of our Cretaceous time series to a linear combination of the precessional and eccentricity cycles reinforces this impression.

The redox and carbonate cyclicity exhibited in our core section appears to have been highly stable over time. The estimated 100-kyr bundling can be followed visually in photographs of core sections for >50 m, or 10 Myr. In addition, outcrop studies[14,16] of the formations above and below the Piobbico core section show the persistence of these periodicities. This stability contrasts sharply with the changes in power of the Milankovitch frequencies in the Pleistocene ice volume record, in particular the 100-kyr cycle[58]. Abrupt shifts in the character of the $\delta^{18}O$ record from earlier higher-frequency to dominant 100-kyr periodicity at ~700 kyr BP have been postulated to be the effects of dicontinuous ice-cap sensitivity to small changes in insolation[54]. The absence of glaciation in the mid-Cretaceous may simplify study of the climate system, in that it removes a potentially large source of internal variability, and account for the regularity of the 100-kyr cycle in our records. Palaeoclimatic studies of the non-glacial past may thus prove to be useful in testing theories of Pleistocene climatic change and in separating glacial effects from other responses of the Earth's climate to orbitally modulated variations in insolation.

T.D.H. has been supported by an NSF graduate fellowship. The project has been financed by NSF grants INT-8105265 and EAR-8306161 to A.G.F. We acknowledge discussions with R. F. Stallard, assistance by Ed Turner in the use of the microdensitometer, help by Ivan Henson and Rob Hawman in computer programming, and Isabella Premoli Silva and her students in Milan for their work in preparing and photographing the Piobbico core and for providing biostratigraphic control.

Received 22 November 1985; accepted 25 April 1986.

1. Arrhenius, G. *Rep. Swed. deep Sea Exped.* **1**, 1–228 (1952).
2. Berger, W. H. *J. foram. Res.* **3**, 187–195 (1973).
3. Hays, J. D., Saito, T., Opdyke, N. D. & Burckle, L. H. *Geol. Soc. Am. Bull.* **80**, 1481–1514 (1969).
4. Rea, D. K., Leinen, M. & Janacek, D. *Science* **227**, 721–725 (1984).
5. Broecker, W. S. & VanDonk, J. *Rev. Geophys. Space Phys.* **8**, 169–198 (1968).
6. Shackleton, N. J. & Opdyke, N. D. *Geol. Soc. Am. Mem.* **145**, 449–464 (1973).
7. Hays, J. D., Imbrie, J. & Shackleton, N. J. *Science* **194**, 1121–1132 (1976).
8. Imbrie, J. *et al.* in *Milankovitch and Climate* Pt 1 (eds Berger, A., Imbrie, J., Hays, J., Kukla, G. & Saltzmen, B.) 269–305 (Reidel, Boston, 1984).
9. Berger, A. L. *Inst. Astr. Geophys. G. Lemaitre Contr.* No. 18.
10. Berger, A. L. *Celest. Mech.* **15**, 53–74 (1975).
11. Van Houten, F. B. *Bull. Kans. Univ. geol. Surv.* **169**, 497–531 (1963).
12. Dean, W. E., Gardner, J. V. & Cepek, P. *Mar. Geol.* **39**, 81–101 (1981).
13. Arthur, M. A. *Init. Rep. DSDP* **42**, 719–751 (1979).
14. de Boer, P. L. in *Cyclic and Event Stratification* (eds Einsele, G. & Seilacher, A.) 456–475 (Springer, New York, 1982).
15. Anderson, R. Y. *J. geophys. Res.* **87**, 7285–7294 (1982).
16. Schwarzacher, W. & Fischer, A. G. in *Cyclic and Event Stratification* (eds Einsele, G. & Seilacher, A.) 72–95 (Springer, New York, 1982).
17. Olsen, P. E. in *Milankovitch and Climate* Pt 1 (eds Berger, A. *et al.*) 129–146 (Reidel, Boston, 1984).
18. Savin, S. M. *A. Rev. Earth planet. Sci.* **5**, 319–355 (1977).
19. Saltzman, E. S. & Barrow, E. J. *Palaeogeogr. Palaeoclimatol. Palaeoecol.* **40**, 167–181 (1982).
20. Frakes, L. *Climate Through Geologic Time* (Elsevier, New York, 1979).
21. Barron, E. J. *Earth Sci. Rev.* **19**, 305–338 (1983).
22. Fischer, A. G. & Arthur, M. A. in *Deep Water Carbonate Environments* (eds Cook, H. E. & Enos, P.) 19–50 (Soc. econ. Paleont. Miner. No. 25) (1977).
23. Barron, E. J. & Washington, W. M. in *The Carbon Cycle and Atmospheric CO_2: Natural Variations Archaean to Present* (eds Sundquist, E. T. & Broecker, W. S.) 546–553 (Am. geophys. Un. Monogr. **32**, 1984).
24. Cirilli, S., Marton, P. & Vigliotti, L. *Earth planet. Sci. Lett.* **69**, 203–214 (1984).
25. Schlanger, S. O. & Jenkyns, H. C. *Geologie Mijnb.* **55**, 179–184 (1976).
26. de Graciansky, P. C. & Gillot, E. *Init. Rep. DSDP* **80**, 885–897 (1985).
27. Cotillon, P. H. & Rio, M. *Init. Rep. DSDP* **77**, 339–376 (1984).
28. McCave, I. N. *Init. Rep. DSDP* **56**, 682–693 (1979).
29. Harland, W. B. *et al. A Geologic Time Scale* (Cambridge University Press, 1982).
30. Odin, G. S. & Kennedy, W. J. *C. r. hebd. Séanc. Acad. Sci., Paris* **294**, 31–54 (1982).
31. Hallam, A., Hancock, J. M., LaBreque, J. L., Lowrie, W. & Chanell, J. E. T. in *Geochronology and the Geological Record* (ed. Snelling, N. J.) 118–140 (Geological Society, London, 1985).
32. Bralower, T. J. & Thierstein, H. R. *Geology* **12**, 614–618 (1984).
33. Arthur, M. A., Dean, W. E., Bottjer, D. & Scholle, P. A. in *Milankovitch and Climate* Pt 1 (eds Berger, A. *et al.*) 191–201 (Reidel, Boston, 1984).
34. Berggren, W. & Hollister, C. D. *Tectonophysics* **38**, 11–48 (1977).
35. Rossignol-Strick, M. *Nature* **304**, 46–48 (1983).
36. Kutzbach, J. E. & Otto-Bliesner, B. L. *J. atmos. Sci.* **39**, 1177–1188 (1982).
37. Prell, W. L. in *Milankovitch and Climate* Pt 1 (eds Berger, A. *et al.*) 349–366 (Reidel, Bolton, 1984).
38. Barron, E. J., Arthur, M. A. & Kauffman, E. G. *Earth planet. Sci. Lett.* **72**, 327–340 (1985).
39. Weissert, H., McKenzie, J. A. & Hochuli, P. *Geology* **7**, 147–151 (1979).
40. Brass, G. W., Southam, J. R. & Peterson, W. H. *Nature* **296**, 620–623 (1982).
41. Fischer, A. G., Herbert, T. D. & Premoli Silva, I. in *Soc. econ. Paleont. Miner. Field Trip Guidebook* No. 4, 1–10 (1985).
42. de Graciansky, P. C. *et al. Init. Rep. DSDP* **47**, 877–907 (1979).
43. Habib, D. in *Origin of Cretaceous Carbon-Rich Facies* (eds Schlanger, S. O. & Cita, M. B.) 113–127 (Academic, London, 1982).
44. Waples, D. W. *Bull. Am. Ass. Petrol. Geol.* **67**, 962–978 (1983).
45. Myers, P. M., Leenheer, M. J., Kawka, O. E. & Trull, T. W. *Nature* **312**, 356–359 (1984).
46. Le Treut, H. & Ghil, M. *J. geophys. Res.* **88**, 5167–5190 (1983).
47. North, G. R., Mengel, J. G. & Short, D. A. *J. geophys. Res.* **88**, 6576–6586 (1983).
48. Pollard, D. P. *Nature* **296**, 334–338 (1982).
49. Weertman, J. *Nature* **261**, 17–20 (1976).
50. Birchfield, G. E. *J. geophys. Res.* **82**, 4909–4913 (1977).
51. Wollin, G., Ryan, W. B. F. & Ericson, D. B. *Earth planet. Sci. Lett.* **41**, 395–397 (1978).
52. Briskin, M. & Harrell, J. *Mar. Geol.* **36**, 1–22 (1980).
53. Moore, T. C., Pisias, N. G. & Dunn, D. A. *Mar. Geol.* **46**, 217–233 (1982).
54. Imbrie, J. & Imbrie, J. Z. *Science* **194**, 943–952 (1980).
55. Oerlemans, J. *Nature* **287**, 430–432 (1980).
56. Kukla, G., Berger, A., Lotti, R. & Brown, J. *Nature* **290**, 295–300 (1981).
57. Wigley, T. M. L. *Nature* **264**, 629–631 (1976).
58. Pestiaux, P. & Berger, A. L. in *Milankovitch and Climate* Pt 1 (eds Berger, A. *et al.*) 417–466 (Reidel, Boston, 1984).
59. Lowrie, W. & Ogg, J. G. *Earth planet. Sci. Lett.* **76**, 341–349 (1986).
60. Priestely, M. *Spectral Analysis and Time Series* Vol. 1 (Academic, New York, 1981).

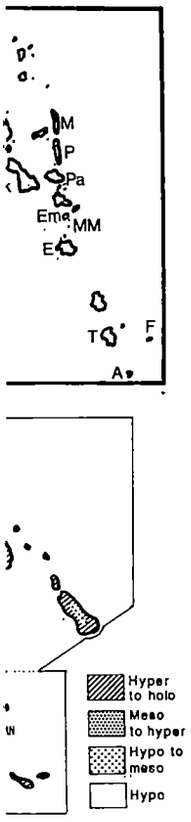
MRC

The frequenc
correlation w
disease is th

THE haemog
vincing dem
frequencies i
lethal disorde
which occur a
areas lying w
that malaria i
loss of thala
homozygotes
malarial envi
sickle cell ar
this hypothes
frequencies
selection[2-7].

Although
regions of th
conform to th
cell disease, t
is responsibl
This reflects i
gene disorde
genome, the
is such that
cally. On the
genes per ha
in α^+-thalas
two α gene
$(-\alpha/\alpha\alpha)$. T
hypochromic
from normal
results in α°
α-globin gen
a mild hypo
gous α^+-thal
α-globin gen
from the sam
somes. Thus
than that of
overall corre

** To whom c



ıria is found west
:alia; PNG, Papua
ıuatu; NC, New
spiritu Santo; M,
; Em, Emae; MM,
ı; A, Aneityum. c,
astal regions from
ern and eastern),
ghlands and Enga
bu Province; EH,
malarial endemic-
en aged 2–9 years:
ndemic, >50%;
ref. 77). Adapted

te strongly with
itude or altitude.
ıer unlinked poly-
: analysis of α-
selection as the
ntal consequences

ution of α-globin
ion deletion forms
3.7 kilobases (kb)
ıoves the α1 gene
removes the entire
pes were identified
lative proportions
only on the north
he $-\alpha^{3.7}$ deletions
found only in the
n than the $-\alpha^{3.7}$I
with locality. No
was found in this
ıia would not have
ver other evidence

suggests tha
are much le

It can be
generally sh
almost 70%
west to les
Because the
with altitud
region that
two groups:
subdivided
ted: Enga
and the Ma
Coastal san
Sepik Provi
and east (M
attempt has
since the ot
highlands a
mates for c
deletion an
figure of 4
highlands.
areas are 1
features of t
of α-thalass
through Me

Malaria

There have
in the Sou
detailed ma
colonized b
that before
programme
confined to
of the disea
coast but is,
Plasmodiun
dominant p
malaria sur
in 1926 in
early surve
and during
in the 1950
be seasonal
but *Plasmo*
archipelago
in the amo
intense mal
south. The
the only isl
island in V
it too may
only *P. ma*
in Melanes
always beer
and east fro
of malaria

α-Thala

The results
with the fin
and two sm
coast[38,39], i
high incide
in Papua N
1,500 m. D
generations
demonstrat

Incidence of α-thalassaemia in Melane

αα/αα	−α/αα
75	6
85	4
143	14
179	11
20	1
502	36
8	24
68	28
8	9
84	61
9	15
72	75
80	67
80	56
9	10
15	9
46	33
23	5
20	11
149	69
51	4
56	10
74	10

bin genotypes and the percentage gene fr
of normals, heterozygotes and homozygc
of 1%, has been included in the table as
according to altitude: coastal samples ar
ger towns from schools and hospitals att
mple as widely as possible. The North S
ast (see Fig. 1). The samples from Van
he New Caledonian samples were collec
re were performed as described previousl

it is reason-
time on the
ean arrival.
ple correla-
emicity (the
conclusion,
h the 1,800–
Peters and
rveys up to
alassaemia
lates with a

between the
quencies of
sia. As one
w Guinea,
Caledonia,
t in Table 1
ity[24]. New
t frequency
of malaria,
len, unpub-
in Vanuatu
alassaemia
e of malaria
ave a higher
ls. The rank
demicity is

ns, $-\alpha^{3.7}$I,
ency of α-
c restriction
enes allows

some insight in
Haplotypes defi
single or multi
investigate the o
eight such polyn
chromosomes[44].
dominant $-\alpha^{3.7}$
not found in ot
with a single re
single origin. –
at least three di
as the haplotyp
mutants (Table

Table 2 Associatio

Island
North coastal PN
South coastal PN
North Solomons
Espiritu Santo
Maewo
Pentecost
Malekula
Efate
Tanna
Futuna
Aneityum
New Caledonia

The percentage –
listed from north-we
both southern and ea
in the south coastal
taken from the earli
had been initiated.
Paama.

(data not shown) showed that at least two different haplotypes are associated with this variant. Hence, subtyping and haplotype analysis of these chromosomes indicate that the three types of α-thalassaemia deletion have had at least six independent origins. However, of particular interest is the observation that these deletion chromosomes have the same haplotypes as the common normal ($\alpha\alpha$) haplotypes in Melanesia (Table 3). These Melanesian $\alpha\alpha$ haplotypes are unusual in being relatively uncommon in other populations[44]. This suggests that the $-\alpha$ deletion chromosomes now prevalent in Melanesia arose locally on the $\alpha\alpha$ haplotypes common in this region, and were not imported from other malarious areas. The implication of these findings is that some local mechanism is responsible for their elevation to the present high frequencies. As shown in Tables 1 and 3, different types of deletions predominate in different Melanesian populations suggesting, for example, that the $-\alpha^{4.2}$ deletion of haplotype $--+$MZ$-$del$-$ may have originated in north coastal Papua New Guinea, and the $\alpha^{3.7}$III deletion in northern Vanuatu.

If malarial selection is solely responsible for the high frequencies of α-thalassaemia, it follows that genetic variation at loci unlinked to the α-globin cluster is unlikely to show the same correlation with malaria endemicity.

There exist a large amount of data on blood groups and protein polymorphisms for the inhabitants of Papua New Guinea[45], and no non-globin locus so far examined has the degree of divergence between highland and coastal populations discovered for α^+-thalassaemia. To confirm that previous observations apply to our samples, we measured allele frequencies for a number of polymorphic DNA loci, unlinked to the α genes. To maximize the detectable heterogeneity, two types of polymorphisms were examined: those due to changes that alter a restriction enzyme cleavage site and are thus dimorphic, and those due to variation in the copy number of tandem repeats of a consensus sequence (hypervariable regions, HVRs). Whereas the heterozygosity of site polymorphisms can never exceed 50%, the HVRs are multiallelic; they are therefore potentially far more informative than site polymorphisms; and allow finer resolution of genetic relationships between populations. Combining linked polymorphisms into a haplotype also increases the heterozygosity obtainable at a specific locus, and eight polymorphic sites in the β-globin gene cluster[43,46] were used in this study in addition to site polymorphisms and HVRs. Two probes of known chromosomal location but unknown function were used to look at site polymorphisms. Neither of these probes is linked to the α-globin cluster: probe 2.30 lies on chromosome 2 (ref. 47) and probe 3.6 on chromosome 4 (ref. 48). We examined a further site polymorphism on chromosome 19 with a fragment of the human third complement gene, C3 (ref. 49). The two hypervariable regions examined are on chromosome 11, one 400 base pairs 5′ to the insulin gene[50] and another 1.5 kb 3′ to the Harvey *ras*-1 oncogene[51]; they are arranged in the order β-globin–insulin–Ha-*ras*, with an estimated recombination of 11.6% between β-globin and insulin, and 3.2% between Ha-*ras* and insulin[52]. Unless these samples are from closely related individuals, there is no reason to expect any redundancy of information from looking at all three loci, and indeed no linkage was observed.

There have been relatively few population surveys in Island Melanesia, so there are few protein data to draw on. We therefore analysed the frequencies of two genetic polymorphisms readily detectable by DNA analysis in the same samples from Island Melanesia as used for the α-thalassaemia study. These are the haptoglobin polymorphism, with alleles Hp^1 and Hp^2 (ref. 53), and the frequencies of the variant γ-globin genotypes: $-\gamma$ and $\gamma\gamma\gamma$ (refs 54, 55). Studies of the phenotypes of these γ-gene variants have shown that they are unlikely to be subject to selection[46]. Tables 4 and 5 summarize the distribution of DNA polymorphisms in Melanesia. A partition of genetic variation[56] showed a highly significant difference between highland and coastal regions of Papua New Guinea for $-\alpha$ gene frequencies ($F_{1,6}=22.04$; $P<0.001$), but not for other loci. There was no significant association between the frequencies of γ genotypes or haptoglobin alleles and malaria endemicity. Clearly, no allele exhibits an altitude- or latitude-dependent variation comparable to that found for α-thalassaemia.

Table 3 Haplotypes of $-\alpha$ and $\alpha\alpha$ chromosomes

Population		No.	Haplotype X	S	B	H	Z	A	R	P
Vanuatu	$-\alpha^{3.7}$III	19	−	−	+	M	Z	−	·	del
	$-\alpha^{4.2}$	2	−	−	+	M	Z	−	del	−
	$-\alpha^{4.2}$	2	+	−	−	S	PZ	+	del	+
	$\alpha\alpha$	13	−	−	+	M	Z	−	−	−
	$\alpha\alpha$	4	+	−	+	M	Z	−	−	−
	$\alpha\alpha$	16	+	−	−	S	PZ	+	−	+
	$\alpha\alpha$	3	+	−	−	S	PZ	+	−	−
	$\alpha\alpha$	1	−	−	−	S	PZ	+	−	+
	$\alpha\alpha$	1	+	+	−	M	PZ	+	+	−
Papua New Guinea	$-\alpha^{3.7}$III	2	−	−	+	M	Z	−	−	del
	$-\alpha^{4.2}$	29	−	−	+	M	Z	−	del	−
	$-\alpha^{4.2}$	7	−	−	+	M	Z	−	del	+
	$\alpha\alpha$	14	−	−	+	M	Z	−	−	−
	$\alpha\alpha$	4	+	−	+	M	Z	−	−	−
	$\alpha\alpha$	2	+	−	−	S	PZ	+	−	+
	$\alpha\alpha$	2	+	−	−	S	PZ	+	−	−
	$\alpha\alpha$	1	−	−	−	S	PZ	+	−	+
	$\alpha\alpha$	1	−	−	−	S	PZ	+	−	−
South-East Asia	$-\alpha^{4.2}$	6	+	+	−	M	PZ	+	del	−

Restriction enzyme haplotype analysis of $-\alpha$ and $\alpha\alpha$ chromosomes from Melanesia. For comparison, data on six deletions from South-East Asians are included. The eight polymorphic sites in the α complex were detected as described in ref. 44. The *Pst*I site 3′ to the α1 gene[44] is not included in these haplotypes. del indicates that the single α-gene deletion removes that polymorphic site. + indicates the presence of a restriction site, − its absence. M and S indicate medium- and small-length alleles, respectively, of the inter-zeta hypervariable region. PZ and Z refer to a $\psi\zeta$1 and ζ1 gene, respectively, detected as described previously[78]. X, *Xba*I; S, *Sac*I; B, *Bgl*I; H, inter-zeta hypervariable region; Z, zeta-pseudozeta polymorphism; A, *Acc*I; R, *Rsa*I; P, *Pst*I. Additional probes used to determine these haplotypes were a 0.6-kb *Bam*HI/*Eco*RI fragment from pJW5, a 1.8-kb *Sac*I fragment from pBRζ, a 1.1-kb *Alu* fragment from pSG21 and a 0.8-kb *Bam*HI fragment from pDH 12 (ref. 44).

Genetic drift and founder effect

The most plausible explanation for the observed geographical distribution of α-thalassaemia is that malarial selection is responsible. Support for the malaria hypothesis thus comes from four lines of epidemiological evidence: (1) α-thalassaemia correlates with malaria across two independent variables, namely latitude and altitude; (2) other polymorphic loci unlinked to the α-globin cluster fail to show equivalent variation; (3) a number of phenotypically similar α-thalassaemia variants are present at high frequencies; (4) these mutations arose within the Melanesian populations and have been amplified to high frequencies, implicating a mechanism operating within Melanesia rather than the large-scale import of the variants from elsewhere.

What alternative explanations might accommodate these observations? Genetic drift and founder effects are undoubtedly important in influencing gene frequency variations in small isolated communities[57–60]. How likely is it that they are responsible for the observed distribution of α-thalassaemia described here?

Examples of the clustering of particular genetic variants on single islands in Vanuatu[13] suggest that, despite their proximity, historically these islands have remained relatively isolated, increasing the potential for genetic drift. Migration of two populations with different genetic compositions into a single area can readily produce a gene frequency cline. For example, had Melanesia been populated from the south-east by a population with little α-thalassaemia and from the north-west by people in whom it was common, a frequency distribution somewhat similar to that observed might have been generated.

Table 4 Distribution of DNA variants in Melanesia

	Papua New Guinea highlands						Papua New Guinea coast			
a, Probe	Madang (Bundi)	Chimbu	Eastern Highlands	Southern Highlands	Western Highlands	Mean gene frequency	Northern region	Southern region	Eastern region	Mean gene frequency
C3	43 (56)*	42 (78)	53 (18)	58 (83)	50 (10)	48 (245)	48 (33)	52 (62)	50 (8)	51 (103)
3.6	10 (80)	21 (82)	10 (111)	5 (148)	0 (13)	10 (434)	9 (53)	7 (97)	11 (14)	8 (164)
2.3	24 (55)	28 (38)	46 (37)	22 (154)	42 (13)	27 (295)	19 (48)	26 (89)	5 (10)	22 (147)
Insulin HVR class										
1	1	2	4	4	0	3	3	0	0	2
2	0	0	0	0	0	0	5	4	0	4
3	0	1	0	4	0	1	0	0	0	0
4	99	97	96	92	100	96	92	96	100	94
	(57)	(42)	(52)	(79)	(18)	(248)	(48)	(26)	(7)	(81)
Ha-*ras*-1 HVR class										
1	21	7	7	21	8	14	24	12		18
2	29	31	26	16	17	23	26	29		28
3	5	2	0	0	0	1	1	1		1
4	0	5	6	8	8	6	7	4		5
5	45	55	61	55	50	55	35	48		42
6	0	0	0	0	0	0	3	3		3
Variants	0	0	0	0	17	1	4	3		3
	(19)	(21)	(52)	(50)	(6)	(148)	(40)	(38)		(78)

b	North coastal PNG	South coastal PNG	North Solomons	Espiritu Santo	Maewo	Pentecost	Emae	Efate	Tanna	Futuna	Aneityum	New Caledonia
$\%-\gamma$	5	1	3	11	10	2	12	3	2	13	10	2
$\%\gamma\gamma\gamma$	1	1	2	3	9	4	2	3	1	0	1	8
$\%\ Hp^1$	64	71	62	73	76	68	63	61	71	69	61	59
$\%-\alpha$	68	22	45	38	33	27	26	25	18	6	8	6

a, Percentage gene frequencies of the presence of site polymorphisms as detected by three unlinked probes, and percentages of allele classes as detected by two hypervariable region probes in samples from Papua New Guinea. Two *Bgl*II polymorphisms were examined using probes from a bank of clones used in genetic linkage studies; their chromosomal location is known but not the function of the genomic DNA they contain; they are therefore referred to by laboratory designations: probe 2.30 lies on chromosome 2, probe 3.6 on chromosome 4 (refs 47, 48). An *Sst*I polymorphism detected by a fragment of the third complement component gene (C3) on chromosome 19 (ref. 49) was also surveyed. The insulin gene in phins214 (ref. 79) on a *Rsa*I digest detected four HVR allele classes. Where two alleles appear on a Southern blot to be the same size, it cannot be assumed that they are the same allele, because the technique cannot resolve differences of one or two repeats in a HVR, and also because alleles that are equal in size can have internal sequence differences[80]. Therefore, we refer here to allele classes rather than discrete allele sizes: class 1, 4.7 kb; class 2, 3.9 kb; class 3, 2.6 kb; class 4, 2.1–2.4 kb. Microheterogeneity was particularly obvious with the smaller (class 4) insulin alleles. A *Bam*HI–*Sst*I fragment from the plasmid pBL116-4 containing the Ha-*ras*-1 HVR[51] resolved six allele classes in a *Hin*fI digest: class 1, 4.3 kb; class 2, 3.8 kb; class 3, 3.0 kb; class 4, 2.8 kb; class 5, 2.7 kb; class 6, 2.6 kb. Seven alleles could not be fitted into these categories: three (two from the coast and one from the highlands of Papua New Guinea) were of equal size, but the remaining four could not be reconciled either with this size or with each other; they are therefore grouped separately as variants. *b*, To determine the γ-globin[54,55] and haptoglobin[53,81] genotypes in Island Melanesians, the nitrocellulose filters with *Bgl*II-digested DNA samples, prepared previously for determination of α genotypes, were rehybridized, in turn, with a 3.2-kb $^{A}\gamma$-gene probe[46] and a 1.5-kb *Pst*I fragment from *Hp*9 (ref. 81). Sample sizes for each island were comparable to those in Table 1 and at least 60 chromosomes were analysed in each case. Some of these haptoglobin, $-\gamma$ and $\gamma\gamma\gamma$ frequencies are reported elsewhere[46,81]. The $-\alpha$ frequencies from Table 1 are included for comparison.

*Numbers of individuals are shown in parentheses.

In Papua New Guinea there are two ways in which α-thalassaemia gene frequencies might increase by genetic drift or founder effects. First, as part of a substantial population movement, α-thalassaemia could have infiltrated the coastal area on a large scale. Second, an initially homogeneous population with a low prevalence of α-thalassaemia might have become divided genetically as drift elevated the frequency of thalassaemia on the coast and depressed it in the highlands, or the division could have occurred because of colonization of the highlands by a subset of the original settlers lacking the mutation. We believe our data favour selection when viewed from any of these standpoints.

The gene frequencies of the $-\alpha$ deletion, particularly in the north of Papua New Guinea, seem too high to attribute to random fluctuations unless the founding population was extremely small. Furthermore, genetic drift should produce uneven variation from island to island, as seen for the $-\gamma$ and $\gamma\gamma\gamma$ frequencies, rather than a frequency cline. Moreover, assuming that the $-\alpha$ chromosome in most of the founding populations of these islands was less common than the normal $\alpha\alpha$ chromosome, in the absence of selection, the deletion chromosome should have been lost completely on some islands through genetic drift, as appears to have happened with the $-\alpha^{3.7}$III mutation when it was carried out into the central Pacific[34], where there is no malaria[24], by the settlers of Polynesia. That this has not occurred in the malarial regions of Melanesia suggests that selection is involved.

With the exception of some recent back-migration from Polynesia, all known migrations into Melanesia have come from the north-west[61]. The 'outlier' islands of Futuna and Emae in Vanuatu have ethnically Polynesian populations and, culturally, there is probably more Polynesian influence in the south than in the north of Vanuatu[61]. Similarly, a relatively recent admixture of Polynesian genes into the south coastal population of Papua New Guinea may, in part, explain the lower overall prevalence of α-thalassaemia there than on the north coast. However, such back-migration has almost certainly been too limited to explain more than a minor part of the observed α-thalassaemia cline. For example, the 'Polynesian' population of Emae has a much higher α-thalassaemia frequency than anywhere in Polynesia[62]. Similarly, although a late migration from the north-west by a very large population with a high frequency of α^+-thalassaemia could have produced a $-\alpha$ gene frequency cline, this is inconsistent with the haplotype data which indicate that most of the $-\alpha$ chromosomes found in Melanesia had local origins and have not been imported from South-East Asia. Furthermore, no simple migration model could explain the generation of a cline made up of different proportions of the various molecular types of $-\alpha$ deletions in different locations.

Similar arguments apply within Papua New Guinea. Here

Table 5 Distribution of β-globin haplotypes in Papua New Guinea highland and coastal populations

Highlands		No.	5′ Haplotype +−−−−	−+−++	−++−+	−+−−+	−−−−+	+−−++	−++++	−−−−−	−−+−−	−+−−−
Southern Highlands		19	69	18	5	5	3	0	0	0	0	0
Eastern Highlands		20	59	7	5	10	3	10	0	3	3	0
	Total	39	64	13	5	8	3	5	0	1	1	0
Coast												
Madang		19	55	16	0	0	0	16	5	5	0	3

Highlands		No.	3′ Haplotype ++−	+v+	+−−	−−+	+−+	+++
Southern Highlands		19	53	18	8	13	5	3
Eastern Highlands		18	56	19	0	6	11	8
	Total	37	54	19	4	10	8	5
Coast								
Madang		16	47	22	0	19	9	3

Percentage frequencies of β-globin gene complex haplotypes in two highland provinces and the north coast of Papua New Guinea. The β-globin haplotype used here consists of five sites reported previously and referred to as 5′ haplotype, and three sites (*Ava*II, *Hin*dIII and *Bam*HI) combined into a 3′ haplotype[43]. 'v' indicates the presence of an additional *Hin*dIII site 11 kb 3′ to the β-globin gene[46].

again three subtypes of α^+-thalassaemia are found at elevated frequencies. Genetic drift or disturbance caused by new population influx should have affected other gene frequencies as well as α-thalassaemia. Unless by chance we, and others, have looked only at unaffected loci, drift acting to divide the population can be excluded as an explanation of the observed distribution of α-thalassaemia. Similarly, immigration leaving existing gene frequencies unaltered would have been possible only if the invaders were genetically similar to the resident Papuans except at the α-globin locus. While this possibility cannot be formally excluded, it runs counter to evidence from other disciplines.

Archaeological and linguistic data indicate a definite but small Austronesian admixture to the Papuan stock[63,64], and this is supported by genetic studies[65,66]. There exist a large amount of data on blood group and serum protein polymorphisms in Papua New Guinea[45]. Markers that distinguish between highland and coastal populations are either common alleles which show minor but significant variation between populations (for example, ABO and MNS blood groups[67]) or alleles occurring at low frequencies in one or other of the populations (MDH[4], ref. 68; or Ge^{a-}, ref. 69). This argues that immigration into coastal areas produced only minor changes in gene frequencies. Hence if α-thalassaemia had been imported it would have resulted in only low frequencies of the condition in the total coastal population.

The most plausible explanation for the observed difference is, therefore, that selection has acted on mutations arising within the original settlers of Melanesia.

Discussion

This microepidemiological study in Melanesia strongly implicates malaria as the selective agent responsible for the high prevalences of α-thalassaemia in certain tropical and subtropical regions. Limited data documenting the absence of α-thalassaemia in populations historically free of malaria support this conclusion[70]. The one apparent exception is the presence of α-thalassaemia at gene frequencies of ~7% in parts of Polynesia[62], all of which is free of malaria[24]. However, detailed molecular analysis of the −α deletion found in Polynesia shows that it is identical to the $-\alpha^{3.7}$III deletion prevalent in Island Melanesia. It seems probable, therefore, that α-thalassaemia was carried out into Polynesia by the original migrants from malarious Melanesia, its present patchy distribution reflecting the influence of genetic drift and founder effects over the past 3,000 years[34,62].

The mechanism whereby α-thalassaemia might confer protection against *P. falciparum* malaria is unclear. *In vitro* culture studies have not demonstrated any abnormality of invasion or growth of the parasites in the red cells of α- or β-thalassaemia heterozygotes, except in cases where the cells were maintained under conditions of unusual oxidant stress[71]. Furthermore, with the exception of the newborn period when the red cells contain increased levels of Hb Bart's, the haematological abnormalities in the α-thalassaemia carrier states are extremely mild and there are no changes in haemoglobin constitution. Thus the protective effect of α-thalassaemia against malarial infection must be extremely subtle and may not constitute a direct deleterious effect on parasite development, such as has been shown in the case of the red cells of sickle cell carriers[71].

Although the mechanism involved remains obscure, the epidemiological data do provide some indication of the magnitude of the apparent selective advantage conferred by α^+-thalassaemia with respect to malaria. It is unclear whether the observed gene frequencies in Melanesia are at equilibrium or whether the single α-gene deletion is still increasing in frequency. If the latter is true, because Island Melanesia has been inhabited for over 3,500 years and Papua New Guinea for much longer[61], the observation that the −α chromosomes have not yet reached their equilibrium frequency would suggest that the selective advantage is relatively small. On the other hand, if the present frequencies are at or near equilibrium, the selective advantage in the presence of malaria must be balanced by some disadvantage associated with homozygosity for α^+-thalassaemia. The mildness of the latter condition, which contrasts markedly with homozygosity for β-thalassaemia or Hb S, would again suggest that the balancing selective advantage of α^+-thalassaemia against malaria is small. This may explain the failure to detect differences between the −α and αα haplotypes in *in vitro* invasion or growth assays using *P. falciparum* in culture[71,72]. It seems that these data on α-thalassaemia in Melanesia provide a remarkable example of how a small selective advantage can lead to large variations in gene frequencies between human populations.

We thank Dr J.-P. Moreau, R. A. Spark and J. Barker for assistance in collecting samples, Drs K. Davies and B. Bakker for the 3.6, C3 and 2.30 probes, Drs D. R. Higgs and R. J. Trent for helpful discussions, Linda Roberts for preparing the manuscript, and the Rockefeller Foundation and Wellcome Trust for financial support. A.V.S.H. is a MRC Training Fellow, and J.F. is supported by his wife.

Received 27 January; accepted 7 May 1986.

1. Haldane, J. B. S. *Proc. 8th int. Congr. Genet.* 267–273 (*Hereditas* Suppl. 35, 1949).
2. Allison, A. C. *Br. med. J.* 1, 290–294 (1954).
3. Allison, A. C. *Trans. R. Soc. trop. Med. Hyg.* 48, 312–318 (1954).
4. Pasvol, G., Weatherall, D. J. & Wilson, R. J. M. *Nature* 274, 701–703 (1978).
5. Friedman, M. J. *Proc. natn. Acad. Sci. U.S.A.* 75, 1994–1997 (1978).
6. Livingstone, F. B. in *Distribution and Evolution of the Hemoglobin and Globin Loci* (ed. Bowman, J. E.) 15–44 (Elsevier, New York, 1983).
7. Livingstone, F. B. *Frequencies of Hemoglobin Variants* (Oxford University Press, 1985).
8. Higgs, D. R. & Weatherall, D. J. *Curr. Topics Haemat.* 4, 37–97 (1983).
9. Higgs, D. R. *et al. Br. J. Haemat.* 46, 39–46 (1982).
10. Old, J. M. & Higgs, D. R. in *The Thalassaemias* (ed. Weatherall, D. J.) 74–102 (Churchill-Livingstone, London, 1983).
11. Black, R. H. *South Pacif. Commn tech. Pap.* 81 (South Pacific Commission, Noumea, 1955).
12. Ewers, W. H. & Jeffrey, W. T. *Parasites of Man in Niugini* (Jacardanda Press, Milton, 1971).
13. Bowden, D. K., Hill, A. V. S., Higgs, D. R., Weatherall, D. J. & Clegg, J. B. *Lancet* ii, 1025–1028 (1985).
14. Willis, C. & Londo, D. R. *Am. J. hum. Genet.* 33, 215–226 (1981).
15. Parkinson, A. D. *Papua New Guin. med. J.* 17, 8–16 (1973).
16. Ratard, R. C. *Trop. Doctor* 9, 212–216 (1979).

17. Buxton, P. A. *Trans. R. Soc. trop. Med. Hyg.* **19**, 420–454 (1926).
18. Buxton, P. A. & Hopkins, G. H. *Researches in Polynesia and Melanesia I-IV*, 225–230 (London School of Hygiene and Tropical Medicine, 1927).
19. Tully, W. J. *Rep. of Finding by Health Compaign Conducted in the New Hebrides from 31 January 1929 to 21 August 1931* (copy in Library, School of Public Health and Tropical Medicine, Sydney, 1931).
20. Herivaux, A. *Annls Méd. Pharm. colon.* **37**, 40–62 (1946).
21. Mauze, J. *med. Trop.* **6**, 109–138 (1946).
22. Levine, N. D. & Harper, P. *Am. J. trop. Med.* (Suppl.) **27**, 119–128 (1947).
23. Harper, P., Levine, N. & Liebour, A. *Proc. 7th Pacif. Sci. Congr. N.Z.* **7**, 375–380 (1947).
24. Lambert, S. M. in *Malariology* (ed. Boyd, M. F.) 820–830 (W. B. Saunders, Philadelphia, 1949).
25. Black, R. H. *South Pacif. Commn tech. Pap.* 60 (South Pacific Commission, Noumea, 1954).
26. Black, R. H. *Aust. Geogr.* **6**, 32–35 (1955).
27. Black, R. H. *Oceania* **27**, 136–142 (1956).
28. Peters, W. *Papua New Guin. med. J.* **3**, 66–75 (1959).
29. Peters, W. *Trans. R. Soc. trop. Med. Hyg.* **54**, 242–260 (1960).
30. Norman-Taylor, W. & Rees, W. H. *South Pacif. Commn tech. Pap.* 143 (South Pacific Commission, Noumea, 1962).
31. Van Dijk, W. J. O. M. & Parkinson, A. D. *Papua New Guin. med. J.* **17**, 17–21 (1973).
32. Embury, S. H. *et al. J. clin. Invest.* **66**, 1319–1325, (1980).
33. Higgs, D. R., Hill, A. V. S., Bowden, D. K., Weatherall, D. J. & Clegg, J. B. *Nucleic Acids Res.* **12**, 6965–6977 (1984).
34. Hill, A. V. S. *et al. Am. J. hum. Genet.* **37**, 571–580 (1985).
35. Mills, A. R. *J. trop. Med. Hyg.* **57**, 99–107 (1954).
36. Laird, M. *Bull. ent. Res.* **45**, 279–283 (1954).
37. Booth, K. *Papua New Guin. med. J.* **24**, 264–266 (1981).
38. Oppenheimer, S. J., Higgs, D. R., Weatherall, D. J., Barker, J. & Spark, B. A. *Lancet* **i**, 424–426 (1984).
39. Yenchitsomanus, P.-J., Summers, K. M., Bhatia, K., Cattani, J. & Board, P. G. *Am. J. hum. Genet.* **37**, 778–784 (1985).
40. Siniscalco, M. *et al. Bull. Wld Hlth Org.* **34**, 379–393 (1966).
41. Breinl, A. *Ann. trop. Med. Parasit.* **9**, 285–334 (1915).
42. Peters, W. & Christian, S. H. *Trans. R. Soc. trop. Med. Hyg.* **54**, 529–536 (1960).
43. Orkin, S. H. & Kazazian, H. H. *A. Rev. Genet.* **18**, 131–171 (1984).
44. Higgs, D. R. *et al. Proc. natn. Acad. Sci. U.S.A.* (in the press).
45. Simmons, R. T. & Booth, P. B. *A Compendium of Melanesian Genetic Data I–IV* (Commonwealth Serum Laboratories, Victoria, 1971).
46. Hill, A. V. S., Bowden, D. K., Weatherall, D. J. & Clegg, J. B. *Blood* (in the press).
47. Povey, S., Morton, N. E. & Sherman, S. L. *Cytogenet. Cell Genet.* **40**, 67–106 (1985).
48. Gilliam, T. C. *et al. Hum. Genet.* **68**, 154–158 (1984).
49. Davies, K. E. *et al. J. med. Genet.* **19**, 259–263 (1983).
50. Bell, G. I., Karam, J. H. & Rutter, W. J. *Proc. natn. Acad. Sci. U.S.A.* **78**, 5759–5763 (1981).
51. Capon, D. J., Chen, E. Y., Levinson, A. D., Seeburg, P. H. & Goeddel, D. V. *Nature* **302**, 33–37 (1983).
52. White, R. *et al. Nature* **313**, 101–105 (1985).
53. Smithies, O. & Walker, W. F. *Nature* **176**, 1265–1266 (1955).
54. Sukumaran, P. K. *et al. Nucleic Acids Res.* **11**, 4635–4643 (1983).
55. Trent, R. J. *et al. Nucleic Acids Res.* **9**, 6723–6733 (1981).
56. Smouse, P. E. & Ward, R. H. *Genetics* **88**, 611–631 (1978).
57. Imaizumi, Y. & Morton, N. E. *Archaeol. phys. Anthrop., Oceania* **5**, 218–227 (1970).
58. Giles, E., Wyber, S. & Walsh, R. *Archaeol. phys. Anthrop., Oceania* **5**, 60–72 (1970).
59. Cavalli-Sforza, L. L. & Bodmer, W. F. *The Genetics of Human Populations* (W. H. Freeman, San Francisco, 1971).
60. Littlewood, R. A. *J. Polynes. Soc.* **75**, 95–106 (1966).
61. Bellwood, P. *Man's Conquest of the Pacific* (Collins, London, 1978).
62. Trent, R. J. *et al. Am. J. Hemat.* **18**, 431–433 (1985).
63. White, J. P. & O'Connell, J. F. *A Prehistory of Australia, New Guinea and Sahul* (Academic, Sydney, 1983).
64. Wurm, S. A., Laycock, D. C., Vorhoeve, C. L. & Dutton, T. E. in *New Guinea Area Languages and Language Study* Vol. 1 (ed. Wurm, S. A.) 935–960 (Australian National University, Canberra, 1975).
65. Kirk, R. L. in *The First Americans: Origins Affinities and Adaptations* (ed. Laughlin, W. S.) 211–237 (Gustav-Fischer, New York, 1979).
66. Kirk, R. L. in *Population Structure and Genetic Disorders* (eds Eriksson, A. N., Forsius, H., Nevanlinna, H. R., Workman, P. L. & Noris, P. K.) 113–137 (Academic, London, 1980).
67. Booth, P. B. & Simmons, R. T. *Papua New Guin. med. J.* **15**, 10–14 (1972).
68. Blake, N. M. *Hum. Genet.* **70**, 1–12 (1978).
69. Booth, P. B. & McLoughlin, K. *Vox Sang.* **22**, 73–84 (1972).
70. Flint, J., Hill, A. V. S., Clegg, J. B., Weatherall, D. J. & Higgs, D. R. *Br. J. Haemat.* (in the press).
71. Pasvol, G. & Wilson, R. J. M. *Br. med. Bull.* **38**, 133–140 (1982).
72. Ifediba, T. C., Stern, A., Ibrahim, A. & Rieder, R. F. *Blood* **65**, 452–455 (1985).
73. Higgs, D. R., Old, J. M. Pressley, L., Clegg, J. B. & Weatherall, D. J. *Nature* **284**, 632–635 (1980).
74. Goossens, M., Dozy, A. N., Embury, S. H. & Kan, Y. W. *Proc. natn. Acad. Sci. U.S.A.* **77**, 518–521 (1980).
75. Trent, R. J., Higgs, D. R., Clegg, J. B. & Weatherall, D. J. *Br. J. Haemat.* **49**, 149–152 (1981).
76. Bonnisseau, G. thesis, Univ. René Descartes, Paris (1975).
77. Manson-Bahr, P. E. C. & Apted, F. I. C. in *Tropical Diseases* 18th edn, 41 (Bailliere-Tindall, London, 1982).
78. Hill, A. V. S., Nicholls, R. D., Thein, S. L. & Higgs, D. R. *Cell* **42**, 809–819 (1985).
79. Bell, G. I., Horita, S. & Karam, J. H. *Diabetes* **33**, 137–181 (1984).
80. Goodbourn, S. E. Y., Higgs, D. R., Clegg, J. B. & Weatherall, D. J. *Molec. Biol. Med.* **2**, 223–238 (1984).
81. Hill, A. V. S. *et al. Am. J. hum. Genet.* **38**, 382–389 (1986).
82. *An Atlas of Papua New Guinea* (Department of Geography, University of Papua New Guinea; Collins Longman, Harlow, 1970).

LETTERS TO NATURE

PKS1345+125: a Seyfert nucleus merging with a powerful radio galaxy

Gerard Gilmore* & M. A. Shaw†

* Institute of Astronomy, Madingley Road, Cambridge CB3 0HA, UK
† Astronomy Department, University of Edinburgh, Blackford Hill, Edinburgh EH9 3HJ, UK

The bright compact radio source PKS1345+125 (4C 12.50) has been optically identified with a magnitude 17 galaxy with a redshift $z = 0.122$ (refs 1, 2) and an unusual spectrum[3]. Here we show it to be an elliptical galaxy with a compact radio source coincident with its optically undistinguished nucleus. An unresolved radio-quiet Seyfert nucleus with the same redshift as the elliptical galaxy is offset by 1.8 arc s from the radio source. The Seyfert nucleus is remarkable for its location in an elliptical galaxy, for its extreme far-infrared flux, and for the very low density in the broad-line region. We present a model of 1345+125 involving the dynamical merger of an elliptical galaxy with a spiral. The merger has stripped the spiral galaxy of its interstellar gas, fuelling the nuclear engines in both galaxies, and allowing the broad-line region to stream out freely. The elliptical has acquired an envelope, and is becoming a radio-loud cD galaxy.

PKS1345+125 is a suspected low-frequency radio variable, showing fractional flux variations of 30% on timescales of 4.5 yr (refs 4, 5) at a frequency of 408 MHz. If these variations are intrinsic to an incoherent synchrotron-emitting source, then relativistic effects are affecting significantly the observed properties of this source[6]. The radio source is in the VLA (Very Large Array) calibration list, so that reliable structural and positional data are available (ref. 7 and J. J. Condon, personal communication). More than 95% of its flux is contained in a region smaller than 0.5, 0.15 and 0.05 arc s at 20, 6 and 2 cm respectively (J. J. Condon, personal communication).

Table 1 Photometric data for PKS 1345+125

Waveband	Wavelength (μm)	log flux (Jy)	log frequency
J*	1.20	−2.61 ± 0.04	14.40
H*	1.64	−2.48 ± 0.02	14.26
K*	2.19	−2.46 ± 0.02	14.14
L'*	3.80	−2.08 ± 0.05	13.90
1†	12	−0.6	13.40
2†	25	−0.17	13.08
3†	60	0.30	12.70
4†	100	0.31	12.48

* 7.5-arc s aperture, 16-arc s chop north–south.
† IRAS point-course catalogue[8].

In a study of the optical spectrum, Grandi[3] noted the very broad forbidden lines, but classified the spectrum as that of a narrow-line radio galaxy because of its excitation level. The order-of-magnitude discrepancy between the velocity width in this object and in other narrow-line radio galaxies was noted, but did not overrule the classification. The absorption-line redshift[3] due to the underlying galaxy is consistent with that of the emission-line source.

The optical identification was classified as an S0 galaxy[1], presumably because the image is noticeably irregular on sky survey plates. To study the morphology in more detail, we

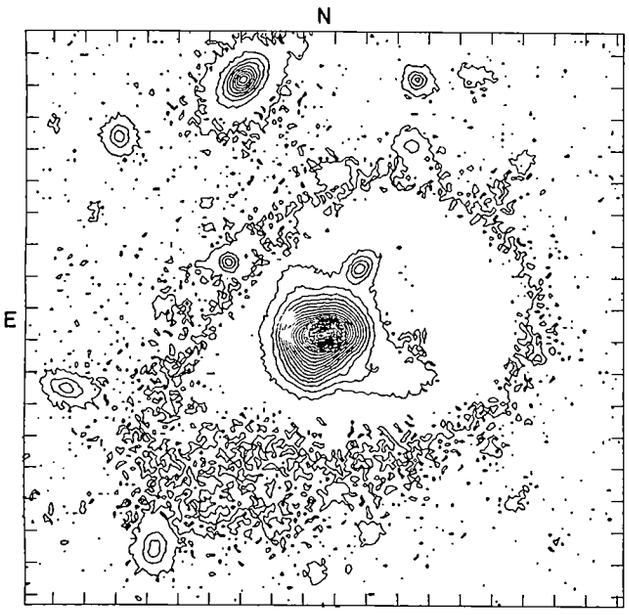


Fig. 1 R-band CCD image of PKS1345+125. North is at the top and East is to the left. The tick marks on the axes occur every 10 pixels, or 4.9 arc s. The eastern nucleus of the dominant galaxy is coincident with the radio source; the western nucleus is the Seyfert source.

obtained B- and R-band CCD (charge-coupled device) frames with an RCA CCD on the Anglo-Australian telescope in April 1985. Several exposures were obtained in each colour with the telescope offset between exposures to remove the effects of bad pixels and cosmic-ray events. All frames in each colour were bias-subtracted, defringed, flat-fielded, offset to a common centre and summed. Part of the resulting R frame is shown in Fig. 1, and shows the galaxy to be a very distorted, double-nucleus, giant elliptical in the centre of a cluster. The important features of this galaxy are its two nuclei, its distorted isophotal structure and its extensive asymmetric envelope.

The outer galactic isophotes in Fig. 1 correspond to a projected linear diameter of 110 h^{-1} kpc, where h is the Hubble constant in units of 100 km s^{-1} Mpc^{-1}. This galaxy then has the physical dimensions of a cD galaxy, consistent with its location at the centre of a cluster. The distorted isophotal structure indicates a recent (on a dynamical timescale) interaction in which the perturbations to the local gravitational potential are comparable to the potential in the outer parts of the galaxy. The luminosity profile is not consistent with an $r^{1/4}$ law.

Coordinates for the two nuclei have been determined relative to the nine compact images on the CCD image which are also visible on a UK Schmidt telescope plate, which in turn were measured relative to a set of AGK3 stars. The resulting positions (RA, dec. (1950.0)) for the two nuclei are: eastern nucleus, (13 h 45 min 06.20 s ± 0.02 s, +12° 32′ 20.06″ ± 0.30″); western nucleus, (13 h 45 min 06.09 s ± 0.02 s, +12° 32′ 20.57″ ± 0.30″). The VLA position (ref. 7 and J. J. Condon, personal communication) of the compact radio source is (13 h 45 min 06.17 s ± 0.01 s, +12° 32′ 20.3″ ± 0.1″). The eastern nucleus is most closely coincident with the centre of the dominant galaxy, is coincident with the compact radio source and is very red. The bluer western nucleus is unresolved in our CCD image, as it was during spectroscopic observations at La Palma, indicating a size of <0.9 arc s.

PKS 1345+125 was detected as a point source by IRAS (the Infrared Astronomy Satellite) at 100, 65, and 25 μm. Only an upper limit to the flux is available at 12 μm (ref. 8). If the infrared flux were from the elliptical galaxy, it would be unique in the IRAS survey; an identification of the infrared flux source with the emission-line source is therefore suggested. Near-infrared photometry was obtained in January 1982 (before the IRAS mission) with the UK Infrared Telescope. This shows substantial excess flux at 3.8 μm relative to that expected from an elliptical galaxy. The observations were obtained through a 7.5-arc s aperture including both nuclei, relative to positions 16-arc s north and south and are detailed in Table 1.

The IRAS data cannot be fitted by a single-temperature black body, with emissivity varying as frequency or (frequency)^2, which encompassess the usual range of assumed parameters. Sufficiently few data points are available for wavelengths longer than 3 μm that it is possible to fit the data with a power law having a break near 50 μm. Such a fit is steeper than usually observed (spectra index = −2.36), and is not required by the data.

The most conservative assumption possible is that a black body with emissivity ε poportional to frequency and fitted to the 60- and 100-μm data represents the total infrared flux. In this case the required temperature is $T = 47$ K, the resulting infrared flux is $F_{IR} = 1.25 \times 10^{-13}$ W m^{-2} and the absolute luminosity is $L_{IR} = 2 \times 10^{45} h^2$ erg s^{-1}, or $L_{IR} = 5 \times 10^{11} h^2 L_\odot$, with $L_\odot$ the solar luminosity. Even with these very conservative assumptions, this source is more luminous than 90% of those in the IRAS catalogue[8].

The minimum possible radius for the source may be calculated to be $r_{IR} = 220\, h^{-1}\, \varepsilon^{-1/2}$ pc, where ε is the emissivity at 60 μm. Assuming that $\varepsilon \simeq 1$, as representative for dust in our Galaxy, leads to a minimum physical size, $r_{IR} \simeq 220\, h^{-1}$ pc, and a corresponding minimum angular size, $\theta_{IR} \simeq 0.1$ arc s. We emphasize that this source is almost certainly coincident with the optical emission-line source.

Optical spectra with a resolution of ~1 Å were obtained in July 1982 and February 1984 with the du Pont telescope and reticon array detector at the Las Campanas observatory, and in May 1985 with the Isaac Newton telescope and an IPCS detector at La Palma. The La Palma observations used a 1-arc s slit in excellent seeing (~0.9 arc s with both nuclei visible) to check for spatially resolved emission. None was found. There is no optical line emission except from the unresolved radio-quiet western nucleus, and no continuum is seen from the line-emitting source.

The remarkable feature of the optical spectrum is the width, complexity and asymmetry of the [O III] 4,959+5,007 Å (Fig. 2*a*) and Hα+[N II] 6,563+6,548+6,583 Å (Fig. 2*b*) emission-line profiles. The half-width at zero intensity of these forbidden lines is ~5000 km s^{-1}. Line fluxes for the important diagnostic lines [O I] 6,300 Å and [S II] 6,716+6,731 Å are available only from the narrow-slit La Palma observations, with consequent large uncertainties, as seen by a comparison of the line fluxes determined here (Table 2) with the large-aperture data of Grandi[3].

The line ratios of Table 2 provide a powerful diagnostic of the ionization mechanism. We can use all five diagnostic

Table 2 Spectral data for the emission-line source

Emission line	Flux* (10^{-16} erg cm^{-2} s^{-1})
[O II] (Å) 3,726, 3,729	85
[Ne III] 3,869	25
[SII] 4,068, 4,076	15
[O I] 4,363	2
Hβ 4,861	20
[O III] 4,959	80
[O III] 5,007	170
[O I] 6,300	10
Hα+[N II] 6,563, 6,548, 6,583	130
[S II] 6,716, 6,731	40

* Due to different slit losses in the source and the flux standard, these values are expected to be accurate to 50% at 5,000 Å, to be systematically too high by ~100% in the blue, and too low by ~100% in the red.

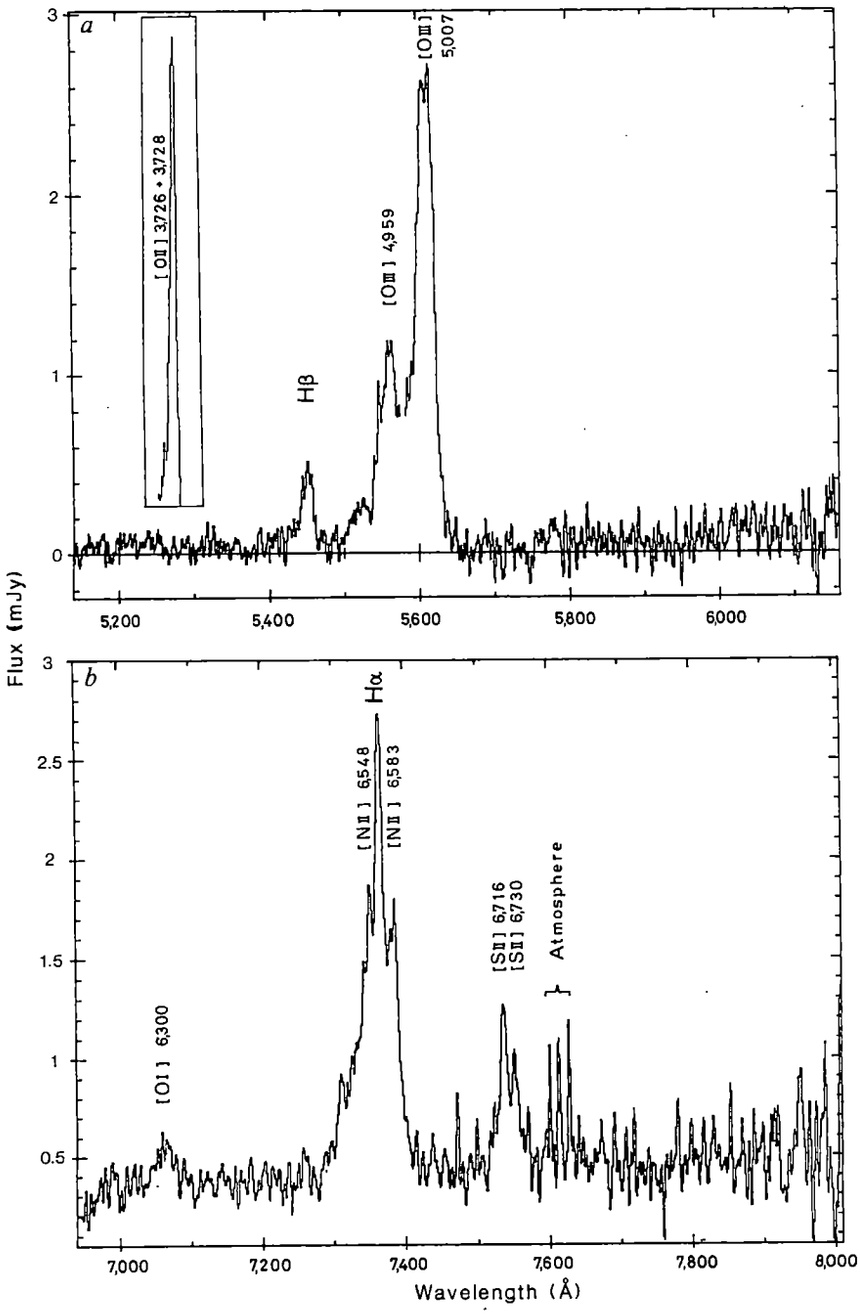


Fig. 2 Two portions of the western nucle Hβ and [O III] 4,959- 3,726+3,728 Å doub The width, complexi line profiles is evident is detected. *b* shows The narrow emission atmospheric A-band a instrumental resolutic tic continuum has n

diagrams discussed by Baldwin *et al.*[9]: two examples are shown in Fig. 3. Clearly, the emission-line spectrum is indistinguishable in line ratios from that of a classical Seyfert galaxy with ionization provided by a central photoionizing source. In this case we can use the various [S II] and [O III] line ratios to derive[10] an electron density $N_e \simeq 300\ \mathrm{cm}^{-3}$ and a temperature $T \simeq 10^4$ K. These values are consistent with our observed line ratios and our null detection of [O III]4,363 Å. The remarkable feature of the emission-line source is therefore not its velocity field, which is typical of other Seyfert galaxies, but its extremely low electron density. We discuss this further below.

The observed Hα luminosity ($\sim 10^{42}$ erg s^{-1}) allows a calculation of the radius of the emitting volume, $r_{H\beta}$, as a function of the filling factor of line-emitting gas, η, to give $r_{H\beta} \simeq 300\ \eta^{1/3}$ pc, and a corresponding upper limit on the source angular size, $\theta_{H\beta} \leqslant 0.2\ h$ arc s, consistent with our observations.

We now outline a self-consistent model of this object. The extreme far-infrared luminosity (unknown for an elliptical galaxy) and the limited photometric evidence suggest the coincidence of the IRAS and the optical they are indeed, then the coincidence size of the line-emitting region and th deduced for the dust source requires the line-emitting gas is of order unity region is ~300 pc, the mass of encl $\sim 10^8\ M_\odot$ (where $M_\odot$ is the solar ma has a range of $\sim 10^4$ km s^{-1}. For this bound requires a mass of $\sim 10^{12}\ M_\odot$ v gas must be expanding. If this expans pressure from a central accreting bla calculated from $L_{Edd} \simeq 10^{46.2}\ (M/10^8$ at the Eddington limit[11]. Our observe $10^{45}\ h^2$ erg s^{-1} then implies a mass of

If the dust and the expanding emis line asymmetry is readily understood[1] the far side (redshifted wing) of the g

Why then does this source have a r broad-line region than do other Sey

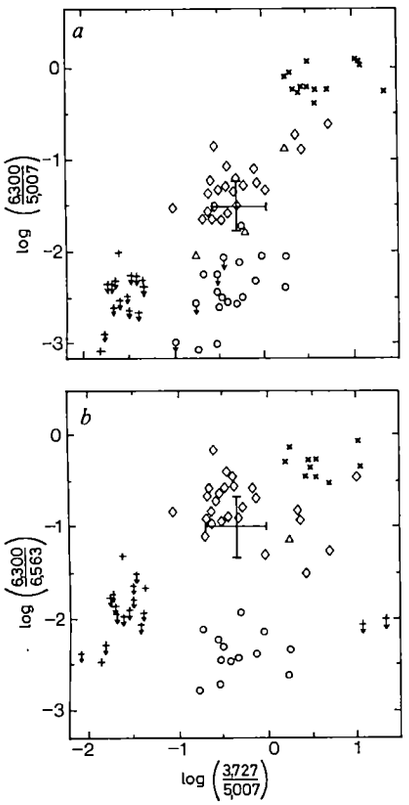


Fig. 3 Diagnostic diagrams showing the relationships between log intensity ratios (see ref. 10): *a*, log (6,300 Å/5,007 Å) versus log (3,727 Å/5,007 Å); *b*, log (6,300 Å/6,563 Å) versus log (3,727 Å/5,007 Å). Plus signs, planetary nebulae; Open circles, normal H II regions; the crosses are thought to be shock-heated galaxies and the diamonds are thought to be photoionized (Seyfert) galaxies. Arrows indicate upper limits. The large cross represents the emission-line source discussed in the text, with the length of the arms indicating a factor of two uncertainty. This source is seen to lie in the Seyfert part of both diagrams.

solution is its location, in transit through the deep potential well of the giant elliptical. Tidal stripping of a spiral galaxy can efficiently remove both the stars and the interstellar medium in such circumstances (this can be estimated from Roche-limit arguments comparing the local potential wells of the two galaxies). There is then no containing medium or potential gradient to resist free expansion of the gas. Similarly, efficient fuelling of the nuclear engine is expected from tidal deformations of the potential well[13,14]. The lack of optical line emission from the compact radio source is also explicable if the accretion rate into the centre of the elliptical is low[15]. This situation will no doubt change dramatically if the Syfert nucleus spirals into the centre of the elliptical.

The disturbed optical isophotes of the elliptical suggest that the interaction has been both violent (perturbations of order unity to the local gravitational potential) and recent. Phase mixing will restore the symmetry of the structure on a timescale D/σ, with D a typical distance and σ a velocity dispersion. For $D \simeq 10$–50 kpc and $\sigma \simeq 400$ km s^{-1}, this time is 10^7–10^8 yr. As the structure becomes symmetric, the galaxy will acquire an extensive, shallow-profile envelope, indicative of a cD galaxy. This system therefore provides an example of the importance of dynamical evolution to radio galaxies and first-ranked cluster ellipticals.

The radio structure of the compact source could be measured by very-long-baseline interferometry. At this redshift, distances of ~1 pc are measurable, allowing a detailed study of a low-frequency radio variable at high physical resolution. I however, the complexity of the system makes it like apparent variability at low radio frequencies is not the source, but is an effect of propagation through the medium of the host galaxy. This hypothesis is amenab observational test, as is the coincidence of the optic line and the far-infrared sources.

The Isaac Newton telescope is operated on the is Palma by the Royal Greenwich Observatory in th Observatorio del Roque de los Muchachos of the I Astrofisica de Canarias. G.G. is a visiting associate Wilson and Las Campanas Observatories, Carnegie of Washington.

Received 4 February; accepted 27 March 1986.

1. Clarke, M. E., Bolton, J. G. & Shimmins, A. J. *Aust. J. Phys.* **19**, 375–387
2. Burbidge, E. M. *Astrophys. J.* **160**, L33–L39 (1970).
3. Grandi, S. A. *Astrophys. J.* **215**, 446–451 (1977).
4. McAdam, W. B. *Proc. astr. Soc. Aust.* **3**, 283–285 (1978).
5. Fanti, C. *et al. Astr. Astrophys. Suppl. Ser.* **45**, 61–75 (1981).
6. Dennison, B. & Condon, J. J. *Astrophys. J* **246**, 91–99 (1981).
7. Perley, R. A. *Astr. J.* **87**, 859–880 (1982).
8. *IRAS Point Source Catalogue* (Jet Propulsion Laboratory, Pasadena, 198
9. Baldwin, J. A., Phillips, M. M. & Terlevich, R. *Publ. astr. Soc. Pacif.* 93,
10. Osterbrock, D. E. *Astrophysics of Gaseous Nebulae*, pp. 97–133 (Freeman 1974).
11. Davidson, K. & Netzer, H. *Rev. mod. Phys.* **51**, 715–766 (1979).
12. Heckman, T. M., Miley, G. K., van Bruegel, W. J. M. & Butcher, H R. 403–418 (1981).
13. Silk, J. & Norman, C. *Astrophys. J.* **247**, 59–76 (1981).
14. Norman, C. & Silk, J. *Astrophys. J.* **266**, 502–515 (1983).
15. Rees, M. J., Begelman, M. C., Blandford, R. D. & Phinney, E. S *Nature* 2

A compact radio source in the nucleus of M87

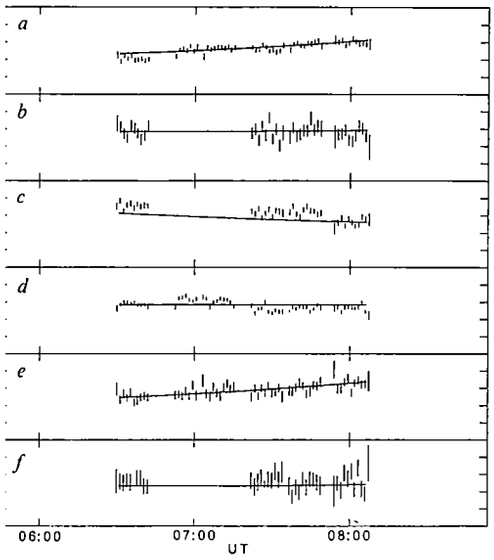
R. E. Spencer & W. Junor

University of Manchester, Nuffield Radio Astronomy Lab Jodrell Bank, Macclesfield, Cheshire SK11 9DL, UK

The nucleus and jet of the giant elliptical galaxy M8 studied at radio wavelengths with resolutions rangi from a few milliarc seconds[1–3]. The higher-resolution that the nucleus consists of a bright central region wi with smoothly decaying brightness pointing in the dire larger-scale radio/optical/X-ray jet. Moreover, these cate that collimation of the jet occurs within 10 m nucleus (that is, within 1 pc of the nucleus, as M87 lies a of 12–20 Mpc[4]). We report here high-resolution, baseline interferometric (VLBI) observations a wavelength, which reveal the existence of a co (≲0.2 marc s) and an associated extended feature (~ again pointing in the same direction as the large-sc observations show that the radio jet is formed on a s $\lesssim 10^{-2}$ pc, thus strengthening the evidence for the pr massive black hole in the nucleus of M87.

Optical observations of the nucleus of M87 (Virgo show a central luminosity spike of size <1 arc s an dispersion which increases towards the centre[5–8]. suggest the presence of a massive compact object $10^9 M_\odot$ (ref. 5), where $M_\odot$ is the solar mass. Acc this object may give rise to intense activity, as d demonstrated by the radio[1]/optical[9]/X-ray[10] jet ex ~30 arc s to the west of the nucleus. The mechanis of the jet (and of extragalactic jets in general) is un its investigation requires the highest available re observe the region where the jet is first produced.

Our observations were made on 8 February 19 VLBI Mk III recording system using 28-MHz band telescopes used were the Max-Planck-Institut fü



ots of correlated flux density on each baseline versus Time on 8 February 1985 for $\lambda = 1.35$ cm observations , Effelsberg (Eff)–Haystack (Hay); *b*, Eff–Owens Valley Hay–Owe; *d*, Eff–Onsala (Ons); *e*, Hay–Ons; *f*, Owe–Ons. Solid lines, model visibilities fitted to the data.

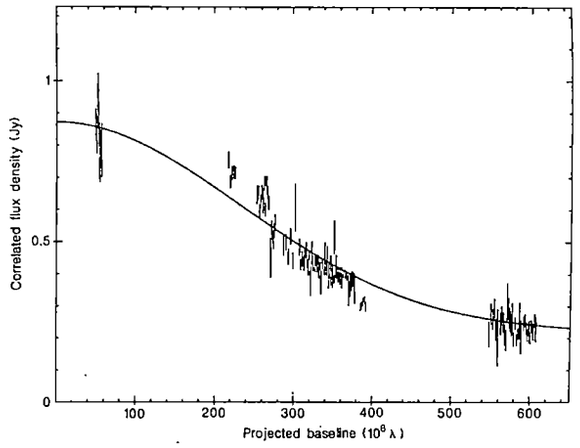


Fig. 2 Plot of the observed amplitudes for M87 against projected baseline length. The solid line superimposed on the data represents the variation of amplitude with projected baseline length for the two-component model derived from model fitting.

MPIfR) 100 m at Effelsberg, FRG, the Onsala Space y 20 m, Sweden, the Haystack Observatory 36 m and ited States the Owens Valley Radio Observatory 0 m, giving a maximum baseline of 6×10^8 λ. M87 ed for 2 hours. Additionally, brief observations of 1611+343 were made; the first as a 'fringe-finder' setting-up of the Mk III analysis package and the librate the fringe amplitudes. The data, recorded on ape, were processed at MPIfR, Bonn, to produce amplitudes and phases (integrated over 16 s). Later, corrected for the individual receiver system tem- nd antenna gains and averaged arithmetically to 80 s. no evidence for a significant systematic decrease of ed fringe amplitude with baseline length for the 1+343, thus indicating that this source was suitable ator. The average flux density of this source was Jy, whereas observations of M87 gave an average flux the shortest baseline (Onsala–Effelsberg, 6.1×10^7 λ) 08 Jy, decreasing with increasing baseline length to Jy for the longest baseline (Effelsberg–OVRO) (see Some idea of the reliability of the calibration can be y noting that, for the calibrator source 1611+343, amplitudes[12] were within 21% of unity and typically closer than this (~8%), showing that this source unresolved. The closure amplitudes for M87 were n 2, reflecting strong resolution effects.

ılar structure of M87 was obtained by fitting the nsform of a model of the sky brightness to the lata using a least-squares method. The model in best vith the observations consisted of an unresolved core s) of flux 0.22 Jy and an extended component in diameter of flux 0.65 Jy, offset from the core by to the west. Figure 2 shows the fit between this model erved amplitudes as a function of projected baseline erved closure phases[12] (Fig. 3) clearly show an offset owing that the source is asymmetric and extended As an independent test of this model, a map of the produced using the 'hybrid mapping' technique of and Wilkinson[12]. This clearly showed a western f the source in spite of the large north–south size of ized beam. Figure 4 shows a contour plot of the map toring beam of diameter 0.15 marc s. This is also a representation of the source structure found by model fitting.

The VLBI observations by Reid *et al.*[2] with a resolution of 8 marc s show that the inner jet lies at a position angle of 288°. The limited hour-angle range of our observations is not sufficient to constrain the position angle of the model to better than about a radian, but the existence of this extension in the same general direction as the larger jet suggests continuity over a size range of more than 5 orders of magnitude, with formation of the jet occurring within <0.2 marc s ($\simeq10^{-2}$ pc) of the nuclear core.

Blandford and Rees[13] suggested that jets may be produced by fluid dynamical processes in high-entropy gas confined by a gravitational potential well. Collimation of the jets would occur via 'nozzles' situated at roughly one scale height from the centre of the well. The potential well could be produced by a dense star cluster or compact massive object. In the former case, we can follow Jenkins[8] and use the optically measured velocity dispersion, ΔV, to estimate the mass M contained within a radius r, that is, $M \simeq 3r(\Delta V)^2/G$ (where G is the gravitational constant). The observations of Stauffer and Spinrad[7] indicate a

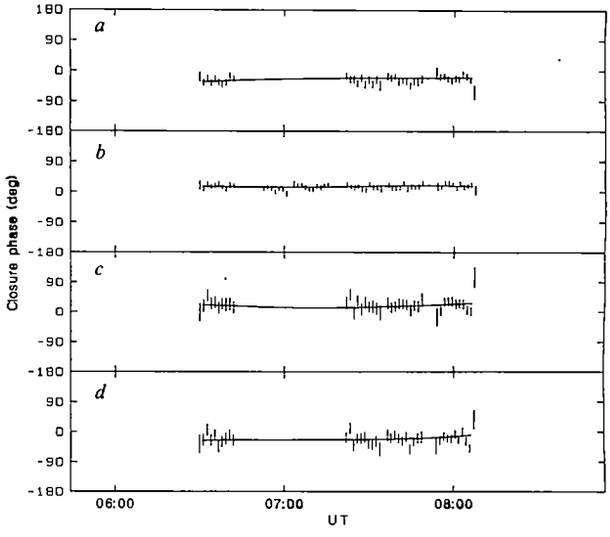


Fig. 3 Plots of closure phase versus Universal Time for 1.35-cm observations of M87. *a*, Eff–Hay–Owe; *b*, Eff–Hay–Ons; *c*, Eff–Owe–Ons; *d*, Hay–Owe–Ons. Solid lines, model closure phases fitted to the data. A symmetric source would give a closure phase of 0°.

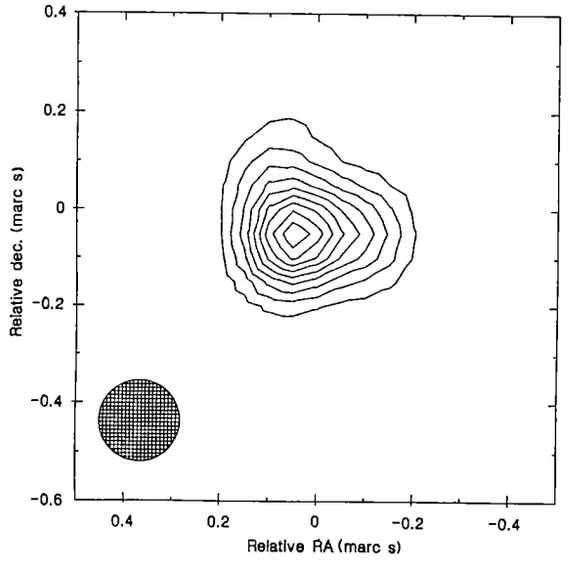


Fig. 4 Contour map of the nucleus of M87 at 1.35 cm wavelength. A circular gaussian restoring beam of diameter 0.15 marc s (shown in the bottom left-hand corner) has been used. Contours are shown at 10, 20, 30, 40, 50, 60, 70, 80 and 90% of the peak brightness of 0.34 Jy per beam.

value of $\sim 400\ km\ s^{-1}$ at 1 arc s from the nucleus, but 'seeing' and any departures from a spherically symmetric gravitational system mean that this is a lower bound on ΔV. Thus, if a star cluster has produced the potential well, then it must contain a mass of at least $10^6\ M_\odot$ within a radius of 10^{-2} pc. The star density within such a cluster would be extremely high (assuming a reasonable mass function for the cluster), and consequently the cluster would have a relaxation time of $\sim 10^5$ yr. This cluster would then evaporate in a time which is brief when compared with the lifetime of the large-scale structure of the source ($\sim 10^8$ yr)[14], suggesting that such a model is unlikely.

Accretion disks orbiting massive black holes have been proposed in order to explain many observed features of active galactic nuclei such as that of M87. In particular, the 'funnels' formed in thick accretion disks can collimate the ejected material to form jets[11]. Such disks may be characterized naturally by Q, the ratio of the outer radius to the inner[15]. Thick accretion disks with large values of Q would produce well-collimated jets. If a massive black hole of mass $5 \times 10^9\ M_\odot$ exists in M87, then, for a funnel size of $<10^{-2}$ pc as suggested by our observations (assuming that the unresolved core encompasses the entire accretion disk), Q must be less than 30. However, much higher values of Q are required for the production of highly collimated jets, such as that of M87.

The radio power in the jet, estimated from the stored energy in the large-scale radio source[14] divided by the lifetime, is $\sim 10^{36}$ W. This amount of power is equal to the Eddington luminosity of accretion onto a black hole of mass $\sim 10^6\ M_\odot$. Our observations indicate a Q value of $\sim 10^3$ for a disk surrounding a black hole of this mass: such an arrangement would be more able to produce a collimated jet. It has been pointed out[11] that if a very massive black hole of mass $5 \times 10^9\ M_\odot$ were present in the nucleus of M87 it would have to be extremely underluminous, and, in view of the uncertainties[16,17] of the existence of such a massive object, a black hole of $10^6\ M_\odot$ surrounded by a thick accretion disk fed from material from a much larger star cluster (>0.1 arc s) is a more likely model. The resolution given by the Space Telescope should enable further studies of this star cluster to be made. Also, the proposed Quasat VLBI satellite may yield more information on the radio jet and perhaps set tighter limits on the massive object in M87.

We thank Paul Burgess and the staff of the participating observatories of MPIfR, Owens Valley, Haystack and Onsala for assistance with the observations, and acknowledge the help of the staff of MPIfR, Bonn, in processing the VLBI tapes. VLBI at Owens Valley Radio Observatory and at the Haystack Observatory of the Northeast Radio Observatory Corporation (NEROC) is supported by the NSF. W.J. thanks SERC for a studentship.

Received 13 January; accepted 4 April 1986.

1. Owen, F. N., Hardee, P. E. & Bignell, R. C. *Astrophys. J.* **239**, L11–L15 (1980).
2. Reid, M. J. *et al. Astrophys. J.* **263**, 615–623 (1982).
3. Charlesworth, M. & Spencer, R. E. *Mon. Not. R. astr. Soc.* **200**, 933–940 (1982).
4. Mould, J., Aaronson, M. & Huchra, J. *Astrophys. J.* **238**, 458–470 (1980)
5. Young, P. J., Westphal, J. A., Kristian, J., Wilson, C. P. & Landaver, F P *Astrophys J* **221**, 721–730 (1978).
6. Sargent, W. L. *et al.* **221**, 731–744 (1978).
7. Stauffer, J. & Spinrad, H. *Astrophys. J.* **231**, L51–L55 (1979).
8. Jenkins, C. R. *Mon. Not. R. astr. Soc.* **192**, 41P–45P (1980).
9. Nieto, J.-L. & Lelièvre, G. *Astr. Astrophys.* **109**, 95–100 (1982).
10. Schreier, E. J., Gorenstein, P. & Feigelson, E. D. *Astrophys. J.* **261**, 42–50 (1982).
11. Begelman, M. C., Blandford, R. D. & Rees, M. J. *Rev. mod. Phys.* **56**, 255–351 (1984).
12. Readhead, A. C. S. & Wilkinson, P. N. *Astrophys. J.* **233**, 25–36 (1978).
13. Blandford, R. D. & Rees, M. J. *Mon. Not. R. astr. Soc.* **169**, 395–415 (1974).
14. Turland, B. D. *Mon. Not. R. astr. Soc.* **170**, 281–294 (1975).
15. Abramowicz, M. A. & Piran, T. *Astrophys. J.* **241**, L7–L11 (1980).
16. Dressler, A. *Astrophys. J.* **240**, L11–L16 (1980).
17. Binney, J. & Mamon, G. A. *Mon. Not. R. astr. Soc.* **200**, 361–375 (1982).

On the depletion of Antarctic ozone

Susan Solomon*, Rolando R. Garcia†, F. Sherwood Rowland‡ & Donald J. Wuebbles§

* National Oceanic and Atmospheric Administration Aeronomy Laboratory, Boulder, Colorado 80303, USA
† NCAR, Boulder, Colorado 80307, USA
‡ Department of Chemistry, University of California, Irvine, California 92717, USA
§ Lawrence Livermore Laboratory, Livermore, California 94550, USA

Recent observations by Farman *et al.*[1] reveal remarkable depletions in the total atmospheric ozone content in Antarctica. The observed total ozone decreased smoothly during the period from about 1975 to the present, but only in the spring season. The observed ozone content at Halley Bay was ~30% lower in the Antarctic spring seasons (October) of 1980–84 than in the springs of 1957–73. No such obvious perturbation is observable in other seasons, or at other than the very highest latitudes in the Southern Hemisphere, and the magnitude of the observed change there far exceeds climatological variability[2]. We present here balloonsonde ozone data[3,4] which show that these ozone changes are largely confined to the region from about 10 to 20 km, during the period August to October. We show that homogeneous (gas phase) chemistry as presently understood cannot explain these observed depletions. On the other hand, a unique feature of the Antarctic lower stratosphere is its high frequency of polar stratospheric clouds[5], providing a reaction site for heterogeneous reactions. A heterogeneous reaction between HCl and $ClONO_2$ is explored as a possible mechanism to explain the ozone observations. This process produces changes in ozone that are consistent with the observations, and its implications for the behaviour of HNO_3 and NO_2 in the Antarctic stratosphere are consistent with observations of those species there, providing an important check on the proposed mechanism. Similar ozone changes are obtained with another possible heterogeneous reaction, $H_2O + ClONO_2$.

Recent satellite observations[6,7] have revealed Antarctic ozone depletions over a very extended region in general agreement with the local ground-based data of Farman *et al.*[1]. It was suggested[1] that the dramatic decreases may arise from a change

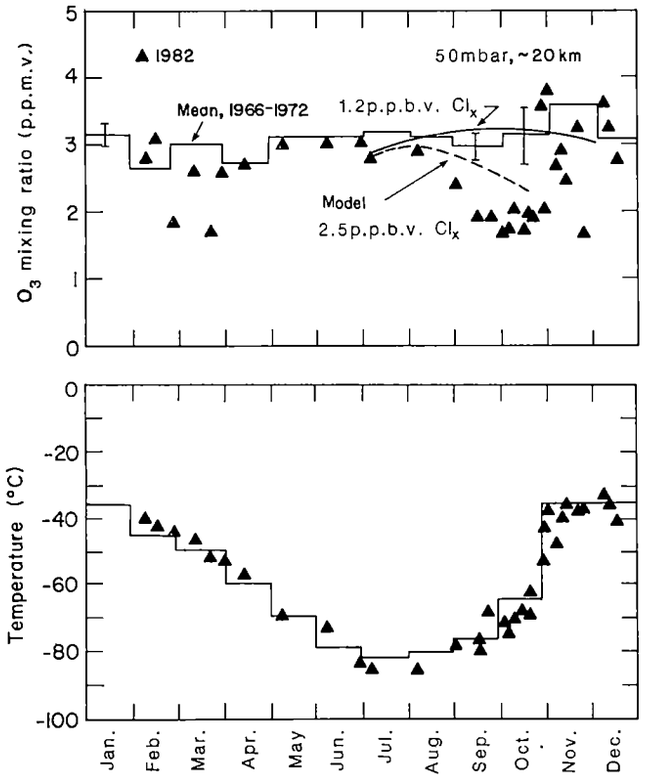


Fig. 1 Temporal behaviour of ozone mixing ratio at the 50-mbar level over Syowa, 69° S, compared with model calculations, for the late 1960s and early 1970s (histogram) and in 1982 (▲)[3,4]. Error bars represent standard deviations of the observations. Temperature observations for the same periods are also shown[3].

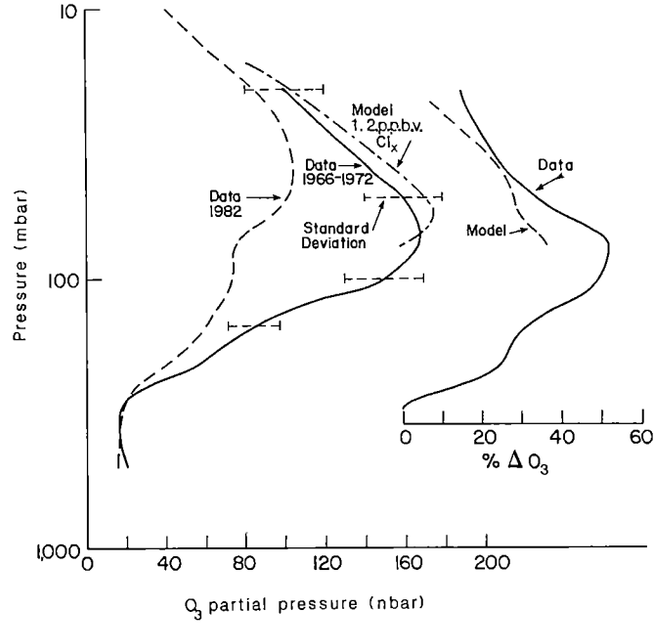


Fig. 2 Vertical profile of the ozone partial pressure observed over Syowa in the late 1960s and early 1970s, and the standard deviation, compared with observations in 1982, for the month of October[3,4]. The model vertical profile in the late 1960s is shown for comparison. Percentage changes of the model and the data for the same time period are also indicated.

in the NO_2/NO ratio due to the reaction

$$ClO + NO \rightarrow Cl + NO_2 \quad (1)$$

(and its relationship to ozone chemistry) which is of particular importance at the very low temperatures characteristic of Antarctic spring (−80 °C). Clearly, this process should be expected to be of increasing importance with time as the chlorofluorocarbon content of the atmosphere increases due to anthropogenic releases. As Farman *et al.*[1] showed, reaction (1) can be effective in perturbing the ratio between NO and NO_2 near 30 km, and hence can influence ozone at those altitudes. However, the bulk of the ozone layer is located well below these levels in Antarctic spring, and so perturbations to ozone near 30 km can have only a modest influence on the total column (see Fig. 2 for a typical ozone profile). Most of the total ozone column at these latitudes and seasons resides near 15–20 km, where the ozone photochemical timescale is of the order of several years[8] using presently accepted homogeneous photochemistry; it is at these low levels that a change must occur for the total column to be perturbed by such a substantial amount. Using a climatology of Antarctic winter temperatures presented by Labitzke[9], we tested the role of reaction (1) in our dynamical-chemical two-dimensional model of the middle atmosphere[10,11]. During the period from 1965 to about 1980 the total chlorine content of the atmosphere is estimated to have increased from about 1.2 to 2.5 p.p.b.v. (parts per 10^9 by volume)[12]. This increase produced a 3–5% change in calculated ozone in Antarctic spring near 30 km, while the calculated changes at 20 km and below were less than 1%. The corresponding change in column-integrated ozone was, therefore, much smaller than that observed.

It is clear that further information regarding the vertical profile of the ozone perturbation is essential to any theory regarding the ozone column change. We present below Antarctic balloonsonde data which show that the observed perturbation is indeed greatest at about 15–20 km, where it develops over a timescale of the order of 2 months. No significant changes in dynamical processes are indicated by the observed temperature structure there[1] (see also Fig. 2), suggesting that the cause of the ozone depletion is chemical rather than dynamical. If the observed depletions are the result of a chemical process, then that process must obey the following constraints: (1) it must be essentially confined to the Southern Hemisphere[2], (2) it must be a strong function of latitude and season; (3) it must produce an acceleration of the ozone chemical loss rate from a timescale of the order of several years to about a month near 15–20 km; and (4) it must increase with time over at least the past 10 yr. Constraint (4) suggests that we examine the photochemistry of atmospheric chlorine.

Chlorine can destroy ozone catalytically in the Earth's atmosphere through the following reactions:

$$Cl + O_3 \rightarrow ClO + O_2 \quad (2)$$

$$ClO + O \rightarrow Cl + O_2 \quad (3)$$

$$\text{Net: } O + O_3 \rightarrow 2O_2$$

At lower altitudes, the following catalytic cycle should also be considered:

$$OH + O_3 \rightarrow HO_2 + O_2$$

$$Cl + O_3 \rightarrow ClO + O_2$$

$$HO_2 + ClO \rightarrow HOCl + O_2$$

$$HOCl + h\nu \rightarrow OH + Cl$$

$$\text{Net: } 2O_3 \rightarrow 3O_2$$

With present chemical schemes, the depletion due to increasing levels of atmospheric chlorine maximizes near 40 km, where much of the available chlorine resides as ClO and Cl. At lower levels, these catalytic free radicals are effectively converted to the 'reservoir' species, HCl and $ClONO_2$, which are inert towards ozone. Both of these reservoirs are expected to be ~100 times

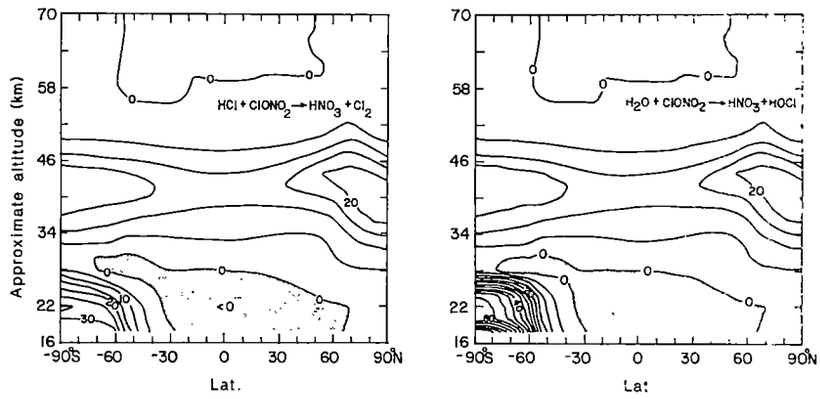


Fig. 3 Contour plot of the calculated change in ozone from the late 1960s to the early 1980s.

more abundant than ClO near 20 km, strongly inhibiting the Cl and ClO densities. Thus, if the densities of the catalytic species in the lower stratosphere are to be appreciably enhanced, both HCl and $ClONO_2$ must be severely reduced. One means of achieving this is the process

$$HCl + ClONO_2 \rightarrow HNO_3 + Cl_2 \quad (4)$$

The Cl_2 will photolyse rapidly in the sunlit atmosphere, producing Cl. Laboratory studies suggest that reaction (4) does not occur rapidly in the gaseous phase, but is much faster on laboratory surfaces[13–15]. To alter the balances between the catalytic species and their reservoirs, which occur on a timescale of a few days, this reaction must proceed in Antarctic spring on a comparable timescale, requiring an equivalent two-body reaction rate of $\sim 2 \times 10^{-14}$ cm^3 s^{-1}. Farman *et al.*[1] suggested that this reaction could be an alternative explanation for their observations, but they did not consider the need for a very rapid rate of this process in order to perturb the equilibrium between ClO and its reservoirs following the return of sunlight. Since reaction (4) is heterogeneous, it presumably takes place only in the presence of stratospheric aerosol, and indeed, the stratospheric aerosol surface area increases substantially in the vicinity of polar stratospheric clouds. These clouds are very common in the cold environment of Antarctic winter and early spring near 10–20 km, where their occurrence frequency is far greater than in the warmer Northern Hemisphere. They are observed predominantly between about July and September, and their presence is closely coupled to the temperature structure. The mean 1-μm aerosol optical depth in Antarctica is about an order of mangitude greater in winter and early spring than it is either during other seasons in Antarctica, or during any season in the Arctic[5], suggesting that reaction (4) should be enhanced specifically during Antarctic winter and spring.

Figure 1 shows balloonsonde temperature and ozone observations from Syowa station, Antarctica (69° S, 39° E), at the 50 mbar (20 km) level[3] (for the complete dataset, see the tape available from Ozone Data for the World). There are several years of historical data covering the period from about 1966 to 1972; the monthly mean of these data is shown as the histogram. In recent years, the station has been operated much less frequently, and virtually the only data available are those of an intense measurement programme carried out in 1982. Chubachi[4] has shown that large changes in ozone were observed there during this period, similar to those obtained by Farman *et al.*[1]. The temperatures obtained at this particular station in 1982 were in general agreement with the historical data, while the ozone exhibited a dramatic departure in September and October.

Figure 1 also shows the results of our model calculations for 1.2 p.p.b.v. and for 2.5 p.p.b.v. including the hypothetical reaction (4) at an equivalent two-body rate as indicated above, imposed uniformly over the region from the model lower boundary at 100 mbar (about 16 km) to 26 km, for latitudes from 61° S to the Pole. The calculated seasonal trend in the unperturbed case, and the timescale of the calculated perturbation, are in reasonable agreement with those observed at the 50 mbar level. Calculated daytime-averaged ClO mixing ratios are about 1.8 and 0.4 p.p.b.v. at this level in September for 2.5 and 1.2 p.p.b.v. total chlorine (respectively), compared with ~0.02 and 0.01 p.p.b.v. when reaction (4) is not considered. Note that although the clouds are expected to be present in July, no ozone perturbation is observed or predicted then. This is consistent with the notion that the perturbation is photochemical, because the sunlight required to drive the photochemistry is present only after about August, when polar night ends at this latitude. Because this chemical perturbation occurs more rapidly (timescale of about a month) than do transport processes in this region (timescale of more than a season), this model can be used to study the problem even at levels near to the lower boundary at 100 mbar without significant bias due to the boundary conditions imposed[10,11]. As mean temperatures rise above −80 °C in October, the polar stratospheric clouds disappear[5]; the ozone remains low throughout October, but returns rapidly to levels much closer to the historical pattern in early November. This recovery is probably dominated by the acceleration of wave-driven transport accompanying the final spring warming of the Antarctic stratosphere, which brings in ozone-rich air from higher altitudes and lower latitudes. Because the behaviour of planetary waves cannot be calculated explicitly with our model, we are unable to simulate this rapid ozone increase.

Figure 2 presents the vertical profile of the October monthly mean of the observed ozone at Syowa for the historical years, as well as that obtained in 1982, along with the associated percentage changes. The observed changes are largest near 15–20 km, where they approach 40%. Figure 2 also shows the vertical profile of ozone obtained in our model for 1.2 p.p.b.v. chlorine and the percentage changes obtained for 2.5 p.p.b.v. when reaction (4) is considered. The vertical profile of the calculated ozone depletions, which agrees well with that observed, is determined by the chemical lifetimes of HNO_3 and $ClONO_2$. The equilibrium between ClO and $ClONO_2$ is established very rapidly if much NO_2 is present, and the ratio between the reservoir and the catalytic agent, ClO, is then so large that it will effectively inhibit the densities of Cl and ClO. Reaction (4) sequesters virtually all of the NO_2 in HNO_3, and the slow photolysis rate of HNO_3 at low levels implies that NO_2 cannot be released quickly enough to appreciably reduce ClO. At higher levels, where the HNO_3 photolysis rate is faster, NO_2 is released more rapidly and $ClONO_2$ formation effectively inhibits the ClO density. Note that large abundances of ClO can occur only if NO_2 levels are extremely low; thus the production of the HNO_3 product in reaction (4) is as important to the overall mechanism as the reactants.

Reaction (4) is not the only possible heterogeneous process capable of perturbing ozone. Indeed, another reaction that is

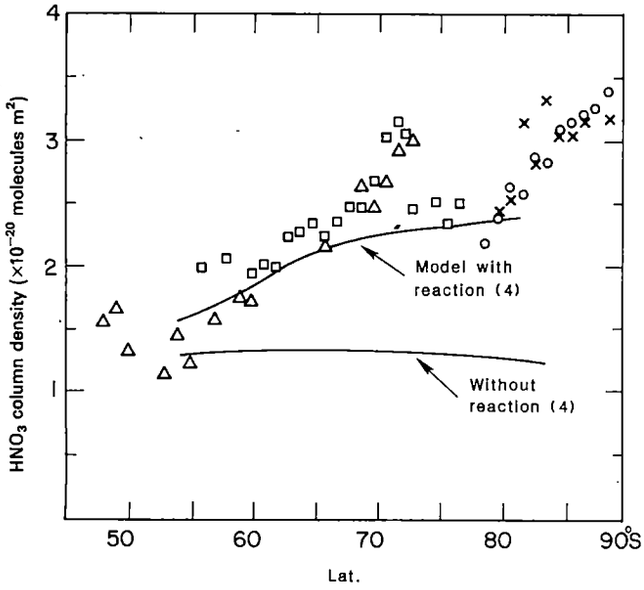


Fig. 4 Latitudinal gradient of total HNO_3 column abundance observed in Antarctic spring[17], along with model calculations with and without consideration of reaction (4). □, 17 November 1978; ○, 20 November 1978; ×, 21 November 1978; △, 27 November 1978.

similar to reaction (4) in its effects on the balance between ClO and its reservoirs, as well as in its effects on HNO_3 (if it proceeds at an equivalent two-body rate of $\sim 1 \times 10^{-17}$ cm^3 s^{-1}) is

$$H_2O + ClONO_2 \rightarrow HNO_3 + HOCl \quad (5)$$

Laboratory studies show that this process also occurs heterogeneously[15]. Figure 3 shows a contour plot of the percentage ozone changes calculated between about 1965 and the early 1980s for both reactions (4) and (5). The high-altitude changes and their structure are due to standard chemistry[8], but should be considered upper limits because of the neglect of the important effects of coupled temperature and CO_2 perturbations[16]. The calculated latitudinal structure in the additional depletions in the Antarctic lower stratosphere is due to the assumption that the clouds occur only poleward of about 60° S, confining the perturbation to high latitudes and low altitudes. A substantial gradient in mean cloud intensity (and hence in ozone depletion) probably occurs over the latitude range 60–90° S because of the strong gradient in temperature over this region, but this has not been included in the present calculations. In the case of reaction (5), the possible production of HOCl leads to hydrogen radical formation, and thus produces even greater ozone depletions than those due to chlorine free radicals alone. The efficiency of reaction (5) in ozone destruction is thus critically dependent on HOCl as a reaction product.

Because HNO_3 is a product of both reactions (4) and (5), observations of odd nitrogen species provide an independent check on the feasibility of these processes. Figure 4 presents HNO_3 column abundance measurements from Antarctica in November[17], along with model-calculated column abundances with and without consideration of reaction (4); reaction (5) produces similar results. Reaction (4) significantly improves the agreement between the model and the observations. Examination of the chemistry and transport of HNO_3 at high latitudes in Northern Hemisphere winter by Austin *et al.*[18] reveals other evidence for an additional source of HNO_3 beyond presently accepted photochemistry, and points out that it is likely to be heterogeneous. This enhancement in HNO_3 should be accompanied by a decrease in other forms of active nitrogen (such as NO_2 and N_2O_5) in the lower stratosphere below about 25 km where the HNO_3 photolysis rate is slow, as discussed above with regard to the vertical extent of the ozone depletion. This implies that the total NO_2 column, and its diurnal variation in the spring, should be smaller in the Antarctic than in the Arctic due to the far greater frequency of polar stratospheric clouds in the Antarctic. McKenzie and Johnston's[19] observations in September at 78° S display a sunset total NO_2 column of ~ 1.5–2×10^{15} cm^{-2}, with a diurnal variation of $< 0.5 \times 10^{15}$, while those of Noxon *et al.*[20] in March at 71° N suggest a sunset total abundance of 3–3.5×10^{15}, and a much larger diurnal variation of about $\sim 2 \times 10^{15}$, consistent with this suggestion.

Reaction (4) is certainly very speculative, and has been modelled only crudely here. However, it is consistent with all of the available features of the observed depletion of ozone, namely its vertical, latitudinal and temporal structure, as well as with observations of HNO_3 and NO_2. The process responsible for Antarctic ozone depletion is probably heterogeneous, and related to odd nitrogen chemistry. In view of these considerations, as well as the lack of direct laboratory data regarding the kinetics and mechanism of reaction (4), we emphasize that other possible heterogeneous reactions, such as $H_2O + ClONO_2$ and $H_2O + N_2O_5$, should also be the subject of laboratory and atmospheric studies. Further observations of polar stratospheric clouds, and in particular, their occurrence frequency, are also badly needed. If the mean temperatures in Antarctic spring decrease (or have perhaps already decreased) by even 1 or 2 °C, it is likely that the cloud frequency will increase, with associated changes in the aerosol surface area and rates of heterogeneous processes. Observations of ClO, or the more easily observable species, NO_2, near Antarctic polar stratospheric clouds would be of considerable value in evaluating the mechanism responsible for the ozone depletion there. If heterogeneous reactions are indeed the cause of the Antarctic ozone phenomenon, these large depletions will be confined essentially to this region in the near future unless there is a very large increase in stratospheric aerosol.

We thank R. J. Cicerone and S. C. Liu for helpful comments. Discussions with J. Angell were critical to the development of this work.

Received 13 January; accepted 21 March 1986.

1. Farman, J. C., Gardiner, B. G. & Shanklin, J. D. *Nature* **315**, 207–210 (1985).
2. Angell, J. K. & Korshover, J. *Mon. Weath. Rev.* **111**, 901–921 (1983).
3. *Ozone Data Wld*, **25**, 192–199 (1984).
4. Chubachi, S. *Mem. natn. Inst. pol. Res., spec. Iss.* **34**, 13–19 (1984).
5. McCormick, M. P. *Adv. Space Res.* **2**, 73–86 (1983).
6. Heath, D. F., Bhartia, P. & Schlesinger, B. *EOS* **66**, 1009 (1985).
7. Krueger, A. J. & Stolarski, R. S. *EOS* **66**, 838 (1985).
8. Solomon, S., Garcia, R. R. & Stordal, F. *J. geophys. Res.* **90**, 12981–12990 (1985).
9. Labitzke, K. *Phil. Trans. R. Soc.* **296**, 7–18 (1980).
10. Garcia, R. R. & Solomon, S. *J. geophys. Res.* **88**, 1379–1400 (1983).
11. Solomon, S. & Garcia, R. R. *J. geophys. Res.* **89**, 11633–11644 (1984).
12. WMO/NASA *The Stratosphere* (in the press).
13. Molina, L. T., Molina, M. J., Stachnik, R. A. & Tom, R. D. *J. phys. Chem.* **89**, 3779–3781 (1985).
14. JPL/NASA *Chemical Kinetics and Photochemical data for Use in Stratospheric Modeling* (JPL 85-37, 1985).
15. Rowland, F. S., Khwaja, H. & Sato, H. *J. Phys. Chem.* (in the press).
16. Groves, K. S. & Tuck, A. F. *Q. Jl R. met. Soc.* **106**, 125–142 (1980).
17. Williams, W. J., Kosters, J. J. & Murcray, D. G. *J. geophys. Res.* **87**, 8976–8980 (1982).
18. Austin, J. A., Garcia, R. R., Russell, J. M., Solomon, S. & Tuck, A. F. *J. geophys. Res.* **90**, 5477–5485 (1986).
19. McKenzie, R. L. & Johnston, P. V. *Geophys. Res. Lett.* **11**, 73–75 (1984).
20. Noxon, J. F., Henderson, W. R. & Norton, R. B. *J. geophys. Res.* **88**, 5240–5248 (1983).

Reductions of Antarctic ozone due to synergistic interactions of chlorine and bromine

Michael B. McElroy, Ross J. Salawitch, Steven C. Wofsy & Jennifer A. Logan

Harvard University, Center for Earth and Planetary Physics, 29 Oxford Street, Cambridge, Massachusetts 02138, USA

The vertical column density of ozone observed in October over Antarctica has fallen precipitously over the past 10 yr. The concentration at Halley Bay (76° S 27° W), expressed conventionally in Dobson units (DU) (1 DU = 10^{-3} atmos. cm = 2.7×10^{16} molecules cm^{-2}), has dropped from about 300 DU in 1975 to <200 DU in 1984 (ref. 1). Values in 1985 were even lower, comparable with the lowest values recorded anywhere on Earth[2]. We suggest here that the loss of O_3 in Antarctica may be attributed to catalysis of O_3 recombination by a scheme in which the rate-limiting step is defined by the reaction $ClO + BrO \rightarrow Cl + Br + O_2$. Concentrations of NO_2 must be low and heterogenous reactions involving particles in the polar stratospheric clouds must be an important element of the relevant chemistry. Industrial sources make important contributions to the contemporary budgets of both BrO and ClO and are likely to grow significantly in the future.

The decline in O_3 at Halley Bay does not simply reflect a local anomaly. It extends over at least 15° in latitude, according to measurements by the Total Ozone Mapping Spectrometer (TOMS) on Nimbus 7 (ref. 3). It is associated generally with air within the polar vortex, in a region offset some distance to the east with respect to the pole. The drop in O_3 begins in early September. The rate of decline in September 1983 averaged ~0.6% per day (ref. 3). The largest reductions in O_3 occur between 14 and 24 km, as evidenced by soundings from Syowa (69 °S, 40° E)[2,4]. The challenge for models is to account for the rate of change in September, and to rationalize the surprisingly short time constant implied by the observational data. It is particularly difficult to explain the large reductions observed at low altitude. A complete theory should account for the trend since 1975.

Several profiles adopted from ozonesonde data taken at Syowa[2,4] are shown in Fig. 1. Curve *a* reflects the mean data for October before 1975. Curve *b* shows the average observed for the winter of 1982, while curves *c*–*e* illustrate conditions with much lower O_3 observed in October of 1982 and 1983. Temperatures were low for cases *c*–*e*, suggesting a significant contribution to the overhead column at these times due to air drawn from within the vortex. As noted above, reductions in O_3 are most striking near the peak at 70 mbar.

Ozone may be removed either by reaction with O,

$$O + O_3 \rightarrow 2O_2 \quad (1)$$

or by reaction with itself,

$$O_3 + O_3 \rightarrow 3O_2 \quad (2)$$

These reactions proceed, for the most part, by indirect paths, catalysed by trace quantities of HO_x, Cl_x, Br_x and NO_x. Reaction (1) can occur through[5–8]

$$\begin{aligned} Cl + O_3 &\rightarrow ClO + O_2 \\ ClO + O &\rightarrow Cl + O_2 \end{aligned} \quad (3)$$

$$\begin{aligned} Br + O_3 &\rightarrow BrO + O_2 \\ BrO + O &\rightarrow Br + O_2 \end{aligned} \quad (4)$$

and

$$\begin{aligned} NO + O_3 &\rightarrow NO_2 + O_2 \\ NO_2 + O &\rightarrow NO + O_2. \end{aligned} \quad (5)$$

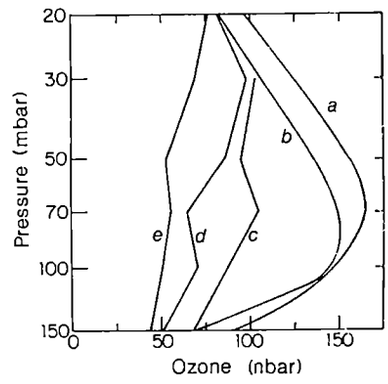


Fig. 1 Vertical distributions of ozone at Syowa (69° S, 40° E). *a*, An average of 26 soundings made between 1968 and 1974, in October. The average column density recorded during this period was 337 DU. *b*, An average of soundings made in June, July and August, 1982; the average ozone column was 320 DU. *c*, *d* and *e* were measured on 23 September 1982, 14 October, 1982, and 17 October, 1983; the ozone columns were 256, 241 and 217 DU, respectively. The mean ozone column for October 1982 was 236 DU; 260 DU for October 1983.

Reaction (2) can proceed by[9,10]

$$\begin{aligned} OH + O_3 &\rightarrow HO_2 + O_2 \\ HO_2 + O_3 &\rightarrow OH + 2O_2 \end{aligned} \quad (6)$$

$$\begin{aligned} Br + O_3 &\rightarrow BrO + O_2 \\ Cl + O_3 &\rightarrow ClO + O_2 \\ BrO + ClO &\rightarrow Br + Cl + O_2, \end{aligned} \quad (7)$$

$$\begin{aligned} OH + O_3 &\rightarrow HO_2 + O_2 \\ HO_2 + ClO &\rightarrow HOCl + O_2 \\ h\nu + HOCl &\rightarrow OH + Cl \\ Cl + O_3 &\rightarrow ClO + O_2, \end{aligned} \quad (8)$$

and

$$\begin{aligned} Cl + O_3 &\rightarrow ClO + O_2 \\ ClO + ClO &\rightarrow 2Cl + O_2 \end{aligned} \quad (9)$$

If we assume that the change in Antarctic O_3 should be attributed to effects of chlorine, we can estimate the maximum possible impact from reactions (3)–(9), as follows.

Assume that Cl_x is present mainly as ClO and consider a profile for ClO corresponding to a total stratospheric chlorine abundance of 3.0 p.p.b. (parts per 10^9), as would be appropriate for 1983. The associated (maximum) rate for removal of O_3 by reactions (3)–(5) is too small by an order of magnitude to account for the reductions implied at lower altitudes by the perturbed profiles of Fig. 1. The abundance of O at low Sun angles characteristic of high southern latitudes in September is insufficient to permit an important role for rection (1) below 26 km.

No such restriction applies for reaction (2). In contrast to reaction (1), reaction (2) allows for significant loss of O_3 near 70 mbar. If we assume that chlorine and bromine are present primarily in the form of the reactive oxides, ClO and BrO, and consider concentrations of ClO and BrO of 3 p.p.b. and 25 p.p.t. (parts per 10^{12}) at high altitude, we find that the column abundance of O_3 could fall by >2% per day, a rate significantly larger than observed by TOMS[3].

High concentrations of ClO and BrO in the lower stratosphere require that the abundance of NO_2 be small. At mid latitudes the concentrations of NO_2 are high enough for ClO and BrO

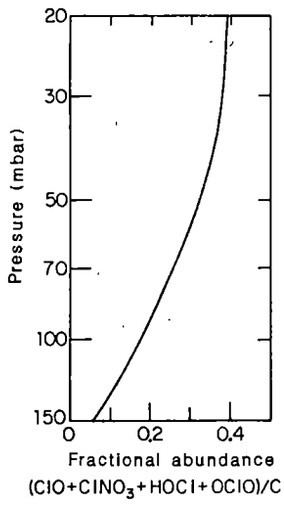


Fig. 2 Vertical distribution of the fraction of Cl_x present as ClO_x ($ClO_x = ClO + ClNO_3 + HOCl + OClO$). The vertical profile of Cl_x was calculated at 30° S using a one-dimensional model, and Cl_x was estimated at 45°, 60° and 80° using slant mixing surfaces[25–27]. The fractional abundances of ClO_x were then calculated for the four latitudes using observed concentrations of ozone and a solar declination of 0°. The results of the four calculations are shown averaged along slant mixing surfaces approximately parallel to the tropopause. All calculations employed the rate constants recommended in ref. 22.

to be efficiently converted to $ClNO_3$ and $BrNO_3$ respectively. The abundance of NO_2 is very low at high latitudes in winter[11–14] and this is usually attributed to an influence of heterogeneous chemistry[15,16] involving particles in clouds which form during the polar night[17,18]. A plausible scheme is

$$NO_2 + O_3 \rightarrow NO_3 + O_2 \quad (10)$$

$$NO_3 + NO_2 + M \rightarrow N_2O_5 + M \quad (11)$$

and

$$N_2O_5 + H_2O\ (\text{particle}) \rightarrow 2HNO_3 \quad (12)$$

Removal of $ClNO_3$ is possible also by[19]

$$ClO + NO_2 + M \rightarrow ClNO_3 + M \quad (13)$$

$$ClNO_3 + H_2O\ (\text{particle}) \rightarrow HOCl + HNO_3 \quad (14)$$

or by

$$HCl + ClNO_3 + \text{particle} \rightarrow HNO_3 + Cl_2 + \text{particle} \quad (15)$$

Reactions (12), (14) and (15) have been observed on the w of reaction vessels in the laboratory[20–22]. Reaction (15 unlikely to occur in the atmosphere in that it requires an inte tion of two minor species present simultaneously on parti composed primarily of H_2O and H_2SO_4.

The high-latitude stratosphere is coupled in autumn to lc latitudes by mixing along slant surfaces oriented roughly par to the tropopause[23,24]. The average abundance of ClO_x (defi as $ClO + ClNO_3 + HOCl + OClO$) relative to HCl along tl surfaces may be estimated using one-dimensional model stu as a guide[25–27]. A mean profile, obtained from an average al the slant mixing surfaces, is given in Fig. 2. This should pro an appropriate representation of air entering the polar vor We expect the abundances of ClO_x and BrO_x (mostly Br $BrNO_3$) to remain essentially constant throughout the p night. A combination of $ClNO_3$ formed by reaction (13), H produced by reaction (14) and OClO derived from

$$ClO + ClO \rightarrow OClO + Cl$$

and

$$BrO + ClO \rightarrow OClO + Br$$

should represent the dominant forms of reactive chlorine. potential importance of reaction (17) in this context was rec ized first by Tung *et al.*[28].

Consider two possibilities as the Sun returns to the h latitude stratosphere in early spring: (I) Suppose that reac chlorine is present mainly as OClO. (The dominant sourc reaction (17).) (II) Suppose that HOCl is more abundant. (implies significant production by the heterogeneous reac (14).) In either case BrO is likely to be the dominant forr reactive bromine. Assume that the initial abundance of] (defined as all forms of reactive nitrogen other than HNO less than that of ClO_x.

In case I, OClO provides an immediate source of ClO. concentration of O_3 begins to fall, as illustrated in Fig Removal is predominantly by reaction (7). Reduction in and high concentrations of ClO and BrO, persist until the l of NO_y is comparable to that of ClO_x. Recovery of NC regulated by decomposition of HNO_3. The associated time stant for NO_y is about 10 days in mid-September.

In case II, photolysis of HOCl provides an immediate so of OH, in addition to Cl. If the subsequent chemistry dominated by gas-phase processes, OH would react with H leading to rapid growth in NO_y with conversion of Cl $ClNO_3$, short-circuiting the potential effect of reaction (7) sink for odd oxygen. A continuing role for reaction (7) req that heterogeneous chemistry maintain a high ratio of Cl $ClNO_3$. We assume that reaction (14) proceeds with

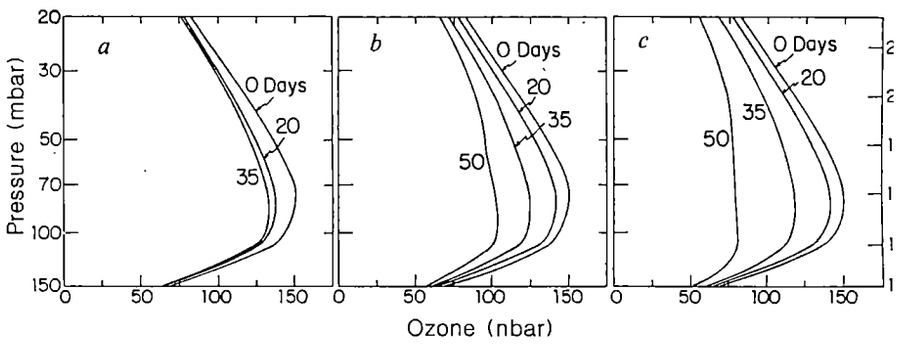


Fig. 3 Vertical distribution of ozone calculated for 20, 35 and 50 days after the end of polar night. The initial distribution of ozone was taken from Fig. 1*b* (320 DU). Chlorine and bromine abundances were 3.3 p.p.b. and 25 p.p.t. respectively, appropriate for 1985 (ref. 30). The initial fraction of Cl_x present as ClO_x was taken from Fig. 2; initial concentrations of NO_y were low, less than ClO_x. Calculations allowed for the diurnal variation of insolation, and ozone values were updated daily. Results are given for latitude 80° S. *a*, Results for case I: ClO_x was assumed to be present as OClO at the end of polar night, and the model allowed for gas-phase process only. Results for 50 days are very similar to those for 35 days. *b*, Results for case IIa in which ClO_x was assumed to be present initially HOCl, and the heterogeneous reactions (12) and (14) were allowed to proceed at a rate of $1.0 \times 10^{-5}\ s^{-1}$. *c*, Results for case IIb, with a fast rate for reactions (12) and (14), $5.0 \times 10^{-5}\ s^{-1}$. At 80° S, days 20, 35 and 50 correspond to 15 September, 1 October and 15 October. Mod results indicate similar reductions in ozone one calendar week earlier at 75° S, two weeks earlier at 70° S.

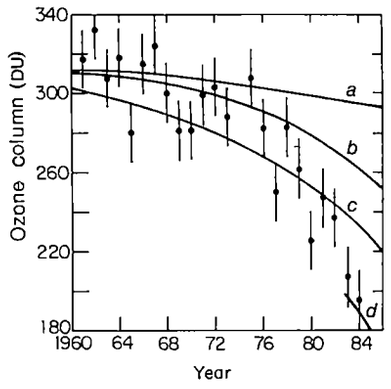


Fig. 4 Trend in the ozone column over Antarctica from 1960 to 1985. The circles correspond to October mean values from Halley Bay (76° S)[1]. Results are given for 80° S, and assume an initial ozone column of 320 DU for each model year (see Fig. 3). The abundance of Cl_x was taken to be 1.0 p.p.b. in 1960, 2.1 p.p.b. in 1975 and 3.3 p.p.b. in 1985 (ref. 30); the abundance of Br_x was held constant at 25 p.p.t. *a–c*, Results for case I, IIa and IIb respectively, for day 50. *d*, Results for case IIb after 60 days. This curve illustrates the dramatic acceleration in O_3 loss which occurs if the aerosol burden persists.

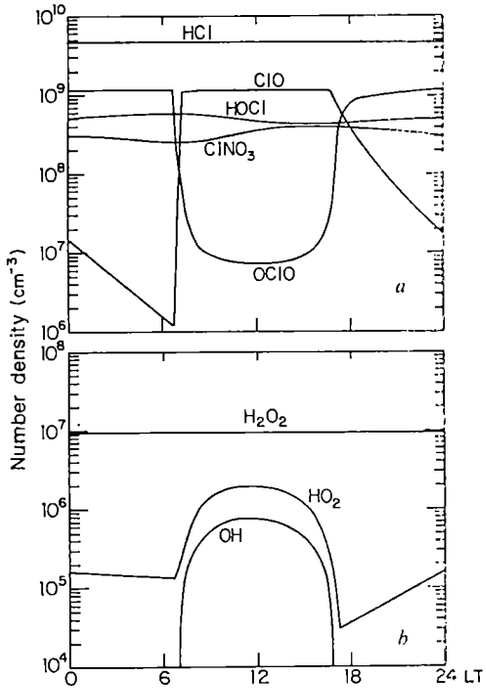


Fig. 5 Diurnal variations of Cl_x (*a*) and HO_x (*b*). Results are shown for case IIa, for day 20, 80° S latitude at 75 mbar (~16 km). The atmospheric density was 2.92×10^{18} molecules cm^{-3}.

accommodation coefficient of 2.5×10^{-2} and select an aerosol surface area appropriate for an extinction coefficient of 2×10^{-3} km^{-1}. The associated reaction rate constant is 1×10^{-5} s^{-1}. Extinction coefficients of 2×10^{-3} km^{-1} were typical for September in the Antarctic stratosphere before 1982 (ref. 17). Optical depths were much larger in 1983 (ref. 29)and 1984 following the arrival of the aerosol cloud associated with eruption of El Chichón (M. P. McCormick, personal communication). To account for additional aerosol loading, calculations were carried out also with a larger rate for reaction (14), 5×10^{-5} s^{-1}. We shall refer to the low- and high-aerosol models as IIa and IIb. The polar clouds dissipate typically in late September when the aerosol burden is low[17]. They persisted longer in 1983 and 1984 when the aerosol burden was higher. The results in Fig. 3*b*, *c* should be interpreted accordingly.

The calculations summarized in Fig. 3 are appropriate for a latitude of 80° S. Sunrise at 80° S occurs at the end of August. Results for Syowa would be similar but the calendar date would be about 2 weeks earlier. With case I (Fig. 3*a*) there is a significant drop in O_3 over the first 2 weeks. The decline is slow thereafter, however, limited by the growth of NO_y and associated immobilization of ClO_x as $ClNO_3$. The drop in O_3 persists longer if we allow for heterogeneous removal of $ClNO_3$ and N_2O_5 (Fig. 3*b*, *c*). The reduction at the peak, primarily due to reaction (7), is as much as 0.5% per day over the initial 30-day period if the rate constant for reaction (14) is as large as 5×10^{-5} s^{-1}. The reduction exceeds 2% per day in the subsequent 15-day period, more than enough to account for the rate of decline observed by TOMS in 1983 (ref. 2). The faster decline at the later time is attributed to an increase in the abundance of ClO_x due to production of Cl by reaction of OH with HCl. If we allowed for heterogeneous removal of N_2O_5 and $ClNO_3$, results for case I would agree with those for case II for times later than about 30 days.

Trends as a function of time are shown for total column O_3 in Fig. 4. The data, reflecting mean values for October at Halley Bay, are from ref. 1. As with Fig. 3, the model results are for a latitude of 80° S and are intended to illustrate the reduction expected 50 days after the end of polar night. The decline in O_3 would commence at the beginning of August in more northerly regions of the vortex. Effects would spread into the interior as the Sun advanced. The actual situation could be complicated by effects of transport, and precise comparison of model and observational data is consequently difficult. The model results in Fig. 4 should be approximately applicable for mean conditions within the vortex at the beginning of October.

The model assumed an initial value of 320 DU for O_3. The predicted year to year decline in O_3 at 50 days reflects the assumed growth of total chlorine, 4.7% yr^{-1} since 1973 (ref. 30). Case I, with only homogeneous processes considered, depicts a relatively small reduction in O_3, about 25 DU in 1984. Reductions with case IIb should be as large as 100 DU for the same year. An intermediate effect is suggested for case IIa, 60 DU.

It is tempting to attribute the large reductions in O_3 observed in 1983 and 1984 to effects, both direct and indirect, of the aerosols from El Chichón. A reduction of 15% in O_3 was observed at northern mid-latitudes in winter and spring of 1983 (ref. 31), coincident with the time of maximum aerosol loading[32]. The reduction then could be associated with heterogeneous processes involving aerosols, enhanced perhaps by chlorine added to the stratosphere by the eruption[33]. These effects could have an impact on Antarctic O_3 in addition to the ClO + BrO contribution emphasized here and could contribute, at least in part, to the low values of O_3 observed since 1982.

The recombination scheme proposed here for O_3 is nonlinear, in the sense that the mechanism depends on the abundance, persistance and height distribution of aerosols. The rate-limiting step, reaction of ClO with BrO, involves a product of concentrations of two trace species each of which may be changing in time. The abundance of ClO is set mainly by decomposition of industrial sources of organic chlorine, notably $CFCl_3$, CF_2Cl_2 and CH_3CCl_3 (ref. 5). The concentration of inorganic chlorine has increased steadily since 1960 (ref. 30). We assumed that the growth rate for inorganic bromine was comparatively small, and used a fixed concentration of 25 p.p.t at high latitude in all calculations (ref. 27 and refs therein). There are reasons, however, to believe that the concentration of bromine may be increasing. Increases in production and use of CH_3Br, a fumigant, and CF_3Br and CF_2ClBr, employed extensively as fire extinguishers, are likely to have an important role in the future

course of stratospheric Br. Prospective levels could rise to as high as 100 p.p.t. (ref. 27).

The surprising results from Antarctica emphasize the potential importance and complexity of processes in the high-latitude stratosphere. Figure 5, for example, illustrates the diurnal variation expected for some of the dominant forms of Cl_x and HO_x. Observations are few and there is a need for additional data. Measurements of the abundance of aerosols, ClO, OClO, HOCl, BrO, NO_2 and HNO_3 in winter and early spring would be valuable and would serve as a check on the model developed here.

We thank R. Stolarski for informative discussions of the TOMS results. This work was supported by NSF grant ATM-84-13153 and by NASA grant NAGW 731 to Harvard University.

Received 21 January; accepted 27 March 1986.

1. Farman, J. C., Gardiner, B. G. & Shanklin, J. D. *Nature* **315**, 207–210 (1985).
2. *Ozone data for the World*, Indexes 6, 14 and 19 (Atmospheric Environment Service, Toronto, Canada, 1985).
3. Stolarski, R. S. *et al. Nimbus 7, SBUV/TOMS Measurement of Antarctica Ozone* (submitted).
4. Chubachi, S. *Mem. natn. Inst. Pol. Res. (Tokyo), Spec. Iss.* No. 34, 13–19 (1984).
5. Molina, M. J. & Rowland, F. S. *Nature* **249**, 810–812 (1974).
6. Wofsy, S. C., McElroy, M. B. & Yung, Y. L. *Geophys. Res. Lett.* **2**, 215–218 (1975).
7. Crützen, P. J. *Q. Jl R. met. Soc.* **96**, 320–325 (1970).
8. Johnston H. S. *Science* **173**, 517–522 (1971).
9. Bates, D. R. & Nicolet, M. *J. geophys. Res.* **55**, 301–327 (1950).
10. Yung, Y. L., Pinto, J., Watson, R. T. & Sander, S. P. *J. atmos. Sci.* **37**, 339–353 (1980).
11. Noxon, J. F. *Science* **189**, 547–549 (1975).
12. Noxon, J. F. *Geophys. Res. Lett.* **5**, 1021–1022 (1978).
13. Noxon, J. F., Henderson, W. R. & Norton, R. B. *J. geophys. Res.* **88**, 5240–5248 (1983).
14. McKenzie, R. L. & Johnston, P. V. *Geophys. Res. Lett.* **11**, 73–75 (1984).
15. Wofsy, S. C. *J. geophys. Res.* **83**, 364–378 (1978).
16. Evans, W. J. F., McElroy, C. T. & Galbally, I. E. *Geophys. Res. Lett.* **12**, 825–828 (1985).
17. McCormick, M. P., Steele, H. M., Hamill, P., Chu, W. P. & Swissler, T. J. *J. atmos. Sci.* **39**, 1387–1397 (1982).
18. Steele, H. M., Hamill, P., McCormick, M. P. & Swissler, T. J. *J. atmos. Sci.* **40**, 2055–2067 (1983).
19. Rowland, F. S. *Pap. at NASA Meet. Current Issues in our Understanding of the Stratopshere and the Future of the Ozone Layer* (Feldafing, FRG, 1984).
20. Atkinson, R., Tuazon, E. C., MacLeod, H., Aschmann, S. M. & Winer, A. M. *Geophys. Res. Lett.* **13**, 117–120 (1985).
21. Molina, L. T., Molina, M. J., Stachnik, R. A. & Tom, R. D. *J. phys. Chem.* **89**, 3779–3781 (1985).
22. DeMore, W. B. *et al. Chemical Kinetics and in Stratospheric Modelling Evaluation* No. 7 (Jet Propulsion Laboratory, Pasadena, JPL 85-37, 1985).
23. List, R. J. & Telegadas, K. *J. atmos. Sci.* **26**, 1128–1136 (1969).
24. Telegadas, K. & List, R. J. *Science* **190**, 882–883 (1975).
25. Logan, J. A., Prather, M. J., Wofsy, S. C. & McElroy, M. B. *Phil. Trans. R. Soc.* **290**, 187–234 (1978).
26. Wofsy, S. C. & Logan, J. A. in *Causes and Effects of Stratospheric Ozone Reduction: An Update*, 167–205 (National Academy of Sciences, Washington DC, 1982).
27. Prather, M. J., McElroy, M. B. & Wofsy, S. C. *Nature* **312**, 227–231 (1984).
28. Tung, K. K., Ko, M. K. W., Rodriguez, J. M. & Sze, N. D. *Nature* (submitted).
29. Hofman, D. J. & Rosen, J. M. *Geophys. Res. Lett.* **12**, 13–16 (1985).
30. *WMO/NASA Atmospheric Ozone: Assessment of our Understanding of the Processes Controlling its Present Distribution and Changes* (in the press).
31. Angell, J. K., Korshover, J. & Planet. W. G. *Mon. Weath. Rev.* **113**, 641–646 (1985).
32. Hofmann, D. J. & Rosen, J. M. *J. geophys. Res.* **89**, 4883–4890 (1984).
33. Mankin, W. G. & Coffey, M. T. *Science* **226**, 170–172 (1984).

Temporal evolution of nitrogen compounds in Swedish precipitation since 1955

H. Rodhe & M. J. Rood*

Department of Meteorology, University of Stockholm, S-106 91 Stockholm, Sweden

Nitrate (NO_3^-) and ammonium (NH_4^+) ions are important determinants of the ionic strength and *p*H of precipitation[1]. The deposition of these ions on vegetation and on the ground also constitutes a significant source of nutrients for plants. This is particularly the case in polluted regions, for example, Europe, where the deposition of nitrogen compounds is enhanced[2]. There are indications (for example, increased run-off of nitrogen[3]) that forests in some parts of Europe have reached saturation levels with respect to nitrogen deposition; and excessive wet and dry deposition of nitrogen compounds has been suggested as a possible cause of the extensive damage to forests in Europe[4]. Data from Rothamsted, UK, indicate that the mean concentration of NO_3^- in precipitation doubled between the 1850s and 1960 (ref. 5); similarly, the NH_4^+ concentration probably increased between the 1880s and 1960. A review of precipitation chemistry data from Europe indicates an approximately threefold increase in NO_3^- deposition between the 1890s and the late 1970s[6]. The present analysis of data from the European Air Chemistry Network reveals that the NO_3^- concentration at most stations approximately doubled between the late 1950s and early 1970s, with a less pronounced increase in NH_4^+. Detailed analysis of data from 12 Swedish stations showed no further increase of NO_3^- or NH_4^+ between 1972 and 1984. In contrast, the sulphate concentration decreased by ~30% for the same locations and time period.

The data that we have analysed are from the European Air Chemistry Network (EACN)[7,8]. These data are obtained from monthly precipitation samples collected in bulk samplers at more than 50 stations in northern and central Europe since 1955. Details about the sampling and chemical analysis of ammonium and nitrate ions as well as a listing of all the data between 1955 and 1979 are presented in refs 9 and 10, respectively.

Table 1 Changes in concentration of NO_3^- and NH_4^+ in northern European precipitation between the late 1950s (median of all months 1955–59) and the early 1970s (1970–74)

Relative change %	No. of stations* (NO_3^-)	No. of stations* (NH_4^+)
> +250	3 (0)	1 (0)
+200–249	3 (0)	0 (0)
+150–199	6 (0)	3 (1)
+100–149	21 (5)	6 (0)
+50–99	20 (4)	12 (2)
0–+49	2 (0)	15 (3)
0–−49	0 (0)	10 (2)
< −50	0 (0)	8 (1)
Total	55 (9)	55 (9)

* Numbers in parentheses refer to Swedish stations.

Almost all (54 out of 55) EACN stations with sufficiently long records exhibit an increase in NO_3^- concentration between the late 1950s and the early 1970s. Table 1 shows the magnitude of the observed changes. At 75% of the stations the NO_3^- concentration increased between 50 and 150% during the 15-yr period, corresponding to an annual increase of 2–6%. Similar analyses have been published by Kallend *et al.*[11] and Horvath[12], who found an averge annual increase of NO_3^- concentration at various sites to be ~6% and 7%, respectively. An increase in the NH_4^+ concentration was observed at 37 out of 55 EACN stations (Table 1). At half of the stations, the NH_4^+ concentration increased by 0–100%. Other previously published data[12] present no clear temporal trend of the NH_4^+ concentration between 1968 and 1981. Also, the variability in the NH_4^+ concentration was greater than that for NO_3^-. Note that the quality of some of the NH_4^+ data is dubious[9], because microbiological activity may have an effect on the concentration of ammonium in the sample after collection.

For a more detailed analysis of temporal changes in nitrogen concentrations, we limited ourselves to the period between 1972 and 1984 and to Swedish stations only. We imposed this limitation mainly because this part of the network has been modified to meet more stringent sampling and analysis criteria[13]. For this period, data are available from 12 stations located in rural areas

* Present address: Department of Civil Engineering, University of Illinois, Urbana, Illinois 61801, USA.

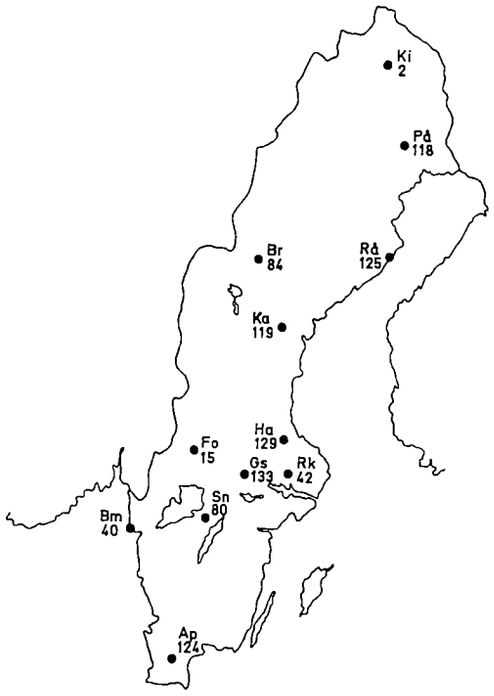


Fig. 1 Locations of 12 Swedish stations used in the statistical analysis.

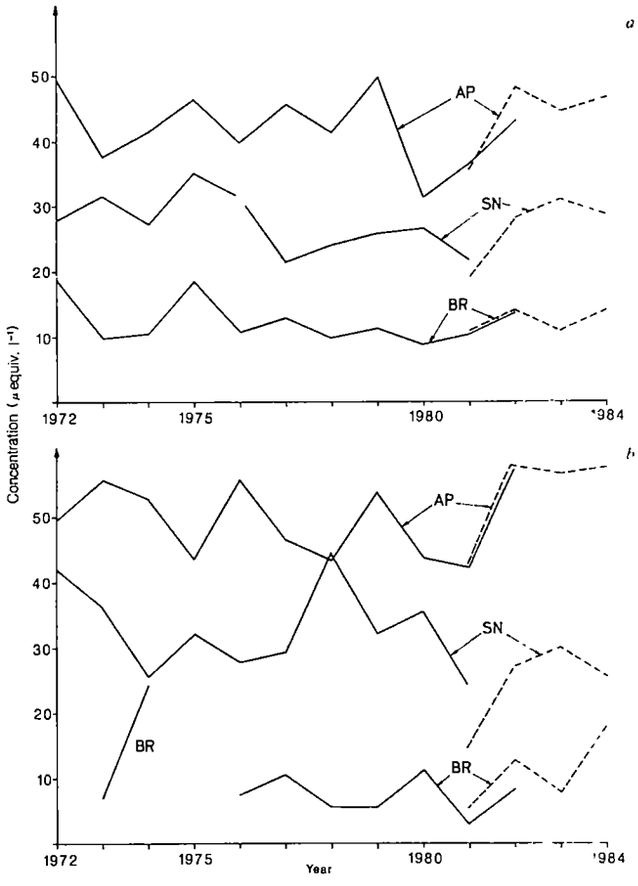


Fig. 2 Annual average concentrations of: *a*, NO_3^-; *b*, NH_4^+ at three Swedish stations (shown in Fig. 1). 'Bulk' and 'wet-only' data are represented by continuous and broken lines, respectively.

and believed to be free of local sources of contamination (Fig. 1). Up to 1982, precipitation sampling was performed with 'bulk' collectors, that is with collectors that remain open during the entire month. Since 1981, sampling has also been performed with collectors that are used only during periods of precipitation ('wet-only' collectors).

Figure 2 shows the NO_3^- and NH_4^+ concentration in precipitation at individual stations located in northern (Br), central (Sn) and southern (Ap) Sweden. The annual values were obtained as precipitation-weighted averages of monthly values. A statistical filter was applied to remove outliers from the monthly values. This filter removed ~1% of the NO_3^- values and 4% of the NH_4^+ values. These stations were selected as examples because they have complete records and represent different geographical locations with different average concentrations. The general shapes of the time series from the other Swedish stations are similar. The values obtained by 'bulk' and 'wet-only' samplers agree quite well during simultaneous operation of both samplers (Fig. 2). No clear positive or negative trend in the nitrate or ammonium ion concentration was evident over the 13-yr period between 1972 and 1984.

To elaborate on the last point, we have performed linear regression analysis on data from all 12 Swedish sites. For NO_3^-, the slope was positive at five sites and negative at seven; at one of the sites, the slope was significantly (90% confidence level) greater than zero. For NH_4^+, the slopes were also positive at five sites and negative at seven; with two of them being significantly different from zero (one greater than and one less than zero).

In contrast to the NO_3^- and NH_4^+ trends, the sulphate concentration showed a negative trend at all of the stations. Nine of the stations had trends significantly less than zero at the 90% confidence level. A decrease in sulphate concentration is consistent with decreasing anthropogenic sulphur emissions in several west European countries during the same time period[14].

The temporal evolution of nitrogen oxides and ammonia emissions is not well established. In Sweden, the emissions of NO_x remained essentially constant between 1970 and 1983 (ref. 15). In France, FRG and the UK, NO_x emissions changed by +4, +15 and −3%, respectively, between 1975 and 1983 (ref. 16). No reliable information seems to be available regarding changes in ammonia emissions.

The results presented here indicate a significant increase in the NO_3^- concentration in precipitation in northern Europe between the late 1950s and the early 1970s. However, since then no significant change has occurred in Sweden. A similar situation holds for the NH_4^+ concentration, although the increase from the late 1950s to the early 1970s was less pronounced than for NO_3^-.

Unless the forest damage that has been observed during the past few years in FRG[17], and suspected to have occurred in Sweden[18], is caused by an unlikely increase in dry deposition, by nitrogen deposition accumulated over several years or by infrequent events of very high concentration/deposition, it is hard to believe that only NO_3^- and NH_4^+ in precipitation are responsible for such damage. This conclusion is based on the lack of correlation during the past decade between the observed forest damage and the concentrations of these ions in precipitation.

We thank L. Granat for useful discussions and the Valle Scandinavian Foundation at the University of Washington, Seattle, Washington for its financial support.

Received 17 December 1985; accepted 17 March 1986.

1. Granat, L. *Tellus* **24**, 550-560 (1972).
2. *Acidification Today and Tomorrow* (Swedish Ministry of Agriculture, Stockholm, 1982).
3. Paces, T. *Nature* **315**, 31-36 (1985).
4. Nihlgård, B. *Ambio* **14**, 2-8 (1985).
5. Brimblecombe, P. & Pitman, J. *Tellus* **32**, 261-267 (1980).
6. Brimblecombe, P. & Stedman, D. H. *Nature* **298**, 460-461 (1982).
7. Eriksson, E. *WMO Tech. Note* 106, 31-54 (World Meteorological Organization, Geneva, 1970).
8. Rodhe, H., Söderlund, R. & Granat, L. *Rep. CM-64* (Department of Meteorology, Univ. Stockholm, 1984).

9. Söderlund, R. & Granat, L. *Rep. CM-59* (Department of Meteorology, Univ. Stockholm, 1982).
10. Söderlund, R., Granat, L. & Rodhe, H. *Rep. CM-69* (Department of Meteorology, Univ. Stockholm, 1985).
11. Kallend, A. S., Marsh, A. R. W., Pickles, J. H. & Proctor, M. V. *Atmos. Envir.* 17, 127–137 (1983).
12. Horvath, L. *Tellus* 35, 304–308 (1983).
13. Granat, L., Söderlund, R. & Bäcklin, L. *Rep. AC-40* (Department of Meteorology, Univ. Stockholm, 1977).
14. Rodhe, H. & Granat, L. *Atmos. Envir.* 18, 2627–2639 (1984).
15. *Rep. PM 1879* (National Swedish Environment Protection Board, 1984). (In Swedish.)
16. *The State of the Environment 1985* (Organization of Economic Cooperation and Development, Paris, 1985).
17. *FRG 1984: Forest Damage Survey* (Federal Ministry of Food, Agriculture and Forestry, Bonn, 1984).
18. Andersson, F. *Water, Air and Soil Pollution* (in the press).

High-temperature fluid–rock interactions in a layered syenite pluton

Ian Parsons & Susanne M. Becker*

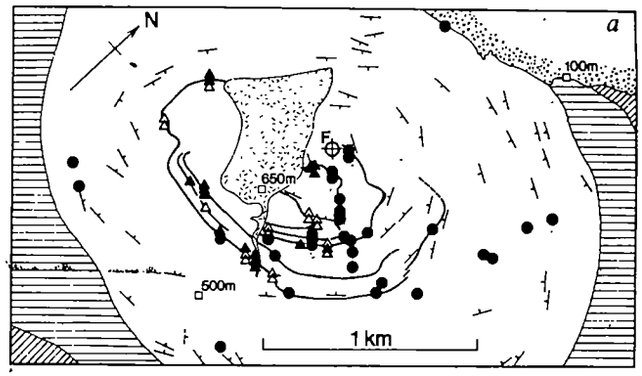
Department of Geology and Mineralogy, University of Aberdeen, Aberdeen AB9 1AS, UK

Variation in mineral composition with stratigraphic height in layered igneous intrusions is generally taken to indicate progressive fractional crystallization, and, following pioneering work on the Skaergaard complex[1], petrologists have used this variation in modelling the evolution of magma bodies. In cooling plutons, however, major chemical changes may occur in circulating deuteric fluids[2,3]. In the Klokken (South Greenland) layered syenite we have discovered that mineral compositions vary both along and normal to the strike of individual layers, and we argue that major chemical changes have occurred in a circulating aqueous fluid constrained to move along relatively permeable high-temperature aquifers in the layered series.

The Klokken intrusion is a predominantly syenitic stock in the Gardar alkaline province in South Greenland (Rb–Sr age 1,139 ± 11 Myr; ref. 4), with an outer sheath of gabbro and an inner ring of structureless unlaminated syenite[5] (Fig. 1). Current work shows that the unlaminated syenites become more evolved inwards, suggesting that they formed by congelation against the chamber wall. They enclose an elliptical chamber measuring 3 × 2 km, in which the more evolved layered syenite series formed. The exposed thickness is ~600 m; modelling using trace elements suggests that the chamber was >1,320 m thick at this stage[6], and both the cryptic variation and studies of cryptoperthite exsolution textures show that the roof was close to the highest present levels of exposure[7]. The layered sequence is cut by a body of more basic biotite-syenodiorite (Fig. 1), which has the form of a feeder dyke which spreads laterally near the topographic summit of the intrusion to form a sheet.

The layered series dips inward at 30–50°, flattening close to a focus (F, Fig. 1*a*). Individual mineral layers may be traced for up to 3 km along strike. The layered series consists of two texturally contrasting syenite types[5]. Layers of fine-grained granular syenite form ~15% of the exposed section, and cryptic variation shows that these represent a roof-chill series, continuing the trend of the unlaminated syenite (Fig. 2*a*), which was stoped in a *lit-par-lit* fashion by the laminated syenites which form the remainder of the succession. These laminated syenites show repeated mineral layering of an unusual, inversely graded type (Fig. 3), in which normal leucocratic syenite gives way upward, characteristically over 2–3 m, to hedenbergite pyroxenite or fayalite-rock[5]. The layering is ascribed to variations in the crystal supply brought about by changes in nucleation and growth rates under a regime of fluctuating P_{H_2O} (ref. 5).

* Present address: Department of Adult Education, University of Leicester, LE1 7RH, UK.



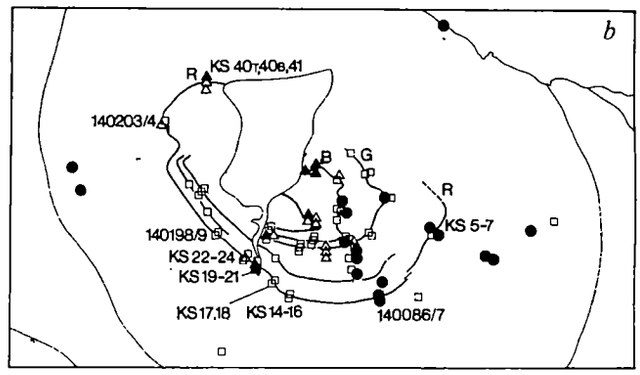


Fig. 1 *a*, Outline geological map of the central part of the Klokken complex. Oblique hatching, gabbro; horizontal hatching, unlaminated syenite; dashed, late syenodiorite. In the northern corner of the map the igneous rocks are obscured by glacial gravels. In the layered series the inward dips are shown (30–50°), with a focus at F. Individual mafic layers in the laminated syenite series which have been traced on the ground are shown as heavy lines. Note that the topography falls steeply towards the north (see spot heights). Symbols show the per cent anorthite component ($CaAl_2Si_2O_8$) in the ternary alkali feldspars: ●, <2%; △, 2–3%; ▲, 3–8%. *b*, As *a*, but illustrating clinopyroxene variation in terms of the scheme shown in Fig. 2: ▲, high-Mg, field 1; △, high-Mg, field 2; □, normal, field 3; ●, high-Na, field 4. The layers B, G and R, which have been studied in detail, are labelled, as are samples from layer R used in the construction of Fig. 2.

The mineralogy of the Klokken layered series comprises alkali feldspar ≫ Fe-rich clinopyroxene > Fe-rich olivine = ilmenomagnetite, with biotite, amphibole, quartz and sphene occurring as intercumulus phases only. The magmatic evolution of the complex is revealed most clearly by the pyroxenes, as summarized in Fig. 2*a*. The granular syenites become systematically more evolved downwards, and generally show considerable compositional contrast with the more evolved, interbedded laminated syenites. 70% of analysed clinopyroxenes in the laminated syenites plot close to the hedenbergite composition (field 3, Fig. 2*b*), showing that the liquid from which they crystallized was the end product of extended *in situ* fractionation, of which the granular syenites represent less evolved stages[5,6].

In detail the laminated syenite sequence is more complex. We collected along and normal to individual layers, selecting three (R, G, B in Fig. 1*b*) for detailed study. We also collected from other layers and from 'normal' massive syenite. Figure 2*b* shows the pyroxene variation along the outcrop of layer R; Fig. 3 shows the variation normal to the layer. (See Fig. 1*b* for sample localities.) Variation on a similar scale was found in the other layers studied. Clearly, intra-layer variation is as large as in the layered series as a whole. To show varation with locality, we have divided the diopside–hedenbergite–acmite triangle (Fig. 2*b*) into four fields, and classified each sample of laminated

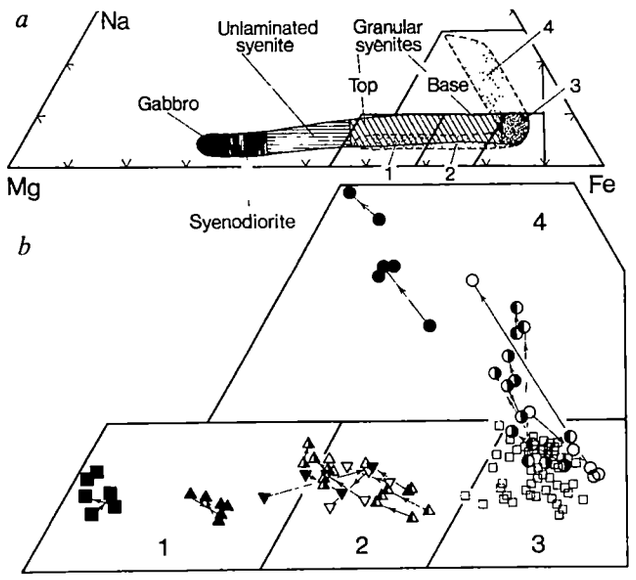


Fig. 2 *a*, Triangular diagram summarizing the range of clinopyroxene variation in all units of the Klokken intrusion (atom per cent Na, Mg and Fe calculated on the basis of 6 oxygens; $Mg = CaMgSi_2O_6$, diopside; $Fe = CaFe^{2+}Si_2O_6$, hedenbergite; $Na = NaFe^{3+}Si_2O_6$, acmite). The stippled area shows the range of all laminated syenites; the majority (>70%) lie in the region of heavy stippling. *b*, Variation within a single layer (R) of the laminated syenite series. Fields 1–4 were used to classify high-Mg and high-Na clinopyroxenes as shown in Fig. 1*b*. Samples which fall predominantly in fields 1, 2 and 4 may be identified by their symbols (●, KS 6; ◐, 140086; ◑, 140087; ○, KS 7; ■, KS 19; ▲, KS 20; ▼, KS 23; ◭, KS 40B; ◮, 140204; ▽, KS 41; △, KS 40T), and their localities found in Fig. 1*b*. All other samples ('normal' laminated syenites) are shown as squares. Tie lines indicate zoned crystals, with arrows pointing towards rims.

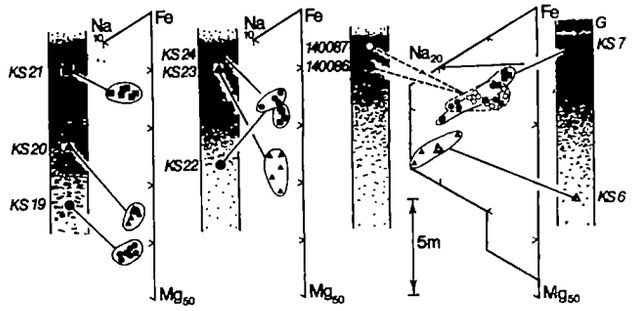


Fig. 3 Relationship between clinopyroxene composition and position relative to bedding in layer R. The layer, which is unusually thick, shows inversely graded mineral layering, with a diffuse top which grades upwards into normal syenite considerably more rapidly than downwards. The sections are arranged from left to right in order of distance from the syenodiorite dyke (Fig. 1). The shading shows the general change in feldspar/pyroxene ratio (light, feldspar; dark, pyroxene) in the inversely graded layer; feldspar primocrysts are not to scale. At the locality of samples KS 5–7 a granular syenite layer (G) appears above the mafic horizon. Note that the most extreme compositions, both high-Mg and high-Na, tend to come from the more leucocratic parts of the layers.

syenite according to the field in which the pyroxene predominantly falls. Figure 1*b* shows the distribution of pyroxene analyses according to this scheme: high-Mg examples (fields 1 and 2) all come from an area south of the focus of the complex, in the vicinity of the late syenodiorite body; the most magnesian come from the sampling points nearest to the syenodiorite. The high-Na pyroxenes (field 4) come from the outer part of the layered series, irrespective of stratigraphic position. Figure 3 shows the relationship between pyroxene composition and lithology for points in layer R, arranged in order of distance from the syenodiorite dyke.

Other primocryst phases show similar variation. Layer G contains olivine in which the Mg/Fe ratio varies sympathetically with that of coexisting clinopyroxene. Subtle variation is found in the alkali feldspars, which have bulk compositions in the range $Ab_{75}Or_{25}$–$Ab_{55}Or_{45}$, with up to 8 mol % An (ref. 7). All samples with >2% An come from the same broad region of the complex, offset from the focus, in the vicinity of the late syenodiorite. Those with >4% An come from localities within 50 m of the diorite, although not all such samples have high An. Away from this central area all samples have <1% An.

Conventional analysis of the cryptic variation would suggest that the outer part of the layered series crystallized from a more evolved liquid than the inner, in marked discordance with the mineral layering, and in an opposite sense to the inward evolution of the sheath of unlaminated syenite. The variation is not related in any direct way to stratigraphic height (Fig. 1), as is the case in the simplest layered intrusions[1], or to the focus of the layering, as might be expected if the discordance were the result of a lateral accretion process[8,9] or of crystallization in a chemically zoned magma body[10]. Ponding of light magma beneath granular layers can be ruled out because the latter become rare and discontinuous towards the margin of the layered series. The complex and variable relationship to lithology within individual layers (Fig. 3) also rules out all these hypotheses.

We suggest that the compositions of the main mineral species in the laminated syenite series have been modified, immediately after crystallization, in a large-scale deuteric fluid system. This system left the granular and unlaminated syenites largely unaffected. Textural evidence consistent with this hypothesis is the reversed zoning observed in the high-Mg proxenes (Fig. 2*b*) and the normal zoning (Na replacing Ca) exhibited by the high-Na examples. In thin section the zoning is patchy, being related to fractures as well as grain boundaries. The most extreme examples of high-Mg pyroxene and high-Ca feldspar come from close to the syenodiorite and we can see no other explanation for this than high-temperature, sub-solidus modification. Exsolution microtextures in the cryptoperthitic alkali feldspars, indicating exsolution by spinodal decomposition at >850 °C in the most An-rich examples, show that Ca exchange occurred at even higher temperatures, before exsolution. Patchy zoning in the alkali feldspars has been demonstrated by transmission electron microscopy, as well as by electron microprobe[7].

Field evidence of the presence of high-temperature, alkaline solutions in the outer part of the layered series is provided by a suite of drusy peralkaline pegmatites which occur as lenses and veins at the boundary between the layered series and the unlaminated syenites. The development of a pegmatitic facies of the laminated syenite in flame structures at the base of granular layers and the presence of druses in the laminated syenites demonstrate the presence of a fluid phase during the final stage of crystallization[11,12].

Persistence of deuteric fluids down to lower temperatures is demonstrated by the turbid alteration of the alkali feldspars[11], which are white and translucent in the laminated syenites, and transparent, often dark green, in the granular and unlaminated syenites. The turbidity is related to the development of patch perthites in place of strain-controlled braid crypto- or microperthites, which occurred at <450 °C (ref. 13). The most turbid samples tend to be those containing the most Na-rich pyroxenes, and these frequently also contain replacive alkali amphibole and acmite. Extensive replacement of magmatic phases by hydrous phases at low temperatures, as is found in the Scottish Tertiary epigranites[2], is not found in Klokken. Granular syenite feldspars have retained radiogenic ^{40}Ar, while the laminated

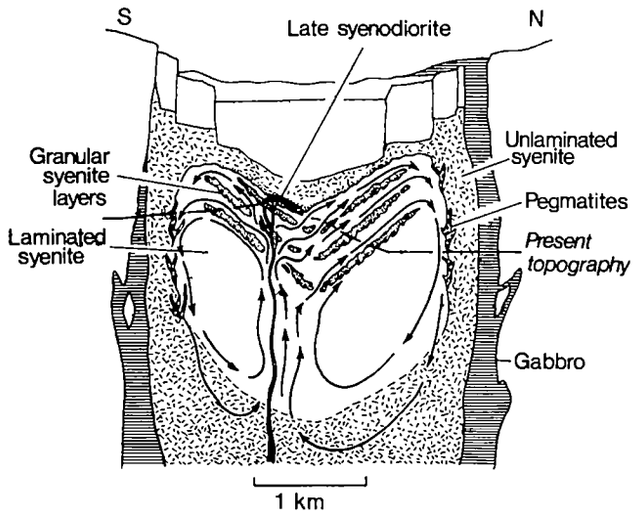


Fig. 4 Stylized section through the Klokken chamber showing suggested flow-lines (arrows) for the deuteric fluid and the disposition of the main rock units. Although the thickness of the layered series (laminated+granular syenites) is approximately correct[4] (equal horizontal and vertical scales), for clarity the thickness of the granular layers is greatly exaggerated (real thickness 0.1–30 m) and their number underestimated (there are ~40 granular layers in the exposed section, and they become thicker and more abundant upwards)[5,12]. The caldera superstructure is speculative.

syenite feldspars have leaked argon in proportion to their turbidity[14]. We conclude that the coarse-grained, drusy laminated syenite layers acted as high-temperature aquifers in the layered complex, over at least the temperature range 850–450 °C, probably corresponding to a cooling interval of $>10^5$ yr (ref. 13). The relatively fine-grained, compact-textured granular layers acted as impermeable horizons. Variable permeabilities account for the irregular relationships observed across layers at single localities (Fig. 3). Generally, the mafic parts of inversely graded layers have feldspars which are less turbid than those in leucocratic parts, suggesting that the mafic layers were less permeable than the leucocratic syenite.

Fluid circulation has been modelled numerically for the Skaergaard intrusion[15], which water is thought to have entered from the well-jointed basalt envelope. In contrast, the Klokken layered series was sealed against the ingress of water by the outer gabbro and unlaminated syenite rings (Fig. 4). Biotites in the gabbros form a series with OH/F ratios different from those in all syenites, suggesting that they were in equilibrium with a different fluid (I.P., R. A. Mason and S.M.B., in preparation).

Although the late syenodiorite intrusion strongly influenced the mineral chemistry in its vicinity, it seems unlikely that this comparatively small body would have provided the heat source necessary to drive kilometre-scale convection in the entire chamber. The summit sheet is thin, and the feeder dyke is only ~3 m wide at its intersection with layer R (Fig. 1). We envisage an initially symmetrical convecting system upon which the thermal effect of the late-arriving syenodiorite was superimposed (Fig. 4), causing a local perturbation in the flow regime.

The roof of the complex was close to the present level of erosion[7], and Fig. 4 shows an axial rise of heated water from the comparatively slowly cooling interior; this water is then constrained to move laterally along inclined laminated syenite aquifers beneath the roof. Pyroxenes in equilibrium with this fluid were more Na- and Fe-rich in the cooler, outer part of the system, and in the inner core the mineralogy of the layered series was modified by the emplacement of the more basic syenodiorite. Klokken is unusual in that its laminated syenites crystallized from a residual magma which was at or near water-saturation[5]. Large-scale modification of mineralogy may be unlikely in more basic intrusions. We note that the discordant mineral variation found in the Skaergaard intrusion[10] occurs at the junction between the Upper Zone and the Upper Border Group, a situation analogous to the granular syenite/laminated syenite boundary at Klokken. Although infiltration metasomatism has been postulated as a post-cumulus source of mineral modification in the Muskox intrusion[16], this is a local re-equilibration with intercumulus silicate liquid. It is improbable that the effects at Klokken could result from kilometre-scale circulation of intercumulus melt, particularly in view of the relatively low temperature and high silica content of the residual liquid. Circulation of residual melt is also unlikely because individual layers tend to have distinctive intercumulus assemblages (for example, quartz is found only in certain layers, as is intercumulus sphene).

In the Klokken intrusion, sub-solidus modification of the consolidated sequence by deuteric fluids appears to have produced compositional variation very similar to that usually ascribed, in layered complexes, to crystal–melt fractionation. Although most salic plutons are not layered, they almost invariably exhibit low-temperature deuteric alteration, and by analogy with Klokken, substantial changes in mineral chemistry may also accompany the circulation of fluids at high temperatures during their cooling history.

We thank George Taylor and John Still for careful microprobe work, and W. L. Brown and P. E. Brown for stimulating companionship in the field. P. E. Brown kindly criticized the manuscript. Samples prefixed 140- were collected by I.P. during mapping of the complex for Grønlands Geologiske Undersøgelse, and this paper appears by permission of the Director. The current research is supported by NERC grant GR3/4639.

Received 6 March; accepted 3 April 1986.

1. Wager, L. R. & Brown, G. M. *Layered Igneous Rocks* (Oliver & Boyd, Edinburgh, 1968).
2. Ferry, J. M. *Contr. Miner. Petrol.* **91**, 283-304 (1985).
3. Taylor, H. P. Jr & Forester, R. W. *J. Petrol.* **12**, 465-497 (1971).
4. Blaxland, A. B. & Parsons, I. *Meddr. dansk geol. Foren.* **24**, 27-32 (1975).
5. Parsons, I. *J. Petrol.* **20**, 653-694 (1979).
6. Mason, R. A., Parsons, I. & Long, J. V. P. *J. Petrol.* **26**, 952-970 (1985).
7. Brown, W. L., Becker, S. M. & Parsons, I. *Contr. Miner. Petrol.* **82**, 13-25 (1983).
8. Wilson, J. R. & Larsen, S. B. *Nature* **299**, 625-626 (1982).
9. Wilson, J. R. & Larsen, S. B. *Geol. Mag.* **122**, 97-124 (1985).
10. Naslund, H. R. *Yb. Carnegie Instn. Wash.* **75**, 640-644 (1976).
11. Parsons, I. *Trans. R. Soc. Edinb.* **71**, 1-12 (1980).
12. Parsons, I. & Butterfield, A. W. *J. geol. Soc. Lond.* **138**, 289-306 (1980).
13. Brown, W. L. & Parsons, I. *Contr. Miner. Petrol.* **86**, 3-18 (1984).
14. Rex, D. C., Guise, P., Halliday, A. N. & Parsons, I. *Eos* **66**, 1116 (1985).
15. Norton, D. & Taylor, H. P. *J. Petrol.* **20**, 421-486 (1979).
16. Irvine, T. N. in *Physics of Magmatic Processes* (ed. Hargraves, R. B.) 325-383 (Princeton University Press, 1980).

Jack Hills, evidence of more very old detrital zircons in Western Australia

W. Compston* & R. T. Pidgeon†

* Research School of Earth Sciences, The Australian National University, GPO Box 4, Canberra, A.C.T. 2600, Australia
† Department of Physics and Geoscience, Western Australian Institute of Technology, Bentley, Western Australia 6102, Australia

The age of the Earth's oldest crustal minerals sets a time-limit on the earliest preservation of buoyant solid crust. The oldest mineral ages reported so far are ~4,180 Myr for detrital zircons from quartzites at Mount Narryer[1], in the Yilgarn Block, Western Australia. The oldest-known intact rocks, as distinct from individual minerals, are substantially younger; they formed ~3,813-Myr ago[2] in the Isua supracrustal belt, West Greenland. We report here a further occurrence of old detrital zircons, again identified using the ion-microprobe SHRIMP[3], in conglomerate from the Jack Hills Metasedimentary Belt[4,5] (26°11′ S, 116°58′ E),

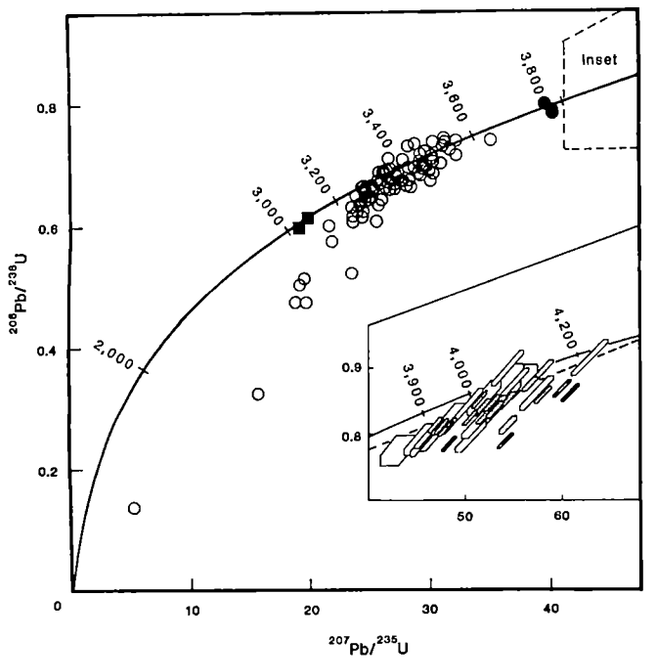


Fig. 1 Conchordia diagram showing U–Pb ages by ion microprobe for 140 grains of detrital zircon from Jack Hills conglomerate sample W74. All points on the main diagram and the open symbols in the inset are reconnaissance analyses. The filled symbols in the main diagram denote concordant ages for the youngest and oldest grains in the younger population, and those in the inset are precise analyses. The inset shows the complete data (Table 1) for the 17 oldest grains. Uncertainties are one standard error. The broken line is a hypothetical early Pb-loss line to 3,500 Myr.

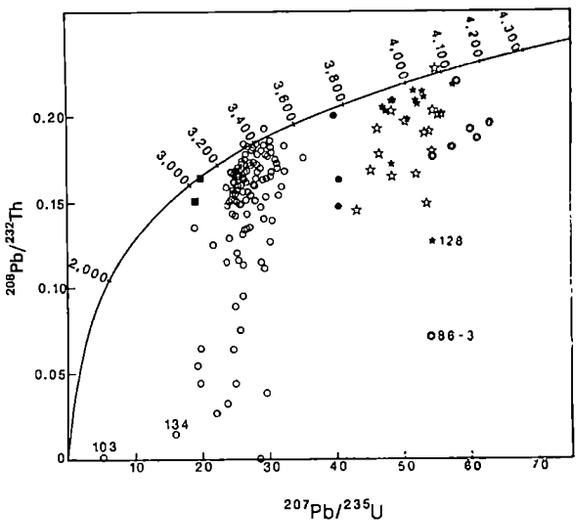


Fig. 2 Concordia-type diagram showing Th–Pb ages. Symbols are as for Fig. 1, except that analyses of the older crystals are shown as stars. ☆, reconnaissance; ★, precise analyses; circled stars, grain 86.

~60 km north-east of Narryer. This discovery is important for several reasons. First, one zircon registers the exceptionally old age of 4,276 ± 6 Myr, which is, moreover, a minimum estimate for its original age; 16 other grains may have the same age or may be slightly younger. Second, the new occurrence considerably extends the area over which the old Narryer suite is known, thus amplifying its geological significance. Third, the frequency of old zircons in the Jack Hills occurrence is 12%, about five times higher than at Narryer, which suggests that the intact ~4,180 Myr-old rocks, if they still exist, might be closer, and facilitates future comparison of the SHRIMP data with conventional analyses of these grains. (Recent conventional U–Pb work[6] on other zircons from the same Narryer concentrate confirmed the younger ages but failed to observe any at ~4,180 Myr, probably because of their low abundance[7]). The likelihood that zircon would dissolve in magmas undersaturated in zirconium[8] argues against its survival in long-term contact with such magmas during the disaggregation and subduction of crust. Consequently, the existence of zircon in the Jack Hills area from ~4,300 Myr ago implies that this part of the crust has been preserved, since then, from recirculation in the mantle through plate-tectonics or any other mechanism.

The Jack Hills Metasedimentary Belt is a narrow belt ~70 km long composed of minor metabasalts and thick chert and banded iron formation interleaved with clastic metasediments[5]. It is broadly similar to the nearby Narryer Metamorphic Belt[9] but lower in metamorphic grade (high greenschist). It is separated from surrounding granites and gneisses by zones of major deformation which prevent direct observation of the relative ages of the granitic rocks and the belt. Some of the granites have been dated using conventional zircon U–Pb techniques as ~3,500 Myr (gneissic granite) and ~2,600 Myr (undeformed granite)[5]. The detrital zircons were concentrated from a chert pebble conglomerate within a thick clastic sequence in the southwestern section of the belt. They vary from almost colourless to deep purplish brown, and are predominantly broken (probably during processing) and rounded. Most of the latter are pitted suggesting transport abrasion. Rare grains have a blunted prismatic form. Only a few are structured into a core surrounded by a distinct rim of younger zircon. Several analysed grains show faintly the euhedral internal zoning that is generally considered to result from magmatic crystallization, but none of the 4,100–4,300-Myr-old zircons (hereafter termed the 'old' zircons) have this feature. Most of the zircons are devoid of inclusions although some, including three old grains, contain a few randomly oriented, transparent, acicular inclusions. The 17 old zircons identified cannot be distinguished on colour or morphological criteria from the other rounded grains.

The U–Pb results are plotted in Fig. 1, which shows that the analyses of most zircons lie either within error of Concordia or slightly below it, signifying only small losses in their uranogenic Pb. In contrast, a few areas within grains have lost much of their radiogenic Pb comparatively recently. For concordant zircons and those having Pb loss at zero-age only, the original ages are calculable from the radiogenic $^{207}Pb/^{206}Pb$. Where the Pb-loss history is more complex, the $^{207}Pb/^{206}Pb$ ages can be interpreted reliably as minimum estimates for the original ages. (We emphasize that Pb isotopic ratios are directly measured without peak-stripping on SHRIMP and are independent of standard comparisons and calibrations; as such they provide straightforward minimum age-determinations for each analysed area.) The $^{207}Pb/^{206}Pb$ age for most grains is ~3,350 Myr, which we interpret as their age of crystallization or high-grade metamorphic recrystallization before deposition in the conglomerate. Those between 3,400 and 3,600 Myr (Fig. 1) probably represent older zircons that formed at different times within that interval, and there are several grains that formed earlier still at ~3,800 Myr. Two zircons are distinctly younger than all the rest with concordant ages at just less than 3,100 Myr. They are detrital, having rounded forms and abraded surfaces, and their age constrains the deposition of the conglomerate to later than that value. The $^{207}Pb/^{206}Pb$ ages that exceed 3,900 Myr belong to a much older population which may have had a single original age close to 4,300 Myr and have undergone early as well as recent Pb loss, or it may be a mixed-age population that formed during discrete events over an extended time period from 4,100 to 4,300 Myr ago.

The details of reconnaissance and precise analyses of the 17 old zircons are listed in Table 1. The five analysed areas within grain 86, which shows the highest minimum ages, exhibit small

Table 1 Ion microprobe analyses for U, Th and radiogenic Pb for 25×35 μm areas within the older zircons from Jack Hills

Grain-area	U (p.p.m.)	Th (p.p.m.)	% Common 206*	208/232	206/238	207/235	207/206	Minimum age (Myr)
22-1R	49	25	3.4	0.180±23	0.880	54.4	0.448±8	
22-1P	56	24	0.6	0.172±6	0.784	48.3	0.446±2	4,072±7
31-1R	55	22	4.2	0.166±26	0.854	51.9	0.441±7	4,055±24
34-1R	217	113	1.0	0.197±8	0.843	50.2	0.432±3	
34-2P	82	34	0.6	0.195±6	0.824	50.4	0.444±2	4,065±7
43-1R	39	27	9.7	0.149±27	0.857	53.6	0.453±12	
43-1P	46	33	1.4	0.206±7	0.826	51.9	0.456±3	4,105±10
46-1R	57	23	4.4	0.165±27	0.821	48.4	0.427±8	4,007±28
51-1R	70	47	3.4	0.178±14	0.797	46.5	0.423±7	
51-1P	71	47	0.2	0.209±5	0.808	47.9	0.430±2	4,017±7
53-1R	32	20	7.2	0.145±33	0.774	43.1	0.403±13	3,920±48
56-1R	149	95	0.6	0.227±9	0.873	54.9	0.456±3	
56-1P	160	104	0.3	0.214±9	0.846	52.7	0.452±2	4,092±7
82-1R	39	25	3.2	0.201±19	0.878	55.6	0.459±8	
82-1P	47	30	0.7	0.211±6	0.836	53.0	0.460±3	4,118±10
86-1R	96	58	2.5	0.182±10	0.861	57.4	0.483±4	
86-1P	115	70	0.5	0.220±5	0.859	58.0	0.490±2	4,211±6
86-2R	174	152	1.0	0.196±6	0.915	62.9	0.499±3	
86-2P	187	156	0.5	0.192±5	0.868	60.0	0.501±2	4,244±6
86-3P	181	327	0.9	0.071±2	0.789	54.1	0.497±2	4,232±6
86-4P	113	87	0.5	0.187±4	0.862	60.9	0.512±2	4,276±6
86-5P	40	20	2.1	0.175±8	0.811	54.4	0.485±4	4,196±12
92-1R	59	26	3.3	0.169±19	0.791	45.1	0.414±6	3,961±22
102-1R	174	77	1.4	0.203±9	0.899	54.4	0.439±3	
102-1P	165	76	0.1	0.215±3	0.852	51.4	0.438±2	4,045±7
119-1R	186	108	0.7	0.193±6	0.801	46.1	0.418±3	
119-1P	198	112	0.2	0.205±3	0.812	46.9	0.418±2	3,975±7
119-2P	182	102	0.5	0.209±4	0.840	51.8	0.447±3	4,075±10
P	177	95	0.1	0.209±4	0.812	48.3	0.431±3	4,021±10
123-1R	61	24	1.9	0.190±18	0.828	52.4	0.459±6	4,115±19
123-1P	70	28	0.8	0.225±10	0.898	58.2	0.470±3	4,150±9
	71	28	0.5	0.212±8	0.877	56.8	0.470±3	4,150±9
128-1R	77	23	2.3	0.182±21	0.816	51.2	0.455±5	4,102±16
128-2P	93	53	1.0	0.123±5	0.850	54.3	0.463±3	4,128±10
	101	54	0.4	0.130±5	0.845	53.4	0.458±3	4,111±10
130-1R	114	41	1.0	0.193±12	0.789	45.7	0.420±4	3,982±14
130-1P	123	44	0.6	0.201±7	0.810	47.2	0.423±3	3,993±11
	127	45	0.3	0.205±5	0.811	47.5	0.425±2	4,000±7
138-1R	91	57	2.3	0.180±11	0.796	50.5	0.461±5	4,121±16

Analytical procedures are described elsewhere[2]. Uncertainties shown are one standard error and refer to the last digits only. Coefficients of variation are 1.5% for precise Pb/U, 3.0% for Th/U and reconnaissance Pb/U, and 10% for U, Th concentrations.

R, Fast reconnaissance analysis using three scans.

P, Precise analysis using 14 scans and lower content of surface-related common Pb.

* Surface-related common Pb, taken as Broken Hill ore; sample 206/204 is 1600/(% common 206).

but real differences in radiogenic $^{207}Pb/^{206}Pb$ that can only have been generated by internal redistribution or loss of radiogenic Pb relative to U at some early time. The slightly discordant distribution of U–Pb data within this grain and all except possibly one of the other old grains (Fig. 1) is similar to that observed in many zircon suites in Archaean rocks elsewhere, and is customarily explained by minor Pb loss during one or more later events. Nevertheless, another conceivable explanation involves an early gain of Pb (or loss of U) followed by recent Pb loss, which would have the effect of increasing the $^{207}Pb/^{206}Pb$ age of the zircons. Redistribution of Pb that resulted in such 'reverse' discordance (points above Concordia) has been reported[10] for three out of seven areas analysed in one exceptional zircon from an orthogneiss at Mount Sones (Napier Complex, Antarctica), but the phenomenon of reverse discordance is very rare. In view of this and the overall consistency of the slightly (normally) discordant data for the old zircons, such a complex and *ad hoc* mechanism involving reverse discordance followed by recent Pb loss is considered most unlikely as an explanation of the observed old U–Pb ages. Grain 86 also shows large differences in Pb/U between areas having the same $^{207}Pb/^{206}Pb$, which indicate recent Pb loss. Because there have been two or more apparently independent Pb loss events, a single Pb loss vector in Fig. 1 cannot be constructed for grain 86 to estimate its original age of crystallization. All that can be said is that 4,276±6 Myr, the highest $^{207}Pb/^{206}Pb$ age listed in Table 1, is most likely a minimum estimate for the original age.

Additional evidence for recent Pb loss from many of the zircons, including grain 86, is shown in Fig. 2, a Concordia plot of $^{208}Pb/^{232}Th$ against $^{207}Pb/^{235}U$. Many of the analysed zircons are close to Concordia on this diagram, but assuming no U or Th movement, many others have lost ^{208}Pb relative to ^{207}Pb. The reliability of Th/U and Pb/U as measured by SHRIMP has been documented elsewhere[3], so that the differential loss of Pb isotopes (which has also been seen elswhere[11]) is a property of particular areas of zircon. The timing of this loss is equal to or younger than the youngest observed $^{208}Pb/^{232}Th$ age, which within error is zero. None of the data fall above Concordia, indicating that only Pb losses are registered rather than both gains and losses. The area showing the greatest loss of ^{208}Pb, 86-3, also has the lowest $^{207}Pb/^{235}U$, and the other zircons that are most discordant in Pb/U such as grains 134 and 103, also

have the lowest $^{208}Pb/^{232}Th$. A plausible hypothesis is that all the old zircons first formed at ~4,300 Myr, then lost Pb during one or more early events such as the known felsic magmatism at ~3,500 Myr and the uplift and weathering of the zircon provenance at ~3,100 Myr. Their present compositions would lie on the hypothetical chord shown in Fig. 1 if no Pb had been lost subsequently. Instead, because Pb loss also occurred recently, they are variably scattered below it.

In the absence of other evidence, we have attempted to use the internal structure, morphology and Th, U contents of the detrital zircons to suggest the nature of their original source rocks. The nearly universal rounding of the zircons is ambiguous, as we cannot ascertain how much of the rounding is due to mechanical abrasion and how much to metamorphic corrosion. The most important genetic features of the 140 analysed zircons are the lack of internal structure and the lack of inclusions in most grains, the blunted euhedral forms of some zircons, and the faint euhedral zoning in the rest. Their mean U, Th, at about 100 and 50 p.p.m. respectively, is distinctly low relative to the average crustal zircon, and zircons with similar morphological features and with low U and Th contents are known in only a few rock types. Zircon populations made up almost entirely of coarse, rounded, uranium-poor, transparent, inclusion-free, unzoned zircon occur in pyroxene granulites[12]. Consequently, we favour mafic rocks that experienced granulite facies metamorphism as the probable sources for most of the detrital zircons from the Jack Hills conglomerate. In contrast to the old zircons from Jack Hills, all but one of those from Narryer have distinctive subhedral forms and pronounced euhedral internal zoning. The Narryer zircons also have significantly higher uranium, but not thorium, contents. These differences suggest that the zircons in the Narryer quartzite came from felsic igneous rocks not recrystallized by granulite grade metamorphism, and provide evidence for considerable geological complexity in the ancient terrain contributing zircons to the two metasedimentary belts.

The ion microprobe analyses were largely made by I. S. Williams and P. D. Kinny who also reviewed the text, and J. J. Foster prepared the diagrams. Geological mapping and sampling in the Jack Hills were done in association with S. A. Wilde and J. L. Baxter assisted by WAIT students. Field work and R.T.P.'s participation in this project were supported by the Australian Research Grants Scheme.

Received 18 October 1985; accepted 27 February 1986.

1. Froude, D. O. *et al. Nature* **304**, 616-618 (1983).
2. Baadsgaard, H. *et al. Earth planet. Sci. Lett.* **68**, 221-228 (1984).
3. Compston, W., Williams, I. S. & Meyer, C. *J. geophys. Res.* **89**, B525-534 (1984).
4. Elias, M. *Geol. Surv. Western Australia Belele Explan. Not.* (1983).
5. Baxter, J. L., Wilde, S. A., Pidgeon, R. T. & Fletcher, I. R. *7th Australian Geol. Conv.* 56-57 (1984).
6. Scharer, U. & Allègre, C. *Nature* **315**, 52-55 (1985).
7. Compston, W. *et al. Nature* **317**, 559-560 (1985).
8. Watson, E. B. & Harrison, T. M. *Earth planet. Sci. Lett.* **64**, 295-304 (1983).
9. Williams, I. R., Walker, I. M., Hocking, R. M. & Williams, S. J. *Geol. Surv. Western Australia Rec.* **5** (1980).
10. Williams, I. S., Compston, W., Black, L. P., Ireland, T. R. & Foster, J. J. *Contr. Miner. Petrol.* **88**, 322-327 (1984).
11. Compston, W., Williams, I. S. & McCulloch, M. T. *Aust. J. Earth Sci.* (in the press).
12. Pidgeon, R. T. & Bowes, D. R. *Geol. Mag.* **109**, 247-258 (1972).

Carbon-14 dates point to man in the Americas 32,000 years ago

N. Guidon* & G. Delibrias†

* Laboratoire d'Anthropologie Préhistorique d'Amérique, Ecole des Hautes Etudes en Sciences Sociales, 44 rue de la Tour, 75016 Paris, France
† Centre des Faibles Radioactivités, Laboratoire Mixte CNRS-CEA, Boite Postale 1, 91190 Gif-sur-Yvette, France

The view that man did not arrive on the American continent before the last glaciation has been supported by the fact that until now the known and dated archaeological sites have not been of very great antiquity. But now we report radiocarbon dates from a Brazilian site which establish that early man was living in South America at least 32,000 years ago. These new findings come from the large painted rockshelter of Boqueirao do Sitio da Pedra Furada, the walls and the ceiling of which are decorated with a rich set of prehistoric paintings. We have excavated a sequence containing abundant lithic industry and well-structured hearths at all levels. Carbon-14 dates from charcoal establish a continuous chronology indicating human occupation from 6,160±130 to 32,160±100 years BP. A date of 17,000±400 BP, obtained from charcoal found in a level with fragments of a pictograph fallen from the walls, testifies to the antiquity of rupestral art in this region of Brazil.

The site of Boqueirao of Pedra Furada is one of the 200 known painted rock-shelters located in a remote region of the Brazilian plateau famous for its richness in prehistoric rupestral art (Fig. 1). This site, discovered in 1973 by the French-Brazilian archaeological mission in Piaui, is a rock-shelter situated on the steep bank of a 100-m non-calcareous sand-stone cliff, standing 20 m above the bottom of the valley of Pedra Furada.

The first excavation campaign at the site of Boqueirao of Pedra Furada was undertaken to date the rupestral art which is abundant in the region, and the first two dates obtained were from 7,640±140 yr (Gif-4928) and 8,050±170 yr BP (Gif-4625)[1]. The excavations were extended in area and depth during the following years. In 1985, the bedrock was finally reached after more than 3 m of sediment had been excavated.

Traces of human occupations succeed one another throughout the stratigraphic sequence. Based upon the distribution and number of artefacts which were in any case associated with the hearths, it appears that the site was occupied only by a small human group on temporary basis. The first traces of human presence in the shelter are a few scattered pieces of charcoal and two lithic pieces, found in the lowest layer A. These were a large pebble bearing the scars of several flakings, and a flake. This lowest level could not be dated.

All of the sedimentary layers contained remains which can be classified, according to the lithic industry and the type of structures of the hearths, in two main stages called Pedra Furada and Serra Talhada[2]. The artefacts unearthed in the surface layer E are different from those found in the lower layers, but not characteristic enough to permit definition of a cultural phase.

During the most ancient cultural phase, Pedra Furada, large circular hearths are found. They are well built with fallen blocks and contain large quantities of charcoal and ash. Lithic industry is abundant and localized around the hearths. The raw materials used for the fabrication of tools were quartz and quartzite, from the pebbles present at the site. Based upon typological and archaeological criteria, this cultural phase has been divided into four stages. In the earlier stage, Pedra Furada I, a lithic collection composed of 560 pieces was found, principally pieces with blunt points obtained by two, three or four convergent flakings, made of pebbles or flakes. Besides these typical tools, pebble-tools (chopping tools and choppers) appear as well as denticulates, burins, notched pieces, retouched flakes and double-edged flakes (Fig. 2).

In addition to the retouched pieces, the collection includes pebble-hammers, flaked pebbles, flakes and fragments produced by flaking. In this level, fragments of painted rock, fallen from the walls, are perhaps evidence of the ancient practice of rupestral art. Two dates, 31,700±830 yr (Gif-6652) and 32,160± 1,000 yr (Gif-6653) have been obtained from charcoal coming from the first hearth found at the site.

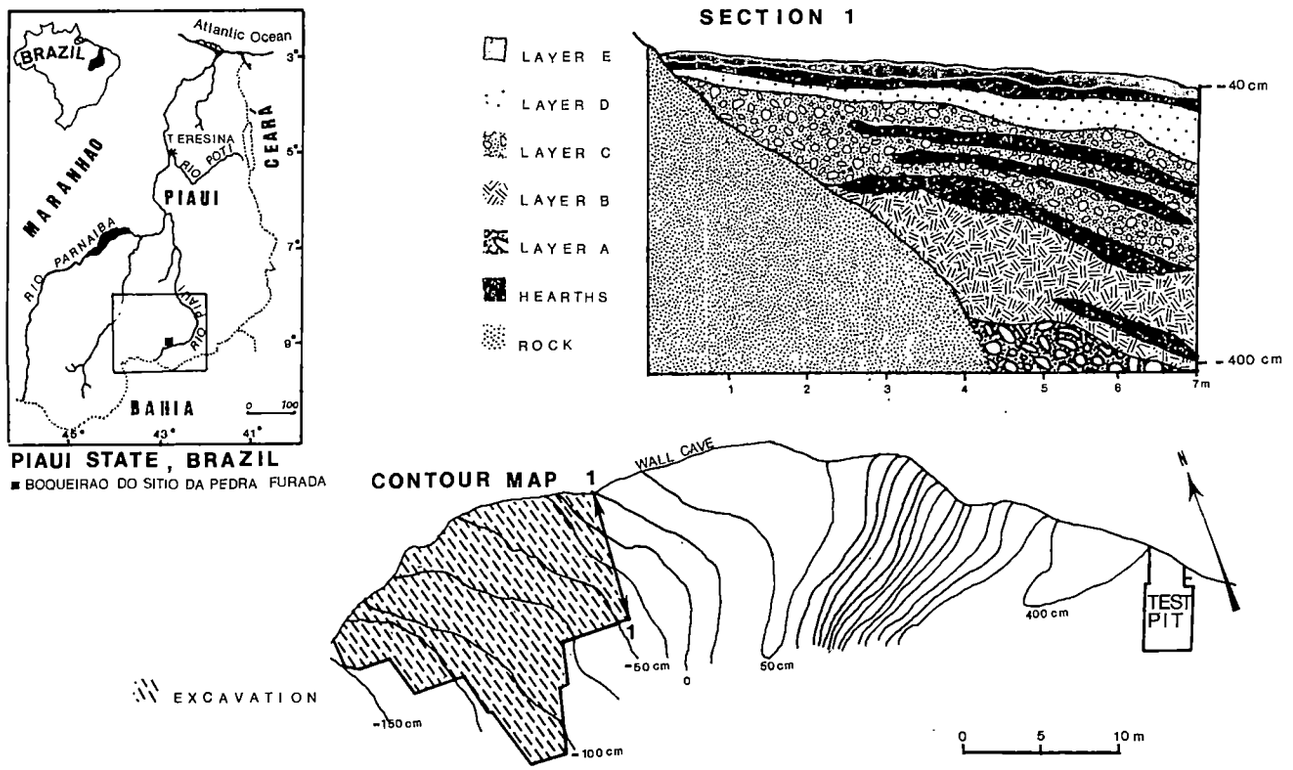


Fig. 1 The shelter 'Toca do Boqueirao do Sitio da Pedra Furada' is situated in the state of Piaui, in northeastern Brazil. This area, known by archaeologists as Sao Raimundo Nonato, is one of the most important in America, with 244 sites discovered there: 186 painted shelters, 13 painted and engraved shelters, 10 sites with only engravings, and 1 site with fossil megafauna. Five distinct sedimentological layers were distinguished, from the bottom to the top: **A**, beige-coloured sand containing coarse grains (≥1 mm): 5% pebbles and silt: 8.5 to 10.5%. The sediment is compact. **B**, compact beige-pink sand with silt: 6 to 8% and lower percentage of coarse grains. Pebbles are more abundant in some places. **C**, pinkish sand with silt, 4 to 6% and with gravels and pebbles in some places. **D**, brown to beige coloured sand with coarse grains (≥1 mm): 8% and gravels and pebble-beds in some places. This layer is rich in organic matter, mostly ash and charcoal. **E**, at the surface, brown-grey coloured layer with composition identical to that of the lower layers. It is very loose and contains numerous organic remains. The layers B, C, D and E contain saucers or lenses-shaped hearths characterized by a heavy concentration of ashes and charcoal.

Table 1 Carbon-14 dates in years BP and correlation between divisions and sedimentological layers for the site of Pedra Furada

Layers	Occupations		Chronology	Rock art
Layer E	Last occupations		Relative: 5,000 BP	Agreste tradition
Layer D	Phase Serra Talhada	IV Final Stage	6,160±130 BP (GIF 5863)	Nordeste tradition
		III Late Stage	7,750±80 BP (GIF 6161)	
			7,640±140 BP (GIF 4928)	
Layer C		II Middle Stage	8,050±170 BP (GIF 4625)	
			8,450±80 BP (GIF 6162)	
		I Early Stage	Relative: 10,000–12,000 BP	
	Phase Pedra Furada	IV Final Stage	17,000±400 BP (GIF 5397)	Fragments of pictographs spalled from the walls
		III Late Stage	21,400±400 BP (GIF 6160)	
Layer B		II Middle Stage	23,500+390 BP (GIF 6158)	Painted fragments spalled from the walls
			≥25,000 BP (GIF 5648)	
			≥25,000 BP (GIF 5398)	
			25,200±320 BP (GIF 6147)	
			26,300±800 BP (GIF 6309)	
			26,400±500 BP (GIF 5962)	
			27,000±800 BP (GIF 6308)	
			29,860±650 BP (GIF 6651)	
		I Early Stage	31,700±830 BP (GIF 6652)	Painted fragments spalled from the walls
			32,160±1,000 BP (GIF 6653)	
Layer A	First occupations		???	

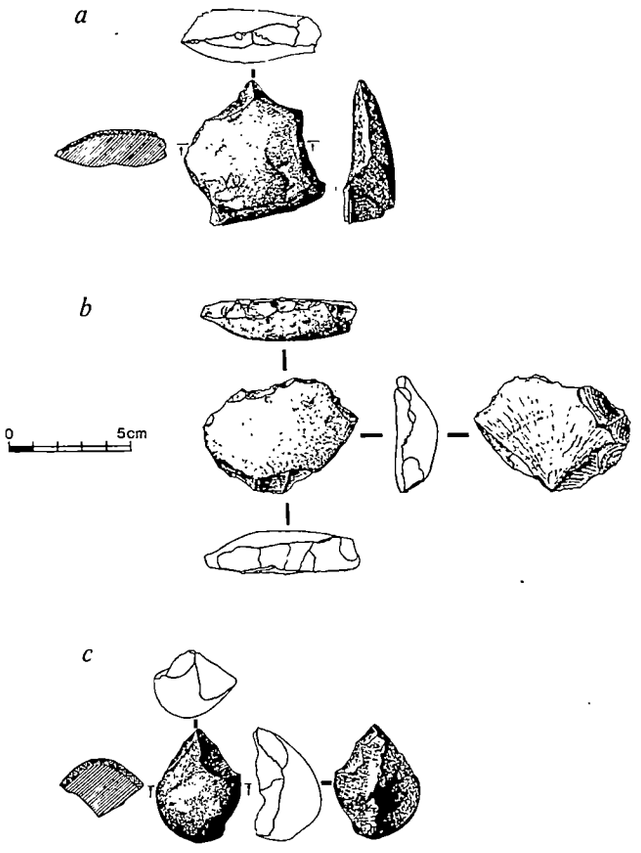


Fig. 2 Large quantities of lithic artefacts were recovered at Pedra Furada I. The lithic pieces are performed by unifacial retouching with a hard hammer although some bifacial pieces are present. *a*, A notched point made from quartz flake; the retouch on edges is flat and regular. *b*, *c*, Blunt points obtained by 2, 3 or 4 convergent flakings. Blunt points are made from flakes or pebbles, they show some traces of utilization.

The next stage, Pedra Furada II, produced 711 lithic pieces. Eight different hearths which correspond to eight distinct periods of occupation have been dated, giving ages from 23,000 ± 390 yr (Gif-6158) to 29,860 ± 650 yr (Gif-6651) (Table 1). Hence the site Pedra Furada was occupied at different times and probably on a temporary basis from 32,000 to 23,000 yr BP. This occupation is supported by the presence of numerous hearths and the abundant evidence of lithic industry.

The characteristic tools of Pedra Furada III are the blunt points made out of pebbles or flakes, along with chopping-tools, denticulates, knives, retouched and unretouched flakes, and pebbles bearing flaking scars. This stage was dated at 21,400 ± 400 yr (Gif-6160). A new series of occupations which represents the final stage of Pedra Furada is characterized by side-scrapers and blunt points. The other retouched pieces are small bifaces, denticulates and double-edged tools.

A carbon-14 date was obtained for one of the hearths and gave the age of 17,000 ± 400 yr (Gif-5397). A piece of rock with two red painted lines was found in the same hearth. This pictograph indicates the practice of rupestral art at that time and makes the site of Pedra Furada the most ancient rupestral art site known in America, and one of the most ancient in the world.

The upper layers of the site have produced artefacts which belong to another cultural unit, Serra Telhada: flint and siltite appear little by little and replace quartz, as the raw material for tools, the retouching of the tools is of better quality, and the hearths are of different types. The absence of hearths and charcoal have precluded the dating of the beginning of this phase. An age of between 10,000 and 12,000 years BP can be suggested based on analogy with lithic material found in a test pit in section E of the site which gave an age of 10,400 ± 180 yr (Gif-5862).

Higher in the stratigraphic column, a level of dense occupation is found. The hearths are surrounded by pebbles and blocks and the base covered by a slab, showing traces of successive utilizations. The lithic industry is quite varied and the flaking of blades is an innovation. The proportion of pieces of flint is important even though quartz and quartzite continue to be employed. Retouched pieces include end-scrapers, side-scrapers, knives, blunt points, planoconvex retouched blades and flakes, chopping-tools, bifaces, notched-pieces and pebble-hammers.

Ochre, which is present in large quantities in this level, as well as fragments of painted rock, suggest that rupestral art has been an important activity during this period, which has been placed between 8,050 ± 170 (Gif-4652) and 8,450 ± 80 yr (Gif-6162). Subsequently, the hearths become larger and more diversified in their structure. Towards the end of the phase Serra Telhada, they become elliptical in outline. Rich in ashes and charcoal, they also contain fragments of bone, wood, leaves, and fruit pits. Nearby are found a large quantity of lithic objects such as flint end-scrapers of three types: discoidal, steep, and nosed. The end of this phase has been dated at 6,160 ± 130 yr (Gif-5863). The uppermost sediments are very disturbed by recent human activity and cannot be used for study.

Thanks to the abundance of charcoal present in almost all of the levels, the occupation of this site has been dated in a systematic manner. The seventeen carbon-14 dates obtained from charcoal samples collected during the excavation of the site, are summarized in Table 1. From bottom to top, their succession is not only internally consistent but also consistent with the stratigraphy. These dates, along with the archaeological remains discovered, make it possible to establish the sequence of the different cultural phases of the site. They also establish the antiquity of the human presence in the region. Most archaeological sites known at present in America are not very old. The most ancient ones, the stratigraphy and the dating of which have not given rise to controversy, are comparatively young: 13,000-yr-old for the site of Monte Verde in Chile[3], 14,200-yr-old for the site of Alice Boer in Brazil[4] and 19,450 yr for Meadowcraft Rockshelter in Pennsylvania[5]. Others, recently claimed as being older, are doubtful since the presence of man has not been proved, or since the methods used for dating are questionable. An example of questionable dates is provided by the very old dates of bones, obtained by aspartic acid racemization[6]. Holocene ages were produced for these same samples when measured by accelerator mass spectrometry[7]. The present findings for the site of Pedra Furada testify to the presence of man in the north of South America 32,000 years ago, and strongly suggest that the migration from Asia to North America occurred earlier.

We thank W. Dudley for translating the French text and N. J. Shackleton, N. Hammond, and J-C Duplessy for helpful reviews of the preprint. CFR contribution no. 758.

Received 3 February; accepted 29 April 1986.

1. Guidon, N. *Proc. 10th Congresso UICPYP Mexico, Commission* XII, 101-110 (1980); in *New Evidence for the Pleistocene Peopling of Americas Orono: Center for Early Man Studies* (ed. Shutler, R. Jr) (Sage, Beverly Hills, in the press).
2. Guidon, N. thesis, Univ. Paris I (1984).
3. Dillehay, T. D. *Scient. Am.* **251**(4), 100-109 (1984).
4. Bryan, A. L. & Beltrao, M. C. *Occasional Papers* I, 303-305 (Department of Anthropology, University of Alberta, Edmonton, Canada, 1978).
5. Adovosio, J. M. & Carlisle, R. C. *Scient. Am.* **250**(5), 104-108 (1984).
6. Bada, J. L. & Helman, P. M. *World Archaeol.* **7**, 160 (1975).
7. Taylor, R. E. *et al. Science* **220**, 1271-1273 (1983).

Synaptosomes possess an exocytotic pool of glutamate

David G. Nicholls & Talvinder S. Sihra

Neurosciences Research Group, Ninewells Medical School, University of Dundee, Dundee DD1 9SY, UK

There is increasing evidence that L-glutamate is a major excitatory neurotransmitter in the central nervous system[1,2]. Immunocytochemical studies indicate that glutamate within nerve terminals may be concentrated in vesicles[3] and glutamate-accumulating vesicles have recently been isolated[4]. Exocytotic release of glutamate from synaptosomes (isolated nerve terminals) has not been convincingly demonstrated, however, and remains highly controversial[5–7]. In order to study the kinetics of release of endogenous L-glutamate from guinea pig cerebral cortical synaptosomes we have devised a continuous enzymatic assay. This has enabled us to identify a pool, equivalent to 15–20% of the total synaptosomal glutamate, which is capable of rapid Ca^{2+}-dependent exocytotic release.

If synaptosomes are incubated in a medium containing glutamate dehydrogenase and NAD^+, then release of the amino acid into the medium should cause an increase in fluorescence due to the formation of NADH. Figure 1 shows that this system has sufficient sensitivity to detect a release within seconds from less than 2 mg of synaptosomal protein. The advantages over existing techniques are considerable: detection is rapid and continuous; there is no need to chromatograph multiple samples to obtain a single time-course; complexities due to isotopic metabolism are avoided and errors due to incomplete isotopic equilibration between intrasynaptosomal compartments cannot arise.

Incubations of synaptosomes with polarized plasma membranes show a decrease in fluorescence once external glutamate has been assayed (Fig. 1*a*). The decrease is sensitive to rotenone and is due to the slow reoxidation of NADH by the small fraction of damaged mitochondria present in the incubation. Although it has been reported that synaptosomes degrade micromolar concentrations of added NAD^+[8], any hydrolysis of the 1mM NAD^+ added was insufficient to affect the sensitivity of the assay to glutamate, even after a 10 min preincubation.

When Ca^{2+}-depleted synaptosomes are depolarized by adding 30mM KCl to the incubation medium, efflux of glutamate is negligible for the first 15–20 s, after which there is a slow efflux (Fig. 1*b*). When KCl is added in the presence of Ca^{2+}, a much more rapid increase in fluorescence results (Fig. 1*c*). The fluorescence lags behind the actual glutamate release due to the finite activity of the glutamate dehydrogenase. This hysteresis may be quantified from the rate at which an added glutamate standard is assayed to completion and used to correct trace 1*c*. The correction is negligible for the slow release in the absence of Ca^{2+}. The corrected trace (Fig. 1*d*) shows that the Ca^{2+}-dependent component of glutamate release is complete by 30–45 s. In five experiments, the mean size of the rapid, Ca^{2+}-dependent component of glutamate efflux was 1.83 ± 0.2 nmol mg^{-1} ($n = 5$). For comparison, the glutamate released by complete permeabilization of the synaptosome with 0.05% Triton X100 was 11.0 ± 1.0 nmol mg^{-1} ($n = 4$).

NAD^+ inhibits evoked synaptic potentials in the guinea pig hippocampus[8]; however it does not appear to inhibit glutamate release from cortical synaptosomes because there is a good agreement between the release seen by the continuous assay in the presence of NAD^+ (Fig. 1*d*) and the release within 30 s of 2.1 ± 0.09 nmol glutamate mg^{-1} as determined by HPLC in the absence of NAD^+ (unpublished data). The fluorometric assay is insensitive to aspartate and any adenine nucleotides released are insufficient to affect the kinetics of the enzyme, since the extent and rate with which a standard glutamate addition is assayed is the same in the presence and absence of synaptosomes.

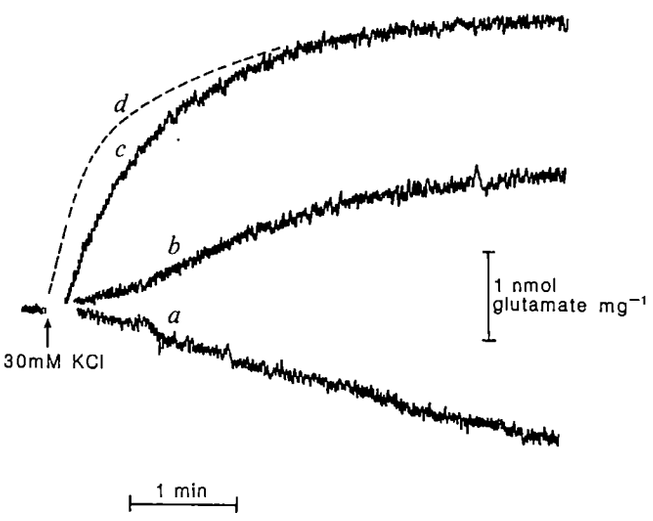


Fig. 1 Ca^{2+}-dependent release of endogenous L-glutamate. *a*, Control (Ca^{2+} present); *b*, KCl added, EGTA present; *c*, KCl added, Ca^{2+} present; *d*, the rate at which a standard addition of 6.5 μM L-glutamate was assayed was used to correct the Ca^{2+} + KCl trace for the hysteresis in the assay of the released amino acid. **Methods.** Synaptosomes prepared from cerebral cortices of Dunkin-Hartley guinea pigs[13] were suspended at 1.2 mg protein ml^{-1} in 1.5 ml medium, (3.1 mM KCl, 122 mM NaCl, 1.2 mM $MgSO_4$, 0.4 mM KH_2PO_4, 5 mM $NaHCO_3$, 20 mM Na-Tes, 10 mM D-glucose, 16 μM albumin, 1 mM NAD^+, 12.5% (w/v) Ficoll, *p*H 7.4 at 30 °C in a cuvette within an Eppendorf filter photometer with fluorescence attachment (excitation 313 + 366 nm; secondary 430–3000 nm). 1.3 mM $CaCl_2$ or 0.5 mM EGTA were added at 2 min, followed at 5 min by the addition of 50 units of L-glutamate dehydrogenase (EC 1.4.1.3). When the initial exogenous glutamate was assayed, the recorder trace was started and 30 mM KCl added where indicated.

In contrast to the results obtained with the fluorometric assay, the KCl-induced release of label from synaptosomes that had accumulated ^{14}C-L-glutamate for 20 min shows only slight dependency upon external Ca^{2+} (Fig. 2). Using HPLC, we determined that more than 90% of the isotope in the synaptosomes depolarized by adding KCl was present as glutamate plus aspartate. The discrepancy between the isotopic and fluorometric results indicate that there are two separate pools of glutamate, one labelled by ^{14}C-L-glutamate, which does not require Ca^{2+} for its release, and the other, inaccessible to labelled glutamate within the timescale of this experiment, which is Ca^{2+}-dependent. Because exogenous glutamate readily exchanges across the synaptosomal plasma membrane[9], we assume that the Ca^{2+}-dependent release detected by the fluorometric assay occurs from a noncytoplasmic compartment that does not equilibrate significantly with exogenous labelled glutamate under the conditions of the experiment.

The entry of ^{45}Ca and the elevation of cytosolic free Ca^{2+} show a sigmoidal dependency upon the extent of synaptosomal plasma membrane depolarization[10,11]. Figure 3 shows that the rate of glutamate release upon depolarization with KCl in Ca^{2+}-containing media is also sigmoidal, with a threshold potential of about 40 mV. In contrast, the Ca^{2+}-independent release of glutamate increases linearly with the extent of depolarization, consistent with release from the cytoplasm by reversal of the electrogenic glutamate transporter[12].

D-Aspartate exchanges across the synaptosomal plasma membrane on the same carrier as L-glutamate[9] and may therefore be used to exchange glutamate out of the cytoplasm. Fig. 4 shows that D-aspartate causes a Ca^{2+}-independent release of

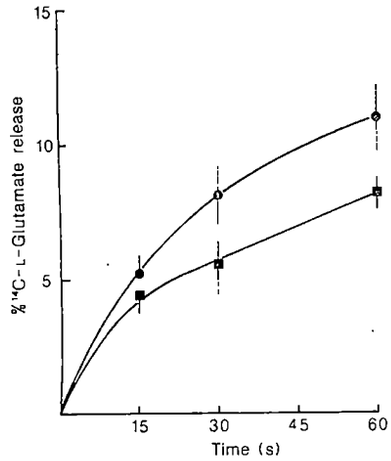


Fig. 2 Release of accumulated ^{14}C-L-glutamate is largely Ca^{2+}-independent. Synaptosomes were incubated at 1.5 mg protein ml^{-1} in the initial medium described in Fig. 1, with the omission of Ficoll and NAD^+. 1.3 mM $CaCl_2$, ^{3}H-sucrose (0.5 μCi ml^{-1}) and 0.35 μM ^{14}C-L-glutamate (0.1 μCi ml^{-1}) were added at 5 min. In one set of experiments 2 mM EGTA was added at 24 min to chelate exogenous Ca^{2+}. 20 mM KCl was added at 25 min, 250 μl aliquots were centrifuged after a futher 15s, 30s or 60s, and the retained ^{14}C quantified[14]. ●, 1.3 mM Ca present; ■, Ca chelated by 2 mM EGTA.

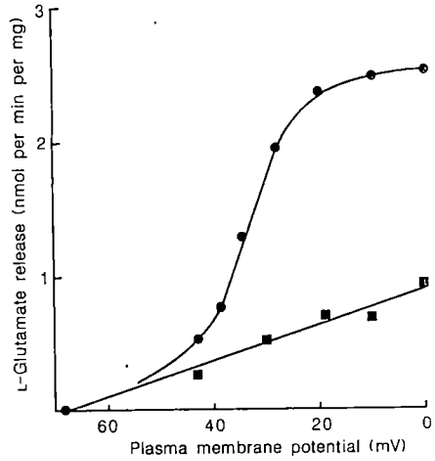


Fig. 3 Release of L-glutamate and plasma membrane depolarization. Synaptosomes were incubated as described in Fig. 1, except that the concentration of KCl added to initiate glutamate efflux varied from 6 to 48 mM. The plasma membrane potential was estimated from the ^{86}Rb distribution across the plasma membrane[15]. ●, 1.3 mM $CaCl_2$ present; ■, 0.5 mM EGTA present

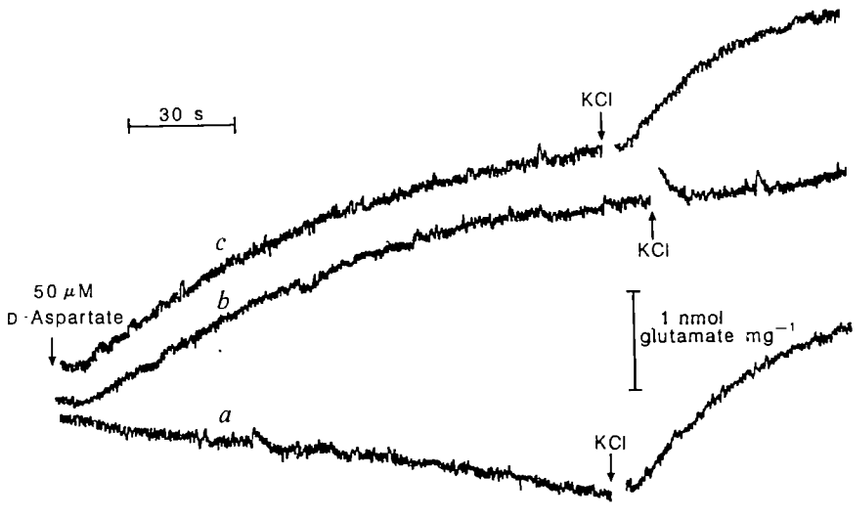


Fig. 4 Depletion of cytoplasmic L-glutamate by D-aspartate. *a*, control (1.3 mM $CaCl_2$ present, no D-aspartate); *b*, 0.5 mM EGTA present, D-aspartate added; *c*, 1.3 mM $CaCl_2$ present, D-aspartate added. Synaptosomes were incubated as described in Fig. 1. 50 μM D-aspartate was added to initiate release of cytoplasmic glutamate. Where indicated 30 mM KCl was added. Note that D-aspartate pretreatment does not inhibit the subsequent Ca^{2+}-dependent release of glutamate by KCl.

the amino acid which is as extensive as that induced by KCl (Fig. 1). If the D-aspartate were exchanging glutamate out of the "transmitter" pool, defined functionally as the Ca^{2+}-dependent component in Fig. 1, one would predict a very substantial diminution of the Ca^{2+}-dependent efflux induced by the subsequent addition of 30 mM KCl. This however is not seen; thus D-aspartate, although exchanging extensively with cytoplasmic glutamate, does not deplete glutamate from the "transmitter pool" within 3 min, providing further evidence for a noncytoplasmic origin for the latter.

The total glutamate in the system (determined with Triton X100) does not increase when D-aspartate is employed to exchange glutamate out of the cytosol. Thus there is no resynthesis of the cytosolic pool within the time course of the experiment in Fig. 4. When D-aspartate and KCl are added simultaneously, the rate of glutamate efflux is equal to the sum of the rates induced by each agent separately. Thus 50 μM D-aspartate released 0.52 nmol glutamate per min per mg protein; 30 mM KCl released 1.05 nmol per min per mg; while the two agents together released 1.58 nmol per min per mg.

These results show that 15–20% of the total glutamate in a preparation of guinea pig cerbrocortical synaptosomes can be rapidly released in a Ca^{2+}-dependent manner from a noncytoplasmic pool by depolarization of the plasma membrane. The continuous enzymatic assay of released glutamate can provide within 5 min the complete kinetics for the release of glutamate from either the cytoplasmic or "transmitter" pool and should prove a powerful tool in the elucidation of the energetic and ionic requirements for the exocytosis of this putative transmitter.

Received 6 November 1985; accepted 18 April 1986.

1. Cotman, C. W., Foster, A. & Lanthorn, T. in *Glutamate as a Neurotransmitter* (eds DiChiara, G. & Gessa. G.) 1–27 (Raven, New York, 1981).
2. Fonnum, F. *J. Neurochem.* **42**, 1–11 (1984).
3. Storm-Mathisen *et al.*, *Nature* **301**, 517–519 (1983).
4. Naito, S. & Ueda, T. *J. biol. Chem.* **258**, 696–699 (1983).
5. DeBelleroche, J. S. & Bradford, H. F. *J. Neurochem.* **29**, 335–343 (1977).
6. Levi, G., Banay-Schwartz, M. & Raiteri, M. *Neurochem. Res.* **6**, 275–285 (1981).
7. Wheeler, D. D. & Wise, W. C. *Neurochem. Res.* **8**, 1111–1134 (1983).
8. Snell, C. R., Snell, P. H. & Richards, C. D. *J. Neurochem.* **43**, 1610–1615 (1984).
9. Logan, W. J. & Snyder, S. H. *Brain Res.* **42**, 413–431 (1972).
10. Nachshen, D. A. & Blaustein, M. P. *J. gen. Physiol.* **76**, 709–728 (1980)
11. Heinonen, E., Akerman, K. E. O., Kaila, K. & Scott, I. G. *Biochim. biophys. Acta* **815**, 203–208 (1985).
12. Kanner, B. I. & Sharon, I. *Biochemistry* **17**, 3949–3953.
13. Nicholls, D. G. *Biochem. J.* **170**, 511–522 (1978).
14. Sihra, T. S., Scott, I. G. & Nicholls, D. G. *J. Neurochem.* **43**, 1624–1630 (1984).
15. Scott, I. D. & Nicholls, D. G. *Biochem. J.* **186**, 21–33 (1980).

Phosphorylation of the nicotinic acetylcholine receptor regulates its rate of desensitization

Richard L. Huganir*, Anne H. Delcour†‡, Paul Greengard* & George P. Hess†

* Laboratory of Molecular and Cellular Neuroscience, The Rockefeller University, New York, New York 10021, USA
† Section of Biochemistry, Molecular and Cell Biology, Cornell University, Ithaca, New York, 14853, USA

Recent studies have provided evidence for a role of protein phosphorylation in the regulation of the function of various potassium and calcium channels (for reviews, see refs 1, 2). As these ion channels have not yet been isolated and characterized, it has not been possible to determine whether phosphorylation of the ion channels themselves alters their properties or whether some indirect mechanism is involved. In contrast, the nicotinic acetylcholine receptor, a neurotransmitter-dependent ion channel, has been extensively characterized biochemically[3] and has been shown to be directly phosphorylated[4,5]. The phosphorylation of this receptor is catalysed by at least three different protein kinases (cyclic AMP-dependent protein kinase, protein kinase C and a tyrosine-specific protein kinase) on seven different phosphorylation sites[6–8]. However, the functional significance of phosphorylation of the receptor has been unclear. We have now examined the functional effects of phosphorylation of the nicotinic acetylcholine receptor by cAMP-dependent protein kinase. We investigated the ion transport properties of the purified and reconstituted acetylcholine receptor before and after phosphorylation. We report here that phosphorylation of the nicotinic acetylcholine receptor on the γ- and δ-subunits by cAMP-dependent protein kinase increases the rate of the rapid desensitization of the receptor, a process by which the receptor is inactivated in the presence of acetylcholine (ACh). These results provide the first direct evidence that phosphorylation of an ion channel protein modulates its function and suggest that phosphorylation of postsynaptic receptors in general may play an important role in synaptic plasticity.

The purified nicotinic acetylcholine receptor is a pentameric complex, which consists of four types of subunits in the stoichiometry $\alpha_2\beta\gamma\delta$ (ref. 3). This pentameric complex is fully functional biologically when reconstituted into phospholipid vesicles[3]. The ion transport properties of the reconstituted receptor can be analysed quantitatively by measuring the ACh-dependent transport of cations into vesicles by rapid kinetic techniques[9]. The nicotinic acetylcholine receptor in *Torpedo californica* postsynaptic membrane preparations was phosphorylated using the catalytic subunit of cAMP-dependent protein kinase in the presence of ATP (see Fig. 1 legend). This kinase phosphorylates a single serine residue in the γ-subunit and δ-subunit of the receptor that we have previously proposed to be serine 354 (γ-subunit) and serine 361 (δ-subunit)[6–8]. Under the standard conditions used, the γ- and δ-subunits were each phosphorylated to a final stoichiometry of 0.6–0.7 mol phosphate per mol of subunit (data not shown). Following the phosphorylation reaction, the postsynaptic membranes were solubilized with 1% Na-cholate and the nicotinic acetylcholine receptor purified by affinity chromatography[10]. Control non-phosphorylated receptor was prepared under identical conditions except that the catalytic subunit of cAMP-dependent protein kinase or ATP or both were omitted from the reaction mixture. (The three types of control preparations gave virtually identical results.) The purified receptor preparations were then reconstituted into phospholipid vesicles by cholate dialysis[10], and quench-flow[11] and stop-flow[12] rapid kinetic techniques were used to analyse the properties of the ACh-dependent ion transport of the non-phosphorylated and phosphorylated receptor preparations.

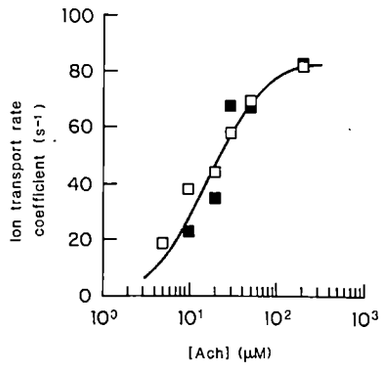


Fig. 1 Rate coefficient of ion transport (J_A) of the phosphorylated (0.6 mol phosphate per mol subunit) (■) and non-phosphorylated (□) receptor preparations as a function of acetylcholine (ACh) concentration.

Methods. Postsynaptic membrane preparations highly enriched in the nicotinic acetylcholine receptor were isolated from the electric organ of *T. californica*[10] and alkali-treated[25] to increase the permeability of the membrane vesicles to exogenous reagents. The postsynaptic membranes were then diluted to 1.4 mg ml^{-1} in the phosphorylation reaction mixture, which contained 20 mM Tris-HCl (*p*H 7.4), 2 mM EGTA, 1 mM EDTA, 10–20 mM $MgCl_2$, 1 mM β-mercaptoethanol, 1 mM ouabain, 1 mM Na_2VO_4, 20 μg ml^{-1} leupeptin, 20 μg ml^{-1} antipain, 20 units ml^{-1} trasylol, 0.5 mM ATP and 100 nM of purified catalytic subunit of cAMP-dependent protein kinase. The phosphorylation reaction was carried out for 60 min at 30 °C, Na-cholate was then added to a final concentration of 0.3% and the mixture incubated for an additional 15 min at 30 °C. After cooling on ice, the receptor was solubilized with a final concentration of 1% Na-cholate and purified from the cholate extract on an ACh affinity column. The control non-phosphorylated receptor was prepared under identical conditions, except that ATP or the catalytic subunit, or both, were omitted from the reaction mixture. The two receptor preparations (~5 mg each) were reconstituted into phospholipid vesicles (asolectin) at a final concentration of ~0.45 mg ml^{-1} receptor and 25 mg ml^{-1} asolectin by cholate dialysis[10], in the following buffer: 20 mM Tris Cl (*p*H 7.4), 100 mM NaCl, 50 mM KCl, 1 mM EDTA, 1 mM EGTA. The vesicles were frozen in liquid nitrogen in the absence (for quench-flow) or presence (stop-flow) of 10 mM 1,5-anthracene disulphonate and thawed before use. The ion transport properties of the reconstituted receptor preparations were analysed at 4 °C by measuring either the direct transport of $^{86}Rb^+$ (quench flow), or the quenching of the fluorescent dye, 1,5-anthracene disulphonate by Cs^+ (stop-flow) as described previously[11,12]. The rate coefficient for ion transport at ACh concentrations smaller than 50 μM was obtained from a nonlinear least-squares fit of Cs^+ influx curves, measured with the stop-flow technique and normalized to the values of J_A at 50 μM or 200 μM ACh which were obtained with the quench-flow technique as described elsewhere[13,14].

We first determined the initial rates of ACh-dependent ion transport by the non-phosphorylated and phosphorylated acetylcholine receptor over a wide range of ACh concentrations (Fig. 1). The rates of ion transport characterized by the rate coefficient J_A of the non-phosphorylated and phosphorylated receptor had the same dependence on ACh concentration. This indicated that the dissociation constant of ACh for the sites that activate the receptor was unchanged by phosphorylation.

In contrast, when the rates of the rapid desensitization of the non-phosphorylated and phosphorylated receptor were measured directly, a striking difference was observed (Fig. 2). The rapid desensitization was measured by the quench-flow technique by preincubation of reconstituted vesicles with ACh for various periods of time (T) before the determination of the rate of ion transport[13,14]. The data in Fig. 2 show the per cent ion transport activity remaining after preincubation of the non-

‡ Present address: Department of Biochemistry, University of Wisconsin-Madison, Madison, Wisconsin 53706, USA.

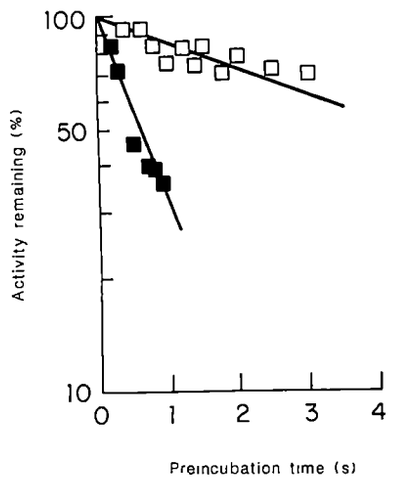


Fig. 2 Desensitization of the non-phosphorylated (□) and phosphorylated (■) nicotinic acetylcholine receptor. The reconstituted vesicles were preincubated with 10 μM ACh for the times indicated and then the ion transport activity was measured for 12 ms with 50 μM ACh using $^{86}Rb^{+}$ (refs 14, 26). The data were fitted to the following equation using a nonlinear least-squares program:

$$(J_A)_T = (J_A)_{T=0}\, e^{-\alpha T} \quad (1)$$

where $(J_A)_T$ is the ion transport rate coefficient after preincubation of the receptor with ACh for the period of time (T) given on the abscissa of the graph, $(J_A)_{T=0}$ is the ion transport rate coefficient prior to desensitization, and α is the desensitization rate coefficient. The 'activity remaining' given on the ordinate is $[(J_A)_T/(J_A)_{T=0}]\times 100$. □, Average data obtained with the three non-phosphorylated preparations ($\alpha = 0.15 \pm 0.02\ s^{-1}$); ■, averaged data obtained with two preparations of receptors phosphorylated to a stoichiometry of 0.6 mol phosphate per mol γ- and δ-subunits ($\alpha = 1.1 \pm 0.1\ s^{-1}$).

phosphorylated and phosphorylated receptor preparations with 10 μM acetylcholine for the indicated times. The ion transport activity of both receptor preparations decreased as the preincubation time was increased and was described by a first-order rate law with the slope of the line proportional to the desensitization rate coefficient (α). The rate of desensitization of the non-phosphorylated receptor was similar to the rate previously described for the rapid desensitization in *Torpedo*[14]. The rate of desensitization of the phosphorylated receptor was 7–8 times faster than the rate of desensitization of the non-phosphorylated receptor. Figure 2 shows only the initial phase of the desensitization reaction to help visualize the difference in desensitization rates between the two preparations.

To investigate the effect of the stoichiometry of phosphorylation of the receptor on the desensitization process, we analysed the desensitization of receptor preparations phosphorylated to different extents. The data in Fig. 3*a* and *b* compare results obtained with receptor preparations that were phosphorylated on the γ- and δ-subunits to a stoichiometry of 0.4 mol phosphate per mol subunit and 0.6 mol phosphate per mol subunit respectively. With each of the preparations, when the time course of desensitization was followed to near completion, the data could not be fit with a single exponential and were best fit to the sum of two exponentials (see Fig. 3 legend). In contrast, control non-phosphorylated preparations displayed only a single exponential decay (data not shown). These results indicate that two different receptor populations existed in both phosphorylated preparations.

From the experiment shown in Fig. 2, we can equate the initial steeper slope seen in Fig. 3 with desensitization of the phosphorylated receptor and the final more shallow slope with that of the non-phosphorylated receptor. The intercept of the final slope with the ordinate represents the per cent of the ion transport associated with the receptors characterized by the slower

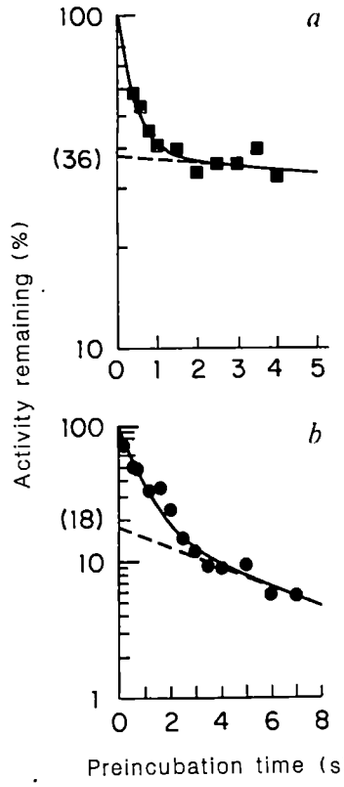


Fig. 3 Double exponential desensitization rate of the phosphorylated acetylcholine receptor. Desensitization of phosphorylated acetylcholine receptor preparations was measured as described in Fig. 2 legend. *a*, Receptor phosphorylated on the γ- and δ-subunits to a stoichiometry of 0.4 mol phosphate per mol subunit. 10 μM ACh was used in the preincubation and 50 μM ACh in the 12-ms influx measurement. *b*, Receptor phosphorylated on the γ- and δ-subunits to a stoichiometry of 0.6 mol phosphate per mol subunit. 50 μM ACh was used in the preincubation and in the 12-ms influx measurement. The 'activity remaining' given on the ordinate is $[(J_A)_T/(J_A)_{T=0}]\times 100$. The rate coefficients of the two exponentials were calculated according to the following equation:

$$(J_A)_T = (J_A)_{T=0}[a\, e^{-\alpha_N T} + b\, e^{-\alpha_P T}]$$

$(J_A)_T$ and $(J_A)_{T=0}$ are defined in Fig. 2 legend and α_N and α_P indicate the constants characteristic of the non-phosphorylated and phosphorylated receptor, respectively; a and b represent the fractions of the preparation associated with the non-phosphorylated and phosphorylated receptors, respectively. All parameters (a, b, α_N, and α_P) were determined from a nonlinear least-squares fit of the data to the above equation.

desensitization rate. In the receptor preparation that was phosphorylated to a stoichiometry of 0.4 mol phosphate per mol subunit, 64% of the preparation desensitized with the increased rate while 36% desensitized with the slow rate (Fig. 3*a*). In the receptor preparation that was phosphorylated to a stoichiometry of 0.6 mol phosphate per mol subunit, 82% of the preparation desensitized with the increased rate while 18% desensitized with the slow rate (Fig. 3*b*).

Assuming that phosphorylation of the γ- and δ-subunits occurs independently, four different populations of receptors would exist: those that are phosphorylated on neither subunit, those that are phosphorylated on only the γ-subunit, those that are phosphorylated on only the δ-subunit, and those that are phosphorylated on both subunits. Given this assumption, and the stoichiometry of phosphorylation of the receptor preparations used for the experiments in Fig. 3, the percentage of receptor molecules that would contain at least one phosphate group would be 64% and 84%, respectively. These values are in excellent agreement with the 64% and 82% calculated (from the intercepts of the final slopes in Fig. 3 with the ordinate) for

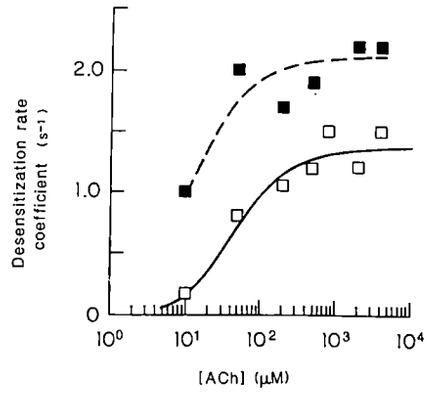


Fig. 4 Rate coefficient for desensitization of the phosphorylated receptor (α_P, ■) and non-phosphorylated receptor (α_N, □) as a function of acetylcholine concentration. Receptor preparations were phosphorylated to a final stoichiometry of ~0.6 mol phosphate per mol γ- and δ-subunits. Desensitization of the nonphosphorylated and phosphorylated receptor was measured at various ACh concentrations. The rate coefficient of the phosphorylated receptor was obtained by analysis of the desensitization data according to the equation given in Fig. 3 legend using the values of α_N determined experimentally and the values of *a* and *b* observed in Fig. 3*b*. Four different phosphorylated and non-phosphorylated preparations were used to obtain the α values over the concentration range shown.

the percentage of receptors that desensitize with the fast rate. The simplest model which accounts for these results is that the ion transport rate is unchanged by phosphorylation (see Fig. 1) and that phosphorylation of either the γ- or δ-subunit or both results in the observed increase in the rate of desensitization.

The dependence on the ACh concentration of the desensitization rate coefficient (α) of the non-phosphorylated and phosphorylated receptor preparations is shown in Fig. 4. The rate of desensitization of the phosphorylated receptor was significantly greater than that of the dephosphorylated receptor over the whole concentration range. The most dramatic differences were seen at low concentrations of ACh, since the ACh concentration required to reach the half-maximal desensitization rate was several-fold lower for the phosphorylated receptor.

The results presented here demonstrate that phosphorylation of the γ- and δ-subunits of the nicotinic acetylcholine receptor increases the rate of the rapid desensitization of the receptor. Our results also indicate that phosphorylation of the receptor does not affect either the rate of ion transport or the apparent dissociation constant of acetylcholine for the activation of ion transport. In addition, preliminary results from patch-clamp studies of reconstituted vesicles[15] indicated that phosphorylation of the γ- and δ-subunits has little or no effect on the single-channel conductance or mean channel open-time (D. W. Tank and R.L.H., unpublished results).

Recent studies with intact muscle preparations have shown that forskolin, an activator of adenylate cyclase, dramatically increases the rate of desensitization of the nicotinic acetylcholine receptor[16,17]. In addition, it has recently been reported that agents that activate protein kinase C increase the rate of desensitization of the acetylcholine receptor in cultured myotubes[18]. These *in vivo* results, together with the *in vitro* results of the present study, suggest that phosphorylation of the nicotinic acetylcholine receptor by either cAMP-dependent protein kinase or protein kinase C increases its rate of desensitization. This is interesting in the light of our proposal[8] that the phosphorylation sites for cAMP-dependent protein kinase and for protein kinase C are located on a common region of each subunit, with the two phosphorylation sites on the δ-subunit being within 16 amino acids of each other. These regions are the major intracellular loops adjacent to the membrane-spanning α-helices that are proposed to form the ion channel in the theoretical models of the receptor[19–23]. Our results suggest that these intracellular loops are intimately involved in the process of desensitization. Desensitization has been proposed to be a form of short-term regulation, in the second to minute time range, of synaptic efficacy (see, for example, refs 3, 9, 24). Although desensitization of the nicotinic acetylcholine receptor clearly occurs in non-phosphorylated receptor preparations, it is also clear that phosphorylation can dramatically modify the desensitization process. In addition, the present results support the idea (see, for example, ref. 3) that phosphorylation of postsynaptic receptors is a plausible although speculative molecular model for short-term and long-term learning at the neuronal level.

We thank Gene Yee and Lisa Moritz for technical assistance. The purified catalytic subunit of cAMP-dependent protein kinase was generously supplied by Dr Angus Nairn, This work was supported by a grant from The Council for Tobacco Research USA Inc. (to R.L.H.) and grant 84-10816 from the National Science Foundation (to G.P.H.) The kinetic experiments presented here were part of A.H.D.'s dissertation, submitted to the Graduate School of Cornell University in partial fulfilment of the requirements for his doctorate.

Received 14 March; accepted 9 April 1986.

1. Levitan, I. B. *J. Membrane Biol.* **87**, 177–190 (1985).
2. Browning, M. D., Huganir, R. L. & Greengard, P. *J. Neurochem.* **45**, 11–23 (1985).
3. Changeux, J. P., Devillers-Thiery, A. & Chemouilli, P. *Science* **225**, 1335–1345 (1984).
4. Gordon, A. S., Davis, C. G., Milfay, D. & Diamond, I. *Nature* **267**, 539–540 (1977).
5. Teichberg, V. I., Sobel, A. & Changeaux, J.-P. *Nature* **267**, 540–542 (1977).
6. Huganir, R. L. & Greengard, P. *Proc. natn. Acad. Sci. U.S.A.* **80**, 1130–1134 (1983).
7. Huganir, R. L., Albert, K. A. & Greengard, P. *Soc. Neurosci. Abstr.* **9**, 578 (1983).
8. Huganir, R. L., Miles, K. & Greengard, P. *Proc. natn. Acad. Sci. U.S.A.* **81**, 6968–6972 (1984).
9. Hess, G. P., Cash, D. J. & Aoshima, H. *A. Rev. Biophys. Bioengng* **12**, 443–473 (1983).
10. Huganir, R. L. & Racker, E. *J. biol. Chem.* **257**, 9372–9378 (1982).
11. Hess, G. P., Cash, D. J. & Aoshima, H. *Nature* **282**, 319–331 (1979).
12. Karpen, J. W., Sachs, A. B., Cash, D. H., Pasquale, R. B. & Hess, G. P. *Analyt. Biochem.* **135**, 83–94 (1983).
13. Aoshima, H., Cash, D. J. & Hess, G. P. *Biochemistry* **20**, 3467–3474 (1981).
14. Hess, G. P., Pasquale, E. B., Walker, J. W. & McNamee, M. G. *Proc. natn. Acad. Sci. U.S.A.* **79**, 963–967 (1982).
15. Tank, D. W., Huganir, R. L., Greengard, P. & Webb, W. W. *Proc. natn. Acad. Sci. U.S.A.* **80**, 5129–5133 (1983).
16. Middleton, P., Jaramillo, F. & Scheutze, S. M. *Proc. natn. Acad. Sci. U.S.A.* (in press).
17. Albuquerque, E., Desparde, S. S., Arcava, Y., Alkondon, M. & Daly, J. W. *Febs Lett.* **199**, 113–120 (1986).
18. Eusebi, F., Molinaro, M. & Zani, B. M. *J. cell Biol.* **100**, 1339–1342 (1985).
19. Noda, M. *et al. Nature* **302**, 528–532 (1983).
20. Claudio, T., Ballivet, M., Patrick, J. & Heinemann, S. *Proc. natn. Acad. Sci. U.S.A.* **80**, 1111–1115 (1983).
21. Devillers-Thiery, A., Giraudat, J., Bentaboulet, M. & Changeux, J. P. *Proc. natn. Acad. Sci. U.S.A.* **80**, 2067–2071 (1983).
22. Finer-Moore, J. & Stroud, R. M. *Proc. natn. Acad. Sci. U.S.A.* **81**, 155–159 (1984).
23. Guy, H. R. *Biophysics J.* **45**, 249–261 (1984).
24. Changeux, J. P. *et al.* Cold Spring Harb. Symp. quant. Biol. **47** (1983).
25. Neubig, R. R., Krodel, E. K., Boyd, N. D. & Cohen, J. B. *Proc. natn. Acad. Sci. U.S.A.* **2**, 690–694 (1979).
26. Cash, D. J. & Hess, G. P. *Analyt. Biochem.* **112**, 39–51 (1981).

Purification and characterization of an FSH releasing protein from porcine ovarian follicular fluid

Wylie Vale, Jean Rivier, Joan Vaughan, Richard McClintock, Anne Corrigan, Wilson Woo, David Karr & Joachim Spiess

Clayton Foundation Laboratories for Peptide Biology, Salk Institute, 10010 North Torrey Pines Road, La Jolla, California 92037, USA

A variety of hypophysiotropic peptides or proteins have been reported to be present in mammalian gonads. Inhibin, a hormone that under most circumstances selectively suppresses the secretion of follicle-stimulating hormone (FSH) but not luteinizing hormone (LH), has been isolated from the gonadal fluids of several species[1–5] and characterized as a heterodimeric protein consisting of α- and β-polypeptides associated by disulphide bonds. The complete amino-acid sequences of the precursors of porcine[6,7] and human[7] inhibin α-subunits and two distinct porcine inhibin β-subunits

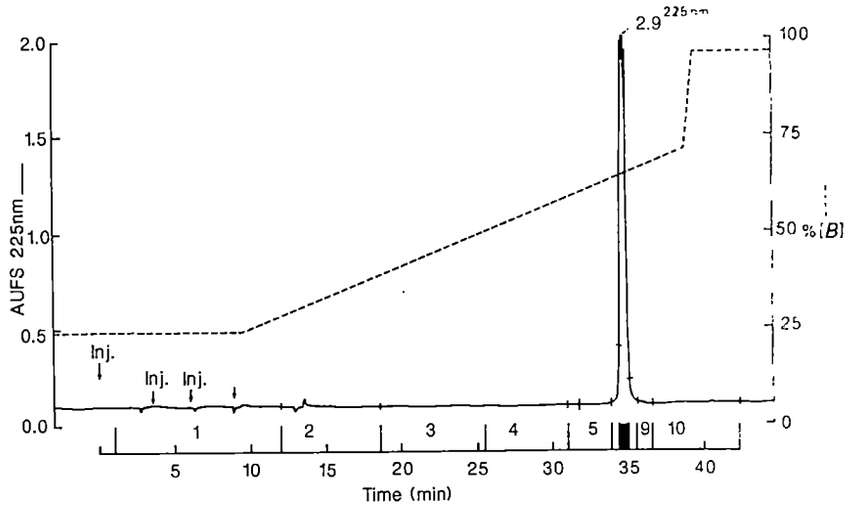


Fig. 1 Elution profile on analytical HPLC of FRP bioassayed and purified as described below. AUFS, absorbance units full scale. **Bioassay:** Rat anterior pituitary glands were dissociated enzymatically and the cells plated as described previously[3,15]. After washing the cells twice, treatments were added and allowed to remain on the cells for 48–72 h, after which fluids were removed and tested for FSH using a radioimmunoassay kit provided by the National Hormone and Pituitary Program of NIADDK. For reverse-phase HPLC columns, aliquots for assays (0.1–1.0% of total fraction volume but never less than 5 μl) were measured with micropipettes and plastic tips and were transferred into polypropylene tubes containing bovine serum albumin (10 μl of 10 mg ml^{-1}) and dried in a Savant rotary evaporator. For gel permeation and ion-exchange columns where desalting was necessary before assay, small aliquots were removed and transferred to glass tubes containing 0.5 ml of 10 mM HEPES + 0.1% bovine serum albumin *p*H 7.5. Squares of dialysis tubing with a M_r cutoff of ~1,000 were secured over the tops with rubber bands. The tubes were inverted and dialysed against 10 mM HEPES, *p*H 7.5. The retentates were then dried using a Savant rotary evaporator. All fractions were resuspended in cell culture assay medium. **Ammonium sulphate precipitation and ultrafiltration:** Porcine follicular fluid (6,050 ml) was made available to us by the Contraceptive Development Branch of NICHD, and thawed and centrifuged at 700*g* for 5 min to separate cell debris. An equal volume of Schwartz/Mann ultrapure 100% saturated ammonium sulphate, adjusted to *p*H 7.8 with ammonium hydroxide, was added dropwise to the crude supernatant over 2–3 h. The mixture was centrifuged at 8,200*g* for 30 min and the supernatant and precipitate were separated. The supernatant was ultrafiltered and concentrated using a Millipore Pellicon Cassette system with 5 square feet of filters of 10,000 M_r cutoff at a rate of 300 ml min^{-1}, using a peristaltic pump with back pressure applied until the filtration rate was 20 ml min^{-1}. The retentate was washed several times with 10 mM HEPES and 0.05% dimethyl sulphide, *p*H 7.5. The final retentate was collected (6,050 ml-equiv. in 2.24 l). **Preparative reverse-phase HPLC[3]:** 500 ml-equiv. or less per run was processed on a Waters Prep 500A using Vydac end-capped C_4 silicas, 15–20 μm particle size in a 5 × 30 cm cartridge The column temperature was thermostated at 60 °C. Buffer A was 0.1% H_3PO_4, 0.28% triethyl ammonium (TEA), *p*H 6.5; buffer B was 60% *n*-propanol in buffer A Columns were loaded at 20% buffer B; gradient used was 20% B to 65% B in 45 min. Flow rate was 75 ml min^{-1}. FSH releasing activity eluted between retention volumes 825 and 1,360 ml from the start of the gradient. **Gel permeation chromatography:** Active zones from preparative reverse-phase HPLC were pooled, lyophilized and brought up in gel permeation column eluant. Column eluant was 6 M guanidine-HCl, 0.1 M ammonium acetate, 0.05% dimethyl sulphide, *p*H 4.75. Eluant was filtered at 0.22 μm and degassed before use. A 10 × 120 cm column (volume 8,600 ml) of Sepharose CL-6B was used at a flow rate of 180 ml h^{-1}. FSH releasing activity eluted between K_{AV} 0.54 and 0.71. **Cation exchange on FPLC:** Active fractions from the gel permeation chromatography were pooled and dialysed against Milli H_2O + 0.01% dimethyl sulphide using tubing with a M_r cutoff of 1,000. The retentate was lyophilized and brought up in buffer A. Buffer A was 50 mM sodium formate, 4 M urea, 1 mM CHAPS (3-[(cholamidopropyl)dimethylammonio]-1-propanesulphonate) in Milli Q H_2O, *p*H 4.3. Buffer B was 1 M NaCl in buffer A. Buffers were filtered at 0.22 μm and degassed before use. FRP fractions were processed in three equal batches using a Pharmacia FPLC system equipped with a Mono S HR 16/10 column, V_t = 20 ml. Flow rate, 8 ml min^{-1}. The sample was loaded in buffer A and the column was then run isocratically at 15% buffer B for 7 min followed by a gradient from 15% to 50% B in 15 min. Two active zones of FRP resulted from cation exchange. The later-eluting zone, which eluted from 0.43 to 0.60 NaCl, was purified further. **Semi-prep reverse-phase HPLC[3]:** FRP was purified further and desalted on a Beckman HPLC using Vydac 1 × 30 cm columns packed with end-capped C_8 silicas, 5 μm particle size. Buffer A was 0.1% trifluoroacetic acid (TFA); buffer B was 80% CH_3CN in 0.1% TFA Columns were thermostated at 40 °C and run at 2.5 ml min^{-1} isocratically at 25% buffer B for 17 min followed by a gradient to 55% B in 30 min. Activity eluted between retention volumes 60 and 65 ml from the start of the gradient. **FPLC gel permeation:** Active zones from analytical reverse-phase HPLC of FRP were processed on a Pharmacia FPLC system using tandem Superose 12B columns, 10 μm, 10 × 300 mm each. Column eluant was 6 M guanidine-HCl, 0.1 M ammonium acetate, 0.05% dimethyl sulphide, *p*H 4.75 in Milli Q H_2O. Buffer was filtered at 0.22 μm and degassed before use. Flow rate, 0.4 ml min^{-1}. Activity was eluted between K_{AV} 0.26 and 0.31. **Analytical reverse-phase HPLC:** The active zone of FRP was processed using a Vydac C_8, 0.46 × 25 cm column using the Beckman system at 40 °C. Buffer A was 0.1% TFA, buffer B was 80% CH_3CN in 0.1% TFA. Approximately 1,000 ml-equiv. was loaded at a time, starting initially at 25% buffer B, 1.2 ml min^{-1}, and running a gradient to 45% B in 30 min with a flow rate of 0.7 ml min^{-1}. The active fractions of FRP were pooled, then concentrated on a steep gradient of 25% B initially to 72% B in 30 min. FSH releasing activity eluted as shown.

(β_A and β_B)[6] have been deduced from complementary DNA sequences. Gonadotropin releasing peptides have also been found in the gonad and have generally been shown to be active in radioreceptor assays for gonadotropin releasing hormone (GnRH) but to exhibit different chromatographic and immunological characteristics from those of GnRH[8–14]. During our purification of inhibin from porcine follicular fluid, we noted fractions that could stimulate the secretion of FSH by cultured anterior pituitary cells[3]. We report here the purification of an FSH releasing protein (FRP) and its characterization by SDS-polyacrylamide gel electrophoresis under non-reducing and reducing conditions and by partial sequence analysis. Our results indicate that porcine gonadal FRP is a homodimer consisting of two inhibin β_A-chains linked by disulphide bonds. FRP is highly potent (50% effective concentration (EC_{50}) ~ 25 pM) in stimulating the secretion and biosynthesis of FSH but not of LH or any other pituitary hormone. In contrast to the effects of GnRH and other reported gonadal gonadotropin releasing fractions, the action of FRP is not mediated by GnRH receptors.

The dialysed supernatant from a 50% ammonium sulphate precipitation of 6 litres of porcine follicular fluid was subjected to preparative HPLC as described previously[3]. FSH releasing activity was observed in the early-eluting, retarded fractions, and was thereby separated from the two major FSH release inhibiting (inhibin) zones, which were either not retarded or eluted later.

We hypothesized that an FSH releasing activity was due to an FSH releasing protein and we decided to purify this (Table 1) and characterize it chemically. The assay for FRP was based on the ability of the protein to stimulate basal FSH secretion by cultured rat anterior pituitary cells[3,15]. The FSH releasing zones from preparative reverse-phase HPLC were subjected to gel filtration on Sepharose CL6B in a strongly dissociating buffer containing 6 M guanidine-HCl. We noted at this point that FRP behaved similarly on gel permeation to the 32,000 (32K)-relative molecular mass (M_r) form of inhibin which had been separated earlier by preparative HPLC. The FSH releasing fractions were then purified further by cation exchange chromatography on fast protein liquid chromatography using Mono-S in a buffer containing urea and the detergent CHAPS at *p*H 4.3, and eluted by a gradient of 0–1 M NaCl. Two regions of FSH releasing activity were detected. The later-eluting zone had the higher specific activity and was purified further by semi-preparative reverse-phase HPLC, gel permeation on FPLC in 6 M guanidine-HCl and two steps of analytical reverse-phase HPLC (Fig. 1). On SDS-polyacrylamide gel electrophoresis (Fig. 2), purified non-reduced FRP showed a major band of M_r ~28,000. Bioassay of fractions that eluted from a similar gel confirmed that FSH releasing activity was associated with this band. Under reducing conditions, FRP converted to a species of M_r ~ 15,000. An aliquot of highly purified FRP was subjected to Edman degradation and the N-terminal sequence (Fig. 3) was found to

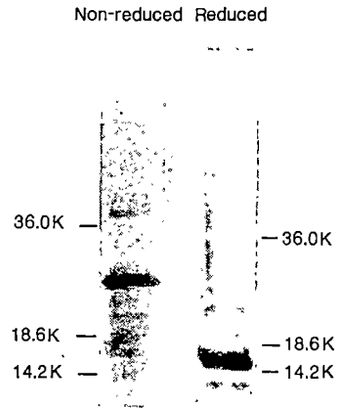


Fig. 2 SDS-polyacrylamide electrophoresis of FRP. Aliquots (0.3–0.8 μg) of the FRP fraction used for Edman degradation (see Fig. 3) were treated with 2% SDS in the presence and absence of 5% (v/v) β-mercaptoethanol for 15 min at room temperature and subjected in separate experiments to electrophoresis in polyacrylamide gels consisting of a stacking gel (5% acrylamide) and a gel of decreasing pore size (10–20% acrylamide). Bands were detected by silver staining. The mobilities of protein markers (glyceraldehyde 3-phosphate dehydrogenase (36K), β-lactoglobulin (18.6K) and α-lactalbumin (14.2K)) are indicated.

be identical to the N-terminal 38 residues of the porcine inhibin β_A-chain[6]. Another aliquot was reduced, *S*-carboxymethylated and purified by HPLC. The major protein zone was digested with clostripain and the fragments were purified by HPLC. The sequences of three such fragments were determined by Edman degradation to be identical to residues 70–85, 88–102 and 103–116 of porcine inhibin β_A (Fig. 3). These results are consistent with the hypothesis that porcine gonadal FRP is a homodimer consisting of two inhibin β_A-chains linked by disulphide bonds.

Both of the β-subunits of porcine inhibin, β_A and β_B, possess significant homology with human transforming growth factor-β (TGF-β)[16] and are considered to be members of the same gene family[6]. It is noteworthy that TGF-β, like FRP, exists as a homodimer linked by disulphide bonds. The presence of the inhibin β_A dimer (FRP) raises the possibility of the existence of an inhibin β_B dimer as well as perhaps inhibin β_A-β_B heterodimers.

Highly purified FRP stimulates FSH secretion by cultured anterior pituitary cells in a dose-related fashion, exhibiting an EC_{50} value of ~25 pM (Fig. 4*a*). FRP does not stimulate the secretion of LH (Fig. 4*b*), prolactin, growth hormone or adrenocorticotropic hormone, and in fact suppresses the basal and stimulated release of the latter two hormones (data not shown). FRP can be distinguished from GnRH in several ways. FRP, which is a potent releaser of FSH, has no effect on the

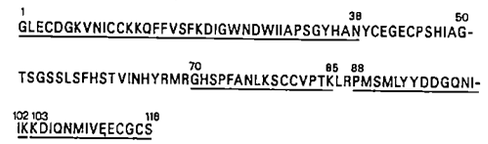


Fig. 3 Sequence analysis of FRP and structural comparison of FRP and the β_A-subunit of porcine inhibin. Identified residues of FRP are indicated by underlining of the porcine β_A-subunit structure[6]. Eighty-three amino acids of the sequence of porcine FRP were established and all were homologous with the corresponding 83 out of 116 residues of porcine inhibin β_A. FRP from the final reverse-phase HPLC was subjected to Edman degradation on an Applied Biosystems 470A gas-phase protein sequencer. Phenylthiohydantoin (PTH) amino-acid analysis was performed by reverse-phase HPLC with a Hewlett-Packard 1084B liquid chromatograph. Repetitive yields of stable PTH-amino acids were >94%. Relative PTH-amino-acid yields of consecutive Edman cycles agreed with corresponding values found by Edman degradation of synthetic peptides. Details of the method of sequence analysis are described elsewhere[22]. The amino-acid sequence of residues 1–38 of FRP was established by analysis of ~0.9 nmol of unmodified peptide. On the basis of the PTH-amino-acid anlaysis, the identified peptide represented >90% of the peptide of the fraction analysed. The FRP fragments, FRP(70–85), FRP(88–102) and FRP(103–116), were analysed after *S*-carboxymethylation[23] of 1.2 nmol of FRP, reverse-phase HPLC of the carboxymethylated FRP, its digestion with clostripain[24] (Substrate enzyme weight ratio, 20:1; 3.5 h at 37 °C; buffer, 0.05 M Quadrol, 5 mM $CaCl_2$, 1 mM dithiothreitol, 6% (v/v) *n*-propanol, *p*H 8.0) and purification of the fragments on reverse-phase HPLC (Vydac C_{18} column, 0.46×25 cm, pore size, 300 Å; elution: 0.05% TFA in aqueous acetonitrile; 1.0 ml min^{-1}, 31 °C). 100% of each purified fragment (corresponding to 200–400 pmol of peptide as estimated on the basis of PTH-amino-acid analysis) was subjected to Edman degradation.

secretion of LH whereas GnRH releases both gonadotropins (Fig. 4*b*). GnRH acts immediately to stimulate gonadotropin secretion; by contrast, the onset of action of FRP is delayed by more than 4 h, and is maximally effective only after 24 h. Pituitary cells treated with the highest concentrations of FRP for 72 h secrete 70–100% as much FSH during that period as do cells exposed to plateau levels of GnRH. On the other hand, FRP is considerably more potent than GnRH, typically exhibiting EC_{50} values of less than 1/25th that of GnRH (Fig. 4*a*). The administration of high concentrations of both FRP and GnRH together stimulates more FSH secretion than does the addition of maximal levels of either substance alone. GnRH receptor antagonists which completely prevent the release of FSH and LH due to GnRH *in vitro* have no effect on the secretion of FSH mediated by FRP. These results indicate that FRP acts independently of the GnRH receptor. Prolonged exposure of pituitary cells to GnRH results in depletion of cellular FSH stores whereas FRP, which releases similar amounts of FSH into the medium, actually increases the amounts of stored FSH (Table 2). FRP therefore appears to have a greater stimulatory effect on the biosynthesis of FSH than does GnRH, when delivered continuously.

Purified porcine inhibin[3] lowers baseline production of FSH

Table 1 Purification of FSH releasing protein

Step	Activity elutes	μg protein per ml-equiv.	Bioassay EC_{50} (ng protein per ml medium)
Starting material: 6,050 ml porcine follicular fluid		65,000	
1. 50% $(NH_4)_2SO_4$	Supernatant	10,000	
2. Preparative HPLC; Vydac C_4; TEA-phosphate, *p*H 6.5/propanol at 60 °C	Retarded	700	2,800
3. Gel filtration; Sepharose CL 6B; 6 M guanidine-HCl, 0.1 M NH_4CH_3COOH, *p*H 4.75	K_{av} = 0.54–0.71	130	730
4. Cation exchange FPLC; Mono S; 4 M urea, 1 mM CHAPS, 0.1 M NaCOOH, *p*H 4.3; 0–1 M NaCl	0.43–0.6 M NaCl	8	96
5. Semi-preparative HPLC; Vydac C_8; 0.1% TFA/CH_3CN	Retarded	0.7	25
6. Gel permeation FPLC; Superpose 12B, 6 M guanidine-HCl, 0.1 M NH_4CH_3COOH, *p*H 4.75	K_{av} = 0.26–0.31	0.3	5
7. Analytical HPLC; Vydac C_8; 0.1% TFA/CH_3CN			
8. Repeat step 7	Retarded	0.02	0.5–1

Ultrafiltration or dialysis following steps 1, 2 and 3. Details and explanation of abbreviations are given in Fig. 1 legend. Results of the bioassay are expressed as the concentration (ng protein per ml) required of a fraction to elicit a half-maximal response in the cell culture bioassay[15].

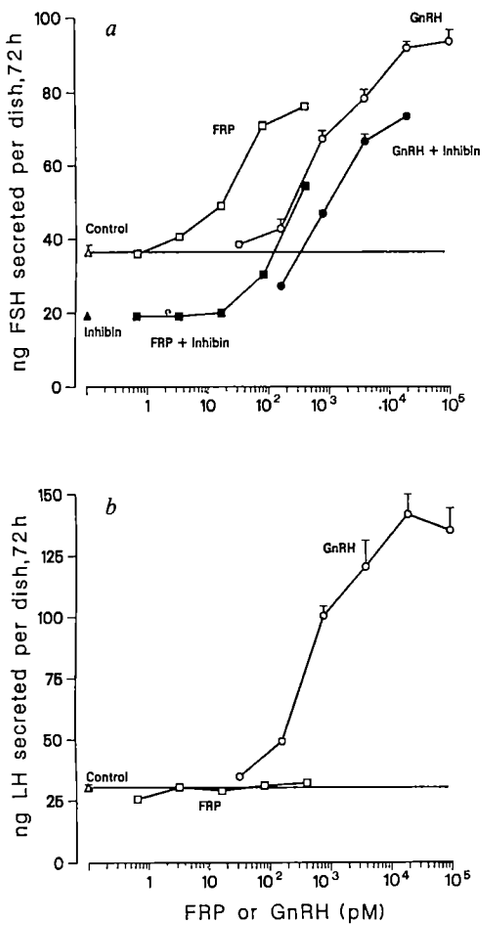


Fig. 4 *a*, Effects of FRP, porcine inhibin and GnRH on FSH secretion by rat anterior pituitary cells in primary culture prepared as described in Fig. 1 legend. All treatments were added simultaneously and incubation was continued for 72 h. Highly purified 32K porcine inhibin was given at 40 pM. *b*, Effects of GnRH and FRP on LH secretion by rat anterior pituitary cells in primary culture.

and will thereby obscure the effects of the lower concentrations of FRP (Fig. 4*a*). The pharmacological interaction between the two proteins is functionally antagonistic although each has effects in the absence of the addition of the other. The existence of gonadal FRP may have been overlooked previously because of the presence of inhibin, whose 32K form is not separated from FRP by gel-permeation chromatographic methods.

The physiological significance and anatomical distribution of FRP remain to be investigated. Previous reports of an FSH releasing factor have assumed its presence in the hypothalamus and partial purification of a hypothalamic FSH releasing factor of smaller size and more rapid action than gonadal FRP has been claimed[17-21]. At this time, we do not know whether FRP is secreted *per se* or is generated by extracellular processing. The high potency of FRP on pituitary cells in modulating hormone secretion and biosynthesis suggests the presence of high-affinity FRP receptors and supports the regulatory potential of this protein. In view of its similarity of sequence and subunit organization to TGF-β, FRP may have a variety of autocrine and paracrine actions within the gonad and perhaps other tissues.

With the information available, we can propose the existence of a novel and complex regulatory system involving differential subunit association giving rise to dimers with biologically opposite effects. It is clearly important to elucidate the conditions that determine whether inhibin β_A-subunits are combined with the dissimilar inhibin α-subunits to yield inhibin, which suppresses FSH production, or with each other, yielding FRP, a potent stimulator of FSH production.

The isolation of FRP was carried out under contract NO1-HD-32826 with the Contraceptive Development Branch of NICHD. The characterization of FRP was supported in part by NIH grants HD-13527 and AM-26741 and contract B85-28A/ICCR from the Population Council and the USAID. The research was conducted in part by the Clayton Foundation, California Division. W.V. and J.S. are Clayton Foundation Investigators. We thank J. Dykert, R. Azad, K. Carlin, S. Cappel and D. Dalton for technical assistance and R. Hensley, B. Connor and S. McCall for preparation of the manuscript.

Received 2 April; accepted 22 May 1986.

1. Robertson, D. M. *et al. Biochem. biophys. Res. Commun.* **126**, 220-226 (1985)
2. Miyamoto, K. *et al. Biochem. biophys. Res. Commun.* **129**, 396-403 (1985)
3. Rivier, J., Spiess, J., McClintock, R., Vaughan, J. & Vale, W. *Biochem. biophys. Res. Commun* **133**, 120-127 (1985).
4. Ling, N. *et al. Proc. natn. Acad. Sci. U.S.A.* **82**, 7217-7221 (1985).
5. Robertson, D. M. *et al. Molec. cell. Endocr.* **44**, 271-277 (1986)
6. Mason, A. J. *et al. Nature* **318**, 659-663 (1985).
7. Mayo, K. *et al. Proc. natn. Acad. Sci. U.S.A.* (in the press).
8. Bhasin, S., Heber, D., Peterson, M. & Swerdloff, R. *Endocrinology* **112**, 1144-1146 (1983).
9. Dutlow, C. M. & Millar, R. P. *Biochem. biophys. Res. Commun.* **101**, 486-494 (1981)
10. Paull, W. K., Turkelson, C. M., Thomas, C. R. & Arimura, A. *Science* **213**, 1263-1264 (1981)
11. Sharpe, R. M. *Biol. Reprod.* **30**, 29-49 (1984).
12. Sharpe, R. M. & Fraser, H. M. *Nature* **287**, 642-643 (1980).
13. Aten, R. F., Wolin, D. L. & Behrman, H. R. *Endocrinology* **118**, 961-967 (1983)
14. Ying, S.-Y., Ling, N., Bohlen, P. & Guillemin, R. *Endocrinology* **108**, 1208-1213 (1981).
15. Vale, W., Grant, G., Amoss, M., Blackwell, R. & Guillemin, R *Endocrinology* **91**, 562-572 (1972).
16. Derynck, R. *et al. Nature* **316**, 701-705 (1985).
17. Mizunauma, H. *et al. Brain Res. Bull.* **10**, 623-629 (1984).
18. Igarashi, M. & McCann, S. M. *Endocrinology* **74**, 446-452 (1964).
19. Igarashi, M., Taya, K. & Ishikawa, J. in *Psychoneuro-endocrinology* (ed Hatotani, N.) 178-186 (Karger, Basel, 1973).
20. Dhariwal, A. P. S., Watanabe, S., Antunes-Rodrigues, J. & McCann, S M *Neuro-endocrinology* **2**, 294-303 (1967).
21. Schally, A. V. *et al. Endocrinology* **98**, 380-391 (1976).
22. Spiess, J. in *New and Improved Methods in Protein Microsequence Analysis* (eds Wittmann-Liebold, B., Salnikow, J. & Erdmann, V. A.) (Springer, New York, in the press)
23. Spiess, J., Villareal, J. & Vale, W. *Biochemistry* **20**, 1982-1988 (1981).
24. Spiess, J., Rivier, J. & Vale, W. *Biochemistry* **22**, 4341-4346 (1983)

Table 2 Effects of GnRH or FRP on amounts of intracellular, secreted or total FSH in anterior pituitary cell cultures over a 48-h period

	ng FSH per well		
	Intracellular	Secreted	Total
Control	135.6±1.9	79.7±2.0	216.3±0.2
100 nM GnRH	46.8±2.1	161.0±0.9	207.8±2.9
0.2 nM FRP	176.4±3.6	165.8±6.4	342.2±3.0

Pituitary FSH is released by a heterodimer of the β-subunits from the two forms of inhibin

Nicholas Ling, Shao-Yao Ying, Naoto Ueno, Shunichi Shimasaki, Frederick Esch, Mari Hotta & Roger Guillemin

Laboratories for Neuroendocrinology, Salk Institute, 10010 North Torrey Pines Road, La Jolla, California 92037, USA

Inhibin is a gonadal protein that specifically inhibits the secretion of pituitary follicle-stimulating hormone (FSH). Two forms of inhibin (A and B) have been purified from porcine follicular fluid[1] and characterized as heterodimers of relative molecular mass (M_r) 32,000 (ref. 2). Each inhibin is comprised of an identical α-subunit of M_r 18,000 and a distinct but related β-subunit of M_r 13,800–14,700 linked by interchain disulphide bond(s). Throughout the purification of inhibins, we consistently observed two fractions which stimulated the secretion of pituitary FSH. We report here the isolation of one of the FSH-releasing proteins; it has a M_r of 24,000 and its N-terminal sequences up to residue 32 are

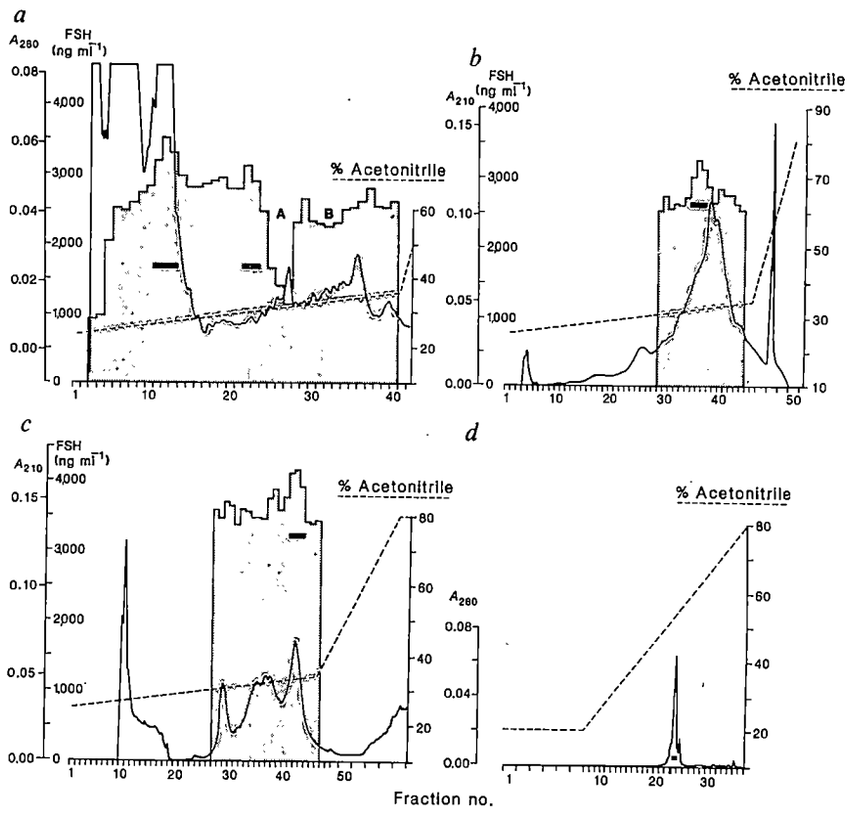


Fig. 1 Purification of the FSH-releasing substance, activin, from porcine follicular fluid. Sequential chromatography of the Sephacryl S-200 purified material was processed through: a Vydac C_4 semi-preparative column and eluted with acetonitrile in Et_3NP buffer (*a*); a Vydac C_4 semi-preparative column and eluted with acetonitrile in trifluoroacetic acid (TFA) solvent system (*b*); a Vydac phenyl semi-preparative column and eluted with acetonitrile in Et_3NP buffer (*c*); and an Aquapore RP-300 C_8 analytical column and eluted with acetonitrile in TFA solvent system (*d*). Solid bars, active material.

Methods. The FSH-releasing substance was purified by a procedure similar to that used in the isolation of inhibins A and B[1]. Briefly, 500 ml of porcine follicular fluid was defrosted and the cell debris removed by centrifugation. The supernatant was diluted to 10 times its original volume with 0.1 M NaCl/10 mM Tris-HCl, *p*H 7, and pumped simultaneously onto eight heparin–Sepharose (Parmacia) columns (3.5×9 cm) at 40 ml h^{-1} per column[1]. The adsorbed proteins were removed by washing with 1 M NaCl/10 mM Tris-HCl, *p*H 7. The protein-containing fractions were pooled and dialysed overnight (Spectrapor No. 3 membrane tubing, M_r cutoff 3,500, Spectrum Medical Industries) against 30% (v/v) acetic acid. The retentate was centrifuged to remove a white precipitate and the supernatant divided into eight equal portions for application to eight 5×100 cm columns of Sephacryl S-200 Superfine (Pharmacia) and developed with 30% acetic acid at 20 ml per 22 min as before[1]. The fractions containing the 32,000-M_r inhibins and FSH-releasing activity, which eluted after inhibin, were pooled and lyophilized (see Fig. 1a in ref. 1). For reverse-phase HPLC, two solvent systems were used. In the Et_3NP system, solvent A consists of 0.25 M triethylammonium phosphate (*p*H 3), and solvent B is 80% (v/v) acetonitrile in solvent A. In the TFA solvent system, solvent A contains 1 ml TFA in 999 ml of water, and solvent B is 1 ml of TFA in 199 ml of water and 800 ml of acetonitrile. The lyophilized material (53 mg) was dissolved in 40 ml 0.2 M acetic acid and filtered through a Millex-HA 0.45 μm filter (Millipore). The filtrate was applied directly to a Vydac 5 μ C_4 column (10×250 mm). After all the filtrate had been loaded, the column was washed with the aqueous solvent A until the ultraviolet absorption reached baseline. The inhibin and FSH-releasing activities were separated with the indicated gradient of acetonitrile in Et_3NP solvent system on a Beckman 322 gradient liquid chromatography system equipped with a Spectroflow 747 UV detector (Kratos Analytical Instruments), a Soltec 220 recorder (Soltec) and a RediRac 2112 fraction collector (LKB) as shown in *a*. Two zones of inhibin activity, designated inhibins A and B, were separated, as were two zones of FSH-releasing activity denoted by the two solid bars. The FSH-releasing fractions denoted by the black bar and eluting at 30% acetonitrile were pooled and, after mixing with an equal volume of 0.2 M acetic acid, pumped directly onto a Vydac 5 μ C_4 column, 10×250 mm, and eluted with the indicated gradient of acetonitrile in TFA solvent system at 6 ml per 2 min as shown in *b*. The active material (denoted by the solid bar) was pooled, diluted to twice its original volume and chromatographed on a Vydac 5 μ phenyl column (10×250 mm) with the indicated gradient of acetonitrile in Et_3NP solvent system at 2 ml per 2 min (*c*). The active material (solid bar) from four chromatographic runs identical to those in *c* was pooled and, after dilution with 0.2 M acetic acid, concentrated by chromatography on an Aquapore 10 μ RP-300 column (4.6×250 mm) using the indicated gradient of acetonitrile in TFA system at 0.5 ml min^{-1} as shown in *d*. From 2 l of follicular fluid, 32 μg of activin was isolated.

identical to those of each β-subunit of inhibins A and B. In the presence of reducing agents, SDS-polyacrylamide gel electrophoresis resolves the FSH-releasing substance into two subunits which are identical in their migration behaviour to the reduced β-subunits of inhibins A and B. Based on the N-terminal sequence data and M_r of the intact and reduced molecules, we propose that the FSH-releasing substance, which is active in picomolar concentrations, is a heterodimeric protein composed of the two β-subunits of inhibins A and B linked by interchain disulphide bond(s). The structural organization of the FSH-releasing substance is homologous to that of transforming growth factor-β (TGF-β)[3], which also possesses FSH-releasing activity in the same bioassay[4]. We suggest that the substance be called activin to signify the fact that it has opposite biological effects to inhibin.

Frozen porcine follicular fluid (collected by J.R. Scientific and procured through the Contraceptive Development Branch, Center for Population Research, National Institute of Child Health and Human Development) was used as starting material for the purification of the FSH-releasing substance. After defrosting, the follicular fluid was diluted with buffer and purified through successive steps of heparin–Sepharose affinity chromatography, size fractionation on Sephacryl S-200 in acidic medium and four reverse-phase HPLC steps as described in Fig. 1 legend. The inhibin and FSH-releasing activities were monitored by an *in vitro* bioassay using a monolayer culture of dissociated rat anterior pituitary cells[1]. Inhibin-containing fractions were identified by their ability to inhibit the 48-h basal release of FSH but not that of luteinizing hormone or other pituitary hormones in comparison with control cultures; FSH-releasing fractions were identified by their ability to release FSH above basal level during the 48-h incubation in comparison with control cultures. Two forms of FSH-releasing substance, eluting at 27% and 30% acetonitrile, were noted in the first reverse-phase HPLC step (Fig. 1*a*). The later-eluting form was purified to homogeneity by three more HPLC steps (Fig. 1*b*–*d*). The purified protein yielded a single band of apparent M_r 24,000 on SDS-polyacrylamide gel electrophoretic (SDS-PAGE) analysis under non-reducing conditions (Fig. 2*a*).

The homogeneous 24,000-M_r material, now called activin, exhibited a half-maximal stimulation of FSH release at a concentration of 3.7±0.5 ng ml^{-1} (~1.5×10^{-10} M) and maximal release at 16 ng ml^{-1} (~6.7×10^{-10} M) or higher. The FSH-releasing activity was inhibited by inhibin. Activin had no effect on the secretion of luteinizing hormone. The FSH-releasing

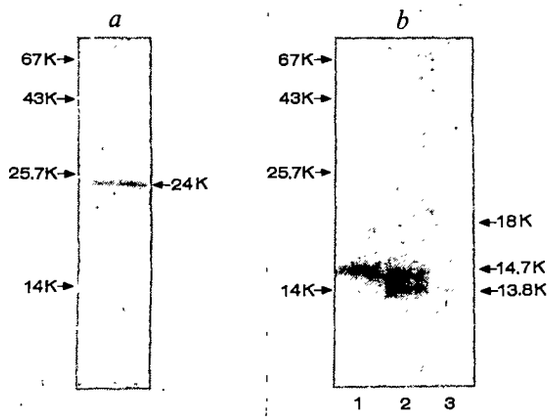


Fig. 2 SDS-polyacrylamide gel electrophoretic analysis of the purified activin under non-reducing (*a*) and reducing (*b*) conditions. Lanes 1 and 3 in *b* denote the purified inhibins A and B, respectively, being analysed simultaneously with activin (lane 2). The high-M_r band at 18K (18,000 M_r) is the common α-subunit of the inhibins and the low-M_r bands at 14.7K and 13.8K correspond to the β-subunits of inhibin A and inhibin B, respectively. The following M_r standards were used to calibrate the gel: bovine serum albumin (M_r 67K), ovalbumin (43K), α-chymotrypsinogen (25.7K) and lysozyme (14K).

Methods. The purified proteins were analysed in 1-mm-thick 15% polyacrylamide gels according to the method of Laemmli[8]. The proteins were revealed by a Coomassie blue staining reagent. For non-reducing conditions, 1 μg of protein in 20 μl of water was incubated with 20 μl of sample buffer (0.125 M Tris-HCl, *p*H 6.8/20% (v/v) glycerol/4% SDS/0.04% bromophenol blue) for 1 h at 37 °C and then loaded onto the gel. Electrophoresis was at constant voltage (200 V) for 6 h at room temperature. For reducing conditions, 1.5 μg of protein was incubated first with 20 μl of 0.02 M dithiothreitol for 15 min at 37 °C, then 20 μl of sample buffer was added and the incubation was continued for 1 h before the sample was applied to the gel. Electrophoresis was carried out as above except that 5 mM dithiothreitol was included in the electrophoretic buffer.

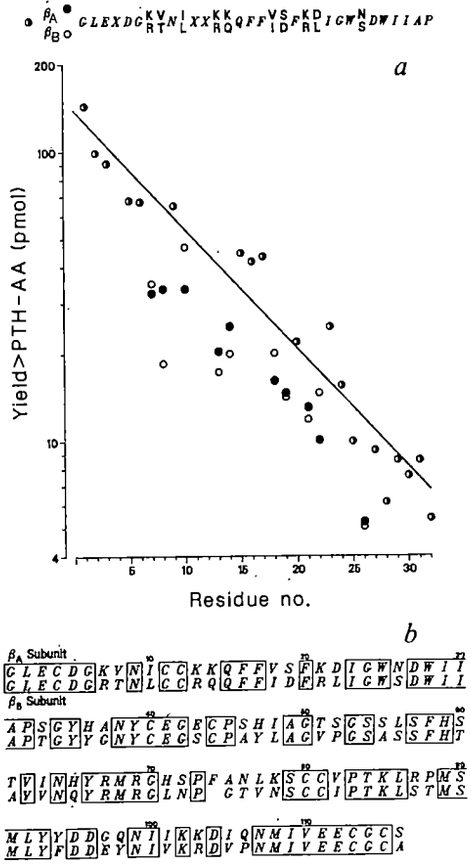


Fig. 3 *a*, N-terminal sequence analysis of activin. Residues determined that are identical to both subunits are denoted by ◑. Unique residues present only in the β_A-subunit are designated by ● and those present only in the β_B-subunit by ○. An X denotes a residue (cysteine?) which is not identified. *b*, Primary structure of the β-subunits of inhibins A and B deduced from molecular cloning[2]. The regions containing identical residues are boxed. A gap is introduced at position 74 of β_B to maximize homology alignment with β_A.

Methods. The protein (200 pmol) was sequenced using an Applied Biosystems 470A protein sequencer as described previously[9] and the released phenylthiohydantoin-amino acids (PTH-AA) analysed by an online Applied Biosystems 120A PTH-amino-acid analyser. The initial yield was 36% and the average repetitive yield 91.1%.

activity requires both subunits to be joined together; reduction of the disulphide bonds by dithiothreitol destroyed bioactivity (as in the case of inhibin[1]).

Microsequencing of the intact activin on an Applied Biosystems model 470A protein sequencer revealed the first 32 N-terminal residues as shown in Fig. 3*a*. These sequence data are identical to the theoretical residues obtained if the two β-subunits of inhibins A and B were sequenced simultaneously (see Fig. 3*b*). To determine the structure of the two activin subunits, the molecule was compared with inhibins A and B by SDS-PAGE under reducing conditions. As shown in Fig. 2*b*, the migration of the two reduced subunits of activin coincides with that of the reduced β-subunits of inhibins A and B, respectively. Thus, based on the M_rs of the reduced subunits and their N-terminal sequences, we propose that activin, one of the FSH-releasing substances present in porcine follicular fluid, is a heterodimer comprised of the two β-subunits of inhibins A and B.

In our original report on the characterization of porcine follicular fluid inhibins[2], we had speculated, based on complementary DNA sequencing, that the β-subunits of inhibins A and B contain 116 and 115 amino acids, respectively. In view of the different sizes of the two β-subunits on SDS-PAGE analysis under reducing conditions (β_A slightly larger than the β_B), it is possible that the mature β_B undergoes proteolytic processing[5] at the C-terminal Lys-Arg sequence of residues 101 and 102 to yield a β_B-subunit ~16 amino acids shorter than the β_A-chain. This would also be the case for the β_B-subunit of activin. We have noted previously[2] the striking homology between the β-subunits of the two forms of inhibins and TGF-β and have recently shown that the homodimer TGF-β has intrinsic FSH-releasing activity[4]. To see FSH-releasing activity in a molecule comprised of the two β-subunits of inhibins A and B is thus in keeping with the TGF-β precedent. What is striking is that when each of the β-subunits of the inhibins is combined with an α-subunit, the resulting molecule inhibits the basal release of FSH, whereas if the two β-subunits are paired together, the resulting molecule acts as an FSH releaser. It is conceivable that a homodimer composed of either of the β-subunits of inhibin A or B could produce similar FSH-releasing activity. Such a precedent can be found in the case of platelet-derived growth factor (PDGF), a heterodimer of two closely related A and B subunits[6], the same PDGF-like biological activity also being exhibited by a homodimer of either the A or B subunit[7].

Our previous report[2] on the structure of inhibins A and B demonstrated that each subunit (α, β_A, β_B) is the product of a different messenger RNA rather than being processed from some unique, very large precursor, and we hypothesized the existence of multiple combinations of the inhibin subunits, including hybrids with subunits of the ubiquitous TGF-β. The characterization of activin as a heterodimer of the two β-subunits of

inhibins A and B reinforces that hypothesis. If such rearrangements of several gene products are the norm, rather than the exception, this process clearly considerably extends the diversity of the final products (and of their biological activity) derived from a limited number of genes. Multiple arrangements of protein subunits through disulphide bridges, leading to mature molecules with totally different biological activities (possibly of opposite biological activities, as here), would seem to extend to the gene products the possibility of reorganizations, as is now well recognized occurs in DNA and RNA.

We thank F. Castillo, R. Schroeder, M. Regno, A. Becker, J. Czvik and D. Angeles for technical assistance; and B. Gayer and W. Collins for preparing the manuscript. This work was supported by NIH Program Project Grants HD-09690 and AM-18811 and a grant from the Robert J. Kleberg Jr and Helen C. Kleberg Foundation.

Received 8 April; accepted 22 May 1986.

1. Ling, N. *et al. Proc. natn. Acad. Sci. U.S.A.* **82**, 7217-7221 (1985).
2. Mason, A. J. *et al. Nature* **318**, 659-663 (1985).
3. Derynck, R. *et al. Nature* **316**, 701-705 (1985).
4. Ying, S-Y. *et al. Biochem. biophys. Res. Commun.* **135**, 950-956 (1986).
5. Docherty, K. & Steiner, D. F. *A. Rev. Physiol.* **44**, 625-638 (1982).
6. Waterfield, M. D. *et al. Nature* **304**, 35-39 (1983).
7. Heldin, C. H. *et al. Nature* **319**, 511-514 (1986).
8. Laemmli, U. *Nature* **227**, 680-685 (1970).
9. Esch, F. *Analyt. Biochem.* **136**, 39-47 (1984).

Inducible cellular transformation by a metallothionein-*ras* hybrid oncogene leads to natural killer cell susceptibility

W. S. Trimble, P. W. Johnson, N. Hozumi & J. C. Roder

Division of Immunology and Neurobiology,
Mount Sinai Research Institute, 600 University Ave, Toronto,
Ontario, Canada M5G 1X5

Natural killer (NK) cells are lymphoid effector cells possessing spontaneous cytolytic activity against a variety of tumour targets[1]. The fact that NK cells pre-exist at high frequency and require no lengthy activation, and the observation that differentiated and metastatic tumour cells often have a decreased sensitivity to NK cytolysis have led to the hypothesis that these cells may be involved in the earliest stages of antitumour surveillance[2]. Central to this model is the prediction that NK sensitivity must arise during cellular transformation. To test this prediction directly, we have constructed a vector containing the transforming gene from the EJ bladder carcinoma cell line under the transcriptional control of the mouse metallothionein-I promoter. When induced with heavy metal ions, mouse fibroblast lines containing this vector become dramatically sensitive to NK-mediated cytolysis concomitant with the expression of the cellular Harvey *ras* (c-Ha-*ras*) p21 protein and with cellular transformation.

To examine the NK sensitivity of cells during the transformation process, we have constructed vectors that permit controlled expression of c-Ha-*ras* (Fig. 1). For constitutive expression of *ras* in fibroblast cells, a 6.6-kilobase (kb) *Bam*HI fragment containing the transforming human c-Ha-*ras* gene[3] (from the EJ bladder carcinoma cell line) under the control of its own promoter was introduced into the *Bam*HI site of pSV2neo (ref. 4) and called pREJ. For inducible *ras* expression, the mouse metallothionein-I promoter[5] was ligated upstream from the coding sequence of the EJ *ras* gene. This zinc-inducible promoter has been used to express a number of heterologous genes both *in vitro*[6] and *in vivo*[7]. The resultant chimaeric oncogene was introduced into pSV2neo and called pMTEJ.

Table 1 NK susceptibility using spleen cells as effectors

Target cells	Vector	Zn^{2+} Induction	No. of expts	Mean cytolysis ±s.e. % Lysis (200/1 E:T)	Mean cytolysis ±s.e. LU/10^6	*P* value
10T1/2	–	–	4	10±4	1.0±0.3	
		+	3	17±3	1.2±0.3	NS
212	pMTEJ	–	15	18±3	1.4±0.4	
		+	17	57±4	9.3±1.2	<0.001
245	pREJ	–	4	46±10	5.7±1.7	
246	pREJ	–	3	33±13	3.5±1.5	
247	pREJ	–	5	38±2	6.0±1.2	
		+	1	40±3	8	NS
YAC1.2	–	–	11	51±4.5	19±3.3	

Target cells were grown for 24–48 h in the presence or absence of 50 μM zinc sulphate and collected by trypsinization. ^{51}Cr-labelled cells were tested in a 6-h cytotoxicity assay against spleen cells pooled from 8–12-week-old CBA mice injected intraperitonealy on day −1 with 100 μg of poly-I:C. Effector titration curves yielded maximum lysis values at a 200/1 effector:target ratio (E:T) as shown and lowest values at 1.5/1. One lytic unit (LU) was defined as the number of effector cells required to lyse 20% of the target cells, and the data are expressed as the mean % lysis±standard error (s.e.) and LU per 10^6 spleen cells in data pooled from 1–17 independent experiments. *P* values represent the probability (Student's *t*-test) that LU values for zinc-induced compared with uninduced cells are not different. NS, not significant.

The vectors were transferred into the murine fibroblast cell line C3H 10T1/2 (ref. 8) via protoplast fusion. Cells were selected for resistance to the antibiotic G418 (neo^+) in the absence of zinc. All of the isolated clones were then tested for their responsiveness to zinc ions in the medium. Each line was plated in the presence or absence of 50 μM zinc and their morphologies were compared. pSV2neo seemed to have no effect on colony morphology, leaving the cells flat and contact inhibited in the presence or absence of zinc. On the other hand, in 5 of the 10 neo^+ pREJ colonies, the cells were rounded and more refractile, and within the colony the cells criss-crossed in a disorganized manner, with no evidence of contact inhibition. Again, zinc had no effect on the morphology of these lines. The vector pMTEJ gave rise to a broader spectrum of morphologies, including normal and fully transformed colonies and some intermediate morphologies not seen with pREJ. These exhibited contact inhibition but were more refractile and more densely crowded than the 10T1/2 parent cells or any pSV2neo lines. Of the 27 neo^+ pMTEJ colonies obtained, 2 were fully transformed and 3 were of intermediate appearance. One of the 27 pMTEJ lines (212), which in the absence of zinc has an intermediate but nearly normal morphology, became highly refractile and formed an irregular criss-crossed pattern of fusiform cells 48–72 h after exposure to zinc (Fig. 2). In all cases, removal of zinc from the medium led to the return of the original morphology within 48 h, indicating that the continued expression of *ras* is required to maintain transformation.

Human *ras*-specific transcripts were detected in the RNA of all lines that exhibited a transformed morphology (data not shown), but inducible transcription was found only in the line showing zinc-induced morphological change. The 212 cell line expressed a low basal level of a 1.2-kb human *ras*-specific sequence not found in the 10T1/2 line (Fig. 3*a*). When induced with 50 μM zinc sulphate, the expression increased six to eight-fold within 24 h to levels higher than those found in the pREJ line 245 or in the human bladder carcinoma line 5637. The slightly reduced size of this transcript compared with controls can be accounted for by the reduced size of the hybrid 5′UT relative to the predicted c-Ha-*ras* 5′UT[9]. RNA blots were washed and rehybridized with a probe specific for β_2-microglobulin, confirming that equal amounts of RNA had been loaded in each lane. Consistent results were obtained when the levels of biosynthetically labelled p21 proteins were examined by immunoprecipitation with monoclonal antibodies specific for c-Ha-*ras* p21[10]. The level of p21 increased dramatically in the

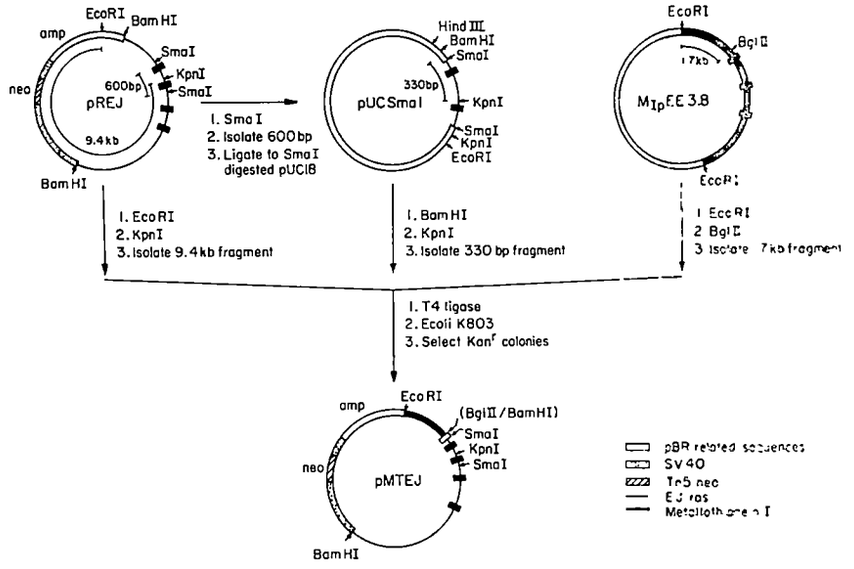


Fig. 1 Construction of Ha-*ras* expression vectors. The 6.6-kb *Bam*HI fragment from pEJ[3] was subcloned into the *Bam*HI site of pSV2neo[4] and the resultant plasmid was termed pREJ. From this a 602-base pair (bp) *Sma*I fragment containing all of the 5'UT as well as exons 1 and 2 was subcloned into the *Sma*I site of pUC 18[17] such that the 5'UT was adjacent to the pUC 18 polylinker *Bam*HI site. A 322-bp *Bam*HI–*Kpn*I fragment from this plasmid was then ligated to a 9.6-kb *Eco*RI–*Kpn*I fragment from pREJ and a 1.7-kb *Eco*RI–*Bgl*II fragment from M1pEE3.8[5], containing the metallothionein promoter and messenger RNA cap site[18] in the construction of pMTEJ. Vectors were transferred into the recipient fibroblasts via protoplast fusion. The cells were detached by trypsin treatment and fused to bacterial protoplasts in suspension as described elsewhere[19] using a 40% polyethelene glycol 1000 (BDH)/10% dimethyl sulphoxide mixture. Cell lines resistant to 1 mg ml^{-1} G418 were isolated and subcloned by limiting dilution.

inducibly transformed line 212 to levels considerably higher than those found in the constitutively transformed line 245 (Fig. 3*b*).

Anchorage-independent cellular transformation was assessed more quantitatively by examining the colony-forming ability of the cells in semi-solid medium. 10T1/2 cells had no detectable colony-forming ability when plated in medium containing 0.3% agar in the presence or absence of zinc. Constitutively transformed pREJ lines 245, 246 and 247 had agar plating efficiencies of 2–3% irrespective of zinc ions. The inducible line 212, however, formed colonies at 0.5% in the absence of zinc but increased to 10% in the presence of 50 μM zinc sulphate. These data demonstrate that the cell line 212 is inducible for c-Ha-*ras* expression and, hence, for cellular transformation.

Cytoxicity assays performed on these cell lines consistently demonstrated that an increased sensitivity to NK-mediated lysis correlated with expression of the transforming c-Ha-*ras* oncogene. The highly lytic NK clone LH49-IIIF6 (ref. 11) lysed 20% of the uninduced 212 cells within 6 h at an effector to target ratio of 5:1, compared with >90% lysis after induction with zinc ions (Fig. 4). In addition, NK clones with intermediate or low lytic activities on the standard NK target (YAC 1.2 lymphoma) had the same rank order of activities on 212 induced with zinc.

Similar results were obtained using murine spleen cells as effectors. The parental line C3H 10T1/2 (H-2^k) was moderately resistant to NK lysis by spleen cells from H-2-identical CBA mice treated with the NK stimulating agent poly-I:C (Table 1) pREJ-transformed lines expressed a much higher sensitivity to lysis, corresponding approximately with levels of *ras* expression. Neither the transformed nor parental lines became more NK sensitive through growth in the presence of zinc. However, 212 cells grown in the presence of zinc became significantly more sensitive to NK cells than those grown its absence, and the level of cytolysis approached that of the YAC tumour line. Equivalent results were obtained with spleen cells from mice not boosted with poly-I:C when assayed for 18 h.

The effector cells were further confirmed to be of NK origin by the observation that lytic activity against zinc-induced 212 was much reduced in spleen cells from NK-deficient beige mice[12]. In addition, lytic activity could be completely abrogated by pretreatment of the spleen cells with complement plus anti-NK1.2 (ref. 13) or anti-asialo GM_1 (ref 14) antisera, indicating that the effector cells, like NK cells, bear these surface antigens (data not shown). In contrast, the T-helper-specific Lyt 1.1 antibody had no effect on this activity. The zinc-induced 212 cells were no more sensitive to lysis by 10T1/2-allospecific or

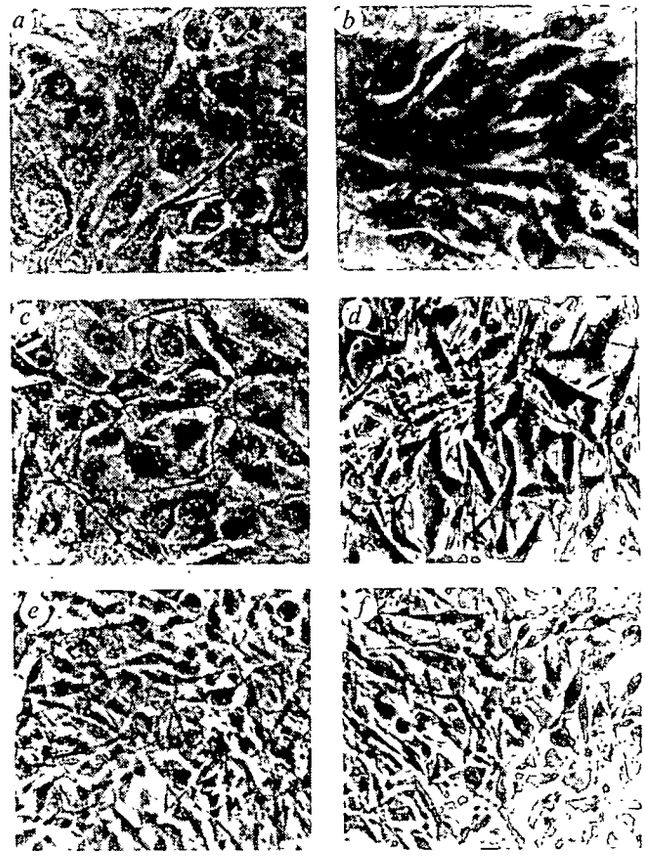


Fig. 2 Induction of morphological change with zinc. Cells were grown to confluence in medium containing 10% fetal calf serum with (*b*, *d*, *f*) or without (*a*, *c*, *e*) 50 μM zinc sulphate, and photographed with phase contrast. Cell lines shown are 10T1/2 (*a*, *b*), the pMTEJ line 212 (*c*, *d*) and a pREJ line 245 (*e*, *f*). ×320

H-2^k-specific cytotoxic T lymphocytes than were uninduced 212. At a 6:1 effector/target ratio, the lysis of uninduced 212 cells by allospecific cytotoxic T cells was 62 ±3% compared with 65±5% for zinc-induced 212 cells. The lytic units per 10^6 lymphocytes (as described in Table 1), calculated at 20% lysis, were 600 and 800, respectively. Similarly, anti-H-2^k-specific cytotoxic T cells from congeneic resistant strains gave 49% lysis

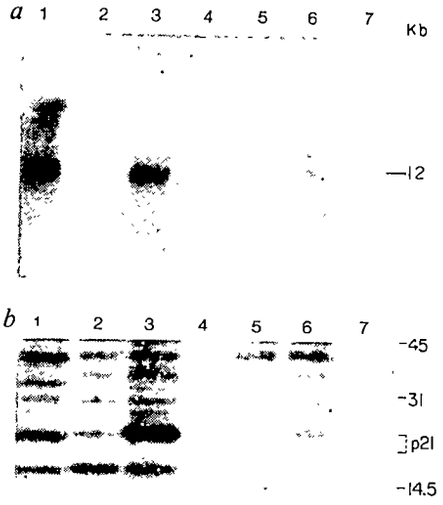


Fig. 3 Induction of *ras* expression in cell line 212. *a*, RNA blot analysis. Total cellular RNA was isolated[2] from cells cultured for 48 h in the presence (lanes 3, 5, 7) or absence (lanes 1, 2, 4, 6) of 50 μM zinc sulphate in Dulbecco's modified Eagle's medium (DMEM) with 10% fetal calf serum. RNA (20 μg per lane) was electrophoresed and transferred to nitrocellulose as described previously[21]. Hybridization was performed as described elsewhere[21] using as probe the 602-bp *Sma*I fragment from the plasmid pUC *Sma*I described in Fig. 1. The cell lines studied are as follows: 5637 (lane 1), 212 (lanes 2, 3), 10T1/2 (lanes 4, 5) and 245 (lanes 6, 7). *b*, p21 immunoprecipitation. Biosynthetic labelling was performed by incubating 50% confluent 60-mm cultures for 24 h in (DMEM) lacking methionine supplemented with 250 μCi ml^{-1} ^{35}S-methionine (Amersham). Labelled cells were washed twice and lysed as described elsewhere[10]. Immunoprecipitation involved the addition of 5 μl of ammonium sulphate concentrated YA6-172 rat monoclonal anti-p21 antibody[10] to 300 μl of lysate containing 10^7 trichloroacetic acid-precipitable c.p.m. and incubation for 4 h at 4 °C. To this was added 25 μl (as a 25% suspension) of protein A–Sepharose beads previously coated with rabbit IgG specific for rat IgG (Cappel) and incubated at 4 °C overnight. The beads were then washed four times in phosphate-buffered saline and four times in lysis buffer before electrophoresis on a 12.5% acrylamide slab gel[22]. The gel was soaked in Amplify (Amersham) before drying and exposure to XAR film (Kodak) at −70° C. The loading order of this gel is identical to that for *a*. The relative molecular masses of the marker proteins are indicated on the right (×10^{-3}).

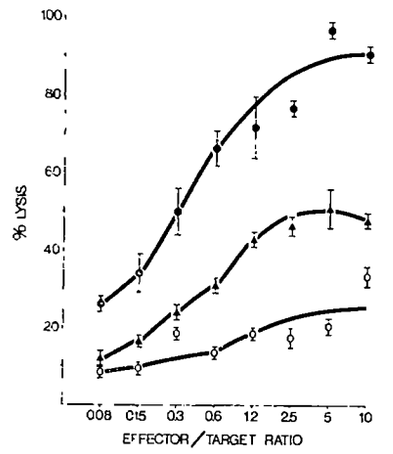


Fig. 4 Increased sensitivity to a cytolytic NK clone. The pMTEJ line 212 was grown for 24 h in the presence (●) or absence (○) of 50 μM zinc added to the culture medium and collected by trypsinization. YAC 1.2 lymphoma cells (▲) or 212 cells were labelled for 2 h with ^{51}Cr and tested in a 6-h cytotoxicity assay against a subclone (IIIF6) of the C57Bl/6 NK clone (LH 49)[11] kindly provided by Dr Colin Brooks (Fred Hutchison, Seattle). As reported for the original clone, the IIIF6 subclone was thyl$^+$, aGM$_1^+$, Lyt1.2$^-$, Lyt2.2$^-$, NK1.2$^+$, Qa4$^-$ as determined by immunofluoresence staining and flow cytofluorometry. Values represent the mean % lysis ± standard error in triplicate wells. Spontaneous release was <10% of total label for the three targets. This experiment was repeated three times with similar results.

of 212 with no induction and 48% with zinc induction at 50:1 effector to target ratios, and the lytic units were the same at 16 lytic units per 10^6 cells. Furthermore, trinitrophenyl (TNP)-haptenated, zinc-induced 212 cells did not lyse more readily with complement plus anti-TNP antibodies than did the unstimulated equivalents (data not shown), thereby demonstrating that zinc induction of 212 cells does not make them more sensitive to lysis in general.

These results demonstrate the potential for a single oncogene with a defined lesion to alter the NK sensitivity of the murine fibroblast cell line C3H 10T1/2. Previous studies with methylcholanthrene (MCA)-transformed BALB/c fibroblasts have demonstrated that the same effect can be acquired during transformation by chemical carcinogens[15]. The fact that MCA-transformed C3H 10T1/2 lines have been found to contain activated *ras* oncogenes[16] suggests that MCA-induced NK sensitivity could result from mutation of the *ras* locus.

The ability to regulate transcription of the c-Ha-*ras* oncogene allows us to mimic the events occurring during cellular transformation. The low level of p21 expressed in uninduced 212 cells does not increase their NK sensitivity relative to the parental line 10T1/2 but, concomitant with zinc-induced transformation, the cells acquire an increased sensitivity to NK cytolysis which could make them targets for anti-tumour surveillance. This effect seems to be an early form of host defence, as other studies have found that tumour progression and metastasis are generally accompanied by the acquisition of NK resistance. Additional studies are under way to determine the molecular changes associated with *ras*-mediated NK sensitivity, and the generality of this phenomenon.

We thank A. Dube and N. Govindji for technical assistance, R. A. Weinberg for plasmid pEJ, R. Palmiter for plasmid MIpEE3.8, R. Goldberg and E. Scolnick for monoclonal YA6-172 and C. Brooks for NK clone LH49. This work was supported by grants from the MRC and NCI of Canada. W.S.T. is the recipient of an MRC Studentship and P.W.J. is the recipient of an MRC Fellowship.

Received 26 February, accepted 8 April 1986.

1. Kiessling, R., Klein, E. & Wigzell, H. *Eur. J. Immun.* **5**, 112-117 (1975).
2. Herberman, R. & Ortaldo, J. *Science* **214**, 24-30 (1981).
3. Shih, C. & Weinberg, R. A. *Cell* **29**, 161-169 (1982).
4. Southern, P. J. & Berg, P. *J. molec. appl Genet.* **11**, 327-341 (1982).
5. Durnam, D. M. *et al. Proc. natn. Acad. Sci. U.S.A.* **77**, 6511-6515 (1980).
6. Brinster, R. L. *et al. Nature* **296**, 39-42 (1982).
7. Palmiter, R. D. *et al. Nature* **300**, 611-615 (1982).
8. Reznikoff, C. A., Brankow, D. W. & Heidelberger, C. *Cancer Res.* **33**, 3231-3238 (1973).
9. Capon, D. J. *et al. Nature* **302**, 33-37 (1983).
10. Furth, M. E. *et al. J. Virol.* **43**, 294-304 (1982).
11. Brooks, C. G., Kuribayashi, K., Sale, G. E. & Henney, C. S. *J. Immun.* **128**, 2326-2335 (1982).
12. Roder, J. C. & Duwe, A. *Nature* **278**, 451-453 (1979).
13. Burton, R. C. & Winn, H. J. *J. Immun.* **126**, 1985-1989 (1981).
14. Kasai, M., Iwamori, Y., Nagai, Y., Okamura, K. & Tada T. *Eur. J. Immun.* **10**, 175-180 (1980).
15. Collins, J. L., Patek, P. Q. & Cohn, M. *J. exp. Med.* **153**, 89-106 (1981).
16. Parada, L. F. & Weinberg, R. A. *Molec. cell. Biol.* **3**, 2298-2301 (1983).
17. Norrander, J., Kempe, T. & Messing, J. *Gene* **26**, 101-106 (1983).
18. Glanville, N., Durnam, D. M. & Palmiter, R. D. *Nature* **292**, 267-269 (1981).
19. Ochi, A. *et al. Nature* **302**, 340-342 (1983).
20. Chirgwin, J. M. *et al. Biochemistry* **18**, 5294-5299 (1979).
21. Thomas, P. S. *Proc. natn. Acad. Sci. U.S.A.* **77**, 5201-5205 (1980).
22. Laemmli, U. K. *Nature* **227**, 680-685 (1970).

Sequence organization and genomic complexity of primate θ1 globin gene, a novel α-globin-like gene

Jon Marks, Jeng-Pyng Shaw & Che-Kun James Shen

Department of Genetics, University of California, Davis, California 95616, USA

The α-like and β-like globin genes have provided a paradigm for the study of molecular evolution and regulation of multigene families in eukaryotes. The human α-globin gene cluster, which is on chromosome 16 (ref. 1), consists of six genes arranged in the order[2–5] 5′-ζ(embryonic)-ψζ-ψα2-ψα1-α2(adult)-α1(adult)-3′. DNA sequencing data have demonstrated that ζ (ref. 6) and α2 (or α1, refs 7–9) are the embryonic and adult genes, respectively, while ψζ (ref. 6), ψα2 (ref. 5) ψα1 (ref. 10) are all inactive pseudogenes. Restriction mapping analysis has shown that the structure of this locus in several anthropoid primates is nearly identical to that of the human[11,12]. Recently, we have isolated the adult α-globin gene region from orang-utan, olive baboon and rhesus macaque by molecular cloning. We report here the complete nucleotide sequence of a gene located immediately downstream from the adult α1-globin gene of the orang-utan, along with its flanking DNA. We designate this gene as θ1, and show that it contains the essential sequence elements required for an expressive gene. The putative polypeptide is 141 amino acids long, identical to that of the α- or ζ-globin, but its predicted amino-acid sequence is nearly as different from the orang-utan α-globin (55 differences) as the human ζ-globin is from the human α-globin (59 differences), suggesting an ancient history for the θ1-globin gene. Results of blot hybridization experiments using the cloned orang-utan θ1 gene sequence as probe demonstrate a similar α2-α1-θ1 linkage map existing in the human genome. Furthermore, multiple copies of sequences homologous to the θ1 gene are detected in both human and orang-utan. These results cast a new light on the primate α-globin gene family, and have intriguing implications for the existence of previously unreported, functional globin-like gene(s) in the primate genomes.

The human α-globin cluster can be used to investigate the processes of gene duplication, insertion, and correction, in addition to the better-known molecular evolutionary processes[13–16]. To study these processes further, we have constructed genomic libraries of three non-human primates (orang-utan, *Pongo pygmaeus*; olive baboon, *Papio anubis*; rhesus macaque, *Macaca mulatta*), and screened with a 1.5-kilobase (kb) *Pst*I fragment containing the human α1-globin gene. One of the positive recombinant phage clones, λ0αG1, isolated from an orang-utan liver DNA library, contains duplicated functional adult α-globin genes, α2 and α1[17] (see map in Fig. 1). Unexpectedly, blot hybridization and partial sequencing of the DNA region flanking the 3′ side of the orang-utan α1-globin gene revealed a previously unreported α-globin-like sequence[17], which we now designate as θ1. The orang-utan θ1 gene contains all the sequence elements necessary for an expressible, protein-coding gene although its actual expression and function are unknown. However, due to its unique promoter organization and predicted amino-acid sequence, we designate it as θ1 following the suggestion of Dr George Stamatoyannopoulos.

Approximately 1.2 kb of DNA sequences containing and flanking the orang-utan θ1 gene have been analysed (Figs 1, 2). Like the adult α1-globin gene, the θ1 gene contains three exons and two introns. The alignment of its sequence with the α1-globin gene (Fig. 2) indicates that their exons are ~75% identical base-for-base without any deletion or insertion. The introns and most of the flanking sequences of the two genes, however, have diverged to the point of virtually random homology. Furthermore, despite the conserved lengths of the exons (exon 1, 95 base pairs (bp); exon 2, 205 bp; exon 3, 126 bp), the lengths of the introns and the untranslated regions of these two genes are significantly different. The sequence features that are required for the expression of protein-coding genes seem to be conserved within and flanking the θ1 gene. These include the upstream CCAAT and ATA boxes, the polyadenylation signal, the polyadenylation site, the splicing junctions, the initiation codons, the termination codon and an open reading frame without premature termination codons.

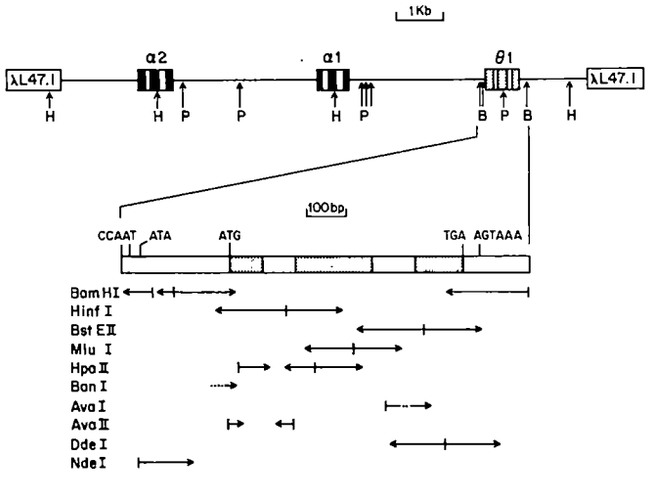


Fig. 1 Above, map of the adult α-globin gene region of the orang-utan. Restriction enzyme sites are as follows: P, *Pvu*II; H, *Hin*dIII; B, *Bam*HI. Below, sequencing strategy of θ1. Presumptive regulatory signals are given above the gene; presumptive coding sequences are stippled. The nucleotide sequences of the orang-utan θ1 gene and its flanking regions were determined by the method of Maxam and Gilbert[28]. Restriction fragments sequenced were labelled with ^{32}P at their 3′ ends by the Klenow enzyme. For the putative coding regions, both strands were sequenced.

However, several features of these controlling elements differ between θ1 and the α1-globin gene. First, whereas θ1 possesses upstream CCAAT and ATA boxes, the spacing between the two promoter elements is 29 bp, instead of 39 bp as in the α1 gene. Second, the ATA box of θ1 is located 157 bp further upstream from the ATG initiation codon. Third, the sequence between the two promoter boxes of θ1 is highly A+T-rich; in α1 the spacer sequence is G+C-rich. Interestingly the spacer region of each gene contains an inverted repeat which starts 7 bp downstream from CCAAT (CGCCCGG CCGGGCG in α1 and GTTTTTACTAGAGACTAAAAAC in θ1). Fourth, the polyadenylation signal of θ1 is AGTAAA, rather than AATAAA. It is known that AGTAAA is functional in other gene systems[18]. Fifth, the termination codon in θ1 is TGA, instead of TAA as in α1.

If θ1 is indeed expressed, at a specific development stage in a specific tissue, it will code for a hitherto unknown α-like globin. The hypothetical polypeptide, whose primary sequence is given in Fig. 2, would be of the same length as α-globin, and bears no greater resemblance to the 'α3 globin' isolated from gorilla and chimpanzee[19] than to the common α1-globin of the orang-utan. The polypeptide would, despite the 55 amino-acid differences from orang-utan α1, nevertheless conserve: (1) all 5 amino acids (Thr 39, Phe 43, Leu 83, His 87, Tyr 140) invariant across all known haemoglobins and myoglobins; (2) all but one (Ser for Asn 97) of the 23 amino acids invariant across all known α-globins; and (3) 42 of the 50 amino acids invariant across all known mammalian α-globins[20]. Of the eight sites not conserved when θ1 is compared with all other mammalian α-globins (Ala for Thr 38; His for Asp 85; Ser for Asn 97; Gln for Lys 99; Ser for Thr 134; Ala for Val 135; Ala for Thr 137; Gln for Lys 139),

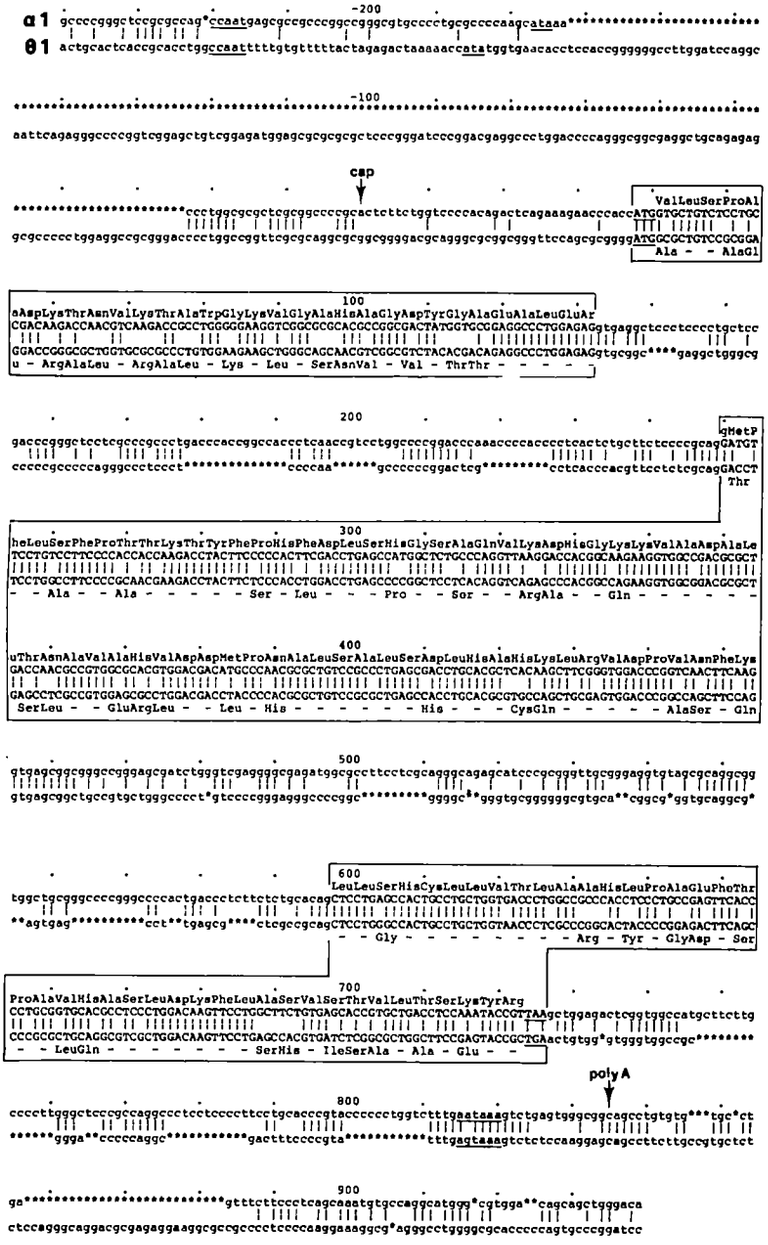


Fig. 2 Alignment of $\theta 1$ and $\alpha 1$ genes of the orang-utan. Sequence begins 20 bp upstream from the 'CCAAT' promoter and extends past the polyadenylation site of $\alpha 1$. Coding sequences are boxed and capitalized; noncoding sequences are given in small letters. The amino-acid translation is given above and below the coding sequence. That of $\alpha 1$ is given in full; where the amino acid in $\theta 1$ is identical, a dash is given below the nucleic acid sequence, otherwise the variant amino acid is given. Promoter, initiation codon, termination codon and polyadenylation signals are underlined. For the orang-utan $\alpha 1$ gene, cap and polyadenylation sites are indicated, based on the homologous sites in the human $\alpha 1$ globin gene. An asterisk indicates a deleted base in the corresponding position. Noncoding sequences are aligned to give maximum base-for-base homology, but these are probably overestimated and should be regarded with caution. Orang-utan $\alpha 1$ sequence is from ref. 17. The nucleotide at position 396 appeared as C when sequenced from the 5′ direction, and as T when sequenced from the 3′ direction. We give it as T for the sake of parsimony, as this is the same nucleotide as in $\alpha 1$; however, as a C the $\theta 1$ codon would change from CTG (Leu) to CCG (Pro).

four are in the carboxy-terminus. Two of these four sites, and eight other amino acids throughout the hypothetical $\theta 1$ protein, are different from those of the most common α-globin amino acid at the position, but identical to those of β-globin. These are Glu 5, Leu 13, Asn 20, Val 21, Ser 67, Leu 76, Gly 102, Gln 122, Ala 135 and Ala 137. A $\theta 1$ protein might thus have properties of both α- and β-globins.

We also note that another ATG codon lies 72 bp downstream from the ATA box of the $\theta 1$ gene. If we consider the possibility that this ATG triplet initiates the translation of $\theta 1$, three possibilities exist for a potential gene product. First, assuming no messenger RNA splicing, translation would be out of phase from α-globin and yield a protein of 126 amino acids until a termination codon is reached. Second, assuming splicing at identical points to the α-globins, out-of-phase translation would yield a protein of 208 amino acids. The last base of the termination codon in this case would be the first of the presumptive $\theta 1$ polyadenylation signal. Third, the mRNA might be spliced at different sites from α-globin, to yield a protein of unknown length. In connection with the latter two possibilities, we have not located an mRNA polyadenylation signal within 200 bp downstream from the AGTAAA sequence (Fig. 2; J.M., results not shown).

Southern blot hybridization experiments have confirmed the genomic $\alpha 2$-$\alpha 1$-$\theta 1$ linkage in the orang-utan, and established a similar linkage in the human. The cloned orang-utan $\theta 1$ gene sequence hybridizes to a number of genomic restriction fragments of human, orang-utan, olive baboon and rhesus macaque (Fig. 3). Under the stringent conditions used for the blot hybridization (see Fig. 3 legend), none of the bands on the autoradiographs of human restriction digests corresponds to those fragments containing either the ζ-[2,6] or the β-globin-like genes[21]. In the orang-utan digests (Fig. 3*c*), all of the restriction fragments containing the $\theta 1$ gene, as mapped in the phage clone $\lambda 0\alpha G1$[17], were visible on the autoradiograph (the bands denoted by asterisks in Fig. 3*c*).

The restriction sites of *Eco*RI, *Bgl*II, *Hin*dIII and *Hpa*I spanning the 3′ region of the human α-globin gene cluster have been mapped previously[2,22]. Using a cloned unique sequence located immediately downstream from the human $\alpha 1$-globin gene as the hybridization probe, we have also established the existence of the 3-kb *Pvu*II fragment located immediately down-

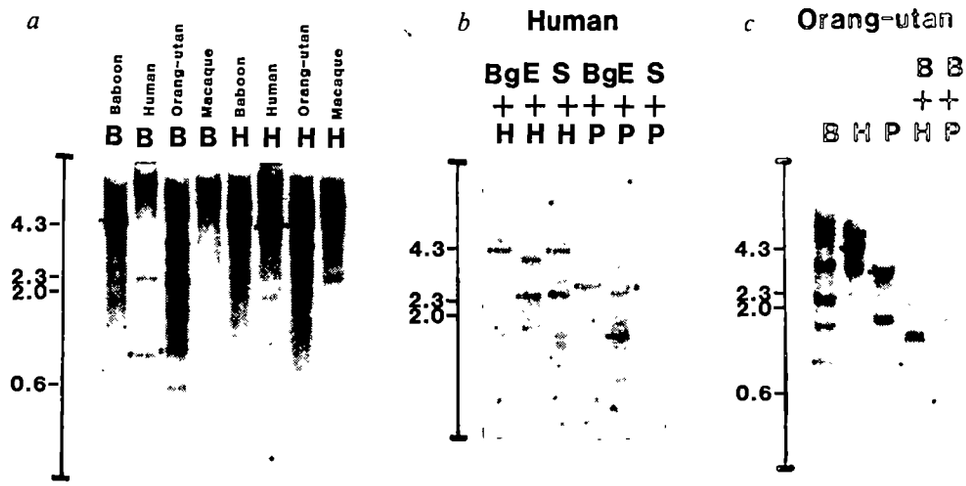


Fig. 3 Genomic blot hybridization of human, orang-utan, macaque and baboon DNAs with the orang-utan $\theta 1$ gene sequence. The lines and numbers on the left side of each panel indicate the lengths (kb) of the markers. Asterisks denote the bands corresponding to the restriction fragments containing the human or orang-utan $\theta 1$ gene located downstream from the $\alpha 1$-globin gene. Their locations and sizes are shown in the maps in Fig. 4*a* and *b*. ***a***, Southern blot of baboon, human, orang-utan or rhesus macaque DNA digested with *Bam*HI (B) or *Hin*dIII (H). ***b***, Southern blot of human chromosomal DNA digested with pairs of the following restriction enzymes: *Bgl*II (Bg), *Hin*dIII (H), *Eco*RI (E), *Pvu*II (P) and *Sac*I (S). ***c***, Southern blot of orang-utan chromosomal DNA digested with *Bam*HI (B), *Hin*dIII (H), *Pvu*II (P), *Bam*HI + *Hin*dIII (B+M), or *Bam*HI + *Pvu*II (B+P).

Methods. Chromosomal DNA samples were digested with different restriction enzymes, electrophoresed in a 1% agarose gel, blotted and hybridized[29] with the 0.9-kb *Bam*HI fragment containing the orang-utan $\theta 1$ gene (see map of Fig. 1). The probe was labelled with ^{32}P by nick translation[30]. The blot was hybridized at 68 °C in a solution containing 0.75 M Na^+ salt, and washed at 68 °C in 50 mM Tris-HCl (pH 7.5) and 1 mM EDTA.

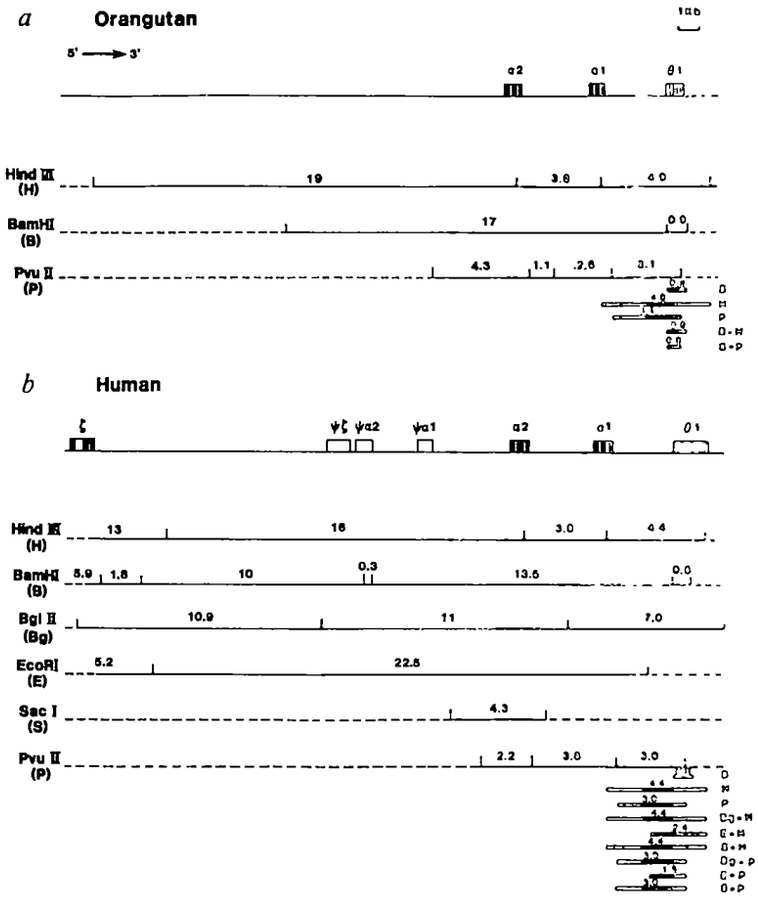


Fig. 4 ***a***, $\alpha 2$-$\alpha 1$-$\theta 1$ linkage map in orang-utan. The arrangement of the $\alpha 2$, $\alpha 1$ and $\theta 1$ genes is derived from the study of Marks *et al.*[17] and the blotting data in Fig. 3. The restriction maps of *Hin*dIII, *Bam*HI and *Pvu*II are shown below the gene linkage map. The genomic fragments that hybridize to the $\theta 1$-specific probes, as denoted by an asterisk in Fig. 3, are represented by the black bars. The numbers above the individual fragments indicate their lengths in kb. ***b***, Linkage map of the human α-globin-like gene cluster. The map is derived from refs 2, 5–10 and the present study (see text). The exons of the functional ζ, $\alpha 2$ and $\alpha 1$ are represented by black boxes while their introns are shown as blank boxes. The three pseudogenes $\psi\zeta$, $\psi\alpha 2$ and $\psi\alpha 1$ are represented by blank boxes and the $\theta 1$ gene by a stippled box. The restriction maps of the gene cluster are derived mainly from refs 2, 22 and the present study, The genomic fragments that hybridize to the orang-utan $\theta 1$ probe, as denoted by asterisks in Fig. 3, are represented by black bars below the restriction maps.

stream from the previously mapped 3.8-kb fragment (see Fig. 4; hybridization data not shown). The hybridization patterns of the human digests (Fig. 3*a*, *b*), combined with the restriction maps mentioned above, demonstrate that as in the orang-utan, a $\theta 1$ homologue also exists ~3 kb downstream from the $\alpha 1$-globin gene. The $\alpha 2$-$\alpha 1$-$\theta 1$ linkage maps of orang-utan and human are shown in Fig. 4*a* and *b*, respectively.

In most digests shown in Fig. 3, there is more than one other band that cannot be explained by hybridization to the known genes of the α- or β-globin gene cluster. The presence of these bands (for example, the 2.7-kb band in the *Hin*dIII digests of orang-utan DNA and the 1.0-kb *Pvu*II band in the *Eco*RI + *Pvu*II digest of human DNA) suggests that additional $\theta 1$-homologous genes exist in the genomes of both species. However, due to lack of available restriction maps and probes, we do not know whether these are located further downstream from the $\theta 1$ gene. Further, the intensities of some of these additional bands, especially in the orang-utan, raise the interesting possibility that there are genomic regions where many $\theta 1$-homologous sequences are tightly clustered together. These regions are being characterized by molecular cloning and sequence analysis.

Although we have not carried out detailed restriction mapping analysis for the macaque and baboon, the genomic hybridization pattern to the orang-utan $\theta 1$ probe (for example, see Fig. 3*a*) and partial sequencing analysis of a recombinant phage clone containing the baboon $\alpha 1$ gene and its 3′-flanking DNA indicate that a $\theta 1$ homologue also exists in these species on the 3′ side of the $\alpha 1$ gene (J.P.S., J.M. and C.-K.J.S., unpublished results).

The $\alpha 2$-$\alpha 1$-$\theta 1$ linkage in human, orang-utan and the Old World monkeys suggests that the $\theta 1$ gene was generated by the tandem duplication of a primordial α-globin gene in a remote ancestor of these anthropoid primates. The duplication may even have antedated the emergence of the primates, since an α-globin-like pseudogene has been reported to exist downstream from the $\alpha 1$ gene of horse[23] and rabbit[24]. In the former organism no sequence data are available[23]; in the latter, no CCAAT and ATA boxes are found within 2 kb upstream from the gene ($\psi\alpha$; ref. 24), and several frameshift deletions in exon 2 create multiple premature termination codons. Nevertheless, there are several indications that the rabbit $\psi\alpha$ gene is indeed an orthologous counterpart of the orang-utan $\theta 1$ gene described here; for example, TGA instead of TAA as the termination codon, and AGTAAA instead of AATAAA as the polyadenylation signal. Further, exons of the rabbit $\psi\alpha$ and orang-utan $\theta 1$ resemble each other more than do orang-utan $\alpha 1$ and $\theta 1$ (Table 1). It thus seems that the $\theta 1$ gene has an ancient phylogenetic history in the mammalian genome.

If we postulate that $\theta 1$ is not, and has not in the recent phylogenetic past, been functional we may predict that the divergence between rabbit $\alpha 1$ and orang-utan $\alpha 1$, under the constraint of natural selection, will be considerably less than the divergence between rabbit $\psi\alpha$ and orang-utan $\theta 1$. While the noncoding segments are so different as to be unreliable in such a quantiative comparison, the percentages of amino-acid replacement mutations in the coding sequences may be compared, and this is done in Table 1. Insofar as the known functional α-globin genes are only very slightly more similar between the two species (12% replacement site divergence) than are the new genes (13%), we interpret this as further indirect evidence for recent or current activity of this gene in at least one of the lineages. Partial DNA sequencing of a cloned baboon $\theta 1$ gene shows that its putative promoter sequences and coding regions are highly homologous to the orang-utan $\theta 1$ reported here (J.M., J.-P.S. and C.-K. J. S., unpublished results).

Table 1 Divergence for amino-acid replacement sites in $\alpha 1$ and $\theta 1$ homologues

Pairwise comparison	% Divergence replacement sites
Orang-utan $\alpha 1$–rabbit $\alpha 1$	12
Orang-utan $\theta 1$–rabbit $\psi\alpha$	13
Orang-utan $\alpha 1$–orang-utan $\theta 1$	25
Rabbit $\alpha 1$–rabbit $\psi\alpha$	27
Orang-utan $\alpha 1$–rabbit $\psi\alpha$	29
Rabbit $\alpha 1$–orang-utan $\theta 1$	29

Calculations were based on the method of Perler *et al.*[27] and data are from refs 17 and 24.

To ascertain that the $\theta 1$ globin gene is functional requires extensive gene transfer experiments, and a search for its corresponding mRNA and protein *in vivo*. Our preliminary studies have indicated that, like the human embryonic ζ-globin gene[25], the promoter of the orang-utan $\theta 1$ gene functions poorly in HeLa cell extract or in transfected Cos cells. Finally, it may be of interest that as yet uncharacterized globin polypeptide(s) exist during the early stages of human embryo development[26].

This research was supported by NIH grant AM 29800, and in part by American Cancer Society grant CD-212. We thank Celia Shen for advice on the calculation of replacement site changes, Ross Hardison for communicating results before publication, Dr G. Stamatoyannopoulos for his suggestion of the $\theta 1$ designation, Candy Miller for typing the manuscript, Yerkes Regional Primate Research Center, Atlanta, for providing the orang-utan tissues, and the Primate Center of University of California, Davis, for the macaque and baboon tissues. C.-K.J.S. is supported by an NIH Research Career Development Award.

Note added in proof: One of the human $\theta 1$-globin-like genes has recently been cloned and mapped to chromosome 22 (J-P.S., T. Mohandas, and C.-K.J.S., manuscript in preparation).

Received 9 January; accepted 4 April 1986.

1. Deisseroth, A. *et al. Cell* **12**, 205-218 (1977).
2. Lauer, J., Shen, C.-K. J. & Maniatis, T. *Cell* **20**, 119-130 (1980).
3. Maniatis, T., Fritsch, E. F., Lauer, J. & Lawn, R. M. *A. Rev. Genet.* **14**, 145-178)1980).
4. Collins, F. S. & Weissman, S. M. *Prog. Nucleic Acid Res. molec. Biol.* **31**, 315-462 (1984).
5. Hardison, R. C., Sawada, I., Cheng, J-F., Shen, C.-K. J. & Schmid, C. W. *Nucleic Acids Res.* **14**, 1903-1911 (1986).
6. Proudfoot, N., Gil, A. & Maniatis, T. *Cell* **31**, 553-563 (1982).
7. Liebhaber, S. A., Goossens, M. J. & Kan, Y. W. *Proc. natn. Acad. Sci. U.S.A.* **77**, 7054-7058 (1980).
8. Liebhaber, S. A., Goossens, M. J. & Kan, Y. W. *Nature* **290**, 26-29 (1981).
9. Michelson, A. M. & Orkin, S. H. *J. biol. Chem.* **258**, 15245-15254 (1983).
10. Proudfoot, N. J. & Maniatis, T. *Cell* **21**, 537-544 (1980).
11. Zimmer, E. A., Martin, S. L., Beverley, S. M., Kan, Y. W. & Wilson, A. C. *Proc. natn. Acad. Sci. U.S.A.* **77**, 2158-2162 (1980).
12. Zimmer, E. A. thesis, Univ. California, Berkeley (1981).
13. Higgs, D. R., Goodbourn, S. E. Y., Wainscoat, J. S., Clegg, J. B. & Weatherall, D. J. *Nucleic Acids Res.* **9**, 4213-4224 (1981).
14. Goodbourn, S. E. Y., Higgs, D. R., Clegg, J. B. & Weatherall, D. J. *Proc. natn. Acad. Sci. U.S.A.* **80**, 5022-5026 (1983).
15. Hess, J. F., Fox, M., Schmid, C. W. & Shen, C.-K. J. *Proc. natn. Acad. Sci. U.S.A.* **80**, 5970-5974 (1983).
16. Hess, J. F., Schmid, C. W. & Shen, C.-K. J. *Science* **226**, 67-70 (1984).
17. Marks, J., Shaw, J.-P. & Shen, C.-K. J. *Proc. natn. Acad. Sci. U.S.A.* **83**, 1413-1417 (1986).
18. Capon, D. J., Chen, E. Y., Levinson, A. D., Seeburg, P. H. & Goeddel, D. V. *Nature* **302**, 33-37 (1983).
19. Boyer, S. H., Noyes, A. N., Boyer, M. L. & Marr, K. *J. biol. Chem.* **248**, 992-1003 (1973).
20. Dickerson, R. & Geis, I. *Hemoglobin: Structure, Function, Evolution and Pathology* (Benjamin/Cummings, Menlo Park, 1983).
21. Fritsch, E. F., Lawn, R. M. & Maniatis, T. *Cell* **19**, 959-972 (1980).
22. Goossens, M. *et al. Proc. natn. Acad. Sci. U.S.A.* **77**, 518-521 (1980).
23. Clegg, J. B., Goodbourn, S. E. Y. & Braend, M. *Nucleic Acids Res.* **12**, 7847-7858 (1984).
24. Cheng, J.-F., Raid, L. & Hardison, R. C. *J. biol. Chem.* **261**, 839-848 (1986).
25. Proudfoot, N. J., Rutherford, T. R. & Partington, G. A. *EMBO J.* **3**, 1533-1540 (1984).
26. Peschle, C. *et al. Nature* **313**, 235-238 (1985).
27. Perler, F. *et al. Cell* **20**, 555-566 (1980).
28. Maxam, A. M. & Gilbert, W. *Proc. natn. Acad. Sci. U.S.A.* **74**, 560-564 (1977).
29. Southern, E. M. *J. molec. Biol.* **98**, 503-517 (1975).
30. Maniatis, T., Jeffrey, A. & Kleid, D. G. *Proc. natn. Acad. Sci. U.S.A.* **72**, 1184-1188 (1975).

Assembly of microtubules at the tip of growing axons

J. R. Bamburg, D. Bray & K. Chapman

MRC Cell Biophysics Unit, King's College, 26 Drury Lane, London WC2B 5RL, UK

The growth of axons in the developing nervous system depends on the elongation of the microtubules that form their principal longitudinal structural element[1,2]. It is not known whether individual microtubules in the axon elongate at their proximal ends, close to the cell body, and then move forward into the lengthening axon, or whether tubulin subunits are transported to the tip of the axon and assembled there onto the free ends of microtubules. The former possibility is supported by studies of slow axonal transport in mature nerves from which it has been deduced that microtubule assembly occurs principally at the neuronal cell body[3,4]. By contrast, the polarity of microtubules in axons, which have their 'plus' or 'fast-growing' ends distal to the cell body[5], suggests that assembly occurs at the growing tip, or growth cone, of the axon. We have addressed this question by topically applying Colcemid (*N*-desacetyl-*N*-methylcolchicine), and other drugs which alter microtubule stability, to different regions of isolated nerve cells growing in tissue culture. We find that the sensitivity to these drugs is greatest at the growth cone by at least two orders of magnitude, suggesting that this is a major site of microtubule assembly during axonal growth.

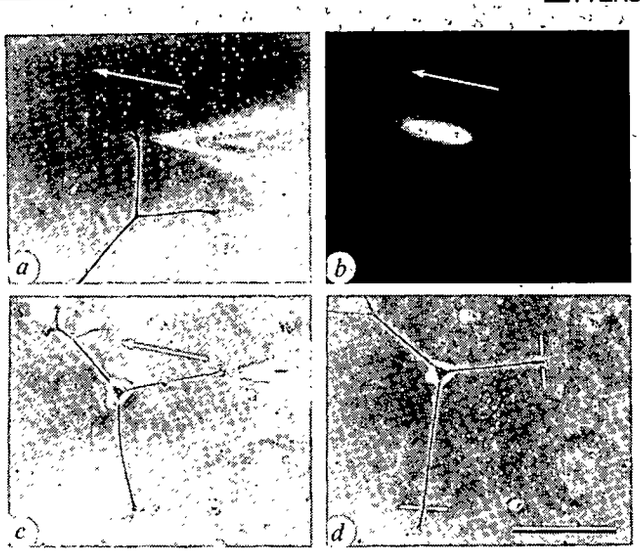


Fig. 1 Response of a growth cone to topically applied Colcemid. Dorsal root ganglia from 8–10-day-old chick embryos were typsin-dissociated and cultured as described previously[17]. Cultures were mounted on the stage of an inverted Zeiss IM35 fluorescence microscope and kept at 37–38 °C by an air-stream incubator. A peristaltic perfusion pump circulated culture medium (total volume 25.6 ml) at a rate of 0.4–1 ml min^{-1}. Dow-Corning silicone fluid (1 ml) was applied to the culture to minimize evaporation. The outflow port of the perfusion system was adjusted so that the direction of flow of the medium (arrow) carried the drug across the cell of interest and removed it from the bulk culture medium. Glass capillary micropipettes (pulled to give tips 1–3 μm in diameter) were back-filled with the desired drug solution, containing 25–50 μg ml^{-1} fluorescein. The micropipette was then placed at the desired point (*a*) and the flow of the drug solution, monitored by the fluorescence of the internal fluorescein marker, applied to the cell (*b*). (For clarity, the micropipette in this panel was raised slightly from the culture substratum and contained a higher concentration of fluorescein.) A typical response of a growth cone to the application of 0.1 μg ml^{-1} Colcemid from a micropipette is shown at zero time (*c*), and after 30 min of application (*d*). Only that growth cone to which the drug was applied ceased its advance over the culture substratum. Scale bar, 100 μm.

Application of drug-containing solutions to localized regions of growing nerves was achieved by means of a pressure-driven micropipette and a background flow of medium to restrict diffusive spread. The localized region of application covered an area ~30 μm in diameter (Fig. 1*a*, *b*). Careful placement of the pipette and adjustment of the background flow allowed us to centre the region of drug application to the growth cone, neurite fibre or cell body.

A typical response of a growth cone exposed to 0.1 μg ml^{-1} Colcemid applied through a micropipette is illustrated in Fig. 1*c*, *d*. The treated growth cone stops its advance within a few minutes. At the same time, a sister neurite from the same cell, but not exposed to the flow of drug-containing solution, continues unabated growth. We observed similar results for sister growth cones from a branched neurite.

A dose-response curve for the application of Colcemid to the growth cone and to the cell body is shown in Fig. 2. A concentration of Colcemid of 0.5 μg ml^{-1} (1.35×10^{-6} M) caused significant inhibition of neurite growth when applied to the growth cone whereas 100 times this concentration had little effect on neurite growth when applied to the cell body.

We tested two other microtubule-active drugs, nocodazole[6] and taxol[7], for their effects on axonal growth in our system (Table 1). Although complete dose–response curves were not obtained, these agents were similar to Colcemid in that they were much more effective when applied to the growth cone than to the cell body. Application of either nocodazole or taxol to

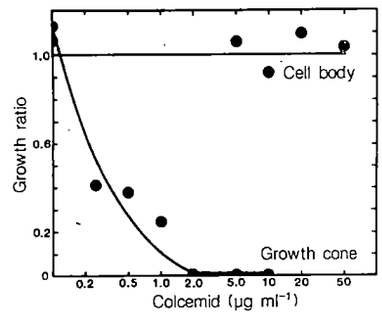


Fig. 2 Dose–response curve for the application of Colcemid to the growth cone and to the cell body. The drug was dissolved in culture medium without methylcellulose and containing 25 μg ml^{-1} fluorescein and 10% Ficoll. These solutions were sonicated and filtered through 0.22-μm filters. Neurite outgrowth in control cultures was unaffected by addition of 50 μg ml^{-1} fluorescein or 10% Ficoll. The response shown here is the ratio of the increase in length over a 20-min period following the application of the drug to the increase in length during 20 min before drug application. Drug was applied for 20 min. An average of 7 cells were observed per point with a minimum of $n = 4$ except for the growth cone application of 2 μg ml^{-1} ($n = 3$) and 10 μg ml^{-1} ($n = 1$). Neurites which retracted were scored as zero.

the growth cone inhibited axonal growth at concentrations at least 150 times lower than those needed to arrest axonal growth when applied to the cell body or neurite fibre. Lumicolcemid, a derivative of Colcemid which no longer binds to tubulin, had no effect on axonal growth when applied to the growth cone (Table 1).

In another series of experiments the time-course of axonal growth was followed for 30 min during drug applications after measurement of growth over a 30-min control period. Continual readjustment of the position of the micropipette was often required in these experiments when growth-cone application was used, as the neurites often retracted or grew beyond the point of application.

Typical time-courses showing the response of growth cones to Colcemid are shown in Fig. 3. A concentration of 2.7×10^{-7} M (0.1 μg ml^{-1}) applied to the growth cone arrests its advance within minutes, whereas a 10-fold higher concentration of this drug (2.7×10^{-6} M, 1 μg ml^{-1}) causes rapid retraction. Again, application of Colcemid at high concentration (4.0×10^{-5} M, or 15 μg ml^{-1}) to the neurite fibre or cell body had no detectable effect on the progress of the elongating axonal tip (Table 1).

Table 1 Concentrations of drugs required to inhibit axonal growth

Drug	Site of application		
	Growth cones (μg ml^{-1})	Neurites (μg ml^{-1})	Cell body (μg ml^{-1})
Colcemid	<0.1	>15	>15
Taxol	<0.1	>15	>15
Nocodazole	<0.1	>5	>15
Lumicolcemid	>5	ND	ND

The concentrations of Colcemid, taxol and nocodazole listed were enough to halt growth cone advance within 10 min of application to the growth cone but had no inhibitory effect on growth when applied to neurites or the cell body. ND, not done. Lumicolcemid was prepared from Colcemid by irradiation of an ethanol solution at 350 nm (ref. 16). Lumicolcemid, nocodazole and taxol were dissolved in dimethyl sulphoxide (DMSO) at a concentration of 1–5 mg ml^{-1} and dilutions prepared as described in Fig. 2 legend. Neurite outgrowth in control cultures was unaffected by 1.5% DMSO (the maximum concentration in any application solution).

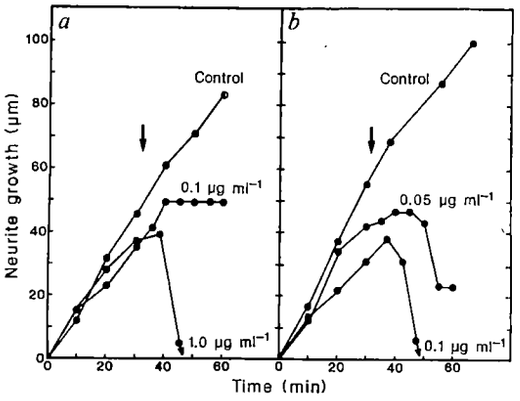


Fig. 3 Time-course for the response of growth cones to Colcemid when applied locally (*a*) or to the whole cell (*b*). The drug was applied at the time indicated by an arrow. Application of the drug to the whole cell was achieved by perfusion of the entire culture.

It was of interest to compare the effect of topically applied drugs, restricted to a small region of the nerve cell, with that of the same drug applied in the bathing medium to the entire surface of the growing nerve cell. Earlier studies of the inhibition of axonal growth by drugs added to the culture medium have shown effects within 6–24 h with as little as 2.5×10^{-8} M (0.01 μg ml^{-1}) colchicine[8] or 7×10^{-8} M (0.06 μg ml^{-1}) taxol[9]. On a shorter timescale (Fig. 3), a significant inhibition of neurite growth was observed at Colcemid concentrations somewhat lower than those which inhibited growth when applied to the growth cone. But, taking into account the dilution of the drug which must occur when it is delivered by micropipette, the inhibitory effects of antimitotic agents on neurite outgrowth probably arise from their effect on the growth cone, the most sensitive site.

The primary target of colchicine and related drugs is the assembly of microtubules[10,11]. Therefore, our finding that sub-stoichiometric concentrations of Colcemid and nocodazole inhibit nerve growth only when they are applied to the growth cone, and not when applied to the cell body or along the length of the axon, suggests that the growing tip of the axon is a major site of microtubule assembly in growing nerve axons. Taxol, on the other hand, promotes microtubule assembly by stabilizing microtubules[7] and cause growth inhibition through an uncontrolled assembly of microtubules at the growth cone[9]. Thus, the controlled assembly of microtubules appears to be tightly coupled to nerve growth, a finding consistent with a recent report suggesting that microtubule assembly proteins are vital regulatory factors in neurite outgrowth from PC12 cells[12]. Although it could be argued that the difference in sensitivity of growth cone and cell body arises because one is much larger than the other, or more active in the uptake of externally applied agents, we are reassured by the more than 100-fold difference in drug sensitivity of these two regions. Moreover, the rapid effects of Colcemid and nocodazole on mitosis show that they readily gain access to microtubules in the cytoplasm of even very large cells[13,14]. Another possible objection is that even though an antimitotic drug is applied to the growth cone, it might act at another site in the cell, being carried there by axonal transport. Against this objection we have clear evidence of restricted action of a topically applied drug (Fig. 1*c*, *d*).

If we are correct in thinking that microtubules assemble at the growing tip of an axon, then tubulin molecules must be available there in an unpolymerized form. Conceivably, tubulin could be polymerized by a Colcemid-resistant mechanism in the cell body, transported through the axon as microtubules and then selectively disassembled near the growth cone to provide subunits for new assembly. But, it seems simpler to propose that tubulin is transported in an unassembled form and that most microtubules in the axon are as stationary as neurofilaments appear to be[15]. The nature of this tubulin-containing precursor, the mechanism by which it is carried in the axon and the regulation of its addition to the ends of microtubules are interesting and intriguing questions.

The idea for these experiments arose in a conversation with Dr Tim Mitchison, whom we thank. J.R.B. is on sabbatical leave from the Department of Biochemistry, Colorado State University, Fort Collins, CO 80523, USA and supported in part by a Senior International Fellowship, Fogarty Centre and NIH grant GM35126.

Received 12 March; accepted 22 April 1986.

1. Yamada, K. M., Spooner, B. S. & Wessells, N. K. *J. Cell Biol.* **49**, 614–635 (1971).
2. Letourneau, P. C. in *Molecular Bases of Neural Development* (eds Edelman, G. F., Gall, W. E. & Cowan, W. M.) 269–293 (Wiley, New York, 1985).
3. Lasek, R. J. *Phil. Trans. R. Soc.* **299**, 313–327 (1985).
4. Heriot, K., Gambetti, P. & Lasek, R. J. *J. Cell Biol.* **100**, 1167–1172 (1985).
5. Heidemann, S. R., Landers, J. M. & Hamborg, M. A. *J. Cell Biol.* **91**, 623–661 (1981).
6. Head, J., Lee, L. L. Y., Field, D. J. & Lee, J. C. *J. biol. Chem.* **260**, 11060–11066 (1985).
7. Schiff, P. B., Fant, J. & Howitz, S. B. *Nature* **277**, 665–667 (1979).
8. Daniels, M. P. *J. Cell Biol.* **53**, 164–176 (1972).
9. Letourneau, P. C. & Ressler, A. H. *J. Cell Biol.* **98**, 1355–1362 (1984).
10. Margolis, R. and Wilson, L. *Proc. natn. Acad. Sci. U.S.A.* **74**, 3466–3470 (1977).
11. Bergen, L. & Borisy, G. G. *J. biol. Chem.* **258**, 4190–4194 (1983).
12. Drubin, D. G., Feinstein, S. C., Shooter, E. M. & Kirschner, M.. W. *J. Cell Biol.* **101**, 1799–1807 (1985).
13. Sluder, G. *J. Cell Biol.* **70**, 75–85 (1976).
14. DeBrabander, M. J., Van de Vein, R. M. L., Aerts, F. E. M., Borgers, M. & Janssen, P. A. J. *Cancer Res.* **36**, 905–916 (1976).
15. Nixon, R. A. & Logvinenko, K. B. *J. Cell Biol.* **102**, 647–659 (1986).
16. Wilson, L. & Friedkin, M. *Biochemistry* **5**, 2463–2468 (1966).
17. Bray, D. & Chapman, K. *J. Neurosci.* **5**, 3204–3213 (1985).

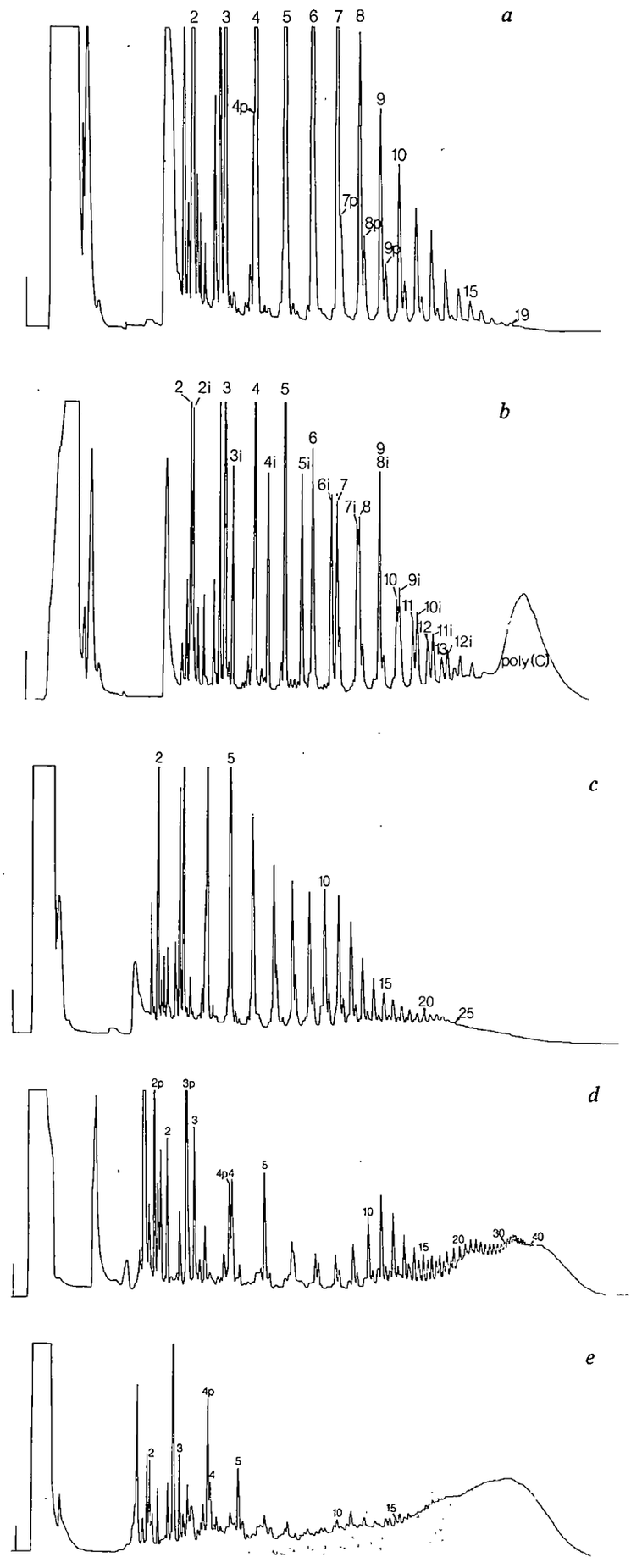
Template-directed oligonucleotide ligation on hydroxylapatite

Oscar L. Acevedo & Leslie E. Orgel

The Salk Institute for Biological Studies, PO Box 85800, San Diego, California 92138, USA

Bernal[1], and subsequently other authors[2], have suggested that the prebiotic synthesis of the precursors of biopolymers could have occurred on a solid surface such as that provided by clay or some other mineral. The separation of products from the other components of the reaction mixture in such a system is reminiscent of modern solid-phase synthesis of polypeptides and polynucleotides. One such scheme envisages that growing polymers were localized by adsorption to a mineral surface where an activating agent or activated monomers were supplied continuously or cyclically[3,4]. We have been trying to test this scheme using reactions which we believe may be related to those that occurred during prebiotic evolution. We have already reported that oligonucleotides adsorbed onto hydroxylapatite provide suitable templates for the oligomerization of (guanosine 5′-phosphor)-2-methylimidazolide (2-MeImpG)[4–7]. However, this is not a suitable test reaction, as 2-MeImpG oligomerization proceeds almost to completion in a single step. Here we report that a sequence of reactions in which initially formed oligo(G)s are reactivated by conversion to phosphorimidazolides in the presence of poly(C) and then allowed to ligate is ideal, in that repeated cycles can be carried out on the surface of hydroxylapatite, whereas in the liquid phase the cycle could be achieved only with considerable difficulty.

To obtain suitable substrates for the reaction, we adsorbed poly(C) (2.5 μmol) on hydroxylapatite (60 mg) and then added 2-MeImpG (7.5 μmol). The pattern of products obtained[7] after incubation for 1 week at 0 °C is shown in Fig. 1*a*. Each reaction



ig. 1 HPLC elution profiles of oligoguanylates on hydroxy-
ıpatite. *a*, Products of standard oligomerization of 2-MeImpG on
oly(C): poly(C) (2.5 μmol) adsorbed on 60 mg hydroxylapatite
BIO-GEL HTP; Bio-Rad Laboratories) and treated with 0.15 M
-MeImpG (7.5 μmol, 0.5 μCi), 0.2 M $MgCl_2$, 0.2 M NaCl, 0.1 M
IEPES, sodium salt buffer, *p*H 8.0, in a 50 μl volume (incubation
or 7 days at 0 °C). *b*, Products of reactivation of oligoguanylates.
eaction mixture contained 1.0 M 1-ethyl-3-(3-dimethyl-
minopropyl)carbodiimide-HCl and 1.0 M 2-methylimidazole,
H 6.0 (25 °C, 4 h, 200 μl volume over hydroxylapatite). The ratio
f the heights of N_i to $N_i + N$ gives the percentage reactivation.
, Products of one cycle of reactivation–ligation. Reaction mixture
ontained 0.2 M $MgCl_2$, 0.2 M NaCl, 0.5 M HEPES buffer (20 h,
7 °C, 200 μl volume over hydroxylapatite) *d*, Products of four
ycles of reactivation–ligation. *e*, Products after 16 cycles. The
otted curve is the elution profile of a 'high-M_r' sample of poly(G)
Sigma). The numbers above selected peaks are the lengths of the
orresponding oligomers; phosphorimidazolides are indicated by
he letter i; pyrophosphate-terminated oligomers are indicated by
the letter p.

cycle is begun by centrifugation, decantation of the supernatant and addition of 200 μl of 1 M 1-ethyl-3-(3-dimethylaminopropyl)carbodiimide in 1 M 2-methylimidazole buffer at *p*H 6 and 25 °C. After 4 h, the suspension is chilled (0 °C) and centrifuged, and the hydroxylapatite then separated from the supernatant. The ligation phase is initiated by adding 200 μl of a solution containing 0.2 M NaCl, 0.2 M $MgCl_2$ and 0.5 M HEPES buffer at *p*H 8. Ligation is allowed to proceed at 37 °C for 20 h, after which the supernatant is removed and the next cycle of reaction initiated as above.

The oligonucleotides, together with the poly(C) template, are eluted from the hydroxylapatite using a solution of 0.5 M EDTA, 0.5 M $K_4P_2O_7$. When necessary, an aliquot of this wash is incubated with pancreatic ribonuclease at *p*H 7.6 to hydrolyse the poly(C) template. HPLC analysis on an RPC-5 column using a gradient of sodium perchlorate at *p*H 12 is carried out as reported previously[7] to provide a profile of the products eluted from the hydroxylapatite.

Figure 1*b* shows the products obtained immediately after the first reactivation step; ~45% of the oligo(G)s had been converted to phosphorimidazolides. Subsequent analyses at later stages of the experiment showed that a similar degree of reactivation was achieved in each cycle.

After one cycle of reactivation and ligation (Fig. 1*c*) short oligomers were depleted and longer ones enriched—oligomers in the size range 20–25 units were present only after ligation. Each successive cycle resulted in a further emphasis of the peaks corresponding to long oligomers at the expense of those corresponding to shorter ones. After four cycles of reactivation and ligation (Fig. 1*d*), peaks corresponding to oligomers up to 30–40 units long were resolved, together with an unresolved tail, found reproducibly, corresponding to oligomers at least 60 residues long. After 16 cycles almost all of the input oligo(G)s had been converted to material of high relative molecular mass (M_r) (Fig. 1*e*). The elution profile of a commercial sample of 'high-M_r' oligo(G)s is included in Fig. 1*e* for comparison. Oligo(G)s adsorbed on hydroxylapatite in the absence of poly(C) were not detectably ligated after four cycles.

The yield of oligomers obtained after several ligation cycles does not decline steadily with increasing oligomer length, but passes through maxima at lengths of 11, 22 and 33 residues. Rhodes and Klug showed that adsorption on calcium phosphate leads to the cleavage of DNA by DNase I, yielding oligomers corresponding to integral numbers of turns of the DNA double-helix[8]. Our observations may have a related explanation, but the details are unclear.

To confirm that the broad absorption peak in the elution profile is due to oligonucleotides, we repeated the experiments described above using [8-^{14}C]2-MeImpG (specific activity 0.06 μCi/μmol^{-1}). After four cycles of reactivation and ligation, the products were applied to an RPC-5 column and fractions of the eluate corresponding to different ranges of oligomer length were collected. The activity of each fraction was determined in a liquid scintillation counter and the percentage of G residues present in each fraction calculated (Table 1). The radioactivity in each sample of the eluate correlated well with the ultraviolet intensity in the appropriate region of the elution profile; this shows that almost all the observed ultraviolet absorption of the HPLC eluate is due to G residues.

Table 1 Distribution of radioactivity by oligoguanylate length

Range of oligomer length (no. of residues):	2–6	7–12	13–19	>19
Before ligation*	73.5†	20.9	4.4	1.2
After four ligation cycles*‡	32.7	23.1	16.9	27.3

* See legend to Fig. 1*a* for details.
† Values represent the c.p.m. in each fraction as a percentage of the total c.p.m. in the sample.
‡ See legend to Fig. 1*b* for details.

We next compared the radioactivity in each region measured for the multiply reactivated sample with that in the same region for a control sample. In the reactivated sample, we found that ~25% of the G residues were present in oligomers more than 20 residues long, while only 1% was present in oligomers of this size range for the control sample. The total recovery of radioactivity after four cycles was ~75% of the original input.

To establish that the products of ligation are 3′–5′-linked oligo(G)s, we used ribonuclease T_1, an enzyme that degrades 3′-5′-phosphodiester bonds only on the 3′ side of G residues. The radioactively labelled product mixture was subjected to paper chromatography in *n*-propanol/ammonia/water (55:10:35 v:v); the material at the origin of the chromatogram included all oligo(G)s ≥ 4 units long. The region at the origin was cut out and degraded with RNase T_1; as anticipated, the only products were Gp, G, pGp, and a small amount of GppGp from pyrophosphate-'capped' chains. This result shows that the condensation is regiospecific and that no C residues were present in our products.

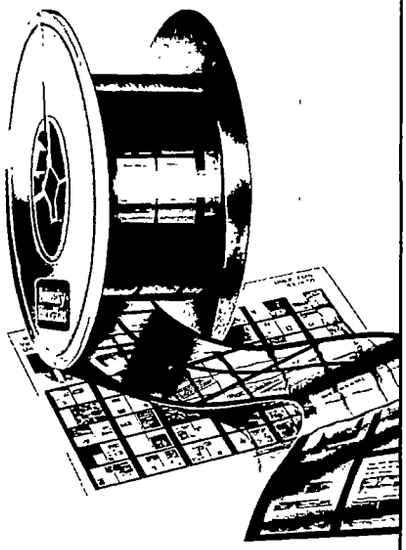
We do not mean to suggest that 2-MeImpG or water-soluble carbodiimides played any part in the origins of life on Earth. Our experiments show only that minerals lining a pond or tide pool could have provided an ideal site for the template-directed elongation and ligation of oligonucleotides in cyclic processes analogous to solid-phase synthesis. It would be premature to try to identify the activating agents or activated intermediates that were important on the primitive Earth; obvious suggestions include cyanamide and related compounds or inorganic trimetaphosphate as activating agents and nucleoside polyphosphates as activated intermediates.

We thank A. R. Hill for technical assistance and S. H. Bailey for manuscript preparation. This research was supported by the NASA grant NGR 05067001.

Received 10 March; accepted 14 April 1986.

1. Bernal, J. D. *The Physical Basis of Life* (Routledge & Kegan Paul, London, 1951).
2. Chang, S., Des Marias, D., Mack, R., Miller, S. L. & Strathearn, G. in *Earth's Earliest Biosphere: Its Origin and Early Evolution* (ed. Schopf, J. W.) 53–92 (Princeton University Press, New Jersey, 1983).
3. Gibbs, D., Lohrmann, R. & Orgel, L. E. *J. molec. Evol.* **15**, 347–354 (1980).
4. Schwartz, A. W. & Orgel, L. E. *J. molec. Evol.* **21**, 299–300 (1985).
5. Bernardi, G. *Meth. Enzym.* **21**, 95–139 (1971).
6. Martinson, H. G. *Biochemistry* **12**, 2737–2746 (1973).
7. Joyce, G. F., Inoue, T. & Orgel, L. E. *J. molec. Biol.* **176**, 379–306 (1984).
8. Rhodes, D. & Klug, A. *Nature* **286**, 573–578 (1980).

nature is available in microform.



University Microfilms International reproduces this publication in microform: microfiche and 16mm or 35mm film. For information about this publication or any of the more than 13,000 titles we offer, complete and mail the coupon to: University Microfilms International, 300 N. Zeeb Road, Ann Arbor, MI 48106. Call us toll-free for an immediate response: 800-521-3044. Or call collect in Michigan, Alaska and Hawaii: 313-761-4700.

☐ Please send information about these titles:

Name _____

Company/Institution _____

Address _____

City _____

State _____ Zip _____

Phone ( ) _____

University Microfilms International



Roland GRUNBERG - NANCY - FRANCE

DO YOU NEED PEPTIDES?

NEOSYSTEM LABORATORIES

PROVIDE
A COMPLETE SERVICE FOR
PEPTIDE SYNTHESIS
PEPTIDE AND PROTEIN SEQUENCING
PEPTIDE ANTIBODY PRODUCTION

WE PROVIDE ALSO
CONTRACT RESEARCH SERVICES
TO INDUSTRIAL AND ACADEMIC
INSTITUTIONS



NEOSYSTEM LABORATORIES
B.P. n° 309 R8
67008 STRASBOURG Cedex
FRANCE - Télex 880 088 F
Tél. : 88.36.96.96

Reader Service No.28

PHARMACOLOGY/ IMMUNOLOGY

IBM PC,XT,AT; APPLE II, II+, IIe & VAX-VMS. Laboratory software for use in research labs. Software products include those for analysis of ligand binding, enzyme kinetics, breast tumor estrogen and progesterone receptor content, and multiple exponential curve analysis. Products are menu driven and include external documentation.

Send for catalog.
Specify computer.

Lundon Software, Inc.
P.O. Box 21820
Cleveland, Ohio 44121
216–371–6220

Reader Service No.6

COMPLETE YOUR NUCLEAR LIBRARY WITH . . .

Continuing the Nuclear Dialogue
Selected Essays
by
ALVIN M. WEINBERG

and

Nuclear Criticality Safety
by
RONALD A. KNIEF

order today
from the
American Nuclear Society
555 N. Kensington Ave.
La Grange Park, IL 60525
(312) 352-6611

Reader Service No.16

novabiochem
SWITZERLAND

A TEAM OF EXPERIENCED SCIENTISTS IS READY TO SUPPLY YOU WITH

BIOLOGICALLY ACTIVE PEPTIDES

- **GRF AND ANALOGS**
  GRF (human) / GRF (rat) / GRF (1-29) amide / [D-Ala^2]-GRF (1-29) amide
- **GASTROINTESTINAL PEPTIDES**
  VIP / PHM / GRP (human) / Gastrin I (human)
- **LH-RH AND FRAGMENTS**
- **NEUROPEPTIDES**
  NPY (porcine and human) / Diazepam Binding Inhibitor Octadecapeptide
- **BRADYKININS AND BRADYKININ ANTAGONISTS**
- **ANF AND RELATED PEPTIDES**
  ANF (human) / ANF (rat) / Atriopeptins I, II and III (rat)

^{125}I-LABELED PEPTIDES

CUSTOM SYNTHESIS IS OUR SPECIALITY

THIS QUALITY SIGN GUARANTEES THAT

- EACH VIAL CONTAINS NET PEPTIDE CONTENT
- EACH BATCH IS DOCUMENTED WITH A CERTIFICATE OF ANALYSIS

NOVABIOCHEM AG

Weidenmattweg 4 · CH-4448 Läufelfingen · Switzerland **phone 062-69 19 22 telex 981 761 nobi ch**

Reader Service No.82

Australia
ORUNDEL PTY. LTD
P.O. Box 93
Terrey Hills, NSW 2084
Phone (02) 4501486
Telex secco aa25486

Austria
DIPL. ING. SZABO KG
Kalbeckgasse 5
1180 Wien
Tel. 222-473195/476411
Telex 116 667 szabo a

France
EMA
2 bis, rue du Logis
95420 Cléry en Vexin
Tél. (1) 34 67 44 44
Télex ccivo a 697 402f
indiquer: attn. ema

Hong Kong
NEW SCIENCE
LABORATORY SUPPLIES
U/9 fl., Valiant Industrial
Centre
2-12, Au Pui Wan Street
Fo Tan, Shatin
N.T. Hong Kong
Phone 0-6055326
Telex 51778 nsls hx

Italy
INALCO S.p.A.
Divisione Labo
Via Calabiana 18
20139 Milano
Tel. 02-5693741-2-3-4-5
Telex 324101-332127

Japan
IWAI KAGAKU
YAKUHIN CO., LTD
7.3-chome,
Nihonbashi-Honcho
Chuo-ku
Tokyo
Phone (03) 241-0376

The Netherlands
BRUNSCHWIG CHEMIE B.V.
Postbus 70213
1007 KE Amsterdam
Tel. 020-11 31 33
Telex 13189 brun nl

Sweden
CHEMICON AB
Box 20524
200 74 Malmö
Tel. 040-10 08 08
Telex 33307 medsca s

Focusing on hormone release

from L. Stephen Frawley, F.R. Boockfor and James P. Hoeffler

Reverse haemolytic plaque assays make possible the microscopic visualization of hormone release at the single-cell level. The method can quantify functional differences among hormone secretors of a given type.

PITUITARY cells that secrete the same hormone do not comprise a homogeneous population but differ from one another according to several morphological and functional criteria. Because of this high degree of heterogeneity, analysis of hormone release at the single-cell level may provide information more meaningful than that derived by evaluating the average response of an entire population of cells.

Such analysis was recently made possible by an adaptation of standard immunological methodologies[1,2]. The technique for analysing single-cell secretions is known as the reverse haemolytic plaque assay and is based on antibody-directed, complement-mediated lysis of indicator eythrocytes in proximity to the hormone secretors (Fig. 1). The assay involves incubating secretor cells with indicator cells in a monolayer. One type of hormone secretor can be distinguished from another because, in the presence of hormone-specific antiserum and complement, it will induce the formation of microscopically identifiable plaques (zones of haemolysis).

In this review, we will summarize our application of plaque assays to endocrine problems and provide examples of experimental findings that demonstrate the power of the technique.

Heterogeneity

The standard version of the plaque assay (Fig. 1), though conceptually simple, is extremely versatile in terms of the information it provides about hormone secretion. Quantification of hormone release is generally achieved by one of two methods. First, the rate at which plaques form can be used as an index of the rate of hormone release because a threshold amount of hormone is required to induce plaque formation; cells that release more hormone molecules per unit time form plaques faster than those which release fewer molecules[3]. Alternatively, the sizes of plaques that develop around individual secretors provide a more cumulative index of the relative amount of hormone released[2,4,5].

Both of these simple methods of quantification have yielded valuable information concerning functional differences among hormone-secreting cells of a given type. For example, discontinuities in the rate of plaque formation among mammotropes

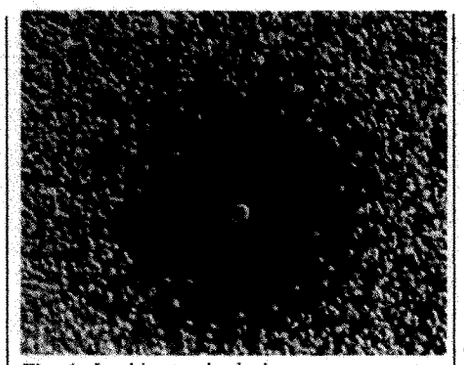


Fig. 1. In this standard plaque assay, monodispersed pituitary cells and protein-A coated ovine erythrocytes are infused into an assay chamber (constructed from a glass coverslip attached to a microscope slide with two pieces of double-sided sticky tape). The monolayer that forms is then incubated with hormone-specific antibody and complement. Hormone released from a pituitary cell binds to antibody which in turn attaches to protein-A on the erythrocyte surface. This facilitates complement fixation, lysis of the indicator cell, and the formation of haemolysis zones or plaques. Shown in this high magnification photomicrograph is a single PRL releasing cell surrounded by a plaque in which ghosts of the lysed erythrocytes are apparent.

revealed that only a small fraction of these cells are maximally responsive to the inhibitory influences of hypothalamic dopamine or to the autosuppressive effects of prolactin (PRL) itself[6]. Likewise, stimulation of pituitary cells with growth hormone (GH) releasing factor shifted the frequency distribution of plaque sizes from unimodal to bimodal, suggesting that not all somatotropes are responsive to this secretagogue[4].

The plaque assay also yields useful information when combined with immunocytochemistry. Studies of this type have shown that subpopulations of hormone secretors exist which contain hormone but do not release it[5], or conversely, release hormone without storing appreciable quantities[7]. Taken together, these examples illustrate the utility of the standard plaque assay for characterizing functional differences among pituitary cells that release the same hormone.

Dual hormone release

By sequentially performing plaque assays for different hormones, it is possible to identify cells that release more than one hormone. The essence of the sequential plaque assay is that only the pituitary cells are attached to the chamber floor; fresh assay components (including indicator cells) are added at the beginning of each sequence. Reidentification of plaque formers is facilitated by using a photoengraved coverslip as the roof of the incubation chamber. This assay has been employed in our laboratory to challenge the prevailing view that GH and PRL are invariably secreted by separate and distinct cell types in rats. We found that in male rats approximately one-third of all GH or PRL secretors actually release both hormones concurrently[8]. Moreover, *in vitro* treatment of these cells with oestrogen causes striking shifts in the ratios of single and dual hormone secretors, indicating these cell types may be functionally interconvertible[9].

We have also employed this assay to monitor the ontogeny of GH and PRL secretors in rats and have observed that the vast majority (98 per cent) of initial PRL cells also release GH[10]. Inasmuch as GH cells precede PRL secretors during development, these results suggest that the former cell type may give rise to the latter. Thus, the sequential plaque assay provides a powerful tool for identifying and quantifying changes in the proportions of cells that release more than one hormone.

Plaque bioassay

While there is compelling evidence that PRL cells differ greatly in the amount of immunoreactive hormone released, the question of whether they are also heterogeneous with respect to the biopotency of secreted hormone has not been resolved. To address this issue, we developed an assay based on the ability of PRL to induce a dose-related release of casein from cultured mammary cells[11]. We call this system the casein plaque bioassay because casein release is quantified by a standard plaque assay for the milk protein.

This system is sensitive enough to assess the bioactivity of PRL released by individual pituitary cells in microwell culture (Fig. 2). In addition, by removing the medium bathing an individual pituitary cell for bioassay and then subjecting the same cell to a standard plaque assay for PRL, it is possible to evaluate both the bio- and immuno-potency of hormone released from one cell.

Using this approach, we were surprised to find that many cells which formed large PRL plaques exhibited low biopotency, and vice versa[11]. These findings show that

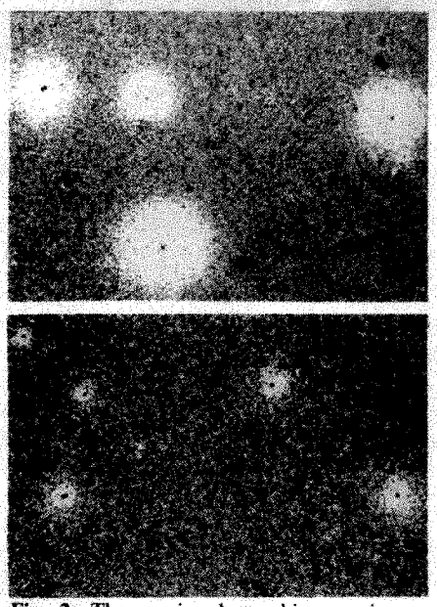


Fig. 2 The casein plaque bioassay is performed by pre-incubating monolayers of collagenase-dispersed mammary cells and indicator erythrocytes in either control medium or medium that previously bathed an individual PRL secretor. The monolayers were then subjected to a standard plaque assay for casein. This low magnification micrograph illustrates the sensitivity of this bioassay; mammary cells exposed to PRL released from a single pituitary cell (top panel) formed larger plaques than controls (bottom panel).

individual cells release forms of PRL which differ in biological and immunological potencies and may indicate a cellular basis for the molecular heterogeneity of secreted forms of hormones.

This review provides just a few examples of how plaque assays can be used to quantify hormone release from single cells. These assays can also be used in more qualitative applications, such as the identification of a hormone secretor for further study in the living state[12,13]. By combining variations of plaque assays with other contemporary methodologies, we should be able to address new levels of questions in cell biology.

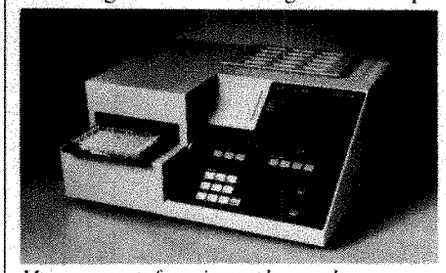
Stephen Frawley, Rick Boockfor and James Hoeffler are at the Department of Anatomy and Cell Biology, Medical University of South Carolina, 171 Ashley Avenue, Charleston, South Carolina 29425, USA.

1. Molinaro, G.A., Eby, W.C. & Molinaro, C.A. *Meth. Enzym.* **73**, 319–338 (1981).
2. Neill, J.D. & Frawley, L.S. *Endocrinology* **112**, 1135–1137 (1983).
3. Jerne, N.K., *et al. Transplantn Rev.* **18**, 130–191 (1974).
4. Frawley, L.S. & Neill, J.D. *Neuroendocrinology* **39**, 484–487 (1984).
5. Frawley, L.S., Hoeffler, J.P. & Boockfor, F.R. *Endocrinology* **116**, 2355–2360 (1985).
6. Frawley, L.S. & Clark, C.L. *Endocrinology* (in the press).
7. Boockfor, F.R., Hoeffler, J.P. & Frawley, L.S. *Endocrinology* **117**, 418–420 (1985).
8. Frawley, L.S. Boockfor, F.R. & Hoeffler, J.P. *Endocrinology* **116**, 734–737 (1985).
9. Boockfor, F.R., Hoeffler, J.P. & Frawley, L.S. *Am. J. Physiol.* **250**, E103–E105 (1986).
10. Hoeffler, J.P., Boockfor, F.R. & Frawley, L.S. *Endocrinology* **117**, 187–195 (1985).
11. Frawley, L.S., Clark, C.L., Schoderbek, W.E., Hoeffler, J.P. & Boockfor, F.R. *68th A. Meet. Endocr. Soc.*, Abstr. No. 919 (1986).
12. Lingle, C.J. & Freeman, M. *J. Neurosci.* (in the press).
13. Ben-Jonathan, N. *Endocr. Rev.* **6**, 564–589 (1985).

Endocrinology outlook

This week's review is aimed at the endocrinologist's needs. Selections include microplate manipulators, probes for chemical labelling and microtomes for sample slicing.

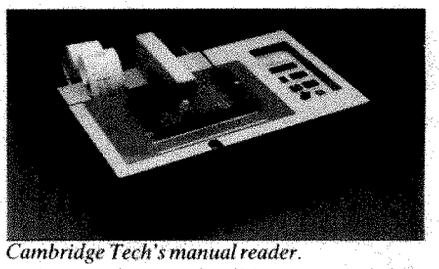
LAST week at the ASBC convention, an **automated microplate reader** from Perkin-Elmer made its market debut (Reader Service No. 100). The Lambda Reader can perform a variety of colorimetric measurements on microscale (less than 300 µl) samples. Its capabilities span enzyme-linked immunoassays (ELISA), protein determinations, antibody sensitivity tests and complement fixation analyses. Perkin-Elmer's instrument has a wave-length range of 380 to 750 nm and, the company claims, 1 per cent linearity for absorbance 0 to 2. The microprocessor-controlled fixed wavelength spectrophotometer will give the absorbance of samples in 96-well microplates or microwell strips within 60 seconds. With an alphanumeric touch panel, the Lambda Reader allows flexibility in data entry, wavelength selection, single or multiple



Measurements for microscale samples.

blanking maps, reading sequences, kinetics and data reduction. There are also several options, such as cartridge programmability, which expand the $7,895 (US) reader's potential applications. The user, however, must supply an Epson printer to render the data in an "easy-to-recognize" format.

A **manual microplate reader** with a built-in printer and RS-232C computer interface comes from Cambridge Technology (Reader Service No. 101). The model 700 densitometer specializes in EIA/ELISA operations to an absorbance of 2 with 1 per cent accuracy, and up to *A* 3.2 with 2 per cent accuracy. The manufacturer supplies filters for 405 and 490 nm wavelengths, but other filters are available and the machine's capabilities extend from 400 to 700 nm. A spring-loaded detent locks in on each well positioned for measurement to aid in correct alignment. The model 700 continuously displays absorbance and well location, but a separate record button must be pressed to send each reading to the printer or an external computer. Cambridge sells the reader for $2,600 (US). It accepts rigid 96-well plates



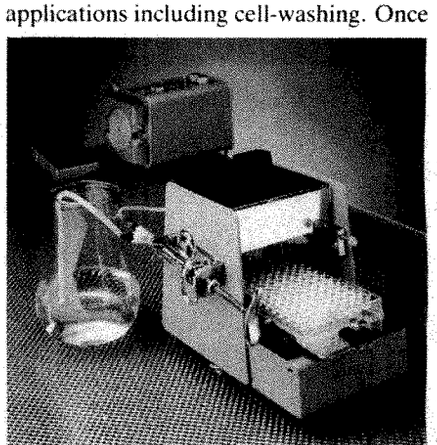
Cambridge Tech's manual reader.

and can adapt to flexible or removable-well varieties with the help of an accessory.

Anyone who buys Labsystems' Uniskan vertical plate reader for enzyme immunoassay (EIA) will also get a **software package** and computer interface cable for free (Reader Service No. 102). The two-part program, which is compatible with the BBC model B, IBM models or IBM 'clones', has provisions for both plate reading and data analysis. The software instructs plates to be read row-by-row or column-by-column; control wells can be positioned randomly, and empty wells can be passed over. Data gets written on a disk from which it can be recalled for threshold, range and standard curve analyses. Labsystem's software also caters to semi-log, log and linear curve preferences in analysis. Written in BASIC in conjunction with a faculty member at Leicester Polytechnic, the program can be customized.

Dispensing devices

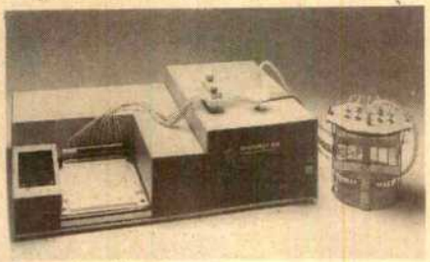
A dispenser from Sterilin, designed for **repetitive multi-well plate procedures**, can carry out filling, inoculation and aspiration operations on all types of standard 96- and 24-well plates (Reader Service No. 103). Sterilin says the Microplater is suitable for numerous sterile and non-sterile applications including cell-washing. Once



Sterilin has relief from repetition.

the dispenser head is positioned above the wells, volumes from 25 to 250 µl per well can be delivered using the 2 ml syringe assembly that comes with the Microplater. A peristaltic pump manufactured by Sterilin will extend the volume range. The company markets Microplater for £530 in the United Kingdom.

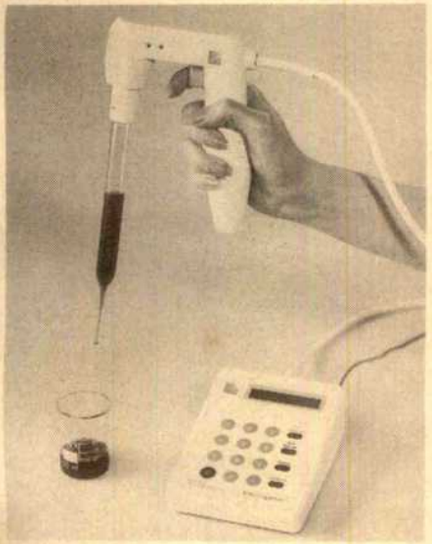
An outgrowth of their manual **reagent dispensing system**, Dynatech's fully automated AM83a Auto Dynadrop system can dispense up to 12 different reagents simultaneously in microplate or strip-well formats (Reader Service No. 104). The latest Dynadrop will fill 8 or 12 wells at a time, depending on user needs, in volumes ranging from 10 to 200 µl. Dynatech says their system guards against reagent contamination with a design that maintains integrity from the reservoir through to the dispense manifold. The plate carriage on



Room for a dozen reagents.

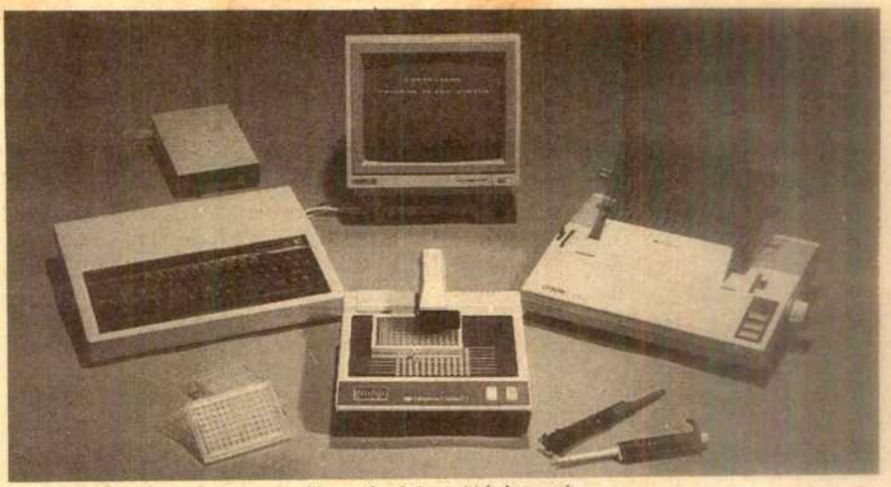
Dynatech's £3,115 (UK) instrument moves via step-less motor drive, but the automatic mode can be halted with a manual over-ride to allow partial plate preparation.

It looks a bit like a pipetting aid, but the Electrapette from Horwell Ltd uses keyboard control and inexpensive ungraduated pipettes to **automatically dispense volumes** between 100 µl and 12 ml



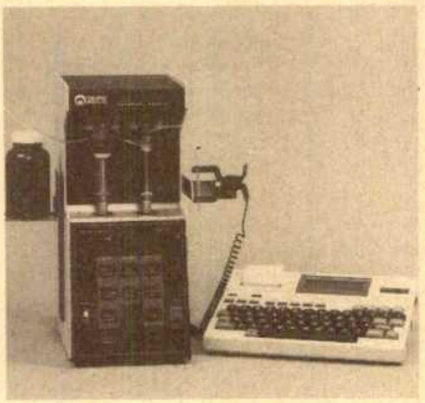
Electrapette set with speed control.

(Reader Service No. 105). Set on automatic or manual mode, the Electrapette can register different fill volumes and dispense volumes independently; dispense volumes can only be set to the nearest 10 µl. Horwell's automatic pipettor also sounds a warning and stops if residual volume in the pipette is insufficient to meet the programmed dispensing volume. The £495 (UK) Electrapette also has a calibration pipette to tailor the Electrapette system to individual liquids.



Labsystems provides complimentary software for their vertical plate reader.

Micromedic Systems, Inc. increased the potential of their **automatic pipette** by providing it with RS-232C computer interface capability (Reader Service No. 106). The Digiflex-CX can be operated from its own



PC power hooks up with Digiflex

keyboard, or the keystrokes can be entered into a personal computer program that will store and run protocols more complex than the keyboard control accommodates. Micromedic's instrument is precise to 0.5 per cent or 0.1 µl standard deviation, whichever is greater. The Digiflex gives readouts in microlitre volumes, and can automatically sense the size of installed syringes, a feature that Micromedic calls unique. The base unit costs $4,300 (US) without the PC.

The tissue section

Reichert–Jung's ergonomically designed **sectioning apparatus** has several interesting features and is available in different versions geared to different budgets (Reader Service No. 107). The company say their Cryostat Frigocut 2800 has a low build that makes operating the machine more comfortable. The Frigocut also incorporates a non-rusting microtome, the Autocut 2040. Housed in a freezing chamber with a heated, mist-free window, the



Frigocut keeps cool to −40°C.

Autocut can be adjusted to a microfeed mode (for thicknesses between 0.5 and 60 µm) or a coarse feed for greater thicknesses. Reichert–Jung's instrument starts at £8,000 (UK). It can automatically defrost, or adhere to a programmed 24-hour timer.

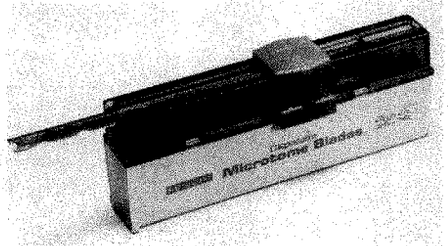
For specimen freezing, an **immersion cooler** from Neslab Instruments can serve as an alternative to dry ice and liquid nitrogen at temperatures reaching down to −75°C (Reader Service No. 108). The CC-70W cooler is compact — Neslab



A compact cooler from Neslab.

made it 60 per cent smaller than any other cooler in their line — for especially crowded quarters. The company is offering their new addition at an introductory price of $495 (US). Its intended uses stretch from vapour trapping and lyophilization to crystallization studies.

Histoline Inc. and Wilkinson Sword Ltd crossed expertise to produce a **disposable microtome blade** that, they say, enhances the consistency of tissue sectioning and improves edge strength (Reader Service No. 109). The new blade, designed for cutting paraffin-embedded human and animal tissue, has a stropped edge free



Microtome blades a cut above.

from grind marks. A triple coating of chromium, chromium nitride and PTFE (polytetrafluoroethylene) imparts strength, wear resistance and corrosion resistance and minimizes friction, according to the companies. A pack of 50 blades cost £40 (UK).

Immunochemicals

Three separate series of **immunohistology kits** have emerged from the laboratories of Bio-Yeda Ltd over the past few months (Reader Service No. 110). The first set was created for the location and identification of human tissue components in routinely-fixed paraffin-embedded sections. These kits targeted human immunoglobulins IgA, IgC, IgM, kappa and lambda. Bio-Yeda is currently producing a second group of kits for desmin, prostatic acid phosphatase, insulin, myoglobin and beta human chorionic gonadotropin. The third group of kits, for intermediate filaments, is still in the works. All the company's kits use the avidin–biotin immunoperoxidase staining technique and provide all the reagents needed for that protocol.

A radioimmunoassay kit for **sexual hormone binding globulin** (SHBG) could be valuable in the diagnosis of sex hormone-related pathological conditions (Reader Service No. 111). Metachem Diagnostics Ltd. say they have a highly specific assay with sensitivity of 5 μg per litre that takes less than 3 hours to complete. SHBG is known to influence the biological activity of circulating androgens. The RIA kit, priced at £135 (UK), includes anti-SHBG, ^{125}I-SHBG, double antibody-PEG, 7 standards of concentrations from 1 to 400 μg per litre, and high and low controls.

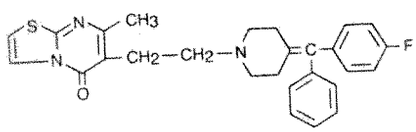


Biosearch's express delivery proteins.

A California-based company is offering **low-cost peptides** that it says it can provide within weeks of ordering (Reader Service No. 112). A technology developed at the Research Institute of Scripps Clinic has given Biosearch, Inc the capability to make hundreds of polypeptides simultaneously, the company says. Biosearch predicts that one of the more useful outgrowths of this technology will be the increased availability of peptide analogues for testing of optimum biological or immunological activity.

A serum **immunoassay for soluble T cell markers** gives a new measure of overall immune system activation (Reader Service No. 113). The Cellfree interleukin-2 receptor test kit from T Cell Sciences determines quantitatively the interleukin-2 receptors (IL-2R) shed from T cells in human sera or culture supernatant. The company's kit allows non-invasive evaluation of activated T cells in organs and tissue. A Cellfree kit uses a sandwich immunoassay with two non-competing monoclonal antibodies, and the results are read colorimetrically from standard 96-well microtiter plates. For $439 (US), T Cell's kit supplies monoclonal antibodies, a full set of standards, diluent, substrate and microplate.

Calcium, a favourite candidate for the second messenger in signal-transducing systems, may now have to vie with **diacylglycerol** for that position. This lipid, according to Janssen Life Sciences Products,

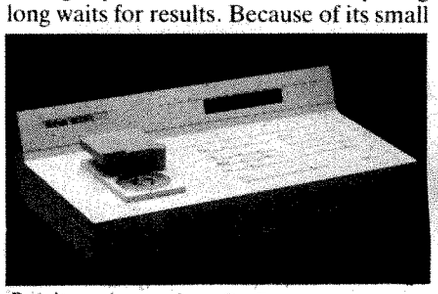


The formula for diacylglycerol kinase inhibition.

has become a contender because elevation of cellular diacylglycerol levels accompanies the phosphoinositide turnover spurred by extracellular stimuli. Janssen now provides an inhibitor to diacylglycerol kinase which potentiates the second messenger effects of diacylglycerol (Reader Service No. 114). Janssen sells 50 mg of R59022, as they call this inhibitor, for £45 (UK).

For the count

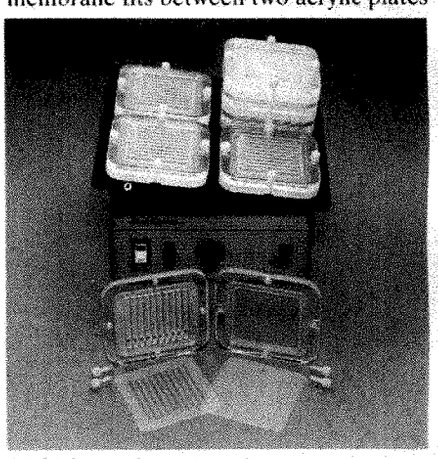
Du Pont's biotechnology division last month introduced a **compact automated radioisotope counter** that takes up only a square foot of bench space (Reader Service No. 115). The Bench-Count detector quantitates ^{32}P and ^{125}I radiolabelled samples without using liquid scintillation cocktails. Du Pont expect their instrument to streamline nick translations, end-labelling, iodination, phosphoprotein analysis and other procedures by giving count data during experiments, rather than imposing long waits for results. Because of its small



Results on the spot from Du Pont.

size, the $2,495 (US) microprocessor-based Bench-Count ought to be able to sit within close range of the experimental procedure itself.

The Mighty Small Deca-Probe is Hoefer Scientific's answer to membrane-cutting for **separate immunotransfers** (Reader Service No. 116). Their new instrument can stain 10 immunotransfers on a single, intact 8 × 8 cm membrane. The membrane fits between two acrylic plates



Multiple transfers, minimal membranes.

which are clamped together and sealed. Parallel troughs, milled in one of the plates, serve as incubation chambers isolated from their neighbours by silicone rubber gaskets. Each trough requires about 0.5 ml of solution, and when staining is complete, the sample lanes can be compared side-by-side. Hoefer ask $195 (US) for their system, complete with reagents and apparatus. □

These notes are compiled by Karen Wright from information provided by the manufacturers. To obtain further details about these products, use the reader service card bound inside the journal.

nature

NATURE VOL. 321 26 JUNE 1986

Social security for students

The dependence of British students on schemes to help the indigent is a sign of sickness in British higher education. The remedy should be radical.

UNIVERSITIES are nothing without students, but in most places operate in a sellers' market and are over full. Not so in impoverished Britain, where an elaborate system for meeting part of students' maintenance costs out of public funds is once again to be scrutinized by a group of civil servants and government politicians bent on removing anomalies and cutting costs. The new inquiry, announced last week, will be the third since the present government came to office in 1979. But this time, the government seems in no particular hurry. The new Secretary of State for Education and Science, Mr Kenneth Baker, said last week that he hoped the inquiry will be completed this year, but that it will be followed by a period of consultation. A conclusion, if any, will certainly be too late for the academic year 1987–88, that in which the next British general election must at the latest be held, which may be part of the government's calculation.

Students' grants have been a nettle too painful to grasp for more than a decade, since the Treasury first told the Callaghan government that Britain could no longer afford them. The new inquiry, like its predecessors, is a damage-control device, probably not the last that Baker will have to cobble together, but the need for it is nevertheless a telling proof of the improverishment of British higher education. The origin of the present scheme was the liberal doctrine thirty years ago that young people able to win places in higher education should not be dissuaded by cost from taking advantage of them. So local authorities were required to pay the tuition fees of British students at British universities, polytechnics and colleges and also to provide them with a maintenance grant, originally just about enough to keep body and soul together and to buy an occasional book.

Over three decades, two trends have been at work: the government has sought to cheapen the cost of keeping students by stiffening the rules by which grants to individuals with well-off parents are reduced, while ingenious students have taken to using the British system of social security to top up their incomes, claiming unemployment pay in the summer vacations, and the bread-line payments called supplementary benefits and housing allowance then and at other times. British governments always boast, as Baker did last week, that the system is the "most generous in the world", which may be true. The system is also among the most cockeyed, which is why it should be changed.

Cover-up

To what? Last week's inquiry is a cover-up for the government's defeat over a mean-minded plan to trim students' entitlement to social security benefits by disqualifying them from housing benefit, entitlement to which is independent of parental income. Two months ago, the government was warned by its own advisory committee on the social services that it would probably be illegal to exclude just one class of claimants from a system of social benefits whose equitable operation requires non-discriminatory rules. Now the government has backed down, and Baker, with plenty on his plate already, has to pick up the pieces. He is prudent not to hurry, for this is the seamy side of British higher education.

The cost of student maintenance, £2,800 million a year, is more than the £2,000 million public subvention of British universities through running costs and tuition fees, which cater for roughly a third of all students. One of the reasons why the government six years ago embarked on a reduction of the number of university students was its fear that maintenance grants were a blank cheque on its dwindling tax revenues. Yet the standard grant (£1,800 a year outside London and Oxbridge) is not enough to keep a young adult reasonably housed and fed, let alone read, while for most students the social security system exploited to the limit will provide only a few hundred extra pounds a year.

The result is that everybody is soured by the problem of student grants. The government is over a barrel, and resents it, while many of its supporters are forever asking why students should be paid to enjoy the privilege of higher education. Students feel impoverished (which they are) and pauperized (which they need not be), and resent that. The universities wring their hands most often about their own impoverishment (four per cent down in real terms next academic year), but extend their self-pity to embrace their students in the sure knowledge that there is nothing they can do about the students' plight and, perhaps, because another bout of student trouble might be the last straw. These are the real reasons why the system needs overhauling.

Solution

Here is how to go about the job. First, whatever government supporters say, there is a need in Britain for a mechanism that will help young people to get themselves a higher education. Britain, which prides itself on being a place that must live by its trained wits, is already desperately short of modern skills, partly because the participation rate among the able children of poorer families is too low. That should be recognized at the outset. But, second, present arrangements do commit the British government to writing blank cheques that it may not be able to afford, whose purposes it does not understand, and whose total amount can be contained only by restricting the total amount of higher education on offer, which is in nobody's interest.

So why not trade the 1950s principle of a grant for every would-be student who can find a place in higher education for the less generous but more realistic and equitable principle that grants will be awarded either on the basis of merit or of national need, but will no longer be mandatory on the government through its proxies, the local education authorities? The short answer is that the shift would trigger a tremendous row. Better that than an endless fudge.

If the government has the stomach for the fight, the outcome will not only put a cap on the cost of higher education but could be immensely beneficial for British higher education, which now differs from that in most other countries not merely in the narrowness of the courses which it offers, and in the pre-shrinking specialization it requires of intending students, but in its almost total lack of scholarship funds. But experience elsewhere shows that educational institutions are both more economical and more humane in their administration of student aid than a central bureaucracy can hope to be. So a large chunk of what the British government now spends on student aid could

usefully be transferred to institutions for them to spend instead. By making deals with individual students about repayment in kind for financial help, to which end they would have an incentive for the first time, much better use would be made of the resources spent on student aid and more students would be helped. So why not give that a try?

But no more than half of what the government spends should be administered by the universities, polytechnics and colleges, for too much power over the fates of students would give them the illusion that their individual sizes had been fixed for good. That is why the greater part of present government aid for students should be spent quite differently, on individual student scholarships that individual students may take to the institutions of their choice. Together, these two components of a different system could contain the present cost of student aid, make more efficient use of what is spent, restore a measure of autonomy to higher educational institutions which have already lost too much of it and restore a sense of independence to students, who cannot wholly welcome the idea of beginning adult life as clients of a creaking system of social benefits.

There are several snags, not the least of which is the government's own predilection towards the notion that business, which benefits from such skill as British higher education engenders, should step in to help, by means of sponsorship schemes for potential employees. This was the general cry when Baker announced his new inquiry in the House of Commons last week. But a scheme that puts students in the pockets of future employers is no better than one that makes them depend on social security. So why not student loans? The Prime Minister's promise that grants would be replaced by loans has twice been defeated by the Treasury's calculation that the short-term cost would be increased, but that objection applies only if the whole of student aid at present is shifted to the banks. There is, however, a need for assistance at the margin by way of loans for students whose opinions of the benefits of higher education to themselves may differ from those of the authorities, as well as for those who seek a second change or a period of retraining. Why should not Britain follow a dozen other countries by making a modest beginning with loans for people in such special circumstances? □

Selling lamb short

The British government's decision to ban the sale of some lambs may yet backfire.

THE British Ministry of Agriculture, Fisheries and Food seems to have had a bad Chernobyl. In the days immediately after the tragic accident in the Ukraine, there was a general complaint that too little had been done too late to monitor the occurrence of radionuclides in British food. Matters were not much helped by the appearance of the Secretary of State, Mr Michael Jopling, on a television programme in the course of which it became clear that he had not previously heard of the notion that doses of radiation smaller than the accepted safety limits could nevertheless be dangerous. Now the ministry has swung from complacency to the other extreme, and has banned for 21 days from last Friday the sale of lamb from North Wales and Cumbria. The decision seems to have been taken on the strength of 100 measurements of ^{137}Cs in lambs born earlier this season, 19 of which showed more than 600 Bq kg^{-1} of total caesium among which were 9 exceeding 1,000 Bq kg^{-1}. The ministry, not now particularly popular among hill farmers for its expressed (and reasonable) wish to reduce the subsidies it pays them, will find that its wish to be seen to be active about fallout from Chernobyl will lose one of the few markets on which its dependent farmers rely.

The circumstances are curious. The ministry is "erring on the side of caution", as one of its spokesmen said this week, to a degree that may prove economically unwise. Although caesium is one of the predominant radioactive components of fission products, it differs from iodine, strontium and plutonium in being a generalized constitutent of the mammalian torso. The result is that, although the radioactive half-life of ^{137}Cs is roughly 30 years, the residence of the material in people and sheep is much less, more like 30 days than 30 years. The highest concentrations of $^{134,137}Cs$ have been found in British sheep where rainfall was heaviest early in May (which is where the agriculture ministry looked for them), and in lambs rather than older animals, a factor to some extent offset by the fact that the biological half-life is even less in lambs than in sheep, perhaps as little as 15 days. Yet the ministry has banned the sale of lambs from Britain's soggiest sheep-farms on the strength of observations of levels of contamination in a proportion of the animals sampled which is much less than the 9,000 Bq kg^{-1} defined as the Emergency Reference Level by the National Radiological Protection Board, an independent public agency. Why the fuss?

Not only domestic politics is involved. Soon after the accident at Chernobyl, the European Commission was stampeded by some of its member governments into an undiscriminating ban on the import of foodstuffs from Eastern Europe. For regulatory purposes, the permissible limit on the radioactive content of food was fixed at 600 Bq kg^{-1}, partly on the grounds that nobody at the outset knew the composition of the fallout, which might have contained more plutonium than appears to have been the case. Now, after the event, the European Commission seems to have been doing its best to justify its decision. A meeting of experts called under the aegis of the Euratom Treaty has apparently recommended that the "action level" for the radioactive content of foodstuffs should be 1,000 Bq kg^{-1}, a factor of nearly ten below that recommended by the radiological protection board. The British ministry seems to have acted on lamb because this limit has been exceeded in some of the animals slaughtered in the past week or so.

Nobody will weep too much for the farmers whose trade will be affected, but the general scare about lamb will have more lasting consequences. It seems to be agreed that the annual dose of radiation arising from an average diet of lamb uniformly contaminated to the 1,000 Bq level would be 0.15 mSv, an estimate already biased on the side of caution because the calculation is based on the physiology of a 10-year-old child. This is a small fraction of the annual dose in Britain due to natural radiation, estimated at 2 mSv, and less even than the fluctuation of the natural dose from one part of the country to another. The International Commission on Radiological Protection allows that artificial doses for members of the general population should not exceed 5 mSv in any year, or more than 2 mSv a year chronically. But to acquire even 0.15 mSv a year from this season's British lamb, people would have to start with heavily contaminated lambs, keep them in a freezer and eat nothing else. The agriculture ministry may have done something to protect a few lamb-gluttons from the small risks of their excesses, and at the same time to suggest that it is an action ministry, but the general effect of its hasty decision will be unwelcome.

The particular danger in the ministry's over-active response is that it will reinforce the general opinion that radiation and radioactivity are mysterious and awesome entities. If it should be necessary to ban British lamb from sale several weeks after the passage of a radioactive cloud, who can hope to be safe from it? The truth, of course, is that calculations of the kind on which the ministry based its decision are by no means uncertain. The notion that caesuim, radioactive or otherwise, travels through soil into grass and from there into the bodies of grazing animals in a relatively slow fashion is well described. The calculation of the radiation doses that result are intricate but relatively precise. The fact that the doses likely to be received by British lamb-fanciers are so much smaller than the internationally agreed limits and the natural background should help people to live with the knowledge that the damage done by radiation is less certainly calculated. Haste will have the opposite effect. □

British astronomy

Greenwich Observatory to move to Cambridge

THE decision to move Britain's oldest observatory has finally been taken by the Science and Engineering Research Council (SERC). The Royal Greenwich Observatory (RGO) is to move from its present site at Herstmonceux Castle in Sussex to Cambridge, where it will sit alongside the university's Institute of Astronomy.

The decision has come as a relief to many of RGO's astronomers who feared that SERC might try to force through a move to the Royal Observatory at Edinburgh, the course of action recommended in an earlier report and bitterly opposed by RGO staff. Worries over the move have been heightened by the apparent unwillingness of SERC to be frank. The week before last, the matter was raised in the House of Lords and the procedures adopted by SERC for dealing with the case described as "grossly inadequate". In particular SERC failed to make public an earlier report spelling out the options for RGO, and failed to canvass adequately astronomers' opinions.

Opinions are now divided at RGO; some, particularly those among the research-orientated staff, feel there may be new opportunities in a close association with Cambridge. For others a move to Cambridge simply means uprooting homes and family and their official reaction has been "decision received with disbelief". Opposition is certain to continue.

Herstmonceux is RGO's second home, Greenwich having been abandoned in 1948 in search of clearer skies. But now the need for even better viewing conditions means that its activities centre on the new 4.2-m William Herschel telescope being built in collaboration with Spain and the Netherlands at La Palma in the Canary Islands. By 1990, its initial instrumentation will be complete and RGO's 190 staff will probably be reduced to around 100 at the observatory and 30 at La Palma. The move to Cambridge will also take place in 1990.

For SERC, that move is dictated by its corporate plan, adopted in December 1985, to operate its establishments in support of universities and polytechnics rather than as independent research institutes. The thinking behind that is simple enough: with present staff numbers there is time for only a little independent research at institutions, 90 per cent of the effort has to go to developing and managing research facilities for the academic community. Without powerful input from the universities, there is a risk they would lose touch with the leading edge of research. Thus, the argument runs, it makes sense for RGO to have a close association with other astronomers at a university. Some RGO researchers agree and see a better chance for spending their 10 per cent of research time profitably at Cambridge.

The risk, of course, is that an observatory closely linked to one university will cease to function as an open national institute. Before making the decision to move RGO, the SERC council apparently did consider, and reject, the alternative of building up the observatory so that it could function as a powerful independent institute. Quite how it has arrived at this decision is unclear for the cost of moving the entire institute might seem to be greater than of increasing research there, especially when disruption to the Herschel project at a critical stage in its development is taken into account.

In rolling out the welcome mat at Cambridge, Professor Martin Rees has been at pains to point out that Cambridge will not gain special rights "through propinquity". Some financial savings can be expected as libraries, computers and the like can be shared. The combined force at Cambridge should then be a match for any of the overseas astronomical competitors, like those at Arizona and Pasadena. That in turn should give Britain a foothold in the next generation of giant telescopes where international cooperation is bound to be necessary on an even bigger scale. Even now, a ten-nation plan for a 15–18m-telescope at La Palma is under consideration.

The loser in the move is the University of Sussex, which, although 20 miles from Herstmonceux, has made considerable use of its facilities and has 7 visiting staff from RGO. The Sussex astronomers — 4 faculty, 6 post-docs and 23 PhD and MSc students — are now very concerned about the future. Although particularly strong in theoretical astronomy, half their work involves observation at RGO. What they will now do has yet to be decided.

One thing not yet clear is how the move to Cambridge is to be paid for. Assurances have been given that the move will be self-financing; that means that the money raised from selling off Herstmonceux Castle will pay for the move. But it is by no means clear that this is really possible; so little information has been released by SERC, and the market for castles is so hard to assess, that the possibility the move will fall through cannot be totally dismissed.

Alun Anderson

Monoclonal antibodies

Kidney rejection at bay

Washington

A MONOCLONAL antibody that reduces kidney transplant rejections last week won approval from the Food and Drug Administration (FDA), marking the first commercialized therapeutic use of the British-born technology in the United States. The drug could benefit over 5,000 transplant patients each year and pave the way for other antibody treatment schemes on the horizon. As a therapeutic tool, monoclonal antibody techniques may, however, involve limitations that have not clouded their success in diagnostics.

The drug, a product of Ortho Pharmaceutical Corporation in Raritan, New Jersey, acts by specifically neutralizing the T cells responsible for renal rejection. In clinical trials, it reversed approximately 94 per cent of rejections in patients receiving antibody intravenously. Conventional steroid treatment ordinarily results in a 75 per cent reversal rate. Because it is targeted to a particular leukocyte, the antibody does not suppress the entire immune system, but it can cause chills, fever and nausea.

Ortho is hoping that its treatment will eventually supplant conventional methods for combating acute rejection. So far, however, the drug cannot be used as a general maintenance immunosuppressive agent (administered over months rather than days) because it is thought that the body may mount an immune response to monoclonals derived from mouse spleen hybridomas. This problem has surfaced before, most notably in cancer treatment, the major focus of monoclonal antibody therapy. Researchers say the only way to circumvent it may be to rely on hybridomas of human cells alone.

Ortho's achievement caps a development drive initiated in 1979, just a few years after the first description of hybridoma culture by Medical Research Council investigators Kohler and Milstein (*Nature* **256**, 495; 1975).

Biotechnology division president Dennis Longstreet estimates a market of between $15 and $20 million annually in the United States for the product, which also received approval in France and Switzerland last winter and is currently awaiting word from Italy.

Monoclonal antibodies for cancer treatment are already in clinical trials, and other immunological therapies seem likely candidates for future testing. Despite potential shortcomings, there is good cause to believe that FDA's action ushers in a new era for monoclonal antibody applications.

Karen Wright

US space science

Centaur bites the dust

Washington

SPACE science suffered a further major setback last week with the announcement by the National Aeronautics and Space Administration (NASA) of its decision to abandon development of the Centaur upper stage for use aboard the space shuttle. The decision was taken because safety studies indicated that Centaur, which carries tens of tonnes of liquid hydrogen fuel and liquid oxygen, would constitute an unacceptable risk to the shuttle crew.

The immediate effect of the decision will be to delay until at least December 1989 two major space exploration missions that were to have been launched last month using the shuttle/Centaur launch combination: Ulysses, the European Space Agency mission to explore the poles of the Sun, and Galileo, the NASA/ West German mission to explore Jupiter and its moons. The Challenger disaster in January had already ensured that Ulysses and Galileo could not fly before 1988.

Other planned science missions that could have used the shuttle/Centaur combination may also be delayed by last week's decision, including the Magellan mission (formerly known as Venus Radar Mapper), CRAF (Comet Rendezvous and Asteroid Flyby), and Cassini, a Saturn orbiter and probe. But Dr Frank McDonald, NASA's chief scientist, said this week that he was confident that launch problems could be solved in time to avoid delaying these later missions.

According to the Federation of American Scientists, several Department of Defense missions, including the "Milstar" communications satellites, were to have used a version of the Centaur upper stage in the shuttle and will probably also face delays. Centaurs used with expendable rockets such as Titans and Atlases are not affected by last week's decision and may provide an alternative means of launching heavy satellites into Earth orbit or into planetary trajectories.

The shuttle/Centaur combination was already under scrutiny at the time of the Challenger accident, which further increased concern about safety; separate studies have been conducted by NASA and by Congress. In a letter to NASA administrator Dr James Fletcher, Congressmen Bill Green and Edward Boland of the House of Representatives' appropriations subcommittee that deals with NASA wrote last week that "since the accident the yardstick against which... risks will be measured has forever changed".

NASA officials interviewed for Green and Boland's study had mixed views about shuttle/Centaur. Some believed it could be made safe, but it was clear that at least another $175–200 million would be needed to do so and to absorb the delays caused by the Challenger accident.

Another new safety worry is that plutonium from the radio isotope thermal generators (RTGs) carried on Ulysses and Galileo could cause 200 cancer deaths and contaminate hundreds of square miles of Florida if it was dispersed in an explosion, according to studies carried out by the Department of Energy. Analyses of the Challenger accident suggest that the overpressures generated in a shuttle explosion are unlikely to rupture the RTGs, but nevertheless special protective shrouds were considered.

The delay to science missions will now depend on how soon the shuttle flies again (not thought likely before December 1987) and on what other launch vehicles can be developed.

Both Ulysses and Galileo were energetically very demanding launches; the Centaur's cryogenic motors represented the most compact and the lightest power source of sufficient capability.

At NASA's Jet Propulsion Laboratory in Pasadena the abandonment of Centaur was no surprise. Staff had been working on alternative launch possibilities for future planetary missions since it became clear after the Challenger accident that the performance of the shuttle would be impaired by the extra weight entailed by safety modifications. An energetically less demanding but more time-consuming delta-vega (ΔV) trajectory was already in prospect for Galileo before last week's decision, and other heavy orbiters of outer planets faced a similar prospect.

According to Allen Wolfe, deputy project manager for Galileo, one possibility for that mission is to use the shuttle with a solid fuel double Inertial Upper Stage. A special third-stage injection module that would be needed has, however, yet to be developed and could not be ready before 1991, according to one estimate. Wolfe had no cost estimates for the re-engineering that would be necessary.

Another possibility would be to use a Centaur with a Titan 34D-7, a new rocket being developed for the Department of Defense. But the new Titans cost more than $200 million each, and as soon as they become available in 1988 they are likely to be fully booked by the military; current plans call for only five to be built each year between 1989 and 1992. And missions to the outer planets launched from a Titan-Centaur would all have to employ delta-vega trajectories, which can increase total journey time by two or three years. Last but not least, a completely new upper-stage design is by no means ruled out.

Tim Beardsley

Chinese rockets

Stealing a march on the West

LAST autumn, China formally announced that it was willing to launch satellites for other countries on a commercial basis, using its Long-March-2 and Long-March-3 rockets. At that time, this was viewed internationally more as a declaration of Chinese confidence in its space programme than as a serious tender for clients. The Challenger disaster and the Ariane failure last month have, however, forced a number of space agencies to think seriously about the Chinese proposal, particularly now that Western insurance companies are refusing to insure satellites. On 6 June, Mr Sun Jiadong, the Chinese Vice-Minister of Astronautics, announced at a press conference that the People's Insurance Company of China will offer "below-market" insurance rates for such launches.

According to Sun, China has so far been approached by eight potential launch customers; Sweden, the United States, the United Kingdom, the Netherlands, Canada, Australia, Pakistan and Indonesia.

The first country to sign an option agreement was Sweden, for its projected *Mailstar* communications satellite, which weighs only 100 kg and so would in any case be too small for Ariane. But the first country actually to use the Chinese facilities, Sun said, will probably be the United States, as the Western Union Corporation signed a memorandum with China last month on the launching of two communications satellites.

At present, China has the capacity to launch 10–12 rockets per year, Sun said. The maximum payload is 1.4 tonnes, but this will shortly be raised to 2.5 tonnes. An obstacle to the conclusion of launch contracts was, according to a US space team which visited China last year, that the Chinese do not provide good ground test data on their vehicles. But what appeared a major obstacle in 1985 may well not seem so in the aftermath of Challenger and Ariane.

Foreign clients will not be able to be present at the launch site at least for the time being. But this, according to Mr Shen Rongjun, vice chairman of the Science and Technology Committee of the Commission of Science, Technology and Industry for National Defence, is simply because there are no facilities for guests at the site. Foreign visitors are welcome, he said, at the Jiuquan centre, which has received more than 30 such delegations in the past few years. As soon as the necessary conditions are provided at the launch site, Shen said, visitors will be welcome there too.

Vera Rich

Environment

Strategy for Earth systems

Washington

ENTHUSIASM is running high for a new report released today that charts a course for government-sponsored efforts to understand global environmental changes in the coming decades. Written by the Earth System Science Committee (ESSC) for the National Aeronautics and Space Administration (NASA) and the National Oceanic and Atmospheric Administration (NOAA), the report lists specific roles for NASA, NOAA and the National Science Foundation (NSF) in reaching a better understanding of how Earth systems interact on a global scale. But even supporters of the report's goals acknowledge that finding the money and political will to achieve its objectives will not be easy.

Francis Bretherton, former director of the National Center for Atmospheric Research in Boulder, Colorado, and now a senior scientist there, was chairman of ESSC. Bretherton says the report was an attempt to provide a strategy for what must be done to look at the Earth as a system. By understanding these interactions, says Bretherton, it will be possible to predict changes that will occur from both natural processes and human activities over the next century.

NASA originally sought the report to provide priorities in its Earth science programmes, in much the same way that previous reports provided direction in astronomy and planetary science. But to achieve an integrated picture of the Earth, it was clear that other agencies would have to become involved, and NOAA administrator Anthony Calio requested that the report be directed to his agency as well.

The report divides the needs of Earth sciences into two periods; the years preceding the launch of the US manned space station, and the decades that follow. In the pre-space station era, a coordinated sequence of missions is proposed for achieving the goals of Earth system science. Some, such as the Upper Atmosphere Research Satellite and the Navy's



Francis Bretherton

Remote Ocean Sensing Satellite, have already received budgetary approval. Others, like the Ocean Topography Experiment (TOPEX) included in NASA's 1987 budget request and the Geopotential Research Mission, proposed as a new start in 1989, still await approval. The ESSC endorsement should have a positive effect on their chances of receiving support.

In the post-space station era, NASA's emphasis will shift to the Earth Observing System (EOS), a series of instruments designed to fly either aboard the space station itself or on polar orbiting platforms serviced by the space station.

The ESSC report calls for greater coordination in the activities of NASA, NOAA and NSF. It suggests the immediate adoption of an advisory body to guide management choices among the agencies. Especially important in the coordination process is the establishment of information storage and retrieval processes for handling the avalanche of data generated by space-based Earth-observing missions as well as *in situ* measurements.

NOAA has traditionally been responsible for gathering and storing such data. But NOAA has not been a favoured agency in the Reagan administration, and many, including Bretherton, have expressed doubts that NOAA's budget will allow it to keep up with the data demands. Administrator Calio is enthusiastic about the goals of the Bretherton report, but also wonders where the money will come from.

Some activities are already under way at different agencies that will dovetail with the recommendations of the ESSC report.

NOAA is developing NOAANET and NOAAPORT, systems for disseminating operational weather satellite data to climate researchers. NOAA is also the lead agency for the Tropical Ocean Global Atmosphere Program (TOGA) designed to gain a better understanding of the El Niño phenomenon. But the administration's proposed budget reduces NOAA's support of TOGA by approximately half in the 1987 budget.

NSF has begun the Global Geosciences programme, seven programmes including the World Ocean Circulation Experiment and the Global Atmospheric Research Program, that represent a major attempt to realize the priorities set by the National Research Council's International Geosphere/Biosphere Program.

For NASA, the Bretherton report comes at a time when the agency is facing many questions about its future. Both the Challenger accident and the decision to abandon the Centaur upper stage rocket for shuttle-launched missions (see p.800) will have a profound effect on NASA's scientific activities.

NASA administrator James Fletcher is well briefed on the concerns of Earth system scientists, but may be unable to spare agency resources to achieve their goals while trying to return the shuttle programme to operational status.

D. James Baker, a member of ESSC and president of the Joint Oceanographic Institutions, argues that the report correctly identifies the good match between emerging technologies and the scientific needs of Earth science. Baker sees the report as non-controversial, scientifically sound, and likely to receive support in Congress. But NASA's internal turmoil and the lack of a strong champion inside the White House may lessen the report's impact. The ESSC report tried to "strike a balance between program needs... and a realistic demand on agency resources and capabilities." The question is, did it succeed?

Joseph Palca

Turkey turns away Israeli scientists

Rehovot

TURKEY is pleased to have Israeli tourists, but seems to discourage visits by Israeli scientists.

This is the conclusion drawn by Professor Mordeckai Magaritz of the Weizmann Institute and three of his professional colleagues from the Israel Geological Survey, all of whom have failed to obtain visas in order to attend an International Union of Geological Sciences Workshop on Late Permian and Triassic in Western Turkey which begins in Istanbul on 14 July.

They sent their $250 registration fee to Turkish scientist Remzi Akkok on 11 April and then, several weeks ago, went to the Turkish Consulate in Tel Aviv to obtain a visa. There was a long line of Israelis already waiting, all of whom obtained visas.

Only Magaritz and his friends were turned down because, the consul explained apologetically, they were scientists, not tourists. Scientists require special permission from the Turkish Foreign Ministry, which has not so far been forthcoming.

As soon as he made his first, unsuccessful application for a visa, Magaritz asked a Swiss member of the organizing committee, Dr Aymon Baud, to intervene. Baud, Magaritz's co-author on a paper that Magaritz had intended to present at the workshop, immediately contacted Akkok, but to no avail. Magaritz has now turned to other members of the organizing committee in the hope that they will be able to influence the Turks. Nechemia Meyers

US defence research

Few second thoughts at MIT

Boston

HALF of the faculty polled at the Massachusetts Institute of Technology (MIT) claim they would discontinue their research if their areas of research became militarily sensitive. Such aversion, however, has not lessened MIT's appetite for contract work from the US Department of Defense (DoD). In a DoD report on university contractors, MIT was identified as the largest on-campus university contractor, a position it has held for five of the past nine years.

Concern over the scale of this involvement has led to the setting up of a faculty/student committee to gather facts about the military presence at MIT. The data gathered, based on student and faculty questionnaires as well as university records, were presented at the faculty meeting last month.

Although DoD funds are expected to increase by 20 per cent from fiscal year 1985 to fiscal year 1987, the committee claims that defence is not the most important source of research backing at MIT. DoD support, in constant 1985 dollar volume and total share, is less than it was twenty years ago. Nor is DoD, with 16 per cent, the primary or even the largest on-campus sponsor: in 1985, support was also provided by the National Science Foundation (NSF, 14 per cent), industry (14 per cent), the National Aeronautics and Space Administration (NASA, 5 per cent) and the Department of Health and Human Services (17 per cent). Very few faculty members rely on just one source.

The Department of Energy (DoE), with 23 per cent, has been the largest source of research support at MIT since 1978. Major recipients of DoE support are the Laboratory for Nuclear Science, the Plasma Fusion Center and the National Magnet Laboratory. DoE, DoD and NASA sponsor nearly half of MIT's research, but only 10–11 per cent of that support is for "specific military application".

Off-campus laboratories involved in military research complicate comparisons between universities as well as judgement about the effect of such research on a given university. Data about these laboratories are inconsistently included in university figures, and defence support of such a laboratory has a variable effect on campus environment. For example, MIT's Lincoln Laboratory, with which Paul Gray, president of MIT, would like to see closer campus interaction, is 97 per cent supported by DoD.

The degree of financial support from different federal agencies has fluctuated by presidential and congressional whim. Thus according to Gray, President Reagan's reversal of President Carter's alternative energy policies has reduced DoE support at MIT. For the most part, however, Gray characterizes federal agency funding at MIT as "stable".

This cannot be said of support from industry, although nobody is downcast by that. Industry has trebled its support of MIT research in the past few years. Gray welcomes that increase, ascribing it to a concerted effort by the university.

Only 5 per cent of the faculty polled think involvement in the Strategic Defense Initiaive (SDI) will be good for MIT, with 40 per cent characterizing it as "generally bad". MIT is a top SDI contractor, with SDI providing 25 per cent of Lincoln Laboratory's $274 million budget in fiscal year 1985. But Gray thinks that $58 million skews MIT's research image: he points out that the percentage of on-campus research supported by SDI, $1 million out of $280 million, is very small. And even if all proposals were funded for next year, that amount will not rise above $5 million, says Gray.

Many faculty members, according to Gray, feel it makes sense to solve the basic and applied sciences issues of SDI regardless of the system's usefulness. Because SDI is as mission-oriented as DoE, however, says Gray, its research support is just as capricious. The fear of an abrupt loss of funding, if SDI is bargained away or declared unfeasible, chills researchers' willingness to rely on the programme.

SDI and military involvement in general evoke a less negative response in the School of Engineering than in other departments. Engineering has a disproportionate share of DoD funding as well as support from major defence contractors. More of that faculty would accept a requirement for security clearances as well as other limitations, and fewer of its students are averse to military work.

Seventy-five per cent of the faculty polled thought that concentration on SDI would channel research away from the civilian economy. This concern was also voiced by Gray in a telephone interview. Basic research garners only 10 per cent of total federal agency funding of the universities. Overall increases in DoD spending can easily mask decreases in that tiny fraction says Gray, resulting in an imbalance harmful to the growth of US science.

At its May meeting, the faculty empowered Gray to appoint a new committee to study the university policy implications of the data reported. The new study will require at least an academic year.

Elizabeth Collins

A prize for Tooze from EMBO

A NEW prize has been launched by the European Molecular Biology Organisation (EMBO). A medal and DM15,000 (£4,500) is to be awarded each year to an outstanding young European molecular biologist:



the aim is to try to help European scientists to gain international recognition as quickly as their US counterparts.

The announcement of the first medal winner at the recent EMBO symposium caused something of a stir: it went not to a research worker but to EMBO's own executive secretary, John Tooze, who from now on will be administering the prize. A somewhat embarrassed Dr Tooze modestly described the decision as "just an interim measure", with the medal to go to young research workers in the future. But there are many scientists who are happy to admit that Tooze's name is one of the best known in European molecular biology.

Tooze joined EMBO in 1973, after a few years as deputy editor of *Nature* and research administrator at the Imperial Cancer Research Fund. In the award ceremony he was particularly thanked for having built up EMBO's fellowship programmes. EMBO now offers 160 long-term fellowships each year, largely within Europe, and 250 short-term fellowships, as well as running 20 practical courses and 20 workshops and symposia. Then there is the *EMBO Journal*, set up by Tooze in 1981, and with all of the 1,200 or so papers submitted each year passing through his hands.

EMBO's total budget is now 4.8 million ECU (European Currency Units, £7.2 million) and the medal, for which funds were raised from private industry, will help to bring EMBO the publicity needed for further expansion. But its chief aim will be to give young molecular biologists the early recognition that will boost their careers.

Alun Anderson

Soviet science

Too many at the top

THE Soviet Union's "sectoral" research establishments — the institutes, laboratories and design centres that belong neither to the universities nor to the Academy network — have failed to respond to Mr Gorbachev's call for streamlining and restructuring. Reporting to the Supreme Soviet last week, Nikolai Ryzhkov, chairman of the USSR Council of Ministers, noted that some of these institutes had virtually ceased to do science altogether and had become little more than "managerial adjuncts" of the ministries to which they are attached.

During the past 20 years, the network of sectoral institutes has proliferated, as Mr Gorbachev pointed out during the General Committee plenary meeting in June 1985. As a rule, interministerial bureaucratic barriers made the sharing of facilities impractical or impossible, while some establishments seem to owe their origin to the empire-building propensities of certain ministries. Mr Gorbachev therefore called for the closure of redundant, inefficient or outdated sectoral institutes, and the establishment of inter-sectoral scientific and technical complexes that would cut across ministerial barriers and, at the same time, link research facilities with production enterprises. At the same time, a massive injection of finance into science was promised. Annual expenditure (excluding capital outlay) is to rise from 24,800 million rubles in 1985 to 33,000 million rubles in 1990. Capital investment in science will rise by 70 per cent over the same period.

The ministries, however, failed to respond to the challenge. Instead, they leapt to the defence of the institutes threatened by Mr Gorbavhev's attack, even if, for years, they had shown no interest in how these institutes were working. In the end, Ryzhkov told the Supreme Soviet, the Council of Ministers had to intervene and close down some of the most blatantly inefficient establishments. He cited two such cases. The All-Union Research and Design Institute for Complex Technological Processes, which belonged to the Ministry of Chemical and Petroleum Machine Building consisted, at the time of its closure, of 71 "ordinary personnel" and no less than 176 "leaders of different ranks", while out of its 130 research projects, only one or two had any scientific relevance. Likewise, one of the design institutes of the Ministry of the Machine Tool and Tool-Making Industry, which employed 600 people at the time of its closure, had managed to produce inventions from only two of its projects.

Vera Rich

Telecommunications

Japanese cable competition

Tokyo

INTERNATIONAL telecommunications in Japan are booming. Annual growth in volume is 20–30 per cent, and in the past few weeks two giant consortia have emerged that hope to grab a slice of this market, currently worth more than 200,000 million yen (£800 million) a year but monopolized until now by Kokusai Denshin Denwa (KDD). KDD, in turn, has announced plans to lay two submarine optical fibre cables to provide high-capacity digital links between Japan and the American and Asian continents by 1990.

Japan's telecommunications laws were liberalized more than a year ago. Five domestic telecommunications companies have been set up to compete with Nippon Telegraph and Telephone Corporation (NTT) in the domestic market, but in the past month a spate of announcements have heralded competition in the international arena.

First off the mark were the three former *zaibatsu* trading houses, Mitsubishi Corporation, Mitsui & Co. and Sumitomo Corporation, which will set up a feasibility study company next month as a first step towards forming their so-called "second KDD". The consortium will lease transponders of Intelsat satellites from KDD, Japan's Intelsat representative.

Next, C. Itoh & Co., a trading house rival of the *zaibatsu* group, announced plans to establish a new international telecommunications company jointly with Toyota, General Motors of the United States and Britain's Cable & Wireless. This consortium intends to lay its own submarine trans-Pacific optical fibre cable in direct competition with that of KDD.

Both consortia have capital investment links with Japan Communication Satellite, one of the five new domestic telecommunications companies, and so will have ready access to a domestic carrier.

The KDD submarine cable network will be built in collaboration with American Telephone and Telegraph, Korea Telecommunication Authority and, surprisingly, Cable & Wireless (Hong Kong) Ltd. Two branching cables will be laid.

The first, trans-Pacific cable 3, to be completed by late 1988, will link Japan, Guam, Hawaii and the US mainland via a submarine branching point about 1,500 km north of Guam. More than 13,000 km of cable will be laid along the seafloor which plunges to depths of over 8000 m in the trenches that rim the western Pacific in an arc between Guam and Japan. The second cable will run off the Pacific coast and split north of Okinawa, with one branch running to South Korea, the other to Hong Kong.

The total cost of the two cables will be a staggering $800 million (£530 million), but with 7,560 channels, the trans-Pacific 3 cable will have about ten times the capacity of the two existing coaxial cables and will be on a par with Intelsat satellites which currently have 6,000 or 12,000 telephone channels. Digitilization will allow high-speed data transmission, video transmission and teleconferencing — capabilities that were formerly the preserve of satellites. At present about 60 per cent of KDD's international transmissions are via Intelsat satellites, but this percentage is expected to drop substantially.

Once in place, maintenance costs for the cables should be low, provided submarine slides, fishing trawls or unwary research vessels do not break them — not uncommon events off Japan's coast. For example, in 1972 turbidity current severed the trans-Pacific cable in Sagami Bay and in 1984 the *Natsushima*, mother ship of Japan's deep-sea submersible *Shinkai 2000*, managed to do the same thing at a cost to KDD of Y52 million (negotiations for compensation are proceeding), while the Japan–China submarine cable has been fished up so often by trawlers it has had to be buried 70 cm below the seafloor using a special cable-laying device equipped with a plough. But barring such accidents, the submarine cable can be expected to have a lifetime of at least 20 years.

The plan of the C. Itoh consortium to lay a competing trans-Pacific optical fibre cable is meeting resistance. KDD considers it to be "unfair competition" because, as a public entity, KDD has a responsibility to maintain parallel systems (satellite and cables) to ensure continuity of service if one system broke down, whereas the "third KDD" plans to use only cable.

KDD further argues that there is simply not enough room for three competitors in Japan's international telecommunications market. Critical in this argument is the future size of the market. Whereas KDD estimates it will amount to 600,000 million yen by 1995, a survey released by the Federation of Economic Organizations (Keidanren) thinks it will be twice that. Competition will influence market value. If rates are slashed, market value growth will not match the growth in telecommunications volume.

The fate of the third KDD thus remains uncertain. Toyota has made no clear commitment to join the consortium, and officials at the Ministry of Post and Telecommunications echo KDD's view that "two's company, three's a crowd". The consortium, however, may simply have been floating a trial balloon.

David Swinbanks

Scientific fraud

New Public Health service policy

Washington

AFTER a delay of four years, the US Public Health Service (PHS) has inaugurated a formal policy for dealing with allegations of scientific misconduct such as fabrication and plagiarism. Scientific staff and officials of organizations receiving PHS funds must in future report alleged misconduct to designated institutional "misconduct policy officers". The new policy also requires institutions that receive its funds to certify that they have in place procedures for investigating allegations of misconduct, and to inform the funding agency when formal investigations are initiated.

The need for a formal PHS policy became apparent after a spate of widely publicized cases of fraud, plagiarism and other misconduct in biomedical research in the early 1980s, of which John Darsee's fabrication of research results was the most infamous. The effort to develop ways of dealing with allegations effectively while minimizing damage to the reputations of those unjustly accused was instigated in 1982. Congress instructed PHS to develop a policy last year.

The new policy has been developed chiefly by the Office of Extramural Research and Training of the National Institutes of Health (NIH), which has in recent years overseen NIH misconduct investigations on an *ad hoc* basis. The deputy director of NIH for extramural research and training, currently Dr William Raub, is "misconduct policy officer" for the whole of PHS. Fifty allegations were received by Raub's office in 1985, of which twenty-four proved substantial; the frequency of allegations has increased markedly since the early 1980s, for reasons not clearly understood.

The policy defines misconduct as either a "serious deviation" from accepted research or reporting practices, or material failure to comply with requirements such as those protecting human subjects or animals. Institutions are required to conduct thorough reviews of any allegation that is "not frivolous or unsubstantiated", preferably within 60 days, and to keep NIH informed about the investigation.

Suggested sanctions range from a simple reprimand to imposition of special reporting conditions and debarment of individuals or institutions. Criminal misconduct such as misappropriation of funds is excluded from the policy and dealt with by separate procedures.

The policy now implemented by PHS is likely to serve as a model for similar policies in other research agencies; the National Science Foundation, for one, expects to implement an almost identical policy. The Office of Management and Budget has recently proposed requiring all federal agencies that award research grants to develop policies for debarment, necessary if debarment is to withstand a court challenge.

The detailed PHS policy guidelines, which include sections for agency personnel and for institutions that receive grants, outline procedures for conducting investigations and for determining administrative action. Individuals under investigation must always be so informed; otherwise, the fact that an investigation is in progress is restricted to those who need to know. As far as possible, informants' identities are kept secret.

Although the announcement of the PHS policy appears to have been somewhat muffled, it was approved by acting assistant secretary for health Donald MacDonald in April and came into force immediately. The policy retains "interim" status until incorporated into standard guidance documents for agency staff.

The interim policy would establish a PHS-wide "alert" system to notify awarding institutions when grant applicants are under investigation for misconduct or are subject to restrictions resulting from adjudged misconduct. Individuals flagged in the "alert" system are not necessarily precluded from receiving an award or participating in review committees; decisions are made according to circumstances.

Although NIH themselves already have an "alert" system, its extension to the whole of the Public Health Service will under the Privacy Act require publication in the *Federal Register*, as it entails maintaining a database referencing individuals.

Details of the responsibilities of institutions receiving funds have also yet to be published for comment before the policy can be put into force; both *Federal Register* notices should be published in August.

The new policy does not answer all the demands of those who have been critical of PHS's existing informal procedures. Institutions are required to inform their awarding agency of an investigation only if preliminary inquiries suggest that the allegations are serious and plausible; some contend that perceived pressure on an institution not to find evidence of wrongdoing will jeopardize impartial scrutiny. But NIH did not want the responsibility of investigating every allegation made, and after long debate decided that primary responsibility should rest with the host institution. NIH can follow up with their own investigation if the institution's appears inadequate.

Daryl Chubin of Georgia Institute of Technology, who has studied scientific misconduct for the National Science Foundation, comments that the existence of guidelines should make it easier for those who suspect misconduct to make their allegations confidentially. But Chubin still sees conflicting pressures on institutions that have to investigate fraud; as employers, they should normally be prepared to give employees the benefit of the doubt.

Ned Feder and Walter Stewart of NIH, in an unpublished manuscript given in testimony to Congress, have supported random audits of all published research. Such random audits are conducted by the Food and Drug Administration to ensure the veracity of data it uses in making regulations, and the agency can impose sanctions on an investigator who is found to be doing careless research. PHS's policy is, however, constrained to scrutinize only the more serious allegations.

Tim Beardsley

JET Britons seek to

BRITISH fusion physicists working at the Joint European Torus (JET) near Oxford take home less than half the pay of other European nationals on the JET project, even though they have equivalent jobs. This is blatant discrimination, the European Court of Justice heard in Luxembourg last week, two-and-a-half years after the British JET staff first instructed European lawyers to take up their case.

Last December, the Court's Advocate General recommended that a subsidiary court accept the Britons' arguments, and award them back pay. However, the subsidiary court referred the case onward to full court, which heard the oral evidence last Thursday. According to the European Commission, the back pay if awarded would amount to some 10–15 million ECU (European Currency Units: roughly 1 ECU=$1, or £0.67). Distributed among the 222 British JET staff involved, this would amount to an average windfall of 45–65,000 ECU (£30–45,000) each, and a salary henceforth of twice present earnings. The Commission estimates that JET costs would rise by 2 million ECU annually, around 2 per cent of current expenditure. This would give the British an average pay rise of £9,000.

Perhaps unsurprisingly, 75 per cent of the Britons working at JET have contributed to a legal fund to pay for the case in Luxembourg, which is based on the argument that the JET statutes discriminate against British employees and so contravene the Treaty of Rome the basic legal text of the European Economic Community (EEC). EEC pays for JET through its Euratom component. The Treaty of Rome demands equal treatment of all EEC nationals, but the JET statutes, agreed (perhaps illegally, it now seems) by the European Council of Ministers in 1978,

US biological weapons

New test facility defended

Washington

DESPITE delays in construction forced on it by the courts, the United States Army has defended its plans to build a biological aerosol test facility (BATF) at the Dugway proving ground. In a report to Congress, the Army calls BATF a "small but critical facility" needed to provide adequate defence against biological weapons. But critics worry that the facility may easily be mistaken for the harbinger of a new offensive biological weapons programme, putting arms control agreements at risk.

Language inserted into last year's defence appropriations bill required the Army to respond to a set of specific questions about the planned uses of the Dugway facility. In its written response, delivered to Congress earlier this month, the Army states that "the United States cannot defend itself adequately against conventional biological warfare agents", making increased defensive efforts crucial. Two factors convince the Army that greater vigilance to the threat of biological warfare is necessary. The United States still maintains that yellow rain in South-East Asia is evidence of Soviet use of biological weapons in violation of the 1972 biological weapons convention.

In addition, new biotechnologies provide cheap and easy methods for production of biological agents that can be used as weapons. BATF is designed to test defensive equipment against a variety of potential biological agents. Despite the fact that Army plans call for a biosafety level 4 facility, the level traditionally associated with recombinant DNA experiments involving virulent agents, the Army has no plans to test genetically engineered material in BATF.

But critics feel the Army's own arguments will force it to resort to testing recombinant DNA organisms. Barbara Rosenberg, a molecular biologist at the Sloan Kettering Institute in Rye, New York, and a member of the committee on the military use of biological research, argues that developing a defence against the many agents formed by recombinant DNA techniques will require similar technology. Indeed, the Army report does not permanently rule out such activities.

The Biological Weapons Convention prohibits signatories from developing, producing or maintaining stockpiles of biological weapons. The Army maintains that BATF does not violate the convention because research on biological agents for "prophylactic, protective or other peaceful purposes" is permitted by the treaty. But critics point out that toxic agents used for testing could quickly be transformed into offensive stockpiles. Possessing such a capability only heightens uncertainty about US intentions, says Rosenberg.

The Dugway facility has faced problems since it was proposed in 1984. At first, the project was held up by Senator Jim Sasser (see *Nature* **312**, 189; 1984). After Sasser's objections were resolved, Jeremy Rifkin successfully thwarted Army plans by convincing a federal judge that the Army had not made an adequate environmental assessment for its facility. The Army has now commissioned a complete environmental impact statement due to be completed at the end of this year. But even an acceptable impact statement may not persuade the court to lift its injunction blocking construction of BATF. **Joseph Palca**

double their pay

have Britons employed by the United Kingdom Atomic Energy Authority on British salaries, while non-Britons (some 162 in all) are employed by Euratom on the very comfortable salaries of a European civil servant.

The European Commission is resisting any change in the JET salary arrangements, however, and an official pointed out on Monday that there were precedents. Euratom helps support a number of other European fusion research centres besides JET, though these are national (such as Britain's own laboratory at Culham, France's at Fontenay aux Roses, and West Germany's at Garching). There are a number of non-nationals (30 at Fontenay, 10 at Garching, but just one at Culham) who are supported at these institutions on Euratom contracts somewhat more favourable than the local, national pay scales. JET is unique, however, in having a roughly 50:50 ratio of local and Euratom-supported staff.

According to a spokesman for the British group at JET, the loyalty and commitment of the Britons to the JET project remains high, and some of the Euratom employees at the laboratory are supporting the case. The late director of the JET project, Hans-Otto Wüster, in fact first suggested the Britons seek legal advice, although he resisted that advice when it proved favourable to the Britons' case. Morale is good at JET, staff insist, and the case is being pursued "without passion". The European Commission hopes for a court decision by the end of this year. Meanwhile, the British at JET are waiting for the recommendations of the new Advocate General appointed to the case; unfortunately for them, the first, who found in their favour in the lower court, has now retired. Robert Walgate

Chernobyl

Eastern bloc reactions

THE chief inspector of the Czechoslovak Atomic Commission, Jiri Beranek, has called for a re-evaluation of all nuclear safety measures, on both a national and an international level. Interviewed on Prague radio, Beranek stressed the need for a longterm study of possible chemical reactions within reactors that would lead to the generation of hydrogen, the presence of combustible material in reactors, and the reliability of the human factor.

The first two points clearly relate to the Chernobyl disaster. Although the Soviet government's special commission on Chernobyl has not yet reported, Soviet experts have already accepted a scenario in which a surge of power led to the production of steam, which reacted with the zirconium fuel-cans to produce hydrogen. Whether human error was directly involved at Chernobyl is unclear. In mid-May, the Soviet media made brief mention of an "experiment" being in progress at the time of the accident, which could mean that someone tried some unorthodox method of dealing with the reactor which was already causing problems.

Beranek's concern for increased nuclear safety coupled with a firm commitment to nuclear power is typical of Comecon officials — although most of them, privately, have a good store of "black" post-Chernobyl jokes. In Poland, where some 300 inhabitants of the Bialystok area signed a petition calling for a halt to construction of the country's first nuclear plant at Zarnowiec, the official reply was that a future without nuclear power would put Poland back in the dark ages.

In Hungary even the dissident ecological "Danube Circle" has refused to condemn nuclear power, which it sees as less threatening than the controversial Gabeikovo-Nagymaros hydroelectric dam. And the Soviet Union itself, of course, is still committed to an energy policy based on the "accelerated growth of nulcear power", which, according to the current five-year plan, should produce an output of 390,000 GW in 1990 (against 167,000 GW in 1985).

It is only the Soviet Union's non-aligned and neutral neighbours that changed their energy strategy in the aftermath of Chernobyl. Yugoslavia, which already had a vocal antinuclear lobby, has postponed any decision on further nuclear power plants "until the long-term programme for the development of the energy industry has been adopted", and has decided to concentrate on energy conservation and hydroelectric power. And Finland has likewise dropped plans for a fifth nuclear power plant. **Vera Rich**

Future of lion tamarins

SIR—On behalf of the International Recovery and Management Committee for the golden-headed lion tamarin, I was delighted to read the News item entitled "Tamarins to go home" (*Nature* **320,** 674; 1986). Tom Milliken, director of WWF Traffic (Japan), is to be complimented on his contribution to the lobbying and diplomacy that has culminated in the announcement that the ten golden-headed lion tamarins imported illegally into Japan three years ago will be returned to the ownership of the Brazilian government. Conservationists well recognize that the case holds great significance for the future development and implementation of CITES in Japan.

With regard to the reference in the news item that captive breeding programmes are under way at the Rio de Janeiro Primate Centre and at the zoo in Jersey, however, Jersey does not at present have this species included in its successful breeding programmes for golden lion tamarins.

Dr Adelmar Coimbra-Filho, director of the Rio de Janeiro Primate Centre, and I are co-chairmen of the international committee. At the inaugural meeting of the committee at San Diego in June 1985, the main objectives were agreed to be illegally exported or illegally held specimens confiscated or voluntarily replaced under the trusteeship of the Brazilian government and to use the world's best resources to establish a viable captive breeding population under scientific management. The committee advises the Instituto Brasileiro de Desenvoluimento Florestal (IBDF) on the management of the species in captivity.

The release into the wild of these already displaced animals is not recommended at this time; the information available on population, distribution and habitat protection in the Brazilian state of Bahia is insufficient to guarantee survival and could well, through disease, impair the survival of the remnant population.

The recent successful re-introduction of the closely related golden lion tamarin species into the Poco des Antes Biological Reserve in the State of Rio de Janeiro required many years of careful preparation. Similar preparatory research must be carried out before such re-introduction is undertaken with the golden-headed lion tamarin and, in the meantime, a captive self-sustaining population must be secured, with breeding programmes being established at a number of different locations, but managed as an overall single unit.

As a result of a recent ballot among the International Management Committee, of which 50 per cent comprises some of Brazil's leading conservationists, it was unanimously agreed that individuals of the golden-headed lion tamarin species should be made available only to institutions that have already had experience with the long-term maintenance and successful propagation of the golden lion tamarin. Priority has been given to selected captive breeding institutions in Brazil, and a list of suitable locations outside Brazil has been drawn up in order to receive individuals that the Brazilian Conservation Authorities consider are surplus to their requirements.

We have great hopes. The golden lion tamarin programme has nurtured a captive population from approximately 70 specimens in 1972 to more than 400 individuals by 1985, recently recording an annual population growth of 50–60 animals, on which was based the successful re-introduction programme for this species.

JEREMY J.C. MALLINSON
Jersey Wildlife Preservation Trust,
Les Augrès Manor,
Trinity, Jersey,
Channel Islands

Is this science?

SIR—In the past few years, we have witnessed in the pages of *Nature* a curious debate between those broadly described as "evolutionist" and "creationist", adopting, the former would have us believe, scientific and unscientific arguments respectively. Leaving aside the deterioration into personal abuse, reminiscent more of discussions in a school playground than reasoned debate in a learned journal, it is particularly disturbing to find those purporting to defend the scientific process haplessly resorting to the same sort of emotional and illogical tirades assumed to be the hallmark of the opposition.

In the latest example, J. Richard Wakefield (*Nature* **320,** 392; 1986) asserts that, in contrast to those who believe in a created order, science "accepts nothing on faith". This naivety requires no other comment than to point to a prime example of the author's own article of faith, that "nothing is potentially beyond science". This happens to be a viewpoint that I share. But let us recognize the ill-defined nature of the belief.

Selective awareness is evident in both the statement that "misrepresentation runs rampant in creationism" and the list of human failings in the last paragraph. Is it possible he really believes that no scientist has ever fallen into this category? Few would argue that scientists are perfect. For those who do, a glimpse at the history of palaeontology and the recent debate about cladistic thought at the British Museum (Natural History) ought to convince them otherwise, so "pure" science is probably rather thin on the ground. It seems to me that if colleagues feel the need to defend science against some of the more bizarre claims levelled at it, they must avoid dual standards. It is our responsibility to counter false logic with rigorous argument, not with personal invective or dubious claims to infallibility.

STUART EGGINTON
University of Birmingham,
Department of Physiology,
Vincent Drive,
Birmingham B15 2TJ, UK

Last word on metric

SIR—My passing remarks mildly critical of metric units (*Nature* **316,** 480; 1985) have provoked your correspondents (**317,** 10; 1985; **318,** 203, 596; 1985; **319,** 8, 93, 716; 1986) to imply that I am in league with those who have opposed printing, telescopes, railways, telephones, motion pictures and so on. That is not quite accurate.

While metric units certainly have some role in science and technology, little purpose is served by compelling their everyday use. One might as well argue that since English is now the lingua franca of science, its use should be made compulsory in households the world over. While that might be a fine idea on its own merits, it would likewise be a *non sequitur*.

Why not simply let people use the units they prefer? Imposing alien units merely fuels the common belief that technocrats seek to control all aspects of life. Such imposition also severs society from its rich linguistic and cultural heritage. It will be remembered that metric units were designed by a group of zealots who hoped to do precisely that, their target being the *ancien régime*.

DAVID C. JOLLY
Box 931,
Brookline, Massachusetts 02146, USA

This correspondence is now closed.
Editor, *Nature*.

Sex discrimination

SIR—Joseph Palca's report (*Nature* **321,** 371; 1986) on the possibility of sequencing the human genome raises the problem of which individual's DNA to use, and suggests possible ways of choosing "him" or "her". While I appreciate this egalitarian phraseology, it is not possible to sequence the whole genome using a female source. Some 2.5×10^7 base pairs of considerable importance to half the world's population would be missing.

Perhaps this conflict between scientific and social requirements could be resolved by selecting an XY female as the source of the DNA.

HOWARD J. COOKE
MRC Mammalian Genome Unit,
Department of Zoology,
University of Edinburgh,
West Mains Road,
Edinburgh EH9 3JT, UK

New technology of medicine

The transformation of basic medical science has been a surprise to all of us, but especially to physicians.

LAST week's *Nature* conference in London was originally planned as one of a series. The intention was that the journal should continue in this vein with its traditional function of acting as a midwife between specialized laboratories and the wider audience outside. Experience has shown that there is a particular need of means by which people who used to be in academic life, but who are now elsewhere, in industry perhaps, may renew acquaintance at first hand with research. Most people were last week surprised that, no doubt more by luck than judgement, a meeting on the biotechnology of medicine appeared to coincide with the fruition of several threads of research in the field.

In retrospect, there is a surprise to be explained. In 1975, when the air was full of reports by government committees (and others) on the promise of biotechnology, the most common prediction was that the pharmaceutical industry would be quickly overwhelmed by a torrent of new products, artificially engineered versions of naturally occurring materials. And, to be sure, human insulin was quickly on the market, although not at such a price that it could hold off competition from chemically modified pig insulin. Since then have come human growth hormone, with an invaluable role to play in the treatment of disease, and the various interferons whose value has still to be defined. There remains a small army of biological materials still waiting in the wings, and there is no reason why the prospectuses of a decade ago will be found to have been bogus. But, inevitably, there is some disappointment in the air.

Much the same is true in the genetic manipulation of plants. Ten years ago, people talked endlessly of the transformation of agriculture that would come about when it proved possible to transplant nitrogen-fixing genes from leguminous plants to those that have evolved without them. There were even academic arguments on the esoteric question whether the effort would be worthwhile in temperate latitudes, where the intensity of sunlight is not enough to make full use of nitrogen-fixing genes. In reality, as events have shown, the nitrogen-fixing genes are a complex too large and well-tuned to be shifted easily from one plant to another. A better hope is that plants at present unable to fix nitrogen directly might, by engineering, be given the facility to form symbiotic associations with soil bacteria (see Jensen, J.S., *et al. Nature* **321**, 669; 1986). But that, too, will not happen the day after tomorrow, especially if modest agricultural experiments with engineered bacteria are held up for regulatory reasons.

None of this implies that last decade's promises on behalf of biotechnology were false. Did it not, after all, take more than a century to bring the steam engine from a dream to a reality? It is no shame that biotechnology has been required to mature. But the surprise is that so much has happened in medicine, in the treatment of patients, when these techniques were overshadowed by the hopes for new pharmaceuticals.

That monoclonal antibodies would be important has, of course been clear since the beginning, just eleven years ago. The principle that it is possible to make by this means a sensitive reagent for almost any antibody is well established now. But did you know that the more distant hope of coupling monoclonal antibodies to toxins so as to kill unwanted cells specifically is already in the early stages of clinical testing? That is what Professor Robert Baldwin (University of Nottingham) explained last week; among the unexpected findings so far is the discovery that the immune system can make antibodies against toxins when these are coupled to antibodies, which is a hurdle to be overcome. The notion that monoclonal antibodies can be used to sterilize the mouth and teeth against infection by streptococci (Professor Thomas Lehner, Guy's and St Thomas's, London) is another dream on the way to coming true.

Vaccines, the classical tools of preventive medicine, naturally featured in the prospectuses of the 1970s, but people had not then thought of the use of vaccinia virus as a means of showing antigens chosen at will to the human immune system. Although there were several at last week's meeting sharing the caution expressed by Dr Geoffrey Schild (director of the British National Institute for Biological Standards and Control) about the potential of vaccinia virus and an all-purpose antigenic vehicle, the plain fact is that this material, the several versions of malaria vaccine now being prepared for trials and the vaccines being worked up as prophylactics of schistosomiasis (Dr André Capron, Pasteur, Lille) would not have been possible without genetic manipulation.

Inevitably, AIDS (Acquired Immune Deficiency Syndrome) crops up in these connections. Who can but be moved to recognize that an infection whose viral character was first demonstrated merely three years ago now has an agent described almost as fully as more or less any other virus? Dr Luc Montagier (Pasteur, Paris) gave such a telling account of this process of discovery last week, with due acknowledgement of the contributions of Gallo and his collaborators in the United States, that many in the audience must have come to share the view that it is a great misfortune that the French and US groups are now separated from each other by their patent suit.

Not surprisingly, AIDS brought into the open an issue lying beneath several of last week's talks. Montagnier had been talking about the rationale of a vaccine against AIDS, which is an awkward concept because it entails the stimulation of lymphocytes which, if already infected, will yield more virus. His chairman, Professor Avrion Mitcheson, raised (by means of a reference to the case of yellow fever) the question whether physicians in earlier days might not have been impelled to see whether a vaccine would cure one or two of their patients otherwise destined for a terminal infection. Earlier Schild had remarked, in passing, that it would have been hard to win regulatory approval for the Sabin live-virus vaccine against poliomyelitis. How great an encumbrance is the regulatory apparatus?

To be fair, nobody seems concerned to sweep away the system that has grown up to regulate the introduction of new pharmaceuticals, for example; what people ask for there is greater efficiency and a plainer understanding on legal implications. (Does licensing imply immunity from some legal suits?) The regulation of new research is more disturbing. Dr French Anderson (National Institutes of Health, Bethesda), describing preparations being made for work with human beings, acknowledged that the present system is probably a necessary way of giving the general public reassurance — even though it will entail a delay of at least six months between application and consent. Anderson is almost certainly right that the public and governments would not be satisfied with less. But how quickly will the apparatus be dismantled when it has served its purpose, and when there is a real danger that regulation will become an impediment to therapy?

John Maddox

Taxonomy

A new class of echinoderms

from David Nichols

WATERLOGGED wood often sinks down to the deep sea-bed, to become an oasis of solidity in a vast expanse of sediment. Its crevices, filled with a soup of bacteria, become a haven for tiny organisms, including, it now emerges, a hitherto unknown echinoderm. So specialized are these 'sea-daisies' that a new class, the Concentricycloidea, has been erected to contain them. An article on page 862 of this issue describes the new genus, *Xyloplax*.

In August 1985, three echinoderm specialists, Alan Baker, Helen Clark and Frank Rowe, met at the National Museum of New Zealand principally to compare species of starfish common to waters off New Zealand and New South Wales. A worker at the museum, Bruce Marshall, was investigating gastropods from crevices in driftwood from a depth of 1,000 m and had put aside capsules with fragments or whole specimens of small caymanostellid starfishes for Rowe to examine during his visit. Sharing the capsules were nine specimens of a tiny animal, clearly an echinoderm, which Rowe and his colleagues could not place in any known group.

The disk-shaped body of the echinoderm is supported by a series of circumferential rings of plates (see Fig. 1) bearing a fringe of spines projecting like the petals of a daisy. The slightly domed dorsal integument contains scale-like plates that imbricate like roofing tiles, and each plate bears several stunted spines. Also visible on top are five large plates equally spaced around the periphery, representing the homologues of the plates at the armtips in starfishes, or those at the top of the radial columns (the so-called 'ambulacra') in sea-urchins.

Towards the circumference on the underside is a ring of hydraulic tube-feet projecting downwards. Each is apparently operated by a bag-like ampulla situated within the body, and all are connected externally by a water-vascular ring. Uniquely for echinoderms there is a second ring beside the first, and the two rings are connected by short inter-radial canals. In known echinoderms there is a functional need for confluence between the water-vascular system and the outside sea water, so that the hydrostatic pressure in the system equates with that of the outside medium. In *Xyloplax* too, this connection is provided at a hydropore on the dorsal surface, connected to the inner water-vascular ring.

The animal has no gut, which takes to the ultimate the reduction in gut feeding of other echinoderms. Some sea-cucumbers, for instance, feed for only part of the year, generally when energy uptake is increased before reproduction. For the rest of the year, the gut remains empty and the organisms rely on the free radicals in sea water, absorbed mainly through a velvet-like 'pile' of microvilli over the external body surface.

The concentricycloids are reported to have a thin velum, which stretches drum-like across the ventral surface, and, further, the tube-feet themselves are thought to have food storage coelomocytes within their lumina. It is interesting to speculate that the suspension of bacteria which share the wood crevices with these animals may aid the nutritional process in a manner similar to that in deep-water pogonophores, which contain symbiotic bacteria in special tissues within their bodies. Perhaps in concentricycloids some bacteria are held beneath the sub-umbrella surface, within the palisade of spines, the radicals they release diffusing through the velum to the interior.

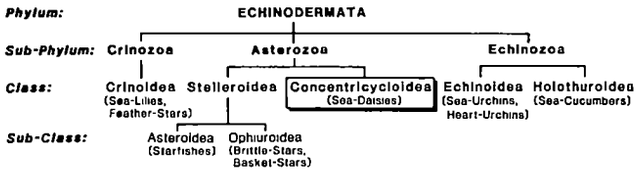


Fig. 2 Classification of echinoderms, showing possible relationships of the concentricycloids.

An exciting find is that the gonads of the animals contain embryos at various stages of development up to juveniles, which look like miniature adults. There are sound reasons for releasing young into the immediate vicinity of the adults when the 'parent' substrate is the only suitable habitat for a considerable distance. But timber, despite its slow decomposition in deep water, does not last for ever, and some mechanism is required for wider deployment of the offspring.

So long as the young concentricycloids are within the gonad, their peripheral spines are tucked under their bodies, but on release the spines open out, and are at this stage longer proportionally than the spines of the adult. This may be a flotation device to assist the juveniles to be carried above the sediment until they encounter another suitably pitted or creviced substrate.

As yet, it is possible to make only the most tentative proposals about relationships of the new class. Suggestions by the authors that *Xyloplax* resembles the cyclocystoids (an extinct class of subcircular echinoderms from the Middle Ordovician to Middle Devonian) may have been based on older reconstructions, now superceded by more detailed studies of almost all known cyclocystoid specimens (Smith, A.B. & Paul, C.R.C. *Phil. Trans. R. Soc.* B**296**, 577; 1982).

Cyclocystoids had a marginal ring of hefty plates with two plate-supported membranes stretched within. But the membranes were closely associated,

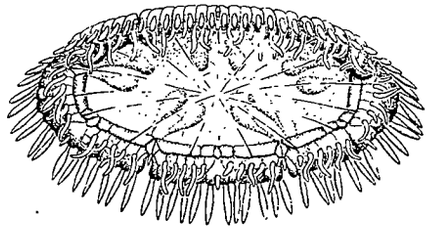


Fig. 1 Conjectural ventro-lateral view of *Xyloplax medusiformis*, a new concentricycloid from deep water off New Zealand.

dorsal to ventral, so that the organism would have resembled, as Smith and Paul put it, "a tambourine, not a drum", and the space between the membranes would have been very limited indeed, unlike the body-cavity in concentricycloids. Further, although earlier reconstructions (for example, Nichols, D. *Palaeontology* **15**, 519; 1972) suggested that a series of cupules in the marginal ring represent anchorages for a ring of tube-feet similar to the arrangement in *Xyloplax*, there are now grounds for rejecting this idea — first, the cupules have tubercles within them; and second, they do not connect up with the most likely seat of the water-vascular system, which provides fluid for tube-foot operation.

What, then, is the nearest known echinoderm relative of this new class? The authors suggest that it belongs to the Asterozoa, the sub-phylum that includes all starfishes and brittle-stars (see Fig. 2). This group already includes some pretty bizarre forms, such as the spherical starfish *Podosphaeraster* (Rowe, F.W.E., Nichols, D. & Jangoux, M. *Micronesica* **18**, 83; 1982; Rowe, F.W.E. *Bull. Mus. natn. Hist. nat., Paris* **7**, 309; 1985).

In the case of *Xyloplax*, a feasible derivation of the marginal ossicles is suggested by the authors, who see the ambulacral tube-feet, normally in a double column and radially arranged, as if having splayed out laterally and come to abut against the adjacent column in a circle. Clearly, a considered proposal about relationships awaits more rigorous study of this animal than has so far been possible. □

David Nichols is Professor of Biological Sciences at the University of Exeter, Exeter EX4 4PS, UK.

Planetary magnetospheres

The double tilt of Uranus

from Fran Bagenal

PERHAPS the biggest surprise of the Voyager 2 fly-by of Uranus was the discovery that the planet's magnetic field axis is tilted as much as 60° with respect to its rotation axis. Moreover, with Uranus tipped on its side, a highly tilted magnetic field produces a particularly unusual magnetosphere. The Voyager science teams have completed preliminary analyses of their data (published in this week's issue of *Science*) which were discussed at a recent meeting*.

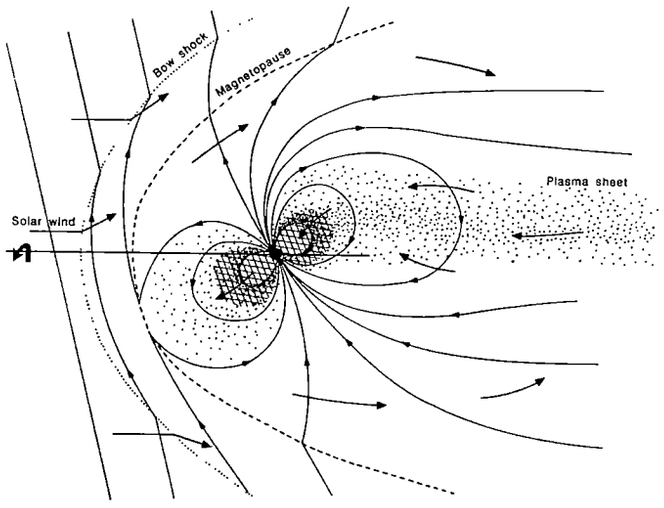
The detection of strong ultraviolet emission from Uranus by the International Ultraviolet Explorer satellite in 1982 provoked speculation of a strong magnetic field, but it was not until Voyager 2 had reached a distance of 275 uranian radii (1 R_U = 25,600 km) from the planet (five days before its closest approach) that the detection of radio bursts established the existence of a uranian magnetic field. Approaching the planet near the sub-polar point the spacecraft first crossed the bow shock at 23.7 R_U and then entered the magnetosphere at 18.0 R_U, where Voyager 2 discovered an unusually complex planetary magnetic field (N.F. Ness, Goddard Space Flight Center, GSFC). To first approximation the magnetic field can be described as a tilted 0.23 Gauss R_U^3 dipole. Higher order terms contribute as much as 70 per cent of the dipole terms and can be represented by displacing the dipole by 0.3 R_U from the centre of the planet away from the sunlit side. Consequently the surface field is much weaker on the sunlit side (<0.1 Gauss) than on the dark side (<1.1 Gauss). By combining magnetic field data with measurements of the periodic radio emission the rotation rate of the interior, dynamo region has been accurately determined at 17.24 ± 0.01 hours (see the paper by M.D. Desch, J.E.P. Connerney and M.L. Kaiser in next week's issue of *Nature*).

Once inside, Voyager 2 found the uranian magnetosphere to be relatively empty compared with Earth, Jupiter and Saturn. The total energy density of all trapped particle populations is much less than the magnetic field pressure ($\beta << 1$) and hence in the inner region ($\lesssim 12\ R_U$) the magnetic field suffers very little distortion from particle loading. Nevertheless for the few high-energy (few MeV) particles, fluxes were comparable to those in Saturn's radiation belts except absorption by the uranian satellites is much stronger (D. Chenette, Aerospace Corp.), which provoked the suggestion that particle bombardment of methane in the satellite's icy surfaces, producing tars, may be partly responsible for their dark appearance (L. Lanzerotti, Bell Laboratories).

The unusual depletion of energetic protons relative to the intense fluxes of electrons of similar energies may be due to preferential removal by charge-exchange reactions with the particularly extensive atomic hydrogen corona of Uranus (S. Krimigis, Johns Hopkins University). The density of low-energy thermal plasma was found to increase towards the planet, reaching a maximum value of ~3 cm^{-3} at closest approach (R.L. McNutt, MIT). The spatial distributions of the two plasma populations (kT~ few keV and kT~10 eV) provide clues to the nature of their sources and their subsequent transport: the cooler (10 eV) population was detected throughout the inner magnetosphere which suggests a source near Uranus (for example, its upper atmosphere or ionosphere), while a sharp inner boundary of the hotter population at ~5 R_U indicates that hot material is brought in from distant sources (for example the solar wind or outer satellites) and prevented in some way from entering the inner region.

The Voyager 2 plasma measurements are consistent with the main plasma motion being that of co-rotation with the planet. In addition, the solar wind is thought to drive a large-scale magnetospheric circulation, similar to that at Earth. Because plasmas are highly electrically conducting we can consider convective motions to consist of the movement of whole tubes of magnetic flux containing a parcel of plasma 'frozen' to the field. The solar wind carries flux tubes from the dayside magnetopause to the nightside. The flux tubes then follow a return flow through the centre of the magnetosphere towards the planet, heating any entrained plasma as the tubes contract. At Earth a point (the plasmapause) is reached where atmospheric drag overpowers the magnetospheric forces and causes the plasma to rotate with the planet.

At Uranus the planet's rotation is orthogonal to the solar wind-driven flow (see figure) so that the two forces are orthogonal. Thus, if one were to watch a parcel of cool plasma it would appear to move in a helical motion through the magnetosphere. Moreover, rotation of the whole magnetosphere guarantees that the planetary and solar wind magnetic fields are anti-parallel at the dayside magnetopause once per rotation. Hence periodic magnetic reconnection may allow the greater efficiency in removal of solar wind energy that is required to power magnetosphere in circulation plus auroral and electroglow emissions (T. Hill and A.J. Dessler, Rice University).



Spots, hot plasma; hatching, cool plasma.

Various features in the Voyager observations ocurred at or were associated with magnetic field lines that cross the magnetic equator at a radial distance of ~5 R_U. This is also the orbital distance of the satellite Miranda, the small, icy body (~480 km diameter) whose bizarre surface features amazed planetary geologists. Could it be that this rather freakish object, like Jupiter's satellite Io, has a major impact on the magnetosphere? The Voyager science teams were quick to make such associations. Although the surface of Miranda shows a history of considerable geological activity there is no evidence of a means of producing material (such as Io's volcanic plumes) and at low temperatures it is unlikely that the satellite is electrically conducting.

Thus the truth may be that Miranda's role is no more exotic than that of other satellites, and that the moon is limited to sweeping up energetic particles. In particular, the ~5 R_U boundary in the plasma data is more likely to be a convection boundary (J. Richardson, MIT). Inwardly increasing plasma densities and temperatures result in significant radial

* American Geophysical Union, Baltimore, Maryland, 19–22 May 1986.

pressure gradients. These essentially deflect the sunward flow and the flux tubes of hot plasma are swept around the inner region to the sunlit side. The plasma inside is then shielded from the electric fields associated with solar wind-driven circulation patterns. Alternatively one can think of the convection boundary being located where there is insufficient energy in the convective process to overcome the atmosphere/ionosphere drag (effectively electrical resistivity) at the ends of the flux tubes.

The solar wind deforms the outer magnetosphere ($>18\ R_U$) 'downstream' of Uranus to produce a magnetotail (cylindrical radius $\sim 42\ R_U$) extending behind the planet. The magnetotail is split into two lobes of oppositely directed field lines separated by a ($\sim 10\ R_U$ thick) central plasma sheet which, as the rotation axis of Uranus is presently pointed essentially sunward, rotates with the planet every 17.24 hours.

Although not observed until the spacecraft was close to the planet, radio emission from Uranus is quite powerful (of the order of megawatts), between Earth and Saturn in emission strength and exhibits a complex spectral morphology with at least 5 different types of emission (M. Kaiser, GSFC). The peculiar geometry at Uranus may also explain why radio emission has not been detected from Earth since Larry Brown's observations in 1971. The most powerful radio bursts are thought to be beamed at low magnetic latitudes so that one would only detect uranian emission on Earth for a small fraction of the uranian 84-year orbital period. The next opportunity arises in 1994. At lower frequencies the plasma wave experiment detected local plasma waves (called Whistler-mode hiss and chorus), familiar from the magnetosphere of Earth, Jupiter and Saturn (F. Scarf, T.R.W. Inc.). These waves are thought to be in cyclotron resonance with energetic electrons which are then scattered by the waves so that they stream along the magnetic field lines into the planet's atmosphere, providing a source of energy for the nightside aurora.

The fundamental question of how the dynamo of Uranus can sustain such a rotational asymmetric magnetic field remains unanswered. Instead, a revised scaling law has been proposed (S. Curtis and N.F. Ness, GSFC) which predicts planetary magnetic fields based on the balance of coriolis and Lorenz forces in the core. A surface field of 0.5 Gauss is predicted for Neptune which would ensure a magnetic sphere large enough to encompass Triton. But after Uranus, serious predictions of the orientation of such a field are much harder to come by. □

Fran Bagenal is in the Blackett Laboratory, Imperial College, London SW7 2AZ, UK.

Oceanography

Predictability of El Niño

from S.G.H. Philander

THE unusually high sea-surface temperatures in the tropical Pacific Ocean during El Niño, and the associated major changes in the atmospheric circulation — which include devastating droughts in some regions and torrential floods in others — can cause economic and ecological disasters[1-5]. Recent calculations indicate that some El Niño events could have been predicted several months in advance, either by statistical analysis of past data[6], or by using a dynamical model to determine whether the inertia of the ocean at a given time predisposes it to certain developments[7]. On page 827 of this issue[8], Cane, Zebiak and Dolan devise a model that extends predictability to approximately one year by taking interactions between the ocean and atmosphere into account. This relatively simple model appears remarkably successful, but its neglect of various physical processes could result in inaccurate predictions under certain circumstances. The predictions made during the first part of 1986 may turn out to be unreliable.

The changes in sea-surface temperatures and other oceanic conditions during El Niño are caused primarily by changes in the surface winds over the tropical Pacific[9]. A general circulation model of the ocean, forced with the winds that prevailed over the tropical Pacific during 1982 and 1983, realistically simulates all the major oceanic changes observed during that period[10]. The changes in the surface winds during El Niño are in turn part of the atmospheric response to the sea-surface temperature variations associated with the event. A general circulation model of the atmosphere realistically reproduces the interannual atmospheric variability (including the El Niño events) observed in the tropics between 1962 and 1976, provided observed sea-surface temperature variation in the tropical Pacific during that period are imposed as a lower boundary condition[11].

There have been similar simulations of the atmospheric changes during the El Niño of 1982–1983 (ref. 12). These circular oceanographic and meteorological results imply that interactions between the ocean and atmosphere are at the heart of El Niño phenomena. Such interactions have not yet been explored with the general circulation models I have just mentioned; but the use of much simpler models[13-15] indicates that the interactions are unstable, as first suggested by Bjerknes[16]. Thus, a slight change in the atmosphere induces an oceanic response which in turn affects the atmosphere in such a manner as to reinforce the original atmospheric change. Relaxation of the trade winds, for example, can cause warming of the central and eastern tropical Pacific which alters the atmospheric heating so as to cause a further weakening of the trades. This is how unstable air–sea interactions amplify a modest initial perturbation into an El Niño.

Once El Niño conditions prevail, another perturbation can initiate unstable interactions that reverse the warming trend, thus re-establishing low sea-surface temperatures in the eastern Pacific[17]. These unstable air–sea interactions depend on the manner in which sea-surface temperature variations affect the heating of the atmosphere. They are strongly modulated by the seasonal cycle because the seasonal movements of the atmospheric convergence zones determine when and where warm sea-surface temperature anomalies can cause a local heating of the atmosphere. It is for this reason that most El Niño events start as an amplification of the warm phase of the seasonal cycle in the eastern equatorial Pacific[2]. The essence of El Niño is therefore the amplification of pertubations by unstable air–sea interactions which are modulated by the seasonal cycle. A simple stochastic model[18] that incorporates these elements produces time-series in which El Niño events are as intermittent as in reality. (The dominant timescale is of the order of four years.) In this model the perturbations are assumed to be random and to represent atmospheric disturbances not attributable to interactions between the ocean and atmosphere. These include waves with a periodicity between 30 and 60 days observed in the tropics; disturbances that propagate into the tropics from higher latitudes; and variability induced

100 years ago

SMALL gelatinous masses that annually, about this time, cause the sea-water to become what fishermen call "foul", are now in great abundance on this coast. A pocket lens makes evident the presence of large specimens of the diatom *Eucampia britannica* that are seen as perfect spirals, some of which have four or five complete turns, and also some filamentous rods. Microscopic examination of the sediment deposited in the course of a few hours enables one to see *Rhizosolenia, Asterionella,* and several other diatoms whose names are not known to me. It will be interesting to know how far round our shores at the present time these organisms extend, and I hope, by thus again directing attention to them, that some one more competent than myself will be led to investigate their life history.

Sheerness W.H. SHRUBSOLE

From *Nature* **34,** 168; June 24, 1886.

by interannual changes in soil moisture and snow cover over continents.

A very different explanation for the irregular period between El Niño events invokes the long memory of the ocean as the principal source of perturbations[19-21], assigning random atmospheric perturbations a minor role. In this model, the oceanic response to wind variations during El Niño does not end when the event ends but continues in the form of waves that slowly propagate westwards in off-equatorial latitudes. On reaching the western boundary of the ocean basin the waves give rise to renewed equatorial disturbances which, through unstable air–sea interactions, again amplify into a new El Niño. The interval between El Niño events is essentially the transit time of the waves, which in models of this type is of the order of three to four years. Some of the models[19,20] are very periodic, but that of Cane and Zebiak[21] is like an irregular nonlinear oscillator and produces time-series almost as aperiodic as those which are observed. But fluctuations with periods less than that of the seasonal cycle are far less energetic in the model than in reality because processes other than air–sea interactions that contribute to atmospheric variability are not considered.

The experimental predictions reported in this issue by Cane, Zebiak, and Dolan[8] indicate that the atmospheric perturbations that are neglected in their model can cause predictions to diverge significantly after approximately one year. This is shorter than the timescale for the memory of the ocean (the waves) to initiate another event and suggests that the memory is not the dominant factor in determining the interval between El Niño events. The memory nonetheless is important in determining the predictability of the tropical oceans and atmospheres because it predisposes the ocean to behave in a certain manner. For a particular model, the behaviour of the ocean at a certain time can be determined by keeping the winds constant from that time onwards: if the ocean is not in equilibrium with the winds then it has a memory of earlier wind variations and continues to adjust. Inoue and O'Brien[7] find that if their model is forced with realistic winds up to April 1982 then El Niño starts to develop during the subsequent months even if the winds are held constant. In other words, the non-equilibrium state of the ocean in early 1982 predisposed it towards the development of El Niño.

The coupled air–sea model of Cane, Zebiak and Dolan[8] simulates the air–sea interactions that amplify the oceanic tendency associated with its non-equilibrium state to provide a forecast of El Niño almost a year in advance. The predictability of the model is limited by its neglect of atmospheric disturbances not attributable to air–sea interactions. These disturbances are particularly important when the ocean is in equilibrium with the prevailing winds and could mean that the prediction of an El Niño for 1986 is inaccurate. (Early in 1986, sea-surface temperatures in the eastern tropical Pacific Ocean were exceptionally high and El Niño appeared imminent. In mid-March the temperatures started to decrease and in May conditions looked essentially normal.) Reliable predictions require not only improved models of air-sea interactions but also a better understanding of and an ability to simulate the high-frequency atmospheric fluctuations. □

S.G.H. Philander is in the National Oceanic and Atmospheric Adminstration/Geophysical Fluid Dynamics Laboratory, Princeton University, Princeton, New Jersey 08542, USA

1. Rasmusson, E.M. & Wallace, J.M. *Science* **222**, 1195 (1983).
2. Philander, S.G.H. *Nature* **302**, 215 (1983).
3. Gill, A.E. & Rasmusson, E.M. *Nature* **305**, 229 (1983).
4. Barber, R.T. & Chavez, F.P. *Science* **222**, 1203 (1983).
5. Schreiber, R.W. & Schreiber, E.A. *Science* **225**, 713 (1983).
6. Barnett, T.P. *Mon. Weath. Rev.* **112**, 1403 (1984).
7. Inoue, M. & O'Brien, J.J. *Mon. Weath. Rev.* **112**, 2326 (1984).
8. Cane, M.A. & Zebiak, S.E. & Dolan, *Nature* **321**, 827 (1986).
9. Wyrtki, K. *J. phys. Oceanogr.* **5**, 572 (1985).
10. Philander, S.G.H. & Seigal, A.D. in *Coupled Ocean-Atmosphere Models* (ed. Nihoul, J.) 517 (Elsevier, Amsterdam, 1985).
11. Lau, N.-C. *Mon. Weath. Rev.* **113**, 1970 (1985).
12. Boer, G.J. in *Coupled Ocean-Atmosphere Models* (ed. Nihoul, J.) (Elsevier, Amsterdam, 1985).
13. Philander, S.G.H. & Yamagata, T. & Pacanowski, R.C. *J. atmos. Sci.* **41**, 604 (1984).
14. Gill, A.E. in *Coupled Ocean-Atmosphere Models* (ed. Nihoul, J.) 303 (Elsevier, Amsterdam, 1985).
15. Hirst, A. *J. atmos. Sci.* **43**, 606 (1986).
16. Bjerknes, J. *Mon. Weath. Rev.* **97**, 163 (1969).
17. Philander, S.G.H. *J. atmos. Sci.* **42**, 2652 (1985).
18. Lau, K.-M *J. atmos. Sci.* **42**, 1552 (1985).
19. McCreary, J.P. *Mon. Weath. Rev.* **111**, 370 (1983).
20. Anderson, D.L.T. & McCreary, J.P. *J. atmos. Sci.* **42**, 615 (1985).
21. Cane, M.A. & Zebiak, S.E. *Science* **228**, 1085 (1985).

Acid rain

Predictions and applications

from Nurtan A. Esmen

ACID rain, a controversial phenomenon which has attracted much recent attention, has nevertheless been ignored by many scientists who are interested in fundamental transport processes. Hence, experimental and theoretical studies of rain acidification have been more or less repetitious, albeit in different locations. Although some rigorous theoretical work has been done in the past decade, field verification of theoretical results has been at best incomplete. This scarcity results from the difficulties associated in measuring simultaneously the size and the acidity of raindrops using the conventional instruments of aerosol physics or meteorology. A new instrumental development reported by S.J. Adams *et al.* elsewhere in this issue (*Nature* **321,** 842; 1986), and the authors' preliminary measurements of raindrop acidity using the instrument, is good news for those interested in the problem of acid rain.

The new instrument, although ingenious, would be of limited interest if it were to apply only to one narrow area of research. Because the instrument, described in fuller detail elsewhere (Bradley, S.G. *J. Tech.* **2,** 190; 1985), can obtain good results under non-ideal conditions, it will be of interest in, for example, agricultural research on effective watering systems, chemical engineering and combustion equipment design.

The preliminary results of droplet size-dependent rain acidity reported by Adams *et al.* are intriguing. Besides the fact that they are the only such measurements that exist, and that they seem to verify qualitatively an existing theory of steady-state raindrop–gaseous pollutant interactions, they also point to significant gaps in our understanding of both local and global influences on rainwater acidity. If the experimental results of Adams *et al.* are found in other sites, several hypotheses could be generated. For example, strong dependence of removal efficiency on raindrop size suggest that interactions between the mainly small drops of a drizzle and acid-producing gases such as sulphur dioxide would have significantly different consequences compared with the interaction between the same gas and the mainly large drops of a rain shower. Such an observation, if verified in different circumstances, opens up new areas of research into the effects of acid rain.

The results of Adams *et al.* also suggest that throughout a period of rainfall there is significant depletion of the local pollutant concentration. Thus, extended measurements using their new method may uncover a relationship between the variables of rain, in-cloud removal and below-cloud removal of contaminants. If such a relationship is found, past and new data can be corrected to factor-out local influences, allowing global transport of contaminants to be reanalysed on a uniform basis. Although we have a fairly good grasp of large-scale transport, important details are still missing and the predictive capacity of the available models is limited. The accident at the nuclear reactor at Chernobyl in the Soviet Union provides an example of the use to which such models, if accurate, could be put. □

Nurtan A. Esmen is Professor of Industrial Environmental Health Science at the Graduate School of Public Health, University of Pittsburgh, Pennsylvania 15261, USA.

Archaean gold

Exploring for magmatic origins

from Neil Williams

ACCORDING to the 6 June issue of *Mining Journal*, gold mining is enjoying a period of accelerating growth, with the production of gold in the Western World reaching a 14-year high of 1,213 tonnes in 1985. This growth has triggered a high-technology gold rush and modern mineral explorers are retracing the steps of the old-time prospectors in the search for new El Dorados. Academics are also catching gold fever, but the findings of their research are often far from academic. For example, the report elsewhere in this issue by D.R. Burrows, P.C. Wood and E.T.C. Spooner (*Nature* **321**, 851; 1986) will leave many explorers wondering about the validity of some of the principles that are used in guiding their search for new gold deposits.

The article is controversial because it concludes that Archaean-age gold–quartz vein systems formed from magmatic fluids that originated from molten granite-like bodies deep beneath the surface of the Earth. This is contrary to the widely held view that the systems were deposited from metamorphic fluids, that is, from fluids that formed during the dehydration of wet sedimentary rocks as they were buried, heated and converted to metamorphic schists and gneisses. The controversy cannot be ignored because it surrounds the origin of a highly prized class of gold deposits that includes the main subject of the article, the Hollinger–McIntyre vein system in Ontario that produced nearly 1,000 tonnes of gold, as well as the fabulous Golden Mile system at Kalgoorlie, Western Australia, that has so far produced around 1,200 tonnes.

Why should someone seeking new Archaean gold–quartz vein deposits need to worry about the origin of mineralizing fluids that flowed through the Earth's crust more than two and a half billion years ago? To answer this question we must consider where new deposits are likely to occur, and how mineral explorers go about finding them. Most of the gold deposits discovered during the original gold rushes were exposed at the Earth's surface and were found because they had shed trails of alluvial gold that were easily traced by simple prospecting methods. Although these same methods still lead to an occasional discovery, most deposits not yet discovered have gone undetected because they are buried and have no surface expression.

The challenge in exploration is therefore to use methods that can unravel the subsurface geology of an area and accurately pin-point the position of buried mineralization. Methods that are widely used today include satellite and airborne images that give a broad geological overview of the areas being explored; various airborne and ground-based geophysical methods that provide data on the magnetic, electrical and mineralogical properties of the rocks being investigated; and sensitive chemical tests that are able to detect the subtle chemical haloes that often envelop mineralization. However, none of these high-technology methods are of any value if the areas in which they are used were never mineralized, and to maximize the chances of discovery the explorer must therefore pay particular attention to selecting the most attractive ground possible. Many methods of ground selection may be used but nearly all rely to varying degrees on conceptual models.

These models attempt to describe, as accurately as possible, the sequence of events that leads to the formation of the type of mineral deposit being sought. The models bring together information from many different sources but are constructed primarily from empirical observations of known mineral deposits and theoretical and laboratory studies of the relevant ore-forming processes. The explorer uses the models to identify those geological features that are critical to the formation of the mineralization being modelled, and he or she tries to select areas for exploration that exhibit as many of the critical features as possible. If the model is accurate, it is clearly of great value in identifying the appropriate geological features, but if it is flawed and misidentifies a critical feature, subsequent exploration may be doomed to failure.

A typical model has three primary elements — a source for the mineralizing components, a site for the deposition of the ore minerals and a transport mechanism that transfers the mineralizing components from their source to the site of deposition. The metamorphic- versus magmatic-fluid debate being fuelled by Burrows *et al.* has an important implications for both the source and transport elements of exploration models for the Archaean quartz–gold vein deposits. If a metamorphic fluid is used it will lead explorers away from intensely metamorphosed terrains, where the fluids would have been generated, and into terrains of weaker metamorphism through which the fluids would have passed as they moved away from their source.

By contrast, if a magmatic-fluid model is used, it will lead explorers to seek out areas that are underlain by the appropriate granitic rocks. These may be the same terrains of weaker metamorphism that were highlighted by the metamorphic model, but they could equally well be the regions of intense metamorphism that would have been avoided using the metamorphic model.

Although we cannot be certain of the final outcome of the magmatic- versus metamorphic-fluid debate, we can be fairly certain that the article by Burrows *et al.* will not be the last word on the subject. As so often happens in stable isotope studies of mineral deposits, the carbon isotope data the authors use are likely to be reinterpreted by those favouring alternate views, and additional research will be needed to refine our understanding of Archaean quartz–gold vein mineralization and enhance our ability to explore efficiently for new examples of this important type of gold deposit. □

Neil Williams is Manager — Consulting Services Carpentaria Exploration Company Pty. Ltd, PO Box 1042, Brisbane, Queensland 4001, Australia.

Mathematics

Counting costs of calculation

from Ian Stewart

THE distinguished computer scientist Donald Knuth once remarked that a major difference between mathematics and computer science is that mathematicians do not, on the whole, worry about the cost of an algorithm — solution of a problem is paramount and the efficiency of the method is a secondary consideration. An entire new subject, complexity theory, has developed on the borders of mathematics and computer science to analyse just these questions. Until recently, the main concern of complexity theory has been discrete problems, although some of the tools used have evolved from continuous mathematics. But now a parallel effort on the complexity of algorithms for continuous problems is appearing. A recent article by Steve Smale (*Bull. Am. Math. Soc.* **13**, 87; 1985) surveys this emerging area and goes so far as to suggest that a new concept of algorithm is required fully to understand such problems.

It has occasionally been suggested that the advent of computers will put mathematics out of business. Presumably the basis for this assertion is the idea that the computer can calculate anything that is

needed more quickly and more accurately than a human mathematician.

This is no doubt true but it has little bearing on the status of mathematics, because most interesting problems require a good deal more than brute calculation. On the contrary, the use of the computer raises new mathematical questions. The work already in existence exhibits a remarkable interaction between the theory of computation and both classical and modern mathematics. Computers enhance the capabilities of the mathematician but they are unlikely to render him or her obsolete.

Smale's survey begins by quoting a remark by Von Neumann made around 1950, to the effect that the then current theory of digital automata was "combinatorial rather than analytical" and calling for a "detailed, highly mathematical and more specifically analytical" theory.

Smale notes that although numerical analysis has made a strong contribution to such questions, it more often concerns itself with the asymptotic efficiency (for example, rate of convergence) of an algorithm than with its average efficiency or total cost. He says: "A study of the total cost for algorithms of numerical analysis yields side benefits. It forces one to consider global questions of speed of convergence, and in so doing one introduces topology and geometry in a natural way into that subject. I believe that this will have a tendency to systematize numerical analysis. This development could turn out to be comparable to the systematizing effect of dynamical systems on the subject of ordinary differential equations over the last twenty-five years."

Smale's previous work on topological dynamics has played a major part in the 'systematization' of differential equations that he refers to, and his remark is an understatement. The topological methods of dynamical systems theory have opened up a vast field of non-linear mathematics, currently a major growth area for research in several branches of science. A comparable development in numerical analysis would be of major importance.

The kinds of problem that Smale has in mind are drawn from numerical analysis, operations research and 'continuous' classical mathematics, for example, finding a zero of a polynomial of a system of non-linear equations. He cites one example which "a numerical analist might give against the theoretization of his subject". The usual way to solve simultaneous non-linear equations is to pick an initial value at random (or by experience), use some iterative approximation method such as Newton's, and apply it for a while. If it doesn't work, pick a new initial guess and repeat, continuing until something does work. At first sight this does not look like a formal procedure amenable to rigorous analysis, but it is possible that a mixture of probability theory and dynamics might be able to do this. Shub and Smale (*SIAM Journal of Computing*, in the press) show that for polynomials in one complex variable, this method requires on average only six random choices.

Another problem is linear programming — maximization of a given linear function of many variables subject to linear constraints. Consider a factory that makes different products subject to various costs trying to maximize profit by varying the quantities made. Until very recently the standard practical method for such a problem was an algorithm developed by George Dantzig, called the simplex method. In practice, it is observed that this algorithm 'usually' runs very efficiently, but that 'occasionally' it can take an enormous time to obtain an answer. Smale has made this observation precise, and proved it (*Math. Programming* **27**, 241; 1983 and *Mathematical Programming, The State of the Art* (eds. Bachem *et al.* Springer, New York 1983). (A more recent algorithm, due to Kamarkar, holds the promise of running efficiently under all conditions.)

In elementary calculus, three standard methods of approximating integrals are often discussed: the Riemann sum; the trapezoidal method; and Simpson's rule. Smale's survey includes an analysis of these methods and their costs, confirming the results of experience. On average, the trapezoidal method costs half as much as the Riemann approximation; Simpson's rule is much cheaper (in a sense that can be quantified precisely) than either.

A topic that is attractive both to the numerical analyst and to the topologist is Newton's method for finding a zero of a function $f(z)$. This takes a guess z and transforms it into $N_f(z)=z-f(z)/f'(z)$. If iteration of this procedure converges, the result is a good approximation to a zero of f. In fact, it does not always converge: this is related to the dynamics of the transformation N_f. A study of such phenomena, even when f is as simple a function as a polynomial, leads into deep and intricate 'pure' mathematics.

In closing, Smale singles out a key test problem for the field: what is the most efficient way to find zeros of a polynomial? He notes that merely to prove the existence of zeros of polynomials requires the development of complex numbers not only to find the zeros, but also to explain what manner of beast they are. A solution to the test problem similarly requires the development of a general concept of algorithm that, because of the way continuity is involved, may well go beyond the current combinatorial concept.

Ian Stewart is at the Mathematics Institute, University of Warwick, Coventry CV4 7AL, UK.

Geophysics

Looking for missing xenon

from Minoru Ozima

How can we determine the bulk chemical composition of the Earth? Analysing the right rocks tells us about the uppermost few hundred kilometres, and below this various indirect techniques can provide some constraints on the bulk physical properties, such as density. But for the past two decades, the composition of the Earth has been derived by analogy with that of meteorites. The method works well for most elements, with the notable exception of xenon. The usual solution to the problem of the missing Xe has been to propose some terrestrial sink such as shales[1] or ice[2]. But successive laboratory work[2,3] argues against this, and now Bernatowicz, Kennedy and Podosek hammer the point home in their report of measurements of Xe trapped in Antarctic ice[4] — far too little exists to make up the missing xenon. Perhaps we should take another look at the meteorite analogy.

The method of meteorite analogy is based on the assumption that the Sun, planets, meteorite parent bodies and all solid materials in the Solar System condensed from the solar nebula, which was once heated to a vaporized state and was therefore well homogenized. Hence, except for non-condensable volatile elements, the relative abundance of elements condensed on solid bodies is assumed to be quite similar to that in the original solar nebula. This assumption has been supported by observational data on the relative abundance of elements in the Sun's photosphere and by analytical data from meteorites. Once the meteorite analogy is accepted the bulk chemical composition of the Earth (at least of the condensable elements) can be equated to the abundance of elements observed in the solar photosphere and in meteorites (or, more precisely, in carbonaceous chondrites).

The noble gases, apart from Xe, are no exception. A remarkable resemblance between the abundance pattern of noble-gas elements in the atmospheres of terrestrial planets and in meteorites (see figure) is regarded as another successful example of the meteorite analogy. But the Xe discrepancy is usually attributed to some kind of sink, and has not been thought to violate the analogy. For example, Canalas *et al.*[1] suggested shales as the sink: Xe is notoriously 'sticky' and can be easily ad-

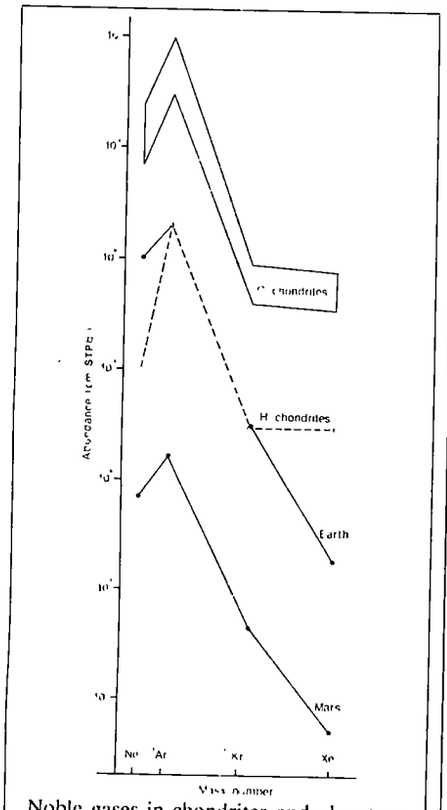
sorbed in porous materials such as shale. But later experiments[3], which examined both the trapped quantities of Xe in shales and the adsorptive capacities of shales for Xe, showed convincingly that this explanation does not account for the missing Xe.

Another suggestion was made by Wacker and Anders[2], who pointed out that because of its highly open structure and large abundance on the surface of the Earth, ice could form a Xe trap. But their own laboratory experiments[2] on adsorption of Xe by ice and the new measurements of Xe abundance in Antarctic glacial ice[4] show that the concentrations of this element fall far short ($<10^{-3}$ in artificial ice and $\sim 10^{-4}$ in Arctic glacial ice) of the amount required for the meteorite analogy to hold. So where is the Xe?

One can still argue that much of the terrestrial Xe remains in the Earth's interior. But because the Xe content in volcanic rocks and in xenoliths is one to two orders of magnitude less than the atmospheric inventory (the total amount of Xe in the air divided by the mass of the Earth), the upper mantle is a very unlikely hiding place. This leaves the deeper mantle or core as the only possible sink.

Yet the whole problem stems from our original assumption of the analogy with meteorites. Perhaps we should therefore question this assumption. It is known that atmospheric Xe isotope composition is distinct from that of the 'planetary' Xe observed in meteorites[5], the latter being thought to represent primordial Xe in the Solar System. Such a large mass-dependent fractionation is very difficult to explain in terms of diffusion loss or gravitational escape. Even more difficult to explain is that although Xe shows such a large isotope fractionation (about 4 per cent per atomic mass unit), lighter noble gases show much smaller (argon) or even opposite (krypton) trends of fractionation. These observations indicate clearly that the origin of noble gases in the Earth is quite different from that in meteorites.

Doubts about the analogy are further augmented by space mission data (see figure) from the atmosphere of Mars: the abundancies of noble-gas elements are quite similar to those for the Earth's atmosphere, with a similar Xe deficiency. An interesting development in this story comes from the observation of Xe in a shergottite meteorite (EETA 79001) which is probably from Mars; the Xe isotope composition is similar to the terrestrial content, but distinct from that of chondrites[6]. At present we do not know the extent of this disparity in the meteorites; but it seems clear that caution should be exercised in applying the meteorite analogy to the terrestrial planets. For example, we may need to question the long-standing 'meteorite game' in which certain types of meteorites are specified as the building blocks of the Earth, as no known meteorites have noble-gas element and isotope compositions that are reasonably related to those in the terrestrial planets. □



Noble gases in chondrites and planetary atmospheres. Planetary atmospheres closely match C-chondrites for Ne–Ar–Kr, but Xe is much depleted in Mars and Earth. C, carbonaceous, H, high-ion; solid circles, planets; open circles, chondrites. (He escapes from the planetary atmospheres and is not shown.) (Ref. 2.)

1. Canalas, R.A., Alexander, E.C. Jr & Manuel, O.K. *J. geophys. Res.* **73**, 3331 (1968).
2. Wacker, J.F. & Anders, E. *Geochim. cosmochim. Acta* **49**, 2561 (1985).
3. Podosek, F., Bernatowicz, T. & Kramer, F. *Geochim. cosmochim. Acta* **44**, 1875 (1980).
4. Bernatowicz, T., Kennedy, B.M. & Podosek, F.A. *Geochim. cosmochim. Acta* **49**, 2561 (1985).
5. Ozima, M. & Podosek, F.A. *Noble Gas Geochemistry* (Cambridge University Press, 1983).
6. Bogard, D.D. & Johnson, P. *Science* **221**, 651 (1983).

Minoru Ozima is at the Geophysical Institute, University of Tokyo, Tokyo 113, Japan.

GTP-binding proteins

One molecular machine can transduce diverse signals

from Henry R. Bourne

ARGUMENT by analogy, like gambling, was once practised behind closed doors. But the increasing recognition of duplicated and diverged genes has elevated it into respectability; it is still a gambler's strategy but, often enough, it works. A prime example of a rich payoff is the understanding of the single molecular machine that mediates vision, olfaction, control of cell proliferation, ribosomal protein synthesis and cellular regulation by a host of hormones and neurotransmitters. In each of its many forms, the machine is a guanine nucleotide-binding protein that mediates signal transduction through the following sequence of events. On stimulation by a receptor protein, it releases GDP and binds GTP. In its GTP-bound conformation, it regulates the function of an effector, usually an enzyme or ion channel. Hydrolysis of bound GTP to GDP terminates the regulatory effect of the G protein.

As was clear from a recent meeting* the power of molecular cloning and site-directed mutagenesis, combined with painstaking biochemistry and considerable luck, is revealing a rapidly expanding list of members of the three related families of GTP binding proteins: the G proteins; the *ras* proteins; and elongation factors (such as bacterial EF-Tu) and related proteins involved in protein synthesis. Moreover, now that the innards of the GTP-binding machine are laid open to inspection, we can begin to understand its action (see bold text opposite).

The heterotrimeric G proteins contain three distinct chains — an α-chain that binds GTP and determines the specificity of the proteins for its detector and effector, and a β/γ complex that probably serves as an anchor to the cytoplasmic face of the plasma membrane. A recent frenzy of molecular cloning in many laboratories has identified complementary (c)DNAs encoding at least eight different α-chains, twice the number of biochemically purified G proteins. One of the latter, transducin, has been purified from outer segments of the photodetector rod cells in bovine retina. Oligonucleotides based on its amino-acid sequence led to isolation of not one, but two transducin α-chain (α_t) cDNAs. Antibodies directed against deduced α_t peptide sequences reveal that one α_t-chain is expressed exclusively in rods (responsible for night vision) and the other in cones, the colour detector cells (J. Hurley, University of Washington). In each case, activated transducin stimulates a cyclic GMP phosphodiesterase (PDE).

Molecular cloning now shows that the two different α-chains of G_s, a G protein that stimulates adenylyl cyclase in response to many hormones and neuro-

*G Proteins and Signal Transduction, 30 May - 4 April 1986, Cold Spring Harbor, New York.

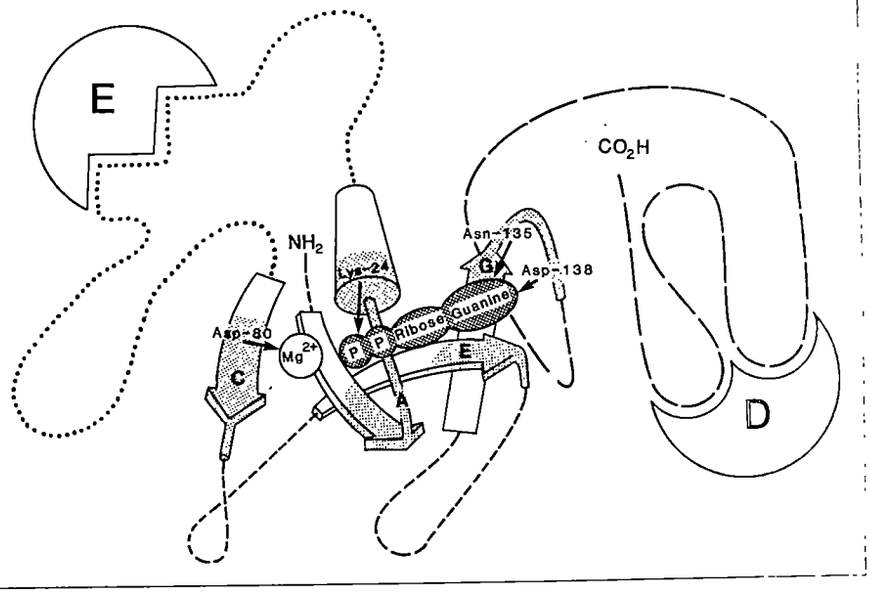
Clues to the mechanism of action

The crystal structure of the guanine nucleotide binding domain of EF-Tu (F. Jurnak, University of California, Riverside; M. Kjeldgaard, Arhus University) reveals a GDP molecule nestled in a partly open site that is bounded by a series of turns between β-strands and α-helices (see figure). Short stretches of amino-acid sequence in four of these regions, cross-hatched in the figure, exhibit close homology with sequences in p21 and the G protein α-chains; following Halliday's[9] nomenclature, the regions are designated A, C, E and G. The bound GDP molecule appears to be fixed in position by the side chains of four key residues. Asp 80 (region C), which fixes the β phosphoryl via an interposed Mg^{2+} ion; Lys 24 (region A), also coordinated with the phosphoryls of GDP; and Asn 135 and Asp 138 (region G), which respectively bind the keto and amino substituents of the guanine ring. Replacement of GDP by GTP is thought to increase the distance between Asp 80 and residues that bind the guanine ring, enhancing the affinity of the protein for effector molecules.

Extrapolated to p21, this picture rationalizes the effects of mutations that affect the handling of guanine nucleotides by the protein. Mutational replacements of Gly 12 in p21 (in the middle of the A region, near the phosphoryls of the bound nucleotide) were already known to stabilize the GTP-bound conformation of the protein to enhance its capacity for malignant transformation. Two additional mutations in p21 (I. Sigal, Merck Sharp & Dohme Research Laboratories) perturb binding of guanine nucleotides in different ways and also enhance its activity: replacement of the lysine corresponding to Lys 24 of EF-Tu by asparagine enhances the rate at which GDP is exchanged for GTP. Replacement by alanine of the aspartate corresponding to Asp 138 of EF-Tu markedly reduces the affinity of p21 for both GDP and GTP, but increases its ability to stimulate yeast adenylyl cyclase, presumably by allowing the mutant protein to relax into an active conformation.

If binding of GTP induces an active conformation of the region that binds effector (E in the figure), where is the effector binding site located? Two clues suggest that it is situated somewhere between regions A and C (dotted line). First, the region between A and C in EF-Tu participates in the GTP-dependent binding of aminoacyl transfer RNA. Second, mutational replacement of residues in a short stretch (between positions 32 and 40 of p21) of the corresponding region of p21 reduces the biological effects of the protein without noticeably altering its known biochemical interactions with guanine nucleotides (Sigal). It is not yet known whether this region constitutes a specific effector recognition site, and whether the much larger domain of the G protein α-chains (140 residues, compared with 40 or less in EF-Tu and p21) interacts with their respective effectors. Comparisons of the sequence of the putative effector region in p21 to deduced sequences in other *ras*-like molecules lead to the prediction (Sigal) that R-*ras* and the p21 products of the three known *ras* oncogenes will be found to interact with a common set of effector molecules, but that *ral* and *rho* will not.

It is attractive to postulate that the detector (D) binding regions of p21 and the G protein α-chains are distal to the G turn in the guanine nucleotide binding site (long dashes). The carboxyterminal 25 residues of the α-chains are a strong candidate for a detector binding region. This region, which I reported to have the predicted secondary structure of an amphipathic α-helix, contains the cysteine whose modification by pertussis toxin prevents coupling of G_i and transducin to their respective receptors.



transmitters such as β-adrenergic amines, result from alternative splicing of the transcript of a single gene (A. Gilman, University of Texas). G_s probably mediates olfactory transduction as well, as odorant stimuli stimulate GTP-dependent cyclic AMP synthesis in olfactory epithelia of the rat (R. Reed, Johns Hopkins School of Medicine) and the frog (D. Lancet, Weizmann Institute). Further evidence for the role of G_s in olfaction comes from a study[1] of patients with pseudo-hypoparathyroidism (PHP), an inherited disease of hormone resistance caused by a generalized partial deficiency of G_s activity[2,3]. Compared with normal subjects, each of five G_s-deficient PHP patients are unable to identify common odorants[1].

Complementary DNAs encoding α-chains of two other purified G proteins, G_i and G_o, have been cloned. G_i mediates inhibition of adenylyl cyclase by receptors for several hormones and neurotransmitters (for example, muscarinic agonists and somatostatin) and is a substrate for pertussis toxin-catalysed ADP-ribosylation, a covalent modification that uncouples G_i from its receptors. Another substrate is G_o, the predominant G protein of mammalian brain. The function of G_o is unknown, except that it can interact with muscarinic receptors *in vitro* (P. Sternweis, University of Texas). Now, comparisons of cDNAs from several laboratories indicate that bovine brain (T. Nukada, Kyoto University; E. Neer, Harvard University) and C6 rat glioma cells (Y. Kaziro, University of Tokyo) express, in addition to α_o, at least two distinct α_i-chains. Furthermore, a cDNA library derived from rat olfactory epithelium contains two cDNAs encoding α-chains not yet identified with any known G protein (Reed).

The unexpected cornucopia of α-chains challenges investigators to determine whether they transduce signals to different effectors. Two prime candidates are ion channels, such as the cardiac K^+ channel that is regulated by ligands via a pertussis toxin-sensitive G protein (G. Szabo, University of Texas) and phospholipase C (PLC), the enzyme that triggers the phosphoinositide cascade which results in increased intracellular Ca^{2+} and activation of protein kinase C (ref.4). G proteins that regulate PLC are sensitive to pertussis toxin in some tissues. Recombinant-DNA produced α-chain polypeptides and chain-specific antisera will help to assign G proteins to specific functions.

Evolution has also produced variants of the other two chains of the G protein heterotrimer. Complementary DNAs from bovine retina (M. Simon, Caltech) and brain (Nukada) predict the primary structure of a β-chain, but fail to account for an immunologically distinct β-polypeptide found in most tissues (but not in rod outer segments). A cDNA encoding the γ-chain of transducin hybridizes to a messenger RNA found only in the retina (Simon) but in other tissues there are at least two more γ-chains, distinguishable immunologically and in apparent size (T. Evans, University of Calgary). Molecular cloning will soon establish whether distinct genes encode the multiple β- or γ-chains. If the sole function of β/γ is to anchor the G protein to the membrane, it is puzzling that there should be two or three versions of each polypeptide.

The *ras* protein family includes two *RAS* proteins that control adenylyl cyclase in yeast and the three p21 proteins that are the products of the mammalian *ras* proto-oncogenes Ha-, Ki- and N-*ras*. Nucleic acid hybridization techniques have recently discovered at least three kinds of *ras*-related proteins, whose functions, like those of several G protein α-chains, are unknown. They include, in descending order of similarity to the known *ras* proteins: human R-*ras*, which has a 26-residue amino-terminal extension not seen in p21 (D. Lowe, Genentech); *ral*, identified in a simian lymphocyte cDNA library (P. Chardin, INSERM); and a subfamily (three genes in man, two in yeast) of *rho* proteins (P. Madaule, Columbia).

Experiments reported by A. Hall (Institute of Cancer Research, London) provide a strong hint that the N-*ras* protein couples receptors for polypeptide agonists to activation of PLC. The date will be published in, and separately commented on, in a subsequent issue of *Nature*.

Of the G protein effector enzymes, PLC is turning out to be harder to handle biochemically than adenylyl cyclase and the PDE of retinal rods, both of which have been purified and functionally reconstituted with the appropriate G proteins and detector components. Fortunately, *Saccharomyces cerevisiae* and the power of yeast genetics may come to the rescue. Feeding glucose to glucose-starved yeast cells causes rapid activation of PLC, production of inositol trisphosphate, and mobilization of intracellular calcium (K. Kaibuchi, DNAX Research Institute). Glucose metabolites, rather than glucose itself, may be the relevant agonists, because non-metabolizable glucose analogues produce no effect. Although preliminary experiments suggest that activation of yeast PLC is GTP dependent, the PLC response is augmented rather than abolished in cells lacking the *RAS* proteins.

Genetic analysis has already elucidated many key features of the yeast adenylyl cyclase signalling system, establishing the G_s-like role of the *RAS* proteins and identifying a potential detector protein, the *CDC25* gene product, which supports Mg^{2+}- and guanine nucleotide-dependent regulation of cyclic AMP synthesis (D. Broek, Cold Spring Harbor Laboratory). Elegant manipulation of the yeast adenylyl cyclase gene (T. Kataoka, Harvard University) has also identified separate catalytic and *RAS*-regulated domains of the catalyst.

Finally, molecular cloning and biochemistry reveal some surprising common structures and turn-off mechanisms among detector components that control mammalian G proteins. The cloning of cDNAs that encode β-adrenoceptors (β-AR), from the hamster (R. Lefkowitz, Duke University)[6] and the turkey (E. Ross, University of Texas; Y. Yarden, Genentech) opens avenues to understanding detector structure and mechanism. Hydropathicity plots of the deduced primary structures of the two β-ARs suggest a common overall structure, shared with retinal rhodopsin[7], in which each protein chain weaves through the plasma membrane seven times, with its carboxy terminus in the cytoplasm and its amino terminus outside.

One would have expected strong conservation of the amino-acid sequence in the putative extracellular and cytoplasmic regions of the two β-ARs, since both mediate interactions with G_s and catecholamines; instead, the transmembrane regions are much more highly conserved than the hydrophilic tails and loops of the two receptors. Because proteolytic studies of rhodopsin show that its third cytoplasmic loop is essential for coupling to transducin (H. Kuhn, Institute for Neurobiology, Jülich), by analogy it is unlikely that the hydrophilic regions of β-AR are irrelevant for signalling between extracellular agonist and intracellular G_s. But perhaps some portions of the agonist or G_s molecules interact directly with hydrophobic intramembrane regions of β-AR, and perhaps intimate contacts in the conserved transmembrane domains are crucial in signalling.

The β-AR also shares with rhodopsin a common biochemical turn-off mechanism, as reported by Benovic *et al.* on page 869 of this issue[8]. Photoexcited rhodopsin (but not dark rhodopsin) was known to be a substrate for phosphorylation by rhodopsin kinase. Now Benovic *et al.* show that an analogous β-AR kinase also phosphorylates photoexcited rhodopsin, probably on the multiple serine and threonine residues that are phosphorylated by rhodopsin kinase in the carboxy-terminal tail of the photon detector protein. To emphasize the homology further, rhodopsin kinase can also phosphorylate β-AR. Each kinase shows some preference for its own signal detector as substrate but both vastly prefer activated detectors (photorhodopsin or agonist-bound β-AR), even in the heterologous reactions.

In retinal rods, phosphorylation of rhodopsin by its kinase promotes its binding to a protein (arrestin or S-antigen) which turns off the photon signal by preventing the detector protein from interacting with transducin. The β-AR kinase probably triggers a similar turn-off of the catecholamine signal, as suggested by a temporal correlation in intact cells between β-agonist-induced phosphorylation of the β-AR and agonist-induced desensitization of the β-adrenergic response. To push the analogy further, is an arrestin-like protein required for turning off phosphorylated, agonist-bound β-AR? Preliminary evidence suggests that the answer is yes: in reconstitution experiments, β-AR kinase-catalysed phosphorylation attenuates coupling of β-AR to G_s; the effect decreases with increasing purity of kinase, however, suggesting that the purification procedure is separating the kinase from an analogue of arrestin (Lefkowitz).

Throughout the meeting, argument by analogy proved a dominant theme. An ideal test for the power of such an approach was provided by the report of a new human oncogene, *mas*. The *mas* open reading frame encodes a protein with a hydropathicity plot that closely resembles that of rhodopsin and β-AR, suggesting that the protein has seven transmembrane domains (D. Young, Cold Spring Harbor Laboratory). Analogy spins from these observations a gossamer web of hypotheses: first, the *mas* protein is a cell surface receptor, like β-AR; second, because its expression produces changes associated with malignant transformation, *mas* detects an extracellular ligand that promotes cell proliferation; third, because its structure resembles those of rhodopsin and β-AR (seven is a powerful cabalistic number), *mas* works by triggering a GTP-binding protein, probably a G, but conceivably a *ras*, protein; protein; and, finally, the GTP-binding protein of *mas* stimulates an effector protein, possibly PLC, that generates second messenger molecules within the cell. Who will bet that *mas* will not fulfill many of these predictions? □

1. Weinstock, R.S., Wright, H.N., Spiegel, A.M., Levine, M.A. & Moses, A.M. *Nature* (in the press).
2. Farfel, Z., *et al. Proc. natn. Acad. Sci. U.S.A.* **78**, 3098 (1981).
3. Spiegel, A.M. & Downs Jr, R.W. *Endocr. Rev.* **2**, 275 (1981).
4. Michell, B. *Nature News and Views* **319**, 176 (1986).
5. Bourne, H.R. *Nature News and Views* **317**, 16 (1985).
6. Dixon, R.A.F. *et al. Nature* **321**, 75 (1986).
7. Newmark, P. *Nature News and Views* **321**, 15 (1986).
8. Benovic, J.L., *et al. Nature* **321**, 869 (1986).
9. Halliday, K. *J. cyclic Nucl. Res.* **9**, 435 (1984).

Henry R. Bourne is in the departments of Pharmacology and Medicine and the Cardiovascular Research Institute at the University of California, San Francisco, California 94143, USA.

Agricultural impact of Chernobyl: a warning

SIR—Since the evening of 30 April 1986, when a series of thunderstorms brought down heavy fallout from Chernobyl along the northern flank of the Alps, we have conducted high-resolution γ spectroscopy measurements on rain water, on a high-efficiency particulate air (HEPA) filter and on various agricultural products from the region around Konstanz (West Germany). Our results on the purely physical aspects of the fallout are comparable to those already published[1,2]. Specifically, from the activity ratio $^{103}Ru/^{106}Ru$ = 4.5(5) and the published values of fission yields, we estimate the age of the Chernobyl core to be 2.0(5) yr. In addition, from a detailed analysis of activities, we infer relative release fractions in six of seven volatility classes and conclude that Chernobyl released core activity in the same proportions as the extensively documented 'reference accident' (PWR2)[3,4]. This putative accident involved core melting and complete loss of containment of a 1,100-MW' (electric) light-water reactor. Our observations are therefore consistent with a core melt at Chernobyl.

In the course of monitoring agricultural products and ground activity around Konstanz, we have noted three aspects of Chernobyl fallout that may have considerable practical importance for agricultural management, both in strongly contaminated regions close to Chernobyl and in many parts of Western Europe.

(1) Fallout from Chernobyl shows extreme geographical variability over short distances, depending on rainfall patterns prevailing when the cloud passed. For example, within the West German state of Baden–Württemberg, a region of ~ 175 × 225 km, gross β activity at ground level, determined uniformly, varied by up to 30-fold (data from the Landesregierung Baden–Württemberg).

(2) Fallout aerosols brought down by rainfall show a high resistance to weathering and drying. In experiments we found that grass dried at 130 ° C for 24 h, followed by vigorous shaking, lost less than 10 per cent of the adhering ^{131}I, $^{132}I/^{132}Te$, ^{134}Cs, ^{136}Cs, ^{137}Cs, $^{140}Ba/^{140}La$, ^{99}Mo, and ^{103}Ru (Fig. 1).

(3) Cutting, drying and storing grass for winter cattle feed will therefore lead to radioactive accumulations in silos and barns. Near Konstanz, where ground activity includes ~ 10^4 Bq m^{-2} of ^{137}Cs (half-life ≃ 30 yr), direct measurement and calculations lead us to expect ~ 0.2–5 mCi of ^{137}Cs in typical small-farm storage facilities. Further east much larger ground activity has been reported and correspondingly larger accumulations are likely.

According to radiation protection laws in most countries, transport and storage of such quantities requires user licences that are normally reserved for a few well-equipped scientific and technological institutions. From a health perspective, the expected accumulations will contaminate barns, lead to significant exposure of farm workers and may pose special threats to children.

The problem of hay accumulation and storage may be all the more acute in view of the recent discovery[1] that fallout aerosols contain 1–2–μm 'hot' β-emitting particles with single-isotope source strengths of 1,000–10,000 Bq. If these are widespread constituents of Chernobyl fallout, they can be expected to be trapped 'permanently' in the lungs of individuals exposed to contaminated hay.

To our knowledge the biological effects of such hot β-emitting particles are not well described. Average dose calculations may not be valid for predicting consequences. Figure 2 shows the results of a sample dose calculation for ^{103}Ru particles of various strengths, and implies a substantial zone of cell lethality at short distances followed by an annulus of very high but non-lethal dose at larger distances. Compared with α-emitting hot particles, the lethal and non-lethal volumes are orders of magnitude larger.

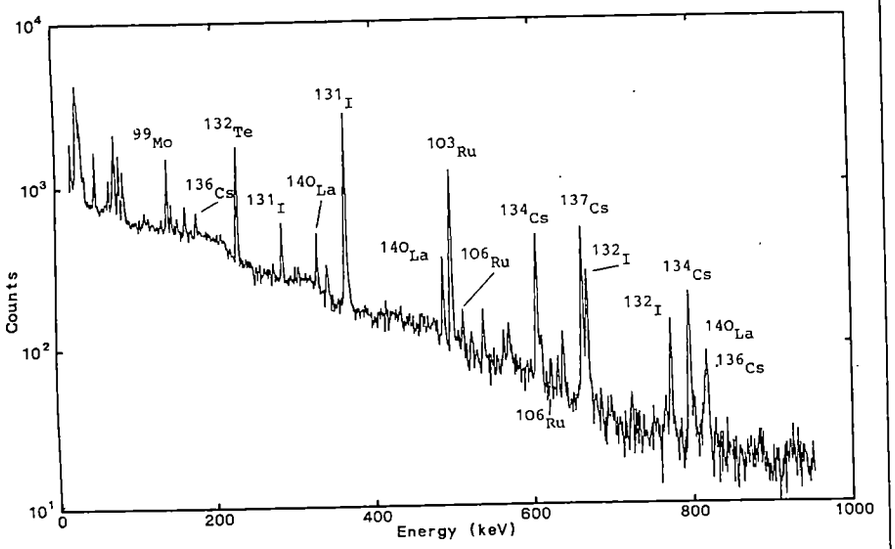


Fig. 1. Gamma-ray spectrum of grass recorded on 10 May 1986 showing dominant isotopes present in adhering particulates.

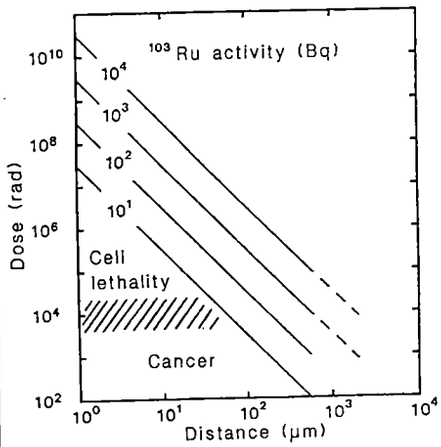


Fig. 2. Local radiation dose as a function of distance from a 1-μm-diameter hot β-emitting particle of ^{103}Ru (half-life ≃ 40 days). The dose assumes integration of the activity over many half-lives, as is appropriate for permanent lung deposition of the particle.

We thank H. Haas of the Hahn Meitner Institute (Berlin) for discussions and the many colleagues and students who participated in recent measurements.

C. HOHENEMSER*
M. DEICHER
H. HOFSÄSS
G. LINDNER
E. RECKNAGEL
J.I. BUDNICK*

Fakultät für Physik,
University of Konstanz,
D-7750 Konstanz, FRG

*Permanent addresses: Clark University, Worcester, Massachusetts 01610, USA (C.H.); University of Connecticut, Storrs, Connecticut 06268, USA (J.I.B.).

1. Devell, L. *et al. Nature* **321**, 192-193 (1986).
2. Fry, F.A., Clarke, R.H., & O'Riordan M.C. *Nature* **321**, 193-195 (1986).
3. US Nuclear Regulatory Commission *Reactor Safety Study* (Wash 1400, NUREG 75/014) (Washington 1975).
4. Lewis, H.W. *et al. Rev. mod. Phys.* **47**, Suppl. 1, S1 (1975).

First assessment of Chernobyl radioactive plume over Paris

SIR—Measurements of the gamma-radioactivity of the surface air in Paris after the Chernobyl accident have shown that the maximum concentrations of ^{137}Cs over a period of three days were 400 times greater than during the worldwide fallout of 1963. Preliminary estimates of ground deposition of ^{137}Cs, amounting to between 2 and 41 mCi km^{-2} (or between 74 and 1,500 MBq km^{-2}), suggest that the recent

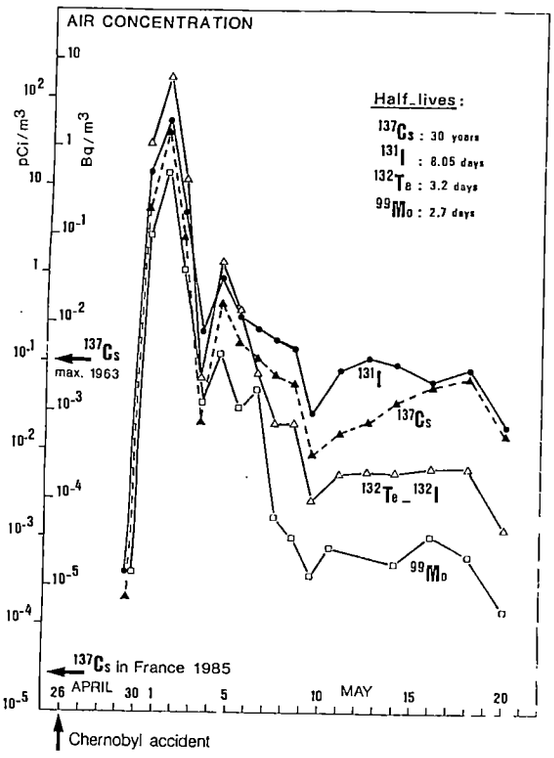


Fig. 1 Concentrations of selected artificial γ-emitters in air filters at Paris.

event is probably comparable in its effects with the global fallout of 1963.

The radioactive plume was first detected over Paris on 29 April (Fig. 1); twenty short-and long-lived nuclides have been detected, and the peak activity (for ^{132}Te) was measured at 170 pCi m^{-3} (6.3 Bq m^{-3}). After three days, the influx of marine air followed by atmospheric washout led to a reduction of the atmospheric activity by three orders of magnitude in the following week. Although some official data were released in France on 8 May, no detailed account of the radionuclide composition of the fallout has previously been published.

In the days after the Chernobyl accident, this institute intensified its routine programme for monitoring air and rain composition. Ground-level air was filtered daily (at 110 m^3 s^{-1}) through Whatman EPM-1000 glass-fibre filters. A rain sample was also collected in a pre-acidified plastic bottle coupled to a 1-m^2 collector and was reduced for gamma spectroscopy to a volume of 30 cm^3. (The slow evaporation used in this treatment probably causes some loss of iodine, but experience has shown that the analysis for other materials is reliable. Similarly, the high percentage of gaseous or desorbable iodine[1] means that the measurements of the activity collected on particle filters probably underestimate the atmospheric content of radioiodine by a factor of between 2 and 5.) Gamma-spectroscopy was carried out with a low-level, high-purity Ge detector (with 32% efficiency and sensitivity of 1.8 keV at 1,332 keV).

Unusual radionuclides (^{99}Mo, ^{131}I) were first detected in the air filters on 29 April. Maximum concentrations were reached between 1 and 2 May, coinciding with the maximum of atmospheric dust (0.11 mg m^{-3}). Between 2 and 4 May, the concentrations of all the measured radionuclides decreased in parallel, at a rate independent of their half-lives; with the arrival of an Atlantic air mass and the rainfall (0.1 mm) associated with a small storm on 3 May, when the atmospheric dust content fell to 0.02 mg m^{-3}. The general decline of activity continued thereafter until 9 May.

The increase in the activity of the long-lived nuclides (^{137}Cs, ^{103}Ru, ^{125}Sb) that we observed between 10 and 19 May probably represents a second passage over Paris of the radioactive plume, with its radioactive content reduced by three orders of magnitude, after a circumnavigation of the Earth. We note, however, that this secondary maximum was not pronounced in respect of ^{99}Mo, ^{132}Te and ^{131}I. Thereafter, atmospheric activity decreased steadily until 21 May, when we ceased our daily monitoring. Throughout our observations, the concentration of cosmogenic ^{7}Be remained constant at 82±22 fCi m^{-3} (3.0±0.8 mBq m^{-3}).

While the largest activities were those corresponding to volatile elements such as iodine, tellurium and caesium, the high concentration of non-volatile elements confirms previous indications[1] that the temperature reached in the reactor must have been very high. Apart from the radioactive elements ^{110}Ag, ^{140}Ba, ^{7}Be, ^{141}Ce, ^{144}Ce, ^{134}Cs, ^{136}Cs, ^{137}Cs, ^{131}I, ^{99}Mo, ^{103}Ru, ^{106}Ru, ^{125}Sb, ^{129m}Te, ^{132}Te and ^{132}I, we also detected short-lived isotopes such as ^{137}U and ^{131m}Te, with activities of 6.3 and 3.1 Bq m^{-3} respectively, and long-lived isotopes such as ^{95}Zr, ^{95}Nb and (probably) ^{51}Cr and ^{124}Sb appeared in the gamma spectra after the decay of the most active short-lived nuclides. Further counting will allow us to make a more accurate determination of the nuclides involved. Although we were not able to arrive at an accurate estimate of the ^{140}Ba/^{140}La activity ratio before equilibrium had been reached, data from early filters confirm the calculation of ref. 1 that the reactor was shut down on 26 April.

During our observations, the radioactive nuclides detected increased and then declined in line with each other. All activities reached a maximum during the period of 23.48 hours spanning 1 and 2 May, but the levels of all the radionuclides increased significantly between the samples collected on 4 and 5 May, usually by a factor of 4 or greater (Fig. 1). This accords with the belief that the original radioactive plume, diluted with the passage of time, was carried over Paris on that second occasion.

Our evidence in support of the suggestion in ref. 1 of the presence of ^{239}Np among the nuclides is more equivocal. Gamma peaks were detected in the 99–106 keV range, but there are many possible sources of interference. Accordingly, we have sought evidence for the presence of the daughter product, ^{239}Pu, by alpha spectroscopy. Our preliminary results suggest that the total concentrations of ^{239}Pu and ^{240}Pu are less than 0.004 mBq m^{-3}. It has separately been reported[2] that during 1984, total 239+240 activity was much smaller (10–40 nBq m^{-3}), so that our preliminary data do not exclude the possibility of a significant enrichment of ^{239}Pu in the air at Paris.

During the sampling period, the activity ratios of pairs of isotopes of the same element showed only small fluctuations about their decay slopes, which has allowed us to calculate the initial ratios ^{132}Te/^{129m}Te=11; ^{135}Cs/^{137}Cs=0.21; ^{141}Ce/^{144}Ce ≃1.4; ^{103}Ru/^{106}Ru=5.4; and ^{134}Cs/^{137}Cs= 0.506. These ratios should provide useful tracers of Chernobyl fallout in future environmental studies.

Deposition during the period of maximum air concentration was estimated from the sample of rain water collected over a period of 86 hours between 29 April and 3 May. Activities in the sampled liquid were particularly high, amounting to 7,400 Bq per litre for ^{132}Te and 700 Bq per litre for ^{137}Cs, for example. We did not attempt to estimate the contribution of dry deposition to these data.

The significance of our measured values of activity of long-lived nuclides such as ^{137}Cs can be estimated by comparison with the maximum atmospheric concentration reached in 1963, after the cessation of major nuclear bomb tests in the atmosphere. Then, ^{137}Cs concentrations at 46° 07′ N reached 3.7 mBq m^{-3} (see ref. 3), less by two orders of magnitude than the

maximum due to the Chernobyl accident at Paris of 1,480 mBq m^{-3}.

Deposition at ground level at Paris during the Chernobyl peak (between 29 April and 3 May) was measured as 74 mBq km^{-2}. Between 29 April and 19 May, a total of 51,786 m^3 of air passed through the filters, giving an average concentration of 90 mBq m^{-3}. During this period, average rainfall was low (18.1 mm). If we assume that the usual deposition velocity of ~1 cm s^{-1} applies, ground deposition at Paris would amount to 1,500 MBq km^{-2}, although it is clear that this result must depend on local weather conditions. In 1963, the average deposition[2] of ^{137}Cs throughout the Northern Hemisphere was ~ 590 MBq km^{-2}. Although this estimate needs to be confirmed by continuing measurements of ground deposition, it seems likely that ^{137}Cs deposition at Paris after the Chernobyl accident will be comparable to that during 1963.

This study was carried out with financial support from CNRS. We thank J. Zhang for help with the gamma spectroscopy.

A.J. THOMAS
J.M. MARTIN
Institute de Biogeochimie Marine,
Ecole Normale Supérieure,
1, rue Maurice Arnoux,
92120 Montrouge, France

1. Devell, L. *et al. Nature* **321**, 192–193 (1986).
2. Cambray, R.S. *et al. Atomic Energy Res. Establ. Harwell Rept.* 11915 (1985).
3. Perkins, R.W. & Thomas, C.W. in *Transuranic Elements in the Environment* (ed. Hanson, W.C.) 53–82 (US Department of Energy, DOE/TIC–22800 (1980).
4. Fry, F.A., Clarke, R.H. & O'Riordan, M.C. *et al. Nature* **321**, 193–195 (1986).

High level radioactive nuclides in Japan in May

SIR—The accidental release of radioactive materials from the Chernobyl nuclear power plant on 26 April 1986 is known to have caused significant pollution in Western Europe at distances as great as 2,000 km. We have been measuring natural and artificial radionuclides in the environment of Japan for the past three decades, chiefly with a network of eleven monitoring stations, from Wakkanai (45.4° N) to Ishigaki (24.3° N), established for the assessment of the effects of atmospheric nuclear bomb tests.

After the detection of radioactivity in Sweden on 28 April, we began to monitor radioactivity in air and water samples. On 3 May, a week after the accidental release, the radioactivity of the surface air and water abruptly increased in the middle of Honshu Island.

Precipitation, airborne particles and gases were collected at the observing station of the Meteorological Research Institute, Tsukuba. Precipitation was collected by a 1-m^2 collector at every precipitation event. Initially, 50-cm^3 portions of the rain were sufficient for the measurement of radioactivity; radioiodine was converted to silver iodide by wet-chemical methods.

Table 1 Activity concentrations in air near ground level at Tsukuba (pCi m^{-3})

Sampling date	Volume (m^3)	Radioactive nuclides ^{137}Cs	^{134}Cs	^{131}I	^{132}I (^{132}Te)	^{103}Ru
26 Apr. – 30 Apr.	5,600	0.00037				
30 Apr. – 3 May	4,600	ND				
3 May – 5 May	2,880	0.64	0.33	4.70	1.65	1.28
5 May – 6 May	1,300	1.53	0.86	6.27	2.60	2.42
6 May – 7 May	1,300	0.50	0.26	2.41	0.76	1.05
7 May – 8 May	1,400	0.87	0.43	3.02	1.01	1.69
8 May – 9 May	1,400	1.46	0.74	4.08	1.36	2.77
9 May – 10 May	1,400	1.64	0.83	3.89	1.47	3.44
10 May – 11 May	1,380	0.09	0.04	0.40	0.04	0.09
11 May – 12 May	1,420	0.25	0.11	0.94	0.10	0.36
12 May – 13 May	1,320	0.16	0.08	0.88	0.06	0.31
13 May – 14 May	1,370	0.28	0.13	1.15	0.10	0.46
14 May – 15 May	1,360	0.27	0.14	0.80	0.07	0.39
15 May – 16 May	1,290	0.00	0.01	0.11	0.00	0.01
16 May – 17 May	1,330	0.07	0.02	0.31	0.00	0.11

Sample was changed at 9:00 a.m., and radioactive decay was corrected to the middle of the sampling period. ND, not determined.

Airborne particles were collected on glass-fibre filters (Toyo GB100R, nominal efficiency 99.9% at 0.3 μm, flow rate 1,000 litres per minute). Filters were changed every morning. Airborne radioactivity, gaseous as well as particulate, was also collected by means of an active charcoal trap (30–60 mesh, 24 mm diameter, 85 mm long, flow rate 8 litres per minute). ^{85}Kr was estimated by cryogenic separation from air samples collected at intervals in an iron cylinder (14 litres, 120 atmospheres) followed by gas-chromatographic purification[1].

Before the abrupt change of atmospheric radioactivity, the concentration of ^{137}Cs ($T_{1/2} \simeq 30$ yr) in the air derived from continuing stratospheric fallout was 0.4 fCi m^{-3} or 14.8 μBq m^{-3}. (In what follows, units of activity have been converted from Ci to Bq by the factor 1 Ci $\doteq 3.70 \times 10^{10}$ Bq.) In the filter sample of 3–5 May, the concentration had increased abruptly to 0.64 pCi m^{-3}, an increase of about a thousandfold, while significant amounts of other radionuclides were detected in the sample. (These were ^{131}I, ^{132}Te, ^{132}I, ^{103}Ru, ^{106}Ru, ^{106}Rh, ^{134}Cs, ^{144}Ce, ^{140}Ba, ^{140}La, ^{99}Mo and ^{99m}Tc.)

The highest concentrations of radioactivity (Table 1), to which ^{131}I was the chief contributor, were found in the sample collected between 5 and 10 May, and persisted for several days. The ^{131}I concentration was about a fiftieth of that observed at Studsvik, Sweden[2]. In the period 3–15 May, the activity ratio $^{137}Cs/^{134}Cs$ was 2.0 ± 0.3, in good agreement with that observed at Studsvik. Airborne radioactivity decreased with an apparent half-life time of three days, until it decreased abruptly after a precipitation event.

The size distribution of particles carrying ^{131}I activity showed a peak at 0.43 μm aerodynamic diameter, and more than half of the total was present in particles smaller than this. Iodine is injected into the atmosphere in gaseous form, and it is of interest to compare the radioactivity of the filter sample with that captured by the charcoal trap. The ^{131}I concentration in the charcoal trap (Fig. 1) in the 5–6 May sample was indeed between 3 and 4 times greater than that of the filter, suggesting that 65–70% of the radioiodine was present in gaseous form eight or nine days after injection, a value slightly less than that derived at Studsvik. In the succeeding 10 days, the ratio of ^{131}I in the trap to that in the filters decreased to ~ 2, suggesting processes for converting gaseous to particulate iodine.

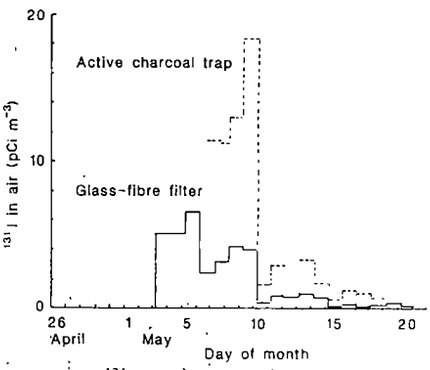


Fig. 1 The ^{131}I concentrations captured by the active charcoal and in the filters.

The level of ^{131}I observed in the surface air is of the same order of magnitude as that seen over Japan[3] after the high-yield nuclear test by the Soviet Union in October 1961, which ranged from 0.02 pCi m^{-3} to 14 pCi m^{-3} (0.74 to 518 mBq m^{-3}).

The concentrations of radionuclides in rain water followed those observed in the atmosphere. During the sampling period, the frontal zone lay along the Japan islands, and the result of the cyclic passage of the pressure drop was that rainfall amounted to 110 mm between 1 and 17 May. The highest concentration of ^{131}I in rain water was found on 5–6 May (163 Bq per litre), after which the concentration decreased steadily. The maximum deposition of ^{131}I was, however, found on 6–7 May, because of the relatively large

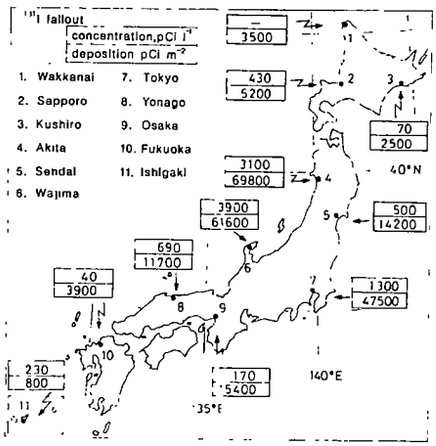


Fig. 2 The ^{131}I concentration in rain water and the deposition at eleven stations in Japan during the period from 1 to 8 May 1986.

amount of precipitation then. It was confirmed chemically that 80% of the dissolved iodine was in the form of iodide, with the remainder as iodate.

The spatial distribution of ^{131}I was determined by the surveillance network of the Japanese Meteorological Agency (Fig. 2). The largest amounts of ^{131}I deposition were on Honshu and amounted to 60 mCi km^{-2} (2,220 MBq km^{-2}). Radioactive material was carried to this region of Japan by the Northern Hemisphere westerlies at a speed of ~ 1,000 km per day, and reached the middle part of Honshu in the west to south-west winds prevailing during this period.

Deposition of ^{137}Cs at Tokyo amounted to ~ 2 mCi km^{-2} (0.074 MBq km^{-2}) from 1 to 17 May, which is ~ 2% of the cumulative ^{137}Cs deposition since 1959 from nuclear tests[4].

Our measurement of ^{85}Kr may be of particular interest because of the large proportions of this radionuclide among the fission products. Before the arrival of the high-level activity from the Chernobyl plant, the atmospheric concentration of ^{85}Kr was 0.93 Bq m^{-3}, but increased to 1.04 Bq m^{-3} on 7 May, falling steadily to the normal concentration within a week. After the Three Mile Island reactor accident, ^{85}Kr was found only in the immediate vicinity; our detection of excess amounts of ^{85}Kr at a distance of 8,000 km from a reactor accident is the first measurement of this kind.

Further information on the accidental release of radioactivity will come from our investigation of alpha and beta emitters in the fallout. The temporal and spatial variation of the radioactivity should give valuable information about transport and scavenging processes in the atmosphere.

We thank the staff of the geochemical laboratory of the Meteorological Research Institute and the weather observation stations of the Japanese Meteorological Agency for their cooperation.

M. AOYAMA
K. HIROSE
Y. SUZUKI
H. INOUE
Y. SUGIMURA

Geochemical Laboratory,
Meteorological Research Institute,
Tsukuba,
Ibaraki 305, Japan

1. Suzuki, Y. *et al. Mem. natn. Inst. pol. Res. spec. Issue* **40**, 462–466 (1986).
2. Devell, L. *et al. Nature* **321**, 192–193 (1986).
3. Miyake, Y. *et al. Pap. Met. Geophys.* **14**, 58-65 (1963).
4. Katsuragi, Y. *Pap. Met. Geophys.* **23**, 1-29 (1983).

Monitoring Minsk and Kiev students after Chernobyl

SIR—In the first few days following the incident at Chernobyl, very little information was available on the size of the release of radioactivity and the potential for further releases. However, the monitoring data from Scandinavia indicated a release significantly greater than that associated with the 1957 Windscale accident. As a consequence, the British Foreign and Commonwealth Office decided to recall British students close to the affected area, mainly from around Minsk and Kiev. The National Radiological Protection Board (NRPB) decided, after consultation with interested parties, to be present at Heathrow Airport, London, to carry out monitoring of the students.

NRPB stressed that the main purpose of the monitoring was to give reassurance to the students, and that we were expecting positive results in our measurements of radioiodine, but at a level that would give no cause for concern. We also hoped that our measurements would provide the first information of activity levels close to the incident area, so permitting some estimate of the severity of the release to be made. The portable radiation monitor for measuring radioiodine in thyroids was demonstrated with an ^{131}I source containing a level of activity equivalent to that which, in a person's thyroid, would give the ICRP annual dose limit for a member of the public.

Travellers from Moscow had their thyroids checked and all were clear of radioiodine. The Minsk and Kiev students were all dressed in British Airways tracksuits with their personal clothing held in polythene bags. It was explained to them that their thyroids would be checked for radioiodine and their clothing for radioactive contamination. When the radiation thyroid monitor was demonstrated and the count rate corresponding to the ICRP annual dose limit indicated, we again stressed that we were not expecting to find this level of activity in their thyroids (see Table 1). The estimates of thyroid radioactivity are given as at the time of measurement, but the original intake of radioiodine has been calculated assuming all of it occurred the same day as the explosion in the reactor. For the Kiev students on the leeward side of the reactor at the time of the accident, this overestimates the initial intake.

In the seven volunteers for monitoring in the mobile laboratory, activity of ^{131}I in the thyroid at the time of measurement varied between 1.9×10^3 and 6.4×10^3 Bq, in good agreement with the estimates of activity made using the hand-held monitors. The committed dose-equivalents to the thyroid were calculated to be in the range of 4 mSv to 14 mSv, or from 8% to 28% of the annual dose limit for the thyroid of members of the public; it was thus possible to tell all the students that the radioiodine content in their thyroids was low and gave no cause for concern.

The monitoring of the clothing for contamination inevitably was more time-consuming. Over 1,000 garments had to be carefully monitored with the monitoring probe in close contact with the surface of the clothing. NRPB staff used Nuclear Enterprise BP7 probes calibrated with a ^{90}Sr source to give 5 counts s^{-1}, corresponding to 1 Bq cm^{-2}. A decision had to be made on the acceptable level of contamination for the particular mixture of fission products concerned, which at that time was unknown. It was thought likely that a significant contribution would arise from the radioiodine and ^{137}Cs and that the critical exposure pathway would be irradiation of skin rather than ingestion. Using published NRPB information[1], an acceptance level of 30 Bq cm^{-2} was adopted.

There remained the problem of determining the count rate for the contamination monitor corresponding to the 30 Bq cm^{-2} for the "unknown" fission product mixture. The equivalent count rate for ^{90}Sr would have been 150 counts s^{-1} and it was decided to reduce this level to 100 counts s^{-1} because of the uncertainties in the exact constitution of the fission-product mixture. Measurements taken since the event have identified the constituents and an assessment of the count rate corres-

Table 1 Thyroid radioactivity of students returning to the United Kingdom

No. of persons	Count rate (counts s^{-1})	Approximate thyroid activity (Bq × 10^3)	Calculated intake at 26 April 1986 (Bq × 10^3)
1	85	6.9	53
1	70	5.6	43
9	50	4.0	30
11	40	3.2	25
33	30	2.4	18
34	20	1.2	9
10	10	0.8	6

ponding to 30 Bq cm^{-2} indicates that 100 counts s^{-1} is appropriate.

A more detailed assessment of the potential hazard presented by the contamination on the clothing, using the known fission products spectrum, has since confirmed that the critical exposure is indeed irradiation of the skin, not the possible ingestion of activity. The monitoring of clothing at Heathrow had established that garments were not extensively contaminated, but that there were isolated spots of contamination. At the clearance limit of 30 Bq cm^{-2}, an isolated spot of activity corresponding to 1.5×10^3 Bq would have passed the screening check for the clothing. This amount of activity if ingested would give rise to a dose of less than 1% of the annual dose limit for a member of the public.

The same spot of contamination on a person's skin would result in exposure to the skin in the immediate vicinity. The Ionising Radiation Regulations 1985, in discussing the assessment of dose from skin contamination, refers to the possibility of averaging the dose over an area appropriate to the circumstances, but in any event not greater than 100 cm^2. The students' contamination was on clothing, not on skin, and the attenuation of the beta radiation by the material, before reaching the skin, would be significant. In addition, the movement of the spot of contamination relative to a specific area of skin would result in lower levels of exposure. In the circumstances, an assumption of 100 cm^2 as an averaging area would seem appropriate. On this basis, the dose to the basal layer of the skin integrated to 12 hours after deposition would result in a dose of 0.5 mSv (or 1/10th the dose received from a dental X-ray to a comparable area of skin) and may be compared with the annual dose limit for a member of the public of 50 mSv.

Most of the clothing showed positive indications of contamination but only 2% of the clothing monitored was in excess of the "clearance" level. Contaminated clothing was put in polythene bags and has since been decontaminated at the Atomic Energy Research Establishment Harwell.

Scientists from Surrey University assisted in the clothing monitoring exercise and it was necessary to calibrate their instruments, which differed from NRPB's, to establish a count rate corresponding to the 30 Bq cm^{-2} clearance level. The monitoring of the students' thyroids and their clothing took approximately 2 hours. The monitoring of the luggage and its contents still at that time in the aircraft clearly would have taken much longer and students were advised to leave these items.

The results of the monitoring enabled NRPB to reassure the students that their levels of dose were low and not a cause for concern. Bearing in mind, however, that Minsk and Kiev are about 300 km and 100 km respectively in opposite directions from Chernobyl, the contamination levels on clothing demonstrate how severe the incident had been. The fact that both the thyroid monitoring and clothing monitoring results for the Kiev and Minsk students showed little variation indicated that the release must have continued for a number of days, during which time it was known that the wind had veered and blown in the direction of Kiev.

After the monitoring of the students, further checks were carried out on other travellers arriving from Eastern Europe. The results of thyroid and clothing contamination checks on a group of twelve employees from a British company working approximately 60 miles from Kiev were very similar to those experienced with the students. Other travellers from Warsaw showed positive but much lower levels of contamination and thyroid activity, while travellers from Moscow gave no detectable contamination. Monitoring facilities were made available to travellers returning from the affected parts of Eastern Europe via the NAIR arrangements[2], which are widely available throughout Britain to cover incidents involving radioactivity. This facility is still available to travellers returning from Eastern Europe but at this stage the justification is primarily the provision of reassurance to those members of the public who have need of it.

Monitoring has also been carried out at Dover of a group of travellers on a coach tour which had included a visit to Minsk, within a few days of the incident occurring, to Leningrad and Scandinavia. No thyroid or clothing contamination was detected.

B. HOLLIDAY
K.C. BINNS
S.P. STEWART
National Radiological Protection Board, Chilton, Didcot, Oxfordshire OX11 0RQ, UK

1. *NRPB Publ.* No. DL2 (1979).
2. *Department of Health and Social Security Health Circ.* HC(76)52.

Radiation levels in Eastern Europe

SIR—Immediately after news of the accident at Chernobyl became available on 28 April, the National Radiological Protection Board (NRPB) was asked by the UK Foreign and Commonwealth Office (FCO) for an appraisal of the radiation situation, on the basis of which advice would be given to embassy staff, residents in affected countries and prospective travellers.

The first Swedish measurements, external gamma dose rates and, later, concentrations of atmospheric and ground radioactivity, were used to estimate the quantity of radioactivity released by means of NRPB's accident consequence code[1], MARC. Our first predictions of 29 April indicated a substantial release of the order of $10^{17} - 10^{18}$ Bq, which was expected to lead to tens of early radiation-induced deaths in the area around the site. On the basis of NRPB's recommended Emergency Reference Levels (ERLs)[1,3], it was thought that there would be a need for evacuation out to 20 or 30 km and for temporary food restrictions out to a few hundred kilometres from the site. FCO accordingly decided to evacuate students from Kiev and Minsk and to advise people not to travel to the western Soviet Union or to north-east Poland unless absolutely necessary.

Because some of the early data were contradictory or not reported in a recognizable way, it was concluded that radiation levels could also be obtained directly through the British embassies in various countries of eastern Europe. Embassies were accordingly equipped to measure external radiation dose rates from gamma rays by means of simple but sensitive instruments consisting either of the Mini Instruments 5.10 environmental exposure rate meter or a hybrid instrument using the same detector. All were calibrated before despatch. The British embassies at Moscow (Soviet Union), Warsaw (Poland), Bucharest (Romania), Budapest (Hungary) and Prague (Czechoslovakia) were the first to be sent instruments, followed after a few days by Sofia (Bulgaria) and Belgrade (Yugoslavia). The embassies were also asked to return samples of tap water, fresh milk, vegetables and grass.

Embassy staff measured gamma dose rates near their embassies and often at other locations (see Table 1). No allowance has been made for the natural background dose, normally between 0.1 and 0.2 μSv per hour. The measured dose rates quoted are the highest known to NRPB, but for some countries, where the first measurements were made about a week after the accident, the measured rates may be less than the peak rates. The estimates in Table 1 of the average external dose from deposited material that will be received in a year are based on the assumptions of a mix of radionuclides, allowing for radioactive decay and natural weathering[4], that people spend 90% of their time indoors[5] and that shielding by buildings reduces exposure by a factor of ten[6]. In all cases, about one third of the dose will be received within the first months, with the remainder delivered over the rest of the year at a fairly uniform rate. Our estimated doses should be compared with the external dose due to natural radiation, typically 0.6 – 0.7 mSv per year. The highest doses outside the Ukraine and Byelorussia are estimated for north-east Poland and Romania, but even

Table 1 External γ-ray doses

Location	Source of data	Highest measured dose-rate (1) ($\mu Sv\ h^{-1}$)	Representative present values on 14 May ($\mu Sv\ h^{-1}$)	Estimated total dose in a year (mSv)
Soviet Union				
Moscow	Brit. Embassy	0.2	0.1	–*
Kiev	Local scientist	30		†
	Official		2	2
Lithuania	Official	–	0.1	0.1
Chernobyl	Official	150	3	‡
Yugoslavia	Yug. authorities	1.6		0.3
	Brit. Embassy		0.4	0.3
Bulgaria	Official	0.7	0.5	0.3
	Brit. Embassy		0.25	0.2
Poland				
North-east	Official	4.5		0.8
	Brit. Embassy		0.8§	0.6
Warsaw	Brit. Embassy	0.4	0.2	0.1
Czechoslovakia				
Prague	Brit. Embassy	0.9	0.5	0.2
Hungary	Official	0.4	0.2	0.1
	Brit. Embassy		0.25	0.1
Romania	Brit. Embassy	3.6	0.9	1

Official figures are from governmental sources in the countries concerned.
* It is likely that dose-rates given here are measurements of fluctuations in natural background radiation in Moscow. However, if the higher reading is taken to indicate the presence of radionuclides from the Chernobyl reactor then the estimated dose over the year is less than 1 mSv.
† If this dose-rate is representative, it suggests a dose over the year of 20 mSv.
‡ It is not clear where in the Chernobyl region these dose-rates were measured. The dose-rates are likely to vary considerably with distance from the reactor so it is unreasonable to estimate a dose at Chernobyl.
§ Measured on 10 May. Earlier measurements indicate that dose-rates in northeastern Poland are falling and so it is likely that the dose-rate here on 14 May is $< 0.8\ \mu Sv\ h^{-1}$.

these are only a fraction of the recommended annual dose limit for members of the public of 5 mSv per year.

The most significant radionuclides in the samples of food from the Soviet Union, Poland, Hungary, Czechoslovakia and Romania measured by NRPB are ^{131}I and ^{137}Cs; levels in tap water were all low, in the range 1 – 100 Bq per litre of ^{131}I. In milk (Table 2), levels of ^{131}I peaked at the end of April or in early May, and have since fallen. The wide variation of measured ^{131}I probably reflects the rainfall pattern and the use of fodder other than grass for some cattle, but the highest levels reported, from Poland and Hungary, are comparable with the Derived Emergency Reference Level (DERL)[3] for the peak concentration of ^{131}I in milk of 2,000 Bq per litre; in both countries, restrictions of milk supplies from cattle grazing pastures were introduced. Concentrations of ^{131}I in milk samples obtained by embassy staff were, however, all well below the DERL and are at present similar to those measured for the northern part of the United Kingdom[7].

Table 2 ^{131}I concentrations in milk

Location	Source of data	Measured concentration (Bq l^{-1})	Date milk obtained
Soviet Union			
Moscow	NRPB	35	3 May
Moscow	NRPB	18	7 May
Yugoslavia	Official	50–150	early May
Poland			
General	Official	30–2,000	29–30 April
General	Official	20–1,000	1–2 May
General	Official	30–600	3 May
Warsaw	NRPB	210	5 May
Czechoslovakia			
Prague	NRPB *	110	8 May
General	Official	100–500	8 May
Hungary			
Fresh milk	Official	100–2,600	1–4 May
Fresh milk	Official	50–1,200	5–9 May
Fresh milk	Official	<600	11 May
Supermarket	NRPB	16	5 May
Romania			
Local market	NRPB	420	4 May

* Polish government source, not Czechoslovakian.

There is a wide variation of the concentrations of ^{131}I and ^{137}Cs (not measured for all samples) in vegetables measured by national authorities and by NRPB, possibly because of the rainfall pattern, the circumstance that some had been grown under cover and the method in which they had been prepared; samples analysed by NRPB show that concentrations in leafy green vegetables can be substantially reduced by the removal of outer leaves, washing and kitchen preparation in general.

Shortly after the Chernobyl accident, FCO advised the avoidance of fresh milk and free-range eggs, the avoidance of surface-grown vegetables and, in any event, washing and peeling (as for fresh fruit) in the Western Ukraine, Byelorussia, Moscow, Lithuania and northeastern Poland. This list was later modified to exclude Moscow and to include Romania. As more evidence becomes available, it should be possible to modify this advice further, although it is likely that precautions will be required for some time in the Western Ukraine and Byelorussia. Other foods, notably meat, from these areas need to be kept under review.

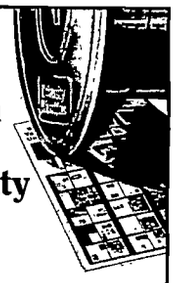
The early appraisal of the situation, based on an estimate of the magnitude of the release, was sufficient to give a reasonable general picture, but far more information is required to give specific advice for individual cities, regions and countries. The data obtained by British embassy staffs, to whom we are grateful, has been invaluable. The situation in Eastern Europe remains under review.

G.A.M. WEBB
J.R. SIMMONDS
B.T. WILKINS

National Radiological Protection Board, Chilton, Didcot, Oxfordshire OX11 0RQ, UK

1. Clarke, R.H. & Kelly, G.N., NRPB R 127 (HMSO, London, 1981).
2. NRPB *ERL 2* (HMSO, London, 1981).
3. NRPB *DL10* (HMSO, London, 1986).
4. Charles, D., Crick, M.J., Fell, T.P. & Greenhaigh, J. R., NRPB, *M74* (1982).
5. Brown, L. *Rad. Prot. Dosim.*, **5**, 203–208 (1984).
6. United Nations UNSCEAR report (United Nations, New York, 1982).
7. Fry, F.A., Clarke, R. H. & O'Riordan, M. C. *Nature* **321**, 193–195 (1986).

nature is available in microform from University Microfilms International.



☐ Please send information about these titles:

Name _____
Company/Institution _____
Address _____
City _____
State _____ Zip _____
Phone (___) _____

Call toll-free 800-521-3044. Or mail inquiry to: University Microfilms International, 300 North Zeeb Road, Ann Arbor, MI 48106.

Neurology

Proceedings of the XIIIth World Congress of Neurology, Hamburg, September 1–6, 1985

Edited by **K. Poeck,** Technische Hochschule Aachen; **H. J. Freund,** University of Düsseldorf; **H. Gänshirt,** University of Heidelberg

1986. 113 figures. Approx. 515 pages.
Hard cover DM 278,–. ISBN 3-540-13750-5

This volume contains an edited collection of papers presented at the XIIIth World Congress of Neurology. The main topics dealt with are the dementias, neuroepidemiology, brain and behavior, and neuroimaging techniques, with special emphasis on their implications for clinical management.

Fundamentals of Sensory Physiology

Edited by **R. F. Schmidt,** University of Würzburg

Translated from the German by M. A. Biederman-Thorson

Springer Study Edition

3rd revised and expanded edition. 1986. 143 figures, mostly in color. XI, 300 pages. Soft cover DM 48,–
ISBN 3-540-15870-7

Contents: General Sensory Physiology, Psychophysics. – Somatovisceral Sensibility. – Neurophysiology of Sensory Systems. – Nociception and Pain. – Physiology of Vision. – Physiology of Hearing. – Physiology of the Sense of Equilibrium. – Physiology of Taste. – Physiology of Olfaction. – Thirst and Hunger: General Sensations. – Suggested Reading. – Answer Key. – Subject Index.

Time, Mind, and Behavior

Edited by **J. A. Michon, J. L. Jackson,** University of Groningen

1985. 69 figures. XII, 313 pages. Hard cover DM 98,–
ISBN 3-540-15444-2

This book examines various aspects of temporal information processing: the nature and development of time from the point of view of natural philosophy and biopsychology; the functional aspects of time processes; the structure and organization of time; and time from a semantic viewpoint.

Electrical Stimulation and Neuromuscular Disorders

Edited by **W. A. Nix,** University of Mainz; **G. Vrbová,** University College, London

1986. 56 figures, 9 tables. Approx. 160 pages.
Hard cover DM 98,–. ISBN 3-540-16700-5

This book describes the role of activity on the development of the mammalian motor unit. Modifications of normal and diseased skeletal muscle induced by electrical stimulation are listed in a series of original papers, and the possible use of these procedures for therapeutic purposes is presented.

Processes of Recovery from Neural Trauma

Edited by **G. M. Gilad,** Rehovot; **A. Gorio,** Abano Terme; **G. W. Kreutzberg,** Planegg-Martinsried

1986. 135 figures, 16 tables. XIV, 370 pages (Experimental Brain Research Series, Volume 13). Hard cover DM 148,–
ISBN 3-540-15781-6

Over the past few years research on neural trauma has witnessed significant progress, despite the fact that recovery is limited by the lack of successful axon regeneration. This book presents a wide range of reports on the latest advances which have resulted from worldwide interdisciplinary research.

Nausea and Vomiting: Mechanisms and Treatment

Edited by **C. J. Davis,** Oxford; **G. V. Lake-Bakaar,** Wantage; **D. G. Grahame-Smith,** Oxford

1986. 39 figures. Approx. 200 pages. (Advances in Applied Neurological Sciences, Volume 3). Hard cover DM 98,–
ISBN 3-540-15436-1

This book considers the biological phenomenon of nausea and vomiting, reviewing the subject with respect to both basic scientific research and clinical aspects. Broadly speaking, the book divides into two halves: the first deals with all of the neuroanatomy, general anatomy, physiology and pharmacology involved in the phenomenon, and the second looks at the mechanisms and treatments of several specific causes of nausea and vomiting.

Springer-Verlag Berlin Heidelberg New York Tokyo

Heidelberger Platz 3, D-1000 Berlin 33
175 Fifth Ave., New York, NY 10010, USA
37-3, Hongo 3-chome, Bunkyo-ku, Tokyo 113, Japan

3335/4/1

Springer

Reader Service No. 7

Oxford University Press

NEW BOOKS

Data for Biochemical Research
Third edition

Rex M. C. Dawson, Daphne C. Elliott, William H. Elliott, and Kenneth M. Jones

This up-to-date and much revised edition of a classic reference work provides factual information about the compounds, reagents, and techniques used most frequently in the laboratory.

0 19 855358 7, 608 pp., illus., Clarendon Press, June 1986 £35

Image Restoration and Reconstruction

R. H. T. Bates and M. J. McDonnell

A comprehensive treatment of the wide variety of techniques available for image restoration and reconstruction.

Oxford Engineering Science Series 16
0 19 856176 8, 304 pp., illus., Clarendon Press, June 1986 £35

Foundations of Colloid Science
Volume 1

Robert J. Hunter

This text is designed as the basis of a one-year course at graduate or senior undergraduate level in colloid science.

0 19 855188 6, 600 pp., illus., Clarendon Press, August 1986 £60

Multiple Parameter Stability Theory and its Applications
Bifurcations, catastrophes, instabilities . . .

Koncay Huseyin

In this book a general non-linear theory concerning the stability, instability, bifurcation, and oscillatory behaviour of autonomous systems is presented from an original engineering point of view which is conceptually simple and applicable.

Oxford Engineering Science Series 18
0 19 856170 9, 304 pp., illus., Clarendon Press, July 1986 £40

Energy Methods in Electromagnetism

P. Hammond

The purpose of this book, which is available in paperback for the first time, is to apply the insights of mechanics to electromagnetic problems.

Monographs in Electrical and Electronic Engineering 12
0 19 859368 6, 200 pp., illus., Clarendon Press, July 1986, paperback £12.50

Diophantine Inequalities

R. C. Baker

This is an overview of the theory of nonlinear Diophantine approximation, the best known example being Heilbronn's theorem on the sequence of squares.

London Mathematical Society Monograph New Series 1
0 19 853545 7, 288 pp., Clarendon Press, June 1986 £32

Strong Solids
Third edition

A. Kelly and N. H. Macmillan

This third edition maintains the high standards and much-praised approach of the previous editions, while bringing the subject up-to-date.

Monographs on the Physics and Chemistry of Materials
0 19 851362 3, 350 pp., illus., Clarendon Press, July 1986 £35

The World of Science and the Rule of Law

John Ziman, Paul Sieghart, and John Humphrey

In 1975, thirty-five nations signed the Helsinki Accords. This book surveys their performance since then, in the context of the rights in the code which are specially important for scientists.

0 19 825516 0, 320 pp., Clarendon Press, March 1986 £19.50

Working Memory

Alan Baddeley

This book is concerned with working memory, the temporary storage of information as required for reading, thinking and comprehension.

Oxford Psychology Series 11
0 19 852116 2, 304 pp., illus., Clarendon Press, July 1986 £30

Biomineralization in Lower Plants and Animals

Edited by Barry S. C. Leadbeater and Robert Riding

A discussion of the controls, processes, products, and functional significance of biomineralization in algae, protozoans, bacteria, and lichens.

Systematics Association Special Volume 30
0 19 857702 8, 416 pp., illus., Clarendon Press, July 1986 £45

Nitrogen Fixation
Volume 4: Molecular biology

Edited by W. J. Broughton and A. Puhler

This fourth volume deals with the underlying molecular biology of nitrogen fixation, and provides basic information on the processes involved.

0 19 854575 4, 336 pp., illus., Clarendon Press, July 1986 £35

The Biochemical Basis of Neuropharmacology
Fifth edition

Jack R. Cooper, Floyd E. Bloom, and Robert H. Roth

0 19 504035 X, 368 pp., illus., OUP USA, July 1986 £25
0 19 504036 8, paperback £12.50

For further information on Oxford Science Publications please write to Elizabeth Bone, Oxford University Press, Walton Street, Oxford OX2 6DP

Readers in the USA should write to Barbara Wasserman, Oxford University Press, 200 Madison Avenue, New York NY 10016, USA.

Living with nature

George Peterken

The History of the Countryside: The Full Fascinating Story of Britain's Landscape. By Oliver Rackham. *Dent/Biblio, Totowa, New Jersey: 1986. Pp.445. £16.95, $35.*
Countryside Conflicts: The Politics of Farming, Forestry and Conservation. By Philip Lowe, Graham Cox, Malcolm MacEwan, Tim O'Riordan, Michael Winter. *Gower/Maurice Temple Smith: 1986. Pp.378. Hbk £19.50, $35; pbk £8.95, $16.*

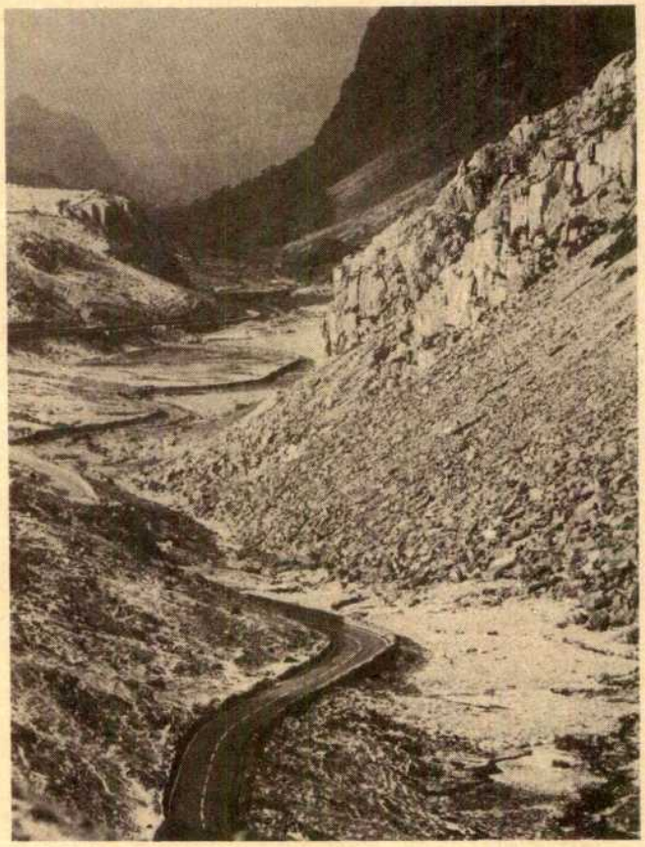
To one who came into countryside conservation in the 1960s, one of the more intriguing developments has been the subsequent demotion of science as an objective. As the authors of *Countryside Conflicts* point out, in Britain ecologists assumed the leadership of the nature conservation movement in the 1940s as part of the British Ecological Society's drive for government recognition. Science became the principal aim of nature conservation — we still call the important sites "Sites of Special Scientific Interest" — and the means by which the behaviour of species and of ecosystems were investigated. With nicely unscientific circularity we reserved sites for scientific research, and conducted scientific research with which the better to reserve and manage these sites. These days we stress other attributes and benefits, such as the seemingly nebulous values of heritage and wilderness, and seek to understand ecosystems more by their history and less by their mechanics. We recognize that science can only be a partial answer even to nature reserve management: even if we could afford the research needed to understand the needs of all species, we would still require other bases for deciding which species to favour.

Both of the books under review testify to this change, but in vastly different ways. Oliver Rackham, already famous as the author of three books on the ecology and history of woodlands, here expands into the countryside at large, though woodlands remain a major theme. Concentrating on the relatively natural elements, his aim is to show how the countryside came to assume its present character. Unlike analogous, but far less detailed works on the making of the English landscape, which apportion history into broad eras then describe the most notable developments within each, Rackham takes each individual element in the landscape separately. Thus, we have chapters on woodland, wood-pasture, fields, hedges and field walls, highways, heath-land, grassland, ponds, dells and pits, and many other features. These chapters follow others on landscape regions, and the use of historical evidence. There is also a short chapter on conservation, and brief conservation sections in other chapters.

Rackham's numerous admirers will once again be delighted with his lucid, precise and non-technical style and illustrations, and his entertaining presentation. Drawing copiously on original historical records, he fascinates the reader with the human interest that runs through the story and with the detail that has survived the centuries. In what other ecological textbook do we learn, for example, that "for his Christmas dinner, 1251, Henry III had 430 red deer, 200 wild swine, 1300 hares... and lampreys without number" as some indication of the produce of wood-pasture? The book also contains important original research, such as the detailed analysis of the ecological content of Anglo-Saxon charters. Numerous myths are demolished, notably the notion that woods, heaths, fens and so on are normally destroyed by use of the native vegetation, when in fact agriculture and plantation forestry have been the main culprits. Throughout, this is essentially a personal statement, which draws its strength from the author's exceptional ability to perceive and express patterns in a mass of detail. Other people's work is used, not to provide syntheses and concepts, but to provide good examples, amplify details, and partially correct Rackham's geographical bias to East Anglia, south-west England and south Wales.

Whereas Rackham covers the full span of countryside history from an ecological standpoint, the authors of *Countryside Conflicts* deal with the recent history of the political, social and economic side of conservation. After reviewing the twentieth-century rural preservation movement, the post-1945 planning system, and the political and economic background to forestry and agriculture over the past 40 years, Lowe and his colleagues are almost wholly concerned with the 1970s and 1980s. They analyse the two "opposing forces" in the countryside — the farming, land-owning and timber-growing "lobbies", and the conservation "movement" (this verbal loading is characteristic) — then describe in some detail the manoeuvrings behind the Wildlife and Countryside Act of 1981 and its subsequent implementation. Then, in what for many will be the most interesting section, they describe the well-known conflicts with farming in Exmoor, West Sedgemoor and the Halvergate Marshes, and with afforestation on the Berwyn Mountains. The final part is a review of needed reforms, more a manifesto than a practical guide, including proposals to merge the Nature Conservancy Council with the Countryside Commissions, and to reform countryside designations such as "Area of Outstanding Natural Beauty".

Rackham's publishers claim that his book is one of the most important on the countryside to appear in recent years, and for once the hype may be right. Certainly, his earlier writings have so fired the interest and imagination that both Parliament and the Forestry Commission dance to his tune, at least in so far as broadleaf woods are



In the wild — Llanberis Pass, in Snowdonia National Park. The picture is reproduced from Wildest Britain: A Visitor's Guide to the National Parks, *by Roland Smith with photographs by Mike Williams. Publisher is Blandford, price is pbk £6.95, $12.95.*

concerned. *Countryside Conflicts*, too, clearly seeks to influence the course of rural events. Where, then, would the two books lead us?

Countryside Conflicts takes the view that conservation should be an operative principle of all land management, not a separate element within reserves and designated sites. This requires a change in direction and purpose of forestry and agriculture. Much of the authors' writing implies a conservative view of the landscape: they seek mechanisms to maintain hill farming and thereby keep the landscape we have. To make this possible they nevertheless show some willingness to sacrifice the wild, for example by advocating grants which would support initial operations such as draining, fencing and planting. They are against conifer afforestation in the uplands, but support broadleaf afforestation in the lowlands, only hinting at how they would avoid setting this woodland on surviving fragments of semi-natural habitat. Indeed, throughout they are vague about what should physically be done on the land.

There is little doubt about Rackham's sense of value. He appreciates the antique features, which have "meaning", particularly the natural elements and time-honoured associations between man and nature. His attitude is exemplified by the claim that "ten thousand oaks of 100 years old are not a substitute for one 500-year-old oak", with the implication that they are less valuable. Inevitably he is scathing about the effects of modern agriculture — "fertility comes in a sack" — and considers not only that it should not be extended but that it should retrench towards more conservative forms of land management.

This is all very well. Many people, including myself, understand these very points and sympathize with his attitudes. Experience has taught us, however, that many others value a single 100-year-old oak above its 500-year-old grandparent, both as timber and scenery. Such people see beauty in order, cultivation and production, and rejoice in increased productivity of farmland and plantations. Others again seek refreshment and beauty in wilderness, and would minimize the effects of man. Rackham sees variety, significance (the latter-day "scientific interest"), permanence and security in traditional conservative use of resources, and thereby rejects both views: it is valuable to have his corner so cogently argued.

Vague though they are on the practicalities, these books converge in their antagonism to much of modern agriculture and forestry, and their support of the semi-wilderness maintained by traditional practices. Living with nature is the modern theme of conservation. □

George Peterken is in the Chief Scientist's Directorate, Nature Conservancy Council, Northminster House, Peterborough PE1 1UA, UK.

The need to know about lipids

Howard Goldfine

Biochemistry of Lipids and Membranes. Edited by Dennis E. Vance and Jean E. Vance. *Benjamin/Cummings:1985. Pp.593. $34.95, £34.95.*

INTEREST in lipids among biochemists and molecular biologists appears to go through cycles ranging from high enthusiasm to near neglect. Recently, a decided upturn in awareness can be detected. Although the phosphatidylinositol cycle has been studied for 30 years, its physiological significance has only recently come to wider notice. Adding to this increase in attention being paid to lipids have been the ripple effects of discoveries on the arachidonate cascade, the regulation of cholesterol biosynthesis and the molecular biology of the low-density lipoprotein receptor, and the finding that the platelet-activating factor is an ether lipid analogue of phosphatidylcholine.

The appearance of a substantial volume devoted to the biochemistry of lipids and membranes will be welcomed not only by those who have long engaged in lipid research, but also by those who have been drawn to it by following leads in such areas as viral tumorogenesis and hormonal regulation, or by a desire to understand how membranes are assembled and how they work. The editors set themselves a double goal — to produce a text for use in advanced biochemistry courses devoted to lipid and membrane biochemistry, and a reference volume for basic and clinical researchers. They have largely succeeded in meeting the second objective by having each of the 15 chapters written by knowledgeable and active specialists. The information is up to date and the subjects are presented in considerable depth, backed up by references to recent reviews and primary publications. As might be expected in a multi-authored work, some contributors show a tendency to advance their own views, but the balance is generally reasonable.

While the need for a text at this level may not extend to many graduate programmes in the biomedical sciences, where such courses exist or are contemplated this volume will prove very useful for both students and their teachers. Most of the chapters begin with a brief historical essay touching on key developments and figures in the field concerned, and end with a discussion of future directions and areas in need of further development. In addition to chapters on traditional areas of lipid metabolism, there are helpful articles on the assembly of membrane lipids and proteins, and a good but somewhat abbreviated discussion of the physical properties and functional role of lipids in membranes.

A recurrent theme in the book is the paucity of information (with a few notable exceptions) that we have on the regulation of lipid metabolism, either at the level of the gene or by modulation of enzyme activities. Students looking for research problems in cell biology will readily find them here. The tools for solving such problems are becoming more sophisticated through the development of methods for solubilizing and purifying membrane proteins, the production of monoclonal antibodies, and the ability to isolate and clone the genes for the proteins of lipid metabolism. Answers may not come easily but, as this volume makes clear, the search should be both stimulating and rewarding. □

Howard Goldfine is a Professor in the Department of Microbiology, University of Pennsylvania School of Medicine, Philadelphia, Pennsylvania 19104, USA.

Dishing the dirt

Richard P. Wayne

Atmospheric Chemistry and Physics of Air Pollution. By John H. Seinfeld. *Wiley: 1986. Pp.738. $59.95, £57.45.*

JOHN Seinfeld defines air pollution as "any atmospheric condition in which substances are present at concentrations high enough . . . to produce a measurable effect on man, animals, vegetation, or materials". Dusts, pollen, smoke and volcanic gases and ash can undoubtedly exert deleterious effects, although they are part of the "natural" atmosphere. Mankind has, however, discovered all manner of means of further polluting the atmosphere on scales ranging from the local to the truly global. Seinfeld's hope is that the scientific study of pollution will provide pointers to finding the optimum way of abating the problem in its manifold forms.

Research into air pollution encompasses several disciplines that are only loosely connected, and Seinfeld makes a determined effort to show how the different facets relate to each other. He first considers the sources of pollution, and the effects that various pollutants have on atmospheric properties, on materials, on vegetation and, above all, on human health. Often, the substances released as primary pollutants are not themselves the agents of damage. Rather, chemical transformations are responsible for the formation of a secondary species that is harmful. Such transformations range from the production of acids from the oxides of nitrogen and sulphur accompanying the com-

bustion of fossil fuels, to complex catalytic cycles in the stratospheric ozone layer that could alter the Earth's protection from solar ultraviolet radiation. Seinfeld has to consider, therefore, atmospheric chemical processes occurring both in the gas phase and within atmospheric liquid water, and he notes that several mass transfer steps must precede such aqueous reaction.

Aerosols, which are suspended particles of solid or liquid, play an important part in pollution studies. They degrade visibility, and can also act as condensation nuclei for the growth of larger liquid droplets. Seinfeld has chosen to present quite a detailed treatment of aerosol behaviour, offering a general review of aerosol physics, with emphasis on the dynamics of individual particles and of populations, and the thermodynamics of aerosols and of nucleation.

The dynamics of the atmosphere itself determine the dispersal and transport of pollutants. Logically, then, discussion of pollution meteorology occupies the next part of the book, and a further main section deals with atmospheric diffusion.

Seinfeld has achieved his objective of providing a comprehensive treatment of pollution processes. He suggests that the work could serve as a textbook for a course on the atmospheric aspects of air pollution, but readers would have to be pretty well equipped with a knowledge of applied mathematics to cope with the second half of the book. Indeed, I have slight reservations about the amount of quantitative detail presented here; the physics is largely relevant to idealized situations, and the implied precision is strangely at variance with the level of our understanding of the sources, effects and chemistry of pollutants.

The final chapter is devoted to a discussion of acid rain, and Seinfeld shows how the topic serves as an elegant summarizing problem which brings in almost all of the features discussed earlier in the book. In many ways, this section would be a good starting point for a beginner. For specialists, this is a most useful reference book, while for those with traditional scientific or engineering backgrounds it will prove a rigorous and trustworthy guide to a complicated subject. □

Richard P. Wayne is University Lecturer in Physical Chemistry, Physical Chemistry Laboratory, University of Oxford, South Parks Road, Oxford OX1 3QZ, UK, and Dr Lee's Reader in Chemistry at Christ Church, Oxford.

• Also published recently by Wiley is *Air Pollutants and Their Effects on the Terrestrial Ecosystem*, edited by Allan H. Legge and Sagar V. Krupa, which is said to be "the first integrated work to present all current research on the effects of pollutants on vegetation, soils, and ecosystems". The book is Vol. 18 in the series *Advances in Environmental Science and Technology;* price is $80, £82.75.

Faith and the ways of science

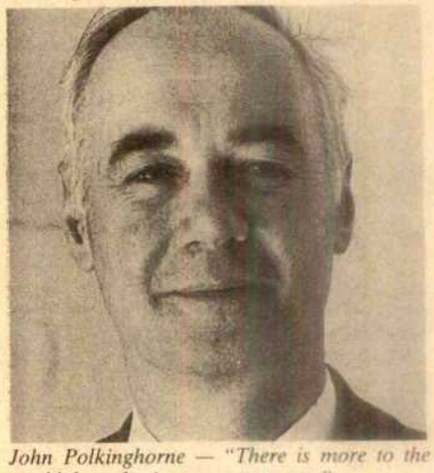
Robert John Russell

One World: The Interaction of Science and Theology. By John Polkinghorne. *SPCK, London/Fortress Press, Philadelphia: 1986. Pp.114. Pbk £4.50, $7.50.*

JOHN Polkinghorne is Honorary Professor of Theoretical Physics in the University of Kent, a Fellow of Trinity College, Cambridge, and the Vicar of Blean, Kent. In his brilliant and artful exposition of contemporary physics (*The Particle Play*, published by W.H. Freeman in 1979), Polkinghorne acknowledged his identity as a "Christian believer", gave his judgement that the world-views of Christianity and science can be in "consonance" and announced that he was leaving his position as Professor of Mathematical Physics to train for the Anglican priesthood. *One World* is not the first of Polkinghorne's books to examine the relationship between religion and science. Appearing in 1983, *The Way the World Is* was a consequence of his "coffee shop" discussions about Christianity with his fellow scientists. Now, in this new book, we see his earlier ideas taking root in the context of contemporary philosophy and theology, though with the same distinctive style, clarity of thought and dry passion which his admirers (myself among them) have come to expect and appreciate.

In *One World* Polkinghorne defends the thesis that science and theology are "capable of mutual interaction" because they both explore "aspects of reality". He espouses a critical realist philosophy and argues against reductionism by the following epistemological claim: that the various fields of study, such as psychology or biology, form a hierarchy in which each field is relatively autonomous from the others. He sets the stage for his case by describing how contemporary physics has overturned the Enlightenment view of the objective and determinate status of the world, and how contemporary philosophy has exposed earlier, simplistic interpretations of the scientific method. Twentieth-century theology, too, has moved beyond dogmatics to a critical analysis of religious experience and so "theology, like science, is corrigible". Hence theologians should seek coherence, economy, adequacy and existential relevance.

Writing with precision and elegance, Polkinghorne captures the majesty and mystery of our current view of nature: elusive (unpicturable but real) and yet intelligible (through mathematics); problematic (for example, the conflicting interpretations of quantum theory); contingent yet lawful; tight-knit (human evolution in an "anthropic" cosmos) and yet futile (given the cosmological scenarios for a lifeless distant future); complete ("the one God who is... truly dead is the God of the Gaps") and incomplete ("There is more to the world than physics can ever express"). Hence Polkinghorne urges that theology and science can intersect without conflict. Regarding origins, theology can see God as the ground of reality rather than a cause among causes, thus allowing Polkinghorne to affirm "God *and* the big bang". Chance, too, is not necessarily a sign of God's absence. Instead "both the lawful necessity of the world and the role that contingent chance has to play within it are aspects of [God's] great creative act". Polkinghorne concludes that "we live in one world and science and theology explore different aspects of it", a world whose "multi-layered unity" is grounded in God.



John Polkinghorne — "There is more to the world than physics can ever express".

This is a satisfying book, though it has some problems. Polkinghorne frequently fails to cite the people whose ideas he seems particularly indebted to (notably Ian Barbour and Arthur Peacocke). More to the point, he does not adequately show how the *contents* of science (and not just its epistemology or methodology) should affect constructive theology and thus how these fields actually address "one world". Still, *One World* offers a balanced, though almost precariously brief, version of the challenges and promise of science and theology. Much to his credit, Polkinghorne never pleads his case, preaches to the reader or draws on fringe arguments, but his personal convictions are clear throughout. As a candid and compelling statement of faith given by an internationally distinguished scientist — now priest and theologian — I welcome Polkinghorne's new book and urge him on in the journey we share. □

Robert John Russell is Associate Professor of Theology and Science in Residence, Graduate Theological Union, and Director of the Center for Theology and the Natural Sciences, 2465 Le Conte Avenue, Berkeley, California 94709, USA.

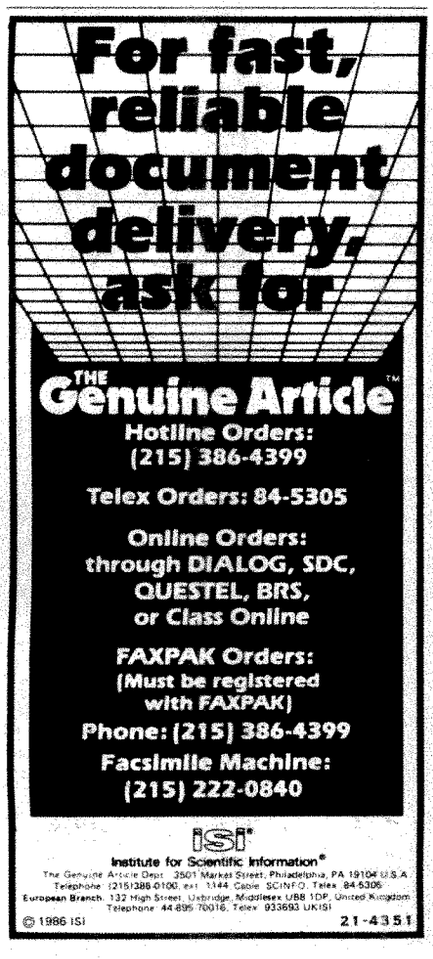
Sound of erudition

James Cullen

Science and Civilisation in China, Vol. 6: Part 1. Biology and Biological Technology: Botany. By Joseph Needham. *Cambridge University Press: 1986. Pp.718. £50, $95.*

DR NEEDHAM'S series *Science and Civilisation in China*, which he began some 30 years ago, needs little introduction here. This latest volume is by Needham himself, with the collaboration of Li Gwei Djen (Cambridge) and Huang Hsing-Tsung (Washington). Part 2 of Vol. 6, *Agriculture*, by Francesca Bray, was published in 1984, and a further part, continuing the subject of botany, is being prepared by Georges Métailié of the Musée d' Histoire Naturelle in Paris.

In covering the history of botany in China from its remote origins to the impact on it of Western science in the late nineteenth century, Needham has surveyed a huge amount of literature. There are three bibliographies — of Chinese and Japanese books before 1800; the same since 1800; and books and articles in Western languages — which altogether occupy 99 pages. This vast quantity of source material is processed with a breath-taking display of erudition.



Throughout, Needham contrasts what was happening botanically in China with corresponding events in the West, and stresses two important differences: first, that the history of botany in China, like that of many of the physical sciences, is more continuous than in the West — in China there were difficult times, but no aching void equivalent to the Dark Ages; second, following the rapid advance of the scientific method in the West, Western botany overtook Chinese in both the pace and scope of its development. Needham categorizes Chinese botanical taxonomy (for the volume is, by necessity, mainly a history of taxonomy) as having reached a "Magnolian" or "Tournefortian" rather than a "Linnaean" or "post-Linnaean" level.

After the introduction, the volume is divided into five large sections. The first, "The Setting: China's Plant Geography", is a brief survey of the floristic divisions of the country as recognized by botanists today, together with a discussion of the development of Chinese ideas on the topic in which the stress is on soils and soil types.

The second section, "Botanical Linguistics", covers Chinese terminology for plant description and nomenclature. This fascinating if complex subject is clearly presented for those who know little about ideographic writing. Needham concludes it with some thoughts on the appropriateness of ideographs for taxonomic purposes. Because they are made up of superimposed radicals, ideographs can convey classificatory ideas very satisfactorily ("it might well be said that a language the dictionaries of which have to be based on taxonomic principles is a language remarkably congruent with the nature of biology" — p.178); indeed, Needham compares them with various coding systems (some of them machine-readable) developed in recent years.

"The Literature and its Contents" follows and is the heart of the volume. A wide variety of texts is surveyed for their botanical content, including lexicographic and encyclopaedic works, medical books, books on wild (emergency) food plants, monographs and tractates, and works on historical and exotic botany. This section is too densely packed to describe in any detail, but one of its most interesting topics is that of the monographs: some little knowledge of these has filtered through to Western botanists, but their age-range and scope are not so well known. Monographs on citrus fruits (*Citrus, Fortunella*), bamboos (*Gramineae Bambusoideae*), peonies (*Paeonia*) and chrysanthemum, among others, are discussed in some detail; the amount of study devoted by the Chinese to cultivated varieties is noteworthy.

The final section deals with a less narrowly taxonomic subject, that of pest control among cultivated plants, and in particular the use of biological control in agriculture. Entitled "Plants and Insects in Man's Service", it is by Huang Hsing-Tsung and contains much of interest, especially the account of the use of a species of ant (*Oecophylla smaragdina*) to control pests in orange orchards, with the use of bamboo bridges from tree to tree to "facilitate migration". This means of control appears to have been in consistent use in South China from AD 300 to 1960. Its effectiveness is, however, doubted by some authorities, both Chinese and Western.



Aquatic frog (wa) — *detail of an illustration in Paul U. Unschuld's* Medicine in China: A History of Pharmaceutics, *newly published by University of California Press. Price is $47.50, £40.50.*

The whole book is a pleasure to read: informative, stimulating and written with a wit and passion that are found more often in historical than botanical texts. Needham expects quite a lot of his readers: on p.373, quoting a long passage from Han Yen-Chih's *Chü Lu*, the footnote to part of it reads:

> The sentences in inverted commas were, as Pelliot recognised, borrowed by Han Yen-Chih from a 'Letter accompanying a Present of Oranges' written by Liu Hsun.... He worked them in, as they were appropriate, just as we might use a few words of Sir Thomas Browne, knowing that all educated readers would respond to the echo.

How many botanists might so respond? However few, the book contains so much valuable "sound" that the loss of a few echoes is not significant. □

James Cullen is Assistant Keeper of the Royal Botanic Garden, Inverleith Row, Edinburgh EH3 5LR, UK.



Wiley

CHICHESTER · NEW YORK
BRISBANE · TORONTO · SINGAPORE

THE ANALYSIS OF EXTRATERRESTRIAL MATERIALS

by **I. Adler,** *University of Maryland*

A summary of the remarkable work being done in the study and analysis of extraterrestrial materials. The book reflects the ingenuity and inventiveness in developing satellite and spacecraft measurement techniques and instruments of high sensitivity and precision, as well as analytical methods for materials which have never been seen before and in which the detection of anomalies is critical to an understanding of the solar system and its origin. It surveys and evaluates detection methods for their reliability, sensitivity and usefulness. The book is also well-illustrated, and contains many tables.

Series: Chemical Analysis, Volume 81

0471 87880 4 368pp April'86 £56.75

DYNAMICS OF EXTINCTION

by **D.K. Elliott,** *Northern Arizona University*

A collection of papers on modern and antediluvian species extinctions presented at a Northern Arizona University symposium at Flagstaff in 1983. Extensively updated, the compilation offers a comprehensive summary of current research and scientific thinking on the possible causes and mechanisms of large-scale periodic extinctions. The book also covers many speculations and controversies on the subject. Topics include the fossil record of extinctions, modern extinctions, theoretical modelling of extinction events, the periodicity of mass extinctions and more.

0471 81034 7 304pp May'86 £47.95

AIR POLLUTANTS AND THEIR EFFECTS ON TERRESTRIAL ECOSYSTEMS

edited by **A.H. Legge,** *University of Calgary, Canada* and **S.V. Krupa,** *University of Minnesota*

A comprehensive presentation of the effects of pollution on vegetation, soils and forestry, describing the interaction of pollutants and their effect on the ecosystem. The book includes evaluation of current research and scientific methods with implications for future study, and stresses both research and regulatory concerns.

Series: Advances in Environmental Science and Technology,

0471 08312 7 682pp May'86 £82.75

PROGRESS IN PESTICIDE BIOCHEMISTRY AND TOXICOLOGY, Volume 5: Insecticides

edited by **D.H. Hutson** and **T.R. Roberts,** *Shell Research Ltd, Sittingbourne*

This book opens with a review of currently available insecticides examined by class and use. The concept of pro-insecticides is then discussed; pro-insecticides are compounds which are converted into bioactivity by the metabolic activity of the target organism or host. By considering several older insecticides which act through bioactivation, rational design methods for suitable new compounds are suggested. Resistance to pyrethroids, and the mammalian toxicology of these compounds is discussed in detail. These subject matters preface consideration of the metabolism and toxicity of insecticides to fish. New areas for research and development which are attractive prospects for future work: chitin synthesis inhibitors and the vast range of natural chemicals which control insect behaviour; are reviewed and their potential explored.

Series: Progress in Pesticide Biochemistry and Toxicology,

0471 90758 8 400pp January'86 £48.00

TOXIC METALS IN THE ATMOSPHERE

edited by **J.O. Nriagu,** *National Water Research Institute* and **C.I. Davidson,** *Carnegie-Mellon University*

This book deals with the origins, behavior and eventual fate of airborne metals — their physical characteristics, interactions, transport and removal from ambient air. Also covered in the book are trends, routine and special monitoring of atmospheric metal levels. Important information on this topic is synthesized, from a wide range of fields, including chemistry, biology, ecology, agriculture, physics, geochemistry, oceanography and meteorology.

Series: Advances in Environmental Science and Technology,

0471 82654 5 650pp April'86 £102.75

INSTRUMENTATION FOR ENVIRONMENTAL MONITORING, Volume 2: Water 2nd Edition

by **Lawrence Berkeley Laboratory,** *Environmental Instrumentation Survey*

Based on information from manufacturers' descriptions and specifications, here is a guide to environmental monitoring that describes water quality constituents and the instruments used to measure them. The book covers analytical methods, instruments and theoretical principles and evaluates available instruments, used in a variety of applications both in and outside the United States.

Series: Instrumentation for Environmental Monitoring,

0471 88567 3 1,014pp May'86 £181.00

TOXIC SUSCEPTIBILITY: Male/Female Differences

by **E.J. Calabrese,** *Division of Public Health, University of Massachusetts*

A critical assessment of the animal models of human clinical and population-based studies that highlight the physiological and biochemical differences between male-female responses to toxic substances. Focuses on the organ systems that are especially sensitive to toxicants and pollutants. Investigates the extent to which the pregnant state may alter a susceptibility to toxic substances, with particular emphasis on alterations in drug metabolism. Shows the significance such findings have for regulatory agencies concerned with environmental health.

Series: Advances in Environmental Science and Technology,

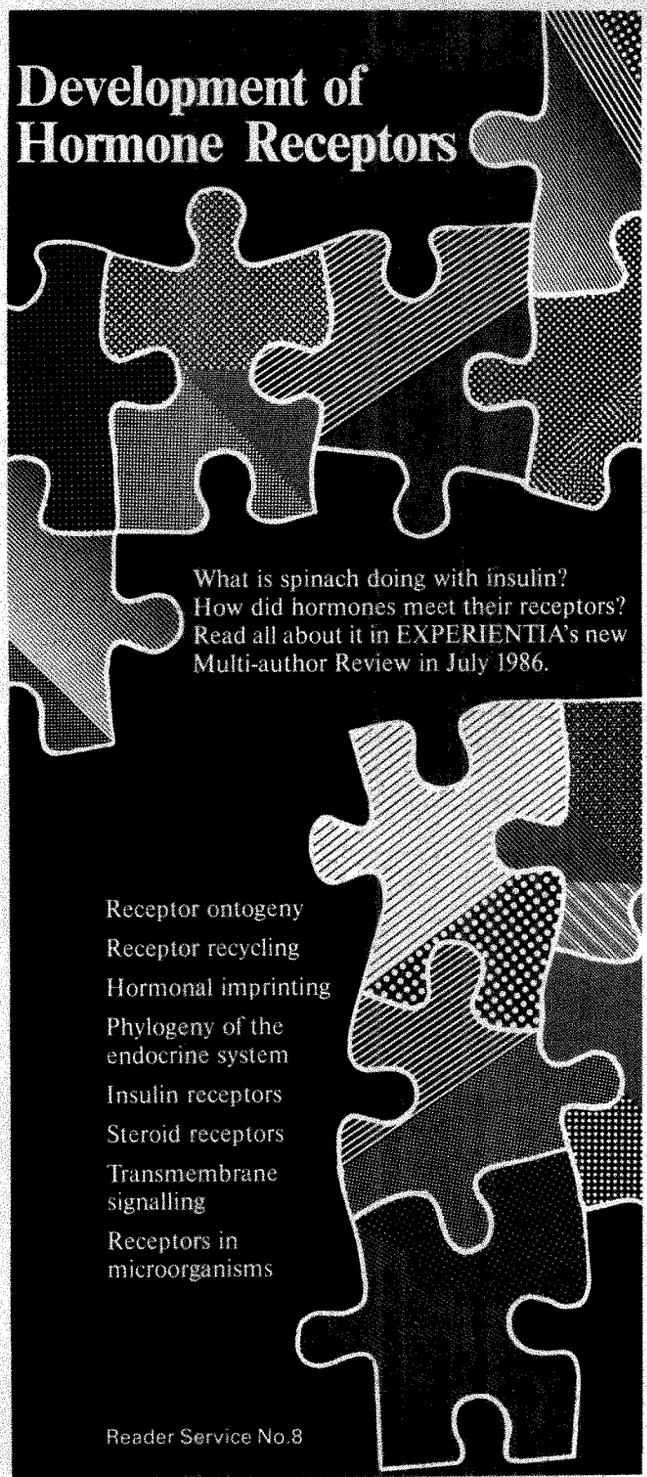
0471 80903 9 352pp October'85 £57.45



John Wiley & Sons Limited
Baffins Lane · Chichester · Sussex PO19 1UD · England

Reader Service No.6

Development of Hormone Receptors



What is spinach doing with insulin?
How did hormones meet their receptors?
Read all about it in EXPERIENTIA's new Multi-author Review in July 1986.

Receptor ontogeny
Receptor recycling
Hormonal imprinting
Phylogeny of the endocrine system
Insulin receptors
Steroid receptors
Transmembrane signalling
Receptors in microorganisms

Reader Service No.8

Order Form

☐ I wish to subscribe to the current (1986) volume of EXPERIENTIA immediately. (Annual subscription: sFr. 455.—)
☐ Please send me further information about EXPERIENTIA.

Name:

Institute or Firm:

Address:

Date, Signature:

Please ☐ bill me ☐ find payment enclosed

*Single issues (sFr. 48.– per issue excluding postage) by pre-payment only.

Note: Extra copies of recent special review issues* are still available! Simply specify the number of copies desired beside each review topic:

___ Ecological Effects of Acid Deposition (double issue)
___ Odor Biology
___ Malaria
___ Evolutionary Significance of Sex
___ Myelinated Nerve Fibers
___ Pancreatic B-cell
___ Contemporary Aspects of Evolution
___ New Trends in Spleen Research

Send to: **EXPERIENTIA**, Birkhäuser Verlag
P.O. Box 133, CH-4010 Basel/Switzerland

SCOTTISH UNIVERSITIES SUMMER SCHOOL IN PHYSICS

The proceedings of the schools provide pedagogical introductions to advanced topics at a level appropriate to research staff and students in high energy physics. All volumes are produced in hardcover editions at reasonable prices and are obtainable directly from SUSSP. Copies purchased through bookshops will be more expensive.

SUPERSTRINGS AND SUPERGRAVITY

1985. 550pp. Editors: Davies & Sutherland. Price £25.

This school was conceived of as a topical survey of supersymmetry and supergravity but developed into an excellent introduction to all facets of superstring theory. The lecture notes provide the first comprehensive presentation of this exciting new subject. Also included are excellent reviews of conventional quantum gravity approaches and cosmology. Contributors: Duff, Ellis, Ferrara, Grisaru, Isham, van Nieuwenhuizen, Schwarz and West.

FUNDAMENTAL FORCES

1984. 540pp. Editors: Frame & Peach. Price £20.

The school was primarily concerned with standard, and non-standard, models of the electro-weak theory, together with a critical assessment of the experimental evidence from the CERN collider (Darriulat, Jarlskog, Walsh, Dowell, Perl, Cashmore, Ledermann). In addition there were excellent reviews of Lattice QCD (Schierholz), Supersymmetry (Llewellyn-Smith) and Composite Models (Harari).

STATISTICAL & PARTICLE PHYSICS

1983. 500pp. Editors: Bowler & McKane. Price £20.

The school was concerned with recent developments in statistical and particle physics which exploit and extend the analogy between statistical fluctuations in thermal systems and quantised field theories of elementary particles. Topics include: The onset of chaos (Feigenbaum); First order transitions (Gunton); Monte Carlo methods (Swendsen); Topological excitations (Goddard); Interface problems (Zia); Random systems (Moore); String theory (Green); Monte Carlo calculations (Rebbi).

GAUGE THEORIES

1980. 640pp. Editors: Bowler & Sutherland. Price £15.

Topics included: Broken gauge theories (Appelquist); Neutrino physics (Barish); GUTS (Ellis); High energy interactions (Giacomelli); High energies (Glashow); Confinement ('t Hooft); QCD (Ross); Surface theories (Wallace); e^+e^- experiments (Wiik).

QUARK MODELS

1976. 500pp. Editors: Barbour & Davies. Price £10.

Seminal articles on strings (Nielsen), Supersymmetry (Zumino), Confinement in lattice gauge theories (Susskind), and Quark models (Close, Pati, Dalitz, Sutherland, Yankielowicz).

SUSSP Publications (N)
Department of Physics
University of Edinburgh
EDINBURGH EH9 3JZ. UK

Reader Service No.9

Experimental forecasts of El Niño

Mark A. Cane, Stephen E. Zebiak & Sean C. Dolan

Lamont-Doherty Geological Observatory of Columbia University, Palisades, New York 10964, USA

Experimental forecasts of El Niño events occurring since 1970, made with a deterministic model of the coupled ocean-atmosphere system, indicate that El Niño is generally predictable one or two years ahead. A forecast for 1986 is also presented.

THE devastating climatic events of 1982–83 were the most recent extreme phase of the irregular cycle of atmospheric and oceanographic changes known collectively as El Niño and the Southern Oscillation (ENSO)[1–5]. If forecasts could provide sufficient warning of an impending episode, appropriate planning could reduce human suffering and economic loss[6,7]. In 1982 the state of information gathering and forecasting activities was clearly inadequate: the event was well under way before it was recognized. Statistical procedures reported more recently[8,9] could have forecast it in the spring of 1982, a few months in advance of the peak warming.

Forecasts of El Niño at longer lead times could be impossible in principle. Perhaps the intrinsic behaviour of the coupled ocean–atmosphere system is such that states which initially differ by a small amount diverge very rapidly. If so, it would be impossible to observe initial conditions with sufficient precision to determine the subsequent evolution over many months. Even if skilful forecasts at longer range are possible in principle, they may be unattainable in practice because of inadequate models or the limitations of available data.

While it leaves many questions unanswered, the work reported here offers grounds for optimism. We have used a deterministic numerical model of the coupled ocean and atmosphere in the tropical Pacific region to make forecasts of all the El Niño events since 1970. The results indicate that the large-scale warmings associated with these events could have been predicted a year or more in advance.

The numerical forecasting model[10,11] is a coupled model for the evolution of the ocean and atmosphere in the tropical Pacific region. Only deviations from the mean are calculated explicitly; mean conditions are specified from monthly climatological data. No statistical procedures are used in the forecasts. Model variables evolve deterministically, according to the physical laws governing the atmosphere and oceans. The model was originally developed for abstract studies of large-scale ocean–atmosphere interactions in the tropics and is far simpler than the numerical models used operationally for weather prediction. Nevertheless, it reproduces much of the characteristic spatial and temporal structure of observed El Niño events, including their recurrence at irregular intervals with an average period of 3–4 yr (refs 10, 11).

In part, the simplifications were designed to serve a didactic purpose: insofar as the model simulations of ENSO are judged to be correct, one may conclude that the omitted processes are not essential for the existence of the ENSO cycle. When the model is to be used for forecasting, however, verisimilitude is clearly desirable and the simplifications are a handicap. The model's predictive skill is probably decreased by the absence of the 30–60-day waves so prevalent in the tropics[12], as well as by the lack of any variability generated in mid-latitudes. The model exhibits too little variability in the western equatorial Pacific and overstates easterly wind anomalies in the east. It cannot reproduce episodes of strong cold anomalies. All of these flaws (and others) reduce the realism of its ENSO simulations.

On the basis of model results, we have suggested a theory for the ENSO cycle[10,11] along lines proposed by Bjerknes[13] almost two decades ago. Many investigators since Bjerknes have substantially advanced our understanding of the tropical atmosphere and oceans, allowing his original framework to be bolstered and elaborated. Our theory and model design draw on this collective progress[1,14], only a brief sketch of which is possible here.

Ocean–atmosphere interaction

Work on equatorial ocean dynamics following the pioneering sea-level studies of Wyrtki[15,16] established that changes in the eastern equatorial Pacific could be caused by remote wind changes to the west, with the signal propagating through the ocean along the equatorial wave guide[17]. Others explored the ways in which ocean dynamics[13,18–20], not surface heating anomalies[4,13,21], accounted for observed anomalies in sea surface temperature (SST). Experiments with atmospheric general circulation models[22–24] showed that tropical Pacific SST anomalies could cause the meteorological changes characteristic of ENSO; other studies showed that simple models could largely account for the tropical aspect of the anomaly pattern[4,25–28].

If the winds alter the SST pattern, which alters the winds, then a coupled ocean–atmosphere model is clearly required. Although highly idealized, the models described in the literature[29–33] provide considerable insight into the mechanics of growing and oscillating modes of the coupled system. (This work has been reviewed by McCreary[34]).

In our model, the atmosphere and ocean both have an active role in ENSO: it is an oscillation of the coupled system. Its consequences are global, but the interactions vital to its existence all occur in the tropical Pacific region.

In the normal state, the tropical Pacific is warmer in the west and colder in the east; a centre of tropical rainfall overlies the pool of very warm water in the far western Pacific. The easterly trade winds blowing towards this atmospheric heating region drive warm surface waters to the west, while drawing colder sub-surface waters upward at the east. Thus, the temperature contrast responsible for the atmospheric circulation is maintained by that circulation—a positive feedback.

If the eastern ocean becomes warmer, then the rainfall spreads eastward with the warm water, and the surface winds slacken. As a result, some of the warm western water moves eastward and less cold water is drawn upwards; hence, the east becomes warmer still. Again, there is a positive feedback, leading to more westerly winds, warmer SSTs and a deeper thermocline in the east. This is an El Niño event.

Bjerknes[13] discussed both of these 'chain reactions' but could not explain why there were transitions from one phase to the other in an endless cycle. The key idea in our theory requires going beyond the vertical plane along the Equator and considering the north–south circulation in the ocean[4,18,29]. Approaching the peak of an El Niño event, water moves not only from west to east, but also poleward[35], emptying the reservoir of warm water at the Equator.

In the aftermath of the event, the heat loss results in colder than normal eastern Pacific SSTs and, consequently, stronger than normal easterlies—an enhanced version of the non-El Niño state. The transition back to the El Niño state cannot take place until enough warm water flows back from higher latitudes to refill the equatorial heat reservoir. Episodes of weak easterlies are frequent, but until the reservoir is refilled there is not enough

warm water available to sustain the 'chain reaction' that generates an El Niño event.

Our focus on the heat content of the equatorial band arose from theoretical considerations and numerical model results. There is also observational evidence supporting these ideas. On the basis of tide gauge data, Wyrtki[36] has independently advanced a similar hypothesis.

The time it takes to restore the equatorial heat content depends on the strength of the coupling between atmosphere and ocean[10]. The phenomenological 'coupling strength' comprises a number of factors, such as the sharpness of the thermocline, advective speeds, oceanic temperature gradients, dissipation rates, oceanic wave speeds and the sensitivity of the surface wind to SST contrasts. All of these vary seasonally and spatially, in addition to changing with the state of the ocean–atmosphere system. In addition, the flow of warm water back to the Equator is affected by higher-frequency events such as the 30–60-day waves[12] in the western Pacific.

The irregularity of the interval between El Niño events reflects the variability of this refill time; it is this variability which makes the prediction of El Niño difficult. It is not known whether it is more a result of high-frequency noise[37] or of the nonlinearities intrinsic to the ENSO cycle[38]. Although either implies that the ENSO cycle cannot be predicted arbitrarily far ahead, neither precludes prediction at useful lead times.

The ENSO scenario outlined here has further implications for the prospects of forecasting an El Niño event. As the essential interactions take place in the tropical Pacific, data from that region alone should be sufficient for forecasting. Also, our model implies that the future evolution of the ENSO cycle could not be predicted without knowledge of the upper-ocean heat content. The radiative relaxation time of the atmosphere is ~1 month, and the thermal damping time of the ocean surface layer is at most a few months (4 months in the model). Evidence that El Niño can be predicted at significantly longer lead times implies an active role for the sub-surface ocean, which has substantially greater thermal inertia.

In the model, the sub-surface thermal structure reduces to a single variable, the anomaly in the heat content of the upper ocean, or, equivalently, the thermocline depth anomaly. (A recent empirical study highlights the same variable[39].) The analysis above implies that this variable is an essential initial input for forecasting. As available observations are insufficient to specify a complete field of thermocline depth anomalies, the following procedure was adopted. A field of monthly mean surface wind stress anomalies was derived from ship observations over the tropical Pacific[40]; a 1–2–1 filter in time, longitude and latitude was then applied to the winds analysed. The anomalies used are the deviations from the average of the same calendar month over the previous 4 years; for example, the May 1985 anomaly is the deviation from the mean of May 1982, 1983, 1984 and 1985.

The period up to the forecast initial time was simulated by forcing the ocean component of the coupled model with wind-stress anomaly fields specified for each month starting with January 1964. The computed SST anomalies were then used to run the atmospheric component of the model. The calculated anomalies in thermocline depth, currents, SST and surface winds were then used as initial conditions for a forecast with the coupled model. Note that the initial SST and wind fields are calculated to be compatible with the initial thermocline displacements within the model framework; they need not agree with observed SST or wind fields. The coupled model runs evolve from the initial conditions as in a true forecast model: no new data are introduced after the initial time.

Forecast results

Figure 1 compares a map of observed SST anomalies during the peak period, January 1983, with that from the forecast initiated in January 1981. The result is typical of the more

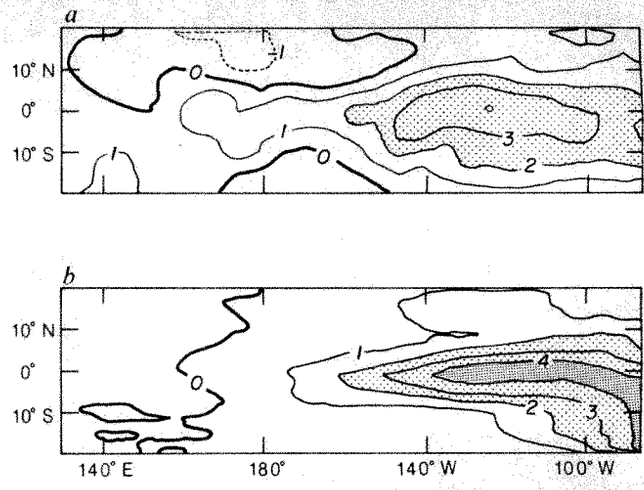


Fig. 1 Sea surface temperature (SST) anomalies (°C) in January 1983. *a*, Observed, based on the analysis of the Climate Analysis Center (CAC) of NOAA. *b*, Predicted by the model forecast initiated in January 1981, 2 years earlier.

successful forecasts. As in earlier work[10], including cases with the same ocean model driven by observed winds[20], the gross character of the eastern Pacific El Niño SST anomaly is reproduced, although its meridional and westward extent is underestimated.

Forecasts were initiated in the periods preceding each of the El Niño events that have occurred since 1970; that is, the events of 1972, 1976 and 1982. An additional set was made for the 'non-event' of 1979. No forecasts were attempted in the years before 1970 because the wind analyses available for these earlier years are of distinctly lower quality. In each period there are six forecasts spaced 3 months apart, with the sequence ending in January of the nominal year. For example, for 1972 forecasts were initiated from October 1970, January, April, July and October, 1971 and January 1972.

The forecast results are summarized in terms of the SST anomaly averaged over the eastern equatorial Pacific area called NINO3 (5° S to 5° N; 90° W to 150° W). The NINO3 index was devised by the Climate Analysis Center of NOAA (National Oceanic and Atmospheric Administration) because a warming in this region strongly influences the global atmosphere[2]. It is probably the best single indicator of an ENSO episode likely to affect global climate.

Figure 2 shows that the model generally succeeds in predicting warmings in those years when they were observed to occur, and

Table 1 Summary of forecast results for past years

Start month	No. right	No. of cases	Chance by coin flips
1-yr forecasts			
October	7	8	0.04
January	8	8	0.004
April	1	4	0.94
July	4	4	0.06
Total	20	24	0.0008
2-yr forecasts			
October	3	4	0.31
January	3	4	0.31
Total	6	8	0.14

Results correspond to the 24 forecasts of Fig. 2. For January, '1-yr forecasts' refers to the same calendar year; for all other start months, to the next calendar year. The last column shows the probability of correctly predicting at least as many cases as the model did by flipping a coin.

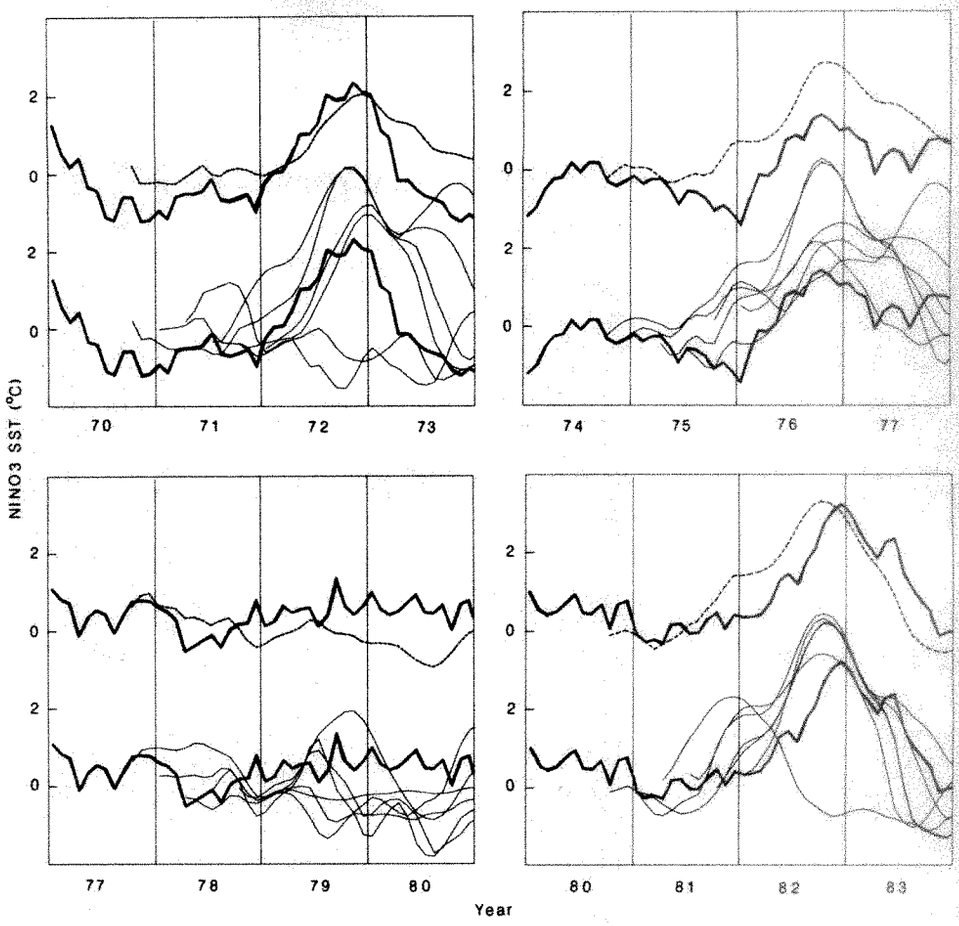


Fig. 2 SST anomalies (°C) averaged over the eastern equatorial Pacific NINO3 region (90° W to 150° W, 5° S to 5° N) for four periods centred on 1972, 1976, 1979 and 1982. Heavy curves, observed values as reported by CAC/NOAA (note repetition of vertical scale). Light curves, values from six forecasts initiated at 3-month intervals from the October two years ahead to the January of the nominal year. Dashed curve, average of the six forecasts (the consensus forecast).

in predicting their absence when they did not occur. As with the observed events, the peaks in the NINO3 index are always forecast to take place at the end of the calendar year. The individual forecasts tend to give too strong an event, especially for the 1976 El Niño. The rise in temperature during 1976 is well predicted, but five of the six forecasts begin the year at least 2 °C too warm. They entirely missed the 1975 cooling trend, which culminated in the coldest NINO3 SST in the entire data record. This failure is present even when the model is forced by observed winds, as in the run creating initial conditions (see, for example, the initial SST for the January 1976 forecast in Fig. 2). On the other hand, the model never predicts an El Niño for 1975, although at the time observers saw enough precursors of an event early in the year to announce an El Niño watch.

It is important to know whether the model's ability to predict whether an El Niño will occur is significantly better than chance. Because the distribution of states in the tropical Pacific is strongly bimodal[1], it is straightforward to distinguish El Niño events from non-events. In terms of NINO3 SST we will say there is an El Niño if there is a rise of at least 2 °C within 12 months, leading to an anomaly of at least +1.0 °C for at least 3 months. These criteria are derived from the observed events; the set of forecasts would score similarly for any other criteria able to separate observed events from non-events.

According to the above criteria, 19 of the 24 forecasts are correct. (The forecasts would be judged to be less successful if more detailed agreement with observation were demanded.) January 1971, April 1971, October 1975 and April 1981 fail to predict the upcoming event, and April 1978 falsely predicts an El Niño in 1979. Of the five failures, three are from April starts. In the spring the Intertropical Convergence Zone is closest to the Equator and the SST in the east is warmest. As a result the coupling between model atmosphere and ocean is such that noise in the initial state is easily amplified, leading to poor results. The real ocean–atmosphere system is also least predictable in the spring: it is the time when the Southern Oscillation index shows the smallest correlation with its future value[41].

Meteorological forecasts are typically evaluated relative to climatology or persistence, but either overestimates the predictive skill for infrequent events like El Niño. Table 1 offers another standard: the random guess. It may seem artificially favourable to compare to a guessing strategy which makes no apparent use of the known 3–4-yr quasi-periodicity of the ENSO cycle[2]; however, we have forecast only for periods 3 or 4 years apart, when events are seemingly due. Hence the occurrence or non-occurrence of an event in any of the years in our sample is roughly equally likely, so that flipping a coin is a reasonable guessing strategy.

In order to establish a rigorous confidence level, the number of independent forecasts must be known. A precise determination of independence would require many more model runs, but estimates adequate for present purposes can be readily made. We treat forecasts that are 3 months apart as independent, based on the observation that qualitative behaviour (such as incorrect forecasts or maintaining high SST in the year after an event) rarely persists longer. Doing this probably overestimates the confidence level. At the other extreme, a very conservative estimate is obtained by assuming that the forecasts within each set are highly correlated. Then there are only four independent forecasts, each given by the majority of the six within each set. As all four are correct, there is 1 chance in 16 of doing as well by coin flipping. Our most plausible estimate is based on the fact that, whereas indices of the Southern Oscillation can be highly correlated for many months, the months preceding April of a given year correlate poorly with months following it[41]. This suggests treating the first October, January and April of a set as one forecast, independent of a second forecast derived from the subsequent July, October and January. There are now eight independent forecasts, the last seven of which are correct. The probability of guessing this successfully is ~0.04.

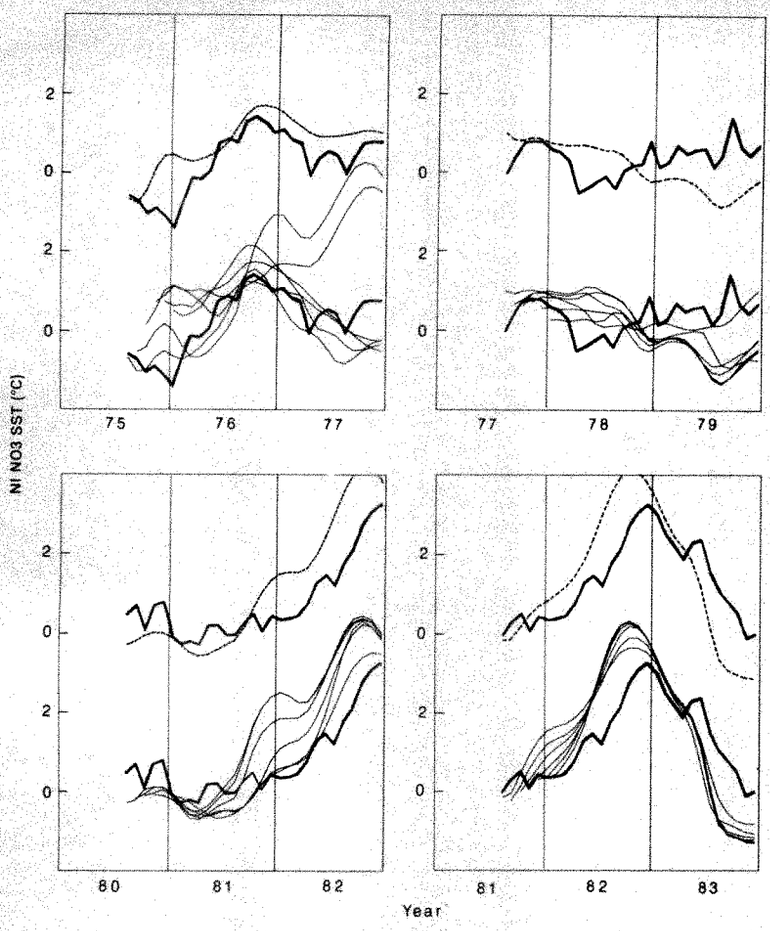


Fig. 3 SST anomalies (°C) for selected periods, averaged over the NINO3 region. Light curves, values from forecasts initiated in the six successive months from August to the following January. Dashed curve, average of the six (the consensus forecast); heavy curves, observed values (note repetition of vertical scale).

Another measure of model performance is obtained by considering events and non-events separately. Altogether, 14 of 18 occurrences of El Niño and 5 of 6 non-occurrences are forecast correctly. The joint probability of getting at least that many of each type right by an optimal random strategy is 0.004. (The optimal random strategy assumes *a priori* knowledge of the number of events and non-events in the sample, as well as the score to beat.) The corresponding joint probabilities for the 'conservative' and 'most plausible' cases are 0.06 and 0.04, respectively.

Forecasts started in the same calendar month in different years differ only in their initial conditions. Their success supports the assertion that the future evolution of ENSO is implicit in the initial conditions. Consider, for example, the eight 1-yr forecasts initiated in January. Even if one knew in advance that there were three El Niño events and five non-events, the chance of matching the model performance by guessing all eight correctly is only 1 in 56.

Rather than considering forecasts at 3-month intervals, we now examine a more useful forecasting strategy. A forecast is initiated in each of the 6 successive months from August to January, to obtain the prediction of the ensemble 1 and 2 years ahead. Table 2 summarizes the results of doing this in every year for which we have data (1970–1984), with the exception of the three El Niño years in the sample. A few examples are shown in Fig. 3. There are twelve sets of 1-yr forecasts: in nine of these all 6 months agree so the interpretation of the model prediction is unambiguous. In all nine the prediction is correct. By the rather stringent standard which scores the other three as wrong, the probability of doing as well or better by chance is 0.07.

It would be more accurate to say that the three latter forecasts provide unclear guidance. In two of the cases, where there was no event in the following year, half of the months forecast correctly and the other half did not. The remaining case is the set from August 1975 to January 1976. As can be seen from Fig. 3, the model actually does a good job of predicting the odd event to come. However, four times out of six our temperature rise criterion is not met because the model SST is too warm at the beginning of 1976. One might quibble with our scoring system, but it would undoubtedly have been difficult to interpret such a forecast at the time.

As might be expected, the 2-yr forecasts are less successful: in five cases all six individual forecasts are correct; in three cases five of six are correct; in the remaining cases one, two or three are correct. Counting eight of the eleven as successes gives

Table 2 Success rates of 6-month sets of forecasts

Forecast from	No. correct (out of 6) 1-yr	2-yr
1970	6	5*
1971	6*	1
1973	6	3
1974	6	6*
1975	2*	5
1977	6	6
1978	6	6
1979	6	2
1980	6	6*
1981	6*	6
1983	3	5
1984	3	?

Summary of the sets of forecasts initiated in the six successive months from August to January of each year from 1970 to 1984 (excluding El Niño years). For example, in the first line of the table, the forecasts are from August 1970 to January 1971; the 1-yr forecasts are for 1971 and the 2-yr forecasts are for 1972.

* Year of El Niño event.

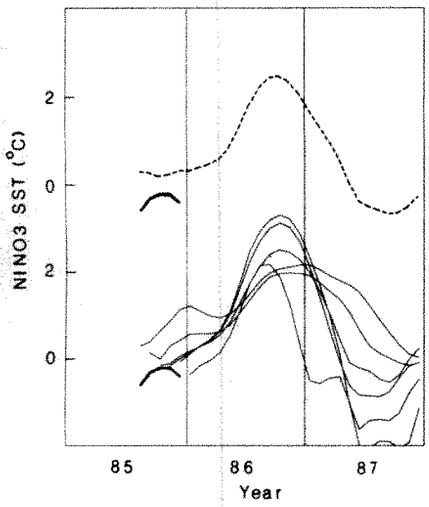


Fig. 4 Forecast for 1986 of SST anomalies (°C) in the NINO3 region. Light curves, values from forecasts initiated in the six successive months from August 1985 to January 1986. Dashed curve, average of the six forecasts; heavy curves, observed values (note repetition of vertical scale).

an 89% confidence level. The most consistent failure is the 1971 set, in which all forecasts predicted the 1972 E Niño but five of the six had the warming persist through 1973. Four of the 1979 forecasts predicted an event in 1981, a year early. The 1983 set is the most ambiguous; note that for the years since the outsized 1982 event both the 1- and 2-yr forecasts have been inconsistent.

We present another case, which cannot be evaluated at the time of writing: the prediction for 1986. Figure 4 shows the forecasts initiated in August 1985 to January 1986: all six predict an El Niño event. The amplitude of the consensus forecast suggests it will be a moderate event, not as strong as the events of 1982, 1972 or 1957. However, the only other moderate event in our study was the peculiar 1976 El Niño; experience with the moderate event of 1965 and the even weaker 1969 one might help in interpreting the present case. For the three events in our sample (1972, 1976 and 1982) the consensus overstated the maximum NINO3 SST anomaly amplitude by 30% (more precisely, by 28%, 36% and 28%, respecitvly). Re-scaling the 1986 forecast accordingly indicates an amplitude of 1.9 °C, well below the 3.2 °C of 1982 or the 2.5 °C of 1972, but above the 1.4 °C of 1976.

How much confidence should be placed in the prediction of a 1986 El Niño? As with all forecasting, there exists the possibility that the present case will put pressure on previously untested weak points in the model. Forecasts since the 1982–83 event have been problematical in some respects, possibly reflecting a shift in circulation regime which could adversely affect model performance. Although all of the 1985 forecasts predict an event for 1986, none of the 2-yr forecasts from 1984 predicts it. This is unprecedented among the limited set of cases we have studied. Also, both the 1983 and 1984 1-yr forecasts lack the consistency which is typical of earlier years. Nonetheless, in no previous case in which all six 1-yr forecasts agreed were they incorrect. Moreover, all eleven forecasts from March 1985 to January 1986 give the same result.

Discussion

The ability of the model to predict at long lead times lends support to the theory outlined above[5], especially the idea that the ENSO cycle owes its existence to interactions in the tropical Pacific. Although the thermal anomalies in the upper layers of the tropical ocean are crucial to the long timescale of the cycle, the ocean alone could not sustain the cycle from event to event. It is an essential part of the ENSO cycle that the two-way coupling between tropical atmosphere and ocean is active in both the El Niño and non-El Niño phases of the cycle.

The results presented here have significant implications for the future prospects of ENSO prediction systems. It seems clear that the predictability limit for ENSO is years rather than weeks or months. We cannot yet state it more precisely, and it cannot be calculated from forecasts alone because the intrinsic lack of predictability of the coupled ocean–atmosphere system is not the only reason for inaccurate forecasts; poor data and model errors also contribute. We presume these failings account for the cases where the forecasts from many consecutive months are both consistent and wrong (for example, the forecasts for 1973 from 1971). It is also likely that the predictability is highly variable: at some times the future evolution of the coupled system is insensitive to small changes; at others, the system passes so close to a bifurcation point that even small-amplitude disturbances may alter its future behaviour substantially, perhaps making the difference between El Niño and non-El Niño states. We conjecture that the latter times are those for which forecasts from consecutive months are inconsistent (for example, the forecasts from 1983). Here we are implicitly assuming that month-to-month variations in initial conditions are sufficient to reveal all of these uncertain times. Further studies may reveal a better indicator of periods of unpredictability.

In view of the sparsity of the observations used to produce model initial conditions, the success of the forecasts is somewhat surprising, and certainly encouraging. Even without any new breakthroughs in understanding, it should be possible to lengthen the lead time of the model predictions, increase their reliability and improve the forecast of features more subtle than NINO3 SST.

Much more could be done to process the initial data for the purpose of forecasting. All operational meterological forecast models have very elaborate procedures for data assimilation and model initialization. The only observations used here are ship reports of surface winds. Available observations of SST, currents and ocean thermal structure should be incorporated in the initial fields. Enhancement of the observing system would increase forecast skill: we expect remote sensing of surface winds from satellites to be especially beneficial.

The model used here was developed for theoretical studies, rather than forecasting. It was deliberately simplified in order to isolate the physics believed to be essential to ENSO, putting it at a level of complexity comparable to numerical weather prediction models of 30 years ago. Because our model is based on physical principles, it can be elaborated to increase the fidelity of its simulations. It seems clear that with better observing networks and more refined models, operational climate forecasts of definite social and economic benefit can be expected in the near future.

We dedicate this paper to the memory of Dr Adrian Gill in appreciation of the encouragement he gave this work, and, more broadly, in recognition of his essential contributions to the understanding of ENSO. We thank Professor J. J. O'Brien and David Legler of Florida State University for providing the surface wind analysis, Dr George Philander for his stimulating comments on an earlier draft, and Professor Harold Sackrowitz for advice on statistical matters. This work was supported by grants NA-84-AA-D-0031 from the US TOGA Office of NOAA, NA-84-RAD-05082 from EPOCS/NOAA, and NAGW-582 from NASA. This is Lamont–Doherty Geological Observatory contribution 4004.

Note added in proof: No indication of El Niño is apparent as of the end of May 1986. There is no known precedent for an event to begin later than June.

Received 10 March; accepted 8 May 1986.

1. Cane, M. A. *Science* **222**, 1189–1194 (1983).
2. Rasmusson, E. M. & Wallace, J. M. *Science* **222**, 1195–1202 (1983).
3. Rasmusson, E. M. *Am. Scient.* **73**, 168–177 (1985).
4. Gill, A. E. & Rasmusson, E. M. *Nature* **306**, 229–234 (1983).

5. Philander, S. G. H. *Nature* **302**, 215-301 (1983).
6. Canby, T. Y. *Natn. geogr. Mag.* **165**, 144-183 (1983).
7. Glantz, M. H. *Oceanus* **27**, 14-19 (1984).
8. Barnett, T. P. *Mon. Weath. Rev.* **111**, 756-773 (1983).
9. Inoue, I. & O'Brien, J. J. *Mon. Weath. Rev.* **112**, 2326-2337 (1984).
10. Zebiak, S. E. & Cane, M. A. *Mon. Weath. Rev.* (in the press).
11. Cane, M. A. & Zebiak, S. E. *Science* **228**, 1085-1087 (1985).
12. Lau, K.-M. & Chan, P. *Mon. Weath. Rev.* **113**, 1889-1909 (1985).
13. Bjerknes, J. *Mon. Weath. Rev.* **97**, 163-172 (1969).
14. Cane, M. A. *A. Rev. Earth planet. Sci.* **14**, 43-70 (1986).
15. Wyrtki, K. *J. phys. Oceanogr.* **5**, 572-584 (1975).
16. Wyrtki, K. *J. phys. Oceanogr.* **9**, 1223-1231 (1979).
17. Busalacchi, A. J. & O'Brien, J. J. *J. geophys. Res.* **86**, 10901-10907 (1981).
18. Gill, A. E. *J. phys. Oceanogr.* **13**, 586-606 (1983).
19. Harrison, D. E. & Schopf, P. S. *Mon. Weath. Rev.* **112**, 923-933 (1984).
20. Zebiak, S. E. & Cane, M. A. *J. phys. Oceanogr.* (submitted).
21. Ramage, C. S. & Hori, A. M. *Mon. Weath. Rev.* **109**, 1827-1835 (1981).
22. Lau, N.-C. *Mon. Weath. Rev.* **113**, 1970-1996 (1985).
23. Shukla, J. & Wallace, J. M. *J. atmos. Sci.* **40**, 1613-1630 (1983).
24. Boer, G. J. in *Coupled Ocean-Atmosphere Models* (ed. Nihoul, J.) 7-18 (Elsevier, Amsterdam, 1985).
25. Gill, A. E. *Q. J. R. met. Soc.* **106**, 447-462 (1980).
26. Webster, P. J. *J. atmos. Sci.* **38**, 554-571 (1981).
27. Zebiak, S. E. *J. atmos. Sci.* **39**, 2017-2027 (1982).
28. Zebiak, S. E. *Mon. Weath. Rev.* (in the press).
29. McCreary, J. P. *Mon. Weath. Rev.* **111**, 370-389 (1983).
30. Anderson, D. L. T. & McCreary, J. P. *J. atmos. Sci.* **42**, 615-628 (1985).
31. Philander, S. G. H., Yamagata, T. & Pacanowski, R. C. *J. atmos. Sci.* **41**, 604-613 (1984).
32. Hirst, A. *J. atmos. Sci.* (in the press).
33. Lau, K.-M. *J. atmos. Sci.* **38**, 248-261 (1981).
34. McCreary, J. P. *A. Rev. Fluid. Mech.* **17**, 359-409 (1985).
35. Cane, M. A. & Sarachik, E. S. *J. mar. Res.* **35**, 395-432 (1977).
36. Wyrtki, K. *J. geophys. Res.* **90**, 11719-11725 (1985).
37. Lau, K.-M. *J. atmos. Sci.* **42**, 1552-1558 (1985).
38. Vallis, G. K. *Science* **232**, 243-245 (1986).
39. White, W. & Pazan, S. *J. phys. Oceanogr.* (submitted).
40. Goldenbert, S. B. & O'Brien, J. J. *Mon. Weath. Rev.* **109**, 1190-1207 (1981).
41. Wright, P. *Bull. Am. met. Soc.* **66**, 398-412 (1985).

Secular variation in carbon isotope ratios from Upper Proterozoic successions of Svalbard and East Greenland

A. H. Knoll*, J. M. Hayes†, A. J. Kaufman†, K. Swett‡ & I. B. Lambert§

* Department of Organismic and Evolutionary Biology, Harvard University, Cambridge, Massachusetts 02138, USA
† Biogeochemical Laboratories, Department of Chemistry and Geology, Indiana University, Bloomington, Indiana 47405-5101, USA
‡ Department of Geology, University of Iowa, Iowa City, Iowa 52242, USA
§ Baas Becking Geobiological Laboratory, PO Box 378, Canberra ACT 2601, Australia

Analyses of stratigraphically continuous suites of samples from Upper Proterozoic sedimentary successions of East Greenland, Spitsbergen and Nordaustlandet (Svalbard) provide an approximation to the secular variation in carbon isotope ratios during a geologically and biologically important period of change from around 900 million years ago to the beginning of the Cambrian period. Late Riphean carbonates and organic material show a stratigraphically useful pattern of enrichment in ^{13}C relative to Phanerozoic or earlier Proterozoic samples. Isotopic compositions of isolated samples from other localities are consistent with a worldwide extended interval of enhanced organic burial and consequent net survival of oxidized material, probably O_2, just before the initial radiation of metazoans.

SECULAR variations in the carbon isotopic composition of sedimentary carbonates and organic materials have been determined with reasonable temporal precision for most of the Phanerozoic eon, and these data have assumed a significant role in discussion of Phanerozoic environmental history[1-4]. Analyses of Precambrian samples show that on a gross scale the earlier record of carbon isotopic variation is not dissimilar to that of the past 570 Myr (ref. 5); however, insufficient sampling density and a lack of stratigraphic control have hindered attempts to continue the curve representing of carbon isotopic abundances in marine carbonates backward into the Proterozoic.

We report here the results of carbon isotopic analyses of stratigraphically continuous suites of samples collected from Upper Proterozoic sedimentary successions in Nordaustlandet (Svalbard), northeastern Spitsbergen and central East Greenland. Stratigraphic position, palaeoenvironmental setting and petrography have been determined for each sample, and a degree of biostratigraphic control is provided by acritarch assemblages that occur in all three sequences. The sections, which represent widely separated localities within a single sedimentary basin, show smoothly covariant carbon isotope records for both carbonate and organic carbon. Here we consider three questions bearing on the interpretation and significance of these isotopic variations:

(1) Are they primary (that is, reflective of changes in the isotopic composition of carbon available for biosynthesis of organic matter)?

(2) Are they of global extent (representative of changes in the isotopic composition of oxidized carbon in the world ocean)?

(3) Do they reflect changes in the Earth's surface environment, especially changes in O_2 concentration, which may have been important in late Proterozoic biological evolution?

Geological setting

The close lithostratigraphic similarities between the Upper Proterozoic and Lower Palaeozoic sequences of the East Greenland Caledonides and eastern Svalbard have long been appreciated[6]. The Spitsbergen, Nordaustlandet and East Greenland sections each contain 7,000-8,000 m of unmetamorphosed, predominantly shallow marine sedimentary rocks, comprising two quartz-arenite-carbonate successions separated by an interval of glaciogenic sedimentation[7-14]. Table 1 summaries the nomenclature of the sampled rock units, and stratigraphic columns are shown in Fig. 1.

Thick sequences of cross-bedded and rippled sandstones with interbedded rippled, often carbonaceous shales grade upward into carbonates with minor siliciclastic intercalations. The limestone and dolostone successions contain abundant stromatolites, cross-bedded oolites and pisolites, and intraformational conglomerates, all of which indicate intertidal to shallow subtidal marine deposition. The carbonates are overlain abruptly by a diamictite-bearing siliciclastic sequence, which is in turn overlain by a quartz-arenite-carbonate sequence of Cambro-Ordovician age. Microfossil assemblages[15-17] and stromatolites[18] indicate that the earlier siliciclastic and carbonate sequence was deposited ~900-700 Myr ago, during the late Riphean interval,

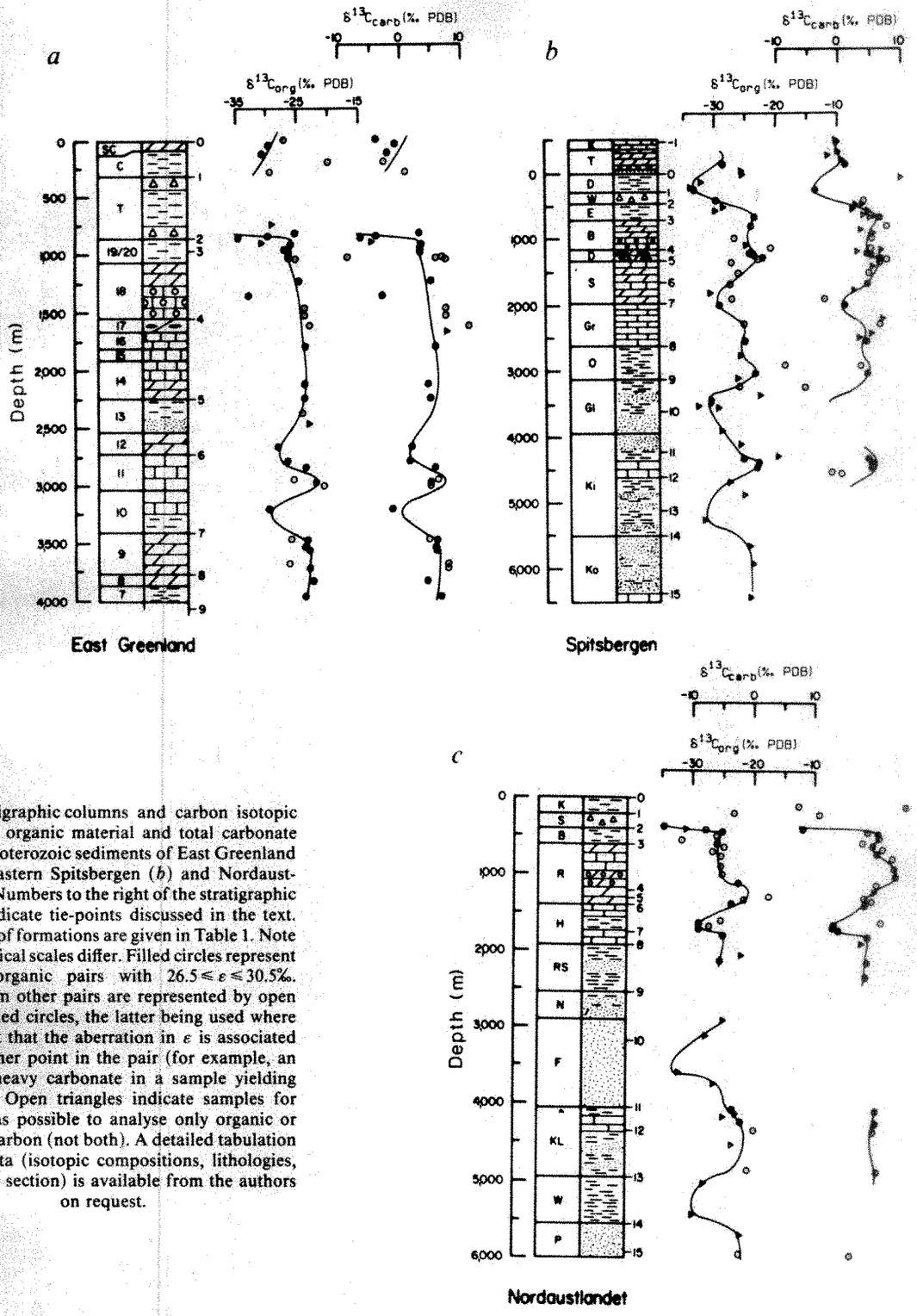


Fig. 1 Stratigraphic columns and carbon isotopic analyses of organic material and total carbonate from late Proterozoic sediments of East Greenland (*a*), northeastern Spitsbergen (*b*) and Nordaustlandet (*c*). Numbers to the right of the stratigraphic columns indicate tie-points discussed in the text. Full names of formations are given in Table 1. Note that the vertical scales differ. Filled circles represent carbonate–organic pairs with $26.5 \leq \varepsilon \leq 30.5‰$. Results from other pairs are represented by open and half-filled circles, the latter being used where it is evident that the aberration in ε is associated with the other point in the pair (for example, an unusually heavy carbonate in a sample yielding $\varepsilon \geq 30.5‰$). Open triangles indicate samples for which it was possible to analyse only organic or carbonate carbon (not both). A detailed tabulation of these data (isotopic compositions, lithologies, locations in section) is available from the authors on request.

and that the diamictite-bearing sequence is Vendian (670–570 Myr) in age. Hiatuses corresponding in time to the latest Riphean and late Vendian to earliest Cambrian occur at the base and top, respectively, of the diamictite-bearing succession[14]. (In Greenland, the stratigraphic break appears to occur not at the Eleonore Bay Group/Tillite Group boundary, but within Bed 19 of the Eleonore Bay Group.)

Petrographic studies reveal further strong parallels in the histories of the Greenland and Svalbard sequences[19], and palaeontological analyses show comparable patterns of microfossil distribution[15–17,20,21]. Based on these observations, 16 tie-points have been identified which can be correlated lithostratigraphically with high confidence among sections: these are shown in Fig. 1 (the tie-point at the Precambrian/Cambrian boundary is designated zero, and numbers increase down-section). The close correlations show that the three successions were deposited contiguously along the margin of a single marine basin[22]. The distance separating the most distant of the successions at the time of deposition was at least 650 km, and possibly much greater. The East Greenland–Svalbard basin apparently constituted the western margin of the expanding Iapetus Ocean during the Cambrian, but debate continues as to whether the thick underlying Upper Proterozoic sequence accumulated intracratonically or on an early-formed passive margin[22,23].

Chemical and isotopic analyses

Field specimens were cleaned, fragmented, etched and ground[24]. Carbon dioxide was produced from carbonates by treatment with H_3PO_4 (density 1.89 g ml^{-1}) at 50 °C for 48 h (ref. 25). For determination of the abundance and isotopic composition of organic carbon, sample powders were treated with hot, concentrated HCl in order to remove carbonates, then mixed with CuO and sealed in evacuated quartz tubes for combustion at 850 °C for 2 h. Recovery and purification of CO_2 formed by combustion of organic matter allowed both quantitative and isotopic analysis. This procedure was tested by application to 49 samples previously analysed by accepted techniques[24], and yielded accurate results for samples similar to those analysed in this work. Isotopic compositions of CO_2 were determined by conventional mass spectrometric techniques[26] and are expressed relative to the PDB standard: $\delta = [(R_x/R_{PDB}) - 1] \times 10^3$, where $R = {}^{13}C/{}^{12}C$ and the subscript x designates the analyte. For compactness, we employ δ_c and δ_o to refer to the carbon isotopic compositions of carbonate and organic carbon, respectively.

Results and discussion

Isotopic variations. Figure 1 summarizes the results of the isotopic analyses: it is evident that the abundance of ^{13}C varies in both carbonate minerals and organic material. Such variations can be primary (reflecting changes in the isotopic composition of carbonate in the water column beneath which the sediments initially accumulated) or secondary (reflecting bacterial reworking of organic material, precipitation and admixture of new carbonates, or isotopic exchange with species in solution). Consideration of the significance of these isotopic variations requires resolution of primary and secondary effects.

Recognition of truly primary isotopic compositions and perfect elucidation of all secondary variations is difficult in the best of circumstances[27]. However, no secondary processes are known (or are, for that matter, conceivable) which always shift the isotopic compositions of carbonate and organic carbon in the same direction at the same rate. Instead, secondary processes commonly alter the isotopic composition either of organic carbon[28] or of carbonate carbon[29], and the magnitudes of the isotopic shifts are controlled by different and unrelated factors. Primary processes (biosynthesis of organic material and formation of carbonate in equilibrium with dissolved CO_2), on the other hand, tend to maintain a constant isotopic difference between carbonate and organic carbon. Systematic consideration of the isotopic fractionation ($\varepsilon \simeq \delta_c - \delta_o$) can therefore assist in the resolution of primary and secondary isotopic variations.

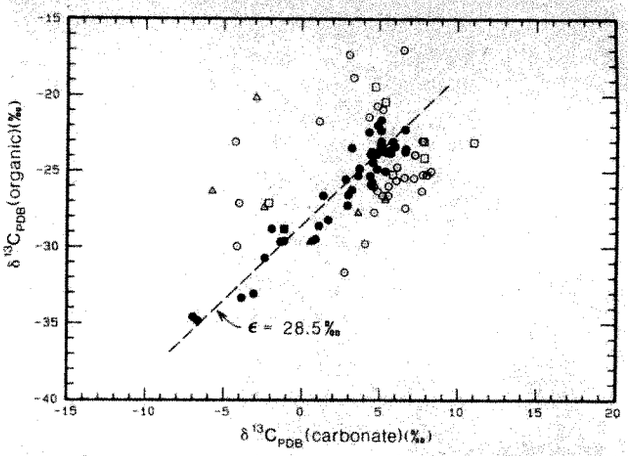


Fig. 2 Carbon isotopic compositions of samples in which it was possible to analyse both organic and inorganic phases. Squares, samples in which the concentration of organic carbon was <0.2 mg C per g sample; triangles, samples containing <10% carbonate (as calcite); filled symbols, samples with $26.5 \leq \varepsilon \leq 30.5$‰.

The data include 92 pairs of measurements from which ε values can be computed; the carbon isotopic compositions of carbonate and organic materials in these samples are compared in Fig. 2. The mode of the distribution of ε values lies near 28.5‰ (dashed line in Fig. 2). Many of the carbonate–organic pairs yielding $\varepsilon > 30.5$‰ or $\varepsilon < 26.5$‰ contain <0.2 mg organic C per g sample or <10% carbonate; because of their low carbon concentrations, the isotopic compositions of these samples are particularly vulnerable to diagenetic alteration. We conclude that samples yielding $\varepsilon = 28.5 \pm 2.0$‰ preserve primary carbon isotopic compositions within a few per mil. We do not contend that isotopic shifts due to diagenesis are absent in these sections, and will return to this point below. We do suggest, however, that measurement of both organic and inorganic carbon isotopic compositions greatly reduces the chance of misinterpretation and allows the recognition of major features in the isotopic records compiled in this work.

Correlations between sections. Comparison of variations observed in the different sections suggests that all three record the same set of primary variations. For example, all are depleted in ^{13}C in the Vendian and show a general pattern of ^{13}C enrichment during the late Riphean. The lithostratigraphic tie-points

Table 1 Stratigraphy and correlation among sections

East Greenland[13,14]		Northeastern Spitsbergen[7–11]		Nordaustlandet[12]		Tie-points* and chronostratigraphy
Group	Formation	Group	Formation	Group	Formation	
		Oslobreen	Kirtonryggen			−1 540 Myr
			Tokammane			Cambrian
	Spiral Creek		Dracoisen		Klackberget	0 560 Myr (hiatus)
Tillite	Canyon	Polarisbreen	Wilsonbreen	Gotia	Sveanor	590 Myr
	Tillite		Elbobreen		Backaberget	Vendian
	Bed 19/20		Backlundtoppen			3 670 Myr (hiatus)
	⋮		Draken		Ryssö	700 Myr
Eleonore Bay	⋮	Akademikerbreen	Svanbergfjellet	Roaldtoppen	Hunnberg	
	Bed 8		Grusdievbreen			
	Bed 7					8 800 Myr
			Oxfordbreen		Raudstup/Sälodd	Upper Riphean
				Celsiusberget	Norvik	
			Glasgowbreen		Flora	
		Veteranen				
			Kingbreen		Kapp Lord	
				Franklinsundet	Westmanbukta	
			Kortbreen		Persberget	15 900 Myr

* Summarizes placement of rock units within chronostratigraphic units and indicates lithostratigraphic tie-points for which ages have been estimated by the authors. Precise placement of tie-points within each section is shown in Fig. 1.

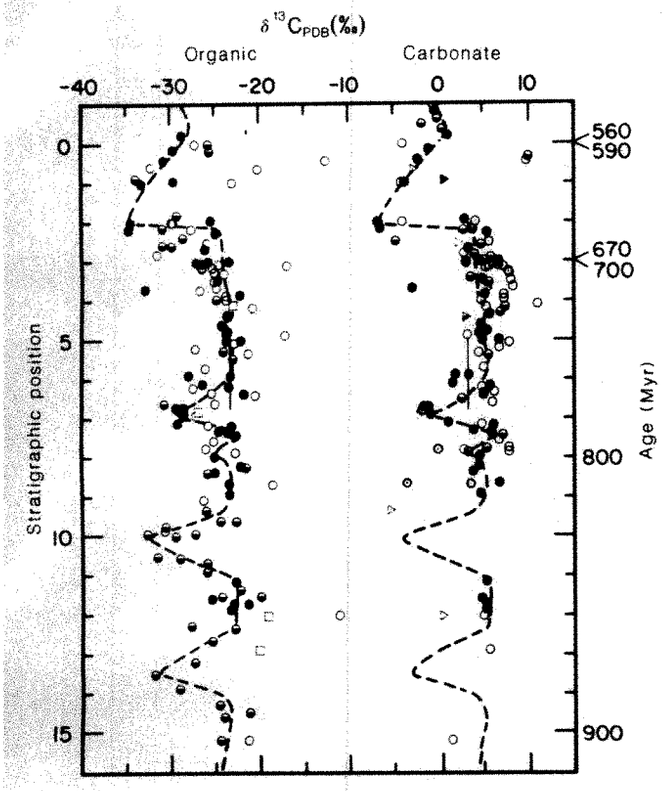


Fig. 3 Isotopic analyses from Fig. 1 pooled and re-plotted on correlated depth scale (numbers at left refer to the tie-points shown in Fig. 1; the scale is thus not linear with respect to either time or thickness of section). Symbols as in Fig. 2 except that half-filled symbols designate samples for which analysis of only one carbon phase (carbonate or organic) was possible. Vertical lines near depth = 6.0 represent a single sample for which stratigraphic placement was uncertain.

already described can be used to plot data from all sections on a single graph, facilitating investigation of isotopic correlations.

In Fig. 3, the ordinate ('stratigraphic position') represents the sequence of tie-points and is thus a scale related to depth. Isotopic compositions of samples collected at stratigraphic levels equivalent to tie-points have been plotted at integer values; others have been placed along the ordinate by linear interpolation between tie-points within each section. The dashed lines are separated by 28.5‰, and were derived by overlaying the carbonate and organic carbon isotopic records (offset by 28.5‰) and considering the trend of both sets of data. The close parallel between the organic and inorganic records is clearly visible in the upper part of the section. Carbonates are rare in the lower part of the section, but strong evidence for additional isotopic variations appears in the organic carbon record. We emphasize that our stratigraphic correlation of the three sections was completed independently of the isotopic analyses; thus, the high degree of congruence seen in Fig. 3 demonstrates the potential of chemostratigraphy based on carbon isotopic compositions for accurate intra-basinal correlation of late Proterozoic sedimentary sequences.

The record of isotopic abundances summarized by Fig. 3 encompasses >300 Myr: the lowermost Cambrian, the Vendian and the Riphean to ~900 Myr. Compared with isotopic compositions prevailing during most of the Phanerozoic (and earlier in the Proterozoic, as far as can be determined[30]), its principal features are a general pattern of strong ^{13}C enrichment during the late Riphean, an extended interval of ^{13}C depletion in the Vendian and, apparently, several episodes of near-'normal' isotopic compositions in the late Riphean.

As enrichment of ^{13}C in carbonates is so prominent in the isotopic record summarized in Fig. 3, the process of methanogenic diagenesis should be considered. Fermentative processes yielding methane, often associated with the formation of carbonates enriched in ^{13}C (ref. 29), apparently have no effect on the isotopic composition of coexisting organic matter. Thus, methanogenic diagenesis shifts points to the right on a graph like that shown in Fig. 2, and it is conceivable that carbonates represented by some of the open points to the right of the broken line in Fig. 2 have been diagenetically enriched in ^{13}C. It is, however, extremely unlikely that this process is responsible for the general enrichment of ^{13}C observed in these sections. To sustain that interpretation, it would be necessary to suggest that, in spite of wide variations in facies (tidal-flat microbial mats, cross-bedded oolites, subtidal dolomitic shales) and carbonate abundance, methanogenesis had, over more than 100 Myr, uniformly affected all of the carbonates that we associate with primary variations in isotopic abundance (filled circles in Fig. 2).

Isotopic compositions within the Vendian Gotia, Polarisbreen and Tillite groups are more variable, reflecting the re-deposition of late Riphean carbonates as detritus[31], as well as primary variations, but horizons of notably 'light' carbon can be correlated among sections. Cambrian values, obtained only from the Spitsbergen section, range from −1.8 to +1.1‰, similar to previously published values for Lower Palaeozoic rocks[1]. In Spitsbergen, the base of the Cambrian is recognized by the first appearance of Lontova-type acritarchs and diverse trace fossils of Cambrian aspect; our Lower Cambrian carbonates are associated with *Salterella* and late-*Holmia*-age acritarchs[21].

Mechanism and scale of primary variations. What might account for the enrichment of ^{13}C in the Upper Riphean sediments of Svalbard and East Greenland? On a basin-wide scale, enrichment of heavy isotopes can be caused by widespread and persistent evaporitic conditions. Isotopically heavy carbonates (δ_c = +3.0–5.6‰) are forming today by this mechanism in Shark Bay, Western Australia (J. Ferguson, L. A. Plumb and M. R. Walter, unpublished data), and the heavy carbon in the sections studied here might have a similar origin (although evaporation does not always lead to marked ^{13}C enrichment; see ref. 32). Two arguments militate against this, however. First, evaporites and indirect sedimentological evidence of evaporitic environments are conspicuously absent in these sections. Second, a clearly evaporitic sequence from the Proterozoic of northwestern Greenland (the Narssarrssuk Formation[33]) has yielded $0.65 \leq \delta_c \leq 2.65$‰ (mean of 12 samples = 1.65‰), somewhat heavy relative to early Palaeozoic mean values, but not comparable to the values recorded for Svalbard and East Greenland sediments.

Primary shifts in the isotopic composition of sedimentary carbon can also be due to changes in the isotopic composition of water-column carbonate caused by preferential biological fixation of ^{12}C into organic material[28,34]. Enhanced rates of burial of organic material lead to greater-than-normal enrichment of ^{13}C in carbonates[35].

The scale of these effects can be global or basinal, and assessment of the geochemical significance of isotopic shifts depends strongly on resolution of these alternatives. In a restricted basin, fixation and burial of organic carbon will cause enrichment of ^{13}C in carbonates if diffusion from the atmosphere and patterns of circulation are unable to maintain isotopic equilibrium with the open ocean. An effect of this kind has been suggested[36] as the explanation for the high levels of ^{13}C enrichment in the early Proterozoic Lomagundi Group, Zimbabwe. Heavy carbonates might alternatively be due to enrichment of ^{13}C in carbonate, not in a restricted basin, but throughout the world ocean. An enhancement in the global rate of burial of organic carbon is required to bring about this effect. In the case of the Lomagundi Formation, correlation with coeval sequences from other areas is difficult, so it has not proved possible to resolve the issue by determining whether enrichment was global. Relatively heavy carbon in the Permian, on the other hand, is demonstrably widespread[1,32].

The possibility that a similar global enrichment occurred in

Table 2 Summary of previous analyses of late Proterozoic carbonates

Rock unit*	Age (Myr)† Min.	Prob.	Max.	δ_c	s.d.	n	Ref.
Yakutsk, Siberia, Yudoma Fm	570	575	670	2.2	1.1	6	38
Yakutsk, Siberia, Yudoma Fm	570	585	670	−0.6	1.0	17	38
Nama Group, Schwarzrand Subgroup	570	590	650	−3.1	0.8	7	57
Yakutsk, Siberia, Yudoma Fm	570	595	670	−3.9	0.7	6	38
Nama Group, Kuibis Subgroup I	570	610	650	−0.9	1.3	5	57
Nama Group, Kuibis Subgroup II	570	610	650	2.2	1.2	8	57
Morocco, Serie Lie de Vin	570	610	670	−2.5	1.3	14	39
Adelaide Geosyncline, Marinoan I	570	650	700	7.4	3.6	3	30
Adelaide Geosyncline, Marinoan II	570	650	700	−6.3	2.4	5	30
Adelaide Geosyncline, Nuccaleena Fm	570	650	700	−2.5	0.7	2	58
Kimberley Reg., Late Proterozoic I	570	650	700	−2.9	0.3	5	58
Kimberley Reg., Late Proterozoic II	570	650	700	0.9	1.3	5	58
Amadeus Basin, Pertatataka Fm	625	675	700	5.2	0.5	2	30
Flinders Range, Umberatana Gp	650	675	725	3.3	2.5	3	57
Eleonore Bay Fm, Bed 18	650	700	725	5.2		1	57
S. Norway, Hedmark Gp, Biri Fm	668	700	750	1.7	0.4	11	59
Eleonore Bay Fm, Beds 14–16	700	720	740	5.7	1.0	4	57
Morocco, Dolomite Inferieur	670	735	800	(−2.1 to	6.9)	10	39
Eleonore Bay Fm, Beds 12–13	720	740	760	4.5	0.7	3	57
Adelaide Geosyncline, Sturtian	650	750	750	2.4	0.8	6	30
Adelaide Geosyncline, Tapley Hill Fm	650	750	750	1.8		1	58
Adelaide Geosyncline, Tapley Hill Fm	650	750	750	−3.0	0.6	10	60
Adelaide Geosyncline, Tapley Hill Fm	650	750	750	−0.7	0.4	2	61
Adelaide Geosyncline, Tapley Hill Fm	650	750	750	−0.2	2.3	20	62
Kimberley Region, Landrigan Tillite	650	750	750	−5.5		1	58
Katanga, Lower Kundelungu Series	640	750	840	1.3		1	57
India, Chattisgarh Basin	700	750	850	3.9	1.1	5	57
Eleonore Bay Fm, Bed 9	750	775	800	5.3	0.2	2	57
Taoudenii Syncline, Atar Gp I-11	725	775	825	−0.4		1	57
Kango and Malmesbury Group I	600	775	950	6.6	2.7	4	57
Kango and Malmesbury Group II	600	775	950	−0.3	1.1	11	57
Otavi Gp, Tsumeb Subgroup I	750	780	800	5.1	2.8	6	57
Otavi Gp, Tsumeb Subgroup II	750	780	800	−1.0	0.2	3	57
Taoudenii Syncline, Tifounka Gp, I12	650	800	950	0.7		1	57
Otavi Gp, Upper Abenab Subgroup	750	810	830	2.5	0.0	2	57
Amadeus Basin, Bitter Springs Fm	750	825	900	3.4		1	5
Amadeus Basin, Bitter Springs Fm I	750	825	900	3.5	1.6	8	30
Amadeus Basin, Bitter Springs Fm II	750	825	900	−0.9	2.1	6	30
Taoudenii Syncline, Atar Gp, I-9	725	825	925	0.5	1.9	2	57
Burra Gp, Skillogalee Dolomite	750	850	850	−2.0		1	57
Burra Gp, Skillogalee Dolomite	750	850	850	4.6		1	5
Burra Gp, Skillogalee Dolomite	750	850	850	2.3	1.0	2	‡
Death Valley, Beck Springs Dolomite	800	850	1200	4.2	0.3	13	65
Taoudenni Syncline, Atar Gp, I-7	800	870	900	0.1		1	57
Adelaide Geosyncline, Burra Gp I	840	875	930	−4.5		1	30
Adelaide Geosyncline, Burra Gp II	840	875	930	4.2	0.7	4	30
Katanga, Mwashia Group	840	875	930	−3.5		1	57
Taoudenii Syncline, Atar Gp, I-6	850	880	920	−2.2		1	57
Taoudenii Syncline, Atar Gp, I-5	850	890	925	1.0	0.4	2	57
Katanga, Lower Roan Gp I	930	1,000	1,200	5.7	1.6	2	57
Katanga, Lower Roan Gp II	930	1,000	1,200	−1.1	2.7	11	57
Lake Superior Basin, Sibley Group	1,000	1,050	1,300	−0.3		1	57
Adelaide Geosyncline, Eurelia Beds	1,000	1,060	1,100	3.5	0.8	30	64
Adelaide Geosyncline, Willouran	1,000	1,060	1,100	2.7	1.2	4	30
Glacier National Park, Middle Belt	910	1,075	1,400	0.5		1	65
Oakway Group	850	1,150	1,450	−1.1		1	57
Arizona, Apache Gp, Mescal Limestone	1,150	1,200	1,500	3.1	0.4	16	66
India, Cuddapah Basin	1,100	1,400	1,600	−0.9		1	57
McArthur Basin, HYC (least altered)	1,400	1,640	1,688	−0.3	0.4	7	67
McArthur Basin, McArthur Group	1,590	1,650	1,690	−1.2	1.9	6	30
McArthur Basin, McArthur Group	1,590	1,650	1,690	−1.0	0.9	6	5
McArthur Basin, Wollogorang Fm	1,590	1,650	1,690	−1.2	1.1	7	§
Birrindudu Basin, Bungle Bungle Dol	1,560	1,650	1,750	−0.7	0.3	7	5

* Roman numerals appended to rock units designate separate modes of bimodal distributions.
† Minimum, probable and maximum ages estimated by the authors.
‡ I. B. Lambert, unpublished data.
§ M. J. Jackson and T. H. Donnelly, unpublished data.

the late Proterozoic can be examined by consideration of all previous reports of carbon-isotopic compositions of middle and late Proterozoic sedimentary carbonates from North America, Africa, India and Australia. Figure 4 shows these data and a summary of carbonate isotopic compositions during the Phanerozoic, together with a curve representative of the isotopic compositions observed in this work. The Phanerozoic and late Proterozoic records differ greatly in temporal resolution, numbers of samples and levels of selectivity. We do not suggest that they can be compared directly in all respects, but contrasts are of such interest that some preliminary consideration is in order.

Comparison (Fig. 4) of the curve representative of isotopic compositions observed in this work with points representing all entries in Table 2 shows that these records are consistent, in that both suggest persistent and significant enrichment of ^{13}C in late Riphean sedimentary carbonates, as well as episodes of ^{13}C depletion or normalcy. The scatter of points representative of other rock units around the East Greenland–Svalbard curve is not significant because the stratigraphic positions of many samples are imprecisely defined, and radiometric and biostratigraphic age determinations for many sequences require further work (age uncertainties are estimated in Table 2). Existing data are thus consistent with the idea that the detailed isotopic records observed in this work reflect global trends, but stratigraphic data are insufficient to establish this point in great detail.

Implications. It should be evident that isotopic studies can assist in the reconstruction of stratigraphic relationships. Margaritz[37] has shown that systematic variations of the carbon isotopic compositions of sedimentary carbonates can be useful in the correlation of Cretaceous sequences, and Margaritz *et al.*[32] have argued that anomalously heavy carbon can be recognized in Upper Permian sections worldwide. Our study of the Svalbard and East Greenland sections indicates that isotopic chemostratigraphy can facilitate correlations within a basin, and comparison of our data with previously published values suggests that stratigraphic patterns of isotope variations will prove useful in making at least gross correlations between sedimentary basins. Particularly encouraging are comparisons between our data and recently published analyses by Margaritz *et al.*[38] and Tucker[38] of sections from Siberia and Morocco, respectively. All three sections show isotopically light intervals in the Vendian, and the Moroccan data, although poorly constrained stratigraphically, show that apparently Upper Riphean beds near the base of the section have highly variable isotopic compositions similar to those assigned to the time interval 645–775 Myr in this work. (Because of this high variability, a point representative of this portion of the Moroccan section is not shown in Fig. 4.) The Moroccan and Siberian rocks also show a short interval of ^{13}C-enriched carbonate deposition in latest Vendian to earliest Cambrian time, but independent biostratigraphic evidence suggests that rocks of equivalent age are absent in Svalbard and East Greenland[21]. Although inter-basinal resolution may be coarse, any additional means of ascertaining stratigraphic position will be useful for the correlation of Upper Proterozoic sections. The present results also demonstrate that carbon isotopic analyses of organic material can assist in the evaluation of the isotopic record, both in the identification of diagenetic alterations and reconstruction of the record itself.

In addition to their use in stratigraphic correlation, the isotopic data have important implications for phenomena as diverse as palaeoclimatology, end-Proterozoic and early Palaeozoic phosphorite deposition[40], atmospheric history and biological evolution. Because a global enrichment of ^{13}C in sedimentary carbonates signals an increase in the rate of burial of organic carbon, it also signals a globally significant shift in oxidation-reduction (redox) processes. Reducing potential flowing to the carbon cycle (in order to allow increased burial of organic carbon, the reduced product in the carbon cycle) must have been diverted from another elemental cycle. The geochemically plausible alternatives are the cycles of sulphur (resulting in an increase in sulphate at the expense of sulphide), iron (resulting in increased precipitation of ferric iron) and oxygen (resulting in accumulation of O_2).

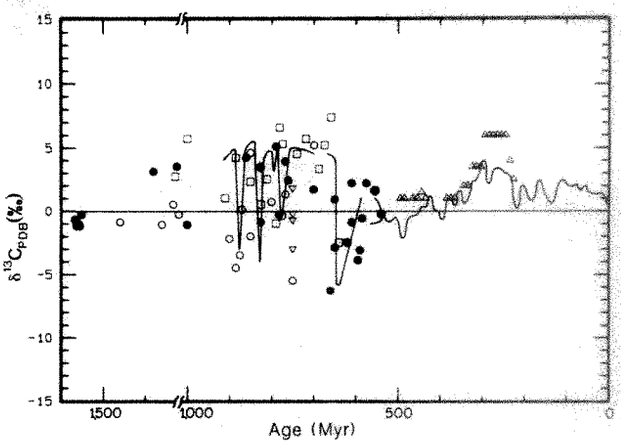


Fig. 4 Carbon isotopic abundances in carbonates with ages of <1,750 Myr. Note compression of age axis, 1,750–1,000 Myr. The continuous curve in the interval 565–0 Myr is the Phanerozoic carbonate curve compiled by Lindh[68]. Triangles in the same interval represent recent measurements of unaltered portions of brachiopods[69]. The broken curve in the interval 915–540 Myr retraces the carbonate line shown in Fig. 3, with allowance for depositional hiatuses at ~700–670 and ~590–560 Myr. Remaining points represent data summarized in Table 2. Open circles, rock units for which a single isotopic analysis is available; open squares, two to four analyses; filled circles, five or more. Triangles at 750 Myr represent the Tapley Hill Formation, which is possibly non-marine[65].

The magnitude of the redox shift can be estimated from the size and duration of the carbon isotopic shift. The flux of carbon in the exogenic cycle in the late Proterozoic is not known. As a point of reference, the present value is $\sim 2.5 \times 10^{19}$ mol C Myr^{-1} (refs 41, 42). In a geochemical carbon cycle characterized by $\varepsilon = 29‰$ (approximately the value observed in this work), precipitation of carbonates with $\delta_c = 0‰$ would correspond (at the modern flux level) to burial of 4×10^{18} mol organic C Myr^{-1} (=17% of total flux, assuming $\delta = 5‰$ for average crustal C). If carbonates instead have $\delta_c = +5‰$, the rate of burial of organic carbon is doubled, and oxidized products (sulphate, O_2, Fe^{3+}) must accumulate at a rate equivalent to 4×10^{18} mol O_2 Myr^{-1}. The present atmospheric inventory of O_2 is 3.8×10^{19} mol. The duration of the late Proterozoic interval of precipitation of carbonates with $\delta_c \simeq +5‰$ was apparently at least 100 Myr. If the flux of carbon in the exogenic cycle was near modern levels, oxidized material produced during that interval would have been ~10 times the present inventory of O_2.

The fate of this oxidizing potential is only partly clear. Interpretation of patterns of covariance in the isotopic records of carbon and sulphur suggests that less extreme episodes of oxidation during the Phanerozoic have been largely accommodated by shifts in the redox balance of sulphur[4]. The sulphur isotopic record for the late Proterozoic is far from complete[43]. Until more is known, quantitative estimates of possible shifts in the redox balance of sulphur will be impossible. We note, however, that the flux of sulphur in the exogenic cycle is about 17 times smaller (on a molar basis[31,42]) than that of carbon. Even if all of the sulphur returned to the system by weathering and erosion were initially in the form of pyrite, this flux would be equivalent (at modern levels) to 3×10^{18} mol O_2 Myr^{-1}. In the absence of any other sink for oxidizing potential, O_2 would thus be expected to accumulate at a rate of at least 10^{18} mol Myr^{-1}. The flux of carbon in the exogenic cycle may have been decreased during this interval by 'tectonic tuning'[44], thus slowing the rate of accumulation of O_2, and a significant portion of the excess might have gone into oxidation[45,46] of materials newly exposed at

spreading centres[47–49], but it seems very likely that the period from 700 to 800 Myr ago was a time of important atmospheric oxygen buildup.

It is interesting to speculate as to what factors controlled the timing of this episode of enhanced burial of organic carbon. Probable eukaryotic phytoplankton appear in the record at least 1,400 Myr ago[50], and must have been well established as important primary producers long before the interval studied here. Morphological changes observed in microfossils from 850–700 Myr ago (ref. 50) might, however, reflect physiological developments which expanded the range of habitable environments by allowing better control of buoyancy or improved interception of nutrients and light. Furthermore, enhanced rates of burial of organic material might be related to tectonic factors. Many of the best known 'Palaeozoic' geosynclinal sedimentary sequences began to accumulate during this interval, including the Iapetus, Adelaidian and Cordilleran, as well as others in India, China and the Soviet Union[48]. Depositional conditions associated with these developments may well have favoured increased rates of burial of organic carbon[51]. At the same time, conditions of high fertility may have been maintained in the marine environment by more efficient recyclcing of phosphorus within and just below the photic zone. In the modern global ecosystem, biomineralization and the rapid sinking of faecal pellets both remove phosphate from the surface layers of the ocean and tend to enhance its burial; however, faecal pellets and biosynthetic phosphates appear only later in the geological record. If late Proterozoic organic materials were exclusively microbial and sank more slowly, and if grazing heterotrophs did not package phosphate for rapid sedimentation, more efficient use of phosphate would seem probable.

The end of this era of enhanced burial of organic carbon coincides with the major Eocambrian glaciation. The periodic returns to 'normal' carbon isotopic compositions within the era may coincide with earlier glaciations[48]. The occurrence of major glaciations implies the existence of a strong climatic gradient which, in turn, is very likely to have affected circulation within the ocean, possibily encouraging the development of deep circulation and reducing rates of burial of organic material. By the close of the Varangian glaciation, evolutionary developments had occurred which countered the factors described above, and very high rates of burial of organic carbon were not re-established. It is also possible, of course, that O_2 pressures equal to or higher than present levels were attained and acted to prevent burial of organic material by establishing a particularly aggressive environment.

An increase in atmospheric O_2 levels 700–800 Myr ago is of great palaeobiological interest because many authors have argued that the time of appearance of macroscopic metazoans was constrained by oxygen tensions sufficient to permit epithelial diffusion of oxygen across multiple cell layers, support metazoan exercise metabolism, and permit collagen synthesis (see, for example, refs 52–56). Until now, there have been no geochemical data to support this idea; however, as the conspicuous fossil record of animals begins just after the interval of heavy carbon deposition, it may be that the late Proterozoic isotopic record is supplying the evidence needed to support this concept. Additional data are required to evaluate this possibility. Detailed secular curves for organic and carbonate carbon need to be established for other Upper Proterozoic sections, and these must be complemented by similar curves for sulphur. It is clear, however, that the carbon isotopic record will be an important part of the evidence on which reconstruction of late Proterozoic evolution, environmental history, and their interaction through the carbon cycle will eventually be based.

We thank the Commission on Scientific Research in Greenland and the Governor of Svalbard for permission to work in national park areas. The Nordaustlandet samples were collected by A.H.K. as a member of the Cambridge Svalbard Expedition (W. B. Harland, director). We thank H. D. Holland, W. T. Holser and J. C. G. Walker for discussions. Research was supported in part by grants from the NSF (A.H.K., K.S.) and NASA (NGR 15-003-118 to J.M.H.). I.B.L. acknowledges support for the Baas Becking Laboratory from BMR, CSIRO and AMIRA.

Received 19 December 1985; accepted 7 May 1986.

1. Holser, W. T. in *Patterns of Change in Earth Evolution* (eds Holland, H. D. & Trendall, A. F.) 123–143 (Springer, Berlin, 1984).
2. Shackleton, N. J., Hall, M. A., Line, J. & Chang Shuxi *Nature* **306**, 319–322 (1983).
3. Arthur, M. A. in *Climate in Earth History* (eds Berger, W. H. & Crowell, J. C.) 55–67 (National Academy Press, Washington, 1982).
4. Veizer, J., Holser, W. T. & Wilgus, C. K. *Geochim. cosmochim. Acta* **44**, 579–587 (1980).
5. Schidlowski, M., Hayes, J. M. & Kaplan, I. R. in *Earth's Earliest Biosphere* (ed. Schopf, J. W.) 149–185 (Princeton University Press, 1983).
6. Kulling, O. *Geogr. Annlr* **16**, 161–254 (1934).
7. Wilson, C. B. *Geol. Mag.* **45**, 305–327 (1958).
8. Wilson, C. B. *Geol. Mag.* **48**, 89–116 (1961).
9. Wilson, C. B. & Harland, W. G. *Geol. Mag.* **101**, 198–219 (1964).
10. Hambrey, M. J. *Geol. Mag.* **119**, 527–642 (1982).
11. Swett, K. *Geol. Mag.* **118**, 225–336 (1981).
12. Flood, B., Gee, D. G., Hjelle, A., Siggerud, T. & Winsnes, T. S. *Norsk Polarinst. Skr.* **146**, 1–139 (1969).
13. Haller, J. *Geology of the East Greenland Caledonides* (Wiley, New York, 1971).
14. Eha, S. *Meddr Grønland* **11**, 1–1095 (1953).
15. Vidal, G. *Grønl. Geol. Unders. Bull.* **134**, 1–40 (1979).
16. Knoll, A. H. *Geol. Mag.* **119**, 269–279 (1982).
17. Knoll, A. H. & Swett, K. *Palaeontology* **28**, 451–473 (1985).
18. Raaben, M. Ye & Zabrodin, V. Ye. *Dokl. Akad. Nauk SSSR* **184**, 676–679 (1968).
19. Swett, K. & Knoll, A. H. *J. sedim. Petrol.* (in the press).
20. Downie, C. *Trans. R. Soc. Edinburgh.* **72**, 257–285 (1982).
21. Knoll, A. H. & Swett, K. *J. Paleont.* (in the press).
22. Harland, W. G. & Gayer, R. A. *Geol. Mag.* **109**, 289–314 (1972).
23. Roberts, D. & Gale, G. H. in *Evolution of the Earth's Crust* (ed. Tarling, D. H.) 255–342 (Academic, London, 1978).
24. Wedeking, K. W., Hayes, J. M. & Matzigkeit, U. in *Earth's Earliest Biosphere* (ed. Schopf, J. W.) 428–442 (Princeton University Press, 1983).
25. Wachter, E. A. & Hayes, J. M. *Chem. Geol.* **52**, 365–374 (1985).
26. Santrock, J., Studley, S. A. & Hayes, J. M. *Analyt. Chem.* **57**, 1444–1448 (1985).
27. Brand, U. & Veizer, J. *J. sedim. Petrol.* **51**, 987–997 (1981).
28. Hayes, J. M. in *Earth's Earliest Biosphere* (ed. Schopf, J. W.) 291–301 (Princeton University Press, 1983).
29. Irwin, H., Curtis, C. & Coleman, N. *Nature* **269**, 209–213 (1977).
30. Veizer, J. & Hoefs, J. *Geochim. cosmochim. Acta* **40**, 1387–1395 (1976).
31. Fairchild, I. J. *Nature* **304**, 714–716 (1983).
32. Magaritz, M., Anderson, R. Y., Holser, W. T., Saltsman, E. S. & Garber, J. *Earth planet. Sci. Lett.* **66**, 111–124 (1983).
33. Strother, P. K., Knoll, A. H. & Barghoorn, E. S. *Palaeontology* **26**, 1–32 (1983).
34. Broecker, W. S. *J. geophys. Res.* **75**, 3553–3557 (1970).
35. Scholle, P. A. & Arthur, M. A. *Bull. Am. Ass. Petrol. Geol.* **64**, 67–87 (1980).
36. Schidlowski, M., Eichmann, R. & Junge, C. E. *Geochim. cosmochim. Acta* **40**, 449–455 (1976).
37. Margaritz, M. *Sedim. Geol.* **45**, 115–123 (1985).
38. Margaritz, M., Holser, W. T. & Kirschvink, J. L. *Nature* **320**, 258–259 (1986).
39. Tucker, M. E. *Nature* **319**, 48–50 (1986).
40. Cook, P. J. & Shergold, J. H. *Nature* **308**, 231–236 (1984).
41. Lasaga, A. C., Berner, R. A. & Garrels, R. M. in *The Carbon Cycle and Atmospheric CO_2: Natural Variations Archean to Present* (eds Sundquist, E. T. & Broeker, W. S.) 397–411 (American Geophysical Union, Washington, 1985).
42. Arthur, M. A., Dean, W. E. & Schlanger, S. O. in *The Carbon Cycle and Atmospheric CO_2: Natural Variations Archean to Present* (eds Sundquist, E. T. & Brocker, W. S.) 504–529 (American Geophysical Union, Washington, 1985).
43. Claypool, G. E., Holser, W. T., Kaplan, I. R., Sakai, H. & Zak, I. *Chem. Geol.* **28**, 199–260 (1980).
44. Worsley, T. R., Moody, J. B. & Nance, R. D. in *The Carbon Cycle and Atmospheric CO_2: Natural Variations Archean to Present* (eds Sundquist, E. T. & Broecker, W. S.) 561–572 (American Geophysical Union, Washington, 1985).
45. McDuff, R. E. & Edmond, J. M. *Earth planet. Sci. Lett.* **57**, 117–132 (1982).
46. Walker, J. C. G. *Mar. Chem.* (in the press).
47. Veizer, J., Compston, W., Clauer, N. & Schidlowski, N. *Geochim. cosmochim. Acta* **47**, 295–302 (1983).
48. Windley, B. F. *The Evolving Continents* (Wiley, London, 1977).
49. Bond, G. C., Nickerson, P. A. & Kominz, M. A. *Earth planet. Sci. Lett.* **70**, 325–345 (1984).
50. Vidal, G. & Knoll, A. H. *Mem. geol. Soc. Am.* **161**, 265–277 (1983).
51. Walter, M. R. *Baas Becking Geobiol. Lab. A. Rep.*, 45–56 (1982).
52. Raff, R. A. & Raff, E. C. *Nature* **228**, 1003–1005b (1970).
53. Runnegar, B. *J. geol. Soc. Aust.* **29**, 395–411 (1982).
54. Runnegar, B. *Alcheringa* **6**, 223–239 (1982).
55. Cloud, P. *Paleobiology* **2**, 351–387 (1976).
56. Towe, K. M. *Proc. natn. Acad. Sci. U.S.A.* **65**, 781–788 (1970).
57. Schidlowski, M., Eichmann, R. & Junge, C. E. *Precambr. Res.* **2**, 1–69 (1975).
58. Williams, G. E. *J. geol. Soc. Aust.* **26**, 377–386 (1979).
59. Tucker, M. E. *Precambr. Res.* **22**, 293–315 (1983).
60. Lambert, I. B., Knutson, J., Donnelly, T. H., Etminan, H. & Mason, M. *Miner. Deposita* **19**, 266–273 (1984).
61. Knutson, J., Donnelly, T. H. & Tonkin, D. G. *Econ. Geol.* **78**, 250–274 (1983).
62. Lambert, I. B., Donnelly, T. H. & Rowlands, M. J. *Miner. Deposita* **15**, 1–18 (1980).
63. Tucker, M. E. *Geology* **10**, 7–12 (1982).
64. Lambert, I. B., Donnelly, T. H., Etminan, H. & Rowlands, N. J. *Econ. Geol.* **79**, 461–475 (1984).
65. Hoering, T. C. *Yb. Carnegie Instn Wash.* **61**, 190–191 (1962).
66. Beeunas, M. A. & Knauth, L. P. *Geol. Soc. Am. Bull.* **96**, 737–745 (1985).
67. Rye, D. & Williams, N. E. *Econ. Geol.* **76**, 1–26 (1981).
68. Lindh, T. B. thesis, Univ. Miami (1983).
69. Popp, B. N., Anderson, T. F. & Sandberg, P. A. *Geol. Soc. Am. Bull.* (in the press).

Enhancement of high-energy cosmic-ray spectrum by type-II supernovae

Yoshiyuki Takahashi*§, Shigeki Miyaji*‖, Thomas A. Parnell*, Martin C. Weisskopf*, Takayoshi Hayashi†, & Ken'ichi Nomoto‡‖

* Space Science Laboratory, NASA Marshall Space Flight Center, Huntsville, Alabama 35812, USA.
† Department of Chemistry, University of Alabama in Huntsville, Huntsville, Alabama 35899, USA
‡ Department of Physics, Brookhaven National Laboratory, Upton, New York 11973, USA
§ Present address: Department of Physics, University of Alabama in Huntsville, Huntsville, Alabama 35899, USA
‖ Permanent address: Department of Natural History, College of Arts and Sciences, Chiba University, Chiba 260, Japan (S.M.); Department of Earth Sciences and Astronomy, College of Arts and Sciences, University of Tokyo, Tokyo 153, Japan (K.N.)

The cosmic-ray spectrum has an intensity enhancement in the energy range 10^{14}–10^{16} eV per nucleus[1] (Fig. 1). Recent observations of heavy cosmic rays in this energy range indicate that the Ca/Fe ratio may be as large as 10 times the solar value. We suggest that pulsars in type-II supernova remnants are the origin of this component of the cosmic-ray spectrum.

The high-energy enhancement in the cosmic-ray spectrum has been suspected to result from rays originating from pulsars[2–4]. For example, Karakura *et al.*[2] explained the feature in the extensive air shower (EAS) energy spectrum in terms of proton-dominated pulsar contributions using the electromagnetic acceleration mechanism proposed by Ostriker and Gunn[5,6]. This analysis agreed reasonably well with the data available at that time. More recent observations[1] indicate a lower intensity of the enhancement, (one-fifth) of that determined by the old EAS data, and the chemical composition in the flux enhancement range has been controversial with some indirect analyses indicating proton dominance[7–9] while the others suggest dominance of iron[10–12]. All of these ambiguities make it difficult to resolve the origin of the enhancement. Recently, however, two new sets of direct observations of chemical composition have led us to propose its origin in type-II supernovae which predicts an overabundance of medium heavy (such as ^{16}O–^{40}Ca) and/or neutron-rich heavy nuclei (such as, ^{48}Ca).

The first of these new observational results were reported by the JACEE collaboration utilizing balloon-borne emulsion chambers[13–15]. These experiments also showed high-energy enhancement and were consistent with the data of Grigorov *et al.*[16] from the PROTON satellite. Of special interest, the JACEE data showed no anomalous proton, helium, and iron abundances. However, they did observe an overabundance of calcium at high energies (Ca/Fe$\gtrsim$2 above 10^{14} eV per nucleus). They also observed some enhancements of medium-heavy nuclei (from C to Si)[13–15]. The second set of observations were obtained by the C3 experiment on the HEAO 3 satellite. Data from this experiment allow an analysis of the abundances of the heavy elements relative to iron at energies up to 10^{12} eV AMU^{-1} (ref. 17), and show a dramatic rise in both the calcium and argon abundances at energies above 500 GeV AMU^{-1} (Fig. 2). Although both these results are subject to large statistical and complicated instrumental uncertainties, we find it significant that a calcium overabundance is implied by two independent experiments and suggest that this anomaly has a direct link with type-II supernova as discussed below.

Cosmic rays are generally thought to originate from supernovae, of which there are two types[18]; type-I (SN-I), which show no evidence for hydrogen at near maximum light and are observed in all types of galaxies, and the type-II (SN-II), which show hydrogen-rich spectrum with various light curves, and are found only in spiral galaxies.

SN-I are thought to involve a mass-accreting white dwarf where carbon deflagration eventually leads to a total disruption of the white dwarf and a significant amount of ^{56}Ni is produced[19,20]. The resulting β-decay of the ^{56}Ni to ^{56}Fe provides a satisfactory explanation for changes in the SN-I light curve. The predicted Ca/Fe ratio in the synthesized elements is less than a half of the solar value[20]. Thus, we can rule out SN-I as a source of the calcium anomaly.

There are, on the other hand, two proposed mechanisms for SN-II: one model, involving 8–11 solar mass stars, invokes core collapse triggered by electron capture on ^{20}Ne and ^{24}Mg in an oxygen-neon-magnesium core[21]. The shock wave, generated when the nuclear matter density core bounces, ejects the overlaying mass and leaves a neutron star[22]. Miyaji *et al.*[21] found that ^{48}Ca could be a most abundant nucleus when nuclear statistical equilibrium (NSE) is realized above 10^{10} g cm^{-3}. Because the NSE region in their model extends further than the sonic point when the bouncing shock wave is formed, one can expect mass ejection even from this region, although the composition ratio is dependent on the expansion velocity and the 'freezing out' density of the nucleus. Hartmann *et al.*[23] have assumed mass ejection from near the surface of a neutron star where NSE has been realized, and showed a normal abundance of iron and an

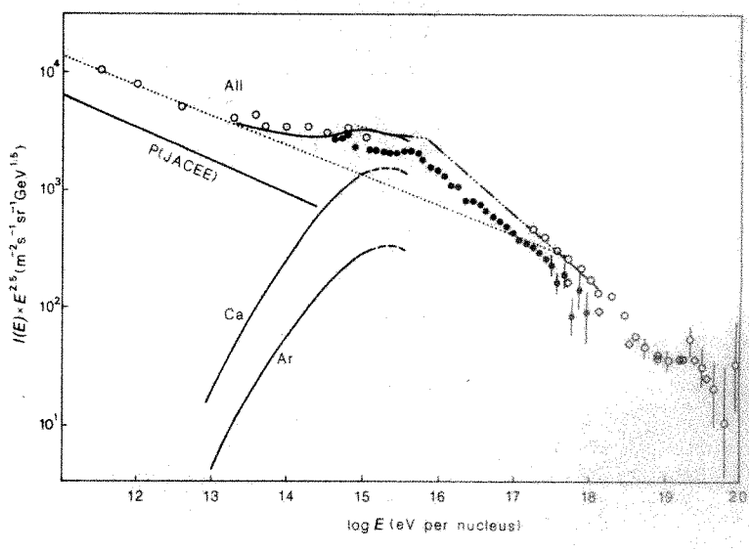


Fig. 1 Differential cosmic-ray energy spectrum of 'all particles' ($I(E)$) multiplied by $E^{2.5}$. Data (points and dash-dotted lines) are taken from refs cited in ref. 1. A straight line (P(JACEE)) denotes proton spectrum from the JACEE experiments[13]. Solid curves (Ca and Ar) illustrate the contributions of calcium and argon nuclei as deduced from the HEAO data and extraporated by the pulsar acceleration mechanism. A sum (uppermost solid curve) of calcium and argon overabundances with $E^{-2.7}dE$ spectrum (dotted line) fits to the observed enhancement.

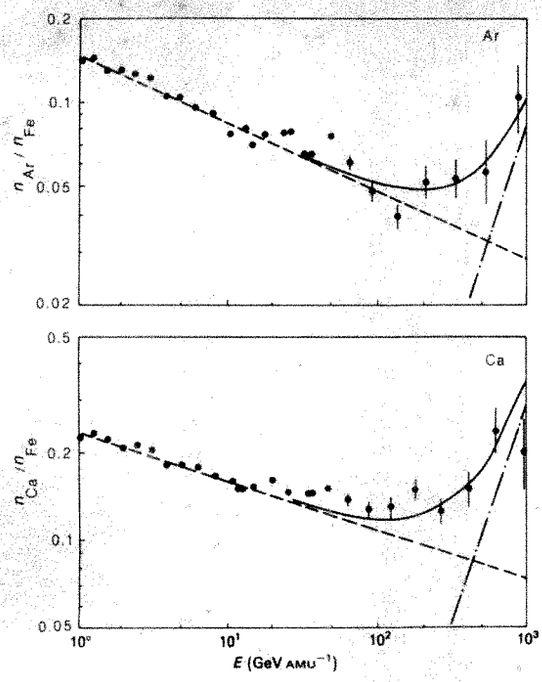


Fig. 2 Ar/Fe and Ca/Fe ratios as observed by HEAO-3C experiment[17]. All lines are fits to the following functions: $0.029\,(E/10^3\ \text{GeV AMU}^{-1})^{-0.24}+0.07(E/10^3\ \text{GeV AMU}^{-1})^{1.5}$ and $0.076\,(E/10^3\ \text{GeV AMU}^{-1})^{-0.126}+0.295\ \ (E/10^3\ \text{GeV AMU}^{-1})^{1.5}$, for Ar/Fe and Ca/Fe, respectively.

overabundance ($\sim 10^5$ solar) of neutron-rich isotopes (^{48}Ca, ^{50}Ti, ^{64}Ni, ^{66}Zn, ^{82}Se...) at the vicinity of a neutron star. We note that this anomaly exists near the surface of the star and should not dominate if all of the SN-II ejecta are considered. It is, however, the material near the neutron star surface that will be accelerated to the highest energies.

The other model for SN-II involves more massive stars ($11 < M < 100\ M_\odot$) and invokes a collapse of an iron core triggered by both photo-disintegration of, and electron capture on, iron group nuclei. These stars do not promptly explode via the bouncing-shock mechanism, except for those in a narrow mass range around 12 $m_\odot$ (ref. 24), but later by neutrino heating[25]. The resulting explosion is relatively weak and leads either to the formation of a neutron star (for $M < 20\ M_\odot$) or a black hole ($M > 20\ M_\odot$) depending on the mass of the remnant core. According to a nucleosynthesis calculation for a 15 $M_\odot$ model[26], the ^{40}Ca/Fe ratio can be as large as $\sim$10 times the solar value because the explosion energy is so small that only the shell material is ejected. This model also predicts a large ratio ($\sim$7) of S/Fe and Ar/Fe, and $\sim$4 of Si/Fe relative to solar abundances. For a more massive progenitor (25 $M_\odot$), the ^{40}Ca/Fe ratio is predicted to be close to solar but here the remnant core may be too massive to remain a neutron star.Thus we associate SN-II that produce neutron stars with the calcium anomaly.

The energy spectrum resulting from supernova shock acceleration is a single power law, and its maximum energy has been estimated by Lagage and Cesarsky[27] at 10^{13} eV AMU^{-1}. Therefore, we can rule out simple supernova shock acceleration as a source of cosmic-ray high-energy enhancements. However, injected particles from a neutron star in SN-II have higher energy, because there should be about three orders of magnitude difference in the surface gravitational potential between a white dwarf (SN-I) and a neutron star (SN-II) from where the remnant is ejected. This difference, together with the strong magnetic field of a neutron star, might affect the shock wave acceleration in SN-II. Thus the high-energy feature in the cosmic-ray spectrum can be associated with SN-II and its neutron star (some entirely different origins are, of course, always possible). Furthermore, if the pulsar acceleration proposed by Ostriker and Gunn[5,6] is applied to the calcium and other nuclei formed in the SN-II, and the upper bound to the intensity deduced from HEAO satellite data is used, we find reasonable agreement between the JACEE observations and the EAS data. The observed rise of both the Ca/Fe and Ar/Fe ratios of the HEAO data (see Fig. 2) are consistent, not only with the JACEE calcium anomaly (Ca/Fe ≥ 2; $E > 10^{14}$ eV per nucleus), but also with the lower energy part of the pulsar acceleration ($E^{-1}\,dE$) which is dominated by magnetic acceleration. Next, applying the pulsar acceleration to the calcium and argon intensities of the HEAO data, we find reasonable agreement of the enhanced 'all-particle' spectrum at 10^{14-16} eV per nucleus (see Fig. 1) with the high-energy side of pulsar component ($E^{-2.5}dE$) which is formed during the gravitational-loss era of a pulsar. Above 10^{16} eV, cosmic rays are believed to escape from the galactic confinement and the observed steepening in Fig. 1 is thought to be a consequence[28]. Note, however, that intensity of the nuclear components from pulsars should start their reduction rapidly above 10^{13} eV AMU^{-1} due to X-ray photo-disintegration and other collision losses in the early stage of the gravitational-loss era, leaving secondary protons for further acceleration and eventual leakage from the confinement volume in the galaxy. This steepening involves various complicated parameters. Here we have used average parameters for typical pulsars[2-6] and which affect slightly the low-energy slopes shown in Fig. 1. The determination of the high energy steepening will be discussed elsewhere.

Verification of our speculations requires the observation of heavy nuclei at energies above 10^{12} eV AMU^{-1}. For further studies, isotope identification would be especially important as one would expect an overabundance of high-energy ^{40}Ca and ^{48}Ca. (^{48}Ca is not only highly abundant in the high density NSE state but also a very stable neutron-rich nucleus.) Experimentally, mass discrimination in this energy range is diffcult, but the average meson multiplicities could be used to evaluate the ratio of ^{48}Ca to ^{40}Ca (ref. 29). Other prominent overabundances we would expect are those of ^{32}S and ^{36}Ar or ^{66}Zn. ^{66}Zn is synthesized at a lower density NSE state, although its abundance in high-energy cosmic rays would be much reduced by photo-disintegration. Additional enhanced species expected would be ^{64}Ni and ^{82}Se. The observation of these specific nuclei in the high-energy cosmic-ray spectrum would be an almost conclusive signature of nucleosynthesis in SN-II and, indeed, could serve as a probe of the physical conditions in the NSE core.

We thank Dr A. J. Dessler for comments. This work was supported in part by NAS-NRC Resident Research Associateships in 1983-85 (Y.T.) and 1985-86 (S.M.).

Received 23 December 1985; accepted 13 March 1986.

1. Hillas, A. M. *A. Rev. Astr. Astrophys.* **22**, 425-444 (1984).
2. Karakula, S., Osborne, J. L. & Wdowczyk, J. *J. Phys.* **A7**, 437-443 (1974).
3. Strong, A. W., Wdowczyk, J. & Wolfendale, A. W. *J. Phys.* **A7**, 1489-1496 (1974).
4. Sitte, K. *Nuovo Cimento* **7B**, 110-118 (1972).
5. Ostriker, J. P. & Gunn, J. E. *Astrophys. J.* **157**, 1395-1417 (1969).
6. Gunn, J. E. & Ostriker, J. P. *Phys. Rev. Lett.* **22**, 728-731 (1969).
7. Linsley, J. in *Proc. 18th int. Cosmic Ray Conf.* Vol. 12, 135-191 (Tata Institute: Bombay, 1983).
8. Acharya, A. S., Rao, M. V. S., Silvaprasad, K. & Sreekantan, B. V. *Proc. 19th int. Cosmic Ray Conf.* Vol. 2, 226-229 (NASA: Washington, DC, 1985).
9. Sood, R. K. *Nature* **301**, 44-46 (1983).
10. Goodman, J. A. *et al. Phys. Rev.* **D26**, 1043-1060 (1982).
11. Thornton, G. & Clay, R. *Phys. Rev. Lett.* **43**, 1622-1625 (1979).
12. Andam, A. A. *et al. Phys. Rev.* **D26**, 23-26 (1982).
13. Burnett, T. H. *et al. Phys. Rev. Lett.* **51**, 1010-1013 (1983).
14. Burnett, T. H. *et al.* in *Cosmic Rays and Particle Physics* (eds Ohsawa, A. & Yuda, T.) 468-479 (University of Tokyo, 1984).
15. Burnett, T. H. *et al.* in *Proc. 19th int. Cosmic Ray Conf.* Vol. 6, 164-167 (and also Vol 2, 48-51) (NASA Publ. No. 2376, Washington, DC, 1985).
16. Grigorov, N. L. *et al.* in *Proc. 12th int. Cosmic Ray Conf. Vol.* 5, 1746-1751 (University of Tasmania, Hobart, 1971).
17. Jones, M. D. *et al. Proc. 19th int. Cosmic Ray Conf.* Vol. 2, 28-31 (NASA Publ. No. 2376, Washington, DC, 1985).
18. Trimble, V., *Rev. mod. Phys.* **54**, 1183-1224 (1982).
19. Nomoto, K. in *Problems of Collapse and Numerical Relativity* (eds Bancel, D. & Signore, M.) 89-116 (Reidel, Dordrecht, 1984).
20. Nomoto, K. *Ann. N.Y. Acad. Sci* (in the press).
21. Miyaji, S., Nomoto, K., Yokoi, K. & Sugimoto, D. *Publ. astr. Soc. Jap* **32**, 303-329 (1980).
22. Hillebrandt, W., Nomoto, K. & Wolff, R. G. *Astr. Astrophys.* **133**, 175-184 (1984).
23. Hartmann, D., Woosley, S. E. & El Eid, M. F. *Astrophys. J.* **297**, 837-845 (1985).

24. Baron, E., Cooperstein, & Kahana, S. *Phys. Rev. Lett.* **55**, 126–129 (1985).
25. Wilson, J. R., Mayle, R., Woosley, S. E. & Weaver, T. A. *Ann. N. Y. Acad. Sci.* (in the press).
26. Woosley, S. E. & Weaver, T. A. in *Nucleosynthesis and Its Implications On Nuclear and Particle Physics*, (eds Audouze, J. & Thanh Van, T.) (Reidel, Dordrecht, in the press).
27. Lagage, P. O. & Cesarsky, C. J. *Astr. Astrophys.* **125**, 249–257 (1983).
28. Peters, B. & Westergaard, N. J. *Astrophys. Space Sci.* **48**, 21–46 (1977).
29. Takahashi, Y. in *Physics in Collision 5* (ed. Montanet, L.) (Editions Frontieres, Gif sur Yvette, in the press).

Are bipolar jets precessing?

Jun Fukue & Takeo Yokoo

Astronomical Institute, Osaka Kyoiku University, Tennoji-ku, Osaka 543, Japan

Whether bipolar jets from the star-forming regions precess or not is indicative of their model of origin and formation. Both the beam model[1] and the model of the shocked interaction between an isotropic stellar wind and a massive isothermal disk[2,3] have difficulty in explaining this precession. Other models[4–7], which admit precession of jets, predict different periods of precession. If the recent observation of L723 (ref. 8) represents precession, then this is probably the orbital precession of a torus (disk) around a central oblate star, or the forced precession of a torus around a central star by its companion. The free precession of a central star as well as the precession of a torus may be responsible in the case of L1551 IRS5 (refs 9–11).

Astrophysical jets have been discovered in various classes of astronomical objects; in extragalactic radio sources[12,13], in SS433 (ref. 14), and in regions of recent star formation[15–18]. Of these, precession of the jet flow has only been confirmed for SS433 (refs 19, 20) and for extragalactic jets[13,21,22]. On the other hand, no explicit evidence of precession has been reported for bipolar jets from star-forming regions. However, if the basic mechanism underlying the phenomena of astrophysical jets is common (at least in part), we can also expect precession of the bipolar jets. Moreover, the discovery of, or even the absence of precession will impose restrictions on models of bipolar jets.

We can now characterize various models proposed for bipolar jets in view of the precession theory. Can they admit precession? If so, how long is a precession period?

Model A. The scaled-down version of the 'beam model' originally proposed for extragalactic double radio sources[23] has been applied to bipolar jets[1]. In this model, an initially spherical flow is collimated and accelerated into the polar directions of a spheroidal gas cloud surrounding a central source like a de Laval nozzle, without the influence on the flow of the gravitational field of any objects. Thus, it seems difficult for the gaseous cloud (and confined flow) to precess due to any gravitational force because it is inconsistent with the assumption of the model.

Model B. In a similar picture, the bipolar jets are caused by the interaction between an isotropic stellar wind from a proto star and a surrounding high-density isothermal disk[2,3], where the shock fronts emanate into the polar directions of the disk. Because the jet caused by this mechanism is essentially non-steady, we can expect no precession.

Model C. An alternative type of model which explains collimation and acceleration of astrophysical jets is the (magneto) hydrodynamical wind-type flow in the funnel formed by a torus around a central object[4,24–26]; the gravity of the central object has the essential role in contrast to the beam model A. In model C, the jet precession can be easily interpreted by precession of the torus. Among several ways that the torus can precess, free precession is excluded because it is difficult for the fluid torus to precess freely without damp. Also, a slaved disk model proposed for Her X-1 (ref. 27) and SS433 (ref. 28) may be inadequate for bipolar jets as rapid mass accretion from the companion cannot be expected. Hence, the remaining solutions are the forced precession of the torus by the companion and the orbital precession by the central oblate star.

The angular speed of the forced precession where the companion exerts torque on the torus[29] is $\Omega_p(r) = -(3/4)(G/M)^{1/2} Mm/(M+m)r^{3/2} \cos\alpha/a^3$, where M and m are respectively the mass of the central proto star and that of the companion, a the separation between them, r the distance of the torus from the central star, and α the angle between the torus equatorial plane and the binary orbital plane. Thus, when the bipolar source consists of a binary system, the possible precession period $\Pi = 2\pi/\Omega_p$ of the torus is

$$\Pi = -4.23\times10^2 \text{ yr } M_{10}^{1/2} m_{10}^{-1} \times (1+m/M) a_{10\text{AU}}^3 r_{\text{AU}}^{-3/2} (\cos\alpha)^{-1} \quad (1)$$

where M_{10} and m_{10} are respectively M and m in units of 10 solar masses, $a_{10\text{AU}}$ and r_{AU} respectively a and r in units of 10 AU and 1 AU. We assume that the central proto star is a zero-age main-sequence of B type[30]. This period depends on r and a, but typically lies within 10–10^4 yr. Although the outer massive molecular disks were found by CS observations[30,31], the tidal forces by them on the inner torus is negligible.

The central star is probably deformed by its rapid rotation. If so, its oblateness also gives rise to precession of a torus orbiting it with a misaligned equatorial plane with angular speed $\Omega_p(r) = -(3/2)(R/r)^2 \Omega_r J_2 \cos\beta$, where R is the radius of the central star, $\Omega_r = (GM/r^3)^{1/2}$ the rotational angular speed of the torus, J_2 the dynamical ellipticity, and β the angle between the star's equatorial plane and the torus plane. For a model of uniform density ellipsoid, $J_2 = (2/5)(5/2)\varepsilon$, where ε is the ellipticity of the Roche model star: $\varepsilon = 0{\cdot}02622 M_{10}^{-1} R_{10} V_{100}^2$. Here R_{10} is R in units of 10 solar radius and V_{100} is the equatorial rotation velocity of the star in units of 100 km s^{-1}. For other stellar models, ε is replaced by $f\varepsilon$ with the numerical factor f of the order of unity. The period of this orbital precession is thus

$$\Pi = -2{\cdot}45\times10^4 \text{ yr } M_{10}^{-1/2} R_{10}^{-2} r_{\text{AU}}^{7/2} (f\varepsilon\cos\beta/0{\cdot}01)^{-1} \quad (2)$$

and strongly depends on r. For typical values of parameters, $\Pi = 1-10^4$ yr ($r = 0{\cdot}1$–1 AU). We emphasize that even if the central star is a single star, this precession mechamism can operate.

Model D. A final category of jet formation is due to magnetic field[5–7,32]. In a Drain's picture[5], the magnetic field is anchored on a proto star and is wound up by the star's rotation to make a magnetic bubble blowing off in opposite directions along the rotational axis. Therefore, when the central star precesses freely, the resultant jet also precesses with the angular speed of $\Omega_p = -\varepsilon\Omega\cos\gamma$, where Ω is the star's angular speed, γ the angle between the rotational axis and the figure axis. This leads to a rather short period precession:

$$\Pi = -1.38 \text{ yr } R_{10} V_{100}^{-1} (f\varepsilon\cos\gamma/0{\cdot}01)^{-1} \quad (3)$$

The problem inherent in this picture of precession is how the fluid star can precess freely.

The forced precession of the rotationally-deformed central star by a companion is also possible in the Draine's picture. The precession period is

$$\Pi = -4.84\times10^5 \text{ yr } m_{10}^{-1}(1+m/M) \times R_{10}^{-1} V_{100} a_{10\text{AU}}^3 (f\varepsilon\cos\delta/0{\cdot}01)^{-1} \quad (4)$$

where δ is the angle between the star's equatorial plane and the binary orbital plane. Unless the binary separation is rather small ($a \lesssim$ a few AU), this gives a relatively long period of precession.

Model E. In another scheme[6,7,32,33], the magnetic field anchored on a disk forms the bipolar jets. Hence, the precession of jets is also possible through disk precession discussed in Model C.

We next discuss the observational appearance of precession for various models. We should bear in mind that the typical age τ of CO bipolar jets is $\sim10^4$ yr. When the precession period Π is much longer than τ, the precessional motion cannot be detected and is, therefore, less interesting; this case corresponds

to the tidal precession of the proto star by the companion [model D, equation (4)]. When $\Pi \sim \tau$ as in the cases of the tidal precession of the torus by the companion [models C, E, equation(1)] or the orbital precession of the torus around the oblate star [models C, E, equation (2)], we can observe the S-(Z-) shapes or the corkscrew pattern often found in extragalactic jets or in SS433 jets (see refs 13, 34). These two cases can be distinguished by the fact that the former needs the companion while the latter does not. Moreover, since the orbital precession of the torus is effective close to the central star [compare the r-dependence of equations (1) and (2)], it will be consistent with a narrow-collimated jet in comparison with the tidal precession of the torus by the companion. For a sufficiently short period of $\Pi \ll \tau$ as in the free precession of the central star [model D, equation (3)], the direct observation of the central source will reveal the periodic change of precession timescale Π in the luminosity or polarization. In addition, we can only observe spread jets with the opening angle not of the jet itself but of the precession angle through CO observations (and also the hollow cylindrical structure).

Finally, we try to interpret the observational data by the precessional hypothesis. The recent observation of L723 by Goldsmith *et al.*[8] clearly shows the Z-shape structure. If this means precession, then $\Pi \sim \tau$ to produce the Z-shape. The age of L723 is estimated as $\tau = 4.7\text{-}3.0 \times 10^4$ yr. Thus appropriate models in this case are (C) or (E).

Another candidate of precession is IRS5 in L1551[9-11,35]. In this case, the orientation of the radio contours gradually changes by about 15° from the innermost to the outermost contours[10]. If this indicates about one turn of the precession axis, we have the period of some 23 yr, assuming the size of IRS5 of 1.1×10^{-2} pc and the jet speed of 500 km s^{-1}. In addition to the precession of the torus [models (C) and (E)], the free precession of a central star [model D, equation (3)] may be also adequate.

Further observations involving the detection of binary nature of the central source (see ref. 11), periodic changes, and high-resolution structures would be desirable to confirm precession: the clue to astrophysical jets.

We thank Dr K. Shibata for discussions and useful comments. This work was supported in part by the Scientific Research Fund of the Ministry of Education, Science, and Culture (60740132).

Received 29 January; accepted 4 April 1986.

1. Königl, A. *Astrophys. J.* **261**, 115-134 (1982).
2. Okuda, T. & Ikeuchi, S. *Publ. astr. Soc. Jap.* (submitted).
3. Sakashita, S., Hanami, H. & Umemura, M. *Astrophys. Space Sci.* **111**, 213-223 (1985).
4. Fukue, J. *Publ. astr. Soc. Jap.* **35**, 539-545 (1983).
5. Draine, B. T. *Astrophys. J.* **270**, 519-536 (1983).
6. Pudritz, R. E, & Norman, C. A. *Astrophys. J.* **274**, 677-697 (1983).
7. Uchida, Y. & Shibata, K. *Publ. astr. Soc. Jap.* **37**, 515-535 (1985).
8. Goldsmith, P. F., Snell, R. L., Hemeon-Heyer, M. & Langer, W. D. *Astrophys. J.* **286**, 599-608 (1984).
9. Cohen, M., Bieging, J. H. & Schwartz, P. R. *Astrophys. J.* **253**, 707-715 (1982).
10. Bieging, J. H., Cohen, M. & Schwartz, P. R. *Astrophys. J.* **282**, 699-708 (1984).
11. Bieging, J. H. & Cohen, M. *Astrophys. J.* **289**, L5-L8 (1985).
12. Begelman, M. C., Blandford, R. D. & Rees, M. J. *Rev. Mod. Phys.* **56**, 255-351 (1984).
13. Bridle, A. H. & Perley, R. A. *Ann. Rev. Astr. Astrophys.* **22**, 319-358 (1984).
14. Margon, B. *Ann. Rev. Astr. Astrophys.* **22**, 507-536 (1984).
15. Snell, R. L., Loren, R. B. & Plambeck, R. L. *Astrophys. J.* **239**, L17-L22 (1980).
16. Lada, C. J. & Harvey, P. M. *Astrophys. J.* **245**, 58-65 (1981).
17. Rodriguez, L. F., Carral, P., Ho, P. T. P. & Moran, J. M. *Astrophys. J.* **260**, 635-646 (1982).
18. Bally, J. & Lada, C. J. *Astrophys. J.* **265**, 824-847 (1983).
19. Milgrom, M. *Astr. Astronphys.* **76**, L3-L6 (1979).
20. Margon, B. *et al. Astrophys. J.* **233**, L63-68 (1979).
21. Ekers, R. D. *et al. Nature* **276**, 588-590 (1978).
22. Lonsdale, C. J. & Morison, I. *Nature* **288**, 66-69 (1980).
23. Blandford, R. D. & Rees, M. J. *Mon. Not. R. astr. Soc.* **169**, 395-415 (1974).
24. Fukue, J. *Publ. astr. Soc. Jap.* **34**, 163-171 (1982).
25. Calvani, M. C. & Nobili, L. *Astrophysical Jets* (eds Ferrari, A. & Pacholczyk, A. G.) 189-199 (Reidel, Dordrecht, 1983).
26. Ferrari, A., Habbal, S. R., Rosner, R. & Tsinganos, K. *Astrophys. J.* **277**, L35-L39 (1984).
27. Roberts, W. J. *Astrophys. J.* **187**, 575-584 (1974).
28. van den Heuvel, E. P. J., Ostriker, J. P. & Petterson, J. A. *Astr. Astrophys.* **81**, L7-L10 (1980).
29. Merritt, D. & Petterson, J. A. *Astrophys. J.* **236**, 255-262 (1980).
30. Kaifu, N. *et al. Astr. Astrophys.* **134**, 7-12 (1984).
31. Takano, T. *et al. Astrophys. J.* **282**, L69-L71 (1984).
32. Blandford, R. D. & Payne, D. G. *Mon. Not. R. astr. Soc.* **199**, 883-903 (1982).
33. Shibata, K. & Uchida, Y. *Publ. astr. Soc. Jap.* **37**, 31-46 (1985).
34. Miley, G. *Ann. Rev. Astr. Astrophys.* **18**, 165-218 (1980).
35. Snell, R. L., Bally, Y, Strom, S. E. & Strom, K. M. *Astrophys. J.* **290**, 587-595 (1985).

Measurements of *p*H versus drop size in natural rain

Stephen J. Adams*, Stuart G. Bradley*, C. David Stow* & Stephen J. de Mora†

* Department of Physics and † Department of Chemistry, University of Auckland, Private Bag, Auckland 1, New Zealand

Results from numerical scavenging models[1-3], which estimate the acidity of precipitation falling through a polluted atmosphere, have previously been compared with *p*H measurements of bulk rain water or of single drops of unknown size[4]. Here we describe results from an instrument which, for the first time, allows the variation of *p*H with drop size to be evaluated. Field measurements show a *p*H minimum for drops with radii near 0.5 mm, consistent with simple mass transfer considerations.

The raindrop spectrometer uses the increase of terminal velocity with drop size to sort drops. It consists of two disks separated by a small vertical rotating shaft. The upper disk has a small sector-shaped aperture through which rain passes, and the lower disk is divided into sectors by radial walls so that water is collected. Because the disks rotate at the same rate, larger drops (falling at higher speeds) intersect the lower disk more nearly beneath the aperture than do smaller drops (see Fig. 1).

The theory, design and testing of the instrument are described in detail in ref. 5. It comprises two perspex disks of 0.25 m radius, separated vertically by 0.5 m, and rotating at 300 r.p.m. By choosing a 20° aperture width, 1-ml samples can usually be obtained in a few minutes. However, a drop of given size may land within a 20° area on the lower disk, depending on where it entered the aperture; therefore, collecting sectors will contain water from overlapping ranges of drop size.

By computing drop trajectories, collection efficiencies are derived for each sector as a function of drop size and wind speed. These collection efficiencies relate the volume and *p*H of water collected in each sector to droplet concentration and *p*H in each drop-radius range. Droplet concentrations and *p*H spectra are obtained from measured volumes and *p*H in each sector by a least-squares method (six drop-radius ranges and seven sectors). When there is zero horizontal wind, samples in each collecting sector are nearly independent (Fig. 2*a*). However, a wind speed of 1 m s^{-1} produces a bimodal collection efficiency for each sector because drops fall further from the aperture when the aperture is moving upwind, and closer to the aperture when the aperture is moving downwind. As shown in Fig. 2*b*, this affects the ability of the instrument to resolve collected water into drop-size classes. By placing a semicircular mask over the top of the spectrometer and aligning the straight edge with the wind, the collection efficiency resolution is much improved (Fig. 2*c*) and sensible results should be obtainable in winds of 3 m s^{-1}.

Tests carried out to validate the theoretical description of the instrument are summarized in Table 1. Tests 1, 5 and 6 show

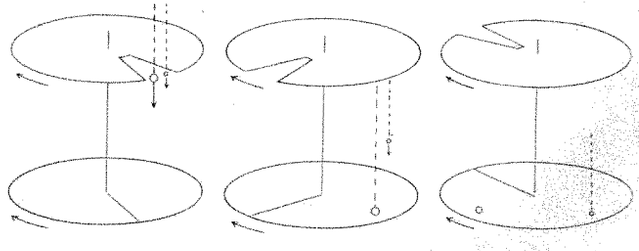


Fig. 1 Schematic of spectrometer operation. The larger drop falls faster, intersecting the lower disk before the smaller drop. The disk rotates during the intervening time, collecting the two drops at different sites.

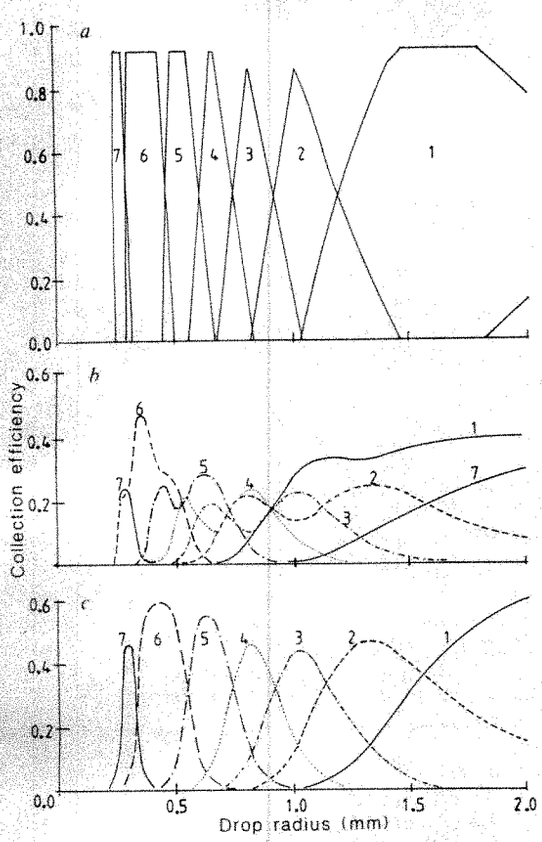


Fig. 2 Collection efficiencies of sectors 1–7 as a function of drop radius: *a*, zero wind speed; *b*, wind speed = 1 m s^{-1}; *c*, wind speed = 1 m s^{-1} but with a semicircular mask placed over the spectrometer.

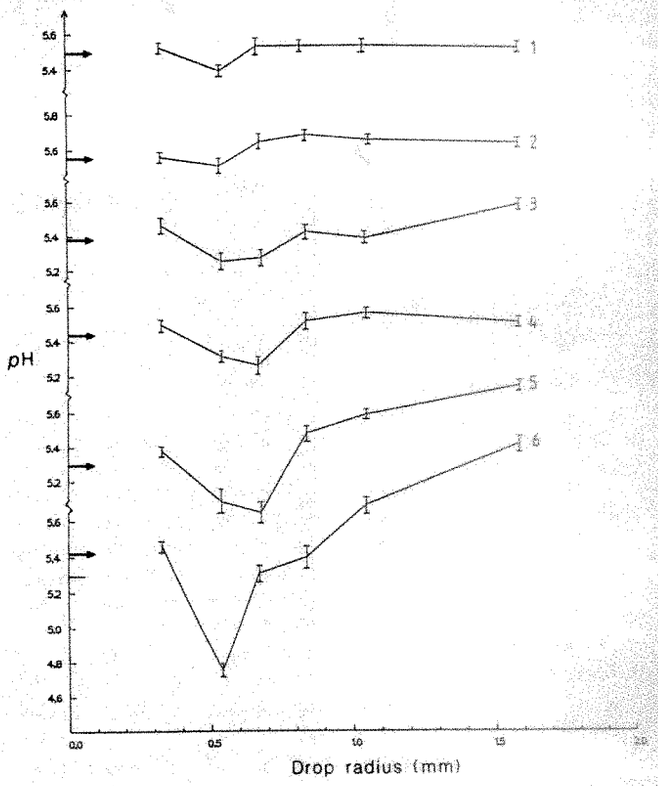


Fig. 3 *p*H versus raindrop size. Bulk-water *p*H values are indicated by arrows at the left.

that drops are collected as predicted, and tests 2 and 3 check that there is no bias in derived drop distributions. Test 4 demonstrates that water is not chemically contaminated by the collection process. Errors in the derived *p*H spectra are therefore almost entirely due to uncertainties in attributing water collected in a sector to drop-size ranges. These errors are estimated as part of the least-squares procedure and include the effect of wind through the collection efficiency matrix.

Figure 3 shows preliminary *p*H spectra from measurements of natural rain; ancillary data are given in Table 2. All spectra exhibit a *p*H minimum near a drop radius of 0.5 mm. The independently measured bulk-water *p*H values, shown by arrows at the left of Fig. 3, are lower than the CO_2 equilibrium values. Rain-bearing systems approaching Auckland are predominantly of maritime origin and will have had little contact with polluted airmasses; in such cases we may assume a flat in-cloud *p*H spectrum, with changes being due to sub-cloud scavenging. The results shown in Fig. 3 suggest that drops with radii near 0.5 mm scavenge more efficiently. The observed spectrum shape is similar to that predicted in detailed models[1,3] for low NH_3 concentrations, but can be interpreted in a simple way as follows: The rate of change of dissolved gas concentration is proportional to both the mass transfer coefficient, k (a function of diffusion coefficient, Reynolds number and Schmidt number), and the surface-area-to-volume ratio, β. For small drops both factors are high and rapid gaseous absorption results. As k and β initially decrease with increasing drop size[6], *p*H should increase rapidly with size for small drops. However, the mass transfer coefficient has a minimum for intermediate drop radii, so that a *p*H maximum results at about 0.1–0.4 mm radius. Thereafter, k increases and β decreases, leading to the observed minimum *p*H near 0.5 mm radius.

Table 2 shows a correlation between both spectrum variance and bulk *p*H, and time since rain shower onset. Only spectra 4 and 6 are directly comparable, having been sampled from the same rainfall system, but the similar bulk *p*H values suggest that

Table 1 Tests of spectrometer performance

Test no.	Quantity tested	Associated error	Comments
1	Angular capture range	±3°	Individual drops in a stream were sized and fall speeds measured before landing on dye-coated paper in each sector.
2	Loss of water	3% volume	Measured quantities of water poured into sectors compared with quantities after spectrometer had been run. Losses are consistent with evaporation into dry laboratory air.
3	Splashing	±0.2% volume	Most splash products fall into the same sector as the parent drop.
4	Contamination	±0.02 *p*H units	*p*H measured before and after passing water through the instrument.
5	Drop-size distribution	±20%	Comparison of distributions derived from dyed filter paper and from the spectrometer, both exposed to rain. Errors were within limits expected from filter-paper counts.
6	Angular capture range	—	The spectrometer was operated in rain with dyed filter paper in each sector. Drops were all within expected sectors (apart from obvious splash products).

Table 2 Data relevant to *p*H spectra in Fig. 3

Spectrum	Wind speed ($m\ s^{-1}$)	Rainfall rate* ($mm\ h^{-1}$)	Start† (min)	Duration (min)	*p*H variation‡	Bulk *p*H
1	1.1±0.2	4±0.5	40	40	0.06	5.50±0.02
2	0.5±0.2	7±0.5	30	30	0.07	5.54±0.02
3	1.6±0.3	5±0.5	20	30	0.12	5.38±0.02
4	1.4±0.2	5±0.5	24	35	0.13	5.44±0.02
5	0.7±0.3	7±0.5	0	22	0.29	5.30±0.02
6	1.9±0.3	8±0.5	0	24	0.43	5.30±0.02

* Rainfall rate derived from water volume collected by spectrometer.
† Time of start of sampling relative to start of rain shower.
‡ Standard deviation computed from the six *p*H spectral points in each spectrum.

all airmasses were comparable. These data suggest that the time constant for spectrum change is ~20 min.

These results are the first test of the drop-size dependence predicted by acid-rain scavenging models; laboratory wind-tunnel experiments are not guaranteed to simulate natural conditions and bulk-water measurements do not allow detailed microphysical inferences. For example, the maritime airmass examples all have comparable bulk-water *p*H values near the CO_2 equilibrium, but when size-fractionated results are plotted, *p*H varies by as much as 1.2 units.

The observed transient *p*H spectra agree qualitatively with present steady-state raindrop scavenging models assuming low NH_3 concentrations[1,3]. There is, however, a need for comparison between time-dependent models and data such as our instrument can obtain. Collection of rain over a wider range of conditions, with a more comprehensive error treatment and chemical analysis of other components, is also desirable to allow closer comparison between theory and measurement.

Received 15 October 1985; accepted 9 April 1986.

1. Overton, J. H., Aneja, V. P. & Durham, J. L. *Atmos. Envir.* **13**, 355-367 (1979).
2. Hill, F. B. & Adamowitz, R. F. *Atmos. Envir.* **11**, 917-927 (1977).
3. Adewuyi, Y. G. & Carmichael, G. R. *Atmos. Envir.* **16**, 719-729 (1982).
4. Esemen, N. A. & Fergus, R. B. *Sci. Total Envir.* **6**, 223-226 (1976).
5. Bradley, S. G. *J. atmos. ocean. Technol.* **2**, 190-200 (1985).
6. *Skelland, A. H. P. Differential Mass Transfer*, 510 (Wiley, New York, 1974).

Palaeolatitude drift history of displaced terranes in southern and Baja California

Lisa Kaplan Morris, Steve P. Lund & David J. Bottjer

Department of Geological Sciences, University of Southern California, Los Angeles, California 90089-0741, USA

The delineation of microplate-tectonic terranes[1] which make up western North America, the timing of their accretions to western North America and the identification of their original geological settings are all topics of debate[2,3]. The most recent addition to this family of terranes is the Santa Lucia/Orocopia allochthon[4,5] (SLOA) (Fig. 1), which is made up of Salinia[6,7] and several other smaller terranes[8] and is located in central and southern California. This composite terrane amalgamated in the Cretaceous and accreted to southern California by the early Palaeogene[4,5]. We describe here new palaeomagnetic results from localities outboard from the SLOA in southern California (USA) and Baja California (Mexico). These results are used to define a newly identified allochthonous terrane in southern and Baja California (Peninsular Ranges terrane[9], PRT) which is outboard from the SLOA, estimate the PRT's palaeolatitude drift history for the past 160 Myr, and infer its original geological setting. PRT and SLOA palaeolatitude drift histories are then combined to produce a new perspective on the tectonic development of southern and Baja California over the past 160 Myr.

Our palaeomagnetic results are based on samples collected from Palaeocene (Silverado Formation), Cretaceous (Ladd and Williams Formations) and Jurassic (Bedford Canyon Formation) sedimentary rocks of the Peninsular Ranges (southern California), and Cretaceous sedimentary rocks of the Santa Monica Mountains (southern California; Tuna Canyon Formation) and El Rosario (Baja California; Punta Baja and Rosario Formations). At each sampling locality, four oriented specimens were collected from each of several sites. The Cretaceous sampling localities and their relations to our proposed terrane boundaries are shown in Fig. 1 (see also Table 1).

All specimens were thermally demagnetized at 50 or 100 °C steps up to at least 500 °C. Zijderveldt diagrams (Fig. 2*a*) were used to estimate the characteristic remanences associated with the primary and any secondary magnetizations. Secondary magnetizations were common and easily removed by 200 °C. Characteristic remanences associated with the primary magnetization (that is, that remanence acquired at the time of initial sediment deposition) were recovered routinely between 200 and 500 °C. Rock magnetic analysis indicated that the primary magnetization was carried by detrital magnetite. If good characteristic remanences could not be discerned, the specimens were discarded from further analyses. Three criteria were then applied to the characteristic remanences to further establish that they were primary in origin. The criteria (see Table 1) were: (1) the presence of well-defined (antipodal polarity) reversals; (2) the passage of a fold test, and (3) *in situ* directions significantly different from the present axial-dipole field. At each of the sampling localities, either two or three of the criteria were satisfied. The results from the Palaeocene and Jurassic rocks of the Santa Ana Mountains should be considered more tentative than the Cretaceous results due to the smaller number of sampling sites at these two localities.

The resultant field vectors for each locality, before (*in situ*) and after bedding correction, are plotted in Fig. 2*b*, and listed in Table 1. The apparent similarity of most *in situ* average field vectors could be interpreted to mean that the rocks were remagnetized after folding while still at lower latitudes. However, the presence of well-defined intervals of reversed and normal polarity in all localities, the fact that the magnetostratigraphies correlate well with the expected magnetic polarity stratigraphy estimated from known biostratigraphical data[10], and the fact that three out of five localities clearly pass fold tests argue convincingly against such a possibility. More detailed analyses of the basic data are presented elsewhere (ref. 10 and L.K.M. and J. G. Fry, unpublished data).

The inclination results were used to estimate palaeolatitudes for each locality based on an axial-dipole mapping. Each locality's palaeolatitude was then normalized to its current latitude to produce the quantity $\Delta\theta$ (palaeolatitude minus present-day latitude) (Table 1).

Our normalized palaeolatitudes, $\Delta\theta$s, and their associated declinations are compared with other previously published results[5,7,8,11-13] of Cretaceous age in Fig. 1. This shows that all localities south of the Oak Ridge Fault (ORF) and its extension into Santa Barbara Basin have small negative $\Delta\theta s$ of about −6°.

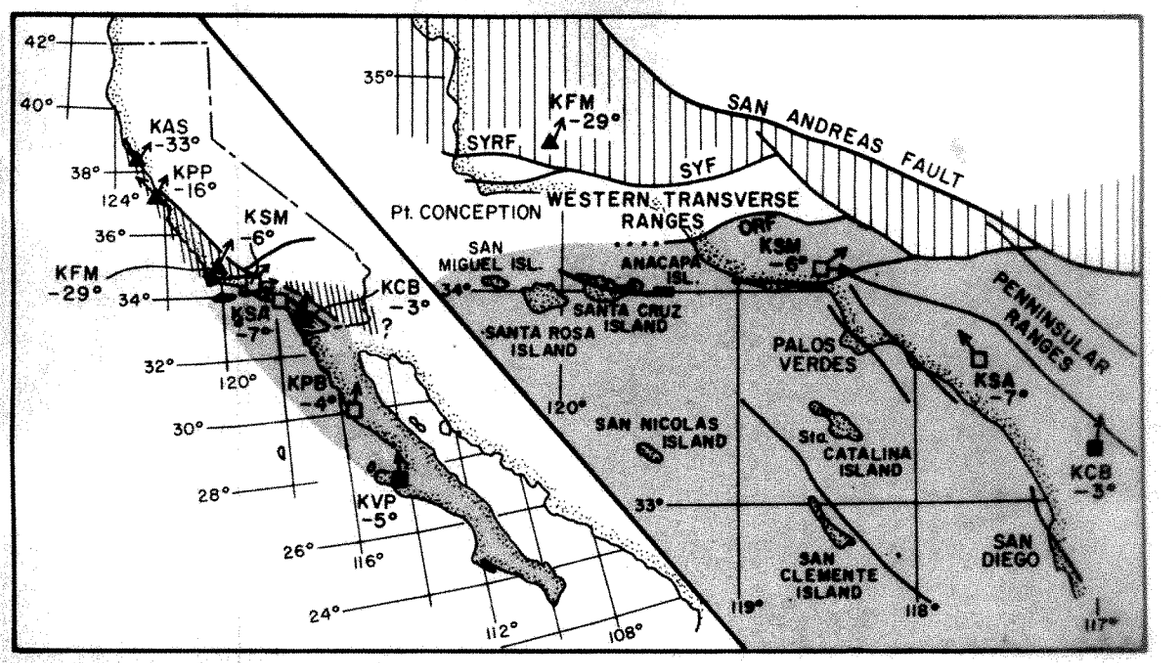


Fig. 1 Cretaceous normalized palaeolatitudes, $\Delta\theta$s, of rocks from southern and Baja California (see Table 1). □, Results from this study; ■ and ▲, previously published results (KPP[5], KFM[7], KAS[8], KCB[11], KVP[12]). □, ■, Results from the PRT; ▲, results from the SLOA. Arrows indicate directions of tectonic-corrected declinations from each locality. The similarity of $\Delta\theta$s south of the Oak Ridge Fault (ORF) and its extension into the Santa Barbara Basin suggest that this region, called the Peninsular Ranges terrane (shading), was spatially coherent in Cretaceous time. The Santa Lucia–Orocopia allochthon is shown by the vertical-lined pattern. Its southern boundary in the Western Transverse Ranges is probably the Santa Ynez (SYF) and Santa Ynez River (SYRF) faults. The normalized palaeolatitudes are also plotted against time in Fig. 3.

Table 1 Summary of palaeomagnetic results

Locality name*	KSM‖	KPB	KSA	JSA	PSA
Locality lat. (°N)	34.1	30.0	33.7	33.7	33.7
Locality long. (°E)	241.4	244.3	242.3	242.3	242.3
Age†	Tur/Maas.	Camp/Maas.	Tur./Camp.	Jurassic	Palaeocene
Confidence criteria‡	A, B, C	A, B	A, B	A, C	A, C
No. of sites§	6, 6‖	17	20	4	4
In situ inclination	37.2, 35.5	46.2	44.6	28.1	45.2
In situ declination	26.4, 104.8	−5.2	5.7	16.6	23.4
In situ α_{95}	9.9, 10.2	13.5	9.2	20.5	9.4
Corrected inclination	45.8, 48.0	44.5	45.1	11.0	43.2
Corrected declination	55.5, 90.8	3.5	−36.4	25.7	−26.0
Corrected α_{95}	7.0, 5.8	8.2	6.7	12.1	8.8
Palaeolatitude¶	28.0 ± 5.0	26.2 ± 6.5	26.6 ± 5.4	5.6 ± 6.2	25.1 ± 6.8
$\Delta\theta$¶	−6.1 ± 5.0	−3.8 ± 6.5	−7.1 ± 5.4	−28.1 ± 6.2	−8.6 ± 6.8

* KSM, Cretaceous Tuna Canyon Formation–Santa Monica Mountains; KPB, Cretaceous Punta Baja and Rosario Formations–El Rosario, Baja California; KSA, Cretaceous Ladd and Williams Formations; JSA, Jurassic Bedford Canyon Formation; and PSA, Palaeocene Silverado Formation—all from the Santa Ana Mountains. KSM, KPB and KSA sampling localities are shown in Fig. 1. JSA and PSA sampling localities are within 10 km of KSA.

† Tur., Turonian; Camp., Campanian, Maas., Maastrichtian; all late Cretaceous stages.

‡ A, Presence of reversals with antipodal polarity, B, passage of fold test, C, *in situ* direction significantly different from the present day field.

§ Four specimens were averaged per site.

‖ Two localities, each with six sites, located on opposite flanks of a large faulted anticlinal structure. Both localities have antipodal reversed sites. Agreement between two localities is markedly improved when corrected for tectonic folding (passes fold test) and declinations agree with previous estimates of large-scale rotation of the Santa Monica Mountains[15], but declinations suggest some residual differential rotation between the two localities.

¶ ±Indicates 95% confidence interval.

These results indicate that this region was about 6° farther south during late Cretaceous time relative to its present geographical position. This region, which has been termed the Peninsular Ranges terrane[9] (PRT) based on geological evidence[9,14], includes the Simi Hills, Santa Monica Mountains, Peninsular Ranges, North Channel Islands and Baja California. The SLOA north of the Santa Ynez Fault (SYF) has much larger negative $\Delta\theta$s which indicate that it was even farther south during the late Cretaceous. The region between the Oak Ridge Fault and the Santa Ynez Fault (SYF) and its extension, the Santa Ynez River Fault (SYRF), has questionable affinities.

In contrast to the negative $\Delta\theta$s of the PRT and SLOA, the $\Delta\theta$ for the North American craton was +9° during the late Cretaceous[15], indicating that the craton was about 9° farther north during this time relative to its present geographical position (Fig. 3). The 95% confidence interval ($\pm 2\sigma$) about the stable craton $\Delta\theta$ estimate for any time interval is ±8.6° (ref. 16) (Fig. 3). The PRT and SLOA $\Delta\theta$s are significantly different from the

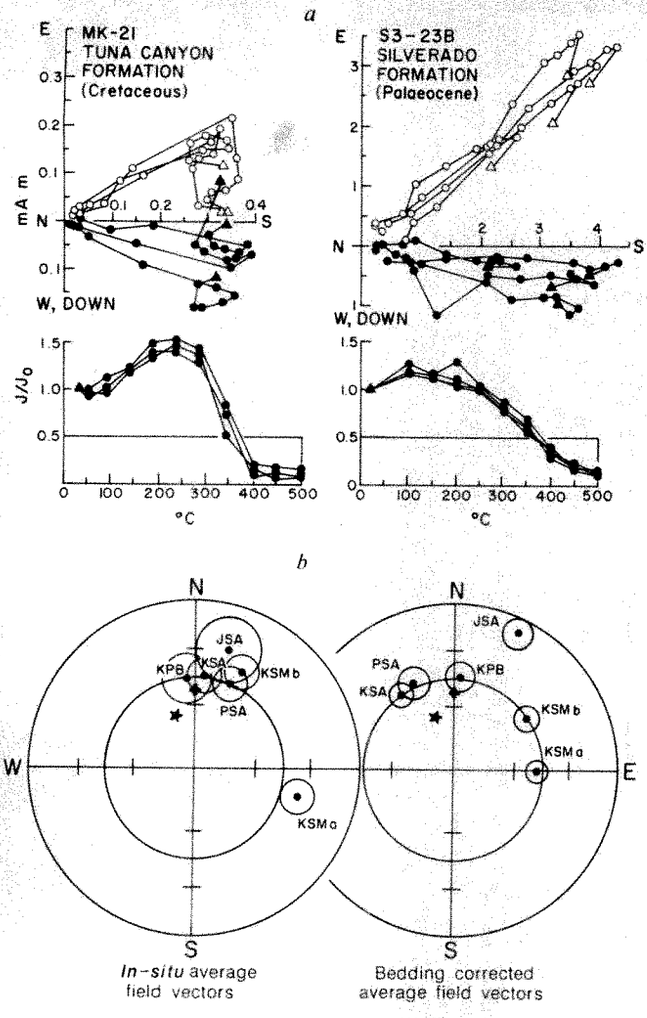


Fig. 2 Zijderveldt diagrams and stereoplots of some results from this study. *a*, Typical Zijderveldt diagrams for two sites of reversed polarity (Upper Cretaceous Tuna Canyon Formation, Palaeocene Silverado Formation) showing intensity loss and vector change with stepwise heating to 500 °C. The filled (open) circles represent the tips of NRM vectors after each heating step plotted in the horizontal (vertical) north, east (north, down) plane. *b*, *In situ* and bedding-corrected average field vectors of the localities listed in Table 1. The present axial-dipole field vector is represented by a cross. The expected late Cretaceous field vector is represented by a star. KSMa and KSMb are each the average of six sites on opposite sides of a large-anticlinal structure in the Santa Monica Mountains.

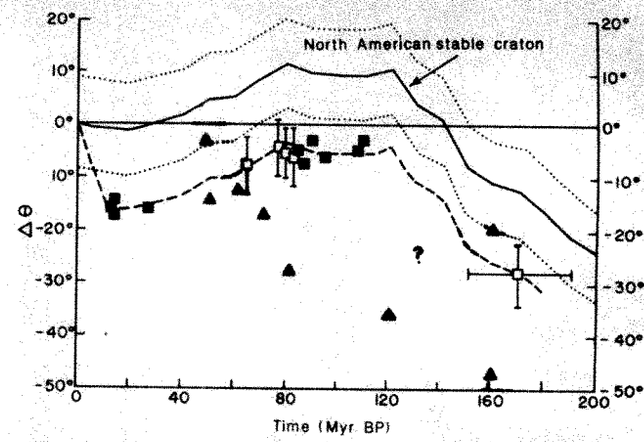


Fig. 3 Normalized palaeolatitudes of the SLOA (triangles) and PRT (squares) plotted against time. The open symbols (with 95% confidence intervals) are results from the present study, the closed symbols are previously published results[5,7,8,11-13,17-19]. The North American stable craton reference curve was derived from Irving and Irving[15] and the $\Delta\theta$ curve for the SLOA (triangles, shading) is from ref. 7. The dotted lines on either side of the stable craton reference curve indicate the 95% confidence interval ($\pm 2\sigma$) about this curve.

stable craton $\Delta\theta$, for they differ by $-15°$ and more than $-23°$ respectively from the stable craton result.

The distinctly different $\Delta\theta$s of the PRT, SLOA and North American stable craton indicate that they were all farther separated in latitude during the late Cretaceous than their present relative geographical positions might indicate. Less uniquely, the similarity of $\Delta\theta s$ within the PRT indicate that it has remained spatially coherent since at least the late Cretaceous, with only minor re-ordering in the late Neogene due to extensional tectonics. This late Neogene tectonic regime has caused a large clockwise rotation of the Santa Monica Mountains[3,17] as noted by the rotated declinations of locality KSM (Fig. 1).

The Cretaceous $\Delta\theta$s and other Mesozoic and Cenozoic age $\Delta\theta$s (refs 5, 8, 13, 17-19) from these terranes are plotted against time in Fig. 3 to estimate each terrane's drift in palaeolatitude over the past 160 Myr. The normalized palaeolatitude, $\Delta\theta$, drift curve for the North American stable craton[15] is plotted for reference. We can see that all the $\Delta\theta s$ from the PRT (squares), all older than 15 Myr, are systematically lower than the stable-craton curve by ~15°. Shifting the stable-craton curve downward 15° produces the dashed curve in Fig. 3 which not only fits all the PRT data but also connects data of different ages from within the PRT. The 95% confidence interval about the 15° offset of the PRT $\Delta\theta$ curve (dashed curve in Fig. 3) is ±6.4°, indicating that the average $\Delta\theta$s of the stable-craton and the PRT were different by more than 4σ before 15 Myr ago. The remarkable match between the offset stable-craton reference curve and these results suggests that this terrane has drifted as part of North America for most of its geological history, but that during this time it was located about 15° lower in latitude relative to the stable craton. This interpretation places the PRT along the western margin of Central America between 15 and 160 Myr ago. The PRT must have moved northward 15° since ~15 Myr ago to reach its present position relative to the stable craton.

The $\Delta\theta$s of the SLOA, on the other hand, are much lower than the PRT results, and their drift pattern[7,8] is significantly different in shape from the stable-craton reference curve. This indicates that the SLOA was not attached to the North American plate until it accreted in early Palaeogene time.

A simple history of these two terranes for the past 160 Myr can be summarized as follows: (1) location of the PRT in Central America as part of the stable craton from 160-15 Myr ago; (2) internal amalgamation of the SLOA in Cretaceous time at lower palaeolatitudes; (3) subsequent drift of the SLOA northward past and outboard from the PRT; (4) accretion of the SLOA with southern California in early Palaeogene time; (5) northward movement of the PRT along the cratonal margin since 15 Myr ago; (6) accretion of this terrane with the SLOA and North American stable craton before 5 Myr ago, (7) continued strike-slip motion along southern California faults in late Neogene time, producing the dispersed terrane pattern that we see today. The SLOA/PRT suture zone is expressed tectonically by the Transverse Ranges of southern California, and recent geophysical studies[20] support this hypothesis. The most notable elements of this history are the location of the PRT in Central America as part of the stable craton until 15 Myr ago, and its subsequent northward displacement in Neogene time. This has never been taken into account in Cenozoic tectonic reconstructions of southern and Baja California[3,21].

These results present a new view of the tectonic history of southern and Baja California and explain several perplexing aspects of the Neogene tectonic development of this region. The

results, however, are inconsistent with some other tectonic reconstructions[21] and require further study of their possible implications.

We thank J. Gilbert Fry, Jeff Bannon, Joseph Bendot, William Gilmour and Robert Morris for assistance during sample collection, the Department of Geological Sciences, University of Southern California, the Society of Sigma Xi, and the NSF (grant EAR-8213202) for support, and Allen Cox and Jack Hillhouse for reviews.

Received 21 November 1985; accepted 2 April 1986.

1. Blake, M. C. Jr, Howell, D. G. & Jones, D. L. *U.S. geol. Surv. Open-File Rep.* 82-593 (1982).
2. Beck, M. E. Jr *J. geophys. Res.* **85**, 715-731 (1980).
3. Luyendyk, B. P., Kamerling, M. J. & Terres, R. *Bull. geol. Soc. Am.* **91**, 211-217 (1980).
4. Vedder, J. G., Howell, D. G. & McLean, H. *Am. Ass. petrol. Geol. Mem.* **35**, 471-496 (1983).
5. Champion, D. E., Howell, D. G. & Gromme, C. S. *J. geophys. Res.* **89**, 7736-7752 (1985).
6. Page, B. *Am. J. Sci.* **282**, 1694-1734 (1982).
7. McWilliams, M. O. & Howell, D. G. *Nature* **297**, 215-217 (1982).
8. Kanter, L. R. & Debiche, M. *CPCEMR Earth Sci. Ser.* No. 1 (1985).
9. Bottjer, D. J. & Link, M. H. *Pacif. Sect. SEPM* **38**, 171-188 (1984).
10. Fry, J. G., Bottjer, D. J. & Lund, S. P. *Geology* **13**, 648-651 (1985).
11. Teissere, R. F. & Beck, M. E. Jr *Earth planet. Sci. Lett.* **18**, 296-300 (1973).
12. Patterson, D. L. *Pacif. Sect. SEPM* **39**, 173-181 (1984).
13. Hagstrom, J. T., McWilliams, M., Howell, D. G. & Gromme, S. *Bull. geol. Soc. Am. Bull.* **96**, 1077-1090 (1985).
14. Abbott, P. L., Kies, R. P., Bochman, W. R. & Natenstadt, C. J. *Pacif. Sect. SEPM* **38**, 151-168 (1983).
15. Irving, T. & Irving, G. A. *Geophys. Surv.* **5**, 141-188 (1982).
16. Lund, S. P. *Geophys. Res. Lett.* (submitted).
17. Kamerling, M. J. & Luyendyk, B. P. *Bull. geol. Soc. Am.* **90**, 331-337 (1979).
18. Hornafius, J. S. *J. geophys. Res.* **90**, 12503-12537 (1985).
19. Luyendyk, B. P., Kamerling, M. J., Terres, R. R. & Hornafius, J. S. *J. geophys. Res.* **90**, 12454-12467 (1985).
20. Bird, P. & Rosenstock, R. W. *Bull. geol. Soc. Am.* **95**, 946-957 (1984).
21. Atwater, T. *Bull. geol. Soc. Am.* **81**, 3513-3536 (1970).

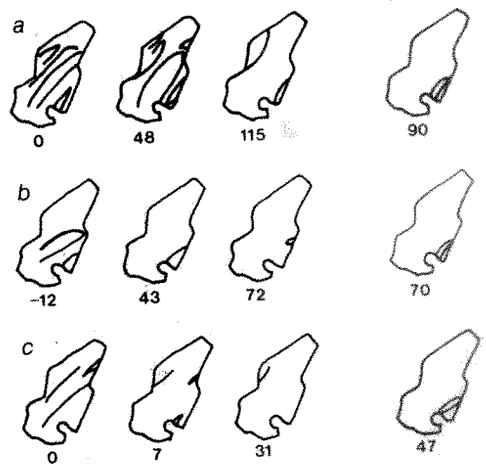


Fig. 1 Domain observations during hysteresis at room temperature (*a*), 50 °C (*b*) and 80 °C (*c*). Numbers refer to magnetic field strengths (in oersteds); positive fields point downwards. At room temperature (*a*), the particle is nearly saturated by 115 Oe and fully saturated at 193 Oe. At 50 °C (*b*), a state of near saturation occurs at 72 Oe, with full saturation at 114 Oe. At 80 °C (*c*), near saturation occurs at 31 Oe, with total saturation at 72 Oe. The final figure in each set shows the first domain pattern observed during ramp-down of the field, and the field value at which it occurred. As temperature increases there is a decrease in the external field values required for saturation and loss of saturation. The particle size is ~35 × 70 μm.

Domain observations of titanomagnetites from room temperature to Curie point and the nature of thermo-remanent magnetism in fine particles

M. Metcalf & M. Fuller

Department of Geological Sciences, University of California, Santa Barbara, California 93106, USA

Single-domain theory[1] has been remarkably successful as a theoretical basis for rock magnetism and hence palaeomagnetism. However, the grain size of much of the magnetic material present in rocks is too large to be single-domain according to classical theory[2]. The resolution of this paradox may lie in the recognition that difficulties in domain wall nucleation[3–10] can preclude the multi-domain state even though it is energetically favoured. Thus, multi-domain particles are observed in a single-domain state in rocks carrying saturation remanence magnetization (IRMs). Inhibition of domain wall nucleation has also been shown to produce high-coercivity materials suitable for permanent magnets[11–13]. Thermo-remanent magnetization (TRM) is one of the most important mechanisms of remanent magnetization for the study of palaeomagnetism, being acquired for example by lavas as they cool on the Earth's surface. We present here domain studies of titanomagnetites showing the increasing importance of the magnetostatic energy in the external field as temperature is increased, and that rocks carrying weak-field TRM, like IRMs, contain multi-domain grains in a single-domain state. These particles contribute very large moments to TRM; indeed, particles of this nature may carry a substantial part of the palaeomagnetic signal. The results also suggest that weak-field cooling of dispersions of suitable fine particles might leave them in a particularly hard magnetic state of some utility.

Domain patterns in titanomagnetites of titanium content $\chi = 0.6$ were investigated during hysteresis at different temperatures and during weak-field thermal cycling, to investigate the role of domain wall nucleation in TRM. The titanomagnetites studied were from DSDP (Deep Sea Drilling Projects) basalts from Leg 49[14], and were mechanically and ionically[15] polished to remove surface stress. The Bitter pattern technique[16] was employed to observe the domain structure, using a special high-temperature colloid. The samples were placed in a brass heating stage and temperature was measured with a thermocouple. The stage was placed between the poles of an electromagnet, so that hysteresis loops could be observed, as well as thermal cycling in a variety of fields. A video camera attached to the microscope, coupled with a video recorder, allowed continuous recording of domain movement and configuration throughout each experiment.

Figure 1 shows the domain patterns resulting during hysteresis at room temperature (*a*), 50 °C (*b*) and 80 °C (*c*). Note the systematic decrease in the field required for saturation, as the temperature increases. Note also that with increasing temperature, the particle remains saturated at lower field strengths during ramp-down of the field. Figures 2 and 3 show heating and cooling cycles of the same particle in external fields of 1 Oe and 45 Oe, respectively. The particle saturates at lower temperature in the higher field. Both cycles carried the particle through its Curie point of 150 °C.

The observed domain patterns attest to the increasing dominance, at higher temperature, of the magnetostatic energy, $M_s H$, where M_s is the saturation magnetization and H the external field. This is to be expected, as other terms are dependent on M_s to higher powers (for example, the demagnetization energy is proportional to M_s^2). As M_s decreases with increasing temperature, the linear term becomes dominant.

No substantial increase in the number of domain walls is seen with increasing temperature. This possibility had been considered because the temperature dependence of the various energy terms should allow nucleation to occur more easily. Neither in these samples, nor in larger particles with numerous walls, have we seen a substantial increase in the number of walls as the sample was heated. This is again consistent with the increasing importance of the magnetostatic energy in the external field relative to the demagnetizing energy.

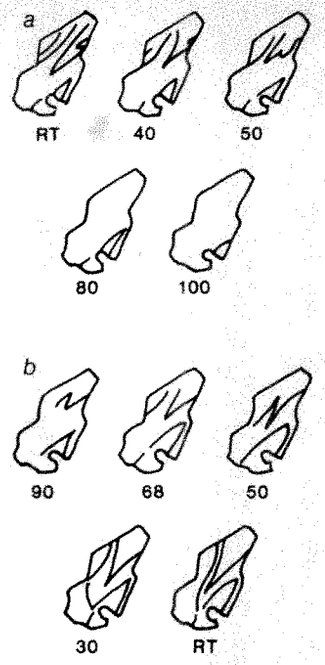


Fig. 2 Domain states during heating (*a*) and cooling (*b*) in the geomagnetic field (1 Oe). Numbers refer to temperature (°C); RT, room temperature. Note the decrease in the number of walls as temperature increases (*a*). A state of near saturation exists at 100 °C, with no domain pattern evident at 120 °C. During cooling (*b*), a faint first wall appears at 110 °C, with definite structure by 90 °C. Again, fewer walls are seen at high temperature.

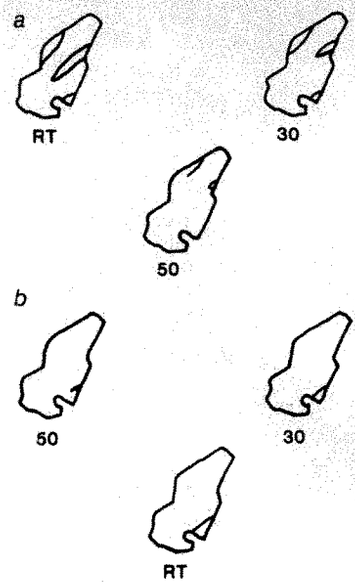


Fig. 3 Domain states during heating (*a*) and cooling (*b*) in an external field of 45 Oe. During heating (*a*), the size of reverse domains decreases rapidly, so that by 50 °C only one reverse domain is left. The particle is saturated by 70 °C. During cooling (*b*), no reverse domains are nucleated until 55 °C, a much lower temperature than in the low-field case (Fig. 2).

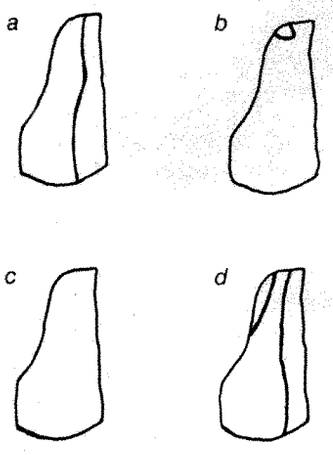


Fig. 4 Domain states of a 14×7 μm titanomagnetite particle. *a*, Before heating in the Earth's field, after a 200 Oe a.f. demagnetization; *b*, After cooling from the Curie point. Note the nearly saturated state of the particle. Another particle of comparable size remained in a single-domain state after a similar experiment. *c*, After cooling from the Curie point in an external field of 30 Oe. Notice the saturated state of the particle. *d*, After application of a 50 Oe a.f. demagnetization.

It has been shown[5-11] that particles larger by orders of magnitude than the classically predicted single-domain size may be found in a single-domain state in saturation remanence. Such a particle has a relatively large moment and hence could be of importance in palaeomagnetic studies if it behaved similarly in TRM. We selected three particles that were able to remain in a saturated or nearly saturated state while in saturation remanence, and subjected them to thermal cycling in the Earth's field. Each particle was demagnetized in an alternating field (a.f.) to 200 Oe before heating, to ensure that the particle was initially in a multi-domain state. On cooling, the first particle showed no domain pattern; on a.f.-demagnetization to 50 Oe a pattern became apparent. Figure 4 shows the second particle before heating (*a*), after cooling in the Earth's field (*b*) and after cooling in a field of 30 Oe (*c*). A nearly saturated state results after cooling in the Earth's field, and the particle is saturated after cooling in the 30-Oe field. The application of a 50-Oe a.f. demagnetization, following cooling in the 30-Oe field, gives rise to the pattern shown in Fig. 4*d*. A third particle also showed a nearly saturated state after cooling in the Earth's field. Grains of the order of tens of micrometres are thus capable of behaving as single-domain particles in weak-field TRM. These particles have large magnetic moments, yet would follow Néel's tanh H field dependence[1].

The results reported here suggest that TRM in small particles is partially controlled by nucleation. As nucleation is grain-size dependent, such TRM should have a similar grain-size dependence. In an assemblage of small particles ranging from true single-domain to true multi-domain, there would be three contributions to the final TRM. First, there will be a single-domain contribution, which obeys Néel's theory. Second, there will be a contribution from particles in a multi-domain state[17]. Note that the multi-domain patterns commonly observed in titanomagnetites are not fully understood. It has been suggested that particularly complicated, finely convoluted patterns are stress-controlled and carry stable TRM[18], but this remains controversial. Third, there will be a contribution from multi-domain grains which have failed to nucleate walls. This TRM should unblock at temperatures near to the Curie point and behave as do large single-domain particles. Stability to a.f.-demagnetization will depend on the nucleation fields of the particular grains, giving a distribution of the microscopic coercivities.

We thank Dr John Wyman of Ferrofluidics Inc. for providing the high-temperature colloid. This work is supported by grants from the NSF.

Received 19 December 1985; accepted 4 April 1986.

1. Neel, L. *Ann. Geophys.* **5**, 99 (1949).
2. Kittel, C. *Rev. mod. Phys.* **21**, 541-583 (1949).
3. Levi, S. & Merrill, R. *J. geophys. Res.* **83**, 309-323 (1978).
4. Becker, J. J. *IEEE Trans. Magn.* **MAG-5**, 211-214 (1969).
5. Becker, J. J. *IEEE Trans. Magn.* **MAG-11**, 965-967 (1976).

6. Boyd, J. R., Fuller, M. & Halgedahl, S. *Geophys. Res. Lett.* **11**, 193-196 (1984).
7. Halgedahl, S. & Fuller, M. *Nature* **288**, 70-72 (1980).
8. Halgedahl, S. & Fuller, M. *J. geophys. Res.* **88**, 6505-6522 (1983).
9. Halgedahl, S. *Eds* **63**, 917 (1982).
10. Fuller, M. *Geophys. Surv.* **7**, 75-87 (1984).
11. Livingston, J. D. *Phys. Status Solidi* **56**, 637-645 (1979).
12. Livingston, J. D. *J. appl. Phys.* **52**, 2544-2548 (1981).
13. Livingston, J. D. *J. appl. Phys.* **57**, 3555-3559 (1985).
14. Day, R. *et al. Init. Rep. DSDP* Leg **49**, 781-791 (1979).
15. Bitter, F. *Phys. Rev.* **38**, 1903-1906 (1931).
16. Soffel, H. & Petersen, N. *Earth planet. Sci. Lett.* **11**, 312-316 (1971).
17. Schmidt, V. A. *Earth planet. Sci. Lett.* **20**, 440-446 (1973).
18. Appel, E. & Soffel, H. *Geophys. Res. Lett.* **11**, 189-192 (1984).

Magnetotactic bacteria and single-domain magnetite in hemipelagic sediments

John F. Stolz*, Shih-Bin R. Chang† & Joseph L. Kirschvink†

* Jet Propulsion Laboratory 125-112, 4800 Oak Grove Drive, Pasadena, California 91109, USA
† Division of Geological and Planetary Sciences 170-25, California Institute of Technology, Pasadena, California 91125, USA

Remanent magnetism in marine sediments has been used extensively over the past twenty years to calibrate the geological timescale, study geomagnetic reversals and secular variation, and measure the rates of seafloor spreading. Although these sediments may contain different magnetic minerals, magnetite is the most commonly observed and magnetically stable phase, and its size, shape and post-depositional fate affect the magnetic remanence of the sediments. Biogenic magnetites are single-domain, with a high natural magnetic remanence (NRM), and have been suggested as a significant source of magnetic remanence in marine sediments. We have studied surface sediments from the Santa Barbara Basin and report the occurrence of living magnetotactic bacteria and the deposition of biogenic ultra-fine-grained, single-domain magnetite. Using a novel extraction technique, transmission electron microscopy and SQUID magnetometry, we show that these bacteria and the magnetite they produce are the major source of stable remanent magnetism in these sediments.

Studies of hemipelagic sediments from several localities in the eastern Pacific show a maximum intensity of magnetic remanence occurring in the surface sediments[1,2]. Rock magnetic studies indicate a dramatic decrease of intensity with depth, correlated with a loss of the fine-grained component[3,4]. However, the limited resolution of the techniques used has so far prevented the specification of the morphology of the fine-grained magnetite, or its mechanism of formation[5]. The high intensity of natural magnetic remanence and bacterial activity in the surface sediments suggested biogenic magnetite as a probable source of the sub-micrometre-sized magnetite.

Our samples were collected from three different sites in the Santa Barbara Basin (34° 14′ N, 120° 1′ W), at a depth of 598 m and a temperature of 8 °C. The top 3 cm of sediment was removed from box cores and either fixed with 2.5% glutaraldehyde immediately after collection or left untreated. All the samples were kept at 8 °C.

We examined the unfixed sediment with a low-power (×160) light microscope by placing a drop of sediment on a glass slide. When the south end of a stirring bar magnet was placed next to the drop, magnetotactic bacteria present in the sediment accumulated at the edge of the drop. To study these bacteria and the ultra-fine-grained magnetite they produce by transmission electron microscopy, we devised a novel extraction technique. Carbon-coated copper grids were placed face down on drops of sediment suspension and the south pole of a cobalt rare-earth magnet was suspended 1 cm above the drops, for 20-30 min. Some grids were treated with 1% uranyl acetate for 1 min to stain the bacteria. The grids were observed with a Phillips 201 transmission electron microscope at 80 kV. Identification of the crystals as magnetite was made by electron diffraction[5,6].

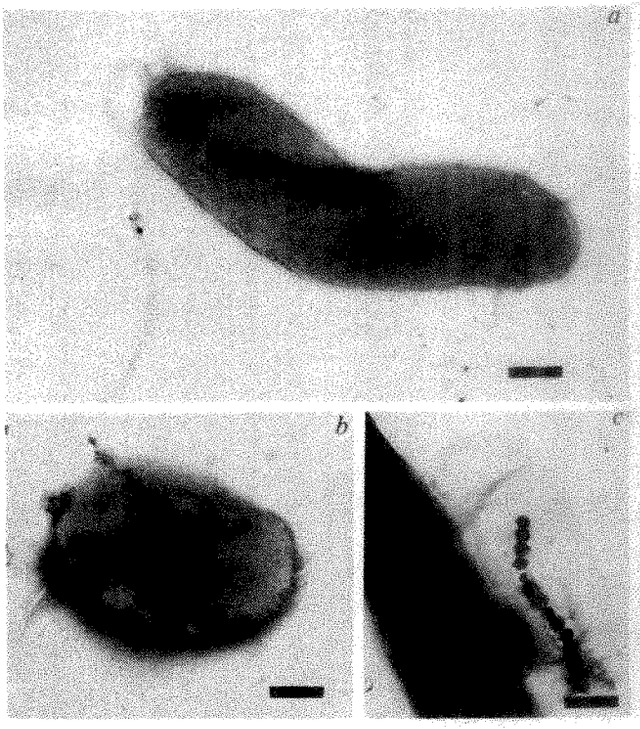


Fig. 1 Transmission electron micrographs of magnetotactic bacteria from the Santa Barbara Basin; all scale bars 200 nm. *a*, Vibrio with chain of 11 crystals of magnetite and one polar flagellum. Note the irregular shape of the crystals. *b*, Coccoid with chain of four crystals. *c*, Rod with chain of 13 crystals.

We observed several morphological types of magnetotactic bacteria in preparations of unfixed sediment samples (Fig. 1). Vibrio and rod-shaped bacteria were seen (Fig. 1*a*, *c*), but the most common morphology was coccoid (Fig. 1*b*). In each case, the crystals of magnetite were arranged in a chain 10-20 crystals long. The individual crystals were between 40 and 60 nm in size and cuboidal, rectangular or irregular in shape. The sizes of all the well-formed crystals fall within the calculated stability field for single-domain magnetite[7]; in fact, to date, all reported sizes of bacterial magnetites fall within this range[8-10]. The irregular crystals may be produced by the dissolution of well-formed crystals (H. A. Lowenstam, personal communication).

Aggregates and chains of ultra-fine-grained magnetite free of bacteria were seen in both unfixed (Fig. 2*a*) and fixed (Fig. 2*b*, *c*) material. Like the magnetite seen in the bacteria, most of the crystals were 40-60 nm in size and cuboidal, rectangular or irregular in shape. In one instance an intact magnetosome was observed (Fig. 2*c*). The gradual increase in crystal size along the chain, with a few much smaller crystals at one end, is characteristic of magnetosomes in many magnetotactic bacteria. Crystals which were roughly teardrop-shaped and larger in size (100-120 nm) were also seen (Fig. 2*d*).

The magnetic properties of the sediment were analysed using saturation isothermal remanent magnetization (sIRM) and alternating-field demagnetization (AF) with a SQUID magnetometer[11]. Both fixed and unfixed sediments were examined, as 0.1-g aliquots in quartz containers. The coercivity spectrum generated (squares in Fig. 3) indicates that the primary remanence carrier is single-domain magnetite. In a previous study, the coercivity spectrum of a marine magnetotactic bac-

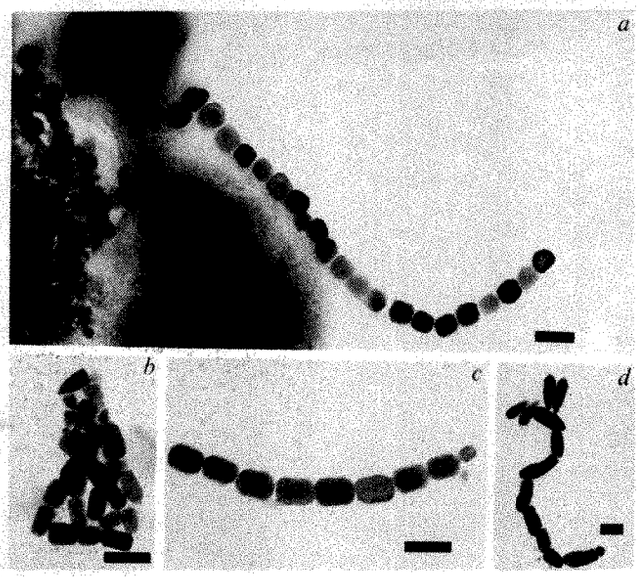


Fig. 2 Transmission electron micrographs of ultra-fine-grained magnetite from the Santa Barbara Basin. All but *a* were from fixed material; all scale bars 100 nm. *a*, Chain of 30 cuboidal crystals extracted from unfixed material. *b*, Cluster of prismatic and irregular magnetite crystals. *c*, Chain of crystals which appears to be an intact magnetosome. Note the smaller crystal at the right-hand terminus. *d*, Chain of irregular and teardrop-shaped crystals.

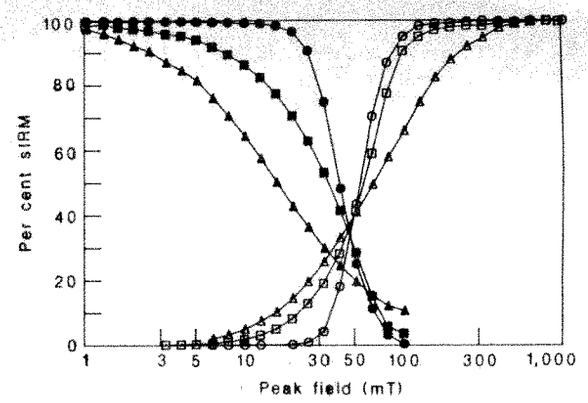


Fig. 3 Coercivity spectra of Santa Barbara Basin surface sediment (squares), pellet of marine magnetotactic bacteria from Laguna Figueroa, Baja California, Mexico[12] (circles) and beach sand with 10% w/v content of coarse-grained magnetite from Laguna Figueroa[12] (triangles). Open symbols, IRM; solid symbols, AF demagnetization.

terium was determined (circles, Fig. 3)[12]. Collected from a salt-water marsh, these bacteria have prismatic crystals measuring 90×120 nm, aligned in a chain of average length 10 crystals. The bacterial crystals saturate at ~100 mT (1 mT = 10 Oe), with an intersection at ~50 mT. The coercivity spectrum of the Santa Barbara Basin material also saturates at ~100 mT and intersects at ~50 mT. Grain-grain interaction and the presence of other magnetic minerals (that is, coarse-grained magnetite and haematite) in the sediment may account for the differences between the two spectra[13]. A few particles of multi-domain magnetite (>1 μm) were seen in sediment extracts. Figure 3 also shows (triangles) the coercivity spectrum of a marine sediment containing mostly coarse-grained magnetite and no bacterial magnetite. Both the saturation values and the intersection point are markedly different. This suggests that the coarse-grained component does not contribute significantly to the magnetic properties of the surface sediments.

The maximum values of sIRM obtained for both fixed and unfixed samples ranged between 2.5×10^{-4} and 1.25×10^{-3} e.m.u. g^{-1} and agree with previously published measurements for hemipelagic sediments[1,2]. A magnetotactic bacterium with a chain of 20 cuboidal 50-nm crystals, such as those seen in the Santa Barbara bacteria, has a calculated saturation moment of 10^{-12} e.m.u. g^{-1} (refs 8, 10). If all the remanent magnetization is attributed to the bacteria, a population density of between 10^7 and 10^8 magnetotactic bacteria per gramme of sediment is predicted. Such a population was not seen in the material we examined; however, direct field counts at the time of collection could not be made. Populations of magnetotactic bacteria from other environments have been observed to decline dramatically within hours or days after collection[12]. The discrepancy in the magnetic remanence and the actual number of live bacteria observed in the Santa Barbara sediments may be explained by episodic increases in population, the persistence of ultra-fine-grained magnetite in the surface sediments, the presence of other magnetic minerals (including some coarse-grained magnetite), and the death of much of the population during sample collection and storage. The bacteria contribute significantly to the natural magnetic remanence because each of the crystals is single-domain and is usually deposited as part of a chain. The discovery of an intact magnetosome and chains of magnetite in the sediment extracts suggests that these crystals remain aligned even outside the bacteria. Unlike bacterial magnetites, coarse-grained magnetites have very little effect on the natural magnetic remanence.

This study has concentrated on the surface sediments of the Santa Barbara Basin, where the conditions of growth for the magnetotactic organisms may be optimal. A microbial mat community, dominated by species of *Beggiatoa*, a sulphur-oxidizing chemolithotroph, thrives on the surface (M. Kastner, personal communication). *Beggiatoa*, along with most magnetotactic bacteria, are microaerophiles, needing trace quantities of oxygen for their metabolism[14,15]. The abrupt disappearance (within the top metre) of the ultra-fine-grained component in sediments from the California continental borderland[2-4] and the Gulf of California[1,3] can be explained by the disappearance of the magnetotactic bacteria and the dissolution of the bacterial magnetites. In these sediments iron oxide reduction is coupled with the diagenesis of organic material[1,3]. The profiles of sulphur, sulphate and oxygen concentration support this explanation[1,3,16].

The results of this study and those we have conducted in two other marine environments (a lagoonal environment in Baja California, Mexico, and a carbonate environment in the Florida Keys, USA)[12] suggest that magnetotactic bacteria are the source of the primary remanence carrier (ultra-fine-grained, single-domain magnetite) in many marine sediments. The eventual fate of this biogenic magnetite depends on a number of post-depositional factors. In environments where there is a strongly reducing zone with abundant sulphide, only greigite pseudomorphs of magnetite have been found[17]. Maghemite pseudomorphs of bacterial magnetite have also been seen in deep-sea sediments[18]. The loss of the ultra-fine-grained bacterial magnetite component with depth in open ocean basins may limit the extent of the biogenic magnetite contribution to rock magnetism to marine sediments with low organic content such as calcareous oozes and limestones.

We thank M. Kastner for providing the samples and H. Lowenstam and K. H. Nealson for helpful discussion. This work was supported by NSF grants EAR8407655 and EAR8351370 to J.L.K. and S.-B.R.C., and by an NRC Research Associateship Award to J.F.S. This is Caltech Division of Geological and Planetary Sciences contribution no. 4328.

Note added in proof: Bacterial single-domain magnetite in deep ocean sediments as old as 50 Myr has recently been reported by Petersen *et al.*[19] and discussed by Frankel[20].

Received 3 February; accepted 3 April 1986.

1. Karlin, R. & Levi, S. *Nature* **303**, 327–330 (1983).
2. Lund, S. P. *et al. Eos* **64**, 683 (1983).
3. Karlin, R. & Levi, S. *J. geophys. Res.* **90**, 10373–10392 (1985).
4. Leslie, B. *et al. Eos* **65**, 957 (1984).
5. Chang, S.-B. R. & Kirschvink, J. L. in *Magnetite Biomineralization and Magnetoreception Organisms* (eds Kirschvink, J. L. *et al.*) 647–669 (Plenum, New York, 1985).
6. Towe, K. M. in *Magnetic Biomineralization and Magnetoreception in Organisms* (eds Kirschvink, J. L. *et al.*) 167–181 (Plenum, New York, 1985).
7. Butler, R. F. & Banerjee, S. K. *J. geophys. Res.* **80**, 4049–4058 (1975).
8. Blakemore, R. P. *A. Rev. Microbiol.* **36**, 217–238 (1982).
9. Towe, K. M. & Moench, T. T. *Earth planet. Sci. Lett.* **52**, 213–220 (1981).
10. Frankel, R. B. *A. Rev. Biophys. Bioengng* **13**, 85–103 (1984).
11. Fuller, M. *et al.* in *Magnetite Biomineralization and Magnetoreception in Organisms* (eds Kirschvink, J. L. *et al.*) 103–151 (Plenum, New York, 1985).
12. Chang, S.-B. R., Stolz, J. F. & Kirschvink, J. L. *Phys. Earth planet. Inter.* (in the press).
13. Cisowski, S. *Phys. Earth planet. Inter.* **26**, 56–62 (1981).
14. Nelson, J. & Jannasch, H. *Archs Microbiol.* **136**, 262–269 (1983).
15. Blakemore, R. P. *et al. Geomicrobiol. J.* **4**, 53–71 (1984).
16. Savrda, C. E. *et al. Bull. Am. Ass. Petrol. Geol.* **68**, 1179–1192 (1984).
17. Demitrack, A. in *Magnetite Biomineralization and Magnetoreception in Organisms* (eds Kirschvink, J. L. *et al.*) 625–645 (Plenum, New York, 1985).
18. Von Dobeneck, T. *et al. Int. Ass. Geomagnetism Aeronomy Meet. Abstr.* **1**, 214 (1985).
19. Petersen, N., von Dobeneck, T. & Vali, H. *Nature* **320**, 611–615 (1986).
20. Frankel, R. B. *Nature* **320**, 575 (1986).

Carbon isotope evidence for a magmatic origin for Archaean gold-quartz vein ore deposits

D. R. Burrows, P. C. Wood & E. T. C. Spooner

Department of Geology, University of Toronto, Toronto, Ontario M5S 1A1, Canada

Archaean gold-quartz vein/shear zone systems constitute one of the most important types of gold ore deposit; however, their origin is controversial. Here we discuss newly obtained $\delta^{13}C$(PDB) values for carbonate associated with the second largest such system in the world (Hollinger–McIntyre, Superior Province, Canada), together with values for fourteen other Au-mineralized locations in the Timmins area[1] and for the largest such system in the world (Golden Mile, Western Australia[2]). All of the data are statistically identical to the $\delta^{13}C$ values, reported here, of proven magmatic carbonate recently found with Au- and W-enriched MoS_2 mineralization in the Mink Lake sodic granodiorite stock, north-west Ontario. The $\delta^{13}C$ values appear to exclude greenschist–amphibolite facies metamorphic processes, a widely accepted genetic alternative[3–6], and granulite facies processes[7,8]. We conclude that currently available carbon isotope data suggest that the H_2O–CO_2 fluid which deposited this type of Archaean Au mineralization was magmatically derived.

The Hollinger (Timmins)–McIntyre (Schumacher)–Coniaurum–Vipond–Moneta–Crown vein system located in the Abitibi greenstone belt, ~550 km north-north-west of Toronto, is ~5 km long, a maximum of ~2 km wide, and has been mined to a depth of 2.4 km (7,875-ft level, McIntyre mine). End-1984 past-production plus reserves total 100.9 million tonnes of ore, at 9.9 g tonne^{-1} recovered/recoverable Au and ~2 g tonne^{-1} recovered/recoverable Ag[9,10]. Of the 994.7 tonnes of contained Au, 60.2% occurred in the Hollinger deposit, which has been in production with some interruptions since 1910. Between 1940 and 1953 it was the principal source of scheelite ($CaWO_4$) of the gold mines in the Archaean of Canada (47,878.1 tonnes ore at 0.78% WO_3)[11–13]. Thus the Hollinger system is an excellent example of the Archaean gold-quartz-(Fe-carbonate-pyrite ± tourmaline ± tellurides ± W (scheelite) ± Mo) type of vein deposit.

The principal type of mineralization in Hollinger is related to quartz-dominated veins with prominent pyrite–Fe-carbonate–muscovite alteration envelopes. The veins are geometrically unusual in that they consist of steeply dipping composite zones containing tabular sections, multiple curves from which extend flats, curved branches, feathers with bifurcations, splits and spurs, and more complicated geometries, all of which largely cross-cut the local fabric. The bulk of the gold (~95%) occurs as small (~5–60 μm) particles within pyrite grains in the alteration selvages. Carbonate (20–60 mol % $CaFe(CO_3)_2$) is very closely related to gold mineralization, occurring with albite as internally projecting fringes on the margins of veins and, particularly, metasomatically dispersed in the mineralized wall-rock. The composition of the carbonate is zoned from Fe-rich in the core of the deposit to Fe-poor around the periphery (Fig. 1). The zone of mineralization and carbonate alteration narrows downwards to the root of the system (Fig. 1). Hollinger, therefore, exemplifies the remarkably ubiquitous association between carbonate and Archaean lode gold mineralization[3–5,14–16]. The remainder of the vein-fill at Hollinger consists of minor sulphides (pyrite, sphalerite, chalcopyrite, pyrrhotite, arsenopyrite and galena), beige scheelite, and minor muscovite, chlorite, tourmaline, tellurides and native bismuth.

Carbon dioxide is known to be a major component of Archaean Au-quartz vein fluids[5]; for this reason, the carbon isotopic composition of the carbonate in the Hollinger deposit has been determined as a source tracer. Analysis of 14 vertically and laterally representative samples (Table 1, Fig. 2) yielded $\delta^{13}C$ values ranging from −4.8 to −0.1‰, with an arithmetic mean of -3.0 ± 1.5‰ (1σ). Data for vein and wall-rock alteration carbonate are statistically identical (Kolmogorov–Smirnov test[17]) at -2.8 ± 1.8 and -3.3 ± 1.3‰, an observation consistent with the two being cogenetic. The histogram in Fig. 2 shows that the Hollinger data are characterized by a marked positive skewness and, consequently, a mode of −4.3‰ which is lower than the arithmetic mean. Thirty previous carbonate $\delta^{13}C$ determinations for the Hollinger system[1] define a higher arithmetic mean of -0.6 ± 0.5‰ and a range of −1.5 to +0.3‰, which overlaps the top end of the range defined in this study. The samples were obtained from only two pits at the surface (55 and 68) and have been described as coming from "stratabound pyritic 'flow-ore', and stratiform pyritic graphitic units"[18], which are not the major ore types in the Hollinger deposit. This study contains data for two samples from pit 55 (Table 1). They are relatively heavy (−1.1 and −1.0‰), and are thus consistent with the determinations in the previous study[1]. It appears, therefore, that the previous data were obtained from samples which were unrepresentative of the system as a whole.

Values (275 data points) for a further 14 Au-mineralized locations in the Timmins area[1] (for example, Aunor, Buffalo Ankerite and Delnite mines, but data for Hallnor not included because of the presence of graphitic inter-flow sediments which could modify the $\delta^{13}C$ values[1]) define a range and arithmetic mean which are very similar to the new Hollinger data: −6.1 to +0.8‰ with an outlier at +2.2‰, compared with −4.7 to −0.1‰ (Hollinger), and -3.1 ± 1.3‰, compared with -3.0 ± 1.5‰ (Hollinger). As the histogram in Fig. 2 shows, the data for the 14 other Au-mineralized localities in the Timmins area are also asymmetrically distributed, with a distinct positive skewness. A χ^2 test confirms that the data are not normally distributed ($\chi^2_{\text{calculated}} = 64.3$; $\chi^2_{0.05,9} = 16.9$) and that, therefore, parametric statistical significance tests are inappropriate. Hence, a two-tailed Kolmogorov–Smirnov test[19,20] was used to verify the hypothesis that the new Hollinger samples and the sample for the 14 Timmins-area Au locations are the same (see ref. 17 for details). A Kolmogorov–Smirnov test was chosen because it is sensitive to any difference in the distributions from which two samples have been drawn.

The $\delta^{13}C$ values for the pooled data (new Hollinger plus 14 selected Timmins-area Au locations: $\bar{x} \pm 1\sigma = -3.1 \pm 1.3$‰; $n = 289$) may be compared with $\delta^{13}C$ values for magmatically derived carbonate found recently[21] in association with Au- and W-enriched MoS_2 mineralization in the Mink Lake granodiorite intrusion. This 1.5×3.25 km stock located ~110 km north-east of Red Lake is an unmetamorphosed, completely post-tectonic

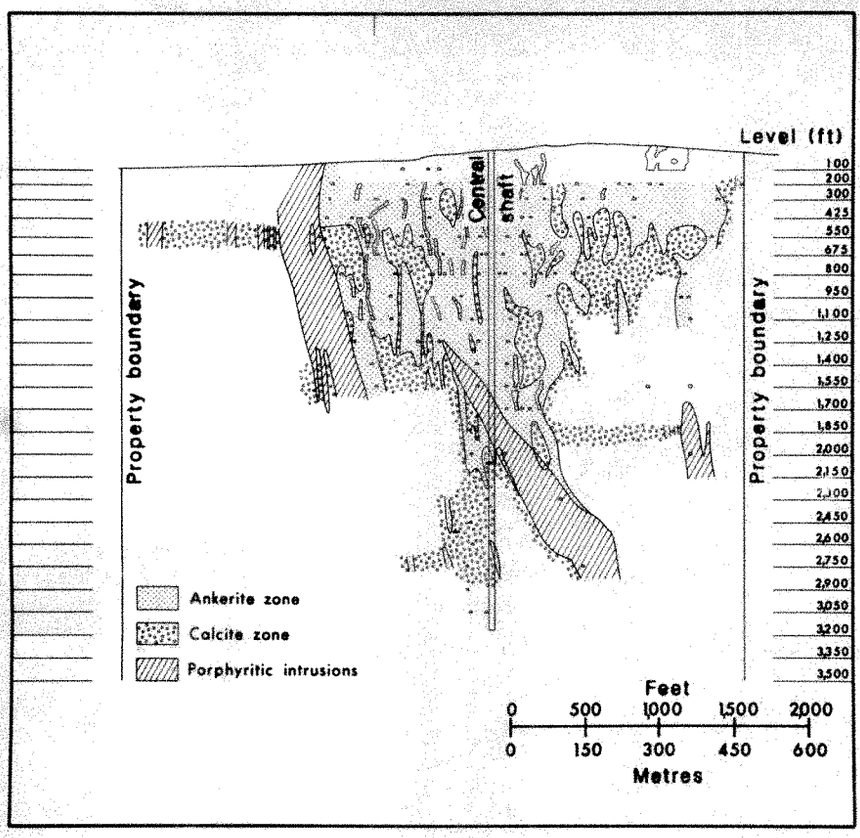


Fig. 1 Vertical cross-section of the Hollinger Au-vein deposit (through 9 cross-cut), showing a zonation from ankeritic carbonate in the core to calcite around the edges, and the narrowing of the mineralized zone downwards to the root of the system.

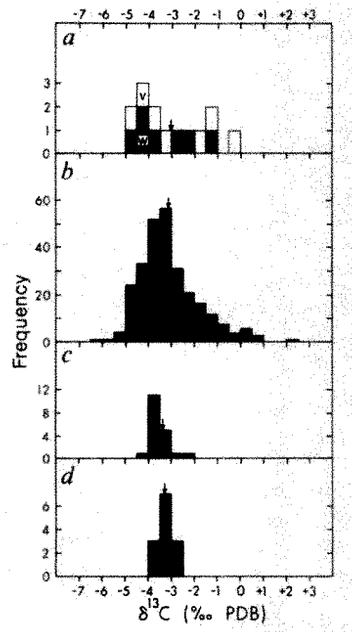


Fig. 2 Histograms of the carbonate $\delta^{13}C$ data. The histogram and statistics for the 14 Au-mineralized locations in the Timmins area[1] do not include the data for Hollinger or Hallnor in ref. 1 because of the presence of graphitic inter-flow sediments in the sampled areas. As suggested in ref. 1, such material could modify $\delta^{13}C$ values. Data for the No. 4 lode, Golden Mile, Kalgoorlie, Western Australia are from ref. 2. v, Vein material; w, altered wall-rock. Arrows denote arithmetic means. *a*, Au vein mineralization, Hollinger mine, Timmins, northern Ontario; $\bar{x} = -3.0 \pm 1.5$ (1σ); $n = 14$. *b*, Au vein mineralization, Timmins area (14 locations, excluding Hollinger); $\bar{x} = -3.1 \pm 1.3$; $n = 275$. *c*, Au vein mineralization, No. 4 lode, Golden Mile, Kalgoorlie, Western Australia; $\bar{x} = -3.4 \pm 0.4$; $n = 19$. *d*, MoS_2 mineralization, Mink Lake granodiorite stock, northwestern Ontario; $\bar{x} = -3.3 \pm 0.4$; $n = 13$.

intrusion in the Archaean Uchi sub-province[21]. It is a sodic granodiorite in composition ($SiO_2 = 64$–71%; $Na_2O/K_2O = 1.6$–3.2), and contains a $350 \times 1{,}000$ m zone of MoS_2 mineralization and associated carbonate metasomatism completely enclosed within its southern end. Carbonate alteration zones occur as symmetrically developed selvages adjacent to aplites ($SiO_2 = 75$–76%) and quartz–carbonate ± K-feldspar–chlorite–pyrite veins, both of which contain MoS_2, and as larger, but localized, sub-horizontal, tabular zones up to 3 m in width also containing MoS_2, but lacking internal veins. The MoS_2 mineralization and carbonate alteration are considered to be magmatically derived for a number of reasons (discussed in detail in ref. 22): (1) they are directly related to an observable silicate melt–hydrothermal fluid(s) transition, as MoS_2 and carbonate occur in, and carbonate occurs adjacent to, aplite veins of granitic composition which represent late melt, as well as quartz-dominated hydrothermal veins; (2) hydrothermal fluids trapped in 5–20-μm fluid inclusions are CO_2-rich and show low aqueous-phase salinities of 5.6 ± 1.2 equiv. wt % NaCl ($n = 48$)[23], both attributes being characteristic of fluids shown to be magmatic in other cases (for example, Boss Mountain Mo deposit, British Columbia[24], Tanco Ta (–Sn) granitic pegmatite, south-east Manitoba[25]); (3) the fluid δD–$\delta^{18}O$ box estimated from the bulk of the δD and $\delta^{18}O$ data shows a ~60% overlap with the general magmatic water field but a significantly smaller overlap (~18%) with the general metamorphic water field, and no relationships to sea water or meteoric water values; (4) the MoS_2 mineralization is completely contained within the stock with no obvious external connections; (5) the intrusion is in any case post-tectonic and post-metamorphic; (6) the mineralization developed marginal to the principal internal zone of fractional crystallization, as shown by contoured Rb, TiO_2, Zr and Li data ($n = 47$); and (7) the aplites, the compositions of which are compatible with derivation by fractional crystallization, are geochemically enriched in Au, Mo and W, thus confirming a link with the subsequent Au- and W-enriched MoS_2 mineralization.

Table 1 $\delta^{13}C$ values for Hollinger and Mink Lake carbonate

Sample no.	Sample description	$\delta^{13}C$ (‰ PDB)
Au-quartz mineralization, Hollinger mine		
33P-S342-v	Vein in volcanic fragmental unit, NE end of pit 33, N part of deposit.	−3.8
33P-S342-w	Wall-rock; as above.	−3.7, −3.6
55P-S330-v	Vein in mafic flow (no. 99), SW end of pit 55, S part of deposit.	−1.0
55P-2-w	Wall-rock; as above.	−0.9, −1.2
4-S124-v	Vein in strained Pearl Lake porphyritic intrusion, 425-ft level, NE part of deposit.	−1.8, −2.0
4-S130-w	Wall-rock in mafic volcanic (M1), 425-ft level, SW part of deposit.	−4.1, −4.0
8-S310-v	Vein in mafic volcanic, 800-ft level, SW part of deposit.	−0.1, −0.1
8-S310-w	Wall-rock; as above.	−2.2, −2.2
12-S166-v	Vein in strained Pearl Lake porphyritic intrusion, 1,250-ft level, NE part of deposit.	−3.3, −3.4
15-22-w	Wall-rock in strained Millerton porphyritic intrusion, 1,500-ft level, SW part of deposit.	−4.3, −4.3
18-83-01-v	Vein in strained Millerton porphyritic intrusion, 1,850-ft level, SW part of deposit.	−5.0, −4.6
18-16-w	Wall-rock; as above.	−4.6
27-S158-v	Vein in strained Millerton porphyritic intrusion, 2,750-ft level, central part of deposit.	−4.5, −4.2
27-S155b-w	Wall-rock in strained Millerton porphyritic intrusion, 2,750-ft level, SW part of deposit.	−2.8, −2.7
$\bar{x}\pm\sigma$		−3.0±1.5
MoS_2 mineralization, Mink Lake stock		
P-75	Fe-calcite in quartz-chl clot in felsic pegmatite vein cut by early aplite.	−3.5, −3.4
S-32	Carbonate alteration selvage on thin MoS_2-bearing aplite.	−3.4, −3.2
		−3.5, −3.4
S-21	Carbonate alteration; no associated quartz vein; cc-chl-MoS_2-py.	−2.7
S-109	Central MoS_2-rich band of 120-cm-wide carbonate alteration zone.	−3.2
S-25/L128	White carbonate from within chlorite haloes; MoS_2-bearing carbonate alteration.	−2.8
L-113b	Light buff carbonate alteration; chl haloes similar to S-25; MoS_2-py, no associated quartz vein.	−2.8
C-29	Unmineralized carbonate alteration.	−3.8, −3.7
S-19	Chl-orthoclase-cc-MoS_2 quartz vein. Py cubes up to 5 mm.	−3.1, −3.1
S-97	Carbonate alteration selvage on quartz vein; MoS_2-chl-py.	−3.9
S-9	Mineralized carbonate alteration.	−3.5, −3.4
S-4/L104	Carbonate alteration selvage on quartz vein with cc, chl, orthoclase, py and MoS_2.	−3.5, −3.4
S-2	Carbonate alteration on MoS_2 quartz vein.	−3.5, −3.4
S-81b	Late muscovite-chl alteration	−3.9, −3.7
$\bar{x}\pm\sigma$		−3.3±0.4

$\delta^{13}C$ analyses were carried out at the Isotope Laboratory, Department of Earth Sciences, University of Waterloo, Waterloo, Ontario N2L 3G1, Canada by standard techniques. The estimated routine uncertainty is ± 0.2‰ (1σ). Precision, as defined by the mean average deviation for the 20 duplicated analyses in this study, is ± 0.1‰ (±3.1%), where mean average deviation is defined as $(\sum_{i=1}^{n}\Delta_i/2\cdot\bar{x}_i)/n$ (n = number of duplicates; Δ_i = difference, regardless of sign, for the ith pair; $\bar{x}_i$ = arithmetic mean of the ith pair)[36].

The samples from Hollinger are equally divided between vein and metasomatic wall-rock carbonate, and were selected to be vertically and laterally representative of the deposit. Hence, samples were obtained from pits 33 and 55 at the surface, and the 425-, 800-, 1,250-, 1,550-, 1850- and 2,750-ft levels underground. Sampling below the 2,750-ft level was not possible because the lower levels, which extend down to 5,450 ft, were no longer accessible. Lateral sample positions on the different levels were variable (see above). Host lithologies are either strained mafic flows or strained porphyritic intrusions (see above). Samples from the high-grade core zone of the Hollinger deposit were very difficult to collect because of inaccessible collapsed workings. One sample (27-S158-v) was obtained. Most samples come from the southwestern (SW), northeastern (NE), southern (S) and northern (N) parts of the deposit. cc, Calcite; chl, chlorite; py, pyrite.

Thirteen $\delta^{13}C$ determinations for Mink Lake carbonate from various associations (Table 1) define a very narrow range from −3.9 to −2.7‰, which is completely enclosed within the pooled Timmins-area Au locality range. More importantly, the modal classes of the two data sets are exactly the same (−3.5 to −3.0‰; Fig. 2), the arithmetic means differ by only 0.2‰, which is equivalent to analytical uncertainty (−3.3 ± 0.4‰ for Mink Lake, compared with −3.1 ± 1.3‰ for Timmins), and a two-tailed Kolmogorov-Smirnov test confirms that the data are drawn from the same population at the 5% significance level[17]. Therefore, as the carbonate in the Archaean Mink Lake stock is magmatically derived, it can be concluded that the identical $\delta^{13}C$ values for the carbonate associated with the Archaean Au mineralization in the Timmins area are compatible with a magmatic derivation[26]. Moreover, currently available data appear to exclude greenschist-amphibolite and granulite facies metamorphic processes as genetic alternatives. CO_2 derived by decarbonation is enriched in ^{13}C by 3-5‰ relative to its starting material[27]. Hence, the $\delta^{13}C$ values of CO_2 produced by decomposition of seafloor carbonate (0 to +2‰; see, for example, refs 28, 29) in greenstone belt sequences is likely to be ~ +3 to +7‰ (modified from ref. 7), values greater than those of Timmins-area Au/Mink Lake MoS_2 carbonate. Organic carbon in inter-flow sediments has markedly lower $\delta^{13}C$ values, mainly between −35 and −20‰ (ref. 30). Mixtures are possible; however, the very narrow ranges and, above all, the recurrence of the Timmins-area Au/Mink Lake MoS_2 carbonate $\delta^{13}C$ values in 16 locations constitute very strong evidence against natural mixing processes which give irregular ranges. Granulite facies metamorphic processes appear to be excluded by fluid inclusion CO_2 $\delta^{13}C$ values, ranging from −21.9 to −4.5‰ (n = 10; ref. 31), and, particularly, by the extremely CO_2-rich fluid compositions which are characteristic of granulites, including those in the Superior Province[22,32,33]. Finally, the carbon species in the fluids are dominated by CO_2, so that intercomparison of carbonate $\delta^{13}C$ values is valid (for example, Hollinger CO_2 melting point (m.p.) = −56.7 ± 0.7 °C (1σ), n = 100 (ref. 34); Mink Lake CO_2 m.p. = −56.4 ± 0.8 °C, n = 57 (refs 21, 22); pure CO_2 m.p. = −56.6 °C). The depositional temperatures are also very similar, so that CO_2-carbonate $\delta^{13}C$ fractionations are comparable (Hollinger, 271 ± 47 °C (ref. 34); Mink Lake, 298 ± 37 °C (refs 21, 22)).

Thus, the weight of the currently available carbon isotope evidence indicates that Archaean gold-quartz vein mineralization is magmatically derived, supporting the suggestion of Wood *et al.*[34] that components of domal tonalite gneiss-granodiorite-quartz monzonite-type material which intrudes the lower parts of Archaean greenstone belts could constitute an indirect, or direct, source region.

This result may have broader applicability. The 1.2 × 3 km set of ~300 shear zone lodes which constitutes the Golden Mile in the Norseman–Wiluna greenstone belt in the Archaean Yilgarn block of Western Australia is the largest known Archaean gold-quartz system in the world, having produced ~1,200 tonnes of Au[35] (compare with the Hollinger system total of 994.7 tonnes Au). The carbon isotopic composition of the associated Fe-carbonate, -3.4 ± 0.4‰ (Fig. 2), as defined by 19 determinations from two traverses of the No. 4 lode (DDH 5027 and DDH 5022)[2], is closely similar to that of the pooled Timmins-area Au locations (-3.1 ± 1.3‰), and remarkably similar to the Mink Lake stock MoS_2-associated carbonate (-3.3 ± 0.4‰). Two-tailed Kolmogorov-Smirnov tests confirm that all of the data are drawn from the same population at the 5% significance level[17]. Hence, the No. 4 lode, Golden Mile $\delta^{13}C$ data are also consistent with a magmatic derivation.

We thank the Noranda Exploration Company Ltd (Mr W. A. Nash) for permission, assistance and financial support to work on the Mink Lake MoS_2 mineralization, and Pamour Porcupine Mines Ltd (Mr. W. W. Holmes) for permission to work in the Hollinger (Timmins) mine; and James Macdonald (Ontario Geological Survey), Mike Cherry (Ontario Geological Survey), Brian O'Donovan (photographer), Subhash Shanbhag (draughtsman), Anne Marie Cooperwhite and Sandra Martin (secretaries) for their help. This research has been financially supported by the Ontario Geological Survey, an Ontario Geoscience Research Grant (GR 236 to E.T.C.S.) from the Ontario Ministry of Natural Resources, the Natural Sciences and Engineering Research Council of Canada (grant A6114 to E.T.C.S.) and Noranda Exploration Company Ltd.

Received 13 January; accepted 22 April 1986.

1. Fyon, A. J., Crocket, J. H. & Schwarcz, H. P. *Ont. geol. Surv. open File Rep. No.* 5464 (1983).
2. Golding, S. D. & Wilson, A. F. *Econ. Geol.* **78**, 438–450 (1983).
3. Kerrich, R. & Fyfe, W. S. *Chem. Geol.* **33**, 265–294 (1981).
4. Fyfe, W. S. & Kerrich, R. in *Gold '82: The Geology, Geochemistry and Genesis of Gold Deposits* (ed. Foster, R. P.) 99–127 (Balkema, Rotterdam, 1984).
5. Groves, D. I. *et al.* in *Gold '82: The Geology, Geochemistry and Genesis of Gold Deposits* (ed. Foster, R. P.) 689–712 (Balkema, Rotterdam, 1984).
6. Phillips, G. N. *Econ. Geol. Res. Unit Inf. Circ.* No. 175 (University of the Witwatersrand, Johannesburg, 1985).
7. Colvine, A. C. *et al. Ont. geol. Surv. open File Rep.* No. 5524 (1984),
8. Fyon, A. J., Schwarcz, H. P. & Crocket, J. H. *Geol. Ass. Can. Progm Abstr.* **9**, 65 (1984).
9. Bertoni, C. H. *Bull. Can. Inst. Min. Metall.* **76**, 62–69 (1983).
10. Pamour Porcupine Mines Ltd *Annual Reports 1982–1984* (Noranda Group, Toronto, 1983–1985).
11. Allen, C. C. & Folinsbee, R. E. *Econ. Geol.* **39**, 340–348 (1944).
12. Ferguson, S. E. *Ont. Dep. Mines geol. Rep.* **58** (1968).
13. Wood, P. C. *Misc. Pap. Ont. geol. Surv.* **116**, 188–190 (1983).
14. Davies, J. F., Whitehead, R. E. S., Cameron, R. A. & Duff, D. in *Geology of Canadian Gold Deposits* (eds Hodder, R. W. & Petruk, W.) 130–143 (Canadian Institute of Mining and Metallurgy, Montreal, 1982).
15. Fyon, A. J. & Crocket, J. H. in *Geology of Canadian Gold Deposits* (eds Hodder, R. W. & Petruk, W.) 113–129 (Canadian Institute of Mining and Metallurgy, Montreal, 1982).
16. Hodgson, C. J. & MacGeehan, P. J. in *Geology of Canadian Gold Deposits* (eds Hodder, R. W. & Petruk, W.) 211–229 (Canadian Institute of Mining and Metallurgy, Montreal, 1982).
17. Spooner, E. T. C., Wood, P. C., Burrows, D. R., Thomas, A. V. & Noble, S. R. *Misc. Pap. Ont. geol. Surv.* **127**, 229–246 (1985).
18. Fyon, A. J., Schwarcz, H. P., Crocket, J. H. & Knyf, M. *Misc. Pap. Ont. geol. Surv.* **103**, 59–64 (1982).
19. Siegel, S. *Nonparametric Statistics for the Behavioral Sciences* (McGraw-Hill, New York, 1956).
20. Till, R. *Statistical Methods for the Earth Scientist* (Macmillan, London, 1974).
21. Burrows, D. R. thesis, Univ. Toronto (1984).
22. Burrows, D. R. & Spooner, E. T. C. (submitted).
23. Burrows, D. R. & Spooner, E. T. C. *Geol. Ass. Can. Prog. Abstr.* **9**, 49 (1984).
24. Macdonald, A. J. thesis, Univ. Toronto (1983).
25. Thomas, A. V. thesis, Univ. Toronto (1985).
26. Burrows, D. R. & Spooner, E. T. C. *Geol. Ass. Can. Prog. Abstr.* **9**, 50 (1984).
27. Sheppard, S. M. F. & Schwarcz, H. P. *Contr. Miner. Petrol.* **20**, 161–198 (1970).
28. Spooner, E. T. C., Beckinsale, R. D., Fyfe, W. S. & Smewing, J. D. *Contr. Miner. Petrol.* **47**, 41–62 (1974).
29. Broughton, D. W. & Gibson, I. L. *Geol. Ass. Can. Prog. Abstr.* **9**, 49 (1984).
30. Schoell, M. & Wellmer, F.-W. *Nature* **290**, 696–699 (1981).
31. Hoefs, J. & Touret, J. *Contr. Miner. Petrol.* **52**, 165–174 (1975).
32. Touret, J. L. R. in *Short Course in Fluid Inclusions: Applications to Petrology* (eds Hollister, L. S. & Crawford, M. L.) 182–208 (Mineralogical Association of Canada, Toronto, 1981).
33. Rudnick, R. L., Ashwal, L. D. & Henry, D. J. *Contr. Miner. Petrol.* **87**, 399–406 (1984).
34. Wood, P. C. *et al. Geol. Soc. Am. Abstr. Prog.* **16**, 700 (1984).
35. Lambert, I. B., Phillips, G. N. & Groves, D. I. in *Gold '82: The Geology, Geochemistry and Genesis of Gold Deposits* (ed. Foster, R. P.) 373–387 (Balkema, Rotterdam, 1984).
36. Skoog, D. A. & West, D. M. *Fundamentals of Analytical Chemistry* (Holt, Rinehart and Winston, New York, 1962).

Significance of a $\delta^{13}C$ anomaly near the Devonian/Carboniferous boundary at the Muhua section, South China

Xu Dao-Yi*, Yan Zheng*, Zhang Qin-Wen†, Shen Zhi-Da‡, Sun Yi-Yin§, & Ye Lian-Fang*

* Institute of Geology, State Seismological Bureau, Beijing, China
† Institute of Geology, Chinese Academy of Geological Sciences, Beijing, China
‡ Guizhou Bureau of Geology and Mineral Resources, Guiyang, China
§ Institute of Geology, Academia Sinica, Beijing, China

The Muhua section of Guizhou Province, South China is one of three candidates for the Devonian/Carboniferous international boundary stratotype[1]. Although palaeontological and stratigraphical data have been published[2,3], no stable isotope study has previously been made. Detailed $\delta^{13}C$ and $\delta^{18}O$ analyses from the Muhua section reveal a significant short-term $\delta^{13}C$ negative anomaly of 8–9‰ at the base of the *Siphonodella crenulata* conodont zone. This is the first $\delta^{13}C$ negative anomaly found near the Devonian/Carboniferous boundary, and is similar to $\delta^{13}C$ anomalies reported from the Permian/Triassic, Cretaceous/Tertiary, and Precambrian/Cambrian boundaries[4,5]. We suggest, therefore, that the $\delta^{13}C$ anomaly at Muhua section provides evidence for major rapid changes in ocean–atmospheric chemistry, and may reflect an important event in geological history.

Muhua town, Changshun County is located ~100 km south of Guiyang, Guizhou Province, South China (Fig. 1). The Muhua section has been investigated by both indigenous and foreign palaeontologists and stratigraphers, including W. Zeigler, C. A. Sandberg, E. Paproth and M. Streel. We have studied Muhua section II. Details of the stratigraphy and fossil zonation of the Muhua section are given in ref. 2 and summarized in Fig. 2.

The section sampled was laid down in an offshore to deep-water facies consisting of grey or black, bedded or nodular limestone and argillaceous limestone, rich in conodonts and with a few ammonoids. During fieldwork in 1984 and 1985, more than 100 samples were collected, in ascending order at intervals of 10–50 cm over a thickness of 16 m.

Fresh samples without late calcite veins were analysed for carbon and oxygen isotopes. All analyses reported in this study were made on whole-rock samples, all of which are carbonates. The analyses were performed using modern techniques[6,7]. The samples were treated under vacuum with 100% phosphoric acid at 75 °C. The evolved CO_2 was separated, purified and analysed

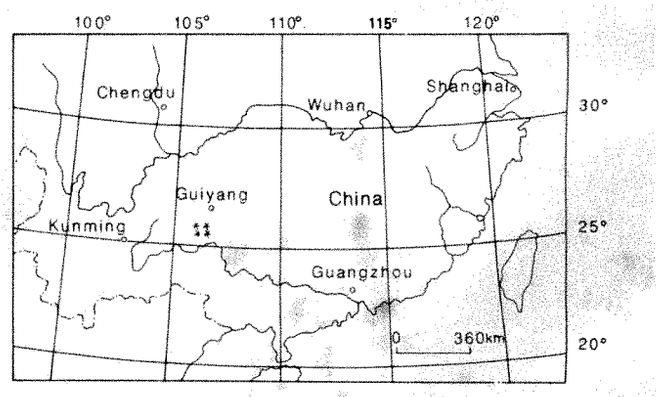


Fig. 1 Sketch map of the location of Muhua section II (**).

for $\delta^{13}C$ and $\delta^{18}O$ in a triple collecting mass spectrometer MAT 251. Reference samples (working standard) used in the analytical procedure were CY1 (carbonate), NBS18 and NBS19. The analytical precision of the C and O isotope data (2σ) was better than 0.1‰ (ref. 7).

Figure 2 shows the changes in $\delta^{13}C$ and $\delta^{18}O$ values in the Muhua section. The $\delta^{13}C$ values in the Daihua and Wangyou Formations are 0–2.3‰ positive, and suddenly decrease to negative values in the lower part of the Muhua Formation. A minimum carbon isotope anomaly with a value of −8.6‰ is found near the base of the Muhua Formation (Bed 65). Thus, the total range of change in $\delta^{13}C$ is ~8–9‰.

The change in $\delta^{18}O$ is positively correlated with that of $\delta^{13}C$ below Bed 57, but above Bed 64 $\delta^{18}O$ values suddenly increase and become negatively correlated with corresponding values of $\delta^{13}C$ (Fig. 2). The sudden change in the relationship of $\delta^{13}C$ to $\delta^{18}O$ after deposition of Bed 64 indicates a severe environmental change during the earliest stage of sedimentation of the Muhua Formation.

The change in $\delta^{13}C$ in the Muhua section is similar to patterns of variation across other important boundaries in the Phanerozoic. Stable isotope data[8,9] indicate a 6–7‰ negative $\delta^{13}C$ anomaly across the Permian/Triassic boundary in the Shangsi section, Sichuan Province, and a 5–6‰ negative shift above the Precambrian/Cambrian boundary has been found[4,5]. Perch-Nielsen *et al.*[10] suggested that there was a 1–2‰ negative $\delta^{13}C$ anomaly above the Cretaceous/Tertiary boundary in a time range of 10^5 yr. Carbon isotope analyses of the Frasnian/Famennian boundary show a drop in overall $\delta^{13}C$ of ~1.5‰ (ref. 11).

The uptake of light carbon by photosynthetic organisms leads to a decrease in ^{12}C in carbonates, and thus a mass extinction of biomass would decrease the $\delta^{13}C$ value. Following a geologically brief period, the surviving community would bloom and the $\delta^{13}C$ value would gradually become positive. Hence, a large $\delta^{13}C$ negative anomaly immediately above a geological boundary suggests a suspension of biotic productivity in the surface water, and a significant change in the biomass of the ancient ocean[2,4].

The $\delta^{13}C$ anomalies at the Cretaceous/Tertiary, Permian/Triassic and Precambrian/Cambrian boundaries coincide stratigraphically with mass extinctions and iridium anomalies, and it has been suggested that they are caused by rare events of short duration[4]. A similar pattern of $\delta^{13}C$ variation in the Muhua section further suggests that an important event occurred near the base of the Muhua Formation.

The sedimentation rate of the Devonian and Carboniferous carbonates in the Muhua section cannot be accurately determined. Playford *et al.*[11] estimate an average time span for an Upper Devonian conodont subzone of ~500,000 yr, and thus suggest an average rate of sedimentation of 1.8 mm kyr^{-1}. The conodont zones in the Wangyou and Muhua Formations are developed in sedimentary units of comparable thickness to those of the Canning Basin zones. We therefore suggest that the 90-cm interval containing the major negative change in $\delta^{13}C$ in the Muhua section may represent ~500,000 yr.

Although the Working Group on the Devonian/Carboniferous boundary has reached a consensus on the biostratigraphical criteria to be used in the identification and correlation of the boundary level, other methods have also been recommended[1], including geochemistry and petrology. A major requirement for defining a natural boundary between systems is the possibility of accurately correlating that horizon with other areas and continents.

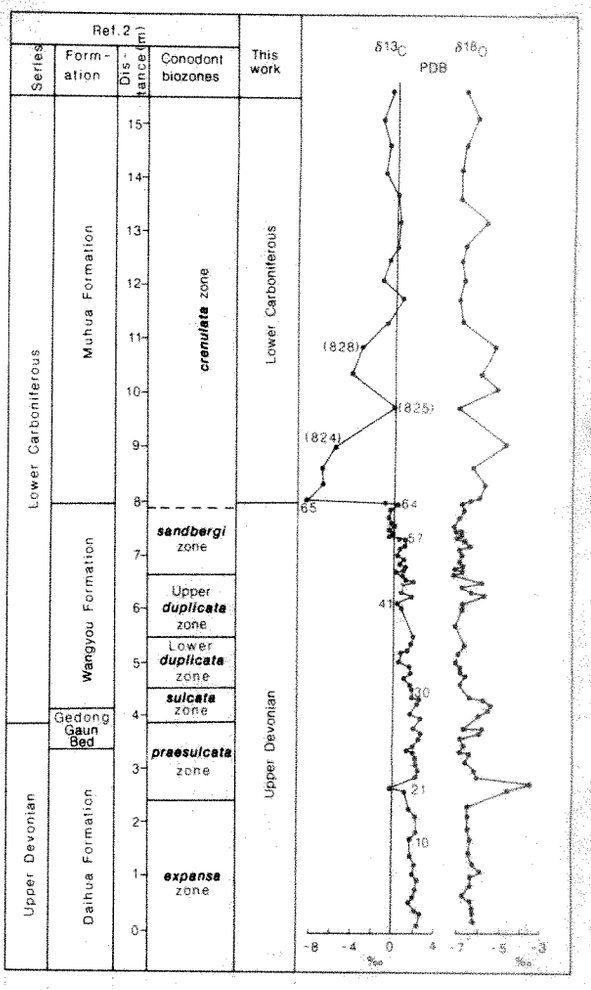


Fig. 2 Stable isotope descriptions of Muhua section II. Numbers on curves are the numbers of the beds from ref. 2. Numbers in parentheses are our sample numbers.

The negative $\delta^{13}C$ anomaly provides evidence of a sudden decrease in fertility of organisms in the ancient ocean, and may satisfy such a requirement. We suggest, therefore, that the results of the present study define a natural boundary at the base of the negative $\delta^{13}C$ anomaly (Bed 65). According to the researches of conodont zonation, the above-mentioned position is probably correlated to the lowest part of *S. crenulata* Zone. Unfortunately, *S. crenulata* has not been found in the Muhua section[3].

More Devonian/Carboniferous sections will be sampled and analysed to verify the anomaly at this horizon.

We thank Dr Hou H. F., Xiong J. F., and Dr Eva Paproth for field assistance, and Professor D. J. McLaren and W. T. Holser for critical reviews. This work was supported by the Scientific Foundation, Academia Sinica.

Received 10 January; accepted 4 April 1986.

1. Paproth, E. & Streel, M. *Episodes* **8**, 110–111 (1985).
2. Hou, H. F. *et al. Muhua sections of Devonian–Carboniferous Boundary Beds* (Geological Publishing House, Beijing, 1985).
3. Hou, H. F., Ji, Q., Xiong, J. F. & Wu, X. H. *Cour. Forsch.-Inst. Senckenberg* **67**, 193–205 (1984).
4. Xu, D. Y., Zhang, Q. W., Sun, Y. Y. & Yan, Z. *Mod. Geol.* (in the press).
5. Hsü, K. J. *et al. Nature* **316**, 809–811 (1985).
6. Yan, Z. *Expl. petrol. Geol.* **6**, 253–261 (1984).
7. Yan, Z. *Donghai Mar. Sci.* **1**, 4, 40–44 (1983).
8. Cheng, J. S., Shao, M. R., Hou, W. G. & Yao, Y. Y. *Scient. geol. Sinica* 1, 88–93 (1984).
9. Holser, W. T. & Magaritz, M. *Geol. Bund. Wien Jhb.* **128**, 75–82 (1985).
10. Perch-Nielsen, K., McKenzie, J. A. & He, Q. *Geol. Soc. Am. spec. Pap.* **190**, 353–372 (1982).
11. Playford, P. E., McLaren, D. J., Orth, C. J., Gilmore, J. S. & Goodfellow, W. D. *Science* **226**, 437–439 (1984).

Organically preserved microbial endoliths from the late Proterozoic of East Greenland

A. H. Knoll*, S. Golubic†, J. Green‡ & K. Swett§

Departments of * Organismic and Evolutionary Biology and ‡ Geological Sciences, Harvard University, Cambridge, Massachusetts 02138, USA
† Department of Biology, Boston University, Boston, Massachusetts 02215, USA
§ Department of Geology, University of Iowa, Iowa City, Iowa 52242, USA

Diverse microorganisms ranging from cyanobacteria to eukaryotic algae and fungi live endolithically within ooids, hardgrounds and invertebrate shells on the present-day sea floor. These organisms are involved in the mechanical destruction of carbonates, and are useful ecological indicators of water depth and pollution[1–3]. The Phanerozoic history of microbial endoliths has been elucidated through the study of microborings (the trace fossils of endolithic microorganisms) and rare cellularly preserved individuals[1,3,4], but nothing was known of the possible Precambrian evolution of comparable microorganisms until Campbell[5] documented the occurrence of microborings in late Proterozoic ooids from central East Greenland. We now report the discovery of large populations of organically preserved endolithic microorganisms in silicified pisolites from the 700–800-Myr-old Limestone–Dolomite Series of East Greenland. This fossil assemblage is significant for three reasons: (1) It confirms the prediction[5] that oolites, pisolites and hardgrounds—the substrates for pre-Phanerozoic endoliths—provide a hitherto poorly explored but rewarding set of environments into which the search for early microfossils must be broadened; (2) the assemblage is diverse, containing about 12 taxa of morphologically distinct and previously unknown endolithic cyanobacteria, plus associated epilithic and interstitial populations; and (3) at least six of the fossil populations are indistinguishable in morphology, pattern of development, reproductive biology and inferred ecology from distinctive cyanobacterial species that bore ooids today in the Bahama Banks.

The Eleonore Bay Group comprises some 7,000 m of unmetamorphosed sedimentary rocks that lie beneath latest Proterozoic glaciogenic beds in the coastal fjordlands of central East Greenland[6–8]. Carbonates occur principally in the upper part of this sequence, particularly in the 1,200-m-thick Limestone–Dolomite 'Series'. The Limestone–Dolomite succession documents a prolonged period of carbonate deposition along an extensive peritidal platform not unlike that of the present-day Bahama Banks. Flat-laminated, hemispherical and columnar stromatolites abound in this sequence, and these are intimately associated with oolites, pisolites, catagraphs, intraformational conglomerates and rippled to flat-laminated carbonate mudstones[9]. On biostratigraphic grounds, the Limestone–Dolomite sequence is considered to be predominantly late Riphean (perhaps 700–800 Myr)[10], although the uppermost beds of the unit, above the horizons of interest here, may be Vendian.

The fossils in question occur in silicified pisolites from Bed 18 of the Limestone–Dolomite Series exposed on Ella Ø (72°53′ N, 25°8′ W) and 87 km to the north in exposures along the east flank of Grejsdalen (73°33′ N, 25°5′ W). Individual pisids within the pisolites average 6–9 mm in diameter, but grains up to 14 mm have been observed. In both localities, the pisolites are cross-bedded, rippled and well-sorted, often grading into conventionally sized oolites. Although the pisids have been affected to various extents by silicification, neomorphism, dolomitization and calcitization, petrographic fabric analysis and strontium content determinations suggest that they consisted originally of concentric laminae of tangentially oriented aragonite crystals[9]. In all sedimentological, petrographic and micropalaeontological aspects, the pisids are essentially large ooids and not diagenetic structures formed in the vadose zone[9]. Chert occurs as irregular nodules that loosely parallel bedding; field and petrographic observations indicate that the silica is an early diagenetic replacement of primary carbonate sediments[9]. All organically preserved endoliths occur within the outer rim of individual pisids, suggesting that preservation was made possible by the rapid burial of pisids following a period of extensive endolithic colonization.

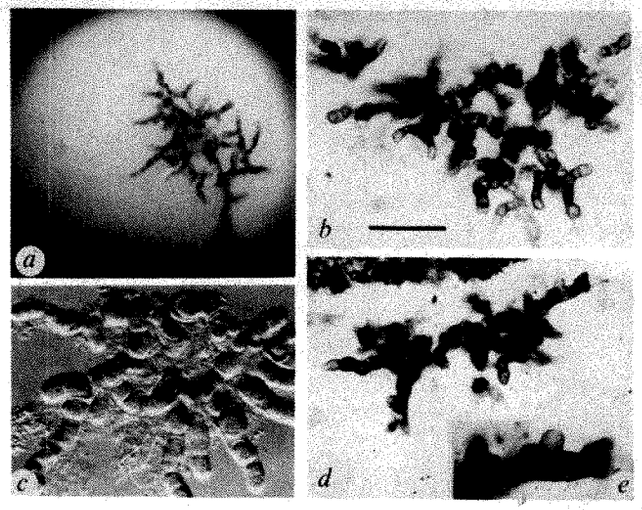


Fig. 1 *a*, Modern endolithic cyanobacterium *Hyella gigas* in ooid from the Bahama Banks (×90; scale bar in *b* = 115 μm). *b*, *d*, Fossil endolithic microorganisms comparable in morphology, development, reproduction and inferred ecology to modern *H. gigas* (×128; scale bar in *b* = 80 μm). *c*, Modern *H. gigas* freed from ooid to show details of morphology (×255; scale bar in *b* = 40 μm). *e*, Detail of *d* showing branch initiation (×500; scale bar in *b* = 40 μm).

Among the more common constituents of the endolith assemblage is a population of relatively large, branching filamentous microfossils that radiate inward from their points of entry into pisoliths (Fig. 1*b*, *d*). Like most other fossils in the Limestone–Dolomite assemblage, these specimens are preserved largely as extracellular envelopes that only rarely contain highly degraded cell contents; however, envelope morphologies preserve a record of divisional patterns and approximate original cell size. Filaments are predominantly uniserial, 8.5–101 μm long (mean 42.5 μm; s.d. 23.8 μm; $n = 37$) by 7.5–21 μm wide (mean 12 μm; s.d. 2.5 μm), and consist of the extracellular envelopes of coccoidal cells 8.5–21 μm long (mean 13 μm; s.d. 3.5 μm; $n = 125$) by 6.5–21 μm wide (mean 11 μm; s.d. 2 μm). Terminal cells may be slightly longer than intercalary cells. Because the cells of endolithic cyanobacteria are constrained by their extracellular envelopes and essentially do not move after division, developmental pattern can be reconstructed from individual specimens[11] and corroborated by observations of younger specimens in the same assemblage. Filaments evidently grew by transverse cell division and branching originated by cell slippage within filaments and by longitudinal divisions of intercalary cells (Fig. 1*e*). Reproduction occurred by the formation of baeocytes (reproductive cells produced by repeated binary divisions without intervening cell growth) from cells near the pisid surface.

In cell and envelope size and shape, branching morphology, developmental pattern and mode of reproduction, these fossils are indistinguishable from populations of the modern endolithic cyanobacterium *Hyella gigas* Lukas and Golubic[12] which occur today as endoliths in oolitic shoals of the Bahama Banks (Fig. 1*a*, *c*). Marine ooids have narrowly circumscribed conditions of formation, and except for the more vigorous agitation implied by their larger size, the East Greenland pisolites appear

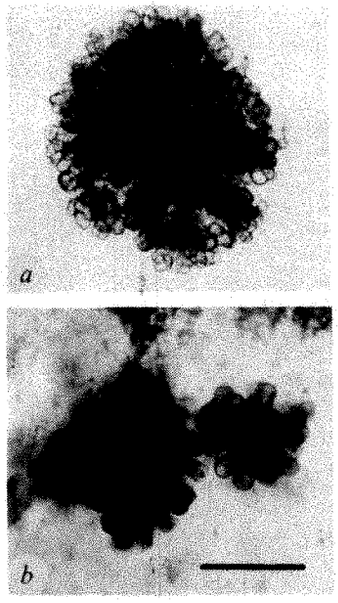


Fig. 2 *a*, Undescribed modern endolithic cyanobacterium freed from Bahamian ooid; view is essentially that seen from the interior of the subtrate (×140; scale bar in *b* = 100 μm). *b*, Two specimens of fossil endolithic microorganisms comparable in morphology, development and inferred ecology to the living population illustrated in *a*; the fossil on the left is seen in longitudinal view, while the smaller individual on the right is viewed from the direction of the pisolith interior (×350; scale bar, 40 μm).

to have accumulated under sedimentary conditions much like those found today in the Bahamas. Thus, the morphological and reproductive similarity between *H. gigas* and its fossil counterpart is paralleled by a close environmental congruence between the modern and Proterozoic sediments in which the two taxa have been found.

Other fossil populations in the Limestone–Dolomite assemblage also compare closely with extant microorganisms that occur in Bahamian ooids. These include fossils resembling the modern taxa *Plectonema terebrans*, *Cyanosaccus* spp., *Solentia foveolarum* and unnamed coccoidal endoliths described by Harris *et al.*[13]. Perhaps the most interesting population is one composed of densely branched microfossils like that shown in Fig. 2*b*. These fossils have a high cell density, giving the appearance of a hemispherical cell cluster from which many short filaments radiate into the pisid. Filaments are uniseriate or biseriate, only a few cells long, and often terminated by a pair of end cells. Branches tend to be club shaped, widening towards the pisolith interior. Filaments are 20–47 μm long (mean 33.5 μm, s.d. 8 μm; $n = 20$) and have a maximum width of 12.5–16 μm (mean 14.5 μm; s.d. 1.5 μm). Cell dimensions are 8.5–21 by 5–19 μm (mean 12.3 × 12 μm; s.d. 3.4 × 3.7 μm; $n = 62$). Baeocyte formation has not been demonstrated for this fossil. This taxon is a common constituent of the East Greenland endolith assemblage, but it has no precise counterpart among described species of modern endolithic cyanobacteria. Our comparative studies of Bahamian ooids have revealed the presence of a locally common and hitherto undescribed blue-green (Fig. 2*a*) that is remarkably similar in morphology and development to the fossil population in question. This demonstrates that palaeobiological knowledge of late Proterozoic microfossils has become sufficiently refined to be of use to systematic and ecological studies of modern coastal marine microorganisms.

Equally well-preserved remnants of at least five other intertidal and shallow subtidal communities occur in silicified carbonates and shales of the Limestone–Dolomite Series[14]. Although the organisms in these assemblages lived contemporaneously with those found in the pisolites, there is essentially no taxonomic overlap between the endolithic and other biotas. Endolithic microfossil assemblages clearly document communities that differed significantly from those of the microbial mat and phytoplankton biotas usually reported from Precambrian rocks; thus, they add significantly to our knowledge of early microbial diversity.

The Limestone–Dolomite fossil endolith assemblage provides new and compelling examples of the close resemblance between Proterozoic prokaryotes and their modern counterparts[15–17], in this case a comparison that begins with morphology and extends to reproductive, developmental and ecological similarity. Most important, the comparisons relate several co-occurring fossils from a single Proterozoic assemblage to taxa that occur today as part of a single community in a physically equivalent environment. Collectively, Limestone–Dolomite fossils demonstrate that endolithic cyanobacteria were abundant, diverse and apparently quite modern in shallow marine environments well before the radiation of either grazing or skeletonized metazoans.

This study was funded in part by NSF grants DPP-83-01226 (K.S.), BSR 85-16328 (A.H.K.) and EAR-83-06179 (S.G.). We thank the Commission on Scientific Research in Greenland for permission to do field work in East Greenland, R. Ginsburg for samples of Bahamian ooids and S. Campbell for helpful comments.

Received 13 January; accepted 7 April 1986.

1. Golubic, S., Perkins, D. & Lukas, K. J. in *The Study of Trace Fossils* (ed. Frey, R. W.) 229–259 (Springer, Berlin, 1975).
2. LeCampion-Alsumard, T. *Oceanol. Acta* **2**, 143–156 (1979).
3. Campbell, S. E. in *Biomineralization and Biological Metal Accumulation* (eds Westbroek, P. & de Jong, E. W.) 99–104 (Reidel, Amsterdam, 1979).
4. Campbell, S. E. *Phycologia* **19**, 25–36 (1980).
5. Campbell, S. E. *Nature* **299**, 429–431 (1982).
6. Eha, S. *Meddr. Grønland* **111**(2), 1–105 (1953).
7. Katz, H. R. *Meddr. Grønland* **111**(1), 1–150 (1952).
8. Haller, J. *Geology of the East Greenland Caledonides* (Wiley-Interscience, New York, 1971).
9. Swett, K. & Knoll, A. H. *J. Sedim. Petrol.* (in the press).
10. Vidal, G. *Grønl. geol. Unders.* **134**, 1–40 (1979).
11. LeCampion-Alsumard, T. & Golubic, S. *Arch. Hydrobiol. Suppl.* **71**(1/2), 119–148 (1985).
12. Lukas, K. J. & Golubic, S. *J. Phycol.* **19**, 129–136 (1983).
13. Harris, P. M., Halley, R. B. & Lukas, K. J. *Geology* **7**, 216–220 (1979).
14. Knoll, A. H., Green, J., Swett, K. & Golubic, S. *Geol. Soc. Am. Abstr. Prog.* **17**(7), 631 (1985).
15. Golubic, S. & Hofmann, H. J. *J. Paleont.* **50**, 1074–1082 (1979).
16. Knoll, A. H., Barghoorn, E. S. & Golubic, S. *Proc. natn. Acad. Sci. U.S.A.* **72**, 2488–2492 (1975).
17. Knoll, A. H. & Calder, S. *Palaeontology* **26**, 467–493 (1983).

More than one event in the late Triassic mass extinction

Michael J. Benton

Department of Geology, Queen's University of Belfast, Belfast BT7 1NN, UK

The recent hypothesis that mass extinctions are discrete phenomena that have occurred with great regularity during the history of life[1,2] is testable in several ways. Two essential elements of the hypothesis are (1) that each extinction event represents a significant departure from normal, or 'background', rates of extinction, and (2) that such mass extinction events are spaced equally in time. The analyses of the cyclicity of mass extinctions so far have concentrated on the past 250 Myr, with the first event occuring at the Permian–Triassic boundary, 245 Myr ago[1–5]. The second event followed 26–33 Myr later[1–6], in the late Triassic. Here I present a detailed analysis of the fossil record of marine and non-marine life during the late Triassic which suggests that there were at least two phases of mass extinction during that time, separated by 12–17 Myr.

The late Triassic has long been recognized as an important time of mass extinction[7–11] (approximately equivalent in magni-

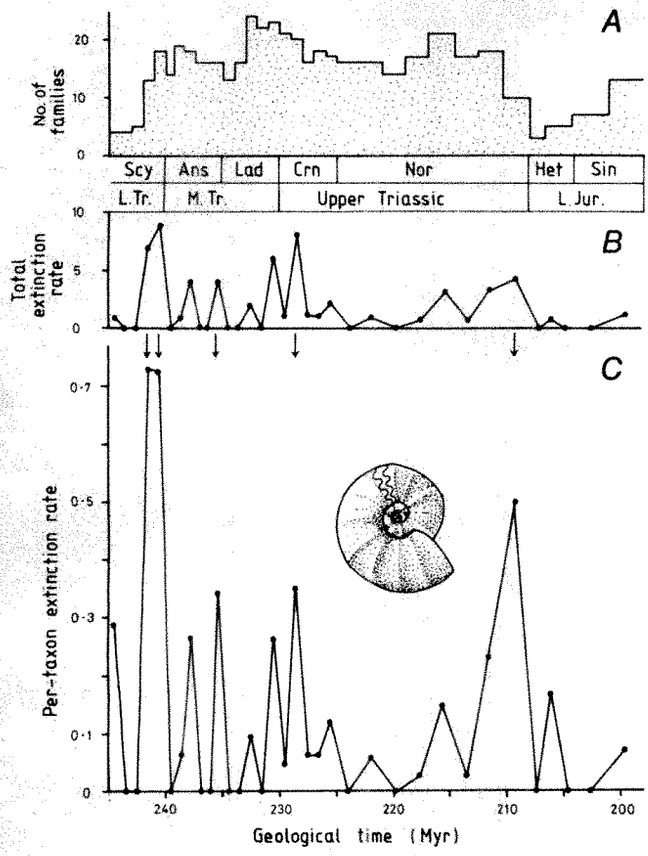


Fig. 1 Total diversity (*A*), total extinction rates (*B*) and per-taxon extinction rates (*C*) of families of Triassic ammonoids. The total extinction rates were calculated as the numbers of families dying out per Myr, and the per-taxon extinction rates were calculated according to the Van Valen metric[23], that is, the total extinction rate divided by the number of taxa at risk.(The latter was estimated as the number of taxa at the beginning of the interval, minus half the extinctions, plus half the orginations in the interval.) The five highest per-taxon extinction rates (possible mass extinctions) are indicated by arrows. Data on ammonoid distributions taken from refs 12 and 22, and the timescale from ref. 21. The Triassic and earliest Jurassic subseries and stages are indicated. Diversity and extinction rate data were calculated by substages (Scythian, Hettangian, Sinemurian) and by zones (Anisian–Norian). The 'Rhaetian' stage is included in the late Norian[12]. The fossil shown is *Ceratites*. Ans, Anisian; Crn, Carnian; Het, Hettangian; Lad, Ladinian; L. Jur., Lower Jurassic; L. Tr., Lower Triassic; M. Tr., Middle Triassic; Nor, Norian; Scy, Scythian; Sin, Sinemurian.

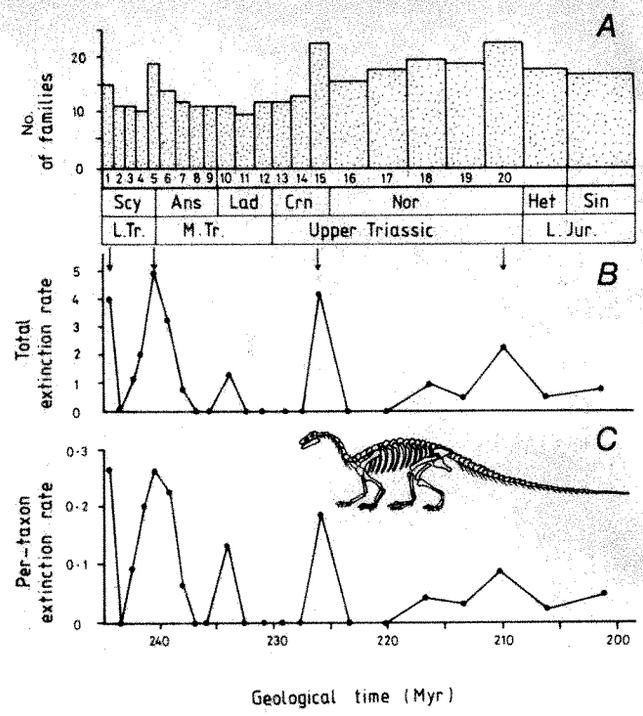


Fig. 2 Total diversity (*A*), total extinction rates (*B*) and per-taxon extinction rates (*C*) of families of Triassic and earliest Jurassic non-marine tetrapods. The four highest total extinction rates (possible mass extinctions) are indicated by arrows. The timescale is subdivided into informal 'substages', numbered 1–20 in the Triassic according to ref. 24. Data on tetrapod distributions are taken from refs 17, 18 and 24, with biostratographic zonations revised according to refs 25 and 26.

tude to the famous event at the end of the Cretaceous[10], when the dinosaurs died out), and involved an overall reduction in the diversity of families in the sea of ~23% (ref. 10) with a similar reduction in diversity of families on the land. The main groups that were affected in the sea were the sponges (loss of 8 families), the gastropods (13 families lost), the bivalves (8), the cephalopods (58), the brachiopods (12) and various marine reptiles (13). The effects on the ceratitid cephalopods, which were abundant and widespread in the Triassic, were dramatic (all 46 late Triassic families died out) and the ammonoids barely survived into the Jurassic[12]. When genera are considered, the Ceratitida reached a peak of ~150 genera in the Carnian, falling to ~100 genera in the Norian, and to single figures in the latest Norian[13]. The extinction rate for bivalve families was not so marked, but the extinction rate for genera was 42%, and the species extinction rate, in Europe at least, was 92% (ref. 11). The last strophomenid brachiopods, conodonts, conulariids, nothosaurs and placodonts also disappeared in the late Triassic.

On land, major extinctions occurred among the insects (35 families lost), the freshwater bony fishes (8) and the thecodontians (8). There was a major faunal turnover amongst non-marine tetrapods in the late Triassic, during which the formerly dominant labyrinthodonts, mammal-like reptiles, thecodontians and rhynchosaurs died out, or were greatly depleted, and new groups, such as the dinosaurs, crocodiles, pterosaurs, turtles, lepidosaurs and mammals, arrived on the scene[14–18].

Several authors have already noted that the extinctions in the late Triassic were either not synchronous in the sea and on land[11,15], or that the extinction lasted for much of the late Triassic, through the Carnian, Norian and Rhaetian stages[5] (the 'Rhaetian' is included here in the late Norian stage[11,12]). A more detailed study of events during this timespan of 18–25 Myr is therefore required.

Here I present data on the rates of extinction of families of marine and non-marine organisms during the late Triassic. Some groups of organisms whose fossil records are relatively well known are examined first, in order to establish the kinds of patterns of mass extinction that occurred in the late Triassic. Then a broader analysis of the fossil record of all plants and animals during that time is attempted.

The ammonoids— cephalopod molluscs with coiled shells— have a relatively good Triassic fossil record[12]; 35 ammonoid zones are recognized in the Triassic, which lasted for 35–41 Myr[19–21]. Tozer[12] has summarized the stratigraphic ranges of the 75 families of Triassic ammonoids accurate to the level of zones. The numbers of families present in each zone (or substage, in the Scythian) are plotted as a simple histogram in Fig. 1*A*; the diagram has been extended into the early Jurassic[22] in order

Table 1 Total numbers of families of marine and non-marine animals and plants present in each stratigraphic stage from the middle Triassic (Ladinian) to the early Jurassic (Sinemurian)

Marine families	Ladinian	Carnian	Lower Norian	Middle Norian	Upper Norian	Hettangian	Sinemurian
Protozoa	43	46	45*	45*	50*	49*	52*
Porifera	33	36	28*	28*	30*	30	30
Coelenterata	19	20	20*	21*	20*	20	21
Ctenophora	1	1	1	1	1	1	1
Priapulida	1	1	1	1	1	1	1
Nematoda	1	1	1	1	1	1	1
Mollusca							
Gastropoda	53*	51*	48*	49*	46*	47*	49*
Bivalvia	49	56	57	57	58	58	57
Cephalopoda	34	37*	23*	29*	22*	13	18
Others	6	6	6	6	6	6	6
Sipunculida	1	1	1	1	1	1	1
Annelida	21	20	20	20	21	21	21
Arthropoda	21	22†	23†	23†	20†	20*	23*
Bryozoa	4	4	5	5	6	6	6
Brachiopoda	17	18	17*	17*	18*	12	14
Chaetognatha	1	1	1	1	1	1	1
Echinodermata	16*	18	19*	19*	21*	31	33
Pogonophora	1	1	1	1	1	1	1
Conodonta	2	2	2	2	2	—	—
Chordata	18	14	8*	9*	11*	13	17
Total:	342*	356*	327*	338*	337*	332*	353*
Non-marine families							
'Thallophyta' (genera/orders)	33	33	33	33	35	39	37
Bryophyta (orders)	4	4	4	4	5	5	5
Charophyta	2	2	2	2	2	2	2
Pteridophyta	11	13	13	13	14	15	15
Gymnospermophyta	6	11	10	10	16	17	15
Mollusca							
Gastropoda	8	8	8	8	8	8	8
Bivalvia	3	4	4†	4†	3†	4†	3†
Onychophora	1	1	1	1	1	1	1
Arthropoda							
Insecta	30	35†	36†	37†	63†	55†	63†
Others	21	20	20‡	21‡	22‡	21	21
Chordata							
'Fish'	24	16*	13‡	13‡	13‡	11	11
Tetrapoda	12	23	16	21	25	18	16
Total:	155	170*	160‡	167‡	207‡	206*	197*
Overall no. of families	497*	526*	487*	505*	544*	538*	550*

The Norian is subdivided into three units which correspond to the Lower, Middle and Upper substages[12]. Data are listed by phyla or other major groups from refs 27–32. Families that have both marine and non-marine representatives are counted once only as 'marine'. In some cases, the precise stage of origination or termination of a family has not been established, and estimates have been calculated on the basis of stratigraphic stage durations and an assumption of equal probabilities through time. Thus, for 'Middle Triassic' originations and terminations, half are assumed to have occurred in the Ladinian. For 'Upper Triassic' originations and terminations, one-quarter are assumed to have occurred in each of the Carnian, Lower Norian, Middle Norian and Upper Norian. For 'Lower Jurassic' originations and terminations, one-quarter are assumed to have occurred in the Hettangian and in the Sinemurian (the remainder of the Lower Jurassic is approximately equal in duration to the Hettangian plus Sinemurian). These uncertain assignments represent ~5% of the total number of families. In addition, certain family extinctions in the Norian stage have not been assigned to the Lower, Middle or Upper Norian divisions. One-third of all such extinctions are assumed to have occurred in each division. In cases where these calculations have been applied, an error estimate is indicated as follows: * < ±5%; ‡ < ±10%; † > ±10%.

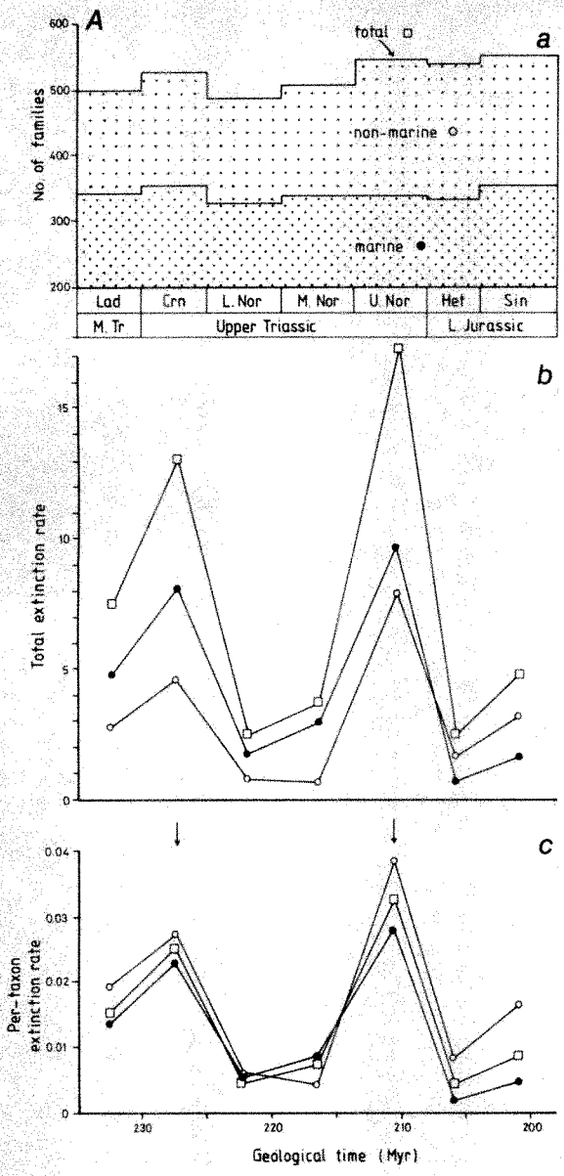
to compare the late Triassic events with those that followed. Several declines in family diversity are evident, the largest occurring in the Carnian and late Norian.

Extinction rates for ammonoid families vary considerably during the Triassic and early Jurassic. Total extinction rates (Fig. 1*B*) show peaks in the late Scythian, the late Ladinian and the early Carnian, with smaller peaks in the Anisian and in the middle and late Norian. The plot of per-taxon extinction rates (Fig. 1*C*), which take account of the numbers of families present and give a measure of the probability of extinction[23], reveals peaks in the late Scythian, the late Anisian, the early Carnian and the late Norian. Thus, the late Triassic 'mass extinction' of ammonoid families was not a single event, but consisted of at least two—one in the Carnian, and a larger one 17–20 Myr later at the end of the Norian (the 'Rhaetian'). The timing and relative sizes of these two peaks are the same when different current timescales are used[19–21].

The fossil record of non-marine tetrapods also lends itself to this type of analysis. The ranges of tetrapod families have been compiled[7,18,24–26] accurate to a number of informal 'substages'[24] that range in length from 1 to 3.4 Myr (mean ~2 Myr). The histogram of Triassic and early Jurassic families of non-marine tetrapods (Fig. 2*A*) shows declines in diversity in the early and late Scythian, at the end of the Carnian, and at the end of the Norian. These declines are matched by peaks in the total extinction rate (Fig. 2*B*) and per-taxon extinction rate (Fig. 2*C*). The mass extinction of non-marine tetrapods at the end of the Carnian was apparently the larger of the two late Triassic events, the extinction rates being approximately twice those associated with the event at the end of the Norian.

The fossil records of non-marine tetrapods and of ammonoids show that at least three mass extinction events occurred in the late Triassic: at the end of the early Carnian (ammonoids: smaller event), at the end of the Carnian (tetrapods: larger event) and at the end of the Norian, at the Triassic–Jurassic boundary (ammonoids: larger event; tetrapods: smaller event).

Below, I attempt to generalize the study to include all families of late Triassic plants and animals. The stratigraphic distributions of families of marine invertebrates and vertebrates[27] and non-marine tetrapods[28,29] have already been compiled. Data on families of non-marine invertebrates and fish were extracted from various sources[30–32], and from an unpublished compilation



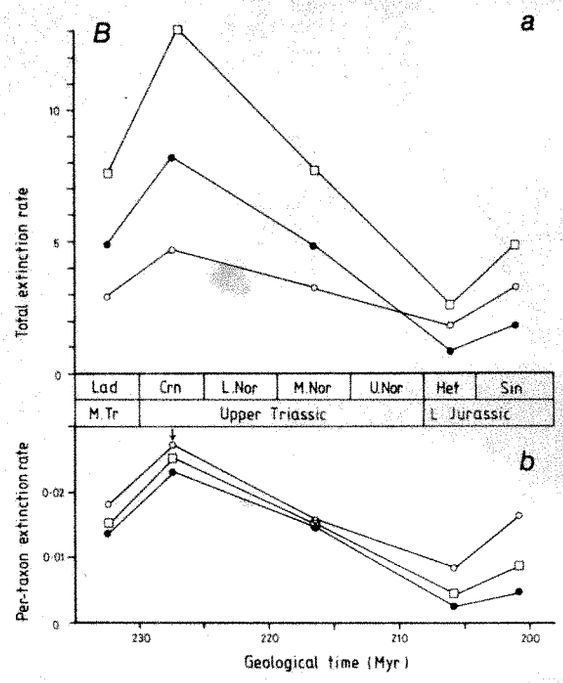


Fig. 3 *A*, Total diversity (*a*), total extinction rates (*b*) and per-taxon extinction rates (*c*) of families of late Triassic and earliest Jurassic plants and animals. The data are plotted separately for marine (●), non-marine (○) and total (□) families. The two mass extinctions (end-Carnian and end-Norian) are indicated by arrows. Data on family distributions from refs 27–32, Sepkoski's unpublished listing of non-marine families, and other sources cited therein. The data were calculated by stratigraphic stage, except for the Norian which was subdivided into Lower, Middle and Upper substages. Each Norian substage was assumed to have the same duration. *B*, Total extinction rates (*a*) and per-taxon extinction rates (*b*) of families of late Triassic and earliest Jurassic plants and animals. When the Norian data are combined, the terminal Triassic extinction event is 'smoothed out' and there appears to have been a single event in the Carnian (arrowed).

by J. J. Sepkoski Jr. Note that, because of the nature of the fossil record, the data on some groups such as insects and plants are rather poor. The time period under study spans from the Ladinian (middle Triassic) to the Sinemurian (early Jurassic), an interval of ~38 Myr[21], and family extinctions have been noted to the level of the stratigraphic stage. The Norian stage is much longer (~17 Myr) than all the other stages (4–6 Myr), and was subdivided into Lower, Middle and Upper units, according to the standard scheme[12]. The stages, and substages, used in this analysis range in duration from 4 to 6 Myr (mean 5.4 Myr).

Table 1 summarizes the diversities of families of plants and animals during the late Triassic; Table 2 summarizes the family extinctions. The present data indicate an average marine diversity of ~340 families, and non-marine diversity of ~190 families. The numbers of family extinctions per time unit range from 3 to 54 (marine; mean 23.0), and from 4 to 45 (non-marine; mean 18.1). Plots of marine and non-marine family diversity (Fig. 3*Aa*) show declines at the end of the Carnian, and smaller ones at the Triassic–Jurassic boundary. In all cases, both the total (Fig. 3*Ab*) and per-taxon (Fig. 3*Ac*) extinction rates show two similar peaks, a slightly higher one in the late Norian, and a lower one in the Carnian.

The two (or more) mass extinctions in the late Triassic have been identified as a single event in most previous studies[1–4,6–10,15–17,23,28,29]. Indeed, when all the extinctions in the Norian are summed, the two mass extinction peaks are 'smoothed out' to give a single broad peak (Fig. 3*B*). Raup and Sepkoski[2,33] have recently noted an extinction peak in the late Carnian in their analysis of fossil marine animal genera, but they regard it as "an artefact of sampling".

If the cyclical models of mass extinction are correct, there should have been a single event in the late Triassic, within the Norian. According to the Harland timescale[19], and a 26-Myr cyclicity pattern[1,2], this event should have occurred at 222 Myr and, according to the Odin timescale[20], at 219 Myr, both in the early Norian. If it is assumed that the mass extinctions occurred at the ends of stages, the late Triassic events documented here occurred at ~225 Myr and ~213 Myr, according to the Harland timescale, at ~220 Myr and ~204 Myr, according to the Odin timescale, and at ~225 Myr and ~208 Myr, according to the 'DNAG' timescale[21]. If the preceding extinction events, at the end of the Permian and at the end of the Scythian[1,2,5,6,16,28,29,34] (see also Figs 1, 2), are considered, the spacings between these events are highly variable, according to each of the present timescales (Table 3).

Table 2 Total numbers of extinctions of marine and none-marine families in each stratigraphic stage from the middle Triassic (Ladinian) to the early Jurassic (Sinemurian)

	Ladinian	Carnian	Lower Norian	Middle Norian	Upper Norian	Hettangian	Sinemurian
Marine families							
Protozoa	—	1	1†	—†	5†	—	—
Porifera	—	8	—	—	—	—	—
Coelenterata	—	1	—†	2†	4†	—	—
Mollusca							
Gastropoda	4	4†	2†	1†	2†	—†	1†
Bivalvia	—	1	—†	1†	6†	1	1
Cephalopoda	8	14	5†	10†	21‡	1	4
Annelida	1	—	—	—	—	—	—
Arthropoda	2†	1†	1†	2†	2†	—	—
Brachiopoda	—	2	1†	1†	8†	—	1
Echinodermata	1	2	—	—	1	1	1
Conodonta	—	—	—	—	2	—	—
Chordata	8	7	—	—	3	—	2
Total:	24*	41‡	10†	17†	54‡	3†	10‡
Non-marine families							
Pteridophyyta	—	—	—	—	2	—	1
Gymnospermophyta	1	—	—	—	2	2†	1†
Mollusca	—	—†	—†	1†	—†	1†	—†
Arthropoda	1	7†	5†	3†	23†	1†	5†
Chordata							
'Fish'	8	4†	—†	—†	4†	1	3
Tetrapoda	4	12	—	—	14	2	9
Total:	14	23‡	5†	4†	45‡	7†	19†
Overall no. of families	38*	66‡	15†	21†	99‡	10†	29‡

The data are listed by phyla, or other major groups, from refs 12, 18, 27–32. Stratigraphic terms and error estimates are explained in Table 1.

Table 3 Gaps (Myr) between consecutive mass extinction events in the late Permian, early Triassic and late Triassic, according to three current timescales

	Harland[19]	Odin[20]	Palmer[21]
Late Permian }	5	6	5
Late Scythian }			
Late Carnian }	18	19	15
Late Norian }	12	16	17

These results indicate that the record of mass extinctions is not as straightforward as has been assumed by some authors: the choice of timescale may be crucial[5], and closer analysis of the fossil data may reveal quite different patterns from those presented so far[1–10,23,28,29]. For example, in a recent study of the two mass extinctions in the Jurassic required by the 26-Myr cyclicity theory (end-Pliensbachian, end-Tithonian), Hallam[35] found that the extinctions were regional, not global, in extent, being restricted largely to Europe.

The record of mass extinctions is not yet well known. It should be possible to obtain more precise data on the stratigraphic and geographical ranges of different taxa, to refine geological timescales, and to revise the systematics of various groups. Many authors have hitherto identified a single late Triassic mass extinction but more detailed studies of particular groups (for example, ammonoids and non-marine tetrapods) and of the whole marine and non-marine fossil record have indicated that there were two quite separate mass extinction events. This conclusion suggests that recent models of bolide-mediated cyclicity of mass extinctions may be incorrect. Cladistic analyses are essential for such studies[29].

I thank A. Hallam and P. E. S. Whalley for information on molluscs and insects respectively, J. J. Sepkoski Jr for supplying unpublished data on marine and non-marine families, and Ms E. A. Lawson for drawing the diagrams.

Received 24 February; accepted 10 April 1986.

1. Raup, D. M. & Sepkoski, J. J. Jr *Proc. natn. Acad. Sci. U.S.A.* **81**, 801–805 (1984).
2. Raup, D. M. & Sepkoski, J. J. Jr *Science* **231**, 833–836 (1986).
3. Rampino, M. R. & Stothers, R. B. *Nature* **308**, 709–712 (1984).
4. Kitchell, J. A. & Pena, D. *Science* **226**, 689–692 (1984).
5. Hoffman, A. *Nature* **315**, 659–662 (1985).
6. Hoffman, A. & Ghiold, J. *Geol. Mag.* **122**, 1–4 (1985).
7. Colbert, E. H. *Proc. natn. Acad. Sci. U.S.A.* **44**, 973–977 (1958).
8. Newell, N. D. *J. Paleont.* **36**, 592–610 (1962); *Spec. Pap. geol. Soc. Am.* **89**, 63–91 (1967).
9. Raup, D. M. & Sepkoski, J. J. Jr *Science* **215**, 1501–1503 (1982).
10. Sepkoski, J. J. Jr *Spec. Pap. geol. Soc. Am.* **190**, 283–289 (1982); *Paleobiology* **10**, 246–267 (1984).
11. Hallam, A. *Paelaeogeogr. Palaeoclimatol. Palaeoecol.* **35**, 1–44 (1981).
12. Tozer, E. T. in *The Ammonoidea* (eds House, M. R. & Senior, J. R.) 66–100, 397–431 (Academic, London, 1980).
13. Kennedy, W. J. in *Patterns of Evolution as Illustrated by the Fossil Record* (ed. Hallam, A.) 251–304 (Elsevier, Amsterdam, 1977).
14. Charig, A. J. in *Studies in Vertebrate Evolution* (eds Joysey, K. A. & Kemp, T. S.) 121–155 (Oliver & Boyd, Edinburgh, 1972).
15. Bakker, R. in *Patterns of Evolution as Illustrated by the Fossil Record* (ed. Hallam, A.) 439–468 (Elsevier, Amsterdam, 1977).
16. Olson, E. C. *Spec. Pap. geol. Soc. Am.* **190**, 501–511 (1982).
17. Benton, M. J. *Q. Rev. Biol.* **58**, 29–55 (1983).
18. Benton, M. J. in *The Beginning of the Age of Dinosaurs* (ed. Padian, K.) (Cambridge University Press, New York, in the press).
19. Harland, W. B. *et al. A Geologic Time Scale* (Cambridge University Press, 1982).
20. Odin, G. S. (ed.) *Numerical Dating in Stratigraphy* (Wiley, New York, 1982).
21. Palmer, A. R. *Geology* **11**, 503–504 (1983).
22. Donovan, B. T., Callomon, J. H. & Howarth, M. K. in *The Ammonoidea* (eds House, M. K. & Senior, J. R.) 101–155 (Academic, London, 1980).
23. Van Valen, L. M. *Nature* **307**, 50–52 (1984).
24. Anderson, J. M. & Cruickshank, A. R. I. *Palaeont. afr.* **21**, 15–44 (1978).
25. Olsen, P. E. & Galton, P. M. *Science* **197**, 983–986 (1977).
26. Olsen, P. E. & Galton, P. M. *Palaeont. afr.* **25**, 87–110 (1984).
27. Sepkoski, J. J. Jr *Milwaukee publ. Mus. Contr. Geol. Biol.* **51**, 1–125 (1982) (with revision sheets dated August 1985).
28. Benton, M. J. *Nature* **316**, 811–814 (1985); *Bull. Soc. géol. Fr.* (in the press).
29. Benton, M. J. *Spec. Pap. Palaeont.* **33**, 185–202 (1985).
30. Moore, R. C. *et al.* (eds) *Treatise on Invertebrate Paleontology* (Geological Society of America and University of Kansas Press, Lawrence, 1953–1985).
31. Harland, W. B. *et al. The Fossil Record* (Geological Society of London, 1967).
32. Whalley, P. E. S. *Bull. Br. Mus. nat. Hist. (Geol.)* **39**, 107–187 (1985).
33. Sepkoski, J. J. Jr & Raup, D. M. in *Dynamics of Extinction* (ed. Elliott, D.) 3–36 (Wiley, Somerset, New Jersey, 1986).
34. Bray, A. A. *Mod. Geol.* **9**, 397–409 (1985).
35. Hallam, A. *Nature* **319**, 765–768 (1986).

A new class of Echinodermata from New Zealand

Alan N. Baker*, Francis W. E. Rowe† & Helen E. S. Clark*

* National Museum of New Zealand, Wellington WN1, New Zealand
† Australian Museum, Sydney, New South Wales 2000, Australia

During examination of echinoderms from sunken wood collected from depths between 1,057 and 1,208 m off the New Zealand coast, we discovered nine specimens of a small flattened discoidal invertebrate. These animals, briefly described here, superficially resemble a cnidarian medusa, but their pentamerous morphology is distinctly echinoderm-like. We consider that the features of these newly discovered echinoderms warrant the recognition of a new class. *Xyloplax medusiformis* n.gen. and n.sp. represents a radical departure in morphology from any other known extant echinoderm. Its obvious tube feet, clearly pentamerous body pattern, and calcite skeleton leave no doubt that the animal is an echinoderm. However, its concentrically arranged skeletal structures and single series of tube feet arranged in a ring are novel. The water vascular system of *Xyloplax* consists of a double ring of canals which service the tube feet in inter-radial positions; in all other living echinoderms the vascular ring (circum-oral) is single, and the tube feet are serviced from it in radial positions. These specimens represent the first new class of living echinoderms to be described since 1821. A full description of the new taxon is in preparation.

Class Concentricycloidea nov.

Diagnosis: A free-living echinoderm characterized by a weakly inflated disk-shaped body, without mouth, anus or radiating arms. Its water vascular system, including tube feet, and supporting skeletal structures are arranged concentrically on the ventral surface. The water vascular canals form a double ring with inter-radial connections to the tube feet; the ventral surface is covered by a complete velum.

Etymology: *concentricus* and *cyclus* are Latin for 'concentric' and 'ring', respectively, alluding to the double water vascular ring and the concentric skeletal structures.

Order Peripodida nov.

Family Xyloplacidae nov.

Diagnoses: The same as for class.

Etymology: *peri* and *podos* are Greek for 'around' and 'foot', referring to the nearly circumferential arrangement of tube feet.

Xyloplax n.gen.

Type species: *Xyloplax medusiformis* n.sp.

Diagnosis: Body medusiform, dorsally plated with peripheral, excavate spines and uniserial, nearly circumferential tube feet.

Xyloplax medusiformis n.sp. (see Figs 1–4)

Etymology: *Xylos* and *plax* are Greek for 'wood' and 'plate' and allude to the habitat and plating of this animal; *Medusa* and *form* are Latin and allude to the animal's superficial resemblance to a cnidarian medusa.

Type material: In the National Museum of New Zealand (NMNZ) and the Australian Museum (AM). The holotype (NMNZ 4240) was collected rom 42°58.6′ S, 168°21.9′ E to 42°57.7′ S, 168°22.6′ E, west of Hokitika, South Island, at a depth of 1,142–1,147 m, on water logged wood, 9 July 1983. There are eight paratypes: four (one sectioned) (NMNZ 4239) collected from 41°09.9′ S, 176°26.5′ E off Castlepoint, North Island, at a depth of 1,174–1,208 m, on waterlogged wood, 4 April 1984; two (one sectioned) (NMNZ 4241) from 41°18.0′ S, 176°18.3′ E off Castlepoint, 1,170–1,152 m, 17 October 1984; one (NMNZ 4242) from 41°25.3′ S, 176°07.6′ E off Castlepoint, 1,110–1,057 m, on waterlogged wood, 26 May 1985; one (AM J19660) from 41°24.7′ S, 176°08.4′ E off Castlepoint, 1,103–1,071 m, on waterlogged wood, 16 October 1984.

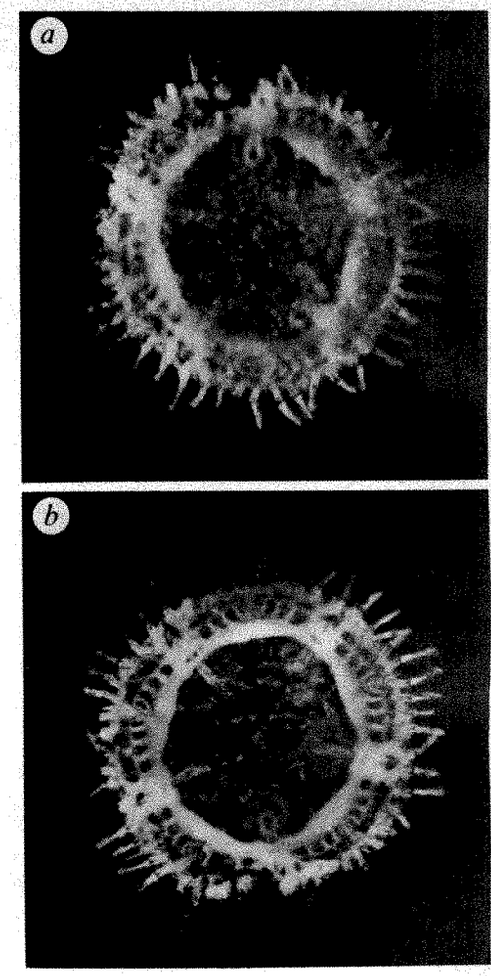


Fig. 1 Holotype (NMNZ 4240) of *Xyloplax medusiformis* n.g. and n.sp. Dorsal (*a*) and ventral (*b*) views. Diameter 3.1 mm.

Description: The following description and figures are based on the type series, four of which had to be sectioned or dissected to obtain the required information. Our terminology must be regarded as provisional at this stage.

The specimens range from 2.1 (2.6) to 7.8 (9.0) mm in diameter (including peripheral spines). The animal is circular or slightly sub-pentagonal, and weakly inflated. The dorsal surface comprises numerous finely perforated, scale-like plates, which bear small, fluted spinelets. In each of the five inter-radii is a large primary plate, the one in inter-radius CD having a hydropore that pierces the plate. The margin of the disk is fringed by small (0.6 mm) excavate spines (Figs 1, 2), and is formed by a single ring of marginal plates interrupted by five large radial plates corresponding to the terminals or oculars of asteroids.

The ventral surface is dominated by a ring of thick skeletal ossicles, the adambulacral and marginal plates (Figs 1*b*, 2*b*). The 'intramarginal' ring comprises ossicles arranged in a pentamerous pattern. Each group of ossicles has four to six elements, the medial pair (each side of the inter-radial line) being the largest. Additional ossicles are developed at the radial positions during growth.

The water vascular system forms a double ring (Fig. 3). The inner water ring runs first in a groove and then in an enclosed duct along the inner side of the ring of ossicles. The 'radial'

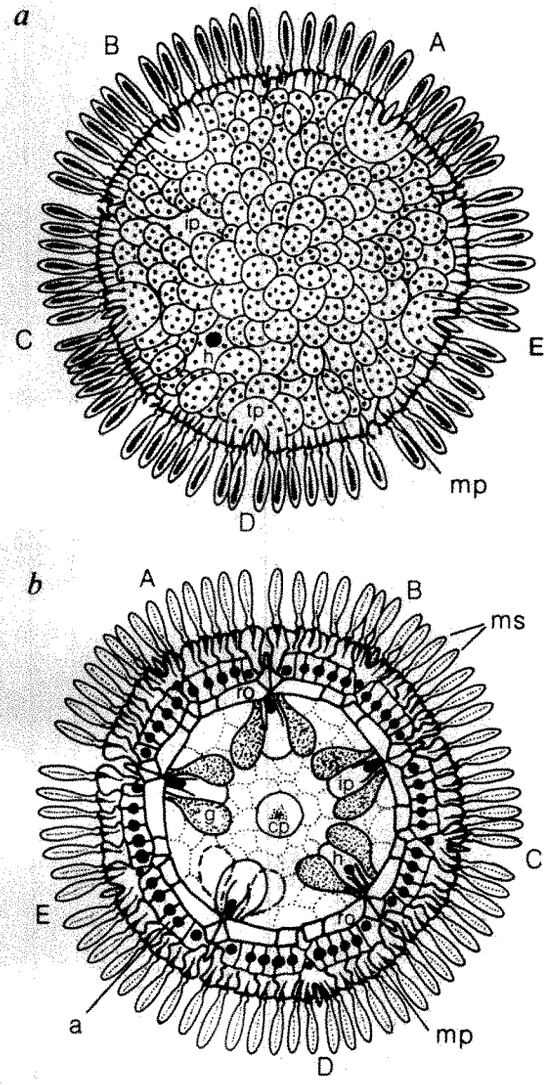


Fig. 2 Semi-diagrammatic representation of paratype NMNZ 4241 of *Xyloplax medusiformis* n.g. and n.sp. Dorsal (*a*) and ventral (*b*) views. Diameter 6.2 mm. A–E, radii; ip, Primary inter-radial plate; mp, marginal plate; tp, terminal plate; h, hydropore; ms, marginal spines; g, gonad; ro, ring ossicle; a, adambulacral plates. cp, central dorsal plate.

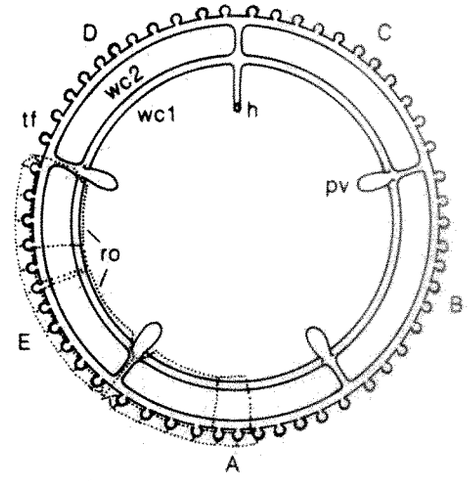


Fig. 3 Diagrammatic representation of the water vascular system of *Xyloplax medusiformis* n.g. and n.sp., determined from histological sections and by dissection. pv, Polian vesicle; tf, tube foot; wc1, circum-oral water canal; wc2, 'radial' water canal. Other abbreviations as for Fig. 2.

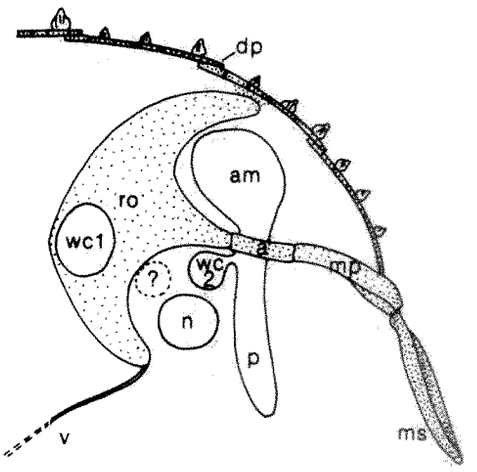


Fig. 4 Semi-diagrammatic section through the margin of *Xyloplax medusiformis* n.g. and n.sp., determined from histological sections and by dissection. am, Ampulla; dp, dorsal plates bearing fluted spinelets; n, 'radial' nerve; p, podium; v, velum; ?, 'radial' haemal canal. Other abbreviations as for Figs 2, 3.

water canals (now outer circumferential) run along a lower, totally exposed groove on the outer side of the ring ossicles and connect with the inner ring at *inter-radial* positions. The 'radial' canal connects with each tube foot below the ampulla (Fig. 4). The tube feet are arranged in a uniserial, circumferential system, just inside the ventral margin of the disk (Figs 1*b*, 2*b*, 4).

There is no gut or mouth: the ventral surface of the animal comprises a complete and thin velum attached to the lower ridge of the ring ossicles below the groove carrying the 'radial' nerve and water canal (Fig. 4). There are five pairs of gonads or bursae which contain embryos at various stages of development, up to plated juveniles, which are similar in form to the adults.

The development of the inner water vascular ring and its protection in a groove/duct within the ossicles of the ring would not, in our view, be evolutionarily difficult to achieve. However, to meet the requirements of the new, circumferential arrangement of tube feet and the obliteration of any prolonged rays, medial splitting of the circum/radial structures, including the water canal (and presumably the nerve and haemal systems—not yet determined), must have occurred. This split could have originated as a lacuna at the junction of the circum-oral and radial canals. The lacuna could then have extended laterally and radially, stopping adjacent to the polian vesicles and terminal tube foot, respectively, and resulting in the water vascular system forming a double ring, with the connection between the two rings becoming inter-radial.

We suggest that the ossicle ring is derived from fusion of the first adambulacral/oral plate with the first two or three ambulacral plates. The tube feet must then have moved sideways and are now situated between the remaining adambulacral plates. The latter have been modified to take over the function previously fulfilled by the ambulacrals. The whole inter-radial mouth frame (ossicle ring) has moved outwards, splitting the ambulacra and taking the associated circum/radial structures with it. The pivotal points are the terminal point of each radius; these points remain fixed so that a disk-like body form is derived.

We propose that the ventral velum of *Xyloplax* derived from the stretching of a simple, sac-like stomach from its original internal position, by opening of the oral frame. Thus, the outer surface of the velum is formed from the inner lining of the stomach.

Only two other classes of echinoderms have been described which have flattened, discoidal or medusiform bodies: Camptostromatoidea (Lower Cambrian) and Cyclocystoidea (Middle Ordovician–Middle Devonian). Recent studies have shown, however, that the camptostromatids do not have a medusiform body[1]. The cyclocystoids do have a body form that is superficially similar to that of *Xyloplax*; a comparative discussion will be published elsewhere.

We believe that *X. medusiformis* is likely to move from niche to niche using a parachute-like mode of locomotion in bottom-water currents.

We include the Class Concentricycloidea within the subphylum Asterozoa, rather than the Crinozoa or Echinozoa; this is justified on the grounds of pattern of growth, which occurs in typical asterozoan fashion[2]. Also, the tube feet occur between, not through, plates and on the underside of the animal. The diagnosis for the Asterozoa will need to be expanded to accommodate the special features of these new echinoderms, which we are also unable to classify within the only other asterozoan Class Stelleroidea[2]. Our discovery supports current views[3–5] that the present higher classification of the Echinodermata requires revision.

We thank the following colleagues for assistance: Mr Bruce Marshall, National Museum of New Zealand, sorted the echinoderms from sunken wood and discussed the habitat with us; Professor D. T. Anderson, University of Sydney, made valuable suggestions during the interpretation of this animal and arranged for Ms Kate Jakes to prepare histological sections; Dr Stephen Clark, Nelson Hospital, sectioned and photographed the tube feet; and Wim Spiekman, National Museum of New Zealand, made scale models of the ring ossicles. F.W.E.R. thanks the Marine Sciences and Technology Committee, Australia, for support. A.N.B. thanks the Zoology Department, Victoria University of Wellington, for the use of photomicrographic facilities.

Received 10 February; accepted 7 April 1986.

1. Paul, C. R. C. *Echinoderms: Proc. int. Conf. Galway* (ed. O'Connor, B.) (Balkema, Rotterdam, 1985).
2. Moore, R. C. (ed.) *Treatise on Invertebrate Palaeontology. Echinodermata* (Geological Society of America and University of Kansas Press, 1966–68).
3. Blake, D. B. *Palaeontology* **25**, 167–191 (1982).
4. Smith, A. B. *Palaeontology* **27**, 431–459 (1984).
5. Paul, C. R. C. & Smith, A. B. *Biol. Rev.* **59**, 443–481 (1984).

Benzodiazepine impairs and β-carboline enhances performance in learning and memory tasks

Patrice Venault*, Georges Chapouthier*, Lia Prado de Carvalho*, Jacques Simiand†, Michel Morre†, Robert H. Dodd‡ & Jean Rossier*

* Laboratoire de Physiologie Nerveuse, Department I and II, and
‡ Institut de Chimie des Substances Naturelles, CNRS,
91190 Gif-sur-Yvette, France
† Sanofi Recherche, 31035 Toulouse, France

Benzodiazepines are widely used anxiolytics and anticonvulsants, and their potent sedative properties are routinely used in presurgical anaesthesia. However, they are also known to induce a strong anterograde amnesia in patients[1]. Specific benzodiazepine antagonists have recently been described[2,3], some of which have intrinsic pharmacological properties that are opposite to those of benzodiazepines. These have been called inverse agonists[4,5] and they have been shown to be proconvulsant or convulsant[6,7] whereas benzodiazepines are anticonvulsants. Inverse agonists are also anxiogenic[8–12] rather than anxiolytic. Since benzodiazepines induce anterograde amnesia, we have investigated the possibility that inverse agonists might also have an opposite effect for this property and so enhance acquisition (learning) and (or) retention (memory). We report here that, in three different animal models, an inverse agonist of the β-carboline group, methyl β-carboline-3-carboxylate (β-CCM), enhances animal performance in three different tasks used to investigate learning and memory.

The first model, habituation to a new environment in rodents, has been used previously to demonstrate the amnesic properties of benzodiazepines[13]. The second model, a passive avoidance task, has been widely used in the study of memory processes in rodents. Finally, to investigate the effects of β-CCM in a very different learning situation, a third model, imprinting in chicks, was used[14]. Imprinting, a phenomenon first described by Konrad Lorenz involves newly hatched birds which are apparently more 'naive' than adult rodents. The effects of β-CCM were compared with those of diazepam, a typical benzodiazepine.

In the habituation model, food-deprived mice were placed in an unfamiliar environment (a different cage) with food *ad libitum*. During this training session, they explored the new cage but ate only a small quantity. When placed in the same environment for a test session a few days later, the same food-deprived animals ate much more than during the training session. This increase in food intake is assumed to indicate that during th

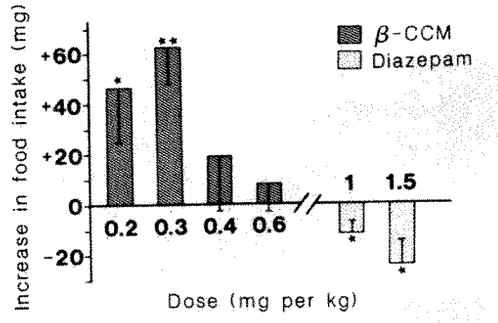


Fig. 1 Effect of β-CCM and diazepam on retention of habituation to a new environment in mice. The results show differences (±s.e.) in the food intake of drug-treated groups compared with saline groups. Hence, ordinate 0 corresponds to the mean of the food intake of saline-treated animals during the 2 min of the test (25 ± 4 mg, $n = 60$). All groups consisted of 10 mice, except for diazepam, 1 mg per kg, where 20 mice were used. * $P < 0.05$; ** $P < 0.01$ (analysis of variance).

Methods. Swiss mice (Iffa-Credo, France, males, 30 g) food-deprived for 24 h, were injected subcutaneously with β-CCM, diazepam or saline. They were transferred to the experimental room 15 min later and placed individually for 30 s in an unfamiliar metallic cage (32 × 24 × 15 cm) containing their usual food. During this very short period, food intake was practically nil for all groups. No differences in locomotor activity could be measured among the groups; this was measured by dividing the floor of the cage into four identical squares and recording the number of times the animals crossed from one square to another during 30 s (number of crossings (mean ± s.e.): controls 2.8 ± 0.4; β-CCM, 0.2 mg per kg: 2.3 ± 0.4; β-CCM, 0.3 mg per kg: 3.6 ± 0.5; diazepam, 1.5 mg per kg: 2.1 ± 0.5). Following this training session, mice were returned to their polystyrene home cage in the animal quarters with no food. Food was provided *ad libitum* at the end of the day. Three days later the mice were once more deprived of food. After fasting for 24 h, they were again placed in the metallic cage for a 2-min test session. Food intake was measured.

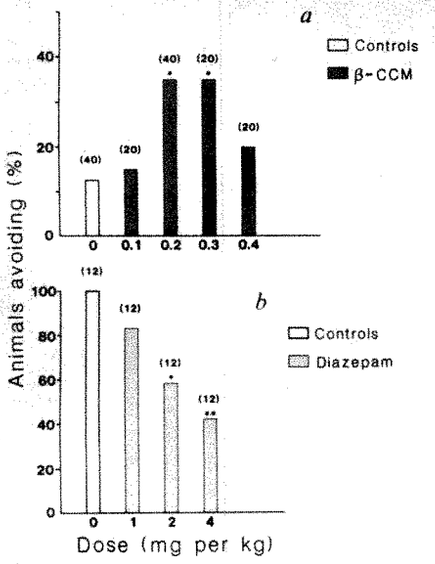


Fig. 2 Effects of β-CCM and diazepam on retention of a passive avoidance task in mice. The number of animals per group is shown in parentheses. * $P < 0.05$; ** $P < 0.01$ between treated and control animals (χ^2 test).
Methods. Swiss mice (Charles River, France, males, 25 g) were injected with saline, β-CCM or diazepam. After 15 min (saline, β-CCM) or 30 min (saline, diazepam), the animals were placed in an illuminated box (10 × 10 × 12 cm) connected to a large dark box (23 × 16 × 12 cm) that had an electrified metallic grid floor. When the mouse stepped into the dark box, a footshock was delivered to its paws. In experiments with β-CCM, where facilitation of retention was investigated, a low shock (0.1 mA for 2 s, unscrambled d.c. current) was delivered. In experiments with diazepam, where impairment of retention was investigated, a high shock (0.6 mA for 2 s, unscrambled d.c. current) was used. Latency to enter the dark box did not differ significantly during the training session, under the influence of the drugs (mean in s, ±s.e.; β-CCM controls: 9·8 ± 1.0; β-CCM, 0.2 mg per kg: 8.8 ± 1.1; β-CCM, 0.3 mg per kg: 10.8 ± 1.1; diazepam controls: 10.5 ± 0.9; diazepam, 2 mg per kg: 15.5 ± 2.6; diazepam, 4 mg per kg: 16.3 ± 4.2). During the test session 24 h later, mice were again placed in the lit box. Mice avoiding the dark compartment for over 60 s were considered as remembering the task. In a control experiment, shock was not delivered in the dark box. Instead, after stepping in the dark box during the first session, mice were returned to their home cages for 5 min; they were then shocked in a different lit box, thus dissociating dark box from punishment. 24 h later, during the test session, no difference was observed between saline and treated subjects. Percentages of animals ($n = 15$ per group) avoiding the dark box were: saline: 8%, β-CCM, 0.2 mg per kg: 0%; β-CCM, 0.3 per mg kg: 17%. This control experiment rules out a nonspecific effect of β-CCM on avoidance of the dark box.

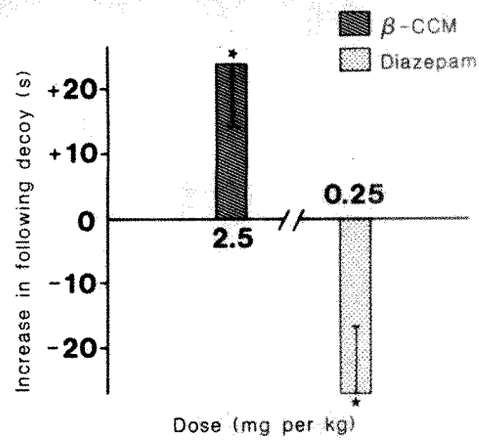


Fig. 3 Effect of β-CCM and diazepam on retention of imprinting (following a ball) in chicks. Results are the differences (±s.e.) in the time the drug-treated chicks spent following the ball compared with saline-treated groups. Hence, ordinate 0 corresponds to the mean of the time spent following the ball by saline-treated chicks (54 ± 8 s, $n = 56$); $n = 17$ and 18 for β-CCM-treated and control groups, respectively; $n = 39$ and 38 for diazepam-treated and control groups, respectively. * $P < 0.025$ between treated and controls (analysis of variance).
Methods. Chicks (24 h old, Hubbard strain, Bas-Bourray, France) were injected i.p. with saline, β-CCM or diazepam, 5 min before imprinting. The imprinting session was performed as described previously[14]. Briefly, the chick was placed for 5 min in a black circular arena (200 cm diameter) facing a decoy (red ball, 11 cm diameter, with yellow stripes). The ball was suspended 5 cm above the floor and moved at a speed of 385 cm min^{-1}. The time the chick spent following the ball was recorded automatically. During this 5-min imprinting session, the average time was 24 ± 3 s with no significant difference between treated subjects and their controls (increase in following behaviour (s) compared with controls ± s.e.: β-CCM, 1.88 ± 6.22; diazepam, 6.04 ± 6.47). 24 h later, a 5-min retention test was performed in the same apparatus.

training session the animals become accustomed to the new environment and that during the test session, they remember it.

In our model, when β-CCM (0.2 and 0.3 mg per kg body weight) was administered to mice before the training session, food intake during the 30 s of the session did not differ from that of controls or diazepam-treated animals. When the same animals were tested 4 days later, by which time all drugs would have been eliminated[7], food intake of the β-CCM group was enhanced compared with that of controls. While the average consumption of the controls was 25 mg during the 2-min test session, the β-CCM group consumed 40–60 mg more (Fig. 1). This effect of β-CCM injected only before the training sessions disappeared when higher doses (0.4 and 0.6 mg per kg), close to those we have shown previously[11] to be anxiogenic doses (1 mg per kg), were used. On the other hand, when diazepam (1.0 and 1.5 mg per kg) was administered before the training session, a reduction in food intake was seen during the test session (Fig. 1).

In the passive avoidance test, mice were trained in a single-trial procedure. The animals were placed in an illuminated box connected to a dark box. Entrance into the dark box usually occurred within 30 s and was punished by an electric footshock. On the next day (test session), the same mice were again placed in the illuminated box. Mice staying in the illuminated box for more than 60 s were considered as remembering the task. Retention was thus quantified by the percentage of animals avoiding the dark compartment.

When facilitation of retention was to be investigated, a low-intensity shock was delivered; when impairment of retention was to be investigated, a high-intensity shock was used. In the low-shock group (Fig. 2*a*), controls showed a poor level of retention and, during the test session, only a small percentage (12%) of subjects avoided the dark box. In this low-shock group, when β-CCM (0.2 and 0.3 mg per kg) was administered before the training session, a much higher percentage (35%) of the animals now avoided the dark box during the test session. Lower (0.1 mg per kg) and higher (0.4 mg per kg) doses of β-CCM were less effective. Hot-plate tests and measurement of latencies of response to shocks showed that β-CCM had no effect on pain threshold[11]. The enhancement of performance by β-CCM in this task is in direct opposition to the amnesic effect of diazepam. Thus, in the high-shock group the percentage of mice avoiding the dark box during the test session was reduced from 100% (controls) to nearly 40% (diazepam-treated) (Fig. 2*b*).

For the imprinting experiments, newly hatched chicks (~24 h

Table 1 Effects of β-CCM and diazepam on performance during a passive avoidance test 30 s after training

Test substance	% Of animals avoiding dark box during test session
Low shock	
Saline	10
β-CCM (0.3 mg per kg)	40*
High shock	
Saline	87
Diazepam (2 mg per kg)	27†

The protocol was the same as for Fig. 2, except that the test session was performed 30 s, instead of 24 h, after the end of the training session ($n = 20$ and $n = 15$ for high- and low-shock groups, respectively).
* $P < 0.05$; † $P < 0.001$ between treated and control animals (χ^2 test).

old) were used. Chicks tend to follow a moving decoy presented to them during the imprinting session. When retested in the same situation 24 h later, imprinted chicks, having memorized the characteristics of the situation and of the decoy, follow the decoy for a longer time than do non-imprinted chicks.

In our experiment, when imprinting was accomplished under the effect of β-CCM (2.5 mg per kg), the time spent by the chick in following the decoy (a ball) during the test session was increased compared with untreated controls (Fig. 3). Thus, in the 5-min period of the test session, controls followed the ball for an average 53 s whereas β-CCM-treated chicks followed it for about 20 s longer. On the other hand, when imprinting was performed under the effect of diazepam (0.25 mg per kg), the time spent following the ball during the test session decreased; treated subjects followed the ball for about 20 s less than controls.

Our results from these three different animal models suggest that β-CCM administered before acquisition enhances the performance of the task during the retention test. We verified that such an effect cannot be obtained when the drug is administered immediately after acquisition or before the retention test. For instance, in the study of habituation to a new environment, when β-CCM (0.3 mg per kg) was administered just after the training session, there was no significant difference in the food intake of these animals during the test session compared with the controls (difference of food intake with the controls -1.3 ± 16.24 mg). Similarly, if β-CCM (0.3 mg per kg) was administered 15 min before the test session, the difference in intake of the treated group as compared with the controls remained non-significant (difference $-15{\cdot}7 \pm 19{\cdot}92$ mg).

In contrast to the improvement of retention when β-CCM was administered before acquisition, diazepam had the opposite effect and, in agreement with previous reports, impaired the performance during the retention test. Such an impairment has been interpreted previously as a demonstration of the amnesic effect of diazepam[1]. However, it has also been suggested that the effect of diazepam is due to 'state dependency'[15]. According to this hypothesis, when learning occurs under the effect of a drug, proper retrieval is achieved only in the presence of the same drug. This hypothesis was tested by reinjecting some of the diazepam-treated subjects from the three models with diazepam before the retention test. No improvement in performance was seen in the three models. The state-dependency hypothesis would thus not explain the impaired performance of diazepam-treated subjects. Our results support the idea that diazepam impairs memory processing, a result consistent with studies using human patients[1]. As β-CCM has opposite effects to those of diazepam, it could be considered as enhancing memory processing. These effects of β-CCM were not seen in the dose range of the anxiogenic or convulsant effects of the drug, as the optimum dose in the present study (0.2, 0.3 mg per kg) is much lower than the anxiogenic (1 mg per kg)[11] or convulsive (1–10 mg per kg)[7] doses in the same strain of mice.

To investigate whether these effects of β-CCM and diazepam are mediated by the benzodiazepine receptor, we attempted to block their actions by using the specific benzodiazepine antagonist Ro 15-1788 (refs 2–3). This experiment was undertaken in the passive avoidance situation described for Fig. 2 and with the same protocol. Thus, low- and high-shock groups were used to study the effects of β-CCM and diazepam, respectively. Groups of mice were injected, before the first session, with β-CCM (0.3 mg per kg subcutaneously (s.c.)), diazepam (4 mg per kg intraperitoneally (i.p.)) or Ro 15-1788 (15 mg per kg, i.p.) or a combination of β-CCM + Ro 15-1788 or diazepam + Ro 15-1788. Results show that Ro 15-1788 had no effect when administered alone. However, the effects of β-CCM or diazepam were completely antagonized by co-administration of Ro 15-1788. This indicates that both the effect of β-CCM and the opposite effect of diazepam are mediated by the benzodiazepine receptor.

The next question was to delineate which stages of learning or memory were being affected by the drug. If memory can be defined as the retention of information, this information needs to be acquired (learning) and eventually recalled (retrieval). Since in our experiments, drugs have no effect when administered just before the retention test, we can rule out an action on retrieval. This agrees with most results obtained with benzodiazepines in human subjects[1]. A possible explanation of the data would be that β-CCM increases the level of arousal during the training session. This explanation would agree with the observation that arousal-enhancing drugs improve learning[16] and that several β-carbolines increase arousal[17]. We tried to confirm this interpretation by using the passive avoidance situation described earlier, the only difference being that the test session was performed 30 s, instead of 24 h, after the end of the training session. The results were the same as with a 24-h interval (Table 1), suggesting an effect on learning rather than memory. Our results with β-CCM could therefore be interpreted as an improvement of performance due to arousal-induced improvement of learning. Conversely, benzodiazepines could act through a reduction of arousal during the training session. However, the effects of benzodiazepines on short-term memory in humans suggest that benzodiazepines not only decrease acquisition (learning) but also seem to interfere with retention (memory). Finally, while it is likely that the observed effects with β-CCM and diazepam are related to the acquisition side of memory processing, the precise mechanisms underlying these effects remain unknown.

P.V. was supported by a Fondation de France fellowship and L.P.C. by a Fyssen Fellowship. This work was supported by CNRS (ATP Pharmacologie des Neuromédiateurs and APS-PIRMED Neurodrogues), INSERM (PRC 121022) and by DRET 84/039. We thank Josette Guitard and Jean-Paul Bouillot for technical assistance.

Received 3 March; accepted 10 April 1986.

1. Lister, R. G. *Neurosci. Biobehav. Rev.* **9**, 87–94 (1985).
2. Hunkeler, W. *et al. Nature* **290**, 514–516 (1981).
3. Braestrup, C., Nielsen, M. & Olsen, C. E. *Proc. natn. Acad. Sci. U.S.A.* **77**, 2288–2292 (1980).
4. Polc, P., Bonetti, E. P., Schaffner, R. & Haefely, W. *Naunyn-Schmiedebergs Archs. Pharmak.* **321**, 260–264 (1982).
5. Braestrup, C., Schmiechen, R., Neef, G., Nielsen, M. & Petersen, E. N. *Science* **216**, 1241–1243 (1982).
6. Oakley, N. R. & Jones, B. J. *Neuropharmacology* **21**, 587–589 (1982).
7. Prado De Carvalho, L. *et al. Eur. J. Pharmac.* **103**, 287–293 (1984).
8. Dorow, R., Horowski, R., Paschelke, G., Amin, M. & Braestrup, C. *Lancet* **2** 98–99 (1983).
9. Ninan, P. T. *et al. Science* **218**, 1322–1334 (1982).
10. File, S. E., Lister, R. G. & Nutt, D. J. *Neuropharmacology* **21**, 1033–1037 (1982).
11. Prado De Carvalho, L., Grecksch, G., Chapouthier, G. & Rossier, J. *Nature* **301**, 64–66 (1983).
12. Corda, M. G., Blaker, W. B., Mendelson, W. B., Guidotti, A. & Costa, E. *Proc. natn. Acad. Sci. U.S.A.* **80**, 2072–2076 (1983).
13. Soubrié, P., Simon, P. & Boissier, J. R. *C.r. hebd. Séanc. Acad. Sci., Paris* (D) **283**, 203–205 (1976).
14. Lecanuet, J. P., Alexinsky, T. & Chapouthier, G. *Behav. Biol.* **16**, 291–304 (1976).
15. Jensen, H. H. & Poulsen, J. C. *Scand. J. Psychol.* **23**, 107–111 (1982).
16. Martinez, J. L. Jr, Jensen, R. A. & McGaugh, J. L. in *The Physiological Basis of Memory* 2nd edn (ed. Deutsch, J. A.) Ch. 2 (Academic, New York, 1983) 49–70.
17. Ongini, E., Barzaghi, C. & Marzanatti, M. *Eur. J. Pharmac.* **95**, 125–129 (1983).

The structural gene coding for myelin-associated proteolipid protein is mutated in *jimpy* mice

A. Dautigny*, M.-G. Mattei†, D. Morello‡, P. M. Alliel*, D. Pham-Dinh*, L. Amar§, D. Arnaud§, D. Simon‡, J.-F. Mattei†, J.-L. Guenet‡, P. Jollès* & P. Avner§

* Laboratoire des Protéines (Unité CNRS 1188 alliée à l'INSERM), Université de Paris V, 45 rue des Saints-Pères, F-75270 Paris Cedex 06, France
† Unité INSERM 242 and Centre de Génétique Médicale, Hôpital d'Enfants de la Timone, F-13385 Marseille Cedex 5, France
‡ Unité d'Immunogénétique des Mammifères and
§ Unité d'Immunogénétique Humaine, Institut Pasteur, 25 rue du Dr Roux, F-75724 Paris Cedex 15, France

Mutations affecting developmental processes may allow some insight into the complexity of the biological processes involved. In mice, two mutants that affect myelin formation in the central nervous system, *jimpy* and *shiverer*, have proved to be useful models for the study of this process[1]. The predominant proteins in myelin are the major myelin proteolipid (PLP) and the myelin basic proteins (MBP), which together account for 80–90% of total myelin proteins[2]. It has recently been shown that the *shiverer* mutation is located in the MBP structural gene[3,4], but the site of the *jimpy* mutation, which is X-chromosome-linked and may be similar to the sex-linked dismyelinization human disease, Pelizaeus–Merzbacher disease[5], remains unclear. Here we provide evidence, based on a combined genetic and biochemical approach, that the sex-linked recessive mutation *jimpy* is located in the structural gene coding for PLP.

P-23, a complementary DNA probe corresponding to a PLP gene transcript, has recently been cloned from a rat brain-specific cDNA library using an oligonucleotide probe corresponding to amino acids 231–235 of bovine PLP[6]. This probe has subsequently been shown to react not only with rat DNA but also with human and mouse DNAs. Southern blotting analysis of *Eco*RI-restricted DNAs from a panel of mouse–hamster somatic cell hybrids, using P-23, revealed a single band whose distribution indicated that the sequence recognized by probe P-23 was on the mouse X chromosome (data not shown). There was no evidence for the presence of crossreacting sequences on other chromosomes.

To localize the PLP gene more precisely and to provide further data to allow correlation of the cytological and genetic X-chromosome profiles, the position of the gene was analysed by *in situ* hybridization and an interspecific mouse cross.

In situ hybridization experiments with probe P-23 were carried out using metaphase spreads from a female WMP mouse, in which all chromosomes other than chromosomes X and 19 are in the form of metacentric robertsonian translocations. From 50 metaphases analysed 55 grains were scored on the X chromosome; 69% of these grains mapped to the F chromsome band (Fig. 1*a*), with a maximal distribution in the proximal part of this band, suggesting that the PLP structural gene maps to XF1 (Fig. 1*b*).

Genetic localization was facilitated when it was found that the P-23 probe detected an *Eco*RI restriction fragment length polymorphism (RFLP) between a B6.CBA.RI strain of the *Mus. musculus domesticus* species and the inbred SPE/Pas strain derived from *Mus. spretus* (Fig. 2), thereby raising the possibility of using an interspecies backcross between the two strains (for details see Fig. 3 legend) to localize the PLP structural gene. Meiotic recombinants from this backcross segregated not only for the X-linked *Tabby* (*Ta*), *jimpy* (*jp*) and *hypoxanthine phosphoribosyltransferase* (*hprt*) markers but also for RFLPs corresponding to six X-linked anonymous unique sequence probes[7] and three X–Y common sequences (P.A. and C. Bishop, in preparation). Figure 3*a* shows the localization of the markers most relevant to the present study.

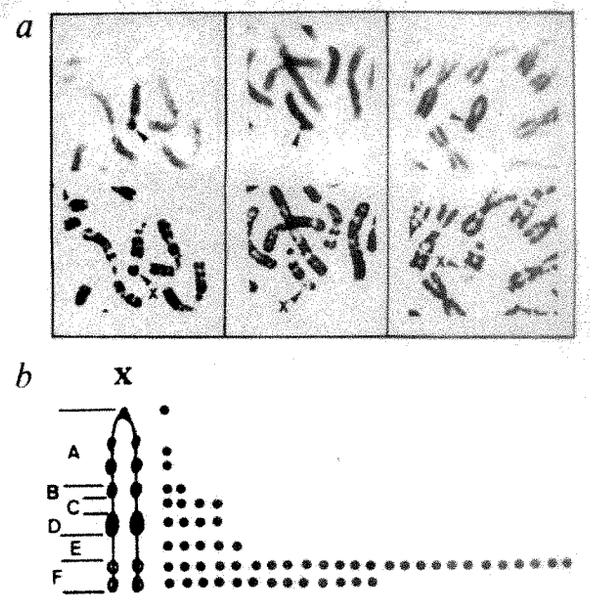


Fig. 1 Localization of the rat PLP probe to the mouse X chromosome by *in situ* hybridization. The pBR322 plasmid containing the P-23 PLP cDNA clone was used to screen R-banded WMP female mouse metaphase preparations using standard procedures[14]. *a*, Ultraviolet light image (upper) and normal light image (lower) of a portion of one such metaphase spread. The arrows indicate grains at position XF1. *b*, Composite grain distribution pattern of the ^{3}H-PLP probe on R-banded metaphase spreads; ●, grains per band. A–F represent the chromsome bands (see ref. 15 for banding nomenclature).

The hybridization profile of backcross progeny from this cross (Fig. 2) confirmed that the probe recognized a restriction fragment in the X chromosome because: (1) a dosage effect was noted when female and male progeny were observed; and (2) whereas male progeny never showed more than one restriction fragment, 57% of female progeny showed a doublet, indicating the simultaneous presence of the two allelic forms. Typing of 90 such backcross progeny with the PLP cDNA probe enabled the gene coding for this sequence to be localized using two approaches; first, by inspection of the pedigrees of the various animals, allowing correlation between the crossover events that occur on the X chromosome of each animal and their PLP haplotype; and second, by estimation of recombination frequencies in the different intervals defined by the markers *hprt*, *Tabby*, *45* and *52* (see Fig. 3*a*).

Figure 3*b* shows the former approach for a limited number of female and male animals. For example, examination of animals 4, 12, 14, 18, 33, 37, 44, 55 and 67 suggests that the PLP gene (*plp*) cannot lie in the region represented by probe *100* between the centromere and *hprt*. Similarly, results with animals 4, 12, 33, 37, 44, 55 and 67 suggest that the PLP gene cannot be proximal to the *Tabby* gene. Overall, the pedigree analysis indicates that the PLP gene must lie between markers *52* and *45*, a region comprising some 26 centimorgans and including the *jimpy* locus[7].

Examination of the recombination frequency data obtained from female progeny is in complete agreement with the above conclusions. The recombination frequencies obtained were: *hprt–plp*, 34%; *Ta–plp*, 20%; *52-plp*, 21%; and *45-plp*, 17%. Thus, the *plp* locus is some 20 centimorgans distal from *Tabby* and 34 centimorgans distal from *hprt*. This latter value is exactly

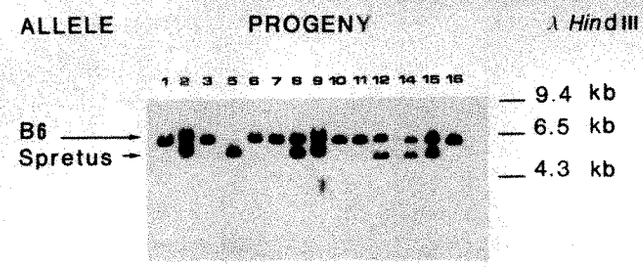


Fig. 2 Progeny haplotype characterization using the PLP P-23 insert on *Eco*RI-restricted genomic DNAs. Washing conditions were 0.2 × SSC and 65 °C. The numbers identify individual backcross mice progeny. kb, kilobases.

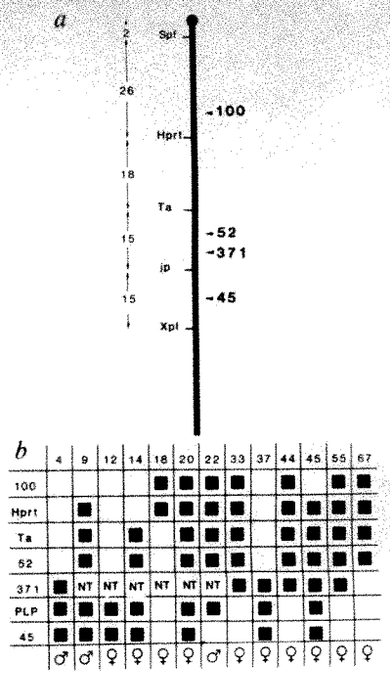


Fig. 3 Pedigree analysis of the R1 RFLP in B6.CBA.RI × Spe/Pas backcross progeny, detected by the PLP P-23 cDNA. *a*, Map localization of the mouse X chromosome markers used in the present study. Localization of molecular probes *100, 52* and *45* is detailed in ref. 7. Details of the localization of the X–Y common 371 probe will be reported elsewhere (P.A. and C. Bishop, in preparation). *b*, Distribution of RFLPs of the *Mus. spretus* type (■) and B6.CBA.RI type (□) detected in individual interspecies backcross progeny using molecular probes *100, 52, 45, 371* and P-23 (*plp*), HPRT allozymic forms and the *Tabby* coat colour marker. The interspecies backcross used was set up by crossing female B6.CBA.RI mice (*hprt*^{b} *Ta jp*/*hprt*^{b}++) with male Spe mice (*hprt*^{a}++/Y). Resulting F_1 females (*hprt*^{b} *Ta jp*/*hprt*^{a}++ or *hprt*^{b} *Ta*+/*hprt*^{a}++) were backcrossed to B6.CBA.RI males (*hprt*^{b}++/Y) and progeny analysed for the *Tabby* and *jimpy* markers. HPRT analysis, DNA extraction, restriction blotting and probing of genomic blots was as described in ref. 7. Only the X chromosome derived from the F_1 female is illustrated. In the region between the centromere and *hprt*, for reasons of clarity, only one of the four possible typed markers has been represented. NT, not tested.

that reported for the distance between *hprt* and the *jp* mutation[8] suggesting that the PLP probe is detecting a locus either identical to or closely linked to *jimpy*. Support for this was obtained by the PLP probe and associated with the B6.CBA.RI strains, although the number of such progeny tested is small (eight animals).

No evidence for the presence of a sizeable deletion within the PLP gene was detected in *jimpy* mice by Southern blot analysis. Probing of genomic blots restricted with a panel of enzymes including *Hin*dIII, *Eco*RI, *Pst*I, *Bgl*I and *Msp*I has failed to reveal a RFLP associated with the *jimpy* mutation (data not shown). In view of this and the fact that even the analysis of very large numbers of such backcross progeny cannot exclude very tight linkage rather than gene identity, the PLP cDNA probe was assumed, on the basis of the mapping data, to be the product of the *jimpy* gene. We therefore attempted to confirm this by using Northern, dot-blot and S_1 mapping techniques with probe P-23 to compare populations of messenger RNA molecules extracted from the brain of male *jp*/Y and female *jp*/+ animals and control male +/Y and female +/+ progeny. No significant difference in overall brain mRNA levels was noted between the different classes of animals. However, quantitative differences in the level of mRNA complementary to P-23 were clearly evident from both Northern blot and dot-blot experiments. The Northern blot in Fig. 4*a* shows that P-23 hybridizes to two classes of mRNA transcripts in +/+ females and +/Y males which are respectivly 3,200 and 2,400 base pairs (bp) long; the smaller transcript is considerably less abundant than the larger one. The presence of two PLP transcripts in normal mouse mRNA[9] and in rat brain has been reported previously[9,10]. Both transcripts are present in heterozygous *jp*/+ females, although in much reduced quantity. In *jp*/Y males these are small amounts of a transcript of similar size to the larger 3,200-bp transcript, the 2,400-bp transcript being either absent or, more probably, present in only trace amounts.

RNA dot hybridization experiments using the P-23 probe (Fig. 4*b*) show that brains of heterozygous *jp*/+ females contain 60–70% of the PLP transcripts present in +/+ females. Brains of male *jp* mice, on the other hand, contain only 15–20% of the PLP mRNA levels found in control males. The slight quantitative discrepancy between the dot-blot and Northern blot experiments over the quantity of RNA in *jp*/Y male hybridizing with the PLP probe may be due either to differential sensitivity linked to the use of poly(A)$^+$ RNA rather than total RNA for the dot-blot experiments, or to accumulation of precursor mRNAs detected only in the latter analysis.

Proof that it is the PLP structural gene that is mutated in *jimpy* mice was provided by S_1 nuclease protection experiments using poly(A)$^+$ brain RNA from *jimpy* and normal wild-type mice. Figure 4*c* shows the results obtained using a probe corresponding to the 5′ end of the PLP mRNA molecule. Two main differences were observed between mutant *jp*/Y male and normal male (+/Y) brain mRNAs. Whereas both +/Y male and *jp*/+ female mouse brain mRNAs protect the probe over a region of some 800 nucleotides, protection by mRNA from *jimpy* mice (*jp*/Y) extends only over ~630 nucleotides, indicating an apparent loss of S_1 protection over a region of some 160 nucleotides in the *jimpy* PLP mRNA molecule compared with the wild type. It is unclear whether the 160-nucleotide band seen only in the *jp*/Y track represents this sequence, but if it does, the deletion occurring in *jimpy* mice must be very limited in extent. The second difference observed with brain mRNA from *jimpy* mice is its failure to protect the 280-nucleotide band otherwise found in both +/Y male and +/*jp* female mRNA tracks. Furthermore, there was no detectable difference between the *jimpy* and wild-type S_1 profiles when a 3′ non-coding PLP fragment (*Pst* 800–*Pst* 1,334)[6] was used instead of the 5′ probe (data not shown).

Although this comparative analysis confirms the presence of a mutation in the PLP structural gene, elucidation of the type of mutation which could account for the differential hybridization pattern is complicated by the presence of two supernumerary bands of 380 and 280 nucleotides in both wild-type and +/*jp* females. These bands cannot be attributed to differences between rat and mouse *plp* sequences because the S_1 profiles

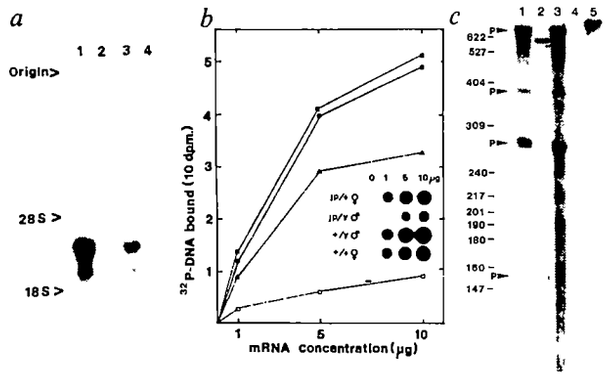


Fig. 4 *a*, Northern blot analysis of RNA from the brains of control (lane 1), hemizygous *jp*/Y (lane 2) and heterozygous *jp*/+ mice (lane 3). Lane 4, purified ribosomal RNA (20 μg). The 5.1-kb and 2.0-kb positions indicate 28S and 18S mouse ribosomal RNAs, respectively. *b*, Dot hybridization analysis of PLP-specific mRNA from mouse brains. ■, Male +/Y control; ●, female +/+ control mice; ▲, heterozygous *jp*/+ female; □, hemizygous *jp*/Y male. The inset shows the autoradiographic spots (2 days' exposure) used for this analysis. Control autoradiographic spots obtained using equal quantitites of *Escherichia coli* transfer RNA gave no signal. *c*, S_1 protection experiment using poly(A)$^+$ RNA from *jimpy* mice. The 795-nucleotide *Pst*I–*Pst*I fragment[6] was subcloned into vector M13mp9. Radiolabelled single-stranded DNA was prepared according to Burke[16]. Aliquots of 60,000 c.p.m. per probe were hybridized with 0.12 μg of poly(A)$^+$ RNA from male +/Y mice (lane 1), 1.4 μg of poly(A)$^+$ RNA from hemizygous *jimpy* male *jp*/Y (lane 2) or 0.5 μg of poly(A)$^+$ RNA from female heterozygous *jp*/+ mice (lane 3), plus 10 μg of carrier yeast tRNA. Lane 4, 5,000 c.p.m. of unhybridized probe which had been digested with S_1. Lane 5, 5,000 c.p.m. of unhybridized probe that had not been S_1 digested. After digestion with S_1 nuclease, the resulting mixture was electrophoresed through 5% acrylamide/8 M urea gel. Autoradiogram exposure was at −70 °C plus intensifying screen for 8 h. Size markers are pBR322 digested by *Hpa*II. P, protected; ND, not digested.

Methods. *a*, Total cellular RNA from 3-week-old mice was prepared, electrophoresed and transferred to nitrocellulose as described elsewhere[17,18]. Blots were prehybridized at 42 °C in 50% formamide, 5×SSC, 5×Denhardt's[19], 20 mM sodium phosphate *p*H 6.8, 250 μg ml^{-1} salmon sperm DNA, 0.1% SDS, then hybridized with nick-translated ^{32}P-labelled probe[20] in the same solution. Blots were washed four times in 2×SSC/0.1% SDS/0.1% pyrophosphate at room temperature and twice in 0.1× SSC/0.1% SDS/0.1% pyrophosphate for 15 min each at 50 °C, then exposed to Kodak X-Omat AR film at −70 °C for 1 day with Cronex Lightning Plus intensifying screen. *b*, Samples of poly(A)$^+$ RNA (1–10 μg) were treated with formaldehyde and spotted onto sheets of nitrocellulose according to the method of White and Bancroft[21], prehybridized and hybridized as for the Northern analysis. Individuals blots were cut out and counted in scintillation fluid and standard curves generated by plotting counts per min of probe bound per dot against μg of RNA immobilized per dot.

observed using the 5′ rat cDNA probe and wild-type mouse brain mRNA are identical to those seen with rat brain mRNA (data not shown). It remains possible that this pattern is related to the presence of a mRNA coding for the DM-20 molecule, which differs from PLP by the deletion of an internal fragment of about 40 amino acids[11], and further experiments are in progress to test this hypothesis and to define the mutational site further. With this finding, mutations in the structural genes coding for at least two different myelin proteins have been shown to lead to myelin deficiency and severe neurological disorders[4]. In both cases, the structural gene mutation leads to lowered steady-state mRNA levels, although it is not known whether this is due to a transcriptional or post-transcriptional event. The correlation reported here between the *jimpy* mutation and the PLP structural gene extends previous findings suggesting that *plp* is on the X chromosome[12,13] and underlines the interest in myelin as a model system for study of gene–gene product interactions.

Received 6 January; accepted 3 April 1986.

1. Hogan, E. L. & Greefield, S. in *Myelin* (ed. Morell, P.) 489–514 (Plenum, New York, 1984)
2. Lees, M. B. & Brostoff, S. W. in *Myelin* (ed. Morell, P.) 197–224 (Plenum, New York, 1984)
3. Roach, A., Boylan, K., Horvath, S., Prusiner, S. B. & Hood, L. E. *Cell* 34, 799–806 (1983)
4. Roach, A., Takahashi, N., Pravtcheva, D., Ruddle, F. & Hood, L. E. *Cell* 42, 149–155 (1985)
5. Ford, F. R. *Diseases of the Nervous System in Infancy Childhood and Adolescence* (ed Thomas, C.) 831–833 (Springfield, Illinois, 1960).
6. Dautigny, A. *et al. FEBS Lett.* 188, 33–36 (1985).
7. Amar, L. C., Arnaud, S., Cambrou, J., Guenet, J.-L. & Avner, P. R. *EMBO J.* (in the press)
8. Davisson, M. T. & Roderick, T. H. *Mouse News Lett.* 83, 7–8 (1985)
9. Milner, R. J. *et al. Cell* 42, 931–939 (1985).
10. Alliel, P. M. *et al. Hoppe-Seyler's Z. physiol. Chem.* 366, 762 (abstr.) (1985)
11. Trifilieff, E. *et al. C.r. hebd. Séanc. Acad. Sci., Paris* 300, Sér. III, 241–247 (1985)
12. Willard, F. & Riordan, J. R. *Science* 230, 940–942 (1985).
13. Dautigny, A. *et al. 616th Meet. biochem. Soc.*, London, Abstr. 10 (1985)
14. Camargo, M. & Cervenka, J. *J. hum. Genet.* 34, 757–780 (1982)
15. Nesbitt, M. N. & Francke, V. in *Genetic Variants and Strains of the Laboratory Mouse* (ed Green, M. C.) 316–324 (Fischer, Stuttgart, 1981).
16. Burke, J. F. *Gene* 30, 63–68 (1984).
17. Kaplan, B. B., Bernstein, S. L. & Gioio, A. *Biochem. J.* 183, 181–184 (1979)
18. Thomas, P. S. *Proc. natn. Acad. Sci. U.S.A.* 77, 5201–5215 (1980).
19. Denhardt, D. T. *Biochem. biophys. Res. Commun.* 23, 641–646 (1966).
20. Rigby, P. W. J., Dieckman, M., Rhodes, C. & Berg, P. *J. molec. Biol.* 113, 237–251 (1977)
21. White, B. A. & Bancroft, F. C. *J. biol. Chem.* 257, 8569–8572 (1982)

Light-dependent phosphorylation of rhodopsin by β-adrenergic receptor kinase

Jeffrey L. Benovic*, Federico Mayor Jr*, Robert L. Somers†, Marc G. Caron* & Robert J. Lefkowitz*

* Howard Hughes Medical Institute, Departments of Medicine, Biochemistry and Physiology, Duke University Medical Center, Durham, North Carolina 27710, USA
† National Eye Institute, National Institutes of Health, Bethesda, Maryland 20892, USA

The structural components involved in transduction of extracellular signals as diverse as a photon of light impinging on the retina or a hormone molecule impinging on a cell have been highly conserved. These components include a recognition unit or receptor (for example, the β-adrenergic receptor (βAR) for catecholamines or the 'light receptor' rhodopsin), a guanine nucleotide regulatory or transducing protein, and an effector enzyme (for example, adenylate cyclase or cyclic GMP phosphodiesterase)[1,2]. Molecular cloning has revealed that the βAR shares significant sequence and three-dimensional homology with rhodopsin[3]. The function of the βAR is diminished by exposure to stimulatory agonists, leading to desensitization[4]. Similarly, 'light adaptation' involves decreased coupling of photoactivated rhodopsin to cGMP phosphodiesterase activation[5–7]. Both forms of desensitization involve receptor phosphorylation. The latter is mediated by a unique protein kinase, rhodopsin kinase, which phosphorylates only the light-bleached form of rhodopsin[8–10]. An analogous enzyme (termed βAR kinase or βARK) phosphorylates only the agonist-occupied βAR[11]. We report here that βARK is also capable of phosphorylating rhodopsin in a totally light-dependent fashion. Moreover, rhodopsin kinase can phosphorylate the agonist-occupied βAR. Thus the mechanisms which regulate the function of these disparate signalling systems also appear to be similar.

Phosphorylation of the β-adrenergic receptor by βARK is almost totally dependent on agonist occupancy of the receptor, as demonstrated in Fig. 1 (compare lanes 1 and 2). βARK is also able to phosphorylate rhodopsin in an almost totally light-dependent manner (Fig. 1, lanes 4, 5). At comparable levels

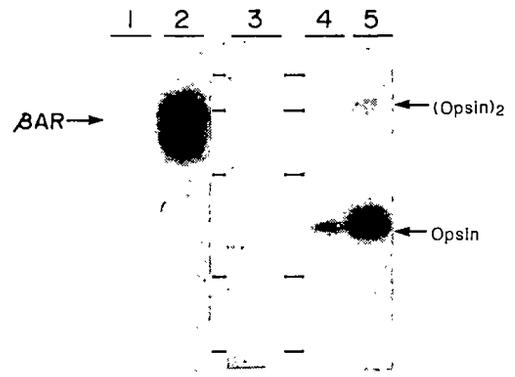


Fig. 1 Phosphorylation of the β-adrenergic receptor and rhodopsin by the β-adrenergic receptor kinase. Lane 1 contains 0.6 pmol βAR; lane 2, 0.6 pmol βAR and 20 μM (−)isoprenaline; lane 3, 0.6 pmol rhodopsin in the light; lane 4, 250 pmol rhodopsin in the dark; lane 5, 250 pmol rhodopsin in the light. The results shown are representative of three experiments. Relative molecular mass (M_r) standards (94,000 (94K), 67K, 45K, 30K and 20.1K) are indicated by marks between lanes 2 and 3 and between 3 and 4.
Methods. Receptors were incubated for 60 min at 30 °C with 20 mM Tris-HCl *p*H 7.5, 20 mM NaCl, 5 mM sodium phosphate, 2 mM EDTA, 5 mM $MgCl_2$, 5 mM NaF, 0.05 mM [γ-^{32}P]ATP, (2,000 c.p.m. per pmol) and 0.3 μg βARK in a total volume of 50 μl. Reactions containing βAR were stopped by adding 1 ml of 100 mM NaCl, 10 mM Tris-HCl *p*H 7.2, 1% digitonin. After incubation for 30 min the samples were centrifuged and the supernatants desalted on Sephadex G-50 using 100 mM NaCl, 10 mM Tris-HCl *p*H 7.2, 0.05% digitonin. βAR was then repurified using an alprenolol affinity resin as described elsewhere[11]. After lyophilization, 100 μl of SDS buffer (8% SDS, 10% glycerol, 5% β-mercaptoethanol, 25 mM Tris-HCl *p*H 6.5) was added to each sample. Reactions containing rhodopsin were stopped by adding 50 μl of SDS buffer. Samples were then electrophoresed on 10% homogeneous SDS-polyacrylamide gels[17]. Gels were dried before autoradiography for 8 h (lanes 1–3) or 15 min (lanes 4, 5). βARK was partially purified from bovine brain by $(NH_4)_2SO_4$ precipitation (13–26%) of a high-speed supernatant fraction. The precipitate was then chromatographed on Ultrogel AcA34, DEAE Sephacel and CM Fractogel. Kinase activity was eluted with 20 mM Tris-HCl *p*H 7.5, 1 mM EDTA, 0.1 mM phenylmethylsulphonyl fluoride, 10 μg ml^{-1} leupeptin, 5 μg ml^{-1} pepstatin, 10 μg ml^{-1} benzamidine (J.L.B., F.M. Jr, R.J.L. and M.G.C., manuscript in preparation). The preparation used was ~20% pure and had a specific activity of ~35 pmol P_i per min per mg using 0.02 μM βAR as substrate. The preparation did not contain any contaminating protein kinase C or cyclic AMP-dependent protein kinase[11]. βAR was purified from hamster lung to >95% homogeneity by affinity chromatography and molecular-sieve HPLC as described elsewhere[18]. Purified βAR was reconstituted into phosphatidylcholine vesicles[11,19] before phosphorylation. Rod outer segments (ROS) were prepared from bovine retinas by stepwise sucrose gradient centrifugation[13]. Rhodopsin kinase-free ROS were prepared by treatment with 5 M urea[10] and consisted of ~95% rhodopsin, as assessed by Coomassie blue staining of SDS-polyacrylamide gels. The urea treatment effectively eliminates the endogenous rhodopsin kinase activity as rhodopsin phosphorylation in our ROS preparations was observed only in the presence of added kinase.

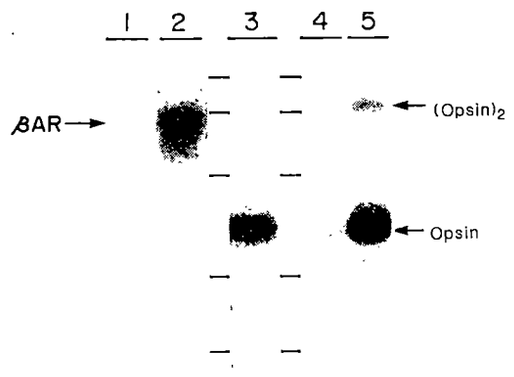


Fig. 2 Phosphorylation of the β-adrenergic receptor and rhodopsin by rhodopsin kinase. Lane 1 contains 0.6 pmol βAR; lane 2, 0.6 pmol βAR and 20 μM (−)isoprenaline; lane 3, 0.6 pmol rhodopsin in the light; lane 4, 250 pmol rhodopsin in the dark; lane 5, 250 pmol rhodopsin in the light. Incubations were identical to those described for Fig. 1, except that they contained 3 μg of rhodopsin kinase instead of βARK. βAR was repurified as described in Fig. 1 legend to remove the rhodopsin kinase autophosphorylation band which runs at M_r ~64K. Reactions containing rhodopsin were stopped by adding 50 μl of SDS buffer before electrophoresis on 10% polyacrylamide gels. Autoradiography of the dried gel was for 24 h (lanes 1–3) or 8 min (lanes 4, 5). The results shown are representative of three experiments. M_r standards are the same as in Fig. 1.
Methods. Rhodopsin kinase was partially purified from bovine ROS extracted with 10 mM potassium phosphate, 3 mM EDTA, 2 mM EGTA *p*H 6.8. The high-speed supernatant from this extract was dialysed against 20 mM potassium phosphate, 0.5 mM EDTA, 0.5 mM EGTA, 20% glycerol *p*H 6.8 before chromatography on a Blue Sepharose column. Rhodopsin kinase activity was eluted with a KCl gradient before dialysis against 0.1 M potassium phosphate, 0.1 mM EDTA, 0.1 mM EGTA, 50% glycerol *p*H 6.8 (R.L.S., manuscript in preparation). The preparation used was ~10% pure and had a specific activity of ~13 nmol P_i per min per mg using 10 μM rhodopsin as substrate. The preparation did not contain any contaminating protein kinase C or cAMP-dependent protein kinase. βAR was purified and reconstituted as described in Fig. 1 legend. Urea-treated ROS were prepared as described in Fig. 1 legend.

(0.6 pmol), βAR is a significantly better substrate for βARK than is rhodopsin (Fig. 1, lanes 2, 3). Figure 2 shows that analogous results are achieved using rhodopsin kinase. Thus, phosphorylation of rhodopsin is almost totally light-dependent (Fig. 2, compare lanes 4 and 5) whereas phosphorylation of βAR is almost totally agonist-dependent (lanes 1, 2). In addition, while βARK preferentially phosphorylates βAR, rhodopsin kinase phosphorylates rhodopsin better than βAR (Fig. 2, lanes 2, 3). The large apparent difference in kinase specificity, with βARK being much better at phosphorylating βAR compared with rhodopsin and rhodopsin kinase being only slightly better at phosphorylating rhodopsin, may reflect the fact that only the bleaching intermediates metarhodopsins II and III can serve as effective substrates for rhodopsin kinase[10,12]. Thus, the actual substrate concentration of rhodopsin in our experiments may in fact be lower than that of βAR. However, this does not alter the fact that βAR is the preferred substrate for βARK while rhodopsin is preferred by rhodopsin kinase.

The striking light dependence of rhodopsin phosphorylation by βARK is demonstrated further in Fig. 3. At the 2-h time point a 60-fold increase in phosphorylation was observed in the presence of light. The low stoichiometry (~0.07 mol per mol) probably reflects the relatively low amount of βARK used in these experiments. To compare the sites phosphorylated by rhodopsin kinase and βARK, HPLC tryptic peptide mapping of phosphorylated rhodopsin was performed. The peptide maps appeared virtually identical, with only a single major peptide. Phosphoamino-acid analysis of this peptide revealed predominantly phosphoserine together with a small amount of phosphothreonine, for both kinases (data not shown).

Rhodopsin kinase phosphorylates rhodopsin at as many as nine different sites[13], with seven of these residues (serines and threonines) being clustered in the carboxy-terminal 15 amino acids[14]. The sequence of the β-adrenergic receptor, deduced recently from the cloned gene, indicates that a similar serine- and threonine-rich region exists in its carboxy terminus[3]. The actual phosphorylation sites on the βAR have yet to be

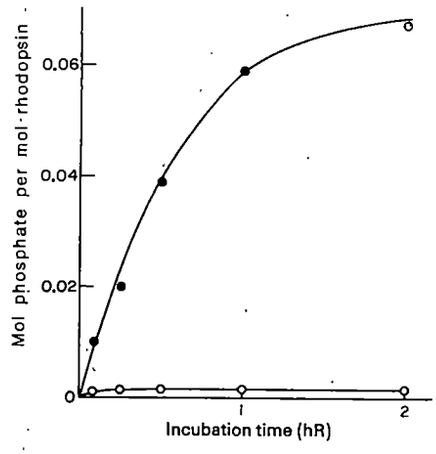
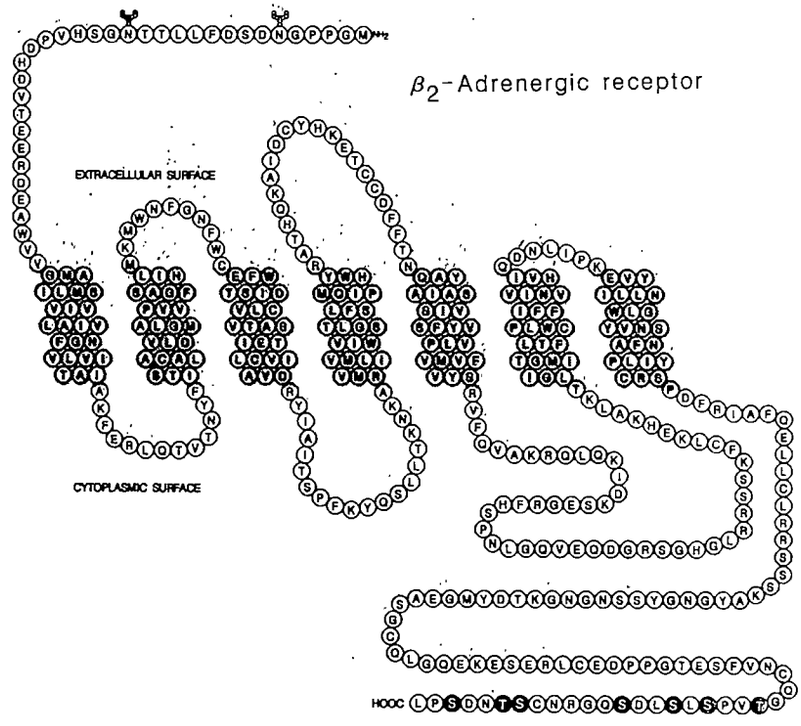


Fig. 3 Time course of rhodopsin phosphorylation by the β-adrenergic receptor kinase. Urea-treated ROS (250 pmol of rhodopsin) were incubated at 30 °C with CM Fractogel-purified βARK (0.3 μg protein) in the dark (○) or under continuous illumination with white light (●) for the times indicated. The incubations also contained 20 mM Tris-HCl pH 7.5, 20 mM NaCl, 2 mM EDTA, 5 mM $MgCl_2$ and 0.05 mM [γ^{32}P]ATP (1,600 c.p.m. per pmol). Reactions were stopped by adding 50 μl of SDS buffer before electrophoresis on a 10% polyacrylamide gel. After autoradiography the rhodopsin bands were excised and counted in a Packard scintillation counter. The results shown are representative of three experiments.



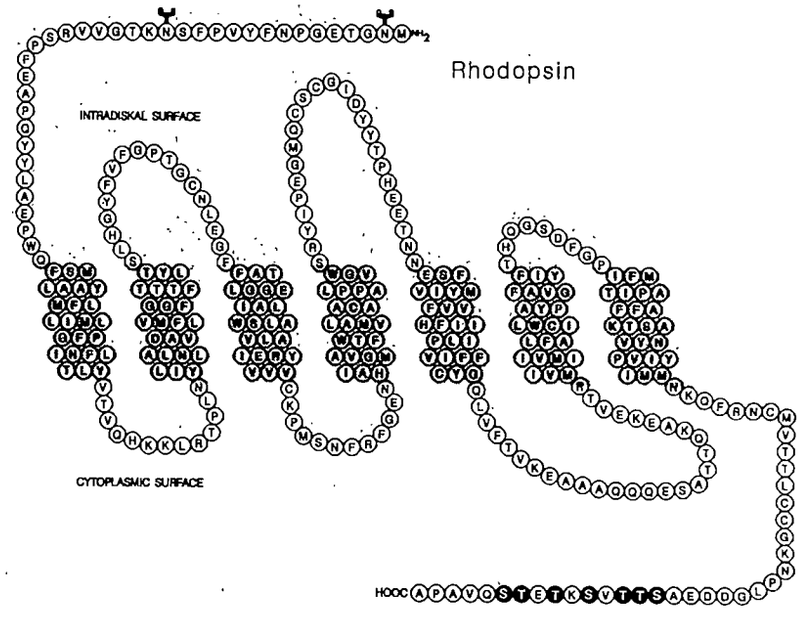


Fig. 4 Structure of the β-adrenergic receptor and rhodopsin polypeptide chains as they may be organized within the membrane. The seven known rhodopsin kinase phosphorylation sites on rhodopsin are represented by solid circles, as is a similar serine- and threonine-rich region near the carboxy terminus of βAR. Amino-acid sequences of the two proteins are taken from refs 3 and 20.

determined, however, the carboxy-terminal domain seems a likely region. Figure 4 compares the structures of the βAR and rhodopsin polypeptide chains as they may be organized within the membrane. The seven known phosphorylation sites on rhodopsin and seven possible sites of phosphorylation on the βAR are shown as solid circles.

We have found that βARK, an enzyme which specifically phosphorylates only the agonist-occupied form of the β-adrenergic receptor, can also phosphorylate the same region on rhodopsin as does rhodopsin kinase, in a light-dependent manner. This result suggests that in addition to the striking homologies in the structure and function of signal transduction components which exist between the two systems, their biochemical mechanisms of regulation are also analogous. Phosphorylation of bleached rhodopsin by rhodopsin kinase appears to lead to the attenuation of its interaction with transducin[15]. Phosphorylation of the β-adrenergic receptor by βARK in response to agonist occupancy of the receptor also appears to lead to an uncoupling of the receptor from the stimulatory guanine nucleotide regulatory protein, and this in turn is associated with attenuation of adenylate cyclase responsiveness (J.L.B., F.M. Jr, M.G.C. and R.J.L., manuscript in preparation).

Because phosphorylation of the receptor appears to be important for physiological adaptation (desensitization) of the responses associated with both the β-adrenergic receptor and the light receptor rhodopsin, phosphorylation may also represent an important control mechanism for other hormone–receptor systems. Recently, we have shown that desensitization of the α_1-adrenergic receptor, a receptor coupled to the phosphatidylinositol-Ca^{2+} signal transduction pathway, is also associated with its phosphorylation[16]. Moreover, desensitization or tachyphylaxis is a phenomenon which is common to many physiologically responsive systems. Thus, phosphorylation of the receptor component of hormone- and drug-responsive systems by a family of specific receptor kinases may represent a major mechanism by which cellular responsiveness to a variety of signals is regulated.

We acknowledge the assistance of Lynn Tilley in the preparation of this manuscript. This work was supported in part by NIH grant HL-16037. F.M. is a recipient of a Fulbright–Spain Ministry of Science postdoctoral fellowship.

Received 10 April; accepted 6 May 1986.

1. Fung, B. K.-K. & Stryer, L. *Proc. natn. Acad. Sci. U.S.A.* **77**, 2500–2504 (1980).
2. Lefkowitz, R. J., Stadel, J. M. & Caron, M. G. *A. Rev. Biochem.* **52**, 159–186 (1983).
3. Dixon, R. A. F. *et al. Nature* **321**, 75–79 (1986).
4. Sibley, D. R. & Lefkowitz, R. J. *Nature* **317**, 124–129 (1985).
5. Liebman, P. A. & Pugh, E. N. *Nature* **287**, 734–736 (1980).
6. Sitaramayya, A. & Liebman, P. A. *J. biol. Chem.* **258**, 1205–1209 (1983).
7. Wilden, U., Hall, S. W. & Kuhn, H. *Proc. natn. Acad. Sci. U.S.A.* **83**, 1174–1178 (1986).
8. Kuhn, H. & Dreyer, W. J. *FEBS Lett.* **20**, 1–6 (1972).
9. Bownds, D., Dawes, J., Miller, J. & Stahlman, M. *Nature new Biol.* **237**, 125–127 (1972).
10. Shichi, H. & Somers, R. L. *J. biol. Chem.* **253**, 7040–7046 (1978).
11. Benovic, J. L., Strasser, R. H., Caron, M. G. & Lefkowitz, R. J. *Proc. natn. Acad. Sci. U.S.A.* **83**, 2797–2081 (1986).
12. Paulsen, R., Miller, J. A., Brodie, A. E. & Bownds, M. D. *Vision Res.* **15**, 1325–1332 (1975).
13. Wilden, U. & Kuhn, H. *Biochemistry* **21**, 3014–3022 (1982).
14. Hargrave, P. A. *et al. Neurochem. Int.* **1**, 231–244 (1980).
15. Shichi, H., Yamamoto, K. & Somers, R. L. *Vision Res.* **24**, 1523–1531 (1984).
16. Leeb-Lundberg, L. M. F. *et al. Proc. natn. Acad. Sci. U.S.A.* **82**, 5651–5655 (1985).
17. Laemmli, U. K. *Nature* **227**, 680–685 (1970).
18. Benovic, J. L., Shorr, R. G. L., Caron, M. G. & Lefkowitz, R. J. *Biochemistry* **23**, 4510–4518 (1984).
19. Cerione, R. A., Strulovici, B., Benovic, J. L., Lefkowitz, R. J. & Caron, M. G. *Nature* **306**, 562–566 (1983).
20. Ovchinnikov, Y. A. *FEBS Lett.* **148**, 179–191 (1982).

Stimulation of haematopoiesis in primates by continuous infusion of recombinant human GM-CSF

Robert E. Donahue*, Elizabeth A. Wang*, David K. Stone*, Robert Kamen*, Gordon G. Wong*, Prabhat K. Sehgal†, David G. Nathan‡ & Steven C. Clark*

* Genetics Institute, Inc., Cambridge, Massachusetts 02140, USA
† New England Regional Primate Research Center, Southborough, Massachusetts 01722, USA
‡ Division of Hematology/Oncology, Dana Farber Cancer Institute and the Children's Hospital, Boston, Massachusetts 02115, USA

Certain proteins are known to play an important part in the proliferation, differentiation and functional activation of haematopoietic progenitor cells *in vitro*[1,2]. These proteins include erythropoietin and various colony-stimulating factors (CSFs), one of which is granulocyte–macrophage colony-stimulating factor (GM-CSF). Recently, both murine[3,4] and human GM-CSF[5–7] have been purified to homogeneity and complementary DNAs encoding them have been cloned. Although the *in vitro* activity of recombinant human GM-CSF has been investigated intensively (refs 5–15; see ref. 8 for a review), little is known about the functional activity of this protein *in vivo*. There is strong evidence that colony-stimulating activities produced by various human and murine tumour tissues and cell lines can stimulate granulopoiesis in mice[16–26], as can human urinary extracts[27,28]. A partially purified preparation of human urinary colony-stimulating factor, however, proved only marginally effective in stimulating granulopoiesis in humans[29]. All these studies suffer from the lack of a homogeneous preparation of colony-stimulating factor. It has recently been shown that recombinant murine multi-CSF or interleukin-3 can stimulate haematopoiesis in mice *in vivo*[30,31]. Large-scale production of recombinant human GM-CSF now permits us to examine its effects *in vivo* using a primate model. We find that the continuous infusion of GM-CSF in healthy monkeys rapidly elicits a dramatic leukocytosis and a substantial reticulocytosis. A similar effect has been observed in one pancytopenic, immunodeficient rhesus macaque. These results suggest that GM-CSF could prove useful in several clinical situations.

To analyse the biological activities of recombinant human GM-CSF on simian progenitor cells, adherence-depleted simian bone marrow mononuclear cells were plated in 0.9% methylcellulose cultures at a cell concentration of 2.5×10^4 cells per ml. In this culture system, picomolar concentrations of purified human recombinant GM-CSF stimulated the terminal differentiation of simian granulocyte/macrophage progenitors (CFU-GM). Eosinophil colonies were not specifically counted (Fig. 1). These results support the earlier observation that conditioned media from the hairy-cell leukaemia cell line Mo can stimulate monkey granulocyte–monocyte colony formation[32]. In the presence of erythropoietin, the hormone also induced the proliferation and differentiation of early erythroid (BFU-E) and multipotential progenitors (CFU-GEM) (Fig. 1). These data confirm previous results obtained with human progenitors which show that GM-CSF is a multi-lineage haematopoietin[11–15]. GM-CSF derived from *Escherichia coli* was as effective in stimulating colony formation as was the glycosylated protein derived from mammalian cells, indicating that carbohydrate modification has little effect on the *in vitro* activity of the haematopoietin (results not shown).

We next analysed the ability of GM-CSF to stimulate the proliferation of enriched populations of simian progenitor cells when plated at low cell densities (data not shown). To determine whether recombinant human GM-CSF acts directly on simian haematopoietic progenitor cells or indirectly through accessory cells, an additional panning step was performed on the adherence-depleted simian bone marrow mononuclear cells so as to remove T cells, B cells, monocytes, natural killer cells and granulocytes. This depletion did not affect the ability of GM-

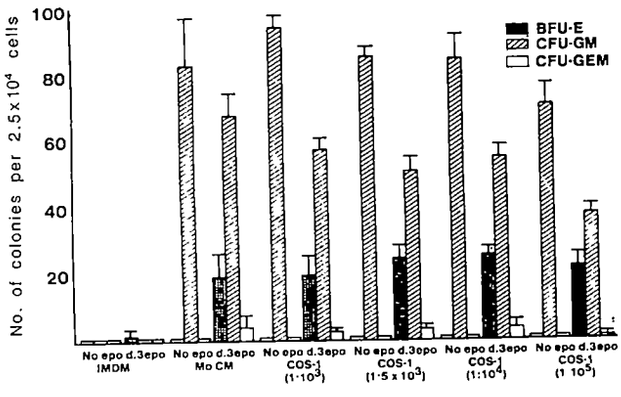


Fig. 1 Biological activity of HPLC-purified recombinant human GM-CSF derived from COS-1 cells on adherent-cell-depleted bone marrow obtained from a cynomolgous macaque (*Macaca fasicularis*) epo, erythropoietin. Bars show the mean (±s:d.) of the colonies in duplicate plates.

Methods. GM-CSF expressed in COS-1 grown in serum-free medium was purified as described previously[6,7]. The GM-CSF expressed in CHO cells grown in serum-free medium was also purified as described elsewhere[6,7]. Heparinized bone marrow was aspirated from the femur of anaesthetized primates, resuspended 1:1 (v:v) in Iscove's modified Dulbecco's medium (IMDM) supplemented with 20% fetal calf serum (FCS) and the mononuclear cell layer was collected after density centrifugation at 20 °C using a Ficoll-Paque (Pharmacia) gradient (specific gravity 1.077). The mononuclear cells were washed three times with IMDM+20% FCS, resuspended at a concentration of 5×10^6 cells ml^{-1}, and depleted of adherent cells by incubating them for 3–4 h on 100×15-mm Lux tissue culture dishes (Miles Laboratories) pretreated with FCS. The non-adherent cells were gently removed and washed twice in IMDM+20% FCS and the adherence depletion step was then repeated overnight. The non-adherent cells were collected, washed twice in IMDM, then resuspended at 2.5×10^4 cells ml^{-1} in 0.9% methylcellulose in IMDM with 30% FCS, 0.9% deionized bovine serum albumin (Sigma fraction V), and 10^{-4} M β-mercaptoethanol[43]. Mo cell-conditioned serum-free medium was added to certain plates as 5% v/v. Highly purified GM-CSF expressed in COS-1 cells was diluted with IMDM so that the protein was at a concentration of 50 $\mu g\ ml^{-1}$. This solution was then diluted still further to final dilutions of $1:10^3$–$1:10^5$ in the methylcellulose cultures. One unit of erythropoietin (Terry Fox Laboratories, Vancouver) was added dropwise in each of the cultures that required the hormone 3 days after the initiation of incubation. The addition of erythropoietin was delayed to minimize or eliminate burst-promoting activity(BPA)-independent erythroid colony formation[12–15].

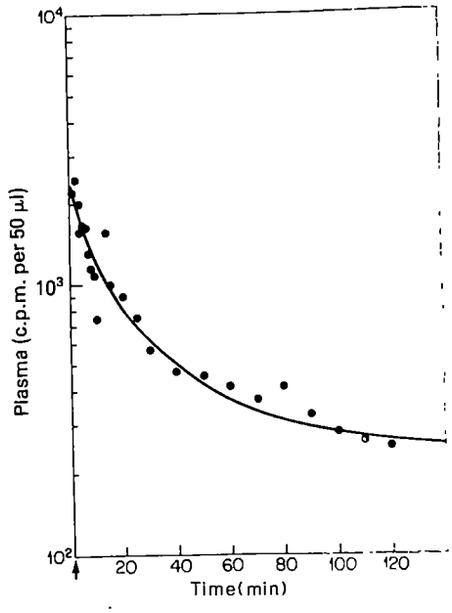


Fig. 2 Circulating plasma clearance of ^{35}S-methionine-labelled CHO-derived recombinant human GM-CSF. The initial, more rapid disappearance of radioactivity from the plasma is called the α phase, while the more prolonged disappearance is the β phase. The phases have a half-life of 7 min and 80–90 min, respectively. **Methods.** ^{35}S-radiolabelled GM-CSF was prepared from CHO cells expressing human GM-CSF by labelling 70% confluent cells with 5 mCi ^{35}S-L-methionine (NEN) in serum-free, methionine-free RPMI (Hazleton Research Laboratories, Denver, Pennsylvania). Supernatants were collected sequentially at 4 and 8 h. The GM-CSF was purified as described above to radiochemical homogeneity and had a specific activity of 0.3 μCi per μg of protein. Approximately 25 μg of GM-CSF metabolically labelled with ^{35}S-methionine, together with ~100 μg of non-radioactive GM-CSF, was inoculated as a single bolus into a cynomolgous macaque. Heparinized blood samples were collected at multiple time points. Aliquots (50 μl) of plasma were added to 1 ml of 5% cold trichloroacetic acid (TCA) and held on ice for 10 min. The samples were filtered through glass-fibre filters, washed with cold TCA, rinsed with cold methanol, dried and counted in anhydrous scintillation fluid (NEN) using a Beckman LS7800 scintillation counter.

CSF to stimulate the formation of any of the different types of colonies when cultured at a low cell density (1,000 cells ml^{-1}). Although these experiments are not definitive, the results are consistent with other studies from our laboratory showing that the pluripoietin activity of Mo cell-conditioned medium acts directly on human progenitors[33] and that antibodies directed against GM-CSF completely neutralize the pluripoietin activity of Mo-conditioned medium (C. Sieff, personal communication).

To assess the importance of GM-CSF in regulating haematopoiesis *in vivo*, we examined the effects of continuous intravenous (i.v.) infusion of the protein on the levels of circulating blood cells in primates. We first analysed the rate of clearance of metabolically labelled haematopoietin from the circulation. The ^{35}S-labelled GM-CSF (0.3 $\mu Ci\ \mu g^{-1}$) was diluted with purified unlabelled GM-CSF (100 μg) and the mixture rapidly injected i.v. into a macaque. The clearance of acid-precipitable GM-CSF from the circulation (Fig. 2) followed the multiphasic kinetics typical of many glycoproteins[34]. Initially, the level of radioactivity in the plasma decreased with an apparent half-life of ~7 min. This initial decay (the α phase) of the protein is probably due largely to the distribution throughout the body fluid of the animal. A second decay component (the β phase) has an apparent half-life of 80–90 min and presumably represents the clearance of the protein by the animal's major organs. Even after 2 h, 10% of the GM-CSF remained in the circulation. Using the apparent half-life of the α phase, we estimated that continuous i.v. infusion at a rate of 50 U per min per kg would maintain the circulating levels of the hormone at a 5–10-fold higher concentration than required to stimulate optimal colony formation *in vitro*.

GM-CSF ($1–2\times10^7$ U per mg) was infused continously at that rate through indwelling venous catheters into seven macaques for varying time intervals and blood samples were drawn daily for complete blood count analysis. Figure 3 shows clearly that the i.v. infusion of GM-CSF (Fig. 3*b*) dramatically increases the leukocyte count, which reaches a level seven times above the preinfusion average, whereas infusion of a control solution (Fig. 3*a*) has negligible effects on blood cell counts. Analysis of a bone marrow aspirate drawn from the monkey's femur on day 7 revealed that the marrow had become hypercellular during the infusion. This rise in leukocyte count was observed within 1–3 days of the start of infusion and was maintained by continued administration of GM-CSF.

Typically, the absolute numbers of neutrophils, band neutrophils, monocytes and lymphocytes all began to increase together. The effects of GM-CSF on circulating neutrophil, monocyte and eosinophil levels were consistent with the demonstrated *in vitro* activities of GM-CSF. This initial rise was usually followed by a 30-fold increase in the eosinophil level. After the infusion was stopped, the haematological profiles returned to normal. Usually, a modest stimulation in the levels of circulating reticulocytes could be observed during the infusion of GM-CSF (Fig. 3*d*) compared with the control infusion (Fig. 3*c*). However, repeated phlebotomy alone had a mild stimulatory effect on erythropoiesis during the control phase of the study, complicating the interpretation of the effect of GM-CSF treatment on this parameter. Results similar to those shown in Fig. 3 have been obtained with all seven animals tested thus far.

The leukocytosis elicted by GM-CSF infusion could be maintained for extended time periods by continued administration of the protein. In one experiment, a macaque infused for 28 days with GM-CSF had leukocyte counts of 30,000–90,000 throughout the infusion (data not shown) without apparent adverse effects. Although the initial leukocytosis obtained during the infusion may result from increased mobilization of mature granulocytes from the marrow, the maintenance of these high levels of circulating blood cells for long periods of time plus the observed marrow hypercellularity suggest that GM-CSF also has a direct effect on haematopoiesis. The maintenance of these high blood cell levels is absolutely dependent on continued administration of GM-CSF because the leukocytosis always resolved on termination of the infusion, usually within several days. In all cases in which we have treated normal animals, the complete haematological profile has always returned to normal.

To test the potential of GM-CSF in the treatment of cytopenias, we administered the protein to a severely debilitated, pancytopenic rhesus monkey (*Macaca mulatta*) that had been naturally infected with a simian type D retrovirus. The animal received ~500 U per min per kg of pyrogen-free recombinant human GM-CSF as a continuous subcutaneous (s.c.) infusion over 7 days. After an initial lag of 3 days, the monkey's leukocyte count began to increase significantly (Fig. 4*a*), rising from an intial level of 1,600 cells μl^{-1} (98% lymphocytes, 2% monocytes) to 23,000 7 days after the start of the infusion (52% neutrophils, 2% band neutrophils, 42% lymphocytes, 4% monocytes). The leukocyte count peaked at 43,700 on day 9 (2 days after the end of GM-CSF administration) and then began to decline, returning to 1,900 cells ml^{-1} by day 18. At the same dose, a healthy rhesus monkey demonstrated a similar response to the s.c. infusion of GM-CSF (Fig. 4*b*), its initial white blood cell count of 6,500 (31% neutrophils, 60% lymphocytes, 6% monocytes, 2% eosinophils, 1% basophils) rising to a maximum level of 64,300 (76% neutrophils, 4% band neutrophils, 7% lymphocytes, 4% monocytes, 8% eosinophils) 9 days after the start of the infusion. On termination of the infusion, the monkey's white blood cell count similarly returned to its initial level.

In the case of the severely pancytopenic monkey, we also observed a dramatic reticulocytosis elicited on infusion with GM-CSF (Fig. 4c). Biologically active erythropoietin was measured in both rhesus monkeys by a ^{3}H-thymidine uptake assay using spleen cells from phenylhydrazine-injected mice[35]. The pancytopenic monkey was found to have higher levels of erythropoietin (320 mU ml^{-1}) than the normal animal (<50 mU ml^{-1}; the assay used was sensitive to ~50 mU ml^{-1}), suggesting that the reticulocytosis observed in the pancytopenic animal may have resulted from a synergy between the infused GM-CSF and the high circulating level of erythropoietin.

Our results demonstrate that GM-CSF is a potent stimulator of haematopoiesis *in vivo*. Because the gene for GM-CSF is highly expressed in activated T cells as well as other cell types, the leukocytosis associated with certain infections may result in part from continued release of this and possibly other

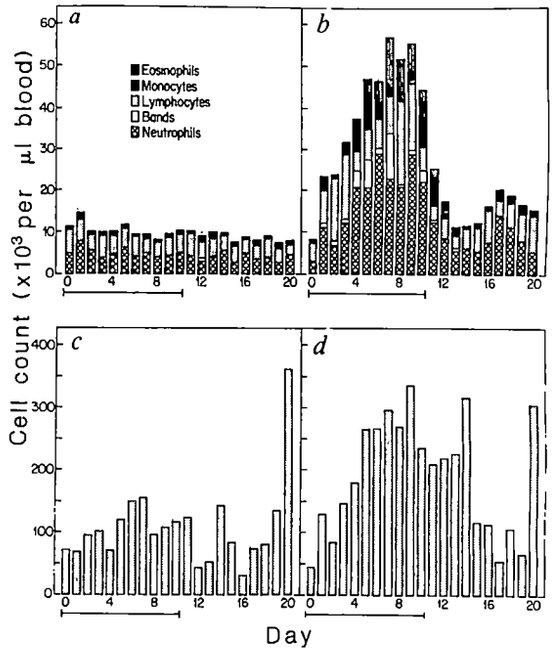


Fig. 3 Serial differential cell counts (*a*, *b*) and reticulocyte counts (*c*, *d*) of a healthy cynomolgous macaque (*M. fasicularis*) continuously infused with carrier alone (*a*, *c*) or recombinant human GM-CSF (*b*, *d*) for 10 days.

Methods. Primates were obtained from and housed at the New England Regional Primate Center. Animals used in this study were maintained in accordance with the guidelines of the Committee on Animals of the Harvard Medical School and those prepared by the Committee on Care and Use of Laboratory Animals of the Institute of Laboratory Animal Resources, National Research Council[44]. GM-CSF expressed in CHO cells grown in serum-free medium was purified as described previously[6,7]. The homogeneous protein from the final reverse-phase HPLC step was prepared for injection by repeated diafiltration against physiological saline (Baxter-Travenol, Deerfield, Illinois). Tween 80 (Rueger Chemical, Irvington, New Jersey) was added to a final concentration of 0.1% in the GM-CSF stock and diluted to 0.01% in 5% dextrose (Cutter Laboratories, Berkeley, California) immediately before infusion. Standard procedures were used to prepare and maintain samples pyrogen-free in the final formulated material. Endotoxin levels were determined by the *Limulus* amoebocyte lysate colorimetric assay (Whittaker Bioproducts, Walkersville, Maryland) and were undetectable (<0.1 endotoxin units ml^{-1}). The activity of the protein was determined by measuring chronic myelogenous leukaemia (CML) peripheral blood myeloblast incorporation of ^{3}H-thymidine in a CSF-dependent proliferation assay which has been described previously[45]. CSF activity was measured relative to a standard preparation to which we had arbitrarily assigned an activity of 20,000 U ml^{-1}. In our assay system, the laboratory standard at a final concentration of 1 U ml^{-1} stimulates half of the maximal possible incorporation of ^{3}H-thymidine by CML peripheral blood myeloblasts. Our laboratory standard also has ~20,000 U ml^{-1} when tested in either the KG-1 or human bone marrow colony-forming assays as described previously[6,7]. The preparation of GM-CSF used had a specific activity of $1–2 \times 10^7$ U per mg. The GM-CSF was infused at a rate of 50 U per min per kg using a continuous infusion pump (Ferring Laboratories, Ridgewood, New Jersey) designed to deliver at a rate of 50–75 $\mu l\ h^{-1}$. Indwelling i.v. catheters were placed in either the iliac or jugular veins. Blood samples were taken after anaesthetizing the animal with ketamine hydrochloride (Bristol Laboratories, Syracuse, New York) and submitted in EDTA for serial blood counts.

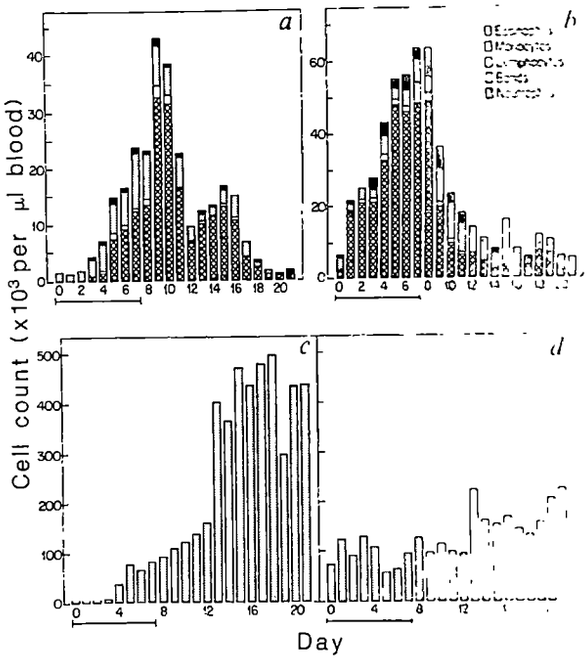


Fig. 4 Serial differential cell counts (*a*, *b*) and reticulocyte (*c*, *d*) counts of a pancytopenic rhesus monkey (*a*, *c*) and a healthy rhesus monkey (*b*, *d*) continuously infused with recombinant human GM-CSF for 7 days.
Methods. GM-CSF was administered s.c. for 1 week using Model 2ML1 Alzet osmotic pumps (Alza, Palo Alto, California) which were surgically implanted. The pancytopenic animal had profuse diarrhoea and was later determined to have been naturally infected with a type D retrovirus by methods previously described[46].

haematopoietins. We are now designing experiments to test this hypothesis. In addition, we are analysing the functional properties of the circulating cells elicited by GM-CSF treatment to assess its role in the activation of mature leukocytes.

The demonstration that GM-CSF is a potent stimulator of haematopoiesis in normal primates provides the opportunity to develop models for testing potential clinical uses of the protein. For example, we have already shown here that virally induced cytopenias, which are a common sequelae of type D infections in simian primates[36-38], may respond to GM-CSF therapy. Moreover, GM-CSF therapy may prove useful in the treatment of other virally induced cytopenias[39], such as is often associated with human AIDS (acquired immune deficiency syndrome)[40,41].The present results also suggest that GM-CSF could prove valuable in patients undergoing bone marrow transplantation or cancer therapy. By shortening and possibly eliminating the leukopenia associated with these treatments, the risk of secondary infections would be reduced. One such approach has already been discussed[42]. The availability of the recombinant human protein should enable us to address these questions.

We thank Drs Mutman Daniel, Norman Letvin, Norval King, R. C. Desrosiers, Ronald Hunt, Mr Mark Metzger, Ms Cynthia Harris, Dorothy Blake, Diane Sawyer and Martha Elliot for assistance; Ms A. Ciarletta, J. Witek-Giannatti, M. Chung and D. P. Luxenburg for purifying and analysing the activity of the protein used; Ms E. Mulkeen for assisting in the analysis of data; Dr Allan Mufson and Ms Jane Aghajanian for the determination of the circulating erythropoietin levels in the two rhesus monkeys; Ms Marybeth Erker for preparation of the manuscript, Drs Steve Emerson, Alan Schwartz and Dr Dagmar Oette for technical advice; and the staff of the Hematology Laboratory at the Children's Hospital of Boston for performing the blood counts. This work was supported in part by Sandoz Ltd, grants from the NIH and the Dyson Foundation, and Division of Research Resources (NIH) grant RR00168 awarded to the New England Regional Primate Research Center.

Received 11 March; accepted 8 May 1986.

1. Stanley, E. R. & Jubinsky, P. J. *Clin Haemat.* **13**, 329-348 (1984).
2. Metcalf, D. *The Hemopoietic Colony Stimulating Factors* (Elsevier, Amsterdam, 1984).
3. Burgess, A. W., Camakaris, J. & Metcalf, D. J. *J. biol. Chem.* **252**, 1998-2003 (1977).
4. Grough, N. M. *et al. Nature* **309**, 763-767 (1984).
5. Gasson, J. C. *et al. Science* **226**, 1339-1342 (1984).
6. Wong, G. G. *et al. Science* **228**, 810-815 (1985).
7. Wong, G. G. *et al.* in *Cancer Cells* Vol. 3 (eds Feramisco, J., Ozanne, B. & Stiles, C.) 235-241 (Cold Spring Harbor Laboratory, New York, 1985).
8. Metcalf, D. *Blood* **67**, 257-267 (1986).
9. Weisbart, R. H., Golde, D. W., Clark, S. C., Wong,. G. G. & Gasson, J. C. *Nature* **315**, 361-363 (1985).
10. Lopez, A. F. *et al. J. clin. Invest.* (in the press).
11. Metcalf, D. *et al. Blood* **67**, 37-45 (1986).
12. Sieff, C. A. *et al. Science* **230**, 1171-1173 (1985).
13. Emerson, S. G. *et al. J. clin. Invest.* **76**, 1286-1290 (1985).
14. Donahue, R. E. *et al. Blood* **66**, 1479-1481 (1985).
15. Sieff, C. A., Emerson, S. G., Mufson, A., Gesner, T. G. & Nathan, D. G. *J. clin. Invest.* **77**, 74-81 (1986).
16. Asano, S. *et al. Blood* **49**, 845-852 (1977).
17. Burlington, H., Cronkite, E. P., Laissne, J. A., Reincke, U. & Shadduck, R. K. *Proc. Soc. exp. Biol. Med.* **153**, 86-92 (1977).
18. Suda, T., Miura, Y., Mizoguchi, H., Kubota, K. & Takaku, F. *Br. J. Cancer* **41**, 980-984 (1980).
19. Lee, M. Y., Sperlin, A. & Dale, D. C. *Expl Hemat.* **8**, 249-255 (1980).
20. Mizoguchi, H., Suda, T., Miura, Y , Kubota, K. & Takaku, F. *Expl Hemat.* **10**, 874-880 (1982).
21. Motoyoshi, K , Suda, T., Takau, F. & Miura, Y. *Blood* **62**, 980-987 (1983).
22. Bessho, M., Hirashima, K., Ando, K., Nara, N. & Momoi, H *Acta haemat. Jap.* **47**, 21 (1984).
23. Yunis, A. A., Jimenez, J. J., Wu, M. & Andreotti, P. E *Expl Hemat* **12**, 843-854 (1984).
24. Lee, M. Y. & Lottsfelt, J. L. *Blood* **64**, 499-506 (1984)
25. Miyanomae, T. *et al. Gann* **76**, 352-358(1985).
26. Johnson, G. R., Whitehead, R. & Nicola, N. A. *Int. J. Cell Cloning* **3**, 91 (1985).
27. Kohsaki, M. *et al. Proc. natn. Acad. Sci. U.S.A.* **80**, 3802-3906 (1983)
28. Metcalf, D. & Stanley, E. R. *Br. J. Haemat.* **21**, 481-492 (1971)
29. Motoyoshi, K., Takaku, F. & Miura, Y. *Blood* **62**, 685 688 (1983)
30. Kindler, V. *et al. Proc. natn. Acad. Sci. U.S.A.* **83**, 1001-1005 (1986)
31. Metcalf, D. *et al.* (in preparation).
32. Golde, D. W. & Hocking, W. G. in *Hematopoietic Cell Differentiation* (ed. Golde D. W. Cline, M. J., Metcalf, D. & Fox, C. F.) 375-383 (Academic, New York, 1978)
33. Linch, D. C. & Nathan, D. G. *Nature* **312**, 775-777 (1984)
34. Shargel, L. & Yu, A. B. C. *Applied Biopharmaceutics and Pharmacokinetics* Appleton-Century-Crofts, Norwalk, Connecticut, 1985).
35. Krystal, G. *Expl Hemat.* **11**, 649-666 (1983)
36. Letvin, N. L. & King, N. W. *Adv. vet. Sci.* **28**, 237-265 (1984)
37. Letvin, N. L. *et al. J. Virol.* **52**, 683-686 (1984).
38. MacKenzie, M. *et al. Lab. Anim. Sci.* **36**, 14-19 (1986)
39. Young, N. & Mortimer, P. *Blood* **63**, 729-737 (1984).
40. Spivak, J. L., Bender, B. S. & Quinn, T. C. *Am. J. Med.* **77**, 224-228 (1984)
41. Zon, L. I. & Groopman, J. E. (in preparation).
42. Gasson, J. C., Chen, I. S. Y., Westbrook, C. A. & Golde, D. W. *Normal and Neoplastic Hematopoiesis* (eds Golde, D. W. & Marks, P. A.) 129-139 (Liss, New York, 1983)
43. Iscove, N. W., Sieber, F. & Winterhalter, K. W. *J. cell. Physiol.* **83**, 309-320 (1974)
44. Committee on Care and Use of Laboratory Animals *DHEW Publ.* NIH 78-23 (rev. 1978)
45. Griffin, J. D. *et al. Blood* **63**, 904-911 (1984).
46. Daniel, M. D. *et al. Science* **223**, 602-605 (1984).

No functional γ-chain transcripts detected in an alloreactive cytotoxic T-cell clone

F. Rupp, G. Frech, H. Hengartner, R. M. Zinkernagel & R. Joho

Institut für Pathologie der Universität Zürich, Universitätsspital, CH-8091 Zürich, Switzerland

Three groups of genes that undergo rearrangements during T-cell maturation have been isolated from T cells[1–13]. Two of them encode the α- and β-subunits of the T-cell antigen receptor and are shared between antigen-specific, major histocompatibility (MHC) class I-restricted cytotoxic T cells and antigen-specific, MHC class II-restricted helper T cells[1–10,14]. The third group of genes, called γ, is preferentially transcribed in cytotoxic T cells[12,15]. This led to the hypothesis that the unidentified γ-gene products could be part of a putative T-cell receptor responsible for MHC class I recognition[16,17]. We report here on the isolation of three different types of γ-gene transcripts of an alloreactive cytotoxic T-cell clone (3F9). Two are derived from two rearrangements that have occurred at the same locus (V_γ 10.8A to J_γ 10.5 and transcribed with C_γ10.5), while the third involves a new V_γ-gene segment that is joined to J_γ13.4 and transcribed with C_γ13.4. All these rearrangements are abortive and lead to the formation of non-functional γ-chain genes because the proper translational reading frame is not maintained. Because the second copy of the C_γ13.4 gene segment is deleted and as C_γ7.5 is considered to be a pseudogene and has not undergone any rearrangements in 3F9, we conclude that the alloreactive cytotoxic T-cell clone 3F9 does not contain a functional transcript of a known γ-chain gene.

3F9 is an alloreactive cytotoxic T-cell clone of BALB/c ($H\text{-}2^d$) origin and is specific for the D^b allele of the murine MHC locus[18]. A complementary DNA library of 3F9 in λgt-11 was constructed[14] and screened with a ^{32}P-labelled oligonucleotide for γ-sequence-bearing clones. Nine γ-positive cDNA clones were isolated, analysed by restriction mapping and sequenced. Three distinct groups of cDNA clones were identified. Figure 1 shows the restriction map of a representative clone from each group (3F9-γ4, -γ6 and -γ7) and the respective sequencing strategy, while Fig. 2 shows the corresponding nucleotide sequence. 3F9-γ4 and -γ7 are transcripts derived from the same gene segments (V_γ10.8A, J_γ10.5 and C_γ10.5) but are different at the variable-joining (V–J) junction (Fig. 2). They therefore represent two rearrangement events involving both copies of the same gene on both chromosomes.

Although 3F9-γ4 and -γ7 use the same V_γ10.8A gene segment, they differ by one nucleotide in the variable region (position 216, Fig. 2). If this difference is not due to a cloning artefact (which we cannot rule out), it might be a somatic mutation, since the T-cell clone 3F9 is derived from a homozygous inbred mouse strain (BALB/c). 3F9-γ6 is a representative of the third group. Although it is not a full-length cDNA clone, it carries nucleotide sequences similar to the already known V_γ genes. The presumptive V_γ region of 3F9-γ6 is ~70% homologous with the three known variable regions V_γ10.8A and B and V_γ5.7 (ref. 13). We therefore conclude that 3F9-γ6 carries part of a new V_γ gene which has not been identified previously at the genomic level. The J_γ region of 3F9-γ6 is identical to the genomic J_γ13.4 gene segment and the constant region is different but highly homologous to the genomic C_γ10.5 and C_γ7.5 (ref. 13). For these reasons we believe that the C_γ gene expressed in 3F9-γ6 is derived from the genomic C_γ13.4. Figure 2 also compares the nucleotide sequences of the C_γ regions of 3F9-γ4 (corresponding to C_γ10.5), 3F9-γ6 (presumably C_γ13.4) and the genomic C_γ7.5 (ref. 13). Both C_γ7.5 and $C_{\gamma 6}$ gene segments have a 15-nucleotide insertion within the coding region at position 776; this insert conserves the original reading frame. $C_{\gamma 6}$ differs from C_γ10.5 and C_γ7.5 by 53 and 37 nucleotides, respectively. Between the 3′ end of V_γ10.8A and the 5′ end of J_γ10.5 in 3F9-γ4, the sequence CCCCG can be found. These nucleotides are not present in the corresponding germline gene segments. In 3F9-γ7 six nucleotides at the 3′ end of the V_γ10.8A gene segment have been deleted and the dinucleotide AT precedes the J_γ10.5 gene segment. These sequences could represent a portion of an as yet unidentified D (diversity) gene segment or the result of a terminal deoxynucleotidyltransferase activity during V–J rearrangement. All these rearrangements, however, produce non-functional RNA transcripts, since the V_γ–J_γ joining did not result in a proper translational reading frame. Stop codons are present in the J segments of 3F9-γ4 and -γ6 and at the V–J junction in 3F9-γ7 (Fig. 2).

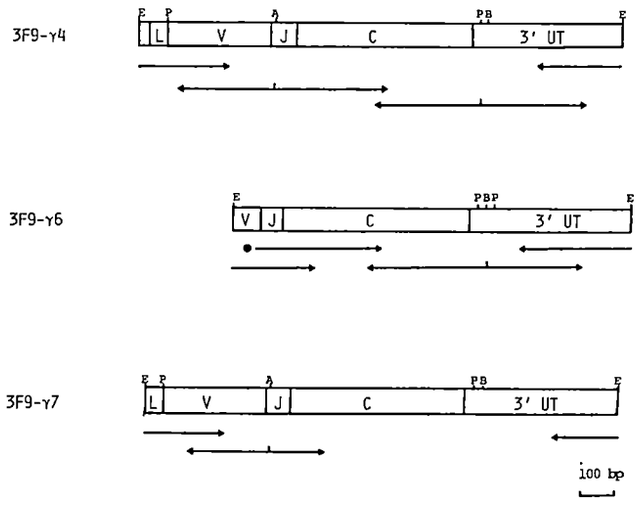


Fig. 1 Restriction map and sequence strategy of the longest inserts from the three different groups of 3F9-γ cDNA clones. Restriction enzyme sites are indicated by small letters: E, *Eco*RI; P, *Pvu*II; B, *Ban*I; A, *Ava*I. Part of the sequence of 3F9-γ6 was derived from a shorter clone of the same group (indicated by •⟶) sharing the same 3′ end of the $V_{\gamma 6}$ gene segment and the same V–J junction.

To evaluate whether the second copy of the C_γ13.4 gene segment located on the homologous chromosome could have been rearranged, we analysed the γ-chain gene rearrangements at the genomic level by Southern blot analysis. Considering the length of the restriction fragments bearing the V_γ and C_γ gene segments, it can be predicted that the rearrangement of V_γ10.8A to J_γ10.5 creates a new band of ~16 kilobases (kb)[13]. The Southern blot (Fig. 3) shows that both chromosomes at the V_γ10.8A and J_γ10.5 loci have undergone rearrangements in 3F9 (as expected from the analysis of 3F9-γ4 and -γ7) since a band at 16 kb can be detected and the germline bands at 10.5 and 10.8 kb are no longer seen. The germline band at 13.4 kb, containing the C_γ13.4 locus, also disappears and a new one at ~20 kb emerges. Hybridization with a ^{32}P-labelled 3F9-γ4 probe (bearing V_γ10.8A and C_γ10.5) or with a 3F9-γ6 probe (bearing part of the new V_γ gene and C_γ13.4) shows that this band is of much lower intensity and probably contains only one rearranged copy of the C_γ13.4 segment (Fig. 3*a*). The 16-kb band containing two rearranged C_γ10.5 gene segments and the 7.5-kb band with the two non-rearranged C_γ7.5 gene segments are clearly more intense than the 20-kb band bearing the rearranged C_γ13.4 locus (this analysis has been done five times with identical results). This finding and the fact that no additional rearranged bands can be detected are strong circumstantial evidence that the second copy of the C_γ13.4 gene segment on the homologous chromosome has been deleted. This conclusion is also strengthened by the cDNA screening results. From the nine

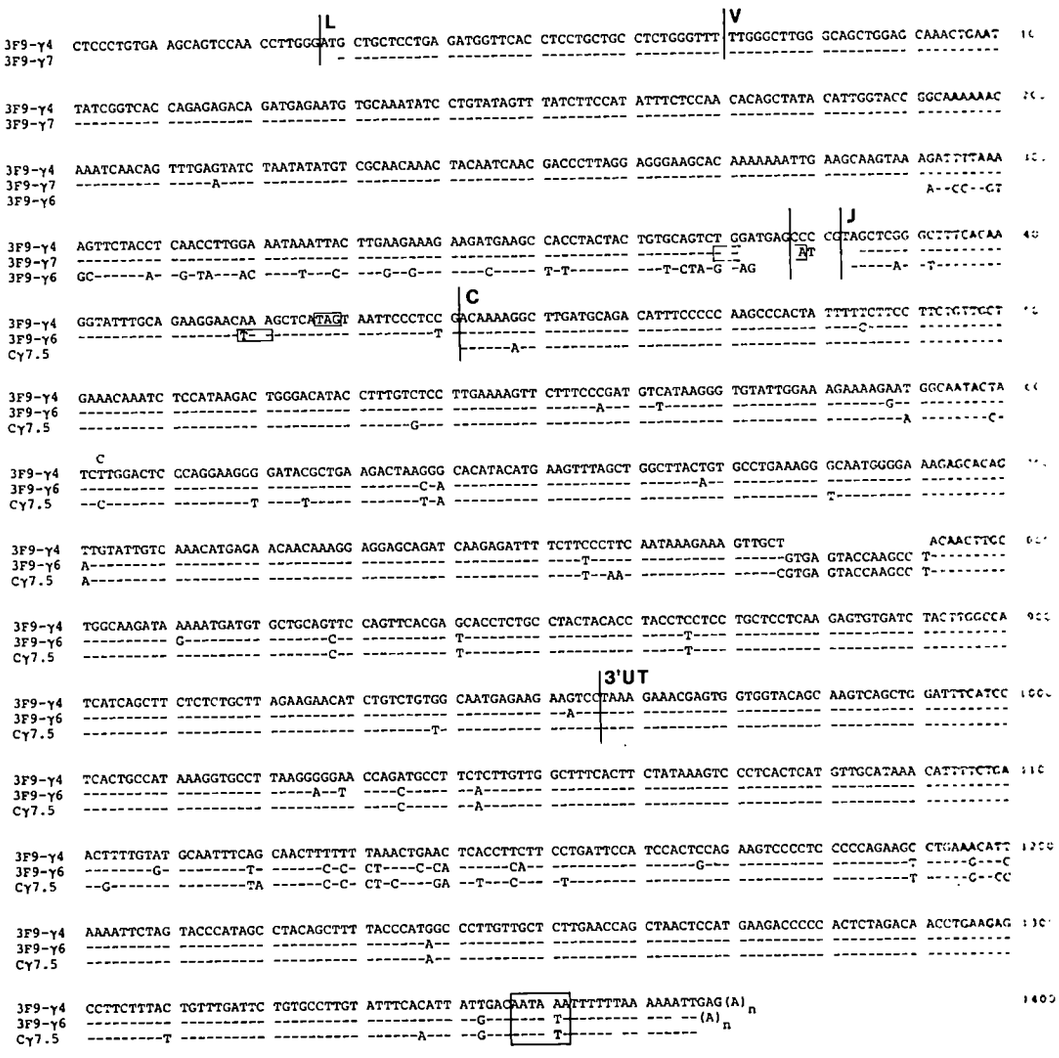


Fig. 2 Nucleotide sequence of 3F9-γ4, γ6 and -γ7 cDNA clones. The sequence of the genomic C_γ7.5 gene segment[13] is also indicated. The synthetic oligonucleotide used for screening was complementary to the C_γ region from position 459 to 482 and was synthesized using an Applied Biosystems 380A DNA synthesizer. The construction of the λgt11-3F9 cDNA library has been described elsewhere[14] and the nucleotide sequence analysis was performed according to the technique of Maxam and Gilbert[22]. The stop codons and the polyadenylation signals of the different C_γ-gene segments are boxed. The 3F9-γ4 cDNA clone and the genomic C_γ10.5 gene segment show a difference at position 603 (T→C).

γ-gene transcripts isolated out of 10^5 recombinant phages, six are derived from the rearranged C_γ10.5 locus (3F9-γ4 and -γ7 types) and the other three, which have all been sequenced, are identical and are exclusively derived from one type of rearrangement event at the C_γ13.4 locus (3F9-γ6 type).

The γ6 probe reveals an additional faint band at 5.0 kb in the germline DNA; this probably represents a genomic V_γ gene segment that cross-hybridizes to the 3F9-Vγ6 gene (Fig. 3*a*, lane 3). The weak signal intensity is probably due to the fact that the 3F9-γ6 probe contains only one-third of the complete V_γ gene segment.

Another observation concerns the pseudogene C_γ7.5 (ref. 13). This gene segment contains an altered splice donor site and carries an unusual polyadenylation signal, AATATA instead of AATAAA. Interestingly, the sequence of C_γ13.4 in 3F9-γ6 shows exactly the same altered polyadenylation signal but, despite this, it is polyadenylated correctly. Therefore, C_γ7.5 should be a pseudogene as a result of its altered splice donor site and not because of its different polyadenylation signal. Also, C_γ7.5 and V_γ5.7 are absent from the genome of B10 mice, and in 3F9 (BALB/c) they are neither rearranged nor transcribed (Fig. 3*b*). The absence in B10 could imply that there is no 'positive' selection pressure on this gene, further indicating that it could represent a non-functional gene.

Our study shows that multiple rearrangement events can occur at different γ loci and that the $V\gamma$10.8A gene segment is always expressed with the J_γ10.5 nd C_γ10.5 genes as described previously[12,15]. From these findings and from the fact that each C_γ gene segment carries its own J_γ gene segment, we believe that the γ-gene family is organized similarly to the immunoglobulin λ-light-chain gene family. In the λ-chain family, two different V_λ regions can only rearrange to a limited number of *J*-gene segments which are associated with their respective C_λ genes[19–21].

The finding that both the C_γ7.5 and the V_γ5.7 gene segments are missing in the C57BL/10 mouse strain indicates that these genes could be associated as a separate set of V_γ, J_γ and C_γ gene segments. Since a functional γ-chain transcript could not be detected in the alloreactive cytotoxic T-cell clone 3F9, we conclude that γ-chains are not necessary for the killing mechanism, at least for alloreactive cytotoxic T cells. Furthermore, if alloreactive and antigen-specific, MHC-restricted cytotoxic T

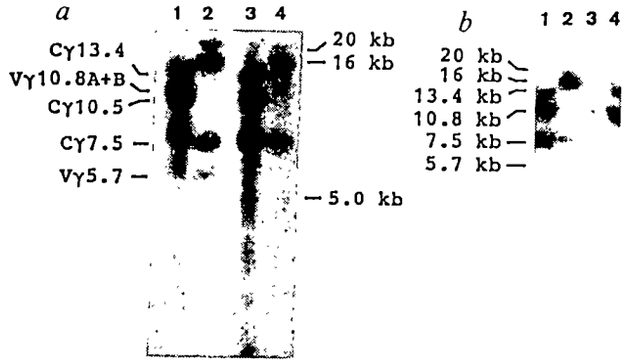


Fig. 3 Southern blot analysis of genomic and 3F9 DNA. *a*, Lanes 1 and 2 probed with ^{32}P-labelled 3F9-γ4, lanes 3 and 4 with 3F9-γ6. BALB/c kidney (lanes 1, 3), 3F9 (lanes 2, 4). *b*, BALB/c kidney, 3F9, C57BL/6 and C57BL/10 kidney DNA (lanes 1-4, respectively) probed with ^{32}P-labelled 3F9-γ4. DNA was extracted from either kidney or 3F9 T cells, digested with *Eco*RI, electrophoresed through 0.5% (*a*) or 0.7% (*b*) agarose gels, treated with 0.25 M HCl and transferred to nitrocellulose[23]. The filters were hybridized to ^{32}P-labelled probes, washed in 0.3 × SSPE, 0.1% SDS at 65 °C and autoradiographed. Each Southern blot analysis was performed five times.

cells use the same recognition mechanism via the αβ T-cell receptor, then the γ-chains are not relevant for recognition. If, however, the still elusive γ-chains are somehow involved in MHC class I recognition in antigen-specific, MHC-restricted cytotoxic T cells, then the recognition mechanism of alloreactive versus antigen-specific, MHC-restricted cytotoxic T cells is different. This could imply that alloreactive cytotoxic T cells either do not need a second receptor for recognition and mediation of effector function or that the determinants functioning as 'restriction' elements of these T cells are recognized by some other unidentified molecules.

We thank Dr Martin Billeter for helpful discussions and Dr Roberto Cattaneo for the synthesis of the γ-oligonucleotide. This work was supported by grants 3.765-0.80 and 3.329-0.82 of the Schweizerischer Nationalfonds and a grant from the Roche Research Foundation.

Note added in proof: Iwamoto *et al.* (*J. exp. Med.*, in the press) have isolated a cDNA clone from a hapten-specific T cell bearing a known V_γ region associated with a new *J-C* region which is similar to, but does not crosshybridize with, any known C_γ region genes. We have isolated similar γ-like transcripts from 3F9, but do not yet know if these clones contain an open reading frame.

Received 16 December 1985; accepted 3 April 1986.

1. Yanagi, Y. *et al. Nature* **308**, 145-149 (1984).
2. Hedrick, S. M., Cohen, D. I., Nielsen, E. A. & Davis, M. M. *Nature* **308**, 149-158 (1984).
3. Chien, Y., Gascoigne, N. R. J., Kavaler, J., Lee, N. E. & Davis, M. M. *Nature* **309**, 322-326 (1984).
4. Siu, G. *et al. Cell* **37**, 393-401 (1984).
5. Gascoigne, N. R. J., Chien, Y., Becker, D. M., Kavaler, J. & Davis, M. M. *Nature* **310**, 387-391 (1984).
6. Siu, G. *et al. Nature* **311**, 344-350 (1984).
7. Hayday, A. C. *et al. Nature* **316**, 828-832 (1985).
8. Winoto, A., Mjolsness, S. & Hood, L. *Nature* **316**, 832-836 (1985).
9. Yoshikai, Y. *et al. Nature* **316**, 837-839 (1985).
10. Saito, H., Kranz, D. M., Eisen, H. N. & Tonegawa, S. *Nature* **312**, 36-40 (1984).
11. Saito, H. *et al. Nature* **309**, 757-762 (1984).
12. Kranz, D. M. *et al. Nature* **319**, 752-755 (1985).
13. Hayday, A. C. *et al. Cell* **40**, 259-269 (1985).
14. Rupp, F., Acha-Orbea, H., Hengartner, H., Zinkernagel, R. M. & Joho, R. *Nature* **315**, 425-427 (1985).
15. Heilig, J. S. *et al. Nature* **317**, 68-70 (1985).
16. Raulet, D. H., Garmann, R. D., Saito, H. & Tonegawa, S. *Nature* **314**, 103-107 (1985).
17. Pernis, B. & Axel, R. *Cell* **41**, 13-16 (1985).
18. Acha-Orbea, H., Zinkernagel, R. M. & Hengartner, H. *Eur. J. Immun.* **15**, 31-36 (1985).
19. Azuma, T., Steiner, L. A. & Eisen, H. *Proc. natn. Acad. Sci. U.S.A.* **78**, 569-573 (1981).
20. Blomberg, B., Traunecker, A., Eisen, H. N. & Tonegawa, S. *Proc. natn. Acad. Sci. U.S.A.* **78**, 3765-3769 (1981).
21. Blomberg, B. & Tonegawa, S. *Proc. natn. Acad. Sci. U.S.A.* **79**, 530-533 (1982).
22. Maxam, M. & Gilbert, W. *Meth. Enzym.* **65**, 499-560 (1980).
23. Southern, E. *J. molec. Biol.* **98**, 503 (1975).

A functional γ gene formed from known γ-gene segments is not necessary for antigen-specific responses of murine cytotoxic T lymphocytes

E. B. Reilly, D. M. Kranz, S. Tonegawa & H. N. Eisen

Center for Cancer Research and Department of Biology, Massachusetts Institute of Technology, Cambridge, Massachusetts 02139, USA

Structural similarities between surface immunoglobulins (s Ig) on B cells and antigen-specific receptors on T cells suggest that a T cell, like a B cell, should express only two immunoglobulin-like genes, one for each subunit of the disulphide-linked, heterodimeric, antigen-specific (αβ) T-cell receptor. However, cytotoxic T lymphocytes (T_c cells) and immature thymocytes also contain RNA transcripts of a third immunoglobulin-like gene, called γ (refs 1-4). A polypeptide corresponding to the γ gene has not yet been identified and the function of this gene remains an enigma. Judging from its nucleotide sequence, the rearranged γ gene is expected to encode an integral membrane polypeptide chain, and γ complementary DNAs from two cloned T_c cell lines have previously been found to have different sequences around the *V-J* (variable region-joining region) junction[1,2], suggesting that, in these cells, the γ-gene product is a clonally diverse surface structure that may form part of an as yet unidentified, antigen-specific receptor. To analyse further the extent of diversity of the γ-gene product, we have determined the partial sequences of 11 γ cDNA clones from three other cloned T_c cell lines, and report here that the sequences are indeed clonally diverse, but in all instances they are out-of-phase in the region of the *V-J* junction. This finding and the pattern of γ-gene rearrangements in these cell lines indicate that a polypeptide product of the previously reported γ gene, *V2J2-C2*, is not expressed in them and is, therefore, not necessary for the antigen-specific cytotoxic and proliferative responses of these mature T cells.

The cloned T_c cell lines examined (described in Table 1) were derived from BALB.B ($H\text{-}2^b$) and BALB.K ($H\text{-}2^k$) mice that had been injected several times ('hyperimmunized') with P815 cells (a DBA/2 ($H\text{-}2^d$) mastocytoma). The cell lines were specific for the class I histocompatibility antigen L^d or D^d and had the L3T4$^-$, Lyt 2$^+$ phenotype expected of T_c cells. cDNA libraries were prepared from these cell lines, γ-positive cDNA clones were identified, and partial nucleotide sequences were determined (see Fig. 1).

Hayday *et al.*[5] previously described three *V*, and *J* and three *C* (constant) γ-gene segments and demonstrated that the J_γ and C_γ gene segments are paired as in the immunoglobulin λ gene family[6,7]. To simplify discussion, these γ-gene segments are referred to here as follows (their previous designations, based on the size, in kilobases (kb), of the *Eco*RI fragment on which each is found, are given in parentheses): *V*1 (10.8B), *V*2 (10.8A), *V*3 (5.7), *J*1-*C*1 (13.4), *J*2-*C*2 (10.5) and *J*3-*C*3 (7.5).

Except for variations in the region of the *V-J* junction, the sequences of the 11 cDNA clones were all identical to the previously described sequence of γcDNA clones (pHDS 4/203)[1] from the T_c cell line 2C (also of BALB.B origin and specific for L^d)[8]. As shown in Fig. 1, in clone pHDS 4/203 from 2C cells, the insertion of an A·T dinucleotide between the *V*2 and *J*2-*C*2 gene segments established an in-frame join; the resulting sequence can encode a full-length γ polypeptide chain[1,2]. However, for all the γ cDNA clones from the three cell lines listed in Table 1, the various sequences in the vicinity of the *V-J* junction result in out-of-frame joins that are not expected to yield full-length γ chains. Thus, for γ cDNA from 3H-2 cells

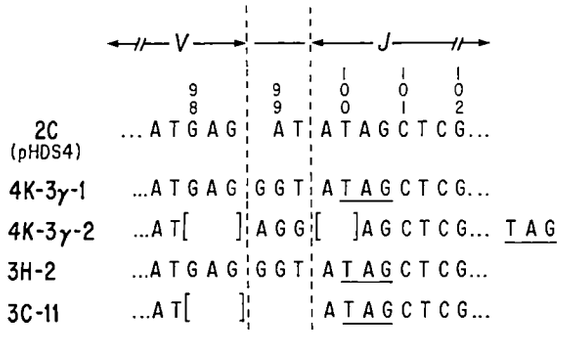


Fig. 1 Nucleotide sequences of γ cDNA clones in the region of the *V–J* junction. Nucleotides shown between the vertical broken lines are not encoded by known V_γ or J_γ gene segments[5]. Brackets indicate deletions. The codons are numbered according to the previously described γ clone pHDS4 from the T_c line 2C[1,2], and premature termination codons are underlined (the termination codon for 4K-3γ-2 occurs ~45 nucleotides downstream).
Methods. cDNA libraries were prepared in λgt10 essentially as described elsewhere[15], and screened with a C_γ probe (pHDS4)[1]. For every 100,000 plaques screened, 3–4 C_γ-hybridizing plaques and 60 C_β-hybridizing plaques were detected, on average. A total of 11 γ cDNA were sequenced by the method of Maxam and Gilbert[16]: 4 of the 4K-3γ-1 type, 2 of the 4K-3γ-2 type (both from 4K-3E), 4 of the 3H-2 type, and 1 of the 3C-11 type.

and for one of the γ cDNA clones from 4K-3E cells (4K-3γ-1), an insert of three nucleotides (GGT) at the *V–J* junction results in premature chain termination. In another γ clone from 4K-3E cells (4K-3γ-2), a different set of three nucleotides (AGG) is inserted at the *V–J* junction and both the last three nucleotides of the *V2* gene segment (GAG) and the first two nucleotides of the *J2* gene segment (AT) are deleted; the result is a termination codon 45 nucleotides downstream of the *V–J* junction. Finally, in the γ cDNA clones of 3C-11 cells, no nucleotides are inserted between the 3′ end of *V2* and the 5′ end of *J2* gene segments and there is a deletion of the last three nucleotides of *V2*; the result is a termination codon in the *J* region (Fig. 1).

The significance of the abberrant γ transcripts in the cell lines listed in Table 1 is apparent on inspection of their respective γ-gene rearrangements. As shown in the Southern blot hybridization patterns (Fig. 2), the 4K-3E cell line, like the previously described 2C cell line[2], has both the 16- and the 22-kb rearranged γ-positive fragments. In 2C cells the 16-kb fragment was shown to contain a rearranged γ gene corresponding to the assembly of *V2J2–C2* gene segments[5]. As there are no differences between the 341 sequenced nucleotides of 4K-3γ-1 (data not shown) and the *V2J2–C2* γ gene of 2C (except at the region of the *V–J* junction), it is probable that this 4K-3E γ cDNA clone represents a *V2J2–C2* γ gene on the 16-kb fragment. Indeed, there are probably two rearranged *V2J2–C2* γ genes in the 4K-3E cell line (one from each chromosome), because these cells do not have the germline configuration of the *J2–C2* γ-gene segments (Fig. 2, lane 5). It is thus of interest that a second γ cDNA clone (4K-3γ-2) from 4K-3E cells also has an out-of-frame *V–J* join (Fig. 1). The rearrangements of some of the other known gene segments also could not encode a γ-chain in these cells: thus, the third C_γ gene segment (*C3*) is defective[5], and a γ gene resulting from rearrangement of V_3 to *J1–C1* or to *J2–C2* would have been detected in Fig. 2 (see ref. 5). The 22 kb rearranged fragment in 4K-3 cells will be discussed below.

Analyses of two other cell lines, 3H-2 and 3C-11, also suggested that a polypeptide chain encoded by the *V2J2–C2* γ gene[2,5] need not be expressed in cytolytically active T_c cells. Southern blots revealed that each of these cell lines has a 16-kb,

Table 1 Cloned cytotoxic T cells

Clone	Strain of origin	Specificity	Lyt 2	L3T4
3C-11	BALB.B (*H-2*^{b})	D^d	+	−
3H-2	BALB.K (*H-2*^{k})	D^d	+	−
4K-3	BALB.K (*H-2*^{k})	L^d	+	−

BALB.B (*H-2*^{b}) or BALB.K (*H-2*^{k}) mice were injected intraperitoneally with ~2.5×10^7 irradiated (3,000 rad) P815 cells (a DBA/2 (*H-2*^{d}) mastocytoma) at 3-week intervals, either three (clones 3C-11 and 3H-2) or four (clone 4K-3) times; 1–2 weeks after the final injection, alloreactive cloned T_c lines were derived from spleen cells as described elsewhere . Specificity in target cell lysis was determined by a standard 4-h ^{51}Cr-release assay[14] using as targets mouse L-cells transfected with D^d (cell line T4.8.3) or L^d (cell line T1.1.1) class I MHC antigens (provided by J. Seidman). At an effector/target cell (ratio of 5:1, the per cent ^{51}Cr-release from the appropriately labelled target cell was 58%, 83% and 39% for lines 3C-11, 3H-2 and 4K-3, respectively. The L3T4$^-$, Lyt 2$^+$ surface phenotype was determined by fluorescence-activated cell sorting (System 50-H, Ortho Diagnostic) using rat monoclonal antibodies against Lyt 2 (536.7; given by F. Fitch) and L3T4 (GK1.5; given by K. Wall).

fragment with a rearranged γ gene (Fig. 2). Moreover, the blots showed that these cells also contain unrearranged germline C_γ gene segments (compare lanes 1–4 of Fig. 2; see ref. 5). Thus it seems that in both the 3H-2 and 3C-11 cell lines there is only a single rearranged *V2J2–C2* γ gene in the γ-positive 16-kb fragment, and in both cell lines this gene is not functional. Thus, four γ cDNA clones from 3H-2 cells yielded the same sequence, which was identical to that of pHDS 4/203 of 2C cells except for the out-of-frame join in the region of the *V–J* junction (Fig. 1). For the 3C-11 cell line only a single γ cDNA clone was analysed and it also had an out-of-frame *V–J* join (Fig. 1). As these cell lines have been found (S. Latt, personal communication) to be predominantly diploid (80–85% of the cells in the 3C-11 clone and 65% of those in 4K-3L are diploid), these results suggest strongly that all of their rearranged *V2J2–C2* γ genes have out-of-frame joins.

Taking all the above results together, all three of the cytolytically active T_c cell lines studied here appear to be incapable of producing a γ-chain that is encoded by the *V2J2–C2* γ gene. Some additional V_γ gene segments, not cross-hybridizing with the *V1*, *V2* and *V3* γ-gene segments, have recently been identified (J. Heilig and S.T., manuscript submitted and ref. 18) and found, when rearranged, to be joined with the *J1–C1* segment; hence they would have been detected by screening libraries with probes that hybridize with the C_γ1 gene segment. Moreover, since both of the *J2–C2* gene segments in 4K-3 cells are rearranged to *V2* in the 16-kb fragment, it seems unlikely that the newly identified V_γ gene segments (or any additional ones) can be expressed in these cells, unless they are rearranged to as yet unidentified *J–C* γ-gene segments; if such gene segments exist, they do not cross-hybridize with the known *J–C* γ-gene segments. The arguments applied here to some cloned T_c cells also apply to certain T-helper (T_H) cells, which do not express the previously described γ-gene segments[9]. Of course, the conclusion that functional T_c and T_h cells need not express γ-chains must be considered provisional for both cell types, because it is possible that as yet unidentified V_γ and J_γ–C_γ gene segments, not cross-hybridizing with the known γ-gene segments, might encode γ-chains in these cells.

Could 4K-3 cells have in-frame γ transcript of a rearranged γ gene of the 22 kb fragment? This fragment has recently been shown to represent an incomplete *Eco*RI digest of a rearrangement in which the newly identified Vγ4 gene segment is joined to the J1–C1 gene segment (J. Heilig and S.T., in preparation). Complete digestion yielded a somewhat smaller fragment not easily resolved from the 16 kb (*V2J2–C2*) fragment. Thus, complete digestion of the *V J1–C1* γ gene may account for the

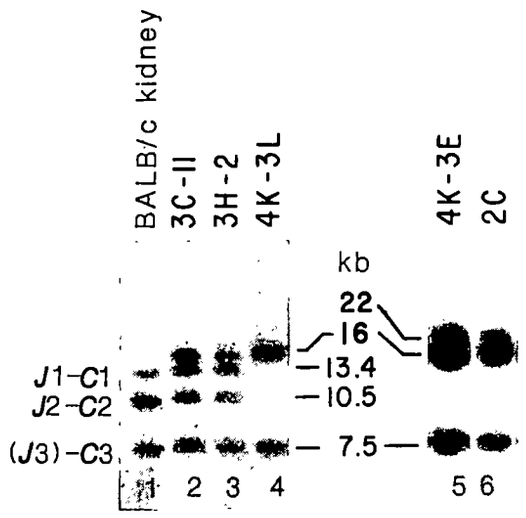


Fig. 2 Southern blot analysis of T_c DNA hybridized to a C_γ probe (pHDS4)[1]. DNA from BALB/c kidney (lane 1) has germline *J1-C1*, *J2-C2* and *(J3)-C3* gene segments on fragments of 13.4, 10.5 and 7.5 kb, respectively. DNAs from T_c lines 3C-11 and 3H-2 (lanes 2 and 3) have germline (that is, unrearranged) 13.4-kb (*J1-C1*) and 10.5-kb (*J2-C2*) fragments. The Southern blot of DNA from the 4K-3 cells (4K-3E) was repeated from cells that had been in culture for about 6 months (4K-3L). The only difference was the presence of a 22 kb fragment in the DNA from 4K-3E cells. This fragment represents an incomplete digest of a *V4J1-C1* γ gene rearrangement. The 4K-3L cells retained specificity for the L^d antigen and were virtually as active cytolytically as 4K-3E cells. DNAs (2–3 μg of each) were digested with *Eco*RI, electrophoresed through 0.8% agarose gels and blotted onto nitrocellulose[17]. Blots were hybridized at 42 °C in 50% formamide and 5×SSC and filters were washed at 65 °C in 0.2×SSC.

absence of the 22 kb fragment in the Southern blot of 4K-3 cells that had been in continuous culture for about six months (designated 4K-3L cells, Fig. 2, lane 4). In any case, the Vγ4 gene segment does not seem to be transcribed in 4K-3 cells or in any of the other mature T cell lines analysed thus far (unpublished observations).

The relative abundance of γ transcripts in immature thymocytes has prompted the speculation that γ-containing, antigen-specific receptors of these cells may be involved in the intrathymic selection of self-MHC (major histocompatibility complex)-restricted T cells, that is, lymphocytes that can distinguish between self- and non-self-MHC[3,4]. This distinction underlies the MHC-restriction of antigen recognition that is characteristic of T_c (and T_h) cells. There are no reasons to doubt that the three cell lines analysed here, although alloreactive (anti-L^d or D^d), are representative of typical MHC-restricted T_c cells. Whether they have ever expressed a functional γ transcript is thus a question of considerable interest. It seems unlikely that the *V2J2-C2* γ gene could have been expressed at any time in 4K-3, 3H-2 or 3C-11 cells because in these cells all copies of this gene are out-of-phase. However it is possible that a functional γ gene could have been expressed in immature progenitors of the cloned 4K-3, 3C-11, and 3H-2 cell lines formed by rearrangement of one of the recently identified *V*γ gene segments to *J1-C1* (J. Heilig and S.T., manuscript in preparation and ref. 18).

Finally, we note that altogether in the four distinct γ cDNA clones analysed here, more than 500 V_γ and J_γ nucleotides were sequenced and, except for those at the *V-J* junction, all are identical to those in the germline *V2* and *J2* gene segments[5]. The absence of nucleotide replacements is notable because the γ cDNA clones analysed were from cloned T_c cell lines that had been derived from hyperimmunized mice. In contrast, a previous analysis of immunoglobulin light-chains (λ1) transcripts from hyperimmunized mice revealed that *V*-domain nucleotide substitutions in these chains occurred with an average frequency of ~0.01 (that is ~3 per 330 nucleotides; ref. 10 and K. Tamoto, E. B. R. T. Azuma and H.N.E., in preparation). If somatic mutations in the transcribed immunoglobulin-like genes in T cells from hyperimmunized mice matched in frequency those in immunoglobulin light chain (λ1) genes in such mice, five nucleotide replacements would have been expected in the γ sequences determined here. As none were seen, our findings support growing evidence that somatic mutations are less frequent in T than in B cells[11,12]. One objection which could be raised is that the absence of somatic mutations in a rearranged γ gene that is not expressed as a polypeptide chain is not relevant for the frequency of somatic mutations in α and β genes, which are expressed as polypeptide chains. However, somatic mutations in a rearranged out-of-phase κ gene have been described[13]. Moreover, it seems reasonable to expect that cells in which somatic mutations have occurred in immunoglobulin and immunoglobulin-like genes that are expressed as polypeptide chains may well also have mutations in rearranged immunoglobulin-like genes that are transcribed but not translated into protein. Indeed, the latter mutations should be particularly informative, because they are not subject to selection by antigen or other agents (for example anti-idiotypes).

We thank Mimi Rasmussen for technical assistance, Haruo Saito for the pHDS 4 γ clone, Samuel Latt and Helene Stroh for determining chromosome numbers in clones 4K-3 and 3C-11, and Ann Hicks for preparation of the manuscript. This work was supported in part by NIH research grants (CA28900, CA15472 and AI-17879 and a NIH Cancer Center Core Grant (CA14051). D.M.K. is a Postdoctoral Fellow of the Medical Foundation.

Note added in proof: Recently another *J*γ*C*γ gene segment (J4-C4) which does not crosshybridize with the previously reported JC segments has been described by Iwamoto *et al.* (*J. exp. Med.*, in the press).

Received 24 December 1985; accepted 21 March 1986.

1. Saito, H. *et al. Nature* **309**, 757–762 (1984).
2. Kranz, D. M. *et al. Nature* **313**, 752–755 (1985).
3. Raulet, D., Garman, R., Saito, H. & Tonegawa, S. *Nature* **314**, 103–107 (1985).
4. Snodgrass, H. P., Dembíc, Z., Steinmetz, M. & von Boehmer, H. *Nature* **315**, 232–233 (1985).
5. Hayday, A. C. *et al. Cell* **40**, 259–269 (1985)
6. Blomberg, B., Traunecker, A., Eisen, H. N. & Tonegawa, S. *Proc. natn. Acad. Sci. U.S.A.* **78**, 3765–3769 (1981).
7. Miller, J., Bothwell, A. & Storb, U. *Proc. natn. Acad. Sci. U.S.A.* **78**, 3829–3833 (1981).
8. Sitkovsky, M. V., Pasternack, M. S. & Eisen, H. N. *J. Immun.* **129**, 1372–1376 (1982).
9. Heilig, J. S. *et al. Nature* **17**, 68–70 (1985)
10. Eisen, H. N. & Reilly, E. B. *A. Rev. Immun.* **3**, 337–365 (1985).
11. Chien, Y., Gascoigne, N. R. J., Kavaler, J., Lee, N. E. & Davis, M. M. *Nature* **309**, 322–326 (1985).
12. Ikuto, K., Ogura, T., Shimizu, A. & Honjo, T. *Proc. natn. Acad. Sci. U.S.A.* **82**, 7701–7705 (1985).
13. Pech, M., Höchtl, J., Schnell, H. & Zachau, H. G. *Nature* **291**, 668–670 (1981).
14. Grabstein, L. in *Selected Methods in Cellular Immunology* (eds Mishell, B. B. & Shiigi, S. M.) 124–137 (Freeman, San Francisco, 1980)
15. Toole, J. J. *et al. Nature* **312**, 342–347 (1984).
16. Maxam, A. M. & Gilbert, W. *Meth. Enzym.* **65**, 499–560 (1980).
17. Southern, E. M. *J molec. Biol.* **98**, 503–517 (1975).
18. Gorman, R. D., Doherty, P. J. & Raulet, D. H. *Cell* (in the press).

Corticotropin releasing factor induction of leukocyte-derived immunoreactive ACTH and endorphins

Eric M. Smith*, Audrey C. Morrill*, Walter J. Meyer III† & J. Edwin Blalock*‡

* Department of Microbiology and † Department of Pediatrics, University of Texas Medical Branch, Galveston, Texas 77550, USA

Human peripheral leukocytes[1,2] infected by virus or treated with endotoxin will, like unstimulated mouse spleen macrophages[3], synthesize immunoreactive corticotrophin (ir-ACTH) and endorphins. The ir-ACTH produced appears to be identical with authentic ACTH[1–6], while enough of the material has been produced in hypophysectomized mice infected with virus to demonstrate a steroidogenic reponse[6]. Because the production of ACTH by *in vivo* pituitary cells and by leukocytes is suppressed by dexamethasone both *in vitro*[7] and *in vitro*[6], suggesting[8] that the production of ACTH and endorphins by leukocytes is indeed controlled, we have investigated the effects of corticotropin releasing-factor (CRF), which is known[9] to regulate the pituitary production of both ACTH and β-endorphin. We now report that the production of ACTH and endorphins by leukocytes is indeed induced by synthetic CRF[10] and, in turn, suppressed by dexamethasone, suggesting that, as in pituitary cells, the pro-opiomelanocortin (POMC) gene may be expressed and similarly controlled in leukocytes.

At the outset, human peripheral leukocytes were incubated in various concentrations of synthetic ovine CRF and then stained by immunofluorescence with antibody monospecific against ACTH (1-13 amide). The proportion of cells positive for ir-ACTH increased linearly with CRF concentrations between 0.7 and 70 nM (with background staining generally about 10%). The percentage of positive cells was generally at a maximum after 48 h, although positive cells were usually observed as early as 24 h (data not shown). The concentrations of CRF required to induce ir-ACTH in leukocytes were within the range of those required to induce production by primary[9–12] and transformed[13] pituitary cells. The chief difference between the induction of ACTH from pituitary cells and leukocytes appears to be kinetic; while the former respond within minutes of stimulation, the latter respond only in hours, which may be explained by the requirement of *de novo* expression in leukocytes.

Because arginine-vasopresin (AVP) both has intrinsic CRF activity[9] and also enhances the activity of CRF itself[12,14–17] on pituitary cells, we also investigated the effects on leukocytes of incubation with AVP with or without CRF. At a concentration of 10 nM, AVP alone increases the production of cells positive for ir-ACTH to a degree equivalent to that by 0.7 nM CRF (see Table 1). Our observation that the presence of AVP (at the same concentration) also augments the response to CRF shows that, with leukocytes as with pituitary cells, the two hormones are similarly synergistic.

Accordingly, we set out to demonstrate that the antigen induced by CRF and detected by immunofluorescence is indeed a peptide resembling ACTH. To this end, we treated human peripheral leukocytes for various times with synthetic ovine CRF and AVP in the presence of tritiated amino acids so as to yield radio-labelled peptides. The ir-ACTH was purified by affinity chromatography on a Sepharose 4B column loaded with a monospecific antibody (1-13 amide) and then sized by gel filtration.

The radiolabelled ir-ACTH (see Fig. 1) has a relative molecular mass, M_r, corresponding to that of authentic ACTH (approximately 4,500). Our experiments show that ir-ACTH was evident after 24 h of treatment with CRF, was at a peak at 48 h and that it had declined by 72 h. In the absence of CRF, no radiolabelled ir-ACTH was detected in the culture fluids. The smaller peak of radiolabelled material (M_r in the range 17,000–20,000) may represent the high-M_r forms of ACTH which have been described previously[18].

In other experiments (Fig. 1), we found that the presence of dexamethasone markedly reduced the amount of ir-ACTH produced by CRF in leukocyte cultures after 48 h. Moreover,

‡ Present address: Department of Physiology and Biophysics, University of Alabama at Birmingham, Birmingham, Alabama 35294, USA.

Table 1 Dose response for CRF induction of ir-ACTH

CRF (nM)	% ir-ACTH-positive cells No AVP	+ AVP (10 nM)
0	13±4	30±7
0.7	28±4	50±14
7.0	38±11	65±7
70	58±11	90±14

Human peripheral leukocytes were prepared on a Ficoll-Hypaque buoyant density gradient[21] and resuspended in Eagle's MEM (supplemented with 2% fetal bovine serum) at 1×10^7 cells per ml. The lymphocytes were incubated with the indicated concentrations of synthetic ovine CRF (Boehringer Mannheim) and arginine vasopressin (AVP, Sigma) for 48 h. The lymphocytes were then washed, fixed with ethanol on coverslips, and stained by a previously described indirect immunofluorescence technique with antiserum made against synthetic ACTH (1-13 amide)[1]. The results are expressed as the percentage of leukocytes staining positively ± the standard deviation between replicate coverslips.

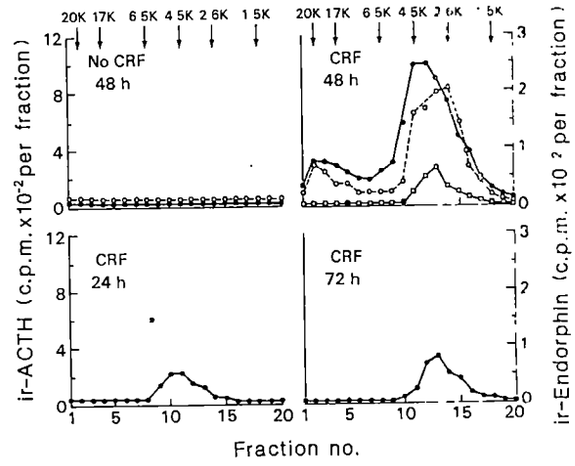


Fig. 1 Kinetics of production and molecular weight determination of CRF induced leukocyte-derived ir ACTH and ir-endorphin. Ficoll-Hypaque prepared HPLs ($1\cdot10^7$ ml^{-1}) were induced for the indicated period of time with CRF (100 ng ml^{-1}) and AVP (100 ng ml^{-1}) in the presence of 1 μCi each of tritiated: glutamic acid (44.1 Ci mmol^{-1}), tyrosine (52.9 Ci mmol^{-1}), lysine (87 Ci mmol^{-1}), methionine (80 Ci mmol^{-1}), and histidine (12.8 Ci mmol^{-1}) purchased from NEN. One 48-h culture was also treated with dexamethasone (0.5 μg ml^{-1}) CRF and AVP. The culture supernatant fluids were passed over an anti-ACTH (1-13 amide) or an anti-γ-endorphin antibody-Sepharose 4B affinity column (1, 4, 7) and eluted with 0.1 M glycine (pH2). A fraction of the radiolabelled material that bound to the affinity columns from each sample was analyzed by gel filtration on a 1 × 16 cm P-10 (Bio Rad, Richmond, CA) column. The column runs were eluted with 0.1 M phosphate buffered saline (pH 7.2) and quantitated by liquid scintillation spectroscopy (42% counting efficiency for ^{3}H). Immunoreactive ACTH and endorphin are represented by closed and open circles respectively. Immunoreactive ACTH produced at 48 h in the presence of CRF, AVP and dexamethasone is represented by open squares.

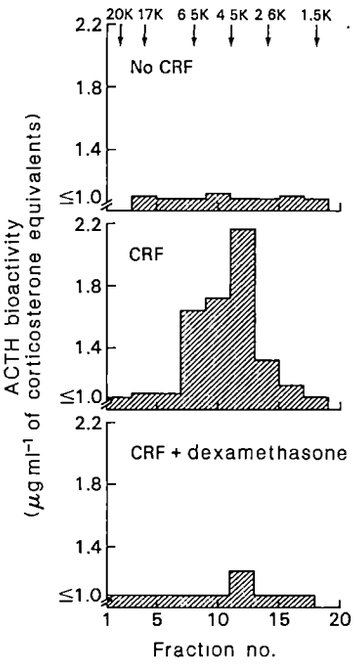


Fig. 2 Steroidogenic activity of CRF-induced leukocyte-derived ir-ACTH. Fractions from the P-10 gel filtration column (Fig. 1) were diluted in F-10 medium and incubated with cultured Y-1 adrenal tumor cells (1-5) for 18 h. The cell culture supernatant fluids were then assayed for glucocorticoid production in a previously described radioimmunoassay for corticosterone (6).

neither the release of ir-ACTH nor the supression of its production by dexamethasone is attributable to cell death; we found, by trypan blue exclusion measurements, that 95% of the cells in our cultures were viable at all times in the range covered by our experiments.

In order to determine the biological activity of the induced ir-ACTH, gel-filtration fractions were assayed for steroidogenic activity in cultured mouse adrenal tumour (Y-1) cells; we found that the peak of steroidogenesis is associated with the 4,500 dalton fraction (Fig. 2), but that samples from the control cultures (with no CRF) and from those treated with dexamethasone have no significant steroidogenic activity. By comparison with the activity of an ACTH standard, we conclude that treatment with CRF for 48 h induces the production of 650 ng of biologically active ACTH from 1×10^9 leukocytes.

We also investigated the possible production by leukocytes of other peptides derived from POMC by examining the radiolabelled culture fluids for immunoreactive endorphins. Fluids from 48 h treated and control (no CRF) cultures of peripheral human leukocytes were passed over a monospecific anti-β-endorphin Sepharose 4B column and the material retained was sized by gel filtration. The treated leukocytes, but not the controls, synthesized an immunoreactive radiolabelled endorphin of M_r approximately that of β-endorphin, or 3,500 (Fig. 1), but the synthesis was inhibited by dexamethasone (data not shown). The two series of experiments together show that CRF induces the production of both ir-ACTH and endorphins from peripheral human leukocytes.

These data strongly suggest that the POMC gene can be expressed in leukocytes, as it is in pituitary cells, and that it is similarly controlled. Our findings have both practical and theoretical implications. We have previously shown[6] that virus-induced spleen ir-ACTH can replace pituitary ACTH, inducing steroidogenesis in hypophysectomized mice; that and our present data suggest that it may be possible to correct pituitary ACTH deficiencies by the administration of exogenous CRF, which may induce ir-ACTH from leukocytes. We also note that the occurrence of hormones and receptors which are common to both the immune and neuroendocrine systems may be a means by which the two systems communicate with each other, providing a regulatory circuit linking the hypothalamus and the immune system which may be coupled with the previously described[6] lymphoid adrenal axis involving leukocyte ACTH and adrenal steroids. We suspect that the immune system may in this way have a sensory function[19], sending signals to the pituitary in response to the presence of somatic stimuli such as viruses, bacteria and tumours. Conversely, the central nervous system may send singals to the immune system by means of hypothalamic hormones such as CRF. These findings may thus provide a biochemical basis for the idea that states of mind may be reflected in states of the immune system[20].

We thank Jeanne Kincaid for technical assistance and Charlene Hoff for typing the manuscript; this work was supported in part by an NIH Biomedical Research Grant Program and by ONR grant N00014-86-K-0486.

Received 16 July 1984; accepted 9 May 1986.

1. Smith, E. M. & Blalock, J. E. *Proc. natn. Acad. Sci. U.S.A.* **78**, 7530-7534 (1981).
2. Blalock, J. E. *Lymphokines* **9**, 1-13 (1984).
3. Lolait, S. J., Lim, A. T. W., Toh, B. H. & Funder, J. W. *J. clin. Invest.* **73**, 277-280 (1984).
4. Blalock, J. E. & Smith, E. M. *Fedn. Proc.* **44**, 108-111 (1985).
5. Blalock, J. E. & Smith, E. M. *Proc. natn. Acad. Sci. U.S.A.* **77**, 5972-5974 (1980).
6. Smith, E. M., Meyer, W. M. III & Blalock, J. E. *Science* **218**, 1311-1312 (1982).
7. Smith, E. M. & Blalock, J. E. *Tex Rep Bio Med.* **41**, 350-358 (1982).
8. Keller-Wood, M. E. & Dallman, M. F. *Endocr. Rev.* **5**, 1-24 (1984).
9. Yasuda, N., Greer, M. A. & Aizawa, T. *Endocr. Rev.* **3**, 123-140 (1982).
10. Vale, W., Spiess, J., Rivier, C. & Rivier, J. *Science* **213**, 1394-1397 (1981).
11. Chan, J. S. D., Lu, C., Seidah, N. C. & Chretian, M. *Endocrinology* **111**, 1388-1390 (1982).
12. Vale, W. *et al. Endocrinology* **113**, 1121-1131 (1983).
13. Hook, V. Y. H., Heisler, S., Sabol, S. L. & Axelrod, J. *Biochem. biophys. Res. Commun.* **106**, 1364-1371 (1982).
14. Yates, F. E. *et al. Endocrinology* **88**, 3-15 (1971).
15. Gillies, G. E., Linton, E. A. & Lowry, P. J. *Nature* **299**, 355-357 (1982).
16. Rivier, C. & Vale, W. *Endocrinology* **113**, 939-942 (1983).
17. Labrie, F., Giguere, V., Proulx, L. & Lefevre, G. *J. Steroid Biochem.* **20**, 153-160 (1984).
18. Eipper, B. A. & Mains, R. E. *Endocr. Rev.* **1**, 1-27 (1980).
19. Blalock, J. E. *J. Immun.* **132**, 1067-1070 (1984).
20. Maddox, J. *Nature* **309**, 400 (1984).
21. Boyum, A. *Scand. J. clin. Lab. Invest. Suppl.* **21**, 31-50 (1968).

The β-subunit of follicle-stimulating hormone is deleted in patients with aniridia and Wilms' tumour, allowing a further definition of the *WAGR* locus

Tom Glaser*, William H. Lewis†, G. A. P. Bruns‡, P. C. Watkins§, C. E. Rogler‖, T. B. Shows¶, V. E. Powers#, H. F. Willard#, J. M. Goguen†, K. O. J. Simola & D. E. Housman*§**

* Center for Cancer Research, Massachusetts Institute of Technology, Cambridge, Massachusetts 02139, USA
Departments of † Surgery and # Medical Genetics, University of Toronto, Toronto, Canada M5S 1A8
‡ Genetics Division, Children's Hospital, Department of Pediatrics, Harvard Medical School, Boston, Massachusetts 02115, USA
§ Integrated Genetics, Inc., Framingham, Massachusetts 01701, USA
‖ Department of Medicine, Albert Einstein College of Medicine, Bronx, New York 10461, USA
¶ Department of Human Genetics, Roswell Park Memorial Institute, Buffalo, New York 14263, USA
** Department of Medical Genetics, University of Helsinki, Helsinki, Finland 00290

One in 10,000 children develops Wilms' tumour, an embryonal malignancy of the kidney[1]. Although most Wilms' tumours are sporadic, a genetic predisposition is associated with aniridia, genito-urinary malformations and mental retardation (the WAGR syndrome)[2]. Patients with this syndrome typically exhibit constitutional deletions involving band p13 of one chromosome 11 homologue[3,4]. It is likely that these deletions overlap a cluster of separate but closely linked genes that control the development of the kidney, iris and urogenital tract (the *WAGR* complex). A discrete aniridia locus, in particular, has been defined within this

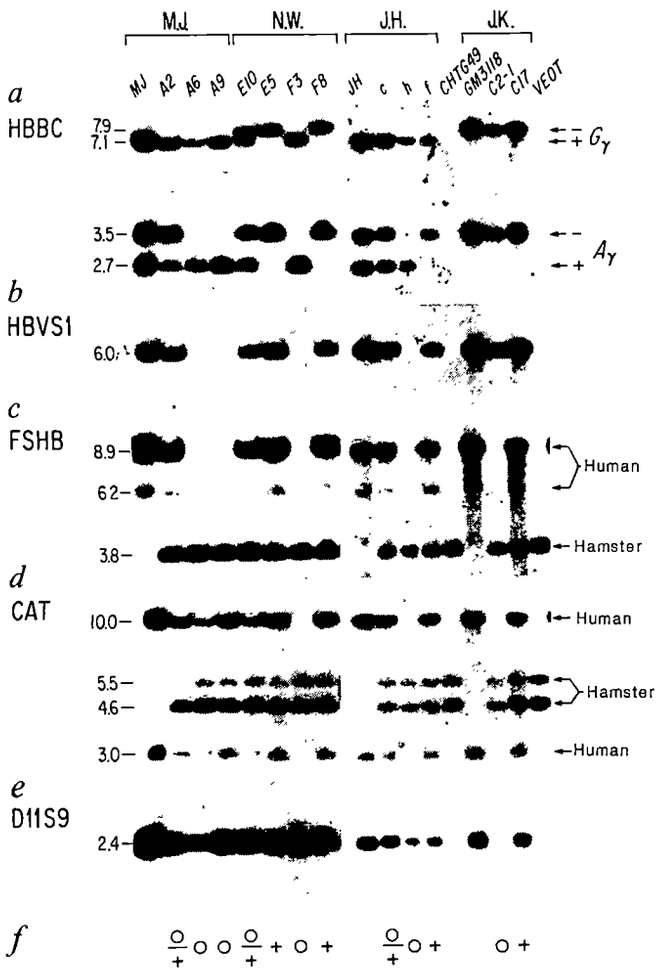


Fig. 1 Southern blot analysis of somatic cell hybrids from four patients with the WAGR syndrome. The panels show *Hin*dIII-digested DNA from hybrid clones and their parental human and hamster cell lines. They represent filters that were sequentially probed with different cloned DNA fragments. Each panel is a composite of two autoradiographs. The results show the segregation of chromosome 11 homologues in the hybrids, and the deletion of four markers in the patients. The size of each hybridizing fragment is given in kilobases to the left of the figure. Cell lines. M.J., an EBV-transformed lymphoblast culture obtained from patient M.J.; J.H. and GM3118, skin fibroblast cultures obtained from patients J.H. and J.K.; CHTG49 and VEOT, Chinese hamster parental cell lines; A2, A6 and A9, hybrid clones derived from patient M.J.[14,50]; E10, E5, F3 and F8, hybrid clones derived from patient N.W.[14,50]; c, h and f, hybrid clones derived from patient J.H.; C2-1 and C17, hybrid clones derived from patient J.K.[15] *a*, Nylon filters hybridized with the 2.7-kb *Eco*RI insert of pγ2.7 (ref. 55). Fragments corresponding to the human $^{A}\gamma$ and $^{G}\gamma$ globin genes are indicated to the right of the figure. This probe reveals a RFLP in both fetal globin genes. In each case, alleles are determined by the presence (+) or absence (−) of a *Hin*dIII site within the second intron[21]. Because patients M.J., N.W. and J.H. are heterozygous at this locus, the chromosome 11 homologues present in the somatic hybrid derivatives can be distinguished. *b*, Identical filters rehybridized with the 1.2-kb *Hin*dIII–*Sca*I insert of pS8-1 (ref. 26). *c*, The same filters rehybridized with the 1.4-kb *Pst*I insert of pFSH-1.4 (refs 24, 25). The human and cross-reacting hamster β-FSH bands are labelled. *d*, The same filters rehybridized with the 0.6-kb *Pst*I–*Ava*I fragment of cDNA clone pC24 (ref. 14). The human and cross-reacting hamster catalase bands are labelled. *e*, The same filters rehybridized with the 0.8-kb *Hin*dIII–*Sac*I insert of pES1-2, a subclone of recombinant phage H11-22 (ref. 22). *f*, The chromosome 11 content of hybrid cell lines, deduced from Southern blot analysis. Chromosomes 11 present in the hybrids are indicated as normal (+) or deleted (−).

Methods. The selection of hybrid clones is detailed in Table 1 legend. Cultured cells were lysed in ice-cold buffer (0.5% Triton X-100, 50 mM HEPES *p*H 8.0, 5 mM $MgCl_2$, 50 mM NaCl, 100 g l^{-1} sucrose), and their nuclei were recovered by centrifugation. Genomic DNA was isolated from the nuclear pellets as described previously[22] and digested with a 3–4-fold excess of *Hin*dIII. The digested DNA (10 μg per lane) was separated by electrophoresis through a horizontal 0.8% agarose gel and transferred to Zetabind (AMF-Cuno) nylon filters[47,66]. Insert fragments from plasmid clones pγ2.7, pS8-1, pFSH-1.4, pC24 and pES1-2 were isolated from low melting-point agarose gels and radiolabelled to high specific activity with [α-^{32}P]dCTP (>10^8 c.p.m. μg^{-1}), using the Klenow fragment of *Escherichia coli* polymerase I and random primers[68]. After transfer, filters were baked in a vacuum oven (80 °C, 2 h), pretreated for 1 h at 65 °C in 0.5% SDS 0.1 × SSC (1 × SSC = 0.15 M NaCl, 0.015 M Na citrate) and prehybridized overnight. Filters were then hybridized for 2 days with 10^6 c.p.m. ml^{-1} radiolabelled probe DNA. Prehybridization and hybridization were at 42 °C in 50% formamide (Nucleic Acid Grade, EM Industries), 1 M NaCl, 50 mM Tris (*p*H 7.4), 6% dextran sulphate, 1 × Denhardt's[69], 0.5% SDS and 1 mg ml^{-1} autoclaved salmon sperm DNA. After hybridization, filters were washed three times in 0.1% SDS 1 × SSC at 55 °C, and exposed to Kodak XAR 5 X-ray film at −70 °C for 3–4 days, using a Dupont Lightning-Plus intensifying screen. Bound probe was removed before rehybridization by bathing the filters in hybridization solution at 70 °C for 1 h.

chromosomal segment by a reciprocal translocation, transmitted through three generations, which interrupts 11p13 (ref. 5). In addition, the specific loss of chromosome 11p alleles in sporadic Wilms' tumours has been demonstrated, suggesting that the *WAGR* complex includes a recessive oncogene[6–9], analogous to the retinoblastoma locus on chromosome 13 (ref. 10). In WAGR patients, the inherited 11p deletion is thought to represent the first of two events required for the initiation of a Wilms' tumour, as suggested by Knudson from epidemiological data[11]. We have now isolated the deleted chromosomes 11 from four WAGR patients in hamster–human somatic cell hybrids, and have tested genomic DNA from the hybrids with chromosome 11-specific probes. We show that 4 of 31 markers are deleted in at least one patient, but that of these markers, only the gene encoding the β-subunit of follicle-stimulating hormone (*FSHB*) is deleted in all four patients. Our results demonstrate close physical linkage between *FSHB* and the *WAGR* locus, suggest a gene order for the four deleted markers and exclude other markers tested from this region. In hybrids prepared from a balanced translocation carrier with familial aniridia[5], the four markers segregate into proximal and distal groups. The translocation breakpoint, which identifies the position of the aniridia gene on 11p, is immediately proximal to *FSHB*, in the interval between *FSHB* and the catalase gene.

Although numerous genes and arbitrary DNA segments have been assigned to chromosome 11p (ref. 12), few sequences have been mapped within the *WAGR* region. The best-characterized example, erythrocyte catalase, has been localized to 11p13 by correlating the level of catalase activity with the dosage of this chromosomal segment in mono- and trisomic individuals[13]. More recently, several investigators have confirmed this result, using complementary DNA clones that code for catalase as molecular probes[14–17]. To define additional DNA markers in this region, we analysed the chromosomes 11 of four WAGR patients whose deletions involve band p13. Cytogenetic findings for three of the patients have been reported previously[18,19] (see Fig. 2). To identify DNA sequences deleted in each patient, we constructed somatic cell hybrids between the patients' primary somatic cells and a Chinese hamster cell line, as described in Table 1 legend. This allowed us to physically segregate the chromosomes 11 from each patient so that the individual homologues could be assayed separately. Several independent hybrid clones were isolated from each fusion, and those hybrids containing one or more chromosome 11 were detected by their expression of human lactate dehydrogenase A (*LDHA*)[20], a marker outside the deleted region, on the short arm[17].

To identify chromosome 11 homologues, we tested the hybrid

clones with DNA markers that exhibit significant restriction fragment length polymorphism (RFLP). At loci where a particular patient is heterozygous, hybrid derivatives segregating a single chromosome 11 homologue should carry only one allele. Figure 1*a* shows an example of this analysis, where genomic DNA from three sources—patients M.J., J.H. and J.K., representative hybrid clones and Chinese hamster parental cell lines—has been hybridized with pγ2.7, a human fetal globin-specific probe. This probe identifies two polymorphic *Hin*dIII sites in the β-haemoglobin gene cluster (*HBBC*), within the $^{A}\gamma$ and $^{G}\gamma$ genes[21]. The β-globin marker has been localized to 11p15 by *in situ* hybridization, meiotic linkage analysis and somatic cell genetic techniques[12]. As shown, the hybridization pattern gives the genotype of each patient, and allows us to identify the chromosome 11 homologues present in each hybrid cell line. For example, patient J.H. is homozygous at the $^{G}\gamma$ site (+/+), giving a 7.1-kilobase (kb) band, but he is heterozygous at the $^{A}\gamma$ site (+/−), and so has both 2.7-kb and 3.5-kb bands. A comparison of hybrid clones derived from J.H. reveals one clone (h) with the 2.7-kb band, one clone (f) with the 3.5-kb band, and one clone (c) with both allelic bands. Therefore, hybrid clones h and f contain different chromosome 11 homologues, and clone c contains both. One hybrid cell line, either h or f, must carry only the del(11) homologue. Analysis of patients M.J., N.W. and J.K. and their hybrid derivatives shows similar patterns of segregation. In the case of patient M.J., however, only one chromosome 11 homologue has been isolated in a hybrid cell line. For patient N.W., total genomic DNA is not available, so the genotype has been reconstructed by the pattern of alleles in hybrid clones.

Table 1 summarizes the results obtained with these cell lines at multiple polymorphic loci on chromosome 11. The markers listed span both chromosome arms and are present in every hybrid tested. These data suggest that the structure of the patients' chromosomes 11 has been preserved in the hybrids, and that the markers listed lie outside the *WAGR* region. The pattern of segregation defines a haplotype for each homologue, but it does not indicate which haplotypes are associated with deletions. This assignment emerged from our analysis of four markers that are deleted (Figs 1*b–e*).

In Fig. 1*e*, we have probed the filters shown in Fig. 1*a* with pES1-2, an arbitrary genomic fragment designated *D11S9* (ref. 22). This marker is present in every hybrid tested except C2-1, which carries the del(11) homologue from patient J.K.[15]. In Fig. 1*d*, we have probed these filters with pC24, a cDNA clone encoding erythrocyte catalase (*CAT*)[14]. This probe recognizes two *Hin*dIII fragments in human DNA and cross-hybridizes with hamster DNA. Hybrid clones from three patients—N.W., J.H. and J.K.—lack the human catalase gene. As expected, these cell lines—F3, h and C2-1—each contain a single chromosome 11 homologue. In contrast, two clones from patient M.J.—A6 and A9—are positive for *CAT*, yet contain only the deleted chromosome 11 (see below). These data are consistent with the finding of Punnett *et al.*[23] that four out of five WAGR patients have decreased catalase activity.

In Fig. 1*c* these filters have been probed with pFSH-1.4, a 1.4-kb *Pst*I fragment containing the structural gene for β-follicle-stimulating hormone (*FSHB*)[24,25]. Like *CAT*, this probe recognizes both human and hamster sequences. *FSHB*, which has been mapped to 11p11-pter (ref. 25), is absent in hybrid clones from all four patients, including M.J. As before, this deficiency is correlated with a particular chromosome 11 haplotype in each patient.

In Fig. 1*b*, filters were probed with pS8-1, a genomic fragment isolated from a hepatocellular carcinoma, flanking a hepatitis B viral (HBV) insertion (Fig. 1*b*)[26]. This marker, designated *HBVS1*, has been localized to 11p13–p14 by *in situ* hybridization. In patients M.J., N.W. and J.H., the *HBVS1* marker is missing from one chromosome 11 homologue, but J.K. has this sequence on both homologues. Provided the four patients' deletions are contiguous, *HBVS1* and *CAT* must flank both *FSHB* and the *WAGR* complex.

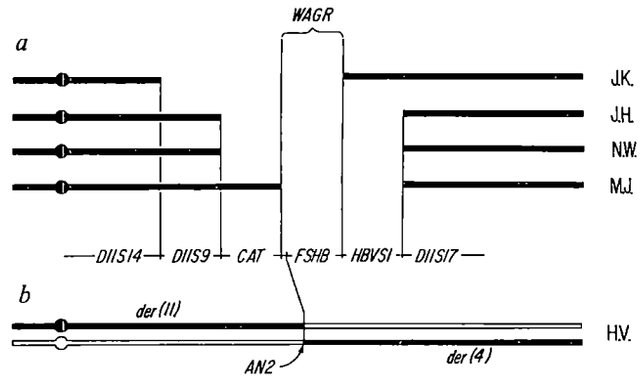


Fig. 2 Genetic map of the *WAGR* region based on five patients. ***a***, Deleted chromosomes 11 of four WAGR patients. Depicted are the short arm and centromere of chromosome 11. The horizontal bars represent chromosomal segments that are retained in the affected homologues. In cytogenetic terms, the deletions in patients J.K. and J.H. are represented as del(11) (p13p11)[18] and del(11) (p14.1p11.2) (R. Nussbaum, personal communication), respectively. Precise cytogenetic breakpoints have not been determined for patients N.W. or M.J.[19]. The four central markers—*D11S9*, *CAT*, *FSHB* and *HVBS1*—are deleted in at least one patient. Loci excluded from the *WAGR* region (Table 1) are represented by *D11S14* and *D11S17*, the nearest outside markers[34,35]. The deleted markers define four discrete intervals in this region. Although seven are predicted from the four deletions ($=2n-1$, for n independent interstitial deletions), three intervals cannot be resolved by the present set of markers. ***b***, Translocation chromosomes associated with familial aniridia. Both derivative chromosomes of patient H.V. are shown. Segments derived from chromosomes 11 and 4 are drawn as solid and open bars, respectively. The detailed karyotype, including G- and R-banded preparations, has been published previously[5]. The translocation, represented as t(4; 11)(q22; p13), serves to orient the deletion map with respect to the centromere. Its breakpoint on 11p lies between *CAT* and *FSHB*, and identifies the aniridia gene (*AN2*). The data presented do not specify the position of *FSHB* in relation to other genes in the *WAGR* complex (for example *WT*).

In the original hepatocellular tumour, the integrated HBV genome itself spanned a deletion of unknown size, exceeding 13 kb. The proximity of this integration site to 11p13 led Rogler *et al.*[26] to propose that the HBV-associated deletion includes the Wilms' tumour locus, and that the loss of one allele at this locus on viral insertion may have contributed to the malignant progression of this liver tumour. When tested, a second probe, which had been isolated from the opposite side of the deletion, was also present in both J.K. derivatives (data not shown). Because J.K.'s deletion spans the *WAGR* complex, these data suggest that the HBV-associated deletion does not overlap the Wilms' tumour gene. The alternative explanation, that one deletion is contained inside the other, is inconsistent with results obtained from the other patients and markers.

Figure 1*f* summarizes the chromosome 11 content of each hybrid as determined from our analysis of haplotypes and deleted markers. By comparing the extent of the deletions, we have ordered four markers in relation to the *WAGR* locus. The resulting map (Fig. 2*a*) reflects our assumption that the deletions are contiguous. Two of the patients—J.H. and N.W.—lack the same set of markers. Presumably, the corresponding end points of their deletions could be resolved by testing additional markers in this region. To orient this map with respect to the centromere, we have used a reciprocal translocation that breaks chromosome 11 at band p13, and disrupts the aniridia gene.

Bilateral aniridia is a rare autosomal dominant trait characterized by rudimentary development of the iris[27–29]. Mutations in

Table 1 Chromosome 11 haplotypes of four WAGR patients

Marker	Probe	Enzyme	M.J.		N.W.		J.H.		J.K.		Ref
Short arm			del	nor	del	nor	del	nor	del	nor	
HRAS1	pEJ6.6	*Bam*HI	8.0	8.0	6.6	6.6	+	+	6.6	8.0	51
INS/IGF2	phins321	*Sac*I	5.8	6.0	5.8	7.6			6.4	6.4	52
CPSD	pCD1.1		+	+	+	+					53
D11S1	pCS1		+	+	+	+					22
D11S26	pα-1b		+	+	+	+					36
D11S25	pγ-6		+	+	+	+					36
D11S12	pADJ762		+	+	+	+					54
HBG2	pγ2.7	*Hin*dIII	7.1	7.1	7.1	7.9	7.1	7.1	7.1	7.1	55
HBG1	pγ2.7	*Hin*dIII	2.7	3.5	2.7	3.5	2.7	3.5	3.5	3.5	55
	pJ1.1		+	+	+	+					36
D11S20	pJ14.1	*Pst*I	1.3	1.3	4.0	1.3					36
CALC1	pTT42	*Taq*I	+	+	+	+			8.0	6.5	56
PTH	pPTH2.5	*Pst*I	2.2	2.2	2.7	2.7					57
D11S21	pE40-4A		+	+	+	+			+	+	58
LDHA	activity		+	+	+	+	+	+	+	+	20
D11S18	pJ24.2	*Sac*I	12.0	4.2	12.0	4.2			+	+	36
D11S17	pJ19.4	*Bam*HI	21.0	21.0	13.0	21.0	+	+	+	+	36
D11S14	pDS1		+	+	+	+			+	+	22
	pJ17.3.5	*Eco*RI	3.1	3.8	3.8	3.8					36
Long arm											
PGA	phpep14-21		+	+	+	+					59
PYGM	pMH11		+	+	+	+					60
INT2	pSS6		+	+	+	+					61
ASSP13	pAS-1		+	+	+	+					62
D11S24	pE4b-TGH2	*Bam*HI	15.0	12.0	12.0	12.0					58
D11S23	pE45-RL4		+	+	+	+					58
PC	phPC1		+	+	+	+					63
APOA1	λApoA1-6	*Sac*I	3.0	4.3	4.3	4.3	+	+	+	+	64
T3D	pPGBS9		+	+	+	+					65

Chromosome 11 haplotypes were determined by the segregation of RFLP alleles in somatic cell hybrids. Where RFLPs have been scored, approximate sizes of the relevant hybridizing fragments are given in kilobases. Otherwise, markers tested are indicated as present (+). Haplotypes were identified as belonging to the deleted (del) or normal (nor) homologue by the absence of various markers from particular cell lines (Fig. 1). The status of markers on M.J.'s normal chromosome 11 was inferred from hybrid A2, which contains both homologues. For each patient, the results represent our analysis of several independent hybrid clones.

Methods: Skin fibroblasts from patient J.H. were fused with thioguanine-resistant CHTG49 hamster cells[48], using polyethylene glycol 1000 (Koch-Light), and hybrid clones were selected in hypoxanthine-aminopterin-thymidine (HAT) medium supplemented with 10% fetal calf serum and 1 μM ouabain[49]. Hybrid colonies were expanded and recloned in HAT medium, and 10–15 recloned cell lines were studied in detail. Somatic cell hybrids derived from the three other patients (N.W., M.J. and J.K.) have been described previously[14,15,50]; hybrids representing N.W. and M.J. were obtained by fusing white blood cells with E36 hamster cells, and hybrids representing J.K. were obtained by fusing fibroblast culture GM3118 (NIGMS Human Genetic Mutant Cell Repository, Camden, New Jersey) with VEOT-3 hamster cells. For each marker, genomic DNA from hybrid cultures was cleaved with the restriction endonuclease shown and analysed by Southern blotting as described in Fig. 1 legend, using the indicated radiolabelled probe. Genetic symbols[12]: *HRAS1* (c-Ha-*ras*-1 oncogene), *INS* (insulin), *IGF2* (insulin-like growth factor 2), *CPSD* (cathepsin D), *HGB1* ($^{G}\gamma$ fetal haemoglobin), *HBG2* ($^{A}\gamma$ fetal haemoglobin), *CALC1* (calcitonin), *PTH* (parathyroid hormone), *LDHA* (lactate dehydrogenase A), *PGA* (pepsinogen A), *PYGM* (muscle phosphorylase), *INT2* (human homologue of a murine mammary tumour virus integration site), *ASSP13* (an argininosuccinate synthetase pseudogene), *PC* (pyruvate carboxylase), *APOA1* (apolipoprotein A1), *T3D* (T3-δ subunit of the T3-T-cell receptor), *CEN* (centromere), TEL (telomere).

at least two separate genes can produce this disorder. One gene (*AN1*) has been assigned to chromosome 2p by linkage to the acid phosphatase locus (*ACP1*)[30] and by the phenotype of a deletion carrier[31]; the second (*AN2*) forms part of the *WAGR* complex on chromosome 11p, as described above. To map the *AN2* gene on 11p, we have analysed a reciprocal translocation that is associated with familial aniridia[5], and which has recombined the short arm of chromosome 11 with the long arm of chromosome 4. As described by Simola *et al.*[5], the grandfather, mother and daughter in this family have bilateral aniridia, but have normal levels of blood catalase and no evidence of genitourinary defects or Wilms' tumour. All affected family members carry the translocation t(4; 11)(q22; p13). We fused a lymphoblastoid cell line, established from the affected grandfather (patient H.V.), with mouse thymidine kinase-negative L-cells (Ltk$^-$), and isolated somatic cell hybrid clones as described elsewhere[32]. Two clones were identified that contain the derivative human chromosomes in the absence of a normal human chromosome 11. Hybrid LHV-3 contains the der(11) chromosome, while hybrid LHV-1 contains both der(11) and der(4) chromosomes (Fig. 2*b*).

To confirm these cytogenetic findings, we tested genomic DNA isolated from the hybrid clones with chromosome 11-specific probes. Table 2 summarizes the results for 10 genetic markers. Two patterns of segregation are evident in the hybrids. Markers present in LHV-1 but absent in LHV-3 are carried on the der(4) chromosome and are distal to the translocation breakpoint. Six markers—*HRAS1, CALC1, LDHA, D11S17, HBVS1* and *FSHB*—segregate with the der(4) chromosome. Markers present in both LHV-1 and LHV-3 are carried on the der(11) chromosome and are proximal to the breakpoint. Recombinant probe pα-11 illustrates the segregation of proximal markers; it detects a family of α-satellite repetitive DNA specific for the centromeric region of chromosome 11 (ref. 33). When probed with pα-11, genomic DNA of both hybrids show hybridizing *Xba*I fragments characteristic of the human chromosome 11 centromeric region (data not shown). Three short-arm markers—*D11S14, D11S9* and *CAT*—and the long-arm marker *INT2* are present in both hybrids, as part of the der(11) chromosome. At polymorphic sites identified by two of these loci (*CAT* and *INT2*), patient H.V. is heterozygous; as expected, only one allele is present in the hybrids, a result consistent with the absence of the normal chromosome 11.

We have positioned the aniridia translocation breakpoint on the *WAGR* deletion map according to these data (Fig. 2*b*). Two of the markers deleted in WAGR patients are proximal to the breakpoint (*D11S9* and *CAT*) and two are distal (*FSHB* and *HBVS1*). In addition, markers excluded from the *WAGR* region (Table 1) are separated by the translocation into proximal and distal groups. We conclude that the break in 11p has occurred between the catalase and β-FSH genes, resulting in the translocation of *FSHB, HBVS1, D11S17, LDHA, CALC1* and *HRAS1* to chromosome 4. The segregation of *LDHA* with the telomeric portion of 11p further supports our conclusion[32,34] that *LDHA* is distal to the catalase gene, and not at 11p12 as previously reported[12].

Together, these data suggest the following gene order for chromosome 11p: *CEN-D11S14-D11S9-CAT-FSHB-HBVS1-*

Table 2 Translocation of chromosome 11 markers in familial aniridia

Marker	Probe	Enzyme	Chromosome der(4)*	Chromosome der(11)†	Chromosome nor(11)	Ref.
HRAS1	pEJ6.6		+	−	+	51
CALC1	pTT42		+	−	+	56
LDHA	activity		+	−	+	20
D11S17	pJ19.4		+	−	+	36
HBVS1	pS8-1		+	−	+	26
FSHB	pFSH-1.4		+	−	+	25
CAT	pCAT-41	*Kpn*I	−	8.0, 3.0	11.0	15
D11S9	pES1-2		−	+	+	22
D11S14	pDS1		−	+	+	22
	pα-11‡		−	+	+	33
INT2§	pSS6	*Bam*HI	−	8.4	5.6, 2.8	61

Reciprocal translocation chromosomes from H.V. (patient 3 in ref. 5) were segregated in somatic cell hybrids. Genomic DNA from the resulting hybrid clones was tested for specific human sequences by Southern blotting[66], using the indicated radiolabelled probes. At polymorphic loci where H.V. is heterozygous, the restriction endonuclease used is shown, and the sizes of the relevant hybridizing fragments are given in kilobases. Otherwise, markers tested are indicated as present (+) or absent (−). The presence of human *LDHA* was determined by cellogel electrophoresis[20]. Hybrids were formed by fusing a lymphoblastoid cell line established from H.V. with mouse Ltk⁻ cells, as described elsewhere[32]. The results shown represent our analysis of two hybrid clones, LHV-3, containing the der(11) chromosome, and LHV-1, containing both der(11) and der(4) chromosomes. In these clones, the presence of the derivative human chromosomes in the absence of a normal human chromosome 11 was determined by detailed karyotyping. At least 15 metaphase spreads were examined at the time of DNA preparation, following trypsin-Giemsa banding[67]. Genetic symbols are defined in the text and Table 1 legend.

* Derivative chromosome 4 (4pter>4q22::11p13>11pter). These data are inferred from hybrid LHV-1.

† Derivative chromosome 11 (11qter>11p13::4q22>4qter).

‡ Detects centromeric α-satellite DNA[33]. A 0.85-kb *Xba*I band, specific for human chromosome 11, was scored.

§ The *INT2* marker has been mapped to 11q13 (ref. 61). All other markers tested are located on the short arm.

(D11S17, LDHA, CALC1, HRAS1)-TEL). This order is consistent with our analysis of other reciprocal translocations (in preparation and ref. 32) and of multi-point meiotic linkage[35,36]. In separate reports (in preparation and ref. 34), we have extended the map shown in Fig. 2 using 11p deletions selected *in vitro*; our results support the *WAGR* deletion series and give an order to markers that have been excluded from the *WAGR* region (Table 1).

The observation that all of the markers tested are present on either the der(11) or der(4) chromosomes suggests that the aniridia translocation has not been accompanied by a large deletion of DNA. The simplest explanation is that the translocation has disrupted or deleted a relatively small area of 11p containing the aniridia gene (*AN2*) but not the Wilms' tumour gene (*WT*). If this interpretation is correct, and no complex rearrangement has accompanied the translocation, the aniridia gene must lie at the breakpoint, in the interval between *CAT* and *FSHB*. This configuration, represented as CEN-*CAT-AN2-FSHB*-TEL, conforms with the findings of Turleau *et al.*[37] and van Heyningen *et al.*[17] which suggest *CAT* is proximal to *WAGR*, but it differs from the orientation proposed by Narahara *et al.*[38].

The exact position of the Wilms' tumour gene is less clear. According to our results, *WT* maps between *CAT* and *HBVS1*, in one of three sub-intervals demarcated by the *AN2* and *FSHB* genes (Fig. 2). If *WT* were distal to *FSHB*, giving the order *CAT-AN2-FSHB-WT-HBVS1*, then the *WAGR* complex would encompass *FSHB*. This arrangement is especially intriguing, since it raises the possibility that the genito-urinary anomalies seen in WAGR patients are caused by a deficiency of β-FSH during embryonic development.

An alternative placement of *WT*, proximal to *AN2*, has been suggested by Turleau *et al.*[37]. These authors describe a patient with a visible deletion of 11p13, reduced catalase activity and Wilms' tumour, but with no evidence of aniridia. Of the four WAGR stigmata, aniridia has the highest penetrance[39,40], particularly when patients at risk are examined thoroughly, so that subtle iris defects can be detected[28,29]. These observations suggest that *CAT* and *WT*, but not *AN2*, are deleted in this patient. If this interpretation is correct, and his deletion spares the β-FSH gene, then the order *CAT-WT-AN2-FSHB* is most likely.

Although the chromosomal rearrangements we have examined are visible in banded karyotypes, the map we present does not depend on cytogenetic data. However, we note that breakpoints carried by patients J.K. and H.V. immediately flank *FSHB* and occur in band p13. These data are consistent with the assignment of *CAT* to 11p13 (ref. 12) and *HBVS1* to 11p13-p14 (ref. 26), and they localize *FSHB* to band 11p13. This segment includes the *WAGR* gene complex and represents approximately 0.1% of the total human genome.

Several closely linked markers bracket the *WAGR* complex (Fig. 2). The nearest marker, *FSHB*, maps either within or distal to *WAGR*. From standard ideograms[41], we estimate that the segment containing *CAT*, *FSHB* and *WAGR* spans 3,000-6,000 kb, the size of an average prokaryotic genome. As the density of markers increases in this interval, the distance separating probes should soon approach the range amenable to restriction mapping using pulsed-field gels[42], and to molecular analysis by so-called 'jumping' techniques[43]. In these studies, cell lines derived from patients with apparent microdeletions[29] and DNA samples from Wilms' tumours should prove especially useful. Despite the close physical linkage between *FSHB* and the Wilms' tumour gene, our attempts to show homozygous loss of *FSHB* in sporadic Wilms' tumours have been unsuccessful (T.G. and D.E.H., unpublished observations).

By segregating individual chromosome 11 homologues, we have gauged in molecular terms cytogenetic lesions associated with familial aniridia and the WAGR syndrome. The hybrid panel we have developed can be used to quickly locate chromosome 11-specific markers in the *WAGR* region. Our approach should be readily applicable to other disorders that are linked to autosomal deletions, including bilateral retinoblastoma[44], and the Praeder-Willi[45], cri du chat[46] and Wolf-Hirshhorn[47] syndromes.

We thank Drs Judy Bader, James Miser, Fred Li, Park Gerald and Robert Nussbaum for providing patient samples, Drs Anthony Beck and Vincent Vellucci for structural information on the β-FSH gene, Dr James Gusella for early contributions to this work, and D. Barker, A. Beaudet, G. Bell, J. Chirgwin, C. Dickson, B. Forget, S. Freytag, J. Gusella, P. Hwang, S. Karanthanasis, H. Kronenberg, B. Nelkin, T. Taggart, P. van den Elsen, T. Vulliamy, J. Waye and R. Weinberg for their gift of DNA probes. T.G. was supported by a predoctoral fellowship from the NSF and NIH Medical Scientist Training Program grant 2T 32 GMO7753-06. This work was supported by NIH grants to D.E.H. (GM27882), G.A.P.B. (GM34988 and HD186588) and T.B.S. (GM20454 and HD05196), by American Cancer Society grant CD62 to T.B.S., and by grants from the NCI and MRC of Canada to W.H.L.

Received 14 February; accepted 7 April 1986.

1. Matsunaga, E. *Hum. Genet.* **57**, 231-246 (1981).
2. Miller, R. W., Fraumeni, J. F. Jr & Manning, M. D. *New Engl. J. Med.* **270**, 922-927 (1964).
3. Riccardi, V. M., Sujansky, E., Smith, A. C. & Francke, U. *Pediatrics* **61**, 604-610 (1978).
4. Francke, U., Holmes, L. B., Atkins, L. & Riccardi, V. M. *Cytogenet. Cell Genet.* **24**, 185-192 (1979).
5. Simola, K. O. J., Knuutila, S., Kaitila, I., Pakola, A. & Pohja, P. *Hum. Genet.* **63**, 158-161 (1983).
6. Koufos, A. *et al. Nature* **309**, 170-172 (1984).
7. Orkin, S. H., Goldman, D. S. & Sallan, S. E. *Nature* **309**, 172-174 (1984).
8. Reeve, A. E. *et al. Nature* **309**, 174-176 (1984).
9. Fearon, E. R., Vogelstein, B. & Feinberg, A. P. *Nature* **309**, 176-178 (1984).
10. Cavenee, W. K. *et al. Nature* **305**, 779-784 (1983).
11. Knudson, A. G. Jr & Strong, L. C. *J. natn. Cancer Inst.* **48**, 313-324 (1972).
12. Grzeschik, K. H. & Kazazian, H. H. Jr *Cytogenet. Cell Genet.* **40**, 179-205 (1985).
13. Junien, C. *et al. Ann. Genet.* **23**, 165-168 (1980).
14. Bruns, G. A. P. *et al. Am. J. hum. Genet.* **36**, 25S (1984).
15. Michalopoulos, E. E. *et al. Hum. Genet.* **70**, 157-162 (1985).
16. Schroeder, W. T. *et al. Am. J. hum. Genet.* **37**, A173 (1985).
17. van Heyningen, V. *et al. Proc. natn. Acad. Sci. U.S.A.* **82**, 8592-8596 (1985).

18. NIGMS Human Genetic Mutant Cell Repository *Catalog of Cell Lines* (NIH Publ. 85-2011, 1985).
19. Bader, J. L. *et al. Proc. Am. Ass. Cancer Res.* **20**, 210 (1979).
20. Khan, M. P. *Archs Biochem. Biophys.* **145**, 470-483 (1971).
21. Jeffreys, A. J. *Cell* **18**, 1-10 (1979).
22. Gusella, J. F. *et al. Proc. natn. Acad. Sci. U.S.A.* **77**, 2829-2833 (1980).
23. Punnett, H. H. *et al. Pediat. Res.* **17**, 217A (1983).
24. Beck, A., Velluci, V. & Curry, K. *DNA* **4**, 76 (1985).
25. Watkins, P. C. *et al. DNA* (submitted).
26. Rogler, C. E. *et al. Science* **230**, 319-322 (1985).
27. Turleau, C. *et al. Clin. Genet.* **26**, 356-362 (1984).
28. Hittner, H. M., Riccardi, V. M., Ferrell, R. E., Borda, R. R. & Justice, J. Jr *Am. J. Ophthal.* **89**, 531-539 (1980).
29. Riccardi, V. M. *et al. J. Pediat.* **100**, 574-577 (1982).
30. Ferrell, R. E., Chakravati, A., Hittner, H. M. & Riccardi, V. M. *Proc. natn. Acad. Sci. U.S.A.* **77**, 1580-1582 (1980).
31. Arias, S., Rolo, M. & Gonzalez, N. *Cytogenet. Cell Genet.* **37**, 401 (1985).
32. Lewis, W. H. *et al. Hum. Genet.* **71**, 249-253 (1985).
33. Willard, H. F. *Am. J. hum. Genet.* **37**, 524-532 (1985).
34. Glaser, T. *et al. Cytogenet. Cell Genet.* **40**, 643 (1985).
35. Gerhard, D. S. & Housman, D. E. *Cytogenet. Cell Genet.* **40**, 640 (1985).
36. Housman, D. E., Gerhard, D. S., Glaser, T. & Jones, C. *Cytogenet. Cell Genet.* **40**, 656 (1985).
37. Turleau, C. *et al. Hum. Genet.* **67**, 455-456 (1984).
38. Narahara, K. *et al. Hum. Genet.* **66**, 181-185 (1984).
39. Cotlier, E., Rose, M. & Moel, S. A. *Am. J. Ophthal.* **86**, 129-132 (1978).
40. Codero, J. F., Li, F. P., Holmes, L. B. & Gerald, P. S. *Pediatrics* **66**, 716-719 (1980).
41. Standing Committee on Human Cytogenetic Nomenclature *Cytogenet. Cell Genet.* **31**, 1-23 (1981).
42. Schwartz, D. C. & Cantor, C. R. *Cell* **37**, 67-75 (1984).
43. Collins, F. S. & Weissman, S. M. *Proc. natn. Acad. Sci. U.S.A.* **81**, 6812-6816 (1984).
44. Yunis, J. J. & Ramsey, N. *Am. J. Dis. Childh.* **132**, 161-163 (1978).
45. Ledbetter, D. H. *et al. Am. J. hum. Genet.* **34**, 278-285 (1982).
46. Carlock, L. R. & Wasmuth, J. J. *Somat. Cell molec. Genet.* **11**, 267-276 (1985).
47. Gusella, J. F. *et al. Nature* **318**, 75-78 (1985).
48. Athwal, R. S. & McBride, O. W. *Proc. natn. Acad. Sci. U.S.A.* **74**, 2943-2947 (1977).
49. Kucherlapati, R. S., Baker, R. M. & Ruddle, F. M. *Cytogenet. Cell Genet.* **14**, 362-363 (1975).
50. Gusella, J. F. thesis, Massachusetts Inst. Technol. (1980).
51. Shih, C. & Weinberg, R. A. *Cell* **29**, 161-169 (1982).
52. Bell, G. I., Gerhard, D. S., Fong, N. M., Sanchez-Pescador, R. & Rall, L. B. *Proc. natn. Acad. Sci. U.S.A.* **82**, 6450-6454 (1985).
53. Faust, P. L., Kornfeld, S. & Chirgwin, J. M. *Proc. natn. Acad. Sci. U.S.A.* **82**, 4910-4914 (1985).
54. Barker, D., Holm, T. & White, R. *Am. J. hum. Genet.* **36**, 1159-1171 (1984).
55. Tuan, D., Solomon, W., Ki, Q. & London, I. M. *Proc. natn. Acad. Sci. U.S.A.* **82**, 6384-6388 (1985).
56. Przepiorka, D. *et al. Biochem. biophys. Res. Commun.* **120**, 493-499 (1984).
57. Vasicek, T. J. *et al. Proc. natn. Acad. Sci. U.S.A.* **80**, 2127-2131 (1983).
58. Glaser, T., Gerhard, D., Payne, C., Jones, C. & Housman, D. *Cytogenet. Cell Genet.* **40**, 643 (1985).
59. Taggart, R. T., Mohandas, T. K., Shows, T. B. & Bell, G. I. *Proc. natn. Acad. Sci. U.S.A.* **82**, 6240-6244 (1985).
60. Hwang, P. *et al. Eur. J. Biochem.* **152**, 267-274 (1985).
61. Casey, G., Smith, R., McGillivray, D., Peters, G. & Dickson, C. *Molec. cell. Biol.* **6**, 502-510 (1986).
62. Su, T. *et al. Am. J. hum. Genet.* **36**, 954-964 (1984).
63. Freytag, S. O. & Collier, K. J. *J. biol. Chem.* **259**, 12831-12837 (1984).
64. Ordovas, J. M. *et al. New Engl. J. Med.* **314**, 671-677 (1986).
65. van den Elsen, P. *et al. Proc. natn. Acad. Sci. U.S.A.* **82**, 2920-2924 (1985).
66. Southern, E. M. *J. molec. Biol.* **98**, 503-517 (1975).
67. Francke, U. & Oliver, N. *Hum. Genet.* **45**, 137-165 (1978).
68. Feinberg, A. P. & Vogelstein, B. *Analyt. Biochem.* **137**, 266-267 (1984).
69. Denhardt, D. *Biochem. biophys. Res. Commun.* **23**, 641-652 (1966).

Ethanol production from sugars derived from plant biomass by a novel fungus

J. F. Wu*‡, S. M. Lastick* & D. M. Updegraff†

* Biotechnology Research Branch, Solar Energy Research Institute, Golden, Colorado 80401, USA
† Department of Chemistry and Geochemistry, Colorado School of Mines, Golden, Colorado 80401, USA

The concept of transforming renewable plant biomass, and in particular organic waste, to fuels or chemicals continues to attract attention as nonrenewable fossil fuel reserves decrease[1,2]. Cellulose and hemicellulose, which comprise more than 70% of plant biomass and are the two most abundant organic compounds in the biosphere, occur in the wastes from agriculture and forestry as well as from vegetable and fruit processing and municipal waste treatment. Recycling of these wastes to useful products helps to prevent pollution. After enzymatic or acid hydrolysis, plant biomass yields mostly cellobiose, xylose and glucose together with mannose, galactose and arabinose. Microorganisms which can ferment such a wide range of sugars, at high concentrations, into a high concentration of ethanol have not been reported previously. Here we report on a novel fungus, *Paecilomyces* sp. NF1, which is capable of fermenting all of the major sugars derived from hydrolysis of plant biomass to ethanol. In xylose fermentation, the ethanol yield of this fungus remained almost unchanged when the concentration of xylose was increased from 20 to 200 g l^{-1}. The fungus also produced good yields of ethanol from glucose, fructose, cellobiose, arabinose, galactose, mannose and ribose, as well as from the simultaneous saccharification and fermentation (SSF) of cellulose with hemicellulose, and from acid hydrolysates of plant biomass.

Paecilomyces sp. NF1 (ATCC 20766) was isolated from compost soil from Denver, Colorado. The medium used for isolation contained (g l^{-1}): yeast extract 3, yeast nitrogen base (Difco) 4, peptone 3, xylose 2 and agar 20 (for plates). The *p*H of the medium was adjusted to 2.5 with dilute hydrocloric acid. The fungus was isolated at 30 °C by the dilution plate method[3]. The composition of the fermentation medium was (g l^{-1}): yeast extract 1.5, KH_2PO_4 1.0, K_2HPO_4 1.0, NaCl 0.5, KNO_3 2.5, $MgSO_4 \cdot 7H_2O$ 0.5, $CaCl_2$ 0.1 and test sugars at the desired concentrations. Tests showed that the fungus would not grow under anaerobic conditions, and would not produce ethanol under aerobic conditions, therefore the fungus was grown under aerobic conditions, and the mycelium was then placed in sealed Bellco tubes containing only a small volume of air (semi-anaerobic conditions). Note that the fungus can tolerate temperatures of up to 43 °C. *Paecilomyces* sp. NF1 can ferment a wide range of substrates, including glucose, galactose, fructose, mannose, maltose, soluble starch, xylose, arabinose, ribose and cellobiose (Table 1); sucrose and inulin yield only small amounts of ethanol. The fungus produced essentially the same amount of ethanol when the *p*H of the initial medium was varied from 2.2 to 7.0, and at either 30 °C or 37 °C. The ethanol yield from xylose fermentation by this fungus remained almost unchanged when the xylose concentration was increased from 15 to 200 g l^{-1} (or 0.38 to 0.39 g per g of xylose)—that is, 75% of the theoretical yield. For a xylose concentration of 200 g l^{-1}, the final concentration of ethanol was 73 g l^{-1} (Fig. 1, Table 2); this is the highest reported yield of ethanol from a xylose fermentation. These data

Table 1 Maximum ethanol yields (g per g of sugar in medium) from sugar fermentation by *Paecilomyces* sp. NF1

Sugar	Sugar concentration (g l^{-1})	Ethanol production (g l^{-1})	Ethanol yield (g per g of sugar in medium)	Time for completion* (days)
D-Cellobiose	100	40.2	0.40	7
D-Fructose	100	39.9	0.40	7
D-Glucose	100	40.9	0.41	7
D-Galactose	100	40.4	0.40	7
D-Mannose	100	38.1	0.38	7
Starch	100	39.8	0.40	7
Xylose	100	39.8	0.40	7
L-Arabinose	50	13.8	0.28	4
Lactose	50	14.1	0.28	4
Maltose	50	21.1	0.42	4
D-Ribose	50	10.2	0.20	4

Fermentation was carried out at 30 °C in anaerobic tubes, shaken at 150 r.p.m. Initial *p*H was 5.0; initial cell density was 6.0 g l^{-1}.
* Number of days taken to completely ferment the individual sugar, as analysed by HPLC and gas chromatography. Higher sugar concentrations did not result in higher ethanol yields.

‡ Present address: Alltech Biotechnology Center, 3031 Catnip Hill Pike, Nicholasville, Kentucky 40356, USA.

Table 2 Ethanol production by various xylose-fermenting microorganisms

	Initial D-xylose concentration ($g\,l^{-1}$)	Maximum ethanol concentration ($g\,l^{-1}$)	Ethanol yield*	Ref.
Candida tropicalis ATCC 1369	75	8.28	0.11	8
Candida XF 217	50	21.0	0.42	9
Candida shehtae CSIR-Y492	50	18.0	0.36	10
Candida shehatae CSIR-Y492	90	26.2	0.29	11
Fusarium oxysporum	50	25.0	0.50	12
VTT-D-80134	50	25.0	0.50	12
Fusarium F5†	100	32.0	0.32	13
	150	43.0	0.29	
	200	40.0	0.20	
Kluyveromyces marxianus SUB-80-S	20	5.60	0.28	14
Kluyveromyces cellobiovorus	100	30.0	0.30	15
Pachysolen tannophilus NRRL-Y2460	20	5.30	0.26	16
Pachysolen	50	15.0	0.30	17
tannophilus	115	27.6	0.24	
NRRL-Y2460	158	33.2	0.21	
Pachysolen	80	21.0	0.26	18
tannophilus	100	23.5	0.24	
RL-171†	120	20.0	0.17	
	160	15.5	0.10	
	200	11.7	0.06	
Paecilomyces sp. NF1	50	19.7	0.39	Present
ATCC-20766	80	31.5	0.39	work
	100	39.8	0.39	
	150	59.7	0.39	
	200	73.5	0.38	

* Ethanol yield: g ethanol produced per g xylose consumed.
† Estimated from the published data.

demonstrated that this fungus can tolerate high concentrations of both xylose and ethanol. *Paecilomyces* sp. NF1 produced high-purity ethanol from $200\,g\,l^{-1}$ of xylose. At the end of fermentation, as analysed by HPLC and gas chromatography, only trace amounts of other chemicals were detected: xylose ($0.00\,g\,l^{-1}$), xylitol ($0.45\,g\,l^{-1}$), acetate ($0.45\,g\,l^{-1}$) and *n*-butyrate ($0.04\,g\,l^{-1}$). Table 2 shows a comparison of ethanol production from xylose by *Paecilomyces* sp. NF1 with that of other organisms known to ferment xylose.

This fungus can produce nearly $60\,g\,l^{-1}$ ethanol from simultaneous saccharification and fermentation of either $150\,g\,l^{-1}$ cellulose or $100\,g\,l^{-1}$ cellulose with $50\,g\,l^{-1}$ hemicellulose (as represented by xylan). The latter result, illustrated in Fig. 1, represents the first report of SSF of both cellulose and hemicellulose to produce ethanol. Among the xylose-fermenting yeasts, only *Kluyveromyces cellobiovorus* is able to convert cellobiose into ethanol; however, the ethanol yield of this yeast was found to decrease when the cellobiose concentration was higher than $40\,g\,l^{-1}$. For example, it produced $20\,g\,l^{-1}$ ethanol from $40\,g\,l^{-1}$ cellobiose, but produced only $21\,g\,l^{-1}$ ethanol from $60\,g\,l^{-1}$ cellobiose[4]. The fungus *Paecilomyces* sp. NF1 also used all the sugars ($30\,g\,l^{-1}$) from an acid hydrolysate of wheat straw to produce $12.5\,g\,l^{-1}$ ethanol, demonstrating that the fungus is not affected by toxic substances in hydrolysates, as are other fermenting microorganisms[4-7].

Thus, *Paecilomyces* sp. NF1 has several unique characteristics with regard to ethanol fermentation. It can produce high concentrations of ethanol from the simultaneous saccharification and fermentation of cellulosics derived from plant biomass. We believe that this fungus is a good candidate for use in the industrial conversion of plant biomass wastes into ethanol.

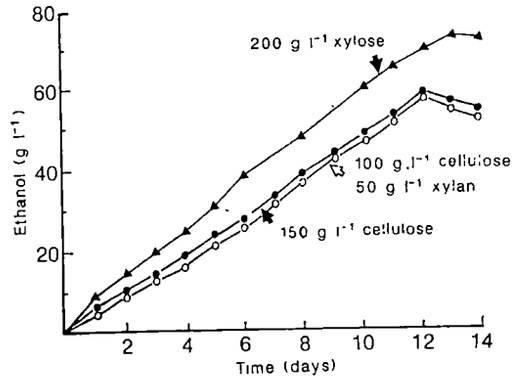


Fig. 1 Ethanol production from xylose (△) and simultaneous saccharification and fermentation (SSF) of cellulose (●) or cellulose with xylan (○) by *Paecilomyces* sp. NF1. Initial *p*H 5.0, temperature 30 °C. The initial cell density was $6.0\,g\,l^{-1}$ for xylose fermentation and $4.5\,g\,l^{-1}$ for SSF. No increase in cell density occurred during the fermentation. In SSF, the cellulose used was Solka Floc BW200 and cellulase (from *Trichoderma reesei*) was added to a concentration equivalent to 8% of the cellulose; xylan was prepared from larch wood and hemicellulase (from *Aspergillus niger*) was used at a concentration of 8% of the xylan.

This work received financial support from the Office of Alcohol Fuels and the Biomass Energy Technology Division of the US Department of Energy.

Received 19 December 1985; accepted 11 April 1986.

1. Hammond, A. L. *Science* **195**, 564-567 (1977).
2. Lubinska, A. *Nature* **314**, 395 (1985).
3. Barron, G. L. *Meth. Microbiol.* **4**, 405-427 (1971).
4. Takasawa, S., Morikawa, Y., Takayama, K. & Masunaga, I. US Patent no. 4472501 (1984).
5. Kurtzman, C. P., Bothast, R. J. & Van Cauwenberge, J. E. US Patent 4359534 (1982).
6. Jeffries, T. W. *Biotechnol. Lett.* **3**, 213-218 (1981).
7. Fein, J. E., Tallim, R. & Lawford, R. *Can. J. Microbiol.* **30**, 682-690 (1984).
8. Gong, C. S., McCracken, L. D. & Tsao, G. T. *Biotechnol. Lett.* **3**, 245-250 (1981).
9. du Preez, J. C. & van der Walt, J. P. *Biotechno. Lett.* **5**, 357-362 (1983).
10. du Preez, J. C., Prior, B. A. & Monteiro, A. M. T. *Appl. microb. Biotechnol.* **19**, 261-266 (1984).
11. Suihko, M. L. & Enari, T. M. *Biotechnol. Lett.* **3**, 723-728 (1981).
12. Margaritis, A. & Bajpai, P. *Appl. envir. Microbiol.* **44**, 1039-1041 (1982).
13. Schnider, H., Maleszka, R., Wang, P. Y., Veliky, I. A. & Chan, Y. K. US Patent no. 4477569 (1984).
14. Slininger, P. J., Bothast, R. J., Van Cauwenberge, J. E. & Kurtzman, C. P. *Biotechnol. Bioengng* **24**, 371-384 (1982).
15. Ueng, P. P. & Gong, C. S. *Enzyme microb. Technol.* **4**, 169-171 (1982).
16. Dekker, R. F. H. *Biotechnol. Lett.* **4**, 411-416 (1982).
17. Leonard, R. H. & Hajny, G. J. *Ind. Engng Chem. analyt. Edn* **37**, 390-395 (1945).
18. Lee, Y. Y. & McCaskey, P. A. TAPPI **66**, 102-107 (1983).

Erratum

Mechanosensitivity of mammalian auditory hair cells *in vitro*

I. J. Russel, G. P. Richardson & A. R. Cody

Nature **321**, 517-519 (1986).

THE first line in this letter should read 'Intracellular responses recorded *in vivo* from the cochleas . . . ', not '*in vitro*'.

Corrigendum

NMDA-receptor activation increases cytoplasmic calcium concentration in cultured spinal cord neurones

A. B. MacDermott, M. L. Meyer, G. L. Westbrook, S. J. Smith & J. L. Barker

Nature **321**, 519-522 (1986).

IN this letter, one of the authors' affiliations was given incorrectly. J.L.B. is at the Laboratory of Neurophysiology, NINCDS, National Institutes of Health, Bethesda, Maryland 20892, USA.

FELLOWSHIPS

IMPERIAL CANCER RESEARCH FUND
Research Fellowship (Edinburgh)

To study the function of Cytochrome P-450 genes which are a multigene family of proteins whose polymorphic expression may be a critical aspect of adverse drug side effects, chemical toxicity and cancer. Using c-DNA probes currently available, it is intended to combine a molecular genetic approach with biochemical methods to identify polymorphic cytochrome P-450 genes in man and to determine whether their function and regulation can be related to individual susceptibility to cancer.

The award will be tenable for three years on the salary range £9,495 to £11,790, entry depending upon qualifications and experience.

For further information please contact: **Dr C R Wolf, Imperial Cancer Research Fund, Laboratory of Molecular Pharmacology, George Square, Edinburgh on 031 668 3343.**

Applications together with a CV and two referees are to be addressed to: The Personnel Officer, ICRF, Lincoln's Inn Fields, London, WC2A 3PX, quoting reference: 101/86 by 25th July 1986. (211)E

Southampton THE UNIVERSITY

INSTITUTE OF CRYOGENICS
POSTDOCTORAL FELLOWSHIP

Applications are invited for a Research Fellowship on high flux heat transfer in cryogenics liquids supported by BOC Cryoplants Ltd.

Salary in range up to £14,000 depending on research experience. USS Superannuation benefits available.

Details from Professor R G Scurlock, Institute of Cryogenics. Tel: 0703 559122 Ext: 2046. (168)E

THE UNIVERSITY OF WARWICK
DEPARTMENT OF BIOLOGICAL SCIENCES
POSTDOCTORAL FELLOWSHIP

Applications are invited from graduates who have obtained or are about to obtain a PhD in Biochemistry or Microbiology to work on the CO_2 uptake system and Rubisco function in Cyanobacteria. The project is funded by the AFRC and will involve collaboration with the Rothamsted Experimental Station.

Salary will be in the range £8,020 to £12,780 pa and the appointment will be for two years in the first instance to commence as soon as possible.

Applicants should send a curriculum vitae with the names of two referees to Ms N A Rowe, Executive Officer/Academic Administration, Department of Biological Sciences, University of Warwick, Coventry, CV4 7AL quoting Ref NGC/AFRC Link. Further particulars can be obtained from Professor N G Carr at the above address or by phoning 0203 523544. (214)E

UNIVERSITY OF NEWCASTLE UPON TYNE
DEPARTMENT OF PATHOLOGY
UNIVERSITY RESEARCH FELLOWSHIP

Applications are invited for a 3 year postdoctoral position to work on the identification of genes involved in the transformation of human breast epithelial cells using DNA transfection techniques. Previous experience in DNA transfection and recombinant DNA techniques would be preferred. Candidates should have the degree of PhD. The appointment which is financed by the University in order to foster and stimulate research projects of outstanding potential, is available to be filled as soon as possible.

Salary will be on the Range 1A salary scale £8,020 — £12,780 per annum according to qualifications and experience.

Further particulars may be obtained from the Senior Assistant Registrar (Establishments) (F.P.), The University, 6 Kensington Terrace, Newcastle upon Tyne, NE1 7RU, with whom applications (3 copies) together with the names and addresses of three referees should be lodged not later than 11th July, 1986. (166)E

UNIVERSITY OF BRISTOL
DEPARTMENT OF PHYSICS AND THE NATIONAL PHYSICAL LABORATORY
POSTDOCTORAL FELLOW

We invite applied physicists and engineers to apply for a Postdoctoral Fellowship at the University of Bristol to further the development of a new device for measuring microwave fields. The proposed work, which won the 1986 National Physical Laboratory Metrology Award, would be carried out under the supervision of Professor J F Nye, FRS; the person appointed would be expected to spend the major part of their time working at the NPL on this topic.

The appointment will be for three years, with a salary in the range of £11,790–£15,700 plus Outer London Weighting. There would be a possibility that a permanent appointment at the NPL could follow.

Applications, with curriculum vitae, details of research and development experience and names and addresses of two referees, should be sent by July 3, 1986 to Professor J F Nye, H H Wills Physics Laboratory, Tyndall Avenue, Bristol, BS8 1TL, who can supply further particulars. (159)E

SEMINARS & SYMPOSIA

CALL FOR PAPERS AND FIRST ANNOUNCEMENT

IMMUNOCYTOCHEMISTRY CLUB
SIXTH MEETING
IN SITU HYBRIDISATION HISTOCHEMISTRY

A one-day symposium on modern microscopical imaging techniques, particularly the development and application of *in situ* hybridisation histochemistry, will take place on

THURSDAY 12th MARCH 1987

at the:

ROYAL POSTGRADUATE MEDICAL SCHOOL
HAMMERSMITH HOSPITAL
DU CANE ROAD
LONDON W12 0HS

Titles for oral and poster presentations are welcomed. The abstracts will be published in a forthcoming issue of *The Histochemical Journal*.

For further details of this meeting and instructions for the preparation of abstracts please contact:

Professor J.M. Polak
Department of Histochemistry
Royal Postgraduate Medical School
Hammersmith Hospital
Du Cane Road
London W12 0HS

Closing date for receipt of abstracts: Friday 31st October 1986 (185)M

MISCELLANEOUS

ALL KINDS OF LOANS ARRANGED, INCLUDING ARBITRAGE TRANSACTIONS. ALSO, ALSO, ALSO FINANCIAL/BUSINESS CONSULTANT TRAINEES INVITED:

If you enjoy helping individuals and firms solve their financial and business needs, and at the same time earn yourself unlimited legitimate and conscionable fees for your service in joining lenders and borrowers and business sales together, including arbitrage and barter trading, then this could be the answer to your dreams and ambitions to become financially independent (after we have taught you our system), without disturbing what you are doing now for a living. EVEN WHILE LEARNING TRAINEES WOULD PARTICIPATE 50% in all fees that they initiate and we help close for you; with access to volumes of all U.S. and foreign banks, private funds, venture capitalists, as tools and your own library to arrange each transaction, including how to appraise a business for value and saleability. Earnings based on loans and business transactions up to $1 million$, 10%, thereafter 5%, $1 BILLION & OVER, 2½%. If you wish to have more complete information, you may call or write, in strictest confidence:

DR. LOUIS BATES SORRENTINO, 123 Maple Ave, Montville, CT 06353
U.S. TELEX: 00562 TEL: 203–848–8552
WE ARE THE ONLY (THAT WE KNOW OF) FINANCIAL BUSINESS CONSULTANTS serving borrowers and firms 24 hrs. per day, 365 days per year (8PM – 9AM, recorded service) (NW474)J

APPOINTMENTS WANTED

advertise your qualities and qualifications through the most influential science weekly in the world at a special reduced cost of ***50p per word, minimum 16 words****. (Personal Box Numbers £2).*

Advertisements must be pre-paid and sent to: Nature Classified (Appts Wtd), 4 Little Essex Street, London WC2R 3LF. (890)B

BIOMATHEMATICIAN MAKES your dynamical modelling (temperature, energy, molecules, cells, population, etc) with differential equations and cellular automata. Send your problem for an estimation to: F D, chez Brejnik, 34 gd Rue, B1210 Ferney-voltaire, France. (W3007)B

TASTE OF IMMORTALITY: retired health physicist needs postmenopausal doctor, GP or psychiatrist favoured, for collaborative employment in ultimately grant-aided research towards potent, vital longevity — Box No: 179 c/o Nature, 4 Little Essex Street, London WC2R 3LF. (179)B

Nick Translation Kit from Boehringer Mannheim



the time & money saving alternative

Nick translation kit, Cat. No. 976 776
contains all reagents ready for use for
50 labeling reactions

Get the detailed protocol from your local representative or

mannheim boehringer

Boehringer Mannheim GmbH
Biochemica
P.O. Box 310120
D-6800 Mannheim
W. Germany
Reader Service No.1